ERIODICAL Calif. Univ. S.I.O.
Contributions
1960
1960

UNIVERSITY OF CALIFORNIA
SCRIPPS INSTITUTION OF OCEANOGRAPHY

1961

CONTRIBUTIONS
1960

THE LIBRARY
UNIVERSITY OF CALIFORNIA
SCRIPPS INSTITUTION OF OCEANOGRAPHY
LA JOLLA, CALIFORNIA

PERIODICAL
Calif. Univ.
SIO.
Contributions

1960

DATE OF MAGAZINE	BORROWER'S NAME	TIME DUE
11/3/65		

PERIODICAL

Calif. Univ. SIO
Contributions

1960

LIBRARY
BUR. OF COMM. FISH.
HON. BIOL. LAB.

UNIVERSITY OF CALIFORNIA
SCRIPPS INSTITUTION OF OCEANOGRAPHY

3073

CONTRIBUTIONS
1960

This volume contains contributions from the Scripps Institution of Oceanography which appeared during 1960 in publications other than *Bulletins of the Scripps Institution of Oceanography.*

THE LIBRARY
UNIVERSITY OF CALIFORNIA
SCRIPPS INSTITUTION OF OCEANOGRAPHY
LA JOLLA, CALIFORNIA

June 1961

PHOTOLITHOPRINTED BY CUSHING - MALLOY, INC.
ANN ARBOR, MICHIGAN, UNITED STATES OF AMERICA
1961

UNIVERSITY OF CALIFORNIA
SCRIPPS INSTITUTION OF OCEANOGRAPHY
CONTRIBUTIONS, NEW SERIES
1960

NUMERICAL INDEX

Contrib. Number		Page Number
1139	INMAN, DOUGLAS L. and JEAN H. FILLOUX. Beach cycles related to tide and local wind wave regime. Journal of Geology, v. 68, no. 2, March 1960. pp. 225-231.	1
1140	NORDSTROM, SVANTE G. and THEODORE R. FOLSOM. Suggestion for eliminating pressure effects on protected reversing thermometers. Deep-Sea Research, v. 6, 1960. p. 169. . . .	11
1141	McGOWAN, JOHN A. The relationship of the distribution of the planktonic worm, *Poeobius meseres* Heath, to the water masses of the North Pacific. Deep-Sea Research, v. 6, 1960. pp. 125-139	13
1142	DAWSON, E. YALE, MICHAEL NEUSHUL and ROBERT D. WILDMAN. Seaweeds associated with kelp beds along southern California and northwestern Mexico. Pacific Naturalist, v. 1, no. 14, March 11, 1960. pp. 1-81	29
1143	LAL, DEVENDRA, EDWARD D. GOLDBERG and MINORU KOIDE. Cosmic-ray-produced silicon-32 in nature. Science, v. 131, no. 3397, February 5, 1960. pp. 332-337.	111
1144	RODEN, GUNNAR I. and GORDON W. GROVES. On the statistical prediction of ocean temperatures. Journal of Geophysical Research, v. 65, no. 1, January 1960. pp. 249-263	119
1145	LAL, DEVENDRA and DAVID R. SCHINK. Low background thin-wall flow counters for measuring beta activity of solids. Review of Scientific Instruments, v. 31, no. 4, April 1960. pp. 395-398	135
1146	ROBINSON, MARGARET K. Indian Ocean vertical temperature sections. Deep-Sea Research, v. 6, 1960. pp. 249-258.	139
1147	TALLING, JACK F. Comparative laboratory and field studies of photosynthesis by a marine planktonic diatom. Limnology and Oceanography, v. 5, no. 1, January 1960. pp. 62-77.	149
1148	LASKER, REUBEN. Utilization of organic carbon by a marine crustacean: analysis with carbon-14. Science, v. 131, no. 3407, April 15, 1960. pp. 1098-1100	167
1149	FISHER, ROBERT L. and ROBERT M. NORRIS. Bathymetry and geology of Sala y Gomez, Southeast Pacific. Geological Society of America, Bulletin, v. 71, April 1960. pp. 497-502.	169

Contrib. Number		Page Number
1150	UCHIO, TAKAYASU. Ecology of living benthonic Foraminifera from the San Diego, California, area. Cushman Foundation for Foraminiferal Research, Special publication No. 5, April 20, 1960. pp. 1-72	177
1151	TYLER, JOHN E. Radiance distribution as a function of depth in an underwater environment. Scripps Institution of Oceanography of the University of California, La Jolla, California, Bulletin, v. 7, no. 5, March 18, 1960. pp. 363-412	*
1152	SCHOLANDER, PER F. Oxygen transport through hemoglobin solutions. Science, v. 131, no. 3400, February 26, 1960. pp. 585-590	259
1153	VAN DORN, WILLIAM G. A new long-period wave recorder. Journal of Geophysical Research, v. 65, no. 3, March 1960. pp. 1007-1012	265
1154	GOLDBERG, EDWARD D. and ROBERT H. PARKER. Phosphatized wood from the Pacific sea floor. Geological Society of America, Bulletin, v. 71, May 1960. pp. 631-632	271
1155	EWING, GIFFORD C. and EDWARD D. McALISTER. On the thermal boundary layer of the ocean. Science, v. 131, no. 3410, May 6, 1960. pp. 1374-1376	273
1156	WOOSTER, WARREN S. and GORDON H. VOLKMANN. Indications of deep Pacific circulation from the distribution of properties at five kilometers. Journal of Geophysical Research, v. 65, no. 4, April 1960. pp. 1239-1249	275
1157	JOHNSON, MARTIN W. Production and distribution of larvae of the spiny lobster, *Panulirus interruptus* (Randall) with records on *P. gracilis* Streets. Scripps Institution of Oceanography of the University of California, La Jolla, California, Bulletin, v. 7, no. 6, May 23, 1960. pp. 413-462	*
1158	HUBBS, CARL L., GEORGE S. BIEN and HANS E. SUESS. La Jolla natural radiocarbon measurements. American Journal of Science Radiocarbon Supplement, v. 2, 1960. pp. 197-223	287
1159	VAN ANDEL, TJEERD H. and DAVID M. POOLE. Sources of recent sediments in the northern Gulf of Mexico. Journal of Sedimentary Petrology, v. 30, no. 1, March 1960. pp. 91-122	315
1160	MILLER, ROBERT RUSH and CARL L. HUBBS. The spiny-rayed cyprinid fishes (Plagopterini) of the Colorado River system. Museum of Zoology, University of Michigan, Miscellaneous Publications, No. 115, July 5, 1960. pp. 1-39	347
1161	ARTHUR, ROBERT S. A review of the calculation of ocean currents at the equator. Deep-Sea Research, v. 6, 1960. pp. 287-297	391

---

* Not available for exchange.

Contrib. Number		Page Number
1162	KNAUSS, JOHN A. Measurements of the Cromwell Current. Deep-Sea Research, v. 6, 1960. pp. 265-286	403
1163	ROSENBLATT, RICHARD H. The Atlantic species of the blennioid fish genus *Enneanectes*. Academy of Natural Sciences of Philadelphia, Proceedings, v. 112, no. 1, June 17, 1960. pp. 1-23	425
1164	BODEN, BRIAN P., ELIZABETH M. KAMPA and JAMES M. SNODGRASS. Underwater daylight measurements in the Bay of Biscay. Marine Biological Association of the United Kingdom, Journal, v. 39, 1960. pp. 227-238	451
1165	LANKFORD, ROBERT R. and FRANCIS P. SHEPARD. Facies interpretations in Mississippi Delta borings. Journal of Geology, v. 68, no. 4, July 1960. pp. 408-426.	465
1166	PHLEGER, FRED B. Ecology and distribution of recent Foraminifera. The Johns Hopkins Press, Baltimore, pp. viii, 1-297.	*
1167	RUDNICK, PHILIP. Small signal detection in the DIMUS array. Acoustical Society of America, Journal, v. 32, no. 7, July 1960. pp. 871-877	487
1168	ANDERSON, VICTOR C. Digital array phasing. Acoustical Society of America, Journal, v. 32, no. 7, July 1960. pp. 867-870	495
1169	BALECH, ENRIQUE. The changes in the phytoplankton population off the California coast. California Cooperative Oceanic Fisheries Investigations, Reports v. 7, January 1, 1958-June 30, 1959. pp. 127-132.	499
1170	BERNER, LEO D. Unusual features in the distribution of pelagic tunicates in 1957 and 1958. California Cooperative Oceanic Fisheries Investigations, Reports v. 7, January 1, 1958-June 30, 1959. pp. 133-135	505
1171	BRINTON, EDWARD. Changes in the distribution of euphausiid crustaceans in the region of the California Current. California Cooperative Oceanic Fisheries Investigations, Reports v. 7, January 1, 1958-June 30, 1959. pp. 137-146	509
1172	HUBBS, CARL L. Quaternary paleoclimatology of the Pacific coast of North America. California Cooperative Oceanic Fisheries Investigations, Reports v. 7, January 1, 1958-June 30, 1959. pp. 105-112.	519
1173	JOHNSON, MARTIN W. The offshore drift of larvae of the California spiny lobster *Panulirus interruptus*. California Cooperative Oceanic Fisheries Investigations, Reports v. 7, January 1, 1958-June 30, 1959. pp. 147-161	527

---

* Not available for exchange.

Contrib. Number		Page Number
1174	REID, JOSEPH L., JR. Oceanography of the northeastern Pacific Ocean during the last ten years. California Cooperative Oceanic Fisheries Investigations, Reports v. 7, January 1, 1958-June 30, 1959. pp. 77-90	543
1175	WOOSTER, WARREN S. *El Niño.* California Cooperative Oceanic Fisheries Investigations, Reports v. 7, January 1, 1958-June 30, 1959. pp. 43-45	557
1176	ROBINSON, MARGARET K. Statistical evidence indicating no long-term climatic change in the deep waters of the North and South Pacific Oceans. Journal of Geophysical Research, v. 65, no. 7, July 1960. pp. 2097-2116	561
1177	RASMUSSEN, ROBERT A. Low frequency wave filters employing thermistors. Review of Scientific Instruments, v. 31, no. 7, July 1960. pp. 747-751	581
1178	ECKART, CARL. Variation principles of hydrodynamics. Physics of Fluids, v. 3, no. 3, May-June 1960. pp. 421-427	587
1179	ECKART, CARL H. Hydrodynamics of oceans and atmospheres. Pergamon Press, New York, pp. xi, 1-290	*
1180	PHLEGER, FRED B. Foraminiferal populations in Laguna Madre, Texas. Science Reports, Tohoku University, Sendai, Japan, Second Series (Geology), Special Volume, No. 4 (Hanzawa Memorial Volume), March 1960. pp. 83-91	595
1181	PARKER, FRANCES L. Living planktonic Foraminifera from the equatorial and southeast Pacific. Science Reports, Tohoku University, Sendai, Japan, Second Series (Geology), Special Volume, No. 4 (Hanzawa Memorial Volume), March 1960. pp. 71-82	607
1182	MASON, RONALD G. Geophysical investigations of the sea floor. Liverpool and Manchester Geological Journal, v. 2, part 3, 1960. pp. 389-410	621
1183	ZoBELL, CLAUDE E. Marine pollution problems in the southern California area. Transactions of the Second Seminar on Biological Problems in Water Pollution, April 20-24, 1959. pp. 177-183	645
1184	SHUMWAY, GEORGE A. Sound speed and absorption studies of marine sediments by a resonance method--Parts I and II. Geophysics, v. 25, nos. 2 and 3, April and June, 1960. Part I, pp. 451-467; Part II, pp. 659-682	653
1185	MENARD, HENRY W. Possible pre-Pleistocene deep-sea fans off central California. Geological Society of America, Bulletin, v. 71, August 1960. pp. 1271-1278	697
1186	O'hEOCHA, COLM and FRANCIS T. HAXO. Some atypical algal chromoproteins. Biochimica et Biophysica Acta, v. 41, 1960. pp. 516-520	705

* Not available for exchange.

Contrib. Number — Page Number

1187 LEIGHTON, DAVID L. An abalone lacking respiratory apertures. The Veliger, v. 3, no. 2, October 1960. p. 48 713

1188 KEELING, CHARLES D. The concentration and isotopic abundances of carbon dioxide in the atmosphere. Tellus, v. 12, no. 2, June 1960. pp. 200-203 717

1189 SCHAEFER, MILNER B. New research required in support of radioactive waste disposal. Proceedings of the Scientific Conference on the Disposal of Radio-active Wastes, Monaco, November 16-21, 1959. pp. 265-282 725

1190 MENARD, HENRY W. Consolidated slabs on the floor of the Eastern Pacific. Deep-Sea Research, v. 7, 1960. pp. 35-41 745

1191 KNAUSS, JOHN A. Observations of irregular motion in the open ocean. Deep-Sea Research, v. 7, 1960. pp. 68-69 755

1192 FILLOUX, JEAN H. and GORDON W. GROVES. A seasonal mean sea-level indicator. Deep-Sea Research, v. 7, 1960. pp. 52-60 757

1193 JENNINGS, FEENAN D. and RICHARD A. SCHWARTZLOSE. Measurements of the California Current in March 1958. Deep-Sea Research, v. 7, 1960. pp. 42-47 769

1194 ISAACS, JOHN D. and GEORGE B. SCHICK. Deep-sea free instrument vehicle. Deep-Sea Research, v. 7, 1960. pp. 61-67 775

1195 JANNASCH, HOLGER W. and GALEN E. JONES. *Caulobacter sp.* in sea water. Limnology and Oceanography, v. 5, no. 4, October 1960. pp. 432-433 783

1196 BARTHOLOMEW, GEORGE A. and CARL L. HUBBS. Population growth and seasonal movements of the northern elephant seal, *Mirounga angustirostris*. Mammalia, v. 24, no. 3, September 1960. pp. 313-324 785

1197 CRAIG, HARMON. The thermodynamics of sea water. National Academy of Sciences, Proceedings, v. 46, no. 9, September 1960. pp. 1221-1225 799

1198 ISAACS, JOHN D. and JOHN E. TYLER. On the observation of unresolved surface features of a planet. Astronomical Society of the Pacific, Publications, v. 72, no. 426, June 1960. pp. 159-166 805

1199 SHOR, GEORGE G., JR. Crustal structure of the Hawaiian Ridge near Gardner Pinnacles. Seismological Society of America, Bulletin, v. 50, no. 4, October 1960. pp. 563-573 815

1200 HAXO, FRANCIS T. The wavelength dependence of photosynthesis and the role of accessory pigments. In "Comparative Biochemistry of Photoreactive Systems," edited by Mary Belle Allen, New York, Academic Press 1960. pp. 339-360 827

1201 FOX, DENIS L. Pigments of plant origin in animal phyla. In "Comparative Biochemistry of Photoreactive Systems," edited by Mary Belle Allen, New York, Academic Press 1960. pp. 11-31 . . 851

Contrib. Number		Page Number
1202	SHEPARD, FRANCIS P. Sediment environments of the northwest Gulf of Mexico. Eclogae geologicae Helvetiae, v. 51, no. 3, December 1959. pp. 598-608	873
1203	FOLSOM, THEODORE R., GOVINDARAJU J. MOHANRAO and PERRIN WINCHELL. Fall-out caesium in surface sea water off the California coast (1959-60) by gamma-ray measurements. Nature, v. 187, no. 4736, August 6, 1960. pp. 480-482	885
1204	RODEN, GUNNAR I. On the nonseasonal variations in sea level along the west coast of North America. Journal of Geophysical Research, v. 65, no. 9, September 1960. pp. 2809-2826	891
1205	GOLDBERG, EDWARD D. Chemists and the oceans. Chymia, v. 6, 1960. pp. 162-179	910
1206	VAN DORN, WILLIAM G. A low-frequency microbarograph. Journal of Geophysical Research, v. 65, no. 11, November 1960. pp. 3693-3698	929
1207	MENARD, HENRY W. The East Pacific Rise. Science, v. 132, no. 3441, December 9, 1960. pp. 1737-1746	935
1208	SHEPARD, FRANCIS P. Mississippi Delta: marginal environments, sediments, and growth. In "Recent Sediments, northwest Gulf of Mexico, 1951-1958," edited by F. P. Shepard, F. B. Phleger, and T. H. van Andel, Tulsa, American Association of Petroleum Geologists, 1960. pp. 56-81	*
1209	SHEPARD, FRANCIS P. Rise of sea level along northwest Gulf of Mexico. In "Recent Sediments, northwest Gulf of Mexico, 1951-1958," edited by F. P. Shepard, F. B. Phleger, and T. H. van Andel, Tulsa, American Association of Petroleum Geologists, 1960. pp. 338-344	*
1210	SHEPARD, FRANCIS P. Gulf Coast barriers. In "Recent Sediments, northwest Gulf of Mexico, 1951-1958," edited by F. P. Shepard, F. B. Phleger, and T. H. van Andel, Tulsa, American Association of Petroleum Geologists, 1960. pp. 197-220.	*
1211	SHEPARD, FRANCIS P. and DAVID G. MOORE. Bays of central Texas coast. In "Recent Sediments, northwest Gulf of Mexico, 1951-1958," edited by F. P. Shepard, F. B. Phleger, and T. H. van Andel, Tulsa, American Association of Petroleum Geologists, 1960. pp. 117-152	*
1212	VAN ANDEL, TJEERD H. Sources and dispersion of Holocene sediments, northern Gulf of Mexico. In "Recent Sediments, northwest Gulf of Mexico, 1951-1958," edited by F. P, Shepard, F. B. Phleger, and T. H. van Andel, Tulsa, American Association of Petroleum Geologists, 1960. pp. 34-55	*

---

*Not available for exchange.

Contrib. Number — Page Number

1213 VAN ANDEL, TJEERD H. and JOSEPH R. CURRAY. Regional aspects of modern sedimentation in northern Gulf of Mexico and similar basins, and paleographic significance. In "Recent Sediments, northwest Gulf of Mexico, 1951-1958," edited by F. P. Shepard, F. B. Phleger, and T. H. van Andel, Tulsa, American Association of Petroleum Geologists, 1960. pp. 345-364 . . . . *

1214 CURRAY, JOSEPH R. Sediments and history of Holocene transgression, continental shelf, northwest Gulf of Mexico. In "Recent Sediments, northwest Gulf of Mexico, 1951-1958," edited by F. P. Shepard, F. B. Phleger, and T. H. van Andel, Tulsa, American Association of Petroleum Geologists, 1960. pp. 221-266 . . . . *

1215 THOMAS, WILLIAM H. and ERNEST G. SIMMONS. Phytoplankton production in the Mississippi Delta. In "Recent Sediments, northwest Gulf of Mexico, 1951-1958," edited by F. P. Shepard, F. B. Phleger, and T. H. van Andel, Tulsa, American Association of Petroleum Geologists, 1960. pp. 103-116 . . . . *

1216 PHLEGER, FRED B. Recent sedimentology, northwest Gulf of Mexico; retrospect and prospect. In "Recent Sediments, northwest Gulf of Mexico, 1951-1958," edited by F. P. Shepard, F. B. Phleger, and T. H. van Andel, Tulsa, American Association of Petroleum Geologists, 1960. pp. 365-367 . . . . *

1217 PHLEGER, FRED B. Sedimentary patterns of microfaunas in northern Gulf of Mexico. In "Recent Sediments, northwest Gulf of Mexico, 1951-1958," edited by F. P. Shepard, F. B. Phleger, and T. H. van Andel, Tulsa, American Association of Petroleum Geologists, 1960. pp. 267-301 . . . . *

1218 PARKER, ROBERT H. Ecology and distributional patterns of marine macro-invertebrates, northern Gulf of Mexico. In "Recent Sediments, northwest Gulf of Mexico, 1951-1958," edited by F. P. Shepard, F. B. Phleger, and T. H. van Andel, Tulsa, American Association of Petroleum Geologists, 1960. pp. 302-337 . . . . *

1219 BOWMAN, THOMAS E. The pelagic amphipod genus *Parathemisto* (Hyperiidea : Hyperiidae) in the North Pacific and adjacent Arctic Ocean. United States National Museum, Proceedings, v. 112, no. 3439, 1960. pp. 343-392 945

1220 REID, JOSEPH L., JR. Pacific Ocean. In "McGraw-Hill Encyclopedia of Science and Technology," 1960. pp. 483-488 995

1221 HUBBS, CARL L. and ROBERT RUSH MILLER. *Potamarius*, a new genus of Ariid catfishes from the fresh waters of Middle America. Copeia, no. 2, June 29, 1960. pp. 101-112 1001

1222 WISEMAN, JOHN D. H. and WILLIAM R. RIEDEL. Tertiary sediments from the floor of the Indian Ocean. Deep-Sea Research, v. 7, no. 3, December 1960. pp. 215-217 1017

---

* Not available for exchange.

Contrib. Number — Page Number

1223 RICHARDS, ADRIAN F. Rates of marine erosion of tephra and lava at Isla San Benedicto, Mexico. International Geological Congress, XXI Session, Norden, 1960, Report, Part X, Submarine Geology. pp. 59-64 1021

1224 FAIRBRIDGE, RHODES W. and HARRIS B. STEWART, JR. Alexa Bank, a drowned atoll on the Melanesian Border Plateau. Deep-Sea Research, v. 7, no. 2, October 1960. pp. 100-116 1029

1225 SHOR, GEORGE G., JR. and RUSSELL W. RAITT. Seismic studies in the southern California Continental Borderland. Congreso Geologico Internacional, XXa Sesión, Mexico City, 1956. Sección IX, Geofisica Aplicada, v. 2, 1958. pp. 243-259 . . . 1053

1226 FOX, DENIS L. Perspectives in marine biochemistry. New York Academy of Sciences, Annals, v. 90, article 3, November 17, 1960. pp. 617-621 1073

1227 FOX, DENIS L. and FRANCIS T. HAXO. Pigments and algal commensalism in the blue oceanic siphonophore *Velella lata*. International Congress of Zoology, 15th, London, 16-23 July 1958, Proceedings. Section 3, Marine Zoology. pp. 280-282. 1079

UNIVERSITY OF CALIFORNIA

SCRIPPS INSTITUTION OF OCEANOGRAPHY

CONTRIBUTIONS, NEW SERIES

1960

AUTHOR INDEX

	Contrib. Number	Page Number
ANDERSON, VICTOR C.		
Digital array phasing	1168	495
ARTHUR, ROBERT S.		
A review of the calculation of ocean currents at the equator	1161	391
BALECH, ENRIQUE		
The changes in the phytoplankton population off the California coast	1169	499
BARTHOLOMEW, GEORGE A.		
(with Carl L. Hubbs) Population growth and seasonal movements of the northern elephant seal, *Mirounga angustirostris*	1196	785
BERNER, LEO D.		
Unusual features in the distribution of pelagic tunicates in 1957 and 1958	1170	505
BIEN, GEORGE S.		
(with Carl L. Hubbs and Hans E. Suess) La Jolla natural radiocarbon measurements	1158	287
BODEN, BRIAN P.		
(with Elizabeth M. Kampa and James M. Snodgrass) Underwater daylight measurements in the Bay of Biscay	1164	451
BOWMAN, THOMAS E.		
The pelagic amphipod genus *Parathemisto* (Hyperiidea: Hyperiidae) in the North Pacific and adjacent Arctic Ocean	1219	945
BRINTON, EDWARD		
Changes in the distribution of euphausiid crustaceans in the region of the California Current	1171	509
CRAIG, HARMON		
The thermodynamics of sea water	1197	799
CURRAY, JOSEPH R.		
(with Tjeerd H. Van Andel) Regional aspects of modern sedimentation in northern Gulf of Mexico and similar basins, and paleographic significance	1213	*
Sediments and history of Holocene transgression, continental shelf, northwest Gulf of Mexico	1214	*

* Not available for exchange.

	Contrib. Number	Page Number
DAWSON, E. YALE		
(with Michael Neushul and Robert D. Wildman) Seaweeds associated with kelp beds along southern California and northwestern Mexico	1142	29
ECKART, CARL H.		
Hydrodynamics of oceans and atmospheres	1179	*
Variation principles of hydrodynamics	1178	587
EWING, GIFFORD C.		
(with Edward D. McAlister) On the thermal boundary layer of the ocean	1155	273
FAIRBRIDGE, RHODES W.		
(with Harris B. Stewart, Jr.) Alexa Bank, a drowned atoll on the Melanesian Border Plateau	1224	1029
FILLOUX, JEAN H.		
(with Douglas L. Inman) Beach cycles related to tide and local wind wave regime	1139	1
(with Gordon W. Groves) A seasonal mean sea-level indicator	1192	757
FISHER, ROBERT L.		
(with Robert M. Norris) Bathymetry and geology of Sala y Gomez, Southeast Pacific	1149	169
FOLSOM, THEODORE R.		
(with Govindaraju J. Mohanrao and Perrin Winchell) Fallout caesium in surface sea water off the California coast (1959-60) by gamma-ray measurements	1203	885
(with Svante G. Nordstrom) Suggestion for eliminating pressure effects on protected reversing thermometers	1140	11
FOX, DENIS L.		
Perspectives in marine biochemistry	1226	1073
(with Francis T. Haxo) Pigments and algal commensalism in the blue oceanic siphonophore *Velella lata*	1227	1079
Pigments of plant origin in animal phyla	1201	851
GOLDBERG, EDWARD D.		
Chemists and the oceans	1205	910
(with Devendra Lal and Minoru Koide) Cosmic-ray-produced silicon-32 in nature	1143	111
(with Robert H. Parker) Phosphatized wood from the Pacific sea floor	1154	271
GROVES, GORDON W.		
(with Gunnar I. Roden) On the statistical prediction of ocean temperatures	1144	119
(with Jean H. Filloux) A seasonal mean sea-level indicator	1192	757
HAXO, FRANCIS T.		
(with Denis L. Fox) Pigments and algal commensalism in the blue oceanic siphonophore *Velella lata*	1227	1079
(with Colm O'hEocha) Some atypical algal chromoproteins	1186	705
The wavelength dependence of photosynthesis and the role of accessory pigments	1200	827

*Not available for exchange.

	Contrib. Number	Page Number
HUBBS, CARL L.		
(with George A. Bartholomew) Population growth and seasonal movements of the northern elephant seal, *Mirounga angustirostris*	1196	785
(with Robert Rush Miller) *Potamarius*, a new genus of Ariid catfishes from the fresh waters of Middle America	1221	1001
Quaternary paleoclimatology of the Pacific coast of North America	1172	519
(with George S. Bien and Hans E. Suess) La Jolla natural radiocarbon measurements	1158	287
(with Robert Rush Miller) The spiny-rayed cyprinid fishes (Plagopterini) of the Colorado River system	1160	347
INMAN, DOUGLAS L.		
(with Jean H. Filloux) Beach cycles related to tide and local wind wave regime	1139	1
ISAACS, JOHN D.		
(with George B. Schick) Deep-sea free instrument vehicle	1194	775
(with John E. Tyler) On the observation of unresolved surface features of a planet	1198	805
JANNASCH, HOLGER W.		
(with Galen E. Jones) *Caulobacter sp.* in sea water	1195	783
JENNINGS, FEENAN D.		
(with Richard A. Schwartzlose) Measurements of the California Current in March 1958	1193	769
JOHNSON, MARTIN W.		
The offshore drift of larvae of the California spiny lobster *Panulirus interruptus*	1173	527
Production and distribution of larvae of the spiny lobster, *Panulirus interruptus* (Randall) with records on *P. gracilis* Streets	1157	*
JONES, GALEN E.		
(with Holger W. Jannasch) *Caulobacter sp.* in sea water	1195	783
KAMPA, ELIZABETH M.		
(with Brian P. Boden and James M. Snodgrass) Underwater daylight measurements in the Bay of Biscay	1164	451
KEELING, CHARLES D.		
The concentration and isotopic abundances of carbon dioxide in the atmosphere	1188	717
KNAUSS, JOHN A.		
Measurements of the Cromwell Current	1162	403
Observations of irregular motion in the open ocean	1191	755
KOIDE, MINORU		
(with Devendra Lal and Edward D. Goldberg) Cosmic-ray-produced silicon-32 in nature	1143	111

*Not available for exchange.

	Contrib. Number	Page Number
LAL, DEVENDRA		
(with Edward D. Goldberg and Minoru Koide) Cosmic-ray-produced silicon-32 in nature	1143	111
(with David R. Schink) Low background thin-wall flow counters for measuring beta activity of solids	1145	135
LANKFORD, ROBERT R.		
(with Francis P. Shepard) Facies interpretations in Mississippi Delta borings	1165	465
LASKER, REUBEN		
Utilization of organic carbon by a marine crustacean: analysis with carbon-14	1148	167
LEIGHTON, DAVID L.		
An abalone lacking respiratory apertures	1187	713
McALISTER, EDWARD D.		
(with Gifford C. Ewing) On the thermal boundary layer of the ocean	1155	273
McGOWAN, JOHN A.		
The relationship of the distribution of the planktonic worm, *Poeobius meseres* Heath, to the water masses of the North Pacific	1141	13
MASON, RONALD G.		
Geophysical investigations of the sea floor	1182	621
MENARD, HENRY W.		
Consolidated slabs on the floor of the Eastern Pacific	1190	745
The East Pacific Rise	1207	935
Possible pre-Pleistocene deep-sea fans off central California	1185	697
MILLER, ROBERT RUSH		
(with Carl L. Hubbs) *Potamarius*, a new genus of Ariid catfishes from the fresh waters of Middle America	1221	1001
(with Carl L. Hubbs) The spiny-rayed cyprinid fishes (Plagopterini) of the Colorado River system	1160	347
MOHANRAO, GOVINDARAJU J.		
(with Theodore R. Folsom and Perrin Winchell) Fall-out caesium in surface sea water off the California coast (1959-60) by gamma-ray measurements	1203	885
MOORE, DAVID G.		
(with Francis P. Shepard) Bays of central Texas coast	1211	*
NEUSHUL, MICHAEL		
(with E. Yale Dawson and Robert D. Wildman) Seaweeds associated with kelp beds along southern California and northwestern Mexico	1142	29
NORDSTROM, SVANTE G.		
(with Theodore R. Folsom) Suggestion for eliminating pressure effects on protected reversing thermometers	1140	11

*Not available for exchange.

	Contrib. Number	Page Number
NORRIS, ROBERT M.		
(with Robert L. Fisher) Bathymetry and geology of Sala y Gomez, Southeast Pacific	1149	169
O'hEOCHA, COLM		
(with Francis T. Haxo) Some atypical algal chromoproteins	1186	705
PARKER, FRANCES L.		
Living planktonic Foraminifera from the equatorial and southeast Pacific	1181	607
PARKER, ROBERT H.		
Ecology and distributional patterns of marine macro-invertebrates, northern Gulf of Mexico	1218	*
(with Edward D. Goldberg) Phosphatized wood from the Pacific sea floor	1154	271
PHLEGER, FRED B.		
Ecology and distribution of recent Foraminifera	1166	*
Foraminiferal populations in Laguna Madre, Texas	1180	595
Recent sedimentology, northwest Gulf of Mexico; restospect and prospect	1216	*
Sedimentary patterns of microfaunas in northern Gulf of Mexico	1217	*
POOLE, DAVID M.		
(with Tjeerd H. Van Andel) Sources of recent sediments in the northern Gulf of Mexico)	1159	315
RAITT, RUSSELL W.		
(with George G. Shor, Jr.) Seismic studies in the southern California Continental Borderland	1225	1053
RASMUSSEN, ROBERT A.		
Low frequency wave filters employing thermistors	1177	581
REID, JOSEPH L., JR.		
Oceanography of the northeastern Pacific Ocean during the last ten years	1174	543
Pacific Ocean	1220	995
RICHARDS, ADRIAN F.		
Rates of marine erosion of tephra and lava at Isla San Benedicto, Mexico	1223	1021
RIEDEL, WILLIAM R.		
(with John D. H. Wiseman) Tertiary sediments from the floor of the Indian Ocean	1222	1017
ROBINSON, MARGARET K.		
Indian Ocean vertical temperature sections	1146	139
Statistical evidence indicating no long-term climatic change in the deep waters of the North and South Pacific Oceans	1176	561

---

*Not available for exchange.

	Contrib. Number	Page Number
RODEN, GUNNAR I.		
On the nonseasonal variations in sea level along the west coast of North America	1204	891
(with Gordon W. Groves) On the statistical prediction of ocean temperatures	1144	119
ROSENBLATT, RICHARD H.		
The Atlantic species of the blennioid fish genus *Enneanectes*	1163	425
RUDNICK, PHILIP		
Small signal detection in the DIMUS array	1167	487
SCHAEFER, MILNER B.		
New research required in support of radioactive waste disposal	1189	725
SCHICK, GEORGE B.		
(with John D. Isaacs) Deep-sea free instrument vehicle	1194	775
SCHINK, DAVID R.		
(with Lal Devendra) Low background thin-wall flow counters for measuring beta activity of solids	1145	135
SCHOLANDER, PER F.		
Oxygen transport through hemoglobin solutions	1152	259
SCHWARTZLOSE, RICHARD A.		
(with Feenan D. Jennings) Measurements of the California Current in March 1958	1193	769
SHEPARD, FRANCIS P.		
(with David G. Moore) Bays of central Texas coast	1211	*
(with Robert R. Lankford) Facies interpretations in Mississippi Delta borings	1165	465
Gulf Coast barriers	1210	*
Mississippi Delta: marginal environments, sediments, and growth	1208	*
Rise of sea level along northwest Gulf of Mexico	1209	*
Sediment environments of the northwest Gulf of Mexico	1202	873
SHOR, GEORGE G., JR.		
Crustal structure of the Hawaiian Ridge near Gardner Pinnacles	1199	815
(with Russell W. Raitt) Seismic studies in the southern California Continental Borderland	1225	1053
SHUMWAY, GEORGE A.		
Sound speed and absorption studies of marine sediments by a resonance method--Parts I and II	1184	653
SIMMONS, ERNEST G.		
(with William H. Thomas) Phytoplankton production in the Mississippi Delta	1215	*
SNODGRASS, JAMES M.		
(with Brian P. Boden and Elizabeth M. Kampa) Underwater daylight measurements in the Bay of Biscay	1164	451

* Not available for exchange.

	Contrib. Number	Page Number
STEWART, HARRIS B., JR.		
(with Rhodes W. Fairbridge) Alexa Bank, a drowned atoll on the Melanesian Border Plateau	1224	1029
SUESS, HANS E.		
(with Carl L. Hubbs and George S. Bien) La Jolla natural radiocarbon measurements	1158	287
TALLING, JACK F.		
Comparative laboratory and field studies of photosynthesis by a marine planktonic diatom	1147	149
THOMAS, WILLIAM H.		
(with Ernest G. Simmons) Phytoplankton production in the Mississippi Delta	1215	*
TYLER, JOHN E.		
(with John D. Isaacs) On the observation of unresolved surface features of a planet	1198	805
Radiance distribution as a function of depth in an underwater environment	1151	*
UCHIO, TAKAYASU		
Ecology of living benthonic Foraminifera from the San Diego, California, area	1150	177
VAN ANDEL, TJEERD H.		
(with Joseph R. Curray) Regional aspects of modern sedimentation in northern Gulf of Mexico and similar basins, and paleographic significance	1213	*
Sources and dispersion of Holocene sediments, northern Gulf of Mexico	1212	*
(with David M. Poole) Sources of recent sediments in the northern Gulf of Mexico	1159	315
VAN DORN, WILLIAM G.		
A low-frequency microbarograph	1206	929
A new long-period wave recorder	1153	265
VOLKMANN, GORDON H.		
(with Warren S. Wooster) Indications of deep Pacific circulation from the distribution of properties at five kilometers	1156	275
WILDMAN, ROBERT D.		
(with E. Yale Dawson and Michael Neushul) Seaweeds associated with kelp beds along southern California and northwestern Mexico	1142	29
WINCHELL, PERRIN		
(with Theodore R. Folsom and Govindaraju J. Mohanrao) Fall-out caesium in surface sea water off the California coast (1959-60) by gamma-ray measurements	1203	885
WISEMAN, JOHN D. H.		
(with William R. Riedel) Tertiary sediments from the floor of the Indian Ocean	1222	1017

* Not available for exchange.

	Contrib. Number	Page Number
WOOSTER, WARREN S.		
El Niño	1175	557
(with Gordon H. Volkmann) Indications of deep Pacific circulation from the distribution of properties at five kilometers	1156	275
ZoBELL, CLAUDE E.		
Marine pollution problems in the southern California area	1183	645

Reprinted for private circulation from
THE JOURNAL OF GEOLOGY
Vol. 68, No. 2, March 1960
Copyright 1960 by the University of Chicago
PRINTED IN U.S.A.

BEACH CYCLES RELATED TO TIDE AND LOCAL WIND WAVE REGIME[1]

DOUGLAS L. INMAN AND JEAN FILLOUX
Scripps Institution of Oceanography, La Jolla, California

ABSTRACT

Along portions of the northwestern coast of the Gulf of California the beaches exhibit a fortnightly cycle of erosion and deposition which is related to the combined effects of the tides and the waves generated by the daily "sea breeze." In this area the higher waters of spring tide occur during the early afternoon when the "sea-breeze" regime is strongest. This coincidence of maximum wave intensity during the times of highest water causes the position of the beach berm to follow the elevation of the envelope of the higher high waters in a fortnightly cycle.

A record of the beach cycle is preserved within the beach face by the bands of heavy minerals that are concentrated by wave action at the level of each high water.

INTRODUCTION

The configuration of the beach profile is determined principally by waves that break on the shore and by the tidal fluctuations that cause periodic changes in sea level. Any systematic repetition in either the wave or tidal regime, or a systematic reoccurrence between the wave and tidal regimes will produce a periodic change or cycle in the configuration of the beach. It is well known

---

[1] Contribution from the Scripps Institution of Oceanography of the University of California, new series. Manuscript received September 25, 1959.

Contributions from the Scripps Institution of Oceanography, New Series, 1139
Reproduced by Permission

that a beach cycle related to the seasonal variation in the character and direction of approach of the waves occurs along many coast lines (Shepard, 1950). In general, the beaches build seaward during the small waves of summer and are cut back by high winter storm waves. There are also shorter cycles of beach cut and fill associated with spring and neap tides, although the wave regime, which is usually more important in the ocean, frequently masks the effect of tide on the more exposed portions of the beach face.

An interesting and often very steady wave regime is created by the "sea breeze" which blows onshore during the warm portion of the day. The sea breeze is caused by unequal heating of the air over land and water. During the day when the land is warmer than the sea a pressure gradient which causes an onshore breeze is produced near the coast. The sea-breeze regime is usually best developed in latitudes of 20° to 35° where permanent large-scale circulations such as the trades are less prevalent. The sea breeze commonly sets in during the forenoon and continues into early evening, reaching a maximum velocity during the afternoon. The sea-breeze wave regime, which frequently exhibits an annual and even a semi-annual cycle of intensity, may combine with the tidal periodicity to produce a beach cycle unique to the particular combination of tides and waves. Such cycles exist along any shore when the sea-breeze regime is effective, although they are often masked by the occurrence of other waves.

WINDS, WAVES, AND TIDES AT ESTRELLA BEACH

A daily sea-breeze cycle is characteristic of part of the year in the vicinity of San Felipe along the northeastern coast of the Gulf of California, Mexico. The effect of the sea-breeze waves on the beach profile was observed at Estrella Beach, approximately ten nautical miles southeast of the town of San Felipe during the six-day period from May 21 through May 26, 1959. This area is an excellent laboratory for studying the effect of the sea-breeze wave regime and its relation to the tidal cycle. The reason is that the area is protected from open ocean waves by the peninsula of Baja California, thus assuring that the waves are of local origin; and the area has a large tidal range so that the effect of the diurnal cycle of wave intensity is easily separated and observed on the beach profile. Also, the area is protected from the northwest winds by a mountain range of 5,000–10,000-ft. elevation, thus favoring the development of a strong sea-breeze regime (fig. 1).

The tidal regime at Estrella Beach is such that the higher high waters of spring tide occur during the early afternoon when the sea-breeze circulation is strongest. This coincidence of maximum wave intensity during the times of highest water causes the beach to exhibit a fortnightly cycle which is dependent upon the elevation of the envelope of the higher high waters. Also, the highest spring tides exhibit a semi-annual cycle such that the highest waters occur near the times of the winter and summer solstice. The reoccurrence of higher high spring waters during the same portion of the day is characteristic of areas where the solar constituents of the tide are significant—a situation which casual inspection indicates is almost general. However, the relation between maximum sea-breeze intensity and the occurrence of higher high water may vary anywhere from full coincidence, as is the case at Estrella Beach, to perfect opposition.

In the vicinity of Estrella Beach the tide has a pronounced diurnal inequality with a maximum diurnal range of about 23 ft. during spring tides. At the time of observations the lower low water directly preceded the occurrence of higher high water, and the height of the higher high water exceeded that of the lower high water by about 5 ft. (fig. 2).

During the observations of May, 1959, the sea breeze in the vicinity of Estrella Beach was usually first observed about 0900, blowing from the northeast (60°) with a velocity of about 6 knots. The direction of approach of the winds rotated in a clockwise direction until about 1400, when the breeze

(2)

reached a maximum velocity of about 15 knots, blowing from the east-southeast (115°). After about 1600 the breeze died rapidly, reaching a calm by 1800. A similar cycle was repeated each day (table 1).

The sea breeze generated waves which on the average reached a maximum significant wave height of about 2 ft. with a period of 3 to 4 seconds. The highest waves observed were about 2½ ft. high and were generated by a 23-knot sea breeze on May 22, which coincided with the time of higher high water of spring tide.

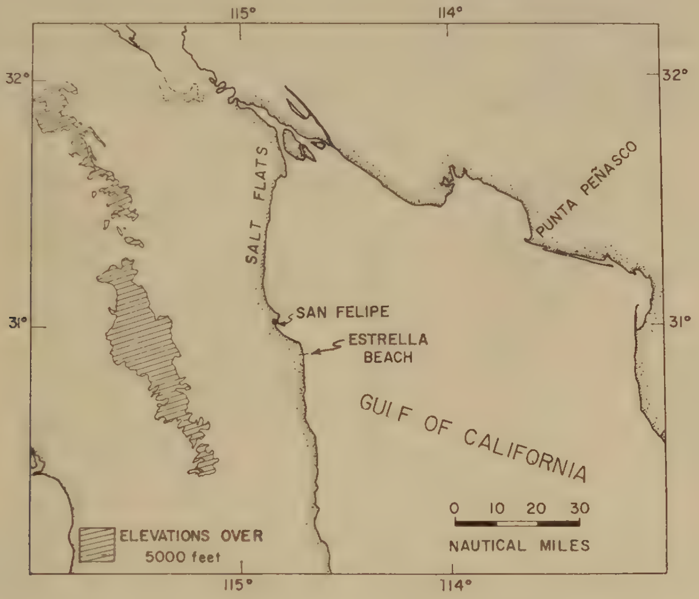

FIG. 1.—Location map giving position of the beach profiles shown in figs. 2 and 3

BEACH CYCLES

The foreshore profile at Estrella Beach is characterized by a relatively steep beach face, which terminates abruptly on a broad low tide terrace (fig. 2). The pronounced discontinuity at the toe of the beach face and the wide low-tide terrace are typical of coast lines where the tidal range is large compared with the wave height. The beach face has a slope of 1:7 and rises about 25 ft. above the low-tide terrace, which extends 4,500 ft. seaward from the toe of the beach face and terminates in an outer bar at a depth of about 10 ft. below mean sea level. Offshore from the bar the sandy bottom has a seaward slope of about 1:20 out to depths of about 30 ft., where the slope becomes gentle. The beach is composed of coarse to medium quartz sand which is derived principally from the extensive fans that slope down from the mountains to the west. The sand on the beach face is a well-sorted coarse sand with a medium diameter of about 700 microns. The sand on the low-tide terrace is coarse and poorly sorted, while the outer bar is composed of fine sand.

Because a brief still-stand in the water level occurs at high and low waters, the energy of the wave action becomes concentrated at these levels. The extreme levels represented by the higher high waters and lower low waters of the spring tides are represented, respectively, by the higher berm crest on the beach face and by the bar at the seaward edge of the low-tide terrace. Near each high water level the waves tend to form a miniature beach or step, complete with berm crest, face, and terrace. The ma-

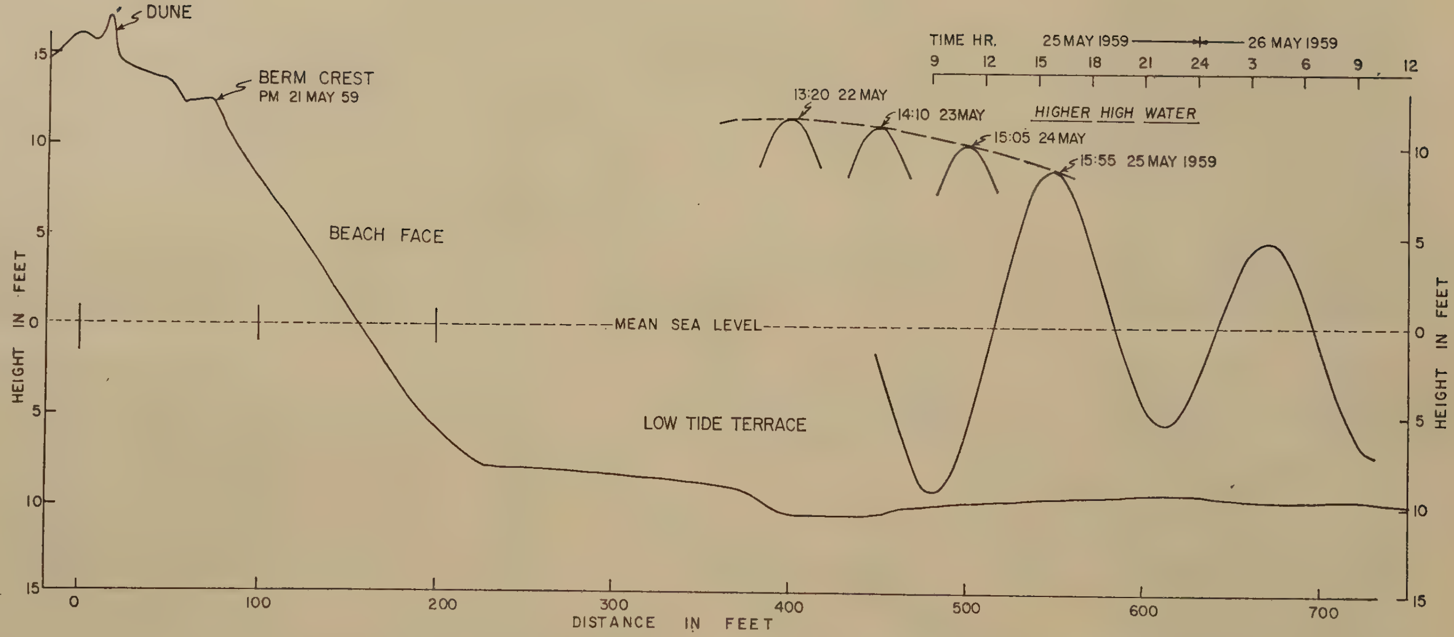

Fig. 2.—Profile of Estrella Beach showing a tidal cycle and the level of higher high water on four consecutive days

terial excavated by the breaking waves is partly carried seaward to form the terrace and partly carried on shore to the level of the maximum run-up to form the crest of the transient beach profile. The extent to which the beach is modified depends upon the intensity of the wave action and the level of the water. The beach face is continually modified and re-sorted by the action of waves superimposed on the rhythmic fluctuations of the tide. The effect of the waves is most dramatic when the water level is near the crest of the beach, because the beach frequently has a slight backslope so that there is no sand above to fill the excavation caused by the waves. The waves are less effective in modifying the mid-sections of the beach face, and the berm crest formed there is less obvious because it tends to merge with the general seaward slope of the beach face.

TABLE 1

TYPICAL DAILY WIND AND WAVE CONDITIONS, MAY 21–26, 1959

	WIND DATA		WAVE DATA		
HOUR	Direction (degrees)	Velocity (knots)	Height (feet)	Period (seconds)	Breaker Angle
0......	Calm		Low	..	....
3......	330	3	Low	..	....
6......	330	3	Low	..	....
9......	60	6	½	1½	5° open S
12......	110	10	1	3	5° open N
14......	115	15	2	4	15° open N
16......	110	10	2	4½	20° open N
18......	Calm		1½	5	15° open N
20......	Calm		Low	..	....
24......	Calm		Low	..	....

The combined effect of the sea-breeze waves and the tide in modifying the beach is shown by the comparisons of the beach profile on five consecutive days (fig. 3). The first profile, that of May 21, 1959, shows the beach configuration resulting from the waves and high water on the day preceding the highest spring water. The high water level on this day was about 11.0 ft. above mean sea level, and the profile shows a slight concavity or terrace at that level, with a pronounced berm thrown up to a height of 12.6 ft. above MSL by the run-up of the waves. On the following day, May 22, the high water level reached its maximum spring elevation of 11.4 ft. MSL. The combination of highest water and the 2½-ft. high sea-breeze waves which overtopped the crest of the berm caused a pronounced terracing centered around the high water level. The waves produced an erosion extending over a horizontal distance of 50 ft. and caused an excavation up to 2 ft. deep under the previous berm crest. A comparison of the profiles for these days shows that the sand eroded from the upper beach face was distributed in a layer averaging 0.4 ft. thick over the lower 90 ft. of the beach face, extending from 9 ft. above mean sea level to 5 ft. below, where the two profiles merge (fig. 3).

The profiles on the two days following highest spring water (May 23 and 24) show a progressive migration of the sands from the lower foreshore face back to the upper, until about two-thirds of the total eroded volume has been replaced. Also by the second day (May 24) the beach in the vicinity of high water level had built out so that the slope of the beach is again approaching its maximum equilibrium steepness of about 1:7 or 8.3°. The water level on succeeding days (May 25) was too low to aid in further berm building, and the action of the waves merely resulted in a slight concavity or terrace near the high water level. The elevation of the small terrace tends to follow the envelope of the higher high water level.

As the tidal range continues to decrease with the approach of the neap tides, the water level becomes more concentrated around mean sea level, and the waves expend their energy near the mid-portion of the beach. However, the occurrence of high water is no longer in phase with the time of occurrence of the maximum sea breeze during neap tides, so that the energy of the waves is not concentrated at a position of still-stand but is distributed over a wider section of beach; hence the waves tend to produce less striking changes in the beach profiles during neap tides. With the approach of the succeeding spring tides, the relation between the maximum sea-breeze intensity and the occurrence of higher high water again approaches full coincidence and the beach cycle approaches completion. The cycle is completed when the sea-breeze waves, riding on the envelope of the rising tide, finally overtop the highest berm and thus produce the maximum terracing on the upper beach face, which heralds the beginning of a new cycle.

HEAVY MINERAL BANDS IN THE BEACH FACE

The quartz sand in the vicinity of Estrella Beach contains about 5 per cent heavy minerals, principally of the amphibole and pyroxene groups, with some olivine. These heavy minerals have a specific gravity aver-

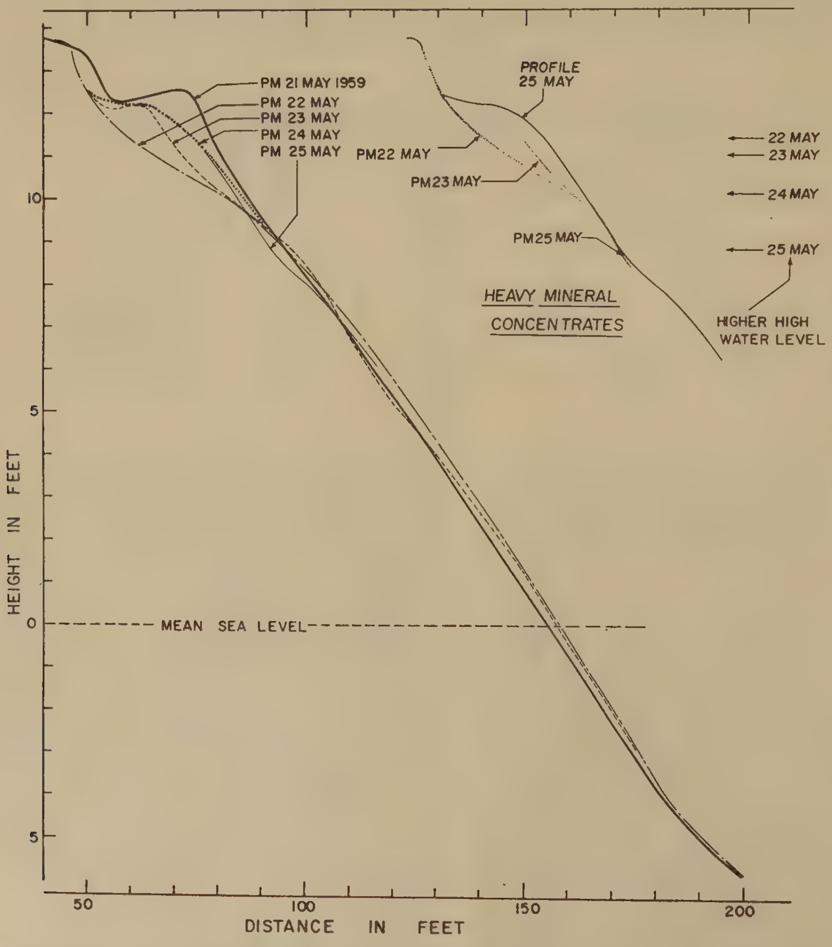

FIG. 3.—Comparison of beach profiles on five consecutive days at Estrella Beach. Each survey was made following the occurrence of higher high water. A photograph of the heavy mineral band formed on May 22, 1959, is shown in plate 1.

(6)

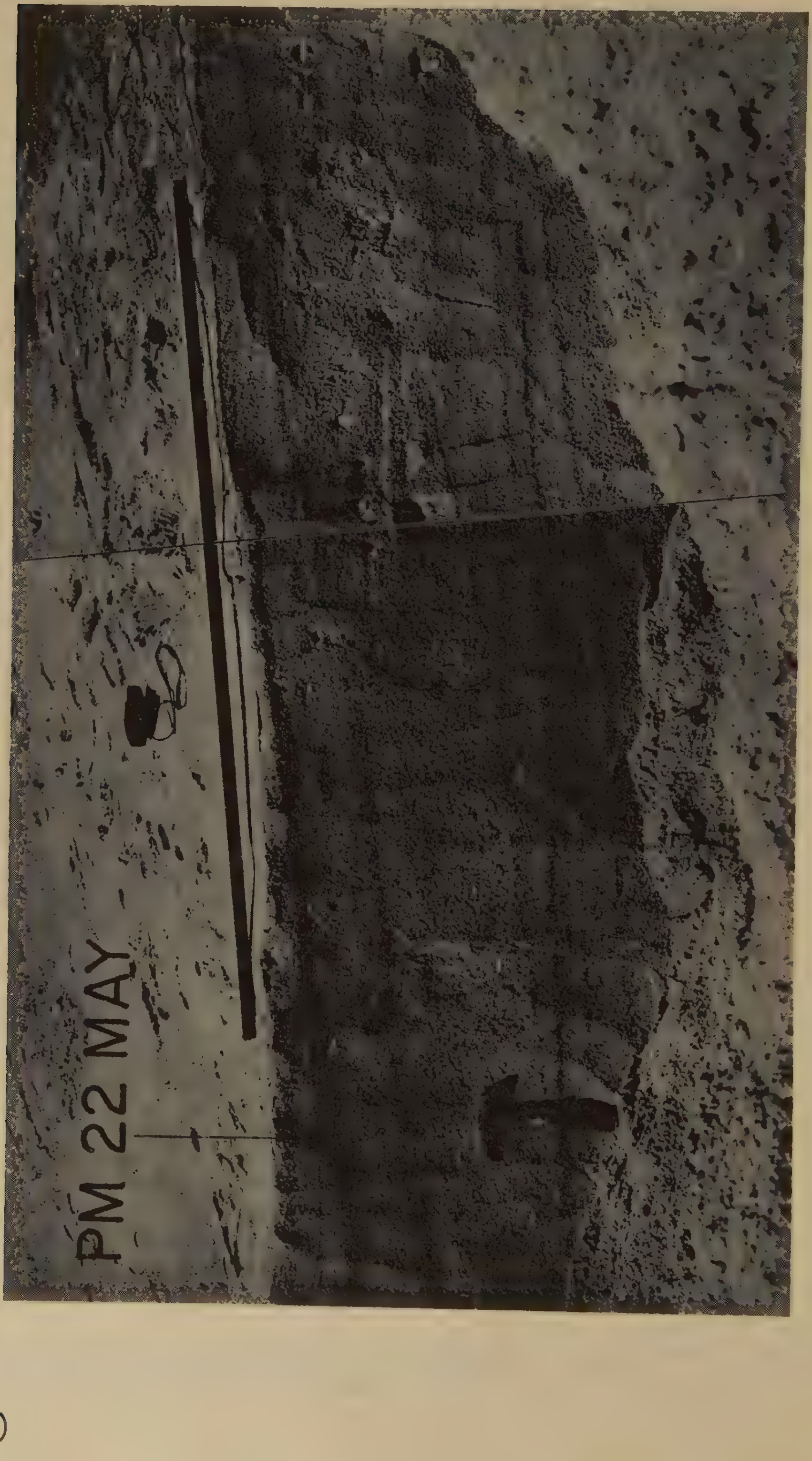

Beach face, Estrella Beach

aging about 3.2 as compared with 2.65 for quartz. In addition to being more dense than quartz, the heavy minerals are somewhat smaller and are mostly dark in color. The heavy and light minerals are easily distinguished from each other in the field on the basis of their color and size.

The smaller heavy minerals settle with approximately the same velocity as the quartz particles; however, the heavy and light minerals behave in a very different manner when moved as bed load. Because of their smaller size and higher density, the heavy minerals naturally migrate deeper into the beach face whenever the sand is stirred or when one layer of sand rolls or slides over another. Also, the larger, lighter quartz grains are more easily rolled or placed in suspension and are thus more easily transported. As a result of their greater susceptibility to transport, the quartz particles are moved back and forth with the cycles of erosion and deposition, while the heavy minerals become concentrated in bands within the beach face (Inman, 1953, p. 37). The relative positions of the bands of heavy minerals provide a record of the beach cycles that is preserved within the beach face. The thickness of the heavy mineral band is a measure of the amount and intensity of erosion.

The nature and distribution of the heavy mineral bands formed at Estrella Beach and their relation to the beach cycles are shown in figure 3 and plate 1. The widest and most extensive band of heavy minerals formed on May 22 as a result of the extensive terracing when the waves overtopped and eroded the berm. Portions of this band were buried and preserved by the deposition associated with the subsiding lower tides. The heavy mineral band formed on May 23 was comparatively thin because the waves accompanying this tide resulted predominantly in accretion. The heavy concentrate marking the still-stand for the high water of May 24 was undercut and caused to merge with that of May 25 because they occurred on the steeper portions of the beach face. Following the terracing and formation of a heavy mineral band on the steeper portion of the beach face, the run-up of the waves riding on the receding tide covers the lower portion with sand so that the bands dip seaward and into the beach face, as illustrated by the concentration of May 25 (fig. 3).

Acknowledgments.—This study was sponsored by the Office of Naval Research and by the American Petroleum Institute, Project 51, under contract with the University of California. The writers express their appreciation to F. P. Shepard and R. S. Arthur for their suggestions and careful reading of the manuscript; to Paul Fleischer, Earl Murray, Wendell Gayman, and the other members of the Oceanography 223 class for their aid in the field; and to Helene Flanders for assistance in the laboratory.

REFERENCES CITED

Inman, D. L., 1953 Areal and seasonal variations in beach and nearshore sediments at La Jolla, California: *Beach Erosion Board, Corps of Engineers*, Tech. Memo. 39.

Shepard, F. P., 1950, Beach cycles in Southern California: *Beach Erosion Board, Corps of Engineers*, Tech. Memo. 20.

PLATE 1

Photograph of heavy mineral bands in the beach face at Estrella Beach. Refer to fig. 3. Scale is 6 ft. long; the right end is 50 ft. from survey "O"; left end is down slope and toward the Gulf. Lower heavy mineral bands repesent previous beach cycles.

(9)

Deep-Sea Research, 1960, Vol. 6, p. 169 Pergamon Press Ltd., London. Printed in Great Britain

INSTRUMENTAL NOTE

Suggestion for eliminating pressure effects on protected reversing thermometers

(*Received* 22 *June* 1959)

It was pointed out recently (Folsom *et al.*, 1959) that present day reversing thermometers appear to be not entirely ' protected ' from the effects of external hydrostatic pressure, and that a correction for the error due to pressure should be considered whenever very precise measurements are to be made at great sea depths. Reasons were given for expecting an average modern protected thermometer to indicate temperatures too high by about 0·002°C for each 1000 m increase in depth ; and it was shown that certain instruments, those overfilled with mercury and those designed with too small an air volume below the cork, could deviate because of pressure by as much as 0·008°C per 1000 m depth change.

The rate of change of apparent temperature with depth varies with the depth ; it is greatest for large depths. Its numerical magnitude depends upon difficult-to-measure details of construction, and it would be difficult to compute for any completed thermometer. Rather elaborate equipment would be required to determine this correction in the laboratory ; however, it might be determined or compensated for at sea by making two successive casts with instruments transposed as to depth. The latter procedure would result also in a precise measurement of the temperature gradient ; it is perhaps only in gradient determinations in very deep water that individual reversing thermometers must be corrected for pressure effects.

It is apparent that some slight changes in the construction of the protected thermometers would diminish the pressure error by at least one order of magnitude, making it insignificant for all oceanographic purposes. In the present instrument, the sea pressure is able to increase the pressure in the small volume of air confined below the cork by an appreciable fraction, because the mercury displaced by the decrease in the whole lower portion of the external shell crowds into this small air space. Obviously, means should be sought for increasing the ratio of the volume confining air to the deformable volume. It is clear that a gas communication through the cork would provide a suitable means, because of the large space above the cork. A simple, open tube through the cork might be sufficient; and the pouring of mercury through this opening when the instrument was upset should not lead to serious new objections. Of course, the present brass fittings would have to be replaced by fittings resistant to mercury.

A much neater solution would be afforded should the maker pierce the present cork with a tube capped at the lower end, or filled with ordinary sintered glass of a pore-size allowing air to pass readily but permitting no mercury passage under the pressures involved here. It would appear that this would add only a few minutes more construction time and might even facilitate the overall manufacture and calibration since it would decrease the likelihood of a slow change in calibration due to diffusion of confined air through the cork.

Scripps Institution of Oceanography
University of California
La Jolla, California

S. G. Nordstrom*
T. R. Folsom

REFERENCE

Folsom T. R., Jennings F. D. and Schwartzlose R. A. (1959) Effect of pressure upon the ' protected ' oceanographic reversing thermometer. *Deep-Sea Res.* 5, 306.

---

*Helsinki, Finland. UNESCO Fellow to Scripps Institution of Oceanography 1958-59.

Printed in Great Britain by The Salisbury Press Ltd., Publicity House, Wilton Road, Salisbury, Wilts. (20256)
ributions from the Scripps Institution of Oceanography, New Series, 1140
Reproduced by Permission

Deep-Sea Research, 1960, Vol. 6, pp. 125 to 139. Pergamon Press Ltd., London. Printed in Great Britain

The relationship of the distribution of the planktonic worm, *Poeobius meseres* Heath, to the water masses of the North Pacific

JOHN A. McGOWAN

(*Received 5 January* 1959)

Abstract—The distribution of a planktonic worm, *Poeobius meseres* HEATH, was determined from an examination of over 1800 quantitative plankton tows taken in the North and South Pacific. This distribution is compared with the distribution of water masses, as defined by temperature-salinity curves. Since the water mass concept involves a three dimensional unit of the ocean, its use in describing the environment of an animal whose distribution is also three dimensional, is preferable to the method of comparing plankton distributions with horizontal isotherms or isohalines.

The distribution of *Poeobius* coincides, for the most part, with that of the Subarctic water mass and the transition region of Subarctic water, the California Current. However, a few specimens were found in the eastern tropical Pacific. A satisfactory explanation for its restricted presence in this latter area is not possible at this time, but there is some evidence to indicate that this southern segment of the population is not endemic but has been carried in from the north. If this is true, then the occurrence of *Poeobius* here must be accounted for in considering the sources of the Intermediate water of the area.

INTRODUCTION

THE environment of most oceanic, zooplanktonic species is generally described in terms of the temperature and salinity ranges to which the animals seem limited. But because zooplankton is distributed three-dimensionally it is frequently difficult to relate the overall horizontal distributions of species to the horizontal distributions of temperature or salinity limits. However, with the development of the water mass concept (HELLAND-HANSEN 1916, SVERDRUP *et al.*, 1942) it has become possible to relate the distributions of species to that of water masses. It is the purpose of this paper to present the distribution of a pelagic organism, *Poeobius meseres* HEATH (1930), and to compare it with the distribution of a water mass.

Poeobius meseres, a small, transparent, planktonic animal ranging in length up to 27 mm, was originally described by HEATH (1930) from Monterey Bay, California. He obtained specimens from a plankton sample taken from a depth of approximately 350 m. HEATH suggested that *Poeobius* was " a connecting link between the Annelida and the Echiuroida." Although Remane (see PICKFORD, 1947) considered it to be an echiuroid, FISHER (1946) excluded it from that Phylum. PICKFORD (1947), after an intensive study of the anatomy and histology of *Poeobius*, came to the conclusion that it was an aberrant Polychaete. Both HEATH and PICKFORD were concerned primarily wth the phylogenetic status of this strange worm, and virtually nothing is known of its ecology and life history. The only information available on the distribution of *Poeobius* is the statement by PICKFORD (1947) that " Pelagic in habit, it has been taken from moderate depths off the coasts of California and in Alaskan waters," the report by BOGOROV (1955) of its occurrence in the North-west Pacific (position not given) and HARTMAN'S (1955) report that " *Poeobius meseres* is known only from the northern Pacific."

Contributions from the Scripps Institution of Oceanography, New Series, 1141
Reproduced by Permission

During the analysis of over 1800 plankton samples taken in the Pacific by the Scripps Institution of Oceanography, the occurrence of *Poeobius* was recorded. These observations were then compared with hydrographic data which had been taken at the same time and place. This comparison revealed that the distribution of *Poeobius* generally coincided with the distribution of the Subarctic Water Mass.

METHODS

The plankton samples used in this study came from several different cruises and expeditions (Fig. 1, Table 1). The routine sampling done by the California Co-operative Oceanic Fisheries Investigations (C.C.O.F.I.), served as a model for all of these cruises

Table 1. Plankton samples used in this study

Expeditions Scripps Institution of Oceanography	*Date*	*Number of tows*	*Depth of tows* (m)
Mid-Pacific	1950	6 12	0-100 0-1000 or greater
Northern Holiday	1951	55 21 trawls (not used in this study)	0-140
Shellback	1952	203 15 trawls	0-300 0-1000 or greater
Capricorn	1953	35	0-140; 0-400; 0-1000
Trans-Pacific	1953	143 135 38 12 16 4 trawls	0-150 150-300 300-450 450-600 0-1000 0-2000 or greater
Troll	1955	85	0-300
EQUAPAC	1956	89	0-280
PAS	1954	14 12 14 13 20 10 12	0-25 25-50 50-75 75-100 100-300 300-500 500-700
CCOFI	1950 to 1954	532 (used in this study)	0-140
CCOFI	1950	8	0-400
Nor-Pac	1955	162 30 20	0-140 140-280 0-700
Downwind	1957	162 30 20 12	0-140 140-280 0-560 0-700 or greater
Tage (Hopkins Marine Sta.)	1951-1952	8	0-700 or greater

and expeditions (Ahlstrom, 1954). The vertical distribution of *Poeobius* was determined, for the most part, from the results of hauls made with an opening-closing net, one metre in diameter, adapted from that described by Leavitt (1935, 1938). This net may be towed obliquely and opened and closed at any desired depth. Occasionally a number of these nets were used in series along a cable, thus sampling several strata simultaneously (Fig. 2).

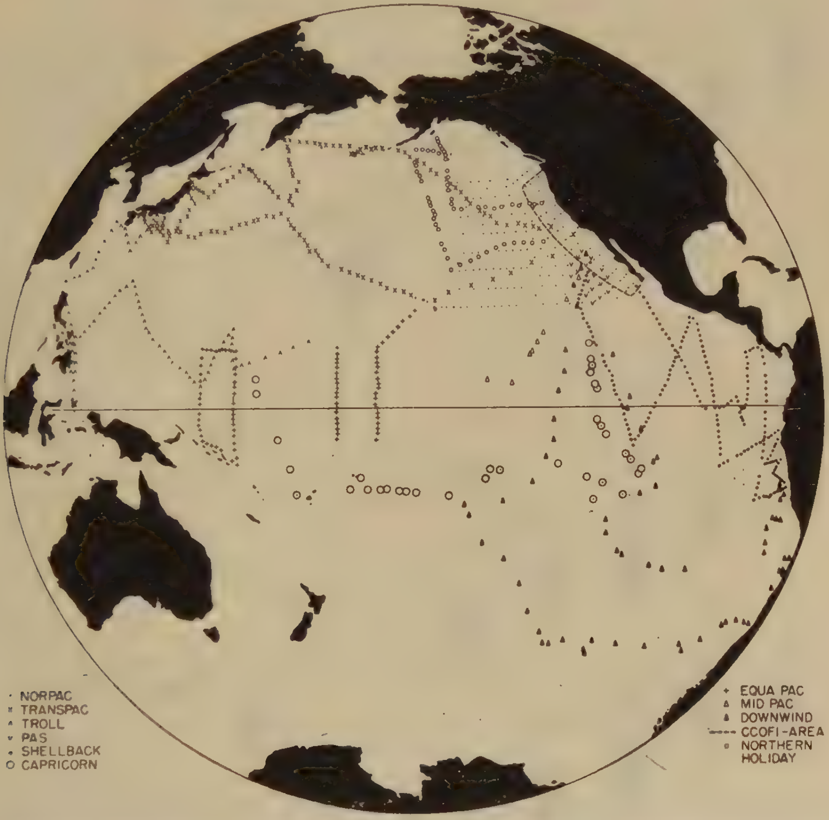

Fig. 1. Scripps expeditions in the North Pacific. Quantitative plankton hauls were taken on every station shown.

DISTRIBUTION

(1) *Geographic distribution*

The greatest density of *Poeobius* was found in the North Pacific in the region of the Oyashio and Subarctic current. Although Dales (1957) did not find it in the surface waters (0-70 m) of the California Current, it does occur at intermediate depths (400 m or greater) in this current and also in the eastern-most part of the tropical Pacific but in greatly decreased numbers (Fig. 3). It is probably present in the Gulf of Alaska but few samples have been taken from that region. *Poeobius* did not occur in any of the 298 plankton hauls taken from the upper 700 m of the

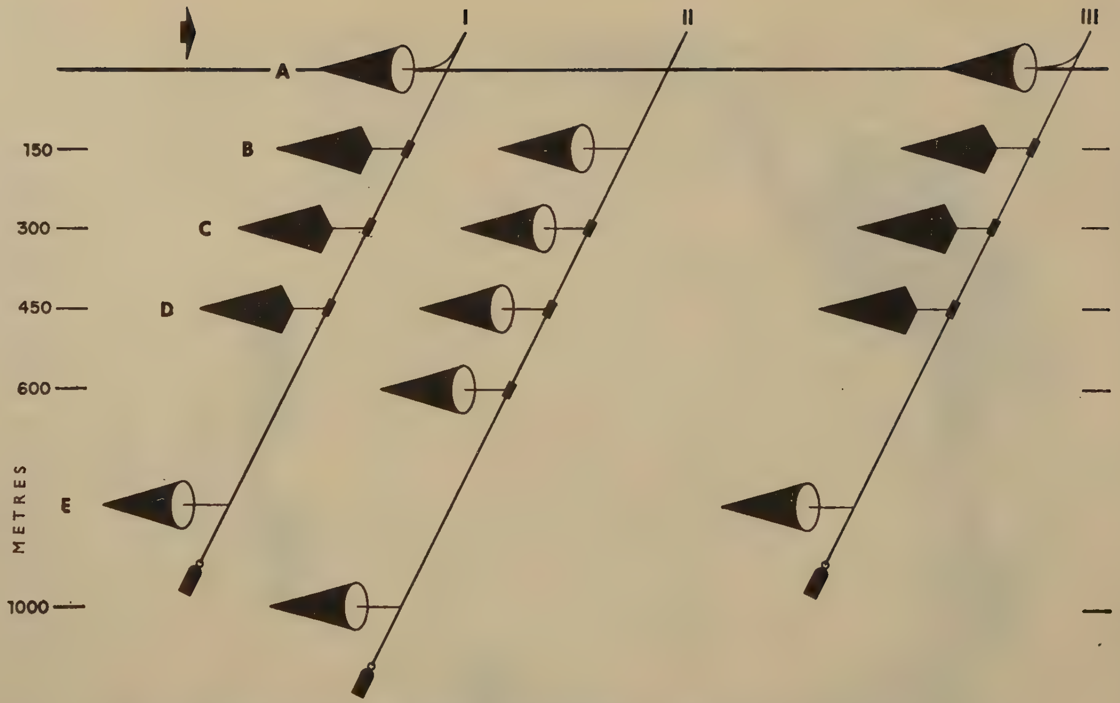

Fig. 2. Diagram illustrating an opening-closing series as taken on the Trans-Pacific Expedition. Nets A and E were standard, quantitative nets. Nets B, C, and D were opening-closing nets. A 600 lb weight was attached to the bottom of the wire. At 1, just before net A entered the water a messenger was sent down to open nets B, C, and D, then the entire series was lowered 150 m (point II). Between points II and III the series was raised 75 m and towed at that depth for approximately 20 minutes. At point III the series was raised another 75 m, net A was removed from the water and a second messenger was sent down to close nets B, C, and D. The entire series was then removed from the water. Nets A, B, C, and D each fished a stratum 150 m thick while net E fished from the surface to depths of 1000 m or more. The ship maintained a speed of 1-1·5 knots during these tows. The entire procedure took approximately 2 hr.

Eastern or Western North Pacific Central waters, nor did Johnson (1956) record it as being present in the Beaufort or Chukchi seas. It apparently does not exist in any other oceans of the world.

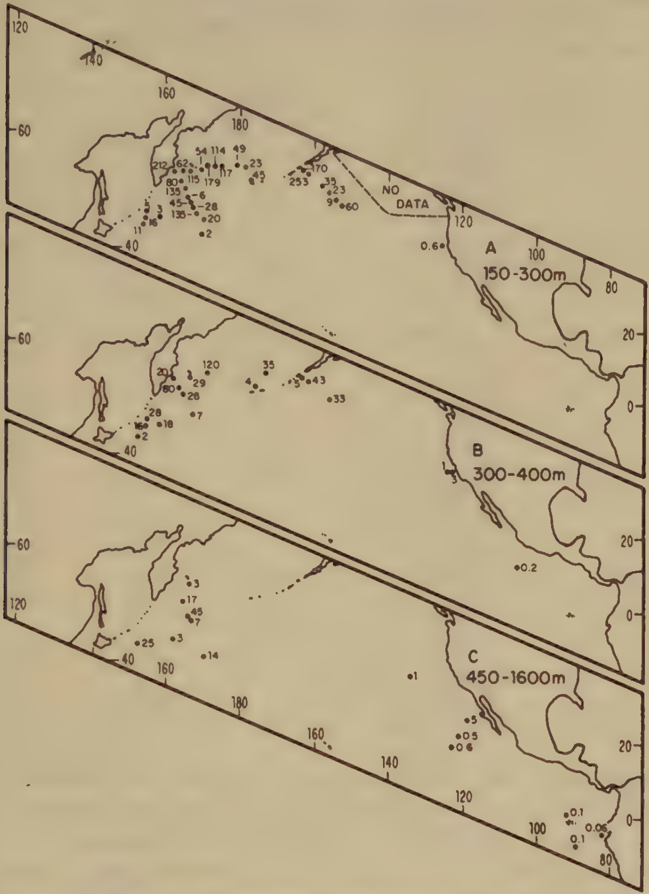
120
140
160
180
60
40
212
62
54
114
49
23
45
117
179
115
80
135
6
45
28
135
20
2
5
3
16
11
170
253
35
23
9
60
NO DATA
120
0.6
A
100
150-300m
80
20
0
60
120
29
28
7
28
16
18
2
40
35
4
5
43
33
B
300-400m
20
0.2
0
60
120
3
17
45
7
25
3
14
40
160
1
C
450-1600m
5
0.5
0.6
20
180
160
140
120
100
0.1
0.06
0.1
0
80

Fig. 3. The geographical distribution of *Poeobius*. The numbers of organisms per 1000 m^3 of water filtered by the net are shown for three strata : A, 150-300 m ; B, 300-450 ; C, 450-1600 m. By increasing the depth of tow, the range is extended to the south in the eastern Pacific, and the abundance of *Poeobius* decreases.

(II) *Vertical distribution*

The opening-closing net tows taken on the Trans-Pacific Expedition show that in its area of greatest abundance in the Oyashio and Subarctic current, *Poeobius* is most commonly found at depths ranging from 150 to 300 m (Table 2 and Fig. 6). Although no systematic use of the opening-closing net has been made in the California Current, the area has been intensively sampled with open, quantitative, one-metre nets towed at various depths (U.S. Fish and Wildlife Service, 1954). In the northern part of this region (Tables 1 and 3), *Poeobius* was found only in those tows that went to a depth of 400 m or more ; in the southern part, which was covered by the Pelagic

Area Studies (P.A.S.) survey (Fig. 1), *Poeobius* was found only at depths of 700 m or more. South of 20° N in the eastern tropical Pacific* it was found, with one exception, only in trawls that reached depths of 1000 m or more (Fig. 3). The exception was the capture of two individuals at a depth of 300 m near Shellback Station 207 (Table 3). WOOSTER and CROMWELL (1958, p. 178) have pointed out that this area near the northern boundary of the Equatorial Countercurrent is characterized by very shallow thermoclines.

Table 2. Selected Trans-Pacific Expedition opening-closing series, showing depth and temperature range of Poeobius

Station	*Depth of tow* (m)	*Numbers per* 1000 m³	*Temperature range* (°C)
25 A	0-150	0	3·5-11·2
B	150-300	170	4·0-4·3
C	300-450	5	3·7-4·0
D	450-600	5	3·4-3·7
40 A	0-150	0	1·4-9·1
B	150-300	179	3·25-3·6
C	300-450	120	3·3-3·6
D	450-600	0	3·1-3·3
42 A	0-150	0	0·6-9·2
B	150-300	115	0·9-3·6
C	300-450	29	3·4-3·6
D	450-600	0	3·1-3·4
46 A	0-150	0	0·7-9·9
B	150-300	135	3·1-3·35
C	300-450	28	3·2-3·4
D	450-600	17	3·0-3·25
48 A	0-25	0	9·2-9·7
B	25-100	0	1·3-9·3
C	35-115	0	1·3-7·0
D	140-320	40	1·7-3 6
59 A	0-150	0	5·6-14·65
B	150-300	0	4·1-5·55
C	300-450	0	3·8-4·1
D	450-600	3	3·55-3·8

Relationship of Poeobius *distribution to water masses*

The water in the top 1000 m north of 45° N in the Pacific has been called the Subarctic Water Mass (SVERDRUP *et al.*, 1942, p. 712). It is generally believed that this water originates mostly from the Oyashio with some slight mixing with water from the Kuroshio Extension. As this Subarctic water approaches the North American continent it splits, some moving northward to form the Gulf of Alaska Gyre, the rest moving southward as the California Current. The temperature-salinity relationship gradually changes as the water moves south and by the time the California Current begins to turn south-west at about 25° N latitude, becoming part of the North

---

* WOOSTER and CROMWELL (1958) have defined this area as " the region lying between the Tropic of Cancer (23° 27′ N) and the Tropic of Capricorn (23° 27′ S) and extending westward from the coast of Central and South America to 130° W.

Equatorial Current (Reid *et al.*, 1958), mixing has considerably altered its properties. Ninety-seven per cent of all *Poeobius* caught were in hauls taken in the area of the Subarctic Water Mass (Fig. 4). Temperature-salinity curves based on data taken at these stations where the depth of *Poeobius* capture was known, fell generally within the range of curves characteristic of this water mass (Fig. 5). Those few curves which fell outside this range were from stations on the edge of the *Poeobius* distribution, and even these curves indicate the presence of a certain amount of Subarctic water. Further evidence that *Poeobius* resides primarily in Subarctic Water is the finding, based on the results of the Trans-Pacific Expedition, that *Poeobius* disappeared abruptly from the plankton when the relatively sharp physical boundaries were crossed from Subarctic to Central waters (Figs. 6 and 7). On the other hand, in the areas where there is a gradual change of properties from the Subarctic Water to the California Current, the numbers of *Poeobius* decreased gradually (Fig. 3).

Table 3. All Poeobius *records excepting the Trans-Pacific Expedition, the Norpac Expedition, and those reported by* PICKFORD (1947)

Cruise station	*Position*	*Date*	*Depth of haul* (m)	*Numbers of organisms caught*	*Water filtered by net* (m^3)
CCOFI 5201 137·40	25° 00′N 113° 25·5′W	1-52	0-147	1	444
CCOFI 5004 47·55	40° 04′N 124° 55′W	4-50	0-421	1	1668
CCOFI 5004 60·70	37° 17′N 124° 21′W	4-50	0-423	3	1945
N. H.	53° 34·5′N 155° 00′W	8-51	0-1200	several	—
Tage 248-B	Monterey Bay	9-52	0-740	25	4721
Tage 242-B	Monterey Bay	3-52	0-910	12	4904
Tage 144-B	Monterey Bay	12-51	0-980	3	4941
PAS 120·90	26° 12′N 118° 30′W	4-54	0-900	1	209
PAS 130·150	22° 30′N 121° 15′W	4-54	0-700	1	2160
PAS 140·180	19° 40′N 122° 15′W	4-54	0-700	2	3475
SB 186-187	1° 1·5′N 91° 45·7′W	8-52	0-938	2	—
SB 108-109	4° 04′S 82° 14′W	7-52	0-1640	1	—
SB 207	12° 13·5′N 106° 07′W	8-52	0-300	2	—
SB 101-102	06° 58′S 88° 35′W	7-52	0-1463	2	—

There is some reason to believe that *Poeobius* might occur in the Intermediate Water of the eastern and western north-central Pacific. UDA (1938), SVERDRUP *et al.* (1942, p. 716) and others have described a convergence zone at about 41° N ,between 150° and 160° E, where mixed Oyashio and Kuroshio water sinks and spreads out

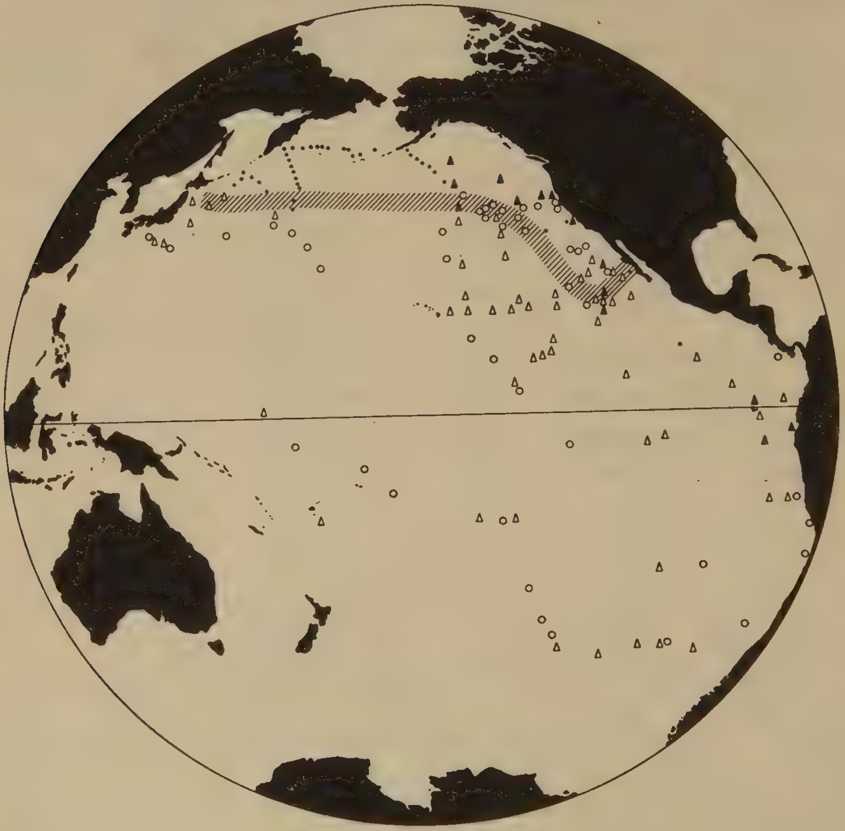

Fig. 4. All known records of *Poeobius*. Circles indicate net tows that reached a depth of 400 m or more, triangles indicate tows that reached a depth of 700 m or more. Those circles and triangles shown in solid black indicate stations where *Poeobius* were captured. Open circles and triangles indicate that no *Poeobius* were found at that station. The hatched portion of the chart is the boundary area of Subarctic and Transition Region water (SVERDRUP *et al.*, 1942, p. 740).

in a clockwise circulation over most of the North Pacific at depths ranging from 200 to 900 m. Although the shallower strata (0-300 m) of this area have been fairly well sampled (Fig. 1), only 21, widely spaced tows reached a depth of 700 m or more in the eastern half of this region (Fig. 4). *Poeobius* was not found in any of these tows. If it is assumed that the animal would be randomly distributed at low densities, the failure to find it in these tows can be used to set an upper 95 per cent confidence level of 1 animal per 11,548 m³ of water for its density in this region (FISHER and YATES, 1938, p.1). This may be compared with an average density of 1 animal per 17 m³ in the Subarctic Water Mass.

If there were no further records of *Poeobius*, its distribution could be simply related to that of the Subarctic Water Mass. However, seven individuals were found in the Intermediate Water of the eastern equatorial Pacific. There is little doubt that some mixing does occur between this water mass and the southern portion of the California Current, but this does not seem sufficient to account for the numbers of *Poeobius* caught here. The source of the Intermediate water of the eastern tropical Pacific is not really known, but SVERDRUP suggests that it is " formed off the coast of South America by the gradual transformation of Subantarctic water " (SVERDRUP *et al.*, 1942, p. 706). If this is true, the presence of *Poeobius* might indicate that it is an antitropical species (HUBBS, 1952) as are several other pelagic organisms in the Pacific Ocean. However, plankton samples taken on the Scripps Downwind Expedition (Fig. 1) and reports of the *Dana* (Wesenburg-Lund, personal communication) and *Discovery* expeditions (MONRO, 1936) indicate that it is not present in either the Central Water or the Subantarctic water of the South Pacific, and TEBBLE (1958) did not find it in the Antarctic or Subantarctic waters of the South Atlantic. It seems therefore that this explanation cannot be used to account for the occurrence of *Poeobius* in the eastern tropical Pacific.

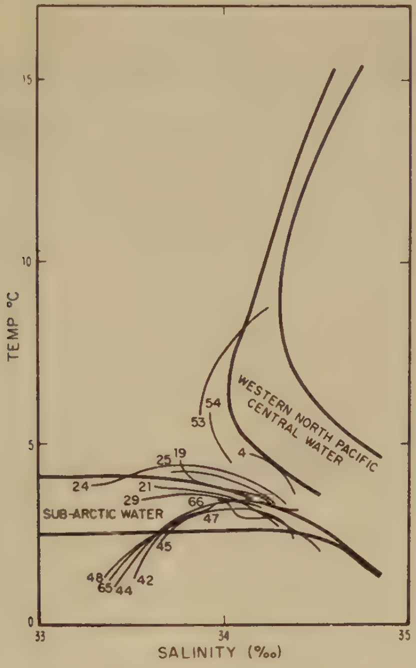

Fig. 5. Temperature-salinity curves from stations where *Poeobius* was taken on the Trans-Pacific Expedition, compared with SVERDRUP's Subarctic and Western North Pacific water. Station numbers are indicated on the fine lines. Only that segment of the curve within the depth range of *Poeobius* is plotted.

Another possible explanation for the presence of *Poeobius* in this area is that these seven individuals represent a second and hitherto undescribed species with different ecological requirements. There are however, only slight morphological bases for this

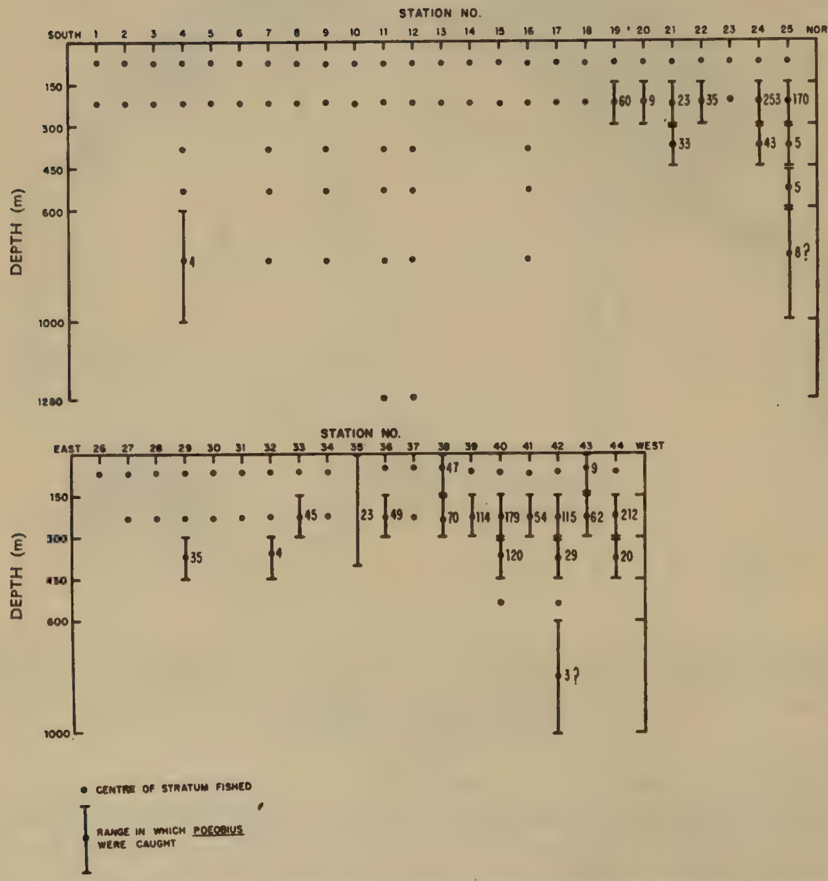

Fig. 6. Trans-Pacific sampling programme, Stations 1 to 44, showing the vertical distribution of *Poeobius*. The numbers to the right of the vertical bars indicate the numbers of organisms per 1000 m^3. The specimens from the deepest tows on Stations 25 and 42 might have come from the shallower depths.

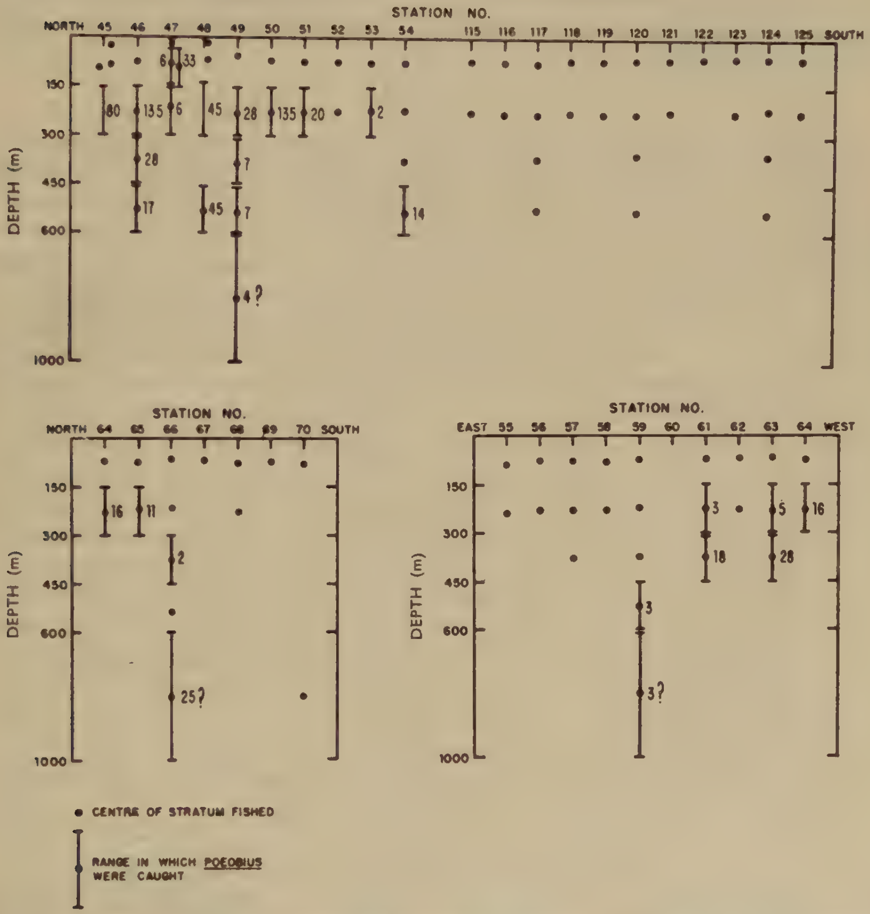

Fig. 7. The Trans-Pacific Expedition sampling programme, Stations 45 to 70 and 115 to 125, showing the vertical distribution of *Poeobius*. The specimens from the deepest tows on Stations 49 and 59 might have come from the shallower depths.

suggestion. All specimens from this area were rather larger than the average of those collected in pure Subarctic water, but despite the large size of these animals, their gonads were either missing or greatly reduced in size (Table 4). These differences do not necessarily indicate that they represent a new species for the resorption of gonads and other internal organs is a well known phenomenon in invertebrates living under unfavourable conditions. One might, therefore, expect to find such a condition in *Poeobius* that had been carried out of their normal environment. If this explanation is correct and the *Poeobius* in this area are sterile expatriates from the north, our ideas on the sources of the Intermediate water of the eastern tropical Pacific will have to be reconsidered.

DISCUSSION

Few attempts have been made to relate the entire distribution of a pelagic planktonic organism to the distribution of water mass*. RUSSELL (1935 and 1939), FRASER (1939 and 1952), PIERCE (1939) and others have shown that the distributions of chaetognaths and certain other organisms in the vicinity of the British Isles are related to the movements of waters from different sources and according to FRASER (1952) " it has now been established that the various species of Chaetognatha are associated each with a more or less specific hydrographical environment, making the group one of the foremost of the biological indicators." JOHNSON (1956) has shown that copepods also may be used as an aid in tracing the water movements in the Chukchi and Beaufort seas. It should be pointed out, however, that most of the species considered by these authors are more widely distributed than the limited areas they have investigated and that until all of the boundaries of their distributions are well known, it will be difficult to define in physical terms the regimen to which they are limited, or to show whether or not their overall ranges coincide with the concept of a physical water mass. HAFFNER's (1952) study on *Chauliodus* is perhaps more extensive, but because he does not have accurate data on depth of capture, it is not certain that his species are really limited to the depth ranges to which he asssign them. Further, his technique of using a single temperature-salinity measurement at the presumed depth of capture is probably not sufficient to identify a water mass, for SVERDRUP *et al.* (1942, p. 143) have pointed out that this may be done only in exceptional cases and that a T-S curve is usually required to define a water mass.

TEBBLE (1958) has reported that certain pelagic polychaetes in the South Atlantic and Antarctic oceans are limited to particular water masses, but at the time of this writing his detailed information has not been published. In a recent study on the chaetognaths of the Antarctic regions, DAVID (1958) has shown that the boundaries of the ranges of some specimens do, indeed, coincide with hydrographic boundaries and that some of these species are endemic to the Antarctic water.

While T-S relationships are used to identify water masses, this does not necessarily mean that the organisms limited to these water masses are limited by temperature and salinity alone. Water having characteristics that would fit certain points of the Subarctic T-S curve may be found in many parts of the world, and yet, so far as is known at present, *Poeobius meseres* occurs only in Pacific Subarctic water or in waters which may have Subarctic components. There are many possible explanations but until more is known of the biology of the animal, they can only be considered

---

* As defined by SVERDRUP *et al.* (1942, p. 143).

(24)

Table 4. Size and gonad condition of Poeobius *from the Subarctic and Eastern Equatorial regions*

Station	*Zone*	*Size of specimens*	*Month*	*Condition of Gonads*
TP 40B	Subarctic	18 mm	Aug.	ovary large 2 mm
		20 mm		ovary large 2 mm
		11 mm		ovary large 2 mm
		15 mm		ovary large 2 mm
TP 36C	Subarctic	17 mm	Aug.	ovary large 2-3 mm
		9 mm		ovary large 2 mm
		12 mm		ovary large 2 mm
		10 mm		ovary large 2 mm
		9 mm		ovary large 2 mm
		16 mm		specimen opaque
		15 mm		ovary large 2 mm
		10 mm		—
		10 mm		ovary large 2 mm
		10 mm		specimen damaged
		13 mm		ovary large 3 mm
TP 41B	Subarctic	18 mm	Aug.	ovary large 2 mm
		16 mm		ovary 1·5 mm
		13 mm		ovary 1·75 mm
TP 47D	Oyashio	13 mm	Sept.	ovary 1 mm
		12 mm		ovary ruptured, eggs diffuse in body cavity
		18 mm		ovary 1 mm
		19 mm		ovary ruptured, eggs diffuse in body cavity
TP 25B	Subarctic	6 mm	Aug.	body opaque
		13 mm		body wall ruptured
		9 mm		ovary 1·25 mm
		14 mm		body opaque
		10 mm		ovary 1·25 mm
		6·5 mm		body opaque
TP 66E	Oyashio	10 mm	Sept.	body opaque
		16 mm		ovary large 2·5 mm
		10 mm		ovary large 2·5 mm
		8 mm		ovary 1·5 mm
		12 mm		ovary ruptured
		12 mm		ovary large 3 mm
		15 mm		ovary large 2 mm
		16 mm		ovary large 2·5 mm
		12 mm		entire posterior half is ovary
SB 101-2	Eastern Tropical Pacific	21 mm	Aug.	viscera degenerate, gonads missing
		20 mm		viscera degenerate, gonads missing
SB 108-9	E.T.P.	10 mm	July	much of viscera missing, gonads missing
SB 207	E.T.P.	10 mm	Aug.	viscera partially gone, gonads missing
		15 mm		ovary present 1·5 mm
SB 186-7	E.T.P.	10 mm	July	gonads missing
		10 mm		gonads missing

(25)

theoretical. One factor which may be of importance is the higher productivity and standing crop of the Subarctic, California Current, and eastern tropical Pacific areas (Holmes, 1958) compared with that of the Central and Equatorial Pacific water masses (Steemann-Nielsen, 1957). Thus the southward extension of the range of *Poeobius* from the Subarctic water mass to the California Current to the eastern tropical Pacific may have a simple relationship to the availability of food.

From the foregoing discussion it appears that water masses, as defined by hydrographers, may also exist as biological entities. The water mass concept, which defines a three-dimensional unit of the ocean, thus provides us with an opportunity to compare plankton distributions with that of circumscribed volumes of water, each of which has a unique set of physical properties.

Acknowledgements—The author wishes to thank Mr. John Knauss for his suggestions and assistance. Drs. Warren Wooster and E. W. Fager also gave valuable help. This study was done under the direction of Professor M. W. Johnson, Scripps Institution of Oceanography. Dr. Eric Barham, working under the Office of Naval Research Contract N6onr 25127, provided the information on the Monterey Bay *Poeobius* catches.

Scripps Institution of Oceanography
California, U.S.A.

Contribution from the Scripps Institution of Oceanography, New Series.

REFERENCES

Ahlstrom E. H. (1954) Distribution and abundance of egg and larval populations of the Pacific sardine. *Fish and Wildlife Service, Fishery Bull.* **93**, (56), 83-140.

Bogorov B. G. (1955) Regularities of plankton distribution in the North-West Pacific. *Proc. UNESCO Symp. Phys. Oceanogr. Tokyo, 1955.* pp. 260-276.

Dales R. P. (1957) Pelagic polychaetes of the Pacific ocean. *Scripps Inst. Oceanog. Bull.* **7** (2), 99-168.

David P. M. (1958) The distribution of the Chaetognatha of the Southern ocean. '*Discovery*' *Rep.* **29**, 199-228.

Fisher R. A. and Yates F. (1938) *Statistical Tables for Biological, Agricultural and Medical Research.* Oliver and Boyd.

Fisher W. K. (1946) Echiuroid worms of the North Pacific Ocean. *Proc. U.S. Nat. Mus.* **96**, 215-292.

Fraser J. H. (1939) The distribution of Chaetognatha in Scottish waters in 1937. *J. Cons. Int. Explor. Mer.*, **14**, 25-34.

Fraser J. H. (1952) *The Chaetognatha and other zooplankton of the Scottish area and their value as biological indications of hydrological conditions.* Scottish Home Department, *Marine Research* (2), 1-52.

Haffner R. E. (1952) Zoogeography of the bathypelagic fish *Chauliodus. System. Zool.* **1**, 113-133.

Hartman O. (1955) Endemism in the North Pacific with emphasis on the distribution of marine annelids, and descriptions of new or little known species. *Essays in the Natural Sciences in Honor of Captain Allan Hancock* pp. 39-61. University of South California Press, Los Angeles.

Heath H. (1930) A connecting link between the Annelida and the Echiuroidea (*Gephyrea armata*). *J. Morph. Physiol.* **49**, 223-249.

Helland-Hansen B. (1916) Nogen hydrografiske metoder. *Forh. Skand. Naturf. Møte* **16**, 357-359.

Holmes R. W. (1958) Surface chlorophyll "A," surface production, and zooplankton volumes in the eastern Pacific ocean. *Cons. Int. Explor. Mer, Rapp. Proc.-Verb.* **144** 109-116.

Hubbs C. L. (1952) Antitropical distribution of fishes and other organisms. *Proc. 7th Pacif. Sci. Congr. Pacif. Sci. Assoc.*, **3**, *Meteorology and Oceanography* 324-330.

(26)

Johnson M. W. (1956) The plankton of the Beaufort and Chukchi Sea areas of the Arctic and its relation to the hydrography. *Arctic Inst. N. Amer. Tech. Pap.* No. 1.

Leavitt B. B. (1935) A quantitative study of the vertical distribution of the large zooplankton in deep water. *Biol. Bull.* **68** (1), 115-130.

Leavitt B. B. (1938) The quantitative vertical distribution of macrozooplankton in the Atlantic Ocean basin. *Biol. Bull.* **74** (3), 376-394.

Monro C. C. A. (1936) Polychaete worms (II). '*Discovery*' *Rep.* **12**, 59-198.

Pickford G. E. (1947) Histological and histochemical observations upon an aberrant annelid *Poeobius meseres* Heath. *J. Morph.* **80** (3), 287-319.

Pierce E. L. and Orton J. H. (1939) *Sagitta* as an indication of water movements in the Irish Sea. *Nature, Lond.* **144**, p. 784.

Reid J. L., Roden G. I. and Wyllie J. G. (1958) Studies on the California Current system. *Progr. Rep. Calif. Oceanic Fish. Invest.*, 1 July 1956–1 Jan. 1958, 27-57.

Russell F. S. (1935) On the value of certain plankton animals as indicators of water movements in the English Channel and North Sea. *Mar. Biol. Ass.* **20**, 309-332.

Russell F. S. (1939) Hydrographical and biological conditions in the North Sea as indicated by plankton organisms. *J. Cons. Int. Explor. Mer.* **14**, 171-192.

Steemann-Nielsen E. and Jensen E. A. (1957) Primary oceanic production, the autotrophic production of organic matter in the oceans. '*Galathea*' *Rep.* **1**, 49-136.

Sverdrup H. U., Johnson M. W. and Fleming R. H. (1942) *The Oceans*, Prentice-Hall, New York.

Tebble N. (1958, July) Distribution of Pelagic Polychaetes in the South Atlantic Ocean. *Nature, Lond.* **182** (4629), 166-167.

Uda M. (1938) Hydrographical fluctuation in the north-eastern sea region adjacent to Japan of North Pacific Ocean. *Jap. Imp. Fisheries Exp. Sta. J.* (9), 64-85 (English Abstract).

Zooplankton volumes off the Pacific Coast, 1949-50. Special Scientific Report: Fisheries No. 125. *U.S. Fish and Wildlife Service (1954).*

Wooster W. S. and Cromwell T. (1958) An oceanographic description of the Eastern Tropical Pacific. *Scripps Inst. Oceanogr. Bull.* **7** (3), 169-282.

Printed in Great Britain by The Salisbury Press Ltd,, Publicity House, Wilton Road, Salisbury, Wilts. (20253)

PACIFIC NATURALIST

CONTRIBUTIONS FROM THE
Beaudette Foundation for Biological Research

VOL. 1, NO. 14 MARCH 11, 1960

SEAWEEDS ASSOCIATED WITH KELP BEDS ALONG SOUTHERN CALIFORNIA AND NORTHWESTERN MEXICO

By E. YALE DAWSON, MICHAEL NEUSHUL
AND ROBERT D. WILDMAN

Box 482, R.F.D. 1 SOLVANG, CALIFORNIA

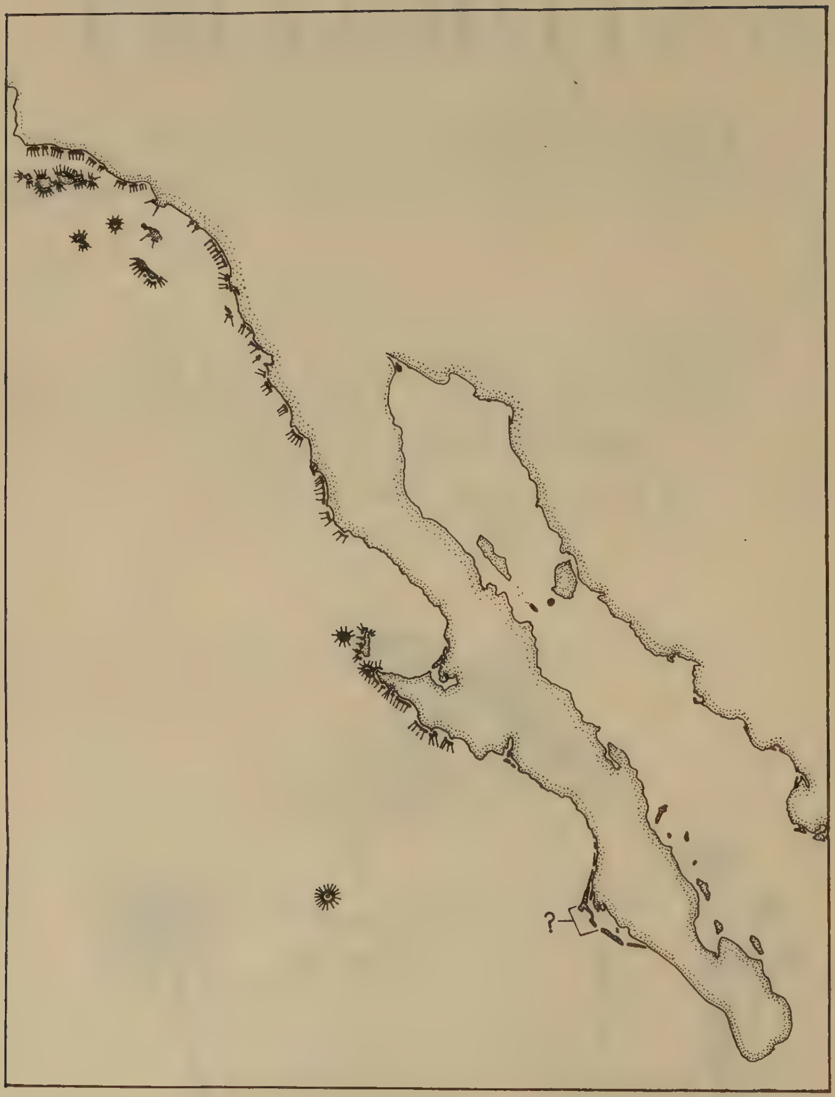

Figure 1. Distribution of kelp beds along the coast of southern California and northwestern Mexico.

SEAWEEDS ASSOCIATED WITH KELP BEDS ALONG SOUTHERN CALIFORNIA AND NORTHWESTERN MEXICO[1]

By E. Yale Dawson[2], Michael Neushul[3], and Robert D. Wildman[4]

1. Introduction

One of the principal benthic marine plant communities of California is that dominated by the largest known marine alga, the giant bladder kelp, *Macrocystis pyrifera.* We have attempted to survey, through a portion of its range, the floristic composition of this community and to distinguish, record and characterize its prominent plants. We present here some of the results of our observations that may be useful to future investigators of various disciplines who wish to gain a general knowledge of these plants in connection with their research problems within this highly productive marine environment.

Increasing interest in the intelligent use and conservation of our marine resources has caused much attention to be focused during recent years on the near-shore marine plant communities. The development of sport fishing as a recreational asset of the nation has brought about increased interest in marine plant resources and, in particular, the *Macrocystis* association. Commercial interest in this remarkable plant has also grown, and a sizeable industry has developed that harvests as much as 100,000 tons of *Macrocystis* annually from California alone.

In accord with the growing attention given to the *Macrocystis* community, a need has been felt for a better understanding of the types of plants that comprise it.[5] Many biologists interested in kelp beds have found it difficult to deal intelligently with their research problems in the absence of a ready means of identifying by name the plants with which

---

[1] These studies were aided by Contract NR104-520 between the office of Naval Research, Department of the Navy, and the Beaudette Foundation for Biological Research. A portion of the publication costs were also defrayed by Mr. Harold A. Fitzgerald. The field collections forming the basis of this work were made largely by M. Neushul while working for the Scripps Institution of Oceanography's Institute of Marine Resources Kelp Investigation Program under agreement K-1 with the California Department of Fish and Game. These collections were incidental to other aspects of the planned field program and were released for study at the Beaudette Foundation. Contribution from the Scripps Institution of Oceanography, New Series

[2] Beaudette Foundation for Biological Research, Solvang, California.

[3] National Science Foundation Post-doctoral Fellow, University of London, Queen Mary College, London, England.

[4] Department of Botany, University of California, Berkeley, California.

[5] Only two reports of underwater work with SCUBA along our coast have given any account of the plant communities. The first of these lists 17 species at La Jolla, California, and the second briefly describes the general composition in profile of the benthic flora at La Jolla: Limbaugh, Conrad. 1955. Fish life in the kelp beds and the effects of kelp harvesting. Univ. of Calif. Inst. of Marine Resources. Multilith 55-9. 155 pp. 9 Sept. 1955. Aleem, A.A. 1956. A quantitative study of the benthic communities inhabiting the kelp beds off the California coast. . . . pp. 149-151 in, Second International Seaweed Symposium. 220 pp. Pergamon Press, London.

Contributions from the Scripps Institution of Oceanography, New Series, 1142
Reproduced by Permission

they are concerned. It is for this reason that the major emphasis in the present work has been placed on the presentation of extensive illustrations of the prevalent plants and of a key to aid in their identification.

Through the generosity of the late Dr. Gilbert Morgan Smith, we have been permitted to draw heavily upon the excellent illustrations from his book, *The Marine Algae of the Monterey Peninsula.* We also thank Dr. H. E. Jaques and the William C. Brown Company, publishers of the Pictured-Key Nature Series, for permission to use illustrations from E. Y. Dawson's *How to Know the Seaweeds.* Illustrations from other sources are acknowledged in the captions.

2. SCOPE AND LIMITATIONS

Macrocystis is a plant of cool to cold waters. It is abundant in the southern hemisphere where its distribution is circumpolar in the subantarctic regions. Under the influence of the cold Humbolt current it extends northward along the coast of western South America to within six degrees of the equator. In the northern hemisphere it occurs only along the western coast of North America, where it occupies a position of dominance over the benthic vegetation of hundreds of miles of coast. The present report is limited geographically to only a portion of this North American range where kelp beds have been studied in relative detail, namely, along the coast of Southern California and Pacific Baja California (Text fig. 1).

Within this restricted range the physical limitations imposed upon the present study have been such that our knowledge of the *Macrocystis* community remains fragmentary compared to a corresponding community of terrestrial plants. Inasmuch as a thorough description of the problems relating to these physical limitations would occupy an inordinate amount of space here, we present the following few comments only as an indication of some of the more prominent factors to which the prospective botanist-diver must become oriented because of the way in which they restrict his effective investigation of this underwater environment.

Until recent years the investigation of the vegetation of the sea floor has been confined to the use of shipboard devices, mainly the biological dredge whose blind scrapings have yielded disconnected fragments of the flora. Now we have self-contained underwater breathing apparatus, SCUBA, a field research tool upon which increasing emphasis is being placed. This emphasis is certainly deserved, but it is often placed without taking into full account the limitations of the equipment as well as those of the environment itself. It must be kept in mind that the observations, collections and measurements upon which such a study as the present one is based are made by botanists working under water in a foreign environment where they are subject to severe restrictions.

The most restricting factor is that of time. On land one can examine the flora of an area quite leisurely on foot or from an automobile, while studies of kelp beds can only be made effectively by descending from boats which are not only expensive and time-consuming to operate, but are also subject to the uncertainties of weather and the state of the sea. Even when adequate ship time is available the diver is limited by the capacity of his SCUBA outfit and, more especially, by his own physiology, to very brief periods of underwater observation.

Because of the hazards and difficulties of work under water the diver finds himself forced to spend a major part of his available time and energy on shore or shipboard in attending to the preparation, care and operation of his equipment. During the execution of a dive, safety precautions and the mandatory presence of a companion hamper orderly observations, for one must continually be aware, because of possible equipment failure, of the condition and position of the other diver, with whom little but visual communication is possible.

The most prevalent handicap underwater is poor visibility. The diver's view of the ocean floor, already restricted by the "blinder effect" of the face plate, is often further limited by darkness or by suspended matter in the water. Thus, under a dense kelp canopy light is commonly reduced to a minute fraction of its surface value, and in the presence of heavy plankton blooms or of sediment in the water the diver may find himself surrounded by an impenetrable gray fog in which successful work is impossible.

More subtle is the effect of the water and suspended matter on the selective removal of parts of the spectrum, to the extent that the colors of various plants become deceiving or absent. Many of the plants which appear brilliantly red in sunlight are dull gray or nearly black at those depths to which red light does not penetrate. As a result of these light and color restrictions, the novice collects only those things that he can readily see, and misses many of the smaller, often abundant and important plants. These more obscure elements of the vegetation can best be collected by bringing loose rocks and shells to the surface where certain plants borne on them can then be seen.

One of the most frustrating handicaps of the marine botanist is his inability to determine readily from the surface the places on the bottom desirable for his work. This is not so true in kelp beds themselves, where the fronds rising to the surface often indicate the presence of a favorable rocky bottom, but otherwise, one often finds it necessary to engage in time-consuming exploration. A general survey of the sea floor over a large area requires repeated dives in many places to locate areas suitable for effective work.

Finally, within the kelp community, the very aspect of the submarine forest with its bewildering array of interesting and beautiful plants and animals, attracting the diver away at every hand from any attempts he may make at methodical investigation, reduces the actual effectiveness of his underwater time and his ability to recall later many details within the scope of his observations. This difficulty can partially be overcome by planning the dive prior to descent and making notations on plastic sheets while underwater.

Despite all of these limitations, a total of some 85 hours of underwater work, during some 240 dives on the part of the junior authors in the kelp beds of Southern California and Northwestern Mexico, has yielded sufficient material to provide for a presentation that we feel may be useful to future investigators of this region.

3. THE KELP BED

The giant kelp, *Macrocystis pyrifera,* grows attached to the ocean floor by a large, root-like holdfast from which arise numerous branches, called stipes. These are floated to the sea surface by many pear-shaped, gas-filled floats borne along their length. On each float is a lanceolate blade. A single stipe with its floats and blades is called a frond. Many fronds, growing from a branching system at the base of the plant rise to the surface in a tangled bundle. Upon reaching the surface they spread slightly and the blades float out to form a layer of vegetation called the canopy. From below, this canopy appears as a vast, golden-brown roof supported by many pillars. (Plate 10)

Groups of *Macrocystis* plants growing together are called beds. These can cover considerable areas of the sea surface. In California alone they occupy approximately 100 square miles of near-shore waters, forming narrow patches in depths of 20 to 60 feet or more along the greater part of the coast and the islands. The major beds vary from an area of a quarter of a square mile to about 13 square miles.

A kelp bed may be compared in some respects to a terrestrial forest. Like the trunks of trees the tangled stipe bundles "support" the light-modifying canopy beneath which there is often deep shade. In open areas on the bottom there may be "glades" of smaller, bottom plants, while within the dense kelp groves the bottom supports only a few shade-tolerant species. The obvious stratification present in many terrestrial forests is, however, almost absent in this submarine forest, for, except for the kelp stipe bundles, the region between the surface canopy and the bottom is usually relatively free of macroscopic vegetation. In some areas, however, young *Macrocystis* plants, or the large, bush-like fruiting portions of *Halidrys* and *Cystoseira,* supported by their many small floats, extend up into this mid-water zone.

To those whose experience with kelp beds has been confined to observations only of the surface, all the beds look very much alike, but divers having seen *Macrocystis* in a number of localities state that no two beds have quite the same aspect. These differences, indeed, are so pronounced from place to place that one finds it difficult to diagram a generalized kelp bed. We have chosen, nevertheless, as representative of the kelp communities most frequently encountered in our area, the kelp bed at La Jolla, California (Fig. 2). Some comparative notes on two dissimilar beds in Baja California are also given below.

It should be pointed out here, in advance of the comments on temperature to follow, that the kelp beds within the range of this study do not change gradually in species composition as one proceeds from north to south. Due to frequent sharp variations in coastal water temperatures, plants common in northern areas reappear at "cold spots" farther south, while certain species characteristic of warm areas, such as *Padina durvillaei* and *Amphiroa zonata*, occur intermittently in those southern kelp beds subject to higher temperatures. At Sacramento Reef, a marked low temperature area, northern forms such as *Calliarthron cheilosporioides, Gigartina binghamiae and Botryoglossum farlowianum* reach the southern limits of their distribution. At La Jolla, California, too, a few plants such as *Agarum fimbriatum* and *Demarestia tabacoides* reach their southern limits, although the flora as a whole is representative of the northwestern Baja California region. Thus, within the La Jolla bed can be found most of the species encountered in the more southern kelp beds.

A. The "typical" kelp bed at La Jolla, California Text fig. 2

As shown in the diagram, the inner kelp bed boundary is usually at a depth of approximately 30 feet and is bounded by the feather boa kelp, *Egregia laevigata*, which extends on into shallow water. On the outer

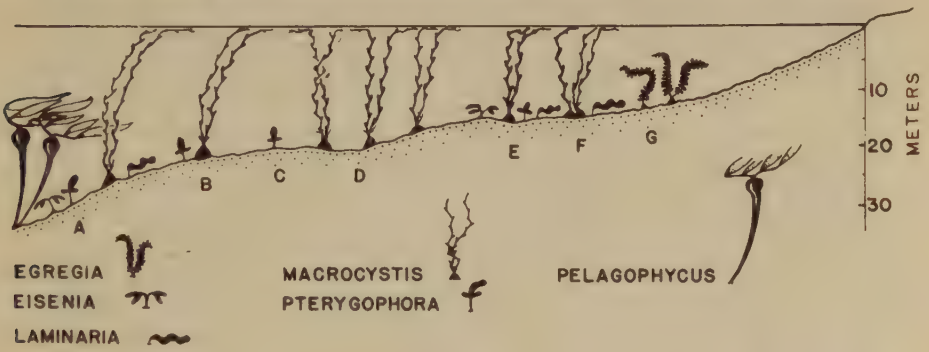

Figure. 2. Diagrammatic cross section of the kelp bed at La Jolla, California. The more conspicuous large brown algae are shown. Smaller plants forming the bottom growth were observed and collected at points A through G. The genera represented are as follows: A. *Agarum, Cystoseira, Desmarestia, Eisenia, Laminaria, Leptocladia, Lithothamnium, Pelagophycus, Plocamium, Pterygophora,* and *Rhodymenia.* B. *Corallina, Cystoseira, Desmarestia, Macrocystis, Pterygophora,* and *Rhodymenia.* C. *Botryocladia, Codium, Lithothamnium, Macrocystis, Pterygophora,* and *Zonaria.* In the dense shade at point D. *Drouetia, Rhodymenia* and *Macrocystis.* E. *Corallina, Cystoseira, Desmarestia, Eisenia, Laminaria, Leptocladia, Pterygophora,* and *Rhodymenia.* F. *Botryocladia, Callophyllis, Dictyopteris, Macrocystis, Nienburgia, Plocamium, Rhodoglossum, Sciadophycus.* G. *Carpopeltis, Chaetomorpha, Cladophora, Dictyopteris, Ectocarpus, Egregia. Eisenia. Gelidium, Gigartina, Gracilaria, Grateloupia, Pachydictyon* and *Pterocladia.* The horizontal scale is greatly compressed, the total distance covered by the transect being slightly over one statute mile.

edge the bull kelp, *Pelagophycus porra*, is commonly found. Both of these plants occasionally grow intermixed with the *Macrocystis*, but, generally speaking, only scattered individuals are present within the bed itself.

The undergrowth present in a kelp bed may be divided generally into those species which are stalked and tree-like and those that lie along the bottom. Of the larger and more conspicuous stalked forms, the southern sea palm, *Eisenia arborea*, and the similarly stalked kelp, *Pterygophora californica*, form what may be called an intermediate layer of vegetation, for their heavy, erect stipes commonly hold the fronds well off the bottom and above the mixed growth of smaller plants there. This tree-like vegetation is usually sparse except in open patches or "glades" in the kelp bed.

Several other large kelps with broad, leathery fronds, such as *Laminaria*, *Agarum* and *Desmarestia*, are frequent to occasional in the kelp beds. In the case of *Laminaria farlowii* the individual broad blades may reach lengths up to 15 feet, and lie out along the bottom like large, undulate strips of leather.

The red algae comprise the greatest number of species in the kelp bed bottom community and are often present in a bewildering array of forms. The most ubiquitous of these are the jointed coralline algae which grow even in the deep shade of the canopy. Crustose forms of coralline algae occur as pink layers on the bottom rocks and often cement together pebbles, shells, and sand to form nodules or even areas of rough "pavement." The variety of animal and plant life that may exist on and within such a coralline algal crust is amazing, and the microscopic examination of a single collection can easily provide one with an afternoon's occupation.

The plants of the bottom community vary greatly in size, and many of the smaller, filamentous or delicate forms remain invisible to the diver except on days of most brilliant sunlight and clear water. The changes in the aspect of the bottom upon the occasion of such favorable illumination are remarkable, for many plants and animals appear that cannot be seen at all under light of different spectral quality.

Some species present within a kelp bed, and most of those inhabiting the inner margins, extend shoreward into the lowest intertidal zone. Others are strictly shade forms that extend toward the other extreme into the lesser known deep zones where light limits the distribution of attached plants. Among those plants that fall into the former category (the common intertidal species) *Eisenia*, *Cystoseira*, *Plocamium*, *Zonaria*, *Dictyopteris*, *Codium*, *Lithothamnium* and *Corallina* are perhaps the most conspicuous. Those plants that exist normally at the lowermost limits of plant distribution are exemplified by *Drouetia rotata* and *Phyllophora clevelandii*, which also extend up into the kelp beds but confine themselves to areas of densest shade. Only a few species appear to be found growing almost exclusively with *Macrocystis*. *Laminaria farlowii* is such an alga, found beneath the *Macrocystis* canopy itself, but rarely extending either inshore or to the lower limits of plant distribution with depth.

B. The Kelp Bed at Sacramento Reef, Baja California

The *Macrocystis* association at this locality presents such a dissimilar aspect to the "typical" situation in the La Jolla area that some observations made during an investigation in August, 1957, are presented. The kelp canopy here was unusually open, and beneath it a rugged bottom of many pinnacles and deep crevasses provided great variability in depth over short distances. The average depth of the pinnacle tops was 40 to 50 feet. The abundance of animals in the area was conspicuous. Many large, colonial tunicates formed crests along the rocks. These animals were often covered by heavy turfs of the minute filamentous red alga *Antithamnion*. Encrusting bryozoans were present on many algae. The more luxuriant plant growth was confined to the slopes or tops of pinnacles where grazing activity of the numerous sea urchins present in the channels and lower areas was apparently not as great. Many young *Macrocystis* plants were observed, also confined to the tops of pinnacles. This limitation prevented the formation of dense groves, and the resulting open nature of the area allowed the establishment of an interesting and diverse bottom flora. *Desmarestia munda*, large foliaceous *Gigartina binghamiae*, *Eisenia arborea*, *Botryocladia pseudodichotoma* and *Botryoglossum farlowianum* grew among the *Macrocystis* on tops of the rocks, while vegetative Halidrys *dioica*, heavily encrusted with bryozoans, and grazed *Plocamium pacificum*, *Nienburgia andersoniana* and *Rhodymena arborescens* grew along the sides of the rocks. Apparently immune to the voracious sea urchins, *Corallina officinalis*, *Calliarthron cheilosporioides* and various encrusting corallines extended down into the crevasses.

C. The Kelp Bed at Isla Asunción, Baja California.

This bed is representative of the southernmost *Macrocystis* associations on this coast, in which a number of warm-water species invade the flora and present a somewhat different aspect than the association of plants characteristic of the beds farther north. The comments are from observations made during the summer of 1957.

Around Isla Asunción a heavy kelp canopy was found between the island and Punta Asunción as well as on the west side of the island. Scattered *Macrocystis* clumps were observed throughout the area although they were not always visible from the surface. The dense bed between the island and the point was characterized by a heavy canopy which reduced the light on the bottom at a depth of nine meters to less than one per-cent of that present immediately beneath the water surface. The bottom was quite irregular, with clumps of rocks alternating with sand- or shell-filled basins. Coralline algae such as *Corallina officinalis* and *Amphiroa zonata* grew, along with the prostrate *Peyssonelia rubra* var. *orientalis* and *Codium setchellii*, under the kelp canopy where some light penetrated. These were gradually replaced along the margins of the sand clearings which were bordered by the ubiquitous *Eisenia arborea. Desmarestia munda* and *Cystoseira*, the latter with epiphytic *Pterochondria pygmaea*, were also present. In open areas where abundant light penetrated, a luxuriant growth of *Codium cuneatum, Padina durvillaei, Phyllospadix torreyi, Colpomenia sinuosa* and *Gelidium cartilagineum* occurred with the flat brown algae *Taonia lennebackerae* and *Dictyota binghamiae.*

In the dense bed on the west side of the island *Macrocystis* formed very dense groves, and the bottom at a depth of 40 feet was quite dark except in areas where sand troughs passed through the otherwise rocky, ridged substrate. In such more lighted places *Eisenia arborea, Codium cuneatum, Codium hubbsii* and *Halicystis ovalis* grew, while under the increasing shade of the overhead canopy these were replaced by the coralline algae, *Amphiora zonata* and *Corallina officinalis* and by *Carpopeltis bushiae, Acrosorium uncinatum, Botryocladia pseudodichotoma* and *Rhodymenia arborescens. The Rhodymenia* persisted farthest into the dark gloom beneath the closely spaced *Macrocystis* stipe bundles, until in some areas no bottom plants at all could be found.

4. FACTORS AFFECTING THE PRESENCE AND COMPOSITION OF A KELP BED COMMUNITY

Along undisturbed portions of our coasts the *Macrocystis* community is distributed according to several limiting factors in the environment, some of the most obviously important being those of substrate, temperature and light. Probably the most markedly limiting of these is substrate. In occasional localities along southern California *Macrocystis* has been observed to form pure stands on sandy bottoms in the virtual absence of other algae. In such places, young plants generally begin growth on worm tubes, their holdfasts spreading widely and penetrating the sand slightly. Anchorage is apparently provided by the accumulation of heavy material within the holdfast. Rocky bottoms, however, especially those constantly swept free of sediment by currents, provide favorable attachment for multitudes of plants, and it is here that the kelp community may find optimum conditions for growth in accord with the factors of temperature and light.

Temperature in the sea markedly influences the geographic distribution of the marine plants by governing, among many things, both the rates of the metabolic processes and the solubility of their metabolic gases. These influences are especially well demonstrated along the coasts of southern California and northwestern Mexico where sea water temperatures vary so markedly with coastal geography and where *Macrocystis* and its associated algae are such effective indicators of this variation.

It has been pointed out that *Macrocystis* is a plant of cool waters. The coast with which we are dealing is a cool water coast, not only because of the general southward drift of water from the north, but because of extensive coastal upwelling of cold, subsurface water as the result of wind-created currents. Coastal configuration, with respect to the direction of the wind, governs the intensity of the cold water upwelling and the consequent temperatures of near-shore waters. We find that along northwestern Baja California strong upwelling occurs all along the coast south to Bahía Vizcaino, but is especially intense south of such headlands as Punta Banda, Punta Baja and Cabo Colnett where low temperatures favorable to the *Macrocystis* community are present. Bays and estuaries such as Bahía de Todos Santos and Bahía de San Quintín are separated from the open sea and, hence, show little influence of upwelling. Such locations are characterized by species of warmer areas. The huge warm water eddy which occurs in the Vizcaino Bay, where upwelling is essentially absent, accounts for high temperatures there and the absence of *Macrocystis*, while at Punta Eugenio and immediately southward, with the reappearance of intense upwelling the kelp beds appear again and continue on south to Punta San Hipólito or beyond.

In Fig. 1, one sees the general distribution of the kelp bed community. *Macrocystis* has been reported as far south of Punta San Hipólito as Isla Magdalena where it may possibly occur sporadically in areas of maximum upwelling such as off Punta Hughes. This area between Punta San Hipólito and Isla Magdalena is, accordingly, one of transition from the cool-water flora of the Californias to the warm water flora of the Mexican tropics.

It is interesting to note that at Alijos Rocks, 180 miles west of Isla Magdalena, a *Macrocystis* community occurs in waters of higher temperature than are normal throughout its coastal range. This seems to be due to conditions of extreme agitation and aeration which would appear to compensate somewhat for the higher temperature by providing greater supersaturation of the water with O_2 and CO_2. At deeper levels, below this highly aerated zone, such characteristic *Macrocystis* community plants as *Phyllospadix*, *Egregia*, and *Cystoseira* are largely replaced by species of tropical affinities.

Light is another critical factor governing the structure and composition of the *Macrocystis* community. The effect of shade on the bottom community is often quite striking.

An "ideal" kelp bed, in terms of light modification, was studied on the west side of Cedros Island in Baja California in August 1957. It had a well-developed, continuous, dense surface layer of fronds. The *Macrocystis* plants were evenly distributed over a smooth rock bottom bordered by sand. Penetration of light was measured in an open area adjacent to the bed where 5% of the surface light reached the bottom at a depth of 51 feet. Within the bed the attenuation of light due to the water, plus the effect of the *Macrocystis* plants, reduced the available light on the bottom below the canopy to less than 0.1% of that measured immediately below the surface in open water.

The bottom flora in the above described area consisted only of a few plants, these being relatively undeveloped. *Leptocladia, Cystoseira, Prionitis, Bossiella, Acrosorium,* and *Lithothamnium* were found. At the same depth in a bed at the San Benitos islands, where an open canopy was formed by scattered *Macrocystis* plants, 28 species were collected. Similarly striking differences in bottom plant abundance and diversity can also be found in different parts of a single kelp bed.

Biological activity, in particular that of herbiverous and encrusting animals, it is of great importance in the modification of kelp bed composition and structure although our present knowledge of their specific effects is limited. The overall importance of this factor was recently demonstrated when a grounded tanker released crude oil into a small bay on the Baja California coast, killing nearly all of the animals, including the major herbivores such as the sea urchins and abalone. The great increase and luxuriance of plant growth that followed upon the removal of grazing pressure, dramatically demonstrated the important part played by these animals in the regulation of the plant association. Attempts to cultivate *Macrocystis* plants in the sea have also demonstrated the importance of animal activity in the establishment and growth of transplants, for grazing damage often results in their complete destruction during certain periods of the year.

5. COLLECTION AND PRESERVATION OF MATERIALS

Marine biologists working with kelp bed plants should keep in mind the great value of preserving identified voucher specimens, both in support of field observations and in connection with any experimental work which, for purposes of obtaining reproducible results, may require precise identification of the organism. Preparation of specimens is relatively easy and should not be neglected.

For most general collecting, the diver will find that a heavy gauge perforated plastic bag of the type used in vascula by terrestrial botanists will serve well under water. An effective underwater collecting kit has been devised, however, which permits several collections to be made and kept separate in accord with field notes which can be made during a dive. This consists of a wire rack to which is attached a series of small bags made of fine nylon netting. The bags are closed by overlapping pieces of netting, but permit specimens to be thrust in through the slit.

Specimens may be kept in the laboratory for considerable periods in dilute formalin (about 2%) in five gallon tins. Dry specimens can easily be prepared by spreading specimens out in water in a sink, slipping a sheet of good rag-content paper under them, draining and pressing in an ordinary plant press, using cloth or waxed paper to prevent specimens from sticking to other than their backing sheets. (For full directions for mounting, labeling, sectioning, etc., see Dawson, 1956, How to Know the Seaweeds.)

6. Use of the Illustrations and Keys

The difficulties of identifying marine plants have been widely acknowledged by marine biologists not trained in algology. In most cases this has been due to the unavailability of local floristic works which permit ready recognition by illustration and avoid the problems of examining internal structures. The few well-illustrated floras which are available for the most part treat rather extensive geographic areas, include the intertidal zone, and generally contain such numerous species of diverse habitats that the algologically untrained worker finds them of little use. Inasmuch as there is no single treatment of the algal flora of southern California and northwestern Mexico, workers in this area have been particularly handicapped. They have used almost exclusively G. M. Smith's Marine Algae of the Monterey Peninsula, California, which is excellent for the region north of Point Conception, but lacks many common and widespread species found within our southern area.

We have felt that a most useful tool for a worker in the kelp areas south of Point Conception would be a fully illustrated manual of the larger, conspicuous, sublittoral forms, selected as a result of our experience with the region to include only those that one is likely to encounter with reasonable frequency in an extensive diving program. By this reduction in the total number of plants involved, we believe that recognition of the species through the use of the illustrations and keys will be practical and relatively easy. In a large majority of cases no microscopic examinations need be made, and in those instances in which internal structures must be relied upon for positive identification, figures have been provided which will enable one to make comparisons by means of a hand section cut with an ordinary razor blade.

Terminology has been kept as simple as possible, and such technical terms as are used may be understood from the illustrations.

Inasmuch as the green, brown and red colors of the larger plants growing in sublittoral waters are in almost all cases readily distinguishable (either in sunlight or artificial light)[6] we have employed this simple color breakdown in the key as an aid to ready identification.

KEY TO THE COLOR GROUPS

Plants distinctly green in color throughout .... Green Algae and Surf Grass, Key I. (text p. 26)

Plants distinctly brown in color throughout .... Brown Algae, Key II. (text p. 30)

Plants in principal parts reddish, pinkish or purplish (sometimes densely so and requiring that they be held up against a strong light to reveal the redness), the spores always red .... Red Algae, Key III. (text p. 38)

---

[6] It has not been possible to use successfully such a color breakdown in keys which include intertidal algae, for in intertidal habitats variations in masking pigments often cause confusing color differences that complicate the problem of recognition on this basis.

I. KEY TO GREEN ALGAE AND SURF GRASS[7]

1. Plants consisting of a single, ovoid cell 1/8 to 3/8 inch in diameter .... *Halicystis ovalis*
1. Plants consisting of more complex structure 2
    2. Plants spongy 3
    2. Plants with slender, elongate parts, not spongy 5
3. Plants prostrate, low, cushion-shaped 4
3. Plants erect, branched .... *Codium cuneatum*
    4. Plants consisting of utricles with pitted end walls .... *Codium hubbsii*
    4. Plants consisting of utricles with smooth, non-pitted walls .... *Codium setchellii*
5. Plants two feet long or more, with long, slender leaves .... *Phyllospadix torreyi*
5. Plants usually less than 6 inches long, the branches of a single row of large cells 6
    6. Plants branched, erect, tufted .... *Cladophora graminea*
    6. Plants unbranched, twining .... *Chaetomorpha torta*

II. KEY TO THE BROWN ALGAE

1. Plants with hollow, float structures 2
1. Plants without hollow, float structures 7
    2. Plants with a single large bulb between the long stipe and the broad blades .... *Pelagophycus porra*
    2. Plants with several to many float structures 3
3. Plants with small float structures joined in series 4
3. Plants with small or large individually separate floats 5
    4. Series of float structures, cylindrical, bead-like .... *Cystoseira osmundacea*
    4. Series of float structures flat .... *Halidrys dioica*
5. Floats less than 1/4 inch in diameter, not bearing a leaf-like part .... *Sargassum agardhianum*
5. Floats about 1 inch long or more, bearing a leaf-like part 6
    6. "Leaves" and floats borne on either side of a flat axis .... *Egregia laevigata*
    6. Leafy parts borne alternately along a cylindrical axis .... *Macrocystis pyrifera*

---

[7] In the annotated list that follows the key, the species are arranged, for convenient reference, alphabetically by genus and species under each color group. The figures making up the plates are arranged in approximate phylogenetic order.

7. Plants hollow, sac-like or bubble-like or convoluted 8
7. Plants differentiated into variously modified holdfast, stipe and blade parts 10

8. Plants sac-like, flattened or expanded, always epiphytic 9
8. Plants bubble-like and smooth or undulate and convoluted, epiphytic or on solid substrate .... *Colpomenia sinuosa*

9. Plants commonly epiphytic on *Halidrys*, flat and semi-rigid .... *Colpomenia rigida*
9. Plants commonly epiphytic on *Cystoseira*, more or less inflated, flabby .... *Coilodesme californica*

10. Plants consisting of a single, unbranched blade (which, however, may become lacerated 11
10. Plants variously branched and divided 17

11. Blades with veins or midrib (sometimes only a diffuse medial thickening) 12
11. Blades without midrib or veins 14

12. Blades with opposite veins from a slender median vein .... *Desmarestia tabacoides*
12. Blades with a single broad midrib or medial thickening 13

13. Blades roughly corrugated, developing performations, the stipe fringed .... *Agarum fimbriatum*
13. Blades smooth, marginally undulate, without perforations, stipe smooth .... juvenile *Egregia laevigata*

14. Plants large, 3-15 feet long, with leathery blades .... *Laminaria farlowii*
14. Plants small, less than one foot long, smooth, thin 15

15. Blades with small lobes along the lower margins .... juvenile *Eisenia arborea*
15. Blades smooth throughout 16

16. Blades expanding gradually above the stipe, developing a longitudinal median slit above the stipe .... juvenile *Macrocystis pyrifera*
16. Blades expanding abruptly above the stipe, not developing a slit .... juvenile *Laminaria farlowii*

17. Plants tree-like, with heavy stalks 18
17. Plants consisting mainly of flat blades 19

18. Stalk forked at the top, bearing two bunches of drooping, strap-like blades .... *Eisenia arborea*
18. Stalk bearing pinnate branches at the top and ending in a blade .... *Pterygophora californica*

19. Plants with midribs or veins 25
19. Plants without midribs or veins 20

20. Plants dichotomously branched, not markedly broader in upper than in lower parts 21
20. Plants having more or less fan-shaped parts, not dichotomously branched 23

21. Blades with small teeth along the margins .... *Dictyota binghamiae*
21. Blades with smooth margins 22

22. Plants usually dark brown, the branches usually over 3/8 inch broad; margins more than 3 cells thick .... *Pachydictyon coriaceum*
22. Plants usually light brown, the branches usually less than 3/8 inch wide; margins only 3 cells thick .... *Dictyota flabellata*

23. Plants broadly fan-shaped, 2-4 inches wide or more, with rolled margins .... *Padina durvillaei*
23. Plants not broadly fan-shaped, without rolled margins 24

24. Terminal branches fan-shaped, but small, about 1/2 inch broad; whole plant of clumping form .... *Zonaria farlowii*
24. Terminal parts not distinctly fan-shaped except in young plants, the whole plant lacerate, thin, flat .... *Taonia lennebackerae*

25. Plants dichotomously branched .... *Dictyopteris zonarioides*
25. Plants pinnately branched, with opposite veins 26

26. Flat blades 1 to 4 inches broad .... *Desmarestia munda*
26. Flat blades 1/4 to 1/2 inch broad; branching abundant .... *Desmarestia herbacea*

III. KEY TO THE RED ALGAE

1. Plants calcareous .... calcareous group, see No. 80
1. Plants firm or fleshy, not calcareous 2

2. Plants prostrate, forming flat, rounded, or lobed crusts more or less closely adherent to rocks 3

2. Plants erect or at least major parts free and not adherent 4

3. Plants closely adherent, firm, somewhat brittle .... *Peyssonelia rubra* var. *orientalis*

3. Plants loosely adherent, membranous, delicate, flexible .... *Amplisiphonia pacifica*

4. Principal and conspicuous parts easily recognized as being distinctly and broadly flat, or distinctly cylindrical, as ▬ or ● 5

4. Principal individual parts of plants only compressed or a little or narrowly flattened, as ⬬ , not more than about 4 times as broad as thick, as ▭ , sometimes the branching so arranged that the whole plant appears to be flat and finely dissected, but the individual parts only compressed or somewhat flattened 62

5. Principal parts of plants distinctly flat, with more or less membranous or thick leafy parts many times as broad as thick 6

5. Principal parts of plants distinctly or nearly cylindrical, either coarse and obviously so, or sometimes filamentous and almost microscopic (use a hand lens on more delicate ones) 45

6. Plants primarily peltate, parasol-shaped 7

6. Plants variously branched and attached, but not peltate 8

7. Blade rotate, the margin smooth .... *Drouetia rotata*

7. Blade with star-like points which later form secondary attachments .... *Sciadophycus stellatus*

8. Plants growing entangled and with frequent hook-like branches .... *Acrosorium uncinatum*

8. Plants attached by some kind of basal holdfasts, without hook-like branches 9

9. Blades with more or less conspicuous lines or veins (easily visible with no more than a 3-power hand lens) 10

9. Blades without conspicuous ribs or veins 16

10. Blades with essentially smooth margins 11

10. Blades with toothed, lobed or crisped margins 12

11. Blades dichotomous, with a single, discontinuous central rib-line .... *Stenogramme interrupta* (female plants)

11. Blades broad, fan-shaped, with many anastomosing veins .... *Polyneura latissima*

12. Blades with teeth along the margins 13

12. Blades with small separate or densely crisped lobes along margins 14

13. Plants large (5-30 cm.) abundantly branched .... *Nienburgia andersoniana*

13. Plants small (under 4 cm.) simple or sparsely branched .... *Anisocladella pacifica*

14. Blades with relatively few, small, marginal lobes .... *Cryptopleura violacea*

14. Blades with crisped margins consisting of densely crowded, small lobe-like outgrowths 15

15. Blades narrow, less than 1 cm. broad, the plants commonly under 10 cm. high; epiphytic .... *Cryptopleura crispa*

15. Blades broader, more than 1 cm. wide, the plants commonly 20 cm. tall or more; usually not epiphytic .... *Botryoglossum farlowianum*

16. Plants with irregular teeth along the margins .... *Leptocladia binghamiae*

16. Plants with margins of blades smooth or with rounded protuberances, lobes, ruffles or papillae, but not teeth 17

17. Plants small, usually less than 2 cm. in height or expanse, usually epiphytic 18

17. Plants larger, 3-60 cm. tall, usually not epiphytic 22

18. Plants always epiphytic on *Phyllospadix* .... *Smithora naiadum*

18. Plants, when epiphytic, not on *Phyllospadix* 19

19. Plants with distinct midrib and lateral veins when viewed with moderate magnification .... *Branchioglossum undulatum*

19. Plants without any midrib 20

20. Plants broadly round-lobed rather than distinctly branched, one cell thick .... *Myriogramme caespitosa*

20. Plants widely branched, the segments strap-shaped, many cells thick 21

21. Cystocarps bearing several crown-like points; tetrasporangia borne embedded in the cortex .... *Fauchea laciniata* (small plants)

21. Cystocarps rostrate but not coronate; tetrasporangia borne in open cavities in the thallus .... *Binghamia forkii*

22. Plants simple or very little branched 23

22. Plants conspicuously and frequently branched 27

23. Surface of broad blades covered with rough papillations or pointed outgrowths 24

23. Surface of blades essentially smooth 25

24. Blades very broad, 10-50 cm. wide .... *Gigartina binghamiae*

24. Blades narrower, mostly under 7 cm. wide, elongate .... *Grateloupia howeii*

25. Blades very broad, rounded .... *Cryptonemia obovata*

25. Blades elongated, much longer than wide 26

26. Plants purplish in color; apices tapered and generally pointed .... *Grateloupia schizophylla* (non-proliferous plants)

26. Plants rose-red; apices rounded ...... *Cryptonemia angustata*

27. Plants distinctly dichotomously branched 28

27. Plants irregularly alternately, flabellately or pinnately branched, but not distinctly dichotomous 37

28. Plants with prominent marginal outgrowths .... *Gigartina volans*

28. Plants without prominent marginal outgrowths 29

29. Ultimate branches commonly becoming congested; interior of thallus densely stuffed with filamentous cells .... *Carpopeltis bushiae*

29. Ultimate branches not becoming congested; interior of thallus of large, relatively thin-walled cells 30

30. Upper segments expanded to over 2 cm. wide; plants to 16 cm. high .... *Phyllophora clevelandii*

30. Upper segments exceeding 1.5 cm. wide 31

31. Tetrasporangia scattered through the cortex, without specialized sori or other structures .... *Gracilaria cunninghamii* (in part)

31. Tetrasporangia borne in special sori or on special branchlets 32

 32. Plants attached by a heavy conical holdfast .... *Rhodymenia arborescens*

 32. Plants attached by a small disc holdfast and often by accessory stolons 33

33. Stolons associated with primary holdfast; tetrasporangial sori on special leaflets 34

33. Attachment only by primary holdfast, without stolons; tetrasporangia borne in irregular sori on middle blade surfaces .... *Stenogramme interrupta*

 34. Terminal segments attenuated or narrowed below tip .... *Rhodymenia attenuata*

 34. Terminal segments rounded, not attenuate 35

35. Tetrasporangia borne in small terminal sori; plants small, usually under 5 cm. tall .... *Rhodymenia californica*

35. Tetrasporangia borne in special leaflets; plants larger, usually over 8 cm. tall 36

 36. Stipe simple, short, with few stolons; tetrasporangial leaflets from uppermost segment margins .... *Rhodymenia pacifica*

 36. Stipe short, sometimes branched, usually with conspicuous stolons; tetrasporangial leaflets from older segments .... *Rhodymenia palmettiformis*

37. Plants with prominent marginal outgrowths, proliferations or pinnae 38

37. Plants with essentially entire segments and without prominent marginal outgrowths, proliferations or pinnae 39

 38. Plants soft and slippery .... *Grateloupia schizophylla* (proliferous form)

 38. Plants coarse, stiff .... *Gigartina volans* (in part)

39. Primary blades long, slender, strap-shaped .... *Prionitis andersoniana*

39. Branching frequent throughout; without long strap-shaped parts 40

40. Central medullary tissue composed of large, thin-walled cells of uniform size 41

40. Central medullary tissue composed of mixed large and small cells 43

41. Plants soft, flabby, without a prominent cylindrical stipe 42

41. Plants coarse, rather stiff, with flat branches from a cylindrical, branched stipe .... *Phyllophora californica*

42. Plants slippery; branching widely divergent; cystocarps coronate .... *Fauchea laciniata*

42. Plants not slippery; branching irregular to dichotomous, but not widely divergent; cystocarps domoid .... *Gracilaria cunninghamii*

43. Cystocarps borne along margins of blades .... *Callophyllis marginifructa*

43. Cystocarps borne over surface of blades 44

44. Cystocarps rostrate 1.0-1.5 (2.5) mm. diameter; segments mostly 0.5-1.5 cm. broad .... *Callophyllis megalocarpa*

44. Cystocarps non-rostrate, 0.6-1.2 (1.5) mm. diameter; segments mostly 1-7 mm. broad .... *Callophyllis violacea*

45. Cylindrical axes bearing swollen branchlets of much larger diameter than their own 46

45. Plants without inflated vesicular branchlets 47

46. Inflated branches many, small, on long branched stalks .... *Botryocladia neushulii*

46. Inflated branches few, large, on short branched stalks .... *Botryocladia pseudodichotoma*

47. Main axes bearing short branchlets which are hollow and divided by transverse partitions into a series of compartments .... *Gastroclonium coulteri*

47. Special hollow, compartmented branchlets absent 48

48. Plants relatively large and coarse, the main branches well over 1 mm. in diameter 49

48. Plants relatively small and delicate, or at least the main axes mostly under 1 mm. in diameter 55

49. Plants dichotomously branched 50

49. Plants variously branched but not dichotomous 51

50. Outer cortex composed only of a layer of large colorless cells with numerous slender 2-3-celled filaments between them .... *Scinaea johnstoniae*
50. Outer cortex consisting of a layer of large colorless cells with numerous slender 2-3-celled filaments between them .... *Gloiophloea confusa*

51. Plants with frequent twining or hooked branches .... *Laurencia subopposita*
51. Plants without twining or hooked branches 52

52. Plants with long, indeterminate branches throughout, without irregular or tufted short branchlets .... *Agardhiella coulteri*
52. Plants with many very short branchlets or papillae or tufts of short branchlets 53

53. Tufts of short branches borne on long, smooth, slender main branches .... *Chondria nidifica*
53. Short branchlets and papillae scattered over upper parts of plants 54

54. Plants short, 8-12 cm. high, the main axes with short segments .... *Gigartina canaliculata*
54. Plants long, lax, 15-30 cm. long, the main axes with infrequent branches, the segments long .... *Gigartina serrata*

55. All branches similar 56
55. Main axes bearing tufts of minute hair-like lateral branches .... *Pogonophorella californica*

56. Branches consisting of a single row of large cells 57
56. Branches consisting of five or more rows of cells 58

57. Plants resembling tufts of fine red hair .... *Spermothamnion snyderae*
57. Plants clumping, not hair-like .... *Griffithsia pacifica*

58. Plants coarse, wire-like, to 20 cm. high or more .... *Gelidium nudifrons*
58. Plants delicate, under 10 cm. high, soft and limp 59

59. Plants dichotomously branched .... *Ceramium pacificum*
59. Plants irregularly alternately branched 60

60. External cells in uniform transverse tiers 61
60. External cells irregularly arranged, not in tiers .... *Chondria californica*

(50)

61. External tiers of cells consisting of 4 cells .... *Polysiphonia mollis*

61. External tiers of cells consisting of 5-6 cells .... *Polysiphonia johnstonii*

62. Principal branching dichotomous 63

62. Branching mainly pinnate or irregular 64

63. Dichotomous branches bearing short, pinnate secondary lateral branches .... *Prionitis cornea*

63. Dichotomously branched throughout .... *Gymnogongrus leptophyllus*

64. Plants coarse, at least in lower parts, seldom epiphytic; ultimate branchlets coarse, at least not reduced to almost microscopic size 65

64. Plants delicate throughout, usually epiphytic; ultimate branchlets very small to almost microscopic 74

65. Plants composed of compressed or flattened parts without marginal teeth 66

65. Plants composed of flat blades with irregular teeth along the margins .... *Leptocladia binghamiae* (in part)

66. Upper branching very dense, in one plane, feathery, with many regularly curved branchlets, pectinate .... *Plocamium pacificum* (in part)

66. Upper branching not particularly feathery, not pectinate; branchlets not regularly curved 67

67. Main axes with series of short, determinate secondary branchlets .... *Prionitis lanceolata*

67. Main axes repeatedly branched in successive orders, without series of short, determinate branchlets 68

68. Ends of branches with a dimple-like terminal depression in which the growing point is located 69

68. Ends of branches without a terminal depression 70

69. Main axes to 5-6 mm. wide; plants to 20 cm. high or more .... *Laurencia diegoensis*

69. Main axes usually 2-3 mm. wide; plants 5-10 cm. high .... *Laurencia splendens* (in part)

70. Ends of branches with a distinct terminal cell microscopically visible 72

70. Ends of branches without a distinct terminal cell; mature plants with spiny outgrowths 71

71. Plants short, 8-12 cm. high, the main axes with short segments .... *Gigartina canaliculata*

71. Plants long, lax, 15-30 cm. long, the main axes with infrequent branches, the segments long .... *Gigartina serrata*

72. Young branchlets not geniculate; mature parts often with terminal branches reduced in diameter and becoming entangled; cystocarps unilocular .... *Pterosiphonia pyramidale*

72. Young branchlets at first geniculate; mature parts with branches more or less uniform throughout; cystocarps bilocular 73

73. Tetrasporangial branchlets with cordate apices .... *Gelidium cartilagineum* var. *robustum*

73. Tetrasporangial branchlets blunt or subacute, not cordate .... *Gelidium purpurascens*

74. Ends of branches with a dimple-like depression in which the growing point is located .... *Laurencia splendens* (in part)

74. Ends of branches acute or at least without a dimple-like depression 75

75. Ultimate branchlets with cells in regular transverse tiers 77

75. Ultimate branchlets with irregularly arranged cells not in tiers 76

76. Branching regularly alternate, distichous .... *Microcladia coulteri*

76. Branching appearing irregular, but in one plane; ultimately pectinate .... *Plocamium pacificum* (in part)

77. Erect branches without percurrent axes; commonly epiphytic on *Cystoseira* 78

77. Erect branches with percurrent axes; variously epiphytic or saxicolous 79

78. Plants less than 2 cm. tall .... *Pterochondria pygmaea*

78. Plants usually over 5 cm. tall .... *Pterochondria woodii*

79. Older branches completely corticated .... *Pterosiphonia baileyi*

79. All branches uncorticated .... *Pterosiphonia dendroidea*

(52)

Calcareous Group

80. Plants crustose, not jointed 90

80. Plants jointed, segmented 81

81. Plants with terminal conceptacles 82

81. Plants without terminal conceptacles 86

82. Plants large, coarse, the segments 4-6 mm. broad in mid-parts 83

82. Plants smaller, the segments less than 2 mm. broad 84

83. Plants with flat segments throughout upper parts .... *Calliarthron cheilosporioides*

83. Plants with flat segments in mid-parts and cylindrical segments in upper parts .... *Calliarthron regenerans*

84. Tetrasporic conceptacles normally antenniferous, at least predominantly so .... *Corallina gracilis*

84. Tetrasporic conceptacles normally non-antenniferous, at least predominantly so 85

85. Segments of main axes mostly .75 mm. broad and 1 mm. long .... *Corallina vancouveriensis*

85. Segments of main axes mostly 1.1-1.3 mm. broad and 1.5-1.7 mm. long .... *Corallina officinalis* var. *chilensis*

86. Segments mostly dorsiventral, not erect .... *Amphiroa dimorpha*

86. Segments not dorsiventral; plants erect 87

87. Upper segments faintly banded; some segments branched .... *Amphiroa zonata*

87. Upper segments not banded; segments not branched 88

88. Segments mainly cylindrical, very short .... *Lithothrix aspergillum*

88. Segments flat, winged 89

89. Segments arrow-head shaped, with acute wings .... *Bossiella orbigniana*

89. Segments wing-nut shaped, with rounded wings .... *Bossiella gardneri*

90. Plants growing on *Phyllospadix* .... *Melobesia mediocris*

90. Plants growing on various algae, rocks or shells 91

91. Plants solid, usually massive, with protuberances 92

91. Plants thin, crust-like, smooth, or at least without protuberances 93

92. Protuberances large, 10-15 mm. high, 5-15 mm. in diameter .... *Lithothamnium giganteum*
92. Protuberances small, often low, 2.5-5 mm. in diameter, 2-10 mm. high .... *Lithophyllum imitans*

93. Plants shingle-like, on rocks, shells or lower parts of some algae .... *Lithothamnium lamellatum*
93. Plants growing as a crust over the surface of various algae .... *Dermatolithon dispar*

SPECIES LIST

FLOWERING PLANTS

Phyllospadix torreyi S. Watson Torrey's Surf Grass Pl. 1, fig. 1.

Northern California to Isla Magdalena, Baja California. This is one of two species of Surf Grass that occur along our Pacific Coast. It grows on rocks from intertidal levels down to as deep as 50 feet. The long, slender, almost filamentous grass-green leaves distinguish it readily. The other species, *P. scouleri*, is usually confined to the surf zone and has thinner, shorter leaves and shorter flowering stems.

GREEN ALGAE

Chaetomorpha torta (Collins) Yendo Pl. 2, fig. 1.

Southern California to Isla Magdalena, Baja California. Grows entwined around other algae in the intertidal zone to a depth of 30 feet. The plant suggests a bluish-green colored tendril. Its large cells are clearly visible to the naked eye.

Cladophora graminea Collins Pl. 1, fig. 4.

Central California to Isla Magdalena, Baja California. Grows as small green tufts of rigid, erect filaments 2-3 inches tall, usually in areas around sand. Occasion, from intertidal to 75 feet.

Codium cuneatum Setchell and Gardner Pl. 5, fig. 2.

Southern California to Isla Magdalena, Baja California. This is a spongy, green plant, 10-12 inches high. Common in depths of 30-60 feet.

Codium hubbsii Dawson Pl. 1, fig. 6

Northern half of Baja California. Forms a greenish-black, spongy patch, 2 inches or more across, on rocks, commonly under the kelp canopy in areas of encrusting coralline bottom at 30-75 foot depths. Distinguished from the next species only by the end-walls of the club-shaped utricles of which the surface of the spongy thallus is composed.

Codium setchellii Gardner Pl. 1, figs. 2, 5.

Alaska to central Baja California. Of the same habit and habitat as *C. hubbsii* and macroscopically indistinguishable.

Halicystis ovalis (Lyngbya) Areschoug Pl. 1, fig. 3.

Alaska to central Baja California. This plant grows as a small, dark green ball, half an inch or less in diameter, on encrusting calcareous algae from intertidal to 75 foot depths. It appears almost black in deeper water and is seen with difficulty.

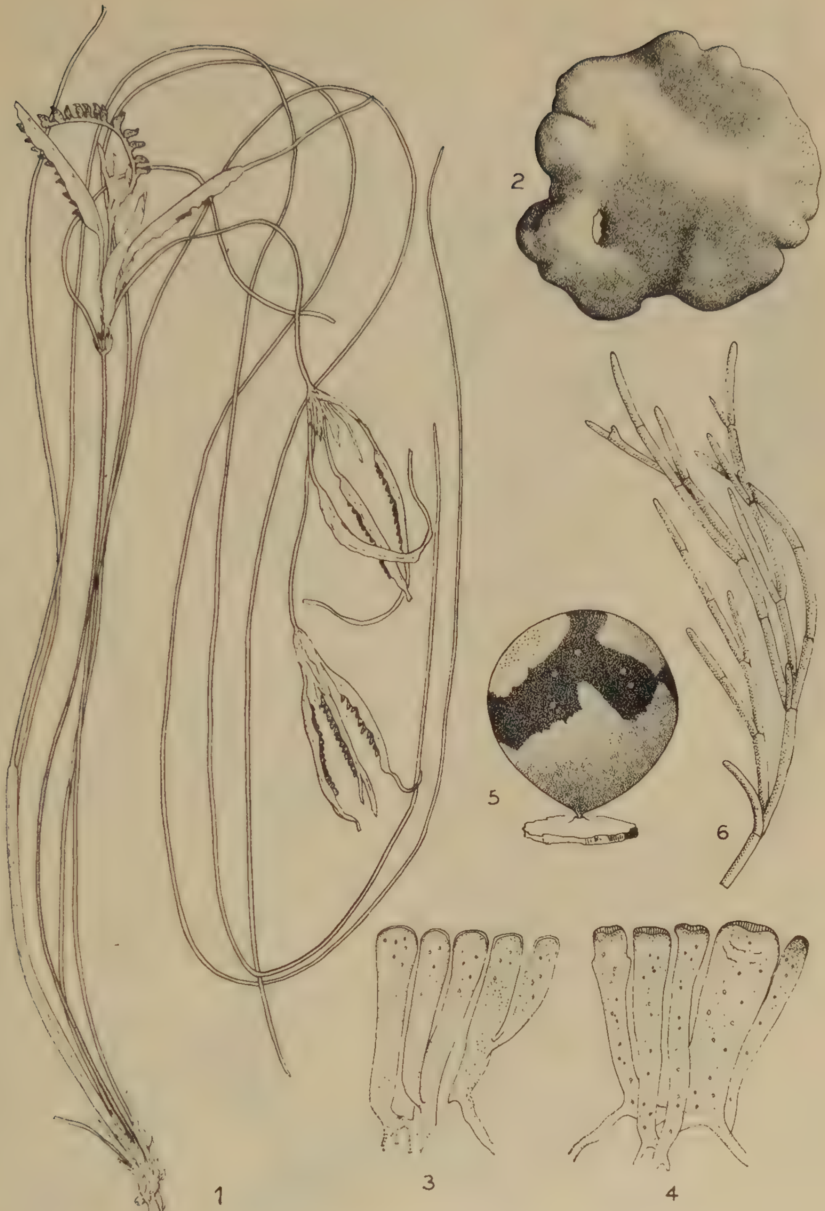

PLATE 1

Fig. 1. *Phyllospadix torreyi,* flowering, × 0.5. Fig. 2-3. *Codium setchellii*: fig. 2, habit, × 0.5; fig. 3, detail of utricles making up exterior of thallus, showing non-pitted end walls, × 28. Fig. 4. *Codium hubbsii,* detail of utricles showing pitted end walls, × 28. Fig. 5. *Halicystis ovalis,* showing attached habit of plant, × 2. Fig. 6. *Cladophora graminea,* upper portion of plant, showing branching, × 6.

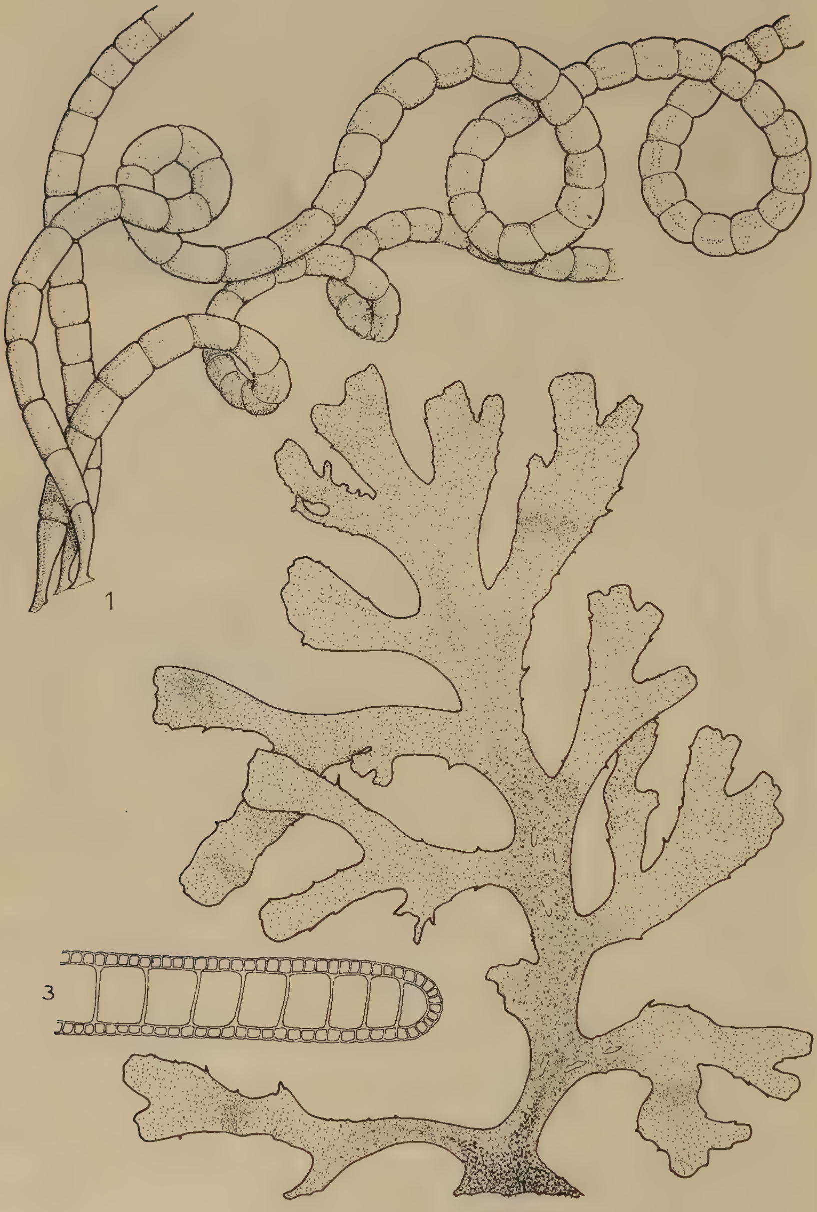

PLATE 2
Fig. 1. *Chaetomorpha torta,* showing twining habit and large cells, × 3. Fig. 2-3. *Dictyota binghamiae*: fig. 2, habit, showing teeth along the margins, × 1; fig. 3, cross-section of blade, × 80.

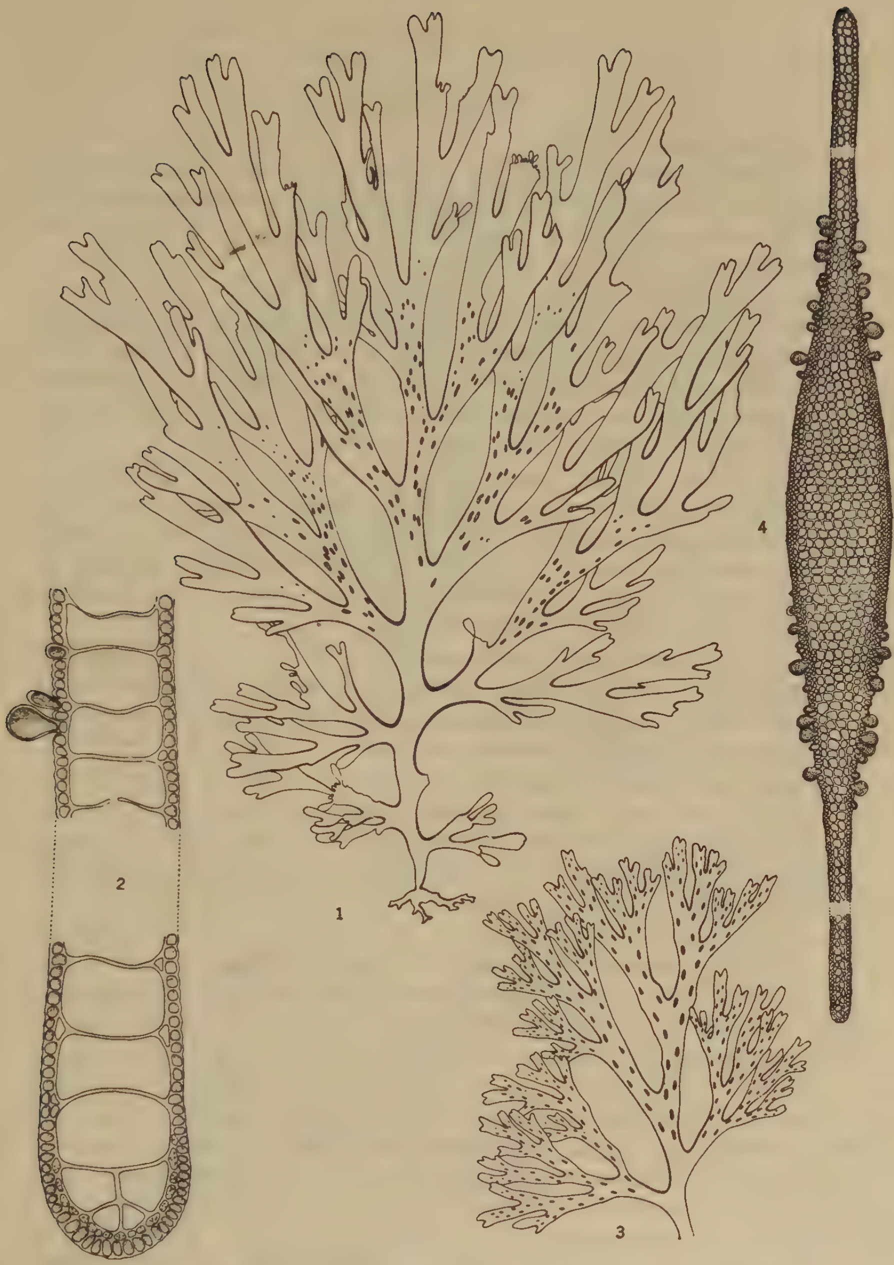

PLATE 3
Fig. 1-2. *Pachydictyon coriacium*: fig. 1, habit, × 0.5; fig. 2, cross-section of a frond showing the character of the cells at the margin, × 125. Fig. 3. *Dictyota flabellata*, portion of frond, × 0.5. Fig. 4. *Dictyopteris zonarioides*, cross-section of frond showing the thick midrib, superficial reproductive bodies and portions (shortened) of the blade, × 45. (after Setchell & Gardner)

BROWN ALGAE

Agarum fimbriatum Harvey Pl. 20, fig. 1.

Southern British Columbia to southern California. The blades are light to dark brown in color, irregularly corrugated and sometimes with holes. A conspicuous midrib is present, and the stipe is fringed. In our region growing at depths of 40-100 feet.

Coilodesme californica (Ruprecht) Kjellman Pl. 9, fig. 3.

British Columbia to central Baja California. Plants hollow, light olive tan in color, somewhat wrinkled when older with terminal portions of the sac-like plant body becoming worn and eroded. Growing on upper portions of *Cystoseira* plants within about 10 feet of the surface, although the host may be attached at depths of 30 feet or more.

Coilodesme rigida Setchell and Gardner Pl. 6, fig. 2.

Southern California to central Baja California. Plants dark brown in color, conspicuously flattened, with a thickening near the margins; small, usually about an inch long. Growing attached to upper portions of *Halidrys*, usually within 10 feet of the surface, although the base of the host may be attached at depths of 30 feet.

Colpomenia sinuosa (Roth) Derbès and Solier Pl. 9, figs. 1, 2.

Alaska to Costa Rica. These hollow plants may be epiphytic, small, and bubble-like, or larger, 2-6 inches in diameter, rough and warty, and broadly attached to rocks. Intertidal to 60 feet.

Cystoseira osmundacea (Turner) C. Agardh Pl. 14.

Oregon to Punta Abreojos, Baja California. The basal portions, habitat and stature (to 20 feet tall) are similar to those of *Halidrys* from which it is distinguished by its conspicuously rounded vesicles in bead-like series. Common, intertidal to 100 feet.

Desmarestia herbacea Lamouroux Pl. 7, fig. 2.

Alaska to central Baja California. Plants light brown, with a conspicuous axial vein running to branch and axis tips, profusely branched, highly acid and sour to the taste. Occasional, intertidal to 30 feet.

Desmarestia munda Setchell and Gardner Pl. 7, fig. 1.

British Columbia to Punta Pequeña, Baja California. Plants light to dark brown, sparsely branched, all the branches stipate at base. The characteristic long blades are often so eaten back by grazing organisms as to lose their distinctive, strap-shaped appearance. Strongly acid to the taste. Frequent in depths of 20-60 feet.

Desmarestia tabacoides Okamura Pl. 8.

Santa Cruz Island, California to La Jolla, California. This strictly sublittoral plant occurs only in depths of 50-135 feet where it appears almost black. Its thick frond contracts to a short stipe at the base and in older individuals is often divided into two main segments. The veins are distinctive but faint.

(58)

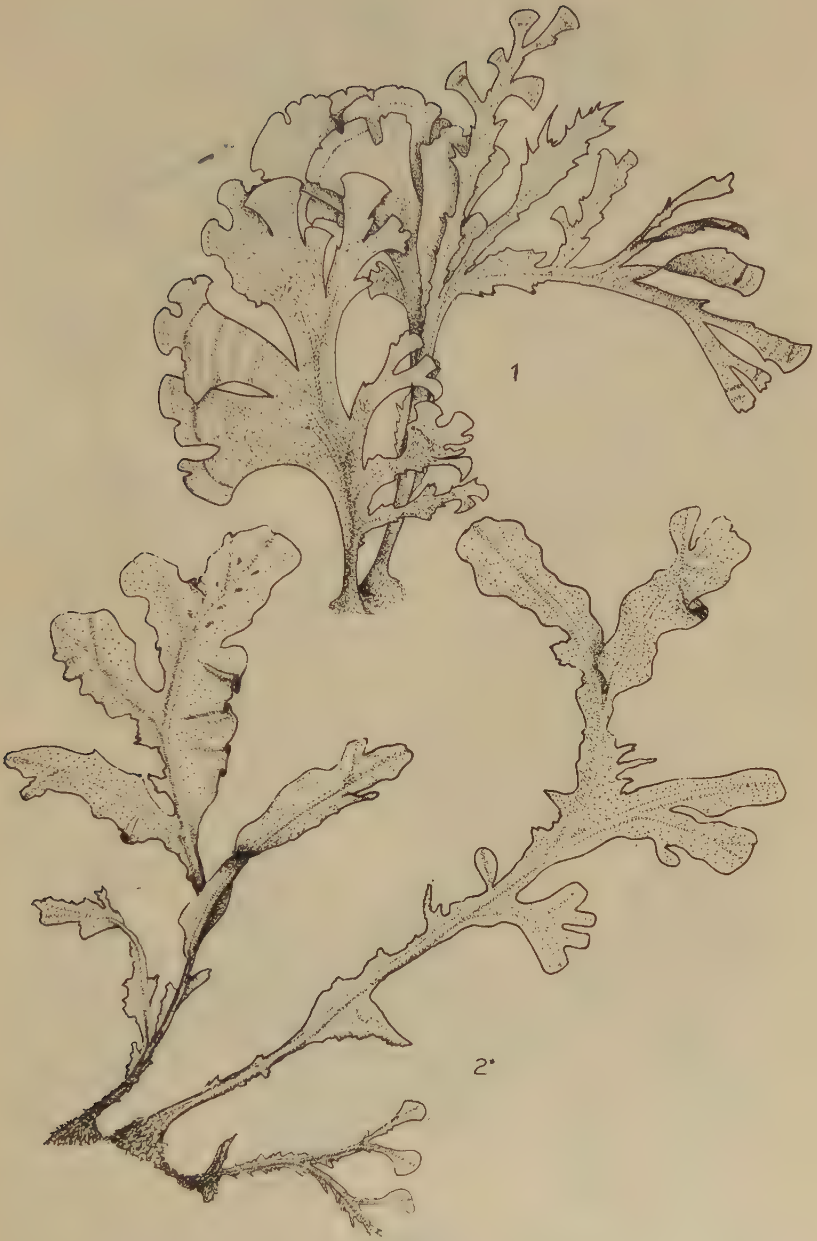

PLATE 4

Fig. 1. *Zonaria farlowii,* habit showing concentric hair lines, × 1. Fig. 2. *Dictyopteris zonarioides,* habit showing distinct midrib, × 1.

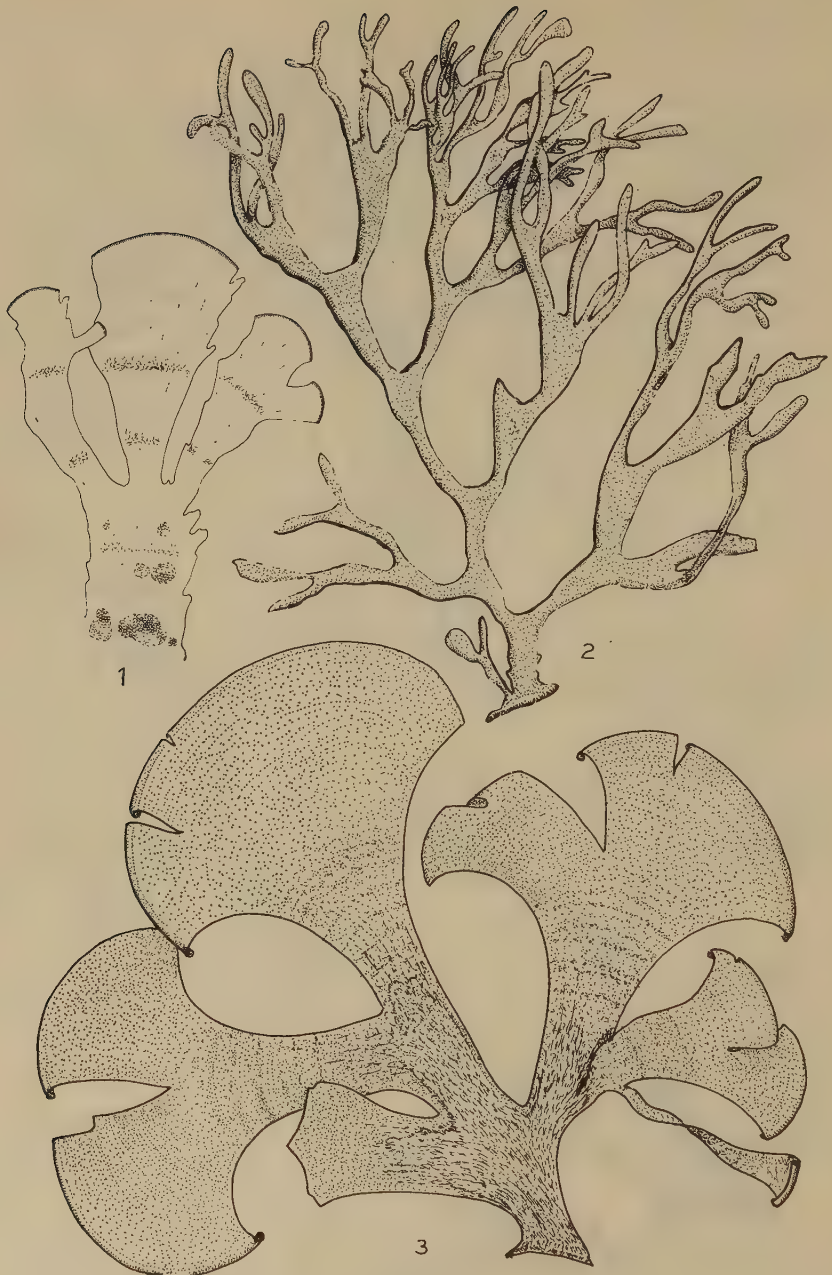

PLATE 5

Fig. 1. *Zonaria farlowii,* upper portion of blade showing sori and hair lines, × 3. Fig. 2. *Codium cuneatum,* habit showing flattened forks, × 0.5. Fig. 3, *Padina durvilliae,* habit, holdfast and upper fan-shaped parts, × 0.5.

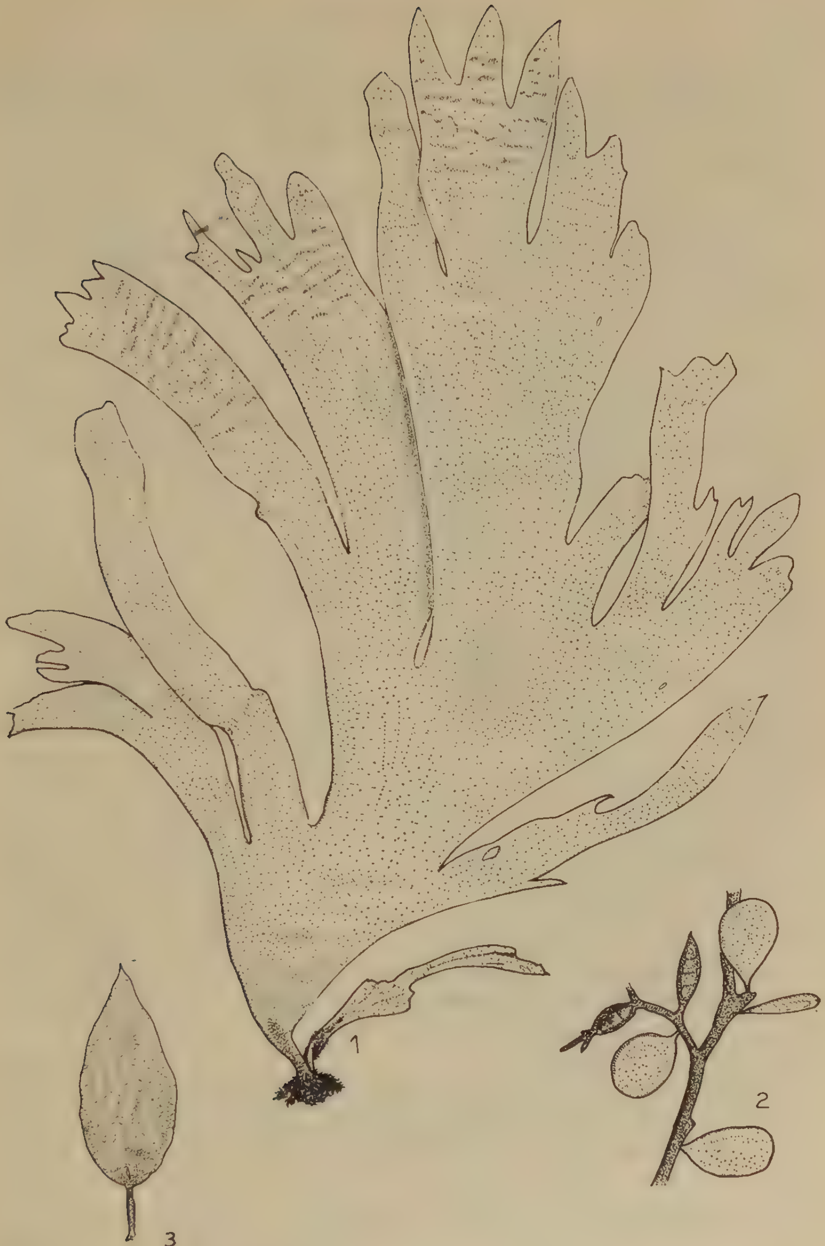

PLATE 6
Fig. 1. *Taonia lennebackerae,* habit, × 0.5. Fig. 2. *Coilodesme rigida,* habit, showing plants epiphytic on *Halidrys dioica,* × 0.5. Fig. 3. *Macrocystis pyrifera,* a juvenile plant showing initial split, × 0.25.

Dictyota binghamiae J. Agardh Pl. 2, fig. 2.

Central California to central Baja California. This brown, dichotomous plant is readily recognized by its small, inconspicuous marginal teeth. Occasional at depths of 30-115 feet.

Dictyota flabellata (Collins) Setchell and Gardner Pl. 3, fig. 3.

Southern California to central Baja California. Among the smooth-margined, dichotomous brown algae, this one is distinguished by its small size (3-5 inches high) and blades only 3 cell layers thick. Occasional, intertidal to 75 feet.

Dictyopteris zonarioides Farlow Pl. 3, fig. 4; Pl. 4, fig. 2.

Southern California to southern Baja California. Although brown in color overall, these plants often exhibit conspicuous blue irridescence in the terminal expanded blade parts. A conspicuous midrib is distinctive and runs to the very ends of the branches. Intertidal to 115 feet.

Egregia laevigata Setchell Feather Boa Pl. 13, fig. 1-3.

Southern California to central Baja California. This is one of the commonest and best known of the large brown kelps on account of its distinctive paired rows of "leaves" and bladders on the long flat axes. Intertidal to 30 feet, seldom deeper.

Eisenia arborea Areschoug Southern Sea Palm Pl. 16, fig. 2, 3.

Southern California to Isla Magdalena, Baja California. These dark brown, tree-like plants have their blades borne in two conspicuous groups at the apex of a stout stipe. Common, intertidal to 115 feet. Plants in deep water or dense shade have more conspicuous marginal teeth on the blades.

Halidrys dioica Gardner Pl. 15, fig. 1, 2.

Southern California to central Baja California. Plants light to dark brown in color, 3 to 20 feet tall, at depths from intertidal to 75 feet. The basal blades of this and the next species are usually quite rigid. The pod-like series of flattened vesicles clearly distinguish this plant from *Cystoseira*. Short, sterile, vegetative plants of *Halidrys* and *Cystoseira* occur at depths of 50-100 feet, and cannot be distinguished in the absence of the distinctive float-bearing portions of the plants.

Laminaria farlowii Setchell Pl. 9, fig. 4, 5.

Central California to northern Baja California. Plants with a single. dark brown, thick, undulate blade reaching lengths up to 15 feet. Common in the kelp beds at La Jolla where it forms a dominant part of the bottom community.

Macrocystis pyrifera (Linnaeus) C. Agardh Pl. 6, fig. 3; Pl. 10.

Monterey, California to Punta San Hipólito, Baja California, intertidal to 100 feet. The plants from La Jolla southward are characterized by relatively few, heavy haptera arising from the erect basal branching system. Plants from Palos Verdes, California, northward generally having haptera arising from a basal branching system which becomes prostrate.

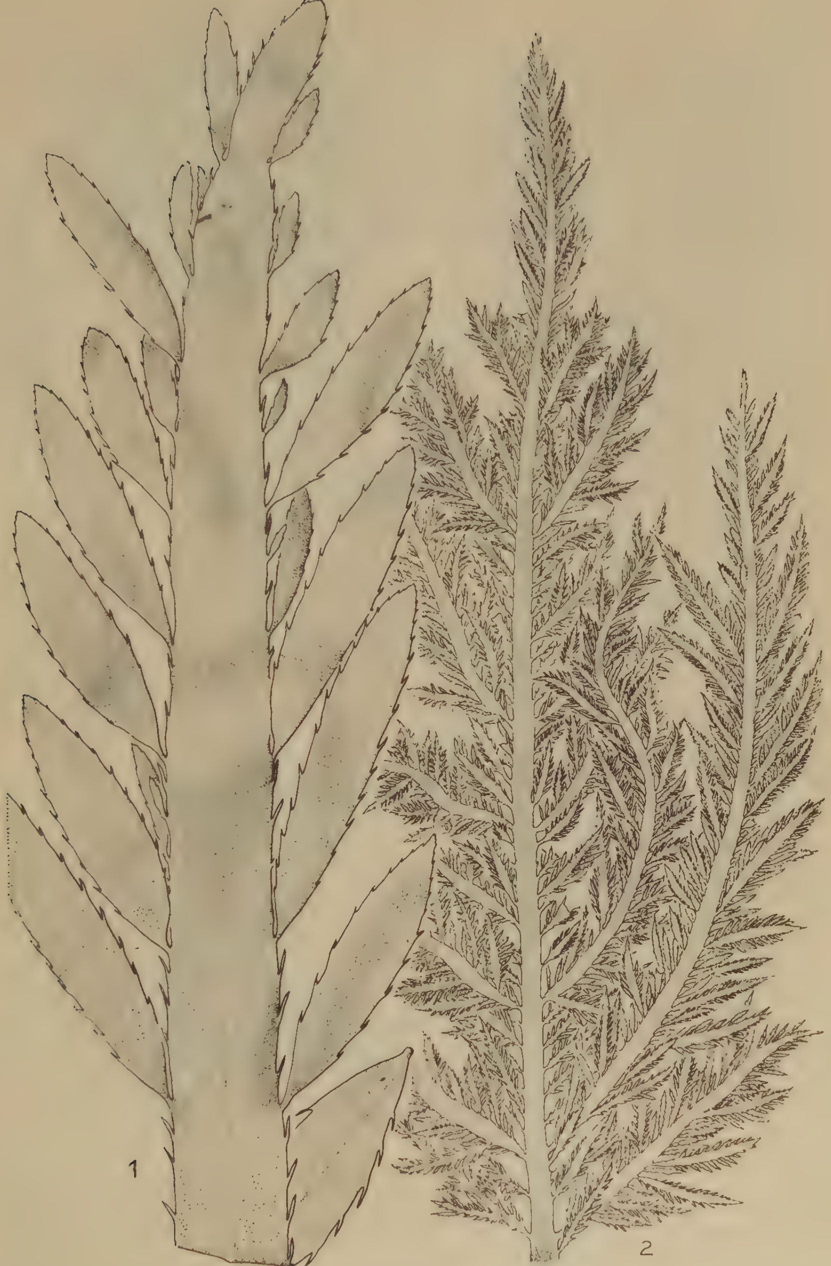

PLATE 7

Fig. 1. *Desmarestia munda,* upper portion of plant showing distinct toothed margins, × 0.33. Fig. 2. *Desmarestia herbacea,* upper portion of plant showing profuse branching, × 0.33.

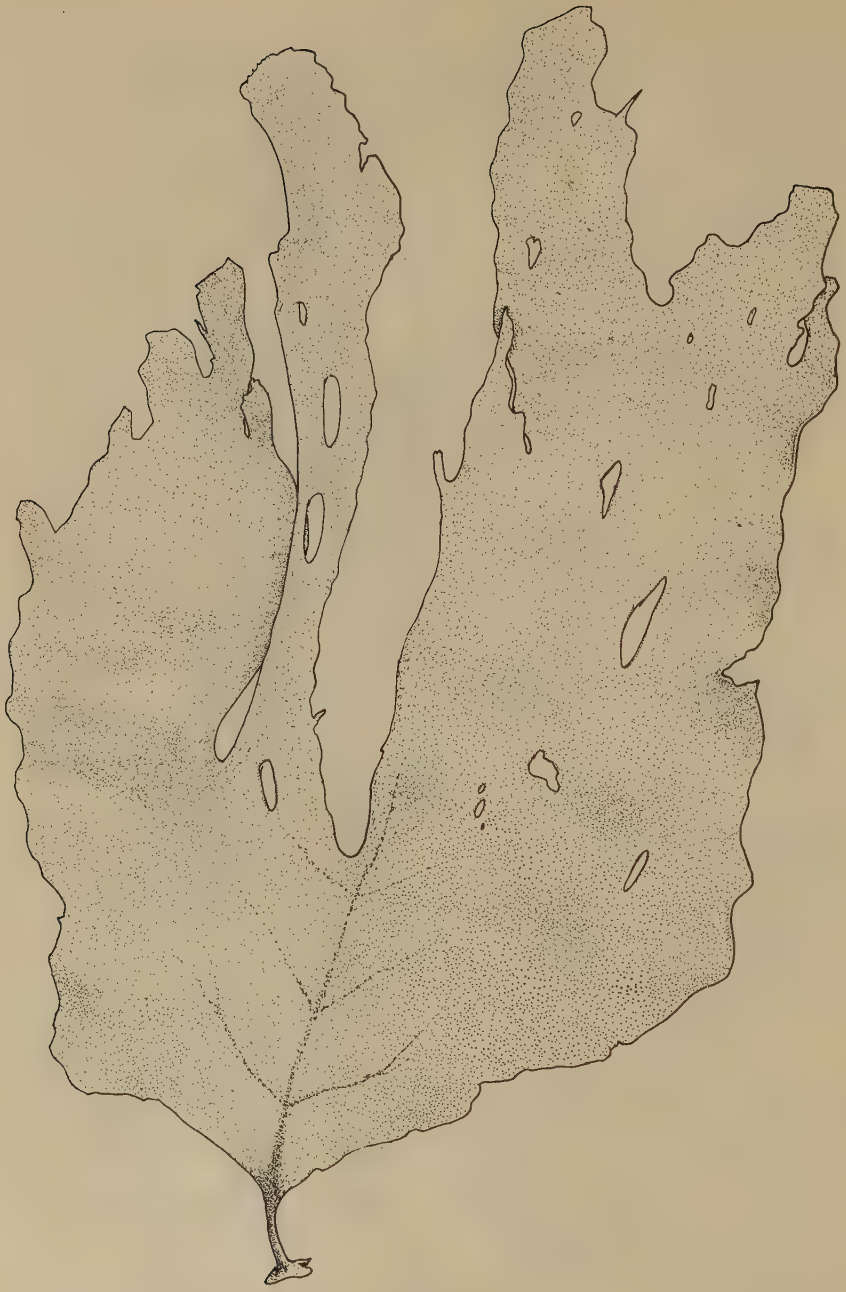

PLATE 8

Desmarestia tabacoides, habit, showing prominent central vein and faint laterals, × 0.5.

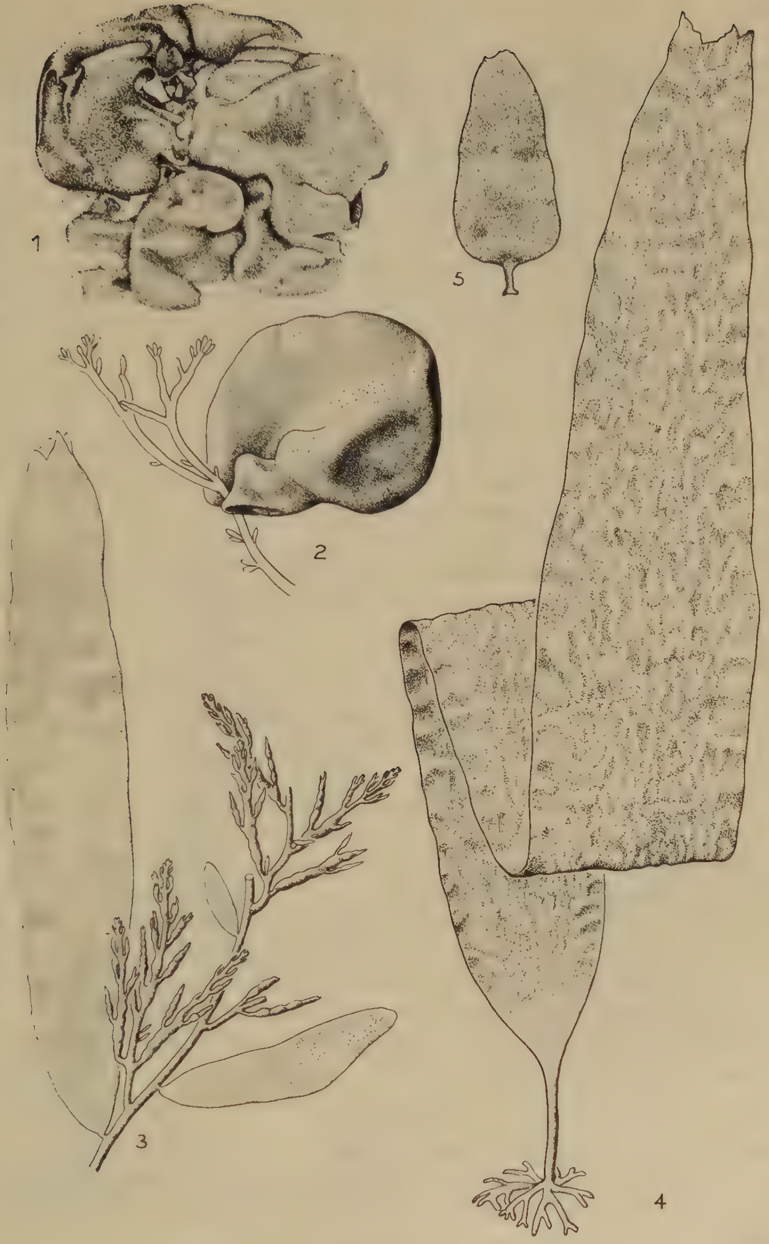

PLATE 9

Fig. 1-2. *Colpomenia sinuosa*: fig. 1, habit of free-living plant, × 0.75; fig. 2, epiphytic habit, × 0.75. Fig. 3. *Coilodesme californica,* on tip of branch of *Cystoseira osmundacea,* × 0.5. Fig. 4-5. *Laminaria farlowii*: fig. 4, entire plant, × 0.25; fig. 5, juvenile plant, × 0.25.

These may be recognizable as a different species, *Macrocystis angustifolia,* according to the most recent taxonomic treatment.

Pachydictyon coriaceum (Holmes) Okamura Pl. 3, figs. 1, 2.

Southern California to southern Baja California. Similar to *Dictyota flabellata,* but darker brown and coarser, often a foot high. Its blades are 5 or more cell layers thick at the margins. Frequent, intertidal to 65 feet.

Padina durvillaei Bory Pl. 5, fig. 3.

Vicinity of Bahía Vizcaino, Baja California and southward. The conspicuous inrolled margins of the coarse, broad, fan-shaped blades clearly set this plant apart from other species of our coast. Common, intertidal to 40 feet.

Pelagophycus porra (Leman) Setchell
Bull Kelp or Elk Kelp Pl. 12, fig. 1, 2

Southern California to central Baja California. Plants reaching 100 feet in length, with individual blades up to 14 feet long, chocolate brown in color, arising from depths of 40-100 feet.

Pterygophora californica Ruprecht Pl. 11, fig. 1.

British Columbia to northern Baja California. Plants dark brown with a conspicuous midrib running through the main blade. Intertidal to 120 feet.

Sargassum agardhianum Farlow Pl. 16, fig. 1.

Southern California to central Baja California. Distinguished by its small size (about 2-3 feet tall), abundant branching and small "leaves" and sperical vesicles. Occasional, intertidal to 30 feet.

Taonia lennebackerae J. Agardh

Southern California to central Baja California. Yellowish-brown, tapering gradually from a wide apex to a rather pointed base, often much split and lacerated. Frequently found in sandy areas, intertidal to 30 feet.

Zonaria farlowii Setchell and Gardner Pl. 4, fig. 1; Pl. 5, fig. 1.

Southern California to Bahía Magdalena, Baja California. The plants are dark brown with areas of light color near the terminal margins. Concentric hair lines are often visible. Mature specimens, 6-12 inches high, are much divided into small, terminal, fan-shaped segments. These show the characteristic "zones of growth" from which the plant derives its name. Intertidal to 50 feet.

RED ALGAE

Acrosorium uncinatum (Turner) Kylin Pl. 34, fig. 1.

Southern California to southern Baja California. Commonly epiphytic and entangled, bright rose red, with frequent hook-shaped branches. The veins are very delicate; intertidal to 125 feet.

Agardhiella coulteri (Harvey) Setchell Pl. 29, fig. 3, 4.

British Columbia to southern Baja California. A common and easily recognized, bright red, feathery plant of attractive appearance. Common and variable in size from 2 to 10 inches tall. Intertidal to 85 feet.

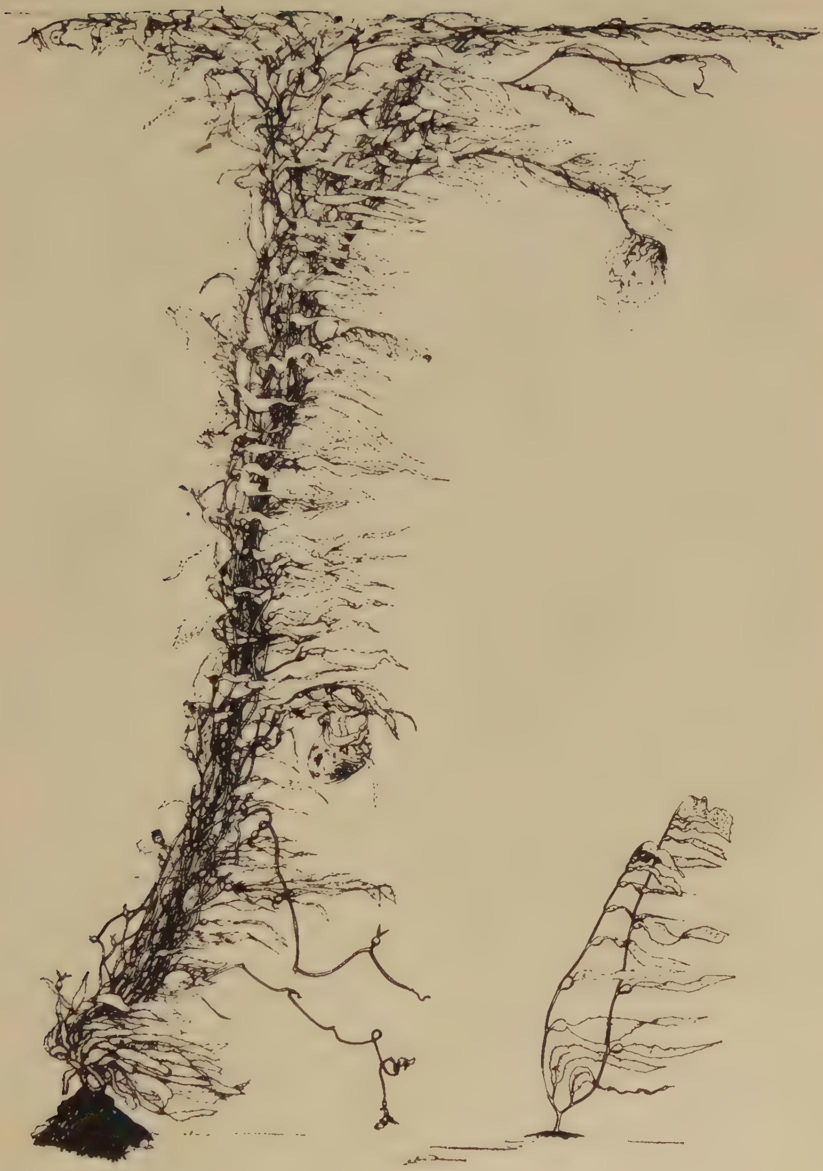

PLATE 10

Macrocystis pyrifera, a mature and a young plant growing under natural conditions in 30 feet of water.

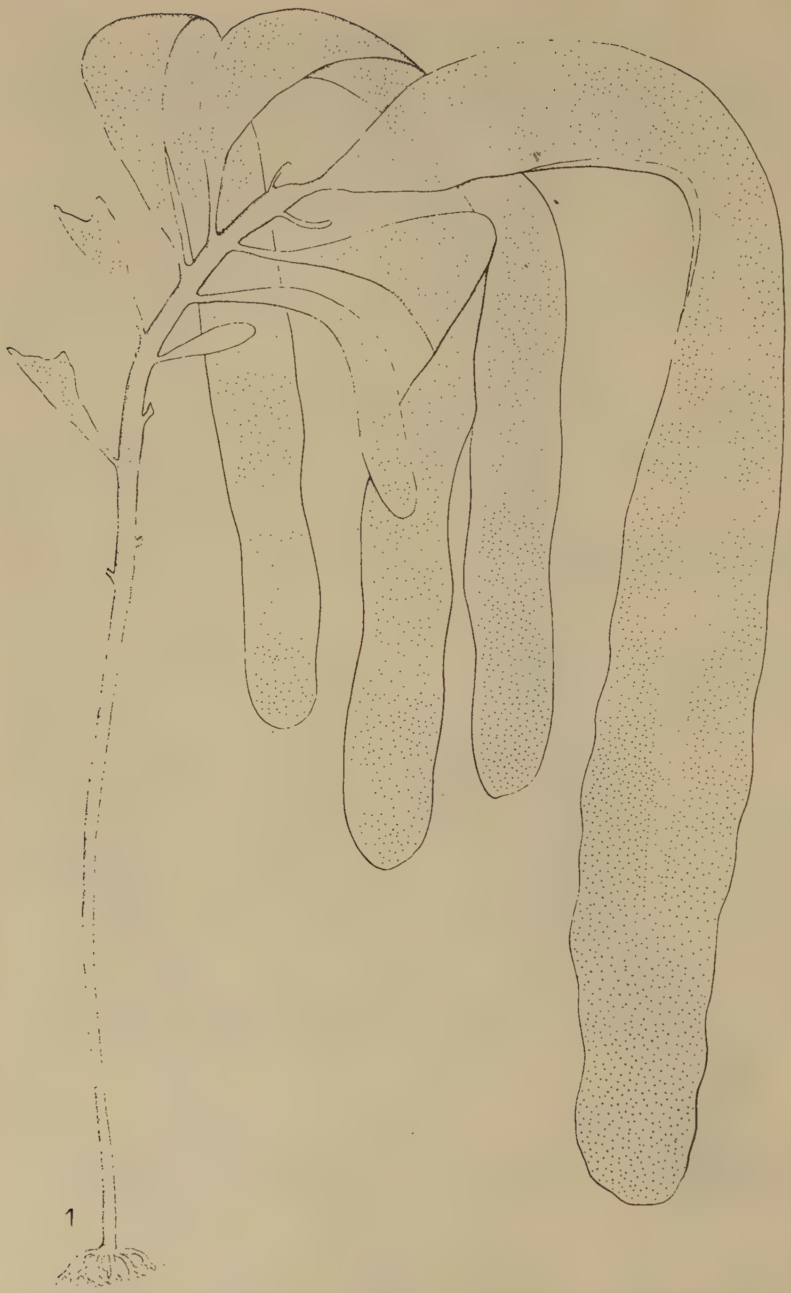

PLATE 11

Fig. 1. *Pterygophora californica,* habit, showing midrib on terminal blade, × 0.25.

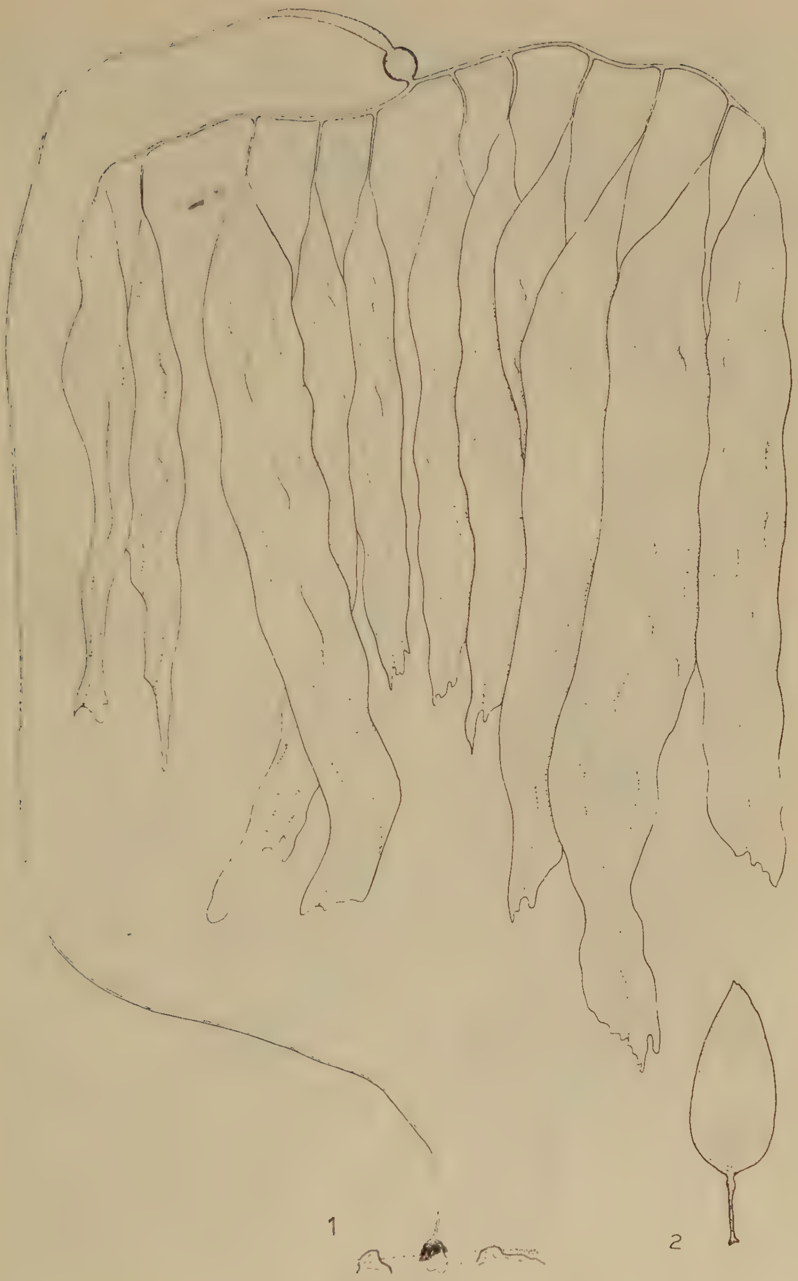

PLATE 12

Fig. 1-2. *Pelagophycus porra*: fig. 1. habit showing large single float and antler-like branching, × 0.04; fig. 2, juvenile plant showing development of float, × 0.25.

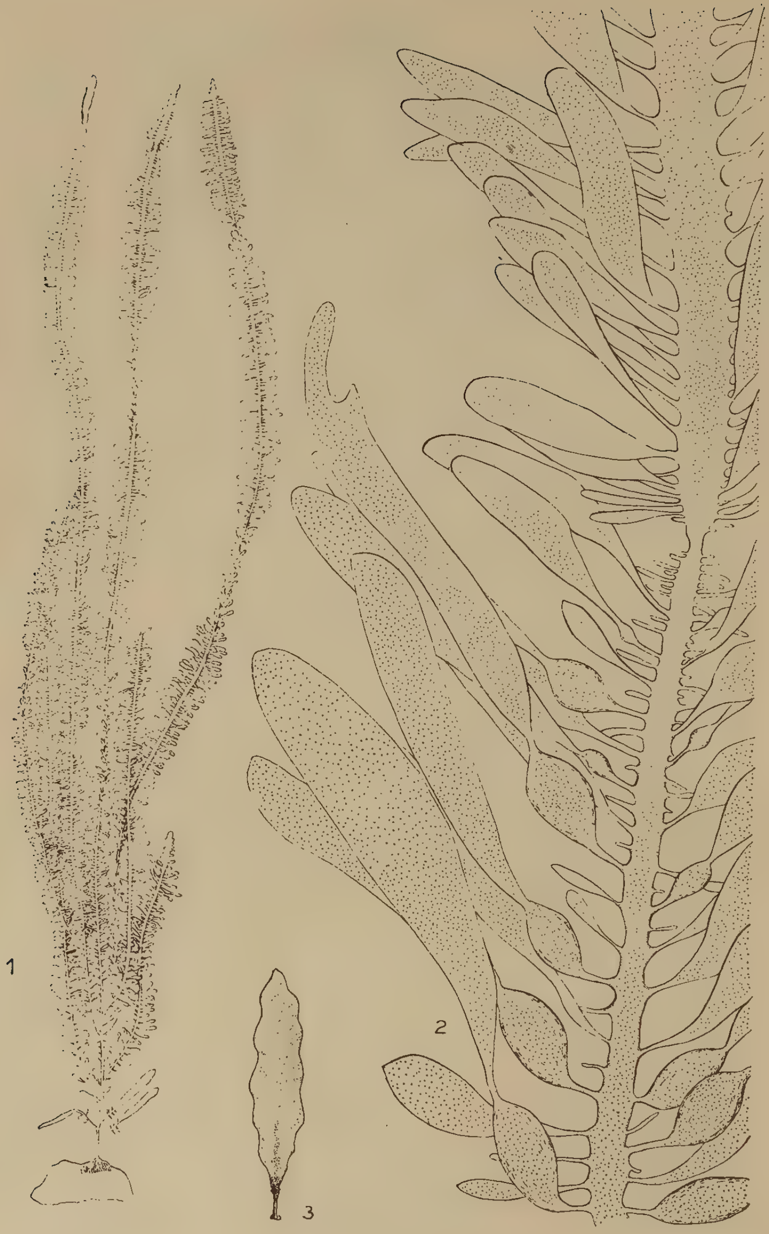

PLATE 13

Fig. 1-3. *Egregia laevigata*: fig. 1, entire plant, × 0.04; fig. 2, portion of flat axis bearing blades and floats, × 0.5; fig. 3, juvenile plant, showing undulate margins, × 0.25.

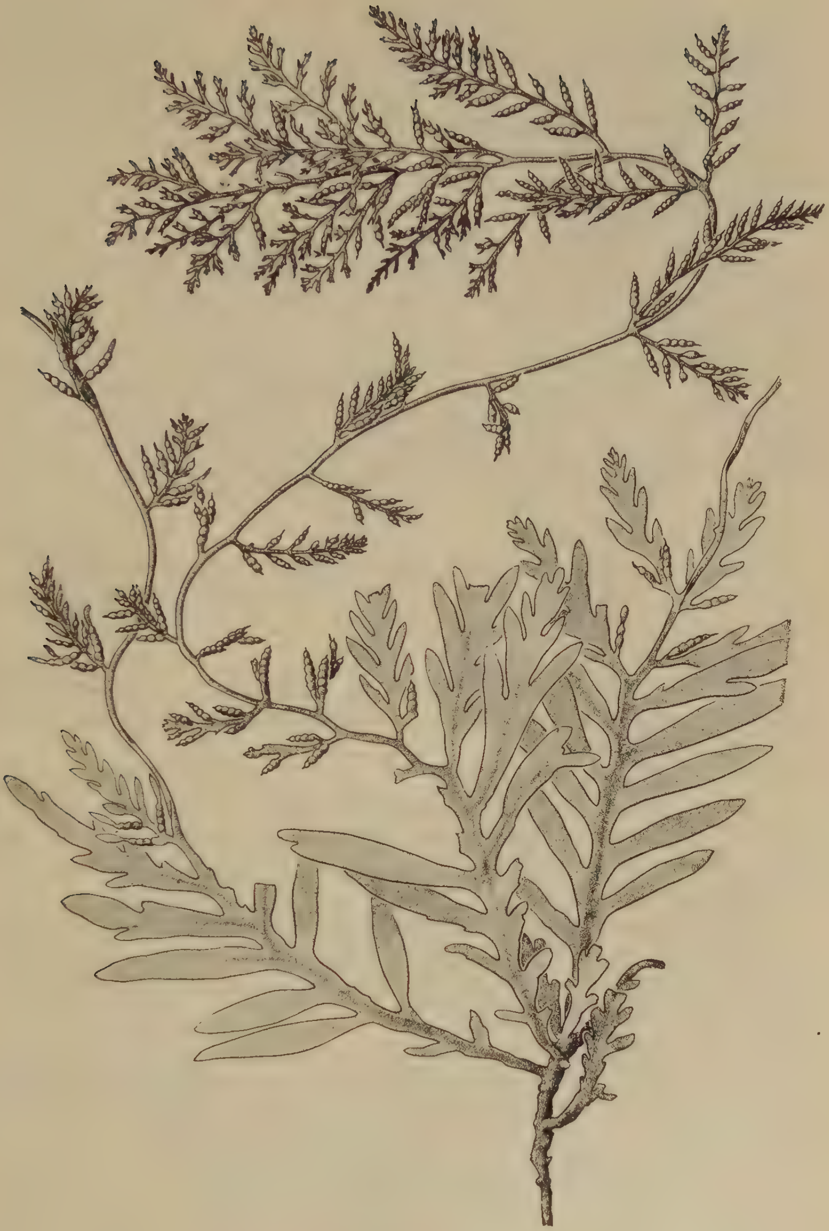

PLATE 14
Cystoseira osmundacea, habit, showing rounded floats, × 0.37.

Amphiroa dimorpha Lemoine Pl. 23, fig. 5.

Central Baja California and southward. This is an exclusively deep-water plant of frequent occurrence at depths of 25-65 feet in the southernmost kelp areas. The small, pinkish branches are usually somewhat appressed to the substrate so that the flat segments have a dorsi-ventral aspect.

Amphiroa zonata Yendo Pl. 23, fig. 6.

Southern California to Tres Marias Islands, Mexico. The elongated and often branched calcareous segments of this small (1-2 inches) loosely-clumping, dichotomously branched plant are distinctive. Occasional at depths of 25 to 65 feet in our area.

Amplisiphonia pacifica Hollenberg Pl. 43, fig. 2.

British Columbia to central Baja California. A small, prostrate plant one to two inches in extent, consisting of overlapping lobes, provided with microscopic veins in a distinctive fan-like pattern. Occasional, on or around holdfasts of larger algae or in algal mixtures on rocks; intertidal to 60 feet.

Anisocladella pacifica Kylin Pl. 38, fig. 2, 3.

Central California to central Baja California. This small plant, about 1 inch high, often grows in mixtures of other small algae from the intertidal down to 40 feet.

Binghamia forkii (Dawson) Silva Pl. 33, fig. 4.

Southern California to southern Baja California. A very small, pink colored, slippery plant occasionally found at 25-40 feet growing congestedly with other small algae.

Bossiella gardneri (Manza) Silva Pl. 23, fig. 7.

Oregon to central Baja California. Similar to *B. orbigniana* but the segments are mostly rounded rather than with pointed wings. Frequent on the inner margins of the kelp beds and inshore into intertidal waters.

Bossiella orbigniana (Decaisne) Silva Pl. 21, fig. 5.

Oregon to central Baja California. The fronds are 3-7 inches long, reddish-pink in color and dichotomously branched throughout. The usually sharply pointed wings of the flat segments are distinctive. Frequent from 25-55 feet.

Botryoglossum farlowianum (J. Agardh) G. DeToni Pl. 40, fig. 1, 2.

Washington to northern Baja California. This plant is rose-purplish, irridescent, to 10 inches high. Much larger than the somewhat similar *Cryptopleura crispa* and usually not epiphytic. Occasional, 20-45 feet.

Botryocladia neushulii Dawson Pl. 32, fig. 2.

Southern California to northern Baja California. This species differs from the following by its much smaller vesicles on the prominent solid branches.

Botryocladia pseudodichotoma (Farlow) Kylin Sea Grapes Pl. 33, fig. 3.

British Columbia to southern Baja California. This plant has so

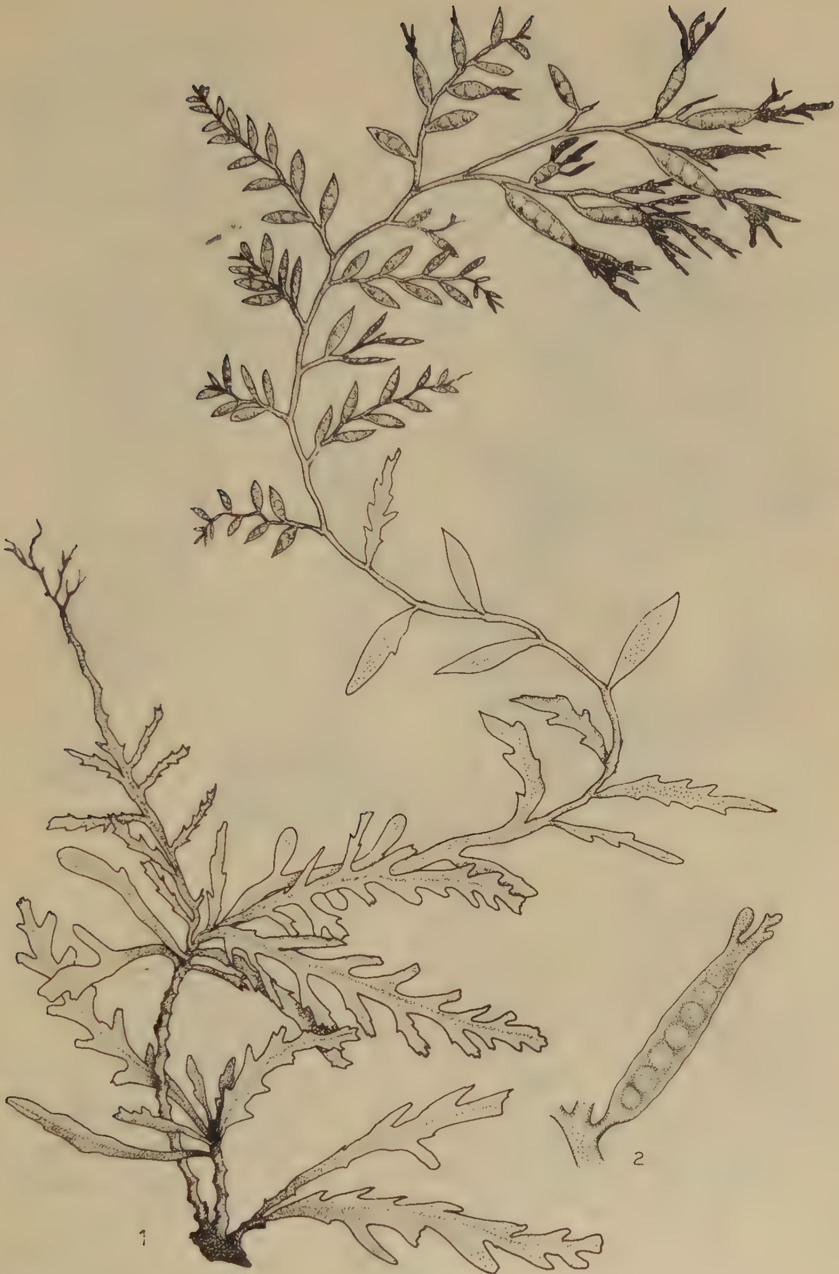

PLATE 15

Fig. 1-2. *Halidrys dioica*: fig. 1, habit, × 0.37; fig. 2, a series of floats showing the flattened character, × 1.

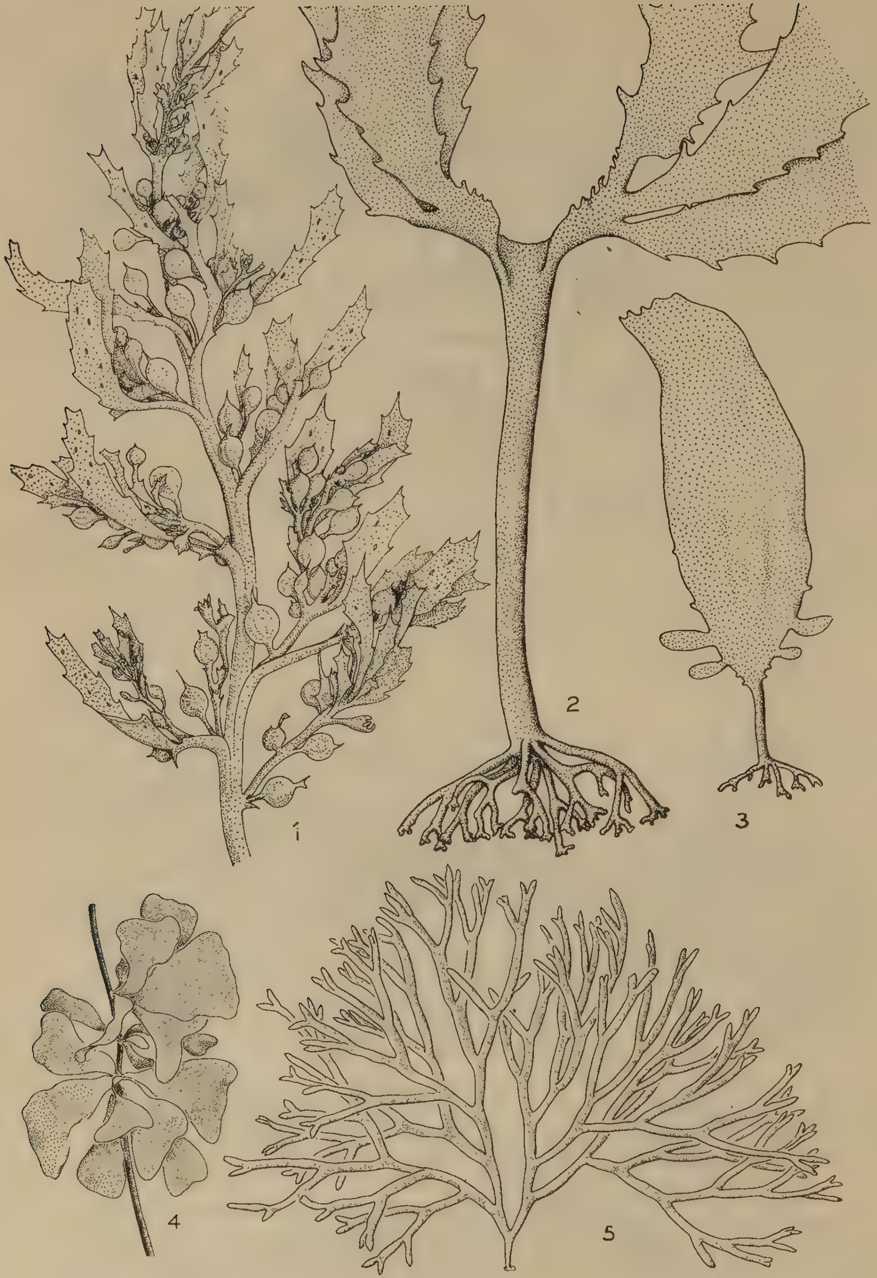

PLATE 16

Fig. 1. *Sargassum agardhianum,* upper portion of plant showing floats and blades, × 1.5. Fig. 2-3. *Eisenia arborea*: fig. 2, lower portion of plant showing holdfast, branching and teeth along blade margins, × 0.4; fig. 3, juvenile plant with proliferations along lower margins of the blade, × 0.4. Fig. 4. *Smithora naiadum,* growing on *Phyllospadix,* × 0.5. Fig. 5. *Gloiophloea confusa,* habit, × 0.75.

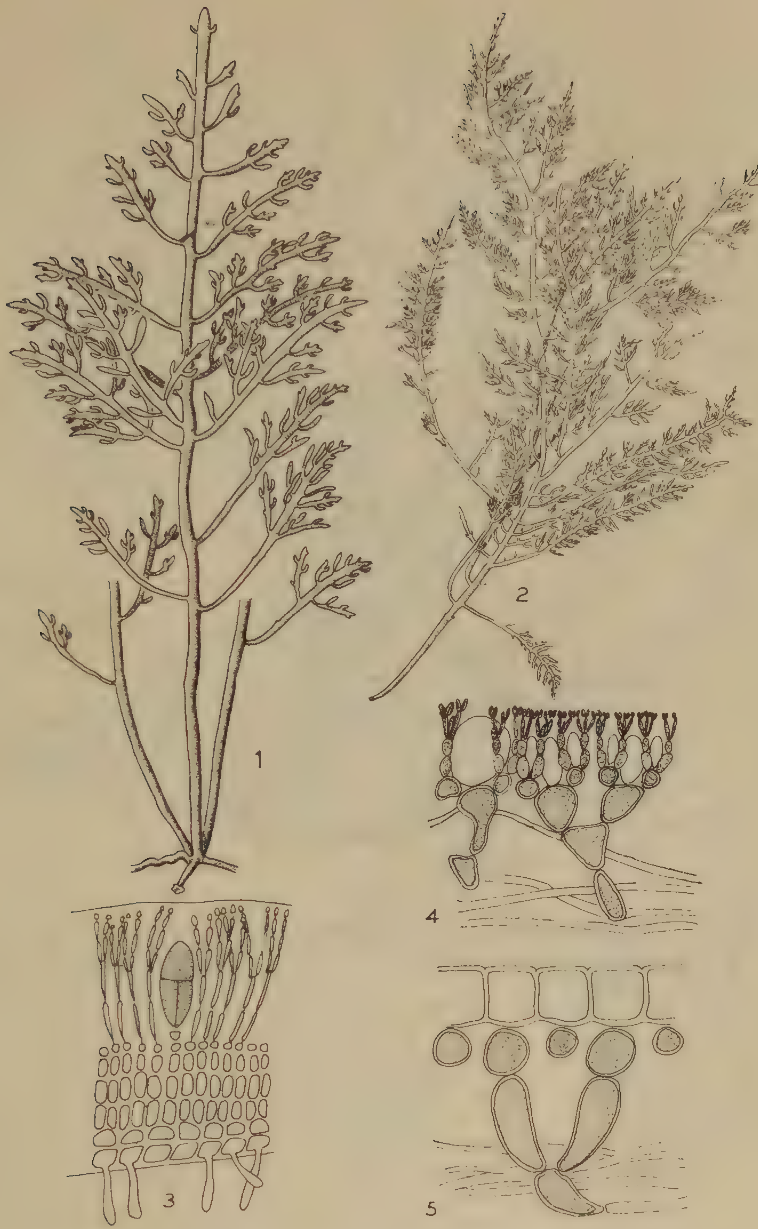

PLATE 17

Fig. 1. *Gelidium cartilagineum* var. *robustum,* habit, × 0.75. Fig. 2. *Gelidium purpurascens,* habit, × 1. Fig. 3, *Peyssonelia rubra* var. *orientalis,* a section through the crust-forming plant body showing rhizoids growing from basal cell layer and a spore group in a special (nemathecial) superficial layer, × 165. Fig. 4. *Gloiophloea confusa,* radial section through branch showing mixture of pigmented filaments and round colorless cells, × 30. (after Setchell)

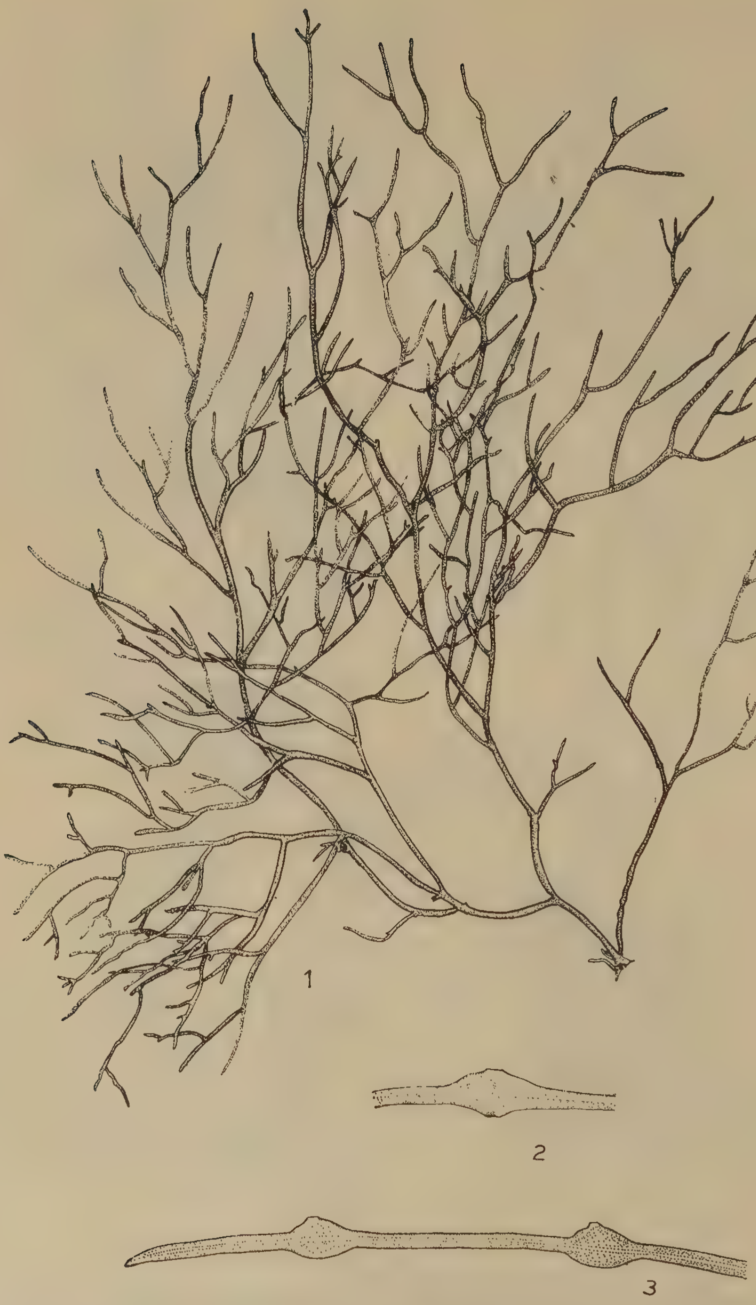

PLATE 18

Fig. 1. *Gelidium nudifrons,* habit, × 0.5. Fig. 2. *Gelidium* sp., cystocarp with two ostioles, × 16. Fig. 3. *Pterocladia* sp., cystocarps, each with a single ostiole, × 16.

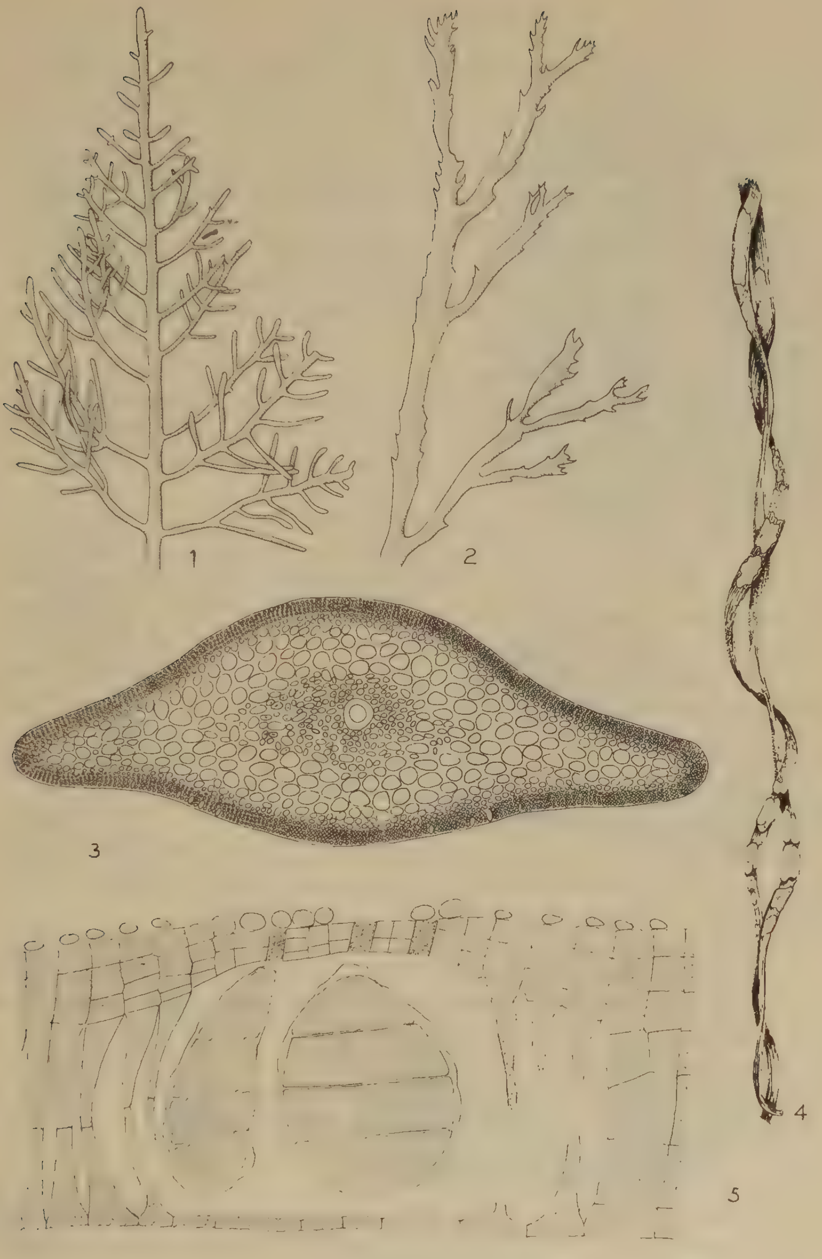

PLATE 19
Fig. 1. *Pterocladia pyramidale,* upper portion of plant, × 2.5. Fig. 2-3. *Leptocladia binghamiae*: fig. 2, small upper portion of plant showing branching, × 2.7; fig. 3, transection of mature apex to show the single large central axial filament, × 46. Fig. 4-5. *Melobesia mediocris*: fig. 4, as found growing epiphytically on *Phyllospadix,* × 1; fig. 5, vertical section through tetrasporic conceptacle, × 430.

distinctive a shape as to be confused with no others. Occasional at 40 to 85 feet.

Branchioglossum undulatum Dawson Pl. 33, fig. 2.

Southern California to central Baja California. A very small species characteristically growing on kelp holdfasts with *Myriogramme caespitosa*.

Calliarthron cheilosporioides Manza Pl. 22, fig. 1.

Northern British Columbia to southern Baja California. This is one of the most common bottom plants of the kelp community, and extends from the intertidal zones to a depth of 75 feet. The erect pinkish shoots sometimes reach a foot in height.

Calliarthron regenerans Manza Pl. 22, fig. 2.

British Columbia to central Baja California. This segmented, chalky-pink, calcareous plant forms erect clumps 3 to 7 inches tall on well-lighted bottoms to depths of 30 feet. It often occupies areas where there are abundant sea urchins.

Callophyllis marginifructa Setchell and Sweezy Pl. 27, fig. 1.

Washington to northern Baja California. The blades are light, rosy red, 3-6 inches high when mature. The female plants are readily recognized by their conspicuous marginal reproductive bodies. Frequent, 10-65 feet.

Callophyllis megalocarpa Setchell and Sweezy Pl. 28, fig. 3, 4.

Washington to southern Baja California. Although the habit illustrations will serve in most cases, good fertile material may be required to distinguish some of these *Callophyllis* species. All are distinctly red in color, mostly between 3 and 8 inches high. These species has large cystocarps on the flat blades. Intertidal down to 45 feet.

Callophyllis violacea J. Agardh Pl. 27, fig. 3.

Oregon to southern Baja California. This species is generally narrower than the other common *Callophyllis* species and is often epiphytic on the lower parts of larger algae. Intertidal down to 75 feet.

Carpopeltis bushiae (Farlow) Kylin Pl. 27, fig. 2.

Southern California to southern Baja California. A common, small, erect, bushy plant, 4 to 5 inches high, with woody holdfast. It ranges from the lowermost intertidal to as much as 75 feet.

Ceramium pacificum (Collins) Kylin Pl. 37, fig. 1, 2.

British Columbia to central Baja California; intertidal to 30 feet. A delicately branched dichotomous plant, often epiphytic, usually under 2 inches high.

Chondria nidifica Harvey Pl. 42, fig. 1.

Southern California to southern Baja California. The cylindrical branches are 6 to 10 inches long, and bear distinctive tufts of short pointed lateral branchlets. Intertidal to 30 feet.

Chondria californica (Collins) Kylin Pl. 42, fig. 4.

Southern California southward. This is a bluish-irridescent small plant usually 2-3 inches tall. It occurs in two forms, an erect, tufted form

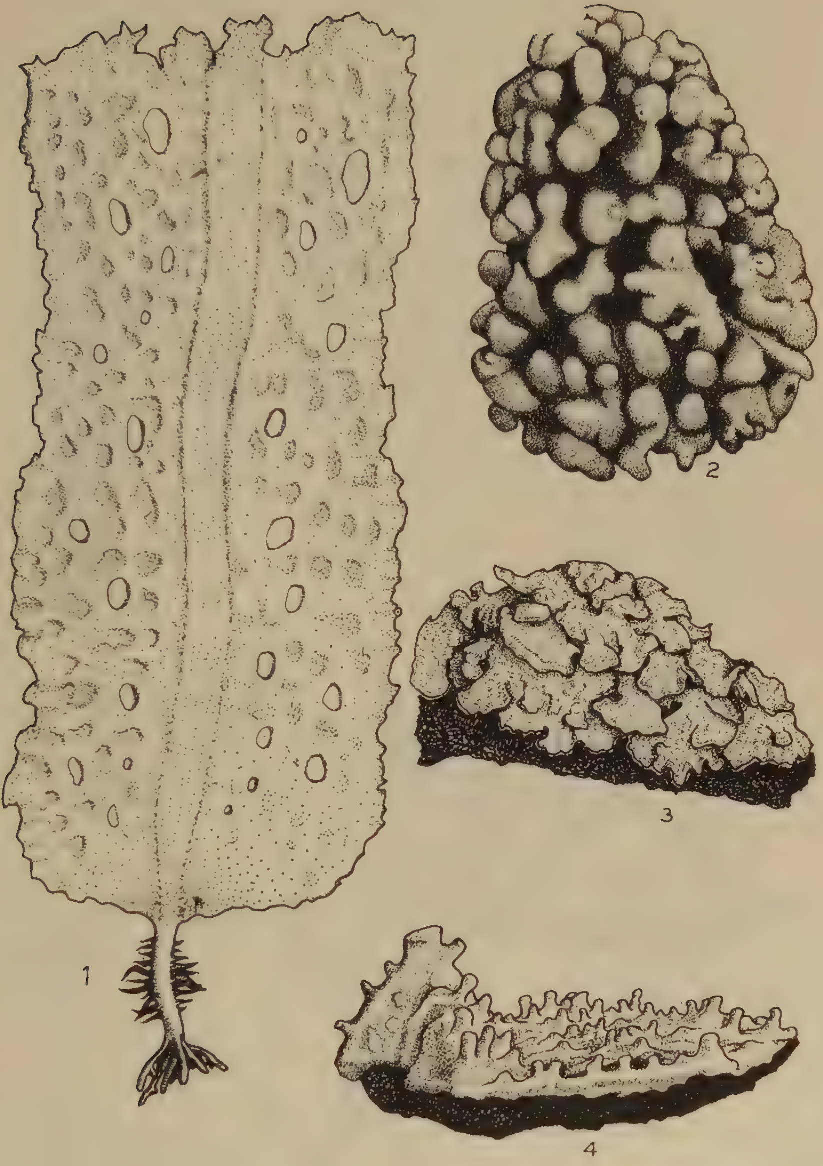

PLATE 20

Fig. 1. *Agarum fimbriatum*, holdfast and lower portion of blade showing midrib, holes and proliferations along stipe, × 0.38. Fig. 2. *Lithothamnium giganteum*, crustose habit showing rounded protuberances, × 1. Fig. 3. *Lithothamnium lamellatum*, crustose habit showing shingle-like surface, × 1. Fig. 4. *Lithophyllum imitans*, crustose habit showing knobby protuberances, × 1.

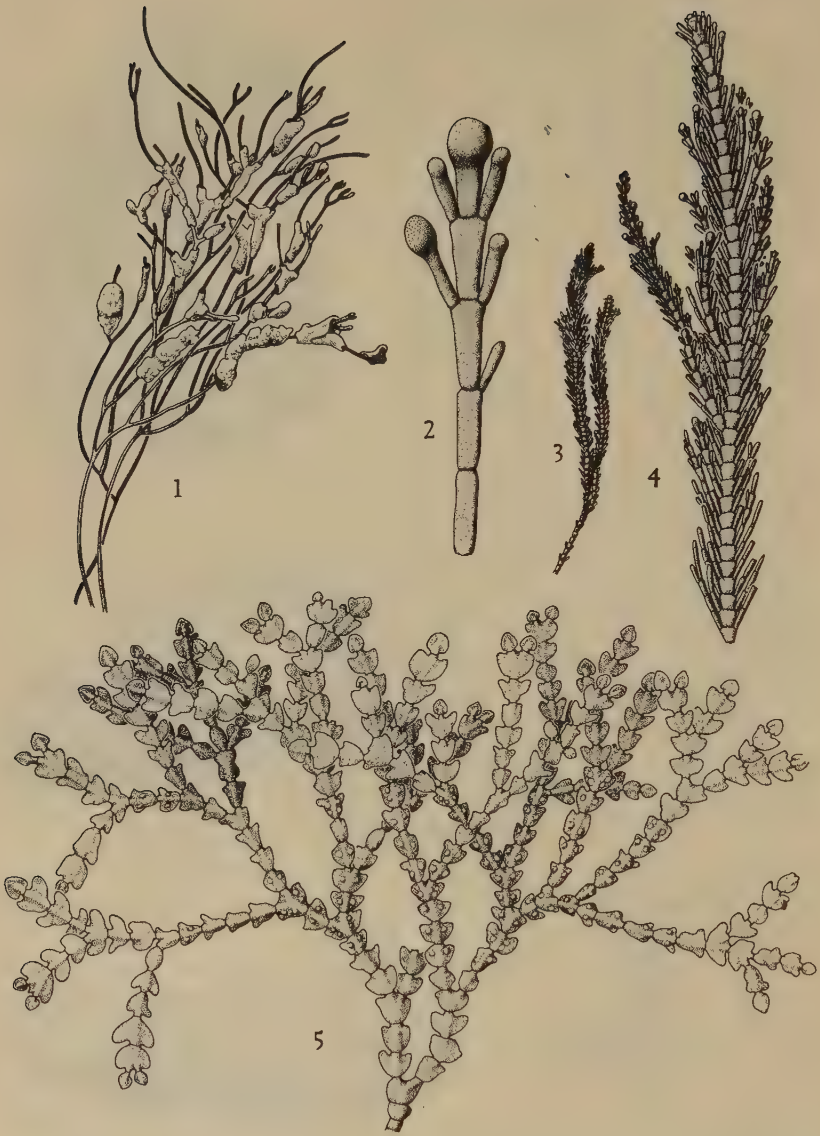

PLATE 21

Fig. 1. *Dermatolithon dispar,* growing epiphytically, × 1.5. Fig. 2-4. *Corallina vancouveriensis*: fig. 2, fertile branchlet, × 14; fig. 3, entire branch, × 1; fig. 4, upper part of branch, × 3. Fig. 5. *Bossiella orbigniana,* branch showing "arrow-head" shaped segments, × 1.5.

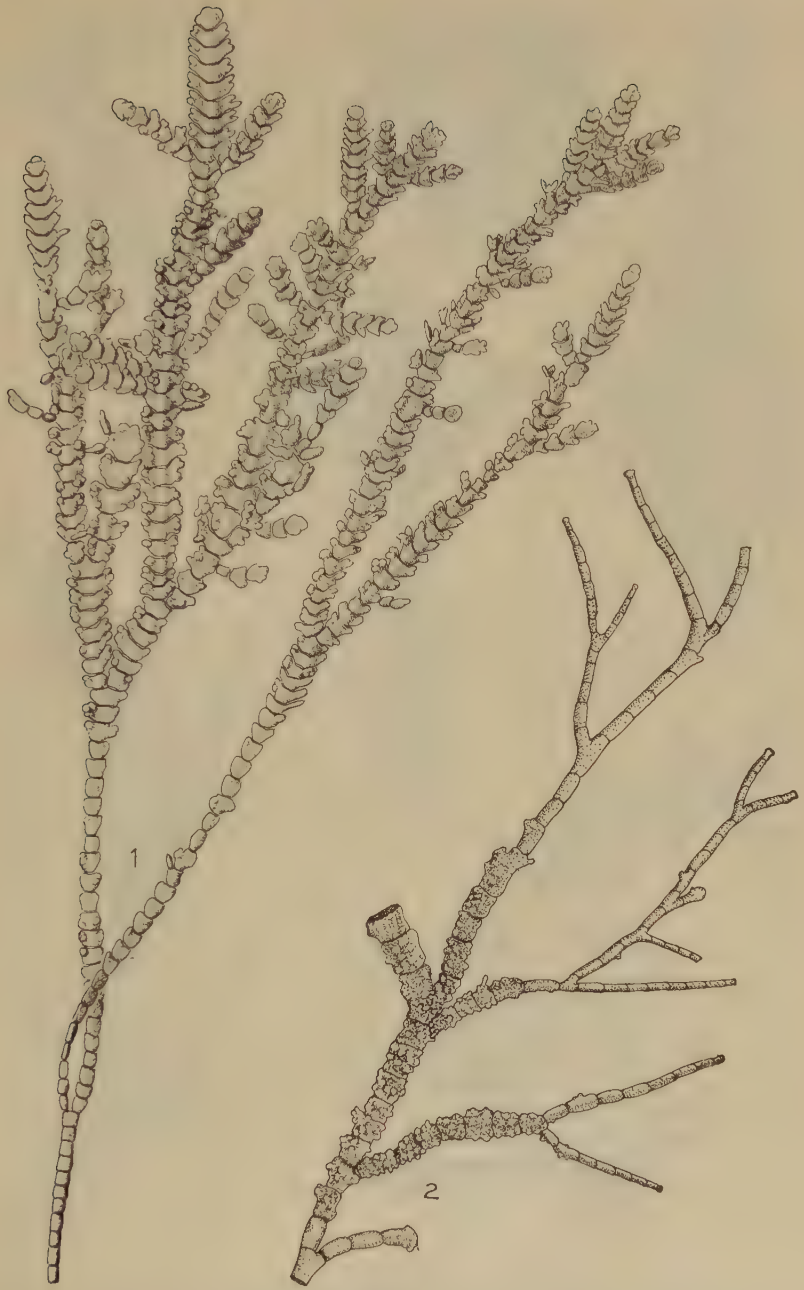

PLATE 22
Fig. 1. *Calliarthron cheilosporioides,* habit, × 1. Fig. 2, *Calliarthron regenerans,* habit, × 1.

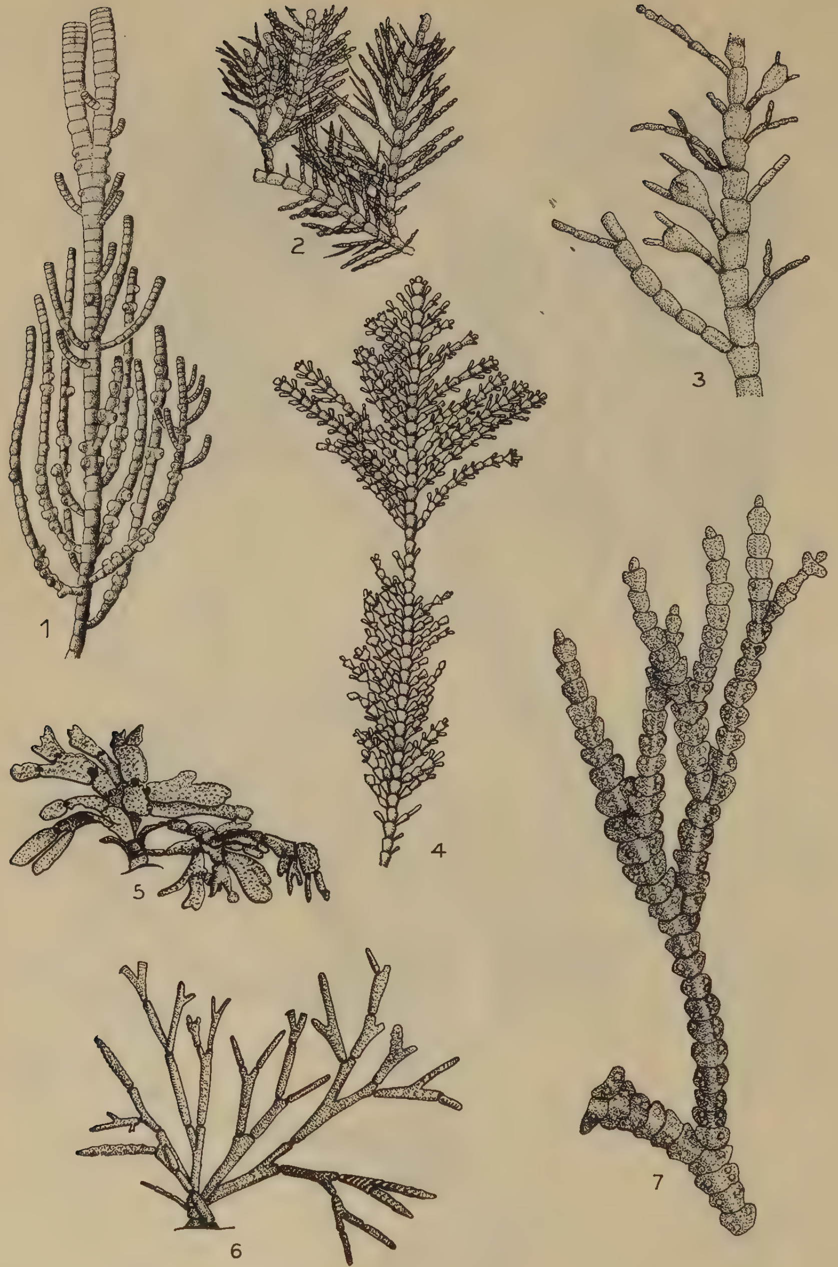

PLATE 23
Fig. 1. *Lithothrix aspergillum,* upper portion of plant, × 3.5. Fig. 2-3. *Corallina gracilis*: fig. 2, upper portion of plant, × 2.5; fig. 3, portion of axis showing antennae-bearing segments, × 5. Fig. 4. *Corallina officinalis* var. *chilensis,* upper portion of plant, × 1. Fig. 5. *Amphiroa dimorpha,* habit, × 1.125. Fig. 6, *Amphiroa zonata,* habit, × 1. Fig. 7. *Bossiella gardneri,* upper portion of plant showing rounded segments, × 1.5.

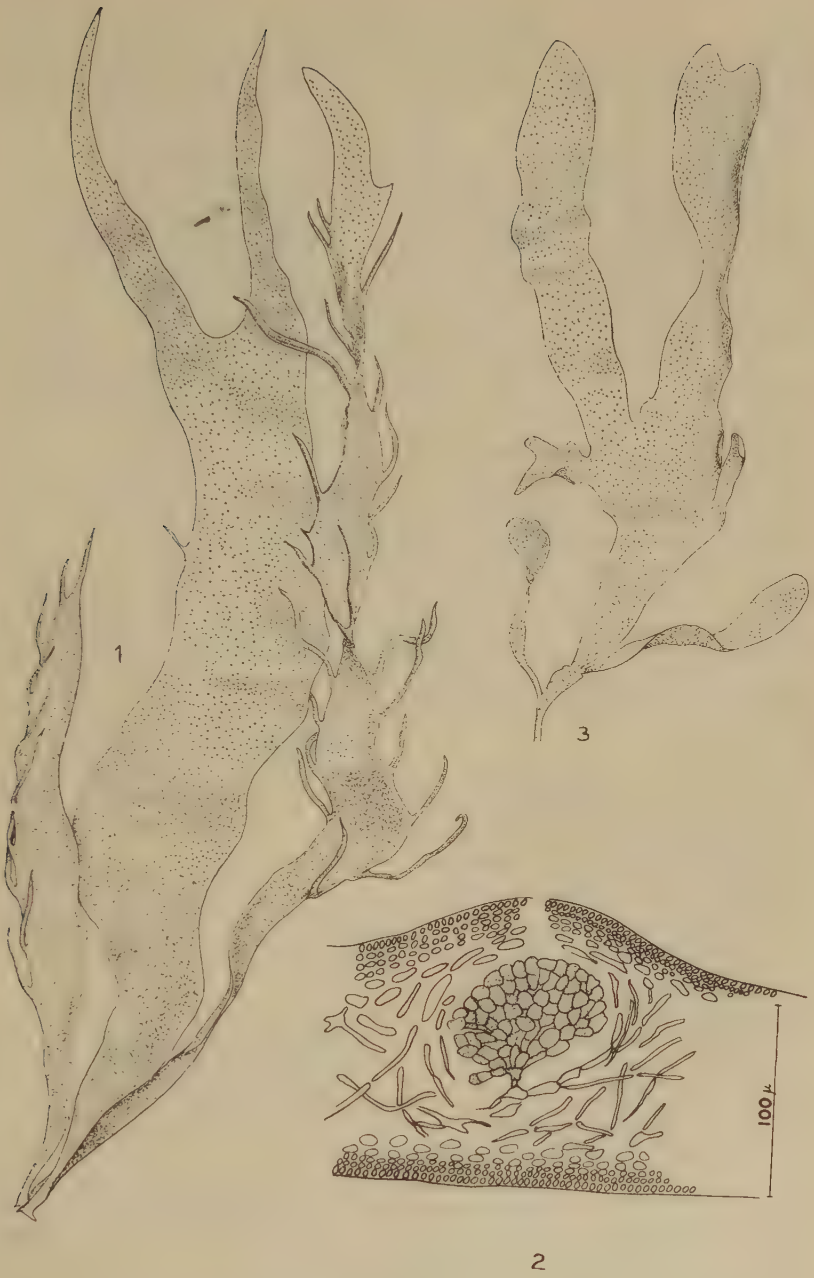

PLATE 24
Fig. 1-2. *Grateloupia schizophylla*: fig. 1, habit, × 0.5; fig. 2, transection through a cystocarp, showing cortical cell rows. Fig. 3. *Cryptonemia angustata,* habit, × 0.5.

attached to rock or shell surfaces, and the more common epiphytic form (in the kelp community) with coiled, tendril-like branches. Intertidal to 30 feet.

Corallina gracilis Lamouroux Pl. 23, fig. 2, 3.

Southern California to central Baja California. This species, and *C. vancouveriensis* are much more delicately branched plants than *C. officinalis*. *C. gracilis* is distinguished by the antenna-like branchlets on the swollen asexual reproductive segments. It is less prevalent and reaches lesser depths (to 30 feet) than *C. officinalis*.

Corallina officinalis var. *chilensis* (Harvey) Kützing Pl. 23, fig. 4.

Northern British Columbia to southern Baja California. This is one of the most common sea bottom plants found in the kelp community, extending from the intertidal zone to depths of 75 feet. The erect shoots often grow to six inches in height.

Corallina vancouveriensis Yendo Pl. 22, fig. 2, 4.

Southern British Columbia to southern Baja California. This species is more representative of the intertidal zone than the deeper waters, but extends down to depths of about 30 feet. The branching is more compact than in *C. gracilis*.

Cryptonemia angustata (Setchell and Gardner) Dawson Pl. 24, fig. 3.

Southern California to southern Baja California. This thin, reddish, membranous plant grows occasionally on small stones and shells at depths of from 25 to 75 feet. It is thinner, narrower and more delicate than *C. obovata*.

Cryptonemia obovata J. Agardh Pl. 25, fig. 3, 4.

Alaska to central Baja California. This is a more amply expanded, membranous, red plant than the last, reaching a foot high, and with lobes to 3 inches broad. Occasional from 10 to 60 feet.

Cryptopleura crispa Kylin Pl. 39, fig. 2.

Oregon to southern Baja California. Distinguished by its abundant small marginal lobes and usually smaller size than the next species. Commonly epiphytic; intertidal to 45 feet.

Cryptopleura violacea (J. Agardh) Kylin Pl. 39, fig. 1.

British Columbia to central Baja California. Unlike the former and the somewhat similar *Botryoglossum farlowianum*, this species bears asexual spores in longitudinal patches along the blade margins and sometimes also in scattered lobes. Intertidal to 30 feet.

Dermatolithon dispar (Foslie) Foslie Pl. 21, fig. 1.

Washington to central Baja California. This small, calcareous, epiphytic plant forms chalky pink crusts to ½ inch in diameter on flat surfaces of host plants, or may completely encase slender branches of such plants as *Gelidium*. At depths to about 30 feet.

Drouetia peltata Dawson Pl. 34, fig. 2.

Southern California and northern Baja California. This is another of the exclusively deep-water plants of the shadowy bottoms under the

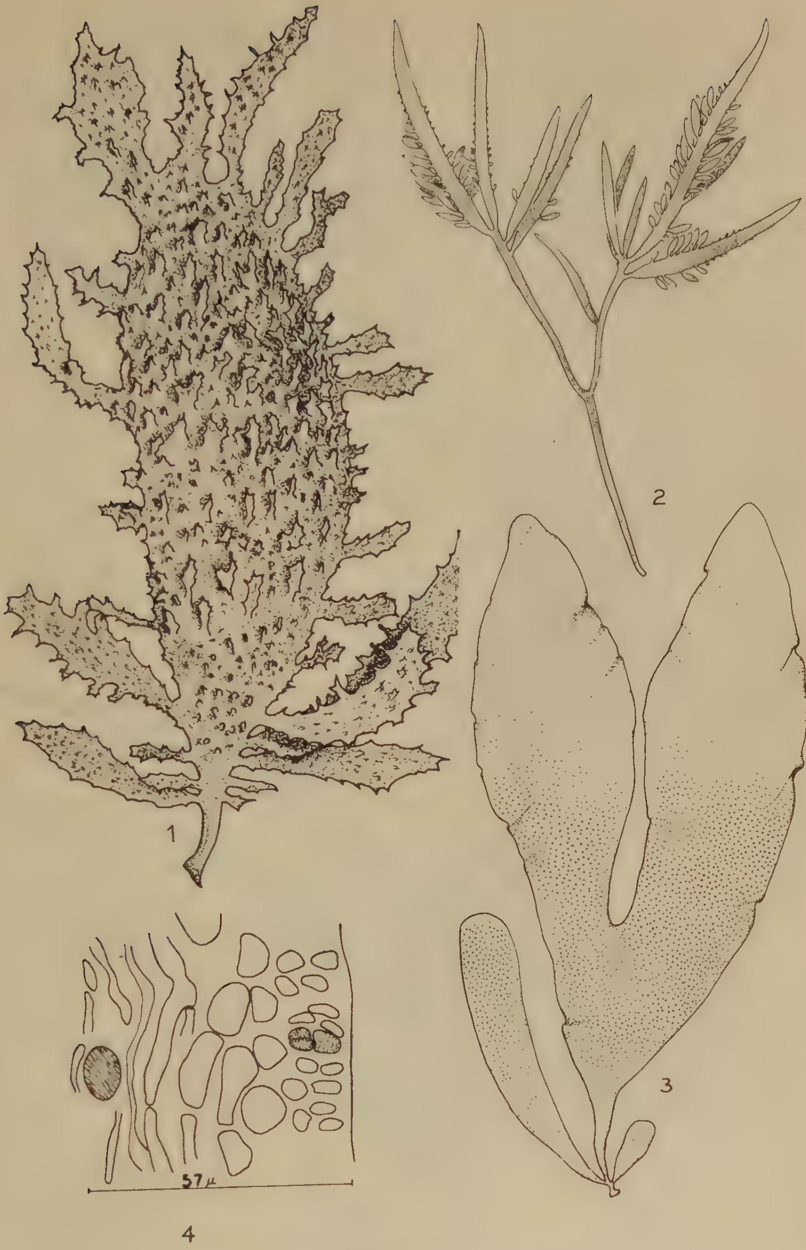

PLATE 25

Fig. 1. *Grateloupia howeii,* habit, × 0.5. Fig. 2. *Prionitis lanceolata,* upper portion of plant, × 0.33. Fig. 3-4. *Cryptonemia obovata*: fig. 3, habit, × 0.5; fig. 4, cross-section of blade showing a characteristic medullary filament with highly refractive contents and a single spore group.

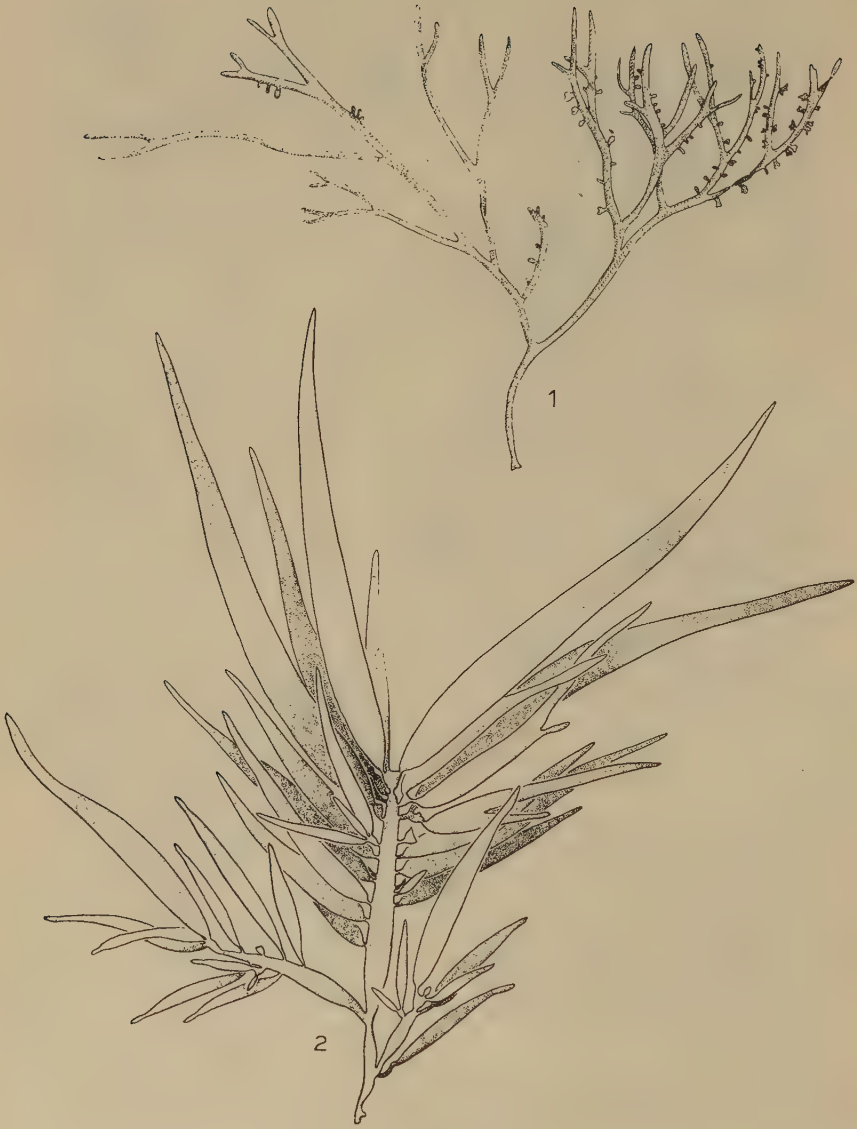

PLATE 26
Fig. 1. *Prionitis cornea,* habit showing sparse lateral branchlets, × 0.5. Fig. 2. *Prionitis andersoniana,* habit, × 0.5.

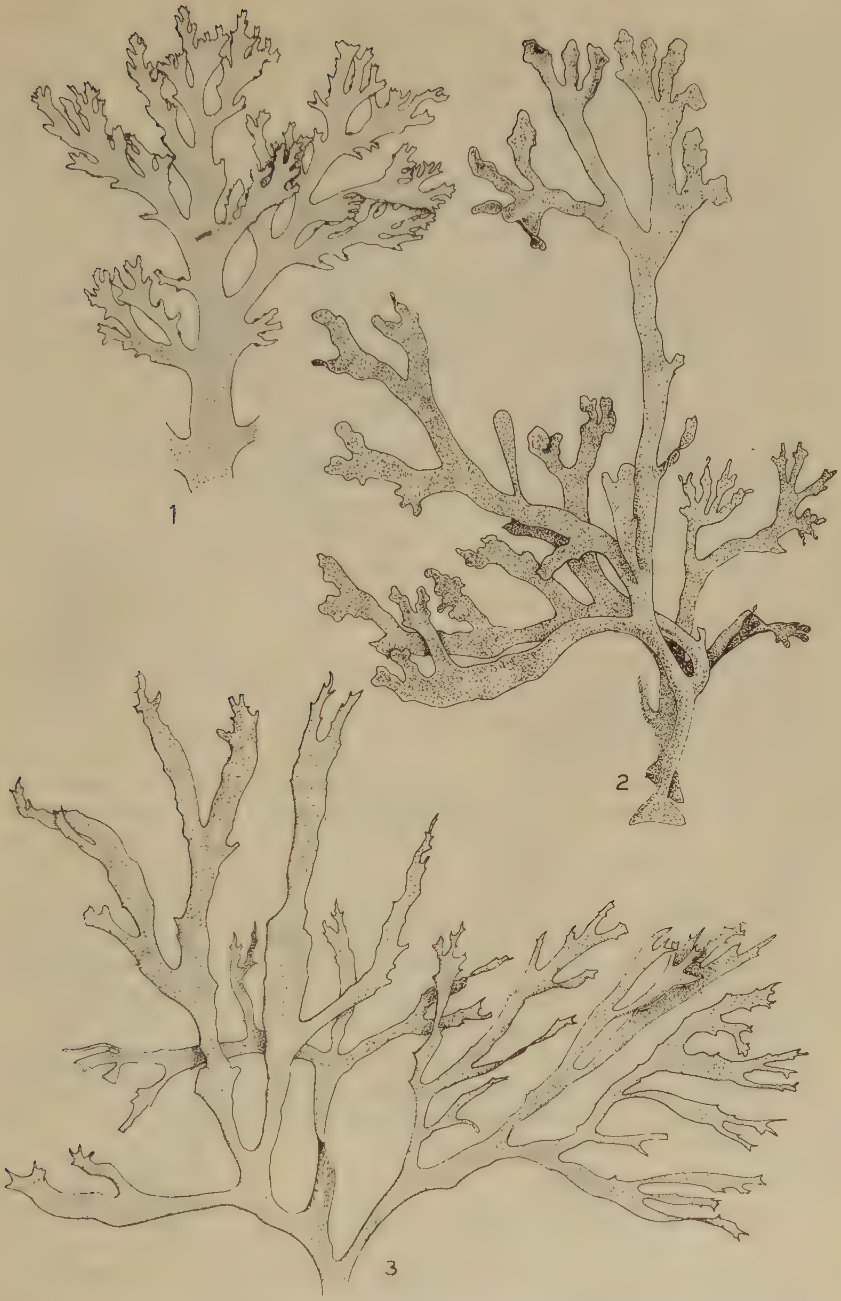

PLATE 27

Fig. 1. *Callophyllis marginifructa,* upper portion of cystocarpic plant, × 1. Fig. 2. *Carpopeltis bushiae,* habit, × 1. Fig. 3. *Callophyllis violacea,* upper portion of plant, × 0.5.

kelp canopy and on out into depths of 100 feet or more. The blades show a distinctive purplish iridescence.

Fauchea laciniata J. G. Agardh Pl. 32, fig. 4, 5.

British Columbia to southern Baja California. A soft, pink-colored, irregularly dissected slippery small plant, sometimes to 6 inches high, often epiphytic on lower parts of larger algae in 30-75 feet.

Gastroclonium coulteri (Harvey) Kylin Pl. 35, fig. 1, 2.

British Columbia to central Baja California. A dull greenish species readily recognized by its partitioned vesicular branchlets, but these are sometimes so few or small in the southern part of the range that one must be careful not to overlook them. Frequent, intertidal to 30 feet.

Gelidium cartilagineum var. *robustum* Gardner Pl. 17, fig. 1.

Southern British Columbia to Isla Magdalena, Baja California. This purplish-red plant often grows to two feet or more in height, and, thus, is a larger, coarser plant than *G. purpurascens* which is otherwise similar. In both of these species the young branchlets have a knee-like bend near their bases so that they are at first almost parallel to the branch bearing them. Common in rocky, well circulated areas from intertidal to 65 feet.

Gelidium nudifrons Gardner Pl. 18, fig. 1.

Southern California to central Baja California. Plants bright red to dark red, the much branched, almost cylindrical fronds of a tough, wiry texture. To 18 inches high, occasional, 10-75 feet.

Gelidium purpurascens Gardner Pl. 17, fig. 2.

Central California to northern Baja California. These dark, purplish-red colored plants are similar in structure and habit to *G. cartilagineum*, but are smaller (1 foot or less high) and more delicate throughout. Frequent, intertidal to 30 feet.

Gigartina binghamiae J. Agardh Pl. 30, fig. 1.

Southern California to central Baja California. This is one of our broadest, bright-red colored algae and is characteristic of depths of 20-45 feet in colder areas. It is similar to the more northern *G. corymbifera*.

Gigartina canaliculata Harvey Pl. 31, fig. 2.

Oregon to Isla Magdalena, Baja California. This is characteristically a clumping, intertidal plant of dark, often greenish color with little red showing through. It extends only occasionally into the inner edges of the kelp community.

Gigartina serrata Gardner Pl. 30, fig. 2, 3.

Southern California to southern Baja California. This plant suggests a large form of *Gigartina canaliculata*, reaching a foot or more in length. It is of a similar dark greenish color with a reddish cast. Occasional from the intertidal to 30 feet.

Gigartina volans (C. A. Agardh) J. G. Agardh Pl. 31, fig. 3.

Oregon to central Baja California. A coarse, tough, dark, greenish-

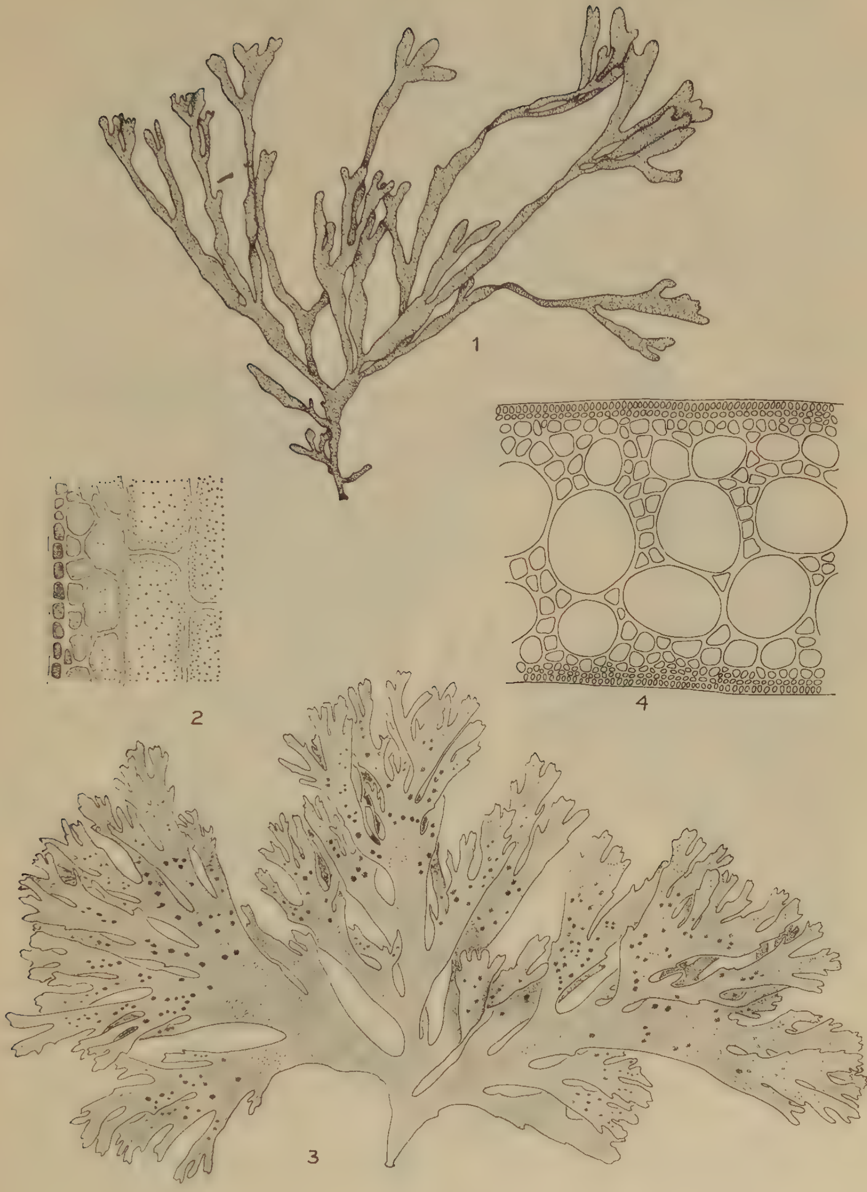

PLATE 28

Fig. 1-2. *Gracilaria cunninghamii:* fig. 1, habit, × 0.45; fig. 2, longitudinal section through frond, × 117. Fig. 3-4. *Callophyllis megalocarpa:* fig. 3, habit showing scattered cystocarps, × 0.5; fig. 4, cross-section through thallus, × 86.

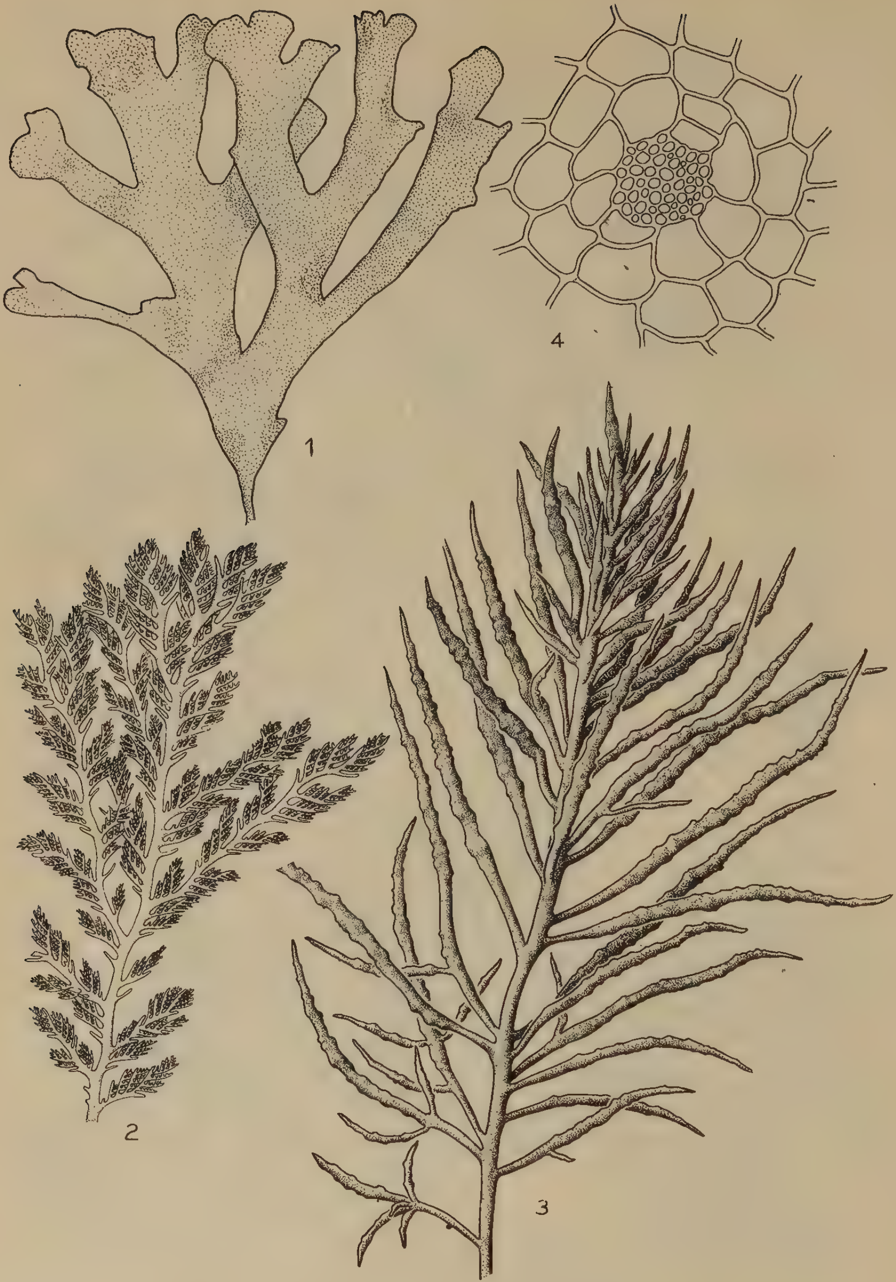

PLATE 29

Fig. 1. *Phyllophora clevelandii,* upper portion of plant, × 0.5. Fig. 2. *Plocamium pacificum,* small portion of branch, × 1. Fig. 3-4. *Agardhiella coulteri*: fig. 3, upper portion of plant, × 0.5; fig. 4, cross-section of inner medullary part of thallus, × 60.

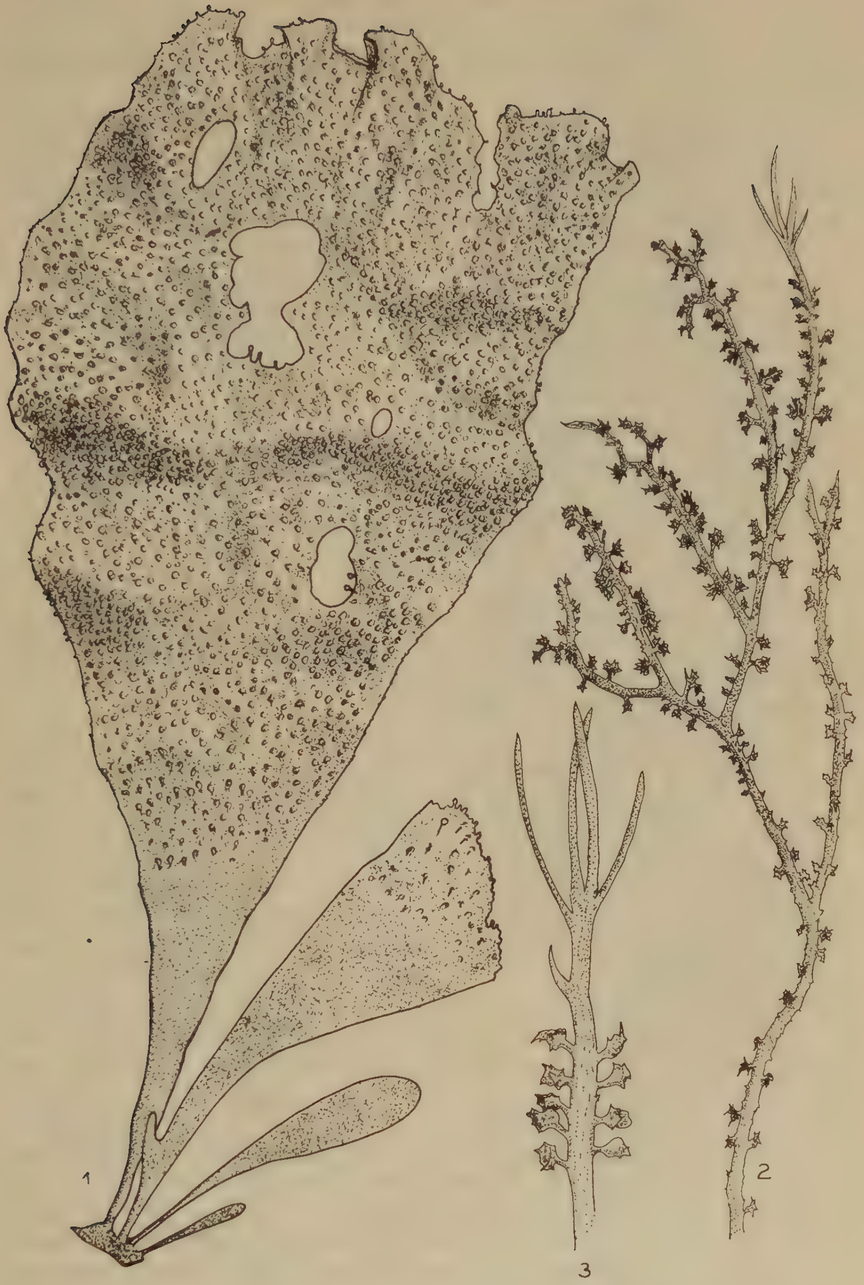

PLATE 30
Fig. 1. *Gigartina binghamiae,* habit, × 0.5. Fig. 2-3. *Gigartina serrata*: fig. 2, habit, × 0.5; fig. 3, branch tip of female plant showing pointed cystocarps, × 2.

red plant characteristic of the lowermost intertidal but extending down to 30 feet.

Gloiphloea confusa Setchell Pl. 16, fig. 5; Pl. 17, fig. 4.

British Columbia to central Baja California. Plants are rose-red to deep red in color, 3 to 5 inches high, of a soft gelatinous texture. Occasional at 20-70 feet. One must examine the structure of the plant in cross section to distinguish it from *Scinaea.*

Gracilaria cunninghamii Farlow Pl. 28, fig. 1, 2.

Southern California to Isla Magdalena, Baja California. The irregular dichotomous branching of this plant and lack of stolons at the base distinguish it from the several *Rhodymenia* species of similar structure and color. Frequent from intertidal to 45 feet.

Grateloupia howeii Setchell and Gardner Pl. 25, fig. 1.

Central and southern Baja California. This species resembles a broad *Gigartina* because of the surface outgrowths, but may be distinguished in this flora by its dull, greenish-purple rather than red color, and more southerly range. Occasional from 10-45 feet.

Grateloupia schizophylla Kützing Pl. 24, fig. 1, 2.

Washington to southern Baja California. The long (1-2 feet), strap-shaped, simple or pinnately branched blades are of slippery texture. Occasional from intertidal to about 30 feet. The female reproductive structure, as illustrated, is distinctive.

Griffithsia pacifica Kylin Pl. 36, fig. 3.

British Columbia to southern Baja California. Plants forming densely branched, small pink clumps 2 to 4 inches high. The large cells of the filaments can be seen with the naked eye. Occasional, intertidal to 100 feet.

Gymnogongrus leptophyllus J. G. Agardh Pl. 32, fig. 1.

Oregon to northern Baja California. This dull, brownish-red plant is distinguished by its small size, 3-5 inches, narrow, abundantly forked branches and dense, small-celled, internal structure. Frequent from intertidal to 30 feet.

Laurencia diegoensis Dawson Pl. 43, fig. 1.

Southern California to northern Baja California. Usually dull greenish-red in color, to 10 inches high, growing on rocks from the intertidal to 30 feet.

Laurencia splendens Hollenberg Pl. 43, fig. 4.

Central California to northern Baja California. Epiphytic and usually only 2 to 4 inches high in our area. Intertidal to 30 feet.

Laurencia subopposita (J. Agardh) Setchell Pl. 43, fig. 3.

Southern California to central Baja California. The coiled, tendril-like, blunt branches which occur on this bright red, epiphytic plant are distinctive. Occasional, 10-50 feet.

Leptocladia binghamiae J. Agardh Pl. 19, fig. 2, 3.

Central California to Isla Magdalena, Baja California. Deep red in

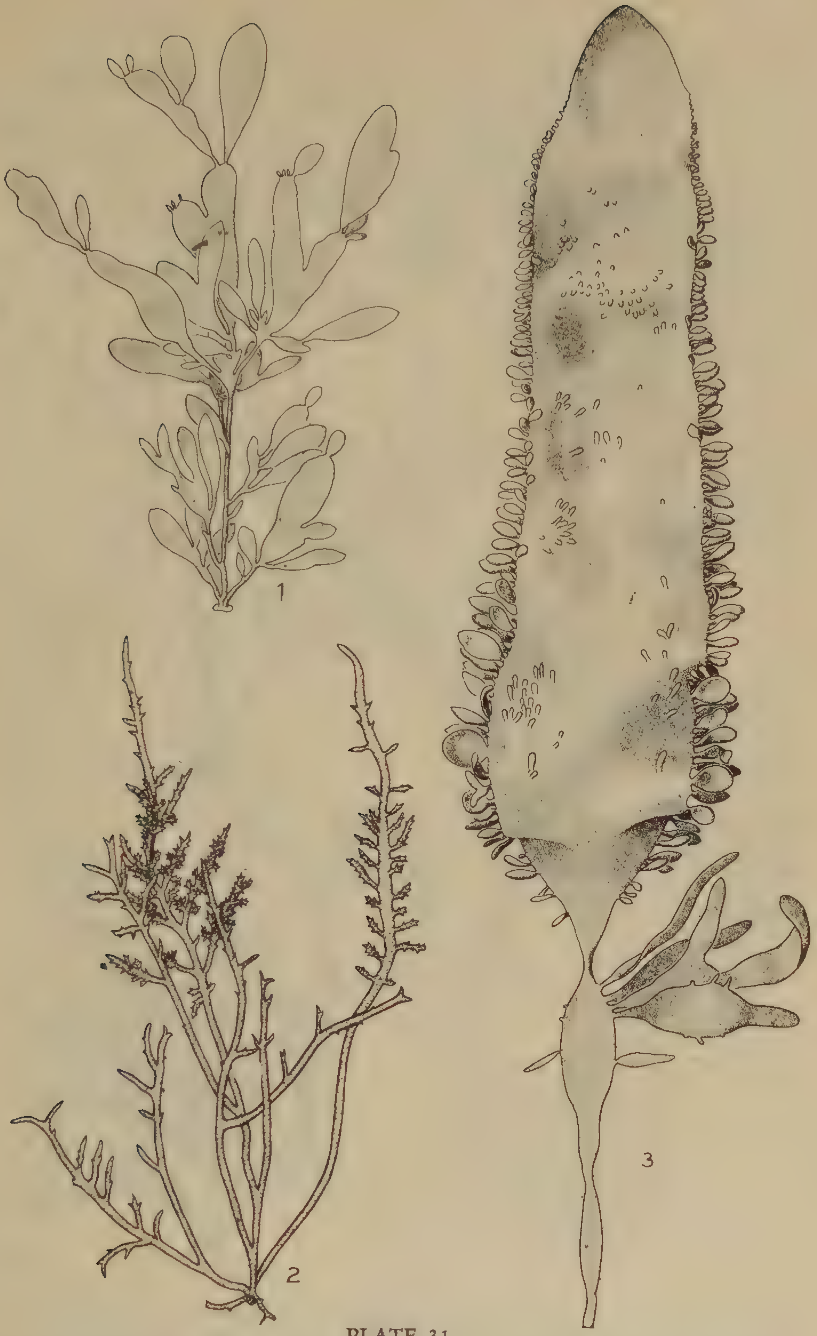

PLATE 31

Fig. 1. *Phyllophora californica,* habit × 0.5. Fig. 2. *Gigartina canaliculata,* habit, × 1. Fig. 3. *Gigartina volans,* habit, × 0.5.

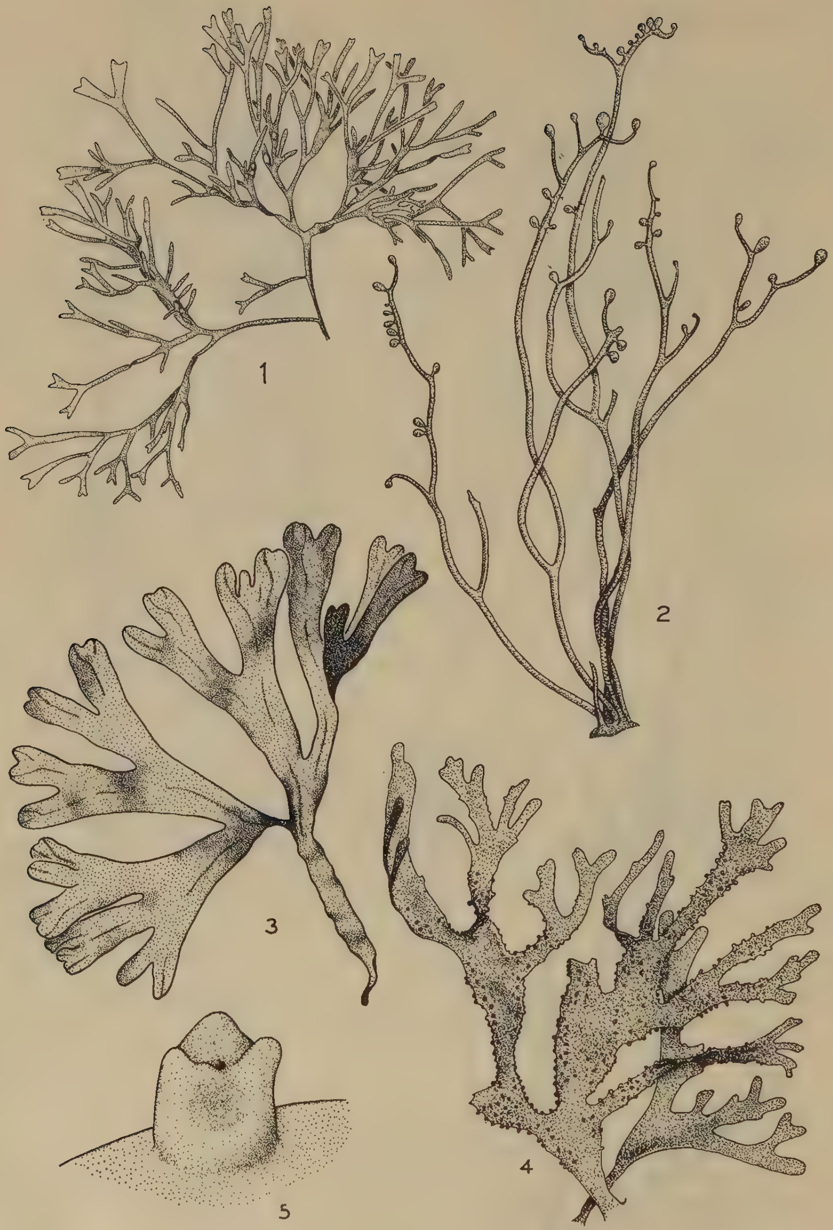

PLATE 32

Fig. 1. *Gymnogongrus leptophyllus,* habit, × 1. Fig. 2. *Botryocladia neushulii,* habit, ×0.5. Fig. 4-5. *Fauchea laciniata*: fig. 4, upper portion of female plant, showing cystocarps, × 1; fig. 5, crown-shaped cystocarps, × 15.

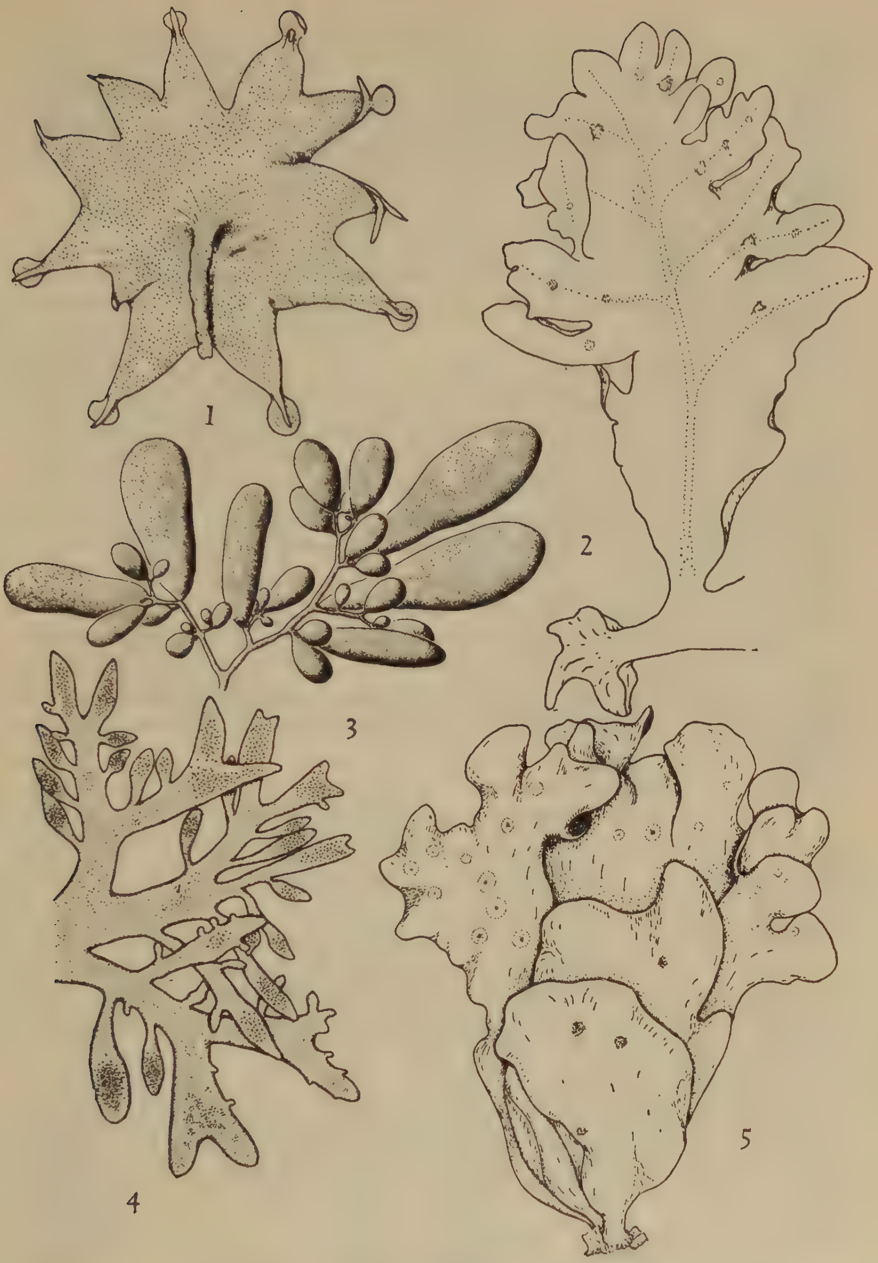

PLATE 33

Fig. 1. *Sciadophycus stellatus,* habit of plant lacking holdfast, × 2. Fig. 2. *Branchioglossum undulatum,* a blade bearing flaired cystocarps, × 7.5. Fig. 3. *Botryocladia pseudodichotoma,* upper portion of plant, × 0.5. Fig. 4. *Binghamia forkii,* upper portion of plant, × 3. Fig. 5, *Myriogramme caespitosa,* habit, × 8.

color, to 1 foot high. The markedly flattened branches and irregular marginal teeth distinguish it externally, but a cross section to show the distinctive structure may sometimes be necessary for confirmation. Occasional, 10-65 feet.

Lithophyllum imitans Foslie Pl. 20, fig. 4.

Central California to central Baja California. The thallus forms a pink colored, coarse, somewhat glossy, hard crust on the surface of rocks or shells in depths of 10-75 feet. The small diameter of the protuberances is distinctive.

Lithothamnium giganteum L. R. Mason Pl. 20, fig. 2.

Southern California to central Baja California. This is the coarsest of our nodular species of *Lithothamnium*. The protuberances are large and have somewhat swollen tips. The pinkish-purple thallus often completely encloses a small stone and lies free on the bottom in depths of 20-60 feet. From a similar species of *Lithophyllum* (*L. grumosum*) it is distinguished microscopically by the presence of many small pores (rather than a single pore) in the cap of the non-sexual reproductive cavities.

Lithothamnium lamellatum Setchell and Foslie Pl. 20, fig. 3.

Central California to central Baja California. The smooth-surfaced, pinkish, shingle-like thallus of lobes about ½ inch in diameter forms loosely attached crusts on rocks and the basal portions of larger algae at depths of 20-75 feet. The crusts are distinctly calcareous, brittle and overlapping, unlike *Peyssonelia*.

Lithothrix aspergillum J. E. Gray Pl. 23, fig. 1.

Southern British Columbia to southern Baja California. The nearly cylindrical thallus and very short segments are distinctive of this bushy little calcareous plant, 4-5 inches high, which is frequent from the intertidal to depths of 40 feet.

Melobesia mediocris (Foslie) Setchell and Mason Pl. 19, fig. 4, 5.

Northern British Columbia to Isla Magdalena, Baja California. This is another epiphyte found exclusively on *Phyllospadix*. The plants are often extremely abundant, forming small, pink crusts on the surfaces of the slender green leaves.

Microcladia coulteri Harvey Pl. 37, fig. 3, 4.

British Columbia to central Baja California. This is a feathery, delicate species 2 to 8 inches high suggesting *Plocamium* but of a darker color. It grows epiphytically on various larger algae from intertidal to 30 feet.

Myriogramme caespitosa Dawson Pl. 33, fig. 5.

Southern California to southern Baja California. A very small clumping species characteristically growing on kelp holdfasts.

Nienburgia andersoniana (J. Agardh) Kylin Pl. 38, fig. 1.

Oregon to southern Baja California, intertidal to 80 feet. This plant varies greatly in size (3-10 inches), branching and breadth of blade, but

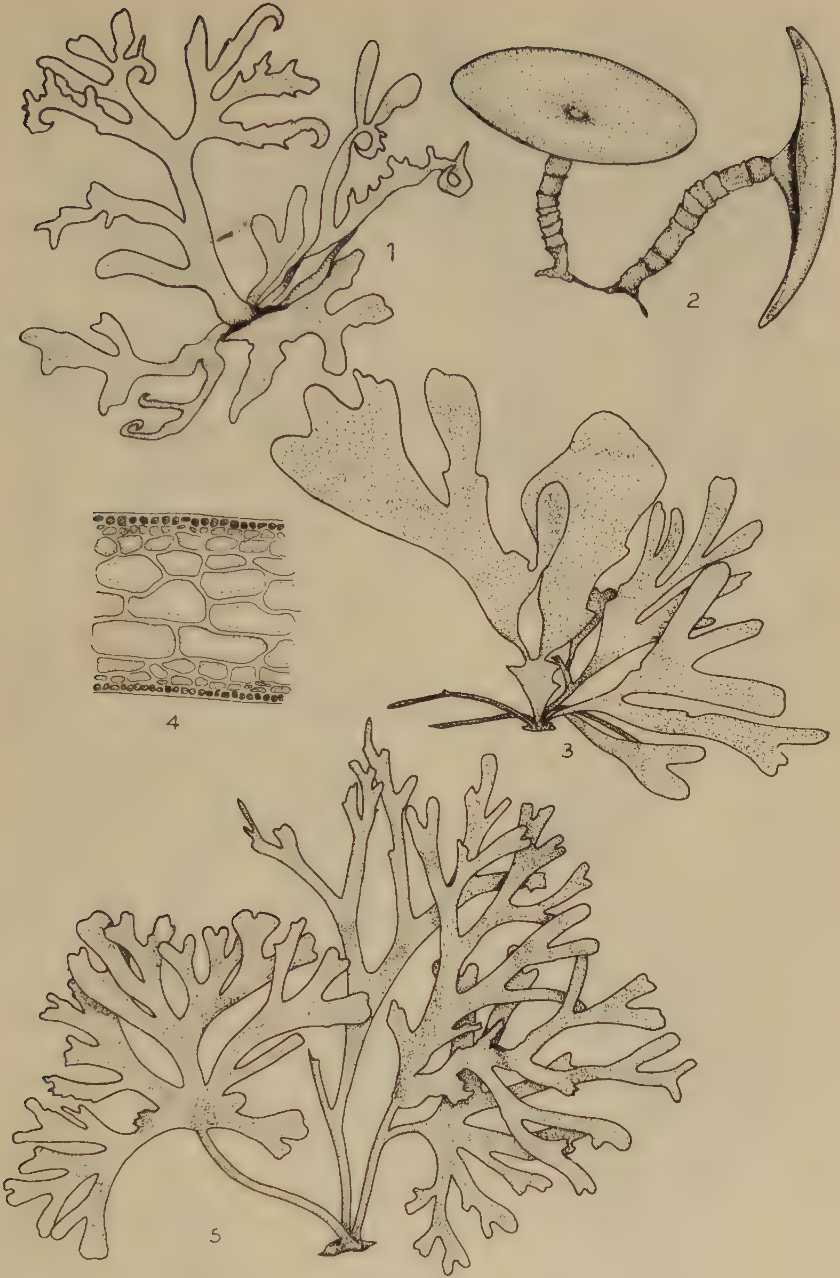

PLATE 34

Fig. 1. *Acrosorium uncinatum,* habit showing hooked tips, × 1.5. Fig. 2. *Drouetia rotata,* habit showing growth scars on stipe, × 0.5. Fig. 3. *Rhodymenia palmettiformis,* habit showing horizontal stolons, × 0.5. Fig. 4. *Rhodymenia pacifica,* longitudinal section through thallus, × 107. Fig. 5. *Rhodymenia arborescens,* habit, × 0.5.

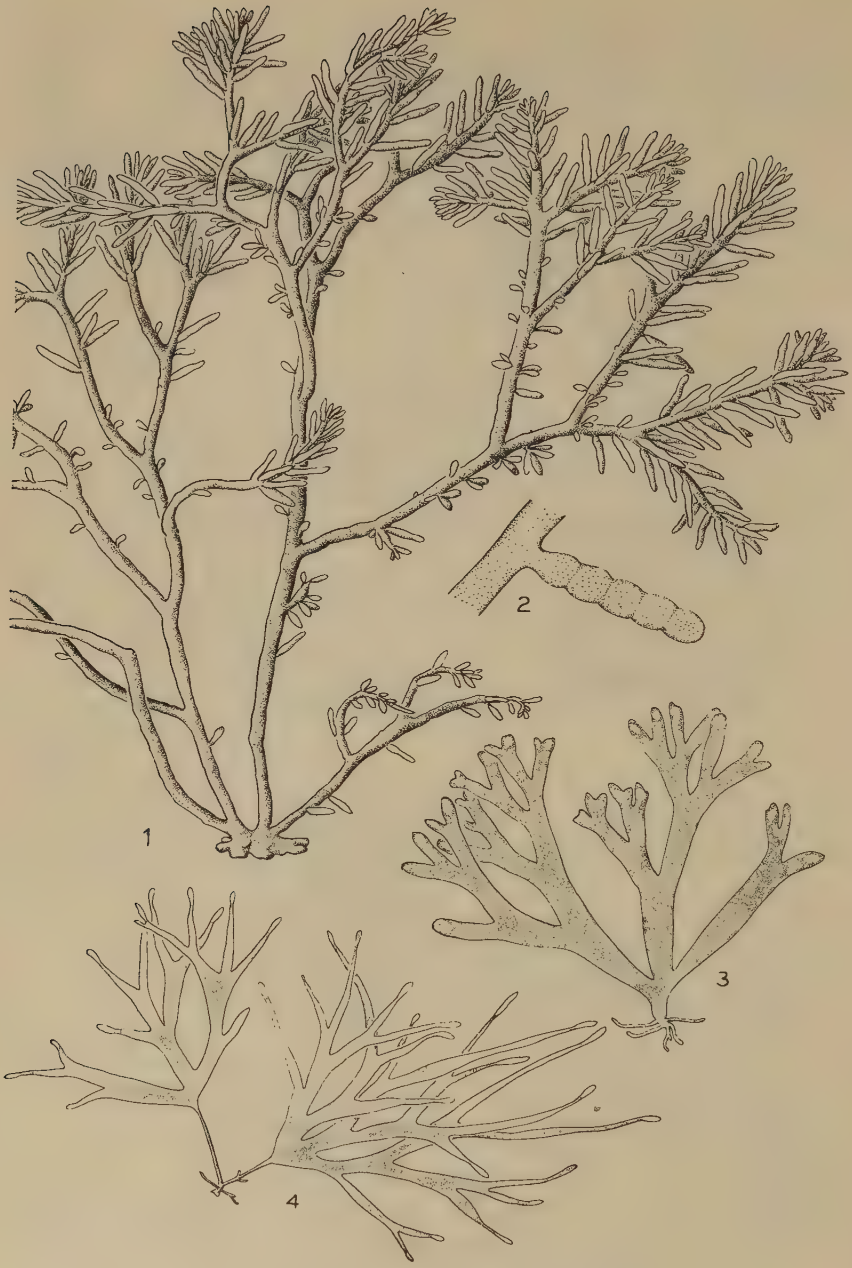

PLATE 35

Fig. 1-2. *Gastroclonium coulteri*: fig. 1, habit showing many-chambered laterals, × 0.75; fig. 2, lateral branchlet showing diaphrams, × 2. Fig. 3. *Rhodymenia californica,* habit showing basal rhizoids, × 0.75. *Rhodymenia attenuata,* habit showing basal rhizoids, × 0.75.

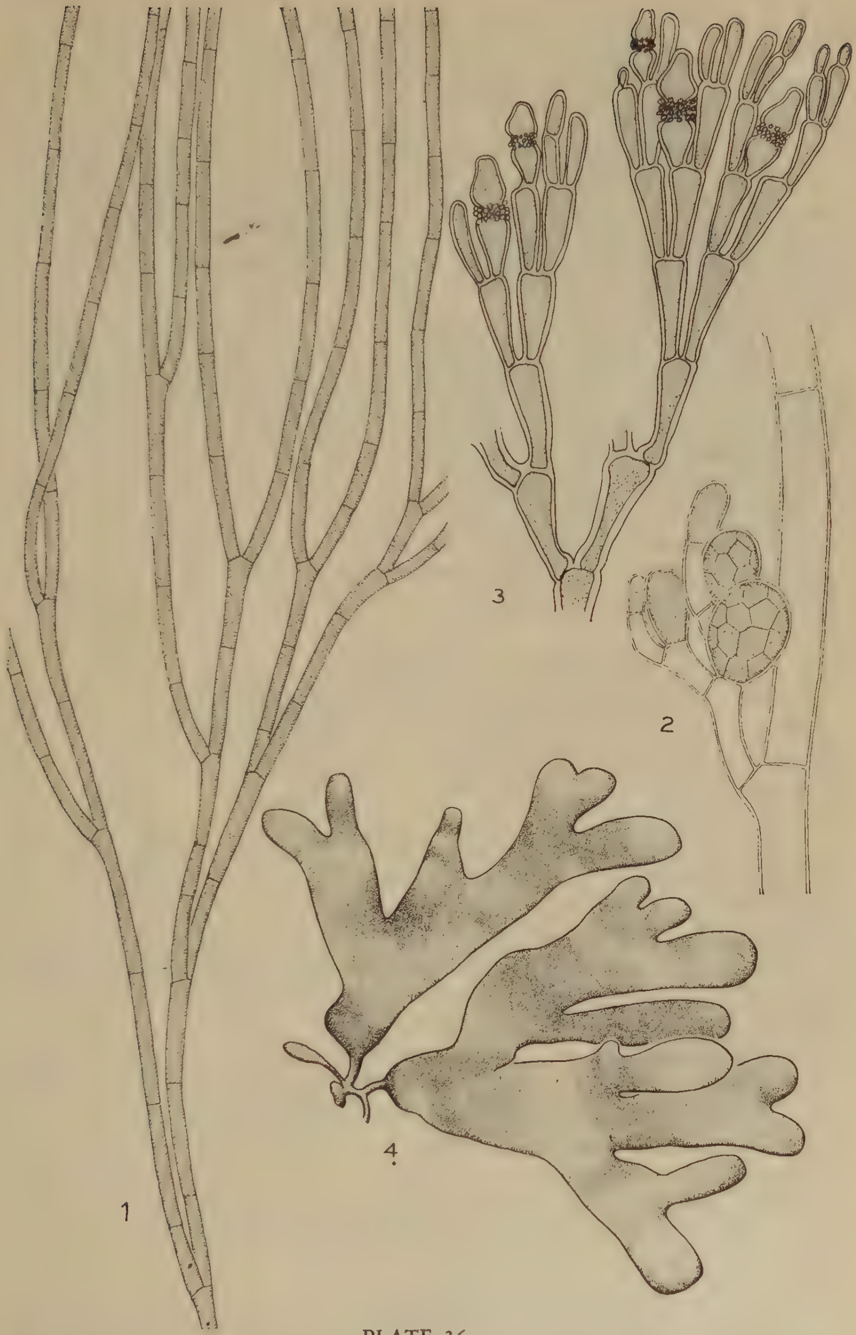

PLATE 36

Fig. 1-2. *Spermothamnion snyderae*: fig. 1, sterile branch, × 8; fig. 2, branch with polysporangia, × 160. Fig. 3. *Griffithsia pacifica*, small upper part of male plant, × 8 Fig. 4. *Rhodymenia pacifica*, habit showing basal stolons, × 0.75.

is recognized by its venation and marginal teeth. It often exhibits patches of bluish iridescence.

Peyssonelia rubra var. *orientalis* Weber van Bosse Pl. 17, fig. 3.

Throughout Pacific Mexico. This is a small, bright red, crust-like plant frequently found closely affixed except at the margins to rocks in shaded intertidal areas to about 60 feet. It is the commonest of several similar species which can be distinguished only by vertical sections through reproductive parts.

Phyllophora californica (J. Agardh) Kylin Pl. 31, fig. 1.

Central California to northern Baja California. The repeated regeneration of flat blades from cylindrical stipes is distinctive of this characteristically sublittoral plant of dull, dark reddish color, which reaches 4-6 inches in height. Occasional at 10-50 feet.

Phyllophora clevelandii Farlow Pl. 29, fig. 1.

Southern California to northern Baja California. This is a characteristically deep water, rose-red colored plant found under the kelp canopy at depths of 50 feet and on out to dimly lighted bottoms at 100 feet or more. None of the other species inhabiting these depths have the distinctively broad branch tips.

Pogonophorella californica (J. Agardh) Silva Pl. 39, fig. 3, 4.

Southern California to central Baja California. This is one of the small species found in mixtures on rocks or around the bases of larger plants. The small tufts of hairs on the upper parts of the erect, cylindrical branches are distinctive. Intertidal to 60 feet.

Plocamium pacificum Kylin Pl. 29, fig. 2.

A common and easily recognized, bright red, feathery plant of attractive appearance. Common and variable in size from 2 to 10 inches tall, intertidal to 85 feet.

Polyneura latissima (Harvey) Kylin Pl. 38, fig. 4.

Northern British Columbia to southern Baja California, intertidal to 60 feet. The anastomosing vein pattern of this rose-red colored species sets it apart from others in our area.

Polysiphonia johnstonii Setchell and Gardner Pl. 41, fig. 5, 6.

Central and southern Baja California. This is probably the most frequent sublittoral species of this genus in which 5 or 6 cells occur per tier. It will be encountered as an epiphyte to depths of about 30 feet.

Polysiphonia mollis Harvey Pl. 41, fig. 7, 8.

Washington to central Mexico. This is the commonest of the several species of this genus having 4 cells per tier. It will be encountered as a slender filamentous epiphyte at depths to 50 feet.

Prionitis andersoniana (Eaton) Dawson Pl. 26, fig. 2.

Oregon to central Baja California. Occasional to 30 feet. The thallus is deep rose-red and is of a smooth, firm, tough texture. The plants may reach a foot or more in length.

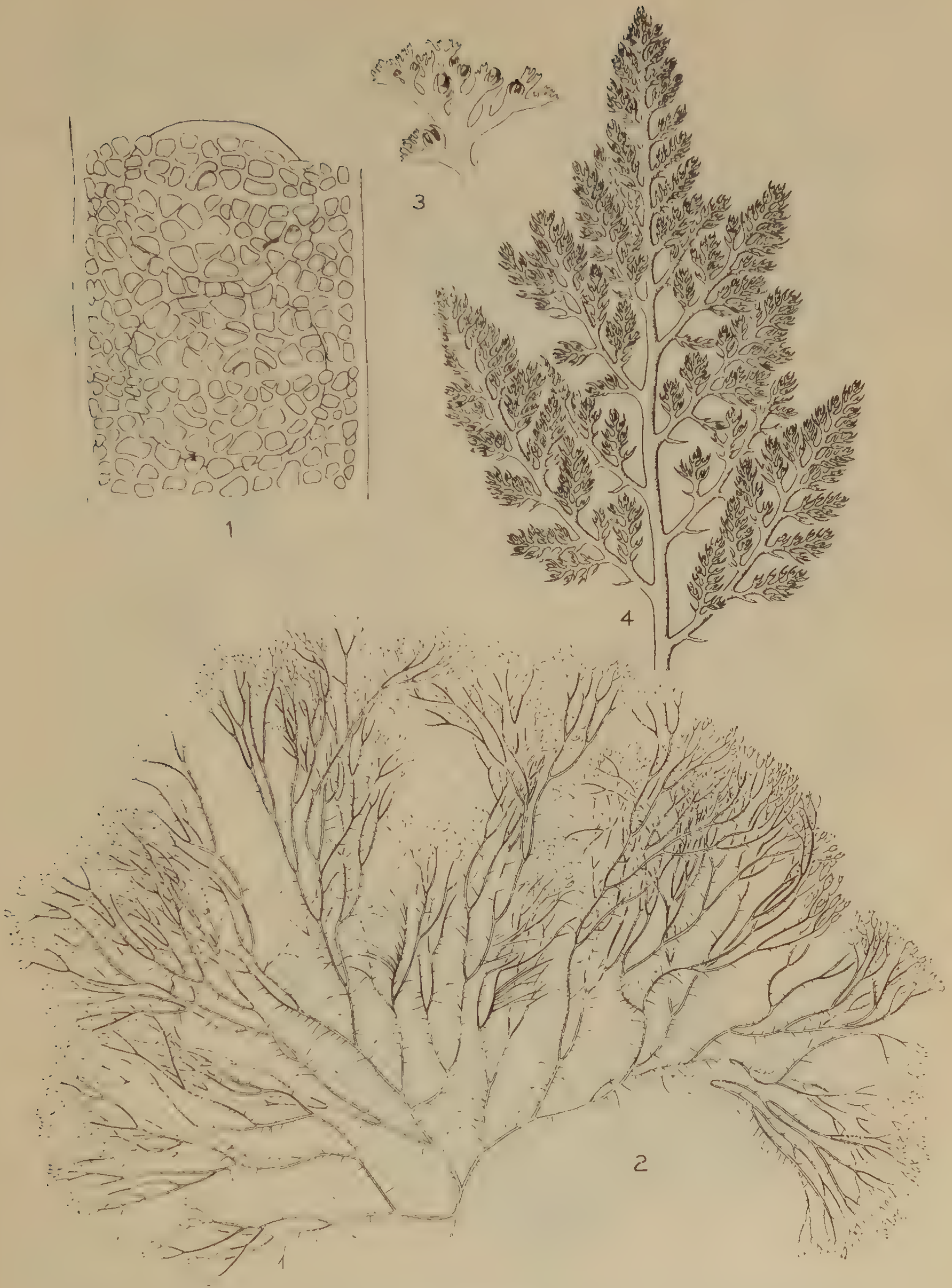

PLATE 37

Fig. 1-2. *Ceramium pacificum*: fig. 1, large portion of plant, × 0.5; fig. 2, small part of a branch to show the irregular arrangement of the cortical cells over the large subspherical cells of the axial filament, × 238. Fig. 3-4. *Microcladia coulteri*: fig. 3, upper portion of branch, × 1.5; fig. 4, branchlet with cystocarps, × 5.

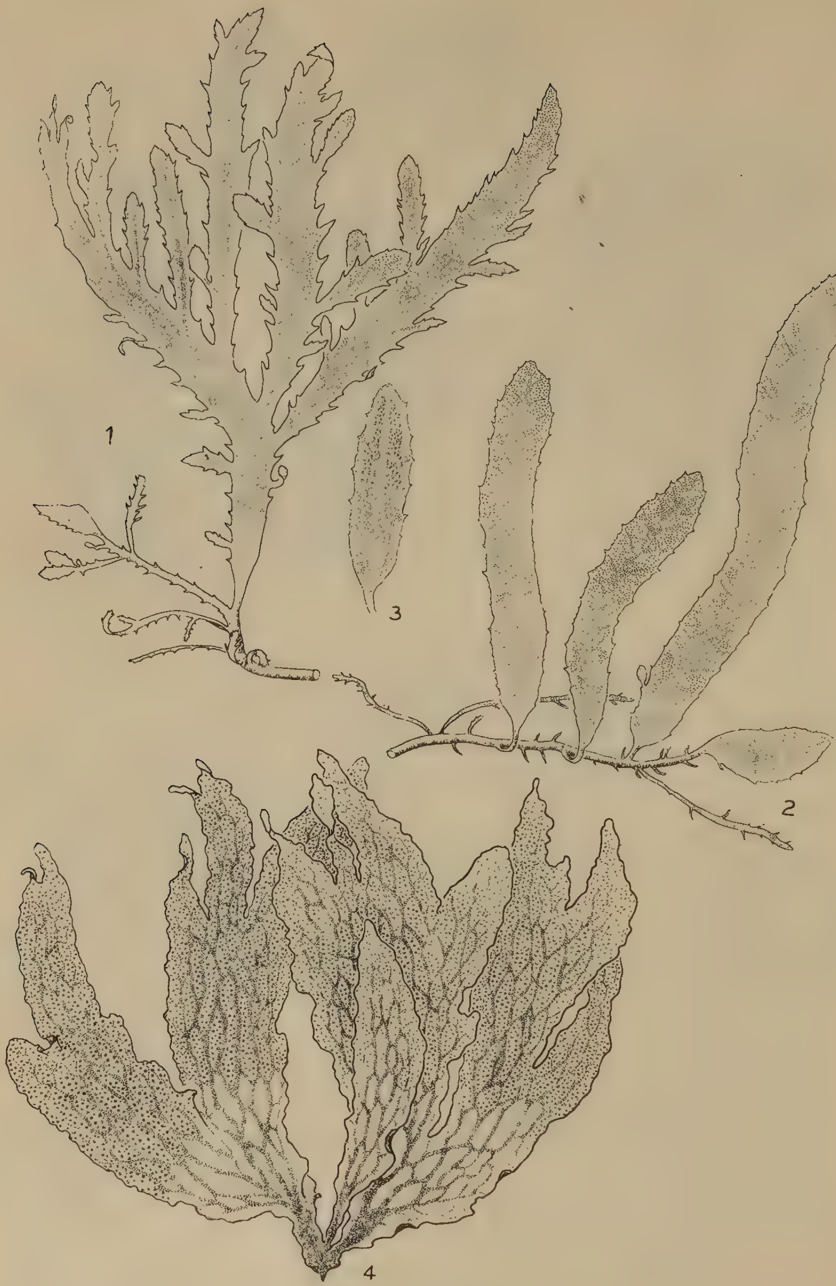

PLATE 38

Fig. 1. *Nienburgia andersoniana,* upper portion of branch, × 1. Fig. 2-3. *Anisocladella pacifica*: fig. 2, sterile plant, × 2; fig. 3, fertile blade of tetrasporic plant, × 2. Fig. 4, *Polyneura latissima,* habit, × 0.75.

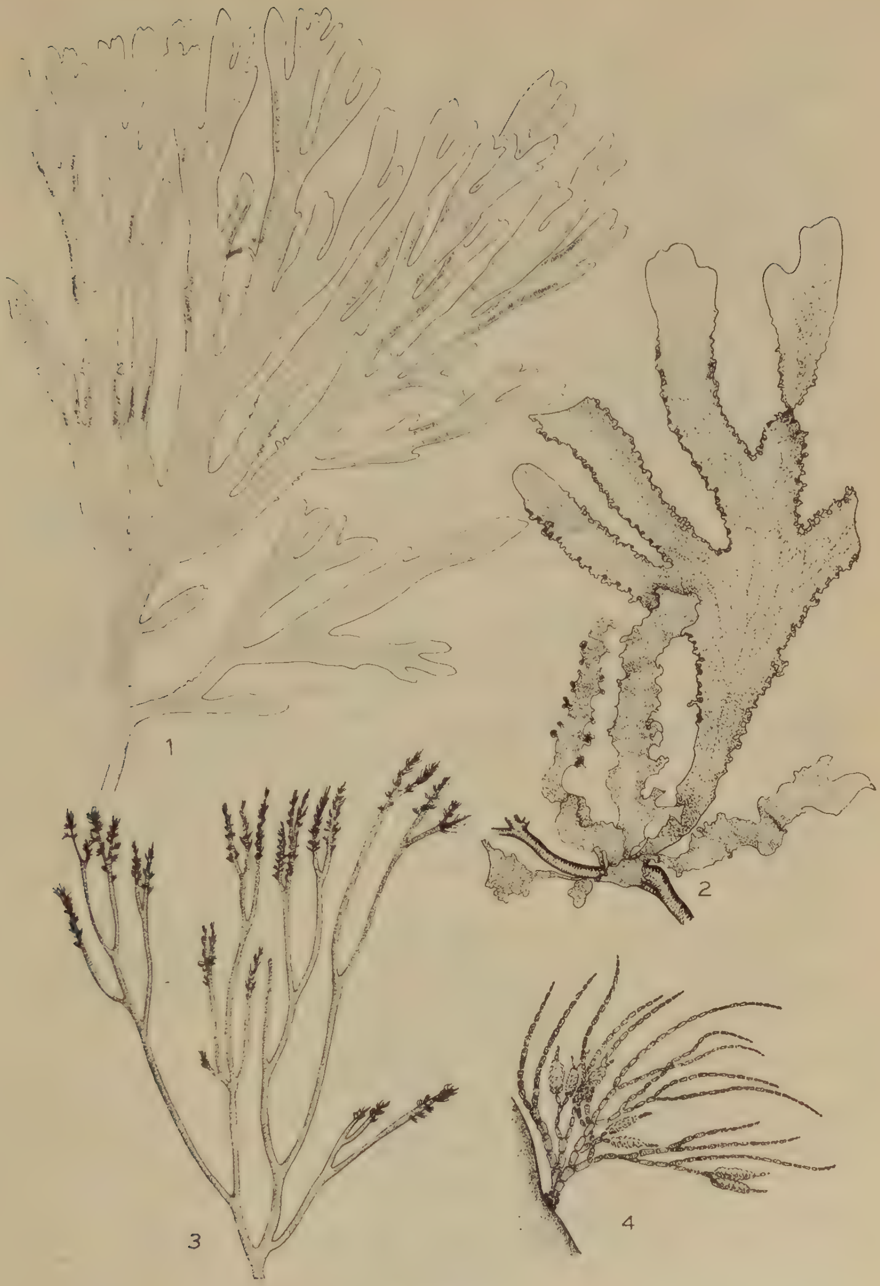

PLATE 39

Fig. 1. *Cryptopleura violacea,* showing lateral tetrasporangia, × 0.5. Fig. 2. *Cryptopleura crispa,* showing tetrasporangia on small lateral lobes, × 0.5. Fig. 3-4. *Pogonophorella californica*: fig. 3, habit showing scattered tufts of hairs near tips of branches, × 1.5; fig. 4, tuft of hairs with spermatangial clumps, × 50.

Prionitis cornea (Okamura) Dawson Pl. 26, fig. 1.

Southern California to central Baja California. The flattened, dichotomous, cartilaginous, deep red fronds, 6-7 inches high, with irregular or scant, very short secondary branchlets, are distinctive. Occasional at 25 to 65 feet, and extending into the lowest intertidal zone.

Prionitis lanceolata Harvey Pl. 25, fig. 2.

British Columbia to northern Baja California. These plants reach 2 feet in height, are dark, dull reddish-purple in color. The texture is firm and coarse. Frequent from 40 feet up into the intertidal.

Pterochondria pygmaea (Setchell) Hollenberg Pl. 42, fig. 3.

Southern California to central Baja California. Similar to the next species but smaller and proportionally broader. Almost always found as an epiphyte on the upper parts of *Cystoseira.*

Pterochondria woodii (Harvey) Hollenberg Pl. 41, fig. 1, 2.

British Columbia to central Baja California. Similar to the former but larger and proportionally narrower. Epiphytic on the upper parts of *Cystoseira.*

Pterocladia pyramidale (Gardner) Dawson Pl. 18, fig. 3; Pl. 19, fig. 1.

Southern California to Isla Magdalena, Baja California. This plant is often confused with the flattened *Gelidium* species, but is macroscopically distinguishable in most cases by its branchlets which extend perpendicularly from the major branches rather than having a knee-like bend toward the major branch apex. The single-pored female reproductive bodies (cystocarps) are distinctive, but these are infrequently found. Mature plants may reach nearly 1 foot in height and often have the upper branches reduced and somewhat matted. Common from the intertidal zone down to 45 feet.

Pterosiphonia baileyi (Harvey) Falkenberg Pl. 42, fig. 2.

Northern California to central Baja California. A dark colored, almost black, small, delicately branched plant to 6 inches high, usually on rocks, intertidal to 30 feet.

Pterosiphonia dendroidea (Montagne) Falkenberg Pl. 41, fig. 3, 4.

British Columbia to southern Baja California. A very common small species 1 to 2 inches high. It grows with other small forms on rocks, shells and holdfasts of larger algae from the intertidal to 50 feet. It is usually very dark dull reddish in color and resembles a minute feather.

Rhodymenia arborescens Dawson Pl. 34, fig. 5.

Southern California to Southern Baja California. This plant is dull red, 5 to 7 inches high. It is one of the common species of the shaded areas under the kelp canopy and on out to depths of 115 feet. The woody conical holdfast is distinctive for this genus. Note that the base may often be covered by animal material.

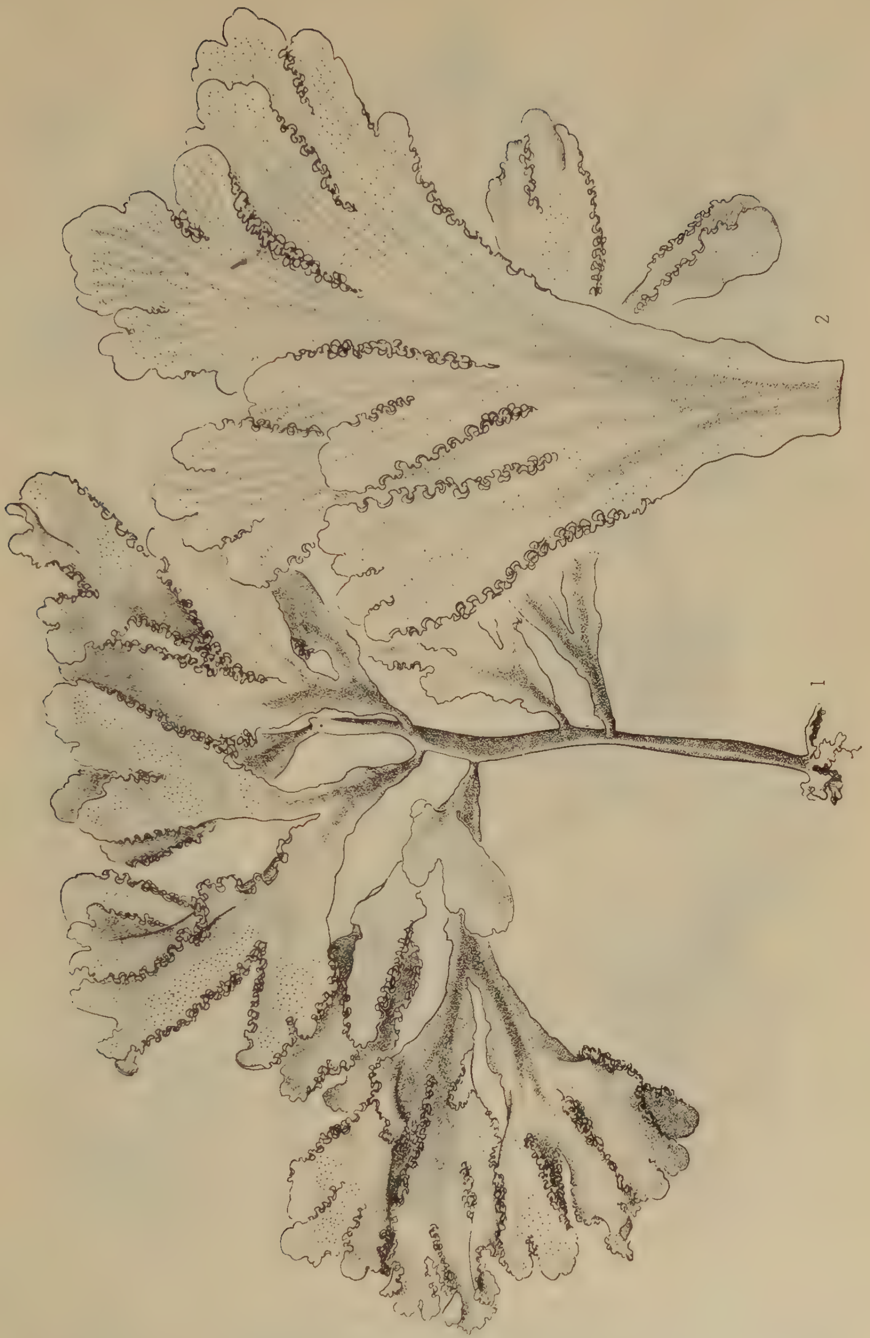

PLATE 40

Fig. 1-2. *Botryoglossum farlowianum*: fig. 1, entire plant, × 0.5; fig. 2, segment of blade, × 1.

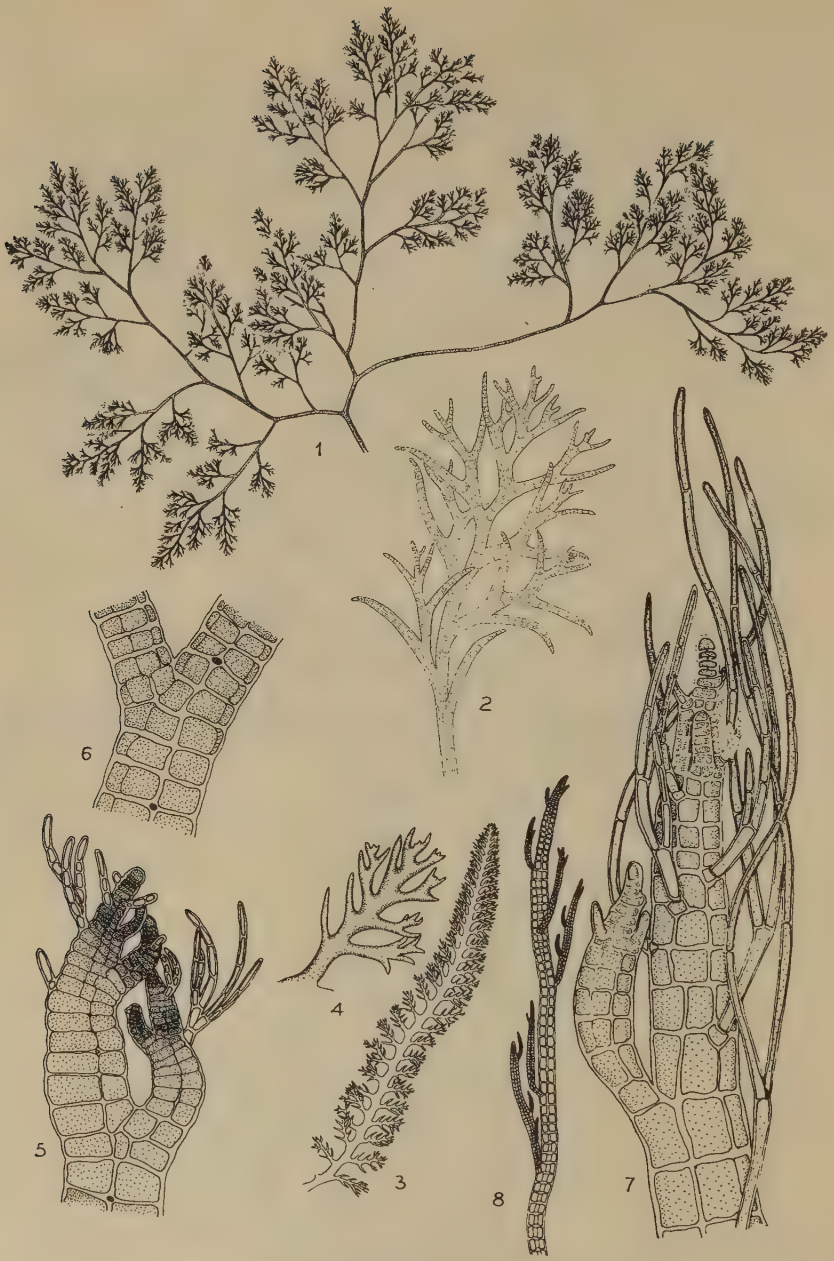

PLATE 41

Fig. 1-2. *Pterochondria woodii*: fig. 1, upper portion of plant, × 0.75; fig. 2, apex of a branch, × 13. Fig. 3-4, *Pterosiphonia dendriodea*: fig. 3, erect axis showing branching, × 3.5; fig. 4, detail of branch tip, × 35. Fig. 5-6, *Polysiphonia johnstonii*: fig. 5, branch tip, × 143; fig. 6, portion of axis showing arrangement of cortical cells, × 98. Fig. 7-8. *Polysiphonia mollis*: fig. 7, portion of branch, × 15; fig. 8, branch tip, × 325. (Fig. 7 after Hollenberg)

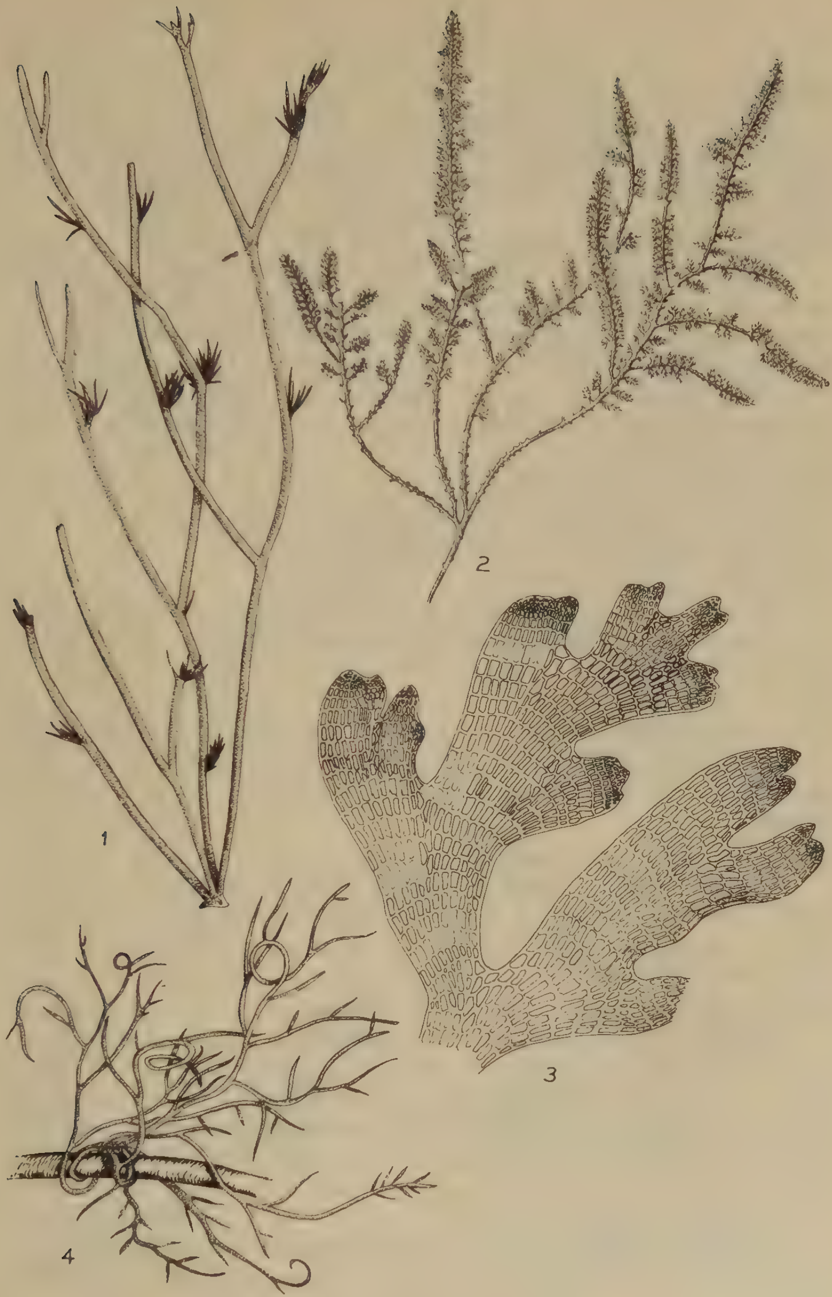

PLATE 42

Fig. 1. *Chondria nidifica,* habit showing tufts on branches, × 1. Fig. 2, *Pterosiphonia baileyi,* habit, × 0.75. Fig. 3. *Pterochondria pygmaea,* cell structure of branch tip, × 15. Fig. 4. *Chondria californica,* entire plant growing epiphytically, × 1.

Rhodymenia attenuata Dawson Pl. 35, fig. 4.

Central California to central Baja California. The attenuate or spatulate blades of this small red plant (2-3 inches high) distinguish it from the several other stolon-bearing *Rhodymenia* species. Occasional, 35-65 feet.

Rhodymenia californica Kylin Pl. 35, fig. 3.

British Columbia to southern Baja California. Plants bright red, sometimes with white blotches, 1-3 inches high. It is the smallest and narrowest species of this genus. Frequent from intertidal to 65 feet.

Rhodymenia pacifica Kylin Pl. 34, fig. 4; Pl. 36, fig. 4.

British Columbia to northern Baja California, 10-50 feet. This and the next species must be distinguished by the characters given in the key and by the illustrations.

Rhodymenia palmettiformis Dawson Pl. 34, fig. 3.

Southern California to northern Baja California, intertidal to 40 feet. Distinguished by key and illustrations.

Sciadophycus stellatus Dawson Pl. 33, fig. 1.

Southern California to central Baja California. This distinctive species is characteristic of deeply shaded bottoms under the kelp canopy or out into deeper water to as much as 150 feet.

Scinaea johnstoniae Setchell Pl. 17, fig. 5.

Southern California to Islas Tres Marías, Mexico. Macroscopically identical with *Gloiophloea*. The two genera are distinguished by the structure of the cortex as shown in Plate 17. Occasional in our area at depths of 20-60 feet.

Smithora naiadum (Anderson) Hollenberg Pl. 16, fig. 4.

Northern British Columbia to Isla Magdalena, Baja California. This is the only small (under 1 inch), membranous red alga to be found growing exclusively on *Phyllospadix* in our area. It is of seasonal occurrence from intertidal to 30 foot depths.

Stenogramme interrupta (C. Agardh) Montagne Pl. 32, fig. 3.

British Columbia to southern Baja California. This plant has a great depth range from just below the intertidal to 135 feet. It is rose red in color, and both morphologically and structurally like *Rhodymenia* and *Gracilaria*, but fertile plants are readily recognized; the female ones, by the broken medial lines, and asexual ones by their blotched spore-bearing areas.

Spermothamnion snyderae Farlow Pl. 36, fig. 1, 2.

Central California to central Baja California. Intertidal to 50 feet. This plant forms patches of soft red hair 1-2 inches long, often mixed with other small algae.

(108)

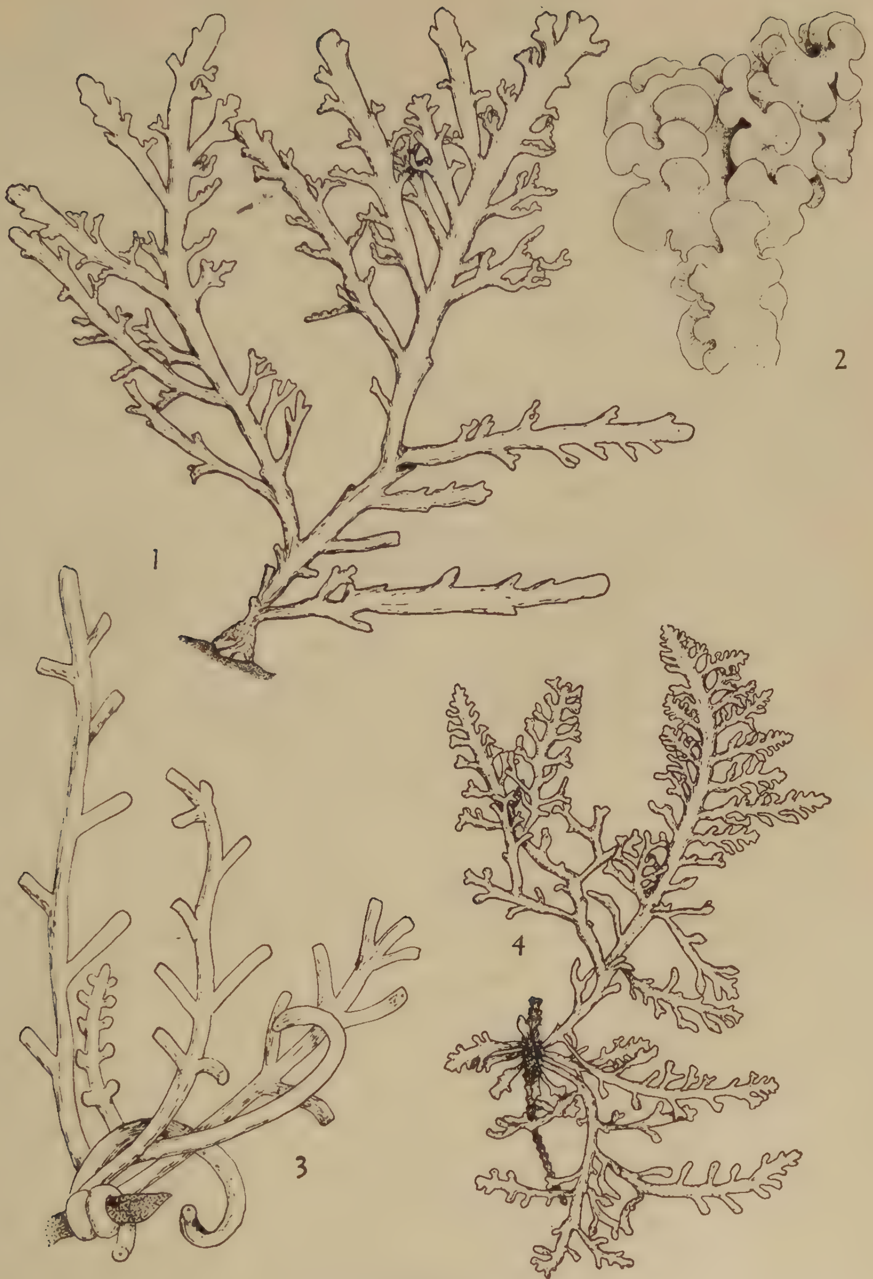

PLATE 43

Fig. 1. *Laurencia diegoensis,* habit, × 0.66. Fig. 2. *Amplisiphonia pacifica,* upper portion of plant, × 1.5. Fig. 3. *Laurencia supopposita,* plant growing entwined around host, × 1. Fig. 4. *Laurencia splendens,* habit, × 1.

Reprinted from Science, February 5, 1960, Vol. 131, No. 3397, pages 332-337

COSMIC-RAY-PRODUCED SILICON-32 IN NATURE

Silicon-32, discovered in marine sponges, shows promise as a means for dating oceanographic phenomena.

Devendra Lal, Edward D. Goldberg, Minoru Koide

Cosmic-Ray-Produced Silicon-32 in Nature

Silicon-32, discovered in marine sponges, shows promise as a means for dating oceanographic phenomena.

Devendra Lal, Edward D. Goldberg, Minoru Koide

The nuclear transmutations resulting from the interaction of cosmic rays with nuclear species in the atmosphere have produced a variety of radioactive products detectable on the surface of the earth. Such isotopes as C^{14}, H^3, Be^{10}, and P^{32} have been found, and their individual distributions and concentrations in the various geological domains have led to many significant concepts and contributions in geochemistry, geophysics, and geochronology (see, for example, *1*).

This article (*2*) concerns still another isotope produced by cosmic rays—Si^{32}, which we have detected in the marine environment. It is thought that this isotope is produced from the nuclear spallations of argon by cosmic rays. It has a half-life of roughly 710 years (*3*). Any Si^{32} that reaches the earth from the atmosphere will be rapidly diluted with stable silicon, and the resulting specific activity of Si^{32} will be very small. However, Si^{32} decays by negatron (β^-) emission to P^{32}, which is a negatron emitter with a half-life of 14.3 days. This makes it possible to detect Si^{32} by milking and by counting the P^{32} daughter from large amounts of silicon.

The principal exchange reservoir for Si^{32} is probably the marine hydrosphere which most likely receives Si^{32} via oceanic rains. The small amounts of silicon in surface marine waters should yield a relatively high specific activity of Si^{32}, whereas the fallout on land will be so diluted by exchange and other chemical interactions with the exposed crustal materials that the detection of this nuclide will be extremely difficult. We estimate the average concentration of Si^{32} to be 2.6×10^{-6} disintegrations per minute, per liter of sea water, or 8 disintegrations per minute, per kilogram of silicon, for a hypothetical thoroughly mixed ocean. The amount of sea water required to yield 1 disintegration per minute, an activity conveniently detectable, is 3.8×10^4 liters. Since the handling of such an amount of water for the extraction of silicon presents many difficulties, Si^{32} was sought initially in siliceous (opaline) sponges, which derive

---

The authors are affiliated with the Scripps Institution of Oceanography, University of California, La Jolla. Dr. Lal is on leave from the Tata Institute of Fundamental Research, Bombay, India.

ontributions from the Scripps Institution of Oceanography, New Series, 1143

Reproduced by Permission

their silicon from sea water and are available in abundance, especially on the sea floors of the continental shelf. Three sponges trawled from the Gulf of California in 1956 were analyzed.

The experimental techniques and the results are presented in the next section. In the third section, an estimate of the rate of production of Si^{32} in the atmosphere from the available cosmic ray and accelerator data is presented. The applications of Si^{32} as a tracer for studying geochemical and geophysical processes with special reference to oceanography are discussed in the last section.

Experimental Techniques and Results

Chemical procedure. The sponges were first cleansed of organic matter and foreign materials, not incorporated in the opaline structure, by digestion with nitric acid, followed by repeated washings with water and acetone. Approximately 200 grams of this material was allowed to stand for 3 months to allow the P^{32} to build up.

The milking procedure was initiated by treating the sample (after grinding) with a 50 percent solution of sodium hydroxide containing a known amount of carrier phosphate, in a polypropylene beaker. The solution was heated to speed up the dissolution. Hydrogen peroxide was added to remove any interstitial organic matter which was released during the breakdown of the opal. At this point approximately 95 percent of the silicon was in solution; the remaining 5 percent was treated with hydrogen fluoride and sulfuric acid, and heated to near-dryness; finally the residue was dissolved in HNO_3.

The dissolved silicon in the NaOH solution was dehydrated to the SiO_2 form by the addition of 400 ml of concentrated hydrochloric acid and filtration through a Büchner funnel. The silica was dried at 130°C and washed thoroughly with dilute HCl to remove any adsorbed phosphorus compounds. The filtrate, washings, and the solution resulting from the treatment with HF and H_2SO_4 were combined and evaporated until the sodium chloride had crystallized out. The salt was removed by filtration through a sintered glass funnel and washed with concentrated HCl. These evaporation steps were repeated twice to remove the bulk of the NaCl. The final filtrate was taken to dryness, digested with 6*N* HCl, and dehydrated. This step was repeated twice to render insoluble any remaining traces of silica. The residue was heated with perchloric acid to dryness, and dissolution was effected in 20 ml of concentrated HNO_3.

The phosphorus was extracted from the above solution and purified by the following steps carried out in accordance with often published standard procedures (*4*): (i) phosphoammonium molybdate precipitation; (ii) magnesium ammonium phosphate precipitation; (iii) elimination of cations by passage through a Dowex-50 cation exchange resin in the H-form; (iv) magnesium ammonium phosphate precipitation; and (v) ignition to magnesium pyrophosphate. This solid was assayed for its radioactivity.

After an initial counting, the sample was subjected to additional chemical purification by a repetition of the last four steps. The silica recovered in the dehydration step was milked again after a period of 28 days.

Counting techniques. The samples were deposited over an area of approximately 6 cm^2 on two split cylindrical copper supports and counted in a cylindrical geometry with a thin-wall, flow-type Geiger tube with "Q gas" (98.7 percent He; 1.3 percent isobutane). The details of the counter have been described by Martell (*5*). The counter was housed in a shield which provided a minimum of 8 inches of steel on all sides and was operated in anticoincidence with a ring of large cosmic ray counters to eliminate the recording of cosmic ray μ-mesons. The background counting rate with blank copper supports was 0.26 count per minute. The counting efficiency for hard beta rays was determined by assaying a weighed sample of potassium chloride for K^{40} β-radiation ($E_{max.} = 1.34$ Mev) under conditions similar to those employed for our samples. The over-all counting efficiency, which includes the counting geometry, back-scattering from the support, and absorption in the counter wall, was found to be 37 percent.

Several blank runs were made to ascertain the amount of contamination arising from chemical reagents and dust in the laboratory. The net counting rates of the blanks varied between 0 ± 0.05 and 0.05 ± 0.04 count per minute. A small, but positive, blank of 0.025 count per minute resulting from man-made or natural activities is indicated.

Results. The chemical yields of phosphorus and the activities of Si^{32} are summarized in Tables 1 and 2, respectively.

Table 1. Chemical yields.

Sample No.	Remarks	Dry sample weight (gm SiO_2)	Amount of carrier added (mg $Mg_2P_2O_7$ eq.)	Yield (%)
1	First milking	200	120	92
1R	First milking recycle			83
2	Second milking	190*	135	66

* Five percent of sample 1 did not dissolve in NaOH treatment. It was treated with HF and H_2SO_4, and therefore was not available for the second milking.

Table 2. Counting data.

Period of milking	Net sample counting rate (count/min)	Time elapsed between end of milking and counting (day)	Estimated No. of disintegrations of Si^{32} per minute, per kilogram of Si *
	Sample No. 1		
3 mo	0.52 ± 0.07	2	20.0 ± 2.7
	Sample No. 1R		
	0.36 ± 0.04	4	19.9 ± 1.7
	0.41 ± 0.05	7	
	0.28 ± 0.04	13	
	0.21 ± 0.04	20	
	0.11 ± 0.03	28	
	Sample No. 2		
28 days	0.26 ± 0.04	2	18.9 ± 2.9
		Mean	19.6 ± 1.3

* Self-absorption in the sample was assumed to be 6 percent in all cases.

The observed activity of the samples can be unambiguously attributed to the presence of P^{32} on the basis of the following four independent checks on the nature of the radiation:

1) *Half-life.* The activity of sample 1R was followed for a period of two half-lives of P^{32}. The counting data are assembled in Table 2. The observed half-life of the activity, 13 ± 4 days, is in good agreement with the literature value for P^{32}, 14.3 days.

2) *Chemical behavior.* Sample 1 was recycled through the purification steps 1 to 4 with the result that the specific activity of the recycled sample remained unchanged within the errors of measurement (Tables 1 and 2).

3) *Beta energy.* Absorption measurements of sample 1, with vinyl acetate absorbers of thicknesses 51 and 102 mg/cm², yield a half-thickness value of 75 ± 20 mg/cm². The P^{32} half-thickness for cylindrical counting geometry had previously been found to be 84.3 mg/cm² of aluminum (*6*). The vinyl acetate half-thickness, in milligrams per square centimeter, is expected to be about 13 percent higher than that for aluminum absorbers. The thinness of the samples, coupled with appreciable backscattered radiation, on the other hand, should yield a slightly smaller half-thickness. In view of this, the energy of the beta radiation is consistent with that of P^{32} (*7*).

4) *Growth of daughter activity.* The estimated disintegration rates of Si^{32} from the first and second milking are concordant.

These results prove conclusively that the observed activity is due to P^{32} and that it arises from the decay of the parent nuclide Si^{32}.

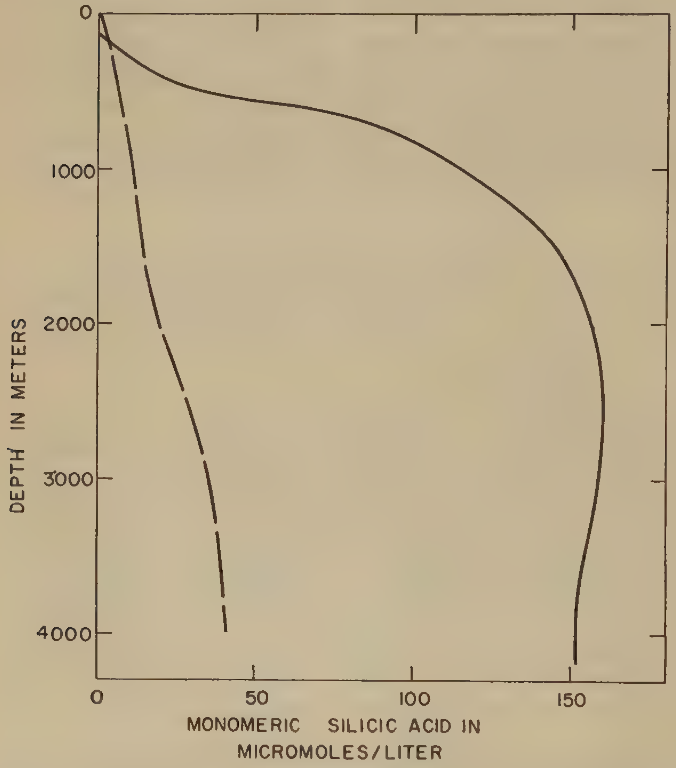

Fig. 1. Vertical distribution of silicic acid in the Atlantic and Pacific oceans. Broken curve: North Atlantic Ocean, latitude 47°24′N, longitude 07°52′W [data from Armstrong (*18*)]. Solid curve: North Pacific Ocean, latitude 26°22.4′N, longitude 168°57.5′W [Goldberg (*19*)].

Rate of Production of Silicon-32

The production rate of Si^{32} can be calculated from the available cosmic ray data, in different regions of the atmosphere, on (i) the star production rates in photographic emulsions and cloud chambers; (ii) the frequency distribution of stars as a function of the number of charged particles emitted; and (iii) the observed variation in the intensity of slow and fast neutrons. Lal *et al.* (*8*) have calculated the production rates of P^{32}, P^{33}, and S^{35} in spallations of atmospheric argon for all regions of the atmosphere from such data. By their procedure, the global production rate of Si^{32} is computed to be 1.7×10^{-4} atom/cm² column per second.

A second estimate can be made by using the observed fallout of cosmic-ray-produced P^{32} and the expected ratio of cross sections for the production of Si^{32} and P^{32} from argon at energies of interest in cosmic rays. The fallout of P^{32} was measured at tropical latitudes during the years 1956–58 (*9*) to be 3.4×10^{3} atoms of P^{32}/cm² per year. This value is shown to be predominantly due to the removal by wet precipitations of activity produced in the troposphere only, with a mean removal period of 40 days. By correcting this figure for the decay of P^{32} in the troposphere and taking a value of 29 percent for the fraction of P^{32} produced below the tropopause (*8*), a production rate for P^{32} of 1.1×10^{-3} atom/cm² per second is obtained. The ratio of the cross sections of Si^{32} and P^{32} is computed to be 0.2 from Rudstam's empirical relation (*10*) describing the cross sections for the formation of nuclides in nuclear spallations.

The ratio of formation cross sections for two isobars, (A,Z) and (A,Z'). depends on two parameters only:

$$\begin{aligned}\sigma(A,Z)/\sigma(A,Z') &\\ &= \exp\{-R[(Z-SA)^2-(Z'-SA)^2]\\ &= \exp[R(Z'-Z)(Z'+Z-2SA)]\end{aligned}$$

The values of the parameters R and S are found to be nearly insensitive to either the bombarding energy or the target nucleus for masses between 51 and 75. In order to approximate our situation, we have used the values observed in the bombardments of vanadium by 60-, 100-, 170-, 175-, and 240-Mev protons: $R = 1.6 \pm 0.1$; $S = 0.468 \pm 0.001$. Therefore the ratio of cross sections is

$$\begin{aligned}\sigma(Si^{32})/\sigma(P^{32}) &= \exp[R(Z+Z'-2SA)]\\ &= 0.2 \pm 0.02\end{aligned}$$

The production rate of Si^{32} therefore amounts to $0.2 \times 1.1 \times 10^{-3} = 2.2 \times 10^{-4}$ atom/cm^2 per second, which is in good agreement with the previous estimate (1.7×10^{-4}).

We take 2.0×10^{-4} atoms/cm^2 per second as the average global production rate of Si^{32} in the atmosphere. The corresponding inventory of Si^{32} on the earth is 28 kilocuries, or 1.75 kg of Si^{32}.

The production of Si^{32} in any significant quantities by nuclear weapons seems quite improbable but cannot be entirely ruled out at present. It cannot result from surface shots by principal neutron capture reactions, (n, γ), (n, p) (n, α), since the target nuclides involved are short lived and do not exist in nature. However, it could be produced in the bomb hardware by successive neutron capture reactions. Unfortunately we cannot estimate this contribution. The total amount of Sr^{90} produced till the end of 1958 has been estimated to be 63.5 kg (*11*). If Si^{32} has been produced in bombs, its natural inventory could be raised by 10 percent if it amounts to as much as ~ 1 percent of Sr^{90} in nuclear weapons.

Geochemical Considerations

The geochemical behavior of silicon has been extensively studied not only because it is one of the principal rock-forming elements but also because it is involved both in the biological and inorganic reactions in the major sedimentary cycle. The following brief summary of present knowledge of silicon geochemistry provides an entry into the problem of the distribution of Si^{32} among the earth's geological domains following its formation.

Crustal rocks are decomposed by various weathering agents, resulting in the solution of silicon, the formation of new minerals containing silicon, and the accumulation of resistant minerals such as quartz, feldspar, and so on (see, for example, Pettijohn, *12*). The two groups of solid phases are transported to the marine environment through the atmosphere and the hydrosphere. The river load of solids is deposited primarily in the near-shore areas, while the eolian minerals, originating mainly from the arid desert areas, fall to the sea floor in mid-latitudinal belts extending across the oceans (*13*).

The dissolved silicon exists nearly entirely as undissociated monomeric silicic acid, $Si(OH)_4$, in both river and marine waters and is in an undersaturated state (*14*). Typical depth distributions in sea water are shown in Fig. 1. The acid is depleted in the photosynthetic zone (upper 100 meters or so) by microscopic organisms such as diatoms, radiolaria and silicoflagellates, which incorporate it into their opaline skeletons. This effect is extended to greater depths by the wind mixing in the upper layers of the oceans, such that waters down to 300 or 400 meters or more can have minimal values of silicon. The combustion of the plant materials which settle from the euphotic zone results in the dissolution of the silicon dioxide at intermediate depths. A maximum in the depth profile arises from the greater amounts of regeneration in warmer waters—that is, depths less than 1000 meters or so.

On the basis of the chemical properties of silicon, it is probable that Si^{32} is involved primarily in the solution geochemistry of silicon. From the chemistry of silicon, we expect that whatever molecular species are formed initially after the production of single atoms of Si^{32}, interactions with water droplets during condensations will finally lead to the formation of $Si(OH)_4$. Single molecular species of silicon such as SiO_2 will be unstable with respect to $Si(OH)_4$ since they cannot form aggregates. Such a situation is probably not too dissimilar to that of cosmic-ray produced Be^7, which is found to exist in rain water as soluble species.

With the foregoing discussions in mind, we can consider the radiosilicon balance in the oceans. Simplified models for oceanic circulation for the case of

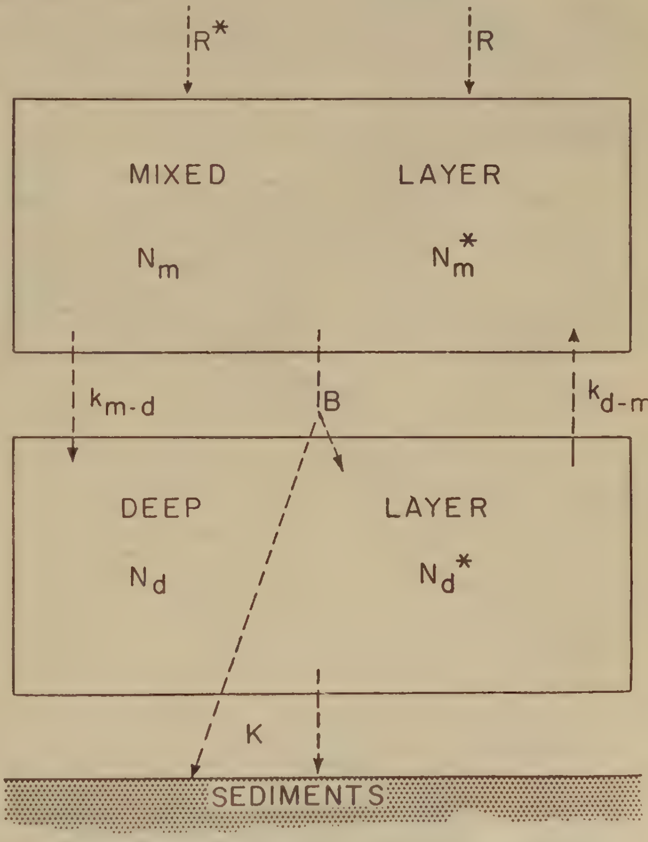

Fig. 2. Simplified model of silicon reservoirs in the exchangeable system.

C^{14} have recently been discussed (*15, 16*). We adopt the model of mixing and transfer processes in the oceans proposed by Craig (*16*). The oceans are divided into two principal reservoirs called the mixed (*m*) and deep (*d*) layers which are assumed to be *well mixed internally.* A steady state is reached by the exchange or transfer of silicon between the reservoirs (Fig. 2). The mixing cycle of *soluble silicon* is considered. As usually is the case in such models, the exchange of isotopes of very low abundance is governed by first-order kinetics, and the exchange rates of dominant species can thus be calculated. The following definitions are used: N_m and N_d are the amounts of silicon in the mixed and deep layers, respectively; N^*_m and N^*_d are the amounts of Si^{32} in the mixed and deep layers, respectively; R and R^* are the rates of introduction of silicon and Si^{32} into the oceans, respectively; $k_{m\text{-}d}$ and $k_{d\text{-}m}$ are the rate constants for the mixing of soluble silicon between the mixed and deep layers, and the deep and mixed layers, respectively; K is the rate constant for removal of silicon from ocean to the sediment; B is the rate constant for removal of silicon from the mixed layer by biological precipitation of solid siliceous phases (part of the precipitated silicon which does not dissolve at greater depths in the oceans reaches the sediments directly; see Fig. 2); and λ is the disintegration constant of Si^{32}. Therefore, $\lambda = 0.693/710 = 1 \times 10^{-3}$ yrs^{-1} (*3*).

By our definitions, we obtain the following relations for a steady state:

$$R = (N_m + N_d)\,K \qquad (1)$$

$$\frac{dN_m}{dt} = O = R - k_{m\text{-}d}\,N_m + k_{d\text{-}m}N_d - BN_m \qquad (2)$$

$$R^* = (K + \lambda)\,(N^*_m + N^*_d) \qquad (3)$$

$$\frac{dN^*_m}{dt} = O = R^* - k_{m\text{-}d}\,N^*_m + k_{d\text{-}m}N^*_d - BN^*_m - \lambda N^*_m \qquad (4)$$

Solving these equations, we find:

$$\frac{N_m}{N_d} = \frac{K + k_{d\text{-}m}}{B + k_{m\text{-}d} - K} \qquad (5)$$

$$\frac{N^*_m}{N^*_d} = \frac{K + \lambda + k_{d\text{-}m}}{B + k_{m\text{-}d} - K} \qquad (6)$$

The ratio of the specific activities in

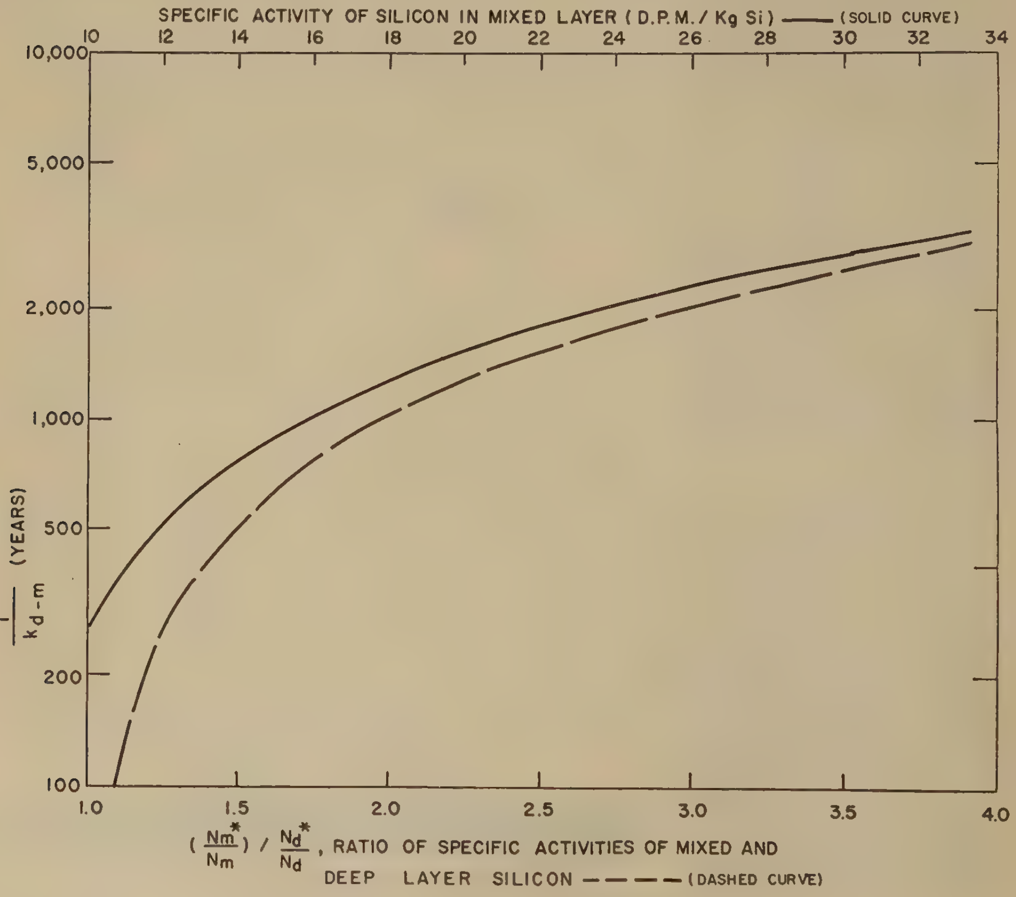

Fig. 3. Calculated specific activities of Si^{32} in the mixed and deep layers as a function of $k_{d\text{-}m}$.

the mixed and deep layers is readily obtainable as:

$$\frac{N^*_m/N_m}{N^*_d/N_d} = \frac{K + \lambda + k_{d-m}}{K + k_{d-m}} \qquad (7)$$

Goldberg and Arrhenius (*17*) have computed a value of 10^{-4} yr^{-1} for K. Since this refers to both the soluble and particulate forms of silicon, a reduction by a factor of 2 of the rate of introduction of silicon based on an induction of Rex and Goldberg (*13*) that up to 50 percent of the silicon enters the oceans in solid phases, gives a more realistic figure of 5×10^{-5} for K. Since K is many orders of magnitudes smaller than other exchange coefficients, uncertainty in K does not affect our model calculations.

A plot of the ratio of the specific activities of Si^{32} in the mixed and deep layers, calculated from Eq. 7, versus $1/k_{d-m}$ is shown in Fig. 3. It is quite clear from the graph that this potentially measurable ratio is a quite sensitive indicator of the rate of mixing of deep waters into the mixed layer. It is of interest to note that this ratio is independent of the production rate of Si^{32}. In the same figure, the expected specific activity of Si^{32} in the mixed layer ($\lambda N^*_m/N_m$, obtained by solving Eqs. 3 and 7, is plotted, taking for R^* a value of 1.7×10^{-4} atom/cm²/per second. The average silicic acid contents of deep and mixed layers are taken as 120 and 15 micromoles per liter, respectively.

The observed specific activity of 19.6 disintegrations per minute, per kilogram of Si, represents principally a value for the mixed layer, inasmuch as the sponges were retrieved from coastal waters of depths under 100 meters. This corresponds to an average mixing time (that is, $1/k_{d-m}$) of more than 1500 years on the basis of the discussed model.

The quantitative significance of a photosynthesizing siliceous organism in the soluble silicon cycle in the sea can be readily seen by solving Eq. 5 for the biological removal constant B:

$$B = \frac{N_d}{N_m}(K + k_{d-m}) + (K - k_{m-d}) \qquad (8)$$

By taking a ratio of 49.6 for the volumes of deep to mixed layers (*16*), a value of 397 for N_d/N_m is found. It is apparent that the second term is trivial compared with the first and can be neglected; furthermore, since K is small compared with k_{d-m},

$$B \approx 397\, k_{d-m} \qquad (9)$$

For likely values of k_{d-m}, say between 2×10^{-3} and 5×10^{-4} yr^{-1}, values of B range between 0.8 and 0.2—that is, the silicon is removed from the mixed layer to deep layers or sediments due to biological activity in mean periods of 1 to 5 years.

In addition to studies of mixing times in the oceans, there are other obvious applications of this isotope as a tracer for studying problems in earth sciences: (i) the rates of accumulation of rapidly growing sediments containing large amounts of biogenous or hydrogenous siliceous phases; (ii) the individual characteristics of water masses within oceans with respect to mixing; (iii) the silicon cycle in the continental hydrosphere; (iv) changes in cosmic ray intensity with time during the last few thousand years; (v) ages of the polar ice caps.

References and Notes

1. H. E. Suess, *Ann. Rev. Nuclear Sci.* **8**, 243 (1958).
2. This work was supported by grants from the Division of Biology and Medicine, U.S. Atomic Energy Commission, and the Air Force Geophysics Research Directorate. We are grateful to Sam Hinton, Robert Parker, and Raymond Ghelardi of the Scripps Institution of Oceanography for supplying the samples. M. Honda suggested many of the steps in the chemical techniques. We are also indebted to James Arnold, Harmon Craig, Gustaf Arrhenius, and Harold C. Urey, as well as to Dr. Honda, for stimulating discussions in the course of the work.
3. M. Lindner, *Phys. Rev.* **91**, 642 (1953).
4. N. H. Furman, Ed., *Scott's Standard Methods of Chemical Analysis* (Van Nostrand, New York, 1939).
5. E. A. Martell, *Rept. A.E.C.U.-3297* (1957).
6. A. D. Suttle, Jr., and W. F. Libby, *Anal. Chem.* **27**, 921 (1955).
7. We could have determined the half-thickness by using commercially available P^{32} but did not consider it safe from the point of view of contamination in the laboratory.
8. D. Lal, P. K. Malhotra, B. Peters, *J. Atmospheric and Terrest. Phys.* **12**, 306 (1958).
9. P. S. Goel, C. Prabhakara, Rama, P. K. Zutshi, *Tellus*, in press; D. Lal, Rama, and P. K. Zutshi, *J. Geophys. Research*, in press.
10. G. Rudstam, "Spallation of medium-weight elements," unpublished thesis, Uppsala (1956).
11. United States Hearings on Radioactive Fall-Out, 5–8 May 1959.
12. F. J. Pettijohn, *Sedimentary Rocks* (Harper, New York, ed. 2, 1957).
13. R. W. Rex and E. D. Goldberg, *Tellus* **10**, 153 (1958).
14. B. Krauskopf, "Silica in sediments," *S.E.P.M. Spec. Publ. No. 7*, (1959), p. 4.
15. J. R. Arnold and E. C. Anderson, *Tellus* **9**, 28 (1957).
16. H. Craig, *ibid.*, p. 1.
17. E. D. Goldberg and G. O. S. Arrhenius, *Geochim. et Cosmochim. Acta* **13**, 153 (1958).
18. F. A. J. Armstrong, *J. Marine Biol. Assoc. United Kingdom* **30**, 149 (1951).
19. E. D. Goldberg, unpublished results.

Journal of Geophysical Research Volume 65, No. 1 January 1960

On the Statistical Prediction of Ocean Temperatures

Gunnar I. Roden and Gordon W. Groves

Scripps Institution of Oceanography
La Jolla, California

Abstracts. Past records of sea-surface temperature are examined and related to wind and solar radiation. There is practically no relation between radiation and sea-surface temperature, but there is a noticeable but small relation between wind and temperature. The best estimate of future values of temperature can be made from past values of temperature, and the use of past wind values slightly improves the prediction. In any case, optimum prediction from statistical considerations alone (Wiener's technique) can account for only about 40 per cent of the variance in the next month's average temperature.

Introduction. The prediction of sea-surface temperature a few months into the future is of interest to both meteorologists and oceanographers and has many practical applications, including fisheries forecasts. In the past, several methods have been used to estimate future temperatures; these are summarized by *Wadsworth* [1951], *Namias* [1953], and *Takenouti* [1957]. In the present investigation we deal with the prediction of temperature from past records of wind, temperature, and radiation, using *Wiener's* [1949] method.

In statistical prediction no attempt is made to use dynamical relations, and an exact value of temperature at any future time cannot be furnished. However, an estimate of the most probable value and the limits within which it is likely to fall can be given. Here it is desired to evaluate the degree of success attainable by the purely statistical approach. Any method based on dynamical considerations which does not give a better estimate than can be obtained by statistical methods (that is, by chance) will not have contained the essential mechanism. Actually, as is shown below, the accuracy of purely statistical prediction of sea-surface temperature is only fair. A similar analysis was carried out by *Pierson* [1958] in the North Atlantic with somewhat better results as to the accuracy of prediction.

Two ocean areas have been selected for testing the method. The first is a 5° square, 45°N to 50°N, 125°W to 130°W, just off the coast of Washington; the other, 25°N to 30°N, 140°W to 145°W, is in the NE trade wind region about halfway between San Francisco and Honolulu, Eighteen-year records of mean monthly sea-surface temperature, cloudiness [*Imperial Marine Observatory, Kobe,* 1921–1938], and sea-level atmospheric pressure [*U. S. Weather Bureau* 1899–1958] were used. The cloudiness was converted into incoming radiation by means of *Budyko's* [1956] tables, and pressure was converted into wind by assuming geostrophic equilibrium. To eliminate seasonal variations, differences from the long-term monthly mean were taken (that is, from any given value the average for the same month in all years was subtracted). The resulting anomalies are shown in Figure 1. Several features are evident in the records: (1) they are somewhat similar in general character; (2) the temperature anomalies do not change their sign as often as do those of wind and radiation; (3) the records appear to be stationary. One can expect that the autocorrelation of temperature will show a slower decay than will that of radiation and wind.

It must be emphasized that taking monthly averages of daily values presupposes a smoothing process. This smoothing generally increases the persistence over that of the original unsmoothed records [*Munk,* 1959].

Analysis of the data. Correlation functions and spectra of the time series shown in Figure 1 were computed on an IBM 704 electronic computer, using the Tukey method [*Tukey,* 1949; *Blackman and Tukey,* 1958]. The analysis

---

Contribution from the Scripps Institution of Oceanography. New Series. 1144

Reproduced by Permission

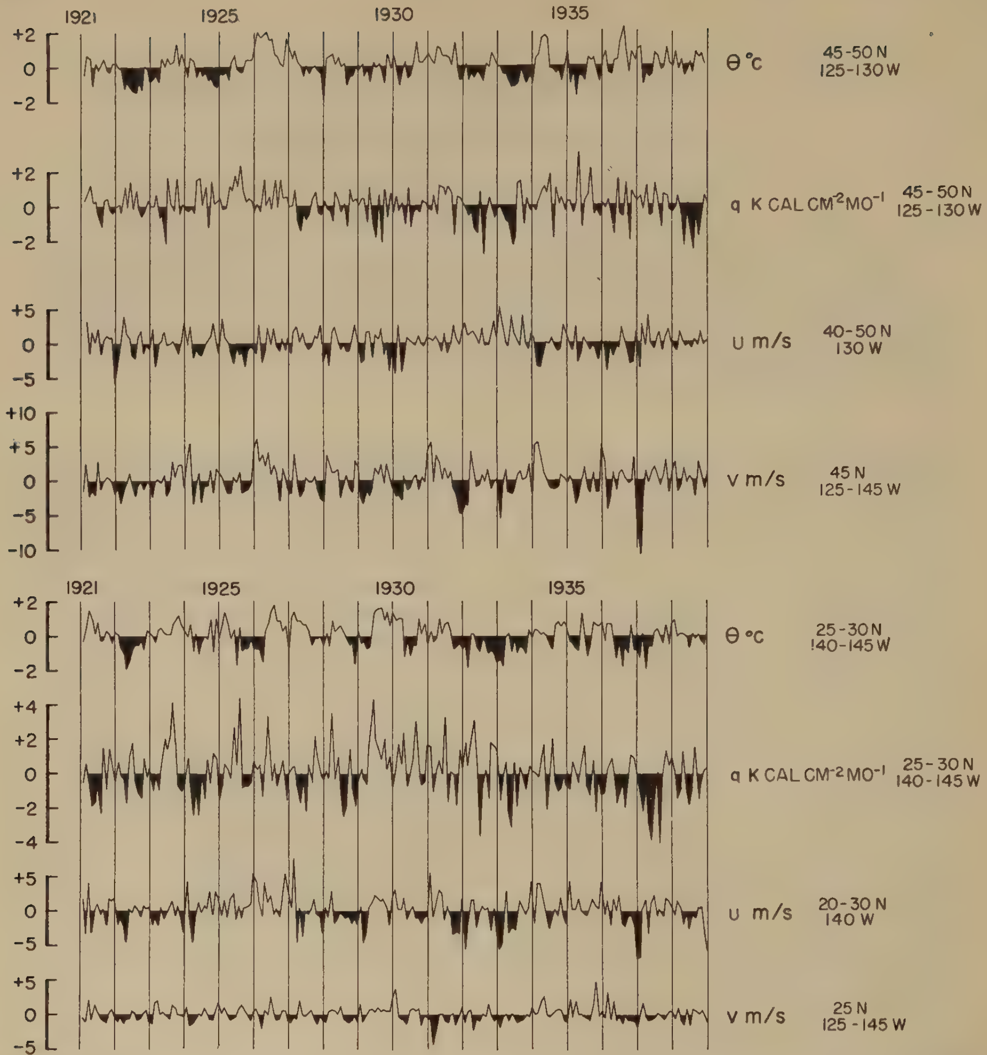

Fig. 1. Time series of anomalies of temperature (θ), east (u), and north (v) components of wind, and radiation (q) for the region off the coast of Washington (top) and the NE trade wind region (bottom).

was carried out for $n = 216$ observations and $m = 24$ lags or spectral estimates. The number of *degrees of freedom,*

$$\nu = 2n/m = 18$$

determines the statistical reliability of the spectral estimates. The definitions of the various functions, autocorrelations, cross correlations, energy spectra, coherence, and phase are given by *Munk, Snodgrass, and Tucker* (in press).

The normalized autocorrelations of temperature, radiation, and east and north wind components and radiation, denoted by $\phi_{\theta\theta}$, ϕ_{uu}, ϕ_{vv}, ϕ_{qq}, are shown in Figures 2*a* and 3*a*.

The statistical reliability of the autocorrela-

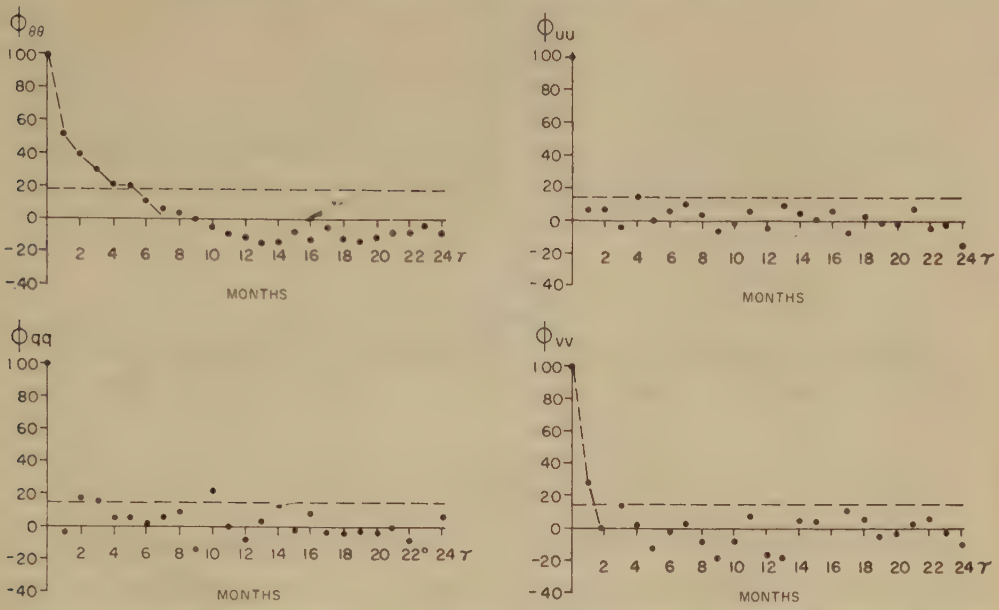

Fig. 2*a*. Normalized autocorrelation of temperature, wind components, and radiation anomalies in the region off the coast of Washington.

tions can be estimated by the inequality

$$\sigma(\tau)^2 \le \sigma_m^2 = \frac{4}{T}\int_0^\infty \phi^2(\tau')\, d\tau'$$

which holds for all τ, where σ^2 is the (normalized) variance in the autocorrelation, determined from random finite samples of an infinite time series [*Laning and Battin*, 1956, p. 163], and T is the record length. The quantity σ_m is indicated by a dashed line on the autocorrelation plots in order to give a rough idea of the significance. It is seen that the autocorrelation of temperature differs significantly from zero for lags of up to 5 or 6 months, indicating a rather high persistence of temperature. The autocorrelation of wind, on the other hand, does not differ significantly from zero for lags greater than 1 month. The autocorrelation of radiation as determined from cloudiness is not very persistent, as could be expected.

The cross correlations between pairs of variables are shown in Figures 2*b* and 3*b*. Significance levels for the cross correlations have not yet been determined, but experience suggests that the erratic variations at large (positive or negative) lag times are not significant. Therefore, we might reason that any peak rising appreciably above the level of those variations might be significant. Such correlations occur only for lag times near zero. Wind and temperature are the best correlated variables; there is hardly a significant relation between any other pair. It should be noted that wind leads temperature for negative lag time. The dotted curves in the correlation graphs show the smoothed correlations that were used in the prediction calculations. The smoothing was carried out by a simple moving-weighted-average, $0.25\ \phi_{-1} + 0.50\ \phi_0 + 0.25\ \phi_1$, applied at each lag in the significant part of the correlation. Outside the significant part the correlations were set equal to zero.

The energy spectra, coherences, and phase relationships are shown in Figures 4 and 5. The energy spectra of temperature show that most of the energy is concentrated in the low-frequency part of the spectrum, between zero and 2 cycles per year (cpy). This is consistent with the slow decay of the temperature autocorrelation; both indicate that future temperatures can be forecast from past temperatures. There are no obvious periodicities in the spectrum

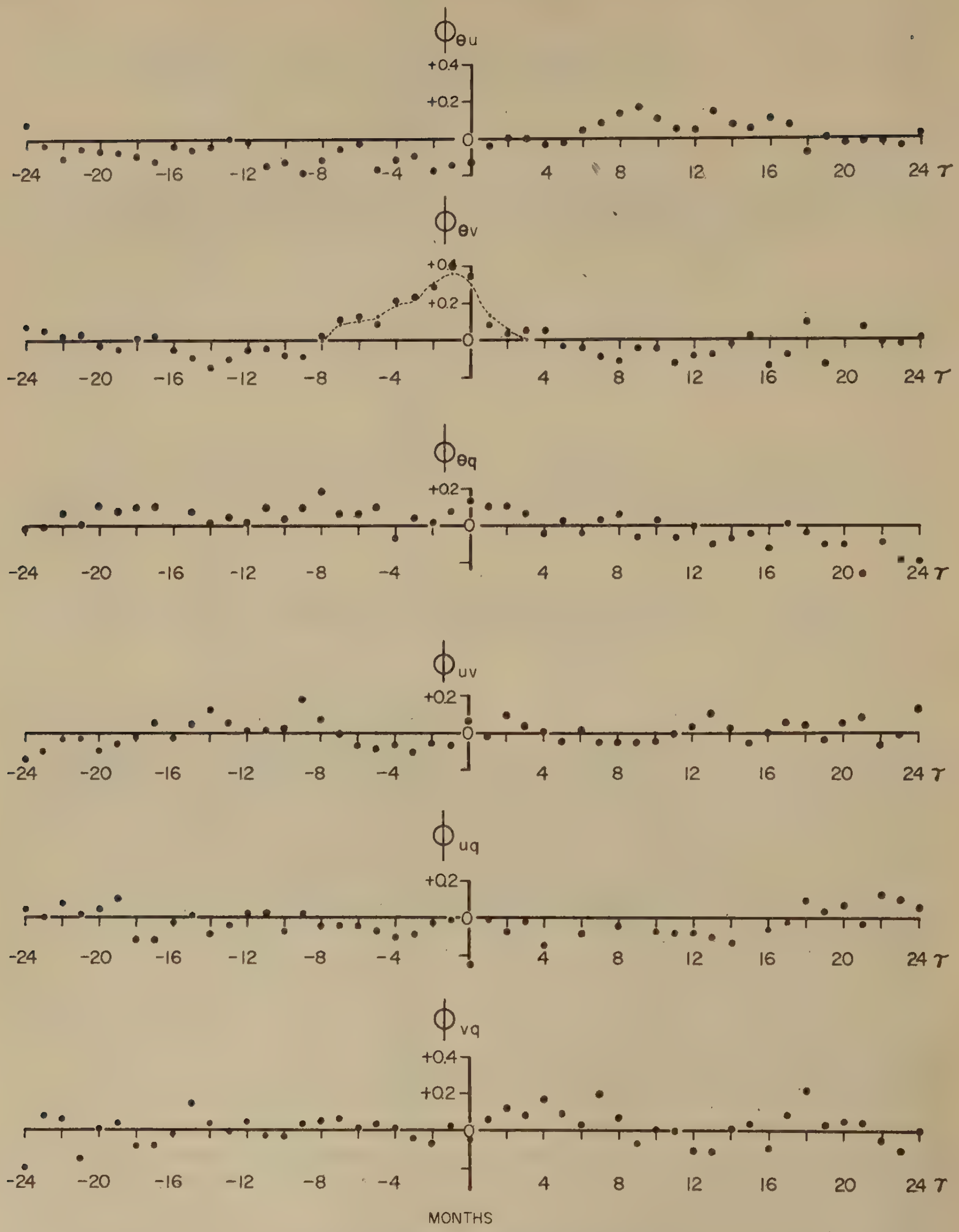

Fig. 2*b*. Normalized cross correlations of temperature, wind components, and radiation anomalies in the region off the coast of Washington.

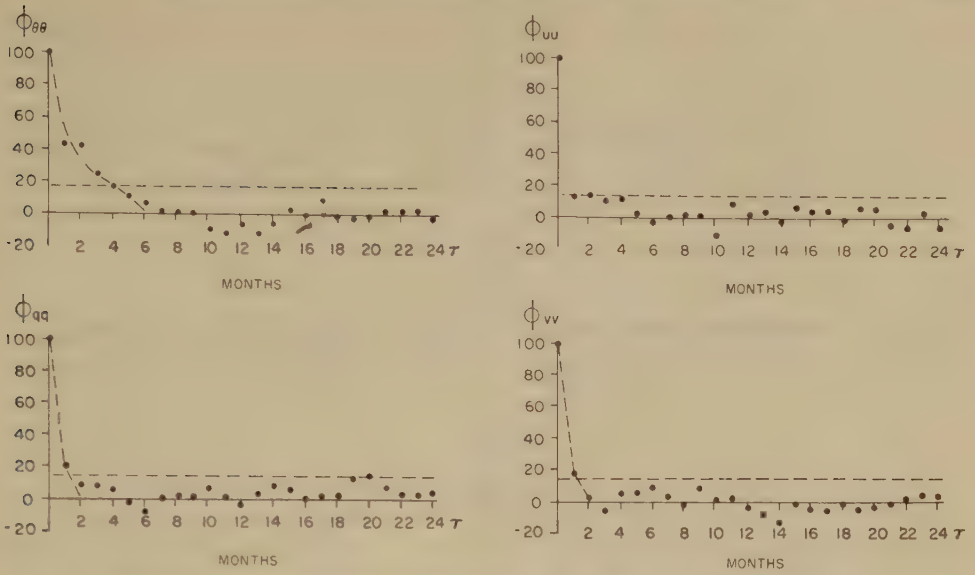

Fig. 3*a*. Normalized autocorrelations of temperature, wind components, and radiation anomalies in the NE trade wind region.

except for a broad-band maximum in the vicinity of 0.25 cpy. The low energy level in the higher-frequency part of the spectrum and the fact that the input data consist of monthly averaged data would indicate that aliasing is not a serious problem.

The spectra of wind are almost constant throughout the frequency range or show only a slight decrease of energy with increasing frequency. In other words, the wind record deviates insignificantly from white noise. This is consistent with the rapid decay of the wind autocorrelation and indicates that prediction of wind from past wind records would yield very poor results. No important periodicities are indicated in the wind spectra except for dubious peaks around 3.0 and 5.5 cpy. The spectrum of radiation appears to be even more white than the wind. The 95 per cent significance level of all the energy spectra lies between 0.57 and 2.20 times the observed value [*Blackman and Tukey*, 1958].

The 95 per cent significance levels for the coherence are indicated by the dashed lines in Figures 4*b* and 5*b*. It is seen that the coherence between temperature and wind is significant in the low-frequency part of the spectrum (zero to 1 cpy). There appears to be significant coherence again in medium frequencies, but this may be doubtful. Perhaps an even better indication of significant coherence between records is given by the continuity in the phase relation as a function of frequency. If the phase values vary considerably, it probably means that the records are not very coherent. It is noted that the only part of the spectrum showing a persistent phase relation between temperature and wind is for low frequencies, for which both are approximately in phase. In the NE trade wind region easterly and southerly winds are associated with high temperatures, for low frequencies. In the Washington region easterly winds are associated with low temperatures, as is indicated by phase difference of about 180° in the low-frequency range, and the southerly wind accompanies higher temperatures.

The coherence between temperature and radiation is generally very poor, although there does appear to be some coherence in the NE trade wind region for very low frequencies, between zero and 0.5 cpy.

Prediction. We shall consider the methods outlined by *Wiener* [1949], taking each time series to be a stationary ergodic process. This

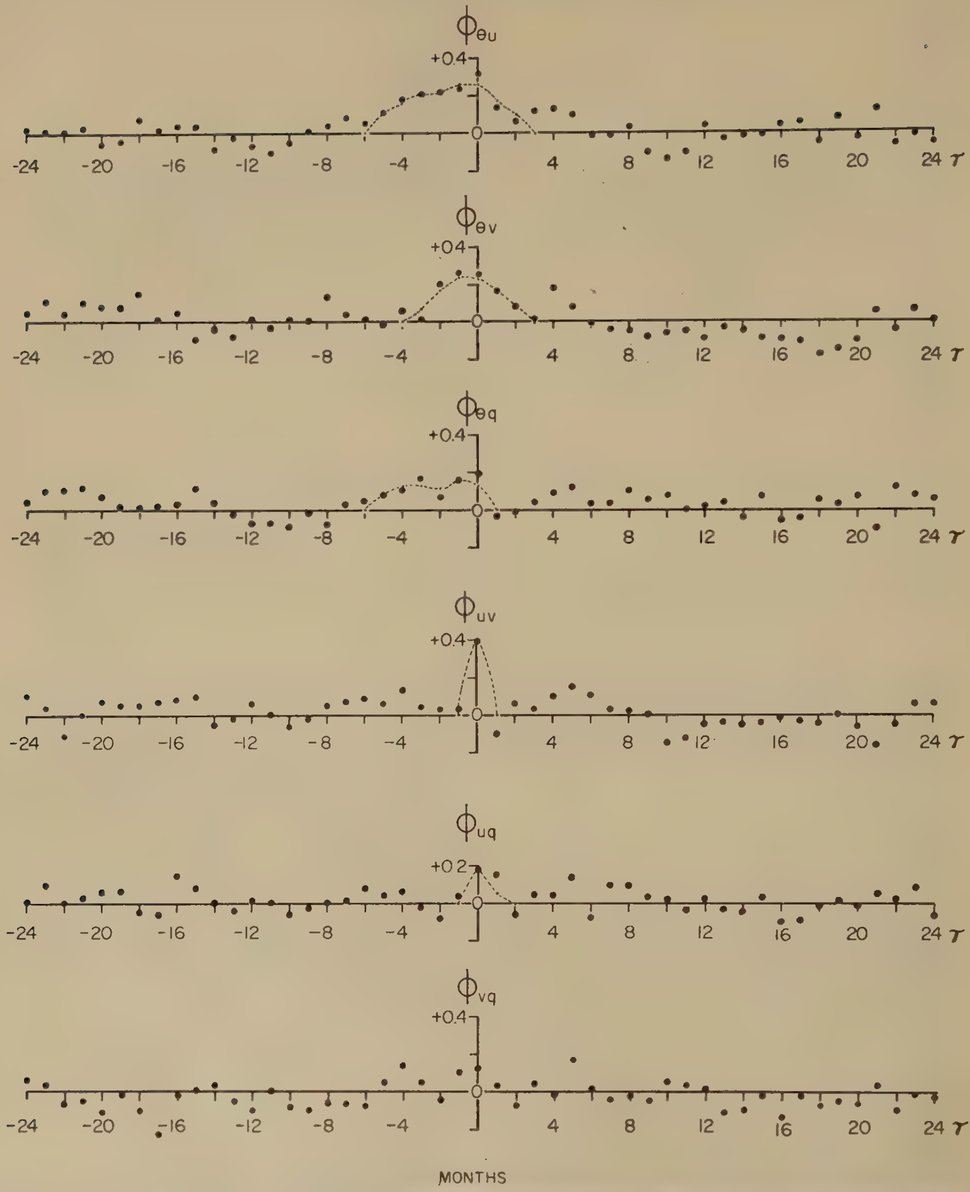

Fig. 3*b*. Normalized cross correlations of temperature, wind components, and radiation anomalies in the NE trade wind region.

allows us to equate ensemble and time averages and assures us that the correlation functions depend only on the time displacement (lag), and not on any particular origin in time. The predicted temperature anomaly θ^* at any future month is taken to be a linear combination of the monthly anomalies of all variables for the present and a few past months. Accordingly,

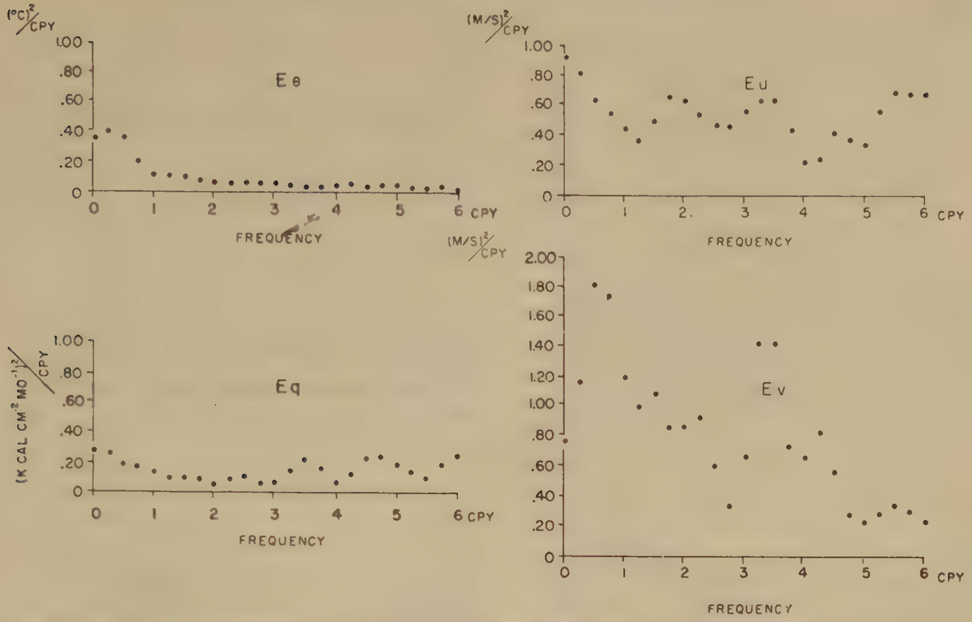

Fig. 4a. Energy spectral density E of temperature, wind, and radiation anomalies, Washington region.

$$\theta^*(t+\alpha) = \sum_{i=0}^{n} [a_i\theta(t-i) + b_i\lambda_{\theta u}u(t-i) + c_i\lambda_{\theta v}v(t-i) + d_i\lambda_{\theta q}q(t-i)] \quad (1)$$

where t is the time measured in months; θ u, v, and q are the observed anomalies of temperature, two wind components, and radiation, respectively; α is the number of months ahead for which the prediction is to be made; and n is the number of past months taken into account. The quantities

$$\lambda_{\theta u} = [\langle\theta^2\rangle/\langle u^2\rangle]^{1/2}, \text{ etc.} \quad (2)$$

are introduced to keep the coefficients a_i, b_i, c_i, and d_i dimensionless. The symbol $\langle\ \rangle$ indicates a long time average, which is approximated, in the present case, by averaging over the available values.

The coefficients are to be determined in such a manner that the mean-square error is minimized. The quantity

$$\epsilon^2 = \langle(\theta^* - \theta)^2\rangle/\langle\theta^2\rangle \quad (3)$$

is a useful dimensionless measure of the prediction error. Note that $0 \leq \epsilon^2 \leq 1$; if $\epsilon^2 = 0$ the prediction is perfect, whereas if $\epsilon^2 = 1$ the prediction scheme does no better than if it always predicted zero anomalies. Combining (1), (2), and (3), ϵ^2 can be expressed in matrix notation,

$$\epsilon^2 = 1 - 2X'N + X'MX \quad (4)$$

where X is the unknown column vector.

$$\left\|\begin{array}{c} a_i \\ \hdashline b_i \\ \hdashline c_i \\ \hdashline d_i \end{array}\right\|$$

N is the column vector

$$\left\|\begin{array}{c} \phi_{\theta\theta}(-\alpha - i) \\ \hdashline \phi_{\theta u}(-\alpha - i) \\ \hdashline \phi_{\theta v}(-\alpha - i) \\ \hdashline \phi_{\theta q}(-\alpha - i) \end{array}\right\|$$

and M is the matrix

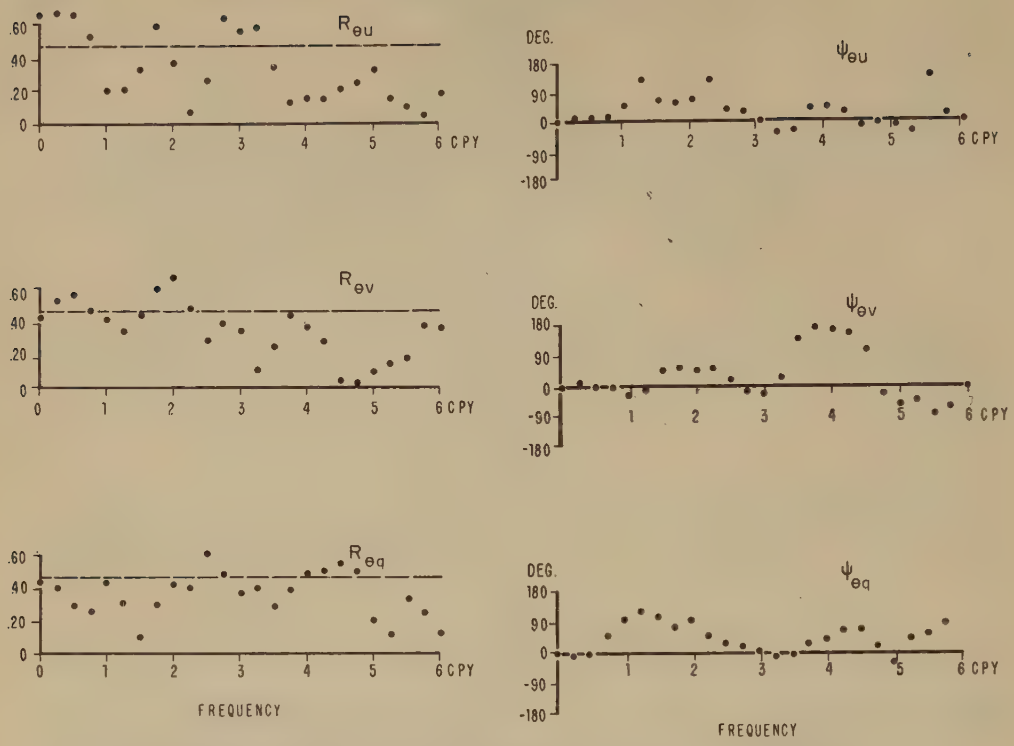

Fig. 4*b*. Coherence and phase relationships off the coast of Washington.

$$\begin{Vmatrix} \phi_{\theta\theta}(i-k) & \phi_{u\theta}(i-k) & \phi_{v\theta}(i-k) & \phi_{q\theta}(i-k) \\ \phi_{\theta u}(i-k) & \phi_{uu}(i-k) & \phi_{vu}(i-k) & \phi_{qu}(i-k) \\ \phi_{\theta v}(i-k) & \phi_{uv}(i-k) & \phi_{vv}(i-k) & \phi_{qv}(i-k) \\ \phi_{\theta q}(i-k) & \phi_{uq}(i-k) & \phi_{vq}(i-k) & \phi_{qq}(i-k) \end{Vmatrix}$$

in which $i, k = 0, 1, \ldots, n$;
and X' is the transpose of X. The ϕ are normalized correlation functions, defined by

$$\phi_{\theta u}(\tau) = \frac{\langle \theta(t) u(t+\tau) \rangle}{\sqrt{\langle \theta^2 \rangle \langle u^2 \rangle}} \qquad (5)$$

For $\tau > 0$ the primary record is related to future values of the secondary record according to (5).

To minimize the mean-square error, expression (4) is differentiated with respect to each unknown coefficient and the result set equal to zero. This may be loosely considered as differentiating with respect to the vector X (like taking the gradient) and equating to zero [*Frazer and others*, 1938, p. 48]. We obtain

$$MX = N \qquad (6)$$

representing a system of linear algebraic equations which can be solved to yield values of the coefficient for optimum prediction. From the solution

$$X = M^{-1}N$$

we can calculate the minimized error by substitution into (4),

$$\epsilon_m^2 = 1 - X'N = 1 - N'M^{-1}N \qquad (7)$$

making use of the fact that M is a symmetrical matrix. It is to be noted that the error and the coefficients depend on the number of past and present values, $n + 1$, upon which the prediction is based, as well as on the number of months ahead, α, for which the prediction is to be made.

Suppose that we are to make a prediction of temperature from its own present and past,

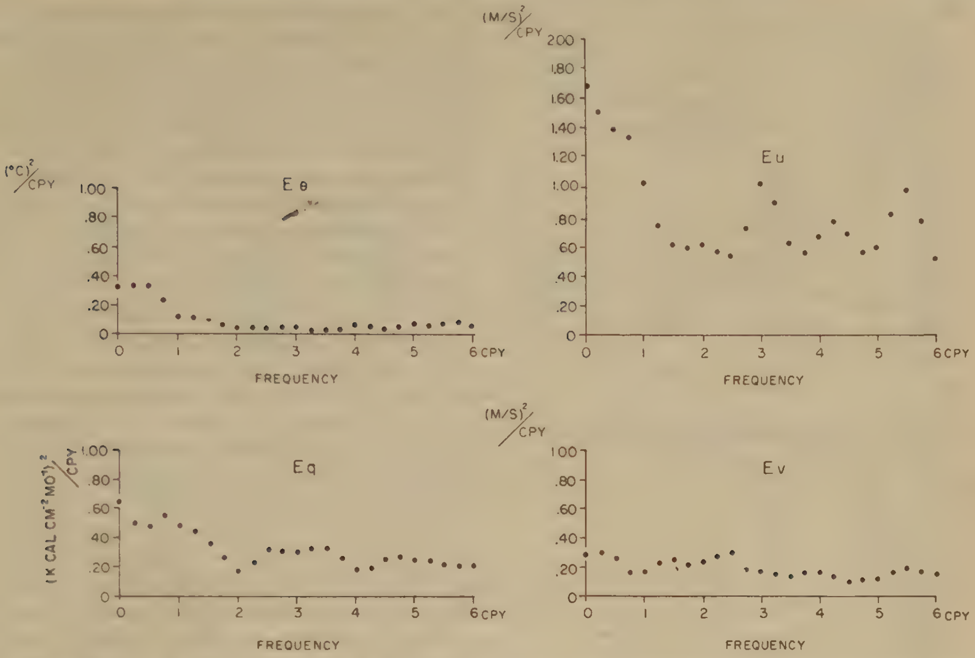

Fig. 5a. Energy spectral density E of temperature, wind, and radiation anomalies, NE trade wind region.

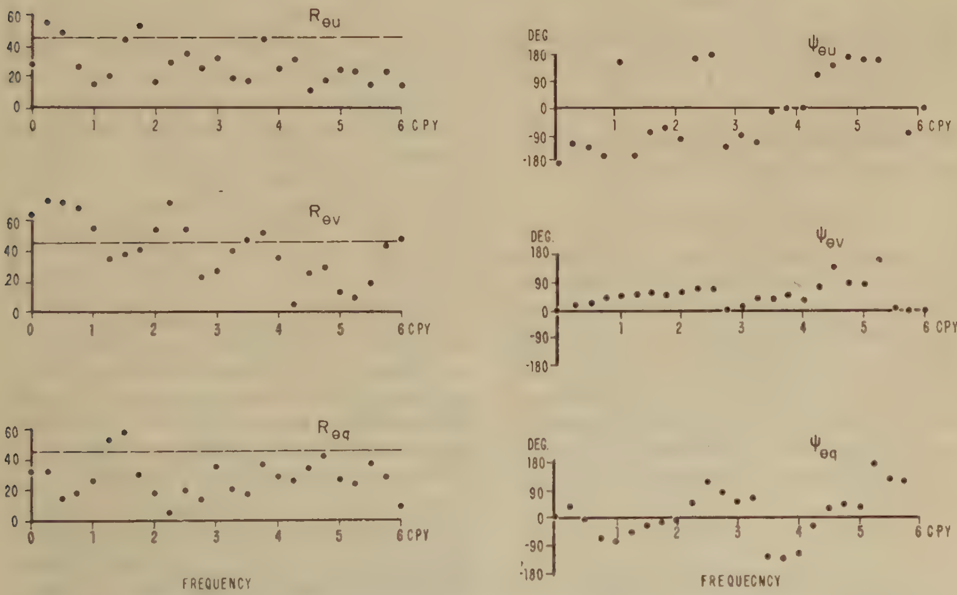

Fig. 5b. Coherence and phase relationships in the NE trade wind region.

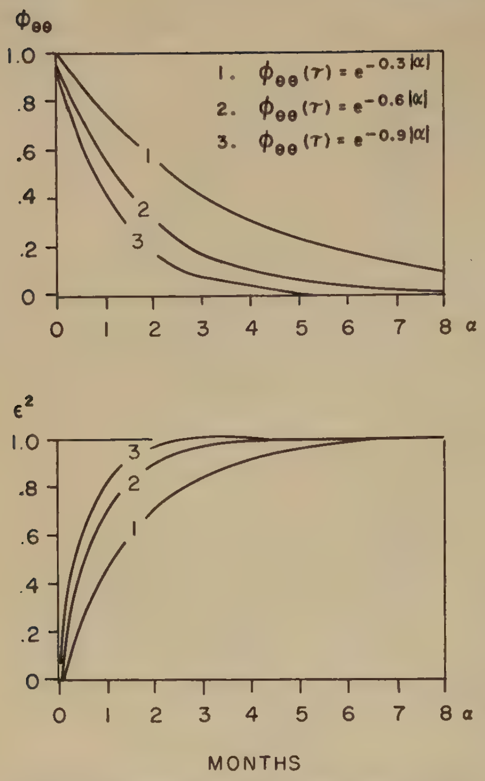

Fig. 6. Autocorrelations and mean-square error for three examples of decay rates in a Markov process.

and suppose also that the autocorrelation of temperature is adequately expressed by

$$\phi_{\theta\theta}(\tau) = e^{-\lambda|\tau|}, \lambda > 0$$

It is evident from Figures 2*a* and 3*a* that the autocorrelations do not differ significantly from the above expression with appropriate decay rates λ. Time series having such exponential autocorrelations are known as Markov processes, and it is well known that taking past values into account in the prediction scheme does not improve the prediction. In fact, the prediction coefficients turn out to be

$$a_0 = e^{-\lambda\alpha} \quad a_1 = a_2 = \cdots = 0$$

and

$$\epsilon_m^2 = 1 - e^{-2\lambda\alpha}$$

Three examples of exponential autocorrelations and the corresponding mean-square errors are shown in Figure 6. The persistence of most temperature records is within the range of curves 1 and 3; therefore, successful prediction cannot be expected far into the future. If the prediction is based on other variables also, even though the autocorrelations and cross correlations are of the simple exponential type, inclusion of past values improves the prediction unless all the decay rates are equal. One must therefore conclude that prediction from temperature alone might as well be based on the present value, whereas prediction from temperature and other variables will be improved somewhat by taking account of some past values of all variables.

Results. The prediction coefficients and the mean-square error were determined for a number of cases. It was desired to find out how the coefficients and the mean-square error depend on α and n and how the number of variables considered in the prediction schemes affects the outcome of prediction. The numerical results of this investigation are given in Tables 1 and 2, and certain important features are illustrated in Figures 7 and 8. Three characteristic aspects stand out immediately: (1) the mean-square error increases rapidly with increasing future month α, (2) the mean-square error rapidly approaches a limiting value with the number of past months taken into account, and (3) the mean-square error is hardly affected by the inclusion of radiation in the prediction scheme. The best prediction can be made by considering both temperature and wind. If only one or the other is considered, temperature can be predicted better from past temperatures than from past winds. There is some improvement in prediction if account is taken of the previous month in addition to the present one, but not much further refinement is gained by including more past data. Useful prediction seems almost to be limited to 1 to 2 months into the future. The smallest mean-square error in our investigation is 0.63 (compared with about 0.5 achieved by *Pierson* [1958] for the North Atlantic); that is, 37 per cent of the temperature variance can be predicted 1 month ahead. The correlation coefficient $R = \sqrt{1 - \epsilon^2}$ between the observed and predicted month is hence 0.61. The smallest mean-square error for 2 months ahead is

TABLE 1. Prediction Coefficients and Mean-Square Error for Washington Region*

Coeff.	α 1	2	3	4	5	6
			$\theta, v, 4$			
a_0	0.32	0.21	0.20	0.11	0.18	0.12
a_1	0.10	0.10	0.01	0.13	0.05	−0.07
a_2	0.08	−0.01	0.09	0.03	−0.10	−0.02
a_3	0.01	0.09	−0.02	−0.12	−0.03	0.00
c_0	0.22	0.22	0.14	0.14	0.07	0.07
c_1	0.09	0.03	0.06	0.01	0.01	0.06
c_2	0.02	0.07	0.01	0.02	0.05	−0.02
c_3	0.05	0.01	0.03	0.04	−0.03	0.01
ϵ^2	0.65	0.78	0.87	0.91	0.94	0.97

Coeff.	α 1	2	3	4
		$\theta, 4$		
a_0	0.42	0.31	0.26	0.16
a_1	0.13	0.13	0.04	0.15
a_2	0.08	−0.01	0.10	0.04
a_3	−0.02	0.06	−0.04	−0.13
ϵ^2	0.71	0.83	0.89	0.93
		$\theta, 2$		
a_0	0.44	0.32	0.27	0.15
a_1	0.16	0.15	0.07	0.12
ϵ^2	0.71	0.83	0.91	0.95
		$\theta, v, 2$		
a_0	0.35	0.30	0.22	0.10
a_1	0.16	0.19	0.06	0.12
c_0	0.21	0.26	0.13	0.14
c_1	0.08	−0.24	0.06	0.02
ϵ^2	0.66	0.80	0.88	0.93
		$\theta, 1$		
a_0	0.52	0.39	0.31	0.21
ϵ^2	0.73	0.85	0.90	0.96

Coeff.	α 1	2	3	4
		$v, 4$		
c_0	0.31	0.28	0.19	0.17
c_1	0.19	0.10	0.12	0.06
c_2	0.12	0.14	0.07	0.07
c_3	0.16	0.09	0.09	0.07
ϵ^2	0.77	0.85	0.92	0.95
		$v, 2$		
c_0	0.29	0.27	0.18	0.16
c_1	0.23	0.14	0.14	0.09
ϵ^2	0.83	0.89	0.91	0.96
		$\theta, v, 1$		
a_0	0.45	0.33	0.26	0.17
c_0	0.22	0.21	0.14	0.14
ϵ^2	0.69	0.80	0.89	0.93
		$v, 1$		
c_0	0.36	0.31	0.22	0.19
ϵ^2	0.87	0.90	0.95	0.96

* Temperature θ; wind u, v; radiation q; $\lambda_{\theta v} = 0.33$°C/m sec^{-1}. The number after the variable refers to the number of past months taken into account; α refers to future time of prediction (in months).

0.76; that is, only 24 per cent of the temperature variance can be accounted for. For 3 months ahead the corresponding values are 0.86 and 14 per cent.

The prediction coefficients a, b, c, and d do not show such simple behavior as does the mean-square error. The temperature coefficients a_i decreases slowly with increasing α, and very rapidly as increasing numbers of past months are taken into account. This suggests that future values of temperature depend primarily on the present value and very little on the past, a result which is characteristic of a Markov process. The prediction coefficients of wind decrease slowly as the number of past months is increased, but their dependence on α is erratic. The coefficients of radiation are negligibly small.

In order to investigate how well the predic-

TABLE 2. Prediction Coefficients and Mean-Square Error for NE Trade Wind Region*

Coeff.	α 1	2	3	4	5
			$\theta, u, v, q, 4$		
a_0	0.37	0.16	0.16	0.14	0.13
a_1	0.00	0.04	0.04	0.05	−0.06
a_2	0.03	0.02	0.04	−0.07	−0.01
a_3	0.03	0.00	−0.07	−0.01	0.00
b_0	0.11	0.13	0.16	0.16	0.10
b_1	0.11	0.16	0.14	0.08	−0.02
b_2	0.13	0.14	0.07	−0.03	−0.01
b_3	0.09	0.06	−0.04	−0.02	−0.01
c_0	0.11	0.08	−0.02	−0.09	−0.06
c_1	0.03	−0.04	−0.09	−0.05	0.00
c_2	−0.05	−0.08	−0.05	0.00	−0.01
c_3	−0.07	−0.03	0.01	0.01	0.01
d_0	0.07	0.05	0.05	0.06	0.05
d_1	0.01	0.03	0.04	0.03	−0.02
d_2	0.04	0.05	0.04	−0.01	0.00
d_3	0.04	0.03	−0.02	−0.01	−0.01
ϵ^2	0.65	0.81	0.87	0.93	0.97
			$\theta, u, v, 4$		
a_0	0.38	0.18	0.17	0.15	0.13
a_1	−0.01	0.04	0.04	0.05	−0.06
a_2	0.03	0.02	0.04	−0.07	−0.01
a_3	0.03	0.00	−0.08	−0.01	0.00
b_0	0.12	0.13	0.17	0.17	0.11
b_1	0.11	0.17	0.15	0.09	−0.02
b_2	0.13	0.15	0.09	−0.02	−0.01
b_3	0.10	0.07	−0.04	−0.02	−0.01
c_0	0.10	0.08	−0.03	−0.09	−0.06
c_1	0.02	−0.05	−0.10	−0.05	0.00
c_2	−0.05	−0.09	−0.05	0.00	0.00
c_3	—0.07	−0.04	0.02	0.01	0.01
ϵ^2	0.67	0.82	0.88	0.93	0.98
			$u, v, 4$		
b_0	0.20	0.18	0.21	0.20	0.13
b_1	0.19	0.22	0.20	0.12	0.00
b_2	0.22	0.20	0.12	0.00	0.00
b_3	0.20	0.12	−0.03	0.00	0.00
c_0	0.15	0.10	0.00	−0.07	−0.05
c_1	0.07	−0.02	−0.07	−0.04	0.01
c_2	−0.01	−0.07	−0.04	0.01	0.00
c_3	−0.08	−0.04	0.01	0.00	0.00
ϵ^2	0.78	0.85	0.91	0.95	0.99
			$\theta, 4$		
a_0	0.52	0.36	0.29	0.23	...
a_1	−0.07	−0.15	−0.12	−0.11	...
a_2	0.10	0.14	0.12	−0.10	...
a_3	0.01	−0.01	−0.09	−0.02	...
ϵ	0.73	0.90	0.94	0.97	...

Coeff.	α 1	2	3	4	5
			$\theta, u, v, q, 2$		
a_0	0.40	0.19	0.15	0.12	0.12
a_1	0.04	0.07	0.04	0.01	−0.07
b_0	0.09	0.11	0.16	0.16	0.10
b_1	0.08	0.15	0.14	0.08	−0.02
c_0	0.14	0.10	0.00	−0.07	−0.05
c_1	0.01	−0.07	−0.10	−0.05	0.00
d_0	0.05	0.04	0.05	0.06	0.05
d_1	0.09	0.09	0.08	0.05	0.00
ϵ^2	0.69	0.84	0.88	0.93	0.97
			$\theta, u, v, 2$		
a_0	0.44	0.23	0.17	0.13	0.12
a_1	0.05	0.08	0.05	0.00	−0.07
b_0	0.12	0.16	0.20	0.17	0.11
b_1	0.13	0.18	0.15	0.10	−0.02
c_0	0.03	−0.03	−0.11	−0.09	−0.06
c_1	−0.11	−0.14	−0.09	−0.06	0.00
ϵ^2	0.71	0.85	0.89	0.94	0.98
			$\theta, u, v, q, 1$		
a_0	0.46	0.26	0.19	0.14	...
b_0	0.08	0.11	0.16	0.15	...
c_0	0.10	0.07	−0.04	−0.09	...
d_0	0.14	0.10	0.10	0.09	...
ϵ^2	0.70	0.87	0.91	0.94	...
			$\theta, u, v, 1$		
a_0	0.48	0.27	0.19	0.14	0.10
b_0	0.10	0.12	0.18	0.17	0.10
c_0	0.08	0.07	−0.04	−0.11	−0.07
ϵ^2	0.70	0.87	0.91	0.95	0.98
			$\theta, 2$		
a_0	0.48	0.27	0.21	0.17	0.14
	0.07	0.10	0.07	0.01	−0.07
a_1	0.73	0.89	0.94	0.97	0.99
ϵ^2			$\theta, 1$		
a_0	0.52	0.32	0.24	0.17	0.10
ϵ^2	0.73	0.90	0.94	0.97	0.99

---

* Temperature θ; wind u, v; radiation q. $\lambda_{\theta u} = 0.35°\mathrm{C/m\ sec^{-1}}$; $\lambda_{\theta v} = 0.74°\mathrm{C/m\ sec^{-1}}$; $\lambda_{\theta q} = 0.55°\mathrm{C/k\ cal\ cm^{-2}\ mo^{-1}}$. The number after the variables refers to the number of past months taken into account; α refers to future time of prediction (in months).

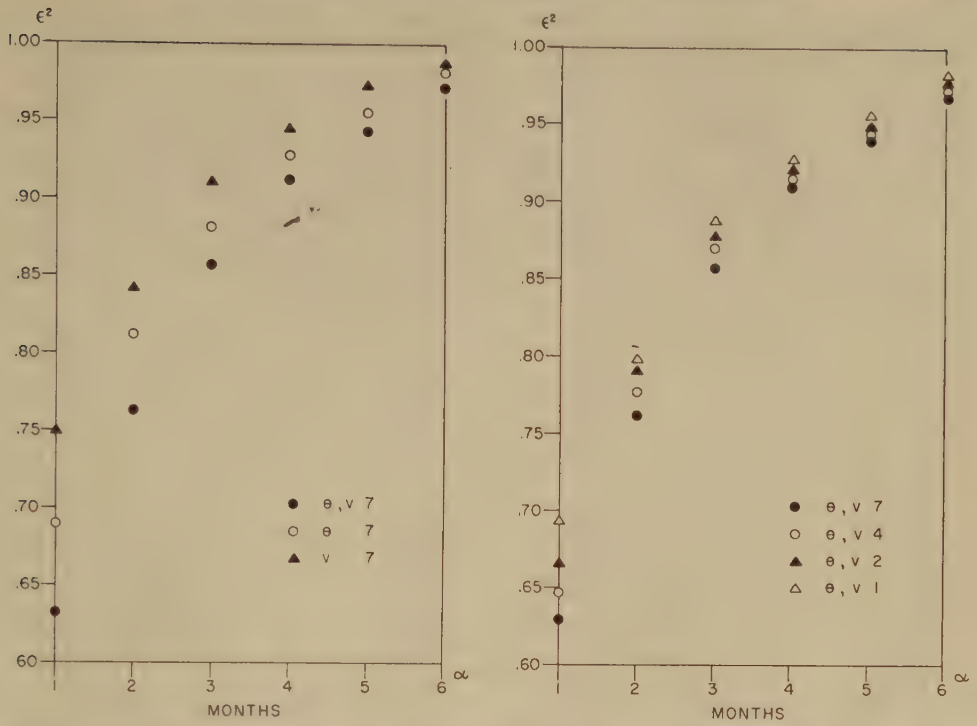

Fig. 7. The mean-square error and its dependence on the number of variables used, number of past months considered, and future time of prediction α for the Washington region.

tion works on independent data, use was made of the temperature records at Amphitrite Point, B. C. (48°55′N, 125°32′W), and north-south wind index along 45°N, 125° to 145°W during the period 1949–1958. The temperature (°C) for the following month was predicted from the temperature and wind (m sec^{-1}) of the present month by the formula

$$\theta^*(1) = 0.45\theta(0) + 0.22\lambda_{\theta v} V(0)$$

where $\lambda_{\theta v} = 0.33$°C/m sec^{-1}. It is seen that the observed and the predicted time series (Fig. 9) agree well with respect to the low-frequency part, but that the high-frequency part cannot be predicted very well. Also, the predicted temperature has a smaller rms deviation from the mean than from the observed, which is a general characteristic of linear regression methods. The computed error is $\epsilon^2 = 0.59$, indicating that 41 per cent of the variance has been accounted for. This is better than the theoretical capability of the prediction, and it must be assumed that an error correspondingly larger than the theoretical value would have been just as likely.

Acknowledgments. The authors benefited considerably from many fruitful discussions with Walter Munk. Maurice Blackburn, John Isaacs, and Joseph L. Reid, Jr., read the manuscript and offered many valuable suggestions. The authors are also indebted to Gaylord Miller and to Convair Astronautics of San Diego, especially to Mr. Bruno Witte of that establishment, who allowed us to use their machine programs and who performed many of the numerical computations on their 704 electronic computer. The remaining desk computations were painstakingly done by Joan Connell.

This work was supported in part by the Scripps Tuna Oceanography Research and the Marine Life Research programs. Funds for the former project were provided by the U.S. Bureau of Commercial Fisheries, Department of the Interior, Contract 14–19–008-9354.

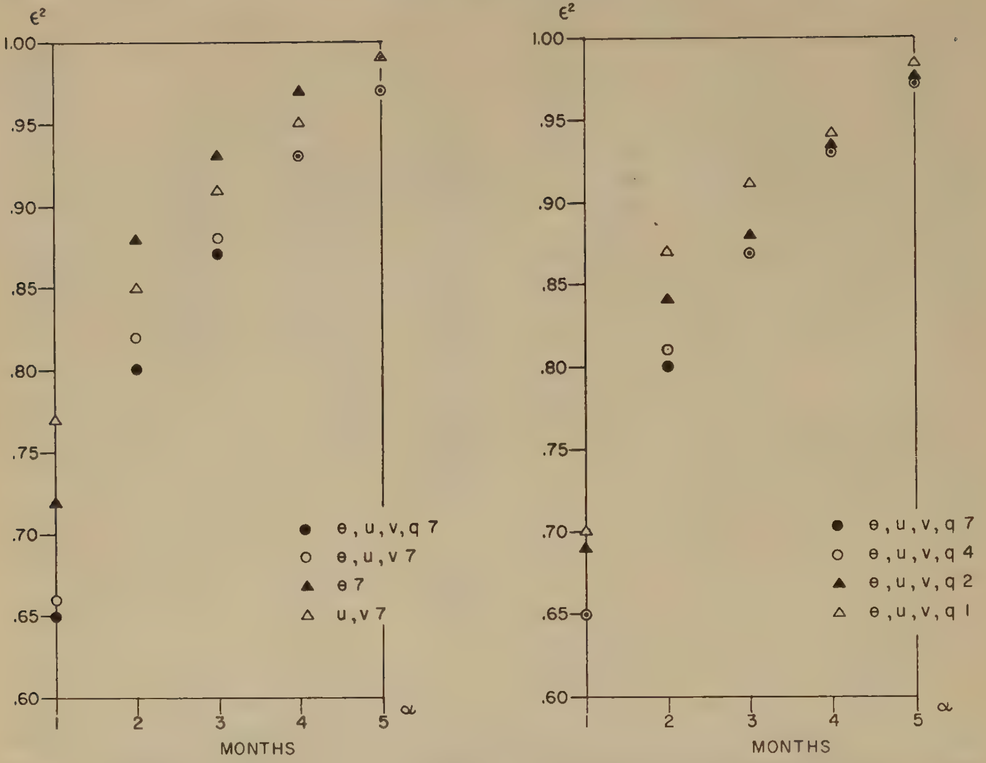

Fig. 8. The mean-square error and its dependence upon the number of variables used, number of past months considered, and future time of prediction α for the NE trade wind region.

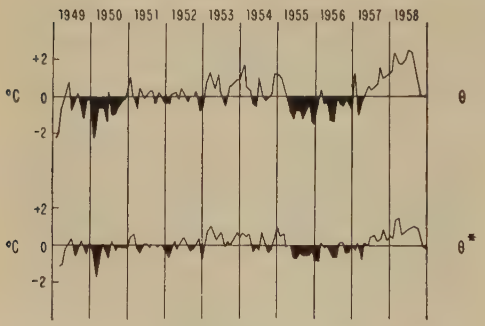

Fig. 9. Observed and predicted temperatures for Amphitrite Point, B. C.

REFERENCES

Blackman, R. B., and J. W. Tukey, The measurement of power spectra from the point of view of communications engineering, *Bell System Tech. J. 37*, Part I, 185–282, Part II, 485–570, 1958.

Budyko, M. I., *Teplovoi Balans Zemnoi Poverkhnosti*, GIMIZ, Leningrad, 256 pp., 1956.

Frazer, R. A., J. A. Duncan, and A. R. Collar, *Elementary Matrices*, Cambridge Univ. Press, 416 pp., 1938.

Imperial Marine Observatory, Kobe, Japan, The mean atmospheric pressure, cloudiness, air temperature and sea surface temperature of the North Pacific Ocean and the neighboring seas, Annual publication of monthly values, 1921–1938.

Laning, J. H., and R. H. Battin, *Random Processes in Automatic Control*, McGraw-Hill Book Company, New York, 434 pp., 1956.

Munk, W. H., Smoothing and persistence, *J. Meteorol.*, in press.

Munk, W. H., F. E. Snodgrass, and M. J. Tucker, *Spectra of Low Frequency Ocean Waves*, Univ. of Calif. Press, Los Angeles, 1959.

Namias, J., Thirty-day weather forecasting: a review of a ten-year experiment, *Meteorol. Monographs, 2*(6), Am. Meteorol. Soc., Boston, Mass., 83 pp., 1953.

Pierson, W. J., *The use of time series concepts and spectral analysis in the study of long range* *forecasting problems,* N. Y. Univ., Dept. Meteorol. and Oceanog., 78–100, 1958.

Takenouti, Y., Long range oceanographic forecast, historical review and future problem, *Oceanog. Mag., Japan, 9,* 1–12, 1957.

Tukey, J. W., The sampling theory of power spectrum estimates, *Symp. Appl. Autocorrelation Analysis to Phys. Probl., NAVEXOS-P-735,* Office of Naval Research, Washington, D. C., 1949.

U. S. Weather Bureau, *Monthly mean sea level atmospheric pressure charts in the Northern Hemisphere,* Extended Forecasting Sect. of U. S. Weather Bureau, Washington, D. C., published monthly, 1899–1958.

Wadsworth, G. P., Application of statistical methods of weather forecasting, *Compendium of Meteorol.,* Am. Meteorol. Soc., Boston, Mass., 849–855, 1951.

Wiener, N., *Extrapolation, Interpolation and Smoothing of Stationary Time Series,* John Wiley & Sons, New York, 163 pp., 1949.

(Manuscript received August 17, 1959.)

Reprinted from THE REVIEW OF SCIENTIFIC INSTRUMENTS, Vol. 31, No. 4, 395–398, April, 1960
Printed in U. S. A.

Low Background Thin-Wall Flow Counters for Measuring Beta Activity of Solids

DEVENDRA LAL* AND DAVID R. SCHINK
Scripps Institution of Oceanography, University of California, La Jolla, California

(Received December 14, 1959; and in final form, January 25, 1960)

The construction and performance of disk-shaped thin-walled flow counters suitable for measuring very small beta activities of solids is described. The circular faces, which serve as the cathode, consist of conducting films. Either a single pear-shaped loop of wire whose plane is parallel to that of the faces, or a group of straight wires stretched across the midplane serves as the anode. The counters are operated in the Geiger region. Samples can be counted against both faces of the counter. Performance data are given for counters having active volumes ranging from 0.2 to 7 cc, and having active areas from 1.6 to 23 cm². Counting efficiencies for natural potassium (mounted on Lucite) vary from 30% to 47%, depending on the relationship of sample area to counter dimensions. Inside a 20-cm steel shield and an anticoincidence ring the background counting rates varied approximately as 1 count/hr/cm² of counting area. Backgrounds as low as 1 count/hr were obtained.

The disk geometry permits the use of a smaller metal and anticoincidence shield than is possible with cylindrical geometry. Counters shielded successively with 1.9-cm mercury, 5-cm steel, and 5-cm lead, and operated with a flat multiple-anode anticoincidence counter (15 cm²), actually gave lower background than with the 20-cm steel and anticoincidence ring assembly. An integral counter assembly, consisting of ∼2-cm diam disk-shaped counter and a disk-shaped guard counter (∼7-cm diam), was constructed and gave satisfactory results.

INTRODUCTION

So far, most of the developments in low-level beta counting have been limited to problems which involve the counting of large samples with low specific activity.[1,2] However, one often is faced with the measurement of very weak activities—of the order of a few disintegrations/hr—in small samples of high specific activity. An obvious approach to this problem is the employment of small size detectors with low enough background so that the sample counting rate is either larger or comparable to the background. Freshly poured nuclear emulsions promise to be the most sensitive means of detection, since they can be used to localize the activity and can thus serve as detectors of arbitrarily small size.[3] But nuclear emulsions have not found much application for beta counting, mainly because absorption and half-life measurements cannot be made conveniently. Geiger counters usually have been preferred over other detectors for beta counting at any level. Small size argon filled end-window counters, and flow-type thin-wall counters, scaled down following the original design of Sugihara *et al.*,[4] have been used in the past.[5–7] The backgrounds of these counters range from 7 to 25 c.p.h. (counts per hour) when operated inside a massive shield and in anticoincidence with large Geiger tubes to eliminate the recording of fast charged cosmic-ray particles. To our knowledge, lower background detectors for beta counting of solids have not been reported. In addition, the use of low level beta-counting assemblies has been limited to a few laboratories because of difficulties in obtaining low background counters.

In this paper, we report on the construction and performance of disk-shaped thin-walled Geiger counters suitable for measuring small beta activities of solids. In its basic form, the counter consists of two thin circular conducting films (cathode) and a pear-shaped loop of thin wire (anode) in the center. The separation of the films is kept as small as possible. The counter is operated in the Geiger region with a mixture[8] of helium (98.7%) and isobutane. The samples can be mounted in proximity with either of the films, thus providing a high ratio of the available counting area to the volume of the counter. Counters of diameters 1.0, 1.9, 2.5, and 3.8 cm have been tested for their plateaus, counting efficiencies, background, and stability. The materials used and the simplicity of construction consistently lead to counters of reproducible low backgrounds. The background counting rates vary with the size of counter approximately as 1 c.p.h./cm² counting area, when operated in a 20-cm steel shield with an anticoincidence arrangement.

Thin-walled counters constructed in this manner combine the merits of the end window and of the cylindrical thin-wall types. The counting efficiency is about 40%. This is about 1.5—2 times larger than for the conventional types scaled down to small sizes. The sensitivity parameter, S^2/B, is therefore 2–4 times larger for this reason alone (S and B are the net sample and background counting rates, respectively). The shape of the counters permits simplification of the anticoincidence shield and reduction in the size of the metal shield.

---

[*] On leave from the Tata Institute of Fundamental Research, Bombay, India.

[1] W. H. Johnston, Science 124, 801 (1956).

[2] E. C. Anderson and F. N. Hayes, Ann. Rev. Nuclear Sci. 6, 303 (1956).

[3] M. Reinharz and G. Vanderhaeghe, Nuovo cimento 12, 243 (1954).

[4] T. T. Sugihara, R. L. Wolfgang, and W. F. Libby, Rev. Sci. Instr. 24, 511 (1953).

[5] D. Lal, "Investigations of nuclear interactions produced by cosmic rays," thesis (1958). P. S. Goel, D. P. Kharkar, D. Lal, N. Narsappaya, B. Peters, and V. Yatirajam, Deep-Sea Research 4, 202 (1957).

[6] E. A. Martell, The Enrico Fermi Institute for Nuclear Studies, Rept. AECU 3262, The University of Chicago (1956).

[7] W. D. Ehman and T. P. Kohman, Geochim. Cosmochim. Acta 14, 340 (1958).

[8] This mixture is commercially available as "Q"-gas. Alternatively, one can use argon bubbled through ice-cooled ethyl alcohol, or isopropyl alcohol (J. R. Arnold and M. Honda, private communication).

Reproduced by Permission

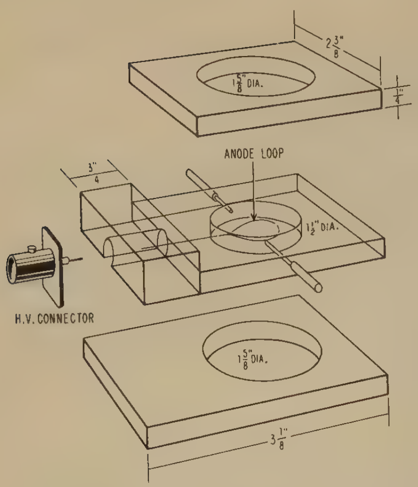

Fig. 1. An exploded view showing the assembly of a 3.8-cm diam (window) counter. Only the chamber in the central piece (B) serves as active volume for the counter.

COUNTER CONSTRUCTION DETAILS

Figure 1 shows an exploded view of a 3.8-cm diam counter, except for the gold-plated Mylar films. The counter body is assembled from three machined Lucite pieces, 1(a), 1(b), and 1(c). The central piece 1(b) houses a 1- or 2-mil tungsten loop (elongated pear-shaped). The wire is supported by a thin stainless steel hypodermic needle (20 mil o.d., 10 mil i.d.) which is held firmly in the Lucite block and provides electrical connection for the anode. The plane of the loop is adjusted so that it is parallel to the broad face. Thin gold-plated Mylar films (0.9 mg cm^{-2}) are then mounted on either side of the piece 1(b), with conducting sides facing each other. The counter is finally assembled by screwing together the pieces 1(a), 1(b), and 1(c). The diameter of the holes in 1(a) and 1(c) is intentionally larger than that in 1(b) so that the sample holder rests against the Lucite surface, rather than directly on the unsupported film. The inlet and outlet tubes for counting gas are shown in Fig. 1.

Photographs of the assembled counters are shown in Fig. 2. The unit in Fig. 2 (center) has two counters of diameter 1.0 and 1.9 cm. The counter shown in Fig. 2 (right) will be explained later in this paper.

COUNTER CHARACTERISTICS

a. Plateau

The counters were operated in the Geiger region. The high voltage unit employed dry cells of 300, 45, 22.5, and 4.5 v in such a manner that any desired voltage—in steps of 4.5 v—could be obtained. The threshold voltages varied between 700 and 900 v, depending on the size of the counter and the anode wire. Most counters were tested only over 45 v above the starting point (knee) of the plateau. The counting rate variations usually were less than 5% over this voltage range, although in some cases they were as large as 25%, showing that the central anode wire was not aligned properly. The pulse heights showed an essentially linear relation to the length of the anode loop. At the plateau knee, the smallest counters gave 50-mv pulses compared to 200-mv for the largest.

Some of the counters were tested over a bigger voltage range. Counters of 1.9 and 3.8 cm diam could be worked over about 70–100 v with reproducible plateaus of 5–10%/100 v. Application of higher voltages in the case of counters of 1.0 and 1.9 cm apparently did not change the counting rates. Actually the counter threshold voltage increased temporarily. This was probably due to a reduction in the effective anode voltage arising from deposition[9] of charge on the Lucite walls of the counter. This effect was found to start ~45 v above the plateau for the small counter 1.0 cm diam, 6 mm thickness), where the wall area was relatively large.

The drift in threshold voltages caused by overvoltages in the case of 1.0- and 1.9-cm counters was overcome (1) by making the walls conducting and (2) by reducing the counter thickness from ~6 to 3 mm. Either technique gave satisfactory plateaus of 5–10% over a range of 45–70 v. It should, therefore, be possible to make still smaller counters.

The small plateau range, 45–70 v, is by no means a handicap. The counter voltages can be maintained constant within a few volts—at least over periods of several months—using units of high voltage batteries.

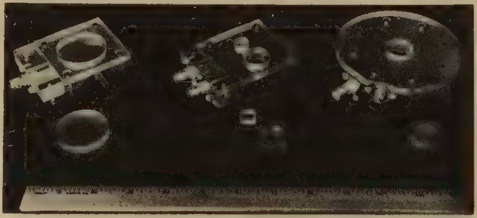

Fig. 2. The assembled, disk-shaped thin-wall counters. Left: A 3.8-cm diam counter. Center: Two separate counters of diameters 1.0 and 1.9 cm. Right: A composite unit with 1.9-cm thin-wall counter and the anticoincidence counter. Sample planchets of the various counters are also shown.

---

[9] For this reason, several attempts to build counters with the cathode on only one face of the Lucite disk failed. These counters continued to show constant counting rates over about 300 v, with the threshold voltage changing in step with increasing voltage. Thus, the application of higher voltages did not result in advances along the plateau curve, but caused instead a displacement of the curve itself. It is conceivable that this property could be put to some use in constructing stable detectors.

Table I. Two-sided thin-disk beta counters.

Counter No.	Approximate diameter (cm)	Thickness (cm)	Available counting area (cm²)	Counting rate (c.p.h.) in 20-cm steel shield Anticoincidence	Counting rate (c.p.h.) in 20-cm steel shield Coincidence	Anticoincidence rate/available counting area (c.p.h./cm²)	R (coincidence rate)/(anticoincidence rate)
1	3.8	0.63	22.8	19.8	430	0.9	22
2	3.8	0.63	22.8	46.0	494	2.0	11
3	3.8	0.63	22.8	19.6	484	0.9	25
4[a]	3.8	0.50	22.8	17.3	418	0.8	24
5	2.5	0.63	9.8	7.8	202	0.8	26
6	1.9	0.63	5.7	4.2	82	0.7	19
7	1.9	0.63	5.7	4.6	102	0.8	22
8	1.9	0.63	5.7	5.4	98	0.9	18
9	1.9	0.63	5.7	4.2	135	0.7	32
10	1.9	0.63	5.7	7.2	113	1.3	16
11[a]	1.9	0.63	5.7	4.3	138	0.7	32
12	1.9	0.32	5.7	3.0	108	0.5	36
13[b]	1.9	0.32	5.7	4.4	72	0.8	16
14	1.0	0.63	1.6	2.4	50	1.5	21
15	1.0	0.63	1.6	2.3	50	1.4	22
16[a]	1.0	0.63	1.6	2.3	38	1.4	16
17[c]	1.0	0.32	1.6	0.9	26	0.6	29

[a] The walls of these counters were coated with a gold film by sputtering.
[b] One straight anode wire was used. Counting efficiency for K^{40} = 42%.
[c] One straight anode wire was used. Counting efficiency for K^{40} was only 26%, which is 35% lower than obtained with loop for this size counter.

b. Background Counting Rates

The counters were operated inside a 20-cm steel shield in anticoincidence with 12 Geiger tubes (70 cm). The operating voltage was usually 10 v above the knee of the plateau. Lucite sample holders were used for counting the background rates. The observed coincidence and anticoincidence rates for the various counters are summarized in Table I. The gross counting rate is the sum of these two rates.

The anticoincidence rate (c.p.h.)/cm² counting area is seen to range within rather narrow limits, 1.0±0.5, except for counter No. 2, showing that the materials and the construction technique used result in consistently clean counters. A very good indicator of the cleanliness of the counter seems to be the ratio of the coincidence to the anticoincidence counting rate R. The former is mainly a function of the counter size, while the latter represents primarily the sum of the counting rates due to contamination of the counter materials, to electrons produced in the wall and gas, and to gamma flux inside the shield. The ratio R varies between 11 and 36 for the 17 counters tested (Table I). Of these, 12 fall in the range 21±5 and five have a ratio greater than 25. To our knowledge, the highest value reported in the literature is 25. Even for the big screen wall counter[10] operated with a 20-cm steel shield, the ratio is 22.

COUNTING EFFICIENCY

The counting efficiency was measured by counting a natural potassium sample (KCl) mounted on a Lucite holder. The disintegration rate of K^{40} was taken to be 0.91 beta/min/mg KCl. Self-absorption in the sample was corrected on the basis of an absorption half-thickness of 59 mg cm^{-2}. The counting efficiency depended mainly on the size of the sample relative to the window area, and to some extent on the size of the counter. The smallest size counters showed lower efficiencies, as would be expected from considerations of geometry. (The samples were located about 1 mm away from the window.) The efficiencies were larger than 30% in each case and were 47% in the case of samples deposited on a 2.5-cm circle and counted with the 3.8-cm diam counter.

In order to examine, in more detail, the sensitivity of the counter at different positions, we prepared a collimated source of P^{32}, such that the incident β particles were confined within an area of $\lesssim$0.7 cm². This source was counted

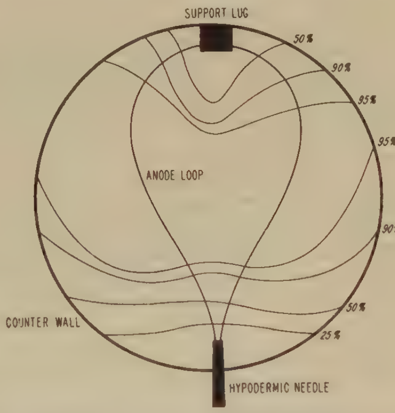

Fig. 3. Contours of constant counting rate for the 3.8-cm diam counter as obtained for a collimated source. The numbers given are relative to counting rate of 100 near the center.

---

[10] W. F. Libby, *Radiocarbon Dating* (University of Chicago Press, Chicago, 1955), 2nd ed.

TABLE II. Anticoincidence rate of counter No. 1 (Table I) with different shieldings. Coincidence rate—430 c.p.h.

Nature of shielding		Anticoincidence rate (c.p.h.)
Anticoincidence	Metal	
12 Geiger counters (70 cm long)	20-cm steel	19.8
Flat multiple anode counter (15×15×2.5 cm)	5-cm steel plus 5-cm lead	22.8
Flat multiple anode counter (15×15×2.5 cm)	Above, plus 1.9-cm mercury below anticoincidence counter only, covering ~0.3×4π solid angle	19.1
Flat multiple anode counter (15×15×2.5 cm)	Above, plus 1.9-cm mercury on top of counter covering ~0.4×4π solid angle	16.6

at different positions on the 3.8-cm counter. The contours of constant counting rate (with respect to 100 near the center, where it was found to be maximum) are shown in Fig. 3. The position of the anode loop also is shown in the figure. It is seen that the efficiency drops rapidly as one approaches either the hypodermic needle or the anode-support lug on the opposite end. The average efficiency over the entire window for a vertically incident, uniform beam of particles was found to be 80% of that in the center. For samples counted in close geometry, the expected variation in efficiency for sources of different sizes should therefore be less than 20%.

More uniform counting efficiencies could be obtained if several straight anode wires were used instead of a loop, and if the protrusion of the hypodermic needle into the counter were kept to a minimum. We have not investigated this point in detail.

STABILITY

Most counters were tested for 10–40 hr each. The long term stability of the counting efficiency and of the background rate was tested for counters No. 1 (300 hr), Nos. 5 and 10 (100 hr each), and No. 9 (70 hr). The background rate varied only within the expected statistical fluctuations. The counting efficiency in a few cases was checked by a KCl source between runs. In most cases, however, the stability of counting efficiency was inferred from the coincidence rate which is due to the charged penetrating component of the cosmic radiation. Day-to-day variations of this component are known to be within ±2.5%, except during infrequent occurrences of solar flares. The counters were stable with respect to background and counting efficiency.

MODIFICATIONS IN METAL AND ANTICOINCIDENCE SHIELDING

Since the counters have the shape of flat disks, it is possible to reduce the size of the anticoincidence counters and the metal shield. For anticoincidence, a flat multiple-anode flow-type counter was built using straight anode wires. The dimensions of the box were 15×15×2.5 cm, the cathodes being 15-cm^2 stainless steel sheets. The anodes were 2-mil tungsten wires separated by about 2.5 cm. The counter had a plateau of more than 300 v with a slope of 2%/100 v.

The largest counter (3.8 cm) was placed in contact with the 15-cm^2 face and operated under different conditions of shielding, as shown in Table II. It is apparent from Table II that successive shielding of the counter with 1.9-cm mercury, 5-cm steel, and 5-cm lead forms a smaller and better shield than 20-cm steel.

The size of the anticoincidence counters used is such that effectively all penetrating particles arriving at the beta counter from zenith angles between 0–80° will be counted by the anticoincidence counter. Because of this, about 0.1% of the μ mesons incident on the beta counter will miss the anticoincidence unit. The angular distribution of μ mesons penetrating 20 cm of steel at sea level has been taken to vary with zenith angle θ as $\cos^3\theta$.[11] The resultant increase in the anticoincidence rate, i.e., the counter background, is $0.1R$%. The highest value of R in our experiments was 36 (Table I) and therefore the use of the small anticoincidence counter causes an increase of less than 3.6% in the background. For sample counters of smaller size the expected rise in background would be negligible.

As a further modification, we have constructed a single counting unit which contains both the thin-wall beta counter and the anticoincidence counters (Fig. 2, right). The diameters of the two counters are 1.9 and 6.8 cm, respectively. A thick, stainless steel sheet is used as a common cathode for the two counters. The anticoincidence counter was about 1 cm thick and was strung with equally spaced straight anode wires. (The anticoincidence counter had a plateau of more than 250 v with a slope of 3%/100 v. Its counting rate was 20 c.p.m. inside the shield.) Since the beta counter is permanently attached to the anticoincidence counter in this arrangement, only one side of the counter is available for counting. The coincidence and the anticoincidence rates were found to be 114 and 6.8 c.p.h., respectively, with a corresponding ratio of 17.

ACKNOWLEDGMENTS

The work was supported by grants from the Cambridge Air Force Geophysics Research Directorate. We are indebted to Dr. J. R. Arnold for suggestions and criticism, and to Dr. R. Sharp, Dr. H. Craig, and Mr. M. Eichen for helpful discussions. We take this opportunity to thank Dr. E. D. Goldberg for his help during the various phases of this work.

Our thanks are due David Randall and H. Hill for machining the counter bodies.

---

[11] J. L. Zar, Phys. Rev. 83, 761 (1951).

Deep-Sea Research, 1960, Vol. 6, pp. 249 to 258. Pergamon Press Ltd. London. Printed in Great Britain

LETTER TO THE EDITORS

Indian Ocean vertical temperature sections*

(*Received* 19 *February* 1960)

THE SCOR Committee for the planning of the multi-ship international oceanographic survey of the Indian Ocean in 1961-62 requested information from the Bathythermograph Section of Scripps Institution of Oceanography concerning the distribution of bathythermograph temperature observations in the Indian Ocean.

The following information and vertical temperature charts were distributed to Committee members in New York in September, 1959. Since these data are unavailable to the large number of scientists who may take part in this expedition, it is hoped that Deep-Sea Research will bring them to the attention of interested persons.

The Scripps Institution of Oceanography, University of California, La Jolla, and the U.S. Navy Hydrographic Office maintain a file of bathythermograph temperature observations in the Pacific and Indian oceans. These observations have been taken between 1942-59 by U.S. and British Navy ships, by U.S. and British research vessels and by a few merchant ships. Figure 1 shows the distribution of bathythermograph observations in the Indian Ocean.

The majority of the observations are in the northern parts of the Indian Ocean along the sea lanes between Singapore, Ceylon and the Red Sea. Another large group fall on the route between Ceylon and the Persian Gulf. There are few latitudinal ship tracks and few longitudinal tracks in the vicinity of the Equator and to the south of it.

From the available data, eleven cross-sections of temperature have been drawn, five of which are latitudinal sections. Figure 2 is a location chart of the sections. Insofar as possible, the sections were selected to show differences between monsoon seasons and between years. The only latitudinal bathythermograph sections which were omitted are those made by the *Vema* of the Lamont Geological Observatory, Columbia University, and the *Atlantis* of the Woods Hole Oceanographic Institution in 1958.

Figures 3, 4 and 5 are latitudinal sections. Figures 6, 7 and 8 are longitudinal sections. Since none of the sections was exactly East-West or North-South, both latitude and longitude scales are indicated on the margins. The inner evenly-spaced scale is the one against which the observations are plotted. The outer irregular scale locates the section with respect to the second coordinate. The inverted ' T ' indicates the depth of the observations whose geographical location is indicated at the top of each section by a tick and the observation number. Dashed lines have been used when isotherms are connected below the depth of the observations, or where distance or time between observations is large. Sections have been broken when distance or time between observations is excessive or when the observations were taken by different ships. All sections have been reproduced on the same scale.

Figures 9a and 9b are charts showing the annual variation in the Arabian Sea. These charts are based on bathythermograph data analyzed by JUNE G. PATTULLO for use in her study of *Seasonal Oscillation in Sea Level* (PATTULLO, *et al.*, 1955). They are reproduced here with her permission. The data have been further smoothed to reduce the effect of erratic distribution in time and space.

Acknowledgements—This paper represents results of research carried out by the University of California, under contract with the Office of Naval Research. Reproduction in whole or in part is permitted for any purpose of the U.S. Government. This research also received support from the

Contributions from the Scripps Institution of Oceanography, New Series, 1146

Reproduced by Permission

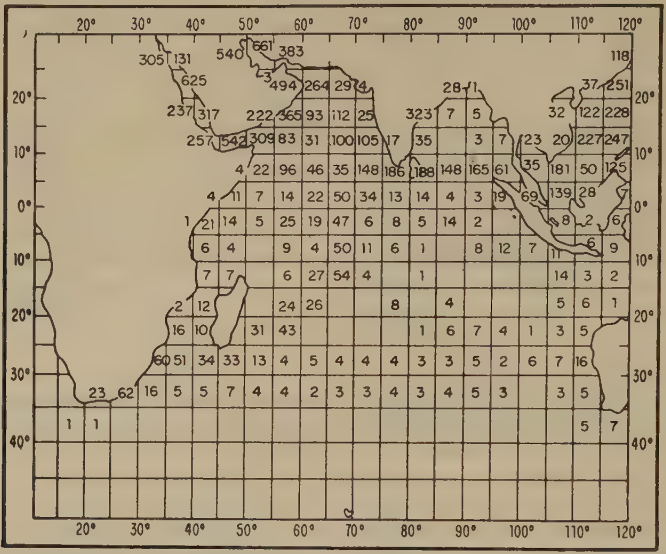
20°
30°
40°
50°
60°
70°
80°
90°
100°
110°
120°
20°
10°
0°
10°
20°
30°
40°
305 131 540 661 383 118
625 494 264 297 28 1 37 251
237 317 222 365 93 112 25 323 7 5 32 122 228
257 542 309 83 31 100 105 17 35 3 7 23 20 227 247
4 22 96 46 35 148 186 188 148 165 61 35 181 50 125
4 11 7 14 22 50 34 13 14 4 3 19 69 139 28 7
1 21 14 5 25 19 47 6 8 5 14 2 8 2 6
6 4 9 4 50 11 6 1 8 12 7 11 6 9
7 7 6 27 54 4 1 14 3 2
2 12 24 26 8 4 5 6 1
16 10 31 43 1 6 7 4 1 3 5
60 51 34 33 13 4 5 4 4 4 3 3 5 2 6 7 16
23 62 16 5 5 7 4 4 2 3 3 4 3 4 5 3 3 5
1 1 5 7

FIG. 1. The total number of bathythermograph observations taken in each 5-degree quadrangle of the Indian Ocean (5,625), Red Sea (1,872), Persian Gulf (1,587) and So. China Sea (1,901), as of January 1, 1960. These include data processed at Scripps Institution of Oceanography, Woods Hole Oceanographic Institution and the U.S. Navy Hydrographic Office in the years 1942-1959.

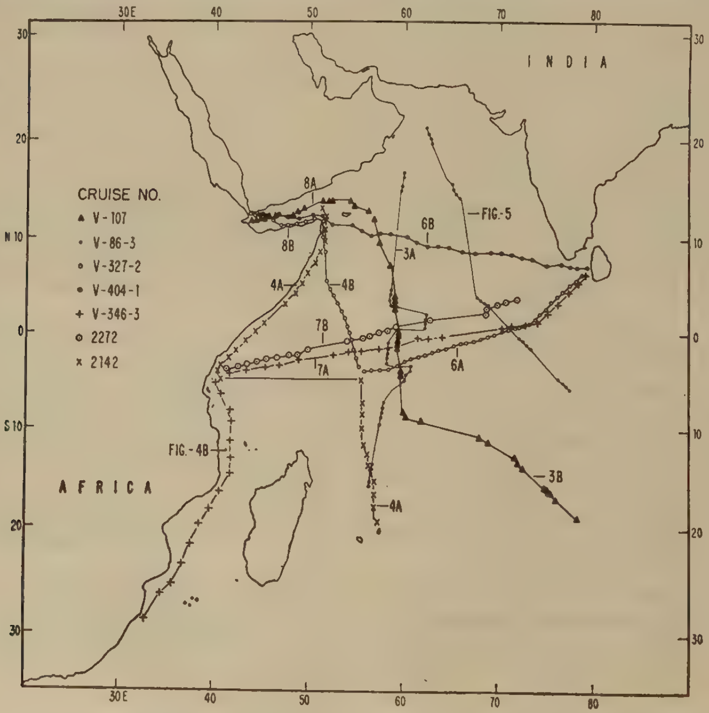
30E
40
50
60
70
80
30
20
N 10
0
S 10
20
30
INDIA
AFRICA
CRUISE NO.
▲ V-107
• V-86-3
○ V-327-2
● V-404-1
+ V-346-3
○ 2272
× 2142
8A
8B
6B
FIG.-5
3A
4A
4B
7B
7A
6A
FIG.-4B
3B
4A

FIG. 2.		
V–107–1	VI, VII–44	S.S. *Francis Lewis*
V–86–3	I, II, III–45	U.S.S. *Fort Niagara*
V–327–2	IV, VII–52	H.M.S. *Challenger*
V–404–1	X, XI–53	U.S.S. *Caperton*
V–346–3	V, VII–54	U.S.S. *Soley*
2272	XII–56	H.M.S. *Cheviot*
2142	V, VI, VII, IX, X, XI–57	H.M.S. *Ceylon*

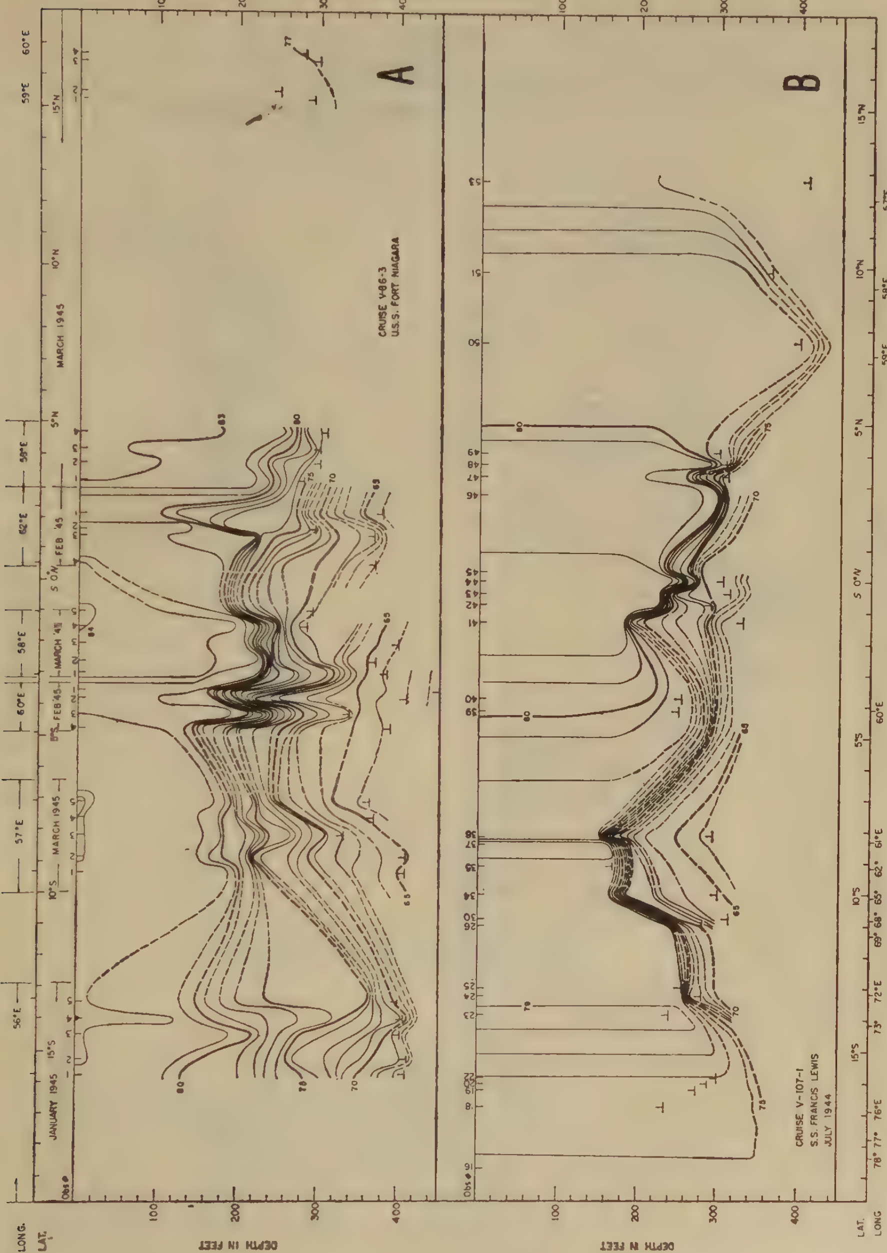

Fig. 3. Latitudinal Sections.

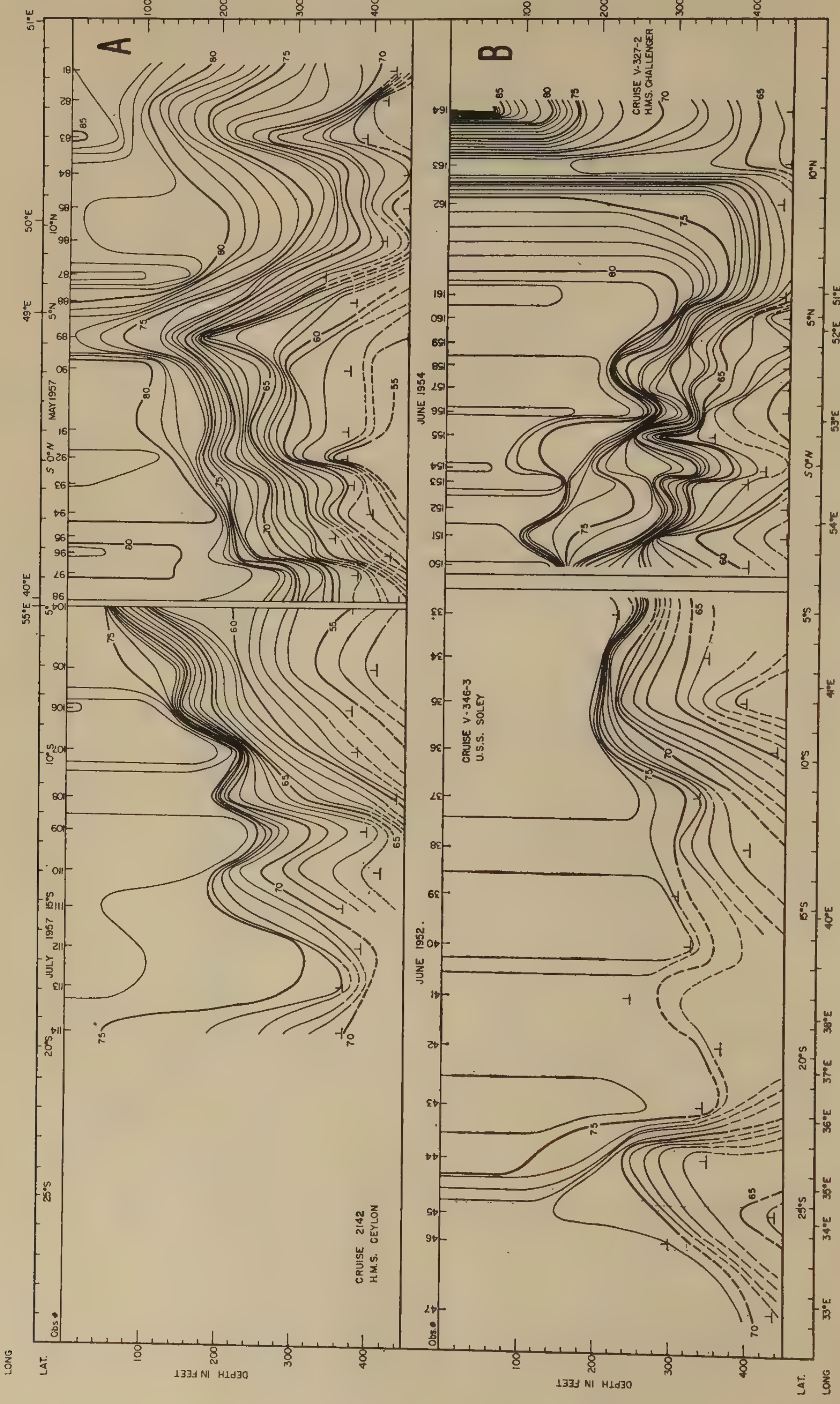

FIG. 4. Latitudinal Sections.

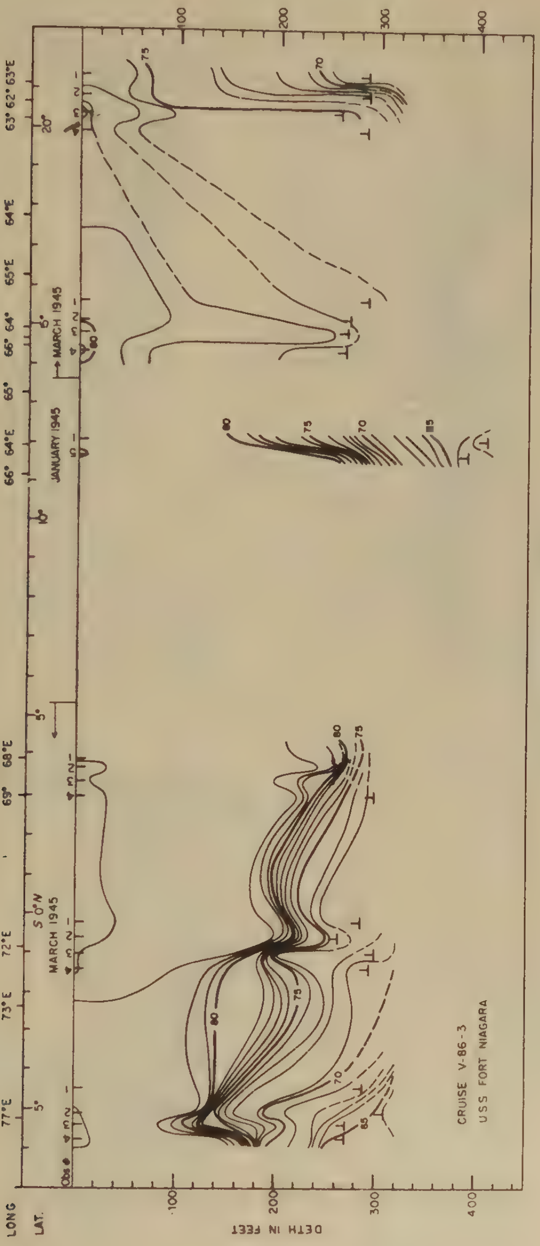

FIG. 5. Latitudinal Section.

(143)

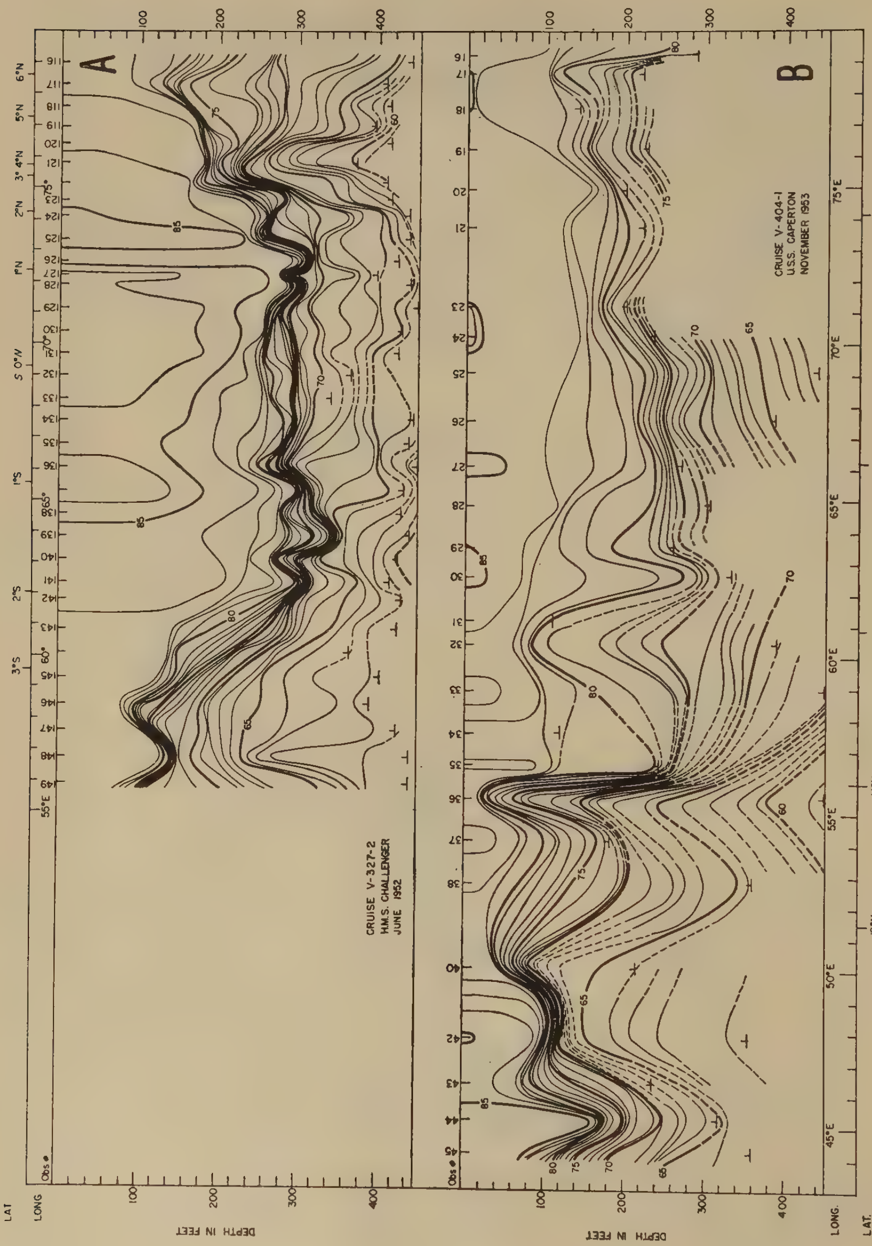

FIG. 6. Longitudinal Sections.

(144)

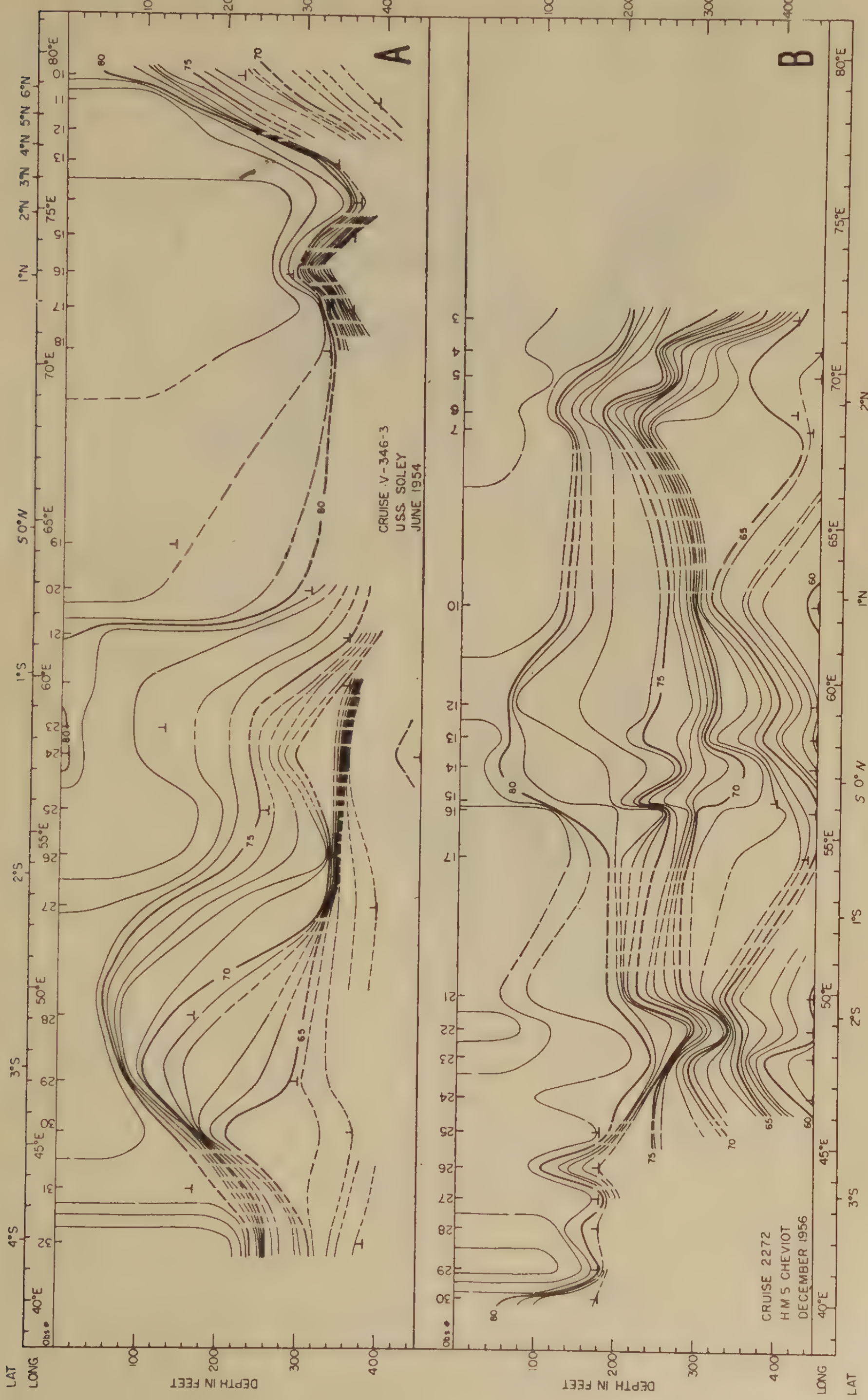

Fig. 7. Longitudinal Sections.

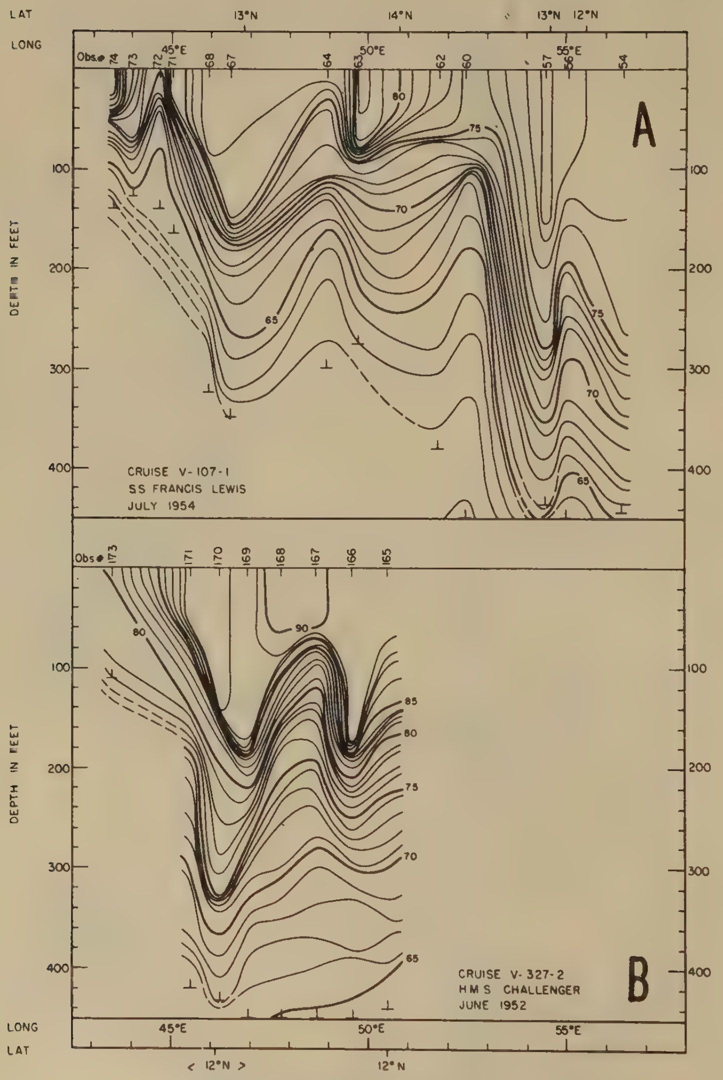

Fig. 8. Longitudinal Sections.

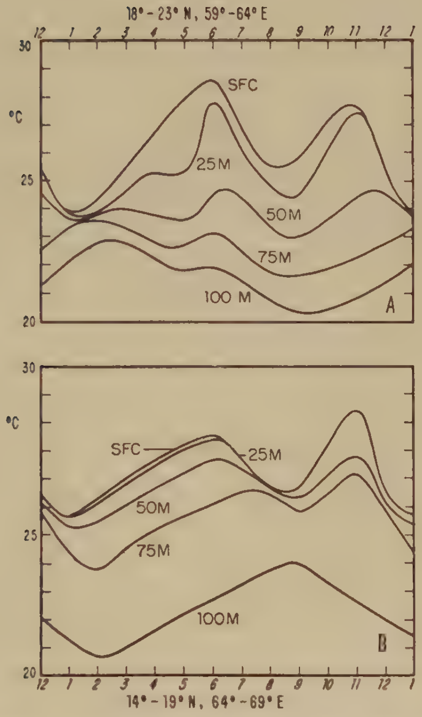

FIG. 9. Annual variation in the Arabian Sea from bathythermograph observations.

California Cooperative Oceanic Fisheries Investigations, a project sponsored by the Marine Research Committee of the State of California.

Scripps Institution of Oceanography,
La Jolla, California.
MARGARET K. ROBINSON

**Contribution from the Scripps Institution of Oceanography, New Series Number.*

REFERENCES

PATTULLO J., MUNK W., REVELLE R. and STRONG E. (1955), The seasonal oscillation in sea level. *Jour. Mar. Res.* **13,** 88–155.

Printed in Great Britain by The Salisbury Press Ltd., Publicity House, Wilton Road, Salisbury, Wilts. (21939)

(148)

Made in United States of America
Reprinted from Limnology and Oceanography
Vol. 5, No. 1, January, 1960
pp. 62–77

COMPARATIVE LABORATORY AND FIELD STUDIES OF PHOTOSYNTHESIS BY A MARINE PLANKTONIC DIATOM

by J. F. Talling

(149)

COMPARATIVE LABORATORY AND FIELD STUDIES OF PHOTOSYNTHESIS BY A MARINE PLANKTONIC DIATOM[1]

J. F. Talling[2]

Division of Marine Biology, Scripps Institution of Oceanography, California

ABSTRACT

A study is described of the factors affecting measurements of phytoplankton photosynthesis by the much used field method, based upon changes of oxygen concentration in clear and darkened bottles as determined by the Winkler method. Unialgal cultures of a marine plankton diatom, *Chaetoceras affinis*, were used with short exposures of 1–3 hours in both laboratory and sea. Indications of a limitation of photosynthetic rate by inadequate CO_2 supply were only found for culture media with pH raised by prolonged photosynthesis. Otherwise photosynthetic rates were unaltered by the bicarbonate concentration over a wide range, including that of unenriched sea-water, or by cell sedimentation in unshaken cultures. A comparison of the Winkler and manometric methods of measuring oxygen production gave very similar results. High rates of photosynthesis were well maintained over the main period of each exposure, despite the development of oxygen supersaturation. Lower rates were however always found during an initial induction phase.

Photosynthetic characteristics deduced from exposures in laboratory and sea, carried out almost simultaneously and with the same algal material, were in general agreement. Data from the experiments as a whole indicated the development of unusually high photosynthetic capacities at light saturation, assessed per unit content of chlorophyll *a*. The onset of light saturation, and the development of photo-inhibition, occurred at intensities similar to those recorded for many other plankton algae. Some ecological implications of the findings are discussed.

INTRODUCTION

Knowledge of the photosynthetic activities of natural populations of planktonic algae has been obtained from experiments in both laboratory and field. Each of these approaches has limitations. The laboratory experiment may provide well-defined data on the photosynthetic characteristics of the organisms, but any deduction of the distribution of photosynthetic activity in the natural environment of sea or freshwater involves uncertain extrapolations, even when given a better knowledge of environmental variables than is usually available. The field experiment, with exposures made in the water-body itself, may appear to give more directly applicable results, and indeed has been the source of most information on the subject. Nevertheless, although the data obtained may be valid for the local conditions of the experiment, they are usually unsuitable for a quantitative analysis of the principal factors involved, and so are difficult to incorporate into a generalized body of knowledge on the photosynthetic behavior of planktonic algae. The obstacles here arise partly from the heterogeneous nature of the populations sampled, and partly from difficulties of measuring the relevant environmental factors, such as light intensity, which may fluctuate considerably during an experiment.

Comparative laboratory and field experiments, using the same well-defined algal material, provide a means of integrating the two approaches. This paper describes such studies. Photosynthesis was followed by measuring the oxygen produced by *Chaetoceras affinis* Lauder during exposures in bottles suspended at various depths in the Pacific Ocean, and was compared with results from almost simultaneous exposures under a range of light intensities in the laboratory. Particular study was made of the relation between photosynthetic rate and light intensity in these two situations. Possible limitations in the method of determining photosynthesis by exposures of algal suspensions in closed bottles were explored,

---

[1] Contribution from the Scripps Institution of Oceanography, New Series. 1147

[2] Present address: Freshwater Biological Association, Ambleside, England.

Reproduced by Permission

(150)

and several photosynthetic characteristics of the diatom used were determined. The results are relevant to similar work in which photosynthetic activity is measured from the uptake of radioactive carbon (C^{14}).

The work was carried out during the tenure of a post-doctoral Rockefeller fellowship at the Scripps Institute of Oceanography, University of California, La Jolla. Grateful acknowledgment is made of the advice and assistance received from various people, particularly Dr. F. T. Haxo, Dr. B. M. Sweeney, Dr. K. A. Clendenning, Mr. M. Neushul, Mr. E. G. Cunnison, Mrs. Anne Dodson and Mrs. Nao Belser of the Department of Marine Botany. Invaluable help in the design and construction of apparatus was given by members of the Division of Special Developments.

MATERIALS AND METHODS

Unialgal cultures of *Chaetoceras affinis* were used throughout. This species had been isolated by Dr. B. M. Sweeney from Pacific coastal water and maintained in culture at the Scripps Institution of Oceanography for several years. It was chosen because of its ease of culture and fast growth of up to at least two cell divisions per day at 15°C. The species is widely distributed in coastal and offshore waters of the Pacific and other oceans. Although pronounced morphological aberrations were not found in healthy cultures, auxospore formation occasionally developed, with corresponding changes in average cell size, during the course of these experiments. Cultures were grown, and most of the following measurements of photosynthesis made, in an enriched sea-water medium containing 75% filtered sea-water. Its composition was based upon that used for *Gonyaulax polyedra* by Sweeney and Hastings (1957), modified by the addition of 5 mg/L of silicon (added as $Na_2SiO_3 \cdot 9\ H_2O$) and of various concentrations of potassium bicarbonate as described later. The large cultures intended for measurements of photosynthesis were grown in 2.5 L flasks at 14–16°C in a constant temperature room. An illumination of approximately 5,400 lux was provided by two fluorescent lamps below the cultures. Cultures were used when they had reached densities of 19,000–46,000 cells per ml, which were still considerably lower than the maxima attainable, about 100,000 cells per ml.

Photosynthesis was followed from changes in the concentration of dissolved oxygen, determined by the Winkler method. Samples of 100 ml were titrated with approximately N/160 thiosulphate, standardized with N/10 potassium dichromate solution. Exposures were made with the algal suspension distributed in ground-glass stoppered bottles of 'Pyrex' glass, capacity about 120 ml, filled from a siphon in a darkened room. Both clear and dark bottles were used in each exposure, and the gross photosynthesis, corrected for respiration, was obtained from the difference between them. Laboratory measurements were carried out with the bottles supported horizontally in a constant temperature water-bath, and illuminated from a bank of five 'daylight' fluorescent lamps placed immediately below the glass base of the bath. Minimum spacing between fluorescent tubes in the bank and between the bank and the bottles gave maximal illumination in the bottles of 2,100–2,500 lux. Each lamp was used with two ballasts connected in parallel to increase its total output. Three lower light intensities could also be obtained in a sequence along the long axis of the water-bath, using neutral filters made from exposed photographic film mounted in glass and placed on the bottom of the bath. The neutral transmission of the filters, in the spectral region 400–700 mμ, was checked spectrophotometrically. Three bottles could be inserted above each neutral filter, in a compartment isolated optically from its neighbors by partitions of blackened plastic. Owing to the extended nature of the light source, differences of light intensity across the depth of each bottle were negligible. Intensities at the levels of the bottles, on a plane perpendicular to the direction of the light source, were measured with a selenium rectifier-cell photometer (Weston model 756) calibrated in foot-candles but here converted to meter-candles or lux. The energy content of the radiation was also measured with a thermopile, yielding an interrelation of 44 ergs/cm^2/sec per foot-candle recorded by the photo-cell or 4.1 ergs/cm^2/sec per lux.

Field exposures were made near a fixed buoy in the ocean about one km. from the shore and laboratory. Bottles were filled with algal suspension in the darkened laboratory and transported in a dark container to this station. Here they were attached by spring clips to metal rings of approximately 60 cm diameter, and the latter fastened to a rope which supported both rings and bottles horizontally at various depths in the sea. The arrangement was devised as a modification of that described by Levring (1947), and enabled up to 9 bottles to be supported horizontally at any desired depth. Dark bottles exposed at several depths yielded almost identical values for respiratory oxygen uptake, which as in dark bottles in laboratory experiments was only a small fraction (0.05–0.2) of the maximum photosynthetic rate. As the sea exposures described here were of short duration, of one to one and a half hours, and were carried out in full sunshine about midday or early afternoon, changes in the intensity of incident solar radiation were small, not exceeding ± 10%. Continuous records were taken with an Eppley thermopile ('pyrheliometer') situated on the roof of the laboratory and used to calculate the mean irradiation on a horizontal surface during each experiment. Radiant energy in the spectral region available for photosynthesis was taken as 0.46 of the total energy recorded (Talling 1957a).

Light intensities at various depths in the ocean were calculated from the surface intensity, reduced by 5% representing surface loss (estimated from the solar elevation and data in Davis 1941 and in Anderson 1952), and measurements of underwater light penetration. The latter were made with a selenium rectifier photo-cell (Weston model 856 RR) in conjunction with red, green and blue Corning glass filters. Measurements were restricted to the linear region of the current-intensity characteristic of the photo-cell, corresponding to photo-currents below 700 μa. The mean extinction midpoints of the cell-filter combinations, in their working depth ranges, were estimated as respectively 450, 525, and 625 mμ; these values were calculated from the spectral sensitivity of the cell, spectral transmission of the color filters, and color-filter action of the sea-water. Values of the percentage transmission (T) per meter were derived from measurements in each spectral region. They were compared with the families of curves obtained by Jerlov (1951, Fig. 48) to describe the variation of T with wavelength in the spectral region 400–700 mμ, from which data for the spectral regions between the experimental points were interpolated. Using the resultant curves for the spectral variation of T, and the data of Taylor and Kerr (1941, Fig. 8, curve D) for the spectral distribution of energy in the surface-incident light, the spectral distribution of energy (400–700 mμ) was calculated for the depths at which photosynthesis was measured. Planimetric integration of the areas under these spectral distribution curves (see, Sverdrup, Johnson and Fleming 1942, p. 105) enabled the total radiant energy (400–700 mμ) at each depth to be expressed as a percentage of the sub-surface intensity. Knowing the latter, the absolute irradiation at each depth could be calculated. The results were very similar to those derived by a more approximate procedure (used by Jenkin 1937 and Talling 1957a) in which the radiant energy is divided between a few spectral blocks whose contributions are summed for each depth. In these field experiments the water-column showed an optical discontinuity, with more turbid water below (Figs. 5 and 6); consequently the calculation outlined above had to be performed in two stages.

Considerable vertical stratification was also shown in the depth-distribution of temperature, which was measured during each experiment with a bathythermograph. Tests were made to determine the rate of equilibration of temperature between the contents of experimental bottles and a colder surrounding medium of flowing water. After 10 minutes exposure the remaining temperature difference was less than 1°C when the initial difference was 7°C; the latter value would not be exceeded under the conditions of the field experiments.

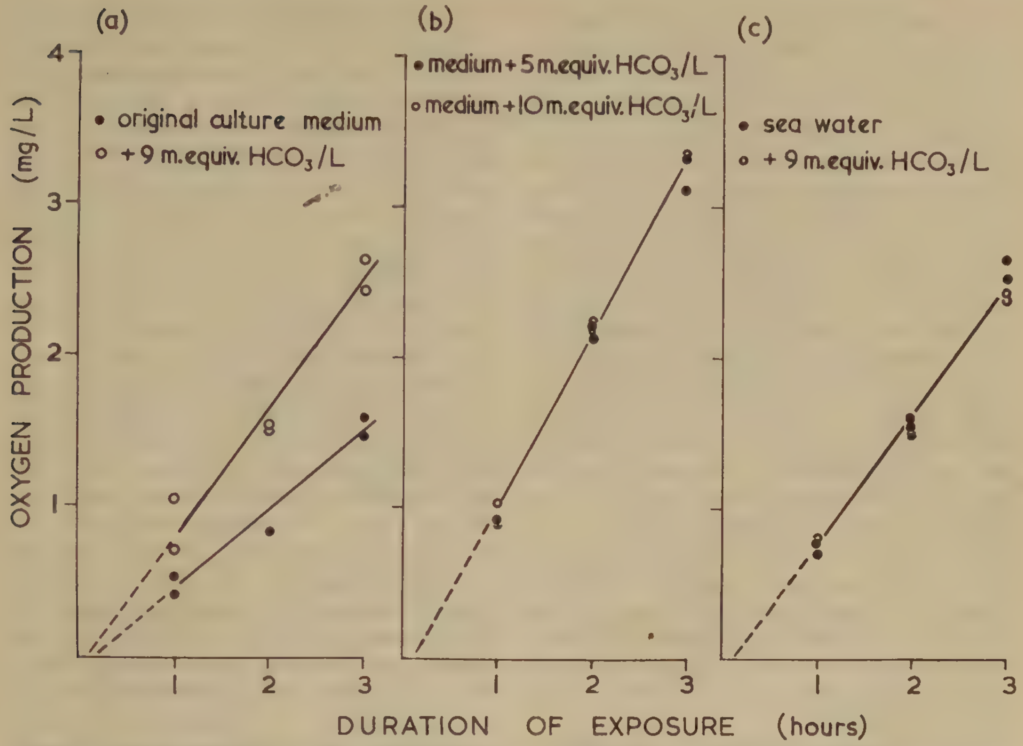

Fig. 1. Photosynthesis in media containing various supplementary additions of bicarbonate. These were made (a) to the original culture medium, (b) to the new culture medium with 5 m equiv of bicarbonate/L, (c) to cells resuspended in filtered sea water.

The densities of the algal suspensions were normally estimated from both cell counts and chlorophyll *a* determinations. Counts were made in duplicate upon volumes of 0.05 ml, counted on a normal microscope slide using the scanning procedure of Utermöhl (1936, Fig. 648). Chlorophyll *a* was estimated by the spectrophotometric method of Richards and Thompson (1952), the cells being first separated by paper filtration. Complete extraction of pigment from the cells was obtained within 3 hours.

FACTORS CONTROLLING PHOTOSYNTHESIS UNDER LABORATORY CONDITIONS

Some knowledge of the factors affecting photosynthesis under laboratory conditions was sought before attempting the analysis of photosynthetic behavior in the sea. Most measurements (in sections i–iii below) were made with high light intensities known to give complete light-saturation of photosynthesis and within a small temperature range (14–16.5°C). The variation of photosynthetic rate with temperature was not determined.

(*i*) *Composition of the medium*—It was clearly desirable to avoid determinations of photosynthesis in unfavorable media, particularly with respect to carbon dioxide and the associated carbonate-bicarbonate buffer system. Figure 1 illustrates comparative measurements of photosynthesis in a number of modifications of the culture medium previously used for the routine subculture of the diatom. The buffer capacity of the original medium was insufficient to prevent a considerable increase of pH (*e.g.* from 8.3 to 9.0) during the growth of cultures to the required density. Photosynthesis in such an alkaline medium (pH 9.0, combined CO_2 1.5–2.0 m equiv/L) is shown in Figure 1a, together with the improved rate obtained by the further addition of 9 m equiv/L of $KHCO_3$ and concomitant reduction of the initial pH to 8.5. Further experiments (Figs. 1b, 2b) showed that this response to added bicarbonate could be eliminated by the addition of 5 m equiv/L of bicarbonate after autoclaving but before inoculation of the cultures. This new culture medium with increased buffering, in which pH was maintained below 8.7, was adopted in all subsequent work. Nevertheless one experiment (Fig. 1c) showed that cells removed from an original culture by filtration, and resuspended in filtered sea-water of pH 8.3, yielded a rate of photosynthesis equal to that of similar cells resuspended in sea-water, enriched by 9 m equiv/L of bicarbonate at pH 8.1. For short exposures, therefore, in which the demands upon the carbon dioxide supply of the medium are small, sea-water without bicarbonate enrichment would appear an adequate medium. Inadequate buffering appears only after the longer exposures used during growth of the cultures to suitably high densities.

(*ii*) *Agitation of the cell suspensions*—Much criticism (*e.g.*, Emerson and Green 1934, Emerson 1935) has been levelled against measurements of photosynthesis by aquatic plants in unshaken and sealed vessels, particularly when large samples of macrophytes were used. Limitations of gaseous diffusion in unstirred media are likely to be minimal for dilute suspensions of unicellular algae, but few tests of this point are recorded in the abundant ecological literature (see, however, Talling 1957a, Doty and Oguri 1958). An experiment was therefore made to test whether rates of photosynthesis differed between unshaken suspensions in which cells were allowed to sediment and suspensions in which shaking by hand every 15 minutes maintained cells in free circulation. Continuous shaking by horizontal movements, with glass beads in the bottles, was also tested but found to be mechanically inadequate for these completely filled bottles. The experimental results (Fig. 2a) show almost identical rates of photosynthesis in shaken and unshaken bottles, despite a considerable sedimentation of cells which occurred in the latter during the three-hour exposure. Several test conditions were more severe than those likely to prevail in ecological field experiments, notably the high algal density (41.7×10^6 cells, or 0.081 mg chlorophyll *a*/L) and high photosynthetic rate (2.37 mg oxygen /L hour). The latter was the highest rate in the present experiments, being probably accelerated by the higher temperature chosen for this exposure (19.7±0.4°C, compared with 14–16.5°C in all other laboratory experiments).

Rates of photosynthesis under light saturation were also compared, using unshaken Winkler bottles and continuously shaken Warburg manometers, at 15.0–15.5°C. The manometric measurements were carried out by Dr. K. A. Clendenning as follows. All cells were derived from the same culture, of which a portion was concentrated by paper filtration to yield the higher cell densities required for the manometric measurements. The cells were centrifuged from this concentrate and resuspended in fresh growth medium with additions of bicarbonate, giving total bicarbonate enrichments of 5–25 m equiv/L at pH 8.3. The cell density so obtained was 24 times higher than that employed for the Winkler determinations. Under the conditions of the Winkler and manometric measurements, the light-saturated rate of photosynthesis was not increased by raising the bicarbonate enrichment above 5 m equiv/L. The rates of photosynthesis observed manometrically with 5 m equiv/L bicarbonate, during the first hour after induction, were within the range of the corresponding Winkler measurements shown in Figure 2b. The agreement between the two methods is noteworthy in view of the very different conditions of shaking and cell concentration which were involved. Manometric measurements of photosynthesis have been made on another species of *Chaetoceras* by Sagromsky (1943), who could not show any injurious effects of the shaking involved. A direct experimental comparison of the two methods, similar to that described above, appears to be lacking in previous work, despite the extensive literature on each method.

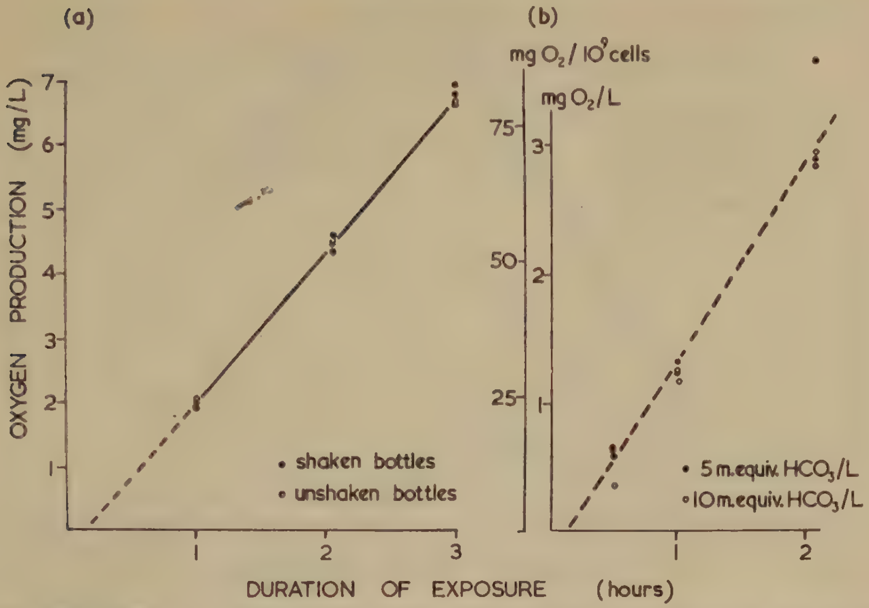

FIG. 2. Photosynthesis in shaken and unshaken cell suspensions, measured by (a) the Winkler method only (b) the Winkler and manometric methods. In (b) the mean rate obtained manometrically is expressed by the gradient of a broken line which is superimposed on Winkler determinations of oxygen production in two unshaken media.

(*iii*) *Variation of photosynthetic activity during exposures*—Measurements of photosynthesis in closed bottles are usually expressed as average rates over the periods of exposure, in which possible short-time changes of activity are not distinguished. Such changes can be followed either by repeated sub-sampling from each bottle, which is impracticable with the Winkler oxygen determination, or by use of replicate bottles which are sampled in succession. Both alternatives are inconvenient in field experiments, but successive sampling of replicate bottles has been used whenever possible in the present laboratory experiments. Results are illustrated in Figures 1, 2 and 3, from which the variation of photosynthetic rate with time can be followed within the exposure limits of 3–3¼ hours used.

In all experiments the time course of photosynthesis shows two general features. An almost constant rate is maintained during the second and third hours of each exposure, despite an increasing supersaturation with oxygen. In the first hour or half-hour the overall rate is lower, and extrapolation shows that it is *equivalent* to a lag of 6–18 minutes succeeded by the rate maintained during most of the exposure. This 'lag-equivalent' is shown by exposures in a wide range of light intensities (Fig. 3), although all these intensities were higher than the very low intensities prevailing when the bottles were being prepared. An induction phase of photosynthesis is therefore likely to occur in all exposures. The 'lag-equivalent' is also seen in exposures involving cells with different photic histories (Fig. 3).

These results clearly imply that rates measured in a single uninterrupted exposure will underestimate the rates finally realized under the same conditions. Thus in the combined laboratory and sea experiments described later with exposures of 1–1½ hours, the probable underestimation is 7–30%. This factor will diminish with increasing length of exposure; its small significance for exposures of 3 hours is illustrated in Figure 3d. Steemann Nielsen and Jensen (1957) have also described lower initial rates of photosynthesis during exposures with a natural

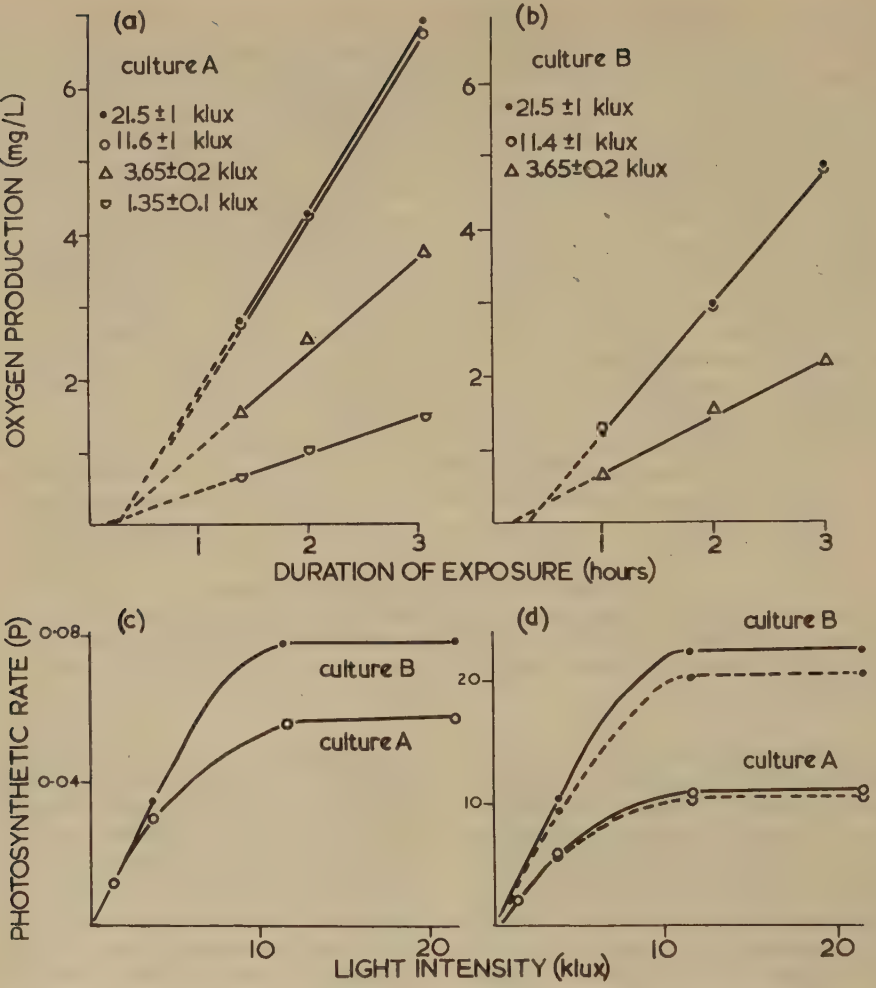

Fig. 3. Photosynthesis–time measurements for two cultures at various light intensities (above), with average gradients inserted and used to derive rate–intensity curves (below). Culture A was grown at 0.97 klux, and B at 5.4 klux, followed by darkness for 2 days. Photosynthetic rates (P) are given in mg oxygen/mm^3 cell volume hour (c) and in mg oxygen/mg chlorophyll *a* hour (d). Broken lines in (d) show the overall rates of photosynthesis during the longest exposures.

population of surface plankton. They attribute this to an after-effect of light-inhibition, an explanation which is not applicable to the present results.

(*iv*) *Light intensity*—Without some knowledge of the relation between photosynthetic rate and light intensity an individual measurement of photosynthesis has little significance, as rates ranging from zero to the light-saturated capacity can be obtained at various intensities. Rates measured at light saturation (here denoted by P_{max}) allow the most direct comparison between laboratory and field experiments. The achievement of such conditions in the laboratory is described below, and the variation of rates with light intensities below saturation is discussed.

The general form of the rate-intensity relation is shown by data from laboratory experiments conducted simultaneously with exposures in the sea (Figs. 5c, 6c). Very similar curves were obtained in four other experiments, not illustrated. An upper

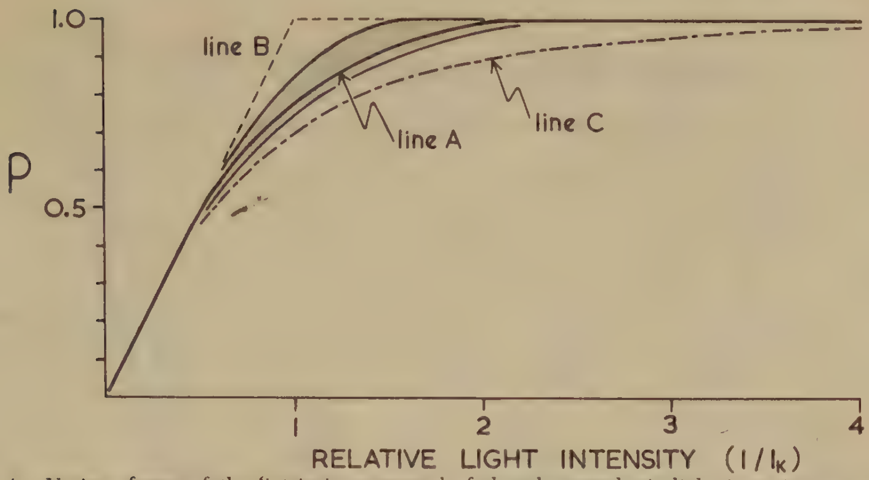

Fig. 4. Various forms of the 'intrinsic curvature' of the photosynthesis–light intensity curves below light saturation. Rates of photosynthesis are expressed as fractions (p) of the rate at light saturation, and light intensities in multiples of the I_K characteristic. The heavy line A indicates the average relation, and the stippled area the range of variation, in the present experiments. Line B shows the initial linear region continued up to the light-saturated rate: line C shows the relationship of Smith (1936, equation 1) here expressed as $p\ (1 - p)^{-\frac{1}{2}} = I/I_K$.

'plateau' on the rate-intensity curves provides good evidence that light-saturation is fully realized at the highest intensities used, 24,000–27,000 lux. The onset of saturation in relation to the light intensity scale can be indicated by the intensity at which extrapolations of the initial linear gradient and final saturation 'plateau' intersect (see Fig. 5c; also Kok 1956a, b, Talling 1957a). This intensity, here denoted by I_K, varied little (between 4,600–6,800 lux) in five experiments, all at temperatures between 14 and 16.5°C.

Considerable interest attaches to the form of the 'intrinsic curvature'—the curvature property independent of the absolute scales used—shown by the rate-intensity curves at intermediate light intensities. With P_{max} and I_K variables, it can be used to summarize much of the rate-intensity characteristic. It has received little attention in ecological work, often being completely neglected (*e.g.* by Ryther 1956). Modifications associated with optically dense suspensions (Rabinowitch 1951, p. 1008) are unlikely to be appreciable with the relatively thin suspensions used in this and most other ecological work. The description of such intrinsic curvature is possible either by the application of a mathematical relation (*e.g.* Kok 1956b, Talling 1957a), or by plotting curves with standard scales for the light-saturated rate (P_{max}) and the initial linear gradient. The latter approach is the more flexible and is illustrated in Figure 4. The same figure (line C) shows the form of curvature implied by the relation proposed by Smith (1936, equation 1) and used in several previous studies (*e.g.* Winokur 1948, Talling 1957a). The approach to light-saturation so derived is clearly more gradual than the experimental data indicate. Similar divergence is shown in some, but not all, of the data of Talling (1957a) obtained from studies of a freshwater plankton diatom. Steemann Nielsen and Jensen (1957) have stated that the equation was inapplicable to their rate-intensity curves for marine phytoplankton, but the type of curvature appears variable and the attainment of complete light-saturation is sometimes not established. Other equations, such as that of the rectangular hyperbola, have been tested here with even less success. Consequently the curvature relation is probably best expressed in a standardized graphical form, as in Figure 4, although errors can easily arise in estimating the initial gradient of the curves.

A further experiment was designed to ob-

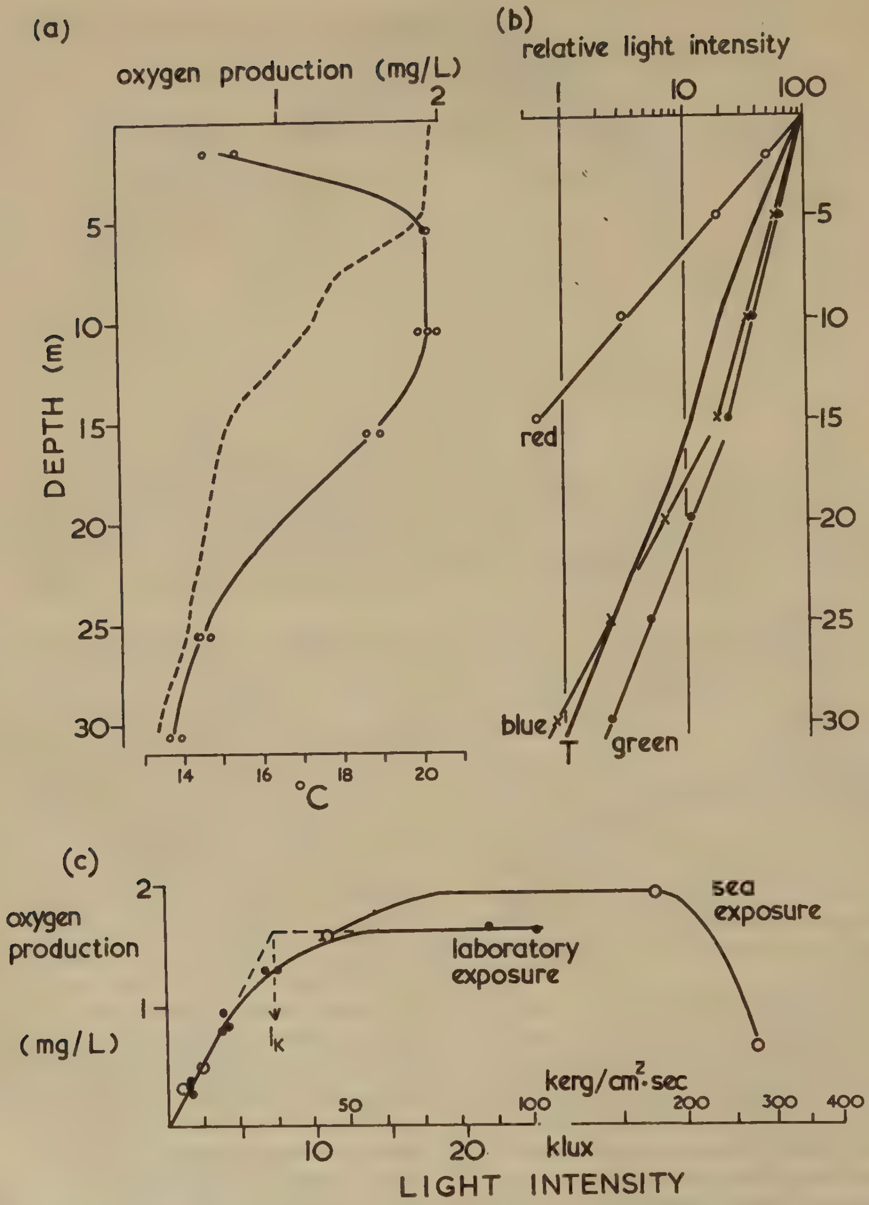

FIG. 5. Combined field and laboratory experiment of 5 Aug., 1957, showing (a) the variation of photosynthetic rate (solid line) and temperature (broken line) with depth, (b) light penetration measured for three spectral regions and of total energy (T) in the region 400–700 mμ, (c) the variation of photosynthetic rate with light intensity (higher intensities shown on a logarithmic scale) obtained from both laboratory and sea exposures.

tain data on the rate-intensity characteristic from exposures in which a time-sequence of determinations enabled the effects of the initially lower rates to be eliminated. The same experiment included a comparison of two sets of cells given different pre-treatments, one being grown at a low intensity of 970 lux, and the other at the normal cul-

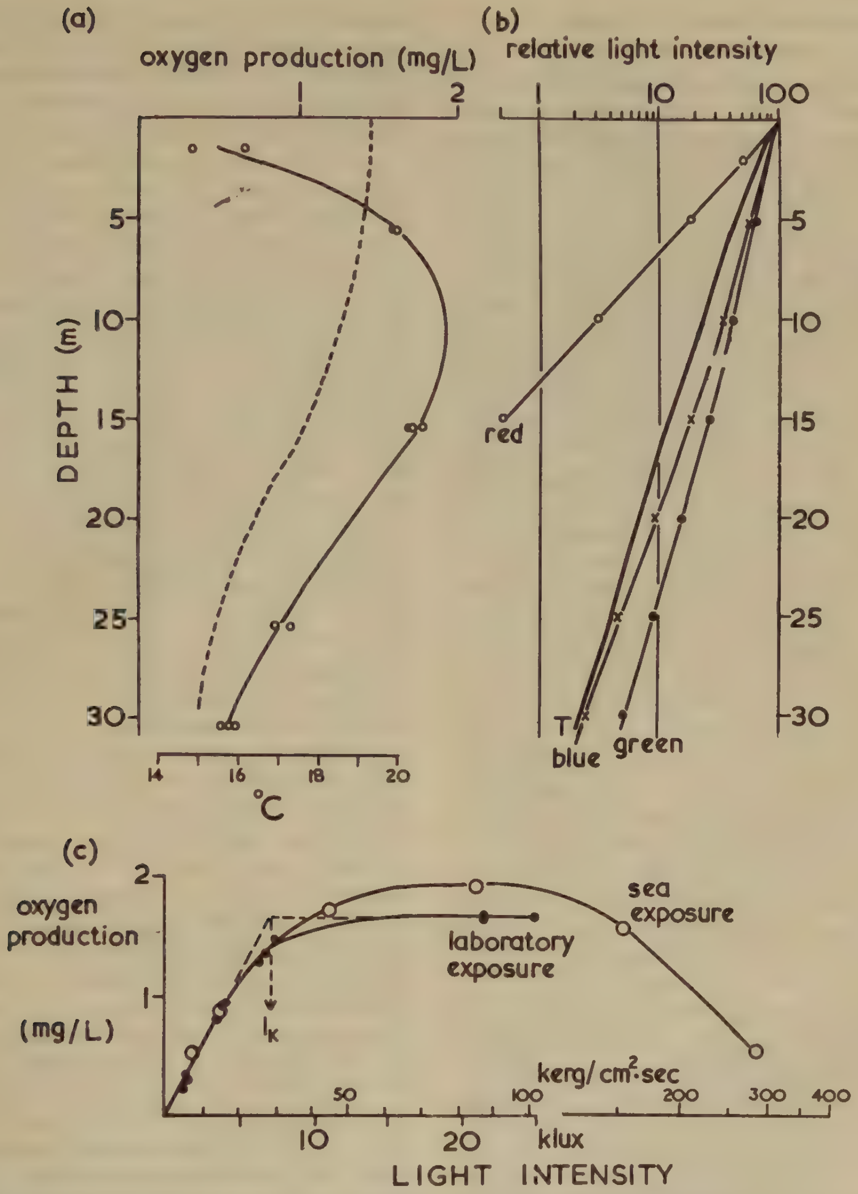

Fig. 6. Combined field and laboratory experiment of 7 Oct., 1957. Representation as in Figure 5.

ture intensity of 5,400 lux but then kept in darkness for two days. Figure 3 illustrates both the original oxygen determinations and the derived rate-intensity characteristics. The latter do not show any appreciable modification in the intensities at which light saturation developed. Similar behavior by cultured populations of several planktonic algae, grown under different types of illumination, is described by Ryther (1956). However, marked modifications have been found in several natural populations, when the characteristics of algae obtained from various depths have been compared (Steemann Nielsen and Hansen 1959, and unpublished experiments of the author).

PHOTOSYNTHESIS IN THE SEA AND LABORATORY COMPARED

Rate-intensity characteristics have been calculated for two experiments, in which simultaneous field and laboratory exposures with the same algal material were made. Figures 5 and 6 illustrate the variation of photosynthetic rate with depth, with the vertical gradient of light intensity expressed for three spectral regions and for the entire visible spectrum (400–700 mμ). From these data the corresponding rate-intensity curves are derived, each depth being replaced by the equivalent light intensity expressed as an energy flux for the 400–700 mμ spectral region. For each experiment direct comparison can be made with the rate-intensity curves obtained in the parallel laboratory exposure with fluorescent illumination. Intensities of the latter are also expressed in terms of energy flux, using the factor noted above; the limits of the spectral region involved (illustrated by Withrow and Withrow 1956, Fig. 3–15) were close to the limits of 400 and 700 mμ adopted in calculating light intensities in the sea. The rate-intensity curves obtained from the sea exposures suffer from various complicating influences connected with the vector distribution and spectral modification of underwater light (see below), so that their correlation with laboratory data is, *a priori*, uncertain. An important difficulty was the presence of vertical gradients of temperature in the sea (see Figs. 5 and 6). The laboratory temperatures, 14.9–16.4°C, were chosen to lie near the centers of the ranges occurring in the photic zone of the sea. Experiments in which the sea surface temperature exceeded 20.5°C are not illustrated.

The variation of photosynthetic rate with depth is of a form familiar from many other studies, both in the sea and freshwater. Much of it can be deduced from the rate-intensity characteristic measured in the laboratory, considered in relation to the almost exponential decrease of photosynthetically active radiation with depth in the sea. The initial linear region of the rate-intensity characteristic corresponds to the lower 'hollow' part of the rate-depth curve; the succeeding 'plateau' region at light-saturation is also reflected, in an abbreviated form, in the depth curve. A partial inhibition of photosynthesis is present at the higher light intensities near the sea surface, which were not attainable with the fluorescent lighting used in the laboratory exposures. The general form of the inhibition, and the intensities under which it developed, resemble those recorded in several other field studies with planktonic diatoms (Jenkin 1937, Talling 1957a). Nevertheless the extent of the inhibition may well depend on the spectral composition of the underwater radiation, particularly in the blue (Kok 1957a) and ultra-violet regions. Consequently the general validity of a calculation of the depth-distribution of photo-inhibition in nature, based on measurements in sunlight reduced by 'neutral' filters (Ryther 1956, Steemann Nielsen 1958, p. 45), is not established. Even direct field measurements of the inhibition may be influenced by the absorption of ultra-violet radiation in the glass walls of the experimental vessels (Gessner and Diehl 1951, Gessner 1955, p. 415). This factor requires further investigation.

Quantitative comparison of the photosynthetic behavior in laboratory and sea exposures can be based upon (i) the rates obtained at light saturation (P_{max}) or (ii) the initial gradients of the rate-intensity curves ($= P_{max}/I_K$). These features have contrasted responses to two factors (Rabinowitch 1951, 1956), temperature and spectral composition of the illumination, which differ between exposures in laboratory and sea. Temperature differences are likely to alter (i) but not (ii), but for spectral differences this situation is reversed. Both characteristics are displayed in Figures 5 and 6, which show considerable agreement between photosynthetic behavior in laboratory and sea. Rates at light-saturation are slightly higher in the sea exposures, but the differences probably result from the higher temperatures present in the upper layers of the sea. As such rates measured in the laboratory have been shown to be uninfluenced by cell sedimentation in unshaken bottles, the limitation of rates measured in field experiments by this factor is very unlikely. At lower light intensities the gradients of the rate-intensity relationship agree between both types of exposure. This similarity, with the small differences between the light-saturated rates, determines the correspondence betwen I_K values measured in laboratory and sea.

SOME PHOTOSYNTHETIC CHARACTERISTICS OF *CHAETOCERAS AFFINIS*

Although not the main object of these experiments, some descriptive information was accumulated on the photosynthetic characteristics of the diatom used. It is discussed below in relation to the few other comparable data which are available for the ecologically important algae of the marine and freshwater plankton.

The onset of light saturation of photosynthesis in relation to light intensity is an important determinant of the depth-distribution of photosynthetic rates; it can be characterized by a single intensity the I_K value. Its variation in natural populations of phytoplankton is poorly understood, but includes the effects of a pronounced, though often neglected temperature dependence. The present laboratory experiments yield I_K values between 4,600 and 7,700 lux, or an estimated equivalent of 19–32 kerg/cm^2 sec, at 14–16·5°C. The results of the sea experiments are similar but involve a greater temperature range. Wider comparison is often difficult, as other work with planktonic algae has frequently involved light fields with different spectral qualities and the use of different instruments or means of calculation for estimating light intensities. There is a general similarity with the values indicated for planktonic algae, particularly diatoms, at comparable temperatures (*e.g.* Jenkin 1937, Sagromsky 1943, Ryther 1956, Talling 1957a). The most conspicuous divergencies are shown by the high saturation intensities obtained for the surface phytoplankton of tropical oceans by Steemann Nielsen (1952) and Steemann Nielsen and Jensen (1957), using fluorescent illumination and an indirect means of assessing the effective light intensities.

The maximum photosynthetic capacity of a unit quantity of algae, measured under light-saturation, is another characteristic useful for analytical and comparative purposes. Three indices of algal quantity were used here: (i) cell numbers, (ii) cell volume, calculated from cell numbers and cell dimensions, and (iii) chlorophyll *a* content. The first is unsuitable as a general measure owing to the variation of cell size, which also contributed to changes of chlorophyll *a* content per cell. Contents measured for 11 healthy cultures grown at 5,400 lux varied from 1.0–3.6 mg chlorophyll $a/10_9$ cells; a single culture grown at 970 lux gave the highest value of 4.6 mg/10^9 cells. Rates based upon cell volume and particularly chlorophyll *a* content have been much used in other studies of phytoplankton photosynthesis and productivity, although the experimental conditions have often been ill-defined especially as regards media, temperature, and light-saturation. The present laboratory experiments, carried out at 14–16°C using adequately buffered media and cells grown at 5,400 lux, yield rates of 29–32 mg 0_2mg chlorophyll *a*/hour for the four longer experiments in which the initially lower rates can be eliminated (Figs. 1, 2 and 3). These values are much greater than those commonly reported for either cultured or natural populations of algae. Ryther and Yentsch (1957) have based a method of calculating photosynthetic production in the sea upon an average value of 3.7 g C/g chlorophyll *a*/hour, which is equivalent, using their value of 1.25 for the photosynthetic quotient, to 12.3 mg O_2/mg chlorophyll *a*/hour. The present experiments provide fewer data for rates based upon cell volume, owing to uncertainties in estimating volume for geometrically complex cells. The values obtained from two laboratory experiments, under the conditions listed above, are 0.048 and 0.073 mg 0_2/mm^3/hour; in the first figure the effect of the initial 'lag' is eliminated. These rates are also higher than most values previously published for natural populations of phytoplankton (Verduin 1956), although higher values are not unknown (Talling 1957c).

Little is known concerning the variation of photosynthetic behavior between cells with different histories, which can be important in other algae (*e.g.* Sorokin 1958). An experiment already described (Fig. 3) compared the behavior of cells grown at a low light intensity of 970 lux with that of cells grown at a higher intensity of 5,400 lux and then kept in darkness for two days. These differing pre-treatments had little effect on the I_K characteristic, but light-saturated rates of photosynthesis were lower in cells cultured at the lower intensity whether expressed in terms of cell numbers, cell volume, or chlorophyll *a* content. The relatively vigorous activity of cells after two days in darkness is ecologically significant, as such dark conditions must often befall cells circulating in nature. A similar response has been obtained with a freshwater plankton diatom (Talling 1957a).

DISCUSSION

Most of the numerous recent measurements of photosynthesis of phytoplankton populations have involved attempts to duplicate, in field experiments, conditions prevailing in a natural water-body during a certain time. As even the field experiments described here involve simplified conditions, such as uniform algal material and short exposures, many factors affecting the populations in nature are not represented. Examples include the possible differentiation of photosynthetic capacities between cells circulating at various depths or photosynthesising at different times of the day. Nevertheless such simplification allows a better resolution of many important factors and permits direct tests of the application of laboratory data to field conditions.

Within these limits, the results generally support the value of measurements based on exposures in closed bottles even when, as in field experiments, effective shaking of the cell suspensions is not possible. The conditions controlling the appearance of secondary effects during long exposures (*cf.* also Ryther and Vaccaro 1954, Vollenweider 1956, Bauer 1957, Rodhe 1958) are not explored, but the photosynthetic rates were shown to be well maintained in exposures of up to three hours. They appeared only slightly modified by lower initial rates, in which induction phenomena were presumably involved. The effectiveness of the method of following photosynthesis by the Winkler oxygen estimation is particularly noteworthy in view of the relatively high algal densities and photosynthetic rates involved. It has been suggested (Steemann Nielsen and Jensen 1957) that uptake of iodine by unsaturated algal constituents may render the Winkler method unusable with dense algal populations. This consequence is not shown in the present experiments or many others described in the literature. The measurements here also show no indications of ill-effects due to the supersaturation with oxygen which resulted from high photosynthetic rates. Similar results were obtained by Vinberg (1934), using the Winkler method with freshwater phytoplankton. In general a marked supersaturation is undesirable, due to its possible effects on bubble-formation and rates of respiration (Gessner and Pannier 1958a,b). Recent unpublished work by the author demonstrates that the Winkler oxygen determination can also be used to detect photosynthetic changes as low as 0.02 mg/L, about two orders of magnitude lower than the changes involved in the present experiments.

Experiments which combine both laboratory and field exposures have relevance for the various recent attempts to use laboratory data for estimating photosynthetic productivity in nature (Ryther 1956, Ryther and Yentsch 1957, Rodhe, Vollenweider and Nauwerck 1958, Cushing 1958). A principal difficulty here is the comparison of light intensities measured in the two situations, particularly in view of the progressive spectral modification of underwater light with depth, which cannot be reproduced by a single color filter as used by Cushing (1957, 1958). A full comparison would require evaluation of the effects of differing qualities of vector and spectral distribution of radiation in laboratory and sea, the latter considered in relation to the action-spectrum of photosynthesis. The present assessment of effective light intensities, by the total energy flux of photosynthetically active radiation, is only an approximation but has value for interpreting field experiments under different conditions. Here it has given

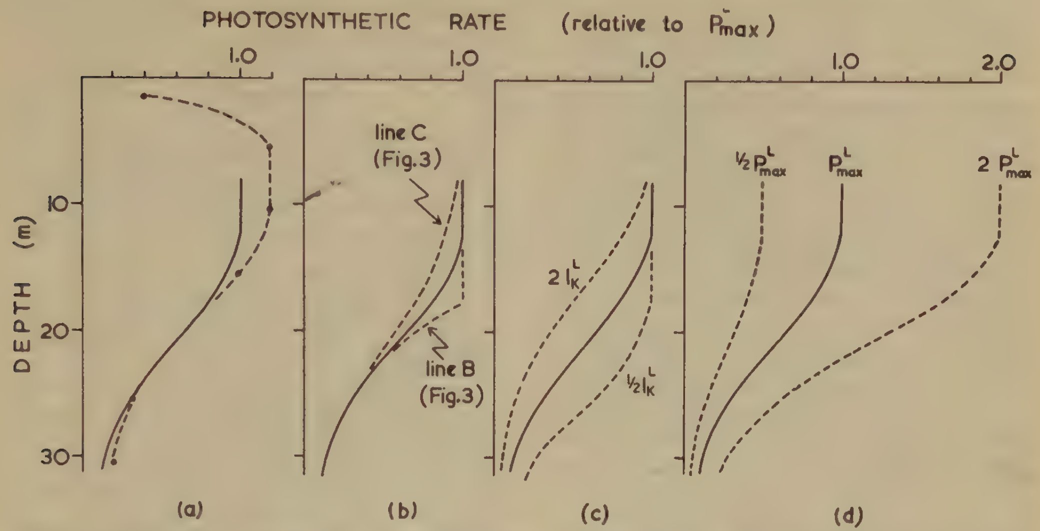

Fig. 7. The depth distribution of photosynthetic rate (full lines) calculated from the laboratory rate–light intensity curve, and the intensity–depth curve, for 5 Aug., 1957. With this depth distribution are compared (a) the photosynthetic rates measured *in situ*, (b) the depth distribution of rates calculated from two variants of the rate–intensity curve (see Fig. 4), (c) the depth distributions calculated for given changes in the I_K characteristic, and (d) for the same changes in the P_{max} characteristic. All photosynthetic rates are expressed relative to the laboratory value at light saturation ($P_{max}{}^L$).

general agreement between rate-intensity characteristics of photosynthesis measured in the laboratory and at sea, so providing some support for the use of such laboratory data in calculating the vertical distribution of photosynthetic rates in nature. Such a calculation is illustrated in Figure 7. Because of the approximations involved, the agreement should be regarded as a working correlation rather than the outcome of a physically and physiologically adequate comparison. However, the type of calculation appears more complete than that involved in any previous comparison of laboratory and field experiments with planktonic algae. Thus the correlative relationship established by Steemann Nielsen (1952) does not include a direct comparison of specific light intensities or their effects. Ryther (1956) has described and compared rate-intensity characteristics of photosynthesis measured in the sea and in sunlight reduced by graded neutral filters. His estimates of underwater light intensities in foot-candles are based upon a single vertical extinction coefficient expressing the diminution in the response of a photo-cell with depth, and suffer from limitations discussed by Lund and Talling (1957) and Strickland (1958).

For many ecological purposes, estimates are needed of the total photosynthetic production below unit area. This can be expressed by the area enclosed by a photosynthesis-depth profile, and can be related to the individual variables controlling the distribution of photosynthetic rate with depth (Talling 1957b). When this depth distribution includes a well-developed region with light-saturation, as illustrated in Figures 5 and 6, it can easily be shown (Fig. 7) that the area mentioned is much more sensitive to variation in the maximum rate (P_{max}) than to similar variation in the onset of light-saturation (expressed by I_K). This feature is expressed in the equations derived by Talling (1957b) to relate the areal production to the P_{max} and I_K variables. With these conditions the experimental errors in determining I_K are less significant than errors in P_{max}, for which measurement of light intensity is not required. The obvious uncertainties in the measurement of I_K, therefore, are unlikely to affect strongly the final calculation of areal production.

Errors or uncertainties in the measurement of I_K, or of the initial gradient of the rate-intensity relation, will tend to become more serious in this connection when the surface intensity (I_o) is low and approaches I_K, and photosynthesis decreases rapidly with depth from the water surface. Another factor affecting the area under the photosynthesis-depth profile, and hence the areal production, is the intrinsic curvature of the rate-intensity curve. However when the effects of the most extreme curvature types of Figure 4 were tested, using a graphical construction of photosynthesis-depth profiles, the changes induced were small (Fig. 7b).

On present knowledge, field experiments involving exposures *in situ* still provide the most direct estimation of photosynthetic productivity by natural populations of phytoplankton. With suitable design, they can also allow the observed behavior to be interpreted in terms of a limited number of variables, from which photosynthetic behavior in other field situations can be estimated (Manning and Juday 1941, Edmondson 1956, Talling 1957a, b). The application of laboratory measurements involves still wider extrapolation, but has been used in recent work with radio-carbon in view of the saving of time and greater ease of measurement. Nevertheless the significance of the measurements is often uncertain, partly on purely physiological grounds such as the unknown effects of temperature on the P_{max} and I_K variables and the incomplete attainment of light-saturation, and partly from uncertainties from the widespread application of formulae (*e.g.* those of Steemann Nielsen 1952, p. 132; Ryther 1956, Ryther and Yentsch 1957) without sufficient testing of the validity of the basic assumptions for local conditions. Other attempts to simplify field conditions of exposure, using photosynthetic rates measured only near the water surface, are still more unsatisfactory in view of the unknown significance of photo-inhibition in such exposures. A need exists for the greater development of analytical studies of photosynthetic productivity by phytoplankton, broadly based upon both laboratory and field experiments, and involving short exposures under conditions better defined than in most previous field experiments.

REFERENCES

Anderson, E. R. 1952. Energy-budget studies. U.S. Geol. Surv., Circ. **229**: 71–119.

Bauer, G. 1957. Die Ausnützung der Sonnenergie durch das Phytoplankton eines eutrophen Sees. Inaugural-Dissertation, Universität München, 77 pp.

Cushing, D. H. 1957. Production of carbon in the sea. Nature, Lond., **179**: 876.

———. 1958. Some experiments using the ^{14}C technique. Rapp. Cons. Explor. Mer., **144**: 73–75.

Davis, F. J. 1941. Surface loss of solar and sky radiation by inland lakes. Trans. Wis. Acad. Sci., Arts & Lett., **33**: 83–93.

Edmondson, W. T. 1956. The relation of photosynthesis by phytoplankton to light in lakes. Ecology, **37**: 161–174.

Emerson, R. 1935. The effect of intense light upon the assimilatory mechanism of green plants, and its bearing on the carbon dioxide factor. Cold Spring Harbor Symp. Quant. Biol., **3**: 128–137.

——— and L. Green. 1934. Manometric measurements of photosynthesis in the marine alga *Gigartina*. J. Gen. Physiol., **17**: 817–843.

Gessner, F. 1955. Hydrobotanik. I. Energiehaushalt. Deutscher Verlag der Wissenschaften, Berlin, 517 pp.

——— and A. Diehl. 1951. Die Wirkung natürlicher Ultraviolettstrahlung auf die Chlorophyllzerstörung von Planktonalgen. Arch. Mikrobiol., **15**: 439–453.

——— and F. Pannier. 1958a. Der Sauerstoffverbrauch der Wasserpflanzen bei verschiedenen Sauerstoffspannungen. Hydrobiologia, **10**: 323–351.

———. 1958b. Influence of oxygen tension on respiration of phytoplankton. Limnol. Oceanogr., **3**: 478–480.

Jenkin, P. M. 1937. Oxygen production by the diatom *Coscinodiscus excentricus* Ehr. in relation of submarine illumination in the English Channel. J. Mar. Biol. Assoc., U.K., **22**: 301-343.

Jerlov, N. G. 1951. Optical studies of ocean waters. Rep. Swedish Deep-Sea Expd., **3**: 1–59.

Kok, B. 1956a. On the inhibition of photosynthesis by intense light. Biochim. Biophys. Acta, **21**: 234–244.

———. 1956b. Photosynthesis in flashing light. Biochim. Biophys. Acta, **21**: 245–248.

———. 1957. Report on some recent results at Wageningen. In: Gaffron, H. (ed.), Research in Photosynthesis, pp. 353–365. Interscience Publishers, New York. xiv + 524 pp.

Levring, T. 1947. Submarine daylight and the photosynthesis of marine algae. Goteborgs

VetenskSamh. Handl., Sjatte Folj. B, **5**(6): 1–90.

Lund, J. W. G., and J. F. Talling. 1957. Botanical limnological methods with special reference to the algae. Bot. Rev., **23**: 489–583.

Manning, W. H., and R. E. Juday. 1941. The chlorophyll content and productivity of some lakes in north-eastern Wisconsin. Trans. Wis. Acad. Sci., Arts & Lett., **31**: 377–410.

Rabinowitch, E. I. 1951. Spectroscopy and fluorescence of photosynthetic pigments; Kinetics of photosynthesis. Photosynthesis and related processes, II, Part 1. Interscience Publ., New York. pp. xi + 603–1208.

————. 1956. Kinetics of photosynthesis (cont'd). Addenda to I and II, Part 1. Photosynthesis and related processes, II, Part 2. Interscience Publ., New York. pp. xvi + 1209–2088.

Richards, F. A., and T. G. Thompson. 1952. The estimation and characterisation of plankton populations by pigment analyses. II. A spectrophotometric method for the estimation of plankton pigments. J. Mar. Res., **11**: 156–172.

Rodhe, W. 1958. The primary production in lakes: some results and restrictions of the ^{14}C method. Rapp. Cons. Explor. Mer, **144**: 122–128.

————, R. A. Vollenweider, and A. Nauwerck. 1958. The primary production and standing crop of phytoplankton. pp. 299–322. *In* 'Perspectives in marine biology,' ed. A. A. Buzzati-Traverso. Univ. of California Press, Berkeley. xvi + 621 pp.

Ryther, J. 1956. Photosynthesis in the sea as a function of light intensity. Limnol. Oceanogr., **1**: 61–70.

———— and R. F. Vaccaro. 1954. A comparison of the oxygen and ^{14}C methods of measuring marine photosynthesis. J. Cons. Int. Explor. Mer, **20**: 25–34.

———— and C. S. Yentsch. 1957. The estimation of phytoplankton production in the ocean from chlorophyll and light data. Limnol. Oceanogr., **2**: 281–286.

Sagromsky, H. 1943. Die Bedeutung des Lichtfaktors für den Gaswechsel planktontischer Diatomeen und Chlorophyceen. Planta, **33**: 299–339.

Smith, E. L. 1936. Photosynthesis in relation to light and carbon dioxide. Proc. Nat. Acad. Sci., Wash., **22**: 504–511.

Sorokin, C. 1958. The effect of the past history of cells of *Chlorella* on their photosynthetic capacity. Physiol. Plant., **11**: 275–283.

Steemann Nielsen, E. 1952. The use of radioactive carbon (C^{14}) for measuring organic production in the sea. J. Cons. Int. Explor. Mer, **18**: 117–140.

————. 1958. Experimental methods for measuring organic production in the sea. Rapp. Cons. Explor. Mer, **144**: 38–46.

———— and E. A. Jensen. 1957. Primary oceanic production. The autotrophic production of organic matter in the oceans. Scientific Results of the Danish Deep-Sea Expedition round the World 1950–52, Galathea Report I: 49–136. Copenhagen.

———— and V. Hansen. 1959. Light adaptation in marine phytoplankton populations and its interrelation with temperature. Physiol. Plant., **12**: 353–370.

Strickland, J. D. H. 1958. Solar radiation penetrating the ocean. A review of requirements, data and methods of measurement, with particular reference to photosynthetic productivity. J. Fish. Res. Bd. Canada, **15**: 453–493.

Sverdrup, H. U., M. W. Johnson and R. H. Fleming. 1942. The oceans, their physics, chemistry and general biology. Prentice-Hall, New York. x +1060 pp.

Sweeney, B. M., and Hastings, J. W. 1957. Characteristics of the diurnal rhythm of luminescence in *Gonyaulax polyedra*. J. Comp. Cell. Comp. Physiol., **49**: 115–128.

Talling, J. F. 1957a. Photosynthetic characteristics of some freshwater plankton diatoms in relation to underwater radiation. New Phytol., **56**: 29–50.

————. 1957b. The phytoplankton population as a compound photosynthetic system. New Phytol., **56**: 133–149.

————. 1957c. Diurnal changes of stratification and photosynthesis in some tropical African waters. Proc. R. Soc. B, **147**: 57–83.

Taylor, A. H., and G. P. Kerr. 1941. The distribution of energy in the visible spectrum of daylight. J. Opt. Soc. Amer., **31**: 3–8.

Utermöhl, H. 1936. Quantitative Methoden zur Untersuchung des Nannoplanktons. *In*: Aberhalden Handb. Biol. ArbMeth., **9**(2): 1879–1937.

Verduin, J. 1956. Energy fixation and utilization by natural communities in western Lake Erie. Ecology, **37**: 40–50.

Vinberg, G. G. 1934. Versuch zum Studium der Photosynthese und der Atmung des Seewassers. Zur Frage ueber Bilanz des organischen Stoffes. (Mitteilung I). (In Russian: German summary.) Arb. Limnol. Sta. Kossino, **18**: 5–24.

Vollenweider, R. A. 1956. Das Strahlungsklima des Lago Maggiore und seine Bedeutung für die Photosynthese des Phytoplanktons. Mem. Ist. Ital. Idrobiol. Marchi, **9**: 293–362.

Winokur, M. 1948. Photosynthesis relationships of *Chlorella* species. Amer. J. Bot., **35**: 207–214.

Withrow, R. B., and A. P. Withrow. 1956. Generation, control, and measurement of visible and near-visible radiant energy. *In* Hollaender, A. (ed.), Radiation biology, vol. **3**. Visible and near-visible light, pp. 125–258. McGraw-Hill Co., New York, Toronto, London. viii + 765 pp.

Reprinted from SCIENCE, April 15, 1960, Vol. 131, No. 3407, pages 1098-1100

Utilization of Organic Carbon by a Marine Crustacean: Analysis with Carbon-14

Abstract. An isotope-dilution technique using carbon-14 was employed to determine quantitatively the carbon budget of a filter-feeding crustacean. The amount of carbon ingested ranged between 0.044 and 0.139 mg. Incorporation of carbon varied between 11.3 and 73.6 percent per day per organism, with an average of 32.5 percent for the animals tested. Values for oxygen consumption are given as they relate to carbon intake and utilization.

Energy and feeding interrelationships have been experimentally determined for some zooplankters. For example, Richman (*1*) determined a calorimetric budget for the fresh water crustacean *Daphnia pulex*, and Marshall and Orr (*2*) used radioactive carbon to determine the filtering rates and the percent of food digested by the marine copepod, *Calanus finmarchicus*. The latter authors made no attempt at a quantitative measure of carbon in their experiments. This report presents a method which utilizes an isotope-dilution technique for quantitative measurements of the utilization and egestion of particulate organic carbon by a planktonic filter-feeding marine crustacean, *Euphausia pacifica*.

The experimental animals *(E. pacifica)* were collected in net hauls (at a depth of about 250 m) off the coast of La Jolla and were brought back at 10°C to the laboratory within a few hours.

A period of 24 hours was usually allowed for the unfed captive animals to void particulate matter from the gut. Eight-day-old, 50-ml, bacteria-free cultures of a green algal flagellate, *Dunaliella primolecta*, grown in a sea water medium (*3*), were labeled with C^{14} (10 μc of $NaHC^{14}O_3$) for 3 to 4 days and were then supplied as food. The amount of carbon in the food offered to the animals in the laboratory ranged between 0.117 and 0.313 mg.

On the day of an experiment the algae were collected by centrifugation, washed free of soluble C^{14}, and suspended in sea water previously filtered through Millipore membranes (0.45 μ porosity). Total organic carbon and C^{14} measurements were determined for aliquots of the algal culture. This information provided the proportion of total carbon to C^{14} in the algae. The culture was suitably diluted to give approximately 0.1 to 0.3 mg of algal carbon in a vessel (about 1 to 3 × 10^5 cells per milliliter). Each vessel was then supplied with an adult euphausiid (dry weight 3 to 5 mg). When euphausiids are put into a heavy suspension of algae, that is, enough cells to tint the sea water green, they quickly filter out enough algae to completely fill the intestine, digestive gland, and crop. Control bottles without animals were included to ascertain the amount of algal respiration. Bottles were usually of 65-ml capacity and contained 40 ml of fluid, but occasionally larger bottles were used. At the start of the experiment an aliquot of the sea water containing the radioactive algae was removed to determine the quantity of organic carbon available to the animals. The method of Kay (*4*) was used for measurement of organic carbon. Another aliquot of algae was retained on a Millipore filter (pore size, 0.45 μ) and analyzed for C^{14}.

The experimental bottles and the contents were kept in the dark at 10°C for 24 hours. Then the animals were removed, washed in filtered sea water, and dissected to remove both their

Contributions from the Scripps Institution of Oceanography, New Series, 1148

Reproduced by Permission

able 1. Fractionation of carbon by radioactivity. In this experiment, the carbon for each fraction as calculated by use of the ratio

$$\frac{27.9 \times 10^3 \text{ cpm}}{0.174 \text{ mg C}} = \frac{\text{Observed cpm}}{x}$$

here cpm is counts per minute.

Material analyzed	10^3 cpm	Total C (mg)
	Time: 0 hours	
0 ml Dunaliella culture	27.9	0.174
	Time: 24 hours	
0 ml Dunaliella culture	5.07	0.032
ngested (by difference)		0.142
gested in fecal pellets	1.27	0.008
viscerated euphausiid	16.7	0.104
atabolized (by difference)		0.030

ntestinal tracts and digestive glands. ecal pellets were removed from the vater with a pipette and washed gently. inally, another aliquot of the algae vas taken out and filtered for C^{14} etermination.

After drying, each eviscerated eu-hausiid was weighed, combusted to arbon dioxide, and assayed for total arbon (*4*). The mean of 16 carbon eterminations is 34.6 percent on a ry weight basis (range 25.4 to 39.0 ercent). The CO_2 thus produced was ecovered as $BaCO_3$ and counted for C^{14} radiation in a windowless propor-onal counter (Nuclear Measurements orporation). The amount of C^{14} ctivity in the barium carbonate was orrected against a self-absorption curve. he radiation emitted by the radio-ctive algae was also counted. No self-bsorption correction was made for ltered algae because of the extremely ow weight of the sample and the lack f measurable absorption of the C^{14} adiation (*5*).

Knowing the C^{14}/total C ratio of an lgal sample permits the calculation of he total carbon contributed by the algae, s shown in Table 1. The constancy f the ratio C^{14}/total C was tested. It ppears that there usually is a change, ue to respiratory processes, of −4 to -5 percent in this ratio over the ex-erimental period. Table 1 presents he results of a typical experiment.

Table 2 gives the carbon balances alculated from the C^{14}/total C ratios ound for eight animals at different hytoplankton densities. Also shown are the calculated efficiencies with which these animals were able to accumulate carbon in their tissues through digestive processes.

Respired CO_2 was not determined directly but was estimated by difference. An indirect gasometric method was used also to calculate the magnitude of total respiratory carbon for comparison with the C^{14} method. Oxygen consumption was found to be linear over several hours at 10°C by tests with the water analyzer devised by Scholander *et al.* (*6*). Q_{O_2} values were based upon eight analyses of individual animals, and showed a range of 0.85 to 1.52 ml/gm per hour, from which the mean of 1.14 was derived. On the assumption that the respiratory quotient was 1.0, CO_2 evolution was calculated from the average oxygen consumption, and was found to have a reasonably close correspondence in some cases with data collected by the C^{14} method (animals Nos. 1 to 4, Table 2).

Some animals (Table 2) showed a larger catabolic carbon fraction than could be accounted for by respiratory processes alone. It is probable that catabolic carbon compounds other than CO_2 are excreted by the animals.

From Table 2 it is also seen that large variations may exist in the efficiency of these zooplankters to incorporate ingested carbon. In the animals tested, this ranged between 11.3 and 73.6 percent. However, the fate of the incorporated carbon was not ascertained. These data may reflect deposition of storage products or actual growth.

The effect of varying temperatures on oxygen utilization was tested gasometrically. The euphausiids were found to have a Q_{10} of approximately 2 between 5° and 12°C. This would imply that when these animals cross the thermocline into warmer water their basal carbon needs increase. However, except those by Fox *et al.* (*7*), few published data exist on the amount of particulate carbon available for zooplankters in the sea.

Application of the method presented in this paper to other organisms, with proper attention to the experimental variables cited here, may permit a direct measurement of the carbon flow through biological systems in aquatic environments. Future investigations call for studies of relative nutritional states and comparative proportions of stored reserves in experimental animals (*8*).

REUBEN LASKER*

Scripps Institution of Oceanography, University of California, La Jolla

References and Notes

1. S. Richman, *Ecol. Monographs* **28**, 273 (1958).
2. S. M. Marshall and A. P. Orr, *Papers in Marine Biology and Oceanography*, supplement to *Deep Sea Research* **3**, 110 (1956); S. M. Marshall and A. P. Orr, *The Biology of a Marine Copepod* Calanus finmarchicus *(Gunnerus)* (Oliver and Boyd, London, 1955).
3. B. M. Sweeney and J. W. Hastings, *J. Protozool.* **5**, 217 (1958).
4. H. Kay, *Kiel. Meeresforsch.* **10**, 26 (1954).
5. E. Steemann-Nielsen, *J. conseil. Conseil permanent intern. exploration mer* **18**, 117 (1952).
6. P. F. Scholander, L. Van Dam, C. L. Claff, J. W. Kanwisher, *Biol. Bull.* **109**, 328 (1955).
7. D. L. Fox, J. D. Isaacs, E. F. Corcoran, *J. Marine Research (Sears Foundation)* **11**, 29 (1952).
8. This study was supported in part by the Rockefeller Foundation and in part by the Lalor Foundation. I am indebted to Dr. D. L. Fox, Dr. W. H. Thomas, and R. W. Holmes for the use of their facilities which materially aided this study. This report is a contribution from the Scripps Institution of Oceanography, New Series.

* Present address: U.S. Bureau of Commercial Fisheries, Scripps Institution of Oceanography, La Jolla, Calif.

7 December 1959

Table 2. Carbon budget of *Euphausia pacifica*. All weights are given in milligrams.

o.	Dry wt. of animal	Wt. C in eviscer-ated animal	% C in animal	Wt. algal C offered to animal	Wt. C ingested by animal	Wt. C incor-porated	% C incor-porated	Wt. C of gut and gland	Wt. C egested	Wt. cata-bolic C, in-cluding CO_2	Wt. C respired (calcu-lated from RQ = 1)
1	4.6	1.66	36.6	0.174	0.139	0.102	73.6	< 0.001*	0.009	0.029	0.033
2	3.7	1.22	33.0	0.156	0.057	0.018	31.6	0.005	0.006	0.028	0.026
3	3.0	1.01	33.6	0.156	0.056	0.021	37.8	0.003	0.007	0.025	0.021
4	3.9	1.49	38.2	0.117	0.044	0.005	11.3	< 0.001*	< 0.001*	0.039	0.028
5	4.1	1.60	39.0	0.276	0.097	0.015	15.5	0.003	0.001	0.079	0.029
6	4.6	1.74	37.8	0.313	0.113	0.020	17.8	0.002	0.002	0.065	0.033
7	3.4	1.27	37.4	0.313	0.147	0.062	42.2	0.011	0.002	0.073	0.024
8	5.1	1.62	31.8	0.313	0.101	0.029	29.7	0.006	0.001	0.065	0.035

* Weight not determinable by the method used.

68)

BULLETIN OF THE GEOLOGICAL SOCIETY OF AMERICA
VOL. 71, PP. 497–502, 3 FIGS., 1 PL. APRIL 1960

BATHYMETRY AND GEOLOGY OF SALA Y GOMEZ, SOUTHEAST PACIFIC

By Robert L. Fisher and Robert M. Norris

Sala y Gomez, charted at 26°27′41″ S., 105°28′00″ W., is a low volcanic islet 415 km east-northeast of Easter Island and 3500 km west of northern Chile (Fig. 1). Like Easter Island, it belongs to Chile. Although it has been visited, and even landed upon, several times since its discovery in 1793, visitors had not collected rock samples systematically. Only one note on the petrology of the islet, from samples, is known to the writers. That note (Falke, 1941) also summarized observations of topography and fauna made during the visit of the Chilean naval training ship General Baquedaño in 1935. Neither had the area near Sala y Gomez been sounded with modern recording echo sounders. Accordingly, on the University of California—International Geophysical Year Expedition "Downwind," a day was devoted to exploring the islet and its bordering platform. Three geologists and two seamen landed to collect rocks while the research vessel Spencer F. Baird engaged in a sight-controlled bathymetric exploration around the islet.

Sala y Gomez lies 750–1000 km east of the axis of the broad, north-trending East Pacific Rise (Fig. 1). This islet (and possibly Easter Island as well) is less closely related to the Rise than to an eastwest structural trend that may extend from 1200 km west of Easter Island eastward beyond San Felix and San Ambrosio nearly to the Chilean coast. Over most of its length this spur or zone appears to be much less active, seismically, than either the East Pacific Rise proper or the swell extending southeast from near Easter Island to southern Chile. However, shallow-focus seismicity is very great in the region west of Easter Island where this trend, projected, intersects the axis of the East Pacific Rise.

Recent soundings from U. S. Navy Operation "Highjump" and from "Downwind" Expedition indicate that the central segment of the structure is a narrow shoal ridge, more than 1200 km long. Several peaks extend to within 500 m of the sea surface. From sounding data now available, it is uncertain whether the main ridge extends westward to Sala y Gomez or whether it swings southwest, as contoured in Figure 1, with the islet an isolated peak off the north slope. It is likewise uncertain whether the ridge extends across the gap near 90° W Long. to join the seamounts and guyots west of San Felix Island. Soundings are practically nonexistent in the region bounded by Lat. 27° and 35° S. and Longs. 80° and 100° W. No shoal areas of comparable size are believed present there; the few soundings available indicate a general sea depth of 3500–4000 m. North of 25° S., between Peru and the East Pacific Rise, the sea floor is generally deeper than 4000–4500 m. It is suggested that this ridge, extending from near Sala y Gomez to at least 90° W. Long., be designated the Sala y Gomez Ridge.

There are similarities between the here-named Sala y Gomez Ridge and Clipperton Ridge in the northeastern Pacific, described by Menard and Fisher (1958). Both separate large areas with a depth difference of several hundred meters. Both are asymmetrical in cross section, steeper on the north, with one or more lines of seamounts capping the rise. In both cases a subordinate less well-defined northwest trend may be discerned. Of comparable widths, Clipperton Ridge has a greater relief, the Sala y Gomez Ridge a greater length. Both ridges appear as segments of large, east-west structural trends. Clipperton Ridge is part of the Clipperton Fracture Zone, more than 4000 km long. The adjacent well-defined Tehuantepec Ridge, off southern Mexico, is similar in trend, dimensions, and position to the Nasca Ridge off southern Peru. In each case, the east-west

Contributions from the Scripps Institution of Oceanography, New Series, 1149

Reproduced by Permission

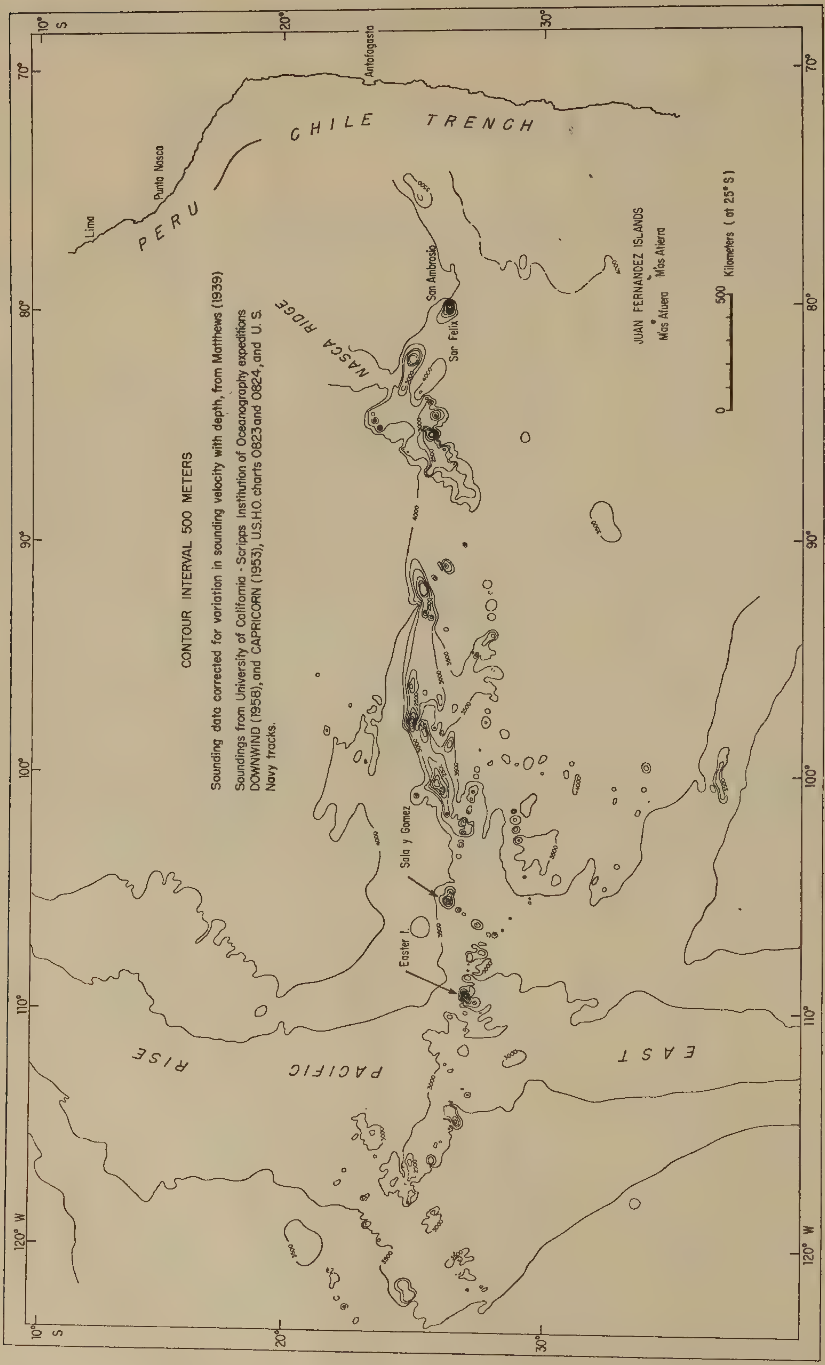

CONTOUR INTERVAL 500 METERS

Sounding data corrected for variation in sounding velocity with depth, from Matthews (1939)

Soundings from University of California - Scripps Institution of Oceanography expeditions DOWNWIND (1958), and CAPRICORN (1953), U.S.H.O. charts 0823 and 0824, and U.S. Navy tracks.

10° S
20°
30°
70°
80°
90°
100°
110°
120° W
Lima
Punta Nasca
PERU
CHILE TRENCH
Antofagasta
NASCA RIDGE
San Ambrosio
San Felix
JUAN FERNANDEZ ISLANDS
Más Afuera
Más Atierra
0
500
Kilometers (at 25° S)
Sala y Gomez
Easter I.
EAST PACIFIC RISE
4000
3500
3000

FIGURE 1.—TOPOGRAPHY OF THE SALA Y GOMEZ RIDGE AND ADJACENT AREA

trend is poorly developed east of the intersection of the northeast-southwest and east-west trends. It might be concluded that the structural trend extending from near the South American coast to Easter Island is another of the "fracture zones" like those described from the northeast Pacific (Menard, 1955). Both zones intersect the East Pacific Rise. Off Mexico, where it is called the "Albatross Plateau", the Rise bisects the Clipperton Fracture Zone. Off South America, it intersects the west portion of the "Sala y Gomez trend"

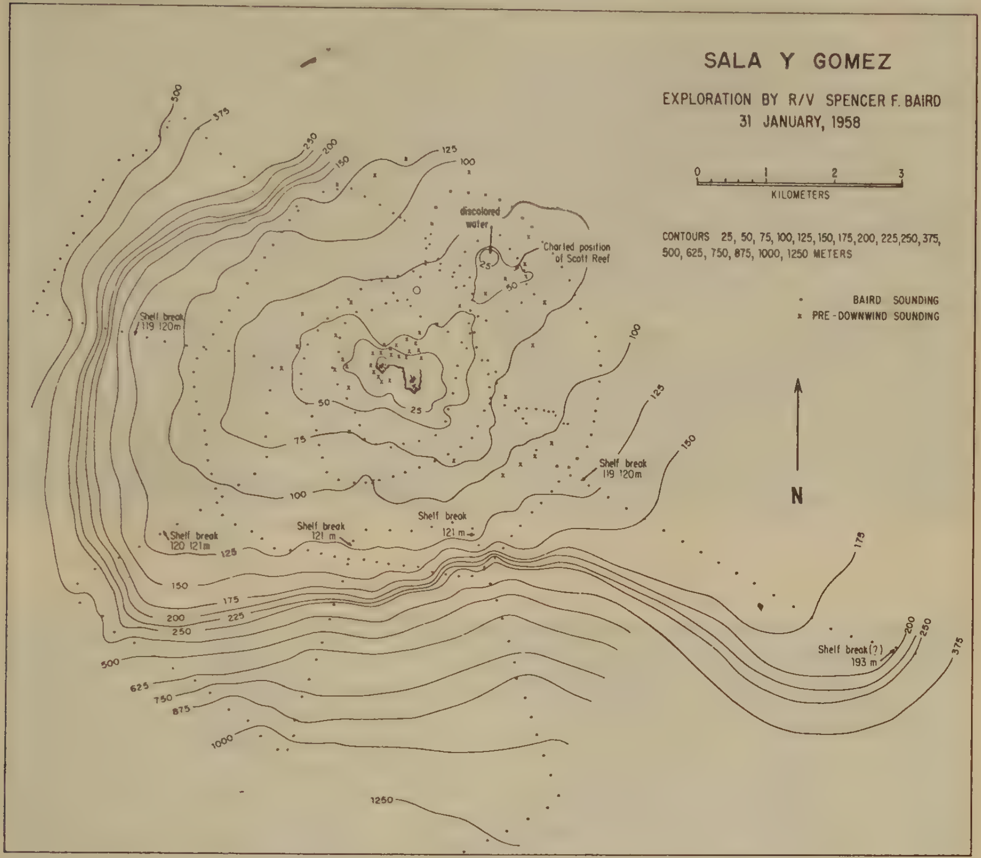
SALA Y GOMEZ
EXPLORATION BY R/V SPENCER F. BAIRD
31 JANUARY, 1958
0 1 2 3
KILOMETERS
CONTOURS 25, 50, 75, 100, 125, 150, 175, 200, 225, 250, 375, 500, 625, 750, 875, 1000, 1250 METERS
• BAIRD SOUNDING
x PRE-DOWNWIND SOUNDING
N
discolored water
Charted position of Scott Reef
Shelf break 119 120m
Shelf break 119 120m
Shelf break 120 121m
Shelf break 121 m
Shelf break 121 m
Shelf break(?) 193 m
25
50
75
100
125
150
175
200
225
250
375
500
625
750
875
1000
1250

Figure 2.—Plot of Near-Shore Topography

Results of near-shore bathymetric exploration by R/V Spencer F. Baird are shown in Figure 2. Soundings taken with a continuously recording echo sounder were recorded on a "precision depth recorder", so that soundings could be read to ± 1 m without difficulty. A sounding interval of 1 minute was used in constructing Figure 2. Slope corrections have not been made. Soundings recorded in fathoms, employing an assumed sounding velocity of 4800 feet/second, were corrected according to the tables of Matthews (1939) and converted to soundings in meters. Positions were taken at 1- or 2-minute intervals, depending upon the ship's speed and the rapidity with which bearings changed. Visual bearings on the highest pinnacle were taken simultaneously with radar ranges to the nearest readily identifiable point on the islet. The accuracy with which the shore line is represented on the available nautical charts is not known.

Sala y Gomez is the subaerial peak of a very large seamount. The extension of this seamount to the west, north, and northeast is not known, but it does extend more than 50 km southeast and 30 km southwest of the islet. Aprons and plains indicative of ponded sediments occur at the base of the slope, near 3500-m depth.

The shelf surrounding the islet is elongated in a northeast-southwest direction, with a minimum width, south of the islet, of 2–2½ km. Its northeast limit was not determined. Five radial lines from "Downwind" show that this platform terminates in a well-defined break west, south, and east-southeast of the islet. The uniformity in this shelf-break depth, 119–121 m, suggests that little or no tilting of the peak has occurred since this platform was cut. East-southeast of the islet, there is a deep break in slope of about 193 m. Above this break the bottom shoals gradually to the platform break of 119–121 m. This gently sloping surface may represent an older tilted shelf or the top of a flow originating east of the present islet. No similar deep break in slope was observed on other radial sounding lines.

The shelf surface is rather smooth, with only broad irregularities, except off the east side of the island. There, narrow sharp pinnacles rise 7–10 m above the platform 30–50 m deep. Larger pinnacles lie north and northeast of the islet; one shoals to less than 50 m. A large patch of discolored water, probably indicating very shoal depths, lay 2 km northeast of the islet, on a bearing 032° from the highest point. An area probably shoaler than 50 m surrounds this pinnacle and extends east-southeast to include the charted position of Scott Reef. However, no discoloration or breaking waves were observed to occur at the latter position.

Sala y Gomez is saddle-bag shaped with a maximum length of 700 m in an east-west direction and a maximum width of 400 m in a north-south direction (Fig. 3). The greatest elevation, according to U.S.H.O. Publication 174 (1952, p. 210a), is 30 m (98 feet). Although no means were available for checking this during the "Downwind" survey, 15 or 16 m would appear to be a more reasonable estimate.

From the sea the islet presents a bleak appearance and seems composed solely of loose black rocks. Once ashore, however, one finds that the islet is made up of several lava flows, with exposed surfaces strewn with loose, apparently water-rounded boulders (Pl. 1, fig. 1) The surface irregularity is accentuated by crude jointing and weathered pillow structure and by the blocky aa type of lava that composes much of the uppermost flow.

The shore line is broken by numerous small inlets 3–30 m wide and up to 100 m long; these appear to have been excavated by waves working along joint planes or other zones of structural weakness. Numerous tide pools are present along the shore; some were observed as much as 3 m above the sea at the time of the visit. These higher pools are almost certainly maintained by spray from breaking waves because the maximum spring-tide range shown on the U. S. Navy H. O. Chart 1119 (1925) is only a little more than 1 m. The numerous rounded boulders on the surface of the islet also suggest that much of the islet is inundated during heavy seas.

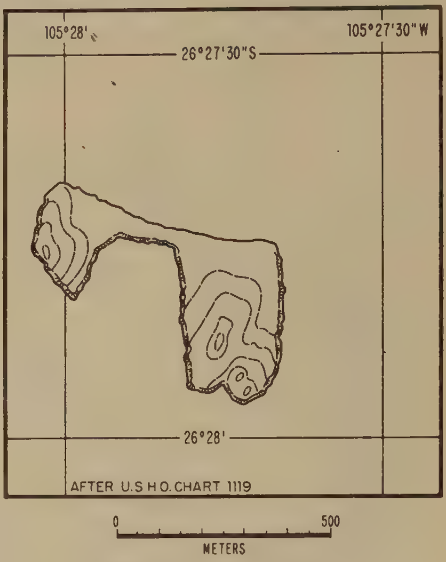

Figure 3.—Sketch of Islet

After U.S.H.O. Chart 1119. Sala y Gomez was reported (1943) to lie 11½ km east of its charted position.

There are no landing places worthy of the name on the islet, although during calm weather a small boat easily can be brought close to the rocky shore. During the survey, in moderate weather, it was necessary to swim the last 50–60 m to shore in order to avoid dashing the boat against the rocks, a not entirely satisfactory procedure owing to the abundance of sharks.

Plate 1.—ROCKS OF SALA Y GOMEZ ISLAND

Figure 1.—Looking southeast, showing highest portion of the island

Figure 2.—Altered zone between the two flows. Note the pillow structure in both flows and the steam pocket or evacuated pillow in the center right. Hammer in lower left gives scale.

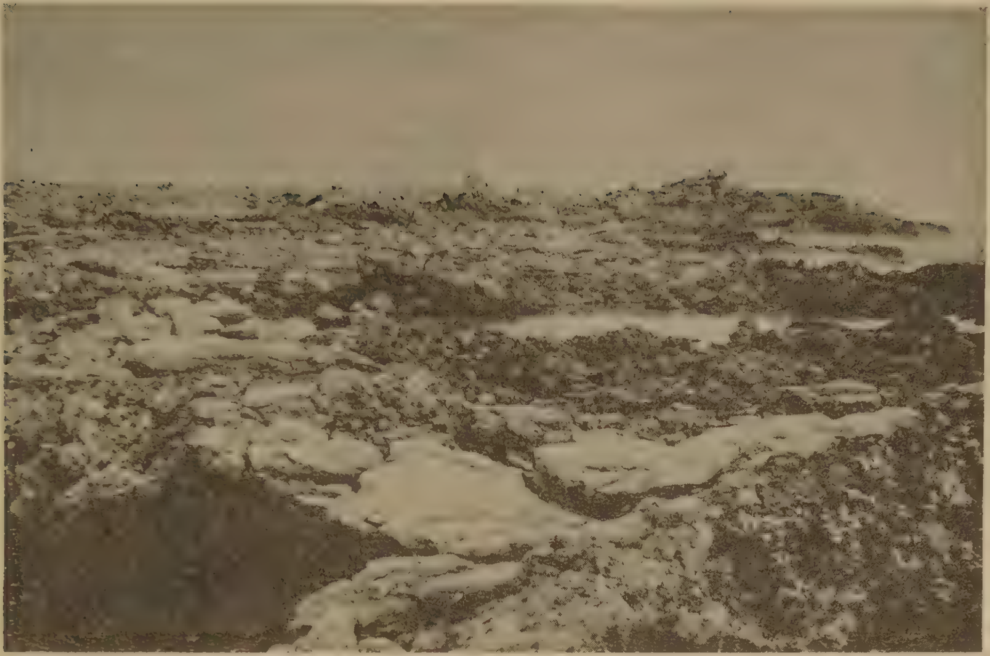

FIGURE 1

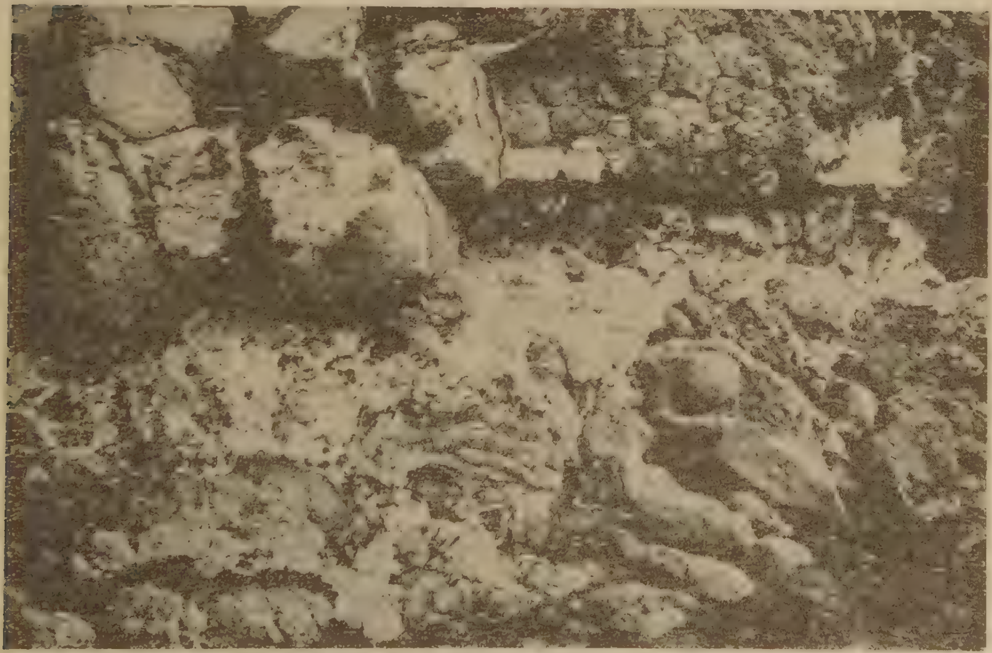

FIGURE 2

ROCKS OF SALA Y GOMEZ ISLAND

No volcanic vents were found on Sala y Gomez, although a vent may have existed in the location now occupied by the embayment on the south side of the islet.

Three distinct rock units are exposed. The lowermost is a vesicular red to dark-gray andesitic olivine basalt. The middle unit, a discontinuous calcareous marine sedimentary deposit, is composed mostly of broken fragments of mollusk shells, Foraminifera, echinoid spines, and corals; this units rests disconformably on the eroded and altered upper surface of the lower basalt. The upper unit is also a vesicular to dense dark-gray andesitic olivine basalt. Both flows show pillow structure. A thin cover of calcareous shell debris is now accumulating on the lowest parts of the islet near the shore, particularly on the northeastern side.

The flows and the included sedimentary unit are probably Pleistocene or Recent. The minor amount of weathering on the surface of the last flow plus the near absence of soil make a greater age unlikely, although soil and other weathering products might be swept away by storm waves on such a low islet.

The lower unit is a reddish to dark-gray andesitic olivine basalt flow, locally scoriaceous and generally showing a well-developed trachytic texture. Vesicles are especially numerous near the upper surface of the flow and commonly show some flattening, which suggests that some movement of the lava occurred just prior to final cooling.

Transition from red to dark gray takes place downward in about a meter, suggesting that only the uppermost portion of the flow was exposed to atmospheric oxidation at the time of formation. Pillow structure and probable steam pockets are well developed in much of the exexposed portion of the flow, indicating a submarine origin for the bulk of the unit (Pl. 1, fig. 2).

Feldspar laths, ranging from oligoclase to andesine (An_{30} to An_{40}) constitute 60–70 per cent of the rock. The laths are roughly parallel, giving the rock a trachytic texture. The feldspar crystals are generally unzoned and unaltered and average about 0.2 mm long.

Ferromagnesian minerals constitute the remaining 30–40 per cent of the rock and include very abundant small granules of iron ore, presumably mostly magnetite. Olivine is common, both as small grains averaging about 0.1 mm in diameter and as scattered large phenocrysts averaging about 1.0 mm in diameter. Associated with the olivine is iddingsite which has replaced nearly all the small olivine grains and which rims the larger phenocrysts. Augite, although present in small grains, is rare. The rarity of augite and other pyroxenes may be due to the relatively sodic character of the parent magma.

Parts of the upper surface of this lower unit are extensively altered. The resulting product is kaolinite, an unidentified zeolite, and a chloritic mineral. Both the groundmass and the included feldspar laths have been altered to the same material. Most of this altered material, which formerly probably covered much of the upper surface of the lower flow, has been removed by erosion before extrusion of the latest flow.

Intercalated between the upper and lower volcanic rocks is a discontinuous calcareous deposit containing subround to angular fragments of scoria, generally of pea size, presumably derived from the lower flow during the erosional period suggested above. The calcareous matrix is composed of Foraminifera tests, echinoid spines, fragments of reef-forming coral, and broken mollusk remains. Most of these organic remains are so badly leached that a reliable age determination is difficult. The freshness of the associated flows, however, suggests a Pleistocene or Recent age.

The deposit is nowhere more than 8 m above sea level and no more than 1 m thick. No great subsidence following formation of the first lava flow would be necessary to produce the requisite shallow-water environment.

The upper unit is a dense, fine-grained andesitic olivine basalt, locally sufficiently vesicular to be considered a scoria. The upper surface, where not destroyed by wave erosion or weathering, is mostly blocky and jagged, resembling a typical aa lava flow. Locally, the upper surface of the flow is smooth ropy pahoehoe. The base of this unit, where it rests on the lower flow or on the middle sedimentary bed, shows crude pillow structure suggesting that this flow too was extruded partly below the level of the sea. The upper flow rests directly on the lower unit in much of the eastern part of the islet and constitutes nearly all the exposed rock in the narrow isthmus.

Composition of the upper and lower units is similar. All specimens of the upper flow have a marked trachytic texture owing to the rough alignment of the abundant feldspar laths. Feldspars range from oligoclase to andesine (An_{28} to An_{37}) as in the lower flow. The crystals average about 0.2 mm long, are normally unzoned and unaltered, and constitute about 60–70 per cent of the rock.

Olivine occurs as large phenocrysts, averaging about 1.0 mm in diameter, and as abundant small grains (average diameter, 0.15 mm), together constituting nearly 20–25 per cent of the total rock. Only a few of the small grains are altered to red iddingsite, and alteration rims and cracks in the larger grains are much less prominent in the upper than in the lower unit. Olivine crystals in both rock units have a 2V near 90°.

Opaque, equant iron-ore granules, probably mainly magnetite, are exceedingly abundant in all samples from the upper flow. Although the grains are generally small, iron ore constitutes not less than 5 per cent of the total rock.

Augite, although not abundant in the upper flow, is not so rare there as in the lower unit. Most augite grains are small (average size about 0.05 mm) and occupy spaces between the feldspar laths. No augite phenocrysts were present. Most of the augite examined was colorless. A few grains are pale greenish and may be aegirine-augite.

The lava flows of Sala y Gomez are considered andesitic basalts on the basis of the abundance of olivine, the dark color of the rocks, and the sodic nature of the feldspars (Williams, Turner, and Gilbert, 1954, p. 43). The varietal name mugearite seems appropriate and conveys an accurate picture of the mineralogical nature of these rocks.

Acknowledgments

The writers are indebted to Gustaf Arrhenius, M. N. Bramlette, and Howel Williams for critical reading of the manuscript.

References Cited

Falke, H., 1941, Die Insel Sala y Gomez: Natur und Volk, Bank 71, Heft 3, p. 146–150

Matthews, D. J., 1939, Tables of the velocity of sound in pure water and sea water for use in echo-ranging and sound-ranging: British Admiralty Hydrog. Dept. H. D. no. 282, 52 p.

Menard, H. W., Jr., 1955, Deformation of the northeastern Pacific Basin and the west coast of North America: Geol. Soc. Am. Bull., v. 66, p. 1149–1198

Menard, H. W., Jr., and Fisher, Robert L., 1958 Clipperton fracture zone in the northeastern equatorial Pacific: Jour. Geology, v. 66, p. 239–253

U. S. Hydrographic Office chart 1119, 8th ed., 1925

U. S. Hydrographic Office Publication 174, 1952, Sailing directions for South America, volume 3 (west coast from Golfo Corcovado to Gulf of Panama, including off-lying islands), 392 p.

Williams, H., Turner, F. J., and Gilbert, C. M., 1954, Petrography: San Francisco, W. H. Freeman Co., 406 p.

Scripps Inst. of Oceanography, Univ. Calif., La Jolla, Calif.; Univ. Calif., Santa Barbara, College, Goleta, Calif.

Manuscript Received by the Secretary of the Society, November 16, 1959

CUSHMAN FOUNDATION FOR FORAMINIFERAL RESEARCH

SPECIAL PUBLICATION NO. 5

ECOLOGY OF LIVING BENTHONIC FORAMINIFERA FROM THE SAN DIEGO, CALIFORNIA, AREA

BY
TAKAYASU UCHIO

APRIL 20, 1960
Price $2.50 postpaid

Contributions from the Scripps Institution of Oceanography, New Series, 1150

Reproduced by Permission

CONTENTS

ABSTRACT 5
PART 1: ECOLOGY 5
Introduction 5
Description of the Area 5
Previous Studies of Recent Foraminifera off California 7
Hydrography 8
Methods of Study 8
Field Methods 8
Laboratory Work 8
Sediments 9
Living Benthonic Foraminifera 12
Depth Distribution of Species 12
Possible Causes of Depth Zonation 13
Size of Living Population 19
Description 19
Discussion 25
Total Populations of Benthonic Foraminifera 29
Depth Distribution of Species 29
Size of Total Population 30
Number of Species and Genera of Living Benthonic Population 31
Planktonic Foraminifera 40
Rates of Sedimentation 42
Change in Sea-Level 46
Vertical Change of Foraminifera Fauna in Cores 47
Lateral Change of Foraminifera Fauna 47
Depth Change of Size of Benthonic Populations 47
Discussion 47
Displaced Foraminifera 48
PART 2: SYSTEMATICS 50
Introduction 50
Systematic Descriptions of Species 50
Saccamminidae 50
Reophacidae 50
Tolypamminidae 51
Lituolidae 51
Textulariidae 54
Verneuilinidae 56
Valvulinidae 56
Ophthalmidiidae 57
Trochamminidae 58
Polymorphinidae 60
Nonionidae 60
Elphidiidae 62
Ceratobuliminidae 62
Buliminidae 63
Discorbidae 66
Cassidulinidae 68
Anomalinidae 69
LITERATURE CITED 70

TEXT FIGURES

1. Locations of stations 6
2. Depth distributions of benthonic Foraminifera 16
3. Depth distributions of benthonic Foraminifera 17
4. Depth distributions of benthonic Foraminifera 20
5. Depth distributions of benthonic Foraminifera 21
6. Depth distributions of benthonic Foraminifera 22
7. Depth distributions of benthonic Foraminifera 23
8. Depth distributions of benthonic Foraminifera 27
9. Depth distributions of benthonic Foraminifera 28
10. Distribution of living *Bolivina acutula* Bandy 29
11. Distribution of living *Nonionella* sp. aff. *N. globosa* Ishiwada 39
12. Distribution of living *Cassidulina delicata* Cushman 40
13. Distribution of living *Bolivina pacifica* Cushman and McCulloch 41
14. Distribution of living populations of benthonic Foraminifera 42
15. Depth distributions of average living and total populations of benthonic Foraminifera 43
16. Distribution of total (living plus dead) populations of benthonic Foraminifera 44
17. Distribution of ratios of total benthonic population to total planktonic population (B/P) 45
18. Distribution of ratios of living population to total population (L/T) 46

TABLES

1. Occurrences of living benthonic Foraminifera 10, 11
2. Occurrences of living benthonic Foraminifera 12, 13
3. Occurrences of living benthonic Foraminifera 14, 15
4. Depth distributions of average populations of living benthonic Foraminifera 26
5. Occurrences of benthonic Foraminifera 32, 33
6. Occurrences of benthonic Foraminifera 34, 35
7. Occurrences of benthonic Foraminifera 36, 37
8. Comparison of living and total faunas 38
9. Depth distribution of average populations of total benthonic Foraminifera 43

PLATES

1. .... opposite page 18
2. .... opposite page 19
3. .... opposite page 24
4. .... opposite page 25
5. .... opposite page 30
6. .... opposite page 31
7. .... opposite page 48
8. .... opposite page 49
9. .... opposite page 54
10. .... opposite page 55

ECOLOGY OF LIVING BENTHONIC FORAMINIFERA FROM THE SAN DIEGO, CALIFORNIA, AREA

Takayasu Uchio

Petroleum Engineering Institute, University of Tokyo, Bunkyo-ku, Tokyo, Japan

ABSTRACT

One hundred and fifty-seven samples from the sea floor off San Diego, California, were studied for both living and total (living plus dead) populations of Foraminifera.

Seven benthonic Foraminifera depth assemblages are recognized on the basis of the living distributions and abundances. The boundaries are at depths of approximately 13, 45, 100, 250, 350, and 450 fathoms. Based on the Scripps Institution's study of hydrography it appears that the 13-fathom boundary may be interpreted as approximating the base of the turbulent zone, the 45-fathom boundary the bottom of the seasonal thermocline, the 100-fathom boundary the bottom of the California Current, the 250-fathom boundary the top of the permanent thermocline, the 350-fathom boundary the oxygen minimum layer, the 450-fathom boundary the bottom of the permanent thermocline. The shallowest assemblage is divided into two facies and difference of sediment types may be one of the principle causes of such differentiation.

Comparison of depth ranges of living and empty tests of 95 species shows that some of the tests of almost all species are transported toward deeper water after death. Total population counts are valid in defining the general composition and distribution where little or no displacement of sediment is expected, but generally these counts are not indicative of distribution of living specimens. Maximum abundance of living benthonic Foraminifera occurs between 55 and 150 fathoms and approximately coincides with the greatest number of species and genera. Temperature, food, and sediment type are considered important factors for depth distribution and size of population of living benthonic Foraminifera.

Ratios of living to total populations from sediment samples appear to be indicative of the rate of sedimentation. The ratios support the suggestion of Dietz (1952) that sediments from the land are deposited either nearshore or on the lower part of the continental slope and in basins, bypassing the outer shelf and upper continental slope. Rates of sedimentation calculated from an assumed rate of reproduction of Foraminifera are 97 years per centimeter of sediment in the San Diego Trough and 0.36 years per centimeter in the nearshore area.

Three methods of calculating the amount of sea-level change by using benthonic Foraminifera are discussed. Five to ten fathoms of deepening is suggested at some time later than the Pleistocene.

The presence of shallow-water Foraminifera and Pleistocene Foraminifera in sand layers of a clayey silt core, and in sandy silt on the surface of the floor of the San Diego Trough, where clayey silts usually are found, proves displacement of sediments from shallow to deep water.

Siltstones were cored at three stations in and near Loma Sea Valley and Coronado Canyon, and are Miocene in age based on assemblages of Foraminifera, diatoms, and Radiolaria.

One hundred and sixty species of benthonic Foraminifera are figured, of which seventy species are discussed as to their ranges of variation of forms and/or synonymies. Two new genera are described: **Paradentalina** and **Recurvoidella**; thirty-four new species are described: **Ammomarginulina sandiegoensis, Arenoparrella oceanica, Asterigerinata pacifica, Bigenerina hoeglundi, Bolivina peirsonae, B. subargentea, Buccella angulata, Cassidulina bradshawi, C. subcarinata, Cassidulinoides waltoni, Cibicides phlegeri, Cornuspira lajollaensis, Eggerella scrippsi, Epistominella sandiegoensis, Globobulimina hoeglundi, Gyroidina quinqueloba, Haplophragmoides neobradyi, H. quadratus, Involutina hoeglundi, Karreriella parkerae, Nonion lankfordi, N. parkerae, Nonionella (?) fragilis, Recurvoidella parkerae, Spiroloculina fragilis, Spiroplectammina bathyca, Textularia sandiegoensis, Trochammina chitinosa, T. discorbinoides, T. labiata, T. rhumbleri, Virgulina apertura, V. delicatula, V. sandiegoensis.**

PART I: ECOLOGY

INTRODUCTION

The submarine geology, oceanography, and taxonomy of the Foraminifera in the San Diego, California, area are relatively well-known. One hundred and fifty-seven samples were studied in this area for the following purposes: 1) to establish the faunal assemblages of living benthonic Foraminifera in various environments and to relate the distribution of the living faunas with known physical and chemical factors and sediment types; 2) to compare the living benthonic faunas with the non-living benthonic faunas at each station; 3) to investigate relative rates of sedimentation and the displacement of sediments by using Foraminifera.

The field work was done on board the research vessels of the Scripps Institution of Oceanography of the University of California. Laboratory facilities were furnished by the Marine Foraminifera Laboratory and the Division of Marine Geology and Geochemistry of the same institution. The laboratory work was supported in part by a contract of the Office of Naval Research with the University of California. The entire work was supervised by Fred B Phleger, and, in addition, R. S. Arthur, M. N. Bramlette, U. S. Grant, IV, M. W. Johnson, H. W. Menard, Miss F. L. Parker, F. P. Shepard and E. L. Winterer read the manuscript and offered suggestions. The writer is especially indebted to J. S. Bradshaw who aided him in numerous ways in the field and laboratory work. R. R. Lankford assisted in collecting samples, and Jean P. Hosmer assisted in the grain size analyses of the sediments. Taro Kanaya identified the diatom flora in a Miocene rock. The writer is also indebted to Dr. C. G. Adams of the British Museum (Natural History), London, for examining type material of *Recurvoides contortus* Earland and lending two topotypes of *Eggerella bradyi* (Cushman) to the writer.

DESCRIPTION OF THE AREA

This area was studied by Emery, Butcher, Gould and Shepard (1952, p. 511-548) who summarized the present state of knowledge of the submarine geology of the area. The main features are as follows (see Text Fig. 1):

(1) The beach consists of sands except in the Point Loma area where there are cliffs of Cretaceous and Eocene rocks.

(2) The Tia Juana River, near the International Boundary, is mostly dry throughout the year and its estuary is relatively wide and is influenced by tides. There is almost no river run-off at present except during floods, but the river had a strong influence on the distribution of sediments during the Pleistocene.

(3) The continental shelf is narrow, approximately 4 nautical miles wide near Point Loma and 10 nautical miles near the Coronados Islands. The shelf break is at a depth of approximately 60 fathoms, and a continental borderland extends seaward.

(4) Loma Sea Valley borders the shelf in the north and extends approximately NW-SE from the head of the Coronado Canyon to the San Diego Trough. Rocks are exposed on the valley wall in many places and the bottom is covered by silt which contains coarse sands and pebbles in many places.

(5) Coronado Bank (and its extension, the Coro-

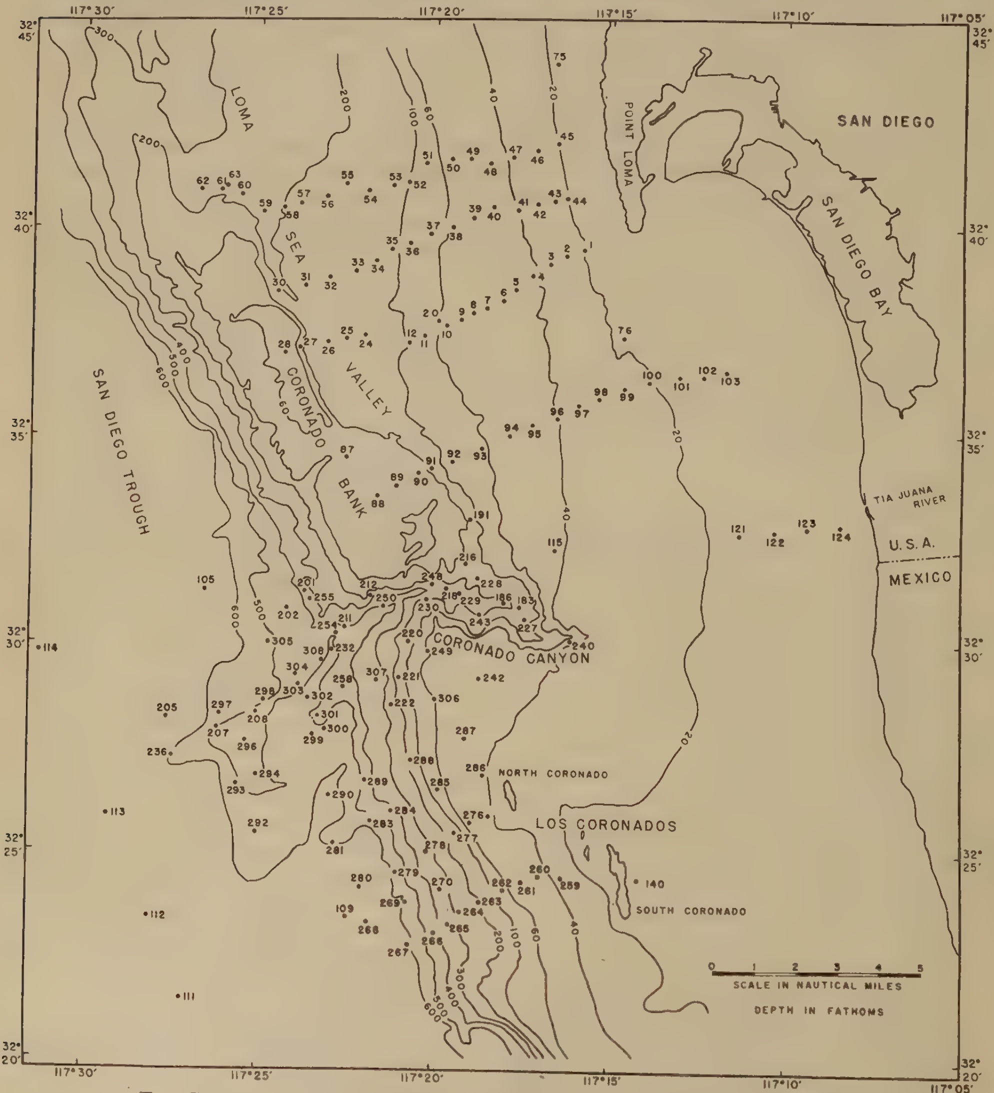
117°30′
117°25′
117°20′
117°15′
117°10′
117°05′
32° 45′
32° 40′
32° 35′
32° 30′
32° 25′
32° 20′
LOMA
SEA
VALLEY
CORONADO
BANK
SAN DIEGO TROUGH
POINT LOMA
SAN DIEGO
SAN DIEGO BAY
TIA JUANA RIVER
U.S.A.
MEXICO
CORONADO CANYON
NORTH CORONADO
LOS CORONADOS
SOUTH CORONADO
300
200
100
60
40
20
400
500
600
1 2 3 4 5 0
SCALE IN NAUTICAL MILES
DEPTH IN FATHOMS
1 2 3 4 5 6 7 8 9 10 11 12 20
24 25 26 27 28 30 31 32 33 34 35 36 37 38 39 40 41 42 43 44 45 46 47 48 49 50 51 52 53 54 55 56 57 58 59 60 61 62 63
75 76 87 88 89 90 91 92 93 94 95 96 97 98 99 100 101 102 103
105 109 111 112 113 114 115 121 122 123 124 140
183 186 191 201 202 205 207 208 211 212 216 218 220 221 222 227 228 229 230 232 236 240 242 243 248 249 250 254 255 258
259 260 261 262 263 264 265 266 267 268 269 270 276 277 278 279 280 281 283 284 285 286 287 288 289 290 292 293 294 296 297 298 299
300 301 302 303 304 305 306 307 308

Text Figure 1. Locations of stations; bathymetry (after Emery *et al.*, 1952).

nado Ridge) trends parallel to Loma Sea Valley, and is separated from the Coronados Islands by Coronado Canyon. The shallowest depth on the bank is less than 60 fathoms and it gradually becomes deeper toward the northwest. The bank consists essentially of rocks but is covered in places by very thin sediments of Recent and Pleistocene age.

(6) Coronado Canyon cuts into Coronado Bank and the shelf and is connected with the head of Loma Sea Valley. The canyon wall is steep and rocks are exposed along it. The upper half of the canyon widens into a broader valley. The floor of the canyon is covered by silty sand and in some places by coarser materials, but the valley is covered by silt. The canyon extends southwest into the San Diego Trough. A delta-like feature at the canyon mouth consists of clayey silt, but fine sands commonly are present which are transported from the nearshore area along the canyon by turbidity currents or some similar mechanism.

(7) The Coronados Islands are the extension of Coronado Bank and Coronado Ridge and probably consist of Miocene rocks.

(8) A prominent slope leads down into the San Diego Trough beyond the break at the outer edge of the shelf and the bank. A series of small and somewhat discontinuous valleys cut the escarpment.

(9) The San Diego Trough, with a maximum depth of approximately 720 fathoms, is wide and flat and is covered by a thick layer of fine-grained sediments. Seismic measurements made by R. W. Raitt (1949) show a fill of 7000-9000 feet above basement rocks in the part of the trough directly off San Diego.

PREVIOUS STUDIES OF RECENT FORAMINIFERA OFF CALIFORNIA*

There are many papers on the taxonomy of the Recent and Pleistocene Foraminifera of the Pacific coast of America. Most of these are listed at the end of this paper.

Walton (1955, p. 958) summarized the ecologic studies of the Recent Foraminifera of the California coast, which were published from 1933 till 1953. These earlier works dealt only with empty tests.

Crouch (1954) analyzed 78 samples (snapper and dredge) taken at depths of 2 to 90 fathoms off San Pedro Harbor, of which 41 are Recent and others are rocks of early Pleistocene to Miocene age. He also dealt only with empty tests of Foraminifera.

Walton (1955) collected and analyzed living Foraminifera assemblages in 215 sediment samples in Todos Santos Bay, Baja California, Mexico, of which many are duplicate samples taken at different times of the year for seasonal study. He also analyzed the dead Foraminifera assemblages of 110 samples. He recognized four geographic assemblages, outer bay, middle bay, inner bay, and marginal bay facies; and five depth facies at less than 30 fathoms, 30-50 fathoms, 50-100 fathoms, 100-350 fathoms, and deeper than 350-400 fathoms. He thought that variation in sediment type, food, etc., might limit the distribution of benthonic Foraminifera, in addition to depth and/or temperature variations. He found that dead population counts are valid to define the faunal composition and general distribution of benthonic Foraminifera faunas but are not indicative of the actual abundances of living faunas. Maximum abundances of living benthonic Foraminifera occurred during the late spring and summer and the maximum populations were at 20-50 fathoms. He suggested that the ratio of living to dead population was indicative of relative rate of sedimentation at each location.

Natland (1957) published a paper on the paleoecology of west coast Tertiary sediments together with the ecology of Recent west coast Foraminifera. His basis of discussion is essentially the same as in his previous paper (1933), although this is supplemented by the work of Crouch (1952) and Bandy (1953) and by his knowledge of the distribution of fossil and Recent Foraminifera species. All the discussions are based on the distribution of empty tests of Foraminifera, not of living ones. He discussed the origin of fossil basins such as Los Angeles, Ventura and San Joaquin based on the distribution of *Bolivina vaughani* Natland. He said (p. 555) "*Bolivina vaughani* is a very hardy species, equally at home in shallow and abyssal waters. It thrives, to the exclusion of most all other species, in deep, stagnant basins with shallow sills. . . . " He also said (p. 549) "The areas where this species dominates may have been the sites of local closed basins with abnormal thermal gradients." For examples of such basins he mentioned the Gulf of California and fossil basins of San Joaquin, Los Angeles, Ventura, and Santa Maria. Living specimens of this species, however, are found at depths ranging from 5 (perhaps shallower) to 105 fathoms in the San Diego area and from 0 to 250 fathoms in Todos Santos Bay, Baja California, Mexico (Walton, 1955). Empty tests are found at many stations in the San Diego Trough (*ca.* 500-650 fathoms). Thus it is possible that Natland's discussion on the origin of such basins is wrong.

Bandy and Arnal (1957) studied the distribution of Recent Foraminifera off the west coast of Central America. They recognized 5 faunal zones based on the distribution of the empty tests from only 36 samples at depths ranging from 1 to 1,045 fathoms and over a distance of approximately 1,200 nautical miles. Their faunal zones are as follows: Inner shelf fauna (0-25 fathoms), Outer shelf fauna (25-66 fathoms), Upper bathyal fauna (66-333 fathoms), Middle bathyal fauna

---

* Editor's note: The paper of Resig (1958) and subsequent papers were not available to the author at the time of writing. References to Resig's species were added later.

(333-666 fathoms), Lower bathyal fauna (666-1,045 fathoms).

HYDROGRAPHY

The following generalizations have been based on data from stations occupied by research vessels of the Scripps Institution of Oceanography ("Physical and Chemical Data" 1949-1957). The temperature at the surface is warmest in August or September (*ca.* 20.00°C.) and coldest in January or February (13.12°C.). The top of the seasonal thermocline is deeper in winter than in summer. It lies at *ca.* 30 m. (17 fathoms) in January, at *ca.* 20 m. (11 fathoms) from February to June, at *ca.* 10 m. (5.6 fathoms) from July to October (except in August when it lies almost at the surface of the sea), and at *ca.* 20 m. (11 fathoms) in November. The depth of the bottom of the seasonal thermocline is at *ca.* 75 m. (42 fathoms) throughout the year. The temperature at the top of the seasonal thermocline is slightly lower than that at the surface of the sea and changes with the seasons (minimum 13.1°C. in January and maximum 19.3°C. in September). The temperature at the bottom of the seasonal thermocline is *ca.* 9.3-11.6°C.

Surface salinity is generally higher in summer and lower in winter, with a minimum of 33.19 o/oo in February and a maximum of 33.79 o/oo in October. Salinity at all seasons decreases slightly with depth to a poorly defined salinity minimum, then gradually increases with increase of depth. The depth of the salinity minimum changes seasonally and yearly but lies below the top and within the seasonal thermocline. It lies between 30 and 75 m. (16.7-42 fathoms). Here the salinity ranges from 33.17 to 33.53 o/oo being highest in April and May and lowest in February and March.

The oxygen minimum layer is at approximately 600-700 m. (333-389 fathoms). The depth of the layer and the amount of oxygen change seasonally and yearly but are approximately as follows:

May-November at *ca.* 367-389 fathoms, 0.25-0.48 ml/L.
November-April at *ca.* 333-367 fathoms, 0.32-0.37 ml/L.

METHODS OF STUDY

Field Methods

The field work was carried out during five cruises as follows:

Date	*Station Number*
July 19-23, 1954	1-103
September 14-15, 1954	104-114
August 16-17, 1955	115-139
November 7-8, 1955	140-200
June 26-28, 1956	201-239
August 13-16, 1956	240-336

Samples were collected along several traverses with an average distance between stations of approximately ½ nautical mile. The traverses were spaced about 1½ nautical miles apart. Stations were located by using sextant angles on known shore positions, dead reckoning, and bathymetry.

All the samples were taken with a small, gravity coring tube except at a few places where the bottom sediments consist of a mixture of very coarse sand, gravel or cobble, where an orange peel dredge was used (see Phleger, 1951b, p. 3-5; 1952, p. 320). The coring tube obtains a short, relatively undisturbed core 1⅜ inches in diameter. As the cores were taken from the tube, the top centimeter was cut off and placed in a sample jar with the sea water above the sediment-water interface and preserved in a 10% solution of neutralized formalin. A small amount of sodium carbonate was added to the samples to maintain an alkaline solution, since neutralized formalin becomes acidic with time. All the samples thus obtained contain approximately the same volume of sediment and represent the same area of surface sediment as those collected by Walton (1955); therefore, the Foraminifera populations of the San Diego and Todos Santos Bay areas can be compared.

In addition to sediment sampling, measurements of sediment temperatures were made during August 13-17, 1956, at 75 stations from depths of 40-630 fathoms. These were obtained on the deck of the vessel when the samples were brought to the surface and do not represent the temperatures *in situ.* Compared with the temperatures *in situ* (measured by Scripps Institution personnel) of water at depths of about 100, 300, and 500 fathoms, the bottom temperatures taken in this manner on the deck of the vessel are approximately 0.5°, 0.7° and 1.5°C. higher respectively.

Laboratory Work

Living populations were counted in 162 samples and dead populations in 156 samples. Sediment size analyses and descriptions of the constituents in the sediment fraction coarser than 0.062 mm. were made on 19 samples.

The living populations were determined by the rose Bengal staining method (Walton, 1952). "Living" is used throughout this paper to indicate those specimens which contained protoplasm when collected as indicated by the rose Bengal stain. The word "dead" refers to those Foraminifera tests which did not contain protoplasm at the time of collection. The reliability of these assumptions is discussed by Walton (*op. cit.,* p. 59). Samples 1-140 were washed through a sieve with an opening of 0.074 mm., and samples 141-326 through a sieve with an opening of 0.062 mm. The residues were stained in a rose Bengal solution for 3-24 hours. All living specimens in each sample were counted while wet.

After the living population count was made the sediment was washed, dried, and then split by using an Otto Microsplit in order to obtain a workable size from which the total population was counted. Five hundred or more specimens were identified in most samples, but in a few only about 150 were counted. The number of planktonic specimens was counted for all the samples, and the ratio of benthonic to planktonic population (B/P) was calculated.

SEDIMENTS

A distribution chart of sediment types was published by Emery *et al.* (1952, fig. 7) based on 1,656 samples. The number of stations occupied during the present study was 337, of which 254 stations were successfully cored. At the other stations sediments were not obtained, but often coarse sands were observed in the core-catcher, or the core-nose was bent which suggests the presence of rock bottom. The sediment distribution shown by these new samples is almost the same as that of Emery *et al.* who divided the modern sediments into three broad groups:

(1) clastic sediments.—subdivided into five major types and four minor ones according to grain size and color.

(2) calcareous organic sediments.—shell sand and Foraminifera sand.

(3) mixed clastic and calcareous organic sediments.—mixture of (1) and (2), each about 50%.

Emery (1952) briefly summarized the continental shelf sediments of southern California from data on Santa Monica Bay (Shepard and Macdonald, 1938), San Pedro Bay (Moore, 1951) and the area off San Diego (Emery *et al.*, 1952). These studies reveal a complex distribution of continental shelf sediments in which there is a notable absence of progressive decrease of grain size with distance from shore. This fact is contrary to the previous concept that the sediments are gradational from coarse-grained near shore to fine-grained off shore. Emery (1952) classified the continental shelf sediments of southern California into five types: (1) authigenic (glauconite, phosphorite); (2) organic (Foraminifera, shell); (3) residual (washed from underlying rock); (4) relict (remnant from a different earlier environment); and (5) detrital (presently supplied chiefly from adjacent river mouths, beaches or sea-cliffs). Representatives of the first four groups occur in such places as banks, hills, and the outer edge of the shelf where they are not masked by the more rapidly deposited detrital sediments. The detrital sediments, taken alone, present a relatively simple gradation from coarse-grained to fine-grained in a seaward direction. The present patchy distribution is evidently the result of insufficient time since post-glacial rise of sea-level for the present supply of detrital sediment to bury completely the irregular topography.

Shale was cored at station 75 at 13 fathoms on the edge of a kelp bed near Point Loma. The rock has been bored by burrowing organisms. It contains no Foraminifera, but may be Cretaceous in age since it has a lithology similar to known Cretaceous rocks which occur nearby.

A siltstone was cored at station 61 at 214 fathoms on the west wall of Loma Sea Valley. The rock is covered by a thin layer of modern sediment. It is rich in diatom remains and is stratified. The Foraminifera are very abundant and very fresh in appearance, and the following species were identified:

Abundant species:
- *Bolivina floridana* Cushman
- *Bolivina* sp. cf. *B. seminuda* Cushman
- *Bolivina woodringi* Kleinpell
- *Bolivina* sp.
- *Buliminella subfusiformis* Cushman
- *Virgulina californica purisima* Bramlette

Common species:
- *Bolivina bramlettei* Kleinpell
- *Bulimina ovula* var. *pedroana* Kleinpell
- *Discorbinella* (?) *valmonteensis* Kleinpell
- *Epistominella* sp.
- *Hopkinsina magnifica* Bramlette
- *Nonion montereyanum* Cushman and Galliher
- *Uvigerina* sp. cf. *U. subperegrina* Cushman and Kleinpell

Rare species:
- *Anomalina hughesi* Rankin
- *Cassidulina* sp.
- *Nonionella miocenica* Cushman
- *Pullenia* sp.
- *Virgulinella* sp. cf. *V. pertusa* (Reuss)
- *Virgulinella* sp.

These Foraminifera show that the age of the siltstone is late Miocene.

The following diatom species were identified by Taro Kanaya:

- *Actinoptychus senarius* (Ehrenberg)
- *Actinoptychus* spp.
- *Asteromphalus* sp.
- *Campyloneis grevillei* (W. Sm.) Grunow var. *argus* Grunow
- *Coscinodiscus aeginensis* A. Schmidt
- *Coscinodiscus asteromphalus* Ehrenberg
- *Coscinodiscus marginatus* Ehrenberg
- *Coscinodiscus denarius* A. Schmidt
- *Coscinodiscus oculus-iridis* Ehrenberg
- *Dicladia pylea* Hanna and Grant
- *Hemiaulus polymorphus* Grunow
- *Hemiaulus* sp.
- *Lithodesmium undulatus* Ehrenberg
- *Melosira sol* (Ehrenberg) Kützing
- *Melosira sulcata* (Ehrenberg) Kützing
- *Navicula californica* Greville
- *Navicula lyra* Ehrenberg
- *Navicula ornata* Schmidt
- *Nitzschia nelsoni* Hanna and Grant
- *Periptera tetracladia* Ehrenberg

TRAVERSE	I																			II															III																		IV		
STATION	45	46	47	48	49	50	51	52	53	54	55	56	57	58	59	60	61	62	63	44	43	42	41	40	39	38	37	36	35	34	33	32	31	30	1	2	3	4	5	6	7	8	9	10	20	11	12	24	25	26	27	28	103	102	101
DEPTH IN FATHOMS	20	33	38	42	47	53	80	99	118	137	157	164	181	194	208	223	214	247	238	20	29	34	39	42	46	53	73	87	104	114	121	135	148	180	19	20	35	40	44	45	47	49	52	56	59	74	92	112	123	157	92	71	15	17	20
LIVING POPULATION	239	1177	869	762	1354	689	894	528	1036	372	712	346	225	183	116	550	171	1252	29	153	1293	1932	731	795	685	680	811	976	412	129	669	861	523	190	195	212	142	96	207	534	800	328	562	761	591	408	83	418	1050	258	406	65	143	79	141
Alliatina primitiva		.1	.1	.5			.7	.2			1	2	1	2	2	.5		1	7		.1		.1	.6		.3	2	2	1		2	.1	3	8							.1	.3	.7	1	1	2		1	1	2		2			
Alveolophragmium advena	2																				.9	.6	.6			.3	2																												
A. columbiense	2	.9	.7	1	2	2	.6	1	.6	1	.6	2	1							3	.1			.5	1	.5		.3	.4	.8	.8	.1		.5	11	2	.7	3	3	8	2		1	1	.7	2	2	.7	.5	.4	.7	1	10	22	.7
Ammobaculites catenulatus						.1	.2	.2	.5	4	6	7	6	6	2	6	2	2						.4	.7	.1	.1	.2	.2	.8	1	2	1	2										.3	.2			1	.5	3					
Ammotium planissimum	2	1	.5	1	.7	1	.9	.2	.6	2	.3		1	2		5	.6	.2			.6	.6	.4	2	1		.6		.2	5	3	.5		2		14		5		1	.1	2	.4	.3	.5	.7		3	.8	2	.7			3	4
Angulodiscorbis charlottensis																																																							
Angulogerina angulosa	3	.4			.7	4	3	1	.3	3	2	.6	1				7	.2		1	.5			.4	1	1	.2	.5	1	3	1	1	.6	2	7	5			1	2		5	2	9	9	3	1	1	.4	.8	6	6			.7
Arenoparrella oceanica		.1		.1	.3	1	.7	.8	.4													.1	.1	.6	2	.7	1	.1		1	.3	.1	.4	2									1	1	.7	1	1	1	.2		1				
Asterigerinata pacifica																																																							
Astrononion viragoensis							.3																																																
Bigenerina höglundi		.1																																							.1	.6	.4		.2						.5				
Bolivina acuminata		.3	.9	.7	9	13	4	5	1	1		.9	1									.6	.3	3	10	11	2	.5	.7	2	3	.7	.6					4	1	8	4	2	7	5	4	8	17	6	.7	1	.5	5			
B. acutula	2	.3	.2	.7	1	.6															.2	.4	.1	.8	.6	.6												1	3	.7	.2		2	5	2	3							2		.7
B. bicostata											.1																																												
B. filocostata																																													.5										
B. minuta											.1	.6	2	4	5	2	5	2												.8		.1	.2													.2			.1	2					
B. pacifica	.8	13	14	13	19	6	12	35	70	18	17	8	6	6	7	.7	15	3	3	.7	5	10	17	16	9	23	21	45	21	18	17	36	29	33		1	4	2	10	8	7	12	15	19	18	30	12	8	21	21	15	11	1		
B. peirsonae																																																							
B. spissa										3		4		6	3	3	13	2																																.4					
B. subargentea									.4	8	6	3	2	2	2	2	.6	29	7											.8	1	2	8	.5															1	9					
B. subexcavata	.4																																											.4											
B. vaughani	1	.4	.7	.1																.7	.5	.3		.3	.2											.5					.2			.3	.2								.7	1	
Buccella angulata		3	2	2	5	12	6	.6													1	3	2	7	16	6	7	1								1	1	4	5	8	2	3	1	2	2	.5	1						.7	1	3
Bulimina denudata		.1	.2	.5	.7	2	4	1	3		.6			.5				.1			.2			.3	1	.9	3	1	4	14	6	2	.8			1	1		2	1	.6	1	.5	.4	.5	.7	7	1	.7	.8					
B. mexicana																																																							
B. pagoda																																																							
B. subacuminata																																																							
Buliminella elegantissima	2	4	2	1	.5	.1														.7	3	3	2	.6	.4	2	.4	.1								2	.7			1	1	.9	1										14		3
B. tenuata																		1										.1																											
Cancris auricula	1	.1		.3	.3	3	3	.8	.1	.3		.3													.6	2	2	.4					.4	4						.2	3		7	8	10	8		.2	.1	3	8	3			
C. inaequalis																	1																																						
Cassidulina bradshawi																																																							
C. californica																													.2															.8		.2									
C. delicata											.1	.3			.9	.2	.6	.6																																.4					
C. depressa	1	.7	.1	1	.4	.1	7	2	3	3	.1									22	1	.5	.4	2	1	3	.9	2	.7	9	8	2	.2								.4			1	2	1		4	1		.7	11			
C. limbata					.2	.6	.5	2	1	5															.2	.1	.9	.7	.7	2	5	.5											.4	3	1	1		2	.6			1			
C. subcarinata													.5			.2	2	.1																																					
C. subglobosa		.1	.1			.7	1	.4	1	3	5	9	19	8	.9		4				.2				.2	.5	4	.5	.2	3	3	2	2	4	8	3		13	2			2	2	9	4	4	4	1	.9	5	.7	3		1	2
C. tortuosa																											.1																	.9		.5									
C. sp. cf. C. orientalis																																																							
Cassidulinoides waltoni								.2		.3		.3	1			.2	.6															.1																			.2				
Chilostomella ovoidea						.1	9	.2	1	1	.3	4				.4		3									6	3				.1	.2	2									.4	.4	.7	4			4	.8	3	6			
Cibicides fletcheri	.4		.1																	.7															2	1					.2	.6	.4												
C. mckannai					.1	2	1	.8	.5	.3														.1	.3	.7	2	.4		4	1				2				2			.6	.4	2		.2	4	.5	.3		2	5			
C. phlegeri																																																							
C. spiralis																																																							
Cornuspira lajollaensis																				2																1					.2	.3												4	
Cornuspiroides foliaceus		.1					.1																																																
Ehrenbergina compressa																		.1																																					
Elphidium spp.																																				2																	4		.7
Epistominella sandiegoensis	1	.2	.2		.1	.9	.8	.2	.1	.3	.1	.3	.5				.6	.1			.8	.2	.1		.3	.9	1			1	.8	.1	.6								1	.6	.2	.4	.2			.5	.1	.4	.2				
E. smithi																		.1																																.4					
Eponides leviculus						.3	2	2	.4	.8	.1	.3	2											.3		.3	.4	.3	.7	3		.2									.2			1	3		4	.2	.2		.7				
E. subtenerus																																																							
Gaudryina arenaria				.1	.6	2	.9	.2																.1	.4	.7	2	.4			.3								.5	.6	.1	1			.3	.5									
G. subglabrata						.4																																							.3										
Goësella flintii		5	8	9	7	2	1		.5	3	2	3	14	10	10	31	14	3	10		1	4	5	20	6	1	.5			.8	.1	.1	.5	28		2	4	25	7	16		.3	2	.5		1		.5	.4	3					.7
Globobulimina barbata																																																							
G. höglundi																																																							
G. pacifica		.1	.8	1	.6	.9	2	13	2	.5	6	6	10	2	2			7			1	1	.3	.6	1	.3	.9	8	8	9	4	17	5	.5			5	1	1	1	2	2	1	.7	.2	.5	4	5	8	6	.2	1			
G. spinifera																																																							
Glomospira gordialis																																																							
Gyroidina gemma																																																							
G. quinqueloba																																																							
Hanzawaia nitidula	3																			8															1	.5								.5	2						1	6			
Haplophragmoides neobradyi					.4	2	1			.3														.1	1		.6	.2																.3	.3										
H. quadratus																																																							
H. sp.																																												.4	.7						.2				
Höglundina elegans										.3							.6																	1																	.5				
Cassidulina sp.																										1		.1				.1									.2		.2												

Table 1. Occurrences of living benthonic Foraminifera in percent of living population.

Rutilaria epsilon Greville
Stephanopyxis antiqua Pantocsek
Stephanopyxis grunowii Grove and Sturt
Thalsionema nitzschioides Grunow
Thalassiothrix sp.
Xanthiopyxis globosa Ehrenberg

Xanthiopyxis maculata Hanna
Xanthiopyxis ovalis Lohman
Xanthiopyxis oblonga Ehrenberg

According to Kanaya (personal communication), *Rutilaria epsilon* and *Navicula ornata* are well-known forms

STATION	45	46	47	48	49	50	51	52	53	54	55	56	57	58	59	60	61	62	63	44	43	42	41	40	39	38	37	36	35	34	33	32	31	30	1	2	3	4	5	6	7	8	9	10	20	11	12	24	25	26	27	28	103	102	101
Involutina pacifica		.1	.3	1	.2	.6	.3	.6	.2	.8	1	2	3	1	.9	.4	1	.3					.3	.8	.2		.3		.2	.8	.3	.5	.8	.5	5				1	2	1			.4	.5	1				.4	.2	1			
Lagena & related spp.	5	.2	.1	.1	.3	.9	1	.4	.3	.9	.7	.6	.5	.5						2		1		1	1	2	.6	.2			.1	.2	.2		2	3	.7	1	1	.2	1	.3	.4	1	.3	.4		.2					4	4	7
Lagenidae (other)	2						.6	.4	.2	.3											.2				.2		.1														.1			.2	.4	.2				.4		2			
Loxostomum bradyi																																																							
L. pseduobeyrichi																.5		4	7																																				
Neoconorbina terquemi																																																							
N. parkeri																																																							
Eggerella advena	.8	1	1		.7	2	1	.8	.1	.3	.1	.3	—	—	—	12	3	1	—	2	3	2	2	1	1	1	.7	.7	—	8	.5	.3	—	2	.5	2	—	—	.5	.2	1	.6	—	.7	8	—	—	—	.1	—		2	1	—	1
E. scrippsi			1	.1	.2																																														.5				
Nonion lankfordi																								.1																		3			.3										
N parkerae																																																							
Nonionella basispinata	15	3	.7	.7																5	9	12	15	1		.6	4	.5		8					1	16	5	4	2	.7	.2		1		1	1			.7	.8			39	26	29
N (?) fragilis																																																							
N stella	21	39	24	25	19	16	19	15	2	9	8	4	.5	2	.1		2	3	3	1	55	39	10	18	10	9	15	10	4	5	2	.3				17	73	28	48	21	46	34	18	7	13	11	8	4	6	3	24		18	23	33
N. sp. aff. N. globosa								.6	.1	3	3	2		3	17	.4		2											.2	.8	.6	.3	1	3																.4					
Nouria harrisii					.1		.2																																					.4	.3										
N polymorphinoides					.1				.5	.3																																													
Patellina corrugata																																																							
Planulina ornata																				.7				.1											.5																				
Placopsilina bradyi																																													6						27				
Polymorphinidae	2																														.1				5																				
Saccammina longicollis		.7	.2						.7	.2	1			.5									1	.1							1	5	2		3	4		1	.5	.7	.1	.6	1	.4	.8	3		2	.7				1	1	.7
Pullenia salisburyi							.1	2	.1																																			.4	.3			.2							
Recurvoides sp.		.2	—	—			2	—	.7	3	2	—	2	—	—	—	4	—	—	1	.5	.2	—	.4	2	3	.7	.1	.2	—	.8	—	—	—						3	3	.6	.2	.3											
Recurvoidella parkerae					.1	.2																			3																														
Remaneica cf. helgolandica																																																							
Reophax excentricus								.2																.1			.4	.2	2														.2							1	.2				
R gracilis	5	.4	20	23	.2	6	2	6	6	.5	22	2	.5	2	0	2		12	10		7	13	29	9	13	14	4	14	51	2	26	19	26	3		.3				5	9	13	16	6	2	4	6	38	37	14	1	18			
R horridus																														.8																		.7	.2						
R micaceous						.4		4	.1		4	3	5	24	.9		2	3							.6	1	3		2		2		7	.5							.1							3	4	2					
R communis		.3	.3	.4	.4	.4	.2														.4	.6	1	.4	2	1															.2	2	.5												
R scorpiurus	2		1	1	1	4	[illegible]	.8	.6	.5	.3	.6	.5				2			.7	.5	.4	.6	4	3	1	1	.4			.5	.1			.5	2	4	4	2	8	4	5	7	.5	.7	3		.7	.2	.4	.5		.7		.7
R subfusiformis																																											.2												
R spp																																				.5			1	.2				.1											
Robertinoides charlottensis	.4																																																						
Rosalina columbiensis																																			25											.2									
R. campanulata	3	.1	.9	.3																23	2	.4			.2	.1									3	3	.7		.5					.5	.5										
R. turbinata																																																							
Seabrookia earlandi					.1		.3	1		.8	.7	.9	1	1		.2	2	.3	4				.1	.1	.2		.2	.6			.6	.3	.4								.2			.8	.7	.5		2	.5	.8	2	2			
Sigmoilina tenuis				.1	.1			.2	.2	.3			.5														.5		.2		.5	.2											.2												
Spiroloculina fragilis																																																							
Spiroplectammina bathyca																																																							
S biformis																																																							
Suggrunda (?) eckis											.6	1																																											
Textularia cf abbreviata			3	.1		.4	2		.1														.1	.3			.2												1																
T earlandi		2	2	.1	.8	.6															.4	1	.6	.1	.6	2	.1			.8					.5	.5			1		.1														
T sandiegoensis		.2	.2	.7	.5	7		.2	.7		.1							1	4			.2	.4	.6	.4	.9	.5	.2	.7		1		1							.4								1	.1						
T schencki		.6																				.4		.1	.3	.3	.2														.1	.3													
Tritaxis bullata																																																							
Trochammina charlottensis	10	.2																		14	.5																																		
T chitinosa																																																							
T conica							.2			1		.6					6										.1	.3						.5										.1	.7										
T discorbinoides																												.1																											
T globigeriniformis																																																							
T kellettae		4	12	9	5	3	5	2	.5	.3	1	3	4	5	5	.9	2	.7	24	2	3	2	9	2	3	2	2	1	1	7	2	2	1	.5		2	2	2	3			4	2	5	2	1	28	1	.6	2	.7				.7
T labiata																																																							
T nitida																																													.2										
T pacifica & var.	.4	.1	.7	.3	.1	.1	2	.2	.7	2	1	1	2	2		1	5	.4	3		.2	.2	.3				1		.2	.8	2	.5	3		18	2				.2				.3	.2			1	.2	2	1				
T rhumbleri	.4	.4	1	1	4	1	1	1	.9	9	2	16	.5		7						.3	.7	.6	2	2	.7	3	4	2		1	7	3							1	1			.3		.7	1	6	6	4					
T squamiformis		.4	.1																	2																																			
Uvigerina auberiana																																																							
U curticosta															2	31		17	14																																				
U juncea					.6	4	.7			.8		.3					.6															.1							1	.2	.6	.6	4	1		1				2	.9				
Valvulineria araucana																	1	.4																																					
V. glabra																	4																																						
Virgulina apertura																																																							
V bramlettei																		.1																																					
V complanata																																																							
V cornuta																																																							
V delicatula											.6	4	.5	4	2			.2														.8																							
V sandiegoensis	.8	2	2	4	6		.1		.1	2	4	2						.7			3	4	.8	3	2	.5	.1	.1	.2	1			1			1					4	3	2	.3	.8			.5	.6	1					2
V seminuda										.1	.7	4	8	6	8			1	4												.6	.6	.4	.5														.5	.5	4	.2				
Miliolidae	8	.6											1	.5	.9					1	.1			.6		.3	.7	.5	.2				.2		3	7				.2	.2	.9	.4	.1	.2			.5	.2				4	12	11
Miscellaneous spp.	9				.2	.4	.1	.6	.3		.2	1	2				5	.2		6					.5			.2	.2		1	.7	.6	.5	2	.5				.8		.3	.7	1	4	.2		2		.4	1	11		1	.7

Table 1 (continued). Occurrences of living benthonic Foraminifera in percent of living population.

in the Monterey shale (Hanna, 1928), with which this rock seems to correlate.

William Riedel examined the radiolarian fauna of the rock, and he also thought the age to be Miocene.

A soft grey siltstone was cored at stations 221 and 312 under a thin layer of Recent sediment. The siltstone at station 221 contains a small patch of sand and pebbles (diameter *ca.* 2 mm.). Foraminifera are rare and most of them are *Cassidulina limbata* Cushman and Hughes and *Cassidulina tortuosa* Cushman and Hughes, which characterize the Pleistocene Foraminifera sand on Coronado Bank. Diatoms are very abundant but were not studied. Radiolaria are common, and indicate that the age of the rock is Miocene or Pliocene, most probably Miocene (W. Riedel, personal communication). The interpretation of these fossil studies is that the age of the siltstone at station 221 is Miocene and the patchy sand, from which the *Cassidulina* fauna appeared to be derived, is a secondary fill in cavities of the siltstone.

TRAVERSE	IV																																																						
STATION	100	99	98	97	96	95	94	93	92	91	90	89	88	87	140	124	123	122	121	259	115	260	240	286	275	242	287	261	306	276	249	262	285	277	191	216	220	227	288	183	228	221	230	243	263	218	229	186	248	212	264	321	323	324	270
DEPTH IN FATHOMS	21	25	30	33	40	45	48	61	80	104	65	63	64	75	5	7	9	11	11	38	39	40	40	41	45	47	50	53	53	55	57	64	67	98	120	125	128	134	140	150	160	167	180	200	213	218	234	248	250	275	280	285	310	328	345
LIVING POPULATION	79	136	228	128	239	296	260	343	394	178	109	437	1237	675	132	203	304	217	283	493	231	693	1548	581	388	818	642	1034	1501	1074	1193	982	417	845	1277	1119	696	171	916	1289	1212	306	598	943	517	808	510	1232	834	240	1379	69	210	119	167
Alliatina primitiva									1		2	5	3	4						.8		5	.3	1	2	.4	.8	3	.7	2	2	2	5	2	2	3	5	1	2	2	3	4	6	4	1	2	8	3	2	6	2				.6
Alveolophragmium advena													.1									.1			.1				.1																									
A. columbiense		1	3	1		1	3	.9	3	1	5	.5	1	3			2	1	12	.2	.4	2	2	.3		.7	.3	.2	.1	1		.3	.2	.5		1	.3	.2	.1		.2			.3									.5	.8	
Ammobaculites catenulatus																			.5			.4	.1								.1		.1			1	.2	3			.2	.2	2	.5	.2			.2	.2	.8	.8	.5		1		
Ammotium planissimum	5	4	.4	2	8	5	2	1	.3		3									.4	.4	.9	.5	.3			.3	.2	.7		.4				.3	.4	.9					.6	.2	1		4	4		6			3	2		.6
Angulodiscorbis charlottensis																																																							
Angulogerina angulosa	8	1	2	3	.4	3	6	4	2	2	5	5	2	2		.5				.2	9	2	.8	2	2	3	1	.1	.1	2	.5	1	.2		2	.2	1	.2			.3	.9	.7		.2			.7	.1			3	.5		
Arenoparrella oceanica												.7	1	.4						2	6	3	5	4	2	2	2	3	3	2	3	1	15	5	4	2	3	3	6	4	5	2	3	1	.2	2	2	5	2	.4	.2				
Asterigerinata pacifica																		1																																						
Astrononion viragoensis												.2	.1																																									
Bigenerina höglundi											.9	.5									.1		.3					.1	.1		.1	.2																					
Bolivina acuminata					1	2	8	8	18	7	9	6	6	5						1	.4	3	2	2	2	3	8	7	9	12	9	8	6		5	.2	2	2	.1	3	.7		.3	.2				6		1					
B. acutula		5	4	2	1	4	3	2			.9	.9	.4							.2		2	1	3	2	2	2	.8	1	2	2	.8	.7											.1											
B. bicostata									.5																																															
B. filacostata							.4	.6	.3	.5	2		.3	.3								.1				1		.1		.5	.1	.2			.1																				
B. minuta								.6	2	2																															.7	1			.5	1		1		.8		1	.8	
B. pacifica				.8	2	3	1	2	5	12	18	14	39	25			.6			12	2	23	17	29	10	44	19	20	24	24	35	28	25	58	39	67	18	27	51	41	24	23	31	58	74	38	19	40	24	47	28	4	4	2	
B. peirsonae																																																							
B. spissa										.5												.1										.1			.1	.5	.9			.1		.7	2	.1	.2				12	3	4		9	3	8
B. subargentea										.5																												.6	1	.9			.5	.3	1	1	.7	.4	3	2		3		28				2
B. subexcavata					.4		.8		.7			3	2	7									.6				.3				.2																						
B. vaughani					.4	.3	.4	.6	.8	1					6	.5	14	2	2	.8		.1	.5									.3								.1										.4					
Buccella angulata		3	4	2	.4	3	4	2	.5							.5	.6	2	2		1															.1																					
Bulimina denudata	6	2	2	2	5	3	6	5	3	6	.9	.2		.9									.3	.2		.2	2	.7	.8	.4	.2	.4			7	2	1	2	.1	1	3		.5	.6		.3		1							
B. mexicana																																																							
B. pagoda																																																							
B. subacuminata																																																							
Buliminella elegantissima							.4					.2	.1			11	34	42	13	.6	.4		.1		.3	.1	.3	.4	.3		.2	.3		.2				.1																	
B. tenuata																																																	.4		.7				.6
Cancris auricula	1		.4	6		.7	2	4	4	9	7	3	5	3						.2		3	.8	1	7	3	3	.4	3	8	2	7	3	.8	.3	.4	.9	.7	5	.7	.7	4	.2	.3				.5	.1				.5		
C. inaequalis																																				.1	.1	.3					9											1	3	
Cassidulina bradshawi												2	.1	1								.1		1		1	.2		.5	.4			.2				.7																	
C. californica												.5	.2												.3				.1														.3				.2								
C. delicata																																													.2		.2				.6	.4	.1		13	9	4
C. depressa				1	2		.8				9		.6	2						3	2	3	4	.5	1	3	.6	.4		.1	.8		.2		.4	.4	2	3		.2	1	2	.8	.5			.2	1	2	.8	1		5	.8	2
C limbata			3	3		3	5	10	9	13	6	2	.8	.7								.1		.3	1	.6	.2	.2		.3		1	.5		2	.5	.1	.1		.2		.6	.2					.9							
C. subcarinata																																																		.1		.2		3	6	4
C. subglobosa	5	6	14	10	6	8	13	15	10	6	2	1	.3	2							2	.3			1	.7	.6	.5	.5	.2	1	1			.6	.9	2	.1			.3	2	.3		.2	.3	.4	.1	.1	.4					.6
C. tortuosa	3		10	7	3	4	.4	1	.3				.1									37				.5	.1						.5	.5																						
C. sp. cf. C. orientalis																																					.3																		
Cassidulinoides waltoni																																					.4		.3						.2										
Chilostomella ovoidea								.9	7	.5			.1	.3								.9				.4	1	.5	1	2	.8	1	2	3	.1	.1	.1	.3	12	.2	.3	.6	.3	.1	.4		.8	.8	4	.4		19	2	3	7
Cibicides fletcheri	9	5		2	.4	1	1	.3				1	.2		.7								.1		.3	.2		.1				.2				.1	.3						4												
C. mckannai			1	4	.4	.3	1	4	5	5		.9	.4	.3							.4		.1			.4		.4	.5	.3	.6	.2	.5		.6	.1		.1		.2		1						.4							
C. phlegeri																																					.9			.2		2	.5						.9					2	
C. spiralis																																																							
Cornuspira lajollaensis					.4			.6																																																
Cornuspiroides foliaceus																												.1																												
Ehrenbergina compressa										.5																																	1											3	
Elphidium spp.	3	3	2			.3	.4										28	12	21	26																																				
Epistominella sandiegoensis					.4	1	3	5	3	1		2	.5	.1									.4	.3			.9	.6	.3	.5	.8	1			.9	.6	.9	.4	.2	.2	.6	.6	6	.5		.4		2	.5	.4	.2		4	3	
E. smithi																																																				.1		.5	3	6
Eponides leviculus												2	.6	2								.4	.1	.7	.5			1	.2	2	.3	.4			2		2	.8	.2	3	.1	.3	2					6	.2				1		
E. subtenerus																																																							
Gaudryina arenaria			3	.8	.4		1						.2	.4							2			.2		.1	.2	.3	.1	.1	.5	.1			.6	.7	.6					1						.2							
G. subglobrata						.3							.1								.1					.2																												
Goësella flintii			5		6	16	2	.3	1	3		.5									2	.3		.2			.2	.2	.1		.2	.1		.1		.3	.3	.2			.8	2	9	3	10	27	37	.4	.6	2		7	3	2	
Globobulimina barbata																																																							
G. höglundi																																																						1	8	
G. pacifica	4	.7		5	1	2	2	2	6	10				.1						4		10	1	4	.8	.4	5	2	.9	1	2	.3	.5	.4	3	.9	2	14		3	6		4	3		2	4	.4	2	5	3	6	2	4	5
G. spinifera																																																							
Glomospira gordialis												.2													.3																	.1	.3													.6
Gyroidina gemma																																																							
G. quinqueloba																																																		.2						
Hanzawaia nitidula	3		2	2		.3					2	2	.6	.6							.4	.6			1	.7	.2		.1	.2	.1	1	2				.4		.4			2	.3						.6						
Haplophragmoides neobradyi						1	.4	.3														.6	.4	.5		.1	.2			.1						.1		.1	.2		.2		.3					1						2	3
H. quadratus													.2	.3												1	.2	.2		.3							.7			.1			2												
H. sp.																						.4	.1	.2		.2																													8	
Höglundina elegans									.5																																	.7										.5	3	
Cassidulina sp.								.6				2	.1	1								.1		1		1	.2		.5	.4		4	.2	.2	.1		.7	.1		.1			.2	.1				.2							

Table 2. Occurrences of living benthonic Foraminifera in percent of living population.

LIVING BENTHONIC FORAMINIFERA

Depth Distribution of Species

Occurrences of the species of living benthonic Foraminifera are listed in Tables 1-3. In addition, the important species have been arranged in diagrammatic form according to depth ranges and frequencies in Text Figs. 2-9. Distribution charts of fifteen significant species were made, of which four are shown in Text Figs. 10-13 as examples (the others are on record at the Scripps Institution of Oceanography and the University of California, Los Angeles). These figures show that each species has a more or less characteristic

STATION	100	99	98	97	96	95	94	93	92	9	90	89	88	87	140	124	123	122	121	259	5	260	240	286	275	242	287	26	306	276	249	262	285	277	141	216	220	227	288	183	228	221	230	243	263	218	229	186	248	212	264	322	323	324	270
Involutina pacifica			.4	.8	.4	1	4	1	2	1		.9	6	1					1	2		6	5			5		.3		1	1	4	2	.2	8	.4	1	.4		.3	4	6	2				2	2	2			10	7	3	4
Lagena & related spp		7	2	2	2	3	8	.9			9	.5	5	7				2	.4	3	.4	2	9		.5	.9	1	5	7	4	8	7	5		.4	5	4	3		.1		.6		4	.2	.1	.2	.2		4	1		.5	.8	1
Lagenidae (other)										.5	.9			.1			3			2		.1	1			.2		2		2		.1			1			2					2					.1							
Loxostomum bradyi																						.1			.3																													3	
L. pseduobeyrichi																																											2						2		3		2	8	4
Neoconorbina terquemi															72																																								
N. parkeri																																																							
Eggerella advena	1		4		1		1		3		9	3	.6	3			6	1	7	2	5	3	5	7	3	1	2	2	6	2	3	2		1	2	8	3	.7	1	3	1	7	8			.1		2	.1		.3	2	.5		
E. scrippsi																				4		4	1	5	3		9	2	3	2	2	5	1	1	.1	3	9	2		2	1	1	.8	6	2		8	3	1	1			1		
Nonion lankfordi						.7	.8	.9					.2	.4						.6		.4			3		.6			1																									
N. parkerae																																																							
Nonionella basispinata	10		3	4	2	.7		.6	1				.7	.4		.1	1	20	22	4	.6		.4	.4	3		1	.7	.9	.5	.3	.8		.1	.1	.2		.2	.1					2				.7							
N.(?) fragilis																																																							
N. stella	9	33	8	26	3	10	6		.5	.5	9	2	2	.6		1	.6	4	.6	5	.3	.2	25	7	22	.8	14	.5	18	10	10	5	7	2	4		3	8	2	7	7	4	2	2	3	1	2	4	1		7	13	2		8
N. sp. aff. N. globosa										1			1																						.2		.1	.2								.3		.1	.4		.3				
Nouria harrisi																				2					.5	2	5		.1	1		.5	.5	.1					.2		.1	7	5												
N. polymorphinoides																												.1						.1		.6		4			.4			.2		.3				.4					
Patellina corrugata																																																							
Planorbulina ornata	4		2	3		3	.4					.5											.1		.3				.1			.1	2															.1						3	
Placopsilina bradyi												5	4												.5					.5		6	3	8			7		2			8													
Polymorphinidae		2	2		.4	3																	.1										.2																						
Saccammina ungicolis			.2	.8	2	3	5	2	1	2	.6						.6											.2				.2													1						2		1		1
Pullenia salisburyi				2		.3		.6	3				.3	.1								.3		.2		.4				2						.1		.2		.1	.1		.2					.1							
Recurvoides sp.													.2								1		1			2	5	1	1	.3			2							1	1														
Recurvoidella parkerae													.7													.2		5		3																							.5	.8	
Remaneica cf. helgolandica												2								.8		.3		.2			2				2																								
Reophax excentricus							.4	2	2	2			.2							.6			.2				.5	.8	.1		.3					.4	.7	.1				.6	.5	.5		1	1								
R. gracilis					1	.3		.3	5	2	3	4	2	4						20	3	8	9	.3	9	7	14	.2	9	6	5	.8	5	9	9	2	.2	2	3	2	1	5	2	7	2	2	2		4	2	2	3	2	2	
R. horridus						.3																.4					2		1	1		.1				.1							.2	.6		.7	2	.1	8	.4	.4	2	.5		.6
R. micaceous																																.4						2			2			.4		1		.3	3	.4		1			
R. communis												.5	.4	.7		.5	3	.5	7		1		5	.5	.3			.4	2	.2	.1		.5							.2															
R. scorpiurus		4	3		12	9	1	5	2	1	3	.7	.3							.8		1		.3	.8	.6	.5	.8	4	.5	.7		.5	.2		.4	.7		.2																
R. subfusiformis																																																							
R. spp		2	2	4	4	7	2			1																	.6				.1						.9				.3		.5			.4		.4	.2						
Robertinoides charlottensis	3				.4	.7														2	.4	.4	.2		3	.2		.3		.1					.1																				
Rosalina columbiensis															12																																								
R. campanulata	10			3	2	2	1	.3				9	2	1	.7	.5	.3				1	.1						.1	.1																										
R. turbinata																																																							
Seabrookia earlandi							.4			.5	4	1	1	2						.2		.6		.3		1	.5			.5	.1	4	1	.4	.8	.3	.7	.5	.5	.2	1	.3	1	.3		.1		.5	.1	1	.1	4		.8	
Sigmoilina tenuis				.8	.4	3		.3															.3			.5		.3		.1	2	.1			.1			.1			.2		.2	.2				.7	.1						
Spiroloculina fragilis																																																							
Spiroplectammina bathyca																																							.1															.8	
S. biformis																																																							
Suggrunda(? eckisi																																				.1		2		1	2		.5	2	.8	.1	.2	.2		.4					
Textularia cf. abbreviata	1	7	2	8	4	3	4						2											.2	.3			2	.3	.1		.1				.3	.7						.3	.2											
T. earlandi						7		3						1						.4		.4	1	.2			.8	.6	.5	1	2		.7	.1	.1	.5	1	.3		.5	.6		1	.2				.7							
T. sandiegoensis												.7	3	1						.2		.4	9	.2	.3	.1	.6	2	.7		1	.4	1	12	.5	1	2	1	8	.9	1	1	2	2	2	.9	2	4	5	.8	4	2	.5		.6
T. schencki																										.4																													
Tritaxis bullata													.4														.2								.8							.7							.2						
Trochammina charlottensis													3				.3		.4		1				1						.1		.5																						
T. chitinosa																																																				13	9	3	
T. conica														.6			.3							.2	.5					.2					.2		1					2													
T. discorbinoides												.5	.2	.4							.4				.5	1	.2			.5			.2	.1			.6		.1																
T. globigeriniformis																																																							
T. kellettae	1				1	.3	1	.3		1		2		.1	3	1	.3			12		2	.1	.9	1	1	2	.6		.3	.7		.7	.2	.1		.6								.8	.3		.1		9	1		2		3
T. labiata																																																							
T. nitida												.2	1	.3						.2				.2			.3		.1	4	.1						.3																		
T. pacifica & var.											3		.4			.5		1	4		.4	4	.3	.2	.5	.8	.5	.3	.1	.2	1	.2			.6	4	1	.2	.2	.3	.3		2	.7		.1		.7	.5			4	3	3	.6
T. rhumbleri												2	.8	.6				1		.2		.4	2	.3	.5		3	1	.2	.7	1	.1	.7	.8	.8	3	.6	2	.7		2	.7	1	.1			.2	.1	.2						
T. squamiformis												2	1	2					.4		.4		2	.3	2	.2	.3	1	1	.2	1		6	.6	.4	.1	2		3			2							.1						.6
Uvigerina auberiana																																																							
U. curticosta																																											.3				.2		3	7	1		2		4
U. juncea							2	3	2	4	4	4	1	2									.1		2		.7	.5		3	2				1	5	3	2		6	2			.6			.8	7	.9						
Valvulineria araucana																																									.1		.2						2		.1				4
V. glabra																																																							
Virgulina apertura												1	2	7								.3	2		.3	2	2	3	8	1	3	.2	4	.4	4	.4	.6	19		17	26	1	2	4		9	7	2	4		4		2	6	13
V. bramlettei																																																	6		.4				2
V. complanata																																								.1															
V. cornuta																																																							
V. delicatula																																		.8	.9	.5	2	.6	.8	.7	1	.6	.7	3	1	2	1	.8	.8	8	4			.8	2
V. sandiegoensis		7										1	2	.9						11		.9	12	6	3	.8	4	8	8	1	2	4	2	.1	.1		.3	.3		.2	.1			.5		.3		.1							
V. seminuda														.1																				.7	.4	.2	2	2	.4		2	1	.7	.8		.7	1	.6	6	.8	1		4	3	6
Miliolidae	1	3	.4		4							.4	.1	.1	5	55	9	.5	3		.4	.4	2	2	1	.1	.6	1	.3			1			.5	.1	.7			.2	.1	.6	2				.4	.1	.1		.1		2	8	
Miscellaneous spp	11	8	8			2	1	1	3	2	9	3		1	7			.5			.6	.1	.2	5	.6	4			4			1			.1	2	.1	.4		.3	4	.2				.2	.5			.2	4	2	2	6

Table 2 (continued). Occurrences of living benthonic Foraminifera in percent of living population.

depth range, but that there are also rather general boundaries between different assemblages. These boundaries are based on upper and lower limits of several species and also on their frequencies. Seven faunas can be recognized with boundaries at 13, 45, 100, 250, 350, and 450 fathoms. The detailed discussions of these faunas and boundaries are not presented for the sake of brevity but are on record at the above-mentioned institutions.

Possible Causes of Depth Zonation

There may be many factors which influence the physiological activities and hence the distribution of living Foraminifera. Temperature and food are considered most important by many workers. Also of possible importance are salinity, sediment type, rate of sedimentation, oxygen content, pressure, light penetration, pH, Eh, turbulence, currents, and submarine topography. These factors are interrelated. For example, pressure, temperature, light penetration and salinity may be entirely or in part related to depth. The food and the nature of the substrate are related to sediment types. It is not known, however, which factor or com-

TRAVERSE																																																
STATION	201	307	265	278	325	255	326	250	211	266	304	258	202	294	303	284	289	296	254	208	308	301	207	298	300	302	292	293	305	232	299	290	297	279	269	283	281	236	109	280	114	267	268	112	205	113	111	105
DEPTH IN FATHOMS	345	350	350	350	350	355	385	390	395	420	430	430	440	450	455	455	460	460	465	473	485	490	505	505	505	515	515	520	525	528	530	550	560	565	570	580	580	585	599	605	608	615	630	635	638	639	640	650
LIVING POPULATION	693	106	621	587	79	1154	269	9300	564	805	421	598	570	335	273	506	351	183	793	300	443	236	253	307	467	712	162	207	689	475	455	146	204	488	433	409	172	198	150	380	90	566	357	252	307	118	192	29
Alliatina primitiva	1	2	1	1	1	2	1	2		.9	.5	.3	5	.9	.7	1	.9		1	1	.2	.9	.4	.7	1	.3		2	.3	.2	5	3		.4	.2	.5		.5	.7	.5		.5	1	1	3	.8	1	
Alveolophragmium advena																																																
A. columbiense												.7	.2					.5	.4	2						.1			.1											.8		.9						
Ammobaculites catenulatus	1	2	1	.9	5	1	3	.1	3	.5	2	4	2	.3		1	.6	1		9		.4	2	2	.4		.6	.5	.4	.2		2	1	2	.7	.2	4		.7	.3	1	.7	.3	4	2	6	2	
Ammotium planissimum	.6			.2		.4		.1	.2																																							
Angulodiscorbis charlottensis																																																
Angulogerina angulosa																																																
Arenoparrella oceanica	.1			.2	1	.2	.7			1	2	1	4	.3	.4	.4	1	.5	1		.2	1	.8	1	2	.8	3		.9	1	2		.5	.2	2	1	1			.5	1	2	3	2		.8	4	
Asterigerinata pacifica																																																
Astrononion viragoensis																																																
Bigenerina höglundi																																																
Bolivina acuminata						.2																																										
B. acutula																																																
B. bicostata																																																
B. filacostata																																																
B. minuta	.9		2	.5	3	.2	.4	.2	4	.6	.5	.8	.7	.3	.4	.6	.3		.4	.1	.6				.2						.4			.4		.5			.7	.3		.5	.3	.4				
B. pacifica	21	10	2	28	27	25	3	33	23	13	4	9	6	3	2	17	17	.5	10	2	7	6	2	1	12	10	6	2	2	20	8	.7	1	5	1	8	1		.7	2		3	.6	2	1	.8	3	
B. peirsonae																																																
B. spissa	11	6	11	6	3	13	16	5	12	10	16	15	16	14	12	12	6	5	6	12	10	7	10	7	8	4		10	4	15	4	3	.5	8	3	3	.6	3	2	4		3	1		2		2	
B. subargentea	2	.9	1	2		.5		12	3			.3	.2			.4			.3		.9									.2				.6														
B. subexcavata																																																
B. vaughani						.1														.1																												
Buccella angulata																																																
Bulimina denudata																																		.2									.3					
B. mexicana																X																X							X		X			X		X	X	X
B. pagoda																																																
B. subacuminata										.9	.7		.7			1	.6				2				.6			.5			.2	.7	3	.2	.5					.8	1	.3	2		1	3	.5	
Buliminella elegantissima																																																
B. tenuata	1	3	1	4		2		4	2			.2	.2						.5							.1			.1	.2																		
Cancris auricula																																																
C. inaequalis	.1						2	.1	.2	.1		2									.2									.4																		
Cassidulina bradshawi										2									.4																													
C. californica																																										.3						
C. delicata	4	3	2	1	6	2	.4	.1	3	6	3	9	3	11	3	2	6	7	4	4	7	9	2	2	5	.7	7	1	3	2	2	4	3	2	3	5	5		2	5	1	7	3	1	1	2	3	14
C. depressa			3	.2		.2					.7	2												.3				3	.9		.4			2	1	.7							.3				.5	
C. limbata																																																
C. subcarinata	3		2	.7		.6			.5	.4		3	.3	.9	3	1	.9	3	.5	3	3	3	.4	2	3	.4	3	1	2	2	4	6	9	4	4	.7	1	1	3	3	2	2	5	3	1	2	3	14
C. subglobosa														.6	.7			3		2		.4	1			.3			.4	.4							1			.5			.3					3
C. tortuosa																																																
C. sp. cf. C. orientalis																																																
Cassidulinoides waltoni																																																
Chilostomella ovoidea	7	3	10	3		11	.4	5	2	5	1		.5	.3		8	6	1	11		4	.9	.8	2	1	2	3	2	3	3	2	3	.5	2	3	3	5	4	2	2	5	2	4	4	2	2	3	3
Cibicides fletcheri																																																
C. mckannai																																												4				
C. phlegeri	.1		.9	.5	4	.3	2		.7	3	1	3	3	.6	1	.8	.3		.3	1	.7		.4		.2				1		.7	1		2	.7	2	3			.5	1	1	.3	2	.7	15	1	
C. spiralis																							.4	2				.5				1	10		.2	.2	1	1	.7	2	9	.9	5	4	2	21	6	14
Cornuspira lajolloensis																																																
Cornuspiroides foliaceus																																																
Ehrenbergina compressa																																																
Elphidium spp.																																																
Epistominella sandiegoensis	6		.8	2	1	.5	1	.1	2	2	.5	2	.3	.6	2	1	.3	1		.7		.9		.3	.9	.1	1	.5	.1	.4	1	.7		4	.5	.2		.5	.7	3		.7	1	.4	2		.5	
E. smithi	2	5	6	2		2		.4	7	.9		1	.5			.4	.3		.3		.5					.1									.2	.5	.6					2						
Eponides leviculus	.1		.2	.2	3	.7	3		.4	2	1	2	1	.3	3	2	1	2	.3	4	1	2		2	.6	.1	1	2	.7	1	.7	3	2	3	.9	3		1		5	1	.3	2	.8	6	11		
E. subtenerus														.3									.8				.6	1				1	3	.6	.5	.7		1	3	2		.7	.3	.4	3		2	7
Gaudryina arenaria																																																
G. subglobrata																																																
Goësella flintii	.4	.9		.3			.7	.1	.2	.2		1	1	2	.7		.3	.5	.3	3	.9		1				2		.3	.6		1	2		.5		1	.5					2	.8	.7	.8	3	
Globobulimina barbata		2	1												.4	.4	.3			.3				.3		.6					.2	.7	1			1								.8	.3		.5	10
G. höglundi	3		.5			.1					.7			.6		.4		1		1	.2			1				.5	.1	1				.4	.7	.2	1		.7			.2						
G. pacifica		8	2	.5		1	1	7	.4				.3	2	3	2	2	2		3	.2		2	3		.1	3	2	.3			4		2			2	1	1	.8	1	.5	.3	.8	1	.8	.5	
G. spinifera	1			.3		.1				.1		.2	8																	.2	.2									.3								
Glomospira gordialis	.3			.5			.7		.2	.7		.5	3	3	2		1	.5	.1	.3			2	2	1	.4		3	.7		.2	4	2	.6	.2	2	2	5		1	1	.3	1		2	2	2	
Gyroidina gemma			.2				.7				1	.8	.2								.2	1		.3				2	.4		.2		2		1							.2	1		3		1	
G. quinqueloba	.1					.1				.1			.3						.3																.2	.2				.3			.9					
Hanzawaia nitidula																																																
Haplophragmoides neobradyi			2				5		1		5	.5	6	5	6	2	.6	1	3	1	.9	2	16	3	.6	.4	1		.7	.2	.2			3	1	3		2		4	2	.3	1	2				.3
H. quadratus																															.2		1		.2							.2			.3			
H. sp.				.3	1		5				2		.7	2	3			7				1	5	10	.2	.4	2	3	.9			1	7	.4		.2		3		3	5		2	.8	.3	2	3	
Höglundina elegans							1			.1	.2	.2	.2	1	1	2	1	2		4	.9		7	4	.2		4	.5	.3	.2	.4	.7	4	.8	.5	.2	1	4		1		1	1	.4	1		.5	
Cassidulina sp.																			.1																													

Table 3. Occurrences of living benthonic Foraminifera in percent of living population.

STATION	201	307	265	278	325	255	326	250	211	266	304	258	202	294	303	284	289	296	254	208	308	301	207	298	300	302	292	293	305	232	299	290	297	279	269	283	281	236	109	280	114	267	268	112	205	113	111	105
Involutina pacifica	.9	2	2	.5		.9	1		.9	3	2	2	3	3	2	1	1	.5	.4	2	.5	.4	.8	3	.6	.3		2	1	.2	1	2	7	4	2	3	1	12	4	2	8		.9	7	6		3	
Lagena & related spp.			.6			.1	.4			.1	.5		.3	.3	.7	.2	.3	.5	.1		.7	.4		.6	.6		1	1	.3	.6		.7	1	.4		.2	.6				1		.6	.8	1	.8		
Lagenidae (other)										.1								.5												.2														.4				
Loxostomum bradyi							3				1	.3								.7	.2					.1																						
L. pseudobeyrichi	.6	.9	.3	3		2		5	5	1	.5	2	.5		.4	.4			4			.9			.2	.1		2	.3	2	.9			.2	4	.2				.3		.3						
Neoconorbina terquemi																																																
N. parkeri																																																
Eggerella advena	.3					.2			.2		.2	.2	.2		.7								.4										.5							.8		.2			.7	.8	.5	
E. scrippsi	.4						10			.9	2	1	2	1	7			2		2		.4	2	2			1	2	2			2	2	.2	.2			.5		.5	1	.3	.9					
Nonion lankfordi																																																
N. parkerae																		.5																														
Nonionella basispinata															.7	.6			.1	.3		.4	2	.3		.1				.4			.5	.4	.5			1				.2						
N. (?) fragilis																																									1					.8		
N. stella	3	17	6	3		2	.4	1	1	.6	.7		2	.9	1	1	6	1	2	2	1	2	2	1	2	2	3	1	3	1	3	3		3	3	13	2	3	14	.8	1	7	1	2	.3		1	
N. sp. aff. N. globosa				.3		.3		.5									.3																															
Nouria harrisii																																																
N polymorphinoides	2	5	4	2		.3		.1	.2	.1	.2	.2	.2			.4	2	1	2		1	.4			2	2	8	4	1		3	3		2	1	3		.5		.3					1			
Patellina corrugata																																																
Planulina ornata							.4		.4		.2	.2								.3																												
Placopsilina bradyi																																																
Polymorphinidae																																																
Saccammina longicollis																						.4			.2			.5						.2									8					
Pullenia salisburyi												.3	.3	.9											.2			.5				.7	1						.7								.5	
Recurvoides sp.			.3											.3				.5						1	.2				.7			.7								.5			.3					
Recurvoidella parkerae							1			7												.9				.1												.5										
Remaneica cf. helgolandica																																										.2			.3	.8		
Reophax excentricus						1	.4							2			.6	.5			.2	.9			.2	.3			.3		.2			.2														
R. gracilis	3		2	3	1	5	.7	.4	1		3	2	2	2	2	2	5	.5	3	3	2	3	4	3	1	2	3	2	.7	6	2	.7	1	2	2	2	1	1	5	1	1	2	3	.8			2	
R. horridus	1	.9	.6	.2		.6		.1	.4	.4		.2		.9		.8	.9		.5		.5					.3							1											.4				
R micaceous	.1		.3	4		3	.4	.2	2		3	.2			1	.8	2	.5	2		.9	11		3		3				.8	2		3		1			2	1		1			1	5			
R. communis																																																
R. scorpiurus										2					1																		.5					1										
R. subfusiformis																																																
R. spp	1				2	2			1	2	3	2	.9		.7						.7	2		.3	1	.2	3		.2	.8	3	.7	2	1	4	2		3			2	.2	2	4	5		1	
Robertinoides charlottensis													.2																																.3			
Rosalina columbiensis																																																
R. campanulata			.2																																													
R turbinata																																																
Seabrookia earlandi	.1		.3			.1	.4		.2	.4		.2	.2	.3	.4	.2						.4		.7		.1			.1					.2	.2							.2	.3					
Sigmoilina tenuis																.2																																
Spiroloculina fragilis																			.1					.7		.1			.4				1		.5	.2							2	2	1	.8	1	
Spiroplectammina bathyca	.1								.9	.7		.3	1		1				.1		.2					.1			.3	.4	.4				.2						2	.5	1	2	2	3		
S. biformis																																2				.2						.2	1	.8		10	.5	.2
Suggrunda (?) eckisi									.2																																							
Textularia cf. abbreviata																																																
T. earlandi												.2																																				
T. sandiegoensis	2	4	2	16		4		11	.9	.6		.2	.2			.2	.3		1		.2	.4			.9	1				.6	3				.2	.2		1					.6		.6			
T. schencki																																																
Tritaxis bullata	.1									3	.2	1		.9		.8														.6					.2								.9			.8	.5	.5
Trochammina charlottensis																																																
T. chitinosa	3		2	.2		.9				.5	7		1	.9	.4	1	3	2	4		3	4		1	2	3	4	3	3	7	4	1		3	8	5	7	1	8	2	1	3	1	.4	.3		2	
T. conica								X		.2		.5	1		.7			2	.3					1	.6	.3					.2			3		.2				1					2			
T. discorbinoides														.3																																		
T globigeriniformis								X					.5																.1				3							2	2		1	.4	.7		1	
T kellettae	2	7	.8	.7					.5	.1	1				.7	3	6	4	.8			2	1	1	6	.1	8	3	2		.4	6	7	2	1	3	7	.5	3	2			5	.4	.3	.8	1	14
T labiata	.1						1		.4	1	.7	6	.2		1				.3		.5	.4		.3					.1	.6		.7	3	.6	1			3		2				4	4	.8		.5
T nitida																																																
T pacifica & var.						.1						.5	.9	.9	1								.8				.6			.4	.4						.6		.7	.3							2	
T rhumbleri	.3					.1	2	2				2	.5		.4								.4	1					.4				.5					3		.5			.9					
T. squamiformis							.4																																			.2					.5	
Uvigerina auberiana																								1	.2							2	3	.4	.5	1		2	1	1	1	.5	2	.4	2		.5	
U. curticosta	.4			.3	1	1	.7	1	2	.4			.9	2	1	.4		1	2	1	6	2	.4		.2	.4		2	.9	3	.2	6		.2		.2		1		.5	4	.2		.4		2		7
U. juncea			.6															.5		.7			.4	.3																								
Valvulineria araucana	.6	3	.5	.9		.6	9	X	.2	1	.5		.2	.9	.4	.4			5	.3		.4	1	2				2	1		2	1	3	2	.9	2		8	.7	1	4	2	1	1	4		3	
V. glabra	.1					.1	.4			1	4	.8	6	7	7	2		9	1	6	.7	.9	11	4	1	.4	6	5	3	.8	2	2	3	6	5	3	2	2	.7	3		3	.6	6	3		2	
Virgulina opertura	.3	8	19	7	3	8	15	7	7		20	17	6	22	17	24	22	31	24	24	32	29	15	24	40	62	22	29	56	25	33	25	2	14	35	21	46	23	32	30	20		14	25	14	.8	28	4
V. bramlettei	.6	.9	1	.2		.5		.6	.4			.2							.5				1							.6				.4	.2		.6		.7								.5	
V. complanata	.1		.5					.9													4	.9																										
V. cornuta	.1		.5					.9														.9																										
V. delicatula	3	.9	1			2	2	.8	3	2	.2	.7				.4	.9		2		.2				2	.1	.6		1		.9			7	.2	3	1			3		9		.4	1			
V. sandiegoensis				.2						.9		.2																																				
V. seminuda	3	4	6	3			2	.5	1	1	.7	.3		4	.7	1	3		.9	.7		.9			.4	.4	1	3		2	1			2	.2		.6		5		6	.5		.8		2	1	3
Miliolidae			.3	.2		.3	.4		.4	.5	.2	.3	.3		1	.8		2			.7		2	2		.4		1	.5		4	1		1	.5	1		.5		2			.9		.6		.5	
Miscellaneous spp.	1				1	1	2	.2	2	2	12	.2	5	1	6	3	.8	.5	1	5		4		1	1	.1		1	.4	.2		1		.4	3	.2	.6	2	2	1	2	1	12	4	.8	9	1	.5

Table 3 (continued). Occurrences of living benthonic Foraminifera in percent of living population.

bination of factors is most important to Foraminifera ecology.

Some workers have attempted by laboratory experiments to evaluate these various factors. The results of such experiments are useful in indicating the relative importance of many factors existing in nature. But the natural environments are always changing, the dimensions are extremely large, and dynamic equilibria may exist among many factors. A laboratory culture, on the other hand, is small in scale and static in nature. One should use care in applying results from experiments to natural phenomena.

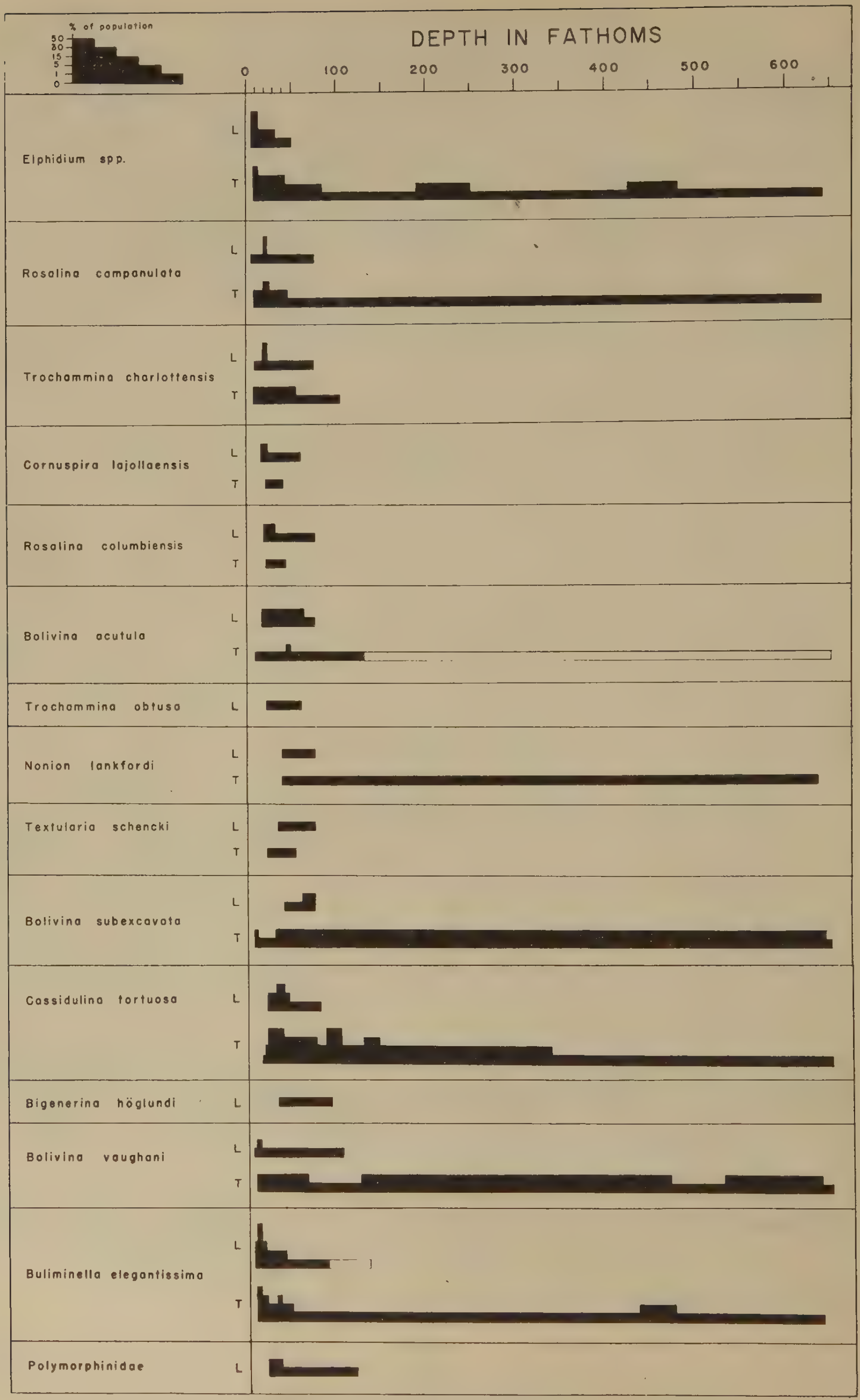

Text Figure 2. Depth distributions of benthonic Foraminifera. L: living population; T: total population. Height of bar: average frequency; solid bar: consistent occurrence; open bar: scattered occurrence.

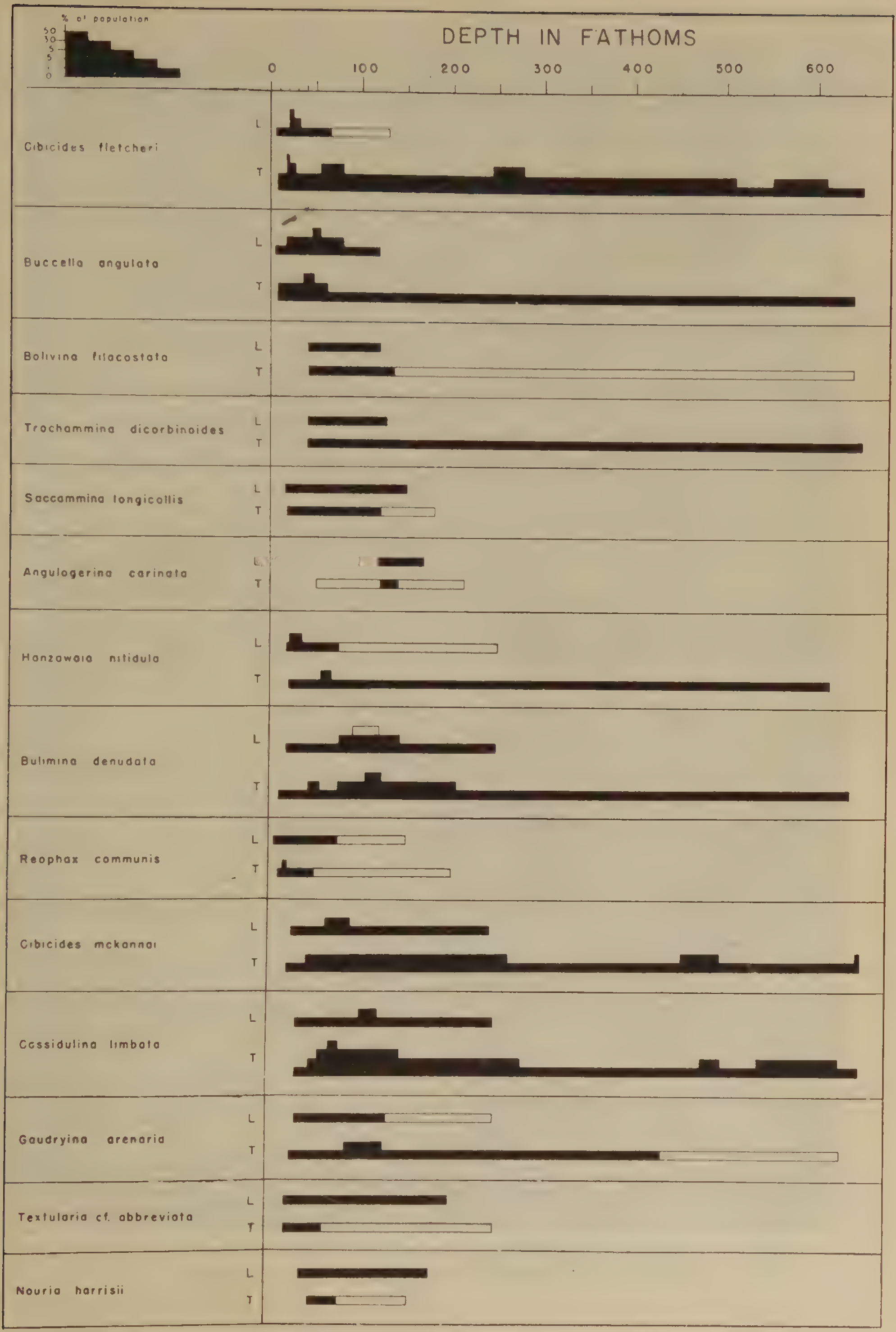

Text Figure 3. Depth distributions of benthonic Foraminifera. L: living population; T: total population. Height of bar: average frequency; solid bar: consistent occurrence; open bar: scattered occurrence.

The differentiation of fauna 1 (shallow-water fauna) into two facies appears to depend on sediment types. Large grains are necessary for attached Foraminifera and the heavier the grains the better for Foraminifera living in the turbulent zone. *Poroeponides cribrorepandus* Asano and Uchio is found only as an attached form in the nearshore zone. *Rectocibicides miocenicus* Cushman and Ponton and *Placopsilina bradyi* Cushman are also found only as attached forms in relatively shallow water.

The boundary at 13-20 fathoms which separates faunas 1 and 2 may be interpreted as the base of the turbulent zone. This appears to be supported by the observation of C. Limbaugh (personal communication) that wave action decreases abruptly at approximately 40 feet (*ca.* 7 fathoms) and has no influence on the bottom at approximately 100 feet (17 fathoms) near the Scripps Institution of Oceanography. Turbulent water brings up nutrient salts from the bottom, but at the same time it carries a portion of phytoplankton continuously down to depths where light is insufficient, and this may affect benthonic Foraminifera which feed on the phytoplankton. Turbulent water also carries organic detritus from the sediments offshore and leaves the sediment barren.

The boundary at 45 fathoms between faunas 2 and 3 may represent the bottom of the seasonal thermocline. Therefore, fauna 2 is influenced by the seasonal thermoclinal layer which includes the salinity minimum. The species in this layer may be considered relatively eurythermal compared with those on the bottom in deep water.

The boundary at 100 fathoms between faunas 3 and 4 may represent the boundary between the California Current and an underflowing current from the southern hemisphere. The current flowing toward the north under the California Current off the west coast of North America is the Equatorial Pacific Water mass, and the Equatorial Water, in turn, probably is formed off the coast of South America by gradual transformation of the Subantarctic Water (Sverdrup *et al.*, 1942, p. 706). The ecological importance of this hydrographic boundary appears to be supported by the fact that characteristic species commonly found shallower than 100 fathoms also occur off British Columbia, Canada, and those deeper than 100 fathoms also occur off South America in deep water. These other occurrences are based on distribution of empty tests. Species shallower than 100 fathoms whose distributions are limited to the northern shallow sea are as follows:

Alveolophragmium advena (Cushman)
Alveolophragmium columbiense (Cushman)
Angulodiscorbis charlottensis (Cushman)
Astrononion viragoense Cushman and Edwards
Cassidulina limbata Cushman and Hughes
Cassidulina tortuosa Cushman and Hughes
Elphidium sp. cf. *E. subarcticum* Cushman
Gaudryina arenaria Galloway and Wissler

EXPLANATION OF PLATE 1

Figs.		Page
1, 2.	*Saccammina longicollis* (Wiesner) Hypotypes (U.S.N.M. Nos. 626572, 626573), ×47, ×48.	50
3.	*Reophax communis* Lacroix. Hypotype (U.S.N.M. No. 626574), ×102.	
4.	*Reophax dentaliniformis* Brady. Hypotype (U.S.N.M. No. 626575), ×19.	
5.	*Reophax excentricus* Cushman. Hypotype (U.S.N.M. No. 626576), ×19.	
6.	*Reophax gracilis* (Kiaer). Hypotype (U.S.N.M. No. 626577), ×44.	
7.	*Reophax horridus* Cushman. Hypotype (U.S.N.M. No. 626578), ×18.	
8.	*Reophax micaceous* Earland. Hypotype (U.S.N.M. No. 626579), ×47	50
9.	*Reophax scorpiurus* Montfort. Hypotype (U.S.N.M. No. 626580), ×17.	
10, 11.	*Involutina flavida* (Höglund). 10, Microspheric form. Hypotype (U.S.N.M. No. 626581), ×5. 11, Megalospheric form. Hypotype (U.S.N.M. No. 626582), ×5.	
12.	*Involutina hoeglundi* Uchio, n. sp. Holotype (U.S.N.M. No. 626583), ×46.	51
13.	*Involutina minutissima* (Cushman and McCulloch). Hypotype (U.S.N.M. No. 626584), ×60.	
14.	*Involutina pacifica* (Cushman and Valentine) Hypotype (U.S.N.M. No. 626585), ×18.	51
15, 16.	*Haplophragmoides neobradyi* Uchio, n. sp. 15, Holotype (U.S.N.M. No. 626587), ×99. 16, Paratype (U.S.N.M. No. 626588), ×103.	51
17.	*Haplophragmoides quadratus* Uchio, n. sp. Holotype (U.S.N.M. No. 626590), ×46.	52
18, 19.	*Recurvoidella parkerae* Uchio, n. gen., n. sp. 18, Holotype (U.S.N.M. No. 626603), ×99. 19, Paratype (U.S.N.M. No. 626604), ×96.	53
20, 21.	*Alveolophragmium advena* (Cushman) Hypotypes (U.S.N.M. Nos. 626594, 626595), ×28, ×29.	52
22.	*Alveolophragmium columbiense* (Cushman) Hypotype (U.S.N.M. No. 626596), ×41.	52
23.	*Alveolophragmium evolutum* (Natland). Hypotype (U.S.N.M. No. 626597), ×22.	
24, 25.	*Alveolophragmium lenticulare* (Natland). Hypotypes (U.S.N.M. Nos. 626598, 626599), ×30, ×26.	
26, 27.	*Recurvoides subglobosus* (G. O. Sars) Hypotypes (U.S.N.M. Nos. 626601, 626602), ×21, ×26.	52

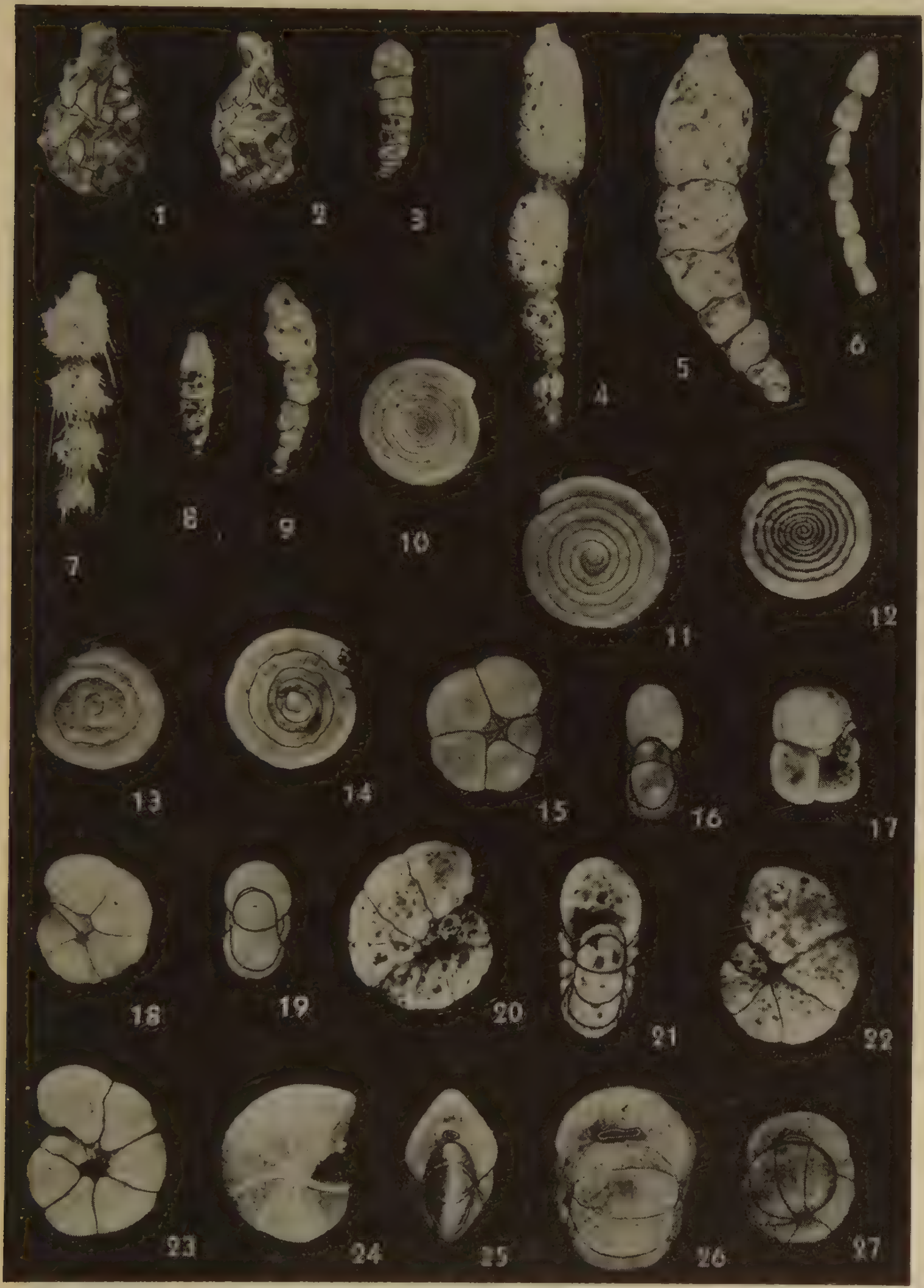
1
2
3
4
5
6
7
8
9
10
11
12
13
14
15
16
17
18
19
20
21
22
23
24
25
26
27

Uchio: Living Foraminifera, San Diego, California

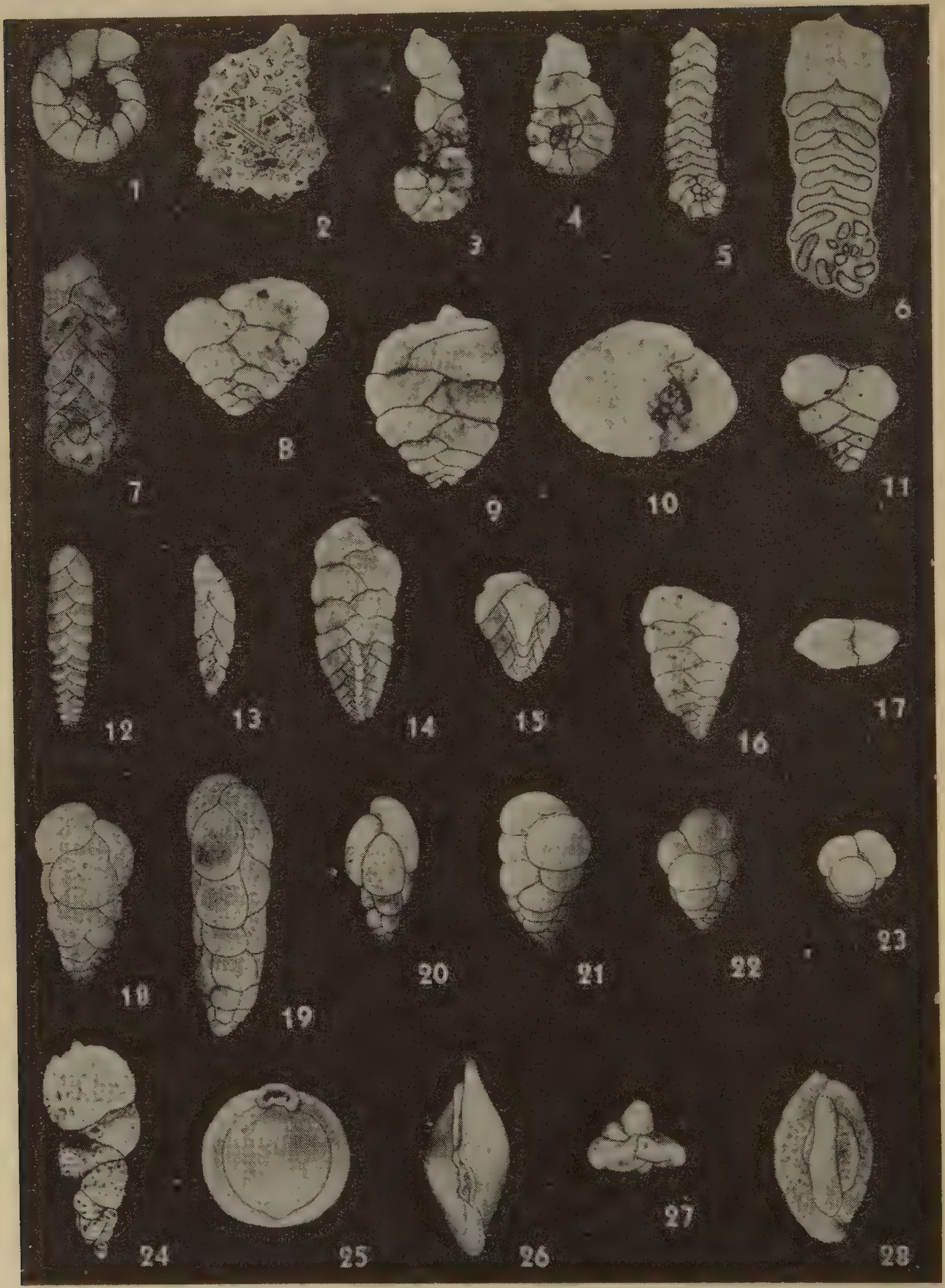
1
2
3
4
5
6
7
8
9
10
11
12
13
14
15
16
17
18
19
20
21
22
23
24
25
26
27
28

Uchio: Living Foraminifera, San Diego, California

Nonionella sp. aff. *N. globosa* Ishiwada
Nonionella stella Cushman and Moyer
Robertinoides charlottensis (Cushman)
Rosalina columbiensis (Cushman)

Species occurring deeper than 100 fathoms and characteristic of South American water as as follows:

Cancris inaequalis (d'Orbigny)
Cassidulina braziliensis Cushman
Valvulineria araucana (d'Orbigny)

The boundary at 250 fathoms between faunas 4 and 5 may represent the top of the permanent thermocline.

The boundary at 350 fathoms between faunas 5 and 6 may be related to the oxygen minimum layer, which may limit the vertical movement of some species. Many workers have discussed the origin of the oxygen minimum layer, but have come to no definite conclusion about it. If, as Wüst (1935) proposes, it is due to minimum replenishment of oxygen due in turn to minimum movement of water at the boundary between two water masses which move in opposite directions, then the oxygen minimum layer represents a boundary of two water masses, and a distinct faunal break can be expected. The ocean on the whole, even in abyssal depths, is well supplied with oxygen for organisms, and oxygen is not a determining factor in the distribution of most marine life except in certain environments.

The boundary at 450 fathoms between fauna 6 and fauna 7 may represent the bottom of the permanent thermocline.

Size of Living Population

Description.—Sizes of the standing crops of living benthonic Foraminifera per standard sample are shown on Text Fig. 14. Several generalizations may be made from these distributions.

There is a population of less than 200 specimens per sample in the shallow areas. This low population occurs at less than 40 fathoms in most of the San Diego area, but is at less than 20 fathoms in the region west of Point Loma.

Intermediate populations of 200-1000 per sample occur seaward from the low population area. The depth ranges from 20-40 fathoms north of Coronado Canyon, but ranges from 35-55 fathoms south of Coronado Canyon. A small area of intermediate population also occurs near the mouth of the Tia Juana River.

A high population area occupies a narrow band along the outer edge of the shelf and in the head of Coronado Canyon. This zone has an average population of more than 1000 per sample. The depth of this zone ranges from 55 to 100 fathoms along the outer shelf and from 60 to 150 fathoms in the head of Coronado Canyon. This narrow band may be expected farther north, on the western side of Coronado Bank, but the present study does not include this area. There is no apparent reason why this highest population band does not exist on the eastern side of Coronado Bank. Several small patchy areas also have more than 1000 specimens per sample.

EXPLANATION OF PLATE 2

FIGS. PAGE

1. *Alveolophragmium veleronis* (Cushman and McCulloch). Hypotype (U.S.N.M. No. 626600), ×29.
2. *Ammotium planissimum* (Cushman). Hypotype (U.S.N.M. No. 626606), ×20.
3, 4. *Ammobaculites catenulatus* Cushman and McCulloch. Hypotypes (U.S.N.M. Nos. 626607, 626608), ×97, ×99.
5, 6. *Ammomarginulina sandiegoensis* Uchio, n. sp. 54
5, Holotype (U.S.N.M. No. 626613), ×46. 6, Paratype (U.S.N.M. No. 626614), ×96.
7. *Spiroplectammina bathyca* Uchio, n. sp. 54
Holotype (U.S.N.M. No. 626616), ×94.
8-10. *Textularia* sp. cf. *T. abbreviata* d'Orbigny 54
(U.S.N.M. Nos. 626619-626621), ×29, ×21, ×35.
11. *Textularia schencki* Cushman and Valentine 55
Hypotype (U.S.N.M. No. 626624), ×42.
12. *Textularia sandiegoensis* Uchio, n. sp. 55
Holotype (U.S.N.M. No. 626623), ×100.
13. *Bigenerina hoeglundi* Uchio, n. sp. 56
Holotype (U.S.N.M. No. 626625), ×60.
14, 15. *Gaudryina arenaria* Galloway and Wissler 56
Hypotypes (U.S.N.M. Nos. 626626, 626627), ×28, ×46.
16, 17. *Gaudryina subglabrata* Cushman and McCulloch. Hypotypes (U.S.N.M. Nos. 626628, 626629), ×33.
18. *Eggerella advena* (Cushman). Hypotype (U.S.N.M. No. 626630), ×100.
19. *Eggerella pusilla* (Goës). Hypotype (U.S.N.M. No. 626631), ×99.
20. *Eggerella scrippsi* Uchio, n. sp. 56
Holotype (U.S.N.M. No. 626632), ×98.
21-23. *Karreriella parkerae* Uchio, n. sp. 56
21, Holotype (U.S.N.M. No. 626633), ×48. 22, 23, Paratypes (U.S.N.M. Nos. 626634, 626635), ×46, ×47.
24. *Goesella flintii* Cushman. Hypotype (U.S.N.M. No. 626636), ×19.
25, 26. *Pyrgo murrhina* (Schwager). Hypotypes (U.S.N.M. Nos. 626639, 626640), ×36, ×45.
27, 28. *Quinqueloculina granulosa* Natland. Hypotypes (U.S.N.M. Nos. 626637, 626638), ×46, ×47.

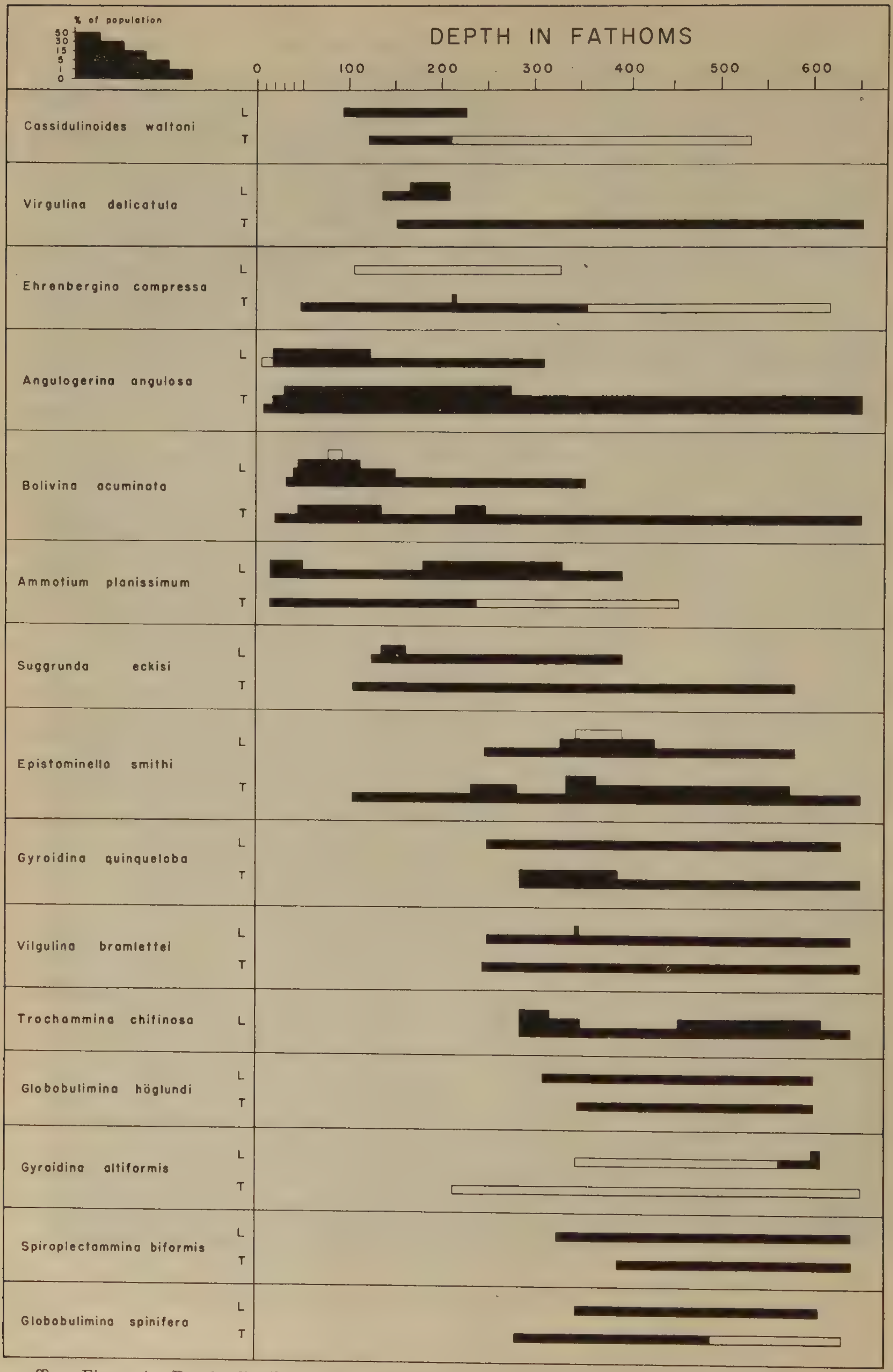

Text Figure 4. Depth distributions of benthonic Foraminifera. L: living population; T: total population. Height of bar: average frequency; solid bar: consistent occurrence; open bar: scattered occurrence.

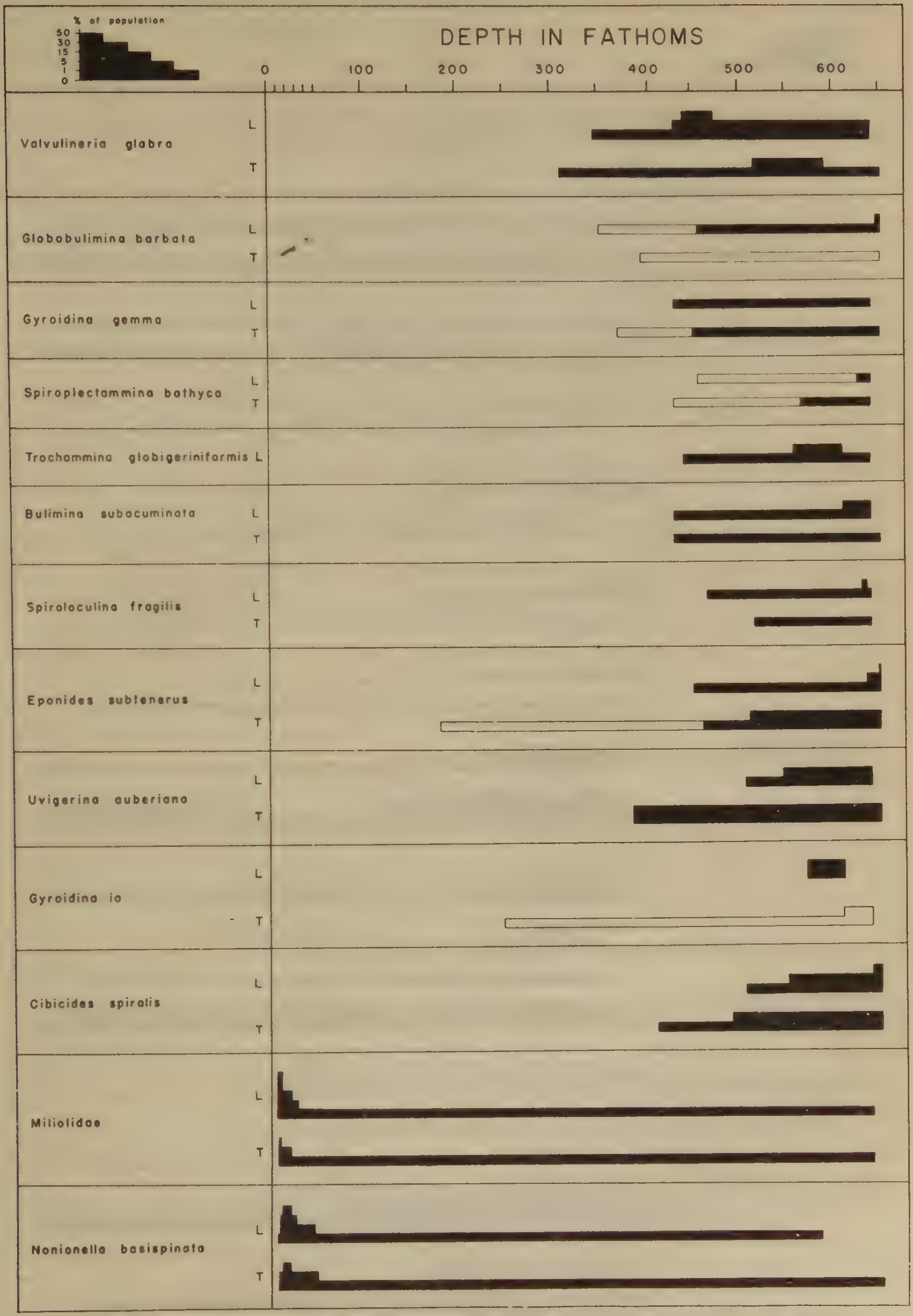

Text Figure 5. Depth distributions of benthonic Foraminifera. L: living population; T: total population. Height of bar: average frequency; solid bar: consistent occurrence; open bar: scattered occurrence.

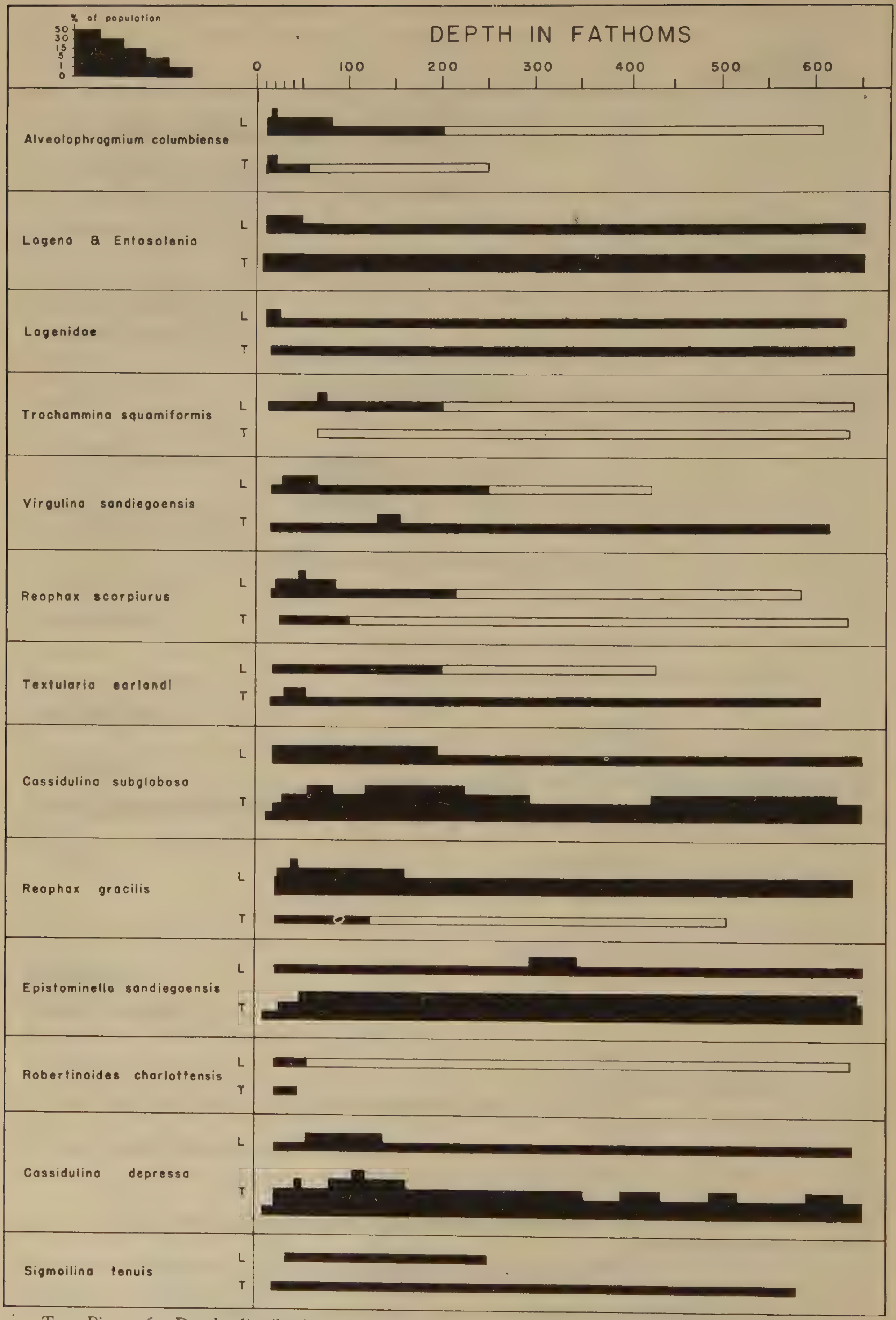

Text Figure 6. Depth distributions of benthonic Foraminifera. L: living population; T: total population. Height of bar: average frequency; solid bar: consistent occurrence; open bar: scattered occurrence.

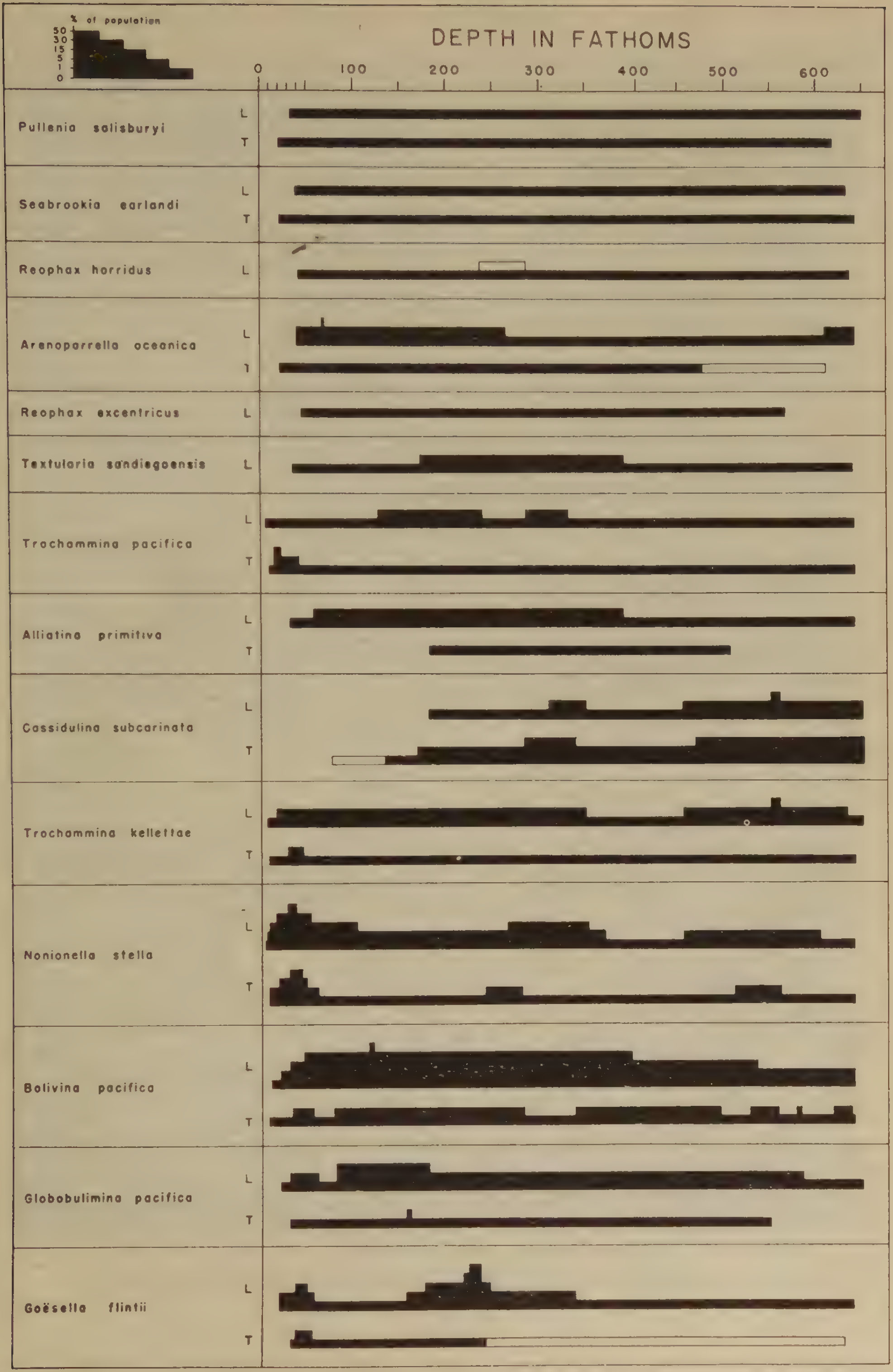

Text Figure 7. Depth distributions of benthonic Foraminifera. L: living population; T: total population. Height of bar: average frequency; solid bar: consistent occurrence; open bar: scattered occurrence.

Deep areas have a moderate population of 200-1000 per sample. The depth ranges from 100-150 to 600 fathoms in Coronado Canyon and the San Diego Trough. In the northern region, however, where there is no large area of high population, moderate populations occur from 20-40 to 200 fathoms.

There is a deep-water low population area of less than 200 per sample. This occurs at deeper than 600 fathoms in the San Diego Trough and deeper than 200 fathoms in the lower part of Loma Sea Valley.

Walton (1955) calculated the frequency distribution of the average population of living benthonic Foraminifera in Todos Santos Bay, Mexico, per 5-fathom interval, regardless of sediment type. This approach does not appear to be reasonable because benthonic Foraminifera populations vary not only with depth, but also with other environmental factors such as sediment type. Also, there is an areal change in the population due to changes in sediment type, submarine topography and amount of food supply, etc. It is of interest, therefore, to relate the population size to some of these factors.

The average population size has been correlated with different sediment types found in the San Diego area and also with all the sediment types combined at 10-fathom intervals respectively. As shown in Table 4, there are some irregularities in the population size within the same sediment type and depth range; nevertheless, some generalizations can be made.

Coarse sands, including brown sands and shell sands (with or without pebbles), and glauconite sands have a relatively small standing crop, regardless of depth. These coarse sands are mostly distributed in the near-shore area (shallower than 35 fathoms), but the glauconite sands (about 80% of the total weight is glauconite) are distributed along the eastern side of the Coronado Ridge (280-390 fathoms). The average population of this group of sediments is 149 specimens per sample. Rocky bottom, which is partly covered by a thin layer of detrital sediments, also has a small standing crop regardless of depth with an average of 146 per sample, almost exactly the same size as that of coarse sands.

Fine sands are much more productive than coarse sands, with an average standing crop of 578 specimens per sample at all depths. The standing crop suddenly increases at 40 fathoms and seems to begin to decrease at approximately 450 fathoms.

Silts are as productive as fine sands with an average standing crop at all depths of 568 specimens per sample. There is also a striking change in the size of population with depth, with an increase at 20-30 fathoms and a gradual decrease deeper than approximately 300 fathoms.

Clayey silts also have relatively large standing crops with an average for all depths of 536 specimens per sample. No clayey silts are found shallower than 30 fathoms. Very large and very small standing crops are found at both shallow and deep stations, but the standing crop seems to be rather constantly small at depths greater than 550 fathoms in the San Diego Trough. This may be due to lower temperature and lower oxygen content in this region.

Foraminifera sands and/or silts are very productive

EXPLANATION OF PLATE 3

Figs.		Page
1, 2.	*Sigmoilina tenuis* (Czjzek) Hypotypes (U.S.N.M. Nos. 626643, 626644), ×45, ×48.	57
3, 4.	*Sigmoilina victoriensis* Cushman. Hypotypes (U.S.N.M. Nos. 626645, 626646), ×48, ×39.	
5, 6.	*Spiroloculina fragilis* Uchio, n. sp. 5, Holotype (U.S.N.M. No. 626641), ×46. 6, Paratype (U.S.N.M. No. 626642), ×47.	57
7.	*Seabrookia earlandi* Wright. Hypotype (U.S.N.M. No. 626863), ×94.	
8, 9.	*Cornuspira lajollaensis* Uchio, n. sp. 8, Holotype (U.S.N.M. No. 626647), ×48. 9, Paratype (U.S.N.M. No. 626648), ×45.	57
10, 11.	*Gordiospira fragilis* Heron-Allen and Earland. Hypotypes (U.S.N.M. Nos. 626650, 626651), ×39, ×40.	
12.	*Cornuspiroides foliaceus* (Philippi). Hypotype (U.S.N.M. No. 626652), ×31.	
13, 14.	*Trochammina charlottensis* Cushman Hypotypes (U.S.N.M. Nos. 626653, 626654), ×46.	58
15-17.	*Trochammina labiata* Uchio, n. sp. 15, Holotype (U.S.N.M. No. 626663), ×94. 16, 17, Paratypes (U.S.N.M. Nos. 626664, 626665), ×94, ×95.	59
18, 19.	*Trochammina discorbinoides* Uchio, n. sp. 18, Holotype (U.S.N.M. No. 626657), ×100. 19, Paratype (U.S.N.M. No. 626658), ×93.	58
20, 21.	*Trochammina kellettae* Thalmann Hypotypes (U.S.N.M. Nos. 626661, 626662), ×65.	58
22, 23.	*Trochammina chitinosa* Uchio, n. sp. 22, Holotype (U.S.N.M. No. 626655), ×96. 23, Paratype (U.S.N.M. No. 626656), ×83.	58
24, 25.	*Trochammina nitida* Brady. Hypotypes (U.S.N.M. No. 626666, 626667), ×104.	
26, 27.	*Trochammina pacifica* Cushman Hypotypes (U.S.N.M. Nos. 626668, 626669), ×47, ×44.	59
28.	*Nouria harrisii* Heron-Allen and Earland. Hypotype (U.S.N.M. No. 626678), ×47.	
29.	*Nouria polymorphinoides* Heron-Allen and Earland. Hypotype (U.S.N.M. No. 626679), ×46.	

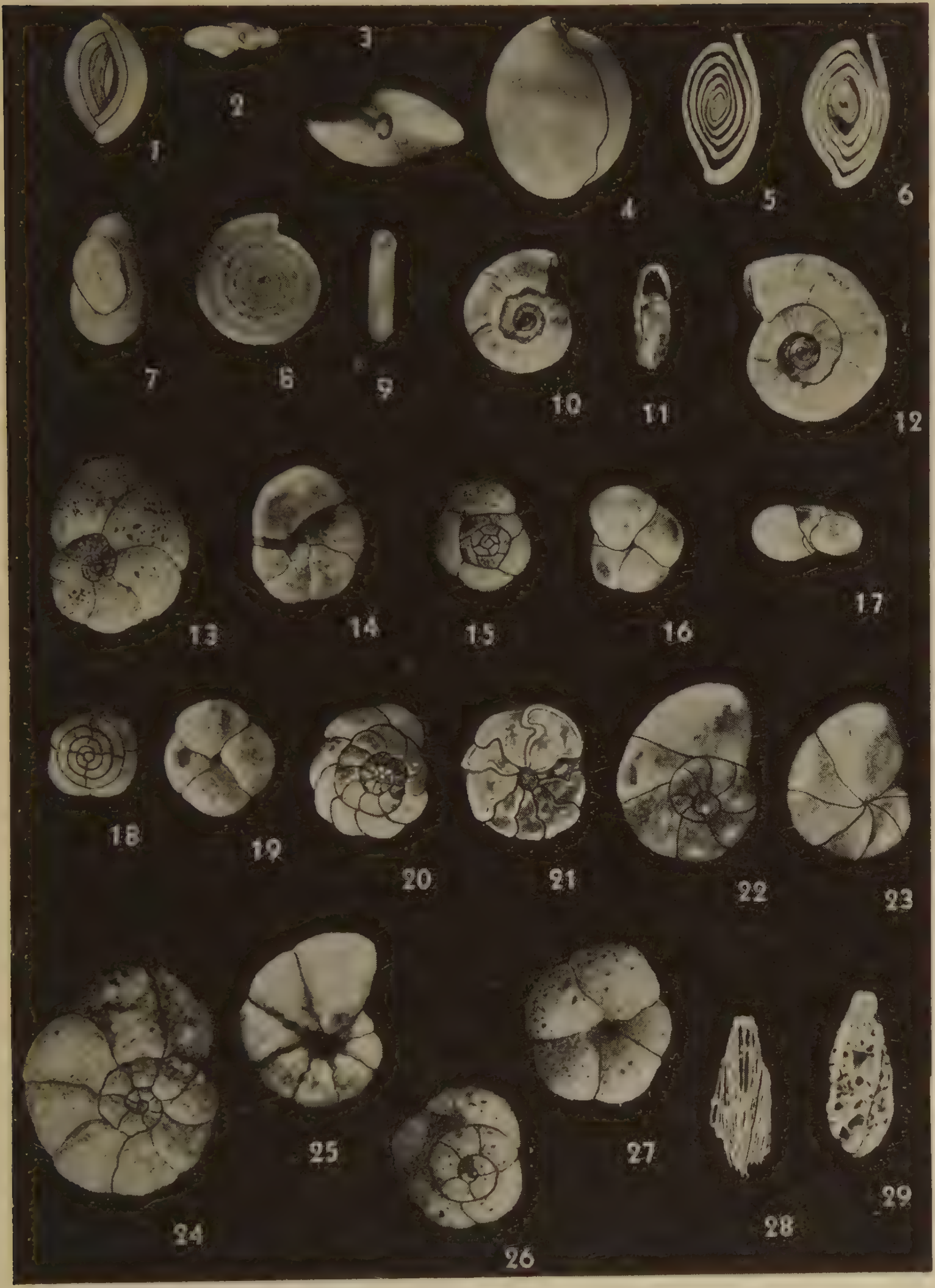
1
2
3
4
5
6
7
8
9
10
11
12
13
14
15
16
17
18
19
20
21
22
23
24
25
26
27
28
29

Uchio: Living Foraminifera, San Diego, California

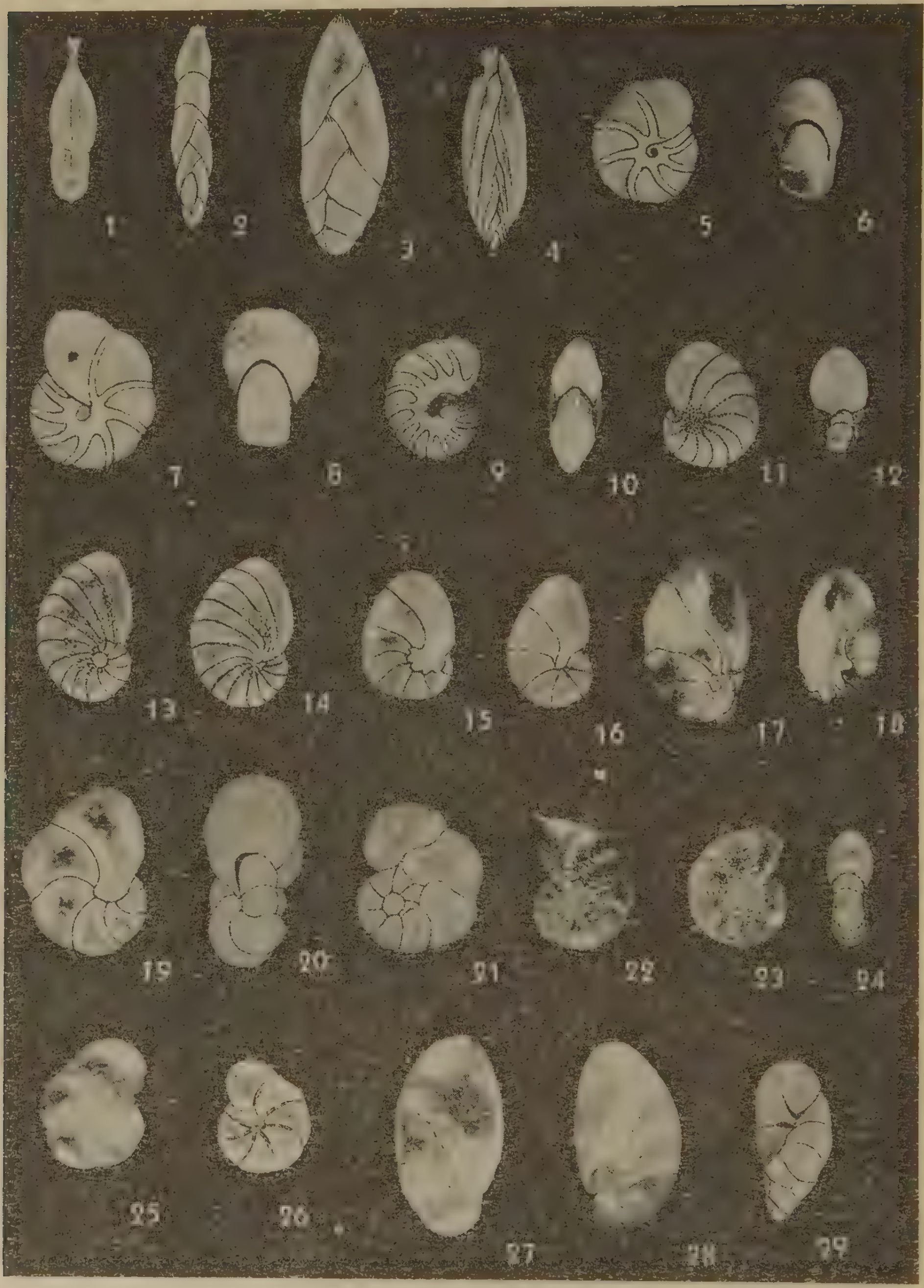
1
2
3
4
5
6
7
8
9
10
11
12
13
14
15
16
17
18
19
20
21
22
23
24
25
26
27
28
29

Uchio: Living Foraminifera, San Diego, California

with an average standing crop at all depths of 629 specimens per sample. No Foraminifera sands and/or silts are found at depths shallower than 45 fathoms or deeper than 167 fathoms. The term "Foraminifera sands and/or silts" is used loosely because often it is difficult to separate this type of sediment from others. The term applies to a type of sediment which contains a high percent of supposedly late Pleistocene residual sediment. Usually this type of sediment appears to be a mixture of coarse and fine sediments owing to a high content of Foraminifera tests, often with coarse sands, pebbles, and shell fragments. There is a considerable variation in the size of the standing crop in sediment of this type, perhaps due to the different amounts of the finer fractions of a sample and the physico-chemical character of the bottom.

The size of the average population plotted at 10-fathom intervals is shown in Table 4 and at 50-fathom intervals in Text Fig. 15. The occurrence of the largest living population at 55-150 fathoms on the eastern escarpment of the San Diego Trough and in an area between Coronados Islands and the head of the Coronado Canyon, and at 100-150 fathoms in the whole area agrees with distributions in the Todos Santos Bay area (Walton, 1955, p. 996).

Discussion.—The low population area nearshore may be due to the presence of coarse sediment and hence little organic material, although the relatively higher temperature found there is favorable for physiological activity. Turbulence may be advantageous in bringing food closer, getting oxygen from the air and taking waste away, or disadvantageous in mechanical agitation, hindering light-penetration, etc., but there is no direct evidence. An area near the Tia Juana River mouth which has a slightly higher population, has micaceous fine sand which may contain more organic matter.

The low population in the San Diego Trough and in the lower part of Loma Sea Valley may be due to low temperature, very fine sediments, and a slight excess of organic matter. Trask (1932) and Emery *et al.* (1952, p. 537, fig. 10) pointed out that the content of organic matter in the sediment is very high in the San Diego Trough, although lower than in marsh areas. Because of this high organic content, oxygen will be used to oxidize organic matter and CO_2 and/or H_2S will be formed and Eh will become lower. Some tests of Foraminifera from this environment were filled with pyrite. These factors may hinder the growth of organisms and thus tend to reduce the size of their populations.

The area which has the highest population occurs at 50-150 fathoms where there are intermediate temperatures. The sediment type seems to be of no importance to the population size since it includes clayey silt, silt, fine sand and Foraminifera sand. The explanation for the narrow zone of exceptionally high population probably is some physico-chemical factor, perhaps intermediate temperature and/or tidal effect. All the stations in this zone lie in the canyon head or at the outer edge of the shelf. According to Fleming and Revelle (1939, p. 134-136), the tidal currents reach a

EXPLANATION OF PLATE 4

Figs.		Page
1.	*Nodosaria* sp. cf. *N. perversa* (Schwager). (U.S.N.M. No. 626681), ×47.	
2.	*Paradentalina muraii* (Uchio), n. gen. Hypotype (U.S.N.M. No. 626682), ×47.	60
3.	*Pseudopolymorphina charlottensis* (Cushman). Hypotype (U.S.N.M. No. 626683), ×19.	
4.	*Sigmomorphina frondiculariformis* (Galloway and Wissler). Hypotype (U.S.N.M. No. 626684), ×33.	
5-8.	*Nonion lankfordi* Uchio, n. sp. 5, 6, Holotype (U.S.N.M. No. 626685), ×98. 7, 8, Paratype (U.S.N.M. No. 626686), ×98.	60
9, 10.	*Nonion parkerae* Uchio, n. sp. Holotype (U.S.N.M. No. 626687). 9, ×47. 10, ×51.	60
11, 12.	*Nonionella atlantica* Cushman. Hypotypes (U.S.N.M. Nos. 626689, 626690), ×33, ×34.	
13, 14.	*Nonionella basispinata* (Cushman and Moyer) Hypotypes (U.S.N.M. Nos. 626691, 626692), ×33.	61
15, 16.	*Nonionella stella* Cushman and Moyer Hypotypes (U.S.N.M. Nos. 626698, 626699), ×45, ×122.	61
17, 18.	*Nonionella* sp. aff. *N. globosa* Ishiwada. (U.S.N.M. Nos. 626696, 626697), ×90, ×92.	
19-21.	*Nonionella* (?) *fragilis* Uchio, n. sp. 19, 20, Paratypes (U.S.N.M. Nos. 626693, 626694), ×100, ×91. 21, Holotype (U.S.N.M. No. 626695), ×97.	62
22.	*Elphidium spinatum* Cushman and Valentine. Hypotype (U.S.N.M. No. 626700), ×47.	
23, 24.	*Elphidium spinatum* var. *translucens* Natland Hypotypes (U.S.N.M. Nos. 626701, 626702), ×40, ×46.	62
25.	*Elphidium* sp. cf. *E. subarcticum* Cushman. (U.S.N.M. No. 626703), ×119.	
26.	*Elphidium* sp. cf. *E. incertum* (Williamson). (U.S.N.M. No. 626704), ×46.	
27, 28.	*Alliatina primitiva* (Cushman and McCulloch) Hypotypes (U.S.N.M. Nos. 626705, 626706), ×104, ×94.	62
29.	*Robertinoides charlottensis* (Cushman) Hypotype (U.S.N.M. No. 626707), ×46.	62

Depth Range (Fathoms)	Coarse Sand		Fine Sand		Silt		Clayey Silt		Foram. Sand		All	
	no. of samples	av. pop.	no. of samples	av. pop.	no. of samples	av. pop.	no. of samples	av. pop.	no. of samples	av. pop.	no. of samples	av. pop.
0 - 10	1	132			2	254					3	213
10 - 20	1	153	1	239	6	179					8	184
20 - 30	4	149	1	239	1	1293					6	355
30 - 40	2	184	2	890	2	593	6	825	3	511	12	688
40 - 50			4	897	6	545	5	643	3	511	18	613
50 - 60			2	296	3	801			5	636	10	873
60 - 70					1	343			5	637	6	588
70 - 80					3	699			3	416	6	541
80 - 90					3	755					3	755
90 - 100							2	305	2	625	5	466
100 - 110							2	295			2	295
110 - 120					1	1277	3	528			4	715
120 - 130			1	1119	1	1277	2	855	1	696	5	962
130 - 140							3	759	1	916	4	799
140 - 150							2	906	1	916	3	909
150 - 160					1	258	3	1071			4	868
160 - 170							2	779	1	306	3	621
170 - 180	1	190			1	598					2	394
180 - 190	1	190			1	598	1	225			3	338
190 - 200					1	943	1	183			2	563
200 - 210					1	943	1	116			2	530
210 - 220					1	517	1	808			2	662
220 - 230					1	550					1	550
230 - 240					1	510					1	510
240 - 250			1	834			2	1242			3	1106
250 - 260			1	834							1	834
260 - 270												
270 - 280					1	1379					1	1379
280 - 290	1	69			1	1379					2	724
290 - 300												
300 - 310	1	210									1	210
310 - 320	1	210									1	210
320 - 330	1	119									1	119
330 - 340												
340 - 350	1	79			5	435					6	376
350 - 360	1	79			3	438					5	509
360 - 370												
370 - 380												
380 - 390	1	269									1	269
390 - 400							1	564			1	564
400 - 410												
410 - 420							1	805			1	805
420 - 430			1	421			2	702			3	608
430 - 440			1	421			2	584			3	530
440 - 450					1	335	1	570			2	453
450 - 460			2	228	1	335	2	429			5	349
460 - 470			1	183			2	572			3	442
470 - 480			1	300							1	300
480 - 490							2	340			2	340
490 - 500							1	236			1	236
500 - 510			1	253	1	307	1	467			3	342
510 - 520							3	360			3	360
520 - 530							4	456			4	456
530 - 540							1	455			1	455
540 - 550							1	146			1	146
550 - 560							2	175			2	175
560 - 570							3	375			3	375
570 - 580							3	338			3	338
580 - 590							3	260			3	260
590 - 600							1	150			1	150
600 - 610							2	235			2	235
610 - 620							1	566			1	566
620 - 630							1	357			1	357
630 - 640							5	247			5	247
640 - 650							2	111			2	111
0 - 650	12	149	15	578	35	568	70	536	21	629	156	523

Table 4. Depth distribution of average populations of living benthonic Foraminifera.

Note. Stations occurring at depth boundaries are calculated for the depth ranges both above and below the boundaries. Station 250 is not included in this table.

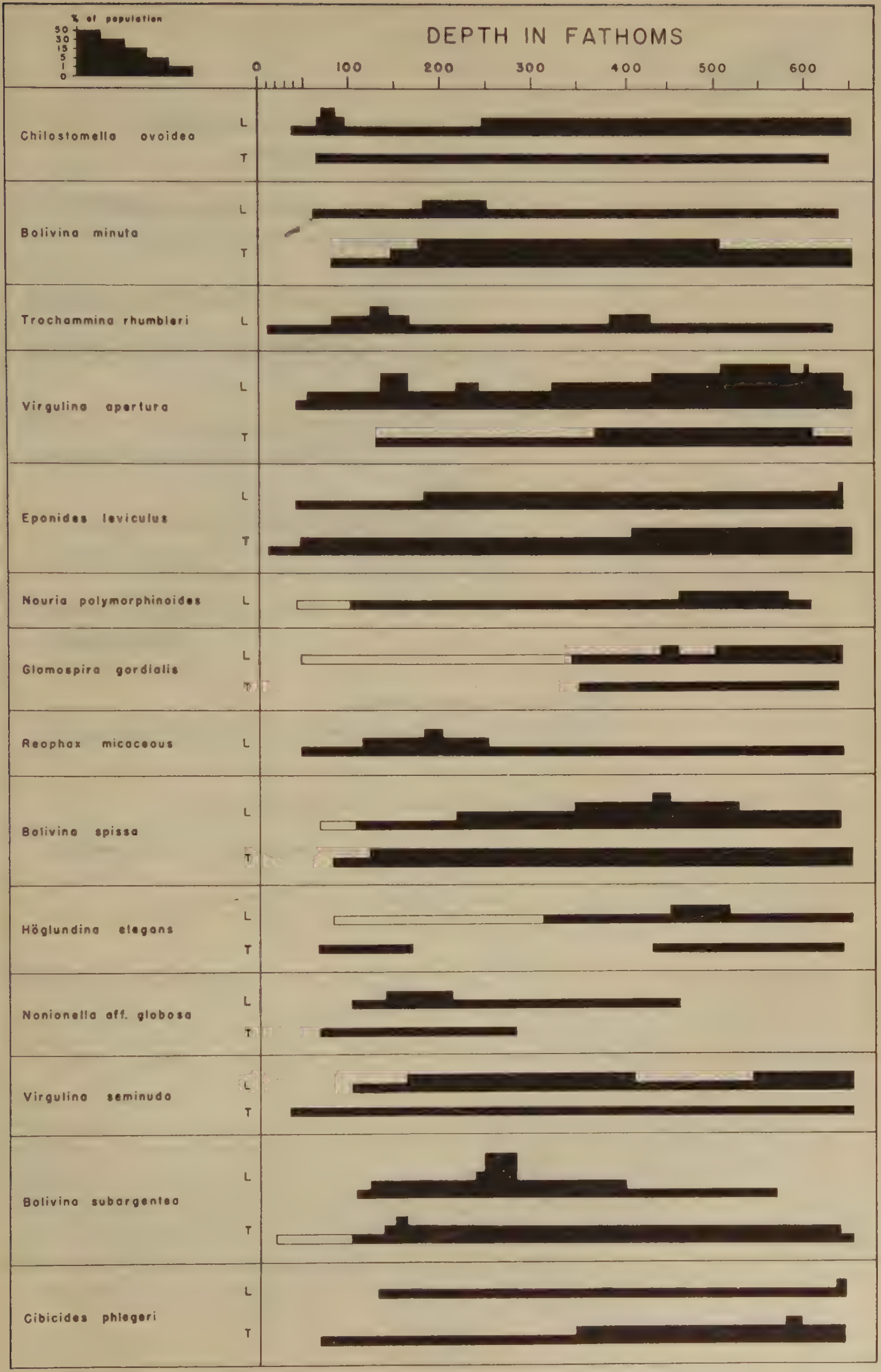

Text Figure 8. Depth distributions of benthonic Foraminifera. L: living population; T: total population. Height of bar: average frequency; solid bar: consistent occurrence; open bar: scattered occurrence.

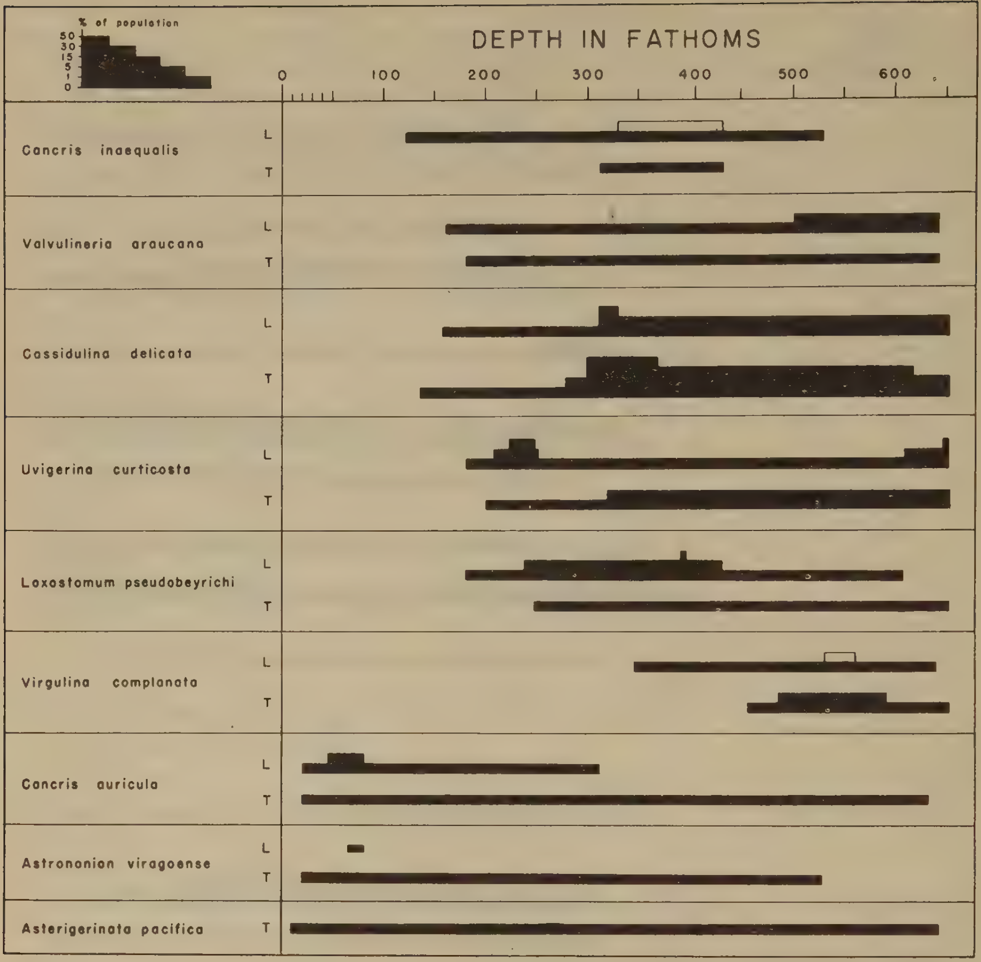

Text Figure 9. Depth distributions of benthonic Foraminifera. L: living population; T: total population. Height of bar: average frequency; solid bar: consistent occurrence; open bar: scattered occurrence.

maximum where they impinge on the outer edges of continental shelves and over banks and seamounts. Such a daily effect may stir up bottom sediments, renew food and oxygen, and remove waste products.

It is difficult to explain why the living population is smaller in Todos Santos Bay than in the San Diego area as shown below.

Average Living Population Per Sample

Location	*Depth Range*	
	0-50 fathoms	*50-100 fathoms*
Todos Santos	104	142
San Diego	502	679

A part of the reason may be that the Todos Santos Bay samples were collected during February and the San Diego samples were collected during the summer months. Walton (1955) shows that the average living populations in August were the highest and approximately three times larger than those in February. Another possible reason why the Todos Santos Bay area has a smaller living population than the San Diego area is that specimens smaller than 0.088 mm. were not counted by Walton. In the deep area (deeper than 350 fathoms) *Virgulina apertura* Uchio, n. sp., a very tiny species, constitutes more than 20% of the population at each station in the San Diego area.

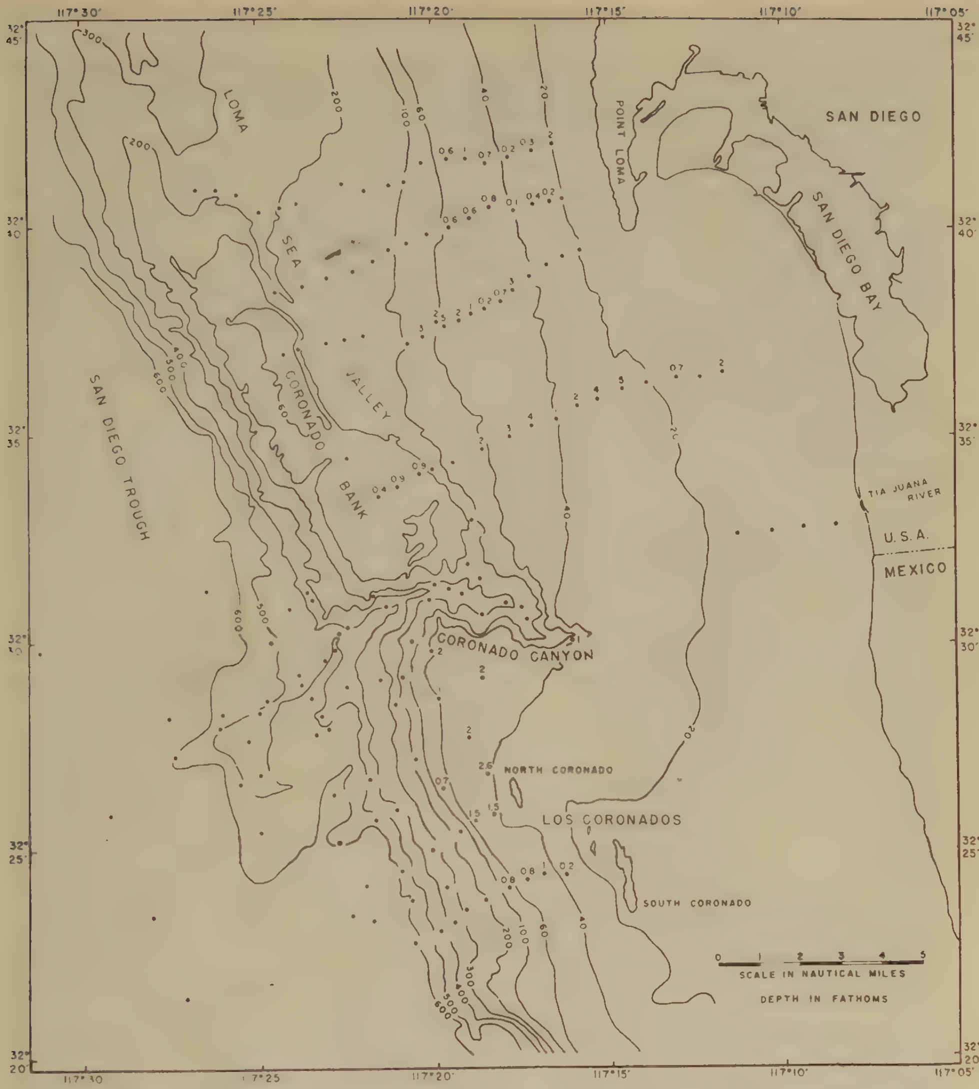
117°30'
117°25'
117°20'
117°15'
117°10'
117°05'
32° 45'
32° 40'
32° 35'
32° 30'
32° 25'
32° 20'
SAN DIEGO
SAN DIEGO BAY
POINT LOMA
LOMA
SEA
VALLEY
CORONADO
BANK
SAN DIEGO TROUGH
CORONADO CANYON
NORTH CORONADO
LOS CORONADOS
SOUTH CORONADO
TIA JUANA RIVER
U. S. A.
MEXICO
SCALE IN NAUTICAL MILES
0 1 2 3 4 5
DEPTH IN FATHOMS

Text Figure 10. Distribution of living *Bolivina acutula* Bandy in percent of living population.

TOTAL POPULATIONS OF BENTHONIC FORAMINIFERA

Depth Distribution of Species

Depth ranges and frequencies of the empty tests of many benthonic species are quite different from those of living ones as shown in Text Figs. 2-9. Comparison of depth ranges of the total Foraminifera fauna (living plus dead) with those of living ones reveals striking differences, particularly at depths greater than 47 fathoms. Total Foraminifera assemblages depend upon the productivity of living Foraminifera and contamination with displaced and/or residual or fossil faunas from other places. Occurrences of the species of benthonic Foraminifera in percent of total (living plus dead) populations are listed in Tables 5-7.

The most remarkable differences between the living and total faunas are that 7 living faunas are recognized in this area while only 4 total faunas are recognized, and the depths of the boundaries of these two faunal types differ from each other.

The following generalizations can be made from the comparison of the depth ranges of the total faunas with those of the living faunas (see Table 8):

The total fauna shallower than 20 fathoms appears to represent the living fauna. The probable reason is that the deeper fauna can not be transported to shallower water (except under very unusual conditions), and few fossil specimens are supplied to the nearshore fauna (in the samples studied) from sea-cliffs where Cretaceous and Eocene rocks are exposed.

The total faunas deeper than 280 fathoms are marked by abundances of *Cassidulina subcarinata* Uchio, n. sp., *C. delicata* Cushman, and *Epistominella sandiegoensis* Uchio, n. sp. Living specimens of *Cassidulina subcarinata* and *C. delicata* begin to occur at 250 fathoms and are important members of deep-sea faunas, although they do not constitute as high percentages as dead specimens in the total fauna. Living specimens of *Epistominella sandiegoensis* are eurybathic, found from nearshore to the bottom of San Diego Trough but in low frequency. The total fauna present deeper than 280 fathoms is represented by living species there, but the frequencies differ.

The total faunas between 20 and 280 fathoms are characterized by an abundance of species of *Cassidulina*. In addition, there are species which are indigenous to those depths and other species whose living specimens are found only in shallow water. The species which are most abundant in the fauna are characteristic of Pleistocene "Foraminifera sand." Thus the total faunas at 20-280 fathoms are quite different from the living assemblages at those depths.

Size of Total Population

There are striking differences in the areal distributions of living and total (living plus dead) populations (see Text Figs. 14, 16). In the San Diego area the distribution of the total population generally can be correlated with distribution of sediment type except on the shelf off Point Loma (see Table 9).

The area which has a relatively low total population, less than 10,000 per sample, is divided into two parts. The first is shallower than 40 fathoms and approximately coincides with the distribution of coarse sediments (fine to coarse grey sand, medium to coarse brown sand, shell sand) and rocky bottom. This zone extends along the shelf west of Point Loma. The second is deeper than about 600 fathoms in the San Diego Trough. Shallower than 20 fathoms the total population usually is less than 2000 per sample.

The highest total population, more than 50,000 per sample, is on Coronado Bank and its southern extension which is separated from the bank by Coronado Canyon. The depth range is about 40 to 300 fathoms. Another high population area is on the shelf between Coronado Bank and Point Loma at about 50 to 75 fathoms. Intermediate total populations between 10,000 and 50,000 per sample occur between the two areas mentioned above.

The size of the population of empty tests (therefore, that of the total population) is primarily a function of: (1) rate of production of tests, (2) dilution of populations by detrital sediments, and (3) preservation of empty tests (Walton, 1955, p. 977). The sediment of high total population areas is composed of relatively pure Foraminifera sands or contains a high

---

EXPLANATION OF PLATE 5

Figs.		Page
1.	*Bolivina acutula* Bandy. Hypotype (U.S.N.M No. 626733), ×95.	
2.	*Bolivina vaughani* Natland Hypotype (U.S.N.M. No. 626747), ×100.	64
3.	*Bolivina lowmani* Phleger and Parker. Hypotype (U.S.N.M. No. 626736), ×128.	
4.	*Virgulina delicatula* Uchio, n. sp. Holotype (U.S.N.M. No. 626724), ×99.	63
5.	*Neoconorbina parkeri* (Natland). Hypotype (U.S.N.M. No. 626765), ×109.	
6.	*Rectocibicides miocenicus* Cushman and Ponton Hypotype (U.S.N.M. No. 626854), ×38.	69
7.	*Textularia earlandi* F. L. Parker. Hypotype (U.S.N.M. No. 626622), ×92.	
8.	*Spiroplectammina biformis* (Parker and Jones). Hypotype (U.S.N.M. No. 626618), ×101.	
9.	*Placopsilina bradyi* Cushman and McCulloch. Hypotype (U.S.N.M. No. 626680), ×31.	
10-13.	*Ammomarginulina foliacea* (Brady). Hypotypes (U.S.N.M. Nos. 626609-626612), 10, ×32; 11-13, ×36.	
14.	*Haplophragmoides quadratus* Uchio, n. sp. Paratype (U.S.N.M. No. 626591), ×67.	52
15.	*Haplophragmoides* sp. (U.S.N.M. No. 626593), ×46.	
16.	*Glomospira gordialis* (Jones and Parker). Hypotype (U.S.N.M. No. 626586), ×123.	
17.	*Cyclammina pusilla* Brady. Hypotype (U.S.N.M. No. 626615), ×24.	
18-20.	*Trochammina rhumbleri* Uchio, n. sp. 18, 19, Holotype (U.S.N.M. No. 626670), ×144 20, Paratype (U.S.N.M. No. 626671), ×150.	59
21, 22.	*Trochammina globigeriniformis* Brady. Hypotypes (U.S.N.M. No. 626659, 626660), ×30.	
23, 24.	*Tritaxis bullata* (Höglund) Hypotypes (U.S.N.M. No. 626672, 626673), ×106, ×107.	59
25-27.	*Arenoparrella oceanica* Uchio, n. sp. 25, 26, Paratypes (U.S.N.M. No. 626675, 626676), ×99, ×149. 27, Holotype (U.S.N.M. No. 626674), ×98.	59

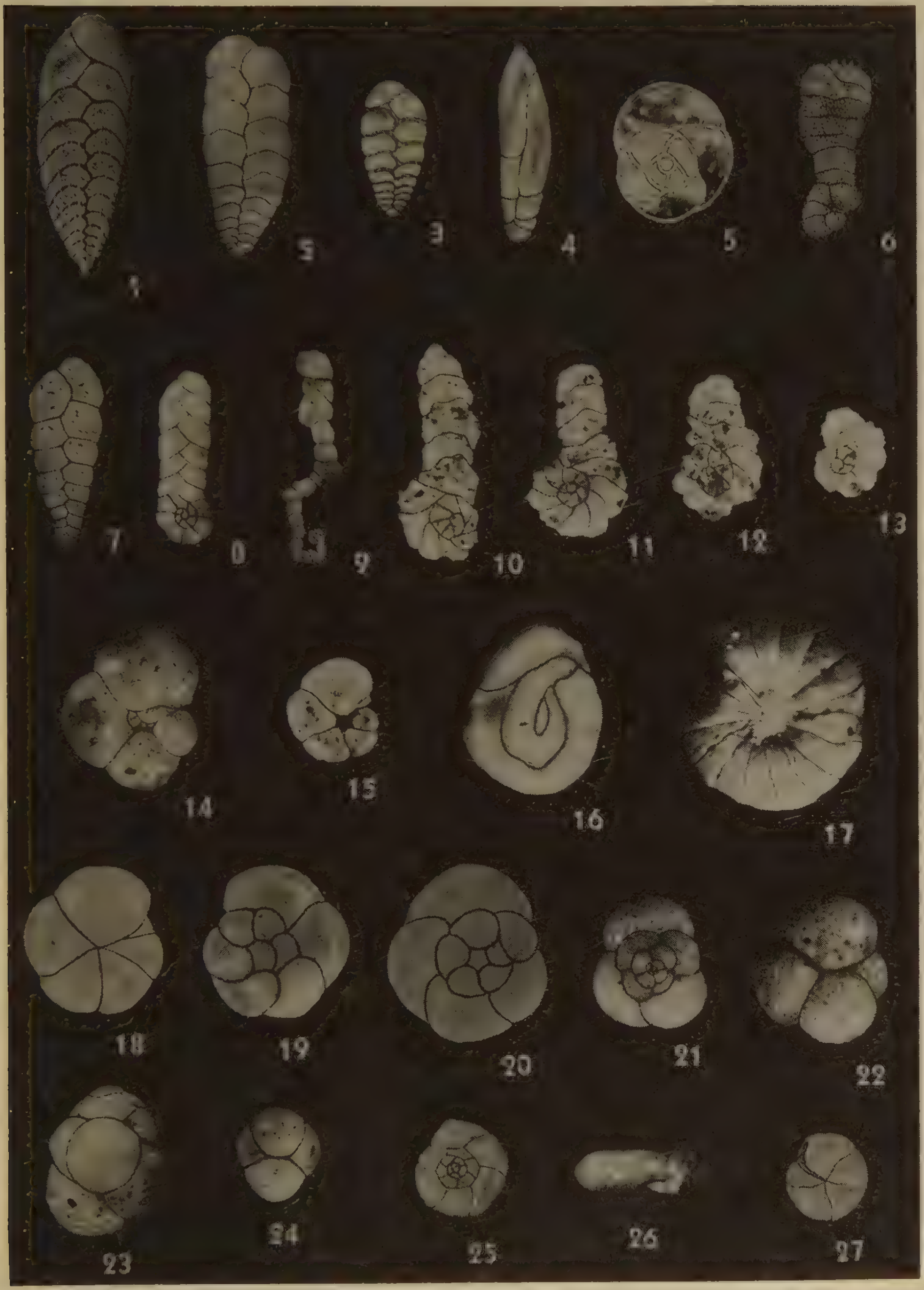
1
2
3
4
5
6
7
8
9
10
11
12
13
14
15
16
17
18
19
20
21
22
23
24
25
26
27

Uchio: Living Foraminifera, San Diego, California

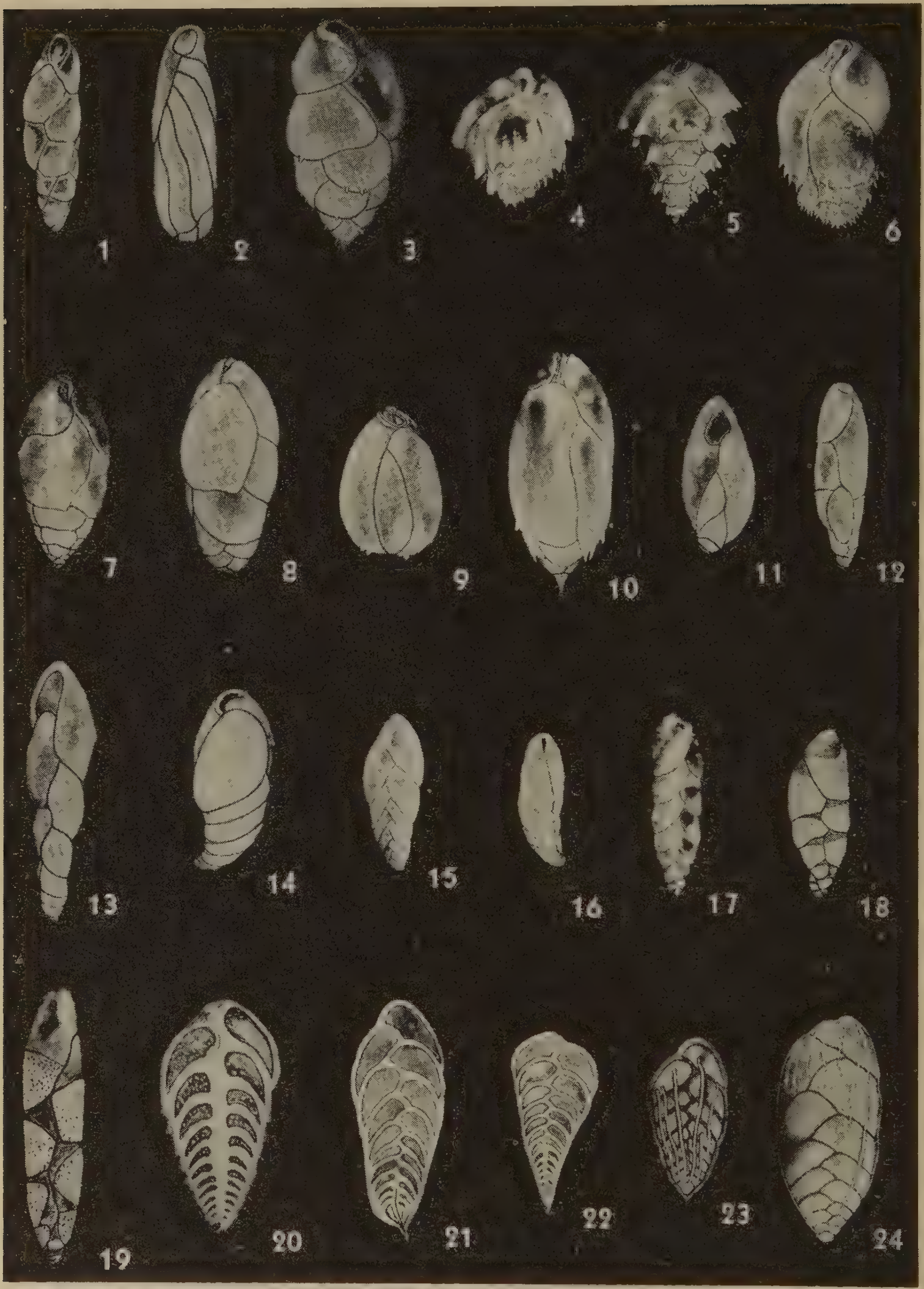
1
2
3
4
5
6
7
8
9
10
11
12
13
14
15
16
17
18
19
20
21
22
23
24

Uchio: Living Foraminifera, San Diego, California

percent of Foraminifera sands which are mostly residual faunas of Pleistocene age. Coronado Bank is a non-depositional area at present, as shown by the very thin cover of Recent sediments and the presence of glauconite and phosphorite nodules. For this reason there is almost no dilution of the Foraminifera tests by detrital sediments. The low total population in the San Diego Trough may be due to low production and low temperature and also to dilution by detrital sediments. The low total population in the nearshore area is explained by low production suggested by the presence of small living populations. The presence of a tongue-like area of intermediate total populations in the San Diego Trough is explained by the presence along Coronado Canyon of fine sand which has been displaced from the intermediate total population area on the shelf.

Usually the size of the living population is very small compared to that of the dead population, and, therefore, the size of the dead population is almost the same as that of the total population (see Walton, 1955, text-figs. 8, 9). For this reason the distribution of the L/T (Living population/Total population) ratios is more influenced by total population than by living population.

Walton (1955, p. 977, text-fig. 12) finds that the frequency distribution of dead population per 5-fathom interval is multimodal, and that the high population of dead Foraminifera does not correspond to the areas or depth of the maximum production of living Foraminifera in Todos Santos Bay at the time of collection. He does not mention the dead benthonic population in the deeper traverse, but his table 4 shows the irregularity down to 490 fathoms. Bandy (1956, p. 185), instead of counting dead or total populations, estimates the weight percentage of the Foraminifera (including benthonic and planktonic) in sediments, and concludes that the percentage fluctuates from less than one percent near the shore to two percent on the outer part of the continental shelf. Deeper, they increase rapidly down the continental slope; this increase coincides with the progressive increase of planktonic tests in the sediments. After examining Bandy's charts (*op. cit.*, charts 3-7) which deal with offshore Foraminifera, the writer finds that Bandy's conclusion is correct in three traverses (*op cit.*, charts 3, 6, 7), but is not correct in two other traverses (*op. cit.*, charts 4, 5).

NUMBER OF SPECIES AND GENERA OF LIVING BENTHONIC FORAMINIFERA

Bandy (1954, p. 135) in his study of shallow-water Foraminifera in the Gulf of Mexico concluded that the number of species increased away from shore because of the more rapid sedimentation near shore and the fairly stable normal chlorinity offshore. Later in his ecologic study of Foraminifera in the northeastern Gulf of Mexico, he also concluded that the number of species generally increased from about 20 in the nearshore area to more than 50 at the outer ends of the deeper profiles (Bandy, 1956, p. 184-185). His conclusion applies to the present study in the San Diego area, but it should be remembered that he dealt with the empty tests of Foraminifera and a different result might have been obtained if he had dealt with living Foraminifera only. If one considers only total populations from dried samples there is no way to distinguish Forami-

---

EXPLANATION OF PLATE 6

Figs.		Page
1.	*Buliminella tenuata* Cushman. Hypotype (U.S.N.M. No. 626709), ×46.	
2.	*Buliminella elegantissima* (d'Orbigny). Hypotype (U.S.N.M. No. 626708), ×103.	
3.	*Bulimina denudata* Cushman and Parker. Hypotype (U.S.N.M. No. 626710), ×100.	
4.	*Bulimina mexicana* Cushman. Hypotype (U.S.N.M. No. 626711), ×50.	
5.	*Bulimina pagoda* Cushman. Hypotype (U.S.N.M. No. 626712), ×47.	
6.	*Globobulimina barbata* (Cushman). Hypotype (U.S.N.M. No. 626713), ×52.	
7, 8.	*Globobulimina hoeglundi* Uchio, n. sp. 7, Holotype (U.S.N.M. No. 626714), ×38. 8, Paratype (U.S.N.M. No. 626715), ×38.	64
9.	*Globobulimina pacifica* Cushman. Hypotype (U.S.N.M. No. 626717), ×18.	
10.	*Globobulimina spinifera* (Cushman). Hypotype (U.S.N.M. No. 626718), ×70.	
11.	*Virgulina apertura* Uchio, n. sp. Holotype (U.S.N.M. No. 626719), ×100.	63
12.	*Virgulina bramlettei* Galloway and Morrey. Hypotype (U.S.N.M. No. 626721), ×35.	
13.	*Virgulina complanata* Egger Hypotype (U.S.N.M. No. 626722), ×96.	63
14.	*Virgulina cornuta* Cushman. Hypotype (U.S.N.M. No. 626723), ×46.	
15, 16.	*Virgulina rotundata* Parr. Hypotypes (U.S.N.M. Nos. 626726, 626727), ×47, ×46.	
17, 18.	*Virgulina sandiegoensis* Uchio, n. sp. 17, Holotype (U.S.N.M. No. 626728), ×155. 18, Paratype (U.S.N.M. No. 626729), ×136.	63
19.	*Virgulina seminuda* Natland. Hypotype (U.S.N.M. No. 626731), ×92.	
20.	*Bolivina acuminata* Natland. Hypotype (U.S.N.M. No. 626732), ×83.	
21, 22.	*Bolivina subargentea* Uchio, n. sp. 21, Holotype (U.S.N.M. No. 626744), ×33, megalospheric form. 22, Paratype (U.S.N.M. No. 626745), ×34, microspheric form.	64
23.	*Bolivina interjuncta bicostata* Cushman. Hypotype (U.S.N.M. No. 626734), ×34.	
24.	*Bolivina tongi filacostata* Cushman and McCulloch. Hypotype (U.S.N.M. No. 626735), ×102.	

TRAVERSE	I																			II															III																		IV		
STATION	45	46	47	48	49	50	51	52	53	54	55	56	57	58	59	60	61	62	63	44	43	42	41	40	39	38	37	36	35	34	33	32	31	30	1	2	3	4	5	6	7	8	9	10	20	11	12	24	25	26	27	28	103	102	101
DEPTH IN FATHOMS	20	33	38	42	47	53	80	94	118	137	157	164	181	194	208	223	214	247	238	20	29	34	39	42	46	53	73	87	104	114	121	135	148	180	19	20	35	40	44	45	47	49	52	56	59	74	92	112	123	157	92	71	15	17	20
TOTAL POPULATION	11600	6600	4700	9400	11200	2100	6700	6600	14200	13900	3400		6100	8300	[illegible]5400	19700	9200	52100		700	6100	5300	2400	7100	2500	7700	24400	23900	11800	28400	52500	14500	19800	20500	2000	6100	7000	12700	16200	2700	7800	28500	55400	152300	184700	261600	22200	16500	24900	24400	11600	547800	3600	2300	1800
Alliatina primitiva													.1			.2																		.2																					
Alveolophragmium advena																																										.1												1	.9
A. columbiense	.1		.4	.3	.4	.8														1	1		1												.8	.5		.1	.2															2	6
Ammobaculites catenulatus					.1	.8					2		1	.2			.7	.5											.5			.5	.6	1															.1	.3					
Ammotium planissimum	.3		.4		.4	1	.2		.1												.3			.5	.5													.3	.2		.2		.1					.2		.8			1	.7	.2
Angulodiscorbis charlottensis																																																							
Angulogerina angulosa	3	2	2	4	6	12	11	6	5	5	6		5	7	8	5	8	7		1	2	3	1	4	10	12		6	7	4	4	5	6	10	.8	4	6	4	2		7	10	14	13	7	14	10	4	5	11	10	10	1	.7	
Arenoparrella oceanica		.2			.1		.1													.6			1															.3	.3		.4		.1												
Asterigerinata pacifica				.3				.7					1									.3																						.2			.1							.7	
Astrononion viragoensis	.1													.2	.8	.2																	.2											.2	.7			.1							
Bigenerina höglundi																																																							
Bolivina acuminata	.3		.4	1	2	5	4	3	3	.8	.2					.2								1	2	3		1	3	2	1	1	.2	.2				.6	1		1	1	.5	.8	4	1	4	3	2	.5	.5	1			
B. acutula		.5	.7	2	1	.8	.6	.2										.5						2	1	.4										.5	.8	.9	.3		1	.5	.5	.5			.1		.3						
B. bicostata																																	.2																	1					
B. filacostata																								.2							.1	.1											.1			.2	.3				.2				
B. minuta									.1	.5	2		10	23	20	15	18	20										.3	.3	.2		1	2	5													.1	1	1	3					
B. pacifica		2	5	2	4	1	4	3	4	3	2		.8	.2	1			.2			1	5	4	5	6	4		3	1	1	.5	1	1	3			.8	4	5		4	.9	.3	.8		.2	2	.4	.9	2	.7		.7		.4
B. peirsonae																																																							
B. spissa									.3	2	3		9	6	6	4	1	2											.3	.6	1	4	4	3													.3	.2	2	4					
B. subargentea									.2	2	8		4	2	2	.8	.3	6												.3	.2	3	7	3														.3	2	9				.4	
B. subexcavata	.7	4	1	1	1	.4	.1	.7	.2	.3	1		.8	1	.2	4		1		.6	1	2	.9	2	.6	.4		.8	1	.3	.6	.4	.3	.5		1	.8	3	2		1	.7	.5	.5	.7	1	3	.7	1	.3	1	.4	.4		1
B. vaughani	.6	2	3	1	2	.4	1	1	.3	.3			.3	1	.4	.3					2	1	.6	2	.8	.4		1		.7	.1	.5	.5	.2		.5	.8	1	1		1	.2		1	.7	.4	4	.5	.1	.3	.2	.2	1	3	2
Buccella angulata	.6	5	9	15	6	6	3	.7	.1	.1	.7		.3			.3					6	8	6	8	13	3		1	.8					.2	.8	6	8	6	22		5	.6	.5	.2		.4	.3						8	6	3
Bulimina denudata	.3	.2	.4	1	2	7	3	4	7	4	1		2	1		.6					.5	.3		2	6	4		4	7	6	8	8	3					1	.9		4	1	1	.5			5	4	3	2			2	1	.4
B. mexicana																																																							
B. pagoda																																																							
B. subacuminata																																																							
Buliminella elegantissima		7	3	2	.7		.4						.1		.2					1	7	8	5	2	1	.4		.3								2	4	3	1		.6	.1	.2				.1	.2					7	5	15
B. tenuata																																																							
Cancris auricula	.1	.2			.4	.8	.5				1		.1	.4		.2					.3		.3		.8	2		.3	.3	.1	.6	.3		2							1	.7	.5	.8		.6	.4	.3	1	.5	.5	.7			
C. inaequalis																																																							
Cassidulina bradshawi																																																							
C. californica																																									.2	.1	.5	.7						3					
C. delicata											.2		.4	1	.6	2	9	9														.1	.6	.3																					
C. depressa	6	8	10	17	14	2	20	44	39	27	15		12	13	10	10	3	8		9	4	2	10	22	8	19		25	37	45	24	27	18	5			9		20		14	13	10	5	13	7	27	43	25		4	4	.9	.7	
C. limbata				.7	6	1	2	6	11	13	3		4	1		.2	2								.8	4		7	10	11	20	9	4	3					.2			13	9	13	11	15	6	10	12	7	28	21			
C. subcarinata										.1	.5		2	2	4	5	6	12														.1	.8	1												.2			.1	.3					
C. subglobosa	3	3	3	4	4	5	14	5	8	21	28		32	25	20	30	34	9		.6	3	2	1	2	6	13		13	7	9	20	20	34	26		7	3	25	2		8	12	17	13	15	19	10	10	20	34	10	23	.7		.2
C. tortuosa	3				5	1	.4						.3				7	.2		37						4								3	14	3	2				1	16	15	17	18	10	.6	.6	.1	1	28	17	.2		
C. sp. cf. C. orientalis																																	.2				2		.2		1												.7		
Cassidulinoides waltoni													.1		.2																.1			.5															.1						
Chilostomella ovoidea							.4		.1	.6			.7	.2	1			.7										.3																				.1	.4	.3					
Cibicides fletcheri	34	5	5	2	4	.8	.5	3	2	.3	1		.7	.8	3	2	.7			9	5	2	.3	2		.8		2		1		.9	1	3	11	23	4	8	.5		.8	3	8	11	4	14	2	1	2	4	4	11	1		
C. mckannai					.6		1		1	.3	.2		.1	.2		2				1						.8		.8	.8	.8	1	.2		.7				.3			.2	4	2	2		4	4	2	1	.5	4	3			
C. phlegeri																		1													.1		.2	.3																					
C. spiralis																																																							
Cornuspira lajollaensis	.1																			.6																																			
Cornuspiroides foliaceus																																																							
Ehrenbergina compressa							.1						.1			.6	2	3										.3		.1		.1	.2	6												.8	.7	.2		1	.5	.9			
Elphidium spp.	.6	6	6	6	4	.4	1	.7		.2	.2		.1		.2	.6				1	10	5	4	8	5	4		.5	.3	.2	.1	.2	.3	.3		5	6	7	5		3	4	2	1		.2		.1	.1			.2	10	9	13
Epistominella sandiegoensis	1	3	1	1	6	10	16	15	8	6	7		10	6	7	6		6		.6	3	2	3	3	6	12		17	7	7	5	7	7	2				.9	2		7	7	10	4	7	3	9	5	7	3	.7	3	.2	.7	
E. smithi													.1					2																															.3						
Eponides leviculus					1	.8	1	2	3	3	4		1	4	5	3	.7	2					.6	.5	3	.4		6	2	3	2	2	2	.8					.5		3	1	.5	.5	2	1	4	2	2		.2	.4			
E. subtenerus																																																							
Gaudryina arenaria					.3	.8	1	.5	.4	.3	.2		.3	.8		.2							.6	.2	.3	2		2	.8	.6	1	1	.3	1			.8				1	.7	.2	.3		.8	2	.8	1	.5	.7	.2			
G. subglobrata	.3																																	.7																	.2				
Goësella flintii		1	1	2	.7	1	.1				.5				.2	.5	1					.9	1	3	2									2			2	1	.5		.6								.1	.3					
Globobulimina barbata																																																							
G. höglundi																																																							
G. pacifica					.6		1	.5	.2	.6	1		.1		.4	.5	.3	.5			.3	.9		.2	.5				1	.6	.2	.7	.8	.8				.3	.2		1	.3					.3	.7	.5	2		.2			
G. spinifera																																																							
Glomospira gordialis																																																							
Gyroidina gemma																																																							
G. quinqueloba																																																							
Hanzawaia nitidula	1				.7												1											.3			.1			1							.4	.3	.2	2	.7	.6	.3			.3	.9	.2			
Haplophragmoides neobradyi				.7	.6	7	.7																	.2	2							.1	.3						.2		1	.3													
H. quadratus																																																							
H. sp.																																																							
Höglundina elegans																																.1		1												.2			.1		.5				
Cassidulina sp.																																												3											

Table 5. Occurrences of benthonic Foraminifera in percent of total (living plus dead) population.

nifera indigenous to an area from those which have come from other environments. One can expect more species in mixed sediments of different origins than in sediments of a single origin.

Bandy (1954, p. 135) also pointed out that there was a correlation between weight percentages of Foraminifera and the number of species. This is probably true, but it should be pointed out also that the greater the number of specimens examined the greater the likelihood of finding rare species. The larger the population, therefore, or the higher the weight percentage of Foraminifera in a sediment, the larger the number of species.

In most of the San Diego area the number of species

(214)

STATION	45	46	47	48	49	50	51	52	53	54	55	56	57	58	59	60	61	62	63	44	43	42	41	40	39	38	37	36	35	34	33	32	31	30	1	2	3	4	5	6	7	8	9	10	20	11	12	24	25	26	27	28	103	102	101
Involutina pacifica			.4		.1		.1		.1	.1	.2		.1			.2							.3					.3			.1						.8	.1	.2		.6							.1							
Lagena & related spp.	.8	3	5	4	2	2	10	1	10	1	.2		2	.8	1	2	2	2			4	3	.3	2	2	1		1	2	1	1	1	1	2			2				2	2	.6	2	4			1	1	.8	.7	2	3	2	2
Lagenidae (other)				.3										.2							.3			.2								.2		.2				.2							.7	.2		.1	.3				.2		
Loxostomum bradyi																																																			.2				
L. pseduobeyrichi																		.2																																					
Neoconorbina terquemi																																																							
N. parkeri	2																																																						
Eggerella advena	.7	.9	7	1	2	7	.6	.2	.2											.6	12	16	13	2	3	.4			.3	.1		.1			.8	2	3	1	2		3	.3	.1	.2			.3	.2					24	31	23
E. scrippsi				.3		.4											.7	.2						.2										.2																					
Nonion lankfordi				.3			.5	.2	.1	.1			.1					.5					.3		.8					.2	.1								.3					.2				.1							
N. parkerae																																																							
Nonionella basispinata	2	.7		.7	.3									.2	2	.2		.2		1	4	5	1	.2	.5				.3					.5		1	2	3	3		2	.1	.1			.2	.9	.2		.8			5	6	9
N. (?) fragilis																																																							
N. stella	.6	19	18	21	13	7	6		.8	.2	.7			.2	.2	.2		1		1	16	15	12	19	5	4		3	2	.4	.1	.1	.5	.5		8	24	13	16		14	3	2	.9		.6	1	.7	.9	.5	.5		14	10	10
N. sp. aff. N. globosa								.2	[illegible]	.5	2		.5		.6	.2														.1	.2	.1		.7																.3	.2				
Nouria harrisii																																									.2		.1							.5					
N. polymorphinoides			.4																																																				
Patellina corrugata	.1							.2																																		.1													
Planulina ornata	3				.6												1			.6	3												.2	.3	.8	2	.8	.6	.2		.6	1		3	2	2	.4	.3		.3	2	.7	.2		
Placopsilina bradyi																																																							
Polymorphinidae	.1																			3				.2											.8			.1			.2	.1								.3	.2				
Saccammina longicollis			.8			1			1				.3							.6		1			3			.3		.2	.1					2		.5			.2							.6	.1						
Pullenia salisburyi	.3						.1		.9	3						.6		.5						.2	8						.2	.2	.5	.3							.4	.3	.8	.5	.7	.2	.4	.5	.1	.5		.2			
Recurvoides sp.		.2			.1	3	.4		.1	.1	.5		.1									.6		.2	3	.4		.3	.3		.1	.2							.2		.8									.3					
Recurvoidella parkerae																																																							
Remaneica cf. helgolandica																																																							
Reophax excentricus																						3				.4																													
R. gracilis	.1	.5							.1													.3																.3										.1	.1						
R. horridus																																																							
R. micaceous																																																							
R. communis	.1	.5			.3	.8															.3	.9	.6		.5																.6	.1											2	2	2
R. scorpiurus		.5	.4			2	.7		.1														.3	.2	1	.4												.4				.1													
R. subfusiformis																																																							
R. spp.																																		.4												.2									
Robertinoides charlottensis	.1																																																						
Rosalina columbiensis					.6																2			1											43	3																			
R. campanulata	21	2	1	2																13	1	2	1			2		.3							23	12	3		.5			.8	.6	.3	.7		.1						.7		.2
R. turbinata	2																																			.5																			
Seabrookia earlandi					.3				.3	.9	.7		1	.2	1	.6	.3	.2										.5	.8	.4	.2	.5	.3						.2					.3			.3	.6	.4	.3	.2				.2
Sigmoilina tenuis			.4							.5	.7		.3	.4	1													.3	1	.3	.7	1	.2	.5		.5		.1				.1	.2	.3	.7	.2	.4	.6	.6						
Spiroloculina fragilis																																																							
Spiroplectammina bathyca																																																							
S. biformis																																																							
Suggrunda (?) eckisi											.2		.1					.2																																.3					
Textularia cf. abbreviata			2		.1																								.3					.2				.1	.3							.2									
T. earlandi		6	6	1	2	3	.1		.1												2	5	6	.7	1											.5	2	3	3		2	.5											.2	.4	.2
T. sandiegoensis																																									.2														
T. schencki	.4					.8																		.2										.3																					
Tritaxis bullata																																									.4														
Trochammina charlottensis	.8		3	2		2														4	4	3	4	.9	1									.2			2																		
T. chitinosa																																																							
T. conica						.4	.4	.2	1								.3																	1																.3					
T. discorbinoides			.4															.2												.1				.3												.2									
T. globigeriniformis																																																							
T. kellettae	.1	.5	3	4	.4		.5	.7													2	2	7	2	.3						.1					.5	.8	.8	1		.6								.1				.7		.2
T. labiata																																																							
T. nitida																					.8																.8																		
T. pacifica & var.	1	4	1		1	1	.3		.1		.5					.2	.7			.6	.8	.3	2	.5	.3			.3		.6	.1	.1		.2			3		.5		.8						1	.5	.1	.5			12	7	6
T. rhumbleri		.2			.1	.4															2		11	.2																															
T. squamiformis																																																							
Uvigerina auberiana																																																							
U. curticosta															.2	2		1																																					
U. juncea					.5	3		1	3				.3												.6							.1		2					.2		1	.3	.3	.6	1	.6			.3	1	.2	.2			
Valvulineria araucana																																		.2																					
V. glabra																																																							
Virgulina apertura																																																							
V. bramlettei																		x																																					
V. complanata																																																							
V. cornuta																																																							
V. delicatula											.5			.4																																									
V. sandiegoensis		2	1	.7	2								.3								.5	1	.3													.5			.2		.4												1	.4	.7
V. seminuda		.2									.5		.7		.4	.2														.8				.2				.8	.5		.2							.1		.3					
Miliolidae	3				.3				.2	1								.2		4			.6	.2	.3	.4		.3	.5			.3	.2	.3	3	.5									2				.1	.3	.2		1	2	
Miscellaneous spp.	5	1		.3	.3		1		.1	5	5		.3	1	3	1	.7	2		7	1	2	.3	.2	2	1		.8	5	2	7	3	2	2	1	11	4	.3	1		1	.1	.3	4	.7	2	1	4	5	1	.6	.4	2	6	4

Table 5 (continued). Occurrences of benthonic Foraminifera in percent of total (living plus dead) population.

is less than 20 at a depth less than 20 fathoms, then gradually increases with increase of depth offshore reaching a maximum of more than 50 species at 60-100 fathoms. There is a gradual decrease in number of species with the increase of depth in the northern part of this area where the slope of the bottom is gentle down to the bottom of the Loma Sea Valley.

In the southern part of the area, where the shelf ends abruptly and there is a steep escarpment down to the bottom of the San Diego Trough, the situation is different from that in the northern part. The number of species is small at a depth shallower than 20 fathoms, then increases with increase of depth reaching a maximum at 45-100 fathoms, and then decreases again. Another maximum is found at 400-600 fathoms. The area of delta-like topography at the lower end of the Coronado Canyon does not show such a second maximum. The true deep floor of the San Diego Trough has a moderate but unexpectedly high number (average 41) of species. There is no positive correlation of the areal distribution of the number of species with that of the size of the living population, the total popula-

TRAVERSE	IV																																																					
STATION	100	99	98	97	96	95	94	93	92	91	90	89	88	87	140	124	123	122	121	259	115	260	240	286	275	242	287	261	306	276	249	262	285	277	191	216	220	227	288	183	228	221	230	243	263	218	229	186	248	212	264	322	323	324	270
DEPTH IN FATHOMS	21	25	30	33	40	45	48	61	80	104	65	63	64	75	5	7	9	11	11	38	39	40	40	41	45	47	50	53	53	55	57	64	67	98	120	125	128	134	140	150	160	167	180	200	213	218	234	248	250	275	280	285	310	328	345
TOTAL POPULATION	19400	8800	14300	1800	12800	13900	6700	24500	43500	22500	186700	467500	505900	247300	2900	700	1900	400	1200	21100	9600	58100	62300	290800	175900	214300	235800	120300	263700	151800	351700	62100	191000	161300	37600	50600	163200	19600	262700	16900	17300	72100	40100	29900	114400	19300	38800	50300	43900	16200	9600	23000	18900	15500	33900
Alliatina primitiva																																															.2			.6			.3		
Alveolophragmium advena																																																							
A. columbiense			.5		.5	.5											.6	1	7			.4	.4														.3					.1							.2							
Ammobaculites catenulatus							.6		.1									.2																							.4				.1				.6	.6	.1		5	4	
Ammotium planissimum	.2	X	.1	.7	.3	.6				.3																											.4						.2		.3	.2								
Angulodiscorbis charlottensis																6	3																																						
Angulogerina angulosa	8	9	11	17	12	10	8	15	9	10	15	18	13	8		.4	.4	.2		3	8	10	5	17	12	20	6	4	8	10	9	9	9	13	13	10	9	3	10	4	4	7	5	7	5	6	5	8	5	7	2	5	9	4	2
Arenoparrella oceanica							.6						.3							.3		.9								.3			.3		.3	.1		.6		1	.5		.2	.4	.1	.3		.2	.3		.2				
Asterigerinata pacifica		.4					.3						.3	.4			.2	2	.7	.6			.6	.3				.8	.4		.3	.3	.3	.3	.7		.4	.2		.4	.5		.2		.1	.3	.2	1	.3					
Astrononion viragoensis				.1	.3			.1			.1		.3											.4	.3														.1			.4	.1		.2	2	.3						
Bigenerina höglundi																																																							
Bolivina acuminata				.1	.1	.4	2	2	5	2	1	2	.3	.8						.9		1	.6	.3	.4	.3		2	2	3	1	1	.6	.9	1	3	.4	1		2	.9		.5	.6		1	2	1	.9	.6	.2				
B. acutula	.4	.2	.8	.9	.9	1	2		.2		.1						.2	.2	.2			.2	2	.2	.7	.4	.6		2									.3	.8																		1	.8	
B. bicostata																																					.4								.2					.5								
B. filacostata							.3	.1			.3			.4											.6	.4					.1	.3												.2									.2				.2
B. minuta									.7																									.7	.8			.4		.5		.7	.4	3	2	3		3	4	8	13	9	5	8
B. pacifica	.3	.7	.2	.4	2	2	2	.5	2	1	3	.6		.4		1	.4	.5		.6	.5	2	1	.3	.4	.3	.4	2	2	.3		.6	.3	2	2	2	.8	6	3	7	6	.5	3	3	2	6	1	3	1	3	3	.4		.4	.2
B. peirsonae																																																	X						
B. spissa									.6	1																									1	.5	1				1	2	.6	2	1	.8	.8	.9	3	3	2	3	3	4
B. subargentea									.2	.3																									.3	.9	.4	.2		.4	.6		1	1	3	4	2	.3	2		8	.7	1		4
B. subexcavata	.4	.4	.1	.3	2	.5	1	.9	1	2	1	2	2	2		2	1	.2	.1	21		7	5	2	5	.9	10	12	10	1	2	4	1	.3	5	2	3	8	2	8	9		6	6	10	9	8	9	8	4	6			.8	2
B. vaughani	2	2	.1		1	.4	1	.8	.4	.3	.3	1			2	2	6	1	2	7	1	5	3	2	.7		3	6	3	2	2	2		.6	2	.8	1	4	.8	4	3		2	2	3	6	3	1	2	6	2	1		.4	
Buccella angulata	4	8	3	2	3	1	1	2	.4	.3						5	6	5	4	.6	.2	2	.2		.4	.3		2		.6	.3	.3			.7	.3		.2		.4			.3			.3		.8	9		.2		.3		.4
Bulimina denudata	.5	1	.3	.5	.4	2	2	1	1	3	.3	.3						.2	.2		.9	.2	.4		.7	.4	.3	.4	.4	3	1	.3	1	.3		6	2	2	3		3	2	3	.8	2	.7	.8	1	1	.6	1	.3				.6
B. mexicana																																																							
B. pagoda																																																						.4	
B. subacuminata																																																							
Buliminella elegantissima	2	1	.1		1	1	1	.1	.2	.3						17	21	27	25	.3		.4	.4				.7	.4				.8				.4	.8	.5		1	.6		.3	.4	.5	.5	.5	1			.5	.4		.4	.6
B. tenuata																																																		.6					
Cancris auricula	.1			.1		.2	2	.1	1	1	.4	3		.8						.3	.3	.9		.3	.4	.6	1	1		.6	.3	1	.6	.6		.5	2		.4	.2	.3	1	.2	.2	.5	.3	.2		.3	.6	.1				.2
C. inaequalis																																																					.3		
Cassidulina bradshawi																																													X									
C. californica					.1				.2		.1		1	.4										.3					.4		.3		.9	.3		.3	.4												.3							
C. delicata																																										.5		.9	.8	.5	.2		.9	.6	6	4	21	20	18
C. depressa		12	2	.8	2	.9	33		22	24	6	6	7	10		.8				22		19	58	10	16	12	26	19	22	12	10	11	8	6	23	15	11	23	3	29	18	.5	10	11	15	15	13	18	8	15	15	15	6	9	16
C. limbata			.7	3	.3	.8	2	6	4	3	11	9	13	21						1	.7	6	.8	4	6	10	6	1	4	16	21	18	24	21	7	6	10	.2	17	1	.7	34	4	4	3	1	3	4	1	2	.2				
C. subcarinata										.6																								.3								1			.3						6	21	15	17	11
C. subglobosa	5	2	17	19	44	41	3	45	19	10	17	13	21	14			2		.1	3	9	3	6	15	11	19	11	3	11	13	19	10	13	10	8	12	11	3	13	7	5	31	17	15	7	3	14	4	9	11	4	6	3	3	3
C. tortuosa	16	1	38	33	5	12	2	4	3	2	14	10	15	16						2	62	3	2	7	13	12	5	.8	4	11	14	8	22	23	2	2	11		22	.6		9	3	3	2		2	1	4	1	.2			1	.2
C. sp. cf. C. orientalis		.3					.3			.3								.2	.3			.4			.7	.3		.4										1			.4		.5	.4	.4	1		1								
Cassidulinoides waltoni																																													.1									
Chilostomella ovoidea									.2	.3				.4																.1				.3				.4	.2	.1		.2											.4	.4			.6
Cibicides fletcheri	11	7	4	5	2	1	2	.4	6	5	17	11	10	7	32	4	3			4	1	9	.8	17	12	4	5	3	2	3	2	6	3	6	4	5	7	2	6	1	.8		8	6	4	4	4	11	8	6	2	.4		1	.4
C. mckannai		X	.4	1	.5	.6		1	2	2	2	4	5	.8						.3	.8	.9		3	4	4	.7	.8	2	4	.7	3	5	3	1	1	.8		4	1	.5	4	1	3		.1	2	.3	2		.4		.7		.2
C. phlegeri																																.1					4	.3			.1		.7		.3		.5		.3	.6	.7	4	.3	.8	.6
C. spiralis																																																							
Cornuspira lajollaensis			.1												2	.2																																								
Cornuspiroides foliaceus																																																							
Ehrenbergina compressa									.3	.8	.1		.3	1												.3				.3				.9	.3	.3	.4		1		.1	.5	.5		2	.2	.6		.3		.3	.4	.7	.4	.2
Elphidium spp.	5	7	3	.8	1	2	2	1	1	3	.5			2		28	29	33	35	.9		1	2	.7			1	2	2	1	1	1			.3	.5	.4	1		.6	1		1	1	3	2	2	2	.3		.9			.4	.2
Epistominella sandiegoensis	.1	1	.2	.6	3	2	7	8	12	10	1	5	2	7		.2		.2		5	.3	2	4	2	2	2	6	12	12	5	6	7	2	2	8	13	8	11		6	13		8	11	11	10	10	8	8	11	16	7	8	6	5
E. smithi										.3																																	.2	.9	.5	.1		2	.6		2	.4	.3	.8	12
Eponides leviculus							2		2	2	.3	1	1	2				.2		.6	.3	2	.6	.7	1	2	1	2	3	1	2	2	.6	.6	3	3	2	3	.4	4	4	1	3	1	3	3	4	2	2	5	2	5	4	9	2
E. subtenerus																																											2						.6						.4	
Gaudryina arenaria		.7	.6	.3	.3	.9	.3	.4	.6	3		.3		.4							.2				.4		.4				.3	.2		.3	2	3	.4	.2	2	.4	.3		.2	.4				.8	.9		.2			.8	
G. subglabrata	.4			.2	.1					.6		.3								.6		.9			.4	.9							.3						.4	.2			.2		.3	.3	.3		.6						
Goësella flintii			.1	.1	.1	.5																																								.8	.2							
Globobulimina barbata																																																							
G. höglundi																																																							
G. pacifica				.2	.1	.5		.3		.8	.1										.4	.2										.1			.7	.1		.5		.2	.1			.2		.8	.2		.6		.2	.7		.4	
G. spinifera																																																			.1				.2
Glomospira gordialis																																																							
Gyroidina gemma																																									.1													.7		
G. quinqueloba																																																				3			
Hanzawaia nitidula	1	.4	1	1	.1	.4			.3		2	2	.7	.4						.3		.4		1				1			.6		.6	1	1	.3	1	.8		.8	.6	.5		.6		.4	.5	.3	.2	.3	2	.5				.2
Haplophragmoides neobradyi				.1	.4	.2	2			.3																		.4											.2				.1								.3						.2
H. quadratus																																	.3																					
H. sp.																																																							
Höglundina elegans												.3		.4																								.4		.4			1														
Cassidulina sp.							.3					2	.3	.8			.2			4	10	.9		.3			2	5	5	1	1	5	2	.9	2	4	2	11	.8	1	8	.5	5	5	6	5	5	2	6	5	.5				

Table 6. Occurrences of benthonic Foraminifera in percent of total (living plus dead) population.

tion, or the L/T ratio. Further study of the deeper area is necessary to establish the relationship of number of species with depth.

A possible reason for the small number of species in nearshore and very deep areas is that the more rigorous the environment the fewer the species which can become established.

The morphological features by which a species is characterized are less fundamental and presumably of more recent origin than those characterizing genera. But when one tries to apply the knowledge of modern distributions to paleoecology, one finds that most of the Recent species are not found in strata older than early Pliocene or late Miocene. In such cases the

STATION	100	99	98	97	96	95	94	93	92	91	90	89	88	87	140	124	123	122	121	259	115	260	240	286	275	242	287	261	306	276	249	262	285	277	19	216	220	227	288	183	228	221	230	243	263	218	229	186	248	212	264	322	323	324	270
Involutina pacifica				.1		.2			.2	.3									.3																			2			.2		.2										1		.4
Lagena & related spp.	3	5	2	1	4	2	1	2	1		.4	1	.3	2			4	2	3	2	1	3	3	2	1	1	3	2	.4	1	1	1	.9	.6	1	2	1	1		1	2		1	2	2	2	2	1	1	2	2	1	2	1	1
Lagenidae (other)		.4								1						.4	.2				.2			.3						.3					3			.2		.6					.1				.6				.3		
Loxostomum bradyi																																																.8							
L. pseudobeyrichi																																											.2										.3		.2
Neoconorbina terquemi															7		.2																																						
N. parkeri																8																																							
Eggerella advena	4	7	1	.5	3	.7	3	.4	.3				.3	.8		.8	3	2	3	.6	.3		.1					1	2		.3	.5	.3	.3		.1	.4	2		.2	2		1	.9	[illegible]	1	.8	1	.9		.2				.2
E. scrippsi																																																							
Nonion tankfordi					X		.3		.7	.8				.8						.3							.4	1				.3		.3																	.3				
N. parkerae																																				.1		.3			.2		.7	.4	.5	.5	1	.8	.6						
Nonionella basispinata	2	5	2	1	2	.8	3	.3	.6	1	.3					1	4	12	10	.3	.3	.9	.8				.4	.4				.2			.3	.3	.4	.2		.8	.1		.7	.2	2	.3	.3	.8	.6	1	.2				
N. (?) fragilis																																																							
N. stella	11	9	2	3	.8	6	6	3	.7	.6		.3	.3	.4		.8	2	2	3	4	2	6	2	1	.7	.6	3	7	2	2	1	.9		.6	1	.5	2	3		3	3	.5	1	.9	1	4	.5	3	2	1	1	.7	.3		.8
N. sp. aff. N. globosa																																.1		.3			.8								.1						.4				
Nouria harrisii							.3		.1																																														
N. polymorphinoides																																																							
Patellina corrugata	1															.2												.4								.1									.1	.1	.2	.2							
Planulina ornata	4	2	2	3	.9	1			.6	.8	4	4	4	.8		.2				.3		.9	1	3	3	5	.7		1	3	2	.8	2	2		.9	2	.5	3	.6	.5	.5	1	.6	.3	.5	.3	.8	.6	1		.4	.3		
Placopsilina bradyi																																																							
Polymorphinidae		.2	.4	.1		.1													.3		.7				.4					.6	.3								.4					.2											
Saccammina longicollis	.2			.1	.1	.7																																																	
Pullenia salisburyi	.3		.1	8	.1		.6	.1		.3	.4	.3		.4							.2			.3	.4	.3		.4	.4	1	.3	.2							.4	.4	.3			.9		.2	.5	.2		.6					
Recurvoides sp.			.3	[illegible]	.1	.1	.3																																																
Recurvoidella parkerae																																				.1		.2			.1														
Remaneica cf. helgolandica																																																							
Reophax excentricus																																																							
R. gracilis	.3				.1			.1				.3																																											
R. horridus																																																			.1				
R. micaceous																																																							
R. communis		.5					.3										.4	.2					.2															.2						.2											
R. scorpiurus		X	1	.1		1	.3																													.1																			
R. subfusiformis																																																							
R. spp				.1																																															.1				
Robertinoides charlottensis	.2					.1																																																	
Rosalina columbiensis	1																10																																						
R. campanulata	4	7	3	.2	2	2	.9	.7	.1	.8	2	2	1	.4	12	3	2	.5	.1	2	.5	.9	.8	3	1		.7	.8	.4	.3		.5		2	.7	.1	.4		2	.2	.2		1	1	1			1			.1				
R. turbinata															10										.4																								2						
Seabrookia earlandi				.1	.3	1	.6	.3		.8	.1	.9														.3	1				.3	.3		.3	.3	.5	2	.3		.4	1		.7		1	2	.5	.3	.9	.6	.9	1	.3		.4
Sigmoilina tenuis				.1				.3	.2	.6	.9											.9		.3			.4	.4	.8	.3		.4		1	1	.5	.4		.4	1	.1		1		.7	.3	.2	.5	.6		.1	.7			.2
Spiroloculina fragilis																																																							
Spiroplectammina bathyca																																																							
S. biformis																																																							
Suggrunda (?) eckisi										.3																												2		2	2			.2	.1	.7	.5								.2
Textularia cf. abbreviata	.2	X	.6		.3	[illegible]		.3														.4				.3							.6		.3														.3						
T. earlandi	.9	.4	.1	[illegible]	1	.2	1													.3		.4	.2			.3	1	.4	.8	.3	.3	.1				.1	.8	2		2	2		1	.6	.2	.2	.5	.5			.2	.4			
T. sandiegoensis																.2																.1																	.6		.1				
T. schencki																																																							
Tritaxis bullata																																			.3	.1					.3		.2	.2		.3									
Trochammina charlottensis										.3						2	.2	2	1																																				
T. chitinosa																																																							
T. conica																									.4	.3											.4																		
T. discorbinoides										.6												.4				.3					.3					.3		.2		.6	.8		.8	.6	.1	.3	.8	.5	.6						
T. globigeriniformis																																																							
T. kellettae	.4	.4		.1	.1	.1	.3									.6						.4	.2					.4				.1						.3			.2		.2												
T. labiata																																																							
T. nitida												.3																																											
T. pacifica & var.		.4									.1					.4	.2	.5	1		.3			.3		.3						.3												.2							.1				.2
T. rhumbleri																		.5																																					
T. squamiformis																																.1							.4		.1								.3						
Uvigerina auberiana																																																							
U. curticosta																																												.2	.2		.5		.3			1	5	5	
U. juncea								.8	.7	2	.3																		.4	.6		.1		.6		3		.2	.4	.2	1		2	1	2	3	2	.8	.6				.3	1	.6
Valvulineria araucana																																			.1								.2	.2					.3		.2			.4	.2
V. globra																																																					.3		.2
Virgulina apertura																																					.4	1			3		.2		.8	1	.6		.6	3	2			.4	.2
V. bramlettei																																																							
V. complanata																																																							
V. cornuta																																																							
V. delicatula																																								.2	.3				.3	.5			.3		.1				
V. sandiegoensis	.2	.4			.1		.6															.4	.2					.8		.6		.1				.3		2		2	.1		.2												
V. seminuda																																									.1			.2		.3					.1				.8
Miliolidae	.5	.4			.1	.5		.5				.6			7	14	2	.5	2	.3		.4	.2	.7	1										.3		.4		.4		.1					.2			.3		.3				.4
Miscellaneous spp.	11	.2	2	2	2	1	1	.3	.4		1	3	1	.4		.6	.2	4	.9	10		7	.4	6	4	.6	2	2		.9	.7	2	1	1	.3	1	3	1	.4	.4	.2	3		2	1		.8	1	8	.6	1	2	5	1	1

Table 6 (continued). Occurrences of benthonic Foraminifera in percent of total (living plus dead) population.

knowledge of genera may be more important than that of species.

On the basis of the *Challenger* data Murray (1913) states that the ratio of species to genera decreases regularly from coastal to offshore deep water, so that in the deepest zone the ratio of species to genera is 5 to 4, whereas in the shallow coastal water it is 3 to 1. Sverdrup, Johnson and Fleming (1942, p. 807) state that a striking characteristic of the deep-sea fauna is the relatively smaller number of species in proportion to the number of genera.

In the San Diego area the distribution of the number of genera coincides, in a general way, with the number of species. The number of genera ranges from 9 to 39, and is less than 15 at depths shallower than 20 fathoms, then gradually increases with increase of depth offshore reaching a maximum of more than 30 at 60-100 fathoms. There is a gradual decrease in

TRAVERSE																																																
STATION	201	307	265	278	325	255	326	250	211	266	304	258	202	294	303	284	289	296	254	208	308	301	207	298	300	302	292	293	305	232	299	290	297	279	269	283	281	236	109	280	114	267	268	112	205	113	111	105
DEPTH IN FATHOMS	345	350	350	350	350	355	385	390	395	420	430	430	440	450	455	455	460	460	465	473	485	490	505	505	505	515	515	520	525	528	530	550	560	565	570	580	580	585	599	605	608	615	630	635	638	639	640	650
TOTAL POPULATION	47900	67200	34600	45800	22000	24400	13700		16000	17000	9700	16300	32900	15500	9900	11400	14900	17600	8100	16300	4700	11100	35000	21000	7700	8500	8000	9800	11500	14000	7400	11300	5600	10400	8900	9500	9300	18900	6400	7000	9600	28500	17100	5600	16700	10000	6000	11000
Alliatina primitiva																			.2					.3																								
Alveolophragmium advena																																																
A. columbiense																																								1								
Ammobaculites catenulatus		.2	1			.6	2				4		1	.4	.7	1	3	.6	1		2	1		.9	.6	1	.6	1	1		1	1	1	.2	.7	6		2	2	4	1	1	2	4	2		2	
Ammotium planissimum							2									.5																																
Angulodiscorbis charlottensis																																																.6
Angulogerina angulosa	.5	2	3	4		.6			4	5	4	4	1	3	.7	5	2	2	4	4	6	3	1	1	3	.4	.6	2	3	5	2	1		2	4	1	2		2	4	1	4	2	4	.5	.5		3
Arenoparrella oceanica		.2		.3					.2			.2							.4	.7																					.2							
Asterigerinata pacifica											.4	.4		.2		.5			.6		.7	.7		.3	.2	.4		.4							.7		.6				.2	.5				.2		
Astrononion viragoensis										.6												.7								.9																		
Bigenerina höglundi																																																
Bolivina acuminata		.8		.3					.6	1	.2	.2		.8				.6	.2	.6	.7			.3	1	2		.4		2	.4			.6					.9	.5		.5	.8					.3
B. acutula						.6									.7																																	.3
B. bicostata																																																
B. filacostata		.2								.6				.2																																	.3	
B. minuta	4	3	6	8	.9	8			8	4	6	5	10	5	8	8	12	6	6	7	5	2	.3	5	5	6	1	6	5	3	5	3	2	5	.7	9	3	4	6	2	5	5	2	3	5	4	5	6
B. pacifica	3	2	1	.3	.9	.6			4		.4	.2	1	2		.5			3	1	2			.6	.2	2	.6	.4	.6		3	1		.9	.7	1	2	.8	.9	.9			2	2		.8	.8	
B. peirsonae			x																													x															x	
B. spissa	6	2	4	2	8	2			2	5	2	3	6	1	3	2	4	6	2	4	3	3	4	3	4	5	2	.3	3	.9	3	2	3	3	2	2	2	3	2	2	.7	2	2		.6	.5	1	4
B. subargentea	2	3	1	3		3			3	1	.7	2	2	.8	1	.5	2		.8		1				.6	.8					1	1		.9	2	.6			2			2	3				.5	.9
B. subexcavata	4	6		3		1			5	4	4	4	2	4	1	1	2	.3	5	5	4		1	2	2	1		.9	3		5	1	1	3	2	4	5	3	.9	5	1	1				.2	1	.3
B. vaughani	1	2	.6	.8		1			2	2	1	.6	1	.8	2	1	1	1	2	.7	.7		.6	.3	.8	1	.6	.4		.9	3	2		2	.7	2	2	3	.4	2	1	1	2	1		.2	.8	.6
Buccella angulata			.2						.4	.6	.2		.5	.2							.3				.4	.4																			.6		.3	
Bulimina denudata		.4	1	.6					.2	2	.2			.4			.6		.6		.3					.8				.9				.9	2				.4		.2	2	.8	3	.5			
B. mexicana																																																
B. pagoda																				.7												3	1															.3
B. subacuminata											2		.5	.6		1	1	1		1	.3	.7	2		.4	1	.6	.4			2		1	.3	.7				.4	.5	2		2		1	.8	2	.6
Buliminella elegantissima	1	.2	.2								1	.2	2	.2	3			1	1	2	.3		.6	.6	.6	.8		.4			.4		1								.3					.2	.3	
B. tenuata	.5	.2				.6												.6								.4								.3						.2								
Cancris auricula		.2				.6						.8		.6		1			.4		.3			.6	.4									.6	.7					.5		.5	2					
C. inaequalis						.6					.2	2																																				
Cassidulina bradshawi					2					1						.5			.8	.7		.7					.6				.4	2				.6											.3	.6
C. californica		.6				1								.2																	.4															.2		
C. delicata	18	5	18	19	25	23	11		7	8	8	15	14	6	9	14	10	14	6	8	6	15	13	9	10	8	13	7	6	7	5	8	4	5	3	7	7	3	7	5	3	6	4	.7	2	4	5	14
C. depressa	3	17	14	8	2	3	2		13	9	8	9	3	10	3	6	3	1	12	3	4	10	5	6	7	5	6	4	3	3	5	4	1	5	4	2	3		5	6	3	6	8	4	2	1	5	2
C. limbata		.4	.4		1	.6	2				.2			.2	.7	1			.8		1	3		.3	.4	1	1			.9	.9	4	1	.6	2							2					.3	.3
C. subcarinata	14	7	8	6	11	10	11		3	6	7	7	5	11	10	11	12	20	4	15	9	15	13	17	15	9	20	22	20	26	12	8	23	14	18	9	8	29	21	11	22	10	23	18	26	21	16	21
C. subglobosa	2	4	4	2		.6	2		3	3	9	3	6	5	4	5	2	6	3	6	7	6	8	10	5	6	4	7	4	9	5	9	9	5	16	3	7	12	9	6	4	9	4	2	7	4	4	7
C. tortuosa		.2		.3			5		.4		.4												.6			.4				6				.6	.7								2			.2		.3
C. sp. cf. C. orientalis	.5										.2					1						.7													.7													
Cassidulinoides waltoni					2																										.4																	
Chilostomella ovoidea		.4	.2			2			.6	.6	.4			.6	1		1		.4		.3	.7			.2	.4	1	.4			.4			.3		.6				.2	.5							.6
Cibicides fletcheri	1	4	3	2					2	5	.9	.8		2			1		2		2			.9	2	.8		.4		.9	.9			2	2					1		.5				.2		1
C. mckannai		.8	.6		11	2			.6			.2	2	.6	1	3					2			.3		.4				3	.4			.6					.9	.2	.7		.8	1		.6	.5	2
C. phlegeri	1	2	.7	3		2			1	3	3	5	2	3	.7	2	2	1	1	1	2	.7	1	3	3	2	4	3	4	3	4	3		2	2	3	9	11	.4	2	4	2	2	5	3	5	3	
C. spiralis					.9													.6					2				.6		.6			1	8	.6	.7				2	.5	3	2	2	3	4	3	5	2
Cornuspira lajollaensis																																																
Cornuspiroides foliaceus																																																
Ehrenbergina compressa		.4	.2	.6						.6		.4													.2																	.5						
Elphidium spp.	.5	1	1	1					.6	.9	3	1	1	1	3				1	1	.7	.7	.6	2	.8	1	.6		1	.9				1	3	.6	.6		.4	.9	.5	.5	.8	.3	.5	.2	1	
Epistominella sandiegoensis	16	13	9	13	3	14	7		11	12	9	13	11	16	19	12	12	11	10	12	9	10	7	8	14	13	9	6	8	9	11	19	6	12	10	12	11	3	4	10	7	11	18	3	7	6	6	4
E. smithi	6	5	7	6	.9	7	2		3	2	.9	4	3	.8	2	3	2	.6	1	3	1	1	4	4	2	1	1	.9		.9				1	4		.6		.4	.7	.3	2	2		.6	.3	.8	2
Eponides leviculus	6	4	4	4	3	2	2		4	9	6	8	5	8	5	5	12	7	5	5	6	6	7	9	8	5	8	10	5	6	7	6	10	6	8	8	11	10	4	6	15	9	11	15	16	16	11	7
E. subtenerus					2		2											1		1		.7		2	.4	.4	3	4	2			1	10	1	.7		.6		1	.9	2	1		1	4	2	3	.6
Gaudryina arenaria			.2						.2	1	.4																													.2			.8					
G. subglabrata																																																
Goësella flintii							2																																				.8					
Globobulimina barbata									.4		.2															.4																						
G. höglundi	.5											.4		.4						.6							.6				.4																	
G. pacifica		.2	.7																										.6			1																
G. spinifera				.3		.6									.7	.5		.6			.3	.7																					.8					
Glomospira gordialis				.3		.6					.2	.2	.5	.2	1													.4	1		.4			.6						.5			.8	.9				
Gyroidina gemma	.5										.4			.2	1		1										.6						1					3			.3		.8	.3		.3	1	.6
G. quinqueloba						1	5		.4				1	.4			1	1				1	.3	.3	.8	.4		.4	1	.9				.9	.7		.6		.4	.5	1	1		1	.6	1	1	.6
Hanzawaia nitidula			.4	.6					.8	.6		.4				.5					.7											1										1						
Haplophragmoides neobradyi			.2				2				.7			.4	.7						.3			.3		.4					.4			1										.3				
H. quadratus																																																
H. sp.																																																
Höglundina elegans					.9						.2	.2		.2				.6			.3			.3		.4	.6			.9												.5			.6	.3	.3	
Cassidulina sp.	1	2		4		2	2		5	2	2	6	1	2		1	3	.6	6	4	6	.7	.6	1	2	3	1			3	2			2		2	2		.4	4	.7	2	3	2	.5	.3	2	.3

Table 7. Occurrences of benthonic Foraminifera in percent of total (living plus dead) population.

STATION	201	307	265	278	325	255	326	250	211	266	304	258	202	294	303	284	289	296	254	208	308	301	207	298
Involutina pacifica			.4						.4				.5					.6	.4		.3			
Lagena & related spp.	.5	2	1	2	4	1			1		2	.8	2	2	1	2	1		1		.7	.7	1	.9
Lagenidae (other)					.9							.2	.5		.7				.2			.7		
Loxostomum bradyi																								
L. pseudobeyrichi	.5	.4	.4						.6		.2	.2		.2	.7				.4		1			
Neoconorbina terquemi																								
N. parkeri																								
Eggerella advena		.2		.3					.8			.6		.2			1		2					
E. scrippsi														.2	.7									
Nonion lankfordi																								
N. parkerae	.5	.4	2		6				.4			.2	.5		.7	.5		.6	.4		.3	1		.3
Nonionella basispinata		.4		.3							.2			.8					.6					
N (?) fragilis											.2													
N. stella		.8	.9	.8					1	.6	.7	.2		.4					2		1	.7	.6	.3
N. sp. aff. N. globosa																								
Nouria harrisii																								
N polymorphinoides																								
Patellina corrugata																								
Planulina ornata	.5	.6	.2		.9	.6	2		.2	1			.5		1				.2			.7		
Placopsilina bradyi																								
Polymorphinidae																								
Saccammina longicollis																								
Pullenia salisburyi		.2			.9						.4										.3		.6	
Recurvoides sp.																								
Recurvoidella parkerae						.6									.7				.6		.3			
Remaneica cf. helgolandica																								
Reophax excentricus														.2										
R gracilis																								.3
R horridus					.9																			
R micaceous																								
R communis																								
R scorpiurus														.2					.2					
R. subfusiformis																								
R. spp																			.6					
Robertinoides charlottensis																								
Rosalina columbiensis																								
R. campanulata			.2						.2			.2									.7			
R. turbinata																								
Seabrookia earlandi		.8	.6	.3					1	1		.2	.5	.2			.6		.8		.3		1	
Sigmoilina tenuis			.2						.4		.2						1							
Spiroloculina fragilis																								
Spiroplectammina bathyca											.4					.5								.3
S. biformis							2				.2				.7									.3
Suggrunda (?) eckisi		.2							.4								.6		.2		.7			.3
Textularia cf. abbreviata																								
T. earlandi																			.2				.6	
T. sandiegoensis									.4		.2								.2					
T schencki																								
Tritaxis bullata																			.2		.7			
Trochammina charlottensis																								
T chitinosa											.2			.2										
T conica											.7								.8					
T discorbinoides			.2								.2								.2	.6				
T globigeriniformis														.4										
T kellettae	.5	.4																.6			.7			
T labiata																								
T nitida																								
T pacifica & var												.2		.4					.2					.6
T rhumbleri														.2										
T squamiformis									.6	.6				.2					.1					
Uvigerina auberiana							2						1		2	1	2	7	.6	2	.3	3	8	.3
U curticosta	2	.9	2	.8	12	.6	9		2	1	2	.4	7	1	4	2	3	4	.8	6	2	.7	6	2
U. juncea		.2								2	2		.5	2					.4					3
Valvulineria araucana	1		.2	.3	3	.6	2		.2			.6			.7			.6	1	1	.3			.3
V. glabra	1	.2	.2	.6	.9	1	4		.2	.6	.4		1	2		1	1	.6	.6		.3	3	.6	.6
Virgulina opertura		.6	.7				2		2	2	1		.5	.8	.7	2			2	1	2		.6	
V. bramlettei	.5		.2	1				X											X					
V. complanata																.5	1				1	2		.9
V. cornuta																								
V. delicatula		.8	.4						.4	1									.8		.7		.6	
V. sandiegoensis									.6									.6						
V seminuda		.6	.6	.3		1			.4		.4	1		2	1					.7	.3	1		.9
Miliolidae											.2									.6		.7		.3
Miscellaneous spp.	1	1	3	1		3	6		1	1	2	2	.5	.2		3			1	1	2	3	.6	1

STATION	300	302	292	293	305	232	299	290	297	279	269	283	281	236	109	280	114	267	268	112	205	113	111	105
Involutina pacifica	.2			4					1			.6		.8			.2	.5						
Lagena & related spp.	1	1	2	2	4	.9	2	4	1	1	.7	2	1	3	3	1	2		2	3		2	1	3
Lagenidae (other)	.6		.6		.6									2	.9	.2	.2				1	.2		
Loxostomum bradyi								1																
L. pseudobeyrichi	.4		.6	.4						.3							.2	.5		.3				.6
Neoconorbina terquemi																								
N. parkeri																								
Eggerella advena	.2			1	.6		.9			.9						.7				1		.2	.3	
E. scrippsi					.6																			
Nonion lankfordi																								
N. parkerae	.2	.4		.4			.9						.6		.4		.5					.3		
Nonionella basispinata	.4				.6	2	.4			.6			.6			.2							.3	.3
N (?) fragilis	.6		.6	.4	2				1		.7	2	7		2	.7	2	2	2	5	2	3	.3	.9
N. stella		1			2		2		1		.7	4	1		.4	3	.2					.3	2	
N. sp. aff. N. globosa																								
Nouria harrisii																								
N polymorphinoides																								
Patellina corrugata																								
Planulina ornata	.2						.9	2		.3						.2			.8					
Placopsilina bradyi																								
Polymorphinidae				.4																				
Saccammina longicollis																								
Pullenia salisburyi										.3								.5				.2		
Recurvoides sp.																								
Recurvoidella parkerae					1					.6		.6												
Remaneica cf. helgolandica																								
Reophax excentricus																								
R gracilis																								
R horridus																								
R micaceous																								
R communis																								
R scorpiurus																				.3				
R. subfusiformis																								
R. spp		.4								.6						.5								
Robertinoides charlottensis																								
Rosalina columbiensis																								
R. campanulata	.2	.4													.4								.3	
R. turbinata																								
Seabrookia earlandi		.8		1	1			1				1	.6					.5	.8				.5	
Sigmoilina tenuis												.6												
Spiroloculina fragilis		.4								.3						.5		.5					.3	
Spiroplectammina bathyca										.3	.7	2								1			.3	
S. biformis										.3						.2	.5		.8	.6	1	.3	.8	
Suggrunda (?) eckisi	.2						.4						.6											
Textularia cf. abbreviata																								
T. earlandi												.6				.5								
T. sandiegoensis																								
T schencki																								
Tritaxis bullata	.2	.4										.6												
Trochammina charlottensis																								
T chitinosa		.4																						
T conica																								
T discorbinoides		.8					.4			.3					.4	2	1		2	3	.5	1	1	.3
T globigeriniformis	.2				.6				1	2					.4	.9	.2	.5		.9	.6		2	
T kellettae	.8	1		.4			.4			.3						.2		1	.8	.3		.2	.3	
T labiata																								
T nitida																		.5						
T pacifica & var		.4	.6												.9				2				.8	
T rhumbleri																								
T squamiformis			.6							.3							.3			.6				
Uvigerina auberiana	.8	1	6	6	5	.9	2	2	11	3	.7	4	1	7	7	5	7	3	2	6	4	13	3	8
U curticosta	.8	2	3	.9			1	3	1	.6		2		.8	2	.5	.8	1		1	.6	1	2	2
U. juncea	.8	.4			1		.9			.3						2							.3	
Valvulineria araucana	.4			.4	.6				1						1	.2	.7			.6		.5		
V. glabra	.6	.8	2	2	2	.9	2	1		.6	2	1	2		.9	.7	.2	.5			.5		.3	1
Virgulina opertura	.2	2	.6	.4	3		2	1		.3		2	3		1	2	.7	1	.8		.5	.5	.3	.3
V. bramlettei																						X	X	
V. complanata	.2	.4	.6	2	2		2			2	.7	3			.9	1	1	.5		1	2	1	.8	.3
V. cornuta													3											
V. delicatula	.2	.4						2					.6											.6
V. sandiegoensis											.7		.6					.5						
V seminuda		.4						1					.6	.8	.9					.6	.6	.3	.3	.3
Miliolidae		.4		.4	.6	.9	.4			.9			1		.4				.8	.3	.5	.2	.3	.3
Miscellaneous spp.		.4	.6	.8	2	3	.4	2	3	.9	1	1			3	.5	3	1	3	3	3	2	4	1

Table 7 (continued). Occurrences of benthonic Foraminifera in percent of total (living plus dead) population.

number with increase of depth in the northern part of the area where the bottom slope is gentle down to the bottom of Loma Sea Valley. In the southern part of the area, where the shelf ends abruptly and there is a steep escarpment down to the bottom of the San Diego Trough, the situation is quite different from that in the northern part. The number of genera is small at a depth shallower than 20 fathoms and then increases with increase of depth, reaching a maximum at 45-100 fathoms, then decreases again. Another maximum is

Depth in Fath.		Living Fauna
0	Fauna 1	Coarse sand *Rosalina columbiensis* *Rosalina campanulata* *Neoconorbina terquemi* *Cibicides fletcheri* Miliolids Fine sand, silt *Elphidium* spp. *Buliminella elegantissima* *Nonionella basispinata*
13	Fauna 2	*Nonionella stella* *Nonionella basispinata* *Reophax gracilis* *Alveolophragmium columbiense*
45	Fauna 3	*Bolivina pacifica* *Bolivina acuminata* *Nonionella stella* *Reophax gracilis* *Chilostomella ovoidea*
100	Fauna 4	*Bolivina pacifica* *Goesella flintii* *Reophax gracilis*
250	Fauna 5	*Bolivina pacifica* *Bolivina subargentea* *Nonionella stella*
350	Fauna 6	*Bolivina pacifica* *Bolivina spissa* *Virgulina apertura*
450	Fauna 7	*Virgulina apertura* *Bolivina pacifica* *Bolivina spissa*
650		

Total Fauna		Depth in Fath.
Coarse sand *Rosalina campanulata* *Rosalina columbiensis* *Cibicides fletcheri* Fine sand, silt *Elphidium* spp. *Nonionella stella* *Buliminella elegantissima*	Fauna 1	0
Nonionella stella *Cassidulina depressa* *Cassidulina quadrata*	Fauna 2	20
Cassidulina depressa *Cassidulina quadrata* *Epistominella sandiegoensis* *Cassidulina limbata* *Cassidulina tortuosa*	Fauna 3	47
Cassidulina subcarinata *Cassidulina delicata* *Epistominella sandiegoensis*	Fauna 4	280
		650

Table 8. Comparison of living and total faunas.

found at 400-600 fathoms. The deep floor of the San Diego Trough has a moderate number (average 25) of genera.

The ratio of number of species to number of genera in the San Diego area ranges from 1.1 to 1.96 and the average is as follows:

Depth Range (fathoms)	*No. of Stations*	*Average ratio*
0-60 (shelf)	51	1.52
60-500 (escarpment, canyon, valley)	82	1.54
500-650 (trough)	24	1.72
0-650	157	1.58

It appears strange that the average ratio of number of species to number of genera increases with increase of depth in this area, which is contrary to the *Challenger* data. In the San Diego area the differences of the ratios at the various stations are very slight, and for this reason the ratio can be considered to be about the same throughout the area. The highest ratio in shallow water does not reach 3, and in deep water is not as small as 1.25 as shown by the *Challenger* data. One reason for this is that the *Challenger* data are based on a larger part of the animal kingdom while the present study is based only on Foraminifera. A more important reason is that genera and species, at least in

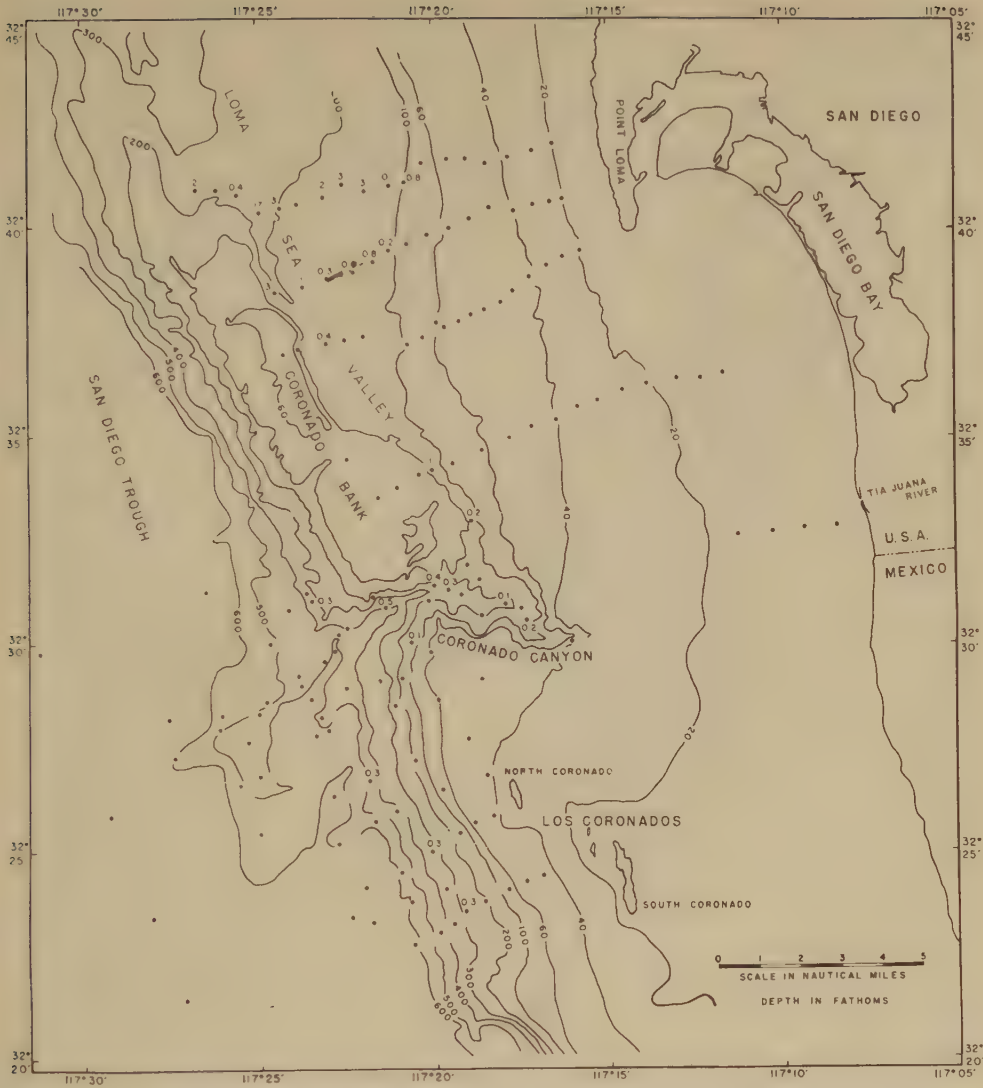
117°30'
117°25'
117°20'
117°15'
117°10'
117°05'
32° 45'
32° 40'
32° 35'
32° 30'
32° 25'
32° 20'
LOMA
SEA
VALLEY
CORONADO
BANK
SAN DIEGO TROUGH
POINT LOMA
SAN DIEGO
SAN DIEGO BAY
TIA JUANA RIVER
U.S.A.
MEXICO
CORONADO CANYON
NORTH CORONADO
LOS CORONADOS
SOUTH CORONADO
0 1 2 3 4 5
SCALE IN NAUTICAL MILES
DEPTH IN FATHOMS

Text Figure 11. Distribution of living *Nonionella* sp. aff. *N. globosa* Ishiwada in percent of living population.

the case of the Foraminifera, are now subdivided more than in the *Challenger* days. If samples are taken much deeper than 650 fathoms, which is the greatest depth sampled for the present study, the ratio may decrease down to 1.25 as shown by the *Challenger* data. Foraminifera are among the most primitive animals and can survive in almost any marine environment, while more advanced animal groups may be less widely distributed.

There is no positive correlation of areal distribution of number of genera, as in the case of species, with that of the size of living and total populations, nor with that of L/T ratio. The depth distribution of the highest living populations (50-150 fathoms), however, generally agrees with that of the greatest number of living species and genera. This can be interpreted in two ways. One is that Foraminifera are more prosperous at those depth ranges than at other depths, and thus the greatest number of species and genera are originated. The other is that the greater the number

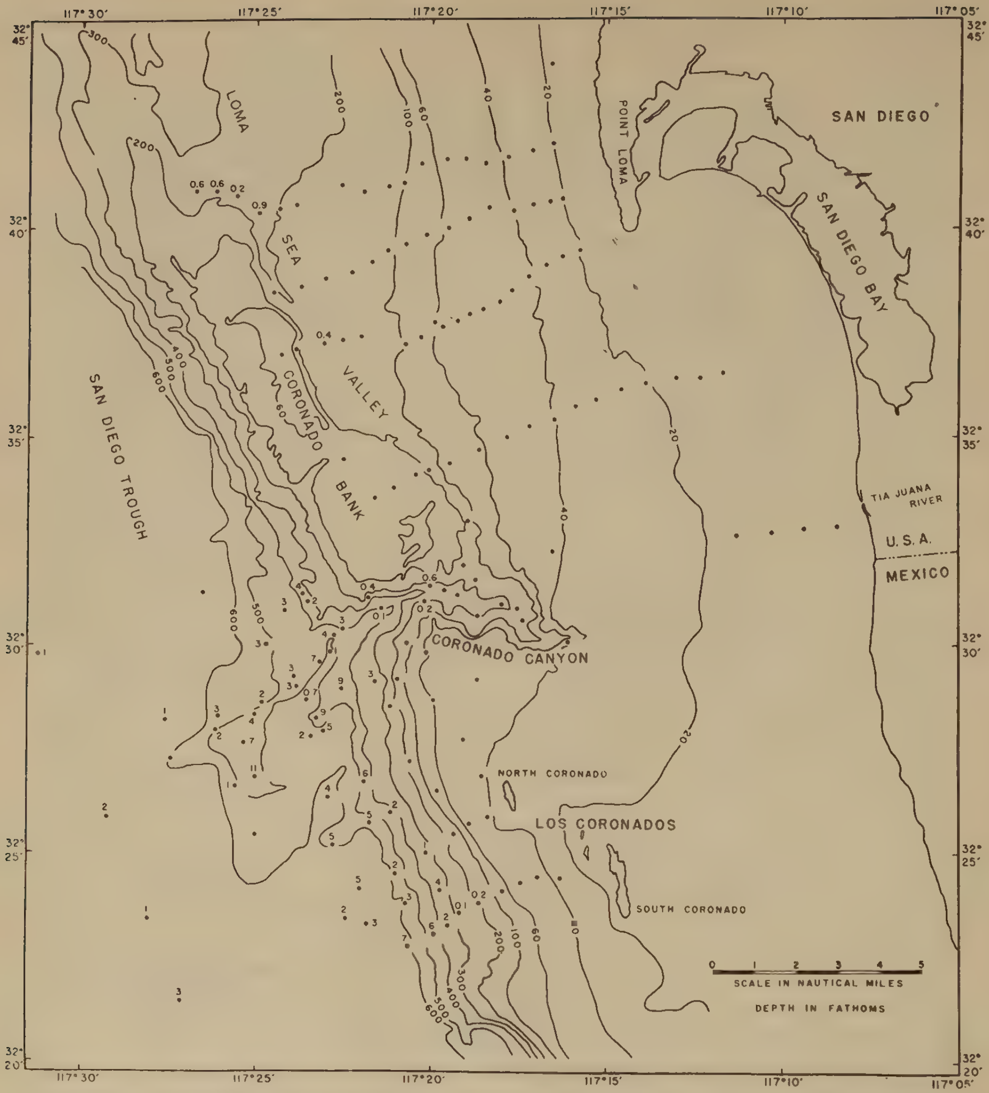
117°30′
117°25′
117°20′
117°15′
117°10′
117°05′
32° 45′
32° 40′
32° 35′
32° 30′
32° 25′
32° 20′
SAN DIEGO
POINT LOMA
SAN DIEGO BAY
LOMA
SEA
VALLEY
CORONADO BANK
SAN DIEGO TROUGH
CORONADO CANYON
NORTH CORONADO
LOS CORONADOS
SOUTH CORONADO
TIA JUANA RIVER
U. S. A.
MEXICO
0 1 2 3 4 5
SCALE IN NAUTICAL MILES
DEPTH IN FATHOMS

Text Figure 12. Distribution of living *Cassidulina delicata* Cushman in percent of living population.

of specimens found the greater the likelihood of finding more species and genera.

Areal as well as depth changes in the number of families were not analyzed because of the differing opinions among workers in the grouping of genera into families.

PLANKTONIC FORAMINIFERA

No detailed study of the planktonic Foraminifera was made. A few specimens of living planktonic Foraminifera were found in some samples while counting living benthonic Foraminifera. Numerous empty tests of planktonic Foraminifera were found in almost every sample studied. They were not identified specifically but were counted together as "planktonics," since the ratio of benthonic to planktonic populations may provide useful information in understanding sedimentary environments.

The areal distribution of the ratio of benthonic population to planktonic population (B/P) shows the following (Text Fig. 17): The B/P value on the northern shelf is high near shore and decreases down to the

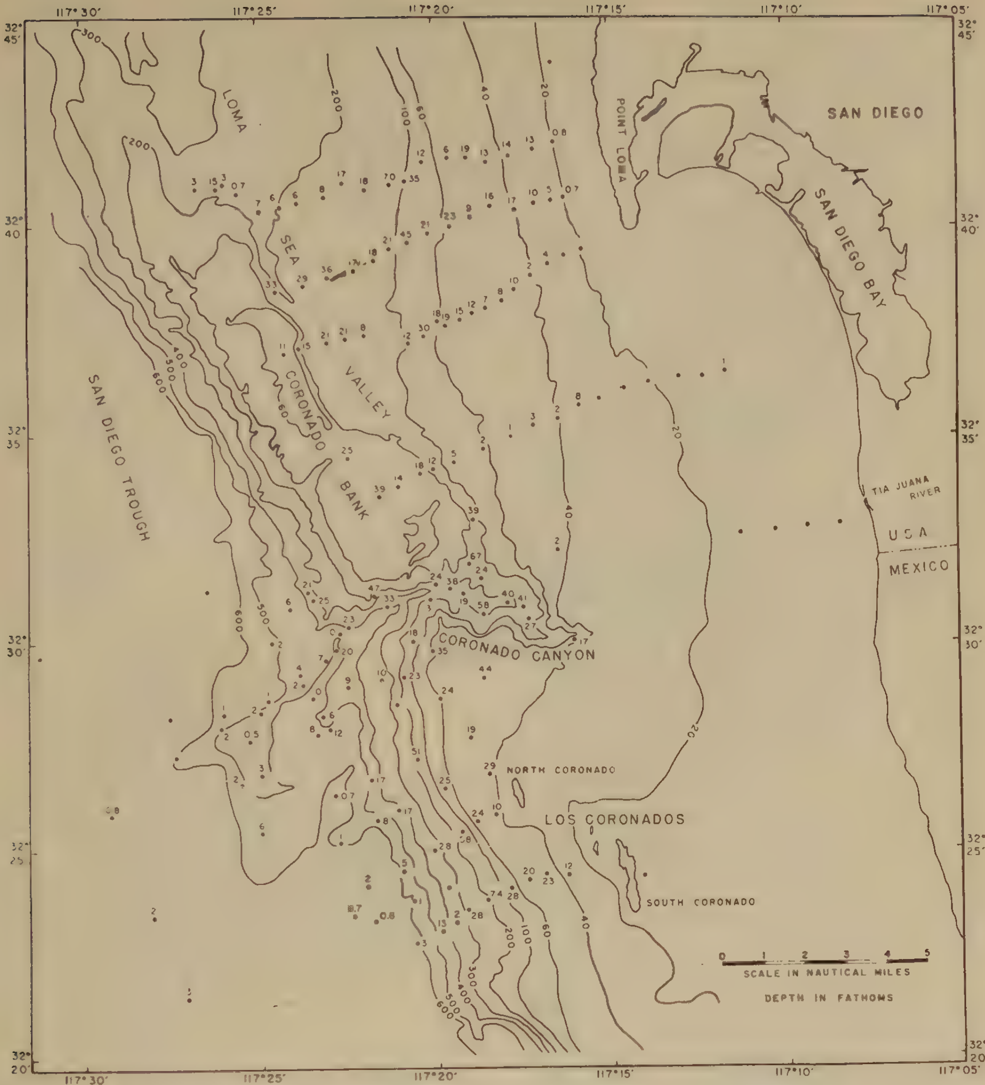
117°30′
117°25′
117°20′
117°15′
117°10′
117°05′
32° 45′
32° 40′
32° 35′
32° 30′
32° 25′
32° 20′
SAN DIEGO
POINT LOMA
SAN DIEGO BAY
LOMA SEA VALLEY
CORONADO BANK
SAN DIEGO TROUGH
CORONADO CANYON
NORTH CORONADO
LOS CORONADOS
SOUTH CORONADO
TIA JUANA RIVER
U S A
MEXICO
0 1 2 3 4 5
SCALE IN NAUTICAL MILES
DEPTH IN FATHOMS

Text Figure 13. Distribution of living *Bolivina pacifica* Cushman and McCulloch in percent of living population.

Loma Sea Valley. The area of the highest B/P value is found between Point Loma and off the Tia Juana River. In most of the area, except on the above-mentioned northern shelf, the B/P value is low and irregular. Four stations have a value larger than 5 and at these Foraminifera sands are exposed. At other stations where Foraminifera sands are exposed, however, the B/P value is not high. One station on the lee side of the South Coronado Island has a relatively high value (9.0).

It is a general concept that the planktonic foraminiferal population increases offshore if there is neither displacement nor residual sediment, hence, the value of B/P decreases in an offshore direction. The data collected in the San Diego area support this concept only in the area very near shore.

The planktonic species which were found are:

Globigerina bulloides d'Orbigny
Globigerina eggeri Rhumbler
Globigerina hexagona Natland

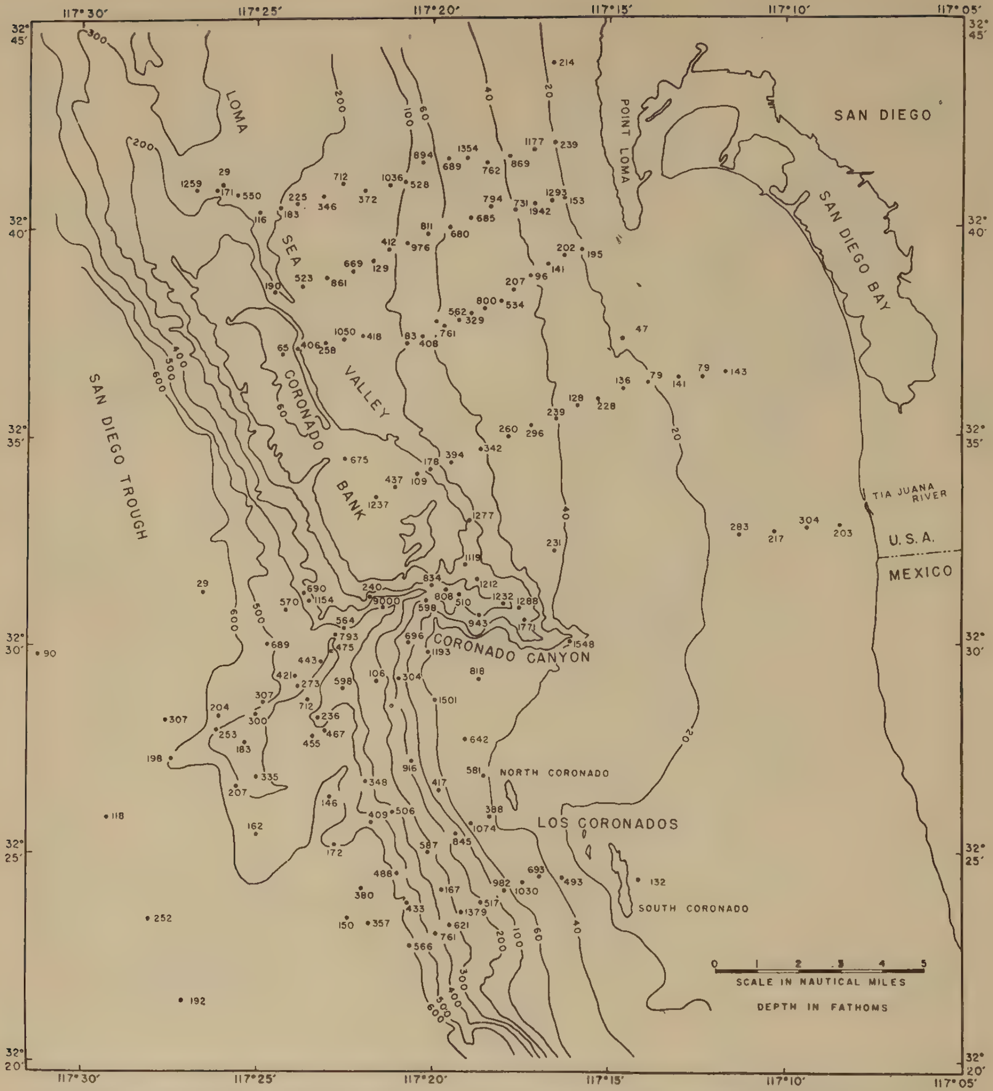
117°30′
117°25′
117°20′
117°15′
117°10′
117°05′
32° 45′
32° 40′
32° 35′
32° 30′
32° 25′
32° 20′
LOMA
SEA
VALLEY
CORONADO
BANK
SAN DIEGO TROUGH
POINT LOMA
SAN DIEGO
SAN DIEGO BAY
TIA JUANA RIVER
U. S. A.
MEXICO
CORONADO CANYON
NORTH CORONADO
LOS CORONADOS
SOUTH CORONADO
SCALE IN NAUTICAL MILES
DEPTH IN FATHOMS

Text Figure 14. Distribution of living populations of benthonic Foraminifera in number of specimens per sample.

Globigerina quinqueloba Natland
Globigerina sp. cf. *G. pachyderma* (Ehrenberg)
Globigerinita glutinata (Egger)
Globigerinoides minutus Natland
Globigerinoides ruber (d'Orbigny)
Globorotalia truncatulinoides (d'Orbigny)
Orbulina universa d'Orbigny

Living specimens of *Globigerinoides minutus* Natland occur in many bottom sediments.

RATES OF SEDIMENTATION

Walton (1955) suggested that the ratio of living population to dead population (L/D) was proportional to the rate of sedimentation. Phleger (1955, pp. 733-734) revised this ratio to the ratio of living population to total (living plus dead) population (L/T). The writer shows living and total populations of benthonic Foraminifera in the top centimeter of short cores in Tables 1-3, 5-7. If one selects stations where there are

Depth Range (Fathoms)	Coarse Sand no. of samples	Coarse Sand av. pop.	Fine Sand no. of samples	Fine Sand av. pop.	Silt no. of samples	Silt av. pop.	Clayey Silt no. of samples	Clayey Silt av. pop.	Foram. Sand no. of samples	Foram. Sand av. pop.	All no. of samples	All av. pop.
0 - 50	6	12.5	6	103.8	16	20.8	10	8.1	3	139.6	41	37.3
50 - 100			2	249.8	8	31.6	2	14.4	15	217.1	27	150.0
100 - 150			1	50.6	1	37.6	12	21.3	2	213.0	16	48.1
150 - 200	1	20.5			3	31.5	5	10.4	1	72.1	10	23.9
200 - 250			1	43.9	4	50.7	4	39.3			9	44.9
250 - 300	1	17.2	1	43.9	1	96.0					4	43.3
300 - 350	3	18.8			3	53.6	2	34.3			8	35.7
350 - 400	2	17.9			2	56.5	3*	25.0			7*	32.0
400 - 450			1	9.7			4	20.4			5	18.3
450 - 500			3	12.6			6	11.0			9	11.5
500 - 550			2	28.0			8	9.8			10	13.4
550 - 600							8	10.0			8	10.0
600 - 650							9	12.4			9	12.4
0 - 650	12	15.3	15	72.2	35	32.8	69*	15.3	21	198.9	152*	50.3

Note. Stations occurring at depth boundaries are calculated for the depth ranges both above and below the boundaries.
* not including Station 250.

Table 9. Depth distribution of average populations of total benthonic Foraminifera in thousands of specimens.

no displaced Foraminifera, and knows the average reproductive period of all the species and the living populations at these stations, one can calculate the number of tests reproduced in a year (assuming all the tests are preserved in the sediments). It is generally accepted that each area sampled has reached its own maximum population, that is, the benthonic population can be considered to be in a steady condition (in equilibrium between environmental factors and population) (Clarke, 1954, p. 340, 485). If these assumptions are correct one can calculate the rate of sedimentation. The equation is: $1 \div R = T \div L/P$ where R = rate of sedimentation (cm./year) and P = average reproductive period (year).

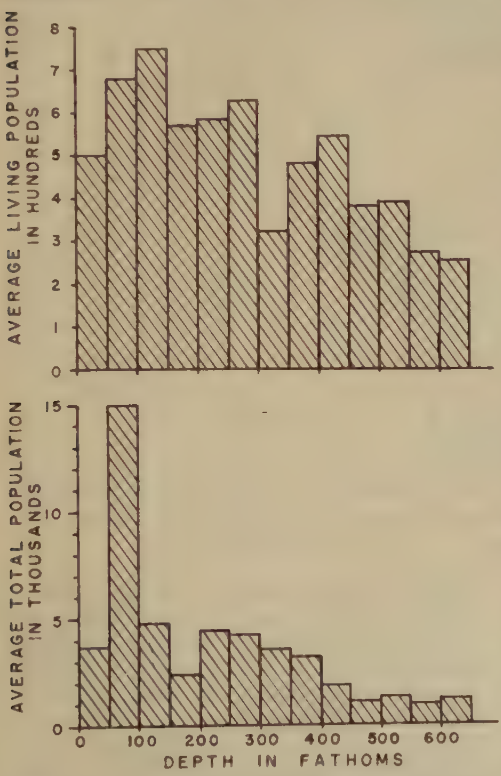

Text Figure 15. Depth distributions of average living and total populations of benthonic Foraminifera.

The average living population of benthonic Foraminifera of 9 samples at 600-650 fathoms in the San Diego Trough is 255, the average total population in the top centimeter of the cores at these stations is 12,400 specimens per sample. The average reproductive period of Foraminifera is not well-known, particularly that of deep-sea species. *Streblus beccarii* (Linné) (Bradshaw, 1957), *Rotaliella heterocaryotica* Grell (Grell, 1954), and *Patellina corrugata* Williamson (Myers, 1935), all nearshore species, reproduce every 2 to 4 weeks in laboratory cultures. *Bolivina* sp. (shallow water species), according to Bradshaw (personal communication), apparently reproduces every 2 months in laboratory cultures (temperature about 20°C). *Elphidium crispum* (Linné) reproduces every 2 years at Plymouth, England, and once a year at La Jolla, California (Myers, 1942). The colder the temperature, the slower the metabolic activity appears to be, hence a longer reproductive period is expected. Assuming a reproductive period of 2 years at the bottom of the San Diego Trough, then the average rate of accumulation of tests would be 128 per year, and the average rate of sedimentation would be 1 cm. per 97 years.

At stations 109, 111, 112, 113 and 114 in the San

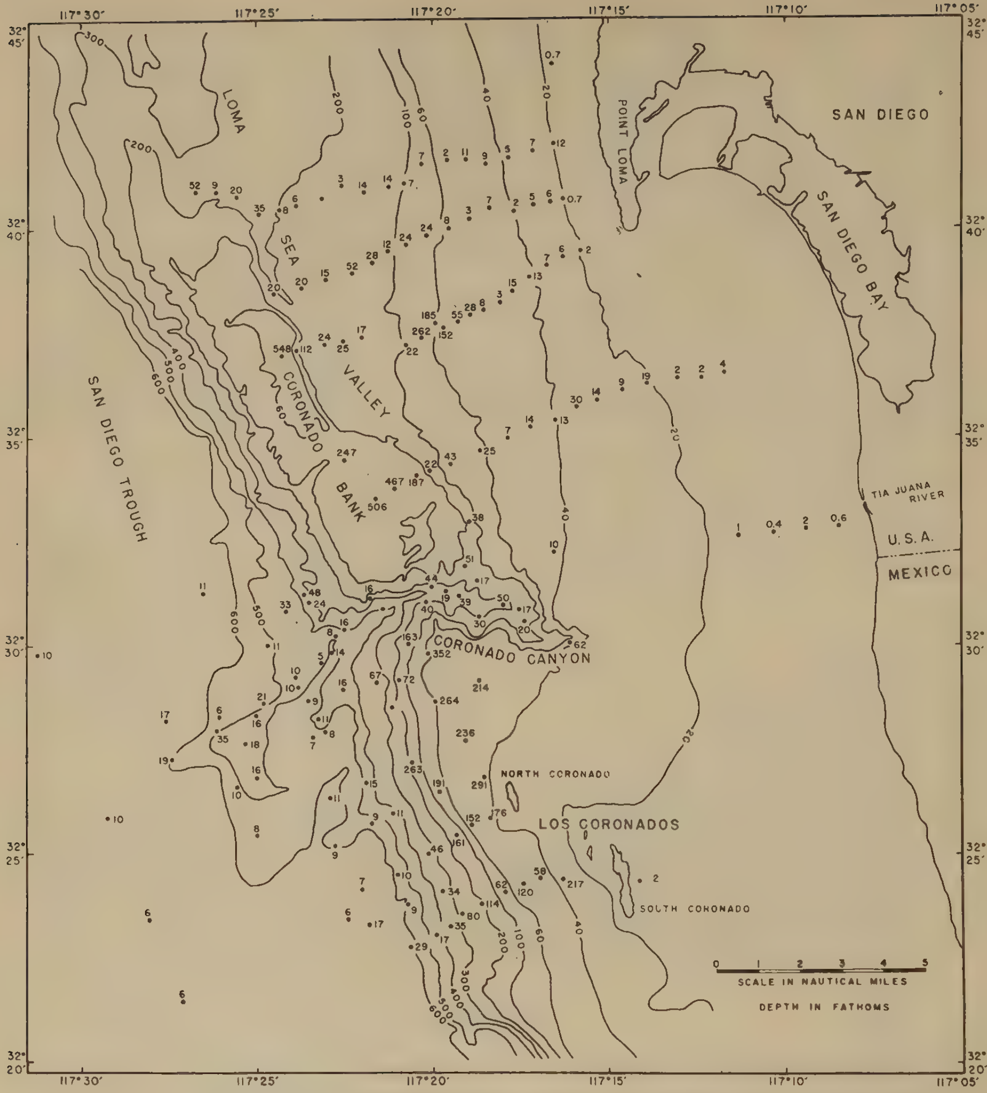
117°30′
117°25′
117°20′
117°15′
117°10′
117°05′
32° 45′
32° 40′
32° 35′
32° 30′
32° 25′
32° 20′
LOMA
SEA
VALLEY
CORONADO
BANK
SAN DIEGO TROUGH
POINT LOMA
SAN DIEGO
SAN DIEGO BAY
TIA JUANA RIVER
U. S. A.
MEXICO
CORONADO CANYON
NORTH CORONADO
LOS CORONADOS
SOUTH CORONADO
0 1 2 3 4 5
SCALE IN NAUTICAL MILES
DEPTH IN FATHOMS

Text Figure 16. Distribution of total (living plus dead) populations of benthonic Foraminifera in thousands of specimens per sample.

Diego Trough at 599-640 fathoms living and total populations are relatively constant and there seem to be no displaced sediments. The average living population at these stations is 160, the average total population in the top centimeter is 7,514 per sample. Assuming a 2-year reproductive period, the rate of sedimentation would be one centimeter per 94 years.

In the nearshore area there are four stations (121, 122, 123 and 124) which do not contain displaced sediments (all fine micaceous sands at 6.5-11 fathoms). The average living population is 252 per sample and the average total population in the top centimeter is 1,048. Assuming a reproductive period for the species at this depth to be one month, the rate of sedimentation would be one centimeter per 0.36 years, that is, about 3 cm. per year at these stations. This rate of sedimentation seems to be very high for the fine micaceous sands at these stations, and the assumed reproductive period may be much shorter than it really is.

Revelle and Shepard (1939) have calculated the rate

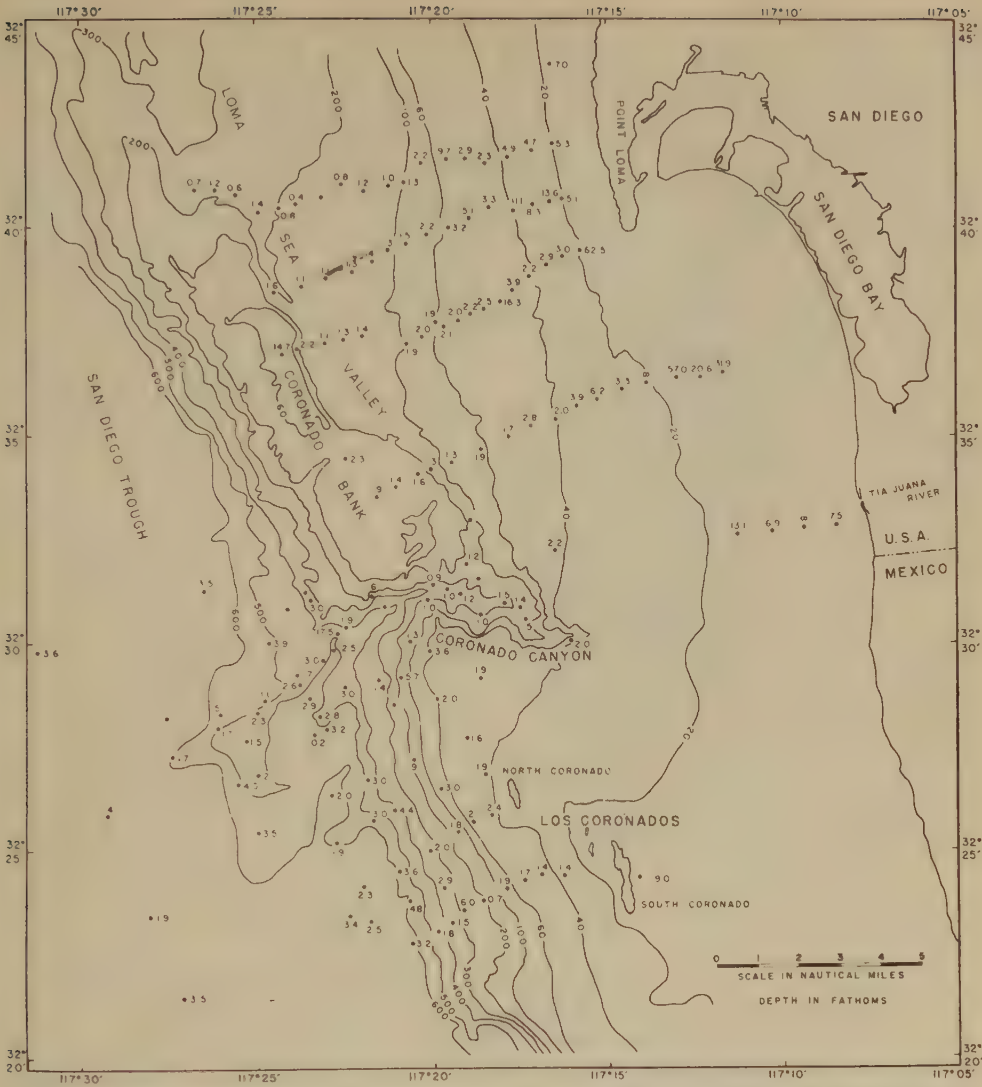
117°30′
117°25′
117°20′
117°15′
117°10′
117°05′
32° 45′
32° 40′
32° 35′
32° 30′
32° 25′
32° 20′
LOMA
SEA
VALLEY
CORONADO
BANK
SAN DIEGO TROUGH
POINT LOMA
SAN DIEGO
SAN DIEGO BAY
TIA JUANA RIVER
U.S.A.
MEXICO
CORONADO CANYON
NORTH CORONADO
LOS CORONADOS
SOUTH CORONADO
SCALE IN NAUTICAL MILES
0
1
2
3
4
5
DEPTH IN FATHOMS
20
40
60
100
200
300
400
500
600

Text Figure 17. Distribution of ratios of total benthonic population to total planktonic population (B/P).

of sedimentation in the offshore basins of southern California, based on the rate of erosion of the local watersheds and the relative areas of erosion and deposition, and obtained a value of about 25 cm. per 1,000 years, that is, one centimeter per 40 years. The value obtained by them shows a rate of sedimentation about 2½ times higher than that based on Foraminifera. It would be necessary for the Foraminifera in the San Diego Trough to reproduce every 10 months if the value of Revelle and Shepard is correct.

The areal distribution of L/T (in %) is shown in Text Fig. 18. Coronado Bank and its southern extension (except Coronados Islands) have a low L/T value (less than 1) and this agrees quite well with the fact that the area appears to be non-depositional at present. Another small area between Coronado Bank and Point Loma also has a very low L/T value. Foraminifera sands are exposed at all these areas.

The highest L/T areas are off the Tia Juana River and off Point Loma, but most of the shelf has an inter-

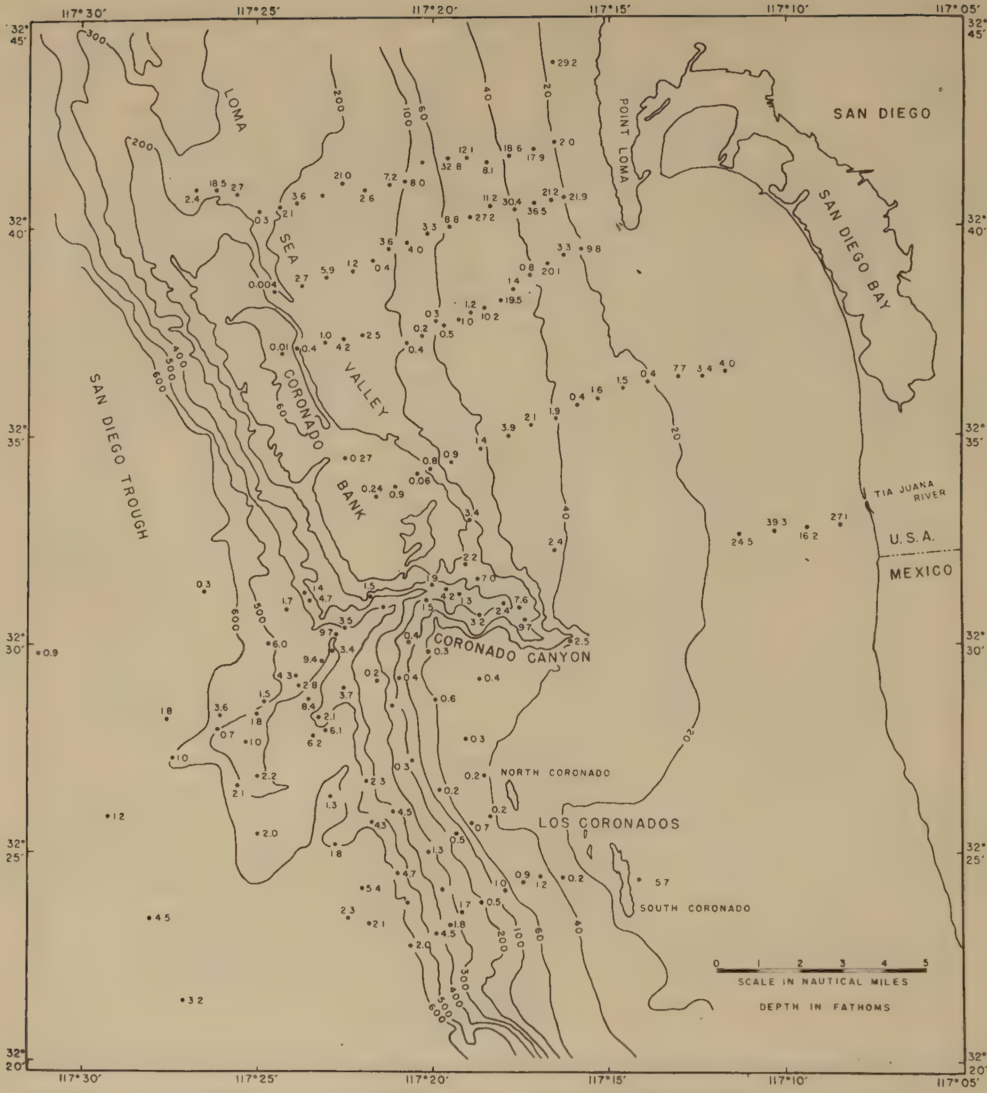
117°30′
117°25′
117°20′
117°15′
117°10′
117°05′
32° 45′
32° 40′
32° 35′
32° 30′
32° 25′
32° 20′
SAN DIEGO
POINT LOMA
LOMA
SAN DIEGO BAY
SEA VALLEY
CORONADO BANK
SAN DIEGO TROUGH
CORONADO CANYON
NORTH CORONADO
LOS CORONADOS
SOUTH CORONADO
TIA JUANA RIVER
U.S.A.
MEXICO
0 1 2 3 4 5
SCALE IN NAUTICAL MILES
DEPTH IN FATHOMS
20
40
60
100
200
300
400
500
600

Text Figure 18. Distribution of ratios of living population to total population (L/T).

mediate L/T value. The bottom of the San Diego Trough and Coronado Canyon and the lower part of the escarpment from Coronado Bank and its extension have intermediate L/T values (between 1 and 10).

These data seem to agree with Dietz's suggestion (1952) that sediments from the land are deposited either nearshore or on the lower part of the continental slope and in basins, bypassing the outer shelf and upper continental slope.

CHANGE IN SEA-LEVEL

During and after the Pleistocene glacial period there is evidence that sea-level rose and fell with melting and freezing of ice-caps in polar regions. The elevation of sea-level after the last glacial age to the present time is relatively well known. In the following the writer discusses methods of estimating the amount of sea-level change using Foraminifera and gives some of the results obtained. There are three ways to estimate the amount of sea-level change using benthonic Foraminifera.

Vertical Change of Foraminifera Fauna in Cores

First, one must assume that the depth distribution of living Foraminifera in an area is known. If the dead Foraminifera fauna is different from the living one, the difference of the depths indicated by the two is the amount of sea-level change. The amount of sea-level change thus obtained is that since the beginning of deposition of the particular sediment sample. In this analysis one assumes no contamination with sediments from other sources. Phleger (1952, p. 360), in his work on the Foraminifera from Portsmouth, New Hampshire, found striking differences between the upper and lower faunas of many cores. His interpretation is that this lower fauna (which indicates a shallow sand facies) was covered rapidly by mud with increase of depth (post-glacial rise of sea-level), and that the amount of the change was at least 60-75 m. Walton (1955, p. 988) found nearshore coarse sands which contained some *Elphidium crispum* (Linné) and large populations of miliolids which indicate a much shallower depth than the depths at which the sediments occur. He interpreted these sands as being "relict" sediments deposited during a time of lower sea-level.

Lateral Change of Foraminifera Fauna

If the distributions of the living and dead faunas in samples taken along a traverse from shallow to deep water are different, the difference of depth of the boundaries of equivalent living and dead faunas is the amount of sea-level change. For example, if there are depth boundaries of living Foraminifera fauna at 30, 50 and 100 fathoms, and those of the representative faunas of dead Foraminifera lie at 40, 60 and 110 fathoms, the amount of sea-level change during the time of deposition of the samples is 10 fathoms.

Depth Change of Size of Benthonic Populations

Walton (1955, p. 977, text-fig. 11) shows that the average size of living populations of benthonic Foraminifera is highest at 30-35 fathoms. In reality there are many irregularities in the depth distribution of living populations as the writer has pointed out (see p. 25). If one smooths out these irregularities by averaging 5-, 10- or 50-fathom intervals, however, one can generalize on the depth distributions of the average living populations. The depth of the highest average dead or total population may be different from that of the living one. The difference of the depths of the highest average populations of living and dead (or total) benthonic Foraminifera is the amount of sea-level change during the time represented by the samples.

Discussion

The writer has tried these methods in the San Diego area. As is shown, however, on the distribution tables (Tables 1-3, 5-7) and the frequency charts (Text Figs. 2-9) many empty tests are transported in a deeper or shallower direction; also many of them come from residual sediments. The only place which has been little influenced by contamination with other sediments is the northeastern part of this area. Medium to coarse sands were sampled at stations 45, 44 and 1, at 20, 20 and 19 fathoms respectively. The main components of the living and total faunas at stations 1 and 44 are essentially the same. At station 45, however, the total fauna has the same main components as that at station 1 and 44 but the living components are different. In the total fauna *Cibicides fletcheri* Galloway and Wissler makes up 34%, *Rosalina campanulata* (Galloway and Wissler) 21%, *Rosalina columbiensis* (Cushman) 3% and miliolids 3%, while the living fauna contains *Nonionella stella* Cushman and Moyer 21%, *Nonionella basispinata* (Cushman and Moyer) 15%, *Trochammina charlottensis* Cushman 10%, miliolids 8% and *Rosalina campanulata* (Galloway and Wissler) 3%. Thus, the living fauna is characteristic of a fine sand or silt fauna at 15-20 fathoms, and the total fauna has the characteristics of a coarse sand fauna at a depth shallower than 20 fathoms, most probably shallower than 13 fathoms. The dead fauna, therefore, lived at a depth approximately 5 fathoms shallower than the present depth.

There are distinct differences between the living and total faunas at stations 101, 102, and 103, the depths of which are 19.5, 17 and 15 fathoms respectively. At all these stations *Nonionella basispinata* (Cushman and Moyer) makes up 26-39%, *N. stella* Cushman and Moyer 12-32% and *Buliminella elegantissima* (d'Orbigny) 0-14% in the living faunas, while *Eggerella advena* (Cushman) occupies 23-31%, *Nonionella basispinata* (Cushman and Moyer) 5-9%, *N. stella* Cushman and Moyer 10-14%, *Buliminella elegantissima* (d'Orbigny) 5-15%, *Buccella angulata* Uchio, n. sp., 3-8%, *Elphidium* spp. 8-13%, and *Trochammina pacifica* Cushman 6-12% in the total faunas. Living specimens of *Eggerella advena* (Cushman) are most abundant at depths shallower than 10 fathoms in Todos Santos Bay, where more shallow samples are available than from the San Diego area. *Elphidium* spp., *Buliminella elegantissima* (d'Orbigny) and miliolids are most abundant shallower than 13 fathoms both in the San Diego and Todos Santos Bay areas. The empty tests at stations 101, 102 and 103 lived at a depth of less than 10 fathoms, approximately 5-10 fathoms shallower than the present depth.

These interpretations suggest that there was a recent rise of sea-level of about 5 fathoms. A change of 5 fathoms may be within a range of error, however, and more extensive study is needed to establish such a small oscillation of sea-level.

The most striking change of sea-level suggested by

Foraminifera assemblages in the San Diego area is the one since the "Foraminifera sand and/or silt" was deposited on the Coronado Bank and its vicinity. The sedimentary environment of the "Foraminifera sand" is complicated. This sediment seems to have been subjected to wave action or strongly agitated water judging from the scratched surfaces of the Foraminifera tests. Relatively pure Foraminifera sands actually are not sands but contain a rather high amount of the finer fractions and should be called sandy silt. The sorting is poor as is shown by the high value (2.25) of ø (phi standard deviation measure of Inman), and perhaps more than two sediment types of different kinds are mixed together. This is supported by the Foraminifera assemblage in the sediments, which is characterized by high percentages of *Cassidulina limbata* Cushman and Hughes (15-28%, average of 9 samples is 19%), *C. tortuosa* Cushman and Hughes (11-28%, average 17%), *C. quadrata* Cushman and Hughes (10-21%), *Angulogerina baggi* (Galloway and Wissler) (including *A. hughesi*) (8-13%), *Cibicides fletcheri* Galloway and Wissler (7-10%) and *Cassidulina depressa* Asano and Nakamura (7-10%). From the frequency distribution of living specimens of these species at least two different faunal associations may be recognized. One is the nearshore fauna represented by *Elphidium* spp., *Poroeponides cribrorepandus* Asano and Uchio, *Cibicides fletcheri* Galloway and Wissler, *Rosalina campanulata* (Galloway and Wissler) and *Asterigerinata pacifica* Uchio, n. sp., etc. The other, which forms the main part of the entire assemblage, is characterized by species of *Cassidulina and Angulogerina* which indicate a depth range of 20 to 130 fathoms, most probably 30 to 60 fathoms. This shows that the sediment was deposited essentially 5-45 fathoms shallower than the present depth. However, the whole block of Coronado Bank and Coronados Islands may have been faulted up from the San Diego Trough and tilted gently toward the north during the late Pleistocene. Therefore, it is very difficult to speculate on the amount of sea-level change which has taken place since the time of deposition of this sediment.

DISPLACED FORAMINIFERA

Phleger (1951a) discussed the Foraminifera faunas in sand layers which are embedded in clay or silt in the San Diego Trough. He studied cores taken at depths of 407-642 fathoms and concluded that the shallow-water species of Foraminifera in these deep sand layers were displaced by turbidity currents or other mechanisms. Judging from his faunal assemblages none of the sand layers mentioned above contained pure, shallow-water faunas but a mixture of several faunas which presently exist between the nearshore area and the San Diego Trough. His discussion was based on the depth distributions of empty tests of benthonic Foraminifera and needs further revision based on the distribution of living Foraminifera.

Ludwick (1950) studied deep water sand layers in a wide area off San Diego, including La Jolla Canyon. Most of the sands are fine grained and well-sorted and differ little in general character from typical fine-grained beach sands. In the present study only one core sample included two thin layers of fine sand be-

EXPLANATION OF PLATE 7

Figs. PAGE

1. *Bolivina minuta* Natland. Hypotype (U.S.N.M. No. 626737), ×130.
2. *Bolivina pacifica* Cushman and McCulloch. Hypotype (U.S.N.M. No. 626738), ×99.
3, 4. *Bolivina peirsonae* Uchio, n. sp. 63
3, Holotype (U.S.N.M. No. 626739), ×33. 4, Paratype (U.S.N.M. No. 626740), ×47.
5, 6. *Suggrunda* (?) *eckisi* Natland. Hypotypes (U.S.N.M. No. 626748, 626749), ×91, ×110.
7, 8. *Bolivina spissa* Cushman. Hypotypes (U.S.N.M. Nos. 626742, 626743), ×42. 7, megalospheric form; 8, microspheric form.
9. *Loxostomum bradyi* (Asano) 64
Hypotype (U.S.N.M. No. 626751), ×47.
10. *Loxostomum pseudobeyrichi* (Cushman). Hypotype (U.S.N.M. No. 626753), ×34.
11. *Uvigerina auberiana* d'Orbigny 65
Hypotype (U.S.N.M. No. 626754), ×98.
12, 13. *Uvigerina curticosta* Cushman 65
Hypotypes (U.S.N.M. No. 626755, 626756). 12, typical form, ×35. 13, *U. dirupta* type, ×34.
14. *Uvigerina excellens* Todd. Hypotype (U.S.N.M. No. 626757), ×42.
15-17. *Uvigerina juncea* Cushman and Todd 65
Hypotypes (U.S.N.M. Nos. 626758-626760). 15, *U. cushmani* type, ×47. 16, typical form, ×45. 17, form with a smooth surface, ×47.
18. *Angulogerina angulosa* (Williamson). Hypotype (U.S.N.M. No. 626761), ×97.
19. *Angulogerina carinata* Cushman 66
Hypotype (U.S.N.M. No. 626762), ×30.
20, 21. *Neoconorbina terquemi* (Rzehak). Hypotypes (U.S.N.M. Nos. 626763, 626764), ×101.
22-25. *Rosalina* sp. 66
Hypotypes (U.S.N.M. Nos. 626766-626769), ×46.
26. *Rosalina campanulata* (Galloway and Wissler) 66
Hypotypes (U.S.N.M. No. 626770), ×46.

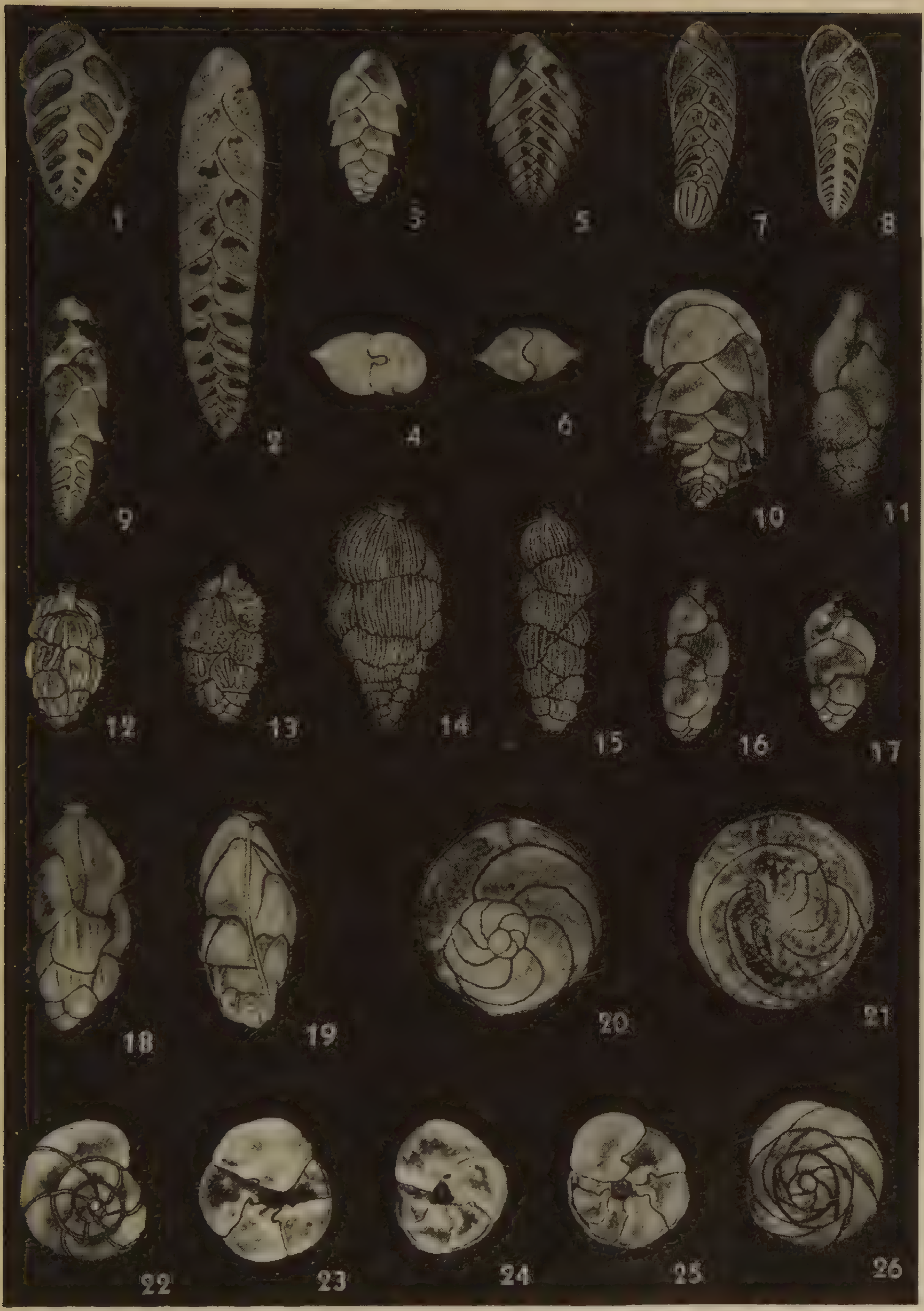
1
2
3
4
5
6
7
8
9
10
11
12
13
14
15
16
17
18
19
20
21
22
23
24
25
26

Uchio: Living Foraminifera, San Diego, California

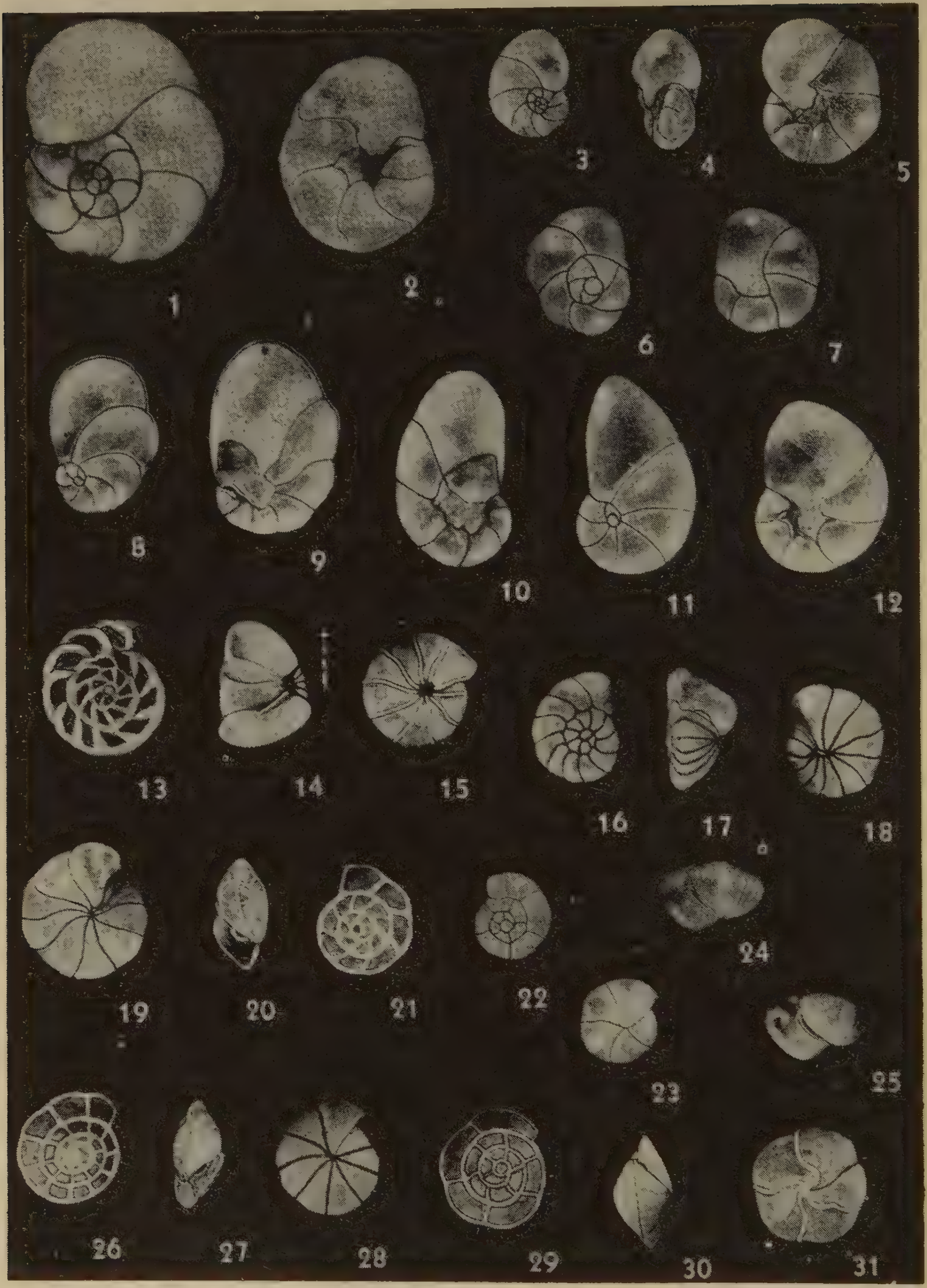
1
2
3
4
5
6
7
8
9
10
11
12
13
14
15
16
17
18
19
20
21
22
23
24
25
26
27
28
29
30
31

Uchio: Living Foraminifera, San Diego, California

neath the typical clayey surface sediment of the San Diego Trough. Most cores taken were not long enough to penetrate any sand layers which might exist in the deep area.

At station 268 in the San Diego Trough a short core was taken at 630 fathoms. The top centimeter was analyzed for living and total counts and the results are listed in Tables 3 and 6. The core consists of clayey silt with two fine sand layers, 0.5 mm. and 3 mm. thick, at 20 cm. and 25 cm. from the top respectively. The entire length of the core is only *ca.* 30 cm. The living and total faunas of the top centimeter differ from each other in the percentage frequencies of the individual species but the faunal compositions are the same. The Foraminifera fauna of the lower sand layer is as follows:

* *Bolivina spissa* Cushman	19%
** *Cassidulina quadrata* Cushman and Hughes	14%
* *Uvigerina curticosta* Cushman	10%
* *Epistominella smithi* R. E. and K. C. Stewart	9%
* *Cassidulina delicata* Cushman	6%
* *Bolivina subargentea* Uchio, n. sp.	5%
* *Eponides subtenerus* Galloway and Wissler	4%
* *Cassidulina subcarinata* Uchio, n. sp.	4%
* *Cassidulina* cf. *C. braziliensis* Cushman	3%
** *Angulogerina* cf. *A. hughesi* (Galloway and Wissler)	3%
** *Cassidulina limbata* Cushman and Hughes	3%
** *Cassidulina tortuosa* Cushman and Hughes	2%
** *Bulimina denudata* Cushman and Parker	2%
* *Bulimina subacuminata* Cushman and Stewart	2%
* *Cibicides spiralis* Natland	2%
* *Gyroidina altiformis* Stewart and Stewart	1%
* *Gyroidina gemma* Bandy	1%
Sigmoilina tenuis (Czjzek)	1%
Epistominella sandiegoensis Uchio, n. sp.	1%
** *Bolivina minuta* Natland	1%
** *Elphidium* spp.	1%
** *Buliminella elegantissima* (d'Orbigny)	0.5%
** *Rosalina campanulata* (Galloway and Wissler)	0.5%
Miscellaneous (8 species)	4.8%

This assemblage, of which 227 specimens were counted, shows that this is a mixed fauna composed of species (*) normal to this depth and amounting to *ca.* 65%, and displaced species (**) from Foraminifera sand amounting to *ca.* 27%. This shallow-water fauna came from a depth of 50-150 fathoms on the upper part of the escarpment west of the Coronados Islands. Vertical displacement of the Foraminifera sand at station 268 is approximately 500 fathoms. Mineral grains are well sorted, mostly with a diameter of 0.12-0.35 mm. They consist mostly of terrigenous material such as angular quartz, some feldspar, hornblende, pyroxene, and biotite.

Other evidence of displaced sandy silt is found in surface sediments at stations 207, 208, 296, 298, 303 and 304, at depths of 505, 473, 458, 505, 485 and 430 fathoms respectively. The living and total Foraminifera faunas are listed in Tables 3 and 6. The latter show the environments of deposition of the sands before they were transported to the present positions. Displaced Foraminifera at stations 207, 208, 296, 298, 303 and 304 are approximately 10, 17, 5, 5, 12 and 15% of the total fauna respectively. These 5 stations are located on a delta-like feature at the mouth of Coronado Canyon, but not in the channel or canyon floor. The sediment in the channel is partly clayey silt which is to be expected at its present depth, while that on the delta-like feature is coarser and is composed of sandy silt. This fact suggests that sandy silt was first deposited at the mouth of the present canyon forming the delta-like feature. Later the canyon cut this delta-like feature and the canyon floor was covered by the clayey silt which is widely distributed at the bottom of the San Diego Trough. Shepard (*in* Emery *et al.*, 1952) suggested that the delta-like feature might represent a true delta when the sea-level was much lower

---

EXPLANATION OF PLATE 8

Figs.		Page
1, 2.	*Rosalina columbiensis* (Cushman). Hypotypes (U.S.N.M. Nos. 626771, 626772), ×96.	66
3-5.	*Valvulineria araucana* d'Orbigny. Hypotypes (U.S.N.M. Nos. 626773-626775), ×28, ×34, ×51.	
6, 7.	*Valvulineria glabra* Cushman. Hypotypes (U.S.N.M. Nos. 626776, 626777), ×95.	
8, 9.	*Cancris auricula* (Fichtel and Moll). Hypotypes (U.S.N.M. Nos. 626778, 626779), ×36.	
10-12.	*Cancris inaequalis* d'Orbigny). Hypotypes (U.S.N.M. Nos. 626780-626782), ×23, ×29, ×39.	
13-15.	*Gyroidina altiformis* R. E. and K. C. Stewart. Hypotypes (U.S.N.M. Nos. 626783-626785), ×40, ×33, ×32.	
16-18.	*Gyroidina io* Resig. Hypotypes (U.S.N.M. Nos. 626786-626788), ×81, ×94, ×98.	
19-21.	*Gyroidina gemma* Bandy. Hypotypes (U.S.N.M. Nos. 626789-626791), ×46.	
22-25.	*Gyroidina quinqueloba* Uchio, n. sp. 22, 23, 25, Paratypes (U.S.N.M. Nos. 626793-626795), ×96, ×117, ×132. 24, Holotype (U.S.N.M. No. 626792), ×107.	66
26-28.	*Eponides subtenerus* (Galloway and Wissler). Hypotypes (U.S.N.M. Nos. 626800-626802), ×42.	
29-31.	*Pseudoeponides umbonatus* (Reuss). Hypotypes (U.S.N.M. Nos. 626803-626805), ×43.	

(*ca.* 400 fathoms) than at present. The displaced Foraminifera at these stations include very shallow (shallower than 20 fathoms) species such as *Buliminella elegantissima* (d'Orbigny), *Buccella angulata* Uchio, n. sp., *Asterigerinata pacifica* Uchio, n. sp., *Nonionella basispinata* (Cushman and Moyer), *Bolivina vaughani* Natland, *B. lowmani* Phleger and Parker, *Elphidium* sp., and *Bolivina acutula* Bandy, etc., but in very small percents. The remaining species are those which are indigenous to the present depths. The empty tests of such very shallow-water species also are found at stations in the canyon floor, and they may be reworked from sediment on the delta-like feature or displaced directly from a nearshore area.

At station 248, in the middle of Coronado Canyon at a depth of 250 fathoms, displaced sands occur at the surface of the sediment. Here displaced Foraminifera forming approximately 45% of the total fauna came from Foraminifera sands on the Coronado Bank and the nearshore area. It is quite reasonable that this station should contain more displaced Foraminifera than other stations, since it is located just below Coronado Bank. The general tendency is for the percent of displaced Foraminifera gradually to decrease with distance from Coronado Bank.

Another example of sediment displacement is found at station 30 below Coronado Bank at 180 fathoms. Displaced specimens form at least 25% of the total fauna. The sediment is composed of very coarse sand with some shell fragments. Apparently most of this sediment came from the top of Coronado Bank.

These displaced sediments are easily recognized by their coarse grain size. Many examples of displacement or mixing of sediments can be found even in fine-grained sediment, however, if the depth distributions of living Foraminifera or other organisms are known. Text Figs. 2-9 show the depth ranges of the main species of living and total (mostly dead) Foraminifera in this area. That the depth range of dead specimens of a species extends much deeper than that of the living specimens is clearly demonstrated.

PART 2: SYSTEMATICS

INTRODUCTION

Many micropaleontologists who are interested primarily in stratigraphy and/or taxonomy tend to split Foraminifera into varieties, subspecies or even species on the basis of minor changes in the morphology of the test. These species, subspecies or varieties, as well as those of the early workers, are based in many cases on a few specimens so that the range of variation is unknown. On the other hand, ecologists, who deal with a large number of specimens, are apt to lump these species, etc., for practical reasons, and also because they have a clear idea of the range of variation of the forms. However, taxonomy is the basis of ecology. It is desirable for workers to understand the point of view of the taxonomist, stratigrapher and ecologist. In the following section the writer briefly discusses his views on the range of variation of significant species used in this study and describes two new genera and thirty-four new species. Complete synonymies are not listed but the original references, in some cases later ones of special interest, are given. In many cases references of synonymous species are also included. The distributions of the living and empty tests of the species are given in Part I: Ecology. All figured specimens are deposited in the U. S, National Museum, Washington, D. C. Duplicate sets of the assemblages are in the collection of the Scripps Institution of Oceanography of the University of California, La Jolla, California. It should be noted that many more species are figured than shown by the plate and figure references in the text.

SYSTEMATIC DESCRIPTIONS OF SPECIES

Family SACCAMMINIDAE

Saccammina longicollis (Wiesner)

Plate 1, figures 1, 2

Proteonina longicollis WIESNER, 1929, Deutsche Sud-Polar-Exped., v. 20, p. 82, pl. 6, fig. 55; CUSHMAN and MCCULLOCH, 1939, Allan Hancock Pacific Expeds., vol. 6, n. 1, p. 42, pl. 1, figs. 7-9.

Proteonina atlantica WALTON (not Cushman), 1955, Jour. Paleontology, vol. 29, p. 1012, pl. 99, fig. 1.

This species was originally described from the Atlantic. The San Diego specimens have a shorter neck than the type specimen, but may represent forms whose long necks have been broken off. The San Diego specimens are also similar to *S. limnetica* (Hada) (1937, p. 342, text-fig. 5), which was originally described from a small lake near Tottori, a western city in Japan on the Japan Sea, but the latter has a more globular test. The San Diego form is transitional between *S. longicollis* and *S. limnetica,* and these three forms may belong to the same species, *S. longicollis*.

Family REOPHACIDAE

Reophax micaceous Earland

Plate 1, figure 8

Reophax micaceous EARLAND, 1934, *Discovery* Reports, London, vol. 10 (1935), p. 82, pl. 2, figs. 37-40.

This species was originally described from the Atlantic (depth not given). *Proteonina* sp. Walton (1955, p. 1012, pl. 99, figs. 2, 3) seems to belong to *R. micaceous*. Walton said that this species had a single undivided chamber, that the chamber wall was chitinous and was covered by small detrital particles, mostly mica. This species seems to have a single chamber at first glance, particularly the young form,

(234)

but in reality has more than two chambers. Walton's figures show an indication of segmentation.

Family TOLYPAMMINIDAE

Involutina hoeglundi Uchio, n. sp.

Plate 1, figure 12

? *Ammodiscus planorbis* Höglund, 1947, (part), Zoologiska Bidrag fran Uppsala, vol. 26, p. 107, 115, 125, pl. 28, fig. 16, text-fig. 92 (not pl. 8, figs. 4, 9; pl. 25, figs. 13-15, text-figs. 91, 105, 109).

Test small, thin, very regularly planispiral; whorls up to 12 in number; spiral suture very distinct; proloculus central; wall finely arenaceous with very small sand grains and an excess of cement, surface with fine radial striations but otherwise smooth and polished, color brownish. Diameter up to 0.5 mm. (average 0.4 mm.); peripheral thickness up to 0.029 mm.; proloculus diameter up to 0.025 mm. (average 0.018 mm.).

Holotype (U. S. N. M. No. 626583) from station SD-337 (Lat. 32° 38′ N., Long. 117° 31′ W.; 610 fathoms). Diameter *ca.* 0.45 mm.

Remarks.—Höglund (1947, *op. cit.*, p. 125, pl. 8, figs. 4, 9; pl. 28, figs. 13, 14, text-figs. 91, 105, 109) described "*Ammodiscus planorbis*" from the Skagerak and included two other forms (one from the Gulf of Mexico, *op. cit.*, p. 125, pl. 28, fig. 16, text-fig. 92, the other from the Atlantic, off Portugal, p. 125, pl. 28, fig. 15) with some hesitation due to differences in proloculus diameter and the size of the test. F. L. Parker (1958, p. 253, pl. 1, figs. 1, 2) in her study of eastern Mediterranean Foraminifera has found *Involutina planorbis* (Höglund) (of the type from off Portugal) from the Aegean Sea and from off Egypt. The San Diego specimens are different from the Mediterranean form in having a much less inflated chamber, and consequently a much thinner test, and a very narrowly rounded periphery. The San Diego specimens are identical to "*A. planorbis*" of the Gulf of Mexico type, but differ from "*A. planorbis*" of the type locality, that is from the Skagerak, by their greater diameter and much larger proloculus.

Involutina pacifica (Cushman and Valentine)

Plate 1, figure 14

Ammodiscus pacifica Cushman and Valentine, 1930, Dept. Geol. Stanford Univ., Contr., vol. 1, no. 1, p. 7, pl. 1, fig. 1.

The differentiation of *I. pacifica* from *I. minutissima* (Cushman and McCulloch) is difficult because *I. minutissima* only differs in its smaller size and in having a polished, chitinous wall. *I. minutissima* may be a young form of *I. pacifica*. So far as known (Cushman and McCulloch, 1939, p. 69, 70) the geographic distribution and depth range of the empty tests of the two species are almost the same. In the population counts of this study the two species were tentatively separated, but in view of probable misidentifications, due to the above reasons, the species were later combined and listed in the tables (Part I: Ecology, Tables 1-3, 5-7) as *I. pacifica.*

I. pacifica is easily separated from *I. flavida* (Höglund) (1947, p. 127, pl. 28, figs. 1, 2; pl. 29, fig. 3; text-figs. 99, 100, 105, 106, 108, 109) by its very much smaller and more inflated test. *I. flavida* is found only in the San Diego Trough, while *I. pacifica* is found in shallow water.

Family LITUOLIDAE

Haplophragmoides neobradyi Uchio, n. sp.

Plate 1, figures 15, 16

Test free, minute, planispiral, much compressed, incompletely involute; chambers inflated, 5 chambers in the last whorl but very rarely 4½ in young specimens, those of the previous whorl slightly exposed in the depressed umbilical region; periphery lobulate in side view, moderately rounded in edge view; sutures distinct, depressed, straight, radiate; wall finely arenaceous, smooth, polished, color brownish yellow; aperture a short slit at the base of the apertural face of the last chamber, with a lip.

Holotype (U. S. N. M. No. 626587) from station SD-337 (Lat. 32° 38′ N., Long. 117° 31′ W.; 610 fathoms). Length *ca.* 0.21 mm.; width *ca.* 0.19 mm.; thickness *ca.* 0.09 mm.

Comparison.—This new species is very similar to *Haplophragmoides bradyi* (Robertson), which was first figured by Wright (1891, p. 469, pl. 20, fig. 4). F. L. Parker (1952, p. 339, pl. 2, fig. 11; 1954, p. 486, pl. 1, fig. 16) figured *H. bradyi* from off Portsmouth, New Hampshire, and from the northeastern Gulf of Mexico. The writer has examined her specimens and British specimens and found that the former are different from the latter and should be referred to a new subspecies. Höglund (1947, p. 134, pl. 10, fig. 1, text-fig. 111) described *H. bradyi* from the Gullmar Fjord and from the Skagerak, but his specimens also differ from the British ones.

Remarks.—The writer has examined 5 specimens of *H. bradyi* from southwest of Ireland at a depth of 53 fathoms. They do not show any variation in morphological features and quite agree with Wright's figure. They seem to represent a nonvariable form. Höglund also mentioned such a lack of variability in external appearance, number of chambers and whorls in his "*H. bradyi.*" The writer has examined 79 specimens of *H. neobradyi* at one station and more at other stations in the San Diego area. The British specimens have 5-5½ chambers in the last whorl (one more than San Diego specimens), are more evolute, always show a part of the previous 2 whorls and hence are more deeply umbilicate, are more firmly built and darker in color. San Diego specimens are completely involute (in young specimens) or slightly evolute (in large specimens) and a part of only one previous whorl can be seen in the umbilical area.

Haplophragmoides quadratus Uchio, n. sp.

Plate 1, figure 17; Plate 5, figure 14

Test free, finely arenaceous, thin, broadly rectangular in side view, planispiral, consisting of 4 chambers in the last whorl, slightly evolute so that the early portion is slightly visible; chambers increasing rapidly in size as added, last one occupying about ½ or ⅓ of the size of the test, inflated but not globose, quadrangular; sutures very distinct, very depressed; periphery distinctly lobulate in side view, moderately broad in apertural view; aperture a long, narrow arched opening at the base of the apertural face of the last chamber, with a distinct lip.

Holotype (U. S. N. M. No. 626590) from station SD-220 (Lat. 32° 30′ N., Long. 117° 20.7′ W.; 128 fathoms). Length *ca.* 0.39 mm.; width *ca.* 0.30 mm.

Remarks.—This new species is easily distinguished from any other species of the genus by the quadrangular shape of the test and chambers, the number of chambers in the last whorl, and the rapidly increasing size of the chambers as added. The holotype is perhaps one of the largest specimens of this species.

Alveolophragmium advena (Cushman)

Plate 1, figures 20, 21

Haplophragmoides advena Cushman, 1925, Cushman Lab. Foram. Research, Contr., vol. 1, p. 38, pl. 6, fig. 1.

According to the original description this species has about 10 chambers in the last whorl and the test is involute and umbilicate. Many specimens in the San Diego area have 9 chambers in the last whorl and are involute to slightly evolute.

Alveolophragmium columbiense (Cushman)

Plate 1, figure 22

Haplophragmoides columbiense Cushman, 1925, Cushman Lab. Foram. Research, Contr., vol. 1, p. 39, pl. 6, figs. 2a, b.

This species always has 6-6½ chambers in the last whorl. Some specimens have a broadly rounded periphery as shown in Cushman's type figures, some an angular one, but adult specimens usually have a narrow periphery. Therefore, it seems that the character of the periphery is not significant in this species. Some specimens are slightly evolute while others are involute and umbilicate. Therefore, *A. columbiense* var. *robustum* (Cushman and McCulloch) is just a variant form of *A. columbiense* and has no ecological significance. It is included with *A. columbiense* in this study.

Genus **Recurvoides** Earland, 1934, emend. Uchio

Type species: *Recurvoides contortus* Earland

The test is free, arenaceous, composed of several convolutions, each containing many chambers. The convolutions are planispiral and partially embracing but arranged in two series, the axis of winding of the second series being oblique (not necessarily at right angles) to that of the previous or earlier series. Therefore, the second series envelops the first, but leaves the peripheral edge of the final convolutions of the first series visible on one of the faces as a raised line of chambers extending across the umbilical portion of the adult test. Composed of sand grains of varying sizes with a considerable amount of ferruginous cement. Aperture a narrow slit slightly above the base of the apertural face of the last chamber, frequently with a distinct lip.

Remarks.—Earland did not describe the apertural character of the genus in detail, nor that of the type species, *R. contortus.* Dr. C. G. Adams, curator at the Foraminifera section, British Museum (Natural History), London, has kindly examined Earland's type material. According to his personal communication to the writer, "Earland's type slide 2F3470 contains 30 specimens, 13 of which are illustrated in the *Discovery* Report volume X, plate X. No holotype was designated, the 13 figured specimens thus becoming syntypes, and the 17 unfigured specimens paratypes." Adams has selected a lectotype and intends to publish a short description, together with photographs. The photograph of the proposed lectotype shows a 30° change in the axis of winding of the second series from that of the first series rather than a right angle change; the aperture is a narrow slit a little above the base of the apertural face of the last chamber, with a protruding lip. The apertural character of the other 5 specimens, which Adams sketched for the writer, shows that the apertures are slightly above the base of the apertural face. Further discussion of the genus is given in the description of *R. subglobosus* (G. O. Sars).

Recurvoides subglobosus (G. O. Sars)

Plate 1, figures 26, 27

Lituola subglobosa M. Sars, 1868 (1869), Forh. Vid. Selsk. Christiania, p. 250 (*nomen nudum*); G. O. Sars, *ibid.*, p. 253.

Haplophragmium latidorsatum Brady, 1884 (not *Nonionina latidorsatum* Bornemann, 1885), Rept. Voy. *Challenger*, Zool., vol. 9, p. 307, pl. 34, figs. 7-10, 14 (?).

Haplophragmoides subglobosum (G. O. Sars), Cushman, 1910, U. S. Natl. Mus., Bull., vol. 71, pt. 1, p. 105, text-figs. 162-164.

Cribrostomoides bradyi Cushman, 1910, *ibid.*, p. 109, text-fig. 167.

Haplophragmoides subglobosus (G. O. Sars), EARLAND, 1934, *Discovery* Rept., vol. 10, p. 89.

Haplophragmoides subglobosum (G. O. Sars), CUSHMAN and McCULLOCH, 1939, Allan Hancock Pacific Expeds., vol. 6, p. 80, pl. 6, figs. 9-11.

Labrospira subglobosa (G. O. Sars), HÖGLUND, 1947, Zool. Bidrag. fran Uppsala, vol. 26, p. 144, pl. 11, fig. 2, text-fig. 126.

Alveolophragmium subglobosum (G. O. Sars), F. L. PARKER, 1954, Mus. Comp. Zool., Bull., vol. 111, no. 10, p. 487, pl. 2, figs. 1-2.

The first figures of this species appeared in Brady's *Challenger* Report, but he did not mention the presence of an apertural lip, nor did he describe the aperture in detail. He said that the aperture was at the base of the apertural face of the last chamber. His figure 7 shows an aperture at the base of the apertural face, but figure 8 shows an aperture that is slightly above the base of the last chamber. His figure 9 shows an irregular aperture and Cushman proposed the new generic and species name "*Cribrostomoides bradyi*" for this form. However, as the result of the study of many specimens of this species Earland and Höglund considered this an abnormal specimen. Höglund, Parker, and Cushman and McCulloch all showed the presence of an apertural lip and the position of the aperture slightly above the base of the apertural face of the last chamber.

Parker says, "This species appears to be intermediate between *Recurvoides* and *Alveolophragmium* but is more closely allied to the latter in adult specimens." From the standpoint of evolution *Recurvoides* seems to be derived from *Alveolophragmium*. However, as Parker mentioned, adult specimens of *R. subglobosus* are more *Alveolophragmium*-like. Therefore, *Alveolophragmium* seems to be derived from *Recurvoides*. This seems to be contradictory, but if the plane of coiling changed again at the *Recurvoides* stage, the form could become of the *Alveolophragmium* type again. Therefore, the young form of this species may show an *Alveolophragmium* stage, then a *Recurvoides* stage, and finally in very large specimens an *Alveolophragmium* stage. This can be proved or disproved by sectioning many specimens. Here the writer tentatively refers the species to *Recurvoides*, because it always shows a change in the plane of coiling.

Genus **Recurvoidella** Uchio, n. gen.

Type species: *Recurvoidella parkerae* Uchio, n. sp.

The test is free, arenaceous, composed of several whorls, each containing many chambers. The whorls are planispiral and partially embracing but arranged in two series, the axis of winding of the second series being oblique (not necessarily at right angles) to that of the first or earlier series. The second series, therefore, envelops the first, but leaves the peripheral edge of the final whorl of the first series visible on one of the faces as a raised line of chambers extending across the umbilical portion of the adult test. The umbilical portion of the opposite face is more depressed. The test is composed of sand grains of varying size with a considerable amount of ferruginous cement. The aperture is small, narrow, at the base of the last chamber, sometimes with a protruding upper lip.

Remarks.—This new genus is very similar to *Recurvoides* Earland (1934, p. 90) in its arrangement of chambers, but differs from it in having the aperture at the base of the apertural face of the last chamber, while that of *Recurvoides* is slightly above the base of the apertural face of the last chamber. This relationship is like that between *Haplophragmoides* Cushman, 1910, and *Alveolophragmium* Stschedrina, 1936 (including *Labrospira* Höglund, 1947).

Recurvoidella parkerae Uchio, n. sp.

Plate 1, figures 18, 19

Test free, small, nearly circular, early portion planispiral, later portion planispiral but with a slightly changed plane of coiling from that of the previous portion, resulting in its being slightly evolute on one side and less so or completely involute on the other side; chambers inflated, numerous, usually 5 (4½ in small specimens and 5½ in large specimens) in the last whorl; periphery broadly rounded in edge view, lobulate in side view; sutures distinct, depressed, straight, radiate from the umbilical area; wall finely arenaceous with much cement, surface smooth, shining, polished; aperture a narrow crescentic slit at the base of the apertural face of the last whorl on the periphery of the involute side, with an upper lip; color yellowish brown. Diameter up to *ca.* 0.18 mm.; thickness up to *ca.* 0.1 mm.

Holotype (U. S. N. M. No. 626603) from station SD-50 (Lat. 32° 41.6′ N., Long. 117° 19.6′ W.; 53 fathoms).

Comparison.—*Haplophragmoides bradyi* and *H. neobradyi* are very similar to this new species, but it has a thicker test than either of them and the chamber arrangement gradually changes from a *Haplophragmoides* type to a *Recurvoidella* type becoming progressively like *H. bradyi*, *H. neobradyi* and *R. parkerae*. The umbilical area is broadest and deepest in *H. bradyi* and least so in *R. parkerae*. Some specimens in the northeastern Gulf of Mexico referred to *H. bradyi* by Parker are almost identical with this new species, but become larger in size. Höglund's specimens from the Gullmar Fjord and the Skagerak are very close to British specimens of *H. bradyi* in side view but have much thicker tests.

Remarks.—It is interesting to note that living specimens of *R. parkerae* seem to prefer shallower water and *H. neobradyi* deeper. A similar phenomenon was noted by Höglund in the Gullmar Fjord and the

Skagerak. *H. bradyi* of Höglund is widely distributed but at scattered depths, being very scarce at intermediate depths in the Gullmar Fjord, and on the contrary increasing with greater depths in the Skagerak. For this reason it may be that Höglund included two very similar species or varieties in one species.

Ammomarginulina sandiegoensis Uchio, n. sp.

Plate 2, figures 5, 6

Test crosier-shaped, complanate, very thin, coarsely arenaceous, flat on both sides; consisting of numerous chambers, early ones forming two or three convolutions of a flat spire, the later ones arranged in a straight, linear series; chambers distinct, earlier ones rectangular, later ones of the linear series with a slightly inverted V-shape; sutures not very clear in dried specimens, but very distinct in Canada balsam or when wet, slightly depressed; periphery slightly lobulate at the sutures in side view; aperture terminal, small, rounded, at the end of a distinct neck.

Holotype (U. S. N. M. No. 626613) from station SD-337 (Lat. 32° 38′ N., Long. 117° 31′ W.; 610 fathoms). Length *ca.* 0.60 mm.; width *ca.* 0.16 mm.

Comparison.—This new species is closely related to *A. foliacea* (Brady), but differs in having chambers with a slightly transverse V-shape, a distinct apertural neck, and fewer chambers in the spiral portion.

Family TEXTULARIIDAE

Spiroplectammina bathyca Uchio, n. sp.

Plate 2, figure 7

Test minute, elongate, much compressed, coarsely arenaceous, broadest at the spiral portion, with the sides of the biserial portion either parallel or slightly increasing in breadth toward the apertural end; chambers distinct, earlier ones planispiral, forming about two coils, later biserial, low and broad, about twice as broad as high, last chamber protruding; sutures slightly depressed, oblique, not distinct in dried specimens, but distinct in specimens mounted in Canada balsam or when wet; periphery lobulate; aperture a low opening at the base of the last chamber.

Holotype (U. S. N. M. No. 626616) from station SD-268 (Lat. 32° 23.3′ N., Long. 117° 21.8′ W.; 630 fathoms). Length *ca.* 0.34 mm.; width *ca.* 0.11 mm.

Comparison.—This species is similar to *S. typica* Lacroix (1931, p. 14, text-fig. 9; 1932, p. 7, text-figs. 2-3), which was described from sands at 30-60 m. near Cape Martin in the Mediterranean Sea, but differs from it by having more oblique sutures, more elongate and lower chambers and by not having a triangular last chamber. The thickness of the test of *S. bathyca* does not increase rapidly but is rather constant although sometimes the spiral portion is a little thicker than the biserial portion. The shallowest depth of living specimens of *S. bathyca* is 345 fathoms.

Textularia sp. cf. **T. abbreviata** d'Orbigny

Plate 2, figures 8-10

Textularia abbreviata Lalicker and McCulloch (not d'Orbigny, 1846), 1940, Allan Hancock Pacific Expeds., vol. 6, no. 2, p. 116, pl. 13, fig. 1.

Textularia cf. *abbreviata* Cushman, 1927, Scripps Inst.

EXPLANATION OF PLATE 9

Figs.		Page
1-3.	*Buccella angulata* Uchio, n. sp. Holotype (U.S.N.M. No. 626806), ×28, ×24, ×24.	67
4, 5.	*Hoeglundina elegans* (d'Orbigny). Hypotypes (U.S.N.M. Nos. 626808-626809), ×21.	
6, 7.	*Epistominella sandiegoensis* Uchio, n. sp. 6, Paratype (U.S.N.M. No. 626813), ×115. 7, Holotype (U.S.N.M. No. 626812), ×94.	68
8-10.	*Epistominella smithi* (R. E. and K. C. Stewart). Hypotypes (U.S.N.M. Nos. 626815-626817), ×47, ×49, ×46.	
11, 12.	*Cassidulina bradshawi* Uchio, n. sp. 11, Holotype (U.S.N.M. No. 626818), ×96. 12, Paratype (U.S.N.M. No. 626819), ×101.	68
13-14.	*Cassidulina braziliensis* Cushman. Hypotypes (U.S.N.M. Nos. 626821, 626822), ×38.	
15, 16.	*Cassidulina subcarinata* Uchio, n. sp. 15, Holotype (U.S.N.M. Nos. 626827), ×94. 16, Paratype (U.S.N.M. No. 626828), ×96.	68
17.	*Cassidulina delicata* Cushman Hypotype (U.S.N.M. No. 626823), ×94.	68
18, 19.	*Cassidulina depressa* Asano and Nakamura Hypotypes (U.S.N.M. Nos. 626824, 626825), ×103, ×100.	68
20.	*Cassidulina limbata* Cushman and Hughes. Hypotype (U.S.N.M. No. 626826), ×46.	
21.	*Cassidulina subglobosa* Brady. Hypotype (U.S.N.M. No. 626830), ×94.	
22.	*Cassidulina subglobosa* var. *quadrata* Cushman and Hughes. Hypotype (U.S.N.M. No. 626831), ×108.	
23.	*Cassidulina tortuosa* Cushman and Hughes Hypotype (U.S.N.M. No. 626832), ×38.	69
24-27.	*Cassidulinoides waltoni* Uchio, n. sp. 24, Holotype (U.S.N.M. No. 626833), ×37. 25-27, Paratypes (U.S.N.M. Nos. 626834-626836), ×38, ×38, ×37.	69
28-31.	*Ehrenbergina compressa* Cushman. Hypotypes (U.S.N.M. Nos. 626838-626841), ×46, ×46, ×48, ×47.	

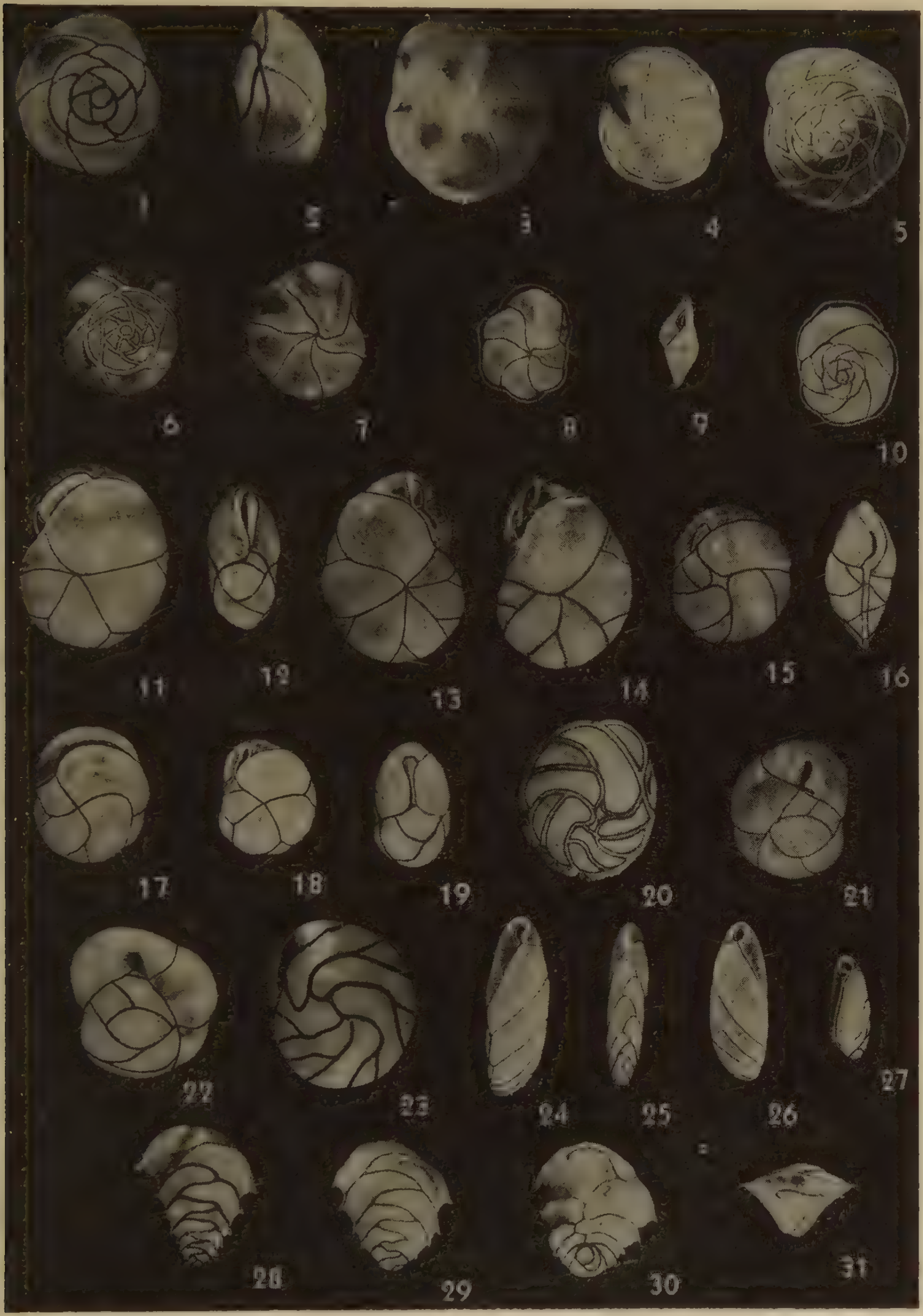
1
2
3
4
5
6
7
8
9
10
11
12
13
14
15
16
17
18
19
20
21
22
23
24
25
26
27
28
29
30
31

Uchio: Living Foraminifera, San Diego, California

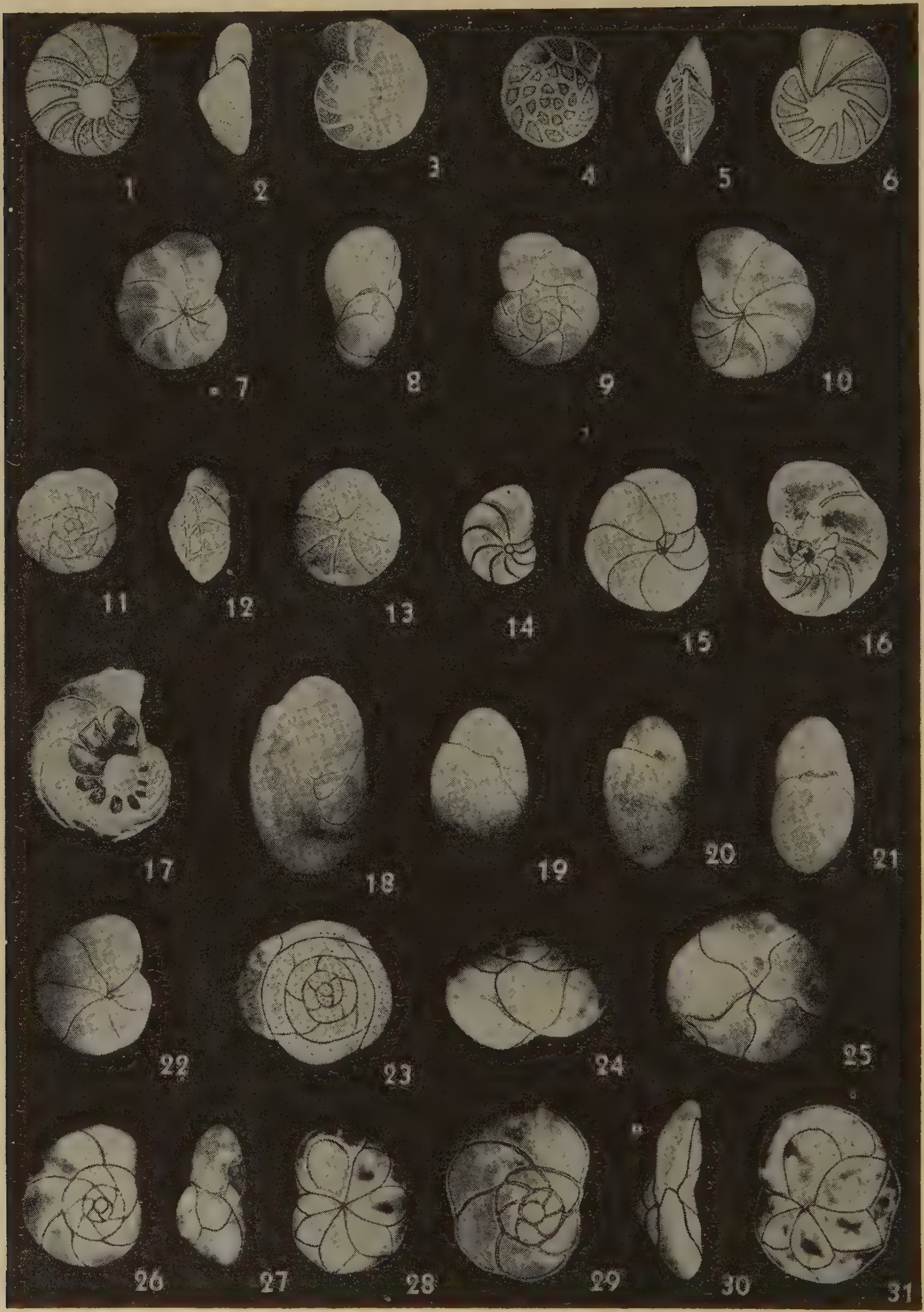
1
2
3
4
5
6
7
8
9
10
11
12
13
14
15
16
17
18
19
20
21
22
23
24
25
26
27
28
29
30
31

Uchio: Living Foraminifera, San Diego, California

Oceanography, Bull., Tech. Ser., vol. 1, no. 10, p. 136 (part).

In the San Diego specimens the side view of young forms is broadly triangular and very similar to that of *T. abbreviata* d'Orbigny (1846, p. 249, pl. 15, figs. 9-12) but the later portion becomes elongate and the sides nearly parallel as in *T. articulata* d'Orbigny (1846, p. 250, pl. 15, figs. 16-18). The periphery is acute but not keeled, becoming round in the adult form, and is, therefore, more like that of *T. abbreviata* than *T. articulata*. *T. articulata* of Lalicker and McCulloch (1940, p. 118, pl. 13, fig. 3) seems to be the adult form of *T. abbreviata* in the San Diego area, but the size of the figured specimen is smaller than that of the figured *T. abbreviata*. *T. conica* Lalicker and McCulloch (not d'Orbigny, 1839) seems to be the same as their T. *abbreviata* but consists of finer grains. *T. conica* d'Orbigny (1839, p. 143, pl. 1, figs. 19, 20) was originally described from the Recent marine sands near Cuba, and seems to be different from *T. abbreviata* or *T. articulata*. *T. calva* Lalicker (*in* Lalicker and McCulloch, 1940, p. 120, pl. 13, figs. 6a-d) and *T. schencki* Lalicker and McCulloch (not Cushman and Valentine, 1930) (1940, p. 140, pl. 16, fig. 23) seem to be the adult form of *T.* sp. cf. *T. abbreviata* in the San Diego area. The Recent distributions of *T. abbreviata*, *T. articulata* and *T. conica*, all of Lalicker and McCulloch, are all about the same, in the shallow waters of southern California to the northern part of South America.

Cushman's specimens referred to *T.* sp. cf. *T. abbreviata* became the types of *T. schencki* Cushman and Valentine. The writer has examined 9 specimens which were collected 2½ miles south of the Scripps Institution's pier at a depth of 200-210 feet, and identified as *T.* cf. *abbreviata* by Cushman (deposited at the Scripps Institution of Oceanography); 8 specimens are conspecific with *T.* sp. cf. *T. abbreviata*, and the other is conspecific with *T. schencki*.

Textularia sandiegoensis Uchio, n. sp.

Plate 2, figure 12

Test minute, very elongate, straight or slightly curved, oval in cross section, early chambers close coiled with the initial end rounded, later ones biserial, consisting of very fine grains and chitinous cementing matter, very fragile, easily broken, about 5 or 6 times longer than broad, sides nearly parallel; periphery slightly lobulate; sutures oblique, slightly depressed when wet, but distinctly so when dried; chambers about 1½ times as broad as high, slightly inflated when wet, smooth except at the lower margins which are slightly thickened, gradually increasing in size as added except in the later portion; aperture a narrow slit at the base of the apertural face of the last chamber.

Holotype (U. S. N. M. No. 626623) from station SD-250 (Lat. 32° 30.9′ N., Long. 117° 20.4′ W.; 390 fathoms). Length *ca.* 0.27 mm.; width *ca.* 0.07 mm.

Comparison.—This species is similar to *T. praelonga* Schwager (1866, p. 252, pl. 7, fig. 104), which was originally described from the Pliocene of Kar Nicobar in the Indian Ocean, but differs from it in having a much smaller (about ⅛ the length), more compressed, smoother test and a less lobulate periphery.

Textularia schencki Cushman and Valentine

Plate 2, figure 11

Textularia schencki CUSHMAN and VALENTINE, 1930, Dept. Geol. Stanford Univ., Contr., vol. 1, no. 1, p. 8, pl. 1, fig. 3.

Textularia cf. *abbreviata* CUSHMAN (not d'Orbigny 1846), 1927, Scripps Inst. Oceanography, Bull., Tech. Ser., vol. 1, no. 10, p. 136 (part).

In their original description of *T. schencki*, Cushman and Valentine included *T.* cf. *T. abbreviata* Cushman as a synonym, and said that this species occurred abundantly off La Jolla. This was later designated as the type locality of *T. schencki* by Lalicker and McCulloch (1940, p. 140). The writer has exam-

---

EXPLANATION OF PLATE 10

FIGS.		PAGE
1-3.	*Cibicides fletcheri* Galloway and Wissler. Hypotype (U.S.N.M. No. 626842), ×29.	
4-6.	*Cibicides mckannai* Galloway and Wissler. Hypotypes (U.S.N.M. Nos. 626843-626845), ×31.	
7-10.	*Cibicides phlegeri* Uchio, n. sp. 7-9, Paratypes (U.S.N.M. Nos. 626846-626848), ×162, ×171, ×159. 10, Holotype (U.S.N.M. No. 626849), ×156.	69
11-13.	*Cibicides spiralis* Natland. Hypotypes (U.S.N.M. Nos. 626851-626853), ×46.	
14-16.	*Hanzawaia nitidula* (Bandy) Hypotypes (U.S.N.M. Nos. 626855-626857), ×30, ×30, ×31.	70
17.	*Laticarinina pauperata* (Parker and Jones). Hypotype (U.S.N.M. No. 626858), ×30.	
18-21.	*Chilostomella ovoidea* Reuss. Hypotypes (U.S.N.M. Nos. 626859-626862), ×43, ×54, ×43, ×41.	
22.	*Pullenia salisburyi* R. E. and K. C. Stewart. Hypotype (U.S.N.M. No. 626864), ×24.	
23-25.	*Eponides leviculus* (Resig) Hypotypes (U.S.N.M. Nos. 626797-626799), ×145, ×155, ×168.	67
26-31.	*Asterigerinata pacifica* Uchio, n. sp. 26-28, Holotype (U.S.N.M. No. 626810), ×171. 29-31, Paratype (U.S.N.M. No. 626811), ×173.	67

ined 9 specimens, which were collected 1½ miles south of the Scripps Institution Pier at a depth of 200-210 feet and identified by Cushman (deposited at the Scripps Institution of Oceanography) and has found that only one specimen can be referred to *T. schencki* (see below), while the other 8 specimens are the same as *T.* sp. cf. *T. abbreviata* as identified by the writer in the San Diego area. The one specimen referrable to *T. schencki* was compared with 12 specimens collected off San Diego, which were in turn compared with the type specimens at the U. S. National Museum by F. L. Parker. According to her (personal communication) these specimens may be *T. schencki,* although they may be a part of a "*T. schencki-T. articulata*" series. The writer has examined specimens identified as *T. articulata* by Parker, and finds that they are conspecific with the adult form of *T.* sp. cf. *T. abbreviata* of the writer. Parker says of them, "They are very close to paratypes of *T. schencki* but not as similar to the holotype." Thus it seems that *T. schencki* has two forms, that is: *T. schencki* (*s.s.*) and the adult form of *T.* sp. cf. *T. abbreviata* of the writer or *T. articulata* of Parker. Little is known at present about the range of variation of *T. schencki.*

T. schencki of Lalicker and McCulloch (1940, pl. 16, fig. 23) is the adult form of *T.* sp. cf. *T. abbreviata* of the writer; however, *T. candeiana* Lalicker and McCulloch (not d'Orbigny) (1940, pl. 13, fig. 7) and *T. aura* Lalicker and McCulloch (1940, pl. 13, fig. 5) are conspecific with *T. schencki* (*s.s.*).

Bigenerina hoeglundi Uchio, n. sp.

Plate 2, figure 13

Textularia bigenerinoides Höglund (not Lacroix), 1947, Zool. Bidrag fran Uppsala, vol. 26, p. 181, pl. 13, fig. 6, text-fig. 159.

Test small, elongate, fusiform, compressed, consisting of fine grains with much cementing matter, surface smooth, rather fragile, broadest part above the middle, tapering gradually towards both ends which are bluntly pointed; chambers biserial but becoming uniserial, very slightly if at all inflated; sutures oblique, slightly depressed but sometimes indistinct; aperture terminal, produced, an elongate oval.

Holotype (U. S. N. M. No. 626625) from station SD-9 (Lat. 32° 37.7′ N., Long. 117° 19.3′ W.; 52 fathoms). Length *ca.* 0.34 mm.; width *ca.* 0.10 mm.

Comparison.—*B. hoeglundi* is similar to *Textularia bigenerinoides* Lacroix (1932, p. 24, text-figs. 27-31), originally described from the Mediterranean (near Cape Martin), but differs from it in having a smoother and more inflated test, a more or less regularly denticulate margin and no distinctly pointed apertural neck. *Textularia* (?) sp. of Cushman and Kellett (1929, p. 3, pl. 1, fig. 4) may be referrable to this new species.

Remarks.—This is a transitional form between *Textularia* and *Bigenerina* in its chamber arrangement but its aperture is that of *Bigenerina.*

Family VERNEUILINIDAE

Gaudryina arenaria Galloway and Wissler

Plate 2, figures 14, 15

Gaudryina arenaria Galloway and Wissler, 1927, Jour. Paleontology, vol. 1, p. 68, pl. 11, fig. 5.

The tests of specimens from deep samples are made of fine sand with silty cementing matter. For this reason their surfaces are smoother than those from shallow samples where coarse sands are available to form tests.

Specimens of the younger stages are triangular in transverse section, while those with later stages become quadrangular.

Family VALVULINIDAE

Eggerella scrippsi Uchio, n. sp.

Plate 2, figure 20

Test small, elongate, tapering, earliest whorl very short with more than three chambers, remainder of test triserial, broadest near the apertural end; chambers inflated, sutures depressed; wall very finely arenaceous with much chitinous material; aperture in a deep depression at the inner margin of the last chamber.

Holotype (U. S. N. M. No. 626632) from station SD-122 (Lat. 32° 32.7′ N., Long. 117° 10.3′ W., 10.5 fathoms). Length *ca.* 0.22 mm.; diameter *ca.* 0.11 mm.

Comparison.—This species is very similar to *E. advena* (Cushman), but differs from it in its much more finely arenaceous test which has a smoother surface. Living specimens of both species are found together in samples but they seem to prefer different types or sizes of material for constructing their tests. When the writer began to count populations he combined both species but later differentiated them, so that they appear in the tables (Part I: Ecology, Tables 1-3, 5-7) either separately or combined.

Karreriella parkerae Uchio, n. sp.

Plate 2, figures 21-23

Test small, a trochoid spiral, later triserial, rarely with a final biserial stage, elongate, usually short, stout, about 1½-2 times as long as broad, tapering to initial end, broadest at apertural end; chambers numerous, distinct, overlapping, inflated particularly in the last few chambers; sutures distinct, depressed particularly near the apertural end, nearly horizontal throughout most of the test; wall finely arenaceous with much cement, smoothly finished, somewhat polished; aperture an elongate opening with a low lip at the base near the middle of, or very slightly above, the base of the apertural face of the last chamber.

Holotype (U. S. N. M. No. 626633) from station

SD-337 (Lat. 32° 38′ N., Long. 117° 31′ W.; 610 fathoms). Length *ca.* 0.48 mm.; breadth *ca.* 0.29 mm.

Comparison.—This species has been identified by many workers as *Eggerella bradyi* (Cushman) or *Karreriella bradyi* (Cushman), which represent two different forms. The writer has examined two topotypes of *Eggerella bradyi* (Cushman) (*Verneuilina pygmaea* Brady, not Egger) through the courtesy of C. G. Adams of the British Museum (Natural History), London. They are identical to Brady's type figure. *K. parkerae* differs from *E. bradyi* in its much smaller test, more globular chambers, and slightly raised apertural lip. The sutures of *K. parkerae* are depressed but flat, while those of *E. bradyi* are depressed. The specimen figured by F. L. Parker (1954, p. 494, pl. 3, fig. 17) is almost identical to *K. parkerae*.

Family MILIOLIDAE

Sigmoilina tenuis (Czjzek)

Plate 3, figures 1, 2

Quinqueloculina tenuis Czjzek, 1848, Naturw. Abh. Wien, Bd. 2, Abth. 1, p. 149, pl. 13, figs. 31-34.

Spiroloculina tenuissima Reuss, 1867, K. Akad. Wiss. Wien, Nath.-Naturw. Cl., Sitzber., Bd. 55, Abth. 1, p. 71, pl. 1, fig. 11.

Sigmoilina elliptica Galloway and Wissler, 1927, Jour. Paleontology, vol. 1, p. 39, pl. 7, figs. 2a, b.

Sigmoilina tenuis (Czjzek), Cushman, 1946, Cushman Lab. Foram. Research, Contr., vol. 22, p. 32, pl. 5, figs. 13-15; Marks, 1951, Cushman Found. Foram. Research, Contr., vol. 2, p. 39, pl. 7, figs. 2a, b; Puri, 1953, Florida Geol. Survey, Bull., no. 36, p. 90, pl. 14, figs. 6-8.

Sigmoilina miocenica Cushman, 1946, Cushman Lab. Foram. Research, Contr., vol. 22, p. 33, pl. 5, figs. 19-22.

Sigmoilina cf. *S. miocenica* Walton, 1955, Jour. Paleontology, vol. 29, p. 1015, pl. 100, figs. 22, 23.

Cushman and Marks considered *S. tenuissima* to be a synonym of *S. tenuis*. Cushman says that *S. elliptica* is very similar to *S. tenuis*, and Recent specimens from the Pacific also are close to *S. tenuis*. He described *S. miocenica* from the Miocene of Florida, but Puri (1953), in his Miocene study of the Florida Panhandle, included Cushman's figure of *S. tenuis* (1929, pl. 12, figs. 12-14), which was later included in *S. miocenica*, as a synonym of *S. tenuis*. According to Cushman *S. miocenica* differs from *S. tenuis* in the relatively broader, more strongly sigmoid test, much less developed apertural neck, and the broader chambers. The young stages resemble *S. tenuis* very much. The writer has examined many specimens at station SD-290 (550 fathoms, dead specimens) off San Diego, which according to Cushman are close to *S. tenuis*, and has found that they show a wide range of variation, having weakly to strongly sigmoid tests, tests varying in width, and necks of varying length. Therefore, *S. miocenica* Cushman is within the range of variation of *S. tenuis*.

Spiroloculina fragilis Uchio, n. sp.

Plate 3, figures 5, 6

Test minute, fragile, less than twice as long as broad, slightly depressed in the central portion, periphery rounded; chambers very distinct, numerous, narrow, arched, tubular, earlier ones very narrow, later ones gradually increasing in size and thickness as added; the successive coils separated or loosely connected by deeply depressed sutures; apertural end projecting, but becoming extended out beyond the normal line of coiling in the larger specimens because of the loose connection between successive coils. Sutures distinct, very strongly depressed in the adult; wall dull white; aperture at the end of a neck, circular, without a tooth, with a lip.

Holotype (U. S. N. M. No. 626641) from station SD-112 (Lat. 32° 23.4′ N., Long. 117° 28.1′ W.; 635 fathoms). Length *ca.* 0.48 mm.; width *ca.* 0.25 mm.

Comparison.—*S. tenuiseptata* Brady (1884, p. 153, pl. 10, fig. 5, *not* fig. 6) is very similar to this new species. In fact, Brady's fig. 6 may represent it. Cushman and Todd (1944, p. 47) also questioned the identification of figure 6. *S. fragilis* is easily separated from *S. tenuiseptata* by its rounded periphery, smooth wall and smaller size (less than 0.5 mm. in length). It is obvious that Brady included two species in *S. tenuiseptata* because he said that the peripheral edge was square or rounded. His figure 5 shows a square periphery, and figure 6 is not shown in apertural view but seems to be rounded. Brady did not say which specimen was the holotype, but the specimen shown in figure 5 has priority, is well figured, and is referred to as the holotype by Cushman and Todd (1944, p. 53).

Family OPHTHALMIDIIDAE

Cornuspira lajollaensis Uchio, n. sp.

Plate 3, figures 8, 9

Test free, thick, circular in side view, very slightly concave on each side except for the umbilical area which is slightly raised; periphery broadly rounded in edge view; chambers inflated, consisting of a proloculus and a long planispiral coiled tube, with up to 6 whorls (in the megalospheric form), the diameter of the tube almost the same throughout except in the last whorl, which is broader, and the proloculus which is very large and inflated in the megalospheric form, each coil considerably overlapping the previous one for about ⅓ of the width of the tube so that only ⅓ of the width shows the translucent wall with the remainder opaque; spiral suture distinct, mostly flush with the surface, but very slightly depressed between the last two whorls; surface smooth, polished, sometimes showing very weak transverse growth lines; color white.

Holotype (U. S. N. M. No. 626647) from station LJ-4, 75 m. north of La Jolla Cove at 22 fathoms. Diameter *ca.* 0.4 mm.; thickness *ca.* 0.1 mm.

Comparison.—This new species is similar to *C. planorbis* Schultze (1854, p. 40, pl. 2, fig. 21) which was originally described from Recent mud off the coast of Mozambique, southeastern Africa, but differs from it by greater overlapping of the whorls leaving a narrower translucent area in each whorl. Specimens from the Atlantic and the Gulf of Mexico show less overlapping of the whorls resulting in a translucent test, and seem to be identical with *C. planorbis*. *C. lajollaensis* is also similar to *C. tasmanica* Parr, which was based on six microspheric specimens. The San Diego specimens are all megalospheric forms and, therefore, the species can not be compared directly to *C. tasmanica*. However, *C. lajollaensis* apparently differs from *C. tasmanica* by the greater overlapping of the whorls, the almost flat surfaces, and the more broadly rounded periphery.

Family TROCHAMMINIDAE

Trochammina charlottensis Cushman

Plate 3, figures 13, 14

Trochammina charlottensis Cushman, 1925, Cushman Lab. Foram. Research, Contr., vol. 1, p. 39, pl. 6, fig. 4; Cushman and McCulloch, 1939, Allan Hancock Pacific Expeds., vol. 6, no. 1, p. 104, pl. 11, figs. 5, 6.

This species was originally described from Queen Charlotte Sound, off British Columbia, together with *T. pacifica*. The former, according to the original description, differs from the latter in having more curved sutures on the dorsal side, a much less umbilicate ventral side, and a somewhat compressed test. However, the type figure of *T. charlottensis* does not show the apertural view, so one can not compare the degree of compression with that of *T. pacifica*. *T. pacifica* also has slightly curved sutures on the dorsal side, and can not be easily separated from the type figure of *T. charlottensis* in this respect. In other words, one can not easily separate these species by their original figures. However, Cushman and McCulloch figured *T. charlottensis*, which is distinct from the type figures of both *T. charlottensis* and *T. pacifica* in having a much compressed test, distinctly curved dorsal sutures and a shallow but sometimes round umbilicus in which the earlier whorl can be seen to a small extent. The San Diego specimens are identical with this form.

Trochammina chitinosa Uchio, n. sp.

Plate 3, figures 22, 23

Test free, medium in size for the genus, chitinous, trochoid, dorsal side slightly inflated, ventral side convex, umbilical area rather flat but deeply umbilicate in well preserved specimens; consisting of about two coils besides the proloculus, the last whorl occupying most of the test; chambers somewhat inflated, usually 6, sometimes 6½ or 7 in the last whorl, increasing very rapidly in size as added; sutures slightly depressed, straight or very slightly curved on both sides; periphery rounded in edge view; aperture a narrow slit at the base of the apertural face of the last chamber. Color light brown. Length up to *ca.* 0.28 mm.; width *ca.* 0.21 mm.

Holotype (U. S. N. M. No. 626655) from station SD-265 (Lat. 32° 23.2′ N., Long. 117° 19.5′ W.; 350 fathoms). Length *ca.* 0.28 mm.; width *ca.* 0.21 mm.

Remarks.—This species has almost no possibility of being preserved as fossil or in Recent dried sediments. The only form that can be compared to it is the specimen figured by Rhumbler (1911, pl. 25, fig. 6, "*T. perforata*" *nom. nud.*).

Trochammina discorbinoides Uchio, n. sp.

Plate 3, figures 18, 19

Test free, small, trochoid, finely arenaceous, surface smooth, not polished, consisting of 5 whorls, all visible from the dorsal side, only the last one from the ventral side, dorsal side moderately convex, ventral side depressed, umbilicus very deep; periphery narrowly rounded in edge view, lobulate in side view; chambers somewhat inflated, elongate, somewhat rectangular in dorsal view, nearly triangular on ventral view, 4 in the last whorl; sutures distinct, depressed, nearly radial on both sides; aperture a narrow slit at the base of the apertural face of the last chamber. Diameter up to *ca.* 0.18 mm.

Holotype (U. S. N. M. No. 626657) from station SD-220 (Lat. 32° 30′ N., Long. 117° 20.7′ W.; 128 fathoms). Diameter *ca.* 0.14 mm.

Comparison.—This new species is similar to *T. discorbis* Earland (1934, p. 104, pl. 3, figs. 28-31), which was originally described from the Recent sediments of the Falkland sector of the Antarctic region, but differs from it in having a lower spiral test, radial sutures on the dorsal side, a narrowly rounded periphery and a much deeper umbilicus.

Trochammina kellettae Thalmann

Plate 3, figures 20, 21

Trochammina peruviana Cushman and Kellett (not W. Berry, 1928), 1929, U. S. Natl. Mus., Proc., vol. 75, art. 25, p. 4, pl. 1, figs. 8a, b.

Trochammina kellettae Thalmann, 1932, Eclog. Geol. Helv., vol. 25, no. 2, p. 313.

The test of this species has an excess amount of cementing or chitinous material and when dried usually shrinks, or sometimes collapses completely. For this reason the description and figures of dried specimens do not always, or perhaps in most cases, represent the true character of the species. This is one of the *Trochammina squamata* group which includes about nine species, eight of which were discussed in detail by Rhumbler (1938) and Höglund (1947).

Living specimens of this species do not stain well with rose Bengal because the test is so compressed that the amount of protoplasm contained in it is very small; since the color of the test is brownish the red color of the stain does not show clearly. The result is that the distribution of living specimens appears to be from all depths in the area studied, but some specimens may have been wrongly identified as living. According to Walton (1955) living specimens of this species are limited to shallow water.

Trochammina labiata Uchio, n. sp.

Plate 3, figures 15-17

Test free, trochoid, spire very low, dorsal side almost flat, ventral side somewhat flat but umbilicus very deep, consisting of 3 whorls besides the proloculus, the last whorl occupying about ¾ of the dorsal surface; periphery broadly rounded in edge view, lobulate in side view; chambers inflated, 4-5 in the last whorl, increasing rapidly in size as added; sutures distinct, depressed, nearly straight and nearly radial or slightly oblique on the dorsal side, radial and nearly straight or slightly curved on the ventral side; wall finely arenaceous with much cement, smooth, not polished; aperture a narrow slit at the base of the apertural face of the last chamber, extending from the umbilicus almost to the periphery, with a distinct lip. Length up to *ca.* 0.18 mm.; width up to *ca.* 0.15 mm.

Holotype (U. S. N. M. No. 626663) from station SD-297 (Lat. 32° 28.3′ N., Long. 117° 26.1′ W.; 560 fathoms). Length *ca.* 0.17 mm.; width *ca.* 0.15 mm.; thickness *ca.* 0.09 mm.

Comparison.—This new species is easily distinguished from others of the genus by the characters described above, particularly the distinct apertural lip and very finely arenaceous, smooth, unpolished test.

Trochammina pacifica Cushman

Plate 3, figures 26, 27

Trochammina pacifica CUSHMAN, 1925, Cushman Lab. Foram. Research, Contr., vol. 1, p. 39, pl. 6, figs. 3a-c.

Trochammina pacifica Cushman var. *simplex* CUSHMAN and MCCULLOCH (not Friedberg 1902), 1939, Allan Hancock Pacific Expeds., vol. 1, no. 1, p. 104, pl. 11, fig. 4.

Trochammina pacifica Cushman var. *simplissima* CUSHMAN and MCCULLOCH, 1948, Cushman Lab. Foram. Research, Contr., vol. 24, p. 76.

Cushman and McCulloch say that *T. simplissima* has a smaller test than the typical form, *T. pacifica.* It is not, however, a variety of *T. pacifica,* but a young form, and has been included in the population counts of *T. pacifica.*

Trochammina rhumbleri Uchio, n. sp.

Plate 5, figures 18-20

Test free, small for the genus, trochoid, dorsal side slightly inflated, ventral side slightly depressed, umbilicate, consisting of 2½ whorls; periphery lobulate in side view, rounded in edge view; chambers somewhat inflated, 4½ or 5 in the last whorl; sutures slightly depressed, curved on dorsal side, radial and almost straight on the ventral side; wall consisting of chitinous material which collapses when dried; aperture a narrow slit at the base of the apertural face of the last chamber. Diameter up to *ca.* 0.17 mm.

Holotype (U. S. N. M. No. 626670) from station SD-35 (Lat. 32° 39.5′ N., Long. 117° 21.2′ W.; 104 fathoms). Length *ca.* 0.16 mm.; width *ca.* 0.14 mm.

Comparison.—This new species is chitinous and there is probably little chance of its being preserved as fossil, even in dried Recent sediments. The only comparable form is "*Haplophragmium nana* Brady var. *truncatulinoides* Rhumbler" (1911, pl. 24, fig. 15), which is a *nomen nudum* according to the Rules of Zoological Nomenclature. Rhumbler's figure is almost identical to the San Diego form but there is no way of confirming this identity since there is no description.

Tritaxis bullata (Höglund)

Plate 5, figures 23, 24

Trochamminella bullata HÖGLUND, 1947, Zoologiska Bidrag fran Uppsala, vol. 26, p. 213, pl. 17, fig. 5, text-figs. 194, 195.

The San Diego specimens are identical to the Höglund species except that they sometimes have a higher spire. In the population counts this species included *Trochammina* cf. *T. inconspicua* Earland because of the similarity of the two, both having a very small, globose test with 4 chambers in the last whorl. Both are deep water forms.

Arenoparrella oceanica Uchio, n. sp.

Plate 5, figures 25-27

Test small, nearly circular in outline, compressed, trochoid, ventral side more inflated than the dorsal side which is almost flat; periphery moderately rounded, all chambers visible from the dorsal side and only those of the last whorl from the ventral side which is umbilicate, chambers very slightly inflated, consisting of equidimensional, fine-grained sands, usually six in the last whorl; sutures depressed on both sides, oblique and almost straight on the dorsal side, radial on the ventral side; aperture a slit-like opening at the base of the last chamber extending from the periphery about half way to the umbilicus, its long axis oriented approximately parallel to the plane of coiling. Diameter up to *ca.* 0.13 mm.

Holotype (U. S. N. M. No. 626674) from station SD-240 (Lat. 32° 30′ N., Long. 117° 16.1′ W.; 40 fathoms). Diameter *ca.* 0.13 mm.

Comparison.—Only one other species belonging to this genus is known, *A. mexicana* (Kornfeld). *A. mexicana* is limited to a brackish marsh environment or to bays near marsh. *A. oceanica* differs from it in its smaller size (about one half), less inflated chambers, more coarsely arenaceous test, oblique sutures on the dorsal side, and the absence of an apertural lip.

Remarks.—According to the emended description of Andersen (1951, p. 96), this genus has supplementary openings at the apex of the final chamber. The writer has examined many specimens of the type species, *A. mexicana,* from Rockport, Texas, but none of them has supplementary openings, nor are they seen in *A. oceanica.*

The test of *A. oceanica* is fragile and usually collapses when dried so that it looks almost flat on both sides and the sutures are not distinct.

Family POLYMORPHINIDAE

Genus **Paradentalina** Uchio, n. gen.

Type species: *Paradentalina muraii* (Uchio)
= *Enantiodentalina muraii* Uchio

Test calcareous, elongate, subcylindrical, straight or slightly arcuate, chambers alternating in the early portion, uniserial in the adult and less embracing, sutures very oblique; aperture terminal, radiate, slightly projecting. Cretaceous to Recent.

Remarks.—The type species of *Enantiodentalina* Marie, 1941, is *Dentalina communis* d'Orbigny, which is also the type species of *Dentalina,* 1826. There has been some confusion about the type species of *Dentalina.* Jones (1883, p. 241) designated *Nodosaria (Dentalina) communis* d'Orbigny as the type species. Cushman (1948, p. 215) and Galloway (1933, p. 246) adopted *N.* (*D.*) *obliqua* d'Orbigny (designated by Galloway and Wissler, 1927). *N. communis,* however, has priority over *N. obliqua* as the type species of *Dentalina,* and *Enantiodentalina* becomes a synonym of *Dentalina.*

There is confusion about *Dentalina communis* d'Orbigny. D'Orbigny's *Dentalina communis* was described from Recent sediment of the Adriatic Sea, and has a uniserial series of chamber arrangement throughout, while Marie's *D. communis* d'Orbigny, which is the type species of *Enantiodentalina,* was described from the Cretaceous of France, and is biserial in the early portion and uniserial in the later portion, and thus can not be the same species as d'Orbigny's. The writer proposes a new genus for the forms which were referred to *Enantiodentalina.*

Paradentalina muraii (Uchio)

Plate 4, figure 2

Enantiodentalina muraii Uchio, 1953, Japanese Jour. Geology Geography, vol. 23, p. 152, pl. 14, figs. 1, 2.

This species was originally described from the Plio-Pleistocene of Japan, and was later found in the late Pleistocene of Japan. No living specimens have been found in the area studied. Clean tests of this species are found at 41, 56 and 64 fathoms at a very low frequency. The writer also has found 3 specimens from Recent sediments of the northeastern Gulf of Mexico at 47 fathoms. Therefore, this species seems to be limited to depths ranging from about 40 to 65 fathoms.

Family NONIONIDAE

Nonion lankfordi Uchio, n. sp.

Plate 4, figures 5-8

Test small, nearly circular in side view, umbilical area deeply depressed with its margin limbate and flush with the surface or slightly raised; wall moderately perforate, not thick; periphery broadly rounded; chambers distinct, inflated, about 8 in the last whorl, increasing in size as added; sutures limbate, flush with the surface in the early portion but depressed, slightly curved in the later portion; aperture a low arched opening at the base of the apertural face of the last chamber extending to the umbilical area.

Holotype (U. S. N. M. No. 626685) from station SD-287 (Lat. 32° 27.7′ N., Long. 117° 19.1′ W.; 50 fathoms). Length *ca.* 0.20 mm.; width *ca.* 0.16 mm.

Comparison.—This species is similar to *N. pacificum* (Cushman) (1942, p. 48, pl. 16, fig. 3) which was originally described from the Island of Samoa, Pacific, but differs from it by having limbate sutures and a limbate umbilical margin.

Nonion parkerae Uchio, n. sp.

Plate 4, figures 9, 10

Nonion umbilicatula (Montagu) var. *pacifica* Cushman (not Cushman, 1942), 1927, Scripps Inst. Oceanography, Bull., Tech. Ser., vol. 1, no. 10, p. 149, pl. 2, fig. 5.

Test small, compressed, nearly circular in side view; wall coarsely perforate, thick, umbilical area deeply depressed with its margin limbate, slightly raised; periphery narrowly rounded in edge view, lobulate in later portion in side view; chambers distinct, slightly inflated, slightly compressed near periphery, about 13 in the last whorl, increasing regularly in size as added; sutures strongly limbate, slightly curved; aperture a low arched slit at the base of the last chamber extending toward the umbilical area.

Holotype (U. S. N. M. No. 626687) from station SD-337 (Lat. 32° 38′ N., Long. 117° 31′ W.; 610 fathoms). Length *ca.* 0.39 mm.; width *ca.* 0.31 mm.

Comparison.—This new species is similar to *Nonion pacificum* Cushman but differs from it by having more chambers in the last whorl, limbate sutures, and a narrowly rounded periphery. It is very similar to *N. barleeanum* (Williamson), which was originally described from the vicinity of the British Isles. The writer has examined 16 specimens of *N. barleeanum* from the southwest of Ireland (N. Lat. 51° 12′, W. Long. 11° 55′, in 661-680 fathoms) and has found that the periphery of that species is rounded and lobulate, the test less coarsely perforate, and the sutures limbate and generally flush with the surface, rarely very slightly raised. *N. parkerae* has a lobulate periphery and less inflated chambers, particularly near the periphery, limbate and raised sutures, and a more coarsely perforate and rough surface. *N. affinis* (Reuss), which was originally described from the Oligocene of Hermsdorf, near Berlin, Germany, has a test which is slightly longer than broad, a broadly rounded and non-lobulate periphery, fewer chambers in the last whorl and slightly depressed and gently curved sutures.

Nonionella basispinata (Cushman and Moyer)

Plate 4, figures 13, 14

Nonion pizarrensis Berry var. *basispinata* Cushman and Moyer, 1930, Cushman Lab. Foram. Research, Contr., vol. 6, p. 54, pl. 7, fig. 18.

The number of chambers in the last whorl is not given in the original description. The figured specimen (holotype ?) has 12 chambers; its greater diameter or length is *ca.* 0.72 mm., and it has a narrowly rounded periphery (The figure in Ellis and Messina's *Catalogue of Foraminifera* has a sharply angular periphery and is a poor reproduction of the original figure). The type specimens were described from off San Pedro at 35-50 fathoms. The San Diego specimens show a wide range of variation. Young specimens have 10 chambers, but the adult (maximum size up to *ca.* 0.96 mm.) specimens usually have 14, rarely 15, chambers in the last whorl. Cushman and Moyer's figured specimen is larger but has fewer chambers in the last whorl, therefore the San Diego specimens can be considered as a subspecies. But it is necessary to determine the range of variation by studying many specimens from off San Pedro in order to determine whether or not the San Diego forms are a new subspecies.

The empty tests at station SD-3 are more inflated and have fewer (*ca.* 10) chambers in the last whorl. They are identical to *N. atlantica* Cushman (1947, p. 90, pl. 20, figs. 4, 5). The writer has examined 16 topotypes of *N. atlantica* deposited at the Scripps Institution of Oceanography and has found that they have about 10-11 chambers in the last whorl, and that most of them have a more inflated test, although a few have compressed tests. Such compressed forms are identical with the original figure of *N. basispinata.* From the above-mentioned facts it may be concluded that *N. atlantica* was present in the San Diego area during the Pleistocene, and that after the Panama Isthmus emerged *N. basispinata* developed from *N. atlantica. N. basispinata,* however, was described earlier than *N. atlantica,* therefore, *N. atlantica* is a subspecies of *N. basispinata.*

Nonionella stella Cushman and Moyer

Plate 4, figures 15, 16

Nonionella miocenica Cushman var. *stella* Cushman and Moyer, 1930, Cushman Lab. Foram. Research, Contr., vol. 6, p. 56, pl. 7, figs. 7a-c.

Nonionella pulchella Hada, 1931, Tohoku Imp. Univ. Sci. Rept., ser. 4, Biology, vol. 6, p. 120, fig. 79 (in text).

Nonionella basiloba Cushman and McCulloch, 1940, Allan Hancock Pacific Expeds., vol. 6, no. 3, p. 18, fig. 3.

Nonionella opima Cushman, 1947, Cushman Lab. Foram. Research, Contr., vol. 23, p. 90, pl. 20, figs. 1-3.

The writer has examined *N. miocenica* collected from the Upper Miocene siltstone at station SD-61. It is quite different from *N. stella* in having more inflated chambers, deeply depressed sutures, and more chambers in the last whorl. *N. stella* is not a variation nor a subspecies of *N. miocenica.*

N. stella has a wide range of morphological variation. The number of chambers in the last whorl varies from 7 to 9, usually 8. In typical *N. pulchella* the more chambers there are in the last coil, the longer and narrower they are, while the opposite is true of typical *N. stella.* The writer has examined many specimens from fine sands off Kushiro, Hokkaido, which is close to the type locality of *N. pulchella,* and from Yokosuka Harbor in Tokyo Bay, and has found that in every instance *N. stella* grades into *N. pulchella.* The stellate character of the inner end of the last chamber on the ventral side is quite variable. The young form has a very round lobe, smaller in proportion to the size of the test; the young adult specimen has a larger but non-stellate lobe; the adult specimen has a large lobe with finger-like processes over the previous sutures as found in typical *N. stella* and *N. pulchella.* Occasionally the last chamber becomes extraordinarily inflated with the end of the lobe reaching almost to the base of the test. Such forms are called *N. basiloba* (in the Pacific) or *N. opima* (in the Gulf of Mexico). F. L. Parker (1954, p. 507, pl. 6, figs. 10-12) showed such variation in *N. opima.* In the San Diego area the *N. basiloba* stage is smaller than typical *N. stella.*

This species occurs from shallow to deep water, but the typical forms are found in fine sands of shallow water.

Nonionella (?) **fragilis** Uchio, n. sp.

Plate 4, figures 19-21

Test free, small for the genus, biconvex, translucent, fragile; periphery broadly rounded in edge view, lobulate in side view; chambers usually 6-7 in the last whorl, rapidly increasing in size and inflation as added, last chamber slightly extended toward the umbilical area; sutures very distinct, deeply depressed, often with a narrow opening like a sutural supplementary aperture developed along the inner side of the sutures and spiral suture; wall very thin, very finely perforate; aperture a wide crescentic opening at the base of the apertural face of the last chamber, extending to the umbilical area.

Holotype (U. S. N. M. No. 626695) from station SD-337 (Lat. 32° 38′ N., Long. 117° 31′ W., 610 fathoms). Length *ca.* 0.23 mm.; width *ca.* 0.18 mm.; thickness *ca.* 0.10 mm.

Comparison.—This species is very easily distinguished from all the previously described ones by its deeply depressed sutures and sutural openings between chambers and whorls. It may belong to a new genus, but the writer prefers to wait until more similar species are known. Its general shape and structure resemble *Valvulineria,* but the aperture is closed off by the umbilical lobe.

Family ELPHIDIIDAE

Elphidium spinatum var. **translucens** Natland

Plate 4, figures 23, 24

Elphidium translucens Natland, 1938, Scripps Inst. Oceanography, Bull., Tech. Ser., vol. 4, no. 5, p. 144, pl. 5, figs. 3, 4.

According to the original description, this species has 12 to 13 chambers in the last whorl, but the many specimens examined by the writer have 9 to 12, usually 9 or 10. This form grades into *E. spinatum* Cushman and Valentine (1930, p. 21, pl. 6, figs. 1, 2) at the same localities, but is more common than the latter. Since *E. spinatum* has priority over *E. translucens,* the latter should be called a variety of the former, although the latter is the normal form and the former is the variant.

Family CERATOBULIMINIDAE

Alliatina and *Robertinoides* are here tentatively placed in this family, though there are some different opinions (*see* J. C. Troelsen, 1954).

Alliatina primitiva (Cushman and McCulloch)

Plate 4, figures 27, 28

Cushmanella primitiva Cushman and McCulloch, 1940, Allan Hancock Pacific Expeds., vol. 6, no. 3, p. 163, pl. 18, figs. 6-8, 10.

The test of this species is aragonitic and very thin and fragile. Therefore, the species is very rare in dried samples, though not rare in wet samples used for population counts of living specimens. In almost all cases the supplementary chambers are broken and consequently there is a large opening at the base of the apertural face of the last primary chamber.

Robertinoides charlottensis (Cushman)

Plate 4, figure 29

Cassidulina charlottensis Cushman, 1925, Cushman Lab. Foram. Research, Contr., vol. 1, p. 41, pl. 6, figs. 6, 7.

Robertina californica Cushman and Parker, 1936, *ibid.,* vol. 12, p. 97, pl. 16, fig. 14.

Höglund described *Robertinoides* which differed from *Robertina* d'Orbigny, 1846, in having a supplementary aperture at the base of the apertural face, which was believed not to be present in *Robertina.* F. L. Parker (1952, p. 416) discussed the relationship of the two genera.

The differentiation of species of this group is difficult, because they never occur abundantly and the range of variation within a species is not known. Therefore, it appears that more than one species has been erected for what in reality is one. Walton's figures of *Robertina charlottensis* (1955, p. 1014, pl. 102, figs. 11, 12) are identical to the young form of the San Diego specimens but do not show a supplementary aperture. *Robertina austriaca* Cushman and McCulloch (not Reuss) (1948, p. 240, pl. 29, figs. 9a-c) is also very close to the young form of the San Diego specimens but again has no supplementary aperture. Their figured specimen seems to be different from figured specimens of *Robertina austriaca* Reuss (Cushman and Parker, 1947, p. 73, pl. 18, figs. 8, 22) from the Miocene of the Vienna Basin.

Robertinoides charlottensis (Cushman) was originally described from Queen Charlotte Sound, British Columbia in 20-25 fathoms and *R. californica* (Cushman and Parker) was from the Pliocene of Santa Barbara, California (also reported from Timms Point, San Pedro, Calif.). The adult form of the San Diego specimens is identical to *R. californica.* Cushman and Parker (1947, p. 74) said that *R. californica* was related to, and probably the ancestral form of, *R. charlottensis.* The present writer believes that they are conspecific, *R. charlottensis* representing an abnormal form and *R. californica* a normal form. Loeblich and Tappan (1953, p. 109) examined holotypes and paratypes of the two species and concluded that they were conspecific.

The specimen figured by Cushman and McCulloch (1948, p. 241, pl. 29, fig. 10) as *Robertina californica* is not referrable to either *Robertina* or *Robertinoides.*

Family BULIMINIDAE

Virgulina apertura Uchio, n. sp.

Plate 6, figure 11

Test very small, inflated, fusiform, both ends gradually tapering, biserial, slightly twisted, about twice as long as broad; chambers numerous, much inflated, increasing very rapidly in size as added, usually the last two chambers occupying *ca.* ¾ - ⅘ of the test, each chamber embracing almost all of the previous chambers; sutures distinct, depressed; wall thin, very finely perforate, translucent; aperture very large, nearly triangular in shape or broadly arched as in *Pleurostomella*, but without teeth at either side of the apertural base.

Holotype (U. S. N. M. No. 626719) from station SD-267 (Lat. 32° 22.8′ N., Long. 117° 20.6′ W.; 615 fathoms). Length *ca.* 0.24 mm.; width *ca.* 0.11 mm.

Comparison.—This new species can easily be distinguished from other species of this genus by its very large aperture and very large *Globobulimina*-like last two chambers.

Virgulina complanata Egger

Plate 6, figure 13

Virgulina schreibersiana Czjzek var. *complanata* EGGER, 1895, Abhandl. k. bay. Akad. Wiss. München, vol. 18, pt. 2, p. 292, pl. 8, figs. 91, 92.

Virgulina davisi CHAPMAN and PARR, 1937, Australasian Antarctic Exped. 1911-1914, Sci. Repts., ser. C, vol. 1, pt. 2, p. 88, pl. 8, fig. 15.

Virgulina concava HÖGLUND, 1947, Zoologiska Bidrag fran Uppsala, vol. 26, p. 257, pl. 23, figs. 3, 4; pl. 32, figs. 4-7; text-figs. 273-275.

Virgulina loeblichi FEYLING-HANSSEN, 1954, Norsk Geol. Tidsskr., Bergen, vol. 33, no. 3-4, p. 191, pl. 1, figs. 14-18; p. 192, text-fig. 3.

Höglund described *V. concava* in detail, but was not sure whether or not his species was a synonym of *V. davisi.* His figures 3 and 4 on plate 23 show the broadest portion to be in the middle of the test, but figures 4-7 and text-figure 273 show it at the apertural end. Feyling-Hanssen shows similar variation in *V. loeblichi.*

The original figure of *V. complanata* is also not complete but the later interpretation of this species seems to be established as shown in the studies of Cushman (1937, p. 26, pl. 4, figs. 14-17, and 13 (?)), Phleger and Parker (1951, pl. 9, figs. 1-3) and Parker (1954, pl. 7, fig. 6). The San Diego specimens are identical to those of *V. complanata* from the Gulf of Mexico and the North Atlantic.

Virgulina delicatula Uchio, n. sp.

Plate 5, figure 4

Test very small for the genus, slightly twisted, triserial stage short, later biserial, elongate, fusiform, tapering toward both ends, sometimes slightly curved, broadest above the middle of the test or near the apertural end, basal end rounded, apertural end pointed, ventral side of initial portion slightly compressed; periphery non-lobulate, rounded; chambers somewhat inflated, increasing somewhat rapidly in size as added; sutures slightly depressed; aperture terminal, broadly loop-shaped; wall thin, very finely perforate, translucent.

Holotype (U. S. N. M. No. 626724) from station SD-250 (Lat. 32° 30.9′ N., Long. 117° 20.4′ W.; 390 fathoms). Length *ca.* 0.30 mm.; width *ca.* 0.09 mm.

Comparison.—This species is closely related to *V. mexicana* Cushman (1922, p. 120, pl. 23, fig. 8), but is much more slender, smaller in size, and has more chambers. *V. delicatula* is also similar to *V. bradyi* Cushman (1922, p. 115, pl. 24, fig. 1), which was originally described from deep water of the western Atlantic, but differs from it in its non-lobulate periphery, less depressed sutures, pointed apertural end, more rapid increase in size, much smaller size (about a half), and thinner, fragile test.

Virgulina sandiegoensis Uchio, n. sp.

Plate 6, figures 17, 18

Test minute, elongate, oval in cross section, broadest near the apertural end, tapering toward the initial end which is rounded and without a spine; chambers inflated, increasing in height and size as added, particularly in the last few chambers, triserial part very short, indistinct, usually 4-6 pairs making up the biserial part; sutures distinct, depressed; periphery slightly lobulate in side view and broadly rounded in edge view; wall of each chamber with a band of clear shell material surrounding a finely perforate and relatively opaque area, the clear shell area iridescent; aperture subterminal, elongately oval.

Holotype (U. S. N. M. No. 626728) from station SD-240 (Lat. 32° 30′ N., Long. 117° 16.1′ W.; 40 fathoms). Length *ca.* 0.26 mm.; width *ca.* 0.07 mm.

Comparison.—This new species has a shape which is transitional between *Bolivina pacifica* Cushman and McCulloch and *Virgulina seminuda* Natland. However, it can be easily distinguished from *V. seminuda* in having the broadest portion near the apertural end, and a slightly lobulate periphery. It differs from *B. pacifica* in having a more inflated and twisted test, a lobulate, broadly rounded periphery, and fewer chambers.

Bolivina peirsonae Uchio, n. sp.

Plate 7, figures 3, 4

Bolivina pygmaea CUSHMAN (not Brady 1881), 1927, Scripps Inst. Oceanography, Bull., Tech. Ser., vol. 1, no. 10, p. 156, pl. 3, fig. 9; CUSHMAN and MCCULLOCH (part), 1942, Allan Hancock Pacific Exped., vol. 6, no. 4, p. 204, pl. 25, figs. 9-12 (not 8).

Test stout, large, slightly twisted; periphery broadly rounded in edge view, serrate in side view; chambers comparatively few, 15 at maximum, distinct, later ones becoming distinctly inflated and terminated by a distinct short spine at the outer posterior angle, early chambers smooth and more compressed; sutures distinct, greatly depressed especially in the later chambers, wall smooth, very finely perforate, translucent; aperture broadly oval, at the base of the last chamber in the median line.

Holotype (U. S. N. M. No. 626739) from station SD-290 (Lat. 32° 26.3′ N., Long. 117° 22.9′ W.; 550 fathoms). Length *ca.* 0.51 mm.; width *ca.* 0.25 mm.

Comparison.—Cushman and McCulloch included this species with *Suggrunda eckisi* Natland. Only one of their figures (*op. cit.* pl. 25, fig. 8), however, represents that species. *B. peirsonae* can be easily distinguished from it by its much larger test, more inflated chambers which are differently shaped, and much more depressed sutures.

Bolivina subargentea Uchio, n. sp.

Plate 6, figures 21, 22

Bolivina argentea CUSHMAN and McCULLOCH (not Cushman 1926), 1942, Allan Hancock Pacific Expeds., vol. 6, no. 4, p. 188, pl. 22, figs. 2-4 (not 5); WALTON, 1956, Jour. Paleontology, vol. 29, p. 1001, pl. 101, figs. 26, 27.

Bolivina interjuncta Cushman var. *bicostata* CUSHMAN and McCULLOCH (not Cushman 1926) (part), 1942, Allan Hancock Pacific Expeds., vol. 6, no. 4, p. 195, pl. 23, fig. 15 (not figs. 9-11, 13, 14, 16).

Test usually triangular, elongate, about 2½ to 3 times as long as broad, very much compressed, periphery acute, usually keeled; chambers very distinct, narrow in the young, in the adult about 2½ times as long as broad; sutures oblique and curved, early ones limbate but somewhat depressed; wall very finely perforate, smooth except for the very basal portion which usually has a short spine and one or more weak costae extending from proloculus to the second or third pair of chambers; aperture an elongate, narrow opening occupying the whole area of the apertural face; color light silvery grey, polished. Length up to 1.29 mm.; breadth 0.50 mm.

Holotype (U. S. N. M. No. 626744) from station SD-62 (Lat. 32° 40.9′ W., Long. 117° 26.7′ W.; 247 fathoms). Length *ca.* 1.01 mm.; breadth *ca.* 0.42 mm.

Comparison.—This is one of the characteristic and abundant forms of the western coast of America, and has been wrongly referred by most workers to *B. argentea* Cushman (1926, p. 42, pl. 5, fig. 5). This species, however, differs from it in having a short spine at the basal end and a keeled periphery. The width of the test increases very gradually with growth in the microspheric form, but in the megalospheric form increases slowly after the first few chambers.

Bolivina vaughani Natland

Plate 5, figure 2

Bolivina vaughani NATLAND, 1938, Scripps Inst. Oceanography, Bull., Tech. Ser., vol. 4, no. 5, p. 146, pl. 5, fig. 11.

There are two forms of *Bolivina* which are very similar and may represent juveniles and adults of the same species. The adult specimens are probably referrable to *B. vaughani* although the writer has not been able to compare them with types. Comparative specimens, however, in the Marine Foraminifera Laboratory collection of the Scripps Institution of Oceanography, have been compared with the holotype by Miss F. L. Parker. The smaller specimens, which may represent juveniles, are conspecific with *B. lowmani* Phleger and Parker.

It is difficult to separate *B. vaughani* and *B. lowmani* in wet samples, and for this reason they have been listed together as *B. vaughani* in the population counts (Part I: Ecology, Tables 1-3, 5-7). The writer has examined Walton's (1955) specimens, which are deposited in the Marine Foraminifera Laboratory, and has found that his *B. vaughani* includes two other species, *B. lowmani* and *B. subexcavata* Cushman and Wickenden. Most of his specimens, however, may be referred to *B. vaughani.*

Loxostomum bradyi (Asano)

Plate 7, figure 9

Bolivina beyrichi BRADY (not Reuss 1851), 1884, Rept. Voy. *Challenger,* Zool., vol. 9, p. 422, pl. 53, fig. 1.

Bolivina bradyi ASANO, 1938, Geol. Soc. Japan, Jour., vol. 45, p. 603, pl. 16, fig. 2.

Loxostomum instabile CUSHMAN and McCULLOCH, 1942, Allan Hancock Pacific Expeds., vol. 6, no. 4, p. 221, pl. 27, figs. 15-17; pl. 28, figs. 1-7.

Bolivina bramlettei CUSHMAN and McCULLOCH (not Kleinpell 1938), 1942, *op. cit.*, p. 189, pl. 22, figs. 7-13.

According to Cushman and McCulloch there is a great deal of variation in this species as was shown by their figures. The San Diego specimens show such variation. Young specimens show a *Bolivina*-like character and are identical with their figures of "*Bolivina bramlettei.*" However, *B. bramlettei* Kleinpell, which was originally described from the Miocene of California, differs from *Loxostomum bradyi* in having a more inflated test and sinuous sutures. *B. bramlettei* is found only in the upper Miocene siltstone at station SD-61 in the Loma Sea Valley.

Globobulimina hoeglundi Uchio, n. sp.

Plate 6, figures 7, 8

Bulimina subaffinis WALTON (not Cushman 1921), 1955, Jour. Paleontology, vol. 29, p. 1004, pl. 102, fig. 14.

Test fusiform in side view and circular in end view, apical end sharply pointed but without a spine in the microspheric form and rounded in megalospheric form, broadest part a little above the middle of the test; sutures sometimes slightly limbate but depressed, particularly in the neighborhood of the aperture, nearly horizontal at the base of the chamber; chambers distinct, moderately inflated, the last one extending half way back to the apical end; wall smooth, thin, hyaline, translucent, finely perforate particularly in the last chamber; aperture a loop-shaped opening filled with a somewhat fan-shaped tooth. Length up to *ca.* 0.76 mm. in the microspheric form and 1.0 mm. in the megalospheric form; breadth up to *ca.* 0.36 mm. in the microspheric form and 0.5 mm. in the megalospheric form.

Holotype (U. S. N. M. No. 626714), microspheric form, and paratype (U. S. N. M. No. 626715), megalospheric form, from station SD-337 (Lat. 32° 38′ N., Long. 117° 31′ W.; 610 fathoms). Length *ca.* 0.76 mm.; width *ca.* 0.36 mm.

Comparison.—Globobulimina sp. C of Höglund (1947, p. 247, pl. 21, fig. 3; pl. 22, fig. 4; text-figs. 243-246) may be conspecific with this new species. *G.* sp. C was originally described from the Gulf of Mexico, based on 10 specimens of which only one is a microspheric form. This species is also similar to *Globobulimina subaffinis* (Cushman) (1921, p. 166, text-fig. 7), which was originally described from Sogod Bay, southern Leyte, Philippines, in 554 fathoms, but differs from it in having a greater number of chambers, the broadest portion above the middle of the test (at the middle in *G. subaffinis*), and nearly horizontal sutures at the base of the chambers.

Uvigerina auberiana d'Orbigny

Plate 7, figure 11

Uvigerina auberiana D'ORBIGNY, 1839, *in* De la Sagra, Hist. Phys. Pol. Nat. Cuba, "Foraminifères," vol. 8, p. 106, pl. 2, figs. 23, 24.

Uvigerina ampullacea BRADY, 1884, Rept. Voy. *Challenger*, Zool., vol. 9, p. 579, pl. 75, figs. 10, 11.

Uvigerina proboscidea Schwager var. *vadescens* CUSHMAN, 1933, Cushman Lab. Foram. Research, Contr., vol. 9, p. 85, pl. 8, figs. 14, 15.

The Pacific species is identical with *U. auberiana* found in many parts of the North Atlantic, in the Gulf of Mexico, and at Culebra Island, north of St. Thomas, West Indies. *U. ampullacea* is within the range of variation of *U. auberiana. U. proboscidea* var. *vadescens*, although it was described from shallow water (21 fathoms), Guam Anchorage, Ladrone Island, is also within the range of variation. *U. auberiana bella* Bandy (a new name for *U. auberiana laevis* Goës, not Ehrenberg) (1956, p. 199, pl. 31, fig. 13) is probably a synonym of *U. auberiana*.

Uvigerina curticosta Cushman

Plate 7, figures 12, 13

Uvigerina pigmea d'Orbigny var. *curticosta* CUSHMAN, 1927, Scripps Inst. Oceanography, Bull., Tech. Ser., vol. 1, no. 10, p. 157, pl. 4, fig. 1.

Uvigerina peregrina Cushman var. *curticosta* Cushman, TODD (*in* CUSHMAN and MCCULLOCH), 1948, Allan Hancock Pacific Expeds., vol. 6, no. 5, p. 266, pl. 34, figs. 2a, b.

Uvigerina peregrina Cushman var. *dirupta* TODD (*in* CUSHMAN and MCCULLOCH), 1948, *ibid.*, p. 267, pl. 34, figs. 3a-c.

Uvigerina peregrina BANDY (not Cushman 1923), 1953, Jour. Paleontology, vol. 27, no. 2, p. 177, pl. 25, figs. 1a, b.

Uvigerina peregrina was described from Albatross Station D2029 in 1168 fathoms off the northeastern coast of the U. S. A. The writer has compared the Pacific specimens of so called *U. peregrina* with topotypes and many other specimens from many parts of the Atlantic and finds that the Atlantic and Pacific species differ from each other and are quite distinct. The Pacific species has on each chamber fewer but more prominent costae, which are more plate-like than those of the Atlantic species. *U. peregrina* var. *dirupta* Todd is not a variety of *U. peregrina*, but is gradational into *U. curticosta* and is included with that species in the population counts (Part I: Ecology, Tables 1-3, 5-7). However, *U. dirupta* is generally found in deep water and *U. curticosta* in relatively shallow water. Thus the two forms are gradational in morphological character but seem to prefer different environments and are worth separating from the ecological point of view.

Uvigerina peregrina Cushman var. *latalata* R. E. and K. C. Stewart (1930, p. 66, pl. 8, fig. 7) may be conspecific with *U. curticosta*.

Uvigerina juncea Cushman and Todd

Plate 7, figures 15-17

Uvigerina juncea CUSHMAN and TODD, 1941, Cushman Lab. Foram. Research, Contr., vol. 17, p. 78, pl. 20, figs. 4-11.

Uvigerina cushmani TODD (*in* CUSHMAN and MCCULLOCH), 1948, Allan Hancock Pacific Expeds., vol. 6, no. 5, p. 257, pl. 33, figs. 1a, b.

Uvigerina hollicki Thalmann (1950, p. 45) was originally described from off the northeastern coast of the U. S. A. (1781 fathoms) under the name of *U. peregrina* Cushman var. *bradyana* Cushman (not Fornasini 1900) (1923, p. 168, pl. 42, fig. 12). It is different from the form which has been called *U. hollicki* in the Pacific. The latter should be referred to *U. juncea*.

U. cushmani is very variable in its morphological character as was shown in the original figures. The costae are weak and often disappear entirely so that the surface, particularly that of the last few chambers, becomes rather smooth. The fully costate form has been called *U. cushmani*, the gradational form *U. juncea*, and the smooth form *U. hollicki* in the Pacific. Todd says that *U. cushmani* has more prominent costae than *U. juncea*, but it should be taken into account that the latter is a fossil form and its costae may be somewhat worn. The forms which Todd (1948) called *U. bradyana*, *U. senticosa* and *U. hollicki*, and which Bandy (1953) called *U. hollicki*, all seem to be referable to *U. juncea*.

The writer has examined 12 paratypes of *U. senticosa* Cushman deposited at the Scripps Institution of Oceanography. They are large in size, brownish in color, and are probably fossils. This species is quite distinct from *U. juncea*.

In the present study the writer has separated three types of *U. juncea* (costate, intermediate, smooth forms), but the separation is quite artificial and there is no definite boundary between them. Therefore they are combined and listed as *U. juncea* in the tables (Part I: Ecology, Tables 1-3, 5-7).

Angulogerina carinata (Cushman)

Plate 7, figure 19

Angulogerina carinata Cushman, 1927, Scripps Inst. Oceanography, Bull., Tech. Ser., vol. 1, no. 10, p. 159, pl. 4, fig. 3.

Angulogerina carinata Cushman var. *bradyana* Cushman, 1932, Cushman Lab. Foram. Research, Contr., vol. 8, p. 45, pl. 6, figs. 9, 10.

Angulogerina carinata Cushman var. *vana* Todd, 1948, Allan Hancock Pacific Expeds., vol. 6, no. 5, p. 287, pl. 35, fig. 10.

This species is omitted from the tables (Part I: Ecology, Tables 1-3, 5-7) since living specimens have been found at only four stations at depths of 118 fathoms (0.1%), 121 fathoms (0.1%), 125 fathoms (0.1%) and 167 fathoms (1%). They are all typical forms. Dead specimens are found widely but in low frequency in Recent sediments in the San Diego Trough and in Pleistocene sediments. They include both typical and variant forms.

Family DISCORBIDAE

Rosalina campanulata (Galloway and Wissler)

Plate 7, figure 26

Globorotalia campanulata Galloway and Wissler, 1927, Jour. Paleontology, vol. 1, p. 58, pl. 9, fig. 14.

Rotalia versiformis Bandy, 1953, *ibid.*, vol. 27, p. 179, pl. 22, fig. 5.

Rotalia lomaensis Bandy, 1953, *loc. cit.*, pl. 22, fig. 6.

Rotalia spp. Walton, 1955, *ibid.*, vol. 29, p. 1014, pl. 103, figs. 18, 19, 24.

This species was originally described from the Pleistocene of Lomita Quarry, San Pedro, California, and is variable in its umbilical character as the original authors mentioned "the umbilicus depressed or sometimes with a rounded knob of clear shell material." The writer has examined topotypes of *R. campanulata* and finds that *R. versiformis* and *R. lomaensis* are synonyms of *R. campanulata.*

Rosalina columbiensis (Cushman)

Plate 8, figures 1, 2

Discorbis columbiensis Cushman, 1925, Cushman Lab. Foram. Research, Contr., vol. 1, p. 43, pl. 6, fig. 13.

This species is very variable in its morphological character. The number of chambers in the last whorl is 4-6, usually 5-6. The shape and size are variable, particularly in the last one or two chambers. When the last one or two chambers are irregular, the number of chambers in the last whorl is only 4. A progressively greater size of the perforations on the dorsal side with growth is characteristic.

It is observed in the tide pools north of The Scripps Institution's pier that a few living specimens of *Tretomphalus bulloides* (d'Orbigny) occur together with many specimens of *R. columbiensis*, and the former seems to be a reproductive stage of the latter. This relationship can be ascertained only by culturing the species in a laboratory.

Rosalina sp.

Plate 7, figures 22-25

Discorbis rosacea Cushman and Valentine (not *Rotalia rosacea* d'Orbigny 1826), 1930, Dept. Geology Stanford Univ., Contr., vol. 1, no. 1, pl. 6, fig. 5.

Discorbis spp. Walton, 1955, Jour. Paleontology, vol. 29, p. 1006, pl. 102, figs. 27-29.

Cushman (1931, p. 31) examined many topotypes of "*Rotalia rosacea*" from the Miocene of Bordeaux, France, and concluded that the species was an *Amphistegina*.

This species is variable in its umbilical character as is *R. campanulata*. That is, the umbilical plug is large or small and sometimes even disappears. This species occurs with *R. campanulata* at many stations and is sometimes difficult to distinguish from it. The two species are combined in the population counts and are listed as *R. campanulata* in the tables (Part I: Ecology, Tables 1-3, 5-7).

Gyroidina quinqueloba Uchio, n. sp.

Plate 8, figures 22-25

Test free, small for the genus, nearly circular in side view, trochoid, consisting of 2½ or 3 whorls, all visible on the dorsal side, only the last one on the ventral side; dorsal side slightly convex but more so in the early portion, ventral side strongly convex, umbilicus slightly depressed but usually hidden by the last chamber; periphery broadly rounded in apertural view; chambers inflated, relatively few, usually 5 in the last whorl, increasing rather rapidly in size as added; wall thin, finely perforate; sutures distinct, depressed, very slightly limbate, nearly radial on the dorsal side, nearly radial but slightly curved on the ventral side; aperture an elongate narrow slit at the base of the apertural face of the last chamber midway between the umbilicus and periphery, with a distinct lip.

Holotype (U. S. N. M. No. 626792), from station SD-326 (Lat. 32° 46.3′ N., Long. 117° 31.2′ W.; 385 fathoms). Length *ca.* 0.14 mm.; width *ca.* 0.13 mm.; thickness *ca.* 0.09 mm.

Comparison.—This species is closely related to *Gyroidina umbonata* (Silvestri) (*Rotalia soldanii* d'Orbigny var. *umbonata* Silvestri, 1898, p. 329, pl. 6, fig. 14), which was originally described from the Pliocene of Italy. The writer has examined 11 specimens of *G. umbonata* from the Pliocene of Ponticello, near Bologna, Italy. *G. quinqueloba* differs from *G. umbonata* in its smaller size (*ca.* ½ in diameter), thinner test, much less convex ventral side, less broadly rounded periphery, and shorter aperture (aperture of *G. umbonata* extends from periphery to umbilicus). This species may be a subspecies of *G. umbonata*.

Eponides leviculus (Resig)

Plate 10, figures 23-25

Epistominella levicula Resig, 1958, Micropaleontology, vol. 4, p. 304, text-fig. 16.

Remarks.—Resig considered this species an *Epistominella*. The present writer has examined many specimens and finds that the aperture is a narrow slit with a lip midway between the umbilicus and the periphery, though the test has a slight indentation of the wall of the last septal face which is parallel to the periphery on the ventral side and has, like *Alabamina*, no opening into the interior of the chamber. This species may be an *Alabamina*, whose geologic range has hitherto been limited to the Tertiary, but it has a lip around the aperture and the wall is rather coarsely perforate. Therefore, the writer has tentatively placed it in *Eponides*.

Buccella angulata Uchio, n. sp.

Plate 9, figures 1-3

Test small, trochoid, biconvex with the dorsal side slightly convex and ventral side convex, with a depressed umbilicus, composed of about 3 whorls with 5 (rarely 6) chambers in the last whorl; periphery angular in edge view, rounded and slightly lobulated in side view; sutures on the ventral side depressed, nearly radial, partly covered with opaque pustulose material, those on the dorsal side limbate, slightly depressed or flush with the surface, oblique and slightly curved; aperture at the base of the apertural face of the last chamber on the ventral side with supplementary apertures along the ventral sutures.

Holotype (U. S. N. M. No. 626806) from station SD-50 (Lat. 32° 41.6′ N., Long. 117° 19.6′ W.; 53 fathoms), living when collected. Diameter *ca.* 0.18 mm.

Comparison.—This species is similar to *B. frigida* (Cushman), but differs from it in having fewer chambers in the last whorl, an angular periphery and nearly plano-convex test. This species is also close to *B. inusitata* Andersen, but differs from it in the smaller size of the test and fewer chambers in the last whorl (*B. inusitata* usually has 9 chambers). Furthermore, the megalospheric form of *B. inusitata* has an equally biconvex test and the microspheric form has a nearly flat ventral side and a very convex dorsal side, while *B. angulata* has a nearly flat dorsal side and very convex ventral side.

Asterigerinata pacifica Uchio, n. sp.

Plate 10, figures 26-31

Test small, compressed, very slightly convex on the dorsal side, slightly concave on the ventral side, with secondary plates forming over the apertures and extending to the periphery to form a star-shaped central portion; periphery narrow, rounded in the megalospheric (?) form, acute and keeled in the microspheric (?) form; chambers 6-6½ in the last whorl, increasing gradually in size as added, uninflated in the microspheric (?) form, slightly inflated in the megalospheric (?) form, each secondary plate successively covering the aperture of the previous chamber; sutures on the dorsal side slightly limbate, slightly curved, on the ventral side slightly depressed; wall thin, finely perforate, often translucent; aperture loop-shaped, large, occupying more than half of the last chamber. Maximum diameter 0.15 mm.

Holotype (U. S. N. M. No. 626810), megalospheric (?) form; paratype (U. S. N. M. No. 626811), microspheric (?) form, from station SD-186 (Lat. 32° 31′ N., Long. 117° 18′ W.; 248 fathoms) (empty tests). Diameter of holotype *ca.* 0.13 mm.; paratype *ca.* 0.15 mm.

Comparison.—This species is similar to *A. pulchella* (F. L. Parker) (Parker, 1952, p. 420, pl. 6, figs. 18-20), which was described from shallow sediments in the Atlantic, but differs from it in having fewer chambers (6-6½ in the former, 7-9 in the latter) in the last whorl, in having the secondary plates extending to the periphery (except in young forms) rather than extending only halfway to the periphery as in *A. pulchella*, and in the larger aperture. The microspheric (?) form of this new species is similar to *A. nitidula* (Chaster) which was described from off the coast of England, but differs from it in having fewer chambers (*A. nitidula* has 8 chambers in the last whorl).

Remarks.—There are two forms of this genus in the San Diego area, one with a rounded periphery and the other with a keeled periphery. The number of chambers in the last whorl is the same in both forms, which were found together at three stations (all specimens dead when collected). Therefore, the writer considers the two forms to be conspecific, one megalospheric (?) and the other microspheric (?). Living specimens were found only at shallow depths, 10.5, 13 and 45 fathoms. Dead specimens were found at 9-430 fathoms. The writer has also found the species in Todos Santos Bay, Baja California, Mexico, at a depth of 28 fathoms.

Heminwayina Bermudez, 1951, seems to be a synonym of *Asterigerinata* Bermudez, 1948, though Bermudez says that the aperture of the former is larger than that of the latter and occupies only the basal area of the last chamber. The aperture of *Heminwayina gallowayi* Bermudez is low, arch-shaped, and the species seems to belong to *Asterigerinata.*

Family CASSIDULINIDAE

Epistominella sandiegoensis Uchio, n. sp.

Plate 9, figures 6, 7

Test free, trochoid, biconvex, slightly umbilicate, nearly circular but slightly truncate on the apertural side; periphery narrowly rounded in edge view, slightly lobulate in side view; chambers distinct, numerous, 4 to 6, usually 6, in the last whorl, slightly inflated on the dorsal side, more so on the ventral side; sutures distinct, slightly limbate, flush with the surface but sometimes very slightly depressed, oblique and straight on the dorsal side, slightly curved and very slightly recurved on the ventral side; wall smooth, finely perforate; aperture elongate, narrow, nearly parallel to the periphery.

Holotype (U. S. N. M. No. 626812) from Station SD-265 (Lat. 32° 23.2′ N., Long. 117° 19.5′ W.; 350 fathoms). Length *ca.* 0.21 mm.; width *ca.* 0.18 mm.

Comparison.—This new species differs from *E. bradyana* (Cushman) in having fewer chambers (*E. bradyana* usually has 8) in the final whorl, a less sharply angled periphery, and straight sutures on the dorsal side. It differs from *E. exigua* (Brady) in its smaller size, more rounded periphery, and in having usually 6 chambers in the last whorl (*E. exigua* has 5). It is possible that a study of the types of *E. exigua* will show that *E. sandiegoensis* bears a subspecific relationship to Brady's species.

Remarks.—Natland (1933), Bandy (1953) and Walton (1955) did not record *E. sandiegoensis.* The writer, however, has found many specimens in samples from Sebastian Vizcaino Bay, Mexico.

Cassidulina bradshawi Uchio, n. sp.

Plate 9, figures 11, 12

Test small, nearly circular in side view, lenticular in edge view; periphery rounded, not lobulated; sutures very slightly depressed, nearly straight except near the periphery; chambers usually 4 pairs, but sometimes 5 pairs, in the last coil; wall thin, transparent, hyaline, smooth; aperture an elongate slit following the curve of the previous chamber, with a tooth.

Holotype (U. S. N. M. No. 626818) from station SD-254 (Lat. 32° 30.2′ N., Long. 117° 22.8′ W.; 465 fathoms). Length *ca.* 0.28 mm.; width *ca.* 0.23 mm.

Comparison.—This new species is similar to *C. islandica norvangi* Thalmann (*in* Phleger, 1952, p. 83, pl. 14, fig. 30), but differs from it by having a nonlobulated periphery, less depressed sutures and a thinner wall.

Cassidulina delicata Cushman

Plate 9, figure 17

Cassidulina delicata CUSHMAN, 1927, Scripps Inst. Oceanography, Bull., Tech. Ser., vol. 1, no. 10, p. 168, pl. 6, fig. 5.

Cassidulina cushmani R. E. and K. C. STEWART, 1930, Jour. Paleontology, vol. 4, p. 71, pl. 9, figs. 5a, b.

The writer has examined many specimens of this species. Cushman's original figure is not representative and for this reason R. E. and K. C. Stewart described *C. cushmani,* the figures of which are like specimens within the range of variation of *C. delicata.* Both types, together with gradational specimens, have been found together at many stations, but most specimens are of the "*C. cushmani*" type. Some adult specimens have a peripheral keel; many have no keel but a sharply angled periphery.

Cassidulina depressa Asano and Nakamura

Plate 9, figures 18, 19

Cassidulina subglobosa depressa ASANO and NAKAMURA, 1937, Japanese Jour. Geology Geography, vol. 14, nos. 3-4, p. 148, pl. 13, figs. 8a-c.

San Diego specimens have been compared with topotypes from Sematanoseki, Shito-mura, Chiba-ken, Japan, and found to be conspecific, although they are a little smaller.

It is difficult to separate this species from young forms of *C. californica. Cassidulina subglobosa* var. *subcalifornica* Drooger (1953, p. 140, pl. 22, figs. 8, 9) seems to be a synonym of *C. depressa.*

Cassidulina subcarinata Uchio, n. sp.

Plate 9, figures 15, 16

Cassidulina laevigata WALTON (not d'Orbigny 1826), 1955, Jour. Paleontology, vol. 29, p. 1004, pl. 104, figs. 2, 7.

Test small, biconvex, lenticular in edge view, periphery slightly lobulate, acute with a narrow keel; central umbilical region mostly clear, showing the chambers of the earlier coils; chambers distinct, elongate, 3-4 pairs but usually 4 pairs in the last coil, slightly inflated; sutures distinct, slightly depressed, slightly curved; wall thin, finely perforate, semi-translucent; aperture

(254)

an elongate, narrow slit parallel to the periphery, with a thin triangular tooth.

Holotype (U. S. N. M. No. 626827) from station SD-290 (Lat. 32° 26.3′ N., Long. 117° 22.9′ W.; 550 fathoms). Length *ca.* 0.21 mm.; width *ca.* 0.18 mm.; thickness *ca.* 0.09 mm.

Comparison.—This new species most closely resembles *C. laevigata* var. *carinata* Silvestri (1896, p. 104, pl. 2, figs. 10a-c) which was described from the Pliocene of Italy. The writer has examined many topotypes from Coroncina, Italy. *C. carinata* has a larger test, more curved sutures, but has not the translucent umbilical area through which chambers of earlier coils are seen, which is characteristic of *C. subcarinata.*

C. subcarinata is similar to *C. neocarinata* Thalmann described from Recent sediments off Florida at 75 fathoms, but differs from it in having a thicker, more coarsely perforate, less translucent wall, and a less distinct keel. Many specimens of *C. neocarinata* from the Gulf of Mexico were studied for comparison.

C. subcarinata is also similar to *C. norcrossi* Cushman (1933, p. 7, pl. 2, figs. 7a-c) and *C. kasiwazakiensis* Husezima and Maruhasi (1944, p. 399, pl. 34, figs. 13a-c) but differs from them in having a tooth in the aperture and differently shaped chambers (*C. norcrossi* and *C. kasiwazakiensis* have wedge-shaped chambers).

Cassidulina tortuosa Cushman and Hughes

Plate 9, figure 23

Cassidulina tortuosa Cushman and Hughes, 1925, Cushman Lab. Foram. Research, Contr., vol. 1, p. 14, pl. 2, figs. 4a-c.

Cassidulina reflexa Galloway and Wissler, 1927, Jour. Paleontology, vol. 1, p. 80, pl. 12, figs. 13a, b.

Cassidulina wakasaensis Asano and Nakamura, 1937, Japanese Jour. Geology Geography, vol. 14, nos. 3-4, p. 149, pl. 14, figs. 7a-c.

Cassidulina tumida Natland, (not *C. laevigata* var. *tumida* Heron-Allen and Earland, 1922), 1938, Scripps Inst. Oceanography, Bull., Tech. Ser., vol. 4, p. 148, pl. 6, figs. 2, 3a, b.

Natland's *C. tumida* is very rare, found only in Pleistocene "Foraminifera sand." It seems to be an irregular variety of *C. tortuosa.*

Cassidulinoides waltoni Uchio, n. sp.

Plate 9, figures 24-27

Cassidulinoides sp. Walton, 1955, Jour. Paleontology, vol. 29, p. 1005, pl. 104, fig. 1.

Test compressed, elongate, slightly convex on the dorsal side; periphery sometimes slightly lobulated, narrowly rounded; earliest portion closely coiled, later portion uncoiled, biserial; initial end rounded in the megalospheric form; chambers elongate, distinct, narrow, depressed, strongly oblique; wall thin, smooth, polished; aperture large, elongately oval and slightly comma-shaped in a depression of the apertural face.

Holotype (U. S. N. M. No. 626833) from station SD-288 (Lat. 32° 27.2′ N., Long. 117° 20.6′ W.; 140 fathoms). Length *ca.* 0.69 mm.; width *ca.* 0.24 mm.

Comparison.—This new species is similar to *C. simplex* Cushman and Todd (1945, p. 63, pl. 10, fig. 15) in side view but the latter has a cylindrical test and indistinct sutures.

Family ANOMALINIDAE

Cibicides phlegeri Uchio, n. sp.

Plate 10, figures 7-10

Test very small, fragile, convex on the ventral side with a slightly depressed umbilicus, flat or slightly convex on the dorsal side; periphery rounded, and slightly lobulated; chambers inflated, numerous, 7-8, usually 8 in the last whorl, all visible from the dorsal side, only those of the last whorl from the ventral side; sutures on the dorsal side distinct, depressed, oblique, slightly curved, on the ventral side slightly curved; wall thin, translucent, very finely perforate on the ventral side, coarsely perforate on the dorsal side, brownish in color in fresh tests; aperture a narrow slit along the base of the last chamber on the ventral side, extending from near the umbilicus to the periphery. Length up to *ca.* 0.15 mm.; width up to *ca.* 0.12 mm.; thickness up to *ca.* 0.07 mm.

Holotype (U. S. N. M. No. 626849) from station SD-326 (Lat. 32° 46.3′ N., Long. 117° 31.2′ W.; 385 fathoms). Length *ca.* 0.15 mm.; width *ca.* 0.12 mm.

Comparison.—The nearest species is *C. robertsonianus* (Brady). The writer has examined many specimens of *C. robertsonianus* from the Gulf of Mexico and North Atlantic both young and adult, but *C. phlegeri* is much smaller than the young of *C. robertsonianus,* is more compressed and has a thinner wall. The number of chambers in the last whorl of *C. robertsonianus* is variable, 6-13. Both species are deep sea forms.

Rectocibicides miocenicus Cushman and Ponton

Plate 5, figure 6

Rectocibicides miocenicus Cushman and Ponton, 1932, Cushman Lab. Foram. Research, Contr., vol. 8, p. 2, pl. 1, figs. 5-7.

This species was originally described from the Miocene of Florida, but living specimens are found in the San Diego area. They are always attached to shell fragments or pebbles, etc., and, therefore, their depth distribution is limited to shallow water (shallower than 20 fathoms). The shape and size of the tests depend upon those of the substrate to which they are attached. Sometimes many specimens crowd on a small pebble or shell fragment and interfere with each other, resulting in changes in growth direction and shape and size of chambers. Such specimens were found near Cedros Island, Baja California, Mexico.

Hanzawaia nitidula (Bandy)

Plate 10, figures 14-16

Cibicidina basiloba (Cushman) var. *nitidula* Bandy, 1953, Jour. Paleontology, vol. 27, p. 178, pl. 22, figs. 3a-c.

The dorsal side of adult specimens is slightly evolute but that of young specimens is involute. The dorsal sutures are strongly limbate and slightly raised in the early portion of test, later becoming limbate and flush with the surface; later still the sutures become depressed and non-limbate.

LITERATURE CITED

Andersen, H. V., 1951, An addenda to *Arenoparrella* and *Arenoparella mexicana* (Kornfeld): Contr. Cushman Found. Foram. Research, vol. 2, p. 96.

Bandy, O. L., 1953, Ecology and paleoecology of some California Foraminifera, Pt. 1, The frequency distribution of Recent Foraminifera off California: Jour. Paleontology, vol. 27, pp. 161-182, pls. 21-25.

———, 1954, Distribution of some shallow-water Foraminifera in the Gulf of Mexico: U. S. Geol. Survey, Prof. Paper 254-F, pp. 125-140.

———, 1956, Ecology of Foraminifera in northeastern Gulf of Mexico: U. S. Geol. Survey, Prof. Paper 274-G, pp. 179-204, pls. 29-31.

———, and Arnal, R. E., 1957, Distribution of Recent Foraminifera off west coast of Central America: Am. Assoc. Petroleum Geologists, Bull., vol. 41, pp. 2037-2053.

Bradshaw, J. S., 1957, Laboratory studies on the rate of growth of the foraminifer, *"Streblus beccarii* (Linné) var. *tepida* (Cushman)": Jour. Paleontology, vol. 31, pp. 1138-1147.

Brady, H. B., 1884, Report on the Foraminifera dredged by H. M. S. *Challenger*, during the years 1873-76; Rept. Voy. *Challenger*, Zool., vol. 9, 814 pp., 115 pls.

Clarke, G. L., 1954, Elements of ecology: New York, N. Y., J. Wiley & Sons, 534 pp.

Crouch, R. W., 1952, Significance of temperature on Foraminifera from deep basins off southern California: Am. Assoc. Petroleum Geologists, Bull., vol. 36, pp. 807-843, pls. 1-7.

———, 1954, Paleontology and paleoecology of the San Pedro shelf and vicinity: Jour Sed Petrology, vol. 24, pp. 182-190.

Cushman, J. A., 1921, Foraminifera of the Philippine and adjacent seas: U. S. Natl. Mus., Bull. 100, vol. 4, 589 pp., 100 pls.

———, 1922, The Foraminifera of the Atlantic Ocean. Pt. 3, Textulariidae: U. S. Natl. Mus., Bull. 104, pt. 3, 149 pp., 26 pls.

———, 1923, The Foraminifera of the Atlantic Ocean. Pt. 4, Lagenidae: *ibid.*, pt. 4, 228 pp., 42 pls.

———, 1924, Samoan Foraminifera: Carnegie Inst. Washington, Publ. 342, pp. 3-75, 25 pls.

———, 1926, Some Pliocene Bolivinas from California: Contr. Cushman Lab. Foram. Research, vol. 2, pp. 40-45, pl. 6 (pt.).

———, 1929, A late Tertiary fauna of Venezuela and other related regions: *ibid.*, vol. 5, pp. 77-101, pls. 12-14.

———, 1931, The Foraminifera of the Atlantic Ocean. Pt. 8, Rotaliidae, etc.: U. S. Natl. Mus., Bull. 104, pt. 8, 179 pp., 26 pls.

———, 1933, New Arctic Foraminifera collected by Capt. R. A. Bartlett from Fox Basin and off the northeast coast of Greenland: Smithsonian Misc. Coll., vol. 89, no. 9, 8 pp., 2 pls.

———, 1937, A monograph of the subfamily Virgulininae of the foraminiferal family Buliminidae: Cushman Lab. Foram. Research, Spec. Publ. 9, 228 pp., 24 pls.

———, 1947, New species and varieties of Foraminifera from the southeastern coast of the United States: Contr. Cushman Lab. Foram. Research, vol. 23, pp. 86-92, pls. 18, 19.

———, 1948, Foraminifera, their classification and economic use (4th ed.): Cambridge, Mass., Harvard University Press, 605 pp., 55 pls.

———, and Kellett, Betty, 1929, Recent Foraminifera from the west coast of South America: U. S. Natl. Mus., Proc., vol. 75, art. 25, 16 pp., 5 pls.

———, and McCulloch, Irene, 1939, A report on some arenaceous Foraminifera: Allan Hancock Pacific Expeds., vol. 6, no. 1, 113 pp., 12 pls.

———, and ———, 1948, The species of *Bulimina* and related genera in the collections of the Allan Hancock Foundation: *ibid.*, vol. 6, no. 5, pp. 231-294, pls. 29-32.

———, and Parker, F. L., 1947, *Bulimina* and related foraminiferal genera: U. S. Geol. Survey Prof. Paper 210-D, pp. 55-176, pls. 15-30.

———, and Todd, Ruth, 1944, The genus *Spiroloculina* and its species: Cushman Lab. Foram. Research, Spec. Publ. 11, 82 pp., 9 pls.

———, and ———, 1945, Miocene Foraminifera from Buff Bay, Jamaica: Cushman Lab. Foram. Research, Spec. Publ. 15, 73 pp., 12 pls.

———, and Valentine, W. W., 1930, Shallow water Foraminifera from the Channel Islands off southern California: Dept. Geology Stanford Univ., Contr., vol. 1, no. 1, 51 pp., 10 pls.

Dietz, R. S., 1952, Geomorphic evolution of continental terrace (continental shelf and slope): Am. Assoc. Petroleum Geologists, Bull., vol. 36, pp. 1802-1819.

Drooger, C. W., 1953, Miocene and Pleistocene Foraminifera from Oranjestad, Aruba (Netherlands Antilles): Contr. Cushman Found. Foram. Research, vol. 4, pp. 116-147, pls. 19-24.

Earland, Arthur, 1934, Foraminifera. Pt. 3: The Falklands sector of the Antarctic (excluding South Georgia): Discovery Repts., vol. 10 (1935), 208 pp., 10 pls.

Emery, K. O., 1952, Continental shelf sediments of southern California: Geol. Soc. America, Bull., vol. 63, pp. 1105-1108.

———, Butcher, W. S., Gould, H. R., and Shepard, F. P., 1952, Submarine geology off San Diego, California: Jour. Geology, vol. 60, pp. 511-548.

Fleming, R. H., and Revelle, Roger, 1939, Physical processes in the ocean: Recent marine sediments, Soc. Economic Paleontologists and Mineralogists, Spec. Publ. 4, pp. 48-141.

Galloway, J. J., 1933, A manual of Foraminifera: Bloomington, Ind., The Principia Press, Inc., 483 pp., 42 pls.

———, and Wissler, S. C., 1927, Pleistocene Foraminifera from the Lomita Quarry, Palos Verdes Hills, California: Jour. Paleontology, vol. 1, pp. 35-87, pls. 7-12.

Grell, K. G., 1954, Der Generationswechsel der polythalamen Foraminifere *Rotaliella heterocaryotica*: Archiv Protistenk., vol. 100, pp. 268-286.

Hada, Yosine, 1937, Studies on the Foraminifera of brackish waters, II. Hachiro-gata, III, Koyama-ike: Zool. Mag. (Japan), vol. 49, pp. 341-347.

Hanna, G. D., 1928, The Monterey shale of California at its type locality with a summary of its fauna and flora: Am. Assoc. Petroleum Geologists, Bull., vol. 12, pp. 969-983, pls. 7-10.

Höglund, Hans, 1947, Foraminifera in the Gullmar Fjord and the Skagerak: Zool. Bidrag. fran Uppsala, vol. 26, 321 pp., 32 pls.

Husezima, R., and Maruhasi, M., 1944, A new genus and thirteen new species of Foraminifera from the core-sample of Kasiwazaki Oil-field, Niigata-ken: Jour. Sigenkagaku Kenkyusyo, vol. 1, pp. 391-400, pl. 34.

Jones, T. R., 1883, Foraminifera: in Griffith, J. W., and Henfry, A., The micrographic dictionary: 4th ed. London, J. van Voorst, vol. 1, 829 pp., pl. 1 (pls. 2-53 in vol. 2).

Lacroix, E., 1931, Microtexture de test des Textulariidae: Monaco Inst. Oceanogr., Bull., no. 582, 18 pp.

———, 1932, Textulariidae de plateau continental mediterraneen entre Saint-Raphaël et Monaco: *ibid.*, no. 591, 28 pp.

Lalicker, C. G., and McCulloch, Irene, 1940, Some Textulariidae of the Pacific Ocean: Allan Hancock Pacific Expeds., vol. 6, no. 2, pp. 115-143, pls. 13-16.

Loeblich, A. R., Jr., and Tappan, Helen, 1953, Studies of arctic Foraminifera: Smithsonian Misc. Coll., vol. 121, no. 7, 143 pp., 24 pls.

Ludwick, J. C., 1950, Deep water sand layers off San Diego, California: Scripps Institution of Oceanography, Univ. of Calif., Ph.D. Thesis.

Moore, D. G., 1951, The marine geology of San Pedro shelf: Univ. Southern Calif., M. A. Thesis.

Murray, John, 1913, The ocean: London, Williams & Norgate, 256 pp.

Myers, E. H., 1932, The life history of *Patellina corrugata* Williamson, a foraminifer: Scripps Inst. Oceanography, Bull., Tech. Ser., vol. 3, pp. 355-392.

———, 1942, Biological evidence as to the rate at which tests of Foraminifera are contributed to marine sediments: Jour. Paleontology, vol. 16, pp. 397-398.

Natland, M. L., 1933, The temperature- and depth-distribution of some Recent and fossil Foraminifera in the southern California region: Scripps Inst. Oceanography, Bull., Tech. Ser., vol. 3, no. 10, pp. 225-230.

———, 1957, Paleoecology of west coast Tertiary sediments: Geol. Soc. America, Treatise on Marine Ecology and Paleoecology, vol. 2, pp. 543-572.

d'Orbigny, A. D., 1839, Foraminifères, in De La Sagra, Ramon, Histoire physique, politique et naturelle de l'Ile de Cuba: Paris, 224 pp., 12 pls.

———, 1846, Foraminifères fossiles du Bassin tertiaire de Vienne: Paris, 312 pp., 21 pls.

Parker, F. L., 1952, Foraminifera species off Portsmouth, New Hampshire: Mus. Comp. Zool., Bull., vol. 106, no. 9, pp. 391-423, 6 pls.

———, 1954, Distribution of the Foraminifera in the northeastern Gulf of Mexico: *ibid.*, vol. 111, no. 10, pp. 453-588, 13 pls.

———, 1958, Eastern Mediterranean Foraminifera: Repts. Swedish Deep-Sea Exped., vol. 8, no. 4, pp. 219-283, 6 pls.

Phleger, F. B, 1951a, Displaced Foraminifera faunas: Soc. Economic Paleontologists and Mineralogists, Spec. Publ. 2, pp. 66-75.

———, 1951b, Ecology of Foraminifera, northwest Gulf of Mexico, Pt. 1: Foraminifera distribution: Geol. Soc. America, Mem. 46, pp. 1-88.

———, 1952a, Foraminifera ecology off Portsmouth, New Hampshire: Mus. Comp. Zool., Bull., vol. 106, pp. 315-390.

———, 1952b, Foraminifera distribution in some sediment samples from the Canadian and Greenland Arctic: Contr. Cushman Found. Foram. Research, vol. 3, pp. 80-89, pls. 13, 14.

———, 1955, Ecology of Foraminifera in southeastern Mississippi Delta: Am. Assoc. Petroleum Geologists, Bull., vol. 39, pp. 712-752.

———, and PARKER, F. L., 1951, Ecology of Foraminifera, northwest Gulf of Mexico, Pt. 2, Foraminifera species: Geol. Soc. America, Mem. 46, 64 pp., 20 pls.

RAITT, R. W., 1949, Studies of ocean bottom structure off southern California with explosive waves (abstr.): Geol. Soc. America, Bull., vol. 60, p. 1915.

REVELLE, ROGER, and SHEPARD, F. P., 1939, Sediments off the California coast: Recent Marine Sediments, Soc. Economic Paleontologists and Mineralogists, Spec. Publ. 4, pp. 245-282.

RHUMBLER, LUDWIG, 1911, Die Foraminiferen (Thalomophoren) der Plankton-Expedition, etc., Pt. 1: Systematik: Ergeb. Plankton-Exped. Humboldt Stiftung, Bd. 3, 331 pp., 39 pls.

———, 1938, Foraminiferen aus dem Meeresand von Helgoland, gesammelt von A. Remane (Kiel): Kieler Meeresforschungen, vol. 2, pp. 157-222.

SCHULTZE, M. S., 1854, Uber den Organismus der Polythalamien (Foraminiferen) nebst Bemerkungen über die Rhizopoden im Allgemeinen: Leipzig, 68 pp., 7 pls.

SCHWAGER, CONRAD, 1866, Fossile Foraminiferen von Kar Nikobar: *Novara* Exped. 1857-1859, Geol. Theil, vol. 2, pt. 2, pp. 187-268, pls. 4-7.

SCRIPPS INSTITUTION OF OCEANOGRAPHY, 1949-1957, Physical and chemical data.

SHEPARD, F. P., and MACDONALD, G. A., Sediments of Santa Monica Bay, California, Am. Assoc. Petroleum Geologists, Bull., vol. 22, pp. 201-216.

SILVESTRI, A., 1896, Foraminiferi Pliocenici della provincia di Siena, pt. 1: Accad. Pont. Nuovi Lincei, Mem., vol. 12, 204 pp., 5 pls.

———, 1898, Foraminiferi Pliocenici della provincia di Siena: *ibid.*, vol. 15, pp. 155-381, 16 pls.

STEWART, R. E., and STEWART, K. C., 1930, Post Miocene Foraminifera from the Ventura quadrangle, Ventura County, California: Jour. Paleontology, vol. 4, pp. 60-72, pls. 8, 9.

SVERDRUP, H. U., JOHNSON, M. W., and FLEMING, R. H., 1942, The oceans: New York, N. Y., Prentice-Hall, Inc., 1087 pp.

THALMANN, HANS, 1950, New names and homonyms in Foraminifera: Contr. Cushman Found. Foram. Research, vol. 1, pp. 41-45.

TRASK, P. D., 1932, Origin and environment of source sediment of petroleum: Tulsa, Okla., Gulf Publishing Co., 323 pp.

TROELSEN, J. C., 1954, Studies on Ceratobuliminidae (Foraminifera): Meddel. Dansk. Geol. Forening, Bd. 12, pp. 448-480, pls. 10, 11.

WALTON, W. R., 1952, Techniques for the recognition of living Foraminifera: Contr. Cushman Found. Foram. Research, vol. 3, pp. 56-60.

———, 1955, Ecology of living benthonic Foraminifera, Todos Santos Bay, Baja California, Mexico: Jour. Paleontology, vol. 29, pp. 952-1018, pls. 99-104.

WRIGHT, J., 1891, Report on the Foraminifera obtained off the southwest of Ireland during the cruise of the "Flying Falcon," 1888: Roy. Irish Acad. Proc., ser. 3, vol. 1, pp. 460-502, pl. 20.

WÜST, GEORG, 1935, Die Stratosphäre: Deutsche Atlantische Exped. *Meteor* 1925-1927, Wiss. Ergeb., Bd. 6, Teil 1, 180 pp.

Contribution No. 30, Marine Foraminifera Laboratory.

Contribution from the Scripps Institution of Oceanography, University of California, New Series.

Reprinted from SCIENCE February 26, 1960, Vol. 131, No. 3400, pages 585-590

Oxygen Transport through Hemoglobin Solutions

How does the presence of hemoglobin in a wet membrane mediate an eightfold increase in oxygen passage?

P. F. Scholander

Evolution from single cells to organisms is linked intimately with the development of a circulatory system. Without this, both size and activity would be severely limited by the slowness of diffusion. But even with a circulatory system, oxygen transport would be hampered by still another "unfitness of the environment"—namely, the very low solubility of oxygen in water. This difficulty was overcome by the evolution of oxygen-carrying pigments, which when circulated to the tissues could carry many times more oxygen than can water alone.

Oxygen-carrying pigments appeared not only in blood, however, but also in a vast area where visible means for transport of the pigment is lacking—namely, as myoglobin in the muscle system. Here it is found within the muscle cells, providing, so to speak, the last leg of the supply line to the oxygen-needy contractile machinery. But how could this myoglobin enhance oxygen transport unless it were circulated within the cell? Simple diffusion could hardly be aided by the pigment. It is true enough that the increased oxygen capacity could help to smooth out a fluctuating demand, as demonstrated by Millikan (*1*), but could it possibly also be that the pigment might

---

The author is professor of physiology at Scripps Institution of Oceanography, University of California, La Jolla.

Contributions from the Scripps Institution of Oceanography, New Series, 1152

Reproduced by Permission

serve as a specific conveyor belt for oxygen, enhancing its rate of delivery?

If we turn from a normally aerated environment to habitats of low oxygen tension we find that many animals develop high concentrations of oxygen-carrying pigments. One may mention mud-dwelling worms or insect larvae (chironomids), certain crustaceans in stagnant pools (*Daphnia*), intestinal nematodes and maggots (*Ascaris* and *Gastrophilus*), and many mammals exposed naturally or experimentally to high altitudes. And again we are drawn to the fundamental question: Is it possible that an oxygen-carrying pigment can enhance oxygen transfer through a stationary solution?

A great deal of penetrating experimental and theoretical work has been done to elucidate the kinefics of situations where oxygen, carbon monoxide, and other gases load and unload hemoglobin solutions (*2*). Unfortunately, however, this approach is not so suitable if one wishes specifically to study what happens in a pure steady-state situation, since the capacity factor can easily obscure the steady-state events.

The primary aim of the investigation under discussion has been to find out what happens when air diffuses through human hemoglobin solutions. Complications from oxygen capacity or storage have been eliminated by adhering strictly to steady-state conditions. It is shown below that the rate of oxygen transport may indeed be enhanced by the presence of hemoglobin, and a few preliminary experiments on myoglobin and other pigments indicate that the phenomenon may have wider applications (*3*).

Methods

Principle. Moist air at various pressures is diffused through a Millipore membrane charged with a hemoglobin solution; on the other side of the membrane a moist vacuum is maintained. When a steady state is reached, the amounts of oxygen and nitrogen gas coming through the membrane in a measured time interval are analyzed. With the nitrogen values as a base line, the oxygen transport can be calculated.

Instrumentation. The diffusion apparatus (Fig. 1) consists of a diffusion chamber which may be divided into two compartments by a wet Millipore filter. The membrane rests on a stainless-steel grid. The upper compartment is connected to a vacuum gauge and a glass-stoppered vent tube (*D*); the lower compartment, to the vacuum chamber by means of a taper joint. Each compartment is kept moist by a piece of wet filter paper.

The vacuum chamber is a 300-ml mercury reservoir connected through a gas trap and stopcock to the leveling bulb. The chamber has one wide-bore (5-mm) stopcock (*A*) to the diffusion chamber and a regular one of narrower bore (*B*) to the vacuum line. The upper end of the vacuum chamber terminates in a 1-mm-bore capillary and cup which can be closed under mercury by inserting into it a polyethylene-tipped wire plug. The capillary carries a movable millimeter scale to measure the total amount of gas.

Gas is transferred to the micro gas analyzer by means of a micro syringe. This is made from a glass tube of 2 mm inside diameter fitted with a fine polyethylene tip and a wire plunger. The latter is made airtight by means of a piece of polyethylene tubing which is flared at the end by heating slightly. This micro syringe is filled with mercury, and the gas is always protected by mercury during handling. From this pipette the gas is introduced into the micro analyzer (*4*).

The Millipore membrane (HA grade) holding the hemoglobin solution has a porosity fine enough so that air pressure of 1 atm will not break the capillarity. This filter, which is 0.15 mm thick, has about 80 percent space for the liquid.

Procedure. The basic data were obtained from heparinized human blood. The cells were washed twice in 0.9 percent saline and hemolyzed by repeated freezing and thawing. The oxygen capacity of the hemoglobin solutions was determined by the syringe method (*5*).

To saturate the dry Millipore membrane with the hemolyzed cell solution, it is placed on top of the solution until it is soaked through, whereupon it is submerged. It is then blotted on both sides and placed on the grid of the lower half of the diffusion chamber, which is kept moist by a ring of wet filter paper. The upper half, also carrying a wet filter paper, is screwed vacuum-tight onto the lower half with the wet membrane in between. A wide rubber band prevents evaporation from the crack. The chamber is put on the taper joint of the vacuum chamber, which is stoppered by the plug, and evacuated through *B*. *B* is closed, *A* is opened momentarily, and the chamber is again evacuated through *B*. This process is repeated twice, and the air pressure on the membrane is adjusted to the desired level through screw clamp *C* and vent *D*.

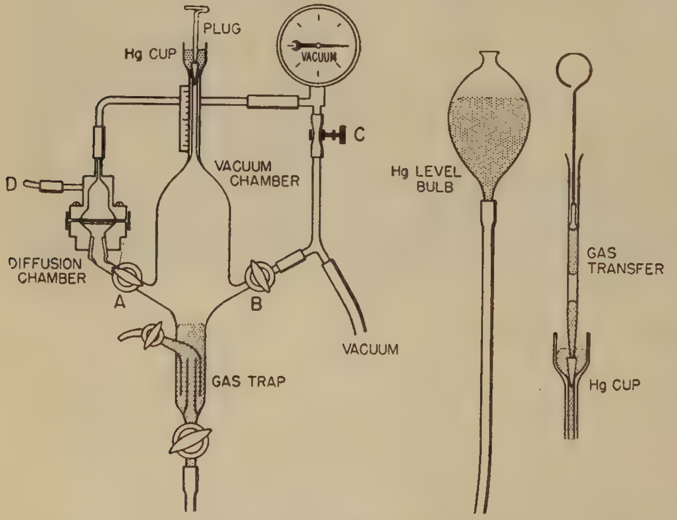

Fig. 1. Apparatus for steady-state diffusion.

Diffusion of gases now proceeds from the upper air compartment through the membrane and into the wide-bore channel to the vacuum chamber. The time of diffusion is clocked by means of a stop watch, and the amount of gas which has moved through the membrane is periodically checked by closing off the diffusion chamber at stopcock *A*, letting the mercury rise, and measuring the volume of the gas bubble in the capillary. Twenty cubic millimeters of gas suffice for an accurate determination of the quantity as well as the composition.

The gas transfer is executed with the gas pressure in the capillary slightly below atmospheric pressure. The plug is removed and quickly replaced by the mercury-filled transfer pipette. The gas is drawn up into this and is followed by mercury, whereupon the pipette is removed and replaced by the plug. The gas sample is now transferred to the cup of the analyzer containing alkaline citrate, and the oxygen and nitrogen are determined by absorption in the conventional way (*4*).

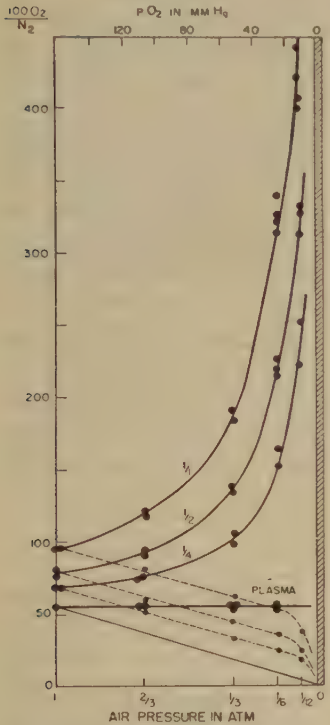

Fig. 2. Diffusion of air through hemoglobin solutions of three concentrations. Curve 1/1 represents oxygen capacity of 22.9 volumes percent; the other curves represent oxygen capacity of ½ and ¼ this amount, respectively. Horizontal line, O_2/N_2 ratio through plasma; lower diagonal line, rate of oxygen diffusion through plasma; three dashed parallel lines, relative rates of oxygen transport calculated from the corresponding O_2/N_2 data; shaded area, water-vapor tension.

Successive samples are analyzed until the O_2/N_2 ratio becomes constant— that is, until the oxygen content of the filter is constant. Under the least favorable conditions (high pressure and high hemoglobin concentration) the membrane contains initially, at most, some 14 to 20 mm^3 of oxygen, but diffusion then proceeds so quickly that some 6 to 8 times this amount goes through before final sampling. At low pressures the membrane holds less than 1/20 of the amount analyzed.

Results

Diffusion of air through a membrane charged with water. The rate of simple gas diffusion through a membrane is proportional to the pressure difference and solubility of the gas and is inversely proportional to the square root of the molecular weight. When air diffuses through a layer of water, the steady-state ratio of oxygen to nitrogen should accordingly be 49.0 percent at 24°C and 48.7 percent at 26°C. In actual fact, our figures for air diffusing through water held in a Millipore filter or a dialyzing membrane come out as 56 ± 1 percent at all pressures. The reason for this quite substantial deviation from the theoretical value is not known, but it may be that a slight diffusion through the membrane substance itself and its 30 percent or so of bound water would favor the oxygen. The oxygen-nitrogen ratio was unchanged by charging the filter with a lampblack suspension or by using the VF grade Millipore filter; both of these procedures give a higher filter-to-water ratio. The same figure was also obtained by diffusing air through blood plasma and methemoglobin solutions (see Figs. 2–4).

In all cases, the total (and partial) amount of the gases diffusing through was proportional to the pressure (Fig. 5).

Oxygen transport through hemoglobin solutions. Typical curves for oxygen transport through hemoglobin solutions are given in Fig. 2. The basic curve (1/1) was obtained from a hemoglobin solution with an oxygen capacity of 22.9 volumes percent. It will be seen that the O_2/N_2 ratio at air pressure of 1 atm is 95 percent instead of 56 percent as it is in water or plasma. The ratio increases rapidly with lowering of the air pressure, reaching over 400 percent at 1/12 atm. But when the rate of nitrogen diffusion is calculated from

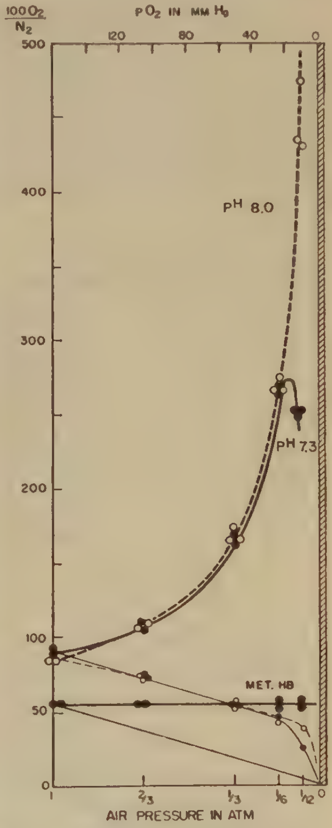

Fig. 3. Diffusion of air through two hemoglobin solutions of the same concentrations (O_2 capacity, 15.8 volumes percent) but with different *p*H's. Horizontal line, O_2/N_2 ratio of diffusion through a methemoglobin solution; lower diagonal line, rate of oxygen diffusion through water; two parallel curves, relative rates of oxygen transport calculated from the O_2/N_2 values; shaded area, water-vapor tension.

the total gas volume and the O_2/N_2 ratio, we find that it is always proportional to the pressure (Fig. 5). Two things follow: (i) the increased O_2/N_2 ratio is exclusively caused by an increased rate of oxygen transport, and (ii) the oxygen transport is proportional to the product of O_2/N_2 and Δp, where Δp is the diffusion pressure.

This enables us to calculate the relative rate curves for oxygen transport in Fig. 2. It will be seen that the transport rates through hemoglobin in all three dilutions are parallel to the diffusion rate through water—that is, numerically the oxygen transport is the result of two additive processes, the one, plain diffusion through the water, the other, a specific transport mediated by the hemoglobin. The latter remains constant over a large gradient of oxygen pressures. This simple relation holds quite precisely for all cases investigated, with various concentrations of hemoglobin or diffusing through intact red cells (Figs. 2–4).

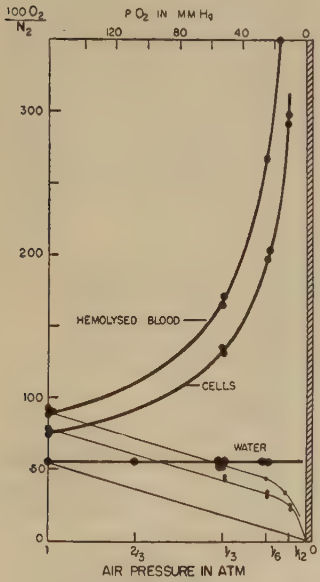

Fig. 4. Diffusion of air through (i) whole blood (O_2 capacity, 21 volumes percent) hemolyzed by HA membrane, and (ii) washed cells smeared on the under side of a dry VF Millipore filter. Horizontal line, O_2/N_2 ratio through water; lower diagonal curve, rate of oxygen diffusion through water; parallel curves above this, relative rates of oxygen transport calculated from the O_2/N_2 data; shaded area, water-vapor tension.

Figure 3 shows the effect of *p*H on the same hemoglobin solution. The only significant difference appears at the very lowest pressure—namely, 1/12 atm where the transport drops off in the acid sample but keeps on undiminished in the alkaline sample.

As would be expected, the hemoglobin concentration has a marked effect on the oxygen transport. In Fig. 2 the decrease in specific transport was proportionately less than the dilution of the hemoglobin. At half strength the rate of transport was reduced to 62 percent and at quarter strength, to 39 percent. When the concentration was doubled there was a marked increase in viscosity and a decrease in the rate of oxygen transport. The rate of nitrogen diffusion through this solution also dropped, and this finding implicates the high viscosity as the cause (*2*, *6*).

The retarding effect of increased viscosity was demonstrated by adding 10 percent of gelatine to the hemoglobin solution, which was enough to make it solidify. This almost halved the specific rate of oxygen transport by the hemoglobin but hardly affected the nitrogen diffusion.

Oxygen transport through red cells. In these experiments the washed red cells were smeared on either the upper or the lower side of the finest Millipore filter (VF grade). It will be seen from Fig. 4 that the oxygen transport was almost doubled at pressure of ⅓ atm. When this procedure was tried on a regular HA filter, the capillary forces in the filter ruptured the blood cells and the hemoglobin solution came through on the other side. This did not happen on a VF filter, and when the filter was soaked afterward in isotonic saline there was little, if any, evidence that hemolysis had taken place. It is therefore indicated that the transport effect displayed by hemoglobin solutions is also operative in the intact red cell.

Oxygen transport through myoglobin and other pigments. A preliminary study was made on oxygen transport through a myoglobin solution. This was prepared from the very dark pectorals of a California sea lion. Thin slices cut across the fibers were repeatedly washed in isotonic saline solution and wrung in a dry towel. The amount of blood left after this procedure is very small compared to the high concentration of myoglobin. The slices were passed through a meat grinder and repeatedly frozen and thawed, and the macerate was ground under a few milliliters of water in a mortar and centrifuged. The fluid was passed through an HA Millipore filter.

This solution at an air pressure of ⅓ atm gave initial O_2/N_2 ratios of 100 percent and 87 percent—that is, there was a substantial oxygen enhancement. After a few hours, and contrary to the finding for hemoglobin solutions, the ratio dropped to that of water. Although this is an unstable preparation, it demonstrates that myoglobin in vitro is capable of implementing a potent steady-state oxygen transport.

A marine sand-dwelling worm, *Thoracophelia,* when cut into pieces and centrifuged, yielded a deep red solution with an oxygen capacity of 5.3 volumes percent. This mixture of blood and body liquid yielded large amounts of CO_2, together with oxygen and nitrogen, but nevertheless showed some 12- to 15-percent enhancement of the oxygen transport when measured at air pressures of 1/6 or 1/12 atm. In view of the loss of oxygen in the membrane, these are clearly minimum figures.

Hemolyzed red cells from fish blood, —mackerel, with an O_2 capacity of 12.1 percent and yellowtail (*Seriola dorsalis*), with a higher O_2 capacity—showed an enhancement of 100 percent at air pressure of ⅓ atm in the mackerel and 110 percent in the yellowtail.

Discussion

We have observed a steady-state rate of oxygen transport which can be attributed to the added effects of two simultaneous processes: one, a diffusion through the solvent; the other, a transport specifically dependent upon hemoglobin. The latter proceeds at a constant rate over a wide range of pressures and depends upon the kinetics and oxygen-binding properties of the hemoglobin molecule.

It therefore seems that when a tension gradient of oxygen is imposed upon a hemoglobin solution, oxygen molecules are handed down from one hemoglobin molecule to the next in a chain or "bucket-brigade" fashion. Provided the "buckets" are emptied at one end and filled at the other, a steady-state system is set up which results in facilitation of oxygen transport through the chain (see Fig. 6).

The steady-state situation requires that the oxygen tension at any level between the upper and lower surfaces of the membrane remain constant. Above, it is near the tension of the gas phase; below, it is near zero. The oxygen saturation at various levels is determined by the oxygen dissociation curve, but the exact relations are here immaterial as long as conditions remain constant. One may tentatively assume that a linear tension gradient exists and that the hemoglobin loses is first oxygen at air pressure of approximately ⅓ atm, its second at ⅙ atm, and its third at 1/12 atm. Near the lower surface only the fourth molecule remains attached to the hemoglobin (Fig. 6). This is the one which jumps off into the vacuum and which is then replenished from the hemoglobin chain above. The maximum rate at which the chain can keep the oxygen moving evidently depends upon the constant kinetic motion of the hemoglobin molecules, for the rate of oxygen transport via this route is constant and independent of the oxygen gradient.

That a rate-limiting factor is located at the vacuum end of the chain is indicated by the *p*H effect. It was found that an increased affinity for oxygen—that is, a high *p*H—is able to maintain the transport unimpaired at very low pressures, whereas lowering of the *p*H slowed it down. A glance at the last column of Fig. 6 will show that at low *p*H and a pressure head of ⅙ atm, the lower half of the chain gets increasingly disrupted by completely reduced hemoglobin molecules, and we may assume that as a consequence of this the delivery slows down.

If the head of pressure is only 1/12 atm to begin with, one would expect a great number of void (unoxygenated) molecules in the lower part of the chain, even at high *p*H; nevertheless, oxygen was delivered at full rate. This seems to weaken the explanation of the *p*H effect just mentioned, unless possibly another factor entered—namely, back pressure of oxygen. From the lower surface of the membrane into the vacuum chamber is a long way for oxygen to go, and this simple diffusion depends, of course, upon a concentration gradient. It is possible that the oxygen back pressure built up sufficiently to keep the chain saturated to the very end. This raises a fundamental question: If the low-pressure side were raised deliberately, would the transport system still work? The answer can be obtained only by the use of a different technical approach.

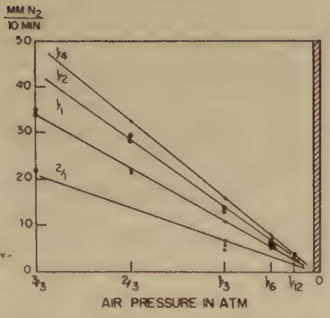

Fig. 5. Rate of nitrogen diffusion through various concentrations of hemoglobin. Curve 1/1 represents oxygen capacity of 22.9 volumes percent; the other curves represent fractions of this amount. Ordinate = vol/min.

What then, one may wonder, is the possible biological significance of this oxygen-specific, steady-state, enhanced rate of oxygen transport?

It will be seen from the various experiments in vitro that the oxygen transport mediated by human hemoglobin may dominate straight diffusion by a factor of 8 or more at low pressures and can at full atmospheric pressure almost double the rate. The effect has also been demonstrated in intact red cells, and it is possible, although this has not been demonstrated, that it plays a role in their normal gas exchange, even when the low-pressure side is not zero.

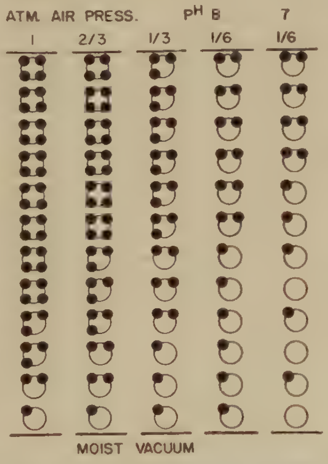

Fig. 6. Schematic presentation of possible mode of oxygen transport via hemoglobin molecules. Solid circles, oxygen molecules; open circles, hemoglobin molecules.

More relevant, however, is the physiological implication of the role of enhanced rate of oxygen transport in the case of myoglobin. One may visualize a system which in addition to its storage function would grease, so to speak, the oxygen transfer from the blood in the capillaries into the metabolic machinery of the muscle fiber. Such a transport would be enhanced even more if the myoglobin were mobile within the muscle cells, somewhat like water in a sponge, rather than held in a viscous medium. But whatever is the case, muscle contractions would undoubtedly favor the transport.

It was found that sea lion myoglobin, indeed, enhances oxygen transport in vitro. The increase in hemoglobin and sometimes in myoglobin observed in many high-altitude mammals fits well into this same line of argument, and the same holds true also for those larvae, worms, intestinal parasites, and other animals which live under low oxygen tension and harbor red hemoglobin-like pigments. A steady-state transport effect of the blood pigment from one such worm has indeed been demonstrated.

Summary

A study has been made of steady-state diffusion of air at various pressures through hemoglobin solutions. Whereas nitrogen diffused in proportion to the pressure, the rate of oxygen transport was greatly enhanced and seemingly proceeded by means of two processes which are additive. One is a regular diffusion through the solvent (water), which is proportional to the pressure; the other is a specific transport mediated by the hemoglobin molecules. The rate of the latter is constant over a wide pressure range, and the process may at low tensions transport over eight times more oxygen than does straight diffusion. Preliminary studies

have established that myoglobin and a few other pigments in vitro have the same property.

References and Notes

1. G. A. Millikan, *Proc. Roy. Soc. (London)* **B123**, 218 (1937); *Physiol. Revs.* **19**, 503 (1939).
2. I. S. Longmuir and F. J. W. Roughton, *J. Physiol. (London)* **118**, 264 (1952); F. Kreuzer, *Helv. Physiol. et Pharmacol. Acta.* **9**, 379 (1951); ———, *ibid.* **11**, suppl. 9 (1953).
3. This investigation was supported by a research grant (No. RG-5979) from the U. S. Department of Health, Education, and Welfare, Public Health Service, and by the Norwegian Research Council. I wish to thank A. Baird Hastings, Denis L. Fox, and Y. Zotterman for their stimulating interest and advice, and I gratefully acknowledge the excellent laboratory facilities extended to me by Edmund L. Keeney and Hastings at the Scripps Clinic and Research Foundation. The effect described here was found in 1956 at the Institute of Zoophysiology, University of Olso, where valuable assistance was rendered by G. Sundnes and H. Leivestad.
4. P. F. Scholander, L. van Dam, C. L. Claff, J. W. Kanwisher, *Biol. Bull.* **109**, 328 (1955).
5. F. J. W. Roughton and P. F. Scholander, *J. Biol. Chem.* **148**, 541 (1943).
6. A. Klug, F. Kreuzer, and F. J. W. Roughton [*Helv. Physiol. et Pharmacol. Acta* **14**, 121 (1956)] exposed thin films (0.1 by 45 mm) of reduced hemoglobin solutions to oxygen pressure of 0.9 atm and studied optically the oxygenation rate. On comparing their findings with earlier determinations of nitrogen diffusion (diffusion into a system much less sensitive to errors from surface disturbance and convection), they estimated an oxygen enhancement of 100 percent at low viscosity vanishing at high hemoglobin concentrations. This effect, attributed to diffusion of oxyhemoglobin, would at a pressure of 0.2 atm amount to 450 percent. This is totally out of the range of our findings and the effect is seemingly, therefore, of a different nature.

JOURNAL OF GEOPHYSICAL RESEARCH VOLUME 65, NO. 3 MARCH 1960

A New Long-Period Wave Recorder[1]

WM. G. VAN DORN

Scripps Institution of Oceanography
La Jolla, California

Abstract. A new long-period wave recorder designed for the study of low-amplitude surface waves of the ocean in the period spectrum intermediate between the swell and the tides ($10 \text{ sec} < T < 10^5$ sec.) is described. The recorder has a limiting resolution in the pass band of about 0.035 cm of water, which is substantially lower than the lowest ambient background found at small island stations in mid-ocean. Two years' experience with temporary installations has proved this equipment to be well suited to continuous observations at such remote stations, and three permanent installations are planned within the coming year.

Introduction. Long-period ocean wave recording is a relatively recent discipline; it dates back to 1947, when the first instrument specifically designed to explore that portion of the oceanic surface-wave spectrum between the wind-generated swell and the tides was installed at the end of the Scripps pier by *Munk* [1948]. Later, *Van Dorn* [1956] developed a somewhat similar portable recorder for temporary observation of long-period waves from nuclear explosions at the Pacific Proving Grounds. This latter instrument, while incapable of resolving finer details of the normal background (wave heights < 2 cm), provided essential data on the order of magnitude of signals to be expected in the low-frequency surface-wave spectrum.

It was determined that an instrument which would resolve wave heights corresponding to an *in situ* pressure amplitude range of 0.5 to 50 cm of water would cover the entire region of interest, provided that both swell and tides could be attenuated to about 3 to 5 per cent of their real amplitudes. The recorder described here has a threshold sensitivity an order of magnitude lower than the lower limit expressed above, although a dynamic range greater than about 100 is proscribed by the limitations of the recording potentiometer.

Recorder installation. Like its predecessors, the new recorder consists of a hydraulic resistance-capacitance wave filter (Fig. 1) connected hydraulically to the sea by a sensing tube and electrically to a strip-chart recorder by a four-wire electric cable. The spatial relationship between the system components is not critical; they can be horizontally displaced from one another by distances as great as a mile.

In previous temporary installations, the tube was a ½-inch (1.27 cm) plastic garden hose extending beneath the sea to a depth of 10 to 20 meters, and the filter was mounted in a protected location below sea level in a hole blasted in the reef. This requirement can be obviated by terminating the tube at depths as great as 300 meters and filling it with fresh water, which will permit the filter to operate in hydrostatic equilibrium at an elevation of about 10 meters above mean sea level. Calculations show that extending the tube to such depths will virtually eliminate short-period waves (swell) from the record and will markedly reduce the 2- to 3-minute surf-beat associated with nonlinear rectification of groups of breaking waves on the reef.

The hydraulic filter. Frequency discrimination against swell and tides is accomplished by the hydraulic filter (Fig. 2). It consists of two capillary tubes, a mercury manometer, and a vertical standpipe arranged to form either of two resistance-capacitance networks, whose electrical analog circuits are shown in the figure. Wave pressure signals passing through the filter are converted to electric signals by a differential pressure transducer. When the trans-

---

[1] Contribution from the Scripps Institution of Oceanography, New Series. 1153

Reproduced by Permission

(265)

TABLE 1. Circuit Constants for the Hydraulic Filter

Symbol	Component	Dimensions		Circuit Constant, 25°C	
		Length, cm	Radius, cm		
R_1	Capillary	1.75	0.070	$8.9 \times 10^{4*}$	$\frac{\text{dynes-sec}}{\text{cm}^5}$
		1.85	0.092	$3,1 \times 10^{5\dagger}$	”
R_2	Capillary	1.75	0.045	$5.3 \times 10^{5*}$	”
		0.5	0.026	$1.4 \times 10^{7\dagger}$	”
C_1	Standpipe	300.	1.27	5.4×10^{-3}	$\frac{\text{cm}^3}{\text{dyne/cm}^2}$
C_2	Mercury manometer	20.	0.86	1.2×10^{-4}	”

* Band-pass when 50 centistoke (0.477 poise) silicone oil is used.
† High-pass when 500 centistoke (4.77 poise) silicone oil is used.

ducer is connected across the manometer (connection A), the filter acts as a single-stage band-pass network discriminating against both swell and tides. When it is connected across the capillary R_2 (connection B), the filter acts as a two-stage high-pass filter and discriminates only against the tides. Although previous installations have always been operated in the band-pass configuration, future instruments will employ high-pass filters and depend upon the extension of the sensing hose to greater depths to provide adequate swell filtering, since the pressure amplitude of swell diminishes as e^{-2kz}, where z is the depth at which pressure is

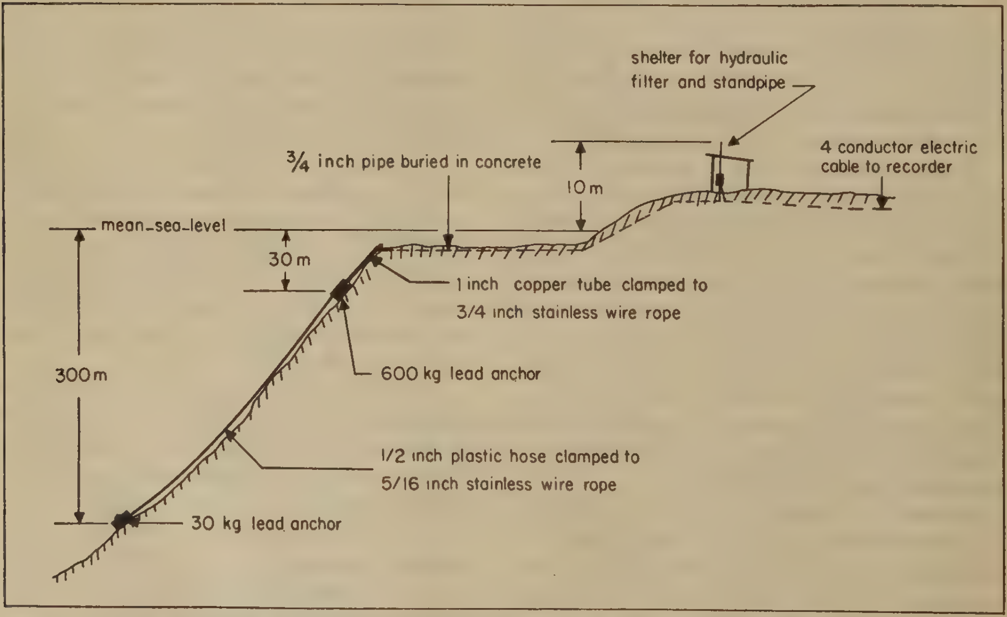
shelter for hydraulic filter and standpipe
3/4 inch pipe buried in concrete
10 m
4 conductor electric cable to recorder
mean-sea-level
30 m
1 inch copper tube clamped to 3/4 inch stainless wire rope
300 m
600 kg lead anchor
1/2 inch plastic hose clamped to 5/16 inch stainless wire rope
30 kg lead anchor

Fig. 1. Typical long-wave recorder installation for high-pass operation; swell filtering obtained by deep hose inlet.

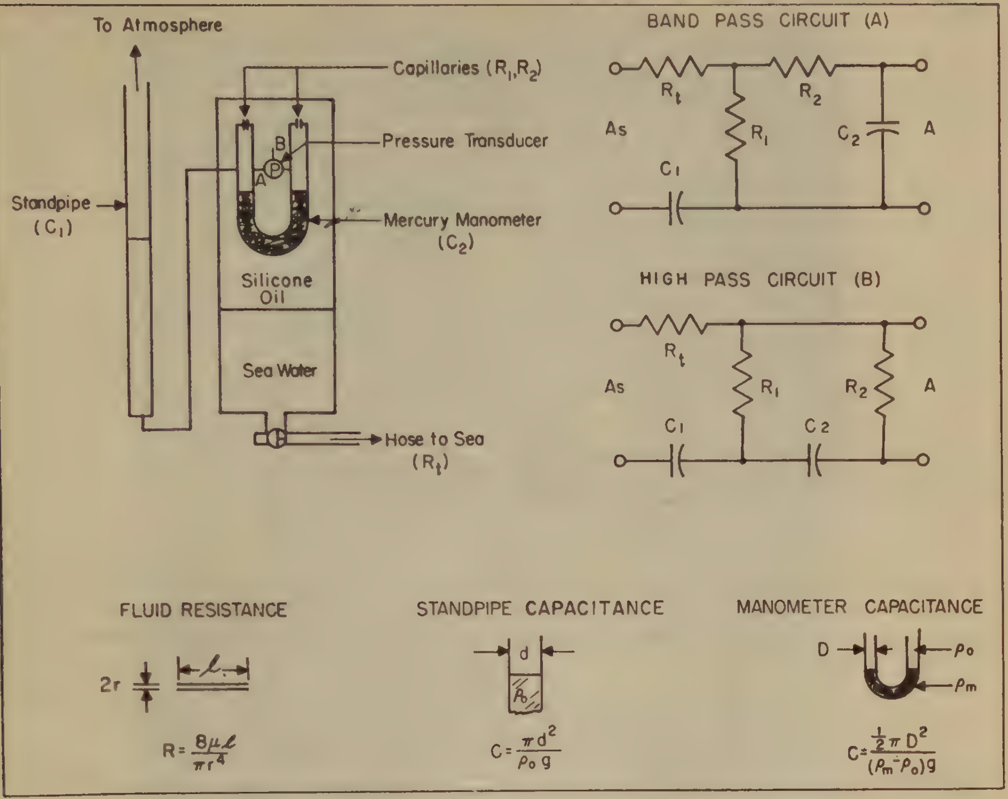
To Atmosphere
Capillaries (R_1,R_2)
Pressure Transducer
B
P
A
Standpipe (C_1)
Mercury Manometer (C_2)
Silicone Oil
Sea Water
Hose to Sea (R_t)
BAND PASS CIRCUIT (A)
R_t
R_2
As
R_1
C_2
A
C_1
HIGH PASS CIRCUIT (B)
R_t
As
R_1
R_2
A
C_1
C_2
FLUID RESISTANCE
2r
ℓ
$R = \frac{8\mu\ell}{\pi r^4}$
STANDPIPE CAPACITANCE
d
ρ_o
$C = \frac{\pi d^2}{\rho_o g}$
MANOMETER CAPACITANCE
D
ρ_o
ρ_m
$C = \frac{\frac{1}{2}\pi D^2}{(\rho_m - \rho_o)g}$

Fig. 2. Schematic circuit for the hydraulic filter and its electrical analogs.

measured and $k = 2\pi/L$ is the wave number. With two-stage, high-pass filtering, the discrimination against tides is so great that the region of unity filter response can be extended to very low frequency without undue tidal interference, thus eliminating the necessity for applying a variable filter correction over most frequencies of interest when analyzing the data.

Physically, the filter is a plexiglass cylinder about 10 cm in diameter and 45 cm long (Fig. 3) enclosed at its upper and lower ends by blocks of plexiglass held in place by brass staybolts. The tube to the sea is connected to a three-way valve which is mounted on the lower block. The pressure transducer and mercury manometer are mounted on the upper block, which is cross-bored to form the appropriate hydraulic fluid passages. The capillaries are bored in small brass screws, which can readily be removed for inspection or cleaning. The standpipe is a brass pipe, 2.54 cm in diameter (1 inch), connected to the filter by a flexible hose. Initially, the entire filter is filled with silicone oil, and water is then admitted through the lower valve until the oil-water interface has risen about 10 cm inside the cylinder. The valve is then opened to atmosphere until pressure equilibrium is established with the sea. Since both the sensing tube and the standpipe are referred to atmosphere, the system does not respond to atmospheric pressure fluctuations.

Amplitude response. The response A/A_s of the hydraulic filter to a sine wave of unit amplitude A_s for both modes of operation is given by the expressions[2]

---

[2] In these expressions the hose resistance R_t in the analog circuits is ignored. This resistance is always small compared with the impedance of the remainder of the network for the values of the circuit constants employed here.

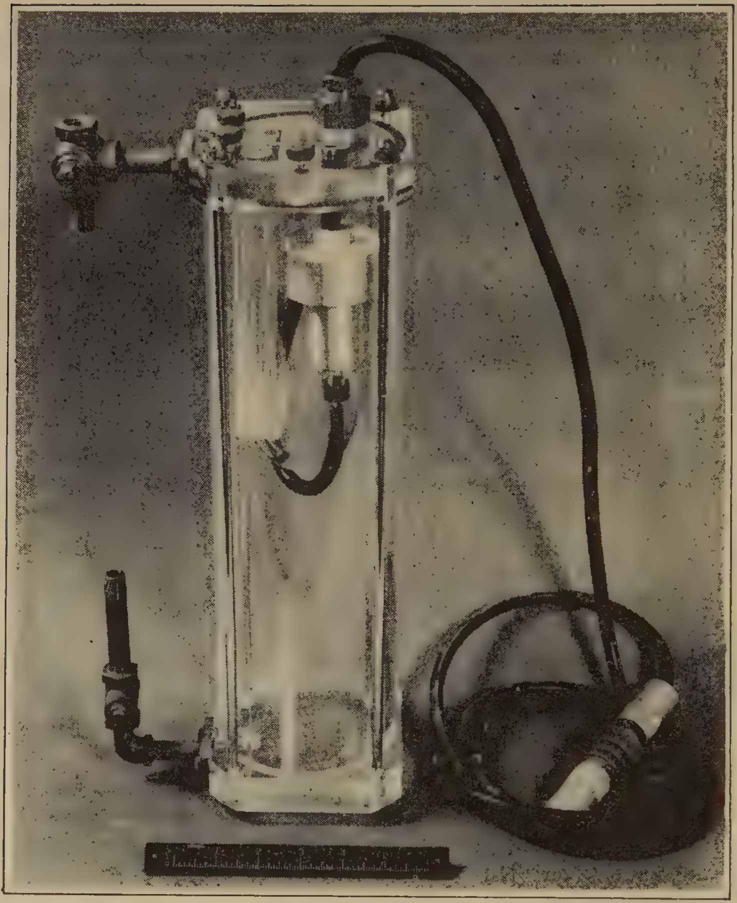

Fig. 3. Hydraulic filter connected for band-pass operation. Standpipe (not shown) is connected to upper valve. For high-pass operation, the pressure transducer can be mounted externally.

$$\text{Band-pass } \frac{A}{A_0} = \left[\left(1 + \frac{C_2}{C_1} + \frac{R_2C_2}{R_1C_1}\right)^2 + \frac{R_2C_2}{R_1C_1}\left(\frac{T}{T_0} - \frac{T_0}{T}\right)^2\right]^{-1/2} \tag{1}$$

$$\text{High-pass } \frac{A}{A_0} = \left[\left(1 + \frac{T^2}{4\pi^2R_1^2C_1^2}\right) \cdot \left(1 + \frac{T^2}{4\pi^2R_2^2C_2^2}\right)\right]^{-1/2} \tag{2}$$

where T is the period (sec) of the input signal, $T_0 = 2\pi(R_1C_1R_2C_2)^{1/2}$ is the period of maximum response for band-pass operation, and the appropriate circuit constants are listed in Table 1. The image impedance reflected from the second filter stage is ignored in equation (2), but the equation is accurate to within 1 per cent for the ratio $C_2/C_1 \doteq 0.02$ employed in the present filter. Both equations (1) and (2) are plotted in Figure 4, together with the swell attenuation provided by a tube terminating at a depth of 300 meters, and it is apparent that two-stage high-pass filtering with adequate swell suppression gives a much more favorable response in the spectrum of interest than the band-pass circuit, with the same discrimination against swell and tides.

The theoretical response of both circuits has been verified in the laboratory by a sine-wave generator which hoists a bucket of water at variable frequency and constant amplitude, or

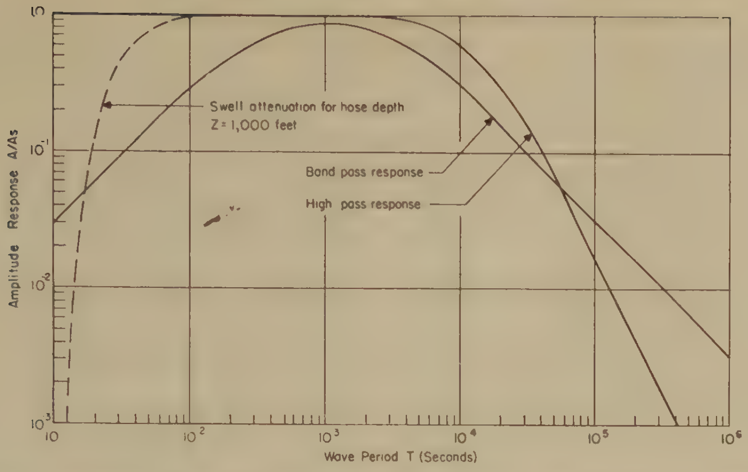

Fig. 4. Amplitude response of the hydraulic filter to a unit sine-wave, for circuit constants given in Table 1.

vice versa. In the field, calibration is more easily checked by applying a step input, for which the response functions are given by[3]

$$\text{Band-pass } \frac{A}{A_s} = \frac{e^{-at} - e^{-bt}}{R_2C_2(b-a)} \tag{3}$$

$$\text{High-pass } \frac{A}{A_s} = \left[1 - \frac{t}{(R_1C_1R_2C_2)^{1/2}}\right] \cdot \exp \frac{-t}{R_1C_1R_2C_2} \tag{4}$$

where

$$a,\, b = \frac{1}{2}\left[\frac{U}{R_2C_2} \pm \sqrt{\left(\frac{U}{R_2C_2}\right)^2 - \frac{4}{R_1C_1R_2C_2}}\right] \tag{5}$$

$$U = 1 + \frac{C_2}{C_1} + \frac{R_2C_2}{R_1C_1} \tag{6}$$

and t (sec) is the time elapsed after applying a step wave of unit height. Equations (3) and (4) are plotted in Figure 5, and the significant response criteria are the maximum amplitude (band-pass) and zero intercept (high-pass), both of which can be determined in the field to an accuracy of 1 per cent.

---

[3] Equation (4) is only strictly valid for the case where $R_1C_1 \doteq R_2C_2$, which was a requirement in the present design.

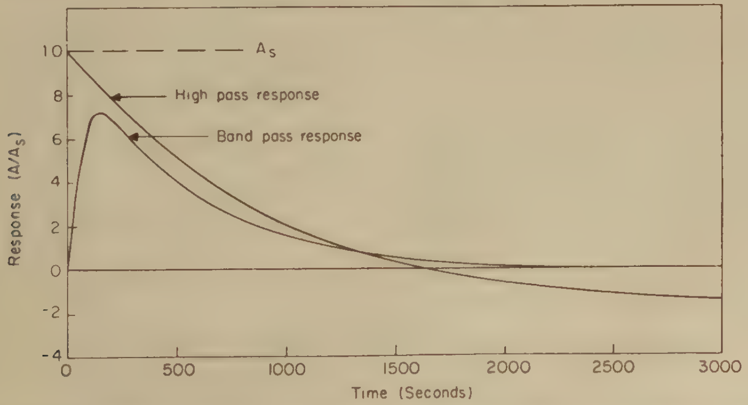

Fig. 5. Amplitude response of the hydraulic filter to unit step-function for circuit constants given in Table 1.

Data recording. Several years' experience in island recording indicates that the pressure amplitudes encountered are never likely to exceed ±30 cm of water, even during very large tsunamis. The pressure transducer selected on this basis is a Statham P5-0.5 psid, unbonded strain-gage unit which has a full scale sensitivity of ±35 cm of water and has been found to be accurate to 0.1 per cent (0.035 cm) of full scale. This transducer has an electrical output in the millivolt range, and in previous installations the signals were amplified by a transistor amplifier described elsewhere [*Van Dorn*, 1959] and recorded on an Esterline Angus 0-1 ma, strip-chart millameter. Since, in future installations, other variables, such as windspeed and direction and microbarometric pressure, will also be recorded, a Leeds and Northrup, 6-channel, multipoint recording potentiometer will be used. It will operate directly from the transducer signal.

Thermal sensitivity. Because the hydraulic filter employs resistance elements (capillaries) whose constants depend on the viscosity of the silicone oil flowing through them, the amplitude response in the region of high spectral discrimination is temperature dependent. This dependency has been investigated by *Snodgrass* [1958], who finds that a temperature change from 25°C to 15°C results in a response change of as much as 30 per cent or about 3 per cent per degree C. This effect is minimized in the high-pass circuit by shifting the temperature-sensitive cutoff region to very low frequencies, and continuous recording of water temperature permits a correction to be applied even though the ambient diurnal temperature change is only about 2°C in the tropical areas where the recorders will operate.

Future installations. The more than 96 months of useful records which have been obtained from twelve Pacific island stations over the past four years indicate that the long-wave recorder is a versatile and useful instrument for exploring the low-frequency surface-wave spectrum. Analysis of these data reveals that there is an abundance of activity throughout the spectrum. In addition to the daily occurrence of 'waves' associated with traveling small-scale barometric pressure fluctuations, long-period waves have been observed from two tsunamis and three large hurricanes. The results of these analyses—to be reported in a forthcoming series of papers—warrant continuing study of those phenomena on a more systematic basis than is possible with temporary installations.

Accordingly, three new permanent installations are planned for the spring of 1960 at Wake, Canton, and Johnston Islands. These recorders will operate in the high-pass configuration and will depend on a deep sea inlet for swell filtering. That portion of the tube which lies below 50-meters depth will again be a plastic hose, but the upper portion will be a rigid metal pipeline encased in concrete. It is expected that these instruments will be essentially free from the maintenance problems experienced with temporary installations, which were susceptible to storm damage and local vandalism.

This paper represents the results of research carried out by the University of California under contract with the Office of Naval Research.

REFERENCES

Munk, Walter H., H. V. Inglesias, and T. R. Folsom, An instrument for recording ultra-low-frequency ocean waves, *Rev. Sci. Instr., 19,* 654–658, 1948.

Snodgrass, Frank E., Shore-based recorder of low-frequency ocean waves, *Trans. Am. Geophys. Union, 39,* 109–113, 1958.

Van Dorn, Wm. G., A portable tsunami recorder, *Trans. Am. Geophys. Union, 37,* 27–30, 1956.

Van Dorn, Wm. G., Low cost dc-amplifier for field use, *Electronics, 33* (1), Jan. 1, 1960.

(Manuscript received November 5, 1959.)

BULLETIN OF THE GEOLOGICAL SOCIETY OF AMERICA
VOL. 71, PP 631–632, 1 FIG. MAY 1960

PHOSPHATIZED WOOD FROM THE PACIFIC SEA FLOOR

BY EDWARD D. GOLDBERG AND ROBERT H. PARKER

A recent expedition of the Scripps Institution of Oceanography, Tuna Oceanographic Cruise TO-58-2, Station D-7, dredged a sample of phosphatized wood from a 410-meter terrace in the Gulf of Tehuantepec (Dredge initiated at Lat. 14° 25′ N. and Long. 93° 05′ W. and concluded at Lat. 14° 27′ N. and Long. 93° 11′ W.). This wood has been identified as a dicotyledon (Elso S. Barghoorn, personal communication). A carbon-14 age determination made by Professor Hans Suess of this Institution on the organic wood phases indicates an age of greater than 28,000 years.

An X-ray diffraction spectrum of the mineralized portion revealed the phosphatic material to be similar to marine carbonate-fluorapatites, $Ca_{10}(PO_4, CO_3)_6F_{2-3}$, in which excess positive charge resulting from substitution of carbonate for phosphate is balanced by excess fluorine or hydroxyl groups. The mineral is a hexagonal network composed of phosphate tetrahedra, with the anions fluorine and hydroxide, and the divalent cation calcium within the structure (Altschuler, Clarke, and Young, 1958). The ratio of the uranium and thorium contents in the fossilized wood, 13 and 0.2 ppm respectively, is in agreement with the values reported by the above authors for marine apatites and is of concern here inasmuch as certain aspects of the marine geochemistry of these elements can be interpreted through studies of their occurrence in phosphatized wood and other calcium phosphates.

The orientation of the wood on the sea bottom is established by clay that adheres to one part of the specimen, the buried portion, but not to the remainder, the portion in contact with sea water. The phosphatization occurred only in that portion of the wood which was above the sediment–water interface; that part of the wood buried in the deposit was essentially free of phosphate infiltration.

The phosphate, as well as the other constituents of the apatite, were clearly derived from the overlying sea water, which at the 400-meter level in this area contains maximal values of phosphorus, of the order of 3 micromoles per liter (Fig. 1). The phosphate content of woods is only about 0.02 grams of P_2O_5 per 100 grams of dry weight material (Specter, 1956). For every molecule of oxygen in the sea water there is a molecule of phosphate and a few thousand molecules of calcium.

This area is notably productive with respect to plant life. The high fertility is reflected in the low values of oxygen below the photosynthetic zone where this gas has been consumed in the combustion of organic matter arising from plant and animal remains. The overlying waters have an exceedingly low oxygen content (between 0 and 0.1 ml. of O_2/liter) or an upper value of about 5 micromoles per liter (Fig. 1). The low oxygen values have a two-fold significance. First, these low tensions probably result in an incomplete combustion of the organic matter to forms less oxidized than CO_2. Hence, only minor contributions to that carbonate content of the sea water can be expected from the oxidation. Second, the absence of the apatite from the buried wood indicates that the combustion did not take place throughout the entire sample. The oxygen was apparently completely used up in the more easily penetratable, exposed portions.

The conditions of phosphatization can be reconstructed from the above evidences and previous investigations of the occurrences and properties of marine apatites. By the time the wood reached the deposit site, it was completely penetrated by sea water. Dissolved oxygen of the sea water reacted with the more readily oxidizable organic components of the wood with a subsequent reduction in Eh. This also leads to a decrease in pH, and this in turn diminishes the carbonate content. Although the hydrogen ion concentrations controlling the precipitation of calcium carbonate and calcium phosphate are remarkably similar, the high phosphate content of the water apparently turns the tide in favor of apatite deposition. Such an event has been postulated by Krumbein and Garrels (1952) who point out that phosphorite may well form in restricted basins in which the pH is relatively low—*i.e.*, deposits near or at anaerobism and with pH slightly lower than normal sea-water values of around 8.

The high uranium/thorium ratio, around 65, provides further evidence for delimiting the physico-chemical conditions of the environ-

ontributions from the Scripps Institution of Oceanography, New Series, 1154

(271)

Reproduced by Permission

ment. Altschuler *et al.* (1958) have demonstrated that the phosphatic nodules from the Pacific Ocean contain predominantly tetravalent uranium which is presumed to substitute directly for calcium in the apatite lattice; the ionic radius of U^{+4} is 0.97 Å, nearly identical to that of Ca^{+2} of 0.99 Å. Uranium enters the ocean in the hexavalent state, probably complexed as the carbonate (Starik and Kolyadin, 1957). The reduction of uranium would be enhanced in those phases of the deposit out of contact with the aerated water and approaching or at anaerobism. The simultaneous reduction of uranium with the formation of the apatite structure which easily accommodates the tetravalent form explains the enrichment of uranium in these nodules. The ionic radius of tetravalent thorium of 1.02 Å explains the capture of this ion from sea water by the apatite structure, in a way similar to that of tetravalent uranium. Whereas the *total* concentration of uranium in sea water is about 3 micrograms per liter, however, thorium concentrations have been delimited to this date only by a maximum value of 10^{-2} micrograms/liter. One can thus conclude that the activities of Th^{+4} and U^{+4} in the reducing environment of apatite formation are of the same order of magnitude as the concentrations of these elements in sea water.

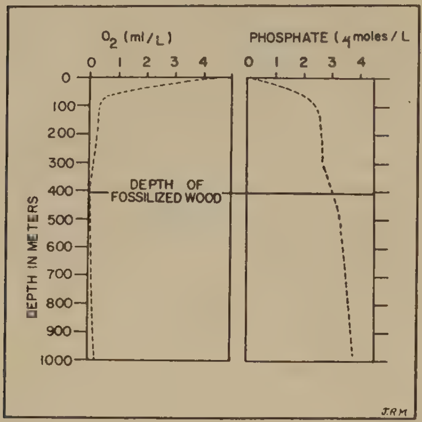

FIGURE 1—TYPICAL PROFILES OF DISSOLVED GASEOUS OXYGEN AND PHOSPHATE IN SEA WATERS FROM THE VICINITY OF THE DREDGED LOG

Data from Tuna Oceanographic Cruise TO-58-2

These views are not in conflict with present opinion on the deposition of phosphate in the marine environment (McKelvey *et al.*, 1953). Marine apatites today are found in eastern oceanic coastal deposits where upwelled waters give rise to high productivity of organic matter. The rapid accumulation of this organic matter on the sea floor can produce an environment similar to that of our wood sample.

This work was supported by the Office of Naval Research under contracts with the University of California.

References Cited

Altschuler, Z. S., Clarke, R. S., and Young, E. J., 1958, Geochemistry of uranium in apatite and phosphorite: U. S. Geol. Survey Prof. Paper 314-D, 90 p.

Krumbein, W. C., and Garrels, R. M., 1952, Origin and classification of chemical sediments in terms of pH and oxidation reduction potentials: Jour. Geology, v. 60, p. 1–33

McKelvey, V. E., Swanson, R. W., and Sheldon, R. P., 1953, The Permian phosphorite deposits of Western United States: 19th Internat. Geol. Cong. (Algiers), C.R., Section XI, p. 45–64

Spector, W. S., *Editor*, 1956, Handbook of biological data: Philadelphia, W. B. Saunders, 584 p.

Starik, I. E., and Kolyadin, L. B., 1957, The conditions of occurrence of uranium in ocean water: Geokhimiya, v. 1957, p. 204–213

SCRIPPS INSTITUTION OF OCEANOGRAPHY, UNIVERSITY OF CALIFORNIA, LA JOLLA, CALIFORNIA

MANUSCRIPT RECEIVED BY THE SECRETARY OF THE SOCIETY, DECEMBER 1, 1959

Reprinted from SCIENCE, May 6, 1960, Vol. 131, No. 3410, pages 1374-1376

On the Thermal Boundary Layer of the Ocean

Abstract. Measurement of the long-wave infrared radiation from the top 0.1 mm of the evaporating ocean demonstrates the existence of a cool surface layer characterized by departures of as much as 0.6°C from the "surface temperature" found by conventional methods. Being very thin, the layer cools sufficiently rapidly to reestablish itself in less than 12 seconds after disruption by a breaking wave.

By means of simultaneous measurements of the radiation temperature and of the conventional thermometric temperature of the ocean, we have found evidence of a persistent cool boundary layer. The equipment used, shown in Fig. 1*A*, consisted of a double-beam radiometer having a spectral sensitivity in the band from 6 to 20 μ, a region in which the absorption in water is so high that 98 percent of the radiant flux originates in the first 0.1 mm. To minimize the necessary corrections for absorption by air and for reflection, the measurements were made at normal incidence at night from a position 2 m above the water. The water was shaded as required. For comparison, the temperature of the water beneath the radiation layer was measured by thermistors encapsuled in 1-mm glass beads, at depths dictated by the surface conditions of swell, waves, and ripples. The system had over-all sensitivity sufficient to discriminate temperatures with an uncertainty of less than 0.1°C, with response of less than 1 second.

Ocean measurements were made from the Scripps pier at a point 200 m off shore in water 7 m deep. A sample traced from the data is shown in Fig. 1*B*, which includes, for comparison, the "surface temperature" obtained by thermistor. The latter was checked by bucket sampling and mercury thermometer. The radiation temperature, when the ocean was shaded from the clear, cold night sky, was more than 0.7°C lower than the thermistor temperature. Since the screen used was at air temperature and therefore cooler than the ocean, a correction of +0.1°C must be applied to the measured value, which leaves a departure of the radiation temperature of more than −0.6°C. It should be noted that the conditions of wind and humidity were not conducive to vigorous evaporation. The effect of exposing the ocean to the night sky by removing the shade is readily seen in the right-hand section of the figure.

In order to evaluate the effect of breaking waves, a small electric rotary pump was submerged beneath the radiometer, positioned so as to draw water from a depth of 15 cm and direct it as a jet which welled up in the radiometer's field of view. It was determined by bathythermogram and thermistor that the water below the upper centimeter was isothermal within measurable limits. The result of intermittent pumping is shown in Fig. 1*C*. When the pump was run sufficiently vigorously to rupture the surface in the manner of a bubbling spring, the radiation temperature rose to approximately the values measured by the thermistor submerged at the level of the pump intake. When the pump was shut off, the radiation temperature dropped to its normal value in about 5 seconds, the cooling rate indicating that the effect takes place in a layer less than 1 mm thick. A remarkable finding was that less intense disturbance of the water failed to produce measurable effects.

Radiometric measurement over a breaking wave gave a concordant result. Coincident with the breaking, a momentary small warm signal was recorded, followed by a longer-lasting, stronger cold signal which seemed to coincide with the life span of the blanket of foam left behind by the wave. The whole disturbance lasted about 12 seconds; then the radiation returned to its normal value. Thus, on the open sea where whitecaps occur at a given point at relatively long intervals, the thermal boundary layer should be present, at least intermittently.

The chief features observed on the ocean were modeled in a controlled laboratory environment. In Fig 1*D* is shown, at the left, the radiation temperature of a salt-water surface being gradually warmed by radiation from the ceiling and walls of the room. Under these conditions, the heat flux was downward, and the water was initially in a state of stable stratification with a warm surface layer. As indicated in the figure, a fan was caused to blow periodically on the surface, the air stream having a velocity of about 1 m/sec and a relative humidity of 55 percent. At the onset of evaporation, the radiation temperature quickly dropped about 1°C in 40 seconds, the polarity of its departure from the bulk temperature reversing from positive to negative. Cessation of the draft produced a return to the initial temperature but at a much slower rate, due, no doubt, to the diminished role of convection in the flow of heat. At the right side of the figure is shown the result of vigorous agitation by a conventional laboratory stirring device positioned so as to produce strong vertical currents in the water. The precipitous drop in temperature coincided with the arrival of cool subsurface water in the radiation layer. Increased evaporation caused by the fan while the stirring continued is plainly shown in the record, though the temperature departures are much reduced in amplitude, probably because of induced changes in the thermal conductivity of the boundary layer.

Additional laboratory experiments were performed with varying conditions of imposed radiation, evaporation, and stability. The general result was that the departure of the radiation temperature from the bulk temperature increased with the flux of heat through the radiation layer, the polarity being positive for downward flow and negative for upward flow. Thermal conditions were steadier in the case of downward heat flux. Moderate vertical stirring reduced but did not obliterate the thermal boundary layer.

It is well known that the ocean, in ice-free latitudes, is heated to a considerable depth by short-wave solar radiation, the heat balance being largely maintained by evaporation and long-wave back radiation from much shallower depths. It follows, therefore, that the heat flux in the superficial layers must, on the average, be upward. Consequently, one may conclude that the radiation temperature of the ocean and other natural bodies of water is usually lower than the ordinary surface temperature.

Because the thermohydrodynamics of a free saline liquid surface have not, as yet, been formulated in detail, it would be premature to attempt a theoretical analysis of the phenomena observed. Neither would it be prudent to identify the phenomena observed too closely with phenomena characteristic of rigid-boundary surfaces. Nevertheless, the experimental results appear consistent with the hypothesis that a boundary layer exists, immediately under the ocean surface, in which transfer of sensible heat is controlled chiefly by molecular conduction rather than by convection or turbulent exchange. In this layer, thermal gradients are maximized.

Contributions from the Scripps Institution of Oceanography, New Series, 1155

Reproduced by Permission

The transition between the boundary layer and the deeper region where turbulent conduction is fully developed is characterized by unsteady thermal conditions which we observed by placing thermistors in vertical arrangement near the surface. Fluctuations appeared, having time constants of less than 1 second. The unsteadiness is much more fully developed when the heat flux is upward than when it is downward. Temperature fluctuations in air heated close to the ground are described in some detail by Sutton (*1*) being attributed to bubbles of overheated air which periodically detach themselves from the thermal boundary layer. In a personal communication, R. W. Stewart, described similar phenomena observed by means of the schlieren method in the cool, unstable thermal boundary of evaporating water. Unsteady thermal conditions in the surface of cooling ponds and sheltered estuaries have been reported by Woodcock and Stommel (*2*).

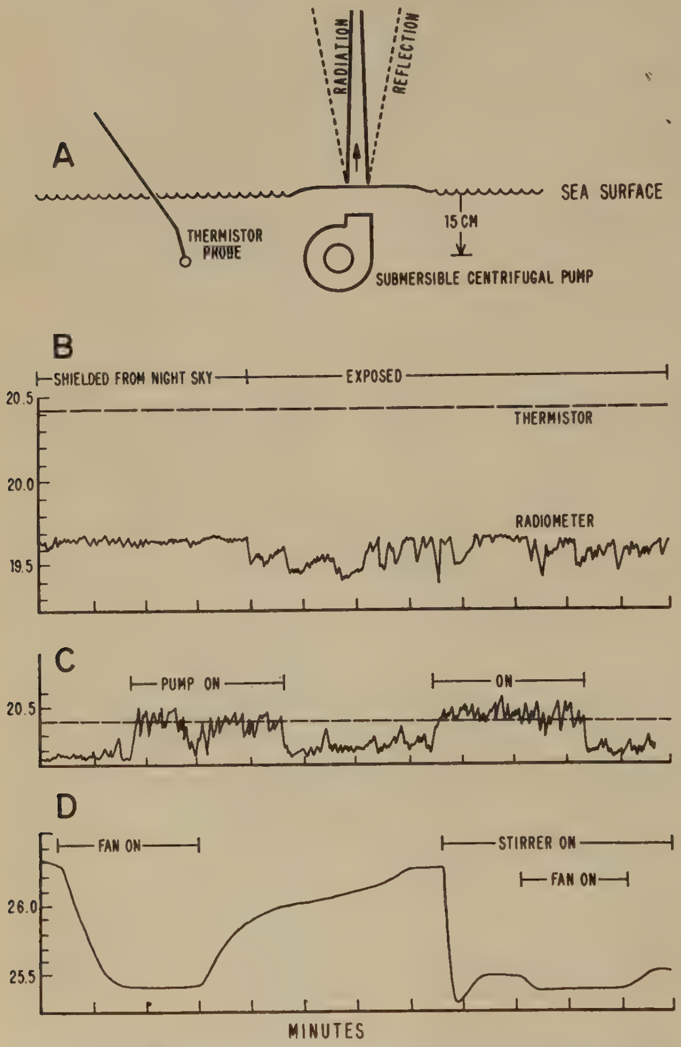

Fig. 1. Simultaneous measurements of the radiation temperature and of the subsurface temperature of evaporating water surfaces. (*A*) Schematic diagram of apparatus. (*B*) Trace of radiometer record in relation to thermistor temperature (dashed line), 2 October, 2300 (P.S.T.); wind, at 10 m above mean sea level, ½ m/sec; sky clear; air temperature 2 m above mean sea level, dry bulb 18.4°C, wet bulb 16.7°C; air temperature 8 m above mean sea level, dry bulb 18.0°C, wet bulb 16.2°C; relative humidity, 83.5 percent at 2 m, 85.0 percent at 8 m. (*C*) Effect of water jetted into surface by submerged pump. (*D*) Effect of induced evaporation and mechanical stirring on water in an insulated container. Air temperature, 32.8°C; fan velocity, 1 m/sec; relative humidity, 55 percent.

Further study of the thermal boundary layer should reveal details of the mechanism by which contaminating surface films reduce evaporation from natural bodies of water. In general, it is to be noted that surface temperatures of the ocean or other wind-swept bodies of water determined by conventional methods are systematically biased in a positive sense (*3*).

GIFFORD EWING
Scripps Institution of Oceanography,
University of California, La Jolla
E. D. MCALISTER
Apparatus and Optics Division,
Eastman Kodak Company,
Rochester, New York

References and Notes

1. O. G. Sutton, *Micrometeorology* (McGraw-Hill, New York, 1953), chap. 4.
2. A. H. Woodcock, *J. Marine Research* (*Sears Foundation*) 4, 153 (1941); ——— and H. Stommel, *J. Meteorol.* 4, 102 (1947).
3. This study was supported by the Office of Naval Research. Credit is due Norman E. Head for technical assistance. This report is a contribution from the Scripps Institution of Oceanography.

21 December 1959

JOURNAL OF GEOPHYSICAL RESEARCH VOLUME 65, NO. 4 APRIL 1960

Indications of Deep Pacific Circulation from the Distribution of Properties at Five Kilometers[1]

WARREN S. WOOSTER

Scripps Institution of Oceanography
La Jolla, California

AND

GORDON H. VOLKMANN

Woods Hole Oceanographic Institution
Woods Hole, Massachusetts

Abstract. A description of the deep Pacific Ocean, based on 145 deep oceanographic stations, is presented, showing the distributions of *in situ* temperature, potential temperature, salinity, and dissolved oxygen at a depth of 5 km. At this depth the open Pacific appears to consist of four major connecting basins. Bottom water is introduced at high southern latitudes from the deep Indian Ocean; initially it has the following characteristics: *in situ* temperature, 0.9°C; potential temperature, less than 0.5°C; salinity, 34.7‰; dissolved oxygen, 5.0 ml/l.

Salinity variations at this depth are little greater than measurement errors, the average value for the whole open Pacific being 34.695‰ with a standard deviation of 0.034‰. *In situ* temperature increases from south to north, the rate of increase being much greater in the central basin than in either the southern or the northern basin. This increase is attributed to heat flow through the sea floor and to mixing with overlying waters. Both the change of temperature and the observed northward decrease of dissolved oxygen content are consistent with a northward drift of bottom water. The deep water of the eastern North Pacific is presumably the 'oldest' water of the open ocean, its properties having been most extensively modified: *in situ* temperature, 1.6°C; potential temperature, 1.1°C; dissolved oxygen, 3.4 ml/l.

Introduction. Classically, the deep ocean circulation has been indirectly studied by inference from the distributions of temperature and dissolved substances at great depths. Our limited knowledge of the deep Pacific is due to the use of this method by *Wüst* [1937] and by *Sverdrup, Johnson, and Fleming* [1942]. Today, promising new techniques are being applied, such as the direct measurement of deep flow [*Swallow*, 1955; *Swallow and Worthington*, 1957] and the use of artificial and natural isotopic tracers for the study of transfer phenomena in the sea [*Craig*, 1957].

Nevertheless, a re-examination of the distribution of properties seems warranted, since (1) the number of deep oceanographic observations in the Pacific has more than doubled since 1942, so that one can now describe abyssal conditions in greater detail than heretofore, and (2) the new techniques, although promising, do not yet give unequivocal answers. Furthermore, the observations are so expensive and time consuming that it will be many years before a systematic body of data is available from the whole Pacific. Meanwhile, knowledge of the characteristics of deep ocean waters provides a framework to which the new measurements can be referred.

Sources and treatment of data. A search of the sources of Pacific oceanographic data yielded 145 stations which reached depths of approximately 5 km and whose data appeared to be sufficiently reliable to provide usable information (Table 1). These observations were made during the last 30 years and, although irregularly spaced, are widely distributed throughout the Pacific basin (Fig. 1).

For each station temperatures were plotted against depth, and salinities and dissolved oxygen concentrations were plotted as functions of

---

[1] Contribution from the Scripps Institution of Oceanography and the Woods Hole Oceanographic Institution. This work was supported by the Office of Naval Research.

Contributions from the Scripps Institution of Oceanography, New Series, 1156
Reproduced by Permission

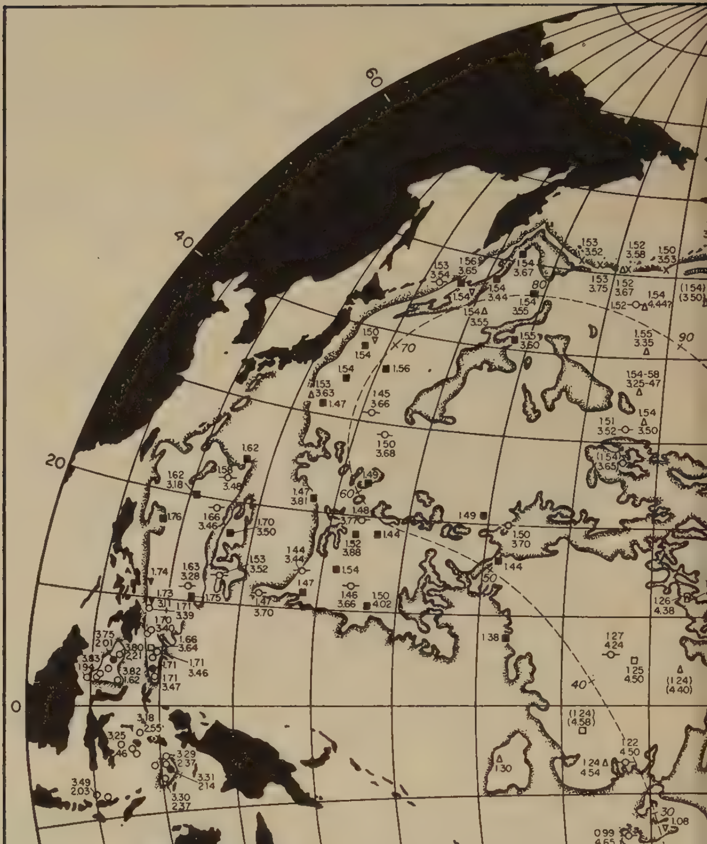
60
40
20
0
20
40
60
60
70
80
90
60
50
40
30
160
140
120
1.53 3.52
1.52 3.58
1.50 3.53
1.53 3.54
1.56 3.65
1.54 3.67
1.53 3.75
1.52 3.67
1.54 4.44?
(1.54) (3.50)
1.54 3.44
1.54 3.55
1.54 3.55
1.52
1.55 3.60
1.55 3.35
1.50
1.54
1.56
1.53 3.63
1.47
1.45 3.66
1.54-58 3.25-47
1.54
1.51 3.52
3.50
1.50 3.68
(1.54) 3.65
1.62
1.58 3.48
1.62 3.18
1.49
1.47 3.81
1.76
1.66 3.46
1.70 3.50
1.48 3.77
1.49
1.44
1.52 3.88
1.50 3.70
1.44
1.44 3.44
1.53 3.52
1.54
1.74
1.63 3.28
1.73 3.11
1.71 3.39
1.75
1.47 3.70
1.47
1.46 3.66
1.50 4.02
1.26 4.38
1.70 3.40
1.38
3.75 2.01
3.80 2.21
1.66 3.64
1.27 4.24
3.83 1.94
3.82 1.62
1.71 3.46
1.71 3.47
1.25 4.50
(1.24) (4.40)
(1.24) (4.58)
3.18 2.55
3.25 2.46
1.22 4.50
1.30
3.29 2.37
1.24 4.54
3.49 2.03
3.31 2.14
3.30 2.37
1.08
0.99 4.65
1.08 4.37
1.07
1.03 4.56
1.08 4.58
1.07 4.50
1.01 4.53
1.02 4.55
1.04 4.46
1.12
1.00
0.90 3.87
0.90 4.16
0.96 4.27
0.95 3.96
0.88 5.02
(0.91)

Fig. 1. Distribution of *in situ* temperature (°C, upper number) and dissolved oxygen (ml/l, lower number, when available) at 5 km. Sources of data are indicated by symbols and listed in Table 1 Dashed line is arbitrary flow line (see text).

(276)

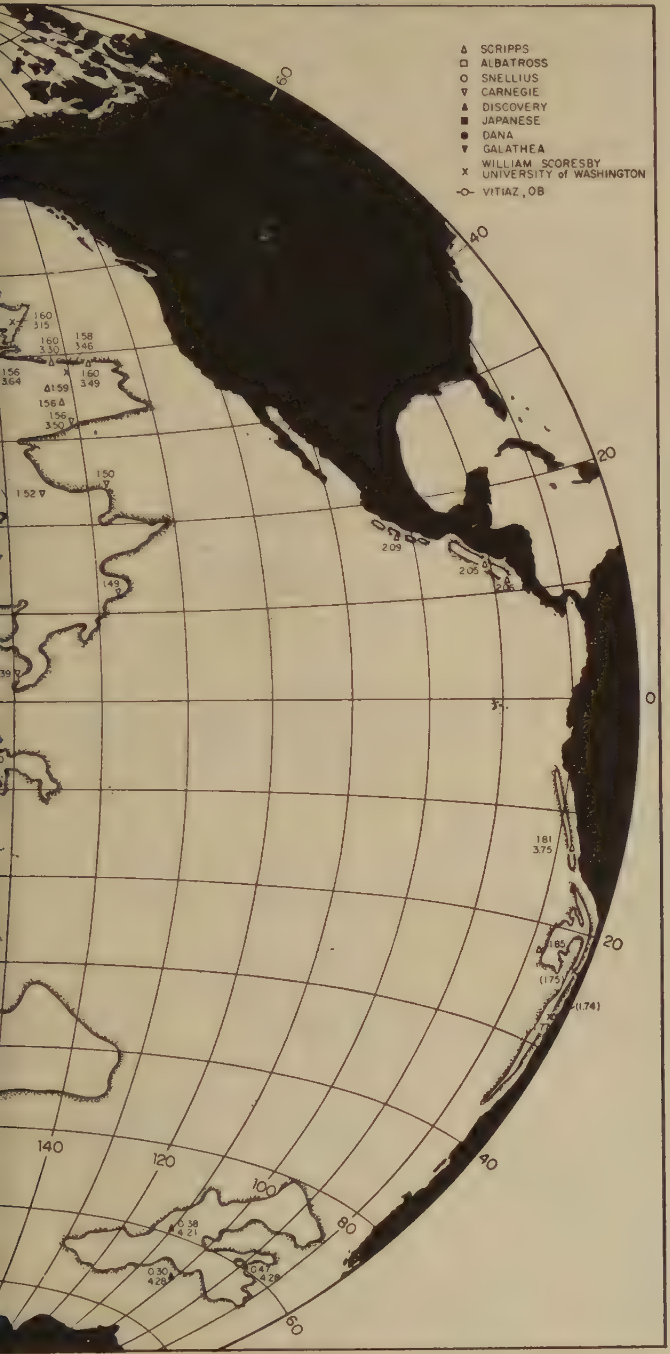
△ SCRIPPS
□ ALBATROSS
○ SNELLIUS
▽ CARNEGIE
▲ DISCOVERY
■ JAPANESE
● DANA
▼ GALATHEA
× WILLIAM SCORESBY UNIVERSITY of WASHINGTON
-○- VITIAZ, OB
60
40
20
0
20
40
60
80
100
120
140
160 315
160 3.30
158 346
156 3.64
160 349
1.59
156
156 350
150
152
149
39
2.09
2.05
2.05
181 3.75
1.85
(1.75)
(1.74)
0.38 4.21
0.30 4.28
0.47 4.28

temperature. In the drawing of the station curves, data from neighboring stations were used to facilitate interpolation. It is estimated that the values read at 5 km are subject to the following random errors: temperature, ±0.03°C; salinity, ±0.04 ppm; oxygen, ±0.05 ml/l.

Values of temperature and dissolved oxygen were plotted on an equal-area chart along with the 5-km isobath (Fig. 1). Salinity values were not plotted, since, as will be discussed later, spatial variations in salinity are little greater than the uncertainty in the reported data.

Configuration of the Pacific abyss. The 5-km

TABLE 1. Sources of Data Used in Study of Five-Kilometer Surface

Identification	Year	Stations	Reference
Albatross	1947–8	105, 123, 128, 133, 138, 162	*Bruneau et al.* [1953]
Carnegie	1929	116, 119, 137, 139, 142, 146, 148, 151, 156, 162	*Fleming et al.* [1945]
Dana	1928–9	3580, 3628, 3676, 3683, 3745	*Carlsberg Found.* [1937]
Discovery II	1932	972, 974, 976	*Discovery Comm.* [1941]
	1938	2217	*Discovery Comm.* [1947]
	1950–1	2735, 2769, 2819, 2823, 2824, 2825	*National Inst. Oceanog.* [1957]
Galathea	1951–2	412, 433, 677	*Bruun and Kiilerich* [1955]
*Japanese**	1933–5	24–15, 28, 68, 83; 27–35; 30–18; 31–88, 95; 32–B77, B84	*Japan, Maritime Safety Agency* [1950]
	1935–7	33–46, 51; 34–107; 35–11, 33; 36–32, 78; 38–92; 42–143; 43–78	*Japan, Maritime Safety Agency* [1951]
	1938	52–24, 94	*Japan, Maritime Safety Agency* [1952]
Ob	1958	361, 393	Data from IGY World Data Center A, College Station, Texas
Scripps	1952–3	*Capricorn* 7, 26	Data on file, Scripps Institution
		Transpac 11, 24, 59, 99	
	1954	*Cusp* B, C	
		Acapulco Trench 8, 12, 15	
	1955	*Norpac* 5, 43	
	1956	*Equapac* 9, 17, 28 *Chinook* 2, 4, 5, 6, 7, 10, 11, 12, 13, 13a, 14	
	1957	*Mukluk* 1, 10	
	1958	*Downwind* 28, 31, 32	
Snellius	1929–30	47, 48, 52, 53, 76, 180	*Van Riel et al.* [1950]
		197, 210, 212, 229, 235, 251, 260, 262, 264, 265, 272, 275, 301, 321, 362, 365	*Postma* [1959]
Vitiaz	1953–5	B, D.	*Brujewicz* [1957]
Vitiaz	1957–8	3625, 3631, 3634, 3686, 3689, 3726, 3728, 3746, 3759, 3778, 3780, 3795, 3805, 3812, 3818, 3823, 3827, 3831, 3876	Data from IGY World Data Center A, College Station, Texas
	1958	4066, 4096, 4120	mss data, courtesy N. N. Sysoev
Washington	1954, 7	64–26; 176–1, 8, 10, 15	Data on file, Univ. Washington
	1958	199–11, 14	
William Scoresby	1931	612, 629	*Discovery Comm.* [1949]

* Oxygen data from these stations were furnished by Dr. Y. Miyake.

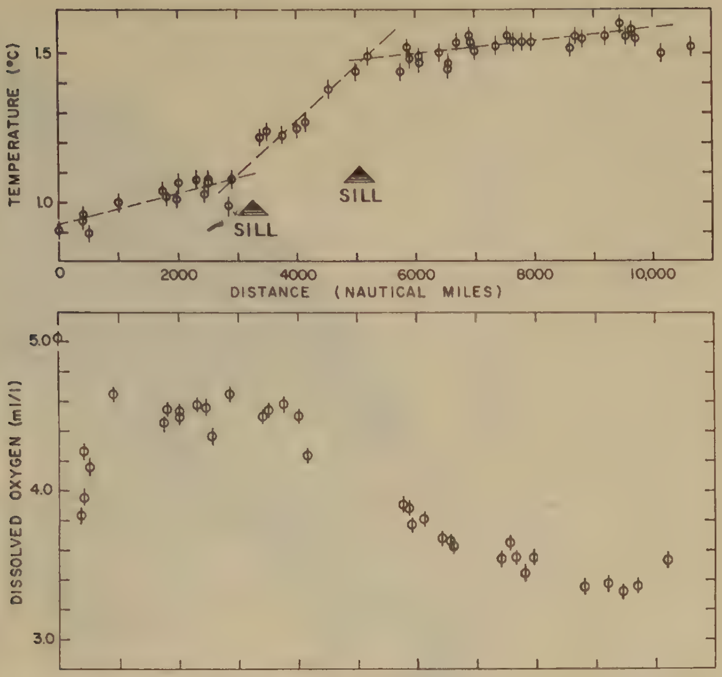

Fig. 2. *In situ* temperature (°C) and dissolved oxygen (ml/l) at 5 km along arbitrary flow line. Distance in nautical miles from origin at 55°S, 170°E. Arrows indicate positions of supposed sills between southern and central basins (at 3200 miles) and between central and northern basins (at 5000 miles.

isobath used in this study (Fig. 1) was derived from an unpublished chart of H. W. Menard. That portion of the open Pacific deeper than 5 km appears to be divided into four major basins: a southern basin extending from 60°S to 10°S, a central basin extending from 10°S to nearly 20°N, a northern basin reaching northward to 50°N from 140°E to 130°W, and an eastern basin lying between 10° and 20°N, east of 170°W. It is possible that the northern basin is further divided into an eastern and western part by a chain of topographic highs extending from Hawaii to Kamchatka.

Division into the four major basins is not always based on detailed soundings, and the existence and character of the dividing sills must be accepted with reservations at this time. However, as will be seen later, the existence of the sills between the southern and central basins and between the central and northern basins does seem to be supported by the temperature data.

Other large areas deeper than 5 km include the Bellingshausen Basin in the eastern South Pacific, and the Philippine Sea Basin in the western tropical Pacific.

Distribution of temperature. The distribution of temperature at 5 km is described in three ways: individual station values are plotted on an equal-area chart (Fig. 1); temperatures on stations near an arbitrary flow line are plotted against distance from the origin of this line at 55°S (Fig. 2); the distribution of potential temperature is shown on an equal-area chart (Fig. 3). The arbitrary flow line (Fig. 1), which we have introduced as a convenience in discussing the distributions of temperature and oxygen, stems from the general picture of circulation in the Pacific abyss, which is discussed later.

The lowest values of *in situ* temperature at 5 km in the Pacific, 0.30° to 0.47°C, are found in the Bellinghausen Basin in the eastern South Pacific; the highest, 3.83°C, occurs in the iso-

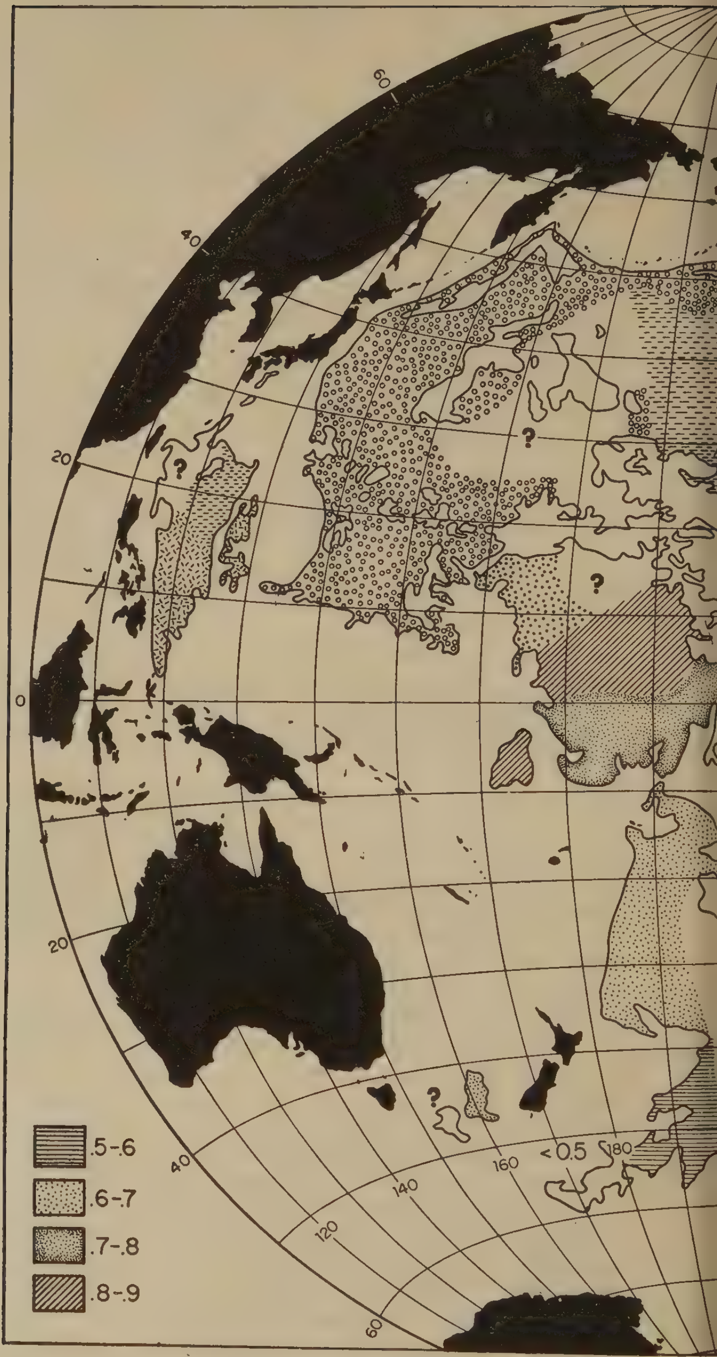
60
40
20
0
20
?
?
?
?
▤ .5-.6
▨ .6-.7
▨ .7-.8
▨ .8-.9
40
120
140
160
<0.5
180
60

Fig. 3. Distribution of potential temperature at 5 km (based on stations shown in Fig. 1).

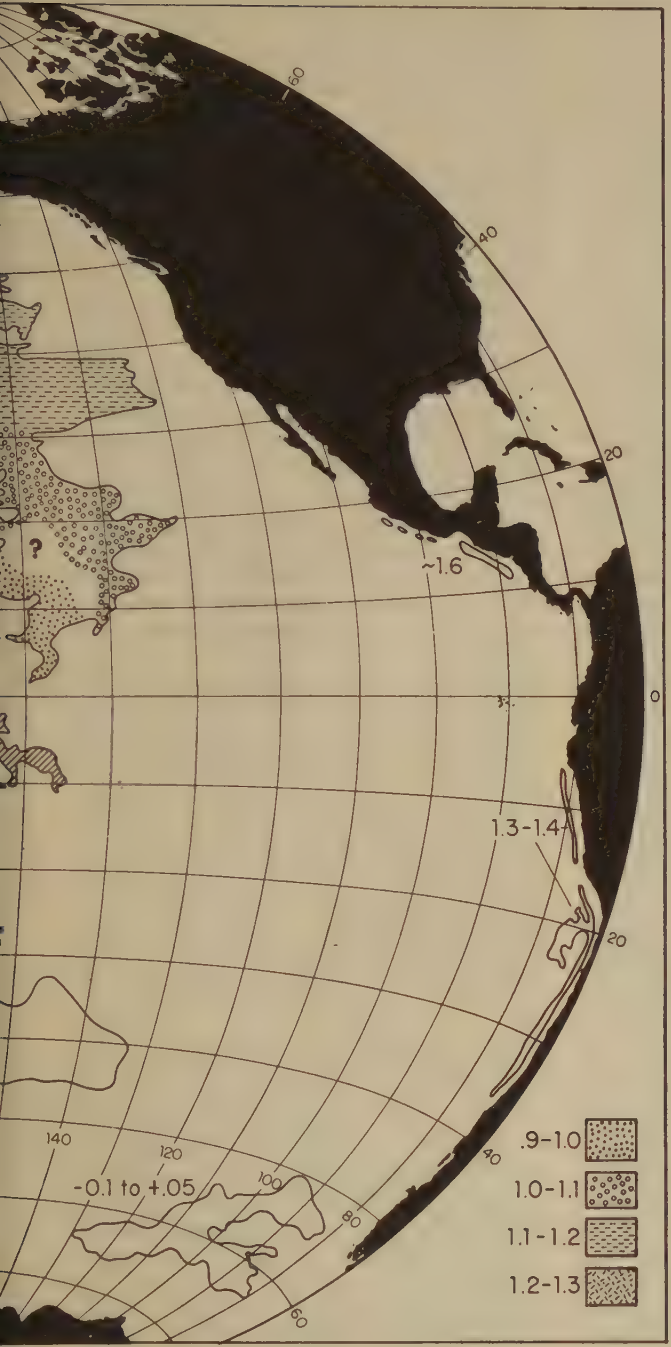
60
40
20
?
?
~1.6
0
1.3-1.4
20
140
120
-0.1 to +.05
100
80
40
60
.9-1.0
1.0-1.1
1.1-1.2
1.2-1.3

lated Celebes Basin of the Malay Archipelago. The range is much smaller in the major basins of the open ocean; the temperature increases from about 0.9°C south of 50°S to 1.6°C in the eastern North Pacific. Along the arbitrary flow line the increase is not uniform (Fig. 2), being about $0.03°/10^3$ km in the southern basin, $0.10°/10^3$ km in the central basin, and $0.01°/10^3$ km in the northern basin. Changes from one rate of temperature increase to another take place near the supposed sills between basins; there is also a suggestion (Fig. 1) of an abrupt increase in temperature (from 1.08° to 1.22°C) across the sill between the southern and central basins, although the data are too sparse to establish this definitely.

In the eastern basin, beyond the arbitrary flow line, the water at 5 km is slightly cooler than it is farther north, the few available values falling between 1.52° and 1.37°C. The temperature in the Aleutian Trench is similar to that in the northern basin with which it connects, whereas in the more isolated Middle America and South America Trenches high average values are found (2.08° and 1.78°C, respectively).

Potential temperatures were computed from an unpublished table of R. B. Montgomery. In order to determine the absolute value of potential temperature, it is necessary to know accurately the coefficient of thermal expansion —the factor which varies more with temperature and pressure than the other pertinent quantities. *Eckart* [1958] pointed out that this value is seriously in doubt, especially at low temperature and elevated pressure. In our use of potential temperature, at constant pressure and with a small horizontal temperature range, this uncertainty presumably does not adversely affect the significance of the distribution (Fig. 3).

The distribution of potential temperature does not, of course, differ markedly from that of *in situ* temperature, the difference between the two values being relatively constant (0.40° to 0.45°C) at this depth throughout the basin. Again it is evident that in the major basins through which the principal circulation takes place the highest temperatures occur in the eastern part of the northern basin.

Although more detailed, the picture is similar in its general features to the 4-km potential-temperature chart of *Wüst* [1937], which was based for the most part on earlier data. Only east of Japan and the Kuriles, where Wüst shows a region of low potential temperature (less than 0.6° to 1.0°C), do the two charts differ markedly. The modern data do not confirm the existence of this low-temperature area even at 4 km, which is the average depth of the deep temperature minimum in the western North Pacific.

Distribution of salinity. The available salinity data are surprisingly similar everywhere in the deep Pacific. On the 86 stations with reliable salinity data in the open Pacific the average value at 5 km was 34.695‰ with a standard deviation of 0.034‰. This range of variation is not much greater than measurement errors in the conventional salinity method. For example, in a recent study based on field data *Wooster and Taft* (in press) concluded that the upper limit of measurement errors could be estimated as 0.018‰ (standard deviation). Until more accurate salinity data are available from the deep Pacific it does not seem profitable to plot salinity values on the 5-km chart.

Salinity data from the various basins were examined for evidence of downstream change (Table 2). Although there appears to be a slight decrease of salinity downstream, the data are inadequate to establish significant differences.

Distribution of dissolved oxygen. The distribution of dissolved oxygen at 5 km is shown as individual station values (Fig. 1) and as a function of distance along the arbitrary flow line (Fig. 2). The extreme range is from 1.62 ml/l in the isolated Celebes Basin (where the highest temperatures were also observed) to about

TABLE 2. Salinity Data

Area	No. of Observations	Average Salinity, ‰	Standard Dev., ‰
Southern Basin	15	34.710	0.043
Central Basin	11	34.710	0.033
Western Northern Basin	25	34.693	0.029
Eastern Northern Basin	33	34.686	0.035
Open Pacific	86	34.695	0.034

5.0 ml/l in the western South Pacific. The open ocean range is, of course, much smaller, from 5.0 ml/l down to low values of about 3.4 ml/l in the eastern North Pacific.

It is evident that a pronounced decrease in dissolved oxygen content parallels the increase in temperature from south to north through the major basins. A region of high oxygen content (more than 4.5 ml/l) extends from 60°S throughout the southern basin and up to the equator in the central basin. It should be noted that within this region there are four anomalous values south of 50°S. All these values are from *Discovery II*, in 1938 and 1951, and are lower than all other oxygen values at 5 km in the western South Pacific.

North of the region of high oxygen content the rate of decrease of dissolved oxygen is large (about 0.15 ml/l per 10^3 km). This sharp decrease appears to begin somewhere beyond the sill between the southern and central basins. In the North Pacific the rate of oxygen decrease from west to east seems to be somewhat smaller. Data from the Scripps *Transpacific* Expedition show a parallel increase in inorganic phosphorus content at 5 km, from 2.51 μg atoms/l on *Transpacific* 99 (at 140°E) to 3.04 μg atoms/l on *Transpacific* 11 (at 140°W). Unfortunately, no deep oxygen data are available from the eastern basin.

Discussion. Knowledge of the Pacific abyssal circulation was summarized by *Sverdrup, Johnson and Fleming* [1942, pp. 751–755]. Deep and bottom waters of high density are formed only in high latitudes; in the North Pacific this does not occur because of low surface salinities. Although it has not been demonstrated conclusively that no bottom water is formed in the Pacific sector of the Antarctic, it is generally accepted that Pacific bottom water originates in the Weddell Sea and to the south of the Indian Ocean [*Deacon*, 1937]. This water then enters the Pacific basin between Tasmania and Antarctica. The Pacific and Indian Oceans are separated by a ridge extending southward from Tasmania, with a greatest depth of about 3500 meters (U. S. Navy Hydrographic Office Chart No. 2562, 1956). Recent carbon-14 measurements in this region [*Brodie and Burling*, 1958] suggest that the entering waters are several thousand years old, but the published observations were taken at too shallow a depth and were too few to be conclusive.

Some fraction of the Antarctic bottom water flows northward into the southern and central basins. Sverdrup suggested that a sluggish northward flow takes place on the western side of the ocean with return flow to the south on the eastern side. The exchange of deep and bottom water across the equator is believed to be very small, the average velocities of flow being estimated as fractions of a centimeter per second.

A somewhat different picture is presented by *Stommel* [1958] in a recent theoretical discussion of abyssal circulation. He envisions a balance between two 'point sources' of deep water (in the North Atlantic and the Weddell Sea) and an oceanwide 'sink' with upward flux everywhere across the 2-km surface. If the sources are connected with this distributed sink in a way consistent with the dynamics of a fluid on a rotating sphere, it appears that the meridional component of velocity in the deep sea is everywhere directed away from the equator, where it vanishes, except in the western parts of oceans where intense boundary currents occur. In the western Pacific such a strong current flowing northward across the equator toward the 30°N parallel is suggested; north of it there is an oppositely directed boundary current [Fig. 2 of *Stommel*, 1958].

Unfortunately, the present description of the distribution of properties on the 5-km surface cannot be used for a direct and convincing test of these ideas of the deep Pacific circulation. We believe, however, that it can contribute to an understanding of some aspects of the problem.

If one assumes that all bottom water enters the Pacific through the passage between Australia and Antarctica, its initial properties in the Pacific at 5 km are those observed south of New Zealand: *in situ* temperature about 0.9°C, potential temperature less than 0.5°C, salinity slightly greater than 34.7‰, and dissolved oxygen content about 5.0 ml/l.

The low values of oxygen content in this region found by *Discovery II* in 1938 and 1951 are not consistent with the two recent *Ob* values or with the widespread presence of more highly oxygenated water north to the equator. A possible explanation is that the oxygen content of the entering water differs from year to year. However, such variation is not reflected in the other values of the southern basin, all of which from 1929 to 1957 are uniformly higher than the *Discovery II* values.

The temperature of bottom water can be expected to increase downstream because of (1) heat flow through the sea floor and (2) mixing with overlying warmer waters. Thus the increase of temperature along the arbitrary flow line on the western side of the deep Pacific is consistent with flow from south to north. As noted before, the rate of increase is not everywhere the same, being much greater in the central basin than it is in either the southern or the northern basin; the changes in rate appear to occur near the supposed positions of the sills between basins. At a lesser depth (4 km) the rate of increase is constant (about 0.05°C per 10^3 km) throughout the southern and central basins; in the northern basin there is no temperature increase at this depth.

The observed changes in rate of temperature increase imply that the speed of flow is not the same in all basins, or that the rate of adding heat, either through the sea floor or from above, is not everywhere the same. The speed of flow in the various basins cannot easily be determined from the present data, but it is obvious that the rate of heating is not uniform everywhere. The available measurements of heat flow through the sea floor show at least 50-fold variation [*Von Herzen*, 1959]. In the northern basin, where the rate of temperature increase is very small, heating from below must be important because at all deep stations in that region *in situ* temperature *decreases* upward to a deep temperature minimum at a depth of about 4 km. Such a temperature minimum is not evident in the central basin, where the rate of temperature increase is greatest, or in the southern basin.

The dissolved oxygen content of bottom water can be expected to decrease downstream because of (1) consumption in oxidative processes (respiration, decomposition) and (2) mixing with overlying, more poorly oxygenated waters. Decreasing oxygen concentrations along the arbitrary flow line tend to support the temperature data in indicating northward flow of the bottom water. The rate of decrease is about the same at both 5 and 4 km, although the oxygen concentration is usually higher at the greater depth.

In the northern basin changes in the properties of bottom water are smaller, and the nature of the circulation is not clear. The slight west-to-east increase in temperature across the North Pacific is compatible with the classical picture of clockwise circulation, as is shown by the arbitrary flow line. A slight decrease in oxygen content (and an increase in that of inorganic phosphorus) is also consistent with the indicated direction of flow. On the other hand, temperature data from the eastern basin suggest that waters there are derived from the central basin rather than from the eastern part of the northern basin. In either case, it seems likely that bottom water of the eastern North Pacific, with the highest temperature and lowest oxygen concentration, is the 'oldest' bottom water of the open Pacific.

REFERENCES

Brodie, J. W., and R. W. Burling, Age determinations of southern ocean waters, *Nature, 181,* 107–108, 1958.

Brujewicz, S. W., On certain chemical features of waters and sediments in northwest Pacific, *Proc. UNESCO Symp. Phys. Oceanog.,* 1955, Tokyo, 277–292, 1957.

Bruneau, L., N. G. Jerlov, and F. F. Koczy, Physical and chemical methods, *Rept. Swed. Deep-Sea Exped., 3*(4), 99–112, I-LV, 1953.

Bruun, A. F., and A. Kiilerich, Characteristics of the water masses of the Philippine, Kermadec and Tonga Trenches, *Papers Marine Biol. Oceanog., Deep-Sea Research, suppl. 3,* 418–425, 1955.

Carlsberg Foundation, Hydrographical observations made during the "Dana" Expedition 1928–1930, *Dana Rept., 2* (12), 1–46, 1937.

Craig, Harmon, Isotopic tracer techniques for measurement of physical processes in the sea and the atmosphere, in *The Effects of Atomic Radiation on Oceanography and Fisheries,* NAS-NRC Publ. no. 551, 103–120, 1957.

Deacon, G. E. R., The hydrology of the southern ocean, *Discovery Rept., 15,* 1–124, 1937.

Discovery Committee, Station list 1931–1933, *Discovery Rept., 21,* 1–226, 1941.

Discovery Committee, Station list 1937–1939, *Discovery Rept., 24,* 197–422, 1947.

Discovery Committee, Station list R. R. S. "William Scoresby" 1931–1938, *Discovery Rept., 25,* 143–280, 1949.

Eckart, Carl, Properties of water, Pt. II, The equations of state of water and sea water at low temperatures and pressures, *Am. J. Sci., 256,* 225–240, 1958.

Fleming, J. A., C. C. Ennis, H. U. Sverdrup, S. L. Seaton, and W. C. Hendrix, Observations and results in physical oceanography, Oceanography I-B. *Carnegie Inst. Wash. Publ. 545,* 315 pp., 1945.

Japan, Maritime Safety Agency, The results of oceanographic observations in the northwestern Pacific Ocean. No. 3. 1931–1935, *Hydrogr. Bull.,* Publ. no. 981, Spec. no., 1–139, 1950.

Japan, Maritime Safety Agency, The results of oceanographic observations in the northwestern Pacific Ocean. No. 4. 1935–1938, *Hydrogr. Bull.,* Publ. no. 981, Spec. no. 8, 1–143, 1951.

Japan, Maritime Safety Agency, The results of oceanographic observations in the northwestern Pacific Ocean. No. 5. 1938–1941, *Hydrogr. Bull.,* Publ. no. 981, Spec. no. 9, 1–194, 1952.

National Institute of Oceanography, Station list 1950–1951, *Discovery Rept. 28,* 299–398, 1957.

Postma, H., Tables. Oxygen, hydrogen ion, alkalinity and phosphate, *Snellius Rept., 4,* 1–35, 1959.

Stommel, H., The abyssal circulation, *Deep-Sea Research, 5,* (1), 80–82, 1958.

Sverdrup, H. U., M. W. Johnson, and R. H. Fleming, *The Oceans, their Physics, Chemistry, and General Biology,* Prentice-Hall, New York, 1087 pp., 1942.

Swallow, J. C., A neutral-buoyancy float for measuring deep currents, *Deep-Sea Research, 3,* 74–81, 1955.

Swallow, J. C., and L. V. Worthington, Measurements of deep currents in the western North Atlantic, *Nature, 179,* 1183–1184, 1957.

Van Riel, P. M., H. C. Hamaker, and L. Van Eyck, Tables. Serial and bottom observations. Temperature, salinity and density, *Snellius Rept., 2*(6) 1–41, 1950.

Von Herzen, R., Heat-flow values from the southeastern Pacific, *Nature, 183,* 882–883, 1959.

Wooster, W. S., and B. A. Taft, On the reliability of field measurements of temperature and salinity in the ocean, *J. Marine Research Sears Foundation, 17,* in press.

Wüst, Georg, Bodentemperatur und Bodenstrom in der pazifischen Tiefsee, *Veroff. Inst. Meeresk. Univ. Berl., Neue Folge, A. Geogr.-naturwiss.,* (35), p. 56, 1937.

(Manuscript received January 11, 1960.)

[AMERICAN JOURNAL OF SCIENCE RADIOCARBON SUPPLEMENT, VOL. 2, 1960, P. 197-223]

LA JOLLA NATURAL RADIOCARBON MEASUREMENTS*

CARL L. HUBBS, GEORGE S. BIEN, and HANS E. SUESS

Scripps Institution of Oceanography, University of California, La Jolla

INTRODUCTION

The recently established low-level radiation laboratory of Scripps Institution of Oceanography has been measuring radiocarbon since August 1957. Through 1959 about 160 samples have been measured.

In the radiocarbon tests the La Jolla laboratory staff utilizes the technique, with acetylene as the counting gas, that was developed at the United States Geological Survey (Suess, 1953, 1954a, 1956, USGS I). Until March 1959 only one set of equipment was in service, with a counter somewhat smaller than either of the two used in Washington, having a sensitive volume of approximately 0.6 liter. Although several counters were constructed and tested, a background as low as that attained in Washington could not be achieved: the background ran about 2.8 counts/min as compared with 2.0 counts/min for each of the 1-liter counters in Washington.

In March 1959 an Oeschger-Houtermans counter, manufactured at the Physical Institute of the University of Bern, Switzerland, was installed. It operates with a background of less than 2.0 counts/min, decreasing with filling pressure, and a sensitive volume of 1.3 liters. The disadvantage of this counter is the large volume of counting gas required, for example, 3.2 l STP for a filling pressure of 850 mm. However, this counter proved to be more stable than the ordinary counters, and it can be operated at pressures as low as 440 mm, at which a background as low as 1.2 counts/min can be attained. Therefore, this counter proves to be superior also in the measurement of relatively small samples. Dates obtained with the Oeschger-Houtermans counter are designated by appending **(B.)**, for Bern, to the serial number of the count.

The installation of one or more additional counters is being considered, with the aim of increasing the annual output of tests.

Shell dates reported in this paper are calculated (as in USGS I) from 19th century wood as a reference standard, without correction for any supposed fractionation of isotopes. This procedure has been adopted because in general, within the errors of measurement, the activity of 19th century wood corresponds to that of modern shell, despite the differences in the equilibrium distribution of the isotopes as shown by C^{13} analyses.

For purposes of calibration and control, numerous tests, not treated in this report, have been run on bituminous coal, on standard oxalic acid, and on dated annual rings of 19th century wood. Numerous other measurements, which will be published elsewhere, have been made: (1) to analyze mixing processes and recent changes in the radioactivity of the sea and the atmosphere; (2) to test changes in the radioactivity of trees, various marine plants and animals, and food items; and (3) to estimate the age of water masses.

---

* Contributions from the Scripps Institution of Oceanography, New Series. 1158

(Bien, Rakestraw, and Suess, in press). A report (Bien and Suess, 1959) has been published on the dating of various annual rings in 20th century wood. Except as just noted, all tests run by the La Jolla laboratory through 1959 are reported below.

In the dating program of the La Jolla laboratory, which has been pursued when the other research projects have afforded the opportunity, particular attention has been paid to the elucidation of past changes in the environment. Most of the samples that have been run were selected for their bearing on such problems, particularly in western North America, both in the coastal waters and in the arid lands of the Southwest. For example, past faunal associations, particularly when bolstered by O^{18} paleotemperature measurements, help in the elucidation of past oceanographic conditions. The environmental changes are being studied not only for their own significance but also for their bearing on the distribution and abundance of organisms, including man. In turn, the data on the organisms are being brought to bear on the environmental changes. The senior author is preparing reports along these lines, and has indicated in the sample accounts below some of the implications that he will discuss in these reports.

ACKNOWLEDGMENTS

The initial equipment, including the 17-ton iron shield, was provided through grants from the Office of Naval Research and the Atomic Energy Commission. A major share of support for the operation of the laboratory has been supplied by the Atomic Energy Commission, under contracts for the study of mixing processes in the sea and the atmosphere. Other support, which has made the laboratory available on a part-time basis for other tests, has stemmed from the California State Water Resources Board, for studies of climatic fluctuations in the California area, and from the National Science Foundation, by a grant to the senior author, for the collection and interpretation of material bearing on past changes in habitat and other ecological conditions, particularly in respect to the effect of these changes on human populations.

We are most grateful for the support received from various sources and to many individuals who have given encouragement and assistance. Paula Sandoval has served effectively as assistant in the laboratory. Laura C. Hubbs has devoted much time to the collecting and recording of data. Jacquelin N. Miller has served as assistant under the senior author's National Science Foundation grant. Robert N. C. Bowen is running O^{18} paleotemperature measurements.

CLASSIFIED SUBJECT INDEX

Many of the natural radiocarbon measurements run at the La Jolla laboratory, especially those reported herein, were selected because of their multiple bearing on various events and processes—geologic, oceanographic, zoogeographic, ecologic, climatologic, and archaeologic. The bearings we envision are listed for each entry in the date list, and the index permits ready reference to the serially listed entries.

I. GEOLOGIC INFERENCES:
  1. Quaternary Changes in Sealevel:
    Raised beaches, Australia and Golfo de California: LJ-128, 130-132
    Buried deposits, Cape Cod: LJ-141, 142
    Submarine shell, Texas and California: LJ-71, 95
    Flooded cave, Florida: LJ-120

Middens sloping or inferred to have sloped to below present sealevel, southern California and Baja California: LJ-19, 20, 34, 37, 38, 78?, 83, 98 (and probably others)

2. Ancient Rise in Sealevel and Elimination of Minor Estuaries, Inferred Chiefly from Faunal Assemblages: LJ-3, 19, 31, 35, 36, 79, 109, 110
3. Quaternary History of Baja California Lagoons: LJ-12, 13, 21, 28, 30, 98
4. History of San Diego Bay, California: LJ-34, 37, 38, 103
5. Periods of Heavy Runoff, Alluviation, and Erosion (see also items I–3 and II-2):
    Basins of ancient lakes LeConte and Clark, California: LJ-7, 15-17, 99, 101, 102, 105, 106
    Coasts of southern California and northwestern Baja California: LJ-3, 19, 25, 27, 78, 83-85, 98
6. Long Continuity of Springs and Streams in Southern California and Northern Baja California: LJ-25, 26, 29, 31, 33-38, 75, 77, 84, 85, 98, 103, 136
7. Age of Last High Stage of Lake LeConte, California and Baja California: LJ-7, 15, 99, 101, 102, 105, 106
8. Age of Ancient Lake Clark, California: LJ-16, 17
9. History of Lake Lahontan and Its Fauna, in California: LJ-76
10. History of Rancho La Brea Tar Pits and Their Faunas, California: LJ-55, 89, 121
11. Rate of Soil Weathering (including clay infiltration and prismatic formation, induration with lime and formation of caliche, and reddening of soil, in southern California and Baja California): LJ-3, 5, 6, 17, 19, 20, 23, 25-27, 29, 31, 33-38, 75, 77-79, 83-85, 98, 103, 109, 110, 136
12. Successive Generations of Dunes, Southern California and Baja California: LJ-6, 16, 17, 20, 28, 30, 108
13. Rate of Sedimentation Due to Turbidity Currents, Northeastern Pacific Ocean: LJ-112
14. Pleistocene History of New England: LJ-141, 142
15. Extinction of Pleistocene Fauna: LJ-55, 121
16. Failure of Wood to Decompose on Ocean Floor, and Rate of Phosphatic Infiltration: LJ-82

II. OCEANOGRAPHIC, ZOOGEOGRAPHIC, ECOLOGIC, AND CLIMATOLOGIC INFERENCES:

1. Past Sea Temperatures and Faunal Changes:
    Southern California and northwestern Baja California: LJ-3, 5, 6, 19, 20, 23, 25-27, 29, 31, 33-38, 75, 79, 83-85, 96, 98, 108-110, 136
    Oregon: LJ-111
    Texas: LJ-71
2. Decreasing Rainfall:
    Desert, southeastern California (see items I–7 and I–8)
    Inferred from abundance of human population, etc., coasts of southern California and Baja California: LJ-3, 5, 6, 12, 13, 19-21, 25, 27, 28, 30, 34, 37, 38, 79, 96, 98, 109, 110, 136
    Inferred from changes in dune structure (northwestern Baja California coast, and southern California coast and desert): LJ-6, 12, 20, 28, 30, 108
3. Continuity of Climatic Pattern:
    Cool (upwelling) areas, southern California and northwestern Baja California: LJ-25, 27, 75, 83-85, 108, 111
    Temperate areas, same region: most other tests from coastal areas.
    Warm area, northwestern Baja California: LJ-20
    Subtropical areas, Baja California: LJ-13, 21, 26, 28-30, 96
4. Age of Sea-water Masses (from CO_2 Analyses): LJ-57-63, 66-69, 88, 90, 91, 93, 94, 123-127, 129, 137, 139, 140, 146, 147, 149-154, 157, 158 (tests to be reported elsewhere)

III. ARCHAEOLOGIC INFERENCES:

1. Data on Early Shellfish-gatherers (7400–4950 B.P., in southern California and northern Baja California): LJ-3, 6, 26, 27, 36, 77, 79, 107, 109, 110
2. Temporal Position of San Dieguitoan Culture, California: LJ-136
3. Man in Rancho La Brea Tar Pits, California: LJ-121 (see also LJ-55 and 89)
4. Data on Cultures Tentatively Appraised as Simple or Retrogressive (3900–<400 B.P., in southern California and northwestern Baja California): LJ-5, 19, 25, 31, 35, 78, 103
5. Data on Somewhat More Complex Cultures, Southern California and Oregon: LJ-34, 37, 38, 111
6. Date on Site in Lahontan Basin, California (2350 B.P.): LJ-76

7. Date on Occupation of Now-flooded Cave in Florida (10,000 B.P.): LJ-120
8. Date on Mayan Ruin, Yucatán: LJ-87
9. Dates on Sites with Flexed Burials (7370–3100 B.P., in southern California and northwestern Baja California): LJ-5, 36, 77, 79, 109, 110
10. Dates on Pottery:
    LeConte Basin, California (960–<200 B.P.): LJ-15-17, 106
    Northwestern Baja California coast (400 B.P.): LJ-33
11. Upper Limiting Date on Submarine Artifact, Southern California (520 B.P.): LJ-95
12. Date on Use of Atlatl, Southern California (4450 B.P.): LJ-121
13. Date on Pishkun (Bison Drive), Montana (550 B.P.): LJ-8
14. Evidence on Conditions Affecting Population Size:
    Especially favorable conditions in desert of southeastern California: LJ-7, 15, 16
    Especially favorable conditions along Pacific coast, Oregon to Golfo de California: LJ-5, 25, 26, 29, 31, 33, 77, 79, 96, 108-111
    Moderately favorable conditions along coasts of southern California and northwestern Baja California: LJ-19, 20, 23, 34, 35, 37, 38, 75, 78, 98, 103
    Conditions rather unfavorable along same coasts: LJ-6, 27, 37
15. Miscellaneous Data on Middens (other than III–2, 3, 6-8, 11-13):
    Oregon: LJ-111
    Southern California coast: LJ-3, 19, 25, 27, 31, 34-38, 77-79, 95, 103, 109, 110
    West coast, Baja California: LJ-5, 6, 20, 28, 33, 75, 83-85, 98, 107, 108
    Golfo de California: LJ-26, 29, 96, 100, 132
    Desert, southeastern California: LJ-7, 15-17, 26, 99, 101, 102, 105, 106

IV. TESTS BEARING ON THE RELIABILITY AND PRECISION OF THE DATES:

1. Orderly, Expected Sequences:
    Midden at Punta Minitas, Baja California Norte: LJ-5 (stratigraphically below W-26 and W-27)
    Two midden layers, Batiquitos Lagoon, California, separated by an unconformity: upper layer, LJ-31; lower layer, LJ-36
    Three occupation streaks, Chollas Creek, California: upper, LJ-37; middle, LJ-34; lower, LJ-38
    Scripps Estates Site I, La Jolla, California: upper level, LJ-110; intermediate level, LJ-79; lower level, LJ-109
    Midden, shore of Santa Rosa Island, California: LJ-27 (stratigraphically below L-257)
    Two occupation streaks, ancient lake LeConte, California: upper streak, LJ-106; lower streak, LJ-105 (other dates for camp sites around Lake LeConte form logical series)
    Rancho La Brea Tar Pits: buried tree, associated with extinct mammals, LJ-55; atlatl foreshaft, with indications of lesser antiquity, LJ-121
2. Agreement between Tests on Contemporary Shell and Charcoal (no corrections were made for C^{13} ratios):
    Occupation streak near La Jolla, California: shell, W-154, 600 ± 200; charcoal, W-155, 580 ± 200 (USGS II)
    Middle of thick midden at Punta Minitas, Baja California Norte: shell, W-26, 2540 ± 200; charcoal, W-27, 2500 ± 200 (USGS I)
    Occupation streak, Valle de Rosario, Baja California Norte: shell, LJ-84, 1060 ± 150; charcoal, LJ-85, 960 ± 150
3. Agreement between Tests on Different Molluscs (from raised beach, Australia): *Turbo* sp., LJ-128, 900 ± 150; *Patella* and *Fissurella*, LJ-130, 900 ± 150
4. Agreement between Datings by Different Laboratories:
    Rancho La Brea, California: LJ-55, 14,400 ± 300; cf. Y-354A, B and Y-355A, B, average 14,470 (Yale IV)
    Chichén-Itzá, Yucatán: LJ-87, 1140 ± 200; cf. Y-626, 1160 ± 60 (Yale IV) and Y-626 *bis*, 1010 ± 100 (Yale V)

SAMPLE DESCRIPTIONS*

LJ-3. Malaga Cove Site, California 6510 ± 200

Clam shells (*Chione californiensis*) from point at N end of Malaga Cove, near Redondo Beach, Los Angeles County (33° 48′ 23″ N Lat, 118° 23′ 32″ W Long), California (from pl. 1, Woodring, Bramlette, and Kew, 1946). Coll. by C. L. Hubbs (sample 1955—XI: 24C); subm. 1957. From the next-to-lowermost soil horizon that contains evidence of human occupation, in the extensive site described by Walker (1951). This is apparently a B soil layer, ca. 2.5 m thick, of rather coarse brownish sand, with considerable clay, well indurated with lime, in places hard to dent, when dry, with a geologist's pick. *Comment*: this soil horizon seems to represent the nonmarine terrace-fill interpreted by Woodring, Bramlette, and Kew as Pleistocene, for it grades downward into the C layer that overlies the Miocene rock and underlies a blackish sand stratum at the base of the overlying dune formation; it also appears to correspond in part with Walker's "microlith"-containing "level 1", although, at the point where our sample was taken, the shells were scattered through a greater depth, rather than being densely congregated, in the uppermost 2 ft of the detritus formation, to form the "Shell Village" of Walker. A few midden shells and a few chips were found in the underlying C soil layer, which seems to correspond with what Walker interpreted as a sterile horizon. Date and circumstances indicate the early occupation of this coast by people with simple cultural traits, subsisting largely on shellfish, and further indicate the time involved in extensive soil weathering. The shell fauna points to temperatures at least as warm as, probably a little warmer than, the present. The circumstances further suggest: (1) physiographic changes, for most of the shells (predominantly *Chione*, with *Pecten circularis aequisulcatus* next in abundance) probably came from a nearby bay or lagoon that existed, presumably during lower and rising sealevels, where none now exists; (2) decreasing rainfall, as the region is now devoid of surface water. The *Chione californiensis* shells from here (and from a deeply buried layer in the cliff in the nearby Clifton section of Redondo Beach) seem unusually flat, suggesting some evolutionary change (J. L. Baily, Jr., personal communication).

LJ-5. Punta Minitas Site, Baja California 3100 ± 300

Charcoal from level 8 (70 to 80 cm below surface) of coastal midden (31° 18′ 50″ N Lat, 116° 26′ 05″ W Long) (from HO Chart 1149, 1948), ca. midway between Punta Cabras and "Punta San Isidro" (as charted, "Punta Piedras Blancas" in local usage), Baja California Norte. Level 8 is ca. opposite the top of a flexed burial and is overlain by denser shell refuse, now exposed on the cliff face. Coll. by C. L. Hubbs and party (sample 1957—VI: 28A); subm. 1957. *Comment*: material from the overlying denser midden has been dated: W-26, 2540 ± 200, *Mytilus* shell; W-27, 2500 ± 200, charcoal (USGS I) (the depth of "3 to 4 ft" there reported was estimated from a higher point). As these earlier datings pertain to the middle of the deposit, which continues about 0.5 m below LJ-5, as the midden was probably occupied for about a millenium, and as very similar, dense middens are semicontinuous for many miles along the coast, a prolonged and extensive occupation is suggested. Conditions were obviously favorable. As fresh water is now very scarce, it seems probable that rainfall was greater during the occupation. Mollusc fauna and the paleotemperature estimate reported for W-26 indicate temperatures somewhat warmer than those presently prevailing. Subsequent soil formation has been slow, for the downward penetration and accumulation of clay and lime has been slight.

---

* Includes measurements of paleoecologic significance (physiography, oceanography, climatology, zoogeography, archaeology) only. Tests of strictly geochemical implication will be published later.

LJ-6. Punta Cabras, Baja California—1 **5020 ± 200**

Mussel shells (*Mytilus californianus*) from 10 to 60 cm below top of consolidated reddish sand (representing a former generation of dunes), which is overlain by unconsolidated white sand; in cove on S side of Punta Cabras (31° 20′ 00″ N Lat, 116° 27′ 15″ W Long), Baja California Norte (from HO Chart 1149, 1948). Coll. by C. L. Hubbs (sample 1955—V: 7C); subm. 1957. Shells here represent a very sparse midden, and artifacts are almost wholly lacking. *Comment*: date and circumstances indicate an early occupation of this coast by a sparse population with a simple culture, living during a period drier than some subsequent period of erosion between the two periods of dune accumulation; and place an upper figure on the time involved in the consolidation and reddening of sand.

LJ-7. Fish Creek, San Diego County, California **1000 ± 200**

Charcoal from hearth site in angle of headwater forks of Fish Creek, arid Fish Creek Mountains, E part of San Diego County (32° 59′ N Lat, 116° 13′ W Long), California (from Carrizo Mountain Quadrangle, 1952). The hearths here contained numerous bones of fishes and of land vertebrates, including bighorn sheep. Coll. by C. L. Hubbs, B. E. McCown, and party (sample 1954—XI: 27B); subm. 1957. *Comment*: date indicates a time when: (1) a rather large settlement of fishing and hunting people with relatively advanced culture existed; (2) rainfall was much greater, because the one nearby spring now existing would not have been adequate, and because the fish eaten and presumably caught here were the young of large fishes (humpback suckers and bonytails) that for spawning almost certainly had run up Fish Creek, which is now bone-dry; (3) Lake LeConte (Hubbs and Miller, 1948) existed, with an abounding human population around its shores, because such fish must have come from the lake. That the lake was then in existence is indicated by LJ-106.

LJ-8. Pishkun (bison drive), Montana **550 ± 200**

Charcoal and charred wood from single intact hearth about midway between Vaughn and Cascade, Cascade County, ca. 30 km SW of Great Falls, in T 19 N, R 1 E (ca. 47° 25′ N Lat, 111° 35′ W Long). The hearth was buried ca. 1.5 m, in close association with numerous bison bones and a considerable number of arrow points, at a "pishkun" site (where bison were stampeded over a cliff for a kill). The hearth was located near the bottom of the trench that was dug through the layer of bison bones. Coll. 1956 and subm. 1957 by T. J. Walker, Scripps Institution of Oceanography. *Comment*: the location was on the migratory route of the bison, the course of which was presumably determined by the only favorable crossing of the Missouri River in this region. Previous attempts to obtain charcoal here for dating had failed because no hearths were found where the Indians are supposed to have camped above the cliff. The hearth site and associated remains are exhibited in the Museum of Plains Indians at Bowman, Montana. An effort is being made to preserve this site.

LJ-9. (See LJ-19)

LJ-12. Scammons Lagoon, Baja California Sur—1 **1900 ± 300**

A thick-shelled gastropod (identification lost) from *Donax* pavement of old shoreline, taken with other molluscs, volcanic metamorphic pebbles, and cobbles, exposed on between-dunes blowout flats, ca. 1 km back of present shore, on the peninsula between Scammons Lagoon (Laguna Ojo de Liebre) and Bahía Sebastián Vizcaíno (ca. 27° 58′ N Lat, 114° 16′ W Long), Baja California Sur (from air-photo compilation map by F. B Phleger). Coll. July 19, 1956 by R. R. Lankford, for F. B Phleger and G. C. Ewing, Scripps Institution of Oceanography; subm. 1957 by Phleger. *Comment*: according to the collectors, date bears on: (1) history of this large lagoon; (2) rapid seaward prograding of barrier island or peninsula; (3) greater rainfall, inferred to have been needed to supply the requisite sand from streams then flowing across the now notoriously arid Vizcaíno Desert. There are no archaeologic implications.

LJ-13. Scammons Lagoon, Baja California Sur—2 **>25,000**

Clam shell (a very large and thick example of *Periglypta multicostata*) found in place in the consolidated shell deposit of a fragment of an old lagoon barrier-island, on "South Brushy Island" of Scammons Lagoon (ca. 27° 44′ N Lat, 114° 14′ W Long), Baja California Sur (from same map, see LJ-12). Coll. and subm. 1957 by F. B Phleger and G. C. Ewing, Scripps Institution of Oceanography. *Comment*: according to the collectors, date bears on: (1) Pleistocene history of this lagoon; (2) probably greater former inflow of river water and sand; (3) persistence of the climatic pattern, for the molluscan assemblage is subtropical, as at present. There are no archaeologic implications.

LJ-15. Lake LeConte, Baja California Norte **300 ± 100**

Charcoal from a shallow, sandy archaeologic site bordering ancient Lake LeConte, W of Mexicali, N of the Mexicali-Tijuana highway, ca. 2 mi S of California border (ca. 32° 36.8′ N Lat, 115° 41.3′ W Long), Baja California Norte. Coll. by C. L. Hubbs, B. E. McCown, and party (sample 1955—X: 15A); subm. 1957. *Comment*: date indicates time when a dense population developed in response to the abundant supply of water and of fish and other food that existed during a late period in the last filling of Lake LeConte.

LJ-16. Clark Dry Lake, California—1 **700 ± 150**

Charcoal from extensive Indian site among the dunes on N side of playa of Clark Dry Lake, along the shore of ancient Lake Clark, San Diego County (33° 22.2′ N Lat, 116° 16.8′ W Long), California (from Clark Lake Quadrangle, 1941). Food remains in this habitation site and in other sites in the basin include terrestrial vertebrates but no trace of fishes. Coll. by C. L. Hubbs, B. E. McCown, and party (sample 1955—III: 5D); subm. 1957. *Comment*: date and circumstances indicate that this enclosed and now-arid basin (Hubbs and Miller, 1948) was probably occupied by an isolated lake, which, although almost certainly fishless, furnished water and attracted food adequate to support a considerable population.

LJ-17. Clark Dry Lake, California—2 **<200**

Charcoal from hearth in sandy soil near SE margin of playa of Clark Dry Lake (33° 19.7′ N Lat, 116° 15.8′ W Long), San Diego County, California (Clark Lake Quadrangle, 1941). Hearth was 4.4 m above the playa. Coll. by C. L. Hubbs, B. E. McCown, and party (sample 1955—III: 5A); subm. 1957. *Comment*: date and circumstances indicate the continued habitation of this basin until very recent time and the support of a population without the fish supply on which the people around nearby Lake LeConte largely subsisted; and further indicate the probable, at least ephemeral, existence of Lake Clark within the last very few hundred yr. The appearance of the sandy soil and the fragmentation of the charcoal suggested greater antiquity but presumably were induced by frequent wetting.

LJ-19. Midden, Torrey Pines Park, California **3700 ± 200**

Mussel shell (*Mytilus californianus*) from occupation layers 2 to 3 m below the top of the low cliff margining N end of the high cliffs of Torrey Pines State Park, San Diego (32° 55′ 33″ N Lat, 117° 15′ 31″ W Long), California (from Air Photo Compilation T-5410, 1934). Charcoal (LJ-9) from the same collection proved insufficient for measurement. The now-buried land surfaces, on which the midden materials accumulated, slope inland at about 1:4 and were formed by talus derived from the high sandstone cliffs. Coll. by C. L. Hubbs, B. E. McCown, and party (sample 1957—VI: 8A); subm. 1957. *Comment*: test suggests that the early shellfish-gatherers who occupied the coasts of southern California and northern Baja California between 7400 and 4950 B.P. (see LJ-3, 6, 26, 27, 36, 77, 79, 107, 109, and 110, this list), or other people with similar food habits and simple culture, persisted until about 3700 yr ago. The steep slope of the old land surface and the rapid truncation of the cliff suggest that the inhabited area continued westward to below present sealevel. A rising sealevel would be consistent with the continued existence of the open estuaries and the rocky foreshore from which the sea-food was presumably gathered (such habitats, which presumably existed during the times of the early shellfish-gatherers, are now nearly lacking in the vicinity). These inferences, along with others indicative of a wetter-than-present climate, will be elaborated by the senior author in other publications. Since the time of occupation and the accumulation of the overlying soil, soil weathering has involved considerable infiltration of clay and induration with lime.

LJ-20. Midden, Estero Beach, Baja California **1170 ± 200**

Pismo-clam shell (*Tivela stultorum*) from a single obvious clambake, enclosed in a former generation of hardened and yellowish dune sand, which is abruptly overlain by loose, whitish sand; at N end of the presumably Pleistocene cliff, Estero Beach, S of Ensenada (31° 47.0′ N Lat, 116° 37.3′ W Long), Baja California Norte (from HO Chart 1149, 1958). Charcoal (LJ-24) from the same compact hearth proved insufficient for measurement. Coll. by C. L. Hubbs and G. E. Lindsay (sample 1956—V: 25B); subm. 1957. *Comment:* the uniformly small size of the clams indicates warm water (along the same general section of the coast large pismo clams seldom occur in water shallow enough for aboriginal gathering; O^{18} paleotemperature estimates from similar small pismo clam shells have indicated warm water—see reports on W-29, 330 ± 160, and W-31, 330 ± 160 (USGS I). Habitation in an area now devoid of fresh water suggests moister-than-present climate. The location of the hearth within reach of storm waves at high tides and the rapid backward retreat of the cliff suggest that the original area of habitation extended to below present sealevel (this inference is consistent with other evidence, as of LJ-19, 34, 37, 38, 83, 98, and probably LJ-78, this list, indicative of the continued, relative rise of sealevel in southern California and northern Baja California into late postglacial time). The data on LJ-20 indicate rapid soil weathering, perhaps accelerated here by salinization.

LJ-21. Black Warrior Lagoon, Baja California **>37,000**

Cockle shell (*Trachycardium panamense*) from an ancient and dense intertidal-flat shell assemblage on salina at head of Black Warrior Lagoon (Laguna Guerrero Negro), near the old airstrip of the salt works (ca. 28° 03′ N Lat, 114° 04′ W Long), Baja California Norte (from air-photo compilation map by F. B Phleger). Coll. 1956 by F. B Phleger and G. C. Ewing, Scripps Institution of Oceanography, subm. 1957. *Comment:* according to the collectors, the date bears on the Pleistocene history of this lagoon and on the development of the salt flats, with their saline deposits. There are no archaeologic implications. The molluscan species are subtropical, as at present.

LJ-23. North Coronado Island, Baja California **<400**

Charcoal from in situ hearths in a rather large camp or village site on high, sharp ridge of North Coronado Island (32° 17.9′ N Lat, 117° 17.8′ W Long), Baja California Norte (from recent relocation of islands by Scripps Institution of Oceanography). Crude pressure-flaked tools abounded in this site, with almost no evidence of higher culture. Coll. by C. L. Hubbs, B. E. McCown, and party (sample 1956—V: 19A); subm. 1958. *Comment:* date and circumstances indicate: (1) long persistence of primitive culture, or a late retrogression, or periodic temporary occupations; (2) the age of associated fauna, which included sea otter; (3) despite the recency of the date, probably more rainfall and more brushy vegetation than now (to supply water needs, and fuel for the abundant fires).

LJ-24. (See LJ-20)

LJ-25. Midden, San Miguel Island, California **1750 ± 200**

Charcoal from a large midden, deeply buried in cliff of Cuyler Harbor, San Miguel Island (34° 03′ 17″ N Lat, 120° 21′ 37″ W Long), California (from USC&GS Chart 5116, 1945). This a deep, rich, solid midden that is being eroded on the face of the sandy cliff. Coll. by C. L. Hubbs and party (sample 1954—IX: 16A); subm. 1957. *Comment:* the date tells when the fauna indicated by the shells and bones lived and when, it is inferred, the flow of the adjacent spring was sufficiently greater than the present trickle to have provided an adequate supply of fresh water for the obviously large population. Here, as elsewhere along the coast, the freshwater supply was probably a major factor limiting the human populations; the midden remains indicate a bountiful supply of molluscs, fishes, birds, and sea mammals. Soil weathering since the accumulation of the midden has been rather slight, except where ocean spray often wets the lower part of the midden (here even the very recent soil is considerably hardened through salinization).

LJ-26. Bahía de los Angeles, Baja California—1 6100 ± 200

Clam shell (*Glycymeris* cf. *maculata*) from dense, almost coquina-like midden deposit, near surface, beside a rather large spring on bajada at foot of the hills behind village of Bahía de los Angeles, Golfo de California (28° 56.4′ N Lat, 113° 34.8′ W Long), Baja California Norte (from HO Chart 0620, 1943). Coll. by C. L. and L. C. Hubbs (sample 1954—II: 17A); subm. 1958. *Comment*: test indicates the occupation of this area on the Gulf of California coast within the period (from ca. 7500 to 5000 B.P. or later) when shellfish-gatherers abounded along the coasts of southern California and northwestern Baja California (see LJ-3, 6, 27, 36, 77, 79, 107, 109, and 110, this list). It seems probable that the vicinity of the springs has been more or less continuously occupied for at least six millenia, as the middens are virtually continuous through several meters about the springs, and evidences of occupation abound in the general region, which is otherwise almost devoid of fresh water, and apparently has long been dry. Sample LJ-29 (this list), yields a date of 2500 ± 300; the occupation of the area continued until historic time (Father Kino mentioned encountering a large *ranchería* on the bay); the more recent middens along the shore contain much pottery. Throughout the long period of occupation the fauna, as repreesnted by midden shells, has remained subtropical, as it is now. The interval of 6000 yr seems rather short for the production of the coquina-like deposit, but the process was presumably accelerated by the action of the spring water.

LJ-27. Midden, Santa Rosa Island, California 7400 ± 200

One red-abalone shell (*Haliotis rufescens*) from 4.6 m below lip of sea-cliff ca. 6.5 km E of Arlington Canyon (between that canyon and "Deer Gulch"), Santa Rosa Island (34° 00′ 20″ N Lat, 119° 10′ 22″ W Long), California (from USC&GS Chart 5116, 1945). Coll. by C. L. Hubbs with P. C. Orr, G. F. Carter, and W. S. Broecker (sample 1955—IX: 11C); subm. 1958. *Comment*: this isolated shell was taken, in the same midden, stratigraphically below the level of the red-abalone shell dated 6820 ± 150 (L-257, Lamont III). Red-abalone shell from a nearby site has been dated 7070 ± 250 (L-290D, Lamont IV). The two Lamont dates have been listed by Orr (1956, p. 5-6). An older midden deposit of red-abalone shells was exposed in an inaccessible part of the midden complex from which this sample was obtained, but still lower (6.0 m below lip of cliff). Date and circumstances indicate, as will be elaborated in a later publication: (1) occupation of island coast by early (initial?) shellfish-gatherers at least 7500 and probably 8000 yr ago, during the latter part of the period of post-Sangamon terrace-fill; (2) rather cold sea temperatures that brought the red abalones within harvesting reach; (3) freshwater supply probably more abundant than at present. The soil has reddened considerably and is moderately infiltrated with clay and indurated with lime.

LJ-28. Dune midden, Baja California Sur—1 **1000 ± 250**

Charcoal from blowout in low dunes near Colina Coyote, on sand strip separating ocean from expansion of lagoon midway between Bahía Santa María and Boca Soledad, N of Bahía Magdalena (25° 10′ 53″ N Lat, 112° 10′ 53″ W Long), Baja California Sur (from HO Chart 1493, 1945). Sample accompanied an abundance of shells of warm-water molluscs. Coll. by F. B Phleger and G. C. Ewing, Scripps Institution of Oceanography (sample 1958—I: 30B); subm. 1958. *Comment*: test was run for Drs. Phleger and Ewing because of its bearing on their studies, to be published elsewhere, of the history of the coastal lagoons of western Mexico; a particular point was to obtain a limiting date for the formation of the barrier sand strip, which they believe was formed when stream inflow greater than at present contributed an adequate supply of sand. The abundant middens in the general vicinity of Colina Coyote suggest that at the time of occupation (see LJ-30, this list) more fresh water and wood fuel were available than at present. The warm-water molluscs in these middens suggest that the present warm regime was established in this region when cold conditions prevailed farther north in Baja California (see LJ-75, 83-85, and 108, this list).

LJ-29. Bahía de los Angeles, Baja California—2 **2500 ± 300**

Charcoal from ca. 0.8 to 1.3 m below surface of exposed, noncoquinized midden, 1.5 m deep, at rim of upper spring at Bahía de los Angeles, Golfo de California (28° 56.4′ N Lat, 113° 34.8′ W Long), Baja California Norte. Coll. by F. B Phleger and G. C. Ewing, Scripps Institution of Oceanography (sample 1957—XII: 31A); subm. 1958. *Comment*: as will be shown in a later publication, date bears on: (1) the prolonged habitation about these permanent springs; (2) continuity of subtropical fauna; (3) time involved in soil weathering.

LJ-30. Dune midden, Baja California Sur—2 **600 ± 150**

Charcoal from low midden halfway between Colina Coyote and larger dune midden (25° 01′ 35″ N Lat, 112° 10′ 50″ W Long), Baja California Sur (from HO Chart 1493, 1945); close to LJ-28. Coll. by F. B Phleger and G. C. Ewing, Scripps Institution of Oceanography (sample 1958—I: 30A); subm. 1958. *Comment*: implications are the same as for LJ-28.

LJ-31. Batiquitos Lagoon, California—1 **3900 ± 200**

Clam shell (*Chione californiensis*) from upper midden level beside marsh on S shore of Batiquitos Lagoon, at W side of westernmost canyon on S side (33° 05′ 01″ N Lat, 117° 17′ 52″ W Long), California (from Air-Photo Compilation T-5411, 1954). Coll. by C. L. Hubbs (sample 1956—X: 27B); subm. 1958. *Comment*: the upper, dark, loose superficial midden, rich in shells and crude artifacts, rests unconformably on a more consolidated stratum containing much older midden shell dated 7300 ± 200 (LJ-36, this list). These dates and preliminary study of the artifacts and shells suggest: (1) long continuation at this site, as elsewhere along the coast, of a simple shellfish-gathering culture; (2) continued existence here, during the same time, of a salt-water estuary, probably during a long period of rise in sealevel; (3) probable long continuity, in the adjacent marsh, of surface or subsurface fresh water, which was probably responsible for the long-continued human population.

LJ-32. (See LJ-35)

LJ-33. Rancho Cuevas, Baja California Norte **400 ± 200**

Charcoal from layer 2 (second dm) below surface, at E end of a rather deep midden deposit in large rock shelter located on Rancho Cuevas, between Rosarita Beach and Punta Descanso, ca. 100 m upstream from low coastal terrace, in third canyon S of basaltic hill known as "Aquajito" (ca. 32° 17.0′ N Lat, 117° 02.0′ W Long), Baja California Norte (from HO Chart 1149, 1948). Coll. by C. L. Hubbs and party (sample 1958—II: 8A); subm. 1958. *Comment*: this is the first date from a potentially important site, in which excavations are being continued. The sample pertains to a late but prehistoric culture with pottery; paleoecologic inferences are expected. The present small water holes in the adjacent canyon bottom probably represent a continuum with a least as adequate surface water in the past. The soil shows little weathering.

LJ-34. Chollas Creek, California—1 **1450 ± 200**

Pismo-clam shell (*Tivela stultorum*) from below high-tide level, in middle of three occupation streaks exposed in bank, here low, of Chollas Creek (a tributary of San Diego Bay), immediately below National Avenue, San Diego (32° 41′ 44″ N Lat, 117° 07′ 17″ W Long), California (from Air Photo Compilation T-5372, 1933). Coll. by C. L. Hubbs, B. E. McCown, and party (sample 1957—I: 12D); subm. 1957. *Comment*: all these occupation streaks, which extend for a considerable distance along the creek, slope to below high-tide level. Dates and positions of the three occupation streaks (see LJ-37 and LJ-38, this list) indicate: (1) rise in sealevel during the past millenium (perhaps as a continuation of a long-established trend)—an idea that seems plausible to us; or (2) subsidence of the land, such as may have been the continuation of the down-faulting of a Mission Bay-San Diego Bay trench; or (3) westward tilting of the strata. The species composition of the molluscs in LJ-34 and LJ-37 (950 ± 200) do not suggest that the temperatures here were colder than at present, during a period when the coastal waters of northwestern Baja California were cold (see LJ-83, 84, 85, and 108, this list). The extensive occupation indicated by the abundant shells in each of the layers suggests that the freshwater supply may have exceeded that of the spring still extant nearby. Abundance of pismo clams in the three occupation layers suggests that the mouth of the creek may have been near the ocean beach (where this clam lives), rather than on the inner side of a broad bay. Artifacts taken from the creek bank indicate culture more advanced than the La Jollan.

LJ-35. Batiquitos Lagoon, California—2 **3500 ± 200**

Clam shell (*Chione californiensis*) from midden in bottom of talus along road beside S shore of Batiquitos Lagoon, San Diego County, across marsh from (E of) location of LJ-31 and LJ-36 (33° 05′ 03″ N Lat, 117° 17′ 44″ W Long), California (from Air Photo Compilation T-5411, 1954). Coll. by C. L. Hubbs, B. E. McCown, and party (sample 1956—X: 27C); subm. 1958. Charcoal (LJ-32) from the same spot proved inadequate for measurement. *Comment*: midden apparently pertains to about the same period of occupation as LJ-31 (3900 ± 200, this list), and, although little in the way of artifacts was seen here, the culture represented was probably similar. Similar physiographic inferences may be drawn.

LJ-36. Batiquitos Lagoon, California—3 **7300 ± 200**

Clam shell (*Chione californiensis*) from the lower of two soil horizons, below that of LJ-31, Batiquitos Lagoon (33° 05′ 01″ N Lat, 117° 17′ 52″ W Long), California (from Air Photo Compilation T-5411, 1954). Coll. by C. L. Hubbs (sample 1957—I: 5B); subm. 1958. Taken about 1 m down in yellowish sand, indurated with lime, overlain unconformably by loose, dark midden soil (LJ-31). There are very few artifacts in the lower layer, but an imperfect human skeleton was found in the same soil horizon (at a slightly higher level). *Comment*: date is conformable with several others along the coasts of southern California and northern Baja California that pertain to the early shellfish-gatherers (see LJ-3, 6, 26, 27, 77, 79, 107, 109, and 110, this list). It bears on inferred Holocene rise in sealevel and on past estuarine condition in the lagoon, which is now silted up and incapable of supporting the molluscs that existed here between three and eight millenia ago; it bears also on the probable temporal continuity of surface or subsurface water in the adjacent marsh (many long-inhabited sites are near springs or other supplies of fresh water).

LJ-37. Chollas Creek, California—2 **950 ± 200**

Pismo-clam shell (*Tivela stultorum*) from uppermost of three occupation streaks exposed in low bank of Chollas Creek, immediately below National Avenue, San Diego (32° 41′ 43″ N Lat, 117° 07′ 19″ W Long), California (from Air Photo Compilation T-5372, 1933). Coll. by C. L. Hubbs, B. E. McCown, and party (sample 1957—I: 12A); subm. 1958. From about 1 to 2 m above high-tide level, but the occupation streak slopes to below that level. Sample taken a few meters downstream from LJ-34. *Comment*: see LJ-34 (this list).

LJ-38. Chollas Creek, California—3 **2100 ± 200**

Pismo-clam shell (*Tivela stultorum*) taken between tidal limits from lowermost of three occupation levels exposed in low bank of Chollas Creek, San Diego, ca. 50 m downstream from LJ-37 (32° 41′ 43″ N Lat, 117° 07′ 19″ W Long), California. Coll. by C. L. Hubbs, B. E. McCown, and party (sample 1957—I: 12B); subm. 1958. *Comment*: inferences are similar to those for LJ-34 (this list), except that the inclusion of *Laevicardium elatum* in this layer suggests that temperatures were probably a little higher than at present.

LJ-55. La Brea Tar Pits, California—1 **14,400 ± 300**

Wood from tree trunk discovered in situ in Pit 3 of Rancho La Brea tar pits (34° 03′ 45″ N Lat, 118° 21′ 25″ W Long), California. Coll. 1913 by L. E. Wyman, Los Angeles County Museum; subm. 1958 for that museum by Hildegarde Howard, who wrote: "This tree was rooted in the sloping bank of the pit (possibly an old gully) at a depth of 12 feet from the surface; the tip of the topmost branch (broken or burned off) was first encountered at a depth of 4 feet; total height of tree as preserved was 8 feet. Bones of typical Pleistocene animals were packed about the tree." Before the wood was analyzed, the tar was removed and run separately (LJ-89). *Comment*: date obtained by the La Jolla laboratory is in almost perfect agreement with four dates (13,890 to 15,390, averaging 14,470) soon afterward announced by the Yale laboratory, for samples (Y-354A, B and Y-355A, B) from the same trunk (Yale IV). Yale, referring to the trunk, noted that "Douglas (1952) cited two unpublished CalTech dates, 16,250 ± 2000 and 16,400 ± 2000, for wood subm. by Chester Stock." The Rancho La Brea datings, which have been discussed by Howard (1960), show that much of the extinct Pleistocene fauna continued into the last millenia of that period. A rather high proportion of the rich bird fauna from Pit 3, as well as of the mammal fauna, is extinct (Howard and Miller, 1939). No definite indications of human occupation have been discovered in Pit 3, but artifacts have been found in other pits (see LJ-121, this list).

LJ-71. Oyster reef, off coast of Texas **2700 ± 100**

Oyster shell (*Crassostrea rhizophorae*) from API Station J468, dredged on continental shelf off Padre Island, at depth of 39 fathoms (26° 46.0′ N Lat, 96° 42.0′ W Long), (from USC&GS Chart 1117, 1956). Coll. June 8, 1956 by R. H. Parker, Scripps Institution of Oceanography; subm. 1958 by J. R. Curray and R. H. Parker. *Comment*: sample submitted for the bearing that the date may have on estimates of changes in sealevel. This species of oyster lives on mangroves, very near sealevel, in tropical waters and is therefore considered to be an excellent indicator of sealevel at a time when surface waters were considerably lower than at present in the same region. The age was predicted at ca. 13,000 yr because of depth of the collection (Curray, 1959, 1960), but such a date would be inconsistent with the inferred temperature. Was there a recession of the sea, or an elevation of the land, about 2700 yr ago, or may the shell have been washed outward? The data of Shepard and Moore (1955) render the first two possibilities unlikely, and also tend to rule out crustal downwarping in this region during the last 10,000 yr.

LJ-75. Near Punta Clara, Baja California **1150 ± 150**

Charcoal from a single hearth at lip of cliff on most prominent point between Punta Clara and Punta China, near (S of) mouth of Arroyo Santo Tomás (31° 31′ 34″ N Lat, 116° 39′ 36″ W Long), Baja California Norte (from HO Chart 1044, 1949). Coll. by C. L. Hubbs and G. F. Carter (sample 1954—V: 7D); subm. 1958. The hearth was in somewhat hardened and reddened soil, barely overlying strongly reddened sand. *Comment*: this is the first dating based on charcoal from the abundant subsurface middens in an area

(300)

where C^{14} and O^{18} analyses of midden shells, bolstering faunal evidence, have indicated a cold period for the NW coast of Baja California from ca. 1600 to ca. 600 yr ago, a period when the climate in the Arctic is reported to have been mild. Other dates on this episode in California are C-659, 889 ± 100 (Chicago III); LJ-83, 1600 ± 150, LJ-84, 1060 ± 150, LJ-85, 960 ± 150, and LJ-108, 1580 ± 100, this list. The date bears on archaeology and on the rate of soil weathering, as well as on paleoclimatology.

LJ-76. Karlo Site, northern California **2350 ± 150**

Charcoal recovered during excavation of the Karlo site (4-Las-7), near Susanville, Lassen County (40° 33′ 45″ N Lat, 120° 19′ 30″ W Long), California (from Karlo Quadrangle, 1954). Coll. 1955 by F. A. Riddell; subm. 1958 by R. F. Heizer, University of California, Berkeley. Sample (#119/323) came from Square 40/21 (same lens as Sq. 40/22), ca. 0.6 to 0.9 m below surface. *Comment*: charcoal contained many rootlets, which were removed as far as possible. The culture disclosed by the excavations here has been interpreted by Riddell (1956, in press) as belonging to the Lovelock Culture, which has been described, with datings between 2000 B.C and A.D. 1000, by Loud and Harrington (1929), Heizer and Krieger (1956), and Grosscup (1958). Heizer comments: "The LJ-76 date falls within the expected time range of the Lovelock Culture as known from a number of other radiocarbon dates, and is of interest in indicating the western extension of the Great Basin culture of Medithermal age." The date bears also on the past fauna of a part of the Lahontan basin, including the fish fauna being studied by W. I. Follett of the California Academy of Sciences.

LJ-77. Zuma Creek Site, California **4950 ± 200**

Black-abalone shell (*Haliotis cracherodii*) from Zuma Creek site, Los Angeles County (LAn–174 of the University of California Archaeological Survey), which lies on the 100-ft (30-m) terrace just above the beach, (ca. 34° 00.1′ N Lat, 119° 49.0′ W Long), California (from USC&GS Chart 5205, 1915.) The shell (174–16) dated came from Pit 6 of the UCLA excavation, at depth of 0.3 to 0.6 m. Coll. spring 1957 by Robert Ascher; subm. 1958 by C. W. Meighan, University of California, Los Angeles. *Comment*: this finding provides another date for the early milling-stone material of the southern California coast, which is associated with an abundance of shellfish, generally crude artifacts, and no pottery (Peck, 1955; Ascher, 1959). The fauna, as reported by Peck, is not much different from that of today (Peck's listing of *Mytilus edulus* (sic) is probably in error).

LJ-78. Near Malibu Beach, California **3460 ± 200**

Mussel shell (*Mytilus californianus*) from the lowest exposed midden streak, buried ca. 4.8 m, in road-cut cliff along Pacific Highway, opposite house no. 20732 (34° 02′ 16″ N Lat, 118° 37′ 31″ W Long), California (from Malibu Beach Quadrangle, 1951). Coll. by C. L. Hubbs (sample 1958—XII: 11A); subm. 1958. According to C. W. Meighan this sample was taken at Site Lan–190 of the University of California Archaeological Survey. *Comment*: Meighan suspects that some of the midden material may have been derived by intermittent slippage, or by inwash of occupation debris, from above, but it appeared during collecting that the midden had accumulated in place on an old land-surface. Several occupation streaks above suggest repeated population on the successive land-surfaces as these were temporarily stabilized. The overlying alluvial fill strongly suggests greater rainfall than now, during and for some time following the dated occupation.

LJ-79. Scripps Estates Site I, California—1 6700 ± 150

Mussel shell (*Mytilus californianus*) associated with Burial 7, near mid-depth of shallow midden near the ocean edge of Linda Vista Terrace, on S rim of Sumner Canyon, at 2504 Ellentown Road, La Jolla (32° 52′ 22″ N Lat, 117° 14′ 54″ W Long), California (from Air Photo Compilation T-5375, 1933, and La Jolla Quadrangle, 1933). Coll. by C. L. Hubbs, J. R. Moriarty, and George Shumway (sample 1958—XII: 13A); subm. 1959. *Comment*: a preliminary account of this ancient, La Jollan site (SDi–525 in the records of the University of California Archaeological Survey; SDMM–9–W of the San Diego Museum of Man) has been published by Moriarty, Shumway, and Warren (1959); the investigations are being continued by these authors and Hubbs. The early date stands in agreement with several other dates for sites in southern California and northern Baja California with similar assemblages of stone tools (other such sites are herein reported as LJ-3, 6, 26, 27, 36, 77, 107, 109, and 110). The molluscan assemblage in LJ-79 suggests water (and air) temperatures probably a little warmer than those prevailing at present, and mass spectrometric O^{18} determinations (by R. N. C. Bowen of Scripps Institution of Oceanography) now yield confirmatory temperature estimates of 21.3° C for *Mytilus californianus* and 20.6° for *Pseudochama exogyra*. As will be detailed in subsequent reports, the fauna and various other data indicate that the site was occupied during a low but rising sealevel. The abundant population that appears to have existed at this site for more than 2000 yr (see also LJ-109, 7370 ± 100, LJ-110, 5460 ± 100) appears to have been too large to have been supported by such limited rain as falls currently. This and other considerations point toward a more humid climate.

LJ-82. Wood from ocean bottom off Mexico >28,000

Wood (log of some dicotyledon), mineralized by phosphatic infiltration, dredged (TO–58–2, D–7) from a 510-m terrace in the Gulf of Tehuantepec, Mexico, near the edge of the Middle American Trench (from 14° 25′ N Lat, 93° 05′ W Long, to 14° 27′ N Lat, 93° 11′ W Long) (from HO Chart 0932, 1956). Coll. November 20, 1958 by R. H. Parker on Scripps Institution of Oceanography Research Ship *Horizon*; subm. 1959 by G. O. S. Arrhenius and R. H. Parker. *Comment*: the wood that abounded on the bottom showed no trace of decomposition. Its exposed portion had become strongly phosphatized, but the part buried in clay had remained essentially unaltered. The overlying waters have an exceedingly low content of dissolved oxygen: between 0 and 0.1 ml/l. G. E. Jones, microbiologist at Scripps Institution of Oceanography, has been unable to cultivate bacteria from the center of this wood, nor any wood-decomposing organisms from the more superficial parts. The radiocarbon determination was made on the organic wood component of the sample.

A report on this discovery, giving consideration to the mechanisms involved in the fossilization, has been prepared by Goldberg and Parker (1960).

LJ-83. Near Punta Baja, Baja California **1600 ± 150**

Mussel shell (*Mytilus californianus*) from cobbly valley-fill truncated by the sea, ca. 2 mi E of Punta Baja (29° 57.3′ N Lat, 115° 46.6′ W Long), Baja California Norte (from HO Chart 1044, 1949). Coll. by C. L. Hubbs and Nobuo Egami (sample 1958—V: 3B); subm. 1958. The midden shells (and a trace of artifacts) were mixed with cobbles, gravel, and sand. *Comment*: material had apparently been deposited at a lower relative sealevel and presumably during a period of heavier rainfall and more intense alluviation. The shells apparently were washed from middens up the canyon (where middens still abound) and therefore may have considerably antedated the valley-fill. Recently the valley-fill has been entrenched to near present sealevel. Inclusion of some *Cryptochiton* valves indicates that the cold period (see LJ-75, this list) had already begun. A confirmatory paleotemperature estimate of 13.6° C was obtained by R. N. C. Bowen, Scripps Institution, through an O^{18} determination on shells of *Mytilus californianus* in this collection. Soil weathering has proceeded to a moderate degree.

LJ-84. Valle de Rosario, Baja California—1 **1060 ± 150**

Mussel shell (*Mytilus californianus*) from occupation streak buried in the sand-and-silt valley-fill of Arroyo Rosario, 2.4 km above mouth (30° 03.3′ N Lat, 115° 45.7′ W Long), Baja California Norte (from HO Chart 1149, 1948). Coll. by C. L. Hubbs and Nobuo Egami (sample 1958—V: 4B); subm. 1958. The continuous midden streak, representing an old land-surface, is buried ca. 150 cm below the present surface and ca. 4.5 m above present floodplain of river; it is exposed in the road cut. *Comment*: some *Cryptochiton* valves place this deposit in the cold period mentioned under LJ-83. The valley, here several mi wide, was probably aggraded when rainfall was greater and sealevel lower. The date exceeds that for charcoal from the same site (LJ-85) by 100 yr. No correction was made for the apparent age of modern shell.

LJ-85. Valle de Rosario, Baja California—2 **960 ± 150**

Charcoal from the same collection as LJ-84. *Comment*: date is close to that obtained from carbonate carbon.

LJ-87. "The Nunnery," Chichén, Itzá, Yucatán **1140 ± 200**

Wood from the ruin known as "The Nunnery," at Chichén-Itzá (ca. 20° 41′ N Lat, 88° 34′ W Long), Yucatán, pertaining archaeologically, we understand, to the Classical Mayan Period A.D. 700 to 1000. Coll. by Theodore Shedlovsky, Rockefeller Institute, who reports: "It was given to me by my guide who detached it as a loosely hanging fragment from what had probably been a substantial beam in the original structure but was no longer supporting any load." By request of the La Jolla Laboratory, the sample was subm. by Julian Shedlovsky in 1959. *Comment*: the agreement of the date with the archaeologic estimate is gratifyingly close. There is also close agreement with the date by the Yale laboratory from Chichén Itzá: Y-626, 1160 ± 60 (Yale IV) and Y-626*bis*, 1010 ± 100 (Yale V).

(303)

LJ-89. La Brea Tar Pits, California—2 **>28,000**

Tar extracted from cavity in trunk of wood run as LJ-55 (this list), Rancho La Brea tar pits (34° 03′ 45″ N Lat, 118° 21′ 25″ W Long), California. *Comment*: run to test whether the tar that impregnated this sample was essentially "dead", since recent tests are said to indicate that some tars may be much younger than previously thought. The count was only slightly above the background.

LJ-95. Submarine artifact, California **520 ± 150**

Oyster shell (*Ostrea lurida*) attached on inside of a gigantic stone bowl found outside the surf, at La Jolla (32° 51′ 15″ N Lat, 117° 15′ 38″ W Long), California (from Air Photo Compilation T-5375, 1933). Coll. by Gary Wickham, Ralph Dam, and Robert Atkinson, La Jolla (sample 1958—IX: 21A); subm. 1959. The bowl was buried in the sand so that only the rim was exposed, but shifting sand may have exposed it more fully in the past. *Comment*: analysis was obtained to give a minimum date for the abundant submarine artifacts in this region (Tuthill and Allanson, 1955). Large numbers of artifacts of relatively recent cultures, mostly smaller bowls, found on the seafloor in southern California, have posed exciting problems. It seems most plausible to attribute their occurrence to a relatively recent rise in sealevel, resulting in a rapid erosion of the shore. As such a heavy object as the bowl here treated, weighing 61 kg, probably would not have shifted greatly in position, it may have stayed near where it was left on shore by man, and the oyster shells on it may not be much younger than the time of its submergence.

LJ-96. Midden, San Felipe, Baja California—1 **1370 ± 200**

Clam shell (*Chione californiensis*) from extensive superficial midden on beach ridge, at edge of coastal terrace, just above and W of air strip occupying a stranded lagoon, close to the San Felipe village well, Golfo de California (31° 01′ N Lat, 114° 51′ W Long), Baja California Norte. Coll. by C. L. Hubbs, F. P. Shepard, and party (sample 1955—XII: 29A); subm. 1959. *Comment*: dates the former dense population, indicated by the abundance of surface middens, in a now-dry coastal area, and dates the greater-than-present precipitation that is inferred to have afforded an adequate water supply.

LJ-98. Estero de Punta Banda, Baja California **1820 ± 200**

Charcoal, mostly from a burned log, in midden buried 1.5 to 4.6 m in alluvial-clay slope along S shore of Estero de Punta Banda (31° 42.3′ N Lat, 116° 38.5′ W Long), Baja California Norte (from insert on HO Chart 1149, 1948). Coll. by C. L. Hubbs and W. J. North (sample 1957—V: 26A); subm. 1959. *Comment*: the character of the alluvial deposits and the evidences of human occupation indicate that the slope, with its midden shells, fire areas, etc., probably accumulated on the shore of the estuary during a period of greater-than-present rainfall, when sealevel was somewhat lower than now. The site is along an active fault with warm springs, which have probably had a long history, and have presumably supplied fresh water for the widespread habitations in this region.

LJ-99. Lake LeConte, California—1 **760 ± 100**

Charcoal from near W shore of ancient Lake LeConte, in recess 1.8 km WSW from Travertine Rock, Imperial County, in south-central part of sec. 6, T 9 S, R 9 E (33° 24.9′ N Lat, 116° 04.4′ W Long), California (from Oasis Quadrangle, 1956). Coll. by G. M. Stanley, Fresno State College, and C. L. Hubbs (sample 1958—IV: 20B); subm. 1959. Taken from a canyon draining toward the NW, between 10.76 and 10.91 m above sealevel, and 0.37 m below surface of foreshore slope of small southward-built gravel spit (altitude 13.38 m), 6 m E, which marks the high shoreline of the last main stage of Lake LeConte (Hubbs and Miller, 1948, p. 103-112. The charcoal, mostly of tules, permeates a layer of lake silt, 7.6 cm thick, that overlies beach gravel, and in turn is covered by sand and gravel. The silt is the thinner and upper of two silt layers, each of which is interbedded between, and is separated by, layers of beach gravel. *Comment*: the silt was formed during the second of three cycles of inundation (due, presumably, to fluctuating lake level) that are indicated in the gully section that exposes the charcoal. The site was occupied well before the termination of the last high stage of Lake LeConte. (Most of these detailed data were kindly supplied by Stanley.)

LJ-100. Midden, San Felipe, Baja California—2 **200 ± 100**

Charcoal from a single hearth in the beach-ridge midden recorded under LJ-96 (this list), San Felipe (31° 01′ N Lat, 114° 51′ W Long), Baja California Norte. Coll. 1955 by C. L. Hubbs, F. P. Shepard, and party; subm. 1959. Only 3.9 g of clean charcoal was secured from the 11.2-g sample. *Comment*: sample dated to confirm the date obtained from shell (LJ-96, this list), but it now appears that the fire was intrusive, and much more recent (very late prehistoric or modern).

LJ-101. Lake LeConte, California—2 **1580 ± 200**

Charcoal from beachline 3.0 km SW×W from Valerie Jean, in NW¼ sec. 24 (close to north–south center line), T 7 S, R 7 E, Riverside County (33° 33.1′ N Lat, 116° 12.4′ W Long), California (from Valerie Quadrangle, 1956). Coll. by G. M. Stanley and C. L. Hubbs (sample 1958—IV: 20C); subm. 1959. In thin silt seams at 10.7 m altitude, where highest beach stand was at 13.4 to 13.7 m (data from Stanley); overlying well-cemented pebbly sand and underlying sand with foreset laminae; ca. 45 cm below top of a broad silt-flat. *Comment*: the silt-flat formed behind a sand-bar on the shore of the last high stage of Lake LeConte, but earlier than the period of greatest population with much pottery. This is the oldest date so far obtained for Lake LeConte.

LJ-102. Lake LeConte, California—3 **220 ± 100**

Charred tules from eastern beachline in Imperial County, ca. 0.6 km NW of Siphon 18 on Coachella Canal, in SW¼ sec. 7, T 9 S, R 13 E (33° 24.1′ N Lat, 115° 39.5′ W Long), California (from Frink NW Quadrangle, 1956). Coll. by C. L. Hubbs and B. E. McCown (sample 1956—XII: 29C); subm. 1959. *Comment*: a sample from one of the extensive tule fires of the shoreline, which appear to have been set in game-drives around the margin of Lake LeConte toward the end of the last stage. The fire baked the underlying clay.

LJ-103. Midden, Sweetwater River, California **760 ± 100**

Charcoal, metamorphosed into almost coal-like hardness and brittleness, from terrace at ca. 13.7 m altitude on S side of Sweetwater River, along the S line of C Street between National Avenue and Date Street, Chula Vista, San Diego County (32° 38′ 49″ N Lat, 117° 05′ 38″ W Long), California (from Air Photo Compilation T-5372, 1933). Coll. by C. L. Hubbs and L. C. Hubbs (sample 1959—IV: 19A); subm. 1959. Accompanying the charcoal are many crudely flaked artifacts. *Comment*: the crudeness of the artifacts, the modification of the charcoal, and the lime induration and the yellowish-to-reddish coloration of the soil in which the artifacts lay, combined to give an impression of very considerable antiquity, but the relatively young date merely shows how recent are some of the crude artifacts that predominate in some Californian sites and how rapid the inferred soil-forming processes can be. Incidentally, this soil grades downward, conformably, in Hubbs' opinion, into the river gravels in which Carter (1952, and 1957, p. 356) found broken cobbles that provided "the major source of data for the initial claim for interglacial man in the San Diego area." No confirmation of this interpretation could be gleaned from the field work of 1959.

LJ-105. Lake LeConte, California—4 **1440 ± 100**

Charcoal from a thin occupation level at 2.0 m depth in an extensive silt deposit behind a bar along E shore of ancient Lake LeConte, Imperial County, in a draw ca. 0.4 km below Siphon 15 of Coachella Canal, in sec. 26, T 9 S, R 13 E (33° 21.7′ N Lat, 115° 35.0′ W Long), California (from Frink Quadrangle, 1940). Coll. by C. L. Hubbs, with B. E. McCown and party of the Archaeological Survey Association of Southern California (sample 1956—XII: 31C); subm. 1959. In a rather continuous and thin occupation streak, with some fish bones, lying ca. 30 cm above a sandy level containing Lake LeConte shells. At a total depth of 3.2 m there was another occupation streak on an older land-surface (with insufficient charcoal for a test). *Comment*: the collectors arrived at the following interpretations: More than 1500 yr ago a lagoon formed behind the barrier-bar on the E shore of Lake LeConte; gradually silt filled this lagoon; when the land surface dried it was widely occupied by man; after further aggradation, a higher land-surface was inhabited ca. 1440 yr ago (LJ-105); then another 2 m of silt accumulated over that land-surface, to form a third surface, which was occupied (see LJ-15, 300 ± 100, and LJ-102, 220 ± 100, this list) by the dense population that developed toward the end of the last high stage of Lake LeConte.

LJ-106. (B.) Lake LeConte, California—5 **960 ± 100**

Charcoal from essentially the same locality as LJ-105, in an adjacent draw. Coll. by same party (sample 1956—XII: 31B); subm. 1959. The very definite habitation streak was 2.5 to 20 cm thick and was buried about 1.7 m. A small potsherd and some fish bone occurred with the charcoal. Very near, at the same level, a large part of a pot was taken by the collectors. *Comment*:

this and other collections show that the earlier inhabitants of the shoreline of the last high stage of Lake LeConte had pottery, though not in the abundance indicated for the terminal period of the lake's existence. This intermediate date confirms the existence of the lake 1000 yr ago, as hypothesized under LJ-7 (this list) and enhances the probability that the lake persisted from at least 1600 B.P. until about 300 B.P.

LJ-107. (B.) Punta Cabras, Baja California—2 6400 ± 200

Rock-scallop shell (*Hinnites multirugosus*) from surface midden near cliff edge at tip of Punta Cabras (31° 20.1′ N Lat, 116° 27.7′ W Long), Baja California (from HO Chart 1149, 1948). Coll. by C. L. Hubbs (sample 1952—VI: 8A); subm. 1959. *Comment*: date provides another indication that the early shellfish-gatherers occupied the NW coast of Baja California. LJ-6 provided a date of 5020 ± 200 for a site 1 km E.

LJ-108. Hearth, Punta Clara, Baja California Norte 1580 ± 100

Black-abalone shell (*Haliotis cracherodii*) from a single definite hearth on the face of the dunes at Punta Clara (first point S of the mouth of Arroyo Santo Tomás) (31° 51′ 54″ N Lat, 116° 39′ 48″ W Long), Baja California Norte (from HO Chart 1044, 1918). The hearth contained many shells, a whale vertebra, some charcoal, etc. Coll. by C. L. Hubbs and party from Great Basin Conference (sample 1955—IX: 3D); subm. 1959. *Comment*: this date is the oldest in the Santo Tomás region for the *Cryptochiton*-bearing middens of a cold period that continued until less than 1000 yr ago. With the date of 1600 ± 150 for LJ-83, it may approach the beginning of this period. This was the first definite hearth located in the shell- and artifact-rich dune area of Punta Clara.

LJ-109. (B.) Scripps Estates Site I, California—2 7370 ± 100

Mussel shell (*Mytilus californianus*), encased in almost cement-like caliche, from the bottom of the shell rich layer of the site, on Lot 24, Scripps Estates Associates, at ca. 107 m altitude (32° 52′ 18″ N Lat, 117° 14′ 55″ W Long), California (from Air Photo Compilation T-5375, 1933, and La Jolla Quadrangle, 1933). Coll. 1954-1957 by C. L. Hubbs; subm. 1959. *Comment*: this sample (1) dates the lower level of main occupation of this significant site, higher levels of which are dated by LJ-79, 6700 ± 150, and LJ-110, 5460 ± 100 (this list), but the initial habitation by a smaller population is still older, though undated; (2) gives a maximal estimate of the time required (under the local conditions) for the production of an extensive caliche limepan; (3) bears on the time of the inferred rise in sealevel and the hypothesized greater-than-present precipitation, and on the time when sea temperatures had become as warm as or warmer than now, as discussed under LJ-79, this list.

LJ-110. (B.) Scripps Estates Site I, California—3 5460 ± 100

Mussel shell (*Mytilus californianus*) from dark, friable A-horizon, superficial soil of site I, Scripps Estates Associates (32° 52′ 18″ N Lat, 117° 14′ 55″ W Long), California (from Air Photo Compilation T-5375, 1933, and La Jolla Quadrangle, 1933). Coll. 1954-1957 by C. L. Hubbs; subm. 1959. *Comment*:

sample dates the upper limit of the probably more than two millenia of occupation and (as discussed under LJ-79) bears on the rate of soil weathering and on past oceanographic and climatic conditions.

LJ-111. (B.) Midden, Cape Arago, Oregon **1500 ± 100**

Charcoal from the upper 2 dm of one of the middens excavated by C. L. Hubbs and party (sample 1957—VII: 10A); subm. 1959. This midden lies at the island end of the footbridge leading to Cape Arago Light, at the E end of the crest of a residual ridge (43° 20′ 27″ N Lat, 124° 22′ 23″ W Long), Oregon (from USC&GS Chart 5984, 1957). *Comment*: date fixes the upper limit of the occupation of this particular midden site; inferred changes in ecologic conditions and in culture will be detailed in a later report.

LJ-112. Mukluk Piston Core B21P **>40,000**

Carbonate ooze (coccoliths and Foraminifera) from piston core taken 1957 by R. J. Hurley in the NE Pacific Ocean, on the Mukluk Expedition of Scripps Institution of Oceanography (52° 32′ N Lat, 141° 44′ W Long); subm. 1959. According to the collector, the core consists of 8.7 m of carbonate ooze interbedded with blue-green mud and with sand layers; the sample was from 42 to 49 cm from top of core and represents the uppermost carbonate-ooze layer; due to disturbances of the bottom materials in the piston coring, the layers in the core cannot be exactly equated with those in an adjacent, shorter gravity core, in which the uppermost 10 cm, consisting primarily of pelagic sediments, overlies sediments of turbidity-current origin that do not extend deep enough to have included the topmost carbonate-ooze layer. *Comment*: a finite radiocarbon date would have confirmed the hypothesis of rapid accumulation of turbidity-current deposits, but, in view of the uncertainties as to the actual depth of the carbonate ooze in the bottom, and in view of the probable variations in the rate of such sedimentation, the test does not negate the hypothesis.

LJ-120. (B.) Flooded cave, Florida **10,000 ± 200**

Strongly charred log taken in close association with human bones and artifacts, buried in sediment on the floor of a now-flooded cave surrounding the opening of Warm Mineral Springs, 11.6 m under water (27° 02′ 30″ N Lat, 82° 15′ 30″ W Long), Florida (from pl.1, Ferguson, Lingham, Love, and Vernon, 1947). Coll. and subm. 1959 by Eugenie Clark, Director, Cape Haze Marine Laboratory. The burned log was uncovered from ca. 2 m of cave deposit, 1.83 m back from the outermost stalactites of the overhanging cave roof. Human bones were found within a few mm of the log. Ca. 6 m from the log there was removed, from the middle of three sedimentary layers, a dolichocephalic human skull containing supposed brain tissue but showing no cellular structure in microscopic sections. *Comment*: a preliminary account of this notable find has been prepared by Clark (ms).

LJ-121. (B.) La Brea Tar Pits, California—3 **4450 ± 200**

Wooden atlatl foreshaft (Los Angeles County Museum no. 385), one of the few artifacts known from the Rancho La Brea tar pits (34° 03′ 45″ N Lat, 118° 21′ 25″ W Long), California. Coll. 1915 by L. E. Wyman, Los Angeles County Museum; subm. 1959 by Hildegarde Howard of the same institution. The test was made of the butt end of the specimen, which was illustrated by Woodward (1937, pl. 18 (*a*)). This specimen, and others described by Woodward, came from Pit 61–67, and bears data "Pit 67, caved wall, SE." Field notes state that several artifacts were found in an area embracing grid sections F, G, H, and I from 8 to 18 ft in Pit 67 and into Pit 61 (pits 61 and 67 were found upon excavation to be continuous). Marine shells were also found where pits 61 and 67 joined. *Comment*: according to Howard (1960), various circumstances suggest a younger age for the evidences of man in the Rancho La Brea tar pits than for the in situ tree trunk (LJ-55, this list). The problem was earlier discussed by Howard and Miller (1939).

LJ-128. (B.) Shell, Long Reef, Australia—1 900 ± 150

A large shell of a presumably intertidal mollusc, *Turbo* sp., from 3.65 m above mean tide, on a "raised beach" at Long Reef, on the coast between Deewhy and Callaroy, near Sydney (ca. 33° 44.6′ S Lat, 151° 19.4′ E Long), Australia (from HO Chart 1904, 1942). Coll. 1959 by H. R. Wanless, University of Illinois, Urbana; subm. 1959 by F. P. Shepard, Scripps Institution of Oceanography. *Comment*: sample was dated to test the evidence for a postglacial high sea-stand, for which perhaps the least assailable evidence seems to stem from Australia. Some authorities, such as Shepard and Suess (1956) and Curray (1959, 1960), believe that the preponderance of evidence argues against such a high stand. Others, particularly Fairbridge (1958), disagree. Possibilities in need of consideration, in this and in similar tests, are whether there has been uplift of the land and whether the shell deposits are really natural. The uniform altitude and broad areal extent of the shell deposit, and the lithified nature of some of the matrix, indicate that the deposit probably represents a "raised beach", but the date and height do not correspond closely with any of the eustatic stages postulated by Fairbridge. Tectonic movement(s) may have been involved.

LJ-130. (B.) Shell, Long Reef, Australia—2 900 ± 150

Shell (intertidal limpets, *Patella* sp. and *Fissurella* sp.) from the same collection as LJ-128, Long Reef, near Sydney (ca. 33° 44.6′ S Lat, 151° 19.4′ E Long), Australia (from HO Chart 1904, 1942). Coll. 1959 by H. R. Wanless, University of Illinois, Urbana; subm. 1959 by F. P. Shepard, Scripps Institution of Oceanography. *Comment*: the reasons for this measurement, and the inferences, are the same as for LJ-128.

LJ-131. (B.) Isla Ceralbo, Golfo de California >42,000

Shell of a single large gastropod (*Strombus galeatus*), from more or less cemented stratum 0.4 to 2.5 m thick, in the lower, marine part of the terrace-fill, just W of the S point of Isla Ceralbo, off Baja California Sur (24° 08.8′ N Lat, 109° 47.1′ W Long) (from HO Chart 1664, 1956). Coll. March 28, 1959, and described by Chao-Siang Wang, National Taiwan University, on a Vermilion Sea Expedition of the Scripps Institution of Oceanography; subm. 1959 by F. P. Shepard. The collector reported the following altitudes: top of terrace-fill [at cliff?], 10 m; fossil bed, 1.5 to 4 m; buried wave-cut platform, 1.5 m. *Comment*: sample was run in an effort to date when, in this unstable region, the fossil bed was at or below sealevel. The date indicates a deposit earlier than late Wisconsin, certainly not Recent. The shell, unlike that of LJ-132, was clearly altered by fossilization.

LJ-132. (B.) Punta Pescadero, Baja California 1700 ± 150

Shell of a single large gastropod (*Strombus galeatus*) from terrace along Golfo de California, at Punta Pescadero (23° 47.6′ N Lat, 109° 42.0′ W Long), Baja California Sur (from HO Chart 1664, 1956). Coll. 1959 by Chao-Siang Wang, National Taiwan University, on a Vermilion Sea Expedition of the Scripps Institution (sample 1959—III: 28A); subm. 1959 by F. P. Shepard. The collector recorded, presumably from the cliff face, the altitude of the terrace [top] as 8 m; the thickness of what he took to be a fossil bed as 0.2 to 0.3 m; the height of the buried wave-cut platform as 6 m; and the thickness of the superficial alluvial fill as ca. 2 m. *Comment*: the late date indicates an unexpected very recent uplift; or, less probably, a recent high eustatic sealevel; or, as now seems almost certain, that the deposit, contrary to the collector's view, is a midden. He reported that the species of molluscs in this deposit are the same as those in the deposit dated by LJ-131, but the two other shells submitted (one each of *Chamma buddiana* and *Muricanthus nigritus*) were not represented in the sample from Isla Ceralbo. All three specimens at hand from Punta Pescadero give the impression of being recent midden shells.

LJ-136. (B.) San Dieguitoan site, California 4720 ± 160

Shell (*Chione californiensis*) from the San Dieguitoan site (SDMM–W–198), extensively studied by M. J. Rogers, San Diego Museum of Man, in the San Dieguito River valley, 12.5 km inland, just above a volcanic dike, in SW¼ sec. 13, T 13 S, R 3 W (33° 02′ 33″ N Lat, 117° 09′ 10″ W Long), California (from Rancho Santa Fe Quadrangle, 1949). This is Site SDi–149 of the University of California Archaeological Survey. Coll. August 1938 and subm. 1959 by M. J. Rogers. *Comment*: the collector reports that *Chione* and *Pecten circularis aequisulcatus* made up about 98% of the shells, which were found in very limited number here (shells are ordinarily lacking in San Dieguitoan, as contrasted with La Jollan, sites). Included also were a few pieces of the warm-water cockle *Laevicardium elatum*, and a few other fragments, possibly of abalone (*Haliotis*). Shells were in a sandy layer, Rogers' Stratum M′, that he interprets as part of an ancient sand-bar. This sandy layer, he states, was in a residual hummock on the floodplain of a now-intermittent stream below a concrete-like layer and, before erosion, was under ca. 5 m of valley-fill. Within the sand Rogers found shells only in the upper part, in contact with the "concrete" and just below [the cemented layer may have prevented the solution of the shells]. From the same sand layer Rogers took artifacts (amulets, notched points, etc.), regarded by him as characteristic of what he has termed San Dieguito III. Rogers originally (1929) indicated that the "Scraper-Maker Culture", which he named San Dieguito in 1939, may have developed from that of the "Shell-Midden People" (which he later called

(310)

La Jollan). After much field work Rogers (1945) reversed the sequence, and theorized that the San Diequitoan people were replaced by the retrogressive La Jollans, who, in turn, graded into the relatively recent Yumans. This sequence has been accepted by Meighan (1959). The evidence for this view, which has not been shared by the senior author of this report, is (1) the stratigraphic relation, at several places, including site SDMM–W–198, of cultural material identified as San Dieguitoan below "La Jollan", and (2) the similarity of the San Dieguitoan stone artifacts to those of other Western sites that appear on artifactual or dated grounds to have preceded the La Jollan. The problem needs further elucidation, especially because stratigraphic relations in reworked floodplain deposits like those at SDMM–W–198 are suspect, and because migrations, cultural deterioration, and independent developments and acquisitions may often affect the apparent cultural sequence. The extent of valley alluviation at this site suggests greater stream flow in the past; the repeated or prolonged occupation of the site may well have resulted from the long persistence of the stream here (prior to the current drought, some surface water persisted perennially here).

LJ-141. (B.) Drilled well, Cape Cod **>42,000**

LJ-142. (B.) **>42,000**

Charcoal from Holdens Well 86, at edge of Holdens Pond, near tip of Cape Cod (42° 03′ 19″ N Lat, 70° 16′ 03″ W Long), Massachusetts (from North Truro Quadrangle, 1948). Coll. September 1959 by J. M. Zeigler, Woods Hole Oceanographic Institution, Massachusetts; subm. 1959 by him through F. P. Shepard. LJ-141 was listed as having come from the charcoal layer at depth 26.0 m; LJ-142, from the mixed layer of charcoal and oxidized clay at 27.0 m. Zeigler reports that this well is being drilled to determine whether or not the four glacial formations, if present, are separated by marine deposits. The well, a 3-in. cased hole, has been handled very carefully; the entire operation has been by staff members. There is no possible way that the charcoal in this sample could have come from elsewhere. The bottom of Holdens Pond is at 1.5 m altitude; the uppermost material is interpreted as fluvio-glacial sands and gravels of Wisconsin age, from the surface; at 6.1 m an oxidized zone tops a layer of clay, probably Gardiners Clay, the age of which is given as Sangamon; this clay extends to 10.8 m and overlies ca. 15.5 m of fine, gray, angular sand, devoid of marine fossils. Below this sand, at ca. 26.2 m depth, is a layer of charcoal, overlying a mixture of charcoal and oxidized clay. *Comment*: Zeigler remarked that "the date of this charcoal could very well be the most important date in New England of this century because: 1. There are no known pre-Wisconsin glacial deposits in New England. 2. The Gardiners Clay is widespread but the correlation is uncertain. Thus no matter what age the carbon gives, it will be very important, whether a pre-Wisconsin age or a stadial age." It is obvious that the charcoal is at the latest early Wisconsin. The date does not further fix the age of either the charcoal or the clay.

REFERENCES

Date lists:

Chicago III.	Libby, 1952
Lamont III.	Broecker, Kulp, and Tucek, 1956
Lamont IV.	Broecker and Kulp, 1957
USGS I.	Suess, 1954b
USGS II.	Rubin and Suess, 1955
Yale IV.	Deevey, Gralenski, and Hoffren, 1959
Yale V.	Stuiver, Deevey, and Gralenski, 1960

Ascher, Robert, 1959, A prehistoric population estimate using midden analysis and two population models: Southwestern Jour. Anthropology, v. 15, p. 168-178, figs. 1-2.

Bien, G. S., Rakestraw, N. W., and Suess, H. E., in press, Radiocarbon concentration in Pacific Ocean water: Tellus.

Bien, G. S., and Suess, H. E., 1959, Increase of C^{14} in the atmosphere from artificial sources measured in a California tree: Zeitschr. Physik, v. 154, p. 172-174, fig. 1.

Broecker, W. S., and Kulp, J. L., 1957, Lamont natural radiocarbon measurements IV: Science, v. 126, p. 1324-1334.

Broecker, W. S., Kulp, J. L., and Tucek, C. S., 1956, Lamont natural radiocarbon measurements III: Science, v. 124, p. 154-165.

Carter, G. F., 1952, Interglacial artifacts from the San Diego area: Southwestern Jour. Anthropology, v. 8, p. 444-456, figs. 1-2, pls. 4-5.

———— 1957, Pleistocene man at San Diego: Baltimore, Johns Hopkins Press, 400 p., 96 figs.

Clark, Eugenie, ms, Florida man dated 8,000 years B.C.

Curray, J. R., 1959, Sediments and history of the Holocene transgression of the continental shelf, northwest Gulf of Mexico: Doctoral dissertation, University of California, La Jolla.

———— 1960, Sediments and history of the Holocene transgression, continental shelf, northwest Gulf of Mexico, *in* Recent sediments, northwestern Gulf of Mexico: Am. Assoc. Petroleum Geologists Special Pub.

Deevey, E. S., Gralenski, L. J., and Hoffren, Väinö, 1959, Yale natural radiocarbon measurements IV: AM. JOUR. SCI. RADIOC. SUPP., v. 1, p. 144-172.

Douglas, D. L., 1952, Measuring low-level radioactivity: General Electric Rev., v. 55, no. 5 (September), p. 16-20, 4 figs.

Fairbridge, R. W., 1958, Dating the latest movements of the Quaternary sea level: New York Acad. Sci. Trans., ser. 2, v. 20, p. 471-482, figs. 1-2.

Ferguson, G. E., Lingham, C. W., Love, S. K., and Vernon, R. O., 1947, Springs of Florida: Florida Geol. Survey Geol. Bull. 31, xii, 196 p., 37 figs., 1 pl.

Goldberg, E. D., and Parker, R. H., 1960, Phospatized wood from the Pacific sea floor: Geol. Soc. America Bull., v. 71, p. 631-632, fig. 1.

Grosscup, G. L., 1958, Radiocarbon dates from Nevada of archaeological interest: California Archaeol. Survey Rept. 44, p. 17-31, map 2.

Heizer, R. F., 1956, Recent cave exploration in the lower Humboldt Valley, Nevada: California Univ. Archaeol. Survey Rept. 33, p. 50-57, 3 figs.

———— 1958, Radiocarbon dates from California of archaeological interest: California Univ. Archaeol. Survey Rept. 44, p. 1-16, map 1.

Heizer, R. F., and Krieger, A. D., 1956, The archaeology of Humboldt Cave, Churchill County, Nevada: California Univ. Am. Archaeol. and Ethnol. Pub., v. 47, no. 1, p. 1-90.

Howard, Hildegarde, 1960, Significance of carbon-14 dates from Rancho La Brea: Science, v. 131, p. 712-714.

Howard, Hildegarde, and Miller, A. H., 1939, The avifauna associated with human remains at Rancho La Brea, California: Carnegie Inst. Washington Pub. 514, p. 39-48, figs. 1-4.

Hubbs, C. L., and Miller, R. R., 1948, The Great Basin, with emphasis on Glacial and Postglacial times. II. The zoological evidence: correlation between fish distribution and hydrographic history in the desert basins of western United States: Utah Univ. Bull., v. 38, no. 20 (Biol. Ser., v. 10, no. 7), p. 18-166, figs. 1-29, 1 map.

Libby, W. F., 1952, Chicago radiocarbon dates, III: Science, v. 116, p. 673-681.

Loud, L. L., and Harrington, M. R., 1929, Lovelock Cave: California Univ. Am. Archaeol. and Ethnol. Pub., v. 25, no. 1, p. i-viii, 1-183, figs. 1-25, pls. 1-68.

Meighan, C. W., 1959, Californian cultures and the concept of an Archaic Stage: Am. Antiquity, v. 24, no. 3, p. 289-318, figs. 1-7.

Meighan, C. W., Pendergast, D. M., Swartz, B. K., Jr., and Wissler, M. D., 1958, Ecological interpretation in archaeology: Part I: Am. Antiquity, v. 24, no. 1, p. 1-23, figs. 1-8.

Moriarty, J. R., Shumway, George, and Warren, C. N., 1959, Scripps Estates Site I (SDi–525): A preliminary report on an early site on the San Diego coast: California Univ., Los Angeles Archaeol. Survey Ann. Rept. 1958-1959, Dept. Anthropology and Sociology, p. 185-216, maps 1-4, figs. 1-5, pls. 1-8.

Orr, P. C., 1956, Radiocarbon dates from Santa Rosa Island, I: Santa Barbara Mus. Nat. History, Dept. Anthropology, Bull. 2, p. 1-10, figs. 1-6.

Peck, S. L., 1955, An archaeological report on the excavation of a prehistoric site at Zuma Creek, Los Angeles County, California: Southern California Archaeol. Survey Assoc. Paper 2, p. i-xiv, 1-87, maps 1-2, chart 1, pls. 1-22.

Riddell, F. A., 1956, Archaeological research in Lassen County, California: California Univ. Archaeol. Survey Rept. 33, p. 44-49.

——— in press, The Karlo Site: California Univ. Archaeol. Survey Rept.

Rogers, M. J., 1929, The stone art of the San Dieguito Plateau: Am. Anthropologist, n. s., v. 31, p. 454-467.

——— 1939, Early lithic industries of the lower basin of the Colorado River and adjacent desert areas: San Diego Mus. Papers 3, vi, 75 p., 1 map, 22 pls.

——— 1945, An outline of Yuman prehistory: Southwest Jour. Anthropology, v. 1, p. 167-198, figs. 1-2.

Rubin, Meyer, and Suess, H. E., 1955, U. S. Geological Survey radiocarbon dates II. Science, v. 121, p. 481-488.

Shepard, F. P., and Moore, D. G., 1955, Central Texas coast sedimentation; characteristics of sedimentary environment, recent history, and diagenesis: Am. Assoc. Petroleum Geologists Bull., v. 39, p. 1463-1593.

Shepard, F. P., and Suess, H. E., 1956, Rate of Postglacial rise of sea level: Science, v. 123, p. 1082-1083, fig. 1.

Stuiver, Minze, Deevey, E. S., and Gralenski, L. J., 1960, Yale natural radiocarbon measurements V: AM. JOUR. SCI. RADIOC. SUPP., v. 2, p. 49-61.

Suess, H. E., 1953, Natural radiocarbon and the rate of exchange of carbon dioxide between the atmosphere and the sea: p. 52-56 *in* Aldrich, L. T., ed., Proceedings of the conference on nuclear processes in geological settings, Williams Bay, Wisconsin: Nat. Research Council Comm. on Nuclear Sci., v. 1, 82 p.

——— 1954a, Natural radiocarbon measurements by acetylene counting: Science, v. 120, p. 5-7.

——— 1954b, U. S. Geological Survey radiocarbon dates I: Science, v. 120, p. 467-473.

——— 1956, Grundlagen und Ergebnisse der Radiokohlenstoff-Datierung: Angew. Chemie, v. 68, p. 540-546, figs. 1-3.

Tuthill, Carr, and Allanson, A. A., 1955, Ocean-bottom artifacts: The Masterkey, v. 28, no. 6, p. 223-232, figs. 1-6.

Walker, E. F., 1951, Five prehistoric archaeological sites in Los Angeles County, California: Southwest Museum, Frederick Webb Hodge Anniv. Pub. Fund, Pub., v. 6, p. 1-116, figs. 1-20, frontisp. + pls. 1-49.

Woodring, W. P., Bramlette, M. N., and Kew, W. S. W., 1946, Geology and paleontology of Palos Verdes Hills, California: U. S. Geol. Survey Prof. Paper 207, p. i-v, 1-145, figs. 1-16, pls. 1-37.

Woodward, Arthur, 1937, Atlatl dart foreshafts from the La Brea Pits: Southern California Acad. Sci. Bull., v. 36, pt. 2, p. 41-60, figs. 17-24.

Journal of Sedimentary Petrology, Vol. 30, No. 1, pp. 91–122
Figs. 1–23, March, 1960

SOURCES OF RECENT SEDIMENTS IN THE NORTHERN GULF OF MEXICO[1]

TJEERD H. VAN ANDEL and DAVID M. POOLE
University of California, La Jolla, California, and The Ohio Oil Company, Littleton, Colorado

ABSTRACT

Sand-size sediments are contributed to the northern Gulf of Mexico by a large number of streams and, to a lesser extent, by marine erosion of coastal deposits, mainly of Pleistocene age. The heavy mineral assemblages and distributive provinces of most sources can be recognized in the Holocene sediments of the northern Gulf of Mexico. Five heavy mineral provinces have been established, the Eastern Gulf, Mississippi, Western Gulf, Texas Coast, and Rio Grande provinces. The Western Gulf province is of complex origin and consists of sediments deposited on the continental shelf during the early Holocene rise in sea level by the Mississippi, Rio Grande, Colorado, Brazos, and Trinity-Neches Rivers. The changing pattern of alluvial plains, deltas, shore deposits, and several major changes in the direction of longshore drift and currents during the transgression can be recognized.

The Texas Coast province consists of a mixture of material contributed by the rivers of the area and of detritus eroded from the Pleistocene deposits of the area by waves. Longshore drift to the west is an agent in the distribution of sediments derived from the Colorado River in the zone between Galveston Bay and Aransas Pass. This material enters the bays from the Gulf side. Barrier island and bay sands are of local origin west of Aransas Pass and consist of a mixture of material derived from the Pleistocene on the land side and material brought in from the shelf during and after the transgression.

INTRODUCTION

The sediments of the northern Gulf of Mexico have been derived from a vast, almost continent-wide, source area and from source rocks ranging in age from Precambrian to Quaternary. They have been weathered under a variety of climates and have been eroded from their source beds by glacial, fluviatile, and marine agents. The sediments are brought to the sea by two large river systems, the Mississippi and the Rio Grande, and by numerous smaller streams. In addition, some material has been derived by marine erosion from the Pleistocene deposits in the coastal area.

In this complex situation an investigation of the sources and transportation of sediments can be expected to contribute much to the understanding of the sedimentation and history of the basin. In addition, it may furnish information concerning the basic laws of sediment supply and transportation in basins with vast and complex hinterlands.

More specifically, the objectives of the present study can be defined as follows:

1.—to define the areas in which sediments directly derived from the Rio Grande and Mississippi are being deposited, and to study the mixing of this material with detritus from other sources;
2.—to identify the sources of sediments on the continental shelf between the distributive provinces of the Mississippi and the Rio Grande, and to study the mechanics and sequence of their deposition; and
3.—to determine the sources of sediments in the bays of the Texas Coast. These sediments may have been derived from local Pleistocene deposits, supplied by local rivers or by longshore drift from the east or west, or brought in from the continental shelf.

Earlier investigations have shown that distribution patterns are not necessarily the same for different size fractions in a single basin and that different sources and different transportation paths may account for the deposition of gravels, sands, and clays (see, for example, van Andel and Postma 1954, p. 155–157). *The present paper deals exclusively with the sources of sand and of the sand fraction of the other sediments. Its conclusions do not necessarily apply to gravels and clays.*

---

[1] The investigation was supported by a grant from the American Petroleum Institute, Project 51, at the Scripps Institution of Oceanography, University of California, La Jolla. Manuscript received July 22, 1959.

Contributions from the Scripps Institution of Oceanography, New Series, 1159

Reproduced by Permission

The gravels in this area are of very minor importance but information concerning the source of clays would be of great value.

The study is based on mineralogical analysis. A clear understanding of the problem of sources and transportation requires additional information, for example, morphological and hydrographical observations and studies of the grain size distribution of the sediments. Some of this information is available in various publications on the sedimentology of the basin (Shepard, 1956; Curray, in press; Rusnak, in press) and will be utilized here.

Traditionally, the mineralogical composition of sands has been studied after separation into a light and a heavy fraction. In order to obtain a quantitative picture of the relative contributions of all sediments, not only the compositions but also the relative proportions of both fractions should be known. The present study is restricted to the heavy minerals only because this method offers a rapid technique for the investigation of large numbers of samples and because a sizeable body of information concerning the heavy mineral distributions of other modern depositional basins is available for comparison. Curray (in press) has made a limited study of the light fraction, which agrees reasonably well with the conclusions of the present investigation.

Restriction to the heavy mineral composition imposes limitations upon the conclusions that can be drawn. Studies of both light and heavy fractions of river sands have shown that different sources may possess great differences in the ratio light/heavy minerals (Koldewijn, 1955). Consequently, the effect of a contribution from a certain source in a mixed sediment can be either exaggerated or minimized depending on the relative percentages of heavy minerals in the source materials. In order to obtain reliable estimates of the relative amounts contributed by multiple sediment sources, a study of the percentages of heavy minerals per unit sediment in each of them is required. For the Gulf of Mexico only a small amount of this information is available.

Various factors modify the mineralogical composition of a sediment between source rock and depositional site. In the present study the most important are the elimination of unstable components by weathering and selective sorting of minerals by size and density. In conclusions concerning sediment sources in the Gulf of Mexico such factors will have to be considered.

The heavy minerals of Gulf Coast sediments have been the subject of various earlier investigations. The results of these investigations will be utilized at various places in this study, and ample use had been made of published analyses. The investigation is based upon approximately 800 new heavy mineral analyses from the Mississippi delta, the continental shelf, the coastal zone of Texas, and the rivers draining into the Gulf. A composite Upper Pleistocene section from several offshore wells south of Grand Isle, Louisiana, has been made available by courtesy of the Humble Oil and Refining Company. A sample location map is presented in figure 1. In this paper a selection of characteristic analyses is included for illustration purposes. A complete copy of all data with detailed location maps has been filed in the Library of the Scripps Institution of Oceanography at La Jolla, California.

METHODS OF ANALYSIS

The methods of analysis used in this investigation have been described in detail in various publications (Doeglas, 1940; van Andel, 1950; Poole, 1958, for heavy mineral analysis; Poole, 1957, for grain size analysis by means of a settling tube). The analyses include only the non-opaque minerals. Small percentage variations and the absence or presence of low frequency minerals have no significance because of the restriction to 100 grains per count (Dryden, 1931; Muller, 1943; van Andel, 1950, 1955). To facilitate comparison with data obtained in the present study analyses published by Dohm (1936), Russell (1937), Hough (1937), Goldstein (1942), and Bullard (1942) have been converted on the basis: sum of non-opaques = 100 percent. Only those analyses that contained more than 100 non-opaque grains were used for the conversion.

The size fraction used here is 0.500 to 0.062 mm. The higher minimum size as compared to standard procedure (0.030 mm approximately) reduces the percentage of zircon. This mineral has little diagnostic value and tends to become concentrated in

(316)

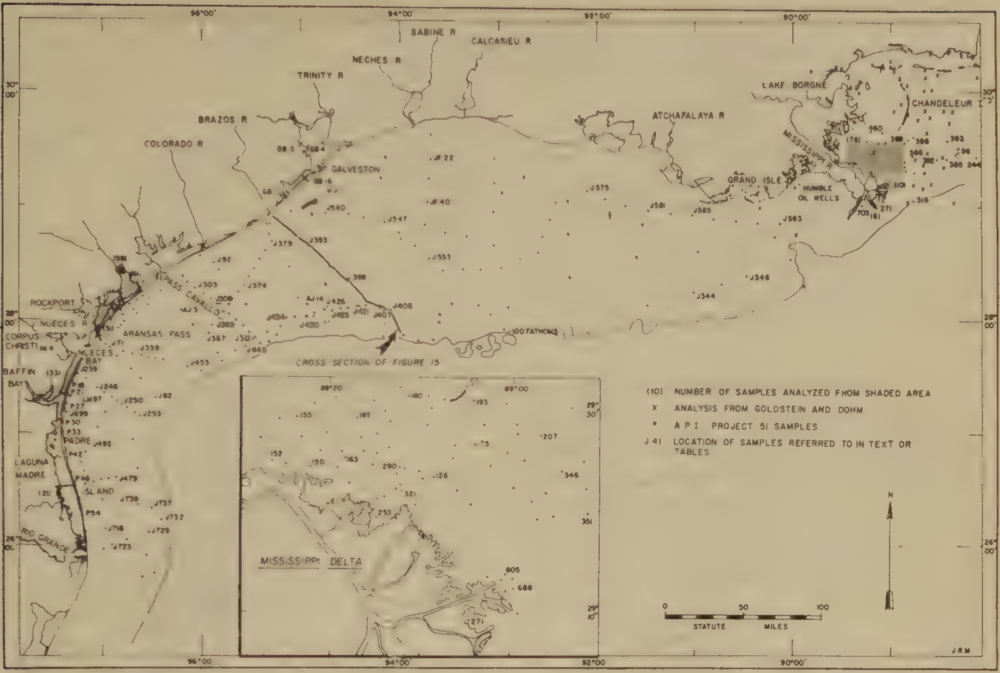
SABINE R
CALCASIEU R
NECHES R
TRINITY R
BRAZOS R
COLORADO R
GALVESTON
LAKE BORGNE
CHANDELEUR I
ATCHAFALAYA R
MISSISSIPPI R
GRAND ISLE
HUMBLE OIL WELLS
ROCKPORT
NUECES R
CORPUS CHRISTI
ARANSAS PASS
PASS CAVALLO
NUECES BAY
BAFFIN BAY
PADRE ISLAND
LAGUNA MADRE
RIO GRANDE
100 FATHOMS
CROSS SECTION OF FIGURE 15
MISSISSIPPI DELTA
(10) NUMBER OF SAMPLES ANALYZED FROM SHADED AREA
x ANALYSIS FROM GOLDSTEIN AND DOHM
• A P I PROJECT 51 SAMPLES
J 41 LOCATION OF SAMPLES REFERRED TO IN TEXT OR TABLES
N
0 50 100
STATUTE MILES
96°00'
94°00'
92°00'
90°00'
30° 00'
28° 00'
26° 00'
JRM

FIG. 1.—Map of place names and sample locations. Numbers indicate samples used in text and tables. See also figure 2 (river samples) and 21 (Rockport area).

fine-grained samples. Table 1 illustrates the difference between analyses of the standard size fraction and analyses of the fraction used here.

SEDIMENT SOURCES

The source areas of the sediments in the northern Gulf of Mexico can be discussed conveniently under four headings: (1) the

TABLE 1.—*Comparison of heavy mineral assemblages obtained by analysis of the 0.500 to 0.030 mm and 0.500 to 0.062 mm grades, respectively, in sands of Texas and Louisiana rivers, in percent of total non-opaque fraction*

	Location at bridge in highway	Size Grade	Hornblende[1]	Tourmaline	Epidote	Zircon	Garnet	Staurolite	Kyanite	Titanite	Rutile	Basaltic Hbl.	Sillimanite	Augite	Hypersthene
Brazos R.	U. S. 79	0.50–0.06		24	5	23	36	4	2	2	4				
		0.50–0.03		15	9	33	32	2		1	8				
Calcasieu R.	U. S. 190	0.50–0.06		22	6	28	3	12	19		9		1		
		0.50–0.03		14	5	61	2	1	5		12				
Colorado R.	U. S. 77	0.50–0.06	82	1	1	2	9	2		2	1				
		0.50–0.03	69	2	7	13	5		1	1	2				
Sabine R.	La. 12	0.50–0.06	8	24	25	12	3	10	13	1	3		1		
		0.50–0.03		7	9	53	3	3	6		19				
Guadelupe R.	U. S. 59	0.50–0.06	2	17	14	33	18	3	4	3	4		2		
		0.50–0.03		6	8	59	6	1	4	5	11				
Trinity R.	U. S. 79	0.50–0.06	2	34	8	19	6	9	11	4	5	1			1
		0.50–0.03		6	12	57	6	5	1		13				

---

[1] Not including basaltic hornblende.

Mississippi basin, (2) the Rio Grande basin, (3) the other rivers of Texas and western Louisiana, and (4) the rivers east of the Mississippi delta. The following brief discussion of the four groups has been based largely on a study of the literature. Some sediments, particularly in the bays of Texas, appear to have been derived to a large extent from local Pleistocene and early Holocene[2] deposits. The evidence for this conclusion will be discussed in connection with the description of the specific depositional areas.

Mississippi River Basin

The heavy minerals of the Mississippi and its major tributaries have been studied in detail by Hough (1937) and Russell (1937). The typical assemblage found along the entire course below the confluency with the Des Moines River consists of augite and hornblende with appreciable percentages of epidote and garnet (table 2). The assemblage is very similar to the suites described by various authors for glacial and outwash deposits in the northern United States and Canada (Doeglas, 1949; Dreimanis and others, 1957; Gravenor, 1951; Kruger, 1937; Murray, 1953). Russell and Hough conclude that at the present time the Mississippi carries to the Gulf of Mexico material essentially derived from glacial deposits. This conclusion may require some modification because the contributions of non-glacial material by the Red, Ouachita, Arkansas, and Yazoo Rivers may be under-represented in the heavy mineral assemblage as a result of a low heavy mineral content of their sands. Nevertheless, it seems plausible to assume that the bulk of the Mississippi sediment deposited in the Gulf of Mexico is of glacial origin.

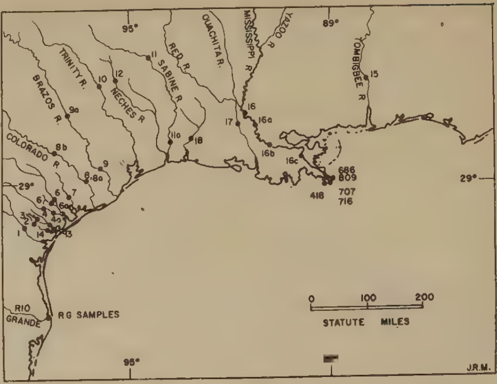

FIG. 2.—Location of river samples listed in tables 2 and 3.

Rio Grande Basin

The Rio Grande contributes to the Gulf of Mexico an assemblage of heavy minerals

---

[2] Throughout this paper the term "Holocene" (synonymous with but preferred to Recent) will be used to designate the series of sediments deposited on top of the last marine unconformity in the Gulf of Mexico.

TABLE 2.—*Heavy mineral composition of selected Mississippi River sands in percent of total non-opaque fraction*[1]

Sample number		Hornblende[2]	Tourmaline	Epidote	Zircon	Garnet	Staurolite	Kyanite	Titanite	Basaltic Hbl.	Augite	Hypersthene
16	Mississippi River	34	6	20	3	16	1		3	3	11	3
16a	Mississippi River	37	1	17	2	7			2	1	32	1
16b	Mississippi River	40	3	16	3	6			3	3	25	1
16c	Mississippi River	32	1	21	3	7			3	1	28	4
716	South Pass	33	5	14	2	13	1		5	1	25	1
707	South Pass	41		12	2	5			2	4	34	
478	Southwest Pass	36	3	16	7	9	1		2	2	22	2
686	Pass a Loutre	38	3	14		8			3	5	28	1
809	Pass a Loutre	30	1	22	3	13		1	4	3	21	2
17	Atchafalaya R.	28		16		32			4	2	18	

[1] For sample locations see fig. 2.
[2] Not including basaltic hornblende.

TABLE 3.—*Heavy mineral composition of sands from Texas and Louisiana rivers,*[1] *in percent of total non-opaque fraction.*

Sample number		Hornblende[2]	Tourmaline	Epidote	Zircon	Garnet	Staurolite	Kyanite	Titanite	Basaltic Hbl.	Augite	Hypersthene	Rutile, Sillim.
RG 1	Rio Grande	21	3	25	3	12	1	2	2	12	16		3
7	Rio Grande	31		19	2	5		5	2	8	25	1	2
9	Rio Grande	19	2	25	15	12	1	2	4	5	12		3
13	Rio Grande	17	3	25	8	5		2	4	10	24	2	
16	Rio Grande	26	2	15	3	4	1	4		10	35		
17	Rio Grande	21		15	3	4		1	4	15	35		2
1	Nueces River	4	15	14	20	15	5	3	5	2	11		6
2	Medio Creek		25	14	33	20		3	3				2
3	Blanco Creek	1	28	14	30	18	4	1					4
4	San Antonio River	6	8	12	40	12	2	13	2				5
4a	San Antonio River		14	13	45	14	1	8	1				4
5	Mile Coleto Creek		13	5	51	13	6	2	2				8
6	Guadelupe River	2	17	14	33	18	3	4	3				6
6a	Guadelupe River	1	13	16	56		9	3	1				1
7	Lavaca River	2	5	34	39	14	1	3		1			1
8	Colorado River	80	1	4	6	5			4				
8a	Colorado River	69	2	7	11	4			4				3
8b	Colorado River	82	1	1	2	9	2		2				1
9	Brazos River		24	5	23	36	4	2	2				4
9a	Brazos River	1	18	9	22	37	8						5
10	Trinity River	2	34	8	19	6	9	11	4	1		1	5
11	Sabine River	1	18	13	23		21	15	1				8
11a	Sabine River	8	24	25	12	3	10	13	1				3
12	Neches River		19	7	29	2	11	15	2				15
13	Mission River		10	8	66	3	8	1					4
14	Aransas River	1	10	16	49	12	4	3	1				4
18	Calcasieu River		22	6	28	3	12	19					10
15	Tombigbee River		12	21	8	8	18	23	2				8

[1] For sample locations see fig. 2.

[2] Not including basaltic hornblende,

which in many respects is similar to that of the Mississippi (table 3). In both rivers there are considerable variations between individual analyses, and single samples cannot always be differentiated. In larger groups the Rio Grande assemblage is found to contain more pyroxene and less hornblende than the Mississippi suite. It is also characterized by small but persistent percentages of basaltic hornblende (probably derived from young volcanics in northeastern Mexico, Sidwell and Renfroe, 1943) and metamorphic minerals, mainly kyanite. Another difference which will be discussed later is in the varietal composition of the hornblendes.

Information is scarce concerning the assemblages of the Rio Grande above the delta and of its tributaries. Rittenhouse (1944) has decribed a suite from the middle course of the river which is quite similar to the assemblage found in the delta. However, the middle course sediments contain less epidote and garnet and a higher amount of hornblende. Addition of Pecos material which contains an abundance of epidote and garnet (Sidwell, 1944) probably accounts for the higher percentages of these minerals in Rio Grande delta sediments.

Rivers of Texas and Western Louisiana

The drainage basins of the rivers between the Mississippi and Rio Grande consist primarily of sedimentary formations of Cretaceous, Tertiary, and Quaternary age. Some Paleozoic is exposed in the headwaters of the Colorado and Brazos rivers. The Nueces and Colorado Rivers also drain relatively small areas of igneous and metamorphic rocks.

The heavy mineral associations (table 3, fig. 2) of most rivers in this area reflect the mineral composition of the Cretaceous and Quaternary as described by Cogen (1940; see also Bornhauser, 1940; Rogers and Dawson, 1958; Rogers and Powell, 1958; Sidwell, 1937, 1947). The influence of Tertiary material is less important. The principal association consists of zircon and tourmaline with minor amounts of epidote, garnet, staurolite, and kyanite. Individual differences between rivers exist, but their significance cannot be inferred from the limited material studied. Higher percentages of kyanite and staurolite are found in the Trinity, Neches, Sabine, and Calcasieu Rivers which drain extensive areas of Paleocene and Eocene sediments which are characterized by a staurolite-kyanite association (Cogen, 1940; Sun, 1954).

The zircon-tourmaline association of the Nueces River contains small but significant percentages of augite and basaltic hornblende which give this assemblage an intermediate position between that of the Rio Grande and those of most other Texas rivers. These minerals may have been derived from Tertiary volcanics in the Uvalde region in the headwaters of this river.

The Colorado River association is completely different from all others in the Texas coastal area. It is characterized by an almost pure blue-green hornblende suite which is found as far upstream as the Llano uplift but is absent above this area of pre-Cambrian rocks (Sidwell and Cole, 1937). The hornblende assemblage delivered to the Gulf of Mexico has been derived either directly from this Precambrian or indirectly from Pleistocene terraces in the Colorado valley (Mathis, 1944).

Area East of the Mississippi River

The heavy mineral suites that characterize shelf sediments in the area east of the Mississippi delta consist of kyanite and staurolite with some zircon and epidote. The very limited information available in the literature (Needham, 1934; Blankenship, 1956; Potter, 1955) and one sample from the Tombigbee River (fig. 2, table 3) suggest that the source of this assemblage is the Cretaceous and younger mantle of the southern Appalachians rather than the old core which, according to the few publications available (for example, Carroll, 1957; Carroll, Neuman, and Jeffe, 1947), would only supply a zircon assemblage.

Summary of Sediment Sources

The heavy mineral assemblages supplied by rivers to the Gulf of Mexico can be divided into several groups, each characterized by a well-defined heavy mineral assemblage. In table 4 and figure 3 the composition and sources of sand-size sediments have been summarized. In addition, some material is derived by marine erosion from Pleistocene deposits of the Texas coastal region.

HEAVY MINERAL PROVINCES OF THE NORTHERN GULF OF MEXICO

Following Edelman (1933) a *sedimentary petrological province* is defined as "a group of sediments which constitute a natural unit by age, origin and distribution." Each province is characterized by a light and a heavy mineral association. Transition zones of mixing, overlap and interfingering normally separate adjacent provinces. Within the boundaries of each province the composition of the individual samples may vary considerably as a result of variations in grain size, sampling and analytical errors, statistical variation, or incomplete mixing of sediment from multiple sources. Consequently, the associations have to be defined in general semi-quantitative terms. A province is best defined when its association contains minerals that do not occur in significant amounts in any of the other provinces of the same basin. An example is the Eastern Gulf province (table 5). Frequently, however, the same minerals are found in many or all of the provinces of a sedimentary basin, and associations have to be defined with the aid of differences in frequency. Under such circumstances the identification of single samples may be difficult, and the establishing of province boundaries and the evaluation of mixed zones become to a certain extent a subjective matter. Since most of the provinces of the northern Gulf of Mexico have to be defined on the basis of quantitative

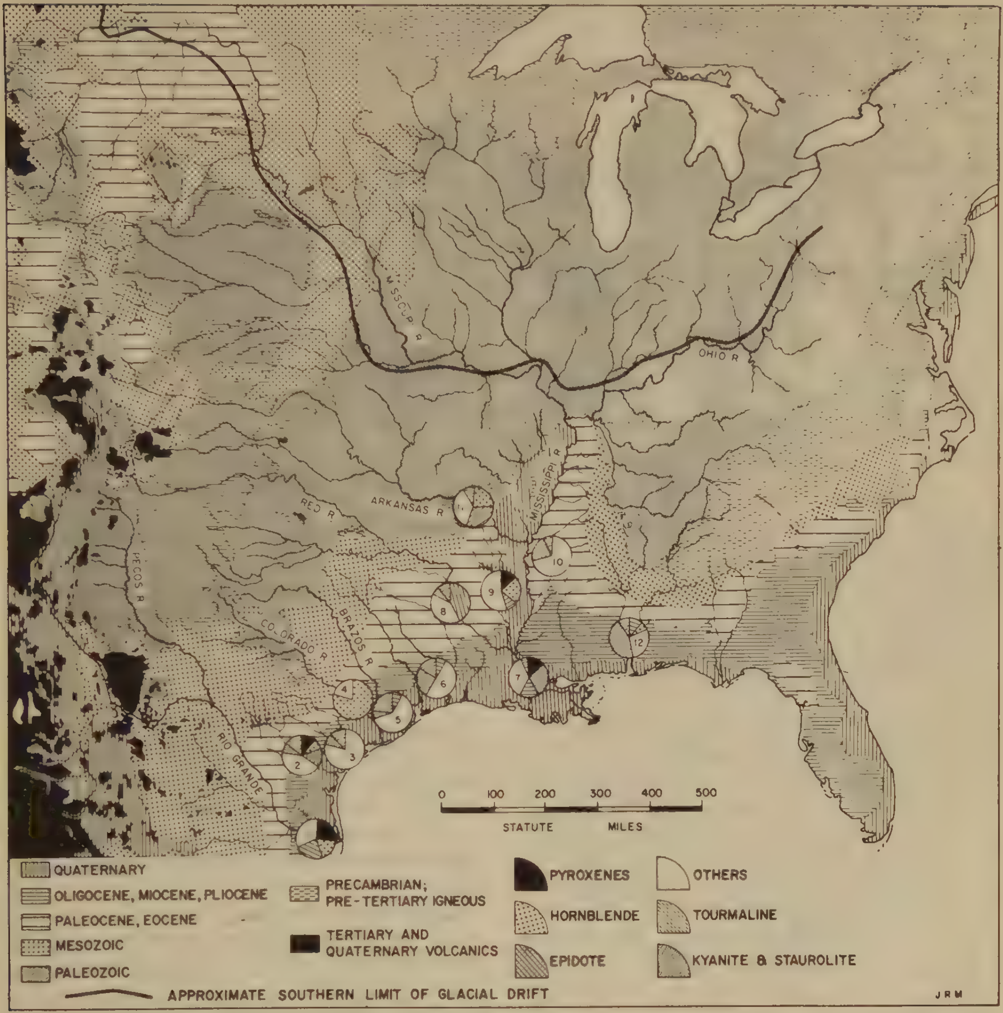
MISSISSIPPI R
OHIO R
ARKANSAS R
RED R
PECOS R
COLORADO R
BRAZOS R
RIO GRANDE
1
2
3
4
5
6
7
8
9
10
11
12
0 100 200 300 400 500
STATUTE MILES
QUATERNARY
OLIGOCENE, MIOCENE, PLIOCENE
PALEOCENE, EOCENE
MESOZOIC
PALEOZOIC
PRECAMBRIAN; PRE-TERTIARY IGNEOUS
TERTIARY AND QUATERNARY VOLCANICS
PYROXENES
HORNBLENDE
EPIDOTE
OTHERS
TOURMALINE
KYANITE & STAUROLITE
APPROXIMATE SOUTHERN LIMIT OF GLACIAL DRIFT
JRM

FIG. 3.—Regional geology of northern Gulf of Mexico source area, and heavy mineral composition of sediments supplied by principal rivers. Geology simplified from "Geological Map of North America," Geol. Soc. America (1946). Mineral assemblages: 1-Rio Grande, 2-Nueces River, 3-composite of streams between Nueces and Colorado, 4-Colorado River, 5-Brazos River, 6-composite of Trinity, Sabine and Neches Rivers, 7-Mississippi River, 8-Red River, 9-Ouachita River, 10-Yazoo River, 11-Arkansas River, 12-Tombigbee River.

differences, the study of sediment sources, transportation, and mixing is particularly difficult. Therefore, an attempt has been made to improve the resolving power of the heavy mineral method by introduction on a large scale of the use of single mineral parameters and mineral ratios. The following five heavy mineral provinces can be distinguished in the northern Gulf of Mexico (fig. 4; table 5). Four of them were defined originally by Goldstein (1942).

Eastern Gulf province: characterized by a kyanite-staurolite association derived from the Cretaceous and younger sedimentary mantle of the Appalachians.

Mississippi province: characterized by a hornblende-pyroxene association with appreciable amounts of epidote and

TABLE 4.—*Composition and source of heavy mineral assemblages supplied to Northern Gulf of Mexico*[1] *in percent of total non-opaque fraction. Averages of all available samples from the lower courses of rivers*

Rivers	No. of samples	Sediment Source	Hornblende[2]	Tourmaline	Epidote	Zircon	Garnet	Staurolite	Kyanite	Basaltic Hbl.	Pyroxenes	Others
Mississippi	16	Glacial of northern U. S.	28	5	16	5	21	1	1	5	18	
Rio Grande	7	Upper Rio Grande, Pecos; volcanics of Chihuahua	20	2	22	5	6	1	3	10	26	4
Nueces	3	Cret., Tert., Quat., and volcanics of Uvalde	4	15	14	20	15	5	3	2	11	11
Rivers between Neuces and Colorado	10	Cret., Tert., and Quat. of Central Texas	1	14	15	44	13	4	4			5
Colorado	5	Llano Uplift, pre-Cambr.	77	1	4	7	6	1				4
Brazos	3	Cret., Tert., and Quat. of Central Texas	1	21	7	22	36	6	1			6
Trinity, Neches, Sabine, Calcasieu	5	Tert. and Quat. of East Texas and West Louisiana	1	17	10	37	4	11	12			8
Area east of Mississippi River	1	Cret., Tert., and Quat. mantle of S. Appalachians		12	21	16	8	18	23			2

[1] For sample locations see fig. 3.
[2] Not including basaltic hornblende.

garnet. The assemblage has been derived from glacial deposits.

Western Gulf province: characterized by a hornblende association with some epidote but little or no pyroxene, garnet, or basaltic hornblende. The origin of this province is very complex and will be discussed below.

Rio Grande province: characterized by a pyroxene-hornblende association with associated epidote and significant percentages of basaltic hornblende. The sediments are supplied by the Rio Grande.

Texas Coast province: characterized by a tourmaline association with abundant zircon and some epidote. Texas rivers, but not the Colorado and Rio Grande, and Pleistocene deposits of the Texas coast supply the material. In many samples small amounts of hornblende are present, which do not belong to the tourmaline association but are the result of admixture of material from the Western Gulf province.

Within the Western Gulf province a group of samples can be distinguished by means of their high zircon content ("Brazos Group"). This group is a mixture of Western Gulf material with another association probably derived from the Brazos and Trinity Rivers. This association has not been observed in a pure form on the shelf.

Except for the Western Gulf province the sources of all sediments in the northern Gulf of Mexico can be established with certainty. The Western Gulf association resembles rather closely the assemblage supplied by the Colorado River, thus suggesting the rather surprising conclusion that this relatively minor river would have supplied sediment for a very large portion of the continental shelf. Goldstein (1942), who first observed the similarity, has offered an alternate explanation for the provenance of the Western Gulf sediments by suggesting that they may have been derived from Mississippi material that had lost its unstable pyroxenes by selective weathering. It will be shown later that the Western Gulf province is a complex system with multiple sources including Colorado sediments and weathered Mississippi and Rio Grande material.

TABLE 5.—*Average heavy mineral composition of associations characterizing Northern Gulf of Mexico provinces, in percent of total non-opaque fraction*

Province	Source	Hornblende[2]	Tourmaline	Epidote	Zircon	Garnet	Staurolite	Kyanite	Pyroxenes	Basaltic Hbl.	Others	No. of samples
Eastern Gulf	Cret., Tert., Quat. S. Appalachians	13	12	16	12	2	16	16	3	t	10	31
Mississippi	Mississippi River	40	2	16	2	9	t	t	25	2	3	116
Western Gulf	complex	58	5	17	4	7	1	1	3	1	3	127
Rio Grande	Rio Grande River	23	3	15	6	10	1	2	24	7	9	41
Texas Coast	Rivers between Nueces and Brazos; reworked Pleistocene	7	28	11	23	9	8	5	3	t	6	54
Brazos Group[1]		32	8	15	20	8	3	3	3	1	7	19

[1] No pure samples available.
[2] Not including basaltic hornblende.

SELECTIVE SORTING OF HEAVY MINERALS

Heavy minerals cover a broad range of densities and sizes. Many minerals, for example zircon, have a marked preference for one specific size. Fine-grained sediments are almost invariably much richer in zircon than coarser deposits from the same source. Many other minerals are concentrated in specific size fractions but the range depends on the source. Consequently, sorting by size can result in strong modification of the mineral assemblage. With a suitable set of preferred sizes a hornblende-pyroxene-epidote suite can be separated into a coarse pyroxene-hornblende and a fine hornblende-epidote assemblage (van Andel, 1955).

This example calls to mind the difference between the pyroxene-hornblende associations of the Rio Grande and Mississippi, and the hornblende association of the Western Gulf province. A test is required to establish whether the difference between these associations is caused entirely or partly by sorting instead of provenance.

In figures 5 and 6 percentages of all diagnostically important minerals have been plotted against the median diameter of the sand fraction. The heavy minerals are compared with the sand fraction only because a light fraction with a lower size limit of 0.10 mm is approximately hydraulically equivalent to the heavy fraction which has a lower limit of 0.062 mm.

The graphs show that except for hornblende none of the mineral species exhibit a correlation with the median of the grain size distribution. Apparently, the percentages of augite, kyanite, epidote, and tourmaline are not controlled by sorting. The hornblende percentages increase slightly with decreasing size. This applies only when samples from all provinces are combined and appears to be due largely to the fact that those provinces that are low in hornblende consist of somewhat coarser sediment than those high in hornblende. The grain size ranges of the individual associations overlap to such an extent that the systematic differences in hornblende content that exist between them cannot be explained by sorting alone.

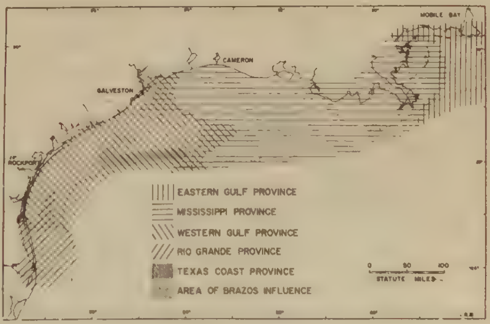

FIG. 4.—Heavy mineral provinces in the northern Gulf of Mexico. Sample locations figure 1. For details concerning Mississippi Delta, Laguna Madre, and the bays of Rockport, Texas, see figures 7, 18 and 22 respectively.

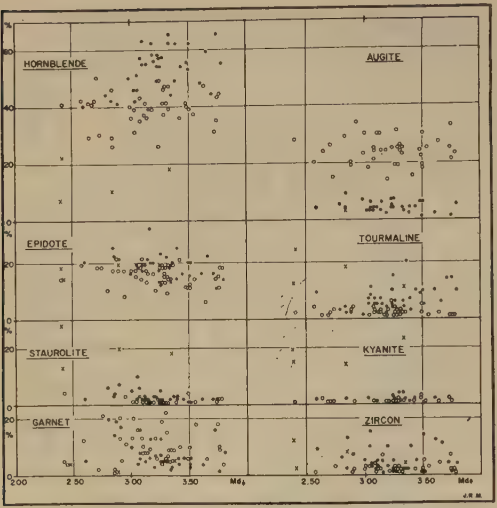

FIG. 5.—Comparison between mineral percentage and median of size distribution of sand fraction in samples from the Mississippi (open circles), Western Gulf (black dots), and Eastern Gulf (crosses) provinces.

Within each individual association grain size and hornblende percentage are not at all or not significantly co-variant. Minor differences in hornblende content may be caused by sorting, but in general it can be concluded that grain size does not control the mineralogical composition.

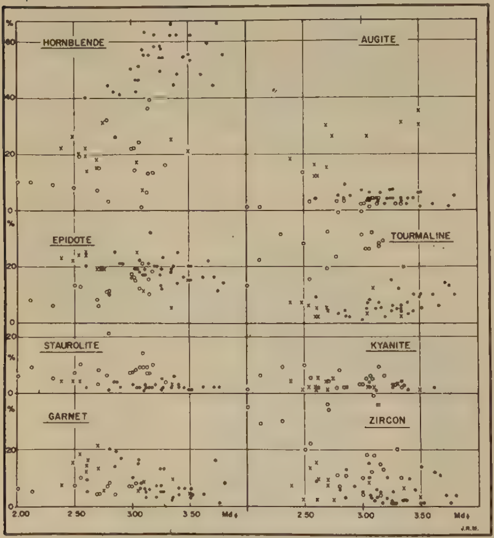

FIG. 6.—Comparison between mineral percentage and median of size distribution of the sand fraction in samples from the Western Gulf (black dots), Texas Coast (open circles), and Rio Grande (crosses) provinces.

HEAVY MINERAL DISTRIBUTION, MISSISSIPPI DELTA REGION

The heavy mineral distribution in the Mississippi delta and on the adjacent shelf (fig. 7, table 6) is the result of the interplay of sediments from two sources, the Mississippi River and the Cretaceous and younger mantle of the southern Appalachians. At present, direct supply of Appalachian sediments is probably restricted to the river estuaries and the nearshore zone east of the Mississippi delta. On the shelf transportation of material from this source appears to be restricted to reworking and redistribution of sediments already present.

From the Mississippi delta the hornblende-pyroxene association spreads east in a broad arc a little beyond the Chandeleur Islands and grades through a narrow transition zone into the Appalachian kyanite-staurolite association. The dividing line runs approximately north and south, cutting obliquely across a major tongue of modern Mississippi sediment extending eastward from the active Pass a Loutre subdelta (Scruton, 1955; Shepard, 1956). The distribution of Mississippi material as inferred by those authors from lithological and petrographical observations does not agree with the heavy mineral distribution (fig. 8). Shepard has explained this discrepancy by the assumption that periodically Eastern Gulf sand containing kyanite and staurolite assemblages is moved westward over the shelf and mixed with Mississippi material supplied from the east.

The heavy mineral boundary of figure 8 is based on single mineral percentages. A similar boundary has been established by Goldstein (1942) on the basis of heavy mineral associations. A parameter more sensitive to changes in relative contribution of Mississippi and Eastern Gulf material is the ratio hornblende/kyanite+staurolite. In the pure associations of the two sources these minerals are mutually exclusive. Contours based on this ratio (fig. 7) reflect better the mixing of Mississippi and Eastern Gulf material than the association map and conform much better to the shape of the Mississippi tongue shown in figure 8. Apparently, Mississippi

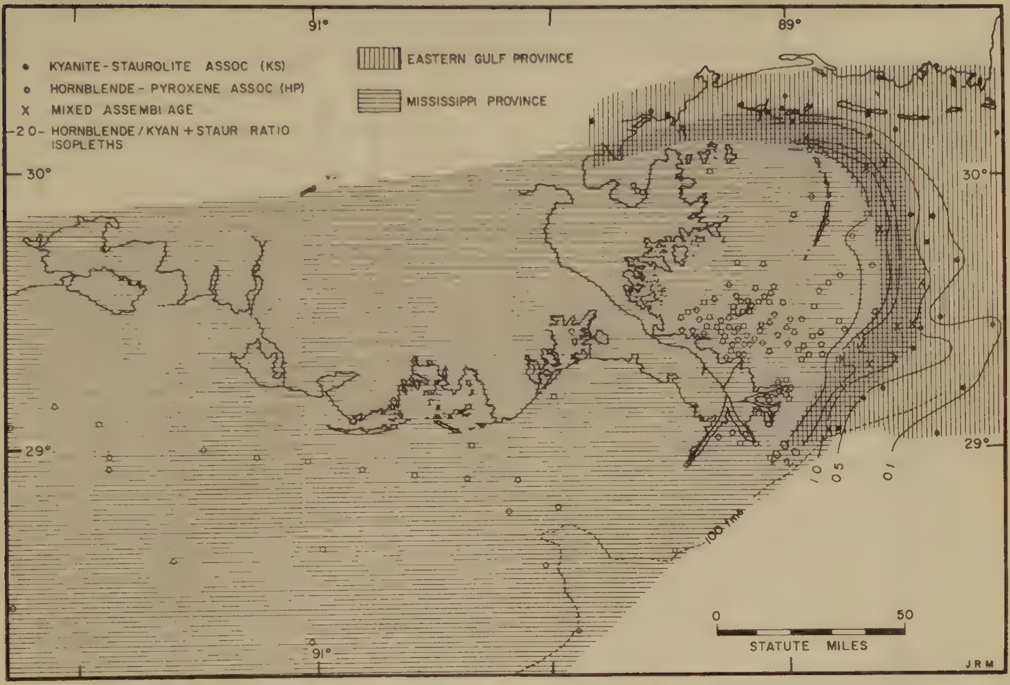
91°
89°
• KYANITE-STAUROLITE ASSOC (KS)
○ HORNBLENDE-PYROXENE ASSOC (HP)
X MIXED ASSEMBLAGE
-2.0- HORNBLENDE/KYAN+STAUR RATIO ISOPLETHS
EASTERN GULF PROVINCE
MISSISSIPPI PROVINCE
30°
29°
1.0
0.5
0.1
100 FM
0
50
STATUTE MILES
JRM

FIG. 7.—Distribution of heavy mineral assemblages, eastern Mississippi Delta area. From 173 samples a total of 96 percent conform to pattern. Samples from Goldstein (1942) included after conversion.

minerals are moved much farther east within the tongue than to either side, although a strong dilution with Eastern Gulf material remains undeniable.

The sediments of the Mississippi tongue consist of almost pure clay with a very small percentage of fine sand. Consequently, the heavy mineral content is low (less than 0.15 percent by weight). The sandy deposits of the Eastern Gulf province on the other hand, contain an average of 0.40 percent heavy minerals (Goldstein, 1942). Thus, even a minor contribution of Eastern Gulf material would greatly change the heavy mineral composition of the sediments of the Mississippi tongue. It can be estimated that in that part of the tongue where the hornblende/kyanite+staurolite ratio is 1.0 the contribution of Eastern Gulf material does not exceed 5 percent.

The Mississippi province overlaps considerably in an eastward direction on deposits of the Eastern Gulf province. Sediments belonging to the Eastern Gulf province have been found in various places under the surface of the Mississippi delta (Shepard, 1956; Shepard and Lankford, 1959), but the precise western limit of the province is not known as far as the author is aware.

HEAVY MINERAL DISTRIBUTION WESTERN GULF PROVINCE

The Western Gulf province has been defined by Goldstein (1942) on the basis of a

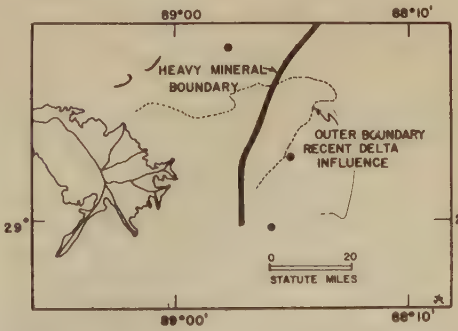
89°00
88°10'
HEAVY MINERAL BOUNDARY
OUTER BOUNDARY RECENT DELTA INFLUENCE
29°
29°
0
20
STATUTE MILES
89°00'
88°10'

FIG. 8.—Relation between modern Mississippi sediment tongue and heavy mineral province boundary in the area east of the Mississippi Delta. Simplified after Shepard (1956, fig. 38).

TABLE 6.—*Representative analyses of samples from the Mississippi and Eastern Gulf Provinces; in percent of total non-opaque fraction*

Sample number	Hornblende[1]	Tourmaline	Epidote	Zircon	Garnet	Staurolite	Kyanite	Titanite	Basaltic Hbl.	Augite	Hypersthene	Others
					Mississippi Province							
MP 126	44	1	18	3	4	2			3	23		2
BS 152	46	1	14	5	2	1		4	2	25		
155	47	7	16	2	6	1		1	2	17	1	
163	50	2	15	2	6	2		2		18	1	2
175	34	3	23		8			3	1	26	2	
180	27	3	14	3	17			2		32		2
185	42	3	12	1	10			6	4	18	3	1
BI 193	41	4	17	2	5		1	4	2	24		
BC 253	43	5	17	1	6			1		27		
BB 271	47		13	2	10		1	5	3	16	1	2
MP 290	48	1	13		3	1		3	5	24		2
321	46	3	14	3	12		2	1	2	13	3	1
PL 346	39	1	15	3	16	1		2	1	18	1	3
351	38		25	2	7			4	4	19		1
GM 366	37	2	19		8			3		29	1	1
398	37	2	21	2	15	1	1	3	2	16		
399	43	3	14	2	8	1		3	2	22	2	
BS 460	49		13	6	5			1	4	18		4
PL 605	44	2	10		10	1		3	1	26	2	1
688	41	1	17		3			5	2	29	1	1
SP 703	39		9	1	4			3		41		3
J 344	44	2	20	4	10			1		18		1
346	49	1	10	5	6				2	26	1	
575	29	2	15	2	16	1		4	1	29		1
581	26	1	19	3	19	1	1	4		22	3	1
585	47	3	9	1	7		1	4	1	26		1
593	31		13	3	21			6		25		1
					Eastern Gulf Province							
GM 244	11	11	13	11	2	19	20	2		4		7
318	11	9	20	23	4	7	12	2		2		10
385	10	19	19	8	1	20	14			4		6
386	7	12	18	12		28	15					8
392	18	11	14	4	5	18	23	1		4		1
393	22	24	14	2	4	13	19					2

[1] Not including basaltic hornblende.

relatively small number of samples. Its hornblende association is characterized by high hornblende percentages and less than 5 percent pyroxene (table 7). The large number of samples available for the present study demonstrates that this province is not a homogeneous unit and that it probably consists of more than one association. A separate group of samples can be distinguished (Brazos Group) which is characterized by a zircon-tourmaline assemblage with some kyanite and staurolite. This group contains highly variable percentages of hornblende, suggesting that all samples contain admixtures of material from the hornblende association.

Theoretically, all rivers emptying in the northwestern Gulf of Mexico could contribute sediment to the Western Gulf province or have done so in the past. The deposits on the shelf may have been derived either directly from the rivers or indirectly from

TABLE 7.—*Representative analyses of samples from the Western Gulf Province, in percent of total non-opaque fraction*[1]

Sample number	Hornblende[2]	Tourmaline	Epidote	Zircon	Garnet	Staurolite	Kyanite	Titanite	Basaltic Hbl.	Augite	Hypersthene	Others
Western Gulf Province												
J 71	66	4	19	2	3				3	3		
82	50	2	17	13	5	2	2		7	2		
92	66	8	12	2	4		1	1	1	4	1	
239	38	12	8	15	12	1	1	3			1	9
246	52	2	19	1	10	3		1	1	6	2	3
250	48	6	19	1	9			1	5	6		5
253	53	5	30		2			1	2	5		2
303	55	5	29	2	5	1			1	1	1	
306	38	5	25	5	10	3	1	7	2	1	2	1
309	42	4	20	7	5	1	7	2	2	4	3	3
310	43	6	15	6	11	3	7	4	1	1		3
312	59	8	4	4	6	2	2	2	3	7		3
359	59	3	19	1	2	1	1	1	3	8	1	1
367	55	10	16	1	8		4	2		3	1	
369	48	5	13	10	9	3	1	3	1	3		3
374	32	6	24	11	13	5	1	2	1	2	1	2
379	55	6	20	1	5	2		1	1	5		4
393	64	4	22		1	1		1	1	4	1	1
399	32	6	27	9	12	4	3	2		1	1	3
406	36	4	18	14	7		2	1	1	13	1	3
445	53	10	11	3	10	3	1	1	1	7		
453	56	3	15	4	6	1	3		5	5	1	1
492	58	5	17		3	1	1	3	4	7	1	
540	58	4	20	3	7			3	2	2		1
547	42	5	19	10	16			1	1	3	1	2
553	41	2	20	5	8	1	2	2		17	2	
699	30	13	16	8	16	3	7	2		1	1	3
AJ 3	54	6	23	1	5	2	2		3	3	1	
14	40	9	20	9	5	2	2	2	2	2	2	5
JF 22	49	4	13	7	5	2	1	1	2	15		1
40	44	2	5	7	17	1	1	3		18	2	
"Brazos Group"												
J 407	24	7	13	32	7	2	4	3	2	2		4
421	40	10	15	9	8	4	4	1	2	4		3
425	21	11	9	34	9	5	2	2	2	4		1
426	14	14	20	29	8	3	4		1	2	1	4
430	11	15	20	23	8	3	6	6			1	7
434	7	5	12	54	5	4	4	1	1	1		5

[1] For sample locations see fig. 1.
[2] Not including basaltic hornblende.

Pleistocene or early Holocene sediments accumulated on the Gulf Coastal Plain or on the shelf. Prior to the post-Pleistocene transgression many of the older deposits have been subjected to substantial weathering on land and on the exposed continental shelf. As a result less stable components may have been removed. Goldstein (1942) has suggested that removal in this manner of the pyroxenes of the Mississippi association may have produced the material for the hornblende association. Similarly, one might assume that selective removal of the pyroxenes from the Rio Grande association

TABLE 8.—*Average composition of Mississippi and Rio Grande suites after removal by computation of all pyroxene in excess of 5 percent, compared with average composition of Western Gulf suite, in percent of total non-opaque fraction. Data from table 5.*

	Hornblende[1]	Tourmaline	Epidote	Zircon	Garnet	Staurolite	Kyanite	Pyroxenes	Basaltic Hbl.	Others
Mississippi	52	2	21	2	11			5	3	4
Rio Grande	29	4	18	8	12	1	3	5	9	11
Western Gulf	58	5	17	4	7	1	1	3	3	3

[1] Not including basaltic hornblende.

would result in an assemblage similar to the hornblende association.

On the average the Western Gulf assemblage contains a maximum of 5 percent pyroxene. In table 8 are listed the assemblages that result when all pyroxene in excess of 5 percent is removed from the Mississippi and Rio Grande associations by computation. The Rio Grande association thus artificially weathered is not similar to the hornblende association; it contains too little hornblende. The Mississippi suite, on the other hand, can be transformed into a suite quite similar to the Western Gulf assemblage.

That such weathering of the Mississippi association actually has occurred with results identical to those predicted by calculation is demonstrated by the heavy mineral sequence of a composite section of the late Quaternary off Grande Isle, Louisiana (fig. 9). The assemblages in the upper part of the section, though variable, are similar to the modern Mississippi association. At the top of the Prairie Formation (Upper Pleistocene), however, a marked and sudden decrease of pyroxene and a concomitant increase of hornblende occur. Samples from the Prairie and the underlying Montgomery Formations have assemblages quite similar to those of the hornblende association. The decrease of pyroxene is accompanied by a strong increase in the degree of etching and alteration of this mineral and an increase of the number of deeply altered minerals (alterites), suggesting that selective weathering is the cause of the disappearance of the pyroxene rather than a change in source. The abundance of fragile hacksaw structures indicates that the weathering took place in place. Thus, weathered Mississippi sediments appear to be a potential source of material for the Western Gulf province. It may be noted that the hornblendes of the Prairie and Montgomery Formations show no signs of weathering.

Both the weathered Mississippi and the Western Gulf suite are quite similar to the Colorado association. Weathered Rio Grande material, though different in a pure form, would be difficult to recognize in mixtures with one of the three others. All of these assemblages contain hornblende as a principal component.

They differ greatly, however, in the vari-

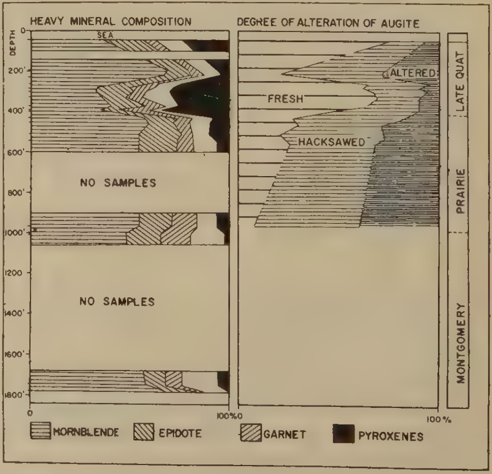

FIG. 9.—Heavy mineral variation in a composite section of the Upper Pleistocene in Humble Oil Company wells, Grand Isle, Block 18, Louisiana. Location of section in figure 1.

TABLE 9.—*Average composition of hornblende fraction in Mississippi, Rio Grande, and Colorado sediments, in percent of total hornblende. Averages of five samples for each river*

	Blue-green	Common	Brown	Basaltic	Others	Ratio blue-green to brown plus common
Mississippi	53	22	16	6	3	1.4
Colorado	89	7	4			8.0
Rio Grande	26	34	14	1	25	0.5

etal composition of the hornblende fraction. The sediments of the northern Gulf of Mexico contain four main types of hornblende: *blue-green* (metamorphic) *hornblende* with strong pleochroism from blue-green to green; *common hornblende*, moderate to weak pleochroism from green and brown to brownish green; *brown hornblende*, weak pleochroism in shades of brown, often deeply colored; and *basaltic hornblende*. In addition small percentages of other amphiboles (tremolite, actinolite) have been found. Percentages of hornblende varieties based on a count of 100 hornblende grains have been obtained for sets of representative samples from the Mississippi, Rio Grande, and Colorado rivers (table 9) and for all Western Gulf samples. In view of the difficulty of identification, in particular of the brown and common varieties, the percentages are approximations only. This may in part explain why the separate percentages of brown and common hornblende do not appear to have diagnostic value. The ratio of blue-green to common plus brown hornblende (called *hornblende ratio* in the following discussion), on the other hand, is a parameter of great value. Basaltic hornblende percentages in general are too low to be of much value.

With the aid of the hornblende ratio it is possible to distinguish between material derived from the Rio Grande, Mississippi, and Colorado Rivers respectively, even where it occurs in minor quantities. The other potential sources of sediment, the Brazos, Neches, Trinity, Sabine, and all other minor Texas rivers, can be distinguished by means of characteristic minerals (zircon, tourmaline, kyanite, and staurolite) which do not occur in significant quantities in the Mississippi, Rio Grande, and Colorado. The percentages of these minerals and the hornblende ratio provide a set of parameters which can be used to identify the relative contributions of the various sources in different parts of the Western Gulf province. These parameters and their characteristic values for all sources are listed in table 10, and the areal distributions are presented in the maps of figure 10–13. Presentation of individual values is impossible on small scale maps, but an estimate of the reliability of the patterns can be obtained with the aid of the percentages of samples that conform to the pattern shown on the map. For every map this criterion is indicated.

Essentially, the patterns have been constructed on the basis of the parameter values alone. In some cases, however, the data allow of two or more slightly different interpretations. In such cases the morphological and grain size observations published by Curray (in press) have been utilized to select the most plausible pattern. In evaluat-

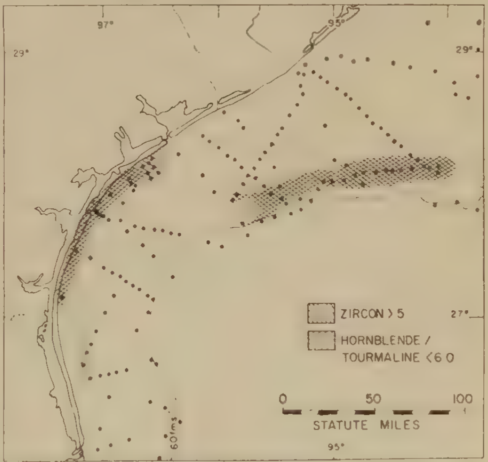

FIG. 10.—Areal distribution of zircon percentages and hornblende/tourmaline ratios in the Western Gulf province; 97 percent of zircon percentages and 99 percent of hornblende/tourmaline ratios conform to pattern.

TABLE 10.—*Mineral parameters characterizing sediments of all potential sources of supply for the Western Gulf Province*

Source	Hornblende[1] %	Pyroxene %	Zircon %	Staurolite plus Kyanite %	Hornblende ratio (see text)	Ratio Hornblende[1] to Tourmaline
Mississippi	40	25	<5	<1	1–2	>20
Mississippi, weathered	52	<5				
Rio Grande	23	24	<5	<5	<1	1–10
Rio Grande, weathered	29	<5				
Colorado	77		<5		>5	>20
Rivers east of Brazos	1		>20	5–10		<1
Brazos, Pleistocene and rivers west of Colorado	1–10		30–40	>10		<1

[1] Not including basaltic hornblende.

ing the maps it must be borne in mind that in some areas the parameter shown pertains to a major portion of the sand-sized sediment but in others the parameter pertains only to a small fraction. In the area close to the shelf edge south of Galveston, for example, the hornblende ratio map (fig. 12) shows a predominance of Colorado derived sediment. Comparison with the hornblende percentage map (fig. 13), however, demonstrates that the sand fraction of this area contains very little of this mineral and that the bulk of the sand must have had other sources. Hence, for a proper evaluation of sediment sources, all maps must be used in combination.

In general the maps show reasonable agreement. The discrepancies that can be observed locally are, in part at least, caused by the relatively high error inherent in an analysis based on counts of 100 grains per sample. The influence of the statistical counting error is particularly great in mineral ratios but has been reduced by omitting all ratios where one or both components occur with less than 5 percent.

The information that can be obtained from the mineral parameter maps has been summarized in figure 14. This sketch map shows the regional distribution of all pure and mixed assemblages in the Western Gulf

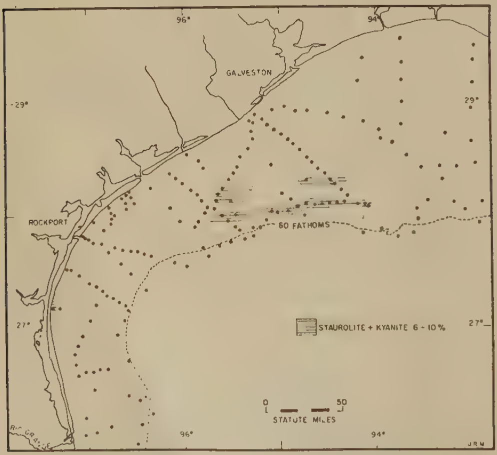
96°
94°
GALVESTON
29°
29°
ROCKPORT
60 FATHOMS
STAUROLITE + KYANITE 6 - 10 %
27°
27°
0 50
STATUTE MILES
Rio Grande
96°
94°
JRM

FIG. 11.—Areal distribution of kyanite+staurolite percentages in the Western Gulf province; 89 percent of samples conform to pattern.

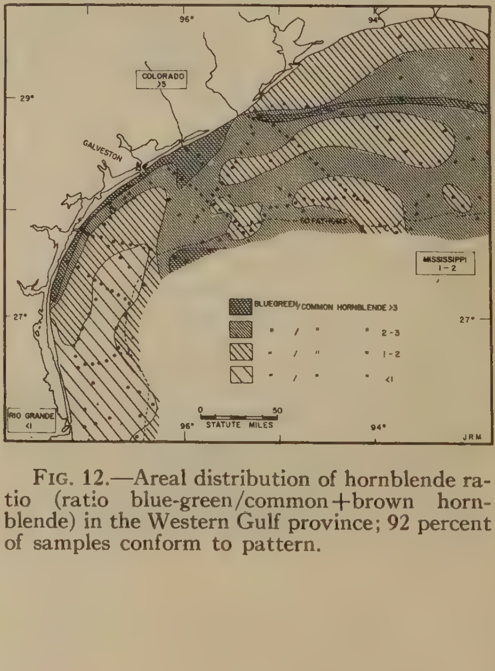
96°
94°
29°
COLORADO >5
GALVESTON
60 FATHOMS
MISSISSIPPI 1 - 2
BLUEGREEN/COMMON HORNBLENDE >3
" / " " 2-3
" / " " 1-2
" / " " <1
27°
27°
RIO GRANDE <1
0 50
96° STATUTE MILES
94°
JRM

FIG. 12.—Areal distribution of hornblende ratio (ratio blue-green/common+brown hornblende) in the Western Gulf province; 92 percent of samples conform to pattern.

(330)

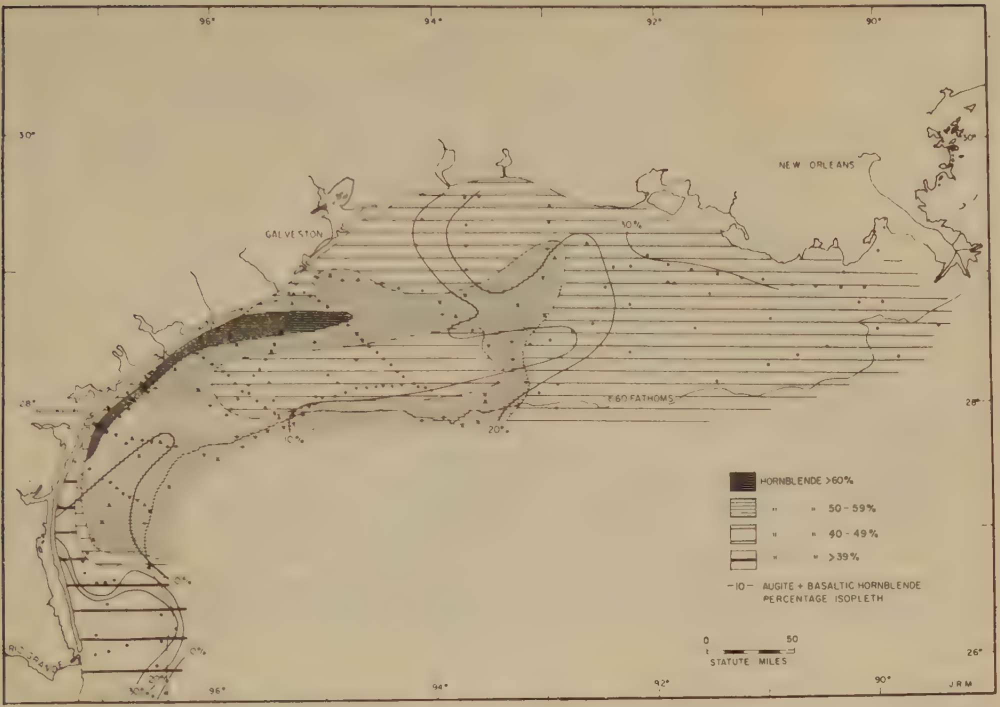

FIG. 13.—Areal distribution of hornblende (not including basaltic) and pyroxene+basaltic hornblende percentages in the Western Gulf province; 86 percent of hornblende percentages and 98 percent of pyroxene+basaltic hornblende percentages conform to pattern.

province and indicates in order of quantitative importance the sources of the sediments in each zone. The conclusions that can be drawn from figures 10–14 can be summarized as follows:

1.—The values of all parameters are lower in the Western Gulf province than in the sediments of the rivers that have contributed the material, thus indicating that all Western Gulf sediments are mixtures in varying proportions of two or more components. Only in a narrow belt close to the shore between the mouth of the Colorado River and Corpus Christi and in the area north of the modern Rio Grande province relatively pure associations derived from the Colorado and from weathered Rio Grande deposits respectively can be observed.

2.—North of the modern Rio Grande province and west of the Mississippi province the sediments appear to have been derived predominantly from older Mississippi and Rio Grande deposits which have lost their pyroxenes by weathering.

3.—In the central part of the Western Gulf province the assemblages occur in belts parallel to the shelf edge or the coast line. Zones of Colorado material or mixed detritus derived from the Colorado, Brazos, and Trinity Rivers alternate with sediments in which the Mississippi element predominates. This zonation is clearly illustrated by figure 15. On the shelf south of the mouth of the Colorado River the zonation is interrupted by a north-south trending belt of almost pure Colorado material extending across the entire width of the shelf and beyond the shelf edge.

4.—Elements derived from Texas rivers exclusive of the Rio Grande and Colorado, or reworked from the Pleistocene of the Texas coast, are concentrated in three areas (figs. 10 and 11). Two of them are situated parallel and relatively close to the shelf edge in the area south of Galveston and the Colorado River. The high zircon percen-

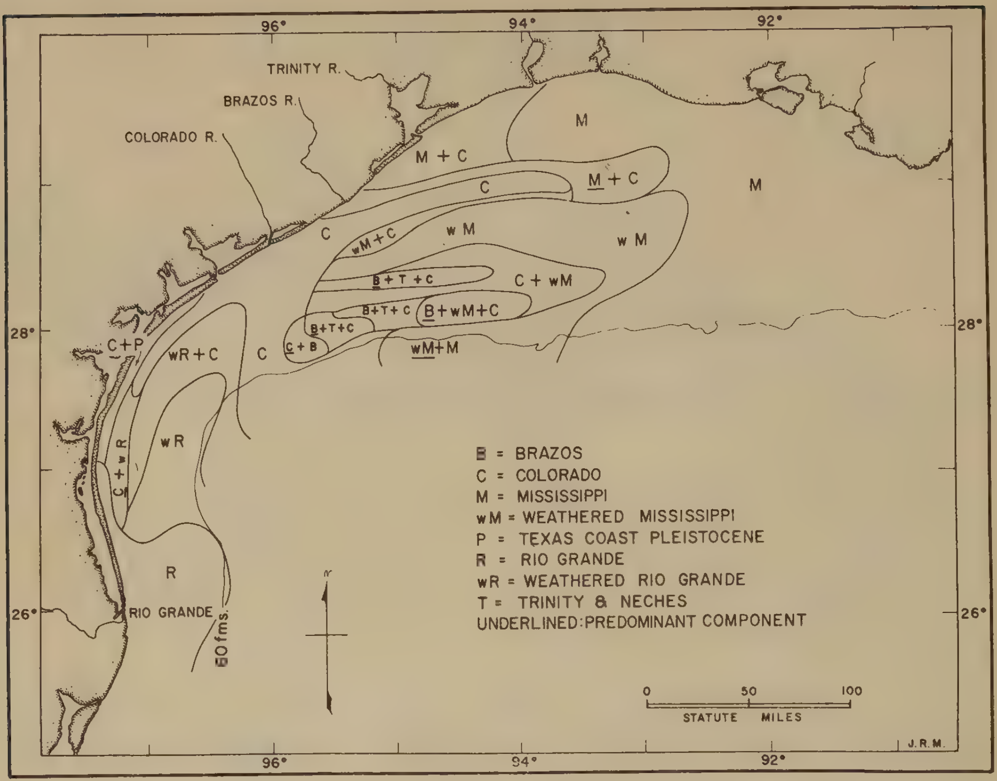
96°
94°
92°
TRINITY R.
BRAZOS R.
COLORADO R.
M
M + C
C
M + C
M
C
wM+C
w M
w M
B+T+C
C + wM
B+T+C
B+wM+C
B+T+C
C+B
wM+M
C+P
wR+C
C
C+wR
wR
R
RIO GRANDE
60 fms.
28°
26°
B = BRAZOS
C = COLORADO
M = MISSISSIPPI
wM = WEATHERED MISSISSIPPI
P = TEXAS COAST PLEISTOCENE
R = RIO GRANDE
wR = WEATHERED RIO GRANDE
T = TRINITY & NECHES
UNDERLINED: PREDOMINANT COMPONENT
0
50
100
STATUTE MILES
J.R.M.

FIG. 14.—Sketch map of sources and mixing of sediments in the Western Gulf province. Boundaries are approximate and based upon figures 10–13. Components for each area are listed in order of quantitative importance.

tages and low hornblende/tourmaline ratios demonstrate considerable influence of Texas river material, probably mainly the Brazos. The influence of the Trinity and Neches Rivers is noticeable in relatively high kyanite and staurolite percentages. The third zone of high zircon percentages and low hornblende/tourmaline ratios occurs along the present coast from Baffin Bay to a point just west of the mouth of the Colorado River. Given the insignificance of the rivers in this area it appears probable that these sediments have been derived largely from outcropping Pleistocene materials. The question of their origin will be discussed further in the next section.

5.—There is no Brazos distributive province off the mouth of this river of a size observable with the available sampling grid. Nienaber (1958) has demonstrated that pure Brazos sediments, relatively uncontaminated with Mississippi and Colorado material, are restricted to a small area in the immediate vicinity of the river mouth. On the other hand, a zone of almost pure Colorado material extends westward from the mouth of this river in an elongated belt parallel to the coast.

The reasons for the mineral distribution pattern shown in figure 14 are complex. Present day deposition of heavy minerals appears to be a factor of importance only in the zone immediately along the coast and off the Rio Grande and Mississippi Rivers. Everywhere else the pattern is controlled by the interplay of three main factors: the post-Pleistocene rise in sea level from a low stand approximately at the edge of the shelf; shifts of current and longshore drift patterns in the Gulf caused by climatic changes during early Holocene time; and the pre-existing drainage patterns of the rivers on the ex-

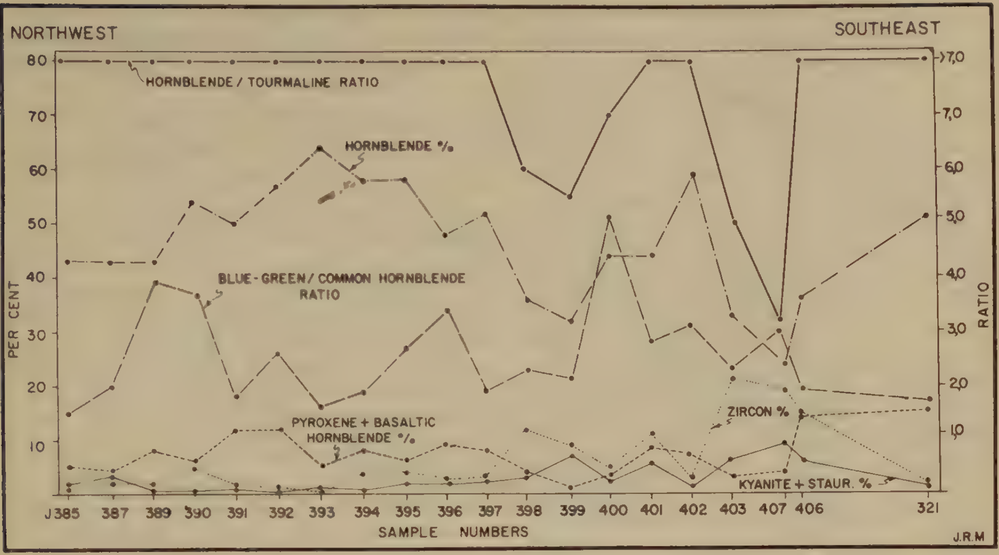

FIG. 15.—Graphic cross section of heavy mineral variation across the continental shelf east of Galveston. For location of section see figure 1. For significance of parameters see table 10.

posed continental shelf. The latter may have been controlled at least in part by tectonic movements.

Curray (in press) has analyzed in detail the Holocene history of the continental shelf on the basis of bathymetrical observations, grain size analyses, and the heavy mineral data of the present paper. A brief summary of this history in terms of sediment sources follows here (fig. 16).

During the period of lowest sea level stand, sediments from all rivers were carried directly downslope across the exposed shelf to deep water. A marine current and drift pattern similar to the one prevailing today is suggested by the northward extension of Rio Grande material and the westward trending tongue of Mississippi sediment. Material from the Colorado, Brazos and Trinity Rivers was deposited in a neutral zone between the areas of eastward and westward drift (fig. 16, stage I).

During the time of early sea level rise this distribution pattern changed appreciably as a consequence of a major reduction in westward drift of the Mississippi material. First, the sediments derived from the Brazos and Trinity Rivers, and a little later also those from the Colorado, were carried eastward over an appreciable distance in channels that are still partially exposed on the shelf (fig. 16, stages II and III).

In the next interval (stage IV) the predominant westward drift of Mississippi sediment and the deposition of Colorado, Brazos and Trinity material in a neutral zone were restored. Rio Grande sands continued to be moved northward as in all previous stages. Mississippi and Rio Grande sediments deposited in the Western Gulf province in this and earlier stages have apparently been derived from weathered deposits or were weathered in place after deposition because they are poor in pyroxene. Younger sediments from both sources contain normal amounts of this mineral.

When sea level reached the 10 fathoms depth contour (stage V), another major shift in the directions of transport occurred. Again the westward drift was reduced and the Colorado and Brazos sediments were carried far east into the area south of the Calcasieu River. How far east the Colorado deposits extended is not known, because in the area east of the Calcasieu River all older deposits are obscured by a blanket of modern Mississippi sediment. At this time Rio Grande sediment was deposited as far north

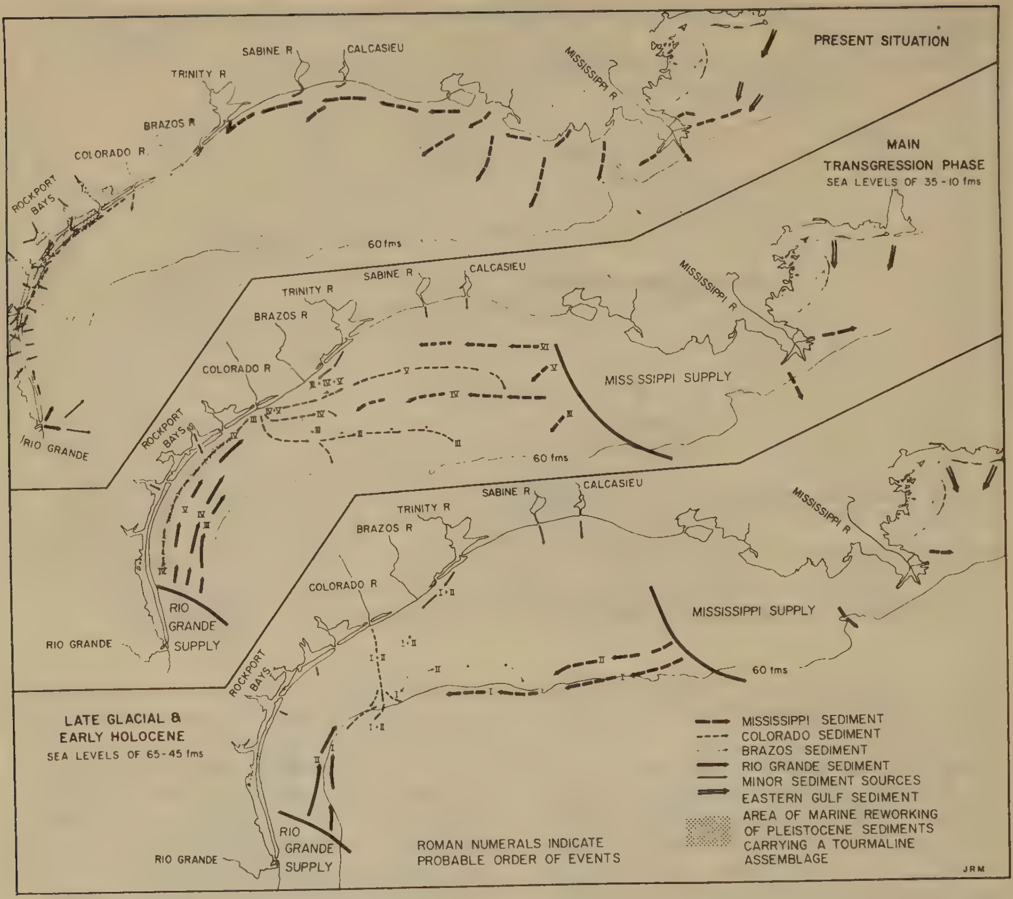
PRESENT SITUATION
SABINE R
CALCASIEU
TRINITY R
BRAZOS R
COLORADO R.
ROCKPORT BAYS
MISSISSIPPI R
60 fms
RIO GRANDE
MAIN TRANSGRESSION PHASE
SEA LEVELS OF 35 - 10 fms
SABINE R
CALCASIEU
TRINITY R
BRAZOS R
COLORADO R
ROCKPORT BAYS
MISSISSIPPI R
MISS SSIPPI SUPPLY
60 fms
RIO GRANDE SUPPLY
RIO GRANDE
SABINE R
CALCASIEU
TRINITY R
BRAZOS R
COLORADO R
ROCKPORT BAYS
MISSISSIPPI R
MISSISSIPPI SUPPLY
60 fms
LATE GLACIAL & EARLY HOLOCENE
SEA LEVELS OF 65-45 fms
RIO GRANDE SUPPLY
RIO GRANDE
ROMAN NUMERALS INDICATE PROBABLE ORDER OF EVENTS
MISSISSIPPI SEDIMENT
COLORADO SEDIMENT
BRAZOS SEDIMENT
RIO GRANDE SEDIMENT
MINOR SEDIMENT SOURCES
EASTERN GULF SEDIMENT
AREA OF MARINE REWORKING OF PLEISTOCENE SEDIMENTS CARRYING A TOURMALINE ASSEMBLAGE
JRM

FIG. 16.—Sediment sources and directions of transportation on the continental shelf of the northern Gulf of Mexico during the Holocene. Roman numerals indicate sequence of events but do not represent a correlation with any stratigraphic system for the Holocene period.

as the area of Rockport.

Major climate changes are assumed to be responsible for the marked change in transport direction in stages II, III, and V.

When sea level rose above the 10 fathom contour the predominant westward drift was restored again (fig. 16, stage VI) as reflected by another shift of the sediments derived from the Mississippi. Virtually the same transportation pattern characterizes present day deposition although, as will be shown in the next section, westward drift is probably not as prominent. At the present time deposition of sand-size material seems to be restricted to the shelf off the Mississippi and the Rio Grande and to a narrow nearshore zone between those rivers. Except for some westward drift of Colorado and Brazos material as far as the area of the Rockport bays, sediments in this nearshore zone appear to have local sources.

Thus, in the Western Gulf province the mineral distribution pattern of the basal part of a transgression has been preserved. It is of interest to note that this pattern is determined almost entirely by nearshore distribution processes operating during various stages of the transgression and has not been significantly modified by the deep water environments following them. Only in the areas immediately off very large rivers do sand-size sediments spread at the present time across the entire width of the shelf.

HEAVY MINERAL DISTRIBUTION, COASTAL ZONE BETWEEN BRAZOS AND RIO GRANDE RIVERS

The mineralogy of the coastal and nearshore sediments of the northwestern Gulf of Mexico has not been examined as systematically as that of the continental shelf deposits. Detailed sample collections are available for Laguna Madre, Aransas, San Antonio, and Mesquite Bays. A few samples have been investigated from Nueces, Copano, and Galveston Bays, and a satisfactory collection is available from Padre, St. Joseph, and Matagorda Islands. No information at all exists for the zone between Galveston Bay and the Mississippi delta.

Five heavy mineral associations can be expected in the sediments of the Texas coastal region: the pyroxene-hornblende association of the Rio Grande, the hornblende association of the Colorado, the tourmaline association of the Brazos and the rivers between the Colorado and Rio Grande and of the Pleistocene, the tourmaline-kyanite-staurolite association of the Trinity, Neches and Sabine Rivers, and the hornblende-pyroxene association of the Mississippi. A large part of the deposits probably consists of mixtures of two or more components.

The heavy mineral variation along the beaches of Texas has been described by Bullard (1942). His principal conclusions follow (fig. 17). The sediments of the beaches and barrier islands have been transported west and southwestward by longshore drift except in the area just north of the Rio Grande where indications of northward movement have been found. The rivers are considered the only important source of sand and the contribution from the erosion of the headlands is supposed to be negligible. Nearly all sediments west of the mouth of the Colorado are supplied by this river although Nueces material is considered an important diluting element in the area of Corpus Christi Bay and the northern part of Laguna Madre. The predominantly stable assemblages occurring east of the Colorado are considered a direct contribution from the Brazos River diluted with material from the Mississippi supplied by longshore drift.

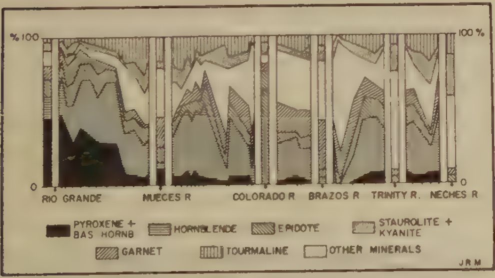

FIG. 17.—Heavy mineral variation diagram for the Texas Gulf Coast beaches between the Rio Grande and the Neches Rivers. Data converted from Bullard (1942). For sample locations see Bullard (1942, fig. 1). Marks on base line are sampling points.

The results of the present study suggest that these conclusions of Bullard require considerable modification.

Laguna Madre

In the southern part of Laguna Madre (fig. 18, table 11) the sediments are characterized by a pyroxene-hornblende associa-

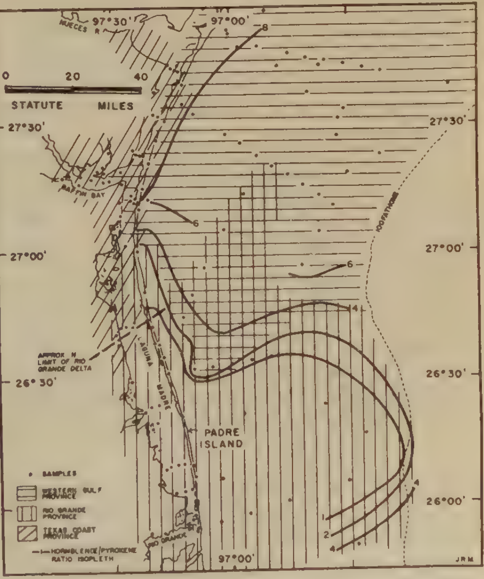

FIG. 18.—Regional distribution of heavy mineral assemblanges in Laguna Madre and on the adjacent continental shelf.

TABLE 11.—*Representative analyses of samples from Laguna Madre, Corpus Christi Bay, and the adjacent continental shelf, in percent of total non-opaque fraction*[1]

Sample number	Hornblende[2]	Tourmaline	Epidote	Zircon	Garnet	Staurolite	Kyanite	Titanite	Basaltic Hbl.	Augite	Hypersthene	Others
Rio Grande Province												
LM 20	22	7	23	7	7	4	4	3	5	18		
65	15	4	19	9	21	2	4	6	5	13	2	1
69	18	5	19	7	13		1	5	1	28	2	1
75	21	3	19	1	10	4	3	5	9	24		1
76	28	8	19	6	4	5	1	4	10	15		
J 479	22	1	14	17	17	1	3	1	7	10	4	3
718	33	2	8	7	7		1	8	3	31		
723	17		4	10	14	3	1	4	3	44		
729	23	1	12	7	11			4	4	34	4	
732	38		4	4	2	1	1	3	5	41	1	
737	29	2	5	9	6	1	1	3	7	37		
739	28	1	19	8	6			1	2	28	5	2
Texas Coast Province (Laguna Madre)												
LM 2	7	32	6	34	4	8	4					5
3	8	22	8	36	4	7	8					7
6	3	39	11	7	8	21	8		1			2
7	1	32	21	18	5	14	5					4
8	5	26	13	29	4	10	5	1				6
11	3	28	18	18	9	7	6	2		1		8
Texas Coast Province (Nueces Bay)												
N 1	5	29	14	16	11	9	6	3		2		5
2	4	32	10	18	9	6	3	3		3		12
3	12	23	10	18	7	8	6	3		1		12
4	1	30	8	14	12	16	3	3	1	3		9
Mixed assemblages												
LM 57	9	8	17	21	25	4	2	6	4			4
78	16	20	12	20	10	4	3	4		2		9
79	6	21	4	36	10	9		4	1	2		7
88	15	19	8	36	4	3		3		2		10
120	36	27	15	4	6	7		1				4
123	32	23	11	11	4	6	2	1	3	3		4
203	2	13	29	15	15	11	3	2		8		2
205	11	9	27	18	17	3	1	3	5	4		2

[1] For sample location see fig. 1, and Rusnak (in press) fig. 27.
[2] Not including basaltic hornblende.

tion and form part of the Rio Grande province. The northern limit of this province in Laguna Madre and on the adjacent shelf coincides almost precisely with the morphological limit of the pre-modern Rio Grande delta (Rusnak, in press). At the present time hardly any sediment from the Rio Grande is brought directly into the lagoon. Consequently, the pyroxene-hornblende assemblages of the southern part of the lagoon must have been derived largely from reworked older deltaic deposits. The transitional zone between the Rio Grande province and the Texas Coast province following

TABLE 12.—*Heavy mineral assemblages from the late Pleistocene (Beaumont Clay) of the Texas Coast, in percent of total non-opaque fraction*[1]

Sample number	Hornblende[2]	Tourmaline	Epidote	Zircon	Garnet	Staurolite	Kyanite	Titanite	Basaltic Hbl.	Augite	Hypersthene	Others
Laguna Madre												
LM 91C	3	29	9	26	6	3	6	4		1		3
97B	13	26	11	18	7	9	7	2		1		6
110A	11	19	12	32	6	6	6	1	1	1		5
189A	1	20	6	48	6	10	4					5
198C		30	9	29	10	7	8	3	1	1		2
213A	25	6	19	6	9	3	6	5	6	14		1
Rockport area												
RA 1	8	18	4	49	4	6	2					9
3	48	27	6	9	4	2	1					3
4	32	19	13	18	3	7	2	1				5
5	23	45	5	14	6		1	2				4
6	7	32	7	20	10	9	4	3				8
Houston (After Rogers and Powell, 1958; Table 1, average values)												
		34		53	3	1	2					7

[1] For sample locations see Fig. 21 and Rusnak (in press), fig. 13.

[2] Not including basaltic hornblende.

to the north is relatively narrow. Apparently, little sediment is at present being transported along the axis of the lagoon.

In the northern part of Laguna Madre, in Corpus Christi Bay, and Baffin Bay the sediments on the land side are characterized by a tourmaline association with varying but generally small amounts of hornblende. This tourmaline association is similar to the assemblages of most smaller Texas rivers (table 3) and also to the heavy mineral suites of the Pleistocene of Laguna Madre and the Rockport Bays (table 12). No rivers of importance drain into Baffin Bay, and the northern Laguna and the distribution of the tourmaline association along the inland shores suggests that reworked Pleistocene may be the principal source of the material. Modern Nueces sands contain small but significant percentages of volcanic minerals (table 3). These minerals are found only in the upper part of Nueces Bay close to the river mouth. Apparently, this river does not contribute much sediment to the outer part of the bay or to the northern Laguna area.[3]

In its purest form the tourmaline association is found on the land side of the northern Laguna Madre. Seaward across the lagoon and the barrier island the percentage of hornblende increases rapidly. This hornblende is to a large extent of the blue-green variety typical for Colorado material, suggesting that the ultimate source of at least part of this material is the Colorado River. This material may either have been transported southwestward by longshore drift as suggested by Bullard (1942) or derived from some older deposit of Colorado material in the vicinity. With the aid of the hornblende/tourmaline ratio it can be estimated that inside Laguna Madre more than 70 percent of the heavy minerals belong to the tourmaline province, and hence were derived locally. The small variable amounts of hornblende present in the Pleistocene sediments make it impossible to obtain a more accurate estimate. The proportion of locally derived material in the total sediment is much higher because Colorado sediments contain at least three times as many heavy minerals per unit sand as the Texas Coast province. Consequently, in a mixture the contribution of Colorado material is heavily over-emphasized.

---

[3] Two samples of Pleistocene beach rock from the western shore of Laguna Madre just north of the entrance to Baffin Bay have been investigated to test the possibility that part or all of the Pleistocene material in this area may represent old Rio Grande delta sediment that has lost its unstable minerals by weathering. In the beach rock such unstable components might have been protected by the carbonate cement. One of the samples contains a normal Texas coast assemblage (hornblende 21 percent, tourmaline 15 percent, zircon 35 percent, kyanite plus staurolite 9 percent, hornblende ratio 1.9) entirely within the range of modern assemblages from this area. The other is also similar to modern samples except for the presence of 2 percent of very badly weathered but recognizable pyroxene and approximately 30 percent of deeply altered grains now consisting of fine micaceous aggregates. These grains might represent completely altered pyroxenes and would thus indicate that the source of this material is a Pleistocene Rio Grande deposit. However, the hornblendes appear to be almost completely fresh and the hornblende ra-

In the discussion of the Western Gulf province use has been made of several parameters characterizing the various sediment sources. The same parameters can be used to unravel the mixtures of sediments in the coastal zone. The parameters used are the hornblende/pyroxene ratio, measuring the relative proportion of Colorado versus Rio Grande or Mississippi material; the hornblende/tourmaline ratio indicating the proportion of Pleistocene or Texas river-sediment; and the hornblende ratio, which gives the proportion of Colorado sediment. For characteristic values in the pure source materials see table 10.

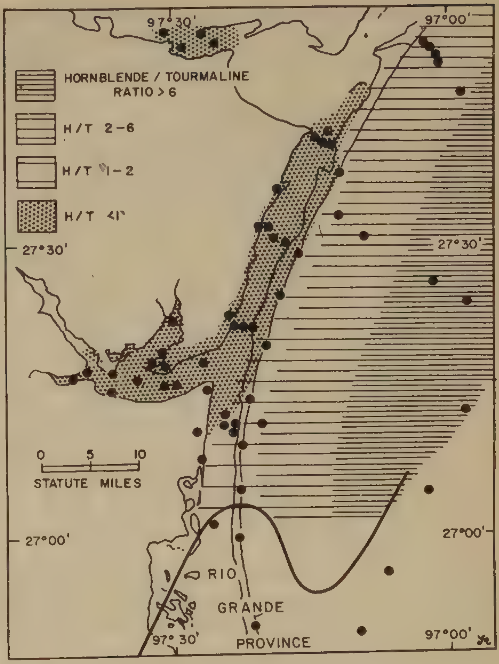

Fig. 19.—Variation of mineral parameters indicating sediment sources in bay and barrier islands deposits between the Rio Grande and Galveston Bay. Black dots indicate barrier island samples; open circles indicate bay samples. curves indicate trends only.

The northern limit of the Rio Grande province is indicated by a sharp increase in the hornblende/pyroxene ratio (fig. 19). Inside the lagoon this increase coincides with the morphological limit of the pre-modern Rio Grande delta but on Padre Island the increase is shifted a little to the north indicating a limited amount of northward longshore drift. North of the Rio Grande delta blue-green hornblende is an important component of the hornblende fraction, but the hornblende ratio remains considerably below the value of 5.0 typical for pure Colorado material (fig. 19). The variety which lowers the value must have been derived from the Rio Grande. Direct northward transportation along the shore appears to be excluded because of the low percentage of associated pyroxene which renders it unlikely that modern Rio Grande material is contributed to this area. The source of the hornblende assemblage which dilutes the tourmaline association in the northern Laguna Madre must be a mixed deposit of Colorado and weathered Rio Grande material. The nearest source of such detritus is found on the continental shelf where according to figures 12 and 13 sediments with the correct pyroxene content and horn-

---

tio of 21 places the sample entirely within the range of modern northern Laguna material, as contrasted with a ratio of 1.0 or less for Rio Grande material. Although this appears to refute the Rio Grande as a source for this sample, the question deserves further study.

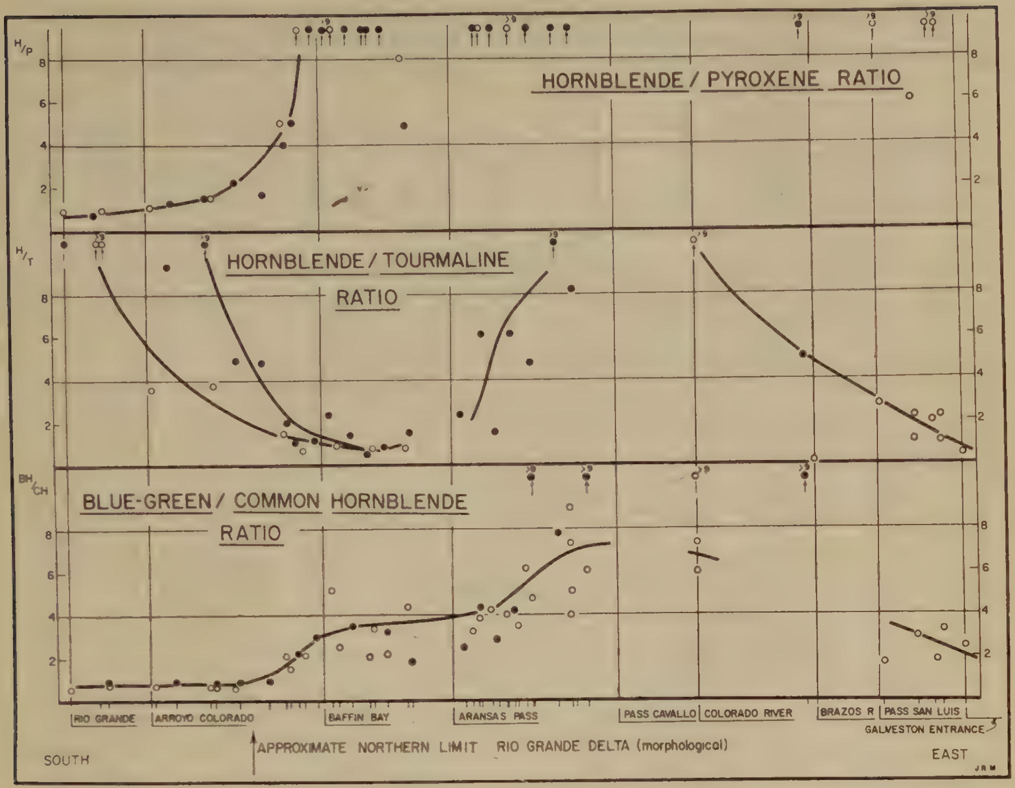

FIG. 20.—Areal distribution of hornblende/tourmaline ratios indicating relative contributions of Colorado and Pleistocene material in the northern Laguna Madre and on the adjacent continental shelf.

blende ratio are present over an extensive area.[4]

Neither the amount of hornblende in the assemblages nor the composition of the hornblende fraction change significantly between the northern limit of the Rio Grande province and Aransas Pass (fig. 19). If, as Bullard assumes, longshore drift in a southwestward direction is the principal mechanism of hornblende supply, a southwestward decrease of this mineral should be expected. This apparently is not the case. The importance of the hornblende admixture increases away from the shore rather than parallel or oblique to it (fig. 20), suggesting, as does the constant presence of Rio Grande components over the entire area between the Rio Grande delta and Aransas Pass, that the shelf off this part of the coast is the source of the hornblende suite.

Contrary to Bullard, it must be concluded that the sediments of the bays and barrier islands between the Rio Grande and Aransas Pass were not brought there by longshore drift with local dilution of river sands, but were locally reworked from preexisting deposits on land and on the continental shelf. Net transportation, instead of parallel to the coast, was predominantly perpendicular to it and probably associated with the Holocene transgression. The prin-

---

[4] An estimate of the amount of Rio Grande sediment present in the assemblage diluting the tourmaline association in Laguna Madre can be obtained with the aid of the characteristic hornblende ratios of the pure Colorado and Rio Grande associations. The hornblende association appears to consist of approximately equal portions of Colorado and Rio Grande sediment, assuming that the heavy mineral contents of both types of material are roughly the same.

TABLE 13.—*Representative heavy mineral analyses of samples from Galveston, Aransas, Mesquite and San Antonio bays, Texas, in percent of total non-opaque fraction*[1]

Sample number	Hornblende[2]	Tourmaline	Epidote	Zircon	Garnet	Staurolite	Kyanite	Titanite	Basaltic Hbl.	Augite	Hypersthene	Others
Galveston Bay												
GB 1	41	15	21	8	10	1	1		1	1		1
4	3	47	2	17	17	10	2					2
5	3	42	8	20	12	3	3					9
16	31	39	13	2	5	4	3	1				2
Aransas Bay												
A 22	76	10	8		2	2		1				1
31	78	8	8		3	3						
40	44	29	15	3	5	2	1					1
60	38	36	11	1	1	5	5	1				2
77	9	58	13	5	1	10	2					2
Mesquite Bay												
M 7	60	13	17	2	2		2	1	1	2		
9	19	56	9	1	2	8	3		1			1
15	61	13	17	3	3	2		1				
22	59	20	15	2	2	1		1				
25	4	52	20	3	5	6	5	1	2	1		1
40	28	51	11	2		3	3					2
44	64	11	13	2	3	3	1	2				1
San Antonio Bay												
S 16	68	16	8	1	1	2	1	1				2
34	38	23	12	12	5	2	2	1	2			3
92	8	38	7	18	7	5	7	2				8
95	22	30	10	15	7	7	4	1	1			3
110	42	27	7	8	7	2	4	2				1
111	64	13	8	10	5							
113	52	30	8	1	3		3	2				1
141	7	37	18	22	4	5	5	1				1
168	44	37	5	1	2	4	2	2		1		2
188	11	44	15	13	7	3	1	2			2	2
191	50	17	11	9	4	3	1	1	1		1	2
270	31	51	3	4	3	4	2					2
340	55	21	8	4	7	2	1	1			1	

[1] For sample locations see fig. 1, and Poole (1958), figs. 2 and 3.
[2] Not including basaltic hornblende.

cipal contributors of sediment are old Rio Grande deposits for the southern part of Laguna Madre, and Pleistocene deposits for the northern Laguna, Corpus Christi Bay, northern Padre Island, and Mustang Island. Mixed Colorado and weathered Rio Grande deposits of early Holocene age on the shelf contributed a mineralogically conspicuous but quantitatively minor amount of material.

Rockport Area, Texas

East of Aransas Pass both the total amount of hornblende and the hornblende ratio increase rapidly in the direction of the Colorado River (fig. 19). Midway between

TABLE 14.—*Representative analyses of samples from Padre, St. Joseph, and Matagorda islands, in percent of total non-opaque fraction*[1]

Sample number	Hornblende[2]	Tourmaline	Epidote	Zircon	Garnet	Staurolite	Kyanite	Titanite	Basaltic Hbl.	Augite	Hypersthene	Others
						Padre Island						
P 54	24	4	17	8	13	1		3	3	25		2
48	40	4	11	2	6	1	2	1	12	20		1
42	28	5	17	1	9	4	4	1	10	20		1
33	29	6	20	6	10	2		6	9	9		3
30	36	26	6	2	8	2	4	4	5	5		2
27	32	31	8	6	5	4	3	1	4	2		4
21	51	21	13		3	6	3	2		1		
18	41	29	7	3	3	5	4	3		2		3
						St. Joseph Island						
SJ 5	51	22	14	3	7	2			1			
20	61	10	6	6	6	1	3	3	1			3
36	61	12	18	3	1	1		1	1			
51	43	16	12	16	4	4	2				2	1
53	41	28	12	1	6	3	2	2	2		3	
						Matagorda Island						
MT 11	53	16	13	5	2	5	2			1	2	1
17	55	9	16	6	6	5	1	2				
26	62	13	9	3	4		2	1	1	2	1	2
33	72	4	5	5	5	3	2	2	2			
42	65	8	8	8	6	2	1	1	1			
45	59	10	11	5	5	6		2				2
53	57	16	14	2	8	2		1				
62	34	13	11	30	6	2	2					2
71	56	14	12	1	6	5	2	2				2
						Sargent Beach (just west of Brazos mouth)						
	28	6	4	38	10	2	2	2	3			5

[1] For sample locations see figs. 1 and 21.

[2] Not including basaltic hornblende.

Aransas Pass and Pass Cavallo (an old Colorado mouth) the coastal sediments are almost entirely derived from the Colorado River. On St. Joseph and Matagorda Islands and in the nearshore zone the eastward gradient caused by gradual replacement of the tourmaline association by deposits rich in Colorado hornblende is very pronounced. The influence of strong westward longshore drift in this area is well substantiated.

Quite extensive heavy mineral information is available for the bays of the Rockport region (Poole, 1958). Two associations, a hornblende and a tourmaline association (tables 13 and 14), and their mixtures in varying proportions can be distinguished. The main components, hornblende and tourmaline, are almost mutually exclusive in the pure assemblages and together make up approximately 75 percent of all suites. Therefore, a map of the hornblende/tourmaline ratios accurately reflects the distribution and mixing of heavy mineral suites (figs. 21, 22).

In its purest form the tourmaline assem-

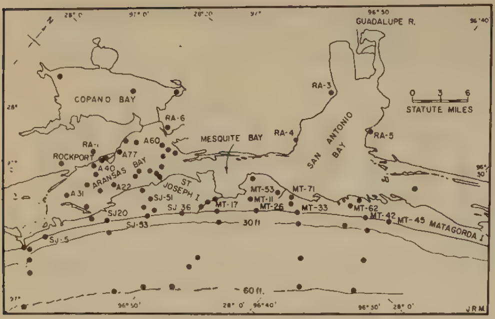
N
28° 0'
97° 0'
28° 20'
97°
96° 50'
GUADALUPE R.
96° 40'
COPANO BAY
28°
RA-3
0 3 6
STATUTE MILES
RA-6
SAN ANTONIO BAY
RA-5
RA-4
MESQUITE BAY
A60
RA-1
ROCKPORT
A77
A40
ARANSAS BAY
96° 30'
A22
ST JOSEPH I
A31
SJ-51
SJ 36
MT-53
MT-71
MT-11
MT-17
MT-26
MT-33
MT-62
SJ20
MT-42
MT-45
MATAGORDA I
SJ-53
30 ft
SJ-5
60 ft.
27°
96° 50'
28° 0'
96° 40'
96° 30'
28° 0'
J.R.M.

FIG. 21.—Place names in Rockport bays and sample location for Aransas Bay, the barrier islands and the adjacent continental shelf. For sample locations in Mesquite and San Antonio bays see Poole (1958, figs. 2, 3).

blage is found in a broad belt along all landward shores of the bays and also off the deltas of the rivers emptying in the bays. Both the rivers and the local Pleistocene deposits (tables 3 and 12) carry this association. The regional distribution suggests that erosion of the Pleistocene shore is probably the most important source of this suite.

Toward the center of the bays and in the direction of the barrier islands the hornblende/tourmaline ratio increases gradually as a result of dilution with the hornblende association. The hornblende ratio in these deposits shows that the hornblende has been derived from the Colorado River (fig. 23).

In detail the mineral distribution patterns of figure 22 are complex and of areally unequal value because of varying sample density. The main trends, however, are clearly established. There is a marked westward decrease of the Colorado component which is also reflected in the nearshore deposits. Farther offshore on the shelf the zone of modern Colorado sediment merges with an older zone of sediments from the same source (see fig. 14). Apparently, the influence of the Colorado River does not extend as far west in the nearshore zone as during the last phase of the Holocene transgression.

A sharply defined tongue of Colorado sediment extends from the near-shore Gulf across the barrier island into San Antonio Bay approximately at the site of a former major inlet. A similar tongue can be observed in Aransas Bay. Apparently, the supply of Colorado sediment to the bays is caused by a sharply localized stream of sediment rather than to washover by storm waves over a broad front, or any other mechanism involving temporary deposition in the barrier island. No Colorado material in appreciable quantity has entered San Antonio Bay from the river by way of Espiritu Santo Bay. Apparently transportation of sand size material between bays is restricted.

Recently, Parker (1959) has postulated a Holocene estuarine phase for San Antonio Bay during which there was an open connection between the bay and the Gulf, possibly similar to the situation at Calcasieu Lake. This would explain the localization of the Colorado sediment tongue as a remnant of an open phase of the bay. Unfortunately, the available subsurface heavy mineral information, although suggestive of a correlation between the first appearance

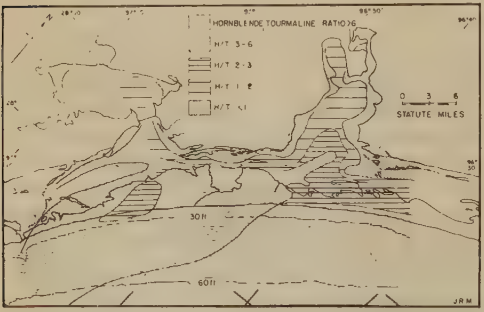
N
28° 0'
97° 0'
97°
96° 50'
96° 40'
HORNBLENDE TOURMALINE RATIO >6
H/T 3-6
H/T 2-3
H/T 1-2
H/T <1
0 3 6
STATUTE MILES
28°
96° 30
30 ft
60 ft
J.R.M.

FIG. 22.—Areal distribution of hornblende/tourmaline ratios in the bays of the Rockport area; 95 percent of samples conform to pattern. For bay names see fig. 21.

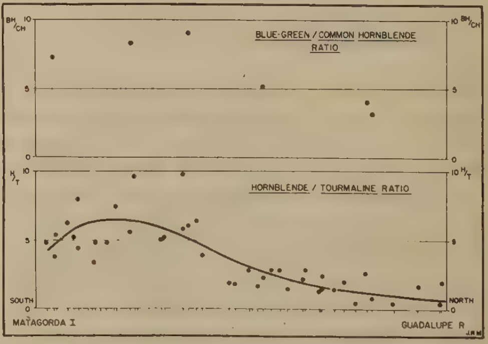

FIG. 23.—Variation of hornblende/tourmaline ratio and hornblende ratio along axis of San Antonio Bay.

of the Colorado tongue and the estuarine phase, does not permit a definite conclusion.

The actual proportion of Colorado sediment in the deposits of the bays cannot be inferred from the heavy mineral assemblage alone. The heavy mineral content per unit sediment of the tourmaline assemblage is not known, but by analogy with other areas in the Texas Coast province it may be assumed that it is at least a few times lower than that of the Colorado sediment. Consequently, the importance of the Colorado contribution to the bay sediments is exaggerated by the heavy minerals.

East Texas Coast

East of Pass Cavallo the information becomes very scarce. Bullard's data (fig. 17) show that as far east as the mouth of the Brazos River relatively high percentages of hornblende persist. This hornblende probably is not derived directly from the Colorado but reworked from older deposits in this area where the mouth of the river has repeatedly migrated. More than 60 percent of the heavy mineral assemblage in this area, however, consists of stable minerals probably supplied by the Brazos and brought by westward longshore drift. The submarine Brazos delta is of very restricted size and contains a mixture of Colorado, Mississippi, and Brazos components (Nienaber, 1958). Only along the shore pure Brazos material is found.

East of the mouth of the Brazos another increase of the hornblende percentage occurs together with a slight increase in the amount of pyroxene. Bullard (1942) has explained this by assuming that Mississippi sediment was carried westward by longshore drift. However, the hornblende/pyroxene and hornblende variety ratios in this area both exceed by an appreciable amount the typical values of the Mississippi association. At least part of this material must, therefore, have been derived from the Colorado. To explain this mixture it is not necessary to assume periodic or temporary replacement of the westward drift by an eastward movement, because not far offshore on the shelf a zone of relatively pure Colorado sediment was deposited during the later part of the Holocene transgression. This zone may have supplied the Colorado element in the coastal deposits, whereas westward drift accounts for the supply of Mississippi material.[5] The mixed assemblages of hornblende and tourmaline are restricted to the barrier islands, beaches, and outer bays. Inside Galveston Bay (fig. 19, table 13) the sediments are characterized by relatively pure assemblages of the tourmaline association derived either directly from the Trinity and Neches Rivers or from older deltaic deposits.

In conclusion it can be said that the sediments of the Texas Coast province are largely of local origin and formed by reworking and dispersal of older deposits present in the coastal zone itself or in the immediate vicinity on the continental shelf. Net long distance transport of Colorado material in the nearshore zone plays an important role in the nearshore area east of Aransas Pass, and its products are being accumulated mainly in the beaches, barrier islands, and outer parts of the bays. Although the Colorado element is conspicuous and quantitatively important in the heavy mineral assemblages, it can be assumed that its importance in the total sand fraction of the sediments in the bays is considerably less.

CONCLUSIONS

The present paper deals with the sources of the sands and the sand fraction of the clays in the northern Gulf of Mexico; its conclusions apply only to this size fraction.

A total of seven sources contributes sediment to the northern Gulf of Mexico: the rivers draining the sedimentary mantle of the southern Appalachians, the Mississippi, the rivers of western Louisiana and east

---

[5] Price (1958) has suggested the possibility that parts of the heavy mineral assemblages in this area may have been derived from old Brazos deposits formed before an assumed capture of the upper course of this river by the Pecos. They would therefore at least partly consist of Rocky Mountain material. Sidwell (1941) has shown that the modern Pecos carries an epidote-tourmaline assemblage. It is possible that some of the tourmaline and epidote in samples from the Galveston area may ultimately have been derived from the headwaters of the modern Pecos, but in view of the evidence for supply of a Mississippi association (based on pyroxene and hornblende, both minerals absent in the Pecos) this does not seem to be a necessary assumption.

Texas, the Colorado, the Brazos and the rivers between the Colorado and the Rio Grande, the Rio Grande, and the Pleistocene deposits of the coast of Texas. Only four of these, the Mississippi, Brazos, Colorado and Rio Grande, are quantitatively of great importance.

In addition to the incompletely studied Eastern Gulf province, four major distributive provinces can be recognized. Two of these, the Mississippi and Rio Grande provinces, have vast and distant source areas. Active deposition of material from the Mississippi extends at the present time from the subaerial delta to the edge of the shelf and beyond. The mineral composition of this province is homogeneous over a very large area. The dispersion of Rio Grande material over the shelf is at the present time probably much more restricted. Beyond the 10 fathom depth contour much of the material in this area may not represent present day deposition.

The Western Gulf province is of complex origin and at present largely inactive as far as the deposition of sand-sized material is concerned. Its formation is associated with the early Holocene transgression and the sediment distribution is primarily caused by nearshore processes. The sediments are derived from virtually all rivers in or near the area, including the Mississippi, partly directly and partly by reworking of older deposits that suffered considerable weathering during the last glacial period. The sediment distribution within this province has been modified very little by the present deep-water environment and essentially is a relict of successive nearshore environments associated with the transgression.

The Texas Coast province is restricted to a narrow belt in the coastal area of Texas and probably also of western Louisiana. Its sediments have been derived largely from local marine erosion and reworking of Pleistocene and early Holocene deposits, partly in connection with the Holocene transgression. In the eastern part of this province, between Galveston Bay and the Rockport bays, longshore drift plays a role in the transportation of sediments, but the quantitative importance of long distance sediment supply is not great.

Radial sediment distribution patterns prevail off the large Rio Grande and Mississippi Rivers. The mineral assemblages around such powerful sediment sources are homogeneous over large areas. Between these loci of active sediment supply, sediment dispersion patterns are complex, and predominantly parallel to the margins of the basin. Sediment supply is less vigorous, and sedimentation is transgressive rather than regressive. Transportation in this zone is caused by nearshore processes, and marine redistributing agents prevail over the forces that tend to build deltas from the shore.

Geologically, the sediment thickness and time interval involved in the present study are small. In an ancient basin the sequence studied here would probably be accepted as an approximately simultaneous series of events. In the light of the results of this study the great difficulties encountered in long range heavy mineral correlation are easily understood.

ACKNOWLEDGMENTS

The samples utilized in the present study have been collected on various field trips for American Petroleum Institute Project 51. The author is indebted to all collaborators for making the material available. The Humble Oil and Refining Company has kindly provided samples from several offshore wells. The assistance of H. N. Fisk and G. C. Harrell in obtaining the material is gratefully acknowledged. Preparation of the samples was carried out by D. M. Poole and H. W. Lusk. W. N. Cogen kindly provided the tables on which his publication of 1940 was based for comparisons between Tertiary and Recent assemblages. J. R. Curray's investigation of the Holocene history of the shelf has provided the basis for many of the conclusions. Discussions with H. W. Menard, G. A. Rusnak, and F. P. Shepard and their comments on the manuscript have been very valuable. J. R. Moriarty has prepared the illustrations.

(344)

REFERENCES

Blankenship, R. R., 1956, Heavy mineral suites in unconsolidated Paleocene and younger sands, Western Tennessee: Jour. Sedimentary Petrology, v. 26, p. 356–362.

Bornhauser, M., 1940, Heavy mineral associations in Quaternary and late Tertiary sediments of the Gulf Coast of Texas and Louisiana: Jour. Sedimentary Petrology, v. 10, p. 125–135.

Bullard, F. M., 1942, Source of beach and river sands on Gulf Coast of Texas: Geol. Soc. America Bull., v. 53, p. 1021–1044.

Carroll, D., 1957, A statistical study of heavy minerals in sands of the South River, Augusta County, Virginia: Jour. Sedimentary Petrology, v. 27, p. 387–404.

Carroll, D., Neuman, R. B., and Jaffe, H. W., 1957, Heavy minerals in arenaceous beds of part of the Ocoee Series, Great Smoky Mountains, Tennessee: Amer. Jour. Sci., v. 255, p. 175–193.

Cogen, W. M., 1940, Heavy mineral zones of Louisiana and Texas Gulf Coast sediments: Am. Assoc. Petroleum Geologists Bull., v. 24, p. 2069–2101.

Curray, J. R., in press, Sediments and history of the Holocene transgression, continental shelf, northwestern Gulf of Mexico, *in* Shepard and others, "Recent sediments, northwestern Gulf of Mexico." Am. Assoc. Petroleum Geologists, Tulsa.

Doeglas, D. J., 1940, The importance of heavy mineral analysis for regional sedimentary petrology. National Research Council, Committee on Sedimentation Report, 1939–40, App. P, Exhibit G, p. 102–121.

Doeglas, D. J., 1949, Loess; an aeolian product: Jour. Sedimentary Petrology, v. 19, p. 112–117.

Dohm, C. F., 1936, Petrography of two Mississippi River subdeltas. Louisiana Geol. Survey Bull., v. 8, p. 339–396.

Dreimanis, A, Reavely, G. H., Cook, R. J. B., Knox, K. S., and Moretti, F. J., 1957, Heavy mineral studies in tillite of Ontario and adjacent areas: Jour. Sedimentary Petrology, v. 27, p. 148–161.

Dryden, A. L., 1931, Accuracy in percentage representation of heavy mineral frequencies: Natl. Acad. Sci. Proc. v. 17, p. 233–238.

Edelman, C. H., 1933, Petrologische provincies in het Nederlandse Kwartair. Centen, Amsterdam, 104 p.

Goldstein, A., 1942, Sedimentary petrologic provinces in the northern Gulf of Mexico: Jour. Sedimentary Petrology, v. 12, p. 77–84.

Gravenor, C. P., 1951, Bedrock sources of till in southwestern Ontario: Am. Jour. Sci. v. 249, p. 66–71.

Hough, L. W., 1937, Petrographic comparison of Mississippi River and tributary bed material sands: Unpublished thesis, Louisiana State University.

Koldewijn, B. W., 1955, Provenance, transport and deposition of Rhine sediments; II, an examination of the light fraction: Geologie en Mijnbouw, v. 17, p. 37–45.

Kruger, F. C., 1937, A sedimentary petrographic study of certain glacial drifts of Minnesota: Am. Jour. Sci. v. 203, p. 345–363.

Mathis, R. W., 1944, Heavy minerals in Colorado River terraces of Texas: Jour. Sedimentary Petrology, v. 14, p. 86–93.

Muller, J. E., 1943, Sediment-petrologie van het dekgebergte in Zuid-Limburg: Mededelingen Geol. Stichting, serie C, II-2, 78 p.

Murray, R. C., 1953, The petrology of the Carey and Valders till of northeastern Wisconsin: Am. Jour. Sci., v. 251, p. 140–151.

Needham, C. E., 1934, The petrology of the Tombigbee sands of eastern Mississippi: Jour. Sedimentary Petrology, v. 4, p. 55–59.

Nienaber, J. H., 1958, Shallow marine sediments offshore from the Brazos River, Texas: Unpublished thesis, University of Texas.

Parker, R. H., 1959, Macro-invertebrate assemblages of central Texas bays and Laguna Madre: Am. Assoc. Petroleum Geologists Bull., v. 43, p. 2100–2166.

Poole, D. M., 1957, Size analysis of sand by a sedimentation technique: Jour. Sedimentary Petrology, v. 27, p. 460–468.

———, 1958, Heavy mineral variation in San Antonio and Mesquite bays of the Central Texas coast: Jour. Sedimentary Petrology, v. 28, p. 65–74.

Potter, P. E., 1955, The petrology and origin of the Lafayette Gravel: Jour. Geology, v. 53, p. 1–38, 115–132.

Price, W. A., 1958, Sedimentology and Quaternary Geology of southwest Texas. Gulf Coast Assoc. Geol. Soc., Trans., v. 8, p. 41–75.

Rittenhouse, G., 1944, Sources of modern sands in the middle Rio Grande valley: Jour. Geology, v. 12, p. 145–183.

Rogers, J. J. W., and Dawson, R. E., 1958, Size distribution of zircon and tourmaline in some samples of the Lissie Formation: Jour. Sedimentary Petrology, v. 28, p. 361–365.

Rogers, J. J. W., and Powell, W. F., 1958, Size distributions of zircon grains in some samples of the lower Beaumont clay. Jour. Sedimentary Petrology, v. 28, p. 36–39.

Rusnak, G. A., in press, Sediments of Laguna Madre of Texas, in Shepard and others, "Recent sediments, northwestern Gulf of Mexico." Am. Assoc. Petroleum Geologists, Tulsa, Oklahoma.

Russell, R. D., 1937, Mineralogical composition of Mississippi River sands; Geol. Soc. America Bull., v. 48, p. 1307–1348.

Scruton, P. C., 1955, Sediments of the eastern Mississippi delta: in, "Finding ancient shorelines," Soc. Econ. Paleontologists and Mineralogists, spec. pub. 3, p. 21–50.

Shepard, F. P., 1956, Marginal sediments of the Mississippi delta: Am. Assoc. Petroleum Geologists Bull., v. 40, p. 2537–2623.

Shepard, F. P., and Lankford, R. R., 1959, Sedimentary facies from shallow borings in the eastern Mississippi delta: Am. Assoc. Petroleum Geologists Bull. v. 43, p. 2051–2067.

Sidwell, R., 1937, Types and sources of sediments deposited by the South Canadian River in New Mexico and Texas: Jour. Sedimentary Petrology, v. 7, p. 80–84.

———, 1941, Sediments of Pecos River, New Mexico: Jour. Sedimentary Petrology, v. 11, p. 80–84.

———, 1944, Red River mineral provenance, Taos County, New Mexico: Jour. Sedimentary Petrology, v. 14, p. 125–130.

———, 1947, Trinity sediments of north and central Texas: Jour. Sedimentary Petrology, v. 17, p. 68–72.

Sidwell, R., and Cole, C. A., 1937, Sedimentation of Colorado River in Runnels and Coleman Counties, Texas: Jour. Sedimentary Petrology, v. 7, p. 104–107.

Sidwell, R., and Renfroe, C. A., 1943, Detrital minerals derived from Recent volcanics in northwestern Chihuahua: Jour. Sedimentary Petrology, v. 13, p. 13–20.

Sun, Ming-Shan, 1954, Heavy minerals from the Jacksonian sediments of Mississippi and adjacent areas: Jour. Sedimentary Petrology, v. 24, p. 200–206.

Van Andel, Tj. H., 1950, Provenance, transport, and deposition of Rhine sediments; I, a heavy mineral study. Veenman en Zonen, Wageningen, Netherlands, 129 p.

———, 1955, Recent sediments of the Rhone delta; II, sources and deposition of heavy minerals. Geol. Mijnbouwkundig Genootschap Nederland, Verhand. v. 15, p. 516–556.

Van Andel, Tj. H., and Postma, H., 1954, Recent sediments of the Gulf of Paria. Koninklijke Acad. Wetenschappen, Verhand., v. 20, 5, 245 p.

(346)

MISCELLANEOUS PUBLICATIONS
MUSEUM OF ZOOLOGY, UNIVERSITY OF MICHIGAN, NO. 115

The Spiny-rayed Cyprinid Fishes (Plagopterini) of the Colorado River System

BY

ROBERT RUSH MILLER
AND
CARL L. HUBBS
University of California

ANN ARBOR
MUSEUM OF ZOOLOGY, UNIVERSITY OF MICHIGAN
JULY 5, 1960

(347)

CONTENTS

PAGE

INTRODUCTION 5

METHODS 5

CHARACTERS AND RELATIONSHIPS 6

DISTRIBUTIONAL RELATIONS 9

SPECIATION 11

ANALYTICAL KEY TO THE PLAGOPTERINI 14

GENUS *Lepidomeda* COPE 18

Lepidomeda mollispinis, new species 18

Lepidomeda mollispinis mollispinis, new subspecies 18

Lepidomeda mollispinis pratensis, new subspecies 21

Lepidomeda albivallis, new species 24

Lepidomeda altivelis, new species 26

Lepidomeda vittata Cope 28

GENUS *Meda* GIRARD 31

Meda fulgida Girard 32

GENUS *Plagopterus* COPE 33

Plagopterus argentissimus Cope 33

SUMMARY AND GENERAL CONCLUSIONS 35

LITERATURE CITED 36

ILLUSTRATIONS

FIGURES IN TEXT

FIGURE PAGE

1. Distribution of the plagopterin fishes 10
2. Pharyngeal arches and teeth of two species of *Lepidomeda* 17

PLATES

(Plates I–III follow page 39)

I. Three new species of *Lepidomeda*.
II. Three species of plagopterin fishes.
III. Radiographs of the Plagopterini.

THE SPINY-RAYED CYPRINID FISHES (PLAGOPTERINI) OF THE COLORADO RIVER SYSTEM*

INTRODUCTION

THE freshwater fish faunas of Western North America, though limited, include a number of distinctive types (Miller, 1946; 1959). One of the endemic groups, the Plagopterini, comprising the cyprinid genera *Lepidomeda, Meda*, and *Plagopterus*, is herein revised. Despite the fact that the three genera have been known for 75 to 100 years, surprisingly little has been written concerning their classification, distribution, or biology.

Research grants from the Horace H. Rackham School of Graduate Studies of the University of Michigan supported much of the field work that made possible the conclusions regarding populations, ecology, and distribution as well as the systematic analyses herein reported. During our field operations of 1934, 1938, 1939, 1942, 1950, and 1959 we enjoyed the hospitality and profited from the assistance of officials and ranchmen too numerous to mention. Permission to study type specimens at the U. S. National Museum was given by Leonard P. Schultz; William Ralph Taylor kindly provided radiographs of the USNM syntypes of *L. jarrovii.* James E. Böhlke, Mrs. M. M. Dick, and Margaret H. Storey sent lists of pertinent material in their respective institutions (the Academy of Natural Sciences of Philadelphia, the Museum of Comparative Zoology of Harvard College, and the Natural History Museum of Stanford University). Ted Frantz of the Nevada Fish and Game Commission forwarded reports on Nevada waters, indicating changes since our 1938 field work, and also furnished a record of *L. mollispinis* from the Nevada portion of Beaver Dam Creek. Vasco M. Tanner of Brigham Young University made his collection available to us. W. L. Brudon took the photographs (Plates I–II), printed the radiograph (Plate III), and drew the pharyngeals (Fig. 2). Betty Anthony drafted the map (Fig. 1).

METHODS

Measurements were made and rays counted according to the criteria outlined by Hubbs and Lagler (1958:19–26).

Some of the diagnostic characters are best portrayed by radiographs (Pl. III). These show well the degree of spinous modification of the rays and the differential enlargement of the last two unbranched dorsal rays. They also yield the distinctive vertebral counts (Table 1). These counts include the hypural complex as one vertebra and the Weberian apparatus as four vertebrae.

---

* Contributions from the Museum of Zoology, University of Michigan, and from the Scripps Institution of Oceanography, New Series.

Contributions from the Scripps Institution of Oceanography, New Series, 1160

Reproduced by Permission

CHARACTERS AND RELATIONSHIPS OF THE PLAGOPTERINI AND CONSTITUENT GENERA

The three genera herein treated are unique among New World cyprinids in the ossification and other spinelike modifications of two anterior dorsal rays and of the pelvic rays. Cope (1874: 130–33) was so impressed with these specializations that he erected a subfamily, Plagopterinae, for these genera. His decision was widely followed, as by Jordan and Gilbert (1883: 148) and Jordan and Evermann (1896*a*: 204). Jordan, Evermann, and Clark (1930: 147), however, went to the extreme of elevating the group to family rank, under the name Medidae. Only Tanner (1936: 157, 171) has accepted this nominal family. Adopting the name Plagopterini, Hubbs (1955: fig. 2) reduced the group to tribal rank, under the subfamily Leuciscinae. We follow this classification.

The characters of the three genera seem to justify their retention in a common group, even though we treat it as of only tribal rank. The distinctiveness of the group receives some confirmation from the circumstance that the constituent genera are among the few North American cyprinids that are not known to hybridize with other genera (Hubbs, 1955).

The specializations of the more extreme members of this group (*Meda* and *Plagopterus*) are striking indeed, but since the less modified forms (comprising the genus *Lepidomeda*) closely resemble other American leuciscines, all three genera, pending the long deferred and much needed critical revision of American cyprinids, are most appropriately classed in the Leuciscinae. There seem to be no valid reasons for separating them from that subfamily. Resemblance is particularly close between *Lepidomeda* and several species referred to the genus *Gila,* and, even more strikingly, with a species of the Bonneville system, *copei,* that has been referred to a monotypic genus, *Snyderichthys* (Miller, 1945).[1] It is not now apparent whether such resemblance, extending even to details of coloration, is indicative of intimate relationship. In all of the obvious distinctive characters of the Plagopterini, *Lepidomeda* is the least modified.

The spinelike modification of the dorsal rays, rather well shown in the radiographs (Pl. III), is least marked in *Lepidomeda* and is variable within this genus, the only one of the three that is polytypic. The modification is strongest in the last unbranched ray, which in the different species is varyingly thickened, vitreous, and expanded on the lateral oblique wings, with the sagittal septum hardly evident by external examination and with the transverse sutures largely obliterated in the thickened portion. The terminal two-fifths to one-fourth of the ray, however, remains typical of soft-rays in structure in that this portion is slender, flexible, and strongly articulated. The preceding unbranched ray is also modified toward a spinelike structure, but remains only about three-fifths as long as the main spine, is less thickened, and is little expanded on the oblique wings basally. Distally it is expanded transversely, and its soft, articulated tip is more or less vestigial. It is not, however, very pungent. The several rays following the main dorsal spine are only slightly dilated and spinelike on the lateral wings basally.

---

[1] Study of the comparative osteology of *Gila* and its relatives, by Teruya Uyeno, convinces us that *Snyderichthys* merits subgeneric recognition only (Osteology and phylogeny of the American cyprinid fishes allied to the genus *Gila*. Ph.D. thesis, Univ. Mich., 1960).

In *Meda* and *Plagopterus* the next to last unbranched dorsal ray is greatly enlarged and extends to a strong, pungent tip just short of the much reduced soft, slender, articulated tip of the last unbranched ray. The outer part of the anterior spine is vitreous and is devoid of evident articulations, but where the ray is thicker, nearer the middle of its length, articulations can be discerned. This ray is more massive than the last unbranched one, which its strong wings largely cover. The last unbranched ray is also very spinelike, except at the extreme tip. Several of the following rays are considerably but decreasingly dilated and spinelike in appearance on the basal half, but distally remain slender, branched, and articulated. The last rays are scarcely modified. The dorsal spines are strongest in *Plagopterus,* but even in this genus no new structures are involved.

In all three genera the branched pelvic rays are thickened, consolidated, vitreous, and otherwise spinelike on the basal half to three-fourths of their lengths, where the articulations are scarcely or not evident. The modification, however, is almost wholly confined to the ventral demitrich; that is, to the left demitrich in the right fin and to the right demitrich on the left pelvic. The two strikingly asymmetrical halves of the anterior branched rays are distinct basally, but posteriorly become fused in the spinous modification. In *Lepidomeda* the spinose demitrich is continued to the fin margin as a slender articulated appendage, and the spinous modification is less extreme than in the other genera. In this character, as in others, the species of *Lepidomeda* are modified to different degrees. In *Meda* and *Plagopterus* the ventral demitrichs are strong spines ending in pungent points on the ventral side of the fin about three-fourths of the way out. The extreme bases of the nearly normal (upper) demitrichs of the first few branched rays are slightly dilated and spinelike (scarcely so in *Lepidomeda*).

Several pectoral rays, behind the first unbranched ray, are somewhat spinelike near their bases in *Meda* and *Plagopterus*, but are only slightly so specialized in *Lepidomeda.* A further distinctive specialization of the pectoral rays is confined to the mature males. In *Lepidomeda* the rays at this stage are only slightly dilated and retain a smooth front edge. In the mature males of *Meda* and *Plagopterus,* in contrast, the anterior several branched pectoral rays are greatly thickened and dilated, with the segments much broadened, and those along the front edge of the anteriormost branch are finely and irregularly denticulate.

The Plagopterini are characterized by having the more or less spinose pelvic fins attached to the belly by a membrane along the osseous part of the innermost ray. In *Lepidomeda* the membrane extends along about half the inner border of the fin; in *Meda* and *Plagopterus,* about two-thirds the length of the border. In all three genera the number of pelvic rays is reduced to seven, occasionally even fewer, very rarely to eight, which is the usual number in American cyprinids.

The primitiveness of *Lepidomeda* is further shown by its retention of scales, which, however, are somewhat degenerate. The entire body is scaly, except, in some species, where covered by the depressed paired fins. The scales of *Lepidomeda* (Cockerell, 1911: 213) are deeply embedded and transversely oval. Unlike those of most American cyprinids with small and not strongly imbricate scales, the scales of this genus lack basal radii (occasionally a few radii extend onto the lateral fields). *Plagopterus* and *Meda* are devoid of scales, unless they are vestigially represented by unsculptured platelets along the lateral line close to the head and, in *Plagopterus,* at the base of the dermal (sensory?) ridgelets on the anterodorsal part of the body (these dermal structures were definitely indicated as vestigial scales by Gilbert and Scofield, 1898: 497, and by Snyder, 1915: 584). If these platelets are remains of scales, *Meda* is the most extreme genus of the Plagopterini in the loss of squamation, which is one trend characteristic of the group.

Another feature of the Plagopterini that *Lepidomeda* exhibits to a less extreme degree than the other genera is the bright silvery coloration. In fact, as already noted, *Lepidomeda* is closely approached in this respect by *Gila* (*Snyderichthys*) *copei,* which is almost as silvery and also has dusky lateral mottlings. *Meda* and *Plagopterus* shine like burnished silver. *Meda* retains dark speckles on the back and on the lateral band. *Plagopterus* is almost uniformly silvery.

The general form of the head and body is also least modified in *Lepidomeda* (Pls. I–III). In that genus the premaxillaries are approximately terminal (varying from slightly prominent to slightly overhung) and the gape is variably oblique. In *Meda* the upper lip is weakly included and the mouth remains oblique. In *Plagopterus* the upper lip is definitely overhung by the snout and the mouth is nearly horizontal. The top of the head and the belly are rounded in *Lepidomeda,* though the contours are

(354)

variably turgid. In *Meda,* and more notably in *Plagopterus,* the top of the head is flattened transversely and longitudinally, the belly is also flattened, and the pectoral fins are lower and more transverse.

Lepidomeda is virtually devoid of conspicuous dermal sense organs. *Meda* has these organs slightly developed on the head, but not noticeably on the body. *Plagopterus,* most extreme in this character also, has the intermandibular region spongy with large, thick-set papillae, and has conspicuous, though short, raised longitudinal dermal ridges on the anterodorsal part of the body.

In conclusion, the Plagopterini are regarded as modified members of the Leuciscinae. Among the three constituent genera, *Lepidomeda* definitely seems to be the most generalized, and *Plagopterus* seems to be the most highly modified, except, perhaps, in squamation. The body form, high development of sense organs, and plain coloration of *Plagopterus* seem to be related to its life in swift, silty waters.

It is obvious that in the evolution of spinelike rays the Plagopterini have taken a course quite independent of that followed by the Old World spiny-rayed cyprinids, such as *Cyprinus* and *Barbus.*

DISTRIBUTIONAL RELATIONS

The singular group Plagopterini constitutes one of the main elements in the highly endemic fauna of the Colorado River system (Miller, 1946; 1959). It is confined, so far as known (Fig. 1), to the lower and middle parts of this drainage, including the remnants of a Pleistocene tributary system, comprising the Pluvial White and Carpenter rivers of southeastern Nevada (Hubbs and Miller, 1948: 96–100). Within this section of the Colorado River system the members of the group exhibit a rather astonishing degree of endemism.

Meda is confined to the clear and more permanently flowing creeks of the Gila River system in Arizona and New Mexico. For this reason, and because of the deterioration of stream flow in Arizona, the range of the species is becoming further reduced.

Plagopterus is seemingly now restricted to the Virgin River system in Utah, Arizona, and Nevada (Miller, 1952: 36), where it lives in the rather swift currents of generally silty streams. Until shortly before the turn of the century, prior to the time when the streams became disastrously reduced as the result of drought, erosion, water storage, and stream diversion, it also inhabited the lower Gila River system, from Tempe, where it lived with *Meda,* to the mouth of the Gila at Yuma (Gilbert and Scofield, 1898: 496; Snyder, 1915: 584).

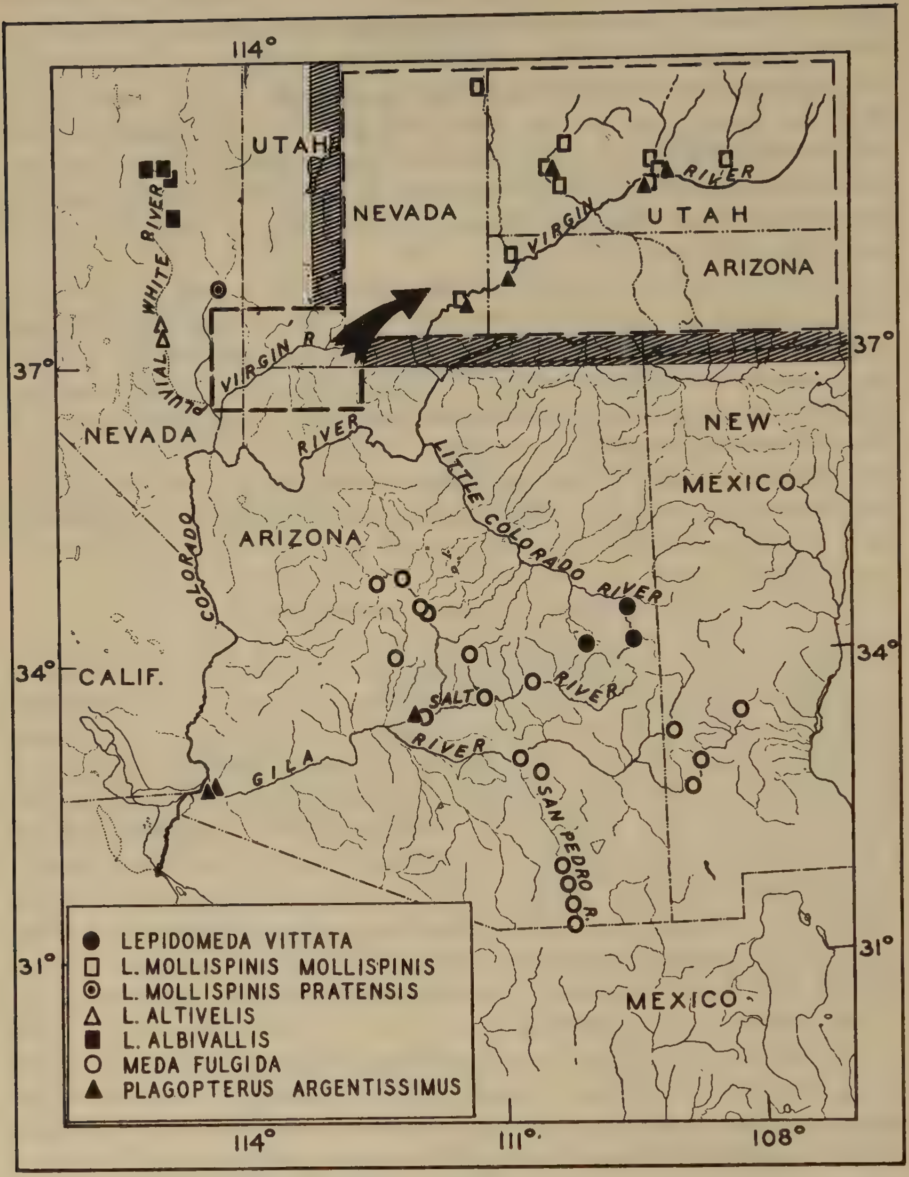
114°
UTAH
NEVADA
UTAH
ARIZONA
VIRGIN
RIVER
WHITE RIVER
PLUVIAL
VIRGIN R
37°
37°
NEVADA
RIVER
NEW MEXICO
ARIZONA
LITTLE COLORADO RIVER
COLORADO
34°
34°
CALIF.
SALT
RIVER
GILA RIVER
SAN PEDRO R.
31°
31°
MEXICO
● LEPIDOMEDA VITTATA
□ L. MOLLISPINIS MOLLISPINIS
⊙ L. MOLLISPINIS PRATENSIS
△ L. ALTIVELIS
■ L. ALBIVALLIS
○ MEDA FULGIDA
▲ PLAGOPTERUS ARGENTISSIMUS
114°
111°
108°

Fig. 1. Record stations showing the distribution of the plagopterin fishes.

Lepidomeda is largely confined to the more or less isolated remnants of the once abundant Pluvial drainage of the middle section of the Colorado River. It is known (1) from the isolated spring waters of the Pluvial White River system, Nevada, where, except for its preference for cool instead of warm waters, its distribution parallels that of *Crenichthys baileyi* (Hubbs and Miller, 1948: 96); (2) from a single spring marsh adjacent to Meadow Valley Wash (Pluvial Carpenter River), Nevada; (3) from the Virgin River and its tributary creeks, in the adjoining parts of Utah, Nevada, and Arizona; and (4) from the upper parts of the Little Colorado River system in east-central Arizona.

Presumably erroneous records for *Plagopterus* and *Lepidomeda* are discussed on pages 34–35 and 30, respectively.

The ranges of the seven forms of the Plagopterini are so limited, and the stream deterioration of the West has been so great, as to put the forms into the category of threatened species. We have just determined, through collecting in 1959 designed to test the point, that the two forms of most restricted range, namely *Lepidomeda mollispinis pratensis* of Big Spring near Panaca, and *Lepidomeda altivelis* of Ash Spring in Pahranagat Valley, both in Nevada, have already been exterminated.

SPECIATION

In line with the facts already presented, we postulate that the Plagopterini were derived in what now constitutes the Colorado River system from a species of *Gila* or from a similar, relatively unspecialized cyprinid genus; that *Lepidomeda* represents the ancestral type of the tribe; and that the more specialized genera, *Meda* and *Plagopterus*, arose from *Lepidomeda* in the same river system.

The origin of the group may have been fairly old, almost certainly as early as the Pliocene period. It is now believed by geologists that the Colorado system dates from a period that old, though the precise stream courses have changed (Repenning and Lance, paper in preparation). We have identified, from the Pliocene Bidahochi formation of northern Arizona, three species that seem referable to genera currently living in the Colorado River system (two to *Gila* and one to *Ptychocheilus*), and these extinct species appear to have been similar to the species of these genera now inhabiting this river system. The high specialization of *Meda* and *Plagopterus* strongly indicates a Tertiary origin for these genera, or for their common ancestor.

The distributional relationships suggest that *Meda* may have been isolated in the Gila River when, and if, the fauna of that stream was geographically separated from that of the main Colorado (Hubbs and Miller, 1948: 94–95). *Meda* has apparently found the big, swift, turbid Colorado River a barrier. In recent years the desiccation of the lower reaches of the Gila and the abundance of introduced predatory fishes in the Colorado have no doubt combined to restrict *Meda* to the Gila system, and to eliminate *Plagopterus* from this basin (Miller, in press).

The highly localized ranges of the five recognizable forms of *Lepidomeda* also indicate limited ecological tolerance, as well as a much more extensive distribution at some past time, presumably Pluvial. The occurrence of perhaps the most distinct species of the genus above the falls of the Little Colorado River suggests considerable antiquity for the period of more extensive and more continuous distribution.

The restriction of the four other forms of the genus to the Virgin River branch of the Colorado River and to the Pluvial tributaries of the Virgin River (Fig. 1) is rather difficult to explain, since the Virgin River has maintained its connection with the Colorado River. Lake Mead, which now floods the lower reaches of the Virgin River, presumably presents a distributional block, and the main river in previous years may have been an equally effective barrier. But at some earlier time the river did not present an insuperable barrier, because the genus occurs on both sides of this river in the region of Grand Canyon.

Within the remnants of the Pluvial Virgin River system, *Lepidomeda* has managed to persist widely in favorable situations. This illustrates two of the zoogeographical and speciational phenomena that are so beautifully exemplified through the arid American West (Hubbs and Miller, 1948), namely, (1) the indications of former, presumably Pluvial, periods of much greater and more continuous distribution—indications provided by chains of now isolated remnant populations of one form or of one series of closely related forms, and (2) the high incidence of differentiation among these isolated forms.

The two main populations of *Lepidomeda* in the Pluvial Virgin River are now well separated by the excessively arid lower parts of the Pluvial White River, and these two populations are now well differentiated. Each, however, is of rather general occurrence in a still more or less integrated stream complex—*L. albivallis* in the rather well-watered present White River Valley in southeastern Nevada, and *L. m. mollispinis* in the presently still largely intact Virgin River system. Within each area the several spring and creek populations remain reasonably consistent in characters, presumably as a result of some interflow of genes and because the habitats in each area are rather similar.

The two other populations which we encountered in our rather extensive field work throughout the area, but which we have just found to have become extinct, were confined to single spring areas. They were differentiated from one another and from the distinctive forms of the White River and the Virgin River. The more strikingly differentiated of the two isolated spring forms was *L. altivelis,* which appears to have been almost wholly confined to the cooled outflow stream fed by the warm waters of Ash Spring, in Pahranagat Valley, Nevada, along the course of Pluvial White River. A few yearlings were also taken in the dirty olive-green, alkaline water of Upper Pahranagat Lake, but the lake population was presumably derived by flood transport from Ash Spring above. Oddly, *Lepidomeda* has not occurred during the period of our explorations in the two other major springs of Pahranagat Valley (Crystal and Hiko) nor in the other springs or lakes that were examined in this valley.

The other isolated form of *Lepidomeda* that we found (on July 10, 1938), namely *L. mollispinis pratensis,* was represented by an extremely meager population in a tiny stream flow in the marsh of Big Spring, along Meadow Valley Wash, near Panaca, Nevada. Assiduous collecting in the most favorable habitats yielded only the seven type specimens. How a local form persisted on such a slender thread until a few years ago is a mystery. This spring is in the drainage of Pluvial Carpenter River (Hubbs and Miller, 1948: 98–100), which joined Pluvial White River along the course of the present Moapa River, about 20 miles above its confluence with the Virgin River. None of the other springs or stream flows in the Meadow Valley Wash or its tributary Clover Valley (both in the basin of Pluvial Carpenter River), nor in Moapa Valley, have yielded *Lepidomeda.*

It is tempting to attribute the differentiation of the four forms of *Lepidomeda* other than *L. vittata* to the interval of about 11,000 years since the end of the Pluvial period. This seems to be a probable, but by no means necessary, conclusion. The present distributional pattern may have resulted from the differential survival in the several localities of forms that had already become differentiated, probably with ecological segregation, within Pluvially integrated waters. We have repeatedly found such ecotypic segregates in western waters. One example, within the general area under discussion, is furnished by two forms of the mountain suckers (*Pantosteus*), of which one, of pool-and-riffle creek type, occurs in the small tributaries of the Virgin River and the other occupies the very swift water of this river where it rushes through the defile in the Beaver Dam Mountains.

ANALYTICAL KEY TO THE PLAGOPTERINI

(Constituting differential diagnoses)

- 1a.—*Lepidomeda*
  - 2a.
    - 3a.
      - 4a.—*L. mollispinis*
        - 5a.—*L. m. mollispinis* (1a)
        - 5b.—*L. m. pratensis* (1b)
      - 4b.—*L. albivallis* (2)
    - 3b.—*L. altivelis* (3)
  - 2b.—*L. vittata* (4)
- 1b.
  - 6a.—*Meda fulgida* (5)
  - 6b.—*Plagopterus argentissimus* (6)

1.

a. *Body* completely covered with scales (except in some species, where covered by the depressed paired fins). Second *dorsal spine* much stronger and longer than first, varying from weak to strong; neither spine pungent (Pl. III). Spiny (lower) demitrichs of branched *pelvic rays* without pungent tips, ending in slender, soft, articulated continuations, extending to margin of fin. Segments of *pectoral rays* in mature males little dilated; those on front margin of ventral demitrichs smooth-edged. *Head and belly* rounded; head about, or more than, two-thirds as deep as long. *Vertebrae* usually 41 to 43—(*Lepidomeda.*) 2

b. *Body* scaleless (except, perhaps, for unsculptured platelets along lateral line near head and, in *Plagopterus*, at base of dermal ridgelets on anterodorsal part of body). First *dorsal spine* much stronger than second and almost as long, always much enlarged, solidified, and strongly pungent (Pl. III). Spiny (lower) demitrichs of branched *pelvic rays* without soft continuations, the pungent tips definitely short of fin margin. Segments of *pectoral rays* in mature males greatly dilated; those on front margin of ventral demitrichs finely denticulate. *Head and belly* flattened; head much less than two-thirds as deep as long. *Vertebrae* usually 40.—(*Meda* and *Plagopterus.*)............ 6

2. (1a).

a. *Anal rays* 9 (not infrequently 8 in *L. albivallis*). Teeth in main row 5–4 (rarely 4–4). *Scales* fewer than 90 (except in *L. altivelis*). *Vertebrae* 42 to 44 3

b. *Anal rays* 8 (rarely 9). *Teeth* in main row 4–4. *Scales* usually more than 90. *Vertebrae* typically 41 or 42 (rarely 43). ADDITIONAL CHARACTERS.—*Mouth* moderately oblique, about as in *L. albivallis*. Second *dorsal spine* about as strong as in *L. altivelis. Dorsal fin* moderately high (depressed length 2.05 to 2.3 in predorsal length) and moderately sharp. *Head* broad (its width 1.45 to 1.65 in its length). *Pigment* on opercles, shoulder girdle, and chin variable. Headwaters of Little Colorado River system, Arizona .... (4) *L. vittata*

3. (2a).

a. *Mouth* less oblique (a line from uppermost tip of premaxillary to middle of caudal peduncle passes below middle of pupil). *Snout* more rounded. *Dorsal spines* variably weaker. *Dorsal fin* low to moderate (depressed length 2.2 to 2.4 in predorsal length, except in *L. m. pratensis*), and varyingly less pointed. *Head* broader (width 1.5 to 1.85 in its length). *Pigment* on shoulder girdle extending variably forward beyond scapular bar.—(*L. mollispinis* and *L. albivallis.*) 4

b. *Mouth* more oblique (a line from uppermost tip of premaxillary to middle of caudal peduncle passes above middle of pupil). *Snout* sharper. *Dorsal spines* stronger. *Dorsal fin* higher (depressed length 1.8 to 2.1 in predorsal length), and more sharply pointed than in any other form. *Head* more compressed (width 1.9 to 2.0 in its length). Almost no *pigment* on shoulder girdle in advance of scapular bar. ADDITIONAL CHARACTERS.—*Pigment* on opercles about as in *L. mollispinis*; a band of coarse pigment crossing chin behind upper lip. *Pelvic-fin length* 1.4 to 1.5 in head. *Upper-jaw length* 1.15 to 1.3 in postorbital. (Formerly) cooled, swift outflow from Ash Spring and Upper Pahranagat Lake, Pahranagat Valley, Nevada (in course of Pluvial White River) .... (3) *L. altivelis*

4. (3a).

a. *Melanophores* confined to upper half of opercle and to upper part of upper limb of preopercle; lower half of outer face of shoulder girdle in adults lacking pigment in front of vertical from pectoral insertion. *Size* smaller (only rarely more than 80 mm. in standard length) and *colors* less bright. *Dorsal spines* weaker. *Pharyngeal arch and teeth* (Fig. 2) much smaller and more delicate (in an average adult about 0.10 per cent weight of fish); the whole arch flatter (more compressed dorsoventrally); anterior angle usually sharp and conspicuous; edge of dorsal surface medially and on anterior limb usually rather sharply ridged (the pharyngeal arch and tooth distinctions are not sharp in the localized form *L. m. pratensis,* of which no large adults are known). Virgin River system in Utah, Nevada, and Arizona, and (formerly) Big Spring in Meadow Valley, Nevada.—(*L. mollispinis*) 5

b. *Melanophores* typically extending across opercle and subopercle, and to angle of preopercle; lower half of outer face of shoulder girdle in adults with considerable pigment in front of vertical from pectoral insertion. *Size* larger (commonly 80–90 mm., largest 103 mm. in standard length) and *colors* particularly bright. *Dorsal spines* stronger. *Pharyngeal arch and teeth* (Fig. 2) much more massive (in an average adult about 0.25 per cent weight of fish); the whole arch thicker (less flattened dorsoventrally); anterior angle usually less conspicuous, more evenly rounded; edge of dorsal surface usually broadly rounded. ADDITIONAL CHARACTERS.—*Pelvic-fin length* 1.4 to 1.8 in head length. *Upper-jaw length* 1.1 to 1.5 in postorbital. Springs and spring-fed creeks in Recent White River Valley (upper headwaters of Pluvial White River system), Nevada .... (2) *L. albivallis*

5. (4a).
   a. *Dorsal fin* lower and more rounded (its depressed length 1.45 to 1.65 in distance from dorsal origin to occiput); when the fin is erected at about 45° the outer edge in the adult usually slopes downward and backward. *Pelvic fin* shorter (length 1.5 to 1.85, usually 1.65 to 1.8, in head length). *Mouth* smaller (upper-jaw length 1.4 to 1.8, usually 1.45 to 1.6, in postorbital), and less oblique (a line from uppermost tip of premaxillary to middle of caudal peduncle passes below pupil). Virgin River system in Utah, Nevada, and Arizona............... .... (1a) *L. m. mollispinis*
   b. *Dorsal fin* higher and more pointed (its depressed length 1.2 to 1.45 in distance from dorsal origin to occiput); when the fin is erected at about 45° the outer edge in the adult is usually about vertical. *Pelvic fin* longer (length 1.35 to 1.6, usually about 1.5, in head length). *Mouth* larger (upper-jaw length 1.25 to 1.4 in postorbital), and more oblique (a line from uppermost tip of premaxillary to middle of caudal peduncle passes through lower part of pupil). (Formerly) outflow of Big Spring, in meadow adjacent to Meadow Valley Wash, in course of Pluvial Carpenter River, Nevada .. (1b) *L. m. pratensis*
6. (1b).
   a. No developed *barbel* (there may be a slight dermal swelling at end of upper lip or at lower posterior corner of maxillary). *Intermandibular region* scarcely papillose. No *dermal ridgelets* on body. Principal *dorsal rays* 7 (rarely 8); *anal rays* usually 9. *Teeth* in main row 4–4 (rarely 5–4). *Mouth* moderately oblique. *Breast region* less flattened. Gila River system, Arizona and New Mexico.—(Genus *Meda*) .... (5) *Meda fulgida*
   b. A well-developed *barbel* pendant from end of upper lip. *Intermandibular region* spongy with coarse, close-set papillae. *Dermal* longitudinal *ridgelets* (overlying minute platelets) on anterodorsal part of

body. Principal *dorsal rays* 8 or 9; *anal rays* usually 10. *Teeth* in main row usually 5–4 (rarely 4–4). *Mouth* nearly horizontal. *Breast region,* including pectoral fins, more flattened. Virgin River system, Utah, Nevada, and Arizona, and (formerly) lower Gila River system, Arizona.– (Genus *Plagopterus.*) ...... (6) *Plagopterus argentissimus*

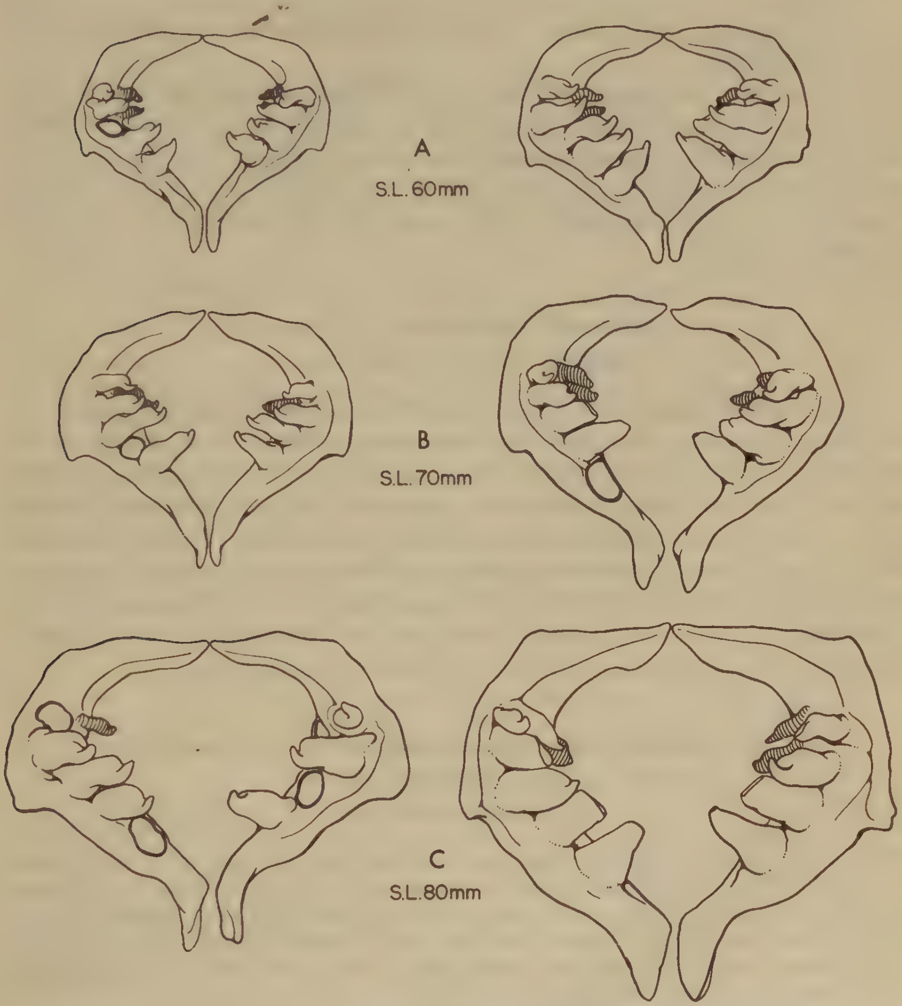

FIG. 2. Pharyngeal arches and teeth of *Lepidomeda m. mollispinis* (left column) and *Lepidomeda albivallis* (right column) at comparable sizes. A, *L. m. mollispinis,* UMMZ 162849; *L. albivallis,* UMMZ 132180. B, *L. m. mollispinis,* UMMZ 162849; *L. albivallis,* UMMZ 124980. C, *L. m. mollispinis,* UMMZ 141674; *L. albivallis,* UMMZ 124980.

GENUS *Lepidomeda* Cope

Lepidomeda.—Cope, 1874: 131 (original description; classification). Cope and Yarrow, 1875: 642 (diagnosis repeated). Jordan and Gilbert, 1883: 148, 251 (comparisons; description). Jordan and Evermann, 1896a: 204, 328 (comparisons; description; key to species). Eddy, 1957: 104 (comparison). Moore, 1957: 94, 138 (characters and comparisons).

TYPE SPECIES.—*Lepidomeda vittata* Cope (designated by Jordan and Gilbert, 1883: 251).

Rubric 1a of the analytical key is the differential diagnosis of this plagopterin genus. Additional characters are the biserial pharyngeal teeth, silvery peritoneum (overlain by sparse to numerous brown puncticulations), moderate intestine with one large S-loop, and no barbel. The four species (five forms) are distinguished in the same key. The range of the genus is outlined on page 11.

Lepidomeda mollispinis, new species

Middle Colorado Spinedace

DIAGNOSIS.—A species of *Lepidomeda* distinguished by having 5–4 teeth in the main row, a relatively weak and soft-tipped (second) dorsal spine, 9 anal rays, typically fewer than 90 lateral-line scales, the depressed length of the dorsal fin less than the head length, the sides of the body mostly silvery, and with melanophores confined to upper half of opercle and to upper part of ascending limb of preopercle (see rubrics 1a, 2a, 3a, and 4a of the analytical key, pp. 14–15). The synonymy and type designation are given below under the heading of the nominate subspecies. An additional subspecies of restricted range, *L. m. pratensis,* is recognized.

Lepidomeda mollispinis mollispinis, new subspecies

(Pl. I, A; Pl. III, B)

Virgin River Spinedace

Lepidomeda vittata (misidentification; not of Cope, 1874).—Tanner, 1932: 135 (Santa Clara Creek, at Veyo, Washington Co., and other localities in the Virgin River drainage, Utah); 1936: 171 (in part; record for Santa Clara Creek only). Wallis, 1951: 87 (from bait tank, Boulder Beach dock, Lake Mead, Nevada; stock originally obtained in Santa Clara Creek, near St. George, Utah). Eddy, 1957: 104, fig. 261 (in part; "Utah" and, in part, "Nevada").

Lepidomeda species.—Miller, 1952: 18, 35, fig. 21 (distribution; habitat; characters in key; use as bait fish). Moore, 1957: 138 (in part; mention of evidently undescribed species in Nevada and Utah related to *L. vittata*).

DIAGNOSIS.—This subspecies is most closely related to *L. m. pratensis,* from which it differs in having the dorsal fin less elevated and more rounded, the pelvic fins shorter, and the mouth smaller and less oblique (see rubric 5a of key).

Types.—The holotype, UMMZ 141673, an adult 88 mm. long, was seined by C. L., L. C., and E. L. Hubbs from Santa Clara River, 3 mi. SE of Shivwitz and 4.5 mi. NW of Santa Clara, Washington Co., Utah, on July 29, 1942. Secured with the holotype were 103 paratopotypes, 23–80 mm. long, UMMZ 141674. An additional 604 specimens were examined from localities in Arizona, Nevada, and Utah as follows: Arizona: UMMZ 141662 (381, 22–77 mm.), Beaver Dam Cr. at U. S. 91 crossing near Littlefield, Coconino Co., July 28, 1942. Nevada: UMMZ 105496 (68, 36–78 mm.), Virgin R., Clark Co. (near Utah border), Sept., 1938; UMMZ 125013 (12, 39–65 mm.), Virgin R. W of Bunkerville, Clark Co., Aug. 31, 1938. Utah (Washington Co.): UMMZ 85955 (2, 48–54 mm.), Santa Clara R., June, 1928; UMMZ 124764 (17, 20–62 mm.), trib. Virgin R. near La Verkin, July 3, 1938; UMMZ 124772 (38, 22–71 mm.), Virgin R. at mouth of La Verkin and Ash creeks, July 3, 1938; UMMZ 162849 (86, 22–74 mm.), Santa Clara R., 2.5 mi. below Gunlock, June 17, 1950. See inset, Fig. 1.

Characters.—Body form and coloration are indicated on Plate I, A. Principal dorsal rays 8 (in 46 specimens); anal rays, 8 (4), 9 (41), 10 (1); pelvics 7–7 (36), 6–7 (1). The dental formula is typically 2, 5–4, 2, varying as follows: 2, 5–4, 2 (19), 2, 4–5, 2 (1), 2, 4-4, 2 (3), and 3, 5–4, 2 (1). Lateral-line scales about 77 to 91, varying as follows: 77 (1), 81 (1), 82 (2), 83 (4), 84 (1), 85 (4), 86 (2), 87 (2), 88 (3), 91 (1). Vertebrae 42 to 44 (Table 1).

TABLE 1
Vertebral Variation in the Plagopterini

Species	Number of vertebrae						No.	Ave.
	39	40	41	42	43	44		
Lepidomeda m. mollispinis	..	..	..	15	12	6	33	42.73
Lepidomeda m. pratensis	..	..	..	1	3	..	4	42.75
Lepidomeda albivallis	..	..	..	1	25	5	31	43.13
Lepidomeda altivelis	..	..	..	3	10	3	16	43.00
Lepidomeda vittata	..	..	10	9	1	..	20	41.55
Meda fulgida	2	20	8	1	..	..	31	40.26
Plagopterus argentissimus	4	19	9	..	..	..	32	40.16

Life colors were noted in the field as follows: body silvery, with a more or less brassy sheen and with sooty specklings on sides; axils of paired fins and basal band on anal fin orange-red to translucent orange-pink; a little spot of golden red at upper end of gill-slit. Younger fish look whitish in the water and some adults have the sides blackish, especially conspicuous in the water.

The nuptial tubercles, best developed on males in a collection of June 17, but evident also in July specimens, are distinctive. Those on the head are almost wholly confined to the dorsal surface, extending onto the sides only in a definite patch across the upper part of the opercle. They are irregularly scattered over the dorsal surface, from near the occipital edge forward to the upper part of the snout and outward to the orbital margins. They are of moderate size, and their spiny tips are weakly curved forward. Tubercles occur on the scales over the entire body, but become obsolescent on the midsides and belly. Those near the margin of the head, between the lateral lines, are considerably strengthened. Here the partly fused tubercles form a single straightish transverse (or vertical) series, with the points essentially erect. On the caudal peduncle the points are smaller and form a more curved series on each scale. On the breast the tubercles are somewhat strengthened, and usually single on each scale. The scales in a band just behind the shoulder girdle, above the pectoral fin, have the soft tissue considerably swollen, and are weakly tuberculate. On the first pectoral ray there is a single file of tubercles, and on the outer part of several succeeding rays a file branched once near the base. Each tubercle has one to several weakly antrorse spiny points. Weak tubercles line pelvic and anal rays. Despite our large collections none of the other species seems to be represented by nuptial males.

This subspecies often attains a total length of nearly four inches. The largest specimen we have seen is the holotype, about 4.25 inches long (88 mm. in standard length). It is the only specimen among 718 that is longer than 80 mm.

HABITAT.—This subspecies is common in the Virgin River and its tributaries in Utah, Arizona, and Nevada (Fig. 1), in moderate to swift current, chiefly in pools. Where the collections were made the bottom was usually sand and gravel, often with stones and occasionally with boulders and some mud. Green algae and sparse pondweed were often associated, and depth of capture varied from 1 to 3 feet. The water was either clear or, as in the Virgin River, very milky; with bottom visibility from about 3 inches to 3 feet.

ASSOCIATES.—Fish species taken with *L. m. mollispinis* include *Pantosteus delphinus utahensis* (Tanner), *Catostomus latipinnis* Baird and Girard, *Rhinichthys osculus* (Girard), and *Plagopterus argentissimus* Cope. *Micropterus salmoides* (Lacépède) was caught at the type locality.

ETYMOLOGY.—The name *mollispinis* is derived from the Latin *mollis,* soft, and *spina,* spine, in reference to the relatively weak and soft-tipped main (second) dorsal spine.

Lepidomeda mollispinis pratensis, new subspecies

(Pl. I, B; Pl. III, C)

Big Spring Spinedace

DIAGNOSIS.—Like *L. m. mollispinis,* but differing in the higher and more pointed dorsal fin, the longer pelvic fins, and the smaller and more oblique mouth (see rubric 5b of key).

TYPES.—The holotype, UMMZ 124799, an adult 55 mm. long, was seined by C. L. Hubbs and family, R. R. Miller, and A. J. Calhoun from Big Spring, about 1 mile NE of Panaca, Lincoln County, Nevada, on July 10, 1938. Taken with this specimen were six paratopotypes, 48 to 56 mm. long, UMMZ 136097.

CHARACTERS.—Plate I, B, shows the general appearance of this localized and now extinct subspecies. Principal dorsal rays 8, anal rays 9, pelvics 7–7 (6), 6–7 (1). The teeth number 2, 5–4, 2 in 3, and the lateral-line scales vary from 82 to 90 (about 89 in the holotype). Vertebrae number 42 or 43 (only 4 specimens countable; Table 1).

In life *L. m pratensis* was bright silvery. Some specimens were lemon to orange in the axils of the paired fins, on the basal part of the anal fin, near the upper edge of the shoulder girdle, on the vertical arm of the preopercle, and above the mouth.

DISTRIBUTION, LOCALIZATION, AND EXTINCTION.—Our field explorations have indicated that this fish has very recently become extinct in the one spring-fed marsh in which the last few individuals persisted until 1938, or a few years later. This marsh is fed chiefly from a single source, Big Spring, which issues from the base of low hills about 1 mile northeast of Panaca, Lincoln County, Nevada. The meadow occupies a basin off the east side of Meadow Valley Wash, which here dissects the remnants of a lacustrine fill. Meadow Valley Wash follows the ancient course of Pluvial Carpenter River, which was the main, eastern affluent of Pluvial White River (Hubbs and Miller, 1948: 96–100) (Fig. 1).

Prior to recent agricultural modifications Big Spring discharged onto and spread over the large wet meadow, and doubtless provided a more favorable fish habitat than presently exists. The natural overflow course can still be followed for about a mile across the meadow. Between 1938, when the seven types of *Lepidomeda mollispinis pratensis* were collected, and 1959, when the subspecies was found to have become extinct, the source was dammed and a contoured ditch was constructed to divert the spring effluent to the upper part of the meadow. In 1938 the outflow followed the natural channel until it spread out. The channel was generally 1 to 3 feet wide and as deep as 2 feet. It contained watercress (*Nasturtium*) above, pondweeds of the *Potamogeton pectinatus* and floating types, and rushes, below. The bottom was of firm to soft clay, with some gravel. The current was slight over most of the course, but occasionally swift. The water was clear, but easily roiled. On July 10, with the air at 94°F., the water temperature was 84°. Here, in 1938, in the stream within the meadow area, we seined, by prolonged effort, along with the seven types of *Lepidomeda mollispinis pratensis,* 31 half-grown mountain suckers, *Pantosteus* sp., and 312 young to adult speckled dace, *Rhinichthys osculus* (Girard), both representing local forms characteristic of the remnants of Pluvial Carpenter River.

By 1959 the generally abandoned natural channel had become very largely clogged with silt and a variety of submerged and emergent plants, chiefly chara, *Nasturtium, Decodon,* a broad-leafed *Potamogeton,* green and blue-green algae, and *Scirpus.* Except for about a half-dozen stretches of 10 to 20 feet the stream was almost completely choked and partially dammed, with silt and weeds filling the stream bed from the original more or less gravelly bottom to the surface. The water was rather clear but very readily roiled. The flow, of seepage origin, was slight; in most places, barely perceptible. On July 4, 1959, when the air was 84.5°F., the water temperature varied from 75° to 81°. In the open-water stretches, where the width averaged 3 to 4 feet, intensive and thorough seining, following removal by hand of the excess of water weeds and muck, yielded only one of the three native species that held out here 21 years previously. This was the *Rhinichthys,* which had not only survived but had even become concentrated—to confirm the ubiquity and adaptability of this dace. In addition we found, in considerable density, a large population of the western mosquitofish, *Gambusia affinis affinis* (Baird and Girard), a scourge of native fishes. Another introduction, the bullfrog, *Rana catesbeiana* Shaw, now also abounded, greatly outnumbering the native *Rana pipiens* Schreber.

The diversion of water, with, no doubt, the occasional stoppage of flow in the ditch (which, furthermore, originates above the former habitat of the native fishes), presumably led to the rapid and catastrophic deterioriation of the original habitat and to the decline in the population of the two more susceptible native fishes, the *Pantosteus* and the *Lepidomeda.* The introduced species almost certainly contributed to the extirpation of the *Pantosteus* and to the extermination of the *Lepidomeda.*

The flow of the Spring is almost surely less than it was formerly. According to Angel (1881: 491), writing of Panaca: "The water supply is abundant, being taken from Warm Spring, which is about one and one-half miles east of the town. A large stream of water, about three feet deep and six feet wide, is thrown out from the spring, and the quantity is not affected by the seasons. This is the principal source of water supply for the whole valley."

Our field studies in 1938 and 1959 indicated, with an approach to certainty, that no populations of *Lepidomeda* have persisted in any other remnants of Pluvial Carpenter River. In July, 1938, about two miles below Panaca, the flow of Meadow Valley Wash was found to contain only a fishless trickle of slightly alkaline seepage from the irrigated fields above. Just above the box canyon, above the section of Meadow Valley in which Caliente lies (about 14 miles southwest of Panaca), enough water issued from springs to restore a stream that averaged eight feet wide, continuing as a surface flow through Rainbow Canyon below Caliente. We fished in this canyon on the same day as at Big Spring, but caught no specimens of *Lepidomeda*; in the lowermost, permanent section of Meadow Valley Wash (13 miles by road above Moapa) we took only *Pantosteus* and *Rhinichthys* in a thorough collection on July 13, 1938. On March 1, 1938, the wash had been subjected to a very severe flood, which may have had a marked effect on the fish fauna.

Absence of *Lepidomeda* was also indicated by our 1938 collections along the former upper course of Pluvial Carpenter River and in Lake or Duck Valley, which may have discharged into this Pluvial stream. Collections from the old stream course were made (1) between Camp Valley and Eagle Valley in the headwaters of the creek of Camp Valley Wash, about 25 miles due northeast of Pioche, (2) in adjacent springs, and (3) in the canyon between Spring Valley and Eagle Valley, about 21 miles northeast of Pioche. Furthermore, thorough collections made in 1950 and 1959 in Clover Creek, the main eastern tributary of Meadow Valley Wash, at two points in Nevada, contained no *Lepidomeda*, and no fish of any kind were visible in the deeply entrenched stream in the northern outskirts of Caliente.

ETYMOLOGY.—The name *pratensis* is derived from the Latin, meaning pertaining to or growing in a meadow, in reference to the extensive meadowland about Big Spring.

NOTE ON SUBSPECIFIC STATUS.—This localized form is accorded subspecific status on the assumption that it was not completely differentiated from the form here named *Lepidomeda mollispinis mollispinis.*

Lepidomeda albivallis, new species

(Pl. I, C; Pl. III, E)

White River Spinedace

Lepidomeda species.—Sumner and Lanham, 1942: 319 (Preston Spring). Miller, 1952: 19, 35, fig. 22 (distribution, habitat, characters in key; use as bait fish). Moore, 1957: 138 (in part; mention of undescribed species in Nevada related to *L. vittata*).

Lepidomeda vittata (misidentification, not of Cope).—La Rivers and Trelease, 1952: 118 (in part; White River). La Rivers, 1952: 97 (in part; White River). Eddy, 1957: 104 ("White River" in vernacular name only).

DIAGNOSIS.—A species of *Lepidomeda* distinguished from others in having 5–4 teeth in the main row, lateral-line scales typically fewer than 90, mouth moderately oblique, dorsal fin of moderate height, melanophores extending well below level of lateral line, and in other details of pigmentation (see key, rubrics 1a, 2a, 3a, and 4b).

TYPES.—The holotype, UMMZ 173781, an adult 69.5 mm. long, was collected by C. L. Hubbs and family from White River, just below the mouth of Ellison Creek, about 5 miles NW of Preston, along the Tonopah–Ely highway (T. 13 N, R. 61 E), White Pine County, Nevada, on September 10, 1934. The 428 paratopotypes, UMMZ 132180 (16–98 mm.), were taken with the holotype. An additional 579 specimens were secured as follows: White Pine Co.: UMMZ 124980 (61, 37–103 mm.), from Preston Big Spring, 2 mi. NW of Preston, Aug. 26, 1938; UMMZ 124984 (17, 17–88 mm.), from Lund Spring at Lund, Sept. 15, 1938; UMMZ 124973 (14, 39–90 mm.), from Nicholas Spring in Preston, Aug. 26, 1938; UMMZ 124977 (371, 24–83 mm.), outflow of Preston Big Spring and Nicholas Spring, Preston, Aug. 26, 1938; UMMZ 138331 (5, 73–93 mm.), from spring near Preston, Sept. 28, 1941 (U. N. Lanham, coll.). Nye Co.: UMMZ 124990 (111, 12–96 mm.), from springs at Hendrix Ranch (southern ranch of Sunnyside group), Aug. 27, 1938.

CHARACTERS.—Pigmentation and general body form are portrayed in Plate I, C. Principal dorsal rays 7 (4), 8 (97); anal rays 8 (24); 9 (75), 10 (2); pelvic rays 7–7 (82), 7–6 (1), 6–7 (5), 7–4 (1). The dental formula is typically 2, 5–4, 2, varying as follows: 2, 5–4, 2 (20), 2, 5–5, 2 (1). Lateral-line scales number about 79 to 92: 79 (1), 80 (1), 82 (5), 83 (3), 84 (2), 85 (5), 86 (3), 87 (2), 88 (1), 89 (2), 90 (3), 92 (2). The vertebrae range from 42 to 44 (Table 1).

This appears to be the most brightly colored of the four species of *Lepidomeda*. Life colors of postnuptial males were noted at the time of collection as follows: The body is bright brassy green to olive above, brassy over bright silvery on sides, and silvery white below, splashed with sooty on the sides. Dorsal and caudal fins pale olive-brown to pinkish brown, with the rays often deep-olive and with the rather clear interradial membranes faintly flushed with rosy color; pectorals yellowish with orange-red axils; anal and pelvic fins bright orange-red, in the young only toward the base anteriorly, but in adults over most of these fins, which otherwise are whitish. Lower edge of caudal peduncle with a speckled diffusion of orange-red in adults. Some coppery-red to red on side of face, at upper end of gill opening, on preorbital just behind mouth, and along upper arm of preopercle. Cheeks and opercles with rather strong gilt reflections; the gular membranes watery yellow. Lateral line more strongly gilt than adjacent parts of body. In females the coloration is similar but less intense.

Remnants of tubercles on postnuptial males collected on August 27 indicate that this pattern in the species is similar to that of *L. m. mollispinis*.

This is the largest species of *Lepidomeda*, commonly attaining a total length over 4 inches; the largest specimen (UMMZ 124980) is nearly 5 inches long (103 mm. S. L.).

HABITAT.—This species occurs in cool springs (65–71°F.), their outflows, and in White River, in the upper part of the ancient White River system of eastern Nevada (Fig. 1). In all the spring habitats the water was clear in the source pools, which varied from about 15 by 25 feet to 60 by 80 feet in major dimensions. The bottom was mostly gravel and sand, with some mud; the fish were generally captured in water not over 2 feet deep (up to 5 feet in Lund Spring); watercress, a fine-leafed *Potamogeton*, and rushes were the common aquatic plants, often dense. The current in the spring-fed ditches and in White River was swift to moderate.

ASSOCIATES.—The following species were associated with *Lepidomeda albivallis*: *Pantosteus intermedius* (Tanner), *Rhinichthys osculus* (Girard), and *Crenichthys baileyi* (Gilbert). *Salmo gairdneri* (Richardson), *S. trutta* Linnaeus, *Salvelinus fontinalis* (Mitchill), and *Archoplites interruptus* (Girard) have been planted in the same waters, and centrarchids, likely bluegill, *Lepomis macrochirus* Rafinesque, and largemouth bass, *Micropterus salmoides*, have been stocked in a reservoir in White River Valley at Sunnyside, according to information received from Ted Frantz.

ETYMOLOGY.—The name *albivallis* is from the Latin *albus*, white, and *vallis*, valley, in reference to the restriction of the new species to the White River Valley, in White Pine and Nye counties, Nevada.

Lepidomeda altivelis, new species

(Pl. I, D; Pl. III, D)

Pahranagat Spinedace

Lepidomeda vittata (misidentification, not of Cope).—Gilbert, 1893: 231 (3 from Pahranagat Valley, Nev., regarded as probably *L. vittata*; former connection with Colorado River). Jordan and Evermann, 1896*a*: 328 and 1896*b*: 265 ("Pahrangat Valley" only). Jordan, Evermann, and Clark, 1930: 147 ("Pahranagat Valley, Nev.," only). Tanner, 1936: 171 (reference to Pahranagat Valley material, evidently that recorded by Gilbert). La Rivers and Trelease, 1952: 118 (in part; Pahranagat Valley). La Rivers, 1952: 97 (in part).

Lepidomeda jarrovii.—Jordan and Evermann, 1896*a*: 328, 1896*b*: 265 (record from springs in desert of southern Nevada only). Jordan, Evermann, and Clark, 1930: 147 (Nevada record only).

Lepidomeda jarrovi.—Eddy, 1957: 104 ("Nevada" only).

Lepidomeda species.—Moore, 1957: 138 (in part, mention of undescribed species in Nevada related to *L. vittata*).

We have examined two juveniles in poor condition (USNM 46118) representing two of the three specimens that Gilbert thought probably referable to *L. vittata* (the other is in the Natural History Museum of Stanford University); they agree with our concept of *L. altivelis*.

DIAGNOSIS.—A species of *Lepidomeda* distinguished by the combination of 5–4 teeth in the main row, 9 anal rays, an oblique mouth, high and sharp dorsal fin, and a compressed head (see rubrics 1a, 2a, and 3b in key). *L. altivelis* has the longer mandible of *L. albivallis*, the silvery coloration of *L. mollispinis*, and is distinctive in its very oblique mouth, high and expansive dorsal fin, more compressed head, and generally finer scales.

TYPES.—The holotype, UMMZ 125004, an adult 56 mm. in standard length, was collected by Carl L. Hubbs and family from the outflow of Ash Spring, from .25 to 2.5 miles (in straight line) below the spring source, in Pahranagat Valley, Lincoln Co., Nevada, on August 29, 1938. Sixteen paratopotypes, UMMZ 125005 (33–66 mm.), were taken with the holotype. Seven other specimens, UMMZ 124813 (33–41 mm.), were seined in Upper Pahranagat Lake, Lincoln Co., Nevada, by Hubbs and party on July 12, 1938.

CHARACTERS.—The form and coloration are portrayed in Plate I, D. Principal dorsal rays 8 (24); anal rays 8 (1), 9 (21), 10 (2); pelvics 7–7 (21), 5–7 (1), 8–7 (1). The pharyngeal teeth number 2, 5–4, 2 in ten specimens, and the lateral-line scales are 84 to 95 in ten (90 or more in six), approximately 92 in the holotype. Vertebrae 42 to 44 (Table 1). This species attains a miximum length of about 3.75 inches (66 mm. S. L.).

DISTRIBUTION, HABITAT, AND ASSOCIATES.—This species was secured by

(372)

us in 1938 at only two localities in Pahranagat Valley, Nevada: (1) the outflow of Ash Spring, about 6 miles north of Alamo, and (2) Upper Pahranagat Lake, on U. S. Highway 93, 6 miles south of Alamo. Thorough collecting in Ash Spring proper and in Crystal and Hiko springs in the same valley failed to reveal the species, and indicated that it shunned constantly warm water (temperatures were 79° to 90°F. at the sources of these springs).

Although the two habitats from which this species is known are strikingly different, the samples from each locality agree well in all diagnostic features. This circumstance strengthens the hypothesis that the observed differences between the recognized forms in this genus are not environmentally induced.

In the outflow of Ash Spring, from .25 to 2.5 miles in a straight line below its head, the water was very clear (bottom clearly visible at 6 feet), the greatly meandering channel 5 to 20 feet wide, and the current generally swift (rarely quiet; in places very swift). The bottom comprised sand, gravel, mud, and boulders; the depth of water was up to 6 feet. Vegetation consisted in general of abundant bulrushes and submerged weeds, but the stream was partly clear of weeds; the banks (about 5 feet high) were wooded, and beyond were grass and farm land. The collection was made between noon and evening on August 29, 1938, using a seine in the upper part, and derris root below (where *Lepidomeda* was taken). In the upper part the water was 88°F., but below was much cooler.

Species taken with *Lepidomeda altivelis* in the outflow from Ash Spring were: *Cyprinus carpio* Linnaeus, *Gila robusta jordani* Tanner, *Rhinichthys osculus velifer* Gilbert, *Pantosteus intermedius* (Tanner), and *Crenichthys baileyi* Gilbert. The native fishes are all endemic as species or subspecies to the immediate region or to the whole Pluvial White River system.

At Upper Pahranagat Lake on July 12, 1938, the water was dirty olive-green and was alkaline to the taste, with bottom visibility about 2 feet. Vegetation comprised a heavy growth of flooded cockleburs. The shore was an alkali flat. The bottom was firm to soft clay soil and we seined to 100 feet from shore, where the water depth did not exceed 3 feet. Associated with *L. altivelis* here were *Pantosteus intermedius* and many carp; the lake was worked between 8:30 and 9:00 A.M., when the water was 74°F., the air 89°F.

The three specimens recorded by Gilbert (1893: 231) from "Pahranagat Valley, Nevada" could have come either from the outflow of Ash Spring or from Pahranagat Lake, since collections were made at both localities by members of the Death Valley Expedition.

EXTERMINATION OF THE SPECIES.—Field study on July 2–3, 1959, undertaken to test the point, indicated that this highly localized species, like

Lepidomeda mollispinis pratensis of Big Spring, near Panaca, had become exterminated during the previous 21 years. The thorough collecting in 1959 failed to reveal a single specimen of *Lepidomeda* in the outlet of Ash Spring or in or about the Pahranagat Lakes, where the species was collected in 1891 and in 1938. A spring-fed ditch in the bed of Maynard Lake, southernmost of the Pahranagat chain, yielded on July 2, 1959, only the local form of *Rhinichthys osculus.* Upper Pahranagat Lake and its outlet on the same day yielded only *Cyprinus carpio.* In the pools of Ash Spring proper, where the water temperature is 89°F., the local (typical) form of *Crenichthys baileyi* still occurred commonly, though for some reason in less abundance than in 1938. In an examination of the outlet stream this cyprinodont occurred down to and into the diversion ditches 5 to 7 miles north of Alamo. Seining at several points in the outlet, supplemented by a visual examination along nearly the whole length of the natural flow and by a thorough application of rotenone in the lower half-mile of the natural creek and the upper mile of the diversion ditch then in operation, on July 3, 1959, indicated the fish population of the outlet, at water temperatures of 86 to 88°F. (air temperature 88.5°F.), to consist of moderate numbers of the *Crenichthys* and of the *Gila,* hordes of carp, and a considerable number of another introduced pest, *Gambusia affinis affinis.* Not a single sucker (*Pantosteus intermedius*) or a single *Lepidomeda* was secured. Since for about 2.5 miles the stream has retained essentially its original bed and condition, with only limited diversions, and since the water source has remained uniform, the probable local extirpation of the *Pantosteus* and the almost certain complete extermination of the *Lepidomeda* is most plausibly attributable largely to the increased abundance of carp and to the establishment of the mosquitofish (*Gambusia*). Both of these introduced species have had a deleterious effect on native fish life in many western waters (Sigler, 1958; Miller, in press). The establishment of bullfrogs, *Rana catesbeiana,* may also have played a role in the modification of the habitat.

ETYMOLOGY.—The name *altivelis* is from the Latin *altus,* meaning high, and *velum,* a sail, in reference to the high, expanded dorsal fin.

Lepidomeda vittata Cope
(Pl. II, A; Pl. III, A)
Little Colorado Spinedace

Lepidomeda vittata.—Cope, 1874: 131 (original description, Colorado Chiquito River, Arizona). Cope and Yarrow, 1875: 642–43, pl. 26, figs. 2–2a (redescription of types). Jordan and Copeland, 1876: 155 (listed; "Colorado, Arizona"). Jordan and Gilbert, 1883: 252 (description, after Cope). Jordan, 1885*b*: 821 (listed). Jordan and Evermann, 1896*a*: 328 (description; range, in part); 1896*b*: 265 (range, in part). Fowler, 1925: 415 (description of syntype). Jordan, Evermann, and Clark, 1930: 147 (reference; range, in part). Eddy, 1957: 104 (characters [from Jordan and Evermann] only). Moore, 1957: 138 (range).

Lepidomeda jarrovii.—Cope, 1874: 132 (original description, Colorado Chiquito River, Arizona). Cope and Yarrow, 1875: 643–44, pl. 26, figs. 1–1a (redescription of types). Jordan and Copeland, 1876: 155 ("Colorado"). Jordan and Gilbert, 1883: 252 (description, after Cope). Jordan, 1885*b*: 821 (listed). Jordan and Evermann, 1896*a*: 328 (description; range, in part); 1896*b*: 265 (range, in part). Jordan, Evermann, and Clark, 1930: 147 (reference; Rio Colorado Chiquito, Arizona, only).

Lepidomeda jarrovi.—Eddy, 1957: 104 (characters [from Jordan and Evermann] and "Arizona" only).

DIAGNOSIS.—A species of *Lepidomeda* differing from its relatives in having 4–4 teeth in the main row, 8 anal rays, usually more than 90 lateral-line scales, and typically 41 or 42 vertebrae (see rubric 2b of key).

SYNONYMY.—An examination of the extant types of *Lepidomeda vittata* and *L. jarrovii*, and of our topotypes (the first specimens of the species taken since these nominal species were described about 65 years previously), yields no indication that more than the one species occupies the Little Colorado River system. We therefore synonymize the species and adopt the name *L. vittata*.

The four syntypes (USNM 15785) of *L. vittata* are in poor condition and one is represented by the head only (a fifth fish, now segregated in a vial, is *Rhinichthys osculus*). All three have 8 anal rays and probably 8 dorsal rays; the teeth number 4, 2 on the right side of one specimen.

The two syntypes (USNM 15786) of *L. jarrovii*, about 53 and 67 mm. in standard length, are in poor condition, but appear conspecific with *L. vittata*. Each has 8 dorsal and 8 anal rays, 7 pelvic rays on each side, 2, 4–4, 2 teeth (with 1 or 2 teeth in each specimen represented by alveoli only), about 90 and 95 lateral-line scales, and 42 vertebrae in the larger specimen (vertebrae abnormal, 41 or 42 in smaller syntype). These counts agree well with those diagnostic of *L. vittata*. The "greater elongation of form, weakness of squamation and peculiarity of coloration" advanced by Cope as distinguishing features of *L. jarrovii* we interpret as phenotypic variations.

There is a syntype of *Lepidomeda vittata* in the Academy of Natural Sciences of Philadelphia (19853), and there are three in the Museum of Comparative Zoology (18816).

A second lot (original number 5X, USNM 15779) referred to *L. jarrovii* by Cope and Yarrow (1875: 644), and also attributed to "Colorado Chiquito River, Ariz.," proves on re-examination to be referable to *Gila robusta* Baird and Girard.

CHARACTERS.—The form of the body, head, and fins is shown in Plate II, A. The principal dorsal rays number 8 (in all 30 specimens counted); anal rays 8 (68), 9 (2); pelvics 7–7 (29), 6–8 (1). The pharyngeal teeth are consistently 4–4 in the main row, but are about as often 1 as 2 in the lesser row. The following formulas were observed: 1, 4–4, 1 (7), 1, 4–4, 2 (2), 2, 4–4, 1 (3), 2, 4–4, 2 (8). The teeth are missing in unusual frequency; many of those listed were represented by alveoli. In three specimens there were no teeth on either arch. Cope recorded the formula as 2, 4–4, 2, as did Fowler for a syntype. The scales in the lateral line number 89 to 105 in twelve specimens, including the syntypes of *L. jarrovii*, but they are embedded and difficult to count and usually appear to be lacking on the body where covered by the depressed paired fins. Vetebrae number 41 to 43 (Table 1).

The life colors were thus described: the axils of the paired fins are bright orange to reddish orange; a trace of these colors shows on the distal part of the anal fin; otherwise the fins are watery white, with the rays white to yellowish-orange. The sides are brilliantly silvery. The scales show light bluish to greenish-brass reflections.

L. vittata attains a total length of about four inches. The largest specimen we have (in UMMZ 131099) is 84 mm. in standard length.

ERRONEOUS RECORDS.—*L. vittata* has been attributed to several other localities, all, we believe, in error. These are entered in the synonymies of the other species. Tanner (1932: 135) reported *L. vittata* from Fremont River, Utah, but in his general report on Utah fishes (Tanner, 1936: 161, 171) he did not repeat the record, and no one else has recorded any plagopterin from above Grand Canyon; nor have we taken any there. We now feel that the Fremont River report should be disregarded, especially since no specimens to support the record have been found in Dr. Tanner's collections by him or by us.

DISTRIBUTION AND HABITAT.—This species seems to be restricted to the upper parts of the Little Colorado River system, eastern Arizona, well above Grand Falls, on and near the northern slopes of the White Mountains (Fig. 1). The types of the two nominal species were recorded only as from the "Colorado Chiquito River." The actual type locality or localities of *Lepidomeda vittata* and *L. jarrovii* has not been specified, but the itinerary of the Wheeler Survey (Wheeler, 1889: 58–77) indicates that the specimens were collected in the headwaters of the Little Colorado somewhere between the mouth of the Zuni River and Sierra Blanca (White Mountain). Our three series bear the following data: UMMZ 124754 (73, 39–69 mm.), Little Colorado R., Apache Co., 7,000 feet, T. 12 N, R. 28 E, July 1, 1938; UMMZ

137082 (130, 21–76 mm.), Little Colorado R., 5 to 6 mi. S of St. Johns, Apache Co., July 16, 1939; and UMMZ 131099 (6, 75–84 mm.), Showlow Cr. below dam at Lakeside, Navajo Co., T. 22 E, R. 9 N, June 13, 1939. At the three stations the water was described as yellow, brownish-white, and murky; current, slight to swift; bottom, thick mud, sand, clay, gravel, and rock; depth of capture, 1 to 3 feet; and vegetation, white water buttercup (rather thick in patches), chara, some rushes, and algae.

ASSOCIATES.—The following were taken with *L. vittata*: four native fishes, *Catostomus latipinnis* Baird and Girard, *Pantosteus delphinus* (Cope), *Rhinichthys osculus* (Girard), and *Gila r. robusta* Baird and Girard, and three introduced species, *Cyprinus carpio, Ictalurus melas* (Rafinesque), and *Lepomis cyanellus* Rafinesque. Hemphill (1954: 41) reported *Gila robusta elegans* Baird and Girard from Lyman Reservoir (near St. Johns), but no specimens are available for checking the identification; however, this subspecies was described from the Zuni River, New Mexico, a flood-tributary to the Little Colorado River. Hemphill also listed five other introduced species: largemouth bass, *Micropterus salmoides* (Lacépède); bluegill, *Lepomis macrochirus* Rafinesque; brown trout, *Salmo trutta* Linnaeus; "several hundred bullhead catfish"; and channel catfish, *Ictalurus punctatus* (Rafinesque). Becker's Lake (near Springerville) contained two additional exotic fishes, the golden shiner, *Notemigonus crysoleucas* (Mitchill) and yellow perch, *Perca flavescens* (Mitchill), which were presumably eliminated by treatment with toxaphene, after which rainbow trout, *Salmo gairdneri* Richardson, were stocked (Hemphill, 1954: 42). Whether the *Lepidomeda* will persist (or has persisted) in competition with such introduced predators and competitors is an open question.

GENUS *Meda* Girard

Meda.—Girard, 1856: 191–92 (original description); 1859: 50 (description and comparisons). Günther, 1868: 263–64 (description quoted; remark on dorsal spine; placed in Leuciscina, not Xenocypridina). Cope 1874: 131, and Cope and Yarrow, 1875: 641 (characters and comparisons). Jordan and Gilbert, 1883: 148, 252 (comparisons; description). Jordan, 1885*a*: 122, and 1885*b*: 821 (*Plagopterus* treated as synonym; species). Jordan and Evermann, 1896*a*: 204, 328 (comparisons; description). Eddy, 1957: 105 (characters). Moore, 1957: 94, 138 (characters and comparisons).

TYPE SPECIES.—*Meda fulgida* Girard (by monotypy).

Meda is one of the two endemic genera of the Gila River basin in Arizona and New Mexico (the other is *Tiaroga*). *Meda* is easily distinguished from the other plagopterin genera by the characters in the analytical key (rubrics 1b and 6a).

Meda fulgida Giard
(Pl. II, B; Pl. III, F)
Spikedace

Meda fulgida.—Girard, 1856: 192 (original description; Río San Pedro, Arizona); 1859: 50, pl. 28, figs. 9–10 (redescription, with figures; list of specimens). Günther, 1868: 264 (after Girard). Cope, 1874: 131, and Cope and Yarrow, 1875: 641–42 (listed). Jordan and Copeland, 1876: 155 (Arizona). Jordan and Gilbert, 1883: 252 (after Girard). Jordan, 1885*a*: 122, and 1885*b*: 821 (characters). Jordan and Evermann, 1896*a*: 329 (description; Río Gila). Jordan and Evermann, 1896*b*: 265 (reference; Río Gila). Gilbert and Scofield, 1898: 497–98 (description of specimens from Chino and Tempe, Arizona). Fowler, 1925: 415 (notes on 2 syntypes and 15 others from San Francisco River, New Mexico). Jordan, Evermann, and Clark, 1930: 147 (listed; reference; range). Winn and Miller, 1954: 282, 284, pls. 1–2 (development of larval characters; photo of postlarva; comparison with associated postlarvae). Illick, 1956: 215–18 (cephalic lateral-line system). Eddy, 1957: 105, fig. 263 (characters and range; compiled). Koster, 1957: 72 (description; habitat). Moore, 1957: 138 (range).

Characters.—Principal dorsal rays 7 (54), 8 (2); anal rays 8 (5), 9 (48), 10 (3); pelvics 7–7 (17), 7–6 (1), 6–7 (2). The pharyngeal teeth typically number 1, 4–4, 1; the following formulas were noted in 24 specimens (12 counts original, remainder from Gilbert and Scofield, 1898, and Fowler, 1925): 1, 4–4, 1 (19), 1, 4–4, 2 (2), 2, 4–4, 1 (1), 2, 4–4, 2 (1), and 1, 5–4, 1 (1). Vertebrae vary from 39 to 42 (Table 1).

In life the sides shine like burnished silver, with bluish reflections; the back is olive to olive-gray, with silvery-white speckles between the sides and dorsum. There are bright cream to yellow-orange spots at either end of the dorsal-fin base, at the upper edge of the procurrent caudal rays, in the axil of the pectoral fin, and on either side of the small spot at the caudal base. There is rather prominent dark mottling on the upper sides and sometimes a bit of rose is mixed with the silvery color of the sides; the abdomen may be tinged yellowish (Koster, 1957: 72). Gilbert and Scofield (1898: 498) described their material as "bright silvery, with reddish brown mottlings along back"; and the "body pale yellowish below."

This is a small species, not attaining a total length of 3 inches; the largest specimen we have seen is 60 mm. in standard length. It spawns in late spring and early summer; individuals as small as 4.0 mm. standard length were caught at night on May 6, 1950.

Distribution.—For nearly 50 years this fish was known only from the San Pedro River, the major southern tributary of the Gila River in southern Arizona. When the stream had a more ample flow, in the nineteenth century, this species presumably occurred also in the headwaters of the San Pedro in México (Miller and Winn, 1951: 84). *Meda* has been reported from numerous places in the Gila River system of New Mexico and Arizona as far downstream as Tempe (Fig. 1).

Syntypes are in the collections of the United States National Museum (No. 154), in the Academy of Natural Sciences of Philadelphia, two (53, 60–61), and in the Museum of Comparative Zoology, one (No. 1959).

HABITAT.—*Meda fulgida* seeks moving water 2 to 4 feet deep, typically inhabiting the swift, deep pools, or the deeper upper parts of long pools, near riffle mouths, over sandy or gravelly bottom. On the Gila River about 6 miles northeast of Redrock, Grant County, New Mexico (May 6–7, 1950), some adults were observed on shallow riffles where the rocks were covered with long streamers of green algae. At Verde River just above Camp Verde, Arizona, on September 2, 1938, adults were common on a very swift riffle over bedrock bottom. Young occur in backwater areas, over silt and sand bottoms, adjacent to swift pools.

GENUS *Plagopterus* Cope

Plagopterus.—Cope, 1874: 130 (original description; classification). Cope and Yarrow, 1875: 640 (description; comparison). Jordan and Gilbert, 1883: 148, 252 (comparisons; diagnosis). Jordan and Evermann, 1896*a*: 204, 329 (comparisons; description). Eddy, 1957: 105 (characters). Moore, 1957: 138 (characters and comparisons).

TYPE SPECIES.—*Plagopterus argentissimus* Cope (by monotypy).

Plagopterus, in most features the most specialized genus of the Plagopterini, is readily distinguished from the other genera by characters given in the key (rubrics 1b and 6b). At the present time its known distribution is limited to the Virgin River system (Fig. 1, insert) and its predilection for a swift-water habitat further restricts it ecologically. Formerly it also occurred in the Gila River (p. 9).

Plagopterus argentissimus Cope
(Pl. II, C; Pl. III, G)
Woundfin

Plagopterus argentissimus.—Cope, 1874: 130 (original description; "San Luis Valley, Western Colorado"; repeated in Cope and Yarrow, 1875: 640–41). Jordan and Copeland, 1876: 155 (locality repeated). Jordan and Gilbert, 1883: 253 (description and record, after Cope). Jordan and Evermann, 1896*a*: 329 (description; Colorado Basin in western Colorado; Fort Yuma); 1896*b*: 266 (reference; same localities). Gilbert and Scofield, 1898: 496–97 (Gila R. at Yuma and Salt R. at Tempe, Ariz., spring of 1890; description of new material). Ellis, 1914: 70 (occurrence in Colorado doubted). Snyder, 1915: 584 (Gila R. near Gila City, Ariz., between 1892 and 1894; brief des-

cription). Fowler, 1925: 415 (notes on 2 syntypes). Jordan, Evermann, and Clark, 1930: 147 (listed; reference; range repeated). Shapovalov and Dill, 1950: 386 (listed from California; woundfin proposed as common name). Miller, 1952: 18, 36, fig. 20 (characters in key; distribution; use as baitfish). Böhlke, 1953: 36 (syntype listed from Colorado Chiquito R., Ariz.). Illick, 1956: 215–18, figs. 31–33 (cephalic lateral-canal system). Eddy, 1957: 105, fig. 262 (characters; range). Moore, 1957: 138 (range).
Meda argentissima.—Jordan, 1885*a*: 122, and 1889*b*: 821 (characters; generic reference).

Characters.—The number of principal dorsal rays varies from 8 to 10, and the anal rays from 9 to 11, as follows: D. 8 (67), 9 (23), 10 (3); A. 9 (9), 10 (73), 11 (11). The pelvic rays number 7 in each fin (in 55 specimens, one had 6–7 and one 7–6). The dental formula is typically 1, 5–4, 1, but varies as follows: 1, 5–4, 1 (14), 1, 5–5, 1 (1), 2, 5–4, 1 (2), 2, 5–4, 2 (2), and 1, 4–4, 1 (2). Fowler (1925: 415) recorded 1, 4–4, 1 or 1, 5–4, 1 for two syntypes; Cope (1874: 130) gave the formula as 2, 5–4, 2. Vertebrae vary from 39 to 41 (Table 1).

This, the most silvery of American cyprinids, was well named by Cope. When taken from the water the body shines like burnished silver, showing blue reflections from the sides. The axil of the pectoral fin was watery yellow on individuals caught on July 3, 1938.

This species attains a somewhat larger size than does *Meda fulgida,* frequently 3 inches; the largest is about 3.5 inches long (71 mm. standard length). It probably spawns in late spring and summer, for specimens 19 mm. in standard length were obtained on July 29 and on September 15 in Arizona and Utah (UMMZ 141669, 124766).

Distribution.—The stated type locality of this species is obviously erroneous. The only fishes known from the isolated waters of San Luis Valley, Colorado (tributary in Pluvial times to the Rio Grande), are *Salmo clarki, Gila nigrescens,* and *Pimephales promelas* (Ellis, 1914: 47; Hubbs and Miller, 1948: 117–18; local testimony). Ellis doubted that *Plagopterus* occurs in Colorado. No type specimen was designated by Cope, who based the species on "numerous specimens"; there are two syntypes in the Academy of Natural Sciences of Philadelphia (19851–52), two in the Museum of Comparative Zoology (18817), three in the United States National Museum (15576), and one in the Stanford Natural History Museum (2003). The syntypes in the National and Stanford collections bear the locality "Colorado Chiquito River," in Arizona, but this is probably also incorrect since the species is not otherwise known from the Little Colorado. Other species collected by naturalists of the Wheeler Survey (1871–1874) also bear erroneous locality data, as, for example, *Ceratichthys biguttatus,* a species native to eastern United States, attributed to "Harmony, Utah" (in the Bonneville basin).

We think it probable that the types were obtained in the Virgin River in Washington County, southwestern Utah, an area from which fishes (e.g., *Gila seminuda* Cope and Yarrow) were collected by Wheeler Survey naturalists. The expedition in 1872 maintained a base at Toquerville, which is on La Verkin Creek, worked the Virgin River valley and canyon, and visited St. George (Wheeler, 1889: 46–57). The species is known today only from the Virgin River system. Our largest collection (192 young to adult, UMMZ 124770) came from the Virgin River at the mouth of La Verkin and Ash creeks (T. 41 N, R. 13 W).

Although Jordan and Evermann (1896*a*: 329) designated USNM 15776 as "type," this does not constitute a lectotype designation since the jar contains three specimens and there are others from the same lot in other museums, as specified above.

HABITAT.—This species frequents swift shallows over stone, sand, or mud bottom, but some adults live in deeper holes, though generally not over 1.5 feet deep. In the Virgin River near Bunkerville, Nevada, it was the only fish found in water described as dirty-orange liquid mud, with swift current, and perhaps it was the only fish capable of tolerating such a "swift mud" environment. In the preserving jar filled with this water nearly one inch of sediment precipitated.

SUMMARY AND GENERAL CONCLUSIONS

The American spiny-rayed cyprinid fishes, revised in this paper, constitute a compact and distinctive group, which was named Plagopterinae by Cope (1874) and Medidae by some recent authors, but which we treat as a tribe, Plagopterini, within the Leuciscinae. It is one of the characteristic elements in the freshwater fish fauna of Western North America. The Plagopterini embrace the monotypic genera *Meda* and *Plagopterus* and the polytypic genus *Lepidomeda*. Of the two previously recognized species of *Lepidomeda*, one (*jarrovii*) is synonymized, and three additional species, one with two subspecies, are now described. The plagopterins are among the few groups of American cyprinids that do not engage in interspecific hybridization.

Lepidomeda appears to be the most generalized as well as the most diverse of the plagopterin genera. It seems to have arisen from *Gila* or some similar genus. *Meda* and *Plagopterus* are strikingly specialized, particularly in the spinelike modification of the dorsal and pelvic rays. The spinose development of the anterior dorsal rays has been independent in the Plagopterini and in such Old World genera as *Cyprinus* and *Barbus*.

Spinosity of the pelvic rays is a unique feature of the plagopterins, and involves only the lower half of each ray—the left demitrich in the right fin and the right demitrich in the left fin (other examples of bilaterally asymmetric modification of fin rays were presented by Hubbs and Hubbs, 1945: 295–96, fig. 2).

Other features of specialization accentuated in *Meda* and *Plagopterus* are loss of scales, intense silvery color, sexual dimorphism in pectoral-ray structure, and, in *Plagopterus,* development of dermal ridges with basal platelets.

The entire group is confined to the Colorado River system, in which it probably arose in Pliocene time. Major differentiation probably continued through Pleistocene time, with isolation and minor speciation during the Postglacial disruptions of the drainage. The highly localized distribution of the species has been accentuated by stream deterioration due to human activities, as well as to the recent drought. The introduction of exotic fishes, particularly *Gambusia* and *Cyprinus,* along with agricultural operations, may have further restricted their distributions. Two forms of *Lepidomeda* (*L. mollispinis pratensis* and *L. altivelis*), which even in 1938 were confined, in reduced populations, to the outlet waters of single isolated springs, were found in 1959 to have become extinct.

LITERATURE CITED

ANGEL, MYRON (Editor)
1881 History of Nevada, with illustrations and biographical sketches of its prominent men and pioneers. Thompson and West, Oakland, California: i–xiv, 15–680, illus. (facsimilie reprod., ed. by David F. Myrick, publ. by Howell-North, Berkeley, Calif., 1958).

BÖHLKE, J.
1953 A catalogue of the type specimens of Recent fishes in the Natural History Museum of Stanford University. Stanford Ichthy. Bull., 5: 1–168.

COCKERELL, T. D. A.
1911 Some notes on fish scales. Proc. Biol. Soc. Wash., 24: 209–13.

COPE, EDWARD D.
1874 On the Plagopterinae and the Ichthyology of Utah. Proc. Amer. Philos. Soc., 14: 129–40.

COPE, E. D., AND H. C. YARROW
1875 Report upon the collections of fishes made in portions of Nevada, Utah, California, Colorado, New Mexico, and Arizona, during the years 1871, 1872, 1873 and 1874. Rept. Geog. and Geol, Expl. and Surv. W. 100th Merid. (Wheeler Survey), 5: 635–703, Pls. 26–32.

EDDY, SAMUEL
1957 How to know the freshwater fishes. Wm. C. Brown Co., Dubuque, Iowa, 253 pp., Figs. 1–615.

ELLIS, MAX M.

1914 Fishes of Colorado. Univ. Colorado Stud., 11 (1): 1–136, 3 maps, 1 fig., Pls. 1–12.

FOWLER, HENRY W.

1925 Notes on North American cyprinoid fishes. Proc. Acad. Nat. Sci. Phila., 76 (1924): 389–416, Figs. 1–23.

GILBERT, CHARLES H.

1893 Report on the fishes of the Death Valley Expedition collected in Southern California and Nevada in 1891, with descriptions of new species. N. Amer. Fauna, No. 7: 229–34, Pls. 5–6.

GILBERT, CHARLES HENRY, AND NORMAN BISHOP SCOFIELD

1898 Notes on a collection of fishes from the Colorado Basin in Arizona. Proc. U. S. Natl. Mus., 20: 487–99, Pls. 36–39.

GIRARD, CHARLES

1856 Researches upon the cyprinoid fishes inhabiting the fresh waters of the United States of America, west of the Mississippi Valley, from specimens in the museum of the Smithsonian Institution. Proc. Acad. Nat. Sci. Phila., 8: 165–213.

1859 Ichthyology of the Boundary. U. S. and Mex. Boundary Surv., 2 (2): 1–85 (sep. pag.), Pls. 1–41.

GÜNTHER, ALBERT

1868 Catalogue of the fishes in the British Museum. London, Vol. 7, xx + 512 pp.

HEMPHILL, JACK E.

1954 Toxaphene as a fish toxin. Prog. Fish-Cult., 16 (1): 41–42.

HUBBS, CARL L.

1955 Hybridization between fish species in nature. Syst. Zool., 4 (1): 1–20, Figs. 1–8.

HUBBS, CARL L., AND KARL F. LAGLER

1958 Fishes of the Great Lakes Region. Cranbrook Inst. Sci., Bull. 26, Pp. xi + 213, Figs. 1–251, Chart 1, Pls. 1–44.

HUBBS, CARL L., AND LAURA C. HUBBS

1945 Bilateral asymmetry and bilateral variation in fishes. Mich. Acad. Sci., Arts, and Letters, 30 (1944): 229–310, Figs. 1–2, Pl. 1.

HUBBS, CARL L., AND ROBERT R. MILLER

1948 The zoölogical evidence: Correlation between fish distribution and hydrographic history in the Desert Basins of Western United States. *In*: The Great Basin, with Emphasis on Glacial and Postglacial Times. Bull. Univ. Utah, 38 (20): 17–166, Figs. 10–29, 1 map.

ILLICK, HELEN J.

1956 A comparative study of the cephalic lateral-line system of North American Cyprinidae. Amer. Midland Nat., 56 (1): 204–23, Figs. 1–39.

JORDAN, DAVID STARR

1885*a* Identification of the species of Cyprinidae and Catostomidae, described by Charles Girard, in the Proceedings of the Academy of Sciences of Philadelphia for 1856. Proc. U. S. Natl. Mus., 8: 118–27.

1885*b* A catalogue of the fishes known to inhabit the waters of North America, north of the Tropic of Cancer, with notes on species discovered in 1883 and 1884. Rept. U. S. Comm. Fish and Fish., 1885: 789–973.

JORDAN, DAVID S., AND HERBERT E. COPELAND

1876 Check list of the fishes of the fresh waters of North America. Bull. Buffalo Soc. Nat. Sci., 3: 133–64.

JORDAN, DAVID STARR, AND BARTON WARREN EVERMANN

1896*a* The fishes of North and Middle America. Part I. Bull. U. S. Natl. Mus., 47: i–lx, 1–1240.

1896*b* A check-list of the fishes and fish-like vertebrates of North and Middle America. Rept. U. S. Comm. Fish and Fish., 1895: 207–584.

JORDAN, DAVID STARR, BARTON WARREN EVERMANN, AND HOWARD WALTON CLARK

1930 Check list of the fishes and fishlike vertebrates of North and Middle America north of the northern boundary of Venezuela and Colombia. Rept. U. S. Comm. Fish., 1928 (2): i–iv, 1–670.

JORDAN, DAVID S., AND CHARLES H. GILBERT

1883 Synopsis of the fishes of North America. U. S. Natl. Mus., Bull. 16 (1882): i–lvi, 1–1018.

KOSTER, WILLIAM J.

1957 Guide to the fishes of New Mexico. Univ. New Mexico Press, vii + 116 pp., illus.

LA RIVERS, IRA

1952 A key to Nevada fishes. Bull. So. Calif. Acad. Sci., 51: 86–102, Pl. 19.

LA RIVERS, IRA, AND T. J. TRELEASE

1952 An annotated check list of the fishes of Nevada. Calif. Fish and Game, 38 (1): 113–23.

MILLER, ROBERT RUSH

1945 *Snyderichthys,* a new generic name for the leatherside chub of the Bonneville and Upper Snake drainages in Western United States. Jour. Wash. Acad. Sci., 35 (1): 28.

1946 The need for ichthyological surveys of the major rivers of Western North America. Science, 104: 517–19.

1952 Bait fishes of the Lower Colorado River from Lake Mead, Nevada, to Yuma, Arizona, with a key for their identification. Calif. Fish and Game, 38 (1): 7–42, Figs. 1–32.

1959 Origin and affinities of the freshwater fish fauna of Western North America. *In*: Zoogeography. Amer. Assoc. Adv. Sci., Publ. No. 51 (1958): 187–222, Figs. 1–19.
187–222, Figs. 1–19.

In press, Man and the changing fish fauna of the American Southwest. Pap. Mich. Acad. Sci., Arts, and Letters, 46.

MILLER, ROBERT RUSH, AND HOWARD ELLIOTT WINN

1951 Additions to the known fish fauna of Mexico: Three species and one subspecies from Sonora. Jour. Wash. Acad. Sci., 41 (2): 83–84.

MOORE, GEORGE A.

1957 Fishes. *In*: Vertebrates of the United States. McGraw-Hill Book Co., New York, Pp. 31–210, Figs. 1–112.

SHAPOVALOV, LEO, AND WILLIAM A. DILL

1950 A check list of the fresh-water and anadromous fishes of California. Calif. Fish and Game, 36 (4): 382–91.

SIGLER, WILLIAM F.

1958 The ecology and use of carp in Utah. Utah State Univ. Agr. Expt. Bull. 405: 1–63, Figs. 1–15.

SNYDER, JOHN OTTERBEIN

1915 Notes on a collection of fishes made by Dr. Edgar A. Mearns from rivers tributary to the Gulf of California. Proc. U. S. Natl. Mus., 49: 573–86, 1 fig., Pls. 76–77.

SUMNER, F. B., AND URLESS N. LANHAM

1942 Studies of the respiratory metabolism of warm and cool spring fishes. Biol. Bull., 82 (2): 313–27, Figs. 1–4.

TANNER, VASCO M.

1932 A description of *Notolepidomyzon utahensis*, a new catostomid from Utah. Copeia, 1932 (3): 135–36.

1936 A study of the fishes of Utah. Utah Acad. Sci., Arts and Letters, 13: 155–83, Pls. 1–3.

WALLIS, ORTHELLO L.

1951 The status of the fish fauna of the Lake Mead National Recreational Area, Arizona-Nevada. Trans. Amer. Fish. Soc., 80 (1950): 84–92.

WHEELER, GEO. M.

1889 Report upon United States geographical surveys west of the One Hundredth Meridian. Vol. I.—Geographical Report, Washington: 1–780, Pls. 1–38, Maps 1–3.

WINN, HOWARD ELLIOTT, AND ROBERT RUSH MILLER

1954 Native postlarval fishes of the Lower Colorado River Basin, with a key to their identification. Calif. Fish and Game, 40 (3): 273–85, Pls. 1–4.

Accepted for publication March 7, 1960

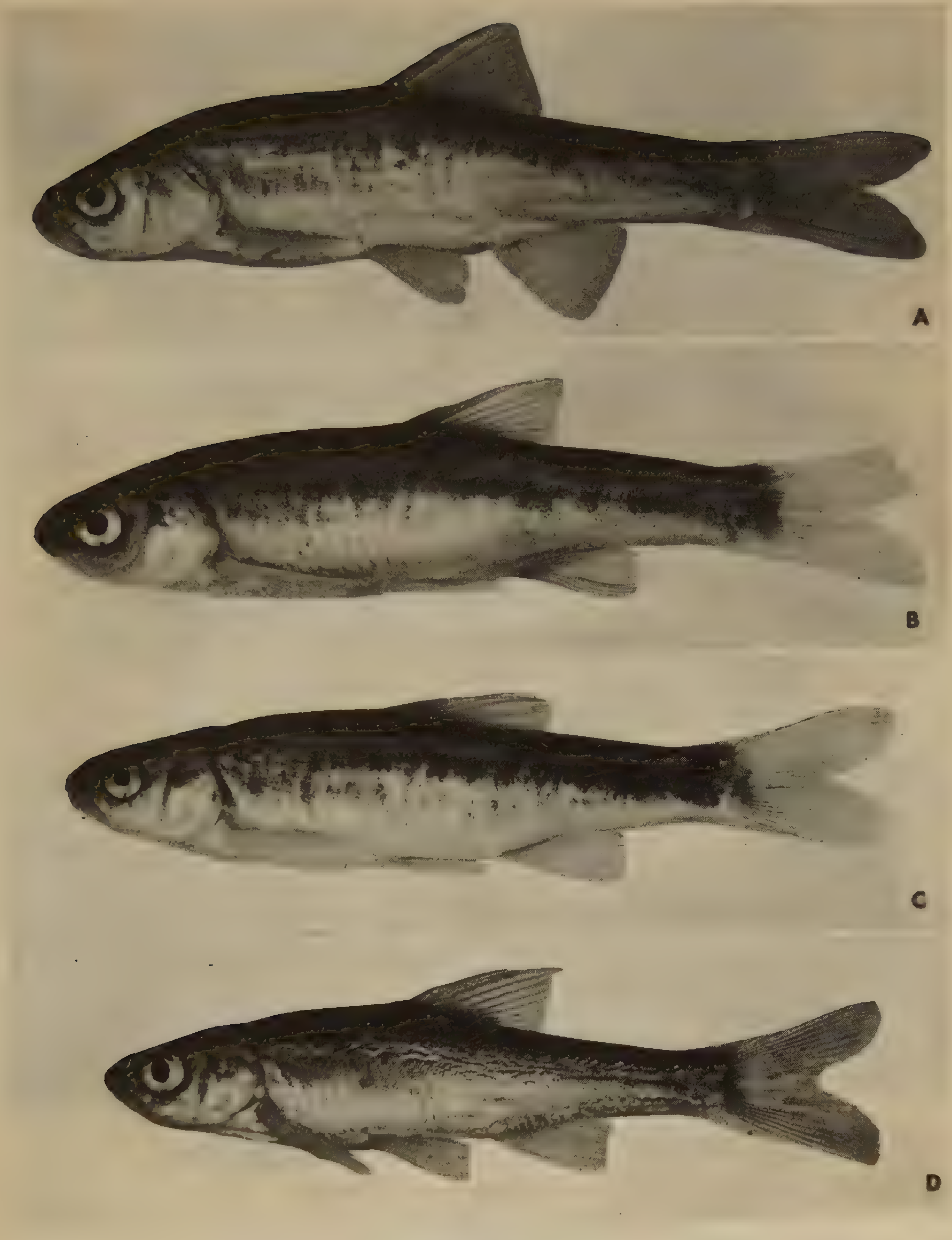

PLATE I

Three new species of *Lepidomeda*

A, Holotype of *L. m. mollispinis,* UMMZ 141673, 88 mm. S.L.
B, Holotype of *L. m. pratensis,* UMMZ 124799, 55 mm. S.L.
C, Holotype of *L. albivallis,* UMMZ 173781, 69.5 mm. S.L.
D, Holotype of *L. altivelis,* UMMZ 125004, 56 mm. S.L.

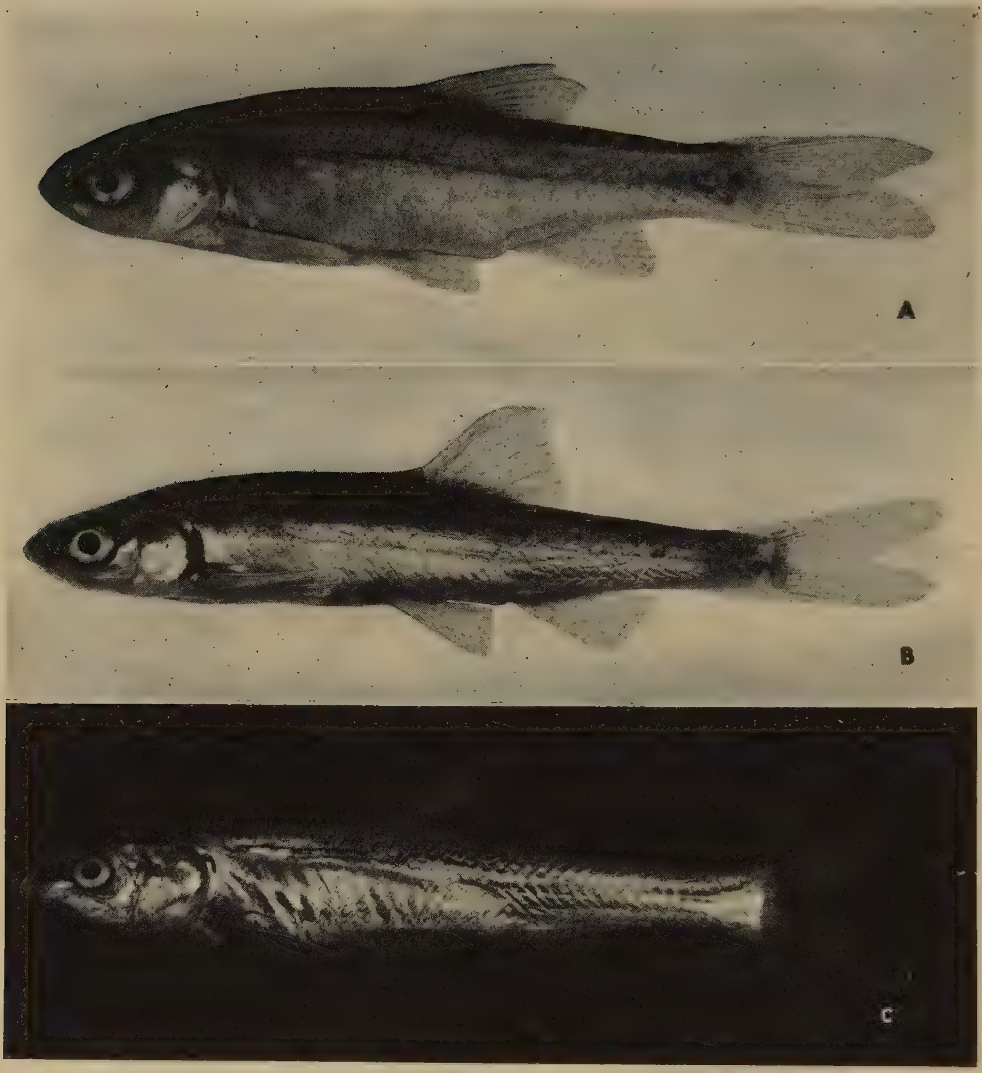

PLATE II

Three species of plagopterin fishes

A, *Lepidomeda vittata*, UMMZ 124754, 62 mm. S.L.
B, *Meda fulgida*, UMMZ 125030, 51 mm. S.L.
C, *Plagopterus argentissimus*, UMMZ 141669, 58 mm. S.L.

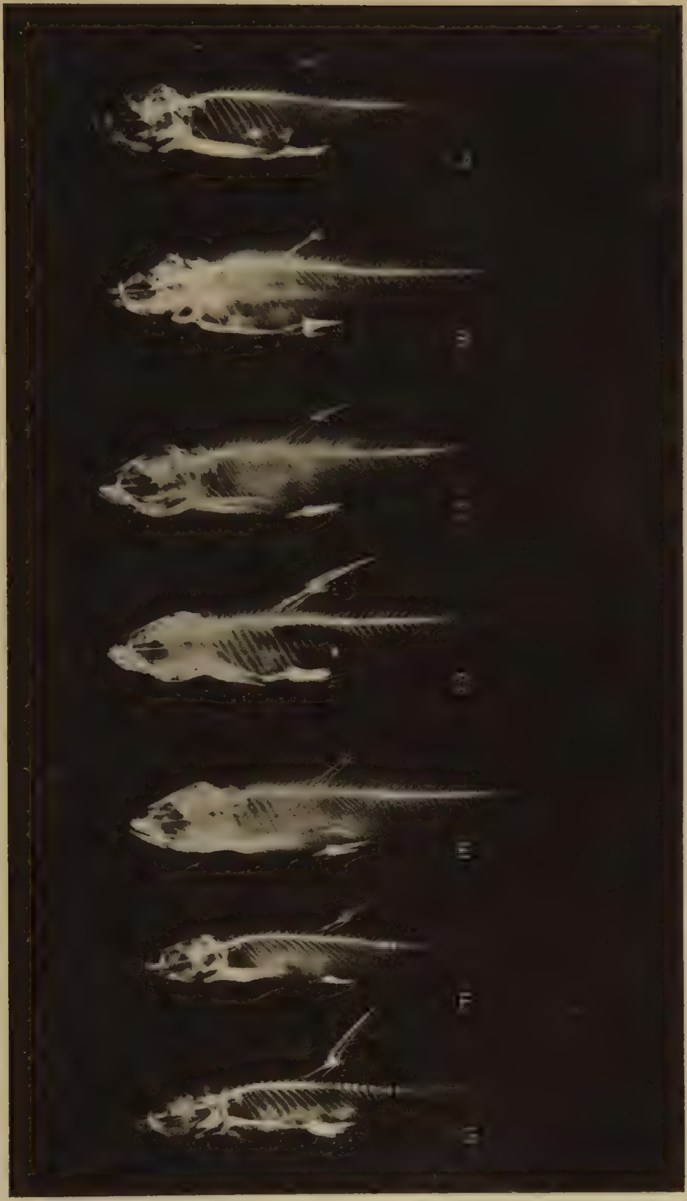

PLATE III

Radiographs of the seven forms of the Plagopterini

A, *Lepidomeda vittata,* UMMZ 137082, 55 mm. S.L.
B, *Lepidomeda m. mollispinis,* UMMZ 162849, 56 mm. S.L.
C, *Lepidomeda m. pratensis,* UMMZ 136097, 56 mm. S.L.
D, *Lepidomeda altivelis,* UMMZ 125004 (holotype), 56 mm. S.L.
E, *Lepidomeda albivallis,* UMMZ 132180, 54 mm. S.L.
F, *Meda fulgida,* UMMZ 162738, 49 mm. S.L.
G, *Plagopterus argentissimus,* UMMZ 141669, 53 mm. S.L.

Deep-Sea Research, 1960, Vol. 6, pp. 287 to 297. Pergamon Press Ltd., London. Printed in Great Britain

A review of the calculation of ocean currents at the equator

ROBERT S. ARTHUR

(*Received* 18 *August* 1959)

Abstract—Wind stress and horizontal pressure gradient at the equator have been used in the calculation of velocity. Various formulae are considered from the standpoint of consistency with an undercurrent. A simple relation between the east-west pressure gradient and the curvature of the velocity profile yields an undercurrent, but application is uncertain because of neglect of accelerations. The most promising formula appears to be that derived from the geostrophic approximation for zonal motion. Both friction and acceleration appear to be important in the dynamics of the Equatorial Undercurrent.

SEVERAL formulae for the calculation of ocean currents at the equator have appeared during the last decade. The purpose of this review is to examine such a calculation in respect to observations of the Equatorial Undercurrent, a narrow, eastward current prevalent in the lower part of the surface layer and in the thermocline layer along the equator in the Pacific. Among the important features observed along the equator are the following (CROMWELL *et al.*, 1954 ; KNAUSS and KING, 1958 ; KNAUSS, 1960) :

(a) surface flow may be directed westward at speeds of 25-75 cm sec^{-1}

(b) current reverses at a depth of from 20 to 40 m

(c) eastward undercurrent extends to a depth of 400 m with a transport of as much as 30×10^6 m^3 sec^{-1}

(d) core of maximum eastward velocity (50–150 cm sec^{-1}) rises from a depth of 100 m at 140 °W to 40 m at 98 °W, then dips down

(e) undercurrent appears to be symmetrical about the equator and becomes much thinner and weaker at 2 °N and 2 °S.

The various calculations of currents at the equator have been made by starting with the dynamic equations in some approximate form (WEENINK and GROEN, 1952; JERLOV, 1953 ; YOSHIDA, *et al.*, 1953 ; WYRTKI, 1956 ; HIDAKA and NAGATA, 1958). In most cases, a surface boundary condition (wind stress) has been introduced, and a bottom boundary condition (zero stress at some depth) has been assumed. The density distribution and resulting pressure distribution have been assumed to be known through observations of salinity and temperature at depth. This last assumption distinguishes the calculation methods from the theories of wind-driven circulation which include the equatorial region. In the theories (e.g., SVERDRUP, 1947 and REID, 1948a) the pressure distribution in integrated form is one of the results from the solution of the equations and is not assumed to be known.

The present paper directs attention primarily toward the calculation methods, but some comments on the theories are included. Except for the results of HIDAKA and NAGATA (1958), little or no indication of the Undercurrent has come from

Contributions from the Scripps Institution of Oceanography, New Series, 1161 (391)

Reproduced by Permission

previous applications of calculation formulae, and no clues to the existence of this current come from the theories. The situation is understandable in the case of calculations in which only a surface current is sought and in the theories which are involved with mass transport only. However, it seems appropriate to examine the bases of previous results to see whether an undercurrent is consistent with the equations and assumptions used.

As a basis for a review of the different methods, a set of dynamical equations for steady-state conditions is introduced.

$$u\frac{\partial u}{\partial x}+v\frac{\partial u}{\partial y}+w\frac{\partial u}{\partial z}=fv-2\Omega\,w\cos\phi-\frac{1}{\rho}\frac{\partial p}{\partial x}+\frac{1}{\rho}\frac{\partial \tau_x}{\partial z}+\frac{A_H}{\rho}\left(\frac{\partial^2 u}{\partial x^2}+\frac{\partial^2 u}{\partial y^2}\right),\tag{1}$$

$$u\frac{\partial v}{\partial x}+v\frac{\partial v}{\partial y}+w\frac{\partial v}{\partial z}=-fu-\frac{1}{\rho}\frac{\partial p}{\partial y}+\frac{1}{\rho}\frac{\partial \tau_y}{\partial z}+\frac{A_H}{\rho}\left(\frac{\partial^2 v}{\partial x^2}+\frac{\partial^2 v}{\partial y^2}\right),\tag{2}$$

$$u\frac{\partial w}{\partial x}+v\frac{\partial w}{\partial y}+w\frac{\partial w}{\partial z}=2\Omega\,u\cos\phi-g-\frac{1}{\rho}\frac{\partial p}{\partial z}.\tag{3}$$

$$\frac{\partial}{\partial x}(\rho u)+\frac{\partial}{\partial y}(\rho v)+\frac{\partial}{\partial z}(\rho w)=0.\tag{4}$$

The rectangular coordinate system has its origin at the sea surface, with x directed eastward, y northward, z upward, and u, v, w represent the corresponding velocity components. The Coriolis parameter is $f=2\Omega\sin\phi$, where Ω is the angular speed of the earth's rotation and ϕ is latitude. The pressure is p, the density ρ, the acceleration of gravity g, and the x- and y-components of shearing stresses across horizontal planes are τ_x and τ_y, respectively. Equations (1) and (2) represent the horizontal component equations of relative motion with the coefficient of lateral eddy viscosity, A_H, taken as uniform. The pressure will be assumed to be *known* from observations of density through the usual hydrostatic form of the approximation (3) of the vertical component equation and assumption of a reference surface. Assumption of a steady density field gives the equation of continuity in form (4).

A detailed analysis of velocity calculation at the equator is made from these equations in simplified form. The terms to be retained in the equations are those which have been suggested to be the important ones in central oceanic areas, i.e., beyond coastal boundary zones (MUNK, 1950 ; STOMMEL, 1956). The object of the analysis is to test the selection of terms against the new piece of observational evidence – the Undercurrent. An inquiry is pertinent in view of the fact that acceleration terms have been neglected at the equator in the calculation methods and theories, although FOFONOFF and MONTGOMERY (1955) have found acceleration to be important near the equator in their model of the Undercurrent.

It will be assumed that the stress and velocity at the surface are known. The applicability of the approximations will be examined, and comparison will be made with other calculations of currents at the equator.

ANALYSIS

STOMMEL (1956 ; 1957) proposes that, in general, the friction layer is limited to the proximity of the sea surface. Below this surface layer, the horizontal currents are approximately geostrophic, but there is vertical velocity which permits steady-state conditions for ρ. If acceleration, lateral friction, and the term $2\Omega\, w \cos \phi$ are neglected in (1)–(4), the horizontal convergence (or divergence) may be obtained without any lateral (coastal) boundary condition, and STOMMEL (1956) used such results to calculate v and w below the friction layer.

At the equator, the layer in which the friction or acceleration terms are important must be as deep as the layer in which the pressure terms are significant, according to (1) and (2). Since an observed distribution of ρ will be introduced, thermohaline forces as well as wind stress may be influencing the pressure gradient calculated from the hydrostatic form of (3). Relatively strong horizontal currents with important vertical shear may occur well below the depth to which the frictional layer is usually limited at higher latitudes. The possibilities for an undercurrent under the assumptions made by STOMMEL and others (e.g., SVERDRUP, 1947) may be examined with only very simple mathematics because at the equator ($\phi = 0°$ and $f = 0$) equations (1) and (2) may be written in the form

$$0 = -\frac{\partial p}{\partial x} + \frac{\partial \tau_x}{\partial z}, \tag{5}$$

$$0 = -\frac{\partial p}{\partial y} + \frac{\partial \tau_y}{\partial z}. \tag{6}$$

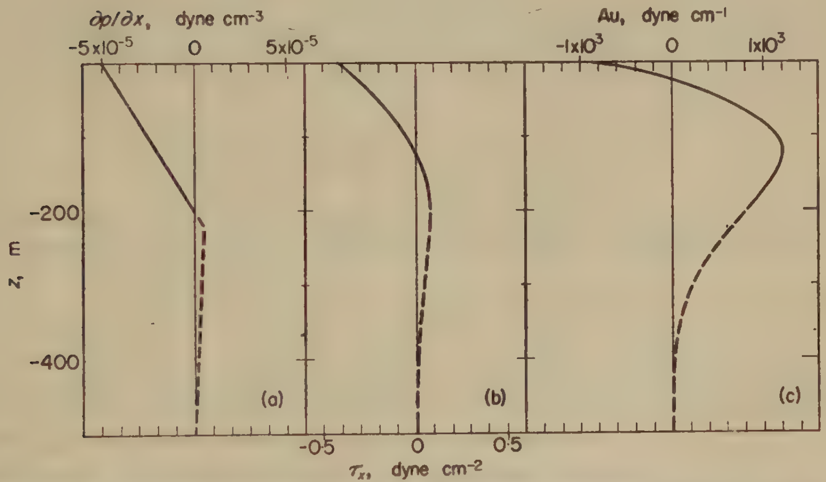

FIG. 1. (a) Assumed distribution with depth of east-west component of pressure gradient. (b) Resulting distribution of stress. (c) Resulting distribution of product of zonal velocity and coefficient of vertical eddy viscosity.

Integration of the x-component equation along the vertical from level z to the surface gives

$$\tau_x = (\tau_x)_0 - \int_z^0 \frac{\partial p}{\partial x}\, dz. \tag{7}$$

A distribution of $\tau_x(z)$ is derived from (7) for a given vertical distribution of $\partial p/\partial x$ (Fig. 1a) and an assumed value of the surface stress. The result is to be regarded as illustrative of a possibility derivable from a longitudinal component of the pressure gradient, the feature which Fofonoff and Montgomery (1955) have shown to be essential for an undercurrent. The sea surface slopes upward toward the west along the equator, so $\partial p/\partial x$, therefore, is negative at the surface. Isotherms in the upper part of the thermocline layer have the reverse slope, and the magnitude of the pressure gradient is reduced to less than 20 per cent of the value at the surface by a depth of some two hundred metres. The solid-line portion of the curve for $\partial p/\partial x$ (Fig. 1a) is representative of the pressure gradient along the equator in the eastern Pacific.

The stress τ_x is seen (Fig. 1b) to increase with depth from the assumed negative value at the surface to a zero value just below a depth of 100 m. Since the stress then becomes positive, the depth at which τ_x becomes zero is of particular significance. The vertical shear in the zonal motion vanishes, and the velocity component must exhibit an extreme value. This depth of zero stress is obviously dependent upon the distribution of $\partial p/\partial x$ and the value of the surface stress.

The conclusion about an extreme value of the velocity component existing at the level of zero stress follows from the expression of shearing stress in the form

$$\tau_x = A\frac{\partial u}{\partial z}, \tag{8}$$

where A is the vertical coefficient of eddy viscosity. The value of A is known only within wide limits, e.g. $1 < A < 300$ in g cm^{-1} sec^{-1}, and it is not independent of z. In spite of the uncertainties, it will be useful to see whether an undercurrent can in fact exist for a uniform, positive value of A. The results may be regarded as representative of an appropriate average value of A. Integration of (8) along the vertical gives

$$u = u_0 - \frac{1}{A}\int_z^0 \tau_x\,dz = u_0 + \frac{1}{A}\left(z\tau_x + \int_z^0 z\frac{\partial p}{\partial x}\,dz\right). \tag{9}$$

The right-hand member is obtained after integration by parts and substitution from (5). If velocity and stress components are negligible at some depth $z = -B$, then

$$u_0 = \frac{1}{A}\int_{-B}^0 \tau_x\,dz = -\frac{1}{A}\int_{-B}^0 z\frac{\partial p}{\partial x}\,dz, \tag{10}$$

which shows how the surface velocity is determined by a bottom boundary condition. Alternatively, a surface boundary condition is used, i.e., u_0 is given in (9).

The distribution of Au with z is determined from (9) for the previous example with the added assumption of a negative value of Au at the surface. Appropriate values for A would lie between 10 and 50. The result (Fig. 1c) shows that an undercurrent is possible with these assumptions.

It is desirable to consider whether a bottom boundary condition can be satisfied, and the dashed portions of the curves in Fig. 1 relate to this inquiry. It has been assumed that at some depth, e.g., 500 m, the quantities $\partial p/\partial x$, τ_x, $\partial \tau_x/\partial z$, u and $\partial u/\partial z$ all become zero. This condition has been considered appropriate for an internal boundary within the fluid because it permits an underlying layer with no pressure gradient and no stress as introduced by Sverdrup (1947), Munk (1950), and others. Equations (7) and (9) show that for τ_x and u to reach zero at some depth $z = -B$, there must be a region of positive values of $\partial p/\partial x$ above the boundary as shown in Fig. 1a. It must, however, be pointed out that in the region where $\partial p/\partial x$ has relatively small numerical values, say $< 0{\cdot}5 \times 10^{-5}$ dyne cm^{-3}, the terms which have been neglected in the equation of motion may become important. Different boundary conditions might also be assumed, as, for example, those appropriate for a rigid boundary, where τ_x could have a small positive value at the bottom. Under such a condition, $\partial p/\partial x$ need not have any positive values ; but if $\partial p/\partial x < 0$ everywhere, then the velocity profile will have negative curvature everywhere between surface and bottom as it does in the solution for the special case of laminar flow in a long channel with wind directed along the axis.

The accuracy in the determination of $\partial p/\partial x$ is not sufficient to guarantee the existence of a region of small positive values of pressure gradient. Pressure is, of course, determined from observations of density by application of the hydrostatic equation. A reference level below 1000 m is desirable in the Pacific. Eckart (1958) has reviewed and analyzed empirical data on the equation of state of pure water and sea water. His results indicate an uncertainty of at least ± 20 dynamic cm in the calculation of dynamic height over a pressure interval of 1000 db as a result of uncertainties in the equation of state. However, Reid (1959) has shown that the effect on calculation of horizontal pressure gradients at the surface may generally amount to an error of less than 5 per cent. Uncertainties in the horizontal temperature and salinity gradients introduce greater errors. Below a depth of 1000 m, the percentage error in the calculation of horizontal pressure gradient may increase to 50 per cent or more as a result of uncertainty in the value of the coefficient of thermal expansion. The distribution of $\partial p/\partial x$ assumed in the upper 200 m is comparable with that used by Montgomery and Palmén (1940) from *Dana* stations along the equator in the Pacific. Hidaka and Nagata (1958) arrive at about the same distribution from more recent observations ; *Albatross* stations 92 and 111 (Bruneau, *et al.*, 1953) to 2000 m give values which are numerically somewhat larger ; Austin (1958) obtains a mean value for $\partial p/\partial x$ of $- 5 \times 10^{-5}$ dyne cm^{-3} at the surface with a reduction to less than 5 per cent of this value by a depth of 200 to 300 m. The first three sources do show a reversal in sign of $\partial p/\partial x$ somewhere below 200 m, but no conclusions can be drawn because of the uncertainties.

Wind stress on the sea surface is not precisely known, and an estimate is now made of the influence of this uncertainty. Equation (7) and the distribution of $\partial p/\partial x$ from Fig. 1a are used to calculate the depth $z = z_m$ at which τ_x becomes zero for given values of $(\tau_x)_0$. Values of $A\,(u_m - u_0)$ at $z = z_m$ are calculated from (9) in the form

$$A\,(u_m - u_0) = \int_{z_m}^{0} z \frac{\partial p}{\partial x}\, dz. \tag{11}$$

Results are shown (Table 1) for a range of values of surface stress.

Table 1. Influence of wind stress

$(\tau_x)_0$ (dyne cm^{-2})	z_m (m)	$A\,(u_m - u_0)$ (gm sec^{-2})
$-0{\cdot}3$	-75	$1{\cdot}1 \times 10^3$
$-0{\cdot}4$	-110	$1{\cdot}9 \times 10^3$
$-0{\cdot}5$	-200	$3{\cdot}3 \times 10^3$

According to HIDAKA's tabulation (1958), the average value of wind stress on the equator (100 °W–135 °W) in summer and fall is about $-0{\cdot}5$ dyne cm^{-2}. For a region farther west HIDAKA and NAGATA (1958, Fig. 1) use an annual mean value of $-0{\cdot}3$. REID (1948a) finds a value near $-0{\cdot}4$ for October–November in a region which extends from near the coast to about 150 °W. A value between $-0{\cdot}3$ and $-0{\cdot}4$ would lead to the best agreement between z_m (Table 1) and the observed depths of the core of the Undercurrent. Observed values of the difference $(u_m - u_0)$ would give a value of A of about 10 g cm^{-1} sec^{-1}.

Analysis of the distribution of τ_y and v with z at the equator would proceed in similar fashion. Observations indicate that the current is mainly zonal which means that τ_y and, therefore, $\partial p/\partial y$ should be relatively small or zero at the equator. This conclusion is supported to a degree by observations since isotherms in meridional sections tend to show a maximum or minimum depth at or near the equator.

If (2) is differentiated with respect to y, after neglect of acceleration and lateral friction the result for $\phi = 0°$ is

$$\beta\rho u = -\frac{\partial^2 p}{\partial y^2} + \frac{\partial^2 \tau_y}{\partial y\, \partial z}, \qquad (12)$$

where $\beta = \partial f/\partial y$. If τ_y is sufficiently small not only at the equator but near the equator, then the last term in (12) may be neglected and the further approximation is

$$\beta\rho u \doteqdot -\frac{\partial^2 p}{\partial y^2}. \qquad (13)$$

APPLICABILITY OF APPROXIMATIONS

The magnitudes of terms neglected in equations (1)–(3) are now considered at the equator. Observations indicate that $\partial u/\partial y$ is zero or very small in the westward flow near the surface at the equator. The Undercurrent appears to be symmetrical about the equator and reasonably steady. For the motion in the meridional plane, the model of CROMWELL (1953) is used, and v is taken as zero at the equator and w positive and symmetrical about the equator. Estimates are made using the following characteristic velocity and distance components:

$U = 10^2$ cm sec^{-1} $\quad L_x = 5 \times 10^8$ cm

$V = 4$ cm sec^{-1} $\quad L_y = 10^7$ cm

$W = 10^{-3}$ cm sec^{-1} $\quad L_z = 10^4$ cm

The value chosen for U is appropriate for the velocity near the core of the Undercurrent. FOFONOFF and MONTGOMERY (1955) have suggested the value 4 cm sec^{-1} for the velocity of flow toward the equator at the depth of the Undercurrent. The value of W is consistent from continuity considerations with the value of V and is a value which has been suggested as appropriate for upwelling at the equator (YOSHIDA, *et al.*, 1953). Distance L_x corresponds to about 50 degrees of longitude along the equator, L_y to about 1 degree of latitude, and L_z to the depth of the core of the Undercurrent.

In the x-component equation (1), the neglected acceleration term $v\,(\partial u/\partial y)$ is certainly negligible at the equator if v is zero and u is symmetrical. However, the

(396)

terms $u\,(\partial u/\partial x)$ and $w\,(\partial u/\partial z)$ may have values of the order of 10^{-5} cm sec^{-2} which is comparable with the longitudinal component of the pressure gradient term in the Undercurrent. The term $(u\,\partial u/\partial x)$ is zero at the core and in the westward surface current which shows relatively constant velocities along the equator. This term is positive in the Undercurrent above the core and negative below because of the rise in the core from west to east. The term $w\,(\partial u/\partial z)$ is zero at the core and at the surface. If w is positive, this term has negative values above the core and positive values below. While these two acceleration terms may not be separately negligible between core and surface, they have a tendency to offset each other. Complete cancellation occurs if the water particles move *without acceleration* along streamlines which are inclined to the horizontal. If the above characteristic velocities W and U are used, the value of the slope of the streamlines is 50 m in 5000 km which is almost identical with the observed rise in the core from west to east.

Actually, the acceleration of the water particles may not be zero at the equator, and an estimate is now made of the separate influence of an acceleration which results entirely from a term of the form $w\,(\partial u/\partial z)$. Calculations are made under the assumption that the right-hand side of (5) equals $w\,(\partial u/\partial z)$. The stress is taken to be zero at $z_m = -100$ m and the distribution of $\partial p/\partial x$ in Fig. 1 is used. Vertical velocity is assumed to decrease linearly from a value of w_m at z_m to a value of zero at the surface. Resulting values of $(\tau_x)_0$ and $A\,(u_m - u_0)$ are given in Table 2 for two values of $\rho w_m/A$ along with comparative values for zero vertical velocity.

Table 2. Influence of vertical velocity

$\rho w_m/A$ (cm^{-1})	$(\tau_x)_0$ (dyne cm^{-2})	$A\,(u_m - u_0)$ (gm sec^{-2})
0	$-0{\cdot}38$	$1{\cdot}7 \times 10^3$
1×10^{-4}	$-0{\cdot}43$	$2{\cdot}0 \times 10^3$
$1{\cdot}6 \times 10^{-4}$	$-0{\cdot}48$	$2{\cdot}2 \times 10^3$

Appropriate values of A would lie in the range of 10 to 20 gm cm^{-1} sec^{-1}, and w_m would then be of the order 10^{-3} cm sec^{-1}. Observed values of $(u_m - u_0)$ and $(\tau_x)_0$ might just be sufficiently accurate to verify the importance of this acceleration term $w\,(\partial u/\partial z)$. Values are changed by about 25 per cent.

The neglected Coriolis term, $2\Omega w \cos\phi$, in equation (1) has a magnitude of about 10^{-7} cm sec^{-2} and is negligible. Any estimates of lateral friction terms are difficult to arrive at because of the arbitrariness in values of lateral eddy viscosity. If these terms are replaced by the single term ku (YOSHIDA, *et al.*, 1953 ; WYRTKI, 1956), then the equation for unaccelerated motion at the equator is

$$A\,\frac{\partial^2 u}{\partial z^2} = \frac{\partial p}{\partial x} + ku, \tag{14}$$

where A has been assumed constant. The left-hand member is negative at the core and $\partial p/\partial x$ is about -2×10^{-5} dyne cm^{-3} and u is about 10^2 cm sec^{-1}. Therefore the maximum value of k is 2×10^{-7} g cm^{-3} sec^{-1}. YOSHIDA, *et al.*, and WYRTKI have used a value of k equal to 5×10^{-6} and A equal to 10^2 g cm^{-1} sec^{-1}. Equation

(14) may be solved with these values and a distribution of $\partial p/\partial x$ given in Fig. 1. For $(\tau_x)_0$ equal to $-0{\cdot}4$ dyne cm^{-2} and u_0 equal to -25 cm sec^{-1}, the value of u increases to -20 at 30 m depth and then decreases. Results bear little resemblance to observations and indicate that lateral friction has been overemphasized.

In the y-component equation (2), the neglected acceleration terms are all zero at the equator if v is zero. Terms neglected in the further approximation (13) are of the order of magnitude 10^{-13} g cm^{-3} sec^{-2}, which is to be compared to 10^{-11}, the order of magnitude of $\beta\rho u$.

In the z-component equation (3), the neglected acceleration terms and the Coriolis term $2\Omega u \cos\phi$ are all zero at the equator or are orders of magnitude smaller than ρg. The derivatives with respect to x and y of the neglected terms are also orders of magnitude smaller than the derivatives of terms retained.

COMPARISON WITH OTHER CALCULATIONS

SVERDRUP (1947) and REID (1948a) introduced the net mass transport from surface to great depth as a variable in place of velocity. Their theory differs from the calculation methods in that the distribution of density is not assumed, but a comparison with observations of the Undercurrent is nevertheless pertinent. Equation (4) and the previously indicated approximations to equations (1) and (2) were integrated along the vertical, and integrated mass transport and integrated pressure were calculated from values of wind stress for the eastern equatorial Pacific. Calculation of the zonal component of mass transport, M_x, requires a boundary condition which was satisfied by taking M_x equal to zero at the coastline on the east. The values of M_x at the equator show a net transport to the west away from the eastern coastline. The question is whether this result implies no undercurrent, and the answer lies in the interpretation of the condition $M_x = 0$. SVERDRUP and REID assume $(\tau_x)_0 \neq 0$ at the eastern boundary, and this means that $\partial p/\partial x \neq 0$ at this boundary at the equator. As a consequence of (1), neither τ_x nor u is zero at all depths, and the boundary is *not* to be interpreted as a vertical wall. Under these circumstances imposition of the condition $M_x = 0$ is somewhat arbitrary and must be interpreted to apply at some distance from the actual coastline with an intervening boundary layer in which terms omitted in equations (1) and (2) are important. An undercurrent may be present at the boundary as long as the *net* transport is zero. The results of SVERDRUP and REID need only imply that the transport of the undercurrent decreases westward from the boundary or that westward flow above or below the undercurrent increases.

WEENINK and GROEN (1952) solved similar approximations to (1), (2) and (3) for the surface velocity at the equator in terms of wind stress. Vanishing velocities at great depth are assumed, and REID's (1948b) model of the density distribution is applied. REID has pointed out certain deficiencies in his model near the equator. YOSHIDA (1955) has examined the results of WEENINK and GROEN and has shown how to remove a discontinuity in the meridional transport and a downward vertical velocity at the surface by application of a more complete density model. As pointed out by YOSHIDA, the method amounts to application of (10) to any vertical distribution of the pressure gradient obtained from observations or a model. Extension of the method to obtain velocities below the surface has been shown in the present paper to lead to an undercurrent.

JERLOV (1953) applied approximation (13) to calculate the zonal component of velocity at the equator. REID (1948a) derived an expression similar to (12) but for integrated mass transport rather than velocity. TSUCHIYA (1955b) concludes that the approximations involved in these expressions are justified. According to (13), the sign of $\partial^2 p/\partial y^2$ should be negative at the depth of the Undercurrent. A trough in the isotherms or isolines of density favours such a sign and, as pointed out by WOOSTER and JENNINGS (1955), is probably related to the Undercurrent. Such a trough at or near the equator occurs in a number of meridional sections including those of KNAUSS (1960) and MONTGOMERY and STROUP (1960).

YOSHIDA *et al.*, (1953) replaced lateral friction terms by the terms $-ku$ and $-kv$ in the right-hand members of (1) and (2), respectively. Accelerations were neglected, and equation (4) was used to determine vertical velocity. Density observations near the equator were introduced into (3) to determine the pressure field. Calculations of u and v from (1) and (2) in terms of stress at top and bottom of the surface layer show no undercurrent. As pointed out previously the reason seems to be the overemphasis on lateral friction through excessively large values of coefficient k. WYRTKI (1956) used essentially the same method to calculate mass transport of the surface layer.

HIDAKA and NAGATA (1958) calculated u and v from (1) and (2) with accelerations neglected. Wind stress and pressure gradients were assumed from observations. The results show an undercurrent, but the method cannot be considered valid because of the magnitude of field accelerations. If the results are used to calculate $v\,(\partial u/\partial y)$ at the equator, the order of magnitude of this neglected term is 10^{-4} cm sec^{-2} which is as large as the magnitudes of terms retained in (1). It should also be noted that the resulting undercurrent is not symetrical with the equator.

FOFONOFF and MONTGOMERY (1955) find the Undercurrent to be consistent with conservation of absolute vorticity in an equatorward flow of a layer of constant thickness. The model assumes a meridional circulation in which the water in the lower part of the surface layer flows equatorward and then moves upward at the equator. The acceleration term $v\,(\partial u/\partial y)$ is found to be important, but the treatment considers the conditions near but not right on the equator. Since this term does not enter the y-component equation of motion, there is no conflict with approximation (13).

SUMMARY AND CONCLUSIONS

1. The assumption is made that two important terms in the x-component (east-west) equation of motion at the equator are the pressure gradient and the frictional stress across horizontal planes. The two terms are equated, and the profile of zonal velocity is calculated from values of surface velocity, wind stress, and horizontal pressure gradient for a constant vertical eddy coefficient. The results give an undercurrent with certain features such as the reversal in direction of current at shallow depths which compare favourably with observations. The calculated depth of the core of maximum eastward velocity is independent of the particular value of the eddy coefficient. The rise of the core toward the east suggests a relatively reduced surface wind stress or an increased pressure gradient.

2. The motion appears to be steady, but two of the field acceleration terms, $u\,(\partial u/\partial x)$ and $w\,(\partial u/\partial z)$, are probably not negligible. FOFONOFF and MONTGOMERY

(1955) have demonstrated the importance of the term $v\,(\partial u/\partial y)$ in the region where water moves toward the equator. This term may be neglected at the equator. However, the implication is that acceleration terms may not be neglected for the determination of currents *both on and near the equator.* This conclusion is important because theories of the surface circulation which include the equatorial regions have neglected acceleration. Conversely, friction is important in the core of the Undercurrent ; and absolute vorticity may not be conserved in the immediate vicinity of the equator. Velocity profiles observed by KNAUSS (1960) would suggest that friction in the core is important to at least 0·5 degrees of latitude north and south of the equator if the value of A appropriate at the equator is used.

3. JERLOV (1953) and others have differentiated the geostrophic formula for zonal motion to remove the indeterminancy at the equator. Indications are that the approximation may have validity, but its usefulness is limited by the difficulty in obtaining sufficiently accurate estimates of $\partial^2 p/\partial y^2$. Nevertheless, this approximation seems to offer the most hope for a successful formula for calculation of currents at the equator, because acceleration and friction terms appear to be negligible in this particular equation.

4. Other formulae include lateral friction. Results are unrealistic because of excessively large friction coefficients or are uncertain because of large accelerations.

Acknowledgements—Contribution from the Scripps Institution of Oceanography. This paper represents the results of research carried out by the University of California under contract with the Office of Naval Research. Reproduction in whole or in part is permitted for any purpose of the United States Government. This study was initiated as a result of discussions with TOWNSEND CROMWELL and JOHN KNAUSS on the various formulae for calculating currents at the equator and their consistency with the Undercurrent. Subsequent discussions with these and other colleagues at Scripps, with R. B. MONTGOMERY of Johns Hopkins University, and HENRY STOMMEL of Woods Hole Oceanographic Institution have also been most helpful.

University of California, Scripps Institution of Oceanography
La Jolla, California

REFERENCES

AUSTIN T. S. (1958) Variations with depth of oceanographic properties along the equator in the Pacific. *Trans. Amer. Geophys. Union* **39**, 1055–1063.

BRUNEAU L., JERLOV N. G. and KOCZY F. F. (1953) Physical and chemical methods. *Rep. Swedish Deep-Sea Exped.* 3, *Physics and Chemistry* **4**, 100–112.

CROMWELL T. (1953) Circulation in a meridional plane in the central equatorial Pacific. *J. Mar. Res.* **12**, 196–213.

CROMWELL T., MONTGOMERY R. B. and STROUP E. D. (1954) Equatorial Undercurrent in Pacific Ocean revealed by new methods. *Sci.* **119**, 648–649.

ECKART C. (1958) The equation of state of water and sea water at low temperatures and pressures. *Amer. J. Sci.* **256**, 225–240.

FOFONOFF N. P. and MONTGOMERY R. B. (1955) The Equatorial Undercurrent in the light of the vorticity equation. *Tellus* **7**, 518–521.

HIDAKA K. (1958) Computation of the wind stresses over the oceans. *Rec. of Oceanogr. Works in Japan* **4**, 77–123.

HIDAKA K. and NAGATA Y. (1958) Dynamical computation of the equatorial current system of the Pacific, with special application to the Equatorial Undercurrent. *Geophys. J.* **1**, 198–207.

JERLOV N. G. (1953) Studies of the equatorial currents in the Pacific. *Tellus* **5**, 308–314.

KNAUSS J. A. (1960) Measurements of the Cromwell Current. *Deep-Sea Res.* **6**, 265–285.

KNAUSS J. A. and KING J. E. (1958) Observations of the Pacific Equatorial Undercurrent. *Nature, Lond.* **182**, 601–602.

(400)

Montgomery R. B. and Palmén E. (1940) Contribution to the question of the Equatorial Counter Current. *J. Mar. Res.* **3**, 112–133.

Montgomery R. B. and Stroup E. D. (1960) (In preparation).

Munk W. H. (1950) On the wind-driven ocean circulation. *J. Meteor.* **7**, 79–93.

Reid R. O. (1948a) The equatorial currents of the eastern Pacific as maintained by the stress of the wind. *J. Mar. Res.* **7**, 74–99.

Reid R. O. (1948b) A model of the vertical structure of mass in equatorial wind-driven currents of a baroclinic ocean. *J. Mar. Res.* **7**, 304–312.

Reid R. O. (1959) Influence of some errors in the equation of state or in observations on geostrophic currents. *Conference on Physical and Chemical Properties of Sea Water, Nat. Acad. Sci.-Nat. Res. Council Pub.* No. 600, 10–29.

Stommel H. (1956) On the determination of the depth of no meridional motion, *Deep-Sea Res.* **3**, 273–278.

Stommel H. (1957) A survey of ocean current theory. *Deep-Sea Res.* **4**, 149–184.

Sverdrup H. U. (1947) Wind-driven currents in a baroclinic ocean. *Proc. Nat. Acad. Sci.* **33**, 318–326.

Tsuchiya M. (1955a) On a simple method of estimating the current velocity at the equator. *J. Oceanogr. Soc. Japan* **11**, 1–4.

Tsuchiya M. (1955b) On a simple method for estimating the current velocity at the equator (II). *Rec. of Oceanogr. Works in Japan* **2** 1–6.

Weenink M. P. H. and Groen P. (1952) On the computation of ocean surface current velocities in the equatorial regions from wind data. *Konikl. Nederl. Akademie van Wetenschappen, Proceedings* (*B*) **55**, 239–246.

Wooster W. S. and Jennings F. (1955) Exploratory oceanographic observations in the eastern tropical Pacific, January to March, 1953. *Calif. Fish and Game* **41**, 79–90.

Wyrtki K. (1956) The computation of oceanic and meteorological fields of motion with friction proportional to the velocity *Penjelidkan Laut di Indonesia* No. 2, 1–26.

Yoshida K. (1955) A note on dynamics near the equator, in view of the recent observations in the eastern equatorial Pacific. *J. Oceanogr. Soc. Japan* **11**, 1–5.

Yoshida K. H. L. Mao and Horrer P. L. (1953) Circulation in the upper mixed layer of the equatorial north Pacific. *J. Mar. Res.* **12**, 99–120.

Printed in Great Britain by The Salisbury Press Ltd., Publicity House, Wilton Road, Salisbury, Wilts. (22851)

Deep-Sea Research, 1960, Vol. 6, pp. 265 to 286. Pergamon Press Ltd., London. Printed in Great Britain

Measurements of the Cromwell Current

JOHN A. KNAUSS

(*Received* 15 *August* 1959)

Abstract—Direct current measurements made along the equator in the central and eastern tropical Pacific during the IGY show that the subsurface eastward flow, first described in 1954, is a fast, thin, but major current. As defined by the 25 cm/sec contour, it is 300 km wide and about two-tenths of a kilometre thick; it is symmetrical about the equator. At 140 °W the core of the current is at 100 m. Velocities up to 150 cm/sec (3 knots) were recorded. The average transport based on four sections is 39×10^6 m^3/sec. The current was traced from 140 °W to the Galapagos Islands at 92 °W. It was not found east of the Galapagos at 89 °W. The core velocity was 100 – 150 cm/sec from 140 °W to the Galapagos; the depth of the core shallowed from 100 to 40 m. At the surface and at 500 m the flow was to the west.

Hydrographic measurements suggest that the flow is in geostrophic equilibrium to within half a degree of the equator. The major features of the Pacific Equatorial Undercurrent (Cromwell Current), including its general shape, the depth of the core, which slopes upward to the east, can be accounted for by assuming a geostrophic flow in response to the perturbation in the horizontal pressure gradients caused by mixing through the thermocline at the equator.

Direct measurements of the Cromwell Current show that the current extends from at least 92 °W to 150 °W (3500 miles). Indirect evidence suggests that the current will be found to at least 170 °W (4700 miles long) and perhaps as far as 160 °E (6500 miles long).

INTRODUCTION

Previous Observations

THE Cromwell Current is a major feature of the oceanic circulation whose presence was unsuspected nine years ago, and whose existence was not predicted by any of the theories of oceanic circulation. Apparently the first indication that there was anything unusual about the currents at the equator in the Pacific was in September, 1951, aboard the *Hugh M. Smith*,* when fishing for tuna at the equator south of Hawaii. The long line gear drifted to the east while the surface drift of the ship was to the west. Further evidence for an eastward subsurface current was gathered at five long line fishing stations (*John R. Manning** and *Charles H. Gilbert**) between January and June 1952. In August of that year an expedition under the leadership of the late Townsend Cromwell made twelve direct current measurements in the vicinity of the equator and 150 °W by observing the rate of drift of deep drags with respect to those at the surface. One of these at 2° 54′S showed no eastward current; four between 0° 14′N and 1° 31′N indicated an eastward subsurface current, and one at 0° 14′N showed an eastward drift of more than a knot. Four observations between 1° 50′N and 2° 43′N showed a westward current. In all nine cases, the surface drag drifted to the west. The remaining three observations were made in the equatorial Countercurrent near 7 °N where both surface and deep drags moved to the east. Although there was no way of knowing the exact depth of the drogue, the eastward current was placed in the ‘ lower part of the surface layer and upper thermocline ’ at a depth of approximately 100 m (CROMWELL *et. al.*, 1954; MONTGOMERY and STROUP, to be published).

*Vessels of the Pacific Oceanic Fisheries Investigation (POFI) U.S. Fish and Wildlife Service.

Contributions from the Scripps Institution of Oceanography, New Series, 1162

Reproduced by Permission

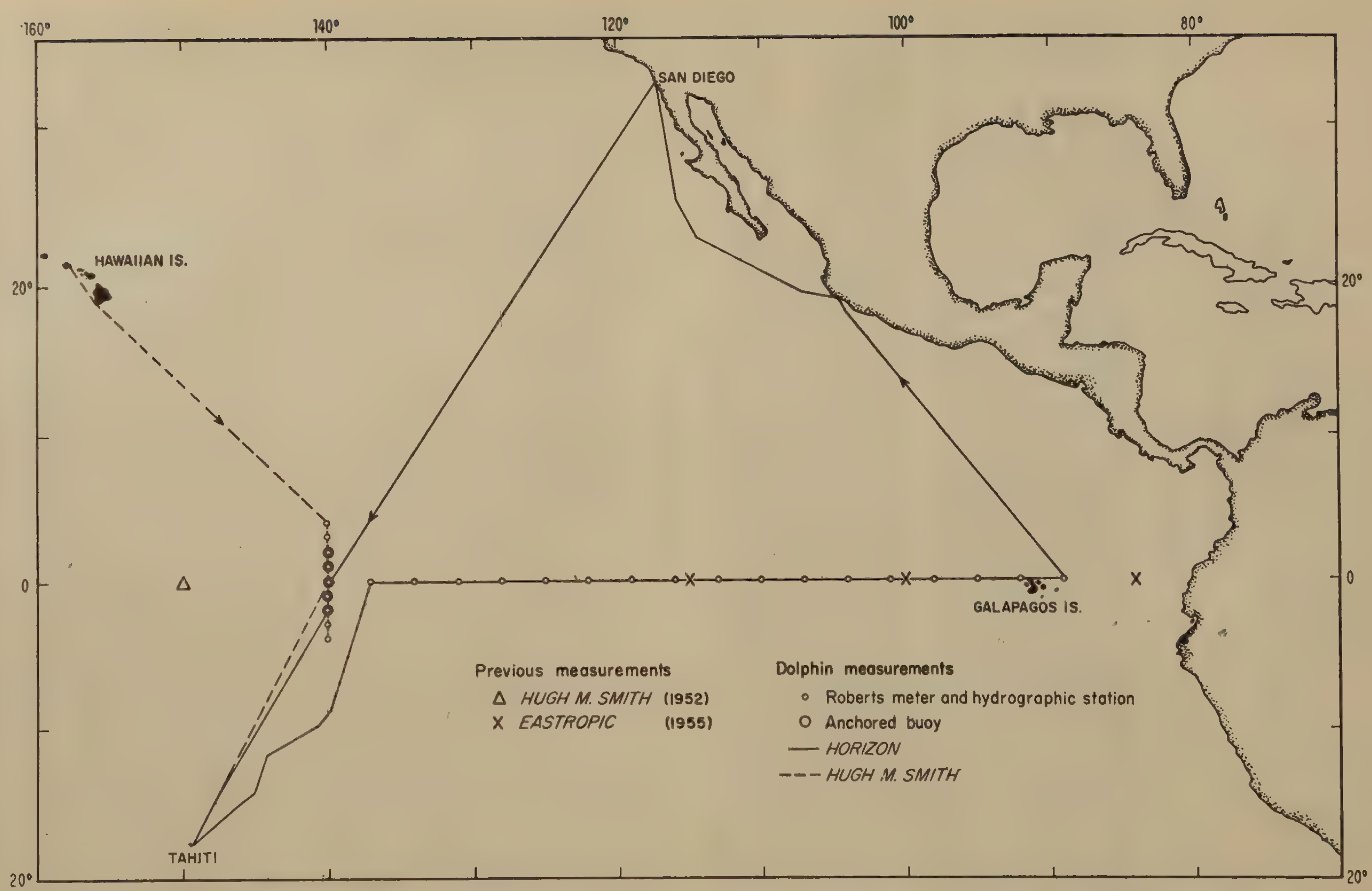
160°
140°
120°
100°
80°
20°
0
20°
SAN DIEGO
HAWAIIAN IS.
GALAPAGOS IS.
TAHITI
Previous measurements
Δ HUGH M. SMITH (1952)
X EASTROPIC (1955)
Dolphin measurements
∘ Roberts meter and hydrographic station
O Anchored buoy
— HORIZON
- - - HUGH M. SMITH

FIG. 1.´ Track chart for the *Dolphin* Expedition and the location of earlier observations of the Pacific Equatorial Undercurrent.

A further attempt to observe this current with free floating parachute drogues (VOLKMANN *et. al.*, 1956), made by Townsend Cromwell and the author in the fall of 1955 (part of the *Eastropic* Expedition) indicated that the east-flowing current was present at 115 °W and 100 °W, but not at 84 °W.

McGary and Rinkel, with an Ekman current meter between 12 °N and 5 °S along 140 °W (*Hugh M. Smith*, Cruise 33, March 1956) found an eastward subsurface current at the equator (RINKEL, personal communication).

Cromwell suggested the name Pacific Equatorial Undercurrent for this east-flowing subsurface current (CROMWELL *et. al.*, 1954). On June 2, 1958, Townsend Cromwell was killed in an aeroplane crash near Guadalajara, Mexico, on his way to join a Scripps Expedition, just as the joint Scripps-Pacific Oceanic Fisheries Investigation, *Dolphin* Expedition, was completing the study of currents at the equator. It has subsequently been suggested that this east-flowing subsurface current be called the Cromwell Current (KNAUSS and KING, 1958).

Dolphin Expedition

The *Dolphin* Expedition in the spring of 1958 (Fig. 1) was planned to answer the following questions : (1) What is the vertical distribution of horizontal current velocity at the equator ? (2) What is the latitudinal variation of this distribution ? (3) How far to the east can the Cromwell Current be traced ? (4) How does the velocity profile of the current change eastward along the equator ? (5) Is there any marked day-to-day change in the current ? (6) How is the Cromwell Current related to the observed distribution of such properties as temperature, salinity, oxygen or phosphate at the equator ?

For this expedition a new technique for measuring currents in the open ocean was developed. A taut wire buoy similar to that described by ISAACS *et. al.* (1957) was anchored to serve as a fixed reference point. A propeller-type current meter equipped with a depth indicator, a modified Roberts Meter (ROBERTS, 1952), was lowered from the ship at different depths to observe the ' apparent current,' i.e., the water flowing by the current meter. The drift of the ship with respect to the anchored buoy was measured by radar. The true current at any depth was then found by vector subtraction of the ship drift from the apparent current.

For some of the observations a free-floating parachute drogue with the parachute suspended at 800–1000 m was used as the reference point. Although such a drogue is in no sense a fixed reference as is an anchored buoy, the drift of these deep parachute drogues is small compared to the currents measured on *Dolphin.*

*Horizon** proceeded directly to the equator at 140 °W to anchor a buoy, where current observations were made twice a day, either by *Horizon* or by *Hugh M. Smith* during the first half of the expedition. At the same time *Hugh M. Smith* made current measurements with reference to deep parachute drogues at stations along 140 °W at 4 °N, 3 °N, 2 °N, 1 °N, 1 °S, 2 °S, 3 °S and 4 °S to determine the approximate boundaries of the Cromwell Current. On completion of this exploratory section, *Hugh M. Smith* took the measurements at the equatorial station and *Horizon* anchored four more buoys at 2 °N, 1 °N, 1 °S and 2 °S along 140 °W. The positions were chosen on the basis of *Hugh M. Smith* measurements which indicated the Cromwell Current was either very weak or missing at all the stations other than at 1 °N and 1 °S.

*Vessel of the Scripps Institution of Oceanography, University of California.

(405)

The equatorial station was monitored continuously by one or the other ship from 6–27 April; the second ship took current observations at the other anchored buoys. Both ships departed for Tahiti, 28 April.

Hugh M. Smith turned to other work after visiting Tahiti, but made a final hydrographic station at the equator, 140 °W on 15 June. *Horizon* returned to the equator and made measurements along the equator between 137 °W and 89 °W at stations 180 miles apart. A 1200 m hydrographic cast and a Roberts current measurement to 300 m were made at each station.

INSTRUMENTATION, TECHNIQUE AND ESTIMATE OF ERROR

Anchored Buoys

Taut wire anchored buoys have been under development at Scripps since 1952 (ISAACS *et. al.*, 1957). Starting at the bottom, the buoy system used on *Dolphin* consisted of a 500 lb anchor, a mooring wire about 4000 m long (0·123 inch diameter, weight 28·8 lbs/1000 ft, 2300 lb breaking strength) attached to a 34 inch steel sphere (positive buoyancy 537 lbs). The length of mooring wire was predetermined to keep the underwater float about 200 m below the surface. Three hundred thirty-five metres of $\frac{3}{16}$ in. wire rope ran from the underwater float to the surface float (an eight foot fibreglass skiff with a light and radar antenna).

By buoying the long length of mooring wire well below the surface, several advantages are gained which help to minimize the extent to which the buoy can swing on its anchor. The first advantage is that the underwater float exerts a buoyant force upon the mooring wire; and if this force can be kept large compared to the horizontal drag forces on the system, there is little horizontal movement of the underwater float. The second advantage of the underwater float over a conventional mooring is that the underwater float is not as subject to forces such as those generated by a heavy sea, and therefore, a light-weight, small-diameter (and consequently low-drag) mooring wire can be used. The surface buoy can also have low-drag characteristics, since it need only be large enough to support the heavier wire used in running from the underwater float to the surface buoy. Finally, the ratio of wire length to water depth of a taut wire mooring can be less than that used with safety in a conventional mooring system.

Roberts meter measurements

A modified Roberts current meter (ROBERTS, 1952) used for these measurements was suspended in a steel bridle with an electric swivel by a single conductor, insulated, steel wire. Twenty-four volts, alternating current, could be sent down the wire and the circuit completed through sea water. Oppositely phased current was led to two contacts through two silicon diodes. One contact (the speed contact) was fixed to the current meter; the other (the direction contact) was attached to a magnetic compass bar and could rotate freely.

The usual procedure in taking measurements aboard the *Horizon* was, when within good radar range (about 1000 m from the anchored buoy), to lower the Roberts meter to a depth of 300–330 m. The meter was allowed to come to equilibrium before taking any readings. More wire had to be let out if the instrument started to rise. Readings inadvertently made while the meter was rising or sinking rapidly were discarded.

Observations were made at depth intervals of 10 to 25 m. The velocity at each depth was recorded for a period of 20 to 150 sec. About every ten minutes the radar range and bearing from the anchored buoy was checked. The time for such a series of observations was between one and two hours. Often a free-floating surface drogue was released next to the anchored buoy before a Roberts meter lowering and picked up on its completion. In this way the surface current was measured.

Estimate of error in Roberts meter measurements

There are several sources of error in current measurements with this technique; some can be estimated with confidence, some cannot. It is believed that the errors are random, and that the various types of error are independent of one another. For those errors which can only be estimated, the values in the following discussion are not the outside limits of error but rather of the standard deviation.

One type of error is introduced in assuming that the anchored buoy is a fixed point. The buoy may move, and this movement can be of two sorts; translational movement caused by dragging the anchor, and random movement because of the swinging of the buoy on its anchor. Movement due to anchor dragging was negligible. Except for the buoy at the equator which dragged five miles during the first 78 hours (less than 0·5 cm/sec), there was no movement of any of the anchored buoys large enough to be detected by celestial navigation, i.e., greater than a mile.

The length of wire between the underwater float and the surface float was in all cases 335 m. The depth of the underwater floats varied between 165 and 225 m. Assuming for a moment no horizontal displacement of the underwater float, the extreme diameter of the circle described by the buoy as it swings on its anchor would be the order of 600 m. Since the line between the surface float and the underwater float is curved rather than straight the circle would be less. On the other hand, any horizontal forces on the underwater float would increase the effective radius, perhaps by a factor of three.

Although no measure of this random buoy movement was taken on the *Dolphin* Expedition, measurements were made with a similar buoy in the Equatorial Countercurrent two months later. Bathymetric sounding lines were run with reference to the buoy. Then by matching different bathymetric surveys, the shift in the buoy position between surveys was determined. Nine such surveys were made around the buoy in a 17-day period, the first being run 36 hours after the buoy was laid. The anchor dragged for the first 150 hours at a speed of about 0·25 cm/sec. There was no net displacement for the remaining ten days. The seven positions of the buoy during this ten-day period fell within a circle of 700 m in diameter.

There were no rapid changes in current or wind observed during the current measurements. For an estimate of the buoy velocity, one might assume a movement of 700 m in six hours. The buoy velocity would be 3 cm/sec.

A second source of error is in the radar ranges. Under the ideal conditions which prevailed during most of the measurements, the precision of reading the Navy-type SU radar used was about ± 100 m and ± 1°. If one assumes that the ship drifted at a constant velocity during the 90 to 120 minutes it takes for a complete set of measurements, the error in measuring ship drift is about 2 cm/sec. Radar readings were taken every ten minutes, plotted and a smooth curve drawn through the points. Usually the ship drift appeared to be steady, but at times it was obvious that this varied. All estimates of ship velocity were made by fitting smooth curves through the plotted points. For the data taken aboard *Horizon*, it is believed that the ship drift relative to the buoy is known between ± 2 and ± 7 cm/sec.

A third source of error is in the current meters themselves. A speed calibration between 5 and 300 cm/sec was made for each instrument in the Convair tow tank, San Diego. Differences between runs with the same meter were as great as the differences between meters. Therefore, a single calibration curve was drawn for the three meters. The standard deviation was 1·5 cm/sec in the 5 to 50 cm/sec range based on 25 points and 7·5 cm/sec in the 50–300 cm/sec range based on 21 points. It is believed that this estimate of error is the largest to be expected. Difficulty was experienced in controlling the calibration at the high velocity end of the scale, and it is believed that at least some of the differences in the two standard deviations are a result of poor calibration control at higher velocities.

A direction calibration was made for each of the three meters, and again there was no significant difference between meters. The standard deviation from the true direction for the three meters was ± 8° based on 280 readings.

There are two other sources of error which are more difficult to estimate. One is ship yaw. As the ship is blown through the water with the wind on the beam, the ship's head swings and the ship begins to sail through the water with the wind abaft the beam. The ship continues to move with increased speed until the resistance of the water becomes too great; then the ship's head falls off, and the process is repeated. A ten-knot wind will cause a variation in *Horizon's* drift rate of 10–15 cm/sec. The period of this yaw is in the order of 20 minutes, which is too short to be detected by radar fixes but probably long enough for a full response of the current meter. It is perhaps possible to minimize this effect by throwing the rudder hard over, so that the ship will sail more easily and come back with the wind on its beam less readily; or steerage way and a constant heading can be maintained by steaming slowly through the water, as was done during most of the second half of the expedition.

The last source of error is the pumping action of the ship as it rides in the sea way causing the meter to ride up and down in the water and further causing it to swing somewhat from side to side. This motion causes the meter to record a higher apparent velocity than it should. It is difficult to guess how big a factor this is, but it must decrease as the amount of wire out increases.

For the second half of the expedition, and for some observations on the first half, the reference point was not a taut wire mooring but a free-floating parachute drogue with the parachute suspended at about 1000 m. Observations of such a drogue system placed near an anchored buoy indicated a westward movement of a few centimetres per second. Measurements made with respect to the free-floating parachute drogues necessarily have a somewhat greater uncertainty than those made with respect to the taut wire anchored buoy.

Ignoring the error caused by the pumping action of the ship and the error due to the drift of a parachute drogue, and summing up the rest of the errors, one can arrive at an estimate of the total error by taking the sum of the squares of the values listed previously. Thus, one arrives at a standard deviation between 11 and 18 cm/sec, depending upon the values used. It is believed that not many errors will exceed ± 30 cm/sec.

As an independent method of estimating the error all the Roberts meter observations from depths between 300 and 365 m were plotted from stations where anchored buoys or deep parachute drogues were used. As expected, the scatter of points for the parachute drogue stations is greater than for the anchored buoys. The average current from the anchored buoy stations is 7·5 cm/sec toward 036 °T, comparable with that determined by a Swallow current float, Table 2. The standard deviation of the vector distance from this mean value to the observed points was 14 cm/sec. For those stations made in reference to the deep parachute drogues the average current was 6·8 cm/sec toward 084 °T; the standard deviation from this average current was 24 cm/sec.

One is not justified in assuming that the current between 300 and 365 m was the same for all 57 stations. The scatter, therefore, reflects not only the errors in the system but changes in the current, and the standard deviation of the error in the Roberts meter must therefore be less than that indicated. On the other hand, the error due to pumping action must be small at this depth, while it may be significant in the top 10 to 20 m.

For the deeper part of the Cromwell Current between 300 and 1000 m, where velocities were too small to be measured with any precision by the modified Roberts meter, observations were made with Swallow current floats (SWALLOW, 1955).

THE CROMWELL CURRENT AS DEFINED BY DIRECT CURRRENT OBSERVATIONS

Representative Observations

The Cromwell Current or Pacific Equatorial Undercurrent is a thin, swift flow, centred on the equator and moving east beneath the west-flowing South Equatorial Current. Its core at 140 °W is at 100 m, where velocities as high as 125–150 cm/sec were recorded (51 cm/sec equals one knot). At 350 m the eastward flow was reduced to 10 cm/sec. At the equator the depth of the change from west to east flow is at about 20 m. The northern and southern limits of the current appear to be at about 2 °N and 2 °S respectively.

The north edge of the South Equatorial Current at the time of the five stations illustrated in Fig. 2 was south of the equator. Appreciable westward components were only found at the two stations at 1 °S and 2 °S. Occasionally a station in the Cromwell Current showed a marked north-south component; however, there appeared to be no consistent pattern to these transverse components.

The high velocity core (Fig. 2) is not very thick and the shear both above and below it is large. Changes of velocity of 150 cm/sec in 70 m or 2×10^{-2}/sec were common. The velocity gradient above the core is nearly always larger than that below it. The upper shear in the east-west component at stations taken along the equator was never less than $1{\cdot}5 \times 10^{-2}$/sec and never as high as 4×10^{-2}/sec.

(408)

Cross Sections and Transport

Four cross sections of the current were made between 8–27 April along 140 °W. These are similar except in detail (Fig. 3). The Cromwell Current appears to be nearly symmetrical about the equator. Its jet-like appearance is misleading (Fig. 3)*; the current more closely resembles a thin ribbon. As defined by the 25 cm/sec contour, it is about two-tenths of a kilometre thick and 300 km wide. The amount of water transported by the current is remarkably high, i.e. between 34 and 42 × 10^6 m^3/sec with a mean value of 39 × 10^6 m^3/sec (Table 1)†.

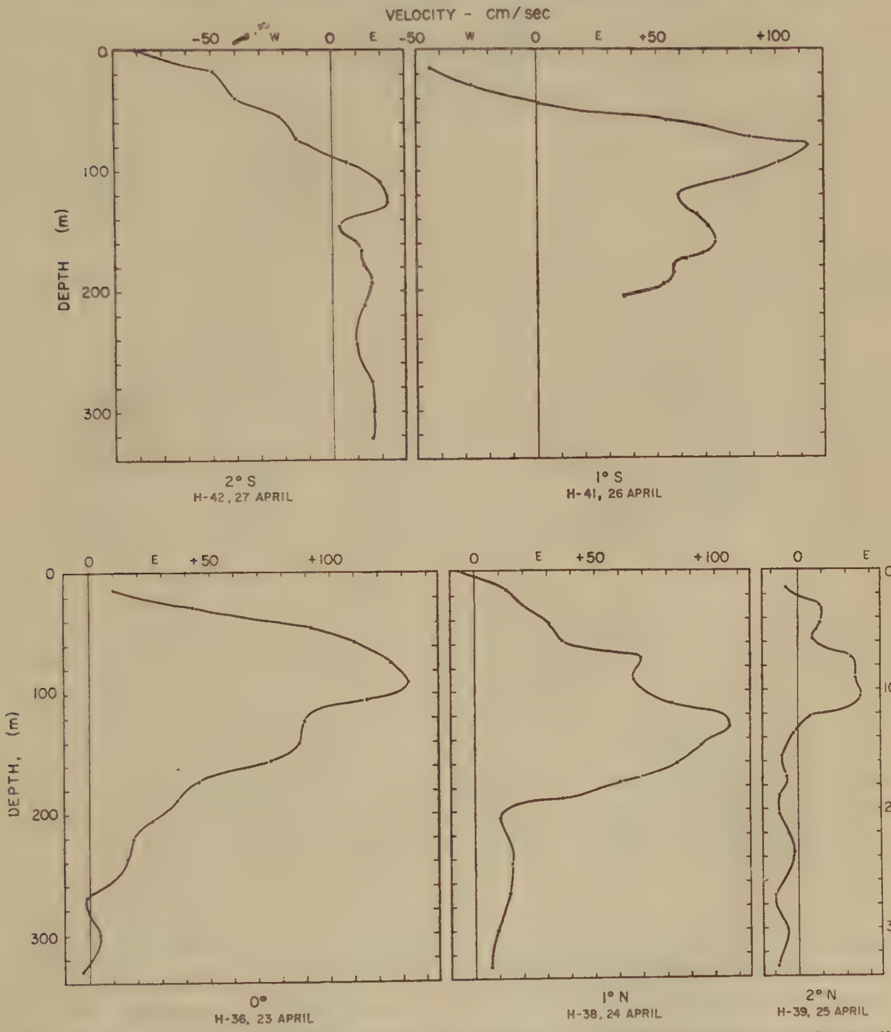

FIG. 2. East-west current profiles, made with Roberts current meter at 140 °W 25–27 April, Section IV.

---

*The vertical exaggeration (Fig. 3) is 2 × 10^4.

†Comparable values for other confined, high-velocity currents are the Gulf Stream 74 × 10^6 m^3/sec; Kuroshio, 65 × 10^6 m^3/sec; and the Florida Current 26 × 10^6 m^3/sec (SVERDRUP *et. al.*, 1942).

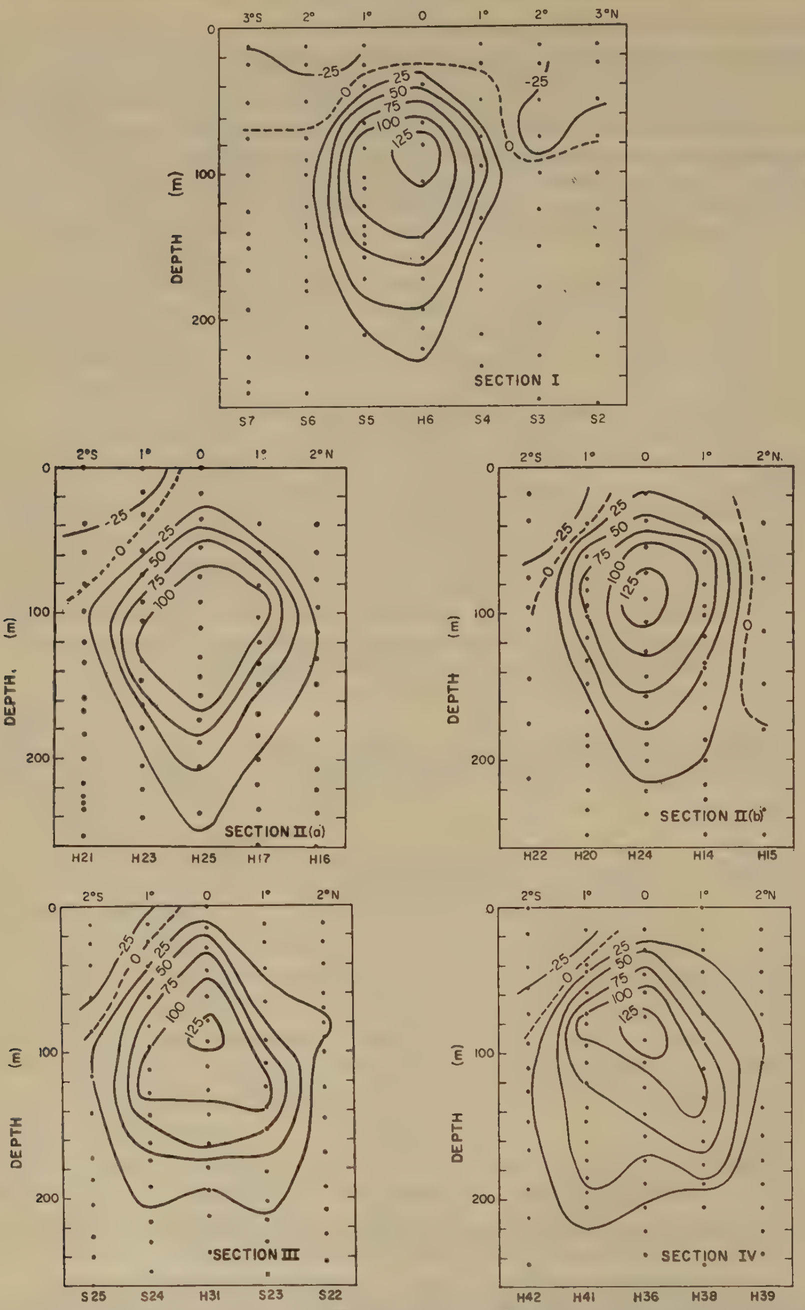

FIG. 3. Velocity cross sections at 140 °W. Dots are observed points, velocity is in cm/sec; plus is eastward and minus is westward flowing current; station numbers are along the bottom. Section I (6–9 April) : all but the equator station were made by *Hugh M. Smith* with reference to deep parachute drogues. Section II (12–18 April) : at least two sets of measurements were made by *Horizon* at each anchored buoy. Section II (a) is drawn from data which give the largest transport; Section II (b) is drawn from data which give the smallest transport. Section III (20–22 April) is drawn from data obtained by *Hugh M. Smith*. Section IV (23–27 April) was made by *Horizon*. The stations are the same as those shown in Fig. 2.

Swallow current floats were used to measure the low velocities at depths greater than 250 m. Four successful measurements were made (Table 2). At 300 m the eastward flow was only 11 cm/sec; at 500 m the direction was reversed; at 700 m it was moving westward at 13 cm/sec, but was again weak at 1000 m. Thus, the Cromwell Current is embedded between two westward-flowing currents (Fig. 4).

Table 1. Cromwell Current mass transport at 140 °W

Date	*Ship*	*Section*	*Transport* (m³/sec)
April 6–9	*Hugh M. Smith*	I	34 × 10⁶
April 12–18	*Horizon*	IIa	42 × 10⁶
April 12–18	*Horizon*	IIb	34 × 10⁶
April 20–22	*Hugh M. Smith*	III	42 × 10⁶
April 23–27	*Horizon*	IV	42 × 10⁶
			39 × 10⁶ Average transport

Table 2. Current velocities from Swallow floats

Date	*Loaded Depth* (m)	*Calculated Depth* (m)	*Hours Tracked*	*Speed* (cm/sec)	*Direction* (*toward*)
April 21	700	670 ± 210	10	14 ± 1	285°
April 22	500	440 ± 125	26	7 ± 0·5	290°
April 23	300	420 ± 135	10	12 ± 1	075°
April 26	1000	1020 ± 365	18	2 ± 0·7	205°

Steadiness of the Cromwell Current

From 11–24 April, 32 usable Roberts meter stations were made on the equator at 140 °W. There was no significant change in the velocity structure during this period (Fig. 5). The peak velocity varied between 120 and 150 cm/sec. Its depth (dotted line, Fig. 5) remained rather constant at 100 ± 12 m.

These results are in marked contrast to the Equatorial Countercurrent which flows eastward along the surface 500 miles to the north of the Cromwell Current. Recent observations there suggest that the Countercurrent can change direction ninety degrees, stop or double its speed all within a three-day period (KNAUSS, unpublished results).

The Eastward Extent of the Cromwell Current

The Cromwell Current was found at all stations from 140 °W to 92 °W inclusive. Sixteen miles east of the 92 °W station and straddling the equator is Isabella Island, the largest island in the Galapagos. The Cromwell Current was weak, but present, sixteen miles west of this island, but it was not found at the single station east at 89 °W. As pointed out in the introduction, Cromwell did not find the current at 84 °W east of the Galapagos.

Velocities in excess of 100 cm/sec are found at all stations through 95 °W. Between 140 °W and 95 °W the core (dotted line, Fig. 6) becomes shallower towards the east. The mean slope is 1·3 × 10^{-5}; however, most of the slope occurs between 140 °W and 116 °W. Between 95 °W and 92 °W the current definitely weakens, and the core slopes downward. What current there is at the station sixteen miles to the west of

Isabella Island is between 80 and 100 m. Except at the eastern terminus of the current, the variation in the velocity profile with longitude is no greater than that observed during the 18 days at the equator, 140 °W. The South Equatorial Current occasionally reached as far north as the equator (131 °W and 122 °W), but its presence appeared to have little effect on the Cromwell Current.

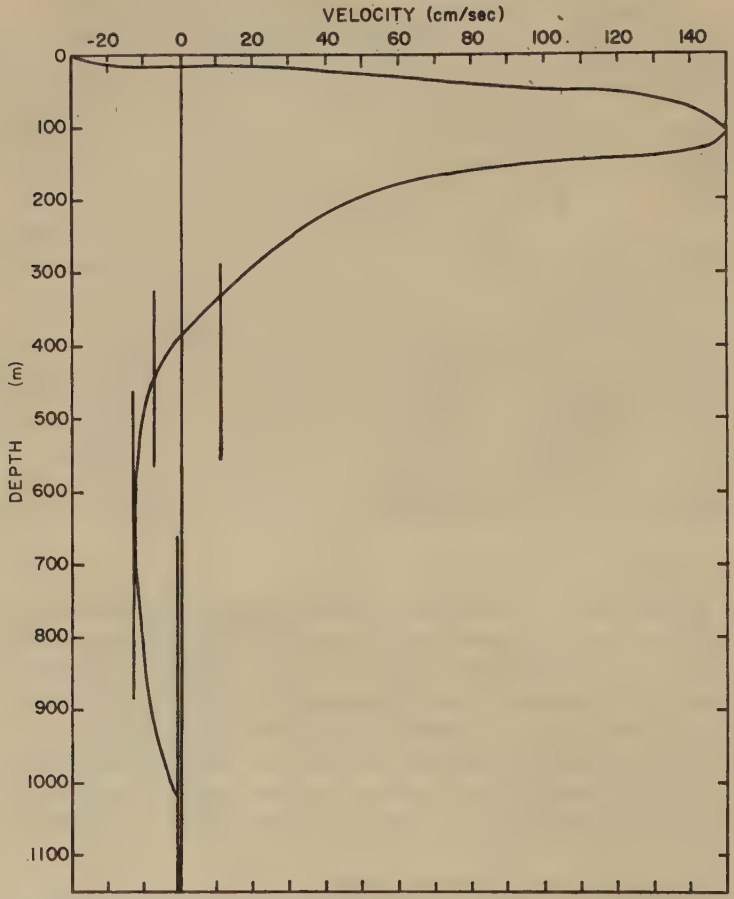

FIG. 4. A composite east-west velocity current profile, 0–100 m, at the equator at 140 °W, based on Roberts current meter and Swallow current floats. Uncertainty in depth of Swallow floats is indicated by vertical lines.

COMPARISON OF THE CROMWELL CURRENT WITH THE HYDROGRAPHIC OBSERVATIONS

One of the objectives of *Dolphin* was to obtain hydrographic measurements to correlate with the Cromwell Current, with the hope that hydrographic observations would provide some insight into the nature and cause of the current. Above the strong thermocline of the eastern tropical Pacific is a layer of warm, well-mixed, almost isothermal water, 10 to 100 m thick with typical temperature values of

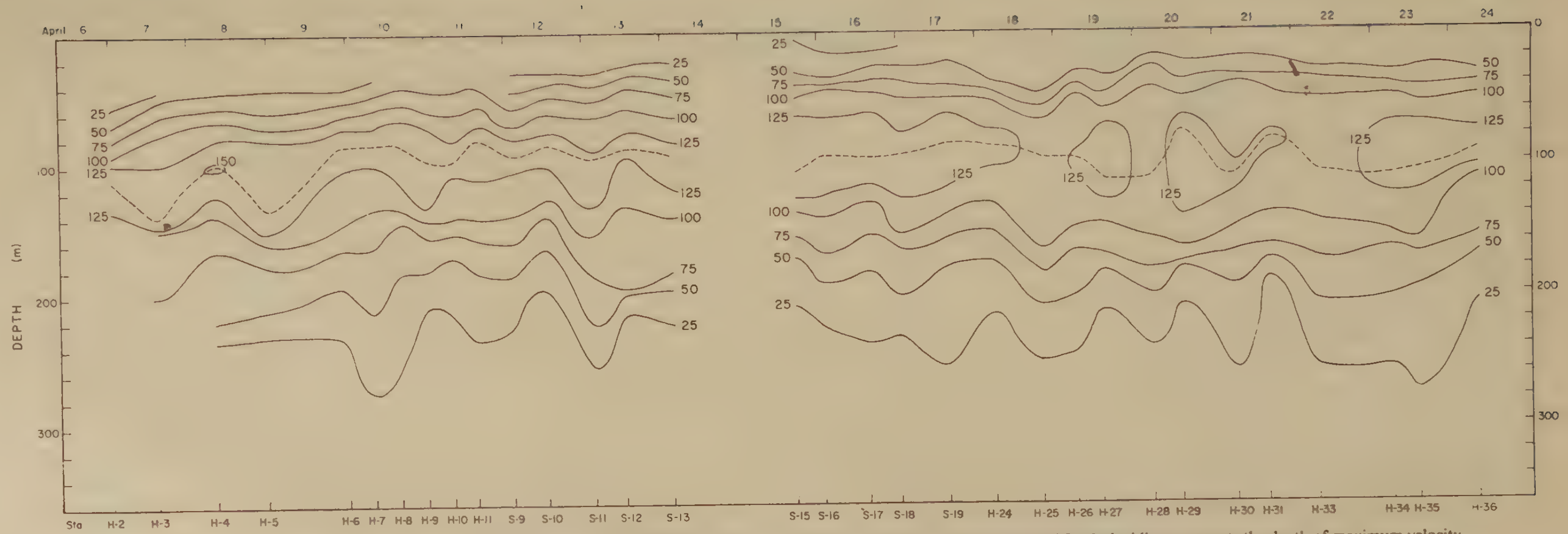

FIG. 5. Variation in east-west velocity component at the equator. Velocity is in cm/sec. Stations are listed along the bottom. The dashed line represents the depth of maximum velocity.

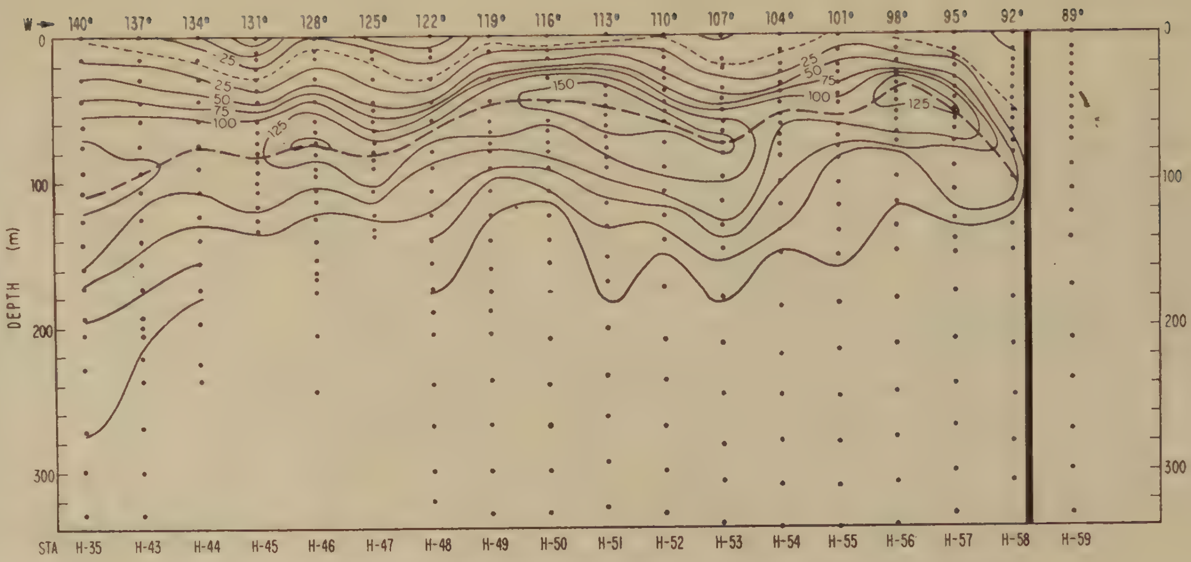

FIG. 6. East-west velocity components along the equator. Stations were made once a day. Dots are observed points. The dashed line is the depth of maximum velocity.

(413)

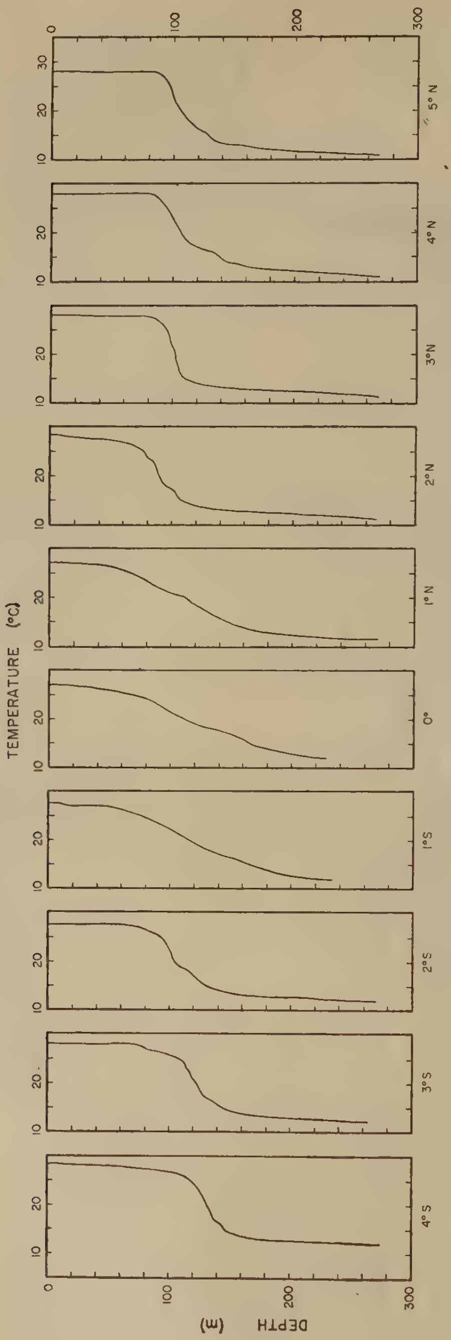

FIG. 7. Bathythermograms, 5 °N–4 °S along 140 °W.

(414)

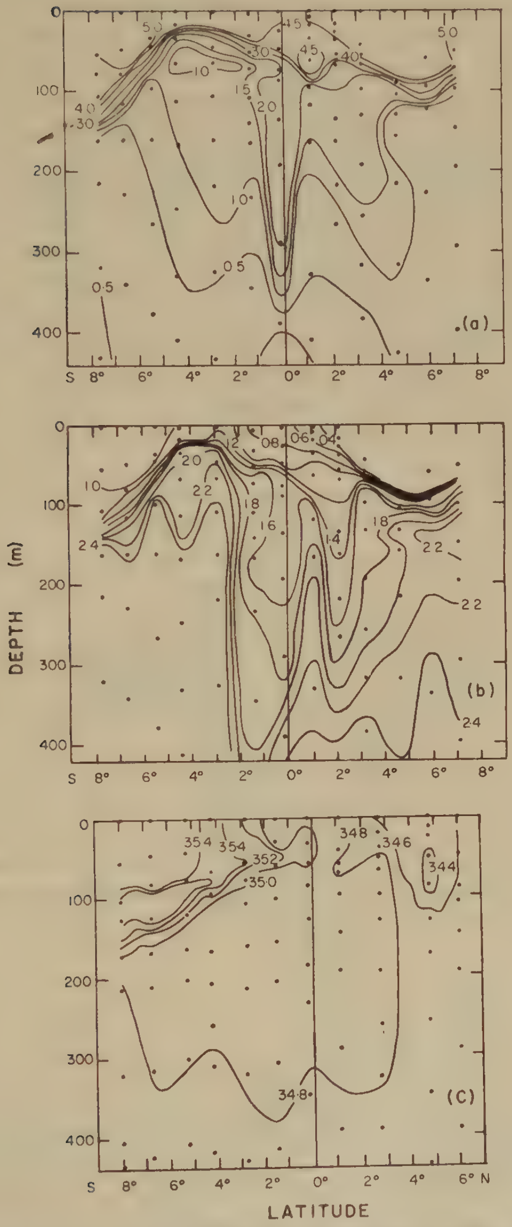

Fig. 8. Cross sections of (a) oxygen, 110 °W; (b) phosphate, 110 °W; (c) salinity, 120 °W (oxygen is in millilitres/litre and phosphate is in microgram atoms/litre). Redrawn from data in King *et al.*, (1957).

25°–28 °C. Just below the mixed layer the temperature can decrease 10 °C within 25 m in some regions. Below the thermocline at 300 m the temperature is 10°–12 °C.

The warm surface layer over a strong thermocline occurred on both sides of the equator on *Dolphin*, but not at the equator (Fig. 7). It would appear that strong vertical mixing takes place in the top few hundred metres. The breakdown of the sharp temperature discontinuity can be seen in the spreading of the isotherms near the equator. Similar changes in distribution can also be seen in the distribution of salinity, oxygen, phosphate and silicate (Cromwell, 1953; Wooster and Cromwell, 1958; King *et. al.*, 1957). The eastern tropical Pacific is characterized by a marked oxygen minimum just below the thermocline. At the equator, however, water of high oxygen content is mixed down from the surface to depths of at least 300 m; near-surface values there are lower than on either side. Similarly, water low in phosphate appears to be mixed downward through the thermocline. The tongue of water with a high salinity which moves up from the south along the thermocline does not cross the equator. Presumably this maximum is dissipated by mixing (Fig. 8).

The colder surface water and the termination of the saline tongue at the equator are suggestive of upwelling (Cromwell, 1953). Presumably the south-east trades would cause a divergence at the equator. From the Ekman wind drift theory, winds with an easterly component would create a northward drift, north of the equator and a southward drift, south of the equator (Cromwell, 1953; Neumann, 1947). The anomalous near-surface distributions (low temperature and oxygen, high phosphate and silicate, and lack of salinity maximum) have been used as criteria for upwelling (Wooster and Cromwell, 1958; Austin and Rinkel, 1957), but do not explain the analogous situation below the thermocline where high temperature and oxygen and low phosphate and silicate values are found. It had been suggested that this ‘ trough ’ in the isopleths might be related to the Cromwell Current (Wooster and Jennings, 1955).

No one seems to have suggested previously that the anomalous distribution of properties in the region of the equator might all be related to a single process—strong vertical mixing at the equator. Similar features can be seen on nearly every meridional section between 90 °W and 180 °. Based on the *Dolphin* observations, the north-south boundaries of the Cromwell Current appear to agree approximately with the limits of mixing indicated by temperature and oxygen data (Fig. 9).

THE CROMWELL CURRENT AS A GEOSTROPHIC CURRENT

The hydrographic data suggest that the water in the upper few hundred metres near the equator is rather well mixed. The sharp vertical density gradient over most of the eastern tropical Pacific that separates high temperature surface water from low temperature water (and acts as a boundary between the surface water which has high oxygen and low phosphate content and the deeper water which is deficient in oxygen but rich in phosphate) is reduced in magnitude at the equator because the gradient is extended over a greater range of depth. Mixing carries water characterized by high temperature, high oxygen and low phosphate to greater depths at the same time that water of lower temperature, lower oxygen and higher phosphate is brought into the surface layer. However, the surface acts as a heat and oxygen source and a phosphate sink (the latter because of increased photosynthesis). For this reason the horizontal temperature, oxygen and phosphate gradient across the equator is less marked at 40 m than at 200 m (Fig. 8–9).

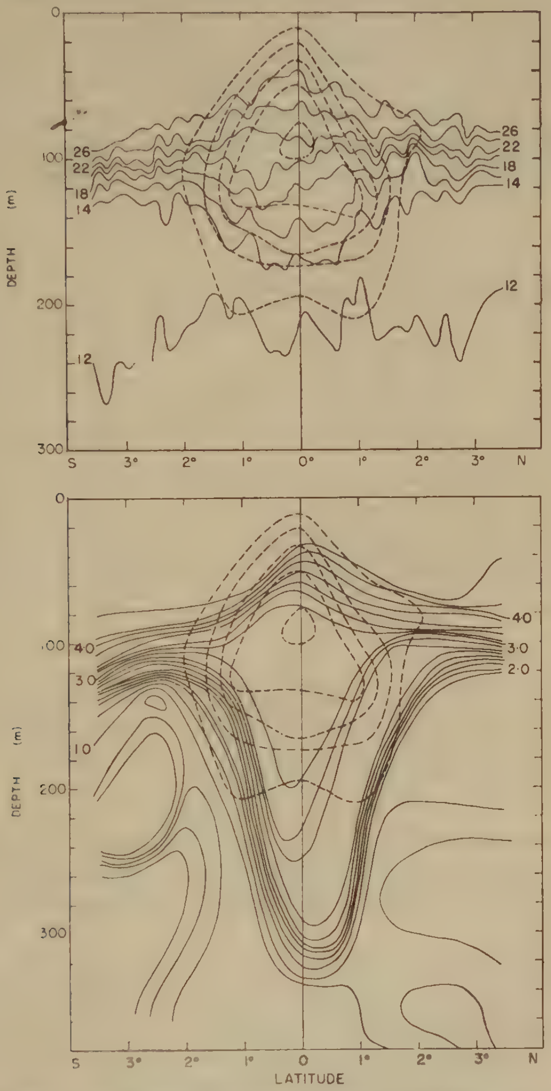

Fig. 9. Velocity cross section (dashed lines) superimposed on temperature and oxygen sections. Velocity contours 25–125 cm/sec identical with Fig. 3, Section III. Temperature is in degrees centigrade, oxygen is in ml/litre. All data taken by *Hugh M. Smith* with Roberts meter, bathythermograph and hydrographic stations on Section III, 140 °W, 20–22 April.

The Cromwell Current is in approximate geostrophic balance (that is, the balance of forces in the north-south direction, except very near the equator is represented by the Coriolis force and the pressure gradient, $fu = \alpha\, \partial p/\partial y$ where u is the eastward velocity, α is the specific volume of sea water, $\partial p/\partial y$ is the north-south pressure gradient, and $f = 2\,\omega \sin \phi$ where ω is the angular rotation of the earth and ϕ is the latitude).

It is suggested that the meridional component of pressure gradient necessary for a geostrophic Cromwell Current is the result of vertical mixing at the equator (see discussion below). To understand how this mixing could result in an eastward subsurface flow, let the density structure of the ocean be represented by a simple two-layer system of constant thickness and imagine this system to extend across the equator. There would be no north-south horizontal pressure gradient under these circumstances and therefore, no geostrophic current. Now, mix the water at the equator. The resulting density structure at the equator and the geostrophic current at 1° are shown in Fig. 10; the unmixed water is at 2°, and it is assumed that the pressure gradient at any given depth is constant between the equator and 2°. The pressure gradient changes sign at the equator, as does the sine of the latitude, so that there is no change in the direction of the current. The current is symmetrical about the equator.

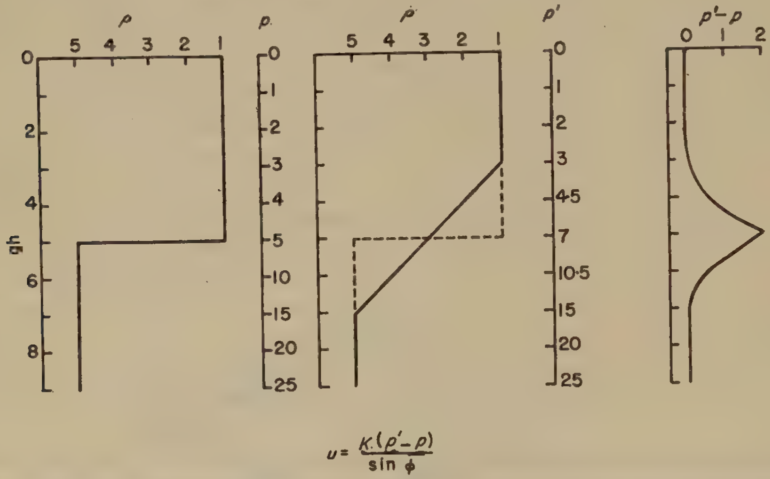

FIG. 10. Two-layer system before and after mixing, and resulting horizontal pressure gradients. $p = \int \rho g \, \partial h$. ρ and gh given in arbitrary units.

The resulting geostrophic current at 1° can be calculated from a more realistic model of the density structure before and after mixing, again assuming that there is no mixing at 2° and a constant gradient between 2° and the equator (Fig. 11). This density model is in excellent agreement with the observed density (Fig. 12). The geostrophic current is of the correct order of magnitude; the core is at approximately the correct depth, and the shape of the current is similar to that observed (Fig. 12). This model is consistent with the rise in the core of the Cromwell Current to the east. If the Cromwell Current is in geostrophic balance, and if the pressure gradient is the result of mixing across the thermocline, then one would expect the core to become shallower to the east in agreement with the shoaling of the depth of the thermocline to the east (AUSTIN, 1958).

The Coriolis parameter approaches zero near the equator, and the question arises as to whether or not one can expect the other terms in the equation of motion to

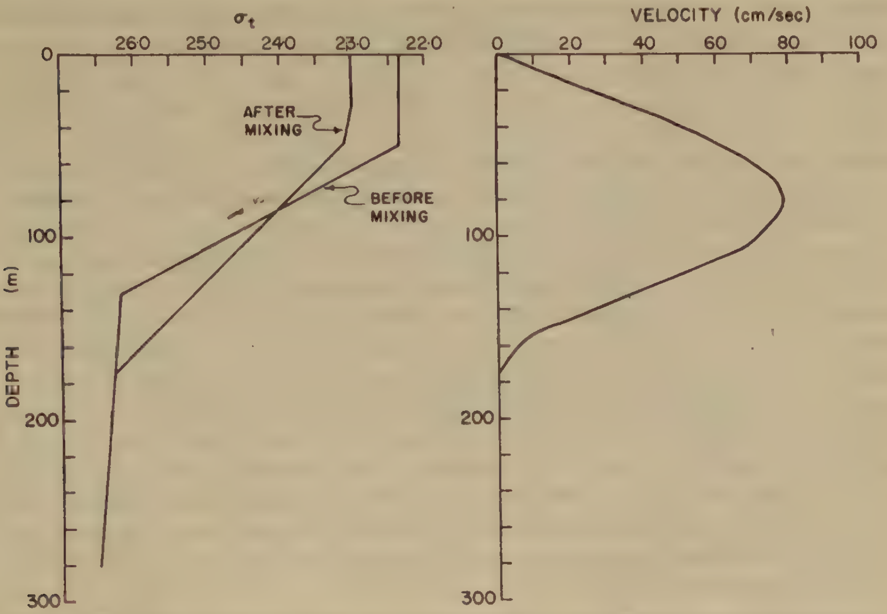

FIG. 11. Realistic density model before and after mixing and the resulting geostrophic current. It is assumed the unmixed water is at 2°, and the mixed water at the equator, and the pressure gradient constant between 0° and 2°. The geostrophic current has been calculated for 1°.

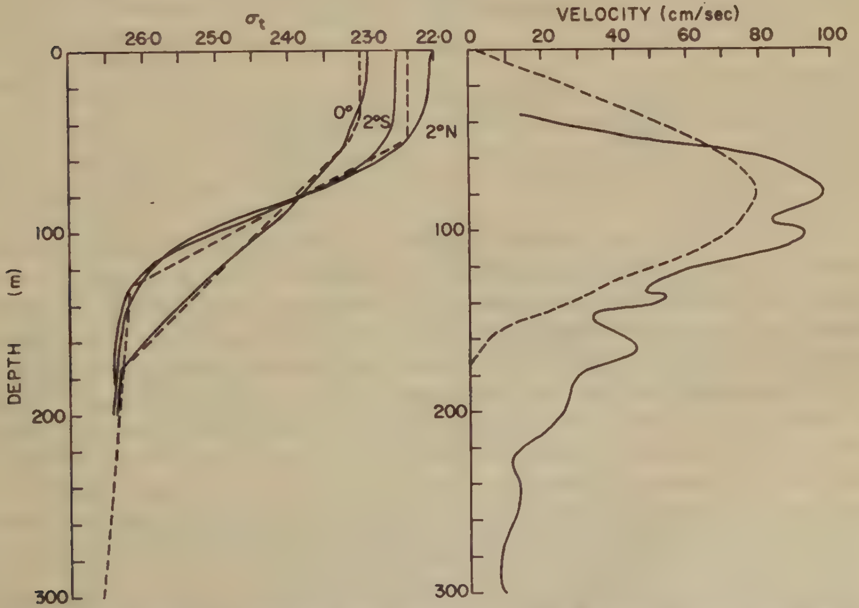

FIG. 12. Comparison of model and geostrophic current with observed velocity and density distribution. The dashed lines are from Fig. 11. The solid lines of σ_t are drawn from hydrographic data along 140 °W at the latitudes indicated. The velocity profile is from a Roberts meter station at 1 °N.

(419)

be small enough to allow the pressure gradient to remain approximately in balance with the Coriolis term. In the meridional plane the equation is:

$$\frac{\partial v}{\partial t} + u\frac{\partial v}{\partial x} + v\frac{\partial v}{\partial y} + w\frac{\partial v}{\partial z} = -\alpha\frac{\partial p}{\partial y} - uf + \alpha A_z\frac{\partial^2 v}{\partial z^2} + \alpha A_h\left(\frac{\partial^2 v}{\partial x^2} + \frac{\partial^2 v}{\partial y^2}\right)$$

where A_z and A_h are vertical and lateral eddy coefficients respectively. The values of uf for $0{\cdot}5° \leqslant \phi \leqslant 2°$ (Table 3) are for a value of u comparable to those observed at 140 °W at a depth of 100 m.

Since little really is known about the nature of the meridional circulation it is not possible to calculate terms other than the pressure gradient with any degree of certainty. However, TSUCHIYA (1955) has shown that if one uses representative values of $v = 5 - 10$ cm/ sec, $A_z = 10^2$ gm/cm/sec and $A_h = 10^7$ gm/cm/sec, the values of the other terms are all less than 10^{-5} cm/sec². This is an order of magnitude less than the Coriolis term corresponding to the observed velocity (Table 3).

For other evidence that geostrophic balance might be expected when the value of the Coriolis term is the order of 10^{-4} cm/sec², it can be pointed out that comparisons in the Equatorial Countercurrent at 5–8 °N of GEK surface current measurements with those calculated from the geostrophic equation are in good order first agreement. The magnitude of the terms is $5-8 \times 10^{-4}$ cm/sec², only two to four times larger than those given in Table 3.

Table 3. *Values of Coriolis terms near equator using representative velocities measured at* 100 *m. The pressure gradient in the last column is that needed for geostrophic balance.*

ϕ	sin ϕ	u (cm/sec)	uf (cm/sec²)	$\frac{\Delta h}{\Delta y}\left(\frac{\text{dynamic cm}}{\text{degree of latitude}}\right)$
0·5	0·009	125	$1{\cdot}6 \times 10^{-4}$	1·8
1·0	0·017	85	$2{\cdot}0 \times 10^{-4}$	2·2
1·5	0·026	50	$1{\cdot}9 \times 10^{-4}$	2·1
2·0	0·035	25	$1{\cdot}3 \times 10^{-4}$	1·5

It is difficult to make a detailed comparison of the geostrophic current and the Cromwell Current using the *Dolphin* data. Differences of one to two dynamic centimetres per degree of latitude are all that are required (Table 3). However, differences of two to four dynamic centimetres were observed on the equator station over a six-day period. This kind of variation in the observed pressure tends to obscure any meridional gradient observed on stations taken on different days. However, the tendency for a pressure gradient to be symmetrical about the equator can be seen in Fig. 13. The necessary pressure gradient of two dynamic centimetres per degree of latitude is approximately realized. A similar picture of the pressure gradient can be seen on the plot of dynamic height at 100 m relative to 1000 m, but the scatter of values is larger. The argument for using the 400 m surface as the ' level of no motion ' is the current reversal at about 400 m (Fig. 4).

It should be noted that the geostrophic balance applies only to the meridional forces; the nature of the balance of the zonal forces is yet to be determined. It should also be noted that the models in Fig. 10 and 11 can be adjusted to include a westward flowing South Equatorial Current at the surface. One need only begin with a mixed layer which is shallower at the equator than at 2°.

From the foregoing, the Cromwell Current is in approximate geostrophic balance. The horizontal pressure gradients appear to result from vertical mixing of the water at the equator, and a breakdown of the sharp tropical thermocline. The mixing creates a meridional pressure gradient symmetrical about the equator; hence, the Cromwell Current is a subsurface eastward flow which balances this gradient. All of the observational data support this idea and the magnitude of the different force terms suggests that a balance between the pressure gradient and the Coriolis term is to be expected even to within half a degree of the equator.

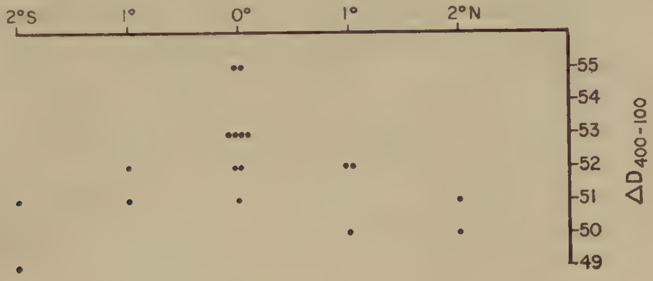

FIG. 13. Distribution of values of dynamic height ($\Delta D_{400-100}$) at 100 m relative to 400 m along 140 °W at all *Horizon* hydrographic stations. Uncertainty of pressure gradients of 1 dynamic centimetre/degree latitude at 1° is equivalent to an uncertainty of 40 cm/sec in the resulting geostrophic current.

The fact that the Cromwell Current is a geostrophic current, does not, of course, explain its existence, nor is this explained by the meridional pressure gradient which appears to result from strong vertical mixing at the equator; because it can be argued that strong turbulence is associated with the high velocities of the current. Thus the Cromwell Current could be the cause of mixing, rather than the result. Hence, one must find a mechanism other than the current itself that will create strong mixing at the equator to depths of 300 m, but not on either side of it.

Little is known or understood about upwelling and vertical mixing processes in the ocean, but it is generally believed that upwelling is a comparatively shallow process and does not extend as deep as 300 m. However, the Cromwell Current might be produced if upwelling created by the wind-induced divergence at the equator could cause vertical mixing to depths of 300 m.

DISCUSSION AND CONCLUSIONS

(1) The observations of the *Dolphin* Expedition have shown that the eastward flow beneath the surface at the equator (CROMWELL *et. al.*, 1954) is a current of major proportions. These data indicate that the Cromwell Current is at least 3500 miles long with a transport at 140 °W of 35–40 × 10^6 m³/sec. This transport is greater than hitherto estimated for any current in the equatorial Pacific and, with the exception of the Kuroshio, for any current in the Pacific (SVERDRUP *et. al.*, 1942).

The existence of a new current with a transport of this magnitude, however, suggests that transport balance in the equatorial Pacific should be re-examined. Further evidence that previous transport estimates are incorrect was found four months later on *Doldrums* (the third IGY Expedition made by the Scripps Institution of Oceanography). Current measurements with the modified Roberts meter and Swallow floats at 7° 52′ N, 107° 30′ W suggested that the transport of the Equatorial Countercurrent is at least twice as great as previously estimated (KNAUSS and PEPIN, 1959). The Cromwell Current and the increase flow in the Countercurrent more than triple the total eastward transport in the equatorial Pacific as given by SVERDRUP *et. al.* (1942).

(2) The length of the Cromwell Current can be inferred by examining hydrographic data.* All available hydrographic sections east of 170 °W show evidence of the current, but none of those examined from the west of 160 °E suggest its presence; some sections between 170 °W and 160 °E are indicative of it. From somewhat similar criteria it appears that '. . . . . upwelling is usually of a comparatively minor nature or may be absent west of 180° ' (AUSTIN and RINKEL, 1957).

However, recent Japanese current measurements in January–February, 1958, suggest the Cromwell Current at 150 °E (YOSIDA *et. al.*, 1959). Their temperature sections also show the characteristic breakdown of the thermocline at the equator.

If the Cromwell Current is a response to the pressure field produced by the wind-induced divergence at the equator, then the easterly component of the south-east trades is a measure of the driving force. The current should be weak or missing east of 180°, since the streamline charts of the mean surface winds for January and July (MINTZ and DEAN, 1952) show no easterly component to the tradewinds along the equator west of 180° during January and only a weak component west of 170 °E during July. The question of the nature and continuity of the Cromwell Current in the western Pacific must be investigated.

(3) Perhaps the biggest problem posed by the data is where does the water go. One possibility is that it is lost to the sides as the current moves downstream. The fact that the core velocity at the equator showed little change between 140 °W and 95 °W does not necessarily imply that the transport is the same throughout this distance. A decrease in the current strength east of 140 °W is suggested by the Mintz-Dean streamline charts of surface winds, as there is a decrease in the easterly component of trades along the equator east of 130 °W. At 90 °W there is no easterly component at all in summer and only a very weak one in winter.

If, on the other hand, the transport is still high at 95 °W, then the current must be deflected either north or south of the equator by Isabella Island. Since water of the Cromwell Current is characterized by high oxygen values, the oxygen content is an excellent tracer. The oxygen distributions on *Shellback* Sections X and XII (July and August, 1952) suggest that the current may be found on both sides of the Galapagos at 91 °W and at the equator at 85 °W (WOOSTER and CROMWELL, 1958). If the *Shellback* oxygen data mean that the current is present east of the Galapagos

---

*One might hope to find evidence of a similar flow in the Atlantic by examining the hydrographic data; however, there are only six meridional sections across the equator in the Atlantic. *Meteor* Profiles IX at 30 °W, Xa at 10 °W and Xb at 0° show evidence of vertical mixing in the oxygen section (WATTENBERG, 1939). *Atlantis* sections at 30 °W, 34 °W and 38 °W (*Bulletin Hydrographique*, 1952, Copenhagen) do not show any clear evidence for vertical mixing at the equator, but it appears possible that such evidence could be obscured because the number of observations in the top 300 m are fewer than on the *Meteor* Expedition.

(422)

in 1952, then either it is not present at all times, or else it is so weak that it was not detected by the parachute drogues used by Cromwell at 84 °W in November, 1955, or by the Roberts meter on *Dolphin* at 89 °W in June, 1958). Perhaps water is entrained as it moves through the islands; hence, there may be only a slow eastward drift east of the Galapagos. This problem cannot be solved until a series of sections east of 140° W become available to determine the transport of the Cromwell Current at successive points along the stream.

(4) It seems likely that the Cromwell Current surfaces at times. Perhaps the most likely place for this is near the Galapagos, where Isabella Island may provide an effective block to further passage of the water and make the current structure unstable. Evidence for this can be found on the Deutschen Seewarte surface current chart which shows the current at the equator 300–600 miles east of the Galapagos to be either east or west in March (SCHOTT, 1943). This region is the only place on the chart where such a variation in the current direction is indicated.

(5) Upwelling at the equator must be re-examined in the light of the Cromwell Current. It may be that upwelling along the equator will be a necessary part of any explanation of the Current. However, if the current can be explained without resorting to upwelling, then one must question whether there is indeed any net upward flow of water at the equator. The evidence for it has been based primarily on the low surface temperatures there. However, as already pointed out, all the hydrographic data suggest that there is strong vertical mixing along the equator. Furthermore, upwelling *per se* cannot account for the high temperatures, high oxygen and low phosphate values beneath the expected depth of the thermocline. The colder surface temperature can be explained by vertical mixing (Fig. 11), and it seems likely that such mixing could be explained by the high velocities and high velocity shears recorded at the equator.

Acknowledgements—Without the assistance of the Pacific Oceanic Fisheries Investigation, the work reported here would be less complete. JOSEPH KING and MURICE RINKEL spent long hard hours aboard *Hugh M. Smith* working with unfamiliar equipment. RINKEL and THOMAS AUSTIN gave freely of their time in helping me analyze their results. The key instrument of this expedition was the modified Roberts current meter. It was developed by JAMES SNODGRASS and was used successfully throughout the cruise.

Dolphin, which was part of the United States oceanographic programme (9.2) of the International Geophysical Year, was supported by the Office of Naval Research, the National Science Foundation and the United States Bureau of Commercial Fisheries.

Scripps Institution of Oceanography
University of California
La Jolla, California

Contribution from the Scripps Institution of Oceanography, New Series.

REFERENCES

AUSTIN T. S. (1958) Variations with depth of oceanographic properties along the equator in the Pacific. *Trans. Amer. Geo. Phys. Union* **39**, 1055–1063.

AUSTIN T. S. and RINKEL M. O. (1957) Variations in upwelling in the equatorial Pacific. Presented at 9th Pacific Sci. Cong. Bangkok, 1957.

CROMWELL T. (1953) Circulation in a meridional plane in the central equatorial Pacific. *J. Mar. Res.* **12**, 196–213.

CROMWELL T., MONTGOMERY R. B. and STROUP E. D. (1954) Equatorial Undercurrent in Pacific Ocean revealed by new methods. *Science* **119**, 648–649.

(423)

Isaacs J. D., Huffer R. P. and Kidd L. W. (1957) Instrument stations in the deep sea. *Science* **125**, 341.

King J. E., Austin T. S. and Doty M. S. (1957) Preliminary report on Expedition *Eastropic. U.S. Fish Wildlife Serv. Spec. Sci. Rept.– Fish.* **201**, 155 pp.

Knauss J. A. and King J. E. (1958) Observations of the Pacific Equatorial Undercurrent. *Nature, Lond.* **182**, 601–602.

Knauss J. A. and Pepin R. O. (1959) Measurements of Pacific Equatorial Countercurrent. *Nature, Lond.* **183**, 380.

Mintz Y. and Dean G. (1952) The observed mean field of motion of the atmosphere. Geophysical Research Directorate, Air Force Cambridge Research Centre, Cambridge, Mass., *Geophysical Research Paper* No. 17, 65 pp.

Neumann G. (1947 Über die Entstehung des äquatorialen Gegenstromes. *Forschungen and Fortschritte*, **21/23**, 177–179.

Roberts E. B. (1952) Roberts radio current meter mod. II, operating manual. Coast and Geodetic Survey, U.S. Dept. of Commerce, 32 pp.

Schott G. (1943) Nachtrag zu dem Aufsatz. ' Die Grundlogen liner Weltkarte der Meerestromungen ' *Ann. Hydrogr. Mar. Meteor.* **71**, 281–282.

Sverdrup H. U., Johnson M. W. and Fleming R. H. (1942) *The Oceans*. 1087 pp. Prentice Hall, New York.

Swallow J. C. (1955) A neutral-buoyancy float for measuring deep currents. *Deep-Sea Res.* **3**, 74–81.

Tsuchiya M. (1955) On a simple method for estimating the current velocity at the equator, II. *Rec. Oceanog. Work in Japan* **2**, 1–6.

Volkmann G., Knauss J. A. and Vine A. C. (1956) The use of parachute drogues in the measurement of subsurface ocean currents. *Trans. Amer. Geophys. Union* **37**, 573–577.

Wattenberg H. (1939) Die Verteilung des Sauerstoffs im Atlantischen Ozean. *Deutsche Atlantische Exped. Meteor.* 1925-1927, *Wiss. Erg.* **9**, Atlas, 72 pls.

Wooster W. S. and Cromwell T. (1958) An oceanographic description of the eastern tropical Pacific. *Bull. Scripps Inst. Oceanog.* **7**, No. 3, 169–182.

Wooster W. S. and Jennings F. (1955) Exploratory oceanographic observations in the eastern tropical Pacific, January to March, 1953. *Calif. Fish and Game* **41**, 79–90.

Yosida S., Nitani H. and Suzuki N. (1959) Report of multiple ship survey in the equatorial region (IGY) Jan.–Feb. 1958 (in Japanese), *Hydrographic Bull.*, Maritime Safety Bd., Tokyo **59** (Publ. 981), 1–30.

Printed in Great Britain by The Salisbury Press Ltd., Publicity House, Wilton Road, Salisbury, Wilts. (22847)

(424)

THE ATLANTIC SPECIES OF THE BLENNIOID FISH GENUS ENNEANECTES

BY

RICHARD H. ROSENBLATT

Proceedings
of
The Academy of Natural Sciences of Philadelphia
Vol. 112, No. 1, pages 1–23
Published June 17, 1960

THE ATLANTIC SPECIES OF THE BLENNIOID FISH GENUS ENNEANECTES[1]

BY

RICHARD H. ROSENBLATT

University of California, Scripps Institution of Oceanography,
La Jolla, California

In connection with his studies on the blennioid fish family Tripterygiidae, the author has completed a revision of the New World genus *Enneanectes*. There are five Atlantic species in the genus, three of which are undescribed. Pending the publication of the monographic study of the family, it is felt desirable to make the names of these species available to workers dealing with the fishes of the western Atlantic. The present paper is therefore limited to descriptions of the Atlantic species and a discussion of problems of nomenclature and identification. A consideration of the relationships of the species is deferred to the presentation of the comprehensive generic revision.

Materials and Methods

The methods of counting and measuring used mostly follow those of Hubbs and Lagler (1958). Only those requiring further amplification are discussed below.

With rare exceptions, the last ray of the dorsal and anal fin is divided through the base, and the two elements have been counted as one ray. In the very few individuals in which the last ray was not so branched, seemingly because the pos-

---

[1] Contribution from the Scripps Institution of Oceanography, N. S. 1163

Proc. Acad. Nat. Sci., Phila., Vol. 112, No. 1, 1960.

Reproduced by Permission

terior element had failed to develop, the total number of rays was recorded. The pelvic spine is reduced to a bony splint and is not recorded in the descriptions. The lateral line count was recorded as pored scales plus notched scales. The scale rows on the back were counted upward and forward, beginning with the first scale back of the head and ending with the scale above the last scale in the lateral-line series, which lies over the hypural plate. Scales below the lateral line were counted in an oblique row between the fourth anal soft-ray and the pored lateral line. In species with a very short pored lateral line the count was continued upward to a posterior projection from it. The scale closest to the fin base is abruptly smaller than the other back scales and was counted as one-half.

The head depth was measured from occiput to isthmus. The length of the snout was taken from the front edge of the orbit, just above the posterior nostril, to the most anterior point of the upper lip. The pectoral length was measured as the length of the longest ray. The length of the fin bases was measured between the actual bases of the first and last rays. The membrane following the last dorsal spine was disregarded. The length of the caudal peduncle was taken as the oblique distance between the base of the last anal ray and the hidden base of the middle caudal ray.

The number of specimens on which the counts and measurements are based are given in a prefatory paragraph in each description. In the body of the description, the meristic and the proportional characters (expressed as thousandths of the standard length) are given first. The first pair of values delimits the range, and the figure in parentheses is the arithmetic mean. It will be noted that little specific mention of the holotype is made in the descriptions of new species, since the intent is to describe species and not specimens. However, unless specified, it may be assumed that the holotype agrees with the species description. Counts and measurements of body parts of holotypes are given in Table II.

ENNEANECTES Jordan and Evermann

Enneanectes Jordan and Evermann in Jordan, Cal. Acad. Sci. Proc. 1895, (2) 5: 50, pl. 53. Type *Tripterygium carminale* (not of) Jordan and Gilbert (= *Gillias sexmaculatus* Fowler 1944); Mazatlan, Mexico (original designation).

Gillias Evermann and Marsh, U. S. Comm. Fish and Fisheries Rept. 1899 (1900): 357, Fig. 95 (type *G. jordani* Evermann and Marsh; Puerto Rico (original designation).

Diagnosis

Lateral line discontinuous, consisting of an anterior row of 10–17 pored scales running back from shoulder above midline, and a posterior section, along midline, formed of 18–22 scales with notched posterior margins, commencing one or two scales before end of pored lateral line. Scales large, 1.5 or 2.5/28–34/4.5 or 5.5. A scale patch on upper portion of opercle. Top of head and upper part of opercular margin spinose. Anterior and posterior orbital flanges well developed and spiniferous. Lateral-line canals on head not covered by bone. No palatine teeth. Dorsal and anal counts low; dorsal III–X to XIII–7 to 10; anal II, 14–17. Soft dorsal usually with some rays branched at tip. Pelvic rays almost completely separate; connected by a membrane for one-eighth the length of the outer ray.

Description

Body robust in most species, varying from chunky (*jordani*) to moderately elongate (*atrorus*). Head varying from pointed (*atrorus*) to very blunt (*jordani*). Head pores in double rows on circumorbitals, preopercle, and mandible. First pore of circumorbital rows enlarged. A median pit on chin, just back of symphysis of lower jaw. Within this pit is a low isthmus. Due to differences in depth of the pit and development of the isthmus (or due to differences in preservation) the median pit is occasionally represented by two pores. A pair of pores just above upper lip, one at lower end of each nasal bone. A pore on the orbital rim, just dorsal to posterior nostrils.

Lateral ethmoid and sphenotic expanded to form flanges at the anterior and posterior border of eye. Posterior orbital flange always spiny; anterior orbital flange smooth in some species, spiny in others.

Posterior nostril on anterior margin of orbit, immediately above anterior orbital flange. Anterior nostril about midway between posterior nostril and upper lip. Anterior nostril in a short tube surmounted by a lobate tentacle about equal in length to distance between nostrils. Posterior nostril with a slightly raised rim. Opening of anterior nostril approximately one-half the size of opening of posterior nostril, except in *E. atrorus*, in which the nostril openings are subequal.

Teeth in jaws conical, recurved, and pointed; arranged in setiform bands. In the upper jaw there is an outer row of more widely spaced, enlarged teeth. In the lower jaw there is a similar outer row of enlarged teeth, except in *atrorus*, in which the teeth of the outer row of the lower jaw are only slightly enlarged. The teeth of the innermost row in the lower jaw are also enlarged. Vomerine teeth slightly larger than inner teeth of upper jaw, arranged in an irregular V-shaped row. Palatine teeth absent. Tongue free marginally and distally, with a very short, bluntly pointed, free projection.

Six or seven stubby gill-rakers on lower limb of first arch (not confirmed for *atrorus*). Each raker bears two or three acicular spines at its tip. Membrane binding first gill-arch to opercle scarcely restricting gill-slit.

Pelvic rays two, connected by a membrane for only one-eighth the length of the outer ray.

Scales large, 1.5 or 2.5/28 to 32/4.5 or 5.5. A patch of ctenoid scales on upper part of opercle. Opercular scale patch well developed in most species, but reduced to four or five scales in the only known specimen of *atrorus*. Cheek naked in most species, but sometimes scaled in *jordani* and always scaled in *pectoralis*. Pectoral base and belly naked in some species, covered with cycloid scales in others. A single row of three large, thin cycloid scales on base of caudal fin. Lateral line discontinuous, consisting of an anterior row of 10–17 pored scales running back from shoulder above midline and ending under second dorsal, and a posterior section, along midline, formed of 18–22 scales with notched posterior margins, commencing one or two scales before, and two scale rows beneath, end of pored lateral line.

Males with a short, conical penis which usually bears a thin tentacle. Females with the periproct much folded and provided with many fleshy processes.

All species have five dark brown bars on the sides. In breeding males the lighter areas of the body are red. Tails of breeding males are black in some (perhaps all) species.

Comparisons

Neither *Enneanectes* nor its synonym *Gillias* has consistently been recognized as valid for American forms (none of the Australian or South African species referred to *Gillias* has anything to do with that genus). Schultz (1950) considered *Enneanectes* (along with a number of other genera) to be a synonym of *Tripterygion* Risso. The species of *Enneanectes* differ from those of that genus, however, in the presence of spines on the head and upper margin of the opercle, the absence of palatine teeth, and in the absence of a membrane between the pelvic rays. In addition the two genera differ in scale size (29–34 scales in *Enneanectes* opposed to 40–45 in *Tripterygion*), and number of fin rays (D_2 X–XIII opposed to XVII–XIX, A II, 14–17 opposed to II, 24–28). The species of *Enneanectes* also have heavier and blunter heads and more robust bodies than do the species of *Tripterygion*, which are elongate and slender.

Enneanectes differs most importantly from *Enneapterygius*, the speciose Old World genus with which it has also been associated, in the presence of spines on top of the head and scales on the opercle, the absence of palatine teeth, and in having two anal spines rather than one. In addition, in *Enneapterygius* the pelvic rays are united by a membrane and the sphenotic is not expanded to form a posterior orbital flange, whereas in *Enneanectes* the pelvic rays are not united by a membrane, and the posterior orbital flange is well developed.

Remarks

The nomenclatural history of the name *Enneanectes* is complex. Jordan and Evermann, in erecting the genus *Enneanectes*, designated *Enneanectes carminalis* (Jordan and Gilbert) (supposedly = *Tripterygium carminale* J. & G.) as the type species (Jordan 1895, p. 501). However, their description was based on a specimen collected at Mazatlan by Gilbert, rather than on the type of *T. carminale*, and it is abundantly clear that this specimen was neither conspecific nor congeneric with the type of *carminale*.

Brock (1940), when informed that the holotype of *T. carminale* could not be located and was presumed lost, designated Jordan and Evermann's Mazatlan specimen as the " neotype " of *T. carminale* and erected a new species, *Enneapterygius storeyae*, for a specimen of the true *T. carminale*. Schultz (1950) located the type of *carminale* and, although he was not able to examine either the " neotype " of *carminale* or the holotype of *Enneapterygius storeyae* Brock, he was able to refer the former to *Gillias sexmaculatus* Fowler 1944 and the latter to *Tripterygium carminale* Jordan and Gilbert. I have examined the holotypes of *Tripterygium carminale* (USNM 20946) and *Enneapterygius storeyae* (SU 35045), as well as Brock's " neotype " of *Enneanectes carminalis* (SU 3854) and fully concur with Schultz's conclusions.

The question then remains, what is the type species of the genus *Enneanectes*. The rules of zoological nomenclature state that a nominal species is the type of the genus, and it is assumed that the type species of a genus has been correctly identified by the author. In this instance, however, that assumption would be unwarranted. The species *Tripterygium carminale* is properly referable to the genus *Axoclinus* Fowler 1944. The specimen of *Gillias sexmaculatus* incorrectly identified as *T. carminale* by Jordan and Evermann is clearly not congeneric, but is related to *Gillias jordani* and the other species here referred to as *Enneanectes*.

It would seem that the most logical course is to recognize as the type of *Enneanectes* the actual species upon which Jordan and Evermann based the generic description, namely *Gillias sexmaculatus* Fowler. The alternative to this would be to replace *Axoclinus* with *Enneanectes*, and refer the species here placed in *Enneanectes* to *Gillias*. This would mean that not one of the species of *Enneanectes* would then agree in any generic character with the original description of the genus. This latter alternative, while admissible nomenclatorially, would create a zoological paradox. It is for this reason that *Gillias sexmaculatus* is here recognized as the type species of the genus *Enneanectes*.

Key to the Atlantic Species of *Enneanectes*

1 Pectoral base and belly covered with scales. Scales in first row above lateral line notably larger than those above *2*

1 Pectoral base and belly naked. Scales in first two rows above lateral line subequal *4*

2 First dorsal spine low, not as high as third spine of second dorsal, .104–.137 of standard length. Anterior orbital flange and usually nasal bones with spines. Pored scales in lateral line 12–14, usually 13. Pectoral rays 14–16, usually 15 .... *3*

2 First dorsal spine high, as long as third spine of second dorsal, .172–.227 of standard length. Anterior orbital flange and nasal bones smooth. Pored scales in lateral line 10–12, usually 11. Pectoral rays 13–15, usually 14 .... *E. altivelis*, sp. nov. (p. 19)

3 Cheek naked or with at most one or two thin, cycloid scales in upper corner behind eye. Orbital tentacle narrow, longer than broad, its tip pointed. Cheek with two bars, the upper very faint, otherwise clear. Anal with six or seven bars .... *E. jordani* (p. 16)

3 Cheek with three to eight less delicate, ctenoid scales in upper corner behind eye. Orbital tentacle broader than long, its tip flat or broadly rounded. Cheek with one bar at lower posterior corner of eye, the remainder evenly pigmented. Anal evenly pigmented.
E. pectoralis (p. 12)

4 Anterior orbital flange and nasal bones spinose in specimens larger than 19 mm. (interorbital and circumorbitals also densely spined in large specimens). First dorsal spine shorter than third spine of second dorsal, .112–.159 of standard length. Distal third of second dorsal lightly spotted with dark brown, never black. Body bars not strongly contrasted, but appearing as brown bars on a tan background. A brown bar below lower posterior corner of eye. Pored scales in lateral line 14–17, usually 15. Snout blunt, its profile steeply sloping .... *E. boehlkei*, sp. nov. (p. 5)

4 Anterior orbital flange and nasal bones smooth. First dorsal spine longer than third spine of second dorsal, .234 of standard length. Distal third of second dorsal black. Body bars strongly contrasted, appearing as dark brown bars on a white background. No bar below eye (a few chromatophores only at lower posterior corner of orbit). Pored scales in lateral line 13 in the type. Snout almost pointed, not blunt, its profile gently sloping.
E. atrorus, sp. nov. (p. 9)

Enneanectes boehlkei, sp. nov.

Figure 1 (p. 8)

Enneapterygius jordani (not of Evermann and Marsh). Hildebrand *in* Longley and Hildebrand, Carnegie Inst. Pub. 535, 1941: 246 (in part, only the specimens described by Hildebrand; Tortugas, Florida).

Description

In the following description, counts are based on 21–23 specimens and measurements on 13–16 specimens.

Table I.—Comparison of certain characters in the Atlantic species of *Enneanectes*. "Spination" refers to the spines on the anterior orbital flange and the nasals. "Black dots" refers to the dots along the base of the second dorsal. "Enlarged scales" refers to the scales on the back and in the axil of the pectoral.

	jordani	*pectoralis*	*altivelis*	*boehlkei*	*atrorus*
L.L. pored scales	12–13 (13)	12–14 (13)	10–12 (11)	14–17 (15)	13
Scale rows	29–31 (29)	28–30 (29)	28–30 (29)	30–32 (31)	32
Scales above L.L.	1½	1½	1½	2½	2½
Pectoral rays	14–15 (15)	15–16 (15)	13–15 (14)	14–16 (15)	15
3rd dorsal rays	7–8 (7)	6–8 (7)	7–8 (8)	7–9 (8)	9
Anal rays	15	14–16 (15)	14–16 (15)	16–17 (16)	16
Scales on cheek	−	+	−	−	−
Scales on pectoral base	+	+	+	−	−
Scales on belly	+	+	+	−	−
Spination	+	+	−	+	−
Black dots	+ (diffuse)	+	−	+	−
Enlarged scales	+	+	+	−	−
Anal color	barred	plain	barred	barred	barred
Length of 1st dorsal spine	.116–.139	.104–.157	.172–.227	.112–.159	.234

First dorsal spines 3; second dorsal spines 11 to 13 (12); dorsal soft rays 7–9 (8.1); anal II, 16–17 (II, 16.0); pectoral 14–16 (15.0); lateral line 14–17 + 18–22 (14.8 + 18.8); scale rows 30–32 (31.0); scales above lateral line 2½; scales below lateral line 4½ or 5.

Head length 295–328 (315); postorbital 136–157 (140); head depth 177–215 (203); head width 223–255 (239); snout 98–123 (106); upper jaw 123–150 (133); eye diameter 80–119 (100); first dorsal spine 127–159 (138); second dorsal spine 116–148 (125); third dorsal spine 94–113 (101); third spine of second dorsal 140–193 (166); third ray of third dorsal 140–180 (164); pectoral 354–400 (375); pelvic 209–278 (249); second dorsal base 292–344 (308); third dorsal base 159–188 (166); anal base 360–436 (378); pelvic to anal 270–304 (286); caudal peduncle length 149–172 (160); caudal peduncle depth 89–112 (104).

Head bluntly triangular when viewed from above. Outline of head strongly convex from opercle to orbit; flat beneath eye; snout bluntly rounded. Snout blunt when viewed from the side. Upper lip little in advance of eye; profile between upper lip and eye steep. Outline of head betwen eyes and dorsal origin with a slight anterior slope.

Upper margin of eye entering outline of top of head, lower margin opposite sixth or seventh pectoral ray. Maxillary ending before hind margin of pupil, but behind midpoint of eye. Upper one-fourth to one-third of preopercle adnate to opercle. Vertical limb of preopercle almost straight, or very slightly convex; slightly inclined posteriorly. Angle of preopercle broadly rounded. Rear margin of opercle weakly concave from upper corner to a point opposite middle of pupil, then evenly rounded. Concave portion of opercular margin spinose; the remainder smooth.

Top of head back of orbits with small, closely set spines. The posterior three-fourths of the interorbital also has a few spines. Superior orbital rim mostly smooth. Posterior orbital flange with a few spines. Anterior orbital flange usually covered with spines as are the nasal bones. The degree of spination of the anterior orbital flange and nasals is dependent on size: all areas are smooth in three specimens smaller than 13 mm. The spination of the anterior orbital flange is developed first, but both bones are spinose in 20 mm. specimens. In the largest specimens the nasals and the anterior orbital flange are densely covered with spines. Circumorbitals spinose (the extent and degree of spination also increasing with size).

Orbital tentacle well-developed, longer than broad, its length slightly greater than interorbital width. Tip of orbital tentacle varying from broadly to narrowly rounded.

Origin of first dorsal over midpoint of opercle. First dorsal low; first spine considerably shorter than third spine of second dorsal. Second dorsal spine slightly shorter than first; third much shorter than first two. Membrane between spines of first dorsal complete to tips.

Outline of second dorsal even, first spine almost as long as highest (third). Third through eighth spines about equal in height; succeeding spines shorter, so that last spine is about one-half as long as third. Second and third rays of third dorsal equal and longest, first ray about three-fourths and last ray about one-half as long as first or second. Usually none of the dorsal rays are branched but occasional specimens may have as many as three branched rays.

Anal spines close together, the first slightly shorter than the second, which is about one-half as long as the first anal soft-ray. Posterior rays of anal slightly higher than anterior rays. Antepenultimate ray longest, about one and one-eighth times as long as first ray. Penultimate ray, when depressed, falls about two scales short of caudal base.

Pectoral moderate, extending almost to third dorsal origin. Pectoral formula quite variable; about equal numbers of specimens have one, two, or three upper unbranched rays, and one had four. This may be partly dependent on size, since most of the specimens with three upper unbranched rays are small and most of those with one are large. All of the specimens have seven lower unbranched rays. Pelvics ending at or before anus.

Sides completely scaled. Scales on back moderate; first two scales above lateral line equal in size, the third smaller. Opercular scale patch only one scale wide, usually extending ventrally to lower margin of eye; occasionally restricted to upper corner of opercle. Cheek, pectoral base, and belly naked. Two uppermost scales in pectoral axilla equal in size.

Color in alcohol.—Body ground color an even light tan. Sides with five brown bars, which do not contrast strongly with the tan body color. First bar lightest and most diffuse, located under space between last spine of first dorsal and fourth spine of second dorsal; second under sixth to tenth spines; third under space between last dorsal spine and second dorsal ray; fourth under fourth to seventh dorsal soft ray; and last covering posterior one-half to two-thirds of caudal peduncle. First three bars extend ventrally to midline; fourth bar extends to anal base. Peduncular bar darker than others, extending from dorsal to ventral surfaces. Anterior edge of peduncular bar straight or slightly inclined posteriorly. Between the bars the pigmentation is even and almost as dense as within the bars. The nape is likewise evenly pigmented.

Top of head lightly and evenly spotted with black, sometimes with underlying brown vermiculations. No large black spot at back of head. Interorbital and median portion of snout lightly and evenly dusted with black. At the side of the snout a faint bar originates just beneath the lower end of the anterior orbital flange and extends downward and forward across the upper lip. Upper lip white except for the above-mentioned bar, a median pigment patch, and a few scattered melanophores at the corner of the mouth. Lower lip with a median pigment patch, which may be faint or absent; chin and brachiostegal membrane otherwise clear. Nasal tentacle lightly spotted with black; orbital tentacle considerably darker.

Lower cheek with a faint brown bar, which begins slightly behind midpoint of eye and ends above and behind rear corner of mouth. This bar is never well developed and may be quite short and indistinct. Above this is another and fainter bar, which extends about one-third of the way to the opercular angle. At the upper corner of the cheek, next to the orbital rim, is a diffuse spot. There are two diffuse spots on the preopercle, one at the upper angle and another on the middle third of the upper limb. The black spot at the angle of the preopercle, characteristic of *E. jordani*, is either absent or represented by a weak aggregation of melanophores. Remainder of cheek unpigmented.

Opercle and pectoral base lightly spotted, but darker dorsally. Pectoral rays lightly and evenly spotted. When the pectoral is folded, the pigment spots tend to form three or four broad, cloudy bars across the lower rays. Pelvic base spotted; pelvic rays clear. Belly lightly dusted with black.

Membrane of first dorsal dark, except after third spine. Distal third of membrane of second dorsal dark, so that fin has a light black margin. There are three black dots along the base of the second dorsal, the first between the second and third spines; the second between the fifth and sixth spines; and the third between the seventh and eighth spines. Third dorsal with some pigment along the rays; membrane clear. Anal evenly and lightly dusted with black. Caudal an even dark brown or with a white band across the proximal one-third. It may be that sexual dimorphism is involved, since all of the specimens with evenly dark caudals are males and the few females in the sample have barred caudals. However, some males also have barred caudals. Perhaps the caudal is evenly colored only in breeding males.

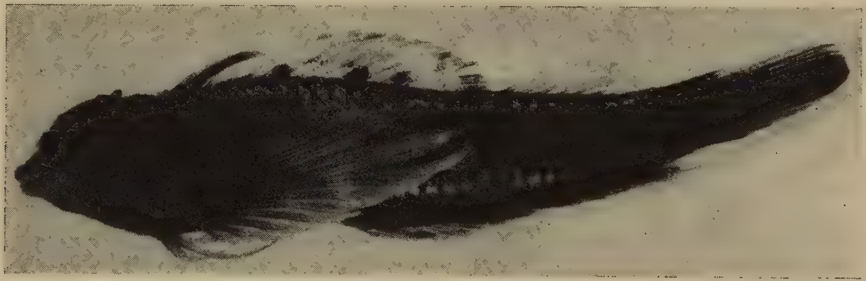

Figure 1. *Enneanectes boehlkei*, holotype, ANSP 74447, a 23.4 mm. male.

Comparisons

In general appearance and gross color pattern, *boehlkei* is quite similar to *jordani* and *pectoralis* and has in the past been confused with the latter. There are, however, certain fundamental differences. In *pectoralis* and *jordani* the belly and pectoral base are scaled; in *boehlkei* these areas are naked. In *pectoralis* and *jordani* the first scale above the lateral line is much larger than the scale above it; in *boehlkei* these scales are equal in size.

While *boehlkei* and *jordani* are similar in color pattern, certain color differences distinguish *boehlkei* from *pectoralis*. In general, *boehlkei* is more evenly colored. The body bars are not as strongly contrasted, the peduncular bar is not as dark, the pigment between the bars is more evenly distributed, and there is no tendency for the formation of secondary bars ventrally. In *boehlkei* the head is also lighter, and the snout bar characteristic of *pectoralis* is very weakly developed. In addition, the spination of the nasals, anterior orbital flange, and circumorbital bones is much stronger in *boehlkei* than in *pectoralis*. *E. atrorus* agrees with *boehlkei* in lacking scales on the pectoral base and belly, but, as indicated in the key and in Table I, the two have little else in common.

Remarks

The Tortugas specimens reported by Hildebrand (*in* Longley and Hildebrand, 1941, p. 246) as *Enneapterygius jordani* are referable to this species. They differ from the other specimens I have examined in the greater development of the head spination, but this may be due to their large size. Other smaller Florida specimens agree well with the Bahama material.

Range

Key West, Sand Key Reef, and Tortugas, Florida; Bahama Islands; Puerto Rico; Martinique.

Derivation of Name

Named for James E. Böhlke, in recognition of his researches on the fishes of the Bahamas, and in thanks for his cooperation and encouragement.

Material Examined

A total of 23 specimens from 11 collections.

Holotype.—ANSP 74447, a 23.4 mm. male; locality—British West Indies, Bahama Islands, Salt Cay (Treasure Island), N. shore about ¼ mi. W. of house, in a small lagoon (25° 06′ 16″ N., 77° 16′ 22″ W.); bottom—rock and sand; depth of capture—to five feet; 22 April 1955; C. C. G. Chaplin.

Paratypes.—British West Indies: Bahama Islands—ANSP 74448, New Providence Island, Delaporte Point, 2 (22.7–23.1). ANSP 85927, Hog Island, 3 (15.8–21.4). ANSP 85928, Andros Island, 6 (13.3–19.1). ANSP 85929, Exuma Cays, 5 (15.0–19.5). ANSP 85930, Rose Island, 1 (21.4).

Additional material.—Florida: Sand Key reef off Key West, USNM 4092, 1 (26.0) and ANSP 74450, 1 (23.5). Florida: Tortugas, USNM 116806, 3 (29.5–30.5). Puerto Rico: Isla Desecheo, CNHM 61803, 1 (16.0). British Virgin Is.: Guana Id., White Bay and North Bay, ANSP 74449, 2 (21.4–23.9). Virgin Is.—USNM 117439, 2 (18–20).

Enneanectes atrorus, sp. nov.

Figure 2 (p. 11)

Description

Following is a description of the holotype and only known specimen:

First dorsal spines 3; second dorsal spines 11; dorsal soft rays 9; anal II, 16; pectoral 15; lateral line 13 + 22; scale rows 32, scales above lateral line 2½; scales below lateral line 5.

Head length 328; postorbital 161; head depth 179; head width 215; snout 106;

upper jaw 161; eye 91; first dorsal spine 234; second dorsal spine 179; third dorsal spine 124; third spine of second dorsal 161; third ray of third dorsal (broken); pectoral 318; pelvic 256; second dorsal base 307; third dorsal base 179; anal base 405; pelvic to anal 277; caudal peduncle length 142; caudal peduncle depth 99.

Head narrowly triangular when viewed from above; outline very slightly convex from opercle to rear margin of orbit; slightly constricted under orbit, then almost straight to tip of snout. Snout conical when viewed from side; upper lip well in advance of eye; outline between upper lip and eyes gently sloping. Outline of head between eyes and first dorsal insertion sloping gently forward.

Upper margin of orbit entering profile of top of head, lower margin opposite seventh pectoral ray. Maxillary ending below a point slightly behind rear margin of pupil. Upper one-third of upper limb of preopercle adnate to opercle, the remainder free. Upper limb of preopercle convex, the angle gently rounded. Margin of opercle weakly concave from upper angle to a point opposite middle of pupil, then evenly rounded. Concave portion of opercular margin with weak spines; the remainder smooth.

Top of head back of mid-interorbital area covered with small prickle-like spines. Posterior orbital flange and fourth circumorbital spinose. Other head bones smooth. Orbital tentacle well developed, about 1.5 times as broad as long, length a little more than equal to interorbital and about equal to pupil diameter.

First dorsal origin slightly in advance of preopercle. First dorsal very high; first and second spines much higher than spines of second dorsal. Spines of first dorsal graduated; the first the longest; the second four-fifths as long as the first; and the third three-fourths as long as the second. Membrane between spines very shallowly incised. Second dorsal damaged, but the outline appears to have been even, with the third or fourth spines longest, and the succeeding spines becoming shorter, so that the last spine is about one-half as long as the third. Third dorsal damaged, but the rays appear to have been unbranched.

Anal spines set close together, the first about three-fourths as long as the second, which is a little more than one-half as long as the first anal soft ray. Outline of soft anal more or less even; posterior rays somewhat longer than anterior rays. Antepenultimate anal ray longest, 1.5 times as long as first ray. Longest anal ray, when depressed, falls one and one-half scale rows short of caudal base.

Pectoral extending to a point under interval between spinous and soft dorsals. Pectoral composed of five upper unbranched rays, three branched rays and seven lower unbranched rays. Longest pelvic ray just reaches vent.

Sides completely scaled; cheek, pectoral base, and belly naked. A patch of three or four ctenoid scales at upper anterior corner of opercle. Scales on back rather large; first two scale rows above lateral line composed of scales of equal size. Scales in axilla of pectoral not enlarged.

Color in alcohol.—Body ground color white. Sides with five dark brown bars. First bar under first to fourth spines of second dorsal; second under seventh to eleventh spines; third under the space between the last dorsal spine and the second dorsal soft ray; fourth under the fourth to ninth dorsal soft-rays; and the last covers the posterior third of the caudal peduncle. The first bar is very diffuse below the level of the upper edge of the pectoral base. The second bar is abruptly narrower below the midline, but extends to within two scale rows of the anal base. The next two bars are almost as wide below the midline as above and also end two scale rows above the anal base. The peduncular bar is complete, but only about two-thirds as wide ventrally as dorsally. In the interspaces between the last four bars, just below the midline, is a thin brown line. In addition to these lines, a few melanophores are scattered over the body. Across the nape a vague band passes through the base of the second dorsal spine.

Top of head vermiculated, due to the presence of large irregular brown chromatophores and a few small melanophores. Snout white, almost immaculate. Lips white, with a few scattered melanophores. Nasal tentacle lightly punctuated with black. Orbital tentacle mottled with brown basally; spotted with black distally. Cheeks mostly clear, with scattered black and brown chromatophores. The bar below the eye, characteristic of all other species of *Enneanectes,* is represented by only a few scattered spots. Opercle with a few pigment spots. Pectoral base lightly dusted with brown; a few black and brown spots on the basal portions of the pectoral rays. Pelvics clear. Belly white.

Membrane of first dorsal dusky behind first two spines, clear behind third. Distal third of second dorsal black. Below this black band the interradial membrane is spotted with brown. The brown spotting is more intense above the bars on the body, so that the bars appear to be continued onto the fin. Third dorsal spotted with brown. Here also the coloration is more intense above the body bars. Anal with five brown to black bars. Caudal clear.

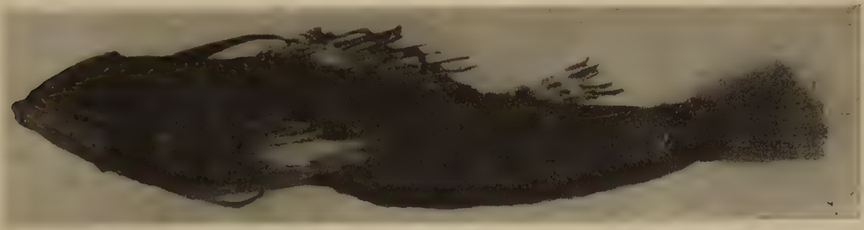

Figure 2. *Enneanectes atrorus,* holotype, ANSP 85931, a 27.4 mm. male.

Comparisons

Enneanectes atrorus differs widely from all its congeners. It is similar to *E. altivelis* only in that both species have a high first dorsal and lack spines on the anterior orbital flange and nasal bones. *E. atrorus* differs markedly from that species in lacking scales on the belly and pectoral base, in having the margin of the second dorsal black, in lacking an enlarged scale in the pectoral axil, and in having the first two scale rows above the lateral line composed of subequal scales. In addition there are meristic differences, notably in the number of scale rows and in the number of pectoral and dorsal rays (Table I). As may be seen in the key and Table I, *atrorus* differs from *boehlkei* in a number of features, and has little besides the generic characters in common with *jordani* and *pectoralis.*

Range

Known only from the type, which was taken at a station north of Green Cay, Bahama Islands, British West Indies.

Derivation of Name

From the Latin *ater,* black, and *ora,* margin, in reference to the striking black margin of the second dorsal.

Material Examined

Holotype.—ANSP 85931, a 27.4 mm. male, locality—British West Indies: Bahama Islands: ⅓ mi. N. of the center of Green Cay (25° 07′ 08″ N., 77° 11′ 17″ W.), on an isolated coral head rising from a white sand bottom; depth of capture—forty-eight feet; 12 May 1957. C. C. G. Chaplin, S. Waterman, J. Böhlke.

Enneanectes pectoralis (Fowler)

Figure 3 (p. 14)

Enneapterygius jordani (not of Evermann and Marsh). Longley *in* Longley and Hildebrand, Carnegie Inst. Wash. Pub. 535, 1941: 246 (in part, only the specimen described by Longley; Tortugas).

Enneapterygius pectoralis Fowler, Proc. Acad. Nat. Sci. Phila. 93, 1941: 96–98, Figs. 10–12 (Sanibel, Florida).

Tripterygion pectoralis Fowler. Schultz, Wash. Acad. Sci. J. 40, 1950: 268 (*pectoralis* placed in synonymy with *jordani*).

Description

In the following description, counts are based on 47–49 specimens. Proportions are based on 30–33 specimens, except for the length of the third dorsal soft ray, for which the number of specimens was 27.

First dorsal spines 3; second dorsal spines 11–12 (11.9); dorsal soft rays 6–8 (7.0); anal II, 14–16 (15.0); pectoral 15–16 (15.0); lateral line 12–14 + 18–21 (12.9 + 19.1); scales above lateral line 1½; scales below lateral line 4 or 4½; scale rows 28–30 (29.1).

Head length 309–348 (331); postorbital 142–168 (159); head depth 182–237 (213); head width 248–284 (265); snout 94–119 (106); upper jaw 142–165 (155); eye diameter 93–128 (109); first dorsal spine 104–157 (133); second dorsal spine 111–151 (133); third dorsal spine 93–122 (108); third spine of second dorsal 156–190 (167); third ray of third dorsal 128–190 (169); pectoral 324–394 (356); pelvic 236–288 (254); second dorsal base 280–340 (305); third dorsal base 133–167 (153); anal base 395–448 (416); pelvic to anal 266–320 (291); caudal peduncle length 136–164 (148); caudal peduncle depth 95–116 (108).

Head broadly triangular when viewed from above. Cheeks tumid; outline of head convex from opercle to tip of snout. Snout blunt when viewed from the side; outline between upper lip and eyes steeply sloping, and flat to slightly convex. Profile between eyes and dorsal origin flat.

Upper margin of eye entering outline of top of head; lower margin opposite ninth pectoral ray. Maxillary ending at or behind a point below rear margin of pupil. Upper limb of preopercle almost completely free from opercle; at most the upper one-fourth adnate. Vertical limb of preopercle straight to slightly curved, the angle gently rounded. Margin of opercle strongly and (usually) evenly rounded, but portion above pectoral base may be weakly concave. Above the pectoral base there are spines on the opercular margin; below the pectoral base there are none.

Top of head back of mid-interorbital area with closely set spines, which vary from sharply pointed to almost blunt. Except for the first, the circumorbitals are spiny, as is the vertical limb of the preopercle. Posterior orbital flange strongly spinose. A few weak spines are usually present on the rim of the anterior orbital flange, but these are occasionally absent. Nasals with a few weak spines, or smooth, the development of the spination increasing with size. The head spination is very weak in 16 mm. specimens, but relatively well developed in those 22 mm. long. Orbital tentacle well developed; about as broad as long; length about equal to interorbital width. Tip of tentacle flat or very broadly rounded.

First dorsal spine inserted slightly behind preopercle. First two dorsal spines about equal in height; the third slightly shorter. Membrane between spines complete, or shallowly incised. All first dorsal spines much shorter than longest spine of second dorsal. Outline of second dorsal even; first spine about three-fourths as long as highest (third or fourth); third through sixth spines about equal in height; succeeding spines becoming shorter, so that first spine is about two-thirds as long as third. Third ray of third dorsal longest; first ray about five-sixths as long as third; last ray about one-half as long as third. Typically the middle five dorsal rays are branched, but occasionally the first six are branched. Infrequently there are fewer than five branched rays (two specimens had four and one had three).

Anal spines set close together; the first a little more than three-fourths as long as the second, which is about half as long as the first anal soft-ray. Outline of soft anal even, becoming higher posteriorly. Antepenultimate ray longest, about one and one-eighth times as long as first ray (when depressed, it reaches caudal base).

Pectoral extending to a point posterior to last dorsal spine. Pectoral typically composed of one upper unbranched ray, seven branched rays and seven lower unbranched rays. This formula is quite constant; one specimen had two upper unbranched rays and two had three, with a corresponding decrease in the number of branched rays. Inner ray of pelvic usually reaches to anal base.

Sides completely scaled. Scales on back large. Anterior to the second dorsal origin the two scales above the lateral line are about equal in size. Under the second dorsal the first scale above the lateral line is much larger than the scale above it. Posterior to the third dorsal origin the scales on the back are again equal in size. A well-developed patch of ctenoid scales on opercle, extending down to a point opposite lower margin of eye. A patch of three to eight ctenoid scales on upper cheek, just behind eye. Pectoral base and belly covered with cycloid scales. An enlarged scale covers the upper two-thirds of the pectoral axil.

Color in alcohol.—Body ground color light tan. Sides with five dark bars. First bar under first to fourth spines of the second dorsal; second under seventh to tenth spines of the second dorsal; third under space between last dorsal spine and first dorsal ray; fourth under the last four dorsal rays; the last covers the posterior half of the caudal peduncle. In addition to the bars on the sides, a narrow brown band runs across the nape, under and between the first two dorsal spines. This band is quite distinct on some specimens, but is often so broad and vague that it merges with the first bar. The first body bar extends ventrally almost to the lower edge of the pectoral base. The second and third bars extend to, or slightly below, the notched lateral line, but become narrower and lighter below the level of the pored lateral line. The fourth bar usually extends to the anal base, but narrows and becomes lighter ventral to the midline. The peduncular bar is the darkest by far, being almost black. Its maximum width is at the midline; hence the anterior edge appears rounded. Between the bars a considerable amount of pigment is arranged so as to outline the scales. As a result the bars do not contrast strongly with the background color. There is a variable number (usually 4–6) of black spots along the course of the pored lateral line.

Top of head densely spotted with punctate chromatophores. At the back of the head, just before the first dorsal base, there is a black spot. Interorbital and median portion of snout lightly dusted with melanophores. At the side of the snout, just beneath the anterior orbital flange, there is a forward-directed bar, which is continued onto the upper lip. Corner of mouth dark; upper lip otherwise evenly and lightly spotted with black. Lower lip and mandible mottled with irregular brown bars. Branchiostegal membrane lightly dusted with melanophores. Nasal tentacle lightly dotted with black; orbital tentacle dark. Lower cheek with a brown bar which starts at a point posterior and ventral to the middle of the pupil and runs back behind the corner of the mouth. There is a dark spot on the upper cheek, beneath and slightly behind the last circumorbital. Remainder of cheek dotted with black, darker dorsally. Preopercular margin with three dark spots, the uppermost at the corner of the vertical limb, the second midway between the first and the angle, and the third at the angle. Opercle mottled with brown. Pectoral base with irregular brown markings. There is a tendency for the formation of irregular bars across the pectorals. Pelvics light. Belly scales outlined in brown.

Membrane of first dorsal dusky, except behind third spine. Second dorsal with three spots basally, the first spot between the second and fourth spines, the second between the fifth and sixth or seventh spines, and the third between the eighth and ninth spines. In addition two very faint bars run obliquely forward away from the fin base; the first originates at the base of the last dorsal spine; the second in the middle third of its length. The last bar is almost always present, but the anterior marking is always faint and often is lacking. Third dorsal rays pigmented, the membrane clear. Anal rays light; the interradial membrane evenly dusky. Caudal with a distal dark band covering the posterior two-thirds, a median light band, and a narrow proximal dark band.

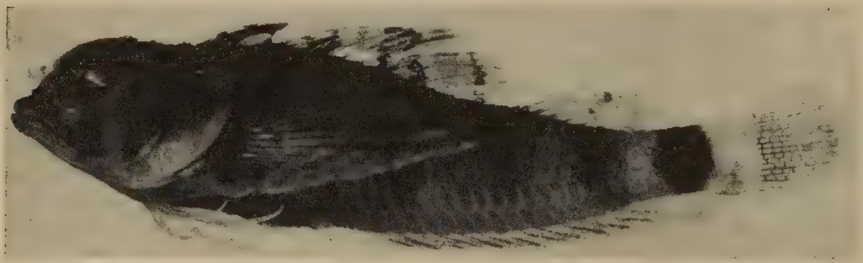

Figure 3. *Enneanectes pectoralis,* a 23.4 mm. male from ANSP 85932.

Comparisons

Since its description, *E. pectoralis* has not been considered by any author to be distinct from *E. jordani.* This circumstance may be ascribed partly to lack of material and partly to the nature of the characters that separate the species. Most of the species of *Enneanectes* are separated by meristic characters. (This is true of almost all the tripterygiid species which I have examined.) *E. pectoralis* and *jordani,* however, can be separated only on the bases of color differences, the presence or absence of large ctenoid scales on the cheek, and the shape of the orbital tentacle. In addition, *jordani* has seldom been collected (the excellent Bahama collections at Philadelphia contain a large number of individuals of

(440)

pectoralis, but only 13 of *jordani*). The differences between the two species are, however, very constant. Of 14 specimens of *jordani*, two have one and one has two small thin scales on the cheek; in the rest the cheek is naked. On the other hand, all of the fifty-odd large juvenile and adult specimens of *pectoralis* examined have well-developed cheek scales. The usual number is four to six; only two have as few as three. Specimens of *pectoralis* smaller than 16 mm. are like *jordani* in this respect, but the cheek scales are developed in 18 mm. specimens.

In addition to the nature of the coloration of the cheek and anal fin, the color patterns of the two species differ in several respects. In *pectoralis* the head is usually dark; the entire snout, most of the upper and lower lips, and the chin are dusky. In addition, there is a rather diffuse bar at the side of the snout. In *jordani*, on the other hand, the head is much lighter. Only the median parts of the snout and lips are pigmented, and the chin is immaculate. Further, *pectoralis* has a series of four or five black dots along the course of the pored lateral line, which are lacking in *jordani*. Although there is some variation in *pectoralis* in intensity of coloration, the general pattern is the same in all specimens. These differences, though small, appear to be constant.

Remarks

The holotype of *Enneapterygius pectoralis* is in very poor condition. It is very soft, almost scaleless, and badly faded. The head is almost torn from the body and most of the caudal peduncle and all of the tail are missing. It does, however, have a well-developed scale patch on the cheek, and it is mainly on this basis that the specimens treated here are regarded as conspecific with it. None of the other features that I was able to confirm for the holotype are inconsistent with this identification.

Fowler's description of *Enneapterygius pectoralis* as well as his figure is extremely misleading. A few of the more important points are listed below:

1. The " head, chest, breast and prepectoral region " are described as naked (there are scales on the cheek, opercle, belly, and pectoral base).
2. The body scales are described as cycloid (they are ctenoid, as in all tripterygiids except for the aberrant Australian genera *Lepidoblennius* and *Notoclinus*).
3. The anal count is given as XVII (there are but two anal spines, the other elements are articulated but unbranched rays).
4. The snout is figured as very narrowly rounded (it is blunt).
5. The vertical fins are all figured as being fantastically high (insofar as I was able to determine, they are normal).
6. The last rays of the dorsal and anal are figured as bound to the caudal peduncle by a membrane (no tripterygiid exhibits this feature).

Material Examined

A total of 95 specimens from 19 collections.

Holotype.—ANSP 69728; locality—Florida: Off Sanibel Island; 21 April, 1940; Mrs. R. Schwengel.

Additional material.—Florida: Patch reef between Margot Fish Shoal and Long Reef, USNM 167667, 3 (29.6–32.4).

Bahamas.—New Providence—ANSP 74434, 5 (18–21.5); 74435, 6 (13–24.9); 74436, 3 (17–20.4); 85932, 36 (14–24.9); 83934, 2 (28.4–28.9). Hog Island—ANSP 72607, 2 (15–21); 74437, 2 (18.1–24.9); ANSP 85933, 10 (14.5–24.5). ANSP 74439, Green Cay, 1 (18.5). ANSP 74452, N. edge of coral between North Cay and small cay W. of Long Cay (25° 05′ 51″ N., 77° 24′ 18″ W.), 1 (22.5). ANSP 85938, San Salvador, Watling Island, 2 mi. N. of lighthouse, 1 (25). ANSP 85937, Rose Island, 7 (21.2–25.5). ANSP 85396, Eleuthera Island, N.E. end of Harbour Island, 4 (12.7–24.4).

U. S. Virgin Islands.—St. Thomas; French Bay—USNM 78149, 1 (20.9).

Antigua.—SU 32033, English Harbor, 2 (22.4–23.4). AHF 932-73, Point Basora, 1 (23.4).

Martinique.—Smith Bay—USNM 117451, 2 (18–18.5).

Enneanectes jordani (Evermann and Marsh)

Gillias jordani Evermann and Marsh, U. S. Comm. Fish and Fisheries, Rept. 1899 (1900): 357 (Puerto Rico, Cardona Lighthouse Reef). Evermann and Marsh, U. S. Fish Comm., Bull. 20, 1900 (1902): 307, Fig. 95 (based on types).

Tripterygion jordani (Evermann and Marsh). Schultz, Wash. Acad. Sci., Jour. 40, 1950: 268 (original description cited).

Description

In the following description, counts are based on 15 specimens, except for the number of lateral-line scales and scale rows, for which the sample sizes were 13 and 12, respectively. Proportional measurements are based on 10 to 12 specimens, except for the length of the first and second dorsal spines, for which the sample size was nine.

First dorsal spines 3; second dorsal spines 11 to 12 (11.9); dorsal soft-rays 7–8 (7.1); anal II, 15 (II, 15); pectoral 14–15 (14.8); lateral line 12–13 + 19–20 (13.0 + 19.7); scale rows 29–31 (29.7); scales above lateral line 1½; scales below lateral line 4½.

Head length 315–339 (329); postorbital 159–172 (165); head depth 205–220 (213); head width 234–266 (250); snout 89–116 (101); upper jaw 136–148 (142); eye diameter 112–127 (119); first dorsal spine 116–139 (123); second dorsal spine 102–132 (115); third dorsal spine 82–118 (100); third spine of second dorsal 140–177 (164); third ray of third dorsal 157–172 (166); pectoral 337–380 (354); pelvic 257–289 (274); second dorsal base 286–350 (320); third dorsal base 141–172 (156); anal base 402–450 (425); pelvic to anal 265–311 (291); caudal peduncle length 153–174 (164); caudal peduncle depth 98–116 (108).

Head broadly triangular when viewed from above. Outline of head evenly convex from opercle to eye; slightly constricted beneath anterior third of eye; snout bluntly rounded. Snout blunt when viewed from the side; upper lip little in advance of eye. Profile between upper lip and eyes steep. Outline between eyes and dorsal origin almost flat.

Upper margin of eye entering outline of top of head; lower margin opposite seventh pectoral ray. Maxillary ending behind midpoint of eye but before rear margin of pupil. Upper one-third of vertical limb of preopercle adnate to opercle. Hind margin of upper limb of preopercle straight to slightly convex, and slightly inclined posteriorly. Preopercular angle gently rounded. Margin of opercle concave from upper corner to a point opposite lower third of pupil, then evenly rounded. Concave portion of opercular margin with spines, the remainder smooth.

Top of head behind mid-interorbital area with numerous closely set spines. Superior orbital rim and orbital flanges spiny. First circumorbital smooth, the others spiny. Nasals usually with a single row of spines, sometimes smooth. Orbital tentacle well-developed, 1.5–2 times as long as broad. Length of orbital tentacle a little more than equal to interorbital width. Tip of tentacle usually pointed, but sometimes narrowly rounded or ragged.

First dorsal insertion just in advance of midpoint of opercle. First dorsal spine low, much shorter than third spine of second dorsal; second dorsal spine either equal to first or very slightly shorter; third spine much shorter than first two. Interspinous membrane damaged on all specimens. Outline of second dorsal even; first spine five-sixths as long as highest (third or fourth). Third through eighth or ninth spines about equal in height; succeeding spines shorter, so that last spine is a little more than one-third as long as longest spine. First or second ray of soft dorsal longest; third ray about seven-eighths as long as first; last ray almost two-thirds as long as first. Typically the middle five rays are branched, but one specimen had two, one had three, and one had four branched rays.

Anal spines set close together; the first three-fourths as long as the second, which is three-fourths as long as the first anal soft-ray. Posterior rays of anal longer than anterior rays. Penultimate ray longest, about one and one-eighth times as long as first (when depressed, it usually falls short of caudal base by one-half of a scale, but in some individuals it does extend to the caudal base).

Pectoral ends under or very slightly behind last dorsal spine. Pectoral formula usually one or two upper unbranched rays, six or seven branched rays and seven lower unbranched rays. One specimen had only six lower unbranched rays, and a correspondingly reduced total pectoral count. Pelvic ending over anus.

Sides completely scaled. Scales on back large. Anterior to the second dorsal origin the two scale rows above the lateral line are composed of scales of equal size; under the second dorsal the first scale above the lateral line is much larger than the scale above it; posterior to the second dorsal the scales on the back are equal in size. Opercular scale patch extends ventrally to a point opposite lower margin of orbit, and is three scales wide dorsally and one scale wide ventrally. Cheek naked or with one or two very thin scales at the upper anterior corner. An enlarged scale covers the upper one-half or two-thirds of the pectoral axil.

Color in alcohol.—Body ground color light yellowish tan. Sides with five brown bars. First bar under first to fourth or fifth spines of second dorsal; second under seventh to ninth spines; third under posterior two-thirds of interdorsal space; fourth under last three rays of soft dorsal; last bar covering posterior half of caudal peduncle. First bar barely reaches midline, second extends below the notched lateral line, ending one scale row above anal base; third and fourth bars reach anal base. Peduncular bar darker than others, and extends from dorsal to ventral surfaces of peduncle. Width of peduncular bar the same throughout its length. Between the bars the pigment cells are aligned so as to outline the scales. This pattern is more distinct below the midline. There is no secondary barring in the interspaces between the main body bars. Nape evenly pigmented; its coloration blending into first body bar.

Top of head peppered with black spots, sometimes with deeper-lying brown vermiculations. No large black spot at back of head. Interorbital and median part of snout lightly dusted with melanophores. At the lower anterior corner of the eye a faint spot is formed by an aggregation of discrete melanophores. The bar found here in *E. pectoralis* is represented by at most a few scattered chromatophores across the suborbital. Upper lip lightly spotted with melanophores medially and at the corner of the mouth, otherwise white. Lower lip punctulate medially; otherwise white. Chin and branchiostegal membrane immaculate. Nasal tentacle lightly and evenly flecked with black; orbital tentacle dark brown.

Lower cheek with a brown bar which begins at the lower posterior corner of orbit and runs down and back, ending above and just behind the corner of the mouth. Above this a faint bar begins at the margin of the orbit and runs across the cheek toward the angle of the preopercle. At the upper rear margin of the eye is a black spot; the remainder of the cheek is clear. There are two spots along the margin of the preopercle, the first at the upper corner and the second covering the middle third. At the angle there is an aggregation of melanophores, but no definite spot, such as is found in *E. pectoralis.*

Opercle lightly spotted with brown and black chromatophores. Pectoral base with superficial black dots and deeper irregular brown markings. Pectoral flecked with black, sometimes with two or three cloudy, diffuse brown bars. Pelvics white; belly white or spotted with brown. Membrane of first dorsal dark between first and third spines; clear behind third spine. Membrane of second dorsal mostly clear, with rather variable barring corresponding to the basal spots present in *E. pectoralis* and *boehlkei.* Third dorsal mostly clear, with a few small, scattered pigment spots. Anal with six or seven brown bars; the first anal fin bar is beneath the second body bar; the remainder are evenly spaced, one under each bar and one under each interspace. The caudal appears to be evenly colored, but in life there may be a darker bar across the middle third.

Comparisons

The primary differences between *jordani* and *pectoralis* are those utilized in the key. Additional differences between the two species are considered in detail in the discussion of *pectoralis. E. jordani* is similar to *boehlkei* in general appearance, and agrees with that species in that the anterior orbital flange and nasals are spinose, but differs significantly in having scales on the pectoral base and belly. *E. jordani* also has fewer anal rays and pored scales in the lateral line (see Table I).

Remarks

Enneanectes jordani, as here interpreted, has until now been known only from the types. The specimens here described are identified with *jordani* on the basis of squamation and color pattern. The holotype of *jordani* has two thin scales on the cheek and a barred anal fin. In this it disagrees with specimens of *pectoralis* and agrees with those that I have called *jordani.* The orbital tentacle is ragged and somewhat shrunken, so that its shape cannot be determined exactly. The characters of anal fin color and weak cheek squamation are, however, sufficient to establish that the Bahama specimens reported here are indeed *jordani* and that most of the earlier records of *jordani* actually pertain to *E. pectoralis.*

Range

Bahama Islands to Puerto Rico.

Material Examined

A total of 15 specimens from 4 collections.

Holotype.—USNM 49368, a 23.4 mm. male; locality—Puerto Rico; Cardona Lighthouse Reef.

Paratype.—USNM 126096, same locality and data as type, 1 (23.4).

Additional material.—British West Indies: Bahama Islands—ANSP 72608, Hog Island, 2 (21.4–24.9). ANSP 74438, New Providence, Delaporte Point, 10 (15.5–21.9). ANSP 74439, about ¼ mi. N. of E. end of Green Cay (25° 07′ 00″ N., 77° 11′ 15″ W.), 1 (18.9).

Enneanectes altivelis, sp. nov.

Figure 4 (p. 21)

Description

In the following description, counts are based on 49–50 specimens, and proportions on 27–31, except for the length of the third spine of the second dorsal, for which the sample size was 24.

First dorsal spines 3; second dorsal spines 10–12 (11); dorsal soft-rays 7–8 (7.7); anal II, 14–16 (II, 14.7); pectoral 13–15 (14.0); lateral line 10–12 + 20–22 (11 + 21); scale rows 28–30 (29.2); scales above lateral line 1½; scales below lateral line 4½.

Head length 319–354 (335); postorbital 154–176 (165); head depth 188–227 (205); head width 221–257 (236); snout 84–112 (97); upper jaw 142–158 (151); eye diameter 98–129 (112); first dorsal spine 172–227 (195); second dorsal spine 143–194 (172); third dorsal spine 98–142 (126); third spine of second dorsal 157–189 (174); third ray of third dorsal 156–185 (169); pectoral 320–398 (365); pelvic 256–336 (279); second dorsal base 274–328 (293); third dorsal base 143–174 (159); anal base 363–435 (391); pelvic to anal 274–333 (306); caudal peduncle length 138–171 (155); caudal peduncle depth 90–114 (103).

Head narrowly triangular when viewed from above; intermediate in this respect between *E. jordani* and *E. atrorus.* Outline of head convex from opercle to orbit, constricted beneath eye, snout rounded. Snout slightly pointed when viewed from side, not blunt; upper lip in advance of eye. Profile between upper lip and eyes sloping. Profile between eyes and dorsal origin flat or with a slight anterior slope.

Upper margin of eye entering outline of top of head, lower margin opposite seventh pectoral ray. Maxillary ending at a point below hind margin of pupil. Upper limb of preopercle almost entirely free from opercle, its hind margin evenly convex, the angle gently rounded. Margin of opercle weakly concave from upper corner to a point opposite lower third of pupil, then evenly rounded. Concave portion of opercular margin with spines, the remainder smooth.

Top of head back of orbits with widely spaced small spines. The posterior third of the interorbital may have a few scattered weak prickles, and the spination of the superior margin of orbit is well-developed. Rim of posterior orbital flange spinose; anterior orbital flange weakly developed and smooth. Circumorbitals and nasals smooth. Orbital tentacle well developed, usually longer than broad; its length a little greater than interorbital width. There is considerable variation in the shape of the orbital tentacle. In most specimens it is triangular, rather than wide and blunt as in most species of *Enneanectes*, but in some specimens the tip may be rounded or even flat. Some but not all of the observed variation appears to be due to injury.

First dorsal origin over anterior third of opercle. First dorsal spine high, as long as or longer than third spine of second dorsal; second dorsal spine only slightly shorter than first; third spine much shorter than first two. Membrane between first two spines complete almost to tip, membrane between second and third spines shallowly incised. Outline of second dorsal even; first spine five-sixths as long as highest (fourth to fifth). Third through seventh spines about equal in height; succeeding spines shorter, so that the last spine is between one-third and one-half as long as the longest spine. Second ray of third dorsal longest; first and third rays nearly as long; last ray about one-half as long as second. Typically three to five rays are branched, but one specimen had no branched rays and another had six.

Anal spines set close together, the first three-fourths as long as the second, which is half the length of the first anal soft-ray. Posterior rays of anal longer than anterior rays. Penultimate and antepenultimate anal rays equal and longest, about one and one-eighth times as long as first ray. Longest ray, when depressed, falls short of the caudal base by one-half to two scale lengths.

Pectoral extending beyond end of second dorsal base, often as far as anterior third of third dorsal. Pectoral formula variable, usually composed of two or three upper unbranched rays, four or five branched rays and six lower unbranched rays. Occasional specimens have four upper unbranched rays, and a single individual had only one. The number of lower unbranched rays is more constant; two specimens had five and one had seven. Pelvic usually ending at anus, but sometimes extending almost to anal base.

Sides completely scaled. Scales on back large. Anterior to the second dorsal origin the two scale rows above the lateral line are composed of scales which are about equal in size; under the second dorsal base the scales of the first row above the lateral line are much larger than those of the row above it; posterior to the third dorsal origin the scales on the back are equal in size. Opercular scale patch extends down to a point opposite lower margin of orbit, and is three scales wide dorsally, and one scale wide ventrally. Cheek naked. Pectoral base and belly covered with cycloid scales. An enlarged scale covers the upper two-thirds of the axil of the pectoral.

Color in alcohol.—Body ground color light, varying from almost white to light tan. Sides with five brown bars. First bar under first to fourth spines of second dorsal; second under sixth to eighth or seventh to ninth spines; third under posterior half of interdorsal space; fourth under last four dorsal soft rays; the fifth covers the posterior half of the caudal peduncle. First bar extends to the midline; second and third bars extend downward slightly below the notched lateral line. Fourth bar reaches anal base. Peduncular bar no darker than others, extending from dorsal to ventral surfaces. Shape of peduncular bar variable; often it is wide at the midline, but it may hold the same width throughout its length. Between the bars the pigment cells are aligned so as to outline the scales. The nape is evenly pigmented. Below the midline, in the interspaces between the second and third and between the third and fourth bars, are two brown blotches. These may be quite faint, but when well developed are elongated vertically, and almost form secondary bars. Even when the secondary pigmentation is well-developed, *altivelis* gives the impression of being strongly barred.

Top of head varying from quite light to dark, dusted with black specks in all specimens. In the dark specimens there are a number of brown vermiculations on the top of the head. No large black spot at the back of the head. Interorbital and snout lightly dusted with melanophores. There is a slight tendency for the formation of a bar at the side of the snout, as in *E. jordani*, but this is never very distinct. Upper lip spotted with black, most densely medially. There may be a light area just anterior to the posterior end of the maxillary. Lower lip and chin dusted with melanophores. Nasal tentacle lightly and evenly spotted; orbital tentacle dark.

Lower cheek with a brown bar, which begins beneath the rear margin of pupil and runs down and back to the corner of the mouth. There is the faintest indication of a second bar just dorsal to the first. Remainder of cheek lightly and evenly spotted. The large dark spots present on the cheek of *E. jordani* are absent, being represented by, at most, slightly more dense aggregations of pigment.

Opercle evenly spotted with brown and black. Some irregular brown markings on pectoral base. Pectoral rays with a few black spots. Pelvics clear, belly with a few dark spots.

Membrane of first dorsal dusky, except after third spine, where it is clear. Membrane of second dorsal mostly clear, sometimes with rather evenly distributed black spots which may form a faint dark border. In addition, there may be two narrow, cloudy, vertical bars, the first extending upward from the base of the fifth spine, the second beginning at the base of the tenth spine. No spots along second dorsal base. Third dorsal rays pigmented, membrane clear. Anal with six or seven brown bars. All of these bars except the last are either below the body bars or below the pigment concentrations between the bars. The last, which is rather faint, is under the middle of the caudal peduncle. Caudal light or faintly brown, apparently never barred or mottled.

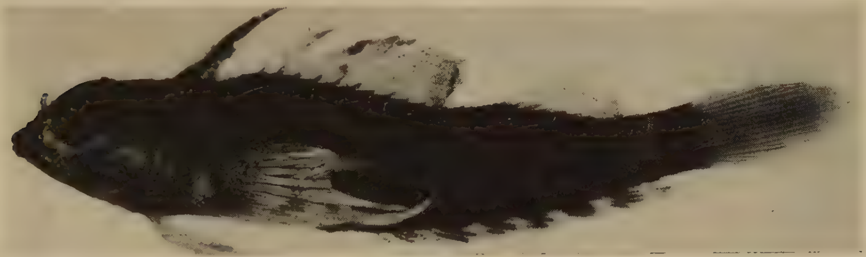

Figure 4. *Enneanectes altivelis*, holotype, ANSP 74446, a 22.6 mm. male.

Comparisons

E. altivelis is similar to *E. jordani* and *E. pectoralis* in that the pectoral base and belly are scaled. *E. altivelis*, however, differs strikingly from those species in having a high first dorsal fin. In addition there are differences in meristic characters (Table I) and in coloration. As indicated in the key to the species, *altivelis* and *boehlkei* differ in a number of characters. *E. altivelis* and *E. atrorus* (the only other Atlantic species with a high first dorsal) are superficially similar, but differ in a number of important features. These are treated in the discussion of *atrorus* and in Table I.

Range

Bahama Islands, British West Indies.

(447)

Derivation of Name

From the Latin *altus,* high, and *velum,* a sail, in reference to the high first dorsal fin.

Material Examined

A total of 71 specimens from 9 collections.

Holotype.—ANSP 74446, a 22.6 mm. male; locality—British West Indies, New Providence Island, an isolated coral head at the W. tip of Lyford Cay (25° 02′ 06″ N., 77° 34′ 08″ W.); bottom—an isolated coral head surrounded by sand; depth of capture—to twenty-five feet; distance from shore—one-quarter mile; 8 May, 1956; C. C. G. Chaplin, S. Waterman, C. Limbaugh, and J. Böhlke.

Paratypes.—ANSP 85924, 7 (18.8–22.4), same collection and data as holotype.

British West Indies.—Bahama Islands—ANSP 74440, New Providence, large coral head offshore and just W. (ca ¾ mi.) of Delaporte Point, 2 (22.7–24.4). ANSP 74441, Athol Island, coral head on S. shore off Quarantine Station (25° 04′ 37″ N., 77° 16′ 26″ W.), 2 (17.5–26.5). ANSP 74442, Rose Island, S. edge of coral head, off small point of N. shore (25° 06′ 04″ N., 77° 12′ 47″ W.), 1 (15.5). ANSP 74443, New Providence Island, reef off Delaporte Point, 21 (12.4–22.5). ANSP 74444, Rose Island, N. of E. end of island (25° 07′ 55″ N., 77° 05′ 32″ W.), 4 (19.2–22.5). ANSP 74445, Green Cay, about ¼ mi. N. of E. end (25° 07′ 00″ N., 77° 11′ 15″ W.), 9 (19.4–22.5). ANSP 85925, Rose Island N. shore, coral

Table II. Counts, and measurements in millimeters, of the holotypes of four Atlantic species of *Enneanectes.*

	Enneanectes			
	boehlkei	*atrorus*	*jordani*	*altivelis*
Standard length	23.4	27.4	29.1	22.6
Head length	7.4	9.0	8.9	7.5
Post-orbital	3.5	4.4	3.9	3.9
Head depth	4.3	4.9	5.9	4.6
Head width	5.9	5.9	4.9	5.4
Snout	2.6	2.9	2.6	2.2
Upper jaw	3.2	4.4	3.8	3.4
Eye diameter	2.0	2.5	2.8	2.4
1st dorsal spine	3.6	6.4	2.5	4.9
2nd dorsal spine	3.0	4.9	3.0	4.0
3rd dorsal spine	2.5	3.4	2.8	3.0
3rd spine of 2nd dorsal	3.9	4.4	...	4.2
3rd ray of 3rd dorsal	3.6	...	...	3.9
Pectoral	8.9	8.7	...	8.4
Pelvic	5.9	7.0	...	6.4
2nd dorsal base	7.4	8.4	8.3	6.5
3rd dorsal base	3.9	4.9	4.3	3.9
Anal base	10.0	11.1	10.0	8.9
Pelvic to anal	6.6	7.6	9.5	7.0
Caudal peduncle length	3.6	3.9	3.9	3.6
Caudal peduncle depth	2.6	2.7	2.8	2.4
1st dorsal spines	III	III	III	III
2nd dorsal spines	XII	XI	XII	XI
Dorsal soft-rays	8	9	7	8
Anal	II, 16	II, 16	II, 15	II, 15
Pectoral	15	15	15	14
Lateral line	14 + 20	13 + 22	12 + 19	11 + 21
Scales above lateral line	2½	2½	1½	1½
Scales below lateral line	5	5	4½	4
Scale rows	31	32	...	29

head off beach bearing 340° from Porpoise Rock, 1 (19.9). ANSP 85926, Green Cay, an isolated coral head rising from a white sand bottom ⅓ mi. N. of center of Green Cay, 23 (13–23).

Acknowledgments

I am grateful to the following individuals and institutions for making specimens available to me: James E. Böhlke, Academy of Natural Sciences, Philadelphia (ANSP); John Garth and Janet Haig, Allan Hancock Foundation, University of Southern California (AHF); Loren P. Woods, Chicago Natural History Museum (CNHM); George S. Myers and Margaret M. Storey, Stanford Natural History Museum (SU); Leonard P. Schultz and Robert Kanazawa, United States National Museum (USNM).

Professors Carl L. Hubbs, Scripps Institution of Oceanography, and Boyd W. Walker, University of California, Los Angeles, have critically read the manuscript and offered many useful suggestions. Dr. James E. Böhlke, Academy of Natural Sciences of Philadelphia, supplied important ecological data.

LITERATURE CITED

BROCK, VERNON E. 1940. Three new blennioid fishes from the west coast of Mexico. Stanford Ich. Bull., vol. 2, no. 1, pp. 266–268.

EVERMANN, BARTON W. AND MILLARD C. MARSH. 1900. Descriptions of new genera and species of fishes from Puerto Rico. Rep't U. S. Fish Comm. for 1899, pp. 351–362.

————. 1902. The fishes of Porto Rico. Bull. U. S. Fish Comm., vol. 20 for 1900, pt. 1, pp. 51–350, 49 pls., 112 text-figs.

FOWLER, HENRY W. 1941. Notes on Florida fishes, with descriptions of seven new species. Proc. Acad. Nat. Sci. Philadelphia, vol. 93, pp. 81–106.

————. 1944. Results of the Fifth George Vanderbilt Expedition. The Fishes. Acad. Nat. Sci. Philadelphia, Monographs, no. 6, pp. 57–529, 20 pls., 268 text-figs.

HUBBS, CARL L. AND KARL F. LAGLER. 1958. Fishes of the Great Lakes region. Cranbrook Inst. Sci., Bull. 26, pp. xiii + 213, 27 pls., 246 figs.

JORDAN, DAVID STARR. 1895. The fishes of Sinaloa. Proc. California Acad. Sci., ser. 2, vol. 5, pp. 377–514, pls. 27–55.

LONGLEY, WILLIAM H. AND SAMUEL F. HILDEBRAND. 1941. Systematic catalogue of the fishes of Tortugas, Florida. Carnegie Inst. Washington, Pub. 535, pp. xiii + 331, 34 pls.

SCHULTZ, LEONARD P. 1950. Notes on the blennioid fish genera *Runula* (subfamily Petroscirtinae) and *Tripterygion* and *Helcogramma* (family Clinidae) of the American tropical Pacific. Jour. Washington Acad. Sci., vol. 40, no. 8, pp. 266–268.

J. mar. biol. Ass. U.K. (1960) 39, 227–238
Printed in Great Britain

UNDERWATER DAYLIGHT MEASUREMENTS IN THE BAY OF BISCAY

By B. P. Boden, E. M. Kampa and J. M. Snodgrass
University of California, Scripps Institution of Oceanography, La Jolla, California

(With Plate I and Text-figs. 1–8)

As modern instrumentation improves the precision of the measurements of underwater light, particularly of monochromatic light, both biological and physical oceanographers are becoming increasingly interested in such measurements in deep water.

Two sets of observations of ambient light to depths of 400 m are presented here. It is suggested that the results were affected by both biological and physical factors.

MATERIALS AND METHOD

The light measurements were made by means of a telerecording bathyphotometer. There have been previous references in the literature (Kampa & Boden, 1956; Boden & Kampa, 1957, etc.) to a manuscript description of this instrument by Snodgrass, Cawley & Devereux. This account was never published and, since the instrument has now been modified, it is here described. This instrument comprises two units—an underwater unit and a deck unit.

The underwater unit (Pl. 1 A, B) is housed in a stainless-steel tube with walls $\frac{1}{2}$ in. thick and consists of a photosensor (RCA 931-A multiplier phototube) with a shutter, a depth sensor, a temperature sensor, control circuits and power supply, and the telemetering circuit by which light, depth, and temperature information are transmitted. It is supported by an insulated, single-conductor cable along which the data are telemetered. There are several advantages to the use of this type of cable. It is extremely strong (breaking strain 2800 lb.) and can be wrapped on a relatively small winch (800 lb. total weight). Due to the buoyancy of the polythene insulation the weight of this cable in water is only 16 lb./1000 ft. In multi-channel cable there is always a danger of short-circuits between the conductors due to mechanical stresses on the winch or block. This is eliminated here. The system uses a sea return.

Signals from the cable are transmitted via slip-rings on the winch to the deck unit.

The deck unit (Pl. 1 C) includes the circuitry that enables the operator to select the function (light, depth or temperature) to be recorded, a number of

Contributions from the Scripps Institution of Oceanography, New Series, 1164

Reproduced by Permission

bias circuits for zeroing the instrument, and a recorder (Pl. 1 D) to which the information is relayed.

The connexions are summarized in Text-fig. 1.

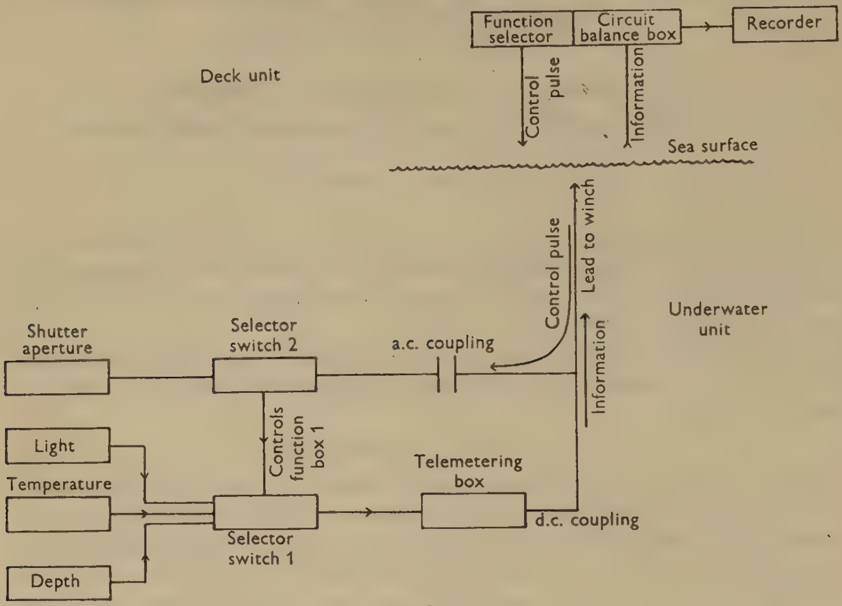
Function selector
Circuit balance box
Recorder
Deck unit
Control pulse
Information
Sea surface
Lead to winch
Control pulse
Underwater unit
Shutter aperture
Selector switch 2
a.c. coupling
Information
Light
Controls function box 1
Telemetering box
Temperature
Selector switch 1
d.c. coupling
Depth

Text-fig. 1

Circuits

Circuit diagrams for the entire instrument are shown in Text-figs. 2–4. The photometric circuitry (modified from Sweet, 1946) gives a logarithmic response over seven decades of light intensity.

The use of a pentode tube as a telemetering coupler (Valley & Wallman, 1948) obviates the interference of various potentials in the earth circuit, such as potentials between the steel hull of the ship and bronze propellor shafts and the water.

Depth

This element is a Bourdon tube coupled to a slide-wire potentiometer. It has been described elsewhere (Boden, Kampa, Snodgrass & Devereux, 1955).

Temperature

Water temperature is measured by a matched pair of 14-A thermistors, which operate in opposite arms of a full-resistance bridge. The bridge unbalance potential is applied directly to the grid of the IV 5 telemetering tube through a stepping switch.

EXPLANATION OF PLATE 1

A, underwater unit of photometer without case. B, underwater unit in case with collimating tube and automatic filter changer in position. The unit is connected by a test lead to C, the deck control unit, which is connected to D, a Leeds and Northrup Speedomax recorder.

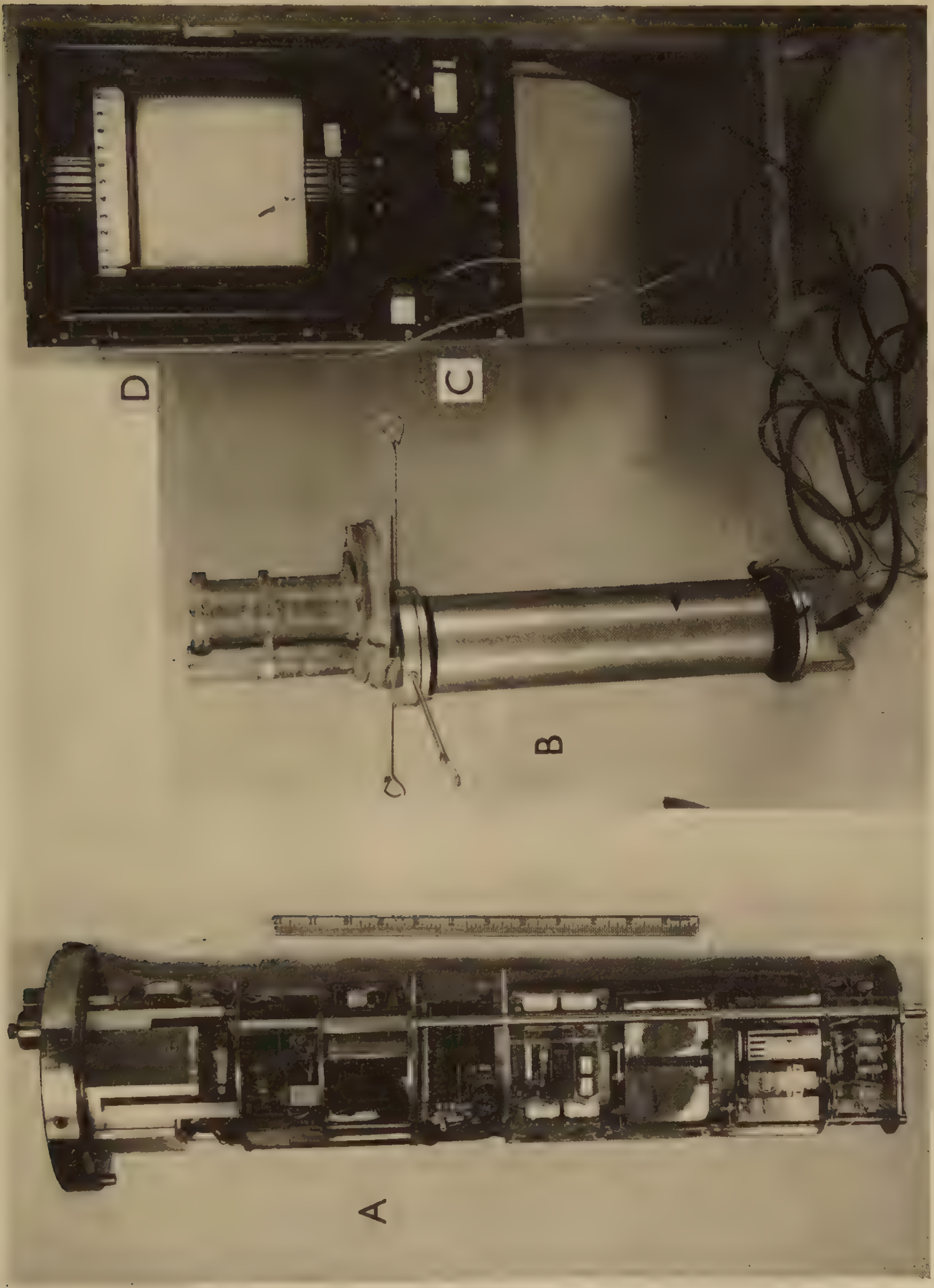

(*Facing p.* 228)

(454)

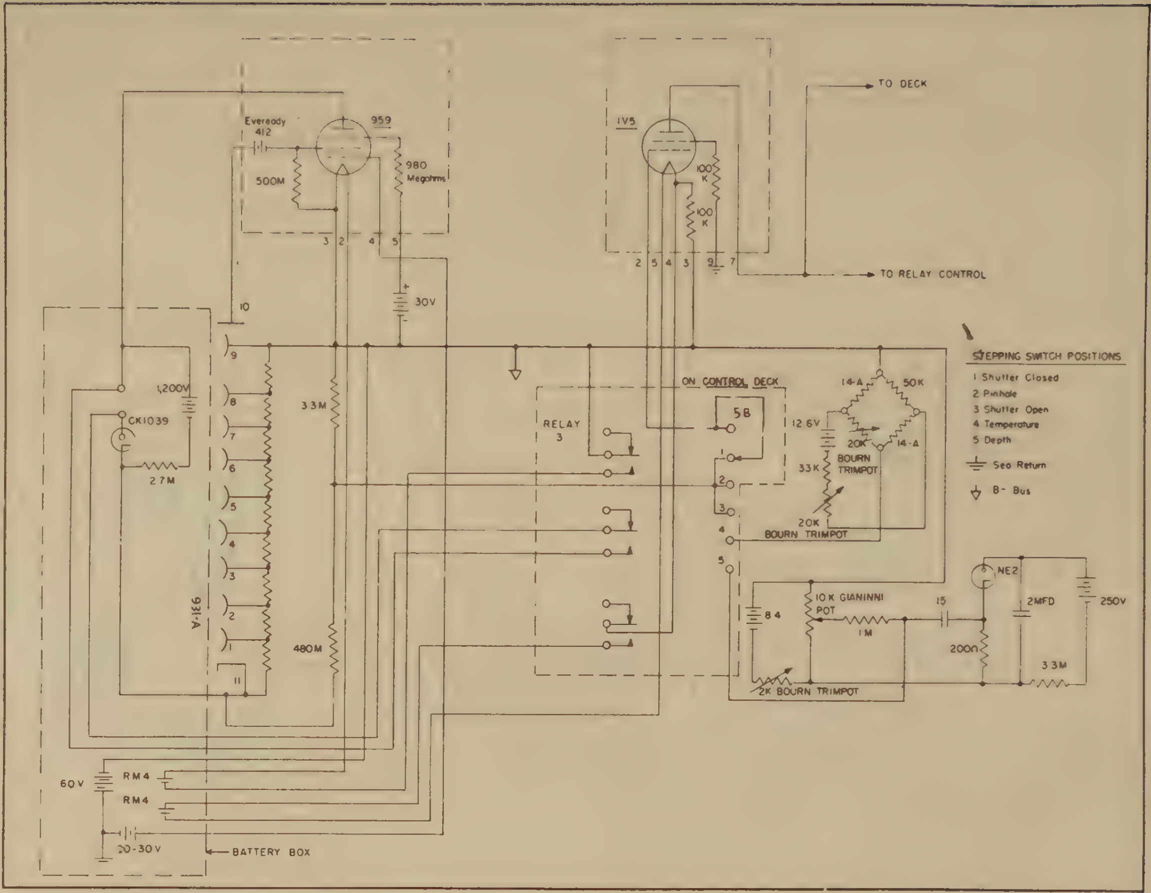
Eveready 412
959
500M
980 Megohms
3
2
4
5
30V
10
9
8
7
6
5
4
3
2
1
11
931-A
1,200V
CK1039
2.7M
3.3M
480M
60V
RM4
RM4
20-30V
BATTERY BOX
IV5
100 K
100 K
2
5
4
3
9
7
TO DECK
TO RELAY CONTROL
RELAY 3
ON CONTROL DECK
5B
1
2
3
4
5
12.6V
14-A
50K
20K
14-A
BOURN TRIMPOT
33K
20K BOURN TRIMPOT
8.4
10K GIANINNI POT
1M
2K BOURN TRIMPOT
15
200Ω
NE2
2MFD
250V
3.3M
STEPPING SWITCH POSITIONS
1 Shutter Closed
2 Pinhole
3 Shutter Open
4 Temperature
5 Depth
Sea Return
B- Bus

Text-fig. 2. Sensing circuits—depth, temperature and light. The assembly consists of the multiplier phototube (931-A) with its associated glow-type regulator (CK 1039) which is coupled to the type 959 control tube. The batteries are turned on and off from the deck unit by means of the multiple contacts on relay 3. The IV 5 tube is the telemetering coupler. The stepping switch relay 5 selects the desired function. The contacts designated under 5 B constitute one deck of this stepping switch. Connected immediately to this deck are the outputs from the photomultiplier control tube, the thermistor temperature bridge, and the depth potentiometer. For interconnexion of controls see Text-fig. 3.

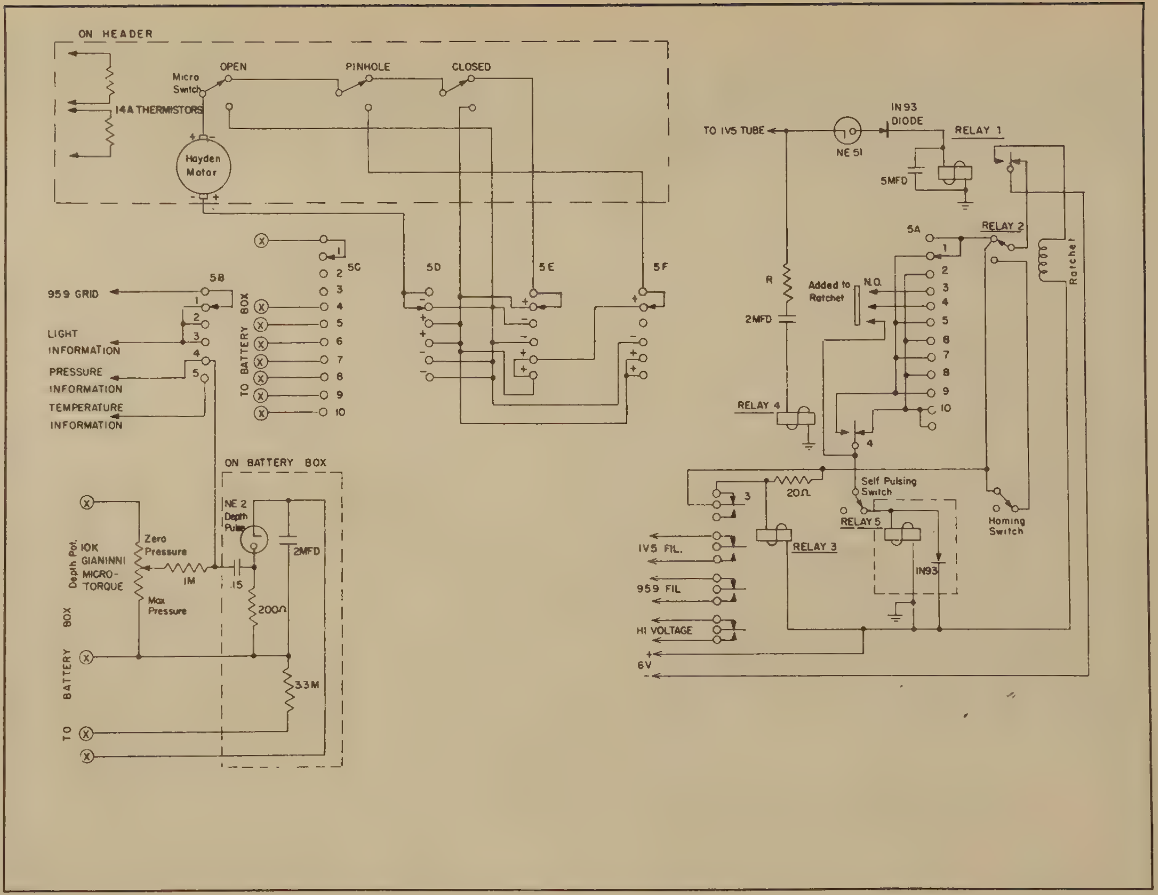
ON HEADER
OPEN
PINHOLE
CLOSED
Micro Switch
14A THERMISTORS
Hayden Motor
959 GRID
LIGHT INFORMATION
PRESSURE INFORMATION
TEMPERATURE INFORMATION
5B
5C
5D
5E
5F
TO BATTERY BOX
ON BATTERY BOX
NE 2 Depth Pulse
2MFD
.15
200Ω
3.3M
Zero Pressure
Max Pressure
1M
10K GIANINNI MICRO-TORQUE Depth Pot.
TO BATTERY BOX
TO IV5 TUBE
NE 51
IN93 DIODE
RELAY 1
5MFD
5A
RELAY 2
Ratchet
R
2MFD
Added to Ratchet
N.O.
RELAY 4
Self Pulsing Switch
20Ω
RELAY 5
RELAY 3
IN93
Homing Switch
IV5 FIL.
959 FIL
HI VOLTAGE
6V

Text-fig. 3. Shutter and relay control circuits in underwater unit. Certain sensing circuit details and relays are shown for convenience. Contact groups relating to a given relay-actuating coil use the relay number as a prefix. The following letter designates the bank of contacts on the relay, e.g. contacts 5E are controlled by relay coil no. 5 and represent the 'E' bank of contacts. Numbers opposite the contacts refer to the sequence of the contacts. A single common wire connects the IV5 telemetering tube and the relay control circuits to the deck unit. The series of contacts designated 'open', 'pinhole' and 'closed' represent limit switches which determine shutter aperture. In order to determine the function being measured and to insure continued synchronization between deck and underwater relays, a small regular pulse is superimposed upon the depth-measuring circuits. This is shown as a simple relaxation oscillator.

(456)

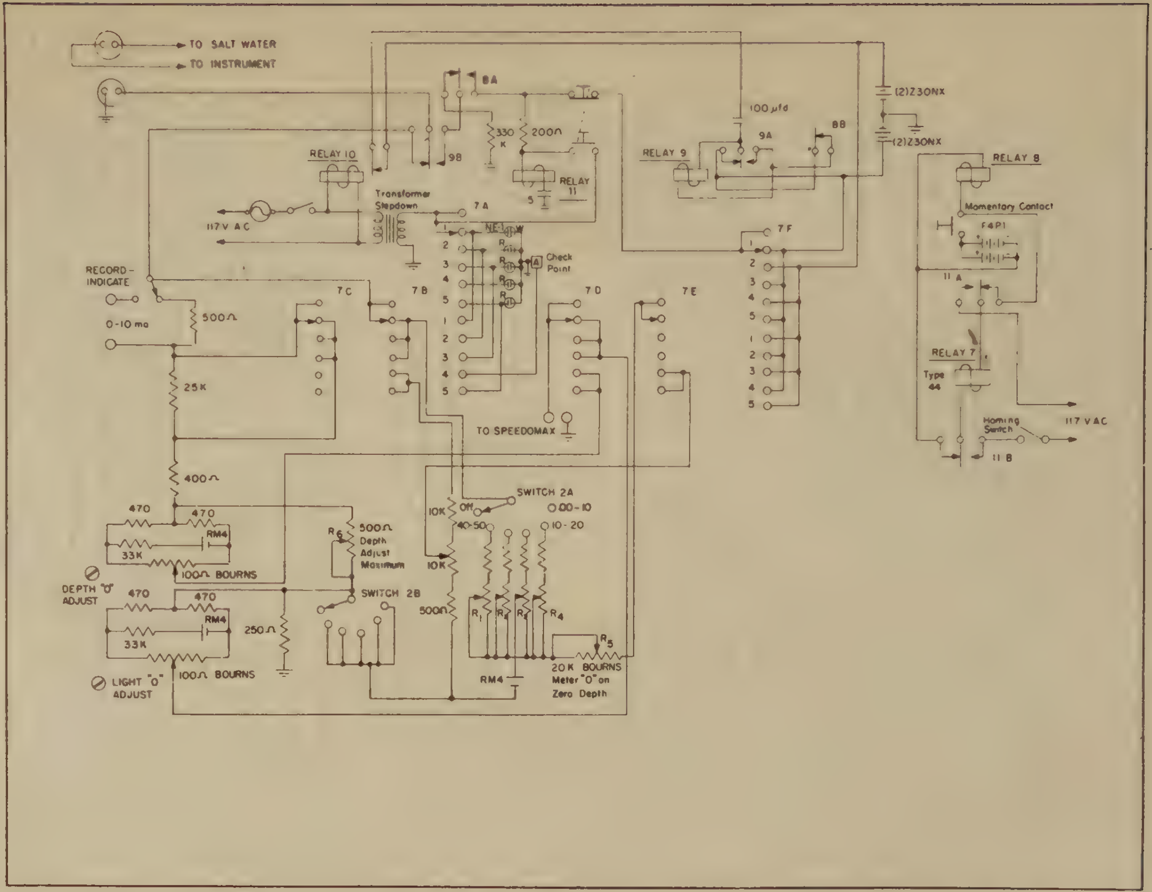
TO SALT WATER
TO INSTRUMENT
8A
330 K
200Ω
98
RELAY 10
RELAY 11
5
Transformer Stepdown
117 V AC
7A
NE-1
Check Point
RECORD-INDICATE
0-10 ma
500Ω
25K
400Ω
7C
7B
7D
7E
7F
TO SPEEDOMAX
100 μfd
9A
8B
RELAY 9
(2)Z30NX
RELAY 8
Momentary Contact
F4P1
11 A
RELAY 7
Type 44
Homing Switch
117 VAC
11 B
SWITCH 2A
OFF
0.00-10
40-50
10-20
10K
R6
500Ω Depth Adjust Maximum
SWITCH 2B
500Ω
R1
R2
R3
R4
R5
20K BOURNS Meter "0" on Zero Depth
RM4
470
33K
100Ω BOURNS
DEPTH "0" ADJUST
250Ω
LIGHT "0" ADJUST

Text-fig. 4. Deck control unit. The same designations are followed as in Text-fig. 3. In order to indicate the function being measured and to insure synchronization between deck and underwater units, two identical stepping switches are pulsed in series. These are relays 5 (in the underwater unit) and 7 (in the deck unit). To insure the operator's safety an isolating step-down transformer is used between the circuits and the 117 V a.c. power supply. Numerous range-adjusting and balancing networks are incorporated for convenience of read-out. A ground symbol indicates a good sea-water contact. The string of neon lamps connected to contacts 7A indicate the function being measured.

The stepping switch controls shutter position and also permits programmed telemetering of light, depth and temperature, or continuous recording of any selected single function.

Light

The 931-A multiplier phototube is selected for high sensitivity and low dark current. About one in five tubes tested will detect intensities as low as $10^{-5}\mu W/cm^2$ at 420 mμ when a narrow band (half-band width 10 mμ) interference-type filter is used.

The 959 electronic control tube automatically adjusts the sensitivity, and prevents damage when the instrument is exposed to bright light.

The photocathode faces outward through a synthetic sapphire window. Between it and the window is an electrically operated ribbon shutter which is controlled from the deck unit. It is possible to select one of three positions: open, closed, or pinhole. The pinhole is 0·001 the size of the open window and permits work near the surface at high intensities. This increases the useful range of the instrument to ten decades of light intensity. With the shutter closed it is possible to measure the dark current of the photomultiplier when the instrument is at depth.

Outside the sapphire window is an optical system through which the sea water passes freely. A battery-operated, automatic filter-changer places interference filters in this system for colour measurements. The filters are placed between the sapphire window and a free-flooding collimating tube that restricts the acceptance angle of the filters to its useful 5° cone. At the distal end of the collimating tube is an integrating disc of opal plastic material with the characteristics of a true cosine collector. Thus the instrument measures irradiance.

Calibration of the photometer

For each filter, curves giving deflexion against incident flux were constructed by attenuating in known steps the light falling on the bathyphotometer from a constant light source and measuring the deflexion of the recorder. The light was attenuated by calibrated neutral filters and by varying the distance between the light source and the instrument. If now for a given filter the deflexions of the recorder are found with the bathyphotometer at the surface of the sea and at a depth z, the diminution of the irradiance from the surface to depth z, for the narrow band of wavelengths transmitted by the filter can be found.

The instrument was also calibrated for absolute energy levels as follows. A calibrated light source (a tungsten filament lamp supplied by the U.S. Bureau of Standards and run at a constant voltage) was used to give a known energy distribution in $W/cm^2/m\mu$ striking the opal of the bathyphotometer. The deflexions given by the recorder of the bathyphotometer were then measured for each of the filters in turn. For any other set of lighting conditions the deflexions given by the bathyphotometer with the same filters can be found. It is now possible, using these results together with the curve showing, for each filter, deflexion against intensity of light, to compare the unknown with the known energy distributions. In this way a curve giving irradiance (H_λ) in $W/cm^2/m\mu$ against wavelength (λ) can be found. The integral $\int H_\lambda d\lambda$ over the spectrum gives the total irradiance. This calibration is valid for lights in which the spectral distribution of energy is broad compared with the narrow bands of transmission of the filters. This is true for the measurements of penetration of light into the sea desired here.

RESULTS

The results reported here were obtained at Station Cavall in the Bay of Biscay (lat. 46° 29′ N., long. 7° 59′ W.) on 25 September 1958, from the Plymouth laboratory R.V. 'Sarsia'. Station Cavall is one of several hydrographic stations established by Dr L. H. N. Cooper during his investigation of this area, and it was occupied for several days at this time.

The bathyphotometer was lowered twice during the day. The morning cast was made between 10.30 and 11.30 h and the afternoon cast between 13.25 and 14.10 h. The interference filters used in the morning cast had pass bands with peaks at 434, 460, 491, 514 and 540 mμ. Those used in the afternoon transmitted maximally at 421, 470, 482, 498 and 528 mμ.

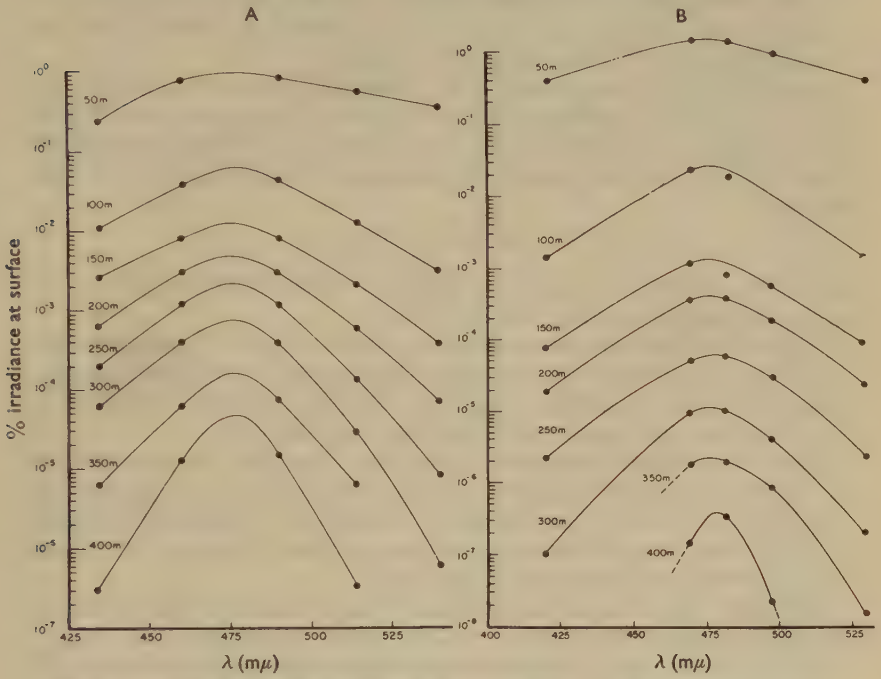

Text-fig. 5. Spectra of transmitted sunlight at 50 m intervals of depth in the Bay of Biscay (lat. 46° 29′ N., long. 7° 59′ W.) on 25 September 1958. A, 10.30–11.30 h G.M.T.; B, 13.25–14.10 h G.M.T.

At this latitude, at this time of the year, differences in degree of underwater irradiance due to differences in the sun's altitude at periods as closely spaced as these during the middle of the day are less than 5%. However, sky conditions changed between the two casts. In the afternoon a light, high haze caused some forward scattering. The afternoon irradiance values are higher than those obtained in the morning, but this is not a matter of importance, since the values have been equated to 1 at the surface, and only relative values are considered.

The spectral composition of the light at 50 m intervals to a depth of 400 m is shown in Text-figs. 5 A, B. The distribution obtained in the morning is very similar to that obtained in the afternoon, although different sets of filters were used. The light becomes steadily bluer with depth until at 400 m the spectrum peaks sharply between 475 and 480 mμ. This is an excellent illustration of the ocean acting as a monochromator as described by Tyler (1959). These results agree closely with those obtained by Jerlov (1951) and the main interest attached to them is: (i) the relatively great depth attained, (ii) the use of a series of interference filters, and (iii) the fact that, with the automatic filter changer, the time intervals between the determinations at different wavelengths were remarkably short (10 s).

Curves depicting the penetration of daylight of various wavelengths are shown in Text-fig. 6 (morning cast) and Text-fig. 7 (afternoon cast). Values of the extinction coefficient (k) for each wavelength at different depths are shown in Table 1. The extinction coefficient at depth z is defined by the equation

$$k_\lambda = \ln H_{\lambda,z} - \ln H_{\lambda,(z+1)},$$

where $H_{\lambda,z}$ and $H_{\lambda,(z+1)}$ represent irradiance values of wavelength (λ) on horizontal surfaces at depths z and $(z+1)$ m.

These results resemble those reported by Kampa (1955). There is a surface stratum in which extinction is rapid. This overlies a thick layer of very transparent water. Somewhere below 300 m a further inflexion suggests that the water becomes optically denser than that just above it.

In the morning cast a layer (between 45 and 60 m) was detected, between the optically dense surface water and the more transparent deeper water, which was very much more opaque than the surface water (for example, $k_{541\,\mathrm{m}\mu} = 0{\cdot}221$, which is about the average extinction coefficient for coastal waters according to Utterback's (1936) data).

This micro-layer was not demonstrated by the afternoon cast, and the break between the surface layer and the middle layer had sunk to about 100 m.

Dr L. H. N. Cooper (personal communication) has kindly supplied us with the data showing the vertical thermal structure (Text-fig. 8) at the time of the casts. Our thermistor circuit failed during the operation, and we did not record temperature. It can be seen that there was a very strong thermocline somewhere between 40 and 97 m. Correlations between attenuation coefficients and thermoclines in the north Pacific have been reported by M. Koslyaninov (Academy of Sciences, U.S.S.R.—personal communication to Mr J. E. Tyler, Scripps Institution).

Between the morning and afternoon casts the wind had increased from force 3 to force 4 and the sea from state 3 to state 5. The ship drifted less than 6 miles between casts and the possibility that this resulted in the sampling of different water masses at an oceanic station is slight.

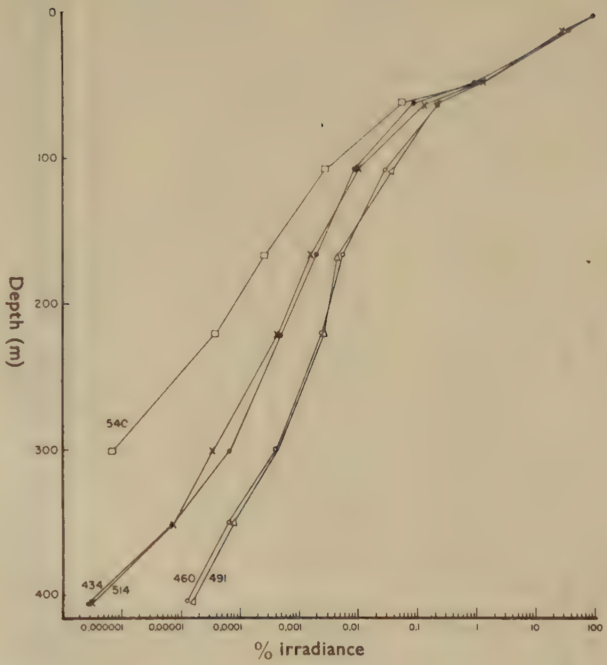

Text-fig. 6. Relation between depth and irradiance at various wavelengths expressed as percentage of irradiance values at the surface. The numbers at the ends of the curves indicate the wavelengths (in mμ) of maximum transmission of the interference filters used.

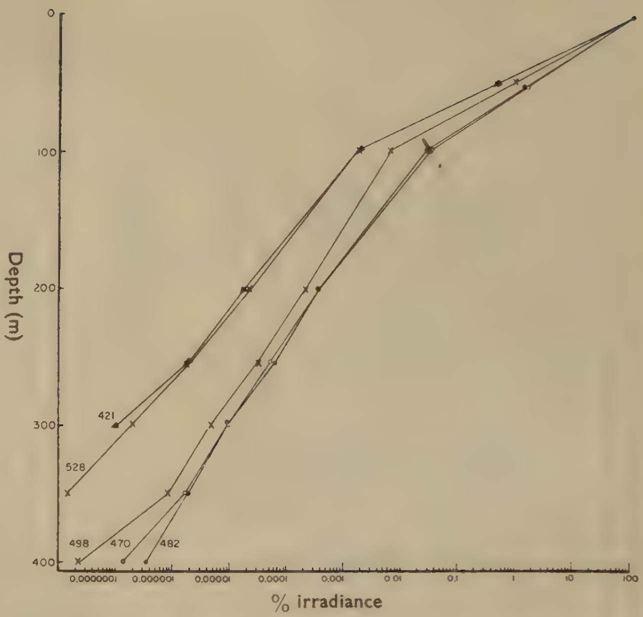

Text-fig. 7. Relation between depth and irradiance at various wavelengths expressed as percentage of irradiance values at the surface. The numbers at the ends of the curves indicate the wavelengths (in mμ) of maximum transmission of the interference filters used

(461)

TABLE 1. EXTINCTION COEFFICIENTS (k) OF LIGHT OF DIFFERENT WAVE-LENGTHS (λ) AT DIFFERENT DEPTHS AT STATION CAVALL

λ (mμ)	D (m)	k	D (m)	k	D (m)	k
			Morning cast			
540	0–60	0·126	60–300	0·047	—	—
514	—	0·112	—	0·034	300–405	0·045
491	—	0·102	—	0·026	—	0·032
460	—	0·101	—	0·026	—	0·033
434	—	0·118	—	0·031	—	0·052
			Afternoon cast			
421	0–98	0·111	98–300	0·048	—	—
470	—	0·081	98–350	0·039	350–400	0·050
482	—	0·083	—	0·037	—	0·035
498	—	0·096	—	0·035	—	0·072
528	—	0·111	—	0·047	—	—

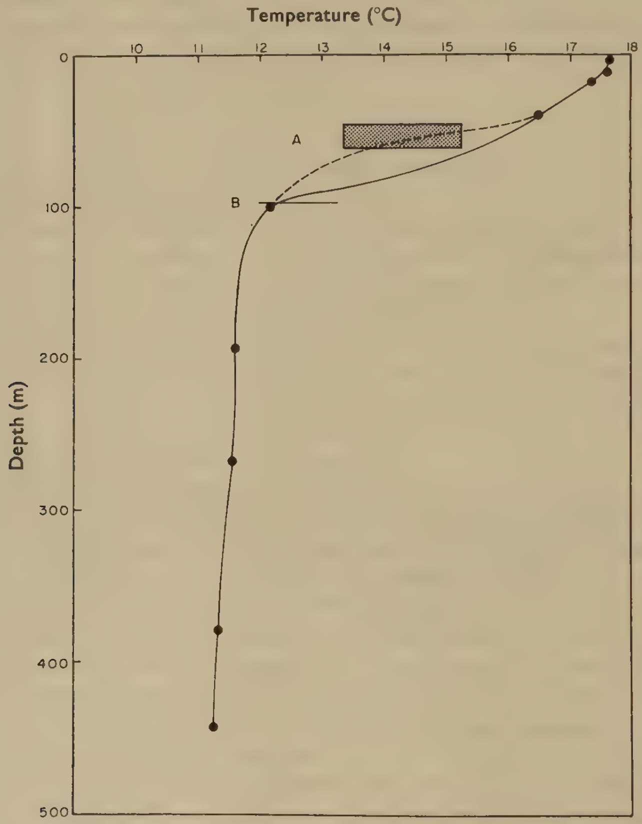

Text-fig. 8. Thermal structure at Station Cavall. The stippled area A shows the vertical position of the turbid micro-layer observed in the morning. The line B shows the vertical position of the inflexion of the sunlight transmission curves in the afternoon. The positions of the thermocline in the morning (broken line) and afternoon (solid line) are inferred from the optical data.

(462)

We interpret this apparent destruction of the optically dense micro-layer and the sinking of the break between the surface and middle layers as being due to turbulence associated with this change in the weather. The high extinction coefficients in the surface layer could well have been caused by particulate matter due to the higher productivity of the layer. The vertical extent of this layer is consistent with the depth of the 'photic' zone (Hedgpeth, 1958) at this latitude. The sharp difference in the optical properties of the two layers was probably due to an accumulation of particulate matter at an interface associated with an apparently long-established thermocline.

TABLE 2. OXYGEN VALUES AT DIFFERENT DEPTHS AT STATION CAVALL

	Oxygen		
D (m)	ml./l.	% sat.	Defect (ml./l.)
97	5·52	93·6	0·37
100	5·45	94·8	0·30
193	5·57	94·6	0·32
268	5·59	95·0	0·29
381	5·38	90·7	0·55
442	5·32	89·6	0·62
537	5·02	83·9	0·96

Such turbulence would cause a slight sinking of the thermocline and this change in thermal structure is summarized in Text-fig. 8. The broken line shows the probable position of the thermocline in the morning, and the solid line the same in the afternoon. The shaded area (A) represents the turbid micro-layer present in the morning, and a line (B) shows the break between the optical properties of the upper and lower layers in the afternoon. This increase in the vertical extent of the surface layer would result in a greater dilution of the particles in it, and this is revealed by somewhat lower extinction values in this layer in the afternoon. The differences in extinction coefficients between the middle and lower layers, somewhere below 300 m, are less pronounced.

In California, Kampa (1955) found that the lower inflexion in the extinction curve was associated with the top of a sonic-scattering layer and inferred that this increased extinction was also of biological origin. We have no evidence of the existence of a sonic-scattering layer at Station Cavall at this time, but this does not preclude the possibility that one was present. The echo-sounder on the 'Sarsia' operates at a much shorter ping-length than most American instruments, and may well have not recorded a layer of the type found in California.

Cooper, who supplied the oxygen data in Table 2, writes 'between 268 and 391 m there was some evidence, particularly from oxygen, of a change in properties. It was not very marked, however'. It is apparent that the photometer entered a water mass with different optical properties at about this depth. Whether such changes in oxygen content and transparency are linked with some biological phenomenon is a moot point. There were no marked changes in temperature, salinity, or other properties at this depth.

This work was done under contract between the U.S. Office of Naval Research and the University of California. A grant-in-aid was made by the U.S. National Science Foundation. Part of the work was supported by the U.S. Bureau of Ships.

We wish to thank the Director, Dr F. S. Russell, F.R.S., for the unfailing hospitality of the Plymouth Laboratory, the scientific staff of the laboratory and the captain, officers and crew of the R.V. 'Sarsia' for their help under rather trying circumstances. Dr L. H. N. Cooper, for whom the cruise was scheduled, was extremely generous in granting us time and in making available the pertinent hydrographic data.

SUMMARY

A telerecording bathyphotometer embodying a multiplier phototube is described and the circuitry is illustrated. Measurements were made of the penetration and spectral characteristics of daylight to a depth of 400 m in the Bay of Biscay. It is suggested that the rapid attenuation of light in the upper 100 m was due in part to biological matter associated with a sharp thermocline. A change in the weather is presumed to have caused a change in the depth of the thermocline and this is reflected in a change in attenuation coefficients.

REFERENCES

Boden, B. P., Kampa, E. M., Snodgrass, J. M. & Devereux, R. F., 1955. A depth telerecording unit for marine biology. *J. mar. Res.*, Vol. 14, pp. 205–9.

Boden, B. P. & Kampa, E. M., 1957. Records of bioluminescence in the ocean. *Pacif. Sci.* Vol. 11, pp. 229–35.

Hedgpeth, J. L. (Ed.), 1958. Treatise on marine ecology and paleoecology. I. Ecology. *Mem. geol. Soc. Amer.*, No. 67, Vol. 1, 1296 pp.

Jerlov, N. G., 1951. Optical studies of ocean waters. *Rep. Swedish deep-sea Exped.*, Vol. 3, *Phys. and Chem.*, Fasc. 1, pp. 1–59.

Kampa, E. M., 1955. A discrepancy between calculation and measurement of submarine illumination. *Proc. nat. Acad. Sci., Wash.*, Vol. 41, pp. 938–939.

Kampa, E. M. & Boden, B. P., 1956. Light generation in a sonic-scattering layer. *Deep-Sea Res.*, Vol. 4, pp. 73–92.

Sweet, M. H., 1946. Logarithmic photometer. *Electronics*, Vol. 19, pp. 106–109.

Tyler, J. E., 1959. Natural water as a monochromator. *Limnol. Oceanogr.*, Vol. 4, No. 1, pp. 102–105.

Utterback, C. L., 1936. Spectral bands of submarine solar radiation in the North Pacific and adjacent inshore waters. *Rapp. Cons. Explor. Mer*, Vol. 101, Pt. 2, No. 4, 15 pp.

Valley, G. E. & Wallman, H., 1948. *Vacuum Tube Amplifiers*. New York: McGraw Hill.

(464)

FACIES INTERPRETATIONS IN MISSISSIPPI DELTA BORINGS

ROBERT R. LANKFORD AND FRANCIS P. SHEPARD

Reprinted for private circulation from
THE JOURNAL OF GEOLOGY
Vol. 68, No. 4, July 1960
Copyright 1960 by the University of Chicago
PRINTED IN U.S.A.

(465)

FACIES INTERPRETATIONS IN MISSISSIPPI DELTA BORINGS[1]

ROBERT R. LANKFORD AND FRANCIS P. SHEPARD[2]

ABSTRACT

A study has been made of samples cut from borings drilled by the Corps of Engineers between New Orleans and the Chandeleur Islands and extending to depths of 60 to 180 feet in the now-abandoned St. Bernard subdelta of the Mississippi River. Interpretations of depositional facies are based on criteria obtained in the study of modern deltaic sediments in and around the presently forming birdfoot delta. The Foraminifera were particularly useful as environmental indicators, but grain-size and coarse-fraction analyses also were diagnostic in many places.

It was possible to correlate many of the facies between borings. The resulting section shows the transgression of Holocene (Recent) marine sediments over an eroded Pleistocene delta. During this initial marine encroachment there was deposition of relatively thin shelf sands containing abundant shells and Foraminifera. Later the Mississippi River shifted its locus of deposition, and the St. Bernard subdelta prograded across the shallow shelf. During this stage the rate of deltaic sedimentation was greater than the rate of rise of post-Pleistocene sea level, resulting in an apparent regressive facies formed during a eustatic transgression. Subsidence of the subdelta and its abandonment by the Mississippi River have permitted the sea to attack and rework the seaward portions with the attendant formation of discontinuous barrier islands and shallow-water sound deposits.

INTRODUCTION

An attempt has been made recently to determine the subsurface sedimentary facies encountered in jet borings made by American Petroleum Institute Project 51 in the modern birdfoot delta of the Mississippi River (Shepard and Lankford, 1959). Applying the same methods of study and criteria developed from the study of recent sediments, the present paper gives the results of an investigation of the depositional environments in the now-abandoned and partly submerged St. Bernard subdelta of the Mississippi River.

The majority of samples studied in this report were supplied by the U.S. Army Engineer Corps. Additional subsurface material has been collected from Breton Island with a Porter Soil Sampler by members of A.P.I. Project 51. All boring locations are shown in figure 1.

Our facies interpretations are based on the results of Holocene sediment investigation in the Mississippi Delta area. Shepard (1956) has divided the deposits into river-channel, natural-levee, marsh, interdistributary-bay, delta-platform, open-sound, and open-shelf sediments. The modern Foraminifera, investigated by Phleger (1955) and Lankford (1959), include the following faunal assemblages: marsh, interdistributary bay, fluvial marine, deltaic marine, sound, and open shelf.

ENGINEER BORINGS, NEW ORLEANS TO CHANDELEUR SOUND

During the past few years numerous reconnaissance borings have been made by the U.S. Army Engineers east-southeast of New Orleans extending across the St. Bernard subdelta and to the Chandeleur Islands. A total of 131 core samples were obtained from 6 of these borings (fig. 1) through the courtesy of the District Engineer of the U.S. Army Engineer District, New Orleans. The borings extend to a maximum depth of 180 feet.

Also supplied were water-content data, a general description of the formations penetrated, and results of compression tests which describe the samples as soft, medium, compact, or stiff. They also sent a generalized cross section (reproduced as fig. 2)

---

[1] Manuscript received November 1, 1959. Contribution from the Scripps Institution of Oceanography, new series; contribution from the Marine Foraminifera Laboratory No. 37.

[2] Scripps Institution of Oceanography, University of California, La Jolla.

(466)

Contributions from the Scripps Institution of Oceanography, New Series, 1165

Reproduced by Permission

based on all the holes along the line from which our samples were selected.

Their section indicates a series of channels with sandy sediments which cut across the general trend of the section. The Pleistocene-Holocene boundary,[3] as interpreted by the Engineers, is based primarily on a large decrease in water content or a change in color indicative of an oxidized zone. Their boundary agrees with our interpretations (figs. 2, 4) except in boring 40-D, where we believe a more marked stratigraphic change occurs at −116 feet than at −90 feet given by the Engineers.

The borings have been studied in detail by the Corps of Engineers (Kolb and Van Lopik, 1958), but their studies are of a different character from those reported here. They give a general lithologic description supplemented by compression test and water-content data to supply information necessary for engineering considerations. On the other hand, we have made sediment-size analyses, diagnosed the coarse fraction con-

---

[3] The definition of this boundary is much disputed among geologists. We are calling "Holocene" those sediments which accumulated during and after the sea-level rise following the unconformity produced by weathering and erosion during the last major glaciation.

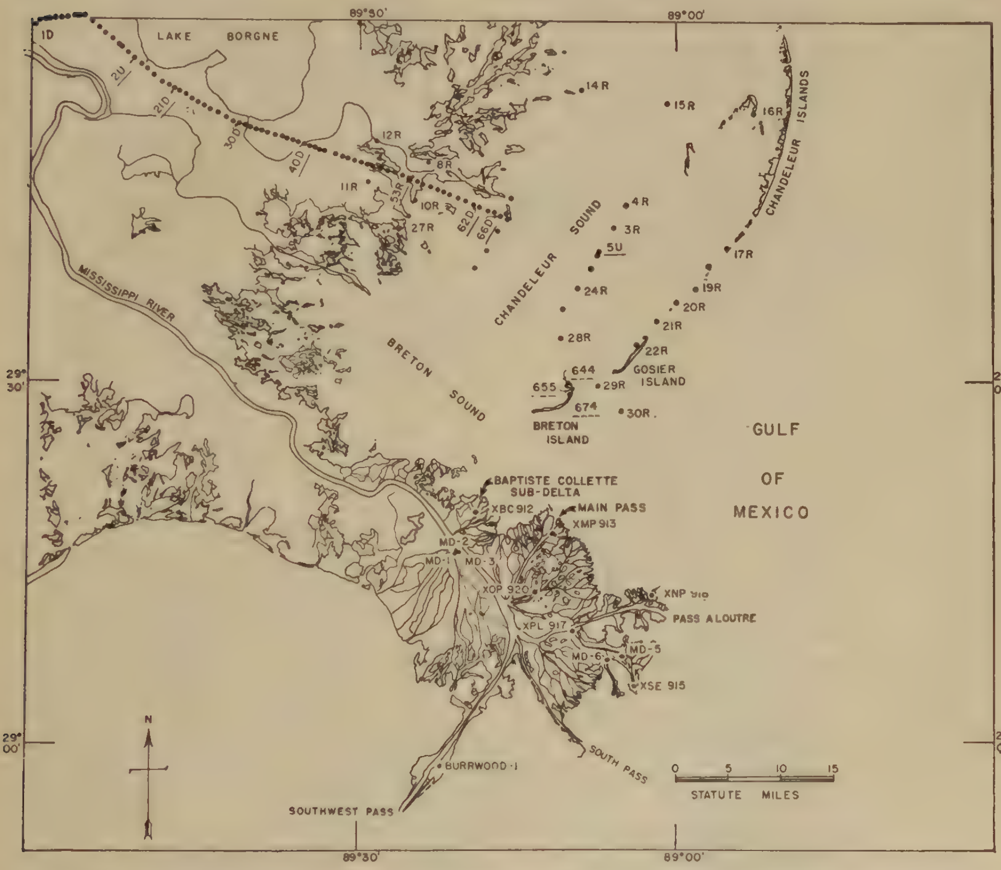
89°30'
89°00'
1D
LAKE BORGNE
21
210
300
400
12R
8R
11R
53R
10R
27R
620
660
14R
15R
16R
CHANDELEUR ISLANDS
4R
3R
5U
CHANDELEUR SOUND
17R
24R
19R
20R
21R
MISSISSIPPI RIVER
BRETON SOUND
28R
22R
644
GOSIER ISLAND
655
29R
674
30R
BRETON ISLAND
GULF OF MEXICO
29° 30'
29° 00'
BAPTISTE COLLETTE SUB-DELTA
XBC 912
MAIN PASS
XMP 913
MD-2
MD-1
MD-3
XOP 920
XNP 919
PASS A LOUTRE
XPL 917
MD-5
MD-6
XSE 915
N
SOUTH PASS
0 5 10 15
STATUTE MILES
BURRWOOD-1
SOUTHWEST PASS

FIG. 1.—Sample locations. Those with underlines are by the Corps of Engineers; those with dashed underlines are by A.P.I. Project 51.

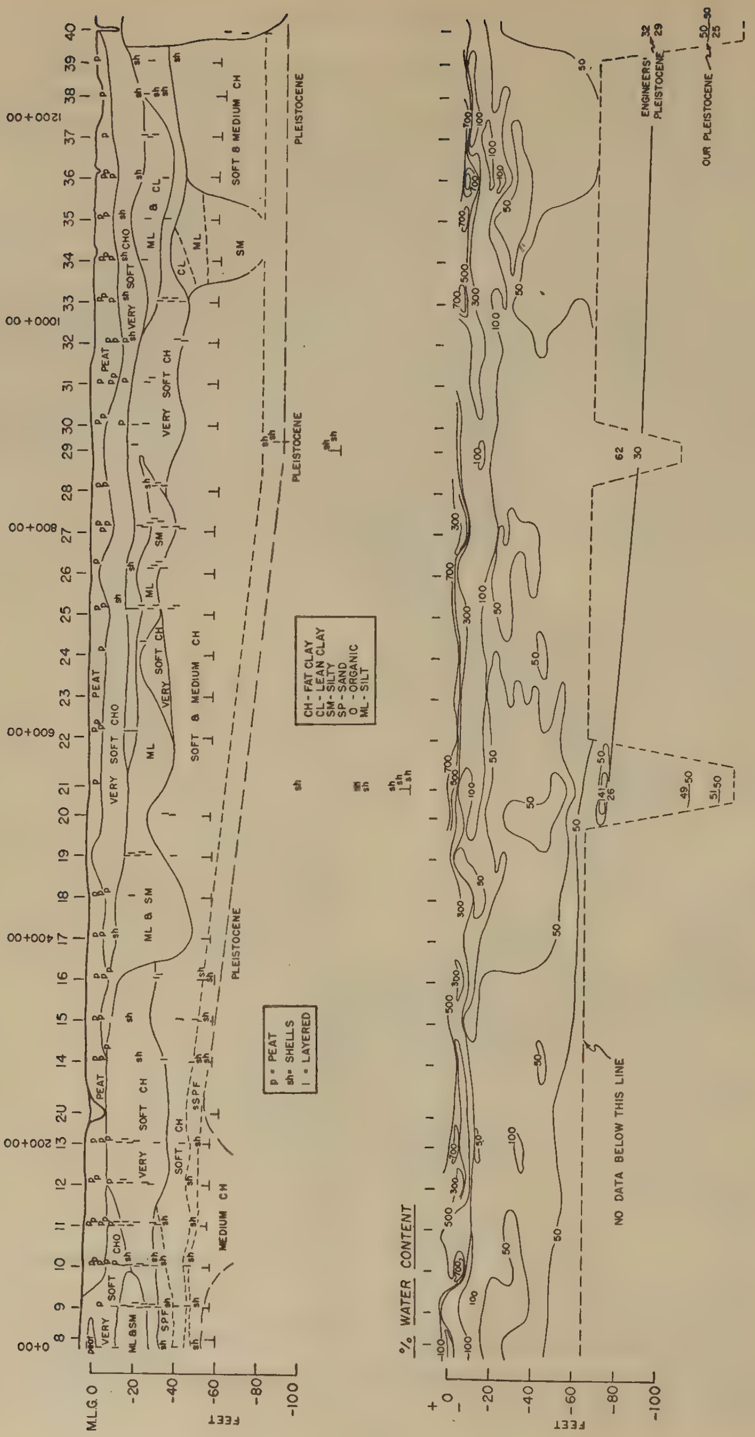
M.L.G.O
-20
-40
-60
-80
-100
FEET
0+00
200+00
400+00
600+00
800+00
1000+00
1200+00
8
9
10
11
12
13
2U
14
15
16
17
18
19
20
21
22
23
24
25
26
27
28
29
30
31
32
33
34
35
36
37
38
39
40
PEAT
VERY SOFT CHO
SOFT CH
VERY SOFT CH
SOFT & MEDIUM CH
MEDIUM CH
ML & SM
ML
SM
CL
SPF
ML & CL
PLEISTOCENE
p = PEAT
sh = SHELLS
l = LAYERED
CH - FAT CLAY
CL - LEAN CLAY
SM - SILTY
SP - SAND
O - ORGANIC
ML - SILT
% WATER CONTENT
+0
-20
-40
-60
-80
-100
FEET
NO DATA BELOW THIS LINE
ENGINEERS' PLEISTOCENE
OUR PLEISTOCENE
50
100
300
500
700

(468)

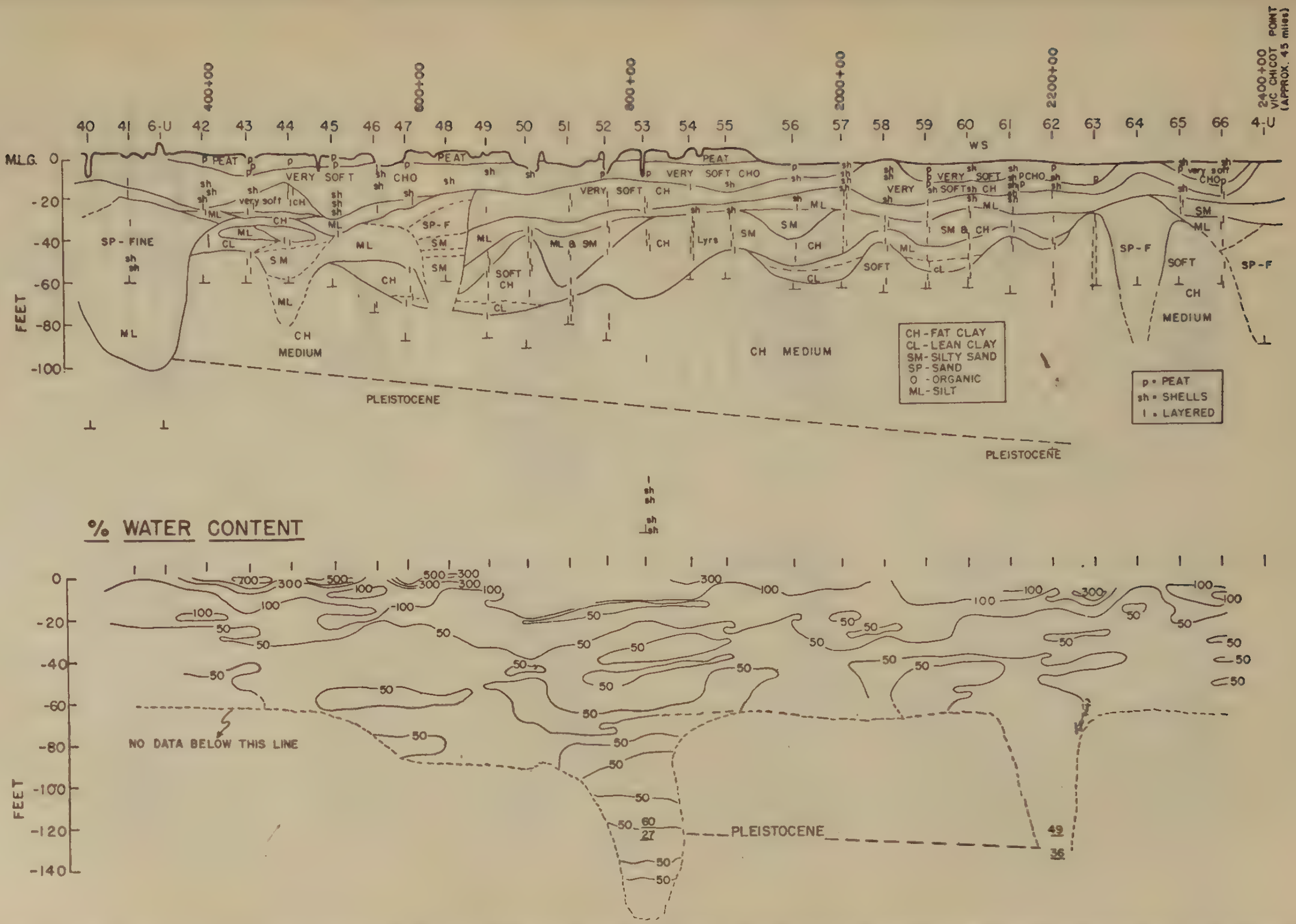
40 41 6-U 42 43 44 45 46 47 48 49 50 51 52 53 54 55 56 57 58 59 60 61 62 63 64 65 66 4-U
400+00
600+00
800+00
2000+00
2200+00
2400+00 VIC CHICOT POINT (APPROX. 45 miles)
WS
MLG. 0
-20
-40
-60
-80
-100
FEET
PEAT
VERY SOFT
CHO
VERY SOFT CH
SP - FINE
ML
CH MEDIUM
SM
CL
SP-F
ML & SM
SOFT CH
Lyrs
SM & CH
SOFT
PLEISTOCENE
CH - FAT CLAY
CL - LEAN CLAY
SM - SILTY SAND
SP - SAND
O - ORGANIC
ML - SILT
p = PEAT
sh = SHELLS
I = LAYERED
% WATER CONTENT
0
-20
-40
-60
-80
-100
-120
-140
FEET
700
500
300
100
50
NO DATA BELOW THIS LINE
PLEISTOCENE
60
27
49
36

FIG. 2.—Gives information from Army Engineers on their complete line of borings from a position near New Orleans to Chandeleur Sound. See fig. 1 for locations. Upper cross section gives the Engineers soil classification and their interpretation of the stratigraphy. Several river channels are indicated as crossing the line of section. The short dashed line gives the upper limit of the sandy layer with abundant shells immediately overlying what was interpreted by the Engineers as the Pleistocene-Holocene boundary. In two of the borings our interpretation of the Pleistocene contact is included. The lower cross section shows the variation of water content, per cent dry weight.

stituents, and identified the ecologic environments of the foraminiferal assemblages contained in the core samples. The generalized cross section made by the Engineers (fig. 2) used data from all the borings. We, on the other hand, have had more limited material, but our methods have enabled us to identify the facies of deposition of most of the formations from which we had samples available. It would have been desirable to make our interpretations apply to all the Engineer borings, but we have found it impossible to do this without much more extensive studies than time permitted.

SAND-SILT-CLAY CONTENT

Our sample analyses provide a generalized picture of the content of sand-silt-clay from these borings (fig. 3, *A*). Two of the borings from which we have samples, 40-D and 66-D, were drilled along the side of one of the supposed channels. The high sand content between −20 and −60 feet in boring 40-D indicates the influence of this channel, but we not find confirmation of the channel deposit in boring 66-D. In the sands of boring 40-D at depths of between −30 and −60 feet, the weight per cent of the $\frac{1}{4}$- to $\frac{1}{8}$-mm. fraction is larger than that of the $\frac{1}{8}$- to $\frac{1}{16}$-mm. fraction, which is also true of channel deposits in the present Mississippi River except near the river mouth. A point bar origin of the sands is more probable than fill of an abandoned channel because the latter should consist predominantly of mud, although few such mud fills have been described—probably because investigators have not recognized them as channel fills.

The same size relationship exists in boring 21-D at −130 and −133 feet, in boring 62-D at −127 and −137 feet (above and below the Pleistocene-Holocene boundary), and in the isolated sample obtained from −55 feet in boring 2-U (west of 21-D). The samples in the last three borings apparently come from a sheet sand rather than a channel.

Aside from boring 40-D the sediments from the Engineer borings have about the same proportions of sand-silt-clay as those in the jet borings made by A.P.I. Project 51 into the distributaries of the birdfoot delta (Shepard and Lankford, 1959). An average of samples from the top 40 feet of the Engineer borings shows sand 16.2, silt 53.2, and clay 30.6 per cent. This compares with averages for the jet borings showing sand 18.4, silt 54.8, and clay 26.8 per cent. This is of interest because the jet borings were put down on the natural levees built, according to Fisk *et al.* (1954), on top of the supposed "bar 'sands,'" whereas the Engineer borings were drilled at equal intervals without reference to natural levees.

There appears to be some indication that a similar variation in clay content in post-Pleistocene formations can be correlated between the borings, particularly if we place the Pleistocene boundary of boring 40-D at −116 feet instead of at −90 feet, where it has been drawn by the Engineers. Assuming this is correct, it will be seen that toward the bottom of the post-Pleistocene section there is a consistent increase in the clay fraction in each boring except in 66-D, which does not penetrate deep enough to approach the Pleistocene. Also, in boring 5-U the Pleistocene is not reached, but there is an increase in clay content at the base, suggesting a correlation with the others.

COARSE-FRACTION STUDIES

The variation of constituents of the coarse fractions with depth is shown in figure 3, *B*. Wood fibers are as abundant in the upper portions of the Engineer borings (to depths of 30 to 50 feet) as in the jet borings in the lower delta. Below that the plant-fiber content is extremely variable but for the most part not very high. A sample from a depth of −75 feet in boring 21-D is completely different from the others at equal depths because the coarse fraction, consisting of 60 per cent of the whole sample, is almost 100 per cent wood fibers. This sample probably represents a peat bog and therefore shows the area was at or above sea level during deposition. Below 50 feet many samples show a high foraminiferal content in

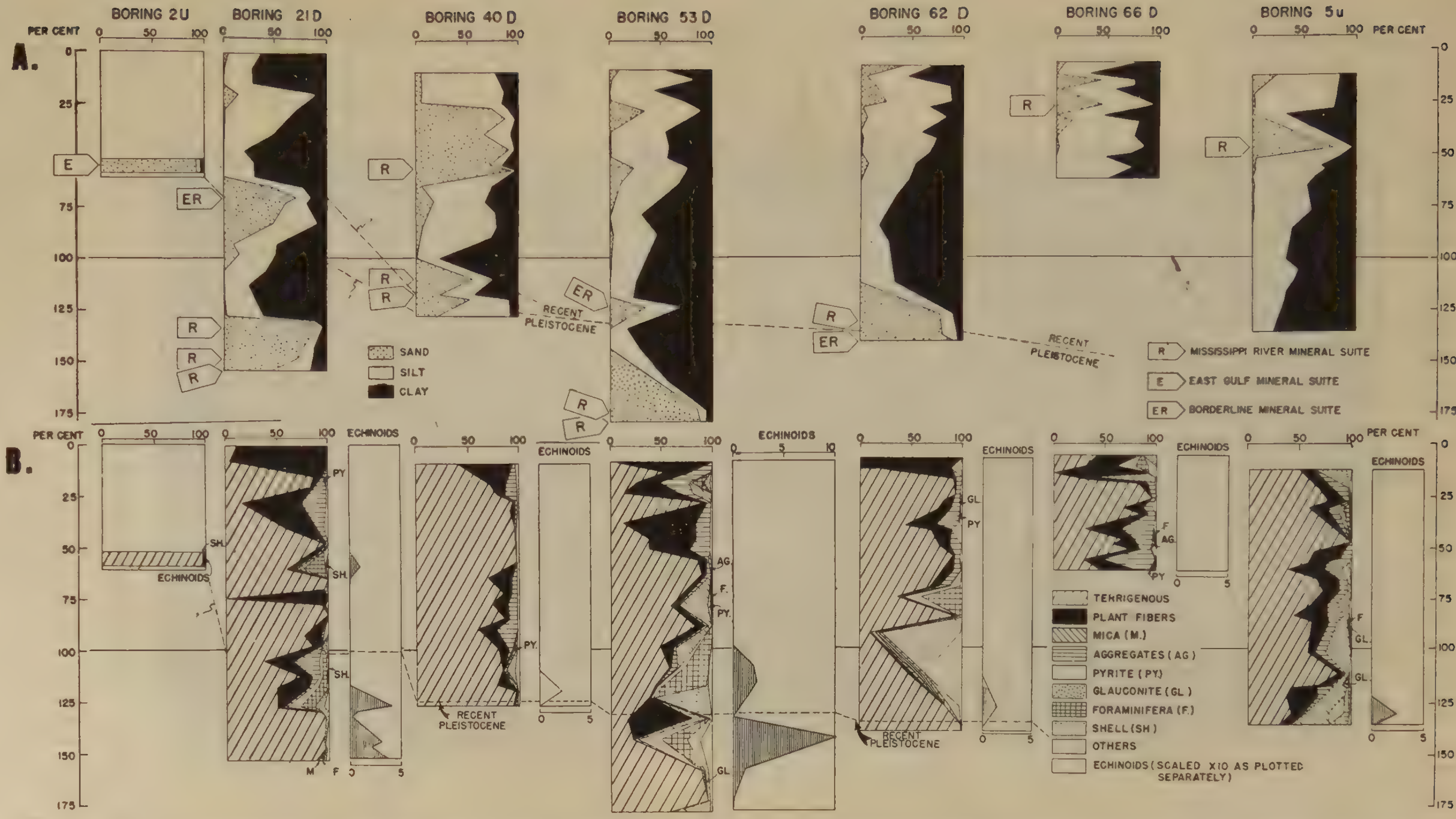

FIG. 3.—Gives analyses of the samples from the Army Engineer borings and our two interpretations of the Pleistocene-Holocene boundary. See fig. 1 for locations. *A* gives the sand-silt-clay percentages. The symbols *E*, *R*, and *ER* give the position and results of mineral grain analyses. *B* gives the percentage of principal constituents in the coarse fraction. The expanded scale gives the echinoid content, except in boring 2-U. Scale indicates depth in feet.

the coarse fraction. Shells also are fairly abundant in a few zones, especially just above the contact with the Pleistocene. A single sample which we have from boring 2-U (5 miles to the northwest of boring 31-D) also had a high content of shells at −55 feet.

Abundant echinoids are usually indicative of open-shelf conditions or barrier-island inlets. A relationship of echinoids to distance from the delta became very evident in previous studies of the Mississippi Delta (Shepard, 1956, fig. 44). In the deeper parts of the borings, samples containing an appreciable quantity of echinoids (fig. 3, *B*) are very low in their content of plant fibers, mica, and aggregates. Comparison with recent sediments marginal to the delta (Shepard, 1956) indicates deposition in the open Gulf at an appreciable distance from the river mouth.

Although pyrite is scarce in the borings from the birdfoot distributaries, it occurs in fair abundance in samples from the deeper portions of the Engineer borings and shows some increase with depth. It is found in equal abundance in the Pleistocene and Holocene.

MINERAL SUITES

There is a striking difference between the sand-mineral suites coming from the eastern Gulf and those from the Mississippi River (Goldstein, 1942). The studies of surficial samples east of the delta showed that some of the East Gulf sands had migrated into what were otherwise Mississippi Delta bottomset beds (Shepard, 1956, p. 2592). A difference between the East Gulf and Mississippi Delta sands is found in both light and heavy minerals. The East Gulf is much higher in quartz, on the one hand, and in kyanite and staurolite, on the other. A group of 15 samples was chosen for study, mostly from the deeper portions of the borings where it was thought more likely that East Gulf minerals would be found because of oral communications from petroleum geologists to that effect, The staurolite, kyanite, and quartz content were determined for each of these samples. The analytical results are shown in figure 3, *A*. Of the 15 samples, 11 contained a Mississippi Delta suite, 1 had an East Gulf suite, and the remaining 3 were borderline cases.

Samples from sands at the bottom of boring 21-D and 53-D, clearly within the Pleistocene, contain the Mississippi Delta suite, and the single sample at −55 feet from boring 2-U, just east of New Orleans, contains the best East Gulf mineral assemblage. The borderline cases are from borings 21-D, 53-D, and 62-D. The East Gulf and borderline assemblages all occur near the Pleistocene-Holocene boundary. The samples from 2-U and 62-D with East Gulf mineral suites are also higher in the $\frac{1}{4}$- to $\frac{1}{8}$-mm. sand size than in the $\frac{1}{8}$- to $\frac{1}{16}$-mm. fraction, which is also true for East Gulf shelf sands (Shepard, 1956). The implication is that, prior to the transgression, the area was not receiving appreciable sediments from the East Gulf. During the early part of the transgression East Gulf sands were introduced, perhaps as partially submerged bars, where the waves could concentrate the shell debris.

LAMINATION

We have no definite evidence concerning the abundance of laminations in the Engineer borings. Their logs give "layered" as a characteristic of the cores at many depths (fig. 2) but refer to only one zone in boring 5-U at 58 feet as being "varved." A sample was cut from this section (pl. 1), and the lamination proved to be well developed, being similar to laminated cores from the delta margin (Shepard and Lankford, 1959). It was not practical to examine many of the other portions of the borings which were called "layered," but a few core sections were extracted from their par-

PLATE 1

Laminated zone at −58 feet in boring 5-U under Chandeleur Sound.

(472)

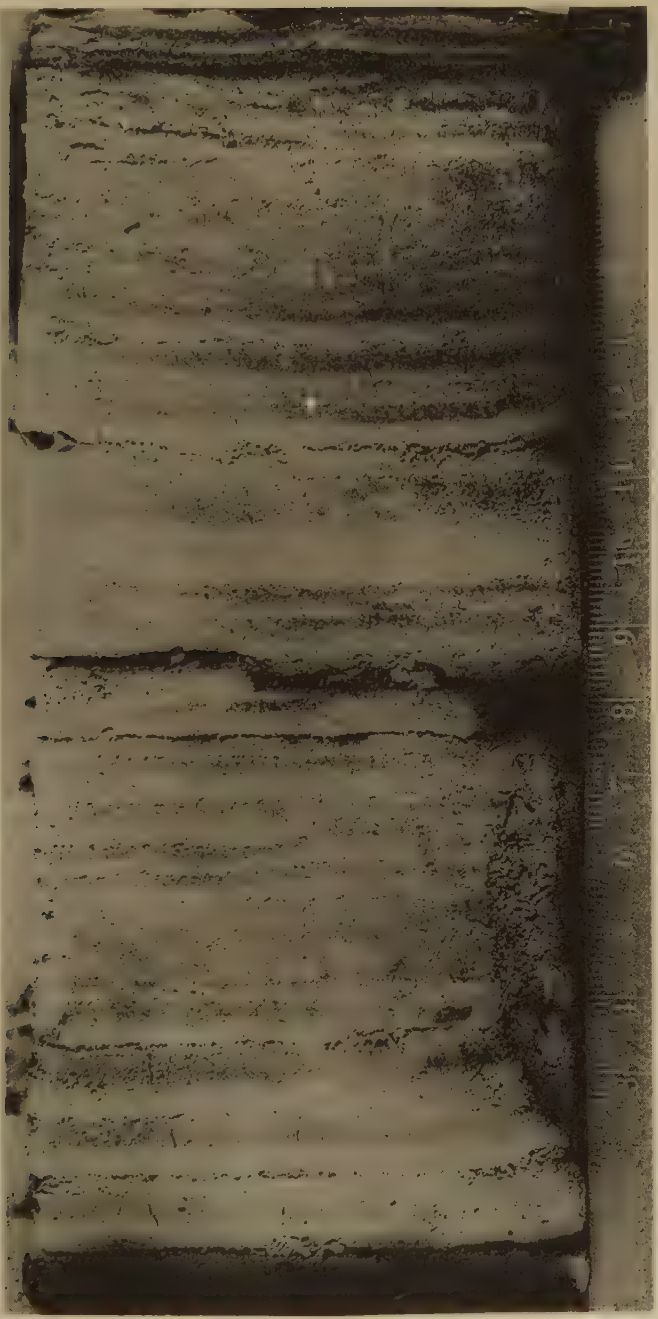

Facies Interpretation

(473)

affin coating for us. In one section rather poor lamination was found, but the others had widely spaced layers. Lamination in the St. Bernard subdelta may not be as well developed as we had found it in the birdfoot delta.

THE THICKNESS OF SAND UNDER BRETON AND CHANDELEUR ISLANDS

Three borings were made with a Porter Soil Sampler (for instrument type see Shepard and Moore, 1955, fig. 57B) into Breton Island (see fig. 1 for location). These were not continuous borings, but the difficulty of penetrating the various sections gave an index of the relative sand contents. In a boring on the beach at the north side of northern Breton Island (644) the sediment was predominantly sand to a depth of 32 feet, where a laminated silty clay was observed. At 8 feet (about 6 feet below sea level) the sand had a roundness index indicative of dune origin (Beal and Shepard, 1956). Some clay lumps were found in the sand at about −20 feet. In this zone the high sand content, the worn Foraminifera, the glauconite, and the echinoid fragments are all indicative of a shallow-water marine environment. At −32 feet the laminated silty clay with abundant plant fibers was a strong indication of an old lobe of the Mississippi Delta. In the boring on the south side of North Breton Island (655) the zone between −18 and −22 feet was a sand, but some of it is probably marine, deposited near a sand island. In the −33- to −37-foot interval, sand content is greatly reduced, and near the bottom an interdistributary bay Foraminifera fauna was encountered. In the other boring (674), which was on the north side of the south island, the sediment appeared to be sand to a depth of 30 feet. Below this, cores showed more sand which was high in plant fibers and mica, like the bar deposits around delta mouths. In the −30-to −34-foot section silt was found with mollusks indicative of a delta margin facies. Thus the three borings all indicate that the old delta is encountered at about −30 feet under the island.

In the strait between Breton Island and Grand Gosier a boring made by the Army Engineers showed that sand and silty sand extended to a depth of approximately 30 feet below sea level. Four miles to the southwest another boring showed sand, silt, and shells which also extend to a depth of 30 feet below sea level, where they are underlain by 4 feet of sandy material with some clay content, below which the sediments are predominantly clay. To the north, for 12 miles along the Chandeleur Islands, scattered borings show the sandy zone extending from the surface down to from 17 to 29 feet below sea level. All the Engineer borings suggest that the sinking of the old St. Bernard subdelta was accompanied by concentration of the sand around the margin and upgrowth of the sand as the submergence proceeded. At the same time there was deposition of typical sound deposits on top of the old delta in Breton and Chandeleur sounds, but the sinking was faster than the sedimentation so that water now averages about 10 feet deep in the sounds.

TABLE 1

FORAMINFERA AND THEIR RELATIVE ABUNDANCES IN SAMPLE −55, BORING 2-U

(Shallow Open-Shelf Environment)

Elphidium advena	VR*
E. discoidale	VR
E. gunteri	C
E. incertum mexicanum	VR
E. matagordanum	VR
E. poeyanum	C
Guttulina cf. *G. australis*	VR
Hanzawaia strattoni	C
Quinqueloculina compta	VR
Q. lamarckiana	R
Q. seminulum	R
Quaternary planktonics	VR

* VR = very rare; C = common; R = rare.

FORAMINIFERAL ENVIRONMENTS IN THE ST. BERNARD SUBDELTA

All the samples from the Engineer borings have been studied for foraminiferal content. Species present in each sample were identified, and their relative abundances were estimated. These data are given in figures 5–10 and in table 1. The species composition of each sample was identified as one of six faunal associations defined in the study of modern Foraminifera in the eastern Mississippi Delta (Lankford, 1959). These faunal associations (fig. 4) are named for their depositional environments, which are thought to limit or control species distribution. The faunal characteristics resulting from recent investigations are summarized below.

OPEN-SHELF ASSEMBLAGE

The present-day fauna occurs on the northern Gulf continental shelf out to a depth of approximately 350 feet and within relatively small limits of temperature and salinity values. It is excluded from or strongly modified in areas of rapid sedimentation. In addition, open-shelf samples characteristically contain both a large number of species and a large number of specimens. The following appear to be restricted to this association or occur only rarely in the adjacent mixed zones: *Amphistegina lessonii; Archaias compressus; Asterigerina carinata; Bigenerina irregularis; Bolivina stiatula spinata; Cancris sagra; Elphidium advena; E. discoidale; Eponides antillarum; Guttulina australis; Hanzawaia strattoni; Massilina* spp.; *Quinqueloculina bicostata; Q. compta; Q. horrida;* and *Textularia mayori.*

Planktonic Foraminifera are found occasionally in several marginal marine associations, but they are most abundant in the open-shelf fauna and increase in abundance with distance from shore.

DELTAIC MARINE ASSEMBLAGE

This assemblage occurs on the rapidly accumulating foreset and bottomset beds of the modern delta and where the bottom water has the same temperature and salinity variabilities as is found in the open-shelf environment. The upper depth limits are controlled by the depth of mixing of gulf and river water. Most of the species characterizing this fauna are found also in the bordering open-shelf fauna. However, certain modifications, probably produced by increased rates of deltaic sedimentation, differentiate the two faunas. The principal criterion for recognizing the deltaic marine association is the large percentages of *Bolivina lowmani; Buliminella* cf. *B. bassendorfensis; Epistominella vitrea;* and *Nonionella opima.* These species seem to be particularly well adapted to the conditions prevailing in rapidly sedimenting areas which exclude or strongly limit the distribution of forms characteristic of the open-shelf environment where deposition rates are much lower.

SOUND ASSEMBLAGE

This association contains species found today in the shallow coastal bays and sounds of the northern Gulf of Mexico. A sparse sound fauna is found also in a narrow-band peripheral to the modern birdfoot delta, where a brackish water and variable temperature environment is produced by mixing river and gulf water. The following species are found in several near-shore environments, but occur in greatest abundances in the sound fauna: *Elphidium gunteri; E. poeyanum; Streblus beccarii; Triloculina sidebottomi.* The species restricted to the sounds and bays include *Bolivina striatula* and *Elphidium matagordanum.* Several species of *Ammobaculites* also appear to be restricted to the sound fauna but were not found in our samples, probably because their delicate arenaceous tests were destroyed by the sample preparation techniques.

FLUVIAL MARINE ASSEMBLAGE

This fauna is limited to that part of the river distributary system which is invaded seasonally by a wedge of dense, saline gulf water along the channel bottoms. The resulting variation in the environmental ecology produces a rather limited suite of species including *Ammobaculites salsus; Elphidium gunteri; Miliammina fusca; Palmerinella gardenislandensis;* and *Streblus beccarii. Palmerinella gardenislandensis,* however, is found in abundance in this environment and only rarely in others. It is considered the diagnostic species of the fluvial marine association.

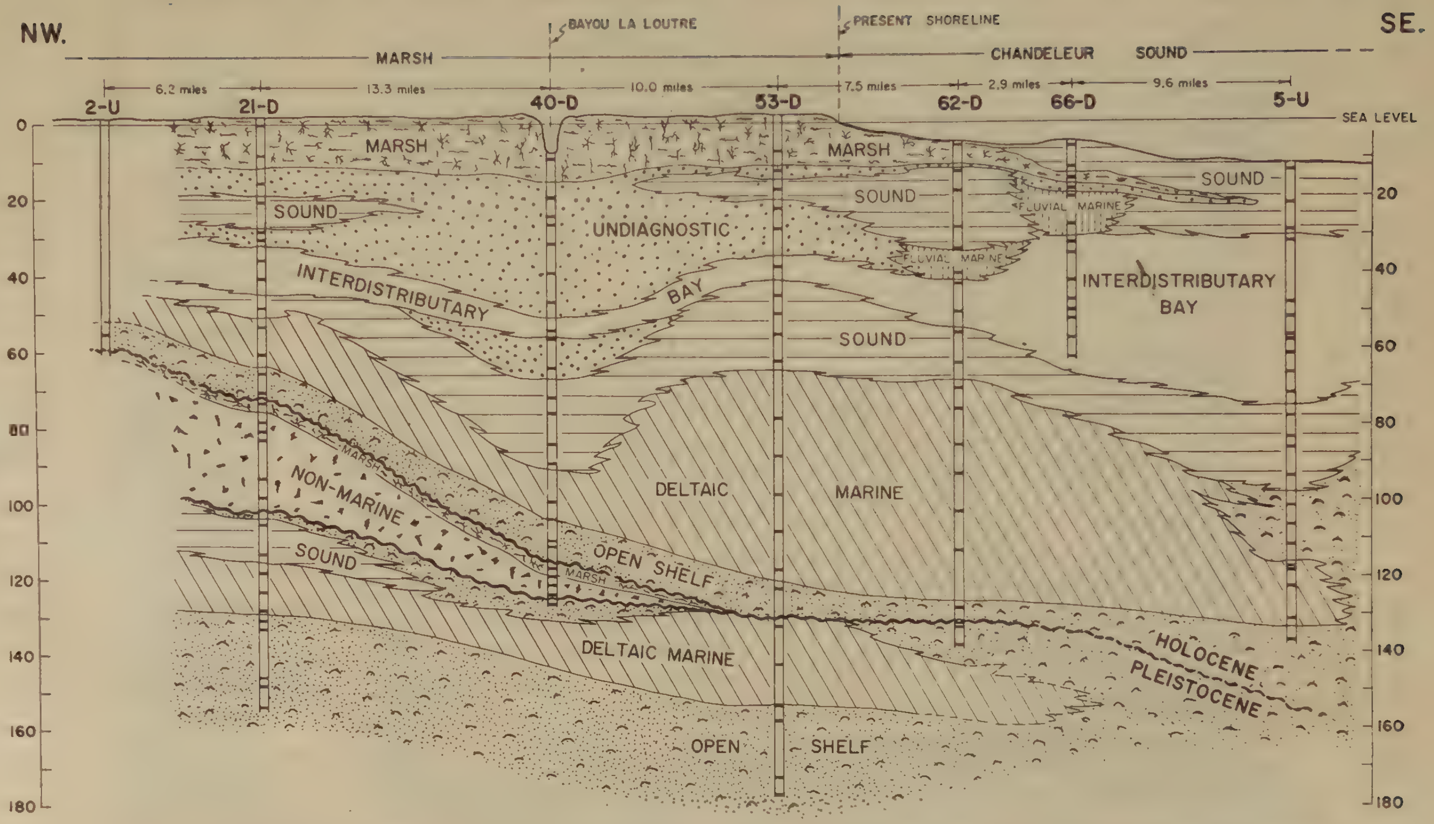
NW.
SE.
BAYOU LA LOUTRE
PRESENT SHORELINE
MARSH
CHANDELEUR SOUND
6.2 miles
13.3 miles
10.0 miles
7.5 miles
2.9 miles
9.6 miles
2-U
21-D
40-D
53-D
62-D
66-D
5-U
SEA LEVEL
0
20
40
60
80
100
120
140
160
180
MARSH
SOUND
UNDIAGNOSTIC
FLUVIAL MARINE
FLUVIAL MARINE
INTERDISTRIBUTARY BAY
INTERDISTRIBUTARY BAY
SOUND
DELTAIC
MARINE
MARSH
NON-MARINE
OPEN SHELF
MARSH
SOUND
DELTAIC MARINE
HOLOCENE
PLEISTOCENE
OPEN SHELF

Fig. 4.—Cross section showing interpretation of environments of deposition along the line of the Army Engineer borings, based only on those borings from which we have samples. Bayou la Loutre is an abandoned distributary channel eroded into pre-existing marsh deposits. Scale indicates depth in feet.

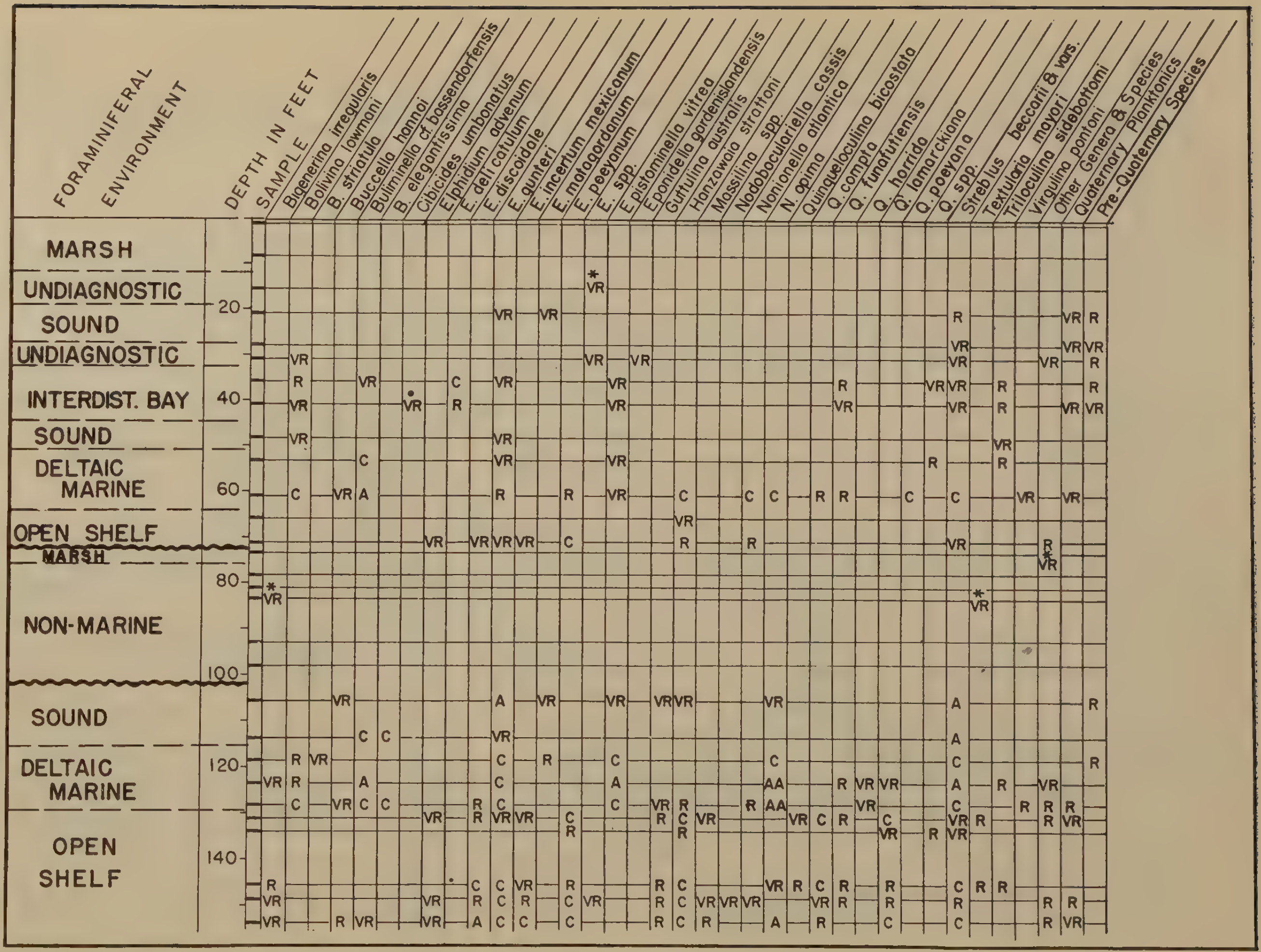

FIG. 5.—Foraminifera found in samples from Engineer boring 21-D. Abundance symbols: VR = very rare, R = rare, C = common, A = abundant, AA = very abundant; * = reworked species, ⁰ = mudlump contamination. The foraminiferal environment of each sample or group of samples is indicated in the left-hand column.

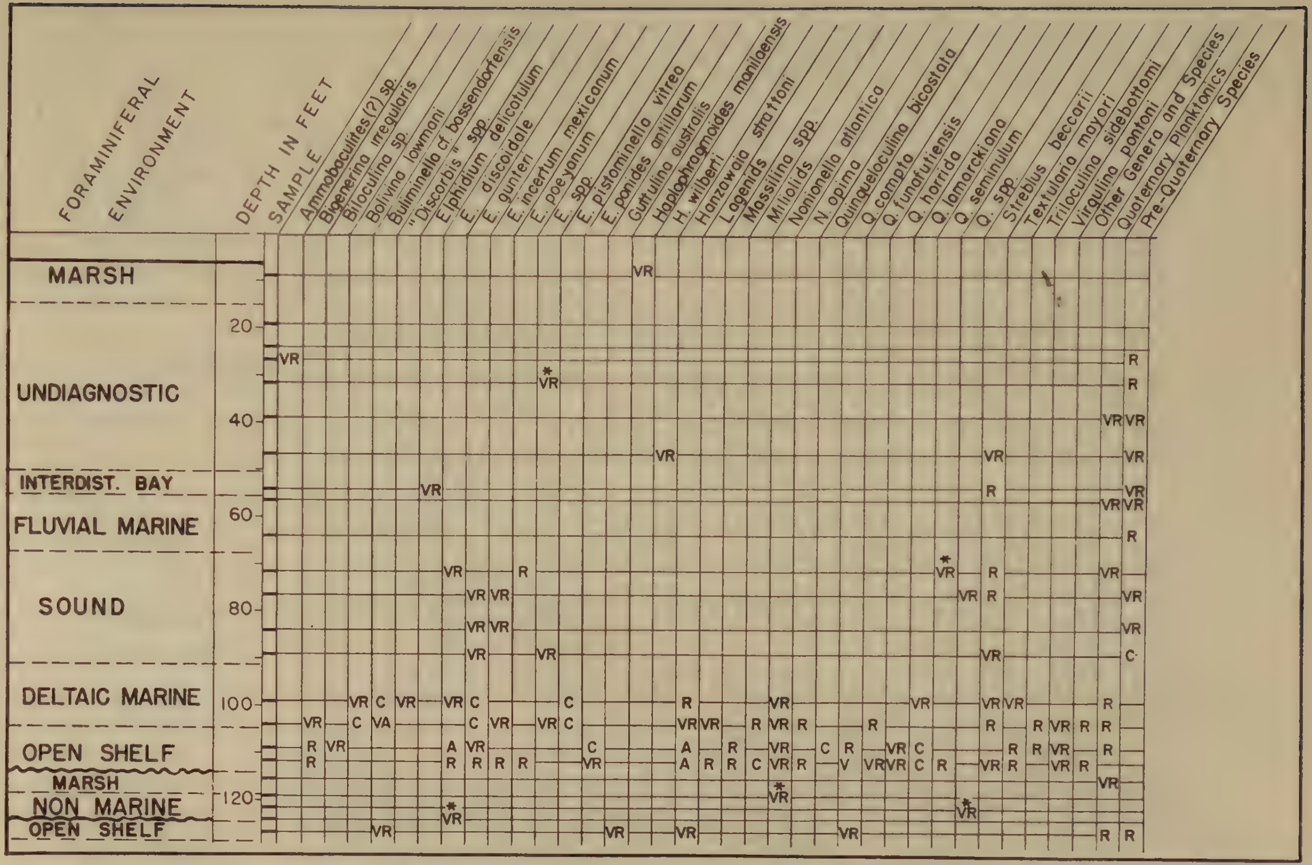

Fig. 6.—Foraminifera found in samples from Engineer boring 40-D. Abundance symbols: VR = very rare, R = rare, C = common, A = abundant, AA = very abundant; * = reworked species, ⁰ = mudlump contamination. The foraminiferal environment of each sample or group of samples is indicated in the left-hand column.

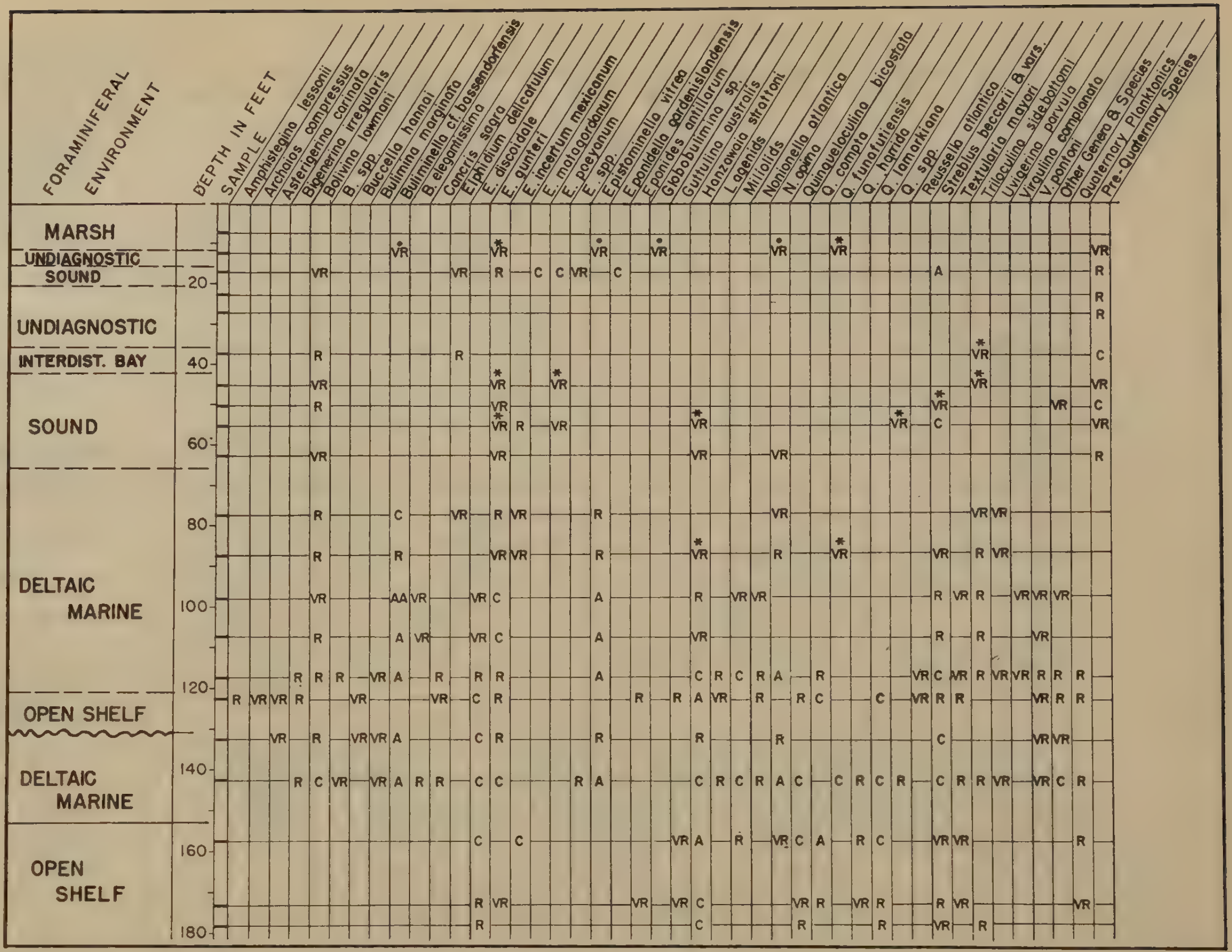

FIG. 7.—Foraminifera found in samples from Engineer boring 53-D. Abundance symbols: VR = very rare, R = rare, C = common, A = abundant, AA = very abundant; * = reworked species, ^{0} = mudlump contamination. The foraminiferal environment of each sample or group of samples is indicated in the left-hand column.

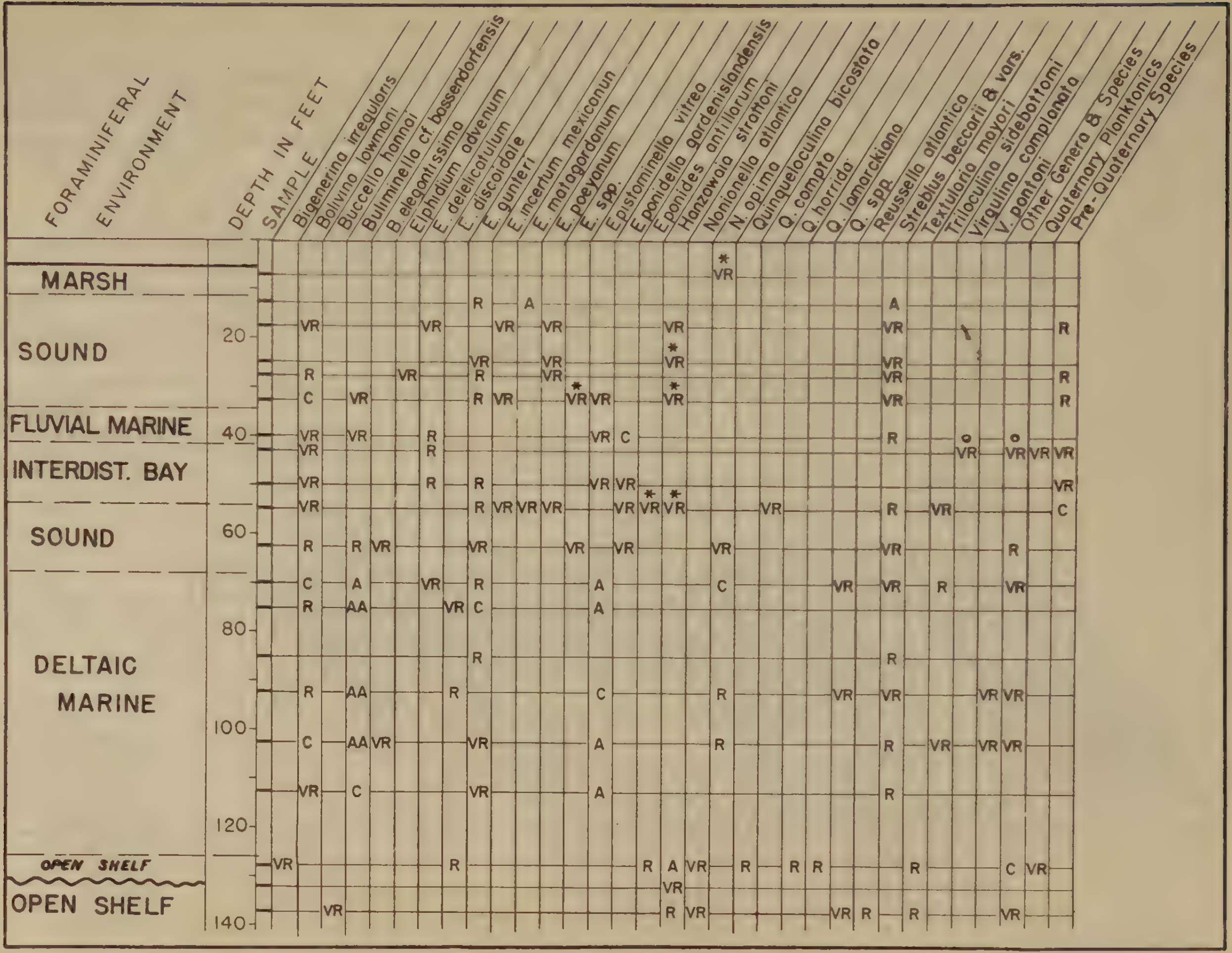

FIG. 8.—Foraminifera found in samples from Engineer boring 62-D. Abundance symbols: VR = very rare, R = rare, C = common, A = abundant, AA = very abundant; * = reworked species, ^{0} = mudlump contamination. The foraminiteral environment of each sample or group of samples is indicated in the left-hand column.

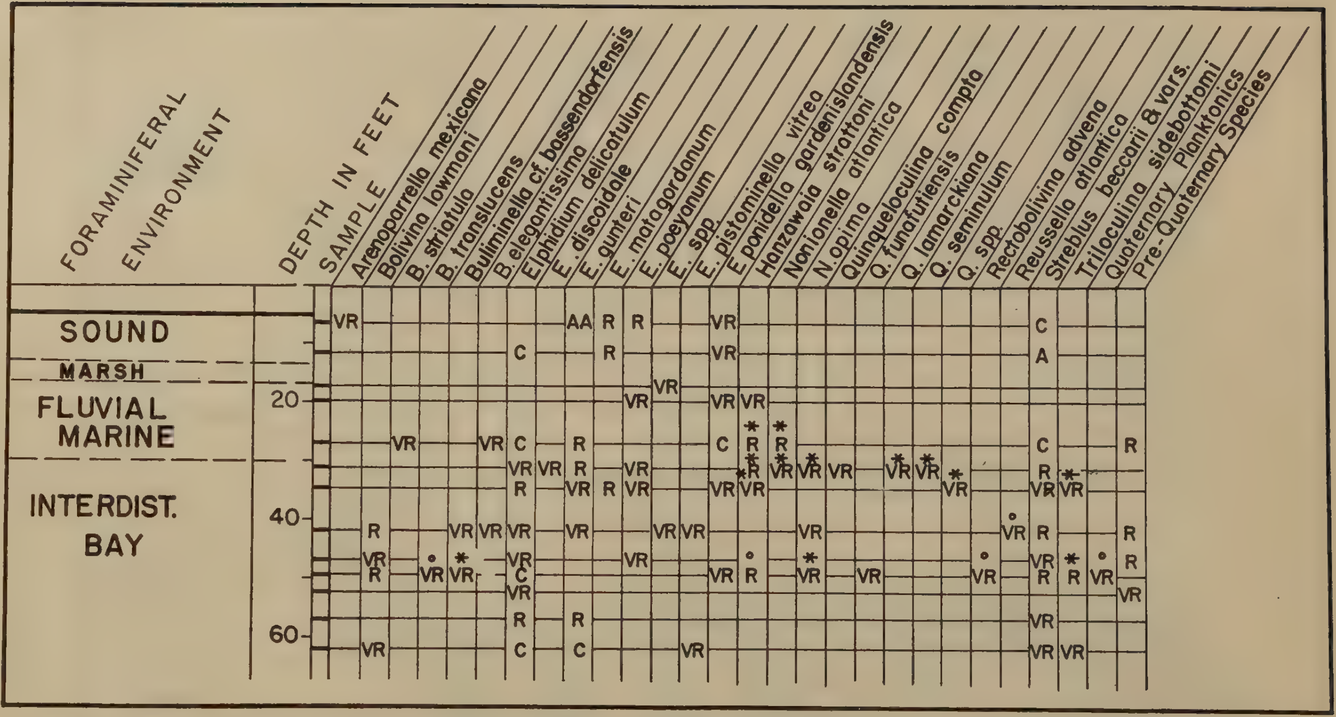

FORAMINIFERAL ENVIRONMENT	Arenoparrella mexicana	Bolivina lowmani	B. striatula	B. translucens	Buliminella cf. bassendorfensis	B. elegantissima	Elphidium delicatulum	E. discoidale	E. gunteri	E. matagordanum	E. poeyanum	E. spp.	E. pistominella vitrea	E. ponidella gardenislandensis	Hanzawaia strattoni	Nonionella atlantica	N. opima	Quinqueloculina compta	Q. funafutiensis	Q. lamarckiana	Q. seminulum	Q. spp.	Rectobolivina advena	Reussella atlantica	Streblus beccarii & vars.	Triloculina sidebottomi	Quaternary Planktonics	Pre-Quaternary Species
SOUND	VR								AA	R	R			VR											C			
							C			R				VR											A			
FLUVIAL MARINE												VR																
											VR			VR	VR													
			VR			VR	C		R					C	*R	*R									C			R
INTERDIST. BAY							VR	VR	R		VR				**R	*VR	*VR	VR		*VR	*VR				R			
							R		VR	R	VR			VR	VR							*VR			VR	*VR		
		R			VR	VR	VR		VR			VR	VR				VR							°VR	R			R
		VR					VR				VR														VR			R
		R		°VR	*VR		C							VR	°R		*VR		VR				°VR		R	*R	°VR	
							VR																					VR
							R		R																VR			
		VR					C		C				VR												VR	VR		

Fig. 9.—Foraminifera found in samples from Engineer boring 66-D. Abundance symbols: VR = very rare, R = rare, C = common, A = abundant, AA = very abundant; * = reworked species, ⁰ = mudlump contamination. The foraminiferal environment of each sample or group of samples is indicated in the left-hand column.

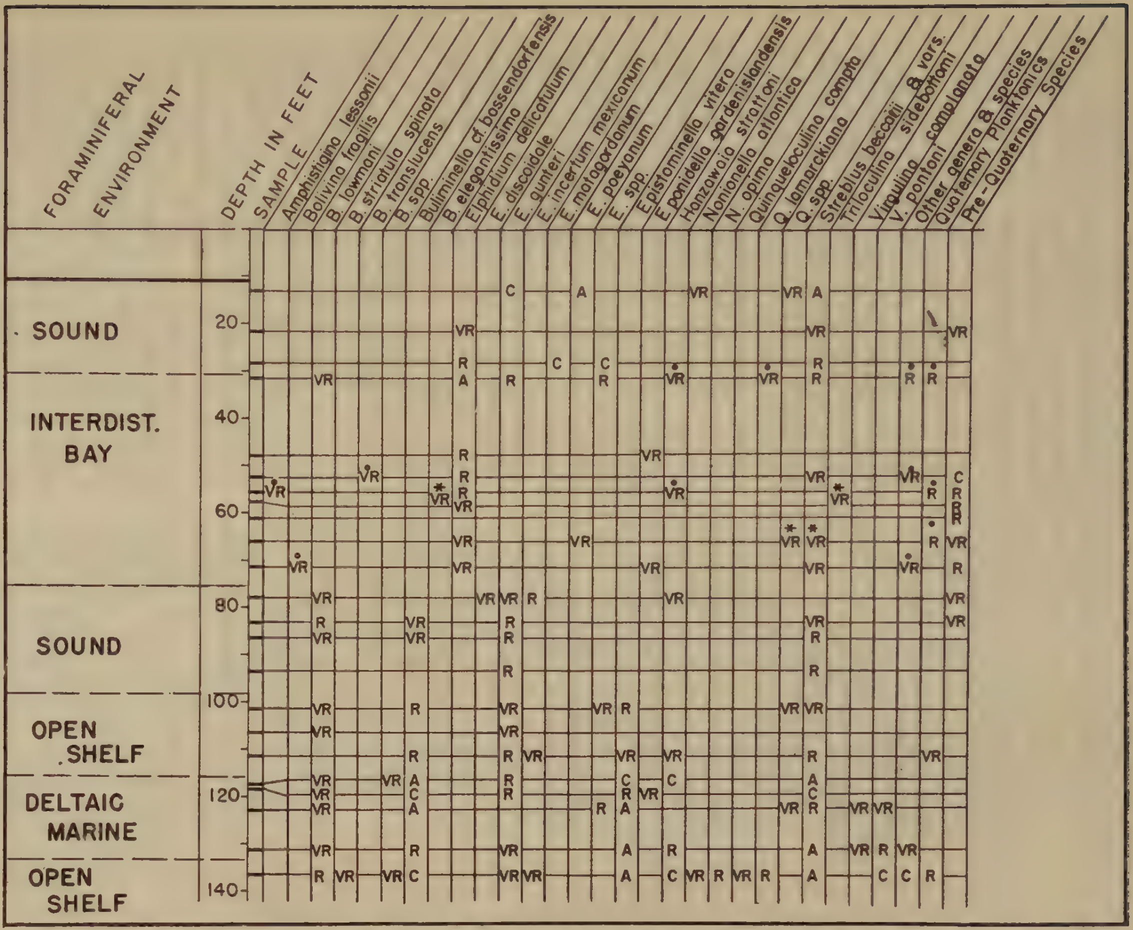

FIG. 10.—Foraminifera found in samples from Engineer boring 5-U. Abundance symbols: VR = very rare, R = rare, C = common, A = abundant, AA = very abundant; * = reworked species, ⁰ = mudlump contamination. The foraminiferal environment of each sample or group of samples is indicated in the left-hand column.

INTERDISTRIBUTARY BAY ASSEMBLAGE

This fauna occurs in those very shallow bays (0 to 6 feet) between the active distributaries of the river. An extremely variable environment exists with short-term changes in temperature, salinity, turbulence, turbidity, etc. Most of the Foraminifera in the interdistributary bay assemblage are found also in the fluvial marine and sound faunas. One species, *Elphidium delicatulum*, occurs in high frequencies in this assemblage but only infrequently elsewhere.

MARSH ASSEMBLAGE

This species suite is characteristically arenaceous and is world wide in its distribution. Though it is one of the most easily recognized of all foraminiferal assemblages, very few of the arenaceous specimens appear to have survived our sample preparation processes. Determination of the marsh environment therefore is based primarily on the large quantities of wood material, plant fibers, and seed cases, and, occasionally, rare charophyte oögonia and non-marine ostracod carapaces.

Many of the samples contained Foraminifera which appear to be natural contaminants reworked from older deposits; these are indicated on the faunal checklists. One reworked category includes specimens of modern species which are stained opaque brown (indicating oxidation), broken and eroded, and sometimes filled with silica, calcite, or glauconite. Most frequently these species are ecologically displaced. A second type of reworking is believed to have resulted from erosion of ancient mud lumps yielding foraminiferal sediments into the interdistributary bays. These mud-lump Foraminifera ordinarily are indistinguishable from the indigenous species; they are neither brown stained nor eroded. However, they are invariably characteristic of deeper-water faunal assemblages (Lankford, 1959, p. 2091).

In many samples from shallow environments having a relatively large sand content, a few fossil Foraminifera were found. Often the fossils were Cretaceous and early Tertiary planktonic species of *Gümbelina*, *Globotruncana*, and *Globigerinella*, but occasional benthonic forms also were found, In addition, large fossil Radiolaria of the *Dictyomitra*-group, believed to be Cretaceous in age, were relatively abundant in most sandy samples.

DEPOSITIONAL HISTORY

Kolb and Van Lopik (1958) have interpreted the Engineer borings from the point of view of engineering practices. Their generalized section (*ibid.*, pl. 4) agrees approximately with our interpretations.

In our attempt to trace the history of sedimentation along the line of borings, we will confine our discussion largely to those borings from which we have had samples available. This overlooks some of the channels which were shown by the Engineers (fig. 2) as existing between some of the borings which we studied. However, these channels do not particularly influence the over-all history of deltaic deposition, since they presumably represent only brief episodes when the river cuts through the sediments which had accumulated on the delta plane.

The lithologic section penetrated by the Engineer borings represents alternate marine, sound, and deltaic deposition. As interpreted in figure 4, there is a boundary representing withdrawal of the sea followed by erosion which is found at −102 feet in boring 21-D, at −120 in 40-D, at −130 in 53-D, at −136 in 62-D. Borings 66-D and 5-U presumably do not go deep enough to reach this boundary. The sediments which underlie the boundary in the other borings show a progression downward from open shelf to deltaic, back to open shelf, with an interfingering of sound deposits in boring 21-D. The younger of the two Pleistocene shelf deposits appears to have been eroded in 53-D but was preserved in 40-D and 62-D.

A wedge of what appears to be nonmarine material occurs between the unconformities in 21-D from −102 feet up to −73 feet. This wedge has feathered out in 40-D, so that it consists of only 5 feet and does not occur in the other borings to the southeast. We consider that this wedge represents a transition zone between Pleistocene and Holocene. The marine deposit overlying the unconformity farther to the southeast may be partly equivalent in age to this transition wedge.

As the sea transgressed during the waning of the last major glaciation, there was deposition of a sheet of shelf sediments which appear to have had shallow-water environments. This is substantiated by the abundant shallow-water shells as well as by the foraminiferal content. The shelly layer is indicated in a series of borings by the Engineers (fig. 2). The delta appears to have built forward, probably advancing to the northeast (Treadwell, 1955, fig. 6), so that it may have covered the shelf sediments in our NW.-SE. section more or less simultaneously. The deltaic deposits consist of foreset and bottomset sediments, which are difficult to differentiate and hence are included together as a phase of deltaic marine deposition. The overlying sound deposits probably include sediments from the active delta.

On top of the sound deposits, deltaic sediments of the shallow marine platform and interdistributary bay types were deposited. In at least two of the borings, 62-D and 5-U, laminated bedding typical of the topset beds was developed. In borings 21-D, 40-D, and 53-D there are sandy sediments which contain no diagnostic organisms and are presumed to be river-channel deposits.

In borings 53-D, 66-D, and 5-U sound deposits reoccur above the topset beds. These deposits interfinger to the northwest with the presumed river-channel deposits. Capping most of the delta mass, there are marsh deposits with a thickness of about 15 feet. Judging from this two-dimensional section, the marsh deposits wedge out to the southeast beneath the sediments of the present Chandeleur Sound.

East of boring 5-U, Breton Island and Chandeleur Islands sand deposits form a cover over the platform deposits which is 30 feet thick in the Breton Island area. The depth to the deltaic beds is therefore of the same order under this island as in boring 5-U.

This section allows several stratigraphic generalizations. The usual effect of a marine transgression is to produce facies characteristic of deepening water. This is reflected in our section only in the thin open-shelf sands lying above the Pleistocene-Holocene boundary. Presumably the rise in sea level at first was sufficiently rapid so that deposition was largely confined to what must have been an entrenched Mississippi River estuary to the north (Fisk and McFarlan, 1955; fig. 9B). At this time, the open-shelf sands accumulated slowly, and, judging from the heavy mineral suites, they were derived from the East Gulf. With the slowing of sea-level rise about 6,000–8,000 years B.P. (Shepard, in press), the river should have been able to fill its estuary and hence supply the shelf area with deltaic sediments. Once deltaic deposition began, sediment accumulated more rapidly than the sea level rose, and the resulting facies are succeedingly shallower as the transgression progressed. Various oscillations of positions of distributaries and concurrent subsidence are indicated.

It is probable that a large portion of the post-Pleistocene time is represented by the thin shelf deposits, since they are known to accumulate at a slow rate, whereas the deltaic deposition occurred quite rapidly (Shepard, 1956). So far as we know, the upper 40 to 60 feet of the section (which represent topset beds, except where overlapped by sound deposits to the southeast) are similar in composition to the topset beds in the birdfoot delta, where there are also at least 40 feet of these deposits in the Pass à Loutre–Southeast Pass area.

ACKNOWLEDGMENTS.—The writers wish to express their appreciation to the Corps of Engineers, U.S. Army, New Orleans District, for furnishing most of the samples and other information, and to R. H. Parker for identifying macro-organisms in the cores. The sediment analyses were made by H. W. Lusk; heavy-mineral determinations were made by D. M. Poole; and the illustrations were drafted by J. R. Moriarity. For critical reading of the manuscript, the writers are indebted to F. B Phleger.

REFERENCES CITED

Beal, M. A., and Shepard, F. P., 1956, A use of roundness to determine depositional environments: Jour. Sed. Petrology, v. 26, no. 1, p. 49–60.

Fisk, H. N., and McFarlan, E., Jr., 1955, Late Quaternary deltaic deposits of the Mississippi River, *in* The crust of the earth: Geol. Soc. America Spec. Paper 62, p. 279–302.

Fisk, H. N., Mc Farlan, E., Jr., Kolb, C. R., and Wilbert, L. J., Jr., 1954, Sedimentary framework of the modern Mississippi Delta, Jour. Sed. Petrology, v. 24, no. 2, p. 76–99.

Goldstein, August, Jr., 1942, Sedimentary petrologic provinces of the northern Gulf of Mexico: Jour. Sed. Petrology, v. 12, no. 2, p. 77–84.

Kolb, C. R., and Van Lopik, J. R., 1958, Geological investigation of the Mississippi River–Gulf outlet channel: U.S. Army Engineer Waterways Expt. Sta., Corps of Engineers, Vicksburg, Miss., Misc. Paper 3-259, 22 p., 11 pls.

Lankford, R. R., 1959, Distribution and ecology of Foraminifera from east Mississippi Delta margin: Am. Assoc. Petroleum Geologists Bull., v. 43, no. 9, p. 2068–2099.

Phleger, F. B, 1955, Ecology of Foraminifera in southeastern Mississippi Delta area: Am. Assoc. Petroleum Geologists Bull., v. 39, no. 5, p. 712–752.

Shepard, F. P., 1956, Marginal sediments of Mississippi Delta: Am. Assoc. Petroleum Geologists Bull., v. 40, no. 11, p. 2537–2623.

——— 1960, The rise of sea level along the northwest Gulf of Mexico, *in* Shepard *et al.*, Recent sediments: northwest Gulf of Mexico: Tulsa, Okla., Am. Assoc. Petroleum Geologists (in press).

——— and Lankford, R. R., 1959, Sedimentary facies from shallow borings in lower Mississippi Delta: Am. Assoc. Petroleum Geologists Bull., v. 43, no. 9, p. 2051–2067.

——— and Moore, D. G., 1955, Central Texas coast sedimentation: characteristics of sedimentary environment, recent history, and diagenesis: Am. Assoc. Petroleum Geologists Bull., v. 39, no. 8, p. 1463–1593.

Treadwell, R. C., 1955, Trafficability and navigability of delta-type coasts; trafficability and navigability of Louisiana coastal marshes: sedimentology and ecology of southeast coastal Louisiana: Louisiana State Univ. Tech. Rept. 6, 78 p.

Reprinted from The Journal of the Acoustical Society of America, Vol. 32, No. 7, 871–877, July, 1960
Copyright, 1960 by the Acoustical Society of America.
Printed in U. S. A.

Small Signal Detection in the DIMUS Array*

Philip Rudnick
University of California, La Jolla, Marine Physical Laboratory of the Scripps Institution of Oceanography, San Diego 52, California
(Received February 9, 1960)

In the DIMUS system for steering an acoustic array, the output of each element is reduced to a sequence of polarity samples and delayed by an integral multiple of the sampling period. Calculations are given to show the effect of this process on the passive detection threshold of an array beam (in isotropic Gaussian noise) both in general and numerically for several examples. In these, over-all losses range from 0.5 to 1.5 db.

I. INTRODUCTION

Anderson[1] has proposed and discussed the use of shift-register delay lines for steering large acoustic arrays. This process, the DIMUS system, differs from conventional steering in that the output of each array element is sampled and infinitely clipped, i.e., is reduced from an analog voltage to a sequence of polarity samples. This paper examines by analysis the ability of an array beam to detect a small plane-wave signal in isotropic noise with Gaussian statistics, comparing DIMUS with conventional steering. Both signal and noise are taken to be stationary processes.

II. OUTLINE OF ANALYSIS

The DIMUS process of forming a beam output contains the following steps:

1. sampling each element output at intervals τ_0,
2. infinite clipping for each element,
3. delaying electrically by an integral multiple of τ_0 for each element,
4. adding the delayed sequences for all elements,
5. squaring,
6. smoothing with a low-pass filter or running average.

For convenience in analysis, these steps will be presumed to be carried out in the following exactly equivalent order: 3, 2, 4, 5, 1, 6.

It is assumed that knowledge of the power spectra of signal and noise is exploited by the incorporation of a suitable linear filter in each array element,[2] and that for detection the only relevant property of the beam output is its power. Detection may occur by observing the dependence of the beam power on bearing, as when the beam is trained across a target, or the dependence on time, as when the target is radiating intermittently. Stated another way, on-target power may be compared with off-target or no-target power. The former alternative will be discussed first and more fully.

Detection capability will be measured by a parameter to be called processing gain which is chosen and defined by the following considerations. As just pointed out, detection is based on a change in the squared smoothed output voltage caused by the target, which will be called the change in dc output. The detectability of any such change will be judged by comparing its amount with the root-mean-square fluctuation in output voltage in the reference condition, either off-target or no-target. (It is assumed that the target signal is small and that its steady presence will not significantly increase the fluctuations.) The nominal threshold signal will be defined by the condition that the dc output change caused by it will be equal to the root-mean-square fluctuation. This would of course not allow very reliable detection, but still leads to useful comparisons. We now define processing gain as the reciprocal of the input power ratio, at any array element, of nominal threshold signal to noise. This definition is employed in Sec. IV and the evaluation of output fluctuations is discussed in Sec. III(d).

The main steps in calculation are the following:

1. A matrix is formed whose elements are the cross-correlation functions of the electrically delayed element outputs.
2. This matrix is modified (or not as the case requires) for the effect of clipping.
3. All elements of the matrix are added to obtain the autocorrelation of the array output (produced by step 4).
4. From this autocorrelation are derived:
    (a) the power into and the dc out of the squarer,
    (b) the correlation time associated with the noise spectrum.
5. Combinations of the foregoing for on-target and off-target cases lead finally to values of processing gain.

III. NOTATION AND PRELIMINARIES

(a) Correlation Matrices

Normalized cross-correlation functions between components of time-delayed outputs from the ith and jth elements in an N-element array are denoted as follows:

---

* This work represents one of the results of research carried out under contract with the Office of Naval Research.

[1] V. C. Anderson, J. Acoust. Soc. Am. 32, 867 (1960), this issue.

[2] Carl Eckart, University of California, Marine Physical Laboratory of the Scripps Institution of Oceanography, SIO Reference No. 52-11 (March, 1952).

Reproduced by Permission

	On-target	Off-target
Isotropic noise alone	$\nu_{ij}'(\tau)$	$\nu_{ij}''(\tau)$
Signal	$\sigma_{ij}'(\tau)$	$\sigma_{ij}''(\tau)$
Noise and signal	$\mu_{ij}'(\tau)$	$\mu_{ij}''(\tau)$

i and j range independently from 1 to N.[3]

All the foregoing are normalized to be correlation coefficients, so that all diagonal elements become unity when $\tau=0$. Thus we have

$$1=\nu_{ii}'(0)=\sigma_{ii}''(0)=\text{etc.} \tag{1}$$

Signal and noise are assumed statistically independent. We may therefore write

$$\mu_{ij}'(\tau)=[n/(n+s)]\nu_{ij}'(\tau)+[s/(n+s)]\sigma_{ij}'(\tau) \qquad \text{(on target)} \tag{2}$$

$$\mu_{ij}''(\tau)=[n/(n+s)]\nu_{ij}''(\tau)+[s/(n+s)]\sigma_{ij}''(\tau) \qquad \text{(off target),} \tag{3}$$

where n and s are power at one array element contributed by noise and signal, respectively.

(b) Effect of Clipping

The statistics of the noise is supposed Gaussian, and the same will be assumed for signal-plus-noise on the basis that the signal is small even if it is not also Gaussian. The effect of clipping each element output is then to replace the matrix $\mu_{ij}'(\tau)$ by[4]

$$(2/\pi)[\sin^{-1}\mu_{ij}'(\tau)]\equiv(2/\pi)[\mu_{ij}'(\tau)+c_{ij}'(\tau)]. \tag{4}$$

Equation (4) serves as a definition of the matrix $c_{ij}'(\tau)$ "added" by clipping in the on-target case. Other matrices $c_{ij}''(\tau)$ and $c_{ij}(\tau)$ for the off-target and no-target cases, respectively, are derived analogously from $\mu_{ij}''(\tau)$ and $\nu_{ij}'(\tau)$. We have, for all i,

$$c_{ii}'(0)=c_{ii}''(0)=c_{ii}(0)=\tfrac{1}{2}\pi-1. \tag{5}$$

Non-diagonal elements in $c_{ij}(\tau)$ (and the two analogs) will ordinarily be quite small since the corresponding elements in $\nu_{ij}'(\tau)$ will usually be well below unity.

More specifically, if we write

$$|c_{ij}(\tau)|<r|\nu_{ij}'(\tau)| \quad \text{whenever} \quad |\nu_{ij}'(\tau)|<m$$

we have corresponding numerical values:

m	0.7	0.5	0.3
r	0.11	0.05	0.016

For small nondiagonal elements the following approximations are useful:
With $i\neq j$,

$$c_{ij}(\tau)\approx\tfrac{1}{6}\nu_{ij}'^{3}(\tau), \tag{6}$$

and for differences between two closely similar matrices,

$$\begin{aligned} c_{ij}'(0)-c_{ij}''(0)&\approx[\{1-\mu_{ij}'^{2}(0)\}^{-\frac{1}{2}}-1][\mu_{ij}'(0)-\mu_{ij}''(0)]\\ &\approx\tfrac{1}{2}\nu_{ij}'^{2}(0)[\mu_{ij}'(0)-\mu_{ij}''(0)]. \end{aligned} \tag{7}$$

(c) Output Power and Autocorrelation

The symbol $\sum$ will denote a sum over all (i,j), containing N^2 terms and $\sum'$ will denote a sum over all (i,j) for which $i\neq j$, containing $N(N-1)$ terms. We then introduce notation for summations as follows:

$$\begin{array}{lll} & \text{Unclipped} & \text{Clipped} \\ \text{On-target power} & V'=(n+s)\sum\mu_{ij}'(0) & W'=\dfrac{2}{\pi}[\sum\mu_{ij}'(0)+\sum c_{ij}'(0)] \\ \text{Off-target power} & V''=(n+s)\sum\mu_{ij}''(0) & W''=\dfrac{2}{\pi}[\sum\mu_{ij}''(0)+\sum c_{ij}''(0)] \\ \text{No-target autocorrelation} & V(\tau)=n\sum\nu_{ij}'(\tau) & W(\tau)=\dfrac{2}{\pi}[\sum\nu_{ij}'(\tau)+\sum c_{ij}(\tau)] \\ \text{No-target power} & V=V(0) & W=W(0) \end{array} \tag{8}$$

Other notation involving sums which will be used for convenience is:

$$\textstyle\sum'\nu_{ij}'(0)\equiv N(N-1)\bar{\nu} \tag{9}$$

$$\textstyle\sum'\sigma_{ij}'(0)\equiv N(N-1)\bar{\sigma}' \tag{10}$$

$$\textstyle\sum'\sigma_{ij}''(0)\equiv N(N-1)\bar{\sigma}'' \tag{11}$$

$$\textstyle\sum'c_{ij}(0)\equiv\frac{1}{6}N(N-1)\langle\nu^{3}\rangle_{\text{av}} \tag{12}$$

$$\begin{aligned} &\textstyle\sum c_{ij}'(0)-\sum c_{ij}''(0)\\ &\quad=\textstyle\sum'c_{ij}'(0)-\sum'c_{ij}''(0)\\ &\quad\equiv\tfrac{1}{2}\langle\nu^{2}\rangle_{\text{av}}''[\textstyle\sum'\mu_{ij}'(0)-\sum'\mu_{ij}''(0)] \end{aligned} \tag{13}$$

---

[3] Each $\sigma_{ij}(\tau)$ is derivable from the autocorrelation of the signal merely by a shift of origin determined by the appropriate geometric and electrical delays. By similar considerations, each $\nu_{ij}'(\tau)$ and $\nu_{ij}''(\tau)$ for isotropic noise is derived from an autocorrelation by superposition of many origin shifts. See, for example, J. J. Faran and R. Hills, Jr., Acoustics Research Laboratory, Harvard University, Tech. Memo. No. 28 (November, 1952).

[4] J. L. Lawson and G. E. Uhlenbeck, *Threshold Signals* (McGraw-Hill Book Company, Inc., New York, 1950), M.I.T. Radiation Laboratory Series, Vol. 24, p. 58, Eq. (63).

$$\sum c_{ij}'(0)-\sum c_{ij}(0)$$
$$\equiv\tfrac{1}{2}\langle\nu^2\rangle_{\text{av}}[\textstyle\sum'\mu_{ij}'(0)-\sum'\nu'_{ij}(0)]. \qquad (14)$$

Though Eq. (12) is an exact definition of $\langle\nu^3\rangle_{\text{av}}$, the form of notation is suggested by the approximation (6). Similar remarks apply to Eqs. (13) and (14), whose form is suggested by Eq. (7).

(d) Output Fluctuations with Sampled Noise

Calculation of processing gain requires a value for the root-mean-square fluctuation in the sampled and smoothed output of the squarer.

For the unclipped Gaussian case, if the autocorrelation of the input to the squarer is $V(\tau)$, the output power spectrum density at zero frequency[5] is $2V^2\tau_1$, in which τ_1 the correlation time is (before sampling) given by

$$\tau_1=\frac{1}{V^2}\int_{-\infty}^{\infty}V^2(\tau)d\tau.$$

Sampling can be considered to alter the autocorrelation $V^2(\tau)$ into a polygonal curve, giving

$$\tau_1=\frac{\tau_0}{V^2}\sum_{j=-\infty}^{\infty}V^2(j\tau_0), \qquad (15)$$

The fluctuation power after smoothing is this spectrum density multiplied by the effective bandwidth of the smoothing filter $(1/T)$. (Both factors are normalized for the frequency range $-\infty\leqq f\leqq\infty$.) In the case of smoothing by an equal-weight running average, T is the averaging time; for any low-pass filter it may be called the effective averaging time. The final root-mean-square fluctuation is then

$$V(2\tau_1/T)^{\frac{1}{2}} \qquad (16)$$

with τ_1 given by Eq. (15).

In the case of clipped noise, the expression analogous to (16) is

$$W(2\tau_2/T)^{\frac{1}{2}}. \qquad (17)$$

The correlation time τ_2 is derived from $W^2(\tau)$ by a relation like Eq. (15), and for convenience in comparison with τ_1, may be expressed as a mean of τ_1 and two times derived from $\sum c_{ij}(\tau)$:

$$\tau_2=\frac{\tau_0}{W^2}\sum_{j=-\infty}^{\infty}W^2(j\tau_0) \qquad (18)$$

$$=[1/(1+\beta)^2][\tau_1+2\beta\tau_c+\beta^2\tau_{cc}] \qquad (19)$$

with

$$\beta=\textstyle\sum c_{ij}(0)/\sum\nu_{ij}'(0) \qquad (20)$$

$$\tau_c=[\tau_0/V\textstyle\sum c_{ij}(0)]\displaystyle\sum_{k=-\infty}^{\infty}[V(k\tau_0)\textstyle\sum c_{ij}(k\tau_0)] \qquad (21)$$

$$\tau_{cc}=\{\tau_0/[\textstyle\sum c_{ij}(0)]^2\}\displaystyle\sum_{k=-\infty}^{\infty}[\textstyle\sum c_{ij}(k\tau_0)]^2. \qquad (22)$$

IV. CALCULATION OF PROCESSING GAINS

(a) Unclipped, On-Off-Target Comparison

The nominal threshold condition for this case, following the definition already given is taken as

$$V'-V''=V''(2\tau_1/T)^{\frac{1}{2}}. \qquad (23)$$

The left member is the change in array power output between on-target and off-target bearings and also the corresponding change in dc output of the squarer. The right member is the fluctuation from (16); the effect of the signal is recognized in V'', but is ignored in τ_1 on the ground that signal and noise spectra will usually be quite similar. Still referring to this nominal threshold condition, we may define the processing gain G_1 as equal to n/s or

$$G_1+1=(n+s)/s. \qquad (24)$$

Combining (23) and (24) gives

$$G_1+1=\{[(V'-V'')/s]/[V''/(n+s)]\}\cdot(T/2\tau_1)^{\frac{1}{2}}. \qquad (25)$$

From (8), (1)–(3), (10), and (11), we have

$$(V'-V'')/s=N(N-1)(\bar{\sigma}'-\bar{\sigma}'') \qquad (26)$$

with neglect of any difference between $\sum\nu_{ij}'(0)$ and $\sum\nu_{ij}''(0)$, these both being responses to isotropic noise.

Again neglecting the influence of signal on the spectrum of noise, we may write

$$V''/(n+s)\approx V/n=N[1+(N-1)\bar{\nu}] \qquad (27)$$

with use of (8), (1), and (9).

Combining (25)–(27) gives finally

$$G_1+1=\left\{\frac{[(N-1)(\bar{\sigma}'-\bar{\sigma}'')]}{[1+(N-1)\bar{\nu}]}\right\}(T/2\tau_1)^{\frac{1}{2}}. \qquad (28)$$

The symbol $\bar{\sigma}'$ differs from unity because the steering delays used are quantized and hence not exactly equal to those ideally required by the array geometry. This effect may be present in unclipped as well as clipped steering systems. We may write

$$\bar{\sigma}'=\frac{1}{N(N-1)}\textstyle\sum'\sigma(\epsilon_{ij})$$

$$\approx1-\frac{1}{2N(N-1)}\langle\omega^2\rangle\textstyle\sum\epsilon_{ij}$$

$$=1-\tfrac{1}{2}\langle\omega^2\rangle\langle\epsilon_{ij}^2\rangle, \qquad (29)$$

---

[5] See footnote reference 4, p. 62, Eq. (75).

where $\sigma(\tau)$ is the autocorrelation function of the signal and ϵ_{ij} the difference between ideal and actual relative delays for the element pair (i,j), so that $\sigma_{ij}'(0)=\sigma(\epsilon_{ij})$, and[6]

$$\langle\omega^2\rangle=\int_{-\infty}^{\infty}(2\pi f)^2S(f)df\Big/\int_{-\infty}^{\infty}S(f)df$$
$$=-[d^2\sigma(0)/d\tau^2] \quad (30)$$

with $S(f)$ the power spectrum of the signal. Equation (29) is the relation underlying Anderson's[1] Fig. 4.

The expression in braces on the right in Eq. (28) represents array gain and the radical is the processing gain from post-rectification integration. The symbols $\bar{\sigma}''$ and $\bar{\nu}$ may be expected to have similar values, as they both are mean interelement correlations, one relating to a single off-axis arrival direction, the other to a mean of all arrival directions. Since $\bar{\sigma}'$ is nearly unity, the term $(N-1)\bar{\nu}$, being ordinarily larger than $\bar{\sigma}''$ will be the more important in Eq. (28).

(b) Clipped, On-Off-Target Comparison

The expression for clipped gain analogous to (25) is

$$G_2+1=(\{(W'-W'')/[s/(n+s)]\}/W'')(T/2\tau_2)^{\frac{1}{2}}, \quad (31)$$

in which factors are regrouped in a way appropriate to the clipped normalization. From (8) and (13) we have

$$W'-W''=(2/\pi)\cdot[s/(n+s)]$$
$$\cdot[(V'-V'')/s][1+\tfrac{1}{2}\langle\nu^2\rangle_{\mathrm{av}}'']. \quad (32)$$

Again neglecting the influence of signal on noise spectrum we replace W'' by W in the denominator of (31). From (8) we have

$$W''\approx W=(2/\pi)(V/n)(1+\beta) \quad (33)$$

with β, already introduced in Eq. (20), given by

$$\beta=[\pi/2-1+\tfrac{1}{6}(N-1)\langle\nu^3\rangle_{\mathrm{av}}]/[1+(N-1)\bar{\nu}] \quad (34)$$

through use of (5), (12) and (27).

Combining (25), (27), (31)–(33), and (19) gives

$$G_2+1=(G_1+1)[(\tau_1/\tau_2)^{\frac{1}{2}}/(1+\beta)][1+\tfrac{1}{2}\langle\nu^2\rangle_{\mathrm{av}}'']$$
$$=(G_1+1)[(1+\tfrac{1}{2}\langle\nu^2\rangle_{\mathrm{av}}'')/(1+2\beta\tau_c/\tau_1+\beta^2\tau_{cc}/\tau_1)^{\frac{1}{2}}]. \quad (35)$$

In the first form of this result the factor $(1+\beta)$ is the loss of array gain by clipping and $(\tau_1/\tau_2)^{\frac{1}{2}}$ is an offsetting improvement in post-detection gain (since $\tau_2<\tau_1$) reflecting the content of higher frequencies in the clipped noise. The second form of the result shows that the combination of these two factors is always a loss (since $\tau_{cc}<\tau_c<\tau_1$). As already noted, the effect of quantized delays in degenerating the signal is already included in G_1, and by (35) appears as a virtually equal factor in G_2.

(c) On-No-Target Comparison

If detection is based on comparison of "on target" with "no target" output, it is convenient to consider three systems: the clipped system, an unclipped system in which automatic gain control maintains constant power output from each array element, and a normal linear unclipped system. Let the processing gains for these three systems be denoted, in order, by G_2', G_1', and G_3'. G_2' and G_1' will replace G_2 and G_1, respectively, in (28) and (35) if $\bar{\sigma}''$ in the former is replaced by $\bar{\nu}$, and $\langle\nu^2\rangle_{\mathrm{av}}''$ in the latter by $\langle\nu^2\rangle_{\mathrm{av}}$. These tend to be very minor changes. Further we have

$$G_3'=\{[(N-1)\bar{\sigma}'+1]/[1+(N-1)\bar{\nu}]\}(T/2\tau_1)^{\frac{1}{2}} \quad (36)$$
$$=(G_1'+1)\{[\bar{\sigma}'+(N-1)^{-1}]/(\bar{\sigma}'-\bar{\nu})\}. \quad (37)$$

Thus, these inequalities hold:

$$G_2'<G_1'<G_3'. \quad (38)$$

V. NUMERICAL ILLUSTRATION

In order to make the foregoing results specific, array geometry and noise power spectrum must be given.

The three-dimensional array described by Anderson[7] was chosen as a basis for some illustrative numerical calculations. The configuration contains 32 elements, of which the inner twelve are the vertices of a regular icosahedron, and the 20 outer ones are apexes of regular tetrahedra whose bases are the faces of the icosahedron. The length of the common edge of these figures is denoted by l.

Each element feeds a delay line with ten taps, providing nine intervals of delay, each equal to τ_0. With these delays, 32 beams are formed, each with its axis parallel to the position vector of one of the 32 array elements, drawn from the array center as origin. Because of the array symmetry, there are just two different forms of beam, associated respectively with inner and outer element directions. For each kind of beam, the ideally desired steering delays must be approximated by integral multiples of τ_0, i.e., $K\tau_0$ with $0\leqq K\leqq 9$. A complete steering scheme consists of 64 values of K, one assigned to each element in each of two beams. Several such sets of integers were formed by inspection. For each there was calculated that value of τ_0 which would minimize the mean squared delay error, and the minimum error so achieved. That set of integers which produced the smallest error was chosen. Results obtained in this way were

$$\tau_0=0.34l/c \quad (39)$$
$$\langle\epsilon_{ij}^2\rangle^{\frac{1}{2}}=0.27\tau_0$$

with c equal to the speed of sound. This root-mean-

---

[6] G. A. Campbell and R. M. Foster, *Fourier Integrals for Practical Applications* (D. Van Nostrand Company, Inc., Princeton, New Jersey, 1958), 1st ed., p. 37, Table I [using pair (208) twice, then (101), and setting $g=0$].

[7] V. C. Anderson, J. Acoust. Soc. Am. 30, 470 (1958).

TABLE I. Numerical factors relating to processing for detection in the presence of isotropic noise. Quantities in parentheses are decibel values; each sign shows the influence of the factor on gain for detection.

Item	Quantity	Lower octave		Upper octave		Both octaves	
1	$N-1$	31.0	(14.9)	31.0	(14.9)	31.0	(14.9)
2	$1+(N-1)\bar{\nu}$	2.19	(−3.4)	1.16	(−0.6)	1.50	(−1.8)
3	$\bar{\sigma}'$	0.973		0.891		0.918	
4	$\bar{\nu}$	0.039		0.005		0.016	
5	$\bar{\sigma}'-\bar{\nu}$	0.934	(−0.3)	0.886	(−0.5)	0.902	(−0.4)
6	$f_c\tau_1$	0.84		0.42		0.35	
7	$(T/\tau_1)^{\frac{1}{2}}$	35.0	(15.4)	49.0	(16.9)	53.0	(17.3)
8	G_1+1	460.0	(26.6)	1160.0	(30.6)	990.0	(30.0)
9	$\frac{1}{2}\langle\nu^2\rangle_{av}''$	0.005		0.001		0.0006	
10	$\frac{1}{2}(N-1)\langle\nu^2\rangle_{av}$	0.006		−0.0002		0.0001	
11	$1+\beta$	1.26	(−1.0)	1.49	(−1.7)	1.38	(−1.4)
12	$(\tau_2/\tau_1)^{\frac{1}{2}}$	0.86	(0.7)	0.84	(0.7)	0.87	(0.6)
13	τ_c/τ_1	0.30		0.49		0.49	
14	τ_{cc}/τ_1	0.21		0.39		0.47	
15	$[1+2\beta(\tau_c/\tau_1)+\beta^2(\tau_{cc}/\tau_1)]^{\frac{1}{2}}$	1.08	(−0.3)	1.25	(−1.0)	1.20	(−0.8)
16	G_2+1	430.0	(26.3)	930.0	(29.7)	830.0	(29.2)
17	$\bar{\sigma}'[1+2\beta(\tau_c/\tau_1)+\beta^2(\tau_{cc}/\tau_1)]^{-\frac{1}{2}}$	0.90	(−0.5)	0.71	(−1.5)	0.76	(−1.2)

square delay error is materially smaller than $0.41\tau_0$ which would correspond to a random relationship between the various $K\tau_0$ and the desired delays.

The input noise spectra were related to a center frequency f_c such that $f_cl/c=0.53$, somewhat less than the value 0.60 chosen by Anderson.[7] Computations were made for one-octave bands $0.5f_c$ to f_c and f_c to $2f_c$, and the two-octave band $0.5f_c$ to $2f_c$. For each band the form of the power spectrum was taken to be

$$\int_{16[(|f|/b)-1]}^{16[(|f|/a)-1]} \operatorname{sech} x\,dx, \tag{40}$$

which represents an approximately flat curve between the nominal limits a and b, with a reasonably realistic cutoff form at each limit. Figure 1 shows the form of the one octave band. The space correlations associated with these spectra are all derivable from the integral

$$\int_0^{2\pi x} \frac{\sin t}{t} \operatorname{sech}\frac{\pi t}{32} dt,$$

which has been computed for x at intervals of 1/36 to 10 cycles, with uncertainty well below 10^{-4}. Because this function is quite special, the numerical table is not being published, but a copy,[8] if available, will be furnished to any worker on request to this Laboratory.

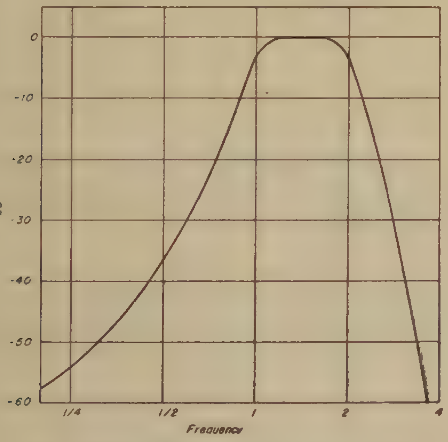

FIG. 1. One octave band with form given by Eq. (40) with $a=1.0$, $b=2.0$.

Post-detection integration time was fixed arbitrarily by the relation $f_cT=1000$.

On the scale on which the array was actually constructed by Anderson,[7] l is 34 in. This leads to $l/c=0.58$ msec $f_c=0.91$ kc, and $T=1.10$ sec. The optimum value of τ_0 is 0.197 msec.

The calculations undertaken were the cross-correlation functions for all element pairs (36 different varieties) for isotropic noise having each of the three spectra before and after clipping. Only one beam, that associated with an inner element, was dealt with. This program was very laborious, and was simplified by approximations or omissions wherever this appeared permissible for the present objectives.

Table I shows numerical values entering the expressions (28) and (35) for unclipped and clipped processing gains for detection.

Item 1 in the table is the ideal array gain in conventional processing. Item 2 is the factor by which this gain is reduced by interelement correlation. Items 3–5 relate to the unclipped signal. Item 3 shows the effect of delay errors. This was evaluated by (29), (30), and (39), taking $\langle\omega^2\rangle$ from the noise spectrum also to apply to the signal spectrum. In item 4, as already suggested,

---

[8] J. Baker and M. Head, University of California, La Jolla, Marine Physical Laboratory of the Scripps Institution of Oceanography, Tech. Memo. No. 111 (September, 1959).

(491)

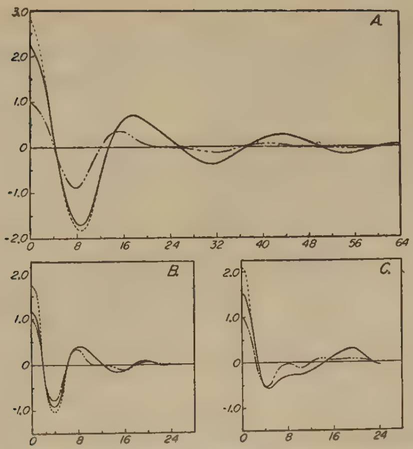

FIG. 2. Autocorrelations. *A* is the lower octave; *B*, the upper octave; *C*, both octaves. In each, the dashed curve is $\nu_{ii}(\tau)$, for the noise at one element; the solid curve is $V(\tau)/nN$, for the unclipped beam output; and the dotted curve (merging with the solid) is $(\pi/2N)W(\tau)$, the clipped beam output. The unit on the horizontal scale is τ_0.

$\bar{\nu}$ is to be considered a rough equivalent to $\bar{\sigma}''$, the mean interelement correlation for the signal when the beam is off-target. Item 5 shows the combination of these two effects which enters (28). Item 6 shows correlation times for the several spectra, and item 7 the corresponding postrectification gains. Item 8 summarizes all of the foregoing, giving over-all unclipped processing gain.

Turning to clipped processing, items 9 and 10 have such small numerical values as to permit their complete neglect in the formulas (32), (34), and (35). Thus, item 15 is the whole factor of disadvantage for clipped as against unclipped gain, and item 16 follows from 8 and 15. Items 11 and 12 are factors of 15 depending on array gain and correlation time, respectively. Items 13 and 14 show the effect of clipping on correlation time in an alternative way, τ_e always being more important than τ_{ee}. The final item 17 combines the results of clipping and delay quantization.

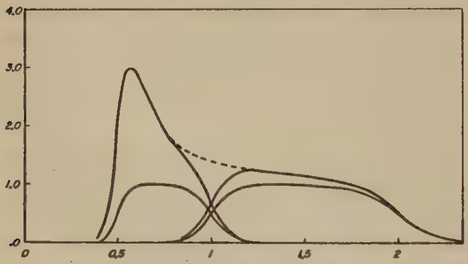

FIG. 3. Noise power spectra. The unit on the frequency scale is f_c. The two flat-topped curves of unit height are the two one-octave input spectra; their smoothly joining sum is the two-octave input. The two upper solid curves are unclipped beam output spectra. These will join smoothly, as shown by the dotted line, for the two-octave case.

In these cases, to a very good approximation the effects on array output of clipping and interelement correlations are independent. The nonlinear effect of clipping is the same in the presence or absence of interelement correlation, and the output due to interelement correlation is the same with or without clipping. (More explicitly interelement correlation is affected in the same way as the signal.) The total adverse effect of clipping is small and is less at lower frequencies. The usual adverse effect of rising interelement correlation at lower frequencies is, however, still the predominant relationship in the clipped system.

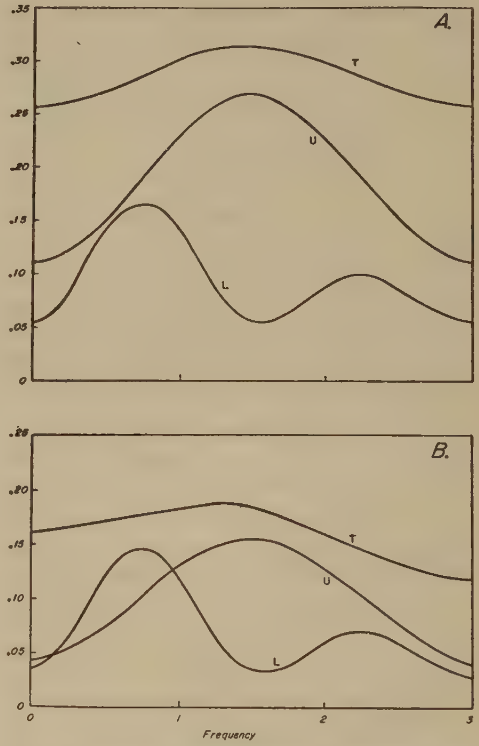

FIG. 4. Power spectra "added" by clipping, transforms of $c_{ii}(\tau)$. Both vertical and horizontal scales are consistent with Fig. 3. *L*, *U*, *T* denote, respectively, lower, upper, and two octave cases. *A* is for sampling rate $6f_c$ and *B* for $18f_c$; in the latter case the spectra actually extend to $9f_c$.

Clipped and unclipped autocorrelations are shown in Fig. 2. Numerical transforms of these have been calculated in order to determine the corresponding power spectra. The finite range of time delay τ over which each

(492)

$V(\tau)$ is known imposes a finite resolution on the calculated power spectra. This resolution is sufficient to display the frequency selectivity of the array within each band, but is insufficient to reproduce well the shape of the sharp cutoff at each band limit. The spectra shown in Fig. 3 have had the cutoffs "restored" by reference to the input spectra. The upper envelope of these spectra indicates the frequency response of the array to isotropic input, which is inversely proportional to the directional gain of the array.

The spectra introduced by clipping, transforms of $c_{ii}(\tau)$, are shown in Fig. 4, both for the present case when the sampling interval is approximately τ_0, and for comparison when the interval is one third as great. The appreciable difference represents power in the unsampled spectrum lying between the two Nyquist limits.

VI. COMMENT ON THE GAUSSIAN ASSUMPTION

The hypothesis of Gaussian noise statistics enters this analysis in two ways, and it seems unwise to conclude this discussion without remarking on its probable importance.

The first occurrence is in connection with the arc sine relation for the clipped correlation coefficient [left member of Eq. (4)]. This coefficient depends merely on the joint probabilities for like and for unlike polarities at two array elements with time delays only of the order of the transit time across the array. Only the second-order distribution is involved and this only through the integral of probability density over pairs of opposite quadrants in the plane. There seems to be no reason to expect this result to be sensitive to the detailed character of the distribution.

The situation appears quite different at the other point where the Gaussian hypothesis is used. This is the evaluation of the spectrum density at low frequencies for the rectifier output, on which expression (16) depends. This depends on a fourth-order moment and involves time delays as long as the total integration time. In practical situations, such as the example discussed above, gains from post-rectification smoothing of more than 15 db will frequently be predicted for Gaussian noise and are doubtless frequently realizable. However, it also is very easy to suppose that actual acoustic detection situations may also occur in which non-Gaussian power fluctuations will eliminate some substantial part of an expected 15 db of post-rectification gain. Under such circumstances the constant-power character of clipped noise might constitute an advantage comparable with or larger than the disadvantage here deduced. An example of this sort has been discussed recently.[9] For this reason, the Gaussian hypothesis should be considered a very real limitation on the applicability of the present analysis.

---

[9] J. B. Thomas and T. M. Williams, J. Acoust. Soc. Am. 31, 453 (1959).

Reprinted from The Journal of the Acoustical Society of America, Vol. 32, No. 7, 867–870, July, 1960
Copyright, 1960 by the Acoustical Society of America.
Printed in U. S. A.

Digital Array Phasing*†

Victor C. Anderson
University of California, La Jolla, Marine Physical Laboratory of the Scripps Institution of Oceanography, San Diego 52, California

The extension of digital techniques to the problem of processing the output of an array of point receiving elements in an acoustic field has given rise to a method of phasing called DIMUS (digital multibeam steering). This digital technique incorporates the use of shift registers as delay line elements which results in a number of operational advantages. A description of the DIMUS technique is given. The effects of amplitude and time quantization imposed by the digital circuits are considered in the light of the relative signal processing gain of the array referred to an exact analog phasing network. The processing gain is computed as a function of sampling frequency for a number of types of signals.

INTRODUCTION

As a result of a program of investigation of the use of underwater acoustic arrays for underwater detection systems,[1] considerable interest has arisen in the past few years in the methods of processing the outputs of the individual elements of such arrays. The vast difference in operating frequency between acoustic arrays and radio or radar arrays, and the difference between the usual broadband acoustic signals, i.e., $\Delta\omega/\omega>1$, and the narrowband radio and radar signals, i.e., $\Delta\omega/\omega<0.01$, have stimulated deviations from the work in the latter fields, leading to innovations in both theoretical approach and in instrumentation.

The basic theory of beam formation, i.e., the calculation of directivity patterns, from an array of elements has been quite well covered for both the single frequency case and the broadband signal case.[2–4] Consideration of the process of beam formation, however, covers only one facet of the application of an array for the purpose of detecting energy from a distant source. The response of the array to sources of noise lying outside of its major lobe is an equally, if not more, important factor in the design of an array for detection applications than is the response on the axis of the major lobe.[5] A third influential design factor in the use of the arrays is the way in which averaging time is utilized for statistical isolation of a signal from a noise background.

As a result of complex interaction of these factors, one is not readily led to a uniquely defined processing technique for a multiple element array, consequently, a number of basically different techniques have been investigated. The use of a compensator plate was one of the earliest approaches to provide electrical compensation in lieu of physically rotating the array.[2] The use of multiple product instead of analog summation processing of the element outputs has also been treated in some detail.[6,7] A combination of the analog summing with a compensator plate followed by a "clipper correlator" processing technique applied to two halves of a split array is shown to have advantages in the presence of nonstationary noise.[8]

The processing technique under discussion in this paper, DIMUS (digital multibeam steering), has resulted from an extension of some of the above concepts in an attempt to obtain optimum processing for an acoustic array designed especially for detection. It is the intent of this paper to present an introductory treatment of the effectiveness of this technique.

The schematic representation of Fig. 1 illustrates the DIMUS technique. The hydrophone elements of an array provide the independent electrical signals e_i which are to be combined in the shift register matrix to form a beam output. Before the e_i's are introduced into the shift register, they are passed through clipping ampli-

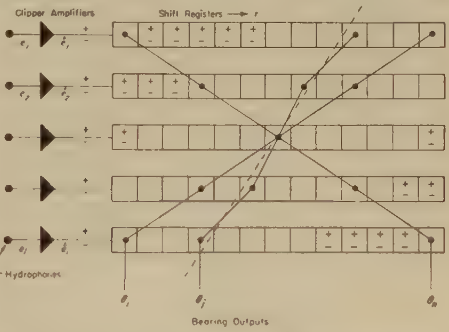

FIG. 1. Schematic representation of the DIMUS technique.

---

* This work represents one of the results of research carried out under contract with the Office of Naval Research.

† Presented at the 58th Meeting of the Acoustical Society of America, October 22–24, 1959, Cleveland, Ohio.

[1] J. M. Ide, Proc. Inst. Radio Engrs. **47**, 864 (1959).

[2] J. W. Horton, *Fundamentals of Sonar* (U. S. Naval Institute, Annapolis, Maryland, 1957), Chap. 5.

[3] R. L. Pritchard, J. Acoust. Soc. Am. **25**, 879 (1953). Note: The reader is referred to the bibliography of this reference which lists a comprehensive selection of references to earlier work including references to the work of Stenzel.

[4] J. J. Faran and R. Hills, Jr., Acoustics Research Laboratory, Harvard University, Tech. Memo. No. 31 (May, 1953).

[5] V. C. Anderson, J. Acoust. Soc. Am. **30**, 470 (1958).

[6] J. J. Faran and R. Hills, Jr., "The application of correlation techniques to acoustic receiving systems," Acoustics Research Laboratory, Harvard University, Tech. Memo. No. 28 (November, 1952).

[7] A. Berman and C. S. Clay, J. Acoust. Soc. Am. **29**, 805 (1957).

[8] J. B. Thomas and T. R. Williams, J. Acoust. Soc. Am. **31**, 453 (1959).

Contributions from the Scripps Institution of Oceanography, New Series, 1168

Reproduced by Permission

fiers which quantize the signals into two amplitude states representing the polarity of the signal. The clipped signals $\hat{e}_i$'s are then used to drive the first stage of their respective shift registers. The shift register operates as a digital delay line, advancing each polarity sample or "bit" through the succession of stages at the clocking pulse rate. In order to form an electrical beam directed at an angle θ_1, the appropriate stage on each shift register is selected which produces a time delay most closely complementing the relative travel-time delay of the signal from θ_1, as it passes across the array. The resulting set of time-delayed signals are then summed in a simple resistive analog summing network to form the θ_1 beam. Inasmuch as the beam output is a combination of the binary or two level voltages of the individual elements, the resultant sum will have $n+1$ possible voltage levels. Similar sums may be formed for other desired directions by merely adding additional summing networks on the appropriate sets of time delays, one network for each desired beam.

Although a simple linear array has been used for the purpose of illustration, it should be emphasized that this technique is not restricted to special geometric array-element distributions, nor is it restricted to a one-dimensional set of beams; arbitrary distributions of elements in three-dimensions, and arbitrary sets of beams in two dimensions (azmuith and elevation) may be accommodated. The technique will also encompass compensation for wave front curvature.

SIMPLE STATISTICS OF THE BEARING OUTPUT

An insight into the nature of the output of a bearing summation matrix and the effects of polarity and time quantization may be obtained by introducing a number of simplifying assumptions. Assume that the sound field is statistically homogeneous, i.e., that the power spectrum of any point in the sound field is independent of position. Further assume that the sound field is made up of an isotropic noise field which has no preferred directional characteristics, plus a signal field which consists of a plane wave arriving from a single distant point source. If the element spacings are made sufficiently large so that the noise pressure signals of the elements in the noise field may be considered to be statistically independent, it is readily demonstrated that the standard deviation of the average of the element outputs from the noise field with the signal absent as it is formed by the bearing summation matrix is,

$$\sigma_N \text{ of } \left(\sum\frac{e_i}{N}\right)=\frac{\sigma_i}{\sqrt{N}}, \qquad (1)$$

where σ_i is the standard deviation of an element output (e_i), N is the number of elements, and σ_N is the standard deviation of the average. This simple expression will be valid as long as the interelement spacing is large enough to insure independence regardless of the statistics of the e_i's. By the central limit theorem,[9] the voltage appearing on the output will approach a Gaussian amplitude distribution for N sufficiently large regardless of the distributions of the e_i's.

From this approach it is easy to see that for large N the statistics of the bearing output signal will be Gaussian and the standard deviation will be given by Eq. (1) whether the inputs to the averaging networks are the e_i's as analog voltages, or the $\hat{e}_i$'s, the clipped voltages. The outputs will be quantized into $N+1$ permissible levels for the clipped case, but this quantization effect is negligible in practical applications for $N>30$.

As far as noise output is concerned, the effect of amplitude quantization will be limited to the general broadening of the noise spectrum by the clipping process. This change in the spectrum will modify the fluctuation of the short time average noise power so as to reduce the relative fluctuation for the sum of the clipped outputs. The magnitude of this reduction is dependent on the spectrum shape and is treated in detail by Rudnick.[10]

SIGNAL RESPONSE OF A CLIPPED AND TEMPORALLY QUANTIZED SYSTEM

The effect of the clipping process on the signal is also most readily demonstrated by considering the process under the simplifying assumption above. In general, if only the spectrum of the signal is known, detection must be made on the basis of an increase in power caused by the presence of the signal. If the $\hat{e}_i$'s are bandpass signals, the power at the bearing output is proportional to

$$W=\left\langle\left(\sum_{i=1}^{N}\hat{e}_i\right)^2/N\right\rangle=\sum_{i=1}^{N}\sum_{j=1}^{N}\frac{\langle\hat{e}_i\hat{e}_j\rangle}{N}, \qquad (2)$$

where the power W, for convenience, has the dimensions of voltage squared and $\langle\ \rangle$ indicates a time average. Actually the e_i's have been delayed in time by an amount τ_i so that Eq. (2) becomes

$$W=1+\frac{2}{N}\sum_{i=1}^{N-1}\sum_{j=i+1}^{N}\langle\hat{e}_i(t-\tau_i)\hat{e}_j(t-\tau_j)\rangle. \qquad (3)$$

The criterion for selection of the τ_i's is to maximize the cross product by establishing time coincidence for the signal at each element pair. Thus, it is convenient to express the bracketed term of Eq. (3) as

$$\langle\hat{e}_i(t-\tau_i)\hat{e}_j(t-\tau_j)\rangle=\hat{\rho}_{ij}(\Delta\tau_i+\Delta\tau_j) \qquad (4)$$

where $\hat{\rho}_{ij}$ is the clipped cross correlation or time averaged displaced product of the two delayed signals and the $\Delta\tau$'s represent the departures from the exact electrical phasing required for perfect coincidence of the arriving signal at the element pair. Equation (4) may be compared with Eq. (29) of Rudnick's more general treatment. The $\Delta\tau$'s of Eq. (4) represent the time quantization errors inherent in the DIMUS system because of the discrete steps in time delay available in the shift registers.

---

[9] H. Cramér, *Mathematical Methods of Statistics* (Princeton University Press, Princeton, New Jersey, 1951), 1st ed., Chap. 17, p. 213.

[10] P. Rudnick, J. Acoust. Soc. Am. 32, 871 (1960).

The clipped correlation function $\hat{\rho}_{ij}(\tau)$ is expressed in terms of the unclipped normalized cross correlation ρ_{ij} by the relation[11]

$$\hat{\rho}_{ij}(\tau)=(2/\pi)\sin^{-1}\rho_{ij}(\tau)\simeq(2/\pi)\rho_{ij}(\tau). \qquad (5)$$

Employing the linear approximation of Eq. (5) which is valid for $\rho_{ij}\ll 1$, as is the case for small signal-to-noise ratios in the e_i's,

$$W=1+\frac{2}{N}\sum_{i=1}^{N-1}\sum_{j=i+1}^{N}\frac{2}{\pi}\rho_{ij}(\Delta\tau_i-\Delta\tau_j). \qquad (6)$$

Relying on the previous assumption of homogeneity of the sound field,

$$W\simeq 1+(N-1)(2/\pi)\langle\rho_{ij}(\Delta\tau_i-\Delta\tau_j)\rangle_{\text{av}}, \qquad (7)$$

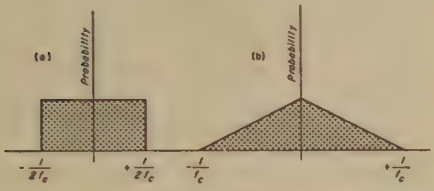

Fig. 2. Distribution of time delay errors for a single element and for a pair of elements.

where the angular brackets signify an average over the set of cross product terms.

At this point one may write for comparison a similar expression obtained as above for an exact analog phasing network where the e_i's have been normalized:

$$W'=1+(N-1)\rho_{ij}(0). \qquad (8)$$

If one now ignores the effect of the broadening of the spectrum by clipping as pointed out earlier, a comparison of the relative signal response, $\mathcal{E}$, of the DIMUS and the exact analog networks is given by the ratio of the contributions of the signal to the bearing powers W and W' as given by the second terms of Eqs. (7) and (8), i.e.,

$$\mathcal{E}=(2/\pi)\langle\rho_{ij}(\Delta\tau_i-\Delta\tau_j)\rangle_{\text{av}}/\rho_{ij}(0). \qquad (9)$$

Numerical evaluation of Eq. (9) may be carried out providing the shape of the autocorrelation of the e_i's, and a set of $\Delta\tau_i$ are established. For the limiting case of N large and arbitrary, irregular geometric distribution of elements, a uniform distribution of the $\Delta\tau_i$ such as that shown in Fig. 2(a) may be assumed. This rectangular distribution is a result of the selection of the nearest delay tap in wiring the summing matrix so that the maximum error is one-half the delay tap spacing, i.e., $1/(2f_c)$ where f_c is the clocking frequency for the shift register. The distribution of the sum of the two delay errors is then the triangular distribution shown in Fig. 2(b). Applying this triangular distribution as a weighting function for the averaging process of Eq. (9), and using the autocorrelation function of the signal to obtain the form of ρ_{ij} the effective signal response as given by Eq. (9) may be calculated. The use of the autocorrelation function instead of the cross correlation function of Eq. (9) is justified for computational purposes in that the two functions are linearly related by signal-to-noise ratio, and thus the ratio of Eq. (9) remains unchanged. This has been done for the two autocorrelation functions shown in Fig. 3, corresponding to a rectangular low-pass spectrum and a line spectrum. The results are represented by Fig. 4 which shows the relative signal response as a function of the clocking

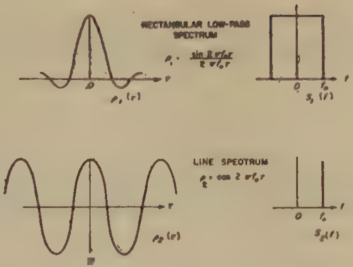

Fig. 3. Signal autocorrelation functions and corresponding rectangular low-pass spectra used for computation of signal processing efficiency.

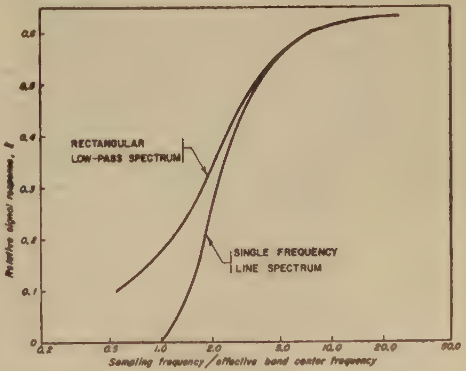

Fig. 4. Relative signal response vs relative sampling frequency.

---

[11] J. L. Lawson and G. E. Uhlenbeck, *Threshold Signals* (McGraw-Hill Book Company, Inc., New York, 1950), M.I.T. Radiation Laboratory Series, Vol. 24, Chap. 3, p. 58.

frequency. The ordinate is plotted versus the ratio of the clocking frequency to the mean effective frequency f_m of the spectrum $S(f)$ where

$$f_m^2=\int_{-\infty}^{\infty} f^2 S(f)df \bigg/ \int_{-\infty}^{\infty} S(f)df.$$

It is interesting to note that the loss due to delay errors is essentially independent of band shape for frequency ratios greater than five.

The asymptotic value of $2/\pi$ or -1.95 db for the loss of signal due to the clipping process will be offset by the lower background fluctuations of the time averaged clipped noise output so as to give a net loss in signal processing efficiency of the order of 1.0 db for practical spectra.

From characteristics of the curve of Fig. 4 one is led to an f_s/f_m ratio of five as a design objective which may be used to determine the required number of shift register stages for a DIMUS compensating matrix. This ratio gives rise to a drop of 0.5 db in signal response from the limiting value of $2/\pi$ at an infinite clock pulse frequency.

CONCLUSIONS

Although the treatment of the effects of quantized processing on the signal has been highly simplified by the initial assumption, it still remains a valid guide to the interpretation of the operation of DIMUS. The complete analysis requires the consideration of the effects of interelement correlations, and the signal loss inherent in the clipping and sampling process in addition to the effect of time delay errors treated here. These effects will be in general superimposed on those of the time delay errors and will be dependent on the spectrum of the noise, and the geometry of the array.

THE CHANGES IN THE PHYTOPLANKTON POPULATION OFF THE CALIFORNIA COAST[1]

ENRIQUE BALECH
(Read by Francis T. Haxo)

Since the studies of the Scandinavian planktologists, particularly those of Cleve at the turn of the century, the microplankton have been recognized as potential indicators of the origin and characteristics of water masses. In the intervening years, the taxonomy of the more important phytoplankton constituents has been advanced and a number of studies have been published in which the distribution of phytoplankton has been carefully correlated with analyses of the chemical and physical features of the surrounding water masses.

Partcularly noteworthy are the studies of Hardy in the South Atlantic and Antarctic (Discovery Expedition), of Steeman Nielsen in the Pacific (Dana Expedition), of Peters and Käsler in the Atlantic Ocean (Meteor Expedition), of Gaarder in the North Atlantic (Cruises of the Michael Sars), and of Graham and Bronikowsky in both the Pacific and Atlantic Oceans (VII Carnegie Cruise). These have provided a great deal of carefully analysed data, especially concerning the dinoflagellates of the genus *Ceratium*. To these we can add my own studies, which have covered the following areas: the south of South America, the Antarctic seas, the Mediterranean, and the Atlantic littoral regions of France and the English Channel.

From these studies it is apparent that, within limits, the broad temperature realms of the oceans have a characteristic flora. While some species are fairly tolerant of wide ranges in temperature, others are restricted in their temperature distribution and are limited, for example, to tropical or to cold waters. Thus the species composition of a given water mass will reflect something of its present and/or previous temperature history. This is particularly valid when assemblages of indicator species are enumerated in characterizing a given water mass.

As background information on the area of present concern, the coastal waters of California, we have among others the studies of Allen extending over a period of more than twenty years, the studies on diatoms by Cupp, the investigation of Sargent and Walker on the relationships between diatom populations and water eddies, and the unpublished studies by Holmes on the phytoplankton of the North and Eastern Pacific. There are also the detailed studies by Kofoid, primarily of a taxonomic nature, on the dinoflagellates and tintinnids, a group of ciliate protozoans.

COMPARISON OF THE QUALITATIVE COMPOSITION OF THE PHYTOPLANKTON IN LA JOLLA DURING THE YEARS 1938-1939 (ALLEN'S COLLECTIONS) WITH 1957-1958

When in December 1957 it became evident that the planktonic populations in La Jolla were of an unexpected warm water, even tropical character, I began a comparative study of recent collections with Allen's samples from the nine month period August 26, 1938 through May 1939, when the water temperature averaged below the long-term mean with the corresponding recent collections in 1957-1958. For this study I have re-examined Allen's collections so that differences in species identification by different observers could be eliminated. Both collections were made from the end of the pier at the Scripps Institution (La Jolla).

Before presenting the results, some mention should be made of the differences in sampling methods employed. Allen was primarily interested in quantitative studies. For that reason he collected small volumes of sea water and the plankton were concentrated by settling. For my studies, the collections were made with a 62μ mesh net. The volume sampled was many times that of Allen for any given day. Because of these differences in methods and in volumes sampled, we can expect that the larger forms would be better represented in my collections. The smaller forms not retained by the net would be better represented in the plankton concentrated by Allen's settling technique. However, because of the greater frequency of Allen's collections (daily), the qualitative differences due to sampling methods might be expected to disappear when collections of a whole month are considered. Notwithstanding the difference in methodology, the differences in composition of the plankton described below were considered to be of real significance.

The results are presented in a somewhat simplified way in figures 113 and 114, in which the more important indicator species of dinoflagellates, diatoms and tintinnidae are listed according to their appearance by months in the two periods under consideration. Such a simplified presentation can give only a rough approximation of the character of the plankton, since stress was placed here on the more persistent species and abundances are not indicated. Considera-

---

[1] Contribution from the Scripps Institution of Oceanography.

Contributions from the Scripps Institution of Oceanography, New Series, 1169
Reproduced by Permission

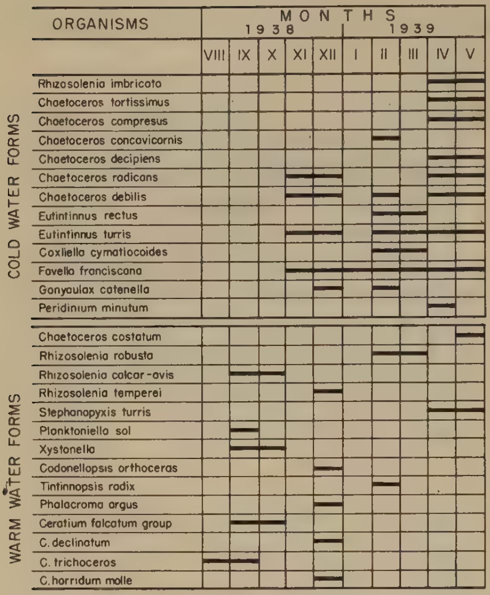

FIGURE 113. Occurrence during 1938-1939 of dinoflagellates, diatoms and tintinnidae in the plankton at La Jolla.

tion of the sporadically occurring species only sharpens the contrast between the two years. The figures do not bring out, for example, the significant differences observed in the planktonic populations of January through the first half of February 1958 and those of March 1958. While the former were relatively homogeneous, the latter showed considerable variability in composition.

The most important general conclusion is that the phytoplankton populations of 1957-1958 were atypical in that, on the one hand, warm water and tropical phytoplankton were abundantly represented (largely absent in 1937-1938) and, on the other hand, the appearance of cold water forms was delayed and restricted. No doubt this is a reflection of the warm water prevailing during the past year.

Looking at the two periods in greater detail, we note that Allen's samples collected during the summer of 1938 contained some warm water species but none of the more rare and tropical species, for example, *Ceratium carriense, C. lunula,* and *C. ranipes,* which are well represented in my pier samples of the past year. By late September of 1938 all but one quite tolerant tropical species of *Ceratium* had disappeared. By contrast, in 1957, many tropical species persisted throughout the first part of autumn. Furthermore, in December of 1957 there was an unexpected development. The planktonic population took on a most tropical character in spite of a relatively low water temperature. This was especially striking for the week of December 8-14, when two tropical species of *Ceratium* were collected for the first time. It is noteworthy that during the period December 19-22 of 1938 there was a slight indication of the same phenomenon in Allen's samples, but very much less marked and involving species less truly tropical in nature.

In the early weeks of 1958, as in 1939, the phytoplankton was not very abundant. In the 1958 samples, however, warm water plankton continued to dominate until the middle of February, at which time some changes were noted. We still found some tropical species, but many noted previously had disappeared. On the whole, the plankton showed a relative abundance of diatoms, including some that thrive in cold

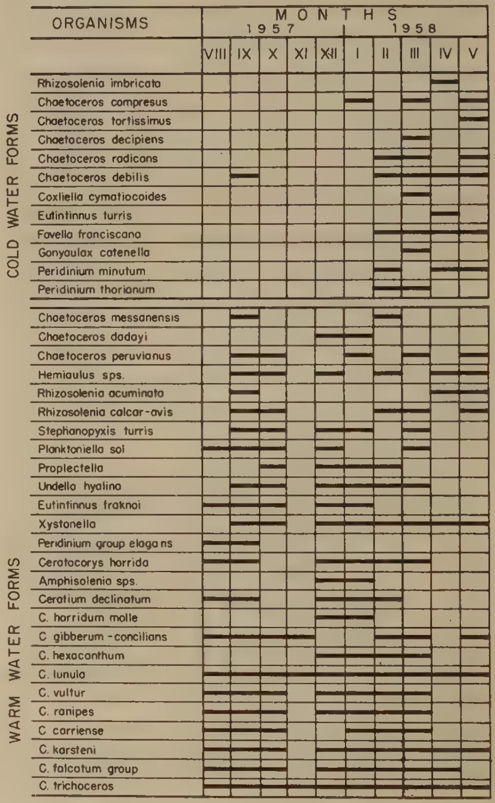

FIGURE 114. Occurrence during 1957-1958 of dinoflagellates, diatoms and tintinnidae in the plankton at La Jolla.

water. Present also were several other protists (*Peridinium* and tintinnidae) that seem to prefer cold and temperate waters. During the last part of the month there were noticeable fluctuations in the character of the plankton from a population typical of warm water to a mixed one, with several northern species. By contrast, in 1939, warm water species were not found in January and the plankton of February was dominated by tintinnidae, generally cold and temperate or cosmopolitan species, a situation which continued through April of that year.

Of particular interest is the characteristic presence in the February 1939 collections, as well as those of December 1938, of chains of *Gonyaulax catenella* and its presence in only a single sample of the 1957-1958 collections (a single chain of two in a sample of March 13). From laboratory experience it is known that this dinoflagellate has markedly lower temperature preferences for growth than other *Gonyaulax* species commonly found in the La Jolla area.

In March of 1958 the collections for the first time showed many common features with those of 1938. In general, the plankton were of a mixed and fluctuating character, dominated by zooplankton, especially larvae, with several of the same cold water species of tintinnidae, diatoms and dinoflagellates.

April 1958 showed a regular increase of temperature but not a very great change in the composition of the plankton. However, some typical warm water species were again present, but these were in general poorly represented.

May 1958 showed significant changes by the middle of the month, with a dominance of dinoflagellates, especially *Gonyaulax polyedra* and *Diplopeltopsis minor*, a truly cosmopolitan species. There were several cold or temperate species of diatoms, but the most conspicuous elements of the plankton are widespread species. Also present was a typical warm water diatom, *Hemiaulus membranacea*. By contrast, May 1939 showed plankton with little changes from that of the preceding month. The last half of May 1939 was dominated by *Prorocentrum micans*.

From all this we gain a strong impression of marked difference in phytoplankton composition in the years under comparison. The difference attenuated after 15th February but did not disappear, as shown by the persistence in 1939 of the typical cold water forms and the almost total absence of warm water species so much in evidence in 1958. The greatest anomaly embraced the period, December to the middle of February.

An interesting feature of the plankton studies is that an invasion of warm water in the San Diego region seems normal for December. This feature was also observed in plankton samples for December 1953, available in the Marine Botany Laboratory at the Scripps Institution of Oceanography. These were largely dominated by *Prorocentrum micans*, but samples of December 17 and 18 contained some typical warm water species. On the whole, the plankton composition was very similar to that of December 1938 and quite different from that of December 1957.

GENERAL SURVEY OF THE CALIFORNIA PLANKTON IN APRIL 1958

Although it was not possible to extend observations during the period of greatest anomaly at La Jolla, opportunity was presented during April of this year to incorporate microplankton collections into the CCOFI cruise program. These were made by vertical and horizontal tows with a 62μ net at stations on the MLR grid extending from Baja to Northern California. Very rough weather restricted the planned coverage, particularly north of San Francisco.

Based upon preliminary examination of the collections, the general character of the plankton distribution is shown in figure 115, that of selected warm water dinoflagellates in figure 116, and that of the genus *Ceratium* in particular, in figure 117. It was indeed found that tropical to warm water forms were commonly present as far north as the 15°C isotherm and in some cases extended to the 14°C isotherm. According to previous investigations, species included

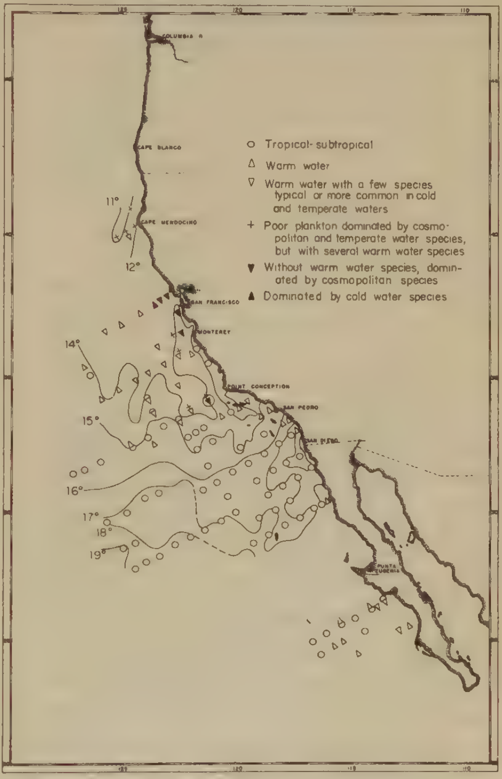
125
120
115
110
COLUMBIA R.
CAPE BLANCO
CAPE MENDOCINO
SAN FRANCISCO
MONTEREY
POINT CONCEPTION
SAN PEDRO
PUNTA EUGENIA
11°
12°
14°
15°
16°
17°
18°
19°
○ Tropical-subtropical
△ Warm water
▽ Warm water with a few species typical or more common in cold and temperate waters
+ Poor plankton dominated by cosmopolitan and temperate water species, but with several warm water species
▼ Without warm water species, dominated by cosmopolitan species
▲ Dominated by cold water species

FIGURE 115. Distribution of micro-nannoplankton, March 29-April 28, 1958 (CCOFI Cruise 5804).

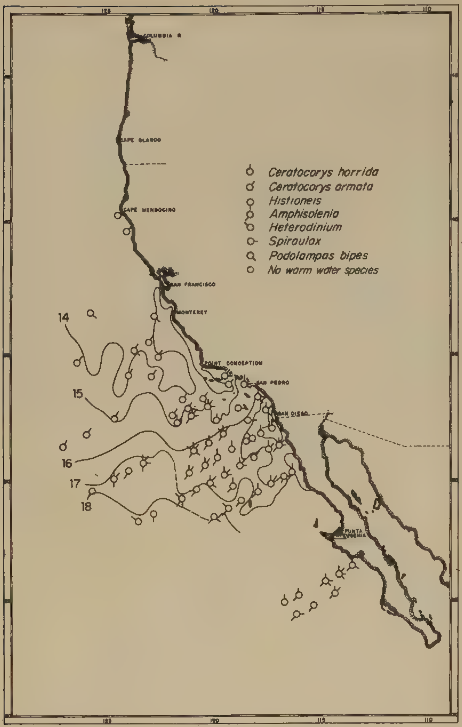
COLUMBIA R
CAPE BLANCO
CAPE MENDOCINO
SAN FRANCISCO
MONTEREY
POINT CONCEPTION
SAN PEDRO
SAN DIEGO
PUNTA EUGENIA
14
15
16
17
18
Ceratocorys horrida
Ceratocorys armata
Histioneis
Amphisolenia
Heterodinium
Spiraulax
Podolampas bipes
No warm water species

FIGURE 116. Distribution of some warm water dinoflagellates, March 29-April 28, 1958 (CCOFI Cruise 5804).

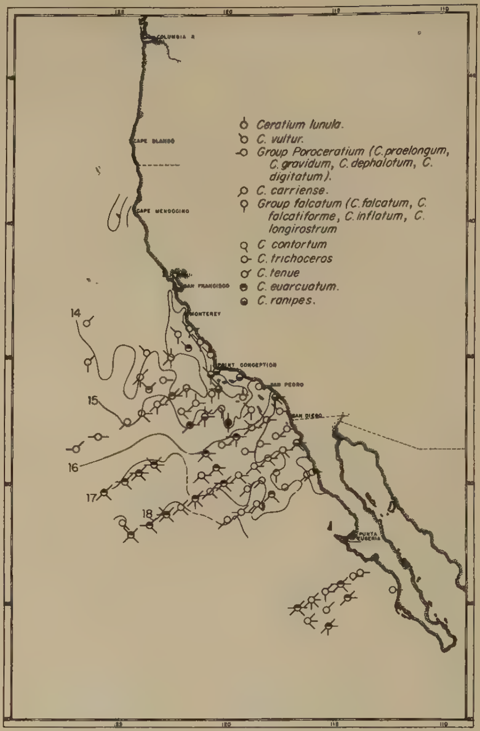
COLUMBIA R
CAPE BLANCO
CAPE MENDOCINO
SAN FRANCISCO
MONTEREY
POINT CONCEPTION
SAN PEDRO
SAN DIEGO
PUNTA EUGENIA
14
15
16
17
18
Ceratium lunula.
C. vultur.
Group Poroceratium (C. praelongum, C. gravidum, C. dephalotum, C. digitatum).
C. carriense.
Group falcatum (C. falcatum, C. falcatiforme, C. inflatum, C. longirostrum
C contortum
C. trichoceros
C. tenue
C. euarcuatum.
C. ranipes.

FIGURE 117. Distribution of Ceratia, March 29-April 28, 1958, (CCOFI Cruise 5804).

in this designation are not normally found in waters cooler than 18-19°C.

Looking to the north off San Francisco and Monterey, we see a different situation. Here the populations are dominated by cold water species; tropical or warm water species were not observed. The collections made farther north off Cape Mendocino, where the temperature was between 11° and 12°, present a surprising picture. Here we note the occurrence of several warm water species of *Ceratium*. Although all of these are tolerant species, they have never previously been found in such cold waters. Perhaps the drift bottle data may shed some light on this anomaly.

In the intermediate area largely delimited to the south by the 14° isotherm, the planktonic populations were of a mixed character. This is probably a reflection of the strong mixing of the water masses.

In conclusion, one is impressed with the striking change in the character of the planktonic populations from south to north and the far northward extension of typically warm water forms. Considering the normal temperature tolerance of these warm water species, it is tempting to ascribe this abnormal distribution to an active transportation to the north and a strong mixing of the waters.

DISCUSSION

Reid: Can you tell if the warm water species are from the south or from the west?

Haxo: I have raised the same question myself, but I believe that Dr. Balech's data do not permit distinguishing between these two alternatives.

Johnson: I am glad that he did not say that this actually established a transport. You are dealing with biological groups which respond to temperature conditions, and they reproduce in large numbers when the factors are favorable. You will notice throughout his paper he indicates the presence of warm water forms in cold water areas, or vice versa, which means that the seed material is really there, and where he speaks of temperature tolerance of a species, this does not necessarily mean that the species cannot get outside those temperature tolerances, but instead, these are the temperature tolerances within which it reproduces in large numbers. I believe we have to think of this when we interpret these things. If the water warmed up sufficiently off Cape Mendocino, we would have many more of these tropical and subtropical forms than are showing up there now. Not because they were carried in, but simply because the conditions became favorable for rapid reproduction; as you know, these organisms reproduce at a geometrical rate, so in a very short time propagate a considerable population. This does not mean that they have not been carried in, but that you have to think of the two things at the same time.

Haxo: Yes, one cannot look at the phytoplankton as simple drift bottles, which they certainly are not. All you need is a basic seed population, and if conditions are suitable for growth the population will increase in size. However, the source of the seed population, whether resident or transported, might be difficult to determine on the basis of present qualitative data. Perhaps the answer will be forthcoming when the collections have been more fully analyzed.

Hubbs: You did mention a few species that have not been found here before, such as tropical species of *Ceratium*. These are examples of temperature restricted distributions, in this case to warm water. The opposite situation is seen in the case of *Gonyaulax catenella*, a cold water form which actually cannot survive in warm water.

Haxo: This is certainly true. Unfortunately, information on temperature restrictions or tolerances is still largerly subjective. It would be very helpful if we had more extensive laboratory information on temperature tolerances of California coastal phytoplankton.

Sette: When you speak of temperature tolerance, do you mean mere survival, or, in addition, the ability to reproduce and maintain a population?

Haxo: Dr. Balech's approach has been that of a phytogeographer. His temperature designations are derived from information obtained at sea from other cruises from which it becomes known that certain species are to be found only in certain temperature realms. Therefore, based on this kind of information, they are thought to have certain temperature requirements and tolerances, presumably for survival and growth. This will remain an uncertain point until more exacting information is available. It is of interest that Dr. Balech has already encountered a number of dinoflagellates four or five degrees colder than previously reported.

Sette: In other words, these are tolerances as they are found to exist in the field.

Haxo: Yes, the tolerances are based upon observed distributions correlated with temperature.

Johnson: In a very few laboratories, cultures have been subjected to experiments to elucidate much of this kind of problem. There has been some work in Braarud's laboratory in which they studied a fair number of dinoflagellates for temperature tolerances. Some were also found to have different salinity tolerances, which may sometimes tend to have a reciprocal influence.

Haxo: Yes, these important studies have provided interesting examples of the complexities in the interaction of environmental factors on the growth of marine organisms and further indicate the desirability of extending efforts to cultivate phytoplankton under controlled laboratory conditions.

Hubbs: A suggestion (I think it is probably true of many of the invertebrates) is that when we have a seeming incursion of the southern forms, (we seem to be certain that it is an actual incursion) they will come up in a warm period and then tend to stay here even if the conditions are so bad that they die during the winter. Some of these that may have come up from the south are now living in water that they would not normally have reached simply because it has turned colder. The second point is a question regarding the 1939 data.

Haxo: The two periods were compared from late August through May. The temperatures of the 1938-1939 series were markedly lower (—0.85°C to —1.89°C) than those of the long term means (1917-1955) only during the months of October, November, February and March.

Johnson: I might mention here I had not realized to what extent Balech was looking at some of Allen's old samples which were concentrated by settling techniques. I have collections made with a No. 20 net which he might look over for some of these rare forms which he did not see before. I am quite sure that Allen did not pay much attention to rare forms, for his opinion was that it was the dominant forms that were important biologically, but they may not be the ones most important from the point of indicating changes in the oceanographic conditions.

Brinton: The phytoplankton reflects rather shallow environment compared to zooplankton forms, so that you can probably define depthwise the environments of these organisms better than you can many zooplankton samples. I seem to recall that Balech did find some forms relatively near to shore which he felt fairly certain were related to tropical waters. How did this compare to offshore?

Haxo: The general distribution of warm water dinoflagellates is brought out by figure 116. *Ceratocorys horrida* is an especially good indicator of tropical conditions and in April was found inshore as far north as San Pedro and far offshore from San Diego at the outermost station made along the 17°C isotherm.

Could I re-emphasize one point? Dr. Balech has dealt in all cases with assemblages of species, single members of which might be absent from adjacent stations. Assemblages of a half dozen or more species were used to indicate a given oceanographic condition.

ADDENDUM BY DR. BALECH

(Prepared following his reading of the transcript of the discussion)

We do not know actually how many species of marine dinoflagellates form cysts, although there is a general belief—far from proven—that most can do so. However, I should stress that these "seed" forms would give active forms with the approach of the conditions most suitable for each species. Thus, for warm water organisms, the main (evidently not the only) factor would be the increase of temperature. In this connection, it is well to remember that there exists what I call "ecological inertia" which delays the development of a population even after the onset of favorable conditions and the disappearance of a population after conditions become unfavorable.

Let us apply what is stated above to the situation at La Jolla during the past year. The theory of the appearance of the warm water population by reproduction (excystment and growth) *in situ* of a seed population requires a very noticeable and protracted increase of temperature, which had not happened. The water temperature at the surface at La Jolla was about 19-20°C. in September. In October it oscillated between 17.5°-18°. In November it was between 16-17°C. and by then the impoverishment of the warm water plankton was plainly noticeable, *i.e., Ceratium vultur, C. ranipes, C. carriense, C. karsteni, C. horridum molle* and the species of the falcatum group were not found in this month. It was the same for some of the most conspicuous warm water tintinnidae. But in December, with the temperature *still decreasing,* all these species plus some others such as *C. hexacanthum,* appeared again and were found consistently from the middle of December to March.

All this supports the conclusion that the populations observed at La Jolla did not arise locally but were transported from a center of subtropical or even tropical water. Whether this center was situated to the south or to the west of La Jolla, we cannot tell.

We tried to get some supplementary information from the samples of the April 1958 cruise (CCOFI Cruise 5804). From the distribution charts we cannot make any clear distinction between a possible southerly or westerly origin of the plankton. However, the distribution of *C. lunula, C. trichoceros* and *Spiraulaux jollifei,* species also found at that time in La Jolla, seems to give some support to a possible west northwest origin. It seems that these species were pushed against the southern coast and then, caught by a current from the south, carried northward, along with forms coming from the south. This explanation seems to fit especially such species as *C. lunula, C. hexacanthum, C. platycorne,* that prefer oceanic oligotropic waters, as shown by distribution data (Steemann Nielsen, Graham and Bronikowsky, and Peters).

The same mechanism, *i.e.,* transportation to the north, may account for the presence of several warm water species near Cape Mendocino, notwithstanding the low temperature of that region. When these species were found in cold waters, they were never far removed from currents having temperatures of at least 16° C.

All these species found near Cape Mendocino are tolerant. By this is meant that under unfavorable conditions, they are able to maintain at least an impoverished population. The species found near Cape Mendocino seem unable to maintain a population if the temperature is below 15°C. These data are derived from the collection studied all over the world. As pointed out by both Dr. Haxo and Dr. Johnson, we have very few data from laboratory experiments. All attempts to cultivate these warm water species have failed as far as I know.

Unfortunately quantitative data on the plankton distribution are not available. However, populations were designated as consisting of warm water plankton only if *many* warm water species were present. The somewhat simplified presentation in the graphs and charts of distribution do not bring forth the full weight of the evidence. For instance, in most of the samples taken at La Jolla in December through February, no less than 25 very definite warm water species were recorded including very intolerant forms such as *Ceratocorys horrida.* Dr. Haxo pointed out the interesting information derived from the distribution of this species.

LITERATURE CITED

Allen, W. E., 1936. Occurrence of marine plankton diatoms in a ten-year series of daily catches in Southern California, *Amer. Jour. Bot.* Vol. 23, pp. 60-63.

________ 1941. Twenty years' Statistical Studies of Marine Plankton Dinoflagellates of Southern California. *The American Midland Nat.* Vol. 26 (3), pp. 603-635.

________ 1945. Vertical distribution of marine plankton diatoms offshore in Southern California in 1940. *Bull. of the Scripps Inst. of Ocean.* Vol. 5 (4), pp. 335-370.

Cleve, P. T., 1900. The seasonal distribution of Atlantic planktonic organisms. *Göteborgs kungl. Vetensk. och Vitt. Handl.* Ser. IV, Vol. 3, pp. 1-368.

Cupp, E. E., 1943. Marine plankton diatoms of the west coast of North America. *Bull. of the Scripps Inst. of Ocean.* Vol. 5 (1) pp. 1-238.

Gaarder, K. R., 1954. Dinoflagellate from the "Michael Sars" North Atlantic Deep-Sea Exp. 1910. *Rep. on the Scient. Results of the M. Sars North Atl. Deep-Sea Exp. 1910.* Vol. II (3).

Graham, H. W., 1941. Plankton production in relation to character of water in the open Pacific. *Jour. Mar. Res.* IV (3), p. 189-197.

________ 1942. Studies in the morphology, taxonomy, and ecology of the Peridiniales. *Publ. Carnegie Inst. Wash.* pp. 1-129.

________, and N. Bronikowsky, 1944. The genus *Ceratium* in the Pacific and North Atlantic Oceans. *Publ. Carnegie Inst. Wash.* pp. 1-209.

Hardy, A. C., and E. R. Gunther, 1935. The Plankton of the South Georgia whaling grounds and adjacent waters, 1926-1927. *Discovery Reports* Vol. XXI (1), pp. 147-291.

Jörgensen, E., 1920. Mediterranean Ceratia. *Rep. on the Danish Ocean. Exp. 1908-1910.* Vol. II, N 6, J.1. pp. 1-110.

Käsler, R., 1938. Die Verbreitung der Dinophysiales im Südatlantischen Ozean. *Wiss. Ergebn. Deut. Atlant. Exped. Meteor, 1925-1927.* Vol. XII (2) pp. 165-237.

Kofoid, C. A. Dinoflagellata of the San Diego region—Description of new species. *Univ. Calif. Publ. Zool.* Vol. 3, pp. 299-340.

________, 1910. The faunal relations of the Dinoflagellata of the San Diego region. *Proc. 7th Intern. Zool. Cong., Boston,* pp. 922-927.

________, 1911. Dinoflagellata of the San Diego region—The genus *Gonyaulax. Univ. Calif. Publ. Zool.,* Vol. 8, pp. 187-300.

________, 1911. Idem—On Spiraulax, a new genus of Peridiniales. *Ebenda,* Vol. 8, pp. 295-300.

Peters, N., 1934. Die Bevölkerung des Südatlantischen Ozeans mith Ceratien. *Wiss. Ergebn. Deut. Atlant. Exp. Meteor,* 1925-1927, Vol. XII. pp. 1-69.

Sargent, M. C., and T. J. Walker, 1948. Diatom populations associated with eddies off Southern California in 1941. *J. Mar. Res.,* Vol. VII (3), pp. 490-505.

Steemann Nielsen, E., 1934. Untersuchungen über die Verbreitung, Biologie und Variation der Ceratien im Südlichen Stillen Ozean. *Dana Report No. 4,* pp. 1-67.

Sverdrup, H. U., and W. E. Allen, 1939. Distribution of diatoms in relation to the character of water masses and currents off Southern California in 1938. *J. Mar. Res.,* II, pp. 131-144.

UNUSUAL FEATURES IN THE DISTRIBUTION OF PELAGIC TUNICATES IN 1957 AND 1958[1]

LEO D. BERNER

Of the zooplankton animals I have studied, two species of the pelagic tunicate group, *Dolioletta gegenbauri* and *Doliolum denticulatum*, are interesting and pertinent to the subject of this meeting. It appears to me that a discussion of only two species rather than a broad group may be a better approach to our problem.

These two species have served as good indicators of cool (California Current or sub-Arctic water) and warm waters (central or sub-tropical water). During several cruises, especially in 1949 and 1950 they were found at adjacent stations but very seldom at the same station.

Both species live almost exclusively in the upper 100 meters of the water column, with their major populations in the upper 50 meters. This is important because, with a vertical distribution such as this, they can be used to interpret happenings in the surface layers where temperature and salinity relationships are confused by annual variations and local modifications.

I have summarized the distributional data for the two species during March, June and September 1949-1952 in figures 118 and 119. These are based on the collections of the oblique meter-net hauls used in the regular fish egg and larvae surveys of the California Cooperative Oceanic Fishery Investigations.

The hauls sampled the upper 70 meter stratum in 1949 and 1950 and the upper 140 meter stratum in subsequent years.*

These figures indicate the percent of successful hauls for the species at any one station and are intended only to give a general idea of where the two animals live. Seasonal changes in distribution have not been taken into account and the shading represents only percentage occurrence, regardless of numbers taken in the hauls. In many cases the distributions of numbers would be quite similar. The percentages south of line 130 (Fig. 1), which extends seaward from Pt. Asuncion, Baja California, are based on only one or two net hauls. To the north most percentages are based on five or more hauls, many on ten or eleven. Although more cruises are included figure 136 gives a good idea of the intensity of sampling over the region.

Figure 118 shows the distribution of the cool water species of the pair, *Dolioletta gegenbauri*, along our coast. It may be seen that its distribution extends rather far south, especially near the coast. In the period since October 1950, when the fishing depth of

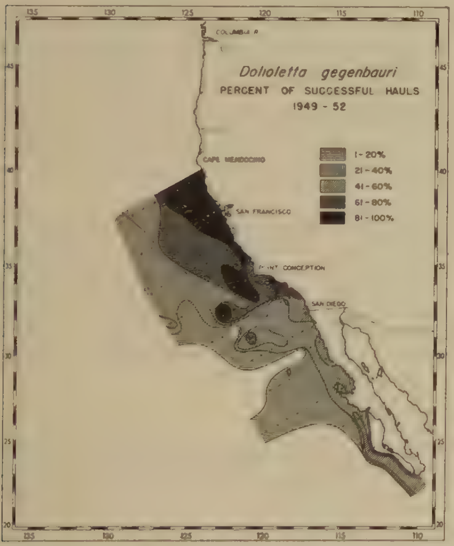
135
130
125
120
115
110
45
40
35
30
25
20
COLUMBIA R
Dolioletta gegenbauri
PERCENT OF SUCCESSFUL HAULS
1949 - 52
1-20%
21-40%
41-60%
61-80%
81-100%
CAPE MENDOCINO
SAN FRANCISCO
POINT CONCEPTION
SAN DIEGO

FIGURE 118. *Per cent of successful hauls for Dolioletta gegenbauri during March, June and September, 1949-1952.*

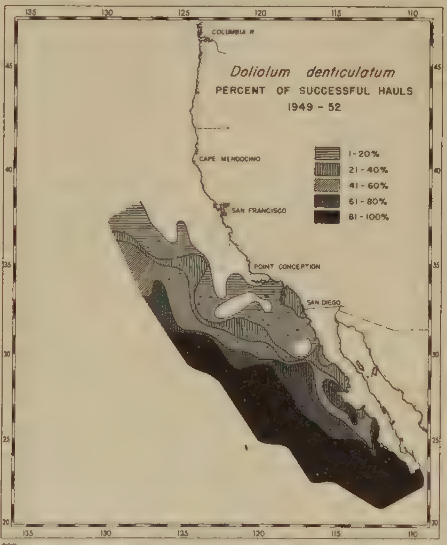
135
130
125
120
115
110
45
40
35
30
25
20
COLUMBIA R
Doliolum denticulatum
PERCENT OF SUCCESSFUL HAULS
1949 - 52
1-20%
21-40%
41-60%
61-80%
81-100%
CAPE MENDOCINO
SAN FRANCISCO
POINT CONCEPTION
SAN DIEGO

FIGURE 119. *Per cent of successful hauls for Doliolum denticulatum during March, June and September, 1949-1952.*

---

[1] Contribution from the Scripps Institution of Oceanography.

* For a description of the nets and method of hauling see Ahlstrom, E. H., 1954.

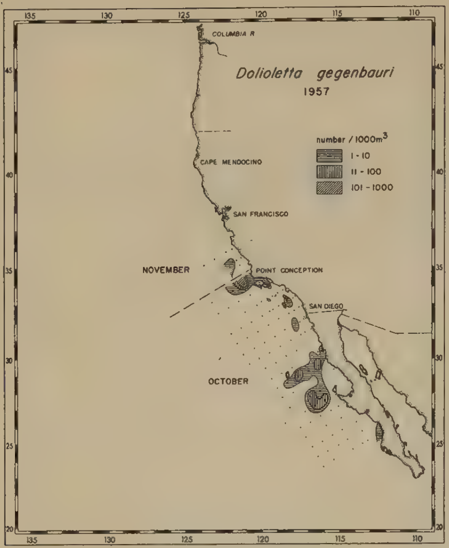
135
130
125
120
115
110
45
40
35
30
25
20
COLUMBIA R
Doliolетta gegenbauri
1957
number / 1000m³
1 - 10
11 - 100
101 - 1000
CAPE MENDOCINO
SAN FRANCISCO
NOVEMBER
POINT CONCEPTION
SAN DIEGO
OCTOBER

FIGURE 120. Distribution of *Doliolетta gegenbauri* during October 4 to November 8, 1957 (CCOFI Cruise 5710).

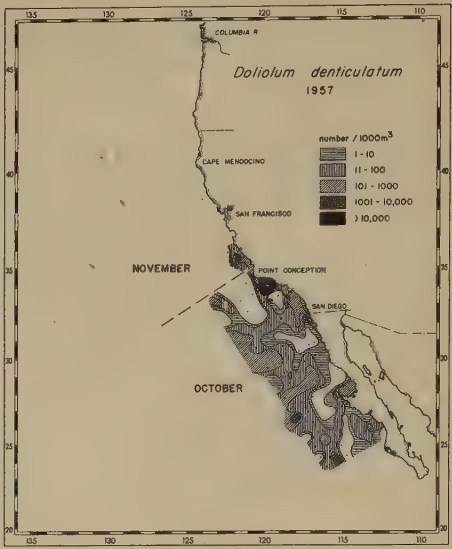
135
130
125
120
115
110
45
40
35
30
25
20
COLUMBIA R
Doliolum denticulatum
1957
number / 1000m³
1 - 10
11 - 100
101 - 1000
1001 - 10,000
> 10,000
CAPE MENDOCINO
SAN FRANCISCO
NOVEMBER
POINT CONCEPTION
SAN DIEGO
OCTOBER

FIGURE 121. Distribution of *Doliolum denticulatum* during October 4 to November 8, 1957 (CCOFI Cruise 5710).

our net hauls was deepened from 70 to 140 meters, this has been a rather typical distribution.

The distribution of the other species, *Doliolum denticulatum,* is shown in figure 119. It may be seen that this species is the warm water analogue of *D. gegenbauri.* During the period 1949-1952, *D. denticulatum* did not occur near shore to the north of the Santa Barbara group of Channel Islands and only rarely north of San Diego.

In October 1957, *D. gegenbauri* appears spottily over the survey area with a rather large group east and south of Guadalupe Island. This might be called a more or less "typical" distribution (Fig. 120). An examination of the distribution of *D. denticulatum* (Fig. 121) however shows a rather marked difference from the "typical" distribution (Fig. 119). It occurred nearshore and north as far as the sampling extended, line 80 off Pt. Conception. In addition to mere occurrence, the maximum numbers were found in the nearshore area around and north of the Santa Barbara group of Channel Islands. The October cruise unfortunately did not sample north of Pt. Conception so I have taken the liberty of superimposing some stations from the November cruise to the north. The fit between the two is rather good at line 80 (Fig. 121). Before leaving the discussion of these two charts it may be of some interest to point out that *D. denticulatum* is missing from several of the stations where *D. gegenbaura* occurred far to the south.

The distributions of these two species during April 1958 again are unusual. *D. denticulatum* is found north almost to Monterey in the nearshore area (Fig. 122). A population center is found in the Santa Monica Bay area where usually at this time of year the species is not found. The offshore distribution is not considered unusual for this time of year. *D. gegenbauri* during April 1958 shows a very patchy distribution, which, to a lesser extent, is seen early in other years (Fig. 123). Samples that have been examined subsequent to the time this chart was prepared indicate the species was also found in patches toward the south.

It is my opinion, on the basis of the biological data, that during 1957, sometime after July, the flow of the California Current for some reason was reduced. During this time upwelling must have also been reduced. At the same time these two processes supplying cool water to the area were reduced, a nearshore countercurrent, as indicated by the distribution of *D. denticulatum,* developed carrying warm water and its contained populations to the north.

DISCUSSION

Isaacs: As a general rule *D. denticulatum* is never in the area north of Pt. Conception near shore. However, it does occur offshore as shown in the October 1957 chart.

Berner: In October 1957 the offshore distribution may have been somewhat closer to shore but was not markedly unusual. The nearshore extension to the north was unusual however. It extended even further in April 1958 while the offshore distribution remained quite "normal." In the same period there were unusually low numbers of *D. gegenbauri* in the area north of Pt. Conception; so it is my feeling that during the latter part of 1957 and early 1958 there was a definite transport northward of *denticulatum* near shore. The individuals were large well-preserved specimens.

Isaacs: Is that not a short period of time for them to grow large?

Berner: We do not know much about growth rates, possibly they could grow this large in a short time. Another interesting thing about these animals is that there are two forms that are readily identifiable. There are animals produced from eggs but which in turn do not produce more animals from eggs. The sexual form and asexual form are usually found together. The egg producing or sexual form of *denticulatum* did not appear in the area. It is my feeling these animals may not have been reproducing. There is another point of interest; at the outer end of line 133 (Fig. 121) a tropical salp, which had not previously occurred in the survey area, was found during the October 1957 cruise.

Marr: Is it an unusual occurrence, having that tropical salp at line 133 in October 1957?

Berner: This is a hard thing to answer. I did not find the species in the NORPAC samples. It has been reported extensively in the POFI material south of Hawaii. From what little can be learned from the literature I would regard it as a warm water form.

Wooster: Are there any specimens in the Shellback Expedition material?

Reid: Is this the first time it has been found north of 20°?

Berner: Yes to Wooster, and yes, as far as I know, to Reid.

Isaacs: Did you look at the samples from those few stations off Mendocino?

Berner: Yes, I did. They look much like those off Monterey—there are no warm water salps or doliolids in them.

Isaacs: It appeared from Balech's data, given by Haxo, that there might have been some remnant of the southern population.

Berner: The animals found north of Pt. Conception looked healthy. One learns to tell when they do not look healthy—the muscle bands are broken down, etc. Some of the cool water forms taken far south were not well preserved while other organisms in the sample were. Another thing I should point out, though not well versed on it, is the distribution of the pelagic crab *Pleuroncodes*. Carl Boyd, who is studying these animals in our laboratory finds that the larvae do not normally occur north of San Diego, certainly not as far north as Pt. Conception. During April 1958, however, they occurred near shore as far north as Monterey.

LITERATURE CITED

Ahlstrom, E. H., 1954, Pacific Sardine (Pilchard), eggs and larvae and other fish larvae, Pacific Coast—1952. *U.S. Fish and Wildlife, SSR Fisheries No. 123*, pp. 5.

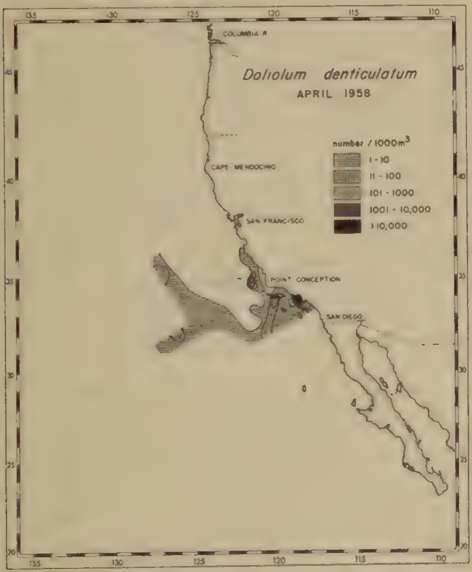
135
130
125
120
115
110
45
40
35
30
25
20
COLUMBIA R
Doliolum denticulatum
APRIL 1958
number / 1000m³
1 - 10
11 - 100
101 - 1000
1001 - 10,000
>10,000
CAPE MENDOCINO
SAN FRANCISCO
POINT CONCEPTION
SAN DIEGO

FIGURE 122. Distribution of *Doliolum denticulatum* during March 29 to April 28, 1958 (CCOFI Cruise 5804).

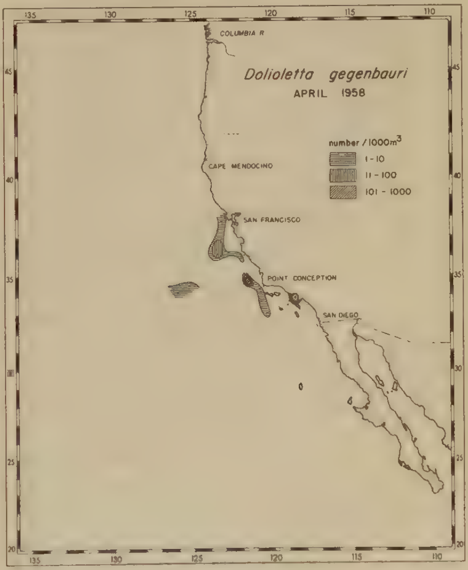
135
130
125
120
115
110
45
40
35
30
25
20
COLUMBIA R
Dolioletta gegenbauri
APRIL 1958
number / 1000m³
1 - 10
11 - 100
101 - 1000
CAPE MENDOCINO
SAN FRANCISCO
POINT CONCEPTION
SAN DIEGO

FIGURE 123. Distribution of *Dolioletta gegenbauri* during March 29 to April 28, 1958 (CCOFI Cruise 5804).

CHANGES IN THE DISTRIBUTION OF EUPHAUSIID CRUSTACEANS IN THE REGION OF THE CALIFORNIA CURRENT[1]

EDWARD BRINTON

Euphausiids are large zooplankton organisms of shrimp-like appearance that make up a high crustacean Order, the Euphausiacea. All species are marine and pelagic; most are oceanic in distribution and appear to have little dependence upon coastal regions. Some euphausiids, for example *Nyctiphanes* and *Meganyctiphanes*, are frequently most abundant in coastal regions, but it is not yet known whether it is essential for any species or assemblage of species to have access to neritic or coastal waters during its life history,—except as such coastal conditions as upwelling may influence the temperature and fertility of the local pelagic environment.

There are approximately 85 euphausiid species distributed over the oceans. Some Pacific species have very wide ranges: fifteen have cosmopolitan ranges from 40°N to 40°S, and six equatorial and twelve antitropical species occupy east-west oceanwide belts in the tropics and mid-latitudes respectively. Twenty-five of these species are numerically important in the California Cooperative Oceanic Fishery Investigation survey area, and an additional eight are occasional indicators of intruding environments. Eight deep-living cosmopolitan species are sometimes sampled by tows reaching deeper than the standard oblique tow from 0-140 meters.

To use a word that is commonly applied to parameters that are the antithesis of biological activity, the euphausiids might be called *conservative* organisms. They are long lived compared to the majority of plankton forms. It is believed that many species live on the order of a year. Some, notably *Euphausia superba* and *Thysanopoda acutifrons* live two to three years (Bargmann, 1945; Einarsson, 1955), but a year may be a reasonable approximation for the euphausiid life span in temperate waters. Species that live in extreme northern or southern regions, where the seasonal effect upon the waters is conspicuous, may be analyzed in respect to their growth rates and life spans. Warm water species, the populations of which may include breeding individuals and larvae at all times, are more difficult to study from the standpoint of the ages of populations sampled by plankton collections.

Euphausiids are deep-living animals relative to the other major components of the zooplankton in the upper layers of the ocean. Many species perform extraordinary diurnal vertical migrations, rising near the surface of the sea at night and descending to depths of 500 to 700 meters during daylight hours. Thus within a 24 hour period, a migrating population may pass through a range of temperature of as much as 16°C.

If one looks at the distributions of euphausiids on a wide geographical scale, it is evident that many species' boundaries can be compared with environmental factors measured by standard oceanographic sampling techniques. Correlations, particularly with temperature and oxygen, appear to be part of the ecological definition of some of the species distributions (Reid, Roden, and Wyllie, 1958). An environmental factor may act at a particular depth to govern or limit the distribution of a vertically migrating species. A temperature-depth value may limit an essential metabolic activity, such as digestion of food at depth or ability to feed at the surface at night as Moore (1952) has suggested. Enough is not yet known about euphausiid distribution to specify limiting factors.

A summary of the typical patterns of distribution found in the Pacific can provide a framework in which to consider the incursion or the occurrence of euphausiids in more local areas such as the CCOFI survey area. These have been derived from collections made during oceanic expeditions carried out by the Scripps Institution, 1949-56 and are described by Brinton (1957). They are essential to a consideration of the California Current as a region of faunal convergence. Northern (subarctic) species are not consistently carried far to the south in the cool current, but appear sporadically along the coasts of California and Baja California. Offshore (central) forms sometimes are found near shore. *Nyctiphanes simplex* and *Thysanoessa spinifera* are adapted to the shoreward part of the California Current, extending variable distances to the north and south, and may be carried to the west in tongues of distribution. (*Nyctiphanes* is the shallowest living local euphausiid, living above 100 meters at night but descending to near that depth in the daytime). Species adapted to an oceanographic transition zone (Sverdrup, Johnson and Fleming, 1942) are the dominant euphausiids in the California Current, while equatorial species are present off Baja California.

Oceanic species distributions have areas of occurrence that approximate the positions of major temperature-salinity water masses. Certain of the factors that operate to maintain species in an area (current systems, intensity of incident radiation) are the same influences that give integrity to large masses of water.

SUBARCTIC DISTRIBUTIONS

Thysanoessa longpipes and *Tessarabrachion oculatus* occur north of about 42°N in the mid-Pacific and sometimes penetrate southward to the latitude of San Francisco (37-38°N) in the California Current. *Euphausia pacifica* has a distribution in the mid-oceanic area which extends south of the two previous species,

---

[1] Contribution from Scripps Institution of Oceanography.

Reproduced by Permission

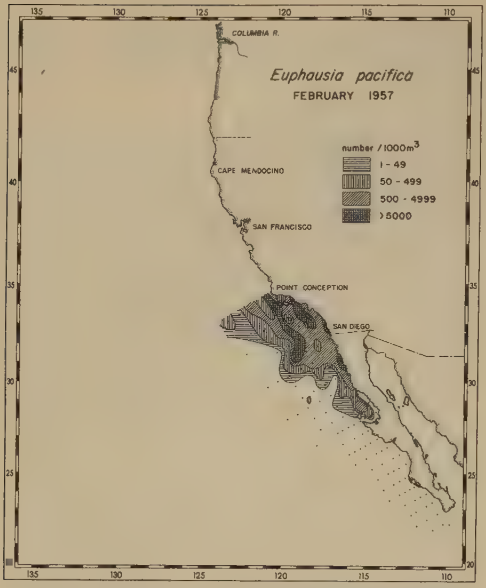
135
130
125
120
115
110
COLUMBIA R.
Euphausia pacifica
FEBRUARY 1957
number / 1000m³
1 - 49
50 - 499
500 - 4999
>5000
CAPE MENDOCINO
SAN FRANCISCO
POINT CONCEPTION
SAN DIEGO
45
40
35
30
25
20

FIGURE 124. Distribution and abundance of the euphausiid *Euphausia pacifica* during February 6 to 20, 1957 (CCOFI Cruise 5702).

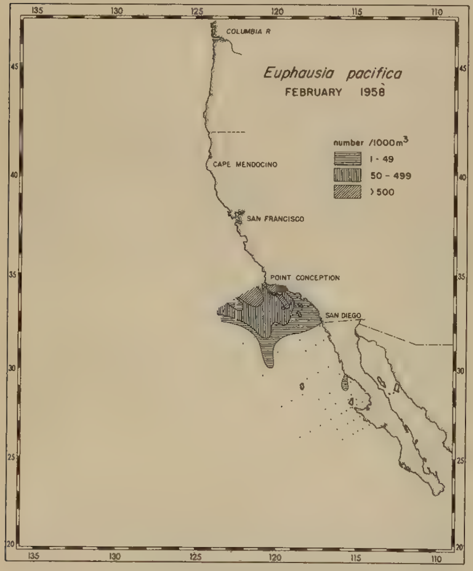
135
130
125
120
115
110
COLUMBIA R
Euphausia pacifica
FEBRUARY 1958
number /1000m³
1 - 49
50 - 499
>500
CAPE MENDOCINO
SAN FRANCISCO
POINT CONCEPTION
SAN DIEGO
45
40
35
30
25
20

FIGURE 125. Distribution and abundance of *Euphausia pacifica* during February 6 to 24, 1958 (CCOFI Cruise 5802).

to near 40°N. It ranges southward in the California Current, terminating off Southern California or Baja California (Figs. 124, 125, 126). *E. pacifica* is frequently abundant, and its distribution may be used as a measure of the southward extension of the cold-water fauna.

TRANSITION ZONE DISTRIBUTIONS

Nematoscelis difficilis and *Thysanoessa gregaria* are present along the boundary between the subarctic and central regions, overlapping both. In the California Current region their distributions bend southward toward equatorial waters. They are dominent off Central California. If plankton sampling were limited to the CCOFI area, these species would be present at nearly all stations, suggesting a wide range. Actually they are present in a narrow (35-44°N) east-west oceanic belt with a southward extension in that part of the California Current which contains semi-permament eddies of Southern California and mid-Baja California.

CENTRAL DISTRIBUTIONS

Euphausia brevis and *E. hemigibba* represent an assemblage that is dominant south of 40°N and north of about 20°S. extending eastward to the offshore waters of central and southern California and Baja California. In these latter waters their presence is regarded as an indication of encroachment of the offshore "central" environment upon the coastal waters (Figs. 127, 128, 129). In order to consider assemblages one must lump together those species that have similar zoogeographical affinities, even though no two species have exactly the same range.

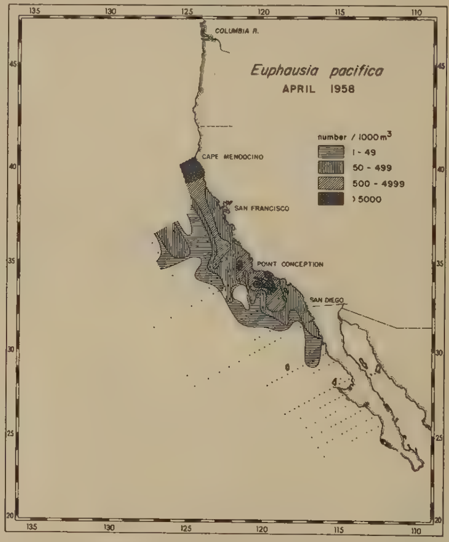
135
130
125
120
115
110
COLUMBIA R.
Euphausia pacifica
APRIL 1958
number / 1000m³
1 - 49
50 - 499
500 - 4999
>5000
CAPE MENDOCINO
SAN FRANCISCO
POINT CONCEPTION
SAN DIEGO
45
40
35
30
25
20

FIGURE 126. Distribution and abundance of *Euphausia pacifica* during March 30 to April 27, 1958 (CCOFI Cruise 5804).

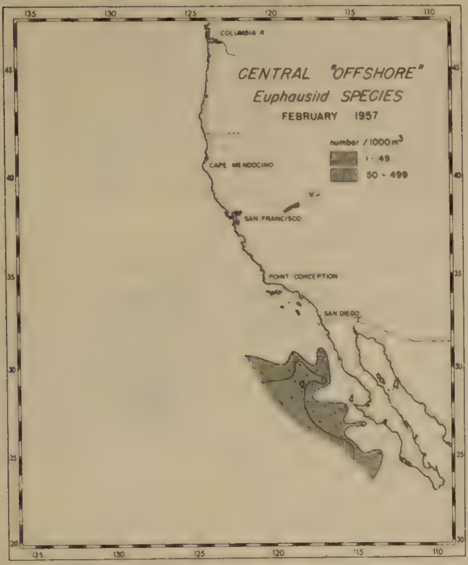
CENTRAL "OFFSHORE"
Euphausiid SPECIES
FEBRUARY 1957
number / 1000 m³
1 - 49
50 - 499
COLUMBIA R
CAPE MENDOCINO
SAN FRANCISCO
POINT CONCEPTION
SAN DIEGO
135
130
125
120
115
110
45
40
35
30
25
20

FIGURE 127. Distribution and abundance of central offshore euphausiid species during February 6 to 20, 1957 (CCOFI Cruise 5702).

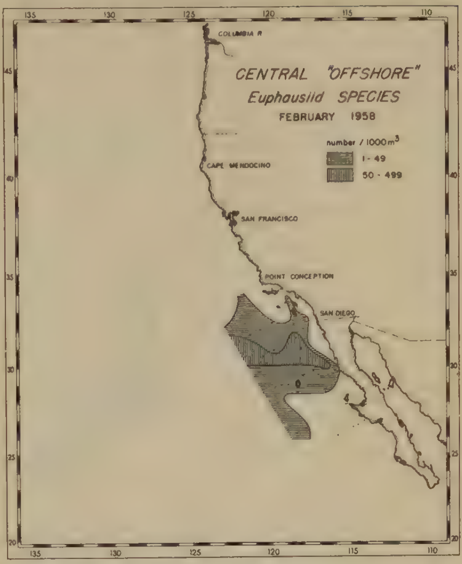
CENTRAL "OFFSHORE"
Euphausiid SPECIES
FEBRUARY 1958
number / 1000 m³
1 - 49
50 - 499
COLUMBIA R
CAPE MENDOCINO
SAN FRANCISCO
POINT CONCEPTION
SAN DIEGO
135
130
125
120
115
110
45
40
35
30
25
20

FIGURE 128. Distribution and abundance of central offshore euphausiid species during February 6 to 24, 1958 (CCOFI Cruise 5802).

EQUATORIAL DISTRIBUTIONS

Euphausia eximia (Figs. 130, 131) is a species which is confined to the Eastern Equatorial Pacific. It has a more restricted type of equatorial distribution than *E. diomediae*, which extends all the way across the Pacific between approximately 20°N and 20°S. *E. eximia* is most numerous in two regions: 1) where California Current waters merge with the equatorial current system, and 2) where the Peru Current contributes to the fertility of an environment near the beginning of the South Equatorial Current. The distribution boundaries of equatorial species undergo changes in their terminal region off Southern California and Baja California. The equatorial assemblage is dominant south of 20-23°N.

We have reason to think that *E. eximia* is deeper than, for example, *Euphausia pacifica* and *Nyctiphanes*. *E. eximia's* vertical distribution indicates that it migrates to a depth of about 300-700 meters in the daytime; adults approach the surface at night, but have not been found at the surface. Off Southern California *Nyctiphanes* migrates within the 0-150 meter layer.

Compared to *E. eximia*, *E. distinguenda* is an eastern equatorial species that is consistently present only south of the latitude of Cape San Lucas (23°N). When it occurs in the California Current off Baja California it is rarely numerous but may indicate northward transport of water. However, in late 1957 *E. distinguenda* was more numerous off Baja California south of Pta. Eugenia than at any previous

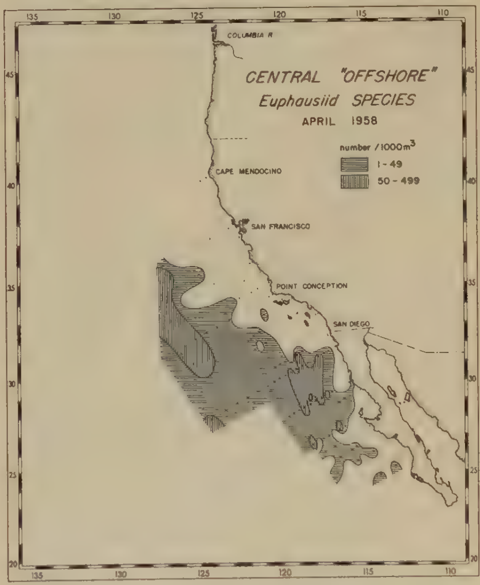
CENTRAL "OFFSHORE"
Euphausiid SPECIES
APRIL 1958
number / 1000 m³
1 - 49
50 - 499
COLUMBIA R
CAPE MENDOCINO
SAN FRANCISCO
POINT CONCEPTION
SAN DIEGO
135
130
125
120
115
110
45
40
35
30
25
20

FIGURE 129. Distribution and abundance of central offshore euphausiid species during March 30 to April 27, 1958 (CCOFI Cruise 5804).

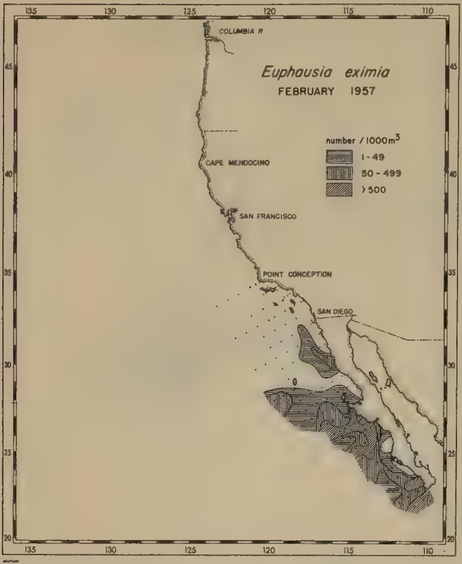

FIGURE 130. Distribution and abundance of the euphausiid *Euphausia eximia* during February 6 to 20, 1957 (CCOFI Cruise 5702).

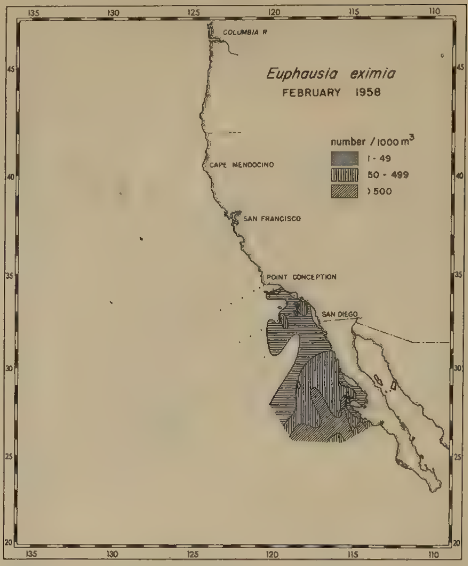

FIGURE 131. Distribution and abundance of *Euphausia eximia* during February 6 to 24, 1958 (CCOFI Cruise 5802).

time, 1949-1956. The population contained many developmental stages, suggesting that an equatorial environment had developed to the north enabling individuals to reproduce there. In addition to being carried north from its eastern equatorial habitat, this species was found to have been carried as far west as 175°W in the latitude of the North Equatorial Current (Equapac Expedition, Sept. 1956). This is one of the dominant species in the Gulf of California; populations live and develop there. But the occurrence of *E. distinguenda* in the waters west of Baja California is exceptional.

The standard oblique plankton tow made in the course of CCOFI sampling is to a depth of 140 meters, using a net one meter in mouth diameter, of 0.6-0.7 mm mesh width. Most euphausiids counted are immature. Tows made below 140 meters indicate that there the adults are dominant, particularly during the daytime. Thus the counts for the CCOFI data are weighted toward small specimens.

If the tows upon which the distributions are based had been made to a depth of 300 meters (as were the tows made by POFI and the Scripps Expedition) some differences in species boundaries would be expected, but differences would be in details. For instance, during the 1953 Transpac Expedition tows were made to at least two different depths at each station. In some cases the 0-700 and 0-1,000 meter strata were sampled. A change in the southern boundary of northern cold-water species was found at only a few stations by deepening the stratum sampled. A good measure of the importance of stratum thickness was derived from sampling done during the Scripps Institution's 1939 cruise off the coast of California, where the series of station lines was similar to the present CCOFI pattern. Changes in apparent distribution brought about by deepening the stratum sampled from 0-70 meters to 0-140 meters or to 0-180 meters were few, qualitatively. The three depths were sampled on the 1939 cruise. If the species was present in—or was absent in—the shoaler tow, the chances that a different record would be shown by the deeper tow were about two or three in fifty. Multiple tows were also made on NORPAC cruise, 1955. The deepest (0-700 meter) tow was not made at every station, but considered on the basis of tows through 0-140 meters and 0-280 meters, species' distribution boundaries were rarely altered by taking the deeper sample into consideration.

Some species (e.g. *Thysanoessa gregaria*) descend to a limited extent as warm waters are approached. There are also warm water mesopelagic species (e.g. *Nematobrachion boopis)*, which ascend as their cool-water distribution boundaries are approached. These are local phenomena and do not greatly alter the broad scale distributions derived from 0-140 or 0-280 meter sampling.

Animals that do not have unlimited depth tolerance might be restricted horizontally by superficial isotherms.

Certain isotherm lines nearly coincide with species distribution boundaries indicating that there are physical properties that have the same type of distribution. For example the 12°C. isotherm at 100 meters

(512)

bounds the southern limit of *Euphausia pacifica*. Certain species relate best to surface or shallow temperatures. Others relate to deeper isotherms, and inasmuch as the vertical ranges of most species are considerable, it is not easy to say how the isotherms could be limiting for each species.

It may be useful, before considering 1957-58 changes, to review the three main zoogeographic features of the coast of California and Baja California—features that may fluctuate from season to season or year to year.

SOUTHWARD EXTENSION OF THE SUBARCTIC AND TRANSITION ZONE DISTRIBUTIONS

Cold water species were consistently present in large numbers off Central California and in small numbers off Punta Eugenia, Baja California, in the years of the CCOFI program 1949-1954. Populations of these species changed quantitatively off Punta Eugenia in 1954-55. *Euphausia pacifica* and *Thysanoessa spinifera* became numerous and widespread in this region in April of 1954, and 1955, related to cooled waters there and an extensive eddy west of mid-Baja California, near the southern limits of the ranges of the species. In April-June of the years 1949-1952 the cold-water populations in this southern region were inconspicuous.

EASTWARD INCURSION OF OFFSHORE "CENTRAL" SPECIES INTO THE COASTAL AREA

This group has a distribution complementary to that shown by the westward tending tongues of cold-water. The central euphausiids may appear close to shore, usually off northern Baja California and Southern California, apparently in relation to the cyclonic circulation there. They are carried eastward as they are caught up in the southern half of this gyre, and sometimes enter the coastal region of Viscaino Bay, overlapping the western boundaries of the cold-water animals.

NORTHWARD EXTENSIONS OF EQUATORIAL DISTRIBUTIONS IN THE COASTAL REGION

Euphausia exima has been consistently abundant off mid-Baja California, 1949-1955. Other species with equatorial affinities *(Euphausia distinguenda, E. tenera, E. diomediae)* sometimes have been present in small numbers south of 27° north; there have been very few records from waters north of Viscaino Bay (28° N).

1957-1958 OBSERVATIONS

February and October, 1957, cruises and February and April, 1958 cruises have been examined for euphausiids. The distribution of *Euphausia pacifica* in February 1957 (Fig. 124) was normal for that month both qualitatively and quantitatively. In contrast, February 1958 (Fig. 125) found this species distribution extremely retracted from the southern part of the coastal area. This is normal for October-December, but not for February. By December *E. pacifica* has usually (1949-55) withdrawn northward to near the latitude of San Diego (33° N).

During April *E. pacifica* was characteristically (1949-55) present in the oceanic area from Guadalupe Island to Pta. Eugenia, sometimes occurring even farther to the south. In contrast, in April 1958 (Fig. 126) this species was sparse in this region and its distribution off Southern California was more inshore than had been previously found for this month of the year. Nevertheless, it must be noted that this cold-water species was *still present* in substantial numbers off Southern California in 1958.

E. pacifica probably lives somewhat deeper than the next species, *Nyctiphanes simplex*, which in 1949-57 occupied the coastal region, usually south of Point Conception. In February 1957 (Fig. 132) *Nyctiphanes* was present in low concentration south of the Point. This was like previous years. In October 1957 all developmental stages of this species were more numerous than usual at the northern limit of its range in the region of the Southern California Channel Islands. I interpret this as meaning that the environment in the upper water layers off Southern California was modified in late 1957, permitting *N. simplex* to reproduce in a relatively northern area. It has subsequently (Figs. 133, 134) reproduced heavily in the areas immediately south and just north of Point Conception, where it had heretofore been rare or absent in April. The April 1958 cruise (Fig. 134) shows that *Nyctiphanes* occurred all the way to Cape Mendocino (40°N) though in very small numbers; but off San Francisco (38°N) concentrations were greater than 50 per 1,000 cubic meters at two stations. I do not think we can regard this northward distribution as necessarily a manifestation of a persistent countercurrent. Drogue measurements made in March showed that the countercurrent was not present at the surface at that time. The large populations of *Nyctiphanes* that were off Northern California in April 1958 must have been residual there, if continuing transport from the south had not been maintained through the winter. These southern animals have, during this 1957-1958 period of change, extended far north of their ''normal'' range.

The offshore occurrence of warm water animals of the central type seems to have undergone little change in the critical region off California. This is the region off San Diego and south of Point Conception. The warm water animals are few here, and while their encroachment toward the east is somewhat greater in February and April 1958 (Figs. 128, 129) than in February 1957 (Fig. 127) or February 1949-55, interpretation in terms of water movements must be speculative. This warm water environment has moved northward and toward shore, but the area *dominated* by the central species is still far offshore.

Another species, *Euphausia eximia* (Fig. 130) is an equatorial type, which occurs in the southern part of the CCOFI survey region and was present north of its usual range, close to shore in 1957-58. It was more numerous to the north, off Southern California in February 1958 (Fig. 131) than during 1949-55. This might be regarded as another indication of the northerly extension of the warm-water environment provided by the current system that distributes the animals.

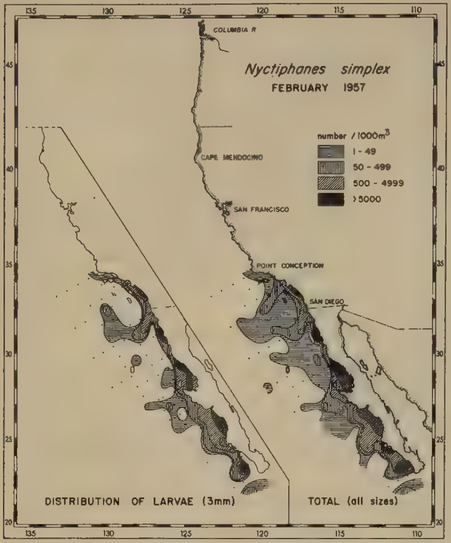
135
130
125
120
115
110
COLUMBIA R
Nyctiphanes simplex
FEBRUARY 1957
number / 1000m³
1 - 49
50 - 499
500 - 4999
>5000
CAPE MENDOCINO
SAN FRANCISCO
POINT CONCEPTION
SAN DIEGO
45
40
35
30
25
20
DISTRIBUTION OF LARVAE (3mm)
TOTAL (all sizes)

FIGURE 132. Distribution and abundance of the euphausiid *Nyctiphanes simplex* during February 6 to 20, 1957 (CCOFI Cruise 5702).

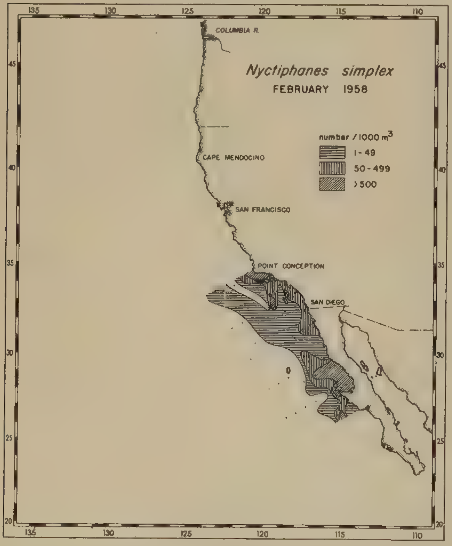
135
130
125
120
115
110
COLUMBIA R
Nyctiphanes simplex
FEBRUARY 1958
number / 1000 m³
1 - 49
50 - 499
>500
CAPE MENDOCINO
SAN FRANCISCO
POINT CONCEPTION
SAN DIEGO
45
40
35
30
25
20

FIGURE 133. Distribution and abundance of *Nyctiphanes simplex* during February 6 to 24, 1958 (CCOFI Cruise 5802).

DISCUSSION

Revelle: Does *E. eximia* occur in the same area where you have *Nyctiphanes simplex?*

Brinton: No, *E. eximia* is in a slightly more offshore region and behaves differently from *Nyctiphanes* because it is a deeper living animal. If there were a very shallow northerly current, you might expect *Nyctiphanes simplex* to be transported farthest, because it would be in the surface layer more continuously than *E. eximia,* which rises into the superficial layers only at night.

Isaacs: Was *E. eximia* found north of Point Conception in April 1958?

Brinton: Yes, it was present at one station off Monterey Bay, and at two other stations north of Point Conception. *E. eximia* had never been previously found north of Point Conception.

Fleming: Practically all your figures show that euphausiids are mostly concentrated near the coast —an example of the Fuglister principle?

Brinton: That is the trouble with our area, I think, rather than with the animals. A feature of our coast is that regions of fertility occur just south of Point Conception, off Punta Eugenia and very close to shore in the intermediate region 28-33°N. All are cool regions as far as the northern species are concerned. The animals might be basically oceanic and still be numerous near-shore because of nutrient renewal expected in the coastal regions.

These animals appear to hug the coast in these regions. I still think they may be regarded as oceanic animals. Euphausiids are primarily phytoplankton-filtering animals that are not found near the surf zone so to speak, but offshore. These small-scale maps are somewhat misleading, particularly where you have heavy concentrations against the shore. Here high euphausiid concentrations are adapted to the cool oceanic waters in coastal regions.

Berner: I think this is true of many species.

Reid: Our region is relatively barren offshore. There are more animals living in the inshore regions which are seasonally rather stable compared to the offshore areas. These animals take advantage of the small seasonal changes in temperature and the cold water masses which are found year round somewhere within the range of 200 miles—a characteristic of this transitional region.

Hubbs: Do you have any collections from the previous warm years, say like 1926, '31 or '41 from Monterey or from anywhere up that way?

Brinton: No. I had intended to make reference to the 1939 cruise. It extended from the Columbia River to south of Punta Eugenia. This is significant from the standpoint of our survey program because the cruise was carried out at a time when many of the subtropical fish were taken off Central California, and when the sardine was spawning there.

Hubbs: What part of 1939?

Brinton: May through July. That is before it got very warm off Southern California. The southern line

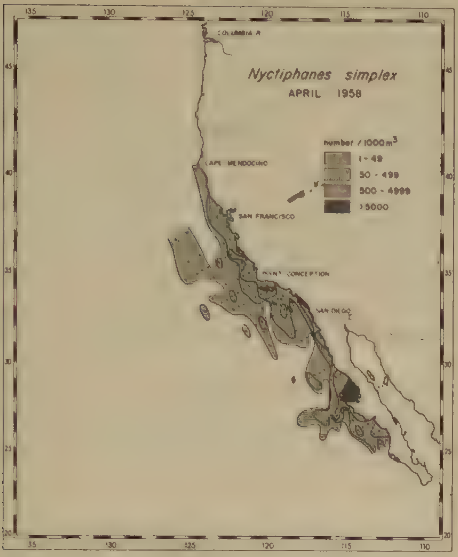

FIGURE 134. Distribution and abundance of *Nyctiphanes simplex* during March 30 to April 27, 1958 (CCOFI Cruise 5804).

of stations, extending westward from Viscaino Bay, was occupied in July.

Hubbs: Then we missed that warm water north of Point Conception that year.

Brinton: Yes. According to the chart of *Nyctiphanes* for 1939, one feature that I think is remarkable, and unique for 1939, is the occurrence of a cool water population off Point Eugenia as late as July, including large numbers of *Nyctiphanes* and *E. pacifica.* Cold eddies in this region in 1954 and 1955 were not observed later than April, I believe. In 1939 they persisted at least until early July. There was a very cold spring that year. The cruise was too late to record what was going on in the winter time, of course. In general the 1939 May through July distributions looked typical, with the exception of this particular area off Point Eugenia.

Sette: As I recall, February was almost a record cool month.

Isaacs: One of the coldest springs on record occurred in 1939, and one of the hottest falls.

Brinton: In February 1957 *Nyctiphanes* (Fig. 132) ranged north of Point Conception where it was present in small numbers near shore. This was not strikingly different from previous Februarys. The countercurrent, which seems to have been conspicuous in April 1958, was already pronounced in the winter of 1957-58 when *Nyctiphanes* was abundant as far north as the survey went (Pt. Conception) and *E. eximia* was well north of its distribution of February 1957 (Fig. 130). Where we have stations to the north of Pt. Conception it is evident that *Nyctiphanes* extended as far north as Cape Mendocino (Fig. 134). The central species had moved nearer than usual to the shore off Southern California in April 1958. This change is not great. Nevertheless we have to look for small changes. Only the northward extension of *Nyctiphanes* was conspicuously different in 1957-58.

Hubbs: The distribution of *Nyctiphanes* in April 1958 (Fig. 134) is the only one that shows numbers offshore at all, north of Pt. Conception.

Brinton: In the waters off Baja California there is an example of a change, which is evident in February 1957, however slight. This change was the northern occurrence of other equatorial species that normally do not occur north of Cape San Lucas except for occasional stragglers. They were not present at all stations, but in February 1957 there were more stations where equatorial animals occurred than is usual off Baja California. Again, these equatorial species were not being swept into the area, but were present in larger numbers at the southern stations in early 1957 than in the first three months of any of the years 1949-55.

Berner: The animals that apparently live in the upper layers show the changes more than those that live throughout deeper layers. Apparently *Nyctiphanes* and *D. denticulatum* are more inclined to the upper layer, and show this northward movement more than the other animals that live at a greater depth.

Brinton: Yes, I would say that of the species I have looked at, the one that shows the strongest northward shift in distribution seems to be restricted to the waters above 100 meters. Some of the deeper ones are slightly farther north than is normal.

Johnson: What are the youngest stages included in your counts?

Brinton: The youngest stages are about 3mm in length, sometimes smaller. Some of the small stages are lost through the net mesh. These larvae are probably two to four weeks old by the time the net retains them.

Johnson: So the count indicates a smaller population than is actually present.

Brinton: Yes, and larvae of *Nyctiphanes* made up some of the population north of Point Conception. The general distribution of larvae is not as extensive as that of adults, as is evident for February 1957 (Fig. 132). Spawning occurs close to shore; the adult population diffuses somewhat seaward. In February 1954 spawning occurred to the northern limit of the adult range. There is always a possibility that only the population of larvae near the surface, may be swept into an area, but, more often, the general population is carried together.

Reid: One thing that seems to stand out is the change in the distribution of the southern types rather than in that of the central types. Is the central type documented well enough to say that it did not move in?

Brinton: It is not documented well enough to be definitive. The central types that I have plotted for California waters in February and April 1958 (Figs.

128, 129) suggest that they all move slightly toward shore. But I feel that this change is not as conspicuous as the northward movement of *Nyctiphanes* and *E. eximia*. The presence of unusually warm water in the California Current could lead to intrusion of both assemblages.

Question: The results might show some on-shore encroachment although they do not swim in but are moved in by the water.

Brinton: They probably do not swim in very actively. Encroachment in the course of a month or two months may be helped by random diffusion of the population in mixed areas. The animals swim up and down—spending most of their lives in swimming up and down. They probably move at random laterally, some of the time, and this could be enough to extend their range into an adjacent region that might be tolerable to them.

Johnson: Directive forces drive them up and down, so they swim straight up or straight down, but the thermal gradients to the right or left are less. Perhaps they do respond to smaller gradients than we think.

Murphy: Do all euphausiids come to the surface during a 24 hour period?

Brinton: No, not all species. I have lumped the species into three bathymetric groups. One group of species lives above 700 meters; these migrate near to the surface at night. A second group lives between 500 and 2,000 meters. These never get to the surface. The third group is bathypelagic—only the larvae live in the upper layers while adults live below 1,500 meters.

If you take the depth distribution of a species which lives in the 0-700 meter environment the youngest vertically migrating stages of development are nearest the surface. The adults would be the deepest. Many of the larvae which are one to two months old live within 20-25 meters of the surface.

Question: Do you suppose sampling of plankton should be switched to the night stations because more adults are found then?

Brinton: Night hauls frequently contain more adults than day hauls. Numbers of larvae and immatures may or may not vary in this way. Most of the animals that are immature seem to be well sampled by the relatively shallow 0-140 meter tows. However, the picture would be much more reliable with a standard time of sampling.

Reid: Your pictures are very coherent.

Brinton: Considering this type of difficulty there still seems to be coherence to the distributions.

Wooster: I would like to borrow Dick Fleming's iconoclastic role for a moment, if I may. We have said before this session started that in many ways the animals might be better oceanographers than the oceanographers, and I am beginning to think that, like many a good oceanographer, they are very difficult to understand. It seems to me the use of zoogeography as an indication of oceanographic circulation has to be calibrated with physical or chemical oceanographic parameters. If species distribution agrees with distribution of temperatures, it is good that this all fits together. Actually, you have not learned anything about circulation; you have learned something about the temperature tolerance or affinity of the organisms. If distribution does not agree with the particular physical parameters with which it is compared, then you are sort of perplexed. One of two things happened: either you chose the wrong physical parameter, such as surface temperature (often it must be that, I think), or something else has happened that you do not really understand. It seems to me that looking at this in general, the comparison of distribution of organisms to those of physical and chemical parameters is likely to show more about the beast than about the ocean.

Johnson: It brings out some points where an oceanographer should look for more information than he has.

Wooster: What he is saying is that where distribution of the physical parameters and the distribution of the beast do not agree, then the oceanographers may have the responsibility of explaining this. It may be something in the biology of the beast, or it might be something not being looked at properly in oceanography.

Isaacs: Euphausiids migrate vertically through a range of 10 to 12 degrees Centigrade, and yet for years they had a distribution that turned out to be consistently limited within 0.2°C by a certain 10 meter isotherm and this all in a moving current. Does anyone think that the temperature of this isotherm was restricting this distribution?

Brinton: It is hard to say. So little is known about the actual physiological requirements of the animals. One temperature might be limiting for feeding, another for reproduction, another for a metabolic function. So it is probably an extremely complex business. One isotherm might be limiting in one area and a different isotherm in another.

Johnson: I think probably while we are on the particular question of temperature requirements and also in the matter of deposition of eggs near the surface, I might point out the case of *Thysanoessa spinifera* washed up on the beach at La Jolla in large numbers. They all turned out to be spent females. What actually happened may have been that they had risen unusually close to the surface to spawn and had been caught in inshore currents and washed up on the shore. Surface temperature might be exceedingly important to spawning.

Ewing: There is one feature that perhaps we are missing or have overlooked, that is the biological edge effect, which we all know, does not affect the extent of distribution, but the density of populations. This is very dependent on boundaries between currents or water masses. On land the transition conditions between dissimilar environments very much increase the carrying capacity of the environment, cutting it up into smaller areas so that the animals have a longer boundary environment. There are cases where this seems to be true in the ocean as well, such as at a front. It is not so much the average temperatures of the water mass itself that determines the carrying capacity of the water as it is the amount of boundary. The albacore is quite sensitive to this. It likes to stay in fairly warm water and feed in cool inshore water. It likes to feed in one environment and live in another. One reason why many so-called warm water animals are at times most abundant along the edge of the California Current, or at least along the cold water, is that they can stay within their temperature tolerance and have access to cold waters which are in general more nutritious. They get as close to their food as they can and still stay in their own temperature range. As an example, the boundary off Cape San Lucas is very nutritious and always full of marine life. Very high gradients are found there. So it is very easy for an animal to pick an optimum area. Many animals must choose environments adjacent to boundaries where there are gradients rather than those areas where optimum conditions prevail.

Ahlstrom: These temperature ranges that I believe we are mentioning, none of these concerns both adults and the larvae. The larvae could have quite different and much smaller temperature ranges, and I think for each stage this has to be established. I think it is a mistake to take the range of an adult and apply it to larvae.

Brinton: Yes, I think there is danger in that too. However, the thing that is remarkable to me is that more often than not, you find very many stages of development together. But of course this is sampling through a long vertical column. In this extreme northern extension of *Nyctiphanes* (Fig. 134) occurring off Mendocino all were adults however. At the stations off San Francisco there were some larvae present. Surface temperatures were 12°C. off Cape Mendocino. I am certain that this species could not survive long there.

Isaacs: What are the comparative ranges of temperature of the distributions of *Nyctiphanes simplex* in the two hemispheres?

Brinton: The temperatures circumscribing the distribution of *simplex* in the Peru Current on Shellback Expedition were very similar to the temperatures found in our CCOFI region: the 20°C. isotherm, normally, I think. But in 1958 it was in colder water at Cape Mendocino, 8 degrees cooler than the usual limiting temperature.

Revelle: What interests the biologists, what interests the organism, what interests the physical oceanographer? The physical oceanographer can measure the temperature very easily and is not interested in using organisms as a thermometer. But he cannot always follow the water masses around by temperature alone; he likes to use organisms as drift bottles. In order to use the drift bottle you have to know where you release it and where you pick it up. These animals are very easy to identify as to where they are picked up, but not as to where they were released. The second difficulty is of course that they apparently migrate vertically as well as horizontally and therefore they are drift bottles that can be used in a kind of hazy way for water at different depths. Looking at this from the standpoint of the organism, the biologist or the physical oceanographer, you have three different things you are concerned about—can the organism swim? How fast can he swim? How far does he swim horizontally? Really, they are no good as drift bottles because they can migrate from that deep scattering layer to the surface in half an hour. This is 400 meters which means they can swim roughly a kilometer an hour or about 20 kilometers a day. They could move extensively in a rather short time.

Brinton: There is no question that they could move into an area that is tolerable as to temperature. It would be nice to know the extent to which they do move laterally, but the observations that have been made on their swimming behavior are only on their vertical movements. They are usually in a sort of spiral path.

Question: What would happen in a boundary region where an animal might be expected to extend his range by random swimming?

Brinton: I do not know what would happen. I do not think there is much likelihood that it would purposefully swim in any given direction horizontally.

Revelle: If you invoke random swimming, though, you would not have as sharp a boundary as you actually have. Look at these February distributions of *Euphausia eximia* (Figs. 130 and 131). A great many are in a certain region, then they stop abruptly. That is true in almost all cases. Your distribution has quite definite boundaries.

Isaacs: This is a strong argument against random dispersion—they do not randomly swim as individuals but as swarms.

Revelle: But it will still cause a dispersion.

Murphy: The map says they are not randomly distributed.

Wooster: Why can not these organisms be spreading, diffusing, or swimming horizontally in a random fashion? In fact, they probably are. They are exerting pressure on the limits of their distribution at all times. Due to physical circumstances the population is tending to spread all the time for one reason or another, and when it goes into an environment that is not favorable, it is dying off or somehow being wiped out. When it spreads out and finds a suitable environment, then it prospers and would develop a tongue by diffusion. On the other hand, a distribution might be reduced around the edge by attrition. A group of parameters rather than a single one, limit its distribution.

Sette: I think we are all agreed that the animals are reacting to something essentially other than temperatures. Nonetheless we use temperature as a marker of water masses or circulation systems. An animal or a group of animals may be an indication of many things—just as temperature is, by the way. The observation of events would not be confined to the physical parameters if other things could as easily be measured.

Murphy: I agree with Warren Wooster; you just do not know the life requirements of these animals, so that finding an animal in a particular place does not say very much about the reasons it was there. We need a better history of it. As to temperature, as it was pointed out before, if you want to know the temperature, you might as well go out and measure it. We do get some data on living things without sending an expedition. Fish kills and unusual distributions of fish are reported by fishermen.

Revelle: I am not arguing; I do not object to the collection of animals. I am simply saying that in the process it is also very easy to measure temperature.

Radovich: Regarding the question of whether or not euphausiids can swim purposefully, I recall that during one of our sardine conferences Dan Miller of the Department of Fish and Game mentioned that schools of gravid *E. pacifica* were seen in Monterey Bay from an airplane. These schools were subsequently sampled from a boat—they were moving similarly to fish schools. I also observed what I thought was a school of euphausiids off Anacapa Island several years ago. I tried to observe the way they were moving.

Question: With the current?

Radovich: No, they were swimming. As we came upon them the school would separate and move away from the boat.

Murphy: This means they do have capacity for coherent motion.

Brinton: Their spawning behavior shows a local peculiarity. For example, these schools have never been observed in the open temperate ocean to my knowledge.

Berner: These schools of *Euphausia pacifica* have been observed at one time or another off central California between Point Conception and Cape Mendocino.

Johnson: Where you have shading on the map—it does not mean that every station yielded animals, does it? There would be zero values in a number of cases.

Brinton: Where the relative numbers of animals belonging to the different assemblages are plotted, for example as the "central offshore" species are plotted (Figs. 127, 128, 129) the zero values for the assemblage would be shown as clear places. There is continuity within these species distributions. Within the distribution there might be smaller dense patches. Often whales actively seek out swarms of euphausiids; that is the only way they can get as many as they do. A plotted record is, of course, a reflection of the situation at a moment, perhaps a week before a species did occur at stations outside of its indicated range. A southern group extending northward as a tongue may be really receding, having had earlier a more extensive distribution.

Isaacs: Some areas of apparently low concentration result from day samples when the euphausiids are at deeper levels as compared with night samples when more of them are in the upper layers.

Brinton: Possibly. I have sometimes in the past tried to correct for day-night differences in apparent concentration. Sometimes numbers are consistently higher in night hauls, sometimes not. If you omit all the day stations on the periphery of a range, it sometimes makes a much improved contour—a smoother one. In other instances there seems to be no reason for concentration irregularity. It would be nice to have all night stations, then you would know that the animals are within the sampling limits.

Revelle: Is it possible to interpret these in terms of onshore movements?

Brinton: Not with certainty. It is impossible to say that there is movement of water in any particular direction. However, I have tried to speak in terms of the environment of the animals being extended in one direction or another. This may be due to local changes or it may not, but I do see examples from time to time where I feel that there are movements of the water.

Revelle: I am talking about the change that we are discussing during this Symposium, that is, whether the water moves from the center of the ocean to the edge, or whether it is actually motion in a north or south direction. I wonder if any light can be thrown on this from the various kinds of critters. I gather the impression that, except for small features and except for coastal species found to the north, the distribution may very well be accounted for by the major movement of the warm offshore waters toward shore, plus the ability of these critters to seek out environments that they like.

Sette: The evidence does not clearly settle the question of whether or not the euphausiids were drifted, or whether they moved by their own effort or a combination of both.

LITERATURE CITED

Bargmann, H. E., 1945. The development and life-history of adolescent and adult krill, *Euphausia superba*. *"Discovery" Rep.* Vol. 23 pp. 103-176.

Brinton, E., 1957. Distribution, Faunistics and Evolution of Pacific Euphausiids. Doctral Dissertation, Scripps Inst., Oceanog., U. Calif.

Einarsson, H., 1945. Euphausiacea 1. Northern Atlantic species. *Dana. Rept.* No. 27: 1-185.

Moore, H. B., 1952. Physical factors affecting the distribution of euphausiids in the North Atlantic. *Bull. Marine Sciences Gulf and Carib.*, Vol. 1 (4): 278-395.

Reid, J. L., Jr., G. I. Roden, and J. G. Wyllie, 1958. Studies of the California Current system. *Progress Rep., California Cooperative Oceanic Fisheries Investigations.* pp. 27-56.

Sverdrup, H. U., M. W. Johnson, and R. H. Fleming, 1942. *The Oceans.* 1087 pp.

QUATERNARY PALEOCLIMATOLOGY OF THE PACIFIC COAST OF NORTH AMERICA[1]

CARL L. HUBBS

We will now deal in a field where facts are disputed and theories are a dime a dozen. A few points in regard to the climate of the past in western North America, however, are reasonably well established.

As a background for a consideration of recent secular changes in climate we may profitably spend a brief—very brief—time reviewing facts and interpretations of climatic changes in this region during Cenozoic time. The earlier periods will be rushed over; increasing emphasis will be accorded data that are accumulating on the more recent, largely Postglacial events, particularly over the past few millenia; in greatest detail, over the past few centuries.

LONG-TERM TRENDS

In western North America, despite enormous fluctuations, there has been, up to the present time, a fairly general climatic trend, which paleobotanists in particular have worked out in some detail. Through all or much of the Tertiary and Quaternary periods the trend in general has been toward cooler temperatures and greater aridity. Harking back momentarily more than a million years, we note that the trend toward aridity seems to have been rather consistent and extensive through Tertiary time. During late Pliocene time the downward trend toward aridity seems to have been reversed, and during Pleistocene time the surface-water supplies fluctuated widely on four main and various minor occasions. During each ice advance the long-term trend toward cooler weather was accelerated, to be reversed during each of the three Interglacial periods, when, in contrast, the trend toward aridity was resumed. With fluctuations again, this combination of drought and warmth characterizes the Recent period, whether or not we class it as Interglacial.

Throughout these complex trends there seems to have been a tendency toward increased fluctuation, from period to period, from year to year, and from season to season; also from region to region. This circumstance, plus the accentuation of some trends along with the temporary reversal of other gradients during Quaternary time, renders difficult and dubious any definite prediction as to future trends. In view of the past, perhaps the highest plausibility can be accorded the hypothesis that climate will change. My own feeling is that there is a very strong possibility, if not a probability, that the trend toward greater aridity will continue, with fluctuations of course.

The complexity of the climatic trends renders difficult not only future predictions, but also an understanding of the causes of past changes. In broad terms, particularly for Tertiary and Pleistocene history, the trends seems to have been largely worldwide, but, as I shall indicate later, some of the more recent fluctuations seem to have been negatively correlated in different regions of the earth.

The trend toward greater aridity in western North America has commonly been attributed to the elevation of the western mountains, which captured rainfall and produced rain shadows to the eastward, but there is some evidence that this was not the only factor. Interglacial aridity could hardly be so explained. Fluctuations in aridity during Recent time seem to have affected coastal regions and offshore islands, as well as the interior of western North America. And at least some of the changes were simultaneous in the diverse regions. Some factor other than local land elevation seems to have been involved.

Though other and broader factors have doubtless operated, it seems obvious that climatic conditions in the West have been greatly influenced by the massive land elevation that began in the Miocene, gained impetus in the Pliocene, and reached a crescendo in early Pleistocene. An important point of vital climatological bearing that has often been neglected is that not only the mountains but also vast plateaus were greatly elevated. In all probability the Great Plains and the Columbia Plateau were elevated, along with the vast Colorado Plateau. The Range and Basin Province, primarily of the Great Basin, was apparently subject not only to the internal ups and downs of fault blocks, but also to a general uplift of perhaps 2,000 or 3,000 feet. There are reasons for believing that in Pliocene time the Great Basin was essentially part of the coastal plain, standing at less than 1,000 feet elevation and draining to the Pacific. One reason that we have advanced to justify this view is that Pliocene fish fossils in the Great Basin represent coastal-plain types.

Though there are conflicting theories, and some would have the major trends of climate alternating in different regions, especially during the Pleistocene, it seems rather obvious now that in general the major climatic trends of Tertiary and Pleistocene times were essentially simultaneous over the earth, at least over Eurasia and North America. Early Tertiary times seem to have been rather uniformly warm and moist over the world, even toward the poles. There were, apparently, no polar ice caps, and, in seeming response, deep ocean temperatures dropped to only about 10°C, according to Emeliani's data from benthic foraminifera. Low elevation of the continents presumably contributed to the uniformity of conditions, but was probably not the only factor. The free passage of currents through the Panama Strait may have played a part. In any event, the Arcto-Tertiary Geoflora reached far south in the West. The warmth of the North Pacific presumably permitted interchange between temperate faunas on the two sides.

---

[1] Contribution from the Scripps Institution of Oceanography.

Reproduced by Permission

New series, 1172 [illegible]

Cooling appears to have continued over the world through late Tertiary, as did desiccation prior to late Pliocene, when there appears to have occurred a reversal that in due time probably led to the first major accumulation of ice. The Panama Strait was closed by the elevation of the isthmus. The Madro-Tertiary Geoflora progressed northward taking over areas previously covered by the Arcto-Tertiary Geoflora.

Enormous fluctuations in precipitation and in temperature, involving the four major glacial periods of the Pleistocene, with their various substages, seem to have been world-wide. Paleontological and paleotemperature studies of bottom sediments confirm the picture in general, but emphasize the multiplicity of substages. Recent paleontological evidence, advanced by Claude W. Hibbard of the University of Michigan, confirms the picture: small fossil mammals of the Great Plains appear to represent all four of the successive cold periods of the Pleistocene, plus, on present evidence, two of the three Interglacial periods. Carbon-14 datings of the recession of the last ice cap about 11,000 years ago, bespeak essential simultaneity over the northern continents and northern oceans. And there is some evidence, as from faunal displacements in the sea, that Wisconsin (Würm) events were simultaneous in the Northern and Southern Hemispheres.

EXTREME COLD IN WISCONSIN TIME?

There are strong indications that the last (Wisconsin) ice stage was one of extreme and far-reaching cold—perhaps emphasizing the long-term trend toward cooler weather. The fact that the continental ice sheet did not advance as far as had the previous glaciers, and the fact that each major ice sheet was less extensive than the preceding one, may well reflect the long-term trend toward greater aridity. The extent of each ice sheet may have depended less on the degree of cold than on the available precipitation. Decreased moisture would have led to less accumulation of ice and less southward flow of the continental ice sheet.

If the Wisconsin was arid, it was dry of course only in comparison with early Tertiary and other ice age periods. Precipitation must have been heavy to have produced the vast ice cap (though less vast than previously) to have formed simultaneously montane glaciers well toward and, some think, almost to the Mexican border; to have produced ponds and marshes in now dry regions on the Great Plains; and to have filled many Western basins with great inland seas. The northern part of the Range and Basin Province had almost as much water as land, and even to the southward at least semipermanent lakes covered the playas. There is much evidence also of increased stream flow, along the coast as well as in the interior. The widespread pimple-mound topography may be interpreted as reflecting greater moisture as well as extreme cold.

Evidence of world-wide coldness during Wisconsin time is rampant. In the East the boreal forest seems to have advanced to the Gulf of Mexico, and the northern biota seems to have been forced into refuges in Florida and Mexico, from which redispersal took place in early Postglacial time. Anadromous fishes were able to move southward through seas now too warm for them: a small salmon became landlocked in Formosa; trout got to Sinaloa, the Atlas Mountains, and the Near East; sticklebacks moved into streams of northwestern Baja California. Disjunct populations of northern freshwater fishes in New Mexico and even in northeastern Mexico almost surely got there in cooler, Wisconsin time. Cool-water mollusks occupied ponds and lakes about which man existed at about the close of the Wisconsin period. The mammoth reached the Valley of Mexico. In New Zealand, I have heard, littoral mollusks dated at about 20,000 years have been dredged, from presumably Pleistocene submarine terraces, farther north than these cool-water species now occur.

It was presumably during Wisconsin time that certain marine plants and animals that now occur in temperate waters to either side crossed the then materially cooled waters of the tropics. One such organism is the giant kelp *(Macrocystis)*, which occurs as the same variants of the same species in Peru and Chile as in California. Another is the Pacific sardine, which is virtually indistinguishable in our waters and in Peru. I have computed that a drop in sea-surface temperature of about 3°C in winter and perhaps 8°C in summer would allow these and distributionally similar species to regain connection off the coast of Middle America, and I am assuming that the seas were cooled about that amount in Wisconsin time. Oxygen-18 temperature estimates from organisms in sea-bottom cores are in essential agreement.

The widespread extinction of large mammals in late Pleistocene time may also be attributed in part at least to extreme cold in Wisconsin time, forcing dispersal far southward into less favorable ranges, and in part to the following period of aridity.

Another line of evidence indicative of the southward extent of Pleistocene cold is furnished by the to-be-sure somewhat controversial pimple-mound or Mima-mound topography. These rather well-aligned mounds cover many thousands of acres in the western half of the United States, from near Canada to the Mexican border, and even, I am told, into the mountains of Sonora. Similar mounds in the far north are attributed to the freezing and thawing of the soil cover overlying permafrost. Farther south, I believe, they were formed by similar seasonal freezing and thawing of waterlogged soil overlying impervious hardpan.

Sea-temperature estimates by the oxygen-18 method from Wisconsin-period mollusks should eventually give us a sounder picture of reduced sea temperatures during that period—and air temperatures were no doubt very closely correlated. But the Wisconsin deposits were laid down when the sea-level was much reduced and, in my belief, the general trend of land elevation (or sea-level depression) has not proceeded far enough since the time of deposit to reveal the fossils of this period. Most of the cold-water fossil-mollusk faunas already exposed at low elevations along the coasts of Southern California and Baja California I believe to be of Illinoian age. From mollusks of one such deposit in northwestern Baja California an oxygen-18 temperature estimate of only about 12°C has been obtained, I have heard.

Great secular fluctuations in sea temperatures—and hence of coastwise air temperatures—are indicated by the Pleistocene faunal assemblages in all temperate regions. Some of these assemblages are indicative of colder-than-present temperatures, others of warmer. Recent claims of mixed cool- and warm-water faunas are in part at least, based on erroneous and doubtful data; and the oceanographic explanation offered does not seem to hold water. Recently I have sampled on Guadalupe Island, only 240 miles south of San Diego, a warm-water late Pleistocene fauna, including reef coral, and mollusks that now inhabit tropical waters extending from the Gulf of California to beyond Panama. With modern isotope methods and other more intensive and critical methods, we should eventually be able to seriate and in part date these findings, and get definite temperature estimates.

POSTGLACIAL TRENDS IN TEMPERATURE

About 7,000 years ago (by carbon-14 determination from shell) the Indians of Santa Rosa Island, California, were feeding chiefly on red abalones *(Haliotis rufescens)*, a species that is available inshore only where the coastal water (and air) is cold. Hence a trace of Glacial cold was presumably persisting. Later the warm-water black abalone, *Haliotis crackerodii* was chiefly consumed.

I have obtained oxygen-18 estimates that indicate, in agreement with faunal data, that the sea-surface temperature along the coast of northwestern Baja California was somewhat warmer than that of the present about 4,000, about 2,500, and about 300 years ago. These estimates were obtained on shells of surf-zone mollusks from Indian middens, from which I also have obtained carbon-14 datings from charcoal and/or shell. But between the 2500-year and 300-year B. P.* datings I have evidence of a cooler-than-present period. Oxygen-18 temperature estimates lie below the present growing-season mean, and the dating is about 900 years ago. In this period the Indians over a long stretch of the Baja California coast fed heavily on the giant chiton *Cryptochiton stelleri*, which now, except for extremely rare deepwater strays off Southern California, is confined to the cold-coastal region from near Pt. Conception in California to Japan. No trace of it has been found along the coast from which it was abundantly harvested about a millenium ago.

A point of prime interest in this connection is that at about the same time it is thought that coastal Greenland had become attractive to and was inhabited by Scandinavians—when Greenland was green. This is one of the bits of evidence of negative correlation in regional temperature regimes. Temperature, like money, may be present in adequate amount but not evenly distributed.

Coming closer to the present, we have evidence of a warm period, along the southern half of the California Coast, just about a century ago, after which this region became cooler while arctic amelioration was proceeding in the far north; again, the ambient temperatures of this coast and of the far north seem to have been negatively correlated. I was led into this interpretation of a warm period approximately a century ago by the faunal evidence. The first zoological survey of the West Coast worthy of that designation, conducted by the naturalists of the Pacific Railroad Survey of 1853-57, disclosed at San Diego a fish fauna of a warmer-water affinity than that of the present—about like that of Turtle Bay, and even of Magdalena Bay (near the middle and southern parts of the Baja California peninsula). And at Monterey this early survey found a fauna containing San Diegan elements that do not now occur in the colder waters of central California. Some of these southern forms at each port were sedentary types not very subject to northward dispersal in isolated warm seasons such as we are now discussing. A seahorse, for example, was one of the fishes taken then, but never recently, at San Diego. Other faunal data keeps fitting into the picture.

To check the indications of warm water in the southern half of California about a century ago, I made a short journey into meteorology. First I showed an extremely high correlation between sea and air temperatures near San Diego. Then I analyzed the weather data, which very fortunately began at San Diego in 1849 and very soon afterward at Monterey. There was indeed a definite trend toward cooler temperatures at these localities through the second half of the nineteenth century, notably in the late-spring and early-summer months, which are of most significance to the fishes.

The weather data for San Diego seemed to indicate a continued cooling trend until about 1910, after which the monthly plots seemed to show a slight rise. But this rise may be attributed at least in part to the effect of urbanization, which, as certain meteorologists have shown, yields temperatures in built-up cities that are somewhat too high for the region. The most marked rise toward the end of the years analyzed is definitely attributable to the moving of the weather station to Lindbergh Field, for test runs showed the temperature there to be about 1.0° F. higher than at the Federal Building, where the weather station had previously been located.

POSTGLACIAL TRENDS IN MOISTURE

There is now, of course, no shadow of a doubt that during the Pluvial period, which accompanied the last Glacial period, the rainfall from the Great Plains to the Pacific Coast and from the ice cap to Middle America must have been vastly greater than at present, and the evaporation must have been much less. Together these factors caused rivers to flow full and basins to fill with great lakes. I have reviewed this evidence in some detail and will not repeat it here.

---

* Before present.

Evidence has been presented to indicate considerable desiccation through the still moist and cool early ("anathermal") portion of Recent time, which was followed by the warm and dry altithermal period (or climatic optimum), around the middle of Postglacial time. A "Little Pluvial" period then is thought to have followed, during which Pluvial lakes and streams were somewhat re-established. Archeological and tree-ring data suggest a severe drought in the thirteenth century.

Obviously there have been marked fluctuations in water supply during Postglacial (Recent) time, but throughout most of the period water was probably much more abundant than it has been over the last few centuries. Archeological and physiographic evidence is replete with indications of more abundant water, at many times during the Postglacial period and at many places from the Pacific Coast to the Great Plains. Indications accumulate of past human populations too large to have been supported by the amount of surface waters presently available. Midden remains are found of fishes and other water-limited animals that could not now exist in the region, and in places the remains of plants indicate vegetation of a more humid period. My own studies keep uncovering confirmatory indications of greater humidity at various dated times in the Postglacial sequence.

In fact, I have for some years thought that the drought of the past three decades has been the most severe of any since the Pluvial period. I have found evidence of the extirpation during this period, as a result of the drought, of wholly isolated fish populations that must have persisted since Pluvial time. Except for isolated introductions by man, fishes occur only in waters that they have at some time reached by normal dispersal.

The "march of the desert" seems to have been continuing right up to the present. In fact I am becoming more and more impressed with the apparent recency of the desert conditions over the southwestern United States. To be sure the desert biota is too distinctive to have suddenly evolved, but the deserts may well have merely been dispersed, with their characteristic biota, northward from some ancient center in Mexico.

Some of the evidence for the recency of the deserts in the Southwest is physiographic. Recent gullying—very striking through the region—is very likely due in part to drought, which has destroyed ground cover. More pointed evidence, in the extreme desert regions of the Colorado Desert and the Colorado Delta, is furnished by the structure of the *bajadas* (the alluvial apron around desert mountains). Typically, sections of *bajada* even against the mountains show fine sediment throughout the greater part of their height. Occasional gravel or cobble streaks tell of flash floods. But the fine sediments are typically capped by desert shingle. Furthermore, secondary fans topping older *bajada* slopes are composed of very coarse rock fragments. The plausible explanation is that over long periods of time until very recently—unfortunately we do not yet have datings—the desert mountains were smooth-topped and largely covered with a mantle of soil, which, from time to time, probably at an accelerating rate, eroded away, to be deposited at the base of the mountains. The abundance of large herbivores until late Pleistocene and early Post-Pleistocene time, and the oncoming drought may have together caused the erosion. Shift of rainfall from a rather even distribution to one of limited but torrential precipitation may have been a major factor. Whatever the cause, the soil on the mountains was largely eroded away, so that subsequent weathering has attacked and broken down the bare rock faces that are now so characteristic of the arid Southwest. I believe that the naked-rock mountain landscape of the West is of much more recent origin than has generally been thought, and that the seas of playa sediments that surround the *Inselbergen* have often accumulated much more rapidly than has generally been assumed. Some radiocarbon dates of buried levels of human habitation in the Southwest confirm this view.

This rapid development of arid landscape may be observed in certain places where the ground cover is being destroyed. Bare rock exposed by landslips in New Zealand mar the mountain slopes that are overgrazed by sheep. The landscape of Santa Rosa Island off California has been transformed over the last two or three decades from one of gentle soil-covered contours to one in which bare rock exposures are becoming more frequent. The soil veneer keeps slipping off to expose these scars. The reason I believe to be a combination of drought plus the foraging and trail-making of many large introduced mammals—elk, deer, and boar, as well as cattle, horses, and sheep. The landscape is beginning to change from one resembling that of the Alleghanies to one beginning to approach that of the desert mountains. What is now happening before our eyes on Santa Rosa Island I believe represents what happened in late Pleistocene or early Recent time over vast areas in the Southwest, very likely from the same causes—drought and over grazing.

The past and present distribution of animals offers much evidence corroborating the view of increasing aridity. For example, the woodchuck over the past few millenia ranged through northern Arizona well south of the range to which it is now limited by reduced moisture and higher temperatures. Fish mummies from caves in Nevada indicate a permanent lake in the Humboldt Sink, in the last few millenia. Now bone-dry canyons in southern Nevada show campsites, pictographs, petroglyphs, and other evidences of human occupation when these water courses contained water. Such evidence abounds throughout the Southwest. My own investigations yield conclusions consistent with the general view.

We are now accumulating evidence of a rather heavy population on the coast of Southern California about 7,000 years ago, in areas where the present water supply would not be adequate. Similar evidence stems from sites dated at about 5,000, 4,000, 3,000, and 2,500 years B. P.

Some of the evidence of more ample water relates to much more recent time. Very extensive middens, predominantly of small Pismo clams, over a long stretch of the Baja California coast, have been dated from a warm period, about 300 years ago, that must also have produced more surface water; carbon-14 dating and oxygen-18 paleotemperature estimates are involved. A rather extensive habitation site on North Coronado Island has been dated at less than 400 years, but there is now not enough fresh water on the islands to supply more than a family or two, and not enough brush to provide fires for any length of time for more than a very few people. But the site carries much evidence of fire, and more rainfall would surely have been needed to grow the wood that was used. Large populations of relatively recent date (to judge from a few radiocarbon tests and from the types of artifacts) existed at points along the Baja California coast, as about San Felipe, Turtle Bay, and San Ignacio Lagoon, where the present available water could not have supported the people.

Evidence of former, much-greater-than-present precipitation in the desert of Southern California was recently obtained on "Fish Creek," in the Fish Creek Mountains on the west slope of the Salton Basin. I went there with archeologists specifically to check on the former fish life of this creek. Some small fish still persisted in water holes in this creek prior to the great flood of 1916, which filled the stream bed with sediment. Since then the rainfall has been insufficient to produce permanent water, in recent years none at all; except for very rare flash floods, the stream bed is bone dry. We travelled up this dry bed by Jeep for about 14 miles, through the defile in Split Mountain, to reach an extensive ancient village site that was already known. On the surface were remains of mountain-sheep horns, suggesting better grazing and more water in former times. Digging in the abundant hearths yielded not only mammal, bird, and lizard bones, but also many fish bones. These represented the humpbacked sucker *(Xyrauchen texanus)* and the bonytail (*Gila robusta elegans*) — species that abounded in Lake LeConte, the vast inland sea that existed until about 300 years ago in the Salton Sink, and that was formed, at least in part, by inflow from a distributary of the Colorado River. These species formed a major—probably the major—part of the diet of the thousands of Indians who lined the shores of the ancient lake. But it was the adults of these large fishes that were caught and eaten about the lake, whereas most of the fish that were eaten at the Fish Creek site far back in the hills were young. The wholly plausible conclusions are that these young fish were caught locally in Fish Creek, and that they had grown from spawn deposited there by big fish that had found sufficient water in the creek to swim up from the ancient lake. To yield such a flow must have required rainfall about equal to that of the coast—say ten inches a year, as contrasted with probably less than five in the same watershed today. The date from charcoal in the hearths is 1,000 B. P.

Surprising as such a rapid decrease in rainfall may appear to be, we may regard the estimate as not at all improbable. The depopulation of the Old World deserts over the past few millenia suggests that the increase in aridity has been very widespread, at least at comparable latitudes.

Other dates of habitations in the desert region over the past few hundred years, about Clark Dry Lake and elsewhere, also suggest that more water was available until very recently, even within the past two to four centuries.

The last few centuries, though almost surely not so excessively arid as the present, have I believe approached the present in desert drought. There has perhaps been no great recovery from the great drought of the thirteenth century (about 700 years B. P.). A bit of physiographic data, for which I am largely indebted to George M. Stanley, bears on this point. The main shore bars of the last stage of Lake LeConte, which I estimate from radiocarbon datings and other evidence to have lasted from at least about 1,000 years B. P. to about 300 years ago, are remarkably unbroken, even where consisting largely of fine sediment in the even sweeps across canyon mouths. Much rainfall during the past 300 years, after the desiccation of the lake, would surely have formed ponds behind the bars, and these ponds on overflowing would have cut much more extensively than they did through these bars (which stand at 45 feet above sea-level). The recession lines representing temporary levels as the lake disappeared also bespeak great aridity about 300 years ago, for they are spaced (or were before the Age of Jeeps) about five feet apart (about half the present rate of evaporation). Earlier Pluvial conditions almost surely yielded enough inflow from the drainage basin to hold the lake levels, without contribution from the Colorado River, but the local rainfall must have been greatly curtailed over the past few centuries.

About five feet higher than these last-formed bars, which give evidence of about three centuries of notable drought, Dr. Stanley found, as remnants only, other bars, representing an earlier lake level. These earlier bars possibly date from a much more ancient, separate lake stage, but my present hypothesis is that they date from an early period during the last lake fill, possibly from about the time Fish Creek provided breeding grounds for the lake fish (1,000 years B. P.). Greater rainfall, in this view, was more responsible than great antiquity for the major destruction of the earlier bars. Archaeological, radiocarbon, and physiographic evidence indicates that in the interval between 1,000 and 300 years ago sedimentary deposits were rapidly formed behind the lake bars, as a result of heavy erosion, before the bars were reworked into the last formation, which has so well resisted erosion during about three centuries of drought.

Historical data confirm the view that the Southwestern deserts have been extremely arid over the past two centuries. Earlier evidence, from the explorers of the coast, dating back more than 400 years, is unfortunately confused. Cabrillo and Vizcaino wrote of forests on Pt. Loma and near Santa Barbara where none have existed more recently, but historians argue over the translations and the meaning. Early Spanish maps of the Central Valley of California show vast expanses of freshwater lakes, ponds, and sloughs, but it is possible that the map maker passed through during a brief flooding. I am inclined to the view, however, that these early observations reflected greater rainfall.

CONSISTENCY IN WEATHER PATTERN

Through all these major fluctuations in climate the general geographic pattern seems to have been maintained throughout the Pacific Coast and Southwestern regions. There have no doubt been north-and-south shifts, as well as general changes in intensity—of rainfall, temperature, wind direction, etc.—but the gradients have been maintained.

The illuminating researches of Axelrod indicate that the pattern was already established in early Tertiary time and persisted throughout that period. Pluvial conditions were graded from north to south in much the same pattern as today, though everywhere the effective precipitation was probably more than twice that of the present. The same pattern almost surely persisted during the greatly reduced rainfall of Postpluvial time.

Along the coast we find evidence of the long duration of the temperature pattern, as indicated by faunal assemblages and some oxygen-18 estimates; and, as I have noted, air temperatures are very strongly correlated with sea temperatures. Though time correlations are questionable, the evidence from Pleistocene deposits strongly indicates a southward increase in temperature with a break near Pt. Conception. Where the coast seems relatively stable, in northwestern Baja California, Pleistocene deposits that I believe will prove to be Illinoian seem to reflect the regions of upwelling that are so striking today; if so, prevailing winds were probably similar to those of the present.

In the middens also we find evidence of the persistence of the temperature pattern. Thus the faunal assemblages of relatively recent middens on the northern Channel Islands show a marked gradient from cold-water types at the western end of San Miguel Island to warm-water types at the southern side of Santa Cruz Island, over a stretch where there is today a gradient of about 10°C in summer sea-surface temperature and a corresponding gradient in the littoral fauna. The region in Baja California where the occurrence of the cold-water *Cryptochiton* in middens indicates, along with isotope determinations, a colder-than-present period about 900 years ago, is precisely the area where upwelling induces today incongruously cold coastal sea-surface temperatures (and cool, moist air). Even within this area the actual points where *Cryptochiton* is found in the middens are those where upwelling is intense (and where ecological conditions were favorable). Other mollusks in the middens confirm the picture. We can feel sure that roughly a millenium ago the winds were predominantly northerly, as now, and that they were, for some reason, sufficiently more intense or persistent to cause even greater upwelling then than now.

Long persistence in available water supplies is indicated by the evidences of especially large aboriginal populations where surface water still remains, or would now exist if the climate turned somewhat more moist. There are many indications through the arid West of ancient and often more or less continuous populations about springs that still flow, or along streams or lakes. Other populations existed, at times as early as 10,000 to 25,000 or more years ago, where streams or lakes are now intermittent, but would contain more or less permanent water if the rainfall were moderately increased. Similar indications can be cited for coastal sites. For instance, radiocarbon dates of approximately 3,500, 3,900, and 7,300 years B. P. have been obtained from camp or village sites along Batiquitos Lagoon in San Diego County, California, right beside a present-day cattail marsh. Along the northern Baja California coast ancient habitation signs dated at about 900 and 2,500 to 3,000 years B. P. tend to be concentrated near the mouths of streams that are still more or less permanent.

POSSIBLE PREDICTIONS

It is obvious that we can venture predictions of future climate only with great uncertainty. Past changes, however, lead us to believe that the climate will almost surely fluctuate widely, perhaps rather abruptly. It is almost certain that the fluctuations, however great or abrupt, will be superimposed on a geographic pattern much like that of the present.

As to temperature, I see no clear suggestion of what we may expect. We have some indication of negative correlation between temperatures along the Baja California coast and in the far north about 900 years ago, and rather definite indication of the cooling of the southern half of California during the recent arctic amelioration. There are suggestions that cool periods as well as warm periods over the past few thousand years were more moist than the present. The general trend since Wisconsin time has been toward warmer weather, but with great fluctuations, and this trend is contrary to the longer-term trend toward cooler conditions. The apparent recency of the evolution of desert conditions in the American Southwest suggests at least continued heat in this area.

As to aridity I feel rather strongly that the long-term trend toward dryness has been continuing, perhaps with acceleration. If so, the trend may well continue into the future. At least, we ought to be prepared, on the existing incidence, to meet the very strong possibility, if not probability, of even increased aridity in the Southwestern regions, including Southern California and Baja California. It would be most unwise to plan otherwise.

DISCUSSION

Isaacs: As I remember, in his book *Two Years Before the Mast*, Dana told about trees on Point Loma.

Schaefer: Dana and some of the others were left on the beach to cure hides and they had to go out to cut the wood. He described it as brush or small trees.

Isaacs: I always thought the storms he described were exaggerated. He was in a small ship and I have always thought that they were probably ordinary storms as we now experience, but some time ago I picked up an edition of *"Two Years Before the Mast"* that I had never seen before. An epilogue in it records a conversation that Dana had with a ship's captain in San Francisco in 1859. Dana came back to this coast in 1859, and in this conversation, the ship's captain said that the storms off Point Concepcion had stopped some time ago. They had not seen anything like them since. I now feel that it is quite possible that these were storms of some significance. I have often wondered about the storms because he described them in quite vigorous terms, as being much more severe than the storms around Cape Horn.

Hubbs: I will have to look into this historical evidence.

One of the things I particularly want to do is to get some botanist to identify the charcoal fragments from ancient hearths so that we can reconstruct the vegetation of various regions at the determined times. There is promise, I think, of our being able to reconstruct the past oceanography, climate, and human occupation.

Namias: Do you have any ideas as to what produces weather regime?

Hubbs: Are you asking me?

Namias: You made a prediction that it would be drier.

Hubbs: Well, over enough millenia, it will be.

Charney: The changes of which you speak are probably part of a word-wide pattern. It would be interesting to see if one could find the same thing, say, on the west coast of Africa.

Hubbs: I have not looked into this, but when Ahlmann was at Scripps, he mentioned that there is some evidence that in Portugal there was cooling during the period of Arctic amelioration.

Charney: The reduction of temperature contrast in the past would probably have weakened the westerlies. This would have slowed down the ocean circulation.

Hubbs: The general pattern has probably long remained the same, because the locations of upwelling are such that if we had had south winds instead of northwest winds, the pattern would have been reversed, so that it would be cold where it is now warm, and warm where it is now cold. However, the evidence from remains of fauna in kitchen maidens is such that reversals could not have taken place along the coast of California and western Baja California since late Pleistocene time.

Charney: What is hard for me to imagine, is how the small change in the same weather pattern could produce enough additional rainfall in the arid regions to enable you to measure it.

Namias: In the climatic pattern of this last winter, we have had storm activity spreading into the southwest with surprising frequency. The smallest disturbances would trigger rains in Arizona and Mexico, for instance. This condition was associated with very warm air in the Labrador area (Fig. 8). The normal temperature contrast between the subtropics and the polar regions was reduced. This increase in precipitation at lower latitudes probably extended over the southern North Atlantic and possibly into the British Isles, Spain and Portugal.

Fleming: Hubbs, what do you mean by this aridity?

Hubbs: Less water for people to drink is the main thing.

Fleming: Do you actually mean to imply that there would be less evaporation from the oceans, too?

Hubbs: That of course goes right with it, and the change has been both in the evaporation and the rainfall.

Fleming: I cannot imagine that there is much change. I would assume that the long-term average evaporation over the ocean must remain relatively constant. Although, obviously, we have had a short term change in the last two years.

Namias: Why should it remain constant?

Fleming: Evaporation amounts to just about a meter of water per year. The thing that brought this to mind, first of all, was this statement made that during the Pleistocene there must have been tremendous changes in the amount of precipitation. Of the estimates I have been able to get out of my geological friends, the total amount of ice accumulated during the glacial period would result in about a millimeter of water evaporated from the ocean per year. This, incidentally, is about the same rate the sea level has risen in the last fifty years. This great change of the evaporation precipitation balance, which gave rise to the glaciers and their subsequent melting therefore resulted from an imbalance of only about 1/1000 of the mean annual evaporation. It reflects a very small annual change in the distribution of water between land and ocean. The change over millenia is, of course, conspicuous, and is essentially a very sensitive thing. I question whether you have to invoke this idea of large changes in precipitation patterns. Certainly you can, but can it be world wide?

Charney: These temperature changes we are speaking of, 2 or 3 degrees decrease in the south and 2 to 3 degrees increase in the north, would produce 10 to 15 percent changes in the wind pattern. Such changes in the mean westerly winds would in turn produce large shifts in the semi-permanent centers of action, and probably even larger changes in the wind-driven ocean circulation patterns.

Hubbs: What would this circulation change then do to north-south temperature gradient?

Fleming: Would it increase it in terms of the ocean as an equalizer?

Charney: I don't know the answer to that. A decrease of wind would perhaps reduce the intensity of the ocean circulation and hence the heat transported northward by the oceans. This change in transport would have to be compatible with the reduced north-south temperature gradient in the atmosphere. The oceanic heat transport across latitudes is usually considered to be small compared with that of the atmosphere, but do we actually know this?

Saur: It is on the order of 10 percent at mid latitudes, according to Jung.

Charney: I have heard this, but does anyone believe it? The oceans certainly transport heat from equatorial to polar regions. The question is: how much do they transport?

Saur: How much? Jung's figures are fairly good, I believe.

Charney: How did Jung arrive at them?

Saur: He took the Atlantic stations and used, I think, latitudinal sections of stations across the Atlantic, balanced each one for the current, and constructed a pattern of currents for the whole Atlantic on the basis of a geostrophic circulation. He also used salt transports in establishing the pattern.

Charney: But how did he know what the deep currents were?

Saur: He took a section of stations and adjusted his levels of no motion till there was essentially no net mass transfer through the section.

Comment: Isn't it so that there is an infinite number of solutions to this problem? Any current assumed will give you the surface topography that will also satisfy continuity, so nobody really knows what the deep currents are unless you measure them. Is he trying to get something for nothing here?

Fleming: But one thing that you do know, is that the heat transfer of that part of the ocean is negligible.

Charney: But do we know this?

Fleming: You can at least set certain limits on it in terms of the heat budget. You can consider how much water sinks from the surface in the higher latitudes and rises at the Equator, and you can set upper limits. We might have violent circulation in the deep ocean, but this will not give you net flux of heat. This water may be circulating very rapidly in the deep water, but it will not give you any net flux across latitudes. Thus the deep currents are not important in the heat budget.

Saur: I agree to your argument that although we do not know accurately how fast the currents are going in the deep ocean, that would not be very important here. We can set some sort of limits.

Charney: Well, put it this way: we know that the atmosphere plus the oceans receive a certain amount of excessive heat in the southern equatorial regions, and deficient heat in the polar regions, therefore this heat has to be transported either by the atmosphere or the ocean. There is no other way. What part of this transport is carried by the oceans? If we had an accurate idea, for example, of how much the atmosphere transferred, exactly how much was coming in and going out, we could then ascribe the difference to the oceans, but we do not have that idea. I think Jung's figure does not contradict anything we know. The oceanic transport could be twice as great as the atmosphere or half as great.

Saur: His figure for oceanic heat transport is twice that given in *The Oceans,* but he still attributes more heat transport to the atmosphere than to the oceans.

Charney: There is probably no point in trying to speculate because in a few years we will be able to get numbers. A difficulty, of course, is, or will be, that a proper climatic theory must consider the atmosphere and the oceans as a coupled dynamical system. A change that takes place in the atmospheric circulation will produce a change in the ocean surface temperatures and thereby produce changes in the atmosphere.

Hubbs: Sometime it would help to have paleotemperature data from Japan at the same periods we are getting it over here. Are there any, Takenouti?

Takenouti: No.

Hubbs: That would be a very interesting thing to do in Japan. If we obtained the same data 1000 years ago here, and 1000 years ago there, it would be extremely interesting comparing them.

Fleming: Three hundred miles off Washington Coast we get into a band of non-calcareous sediments. What is interesting in making a time reference is that we can find this band of non-calcareous sediments, which is an indication of warmer water conditions, extending all the way up the Gulf of Alaska, where there it is about a foot or 18 inches of non-calcareous sediment material. Considering a reasonable rate of sedimentation, this appears to represent a few thousand years. Definitely there must have been some change in the character of the circulation and of the temperature from roughly 50° to 55° or 56° N. We are going to try to get some carbon-14 dates from that layer.

Hubbs: Oxygen-18 determinations too would be tremendously significant. The deposit might be interglacial.

Fleming: Another thing we have that makes a good marker, is the ash fall, ash layers that occurred about 6000 years ago. They constitute a very useful sort of marker.

Hubbs: Apparently the volcano that went off with a big bang was Mount Mazama. There were Alaskan volcanoes too. The ash falls certainly could help.

THE OFFSHORE DRIFT OF LARVAE OF THE CALIFORNIA SPINY LOBSTER *PANULIRUS INTERRUPTUS*[1]

MARTIN W. JOHNSON

The information that I have to offer regarding the drift of the larvae of the California spiny lobster *Panulirus interruptus* (Randall) will perhaps not contribute much directly toward indicating the relative strength of the northward components of water flowing along our coast during the past year. It will, however, point up some interesting questions regarding water currents and recruitment of lobster stock. I will be able to show you in a way that has not been done before, what happens to a floating population of larvae originating near the coast of Southern and Baja California.

For the discussion to follow it is important to note that the adult *Panulirus interruptus* is reported to range from slightly north of Point Conception southward to Manzanillo, Mexico. From the present study it appears that the main centers of concentration are in the regions of the Channel Islands and of Cedros Island off Baja California.

For those of you who are not familiar with the life history of the spiny lobster, it should be said here that the adult female carries its eggs attached to the swimming feet. The larvae, which hatch from the eggs, are thoroughly transparent, flat and thin as a bit of paper, and are known as "phyllosoma." The first stage is about 1½ mm long and the last stage is about 30 to 32 mm long. Between each stage, of which there are eleven, there is a shedding of the old skin to allow for increased growth.

When released in the water, these larvae float about with prevailing currents like so many tiny drift bottles. The last phyllosoma stage metamorphoses into a "purulus" stage which, though still transparent, resembles the adult and soon seeks the bottom to assume the adult habit.

With this brief background we can now discuss in a summary way, when and where these larvae first appear in the plankton as Stage I, and when and where they are found in subsequent stages. A much more complete analysis will be published in the Bulletin, Scripps Institution of Oceanography, University of California, 1960. Here, it will suffice to give only a few typical examples selected from seven years of study based on the monthly plankton collections made by the California Cooperative Oceanic Fisheries Investigation. Involved are a great number of stations extending along the coast from above Cape Mendocino to well below Cape San Lucas, and seaward to distances up to 200 to 300 or more miles (Fig. 1). The collections were made with a one-meter net towed obliquely usually from 70-0 meters or 140-0 meters.

Figure 135 shows the periods of the year in which each of the phyllosoma stages I to XI were found during each year of the seven-year study period. The first stage occurs only from about mid-June to mid-November (once in early December). A line drawn through the mid-period of occurrence of the successive stages, indicates that the total larval life, Stages I to XI, requires about 7¾ months. Hence, for this long period the larvae are presumably drifted about at the mercy of prevailing water currents.

In a summary (Fig. 136) of many samples, it can be seen that the source of larvae is at the immediate coast or in the vicinity of islands. This is, of course, in keeping with the known distribution of the adults.

The later larval stages occur in diminishing numbers and usually at greater distances from the coast (Fig. 137). In general, there is a drift of larvae to the south and southwest. This is to be expected in view of the prevailing southward flow of the California Current.

Rarely are larvae found to the north of Point Conception. There is a notable exception shown in figure 138. A Stage X larva was caught in May 1954 about 200 miles at sea in the latitude of Monterey Bay. It is difficult to account for this specimen on the basis of the calculated prevailing currents. It was found in water characterized as Southern or Central Pacific by the presence of only one variety, (i.e. *californicus)* of the copepod *Eucalanus bungii,* in contrast to the inshore tongue of colder water where the northern variety *Eucalanus bungii bungii* constituted up to 28 percent of this species. There is also a record of a Stage I larva taken August 1954 near the coast just north of Monterey Bay in 14°C water in which only *Eucalanus bungii californicus* was found.

Evidence of flushing of larvae from a restricted area is shown in figures 139 and 140. The area around the Channel Islands was surveyed by a cruise, the second half of which immediately resampled the stations visited during the first half. During the first sampling 41 percent of the stations located inshore of the dashed line shown in the figures yielded Stage I larva, whereas none were found there during the second sampling.

Despite these instances of larval dispersal, it is amazing that when the whole area is considered, there is so little direct evidence of larvae being flushed wholesale from the area. Evidently there prevail along the coast countercurrents, long back swirls, and eddies that effectually retain a good number of larvae up through the later stages within or near the area of adult distribution even for so long a period as 7¾ months. The calculated dynamic anomalies, which

---

[1] Contribution from the Scripps Institution of Oceanography.

Reproduced by Permission

were here kindly provided by the Hydrographic Section, describe patterns of flow tending to support this view. The charts shown in figures 141 to 147 illustrate such back currents as are at times detected from hydrographic studies. Some of these charts also show sections as having currents which, if continuous for long periods, would flush all surface living larvae from the area.

Doubtless many, if not most, of the later stage larvae which we have caught at stations distant from the shore or south of the heavy dashed line shown in figures 136 and 137 are on their way out on currents that will sweep them into uninhabitable areas. What portion of the larval population this loss may represent we cannot estimate with any certainty without further extension of our collecting methods to include more sampling at or near the bottom in both shallow and deep water. For it is not entirely clear just what hydrographic mechanisms combined with larval behavior make possible a recruitment of lobsters sufficient to support the rather stable lobster fisheries that we enjoy.

DISCUSSION

Sette: Dr. Johnson, I am going to ask the first question. Do you have some data on larvae for the last year or two?

Johnson: We have not sorted all of the 1957 material as yet but we have made certain spot tests to give some idea of what is taking place with regards to larval distribution in 1957. At least some significant data seem to be emerging. In the first place, the larvae appear not to have been swept in detectable numbers to the north of Point Conception, or if they are swept to the north they quickly succumb to changing conditions. But as shown in figure 147 for the July 1957 cruise, there is an unusually large number of early-stage larvae in the region of the Channel Islands. The number of Stage I larvae taken in that area was far above average for the area for past years, and furthermore these larvae were present in numbers greater than ever before during the month of July, which appears to indicate that hatching had begun about a month earlier than usual.

Another unexpected feature of this cruise is the almost complete absence of larvae from the collections south of Punta Eugenia as if there had been an intrusion of phyllosoma-free water from offshore. The dynamic height anomalies seem also to bear this out. It can also be said that more late stage larvae were taken between February and July than for that period in any previous year. Thus, while the data do not show more drift out of the area, there appears to have been some earlier hatching in the northern part of the range and probably a better survival to later stages or better retention, especially in the Baja California area.

Isaacs: Would you say that most of the population has shifted to the north?

Johnson: No, larvae are still abundant in the central Baja California area, but there might have been some shift northward from below Punta Eugenia during July. However, for other months, especially October 1957, this is not borne out.

Berner: Could the larger number of Stage I larvae in the Channel Islands area be explained by a water movement along the coast carrying larger numbers from the south into the Channel Islands area?

Johnson: Yes, this could be so, since the larvae apparently remain in Stage I for a matter of two to three weeks. However, the presence of so many as 76 larvae at one station argues against the idea that there had been much opportunity for dispersal prior to the catch. But still it is probable that the lobsters in that area are largely restocked by settlement of larvae that have drifted in from the south. The extent of adult migration into the area is not known.

Radovich: Regarding the possibility of the lobsters getting back to the Channel Islands area, I talked with a gentleman from the cannery at San Quentin who mentioned a rather interesting phenomenon. He had observed a school of full-sized, 12-16-inch lobsters swimming at the surface. He had never seen this before but in talking with other lobster fishermen in the area, they told him they had witnessed this phenomenon some few months before. One fisherman has used scoop nets to fill this boat with lobsters. This sounded peculiar to me and I mentioned it to Mr. W. L. Scofield at the California State Fisheries Laboratory. He said that about 20 years ago he interviewed a fisherman who had observed the same phenomenon.

Johnson: On the whole, I have considerable respect for observations made by fishermen, but sometimes they do make mistakes.

Davies: This is similar to a report from one of our South African lobster fishermen, who witnessed thousands of lobsters swimming all in one direction.

Marr: There is a record of marked spiny lobsters at Bermuda having been released offshore at the surface over deep water and fifty miles from the island. Subsequently, they were recovered at approximately the same place from which they were taken originally. The supposition was that they swam back instead of sinking.

Johnson: There have been tagging experiments on our local lobster which show some short migrations but mostly random movements so far as we know.

Sette: I suppose the question before us is whether or not the drift of larvae differed in 1957 from previous years. According to conclusions you have drawn from your charts, they drift with no swimming effort and should reflect changing conditions. We will look forward to a more complete story when more data have become available.

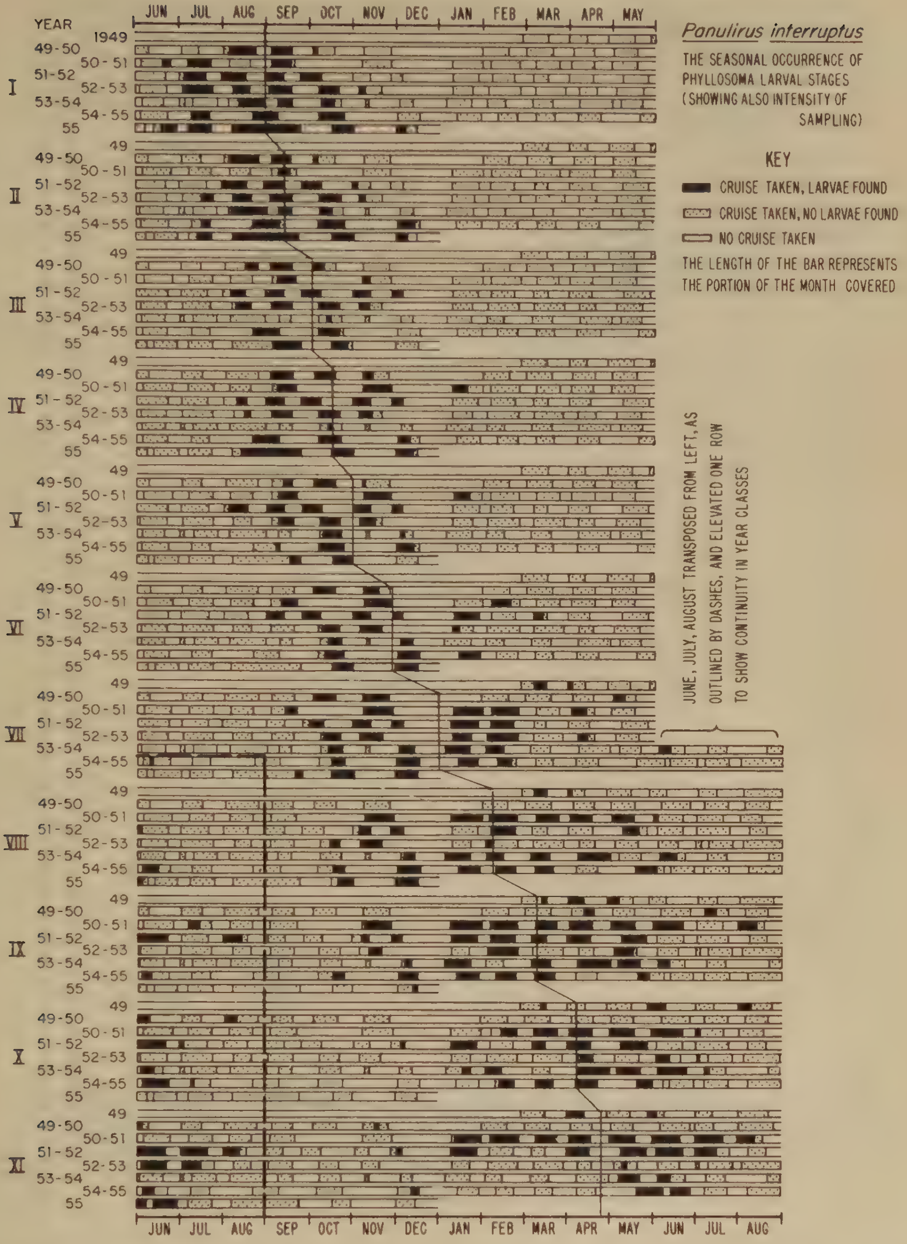

FIGURE 135. Seasonal occurrence and duration of larval stages of *Panulirus interruptus*, with indication of the intensity of sampling.

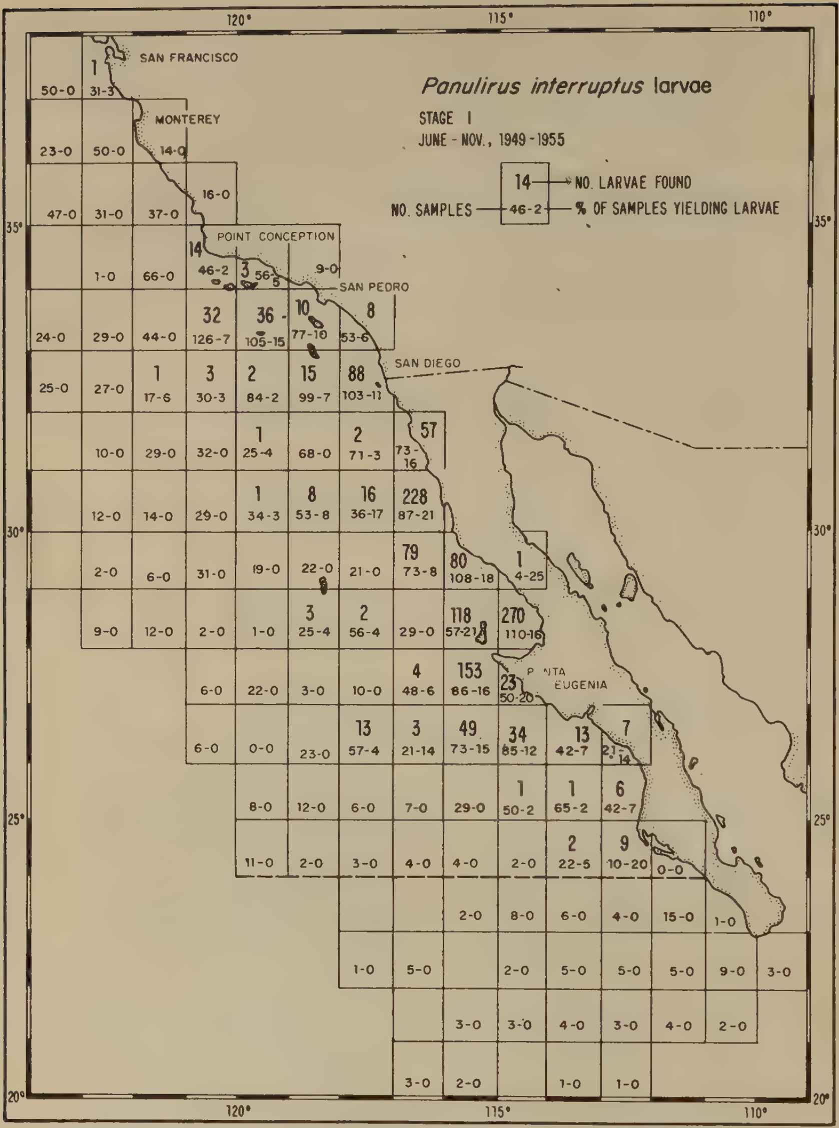
Panulirus interruptus larvae
STAGE I
JUNE - NOV., 1949 - 1955
14 → NO. LARVAE FOUND
NO. SAMPLES — 46-2 — % OF SAMPLES YIELDING LARVAE
SAN FRANCISCO
MONTEREY
POINT CONCEPTION
SAN PEDRO
SAN DIEGO
PUNTA EUGENIA
120°
115°
110°
35°
30°
25°
20°
50-0, 1 31-3
23-0, 50-0, 14-0
47-0, 31-0, 37-0, 16-0
1-0, 66-0, 14 46-2, 3 56-5, 9-0
24-0, 29-0, 44-0, 32 126-7, 36 105-15, 10 77-10, 8 53-6
25-0, 27-0, 1 17-6, 3 30-3, 2 84-2, 15 99-7, 88 103-11
10-0, 29-0, 32-0, 1 25-4, 68-0, 2 71-3, 57 73-16
12-0, 14-0, 29-0, 1 34-3, 8 53-8, 16 36-17, 228 87-21
2-0, 6-0, 31-0, 19-0, 22-0, 21-0, 79 73-8, 80 108-18, 1 4-25
9-0, 12-0, 2-0, 1-0, 3 25-4, 2 56-4, 29-0, 118 57-21, 270 110-16
6-0, 22-0, 3-0, 10-0, 4 48-6, 153 86-16, 23 50-20
6-0, 0-0, 23-0, 13 57-4, 3 21-14, 49 73-15, 34 85-12, 13 42-7, 7 21-14
8-0, 12-0, 6-0, 7-0, 29-0, 1 50-2, 1 65-2, 6 42-7
11-0, 2-0, 3-0, 4-0, 4-0, 2-0, 2 22-5, 9 10-20, 0-0
2-0, 8-0, 6-0, 4-0, 15-0, 1-0
1-0, 5-0, 2-0, 5-0, 5-0, 5-0, 9-0, 3-0
3-0, 3-0, 4-0, 3-0, 4-0, 2-0
3-0, 2-0, 1-0, 1-0

FIGURE 136. Summary of geographic distribution of Stage I phyllosoma larvae of *Panulirus interruptus* for the hatching periods June-November of 1949-1955 inclusive. The number of larvae caught, the number of samples taken, and the percentage of samples yielding larvae are shown for each one-degree square.

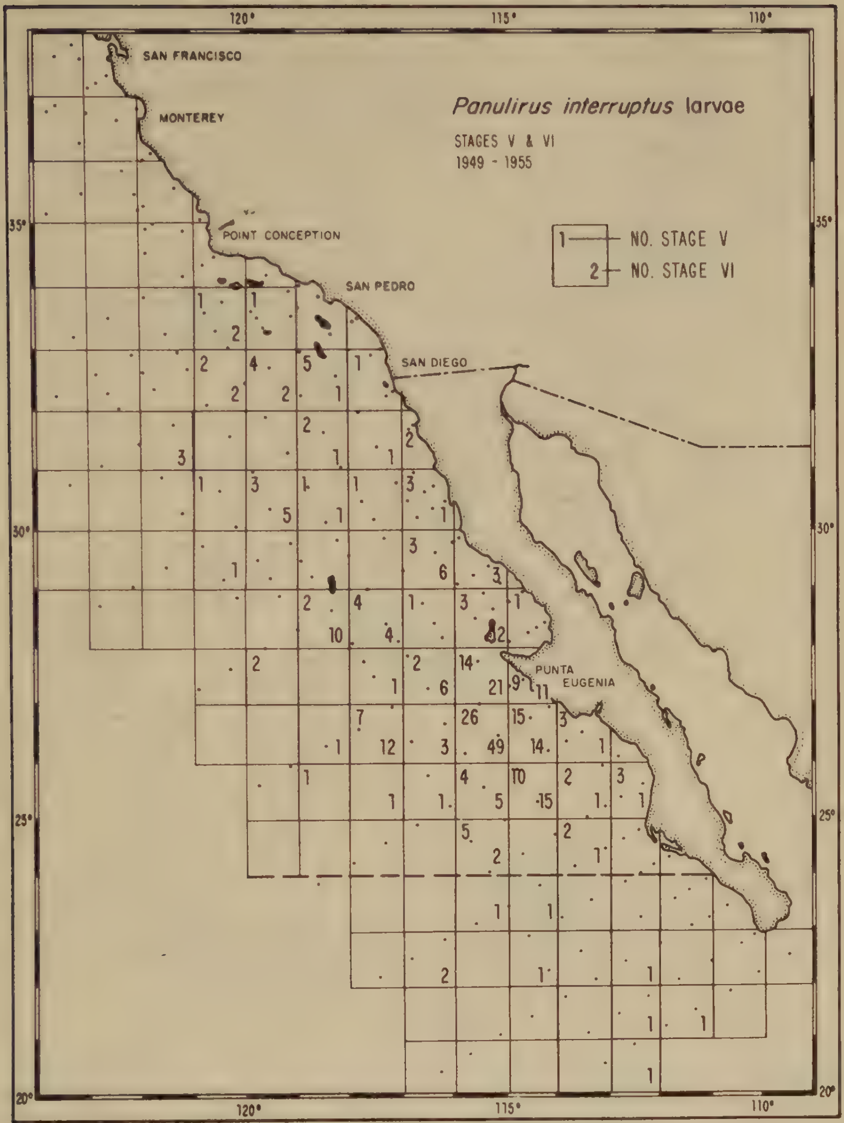
Panulirus interruptus larvae
STAGES V & VI
1949 - 1955
1 NO. STAGE V
2 NO. STAGE VI
SAN FRANCISCO
MONTEREY
POINT CONCEPTION
SAN PEDRO
SAN DIEGO
PUNTA EUGENIA
120°
115°
110°
35°
30°
25°
20°

FIGURE 137. Summary of geographic distribution of Stages V and VI larvae of *Panulirus interruptus*, 1949-1955 inclusive. The numbers of larvae caught are shown for each one-degree square.

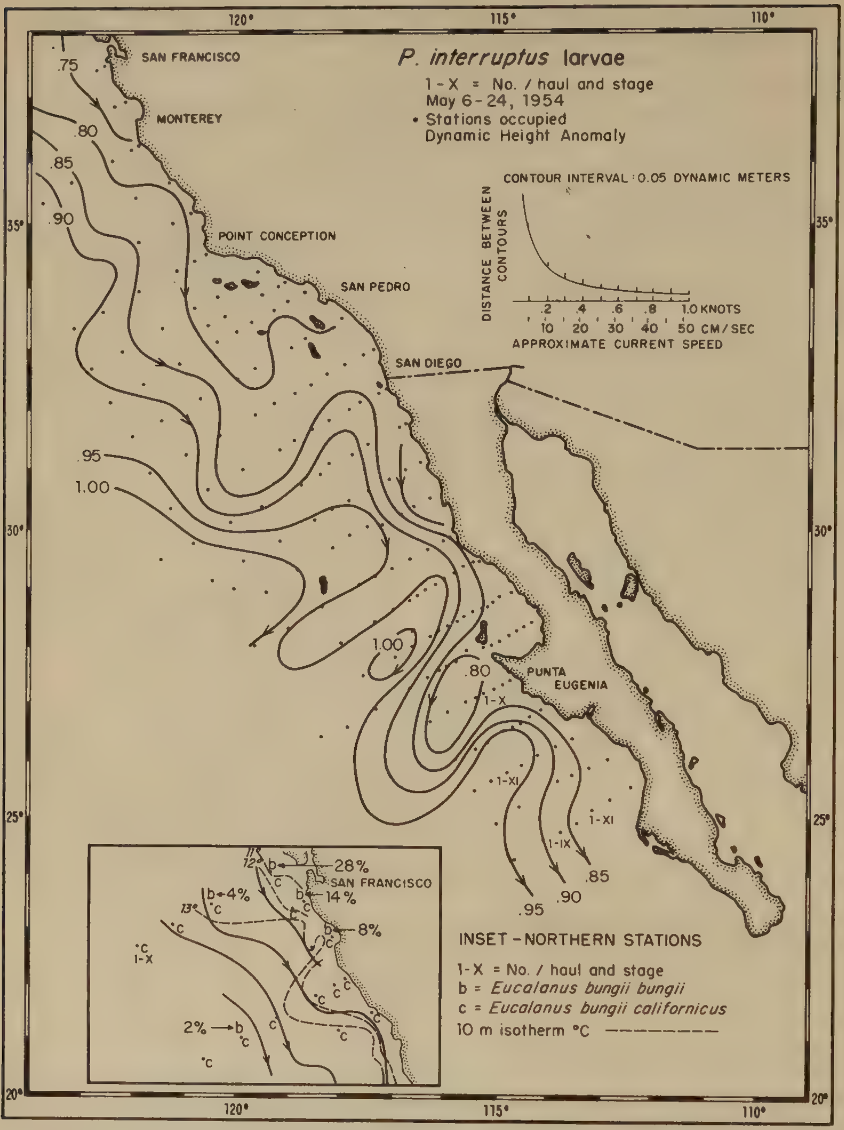
P. interruptus larvae
1-X = No. / haul and stage
May 6-24, 1954
• Stations occupied
Dynamic Height Anomaly
CONTOUR INTERVAL : 0.05 DYNAMIC METERS
DISTANCE BETWEEN CONTOURS
.2 .4 .6 .8 1.0 KNOTS
10 20 30 40 50 CM/SEC
APPROXIMATE CURRENT SPEED
SAN FRANCISCO
MONTEREY
POINT CONCEPTION
SAN PEDRO
SAN DIEGO
PUNTA EUGENIA
.75
.80
.85
.90
.95
1.00
1.00
.80
1-X
1-XI
1-XI
1-IX
.85
.90
.95
120°
115°
110°
35°
30°
25°
20°
INSET - NORTHERN STATIONS
1-X = No. / haul and stage
b = Eucalanus bungii bungii
c = Eucalanus bungii californicus
10 m isotherm °C
11°
12°
13°
28%
14%
8%
4%
2%
b
c
1-X

FIGURE 138. Locality records for *Panulirus interruptus* larvae and dynamic height anomaly (0 over 500 decibars) during May 6-24, 1954 (CCOFI Cruise 5405).

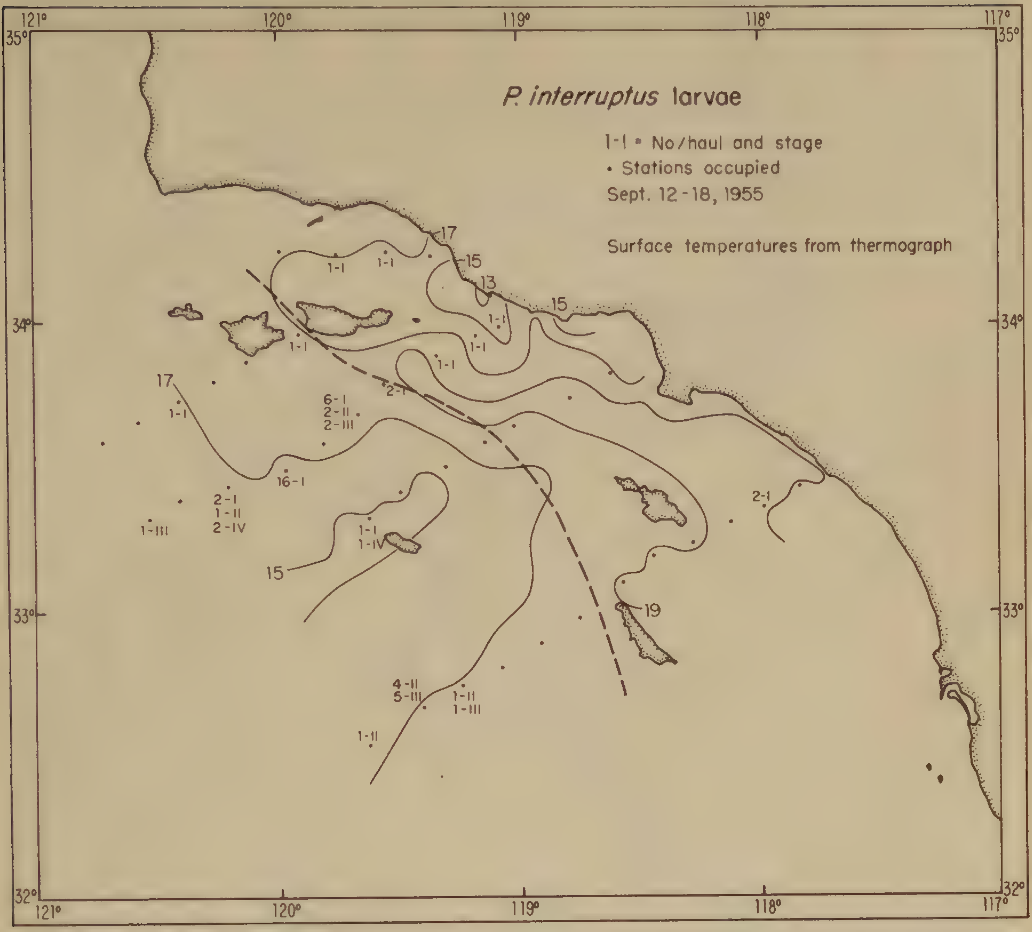
121°
120°
119°
118°
117°
35°
34°
33°
32°
P. interruptus larvae
1-1 = No/haul and stage
• Stations occupied
Sept. 12-18, 1955
Surface temperatures from thermograph
17
15
13
15
17
15
19
1-1
1-1
1-1
1-1
1-1
1-1
2-1
6-1
2-II
2-III
1-1
16-1
2-I
1-II
2-IV
1-III
1-I
1-IV
2-1
4-II
5-III
1-II
1-III
1-II

FIGURE 139. Locality records for *Panulirus interruptus* larvae and surface isotherms in the Channel Islands area during September 12-18, 1955 (CCOFI Cruise 5509). Inner and outer areas separated by dashed line.

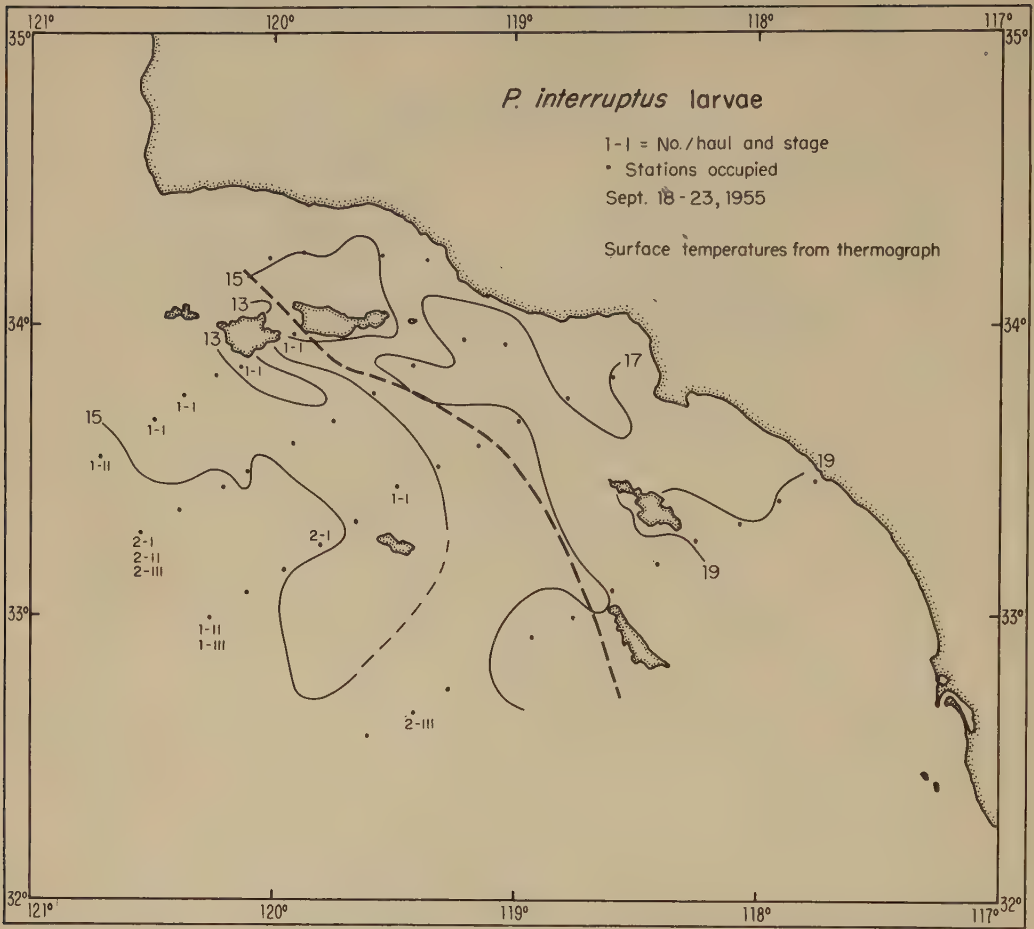
P. interruptus larvae
1-I = No./haul and stage
• Stations occupied
Sept. 18-23, 1955
Surface temperatures from thermograph
121°
120°
119°
118°
117°
35°
34°
33°
32°
15
13
13
15
17
19
19
1-I
1-I
1-I
1-I
1-II
2-I
2-II
2-III
1-I
2-I
1-II
1-III
2-III

FIGURE 140. Locality records for *Panulirus interruptus* larvae and surface isotherms in the Channel Islands area during September 18-23, 1955 (CCOFI Cruise 5509).

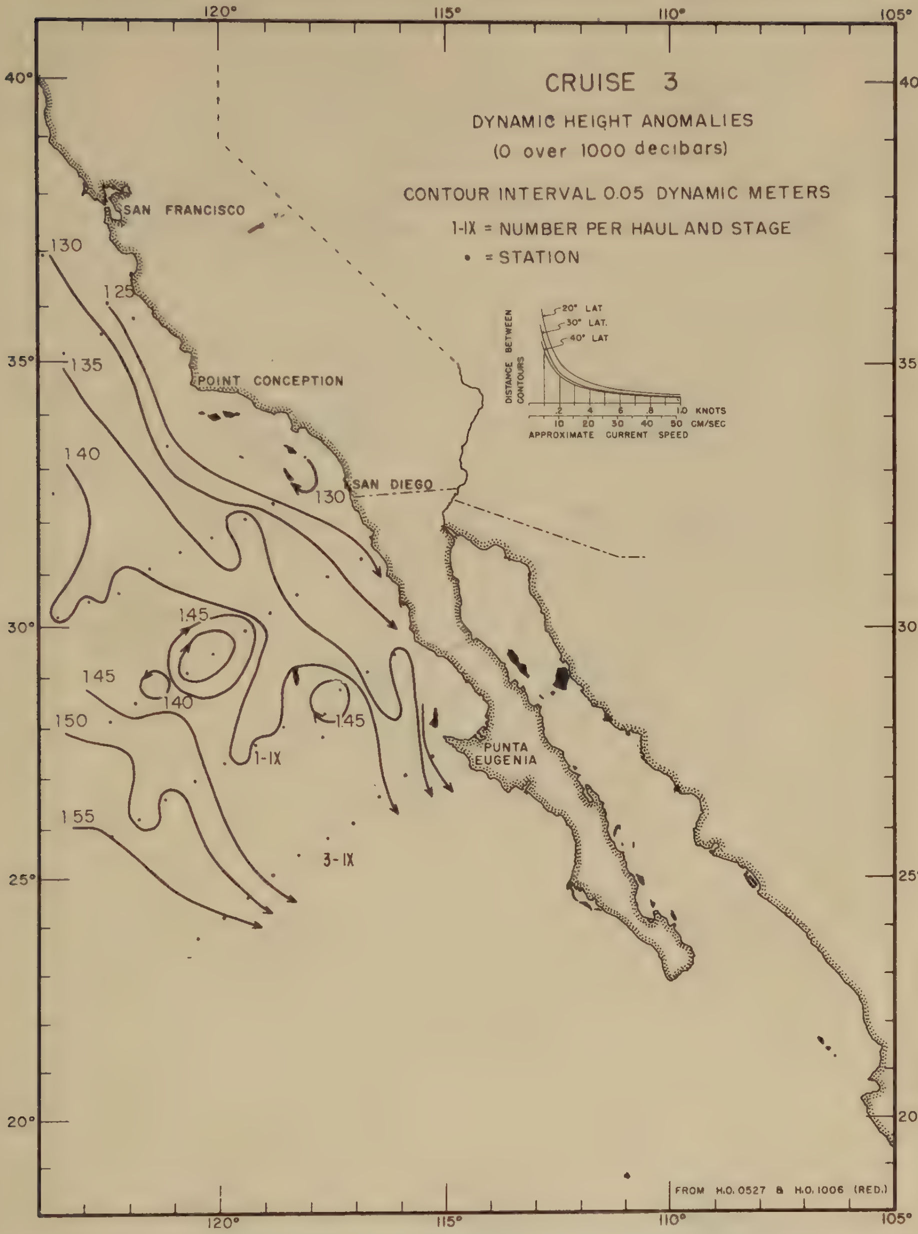
CRUISE 3
DYNAMIC HEIGHT ANOMALIES
(0 over 1000 decibars)
CONTOUR INTERVAL 0.05 DYNAMIC METERS
1-IX = NUMBER PER HAUL AND STAGE
• = STATION
DISTANCE BETWEEN CONTOURS
20° LAT
30° LAT.
40° LAT
.2 .4 .6 .8 1.0 KNOTS
10 20 30 40 50 CM/SEC
APPROXIMATE CURRENT SPEED
SAN FRANCISCO
POINT CONCEPTION
SAN DIEGO
PUNTA EUGENIA
130
125
135
140
145
150
155
1-IX
3-IX
120°
115°
110°
105°
40°
35°
30°
25°
20°
FROM H.O. 0527 & H.O. 1006 (RED.)

FIGURE 141. Locality records for *Panulirus interruptus* larvae and dynamic height anomaly (0 over 1000 decibars) during April 28 to May 14, 1949 (MLR Cruise 3).

(535)

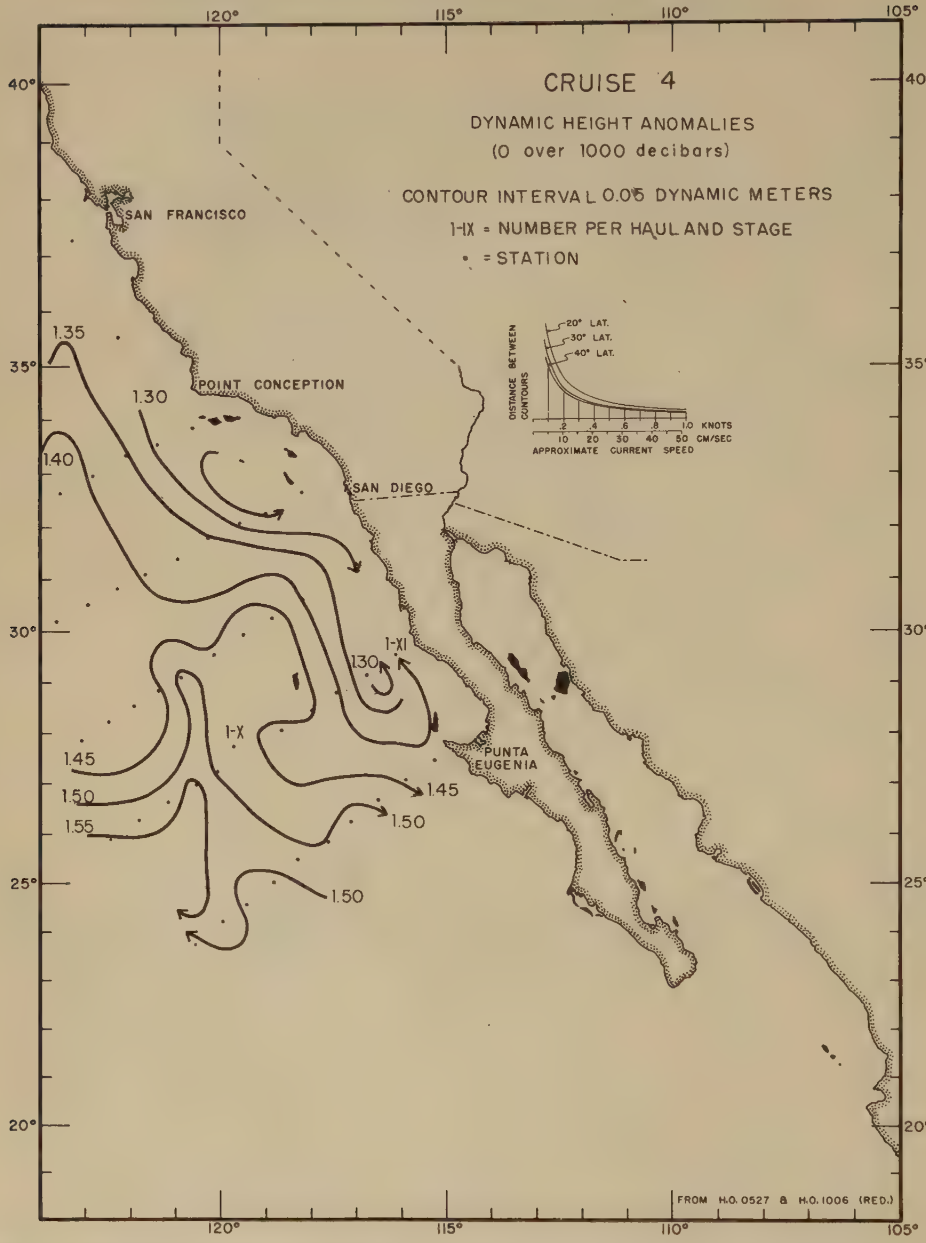
CRUISE 4
DYNAMIC HEIGHT ANOMALIES
(0 over 1000 decibars)
CONTOUR INTERVAL 0.05 DYNAMIC METERS
1-IX = NUMBER PER HAUL AND STAGE
• = STATION
DISTANCE BETWEEN CONTOURS
20° LAT.
30° LAT.
40° LAT.
.2 .4 .6 .8 1.0 KNOTS
10 20 30 40 50 CM/SEC
APPROXIMATE CURRENT SPEED
SAN FRANCISCO
POINT CONCEPTION
SAN DIEGO
PUNTA EUGENIA
1.35
1.30
1.40
1-XI
1.30
1-X
1.45
1.50
1.55
1.45
1.50
1.50
120°
115°
110°
105°
40°
35°
30°
25°
20°
FROM H.O. 0527 & H.O. 1006 (RED.)

FIGURE 142. Locality records for *Panulirus interruptus larvae* and dynamic height anomaly (0 over 1000 decibars) during May 28 to June 9, 1949 (MLR Cruise 4).

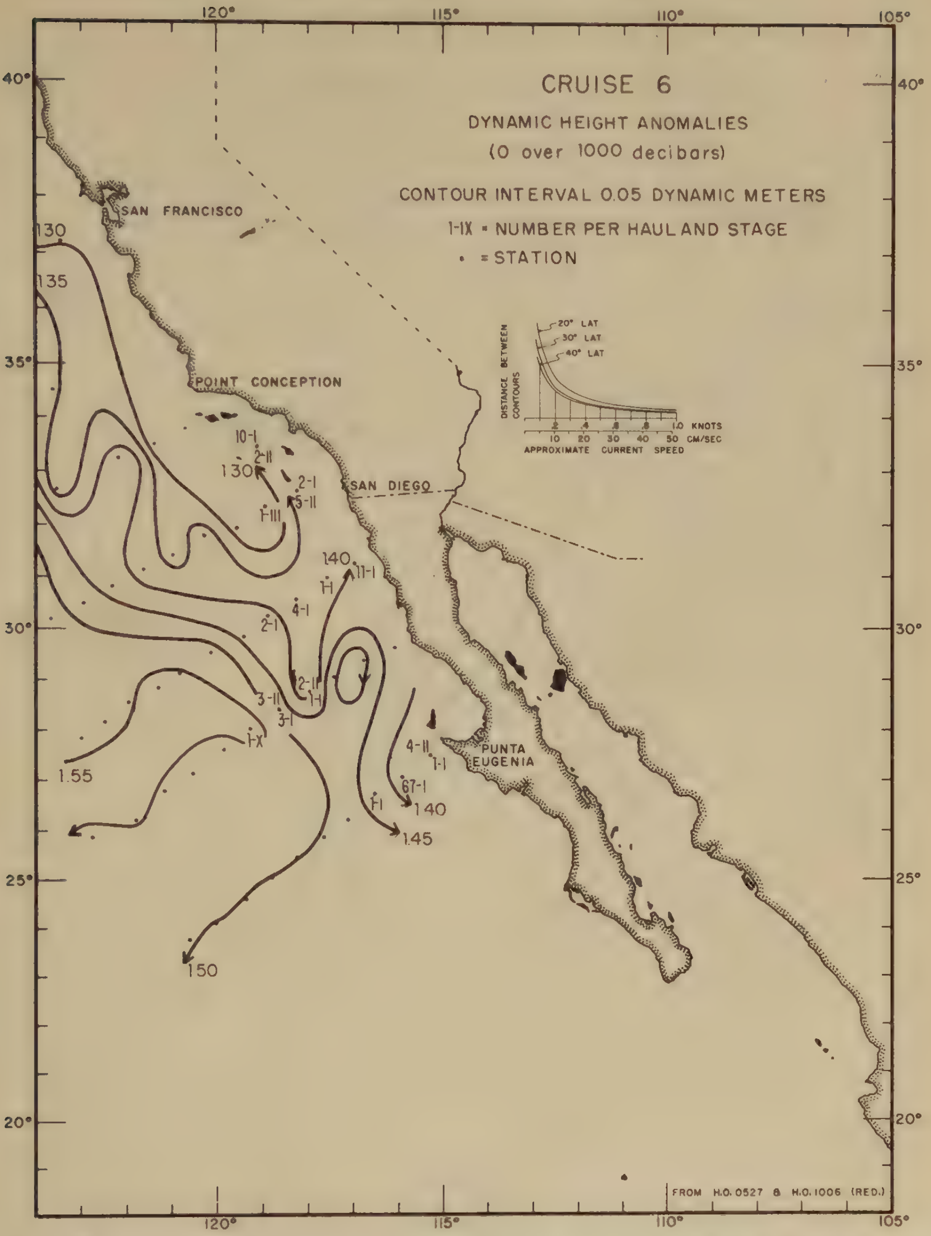
CRUISE 6
DYNAMIC HEIGHT ANOMALIES
(0 over 1000 decibars)
CONTOUR INTERVAL 0.05 DYNAMIC METERS
1-IX = NUMBER PER HAUL AND STAGE
• = STATION
DISTANCE BETWEEN CONTOURS
20° LAT
30° LAT
40° LAT
.2
.4
.6
.8
1.0 KNOTS
10
20
30
40
50 CM/SEC
APPROXIMATE CURRENT SPEED
120°
115°
110°
105°
40°
35°
30°
25°
20°
SAN FRANCISCO
POINT CONCEPTION
SAN DIEGO
PUNTA EUGENIA
130
135
10-I
2-II
1 30
2-I
5-II
1-III
140
11-I
1-I
4-I
2-I
2-II
1-I
3-II
3-I
1-X
4-II
1-I
67-I
1-I
1 40
1.45
1.55
150
FROM H.O. 0527 & H.O. 1006 (RED.)

FIGURE 143. Locality records for *Panulirus interruptus* larvae and dynamic height anomaly (0 over 1000 decibars) during August 2 to 22, 1949 (MLR Cruise 6).

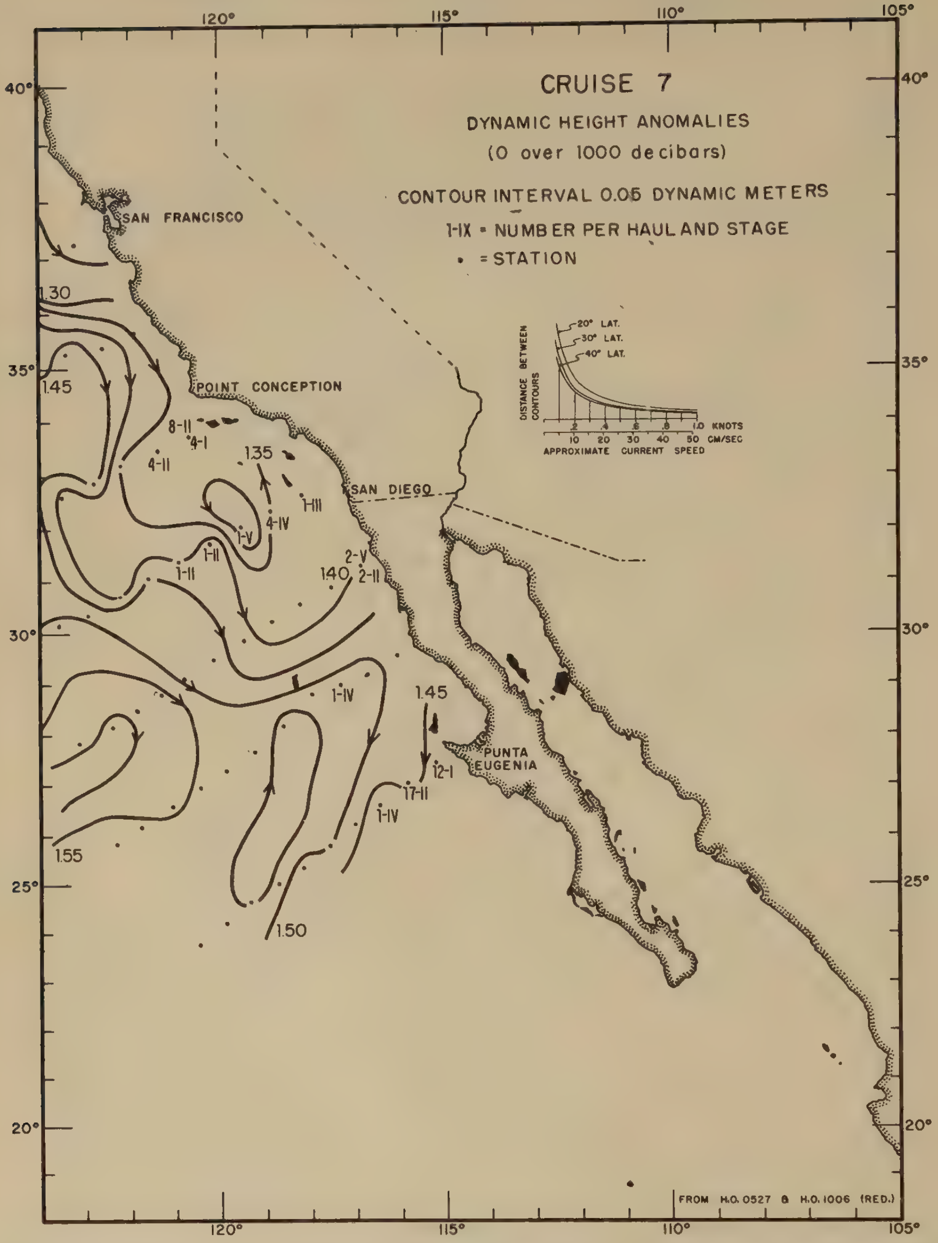
CRUISE 7
DYNAMIC HEIGHT ANOMALIES
(0 over 1000 decibars)
CONTOUR INTERVAL 0.05 DYNAMIC METERS
1-IX = NUMBER PER HAUL AND STAGE
• = STATION
DISTANCE BETWEEN CONTOURS
20° LAT.
30° LAT.
40° LAT.
.2 .4 .6 .8 1.0 KNOTS
10 20 30 40 50 CM/SEC
APPROXIMATE CURRENT SPEED
SAN FRANCISCO
POINT CONCEPTION
SAN DIEGO
PUNTA EUGENIA
1.30
1.45
1.35
1.40
1.45
1.55
1.50
8-II
4-I
4-II
1-II
4-IV
1-V
1-II
1-II
2-V
2-II
1-IV
12-I
17-II
1-IV
120°
115°
110°
105°
40°
35°
30°
25°
20°
FROM H.O. 0527 & H.O. 1006 (RED.)

FIGURE 144. Locality records for *Panulirus interruptus* larvae and dynamic height anomaly (0 over 1000 decibars) during September 4 to 18, 1949 (MLR Cruise 7).

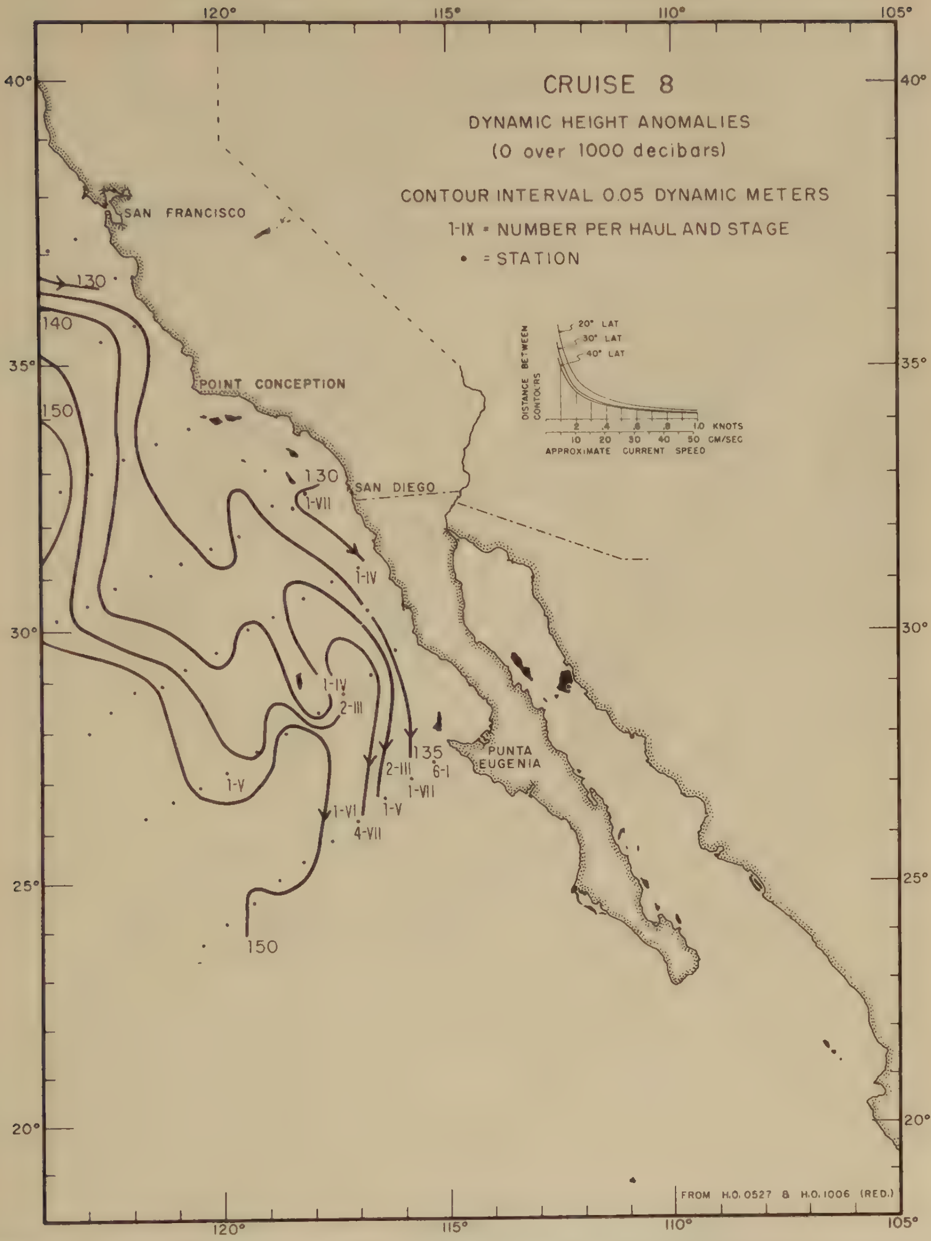
CRUISE 8
DYNAMIC HEIGHT ANOMALIES
(0 over 1000 decibars)
CONTOUR INTERVAL 0.05 DYNAMIC METERS
1-IX = NUMBER PER HAUL AND STAGE
• = STATION
DISTANCE BETWEEN CONTOURS
20° LAT
30° LAT
40° LAT
.2 .4 .6 .8 1.0 KNOTS
10 20 30 40 50 CM/SEC
APPROXIMATE CURRENT SPEED
120°
115°
110°
105°
40°
35°
30°
25°
20°
SAN FRANCISCO
POINT CONCEPTION
SAN DIEGO
PUNTA EUGENIA
130
140
150
130
135
150
1-VII
1-IV
1-IV
2-III
1-V
2-III
6-I
1-VII
1-VI
1-V
4-VII
FROM H.O. 0527 & H.O. 1006 (RED.)

FIGURE 145. Locality records for *Panulirus interruptus* larvae and dynamic height anomaly (0 over 1000 decibars) during October 4 to 19, 1949 (MLR Cruise 8).

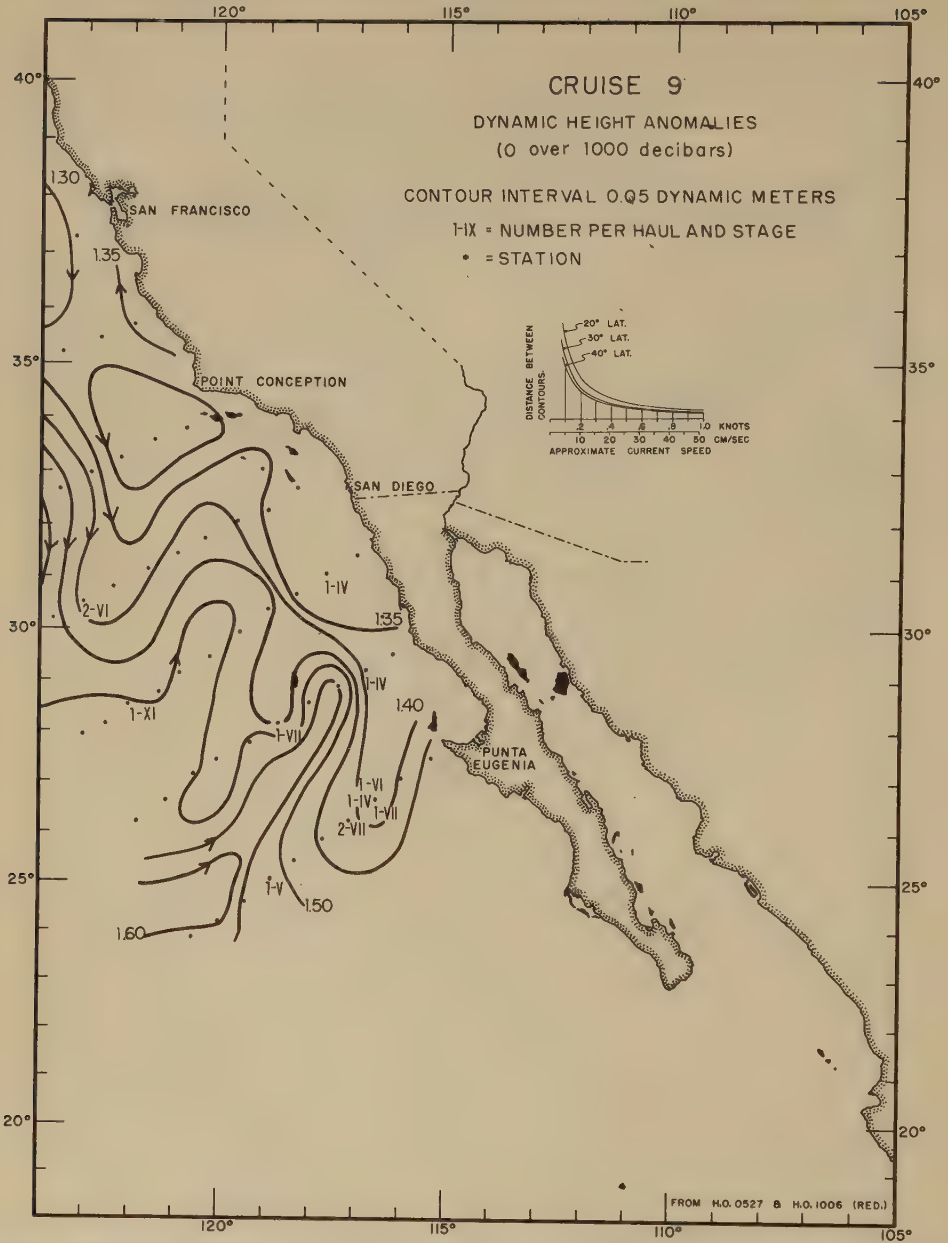
CRUISE 9
DYNAMIC HEIGHT ANOMALIES
(0 over 1000 decibars)
CONTOUR INTERVAL 0.05 DYNAMIC METERS
1-IX = NUMBER PER HAUL AND STAGE
• = STATION
120°
115°
110°
105°
40°
35°
30°
25°
20°
SAN FRANCISCO
POINT CONCEPTION
SAN DIEGO
PUNTA EUGENIA
1.30
1.35
1.35
1.40
1.50
1.60
1-IV
2-VI
1-IV
1-XI
1-VII
1-VI
1-IV
1-VII
2-VII
1-V
DISTANCE BETWEEN CONTOURS.
20° LAT.
30° LAT.
40° LAT.
.2 .4 .6 .8 1.0 KNOTS
10 20 30 40 50 CM/SEC
APPROXIMATE CURRENT SPEED
FROM H.O. 0527 & H.O. 1006 (RED.)

FIGURE 146. Locality records for *Panulirus interruptus* larvae and dynamic height anomaly (0 over 1000 decibars) during November 8 to 25, 1949 (MLR Cruise 9).

(540)

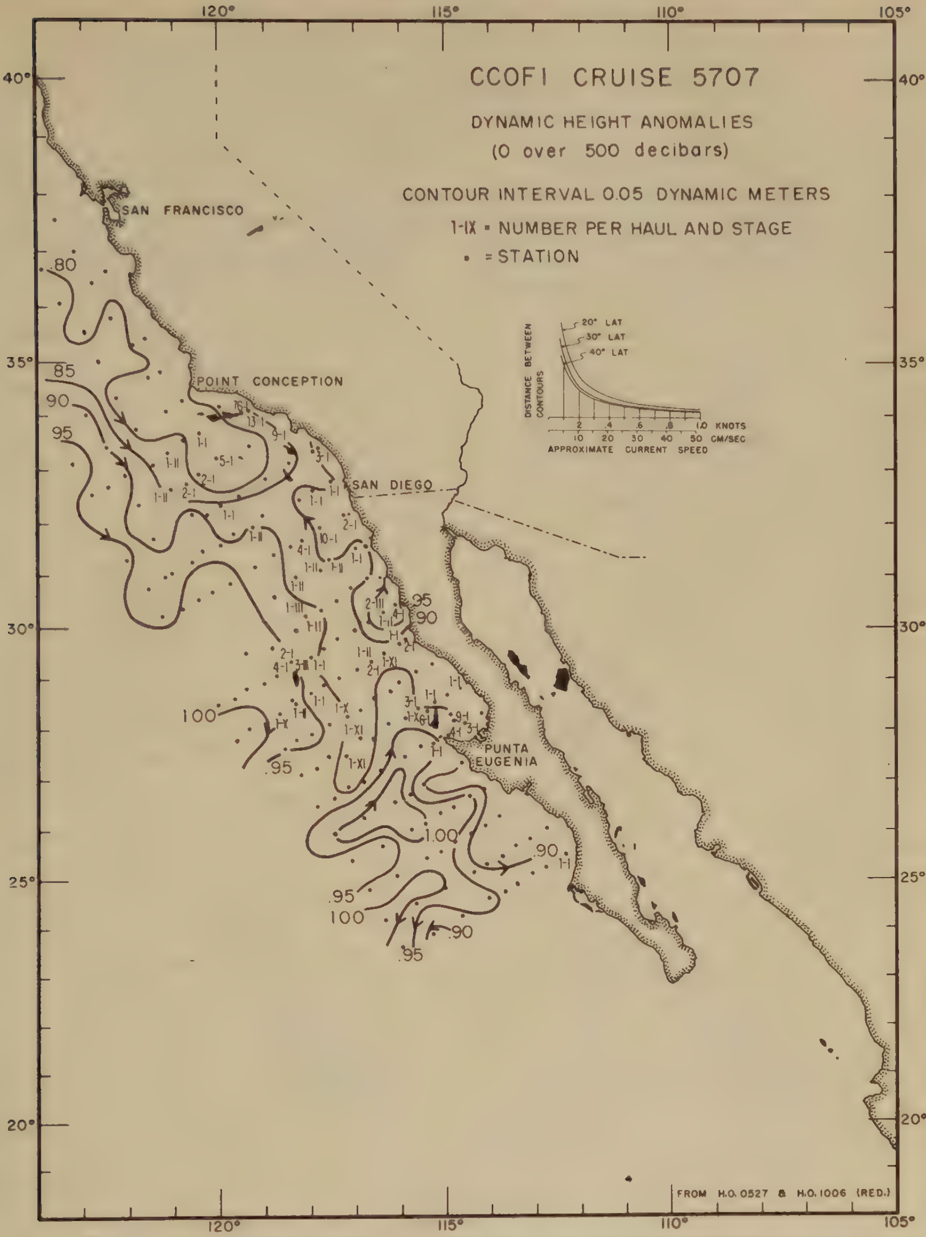
CCOFI CRUISE 5707
DYNAMIC HEIGHT ANOMALIES
(0 over 500 decibars)
CONTOUR INTERVAL 0.05 DYNAMIC METERS
1-IX = NUMBER PER HAUL AND STAGE
• = STATION
DISTANCE BETWEEN CONTOURS
20° LAT
30° LAT
40° LAT
.2 .4 .6 .8 1.0 KNOTS
10 20 30 40 50 CM/SEC
APPROXIMATE CURRENT SPEED
SAN FRANCISCO
POINT CONCEPTION
SAN DIEGO
PUNTA EUGENIA
.80
.85
.90
.95
1.00
120°
115°
110°
105°
40°
35°
30°
25°
20°
FROM H.O. 0527 & H.O. 1006 (RED.)

FIGURE 147. Locality records for *Panulirus interruptus* larvae and dynamic height anomaly (0 over 500 decibars) during July 8 to August 3, 1957 (CCOFI Cruise 5707).

OCEANOGRAPHY OF THE NORTHEASTERN PACIFIC OCEAN DURING THE LAST TEN YEARS[1]

JOSEPH L. REID, JR.

Since 1949 the California Cooperation Oceanic Fisheries Investigations have made hydrographic cruises over the California Current system nearly every month. From these measurements we have been able to construct averages from the first few years' data. We have compared some of the last year's measurements with these longer term averages and the differences are remarkable.

It will be necessary to review briefly the oceanography of the California Current system in order to discuss the recent deviations. I shall draw upon a recent paper (Reid, Roden, and Wyllie, 1958) published in the latest CCOFI Progress Report for this general discussion and for the first five figures, and then proceed to the more recent work.

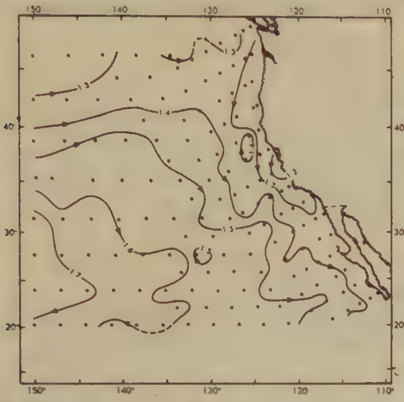

150
140
130
120
110
40
30
20
150°
140°
130°
120
110°

FIGURE 67. Surface current off the western coast of North America in August, 1955. Dynamic height anomalies, 0 over 1000 decibars, in dynamic meters.

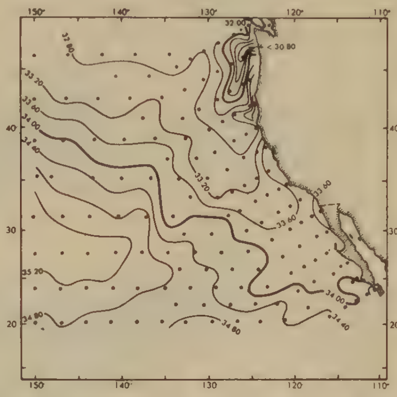

150°
140°
130°
120°
110°
32.00
< 30.80
33.20
33.60
34.00
34.40
35.20
34.80
34.00
40
30
20

FIGURE 69. Salinity at 10 meters, in parts per mille. August 1955.

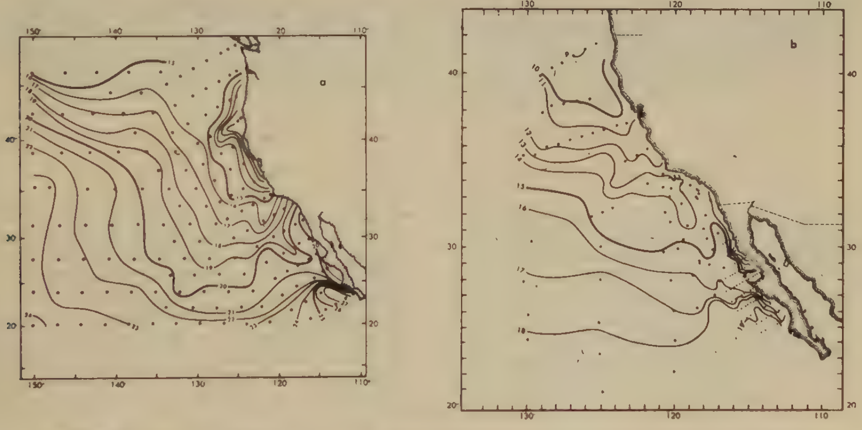

a
b
150
140
130
120
110
40
30
20

FIGURE 68. Ocean temperatures at 10 meters (degrees Centigrade). (a) August 1955. (b) March (composite).

---

[1] Contribution from the Scripps Institution of Oceanography.

Reproduced by Permission

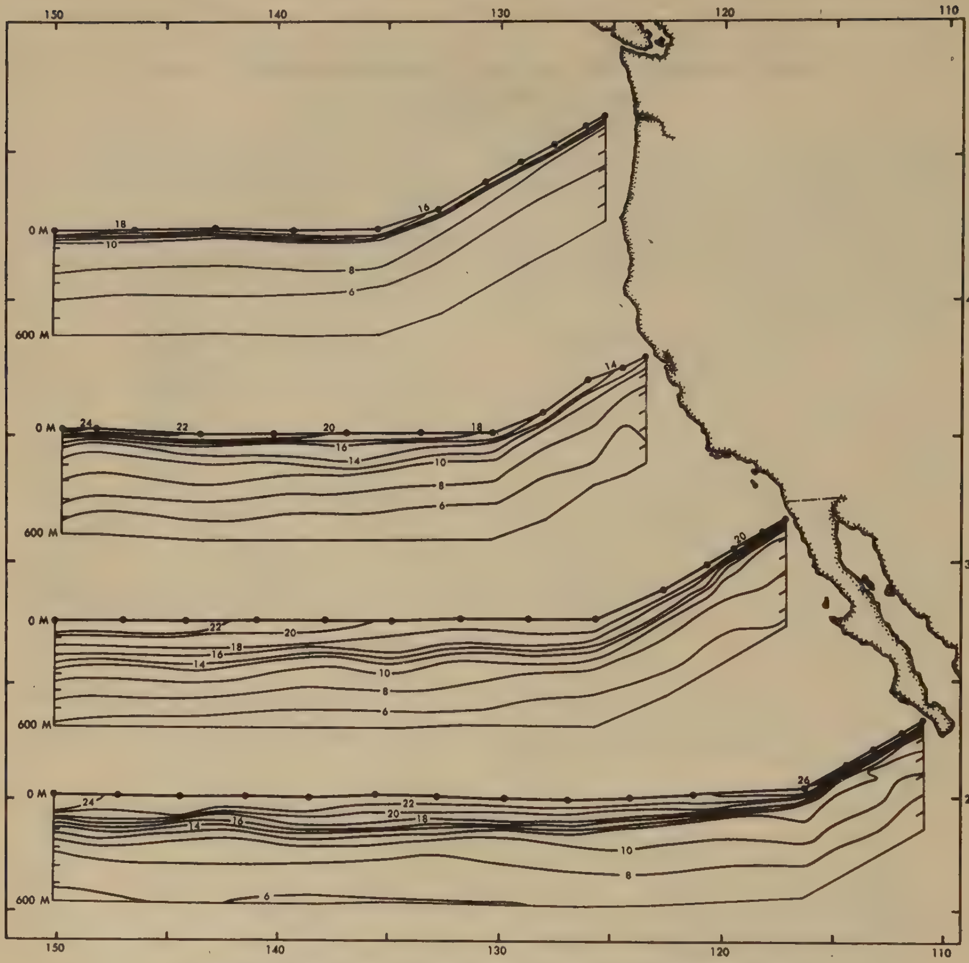

FIGURE 70. Vertical profiles of temperature from the surface to 600 meters, August 1955.

The currents, temperature, salinity and oxygen as they have appeared during most years of the last decade, and the seasonal variation of temperature and salinity are illustrated by the first few figures. The geopotential anomaly in August of 1955 from North America to 150°W and between 20° and 46°N is shown in figure 67. This is the eastern edge of the great oceanic anticyclone which fills most of the temperate zone of the North Pacific. A small eddy is seen south of Point Conception. At 200 meters below the surface a narrow current next to the coast runs counter to the surface flow, and in the winter months the surface waters also run northward near the coast.

The south-flowing current brings water from high latitudes which is both colder and less salty than that farther offshore in the center of the anticyclone. The north-flowing current brings water which is saltier than that offshore. In addition, the deeper waters from the south are very low in dissolved oxygen content.

(544)

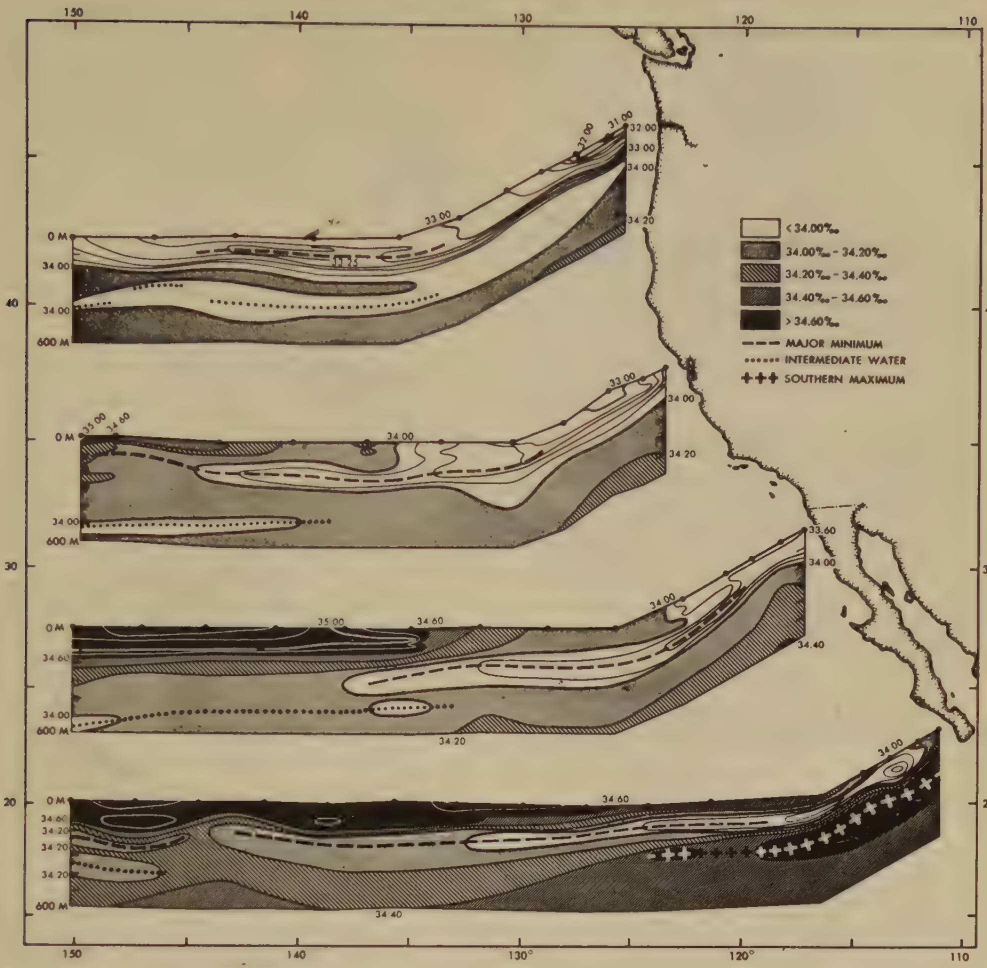

FIGURE 71. Vertical profiles of salinity, parts per mille, from the surface to 600 meters, August 1955.

A remarkable consequence of the strong northwesterly winds of spring and summer is the upwelling which occurs along most of the West Coast. The winds move the surface waters offshore, and they are replaced by the colder and more saline waters from below. Note the enclosed low in temperature from 35° to 46°N in August (Fig. 68a), with a minimum off Cape Mendocino less than 11°C. Note also the strong gradient in the extreme southeast. In March, when there is no upwelling but the seasonal cycle of temperature is at or near its minimum, the temperature off Cape Mendocino is still between 10° and 11°C (Fig. 68b). In the southeast, however, where there is no August upwelling, the seasonal difference in temperature may be as much as 8°C.

The 10 meter salinity in August (Fig. 69), shows the effect of a thin layer of fresh water from the Columbia River as well as the effect of the upwelling off Cape Mendocino. High values of salinity are seen to the west and south.

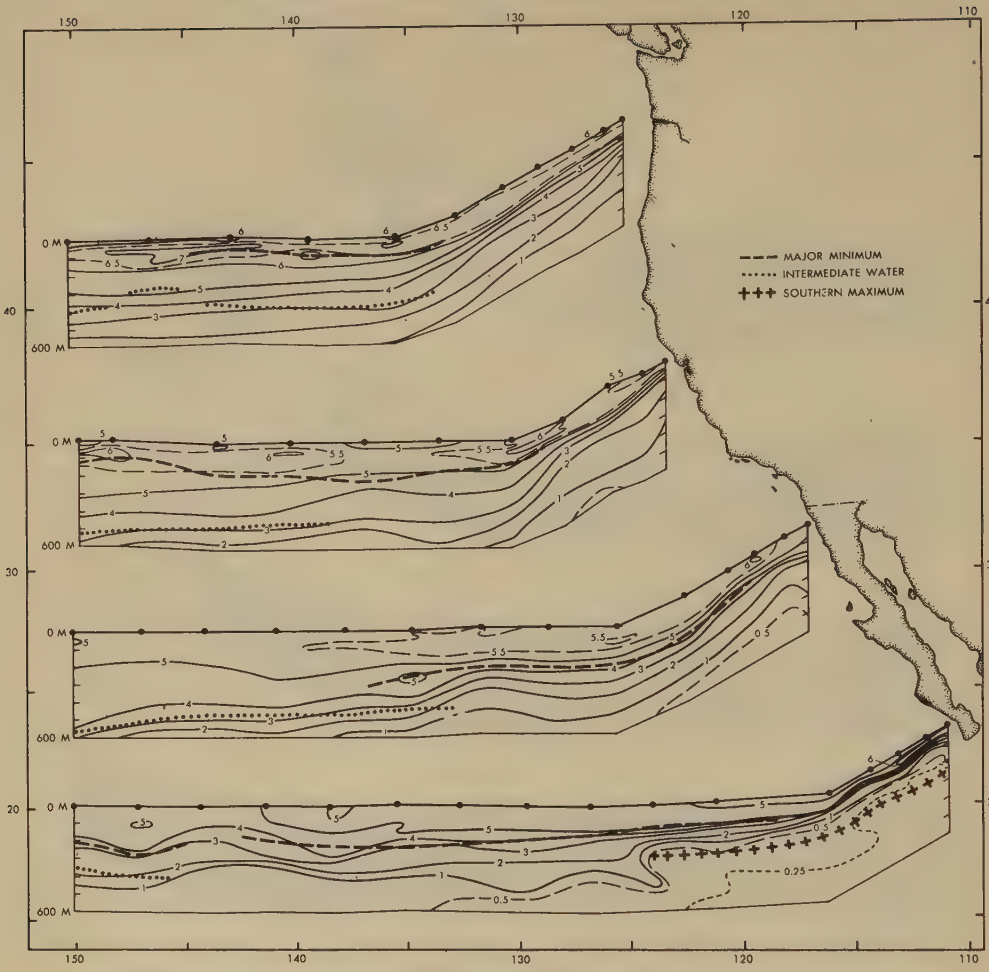

FIGURE 72. Vertical profiles of dissolved oxygen content, milliliters per liter, from the surface to 600 meters, August 1955.

Vertical sections of temperature, salinity, and oxygen in the upper 600 meters in a direction normal to the current are shown in figures 70, 71, 72. Note that at the surface the higher temperatures occur offshore in the north, and in the south they occur at the extreme offshore ends of the section. The vertical sections of salinity show the water of low salinity coming in at the surface in the north. As the water moves south the upper layers are strongly mixed with the more saline water from the west with the result that a subsurface minimum (the dashed line) lies beneath the pycnocline over most of the area. The deeper minimum (the dotted line) is North Pacific Intermediate Water, which is too deep to be of influence in the present problem. In the southeast beneath this subsurface salinity minimum in water from the north lies a salinity maximum in water from the Equatorial regions. The effect of this intrusion of very saline water can be seen to the northward on all of the profiles.

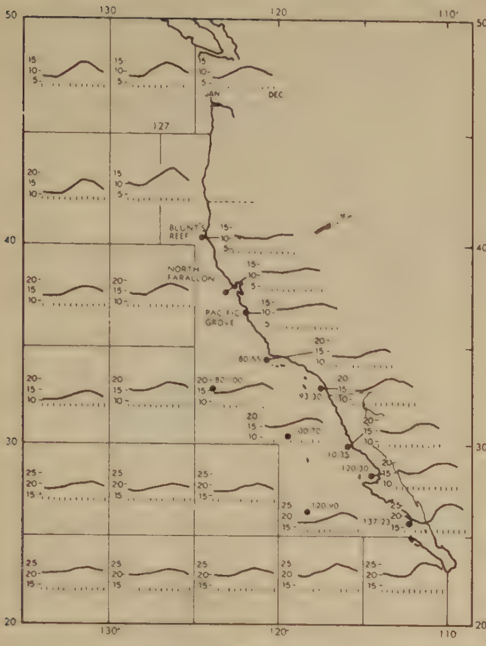

73a

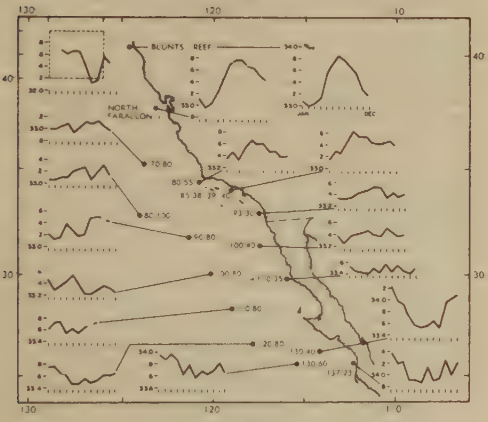

73b

FIGURE 73. Seasonal variation of temperature and salinity at the surface off the western coast of North America.

(a) Temperature in degrees Centigrade. Values over five-degree squares are from Robinson (1957); values at Blunt's Reef, North Farallon Island and Pacific Grove are from U. S. Coast and Geodetic Survey (1956); values at numbered stations are from CCOFI data, 1949-55.

(b) Salinity in parts per mille. Values at Blunt's Reef and North Farallon Island are from U. S. Coast and Geodetic Survey (1954); all other values are from CCOFI data, 1949-55.

The upper waters are saturated with dissolved oxygen or nearly so. The most remarkable feature at depth is the extremely low value found near the coast —especially in the southeast where the water of higher salinity is seen to be of low oxygen content as well.

The extent of seasonal variation of surface temperature over the region is shown in figure 73a. Far offshore the variation, which is principally the result of variation in radiation and exchange with the atmosphere, has a simple pattern with the greatest range in the highest latitude. Near the coast in the region of strong upwelling north of 34°N the seasonal range is reduced and the cool period lengthened by upwelling. Between 28°N and 34°N the upwelling occurs earlier in the year, more nearly at the period of the offshore seasonal minimum, and increases the seasonal range. South of 28°N it is the fall and winter countercurrent which accounts for the high range and delays the low until late spring.

The seasonal variation in surface salinity (Fig. 73b) indicates that the direct effect of evaporation and precipitation is small and, indeed, there is little coherence in the variation of the northern offshore stations. Inshore it is again the processes of upwelling in the north and the countercurrent in the south which dominate the seasonal variation. The effect of the spring and summer upwelling of deeper water to the surface in the north causes a wide range with the maximum value of salinity in summer. In the south the winter countercurrent brings highly saline water northward along the coast giving a maximum in winter. The two effects tend to cancel each other in the middle region between 28°N and 34°N latitude.

The seasonal variation of oxygen is generally in response to the seasonal change in temperature, which causes a change in saturation value.

It has been necessary to give this material as a brief background in order that the variation within the last ten years can be discussed; and again it is necessary to have some idea of the last decade in terms of previous temperatures if we are to think in terms of disturbances of a steady state.

A time-series of temperature anomaly from 1921 to the present and the anomaly of the northerly wind components determined from the pressure difference along 30°N between 110° and 130°W (Fig. 74) indicates that the anomalies of surface temperature along the coast and over the California Current have been remarkably coherent over this period. Certain periods stand out as quite cold and certain other periods as quite warm. The warm periods are seen in 1926, 1931, 1939-40, and 1941. The cold periods are seen in 1924 and 1933. A period of not excessive cold but well below normal values is found from somewhere in the late 1940's through 1956.

The difference is seen more clearly when the mean monthly temperature averaged from 1949-1956 is compared with the 1920-1938 data (Fig. 75). The major differences are seen to occur from March through August. (The gap between 1938 and 1949 is not deliberate. No offshore temperature data were available during this period.)

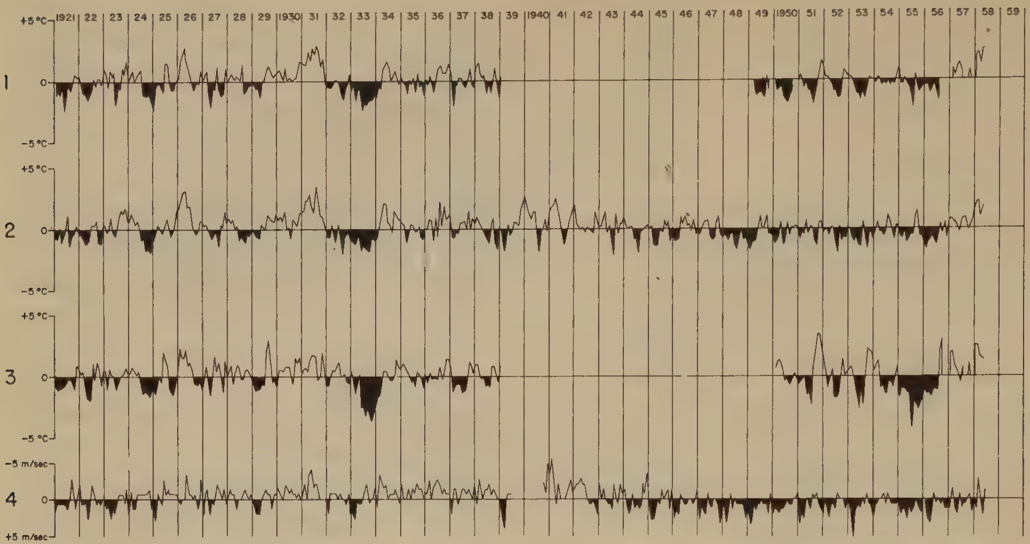

FIGURE 74. Monthly differences from average sea surface temperatures (degrees Centigrade) at (1) 30°-35°N, 115°-120°W, (2) Scripps Pier, and (3) 25°-30°N, 110°-115°W; and (4) monthly differences from average northerly wind component (in meters per second) at 30°N, 110°-130°W. The period 1921-1938 was taken as the average.

However, by early 1957 a substantial difference from the previous eight years had been noted in that the surface waters had become substantially warmer. The recent history of this warming is traced by comparing the weekly averages of temperature for 1957 and 1958 to the present with the longest term means available at each of six positions (Fig. 76). I believe that in the invitations to the Symposium certain anomalies of sea surface temperature over the California Current were presented. I shall refer to those, and more recent ones through May of 1958 (Fig. 77). Let me emphasize that these anomalies are from the mean measured by the CCOFI program period for 1949 through 1954 or 1955, depending upon the stage of data processing. Previous figures (74 and 75) have indicated that this is a period which is different from the long term mean in that February through August temperatures are low and the remainder normal or somewhat high. However, in this series of surface temperature anomalies all of the months since early 1957 have high temperatures relative to the CCOFI mean. It has also been possible to prepare charts of the anomaly of salinity. Here we have selected 10 meters rather than the surface because in the northern regions the outflow from the Columbia River and various other rivers brings into the upper few meters water of low salinity whose values, however, vary from station to station so severely that both an average chart and an anomaly chart are difficult to interpret. By taking the values at 10 meters, rather than at the surface, this incoherence is largely eliminated. These anomaly charts of salinity have also since early 1957 shown consistently high values (Fig. 78).

Another approach is to examine the hydrography of the region with the aim of identifying the source of the anomalous water. Unfortunately when temperature and salinity are both high, suitable sources are found both to the west and to the south. Our ordinary hydrographic casts reach to 600 meters beneath the surface and we can examine the depth of penetration of the anomaly. We find that it reaches to a depth somewhat below the bottom of the mixed layer and is generally not significantly present at depths much below 150 meters. This, however, at first gave some hope of using a third indicator of the source of the anomaly—the dissolved oxygen content. We have prepared vertical sections along three lines extending out from the coast at intervals of 320 miles. These sections show temperature, salinity and oxygen anomalies in the upper 500 meters for July and October of 1957 and for January of 1958.

I shall not present all of the data we have examined but shall discuss briefly the nature of the anomalies in January 1958 (Fig. 79). We find temperature

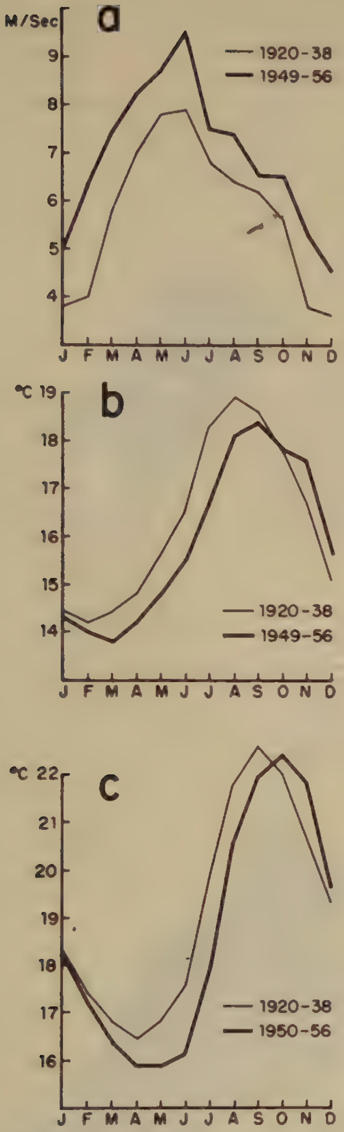

FIGURE 75. Average northerly wind component and temperature in the recent period compared to averages for 1920-38. No data available 1939-48.

(a) Northerly wind component in meters per second at 30°N, 110°-130°W.

(b) Temperature in degrees Centigrade at 30°-35°N, 115°-120°W.

(c) Temperature in degrees Centigrade at 25°-30°N, 110°-115°W.

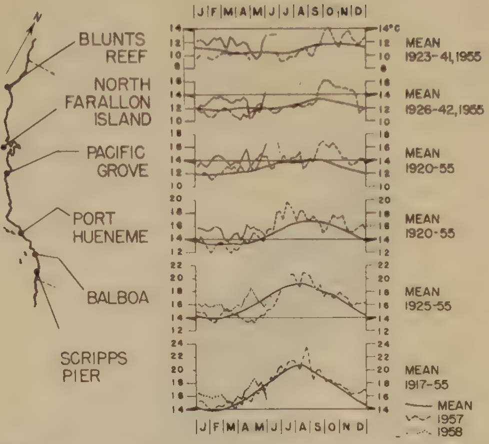

FIGURE 76. Temperature in 1957 and 1958 at six locations along the coast compared to long term means.

anomalies of from 1°C to 3°C at the surface. They generally increase to a high of from 2°C to 4°C in a narrow layer perhaps 10 to 30 meters thick and below the ordinary depth of the thermocline. This depth is from 50 to 100 meters depending upon the distance from the coast, 50 meters being a typical depth inshore and 100 meters more typical at the outer end of the lines. Below this maximum the anomaly dies away to less than 0.5°C nearly everywhere. This would be consonant with a slight warming of the mixed layer and an increase in its depth of 10 to 30 meters.

The salinity anomalies show a somewhat similar picture. The minimum beneath the pycnocline, which we measure at only a few discrete points along the vertical, causes some small confusion, but the general anomaly picture includes a maximum in the pycnocline. The salinity minimum is still present but is somewhat deeper and is higher in salinity.

In the upper layers the change of oxygen should correspond to that of temperature. As the mixed layer temperature has risen, the oxygen should decrease slightly. But if the mixed layer has deepened also, the upper oxygen value should remain constant with depth for another few meters, and the result should be a positive oxygen anomaly in the pycnocline. This situation is indeed found in a great many of the stations.

The deeper oxygen values—those at 200 meters—show something more complex. Both high and low values are found at various stations and at this time no interpretation can be offered.

The data indicate that by January 1958 enough warmer water (or heat) and more saline water have been added to the mixed layer to raise its temperature by about one and one-half degrees and its salinity by about 0.2 parts per mille. The depth of the mixed layer has increased by from 10 to 30 meters. This

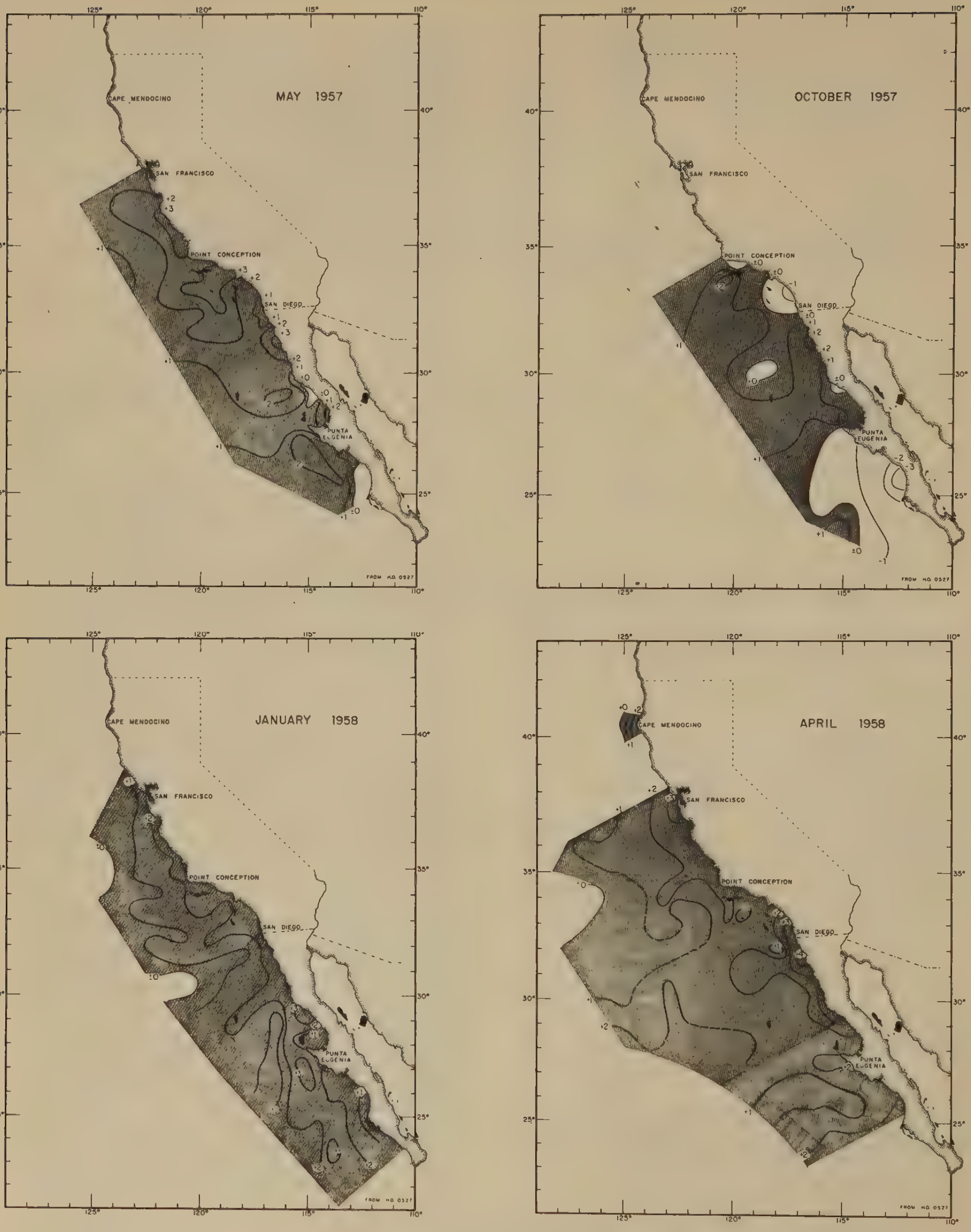
MAY 1957
OCTOBER 1957
JANUARY 1958
APRIL 1958
CAPE MENDOCINO
SAN FRANCISCO
POINT CONCEPTION
SAN DIEGO
PUNTA EUGENIA
125°
120°
115°
110°
40°
35°
30°
25°
+1
+2
+3
±0
-1
-2
-3
FROM H.O. 0527

FIGURE 77. Sea surface temperature anomalies from the CCOFI mean, in degrees Centigrade. Shaded areas are above normal.

(550)

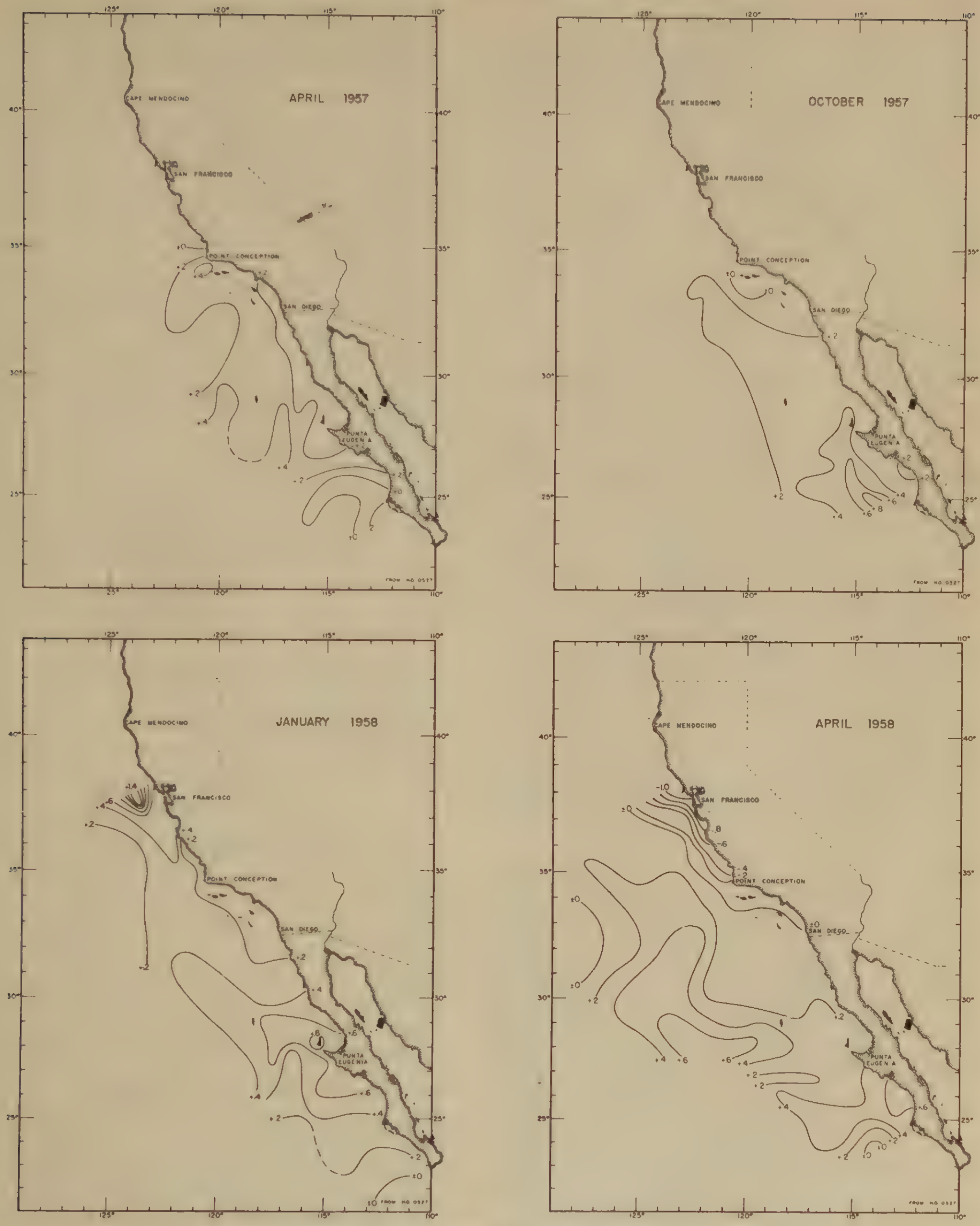
APRIL 1957
OCTOBER 1957
JANUARY 1958
APRIL 1958
CAPE MENDOCINO
SAN FRANCISCO
POINT CONCEPTION
SAN DIEGO
PUNTA EUGENIA
125°
120°
115°
110°
40°
35°
30°
25°
FROM H.O. 0527

FIGURE 78. Ten-meter salinity anomalies from the CCOFI mean, in parts per mille.

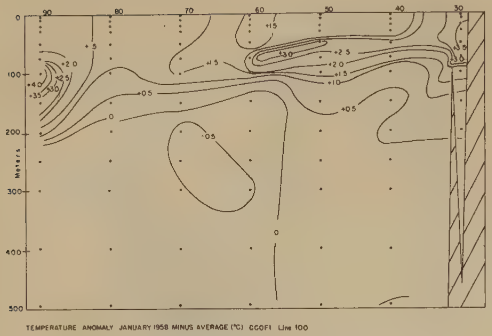

FIGURE 79. Temperature anomaly on a vertical section extending 250 miles offshore. The values are those measured in January 1958 less the CCOFI mean.

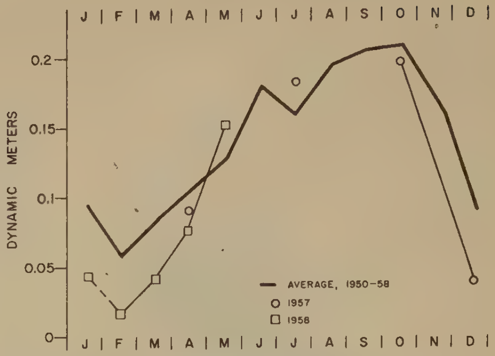

FIGURE 80. Difference in dynamic height (0 over 500 decibars) between a station 140 miles offshore and one 20 miles offshore.

means a net gain of about 10,000 calories per square centimeter and about 1.4 grams of salt. The result of the extra heat is a steric rise of sea level of an average of about 5 cm.

It is not possible at this time to show steric anomalies over the whole area, but a pair of stations, one near the coast and one 140 miles offshore have been compared with each other and with the long-term mean (Fig. 80). Their dynamic heights at the surface relative to 500 decibars are above normal by several centimeters. The difference corresponds to a strong surface flow to the south. The two stations span the region of the countercurrent, with the offshore one so far out as to be always higher than the inshore one. In winter the countercurrent flows north and the difference is reduced. The 1957-58 winter values are about 5 centimeters below the 1950-56 mean. That this really corresponds to a countercurrent is shown by the dynamic topography in January 1958 (Fig. 81) and by the movement of drift bottles to the northward (Fig. 82).

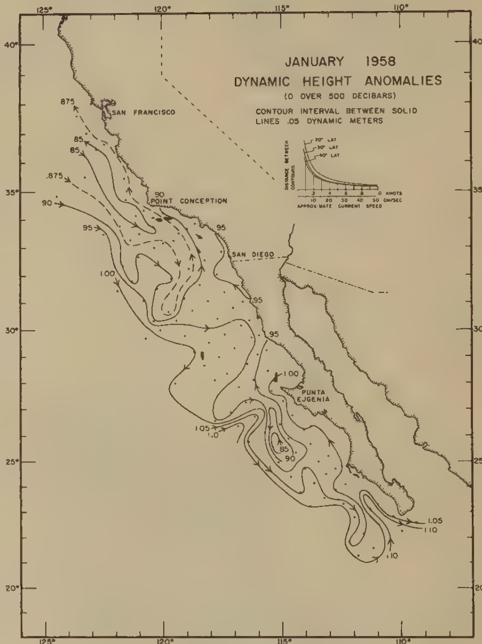
125°
120°
115°
110°
40°
35°
30°
25°
20°
JANUARY 1958
DYNAMIC HEIGHT ANOMALIES
(0 OVER 500 DECIBARS)
CONTOUR INTERVAL BETWEEN SOLID LINES .05 DYNAMIC METERS
20° LAT
30° LAT
40° LAT
DISTANCE BETWEEN CONTOURS
KNOTS
CM/SEC
APPROXIMATE CURRENT SPEED
SAN FRANCISCO
POINT CONCEPTION
SAN DIEGO
PUNTA EUGENIA
875
85
85
.875
90
90
95
95
1.00
95
95
1.00
1.05
1.0
85
90
1.05
1.10
1.10

FIGURE 81. Surface currents in January 1958. Dynamic height anomalies 0 over 500 decibars.

Mr. Roden and I are trying to establish the cause of the anomalous conditions I have described. Our first thought was that in the California Current, coastal upwelling might vary as a result of varying winds. Stronger winds might cause more upwelling, and lower temperatures would result. Under weaker winds upwelling might be weaker and higher temperatures would result. The component of wind from the north along this coast has been higher in the period 1949 through 1956 than the long term mean, and we have seen the sudden change to below-average values from early 1957 to the present. We have also seen the large positive anomalies of temperature and salinity which have occurred at the same time as this change in the wind. Without placing too much confidence at this stage in the hypothesis we have prepared a plot of the north component of wind at 30°N and 110°W-130°W and the surface temperature in the 5° square north of 30°N, east of 120°W and bounded on the north and east by the coast (Fig. 83). We have included all of the available data for the month of May, using CCOFI data for the temperature values from 1949 to the present and values measured by Japanese merchant vessels and averaged and published by the Kobe Imperial Marine Observatory for the years 1916 through 1938. Temperature data are not available in the intervening years and for some of the years pressure data are not available. It would be interesting to have comparable values for 1941 during which period we have good reason from coastal measurements to believe temperatures were high.

Mr. Namias has already described the anomalous wind field of the last year and has presented charts considerably more detailed and accurate than those which Mr. Roden and I have been able to prepare from the data available to us. However, the pressure differences have been so severe that even our limited data have not caused our charts to be substantially different from his.

By looking back into previous years we have found other large anomalies (Fig. 84). January of 1931 was characterized by a severe negative pressure anomaly in the central North Pacific and a temperature anomaly which was negative in the center and positive around the edges. The converse obtained in January of 1933 when the pressure anomaly was positive and large in the center. The temperature anomaly was positive in the center and negative around the edges.

Our own data do not extend far enough offshore to test the effect of the large negative pressure anomalies of the Central Pacific which have obtained during the last year, but by combining them with the ten-day anomaly charts recently prepared by the Pacific Oceanic Fishery Investigations, of which the most recent is for May of 1958, we learn that the anomaly is very similar to that observed in 1931, with low temperatures in the central North Pacific and high temperatures around the edge.

It is thus obvious that even if our first hypothesis of coastal upwelling could account for the temperature variations over the California Current region, there are other and larger area anomalies well offshore for which it could not account. The concurrent large area pressure anomalies suggest that a relation may exist between pressure and temperature anomalies over vast areas of the North Pacific.

The mechanism of the relation could be the intensification or shift of the wind-driven circulation. Over the greater part of the ocean the surface currents are approximately parallel to the winds, yet the isotherms are not everywhere parallel to the currents. They deviate especially on the eastern and western edges of the circulation, along the coasts. Any change in the speed of the current will thus displace the isotherms and result in temperature anomalies. Such an explanation might fit the California Current system as well as that of coastal upwelling, but in itself cannot account for the changes in the central North Pacific temperatures.

Another aspect of the same relation might be a lateral movement of surface waters under increased wind stress, which might account for changes independent of coastal effects. This might be more apt to account for the central North Pacific temperature anomalies.

A third aspect of the relation is the gradual adjustment to a new state of geostrophic equilibrium. If the recent weakened wind circulation over the eastern

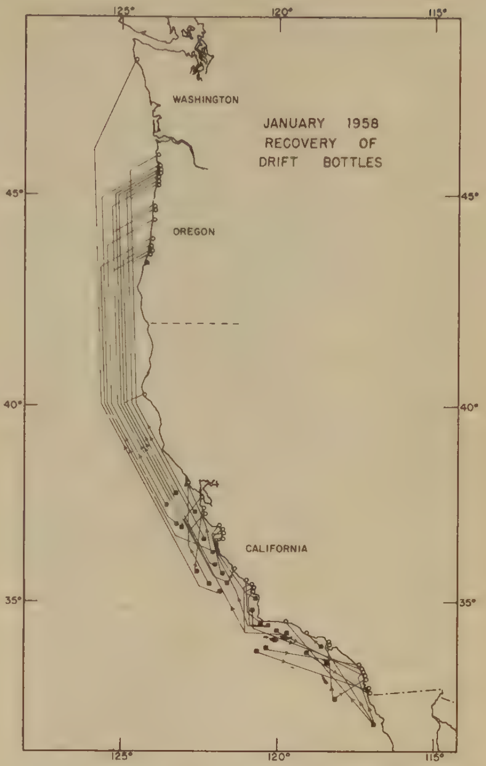

FIGURE 82. Recoveries of some drift bottles released in January 1958. Black squares show the release points, circles show the recovery points.

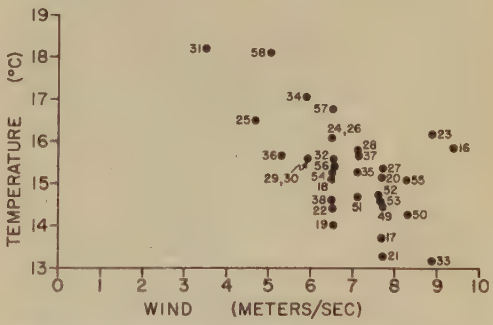

FIGURE 83. May sea surface temperature plotted against May wind for the years 1916-38 and 1949-58. Temperature is measured in the five-degree square 30°-35°N, 115°-120°W. Wind is computed from the pressure difference between 110° and 130°W along 30°N, and represents the component of wind from the north.

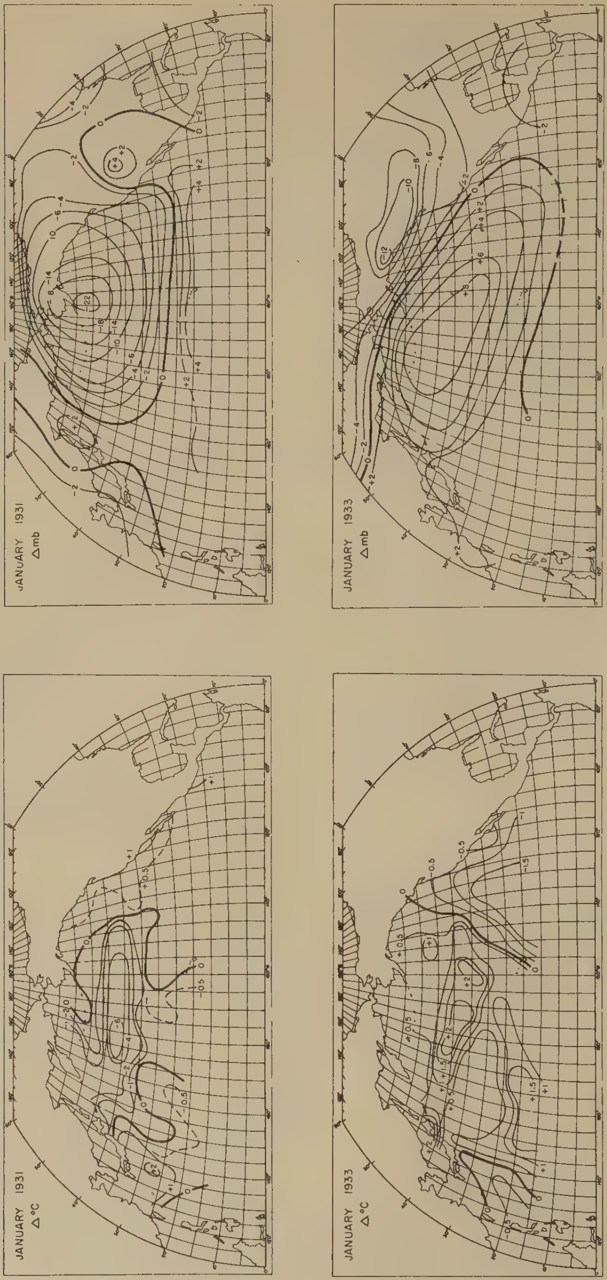
JANUARY 1931
Δmb
JANUARY 1933
Δmb
JANUARY 1931
Δ°C
JANUARY 1933
Δ°C

FIGURE 84. Sea surface temperature anomalies and sea level atmosphere pressure anomalies from the long term January means in January of 1931 and January of 1933.

North Pacific has caused a weakened ocean circulation, and a year has passed since the wind pattern changed, some alterations in the height and slope of the sea surface might be expected. We know of at least one location where the slope has decreased (Fig. 80), and the temperature and salinity anomalies have accounted for a steric rise of about five centimeters averaged roughly over the California Current system. The sea level rise at the coast has been about twice the steric rise. Both of these features are consistent with all three of the possible mechanisms I mentioned, that is, with reduced coastal upwelling, reduced lateral flow from the effect of wind stress, and geostrophic readjustment by moving new surface water from the west and south into the region. The latter two, however, might also account for the central North Pacific anomalies.

DISCUSSION

Fleming: Tell us more about your drift bottle program and the countercurrent.

Reid: The drift bottle program began in the fall of 1954. Before January 1958 we released drift bottles from south of Point Conception on the winter cruises. Each time several of the bottles moved northward past Point Conception. In 1958 bottles were dropped north of Point Conception in January for the first time (Fig. 82). Many went northward with velocities as high as 0.5 knot. Some of these bottles traveled over 600 miles northward along the coast.

Isaacs: When you say 0.5 knot, this is only a minimum?

Reid: Yes. This is computed from the time we put them out until the time they are found on the beach. The number of bottles that went past Point Conception was not larger than in the past years. It was principally those we put north of Point Conception that had this tremendous movement to the north.

Wooster: Are you implying that this countercurrent is a double one? And the ones that you put out south of Point Conception did not commonly go north of the Point?

Reid: A few of them did. I have not said that this was a different countercurrent.

Stommel: The deep countercurrent you have mentioned is hard to define.

Reid: You do it essentially by the distribution of the properties. Equatorial Pacific water is identified by certain temperatures, salinities, and a certain temperature-salinity relationship. It extends up from the Equator all along the coast.

Stommel: How deep is it?

Reid: It is found at 200 meters below the surface. The thickness is uncertain since we use as a reference level the 1000 decibar surface, but it is at least 200 or 300 meters thick. Near the coast the deep salinities are higher than those offshore, and at lower latitudes we have a maximum in salinity that shows the northward intrusion of the high salinity water from the Equatorial Pacific.

Question: Low oxygen is a pretty good identifier?

Reid: Yes, it is. The lowest oxygens are along the coast. Offshore the minimum oxygen value is higher and there is a tongue of high salinity and low oxygen water all the way to the Aleutian Islands. Whether it is a movement along the coast or movement upward from deep water, I do not know.

Saur: This is year around?

Reid: Probably, since it is below 200 meters in depth. I have examined it only for July and August.

Fleming: The Davidson Current was well known about ninety years ago, so it is not an original discovery of the Marine Life Research Program. And presumably the knowledge was based in part upon the experience of sailing vessels operating along the coast and from surface temperatures that were available at the time. In other words, it shows up on the surface in the winter when we do not have much northerly wind. We might say that when we have a northerly component of wind it disappears at surface but persists at depth.

Reid: One of the reasons we have had so much trouble obtaining historical data about the Davidson Current is that when Davidson discussed it, he based a good part of his argument on the location of drifting redwood logs. Such information would of course not be available for Southern California since no redwood logs drift into the ocean here, and we cannot draw any information about continuity of northward flow past Point Concepcion from his work.

Schaefer: I think we are talking about three different things: first the Davidson Countercurrent, that is somewhere up the northern coast. The second is this movement of water near the surface from somewhere down off the Mexican-Baja California coast, shown very well by MLR studies. This is near the surface. And the third thing, is the general movement of deeper water off the southern Mexican and Baja California areas. I think they are not quite the same.

Charney: This water has to come from some place —presumably from beneath the thermocline. This would produce vertical motion. And if this is going to be balanced, from considerations of continuity, you have to have northerly flow. This, in a sense, is what you are arguing about.

Reid: This may be perfectly right. I have nothing against your explanation, except that it would have upwelling off California moving water northward from a position 2,000 miles to the south of the upwelling. This may be perfectly right, however.

Fleming: What is your southern boundary on the chart (figure 67)?

Reid: These data were from the NORPAC Expeditions, which extended from 45°N to 20°N.

Wooster: You show the thermocline is getting shallower as it approaches the coast. Some of the profiles also show something I feel is very common on approaching an upwelling coast—a weakening of the thermocline and the presence of a trough in the isopleths. You have shown one profile, and I have seen others across the Peru Current that show this sort of thing, the isopleths separating near the coast. Do you think this trough has anything to do with the countercurrent?

Reid: Certainly. The trough in temperature and salinity means a trough in the density distribution. The integral of the density shows a cyclonic circulation.

Wooster: There are two classical explanations of the trough. One is that you have horizontal advection of water coming in from the south giving these properties, which apparently cause troughs.

Fleming: I do not think you even have to have upwelling. Obviously at the ocean boundaries you have a source of energy for mixing. Temperature structures not unlike what you have drawn on the board might appear in the absence of any permanent flow along the coast, purely by mixing at the ocean boundaries. If you did get this kind of mixing, then you would have some kind of circulation set up. It is a little difficult to understand the characteristics of this circulation that might result from this vertical mixing.

Wooster: Is it not characteristic of upwelling that the deeper isopleths slope downward toward the coast?

Schaefer: You show the countercurrent there. How deep do you put it at its deepest point? What is the greatest depth for this countercurrent off Baja California? Do you put the center of it at 600 meters?

Reid: The basis of computation for these currents is the geopotential above 1,000 meters. The bottom limit of this flow is probably uncertain with the present methods.

LITERATURE CITED

Reid, Joseph L. Jr., Gunnar I. Roden, and John G. Wyllie, 1958. Studies of the California Current System, *California Cooperative Oceanic Fisheries Investigations Progress Report* 1 July 1956—1 January 1958. pp. 27-56.

Robinson, M. K., 1957. Sea Temperature in the Gulf of Alaska and in the Northeast Pacific Ocean, 1941-1952. *Bull., Scripps Inst. of Oceanography*, Berkeley, Calif.

U.S.C.&G. Survey, 1954. Density of Sea Water at Tide Station, Pacific Coast. *Sp. Pub. No. 281*, 4th Ed. U. S. Dept. of Commerce.

U.S.C.&G. Survey, 1956. Surface Water Temperature at Tide Stations, Pacific Coast. *Sp. Pub. No. 280*, 5th Ed., U. S. Dept. of Commerce.

EL NIÑO[1]

WARREN S. WOOSTER

One of the most celebrated of oceanic disturbances is that known as *El Niño*, an occurrence of the first half of the year which is reported at irregular intervals from the coast of Northern Peru. Conspicuous outbreaks were reported in 1891 (Schott, 1931) and 1925 (Murphy, 1926) and more recently in 1941 (Lobell, 1942), 1953 (Posner, 1957) and 1957-1958. Similarities between this phenomenon and conditions observed off the California Coast and in other coastal upwelling zones suggest that the underlying causes of the observed abnormalities are the same in such regions.

Unfortunately it is not easy to discuss the Peruvian *Niño* in quantitative terms. The lack of a long record of systematic observations throughout the year makes it difficult to determine satisfactory averages with which to compare observations believed to be abnormal. Although it has been possible to establish a crude picture of the seasonal march of surface temperature along the Peruvian Coast (see later), little is known about changes in surface salinity; subsurface conditions are even less well known. In order to look for meteorological changes which might produce *El Niño* one would like a set of average pressure charts such as Dr. Namias has prepared for the Northern Hemisphere—but no such information is readily available.

With such a paucity of quantitative information it is not surprising that the characteristics of *El Niño* have never been well defined. One symptom is common to all reports—the presence of unusually high sea surface temperatures. Other frequently mentioned features include a southward coastal current, heavy rainfall, red tide *(aguaje)*, invasion by tropical nekton, and mass mortality of various marine organisms including guano birds, sometimes with subsequent decomposition and release of hydrogen sulfide (known as *El Pintor*).

Before attempting to define *El Niño* or to hypothesize as to its origin, it is of interest to examine some of the conditions observed during the events of 1957 and 1958.

As early as December 1956 unusually high sea temperatures were observed off Northern Peru. The summers (Southern Hemisphere) of both 1957 and 1958 were marked by heavier than usual rainfall in the north, and as far south as Lima (12°S) the winter of 1957 was warmer and less overcast than usual, this condition lasting until early September. There were, to my knowledge, no reports of a southward coastal current, but there were some indications that the northward flow of the Peru Current was much reduced. The guano birds, which were nesting on the northern islands in December 1956, abandoned their fledglings as they did again during the summer of 1957-1958. During the winter of 1957 large numbers of guanay *(Phalacrocorax bougainvillii*, the principal producer of commercial guano) died along the beaches, apparently from starvation. This did not happen in 1958, but adult birds were uncommonly scarce. Anchoveta *(Engraulis ringens)*, the main food of the guano birds, although caught by fishermen, were unavailable to the birds. There was no evidence of excessive mortality of these fish, but rather indications that they were no longer present at the shallow depths where they are usually abundant. Coastal waters were invaded by tropical forms, the yellowfin tuna fishery extending farther southward than usual, and hammerhead sharks, manta rays, and dolphin fish were common at least as far south as Lima.

Evidence for the conditions described above, although credible, is difficult to document. However, early in 1958 it was possible to make some measurements from *Bondy*, a Peruvian naval vessel attached to the Servicio Hidrográfico. The scientific work was carried out by scientists of the Consejo de Investigaciones Hidrobiológicas. During the period 24 February to 9 March a systematic survey was made of the region between 12°S and 4°S, extending offshore about 60 miles. Observations included 78 bathythermograph and surface-salinity measurements, and hourly surface-temperature readings were made along the track of the vessel.

As is usual along the Peruvian Coast, lowest temperatures (21.5-23.0°C) were found just offshore. However, the areas of cold water were small and isolated, and most of the region was covered with water whose temperature was greater than 25°C. When these values are averaged by one-degree squares they can be compared with the February average latitudinal variation of surface temperature in the same squares, as computed from data in the period 1939-1956 published in the *Mapas Mensuales* of the Compañia Administradora del Guano (Fig. 11). During this period lowest February temperatures were observed in 1950, highest in 1941. Averages from the 1958 *Bondy* cruise are similar to those of 1941, or from 2°C to 4°C higher than the long term mean.

Off upwelling coasts, such as that of Peru, subsurface temperature measurements usually show a moderately strong and deep thermocline offshore, which becomes shallower and less intense as it approaches the coast (Wooster and Cromwell, 1958). Weakening of the thermocline near the coast is associated with the enhanced vertical-mixing characteristic of upwelling. During the February *Bondy* cruise, most of the region was covered by a shallow (less than 30 meters) layer of warm (greater than 25°C) water underlain by a strong thermocline lying offshore a distance of 20 to 60 miles, and only in a few places were the ascending isotherms and weak thermoclines of upwelling encountered.

---

[1] Contribution from the Scripps Institution of Oceanography.

New series, 1175

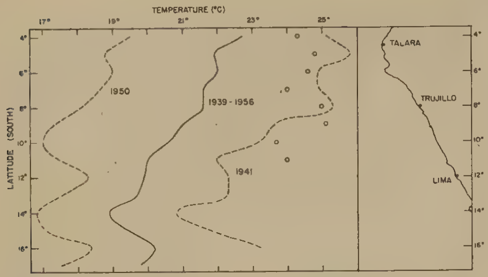

FIGURE 11. February values of average sea surface temperature along the coast of Peru. Curves are based on one-degree square averages from *Mapas Mensuales*. Circles are values for the same squares computed from *Bondy* data of February-March 1958.

Surface salinities in most of the region were 35°/₀₀ or greater, with lower values (to 34.92°/₀₀) only off Talara (4°30′S) and Paita (5°S). South of 7°S, there was a general increase of salinity with increasing temperature (Fig. 12), and also with increasing distance offshore. Only north of 7°S, and especially off Talara, were low salinities associated with high temperatures. Therefore it appears that the warm waters observed off northernmost Peru were of different origin than those present south of 7°S.

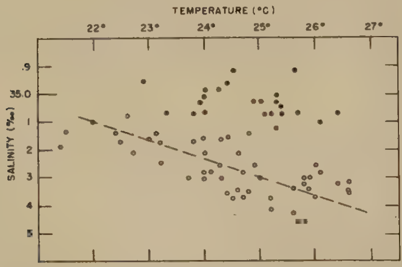

FIGURE 12. Surface temperature-salinity diagram for *Bondy* cruise of February-March 1958. Observations north of 7°S shown by filled circles, south of 7°S by open circles.

I would like to propose the following hypothesis concerning the cause of *El Niño*. Usually a southerly wind blows parallel to the Peruvian Coast, causing a net transport of surface water away from the coast, with replenishment from greater depths. For some reason, as yet unknown, the Peru Current swings westward a few degrees south of the equator. To the north are found the warm and relatively low saline waters of Panama Bight (Wooster, 1959).

Each year during southern summer highest temperatures are found along the Peruvian Coast from 4° to 17°S (Fig. 13). During *Niño* years, there is a general weakening of the atmospheric circulation, and reduction of the wind-stress component parallel to the coast is responsible for a weakening or cessation of upwelling. Higher than normal temperatures then result from *in situ* heating (as suggested by Sears, 1954) and from a coastward drift of open-ocean surface waters. In Northern Peru, the northern boundary of the Peru Current lies farther south than usual, and the tropical waters usually found north of this boundary may reach as far south as 7°S.

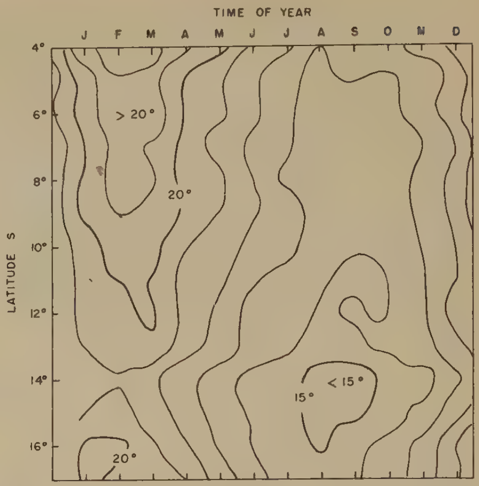

FIGURE 13. Average sea surface temperature along the coast of Peru, based on one-degree square averages for the period 1939-1956 from *Mapas Mensuales*.

It has been suggested that red tides *(aguaje)* are more frequent during *Niño* periods (Schweigger, 1958). This would be consistent with the model if one accepted the theory that red tides are associated with reduced horizontal and vertical circulation, and thus with reduced dispersal of rapidly growing flagellate populations. This theory is implicit in the discussion of Kierstead and Slobodkin (1953).

In the light of this hypothesis, *El Niño* can be defined as the set of conditions developing off an upwelling coast when reduction of the wind stress causing upwelling during an extended period of time leads to weakening or cessation of vertical mixing. The resulting conditions include an increase in surface temperatures, the development of a thin layer of light water offshore, a modification of the surface circulation depending on the nature of the variation in the wind stress, and the biological changes associated with the altered environment. At the same time, in a region such as the Peruvian offing, where a cold coastal current turns away from the coast at low latitudes, the well-defined zone of transition to warmer waters may be at higher latitudes than usual.

El Niño as thus defined is a generic term applicable not only to Peruvian coastal waters but also to similar regions off California, Southwest Africa, Western Australia, and the coast of Vietnam.[1] In the last two regions the monsoonal changes in wind stress lead to annual *Niños.*

Testing of the proposed hypothesis requires a much better set of oceanographic and meteorological observations than are presently available from Peru. Although the *Niño* phenomenon is less well developed in California waters, the extensive body of data from that region might make it possible to examine the hypothesis during years such as 1957 and 1958.

DISCUSSION

Stommel: What I have to say is only to offer some more or less obvious remarks based on Schott's charts of mean summer and winter winds and sea surface temperatures in the *Geographie des Indischen und Stillen Ozeans* (February and August). First we note that there is a considerably greater variation in the winds over the California Current than over the Peru Current. In February the high pressure area over the California Current is weaker than in August; whereas over the Peru Current the high pressure region is strong in both seasons. Looking now at the corresponding charts of the surface temperature, we see that the isotherms are bent toward the Equator on the eastern side of the Pacific in both seasons off Peru, but off California, they are bent toward the Equator only during August. In February, when the atmospheric high is not strong, they extend almost parallel to latitude circles much of the way to the California Coast. If we can assert that the distortion of the isotherms is produced by the winds, then we can see that there is a powerful "thermostatic" action off California, which reduces the seasonal variability of temperature but that this is not so developed off Peru, because there the winds distort the temperature field throughout the whole year. Depending upon how we like to talk of things, therefore, we might say that there is normally an *El Niño* off California every winter, when the winds die down as a rule each winter, whereas in the Peru Current, the *El Niño* is by definition, an abnormal event, because there the winds do not normally change much with season. Of course, this is only a playing with words, but it does point up, I think, a rather important difference between the two current systems. I wonder if more recent studies of oceanic climatological data substantiate the general features of Schott's Charts?

Namias: Although I am not ready to propose anything deserving the designation of a theory, I believe that there are interactions between the North Pacific Anticyclone on the one hand and its Southern Hemisphere counterpart, the South Pacific Anticyclone, whose air circulation affects Peru and its coastal waters. We recognize interrelationships of this sort (called teleconnections) between the semi-permanent high pressure areas of the Northern Hemisphere, and it is quite conceivable that there are similar coupling mechanisms operating between the Northern and Southern Hemisphere cells. In the present case, especially during winter of 1958, the dislocation of the North Pacific High and the westerlies as well (both far south of normal over the eastern North Pacific) was so great it would surprise me if the doldrum belt as well as the position and strength of the South Pacific High were not influenced. In fact, if the southward displacement of wind systems observed in the North Pacific carried into the South Pacific one could account for the weakened (or absent) prevailing southerly winds off the Peruvian Coast which appear to be responsible for *El Niño.*

LITERATURE CITED

Kierstead, H. and L. B. Slobodkin, 1953, The size of water masses containing plankton blooms. *J. Mar. Res., 12*: 141-147.

Lobell, M. J., 1942, Some observations on the Peruvian Coastal Current. *Trans. Amer. Geophys. Un., 1942* (2) : 332-336.

Murphy, R. C., 1926, Oceanic and climatic phenomena along the west coast of South America during 1925. *Geogr. Rev., 16* (1) : 26-54.

Posner, G. S., 1957, The Peru Current. *Bull. Bingham Oceanogr. Coll., 16* (2) : 106-155.

Schott, G., 1931, Der Peru-Strom und seine nördlichen Nachbargebiete in normaler und anormaler Ausbildung. *Ann.D. Hydrogr.U.Mar.Met., 59*: 161-169, 200-213, 240-252.

Schweigger, E., 1958, Aguajes rojos y sus consecuencies. *Bol. Comp.* Adm. Guano, *34* (7) : 11-17.

Sears, M., 1954, Notes on the Peruvian coastal current. 1. An introduction to the ecology of Pisco Bay. *Deep-Sea Res., 1*: 141-169.

Wooster, W. S. and Cromwell, T., 1958, An oceanographic description of the eastern tropical Pacific. *Bull. Scripps Instn. Oceanogr.,* 7 (3) : 169-282.

Wooster, W. S., 1959, Oceanographic observations in Panama Bight. Askoy Expedition, 1941. *Bull. Amer. Mus. Nat. Hist. 118* (3) : 113-152.

---

[1] Some readers of this manuscript have objected to the use of the name *El Niño* to identify the general phenomenon, feeling that previous usage restricts the term to the Peruvian Coast. If a more appropriate generic term can be found, I would recommend its use. I have used *El Niño* in a broad sense to emphasize that the Peruvian *Niño* is *not* a unique phenomenon, but is rather merely a striking example of a wide-spread occurrence.

Journal of Geophysical Research Volume 65, No. 7 July 1960

Statistical Evidence Indicating No Long-Term Climatic Change in the Deep Waters of the North and South Pacific Oceans[1]

MARGARET K. ROBINSON

Scripps Institution of Oceanography
University of California, La Jolla, California

Abstract. No inference of climatic change appears to be warranted from an analysis of temperature and salinity values below 100 meters at 189 oceanographic stations in the North and South Pacific oceans. Data collected in the period 1929–1932 by the *Carnegie, Dana, Scoresby, Discovery II,* and International Fisheries expeditions were used as reference stations. These reference stations were paired with data collected between 1824 and 1958. Fifty per cent of the stations were within 60 nautical miles of their reference stations, 30 per cent were between 60 and 120 nautical miles, and 20 per cent were between 120 and 568 nautical miles. The stations that were more than 120 nautical miles from their reference stations were included in order to obtain additional deep-station values, but they were limited to the same water mass as the reference stations. The analysis showed large random individual differences in both fields down to 1000 meters, and smaller but significant anomalies in several instances between 1000 and 5000 meters. For the data grouped by years or by water mass, scattered significant differences were observed at all levels and in all groups. Much larger samples are needed to separate statistically the short-period variability and the instrumental, processing, and interpolation errors from long-period change in deep waters.

Introduction. In recent years there has been great interest in climatic changes in ocean temperatures, particularly at the sea surface. *Worthington* [1953, 1954, 1955, 1956] has also examined data taken below the surface in the Arctic and Atlantic oceans and in the Caribbean Sea. He found evidence of warming during the past 30 years. In this study, hydrographic data from the North and South Pacific oceans have been examined to determine whether similar long-term trends could be found in the Pacific Ocean.

Sample. Hydrographic-station data from the *Carnegie* cruise, taken during 1929, were used as climatic points of reference for comparisons with data taken between 1824 and 1955 in the North Pacific Ocean. In the South Pacific, in order to increase the size of the sample, the period of reference was 1928–1932, and the data used were taken on *Carnegie, Dana, Scoresby,* and *Discovery II* cruises. The South Pacific reference-station data were paired with data taken between 1875 and 1958.

This particular period centered on the year 1929, and these particular cruises were selected as climatic reference stations because they represent the first comprehensive surveys of the Pacific Ocean in which modern reversing thermometers were used. They furnished the main source material for Sverdrup's water-mass analysis of the Pacific Ocean [*Sverdrup, Johnson, and Fleming,* 1942].

The date, ship, cruise, numbers of paired stations, and source of the data in both the North and South Pacific oceans are given in Table 1. There were 81 climatic reference stations. These station data were paired with 108 sample stations. The original selection of paired stations limited the pairs to stations within 60 nautical miles of each other, and to the same water mass. Only 54 such pairs were available. The allowable distance between stations was therefore extended, but the water-mass restriction was maintained. The sample was restricted in this manner to minimize temperature and salinity variability between paired stations, due to geographical and water-mass differences. Surface values were not considered because of the large seasonal variation at the surface and the small number of stations that could be paired seasonally.

---

[1] Contribution from the Scripps Institution of Oceanography, New Series No. 1176

Reproduced by Permission

TABLE 1. List of Paired Stations

A. North Pacific Paired Stations

Cruise	Ship	Ship Year	*Carnegie* (CA) 1929	*Dana* (DA) 1929	Int. Fish. (IF) 1929	N. Holiday (NH) *Horizon* (HO) 1951	Capricorn (CP) *Horizon* (HO) 1953	NORPAC (NP) *Stranger* (ST) 1955	MLR *Stranger* (ST) 1957	Ref.
	Predpriatie (P)	1824	1							1, 2
	Blossum (BL)	1827							1	2, 3
	Herald (HE)	1846						1		2, 3
	Tuscarora (T)	1874	2							1, 5
	Challenger (CH)	1874		1						6, 7
	Challenger (CH)	1875	5	3		1				1, 4, 6, 7
	Vitiaz (V)	1887	2							1, 2
	Bushnell (BU)	1934	1							1, 8
	Oglala (OG)	1935	1							1, 9
	Louisville (L)	1936	9							1, 8
	Fieberling (F)	1947	1							1, 8
	Serrano (SE)	1949			2					10, 11
Mar. Life Res.	*Black Douglas* (BD)	1950	3							1, 3
N. Holiday	*Horizon* (HO)	1951	4							1, 4
Shellback	*Horizon* (HO)	1952					2			4
NORPAC SIO	*Stranger* (ST)	1955	5							1, 3
NORPAC SIO	*Spencer F. Baird* (SFB)	1955	3							1, 3
NORPAC SIO	*Horizon* (HO)	1955	2							1, 3
NORPAC SIO	*Black Douglas* (BD)	1955	5							1, 3
NORPAC POFI	*Hugh M. Smith* (HMS)	1955	3							1, 12
NORPAC U.W.	*Brown Bear* (BB)	1955	2							1, 13
NORPAC POG	*Ste. Therese* (StT)	1955	1							1, 14
NORPAC Jap.	*Umitaka-Maru* (UM)	1955	1							1, 15
NORPAC Jap.	*Ryofu-Maru* (RM)	1955	4							1, 16
NORPAC Jap.	*Satsuma* (SA)	1955	2							1, 17
NORPAC Jap.	*Tenyō-Maru* (TM)	1955	6							1, 18
	Total		63	4	2	1	2	1	1	
	Grand Total	74								

B. South Pacific Paired Stations

Cruise	Ship	Ship Year	*Carnegie* (CA) 1928	*Carnegie* (CA) 1929	*Dana* (DA) 1928	*Scoresby* (SC) 1931	*Discovery* II (DII) 1932	Downwind (DW) 1957	Ref.
	Gazelle (G)	1875			1				6, 19
	Challenger (CH)	1875	1						1, 7
	Gazelle (G)	1876					1	1	4, 19, 20
	Vitiaz (V)	1887		1	1	1			1, 2, 6, 21
	Dana (DA)	1928		1					1, 6
Shellback	*Horizon* (HO)	1952	1						1, 4
Capricorn	*Horizon* (HO)	1953		3	1				1, 4, 6
Equapac	*Hugh M. Smith* (HMS)	1956		4					1, 22
Downwind	*Horizon* (HO)	1957		2	3	2	1		1, 4, 6, 20, 21
Downwind	*Horizon* (HO)	1958	3	4		2			1, 4, 21
	Total		5	15	6	5	2	1	
	Grand Total	34							

---

1. *Carnegie Inst. Wash. Publ. 545* [1945]; 2. *Makaroff* [1894]; 3. *Scripps Inst. Oceanog. MLR* [1951–1958]; 4. *Scripps Inst. Oceanog. MSS* [1951–1958]; 5. *Belknap* [1874]; 6. *Dana Rept.* [1937]; 7. *Challenger Repts.* vol. 1 [1884]; 8. *U. S. Navy MSS* [1934–1947]; 9. *Goodman and Thompson* [1940]; 10. *Scripps Inst. Oceanog., Oceanog. Obs. Pacific 1949* [1957]; 11. *Thompson, McEwen, and Van Cleve* [1936]; 12. *McGary, Jones, and Austin* [1956]; 13. *Fleming and Staff* [1956]; 14. *Can. Joint Comm.* [1956]; 15. *Tokyo Univ. of Fisheries* [1956]; 16. *Central Meteorol. Obs.* [1956]; 17. *Japan. Hydrograph. Office* [1956]; 18. *Tokai Regional Fisheries Research Lab.* [1956]; 19. *Von Schleinitz* [1888]; 20. *Discovery Rept.* [1941]; 21. *Discovery Rept.* [1949]; 22. *Austin* [1957].

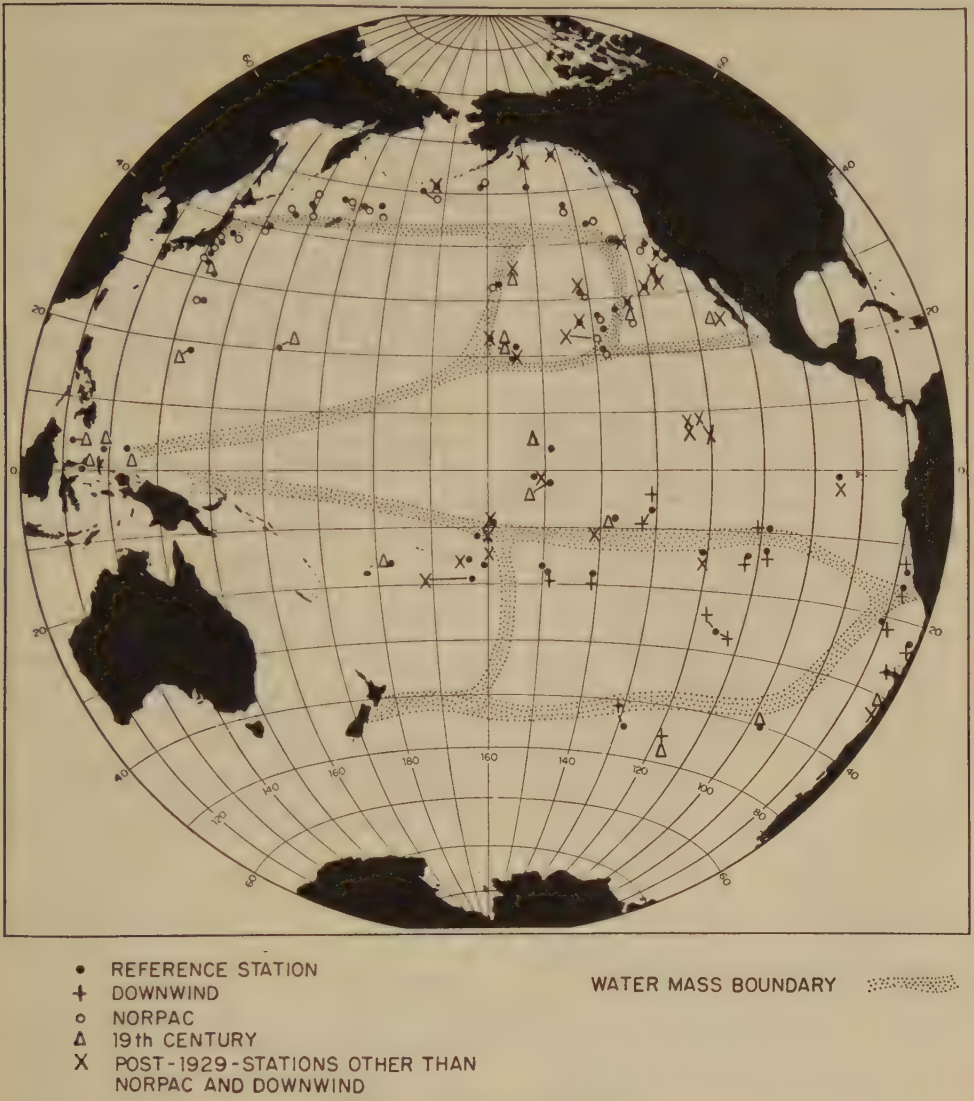
80
40
20
0
20
40
180
160
140
120
100
80
60
● REFERENCE STATION
+ DOWNWIND
○ NORPAC
Δ 19th CENTURY
X POST-1929-STATIONS OTHER THAN NORPAC AND DOWNWIND
WATER MASS BOUNDARY

Fig. 1. Station location chart.

Figure 1 shows the station locations. Fifty per cent of the stations selected were within 60 nautical miles of their reference stations, 30 per cent were between 60 and 120 nautical miles, 13 per cent were between 120 and 210 nautical miles, and 7 per cent were between 210 and 568 nautical miles. Stations more than 120 nautical miles from reference stations were included in order to obtain additional values below 2000 meters and additional 19th-century stations. At 100 meters, there were 108 pairs of stations with temperature data and 80 with salinity data; at 1000 meters, the sample had decreased to 89 with temperature data and 68 with salinity data; at 3000 meters, to 16 and 12, respectively; and at 5000 meters, only a single temperature comparison was possible.

The paired stations were compared both

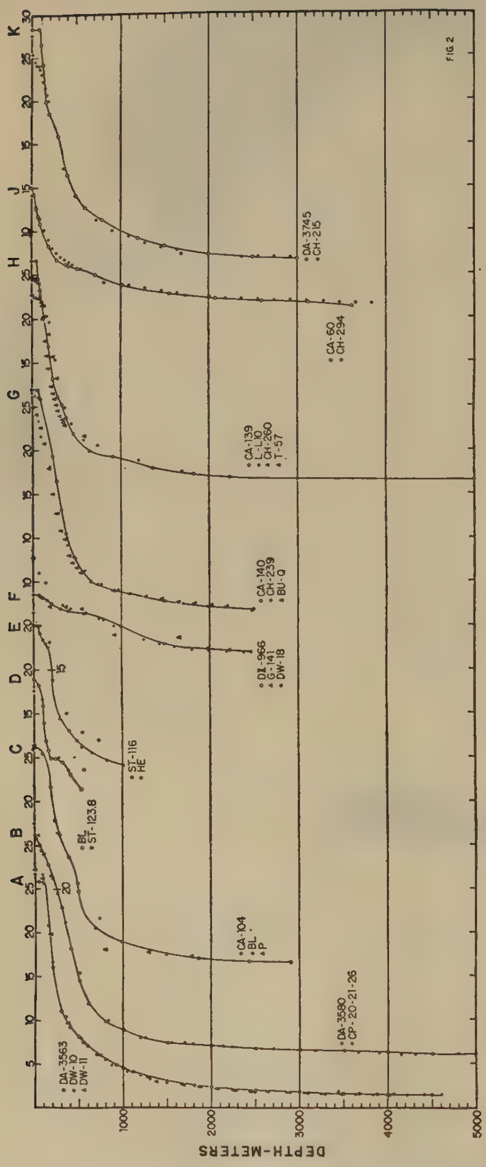

FIG. 2

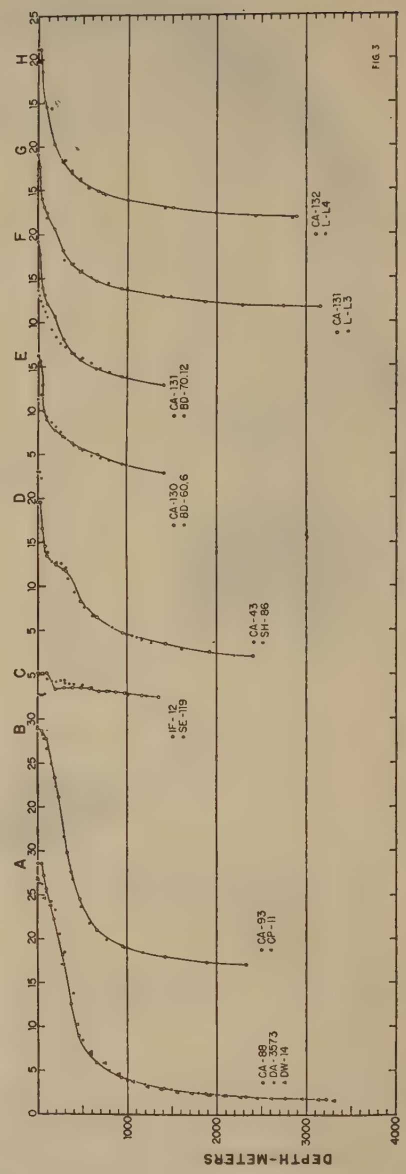

FIG. 3

Figs. 2 and 3. Temperature-depth curves.

(564)

graphically and statistically. Temperature-depth (T-D) curves were drawn for each pair, and temperature-salinity (T-S) curves were drawn for those pairs with complete salinity data.

Temperature-depth curves. A selection of T-D curves is shown in Figures 2 and 3. The reference-station curve is drawn connecting observed values. The paired-station observed values are plotted, but no curve is drawn. Stations are identified by the abbreviation of the cruise or ship name and station number.

Differences found at the deepest and most distant stations in the sample, but within the same water mass, are shown in Figure 2, curves *A* and *B*.

A selection of 19th-century stations is shown in Figure 2, curves *C* through *K*. These show poor agreement for some stations that are close together (Fig. 2, curve *D*) and good agreement for other stations that are more than 60 nautical miles from the reference stations (Fig. 2, curve *J*).

Curves *F*, *G*, and *H* (Fig. 2) show both 19th- and 20th-century stations paired with the same reference stations. Differences between paired stations and reference stations appear to be related neither to time interval nor to distance between stations in these multiple comparisons.

Differences in depth and shape of the thermocline are the primary causes of large anomalies down to 1000 meters (Fig. 2, curves *G*, *H*; Fig. 3, curves *C*, *F*).

An example of stations 167 nautical miles distant from each other, but in close agreement, is shown in Figure 3, curve *B*. The time interval was 24 years.

Conversely, Figure 3, curve *C*, shows stations within 21 nautical miles of each other with poor agreement. The time interval in this instance was 20 years.

Figure 3, curves *E* and *F*, shows two sets of comparisons between the data of 1929 *Carnegie* and 1950 *Black Douglas;* the data demonstrate random differences between pairs of stations for the same years. Curves *G* and *H*, (Fig. 3) are similar sets for 1929 *Carnegie* and 1936 *Louisville* stations.

The *Black Douglas* stations were 32 and 13 nautical miles distant from their reference stations; the *Louisville* stations, 0 and 8 miles, respectively.

These curves in Figures 2 and 3 typify the findings of the entire sample: the size and sign of the anomaly was related neither to the time interval nor to the distance between stations (provided that paired stations were within the same water mass); differences in depth and shape of the thermocline were the primary cause of large anomalies down to 1000 meters; these differences in thermocline depth, however, appeared to be related neither to time interval nor to distance between stations; and the sign of the anomalies changed with depth in random fashion.

Temperature-salinity curves. Figures 4 through 10 present T-S curves of the reference stations with their paired stations. They are grouped by water masses, and within groups they have been ranked by the distance between paired stations. When more than one station is paired with the reference station, the order in the figure depends on the pair with the shortest distance. The scale of these curves is the same as that used in *Carnegie Publ. 545* [1945] and *Sverdrup, Johnson, and Fleming,* [1942]; i.e., the temperature unit 1.00°C and the salinity unit 0.10‰ have the same linear value.

In all water masses the random differences between the paired-station T-S curves (Figs. 4–10) are similar to the random differences in the T-D curves (Figs. 2–3).

The T-S curves frequently cross each other, resulting in higher salinities for given temperatures in some portions of the curve and lower salinities in others (Fig. 4, curve *F*, etc.).

When sample stations from different years are paired with the same reference station, the random differences between sample stations are found to be similar to those between sample stations and reference stations (Fig. 5, curves *A*, *B*, *E*; Fig. 6, curves *B*, *C*, *E*, *J*, etc.).

The T-S curves reveal distant stations in good agreement (Fig. 6, curve *E*; Fig. 9, curve *E*), near stations in poor agreement (Fig. 5, curves *B* and *F*), and stations in the same year having anomalies of different signs (Fig. 10, curves *B* and *C*).

At closely spaced stations there are large differences in T-S curves between 100 and 500 meters in current-boundary regions (Fig. 7, curves *A* and *B*), in transition regions (Fig. 5, curve *B*; Fig. 8, curve *C*), and in areas of large

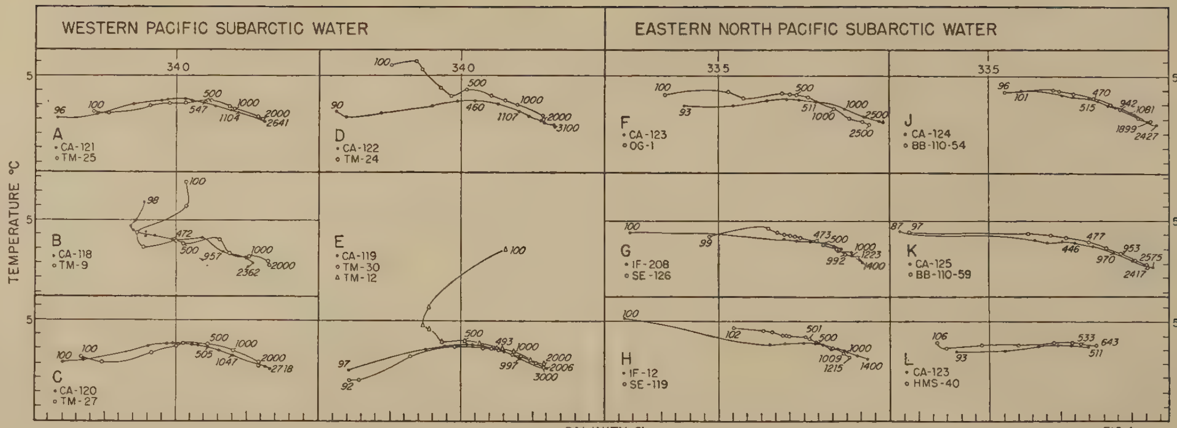

FIG. 4

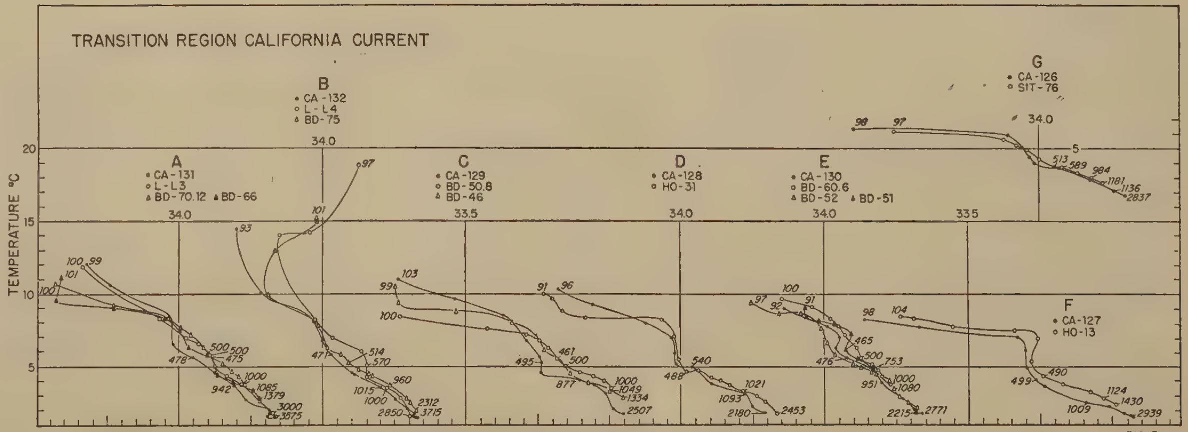

FIG 5

Figs. 4 and 5. Temperature-salinity curves.

(566)

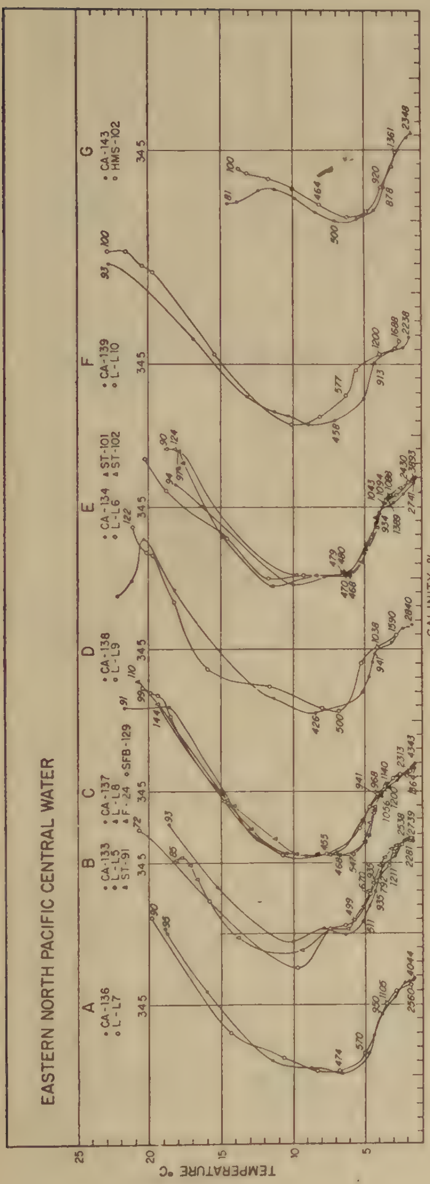

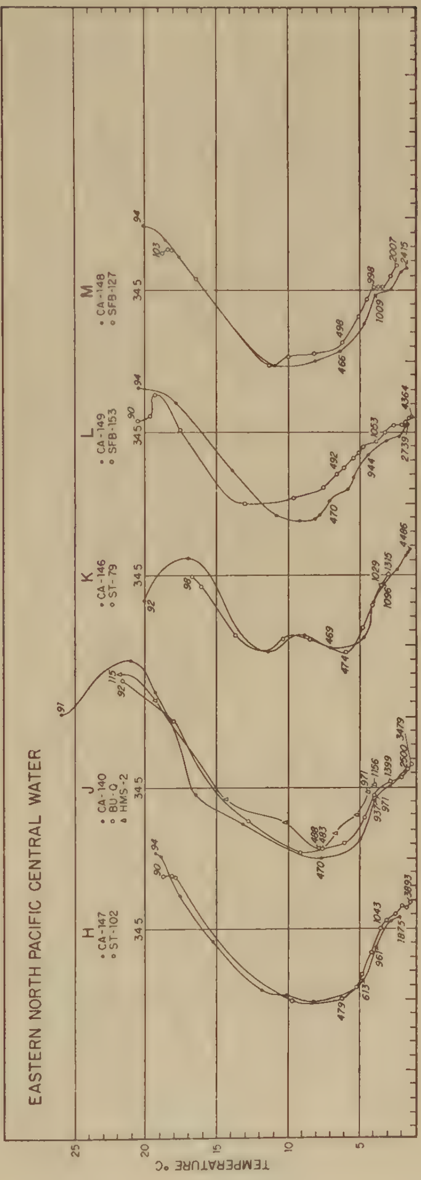

Fig. 6. Temperature-salinity curves.

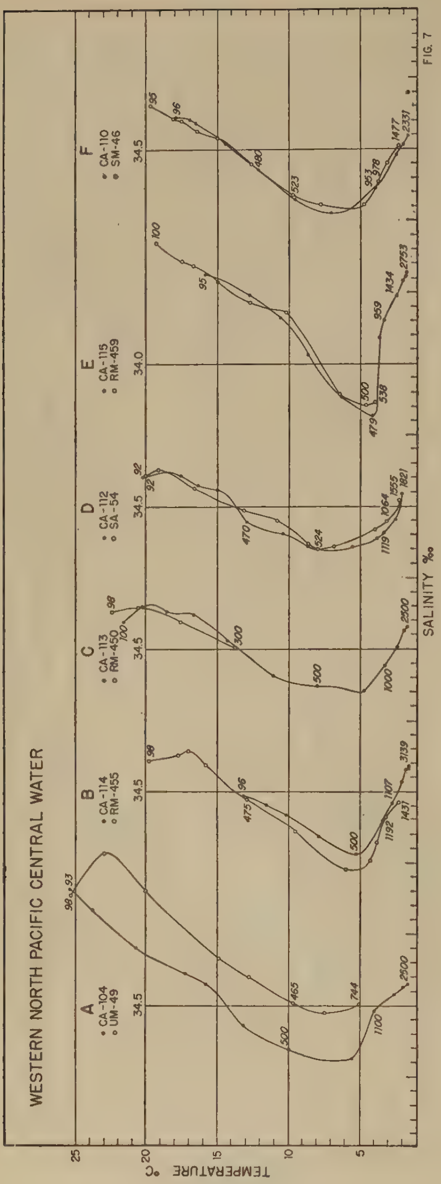

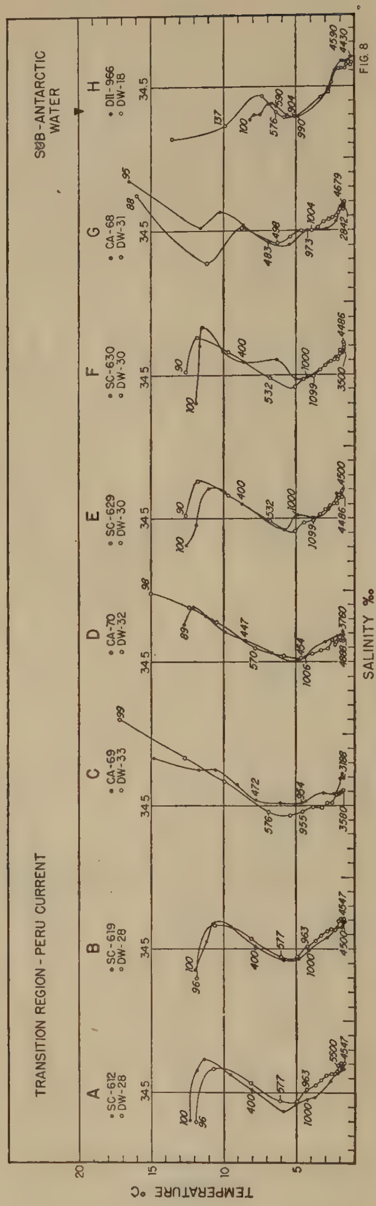

Figs. 7 and 8. Temperature-salinity curves.

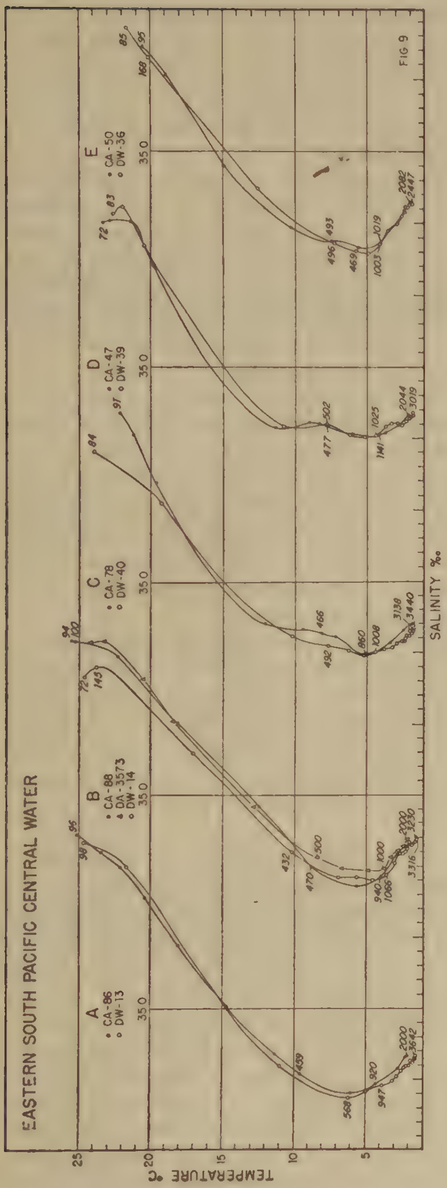

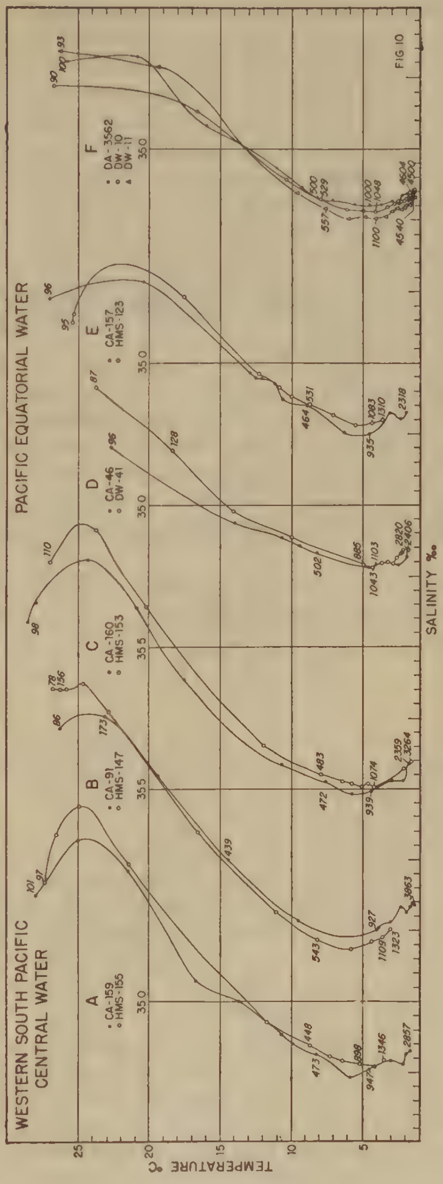

Figs. 9 and 10. Temperature-salinity curves.

(569)

seasonal precipitation and runoff (Fig. 4, curves G and H).

The occurrence of these large positive and negative temperature and salinity differences is usually associated with differences in thermocline or halocline depths at the paired stations. They result from real water-mass differences in the water above 800 meters, and for this reason these pairs of stations might well have been excluded from the sample. They were retained, however, because the station pairs were less than 30 nautical miles apart. They are thus typical of the extreme differences which may occur in random samples of geographically closely spaced observations.

Both T-D and T-S curves suggest that the differences between paired-station curves are random rather than systematic. In the following section a detailed description is given of the attempt, by statistical analysis of the temperature and salinity anomalies, to isolate evidences of climatic change from random, short-period variation.

Statistical analysis. Temperature and salinity anomalies were computed as follows:

$$T_{sa} - T_{ref} = d_T$$

$$S_{sa} - S_{ref} = d_S$$

where T_{sa} and S_{sa} refer to sample temperature and salinity values at standard depths, and T_{ref} and S_{ref} are corresponding temperatures and salinities for the reference stations.

The anomalies were computed for the following standard depths: 100, 200, 300, 400, 500, 800, 1000, 1500, 2000, 2500, 3000, 3500, 4000, 4500, and 5000 meters. Published interpolated values were used when they were available. Eight hundred meters was not a standard depth on all cruises, especially on the cruise of the *Carnegie*. When interpolated values were not available, temperatures were read from the T-D curves and salinity values were read from the T-S curves at the point corresponding to the temperature of the standard level. Interpolated temperature and salinity values were obtained in this way for the following groups of data: *Challenger*, *Tuscarora*, *Gazelle*, Capricorn, Downwind, Equapac, and *Carnegie* (800 meters only).

The anomalies for individual standard depths were grouped and averaged for the sample as a whole and for the following subclasses: North Pacific, South Pacific, 20th century, 19th century, individual years, water masses, and selected cruises.

The magnitude and dispersion of the individual anomalies is illustrated in Figures 11 through 16.

Histograms of the temperature anomalies (d_T) for the 20th-century data are shown in Figure 11. These include anomalies between station data taken in the years 1934 to 1958 and reference-station data taken in the years 1928 to 1932. It can readily be seen that the distribution of the anomalies at all levels is essentially normal, with approximately zero mean.

For convenience, the same class interval was used for all depths, but, since variance decreases with depth, the use of the same class interval distorts the shapes of the histograms so that they look somewhat flat in the upper levels and peaked in the deeper levels. This does not affect the normality of the distributions which are related to the standard deviations and not to the selected class interval.

The stippled area represents the portion of the sample within 60 nautical miles of the reference stations. A comparison of the stippled and solid portions of the histograms shows that the magnitude and dispersion of the anomalies is independent of the distance between sample stations and reference stations within water masses.

The following additional features shown on Figures 11 through 16 are discussed in later sections: error (see also Table 2); anchor-station standard deviations (Table 3); standard deviations for the entire sample; and the criteria for the underlined mean deviations.

Figure 12 shows the histograms of the salinity anomalies (d_S) for the same 20th-century data that is shown in Figure 11. The distributions of the salinity anomalies are essentially normal at all levels, with approximately zero mean. Again, owing to the use of the same class interval for all levels, there is distortion in the shapes of the histograms.

The magnitude of the salinity anomalies is also independent of distance between stations, as is shown by the relationship of the stippled to the solid portions of the histograms.

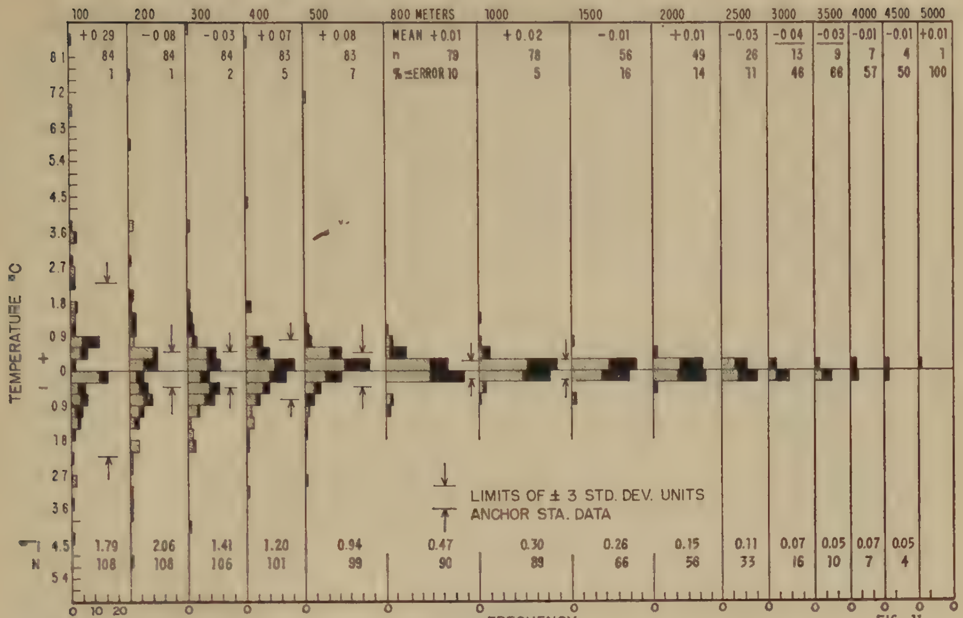

FIG. 11

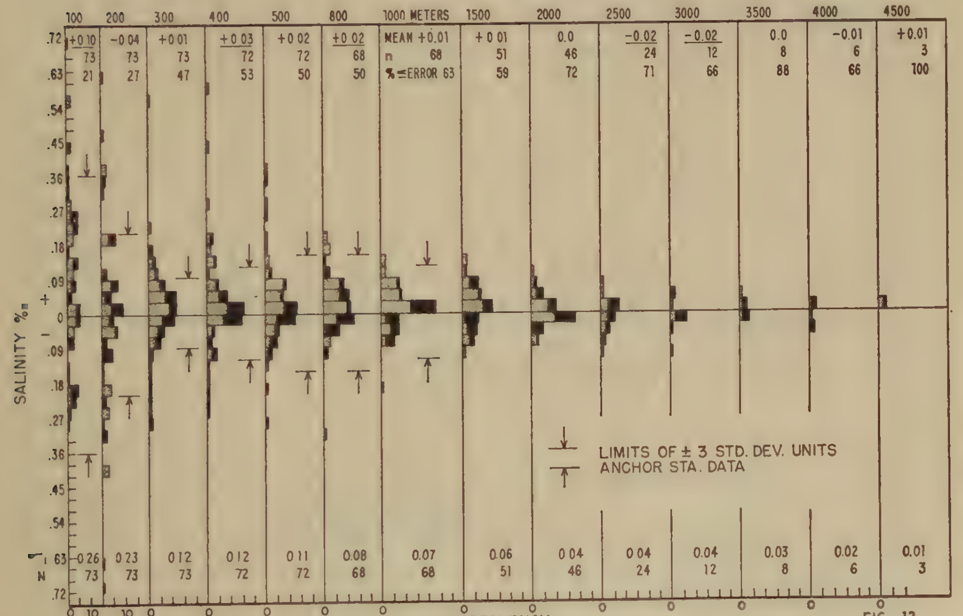

FIG. 12

Figs. 11 and 12. Frequency histograms of 20th-century data. Underlined means exceed $\sigma_i/\sqrt{n}$ at the 5 per cent probability level. n is number of observations in frequency histograms. N is number of observations on which standard deviations (σ_i) are based. Stippled areas show the portion of the sample within 60 nautical miles of reference station.

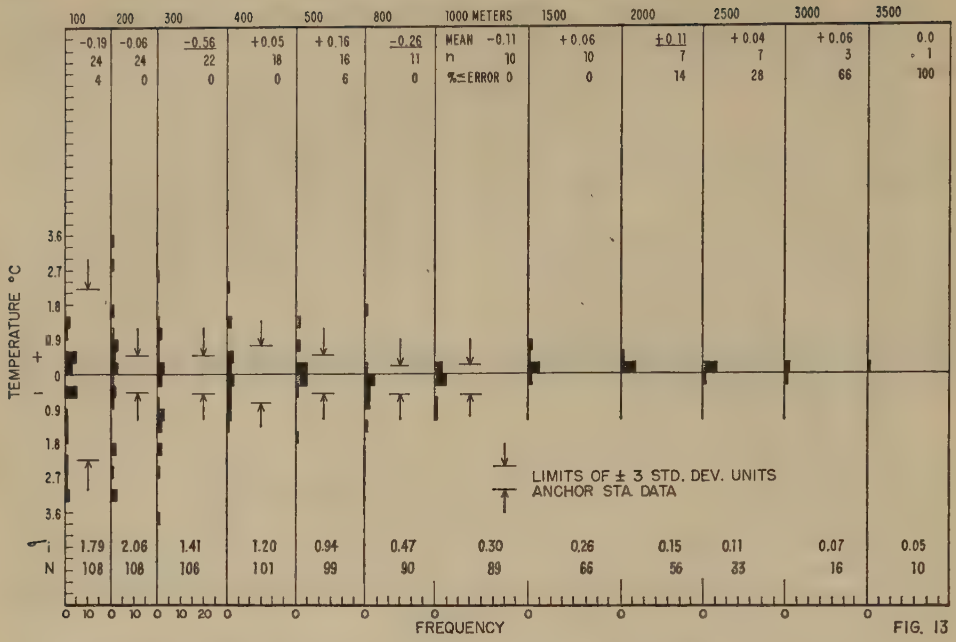

FIG. 13

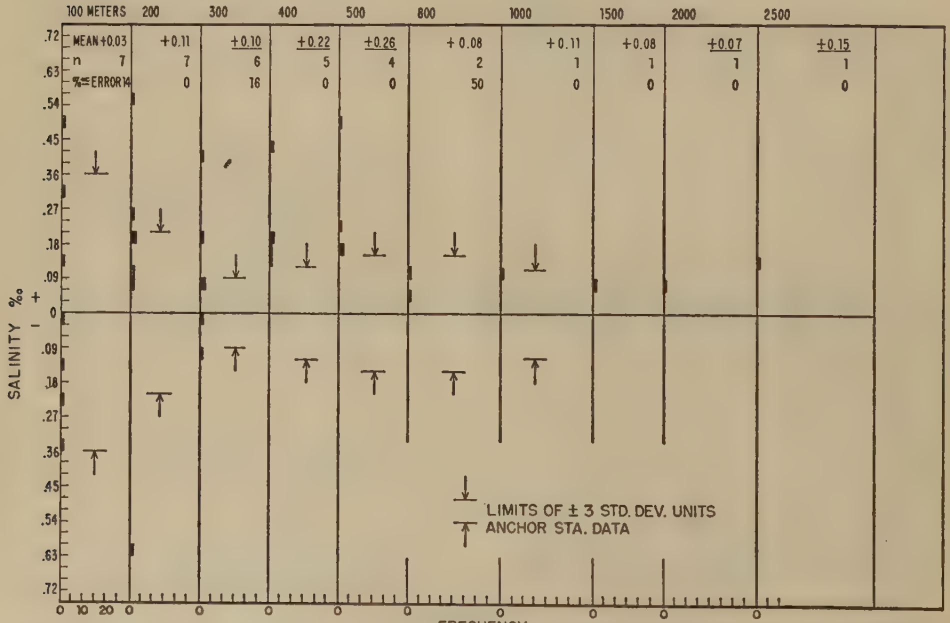

FIG. 14

Figs. 13 and 14. Frequency histograms of 19th-century data. Underlined means exceed $\sigma_i/\sqrt{n}$ at the 5 per cent probability level. n is number of observations in frequency histograms. N is number of observations on which standard deviations (σ_i) are based. Stippled areas show the portion of the sample within 60 nautical miles of reference station.

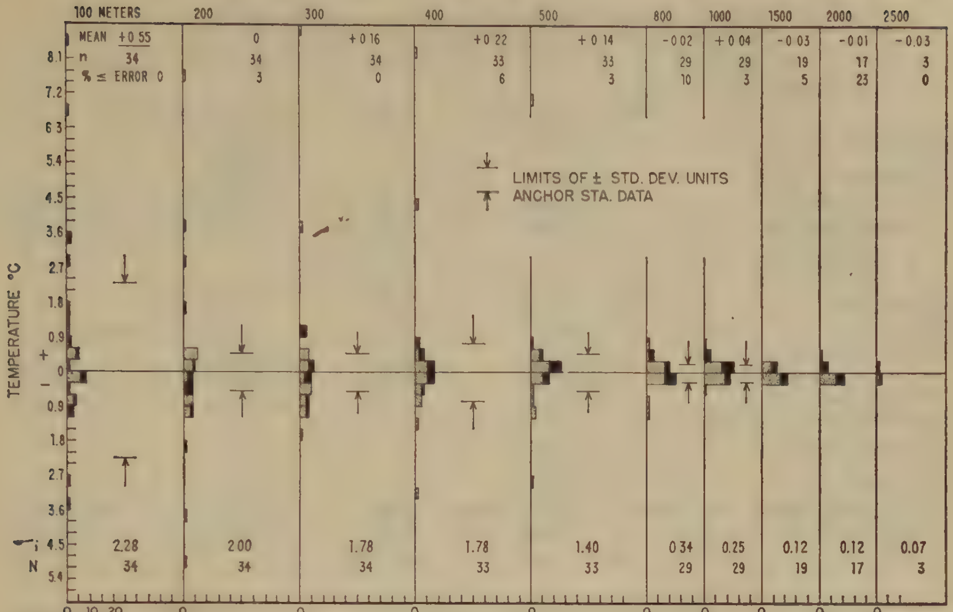

FIG. 15

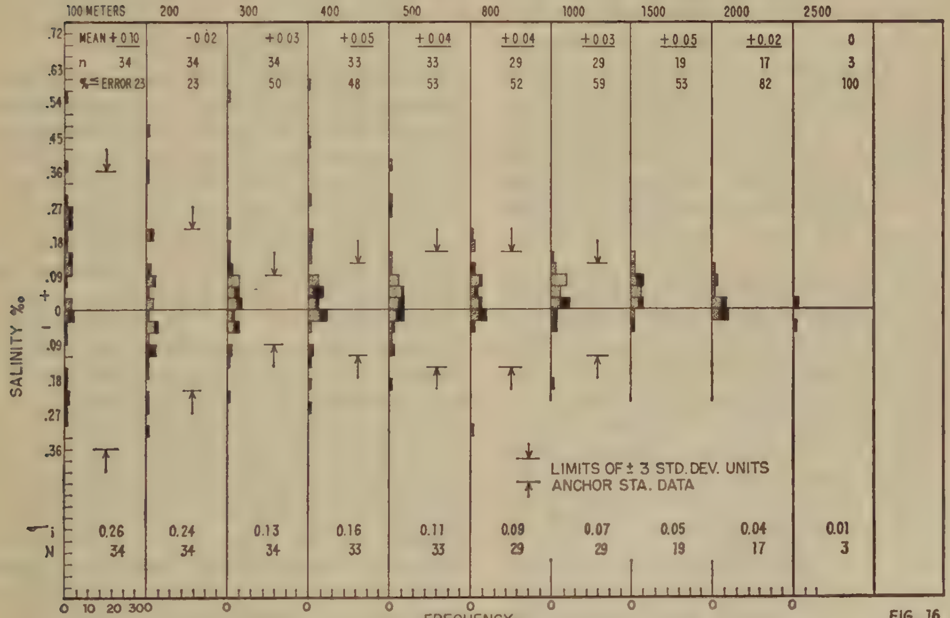

FIG. 16

Figs. 15 and 16. Frequency histograms of *Carnegie*-NORPAC sample. Underlined means exceed $\sigma_i/\sqrt{n}$ at the 5 per cent probability level. n is number of observations in frequency histograms. N is number of observations on which standard deviations (σ_i) are based. Stippled areas show the portion of the sample within 60 nautical miles of reference station.

TABLE 2. Estimate of Temperature and Salinity Error in Post-1928 Data in Terms of Variances and Standard Deviations, after Wooster and Taft [1958]

A. Temperature error	Upper limit $S_t^2(0°C)^2$	$S_t(0°C)$	Lower limit $S_t^2(0°C)^2$	$S_t(0°C)$
Thermometer	0.000196		0.000121	
Depth	1.0000		0.000025	
Interpolation (est.)	0.0025		0.0001	
Total single obs.	1.002696	1.001	0.000246	0.016
Total paired obs.	2.005392	1.416	0.000492	0.022
B. Salinity error	Upper limit $S_s^2(‰)^2$	$S_s(‰)$	Lower limit $S_s^2(‰)^2$	$S_s(‰)$
Determination	0.000324		0.000324(max)	
Depth	0.0064		...	
Interpolation (est.)	0.0009		0.0001	
Total single obs.	0.007624	0.082	0.000424	0.021
Total paired obs.	0.015248	0.123	0.000824	0.029
Error variance in *Carnegie* salinities	0.0016		0.0016	
Depth	0.0064		...	
Interpolation (est.)	0.0009		0.0001	
Total single obs.	0.0089	0.094	0.0017	0.041
Total paired with *Carnegie*	0.016524	0.129	0.002124	0.046

Figures 13 and 14 show frequency histograms of the 19th-century temperature and salinity anomalies, respectively. Few of these sample stations were within the 60-nautical-mile limit, yet the distribution and magnitude of the temperature anomalies is similar to, and consistent with, those of the 20th-century data shown in Figure 11. The addition of these 19th-century anomalies to the 20th-century histograms would materially affect neither the normality of the distributions nor the approximately zero means, nor would they increase the extent of the dispersion.

These distributions suggest that, whatever the depth, instrumental error, or observational error may be in the 19th-century data, it is neither large enough nor systematic enough for the temperature anomalies to exceed the limits of the random variation found in the modern data.

The few salinity anomalies, on the other hand, do show a positive bias. In only two cases do individual anomalies exceed the range of the 20th-century salinity anomalies; however, the positive mean anomalies cannot be accepted at face value because the salinity-determination error in the 19th-century salinity data is high (see following section on evaluation of errors). The 19th-century salinity anomalies are included in Figure 14 for historical interest only, since their climatic significance is doubtful.

We have thus far seen that there appear to be no essential differences in the distributions of the 20th-century and 19th-century anomalies when each is considered as a whole.

Next, let us look at the thirty-four 1929–1955 *Carnegie*-NORPAC North Pacific comparisons whose frequency histograms of temperature and salinity anomalies are shown in Figures 15 and 16. The *Carnegie*-NORPAC sample is the best for any individual-year class. The station pairs are well distributed over the North Pacific, north of 20°N. Sixty-eight per cent of the pairs are within 60 nautical miles of each other.

Both temperature- and salinity-anomaly distributions are again essentially normal, and the temperature means, with one exception, are approximately zero. The salinity means are positive, though small, at 8 of the 10 standard levels.

The excessively large positive and negative anomalies (also seen in Figs. 11 and 12) are derived from those comparisons pointed out in the discussion of the *T-D* and *T-S* curves, where large anomalies, at 100 to 500 meters, are associated with current or water-mass boundaries and excessive precipitation and runoff. These large anomalies increase the dispersion in the depths associated with the thermocline and halocline, yet they do not violate the symmetry

TABLE 3. Unbiased Temperature and Salinity Variances, (°C)^2 and (‰)^2, and Standard Deviations, (°C) and (‰), for Three Anchor Stations

		Standard Depth, meters						
		100	200	300	400	500	800	1000
E. W. Scripps, Sta. 72.60, Oct. 12–18, 1950	$n/(n-1)\sigma_t^2$	0.0777	0.0205	0.0193	0.0531	0.0300	0.0033	0.0025
	σ_t	0.28	$\underline{0.14}$*	$\underline{0.14}$	$\underline{0.23}$	$\underline{0.17}$	0.06	0.05
35°35.5′N, 122°07.5′W	No. obs.	52	50	49	13	13	13	13
(MLR)	$n/(n-1)\sigma_s^2$	0.0038	0.0010	0.0008	0.0011	0.0012	0.0011	0.0012
	σ_s	0.06	0.03	0.03	0.03	0.04	0.03	0.04
	No. obs.	51	47	45	13	13	13	13
Crest, Sta. 70.90, Oct. 11–19, 1950	$n/(n-1)\sigma_t^2$	0.0248	0.0032	0.0045	0.0091	0.0127	0.0051	0.0033
	σ_t	0.16	0.06	0.07	0.10	0.11	$\underline{0.07}$	$\underline{0.06}$
34°51′N, 124°33′W	No. obs.	64	64	64	16	16	15	16
	$n/(n-1)\sigma_s^2$	0.0071	0.0007	0.0007	0.0006	0.0007	0.0020	0.0006
	σ_s	0.08	0.03	0.03	0.02	0.03	$\underline{0.05}$	0.02
	No. obs.	64	64	64	16	16	16	16
Black Douglas, Sta. 70.130, Oct. 11–19, 1950	$n/(n-1)\sigma_t^2$	0.5586	0.0137	0.0191	0.0246	0.0275	0.0001	0.0012
33°33′N, 127°16.5′W	σ_t	$\underline{0.75}$	0.12	0.14	0.16	0.17	0.01	0.04
	No. obs.	64	62	60	16	16	9	14
	$n/(n-1)\sigma_s^2$	0.0140	0.0046	0.0009	0.0020	0.0021	0.0013	0.0016
	σ_s	$\underline{0.12}$	$\underline{0.07}$	$\underline{0.03}$	$\underline{0.05}$	$\underline{0.05}$	0.04	$\underline{0.04}$
	No. obs.	63	61	59	16	16	14	11

* Underlined values are maxima.

of the normal distributions. Because of the lack of systematic bias and the locations in which the large anomalies were found, they can surely be attributed to short-period variation.

With the exception of Figure 14 (the 19th-century salinity histograms), Figures 11 through 16 show that, whether we look at the sample as a whole or in parts, we find evidence of random variation rather than systematic trends at all levels.

Histograms of the remaining subgroups of the sample are not presented, since further evidence of random variation appears unnecessary and the numbers of observations in the remaining subsamples by years is small.

Before we look at the mean anomalies by individual years and by other subgroups for evidence of long-period trends, we must establish some quantitative limits for errors and variance in the data.

Wooster and Taft [1958] recently examined the problem of error in field measurements of temperature and salinity. They considered errors due to temperature reading, salinity determination, and depth determination and gave upper and lower limits for temperature error and upper limits for salinity error. The temperature errors apply to a temperature determination based on the mean of two reversing-thermometer readings at a single depth.

Since the statistical analysis of these data has been made for standard depths, it has been necessary to allow for interpolation errors, which arise from the methods used to obtain values at standard depths from observed values of temperature and salinity. Wooster and Taft did not evaluate interpolation errors. The author has added an estimate of such errors to Wooster and Taft's values.

Wooster and Taft [1958] gave no lower limit for salinity-determination error. A practical lower limit was obtained by subtracting the error in salinity, due to error in depth determination, from the calculations. The resulting limits may then be considered to be maximal for those portions of the water column which are isohaline, but minimal where there is a salinity gradient.

The upper limits include the errors which may result from a standard deviation in depth determination of 2 meters in a temperature gradient of 0.5°C per meter and a salinity gradient of 0.02‰ per 50 meters.

A separate calculation has been made of the salinity error to be expected for data paired with *Carnegie* data. The *Carnegie* salinity data are reported to have an accidental error of ±0.04‰, due to the effect of temperature on the conductivity bridge. The assumption is made that the 0.04‰ error is equal to 1 standard-deviation unit. *Carnegie* deep-salinity values between 34.6‰ and 35.0‰ were reported to have a systematic error of −0.03‰. All deep values in question were corrected by this amount before being used in this study.

The estimates of upper and lower limits of temperature and salinity error applicable to the post-1928 data are listed in Table 2.

The magnitude and dispersion of the 19th-century temperature anomalies, on the other hand, as mentioned in the discussion of Figure 13, were not in excess of those found in the modern data. This would lead us to think that, whatever the observational error in the old data, it was small relative to the true temperature variation. For this reason, and also because it is impossible to give a quantitative estimate of the temperature error in the 19th-century data, we shall use the same criteria for evaluating these data as for the 20th-century sample.

Only 1875 *Challenger* and 1887 *Vitiaz* salinities are tabulated. The *Challenger* salinities may be in error by as much as 0.13‰ because of errors in the determination of specific gravity [*Challenger Repts.*, 1884].

The error in the *Vitiaz* specific gravity determinations may be somewhat smaller, though *Makaroff* [1894] reported that his results were reproducible only to the third decimal. This would mean accuracy to tenths of a part per thousand when the specific gravity values are converted to salinities. Therefore, claims of long-period decreases in salinity from 1875 and 1887 to 1929 do not appear to be justified on the basis of comparisons of the *Challenger* and *Vitiaz* salinities with those of the *Carnegie*.

Reference is again made to Figures 11 through 16. At the top of each figure, for each depth, is listed the percentage of the individual anomalies which was less than or equal to the lower limits of instrumental or determination error listed in Table 2. These figures show that down to 2500 meters a very large percentage of the temperature anomalies exceeds the limits of error. Below that level, less than 50 per cent exceed the limit of error.

For salinity it is quite the opposite. Below 200 meters, for the 20th-century data, more than 50 per cent of the anomalies are less than or equal to the determination error. The percentages increase with depth to 100 per cent at 4500 meters, based on three samples.

The upper limits of error, which are applicable in the thermocline or halocline, account for some of the temperature and salinity variations between 100 and 1000 meters, but it is unlikely that all the variations are due to depth error. Unfortunately, it is impossible to determine which is responsible—error in depth determination or real difference in thermocline or halocline depth. Since the amplitudes of probable depth-errors are less than the known amplitude of short-period internal waves, it is safe to assume that most of the variation is real, but an individual temperature anomaly in the thermocline and an individual salinity anomaly in the halocline might be in error by as much as 1.4°C and 0.13‰, respectively.

A second criterion for evaluation of the sample anomalies was derived from anchor-station data. In October 1950, the *E. W. Scripps*, *Crest*, and *Black Douglas* collected serial-hydrographic data for a period of 72 hours at three anchor stations in the California Current, southwest of Point Conception, as part of the Marine Life Research Program (California Cooperative Oceanic Fisheries Investigations). The variances and the standard deviations computed for each of the anchor stations for both temperature and salinity at standard depths are listed in Table 3. These values include the instrumental and observational error shown in Table 2.

Lower limits of the error variances in Table 2 appear to be applicable to these data. When these limits, 0.0002 $(°\mathrm{C})^2$ and 0.0004 $(‰)^2$, are compared with the variances listed in Table 3, it is seen that in all but one instance these errors are but a small portion of the total variance. At *Black Douglas* Anchor Station 70.130, the total temperature variance at 800 meters, 0.0001

$(°C)^2$, is less than the expected instrumental error.

If the error variances in Table 2 are subtracted from the total variances at the anchor stations, the residual variances may be considered to be true temperature variation. The root mean square of these residual variances would be, at most, only 0.01°C or 0.01‰ less than the standard deviations listed in Table 3.

The variances computed for the different levels from these anchor-station data measure the short-period variation which can be expected at one location. They may be typical only of the California Current region; unfortunately, no others are available at present.

Limits of ±3 maximum anchor-station standard-deviation units for the corresponding depths are indicated in Figures 11 through 16. These limits should include 99 per cent of the short-period variation that could be expected at *one* location. It is of considerable interest to note that a very large proportion of the anomalies, which represent variation occurring within the same water mass over time intervals of 5 to 105 years, also falls within these limits.

At 200 and 300 meters, 40 per cent of the 20th-century temperature anomalies falls within the anchor-station limits. At other depths, roughly 60 per cent comes within these limits. This suggests that the temperature gradient and variance at 200 and 300 meters at the anchor station may not be typical of the Pacific Ocean as a whole.

A much larger percentage of the salinity anomalies falls within the anchor-station limits: at 200, 300, and 400 meters, roughly 70 per cent; at other levels, 90 per cent. Thus, we are forced to conclude that a very large percentage of the variation which we find for single pairs of observations can be attributed to short-period variation.

For the purpose of testing the significance of the departures of the mean anomalies by year classes, from zero, standard deviations were computed.

At the bottoms of Figures 11 and 13, the standard deviations of the temperature anomalies, computed for the entire sample, have been entered. The standard deviations of the salinity anomalies (excluding the 19th-century data) are shown at the bottom of Figure 12. At the bottoms of Figures 15 and 16 are entered the standard deviations of the temperature and salinity anomalies, respectively, computed for the *Carnegie*-NORPAC sample.

Standard deviations of temperature and salinity anomalies were also computed for the following subsamples to determine whether variability was approximately equal in the different subsamples: North Pacific, South Pacific, water masses, *Carnegie*-NORPAC entire sample, *Carnegie*-NORPAC water-mass subsamples, and *Carnegie-Louisville* subsample.

The variance (σ^2) of each subsample was tested for equality with that of the entire sample by use of the F, or variance-ratio, test [*Hoel*, 1947].

The subsample standard deviations of the temperature anomalies were significantly higher than those of the entire sample only in the Western North Pacific Central Water and at a depth of 1000 meters in the Peru Current region. The subsample standard deviations of the salinity anomalies were significantly higher than those of the entire sample in the upper levels of the Eastern North Pacific Subarctic Water and between 300 and 500 meters in the Western North Pacific Central Water.

In a large number of cases the standard deviations of both temperature and salinity in the water-mass subsamples were significantly smaller than those of the entire sample. In many subsamples the maximum values were at 100 meters rather than at 200 meters. The locations of the maximum standard deviations are related to the mean locations of the thermoclines.

A comparison of the standard deviations computed for the entire sample (Figs. 11 and 12) with those of the anchor stations in Table 3 shows that at 100 meters the maximum anchor-station value is about one-half the sample value; at 200 and 300 meters it is less than one-tenth and at 400 to 1000 meters it is roughly one-sixth the value of the paired-station standard deviations. As was pointed out above, the gradient and the depth of the thermocline at the anchor station are not typical of the Pacific Ocean as a whole, and the anchor-station standard devia-
can be expected at single locations elsewhere.
tions at 200 and 300 meters are thus lower than

The mean anomalies shown at the tops of Figures 11 through 16 have been underlined if the

TABLE 4. Mean ∇S for Constant Temperatures

		Central Water				Intermediate and Deep Waters		
	Date	No. of Stations	Temp. Limits, °C	Mean, ‰	Range, ‰	Temp. Limits, °C	Mean, ‰	Range, ‰
Louisville	1929–1936							
ENPCW*		8	9–20	−0.02	0.62	2–8	+0.03	0.32
NORPAC	1929–1955							
ENPCW*		6	9–20	0.00	0.46	2–8	+0.03	0.39
Transition Reg. Calif. Current		7	9–20	−0.07	0.88	2–8	+0.05	0.92
Downwind	1928–1929 1957–1958							
ESPCW†		3	8–14 15–25	−0.04 −0.08	0.24 0.30	2–7	−0.05	0.10
Transition Reg. Peru Current		6	8–14	+0.01	0.41	2–7	−0.01	0.24

* Eastern North Pacific Central Water.
† Eastern South Pacific Central Water.

mean exceeds $\sigma_t/\sqrt{n}$ (deviation of the mean) at the 5 per cent probability level, when the standard deviations for the entire sample, for the appropriate depths, were used as the significance criteria.

Detailed examination of the means for individual years reveals that very few means are significantly different from zero at the 5 per cent level, and these are so scattered in time and depth that their meaning is ambiguous. Much larger samples are needed before we can hope to filter long-term trends from shorter-period variability, since short-period variance is large and $\sigma_t/\sqrt{n}$ is approximately equal to σ_t for the small samples for individual years. Not only do we have considerable short-period variation in terms of days, as is seen in the anchor-station data, but there are also differences from one year to the next as great as the differences over periods of several or many years. (See data for the 1928 *Carnegie* station compared with data for the 1929 *Dana* station and the 1958 Downwind station, Fig. 9, curve *B*.)

The detailed tabulations of the means for individual years and of the standard deviations for the subclasses mentioned above are not given here. They may be obtained from the author upon request.

Thus, in general, we were unable to relate the magnitude and sign of the anomalies to time interval, just as we were unable to relate distance between stations within a given water mass to magnitude and sign of the anomalies. In the particular case of the *Carnegie*-NORPAC sample, however, the NORPAC mean salinity anomalies at all but three levels are significantly higher than the *Carnegie* values. The paramount question is whether this difference between the *Carnegie* and NORPAC salinities is due to a long-period (26 years) increase in salinity or to short-period variation. The lack of systematic trend in the salinity anomalies for the years between 1934 and 1955 points to short-period variation as the probable cause.

For further light on this problem, the three most numerous subsamples, 1936 *Louisville*, 1955 NORPAC, and 1957–1958 Downwind, were examined for possible systematic shifts in the T-S correlation and their relation to time interval. Tables 4 and 5 confirm the occurrence of such shifts, which appear to be of short period.

Salinity changes (∇S) for constant temperatures are within the limits of determination error. Temperature changes (∇T) for constant salinities are much greater. They range between −0.6°C and +0.8°C and appear to represent short-period, random changes rather than long-period, systematic trends. For example, the

TABLE 5. Mean ∇T for Constant Salinities

		Central Water				Intermediate and Deep Waters		
	Date	No. of Stations	Sal. Limits, ‰	Mean, °C	Range, °C	Sal. Limits, ‰	Mean, °C	Range, °C
Louisville	1929–1936							
ENPCW*		8	34.1–35.1	+0.4	5.0	34.0–34.6	+0.3	2.6
NORPAC	1929–1955							
Transition Reg. Calif. Current		9	34.1–35.1	−0.3	3.8	34.0–34.6	+0.4	2.6
ENPCW*		7	34.1–35.1	−0.2	5.0	34.0–34.6	+0.4	2.8
Subarctic		3	33.0–33.9	+0.2	0.4	34.0–34.6	+0.4	0.6
Downwind	1928–1929 1957–1958							
ESPCW†		3	34.5–35.5	+0.6	3.2			
			35.6–36.2	+0.8	4.3	34.5–34.6	−0.6	0.4
Transition Reg. Peru Current		6	34.2–34.6	+0.06	3.8	34.5–34.6	−0.1	2.4

* Eastern North Pacific Central Water.
† Eastern South Pacific Central Water.

Carnegie-Louisville 7-year comparisons and the *Carnegie*-NORPAC 26-year comparisons show practically identical mean temperature increases at constant salinities in intermediate and deep waters. Conversely, the *Carnegie*-Downwind data, with a 29-year interval, show a mean decrease of large magnitude. The range of individual differences was so great, however, that mean increases or decreases in the *T-S* correlation cannot be considered to be significant on the basis of small samples.

Summary and Conclusions. Although no long-period climatic trends were revealed in this analysis, the results indicate real temperature and salinity variations at all levels. Short-period changes are of such magnitude, however, that long-period trends, if present, cannot be found with the data at hand. We need continuous hydrographic data at single locations.[2] The Pacific Oceanographic Group of Canada have started such a program at Weather Station PAPA. Within the next few years their data should provide the answers to the problem: causes and time scale of the variations of temperature and salinity below the layers of seasonal influence.

Acknowledgments. This paper represents results of research carried out by the University of California, under contract with the Office of Naval Research. Reproduction in whole or in part is permitted for any purpose of the U. S. Government. This research also received support from the California Cooperative Oceanic Fisheries Investigations, a project sponsored by the Marine Research Committee of the State of California.

References

Austin, T. S., Summary, oceanographic and fishery data, Marquesas Islands area, Aug.-Sept., 1956 (Equapac), *U. S. Fish Wildlife Serv. Spec. Sci. Rept., Fisheries Ser., 217* (mimeo.), 1957.

Belknap, G. E., Deep-sea soundings in the North Pacific Ocean obtained by USS *Tuscarora, U. S. Hydrograph. Office, 54,* Govt. Print. Office, Wash. D. C., 51 pp., 1874.

Canadian Joint Commission on Oceanography, Pacific Oceanographic Group, Nanaimo, B. C., *Physical, chemical and plankton data record,* NORPAC, July 26-Sept. 1, 1955, *File N 6-17-4,* (mimeo.), 1956.

Carnegie: Scientific results of cruise VII of the *Carnegie* during 1928–1929, Oceanography I-A and I-B, *Carnegie Inst. Wash. Publ. 545,* I-A, 156 pp., 1944, and I-B, 315 pp., 1945.

---

[2] Håkon Mosby has just published an article, "Deep Water in the Norwegian Sea," in Geofysiske Publikasjoner, Geophysica Norvegica, Vol. XXI, Nr 3, Sept., 1959. It is an analysis of deep temperature and salinity observations at Weather Ship Station M (66°N, 2°E), His sample was adequate in number to detect minor fluctuations of salinity in 10-day means and to detect small annual variations of temperature, salinity and oxygen content in the deep waters. Maxima and minima occur simultaneously at all deep water levels below 800 meters, but they are out of phase with the seasonal variations of the surface layers.

Central Meteorological Observatory, Tokyo, Japan, *The results of marine meteorological and oceanographic observations, 17,* NORPAC Exp. Spec. No., July-Sept. 1955 (mimeo.), 1956.

Challenger: Report on the scientific results of the voyage of HMS Challenger, during years 1873–1876, Physics and chemistry, 1, Neill & Co., Gr. Br., 299 pp., 1884.

Dana Reports, 12, Hydrographical Observations, Carlsberg Foundation, C. A. Reitzels Forloag, Copenhagen, Denmark, and Oxford Univ. Press, London, pp. 1–46, 1937.

Discovery Reports, 21, Cambridge Univ. Press, Cambridge, pp. 1–226, 1941.

Discovery Reports, 25, Cambridge Univ. Press, Cambridge, pp. 143–280, 1949.

Fleming, R. E., & Staff, *University of Washington Special Report 22,* NORPAC, 1955, Prelim. data rept. UW ref. *56-4* (mimeo.), 1956.

Goodman, Joe, and Thomas G. Thompson, Characteristics of water in sections from Dutch Harbor, Alaska, to Strait of Juan de Fuca and from Strait of Juan de Fuca to Hawaii, *Univ. Wash. Publ. in Oceanogr., 3*(3), 81–103, 1940.

Hoel, Paul G., *Introduction to Mathematical Statistics,* John Wiley & Sons, New York, 246 pp., 1947.

Japanese Hydrographic Office, NORPAC *oceanographic and meteorological data,* (mimeo.), 1956.

Makaroff, S., *Le Vitiaz el l'ocean Pacifique, 1, 2,* St. Petersburg, Russia, 515 pp., 1894.

McGary, J. W., E. C. Jones, and T. S. Austin, *Mid-pacific Oceanography, 9* (NORPAC), *U. S. Fish Wildlife Serv. Spec. Sci. Rept., Fisheries Ser., 168* (mimeo.), 1956.

Scripps Institution of Oceanography, Univ. Calif., Marine Life Research Program, *Physical and Chemical Data* (mimeo.):
  Cruise 11, Jan.-Feb. 1950, 61 pp., 1951.
  Cruise 12, Mar. 1950, 58 pp., 1951.
  CCOFI Cruise 5508, NORPAC, SIO ref. *56-4,* 94 pp., 1956.
  CCOFI Cruises 5703 and 5704, SIO ref. *58-24,* 118 pp., 1958.

Scripps Institution of Oceanography, Univ. Calif., *Oceanic Observations of the Pacific, 1949,* Univ. Calif. Press, 363 pp., 1957.

Scripps Institution of Oceanography, Univ. Calif., Unpublished temperature and salinity data on file at Scripps Inst. Oceanog.
  Northern Holiday Expedition, Aug.-Sept. 1951.
  Shellback Expedition, May-June 1952.
  Capricorn Expedition, Oct. 1952-Feb. 1953.
  Downwind Expedition, Oct. 1957-Feb. 1958.

Sverdrup, H. U., M. W. Johnson, and R. H. Fleming, *The Oceans: Their Physics, Chemistry and General Biology,* Prentice-Hall, New York, 1087 pp., 1942.

Tokai Regional Fisheries Research Laboratory, Tokyo, Japan, NORPAC *Data of Hydrographic Observations by R. W. Tenyō-Maru,* July 18-Sept. 8, 1955 (mimeo.), 1956.

Tokyo University of Fisheries, *Oceanographic and Meteorological Data,* NORPAC *Project* (mimeo.), 1956.

Thompson, G. G., G. F. McEwen, and R. Van Cleve, Hydrographic sections and calculated currents in the Gulf of Alaska, *Rept. Int. Fish. Comm., 10,* 32 pp., 1936.

U. S. Navy
  USS *Bushnell,* Unpublished temperature and salinity data on file at Scripps Institution of Oceanography, 1934.
  USS *Louisville,* Unpublished temperature and salinity data on file at Scripps Institution of Oceanography, 1936.
  USS *Fieberling,* Unpublished temperature and salinity data on file at Scripps Institution of Oceanography, 1947.

Von Schleinitz, Georg, *Die forshchungreise SMS Gazelle, 1874–1876, Physik und Chemie, 2,* Ernst S. Mittler & Sohn, Berlin, 265 pp., 1888.

Wooster, W. S., and B. A. Taft, Reliability of field measurements of temperature and salinity in the oceans, *J. Marine Research, Sears Foundation, 17,* 1958.

Worthington, L. V., Oceanographic results of project Skijump I and Skijump II in the Polar Sea, 1951–1952, *Trans. Am. Geophys. Union, 34,* 543–551, 1953.

Worthington, L. V., A preliminary note on the time scale in North Atlantic circulation, *Deep-Sea Research, 1,* 244–251, 1954.

Worthington, L. V., A new theory of Caribbean bottom-water formation, *Deep-Sea Research, 3,* 82–87, 1955.

Worthington, L. V., The temperature increase in Caribbean deep water since 1933, *Deep-Sea Research, 3,* 234–235, 1956.

(Manuscript received March 21, 1960; revised April 20, 1960.)

Reprinted from THE REVIEW OF SCIENTIFIC INSTRUMENTS, Vol. 31, No. 7, 747–751, July, 1960
Printed in U. S. A.

Low Frequency Wave Filters Employing Thermistors*

ROBERT A. RASMUSSEN
University of California, La Jolla, Marine Physical Laboratory of the Scripps Institution of Oceanography, San Diego, California

(Received February 29, 1960; and in final form, May 2, 1960)

A review of the general properties of thermistors and analyses of their small signal characteristics are presented. Measurements of their ac properties and response curves obtained for the simplest filter circuit configurations are then described and the results analyzed.

INTRODUCTION

THERMISTORS are temperature-sensitive resistors manufactured from semiconductor solids. In addition to a negative resistance characteristic, they exhibit an apparent inductance over a wide range of very low frequencies. The apparent inductance is a measure of the time lag between variations of power dissipation and resultant changes in thermistor temperature. The thermal time lag is, of course, governed by the heat transfer characteristics of the medium surrounding the thermistor.

Apparent inductances of the order of 10^4 h have been measured, and several investigators have resonated the apparent inductance with capacitance in V. L. F. oscillator circuits.[1,2]

This investigation is concerned with the possible application of thermistors to very low frequency filters, e.g., filters for use in measurements of phenomena exhibiting periodicities of the order of minutes.

THERMISTOR CHARACTERISTICS AND PARAMETERS

The resistance of a thermistor is given by the relation[3]

$$R = R_0\, e^{B(1/T - 1/T_0)}, \tag{1}$$

where R is the resistance at the absolute temperature T, R_0 is the resistance at the reference temperature T_0, and B is a positive constant depending upon the semiconducting material from which the thermistor is manufactured. The temperature coefficient of resistance is, by definition,

$$\alpha = 1/R\,(dR/dT).$$

Then,

$$\alpha = -(B/T^2). \tag{2}$$

When a thermistor is heated to a temperature T_0 well above that of its surroundings and then permitted to cool, the rate of cooling is found to be proportional to the instantaneous temperature difference $T - T_x$, T_x being the surrounding temperature. Then if C is the heat capacity of the thermistor

$$-C(dT/dt) = K(T - T_x),$$

or

$$T = T_x + (T_0 - T_x)\, e^{-t/\tau}, \tag{3}$$

where T is the instantaneous temperature and K is termed the dissipation constant. It is dependent upon the geometry of the thermistor, the manner in which it is coupled to its surroundings, and the thermal properties of both the thermistor and its surroundings. τ is called the thermal time constant and

$$\tau = C/K. \tag{4}$$

A static characteristic curve typical of most thermistors is shown in Fig. 1(a). For small currents, the slope of the VI curve is positive, indicating a positive dynamic resist-

---

* This work represents one of the results of research carried out under contracts with the Bureau of Ships and with the Office of Naval Research.

[1] R. A. Rasmussen, "An ultra-low-frequency oscillator," thesis for Master's Degree, University of Texas, June, 1952.

[2] J. E. Stone, Electronics 23, 94 (January 1950).

[3] For a more complete account of physical, electrical, and thermal properties see J. A. Becker, C. B. Green, and G. L. Pearson, Trans. AIEE 65, 711 (1946).

Contributions from the Scripps Institution of Oceanography, New Series, 1177

Reproduced by Permission

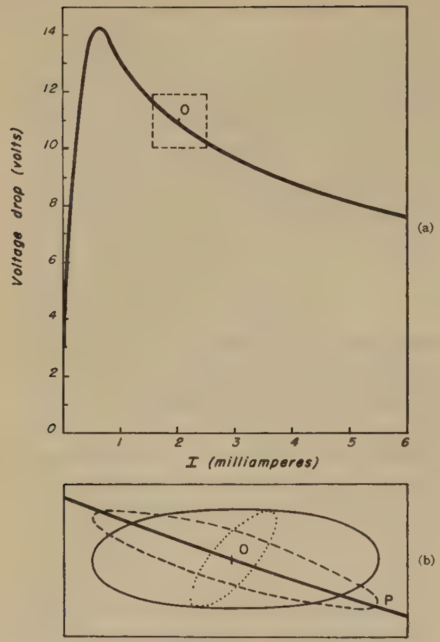

Fig. 1. Thermistor characteristics. (a) Static characteristics; (b) dynamic characteristics.

ance. For larger currents dV/dI, and hence the dynamic resistance, is negative. If the thermistor is biased to the operating point (V_0,I_0) and a sinusoidal current i of very small amplitude is superimposed on the bias current, the phase and amplitude of the resulting voltage variation v will depend upon the frequency of the current. At extremely low frequencies, variations in current and voltage take place along the static curve. The voltage is 180° out of phase with the current, the variations occurring so slowly that the process is effectively quasistatic, each point of the path representing a state of thermal equilibrium between the thermistor and its surroundings. As the frequency is increased, the voltage begins to lead the current by less than 180°. This may be explained qualitatively as follows: Referring to Fig. 1(b), assume the instantaneous operating point to be at P. As the current decreases, the thermistor begins to cool. However, heat is not transferred away from it rapidly enough to allow a decrease in resistance to a value where IR corresponds to a voltage on the static curve. The voltage is therefore higher than the value indicated by the static curve. The locus of dynamic V, I points depicting the behavior at lower frequencies is indicated by the dashed elliptical curve in Fig. 1(b). At a frequency f_{90} the voltage will lead the current by exactly 90°. The dynamic operation at f_{90} is indicated by the solid ellipse in Fig. 1(b). At frequencies much higher than f_{90} the path of operation is along the dotted ellipse and in the limit the path is along a segment of the straight line from the origin through O. At these very high frequencies the variations occur almost adiabatically, e.g., an infinitesimal amount of heat is transferred during one cycle of the current.

From the foregoing description, the equivalent ac impedance for the thermistor may be specified according to the definition

$$\bar{z}=\frac{\bar{v}}{\bar{i}}=\frac{v}{i}\,e^{-j\theta}=r+j\omega L_a, \tag{5}$$

where θ is the angle of the current relative to the voltage. This equation suggests that the equivalent circuit for the thermistor is a resistance in series or in parallel with an inductance, the series representation being indicated directly by Eq. (5).

It is to be noted that, although the analogy of the ac thermistor impedance with real electrical impedances permits application of electric circuit analysis techniques, there are no electrical components analogous to r which may be positive or negative, or to L_a which varies considerably with frequency. In the following analysis expressions for $\bar{z}$, θ, and f_{90} are derived for the case of small signals:

Referring to Fig. 2, T_x= temperature of medium surrounding thermistor; T_0= thermistor temperature at static operating point; T= instantaneous thermistor temperature; $V=V_0+v(t)$ instantaneous voltage drop; $I=I_0+i(t)$ instantaneous current; and $P=VI$= instantaneous power. It will be assumed that

$$v(t)=v_0\sin\omega t,\quad v_0\ll V_0\quad\text{and}\quad |i(t)|\ll I_0,$$

so that the variational power is small compared to the static power, V_0I_0.

The thermistor resistance is expressed as

$$R=V/I=R_0\,e^{B(1/T-1/T_0)}, \tag{6}$$

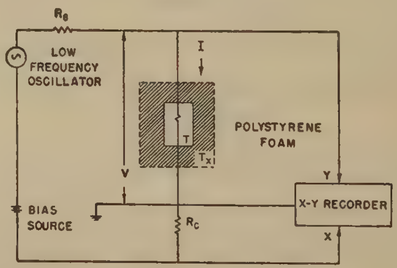

Fig. 2. Arrangement of apparatus employed to study ac properties.

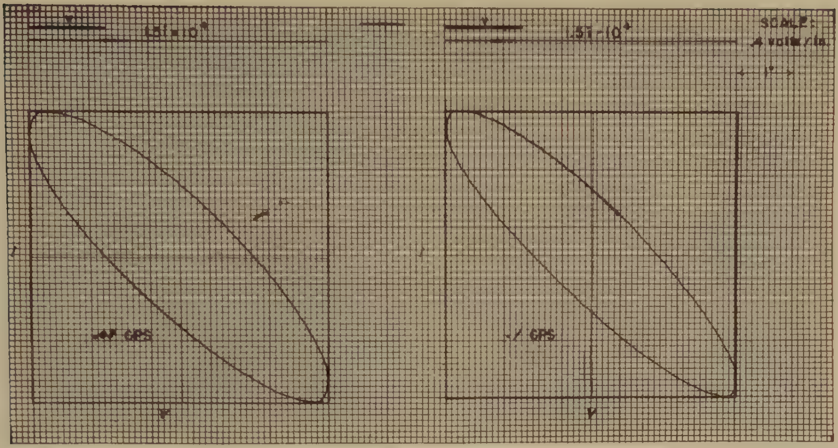

FIG. 3. A typical data record.

and the temperature coefficient of resistance is defined as

$$\alpha=\frac{1}{R}\frac{dR}{dT}=\frac{B}{T^2}. \tag{7}$$

Since the variational power is small, temperature variations will also be small and

$$\alpha \doteq -\frac{B}{T_0^2}=\text{const.}$$

Then

$$R=R_0[1+\alpha(T-T_0)],$$

or

$$T=(R-R_0/\alpha R_0)+T_0. \tag{8}$$

It is next assumed that heat is transferred away from the thermistor at a rate proportional to the temperature difference $T-T_x$ so that the heat transfer equation may be written as

$$C(dT/dt)=P-K(T-T_x), \tag{9}$$

where C is the heat capacity of the thermistor and K is the dissipation constant representative of the system coupling the thermistor and its surrounding medium.

If we substitute Eq. (8) in (9) and rearrange terms, we obtain

$$(dR/dt)+R/\tau=bP+h, \tag{10}$$

where

$$1/\tau=K/C$$
$$b=R_0\alpha/C$$
$$h=(R_0/\tau)[1-\alpha(T_0-T_x)].$$

In terms of the static and variational voltages and currents, Eq. (10) may be written as

$$I_0\frac{dv}{dt}-V_0\frac{di}{dt}+\frac{1}{\tau}(V_0+v)(I_0+i)$$
$$=[b(V_0+v)(I_0+i)+h](I_0+i)^2. \tag{11}$$

By neglecting terms of the second and higher orders in v and i, Eq. (11) reduces to

$$I_0\frac{dv}{dt}+\left(\frac{I_0}{\tau}-bI_0^3\right)v+\frac{V_0I_0}{\tau}=V_0\frac{di}{dt}$$
$$+\left[3bV_0I_0^2+2hI_0-\frac{V_0}{\tau}\right]i+I_0^2(bV_0I_0+h). \tag{12}$$

The symmetry of this linear equation suggests the functional form for i of $i_0 \sin(\omega t+\theta)$. By substituting for v and i in Eq. (12), expanding and equating the constant terms

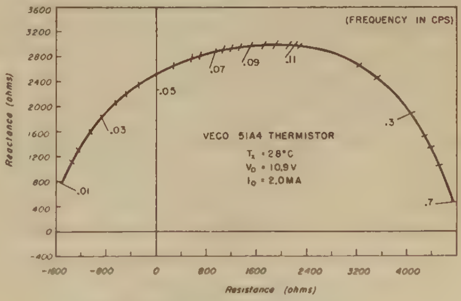

FIG. 4. Impedance diagram.

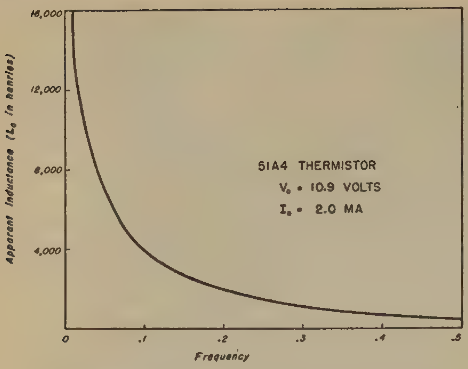

FIG. 5. Apparent inductance as a function of frequency.

and the coefficients of like phase, the following three equations are obtained:

$$\frac{1}{\tau}V_0I_0=I_0^2(bV_0I_0+h) \tag{13}$$

$$\left(\frac{1}{\tau}-bI_0^2\right)\frac{v_0I_0}{i_0}=\left[3bV_0I_0^2+2hI_0-\frac{V_0}{\tau}\right]\cos\theta-\omega V_0\sin\theta \tag{14}$$

$$\frac{\omega v_0I_0}{i_0}=\left[3bV_0I_0^2+2hI_0-\frac{V_0}{\tau}\right]\sin\theta+\omega V_0\cos\theta. \tag{15}$$

Upon solving Eq. (14) and (15) for θ and resubstituting for b and h from Eq. (10),

$$\theta=\tan^{-1}[2\omega\alpha\tau(T_0-T_x)/(\omega\tau)^2+1-\alpha^2(T_0-T_x)^2]. \tag{16}$$

The ratio v_0/i_0 is then determined from either Eq. (14) or (15). On defining this ratio as the modulus of the complex impedance vector $|z|=v_0/i_0$,

$$z=\frac{v_0}{i_0}=R_0\left(\frac{(\omega\tau)^2+[1+\alpha(T_0+T_x)]^2}{(\omega\tau)^2+[1+\alpha(T_0-T_x)]^2}\right)^{\frac{1}{2}}. \tag{17}$$

The frequency at which z is a pure reactance is the frequency for which the denominator of Eq. (16) vanishes, or

$$f_{90}=\frac{1}{2\pi\tau}(\alpha^2(T_0-T_x)^2-1)^{\frac{1}{2}}. \tag{18}$$

From Eqs. (16), (17), and (18) it is apparent that τ and L_a are dependent upon the static operating point and the temperature of the surrounding medium as well as the frequency. The assignment of a characteristic value of inductance to a thermistor is therefore a complicated, if not meaningless, task. However, the value of the apparent inductance at f_{90} is simply obtained both experimentally and analytically, and since this value is indicative of the magnitude of the inductance, it serves as a useful index.

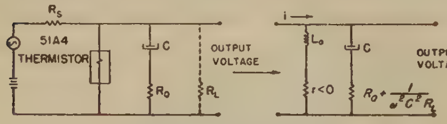

FIG. 6. Parallel thermistor-capacitor configuration and approximate equivalent circuit.

MEASUREMENTS

Ac Thermistor Characteristics

The apparatus employed to study the ac properties of thermistors is shown diagramatically in Fig. 2. The thermistor at temperature T is enclosed in a compartment formed from polystyrene foam to minimize the effects of air currents. The temperature of the air in the compartment is indicated as T_x. R_s is a large resistance placed in series with the thermistor of resistance R and the resistor R_c to provide a constant thermistor current. The bias source is a regulated high voltage power supply, and the low frequency generator is a very low frequency oscillator. Instantaneous thermistor current and voltage drop are I and V, respectively. Voltages V and IR_c are directed to the input terminals of an x-y recorder, the resulting records being Lissajous figures from which $\tan\theta$, $|v|$, and $|i|$ can be measured. From these quantities $|z|$ and L_a may be computed. A typical set of recorded patterns is shown as Fig. 3.

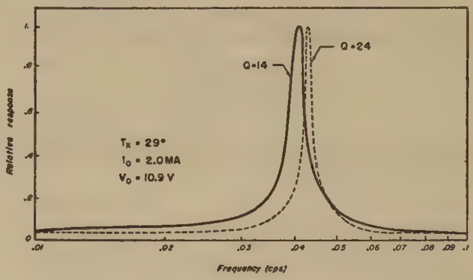

FIG. 7. Transmission response—51A4 thermistor bandpass filter.

Figure 4 is an impedance diagram obtained for the 51A4 thermistor. The behavior of the impedance with frequency is seen to be generally in accord with the qualitative description presented previously. Figure 5 shows the variation of L_a with frequency. In Fig. 4, f_{90} is indicated as 0.05 cps and the apparent inductance L_{90} at this frequency is, from Fig. 5, 7000 h.

RESONANT CIRCUITS COMBINING THERMISTORS AND CAPACITORS

The simplest resonant configuration to investigate is the parallel circuit formed by connecting a capacitor across the thermistor terminals in the measurement circuit of Fig. 2. The problem of capacitor volume was minimized by employing high quality electrolytic capacitors. To offset the leakage resistance R_L of these capacitors, operating frequencies corresponding to thermistor impedances lying near f_{90} in the second quadrant (Fig. 4) were selected, the negative thermistor resistance effectively canceling a part of the leakage resistance. To permit control of the circuit Q, a variable resistance R_q was added in series with the capacitor. This thermistor-capacitor configuration and its equivalent circuit are shown in Fig. 6. With the 51A4 thermistor biased to the same point employed for the impedance measurements, constant current response curves were measured for various Q at each of several resonant frequencies. The value of capacity necessary to resonate with a given L_a was determined from the equation

$$C = 1/4\pi f_0^2 L_a, \tag{19}$$

f_0 being the frequency corresponding to the apparent thermistor inductance. Figure 7 shows the response curves for $Q=14$ and $Q=24$ when $f_0=0.04$ cps. Values of Q are determined experimentally from the definition

$$Q = f_0/f_2 - f_1, \tag{20}$$

where f_2 and f_1 are the half-power frequencies. The similarity of these curves to those of ordinary turned, bandpass filters is very evident. Closer inspection reveals that the thermistor filter response falls more sharply above resonance, a result which can be traced to the fact that the thermistor impedance modulus is very nearly constant for frequencies above f_0, whereas the impedance of an ordinary inductor continues to increase at higher frequencies. Higher Q than those indicated in Fig. 7 are obtainable, the upper limit in these measurements being restricted to Q of approximately 40 due to inadequate control of the ambient temperature T_x.

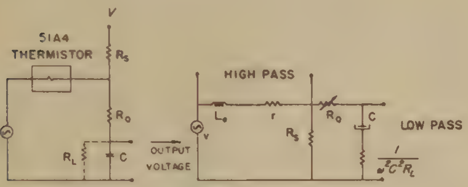

Fig. 8. Series thermistor-capacitor configuration and approximate equivalent circuit.

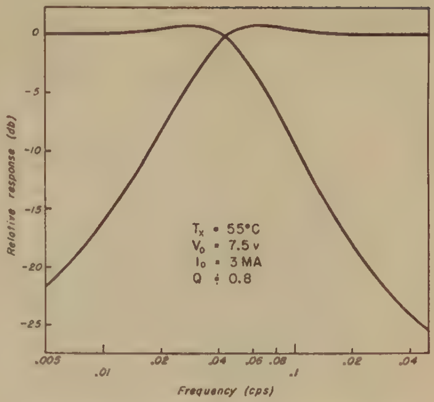

Fig. 9. Response curves obtained with series tuned filters.

Studies of simple series tuned filters were conducted using the circuit diagramed in Fig. 8. As indicated in the equivalent circuit, this configuration may be employed either as a high pass or low pass filter depending upon the location of the output terminals. Transmission response curves typical of this configuration appear in Fig. 9. The parameters employed in the measurements are tabulated in the figure. It is interesting to observe that these curves lie somewhere between those which would be measured for analogous LCR and RC filters. This result is suggested in the impedance diagram. At very high frequencies the thermistor appears resistive while at frequencies near f_{90} it appears mainly inductive. Hence, in the low pass response curve, one would expect the rate of attenuation to be large initially (depending upon the circuit Q) and to approach a value of 6 db per octave at very high frequencies. A similar argument applies to the high pass response curve.

DISTORTION

The linearity of the filter is dependent upon the thermistor bias point and the amplitude of the current variations about this point. Referring to the static characteristics in Fig. 1, it is evident that larger values of bias current and smaller signal currents yield improved linearity. Although no extensive distortion measurements have been made, it may be stated that the total harmonic distortion generated in a thermistor driven by a signal current whose amplitude is less than a tenth of the bias current is, at most, on the order of a few percent.

Reprinted from *Printed in U.S.A.*

THE PHYSICS OF FLUIDS VOLUME 3, NUMBER 3 MAY-JUNE, 1960

Variation Principles of Hydrodynamics

CARL ECKART
University of California, La Jolla, California
(Received March 7, 1960)

It is shown that the Lagrangian equations for the motion of both incompressible and compressible fluids can be derived from variation principles. As has been pointed out by C. C. Lin, an important feature of these principles is the boundary condition: The coordinates of each particle (and not merely the normal component of its velocity) must be specified. A systematic application of known results from the calculus of variations reveals new interrelations between such hydrodynamic results as Bernoulli's principle and the circulation theorem. Their derivation is both simplified and systematized. Clebsch's transformation is found to have an important relation to the problem of integrating the vorticity equation. The general solution of this problem for nonbarotropic flow is obtained. This reduces the second-order Lagrange equations to a set of first-order equations, in which the potential of the irrotational component replaces the pressure. The entropy gradients and a remarkable quantity, defined as the time-integral of the temperature of a particle of the fluid, also appear.

1. INTRODUCTION

ALTHOUGH it was known to Lagrange that the equations of hydrodynamics can be derived from a variation principle, and others[1] have studied the matter, this fact has not been fully exploited. Most probably this is because the Eulerian system of hydrodynamic equations is so much more popular than the Lagrangian system. In the Eulerian system, it is not easy to find a variation principle that is fully general,[2] and the basic principles have been formulated in other ways.

In other fields (e.g., celestial mechanics), the existence of a variation principle has not only resulted in a unification of the subject, but has led to the development of new methods for the integration of the equations[3] (e.g., The Hamilton-Jacobi transformation theory and the Rayleigh-Ritz method). It has therefore seemed of importance to reexamine the foundations of hydrodynamics from the standpoint of the calculus of variations.

In the present paper, few results will be obtained that are completely new, but the relations between known results are clarified by reference to the general Lagrangian problem of the calculus of variations. Equations (4.12) and (6.20) appear to be novel, although even they are related to Clebsch's transformed equations of hydrodynamics.

2. THE GENERAL LAGRANGIAN PROBLEM

To avoid needless repetition, a somewhat abstract and generalized problem will be treated first: Let x^m $(m = 1 \cdots M)$ be functions of the independent variables t^i $(i = 1 \cdots N)$. The notation

$$x_i^m = \partial x^m/\partial t^i \tag{2.1}$$

will be used, and, if L is any function of x^m, x_i^m, t^i, its total derivative with respect to t^i will be defined as

$$\frac{dL}{dt^i} = \frac{\partial L}{\partial x^m}\frac{\partial x^m}{\partial t^i} + \frac{\partial L}{\partial x_j^m}\frac{\partial x_j^m}{\partial t^i} + \frac{\partial L}{\partial t^i}. \tag{2.2}$$

The summation convention is used here and throughout. It is noteworthy that the N total derivatives commute. Let

$$I = \int \cdots \int_S L\, dt^1 \cdots dt^N, \tag{2.3}$$

the integral being extended over the N-dimensional volume bounded by the closed $(N - 1)$-dimensional surface S. Let it be required to find those functions $x^m(t^i)$ that (a) make I stationary, and (b) assume given values $X^m(t^i)$ on the boundary S. Then the necessary Euler-Lagrange equations of condition are known to be

$$\frac{d}{dt^i}\left(\frac{\partial L}{\partial x_i^m}\right) - \frac{\partial L}{\partial x^m} = 0. \tag{2.4}$$

One known consequence of these equations is of enough importance to warrant explicit derivation here:

---

[1] A bibliography and summary of this work is to be found in the article by James Serrin, *Handbuch der Physik* (Springer-Verlag, Berlin, Germany, 1959), Bd VIII/1, Pp. 145–150, 203–206.

[2] C. Eckart, Phys. Rev. 54, 920 (1938); J. W. Herivel, Proc. Cambridge Phil. Soc. 51 344 (1955). The source of this difficulty has now been found by C. C. Lin (private communication, to be published).

[3] J. von Neumann, in a memorandum addressed to O. Veblen, dated March 26, 1945, conjectured that the difficulty of solving the hydrodynamic equations arises, not from their nonlinear character, but from the lack of a variation principle. This memorandum is to be published in the collection of von Neumann's papers which is being prepared by A. H. Taub.

$$\frac{dL}{dt^i} = \frac{\partial L}{\partial x^m}\frac{\partial x^m}{\partial t^i} + \frac{\partial L}{\partial x_j{}^m}\frac{\partial x_j{}^m}{\partial t^i} + \frac{\partial L}{\partial t^i}$$

$$= \left[\frac{d}{dt^j}\left(\frac{\partial L}{\partial x_j{}^m}\right)\right]x_i{}^m + \frac{\partial L}{\partial x_j{}^m}\frac{\partial x_i{}^m}{\partial t^j} + \frac{\partial L}{\partial t^i}$$

$$= \frac{d}{dt^j}\left[x_i{}^m\frac{\partial L}{\partial x_j{}^m}\right] + \frac{\partial L}{\partial t^i}.$$

This may be written

$$\frac{dL_i{}^j}{dt^j} + \frac{\partial L}{\partial t^i} = 0, \qquad (2.5)$$

provided the energy-momentum tensor is defined to be

$$L_i{}^j = x_i{}^m(\partial L/\partial x_j{}^m) - L\,\delta_i{}^j. \qquad (2.6)$$

Equations (2.5) are known as the conservation laws associated with Eq. (2.4).

Sometimes the Lagrangian problem is modified by imposing additional restrictions, called subordinate conditions, that have the form

$$F(x^m, x_i{}^m, t^i) = 0. \qquad (2.7)$$

These may be introduced in various ways and always modify the Euler-Lagrange equations. A particularly elegant way to deal with subordinate conditions is Lagrange's method of undetermined multipliers. Additional unknowns, $x^{M+1} \cdots$ (one for each subordinate condition) are introduced, and a new Lagrangian L_1 is defined by

$$L_1 = L + x^{M+1}F + \cdots. \qquad (2.8)$$

Since L and F are independent of x^{M+1} and its derivatives, Eq. (2.7) is precisely the Euler-Lagrange equation for $m = M + 1$. The equations for $m \leq M$ then are linear in the multipliers and their derivatives. The existence of subordinate conditions therefore requires no modification of the preceding formalism, except the replacement of L by L_1.

3. THE INCOMPRESSIBLE FLUID

The index notation used above is best modified for special problems, but serves to outline the calculations to be made. In the case of a homogeneous incompressible fluid of density ρ, let the coordinates of a "particle" be $x^1 = x$, $x^2 = y$, $x^3 = z$. The trajectory of the particle is described by specifying three functions

$$x = x(t, \alpha, \beta, \gamma), \qquad y = y(t, \alpha, \beta, \gamma),$$
$$z = z(t, \alpha, \beta, \gamma), \qquad (3.1)$$

the variables α, β, γ identifying the particle, and t being the time; the trajectories are found by holding α, β, γ constant in Eq. (3.1), and letting t vary. In the preceding formalism, $t^1 \cdots t^4 = t, \alpha, \beta, \gamma$.

By using, now, the notation

$$x_t = \partial x/\partial t, \quad \text{etc.},$$

the kinetic energy (per unit-mass) of the fluid is

$$T = \tfrac{1}{2}(x_t{}^2 + y_t{}^2 + z_t{}^2). \qquad (3.2)$$

If the subordinate condition

$$dm = \rho\, dx\, dy\, dz = d\alpha\, d\beta\, d\gamma,$$

or

$$\partial(xyz)/\partial(\alpha\beta\gamma) = (1/\rho), \qquad (3.3)$$

is imposed, the equations of motion are derivable from the Lagrangian problem with

$$I = \int \cdots \int \{T + P[\partial(xyz)/\partial(\alpha\beta\gamma) - (1/\rho)]\}\, dm\, dt, \qquad (3.4)$$

P being a Lagrangian multiplier that turns out to be the pressure.

This variation principle is closely related to Kelvin's principle,[4] from which it differs primarily in respect to the boundary conditions. As pointed out by Lin,[2] Kelvin's boundary conditions specify the normal component of the velocity, and this is less stringent than the condition that x, y, z be given. Consequently Kelvin's principle, in its original form, applies only to irrotational motion. In the present form, it governs all possible motions of the fluid, as will appear later.

The Euler-Lagrange equations of this problem are Eq. (3.3) and

$$\frac{d^2x}{dt^2} + \frac{d}{d\alpha}\left(P\frac{\partial(yz)}{\partial(\beta\gamma)}\right) + \frac{d}{d\beta}\left(P\frac{\partial(yz)}{\partial(\gamma\alpha)}\right) + \frac{d}{d\gamma}\left(P\frac{\partial(yz)}{\partial(\alpha\beta)}\right) = 0, \qquad (3.5)$$

together with two others obtained from Eq. (3.5) by cyclic permutation of x, y, z.

By using the identity

$$\frac{d}{d\alpha}\left(\frac{\partial(yz)}{\partial(\beta\gamma)}\right) + \frac{d}{d\beta}\left(\frac{\partial(yz)}{\partial(\gamma\alpha)}\right) + \frac{d}{d\gamma}\left(\frac{\partial(yz)}{\partial(\alpha\beta)}\right) = 0, \qquad (3.6)$$

Eq. (3.5) becomes

$$\frac{d^2x}{dt^2} + \frac{\partial(Pyz)}{\partial(\alpha\beta\gamma)} = 0; \qquad (3.7)$$

---

[4] See reference 1, p. 161.

this and its companions are equivalent to the usual Lagrangian equations of hydrodynamics. The usual form is Eq. (3.15) and will be derived.

Turning now to the energy momentum tensor, typical components are

$$\begin{aligned} L_t^{\,t} &= T, \\ L_t^{\,\alpha} &= P\,\partial(xyz)/\partial(t\beta\gamma), \\ L_t^{\,\beta} &= P\,\partial(xyz)/\partial(\alpha t\gamma), \\ L_t^{\,\gamma} &= P\,\partial(xyz)/\partial(\alpha\beta t), \end{aligned} \qquad (3.8)$$

and

$$\begin{aligned} L_\alpha^{\,t} &= x_t x_\alpha + y_t y_\alpha + z_t z_\alpha \qquad (=u_\alpha), \\ L_\alpha^{\,\alpha} &= (P/\rho) - T \qquad (=\Phi), \\ L_\alpha^{\,\beta} &= L_\alpha^{\,\gamma} = 0. \end{aligned} \qquad (3.9)$$

The conservation laws are

$$\frac{dT}{dt} + \frac{d}{d\alpha}\left(P\,\frac{\partial(xyz)}{\partial(t\beta\gamma)}\right) + \frac{d}{d\beta}\left(P\,\frac{\partial(xyz)}{\partial(\alpha t\gamma)}\right) + \frac{d}{d\gamma}\left(P\,\frac{\partial(xyz)}{\partial(\alpha\beta t)}\right) = 0, \qquad (3.10)$$

and

$$(du_\alpha/dt) + (d\Phi/d\alpha) = 0, \qquad (3.11)$$

together with the two companions of Eq. (3.11).

Equation (3.10) expresses the conservation of energy. It can be transformed in an interesting manner, using the identity

$$\frac{d}{dt}\left(\frac{\partial(xyz)}{\partial(\alpha\beta\gamma)}\right) - \frac{d}{d\alpha}\left(\frac{\partial(xyz)}{\partial(t\beta\gamma)}\right) - \frac{d}{d\beta}\left(\frac{\partial(xyz)}{\partial(\alpha t\gamma)}\right) - \frac{d}{d\gamma}\left(\frac{\partial(xyz)}{\partial(\alpha\beta t)}\right) = 0. \qquad (3.12)$$

[The first term vanishes because of Eq. (3.3), but this is not immediately essential.] Hence Eq. (3.10) may be written

$$\frac{d}{dt}\left[T + P\,\frac{\partial(xyz)}{\partial(\alpha\beta\gamma)}\right] - P_t\,\frac{\partial(xyz)}{\partial(\alpha\beta\gamma)} + P_\alpha\,\frac{\partial(xyz)}{\partial(t\beta\gamma)} + P_\beta\,\frac{\partial(xyz)}{\partial(\alpha t\gamma)} + P_\gamma\,\frac{\partial(xyz)}{\partial(\alpha\beta t)} = 0 \qquad (3.13)$$

or

$$\frac{d}{dt}\,[T + (P/\rho)] = \frac{\partial(Pxyz)}{\partial(t\alpha\beta\gamma)}. \qquad (3.14)$$

This is the general form of Bernoulli's theorem. In the case of steady motions, P can be expressed as a function of x, y, z alone, independent of the time. The Jacobian on the right will then vanish, and Eq. (3.14) integrates at once into the usual form of the principle.

When the differentiations of u_α and T indicated in Eq. (3.11) are performed, a number of terms cancel, and it reduces to

$$\rho(x_{tt}x_\alpha + y_{tt}y_\alpha + z_{tt}z_\alpha) + P_\alpha = 0; \qquad (3.15)$$

this and its companions are Lagrange's equations in their usual form.[5]

All of these equations are invariant when the variables α, β, γ are transformed to

$$\alpha' = f_1(\alpha\beta\gamma), \quad \beta' = f_2(\alpha\beta\gamma), \quad \gamma' = f_3(\alpha\beta\gamma), \qquad (3.16)$$

provided only that

$$\partial(\alpha'\beta'\gamma')/\partial(\alpha\beta\gamma) = 1. \qquad (3.17)$$

This remark will be utilized below; transformations having this property are called unimodular, or measure-preserving.

4. THE CIRCULATION THEOREM AND VORTEX COORDINATES

Consider a closed curve, Γ, in α, β, γ space, whose shape and position does not vary with t, and let

$$C(t) = \int_\Gamma (u_\alpha\,d\alpha + u_\beta\,d\beta + u_\gamma\,d\gamma). \qquad (4.1)$$

Because of Eq. (3.11) and the constancy of Γ,

$$dC/dt = \int_\Gamma d\Phi = 0. \qquad (4.2)$$

Using Eq. (3.1), Γ can be projected into x, y, z space: Here, however, it changes shape and position with time: let $\Gamma(t)$ designate it at a given instant t. Then $\Gamma(t)$ is the instantaneous position and shape of a moving curve that is always composed of the same particles (i.e., is "fixed in the fluid"), and Eq. (4.1) becomes

$$C = \int_{\Gamma(t)} (x_t\,dx + y_t\,dy + z_t\,dz). \qquad (4.3)$$

This is recognized as the circulation around $\Gamma(t)$, while Eq. (4.2) is seen to be the Kelvin-Helmholtz circulation theorem.[6]

In differential form, Eq. (4.1) becomes

$$C_\alpha = (du_\gamma/d\beta) - (du_\beta/d\gamma), \quad \text{etc.}, \qquad (4.4)$$

and Eq. (4.2):

---

[5] H. Lamb, *Hydrodynamics* (Dover Publications, New York, 1945), p. 13.

[6] See reference 1, p. 162.

$$dC_\alpha/dt = 0, \quad \text{etc.} \tag{4.5}$$

Hence C_α, C_β, C_γ are functions of α, β, γ only, independent of t. Now, given any three-dimensional covariant vector u_α, Clebsch's theorem (see Appendix) asserts that it is always possible to find three scalars, A, B, and ϕ, such that

$$u_\alpha = A(\partial B/\partial\alpha) - (\partial\phi/\partial\alpha), \quad \text{etc.} \tag{4.6}$$

Using this definition of A and B, Eq. (4.4) becomes

$$C_\alpha = \partial(AB)/\partial(\beta\gamma), \quad \text{etc.} \tag{4.7}$$

Since the C_α are independent of t, Eq. (4.7) shows that A, B may also be determined so that they are independent of t, and functions only of α, β, γ. The scalar, ϕ, however, will usually depend on all four Lagrangian variables.

By using Eq. (4.6) and this remark, Eq. (3.11) integrates to

$$(P/\rho) - T = \Phi = (\partial\phi/\partial t), \tag{4.8}$$

an equation that enables the pressure to be found, once the velocities and ϕ have been determined.

Equations (4.7) do not determine A and B uniquely; as shown in the Appendix, or as can be seen by inspection of Eq. (4.7), A and B are determined only up to a unimodular transformation. This is a contact transformation, and when A and B are thus transformed, ϕ must be changed by the addition of the generating function of the transformation; this is analogous to a gauge transformation.

Once A, B, and ϕ have been decided upon, the coordinates α, β, γ may be transformed so as to simplify Eqs. (4.6) and (4.7). For there will always be a unimodular transformation of α, β, γ such that in the new system,

$$A = \alpha, \qquad B = \beta. \tag{4.9}$$

These coordinate systems will be called vortex coordinates, for a reason that will become apparent below. In such systems

$$C_\alpha = C_\beta = 0, \qquad C_\gamma = 1, \tag{4.10}$$

while

$$u_\alpha = -(\partial\phi/\partial\alpha), \qquad u_\beta = \alpha - (\partial\phi/\partial\beta), \tag{4.11}$$
$$u_\gamma = -(\partial\phi/\partial\gamma).$$

The vortex lines of the fluid are everywhere parallel to the vector C; in the present α, β, γ space, they are therefore the straight lines parallel to the γ axis. In x, y, z space, they are obtained from Eq. (3.1) by holding α, β, and t constant, and allowing γ to vary.

Equation (4.11) may be solved for x_t, y_t, z_t; the result is that

$$\frac{dx}{dt} = \rho\left\{\alpha\,\frac{\partial(yz)}{\partial(\gamma\alpha)} - \frac{\partial(\phi, y, z)}{\partial(\alpha\beta\gamma)}\right\}, \quad \text{etc.} \tag{4.12}$$

When this is compared with Eq. (3.7), it is seen that the two equations contain the same number of unknowns (namely four) and have the same degree (namely three), but that Eq. (4.12) contains no second derivative. A marked advance toward the integration of the equation of motion has thus been achieved. In fact, Eq. (4.12) is the solution of the problem that is sometimes called "the integration of the vorticity equation."

These results can also be transformed into the Eulerian system of hydrodynamic equations; without going into details, Eq. (4.11) becomes

$$\mathbf{u} = \alpha\nabla\beta - \nabla\phi, \tag{4.13}$$

and the fact that α and β depend only on the particle, not on the time, is expressed by

$$\left(\frac{\partial\alpha}{\partial t}\right) + \mathbf{u}\cdot\nabla\alpha = 0,$$
$$\left(\frac{\partial\beta}{\partial t}\right) + \mathbf{u}\cdot\nabla\beta = 0. \tag{4.14}$$

Equation (4.8) becomes

$$\rho[(\partial\phi/\partial t) + \mathbf{u}\cdot\nabla\phi] = P - \tfrac{1}{2}\rho\mathbf{u}^2, \tag{4.15}$$

and Eq. (3.3),

$$\nabla\cdot\mathbf{u} = 0. \tag{4.16}$$

In this form, they are equivalent to Clebsch's transformed equations of hydrodynamics.[7] These are also first-order equations, of third degree, but with three unknowns, α, β and ϕ. The vector $\mathbf{u}$ may be considered to be an abbreviation and can easily be eliminated.

5. GRAVITATIONAL FORCES

The equations of the preceding sections have ignored the gravitational forces. Let $g\chi$ be the Newtonian (i.e., nonrelativistic) potential. Then χ is the gravitational altitude, and may often be identified with the coordinate z; in other geophysical problems, χ is the radial height above mean sea level. In all these cases, χ is independent of the time variable, and a known function of x, y, z.

---

[7] See reference 5, p. 248.

In tidal problems, however, χ also depends on the time variable t.

The Lagrangian function is altered to

$$L = T - g\chi, \tag{5.1}$$

but the subordinate condition [Eq. (3.3)] remains unaltered. The Euler-Lagrange equations are then

$$x_{tt} + [\partial(Pyz)/\partial(\alpha\beta\gamma)] + g(\partial\chi/\partial x) = 0, \quad \text{etc.} \tag{5.2}$$

Only the diagonal components of the energy-momentum tensor are changed; they become

$$L_t^{\,t} = T + g\chi, \tag{5.3}$$

and

$$L_\alpha^{\,\alpha} = (P/\rho) - T + g\chi, \quad \text{etc.} \tag{5.4}$$

Of the terms $\partial L/\partial t^i$ in the conservation laws, Eq. (2.5), at most $\partial L/\partial t$ is different from zero. The conservation of energy is thus

$$(d/dt)[T + g\chi] + \cdots = g(\partial\chi/\partial t),$$

the omitted terms being the same as in Eq. (3.10). They can be transformed to yield the analog of Eq. (3.14).

The circulation theorem and its associated calculations are altered only in that Φ must now conform to Eq. (5.4).

6. THE ADIABATIC MOTION OF A COMPRESSIBLE FLUID

Many of these results apply equally to the adiabatic motion of a compressible fluid whose thermodynamic properties are determined by a general internal energy function, $\epsilon(V, \eta)$, V being its specific volume and η its entropy. Its pressure, P, and temperature, θ, are then

$$P = -(\partial\epsilon/\partial V), \qquad \theta = (\partial\epsilon/\partial\eta). \tag{6.1}$$

Let the Lagrangian variables be as in Sec. 3; then the Lagrangian function is

$$L = T - \epsilon(V, \eta), \tag{6.2}$$

while the subordinate condition now turns into a definition

$$V = \partial(xyz)/\partial(\alpha\beta\gamma). \tag{6.3}$$

The requirement that the motion be adiabatic is formulated by the new subordinate condition

$$d\eta/dt = 0. \tag{6.4}$$

This is most elegantly treated by the method of Lagrangian multipliers. However, since one of the resulting equations is unusual, it will here be treated by a slightly longer method.

Equation (6.4) shows at once that η is a function only of α, β, γ; this is one of the arbitrary functions that enter into the solution of the Lagrangian problem.[8] It may be introduced into L at the beginning, so that η is not a dependent variable, but a given function of α, β, γ, independent of t.

There are additional requirements imposed by physical considerations; thus, V and θ must both be positive quantities, and perhaps P as well. These requirements cannot always be satisfied without abandoning the requirement that x, y, z, η be continuous functions, with continuous derivatives. The physical phenomena are shock waves and changes of state. These phenomena will be ignored in this paper.

The Euler-Lagrange equations of the problem thus formulated are identical with Eqs. (3.5), but now P is not an independent variable, but is specified by Eqs. (6.1) and (6.3). The analog of Eq. (3.7) can be derived as before.

The energy momentum tensor is altered, and typical components are

$$\begin{aligned} L_t^{\,t} &= T + \epsilon, \\ L_t^{\,\alpha} &= P[\partial(xyz)/\partial(t\beta\gamma)], \quad \text{etc.,} \end{aligned} \tag{6.5}$$

while

$$\begin{aligned} L_\alpha^{\,t} &= x_t x_\alpha + y_t y_\alpha + z_t z_\alpha \qquad (= u_\alpha), \\ L_\alpha^{\,\alpha} &= h - T \qquad (= \Phi), \end{aligned} \tag{6.6}$$

and

$$L_\alpha^{\,\beta} = L_\alpha^{\,\gamma} = 0. \tag{6.7}$$

In the expression for $L_\alpha^{\,\alpha}$, h is the enthalpy:

$$h = \epsilon + PV. \tag{6.8}$$

Since L now depends explicitly on α, β, γ, (through η) the second term of Eq. (2.5) must again be taken into account: The conservation equations are thus

$$(d/dt)(T + \epsilon) + \cdots = 0, \tag{6.9}$$

and

$$(du_\alpha/dt) + (d\Phi/d\alpha) - \theta(d\eta/d\alpha) = 0. \tag{6.10}$$

The terms indicated by dots in Eq. (6.9) are the same as in Eq. (3.10), and Eq. (6.9) can therefore be written in the Bernoulli form

---

[8] In many laboratory motions, the entropy may be supposed independent of all four of the independent variables. These will be called isentropic motions. In geophysics, this supposition is usually not justified. The distinction between the general adiabatic and the isentropic motions is often, but not always, equivalent to the distinction between baroclinic and barotropic motions. A baroclinic motion can never be isentropic.

$$(d/dt)(T + h) = \partial(Pxyz)/\partial(t\alpha\beta\gamma). \qquad (6.11)$$

Equation (6.10) can be transformed by noting that

$$h_\alpha = VP_\alpha + \theta\eta_\alpha \qquad (6.12)$$

and, since $\Phi = h - T$, it becomes

$$(du_\alpha/dt) + V(dP/d\alpha) = (dT/d\alpha). \qquad (6.13)$$

The ordinary form of Lagrange's equations is now obtained on carrying out the differentiation of u_α and T. If C_α is again defined by Eq. (4.4), the analog of Eq. (4.6) is

$$dC_\alpha/dt = [\partial(PV)/\partial(\beta\gamma)], \quad \text{etc.} \qquad (6.14)$$

Hence the motion will be irrotational whenever the pressure can be expressed as a function of specific volume only—i.e., whenever the motion is barotropic. This is the Helmholtz-Bjerknes theorem.

Returning to Eq. (6.10); the somewhat remarkable definition of κ,

$$d\kappa/dt = \theta, \qquad (6.15)$$

converts it into

$$[d(u_\alpha - \kappa\eta_\alpha)/dt] + [d\Phi/d\alpha] = 0. \qquad (6.16)$$

It is to be noted that, since θ is positive, the κ of any particle will be a monotonically increasing function of time. If one now defines the thermodynamic circulation around the curve Γ (of Sec. 4) as

$$C_{Th} = -\int_\Gamma \kappa\, d\eta, \qquad (6.17)$$

and the kinematic circulation as

$$C_{Ki} = \int_\Gamma (u_\alpha\, d\alpha + u_\beta\, d\beta + u_\gamma\, d\gamma), \qquad (6.18)$$

then Eq. (6.16) leads to[9]

$$d(C_{Th} + C_{Ki})/dt = 0. \qquad (6.19)$$

The total circulation, defined in this way, thus remains constant for any closed curve fixed in the fluid.

Vortex coordinates and the integral of the vorticity equation can be obtained as in Sec. 4, except that u_α must everywhere be replaced by $u_\alpha - \kappa\eta_\alpha$. The analog of Eq. (4.12) is therefore

$$x_t \frac{\partial(xyz)}{\partial(\alpha\beta\gamma)} = \alpha\frac{\partial(yz)}{\partial(\gamma\alpha)} + \kappa\frac{\partial(\eta yz)}{\partial(\alpha\beta\gamma)} - \frac{\partial(\phi yz)}{\partial(\alpha\beta\gamma)}. \qquad (6.20)$$

The presence of the monotonically increasing quantity κ suggests that even very small entropy gradients (i.e., small departures from barotropic conditions) will initiate secular changes and ultimately cause great departures from the corresponding barotropic motion. In contrast to their analog in the case of an incompressible fluid, these first-order equations are of fourth degree, and contain the fifth unknown, κ.

They are independent of the thermodynamic properties of the fluid, but must be solved simultaneously with equations that do depend on these properties; these are Eq. (6.15) and

$$h - T = \Phi = \partial\phi/\partial t. \qquad (6.21)$$

The integration of the vorticity equation thus leaves one with a much more difficult problem than in the case of an incompressible fluid.

7. APPENDIX: AN EXTENSION OF CLEBSCH'S THEOREM

This theorem[10] is most conveniently proven in the ordinary notation of vector analysis. If $\mathbf{u}$ is any three-dimensional vector field, it is to be shown that three scalars, A, B, ϕ, can always be found such that

$$\mathbf{u} = A\,\nabla B - \nabla\phi. \qquad (7.1)$$

Let

$$\mathbf{C} = \nabla \times \mathbf{u}; \qquad (7.2)$$

if $\mathbf{C} \equiv 0$, it is known that Eq. (7.1) holds with $A = 0$, and ϕ determined except for an additive constant. If $\mathbf{C}$ does not vanish, and Eq. (7.1) holds,

$$\mathbf{C} = \nabla A \times \nabla B, \qquad (7.3)$$

whence

$$\mathbf{C}\cdot\nabla A = \mathbf{C}\cdot\nabla B = 0. \qquad (7.4)$$

Given $\mathbf{C}$, these are differential equations for A and B, that can always be solved in such a way that Eq. (7.3) is satisfied. For, they also imply that

$$\mathbf{C} = \lambda\,\nabla A \times \nabla B.$$

Since $\nabla\cdot\mathbf{C} = 0$, it follows that

$$\mathbf{C}\cdot\nabla\lambda = 0;$$

hence, λ is a function only of A and B and can be taken equal to unity without loss of generality. This returns one to Eq. (7.3).

---

[9] The relativistic generalization of this theorem has already been obtained by A. H. Taub, Arch. Rat. Mech. Ana. 3, 312 (1959).

[10] See reference 5, pp. 248, 249.

Now,

$$\nabla \times (\mathbf{u} - A\nabla B) = \mathbf{C} - \nabla A \times \nabla B = 0; \tag{7.5}$$

hence $\mathbf{u} - A\ \nabla B$ is a gradient and Eq. (7.1) has been established.

The three scalar fields are not uniquely determined by these considerations; let A', B', ϕ' be a second set. Then Eq. (7.1) implies

$$A\nabla B - A'\nabla B' = \nabla(\phi - \phi'). \tag{7.6}$$

This will certainly be true if

$$\phi' - \phi = S(B, B') \tag{7.7}$$

and

$$A = -\partial S/\partial B, \qquad A' = \partial S/\partial B'. \tag{7.8}$$

Thus A and B are determined only up to a contact transformation, and ϕ transforms by the addition of the generating function S.

It is known (Liouville theorem) that Eq. (7.8) is equivalent to

$$\partial(A'B')/\partial(AB) = 1, \tag{7.9}$$

which can also be derived directly from Eq. (7.3).

ACKNOWLEDGMENTS

Constructive suggestions for this paper were received from C. C. Lin and his seminar group at Princeton, from A. H. Taub, and from M. Rosenbluth. It is a pleasure to acknowledge this indebtedness.

Fred B Phleger

Foraminiferal Populations in Laguna Madre, Texas

Reprinted from the Science Reports of the Tohoku University,
Sendai, Japan, Second Series (Geology), Special
Volume, No. 4 (Hanzawa Memorial Volume),
March, 1960

Science Reports, Tohoku University, Sendai, Japan, 2nd Ser. (Geol.), Spec. Vol., No. 4,
pp. 83-91, 9 text-figs., 1960

Foraminiferal Populations in Laguna Madre, Texas

Fred B Phleger

Scripps Institution of Oceanography, La Jolla, California, U.S.A.

ABSTRACT

Foraminiferal populations in Laguna Madre are large, indicating high organic productivity. The fauna is dominated by Miliolidae, believed to be due to general abundance of sand in the substrate. It is a modified lower lagoon fauna with abundant *Elphidium* and *Streblus beccarii* variants. Live-total population ratios indicate the lagoon barrier as a source of most of the sediment.

INTRODUCTION

Laguna Madre is on the south coast of Texas between approximately 26°00′ and 27°40′N. Lat. and 79°10′ and 97°40′W. Long. It is a coastal lagoon separated from the Gulf of Mexico by Padre "Island", a lagoon barrier 110 mi. long. The northern end is at Aransas Pass and the southern at Brazos Santiago.

The purpose of this report is to record foraminiferal distributions within Laguna Madre and to interpret their possible sedimentary significance. Locations of stations are on Figure 1. The samples are composed of surface sediment approximately 10 sq. cm. in area and 1 cm. thick. Living populations (fig. 2) were determined using rose Bengal stain (Walton, 1952) and total populations also were recorded (fig. 3). The samples were collected by Gene A. Rusnak and were analyzed by C.R. Haller.

DESCRIPTION OF THE AREA

The oceanography and sedimentology of Laguna Madre have been discussed by Rusnak (1960) and the sedimentology of Padre Isalnd and the Laguna Madre flats by Fisk (1959). The lagoon is separated into northern and southern basins by a land bridge of low sand and mud flat extending from Padre Island to the mainland. The average width of the basins, which trend parallel to the coast, is 2½–5 mi. and each basin is approximately 50 mi. long. The basins have an average depth of about 2½ ft. Baffin Bay extends inland from the northern basin for 15 mi. and has an average depth of 5 ft. The sediments range from sand to clay and are described by Rusnak (1960).

The climate is semi-arid with an average rainfall of 27 in. and a reported 21 in. of evaporation in excess of rainfall. The water in the lagoon is generally hypersaline, with salinities in the northern basin ranging from 22–45 ‰ Cl and in Baffin Bay from 1–45 ‰

Contributions from the Scripps Institution of Oceanography, New Series, 1180

Reproduced by Permission

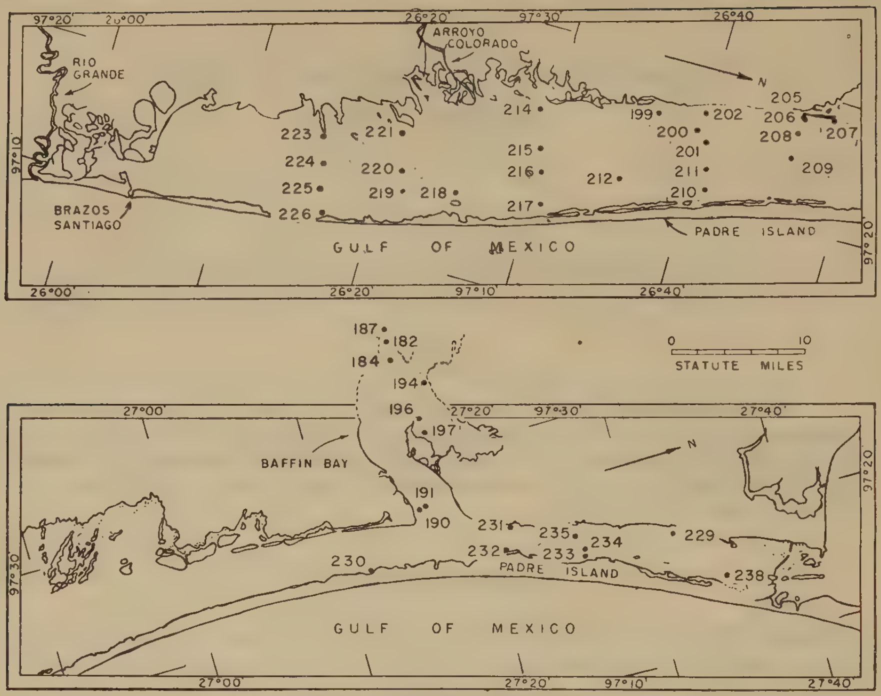
RIO GRANDE
ARROYO COLORADO
BRAZOS SANTIAGO
PADRE ISLAND
GULF OF MEXICO
N
223
224
225
226
221
220
219
218
214
215
216
217
212
199
200
201
202
211
210
205
206
207
208
209
BAFFIN BAY
187
182
184
194
196
197
191
190
231
235
234
232
233
229
230
238
0 10 STATUTE MILES
97°20'
26°00'
26°20'
97°30'
26°40'
97°10'
27°00'
27°20'
27°40'

Fig. 1. Locations of stations.

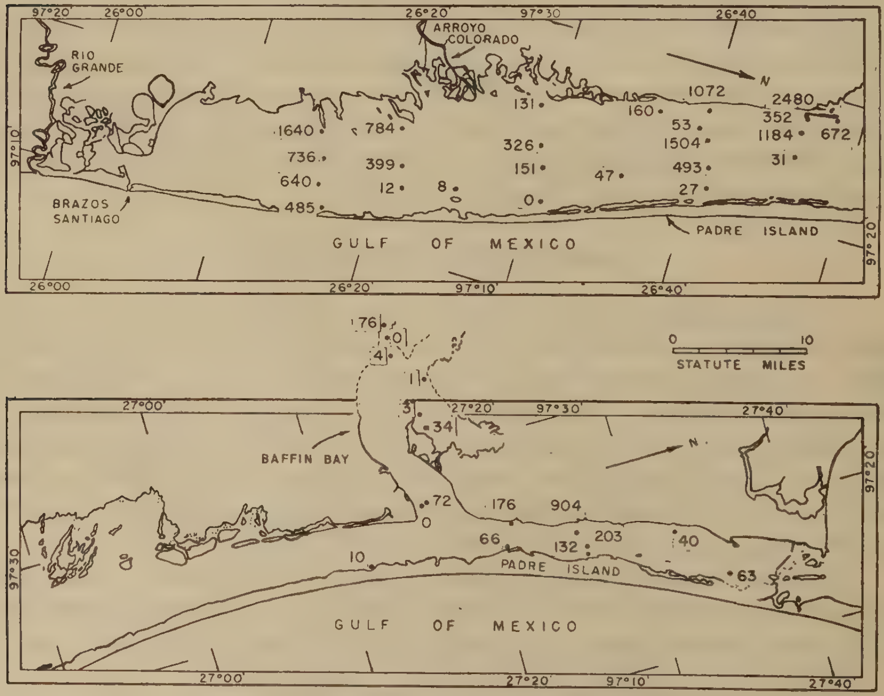
RIO GRANDE
ARROYO COLORADO
BRAZOS SANTIAGO
PADRE ISLAND
GULF OF MEXICO
N
1640
736
640
485
784
399
12
8
131
326
151
0
47
160
1072
53
1504
493
27
2480
352
1184
672
31
BAFFIN BAY
76
0
4
1
3
34
72
0
176
904
66
132
203
40
10
63
0 10 STATUTE MILES
97°20'
26°00'
26°20'
97°30'
26°40'
97°10'
27°00'
27°20'
27°40'

Fig. 2. Living populations of Foraminifera.

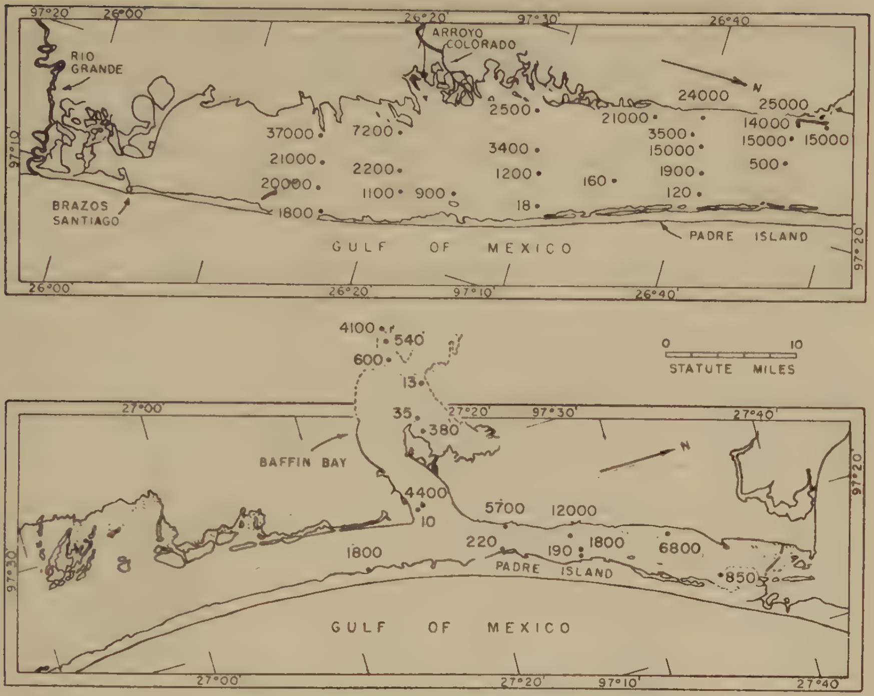
97°20'
26°00'
26°20'
97°30'
26°40'
ARROYO COLORADO
RIO GRANDE
N
24000
25000
2500
21000
14000
37000
7200
3500
15000
15000
15000
3400
21000
500
2200
1200
1900
160
20000
1100
900
120
18
BRAZOS SANTIAGO
1800
PADRE ISLAND
GULF OF MEXICO
97°10'
97°20'
26°00'
26°20'
97°10'
26°40'
4100
540
600
13
0
10
STATUTE MILES
35
27°00'
27°20'
97°30'
27°40'
380
N
BAFFIN BAY
4400
10
5700
12000
220
1800
1800
190
6800
PADRE ISLAND
850
97°30'
97°20'
GULF OF MEXICO
27°00'
27°20'
97°10'
27°40'

Fig. 3. Total populations of Foraminifera.

Cl. The southern basin has lower salinities, but up to 35 ‰ Cl has been observed. Water temperatures reflect the air temperatures and yearly ranges average approximately 10–35°C with occasional extremes higher and lower than these values. The northern basin is reported by E. Simmons (personal communication) to be an area of very high organic production.

FORAMINIFERAL POPULATIONS

Occurrences of Foraminifera are listed in Table 1. Most identifications are referred to those reported by Parker, *et al.* (1953). Samples and additional data are on file at the Marine Foraminifera Laboratory.

Total populations (fig. 3) are generally high in Laguna Madre except at the marginal stations near the lagoon barrier and at some stations in Baffin Bay. The largest populations occur in the southern basin where they range up to 37,000 specimens/10 ml. of wet sediment. Near the barrier populations range from 18 to 1800/sample. In Baffin Bay there were no Foraminifera found at one station, but most of the stations have an appreciable number of specimens and 4,100 are reported from one.

Fisk (1959, p. 108) found that in the Laguna Madre waters "the invertebrate fauna is impoverished and includes only a few foraminifers, ostracodes, and dwarfed molluscs."

Table 1. Distribution of Foraminifera in per cent of living and total population.

STATION	182	184	187	190	191	194	196	197	199	200	201	202	205	206	207	208	209	210	211	212	214	215	216	217	218	219	220	221	223	224	225	226	229	230	231	232	233	234	235	238
L/T		0.6	2		2	8	9	9	0.9	2	10	4	10	2	4	8	6	22	26	29	5	10	13		0.9	1	18	11	4	3	3	27	0.6	0.6	3	31	68	11	8	7
LIVING POPULATION	0	4	76	0	72	1	3	34	160	53	1504	1072	2480	352	672	1184	31	27	493	47	131	326	151	0	8	12	399	784	1640	736	640	485	40	10	176	66	132	203	904	63
Ammotium salsum							33		4	23	X					1																					2		X	
Bolivina cf. striatula																					X						1	1	X	2										
Elphidium galvestonense								6		2	4	2			2	4			1		X	2						3	1		3	6			9	8	7	1	3	
gunteri									4	4		10	10			4	3				3						X	4	X								X	2	1	
koeboeense										4	1								X		2	X					X	1	2			X						1		
matagordanum													3								2							41	X									1		
poeyanum								3	8	15	2	31	8	11	12	11			1			2					2	10	3			X		10		28	12	3	6	2
Palmerinella palmerae										4		9									X																			
Quinqueloculina funafutiensis																					2										3									
poeyanum											3		X		7	5			X		2						1		3		2	1						X	3	2
rhodiensis											11		4	2	5	16			2		2	5			12		X		2		3	X					3	6	7	
wiesneri									4		20			18	2	7	3		X		13	17					6		4	7	8	1			18				1	2
spp.			11						4	2	18		10	28	2	11	10	70	16	4	8	16	X		38	8	22		10	15	2	1		10	4	6	10	17	6	14
Rosalina spp.																					3						1													3
Streblus beccarii vars.		75			100	100	67	91	54	30	4	46	23	16	41	23	3		X		18	6			13	25	4	37	4	22	20	X	70	70	64	24	39	60	51	
Triloculina oblonga			5						13	4	9	2	13	14	2	4	3	4	4	4	5	12	1		25	17	4	1	21	6	15	61	20			3	9	3	8	24
Triloculinella obliquinoda		25	84						8	4	26		19	11	27	12	39	26	75	92	31	38	98			42	54	2	35	48	42	27	10			31	17	2	14	53
miscellaneous spp.										8	1		10			2	39				9	1			12	8	4		14		2	1		10	5			3		
TOTAL POPULATION	540	600	4100	10	440	13	35	380	21000	3500	15000	24000	25000	14000	15000	15000	500	120	1900	160	2500	3400	1200	18	900	1100	2200	7200	37000	21000	20000	1800	6800	1800	5700	220	190	1800	12000	850
Ammotium salsum	X						3	1	1	3	X	2	X	X		X												1		X			X				6	X	X	X
Bolivina cf. striatula			X						X	X		X		X							X					X	X	X	X	X										
Elphidium galvestonense	X		2		1			3	1	1	4	2	6	1	3	6	3	3	2	2	X	4	X	11	2	2	X	6	1	8	1	6	2	2	10	2	6	6	2	6
gunteri	17	23	1	30	8	8	43	4	5	3	X	4	2	1	X	3	2				5	X			1	5	1	8	2	4	X	X	X	4	1		X	3	X	X
koeboeense		X	X		6				2	5	X	X	X	X	1	1	4	X	2	X	7	1	1		1	X	X	6	3	5	2	X	2	X	X			1	X	X
matagordanum	X		X		1				1	X			1	X	1	X		2			2				X			14	X	1		X	1	X	X			1	X	X
poeyanum	20	12	3	10	23			6	2	50	3	36	6	5	5	8	4	10	1	6		4	3	5	1	8	1	6	4	8	2	X	6	17	X	18	11	9	3	4
Palmerinella palmerae		X						1	X	1		2		X		X					1	X	X					1	X	X				X				X		3
Quinqueloculina funafutiensis															1						1										2					4	4			1
poeyanum			6						1	X	7		X	X	15	7	1	2	2	3	1	2	2		3	4	4	2	2	2	5	3	9	4	16	4		1	6	4
rhodiensis	X	X	8				3	1	8	2	11	3	11	20	10	17	X	3	8	3	6	7	X	28	3	5	2	4	7	8	2	X	25	16	16	7	4	8	21	8
wiesneri			2					X	1	X	18	X		13	12	9	11	7	4	2	14	25	8		7	3	10	X	8	10	18	7	12	3	9	1		X	8	5
spp.			14		X			X	7	X	12	X	15	17	2	8	11	39	25	12	4	7	9	17	8	6	32	1	12	13	22	2	16	23	4	16	11	8	21	8
Rosalina spp.							3			X											X					X	X	X		X		X								2
Streblus beccarii vars.	55	64	2	40	59	92	34	80	52	29	4	48	12	13	8	13	5	2	2	3	7	6	2	16	6	12	4	28	4	19	4	1	14	14	11	21	36	56	17	25
Triloculina oblonga			11		X				4	X	7	X	4	5	2	6	5	6	5	5	2	6	6		43	15	3	2	5	2	2	46	6	7	5	4	8	2	4	8
Triloculinella obliquinoda	7	X	46	20			14	3	14	2	33	2	36	22	39	21	45	25	48	63	44	34	67	17	24	37	34	20	40	18	34	31	6		22	21	14	3	17	24
miscellaneous spp.	X		4		1				X	3		X	6	1		X	8		X	X	4	3	1	6	X	2	8	X	11	1	5	3	X	10	3	2		1	X	X

Based on the present samples, the foraminiferal fauna is not at all "impoverished" but is relatively abundant in numbers of species and specimens. The contrasting results may be due to differences in methods of sampling or locations of stations.

The living foraminiferal populations in the present samples are very large, especially in the southern basin where they range up to 1640 specimens per sample (fig. 2). Most of the samples from near the barrier in the southern basin have very small living populations. However, the majority of the living populations in the southern basin are much larger than those reported from any comparable area. In Breton Sound in the Mississippi Delta area, for example, there are generally about 100 specimens per sample or less (Phleger, 1955). In Aransas, Mesquite, and lower San Antonio bays most living populations range from less than 100 to 200 per sample. The populations on the continental shelf off central Texas also are much smaller than those in southern Laguna Madre. Living populations in the northern basin are large at some stations but at most are within the ranges of those found in Aransas, Mesquite, and lower San Antonio bays and Breton Sound.

Populations comparable in size to the large ones in the southern Laguna Madre

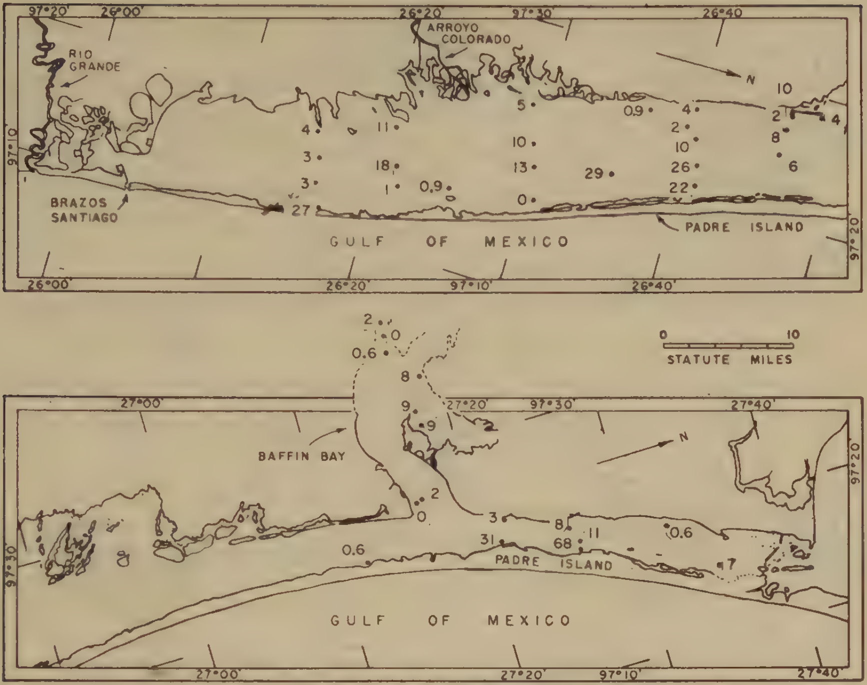
97°20'
26°00'
26°20'
97°30'
26°40'
ARROYO COLORADO
RIO GRANDE
N
BRAZOS SANTIAGO
4
11
3
18
3
1
0.9
27
5
10
13
0
29
0.9
4
2
10
26
22
10
2
4
8
6
PADRE ISLAND
GULF OF MEXICO
97°10'
97°20'
0 10
STATUTE MILES
2
0
0.6
8
9
9
27°00'
27°20'
97°30'
27°40'
BAFFIN BAY
N
2
0
3
8
11
0.6
31
68
0.6
7
PADRE ISLAND
GULF OF MEXICO
97°30'
97°10'

Fig. 4. Living-total population ratios × 100.

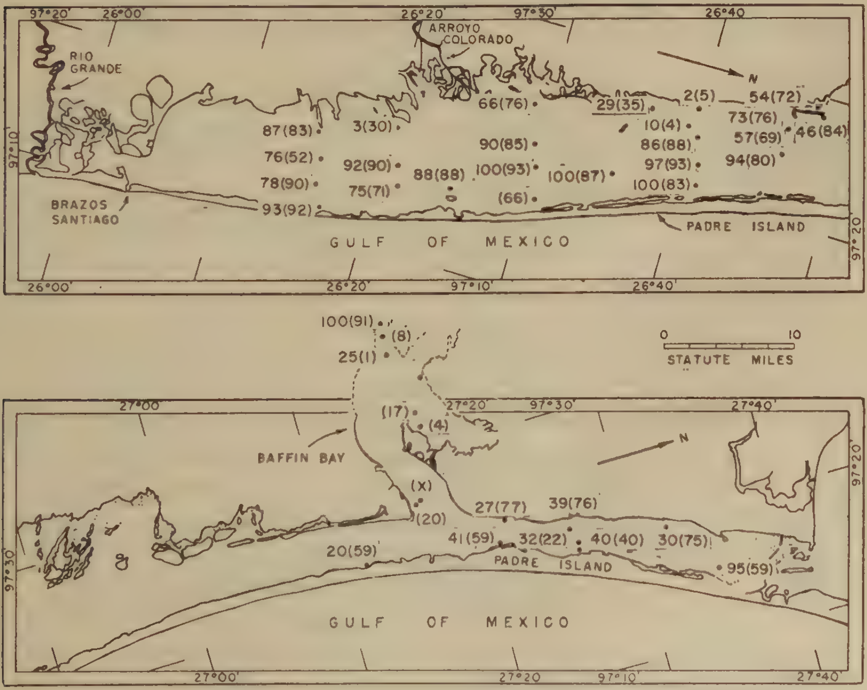
97°20'
26°00'
26°20'
97°30'
26°40'
ARROYO COLORADO
RIO GRANDE
N
66(76)
29(35)
2(5)
54(72)
87(83)
3(30)
10(4)
73(76)
57(69)
46(84)
90(85)
86(88)
76(52)
92(90)
97(93)
94(80)
88(88)
100(93)
100(87)
78(90)
75(71)
100(83)
BRAZOS SANTIAGO
93(92)
(66)
PADRE ISLAND
GULF OF MEXICO
97°10'
97°20'
100(91)
(8)
25(1)
0 10
STATUTE MILES
27°00'
27°20'
97°30'
27°40'
(17)
(4)
BAFFIN BAY
N
(X)
(20)
27(77)
39(76)
41(59)
32(22)
40(40)
30(75)
20(59)
95(59)
PADRE ISLAND
GULF OF MEXICO
97°30'
97°10'

Fig. 5. Miliolidae in per cent of living population (not in parentheses) and total population (in parentheses).

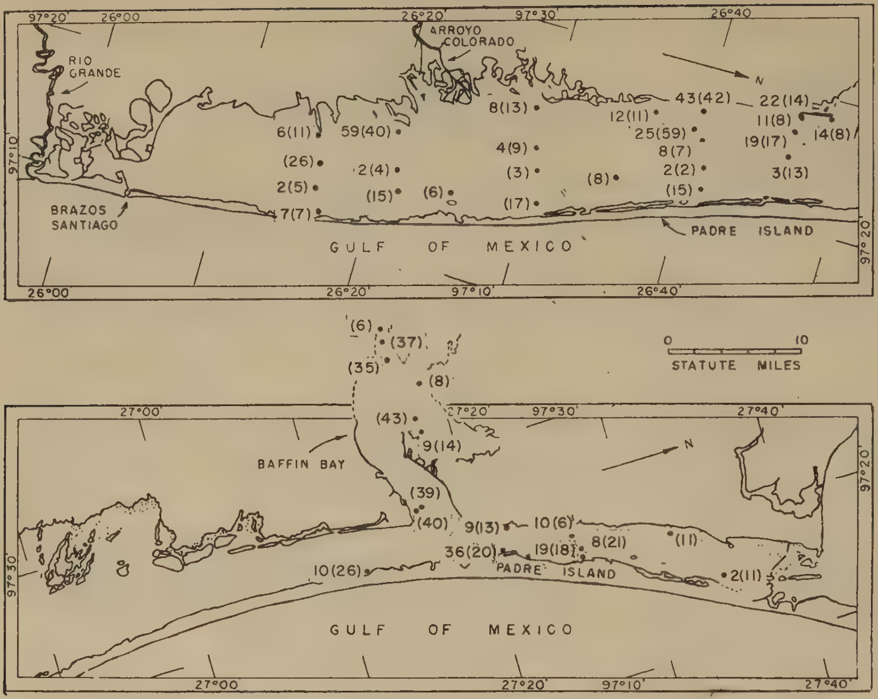
97°20'
26°00'
26°20'
97°30'
26°40'
RIO GRANDE
ARROYO COLORADO
N
97°10
BRAZOS SANTIAGO
6(11)
59(40)
8(13)
43(42)
22(14)
12(11)
11(8)
25(59)
19(17)
14(8)
4(9)
8(7)
(26)
2(4)
(3)
(8)
2(2)
3(13)
2(5)
(15)
(6)
(17)
(15)
7(7)
PADRE ISLAND
GULF OF MEXICO
97°20'
26°00
26°20'
97°10'
26°40'
(6)
(37)
(35)
(8)
0
10
STATUTE MILES
27°00'
27°20'
97°30'
27°40'
(43)
9(14)
BAFFIN BAY
N
97°20'
(39)
(40)
9(13)
10(6)
8(21)
(11)
36(20)
19(18)
97°30
10(26)
PADRE ISLAND
2(11)
GULF OF MEXICO
27°00
27°20'
97°10'
27°40'

Fig. 6. *Elphidium* in per cent of living population (not in parentheses) and total population (in parentheses).

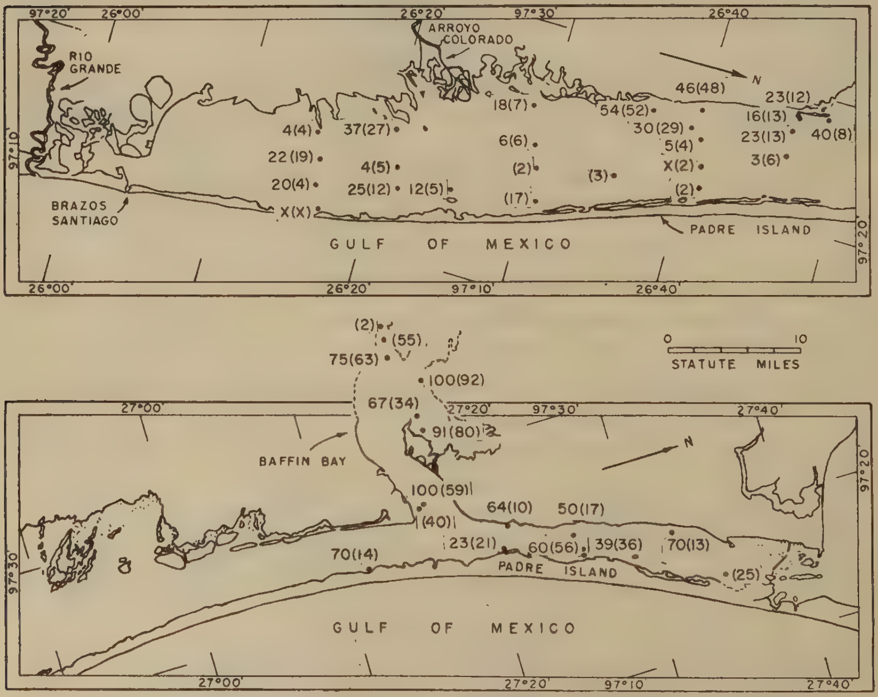
97°20'
26°00'
26°20'
97°30'
26°40'
RIO GRANDE
ARROYO COLORADO
N
46(48)
23(12)
18(7)
54(52)
16(13)
97°10
4(4)
37(27)
30(29)
23(13)
40(8)
6(6)
5(4)
22(19)
X(2)
3(6)
4(5)
(2)
(3)
20(4)
25(12)
12(5)
(2)
(17)
BRAZOS SANTIAGO
X(X)
PADRE ISLAND
GULF OF MEXICO
97°20
26°00'
26°20'
97°10'
26°40'
(2)
(55)
75(63)
0
10
STATUTE MILES
100(92)
27°00'
67(34)
27°20'
97°30'
27°40'
91(80)
BAFFIN BAY
N
97°20
100(59)
64(10)
50(17)
(40)
23(21)
60(56)
39(36)
70(13)
70(14)
PADRE ISLAND
(25)
97°30
GULF OF MEXICO
27°00'
27°20'
97°10
27°40'

Fig. 7. *Streblus beccarii* (Linne) variants in per cent of living population (not in parentheses) and total population (in parentheses).

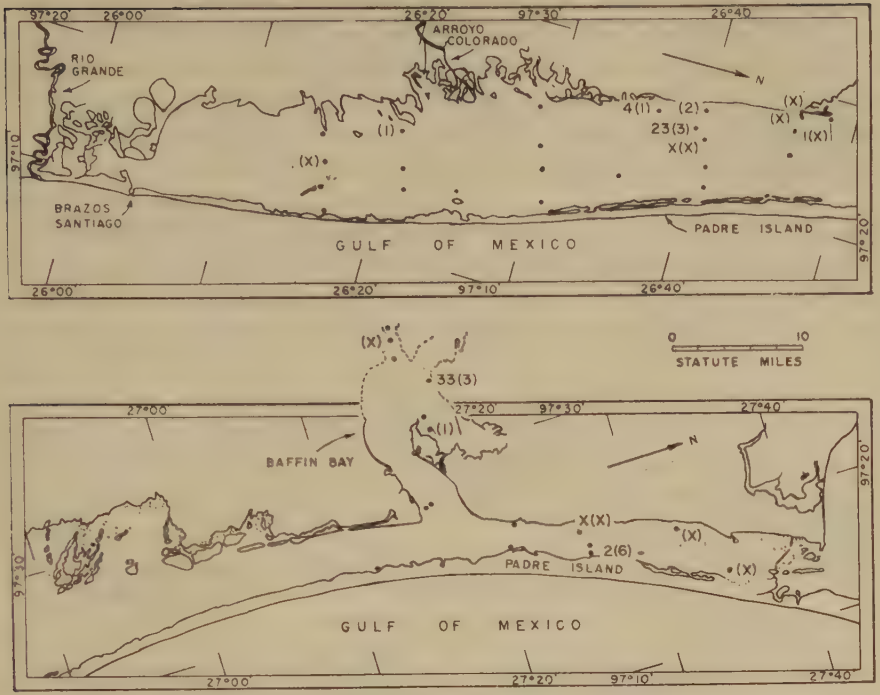
97°20'
26°00'
26°20'
97°30'
26°40'
ARROYO COLORADO
RIO GRANDE
N
4(1)
(2)
(X)
(X)
23(3)
X(X)
1(X)
(1)
(X)
97°10'
BRAZOS SANTIAGO
PADRE ISLAND
GULF OF MEXICO
97°20'
26°00'
26°20'
97°10'
26°40'
(X)
33(3)
0 10
STATUTE MILES
27°00'
27°20'
97°30'
27°40'
(1)
BAFFIN BAY
N
97°20'
X(X)
(X)
2(6)
PADRE ISLAND
(X)
97°30'
GULF OF MEXICO
27°00'
27°20'
97°10'
27°40'

Fig. 8. *Ammotium* in per cent of living population (not in parentheses) and total population (in parentheses).

have been found only in the deltaic marine or deltaic lagoon environment (Lankford, 1959). These populations occur near the mouths of rivers where they enter a lagoon or the open ocean and where sedimentation is rapid. It seems obvious that largest standing crops of Foraminifera reflect abundance of food and thus very high organic productivity in these environments. The small standing crops in the barrier margin samples in the southern basin appear to correlate with distribution of high salinity in the shallow water at these stations (Rusnak, 1960), although high salinity in itself may not be a critical factor.

The foraminiferal fauna is dominated by the Miliolidae which average 40–90% of the total and living populations at most stations (fig. 5). *Elphidium* (fig. 6) and *Streblus beccarrii* variants (fig. 7) are the other abundant elements of the fauna and are dominant at stations having low frequencies of miliolids such as at most stations in Baffin Bay. *Ammotium* (fig. 8) occurs at lower frequencies in Laguna Madre than in adjacent Aransas, Mesquite and San Antonio bays, but does constitute a small part of the total population at approximately one-half the stations. Another group of species which are considered to be typical of the nearshore, open ocean but which also occur in lower lagoons are :

Bolivina cf. *B. striatula* Cushman
Buliminella elegantissima (d'Orbigny)
Rosalina spp.

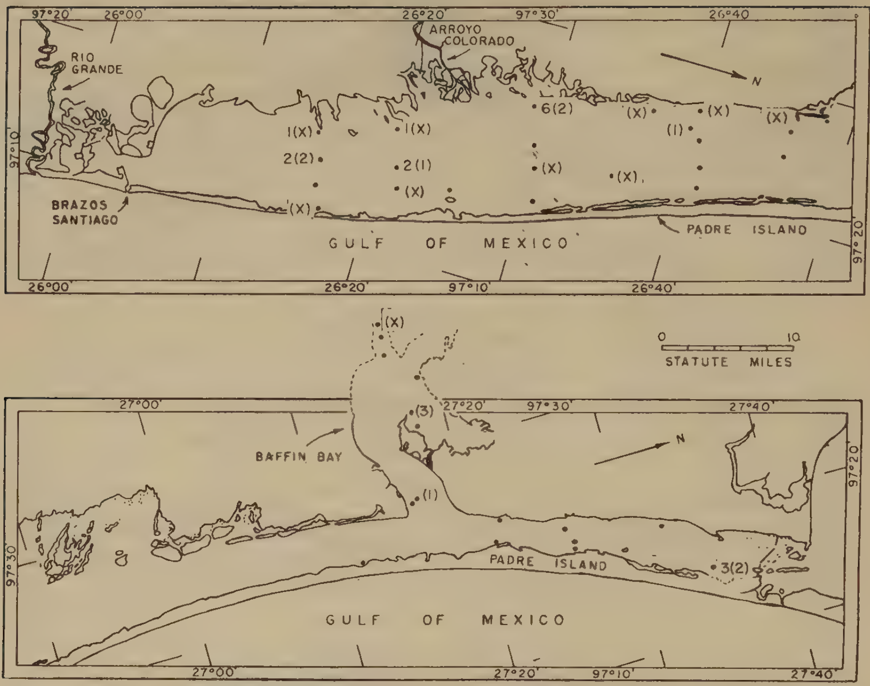
RIO GRANDE
ARROYO COLORADO
BRAZOS SANTIAGO
PADRE ISLAND
GULF OF MEXICO
N
0 10
STATUTE MILES
BAFFIN BAY
PADRE ISLAND
GULF OF MEXICO
97°20'
26°00'
26°20'
97°30'
26°40'
97°10'
27°00'
27°20'
27°40'
97°30'
97°20'
1(X)
2(2)
1(X)
2(1)
(X)
6(2)
(X)
(X)
(X)
(1)
(X)
(X)
(X)
(X)
(3)
(1)
3(2)

Fig. 9. "Open-ocean" benthonic Foraminifera in per cent of living population (not in parentheses) and total population (in parentheses).

Textularia earlandi Parker

These occur in very low frequencies and most are from the southern basin which may have more widespread invasion of gulf water than the northern basin (fig. 9).

The Laguna Madre foraminiferal fauna may be characterized generally as a lower lagoon, or bay, fauna which is dominated by the Miliolidae. The general dominance of the Miliolidae in the Laguna Madre distinguishes it from any other area of comparable size which has been studied in the northern Gulf of Mexico. Post (1951) reports abundant miliolids at three stations in Redfish Bay and they are abundant at four stations in adjacent lower Aransas Bay (Phleger and Lankford, 1957). The latter authors interpreted abundant miliolids as being related to substrate: "They appear to prefer a sand or shell bottom, and numerous instances of living forms with their pseudopods attached to sand grains have been observed in the preserved samples" (*op. cit.*, p. 96). Rusnak's (1960) data show that sand is an important constituent of the sediment at most stations in Laguna Madre. Where the sediment is silt and clay the fauna is dominated by *Elphidium* and *Streblus beccarii* variants and the miliolids are less abundant.

LIVE-TOTAL RATIOS OF FORAMINIFERA

It has been shown that live-total ratios of foraminiferal populations suggest relative rates of deposition of sediment. These ratios (fig. 4) in Laguna Madre are generally much larger than in nearby Aransas, Mesquite and San Antonio bays (Phleger, 1956) and not as large as in the Mississippi Delta area (Phleger, 1955). The implication is that relative sedimentation rates are somewhat faster here than in Aransas, Mesquite and San Antonio bays and considerably slower than in the Mississippi Delta area. There is no certainty that the differences in values between Laguna Madre and the other Texas bays are significant, and it is always possible that the standing crop was unusually large at the time of sampling although this is not likely.

Fisk (1959) has suggested that sedimentation rates are high on the flats and that the rate is approximately 1 ft. in 50 yrs. Rusnak (1960) believes that the rates are much slower on the basis of the thickness of "Recent" deposits. The total thickness of sediment deposited during the Recent cycle, however, does not necessarily indicate present rates of deposition.

The live-total population ratios are higher in most places near the lagoon barrier than elsewhere in the lagoon. This suggests that the source of sediment is from the barrier. This is in agreement with Fisk (1959) and Rusnak (1960) who point out that most or all of the sediment is being introduced into the lagoon from the barrier by wind action and storm wash-over.

REFERENCES

Fisk, H.N. (1959) : Padre Island and the Laguna Madre flats, coastal south Texas, *in* Second Coastal Geography Conference, Coastal Studies Inst., La. State Univ., pp. 103–151.

Lankford, R.R. (1959) : Distribution and ecology of Foraminifera from the east Mississippi Delta margin. Bull. Amer. Assoc. Petrol. Geol., Vol. 43, pp. 2068-2099.

Phleger, F.B (1955) : Ecology of Foraminifera in southeast Mississippi Delta area. Bull. Amer. Assoc. Petrol. Geol., Vol. 39, pp. 712–752.

————, (1956) : Significance of living foraminiferal populations along the central Texas coast. Contrib. Cushman Found. Foram. Res., Vol. 7, pp. 106–151.

————, and Lankford, R.R. (1957) : Seasonal occurrences of living benthonic Foraminifera in some Texas bays. Contrib. Cushman Found. Foram. Res., Vol. 8, pp. 93–105.

Post, R.J. (1951) : Foraminifera of the south Texas coast. Publ. Inst. Marine Sci., Vol. 2, No. 1, pp. 165–176.

Rusnak, G.A. (1960) : The sediments of the Laguna Madre, Texas, in "Recent sediments, Northwestern Gulf of Mexico, in Press.

Walton, W.R. (1952) : Techniques for recognition of living Foraminifera. Contrib. Cushman Found. Foram. Res., Vol. 3, pp. 56–60.

Contribution from the Scripps Institution of Oceanography, New Series. Contribution No. 35, Marine Foraminifera Laboratory.

Frances L. Parker

Living Planktonic Foraminifera from the Equatorial and Southeast Pacific

Reprinted from the Science Reports of the Tohoku University,
Sendai, Japan, Second Series (Geology), Special
Volume, No. 4 (Hanzawa Memorial Volume),
March, 1960

Science Reports, Tohoku University, Sendai, Japan, 2nd Ser. (Geol.), Spec. Vol., No. 4,
pp. 71-82, 20 text-figs., 1960

Living Planktonic Foraminifera from the Equatorial and Southeast Pacific

Frances L. Parker

Scripps Institution of Oceanography, La Jolla, California, U.S.A.

SUMMARY

1. A study was made of 81 plankton samples, mostly from the equatorial and southeast Pacific Ocean. The distribution patterns of 16 of the more common planktonic species of Foraminifera are as follows : 1) Widespread – *Globigerinella aequilateralis*, *Globigerinoides ruber*, *Hastigerina pelagica*, *Orbulina universa*; 2) Equatorial and southeast-central – *Globigerina eggeri*, *Globigerinoides conglobatus*, *G. sacculifer*; 3) Equatorial – *Globigerina conglomerata*, *G. hexagona*, *Globorotalia menardii* (few exceptions), *Pulleniatina obliquiloculata* (one exception) ; 4) Southeast central and subantarctic – *Globigerina bulloides*, *G. inflata*, *Globorotalia punctulata*, *G. truncatulinoides*; 5) Subantarctic – *Globorotalia scitula*.

2. Temperature may be more critical than salinity in controlling these distributions. No conclusions about the physical limits for survival of the planktonic species can be formed until it is known exactly at what water levels they live.

3. Total populations were largest in the equatorial region, in a small area close to the coast of South America, and at a few stations in the northern part of the subantarctic region. These are the regions richest in nutrients.

4. The largest populations were found in the upper 200 m. In addition, the populations from daytime oblique tows from various depths exceeded by a factor of ten the number found in corresponding night tows at the same station. The possible dependence of the planktonic Foraminifera on symbiotic algæ is suggested as the reason for the apparent preference for the euphotic zone. Nothing further can be said until more is known about the habits of the planktonic Foraminifera.

INTRODUCTION

This paper supplements that of Bradshaw (1959) on the North and equatorial Pacific. It extends the study of living planktonic species into the southeast Pacific as well as confirming some of the earlier observations in the equatorial and, to a lesser extent, the northeastern Pacific. The work was supported by the University of California under contract with the Office of Naval Research. John S. Bradshaw made valuable suggestions; Jean Peirson Hosmer drafted the figures.

Contributions from the Scripps Institution of Oceanography, New Series, 1181
Reproduced by Permission

LOCATION OF SAMPLES AND SAMPLING METHODS

Eighty-one planktonic samples collected from the R/V *Horizon* on the Downwind Expedition of the Scripps Institution of Oceanography (October, 1957–February, 1958) were analyzed (*see* Fig. 1). The area covered extends south of the equator to Lat. 46°45′S., between South America and Long. 149°21′W. Six stations north of the equator lie between Longs. 115°50′W. and 130°31′W., the most northerly being at Lat. 29°25.5′W.

Four types of samples were studied: 1) oblique tows (66) taken with a standard meter net (mesh openings *ca.* 0.65 mm.) from depths of 140 m., 280 m., and 560 m. to the surface; 2) vertical tows (8) from depths of 280–300 m. to the surface taken with a half-meter net (mesh openings *ca.* 0.33 mm.); 3) vertical tows (3) from depths of 740 m., or more, to the surface taken with a coarse-mesh net having a fine-mesh cod end (mesh openings *ca.* 0.33 mm.); 4) opening-closing net (mesh openings *ca.* 0.67 mm.) samples (4) taken at various depths.

Table 1 lists the stations, locations, types of tows (given by number as listed above), and the depths fished.

The samples were preserved in a 5–10% solution of formalin. The concentrated formalin had been previously saturated with hexamethylenetetramine to prevent solution of the foraminiferal tests.

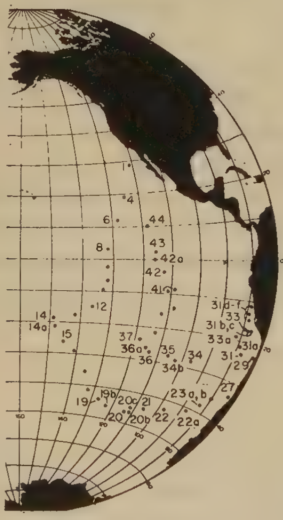
1
4
6
44
43
8
42a
42
41a
12
14
14a
15
31d-f
33
31b,c
33a
31a
37
36a
35
36
34
34b
31
29
27
19b
23a,b
19
20c
21
20
20b
22
22a

Fig. 1. Station locations

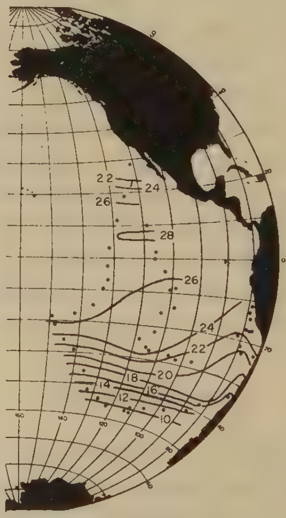
22
24
26
28
26
24
22
20
18
16
14
12
10

Fig. 2. Surface temperatures (°C)

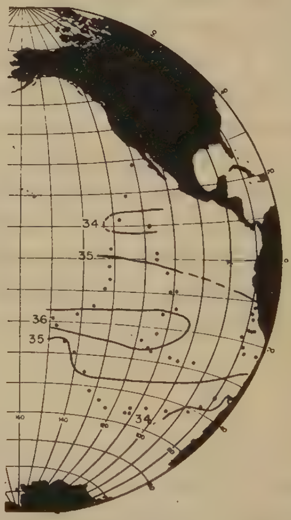
34
35
36
35
34

Fig. 3. Surface salinities (‰)

Table 1

Station	Location		Type of tow	Depth sampled in meters
	Latitude	W. Longitude		
1	29°25.5′N.	120°26.5′	1	301
4	19°34.5′N.	125°00′	1	353
6	11°00′N.	128°30′	1	230
8	3°14′N.	130°31′	1	230
9	2°08′S.	131°27′	1	306
10	6°05′S.	131°31′	1	386
11	9°59′S.	133°20′	1	452
12	14°27′S.	135°25.5′	1, 3.	301, 740
13	18°16.5′S.	141°22′	1	258
14	19°22′S.	149°21′	1	346
14 a	21°26′S.	148°21′	1	514
15	24°57′S.	145°01.5′	1	298
16	29°53′S.	140°06′	1, 1	123, 424
17	34°50′S.	135°53′	1, 1	287, 575
18	40°33′S.	131°50′	1, 1	283, 565
19	44°20′S.	127°15′	1, 1	283, 565
19 b	46°25′S.	123°38′	1	565
20	46°44′S.	113°09′	1	848
20 b	46°45′S.	112°50′	1	283
20 c	44°36′S.	112°08′	1	565
21	43°50′S.	105°30′	3, 1	1250, 306
22	42°54′S.	97°08′	1, 1	283, 565
22 a	40°39′S.	88°02′	1, 1, 1	129, 257, 612
23 a	38°46′S.	83°20′	2	352
23 b	35°02′S.	80°01.5′	2	338
27	33°10.5′S.	73°10′	2	355
29	22°38′S.	72°00′	1, 1	258, 515
31	22°27′S.	78°26′	1	278
31 a	21°19′S.	79°09.5′	2	326
31 b	17°18.5′S.	78°18′	1	283
31 c	17°10′S.	77°01′	2	347
31 d	14°02.5′S.	78°25′	2, 4	347, 141- 283
31 e	12°53′S.	79°43.5′	1	339
31 f	11°49.5′S.	79°05.5′	1	141
33	17°15′S.	79°00′	1	283
33 a	19°02.5′S.	80°21′	1	257
34	28°00′S	96°54′	2, 1, 1	358, 368, 536
34 b	29°15′S.	102°25.5′	1, 1	136, 273
35	28°45.5′S.	106°07′	1, 1, 3	136, 273, 2680
36	27°23.5′S.	113°43′	1, 1	292, 585
36 a	26°41′S.	114°45′	1	1830
37	23°39′S.	118°12′	1, 1, 1	141, 283, 514
38	21°10′S.	113°45.5′	1, 1	283, 565
39	15°45′S.	112°07′	1, 1	153, 306
40	14°17′S.	108°52′	1, 1	173, 346
41 (day)	9°42′S.	110°11′	1, 1, 1	141, 283, 555
41 (night)	9°13′S.	109°42′	1, 1, 1	158, 283, 555
42	4°05′S.	113°13′	1, 1	164, 328
42 a	00°00′S.	116°32′	1, 4, 4	71, 64-129, 100-258
43	2°01′N.	115°50′	4	141- 283
44	10°01.5′S.	118°58′	1	141

LABORATORY METHODS

Most of the samples were examined completely and all the Foraminifera counted. A few contained very large numbers of Foraminifera or other plankters; half of these were examined and the totals estimated. The data on total populations (*see* Fig. 20) are given in

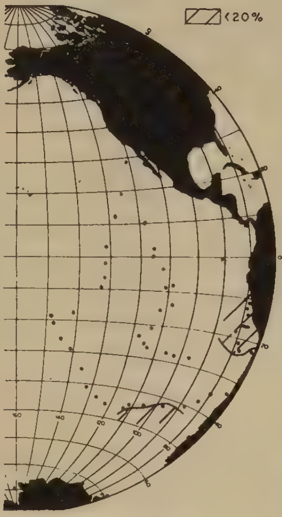

Fig. 4 Globigerina bulloides

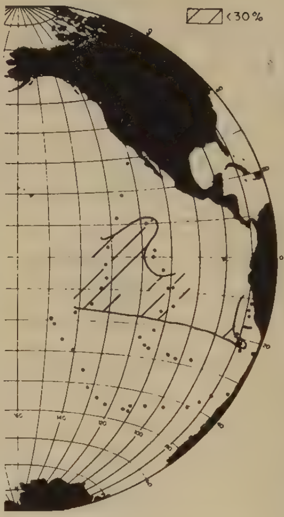

Fig. 5. Globigerina conglomerata

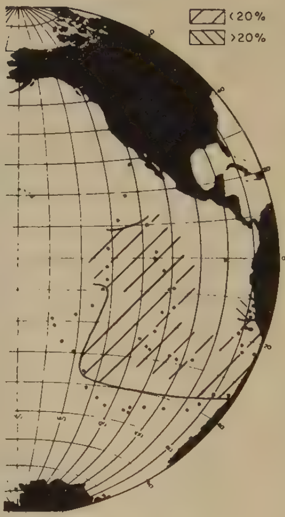

Fig 6 Globigerina eggeri

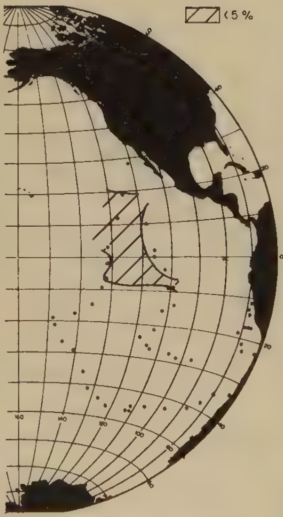

Fig 7. Globigerina hexagona

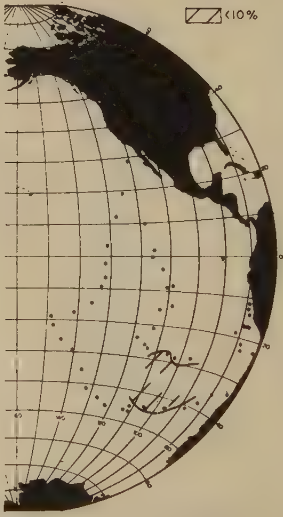

Fig. 8. Globigerina inflata

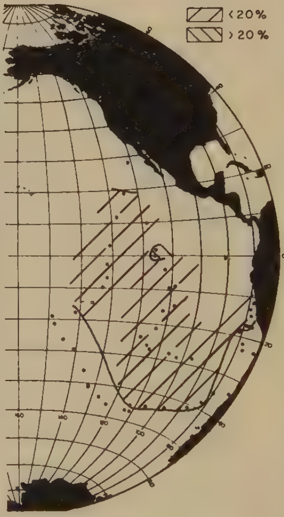

Fig. 9. Globigerinella aequilateralis

numbers of individuals per 1000 cubic meters, since this is the standard method of presenting plankton data. The specimens from all the tows at any one station were used in calculating the percentage frequencies of species (*see* Figs. 4–19). This adds to the validity of the percentages, since the number taken in any one tow was frequently small. For discussions of the problems involved in different sampling methods, variations due to patchiness, etc., the reader is referred to the papers of Bé (1959) and Bradshaw (1959).

DESCRIPTION OF THE AREA

Many diverse upper water masses were traversed in the course of the expedition. Sverdrup *et al.* (1942, fig. 209b) show the temperature-salinity relationships of these water masses in the Pacific Ocean (*see* also Bradshaw, 1959). Each follows a characteristic pattern. By analyzing the data obtained at the Downwind hydrographic stations, it is possible to get at least a general idea of the conditions at the time of sampling. Station 1 appeared to be in water that was transitional from subarctic to equatorial water; stations 4–11, 31b–f, 33, 41–44 in equatorial water; stations 12–17, 28–31a, 34–40 in southeast central water; stations 23a ?, 23b, and 27 in water that was transitional from southeast central to subantarctic water, at least in the upper few hundred meters; stations 18–22a in subantarctic water (also probably somewhat transitional in character).

The surface temperatures taken on the Downwind Expedition are illustrated (*see* Fig. 2). At station 1 the temperature was 20.6°C. Surface temperatures increased to the south reaching 27°C. between stations 4 and 6. In the central area, including stations 8–14, 42–44, they were 27–28°C. To the south there was considerable variation between the eastern and western stations. The central group, stations 36–41, registered 24–26°C. The western group registered decreasing temperatures to the south, stations 19b, 20, and 20b being in water colder than 10°C. at the surface. The eastern group of stations was in relatively colder water than the central or western group due to the cold Peru Current flowing north along the coast of South America. An exception to this occurred at station 29, which was in a warm tongue of water close to the coast.

The surface salinities obtained on the expedition (*see* Fig. 3) varied from 34–35 ‰ between Lats. 0–30°N,. except for a narrow tongue of lower salinity water (less than 34 ‰) along Lat. 10°N. South of the equator the surface salinities were higher, 35–36 ‰, with even higher values of over 36 ‰ in a tongue of water between Lats. 15–25°S. South of Lat. 25°S. in the western part of the area, Lat. 35°S. in the central part, and Lat. 25°S. in the eastern, the surface salinities were 34–35 ‰.

DISTRIBUTION OF SPECIES

The distributions of the various species are given below. Only the larger specimens are represented due to the relatively coarse-mesh nets used in collecting. These distributions, therefore, do not represent the complete foraminiferal faunas to be found in the waters of the area studied.

The frequency data are given (Figs. 4–19) in most cases using Bradshaw's (1959)

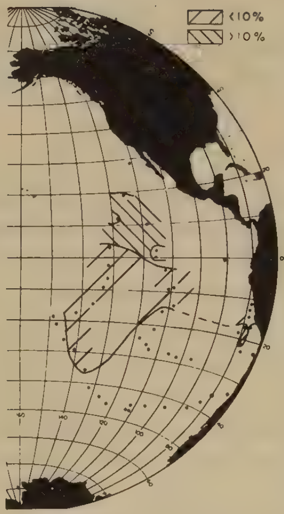

Fig 10 Globigerinoides conglobatus

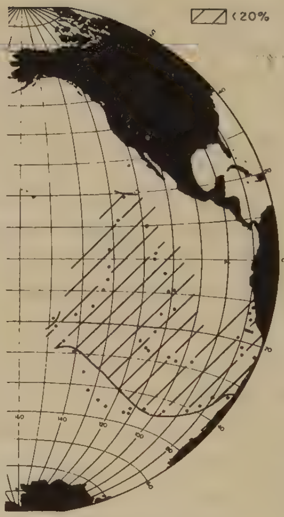

Fig. 11 Globigerinoides ruber

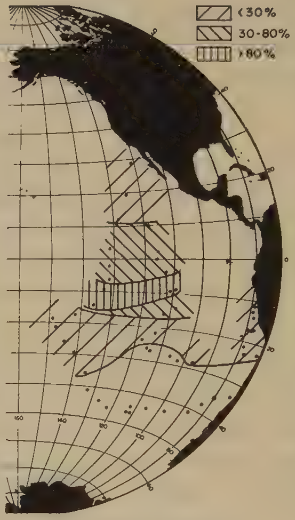

Fig. 12. Globigerinoides sacculifer

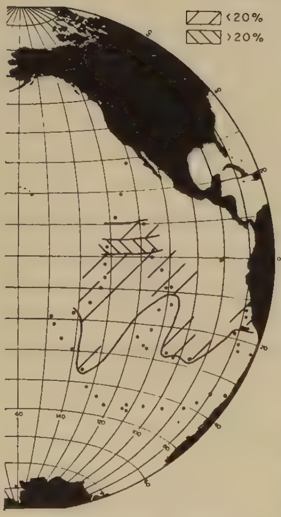

Fig 13. Globorotalia menardii

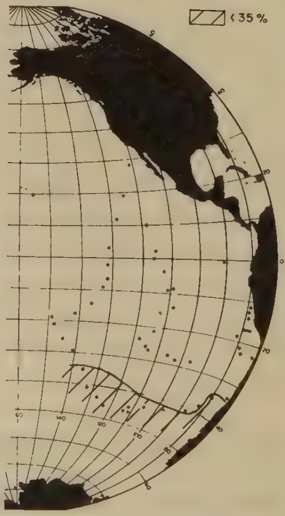

Fig 14 Globorotalia punctulata

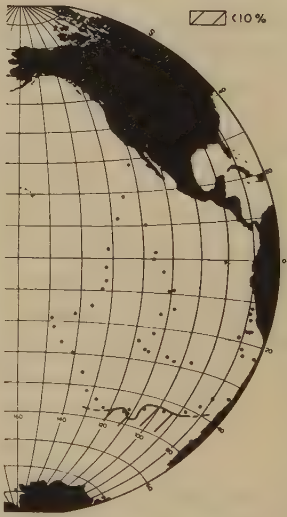

Fig. 15. Globorotalia scitula

figured percentage groups, for convenience of comparison. His identifications are repeated here and reference is made to his figured specimens. The writer is presently working on the taxonomy of the planktonic species in the Pacific sediments and this will probably lead to some changes in this nomenclature. Hofker (1959) has expressed the opinion that some of the presently accepted genera are polyphyletic and that others are based on reproductive stages only. A careful study of large suites of specimens, including developmental stages, is necessary to understand the variation to be expected within a species or genus. The plankton samples taken in the Pacific have not provided these.

Globigerina bulloides d'Orbigny (Bradshaw, 1959, p. 33, pl. 6, figs. 1–4) (*see* Fig. 4) was found at two stations south of Lat. 40°S. and at several stations near the coast of South America between Lats. 10–25°S. (up to 11%). Surface salinities at these stations range from 34–35.3 ‰, surface temperatures from less than 10–24°C. The northern group near the South American coast appeared to be in equatorial water and the southern group in subantarctic water. Bradshaw found a similar distribution along the South American coast and suggests that occurrences here may be due to life at greater depths. The Downwind specimens were from tows taken from depths of 283–347 m. to the surface. It is possible that study of a larger number of specimens from the sediments of these regions will show that there are two species or subspecies.

Globigerina conglomerata Schwager (Bradshaw, 1959, p. 33, pl. 6, figs. 6, 7) (*see* Fig. 5) occurred in the equatorial region and at three stations near the northern limit of what appears to be southeast-central water, north of Lat. 22°S. near the coast of South America and of Lat. 15°S. to the west (up to 7%). Surface salinities at these stations ranged from *ca.* 34–36 ‰, surface temperatures from *ca.* 26–28°C. The distribution extended farther south than the southern limit found by Bradshaw (*ca.* Lat. 6°S.).

Globigerina eggeri Rhumbler (Bradshaw, 1959, p. 35, pl. 6, figs. 5, 10) (*see* Fig. 6) was found from Lat. 10°N. to Lat. 35°S., the most westerly occurrence being at Long. 135°53′W. (up to 52%). It was most abundant near the coast of South America. The species, therefore, occurred in equatorial, southeast-central and transitional (to subantarctic) waters. Surface salinities at the stations ranged from *ca.* 34–36.4 ‰ and surface temperatures from *ca.* 16–27°C. The species, as defined here, is the "typical adult *G. eggeri*" of Bradshaw. Since he also included small forms which may not be referrable to this species, the present distributions cannot be compared with his, although for the typical form recognized here they appear to be similar.

Globigerina hexagona Natland (Bradshaw, 1959, p. 36, pl. 6, figs. 11–15) (*see* Fig. 7) was confined to equatorial water between Lats. 20°N. and 10°S. (up to 3%). Surface salinities at the stations ranged from 34.7–35.7 ‰, surface temperatures from 24.4–26.7°C.

Globigerina inflata d'Orbigny (Bradshaw, 1959, p. 36, pl. 6, figs. 16–18) (*see* Fig. 8) occurred at two stations in subantarctic water and one in southeast-central water, all south of Lat. 25°S. Surface salinities at the stations ranged from 34–35.7 ‰, surface temperatures from *ca.* 10–23.4°C. Bradshaw found the species in the North Pacific, north of Lat. 25°N.

Globigerinella aequilateralis (Brady) (Bradshaw, 1959, p. 38, pl. 7, figs. 1, 2) (*see*

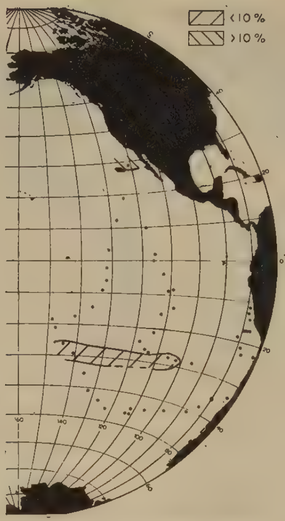

Fig 16. Globorotalia truncatulinoides

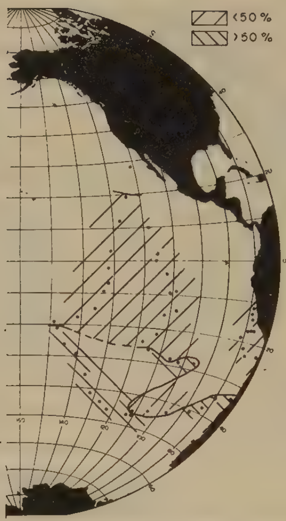

Fig 17 Hastigerina pelagica

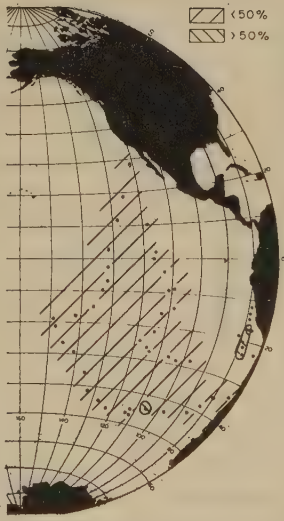

Fig. 18. Orbulina universa

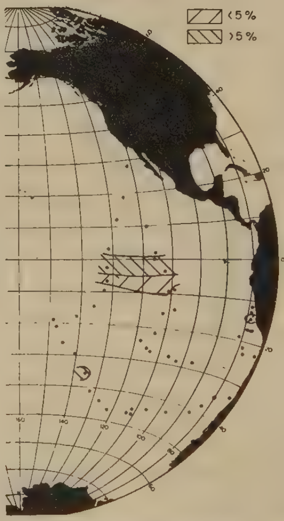

Fig. 19. Pulleniatina obliquiloculata

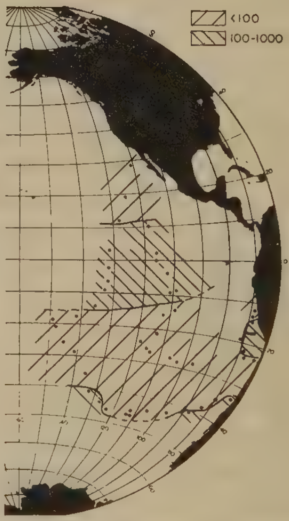
<100
100-1000

Fig. 20. Total populations / 1000 m^3

Fig. 9) had a widespread distribution, with the highest frequencies at the equator (up to 33%). It occurred in equatorial, southeast-central, and subantarctic waters from Lats. 20°N. to 40°S. Surface salinities at the stations ranged from *ca.* 34–36 ‰, surface temperatures from *ca.* 10–24°C.

Globigerinoides conglobatus (Brady) (Bradshaw, 1959, p. 40, pl. 7, figs. 5, 6, 16, 17) (*see* Fig. 10) was confined to equatorial and southeast-central waters (Lats. 20°N. to 35°S.) with the highest frequencies in the former (up to 32%). Surface salinities at the stations ranged from 34.7–36.3 ‰, surface temperatures from 17.7–27.3°C. Bradshaw's form "*Globigerinoides* sp." (pl. 7, figs. 16, 17) is considered to be synonymous with *G. conglobatus* since there appears to be a complete series of specimens from those with narrow apertures to those with widely opened ones.

Globigerinoides ruber (d'Orbigny) (Bradshaw, 1959, p. 42, pl. 7, figs. 12, 13) (*see* Fig. 11) was found in equatorial and southeast-central waters, and at the most northerly stations in subantarctic water (Lats. 20°N. to 44°S.) Surface salinities at the stations ranged from *ca* 34–36.5 ‰, surface temperatures from 10–27.3°C. The species, as defined here, includes both typical and high-spired specimens, the latter possibly referrable to *G. elongata* (d'Orbigny) or *G. pyramidalis* (vanden Broeck).

Globigerinoides sacculifer (Brady) (Bradshaw, 1959, p. 42, pl. 7, figs. 14, 15, 18) (*see* Fig. 12) was one of the most abundant species. It occurred in transitional (to subantarctic), equatorial, and southeast-central waters, with the highest frequencies in the southern part of the equatorial region (up to 97%). Surface salinities at the stations ranged from 34.7–36.5 ‰, surface temperatures from 17.7–28°C.

Globorotalia menardii (d'Orbigny) (Bradshaw, 1959, p. 44, pl. 8, figs. 3, 4, 10–12) (*see* Fig. 13) was found in equatorial and southeast-central waters (Lats. 10°N. to 35°S.) with the highest frequencies at the equator (up to 21%). Surface salinities at the stations ranged from *ca.* 34–35.9 ‰, surface temperatures from 17.7–27.3°C. (with one exception all were higher than 22°C.). The minimum of 17.7°C. was at station 17 where *Pulleniatina obliquiloculata* also was found. No specimens of typical *Globorotalia tumida* (Brady) were observed. Specimens having the shape of this species, but lacking the typically coarsely crystalline test walls, were included with *G. menardii* and occurred in the western part of the area of distribution (*see* Bradshaw, 1959, pl. 8, figs. 10–12).

Globorotalia punctulata (d'Orbigny) (Phleger *et al.*, 1953, p. 20, pl. 4, figs. 8–12) (*see* Fig. 14) occurred in its typical form in subantarctic, transitional (from subantarctic to southeast-central, one station), and southeast-central (one station) waters. The species was confined to the region south of *ca.* Lat. 35°S. (up to 34%). Surface salinities at the stations ranged from *ca.* 34–35 ‰, surface temperatures from *ca.* 9–18°C.

This species appears to be identical with Atlantic specimens. It is reported by Bé (1959) in the plankton of the western North Atlantic as a "warm-tolerant species". It was not observed by Bradshaw (1959) in the North and equatorial Pacific.

Globorotalia scitula (Brady) (Bradshaw, 1959, p. 44, pl. 8, figs. 5, 6) (*see* Fig. 15) was confined to subantarctic water south of Lat. 40°S. Surface salinities at the stations were *ca.* 34 ‰; surface temperatures ranged from 9.2–11.5°C. No specimens were observed in the equatorial region, as reported by Bradshaw.

Globorotalia truncatulinoides (d' Orbigny) (Bradshaw, 1959, p. 44, pl. 8, figs. 7, 8) (*see* Fig. 16) was found in southeast-central water from Lats. 25–30°S. and at station 1 in water transitional from equatorial to subantarctic. Surface salinities at the stations ranged from 34.8–35.7 ‰, surface temperatures from *ca.* 20.6–23.5°C. This distribution agrees with that found by Bradshaw in the North Pacific. There were insufficient specimens to determine coiling-direction ratios but most specimens were right-coiling.

Hastigerina pelagica (d'Orbigny) (Bradshaw, 1959, p. 47, pl. 8, figs. 14, 15) (*see* Fig. 17) was found in most of the area except station 1, occurring in comparatively large numbers especially south of Lat. 20°S. (up to 99%). This is in great contrast to its relative scarcity in the sediments, due probably to its extreme fragility. Surface salinities at the stations ranged from *ca.* 34–36.5 ‰, surface temperatures from *ca.* 9–27°C.

Orbulina universa d'Orbigny (Bradshaw, 1959, p. 49, pl. 8, fig. 18) (*see* Fig. 18) was an ubiquitous species like *Hastigerina pelagica* but occurred in smaller numbers. It was found at more stations north of the equator and fewer in the subantarctic region than *H. pelagica* (up to 88%). Surface salinities at the stations ranged from 33.6–36.5 ‰, surface temperatures from 9.2–27.6°C. It is possible, as suggested by Hofker (1959), that this "species" represents reproductive stages of several forms. This would account for its wide distribution. No bilobate specimens were seen.

Pulleniatina obliquiloculata (Parker and Jones) (Bradshaw, 1959, p. 49, pl. 8, figs. 19, 20) (*see* Fig. 19) was confined to a narrow belt at the equator, one station off the coast of South America north of Lat. 15°S., and at station 17, which was mentioned previously as containing an unusual fauna. Surface salinities at the stations ranged from *ca.* 34.5–35 4 ‰, surface temperatures from *ca.* 24–27°C. (excluding station 17 where the surface temperature was 17.7°C.).

Rare species. There were a few rare species. These included: *Candeina nitida* d'Orbigny (Bradshaw, 1959, pl. 7, fig. 9), station 4; *Globigerina digitata* Brady (1884, pl. 80, figs. 6–10; *not* pl. 82, figs. 6, 7), station 19; *Globigerinella* sp. (Bradshaw, 1959, pl. 7, figs. 3, 4), stations 40, 42; "*Globigerinita*" *glutinata* (Bradshaw, 1959, pl. 7, figs. 7, 8), stations 8 ?, 21, 23b ?; *Sphaeroidinella dehiscens* (Parker and Jones) (Bradshaw, 1959, pl. 8, figs. 21–23), stations 3, 44; *Globigerina* spp. (juvenile ?), stations 4, 17, 20, 37. In addition, a presently unidentified form of *Globigerina* was widespread; it is possible that more than one species was represented but the specimens were too few to determine this. Some of the specimens resemble the form figured by Bradshaw (1959, pl. 6, figs. 19, 26–28).

POPULATION VARIATIONS

Total populations (*see* Fig. 20) were smaller, in general, than those recorded by Bradshaw (1959). The largest populations (100–1000 specimens/cu.m.) were found along the equator from Lat. 10°N. to Lat. 15°S., in a small area along the coast of South America from *ca.* Lats. 15–20°S., and at a few stations south of Lat. 40°S.

The largest populations obtained by the standard meter net were usually in the oblique tows from *ca* 0–200 m., the next largest from *ca.* 0–400 m., and the smallest from *ca.* 0–800 m. The largest populations, therefore, were in tows which fished for a longer period at the shallower depths. This was shown also by a series of opening-closing net tows at station 42a, where 309 specimens were obtained from 64–129 m. and 163 specimens from 100–258 m. The same species were obtained in both these tows with the exception of single specimens of *Globigerinoides ruber* in the shallower one and *Globigerina eggeri* in the deeper. There were more specimens of *Globigerinoides sacculifer* in the shallower tow and more *Globorotalia menardii* and *Hastigerina pelagica* in the deeper one. *Globigerinella aequilateralis* and *Pulleniatina obliquiloculata* were fairly evenly distributed. Two additional opening-closing net tows from 141–283 m. contained : *Globigerina eggeri*, *G.* sp., *Globigerinella aequilateralis*, *Globigerinoides ruber*, *G. sacculifer*, *Globorotalia menardii*, and *Hastigerina pelagica.*

Most of the tows were made at night since this is the time when much of the zooplankton is near the surface. At station 41, however, a series of day and night oblique tows from various depths was made. The day group consistently contained about ten times as many Foraminifera as the night group (when comparing tows from equal depths).

DISCUSSION

The species distributions may be divided approximately into five groups as follows :

1. Widespread (surface salinities 33.6–36.5 ‰, surface temperatures 9–27.6°C.) : *Globigerinella aequilateralis*, *Globigerinoides ruber*, *Hastigerina pelagica*, *Orbulina universa.*

2. Equatorial and southeast-central (surface salinities 34–36.5 ‰, surface temperatures 16–28°C.) : *Globigerina eggeri*, *Globigerinoides conglobatus*, *G. sacculifer.*

3. Equatorial (surface salinities 34–36 ‰, surface temperatures 24–28°C.) : *Globigerina conglomerata*, *G. hexagona*, *Globorotalia menardii*, *Pulleniatina obliquiloculata.* The last two species occurred rarely elsewhere.

4. Southeast-central and subantarctic (surface salinities 34–35.7 ‰, surface temperatures 9–24°C.) : *Globigerina bulloides*, *G. inflata*, *Globorotalia punctulata*, *G. truncatulinoides.*

5. Subantarctic (surface salinities *ca.* 34 ‰, surface temperatures 9.2–11.5°C.) : *Globorotalia scitula.*

These groups agree in general with Bradshaw's (1959) distributions although there are minor differences, already pointed out in the species discussions. A study of the physical conditions leads to the suggestion that temperature may be more critical than salinity but no definite conclusions concerning the physical requirements to the species can be arrived at until more is known concerning the exact levels at which they live. Surface salinities and temperatures are given to provide some basis for discussion; an entirely different set of data may be the critical one.

The largest populations occurred in the regions which were richest in nutrients. Inorganic phosphate can be used as an index of the relative presence of nutrients (Bradshaw, 1959). Phosphate measurements at stations 1–23 showed the highest values between

Lats. 0–10°S. and south of Lat. 40°S. No measurements were made off the coast of South America but it is well-known that upwelling, bringing nutrient-rich water to the surface, occurs in that region.

The observation of larger populations at the shallower depths (and during the day at station 41) agrees with those of most earlier workers and suggests the dependence of planktonic Foraminifera on the abundant plant life in the euphotic zone. Whether it is a purely mechanical process (Bradshaw, 1959), a food necessity, or a dependence on a symbiotic relationship is a matter of speculation. The writer suggests that the symbiotic relationship of the Foraminifera with the various forms of plant life observed in the protoplasm of many species may be the critical factor. It must be emphasized, however, that much more work must be done before the habits of the planktonic Foraminifera are known and conclusions concerning them drawn.

REFERENCES

Bé, A.W.H. (1959): Ecology of Recent planktonic Foraminifera. Pt. 1, Areal distribution in the western North Atlantic. Micropaleontology, Vol. 5, No. 1, pp. 77–100, pls. 1, 2.

Bradshaw, J.S. (1959): Ecology of living planktonic Foraminifera in the North and equatorial Pacific Ocean. Contr. Cushman Found. Foram. Research, Vol. 10, pt. 2, pp. 25–64, pls. 6–8.

Brady, H.B. (1884): Report on the Foraminifera dredged by H.M.S. "Challenger", during the years 1873–1876. Rept. Voy. *Challenger*, Zoology, Vol. 9, 814 pp., 115 pls.

Hofker, Jan. (1959): On the splitting of *Globigerina*: Contr. Cushman Found. Foram. Research, Vol. 10, pt. 1, pp. 1-9.

Phleger, F.B, Parker, F.L., and Peirson, J.F. (1953): North Atlantic Foraminifera. Repts. Swedish Deep-Sea Exped., Vol. 7, No. 1, pp. 1–122, pls. 1–12.

Sverdrup, H.U., Johnson, M.W., and Fleming, R.H. (1942): The oceans, their physics, chemistry and general biology. Prentice Hall, New York, 1087 pp.

Scripps Institution of Oceanography Contribution, New Series. Marine Foraminifera Laboratory, Contribution No 31.

Reprinted from
LIVERPOOL AND MANCHESTER GEOLOGICAL JOURNAL
VOL. 2. PART 3. 1960

(621)

GEOPHYSICAL INVESTIGATIONS OF THE SEA FLOOR

BY R. G. MASON

(Read at Liverpool, 2nd January, 1960)

SUMMARY

Seismic refraction measurements show that the earth's crust thins from about 35 km. under the continents to 6 km. under the oceans, also that the oceanic crust has a layered structure. The sediments that cover it are much thinner than expected, which suggests that the oceans are perhaps younger than was thought, or perhaps the sediments have become engulfed in lavas. Great fracture zones cross the floor of the north-east Pacific and there is evidence for strike-slip movements of more than 200 km. along them. The discovery that heat flow rates for continents and oceans are approximately equal upsets previous ideas about radioactive heat sources. A pattern has been observed in the heat flow associated with an oceanic rise. It has been suggested that both are related to convection in the mantle. Subcrustal drag by convection currents may explain the fracture zones.

1. INTRODUCTION

Although the oceans cover two-thirds of the surface of the earth, we know very little for certain about the rocks under them. This is mainly because almost the whole of the ocean floor is covered by Recent sediments and because with existing free-falling coring techniques we cannot probe more than about 30m. into those sediments. We have no direct knowledge of the solid rocks underneath, and the only way of obtaining samples from exposures is by the relatively crude process of dredging. Thus the methods that have been used to piece together the story of the continents, depending largely on examining the succession of rocks exposed at the surface, or in mines and boreholes, are almost completely denied to us in the case of the oceans.

Other, less direct, approaches are possible. For example, a fundamental difference has long been known to exist between the volcanoes of the continents and the volcanic islands of the deep oceans. Though mainly basaltic, the continental volcanoes extrude large proportions of acidic rocks, such as andesite and rhyolite, which are commonly thought to arise from contamination of the basaltic magma by the granitic rocks of the continental basement. The volcanic islands, on the other hand, are almost entirely basaltic and this is considered to be strong evidence for the absence of granitic rocks from the oceanic crust. Until such time as deep borings are made through the ocean floor, it does not seem likely that the purely geological approach will advance much beyond this general type of reasoning.

Contributions from the Scripps Institution of Oceanography, New Series, No.1182
Reproduced by Permission

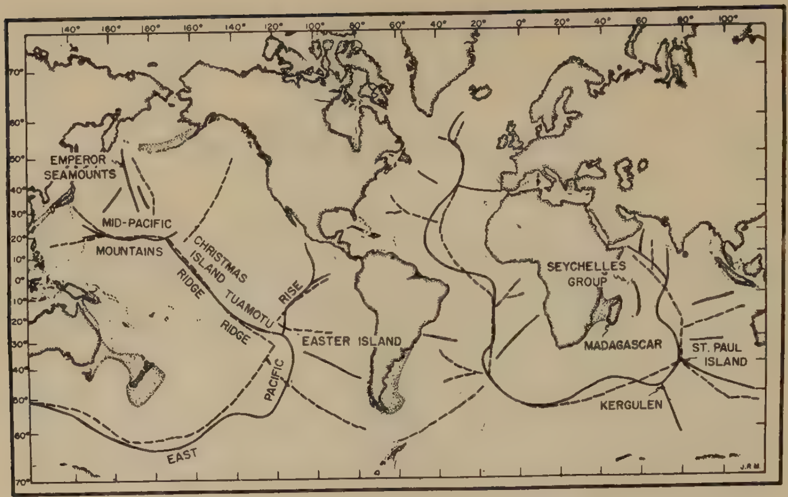

Fig. 1.—Location of the crests of the mid-oceanic ridges and rises (solid line) and of the geometrical median lines (dashed). (From Menard, 1959).

In spite of the difficulties of direct observation, very significant advances in the study of the oceanic crust have been made during the past few years. These stem mainly from the increased effort that has been put into making geophysical measurements at sea, including the allied technique of topographic mapping with the echo sounder. A basis of fact is now being produced for the discussion of topics that were previously a matter of pure speculation.

2. TOPOGRAPHY

The taking of soundings and the mapping of submarine topography are generally considered to belong to the domain of the hydrographer. However, because of the almost complete absence of weathering in the deep oceans mountains, escarpments, trenches and other topographic consequences of the forces operating in the crust, retain their form almost indefinitely, apart from the coating of sediment that eventually drapes over them. A knowledge of the topography of the sea floor is therefore as important to the marine geologist as a knowledge of the configuration of the deeper layers. It is also important in defining problems and areas suitable for geophysical investigation, and in most cases it is essential to the interpretation of such investigations.

The broad features of the ocean basins are now well established. The average depth of the oceans, excluding marginal seas, is a little over 4 km., and more than 80% of the ocean floor consists of broad elevations and depressions lying at depths of between 3 and 6 km. Characteristically, the median areas of all the oceans are relatively shallow (Menard, 1958, p. 1179) and the mid-oceanic ridge system, which is best developed in the Atlantic and Indian Oceans, is one of the major topographic features of the earth's surface. The Mid-Atlantic Ridge, for example, stretches from Iceland in the north to about 55° S, where it swings towards the east and connects with similar ridges in the Indian Ocean. It has a relief comparable with that of the Himalayas and is marked by a belt of shallow seismic activity. On a smaller scale, the floors of the ocean are far less smooth and regular than had once been supposed, except in special areas where turbidity currents have blanketed the bottom with sediments of shallow water origin, and individual seamounts and abyssal hills of all sizes are found distributed irregularly throughout them.

Although the echo sounder is now being used, with precision methods of navigation, to make detailed maps of limited areas of the ocean floors, it has found its widest application in reconnaissance type surveys. Among the most noteworthy of its achievements have been the charting of seamounts and the discovery and surveying of various types of linear topographic structures, such as trenches, rifts and escarpments. The seamounts are particularly interesting. It is possible that their exact number will never be known, but Menard (1959, p. 211) has estimated that the total number in the Pacific is of the order 10^4. By continental standards some of them are very large indeed, rising to heights of more than 10,000 ft. above the sea floor. From their shapes, and from the volcanic materials dredged from their summits and slopes, it is generally concluded that they are of volcanic origin, and this is borne out by magnetic surveys made over them. Their widespread occurrence, at least throughout the Pacific, is evidence for the widespread occurrence of volcanic activity over the ocean floors.

Within the last ten years, four great, almost east-west, fracture zones have been discovered in the north-east Pacific between about 10° N and 40° N (Menard, 1955). These fracture zones are up to 100 km. wide and at least 2,000 km. long, and are characterized by asymmetrical ridges, escarpments up to 3,000 m. high, deep narrow troughs, and occasional seamounts. They normally separate regions of different depth. Thus the most prominent of them, the Mendocino fracture zone, separates regions whose depths differ by 1½ km. A magnetic survey across another, the Murray fracture zone (Mason 1958), indicates a lateral displacement of 160 km. between opposite sides, which makes it one of the largest fault displacements known. Menard has suggested that the fracture zones and the San Andreas

Fault form part of a single integrated fracture system having its cause in the stressing of the crust by a convection current, rising deep within the mantle under the Hawaiian Ridge and sinking near the continental margin. It is possible that improvements in topographic coverage will lead to the discovery of further fracture zones in other parts of the oceans.

3. THE BROAD STRUCTURE

Before discussing the oceanic crust it would be helpful to consider briefly the main characteristics of the continental crust. Until recently, seismologists and geologists were inclined to give the continental crust a layered character, but today opinion seems to be moving away from this concept. On geological grounds it seems unlikely that there could be anything approaching world-wide, uniform layering, and the seismic results do not require that there should be. Repeated deformation in the course of time will have caused much of the crust to have steeply dipping, gneissic structure. Rock types everywhere may be expected to resemble the granite intrusions, schists, etc., of the exposed Pre-Cambrian, but as a result of the tendency of the more volatile constituents to concentrate upwards and the more refractory downwards, the proportion of basic rock, and hence both density and the velocity of propagation of seismic waves, will tend to increase with depth. On a small scale the continental crust will be heterogeneous, but on a scale measured in thousands of kilometres, homogeneous. At a depth of between 30 and 40 km. there is an abrupt seismological discontinuity, the Mohorovicic discontinuity. The contrast between the uniformity, observed everywhere, of the seismic velocity beneath this discontinuity and the variability of that in the overlying materials is most striking. Because of the abrupt change from complexity to simplicity, the Mohorovicic discontinuity is usually taken to mark the lower boundary of the crust.

One of the earliest indications that the oceanic crust might be quite different from the continental came from some very simple gravity measurements made at sea by Hecker during the early years of the century. By the relatively crude method of measuring the height of a mercury barometer, which depends on the acceleration of gravity, and comparing it with the true atmospheric pressure determined from the boiling point of water, he was able to demonstrate that g is approximately the same over the oceans as over the continents. The oceanic crust is therefore roughly in isostatic equilibrium with the continental. This means that the average weight of a vertical column of oceanic rock above some arbitrary datum level below the deepest part of the crust is about the same as for a similar column of continental rock above the same datum level. The mass deficiency of the oceans,

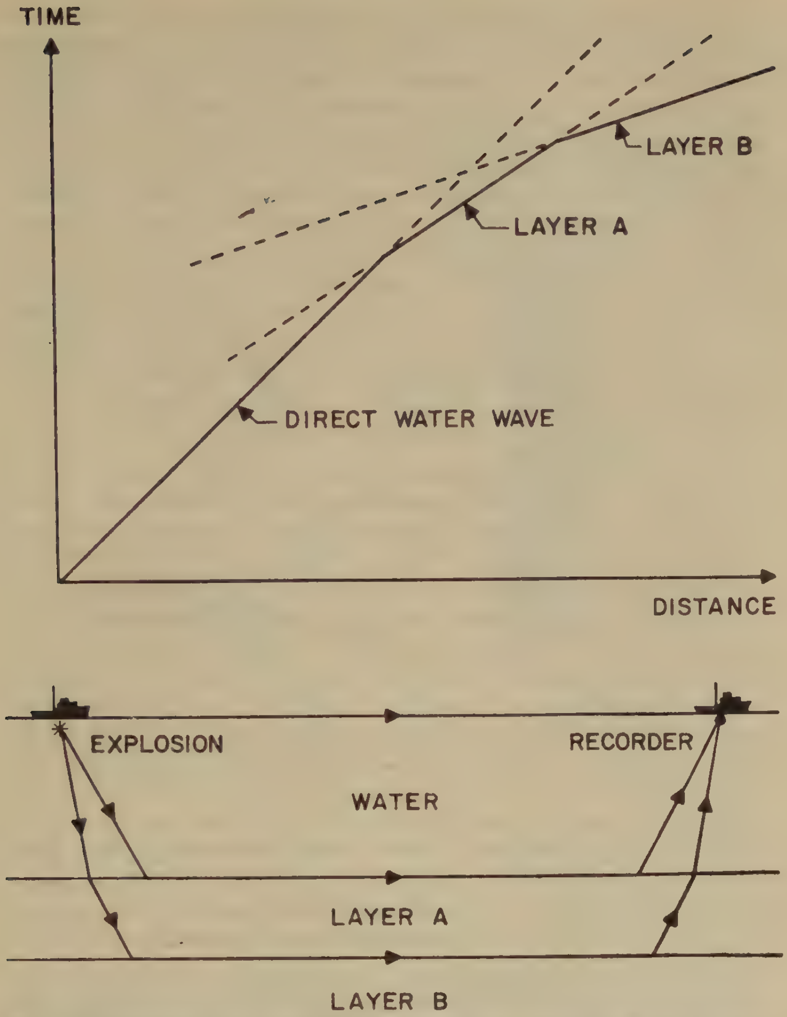
TIME
LAYER B
LAYER A
DIRECT WATER WAVE
DISTANCE
EXPLOSION
RECORDER
WATER
LAYER A
LAYER B

Fig. 2.—Illustrating the principle underlying the seismic refraction method. The lower part shows typical travel paths between two surface points and the upper part shows how each layer is observed in turn over a certain range of distances.

compared with continental rocks at the same depth, must therefore be compensated for by denser rocks beneath the ocean floor. Exactly how this compensation is brought about cannot be determined from the gravity measurements alone, because gravity data are not capable of unique interpretation.

The most informative methods of studying the structure of the ocean floors have proved to be the seismic. The value of these methods lies not only in the direct information that they give about the structure, but also in that they provide the framework essential for the planning and interpretation of other methods of investigation. Of the two techniques available, the reflection and the refraction, the latter has proved the more useful, mainly because it is a self-contained method. Under ideal conditions, given an approximately horizontal layered structure, one set of refraction observations at one station will provide not only the thicknesses of the various layers but also the velocities of the seismic waves in them. By narrowing down the range of possibilities, the velocity measurements help in identifying the material of the layer. The reflection method, on the other hand, is restricted in that for an accurate measurement of the depth of a reflecting horizon the intervening velocity structure must be known, and vice versa.

The refraction method depends on measuring the time taken for a disturbance to travel from its source to a distant point at the surface. A number of paths are open to it between the two points. It can travel direct through the water and it can travel along various refracted paths through the layers under the sea floor. What is observed is the travel time along the quickest of these paths. At short distances the direct wave arrives first. At greater distances some of the energy finds a quicker path through the floor of the ocean, and with increasing distance the quickest path moves to successively deeper layers. Thus each layer is observed in turn over a certain range of distances. By measuring the travel time for various distances, the thicknesses and velocities of the various layers can be determined. The method fails either if the velocity in any layer is less than in the layer above or if the thickness of a layer is less than a certain critical value, depending on the relation of its velocity to those of the adjacent layers and also on the thickness of the layer above. In both cases the layer fails to produce a first arrival and the interpretation breaks down.

In general, the deep-sea seismic stations are poorly distributed throughout the oceans. There is a marked shortage of information from the Indian Ocean, from the Pacific south of a line running from about 25° S in the south-west to about 45° S in the south-east, and from all areas in high latitudes. However, within those areas that have been studied the structure is remarkably uniform and there is no good evidence for any major differences in structure between them.

By contrast with the continents, there seems little doubt that the oceanic crust has a definite layered structure. Although the total number of observations is not large (for all the oceans the total number

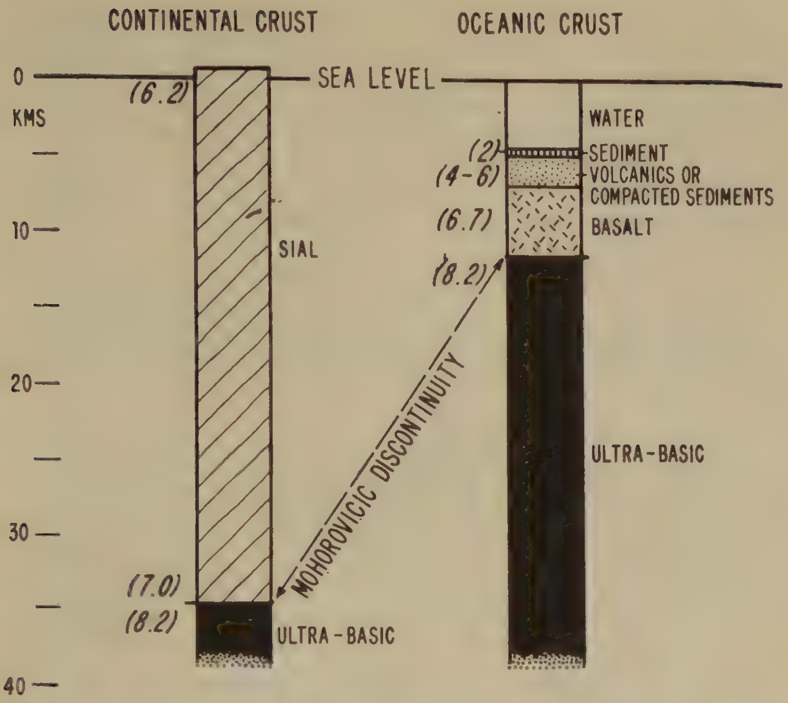
CONTINENTAL CRUST
OCEANIC CRUST
0
KMS
10
20
30
40
SEA LEVEL
(6.2)
SIAL
(7.0)
(8.2)
ULTRA-BASIC
WATER
(2)
SEDIMENT
(4-6)
VOLCANICS OR
COMPACTED SEDIMENTS
(6.7)
BASALT
(8.2)
MOHOROVICIC DISCONTINUITY
ULTRA-BASIC

Fig. 3.—Continental and oceanic crustal sections determined by the seismic refraction method. The figures in brackets are seismic velocities in km./sec.

of deep-sea stations so far occupied is less than 200) it is now sufficient for statistical processes to be applied. The significant fact has emerged that, disregarding the results from anomalous areas near the continents, islands, seamounts, ridges and trenches, the average oceanic structure represents, within surprisingly narrow limits, the structure under most of the deep oceans. Thus it is possible to define a standard, or typical, oceanic structure with which anomalous areas can be compared.

Hill (1957, p. 149) has presented a summary of the results from all oceans up to 1956, and Raitt and Shor (1959) have summarized all Pacific data up to 1959. There is no very great difference between the two sets of results, and it is reassuring that the addition of new data does not seem to alter the average picture very much. According to Hill, the average oceanic structure, for water depths greater than 4 km, is roughly as follows:

	Thickness (km.)	Velocity (km./sec.)
Sea water	4.5	1.5
Layer 1 (Unconsolidated sediments) ..	0.45	2
Layer 2 (Volcanics or consolidated sediments)	1.75	4 - 6
Layer 3 (Basaltic rocks)	4.7	6.71
Layer 4 (Ultrabasic rocks)	—	8.09

There is some doubt about the universal existence of layer 2. In the Atlantic, in particular, it has not always been observed, but in some cases reassessment of the data shows evidence for its existence and in general there are no grounds for saying positively that it does not exist.

The facts that velocities in layer 4 are about the same as in the mantle under the continents, and that the scatter of measured values is small, are considered sufficient justification for identifying the layer with the upper part of the mantle. Its upper boundary is therefore the Mohorovicic discontinuity. The total crustal thickness is, by definition, the sum of the thicknesses of layers 1 to 3. From Hill's data the thickness of the crust is therefore about 6.9 km. and the depth of the Mohorovicic discontinuity about 11.6 km.; the corresponding figures for the Pacific are respectively 6.26 km., with a standard deviation of 1.06 km., and 10.60 km., with a standard deviation of 1.28 km., and a range from 8 to 14 km. Thus the Mohorovicic discontinuity rises from a depth of about 35 km. under the continents to about 6½ km. below the sea floor or 11 km. below sea level. This is probably the most important discovery that has been made about the oceanic crust; it has changed drastically ideas held as recently as 1950 (see for example Kuenen, 1950, p. 116) and has made it necessary to think afresh about the origin of the oceanic crust and the nature of the forces that can operate in it.

When the mean values are compared, the velocities in the mantle under the oceans and under the continents are found to be almost identical. For the oceans, Hill finds a mean value of 8.09 km./sec. with a standard deviation of 0.30 km./sec., and Raitt and Shor 8.20 km./sec. with a standard deviation of 0.18 km./sec. For the continents, Bullard (1954a, p. 67) obtains a mean value of 8.18 km./sec. These values are so close that it seems reasonable to suppose that the rocks are identical, in spite of the differences that must exist between the temperatures and pressures 11 km. under the oceans and 35 km. beneath the continents. Independent evidence for this comes from the work of Ross *et al.* (1954, p. 693-737) who have examined a number of peridotite blocks brought to the surface as foreign bodies in basaltic volcanoes. These specimens came from a variety of sources, from volcanic islands and from three of the continents, and are practically identical. They are also almost identical to a peridotite which outcrops at St. Paul's Rock in the Atlantic Ocean off Brazil, and Hess (1955, p. 426) believes that all these materials represent rock from below the Mohorovicic discontinuity. It has been suggested that the velocity change at the Mohorovicic discontinuity might represent a phase change rather than a change of material, but there is as yet no evidence to support this hypothesis.

An important consequence of the rise of the Mohorovicic discontinuity under the oceans is that, by bringing the denser rock of the mantle closer to the surface, an explanation is offered for how isostatic compensation is brought about under the oceans. Within the limits imposed by uncertainties as to densities, the standard oceanic crust just balances the continental crust. It might be expected that, in order to maintain isostatic equilibrium, the depth of the water would show inverse correlation with the thickness of the crust, that is, where the crust is thinner, the water depth might be greater to compensate for it, and vice versa. Raitt and Shor have examined this possibility, but find no evidence to support it. Thus elevations of the crust do not seem to be the result of thickening processes and their cause must be sought elsewhere. For example, a region may be uplifted above adjacent regions because the upper few hundred kilometres of mantle has a slightly lower density.

4. THE CRUSTAL LAYERS

The first layer is rarely observed by its refracted wave because it is too thin to give rise to first arrivals. Its velocity has been measured by reflection techniques and is found to increase with depth. The mean values usually adopted range from 1.7 to 2.15 km./sec. There can be little doubt that the layer consists of unconsolidated sediments, but there is no evidence as to what these sediments may be. Laboratory experiments on artificially compacted sediments (Laughton, 1954, p. 336) suggest that within the range from red clay to highly calcareous ooze there will be insufficient velocity differences to provide any evidence for composition.

According to Hill (1957, p. 142), the mean thickness of the unconsolidated sediments, from all available sources up to 1956, ranges from 1.0 km. for water depths less than 4 km. to 0.38 km. for depths greater than 5 km. There appears to be a real reduction in sediment thickness

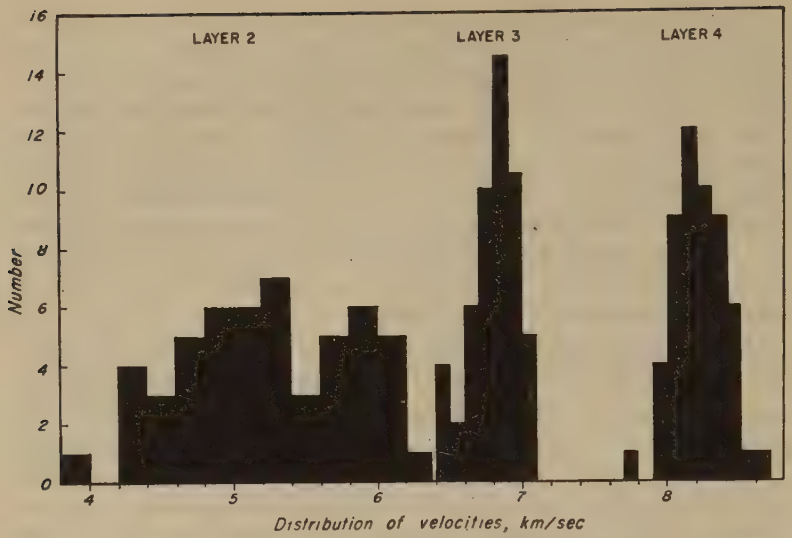

Fig. 4.—Showing the distribution of observed seismic velocities for fifty-three Pacific stations. Layers 3 and 4 show a strong central tendency. Layer 2 velocities are widely scattered, with a tendency to form two groups. (From Raitt and Shor, 1959).

with increasing depth of water, which is to be expected since sediments of continental origin will tend to collect in shallower water near the continental margins. Furthermore, at the greater depths, other things being equal, the increasing solubility of calcite leads to a reduction in the amount of calcareous material deposited. The variation of thickness from ocean to ocean is not large, but it does appear that in the Pacific the sedimentary layer is slightly thinner than in the Atlantic. Thus Raitt and Shor (1959), in summarizing results from 53 Pacific stations selected as representing the normal deep oceanic environment, find a mean thickness of 0.30 km., with more than 80% of the values lying between 0.10 and 0.45 km. This is perhaps because the length of the continental boundary, from which the sediments are mostly derived, is less in proportion to the area of the Pacific. The probable error of the estimated thickness is about 100 m.

Perhaps the most striking feature of these sediment thicknesses is their smallness, and even so they are likely to be over-estimates because of the tendency in refraction work to choose smooth-bottom areas, where the sediments are likely to be thicker, in preference to rough in order to reduce the corrections that have to be applied for bottom topography. These thicknesses are very much less than had been predicted for the average deep-sea sediments. Thus Kuenen (1950, p. 386), from the present rate of sedimentation and the probable age of the oceans, arrives at an average deep-sea sediment thickness of about 3 km.; other lines of reasoning lead him to a similar conclusion. This value is almost one order greater than the observed thickness. It seems that either the rate of sedimentation was less in the past than it is today, or the oceans are younger than is generally believed. Alternatively, most of the sediment laid down in the past may have become incorporated in the second layer, either by consolidation or by interbedding with volcanic rock.

Velocities in the second layer are difficult to measure, principally because of the short range of distances over which it is observed as a first arrival, and for the same reason the layer has sometimes been overlooked; they are also extremely variable and values have been reported ranging from 4 up to 6 km./sec. In the Pacific, Raitt and Shor report a mean value of 5.23 km./sec., with a tendency for the values to form two groups centred about 5.0 and 5.9 km./sec. respectively. The variability of velocities is such that it is impossible to identify the layer with any particular rock. Measurements made near volcanic islands show that basaltic lavas have velocities well within the observed range. So also do the majority of consolidated sediments. If the material of layer 2 is of sedimentary origin, then the missing sediments would be largely accounted for. On the other hand, recent magnetic measurements in the Pacific (Mason, 1958, p. 324–326) showed anomalies which can be explained only by the presence of highly magnetic rocks in layer 2. These results will be discussed more fully later. There are no known sediments sufficiently magnetic to account for the anomalies and it is concluded that the anomalies are most probably caused by basaltic lava flows. The wide scatter of velocities gives good grounds for believing that both explanations are in part correct, that the layer comprises varying proportions of extrusive volcanics and consolidated, sometimes matamorphosed, sediments. This may perhaps explain the tendency of the seismic velocities to form two groups.

The average of all estimated thicknesses of the second layer is 1.9 km., and in the Pacific, where it is best observed, Raitt and Shor report a mean value of 1.18 km., with three-quarters of the values lying between 0.6 and 1.4 km. These thickness estimates are not very reliable, mainly because of the uncertain velocities, and could be in error by as much as 200 m.

The third layer is observed in all areas where measurements have been made. It is the thickest of the layers and forms the main constituent of the oceanic crust. Hill reports a mean velocity from all the oceans of 6.71 km./sec., with a standard deviation of 0.28 km./sec., and Raitt and Shor a mean value of 6.81 km./sec., with a standard deviation of 0.16 km./sec. The smallness of the scatter represented by these values suggests that there are no large variations in the constitution of the layer. The velocities are such as might be expected for a massive basic igneous rock and are in excess of the values found for any acidic or sedimentary rocks, except for highly compacted limestones, which are an extremely unlikely possibility. The thickness of the layer shows a wide variation and Raitt and Shor report values for the Pacific ranging from 2.8 to 8.1 km., with a mean value of 4.8 km. Three-quarters of their values lie between 4.0 and 5.5 km. These thicknesses may be in error by as much as 1 km., and are the main source of error in estimating the total crustal thickness. The reason for this large error is that the thickness determination depends on the observation of disturbances which have travelled large distances through the mantle and so small errors in mantle velocity can lead to large errors in thickness.

5. HEAT FLOW THROUGH THE OCEAN FLOOR

The generation and distribution of heat enters into a number of tectonic hypotheses. It may play an active part, as in convection, or it may be a by-product of a process such as the serpentinization of peridotite. In either case some disturbance of the surface heat flow might be expected. Apart, therefore, from the direct problem of the distribution of radioactive materials, which are commonly supposed to be the main source of the heat reaching the surface, heat flow measurements have the added interest that they may throw some light on processes at work under the ocean floor.

Sixty-nine values of heat flow in oceanic areas have been published, sixty-one from the Pacific and eight from the Atlantic. These measurements reveal the surprising fact that the rate of heat flow through the floor of the ocean is roughly the same as through the continental surface, that is a little over 1×10^{-6} cal./cm.^{2}/sec. This result is unexpected because it has always been supposed that most of the surface heat flow in continental regions comes from radioactive decay in the relatively radioactive rocks of the continental crust. Thus, since the oceanic crust is thinner and its rocks more basic, and therefore probably less radioactive, a considerably reduced rate of heat flow was expected through the floor of the ocean. Apparently most of the heat reaching the sea floor comes from under the crust.

The usual method of determining the rate of heat flow is to make independent measurements of the temperature gradient in the upper few feet of the ocean bottom, and the thermal conductivity of the material involved in the temperature gradient measurement. The temperature gradient is measured directly by two temperature-sensitive elements driven into the bottom on a free-falling probe, which is attached to a container housing the temperature recording equipment. The thermal conductivity measurement is made in the laboratory on a core taken from as close as possible to the probe.

If radioactive processes are accepted as the major source of the heat which flows through the crust, then the very different distributions of rock types in the continental and oceanic columns will lead to correspondingly different temperature distributions under continents and oceans. Unfortunately, reliable figures are lacking for the radioactive heat production in the major rock types and it is not possible to make other than a very rough estimate of what temperature differences may be expected. Birth (1955, p. 112-114) gives some values for the rate of radioactive heat production in typical rocks, with a warning as to the uncertainties surrounding them. Granite is by far the most radioactive of the common rock types. Its rate of heat production is about six times the rate for basalt and gabbro and more than a hundred times the rate for ultrabasic rocks.

Using these values, Birch has investigated the variation of temperature with depth for a number of crustal models. Considering, for example, a continental-type crust 30 km. thick, if it is assumed that about a quarter of the observed heat flow comes from the original heat of the earth, then 10 km. of granite and 20 km. of gabbro will supply the remaining three-quarters and the temperature at the base of the crust, at 30 km., will be about 300°C. In the case of a 5 km. thick basaltic ocean crust, less than 5% of the average heat flow comes from the crust and if, to simplify the problem, it is assumed that all the heat comes from below 30 km., then the temperature at 30 km. beneath the oceans will be about 430°C. Although these estimates are based on uncertain data and over-simplified models, it is quite clear that substantial temperature differences may exist between points at the same depth between continents and oceans.

One problem that has to be faced in placing the radioactive heat source of the ocean floors in the mantle is that, as Bullard *et al.* (1956) have shown, if the radioactivity is distributed over more than a certain range of depths in the mantle, melting will occur. Taking the thermal conductivity in the mantle to be about equal to the value obtained from laboratory measurements on ultrabasic rocks, and there are no definite

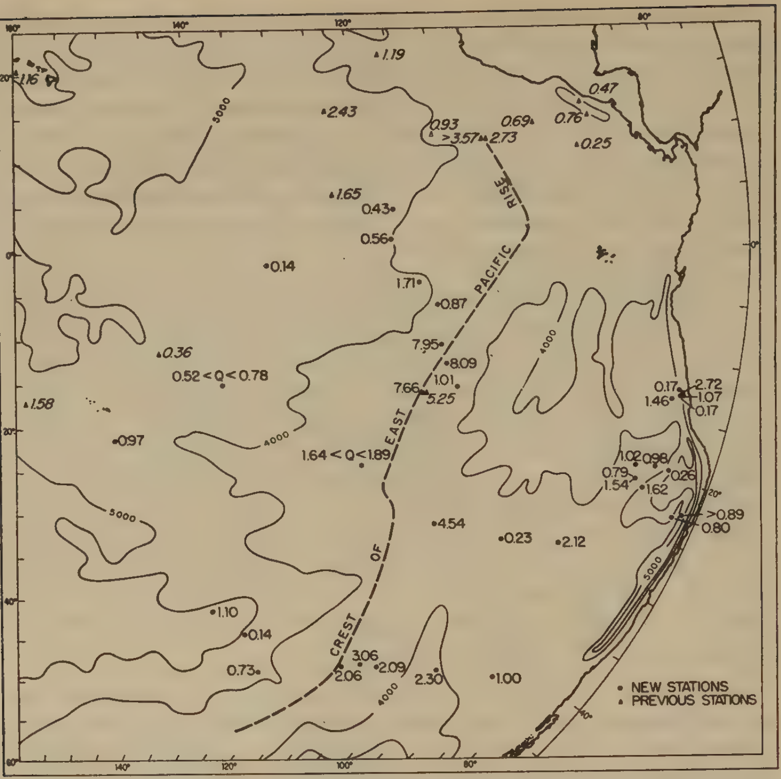
160°
140°
120°
80°
20°
0°
20°
40°
60°
100°
1.16
1.19
2.43
5000
0.93
>3.57
2.73
0.69
0.76
0.47
0.25
1.65
0.43
0.56
0.14
1.71
0.87
EAST PACIFIC RISE
CREST OF
0.36
0.52 < Q < 0.78
7.95
8.09
1.01
7.66
5.25
1.58
0.97
4000
1.64 < Q < 1.89
0.17
1.46
2.72
1.07
0.17
1.02
0.98
0.79
1.54
0.26
1.62
>0.89
0.80
5000
4.54
0.23
2.12
1.10
0.14
0.73
3.06
2.09
2.06
2.30
1.00
4000
• NEW STATIONS
▴ PREVIOUS STATIONS

Fig. 5.—Heat flow values (in cals./cm.^{2}/sec.) and bottom depth contours (in fathoms) for the East Pacific Rise, showing the narrow band of high heat flow associated with its crest (From von Herzen, 1959).

grounds for supposing that it would be substantially different, leads to a maximum depth range of about 200 km. If Birch's figures for the radioactive production of heat in ultrabasic rocks are correct, the radioactivity would have to be spread over a very much greater range of depths than this.

Bullard (1954b, p. 408) has suggested that the higher temperatures at given depths under the oceans might lead to convection currents extending deep within the mantle, rising under the oceans and sinking under the continents. This is in the opposite direction to that normally assumed. Such convection currents present a means for bringing the original heat of the earth to comparatively shallow depths and it is possible that the mechanism provides much of the heat that flows through the oceanic crust. It would also allow a much deeper distribution of radioactive heat sources without leading to melting.

Most of the early heat flow measurements were made at widely separated points and showed no particular relationship to structural features of the crust. Von Herzen (1959, p. 882) has recently published an important new series of comparatively closely spaced measurements from the south-east Pacific which, with other measurements made earlier in the same area, reveal indisputable trends in the heat flow pattern. Thus the East Pacific Rise, an elevated region of the eastern Pacific sea floor, appears to be associated with a relatively narrow band of high heat flow for at least 6,000 km. along its length and there is fair evidence for roughly parallel areas of low heat flow on either side. Along the axes of the trenches bordering the eastern Pacific Ocean the heat flow values are abnormally low, but the overall density of observations in the area is not sufficient to establish a direct correlation between the heat flow pattern and the roughly parallel trenches and rise.

An interesting feature of the measurements is the large range of values obtained, extending from a low of 0.14 x 10^{-6} to a high of 8.09 x 10^{-6} cal./cm^2./sec., representing a range of 1 : 50. Some of the variation can be accounted for by irregularities in bottom topography, or by topographic irregularities in the basement underlying the sediments, but it is unlikely that these irregularities could affect the measured heat flow by a factor of more than two. Undoubtedly, most of the variations observed are due to real differences in the flow of heat from the mantle of the earth.

Hess (1959) has considered the possibility that the elevation of the area and the high heat flow have a common cause in the serpentinization of the olivine in the ultrabasic rocks of the mantle. The process can be represented by the relation:

$$\text{olivine} + \text{water} \leftrightarrows \text{serpentine} + \text{heat}$$

The process goes to the right at temperatures below 500°C. and is accompanied by a 25% increase in volume. It could account for the elevation but fails to explain the high heat flow by about two orders of magnitude. Hess advances the hypothesis that oceanic ridges in general represent the trace on the earth's surface of upward flowing limbs of convection cells in the mantle. Water released at the top of the column produces the serpentinization, subcrustal drag of the horizontal flow produces extension and the graben which has been found to occur along the crests of many of the ridges. Heat moving slowly upwards by convection accounts for the high heat flow and ultimately for deserpentinization and subsidence of the ridge. The hypothesis has the attraction of being able to provide both upward and downward movement, at different stages of the cycle, and offers an explanation for the guyots, or flat-topped seamounts, of the Pacific.

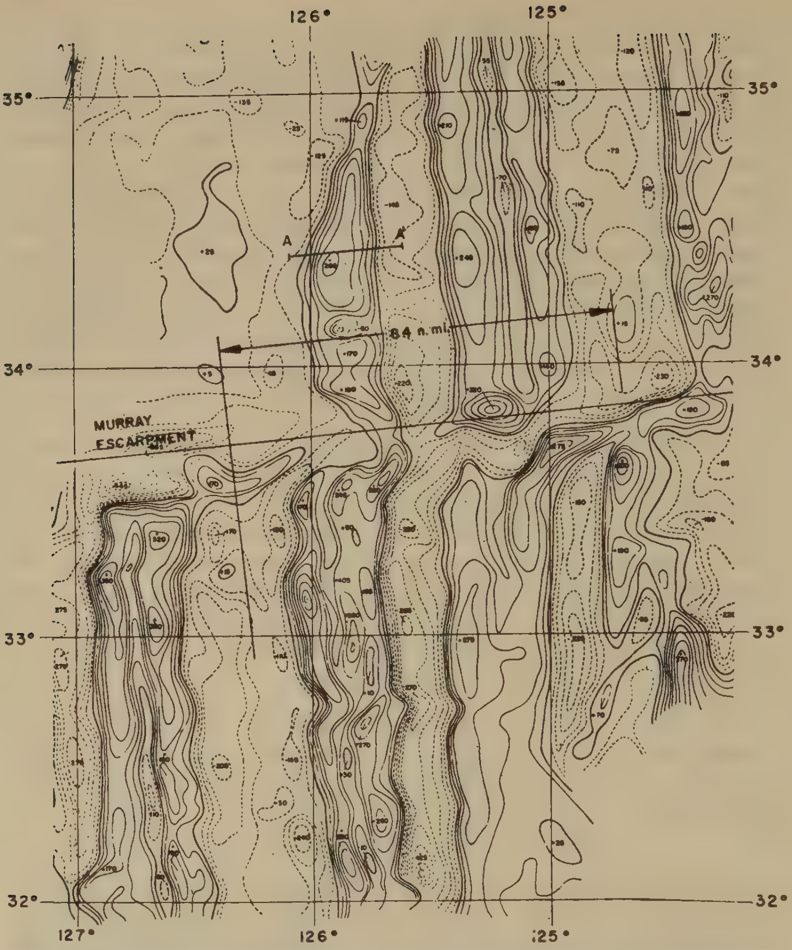

Fig. 6.—Part of the magnetic anomaly map of the north-east Pacific, showing the lateral displacement across the Murray Fracture Zone. The contour interval is 50 gammas.

6. MAGNETIC SURVEYS AND CRUSTAL DISPLACEMENTS

Magnetic mapping with the airborne magnetometer has been used extensively for studying the continental basement. The method depends on the large differences that exist between the magnetic properties of different types of rock. Basic rocks in particular tend to be more magnetic than others, and any situation involving local excesses or deficiencies of basic rocks will lead to anomalies in the earth's magnetic field.

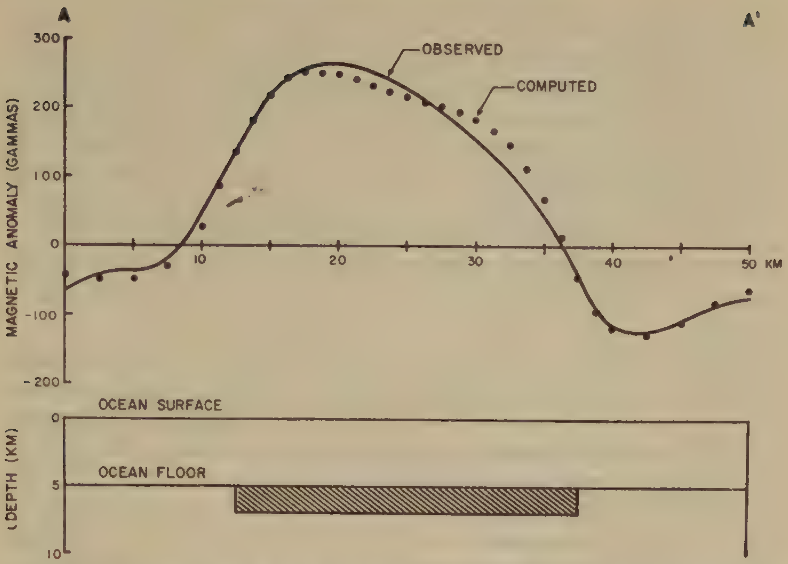

Fig. 7.—Magnetic profile along the line A-A' of Fig. 6 and its interpretation in terms of an infinite slab of rectangular cross section. A magnetic susceptibility of 0.01 is assumed, and normal magnetization in the present direction of the earth's field.

The airborne magnetometer can easily be adapted for towing behind a ship, and in the last ten years many thousands of miles of magnetic profile have been obtained in this way in both the Atlantic and Pacific Oceans. However, it has not proved easy to exploit the data, mainly because most of it is in the form of long, unrelated, profiles which give no indication of the lateral extent, or direction, of anomalous magnetic trends. The chief obstacle to the making of magnetic maps over the oceans is the difficulty of providing the necessary accuracy of navigation and, as far as is known, the only area of any appreciable extent to have yet been surveyed in detail is a strip of the north-east Pacific about 250-300 miles in width from the foot of the continental slope outwards and extending along the whole of the west coast of the United States. This area includes parts of two of the four major fracture zones of the north-east Pacific, the Mendocino and the Murray.

The map of the first section (Mason, 1958) is unusual in several respects. It shows a series of narrow anomalies, each about 40 km. wide and about the same distance apart, trending north-south from top to bottom of the map, a distance of about 450 km. These anomalies, which have now been followed for a further 500 km. in a northerly direction, are quite unlike any which have been observed over the continents. An even more unexpected feature of the map, because there is no evidence for it in the topography, is that where they cross the Murray fracture zone the anomalies are offset by about 160 km. in a right lateral sense. As was mentioned earlier, this is one of the largest fault displacements known, but more recently Vacquier (1959, p. 452), by means of very long lines extending several hundred miles to the west of the area, has discovered an even greater displacement, in excess of 200 km., parallel to, and between, the Mendocino and Murray fracture zones. These displacements imply an unexpected ability of sections of the earth's crust to move large distances relative to one another.

The anomalies themselves are remarkable in extent, uniformity and amplitude. They are what would be expected of flat, slab-like, structures, tapering at the edges and corresponding approximately in lateral extent to the area of the anomalies. Although magnetic data are not capable of unique interpretation, some general conclusions can be reached about these slabs. In the first place, even if they were at the shallowest possible depth in the crust, and if they were of a highly magnetic material such as basalt, they would have to be at least 1 km. in thickness. At the most, they could lie no more than 6 km. below sea level. If they were thicker slabs of less magnetic material they would have to come even closer to the surface. Seismic data indicate a typical oceanic crust throughout most of the area and the slabs would lie at least partly in the second layer. Since the main crustal layer is itself supposedly basaltic, and therefore highly magnetic, it seems probable that the anomalies arise entirely from within the second layer.

Turning to the geological implications, there appear to be at least two possibilities, folding or block faulting of the main crustal layer, and the outpouring of vast quantities of basaltic lavas on to an earlier ocean floor, possibly filling pre-existing troughs. Such lavas would represent 10% of the local crustal volume. Both processes imply remarkably straight continuous lines of weakness in the oceanic crust, though no more so than for the east-west fracture zones, which is supporting evidence for the lateral homogeneity of the main crustal layer.

As far as can be judged from the best available topographic maps, the anomalies show little or no correlation with topography, and there is no indication of any systematic differences between seismic velocities in the anomalous areas and in the areas between, though the amount of data is not yet sufficient to demonstrate this point conclusively. It must be presumed that the areas between the blocks, or the lava flows, are occupied by consolidated or metamorphosed sediments.

7. THE MID-OCEANIC RIDGE SYSTEM

The mid-oceanic ridge system is the most spectacular topographic feature of the ocean floors. It rises as high as 10 km. above the adjacent sea floor and appears to extend, more or less continuously, for more than 60,000 km., following very closely the geometrical median lines of the North and South Atlantic, Indian and Pacific Oceans. Along most of its length it is seismically active, and the belt of shallow earthquakes associated with it constitutes the second most active seismic system of the earth. Perhaps the best developed, and certainly the best known, part of the system is the Mid-Atlantic Ridge.

The Mid-Atlantic Ridge (Heezen *et al.*, 1959)[1] consists of a broad, fractured arch which occupies approximately the central third of the ocean. Between 17° N. and 54° N., where it has been most closely studied, it is between 800 and 1,400 km. wide and 2½ to 4 km. high. It rises, from almost the deepest parts of the adjacent basins, in a series of steps which become progressively more rugged towards the crest. The crest itself is marked by a deep valley, or rift. This valley is from 25 to 50 km. wide, between adjacent peaks, and from 1 to 4 km. deep, and has a rough floor, almost mountainous in the widest parts. It is the most striking feature on the average profile across the Mid-Atlantic Ridge and seems to be a characteristic of the mid-oceanic ridge system in general.

The crustal structure of the Mid-Atlantic Ridge has been determined at a number of places by the seismic refraction technique. The results indicate an average section consisting of 0.4 km. of sediment and 2.8 km. of a rock with a velocity of 5.1 km./sec. overlying a substratum in which the velocity is 7.3 km./sec. The thickness of the sediment varies considerably from place to place. Near the crest the 5.1 km./sec. layer is commonly exposed; on the flanks thicknesses of up to 1 km. of sediment have been measured. The 5.1 km./sec. layer apparently corresponds to the second layer of the normal oceanic crust. The velocity of the underlying rock is intermediate between those of the normal main crustal layer (6.7 km./sec.) and the upper mantle (8.1 km./sec.). Intermediate velocities are common under other elevated areas in both the Atlantic and the Pacific. It is not clear whether this represents an abnormally low mantle velocity, or a physical mixing of mantle and crustal rocks brought about by extensive vulcanism and intrusion, or a distinct crustal layer characteristic of uplifted areas, as for example Hess's serpentinized peridotite.

---

[1] HEEZEN, B. C., THARP, MARIE AND EWING, M., 1959. The Floors of the Oceans, I. The North Atlantic, *Geol. Soc. Amer. Spec. Pap.*, **65**, 83.

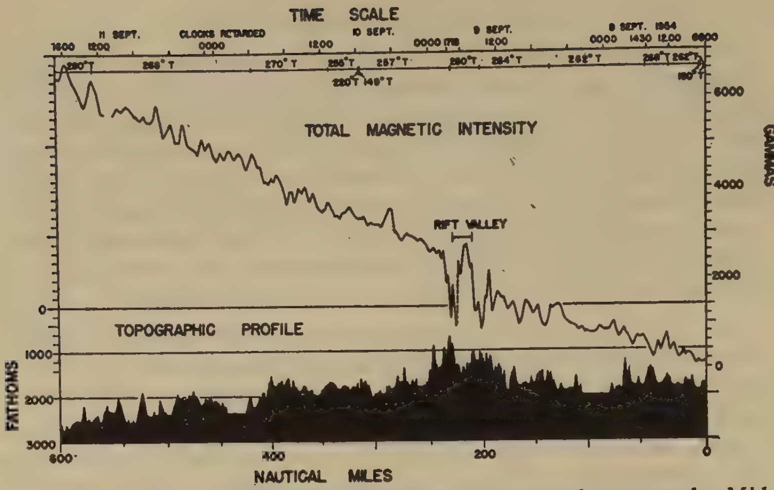

Fig. 8.—Profile of total magnetic intensity and topography across the Mid-Atlantic Ridge. Magnetic values are relative to an arbitrary zero. (From Heezer *et al.* 1959).

The rift valley appears to be a graben-like structure. Magnetic profiles over it indicate a large positive anomaly, which suggests that its floor is underlain by highly magnetic intrusive rocks. Gravity measurements show a small negative free-air anomaly over it. The one heat flow measurement made in the floor of the valley shows a value about six times the average oceanic value (Bullard *et al.*, 1956). Taken with the high heat flow of the East Pacific Rise, this suggests that perhaps high heat flow is characteristic of the entire mid-oceanic ridge system.

Thus far, no single hypothesis has been proposed that will account satisfactorily for all the observed facts. There seems to be no doubt as to the tectonic significance of the ridge system, but on the basis of present evidence it does not seem possible to say whether it is primarily of folded or faulted origin. Heezen and Ewing (in press) have made a detailed comparison of the African rift valleys and the rift valley of the Mid-Atlantic Ridge and conclude that the two are basically similar. Since the former are commonly held to be tension features, it is concluded that so also is the Mid-Atlantic Ridge, though there is as yet insufficient evidence as to whether this could apply to the oceanic ridge system as a whole. Whether the forces are the result of a general horizontal extension of the earth's crust, or of local extension due to convection currents, or of vertical uplift of limited areas of the crust, is one of the most important unsolved problems of the ocean floor.

8. ACKNOWLEDGEMENTS

This paper was written while the author was a member of the staff of the Scripps Institution of Oceanography, on leave of absence from Imperial College, London. He is indebted to various of his colleagues at Scripps for helpful discussions of the various topics dealt with, in particular to Drs. R. L. Fisher, H. W. Menard, R. W. Raitt, R. Revelle, G. G. Shor and R. Von Herzen.

J

(643)

9. REFERENCES

BIRCH, F., 1955. Physics of the Crust. *Geol. Soc. Amer. Spec. Pap.* **62**, 112.

BULLARD, E. C., 1954a. The Interior of the Earth. The Solar System. **2**, The Earth as a Planet, Ed. G. P. Kuiper, Chicago, 67.

—— 1954b. The flow of heat through the floor of the Atlantic Ocean. *Proc. Roy. Soc.* **A22**, 408.

MAXWELL, A. E. and REVELLE, R. 1956. Heat Flow through the Deep Sea Floor. *Adv. in Geophys.* **3**, 153.

EWING, M., HIRSHMAN, J. and HEEZEN, B. C., 1959. Magnetic Anomalies of the Mid-Oceanic Rift. Unpublished paper read at the 1st International Oceanographic Congress, New York, 1 September, 1959.

HESS, H. H., 1955. The Oceanic Crust. *Sears Found. Jour. Mar. Res.* **14**, 426.

—— 1959. Nature of the Great Oceanic Ridges. Unpublished paper read at the 1st International Oceanographic Congress, New York, 1 September, 1959.

HILL, M. N., 1957. Recent Geophysical Exploration of the Ocean Floor. *Physics and Chemistry of the Earth*, **2**, 129.

KUENEN, Ph. H., 1950. Marine Geology, John Wiley, New York, 386.

LAUGHTON, A. S., 1954. Laboratory measurements of seismic velocities in ocean sediments. *Proc. Roy. Soc.* **A222**, 336.

MASON, R. G., 1958. A magnetic survey off the west coast of the United States. *Geophys. Jour.* **1**, 320.

MENARD, W. H., 1955. Deformation of the north-eastern Pacific basin and the west coast of North America. *Geol. Soc. Amer. Bull.* **66**, 1149.

—— 1958. Development of median elevations in ocean basins. *Geol. Soc. Amer. Bull.* **69**, 1,179.

—— 1959. Geology of the Pacific Sea Floor. Experientia. **15**, 205.

RAITT, R. W. and SHOR, G. G., 1959. Pacific Ocean Crust. Unpublished paper read at the 1st International Oceanographic Congress, New York, 31 August, 1959.

ROSS, C. S., FOSTER, M. D. and MYERS, A. T., 1954. Origin of dunites and olivine rich inclusions in basaltic rocks. *Amer. Mineral.* **39**, 693.

VACQUIER, V., 1959. Measurement of horizontal displacements along faults in the ocean floor. *Nature*, **183**, 452.

VON HERZEN, R., 1959. Heat Flow Values from the South-Eastern Pacific. *Nature*, **183**, 882.

DEPARTMENT OF GEOPHYSICS,
IMPERIAL COLLEGE OF SCIENCE
AND TECHNOLOGY,
LONDON, S.W.7.

Reprinted from the Transactions of the Second Seminar on Biological Problems in Water Pollution, April 20-24, 1959, U. S. Public Health Service, Robert A. Taft Sanitary Engineering Center, Cincinnati 26, Ohio. pp. 177-183.

MARINE POLLUTION PROBLEMS IN THE SOUTHERN CALIFORNIA AREA

Claude E. ZoBell - Professor of Microbiology & Chairman Marine Biology Division
Scripps Institution of Oceanography, University of California, La Jolla

ABSTRACT

More than a billion gallons of sewage is discharged daily into the ocean along the coast of California. Nearly two-thirds of this finds its way into the sea in a few highly localized areas in the southern part of the State. Those charged with the responsibility of sewage disposal have experienced difficulty in keeping pace with the rapid and unanticipated increase in population--nearly 4% gain per year during the last decade. Nevertheless, engineers and health authorities alike are dedicated to the proposition that sewage should neither jeopardize human health nor unduly destroy natural resources. The latter include harvestible seaweeds, fish and other marine fauna, and beneficial uses of beaches, bays and sea water.

The beneficial uses include swimming, skin diving, surf boarding, fishing, boating, aesthetic enjoyment, commercial shipping, naval vessels, and water for industrial cooling, cleaning, fluming, flushing, etc. Though difficult to assess in terms of dollars, some people place the premium upon aesthetic values--the sense of satisfaction derived from seeing and smelling good, clean, clear, blue sea water. It seems, though, that part of the price to be paid for the privilege of living in populous areas on the sea coast is the modification of adjacent waters. Not only does sewage itself contribute to the discoloration of sea water, it promotes the growth of plankton organisms. However, the health and economy of populous communities must be protected.

The California State Pollution Control Board recommends that the concentration of coliform bacteria shall not exceed 10 per ml in water from recreational beaches or bays. Certain coastal communities have experienced difficulty in complying with this standard of sanitation owing to rapid population increases, mechanical failures of sewage processing plants or pipelines, adverse meteorological or oceanographic conditions, and the prolonged survival of coliform bacteria in the sea.

Remote from the influences of man, bacteria of sanitary significance do not appear to be normal inhabitants of the sea. Only small numbers of such bacteria were found in 103 out of 2,167 samples of sea water and bottom deposits collected at stations many miles from land. Even here, man may have been responsible for the occurrence of such bacteria. They occur commonly and abundantly, however, in coastal waters and bottom deposits in the vicinity of sewage outfalls and around ships in harbors. From a few to nearly a million coliform bacteria per ml. have been demonstrated in bottom deposits collected within a radius of 5 to 10 miles of submarine sewage outfalls and in bays.

Following sewage fields at sea with dye patches and with radioactive tracers (scandium-46) while determining the abundance of coliform bacteria, it has been found that the T-90 of such bacteria ranges from 2 to 20 hours, the average range being 3 to 8 hours. T-90 is the time required for a 90% reduction in the number of coliform bacteria detected by Standard Methods. Under laboratory conditions, the T-90 of coliform bacteria suspended in sea water ranges from 10 to 100 hours. This shows that forces or factors are operative under natural conditions in the sea that are not revealed by laboratory observations alone. Most important of these factors are dilution or dispersion of the sewage bacteria in sea water, aggregation or flocculation of bacteria into clumps, sedimentation, and predation. In progress are monitoring and research programs designed to determine the effects of domestic and industrial wastes on marine plant and animal life.

The daily discharge of sewage into the ocean along the coast of California exceeds a billion gallons (Pearson, 1956). Nearly two-thirds of this finds its way into the sea in a few highly localized areas in the southern part of the State. The City of Los Angeles discharges about 300 million gallons per day into Santa Monica Bay. Los Angeles County outfalls carry somewhat more than 250 million gallons per day into San Pedro Channel. San Diego Bay receives nearly 45 million gallons per day. Santa Barbara and Orange County each dump about 25 million gallons per day into coastal waters.

The southern California sewage problem is unique in several ways. First, there is virtually no natural runoff along the coast to provide for the dispersion or dilution of the sewage. The average annual rainfall ranges from 10 to 20 inches, most of which falls during the winter months. Since as much water as practical is impounded in storage reservoirs, only rarely do

Reproduced by Permission

the rivers carry much into the sea. Either raw, primary or secondary-treated, and/or chlorinated sewage is carried into the sea by submarine outfalls ranging from a few hundred feet to a few miles in length.

More than 90 percent of the southern California population is concentrated in little pockets along the coast, from which foothills or high mountains rise precipitously. Thus proposals for pumping the watery wastes inland for disposal are generally discouraged by the added expense of elevating the sewage several hundred to a few thousand feet.

In the interests of current economy and guided by precedent, most sanitary districts in southern California gather domestic wastes from rather extensive geographic areas for treatment in central plants and disposal at sea. While this may be more economical than constructing numerous smaller plants and ocean outfalls, bringing the sewage to a central plant does pose the problem of dispersing the effluent safely in the sea near the place where the population pattern is densest.

Another unique feature of the sewage problem is the rapid and unanticipated population increase in California,--nearly 4 percent gain per year during the last decade. As a result, certain sewage disposal systems have become obsolete or inadequate more rapidly than they can be designed, financed, and constructed. Unlike older populous centers along the east coast of U. S. A. or in western Europe, where sewage has been discharged into the sea for centuries, the pollution problem in southern California has become increasingly more acute only relatively recently. Engineers and health authorities alike are dedicated to the proposition that the effluent should neither jeopardize human health nor unduly destroy natural resources.

BENEFICIAL USES OF COASTAL WATERS

In San Diego and in San Pedro harbors, large volumes of sea water are used for fluming and thawing fish in the vicinity of canneries and for flushing fish wells aboard fishing vessels. Seaweed processing plants use millions of gallons of bay water per day for washing, leaching, and fluming chopped kelp. Reduction companies make use of bay water for converting fish and other animal wastes into various products. One of the largest marine salterns in the world obtains salt by the evaporation of water from upper San Diego Bay. Power and electric companies use tremendous volumes of sea water for cooling condensers in steam plants. In most of these as well as in other commercial applications, there is concern for the corrosive and toxic characteristics of sea water and also for sanitation, which may be aggravated by domestic and industrial wastes dumped into the sea.

Thousands of fishing, military, and commercial vessels of many types make use of coastal harbors and bays every month. Many such vessels make extensive use of sea water for cooling and flushing purposes. As one of the major U. S. Naval harbors on the West Coast, the floating population on San Diego Bay alone often exceeds 25,000 persons. Many more people use beaches, bays, and coastal waters for boating, bathing, fishing, clamming, skin-diving, surfboarding, aquaplaning, and other recreational pursuits.

Some people place the premium upon aesthetic values, --the sense of satisfaction derived from seeing and smelling good, clean, blue sea water. It seems, though, that part of the price one must pay for the privilege of living on the coast is having nearby waters discolored as a result of so many people being there. The health and economy of the community must be protected.

PUBLIC HEALTH ASPECTS OF PROBLEM

The California State Water Pollution Control Board recommends that the density of coliform bacteria shall not exceed 10 per ml. in excess of 20 percent of the samples taken along recreational beaches. The maximum allowable limit is 100 per ml. beyond the 1500-ft. line, exclusive of certain defined areas near the sludge or effluent outlets, which for most sanitary districts are located several thousand feet from shore (Figure 1).

Most of the time the concentration of coliform bacteria is well below the prescribed limits. Occasionally, however, mechanical failures or a combination of adverse meteorological, hydrographic, and hydrodynamic conditions have resulted in excessive concentrations of coliform bacteria on beaches in the surf zone. In some cases the affected beach areas have been quarantined, or the effluent has been chlorinated to safeguard human health. Considerable oceanographic, bacteriological, and engineering research work has been directed towards trying to find ways of precluding possibilities of even temporary pollution of coastal areas (California State, 1943; Hartmen, 1956; Gunnerson, 1958; Rittenberg, 1956; Rittenberg, et al., 1958).

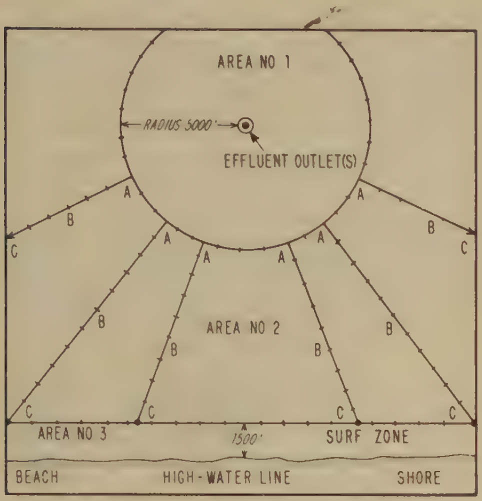

Figure 1. MPN of coliform bacteria shall not exceed 10 per ml. in any three consecutive samples or in more than 20% of any 20 consecutive samples in Area No. 3 (shoreline stations); 100 per ml. for Area No. 2 (samples taken along 8 "B" and "C" traverses).

SURVIVAL OF COLIFORM BACTERIA IN THE SEA

An important desideratum is the natural occurrence and fate of coliform bacteria in the sea. During the last two decades we have collected for bacterial analyses several thousand samples of sea water, bottom deposits, and plankton hauls from the Pacific Ocean. The production of acid and gas in lactose broth was taken as presumptive evidence for the presence of coliform bacteria, as outlined by Standard Methods (A. P. H. A., 1955). Positive cultures were enriched in brilliant green lactose broth and confirmed on eosin methylene blue agar. From finding few or no coliform bacteria in marine materials collected at places remote from possibilities of terrigenous or human contamination, it appears that Escherichia coli and allied enteric forms are not normally marine. This conclusion is based upon observations as follows:

Total tests	Kind of marine material examined	Total number positive		
		0.1 ml.	1.0 ml.	10 ml.
1,468	Sea water collected from open ocean	3	12	43
585	Bottom deposits from open ocean stations . .	0	5	40
114	Plankton hauls from open ocean	0	0	3
630	Intestinal contents of marine fish	42	206	474
9	Intestinal contents of marine mammals . . .	0	2	4
61	Intestinal contents of marine birds	11	21	39
3,850	Sea water collected near shore	248	693	1,388
968	Bottom deposits from near shore areas	36	83	260
114	Shellfish collected from near shore areas	9	25	82

Less than 1 percent of the samples of open ocean materials gave positive presumptive tests; the presence of E. coli was confirmed in none. That such enteric bacteria do occur in marine materials, though, is indicated by positive results with numerous samples from fish, sea lions, and shellfish as well as sea water and bottom deposits collected near shore. Only 9 percent of the lactose-fermenting enrichment cultures from the intestinal contents of marine animals were found to contain E. coli, approximately 75 percent of the gas-producers being Aerogenes species. The circumstances suggest that E. coli is not normally an inhabitant of the gut of marine fish, sea lions, or sea gulls. Those having appreciable numbers of coliform bacteria may have been feeding recently in polluted waters. The period of time that E. coli and allied enteric organisms may remain viable in the gut of marine animals has yet to be determined.

Coliform bacteria concentrations as high as 10^3 to 10^5 per ml of water or mud have been found in the vicinity of certain ocean outfalls. Rittenberg et al., (1958) found coliform bacteria as follows around three marine sewage outfalls:

Location of Outfall	Total samples	Number positive	Range of MPN coliforms/cm^2
Orange County . .	100	83	nil to 25,000
White's Point . . .	106	72	nil to 92,000
Santa Monica Bay	109	9	nil to 250

Although such concentrations occur mostly within a radius of a few thousand feet of the sewage effluent or sludge outlets, large numbers of coliform bacteria have been found in water as well as in bottom deposits 5 to 10 miles from the nearest outlet.

In view of the vast numbers of coliform bacterial discharged into the sea with domestic sewage, it is hardly surprising to find such bacteria in the vicinity of boat harbors and sewage outfalls. California sewage contributes an estimated 2 x 10^{18} coliform bacteria per day. If evenly distributed in all offshore water on the continental shelf to a depth of 100 meters, this would create a coliform concentration of approximately 50 per ml. Such bacteria are found, though, only within a radius of a few miles of place where they were introduced. Their paucity or absence from remote regions is indicative of the relatively rapid rate at which coliform bacteria disappear from the sea.

The survival of coliform bacteria in the sea is influenced by a multiplicity of interrelated factors (Beard and Meadowcroft, 1935; Greenberg, 1956; Nusbaum and Garver, 1955; Orlob, 1956; Vaccaro et al., 1950; Weiss, 1951; ZoBell, 1936; 1946). While laboratory investigations on the effects of salinity or mineral content, kind and concentration of organic matter, temperature, age, and abundance of coliform bacteria in sea water suggest a T-90 ranging from 10 to 100 hours, field observations indicate a much more rapid disappearance. This is probably because sedimentation, dilution, flocculation, aggregation, adsorption, predation, antibiosis, antagonism, phage, sunlight, and other mechanisms, ordinarily not operative in test tube experiments, contribute substantially to the disappearance of coliform bacteria in the sea (Figure 2). The T-90, or time required for a 90 percent reduction in the MPN of coliform bacteria, ranges from 2 to 20 hours in the sea near different outfalls; the average range being 3 to 8 hours.

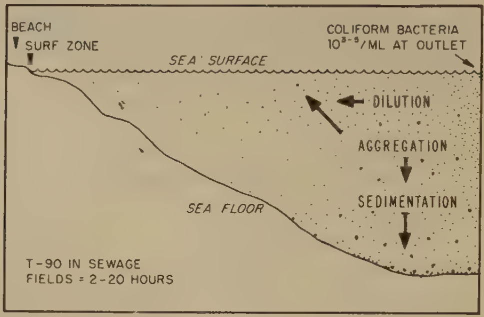

Figure 2. Dilution, aggregation, sedimentation, and predation are believed to be most important factors responsible for decrease in the MPN of coliform bacteria around outlets of sewage outfalls in the sea where average T-90 values range from 2-20 hours, as compared with average T-90 values of 10-100 in sea water under laboratory conditions. Buoyant aggregates may float to surface of sea and be washed ashore.

By following the shoreward movement of sewage fields with dye patches and with radioactive tracers (scandium-46) while determining the MPN of coliform bacteria, Rittenberg (1956) estimated the average T-90 for Hyperion primary effluent in Santa Monica Bay to be about 3 hours for the first few hours after discharge. This value is in good agreement with a T-90 value of 3.4 hours reported by Gunnerson (1958), who found a T-90 of 6.5 hours for Hyperion secondary effluent. Nine hours after discharge of the sewage, the T-90 increased to about 15 hours. This sharp increase may be a reflection of the greater resistance of bacteria that had already survived in the sea for several hours, or it may be an anomaly in the surf zone caused either by disaggregation of bacterial clumps or by the more rapid movement of bacteria shoreward in the surface film of water.

The rather rapid initial decrease in concentration of coliform bacteria after being discharged into the sea is believed to be attributable primarily to dilution, sedimentation, and aggregation or flocculation. Needed is more information on the fate of such bacteria in sediments and aggregates. Do the majority of bacteria in aggregates or clumps die off rapidly or may they be protected long enough to wash ashore to be disaggregated or broken apart in the surf zone, where viable enteric organisms may be of public health significance?

The occurrence and disaggregation of clumps of coliform bacteria in sea water has been demonstrated by laboratory experiments. For example, treating mixtures of sewage and sea water with 10 p.p.m. Tween 80, a dispersing agent, resulted in MPN's that were from 1.7 to 3.9 times higher than untreated controls. Similarly, 10 seconds' treatment in a Waring blendor increased the MPN's of such mixtures by as much as fourfold after different periods of storage. Prolonged agitation, as in the Waring blendor, or prolonged treatment with dispersing agents decreased the MPN's, ostensibly because dispersed cells are more vulnerable to adversity than those in clumps or aggregates.

There is some evidence that the bacterial population in the surface film of water may be considerably larger per unit volume than in the underlying water. Technical difficulties of skimming off surface film for analysis have hampered attempts to obtain accurate estimates. The surface film is the uppermost one-millionth to one-tenth of an inch (Ewing, 1950). Certain bacteria appear to be concentrated in the surface film of water (1) by its surface tension, (2) by the low specific gravity of the bacteria, and (3) by the buoyancy of lipids or gases with which the bacteria are associated. Horrer (1956) gives four reasons why the surface film may be of public health importance:

(1) Bacteria tend to concentrate there.

(2) The film moves with the wind at speeds in excess of measured ocean currents.

(3) Internal waves, wind, and currents cause horizontal compaction (and thus concentration) of materials in the surface film.

(4) Dispersion or diffusion of these surface film materials in the underlying water appear to be surprisingly small.

ECONOMIC ASPECTS OF POLLUTION

Much more controversial than standards of sanitation required to safeguard human health are the effects of sewage on marine resources; aesthetic values in particular. Small quantities of sewage, properly dispersed in the sea, may actually be beneficial for marine plants and animals of economic significance. Excessive amounts may adversely affect food chains, seaweeds, fin fish, shellfish, and other animals in localized areas. The discoloration of water, the appearance of floating solids or debris of sewage origin in the water or on beaches, the presence of grease or oil slicks, and the occurrence of offensive odors constitute nuisances or unaesthetic conditions. Those charged with the responsibility of disposing of sewage attempt to minimize objectionable conditions by adequate sewage treatment (screening, skimming, settling, holding, etc.) and by discharging the effluent or sludge as far from beaches and as dispersed as is economically practical.

Offensive odors and unsightly objects in the water or on beaches have been largely eliminated in most sanitation districts. More troublesome is discoloration of water. Experiences at Hyperion indicate that adequate treatment of sewage and discharging the sludge in submarine outfalls can minimize turbidity. Nutrient-rich effluents may not initiate plankton blooms (Stephenson and Grady, 1956), but they may promote the growth of plankton. Greatly increased numbers of phytoplankton at certain times of the year increase the turbidity of water and decrease its transparency within a radius of a few miles of certain sewage outfalls in the southern California area.

Although neither the mechanism nor the extent of injury has been established, there is some evidence to suggest that kelp beds (Macrocystis pyrifera) of commercial importance may have been adversely affected by discharged wastes. Several different postulates have been advanced to account for the damage: (1) Increased turbidity may restrict the development of young kelp plants on the sea floor at depths of 30 to 90 feet below the water surface. (2) Either reduced oxygen tension of slime formation at the mud-water interface may inhibit the development of kelp sporophytes. (3) Detergents or other toxic ingredients in sewage may be harmful to kelp. (4) Organic substances in sewage may render the seaweeds more vulnerable to invasion by infectious microbes.

There is no direct evidence for adverse effects of sewage on fish in the vicinity of ocean outfalls, despite claims to the contrary by adversaries of sewage disposal at sea. Certain bottom-dwelling forms, including flatfish, abalone, and crabs, seem to have disappeared in places, but it has not been ascertained whether pollution, overfishing, or other factors have been responsible. Nevertheless, most citizens view with considerable concern what effect the continued discharge of increasing amounts of domestic and industrial wastes may have on aquatic life. Hartman (1956) has indicated some of the changes in size, abundance, and kinds of species of bottom fauna that occur in the neighborhood of the Hyperion outfall.

Underway are various long-range programs designed to obtain information that may be useful in assessing the effects of pollution on marine resources and the affairs of man along the coast of southern California. The "monitoring" programs in the vicinity of certain sewage outfalls include frequent determinations of (1) the MPN of coliform bacteria in water and in bottom sediments, (2) dissolved oxygen, (3) transparency, (4) plankton population, (5) grease and oil, (6) salinity, (7) temperature, and (8) bottom fauna. Additionally, an extensive survey is being conducted to determine the numbers and kinds of marine organisms inhabiting coastal waters in areas as yet unaffected by discharged wastes. One research project is concerned specifically with the effects of such wastes on seaweeds.

REFERENCES

American Public Health Association. 1955. Standard Methods for the Examination of Water, Sewage, and Industrial Wastes. A. P. H. A., Inc., New York, 522 pp.

Brooks, N. H. 1952. Some ocean outfall studies. Los Angeles County Sanitation Districts, Sept., 55 pp.

California State Bureau of Sanitary Engineering. 1943. Report on a pollution survey of Santa Monica Bay beaches in 1942. Calif. State Printing Office, Sacramento, 69 pp.

California State Department of Public Works. 1952. Reclamation of water from sewage and industrial wastes. Calif. State Dept. Pub. Works Publ., Sacramento, 63 pp.

Ewing, G. 1950. Slicks, surface films and internal waves. Jour. Mar. Res., 9: 161-187.

Garber, W.F. 1956. Bacteriological standards for bathing waters. Sew. & Ind. Wastes, 28: 795-808.

Greenberg, A. E. 1956. Survival of enteric organisms in sea water. Public Health Reports, 71: 77-86.

Gunnerson, C. G. 1958. Sewage disposal in Santa Monica Bay, California. Jour. San. Eng. Div. Proc. Amer. Soc. Civil Eng., 84 (SA 1): Paper 1534, 28 pp.

Harris, E.K. 1958. On the probability of survival of bacteria in sea water. Biometrics, 14: 195-206.

Hartman, Olga. 1956. Contributions to a biological survey of Santa Monica Bay, California. Final report submitted to Hyperion Engineers, Inc. by the Geol. Dept., Univ. Southern Calif., Sept., 161 pp.

Handerson, W. L. and Nelson, L. M. 1957. Bacterial studies related to disposal of sewage through ocean outfalls. Progress Rept. from Orange County Sanitation Districts, Santa Ana, Calif., 37 pp.

Horrer, P.L. 1956. Sewage in Santa Monica Bay: A critical review of the oceanographic studies. Marine Advisors, P. O. Box 1001, La Jolla, Calif., 95 pp.

Johannesson, J.K. and Martin, R. E. 1957. The determination of Escherichia coli I in sea water. Jour. Appl. Bact., 20: 151-157.

Ketchum, B. H., Ayers, J. C., and Vaccaro, R. F. 1952. Processes contributing to the decrease of coliform bacteria in a tidal estuary. Ecology, 33: 247-258.

McKee, J. E. 1952. Water quality criteria. Calif. State Water Pollution Control Board, Publ. 3, Sacramento, 512 pp.

Moore, B. 1954. Sewage contamination of coastal bathing waters. Bull. Hygiene, 29: 689-704.

Nusbaum, I. and Garver, R. M. 1955. Survival of coliform organisms in Pacific Ocean coastal waters. Sew. & Ind. Wastes, 27: 1383-1390.

Nusbaum, I. and Miller, H.E. 1952. The oxygen resources of San Diego Bay. Sew. & Ind. Wastes, 24: 1512-1527.

Orlob, G. T. 1956. Evaluating bacterial contamination in sea water samples. Public Health Reports, 71: 1246-1252.

Orlob, G. T. 1956. Viability of sewage bacteria in sea water. Sew. & Ind. Wastes, 28: 1147-1167.

Pearson, E. A. 1956. An investigation of the efficacy of submarine outfall disposal of sewage and sludge. Calif. State Water Pollution Control Board, Publ. 14, Sacramento, 154 pp.

Rawn, A. M. and Bacon, V. W. 1957. Organization and accomplishments of the California water pollution control system. Sewage & Indus. Wastes, 29: 201-209.

Rawn, A.M., Caldwell, D. H., and Hyde C.G. 1952. Report on the collection, treatment and disposal of the sewage of San Diego County. S. D. County Sewerage Survey, San Diego, Calif., 515 pp.

Rittenberg, S. C. 1956. Studies on coliform bacteria discharged from the Hyperion outfall. Final report submitted to Hyperion Engineers, Inc., by the Geol. Dept., Univ. Southern Calif., Sept., 51 pp.

Rittenberg, S. C., Mittwer, T., and Ivler, D. 1958. Coliform bacteria in sediments around three marine sewage outfalls. Limnol. & Oceanogr., 3: 101-108.

Rosenfeld, W.D., and ZoBell, C. E. 1947. Antibiotic production by marine microorganisms. J. Bact., 54: 393-398.

San Diego Regional Water Pollution Control Board. 1952. Report upon the extent, effects and limitations of waste disposal into San Diego Bay. State of California, San Diego, Calif., 95 pp.

Stevenson, R. E., and Grady, J. R. 1956. Plankton and associated nutrients in the waters surrounding three sewer outfalls in Southern California. Univ. Southern Calif., Allan Hancock Foundation Report, 18 Sept., 48 pp.

Theroux, R. J. 1957. Enlarged sewage disposal facilities for Los Angeles. Sew. & Indus. Wastes, 29: 124-133.

Terry, R. D. 1956. An annoted bibliography on bacteriology, oceanography, and Marine Geology as they relate to the disposal of waste material into the sea. Allan Hancock Foundation, Univ. Southern Calif., 112 pp.

Vaccaro, R.F., Briggs, M.O., Carey, C.L., and Ketchum, B. H. 1950. Viability of Escherichia coli in sea water. Amer. Jour. Pub. Health, 40: 1257-1266.

Warren, A.K. and Rawn, A. M. 1938. Disposal of sewage into the Pacific Ocean. Ch. 18 in Modern Sewage Disposal, Fed. Sew. Works Assoc., New York, pp. 202-208.

Weiss, C. M. 1951. Adsorption of E. coli on river and estuarine silts. Sew. & Ind. Wastes, 23: 227-237.

ZoBell, C. E. 1936. Bactericidal action of sea water. Proc. Soc. Exper. Biol. & Med., 34: 113-116.

ZoBell, C. E. 1946. Marine Microbiology. Chronica Botanica Co., Waltham, Mass., 240 pp.

ZoBell, C.E. 1958. Occurrence and fate of coliform bacteria in the sea. Proc. I Congreso Latinoamericano, Mexico, D. F., pp. 58-68.

SOUND SPEED AND ABSORPTION STUDIES OF MARINE SEDIMENTS BY A RESONANCE METHOD—PARTS I AND II

BY

GEORGE SHUMWAY

Reprinted for private circulation from
Geophysics
Vol. XXV, Nos. 2 and 3, April and June, 1960

(653)

GEOPHYSICS, VOL. XXV, NO. 2 (APRIL, 1960), PP. 451-467

SOUND SPEED AND ABSORPTION STUDIES OF MARINE SEDIMENTS BY A RESONANCE METHOD*

PART I

GEORGE SHUMWAY†

ABSTRACT

Laboratory measurements of compressional sound speed, and absorption, have been made on 111 unconsolidated marine sediment samples, ranging from shallow water sands to deep-sea clays. In addition, determinations were made of porosity, wet density, and grain size distributions. Frequencies between 20 kc/sec and 37 kc/sec were used for the acoustic studies.

Sound speed values at room temperature range from 1.474 km/sec for a red medium clay to 1.785 km/sec for a medium sand. More than one-third of the values are lower than the value for sea water alone. Variations in the speed of sound in unconsolidated sediments as found in nature are caused by the following factors, in order of importance: (1) porosity, because of the great difference in compressibility of water and mineral grains; (2) the factor which produces rigidity, which appears to be related to the abundance of coarse grains; (3) pressure; (4) temperature; (5) compressibility of the grain aggregate, determined from compressibilities of individual minerals.

Sound absorption measurements ranged from 0.5 db/m for a medium clay (28.4 kc/sec) to about 20 db/m for silts and fine sands (between 30 and 37 kc/sec). An absorption maximum occurs for sediments of intermediate porosity (0.45–0.6) and intermediate grain size (0.031 mm–0.25 mm). The expression $\alpha = MA_s$, where α is the linear absorption coefficient, M is a frequency-dependent factor related to the sediment volume fraction of grains in mutual contact, and A_s is a computable total acoustically effective grain surface area, predicts the absorption values and the absorption maximum.

Absorption measurements at more than one frequency between 20 kc/sec and 37 kc/sec were obtained for 65 samples. Assuming that absorption is directly proportional to frequency raised to a power n, the data yield an average value of n equal to 1.79, with a standard deviation of 0.98.

INTRODUCTION

The general sediment, as found in nature, is a mixture of water, ions, colloidal particles, and mineral grains. Many particles, particularly those of clay and silt size, essentially are in suspension, while others, particularly those of sand size, are in contact with one another. Each particle has an irregular shape. Although certain minerals predominate in sediments, each sediment sample has a unique mineral grain composition. The acoustic properties of sediments are determined by such properties as these, and any general theory for acoustic wave propagation in sediment-like mixtures must account for these variables in one way or another. Experimental data concerning the acoustic properties of sediments and their relations to other physical properties are not abundant. The difficulties of developing useful acoustic theory for sediments make it necessary to have an ample body of experimental data at hand for checking and guiding the theoretical developments.

This study presents compressional sound speed and sound absorption data for 111 unconsolidated marine sediment samples, ranging from shallow-water

---

* This paper is a portion of a doctoral dissertation with the same title submitted to the University of California at La Jolla (1958). Manuscript received by the Editor May 14, 1959.

† U. S. Navy Electronics Laboratory, San Diego 52, California.

Contributions from the Scripps Institution of Oceanography, New Series, 1184

Reproduced by Permission

sands to deep-sea clays. This suite includes most of the common marine sediment types, hence these measurements provide the general range of values to be expected for sea floor sediments. Measurments of porosity and wet density were made also, and grain size distributions were determined.

Previously published studies of a similar nature have not involved such a large and varied group of sediments. Hamilton et al. (1956) in a study preliminary to the present one, measured sound velocity and absorption in a group of shallow-water sediments from the region of San Diego. Sutton et al. (1957) measured sound velocity and certain other physical properties in samples from 26 cores taken in the Atlantic Ocean from water depths between 840 m and 4,780 m. Only a few of their samples had median diameters in the sand range, and all of these were oozes with calcium carbonate contents higher than 85 percent. Sound velocities, and rarely, sound absorptions, have been measured in smaller groups of sediments by a number of workers. Mifsud (1953) made acoustic studies on sands in a laboratory tank. Paterson (1955, 1956) reported sound velocities for porous sands measured in the laboratory. Laughton (1954, 1955, 1957) studied the effects of hydrostatic pressure and compacting pressure on compressional velocity in a few ocean sediments. Busby and Richardson (1957) published some sound absorption data for water-filled sands.

MEASUREMENT METHODS

Sound speed and sound absorption were measured by a resonance technique: for a non-rigid, compliant-walled cylinder, resonant frequency is directly proportional to sound speed, and mechanical Q is inversely proportional to the linear absorption coefficient. Sediment samples were driven to resonance at frequencies between 20 kc/sec and 37 kc/sec while held in thin-walled cylindrical plastic (Lucite) containers 5.08 cm in diameter and 12.7 cm long with a wall thickness of about 0.89 mm. The sound speed measurements are considered accurate to ±10 m/sec in low-loss sediments (clays and fine silts), and to ±15 m/sec for other sediments. Measurements on a given sample are reproducible to within 1 m/sec. Pertinent theory for this resonant technique was developed by W. J. Toulis (1956). A description of the technique of measurement and an evaluation of the accuracy to be expected was given in an accompanying paper (Shumway, 1956).

Immediately after completion of the resonance measurements on a sample, the sample temperature was determined. Then the following steps were taken. The mass of wet sediment in the container and the container volume were determined, and from these wet density was obtained. On some samples the static shear strength was measured by D. G. Moore using his published technique (in press), with the sediment still in the container. Then the sediment was removed and placed in an oven at a temperature between 105°C. and 110°C. until water loss ceased. From the mass of water lost the sediment porosity was calculated. Lastly, standard methods were used to determine the grain size distribution: sieve for coarser sands; settling tube (Poole, 1957) for materials of intermediate size; pipette for the finest materials. Cumulative frequency tables for grain size distributions for all of the samples are presented in the dissertation of which this study is a part (Shumway, 1958), so for the sake of brevity need not be included here.

SEDIMENTS

Sampling techniques

The acoustic measurements were made with the sample held in thin-walled cylindrical plastic containers. In shallow water, these containers were taken to the sea floor by SCUBA diving, and filled with sediment by gently pushing them into the bottom (Shumway, 1956, p. 309). In deeper water, sediments first were obtained by coring or dredging, and then the plastic containers filled from this material.

Diver sampling was done for water depths less than about 45 m. In addition to the fact that diver-sampling allows the sample to be initially collected in the plastic container, it is advantageous because the diver may pick a representative location for the sampling. Often considerable variation in sediment composition is found on the sea floor within a meter laterally, and within even a few centimeters vertically. In many such places on the continental shelves, and in harbors, a randomly taken core or grab sample could misrepresent completely the general environment.

Shallow-water (harbor and shelf) sediments

The shallow waters of San Diego Bay and the adjacent continental shelf were readily available for sampling and for direct observation by diving, hence a large number of samples were taken there. The term "shallow-water" as used here means water shallow enough for diving, i.e. less than about 45 m.

In the preliminary studies reported by Hamilton et al. (1956), 33 shallow-water stations were made and a total of 67 individual samples were studied. An entirely new series of stations was made to provide samples for the present study. Twenty-six new shallow-water stations were made, with two samples generally being taken at each station, to give a total of 55 new shallow-water samples. A chart showing the location of the shallow-water samples from the San Diego area is kept on file by the Navy Electronics Laboratory and does not appear here for reasons of military security. The geologic nature of sediments of the San Diego region has been studied by Emery et al. (1952).

In Table Ia these samples are identified by a prefix of SD (denoting San Diego area) and PC (denoting Panama City, Florida), a station number, and a lower case letter to distinguish samples taken at the same station.

Intermediate depth (continental shelf, slope, and borderland) sediments

Several suites of samples were obtained from waters of intermediate depth. One group of six samples came from the continental slope east of Point Barrow,

(*Text continued on page 464*)

Table Ia. Acoustic, Geologic, and Physical Properties of Shallow-Water Sediments
(Bay and shelf to 50 meter depth)

Sample Number	Sediment Type	Median Diameter Phi (mm)	Mean Diameter Phi	Phi Deviation Measure	Wet Density	Porosity	Sound Speed, km/sec (Temp. ° C.)	Sound Absorption, db/ft at c/s		Acoustic Surface Area, m²/g wet sed.
SD35a	sandy coarse silt	4.20 (.054)	5.16	1.90	1.60	.645	1.496 (19.0°)	1.779 3.692	23,051 30,439	.0434
SD35b	sandy coarse silt	4.10 (.058)	4.93	1.68	1.65	.605	1.512 (18.9°)	1.667 3.708	23,038 30,612	.0409
SD35c	sandy coarse silt	4.10 (.058)	5.00	1.75	1.67	.579	1.512 (19.1°)	2.614 3.897	23,360 30,792	.0437
SD36a	clayey sandy coarse silt	4.45 (.046)	5.98	2.28	1.56	.663	1.490 (19.2°)	2.004 4.036	23,012 30,461	.0403
SD36b	sandy coarse silt	4.45 (.046)	5.83	2.02	1.64	.696	1.526 (19.5°)	1.559 3.516	23,038 30,558	.0388
SD37a	medium sand	1.95 (.259)	1.72	0.75	1.96	.417	1.678 (23.6°)	3.60	25,807	.0146
SD27b	medium sand	2.00 (.250)	1.89	0.62	1.94	.432	1.785 (23.4°)	5.72	31,406	.0162
SD38a	medium sand	1.82 (.284)	1.65	0.91	1.99	.391	1.710 (22.4°)	4.23	26,076	.0129
SD38b	medium sand	1.30 (.407)	0.97	0.96	2.00	.393	1.725 (23.4°)	3.19	26,470	.0103
SD39a	fine sand	2.50 (.176)	2.42	0.46	1.96	.429	1.700 (22.2°)	2.79	26,049	.0187
SD39b	fine sand	2.12 (.230)	1.90	0.22	1.95	.481	1.695 (23.4°)	2.73	25,975	.0120
SD40a	coarse silt	4.25 (.053)	5.14	1.99	1.64	.630	1.510 (21.0°)	2.922 3.873	23,286 31,205	.0416

SD40b	coarse silt	4.20 (.054)	5.23	1.89	1.62	.604	1.514 (21.0°)	2.202 3.811	23,214 30,965	.0445
SD41a	medium sand	1.64 (.320)	1.31	1.07	1.995	.388	1.735 (22.0°)	4.17 2.90	23,435 26,443	.0107
SD41b	medium sand	1.75 (.298)	1.55	0.87	1.99	.362	1.712 (22.0°)	3.65 3.04	23,335 26,218	.0120
SD42a	fine sand	2.92 (.132)	3.37	1.20	1.82	.493	1.548 (19.8°)	6.81	31,445	.0352
SD42b	very fine sand	3.14 (.114)	3.65	1.40	1.81	.498	1.550 (20.6°)	6.38	31,576	.0396
SD43a	fine sand	2.27 (.208)	2.29	0.33	1.95	.424	1.691 (22.8°)	2.75 2.63	23,342 25,987	.0169
SD43b	fine sand	2.27 (.208)	2.30	0.27	1.94	.429	1.696 (22.9°)	2.51 2.78	23,257 26,013	.0170
SD44a	medium sand	1.24 (.425)	1.13	0.82	2.02	.383	1.748 (22.1°)	2.60 3.41	26,851 36,077	.0090
SD44b	medium sand	1.78 (.290)	1.69	0.51	2.03	.397	1.748 (22.6°)	3.16 4.55	26,949 36,546	.0117
SD45a	fine sand	2.75 (.148)	2.77	0.20	1.92	.454	1.68 (21.4°)	4.07	29,227	.0219
SD45b	fine sand	2.71 (.153)	2.75	0.20	1.92	.458	1.67 (21.8°)	3.88	29,338	.0213
SD46a	medium silt	5.48 (.0225)	6.63	2.42	1.42	.745	1.484 (20.3°)	2.63	30,179	.0462
SD46b	medium silt	4.99 (.031)	5.96	3.74	1.44	.724	1.492 (20.9°)	3.52	30,403	.0467
SD47a	sandy coarse silt	4.03 (.061)	4.74	1.91	1.69	.578	1.530 (21.5°)	3.04 4.16	23,457 31,070	.0424
SD47b	sandy coarse silt	3.98 (.063)	4.68	1.86	1.70	.577	1.525 (21.5°)	3.59 4.51	23,449 31,061	.0417

(Continued)

TABLE Ia. (*Continued*)

Sample Number	Sediment Type	Median Diameter Phi (mm)	Mean Diameter Phi	Phi Deviation Measure	Wet Density	Porosity	Sound Speed, km/sec (Temp. ° C.)	Sound Absorption, db/ft at c/s		Acoustic Surface Area, m²/g wet sed.
SD48a	fine sand	2.22 (.215)	2.25	0.37	1.96	.422	1.722 (22.6°)	3.04 2.73	23,362 26,263	.0164
SD48b	fine sand	2.22 (.215)	2.25	0.29	1.97	.414	1.702 (22.7°)	2.99 2.67	23,371 26,175	.0165
SD49a	medium sand	1.82 (.284)	1.78	0.64	1.99	.402	1.742 (22.6°)	3.93 2.66	23,573 26,515	.0148
SD49b	medium sand	1.98 (.254)	2.02	0.67	1.99	.357	1.725 (22.2°)	2.66	26,547	.0164
SD50a	very fine sand	3.05 (.121)	3.74	1.68	1.82	.519	1.540 (22.8°)	4.22 4.72	27,934 31,242	.0334
SD50b	fine sand	2.68 (.156)	3.15	1.39	1.80	.526	1.550 (22.6°)	6.27 7.28 5.89	23,943 27,153 31,194	.0307
SD51a	sandy coarse silt	4.05 (.060)	5.46	2.43	1.65	.600	1.521 (20.7°)	2.58 2.35 3.88	23,344 26,831 31,057	.0385
SD51b	sandy coarse silt	3.96 (.064)	5.29	2.17	1.69	.561	1.525 (21.0°)	2.47 3.21 5.24	23,350 27.002 31,045	.0436
SD52a	medium sand	1.13 (.458)	1.10	0.50	2.05	.379	1.766 (22.6°)	2.51	27,048	.0082
SD52b	medium sand	1.27 (.415)	1.05	0.57	2.05	.376	1.756 (22.9°)	2.44	27,032	.0086
SD53a	medium sand	1.28 (.413)	1.25	0.55	2.00	.387	1.760 (22.5°)	2.00	27,013	.0096

SD53b	medium sand	1.17 (.466)	1.25	0.62	2.00	.394	1.760 (22.6°)	1.99 2.71	26,925 36,177	.0083
SD54a	fine sand	2.62 (.163)	2.48	0.38	1.88	.482	1.770 (20.3°)	4.5	31,192	.0181
SD54b	fine sand	2.62 (.163)	2.48	0.39	1.89	.479	1.773 (20.7°)	4.43	31,239	.0181
SD55a	fine sand	2.72 (.152)	2.71	0.35	1.96	.426	1.680 (23.4°)	3.05 4.01	25,853 29,603	.0235
SD55b	fine sand	2.68 (.157)	2.64	0.33	1.97	.426	1.685 (22.0°)	2.88 3.91	25,885 29,751	.0223
SD55c	fine sand	2.68 (.157)	2.64	0.32	1.95	.432	1.686 (23.8°)	2.65 2.86 3.88	23,219 25,885 29,719	.0220
SD55d	fine sand	2.72 (.152)	2.70	0.31	1.96	.432	1.685 (22.2°)	2.91 3.74	25,876 29,681	.0229
SD55e	fine sand	2.74 (.150)	2.67	0.32	1.98	.427	1.693 (24.7°)	3.59	26,090	.0223
SD55f	fine sand	2.72 (.152)	2.65	0.35	1.98	.427	1.684 (24.3°)	2.22 3.03 4.20	23,078 25,899 29,914	.0227
SD56a	fine sand	2.02 (.247)	2.76	1.49	1.95	.426	1.685 (23.5°)	5.0	29,678	.0300
SD56b	fine sand	2.34 (.197)	2.97	1.13	1.96	.431	1.684 (19.8°)	3.37 5.24	25,881 29,784	.0296
PC1	fine sand	2.12 (.230)	2.11	0.39	1.93	.440	1.735 (25.8°)	6.31 4.90	26,650 31,044	
PC2	fine sand	2.28 (.206)	2.16	0.34	1.92	.445	1.745 (25.25°)	6.33	26,786	
PC3	fine sand	2.20 (.218)	2.19	0.30	1.95	.424	1.725 (25.2°)	7.64 8.00	26,540 30,799	

(Continued)

TABLE Ia. (*Concluded*)

Sample Number	Sediment Type	Median Diameter Phi (mm)	Mean Diameter Phi	Phi Deviation Measure	Wet Density	Porosity	Sound Speed, km/sec (Temp. ° C.)	Sound Absorption, db/ft at c/s		Acoustic Surface Area, m²/g wet sed.
PC5a	fine sand	2.25 (.210)	2.19	0.44	1.98	.397	1.715 (22.6°)	2.83 2.83	26,364 30,448	.0168
PC5b	fine sand	2.12 (.230)	2.11	0.29	1.99	.399	1.725 (23.8°)	2.55 2.82	26,485 30,560	.0158
PC5c	fine sand	2.12 (.230)	2.10	0.35	1.996	.397	1.731 (23.8°)	2.54 2.79	26,549 30,525	.0150

TABLE Ib. ACOUSTIC, GEOLOGIC, AND PHYSICAL PROPERTIES OF SEDIMENTS FROM INTERMEDIATE DEPTH

(Continental shelf, continental slope, continental borderland)

Sample Number	Sediment Type	Median Diameter Phi (mm)	Mean Diameter Phi	Phi Deviation Measure	Wet Density g/cm³	Porosity	Sound Speed, km/s (Temp. ° C.)	Sound Absorption, db/ft at c/s		Acoustic Surface Area, m²/g wet sed.	Water Depth, meters	Location, N. Lat. W. Long.
				CONTINENTAL SLOPE, ARCTIC OCEAN								
AO8	Clayey medium silt	5.8 (.0173)	6.83	2.85	1.67	.604	1.551 (26.4°)	2.193 1.668	23,263 31,030	.0604	174	71°09′ 150°24′
AO7	clayey fine silt	6.4 (.0114)	6.95	2.82	1.55	.671	1.521 (26.8°)	2.413 1.91	23,802 27,125	.0560	232	71°08′ 150°24′
AO6	clayey very fine silt	7.4 (.0058)	7.5	2.6	1.41	.764	1.493 (26.8°)	0.608 0.956	22,796 30,313	.0404	439	71°10′ 150°24′
AO5	silty coarse clay	8.05 (.0038)	8.35	2.4	1.32	.812	1.491 (25.7°)	0.435 0.401 1·315	20,500 22,768 30,225	.0327	1,024	71°11′ 149°54′

AO3	silty coarse clay	8.7 (.0025)	7.10	2.7	1.305	.826	1.486 (25.0°)	0.201 0.560 0.918	20,395 22,766 30,300	.0282	2,203	71°29′ 149°39′
AO2	silty medium clay	9.06 (.0019)	9.75	2.1	1.306	.834	1.486 (26.2°)	0.649 0.582 0.644	20,496 22,714 30,185	.0226	2,780	71°46′ 148°41′
					PIGEON POINT SHELF							
PP7	coarse silt	4.9 (.033)	5.78	1.35	1.63	.646	1.676 (26.2°)	1.722 2.923 4.491	21,099 25,832 34,020	.0364	77	37°07′ 122°28′
PP6	coarse silt	4.9 (.033)	5.56	1.06	1.68	.604	1.559 (27.4°)	2.77	27,283	.0475	88	37°05′ 122°26′
PP16	medium silt	5.0 (.031)	5.22	0.61	1.73	.550	1.526 (24.3°)	6.71	31,053	.0577	105	37°12′ 122°30′
PP2	silty very fine sand	3.9 (.067)	3.96	0.59	1.88	.464	1.756 (27.8°)	4.51	30,775	.0503	88	37°07′ 122°33′
				CONTINENTAL BORDERLAND OFF SOUTHERN CALIFORNIA								
CB1a	clayey very fine silt	7.18 (.0069)	7.27	2.25	1.39	.796	1.518 (21.75°)	1.772 2.45	23,169 30,881	.0285	1,000	for locations see Appendix
CB1b	clayey very fine silt	7.20 (.0068)	7.22	2.30	1.41	.744	1.516 (22.1°)	2.47	23,139	.0344	1,000	
CB2a	clayey very fine silt	7.20 (.0068)	7.36	2.40	1.45	.730	1.504 (22.0°)	0.625 0.846	22,916 30,518	.0371	890	
CB2b	clayey very fine silt	7.10 (.0073)	7.39	2.25	1.40	.748	1.494 (21.4°)	0.267 0.423 0.596	21,264 22,829 30,359		890	
CB3a	clayey fine silt	6.98 (.0071)	7.11	2.23	1.303	.811	1.484 (22.4°)	0.206 0.437 0.756	20,455 22,767 30,209	.0270	1,142	
CB3b	clayey very fine silt	7.50 (.0055)	8.15	2.65	1.335	.794	1.488 (22.4°)	0.190 0.318 0.732	20,437 22,750 30,225	.0268	1,142	

(*Continued*)

TABLE Ib. (*Continued*)

Sample Number	Sediment Type	Median Diameter Phi (mm)	Mean Diameter Phi	Phi Deviation Measure	Wet Density g/cm³	Porosity	Sound Speed, km/s (Temp. ° C)	Sound Absorption, db/ft at c/s	Acoustic Surface Area, m²/g wet sed.	Water Depth, meters	Location, N. Lat. W. Long.
CB3c	clayey very fine silt	7.24 (.0066)	7.73	2.35	1.346	.792	1.489 (20.5°)	0.296 20,391 0.514 22,690 0.687 30,206	.0343	1,142	
CB4a	clayey very fine silt	7.36 (.0061)	7.91	2.29	1.292	.856	1.489 (22.0°)	0.441 20,425 0.458 22,757 0.810 30,233	.0244	1,173	
CB4b	clayey very fine silt	7.20 (.0068)	7.75	2,31	1.355	.796	1.498 (21.4°)	0.217 20,414 0.378 22,753 0.544 30,249	.0404	1,173	
CB4c	clayey very fine silt	7.20 (.0068)	7.83	2.25	1.352	.785	1.499 (22.5°)	0.854 22,912 1.309 30,509	.0436	1,173	
CB5a	clayey fine silt	6.90 (.0084)	7.36	2.05	1.289	.745	1.500 (22.8°)	0.283 20,483 0.554 22,802 1.148 30,260	.0554	1,198	
CB5b	clayey very fine silt	7.10 (.0073)	7.66	2.25	1.334	.799	1.492 (23.2°)	0.295 20,504 0.591 22,847 0.914 30,334	.0399	1,198	
CB5c	clayey very fine silt	7.26 (.0065)	7.81	1.95	1.348	.782	1.495 (23.2°)	0.434 20,658 0.445 22,801 0.634 30,337	.0429	1,198	
CB6a	clayey fine silt	6.96 (.008)	7.49	2.20	1.301	.814	1.517 (22.6°)	1.01 21,256 1.90 23,122 1.03 30,712	.0375	1,218	
CB6b	clayey fine silt	7.00 (.0078)	7.68	2.36	1.345	.789	1.493 (23.7°)	0.323 20,496 0.412 22,842 0.630 30,278	.0414	1,218	
CB6c	clayey medium silt	7.45 (.0057)	7.95	2.45	1.370	.778	1.525 (23.0°)	1.009 23,428 1.200 30,746	.0416	1,218	

CB7	coarse silt	4.58 (.042)	5.34	1.20	1.729	.516	1.534 (23.8°)	2.543 3.937	23,551 31,218	.0628	132
CB8a	coarse silt	4·90 (.0425)	6.38	2.02	1.578	.663	1.510 (23.9°)	1.427 1.168	23,269 30,752	.0529	183
CB8b	clayey medium silt	5.22 (.0265)	6.66	2.30	1.590	.656	1.506 (23.9°)	0.762 1.773	23,083 30,663	.0517	183
CB8c	clayey medium silt	5.60 (.0206)	7.17	2.52	1.594	.651	1.506 (24.5°)	0.569 1.364	23,068 30,655	.0539	183
CB9a	coarse silt	4.70 (.039)	5.64	1.45	1.597	.634	1.545 (23.9°)	2.49 3.89	23,861 31.203	.0420	179
CB9b	clayey medium silt	5.40 (.024)	6.80	2.28	1.590	.659	1.512 (23.2°)	0.902 0.836 1.590	20,818 23,324 30,603	.0409	179
CB10	clayey coarse silt	4.86 (.034)	6.69	2.40	1.645	.622	1.518 (23.6°)	1.222 2.301	23,329 30,957	.0503	205
CB11a	coarse silt	4.38 (.048)	4.33	0.45	1.827	.522	1.532 (24.1°)	5.718	31,226	.0550	84
CB11b	sandy coarse silt	4.28 (.051)	4.34	0.66	1.838	.512	1.556 (24.0°)	5.203 5.364	23,958 31,240	.0554	84
CB12	sandy coarse silt	4.34 (.050)	4.35	0.50	1.816	.524	1.556 (24.0°)	5.40 5.53	24,200 31,250	.0548	84
CB13a	sandy coarse silt	4.27 (.052)	2.77	2.65	1.904	.458	1.63 (25.2°)	5.549	31,281	.0511	99
CB13b	sandy coarse silt	4.44 (.046)	2.89	2.60	1.900	.463	1.60 (25.4°)	4.975	31,264	.0506	99
CB13c	sandy coarse silt	4.44 (.046)	3.27	2.72	1.882	.481	1.60 (25.0°)	6.01 5.74	24,653 31,175	.0497	99
CB14	sandy coarse silt	4.33 (.050)	4.14	0.86	1.895	.487	1.586 (24.6°)	4.778 5.922	24,376 31,182	.0536	99

(Continued)

TABLE Ib. (*Concluded*)

Sample Number	Sediment Type	Median Diameter Phi (mm)	Mean Diameter Phi	Phi Deviation Measure	Wet Density g/cm³	Porosity	Sound Speed, km/s (Temp. ° C)	Sound Absorption, db/ft at c/s		Acoustic Surface Area, m²/g wet sed.	Water Depth, meters	Location, N. Lat. W. Long.
CB15	coarse silt	4.73 (.038)	5.57	1.66	1.747	.570	1.560 (24.7°)	1.786 1.786	21,440 23,689	.0558	137	
CB16a	sandy coarse silt	4.26 (.052)	3.68	1.00	1.800	.554	1.550 (25.4°)	4.910 5.737	23,848 31,291	.0417	137	
CB16b	sandy coarse silt	4.60 (.041)	5.62	2.60	1.779	.540	1.545 (25.1°)	4.711 5.324	23,826 31,181	.0488	137	

TABLE Ic. ACOUSTIC, GEOLOGIC, AND PHYSICAL PROPERTIES OF DEEP-SEA SEDIMENTS

Sample Number	Sediment Type	Median Diameter Phi (mm)	Mean Diameter Phi	Phi Deviation Measure	Wet Density	Porosity	Sound Speed, km/s (Temp. ° C.)	Sound Absorption db/ft at c/s		Acoustic Surface Area, m²/g wet sed.	Water Depth, meters	Location, N. Lat. W. Long.
PO1	red coarse clay	8.96 (.002)	9.06	0.93	1.446	.689	1.596±.02 (18.7°)	0.52	25.4 kc/s	.0333	5,706	27°32′ 154°06′
PO2	red very fine silt	7.16 (.007)	7.45	2.9	1.44	.710	1.60 ±.02 (20.6°)	0.70 1.37	26.3 kc/s 30.5 kc/s	.0478	4,122	21°32.8′ 157°08.8′
PO3	red coarse clay	8.38 (.003)	9.01	1.9	1.50	.743	1.52 ±.02 (19.7°)	1.29 1.99	29.8 kc/s 26.2 kc/s	.0287	4,254	23°21.5′ 156°28.7′
PO4	red coarse clay	8.96 (.002)	—	—	1.30	.804	1.52 ±.02 (24.7°)	0.31	35,660		4,208	31°51.9′ 121°30.8′
PO5	green very fine silt	7.6 (.005)	8.03	2.45	1.43	—	1.51 ±.02	0.8	24,014		3,620	35°52.5′ 123°16′

PO6b	silty medium clay	9.04 (.0019)	9.1	2.64	1.310	.823	1.540 (21.2°)	0.544 1.28 1.42	20,583 23,347 31,470	.0233	3,750	32°27′ 120°41′
PO6d	silty coarse clay	8.94 (.002)	9.0	2.70	1.319	.806	1.493 (23.7°)	0.189 0.478 0.500	20,481 22,810 30,325	.0265	3,750	32°27′ 120°41′
PO7	calcareous silty coarse clay	8.05 (.0038)	7.42	2.90	1.485	.694	1.518 (23.6°)	1.057 1.245 1.907	21,515 23,690 30,640	.0392	3,720	13°29′S* 108°33.5′
PO8	calcareous clayey very fine silt	7.60 (.0052)	7.21	2.65	1.369	.783	1.493 (23.4°)	0.958 1.103 1.265	20,388 22,764 30,269	.0328	4,610	03°42′S* 114°09′

Table Id. Acoustic, Geologic, and Physical Properties of Miscellaneous Sediments

Sample Number	Sediment Type	Median Diameter Phi (mm)	Mean Diameter Phi	Phi Deviation Measure	Wet Density g/cm³	Porosity	Sound Speed, km/s (Temp. ° C.)	Sound Absorption, db/ft at c/s		Acoustic Surface Area, m²/g wet sed.	Water Depth, meters	Location, N. Lat. W. Long.
SP1	fine sand	—	—	—	2.065	.363	1.744 (20°)	1.939 3.194	26,381 36,151	.0408	—	—
All particles between 0.25 and 0.125 mm; distilled water; from disaggregated St. Peter sandstone												
SP2	sandy coarse silt	4.56 (.046)	4.89	1.25	1.79	.623	1.540 (20°)	2.280 4.777	23,684 31,267	.0487	82	32°41′27″ 117°18′30″
SP3	calcareous sandy coarse silt	4.75 (.037)	5.87	2.95	1.57	.666	1.483 (20°)	4.996	30,240	.0411	1,700	17°07′ 117°17′
SP4	red medium clay	9.40 (.015)	9.40	1.53	1.338	.809	1.474 (20°)	0.149	28,413	.0215	5,220	37°15′ 143°07′

Editor's Note: Part II of this paper will appear in the next issue of Geophysics.

* South Latitude.

in the Arctic Ocean. These are designated by the prefix AO. Locations are given in Table I.

A group of samples were taken by core, dredge, and snapper from the continental shelf off Pigeon Point, California. These are designated by the prefix PP. A discussion of the sediments of the Pigeon Point shelf and their geologic setting is given by Moore and Shumway (1959).

Additional sediments from intermediate depth were obtained from the continental borderland area off San Diego, where a varied topography provides a variety of sediments ranging from sands to clays. These are designated by the prefix CB.

Deep-sea sediments

All of these samples were obtained from cores collected in the eastern Pacific Ocean, and are identified by the prefix PO. Two of the cores were from the southeast Pacific Ocean, the remainder being from the northeast Pacific Ocean.

THEORIES OF SOUND PROPAGATION IN COMPOSITE MEDIA

The gamut of sedimentary materials found in nature has, at one extreme, high-porosity suspensions of colloidal clay particles and, at the other, low-porosity porous solids. Natural unconsolidated sediments in the sea range from suspensions of particles with diameters of the order of one micron to tightly packed aggregates of sand grains and granules with diameters of the order of 1,000 microns. In the development of sound propagation theory, models representing these extreme cases generally have been used. The case of the general unconsolidated sediment, in which are present both small suspended particles and relatively large particles in various degrees of mutual contact, has been neglected, due to its complexity and to the fact that in science and industry the extreme cases find broader application than does the general case.

The acoustic behavior of natural unconsolidated water-saturated sediments is essentially that of a suspension of particles in a fluid, but a small rigidity is present that cannot be neglected. Theories for suspensions and for granular aggregates are more pertinent for these sediments than are theories for porous solids; however, certain aspects of porous solid theory are applicable. A brief review of some theoretical developments which most directly relate to the present studies is given below, to provide a background for viewing the experimental results.

A. B. Wood (1930, p. 326–329) noted that in a dispersion of one or more fluids in another the bulk adiabatic compressibility equals the sum of the compressibilities of the individual components multiplied by their proportional volumes in the total volume. A corresponding relation holds for bulk density. A simple expression then, can be written for sound velocity, C_{ws}, in the mixture in terms of the properties of the components:

$$C_{ws}^2 = \frac{1}{[\Sigma f_{si}\beta_{si}][\Sigma f_{si}\rho_{si}]}, \qquad (1)$$

where f_{si} are the volume fractions for the i components, β_{si} the compressibilities of the i components, and ρ_{si} the densities of the i components. Urick (1947, p. 983–987) applied this equation to the case of suspensions or emulsions under the assumption that the suspended particles are infinitesimally small compared with the wave length of sound, hence scattering effects can be neglected.

Urick and Ament (1949) suggested an improvement to the homogenous assumption theory equation (1) with the development of a first order theory, which, in allowing for first order scattering effects, gives a complex propagation constant whose real part yields a velocity that reduces to the homogenous case for very small particles. Ament (1953) carried the work further by determining effective dynamic densities for gross mixtures in the form of either a porous solid or a suspension.

In the case of the somewhat rigid structure of solid grains with fluid-filled channels, compressional waves and shear waves are transmitted by the frame, and compressional waves also are transmitted by the fluid. If coupling between the two phases is good, as in a water-filled sediment, compressional velocity, C_{ws}, may be related to the bulk properties of the sediment by the well-known equation

$$C_{ws}^2 = \frac{K_{ws} + (4/3)\mu_{ws}}{\rho_{ws}}, \qquad (2)$$

where μ_{ws} is the rigidity modulus of the aggregate, ρ_{ws} is the bulk density and equal to $f_w\rho_w + \Sigma f_{si}\rho_{si}$, and K_{ws} is the bulk modulus of the aggregate. For perfect coupling, Gassmann (1951a) showed that the aggregate bulk modulus is a function of the fluid bulk modulus, the particle bulk modulus, and the frame bulk modulus.

Laughton (1957) investigated the justification of using the relation

$$1/K_{ws} = f_w\beta_w + \Sigma(f_{si}/K_{si}). \qquad (3)$$

He introduced a structure bulk modulus, K_c, so that for a two-component system the aggregate modulus is

$$K_{ws} = \frac{K_s K_w (1 + f_w/f_s)}{K_w + (f_w/f_s)K_s} + K_c. \qquad (4)$$

Through static decompression measurements Laughton obtained values for K_c. Then by using equation (4) together with equation (2) he showed that for the two fine-grained deep-sea sediments he studied, at compacting pressures below about 490 bars, rigidity is negligible.

For the general sediment the most useful equation for predicting sound speed is the following,

$$C_{ws}^2 = \frac{K_{ws} + 4\mu_{ws}/3}{\Sigma f_{si}\rho_{si} + f_w\rho_w}, \qquad (5)$$

where K_{ws} is determined as in equation (3).

A number of other theoretical studies with regard to granular materials and porous solids have been made and it will suffice here to mention some briefly. Gassmann (1951b) dealt with spheres in hexagonal close packing and showed that compressional velocity should increase in proportion to the sixth root of the depth of burial. This same result was obtained earlier by Iida (1938, 1939) and by Takahashi and Sato (1949). The theory was extended by White and Sengbush (1953). Brandt (1954, 1955) developed theoretical expressions to explain the influence of pressure, porosity, and liquid saturation on sound speed in a porous granular medium, using as a model an aggregate of randomly stacked spherical particles of four different sizes. Sato (1952) gave expressions for compressional wave propagation in media with small holes and in media containing small obstacles, as an extension of the theory of Mackenzie (1950) for a solid containing spherical holes. Kerner (1956) determined theoretically the gross elastic moduli of a composite medium in terms of the properties of its components.

Biot's general treatment of elastic wave propagation in porous solids (1956a) at low frequencies (where Poiseuille flow holds) predicts a rotational wave whose phase velocity increases slightly with frequency and whose absorption coefficient is proportional to the square of the frequency. It predicts a dilatational wave which has practically a negligible dependence of phase velocity on frequency and an absorption coefficient proportional to the *square of the frequency*. In a second paper Biot (1956b) treats the frequency range high enough that Poiseuille flow does not hold but not so high that wave length is smaller than pore size. A structure factor is introduced to account for pore shape, and it is shown that this is not a very significant parameter. The dilatational wave is found to have a velocity which increases slightly with frequency, and an absorption coefficient proportional to the *square root of frequency*. The rotational wave velocity increases somewhat with frequency, and the absorption coefficient is proportional to the square root of frequency.

Relatively little work has been done on the absorption of sound in aqueous suspensions and in water-filled granular aggregates. Sewell (1910) considered the case of small rigid particles which are immobile in the sound field—a condition satisfied for water droplets in air at audio frequencies, but not for aqueous suspensions. Lamb (1945, p. 657–661) condensed Sewell's treatment and extended it to include the case of rigid incompressible particles free to move in the sound field. Urick (1948) discussed Lamb's theory and rewrote his result in the form of an intensity absorption coefficient for a unit volume, α, defined by $I = I_0 \exp(-\alpha x)$ as:

$$\alpha = \frac{4}{3}\pi a^3 n\left[\frac{1}{6}k^4 a^3 + k(\sigma - 1)^2 \frac{s}{s^2 + (\sigma + \tau)^2}\right], \tag{6}$$

where a is the particle radius, n is the number of particles per unit volume, k

is the wave number and equal to $2\pi/\lambda$, λ is the wave length, σ is the ratio of particle density ρ_s to fluid density ρ_w, i.e. $\sigma = \rho_s/\rho_w$, and where the following relations hold when ω is the angular frequency and μ is the kinematic viscosity of the fluid:

$$a = (9/4a)(1 + 1/\beta a); \qquad \beta = (\omega/2\mu)^{1/2}; \qquad 1/2 + 9/4\beta a.$$

The first term on the right side of equation (6) is the scattering loss by small rigid spherical particles free to move in the sound field; the second term is a frictional loss due to the fluid viscosity. It is the second term which accounts for most of the observed absorption in aqueous suspensions.

SOUND SPEED AND ABSORPTION MEASUREMENTS

Sound speed and absorption measurements by the resonance method are given in Table I together with other physical data. All measurements were made at "room temperature," which was anywhere between 19°C. and 28°C., hence the temperatures at which the measurements were made are recorded along with the sound speed values. Inasmuch as absorption is a frequency-dependent process, the resonant frequency is given for each value. For most samples more than one resonant mode was detected and absorption data taken.

GEOPHYSICS, VOL. XXV, NO. 3 (JUNE, 1960), PP. 659–682, 12 FIGS.

SOUND SPEED AND ABSORPTION STUDIES OF MARINE SEDIMENTS BY A RESONANCE METHOD—PART II*

GEORGE SHUMWAY†

RELATION OF SOUND SPEED TO SEDIMENT PHYSICAL PROPERTIES

Introduction

The relationships between sound speed and the more important physical properties of unconsolidated sediments have become known in recent years largely as a result of the studies of Hamilton, 1956; Hamilton et al., 1956; Shumway, 1956, 1958; Nafe and Drake, 1957; Sutton, Berckhemer and Nafe, 1957; and Laughton, 1954, 1957. The suite of samples used in this study is larger and more varied than the suites used in any of the earlier studies, and the measurements probably were more carefully taken. A large number of shelf and harbor sediments were used in addition to sediments from deeper water in the Pacific and Arctic Oceans.

Porosity stands out as the most important single factor causing variations in compressional sound speed in unconsolidated sediments; this is because the difference in compressibility between water and mineral grains is so great, and porosity is a measure of the relative amounts of fluid and solid present. Second in importance is the factor which produces a rigidity in the sediment; this appears to be related to the abundance of coarse grains. Pressure and temperature rank third and fourth, respectively. Next in importance is the compressibility of the grain aggregate, determined from compressibilities of individual minerals. Differences in densities of the mineral grains most abundantly found in sediments are small; hence the aggregate sample grain density changes little from sample to sample. The effect of grain density variations are not negligible, however. Grain shape and the spatial inter-relationship of grains are factors undoubtedly of importance, for they not only determine the characteristics of fluid flow past the grains, but also they determine (along with grain size) the extent to which a frame incompressibility and a rigidity develop between grains. Unfortunately, it is next to impossible to describe the spatial distribution of particles and the nature of the pore space between them for a given natural sediment.

Considering the extremes of porosity (0.85–0.40), hydrostatic pressure (0–1100 bars), temperature (−2°C.–35°C.), and mineral composition (all quartz —all kaoline-like clay) which nature might provide in the marine sediment en-

---

* This paper is a portion of a doctoral dissertation with the same title submitted to the University of California at La Jolla (1958). Manuscript received by the Editor May 14, 1959. Part I of this paper was published in the preceding issue, v. 25, n. 2, p. 451–467. Contribution from the Scripps Institution of Oceanography, New Series.

† U. S. Navy Electronics Laboratory, San Diego, California.

(673)

vironment, sound speed is affected by individual factors as follows:

Factor	*Percent change in sound speed*
Porosity	16
(Rigidity)	(10–20)
Pressure	11
Temperature	7
Grain aggregate compressibility	3

Pressure and temperature effects

Temperature and pressure changes occur in a sediment sample when it is brought from the sea floor to the laboratory. If the acoustic properties of sediments *in situ* on the sea floor are to be inferred from laboratory measurements, then it is necessary to appreciate the effects of these factors. With the knowledge at hand of how to relate laboratory measurements at atmospheric pressure and room temperature to probable *in situ* values, it becomes possible to understand the interrelationships of acoustic, sediment texture, and other physical properties of sediments *in situ*, on the basis of laboratory studies.

The effects of hydrostatic pressure on the speed of sound in unconsolidated ocean sediments are considered by Laughton (1957). His results showed a compressional velocity increase of about three or four percent in going from one bar pressure to 390 bars; this change is about the same as for sea water alone.

Pressure studies were not undertaken as part of this study because the compliant-walled resonant chamber is not adaptable to pressure work. The resonant chamber could be placed in a pressure vessel of larger volume, but a liquid such as water would be unsuitable as a pressure medium because the external walls of the resonant chamber must be unloaded; even gas, such as nitrogen, under pressures of a few hundred bars, is dense enough to complicate the system greatly.

The effect of temperature on compressional speed is considerable, amounting to an increase of 10 percent to 15 percent in going from 0°C. to about 60°C. This is readily determined by using equations (1) or (2) with appropriate densities and compressibilities, and it has been verified experimentally by the writer (1958) for a number of typical sea floor sediments.

Effects of other physical properties

Introduction.—The interrelationships of wet density, porosity, and the more important textural properties of sediments have been discussed at some length by Hamilton et al. (1956), Hamilton and Menard (1956), Nafe and Drake (1957), Sutton, Berckhemer and Nafe (1957), and others; hence a general discussion is not called for here. The relationships between sound speed and those parameters which appear to be most important on the basis of the earlier work can be considered immediately.

Porosity.—Data for 110 samples are used to show the relationship of porosity to sound speed (Figure 1). The mean temperature at which these samples were

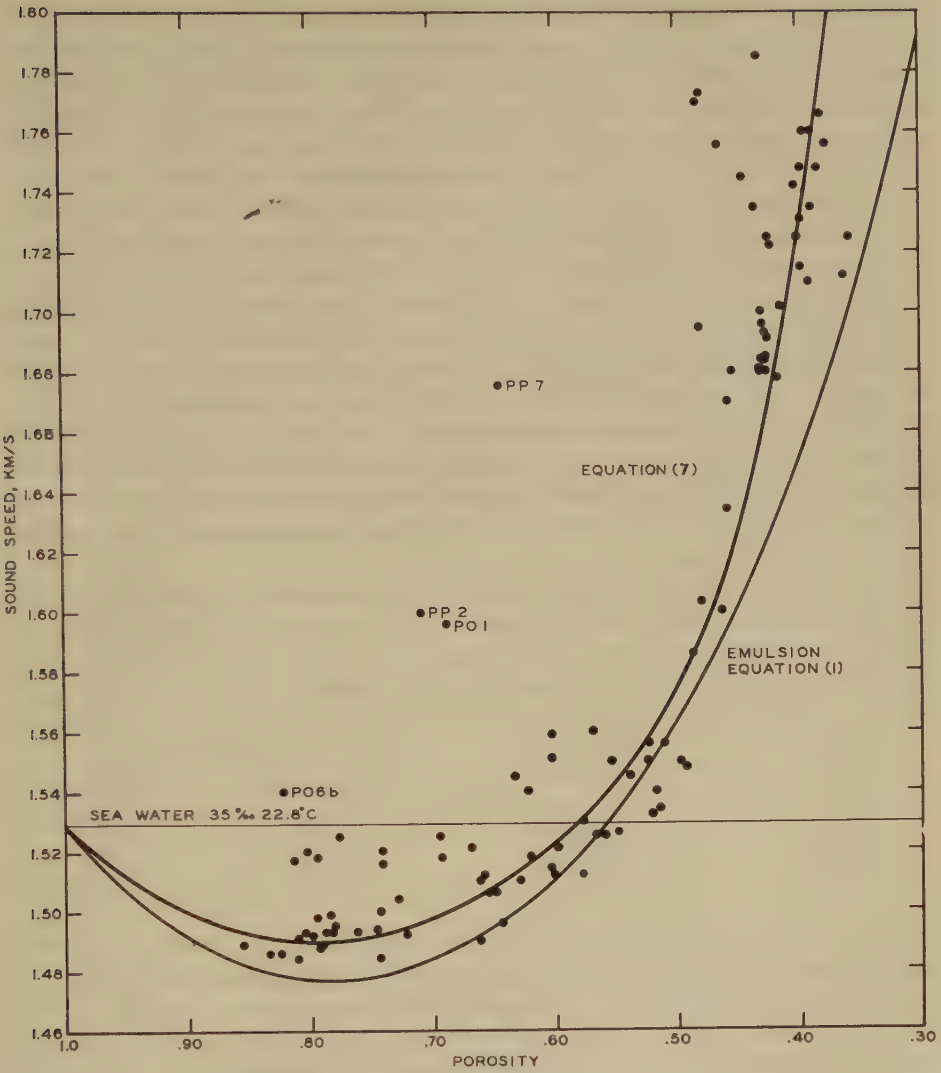

FIG. 1. Sound speed vs. porosity for unconsolidated marine sediments.

measured was 22.79°C. and the standard deviation of temperatures from this mean was 2.064°C. Sound speed in sea water of 35°/₀₀ salinity at this temperature is 1.5293 km/sec (Del Grosso, 1952). More than a third of the sediment speed values lie below this water value. Measured speeds ranged from 1.484 km/sec to 1.785 km/sec; measured porosities ranged from 0.357 to 0.856. It is evident that although sound speed increases as porosity decreases, the relationship is not linear.

Urick (1947) was one of the first to take experimental data on the relationship between sound velocity and porosity. He measured velocity in dilute suspensions of kaolin, by means of an interferometer, and found results which agreed well with predictions using the emulsion equation of Wood (equation 1). This equation predicts a parabolic curve with a minimum sound speed at a porosity of about 0.8, this minimum speed being about three percent below the speed in water alone.

The effect of porosity alone on sound speeds in sediments is given by equation (1), with all grains consisting of one mineral. Using quartz as the mineral, speeds range from 1.476 km/sec at a porosity of about 0.79 to a value 16 percent higher, 1.71 km/sec at a porosity of about 0.35 (Figure 1). The speed variation is similar if typical minerals other than quartz are considered (Hamilton, 1956).

The curve representing equation (1), with quartz as the mineral, lies significantly below the measured values of the sands, in the porosity range 0.35 to 0.45, because rigidity has been neglected. The curve lies significantly below the measured values of the clays and finer silts, in the porosity range 0.65 to 0.85 because here the sediment particles consist dominantly of clay minerals rather than quartz, and the compressibilities of clay minerals are appreciably smaller than the value for quartz.

Mineral grain compressibilities.—The effects of mineral grain compressibility on sound speed are predicted by equation (1), if grain density is held constant. Using a grain density of 2.7 g/cm^3 for quartz, calcite, and "clay," the following sound speeds are predicted by equation (1) for grains in sea water at 22.8°C:

Mineral	Compressibility cm^2/dyne	Sound Speed, km/sec	
		0.70 porosity	0.40 porosity
quartz	2.70×10^{-12}	1.476	1.639
calcite	1.35×10^{-12}	1.486	1.677
"clay"	$1.0\ \times10^{-12}$	1.488	1.687

At 0.40 porosity the difference between the values for quartz and "clay" sediments is about three percent, and at 0.70 porosity it is less than one percent.

Rigidity and grain size.—In the writer's (1958) study on the effects of temperature on sound speed a small, but not negligible, rigidity had to be introduced to make the theoretical curves fall near the experimental data. The existence of this rigidity is acknowledged by a number of papers already mentioned, but no attempt has been made to relate it to the textural properties of the sediment. In addition to rigidity, a frame bulk modulus is involved here. The two are difficult to separate in this case, and in the following discussion they are considered together under the name of rigidity.

The rigidity of a given sediment increases as it consolidates, loses water, and develops intergranular cementation. These are the changes that take place as a sediment ages and becomes buried under younger materials. Laughton (1955, 1957) made laboratory compaction studies of sediments and the changes in the

(676)

acoustic properties of the sediments as compaction proceeded. Consolidation effects are not considered in the present study.

This study deals only with unconsolidated surface sediments—sediments which are compacted only to the extent that is natural as they accumulate at the surface of the sea floor and become buried by no more than about one meter of sediment. In these materials the rigidity modulus must be related to the textural properties of the sediment.

For sediments in general it may be said that as median, mean or mode grain size diameter increases, porosity decreases. The suite of samples used in this study exhibit this relationship well. The relationship is approximately linear when grain size is measured in phi units. (Diameter in phi units equals $-\log_2 r$ where r is diameter in mm.) The porosity-median diameter relationship has a positive correlation coefficient of 0.948. The porosity-mean diameter relationship (Figure 2) has a slightly higher positive correlation coefficient, 0.959.

As a result of this marked correlation between porosity and central tendency, a distinctive relationship between sound speed and mean grain diameter is found (Figure 3). It may be said that, in general, the smaller the median or mean di-

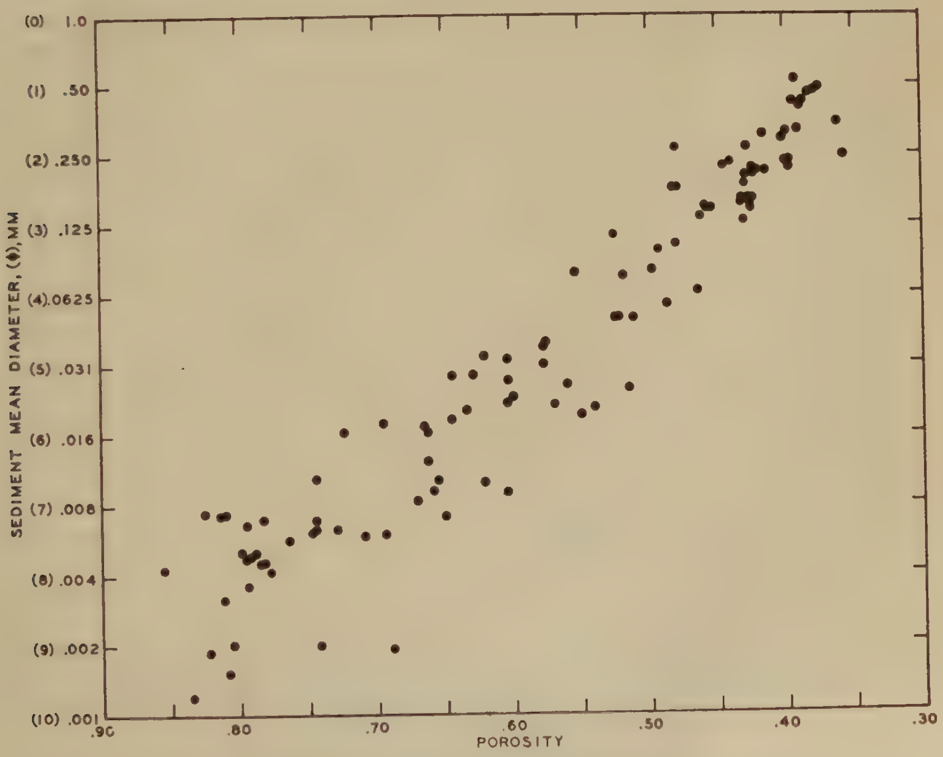

Fig. 2. Mean diameter vs. porosity for unconsolidated marine sediments.

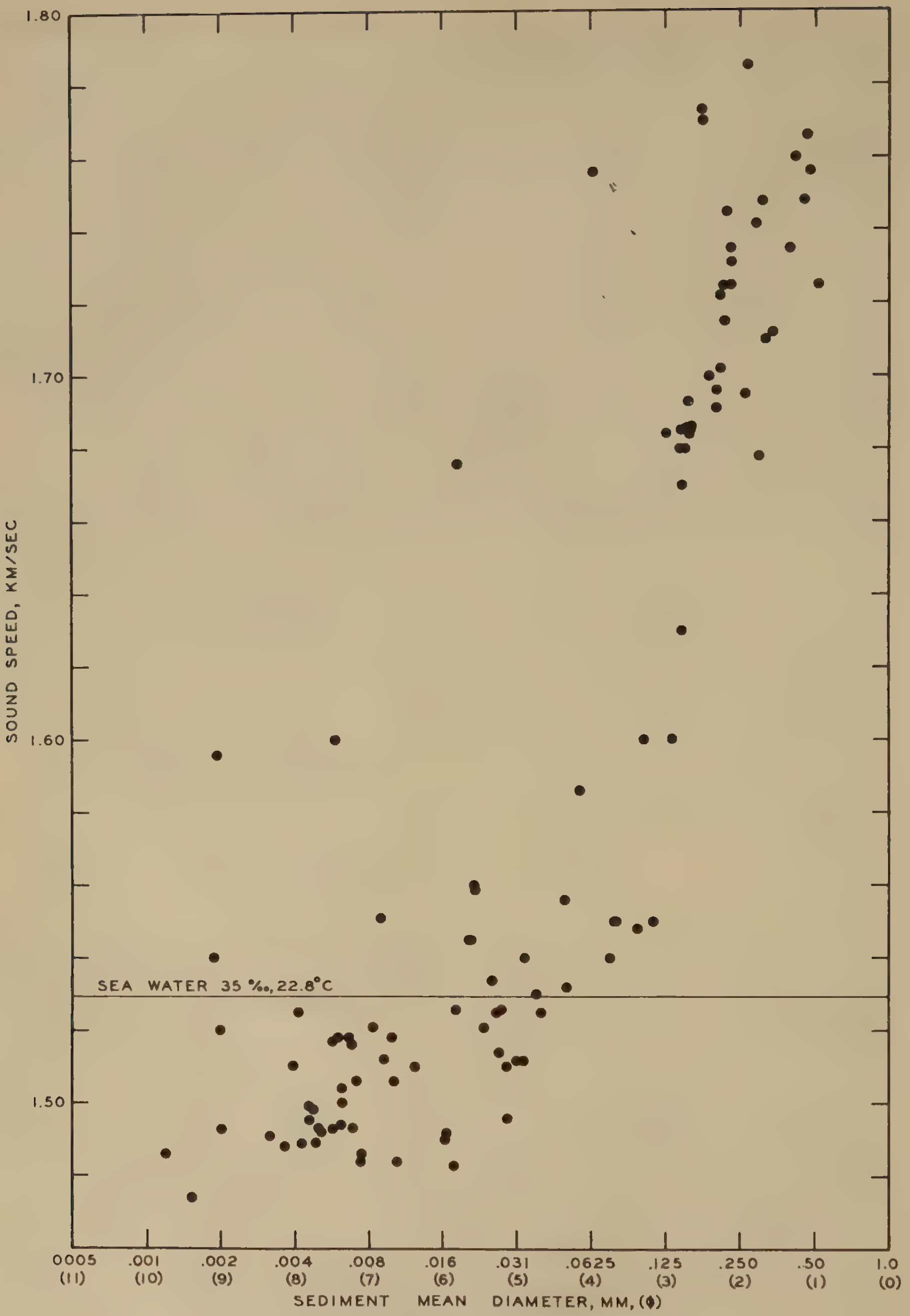

FIG. 3. Sound speed vs. sediment mean diameter.

ameter, the lower the sound speed. The relationship is more pronounced for mean than for median diameter. The relationship is not linear, for it is mainly due to the non-linear sound speed-porosity relationship. In addition to the porosity effect is the effect of the rigidity, which apparently increases as porosity decreases and grain size increases.

The degree to which the distribution of grain sizes in a sediment is sorted can be expressed by phi deviation measure (Inman, 1952). The relationship between this measure and grain size central tendency for the suite of sediments used in this study (Figure 4) is typical for sediments in general (e.g. Inman and Chamberlain, 1955). The sediments with poorest sorting are in the silt group. The sediments with best sortings are the sands. The number of clay samples is relatively small, but the few samples available suggest that the clay group of sea-floor sediments may be better sorted than the silts.

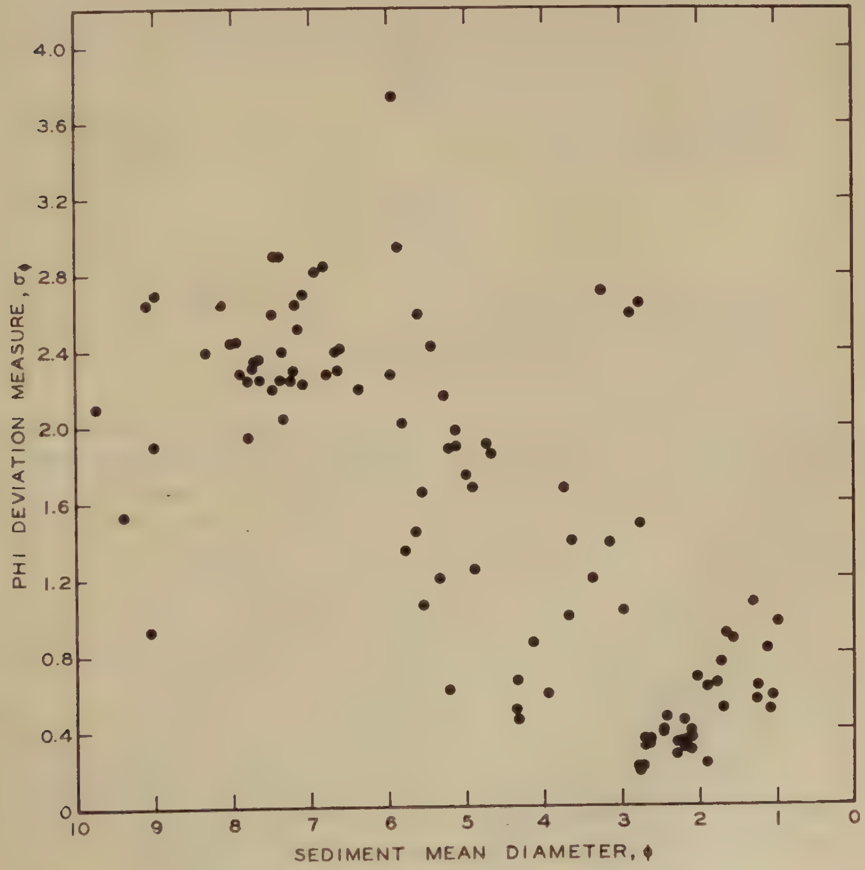

FIG. 4. Phi deviation measure vs. sediment mean diameter.

The general sediment contains both particles in suspension and particles in contract. Throughout the sediment isolated groups of particles-in-contact are found which give local regions where rigidity is important. The effective rigidity of the sediment, therefore, should be a function of the volume fraction occupied by these particles-in-contact and their enclosed interstices. In general it is the larger particles, i.e., the sands and coarser silt particles, which contact one another, while the finer particles, many of which are in the colloidal state, remain effectively in suspension. The volume fraction or weight fraction of coarse grains in the sample therefore might, in itself, be related to the rigidity.

For the sediments involved in this study the volume fraction of the wet sediment occupied by grains coarser than silt size, i.e. coarser than 0.0625 mm, was determined by multiplying the particle concentration, $(1-\eta)$, by the weight fraction of grains coarser than this diameter, ψ, as given by the mechanical analysis. This assumes that there is little difference between weight fractions and volume fractions for the grains alone. For the sediments involved this assumption is valid. A pronounced inverse relationship between porosity and the sand volume fraction is exhibited by the data (Figure 5).

Assuming that the sediment volume fraction of sand grains is proportional to the rigidity modulus, equation (5) can be written in the form

$$C_{ws}^2 = \frac{K_{ws} + b(1-\eta)\psi}{\sum f_{si}\rho_{si} + f_w\rho_w}, \tag{7}$$

where b is a constant. This equation fits the experimental data considerably better than does equation (1), when a value of 0.8 is used for b, appropriate mineral densities and compressibilities are used, and when ψ is given values of 1.0 at $\eta = 0.4$, 0.3 at $\eta = 0.525$, and zero at $\eta = 0.8$ (Figure 1).

Discussion.—Sutton et al. (1957) performed an elaborate statistical analysis on the data from 37 samples they studied. By use of the multiple linear regression statistics they developed an equation relating the dependent variable, sound velocity in km/sec (C_{ws}), to the independent variables phi median diameter (Md_ϕ), percentage of material soluble in HCl (γ), and porosity (η):

$$C_{ws} = 2.093 - (.0414 \pm .0060)Md_\phi + (.00135 \pm .00038)\gamma - (.44 \pm .15)\eta. \tag{8}$$

A multiple correlation coefficient of 0.90 was found for sound velocity in relation to the three independent variables.

An analysis of this type must be viewed with caution. The interrelationships between the variables in a multiple linear regression equation should be linear, yet the ones used are not all linear. Although the analysis accounts for the interdependence of the variables involved, there is no assurance that the variables used are the significant ones. For instance, in the present study the good correlation between porosity and mean (or median) diameter (Figure 2), and between porosity and sand content (Figure 5) result in a strong correlation between

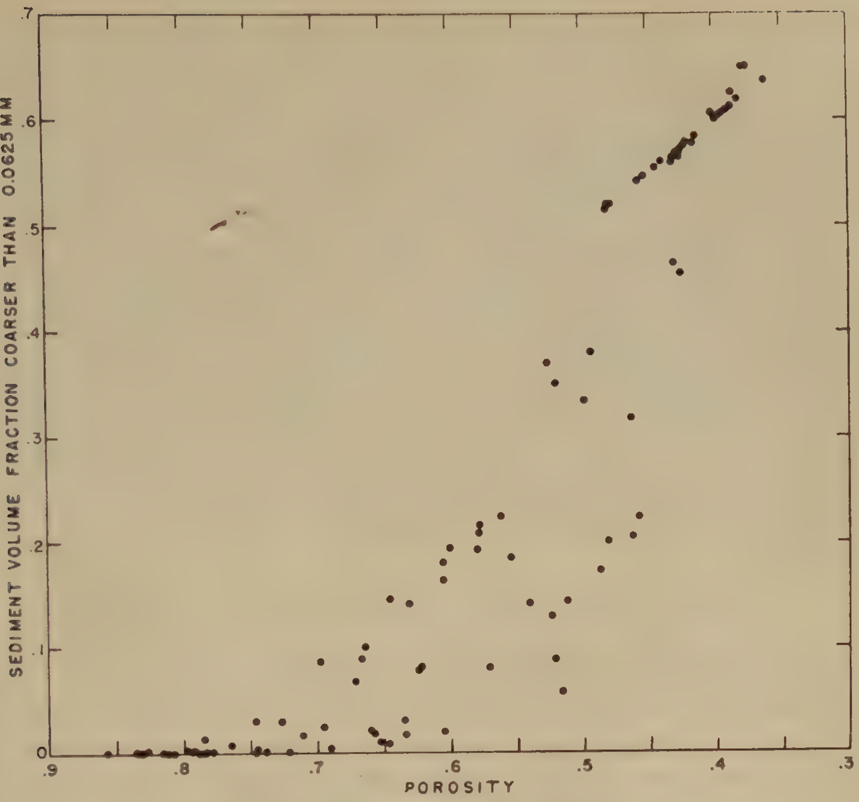

FIG. 5. Sediment sand content vs. porosity.

mean (or median) diameter and sand content. Thus, the median diameter effect implied by equation (8) may in truth be the rigidity effect related to the content of coarse grains and probably also other factors related to the content of coarse grains.

In spite of such objections, there may be some merit in determining a multiple linear regression equation; hence an analysis similar to that of Sutton et al., but not as comprehensive, was made using data from 108 samples of the present study. The independent variables used differed somewhat from those of Sutton et al. Sound speed in km/sec (C_{ws}) again was taken as the dependent variable; independent variables consisted of porosity (η), phi mean diameter (M_ϕ), and phi deviation measure (σ_ϕ). Statistical data are summarized in Table II.

Phi mean diameter rather than phi median diameter was used because it correlates better with sound speed and with porosity. Phi median diameter, however, correlates slightly better with phi deviation measure than does phi mean diameter. The resulting multiple linear regression equation is

$$C_{ws} = 1.5955 - 0.0287(M\phi - \overline{M_\phi}) - 0.3658(\eta - \bar{\eta}) + 0.0472(\sigma_\phi - \bar{\sigma}_\phi), \quad (9)$$

or

$$C_{ws} = 1.87295 - 0.0287M_\phi - 0.3658\eta - 0.0472\sigma_\phi. \tag{10}$$

The multiple correlation coefficient, $R_{C^0M_\phi\eta\sigma_\phi}$, equals 0.959, which is higher than the value of 0.90 obtained by Sutton et al. The standard error of estimate, S_e, equals $(0.0007744)^{1/2}$ or 0.027828, which is lower than the value of 0.054772 obtained by Sutton et al. This means that the standard error for the prediction of sound speed by means of equation (10) is about 28 m/sec.

The best expression relating sound speed to the more important independent variables is equation (7). The problem of relating the rigidity modulus (and frame incompressibility) to measurable sediment variables remains unsolved, however. In equation (7) it is assumed that the combined effect of these moduli is proportional to the content of sand in the sample. This simple assumption is merely a step in the right direction, for undoubtedly a number of factors are involved. The problem has been avoided in the development of existing published theories on sound propagation in composite media. The effect of frequency on sound speed (Laughton, 1957) is so small that it can be neglected for any practical application of equation (7).

RELATION OF ABSORPTION TO SEDIMENT PHYSICAL PROPERTIES

The relationship between absorption and porosity (Figure 6) exhibits an absorption maximum for sediments of intermediate porosity; absorptions are highest in the porosity range 0.45 to 0.60, where the dominant sediment type is coarse silt. The highest absorption measured was 25.1 db/m, and the lowest was 0.66 db/m. In general, the lowest absorption values were found in those sediments which had the highest porosity, the clays and finer silts. Due to the high degree

TABLE II

Statistical Data

Number of observations, $N=108$ S designates a sum

Sound Speed km/sec	$S(C)=172.317$	$\overline{C}=1.595527$
Phi Median Diameter	$S(Md_\phi)=483.28$	$\overline{Md_\phi}=4.4748$
Phi Mean Diameter	$S(M_\phi)=515.51$	$\overline{M_\phi}=4.77324$
Porosity	$S(\eta)=62.294$	$\overline{\eta}=0.57680$
Phi Deviation Meas.	$S(\sigma_\phi)=161.61$	$\overline{\sigma_\phi}=1.49639$
Standard deviations	$\sigma_C=0.098.5$	$\sigma_{M\phi}=2.4446$
$\sigma\eta=0.15028$	$\sigma_{\sigma_\phi}=0.91823$	$\sigma_{Md_\phi}=2.2894$
Correlation coefficients		
$r_{CM\phi}=-0.914$	$r_{M\phi\eta}=+0.959$	$r_{Md_\phi}3=-0.815$
$r_{C\eta}=-0.891$	$r_{M\phi\sigma_\phi}=+0.766$	$r_{Md_\phi\eta}=+0.948$
$r_{C\sigma\phi}=-0.556$	$r_{\eta\sigma_\phi}=+0.803$	$r_{Md\phi\sigma_\phi}=+0.804$
Standard error of estimate	$S_e=(0.0007744)^{1/2}=0.027828$ km/sec	
Multiple correlation coefficient	$R_{C^0M_{\phi\eta\sigma\phi}}=0.959$	
$S(C^2)=275.97712$	$S(\sigma_\phi{}^2)=332.8909$	$S(C\sigma_\phi)=252.44093$
$S(Md_\phi{}^2)=2713.9828$	$S(\eta\sigma_\phi)=105.19227$	$S(Md_\phi\eta)=313.50702$
$S(M_\phi{}^2)=3106.0714$	$S(C\eta)=97.71919$	$S(\eta M_\phi)=335.39041$
$S(\eta^2)=38.36993$	$S(CM_\phi)=799.57545$	$S(M_\phi\sigma_\phi)=975.0575$
		$S(Md_\phi\sigma_\phi)=905.6357$

of correlation between porosity and grain size central tendency, the relationship between median grain diameter and absorption also shows a maximum (Figure 7).

In addition to the sediment data plotted on the absorption-porosity diagram (Figure 6), four absorption values for rocks of essentially zero porosity and a value for quartz have been plotted. These rock values were obtained from Ide's (1937) measured the values of mechanical Q through the relation $\alpha = \pi(\lambda/Q)$ where α is sound absorption in nepers per unit length and λ is the wave length. His measurements were made on rock cylinders 5.08 cm in diameter and 25.4 cm long driven as bar resonators; hence the fundamental resonances were in the audio range. For comparison with the resonant chamber measurements, his reported values were corrected to a frequency of 24 kc/sec by assuming a first power frequency dependence (Knopoff and MacDonald, 1958). Unfortunately, similar measurements have not been made for water-saturated sedimentary rocks, to fill in the gap between zero and 0.35 porosity values.

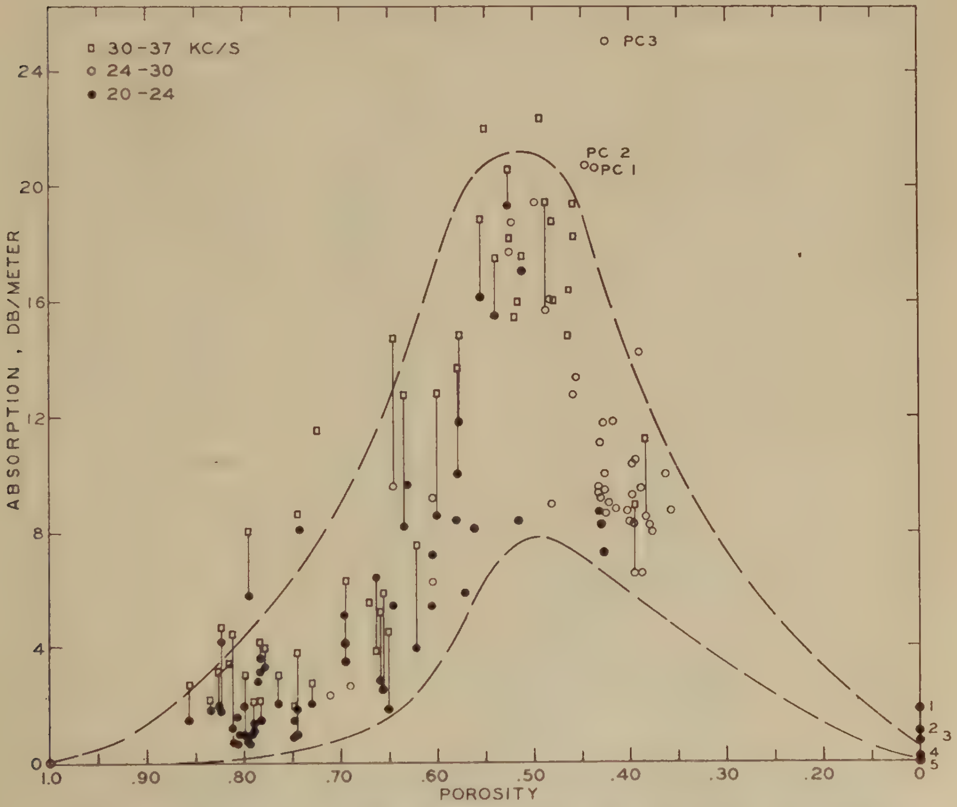

FIG. 6. Sound absorption vs. porosity for unconsolidated marine sediments. Numbered values at zero porosity are (1) Quincy granite, (2) quartzite sandstone, (3) French Creek norite, (4) Vinal Haven diabase, (5) quartz, of Ide (1937), corrected to a frequency of 24 kc/s.

(683)

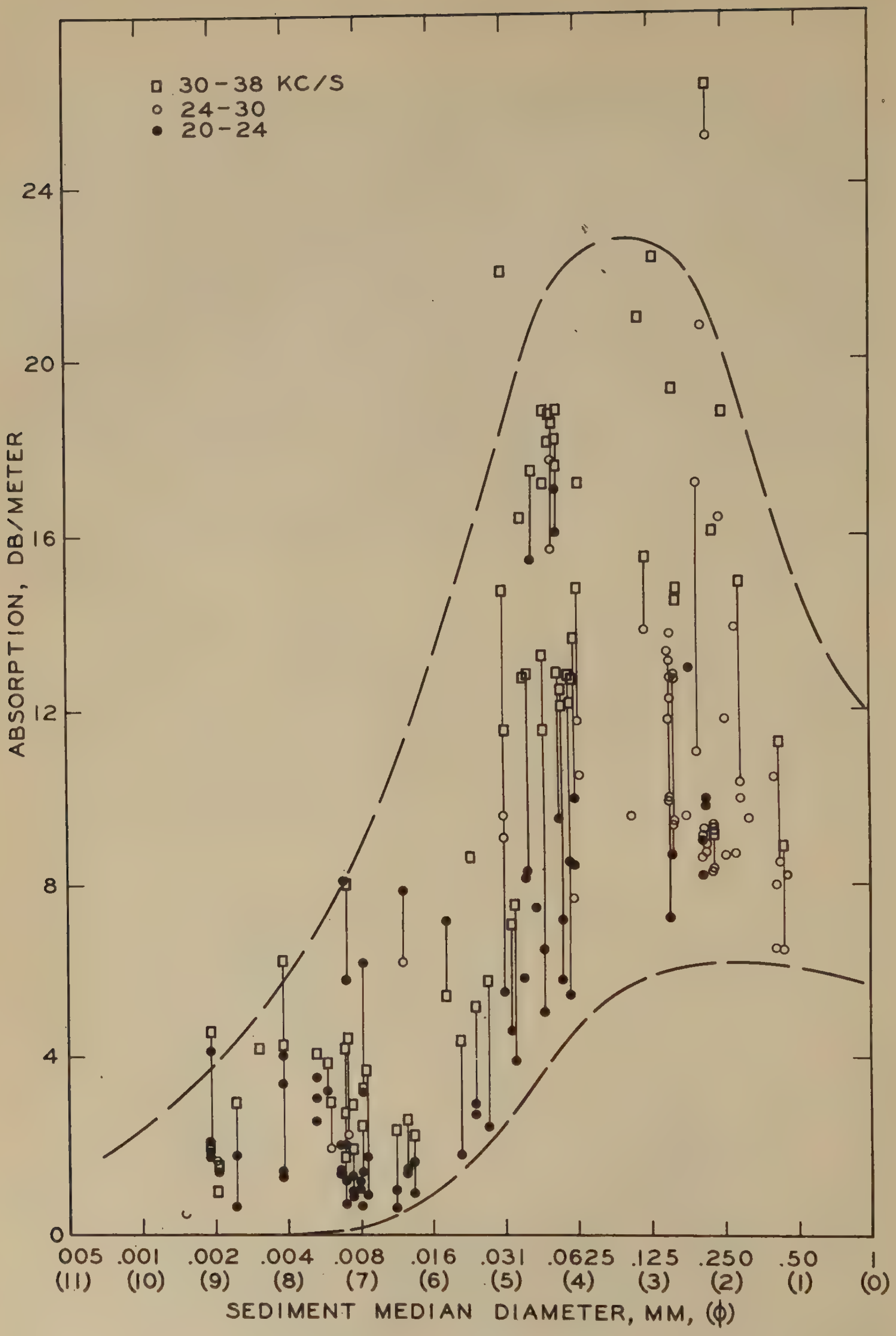

Fig. 7. Sound absorption vs. median diameter for marine sediments.

Most absorption values lie within the two arbitrarily drawn dashed curves on Figure 6. At frequencies between 20 kc/sec and 40 kc/sec most natural sea floor sediments probably have absorption values within the limits defined by these curves. The curves have been drawn to include the porosity region below 0.35, where lithified sediments rather than unconsolidated ones are found. For reasons that will be given below, it is suggested that this curve may predict the general range of values for these lithified sediments also.

Particularly high absorption values were found for three Panama City samples, PC1, PC2, and PC3, whereas normal values were found for the other samples from the same locality, PC5a, PC5b, PC5c. The three samples with high absorption contained numerous gas bubbles along the side of the container and contained many roots scattered throughout the sample. These roots were hollow and contained gas bubbles. When pieces of these roots were squeezed between the fingers visible bubbles were released. The samples with normally low absorption values were samples from which these roots had been removed and from which had been removed any gas bubbles that would float to the surface as a result of agitation of the sediment under water.

An explanation for the absorption maximum found for sediments of intermediate porosity and intermediate grain size can be found through consideration of "accoustically effective" surface areas of particle aggregates. Urick (1948) studied absorption in suspensions of irregular particles, and noted that theory would have this absorption be due primarily to viscous losses resulting from relative motion of particles and fluid (equation 6). He found experimentally that for particles of a given size, absorption increases linearly as the volume concentration increases from zero to about 15 percent, but then drops off as concentration increases further, presumably as a result of particle interaction. Using particle concentrations of one percent by volume, and making measurements in the megacycle range, he found that as particle diameter decreases linearly from 10 to 0.9 microns, absorption increases linearly. According to theory (second term of equation 6) this linear relationship would fail to hold for smaller particles, Urick's explanation being that very small particles undergo less motion relative to water than do somewhat larger particles. Urick comments: "Extremely small particles tend to move to and fro along with the liquid in the sound field. . . . As the particle size increases the particles lag more and more behind the movement of the fluid; but at the same time the total surface area of particles decreases with increasing size if the volume concentration remains constant. These opposing factors result in an absorption maximum." Two important principles thus are suggested: (1) absorption is an additive process; (2) absorption depends on the total acoustically effective surface area of particles in suspension.

In the lower porosity materials considered in the present study, namely sands and lithified sands, suspended particles are of negligible importance. Fluid exists in a framework of grains, and moves relative to this framework under sonic agitation, producing viscous losses. This absorption will depend on the acoustically effective channel wall area and will be approximated closely by the total surface area of the particles. The acoustic surface area for a fluid-filled granular aggregate or a porous solid is here defined as the area of a flat plate lying parallel to the direction of propagation which yields an energy loss due to viscosity equivalent to the viscous loss in the porous material.

For any sediment the total acoustic surface area, A_s, can be computed by dividing the sediment into size fractions, determining the number of particles in each fraction assuming spherical particles, determining the total particle surface area of each fraction, and then applying a correction factor for acoustically small particles based upon the second term of equation (6).

For a volume, v, of wet sediment of porosity η consisting entirely of grains of radius r_i, the surface area, A, is

$$A_i = \frac{(1-\eta)v4\pi r_i^2}{(4/3)\pi r_i 3} = \frac{3(1-\eta)v}{r_i}. \tag{11}$$

The total grain volume is $(1-\eta)v$. If grains of a number of sizes are present rather than grains all of one size, and the volume fraction of grains of radius r_i is represented by $(1-\eta)vf_i$, then the total surface area for a sediment is

$$A = \sum_{i=1}^{n} \frac{3(1-\eta)vf_i}{r_i}. \tag{12}$$

After a grain size analysis has been done for a sediment, the surface area computation can be done fairly easily. In the size analysis the sediment is divided into size fractions and the relative proportions by weight of these fractions are determined. For various size fractions, weights and volumes will be proportional if all grains are of the same material; inasmuch as the densities of quartz, calcite, and "clay" are close to each other, the proportionality will be practically valid for sediments composed of any of these materials. Therefore the weight fractions determined in the size analyses may be used for the f_i values. Values of r_i are taken from the mean radii of the size fractions, which lie midway between the extreme radii of the fractions. Size fraction radii limits usually are taken at whole or half phi intervals, and mean values in millimeters rather than mean phi values should be used.

For equation (12) to be useful for all sediments, factors F_i must be introduced to give "effective" areas for the smaller particles. The equation, for acoustic surface area, A_s, is

$$A_s = \sum_{i=1}^{n} \frac{3(1-\eta)F_i f_i v}{r_i}. \tag{13}$$

Values for the F_i are determined in the following manner. The second term of equation (6) is used in the form which follows to determine the absorption per unit volume for suspensions of constant composition but of varying particle size:

$$\alpha = \frac{4\pi r^3 n}{3}\left[\frac{2\pi}{\lambda}\left(\frac{\rho_s}{\rho_w} - 1\right)^2 \frac{s}{s^2 + (\rho_s/\rho_w + \tau)^2}\right]. \tag{14}$$

If, for acoustically large particles, absorption is directly related to surface area, then using equation (11) yields

$$\begin{aligned} \alpha &= KA \\ &= K[3(1 - \eta)v/r_i], \end{aligned} \tag{15}$$

where K is an undetermined constant. For particles not large acoustically a factor F_i would appear on the right side of (15). By dividing equation (14) by equation (15) with the F_i factor introduced, the F_i values are obtained with the expression

$$F_i = K' \frac{(\sigma - 1)^2(1 + 1/r\beta)}{\beta[s^2 + (\sigma + \tau)^2]}, \tag{16}$$

where K' is another undetermined constant.

Actual values for the F_i were found graphically. Equation (14) was plotted for quartz particles with a constant concentration of one percent, a frequency of 30,000 c/sec, a wave length for sound of 5 cm, and a kinematic viscosity of 0.01 cm²/sec (Figure 8). On the same graph, equation (14) is represented by the straight line which is asymptotic to equation (13) in the region of large particle diameters. For given values of particle diameter the ratio of the ordinates of these two curves provides the F_i. The following values were obtained:

Size range phi	*Mean diam. mm*	*Sediment name*	*F*
4–5	0.04688	Coarse silt	0.91
5–6	.023438	Medium silt	0.78
6–7	.011718	Fine silt	0.67
7–8	.005859	V. fine silt	0.33
8–9	.0029297	Coarse clay	0.089
9–10	.0014648	Medium clay	0.0125
10–11	.0007324	Fine clay	0.00214

Using the F_i thus obtained, acoustic surface areas were computed for the sediments of this study (Table I). Surface areas computed in this manner for the finer sediments are considerably smaller than the values obtained without use of the correction factors. For silts and clays it is difficult to compute a surface area without these correction factors because a significant portion of the total area of such sediments is contributed by particles smaller in diameter than the limiting diameter of the usual grain size analysis. The total surface areas of some deep-sea sediments were measured by Kulp and Carr (1952) using a gas-absorption method. Their values ranged between about 5 and 50 m²/gm of dry sediment. Nelson and Hendricks (1943) and Diamond and Kinter (1958) measured by an absorption method the surface areas of some clay soils and obtained results of the same order of magnitude. In comparison, the acoustic areas computed in the present study have values of about 0.05 m²/gm of dry sediment. Thus total sur-

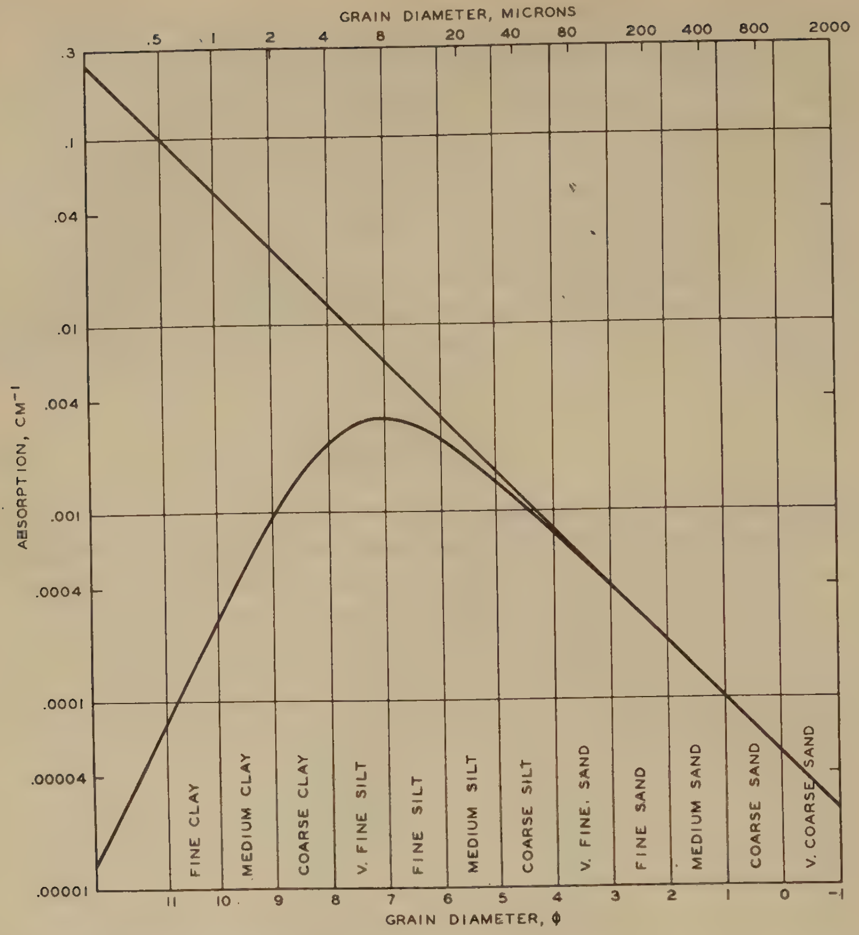

Fig. 8. Absorption per cm at 30 kc/s for a 1 percent by volume suspension of quartz particles in water as a function of grain diameter. The curve is a plot of equation (14). The straight line is asymptotic to the curve.

face areas for silts and clays are about 100 to 1000 times larger than acoustic surface areas, at a frequency of 30 kc/sec. At lower frequencies the acoustic areas would be smaller still.

The computed acoustic surface areas exhibit maxima for sediments of intermediate porosity (Figure 9) and intermediate grain size (Figure 10). These maxima, however, do not coincide exactly with the absorption maxima, but lie somewhat on the high-porosity, smaller-median-diameter side. Furthermore, the acoustic surface areas for the sands are smaller than for the clays and fine silts, yet sand absorption values are higher. These features suggest that absorption and acoustic surface area may be related through an additional factor, or factors, and

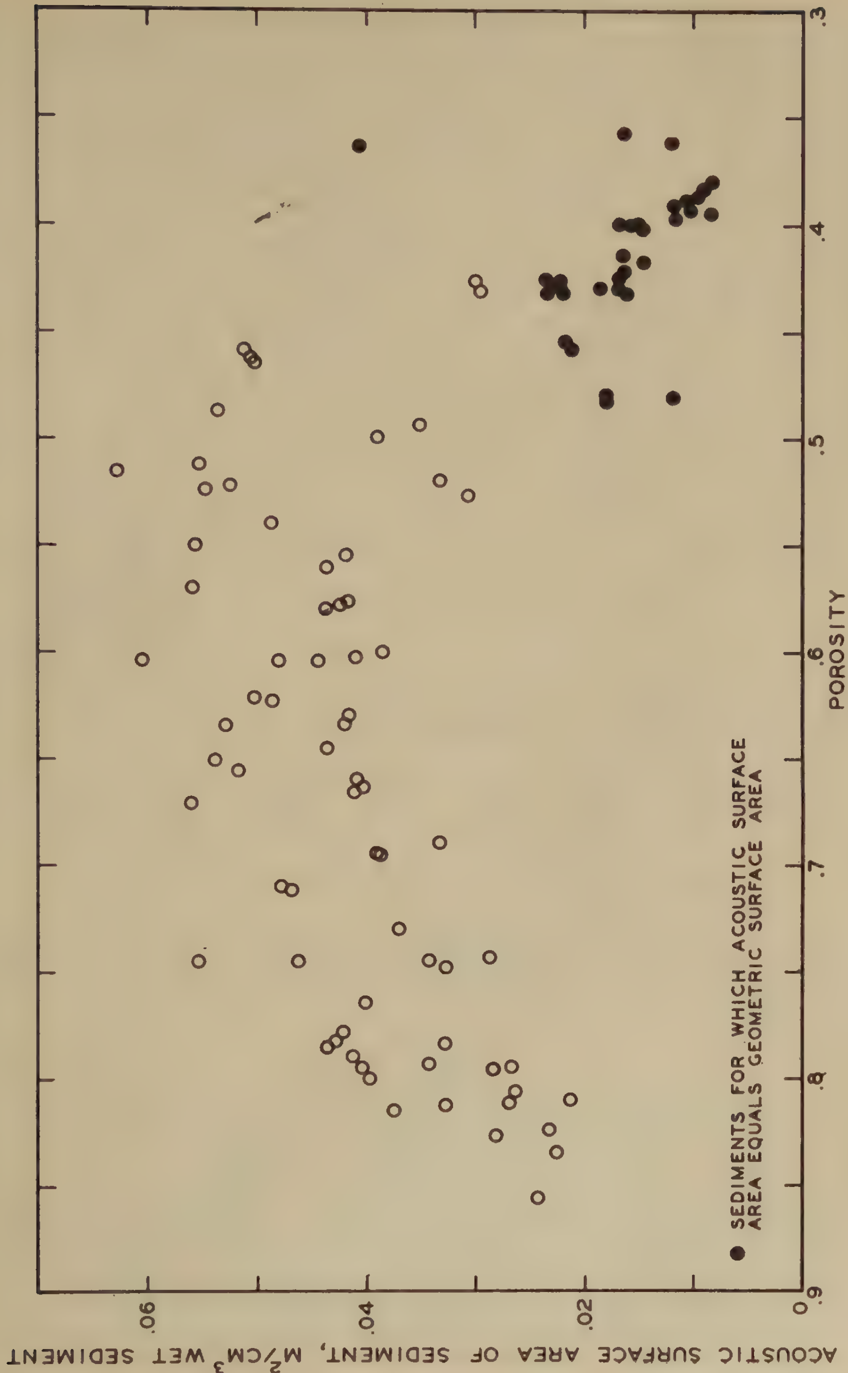

FIG. 9. Acoustic surface area of sediments vs. porosity, at 30 kc/s.

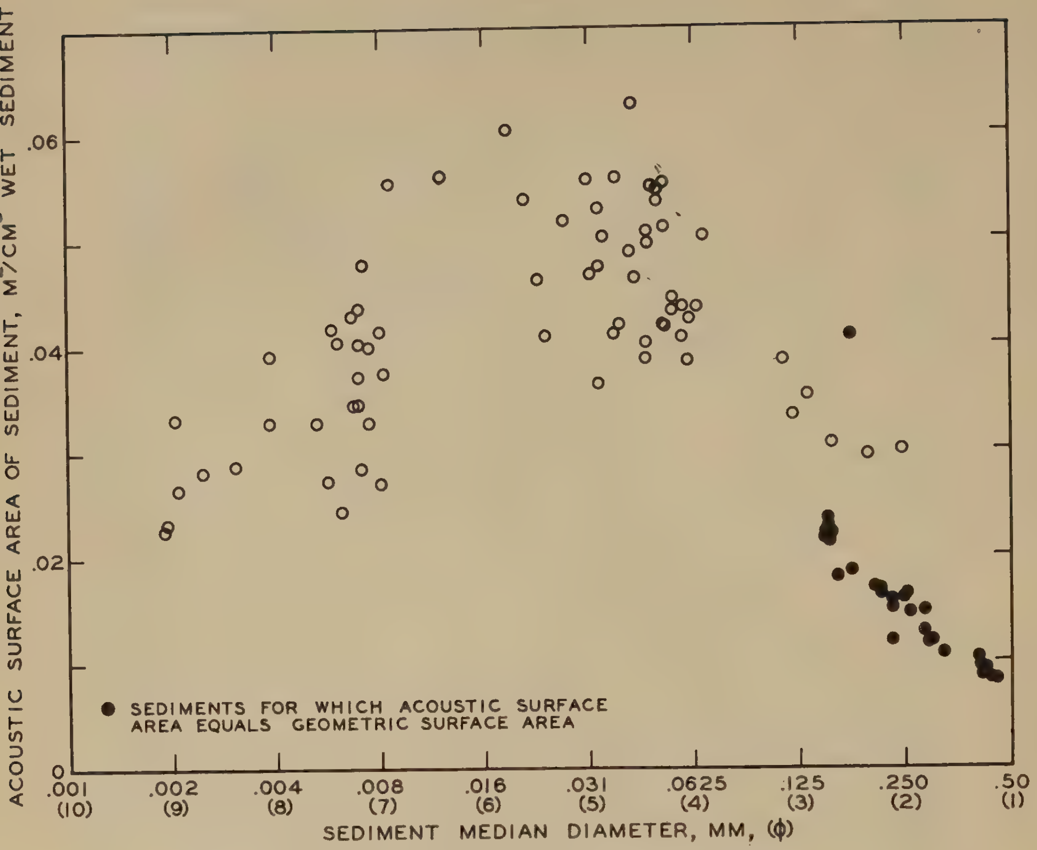

FIG. 10. Acoustic surface area of sediments vs. median diameter, at 30 kc/s.

that this factor may vary with porosity and grain size in a systematic manner.

Let M be the factor relating absorption and acoustic surface area in the following manner:

$$\alpha = MA_s. \tag{17}$$

Values of M were determined from measured absorption and computed acoustic surface area values (Figure 11). The M values increase in a regular manner as porosity decreases, and are frequency-dependent.

The similarity of the M-porosity relationship, and the sand-content-porosity relationship (Figure 5) suggests a possible physical explanation for M. In dry crystalline rocks elastic wave energy absorption is considerably higher than it is in isolated crystals of the minerals involved (Ide, 1937; Birch and Bancroft, 1938a, b; Birch et al., 1942). Crystalline rocks and lithified sedimentary rocks

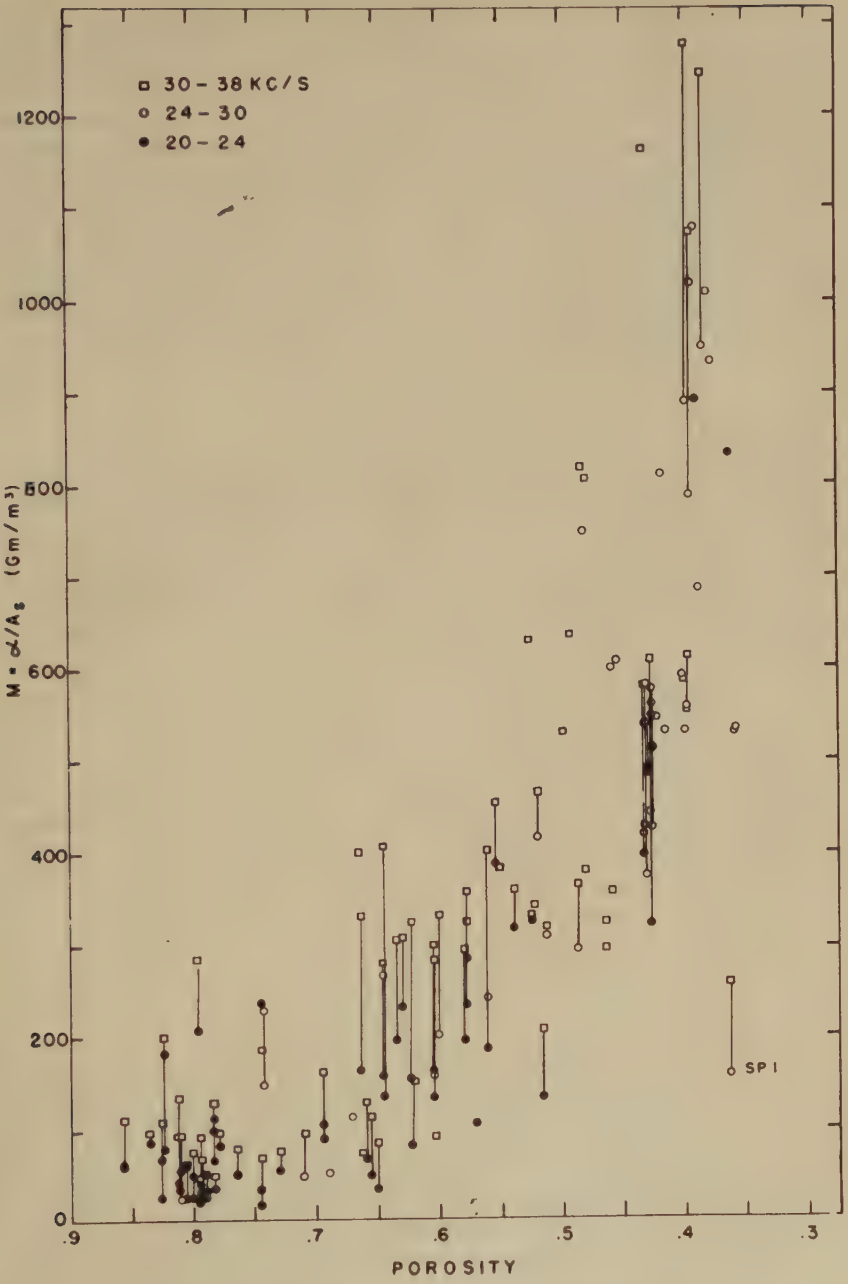

Fig. 11. Absorption factor, M, vs. porosity.

have mechanical Q values of the order of 10^2 at atmospheric pressure, while isolated quartz crystals have yielded Q values as high as 10^7 (Green, 1955). Absorption in the rock materials is due mainly to processes at mineral grain boundaries. By applying a pressure of about 4,000 bars to a rod of granite, Birch and Bancroft (1938b) increased the experimental Q from 180 to 1,200. In an unconsolidated sediment containing grains in mutual contact similar inter-grain losses are to be expected, whereas such losses would almost be non-existent in a suspension of colloidal clay particles. The total of inter-grain losses in a sediment should be approximately a function of the fractional volume of the sediment occupied by grains-in-contract, and this in turn is approximated by the content of coarse grains, ψ. Thus absorption values might be predicted by the expression

$$\alpha = a\psi A_s, \tag{18}$$

where a is a frequency-dependent number.

The M-porosity relationship is pronounced, and this adds considerable support to the contention that acoustic losses in unconsolidated water-saturated sediments are due in large part to viscous losses occurring at grain boundaries, and in channels between grains. The factor M is important also, however, in determining the total absorption. Probably M is a more complicated function than that suggested by equations (17) and (18), and ψ gives only a rough measure of it.

ABSORPTION DEPENDENCE ON FREQUENCY

A theory of absorption applicable to a general sediment containing both suspended particles and "particles-in-contact" probably does not exist. However, due to the additive nature of the absorption process, some general predictions about the dependence of absorption on frequency in a general sediment can be made by adding the effects due to particles in both conditions.

Equation (14), derived for suspended particles assuming energy loss through viscosity, calls for a frequency dependence of the form

$$\alpha = \frac{m + nf^{1/2}}{a + bf^{-1/2} + cf^{-1} + df^{-3/2} + hf^{-2}}, \tag{19}$$

where $\alpha, f, a, b, c, d, h, m,$ and n are, respectively, the absorption factor, frequency, and constants. Biot's (1956a, b) theories for fluid-filled porous solids at frequencies high enough that Poiseuille flow does not hold call for an absorption coefficient proportional to the square root of frequency, and for lower frequencies, where Poiseuille flow does hold, for absorption proportional to the square of frequency. However, in a porous granular material the pore space is irregular in shape, so that at a frequency high enough that Poiseuille flow does hold for the main part of the larger pores there will be regions where it does not hold, such as the space which immediately surrounds the contact area between grains. For the general sediment, the suspended particle theory would apply in part, together with both the high and low frequency theories of Biot.

If these three theories are simultaneously valid for the general sediment, the consequences would be that: (1) for a given material the frequency dependence of absorption changes with frequency because (a) the acoustic surface area of suspended particles is frequency dependent, and (b) because in pores of irregular shape the relative amounts of energy lost through Poiseuille flow and non-Poiseuille flow are frequency dependent, (2) the frequency dependence of absorption for each fluid-grain aggregate is unique. It is probable that for any sediment the change of absorption with frequency lies between the extremes of frequency-squared dependence and square-root-of-frequency dependence.

The absorption measurements of this dissertation provide data which fit within these relatively broad theoretical limits. The resonant technique used for the measurements provided values at two and sometimes three frequencies for individual samples. Occasionally one of the resonant modes gave a value inconsistent with other values for a particular sample, assuming an increase of absorption with frequency. Omitting such inconsistencies, the relation of absorption to frequency was examined for 65 samples. This is shown graphically in Figure 12, where, in addition to the measurements, typical curves for absorption proportional to the first and second power of frequency are given.

For the frequency range involved in the measurements the relation between absorption, α, frequency, f, and a constant, K, can be approximated by the expression $\alpha = Kf^n$. If it is assumed that this expression holds down to zero frequency, then values of n may be determined from absorption measurements at two frequencies. An individual value of n so determined carries little weight by itself because of the possibilities of experimental error. An average n for a number of samples is more meaningful. For the 65 samples used, this average n equals 1.79. The standard deviation of n is 0.98.

ACKNOWLEDGMENTS

Dr. W. J. Toulis of the Navy Electronics Laboratory was my outstanding benefactor in this study, for he developed the theory for the resonant chamber method, helped to set up the basic equipment, and offered advice and encouragement throughout the work. Dr. E. L. Hamilton of NEL encouraged this study by supporting it wherever possible and by being a diving partner in the collection of samples. Drs. R. J. Christensen, G. H. Curl, and Mr. K. V. Mackenzie of NEL provided helpful suggestions throughout the work. Others at NEL who have helped in one way or another include Mr. G. Prible and Miss M. L. Hagar who did the drafting; Mr. John Newton and Mr. Kim Igelman who made the grain-size analyses; Mr. R. F. Dill, Mr. D. G. Moore, and Mr. C. J. Shipek who assisted in sample collecting.

Particularly helpful discussions of this study were provided at various times by Professor R. W. Raitt of the Scripps Institution of Oceanography of the

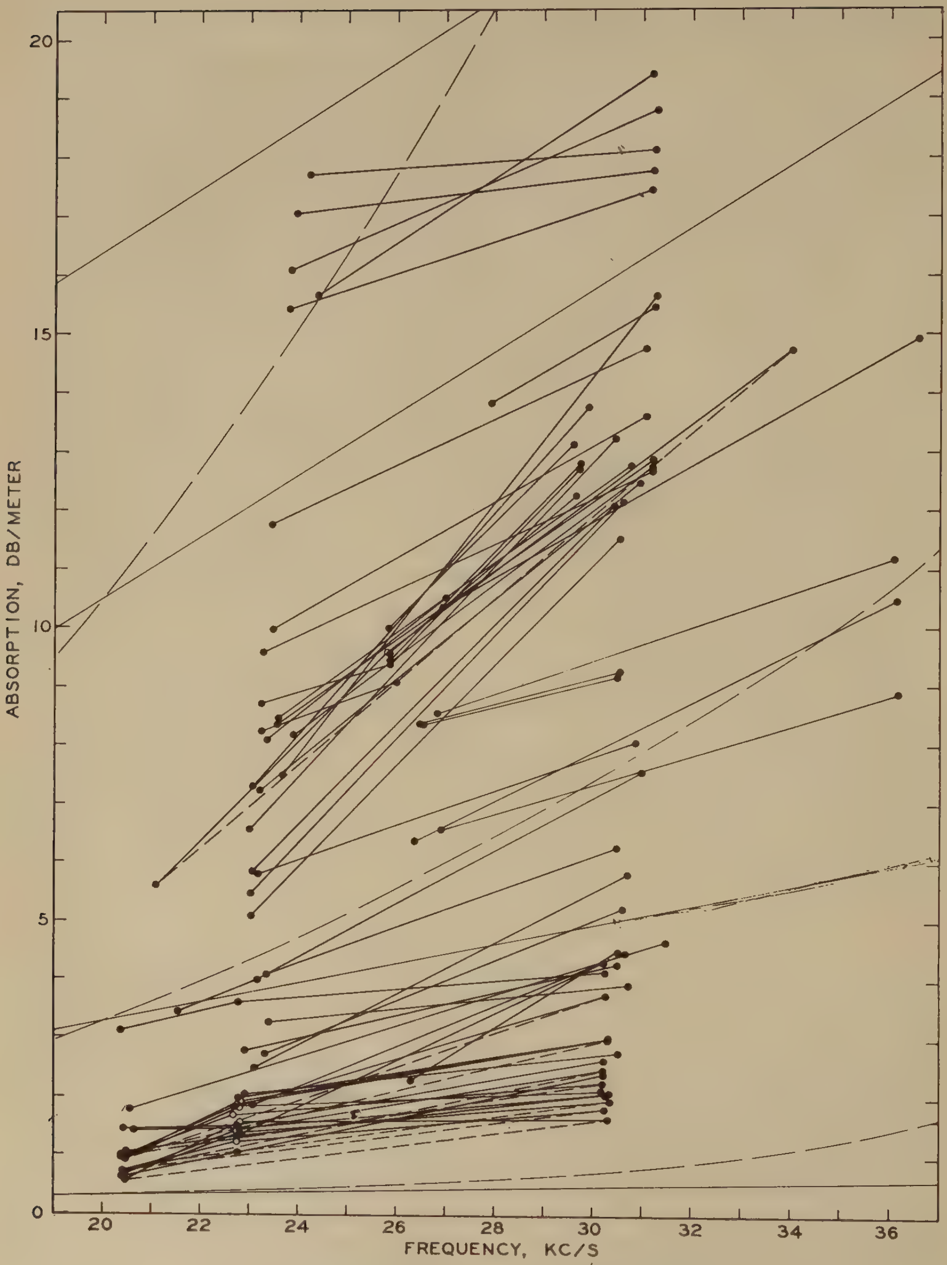

FIG. 12. Sound absorption in sediments vs. frequency.

University of California. Others at Scripps Institution who have given advice include Professors D. L. Inman, L. N. Lieberman, and H. W. Menard. Dr. R. L. Fisher, Mr. M. A. Beal, and Mr. J. H. Sherman III helped in the collection of samples.

REFERENCES

Ament, W. S., 1953, Sound propagation in gross mixtures: Jour. Acoustical Soc. Amer., v. 25, p. 638–641.

Biot, M. A., 1956a, Theory of propagation of elastic waves in a fluid-saturated porous solid. I. Low-frequency range: Jour. Acoustical Soc. Amer., v. 28, p. 168–178.

——— 1956b, Theory of propagation of elastic waves in a fluid-saturated porous solid. II. Higher frequency range: Jour. Acoustical Soc. Amer., v. 28, p. 179–191.

Birch, F., and Bancroft, D., 1938a, Elasticity and internal friction in a long column of granite: Bull. Seismological Soc. Am., v. 28, p. 243–254.

——— 1938b, The effect of pressure on the rigidity of rocks: Jour. Geology, v. 46, p. 59–87, 113–141.

Birch, F., Schairer, J. F., and Spicer, H. C., 1942, Handbook of Physical Constants: Geol. Soc. Amer., Special Paper 36.

Brandt, H., 1954, A study of the speed of sound in porous granular media: unpublished Ph.D. Dissertation, U. Calif., Berkeley.

——— 1955, A study of the speed of sound in porous granular media: Jour. Appl. Mech., Trans. A.S.M.E., v. 77, p. 479–486.

Busby, J., and Richardson, E. G., 1957, The absorption of sound in sediments: Geophysics, v. 22, p. 821–828.

Del Grosso, V. A., 1952, The velocity of sound in sea water at zero depth: U. S. Naval Research Laboratory Report 4002.

——— Sumra, E. J., and Fougere, P. F., 1954, Accuracy of ultrasonic interferometer velocity determinations: U. S. Naval Research Laboratory Report 4439.

Diamond, S., and Kinter, E. B., 1958, Surface areas of clay minerals as derived from measurements of glycerol retention: Clays and Clay Minerals, 5th Nat. Conf. on Clay and Clay Minerals, Nat. Acad. Sci., Nat. Res. Council, Pub. 566.

Emery, K. O., Butcher, W. S., Gould, H. R., and Shepard, F. P., 1952, Submarine geology off San Diego, California: Jour. Geology, v. 60, p. 511–548.

Gassmann, F., 1951a, Über die Elastizität poroser Medien: Vierteljahrsschrift der Naturforschenden Gesellschaft in Zürich, Heft 1.

——— 1951b, Elastic waves through a packing of spheres: Geophysics, v. 16, p. 673–685.

Green, E. I., 1955, The story of Q: American Scientist, v. 43, p. 584–594.

Hamilton, E. L., 1956, Low sound velocities in high-porosity sediments: Jour. Acoustical Soc. Amer., v. 28, p. 16–19.

——— and Menard, H. W., 1956, Density and porosity of sea-floor surface sediments off San Diego, California: Bull Amer. Assoc. Petroleum Geol., v. 40, p. 754–761.

——— Shumway, Geo., Menard, H. W., and Shipek, C. J., 1956, Acoustic and other physical properties of shallow-water sediments off San Diego: Jour. Acoustical Soc. Amer., v. 28, p. 1–15.

Ide, J. M., 1937, The velocity of sound in rocks and glasses as a function of temperature: Jour. Geology, v. 45, p. 689–716.

Iida, Kumizi, 1938, The velocity of elastic waves in sand: Bull. Earthquake Res. Inst., Tokyo Imperial Univ., v. 16, p. 131–144.

——— 1939, Velocity of elastic waves in a granular substance: Bull. Earthquake Res. Inst., Tokyo Imperial Univ., v. 17, p. 783–808.

Inman, D. L., 1952, Measures for describing the size distribution of sediments: Jour. Sediment, Petrology, v. 22, p. 125–145.

——— and Chamberlain, T. K., 1955, Particle-size distribution in near-shore sediments: Finding Ancient Shorelines, Spec. Pub. 3, Soc. Econ. Paleontologists and Mineralogists, p. 106–129.

Kerner, E. H., 1956, The elastic and thermo-elastic properties of composite media: Proc. Phys. Soc. (London) B 69, p. 808–813.

Knopoff, L., and MacDonald, G. J. F., 1958, Attenuation of small amplitude stress waves in solids: Rev. Modern Physics, v. 30, p. 1178–1192.

Kulp, J. L., and Carn, D. R., 1952, Surface area of deep-sea sediments: Jour. Geology, v. 60, p. 148–159.

Lamb, H., 1945, Hydrodynamics: Dover Publications, 6th ed.

Laughton, A. S., 1954, Laboratory measurements of seismic velocities in ocean sediments: Proc. Royal Soc., A, v. 222, p. 336–341.

——— 1955, The compaction of ocean sediments: unpublished Ph.D. Dissertation, Cambridge Univ.

——— 1957, Sound propagation in compacted ocean sediments: Geophysics, v. 22, p. 233–260.

Mackenzie, J. K., 1950, The elastic constants of a solid containing spherical holes: Proc. Phys. Soc. (London) B, v. 63, p. 2–11.

Mifsud, J. F., 1953, Experimental study of the acoustic properties of water filled sands: Univ. of Texas, Defense Res. Lab., Acoustical Report 72.

Moore, D. G., in press, Vane shear strength, porosity, and permeability relations of some sieved cohensionless sands: Proc. XX Internat. Geol. Cong.

Moore, D. G., and Shumway, Geo., 1959, Sediment thickness and physical properties, Pigeon Point Shelf, California: Jour. Geophys. Res., v. 64, p. 367–374.

Nafe, J. E., and Drake, C. L., 1957, Variations with depth in shallow and deep water marine sediments of porosity, density and the velocities of compressional and shear waves: Geophysics, v. 22, p. 523–552.

Nelson, R. A., and Hendricks, S. B., 1943, Specific surface of some clay minerals, soils and soil Colloids: Soil Sci., v. 56, p. 285–296.

Paterson, N. R., 1955, Seismic wave propagation in porous granular media: unpublished Ph.D. Dissertation, Univ. of Toronto.

——— 1956, Seismic wave propagation in porous granular media: Geophysics, v. 21, p. 691–714.

Poole, D. M., 1957, Size analysis of sand by a sedimentation technique: Jour. Sedimentary Petrology, v. 27, p. 460–468.

Sato, Y., 1952, Velocity of elastic waves propagated in media with small holes: Bull. Earthquake Res. Inst., Tokyo Univ., v. 30, p. 179–190.

Sewell, C. T. J., 1910, The extinction of sound in a viscous atmosphere by small particles of cylindrical and spherical form: Phil. Trans. Roy. Soc. London, v. 210, p. 239–270.

Shumway, Geo., 1956, A resonant chamber method for sound velocity and attenuation measurements in sediments: Geophysics, v. 21, p. 305–319.

——— 1958, Sound velocity vs. temperature in water-saturated sediments: Geophysics, v. 23, p. 494–505.

——— 1958, Sound speed and absorption studies of marine sediments by a resonance method: Unpuglished Ph.D. dissertation, University of California at La Jolla.

Sutton, G. H., Berckhemer, H., and Nafe, J. E., 1957, Physical analysis of deep sea sediments: Geophysics, v. 22, p. 779–812.

Takahashi, T., and Sato, Y., 1949, On the theory of elastic waves in granular substances: Bull. Earthquake Res. Inst., Tokyo Univ., v. 27, p. 11–16.

Toulis, W. J., 1956, Theory of a resonance method to measure the acoustic properties of sediments: Geophysics, v. 21, p. 299–304.

Urick, R. J., 1947, A sound velocity method for determining the compressibility of finely divided substances: Jour. Acoustical Soc. Amer., v. 18, p. 983–987.

——— 1948, The absorption of sound in suspensions of irregular particles: Jour. Acoustical Soc. Amer., v. 20, p. 283–289.

——— and Ament, W. S., 1949, The propagation of sound in composite media: Jour. Acoustical Soc. Amer., v. 21, p. 115–119.

White, J. E., and Sengbush, R. L., 1953, Velocity measurements in near-surface formations: Geophysics, v. 18, p. 54–69.

Wood, A. B., 1930, A Textbook of Sound: G. Bell and Sons, London.

(696)

Short Notes

BULLETIN OF THE GEOLOGICAL SOCIETY OF AMERICA
VOL. 71, PP. 1271–1278, 3 FIGS., 1 PL. AUGUST 1960

POSSIBLE PRE-PLEISTOCENE DEEP-SEA FANS OFF CENTRAL CALIFORNIA

BY H. W. MENARD

The deep-sea floor off central California has been surveyed from the base of the continental slope to a distance of about 250 miles from shore by the Coast and Geodetic Survey for the Navy using the Survey ship PIONEER. A Precision Depth Recorder gave depths accurate to within 1 fathom, and an Electronic Position Indicator system yielded positions accurate to within a few hundred feet. Sounding lines were spaced about 5 miles apart, and the depth was continuously recorded with a 1-second interval between soundings. Boat sheets available to the writer have soundings plotted with an average spacing of 1 mile on a scale of about 1/300,000.

Adequate description of California submarine canyons was not possible until the Coast Survey made detailed soundings in the 1930's (Shepard and Emery, 1941). For 20 years the shapes of the canyons have been known, but any discussion of their origin has suffered because the sedimentary deposits resulting from the erosion were unsurveyed. The PIONEER survey has filled this gap, and certain relatively firm conclusions can be drawn from the topography alone.[1] The writer has not attempted to discuss some aspects of the data because they will become clearer within the next few years after further coring and seismic observations are made.

The PIONEER towed a magnetometer which was operated by various Scripps scientists, chiefly A. D. Raff and Ronald Mason who headed the group (Mason, 1958). Consequently a magnetic map is available for the whole area of the topographic survey. A few seismic-refraction stations were made in the southeastern corner of the area by R. W. Raitt, and a line of gravity stations was taken by J. C. Harrison and colleagues of the Institute of Geophysics.

The PIONEER survey stops just short of the edge of the deep-sea fans off California, but soundings have been taken to and beyond the edge by the Scripps Mid-Pacific, Northern Holiday, Cusp, Transpac, and Mukluk expeditions and by the American Telephone and Telegraph Company on the M/V HUDDLE. Echograms from these cruises have been used to clarify details in the area surveyed by the PIONEER.[2]

Many large submarine canyons dissect the continental slope off central California. Gigantic deep-sea fans spread out from the mouths of Delgada and Monterey canyons, and a smaller fan from Arguello Canyon. Delgada and Monterey deep-sea fans are confined within a very broad trough bounded north and south by the Mendocino and Murray fracture zones respectively (Figs. 1, 2). Another province of fans and abyssal plains lies north of the Mendocino fracture zone, but it is almost 800 fathoms shallower than the central California fans. The regions are separated by the Mendocino Ridge which acts as a dam preventing north-south movement of sediment on the deep-sea floor. Murray fracture zone has a relatively low relief, and Arguello deep-sea fan has buried it in one place and filled a few small basins in the Baja California seamount province to the south.

Delgada and Monterey deep-sea fans merge imperceptibly and terminate to the west in a group of connected smooth-bottomed basins. Many hills rise out of the fans, although there are no large volcanic mountains like those in the Baja California seamount province to the south (Menard, 1955b). In addition there are low north-trending ridges with associated shallow troughs in the southwest corner of the area. The best surveyed group of ridges and troughs is about 100 miles long, 20 miles wide,

---

[1] A 20-fathom contour-interval chart of the region prepared by the writer from this survey has been given a security classification by the Hydrographic Office. A more generalized chart based on earlier soundings has been published (Menard, 1955a, Fig. 6). A 50-fathom contour-interval chart of part of the region is based on the PIONEER survey (Menard and Vacquier, 1958, Fig. 4).

[2] The FANFARE expedition in July, 1959, made five seismic stations on parts of the Monterey and Delgada fans at localities chosen to determine any changes in thickness of sediment. The fans were cored extensively, and channels were surveyed. Final conclusions based on FANFARE will not be available for some time, but preliminary shipboard results confirm the calculations and conclusions presented here.

(697)

ntributions from the Scripps Institution of Oceanography, New Series, 1185

Reproduced by Permission

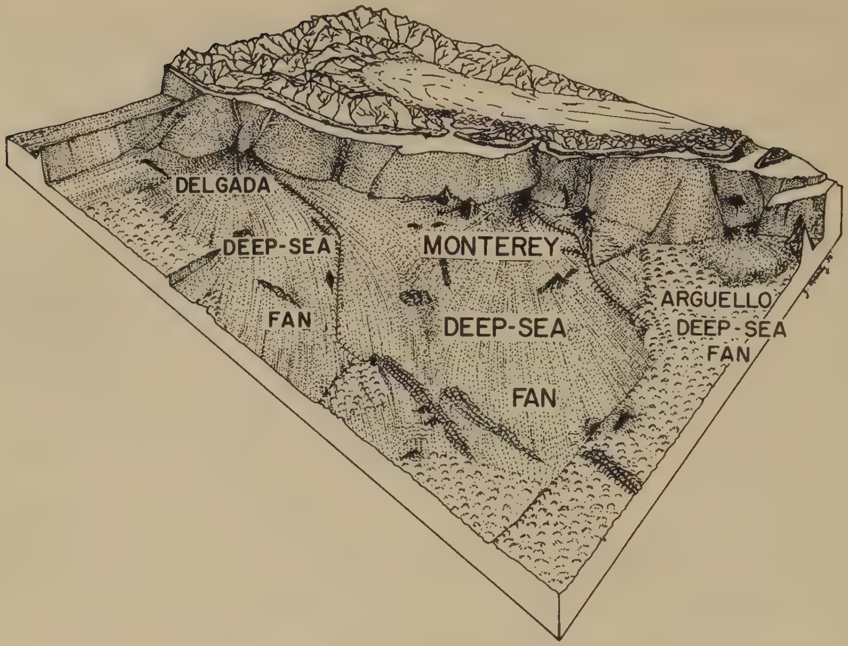

Figure 1.—Block Diagram of the Sea Floor and Coast of Central California

Deep-sea fans spread out from the mouths of Delgada, Monterey, and Arguello canyons. The first two fans are confined in a broad trough between the Mendocino and Murray fracture zones.

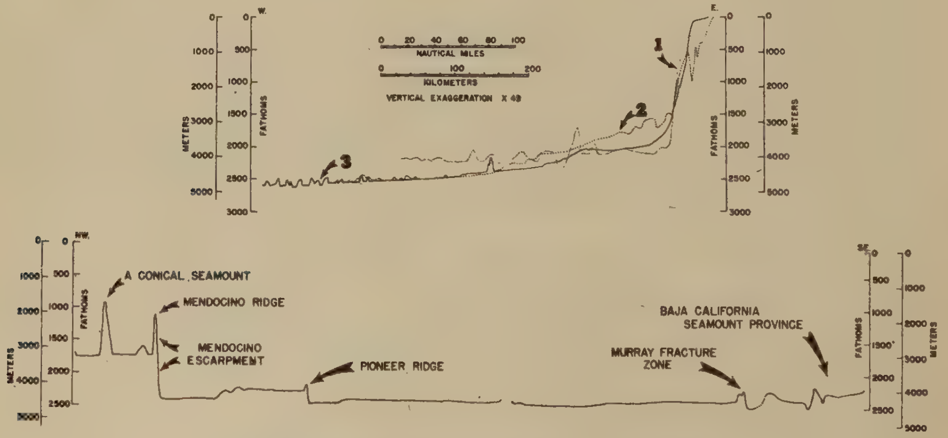

Figure 2.—Profiles Along Coast of California

Above, profiles perpendicular to the coast off (1) the continental borderland of southern California, (2) Monterey Canyon, and (3) Delgada Canyon. Below, profile parallel to the coast of central California about 200 miles from land.

and 100 fathoms high (Menard and Vacquier, 1958, Fig. 4). The relief is so subdued it could not be contoured with confidence except that the surrounding abyssal plain is such a smooth datum. Similar groups of low, north-trending ridges and troughs appear to be present south of the Murray fracture zone, but they are obscured by other hills and mountains These groups have the same dimensions and trends as anomalies of the total magnetic field in the area (Mason, 1958). The magnetic anomalies have sharp boundaries and are roughly 400 gauss. They can be contoured with much more confidence than the low hills and troughs and support the existence of the latter features, especially south of the Murray fracture zone.

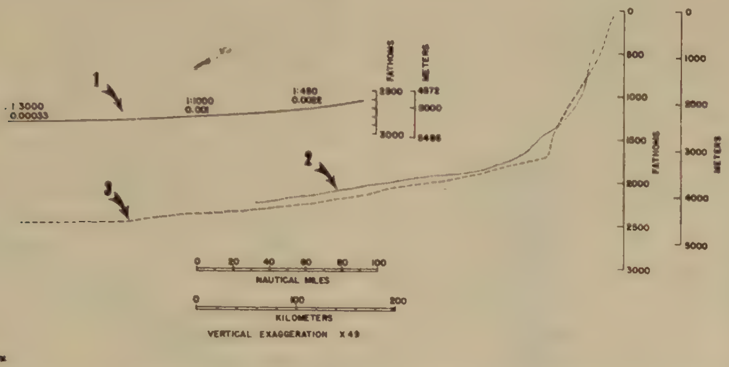

FIGURE 3.—COMPARISON OF ABYSSAL-PLAIN SLOPES AND DEEP-SEA CHANNELS

(1) Abyssal-plain slopes (after Heezen *et al.*, 1954) and longitudinal profiles of (2) Monterey Canyon and deep-sea channel and (3) Delgada Canyon and deep-sea channel.

A newly discovered ridge, here named Pioneer Ridge, trends west for at least 100 miles along latitude 38°45′. The region south of the ridge is about 200 fathoms deeper than to the north. A very similar and possibly connected ridge with a similar regional change in depth lies about 90 miles to the west and extends along the same latitude for at least 230 miles. The ridges are similar to the parallel Mendocino Ridge to the north in all respects but size.

Delgada deep-sea fan radiates from the mouth of Delgada submarine canyon at a depth of about 1500 fathoms. Sediment has spread northwest across the fan into a trough at the base of the Mendocino Escarpment and to the edge of the surveyed area. The spreading probably has continued in the trough to the smooth bottom found by the Mid-Pacific Expedition 420 miles from the head of the fan. Sediment transported southwest from the canyon mouth enters a similar trough at the base of Pioneer Ridge and probably continues in this trough for a total distance of about 400 miles. One major deep-sea channel extends 240 miles from the mouth of the canyon. The slope decreases from about 0.006 to 0.0004 (2.4 feet per mile), but local variations exist like those in most rivers (Fig. 3).

Monterey deep-sea fan is a remarkably uniform feature with a radius of about 200 miles although it is restricted on the south by the Murray fracture zone. A major deep-sea channel has been traced for about 170 miles to the south of the fan head, and a small secondary fan occurs where the channel crosses a ridge.[3]

Both large fans show the influence of low north-trending ridges which act as dams. The effect is most noteworthy on the western edge of the Monterey fan where it is ponded beside the ridges and slopes around the ends (Menard and Vacquier, 1958, Fig. 4). It is not unreasonable to assume that ridges nearer the sediment source have been buried because north-trending magnetic anomalies with the same trend and dimensions as the ridges exist under the smooth parts of the fans. Buried ridges would also account for the observed changes in slope of the fans and deep-sea channels (Pl. 1). There is some suggestion that the channels are entrenched where they cross what may be buried or partially buried ridges, particularly at the intersection of Monterey channel and a line of seamounts and low ridges. The apparent trenching may be erosional or nondepositional in origin.

Volume relationships may be useful in separating trivial processes from important ones. For this reason an attempt is made to estimate volumes eroded and deposited off central California even though the calculations are necessarily rough and mostly deal with orders of magnitude. Extreme values are compared in most calculations because they are usually more illuminating than averages. Thus, it may be convincing to demonstrate that the maximum volume eroded by some process is only a small fraction of the minimum volume of a sedimentary deposit so that the first did not produce the second. It may be less convincing to deal with averages because they are not so definite as extremes in this type of comparison.

---

[3] Sand, pebbles, and shell fragments were cored from this channel on the FANFARE expedition. This coarse material had been transported 160 miles from the head of Monterey canyon .

The total area of the deep-sea fans off central California is roughly 2.4×10^5 km^2 of which about 2×10^5 km^2 is surveyed and about 0.4×10^5 km^2 is estimated from expedition echograms beyond the limits of the survey. Abyssal hills probably have been buried under any smooth area (Menard, 1956, p. 2195), and a minimum volume of the fans can be calculated if the height of the hills is known. The hills immediately west of the fans have an average relief of 300 m which is the same as the average for the whole Pacific Basin. The unusual groups of low ridges and troughs also have a relief of 300 m so that the minimum thickness of sediment in the fans may be taken as 300 m with some confidence. Some of the sediment certainly is of pelagic origin, but it can be neglected because the same pelagic sediment rains on the hills as on the fans, and the smoothing results from the difference in the rates of sedimentation in the two environments. Rates of sedimentation of Pacific pelagic clays (Goldberg, 1958) and of turbidity currents in the Hudson deep-sea fan (Ericson *et al.*, 1955, p. 216) have a ratio of 1/100 which also suggests that pelagic sedimentation can be neglected although turibidity-current deposition may be only intermittent. Granting 300 m thickness, the blanket of sediment produced by turbidity-current deposition of continental material is 7.2×10^4 km^3 minus the initial hilly relief above a datum which has the same general shape as the present surface of the fans. Whether the hills were adjacent cones or groups of ridges and troughs separated by smoother areas, their volume was about a quarter of the layer, leaving a sedimentary fill of 5.4×10^4 km^3.

Inasmuch as the initial general relief of the sea floor under Delgada and Monterey fans is unknown, with regard to sedimentary volume it can be considered to have ranged between approximately the shape of the present surface and the shape of a trench. The volume calculated above would approximate the irreducible minimum. A trench, which would have to be filled, would require a maximum sedimentary volume to produce the present surface of the fans. There is no evidence for a filled trench. However, a volume much larger than the minimum is suggested by comparison of the deep-sea fan province with the adjacent topographic provinces to the north and south. The ridge and trough province to the north features a very broad, smooth-bottomed trough at the base of the continental slope and a range of low mountains west of the trough. The Baja California seamount province to the south is hilly and mountainous, but for several hundred miles off shore the regional depth is relatively constant. Therefore, in either of the adjacent provinces, it would be necessary to build up a thick wedge of sediment to produce the type of topography of Delgada and Monterey fans. The inner portions of these two fans, between the depths of 1800 and 2500 fathoms, may be considered as such a wedge with a base at 2500 fathoms and a volume of 1.4×10^5 km^3. If the fans are isostatically compensated, a downbowing of the crust would result in doubling the thickness and volume to yield a continuous westward slope. Downbowing is suggested by echograms (Pl. 1) in that the general level of the peaks of abyssal hills appears to dip under the edge of the fans. The same effect occurs at the outer edge of some archipelagic aprons (Menard, 1956, p. 2204). The volume of the buried hills can be neglected in this calculation, and the volume of the fans is 2.8×10^5 km^3.

It appears that the volume of Delgada and Monterey fans is of the order of 10^5 km^3. A volume of 5×10^4 km^3 may be considered as minimum.[4]

The volume of the continental slope eroded to form a submarine canyon has been established by computing the volume of similar regular polyhedrons. By this method Delgada submarine canyon has a volume of 300 km^3, and the volume of Monterey submarine canyon is 450 km^3. This compares with a figure of 320

---

[4] R. W. Raitt has been kind enough to calculate the volume of the fans on the basis of his preliminary shipboard results from seismic stations on the FANFARE expedition. The volume of sediment in the area of the fans is roughly 1.6×10^5 km^3. The volume of sediment which would be anticipated in an equal area of the Pacific with normal hilly relief is 0.7×10^5 km^3, and the difference of 0.9×10^5 km^3 is the excess of sediment which has produced the fans. The order of magnitude of calculations used in this paper may be accepted without reservation on the basis of Raitt's preliminary seismic results.

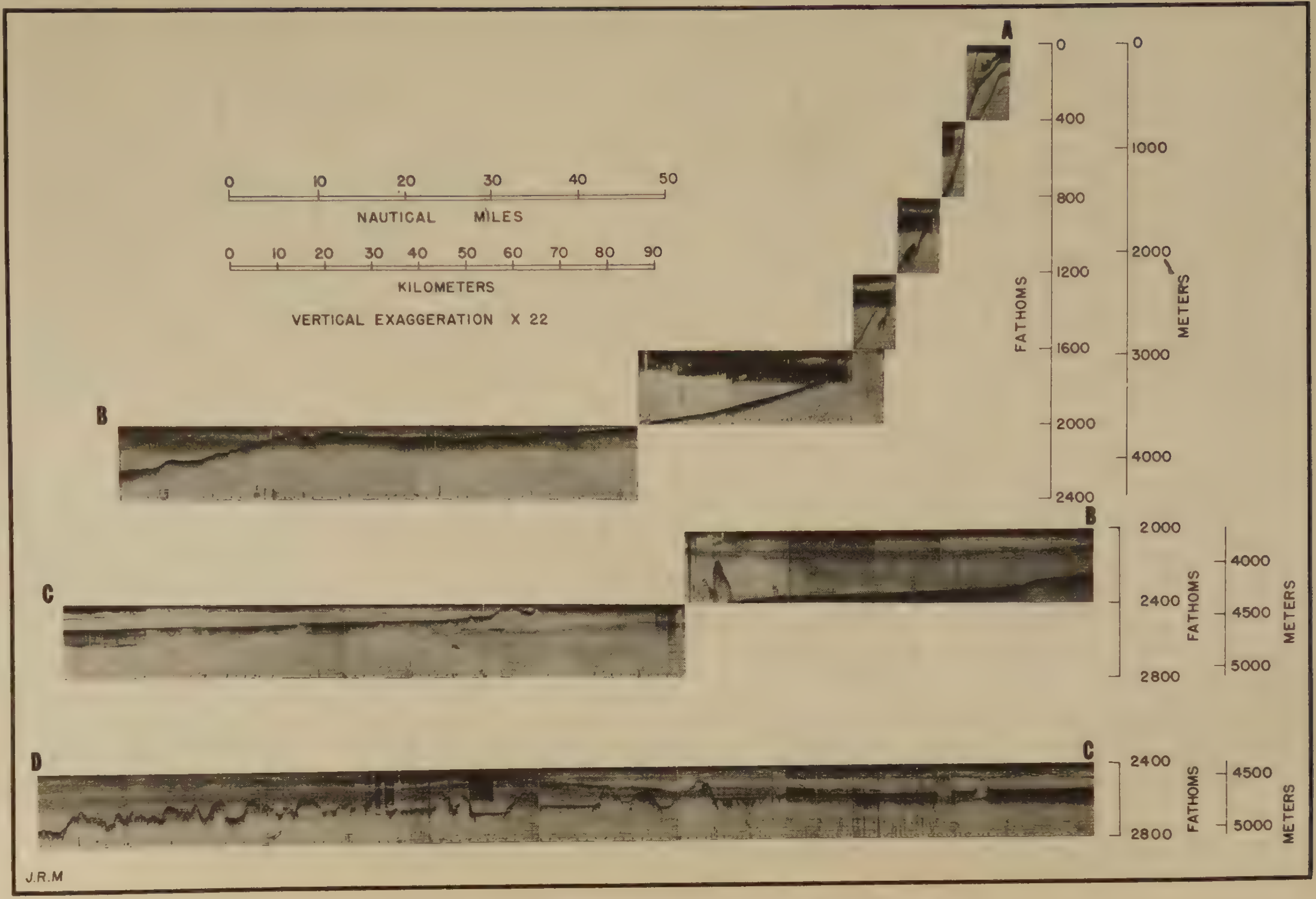

ECHOGRAM FROM PT. ARENA WEST-SOUTHWEST ACROSS DELGADA DEEP-SEA FAN TO ITS WESTERN EDGE WHERE IT FILLS BASINS BETWEEN ABYSSAL HILLS

km³ for the latter canyon, calculated by Dill, Dietz, and Stewart (1954, p. 191), and gives a measure of the uncertainty. The total volume of all submarine canyons between Cape Mendocino and Point Conception is roughly 1.5 × 10³ km³, or about one-thirtieth of the minimum volume of the fans. Therefore the fans contain sediment eroded from places other than submarine canyons.

One such place is the continental shelf off central California which has outcrops of rock and may be considered as a predominantly erosional feature. The volume removed to sea level is about 10³ km³. Assuming that an initially mountainous terrane like the Coast Ranges had an average relief of 300 m above sea level, roughly 5 × 10³ km³ would be eroded to form the present shelf.

The volume of material eroded from the continental slope and shelf amounts to litle more than one-tenth of the minimum amount deposited in the deep-sea fans. Consequently most of the sediment in the fans must have been eroded and transported to the continental shelf by rivers and mass wasting. The predominance of river erosion over sea-cliff erosion is again confirmed (Lyell, 1873, p. 572).

Deep-sea fans head at the mouths of Delgada and Monterey submarine canyons, but a few other tributary or adjacent canyons may contribute sediment. Spanish Canyon is a tributary of Delgada, and Noyo Canyon debouches near the head of Delgada fan. Monterey Canyon has several important tributaries, and Sur, Partington, and Lucia canyons appear to lead out to Monterey fan. The canyons between these two groups do not have large fans at their mouths although there is a sedimentary apron which may have been formed by the lateral merging of relatively small fans. The only obvious difference between the canyons with and without fans is that the former cut the continental shelf almost to the shore line, and the latter barely notch the edge. This relationship confirms the significance of similar observations in the continental borderland off southern California (Gorsline, 1958).

The relationship between types of canyons and fans appears to be meaningless unless the dominant direction of transport of sediment on the continental shelf is parallel to the shore line so that one type of canyon traps all the sediment. Granting this conclusion, the central California region is a relatively self-contained sedimentary province because little sediment can pass Mattole canyon at Cape Mendocino, although some sediment is lost around Point Conception (Trask, 1955, p. 2). The volume of long-shore transport in southern California is of the order of 10⁵–10⁶ m³/year (Handin, 1951). It is unmeasured in central California but probably tends toward 10⁶ m³/year (D. L. Inman, personal communication, 1958).

The material eroded away to form all central California submarine canyons is less than 1.5 × 10³ km³. The material deposited in the fans is at least 5 × 10⁴ km³ or roughly 30 times as great. The location of the fans at the mouths of Delgada and Monterey canyons indicates that most of the sediment has been channeled through these canyons alone. Consequently the ratio of volumes is even larger. It is evident that the dominant role of these canyons is to funnel sediment from the continental shelf to the deep-sea floor.

Sediment is deposited in the heads of submarine canyons because they are traps intersecting long-shore drift (Shepard and Emery, 1941, p. 93). Similarly the sides of canyons intercept sediment moving laterally on the shelf. The sediment eventually slumps into the canyons. When it emerges on the fan at the mouth of the canyon it may be suspended in a turbidity current capable of transporting sediment for hundreds of miles across very gentle slopes and around topographic barriers. The transformation from observed slump to circumstantially evident turbidity current occurs somewhere in the canyon.

One of the important questions regarding submarine canyons is whether they were cut in Pleistocene time. Data from the relatively self-contained sedimentation system of central California can be brought to bear on this question because Delgada and Monterey canyons have existed while sediment was channeled through them from the continent to the deep-sea fans. The minimum volume of the fans, therefore, can be equated to the drainage area to determine the denudation necessary for a Pleistocene age.

The recent geological history of central California is characterized by intense orogeny and erosion, but the present drainage pattern may be taken as an approximation of the Pleistocene one. Many small, short rivers drain the west slope of the Coast Ranges, and the greater Sacramento and San Joaquin rivers drain the Sierra Nevada and the east slope of the Coast Ranges. The total drainage area is 1.8 × 10⁵ km². In most of the area, however, the coarse products of rapid erosion of steep slopes were deposited locally. The end result was a shifting of sediment within the continental area rather than a loss to the deep sea. Perhaps the western slope of the Coast Ranges may be taken as the area from which material was transported to deep-sea fans. This area is 3 × 10^4 km^2; the minimum volume of the fans requires almost 2 × 10^3 m of denudation. Local erosion of mountain ranges occurred on this scale during the Pleistocene in California (Eaton, 1941, p. 206), but deposition was widespread, and locally it was also very thick. For regional denudation the ridges between valleys must be eroded away, and all the sediment produced must be transported out of the region. The geological record of the Coast Ranges does not show any such enormous regional denudation in Pleistocene time. Consequently it appears that initial deposition of Delgada and Monterey fans was pre-Pleistocene.

The rate of construction of the fans in pre-Pleistocene time is barely amenable to quantitative estimation. The drainage area leading to the open ocean is ill-defined; boundaries between land and smaller continental arms of the sea fluctuated rapidly; and an indefinite fraction of the products of subaerial erosion was retained within the drainage area in local basin deposits. These various factors suggest that the rate of construction of the fans was much slower than in the Pleistocene. Extrapolation of the present rate of denudation (Salisbury, 1913, p. 154; Revelle and Shepard, 1939, p. 273) as a rough average for both Pleistocene and Tertiary yields fan ages of 4 × 10^6 to 2 × 10^7 years depending on the assumed area of the drainage basin that was denuded.

The largest measured slump at the head of a California submarine canyon had a volume of 1.5 × 10^5 m^3 (D. L. Inman, personal communication). The slump extended beyond the area of the original survey and consequently was somewhat larger than the measurements indicate. Although accurate surveys are not available in most places, it appears improbable that many slumps exceed 10^7 m^3. Such a slump, perhaps 1 km square and 10 m deep, would be unlikely to escape notice off heavily populated areas.

The effective density of a turbidity current in Lake Mead graded from 10^{-3} gm/cm^3 at the top to 0.2 gm/cm^3 near the bottom with an average of about 0.05 gm/cm^3 (Gould, 1951, p. 45). In terms of volume, the water–sediment ratio was roughly 1/40. Application of this ratio to the slumps in California submarine canyons suggests that the volume of a turbidity current rarely exceeds 4 × 10^8 m^3. Inasmuch as the cross section of Monterey deep-sea channel is as great as 10^6 m^2, the channel is easily capable of containing the current provided the slug of turbid water is as long as the original slump.

When the shore line receded in Pleistocene time of lowered sea level, Monterey and Delgada canyons became long deep embayments with steep subaerial and submarine slopes. The area of accumulation of sediment in canyons was much increased. At that time slumps may have been much larger than at present. At some time turbidity currents were capable of filling deep-sea channels to overflowing, building natural levees, and of spreading as sheet flows to form fans.

Slumps are common around submarine canyon heads (Shepard and Emery, 1941, p. 93–103). Off La Jolla where surveys are repeated frequently, slumping and filling occur constantly (Shepard, 1951, p. 58). An average of at least one slump per year is required if long-shore drift is in short-term equilibrium with slumping because the drift is roughly equal to the largest observed slump. Granting that unobserved slumps may be as large as 10^7 m^3, one slump in 10 years would be the minimum in central California. These figures suggest that roughly 10^6 slumps have passed into the heads of Delgada and Monterey canyons—presumably resulting in a similar number of turbidity currents emerging at the mouths. Lateral transport on the continental shelf also introduces sediment into canyons and produces slumps, but this contribution cannot be evaluated at present. The preponderance of silt in fans suggests that the contribution is large.

Evidence has been presented suggesting that some central California submarine canyons are primarily conduits for sediment poured into their heads by long-shore drift. Are the canyons cut by the passage of the sediment?

The volume of a submarine canyon removed by downcutting is small compared with the whole. The triangular cross section of canyons probably results from the same mass wasting that produces the same cross section on land. These canyons are submerged, however, and some of the widening upward may be caused by deposition of unconsolidated sediment on the surrounding shelf (Shepard, 1952, p. 85). Lithification would be expected during the time available so that canyons might appear to cut rocks that were actually deposited on each side of them. Pleistocene loess deposits on opposite sides of pre-Pleistocene rivers are analogous. If downcutting is taken as 100 m wide, the volume of Monterey canyon so eroded is only 2.8 km^3. Even with tributaries and adjacent canyons the volume is roughly 5 km^3. The minimum volume of Monterey deep-sea fan indicates that at least 5000 times as much sediment has flowed along the axis of the canyon as has been removed by downcutting.

The tentative conclusions about Monterey and Delgada canyons are as follows:

(1) Sediment is deposited around and in the head of the canyons by long-shore drift and by lateral transport on the continental shelf

(2) Sediment slumps into the canyons and emerges as turbidity currents.

(3) This process may have occurred more than a million times beginning in pre-Pleistocene, and possibly even pre-Pliocene time.

(4) The sediment so transported is 5000 times greater than the amount removed by downcutting.

(5) Millions of years were available for mass wasting to produce the triangular cross section of the canyons.

It appears that more time has been available for cutting these canyons than previously had been supposed. Qualitatively, marine slumps, turbidity currents, weathering, and mass wasting have been known to be active (Shepard and Emery, 1941; Woodford, 1951; Crowell, 1952), and the numbers presented here stress the importance of these processes.

Acknowledgments

The writer is indebted to the Navy Hydrographic Office for making the results of the PIONEER survey available and to the officers and men of the Coast and Geodetic Survey who collected them. R. W. Raitt and R. G. Mason kindly discussed their seismic and magnetic measurements prior to publication. D. G. Moore and F. P. Shepard critically reviewed the manuscript, and D. C. Krause independently duplicated the writer's measurements and calculations. The study was supported in part by the Office of Naval Research.

References Cited

Crowell, J. C., 1952, Submarine canyons bordering central and southern California: Jour. Geology, v. 60, p. 58–83

Dill, R. F., Dietz, R. S., and Stewart, H. B., 1954, Deep-sea channels and delta of the Monterey submarine canyon: Geol. Soc. America Bull., v. 65, p. 191–194

Eaton, J. E., 1941, The Pleistocene in California: Calif. Div. Mines Bull. 118, p. 203–206

Ericson, D. B., Ewing, M., Heezen, B. C., and Wollin, G. W., 1955, Sediment deposition in the deep Atlantic, p. 205–220 *in* Poldervaart, A., Editor, Crust of the earth: Geol. Soc. America Special Paper 62, 762 p.

Goldberg, E. D., 1958, Ionium-thorium chronology in deep-sea sediments of the Pacific: Science, v. 128, p. 1003

Gorsline, D. S., 1958, Turbidity current-deposits and the search for oil: Paper presented before 43d Annual Meeting Am. Assoc. Petroleum Geologists

Gould, H. R., 1951, Some quantitative aspects of Lake Mead turbidity currents, p. 34–52 *in* Turbidity currents: Soc. Econ. Paleontologists and Mineralogists Special Pub. no. 2, 107 p.

Handin, J. W., 1951, The source, transportation, and deposition of beach sediment in southern California: U.S Corps of Engineers Beach Erosion Board Tech. Memo. no. 22, 113 p.

Heezen, B. C., Ewing, Maurice, and Ericson, D. B., 1954, Reconnaissance survey of the abyssal plain south of Newfoundland: Deep-Sea Research, v. 2, p. 122–133

Lyell, C., 1873, Principles of geology: v. 1, 11th ed., New York, D. Appleton and Co., 671 p.

Mason, R. G., 1958, A magnetic survey off the west coast of the United States between latitudes 32° and 36°N, longitudes 121° and 128°W: Geophys. Jour., v. 1, p. 320–329

Menard, H. W., 1955a, Deep-Sea channels, topography, and sedimentation: Am. Assoc. Petrol. Geol. Bull., v. 39, p. 236–255

—— 1955b, Deformation of the northeastern Pacific Basin and the west coast of North America: Geol. Soc. America Bull., v. 66, p. 1149–1198.

—— 1956, Archipelagic aprons: Am. Assoc. Petrol. Geol. Bull., v. 40, p. 2195–2210

Menard, H. W., and Vacquier, V., 1958, Magnetic survey of part of the deep sea floor off the coast of California: Research Reviews, Office Naval Research, June, p. 1–5.

Revelle, R. R., and Shepard, F. P., 1939, Sediments off the California coast, *in* Trask, P. D., *Editor*, Recent marine sediments: London, Thomas Murby and Co., 736 p.

Salisbury, R. D., 1913, Physiography: 3d ed., New York, Henry Holt and Co., 770 p.

Shepard, F. P., 1951, Transportation of sand into deep water, p. 53–65 *in* Turbidity currents: Soc. Econ. Paleontologists and Mineralogists Special Pub. no. 2, 107 p.

——, 1952, Composite origin of submarine canyons: Jour. Geology, v. 60, p. 84–96

Shepard, F. P., and Emery, K. O., 1941, Submarine topography off the California coast: Geol. Soc. America Spec. Paper 31, 171 p.

Trask, P. D., 1955, Movement of sand around southern California promontories: U. S. Corps of Engineers Beach Erosion Board Tech. Memo. no. 76, 60 p.

Woodford, A. O., 1951, Stream gradients and Monterey sea valley: Geol. Soc. America Bull., v. 62, p. 799–852

INSTITUTE OF MARINE RESOURCES AND SCRIPPS INSTITUTION OF OCEANOGRAPHY, UNIVERSITY OF CALIFORNIA, LA JOLLA, CALIF.

MANUSCRIPT RECEIVED BY THE SECRETARY OF THE SOCIETY MARCH 11, 1959

CONTRIBUTION FROM THE SCRIPPS INSTITUTION OF OCEANOGRAPHY

(704)

SOME ATYPICAL ALGAL CHROMOPROTEINS

C. ÓhEOCHA AND F. T. HAXO
Scripps Institution of Oceanography, University of California, La Jolla, Calif. (U.S.A.)

ELSEVIER PUBLISHING COMPANY
AMSTERDAM

(705)

SOME ATYPICAL ALGAL CHROMOPROTEINS*

C. ÓHEOCHA** AND F. T. HAXO

Scripps Institution of Oceanography, University of California, La Jolla, Calif. (U.S.A.)

(Received December 24th, 1959)

SUMMARY

1. The biliproteins of two varieties of *Smithora* (*Porphyra*) *naiadum* were compared under identical conditions of extraction and chromatographic isolation. Fresh extracts of var. *australis* contain B-phycoerythrin, allophycocyanin and a purple complex having absorption maxima at 565 and 610 mμ. Upon standing, C-phycocyanin was released from this purple pigment fraction. Fresh extracts of var. *naiadum* contain B-phycoerythrin, allophycocyanin and C-phycocyanin. Upon standing, C-phycocyanin of the fresh var. *naiadum* extracts apparently becomes incorporated in a purple fraction resembling that in fresh extracts of var. *australis*.

2. The *in vivo* phycoerythrin of the three examined *Phormidium* species appeared to be C-phycoerythrin, absorption maximum approx. 565 mμ. This phycoerythrin was also obtained *in vitro* when extracted rapidly. On standing, extracts of these three algae yielded phycoerythrins having two absorption maxima (approx. 542 and 566 mμ). The formation of these artifact phycoerythrins appeared to be enzymically accelerated.

INTRODUCTION

The presence in red and blue-green algae of four spectrally distinct biliproteins has long been recognized. These are the R- and C- variants of phycoerythrin and phycocyanin, so designated by SVEDBERG AND KATSURAI[1] on the basis of their usual occurrence in the Rhodophyta or in the Cyanophyta. More recently attention has focused on unusual biliproteins which may occur as dominant or as minor components; *e.g.*, B-phycoerythrin[2,3], allophycocyanin[3–5], and biliprotein complexes[3,6].

The biliproteins of *Smithora* (*Porphyra*) *naiadum****, an aberrant member of the Bangiales, are of particular interest. DAWSON[8] distinguished between two varieties of this species found on the Pacific Coast of North America. Both are epiphytes on sea grasses; var. *naiadum*, the larger plant of the two, grows north of Point Conception, California, while var. *australis* is found south of this location. AIRTH AND BLINKS[2,3] have worked extensively on the biliproteins of the northern variety and have isolated in crystalline purity a new phycoerythrin which they designate B-phycoerythrin. That this pigment is also present *in vivo* is apparent from the thallus

---

* Contribution from the Scripps Institution of Oceanography, New Series. 1186

** Present address: Chemistry Department, University College, Galway, Ireland.

*** HOLLENBERG[7] very recently placed this alga in the new genus *Smithora* because of its unusual method of reproduction.

Reproduced by Permission

Biochim. Biophys. Acta, 41 (1960) 516–520

absorption curves for the northern variety determined earlier by HAXO AND BLINKS[9]. B-phycoerythrin or a pigment with a very similar absorption curve also occurs in some other red algae; *i.e.*, *Porphyridium cruentum*[4,10], *Rhodosorus marina*[11], and *Rhodochorton floridulum*[12].

In this laboratory the biliproteins of the southern variety of *Smithora naiadum* were found to differ in some respects from those reported for the northern variety[13]. Through the courtesy of Professor L. R. BLINKS, one of us (C. Ó.) was afforded the opportunity of working at the Hopkins Marine Station, Pacific Grove and of comparing the biliproteins of the northern and southern varieties.

MATERIALS AND METHODS

Smithora naiadum var. *australis* (southern form) was collected at La Jolla, California, and var. *naiadum* (northern form) was obtained at Pacific Grove, California. Both were growing epiphytically on the sea grass *Phyllospadix*. The *Smithora* thalli were extracted overnight in distilled water at 3–5°. The extracts were centrifuged at 30,000 $\times g$ in the cold for at least 30 min, and the supernatant biliproteins were then separated by chromotography on tricalcium phosphate gel[4,14]. The column was developed with 1 % NaCl followed by phosphate buffer pH 6.0–6.5 of increasing concentrations.

The *Phormidium* spp. were cultured in sea water enriched with nutrient salts[15] and with trace elements[16]. The cultures were grown at 20–25° in a window receiving a northern exposure. We are indebted to Dr. L. PROVASOLI for supplying the culture of *P. persicinum*.

RESULTS

B-phycoerythrin

Four colored bands were obtained when the fresh aqueous extracts of *Smithora naiadum* var. *australis* (southern form) were chromatographed on tricalcium phosphate with 1 % NaCl. The leading pink band was eluted with 0.0025–0.01 *M* phosphate. Its principal absorption peak was at 542 mμ, while there was a smaller one at 560–562 mμ (Fig. 1); its spectrum corresponds with that of B-phycoerythrin. The second band contained a purple pigment which was eluted with 0.05 *M* phosphate. This purple pigment ($\lambda_{\max}$ 565 and 610 mμ) is somewhat reminiscent of R-phycocyanin ($\lambda_{\max}$ approx. 555 and 615 mμ) but differs from the latter in the shape of its absorption curve, as well as in its instability, which is discussed below. The third band had a diffuse pink color and was not studied further. The fourth band contained a strongly adsorbed blue pigment which was eluted with 1 *M* phosphate. This pigment was allophycocyanin, with an absorption maximum at approx. 650 mμ.

Immediate rechromatography of the second, purple fraction (Fig. 1) indicated it to be homogeneous and apparently stable; it again formed a single band and its absorption spectrum remained unaltered. However, solutions of the chromatographically purified purple pigment, which had been stored at 3–5° for a week, were found to be heterogeneous. Chromatograms of such aged solutions contained several poorly separated purple zones plus a leading blue eluate with an absorption maximum at 610 mμ and a slight "shoulder" at 565–575 mμ. The latter spectrum is suggestive of slightly impure C-phycocyanin.

In contrast to chromatograms of fresh extracts, those obtained with whole extracts that had aged for more than a week in the refrigerator presented a quite different picture. Under these conditions the leading zone was C-phycocyanin (maximum at 610 mμ) and this was followed by B-phycoerythrin and allophycocyanin.

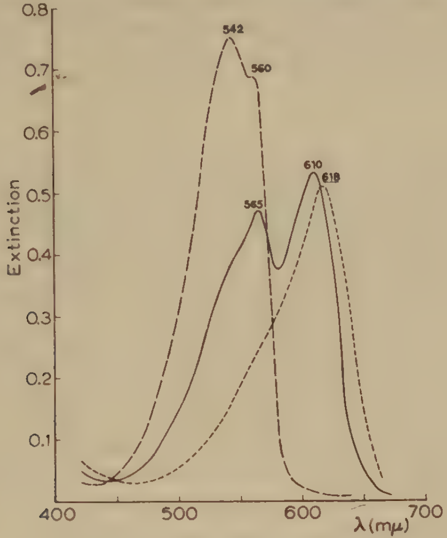

Fig. 1. Absorption spectra of *Smithora naiadum* biliproteins: ------, B-phycoerythrin *ex S. naiadum* var. *australis*; ———, purple fraction *ex S. naiadum* var. *australis*, both in phosphate buffer pH 6.5; ---'----, C-phycocyanin *ex S. naiadum* var. *naiadum*, in dilute saline.

Three main bands were obtained when the fresh aqueous extract of *Smithora naiadum* var. *naiadum* (northern form) was similarly prepared and chromatographed. Here the first pigment to be eluted was not B-phycoerythrin but C-phycocyanin (absorption maximum at 618 mμ, Fig. 1). B-phycoerythrin and allophycocyanin were the other principal biliproteins obtained from this alga. The comparison of the fresh extracts thus revealed the presence of free C-phycocyanin in the northern but not in the southern form. In var. *australis*, C-phycocyanin apparently occurs in the freshly prepared extracts as a purple complex from which it is released when the extract is aged for a week or more. When the var. *naiadum* extract was aged for four days, C-phycocyanin no longer appeared on the chromatogram. B-phycoerythrin now was eluted first, followed by a purple eluate resembling the purple complex in fresh extracts of the southern form. The $\lambda_{max.}$ were similar (567 and 615 mμ), but the relative heights of the two peaks differed.

Blinks[6] speculated that the purple pigment from var. *naiadum* might be a phycoerythrin–phycocyanin complex. Airth and Blinks[3] have recently discarded this idea and conclude that their data can be more readily interpreted by assuming that both B-phycoerythrin and C-phycocyanin exist in fresh extracts in two different forms, characterized by their electric charge and adsorptive properties respectively. However, the present chromatographic evidence suggests that in the var. *naiadum* examined by us, the "complex" is an artifact formed during storage of an aqueous extract, while the purple pigment of fresh var. *australis* extract may represent a native complex.

Airth and Blinks[2] found that B-phycoerythrin of var. *naiadum* was spectrally altered when the chromoprotein was recrystallized three times at pH 4.5, the shoulder at 565 mμ being lost. A similar spectral change was noted in the present study with the B-phycoerythrin of var. *naiadum* but not of var. *australis*. When the extract of var. *naiadum* was chromatographically fractionated by elution with acetate (pH 5.1) rather than phosphate buffer (pH 6.0), the spectrum of its B-phycoerythrin lacked a 565-mμ peak, but the spectrum of B-phycoerythrin form the southern form was unaltered.

C-phycoerythrin and artifacts

Haxo, ÓhEocha and Norris[4] reported that *Phormidium ectocarpi* contained a two-peaked phycoerythrin (maxima at 544 mμ and 564 mμ). Reexamination has shown that the spectral characteristics of the phycoerythrin obtained from this and two other *Phormidium* species (*P. persicinum* and *P. fragile*) vary with the extraction method. When extracted for a few hours in distilled water, *P. ectocarpi* gave a brilliantly fluorescing single-peaked solution, having only one absorption maximum (565 mμ). When extraction was continued overnight, the absorption spectrum of the extract was now two-peaked, as previously reported[4]. This extract also fluoresced brilliantly and on chromatography yielded only one fraction, which was still double-peaked (the ratio of the extinctions at the maxima remained constant). Intact *P. ectocarpi* filaments possess only one pronounced absorption peak (at approx. 565 mμ). It would seem, therefore, that the native phycoerythrin of this alga is the C-variety.

The two peaked phycoerythrin, apparently an artifact not present *in vivo*, was also found to occur in extracts of *P. persicinum* and *P. fragile* under certain conditions. When examined earlier[4], *P. persicinum* appeared to contain only C-phyco erythrin (maximum at 560 mμ). Upon reexamination it was noted, however, that extracts which had been prepared by steeping filaments for 6–18 h in distilled water at 3° now exhibited two maxima at 542 and 568 mμ. Fractionation by chromatography or ammonium sulphate precipitation yielded a two-peaked phycoerythrin. A brownish-black, non-fluorescent dialysable substance which was also present gradually increased in amount when the extracts were stored in the cold. After about four days the phycoerythrin was replaced by such a brown pigment. The nature of this reaction has not been determined; however, it resembles melanization of proteins, an enzymically accelerated reaction[17, 18]. Extracts of other algae examined by us are generally stable under these conditions.

The C-variety also appears to be the main if not the only phycoerythrin of *P. fragile*. When held for a few hours at 0°, its extract appeared to contain a single-peaked phycoerythrin and a trace of phycocyanin. However, chromatography revealed a heterogeneity in the phycoerythrin. The first relatively faint zone from a 6-h extraction was double-peaked (545 and 567 mμ) and the remainder of the phycoerythrin was single-peaked (maximum at 563 mμ, Fig. 2). The relative amount of the two-peaked phycoerythrin increased when the extract was held for 36 h at 0°.

The original 6-h extract of *P. fragile* was precipitated with ammonium sulphate and kept in the dark at 0° for 3 weeks. This precipitate was dialysed against distilled water in the cold. Some of the pigment did not redissolve and was centrifuged off; the absorption spectrum of the fluorescing supernatant was two-peaked, as was the single red zone it formed on the column. On the other hand, the single-peaked C-

(710)

phycoerythrin obtained by chromatography from 6-h extracts of *P. fragile* (Fig. 2) remained stable in phosphate buffer (pH 6.8; 0°) for days.

It appears, therefore, that the two-peaked phycoerythrin obtained from this and possibly the other two species of *Phormidium* does not exist *in vivo* but is formed in whole aqueous extracts by the action of enzyme(s) which can be removed by chromatography. The formation of the two-peaked phycoerythrin was not retarded by approx. 20 % ammonium sulphate.

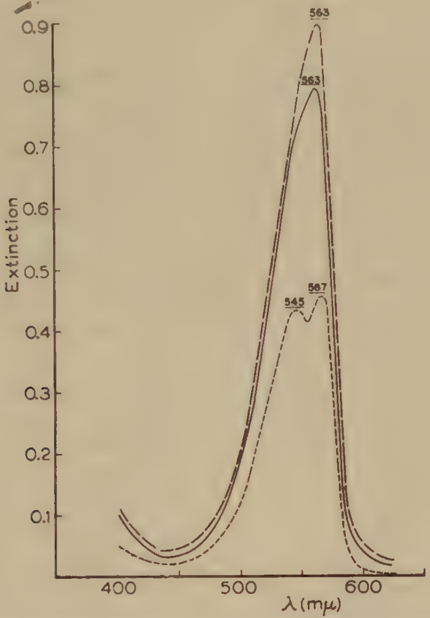

Fig. 2. Absorption spectra of chromatographic fractions of *Phormidium fragile* extracts: -------, 1st fraction; ———, 2nd fraction; – – – – –, 3rd fraction (pure C-phycoerythrin).

REFERENCES

[1] T. Svedberg and T. Katsurai, *J. Am. Chem. Soc.*, 51 (1929) 3573.
[2] R. L. Airth and L. R. Blinks, *Biol. Bull.*, 111 (1956) 321.
[3] R. L. Airth and L. R. Blinks, *J. Gen. Physiol.*, 41 (1957) 77.
[4] F. Haxo, C. ÓhEocha and Phyllis Norris, *Arch. Biochem. Biophys.*, 54 (1955) 162.
[5] C. S. French, J. H. C. Smith, H. I. Virgin and R. L. Airth, *Plant Physiol.*, 31 (1956) 369.
[6] L. R. Blinks, in B. A. Fry and J. L. Peel, *The Role of Accessory Pigments in Photosynthesis in "Autotrophic Micro-organisms"*, Cambridge, 1954.
[7] G. J. Hollenberg, *Pacific Naturalist*, 1 (1959) 1.
[8] E. Y. Dawson, *Alan Hancock Pacific Expd.*, 17 (1952) 1.
[9] F. T. Haxo and L. R. Blinks, *J. Gen. Physiol.*, 33 (1950) 389.
[10] W. Koch, *Arch. Mikrobiol.*, 18 (1953) 232.
[11] G. Girard, *Compt. rend.*, 248 (1959) 277.
[12] P. ÓCarra and C. ÓhEocha, Unpublished observations.
[13] C. ÓhEocha, *Doctoral thesis*, University of California, Los Angeles, 1955.
[14] S. M. Swingle and A. Tiselius, *Biochem. J.*, 48 (1951) 171.
[15] B. H. Ketchum and A. C. Redfield, *Biol. Bull.*, 75 (1938) 165.
[16] P. L. Burkholder and L. G. Nickell, *Bot. Gaz.*, 110 (1949) 426.
[17] M. Thomas, in W. Ruhland, *Melanin, In Encyclopedia of Plant Physiology*, Vol. VIII, Springer, Heidelberg, 1958, p. 1076.
[18] D. L. Fox and N. Millott, *Proc. Roy. Soc. (London) B*, 142 (1954) 392.

Biochim. Biophys. Acta, 41 (1960) 516–520

(711)

Printed in The Netherlands

An Abalone Lacking Respiratory Apertures

by

David L. Leighton

(Contribution from the Scripps Institution of Oceanography, New Series)
University of California, La Jolla, California

(Plate 9)

The discovery of a juvenile red abalone, Haliotis rufescens Swainson, 1822, characterized by a complete absence of respiratory apertures seems worthy of a published note. The imperforate specimen was collected together with a number of normal specimens on a beached kelp holdfast [Macrocystis pyrifera (Linn.) Agardh, 1771] at Pacific Beach, California, in October, 1959 (Figure 1, top). Normally, a pallial cleft develops and aperture formation commences when the juvenile abalone is approximately two millimeters long. Dissection of this specimen, however, revealed that no cleft had been formed in the mantle. The general perfect condition of shell and body tissue lends support to the interpretation that the absence of apertures and pallial cleft is the result of mutation rather than local injury.

Specimens of various abalone species have been collected which apparently had lost the ability to create apertures. In all cases, however, the cessation of aperture formation was found to have been brought about by a mechanical injury to the mantle and shell. In such specimens apertures had been formed in the young stages but were not formed subsequent to injury. Observation of this phenomenon in occasional specimens of the black abalone has led some investigators to describe subspecies of the form (Keep, 1935). Haliotis cracherodii holzneri Hemphill, 1907, and H. c. imperforata Dall, 1919, are two of the so-called subspecies appearing in older literature (Abbott, 1954).

Prosobranch gastropods possessing respiratory apertures or slits (archaeogastropodan families Pleurotomaridae, Scissurellidae, Haliotidae, and Fissurellidae) are considered primitive types (Yonge, 1947). These gastropods create a water current which enters the mantle cavity from beneath the shell and which, after bathing the gills and picking up wastes or sex products, leaves via the respiratory apertures. An abalone lacking apertures must elevate the shell considerably to maintain a respiratory current. A mutation of the kind responsible for the loss of the ability to create apertures through the disappearance of the pallial cleft may have provided the necessary step leading to the evolution of the more advanced non-apertured gastropods.

LITERATURE CITED

Abbott, R. T.
1954. American seashells. D. Van Nostrand Co., Inc., New York.

Keep, J. and J. L. Baily, Jr.
1935. West Coast shells. Stanford University Press, Stanford, California.

Yonge, C. M.
1947. The pallial organs in the Aspidobranch Gastropoda and their evolution throughout the mollusca. Philosoph. Trans. of the Royal Society. Ser. B, vol. 232, pp. 443-518.

Explanation of Plate 9

Figure 1: Imperforate shell of *Haliotis rufescens*.

Figure 2: Foot and viscera of the same specimen.

Figure 3: Normal shell of the same species of abalone.

Figure 4: Foot and viscera of the normal specimen. Note the pallial cleft (arrow). It is non-existant in the imperforate specimen. Illustrations four times natural size.

Contributions from the Scripps Institution of Oceanography, New Series, 1187 (713)

Reproduced by Permission

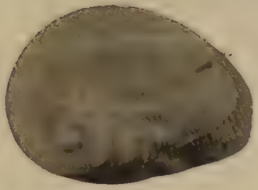

Figure 1

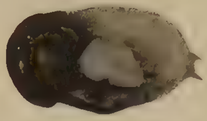

Figure 2

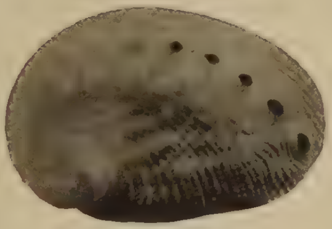

Figure 3

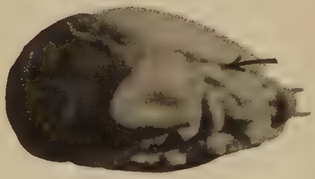

Figure 4

The concentration and isotopic abundances of carbon dioxide in the atmosphere

By

C. D. KEELING

Reprinted from Tellus Volume 12, Number 2

June 1960

Särtryck ur Tellus nr 2, 1960

The Concentration and Isotopic Abundances of Carbon Dioxide in the Atmosphere

By CHARLES D. KEELING, Scripps Institution of Oceanography, University of California,
La Jolla, California

(Manuscript received March 25, 1960)

Abstract

A systematic variation with season and latitude in the concentration and isotopic abundance of atmospheric carbon dioxide has been found in the northern hemisphere. In Antarctica, however, a small but persistent increase in concentration has been found. Possible causes for these variations are discussed.

The content of carbon dioxide in the atmosphere, in contrast to oxygen, nitrogen, and the rare gases, has been found to be significantly variable (GLUECKAUF, 1951). New data indicate, however, that the degree of variability is smaller and the variations are more systematic than previously believed (STEPANOVA, 1952, SLOCUM, 1955, FONSELIUS ET AL., 1956, CALLENDAR, 1958, BRAY, 1959).

Three gas analysers, as described by SMITH (1953), equipped with strip chart recorders, have been employed to measure the concentration of carbon dioxide continuously at stations in Antarctica, Hawaii, and California. A fourth analyser has been used in the laboratory to analyse samples of air collected in glass flasks at various places. These analysers provide direct comparisons of the partial pressure of carbon dioxide in air relative to that in prepared mixtures of carbon dioxide in nitrogen gas. The concentration of carbon dioxide in these reference mixtures is determined manometrically (KEELING, 1958).

The relative accuracy of the data presented here is approximately ± 0.3 p.p.m. (parts per million by volume). The uncertainty in the absolute values is considerably larger, however, since only a preliminary calibration of the reference mixtures has been made. When an accurate manometric calibration is completed, the absolute accuracy is expected to approach ± 0.1 p.p.m.

Monthly averages of the data from the continuously recording stations and from collections in flasks are presented numerically in Table 1 and plotted in figures 1 and 2. The locations of the sampling stations and tracks are shown in figure 3.

Local contamination has been found to occur at all three continuous recording stations. At

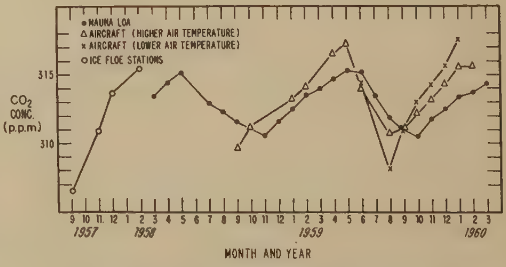

Fig. 1. Variation in concentration of atmospheric carbon dioxide in the Northern Hemisphere.

Contribution from the Scripps Institution of Oceanography, New Series. This paper represents preliminary results of research carried out as part of the International Geophysical Year and its extension. Support was provided by the National Science Foundation, United States Weather Bureau, and the Office of Naval Research.

Contributions from the Scripps Institution of Oceanography, New Series, 1188

Reproduced by Permission

Table 1. Monthly Average Concentrations of Atmospheric Carbon Dioxide at Various Stations in Parts per Million of Dry Air by Volume.

Month	Year	Continuous Recording Stations			Surface Flask Samples			Flask Samples from Aircraft[2]		
		Little America	Mauna Loa	La Jolla[1]	South Pole	Arctic Ice Floes	Down-wind Cruise	Data at Lower Air temp.	Data at Higher Air temp.	Limiting Air temp. (°C.)
Sept.	1957				311.1	306.5				
Oct.							310.9[1]			
Nov.						310.8	311.9			
Dec.					312.0	313.6	311.6			
Jan.	1958									
Feb.		310.8								
Mar.		311.0	313.4		311.9	315.5				
Apr.		311.4	314.4	314.3					314.9[1]	—27
May		311.7	315.1	315.3						
Jun.		311.9			312.5				314.9[1]	—21
Jul.		311.8	312.9	311.1						
Aug.		313.0	312.3	308.4						
Sept.		312.9	311.6	308.7	313.3			308.3[1]	309.6	—18
Oct.		313.0		310.8				312.8[1]	311.2	—27
Nov.			310.6	313.2						
Dec.			311.6	314.3						
Jan.	1959		312.5	314.9	312.8				313.2	—36
Feb.			313.5	314.4	313.4				314.1	—36
Mar.			314.0	315.4	312.7					
Apr.			314.7	315.0	314.3			316.6[1]	316.6	—27
May			315.3	315.0	314.3				317.3	—24
Jun.			315.2	315.2	314.4			314.3	314.1	—21
Jul.			313.5	311.5	314.2					
Aug.			311.9	308.1	314.2			308.1	310.7	—18
Sept.			311.1	308.7	314.0			311.0	311.1	—27
Oct.			310.5	312.1				313.0	312.1	—27
Nov.			311.8	313.7	313.9			314.2	313.2	—36
Dec.			312.5	313.5				315.6	314.3	—36
Jan.	1960		313.4	314.7				317.6	315.6	—36
Feb.			313.7	315.4					315.6	—36
Mar.			314.4	314.7						

[1] Data not shown in Figures 1 or 2.

[2] Data have been separated into two groups based upon the temperature of the air at the point of sampling. Limiting air temperature refers to the temperature separating lower air temperature from higher. It has been chosen so that, for each period of sampling, the boundary between warmer and colder air lies at approximately 50° North (see figure 3).

Little America, Antarctica, it was evidently due solely to combustion of fuel in the immediate vicinity of the station. It could be readily spotted from the significant fluctuations in the otherwise steady trace of the recorder pen and was eliminated from consideration in the initial reading of the charts. At Mauna Loa Observatory, Hawaii, a less prominent variability has been found in approximately half of the records. This is attributed to release of carbon dioxide by nearby volcanic vents; combustion on the island associated with agricultural, industrial, and domestic activities; and lower concentra-

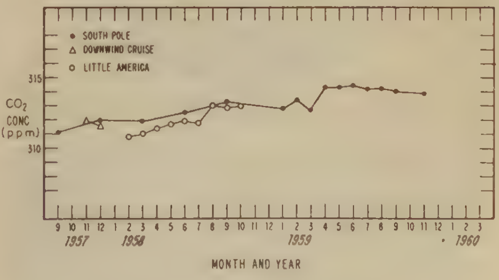

Fig. 2. Variation in concentration of atmospheric carbon dioxide in the Southern Hemisphere.

tion of carbon dioxide in the air transported to the station by upslope winds. The values reported here are averages of data for periods of downslope winds or strong lateral winds when the concentration remained nearly constant for several hours or more. At La Jolla, California, the concentration has been found to be highly variable. Highest concentrations occur during light winds from the north, from the direction of Los Angeles; lowest concentrations when the wind is from the west or southwest and of moderate force or greater. Lowest weekly values usually do not differ by more than ± 1 p.p.m. during any month, and, within a range of 2 p.p.m., agree with other data for the northern Pacific ocean. Monthly averages of these data, which presumably indicate nearly uncontaminated air, are cited here.

Data for air collected in flasks from aircraft flying at 5 to 6 kilometers above the Pacific and Arctic oceans and from surface stations at the South Pole and on Arctic ice floes show a high degree of regularity.

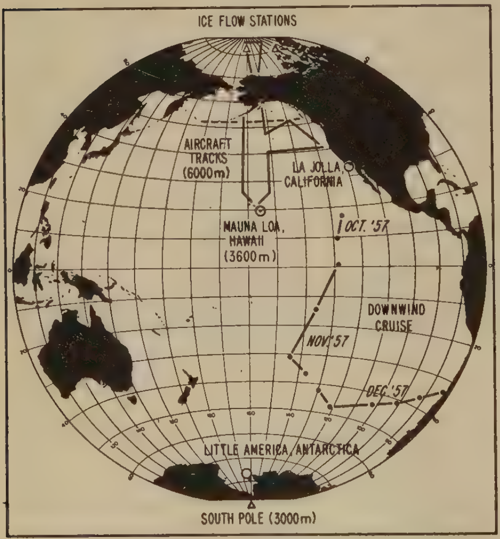

Fig. 3. Location of stations and tracks for sampling of atmospheric carbon dioxide. Circles denote continuous recording stations. Triangles denote flask sampling stations. Elevations in meters are given for locations more than 100 meters above sea level. The approximate mean position of the limiting temperature isotherm, used to separate the aircraft data into groups associated with higher and lower air temperature, is shown by a dotted line.

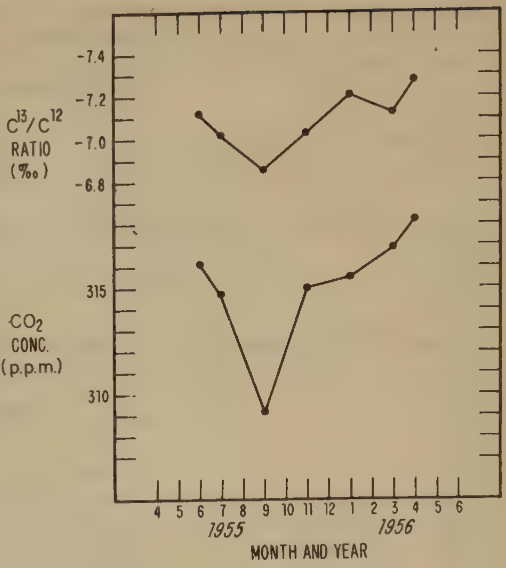

Fig. 4. Variation in concentration and C^{13}/C^{12} ratio of atmospheric carbon dioxide, based on Keeling (1961) for various locations near the Pacific coast of the United States.

A clearly defined seasonal trend in concentration is found at all locations in the northern hemisphere. Going from south to north, the annual range of concentration becomes greater and the month of minimum concentration occurs earlier. Separating the samples from aircraft into two groups based upon the temperature of the air at the point of sampling (see table 1), the values for the high latitude, or polar, air are seen to have a greater seasonal range than the comparable values for air of the temperate zone. In contrast, data for the southern hemisphere do not indicate any seasonal variation. Data from Downwind Cruise in November and December, 1957, suggest that the concentrations observed over Antarctica prevail at all southern latitudes of the Pacific ocean.

A seasonal variation in the isotopic abundance of carbon 13 in atmospheric carbon dioxide may also exist (Keeling, 1961). In figure 4 are plotted the observed seasonal variations in isotopic abundance and concentration, based upon samples collected at various stations near the Pacific coast of the United States during 1955 and 1956. Changes in relative abundance of carbon 13 with concentration obey a relationship found for air near plants (Keeling, 1958). The isotopic composition of the carbon dioxide associated with the change in concentration, according to this relationship, is approximately —22 per mil, in good agreement with the value found for air of forests (Keeling, 1958) and for the carbon of plants growing on land (Craig, 1954, Wickman, 1952). These data, therefore, indicate that the seasonal trend in concentration observed in the northern hemisphere is the result of the activity of land plants. This interpretation receives further support from the fact that maximum concentrations have been found to occur in spring at the outset of the summer growing season for plants in the temperate zone; that minimum concentrations occur in the fall, approximately at the end of the growing season. The observed absence of a seasonal trend in the southern hemisphere is then to be explained by the smaller area of growing plants found in the southern hemisphere at temperate and polar latitudes. These conclusions should be considered tentative, however, since they are based on relatively few isotopic measurements.

Where data extend beyond one year, averages for the second year are higher than for the first year. At the South Pole, where the longest record exists, the concentration has increased at the rate of about 1.3 p.p.m. per year. Over the northern Pacific ocean the increase appears to be between 0.5 and 1.2 p.p.m. per year. Since measurements are still in progress, more reliable estimates of annual increase should be available in the future. At the South Pole the observed rate of increase is nearly that to be expected from the combustion of fossil fuel (1.4 p.p.m.), if no removal from the atmosphere takes place (Revelle and Suess, 1957). From this agreement, one might be led to conclude that the oceans have been without effect in reducing the annual increase in concentration resulting from the combustion of fossil fuel. Since the seasonal variation in concentration observed in the northern hemisphere is several times larger than the annual increase, it is as reasonable to suppose, however, that a small change in the factors producing this seasonal variation may also have produced an annual change counteracting an oceanic effect.

Acknowledgements

The extensive sampling reported here was made possible through the generous cooperation of the United States Weather Bureau whose personnel carried out the sampling at Little America, the South Pole, Mauna Loa Observatory, and Arctic ice floes "A" and "B"; the 55th Weather Reconnaissance Squadron of the United States Air Force who collected the samples from aircraft; and Dr. Norris W. Rakestraw and Mr. Lee Waterman who collected samples from Downwind Cruise. Special thanks are due Messrs. Charles E. Williams and Jack C. Pales who operated the continuous recording instruments and who reduced the data to preliminary tabular form at Little America and Mauna Loa Observatory, respectively; and to Maj. George T. McClelland, Maj. Bernard M. Rose, Lieut. H. T. Fukuda, and Capt. J. D. Sharp for special effort in planning and executing the sampling from aircraft.

REFERENCES

Bray, J. R., 1959: An analysis of the possible recent change in atmospheric carbon dioxide concentration. *Tellus* **11**, pp. 220—230.

Callendar, G. S., 1958: On the amount of carbon dioxide in the atmosphere. *Tellus* **10**, pp. 243—248.

Craig, H., 1954: Carbon-13 in plants and the relationship between carbon-13 and carbon-14 variations in nature. *J. Geol.* **62**, pp. 115—149.

Fonselius, S., Koroleff, F., Wärme, K. E., 1956: Carbon dioxide variations in the atmosphere. *Tellus* **8**, pp. 176—183.

Glueckauf, E., 1951: The composition of atmospheric air. *Compendium of Meteorology*, Amer. Meteorol. Soc., Boston, pp. 3—10.

Keeling, C. D., 1958: The concentration and isotopic abundances of atmospheric carbon dioxide in rural areas. *Geochim. et Cosmochim. Acta* **13**, pp. 322—334.

Keeling, C. D., 1961: The concentration and isotopic abundances of carbon dioxide in rural and marine air. *Geochim. et Cosmochim. Acta*, in press.

Revelle, R., Suess, H. E., 1957: Carbon dioxide exchange between atmosphere and ocean and the question of an increase of atmospheric CO_2 during the past decades. *Tellus* **9**, pp. 18—27.

Slocum, G., 1955: Has the amount of carbon dioxide in the atmosphere changed significantly since the beginning of the twentieth century? *Month. Weath. Rev.* **83**, pp. 225—231.

Smith, V. N., 1953: A recording infrared analyser. *Instruments* **26**, pp. 421—427.

Stepanova, N. A., 1952: A selective annotated bibliography on carbon dioxide in the atmosphere. *Meteor. Abs. Bibl.* **3**, pp. 137—170.

Wickman, F. E., 1952: Variations in the relative abundance of the carbon isotopes in plants, *Geochim. et Cosmochim. Acta* **2**, pp. 243—254.

PRINTED IN SWEDEN
ESSELTE, STHLM 60

NEW RESEARCH REQUIRED IN SUPPORT OF RADIOACTIVE WASTE DISPOSAL

MILNER B. SCHAEFER
INTER-AMERICAN TROPICAL TUNA COMMISSION
SCRIPPS INSTITUTION OF OCEANOGRAPHY
LA JOLLA, CALIF.
UNITED STATES OF AMERICA

Reprinted from
"DISPOSAL OF RADIOACTIVE WASTES"

INTERNATIONAL ATOMIC ENERGY AGENCY
VIENNA 1960

(725)

NEW RESEARCH REQUIRED IN SUPPORT OF RADIOACTIVE WASTE DISPOSAL

Abstract

Numerous physical, chemical and biological processes influence the distribution of radioactive materials and their return to man. These include vertical and horizontal advection, turbulent diffusion, precipitation and sedimentation, uptake concentration, and transport by organisms, and transfer to man through his food from the sea.

Research is urgently needed on the flushing characteristics of typical harbours, estuaries and open coastal waters, on diffusion and sedimentation processes in inshore waters, and on the passage of radioactive elements through the food web in this portion of the sea.

Research is needed to delineate present and potential fishing areas, and non-fishing areas, by basic studies of biological productivity and other means. Studies are also required to determine rates of transfer of radioactive materials between areas by horizontal advection and turbulent diffusion, rates of dilution by diffusion, sedimentation, and vertical transport, and rates of uptake and transfer by the biota.

Research is required on efficient means of monitoring waste disposal areas. The ability of certain organisms selectively to concentrate particular elements offers a possible economical basis of monitoring radioactive wastes in the sea at very low concentrations.

Specific research proposals have been recently developed by several groups of oceanographers in the United States. These are summarized, together with cost estimates.

RECHERCHES NOUVELLES NECESSITEES PAR LE PROBLEME DE L'ELIMINATION DES DECHETS RADIOACTIFS

Résumé

De nombreux processus physiques, chimiques et biologiques influent sur la répartition des matières radioactives et sur leur retour à l'homme. Parmi ces processus, il y a notamment l'amenée verticale et horizontale, la diffusion turbulente, la précipitation et la sédimentation, l'entraînement, la concentration et le transport par des organismes, et leur transfert à l'homme par les aliments qu'il retire de la mer.

Des recherches s'imposent d'urgence sur les caractéristiques de curage des eaux dans les ports, estuaires et rades foraines typiques, sur les processus de diffusion et de sédimentation dans les eaux proches du rivage et sur le passage des éléments radioactifs tout le long de la chaîne alimentaire dans cette partie de la mer.

Il faut entreprendre des recherches pour délimiter les zones de pêche présentes et éventuelles et les zones où la pêche ne se fait pas, en procédant à des études fondamentales sur la productivité biologique ou en recourant à d'autres moyens. Des études sont également nécessaires pour déterminer les taux de transfert de matières radioactives entre les diverses zones par amenée hori-zontale et par diffusion turbulente, les taux de dilution par diffusion,

Contributions from the Scripps Institution of Oceanography, New Series, 1189

Reproduced by Permission

sédimentation et transport vertical, et les taux d'entraînement et de transfert par les organismes.

Une recherche s'impose en ce qui concerne les moyens efficaces de contrôle des zones d'évacuation des déchets. Certains organismes sont capables de concentrer sélectivement des éléments déterminés; cette capacité constitue une base économique éventuelle pour le contrôle des déchets radioactifs existant dans la mer à des concentrations extrêmement faibles.

Des propositions précises de recherche ont été récemment mises au point par plusieurs groupes d'océanographes aux Etats-Unis. Ces propositions ont été résumées en même temps que les estimations de dépenses y afférentes.

НЕОБХОДИМЫЕ НОВЫЕ ИССЛЕДОВАНИЯ В ОБЛАСТИ УДАЛЕНИЯ РАДИОАКТИВНЫХ ОТХОДОВ

Резюме

Многочисленные физические, химические и биологические процессы влияют на распределение радиоактивных материалов и их возвращение к человеку. Сюда входят вертикальная и горизонтальная адвекция, турбулентная диффузия, выпадения осадков и отложения, поднятие, концентрация и перемещение организмами, а также перемещение к человеку через его пищевые продукты из моря.

Настоятельно необходимо исследовать связанные с приливами данные в типичных гаванях, эстуариях и в открытых береговых водах, а также прохождение радиоактивных элементов через пищевые ткани в эту часть моря.

Необходимо провести исследования для того, чтобы разграничить потенциальные рыболовные и не рыболовные районы с помощью теоретического изучения биологической продуктивности и другими способами.

Необходимо изучить эффективные средства контроля за районами удаления отходов. Способность некоторых организмов концентрировать лишь отдельные элементы порядка нескольких тысяч может послужить экономичной основой для контроля за радиоактивными отходами в море при очень низких концентрациях.

Недавно несколько групп океанографов в Соединенных Штатах разработали специальные исследовательские предложения. В документе они обобщаются и приводятся вместе со сметой расходов.

NUEVAS INVESTIGACIONES NECESARIAS PARA LA EVACUACION DE DESECHOS RADIACTIVOS

Resumen

Numerosos son los procesos físicos, químicos y biológicos que influyen en la forma en que las sustancias radiactivas se distribuyen y vuelven al hombre. Entre ellos figuran la convección vertical y horizontal; la difusión turbulenta; la precipitación y sedimentación; la captación, concentración y transporte de los materiales radiactivos por organismos, y su paso al hombre por ingestión de alimentos de origen marino.

Hay que estudiar urgentemente las características del flujo y reflujo de las aguas en puertos típicos, estuarios y aguas costeras abiertas; los procesos

de difusión y sedimentación en las aguas costeras, y el paso de los elementos radiactivos a través de la cadena alimenticia que se encuentra en esta parte del mar.

Es necesario efectuar investigaciones para poder delimitar las zonas de pesca presentes y futuras, y las zonas en que la pesca no es posible, mediante estudios básicos sobre la productividad biológica, etc. También es preciso realizar estudios para determinar la velocidad de traslado de las sustancias radiactivas de una zona a otra por convección horizontal y por difusión turbulenta; la velocidad de dilución por difusión, sedimentación y transporte vertical, y la velocidad de captación y transmisión por los organismos vivos.

Es necesario realizar investigaciones sobre los medios más eficaces para someter a monitoraje las zonas de evacuación de desechos. Algunos organismos pueden concentrar selectivamente determinados elementos; esto ofrece la posibilidad de efectuar, en condiciones económicas, el monitoraje de desechos radiactivos de baja concentración eliminados en el mar.

Varios grupos de oceanógrafos de los Estados Unidos han propuesto recientemente algunos trabajos específicos de investigación cuyo resumen aparece en esta memoria, junto con un cálculo de su costo.

NEW RESEARCH REQUIRED IN SUPPORT OF RADIOACTIVE WASTE DISPOSAL

Milner B. Schaefer
Inter-American Tropical Tuna Commission
Scripps Institution of Oceanography
La Jolla, Calif.
United States of America

Introduction

Safe disposal of radioactive materials in the sea depends on limiting the resulting radiation dose to man, received either directly or through his food from the sea, to tolerable levels. This may be accomplished by either of two means, or by a combination of them—isolation and dispersion. Radioactive materials introduced, or subsequently deposited by physical, chemical or biological processes, into regions of the sea not frequented by man, or not furnishing his food, are *isolated*. During the period of such isolation, they diminish by radioactive decay. Radioactive materials which enter into those parts of the sea used by man may be so diluted by *dispersion* throughout the environment that the quantities of resulting radiation reaching man are tolerable.

Exposure to external radiation in some circumstances (such as accidental recovery of solid wastes during fishing or salvage operations, or where certain isotopes are concentrated in beach sands or sediments) might constitute a direct hazard from atomic wastes placed in the sea; but in general the hazard from contaminated food organisms will be the critical consideration. Revelle *et al* (1) concluded:

"The most serious potential hazards to human beings from the introduction of radioactive products into the marine environment are those that may arise through the uptake of radioisotopes by organisms used for human food. There are several reasons why these indirect hazards are more critical than the direct hazards: (1) the radiation received from a given quantity of an isotope ingested as food is much greater than the dose from the same quantity in the external environment; (2) many elements, including some of those having radioactive isotopes resulting from nuclear reactions, are concentrated by factors up to several thousand by the organisms in the sea; (3) the vertical and horizontal migrations of organisms can result in transport of radioactive elements and thereby cause distributions different from those that would exist under the influence of physical factors alone; for example, certain elements may be carried from the depths of the sea into the upper mixed layer in greater amounts than could be transported by the physical circulation.

"It is quite certain that the direct hazard to man through danger of contamination of food from the sea will require limiting the permissible concentration of radioactive elements in the oceans to levels below those at which there is any direct hazard. Any part of the sea in which the contamination does not cause dangerous concentrations of radioactive elements in man's food organisms will be safe for man to live over or in."

In evaluating the suitability of any marine locale as a receiver of atomic wastes, we must consider numerous chemical, physical and biological processes which affect the distribution of the radioactive materials and their eventual return to man through various routes, including the marine food harvest. PRITCHARD *et al* (2) have diagrammed the various processes which must be considered in the step-by-step evaluation of a portion of the sea as a receiver of nuclear wastes. This is reproduced here as Fig. 1. In this

Schematic Presentation of the Step by Step Considerations which Should be made in Evaluating the Suitability of Any Marine Locale as a Receiver of Nuclear Wastes

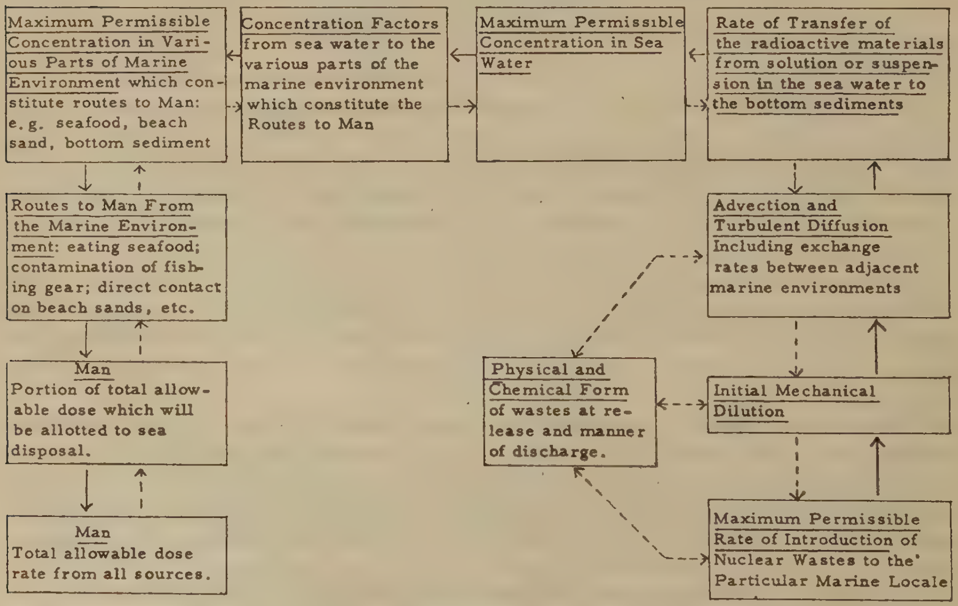
Maximum Permissible Concentration in Various Parts of Marine Environment which constitute routes to Man: e.g. seafood, beach sand, bottom sediment
Concentration Factors from sea water to the various parts of the marine environment which constitute the Routes to Man
Maximum Permissible Concentration in Sea Water
Rate of Transfer of the radioactive materials from solution or suspension in the sea water to the bottom sediments
Routes to Man From the Marine Environment: eating seafood; contamination of fishing gear; direct contact on beach sands, etc.
Advection and Turbulent Diffusion Including exchange rates between adjacent marine environments
Man Portion of total allowable dose which will be allotted to sea disposal.
Physical and Chemical Form of wastes at release and manner of discharge.
Initial Mechanical Dilution
Man Total allowable dose rate from all sources.
Maximum Permissible Rate of Introduction of Nuclear Wastes to the Particular Marine Locale

Fig. 1

figure the solid arrows between blocks indicate the route taken by the radioactive material in returning to man, while the dashed arrows indicate the reverse course taken in making the evaluation.

It may readily be seen from this diagram that the evaluation requires quantitative consideration of the following:

1. Uptake and concentration of radioactive isotopes by organisms from sea-water and from sediments.
2. Exchange between bottom sediments and material suspended or dissolved in sea-water.
3. Advection and diffusion (by both physical and biological processes) both within a given marine environment and between adjacent environments.
4. Site of initial release, initial mechanical dilution, and physical and chemical form of the waste at time of release.

Unfortunately, knowledge of most of the processes involved is quite limited. Therefore, to be on the safe side, we make "conservative" assumptions—that is, when doubt exists about a particular process, one takes a resulting value which would certainly be more hazardous to man than the (unknown) true value. This is, of course, a safe procedure, but it leads to more restrictive practices than would be imposed if better information were available. This over-restriction due to ignorance has an economic cost which will mount rapidly with the increasing use of nuclear energy, and can be decreased by the results of additional research.

In order to provide an adequate basis for controlling the sea disposal of radioactive wastes with optimum benefits to mankind, it is necessary to learn much more about the processes listed above, in various parts of the sea, than we now know. This requires an adequate long-range programme of research on the physics, chemistry and geology of the sea, and on the biology of its contained organisms, with particular reference to the radioactive waste disposal problem.

Research required in estuarine and coastal waters

Of the various parts of the sea, that of most immediate concern from the standpoint of radioactive waste disposal is the region which includes the harbours and estuaries and the shallow coastal waters over the continental shelf. It is, of course, generally recognized that high-level wastes cannot safely be introduced into these waters; but some quantities of low-level wastes are being, and will surely continue to be, liberated there. Such wastes arise from a variety of sources: low-level liquid wastes from shoreside power reactors, such as the United Kingdom establishment at Windscale on the Irish Sea; low-level solid and packaged wastes from hospitals, laboratories, etc; low-level liquid wastes from nuclear-powered ships. It is also in harbours and approaches to harbours that accidental sinking of nuclear-powered vessels is most likely to occur, with possible release of fairly large quantities of fission products. The potentialities of nuclear explosions for deepening and widening channels and for creating artifical harbours are being explored. The effects of the resulting radioactivity are of primary importance in evaluating the feasibility of such operations.

At the same time, this is the region of the sea most used by man for a variety of purposes, and from which he obtains a large share of his marine food, including some of the organisms low in the food chain, such as seaweeds and molluscs, which most highly concentrate some of the hazardous radioisotopes.

Safe disposal of radioactive materials in estuarine and coastal waters relies primarily on dilution (dispersion) rather than on isolation, since few parts of this environment are isolated from man, and these imperfectly. Wastes in impervious containers may be isolated from the water and its contained organisms for a time, likewise isotopes precipitated in bottom sediments may be at least partially isolated, particularly where they are in areas with no commercial fishing. Dilution is accomplished by mixing the estuarine and coastal area, and by exchange (flushing) to the larger volume of the open sea offshore.

Outstanding characteristics of the inshore environment are its complexity and variability. Although the basic principles remain the same from one place to another, at the present state of our knowledge each locality presents a nearly unique problem. What is needed is a better understanding of important parameters of estuarine and coastal situations, so that evaluation based on general principles can be made realistic, and so that detailed studies of waste-receiving capabilities of particular localities can be carried out more efficiently and precisely than is now the case.

Circulation and mixing

The rate of removal of dissolved materials from an estuary or coastal environment by the motion of the waters, that is the flushing rate, and also the distribution in space and time of materials introduced into such an environment, depend on the character of the circulation and mixing, which is determined by a number of internal and external factors. Studies of a single estuary, or of a single coastal area, will not be sufficient to provide general basic concepts. Present knowledge of the hydrography of estuaries indicates, however, that they may be classified into types on the basis of (1) physical structure (i.e. length, width, depth, shape, etc.), (2) the net water gain or loss due to the difference between fresh-water inflow and evaporation, and (3) the character of the tidal circulation. Similarly, coastal areas may be fitted into a broad classification scheme. The required research programme should include detailed studies of a number of representative estuaries and coastal environments, encompassing the range of variation of environmental factors. Four types of estuaries which should be studied have been listed by Brown *et al* (3) as follows:

1. *Coastal plain estuaries*: These estuaries are shallow, elongated indentures on the coast-line, having free connexion with the open sea, and within which sea-water is measurably diluted by land drainage.
2. *Inverse estuaries*: Embayments in which evaporation exceeds precipitation and fresh-water inflow.
3. *Fiord-type estuaries*: Deep coastal indentations in which fresh-water inflow exceeds evaporation. One important case is that in which the entrance is so restricted as greatly to limit the replacement of water in the deeper parts of the estuary.
4. *Bar-built estuaries*: Shallow embayments with restricted connexion to the open sea, within which tidal motion is hence small compared to wind-induced motion.

Methods of studying the circulation and mixing of typical estuaries should include: (1) field studies of the time and space distribution of current, temperature, salinity and other chemical components in relation to other parameters such as morphology, tidal effects, river inflow and evaporation, and winds; (2) tracer studies utilizing both (a) wastes introduced by existing industrial outfalls; and (b) planned release of suitable tracer chemicals, both non-radioactive and radioactive; (3) studies of hydraulic models, particularly in conjunction with the foregoing tracer studies.

Both vertical and horizontal advection are important in coastal waters, the former being brought about where there is convergence or divergence of the surface drift in relation to the land boundary. Mixing processes are effected by a number of factors, including effects of bottom topography on current, internal waves and inertial currents, fresh-water run-off from the land, and wind stress. The various mixing and advective processes are often subject to large changes related to climatic variations over the adjacent coastal area; consequently studies need to be continued over sufficient time to establish seasonal and longer-term variations.

Although coastal regions are difficult to fit into any classification scheme, it is at least possible to divide coastal waters into relatively homogeneous regions for study purposes, as has been indicated for North-American coastal waters by Brown *et al* (3). Considerable research has already been done on the physical oceanography of many of these regions, but there appear to be in nearly all cases large deficiencies in our knowledge of seasonal and other temporal variations, and in our understanding of mixing processes and of vertical advection. Research in coastal waters needs particularly to include:

1. Studies of time variations in the circulation and mixing, through periodic surveys and more especially by the employment of moored buoys or other fixed stations for giving quasi-continuous records of currents and of physical and chemical properties.
2. Comprehensive studies of the distribution of properties and current measurements covering a wide spectrum of scales in space and time as a basis for better understanding of mixing processes.
3. Investigation of the utility of model studies, which may be effective, as they have already been in studies of estuaries, in helping to evaluate regions with complex boundary effects.

An additional important line of research is the development of a suitable theory into which to fit the observational data for coastal waters to arrive at a useful understanding of the physical regime of this complex environment intermediate between the estuaries and the open sea. Such theory is needful for attaining precision in predicting the space and time distribution of dissolved waste materials.

Sedimentation processes

Radioactive materials may be deposited on the bottom in estuarine and coastal areas by precipitation, by sorption on clays and other inorganic sediments, or by the deposition of organic materials in which they have been incorporated or on which they are adsorbed. The deposition does not necessarily remove them from the direct route to man, since in such waters there occur also both vertebrate and invertebrate benthic and bottom-feeding organisms which are part of the food-fish harvest. If the radioactive elements are readily taken up from the sediments by such organisms, such sedimentation may, by concentrating certain isotopes in a smaller volume of sediments than the original volume of water in which they were dispersed, actually lead to increased transfer to man through his food. As has been noted by CARRITT *et al* (4), we are now unable to make any quantitative estimates of the effects of sedimentation processes, although it is believed on the basis of experience at Windscale, Chesapeake Bay and elsewhere that (except where sources of marine food products are directly adjacent to waste disposal sites) the net effect is to reduce the transfer of hazardous radioisotopes to man.

It is evident that additional research, both in the laboratory and in the field, on the nature of sedimentation processes, and on sorption and exchange of radioisotopes between water, sediments, and organisms in estuarine and coastal environments is required as a basis for more precise consideration of waste disposal in these environments.

A further important aspect of sorption and sedimentation processes is the possibility of employing selected clay minerals in decontaminating the water around a nuclear-powered vessel involved in a reactor accident, or following nuclear detonations. Some research has recently been commenced, according to CARRITT *et al* (4) and WALLEN (5).

Biological effects

The role of organisms in estuarine and coastal waters is of paramount importance to the consideration of disposal of radioactive waste materials, for two reasons: firstly, because the uptake and excretion of organisms, together with their migrations, can result in a great difference of circulation and mixing between those elements which enter into the biological cycle and those elements which do not; secondly, because the concentration of radioisotopes by organisms used by man for food is the principal route by which he is exposed to the radioactivity entering these waters, which, as noted above, provide a large share of the seafood harvest.

Many elements, including some which have important radioisotopes, are concentrated by large factors by organisms (see, for example, the tables in REVELLE (1), and PRITCHARD *et al* (2). These may be taken up directly from the water or bottom sediments, or, in the case of the organisms above the plants, passed through the food chain. The uptake of radioactive elements by sessile plants and animals "hold up" the circulation of these elements, so that the flushing rate for them is slower than the flushing rate of the water. For those isotopes with large biological concentration factors, high concentrations may develop locally, for example on heavily fouled pilings or in clam and oyster beds. Also, as noted by KETCHUM (6), the combination of uptake by organisms in the overlying water and gravity effects on their excreta and dead bodies, in an area with estuarine-type circulation or in regions of coastal upwellings, will result in hold-up in the circulation of elements concentrated by such organisms. In addition, the migrations of organisms will modify the distribution of the radioactive elements which they take up.

In order properly to evaluate the distribution of radioactive waste materials in estuarine and inshore waters, and in order to estimate the share of radioactivity which will appear in man's food from this part of the sea, it is necessary to know a great deal about the uptake by different kinds of organisms of various radioactive elements, both from the water and the sediments, the rates of subsequent excretion, and the transfer rates from prey organisms to their predators, and also to know a good deal about the vertical and horizontal migrations of the organisms and about their rates of mortality and rates of fallout of their excreta and dead remains. Such information can be obtained by three approaches:

1. Field studies of the ecology, behaviour, and biochemistry of the organisms, using classical methods. Such studies should be conducted simultaneously and in co-ordination with field studies of the circulation and distribution of properties of typical estuarine and coastal areas described above under "Circulation and mixing".
2. Laboratory studies of uptake and excretion of radioisotopes in water and sediments and of passage from prey to predator. Such studies are now being carried on in several laboratories (5), but need to be much intensified.
3. Field studies using radioactive tracers to measure the flux of elements through the various parts of the ecological system. Such studies are essential because the complete ecological system cannot yet be reproduced in the laboratory. Some such studies may be conveniently conducted in connexion with existing waste-disposal operations. However, controlled field experiments in small lagoons or other semi-enclosed bodies of water are desirable because more precision can be achieved by such planned experiments (3, 7).

Research required in the open sea: The near-surface layer

The waters of the ocean are stratified. The near-surface layer, from which most of man's food harvest is taken, is a relatively thin stratum, varying in thickness in different places but averaging about 75 m, within which vertical mixing by wind-stirring is relatively rapid and complete, wherefore it is often called the "upper mixed layer". Below this is a zone within which temperature decreases, and density increases, rapidly with depth. This thermocline, or pycnocline, separates the upper mixed layer from the layers of intermediate and deeper water, the latter extending to the bottom, within which there are gentle gradients of decreasing temperature and increasing density and salinity with depth. The upper layer is characterized by relatively rapid currents and mixing. In the intermediate and deep layers, vertical movements and horizontal currents are more sluggish. The strong density gradient through the pycnocline acts as a partial barrier between the upper layer and the lower layers. There is, however, exchange of elements across the pycnocline by upwelling and downwelling, by vertical diffusion, by sinking of organic and inorganic sediments, and by vertical migrations of organisms.

The principal source of radioactive materials introduced into the upper mixed layer of the open sea has been fallout from weapons tests. Sources from peaceful uses of atomic energy are wastes from nuclear-powered ships, and wastes from shoreline reactors and other establishments which may be dumped there.

Because of its greater water volumes and often more rapid and extensive mixing, the upper layer of the open sea has a greater capacity safely to receive radioactive wastes than estuarine and coastal waters. Furthermore, materials which fall out of this layer by sedimentation processes have a much smaller chance of being returned to man. The waste-receiving capacity of these waters is, however, much less than that of the deep sea. Especially in and near commercial fishing areas, there can be returned to man an important fraction of some of the radioactive elements through the pelagic foodfish harvest. Our present knowledge is fairly adequate for directing the safe disposal in the open sea during the next decade of quantities of low-level wastes likely to be generated by nuclear-powered ships, and low-level wastes likely to be introduced into this environment from other industrial sources (shoreside reactors, laboratory wastes). The safe disposal of much larger volumes of low-level wastes, or the disposal of even small quantities of high-level wastes will, however, require much improvement of our knowledge of this part of the sea. Some of the more important directions for such research are mentioned below.

Location of existing and potential commercial fishing areas

The important hazard to man from radioactive wastes in the open sea lies in their return to him through the food-fish harvest. All parts of the open sea, however, do not and cannot support commercial fisheries. The ocean, like the land, has areas where the biological production is high, where the environmental conditions cause an abundant growth of plants and animals which, in turn, support large populations of harvestable fishes. Other areas, veritable biological deserts of the sea, are incapable of supporting harvestable fish populations. Now, some areas of high basic biological production which have large harvestable fish stocks are not yet exploited [see for example Fig. 4.3 of SCHAEFER and REVELLE (8)]; other regions of high basic production may not support commercial fisheries because of the behaviour characteristics of the fish and other causes. We can be confident, however, that areas of very low basic production do not and will not support significant commercial fisheries. It is desirable so far as possible, obviously, to restrict the disposal of atomic wastes to such desert areas.

We know how to characterize the productivity of the sea by some relatively simple techniques, including measurements of C^{14} uptake, chlorophyll content of the water as a measure of standing crops of phytoplankton, zooplankton volumes, and certain physical and chemical characteristics. The mapping of the oceans with respect to these parameters, together with the preparation of maps of present commercial fishing areas, can provide a most useful guide to areas of relatively least hazardous disposal of atomic wastes.

Currents and mixing

The upper layer of the open sea is characterized by relatively swift currents, and by rapid horizontal mixing through eddy diffusion. Both these phenomena are of importance to atomic waste disposal, because they are primary processes determining the amount of material deposited in one area that will arrive in other areas. The eddy diffusivity, of course, is also important in determining the rate of dilution of the dissolved or suspended radioactive materials.

Average surface currents of the ocean are quite well mapped. Their variability and their fine structure are not well understood, however. It seems important, therefore, at least in and near those places where disposal of significant quantities of radioactive materials may be contemplated, to study the horizontal currents in some detail, in order to insure that the materials are not carried into other places where they might constitute a hazard.

The process of turbulent diffusion in the sea is not well understood. It is often considered, for a first approximation, to be Fickian (i.e. the coefficient of diffusivity is assumed to be isotropic and uniform throughout the water). Measurements indicate, however, that the rate of spreading of trace substances is more rapid than it should be under the assumption; this means that an ato-

(736)

mic pollutant would be more rapidly diluted, but it also means more rapid spreading to adjacent areas. JOSEPH and SENDNER (9) have recently published a diffusion equation, on the assumption that the dispersion increases linearly with distance, which seems to describe better the existing observational data. This whole matter, however, requires more investigation, both experimental and theoretical.

Sedimentation processes

Solid fractions of atomic wastes tend to be removed from the upper mixed layer by gravity effects. Such solid fractions may occur as precipitates of those elements which exist in sea-water as solid phases—e.g. ruthenium, niobium, and cerium. Others may result from sorption on to organic or inorganic particles, or by accumulation in organisms which later die.

Experimental work appears to be needed to determine the physical states of elements with important radioisotopes in sea-water, the absorption characteristics of the particulate matter occurring in the upper layers of the open sea, and the rates of settling of particles of different kinds.

It needs to be noted that uptake by organisms may greatly impede the settling of some particulate matter. This is suggested, for example, by the observation that Ce^{144}, which is present in sea-water in particulate form, and its daughter Pr^{144}, were found by HARLEY (10) to amount to 80 to 90% of the fission-product activity in plankton samples from the Pacific, a considerable time after their introduction into the sea.

Biological processes

Some biological phenomena and processes important to the radioactive waste problem in the upper layer of the open sea have been mentioned above—the charting of existing and potential fishing areas, and the effects of the biosphere on sedimentation processes. The organisms in the sea, however, also affect the distribution of radioactive wastes in other ways, which need to be properly understood for effective waste-disposal planning.

As noted earlier, the organisms of the sea concentrate certain elements in their bodies, either by direct uptake or by accumulation from their food. Although some studies have been and are being made to determine the factors by which various elements are concentrated by organisms, a great deal yet needs to be done. Concentration factors for some important elements having radioactive isotopes, such as chromium, tantalum, and tungsten, are not available for any organisms. For other elements, concentration factors have been determined for a few organisms, but not for any used as human food. For no elements have we good estimates of transfer rates from one part to another of the food chain.

It is also important to determine to what degree some elements can be substituted for others in the organisms' metabolism. It is known, for example, that calcium and strontium are metabolized in similar fashion, so that the former acts as a diluent for the latter—thus the *ratio* of radiostrontium to calcium is important rather than the absolute amount of radiostrontium. It is suspected that other elements may be similarly related, but this requires investigation for marine organisms.

The migrations of organisms may also have a profound effect on the distribution of those radioactive wastes which they incorporate in their bodies. Vertical migrations of organisms, many of which readily cross the pycnocline, can easily transfer radioactive material across this density barrier to physical circulation. Horizontal migrations can transfer such materials from the area of introduction to other areas. More important, fish contaminated in one area may be caught in far distant uncontaminated areas. Thus, additional study of the extent and range of both vertical and horizontal migrations of the animals in the sea is important for the precise evaluation of the effects of waste disposal.

Research required in the open sea: The deep and intermediate layers

Since the waters of the deeper parts of the ocean, below the pycnocline, exchange only slowly with those of the upper mixed layer, radioactive materials introduced into the deep sea will be isolated for some time, at least for several decades and perhaps for several hundred years, from the upper layer where they can be returned to man. During this time they will be diminished by radioactive decay, and will be diluted by dispersion. Some part of the material will be deposited in deep sea sediments, where it may remain for a very long time, perhaps almost permanently for some elements. It can be confidently stated that much greater quantities of wastes can be safely placed in the deep sea than anywhere else in the oceans. Quantitative assessment of the capacity of the depths of the ocean for receiving such wastes and the best manner and places of introduction can, however, now be made only in the most general fashion. Certainly the deep sea can be used for a considerable quantity of such wastes, including high-level wastes. If, however a very large quantity of high-level wastes, such as the 1,000 tons per year estimated by CRAIG (11) as possible within a few decades, is to be placed in the deep sea, it is necessary to learn a great deal more about this part of the ocean than we now know as a basis for guiding such operations. It is understood that all nations now developing power reactors plan to accommodate the high-level fuel reprocessing wastes by treatment and storage on land. In the foreseeable future, however, it may prove to be desirable for certain nations with easy access to the sea and no good land-storage sites to use the depths of the ocean for this purpose.

In order to assess the effects of radioactive materials introduced into the deep sea, we need to be able to determine how these materials are dispersed throughout the deep waters, what share will be deposited and retained in the bottom sediments, and what amounts of activity will eventually reach the upper layers of the sea and the organisms in this part of the ocean through which the activity is returned to man. For these purposes certain lines of research, in addition to those mentioned above for the upper layer, need to be pursued:

Circulation, mixing, and exchange with the surface layer

The mean currents and mixing processes in the deep sea are poorly known. Calculations from the distribution of properties and the few direct current measurements indicate that the mean current is small in most parts of the deep sea, of the order of a few cm/sec. WÜST'S (12) calculations have, however, indicated meridional currents up to 17 cm/sec along the western margin of the western trough in the Atlantic; and DIETRICH (13) has calculated velocities of about 10 cm/sec for the deep Antarctic Circumpolar Current, and for the Subarctic Bottom Current in the North Atlantic, the latter perhaps increasing to 40 cm/sec across the Greenland—Scotland Ridge. Recent direct measurements by Stommel and Swallow have indicated a rapid deep current

(738)

along the western boundary of the Atlantic, under the Gulf Stream—which had been predicted by theory.

According to the most recent and comprehensive theory of deep ocean circulation, developed by H. Stommel (14), the deep and bottom waters of the ocean are carried from high-latitude, near-surface source regions to low latitudes in narrow, fast-flowing western boundary currents at depths of several thousand metres. At all latitudes lateral mixing occurs between the water in these currents and waters of the same density in the central and eastern parts of the oceans. Over most of the ocean the deep water moves up slowly—at an average rate of perhaps 5 m a year—to the region of the thermocline, and the return flow to high latitudes takes place in the upper water layers. Using Stommel's estimate of total transport of the western boundary currents of 60 million cm per second, we would have an average residence time of the water in the deep ocean of about 700 years.

Calculations by Wooster and Ketchum (15) and Craig (11) based on the distribution of properties, including the distribution of radio-carbon, have given other estimates of mean residence time. Estimates by various methods for the water in the Atlantic below 2,000 m vary from 50 years to 1,000 years. An estimate for the Pacific based on measured heat flow through the sea floor suggests a residence time of less than 1,000 years. Whether thorough mixing of the deep water is accomplished during the average residence time of a water particle is still a moot point, although C^{14} data from the Atlantic tend to indicate that it is.

In order to improve our knowledge of circulation and mixing in the deep sea, and the rate of exchange with the surface layer, several lines of research suggest themselves. It is of importance to test Stommel's model, which can be first approached by making direct measurements of the western boundary currents in both the Atlantic and the Pacific ocean. Zonal sections of temperature and salinity, from surface to bottom, at every 10° or so of latitude across the Pacific, like those now being made in the Atlantic, will give a further check (from geostrophic calculations) of the western boundary currents, and will provide a basis for calculating the net transfer upward across the thermocline between sections. Mixing and vertical exchange across the thermocline can be studied by tracer techniques, using the existing fallout from weapons tests, as suggested by Brown, *et al* (3), naturally-occurring radioactive materials (C^{14}, radium, etc.), and, perhaps most effectively, by purposive experiments with radioactive materials, which has been suggested by, among others, Folsom and Vine (16) and Brown *et al* (3).

Sedimentation in the deep sea

As mentioned above, some fraction of the radioactive wastes in the deep sea will be deposited in the bottom sediments, which may retain them for very long periods of time, thus effectively isolating them. This would be especially true in the case of disposal in packages which would sink to the bottom. In this case, dispersion of the activity would be by slow diffusion from concreted wastes, or would be delayed until the disintegration or rupture of an impermeable container. Since the deep-sea sediments have high exchange capacities, much of the waste would be retained, at least until the upper layers of the sediments became saturated. Goldberg and Arrhenius (17) have also shown that in the deep-sea sediments some elements which have radioactive isotopes are removed from the water by ferromanganese oxide minerals, zeolite phillipsites, and the micro-crystalline skeletal apatite from the remains of marine vertebrates.

The processes, both inorganic and biochemical, bringing about bottom-deposit accumulation of elements having radioisotopes are not well understood, and should be investigated by both field studies and laboratory experiments. Further, it is desirable to determine the average time an element spends in the water of the deep sea before being removed by sedimentation processes. This has been roughly estimated for a variety of elements from concentrations in sea-water, concentrations in sediments, and rate of accumulation of sediments, assuming a steady-state system and uniform mixing of the oceans. These estimates are, however, not very reliable because the basic data on the sediments are sparse and because the assumption of steady-state and uniform mixing may not be correct. More extensive studies of the composition and rates of deposition of sediments in different parts of the sea are called for.

Biological aspects

Radioactive waste materials in the deep sea may be returned to the upper mixed layer, and thence to man, by the circulation and mixing of the water in which they are dissolved. They may also, in some instances, be returned by organisms. This can happen in two ways. First, some of the animals of the upper layer which are used by man feed in the depths of the sea where they could obtain radioactive materials taken up by their food organisms. The feeding of sperm whales on deep-sea cephalopods is a case in point. Second, some elements of the biosphere perform regular migrations between the intermediate depths, at least, and the surface layer, readily crossing the thermocline. Such organisms might take up radioactivity in the deep water and liberate it in the surface water. Elements most effectively transported by this means would be those which are readily and rapidly exchanged with the water. KETCHUM and BOWEN (18) have calculated that this biological transport can be more rapid than that due to physical processes. On the other hand, if the vertical migrants are eaten by fish in the surface layer, and these are, in turn, taken by man for food, those elements which are concentrated and retained by the migrants, but which are incorporated in the bodies of their predators, would be readily returned to man by this route.

Research is required to measure the uptake and excretion rates of elements important in radioactive waste materials by deep-sea organisms, especially those which migrate between the surface layer and the deeper layers, on rates of migration of such organisms, and on the efficiency of ingestion and digestion of food by organisms at different trophic levels. Much of this work can be done by classical methods of biological oceanography, but experiments using moderately large quantities of radioactive materials as tracers in experiments in the open sea, some of which have been suggested by SCHAEFER (7), also constitute a powerful new approach.

Research for monitoring

Introduction into the marine environment of radioactive materials in amounts that might, by any possibility, constitute a hazard should be accompanied by careful and systematic monitoring in and near the disposal

(740)

areas to measure the concentration and distribution of such materials. Thus Carritt *et al* (4), discussing the disposal of low-level wastes in coastal waters of the American Atlantic seaboard, have stated, "Monitoring of a disposal area at intervals following the start of disposal operations will be essential to the safe and efficient use of an area". Pritchard *et al* (2) have recommended that "It is essential that a systematic monitoring programme be initiated as soon as possible to determine the consequences of the release of radioactive wastes from nuclear-powered vessels, both civilian and military", and have further recommended that "The monitoring should cover all harbours in the United States and its territories entered by nuclear vessels to the extent required by such use. It should be flexible enough to encompass, when circumstances require, all marine environments where organisms are exploited by man. It should be directed towards the detection of the radioactive isotopes produced by both corrosion and fission processes, distinguishing the quantities originating from fallout, from land-based reactors and from nuclear vessels". The National Academy of Sciences Committee on Oceanography (3) has likewise placed heavy emphasis on the need for careful monitoring.

Monitoring of radioactive wastes in the sea requires their measurement in sea-water at exceedingly low concentrations, since some isotopes can constitute a hazard in dilutions of the order of 1×10^{-6} μc/l. The efficient detection, identification, and measurement of these materials at such low concentrations require research into improved instrumentation and chemical techniques for the purpose.

A promising tool for monitoring is the use of organisms as detectors. As we have noted previously, it is not the concentration in the water but in the organisms which is the controlling factor for safe waste disposal, since the organisms often concentrate the materials by several orders of magnitude over the concentration in the water. It is thus obvious that the simplest way to monitor nuclear wastes in the marine environment is through measurements in the biota. Furthermore, selected kinds of organisms are known to concentrate certain elements especially. For instance, some molluscs concentrate cobalt by a factor of at least 10^4, and certain tunicates concentrate niobium by very large factors. A systematic search for organisms which concentrate particular elements heavily is therefore a primary line of research towards the development of rapid and simple "bio-assay" methods in a monitoring programme.

Specific research proposals

The National Academy of Sciences—National Research Council's Committee on the Effects of Atomic Radiation on Oceanography and Fisheries during 1956 extensively reviewed the problems of disposal of radioactive wastes in the sea, and considered the present status of knowledge and additional information required in this connexion (1). Its recommendations included suggestions for research in physical, chemical, and biological oceanography, including field investigations, experimental studies in the sea using tracer techniques, and laboratory studies. At a meeting with scientists of the United Kingdom in the autumn of 1956 (19), questions needing answers through additional research were further discussed. Finally, a working group of the Committee on Effects of Atomic Radiations on Oceanography and Fisheries, operating as a panel of the Committee on Oceanography, has made specific recommendations for a five-year research programme for the United States, together with cost estimates (3), which may be outlined as follows:

Estuarine and coastal studies

The recommendations under this heading involve studies of circulation and mixing in estuarine and coastal environments, encompassing essentially the research of this sort discussed earlier in this paper. It was recommended that $ 1,400,000 per year be provided for such studies in estuaries, and an equal sum for studies in coastal waters.

Research in the open ocean

The Committee has recommended studies of circulation and mixing in the open ocean, including:

1. Tests of the Stommel theory of the deep circulation in the ocean, including direct measurements of the western boundary currents, and the completion of zonal profiles across the Pacific at each 10° of latitude for calculation of transport and upward transfer across the thermocline;
2. Estimates of vertical exchange across the thermocline, employing measurements of the distribution in the sea of naturally-occurring radioisotopes and of the artificially-created radioisotopes now present in the sea from past weapons tests; and
3. Studies of mixing within the deep waters by the tracing of radioactive materials introduced in the deep sea in a line along the deep margin of a western boundary current.

The estimated cost of this research is $ 1,400,000 per year. It was recognized that international collaboration would be most helpful in conducting these studies.

Sedimentation processes in estuarine and coastal waters and in the deep sea

Research recommended under this heading includes studies aimed at measuring the concentration of elements of the fission-product spectrum in both deep and shallow waters, and rates of sedimentation in various environments. Studies were also recommended to investigate the exchange characteristics of organic and inorganic components of the sediments.

It was suggested that about $ 350,000 be devoted to the support of these researches during the first year and $ 165,000 per year thereafter.

Effects of the biosphere on the distribution and circulation of radioisotopes in the sea

The research programme on biological aspects, both in inshore and open-sea areas, includes studies of basic productivity, investigations of abundance, species composition, migrations and food-chain relationships of zooplankton organisms, studies of benthic populations with respect to their abundance in various habitats, sources of food and feeding habits and food-chain relationships, studies of commercially-important fish and marine mammals with respect to their distribution and migrations, sources of food and feeding habits and uptake and sites of deposition of radioactive isotopes, elemental analyses of representative invertebrates and vertebrates, and ecological studies of representative waste-disposal areas.

For these purposes it was estimated that $ 838,000 per year will be required. In addition it was recommended that studies of genetic effects of radiation on marine organisms be given additional support in the amount of $ 100,000 per year.

Field experiments using radioactive isotopes

It was recognized that the use of radioisotopes as tracers in field experiments is an important new tool for studies of both physical and biological processes in the sea.

It was recommended that tracer experiments be conducted in a small lagoon to measure the distribution and transfer rates of radioisotopes throughout a marine ecosystem. A budget of $ 100,000 per year was proposed for this work.

Several large-scale field experiments in the open sea were also considered appropriate, including: (1) an experiment in tagging surface-water of the open sea to measure lateral mixing in the mixed layer above the thermocline; (2) an experiment in mid-depth in the main thermocline, to measure the rate of lateral spreading of water within the thermocline, and to determine how effectively the thermocline seals the deep water from the surface water; (3) an experiment in tagging bottom water. It was again recognized that such large-scale experiments should involve international collaboration.

Budget estimates for such large-scale experiments are difficult to make, since there is little previous experience to refer to, but each test might cost from $ 400,000 to $ 5,000,000 depending on location, duration, and complexity.

Excluding the large-scale field tests mentioned immediately above, the recommended research programme would cost a total of about $ 30 million over a five-year period. About one-third of this represents work now under way, leaving some $ 20 million for new effort.

The research recommended by this Committee, while not including all the new studies which I have discussed in this paper, encompasses a substantial share of them, and would constitute a good start on the accumulation of the knowledge which will be required for safe and efficient use of the sea as a receiver of radioactive waste materials.

REFERENCES

(1) REVELLE, R. R. *et al.*, National Academy of Sciences—National Research Council Publication No. 551 (1957).
(2) PRITCHARD, D. W. *et al.*, National Academy of Sciences—National Research Council Publication No. 658 (1959).
(3) BROWN, H. *et al.*, "Oceanography 1960 to 1970" Chap. 5, National Academy of Sciences—National Research Council, 1 (1959).
(4) CARRITT, D. E. *et al.*, National Academy of Sciences—National Research Council Publication No. 655, (1959).
(5) WALLEN, I. E., TID-5550, Appendix C, 43 (Mimeographed), (1959).
(6) KETCHUM, B. H., National Academy of Sciences—National Research Council Publication No. 551, 52 (1957).
(7) SCHAEFER, M. B., National Academy of Sciences—National Research Council Publication No. 551, 133 (1957).
(8) SCHAEFER, M. B. and REVELLE, R. R., "Natural Resources", McGraw-Hill, New York, 73 (1959).

(743)

(9) JOSEPH, J. and SENDNER, H., *Deutsche Hydrographische Zeitung* **2**, 49 (1958).

(10) HARLEY, J. E. (ed.), "Operation Troll", US Atomic Energy Commission, New York Operations Office (1956).

(11) CRAIG, H., National Academy of Sciences—National Research Council Publication No. 551, 103 (1957).

(12) WÜST, G., "Report on the current velocities, volume transports and mixing effects in the Atlantic deep sea as physical processes important to the transport and disposal of radioactive wastes", MS (Mimeographed) (1957).

(13) DIETRICH, G., "Selection of suitable ocean disposal areas for radioactive waste" (A preliminary report with 6 charts), MS (1957).

(14) STOMMEL, H., *Deep Sea Research* **4**, 3, 149 (1957).

(15) WOOSTER, W. S. and KETCHUM, B. H., National Academy of Sciences—National Research Council Publication No. 551, 43 (1957).

(16) FOLSOM, T. R. and VINE A. C., National Academy of Sciences—National Research Council Publication No. 551, 121 (1957).

(17) GOLDBERG, E. and ARRHENIUS, G. O. S., *Geochim. Cosmochim. Acta* **13**, 153 (1958).

(18) KETCHUM, B. H. and BOWEN, V. T., Proc. 2nd UN Int. Conf. Peaceful Uses of Atomic Energy, A/Conf. 15/P/402 (1958).

(19) Report of a meeting of United Kingdom and United States Scientists on biological effects of radiation on oceanography and fisheries (September 27—28, 1956). National Academy of Sciences—National Research Council (Mimeographed).

Deep-Sea Research, 1960, Vol. 7, pp. 35 to 41. Pergamon Press Ltd., London. Printed in Great Britain

Consolidated slabs on the floor of the Eastern Pacific

H. W. MENARD

(*Received* 13 *April*, 1960)

Abstract—Tabular masses, largely phillipsite coated with manganese oxide, are abundant on the floor of the eastern Pacific. They appear to be remnants of layers of volcanic ash derived in large part from volcanoes within the basin. Some of the ash may correlate with the Worzel ash off Central and South America.

INTRODUCTION

SEMI-CONSOLIDATED angular tabular masses, or slabs, with areas of hundreds of square centimetres and thicknesses of a few centimetres are very abundant in large regions of the eastern Pacific Basin. The material in the slabs consists in large part of phillipsite and other alteration products but unaltered mineral grains in some places indicate a volcanic origin. Consideration of the possible sources and the history of the slabs may shed some light on sea floor processes.

SLABS IN THE NORTHEASTERN PACIFIC

The distribution of semi-consolidated slabs in the northeastern Pacific (Table 1, Fig. 1) is based on dredge hauls and bottom photographs. The noteworthy characteristics of the occurrence are the following :

1. The slabs are large, thin, relatively uniform in thickness, and commonly very angular (Fig. 2).
2. They are coated with a few millimetres to several centimetres of ferromanganese oxides, suggesting that they have been exposed on the sea floor for 10^4–10^5 years (Fig. 3).
3. They contain some unaltered minerals and fragments of volcanic glass but phillipsite and other alteration products are the most common constituents.
4. Slabs cover as much as 40 per cent of the bottom in some areas.
5. They appear to decrease in thickness to the west.
6. None of the slabs is on top of others.
7. Some slabs appear to lie in a reticulate pattern rather than being randomly distributed.
8. Manganese nodules cover much of the bottom between slabs in many places.
9. The nodules were formed after the slabs were deposited.
10. The fraction of the bottom covered by nodules and slabs varies systematically over an area of more than 10^6 km^2.

Contributions from the Scripps Institution of Oceanography, New Series, 1190

Reproduced by Permission

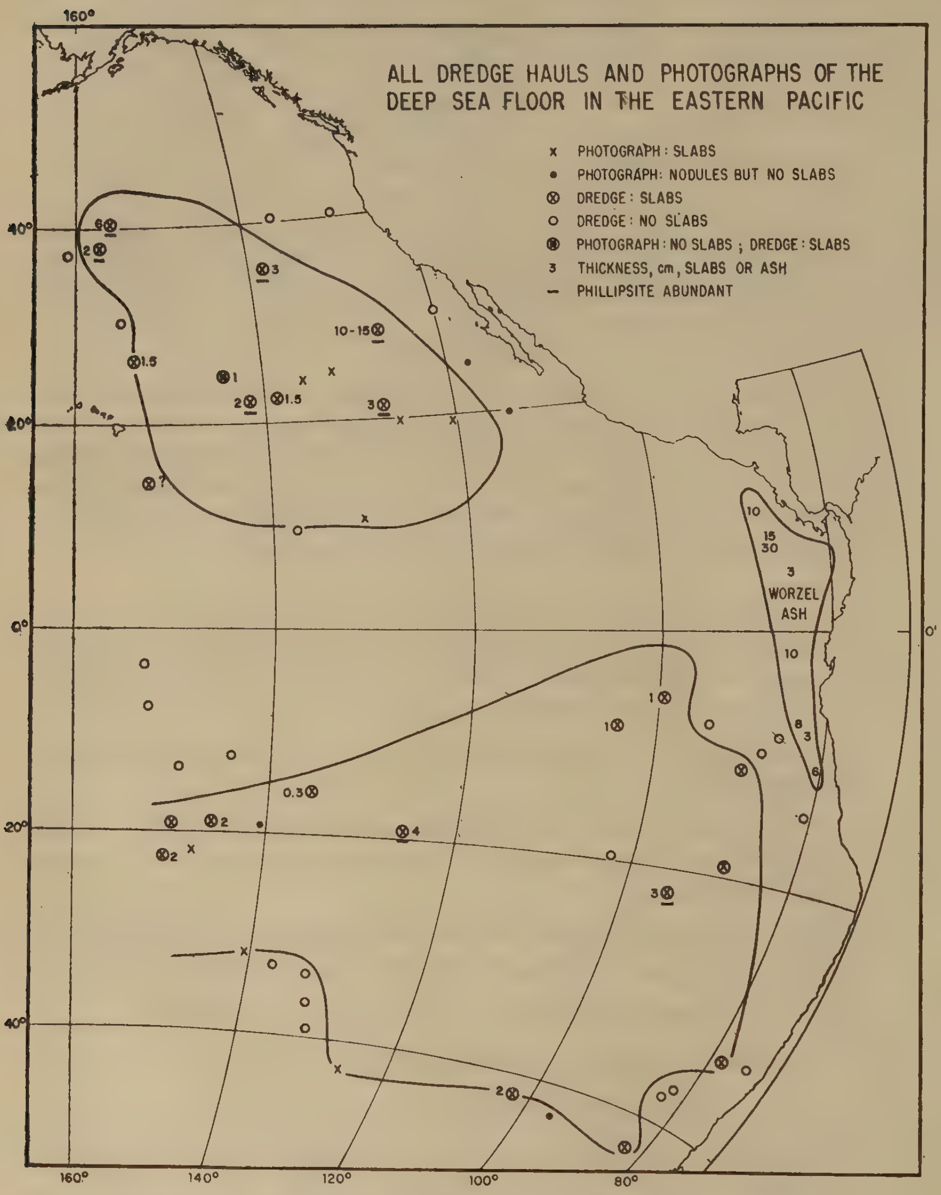
ALL DREDGE HAULS AND PHOTOGRAPHS OF THE DEEP SEA FLOOR IN THE EASTERN PACIFIC
x PHOTOGRAPH : SLABS
● PHOTOGRAPH: NODULES BUT NO SLABS
⊗ DREDGE : SLABS
○ DREDGE : NO SLABS
⊛ PHOTOGRAPH : NO SLABS ; DREDGE : SLABS
3 THICKNESS, cm, SLABS OR ASH
— PHILLIPSITE ABUNDANT
WORZEL ASH
160°
40°
20°
0°
20°
40°
160°
140°
120°
100°
80°
0'
6
2
3
10-15
1.5
1
2
1.5
3
?
0.3
2
2
4
1
1
3
2
10
15
30
3
10
8
3
6

Fig. 1. Occurrence of slabs and of the Worzel ash in the eastern Pacific.

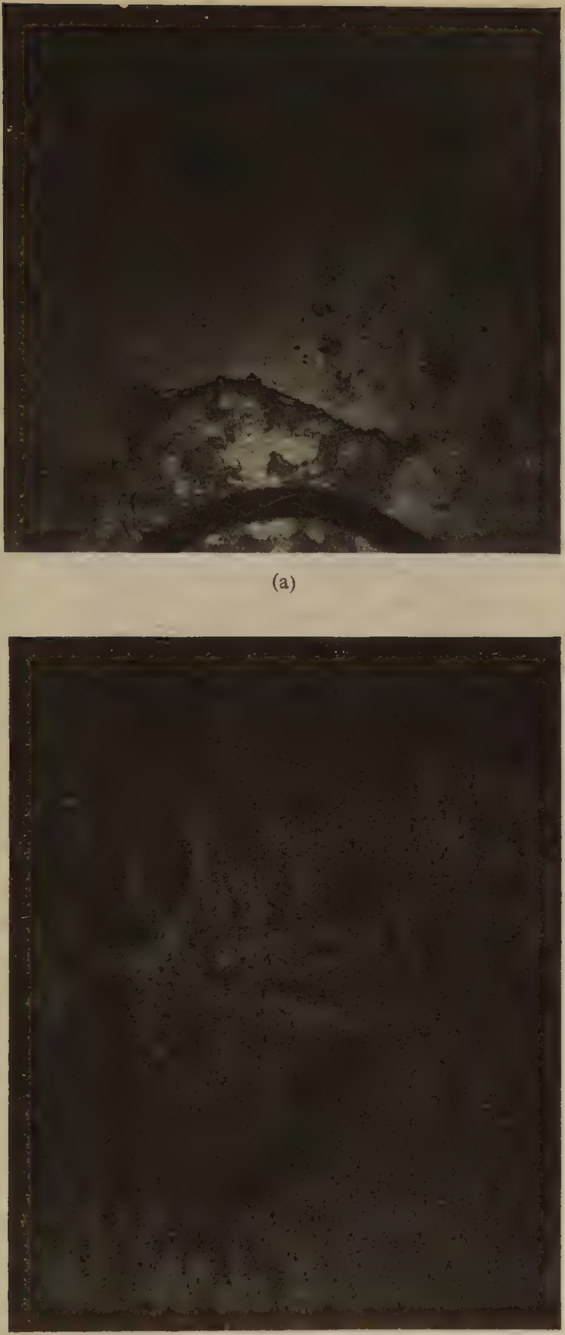

(a)

(b)

FIG. 2. Photographs of slabs on the sea floor of the northeastern Pacific.
(a) Naga 6 C. Photo by C. J. SHIPEK. (b) *Vitiaz* 4279. Photo by N. L. ZENKEVITCH. Note reticulate pattern of slabs. Abundant organisms around the slabs are visible on the stereo-pair of which this is one photo.

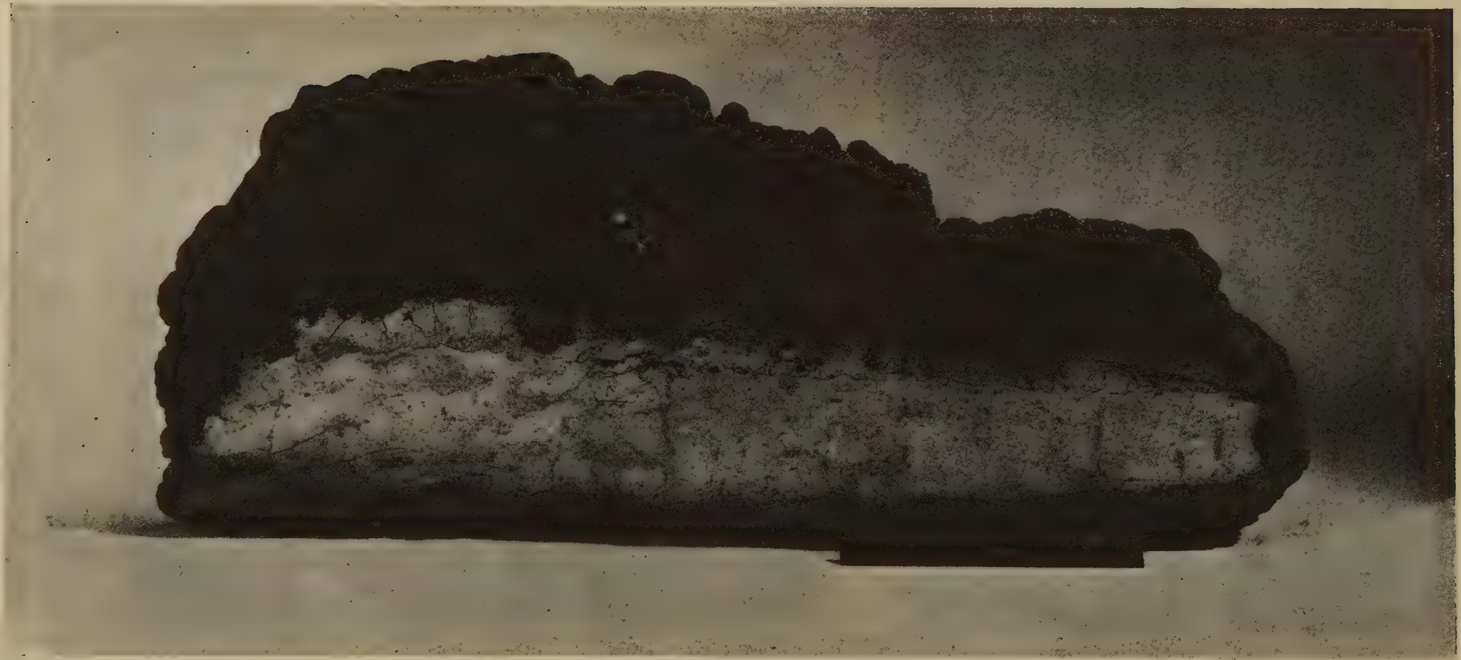

FIG. 3. Cross section of very large nodule from Northern Holiday C-10 showing abrupt termination of layer of phillipsite in nucleus, and thick coating of ferro-manganese oxides on top with thin coatings on bottom and sides.

ORIGIN OF SLABS

Two possible origins for the slabs may be considered : first, that they were emplaced as they now occur, and second, that they are remnants of a continuous layer. The first possibility requires that the slabs are altered blocks of pumice. Certainly pumice is now being distributed through much of the north equatorial Pacific where the slabs are found (RICHARDS, 1958) and the ferro-manganese crusts on top of large slabs contain small equi-dimensional pieces of pumice. However, pumice is very fragile and almost always is rounded by impact with other pieces in the throat of the volcano, in the air, or when floating on the wave-stirred ocean. Floating pumice is quite unlike the large, thin, angular slabs of the northeastern Pacific. Moreover, if the slabs are pieces of pumice, a random distribution with some pieces on top of others would be expected; and the apparent decrease in thickness toward the west and the regional variation in coverage of the bottom are unexplained. For these reasons it appears unlikely that the slabs are blocks of pumice.

All the features of the occurrence of slabs are explained if they are remnants of more or less continuous layers of altered ash. Ash layers vary in thickness systematically, and none of the fragments would lie on top of others. The angularity of the slabs indicates cracking by some physical-chemical process. Numerous dredge hauls show that unaltered ash layers, slabs of zeolites, and manganese nodules have layers with truncated edges and have been split in some way on the sea floor. After splitting or cracking, the edges sometimes are recemented to form septaria, but more commonly the edges are covered with a layer of ferro-manganese oxides, as much as several centimetres thick, thereby proving that some separation has occurred between adjacent slabs of cracked material. However, none of the adjacent angular slabs seen on bottom photographs can be matched as would be anticipated if they were fragments which formerly had been joined and simply moved apart. Consequently it appears that the material on one side of a crack is commonly removed or comminuted. The nuclei of small manganese nodules which are associated with the slabs, but at least in the northern equatorial Pacific, were formed later, may be fragments of the missing pieces of the ash fall.

Various mechanisms are capable of destroying a continuous layer on the sea floor, namely mass movements, erosion by currents, solution, and stirring by organisms, but only the last of these seems to explain the observations. Moreover the slabs themselves show evidence of biological stirring. ' Worm borings ' cut through most slabs, and organisms as well as their trails, mounds, and burrows are visible on most photographs of slabs and manganese nodules. The organisms tunnel under slabs, circle them with trials, and stir up the sediment around them so that small manganese nodules do not form (Fig. 2).

The emplacement and fragmentation of the ash may be reconstructed as follows :

1. Where the ash was very thick the benthos was exterminated and no stirring occurred.
2. Where the ash was thinner and the benthos was large, as in the equatorial belt of rapid sedimentation (compared to red clay) the ash was thoroughly mixed but still detectable (ARRHENIUS, 1952).
3. In the areas of red clay, the scarcer benthos was almost exterminated even though the ash was only a few centimetres thick. Because of the very slow

Table 1. Occurrence of slabs on the sea floor of the eastern Pacific.

Station	*Latitude*	*Longitude*	*Depth (m)*	*Description*
Northeast Pacific Albatross 2	28–23 N	126–57 W	4340	Slabs 45 cm long, 15 cm thick, angular, many worm borings. Nucleus fairly pure zeolite partially replaced by ferro-manganese oxides, 1% oligoclase, volcanic glass, and magnetite. (1)
Challenger 253	38–09 N	156–25 W	5710	Slab 31 × 20 × 6 cm. Nucleus 2 cm thick, earthy with some zeolites. Annelid attached to bottom. (2)
Downwind BD-1	21–27 N	126–43 W	4300	Angular slabs to 31 × 24 × 5 cm. Some coated on all sides with a few mm of mn. Two layers, both with worm borings.
Downwind BD-2 P-2	10–25 N	130–35 W	4712	Photo shows slabs and spherical nodules partially buried. Only nodules dredged. Visible organisms. (3)
Naga 6 C	24–27 N	135–17 W	4300	Photos of angular flat slabs. No organisms or traces. (3)
Naga 8 C	23–17 N	138–15 W	4890	Slabs 3 × 5 × 2 cm. Nucleus 2 layers, earthy, 1·5 cm thick.
Naga 10 C	23–17 N	141–13 W	5400	Rounded slabs 3 × 4 × 2 cm. Nucleus almost pure phillipsite, 2 cm thick.
Northern Holiday C-10	40–14 N	155–06 W	5100	Slab 61 × 61 × 32 cm. Nucleus phillipsite 6 cm thick.
Vitiaz 3630	22–00 N	153–55 E	5733	Photo of sub-angular slab. Organisms, tracks and mounds abundant. (4)
Vitiaz 3632	17–38 N	154–54 E	5718	Photo of very abundant sub-angular slabs. Organisms and mounds. (4)
Vitiaz 4199	35–06 N	137–56 W	5035	Dredge haul. Slab 9 × 9 × 5 cm, angular. Nucleus 2 layers, earthy, in part vesicular, phillipsite abundant. Bottom layer 3 cm thick.
Vitiaz 4239	24–55 N	144–12 W	5190	Slab 7 × 7 × 3 cm. Nucleus 1 cm thick, red clay (?). Photo shows a few small nodules, organisms and mounds. (4)
Vitiaz 4249	24–55 N	132–18 W	4975	Slabs 7 cm long. Nucleus altered volcanic ash. (5). Photo shows small nodules on consolidated bottom. (4)
Vitiaz 4279	19–48 N	120–16 W	4104	Slabs encrusted on top with ferro-manganese oxides. Slabs of altered volcanic ash. (5). Photos of abundant slabs, organisms, and mounds. (4)
Vitiaz 4285	19–57 N	126–06 W	4545	Photo of angular slabs, mounds. (4)
Vitiaz 4370	26–12 N	153–44 W	6120	Slabs 4 × 4 × 2 cm. Thin ferro-manganese crust on earthy centre with abundant worm tubes. Quartz abundant, phillipsite rare.

(750)

Table 1—*contd.*

Station	*Latitude*	*Longitude*	*Depth (m)*	*Description*
Southeast Pacific				
Albatross 173	18–55 S	146–32 W	4460	Slabs 15 cm long, 4 cm thick, rounded. Palagonite tuff nucleus. (1)
Albatross 4662	11–14 S	89–35 W	4460	Nodules of ash and palagonite altered by and coated with ferro-manganese oxides. (1)
Albatross 4681	18–47 S	89–26 W	4390	Slabs 7·5 cm long. Nucleus of altered palagonite and clay. (1)
Albatross 4685	21–36 S	94–56 W	4040	Slabs 15 cm long, 3 cm thick. Volcanic ash slightly impregnated and coated with ferro-manganese oxides. (1)
Albatross 4717	5–10 S	98–56 W	3940	Flat nodules 2 × 2 × 1 cm. No concentric layering. (1).
Albatross 4721	8–08 S	104–11 W	3820	Flat nodules 2 × 2 × 1 cm.
Albatross 4736	19–00 S	125–05 W	4190	Slabs 20 × 10 × 4 cm of zeolites and palagonitic tuff coated with ferro-manganese oxides. (1) Broken on sea floor.
Challenger 280	18–47 S	149–52 W	3550	Nodules 5 cm long. Nucleus ‘ portions of the bottom ’ perforated by worm tubes. (2)
Challenger 281	22–21 S	150–17 W	4370	Slab 45 × 30 × 7·5 cm. Nucleus 2 cm volcanic tuff with graded bedding above consolidated red clay. (2)
Challenger 300	33–42 S	78–18 W	2520	Slabs. Nucleus of hardened volcanic tuff. (2)
Challenger 302	42–43 S	82–11 W	2650	Large flat fragments.
Downwind HD-15	15–23 S	136–18 W	4480	Nodules 3 × 3 × 0·3 cm. Nucleus earthy.
Downwind HD-47	41–59 S	102–01 W	4200	Slab 20 × 10 × 3 cm. Top, ferro-manganese oxide crust 1 cm. Nucleus 2 cm volcanic ash, euhedral quartz and alcalic feldspar crystals to 1 mm diameter.
Downwind P-8	21–37 S	147–40 W	4684	Photo of slabs and spherical nodules capped with sediment. No visible organisms. (3)
Downwind P-10	32–08 S	140–30 W	4754	Photo of angular slabs and spherical nodules. Mounds produced by burrowing. (3)
Downwind P-11	42–50 S	125–32 W	4560	Photo of rounded slabs and smaller nodules. Organisms, trails and mounds abundant. (3)

(1) Murray and Lee (1909).
(2) Murray and Renard (1898).
(3) Photo by C. J. Shipek
(4) Photo by N. L. Zenkevitch.
(5) Personal communications (1960) N. S. Skornyakora and N. L. Zenkevitch.

rate of deposition, the ash was altered to zeolites and clay, partially cemented in some places, and cracked into angular slabs.

4. As the benthos repopulated the region, the more shattered and less cemented parts of the ash were stirred and ingested. Initially the process was random, but gradually the animals created micro-environments with thoroughly stirred small areas separated by vague lines of undisturbed residual slabs which continued to become harder and more coated with ferro-manganese oxides.

This sequence of events offers an explanation for the regional variation in the fraction of the bottom covered by manganese nodules and slabs which is otherwise puzzling. The occurrence of nodules at the sediment surface may be correlated with rate of sedimentation, but, if no other factors were important, a layer of abundant nodules would either be at the surface or buried. If a continuous ash layer, which would act as a locus for ferro-manganese deposition, were partially destroyed by organisms, the fraction of the bottom covered by ferro-manganese concretions would depend on the intensity of stirring by organisms. In the region under consideration, the abundance of the benthos probably is a function of the abundance of pelagic organisms in the surface water which provide food by sedimentation. The pelagic organisms vary in productivity with latitude and reach a peak near the equator which gives a positive correlation with the fraction of the bottom covered by slabs and manganese nodules.

SOUTHEAST PACIFIC SLABS

The evidence for a widespread occurrence of slabs in the southeastern Pacific is consistent although it is by no means as abundant as in the northeastern Pacific. No photographs are available, but ten of eleven dredge hauls in the region (Fig. 1) contain slabs. Several dredge hauls and photographs in the region of French Oceania show slabs, however; one slab is composed of coarse, graded, unaltered volcanic ash (MURRAY and RENARD, 1891) indicating that it was derived from one of the many local volcanic islands. Most of the slabs in the large region to the east are on the East Pacific Rise which is covered with calcareous sediments. It is not known whether the slabs are at the sediment surface or are buried (but still accessible to the dredge). The high $CaCO_3$ content of these sediments results from slow solution on the bottom (BRAMLETTE, pers. comm., 1959). The productivity of plankton in surface waters is not high as in the equatorial regions; indeed, it appears to be exceptionally low (FISHER *et al.*, 1958). Consequently this may be a region where few organisms would be available to stir an ash layer and where the ash would be buried more rapidly than in a region with red clay sediment. The volcanic ash slabs slightly impregnated with ferro-manganese oxides found at Albatross No. 4685 (MURRAY and LEE, 1909) (TABLE 1) may be typical of this environment.

SOURCE OF MATERIAL IN SLABS

More than one layer occurs in some of the northeastern Pacific slabs, and the thickness of ferro-manganese oxide coatings is quite variable suggesting different ages for the original ash layers. The decrease in thickness from east to west implies a source to the east. However the atmospheric circulation at the latitude of the ash deposit is entirely westerly and the ash cannot have been emplaced by falling vertically through the ocean after lateral movement through the air. The only remaining possibility is lateral movement in the ocean which circulates in a pattern which could produce the gradient in ash thickness in this region. Only the top few hundred metres of the ocean move with appreciable velocity, and large lateral movement is possible only if the ash particles are small and only slightly denser than water. For an excess density of 0·1 gm/cc, 12 μ particles could be transported by surface currents throughout the northeastern Pacific. Ash particles of this character are not rare. The particles of oligoclase with a diameter of 0·15 mm found by CASPARI (*in* MURRAY and LEE, 1909) in slabs in this region cannot have been transported much more than 10 km, however. In sum, the ash was derived at least in part from the submarine volcanoes which are characteristic of the region (MENARD, 1955) and transported laterally by surface water currents.

In the southeastern Pacific also, some of the slabs were deposited as ash layers derived from near-by volcanoes. The slabs do not show any regional gradient in thickness and all may have local sources.

This investigation began as a search for the Worzel ash in the eastern equatorial Pacific. The ash has a relatively uniform thickness of 10 cm in the type region (WORZEL, 1959) and must extend over a much larger area (EWING *et al.*, 1959). The ash is buried under several metres of green mud in some places but in much of the northeastern Pacific, where sedimentation is very slow, it would be at or near the sediment surface. However, the distribution of the slabs, multiple layering and coarse texture in some places argue against the possibility that much of the material in the slabs is related to the Worzel ash.

Acknowledgements—The writer is indebted to M. N. BRAMLETTE, W. R. RIEDEL and E. D. GOLDBERG for critical discussions on the origin of the slabs and for identification of minerals in the slabs by optical and X-ray techniques. Unpublished photographs of the sea floor were made available by C. J. SHIPEK and N. L. ZENKEVITCH. *Vitiaz* samples were provided by P. L. BEZRUKOV, N. S. SKORNYAKOVA and N. L. ZENKEVITCH. Support was given by the Office of Naval Research under contract Nonr–2216 (01).

Institute of Marine Resources and
Scripps Institution of Oceanography,
University of California,
La Jolla, California.

Contribution from the Scripps Institution of
Oceanography, New Series.

REFERENCES

ARRHENIUS, G. (1952) Properties of the sediment and their distribution. *Repts. Swedish Deep-sea Expedition* **5**, Pt. 1.

EWING, M., HEEZEN, B. C. and ERICSON, D. B. (1959) Significance of the Worzel deep-sea ash. *Proc. Nat. Acad. Sci.* **45**, 355–361.

FISHER, R. L. *et. al.* (1958) Preliminary report on Expedition Downwind *I.G.Y. General Report Series* 2. (Unpublished manuscript).

MENARD, H. W. (1955) Deformation of the northeastern Pacific Basin and the west coast of North America. *Geol. Soc. Amer. Bull.* **66**, 1149–1198.

MURRAY, J. and LEE, G. V. (1909) The depth and marine deposits of the Pacific. *Mem. Mus. Comp. Zool.* **38** (1).

MURRAY, J. and RENARD, A. F. (1898) Deep-Sea deposits. H.M.S. *Challenger, Sci. Results.* 525 pp.

RICHARDS, A. F. (1958) Transpacific distribution of floating pumice from Isla San Benedicto, Mexico. *Deep-Sea Res.* **5**, 29–35.

WORZEL, J. L. (1959) Extensive deep sea sub-bottom reflections identified as white ash. *Proc. Nat. Acad. Sci.* **45**, 349–355.

Printed in Great Britain by The Salisbury Press Ltd., Publicity House, Wilton Road, Salisbury, Wilts. (24152)

Deep-Sea Research, 1960, Vol. 7, pp. 68 and 69. Pergamon Press Ltd., London. Printed in Great Britain

LETTER TO THE EDITORS

Observations of irregular motion in the open ocean

(*Received* 29 *February* 1960)

It is believed that the following observations are examples of turbulent motion in the open ocean at depths well below the wind stirred layer. The depth of the mixed layer in the area where these measurements were made is 50–100 metres. Observations with neutral buoyant current floats have often indicated irregular movement (Swallow, 1955, 1957); but since these observations have always been made with reference to anchored buoys, it has usually been impossible to determine how much of this erratic movement is real and how much is an artifact resulting from the swinging of the buoy on its anchor.

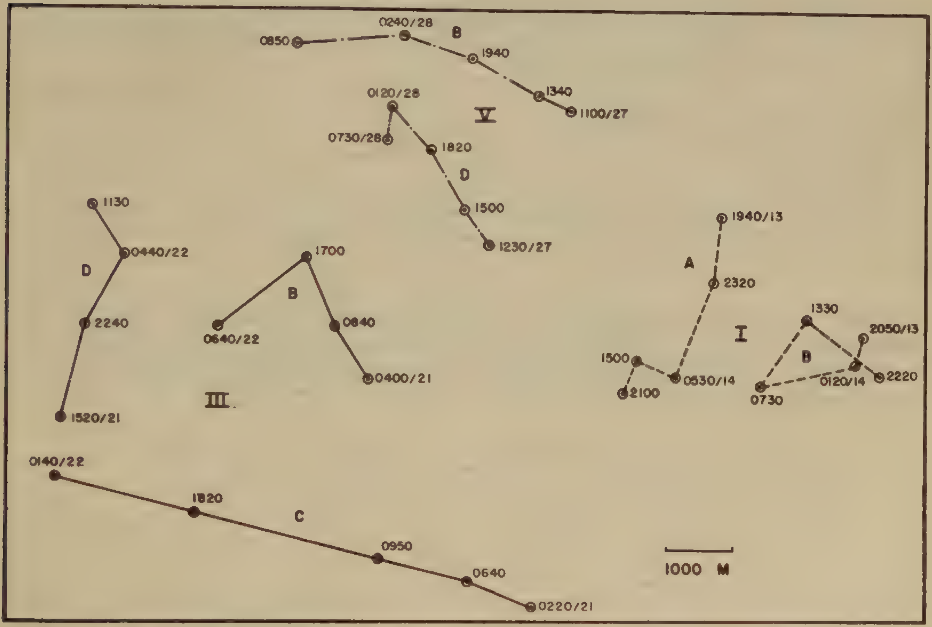
0240/28
B
0850
1940
1340
1100/27
0120/28
V
0730/28
1820
D
1500
1230/27
1130
0440/22
D
2240
1520/21
1700
B
0640/22
0840
0400/21
III.
1940/13
A
2320
I
1500
0530/14
2100
1330
2050/13
B
0120/14
2220
0730
0140/22
1820
C
0950
0640
0220/21
1000 M

Fig. 1. Simultaneous observations of float movement. The time and date of each fix is given. At buoy III, float C (300 m) moved steadily on a course of 285°, while float B (1,170 m) changed course some 90° and float D (1,720 m) changed about 45°. At buoy V, float B (1,070 m) moved in a slightly curving path toward the west while float D (810 m) turned almost completely back upon itself. At buoy I, both floats A (720 m) and B (2,140 m) executed irregular movement, apparently independent of one another.

On a recent cruise it was possible on several occasions to follow two or more floats simultaneously Under these circumstances if one float moves steadily and the other irregularly, or if both should move irregularly but differently from one another, it is difficult to assign any explanation to this movement, other than that such erratic motion is real.

Contributions from the Scripps Institution of Oceanography, New Series, 1191

Reproduced by Permission

Three examples of such motion are given (the pertinent data on the floats in Table 1, that portion of the tracks which best show the turbulent motion in Fig. 1). All positions are based on three bearing fixes. The accuracy of the individual fixes is about 200 metres. All measurements were made with reference to a taut wire mooring whose radius of swing is about 350 metres (Knauss, 1960). It is believed that these observations are examples of turbulence (or possibly, internal waves). If the motion were either barotropic or tidal, then the non-steady portion of the movement should be the same for all floats independent of depth.

Table 1.

Position					*Hrs.*	*Mean Velocity*	
N	*W*	*Date*	*Float Number*	*Depth*	*Tracked*	*(cm/sec)*	*(toward)*
15° 08′	120° 02′	12 July	I–A	720 ± 270	57	2·5 ± 0·2	183° ± 6°
		13 July	I–D	2140 ± 440	38	1·2 ± 0·3	150° ± 17°
7° 30′	120° 00′	20 July	III–B	1170 ± 310	49	4·3 ± 0·3	300° ± 4°
		20 July	III–C	500 ± 230	40	6·6 ± 0·3	270° ± 3°
		21 July	III–D	1720 ± 300	31	4·7 ± 0·4	004° ± 5°
5° 32′	120° 05′	26 July	V–B	1070 ± 270	43	5·3 ± 0·3	268° ± 3°
		27 July	V–D	810 ± 220	19	3·4 ± 0·7	314° ± 12°

Data on seven neutrally-buoyant floats tracked on the Dorado Expedition, July-August, 1959.

John A. Knauss.

Scripps Institution of Oceanography,
University of California,
La Jolla, California.

Contribution from the Scripps Institution of Oceanography, New Series. This work was supported by the Office of Naval Research and the National Science Foundation.

REFERENCES

Knauss J. A. (1960) Measurements of the Cromwell Current. *Deep-Sea Res.* 6, 265–286.

Swallow J. C. (1955) A neutral buoyancy float for measuring deep currents. *Deep-Sea Res.* 3, 74-81.

Swallow J. C. (1957) Some further deep current measurements using neutrally-buoyant floats. *Deep-Sea Res.* 4, 93-104.

Printed in Great Britain by The Salisbury Press Ltd., Publicity House, Wilton Road, Salisbury, Wilts. (24157)

Deep-Sea Research, 1960, Vol. 7, pp. 52 to 60. Pergamon Press Ltd., London. Printed in Great Britain

INSTRUMENTAL NOTE

A seasonal mean sea-level indicator†

(*Received* 4 *January* 1960)

Abstract—By means of oil capillaries the indicator attenuates the tidal rise and fall of the sea surface, as well as all fluctuations of higher frequencies. The time constant of the response is chosen so that the smaller, slower fluctuation of sea level is transmitted with very little change of amplitude and phase. There is no recorder. Visual readings of the oil level in a burette should be tabulated twice a week. Installation of the instrument is much easier and cheaper than a recording tide gauge.

INTRODUCTION

THE STUDY of day-to-day, or longer period, variation of sea level is usually carried out by making suitable averages of tidal data to eliminate the amplitude of the large tidal ' noise.' Such a method of elimination is generally known as mathematical filtering and has recently been refined to a high degree of accuracy by systematic computation of the most efficient weight factor averaging (GROVES, 1955). The instrument described here accomplishes essentially the same thing by an analog method. It consists of a two-stage low-pass hydraulic filter which attenuates the diurnal and semidiurnal tides to a negligibly small amplitudes while the long-term variations, say month to month, are transmitted with practically no attenuation or phase shift. Intermediate frequencies, such as the day-to-day variation, suffer a small attenuation and phase shift, according to the time constant of the instrument. The height of oil in a burette represents the mean sea level. The simplicity in taking the readings can be advantageous with untrained observers. Since the instrument does not respond to rapid fluctuations, a reading twice a week is adequate.

The installation of the mean sea-level indicator is very simple as compared to that of a tide gauge. There is the additional advantage that no subsequent data reduction is required. The instrument and its installation are not costly. These advantages, together with its simplicity of operation and reading, make the indicator suitable for use on any inhabited island or coast.

Table 1. *Relationship between the hydraulic and electrical parameters.*

Hydraulic	*Electric*
$g\,\rho_w\,N_w$	E_1
$g\,\rho_0\,N_o$	E_0
R_1	R_1
R_2	R_2
$Am/g\,P$	Cm
$A_1/g\,\rho_o$	C_1
$A_2/g\,\rho_o$	C_2

$g \rightarrow$ *Acceleration of gravity*
$P = 2\,\rho_m - \rho_w - \rho_o$

---

†Contribution from the Scripps Institution of Oceanography, New Series. 1192

Reproduced by Permission

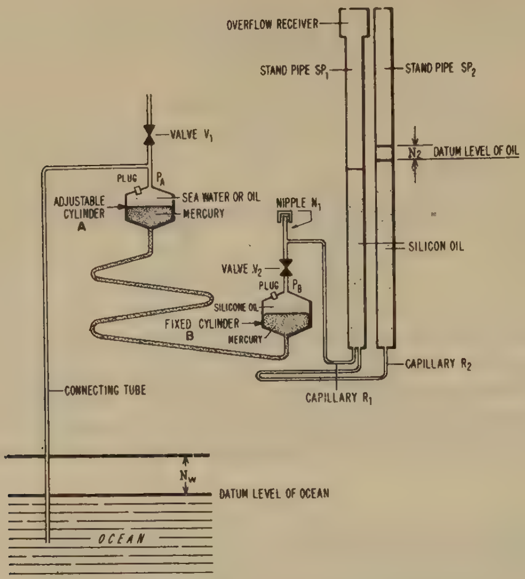
OVERFLOW RECEIVER
STAND PIPE SP_1
STAND PIPE SP_2
VALVE V_1
N_2
DATUM LEVEL OF OIL
PLUG
P_A
ADJUSTABLE CYLINDER A
SEA WATER OR OIL
MERCURY
NIPPLE N_1
SILICON OIL
VALVE V_2
PLUG
P_B
SILICONE OIL
FIXED CYLINDER B
MERCURY
CAPILLARY R_2
CONNECTING TUBE
CAPILLARY R_1
N_w
DATUM LEVEL OF OCEAN
OCEAN

FIG. 1a. Schematic of the mean sea level indicator.

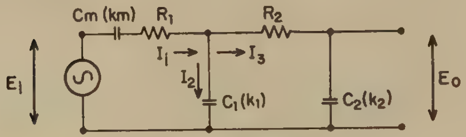
Cm (km)
R_1
R_2
I_1
I_3
I_2
E_I
$C_1(k_1)$
$C_2(k_2)$
E_O

FIG. 1b. Electrical analogy.

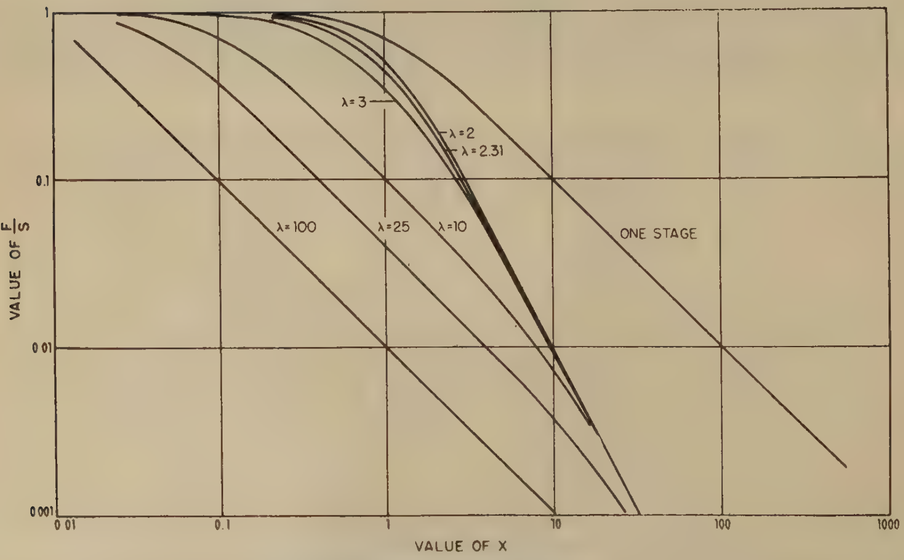

FIG. 2. Response charactertics.

DESCRIPTION

The sea-level indicator (Fig. 1a) consists of a tube of small diameter, filled with sea water or with oil, running from the ocean to a manometer of heavy fluid (mercury). The manometer in turn is connected through two capillary tubes to two open, oil-filled standpipes.

The instrument can be represented equally well by an analogous electrical circuit (Fig. 1b). Potential differences in the electrical analogy correspond to pressure differences in the actual instrument; electric current corresponds to volumetric flow of fluid (cm^3 sec^{-1}); and electrical resistance corresponds to hydraulic resistance. The latter is defined as the ratio of the pressure difference across a capillary to the volumetric flow through it. For a given capillary and given oil, this hydraulic resistance can be taken as constant if the resistance to viscous flow is much greater than the ' form resistance ' or ' end effect.' (This condition is satisfied in the model described). Electrical capacitances are analogous to the capacitances of the various containers, i.e., mercury manometer and oil standpipes defined as the ratio of volume displacement to corresponding pressure change. Then, if the densities of sea water, mercury, and oil are ρ_w, ρ_m, ρ_o the resistance of capillaries R1, R2, the cross-sectional areas of the manometer and standpipes Am, A1, A2, the instantaneous height of sea level N_w, and that of the oil in the second standpipe N_o above their mean positions, then the analogy between the hydraulic and electrical components shown in Fig. 1a and Fig. 1b is given in Table 1. A somewhat similar instrument for recording ultra low frequency ocean waves using a hydraulic and pneumatic filter has been satisfactorily used at Scripps Institution of Oceanography (MUNK, IGLESIAS and FOLSOM, 1948).

FREQUENCY RESPONSE

Writing Kirshoff's equations for the circuit of Fig. 1b gives

$$(Km + R_1)\, I_1 + K_2\, I_2 = Ei$$

$$I_1 = I_2 - I_3 = 0$$

$$-\, k_2\, I_2 + (R_2 + K_1)\, I_3 = 0$$

Solving for I_3 and replacing in the expression $E_0 = -\, K_2\, I_3$ yields :

$$E_0 = \frac{E_i}{\dfrac{Cm + C_1 + C_2}{Cm} - R_1\, R_2\, C_1\, C_2\, \omega^2 + j\omega \left(R_2 \dfrac{C_1\, C_2}{Cm} + R_1\, C_1 + R_2\, C_2 + R_1\, C_2 \right)} \tag{1}$$

If F is the filter factor and ϕ the phase difference between E_0 and E_i we may write in a simplified parametric form

$$|E_0| = F\, |E_i| \tag{2}$$

$$F = S\, [(1 - X^2)^2 + \lambda^2\, X^2]^{-\frac{1}{2}} \tag{3}$$

$$\tan \phi = -\, \frac{\lambda X}{1 - X^2} \tag{4}$$

with

$$S = \frac{Cm}{Cm + C_1 + C_2} \tag{5}$$

$$\Gamma = \sqrt{R_1\, R_2\, C_1\, C_2\, S} \tag{6}$$

$$X = \Gamma \omega \tag{7}$$

$$\lambda = \frac{Cm\, (R_1\, C_1 + R_1\, C_2 + R_2\, C_2) + R_2\, C_1\, C_2}{Cm \sqrt{R_1\, R_2\, C_1\, C_2}} \sqrt{S} \tag{8}$$

S is the sensitivity or asymptotic value of the filter factor for infinitely slow changes. It is noted that the filter factor and the phase difference are given by the three nondimensional numbers, S, λ and X, the latter being a nondimensional frequency. Therefore, the complete characteristics of the instrument is given by the three parameters, S, λ, and Γ, the latter having dimensions of a time constant. The function F/S is plotted as a function of X for various values of λ in Fig. 2. The one-stage curve is obtained as the special case when $Cm = \infty$ and $R_2 = 0$, $C_2 = 0$. The case of two identical stages $R_1 = R_2$; $C_1 = C_2$; $Cm = \infty$ gives the $\lambda = 3$ curve.

It is noted from Fig. 2 that the best cut-off characteristics are obtained from the smallest possible values of λ. If λ is too large, the two-stage instrument has little advantage over a one-stage instrument. It can be shown that λ can never be less than two. If we write

$$\frac{Cm}{C_1} = a \qquad \frac{Cm}{C_2} = b \qquad \frac{R_1}{R_2} = p \qquad (a, b, p, \text{all} > 0)$$

then

$$\lambda = \frac{p\,(a + b) + a + 1}{\sqrt{p\,(a + b + ab)}} \tag{9}$$

If we now hold a and b constant while minimizing with respect to p we find that the minimum value is

$$\lambda = 2\sqrt{\frac{(a + 1)\ (a + b)}{a + b + ab}}$$

which occurs for $p = a + 1/a + b$ (11). This expression further minimized with respect to a and b requires $a + b + ab \gg a^2$ (12) from which the limiting value $\lambda = 2$ is obtained.

SELECTION OF DESIGN PARAMETERS

The choice of the sensitivity of the apparatus essentially depends upon two factors : the expected maximum range of seasonal sea level variation and the necessity for practical dimensions for the enclosing cabinet. For the latter we may accept one metre as the maximum desirable vertical dimension. Due to the uncertainty of the actual position relative to mean sea level at installation time and to the need to contain within the first standpipe the residual tidal oscillation, the range of significant oil level variation cannot be more than approximately one-third of the full standpipe length : thus 33 cm.

A sensitivity of one-third would then accommodate a variation of one metre in the mean sea level. Hence, we take $S = \frac{1}{3}$. It is convenient to take $a = b$ in order that both standpipes have the same diameter, in which case $a = b = 1$, $p = 1$ and $\lambda = 2\sqrt{4/3} = 2{\cdot}31$.

Table 2. Cut off characteristics.

$X = 18$	$T = \frac{1}{2}$ *day*	$\frac{F}{S} = 0{\cdot}0031$	*Residual for* 100 cm, *Semi-diurnal Tide* = ·1 cm
9	$T = 1$ *day*	0.0115	*Residual* for 100 cm, *Diurnal Tide* ·38 cm
4·5	2	0·046	
1·8	5	0·22	
0·9	10	0·49	
0·45	20	0·78	
0·30	30 *days*	0·89	

There is much to lose and only very little to gain by attempting to reduce λ further. This would suppose either reduction of S or choice of b significantly larger than a. The cut-off characteristic, however, would not be appreciably improved. The final choice of Cm C_1, C_2, depends upon the following considerations : We want the standpipes large enough to permit ease of construction and a flow of oil high enough to avoid an extremely small capillary; we also want these standpipes small enough to limit the cross sectional area of the manometer and thus reduce the required quantity of mercury.

If

$$A_1 = A_2 = 1\ \text{cm}^2$$

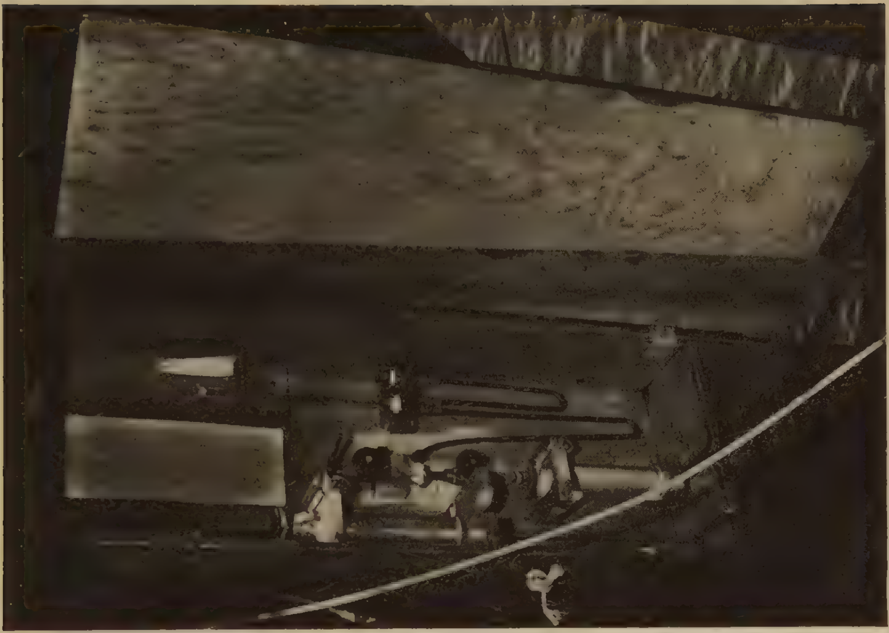

Fig. 3. Prototype of the mean sea level indicator in use at Scripps Institution of Oceanography, La Jolla. (The white plastic tube on the foreground does not belong to the apparatus).

then

$$Am = \frac{2\rho m - \rho_o - \rho_w}{\rho_o} = 26\cdot7 \text{ cm}^2$$

The final choice of R_1 and R_2 is dependent upon the chosen cut-off characteristics. The choice is made from the curves of Fig. 2.

For $\lambda = 2\cdot31$ if we take $X = 9$ when ω corresponds to the diurnal tide, then we get for the passing band characteristics the values tabulated in Table 2. Monthly changes pass with a relative error in amplitude of $(1 - F/S)\,100 = 1\cdot2\%$. Cutting at a lower frequency would reduce the tidal residue but increase badly the error in month-to-month variation. From the above selection

$$X = \Gamma\omega = 9$$

for

$$\omega = \frac{2\pi}{24 \times 3600} = 7\cdot26 \times 10^{-5}\, s^{-1}$$

we obtain

$$\Gamma = 1\cdot3 \times 10^5 \text{ sec}$$

since

$$R_2 = R_1; \quad S = \tfrac{1}{3} \quad \text{and} \quad C_2 = C_1 = \frac{A_1}{\rho_o g} = 1\cdot05 \times 10^{-3} \text{ cgs}$$

then

$$R_1 C_1 = \tau = \frac{9\sqrt{3}}{\omega} = 2\cdot16 \times 10^5\, s$$

$$R_1 = \frac{\tau}{C_1} = 2\cdot07 \times 10^8\, c\,g\,s$$

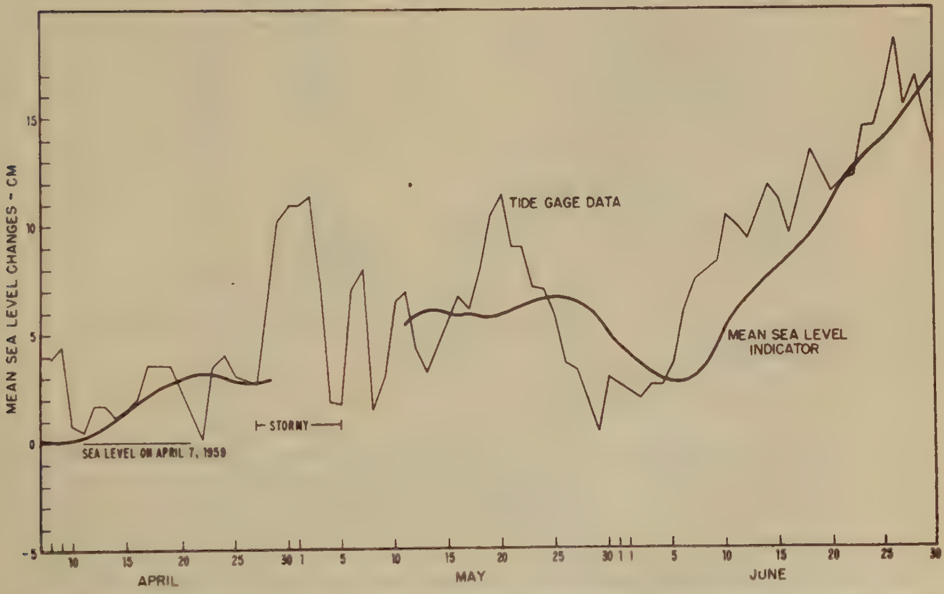

FIG. 4. Variation of the mean sea level at Scripps Institution of Oceanography, La Jolla from April 7 to June 30, 1959.

1. Fine line – according to processed data of the nearby tide gage.
2. Heavy line – from mean sea-level indicator.

Poiseulles' law $R = 8nl/\pi r^4$ permits a preliminary choice of the capillary dimensions l and r, the length and inside radius, respectively. Because of the critical dependence of resistance on inside adius of a capillary, the capillaries should be experimentally adjusted to the accurate value of the time constant $\tau = 2{\cdot}16 \times 10^5$. Due to the very high viscosity of the silicone oil used (1000 cstk at 25° C) the capillary end effect is completely negligible.

CONCLUSION

A prototype of the mean sea-level indicator was installed at the end of the pier of the Scripps Institution of Oceanography, La Jolla, California, at the beginning of April 1959 and has worked satisfactorily ever since (Fig. 3). Fig. 4 shows the mean sea-level changes which have been obtained both from the mean sea-level indicator and from the tide gage located a few feet away. The tube to sea is ¼ in. copper tube. The apparatus is 22 ft above lower low water. No air accumulation in the tube has been observed, and no fouling of the tube hole has interrupted its continuous running.

In case of limited attendance of such a station, it might be advisable to use oil in the tube to sea and to end it in a larger cylinder as shown on Fig. 5. Periodically, say every year, it might be advisable to flow oil through the tube to eliminate any possible bubbles. This can be accomplished most easily by the method described in Fig. 6. The use of oil has also the additional advantage of increasing somewhat the maximum allowable installation height because of the lower density of oil and the lower vapour pressure of some available oils.

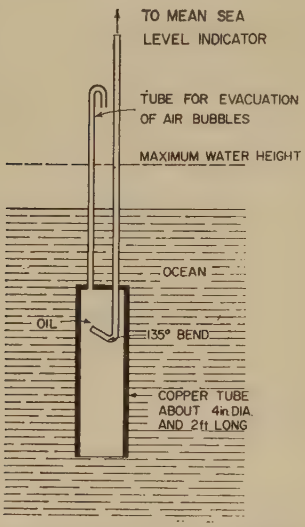

FIG. 5. End protection of the connecting tube against:
(1) Bubble access.
(2) Sediment plugging.
(3) Escaping of oil.

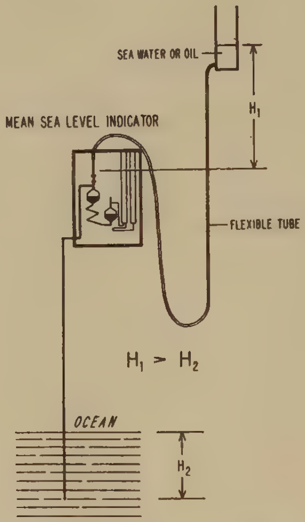

FIG. 6. Priming of the mean sea-level indicator.

A new version of the mean sea-level indicator (Fig. 7) has benefited from experiments with the prototype. Particular attention was taken to preserve a permanent datum level. This was solved by putting a container at the end of the standpipe 1 to receive and retain the oil without any overflow were air accidentally admitted in the sea tube. After reparation of the sea tube the apparatus is primed again; the oil and mercury volumes remain unchanged and the basic equilibrium is preserved. This precaution is particularly useful for records taken over a long period. For the same reason the dimensions of the apparatus must not change with time; this was taken into account in the final design.

APPENDIX

Installation, Starting and Tabulation of Readings

The instrument cannot be located higher than about 30 ft above the lower low water unless a lighter fluid is used in the tube connecting to the sea. The vapour pressure of water at 30 °C : 31 mm

Hg or 4/100 of one atmosphere. Maximum theoretical height : 100 − 4/100 × 76 × 13·6 cm or H_m = 30·8 ft (with light oil in the tube to sea H_m = 34 ft). This requirement eliminates the possibility of using the mean sea-level indicator in cases with an extreme tidal range. The cabinet has to be secured at a steady level, and the tube to the sea should dip enough so that its end is not uncovered in the trough of the deepest waves at the lowest tides. Due to the extremely slow response of the apparatus, a lot of time can be required at the start if a careful schedule and a definite procedure are not followed. There are two phases : filling and zeroing.

Filling.

Pour a few cubic centimeters of the mercury into cylinder B. Fill it with oil and put back plug P_B. Plug the upper end of the standpipe SP_1 and close the valve F_2. The nipple N_1 is capped. Pour the balance of the mercury into cylinder A and replace the plug P_A. Open V_2. The oil is forced through the capillary R_1 into SP_1; it compresses the air above it and is forced into SP_2 through R_2. This requires several hours. When a few centimeters of oil appear in SP_2, close V_2. Unplug SP_1 (SP_2 is already unplugged). Pour oil into both SP_1 and SP_2 until they are half full ±½ cm. Remove the cap of nipple N_1. Pass over a transparent plastic tube about 3 to 4 ft long. Open V_2. The oil flows out slowly under the manometer pressure. Close V_2 when the mercury levels in both A and B reach the marks (cylinders A and B are made of Plexiglas). Remove 8 or 10 cm of oil from the end of the plastic tube to make the interface between oil and air clearly visible. Hang tube end at top of cabinet.

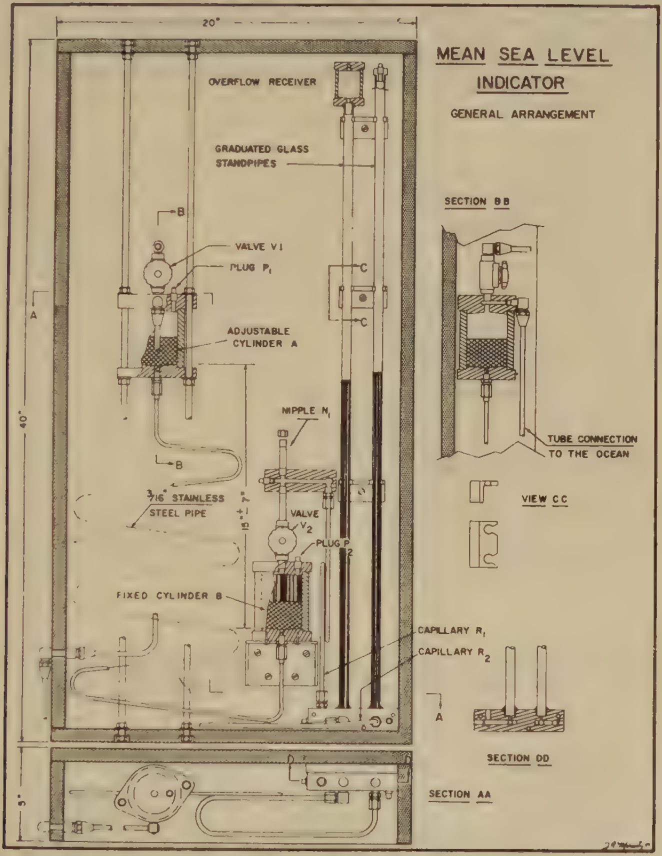
MEAN SEA LEVEL
INDICATOR
GENERAL ARRANGEMENT
20"
40"
5"
OVERFLOW RECEIVER
GRADUATED GLASS STANDPIPES
VALVE V1
PLUG P1
ADJUSTABLE CYLINDER A
NIPPLE N1
3/16" STAINLESS STEEL PIPE
VALVE V2
PLUG P2
FIXED CYLINDER B
CAPILLARY R1
CAPILLARY R2
SECTION BB
TUBE CONNECTION TO THE OCEAN
VIEW CC
SECTION DD
SECTION AA
A
B
C

FIG. 7. Design of the final version of the mean sea-level indicator.

Starting

Determine as accurately as possible the position of mean sea level. The following method is sufficiently accurate : Install a tide staff (pole with graduations). Make 3 readings at 8-hour, 16-min. intervals or better, 6 readings at 4-hr, 8-min. intervals smoothing by eye the waves if any and average them. This will give a sufficiently good approximation for the mean sea level; make a visible mark on the staff; determine the height of the apparatus above mean sea level and set up the cylinder A to the corresponding compensated height. Then prime the apparatus. The diagram in Fig. 6 illustrates one of the most suitable methods.

The following and last step has to be performed with the greatest care. The zeroing will then be easy, fast, simple; but any carelessness may lose many days and may necessitate further handling of oil and mercury. All valves are closed. The oil in both standpipes is half way up $\pm \frac{1}{2}$ cm. The tops of both standpipes are open. The apparatus is primed. Mark location of oil-air interface in the plastic tube.

Wait until the sea comes close to mean sea level, rising (or falling). When it is 30 cm below (or above), set up the oil level in the plastic tube 30 cm $\times S = 10$ cm below (or above) mean height of standpipe. Open valve V_2 and check the oil level in the tube. It should not move at first but slowly rises (or falls) as the tide comes up (or down). Elevate (or lower) the plastic tube to keep the oil level at the same place in the tube. As the tide height reaches mean sea level, close valve V_2 and note the height difference between the oil in the first standpipe and the oil in the tube: $+\Delta l$ if oil level in tube is higher, $-\Delta l$, if lower.

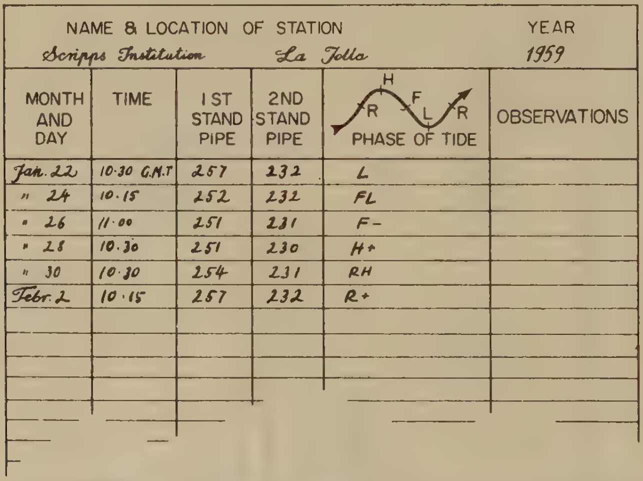

NAME & LOCATION OF STATION					YEAR
Scripps Institution			La Jolla		1959
MONTH AND DAY	TIME	1 ST STAND PIPE	2ND STAND PIPE	PHASE OF TIDE	OBSERVATIONS
Jan. 22	10·30 G.M.T	257	232	L	
" 24	10·15	252	232	FL	
" 26	11·00	251	231	F–	
" 28	10·30	251	230	H+	
" 30	10·30	254	231	RH	
Febr. 2	10·15	257	232	R+	

FIG. 8. Data sheet suggestion : it should include in addition to the basic data a reading of the first standpipe and an indication of the state of the tide.

If $|\Delta l| > \frac{1}{2}$ cm, the apparatus is sufficiently close to equilibrium and no further adjustment is required. If $|\Delta l| < \frac{1}{2}$ cm correct position of cylinder A. (Correction : opposite sign to Δl and equal $\Delta l \, \rho_o/\rho m - \rho w$). Valve V_2 must be reopened at high or low tide, after installing the cap on nipple N_1. This cap should be tightly sealed and never reopened; any leak or reopening would lose the datum.

For frequencies of the order of the tides the phase shift is close to π. The diurnal tide being much less attenuated than the semi-diurnal, reading the instrument at zero amplitude of the diurnal tide offers a way to increase the filter effectiveness. If such a schedule of the observation could be kept, this should be possible in several stations, it might be advisable to reduce the time constant τ by using shorter capillaries in order to extend the pass band to shorter period changes.

In any case a column should be reserved in the data sheet for entering the tide state at the time of every reading. Fig. 8 shows a suggested way to symbolize this data. Furthermore, meteorologic and sea-state observations might in many circumstances become very valuable in the interpretation of the data from the sea-level indicator.

JEAN FILLOUX*
GORDON GROVES†

Acknowledgments—The authors acknowledge the valuable advice and criticisms of Drs. ROBERT S. ARTHUR, JUNE G. PATTULLO, CHARLES S. COX. The capillaries for the test model were calibrated by Mr. HARRY LUSK.

A portion of construction of equipment was carried out with support from the Office of Naval Research (NONR 2216 (01), and the National Science Foundation (NSF – Y/9. 1/51 IGY).

REFERENCES

GROVES, G. W. (1955) Numerical filters for discriminating against tidal periodicities. *Trans. Amer. Geophys. Union*, **36**, 1073–1084.

MUNK, W. H., IGLESIAS, H. V. and FOLSOM, T. R. (1948) An instrument for recording ultra low frequency ocean waves. *Rev. Sci. Instr.*, **19** (10), 654–658.

*Scripps Institution of Oceanography, University of California, La Jolla, California.
†Instituto de Geofisica, Universidad Nacional Autonoma de Mexico.

Printed in Great Britain by The Salisbury Press Ltd., Publicity House, Wilton Road, Salisbury, Wilts. (24155)

(767)

Deep-Sea Research, 1960, Vol. 7, pp. 42 to 47. Pergamon Press Ltd., London. Printed in Great Britain

SHORTER COMMUNICATION

Measurements of the California Current in March 1958

Feenan D. Jennings* and Richard A. Schwartzlose†

(*Received* 25 *February* 1960)

Abstract—Two sets of drogues were placed approximately normal to the usual flow and followed for one and three days respectively. The first set, which extended thirty miles offshore, drifted southeastward. The second set, which extended from thirty to seventy miles offshore, also moved southeastward but with considerable variation in speed and direction along the line. In the latter set two rapidly moving streams appeared with a body of slower water between.

INTRODUCTION

Direct measurements of the California Current have been made at various times and with various techniques (Reid, 1958; Knauss and Reid, 1957; Reid, Roden and Wyllie, 1958). As newer equipment has become available, especially radar and radar reflectors it has become possible to follow many drogues at one time and thus measure the currents over wider areas with only one ship. This paper describes the drogues used and the techniques followed on a cruise in March 1958 and presents the results of the measurements.

DROGUES

Drogues using a parachute as a sea anchor were used and described by Volkmann, Knauss and Vine (1956). The drogues used here were suspended from a bamboo pole some twenty feet long which was held up by an inner tube and counter-weighted to remain nearly upright. The parachute was attached to the pole at the inner tube by a ten metre wire. High on each pole was a light, a radar reflector, an orange flag, an identification number and a drift bottle (Fig. 1). It should be mentioned that in the first part of the survey the parachute was attached at the bottom of the pole. In high winds, this caused the pole to lean very close to the water surface, thus making it difficult to locate the drogue visually or by radar. Attaching a ten metre wire from the parachute to the water line alleviated this fault. The parachutes were in the upper portion of the mixed layer, which was about 60 metres deep as indicated from BT data.

POSITIONING AND LOCATING DROGUES

For a survey of this duration accuracy of navigation is of extreme importance. The position of the drogues on each run was determined from Loran and by radar observation of the coastline when the ship was within thirty miles of the coast. Further offshore the positions were determined from a combination of Loran and radar fixes from one drogue to the next and by extrapolation of the ship's courses and speed (dead reckoning).

Although the Loran receiver was in perfect operating condition, only one Loran system, 2-H-2, could be used with confidence in this region. This gave excellent positions as lines bearing 240° true from the coast, and was used to correct the southeasterly set of the ship by the current. Three other Loran systems could be received in this area but none of these was located to give satisfactory results in this area.

The radar was used extensively during the cruise, not only for locating the drogues, but also for positioning each drogue from the previous one, in a leap-frog fashion. Many times three or four

---

*Present address: Office of Naval Research, Code 416, Washington 25, D.C.

†University of California, Scripps Institution of Oceanography, La Jolla, California.

Contributions from the Scripps Institution of Oceanography, New Series, 1193

Reproduced by Permission

drogues could be seen on the screen at one time and in these cases, the plotted positions were checked against each other for accuracy of positioning. By this method, the range and bearing indicators on the radar were shown to have very good accuracy. When two drogues became too far apart to position one from the other, a new drogue was put between the two. It is felt that the position of each drogue was accurately determined to within one mile of its true geographic position.

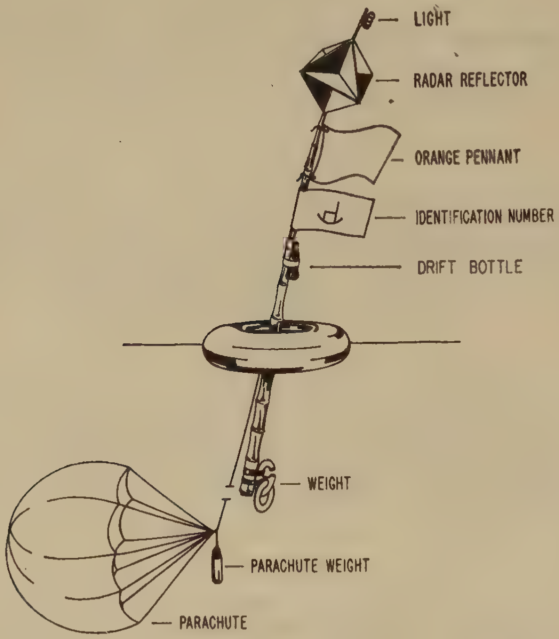

FIG. 1. Construction of the parachute drogue.

Some additional mention should be made concerning the effectiveness of the radar, which was a U.S. Navy type AN/SPS–5. The high degree of success of the entire survey was mainly due to the fine performance of this equipment. In calm weather, some of the drogues could clearly be located at distances up to nine miles. The usual range was between four and seven miles. Even in winds of ten to fifteen knots they still gave contacts at four to seven miles and in thirty knot winds, with the resultant heavy seas, the drogues were still being located and positioned at three miles.

SURVEY

On the morning of 19th March, in calm weather, fourteen drogues were set along a line bearing 240° from Pt. Pinos light, Monterey, from five miles to thirty miles from the coast. The two drogue closest to the coast were set by Scripps personnel from the R/S *Tage*. The *Tage's* personnel positioned these two plus the innermost drogue launched from USS *Thrasher*, until dark, at which time the *Tage* returned to port. The *Thrasher's* personnel spent the day, until 2200 hrs., positioning the outermost eleven drogues and during this time managed three complete runs along the line. The morning of the 19th began with winds from WSW at two knots. In the late afternoon the wind rose to fifteen knots from WSW. The wind continued to increase from late afternoon until the survey was no longer possible at 2200 hrs. At that time the wind was from the south at forty knots. The high seas and winds that developed during the night of the 19th severley disrupted the drogue pattern and only one of the fourteen was located afterwards. This was positioned from the shoreline along the coast at 1130 hrs. of the following day.

(770)

After the storm the drogues were set between 1900 hrs. March 23rd and 0700 hrs. March 24th. They were launched three miles apart between 30 miles and 100 miles from the coast along a line bearing 240° true from Pt. Pinos light. During the next three days, six positioning runs were made along the line. At three places along the line of drogues a group of three drogues were tied together, 1000 yards apart, with sixty thread cotton seine twine. This was done to determine whether drogues, tied in this fashion, would react to the currents differently to the individual drogues.

Of the 34 drogues launched, 31 were still being positioned after a period of 13 hours, 27 after 38 hours, and 22 after 63 hours. The maximum distance travelled by any drogue during the survey was 40 miles. Nine of them traversed more than 25 miles.

The wind from the evening of March 23rd through the morning of March 26th was from WSW, eight to ten knots and by 2100 hrs. it was from the south, 35–40 knots. At this time disintegrating radar reflectors on the drogues, the high seas and rain squalls made it impossible to find the drogues.

The effect of the wind on the radar reflector, flag, number board, bamboo pole and inner tube assemblage has been measured by DAN BROWN. With this information and the data on the drag force of parachutes from VOLKMANN, KNAUSS and VINE (1956), the effect of the wind (March 23rd—26) on the drogue was calculated to have been 0·02 knots, an insignificant amount. Only during the last four to six hours of the survey was the wind strong enough to affect the drogues a measurable amount. During the last few hours of the survey the wind was 35–40 knots, which affected the measured velocity of the drogues about 0·08 knots.

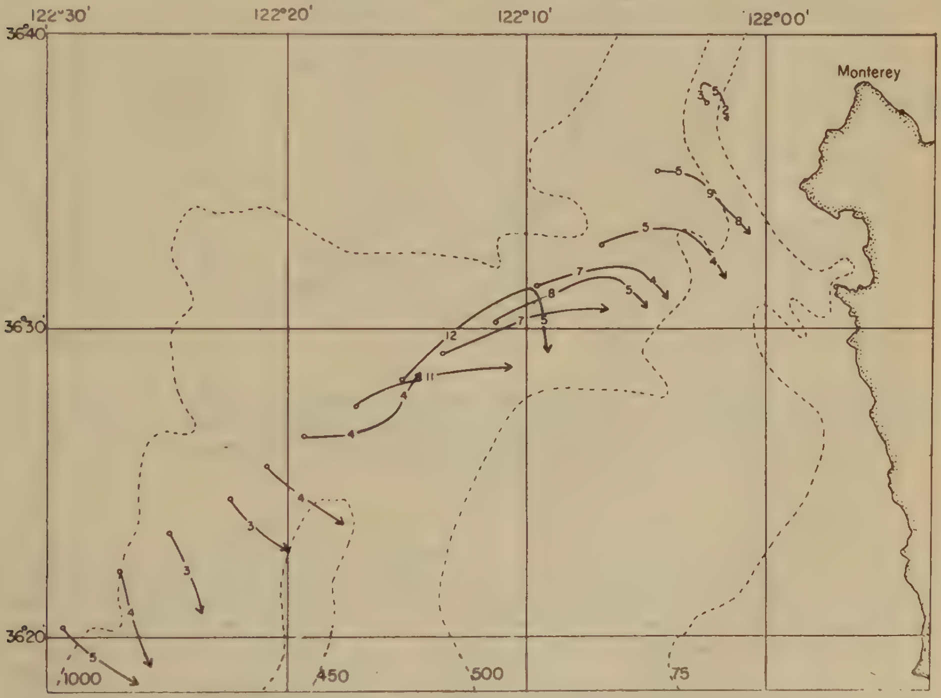

FIG. 2. March 19th, 1958, survey. The velocities are indicated in tenths of knots, and are plotted as the midpoint between the observed drogue positions of each run. Dashed lines are bottom depths in fathoms.

RESULTS

The drogues launched on 19th March were tracked for fifteen hours. The paths, taken by those drogues set within twenty miles of the coast, indicate that there may have been some influence by the tide. The movement of the drogues was to the east or southeast with speeds between 0·3 knots and 1·2 knots (Fig. 2).

The farthest offshore drogues, released 23rd–24th March, indicated that the flow was to the east. In the middle area were measured two streams at high speed with a slower moving body of water between, all moving southeastward (Figs. 3 and 4).

The current streams shown in Fig. 3 are the deduced paths of the individual drogues. The velocities are indicated by numbers, in tenths of knots, and are plotted approximately at the midpoint between the observed drogue positions of each run.

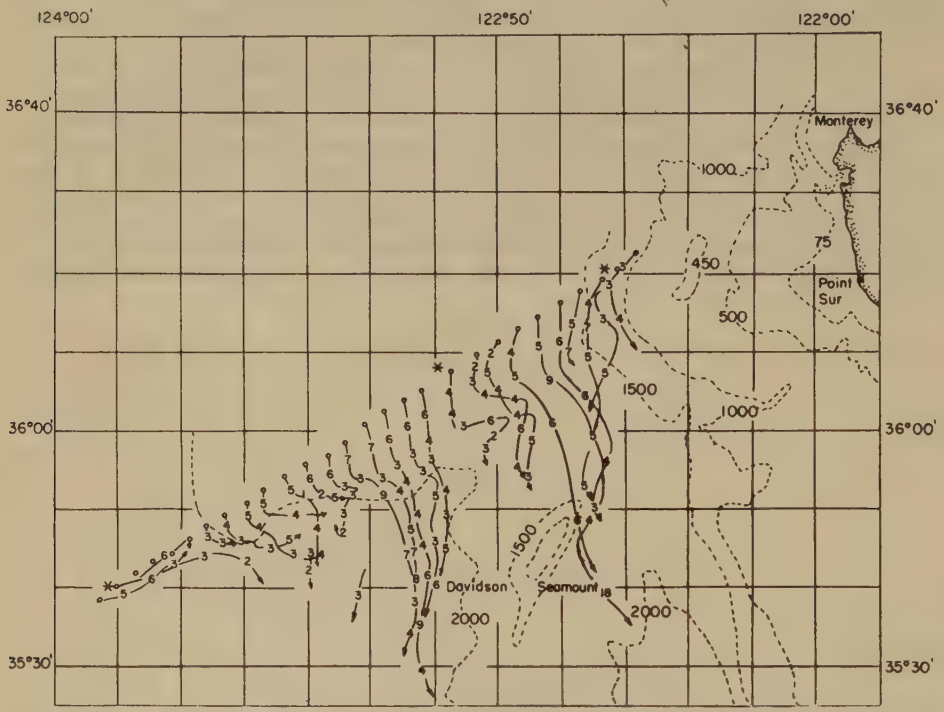

Fig. 3. March 23rd–26th, 1958, survey. The velocities are indicated in tenths of knots, and are plotted at approximately the midpoint between the observed drogue positions of each run. * denotes the positions where three drogues were tied 1,000 yards apart. Dashed lines are bottom depths in fathoms.

The development of the current pattern can be seen in Fig. 4, where the position has been plotted at constant time intervals. To derive the contours, the position was calculated for each drogue at noon and midnight of each day of the survey. Points of equal times were joined giving the distance each particle of water travelled during the twelve hour interval. The splitting of the current can plainly be seen in this figure as can the easterly flowing water at the west side of the pattern.

The average velocity of all drogues was about 0·5 knots. At the centre of the east stream, the average velocity over the 60 hour period was about 0·7 knots, while at the centre of the west stream, the average velocity over the same period was about 0·6 knots. The maximum observed velocity was 1·8 knots, which occurred late in the survey, at the centre of the eastern stream.

The reaction to the current on the three groups of drogues tied together was as follows :—

(1) The behaviour of each group seemed the same as the individual drogues in the same region.

(2) After one day, the three drogues in each group pulled together until they were less than 300 yards apart. They showed no tendency to remain lined up but assumed a random relationship to each other.

(3) After one and one-half days, one of the drogues was lost from each group. Only one of these strays was located again.

CONCLUSIONS

A detailed picture of a part of the California Current, during a period of a few days, has been obtained. These data are too particular to be compared usefully with the Atlas of Currents of the Northeastern Pacific Ocean (H.O. 570) which gives data averaged over larger areas and longer periods. Hydrographic casts were not made in the area this month. A detailed hydrographic survey in the same area at the same time, of such a cruise as this, would be of value in determining the relationship between the dynamic topography and direct current measurements.

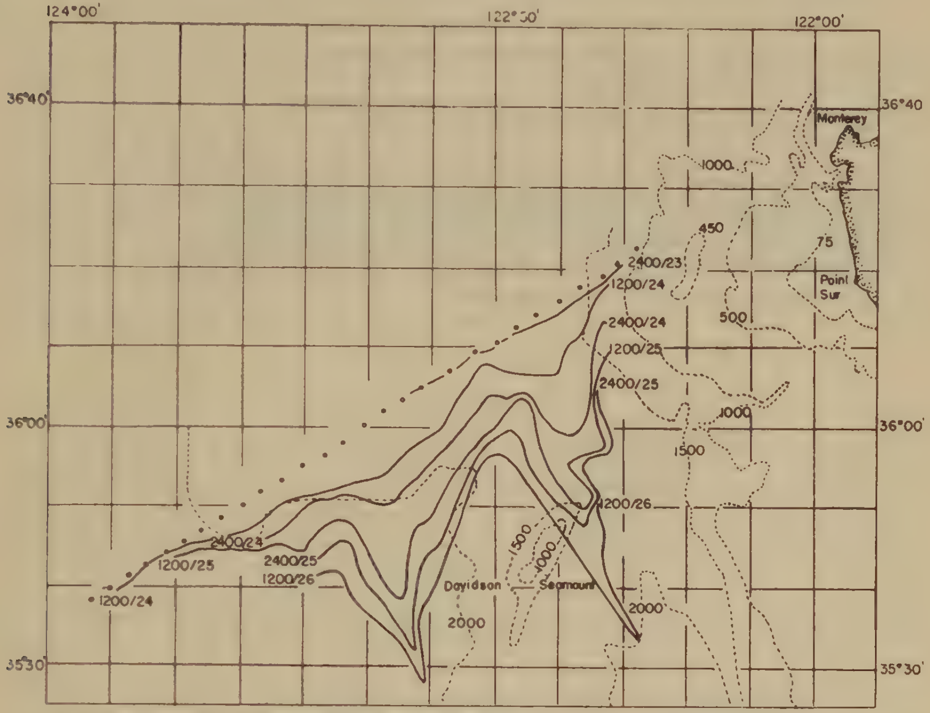

FIG. 4. March 23rd–26th, 1958, survey. The calculated distance each particle of water moved during a twelve hour interval. Dashed lines are bottom depths in fathoms.

It would be of interest to know whether the intensification of flow observed here near the coast, is a regular occurrence in March, and especially whether the two fast streams are part of a single one to the north which has been split by the Davidson Seamount.

The major immediate conclusion from this brief survey is that the technique is a very powerful one and that it will be possible to extend it to wider areas and over longer periods of observations, with no major changes in either equipment or method.

Acknowledgments—This paper represents one of the results of research conducted under the Marine Life Research Programme, the Scripps Institution's component of the California Cooperative Oceanic Fisheries Investigations, a project sponsored by the Marine Research Committee of the State of California; and research conducted for the Office of Naval Research under Contract Nonr 2216 (01). The authors are indebted to the U.S. Navy for supplying the USS *Thrasher* to conduct this research. The captain (Lieutenant C. J. LIMERICH) and crew are both to be thanked for their excellent cooperation and navigation. For the inshore work, the Hopkins Marine Station supplied its small boat the R/S *Tage*. Captain J. BALESTERI and technician B. FINKS were most helpful. From the Scripps Institution of Oceanography, the Programme Director of Marine Life Research, Professor

JOHN D. ISAACS, was one of the initiators of this survey and his advice and assistance has been most helpful. Also from Scripps, J. L. FAUGHN, D. M. BROWN and C. D. JENNINGS assisted greatly in gathering this data; J. L. REID, Jr. and GARTH I. MURPHY have read the manuscript and offered helpful suggestions.

The Scripps Institution of Oceanography,
La Jolla, California.

Contribution from the Scripps Institution of Oceanography.

REFERENCES

KNAUSS J. and REID Jr. J. L. (1957) The effects of cable design on the accuracy of the GEK. *Trans. Amer. Geophys. Union*, **38** (3) 320-325.

REID, J. L. Jr. (1958) A comparison of drogue and GEK measurements in deep water. *Limnology and Ocean* **3** (2) 160-165.

REID J. L. Jr., RODEN G. I. and WYLLIE J. G. (1958) Studies of the California Current System. *Calif. Cooper. Ocean. Fish. Invest. Progress Report* 1*st July* 1956–1*st January* 1958 27-56.

U.S. Hydrographic Office (1947) Atlas of surface currents Northeastern Pacific Ocean.

VOLKMANN G., KNAUSS J. and VINE A. (1956) The use of parachute drogues in the measurement of subsurface ocean currents. *Trans. Amer. Geophys. Union*, **37** (5) 573-577.

Printed in Great Britain by The Salisbury Press Ltd., Publicity House, Wilton Road, Salisbury, Wilts. (24153)

(774)

Deep-Sea Research, 1960, Vol. 7, pp. 61 to 67. Pergamon Press Ltd., London. Printed in Great Britain

INSTRUMENTAL NOTE

Deep-sea free instrument vehicle

(*Received* 11 *April* 1960)

Abstract—A number of free instrument vehicles have been designed and tested. These are simple, reliable, inexpensive devices that transport recording instruments or sampling equipment to the deep-sea bottom, or to intermediate depth, and return them to the surface. Vehicles are provided with radar reflectors and other location devices. In the first tests the vehicles bore fish traps and were successfully operated to 2,000 fathoms. Other instruments designed to make use of the free vehicle's unique capabilities are under development.

INTRODUCTION

THE difficulty of measuring and sampling in deep ocean waters greatly limits the conduct of oceanographic research. Oceanographers traditionally have suffered from inefficiency in their operations because of their dependence upon conventional long-wire techniques for most deep measurements. Freely descending vehicles have been used on occasion (EWING and VINE 1938), (ISAACS and KIDD 1957). These have not previously been brought to the level of design that would allow their routine mass use as general purpose oceanographic tool, however.

Development of the Deep Free Vehicle (DFV) system was undertaken to overcome some of these difficulties, to permit the small vessel to participate in deep investigations, and to add versatility and effectiveness to the large vessel. As examples, with the DFV, small vessels without heavy winches can now be used to collect water samples and benthic organisms on the deep-sea bottom, and many deep-water investigations can be added to the expedition programme of large vessels.

Thus, an expedition with a heavy programme of piston coring or other operations necessitating long-wire techniques, can simultaneously obtain other related or independent measurements by the DFV technique, and small unspecialized vessels can engage in such studies as sampling water and organisms in deep atomic waste disposal areas.

GENERAL DESCRIPTION

In brief, the system (Fig. 1) consists of :

(1) a flexible plastic float filled with gasoline that provides positive buoyancy at any depth;

(2) a separate submersible marker buoy, which enables the system to be located when it arrives at the surface;

(3) a depressing ballast weight with a release device that releases ballast at a predetermined time or depth; and

(4) one or more recording or sampling instruments, whose point of attachment in the line is adjustable.

Reproduced by Permission

OPERATION

In operation, the system is launched freely from a ship. It descends to the bottom where it remains until the ballast weight is released. By use of the pressure release, the system can also be programmed to descend to an intermediate depth and return to the surface.

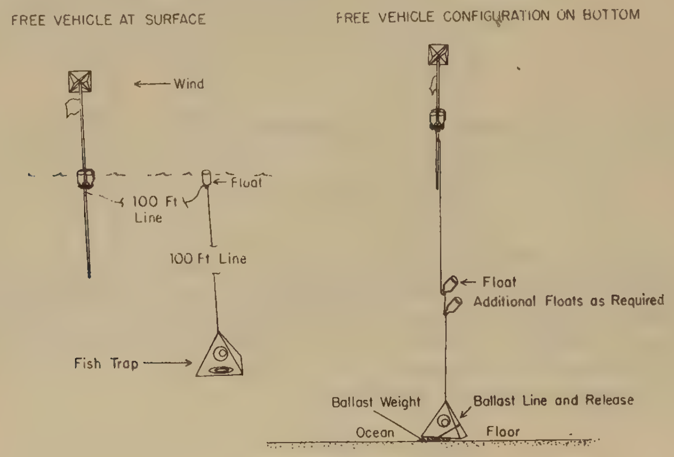
FREE VEHICLE AT SURFACE
Wind
Float
100 Ft Line
100 Ft Line
Fish Trap
FREE VEHICLE CONFIGURATION ON BOTTOM
Float
Additional Floats as Required
Ballast Weight
Ballast Line and Release
Ocean
Floor

FIG. 1.

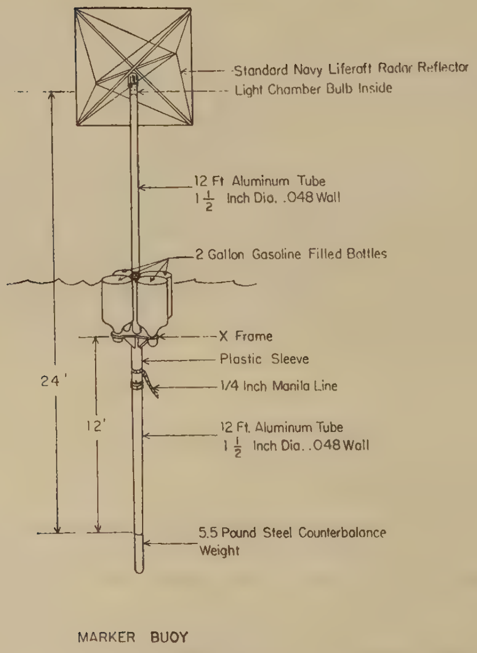
Standard Navy Liferaft Radar Reflector
Light Chamber Bulb Inside
12 Ft Aluminum Tube
1 1/2 Inch Dia. .048 Wall
2 Gallon Gasoline Filled Bottles
X Frame
Plastic Sleeve
1/4 Inch Manila Line
24'
12'
12 Ft. Aluminum Tube
1 1/2 Inch Dia. .048 Wall
5.5 Pound Steel Counterbalance Weight
MARKER BUOY

FIG, 2.

The present system has been used to depths of 2,000 fathoms (although it is not limited to this), and has remained on the bottom for periods longer than ten hours, carrying as much as 25 pounds of payload.

Table 1

No.	Launching Date	Depth Fm.	Location (see map)	Launching time	Sighting time	Catch
1	4/23/59	450	Test 1	11.30	14.30	6 sable fish – *Anoplopoma fimbria*; 6 hagfish – *Myxine circifrons*;
2	5/19/59	746	Test 2	11.00	15.41	3 sable fish; 3 hagfish; 1 lithodid crab; 1 Copepod; 1 octopus (partially digested)
3	6/21/59	650	Test 3	11.00	18.45	Over 50 hagfish (3 species); 5 sable fish; 1 brittlestar; 1 Pacific rattail – *Coryphaenoides acrolepis*
4	7/24/59	1107	Test 4	19.39	14.40	2 rosy snailfish – *Paraliparis rosaceus*; hagfish 5 eelpout – *Lycodes* sp. assorted small Amphipods. (Experimental model)
5	7/24/59	1107	Test 4	20.03	10.30	
6	9/9/59	1855	Test 5	11.40	not recovered	
7	9/9/59	1840		12.25	8.20	no specimens
8	9/9/59	1970	High seas difficult navigation	13.00	21.52	no specimens, trap damaged
9	9/9/59	2050		13.35	not recovered	
10	9/9/59	630	first large scale experiment	10.50	21.10	5 sable fish
11	9/9/59			11.40	not recovered	
12	9/9/59			11.10	not recovered	experimental model
13	10/27/59	950	Test 6	2.10	14.15	3 lithodid crabs; 3 hagfish; 1 rosy snailfish 1 Pacific rattail
14	10/27/59	945		2.20	15.00	3 crabs; 1 eelpout – *Lycodes* sp.; assorted Amphipods
15	10/28/59	1170		21.00	7.35	1 hagfish; 1 flatnose codling – *Antimora rostrata*; 5 eelpouts – *Lycodes* sp.
16	10/28/59	1170		21.15	8.36	2 hagfish (1 albino); 1 eelpout – *Lycodes* sp.
17	3/9/60	105	Test 7	1.15	6.30	1 *Sebastodes eos*
18	3/9/60	120		1.30	6.30	3 *Sebastodes eos* 1 ,, *macdonaldi*

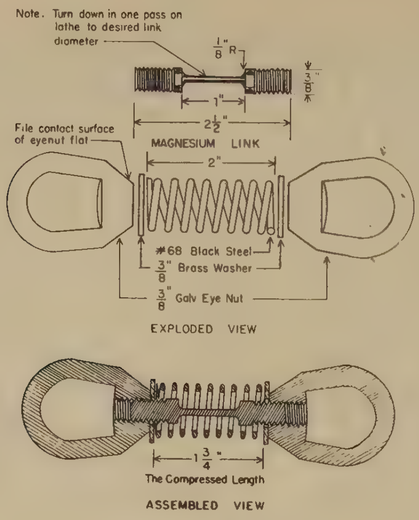
Note. Turn down in one pass on lathe to desired link diameter
1/8" R
3/8"
1"
2½"
File contact surface of eyenut flat
MAGNESIUM LINK
2"
#68 Black Steel
3/8" Brass Washer
3/8" Galv Eye Nut
EXPLODED VIEW
1¾"
The Compressed Length
ASSEMBLED VIEW

MAGNESIUM TIME RELEASE

FIG. 3.

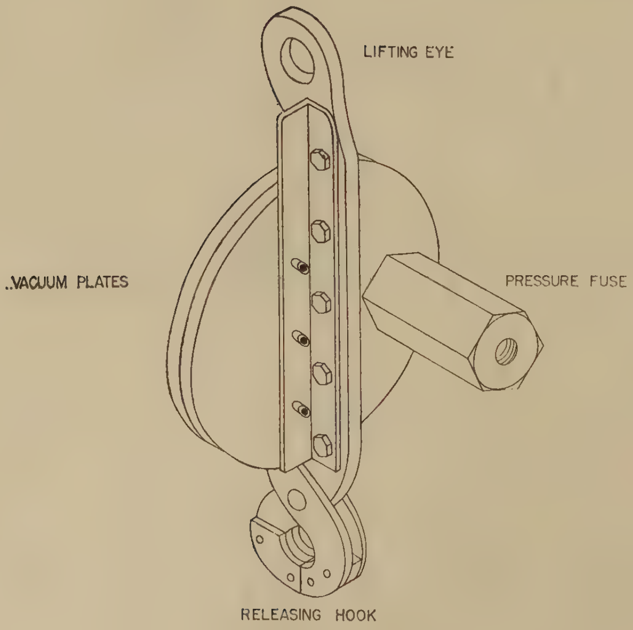
LIFTING EYE
VACUUM PLATES
PRESSURE FUSE
RELEASING HOOK

PRESSURE RELEASE MECHANISM

FIG. 4.

DEVELOPMENT

The DFV was designed for use on two different types of operations. Primarily the vehicles should supplement conventional oceanographic techniques. They should be suitable for quick launching and the ship should be allowed to proceed with other measurements until the vehicles resurface, with a minimum amount of time devoted both to launching and recovery. Secondly, the vehicle system should lend itself to mass deployment and large-scale sampling of the physical or biological characteristics of an area.

The type of instrumentation that the vehicle is intended to transport determines the necessary buoyancy and fixes the size and weight to a great extent.

Other factors considered in the preliminary design are: ease of handling, simplicity of fabrication and assembly, reliability of operation, and versatility.

Since ease of handling was important, the vehicle was designed to accommodate light instruments. The main buoyancy was separated from the marker buoy to reduce the size of the loads to be handled.

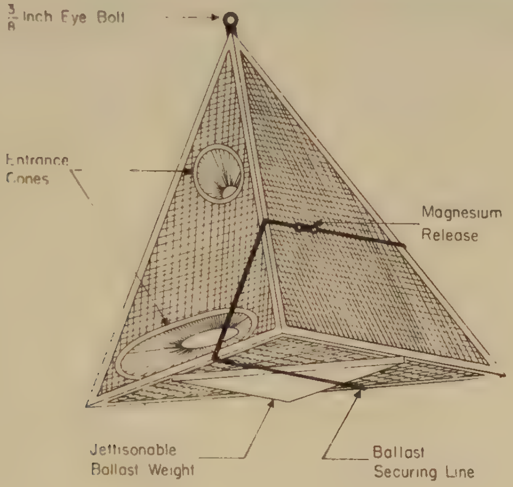

EXPERIMENTAL BOTTOM TRAP

FIG. 5.

Buoyancy

Polyethylene carboys filled with gasoline are used to provide the main buoyancy of the system. These 13 gallon (nominal size) containers weigh 90 pounds in air when filled with regular gasoline, and provide 31 pounds of buoyancy in sea water. Flexible containers of this type are necessary to allow for the expansion and contraction of the gasoline with temperature and pressure changes. For light weight instruments, one carboy provides sufficient buoyancy. For heavier instruments two or more carboys can be tied to the line at intervals to provide the necessary buoyancy.

Marker Buoy

Four gasoline filled polyethylene bottles (two gallons each) provide the buoyancy of the marker buoy (Fig. 2). These are assembled in a cluster around the mast and clamped to an X-shaped plastic frame. The aluminium mast is made of two 12-foot sections of $1\frac{1}{2}$ in. tubing. Each of these is plugged into the plastic centre sleeve and secured with hose clamps. A standard life boat radar reflector is fitted to the top of the mast, and a six pound counter balance to the bottom. The reflector has provided radar contact to 4 miles.

Ballast Release

The DFV system can be provided with a time delay release, a pressure (depth) release, or a bottom contact release (Figs. 3 and 4).

Early tests were carried out with a magnesium time delay release. This device makes use of the electrochemical deterioration of a magnesium weak link in sea water. The release delay time can be predicted with reasonable accuracy, and can be adjusted for from 4 to 40 hours delay by varying the diameter of the magnesium link (VAN DORN, 1953). A clock actuated release is currently under development, which will extend the release time to a year or more.

The pressure release (Fig. 4) releases the ballast weight at a predetermined depth.

Instruments

The first sampling instrument developed for use with the free vehicle was a bottom fish trap (Fig. 5). This device consisted of a pyramid shaped aluminium frame, 6 ft on a side, covered with a plastic screen. The fish are retained in the trap by virtue of the maze effect provided by the design of the entrance cones. These traps are quite successful in capturing bottom and near bottom organisms, and have been launched on seven different cruises in widely scattered areas off the coast of Southern California. The results of these launchings are tabulated below and in Fig. 6. The specimens are most often captured alive, but die soon after reaching the surface, due mainly to temperature changes. On one occasion, sable fish were kept alive for about 4 hours. It is believed that the use of equipment designed to maintain the proper temperature would enable many rare specimens to be preserved alive for further laboratory study.

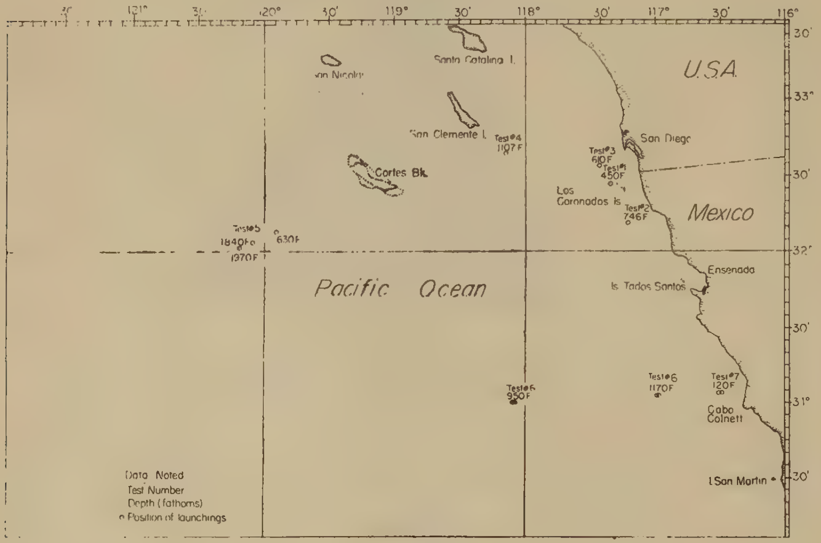
121°
30'
120°
30'
119°
30'
118°
30'
117°
30'
116°
30'
33°
30'
32°
30'
31°
30'
Santa Catalina I.
San Nicolas
San Clemente I.
Cortes Bk.
U.S.A.
San Diego
Mexico
Los Coronados Is
Test#4 1107F
Test#3 610F
Test#1 450F
Test#2 746F
Test#5 1840F 630F 1970F
Pacific Ocean
Ensenada
Is. Todos Santos
Test#6 950F
Test#6 1170F
Test#7 120F
Cabo Colnett
I. San Martin
Data Noted
Test Number
Depth (fathoms)
Position of launchings

FIG. 6.

A larger folding version of the bottom trap is presently under development, which is designed to prevent any possible escape of the trapped creatures, and to retain a sample of cold bottom water to help preserve specimens alive until transferred.

Other instruments under development or test for use with the free vehicle include: a recording deep current meter, sedimentation measuring and collecting devices, water and gas sampling gear, and multiple short coring tubes.

Acknowledgments—This paper represents one of the results of research conducted under the Marine Life Research Programme, the Scripps Institution's component of the California Co-operative

Oceanic Fisheries Investigations, a project sponsored by the Marine Research Committee of the State of California.

Scripps Institution of Oceanography
University of California
La Jolla, California

John D. Isaacs
George B. Schick

Contribution from Scripps Institution of Oceanography

REFERENCES

Ewing, M., and Vine A. C., (1938) Deep sea measurements without wires or cables. *Trans. Amer. Geophys. Un. Meet.*, 248–251.

Ewing, M., Woolard G. P., Vine A. C. and Worzel J., (1946) Recent results in submarine geophysics. *Bull. Geol. Soc. Amer.*, 57, 909–934.

Isaacs, J. D. and Kidd, L. W. (1957) (Personal Coummunication).

Richardson, W. S. (1960) Woods Hole Oceanographic Inst. Ref. No. 60 7, Atlantic Oceanography conducted during the period July 1 Dec. 31, 1959, p. 10. (Unpublished manuscript).

Van Dorn, W. G. (1953) The marine release-delay timer. *Oceanographic Equipment Report No.* 2, SIO Ref. 53–23. (Unpublished manuscript).

Vine, Allyn, Woods Hole Oceanographic Inst. (Personal communication).

Printed in Great Britain by The Salisbury Press Ltd., Publicity House, Wilton Road, Salisbury, Wilts. (24156)

Limnology and Oceanography, v. 5, no. 4, October 1960. pp. 432-433.

NOTES AND COMMENT

CAULOBACTER SP. IN SEA WATER

Jannasch and Jones (1959) reported finding "spirilli-like" bacterial forms in sea water using a direct microscopic method. At one station the "spirilli-like" organisms comprised from 13 to 45% of the open ocean bacterial population as determined by the Cholodny method. Their abundance was inversely proportional to the remaining bacterial population. We now present evidence to identify these organisms as members of the genus *Caulobacter*. The only previous indication that others may have observed *Caulobacter* in the sea was the statement by ZoBell and Upham (1944 p. 253) that stalked bacteria exist in sea water.

Caulobacter is a common freshwater microorganism, having been observed in nonpolluted waters by various investigators using the submerged slide technique. The identification of Caulobacteraceae is possible by a morphological feature of remarkable constancy, the stalk formation. On this basis, Henrici and Johnson (1935) established the taxonomy of the group without pure cultures or extensive cultivation on differential media. Their concept has been accepted and is still valid (Bergey 1957). In the earliest observations of these microorganisms, Jones (1905) was able to observe the stalks, and, after common staining, decided they were true flagella. From microscopic examination of submerged slides, Henrici and Johnson (1935) concluded that "ferric hydroxide or other material is secreted from one side or one end of the cell to form the stalk." Houwink (1955), however, after detailed examination under the electron microscope, suggested that the stalk was part of the living cell.

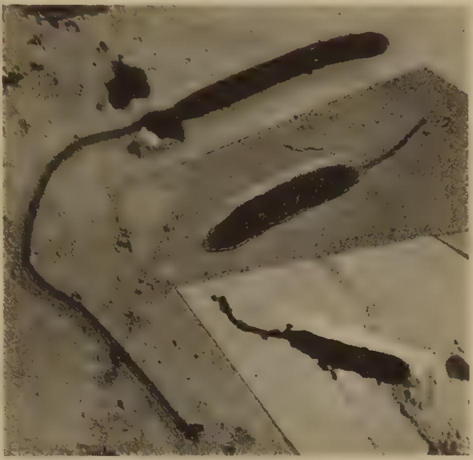

Fig. 1. Electron micrograph of *Caulobacter sp.* concentrated by the cholodny technique from sea water taken 16 miles off San Diego at a depth of 75 m. Magnification × 9000.

Electron photomicrographs (Fig. 1) were prepared from concentrated and desalted samples of sea water, using a protein monolayer technique (Hartman *et al.* 1953). The morphological features of the "spirilli-like" organisms clearly resembled the electron photomicrographs of *Caulobacter* presented by Houwink (1955). Stalks of different lengths in our electron photomicrographs suggested fragmentation of the cells, possibly during preparation. "Button-like" holdfasts such as those reported associated with *Caulobacter* in fresh water were not observed in our preparation. We observed nothing to indicate that *Caulobacter* was parasitized in the open ocean; it was numerous, and other microorganisms were not attached as observed in the electron photomicrographs. We believe that the morphology of the "spirilli-like" microorganisms in our preparations is sufficient to classify them as *Caulobacter*. Additional work is needed on the physiology, geographical distribution, and ecology of these prominent members of the marine environment.

The authors would like to thank Dr. Paul Desjardins of the University of California at Riverside for instruction and use of the electron microscope. This project was supported in part by a grant, E-1768, from the National Institute of Allergy and Infectious Diseases of the National Institutes of Health, Bethesda 14, Maryland.

HOLGER W. JANNASCH
Institut fur Mikrobiologie
Gottingen, Germany

Contributions from the Scripps Institution of Oceanography, New Series, 1195

Reproduced by Permission

GALEN E. JONES

Scripps Institution of Oceanography
University of California
La Jolla, California

REFERENCES

BERGEY'S MANUAL OF DETERMINATIVE BACTERIOLOGY (1957). 7th ed. Edited by Breed, Murray, and Smith. Williams and Wilkins Co., Baltimore, Md., pp. 212–214.

HARTMAN, R. E., T. D. GREEN, J. B. BATEMAN, C. A. SENSENEY, AND G. E. HESS. 1953. Preparation of uniformly dispersed specimens of particulate matter for electron microscopy. J. Appld. Physics, **24**: 90–92.

HENRICI, A. T. AND D. E. JOHNSON. 1935. Studies of freshwater bacteria II. Stalked bacteria, a new order of Schizomycetes. J. Bacteriol., **30**: 61–94.

HOUWINK, A. L. 1955. *Caulobacter*, its morphogenesis, taxonomy and parasitism. Ant. van Leeuwenhoek, **21**: 49–64.

JANNASCH, H. W. AND G. E. JONES. 1959. Bacterial populations in sea water as determined by different methods of enumeration. Limnol. Oceanogr., **4**: 128–139.

JONES, M. 1905. A peculiar microorganism showing rosette formation. Centralbl. f. Bakt. II, **14**: 459–463.

ZOBELL, C. E. AND H. C. UPHAM. 1944. A list of marine bacteria including descriptions of sixty new species. Bull. Scripps Inst. Oceanogr., **5**: 239–292.

(784)

EXTRAIT DE MAMMALIA TOME 24 N° 3 Septembre 1960

POPULATION GROWTH AND SEASONAL MOVEMENTS OF THE NORTHERN ELEPHANT SEAL, *MIROUNGA ANGUSTIROSTRIS* (1)

by

George A. **BARTHOLOMEW** and Carl L. **HUBBS**

University of California, Los Angeles and La Jolla

Cet article rend compte de la croissance de la population de *Mirounga angustirostris* depuis la « redécouverte » de l'espèce, en 1892, jusqu'en 1958, ainsi que de la recolonisation de plusieurs îles depuis 1935 environ. Les mouvements saisonniers sont également étudiés, ce qui fait ressortir de grandes différences entre le cycle annuel des mâles et celui des femelles. Enfin, quelques précisions sur le statut actuel des populations de *Zalophus californianus* et d'*Arctocephalus townsendi*, dans les îles au large de la Basse-Californie, terminent ce travail.

The northern elephant seal *Mirounga angustirostris* (Gill) is one of the few phocids that is largely confined to subtropical and warm-temperate waters and, except for its southern hemisphere congener, *Mirounga leonina* (Linnaeus), it is the largest of the pinnipeds. It is of especial interest from the point of view of population dynamics because it has recovered from virtual extinction and because it has remained in the logarithmic phase of population growth for more than half a century. It is now apparent that the numbers of elephant seals at any given locality fluctuate widely on a seasonal basis and that breeding populations have become established at several localities in addition to Guadalupe Island, its chief refuge.

Before its exploitation by hunters and sealers, the northern elephant seal occupied the coast of western North America through about 14 degrees of latitude from Point Reyes near San Francisco, California to Magdalena Bay, Baja California (then as now adult male stragglers probably wandered commonly as far north as British Columbia and southeastern Alaska). In pre-columbian times

---

(1) Contribution from the Scripps Institution of Oceanography, New Series. 1196

Reproduced by Permission

the elephant seal was undoubtedly a common coastal animal and it was occasionally taken by the seafaring coastal indians (Lyon, 1937). Commercial exploitation began at least as early as 1818 when elephant seals were known to be « very plentiful » on Cedros (« Ceres ») Island (Corney, 1896, p. 125). Its abundant store of blubber, its almost complete indifference to the presence of man, its habit of hauling out in enormous numbers at well defined rookeries, and its slow locomotion on land led to the rapid extermination of the elephant seal during the nineteenth century. The hunting methods used were vividly described by Captain C. M. Scammon (1874). By 1860 the species had become so scarce that it was no longer an important source of oil.

The species was virtually extinct before it was recognized as separate from the southern hemisphere elephant seal by Gill (1866). Except for a small herd found in 1880 at Bahia de San Cristobal, on the coast of Baja California south of Cedros Island, in an area that remains difficult of access even today, after 1865 the seals were found only as occasional stragglers on the hauling grounds of Guadalupe and San Benito islands. At Bahia de San Cristobal between 1880 and 1884, 355 elephant seals, all that could be found, were taken (Townsend, 1885). The last 16 killed were taken by Townsend himself as scientific specimens. In 1883, 80 elephant seals were taken under the towering cliffs on the northwest side of Guadalupe Island, according to Captain Hunt of the Schooner Santa Barbara (Townsend, 1912). No further records of the elephant seal are known for any year until 1892, when C. H. Townsend who was taken by Captain Hunt to Guadalupe Island, found, on the beach just mentioned, 8 elephant seals, of which 7 were taken as specimens (Townsend, 1899).

By 1890 the species consisted of a single herd which hauled out on the exposed northwest coast of Guadalupe Island and its total population can hardly have exceeded 100 animals and may have been as small as 20. It is from this remnant population that the entire species has been reconstituted. The history of this herd was not systematically followed for the first 50 years following the discovery of the few survivors in 1892 by Townsend, but it was visited by scientific collectors at intervals of several years until 1929 (see Huey, 1930 for a review). No published population data are available from 1930 until after World War II. During the last decade, repeated systematic surveys of the elephant seal population

(786)

have been made by the authors (Bartholomew and Hubbs, 1952, and subsequent observations). A reasonably accurate reconstruction of the population growth of the species can now be made.

The smallness of the total elephant seal population, the inaccessibility of the hauling grounds on Guadalupe Island and changing economic conditions made it unattractive to sealers, and the herd began to grow. In 1922, before the population became large enough to attract commercial exploitation, it was afforded virtually complete protection by the Mexican Government. For some time adult males were killed for the shipment to China of the genitalia which were used in the manufacture of a supposedly aphrodisiac drug. Occasional individuals are still shot illegally by fishermen. Collectors for zoos take a few and a few animals are poached. It may be assumed, however, that none of these activities have had significant depressing effects on the growth of the population. Most of the animals taken are males, only a fraction of which are needed for the realization of the full reproductive potential of this highly polygynous species.

In order to trace the recovery of the population of this species from near extinction — a rather unique venture — all published and available unpublished numerical data on population size (except for miscellaneous records of small groups seen since 1935, which have no important bearing on the total picture) have been summarized in Table 1. The figures used are actual counts or careful estimates and indicate minimal numbers present. Because of the fact that from 1884 until the middle 1930's the species apparently bred only on Guadalupe Island and today is known to breed only on Guadalupe, San Benito, San Nicolas and San Miguel islands, the data represent the entire population of the species, except for wanderers at sea. The data reveal large seasonal changes in the numbers of seals on the hauling grounds, as well as a rapidly expanding population. The animals breed during the winter and it is during this period, and more especially in the early spring, that the greatest concentrations of animals are ashore. Unfortunately, most of the counts have been made during the summer. Despite this sampling bias the rate of population increase has been sufficiently great so that when population size is plotted on semi-log coordinates, a straight line can be fitted to the higher points for the years from 1892 through 1957 (Fig. 1).

By correcting for seasonal changes in population and estimating the total population of males, a reasonably accurate estimate of rate of population growth for an entire species can be constructed. It seems certain that the point of inflection for the curve of population growth has not yet been reached. Scammon's (1874) estimates suggest that in the early years of the 19th century the species numbered many thousands and today there are large areas of suitable coastal habitat on which elephant seals formerly hauled out that

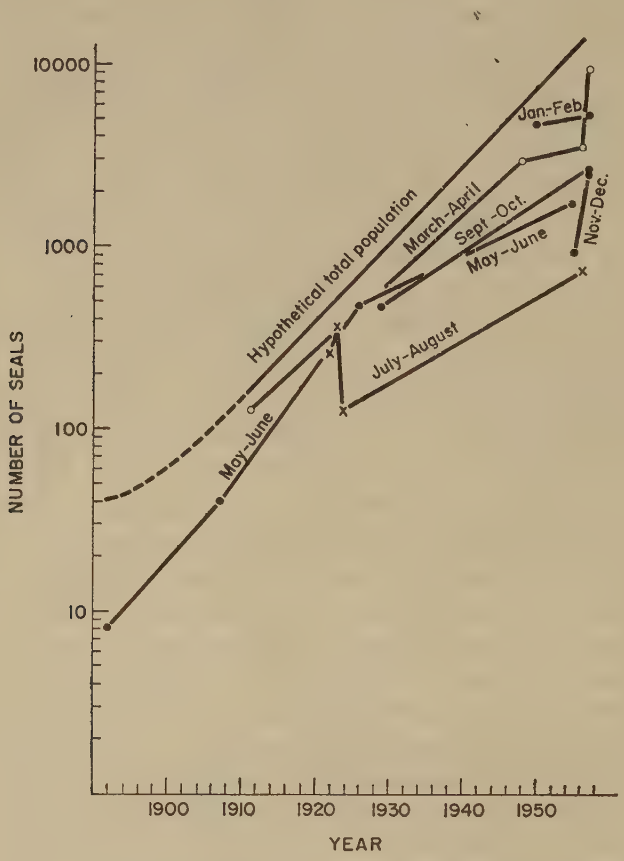

Fig. 1. — The growth of the population of the northern elephant seal. The points are for the Guadalupe Island population only. The methode of estimating the total population is described in the text. A summary of the population data available for the species is given in Table I. The lines connect censuses taken at comparable times of the year. The data since 1950 are plotted by month in Figure 2.

have not been reoccupied despite the spread of the species during the past three decades.

The northern elephant seal is highly polygamous. In the congested rookeries on Guadalupe and San Benito islands, the dominant bulls hold an average of about 13 cows in their harems (Bartholomew, 1952). In less crowded rookeries the harem size is somewhat greater, and under circumstances where local topography makes the females relatively inaccessible to subordinate males stable harems of as many as 40 cows have been recorded (Bartholomew and Boolootian, 1960). Male elephant seals are extremely aggressive toward each other during the breeding season, and the largest and most aggressive males keep the other bulls from having access to the females. The highly polygynous breeding structure that results makes it appear possible that the entire present population of the species may have been derived from a single breeding unit (bull plus harem), and makes it highly probable that the population has been derived from five or fewer such units. The reconstruction of a species from such a small number of breeding units offers excellent opportunity for genetic change. It should be possible to investigate the evolutionary effects of the profound fluctuation in the population of elephant seals during the past century by comparing the specimens taken by C. H. Townsend when the species was in the final stages of the population decline with comparable specimens taken from the present population. No one has undertaken such an investigation.

It is notable that the elephant seals of Guadalupe Island have shown almost explosive population growth during the past half century, but that two other species of pinnipeds occupying this island have responded very differently. The resident population of California sea lion, *Zalophus californianus* (Lesson), has remained essentially stable and apparently has never numbered over a few hundred during the known history of the population. As pointed out by Bartholomew and Hubbs (1952) this may be related to the fact that the California sea lion is primarily a coastal species while Guadalupe is a true oceanic island. The Guadalupe fur seal, *Arctocephalus townsendi* (Merriam) which, judging from the extent of the abandoned rookeries on Guadalupe Island (see Bartholomew and Hubbs, 1952 for a description and photographs), was an extremely abundant species before its decimation by the fur trade, has remained on the brink of extinction during the decades that the elephant seal population has been increasing exponentially. Why the fur seal has not recovered similarly, despite its release from human depredations and despite the availability of an apparently favorable environment, remains an enigma. Counts of the fur seals about Guadalupe Island since their rediscovery there in 1954 (Hubbs, 1956) have ranged from 14 to 107, and the species has not been observed elsewhere in recent years except for one male seen on San Nicolas Island in 1949 (Bartholomew, 1950).

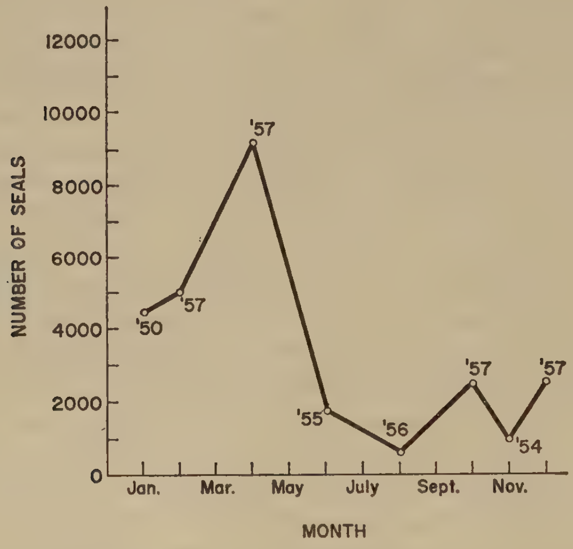

Fig. 2. — Seasonal fluctuations in the elephant seal population on Guadalupe Island. The figures near each point represent the year. The sources are listed in Table I.

Our analysis of the available data indicates that the total population of *Mirounga angustirostris* has increased from about 50 in 1892 to approximately 13,000 in 1957. Since until the 1930's the species apparently bred only on Guadalupe Island, the total population of the species until that time is estimated to have been somewhat in excess of the highest counts made on that island. Since the middle thirties the species has begun to establish additional rookeries. Therefore, for the years since 1935 we have added our estimate of numbers breeding on the San Benito islands of Baja California and the Channel Islands of California. For 1957 the population of 13,000 has been computed as follows : to the maxi-

TABLE I

Population history of the northern elephant seal. The number in parenthesis indicates animals killed or collected. All known counts prior to 1935 are listed. Reports of small groups seen since 1935 which have no important bearing on total population or distribution are not included.

Year	Month	Location	Number	Source
1880	Fall and Winter	San Cristobal Bay	30 (30)	Townsend, 1885
1882	—	» » »	46 (46)	» »
1883	Oct.-Dec.	» » »	110 (110)	» »
1883	—	Guadalupe Is.	80 (80)	Townsend, 1889, 1912
1884	Jan.-Mar.	San Cristobal Bay	93 (93)	Townsend, 1885
1884	May	» » »	40 (40)	» »
1884	Nov.-Dec.	» » »	16 (16)	» »
1884	—	Guadalupe Is.	4 (4)	» »
1892	May	» »	8 (7)	Townsend, 1899
1904	—	» »	4 (4)	Townsend, 1912
1907	June	» »	40 (14)	» »
1911	March	» »	125 (10)	» »
1922	July	» »	264 (1)	Hanna and Anthony, 1923
1923	July	» »	366 (3)	Anthony, 1924
1924	August	» »	124 (5)	Huey, 1930
1926	June	» »	465 (3)	» »
1929	Sept.	» »	469 (4)	» »
1938	Summer	San Miguel Is.	13	Bartholomew, 1951
1946	Summer	» » »	21	Fitch and Wilson, 1949
1948	March	West San Benito Is.	700	Fitch and Wilson, 1949
1948	March	Guadalupe Is.	2891	Fitch and Wilson, 1949
1949	April	Los Coronados Is.	73	Bartholomew, 1950
1950	April	San Nicolas Is.	168	Bartholomew, 1951
1950	Jan.-Feb.	Guadalupe Is.	4548	Bartholomew and Hubbs, 1952
1950	Feb.	San Benito Is.	908	Bartholomew and Hubbs, 1952
1951	March	Middle San Benito Is.	187	Wisner (personal communication)
1951	Dec.	» » » »	83	Wisner (personal communication)
1954	Aug.	San Miguel Is.	190	A. Allanson (personal communication)
1954	Nov.	Guadalupe Is.	899	present paper
1955	June	» »	1786	» »
1956	April	Guadalupe Is. (census incomplete)	3466	Berdegue, 1956
1956	Aug.	Gadalupe Is.	623	present paper
1957	Feb.	» »	5044	» »
1957	April	» »	9143	» »
1957	Oct.	» »	2540	» »
1957	Dec.	» »	2495	» »
1958	Feb.	San Miguel Is.	375	Bartholomew and Boolootian, 1960
1958	April	San Nicolas Is.	207	Bartholomew and Boolootian, 1960
1958	April	Santa Barbara Is.	101	Bartholomew, and Boolootian, 1960

mum count (April) of slightly more than 9,000 elephant seals on Guadalupe Island we add 10 per cent for animals missed, and 15 per cent as a conservative estimate for the adult males since this class was completely absent from the hauling grounds at the time of the census ; to this total we add 1000 animals as our best estimate of the San Benito population and 600 for the animals in the Channel Islands. The supporting data appear in Table I and Figure 1.

The census figures for the years from 1950 to 1957, inclusive, indicate a more than ten-fold seasonal fluctuation in the numbers of elephant seals on their main refuge of Guadalupe Island (Fig. 2). Similar fluctuations have been observed for other species of pinnipeds, including the southern elephant seal (Laws, 1956). The April, 1957 census which found the greatest concentrations of the northern elephant known since the species' presumed extermination (Plates III and IV), revealed no adult males whatsoever ; animals ashore were all females and young males. A similar paucity of adult males has been found in the spring on the California Channel Islands (Bartholomew, 1951 and Bartholomew and Boolootian, 1960). Thus, the adult males have a seasonal cycle, as yet not understood, which differs from that of the females and young males. It seems probable that the animals which leave the coastal islands range far to sea, for some have been seen far off shore along the coasts of Oregon and Washington. Several dozen goose-neck barnacles were found on an immature female hauled out on San Nicolas Island in May, 1949 ; Laws (1956 : 18) similarly reports the presence of large barnacles on southern elephant seals. These findings suggest that both species spend protracted periods at sea.

SUMMARY

Although the data are fragmentary, they clearly reveal the principal features of the history of the population of the northern elephant seal. Prior to its commercial exploitation the elephant seal was a common resident of the coasts of California and Baja California. It was virtually exterminated by the middle of the nineteenth century and was reduced to a single pitiful remnant on Guadalupe Island. With the cessation of commercial hunting and the protection of the Mexican government the species has prospered. During the past 65 years its population has increased more than 250 fold and now stands at approximately 13,000. The species has reoccupied many of its abandoned rookeries and is once again establishing itself as a conspicuous element in the marine fauna of the Pacific coast of North America.

(792)

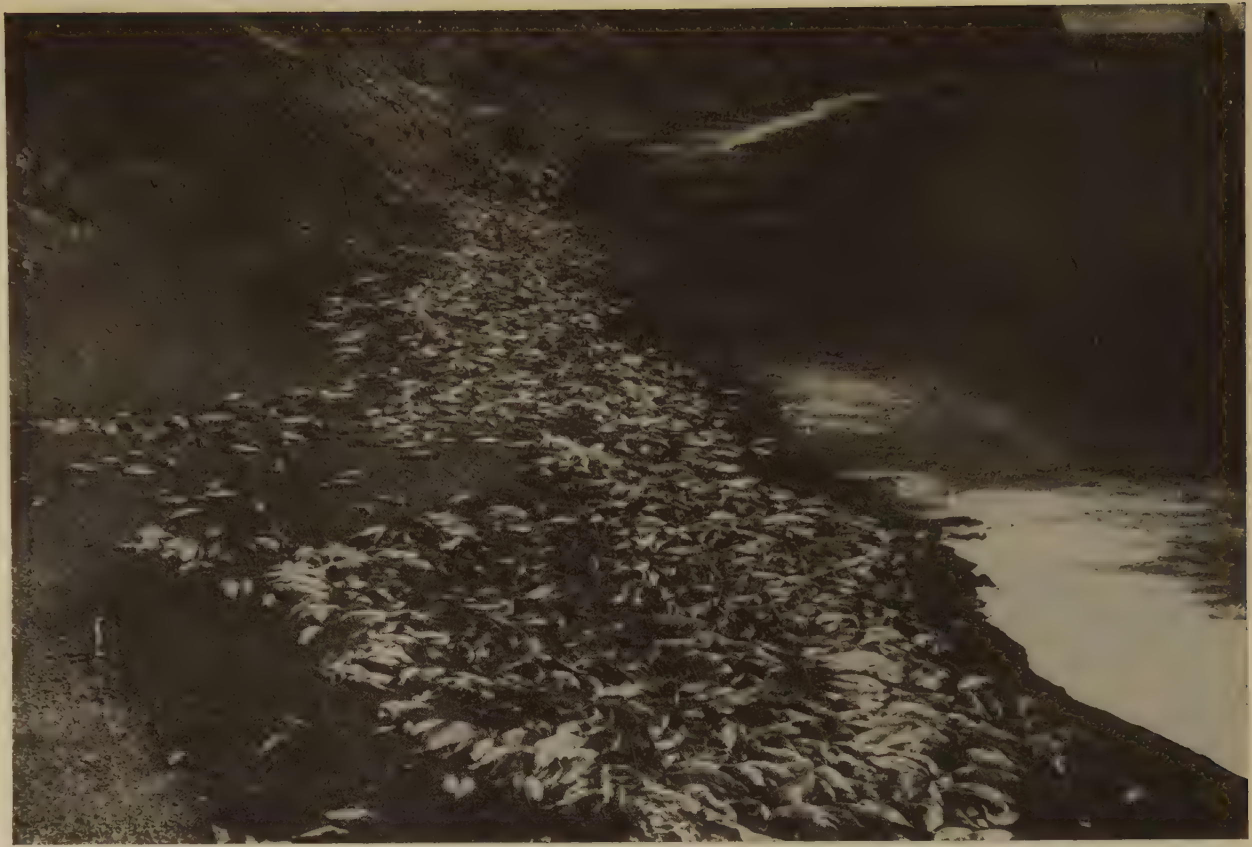

A herd of over 2,000 northern elephant seals on the beach south of Pilot Rock, Guadalupe Island, April 1957. This is the largest aggregation of the species which has been seen during the past century.

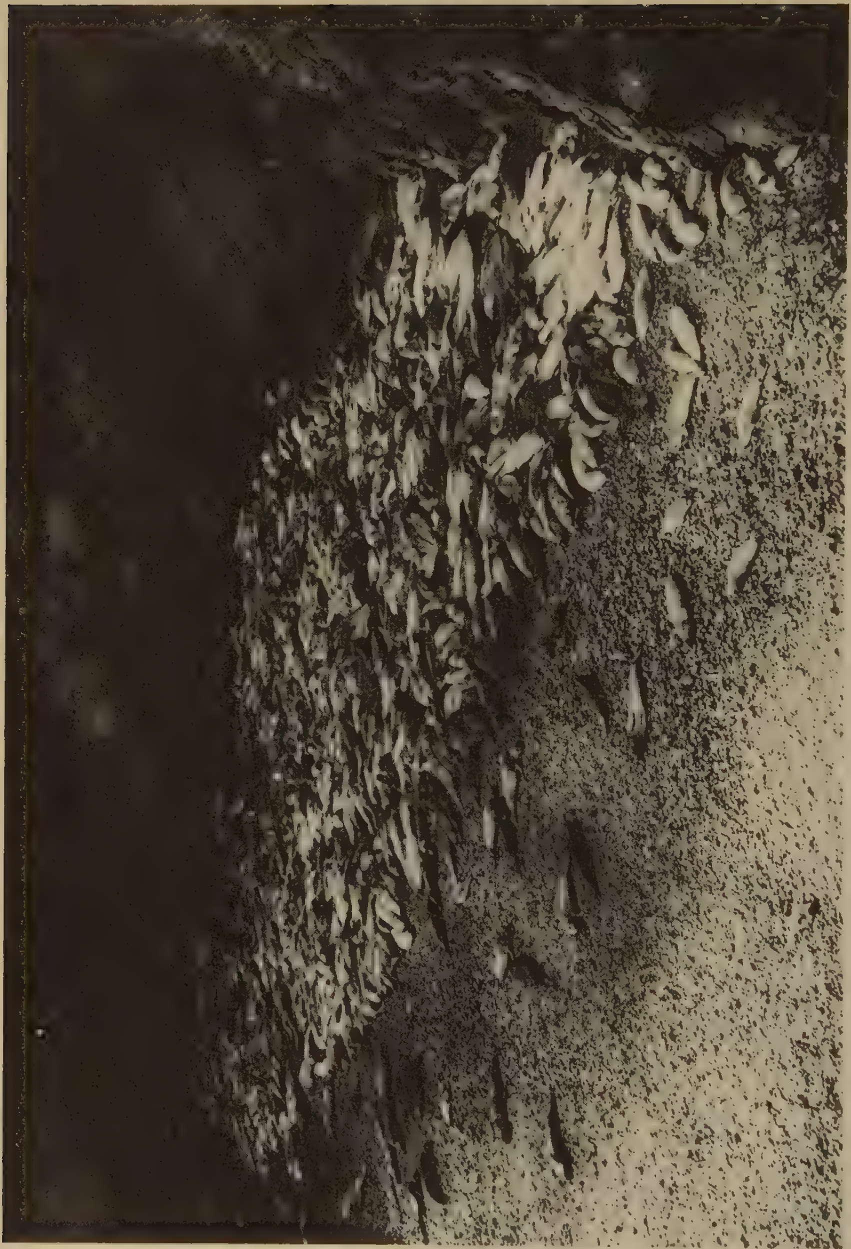

An unusually congested aggregation of slightly more than 1,100 elephant seals on Barracks Beach, Guadalupe Island, April 1957. Note the complete absence of adult males.

⁂

G. A. Bartholomew et C. L. Hubbs. — Croissance de la population et mouvements saisonniers de l'Eléphant de Mer du Nord (*Mirounga angustirostris*)

Résumé

Dans cet article les auteurs étudient la croissance de la population et les mouvements de *M. angustirostris*. Après avoir parlé de la répartition de cette espèce avant le début de la chasse (au début du XIX^e siècle) et de sa quasi-extinction vers 1880, les auteurs mentionnent la « redécouverte » de cet Eléphant de mer en 1892 par Townsend à l'île Guadalupe. Le nombre des survivants n'excédait certes pas 100 et ne dépassait peut-être pas 20.

La croissance, sous protection du gouvernement mexicain dès 1922, a été prodigieusement rapide. Les chiffres de recensements de 1892 à l'heure actuelle (recensements réguliers depuis la dernière guerre) permettent de tracer la courbe de l'accroissement de population, courbe approchant de la verticale de 1892 à 1957 (fig. 1). Il paraît certain que le point d'inflexion de la courbe n'est pas encore atteint. D'ailleurs on pense (avec Scammon, 1874) qu'au début du XIX^e siècle la population de *M. angustirostris* était forte de nombreux milliers d'individus et elle occupait alors 14 degrés de latitude le long du littoral, de Point Reyes (juste au nord de San Francisco) à Magdalena Bay, en Basse Californie, sans parler des îles.

La population est passée de 50 (approximativement) en 1892 à 13.000 en 1957, corrélativement l'aire de dispersion de l'espèce s'étend. En 1892 il n'existait plus qu'une petite colonie sur l'île Guadalupe. A l'heure actuelle *M. angustirostris* recolonise peu à peu son ancien habitat : en plus de l'île Guadalupe (plus de 11.000 en 1957), l'espèce se reproduit depuis 1935 environ sur les îles San Benito (1.000 en 1957), San Miguel et San Nicolas (600 en 1957).

La population présente des fluctuations saisonnières fort importantes. En avril 1957 par exemple, le recensement sur l'île Guadalupe (9.143 individus) ne révèle que des femelles et des jeunes mâles, à l'exclusion de tout mâle adulte. Les mâles adultes ont un cycle saisonnier, encore mal connu, qui diffère complètement de celui des femelles et des jeunes mâles. Les mâles adultes peuvent aller loin en mer ; il existe des records des côtes de l'Orégon et de

Washington et même de la Colombie britannique et du Sud-Est de l'Alaska. La découverte à l'île San Nicola de Cirripèdes (Anatifes) bien développés, fixés sur la peau d'une femelle immature, phénomene signalé par Laws (1956) pour *M. leonina,* prouve que ces deux espèces peuvent effectuer de très longs séjours en mer.

Du fait que la population actuelle ne provient que d'un nombre très faible de geniteurs (les survivants de 1892), le patrimoine génique n'est sans doute pas le même qu'autrefois et des changements dans la morphologie de l'espèce peuvent se produire plus facilement. Il serait intéressant à ce sujet de comparer des crânes collectés au XIX^e siècle et des crânes actuels.

Il faut souligner que si *M. angustirostris* a remarquablement résisté et se multiplie rapidement, il n'en est pas de même des deux Otaries : *Zalophus californianus* a des effectifs actuels voisins de ceux d'autrefois (quelques centaines) et *Arctocephalus townsendi,* qui fut jadis si abondante (cf. Bartholomew et Hubbs, 1952), n'a pas remonté la pente, les effectifs connus ne dépassent pas 107 individus !

⁂

ADDENDUM

Since this manuscript was completed, additional counts have been made and as of January, 1960, the total population of the species appears to have increased to at least 15,000. In January, 1960, a single rookery south of Pilot Rock Beach on Guadalupe Island supported 4,600 elephant seals — a population approximately equal to that of the entire island at the same time of year in 1950.

The figure of 15,000 was derived as follows : To the estimate of 1,600 for the San Benito and Channel Islands and a count of 9,000 for the east side of Guadalupe Island, we added 2,000 for the west side of Guadalupe which could not be closely approached, and 20 per cent more for the immature animals which must have been at sea. (The animals ashore were virtually all breeding adults and pups.)

(796)

LITERATURE CITED

ANTHONY, A. W. (1924). — Notes on the present status of the northern elephant seal, *Mirounga angustirostris*. *J. Mamm.*, 5 : 145-152.

BARTHOLOMEW, G. A. (1950 *a*). — Reoccupation by the elephant seal of Los Coronados Islands, Baja California. *J. Mamm.*, 31 : 98.

— (1950 *b*). — A male Guadalupe fur seal on San Nicolas Island, California. *J. Mamm.*, 31 : 175-180.

— (1951). — Spring, summer, and fall censuses of the pinnipeds on San Nicolas Island, California. *J. Mamm.*, 32 : 15-21.

— (1952). — Reproductive and social behavior of the northern elephant seal. *Univ. Calif. Publ. Zool.*, 47 : 369-472.

BARTHOLOMEW, G. A. and HUBBS, C. L. (1952). — Winter population of pinnipeds about Guadalupe, San Benito, and Cedros Islands, Baja California. *J. Mamm.*, 33 : 160-171.

BARTHOLOMEW, G. A. and BOOLOOTIAN, R. A. (1960). — Population structure of the pinnipeds of the California Channel Islands. *J. Mamm.*, 41 (in press).

BERDEGUE, J. (1956). — La foca fina, el elefante marino y la ballena gris en Baja California, y el problema de su conservación. *Ediciones del Instituto Mexicano de Recursos Naturales Renovables*, A. C., 14 : 1-38.

CORNEY, P. (1896). — Voyages in the northern Pacific. Narrative of several trading voyages from 1813 to 1818 between the northwest coast of America and the Hawaiian Islands and China with a description of the Russian establishments on the northwest coast... *Thos. G. Thrum*, Honolulu, xi + 138 + v pp. (reprinted from the *London Literary Gazette*, 1821).

FITCH, J. E. and WILSON, R. C. (1949). — Observations on the northern elephant seal, *Mirounga angustirostris*. *J. Mamm.*, 30 : 192-194.

GILL, T. (1866). — On a new species of the genus *Macrorhinus*. *Proc. Chicago Acad. Sci.*, 1 : 33-34.

HANNA, G. D., and ANTHONY, A. W. (1923). — A cruise among desert islands. *Nat. Geogr. Mag.*, 44 (1) : 71-99.

HUBBS, C. L. (1956). — Back from oblivion. Guadalupe fur seal : still a living species. *Pacific Discovery*, 9 : 14-21.

HUEY, L. M. (1930). — Past and present status of the northern elephant seal with a note on the Guadalupe fur seal. *J. Mamm.*, 11 : 188-194.

LAWS, R. M. (1956). — The elephant seal (*Mirounga leonina* Linn.) II. General, social, and reproductive behavior. *F. I. D. S., Sci. Rep.*, 13, 88 p.

LYON, G. M. (1937). — Pinnipeds and a sea otter from the Point Mugu shell mound of California. *Publ. Univ. Calif. at Los Angeles in Biol. Sci.*, 1 : 138-168.

SCAMMON, C. M. (1874). — The marine mammals of the northwestern coast of North America. *John H. Carmany and Co.*, San Francisco.

TOWNSEND, C. H. (1885). — An account of recent captures of the California sea-elephant, and statistics relating to the present abundance of the species. *Proc. U.S. Nat. Mus.*, 8 : 90-93.

— (1899). — Notes on the fur seals of Guadalupe, The Galapagos, and Lobos islands. The fur seals and fur-seal islands of the North Pacific Ocean. Part 3, pp. 265-270.

— (1912). — The northern elephant seal *Macrorhinus angustirostris* Gill. *Zoologica*, 1 : 159-173.

Reprinted from the Proceedings of the National Academy of Sciences
Vol. 46, No. 9, pp. 1221–1225. September, 1960.

THE THERMODYNAMICS OF SEA WATER

By Harmon Craig

DEPARTMENT OF EARTH SCIENCES AND SCRIPPS INSTITUTION OF OCEANOGRAPHY,
UNIVERSITY OF CALIFORNIA, LA JOLLA

Communicated by Walter H. Munk, July 15, 1960

In a recent volume dealing with the physics and chemistry of sea water,[1] Fofonoff[2] presents a systematic application of the equations of thermodynamics to an ocean water system. Few subjects are more fundamental to the study of the sea and more neglected in application, reflecting the inherent difficulties in treating a

Contributions from the Scripps Institution of Oceanography, New Series, 1197

multicomponent system in natural surroundings and in treating nonequilibrium systems. Confronted with these obstacles, it seems only reasonable to hope that oceanography, in contrast to meteorology which presents much simpler problems, might refrain from attempting to establish a unique thermodynamic jargon of its own. Especially in dealing with natural systems, a clear and precise formulation according to established theory is necessary to prevent isolation from scientists in other fields, and indeed to insure the correct development of the subject.

Fofonoff's treatment seems to me to be erroneous in several respects, and to be misleading in the development of terminology which obscures the formal simplicity of general usage. In what follows, I discuss in particular two aspects of Fofonoff's paper: the ocean as a thermodynamic system in a gravitational field, and his treatment of the chemical potential in dealing with the components of sea water.

Gravitational Field Treatment.—Fofonoff points out that the ocean is a complex thermodynamic system in a gravitational field, consisting of infinitely many phases in vertical extent. To describe the changes in internal energy of a general sea water system, he states the "First Law" as

$$dU = TdS - PdV + \sum (\mu_i + \phi)\, dm_i \tag{1}$$

an equation which he quotes from Guggenheim.[3] (I use Guggenheim's terminology, rather than Fofonoff's, throughout this paper, except that m_i is the mass of component i and μ is the "specific" chemical potential referred to mass units instead of moles.) ϕ is the gravitational potential gh. Integrating (1) in the usual way gives:

$$U = TS - PV + \sum m_i\mu_i + m\phi \tag{2}$$

where $m = \sum m_i$. (Fofonoff uses intensive form from this point on, but this does not affect the argument.) Differentiating (2) and subtracting (1), Fofonoff derives what he proposes as the "Gibbs-Duhem relation" for sea water,

$$SdT - VdP + \sum m_i d\mu_i + md\phi = 0 \tag{3}$$

and states that the partial derivative of specific "internal" entropy with respect to salinity can be calculated from this relation when the chemical potential of water is known.

Fofonoff's relation (3) is, however, incorrect because equation (1) actually applies only to a specific *phase*, i.e., to matter at a fixed gravitational potential. Thus in the differentiation of (2), the term $md\phi = 0$, and this term will not appear in (3), as indeed it should not. Gibbs, on the other hand, in his discussion of the gravitational field,[4] treats an arbitrary element of mass within the system; here there is an additional term $md\phi$ in (1) as applied to the mass element. This term will also occur on differentiating (2), so that it cancels in the subtraction. In either case we obtain the correct Gibbs-Duhem equation:

$$SdT - VdP + \sum m_i d\mu_i = 0$$

which is therefore invariant in the gravitational field. Gibbs himself stated that this relationship (which he derived without considering the gravitational field) is true for any continuous variations of phase, which is the reason that the equilibrium conditions in a gravitational field are overdetermined.[4]

Equation (2) is always true for an arbitrary mass element and therefore is also true in the special case of fixed ϕ treated by Guggenheim. The difficulty only occurs when we try to integrate Guggenheim and differentiate Gibbs. To describe a general sea water system at equilibrium, as Fofonoff wishes to do, the correct Gibbs-Duhem equation must be integrated over all mass elements (Gibbs) or all phases (Guggenheim), under the equilibrium constraint $dT = 0$ (neglecting the insignificant relativistic gradient). This simply gives the condition for hydrostatic equilibrium, as was shown by Gibbs.

Chemical Potential.—Considering sea water as a system of water and "salinity," Fofonoff defines:

$$\mu = \mu_s - \mu_w$$

where

μ_w = chemical potential of water (mass units);

μ_s = chemical potential of dissolved salts ("salinity"), assuming the components of salinity occur in fixed proportions; and

μ = "chemical potential of sea water."

(Fofonoff actually calls all these functions "partial chemical potentials" in contrast to an ordinary chemical potential which he attributes to a pure phase. This is equivalent to partial Gibbs free energy, a term which has no meaningful definition.)

On page ix of the volume referred to,[1] we find that the Committee on Physical Properties considers the "chemical potential of sea water" to be an important property which should be measured and computed. It is therefore somewhat discouraging to note that the μ defined above is not by any possible definition a chemical potential. If we consider salinity to be a pure salt of fixed composition, then this function is:

$$\mu = \left(\frac{\partial g}{\partial x_s}\right)_{P,\,T} = \frac{g - \mu_w}{x_s}$$

where x_s is the mass fraction of salinity and g is the specific Gibbs free energy per unit mass of sea water.

Gibbs used specific chemical potentials in terms of mass units, but he did not treat the thermochemistry of solutions. Fofonoff does not discuss the concentration dependence of his potentials in terms of the mass fractions he uses, but the greatest difficulty in actually using such functions is that the chemical potential of a component of an ideal solution is no longer linear in the logarithm of concentration. Thus in Fofonoff's units, we have for the chemical potentials of water and "salinity":

$$\mu_w = \mu_w^* + R_wT \ln x_w - R_wT \ln \left[x_w\left(1 - \frac{M_w}{M_s}\right) + \frac{M_w}{M_s}\right]$$

$$\mu_s = \mu_s^* + R_sT \ln x_s - R_sT \ln \left[x_s\left(1 - \frac{M_s}{M_w}\right) + \frac{M_s}{M_w}\right]$$

where M_w and M_s are the molecular weights of water and "salinity," and R_i =

specific gas constant, $= R/M_i$. These expressions involving mass functions are to be contrasted with the simple ideal solution dependence in terms of molal functions and mole fractions:

$$(\mu)_i = (\mu)_i^* + RT \ln (x)_i$$

where the parentheses signify molal chemical potentials and mole fractions.

The use of Fofonoff's function μ puts standard equations in a form difficult to use. For example, Fofonoff's equation (12) for the freezing point depression in sea water in equilibrium with ice (assuming the ideal solution law) is:

$$[s_w - s_{ice}]\left(\frac{\partial T}{\partial x_s}\right)_P = -x_s\left(\frac{\partial \mu}{\partial x_s}\right)_{P,\,T}$$

where s_i is specific entropy of phase i and his μ is as defined above. One may ask what the right hand side of this equation is, in terms of usable functions. In Fofonoff's units, the equation as it must be used becomes:

$$[s_w - s_{ice}]\left(\frac{\partial T}{\partial x_s}\right)_P = \frac{-R_w T}{[1 - x_s]\left[\dfrac{M_s}{M_w}(1 - x_s) + x_s\right]}.$$

This equation and the previous one are to be compared with the simple expression given in molal units and mole fractions:

$$[(s)_w - (s)_{ice}]\left(\frac{\partial T}{\partial (x)_s}\right)_P = \frac{-RT}{[1 - (x)_s]}.$$

Fofonoff comments that he uses specific chemical potentials in mass units in order to use salinity as a state variable. It will be noted, however, that both here and above the molecular weight of "salinity" enters his equations whenever one puts them into the form in which they are actually used. Salinity can be used as a variable in any type of units, depending on the problem. However, in considering the properties of sea water, the function μ is only an apparent convenience which actually obscures the simplicity of most of the thermodynamic equations, regardless of the type of units used for salinity.

In reality, of course, μ_s cannot be defined without treating salinity as NaCl, for if the proportions of dissolved salts are not constant, the Gibbs function changes even though x_s may be constant. Since G is also a function of components not included in salinity, such as dissolved gases, combined CO_2, and dissolved organic matter, the concept of μ_s as a summation involving fixed multipliers is not very useful. One either treats the ocean directly as a two-component system or one doesn't, but in either case the molecular functions are always the more useful when even the simplest chemistry is involved.

The "chemical potential of sea water" could be correctly defined by treating a system whose components are sea water (of a fixed composition), pure water, and any other components desired, using a three or more component system to treat the effects of any particular species. For example we could take standard Copenhagen sea water as a component of sea water and compute or measure μ for this component in simple systems. It is doubtful whether much would be gained compared to treating the ocean simply as water and sodium chloride. Still, the nomenclature should be preserved for an actual component of the system in case such a treatment becomes useful.

[1] *Physical and Chemical Properties of Sea Water*, National Academy of Sciences–National Research Council (Washington, D. C.), Pub. 600 (1959).

[2] Fofonoff, N. P., "Interpretation of Oceanographic Measurements—Thermodynamics," *ibid.*, 38–66.

[3] Guggenheim, E. A., *Thermodynamics*, (North-Holland Publishing Company, 1957), p. 404.

[4] Gibbs, J. W., *Collected Works*, (Yale University Press, 1928), Vol. 1, p. 146.

Publications of the Astronomical Society of
the Pacific, Vol. 72, No. 426, June 1960.

ON THE OBSERVATION OF UNRESOLVED SURFACE FEATURES OF A PLANET

John D. Isaacs and John E. Tyler

Scripps Institution of Oceanography
University of California

The detailed nature of the unresolved features of an illuminated surface exercises a profound influence on the brightness and color of the light that it scatters.

A particular relieved surface will display surface brightness changes and color changes at various angles of illumination and observation that are related to: (1) the nature of the surface slopes, (2) the degree of organization of the slopes, and (3) the distribution of color in relation to the slopes.

Figure 1 presents the calculated brightness changes of three idealized surfaces: (*a*) hemispheres placed two diameters apart; (*b*) a surface, 20% of which is covered by vertical cylinders of diameter/length ratio equal to 1:56; and (*c*) a screen (checker-

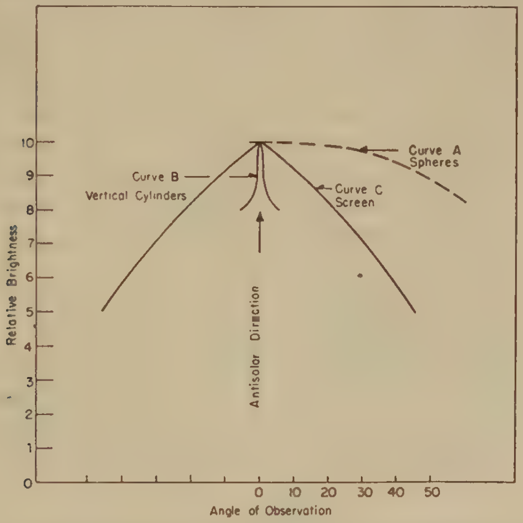

Fig. 1.—Calculated brightness changes of three idealized surfaces (see text).

Contributions from the Scripps Institution of Oceanography, New Series, 1198

Reproduced by Permission

board) with alternate transparent and opaque openings held at a distance of one square above a surface.

All of these surfaces show a maximum brightness in a direction 180° from that of the incident light; that is, in the antisolar direction. Varying the parameters of these surfaces results in broadening or narrowing the bright regions. In particular, the screen can be raised to yield a much narrower bright region than that chosen.

These three surfaces are idealized examples of the three principal types of surface relief on the earth's solid surface: (*a*) low, stubby relief with slopes less than 90° (cobbles, dunes, hummocks, etc.); (*b*) thin, narrow relief with slopes of about 90° (grass, stalks, etc.); and (*c*) relief with slopes greater than 90° (that is, overhangs, such as are found for most erect vegetation, angular sand, etc.).

The effect of such relief on the variation of surface brightness with the angle between the direction of observation and illumination is readily apparent to an occupant of a high-flying aircraft on a clear sunny day. As the aircraft reaches an elevation where its shadow is a widely diffuse penumbra, the "shadow" or antisolar point is occupied by a "bright spot" that expands, contracts, changes color, and occasionally changes to a bright streak, as the antisolar point moves across the various types of surface cover. In each case the color changes and width of the bright spot or streak contain quite discriminating information on the nature of the unresolved surface features.

Figures 2 and 3 demonstrate two simple fundamental relationships of *oblique* observation and illumination. Figure 2 shows that relief of less than 90° slope gives rise to the appearance of a bright *streak* stretching away from the sun from the antisolar point toward the horizon. Figure 3 shows that slopes greater than 90° (i.e., overhangs) give rise to only a bright *spot* at the antisolar point.

Observations show that almost all of the earth's solid surface displays only a bright spot, and only rarely a bright streak appears. Thus, surprisingly, the unresolved surface slopes of the earth, as they affect brightness changes, are dominantly overhangs!

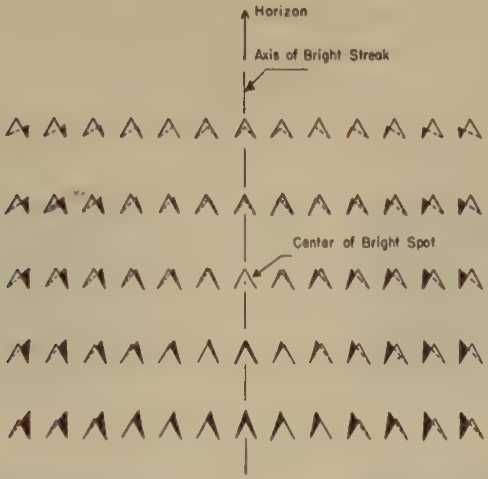
Horizon
Axis of Bright Streak
Center of Bright Spot

FIG. 2.—Bright streak and spot for slopes less than 90°. The symbols represent inverted cones and shadows.

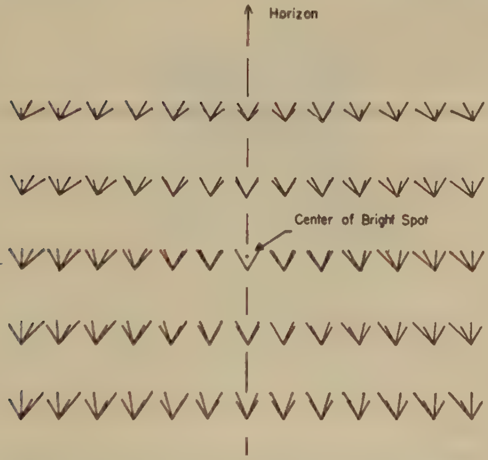
Horizon
Center of Bright Spot

FIG. 3.—Bright spot only, for slopes greater than 90°. The symbols represent idealized grass blades and shadows.

The center of the bright spot is, demonstrably, the point on the earth's surface where every object completely obscures its own shadow.[1,2] Thus all of the surface visible at this point is completely illuminated. The brightness at a given angle of observation away from the bright spot is a function of the amount of shadow that becomes visible to the observer at that angle. Since this shadow falls on the background material, the color components that decrease away from the bright spot are those of the background, that is, the lower-lying portions of the relief.

Many interesting observations can be made that clearly define parameters of the relief. For example, erect green vegetation on yellow soil produces a small yellow-green bright spot at high sun angles. At some low sun angles, more of the shadow falls on the vegetation, and then the bright spot is greener. Therefore, in principle, the observations determine the slopes and sparsity of the relief and the colors of its upper and lower parts.

Orchards, forests, and brush land display two concentric bright spots, an outer spot where the soil color is enhanced, and an inner one where the vegetation color is enhanced. These spots result first from obscuration of the shadows of whole trees and then from obscuration of the shadows of individual leaves as the antisolar point is approached.

A stubble field is a uniquely organized surface that shows a bright streak at all sun angles. Otherwise clearly defined bright streaks are rare. Sand dunes display a streak only when the sun angles are so low as to be comparable with the dune slopes.

These few cases exemplify the variety of this phenomenon.

In view of the above considerations, the writers have conjectured on the possible application of the preceding principles to the study of the unresolved surface features of a planet such as Mars. As an example and test, we have constructed a simple cylindrical model of a planet with asymmetric sand dunes and observed the effect of these dunes on the unresolved brightness. (The optical resolution of the surface was destroyed by rapidly rotating the model.)

The expected relationships and results of the observation of this simple model are shown in Figures 4 and 5, and in Plate I.

PLATE I

Post Opposition
Morning Side

Pre - Opposition
Evening Side

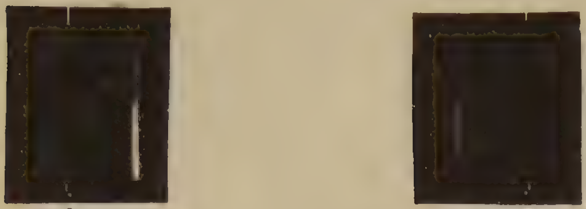

β=120°
The Dark Band is Barely Separated

β=135°
The Dark Band Already is Well Separated

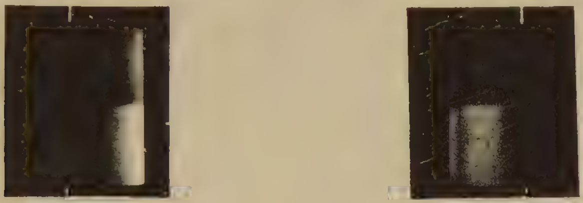

β=85°
Dark Band at Point D (Figure 6)

β=95°
Dark Band at Point B (Figure 6)

β=15°
Asymmetry of Brightness of the Limbs

PHOTOGRAPHS OF MODEL OF A PLANET HAVING ASYMMETRIC DUNES

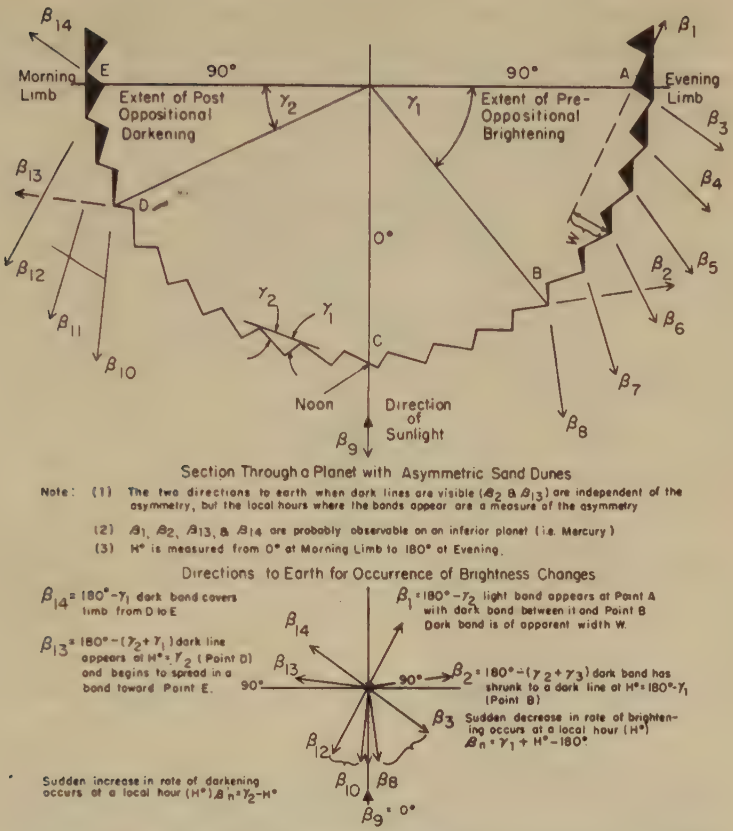
β_{14}
Morning Limb
E
90°
Extent of Post Oppositional Darkening
γ_2
90°
A
γ_1
Extent of Pre-Oppositional Brightening
β_1
Evening Limb
β_3
β_4
β_{13}
D
β_{12}
β_{11}
β_{10}
0°
B
β_2
β_5
β_6
γ_2
γ_1
C
β_7
Noon
Direction of Sunlight
β_9
β_8
Section Through a Planet with Asymmetric Sand Dunes
Note: (1) The two directions to earth when dark lines are visible (β_2 & β_{13}) are independent of the asymmetry, but the local hours where the bands appear are a measure of the asymmetry
(2) β_1, β_2, β_{13}, & β_{14} are probably observable on an inferior planet (i.e. Mercury)
(3) H° is measured from 0° at Morning Limb to 180° at Evening.
Directions to Earth for Occurrence of Brightness Changes
$\beta_{14} = 180° - \gamma_1$ dark band covers limb from D to E
$\beta_{13} = 180° - (\gamma_2 + \gamma_1)$ dark line appears at $H° = \gamma_2$ (Point D) and begins to spread in a band toward Point E.
β_{14}
β_{13}
90°
β_{12}
Sudden increase in rate of darkening occurs at a local hour (H°) $\beta'_n = \gamma_2 - H°$
β_{10}
β_8
$\beta_9 = 0°$
$\beta_1 = 180° - \gamma_2$ light band appears at Point A with dark band between it and Point B Dark band is of apparent width W.
90°
$\beta_2 = 180° - (\gamma_2 + \gamma_3)$ dark band has shrunk to a dark line at $H° = 180° - \gamma_1$ (Point B)
β_3 Sudden decrease in rate of brightening occurs at a local hour (H°) $\beta_n = \gamma_1 + H° - 180°$

FIG. 4.—Relationship of brightness changes due to dunes on a planet, with direction to the earth. At $\beta_9 = 0°$, the planet has reached uniform brightness for effects of low relief.*

Dark bands and lines were found to appear close to the expected locations.

Knowledge of the slopes and asymmetry of dunes in areas of the Martian surface would provide evidence on the climate, geology, and atmospheric circulation of the planet. Figure 6 represents the implications of the results of the observations of our cylindrical model to Mars. If bands or lines and brightness changes were observed on areas of the Martian surface in a sequence compatible with this model, this would definitely demonstrate the existence of dunes and would measure their slopes and orientation.

---

* β_2 should equal $180° - (\gamma_2 + \gamma_1)$, not $180° - (\gamma_2 + \gamma_3)$.

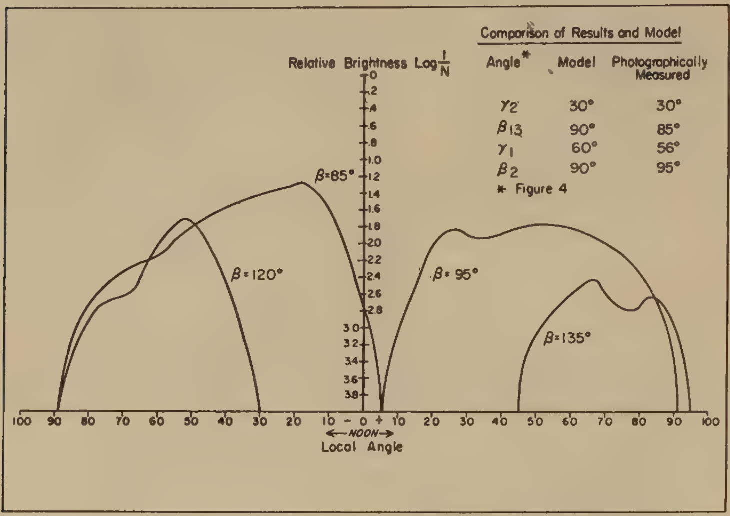

Comparison of Results and Model

Angle*	Model	Photographically Measured
γ_2	30°	30°
β_{13}	90°	85°
γ_1	60°	56°
β_2	90°	95°

* Figure 4

FIG. 5.—Relative brightness of model (corresponding to photographs in Plate I).

Many such results could be expected from analysis of a carefully controlled series of color photographs of Mars during a passage through opposition. Quantitative studies of recognizable areas on such photographs might lead to a better understanding of such problems as:

1. The general nature of the slopes of surface features.
2. The manner in which the seasonal color change is related to relief. (If the dark parts were found to be elevated, the mineral hydration-efflorescence model would appear untenable.)
3. The presence or absence of erect or rugose, encrusting vegetation.[8]
4. The presence or absence of highly organized slopes such as sand dunes, lava needles, etc.
5. The relationship of the snow of the polar caps to the relief.
6. The presence or absence of dew at the morning limb.

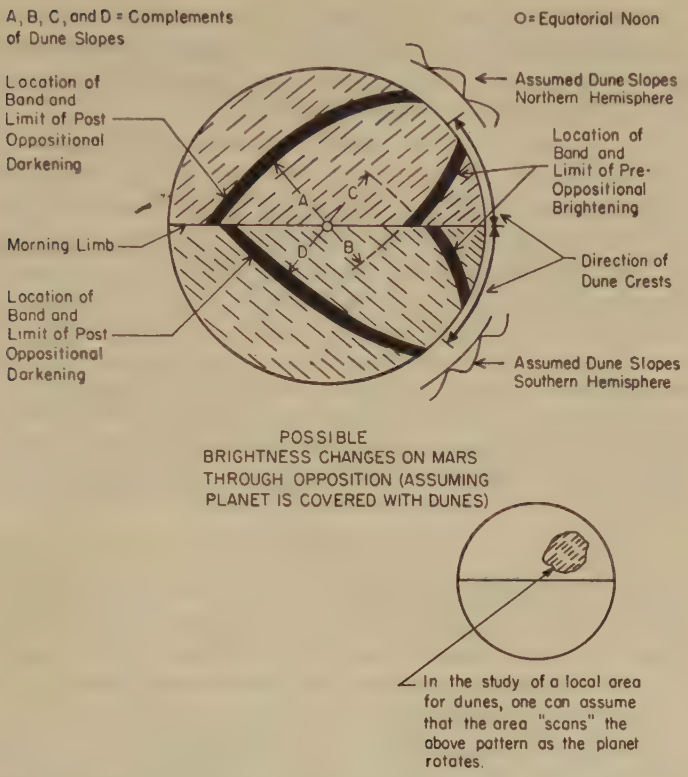
A, B, C, and D = Complements of Dune Slopes
O = Equatorial Noon
Assumed Dune Slopes Northern Hemisphere
Location of Band and Limit of Post Oppositional Darkening
Location of Band and Limit of Pre-Oppositional Brightening
A
C
D
B
Morning Limb
Direction of Dune Crests
Location of Band and Limit of Post Oppositional Darkening
Assumed Dune Slopes Southern Hemisphere
POSSIBLE BRIGHTNESS CHANGES ON MARS THROUGH OPPOSITION (ASSUMING PLANET IS COVERED WITH DUNES)
In the study of a local area for dunes, one can assume that the area "scans" the above pattern as the planet rotates.

FIG. 6.—Possible brightness changes on Mars through opposition, on the assumption that the planet is covered with dunes.

Such a program appears potentially rewarding. Not only are shadows much sharper on Mars than on the earth (the sun's apparent diameter is smaller and skylight less), but the various local sun angles can be observed in one photograph, and all angles of observation and all areas at all sun angles can be observed in a series of photographs.

Some of the suggested observations of low relief are applicable to the planet Mercury (see note 2, Fig. 4), and all are applicable to the asteroids.

Qualitative relationships between brightness and direction of observation have long been recognized as the cause of the increased brightness of the moon and Saturn's rings near opposition.

The moon, of course, is eclipsed at the time that narrow-angle observations might be carried out, but the particulate nature of Saturn's rings has been demonstrated by observations of increased brightness in the narrow-angle direction.[4]

As a matter of further interest, from a high-flying aircraft clouds display faint red and yellow rings about the antisolar point. These effects are probably diffractive as well as dispersive. Similar color changes in the cloudy planets at the proper angle from opposition might be observable, and should supply evidence of the nature of the particles in their clouds.

---

[1] M. Minnaert, in his book *The Nature of Light & Colour in the Open Air* (New York: Dover Publications, 1954), pp. 230–34, describes a halo about the shadow of his head on "bedewed" grass. This he attributes to internal specular reflection in water droplets. Since the observations that we report were made in arid regions, it is thought that Minnaert's effect did not contribute to them. Such specular reflection may identify dew drops, however.

[2] The diffuse shadow of another aircraft near the observer shows no bright spot. Therefore diffraction about the aircraft does not contribute to the bright spot as has been suggested.

[3] Mars may possess areas of plants that turn their leaves to face the sun (as many plants do on earth and possibly more on Mars). If so, at opposition these areas will display a narrow-angle brightness increase at all local sun angles that cannot be explained by any model of nonmoving relief.

[4] E. Schoenberg, in *Handbuch der Astrophysik,* Vol. II/1 (Berlin: Springer, 1929), pp. 4 and 148–54; and H. N. Russell, R. S. Dugan, and J. Q. Stewart, *Astronomy,* Vol. I (Boston: Ginn and Co., 1945), pp. 389–90.

Bulletin of the Seismological Society of America. Vol. 50, No. 4, pp. 563–573. October, 1960

CRUSTAL STRUCTURE OF THE HAWAIIAN RIDGE NEAR GARDNER PINNACLES

By George G. Shor, Jr.

ABSTRACT

A series of seismic refraction profiles has been made across a flat bank at Gardner Pinnacles (a pair of volcanic islets on the western Hawaiian Ridge) down the side of the ridge and across the adjacent deep to the floor of the Pacific basin. The ridge is composed principally of material with velocities typical of volcanic islands. The high-velocity oceanic crust, found in the oceanic areas adjacent, extends beneath the ridge and up into the center of the rise. The total crustal section is thickened and the Mohorovičić discontinuity depressed beneath the deep as well as beneath the ridge.

The smooth "archipelagic apron" on the north side of the ridge has at most 20 meters of sediment over a layer with a velocity of 3 km/sec, which could be volcanic and is definitely of higher velocity than normal oceanic sediments.

Introduction

Gardner Pinnacles are two volcanic islets, the larger of which is 60 meters high and about 180 meters in diameter. The larger pinnacle is at 25° 00′ N latitude, 168° 00′ W longitude, halfway between Kauai and Midway Islands in the Hawaiian chain (fig. 1). Gardner Bank, on which the pinnacles stand, has a flat top about 30 meters below sea level. This flat portion is approximately 100 km from north to south, 40 km east to west at the widest point. The bank has steep slopes on all sides except the northwest, and is separated from the adjoining portions of the Hawaiian Ridge by water over 3000 meters deep. The area was chosen for study because it has a long unobstructed section of shallow flat bottom perpendicular to the strike of the Hawaiian Ridge, and what appears on the charts to be a gentle slope down its northwest side to the Hawaiian Deep. This appearance on the chart proved to be somewhat deceptive and was due to the wide spacing of the soundings used. The actual topography (fig. 2) consists of a series of gently sloping steps with steep slopes between. The principal topographic features, as described by Dietz and Menard (1953) and Hamilton (1957), are the Hawaiian Ridge, Hawaiian Deep and Hawaiian Arch. The last is surfaced by a typical archipelagic apron (Menard 1956).

A set of continuous seismic refraction profiles was shot on August 8 and August 9, 1956 and comprises stations 15 to 19 of Expedition CHINOOK of the Scripps Institution of Oceanography. Receiving station 15 was located on the Hawaiian Arch, station 16 at the bottom of the Hawaiian Deep, 17 halfway up the slope, 18 on the Hawaiian Ridge at the north end of Gardner Bank, and 19 at the south end of the bank. The research vessels STRANGER and SPENCER F. BAIRD were used, each one serving alternately as shooting and recording ship. The lines were continuous, with the receiving station for each line placed at the site of the final shot on the preceding one. Shots ranged from ½ lb to 320 lbs of TNT and tetrytol demolition

---

Manuscript received for publication March 24, 1960, and, as revised, May 23, 1960.

This work represents one of the results of research carried out under contracts NObsr-72512, Bureau of Ships; Nonr 2216 (05), and Nonr 23343, Office of Naval Research, Department of the Navy.

Contributions from the Scripps Institution of Oceanography, New Series, 1199 (815)

Reproduced by Permission

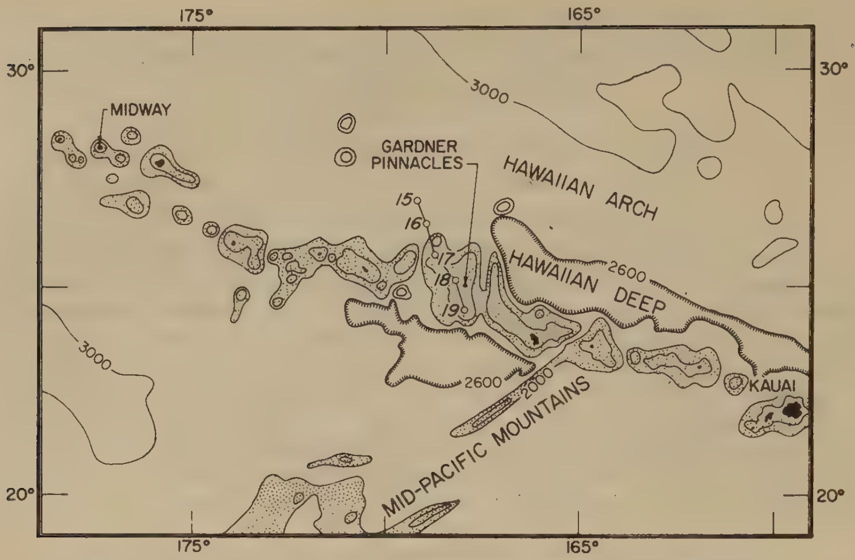
175°
165°
30°
30°
MIDWAY
3000
GARDNER
PINNACLES
HAWAIIAN ARCH
15
16
17
18
19
HAWAIIAN DEEP
2600
3000
2600
2000
MID-PACIFIC MOUNTAINS
KAUAI
20°
20°
175°
165°

Fig. 1. Location of Gardner Pinnacles on the western Hawaiian Ridge. The ridge is shaded within the 2000 fm (3750 meter) contour. Contours are at 1000, 2000, and 3000 fathoms, with an extra 2600 fathom closed contour to show the location of the Hawaiian Deep. Depths are in nominal fathoms; conversion to true meters can be approximated by multiplying by 1.875. Modified from Dietz and Menard (1953).

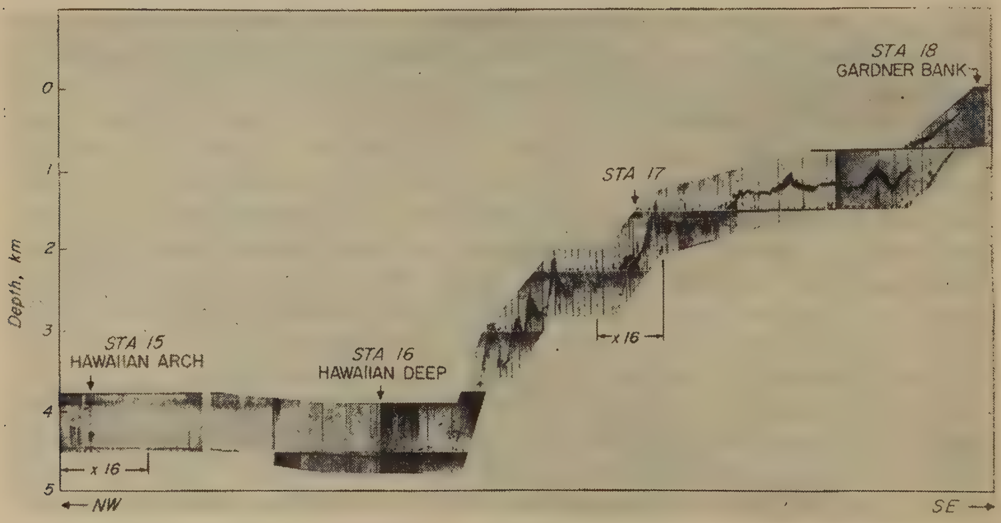

Fig. 2. Fathometer records from station 15 to 18 along the line of seismic profiling. Precision Depth Recorder records (400 fathoms full scale) have been spliced together in proper depth relationship. Vertical exaggeration is 22× except where otherwise noted.

blocks, fired with time fuses at depths chosen to be approximately one-quarter wavelength for the bubble-pulse period. Hydrophones (three from the STRANGER, one from the BAIRD) were streamed on neutrally buoyant suspensions at 50 meters depth. At stations 18 and 19 the above system was modified because of the shallow water, and hydrophones were placed on bottom or a very few meters above. Most of the charges on profiles 18-south and 19-north were on bottom. Instrumentation was generally as described by Raitt (1952).

In the sea phase of the work Alan Jones prepared and maintained the equipment and took records on the BAIRD. Max Silverman was in charge of operations on the BAIRD and fired charges. George Hohnhaus fired charges and David Fogelson recorded on the STRANGER. Other members of the scientific parties and the officers and crews of the two ships provided help in various stages of the operations. Computational work ashore was aided by Gloria Slack and Wanda Willson. This work is part of a continuing program under the direction of Russell W. Raitt. The help and cooperation of all the aforementioned are here gratefully acknowledged. The author is indebted to Russell Raitt and Edwin L. Hamilton for critical reading of the manuscript.

DATA

Travel time plots for all profiles are shown on fig. 3. The horizontal scale is in seconds of direct water wave travel time, either observed or computed from bottom reflection time in cases where the direct water wave was not observed. On the farthest shot of profile 18-south and the farthest two shots of 19-north all water-borne sound had disappeared, and these ranges depend on the combined navigation of the two ships.

All data have been corrected to bottom to remove effects of varying water delays, using the observed slope of the travel time curve for correction. Topographic corrections, other than those for water, have not been used because of the doubt as to which layer contains the irregularities and because they do not decrease the scatter of the points appreciably.

Lines have been fitted to the observed points by eye, giving extra weight to points representing good arrivals. An effort has been made to reconcile either intercept times, reverse times, or both wherever this could be done without going outside the normal scatter of the observed points. In a number of cases, as is obvious on fig. 3, it has been impossible to reconcile both intercept and reverse points simultaneously; in some cases it has been impossible to reconcile either.

Station 15—Station 15 was shot in one direction, and was reversed by the north half of 16. The bottom is smooth, sloping gently from 4.44 kilometers at 15 to 4.57 kilometers at 16. The shooting profile was transverse to the strike of the Hawaiian Deep, ending in the bottom of the deep. Layers with apparent velocities of 7.6, 6.7, 4.3 and 3.0 km/sec are found on the profile with sharp changes of slope and well-defined velocities in all cases except the 4.3 km/sec line. This line is introduced to fit two observed points and the reverse time from a line on profile 16-north.

The strength of bottom reflections at incidence near vertical was striking and unusual on this station. Reflections up to the 5th order were present on all records, and were continuing to arrive at the time the records were cut off. In one case where recording equipment was left on between shots, reflections up to the 22nd have been identified, primarily on the low frequency (below 16 cps) traces. A slight discrepancy between the reflection time as shown by fathometer and that shown by the intervals between successive reflections on each shot was noted, amounting to 0.03 second.

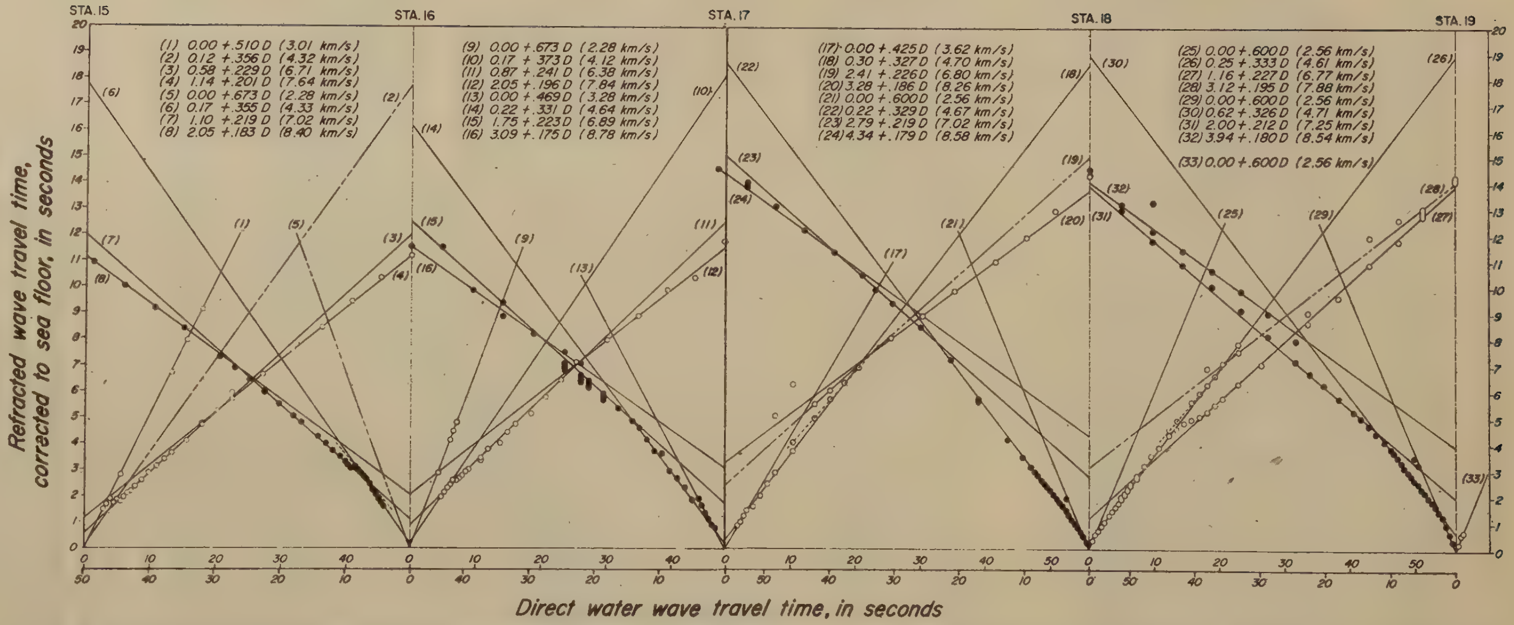

Fig. 3. Travel time plots with refracted arrivals corrected for water delay to the sea floor. Solid lines are fitted to observed data; dashed lines are based on inadequate data but introduced to fit reverse and intercept times; dotted lines are observed arrivals from a possible 5 km/sec layer not used in the layer solutions.

There are numerous small inaccuracies in timing control of the oscillograph, zero-setting of the fathometers, small variations of depth between the shooting and recording ships, and reading of the reflection time from the records, any of which might amount to as much as 0.005 second. A fortuitous combination of these might result in this discrepancy on a single reflection interval on a single record. The discrepancy exists on a number of short-range records from this station. The seismic shots contain lower frequencies than the echo sounder pings, and should therefore penetrate the bottom better. These delays could, then, be explained by reflection of the seismic shots from the base of a layer of about 20 meters of soft sediment rather than from the base of the water column. A weak sub-bottom echo corresponding to this is faintly visible on the original fathometer record. No strong sub-bottom reflections other than these were visible on records from station 15.

Station 16—Station 16, located over the bottom of the Hawaiian Deep, was shot two ways: the north profile reverses 15, the south profile reverses 17-north. Smooth bottom continues south of 16 for 10 kilometers, at which point rapid shoaling begins. The bottom is rough for the remainder of the line.

Profile 16-north, reversing 15, shows layers with apparent velocities of 8.4, 7.0, and 4.3 km/sec, which correspond to the lines on 15 with apparent velocities of 7.6, 6.7, and 4.3 km/sec respectively, with well-matched reverse points. No refracted arrival is found corresponding to the 3.0 km/sec layer on 15, but extremely strong sub-bottom reflections were recorded. Analysis of these for velocity and layer thickness gives a mean vertical velocity for the first 0.23 km of 2.29 km/sec. This is well outside the errors of determination of the first-layer velocity at 15. A few points could be interpreted as showing a layer with velocity near $5\frac{1}{2}$ km/sec, but as this layer does not appear on other profiles it has been omitted from the interpretation.

Profile 16-south shows two layers on the flat portion of the line, with apparent velocities of 2.3 and 4.1 km/sec. The 2.3 km/sec velocity corresponds with the determination from the reflection data on the north side. The agreement between the reflection and refraction velocities is unusual; normally it can be expected that the reflection velocity will be the higher because of compaction with depth. A core, 1.6 meters long, taken at station 16 consisted of red clay interlayered with graded layers of carbonate ooze. Paleontological study of the cores (Robert Hurley, personal communication) disclosed that individual graded layers of carbonate ooze consisted of mixtures of materials from Miocene to Recent, suggesting that they represent individual flows of material from higher up the slope of the ridge. This mixing would be sufficient explanation of the identity of the vertical and horizontal velocities.

The 4.1 km/sec velocity matches the apparent velocities of the second layer at both 15- and 16-north. Within the accuracy of the data, the second layer can be fitted to either the intercept on 16-north or the reverse point on 17-north, but not to both. Reflections from this horizon are present but not well defined on 16-south. Probably, the first layer varies in thickness in the first few kilometers south of station 16.

On the outer portion of 16-south arrivals with apparent velocities of 6.4 and 7.8 km/sec are observed, with larger scatter than on the preceding profiles.

Station 17—Station 17 is half-way up the slope between the Hawaiian Deep and the edge of Gardner Bank. There were abrupt changes of depth and slope in the shooting run, and even changes of over 400 meters at the receiving ship during the run. The topography along this line appears as a series of sloping steps. Because of numerous side reflections, the depths obtained from the fathometer are ambiguous, and the fathometer depths often disagree with the depths obtained from the bottom reflections of the shots as recorded at the shooting ship. Some of the corrected arrival times are, therefore, to an accuracy no better than 0.2 second. A group of shots in the center of 17-north gave weak and dubious first arrivals followed by stronger arrivals slightly later, shown on the travel time plots by a bar rather than a circle. While these may be due to the usual difficulties of reading the beginning on a weak record, they might be due to the arrival of the refracted wave by more than one path with differing water delay corrections applicable. In the interpretation the later arrivals have been used, as they give the better agreement with other data.

Station 17-north shows the same four layers. The deepest, with apparent velocity 8.8 km/sec, is determined by six scattered points, and has been drawn to match the reverse time from 16-south and the observed points, which it does without forcing. The crustal layer, with apparent velocity 6.9 km/sec, appears as a first arrival in the zone in which water delay corrections are doubtful, and has been drawn to fit the reverse time and the best observed points. There is no evidence for a layer with velocity near 5½ km/sec; layers with apparent velocities of 4.6 and 3.3 km/sec are well determined.

Station 17-south presents more difficulty of interpretation. Layers with apparent velocities of 3.6, 4.7, and 8.3 km/sec are observed with reasonable fits of intercepts and reverse times; to force agreement with the stations on either side a line with apparent velocity 6.8 km/sec has been introduced as a masked layer fitting two second arrivals and the reverse time of 18-north. The last two points on the 8.3 km/sec line are weak and late; the agreement of reverse points on this line is poor. There are five points that could be interpreted as lying on a line with velocity 5.3 km/sec.

Station 18—Station 18 was an anchor position in 35 meters of water, one-half kilometer inside the edge of the flat portion of Gardner Bank. Profile 18-north is over the same rough bottom as 17-south. Profile 18-south is in water that varies only between 29 and 38 meters over the entire length of the run. The hydrophone was on bottom, and when retrieved carried small amounts of mud. All shots on 18-south were either on bottom or so close to it that water delay corrections were less than 0.01 second.

Profile 18-north has four layers. The mantle apparent velocity of 8.6 km/sec is determined by five shots. Layers with apparent velocity of 7.0 and 4.7 km/sec are well determined; there are small wobbles on the latter line, probably due to variations in the amount of sediment fill. Sediment velocity, not well determined, is near 2.6 km/sec.

On 18-south, across the flat bank, there are two well-defined lines with apparent velocities of 4.6 and 6.8 km/sec. In addition there are scattered second arrivals through which a line has been drawn on the flimsiest of evidence to fit the reverse point from 19-north and give a layer velocity of 8.2 km/sec. The agreement of intercept times between 18-north and 18-south is extremely poor; the greatest mismatch is on the crustal arrival, with an intercept time of 2.79 seconds on the north profile and 1.16 seconds on the south. This difference cannot be reconciled by any method of drawing lines on the travel-time plot, and must represent some structural change near station 18. A zone of late arrivals about 20 km (13 seconds) south of station 18 could be interpreted as showing a rapid rise, except that no such delay is found in shots at the same location recorded at 19. The shots showing the delay at 18 were generally weak, and the delays were probably caused by failure to detect a weak first arrival preceding a strong second arrival. Only a single shot appears on a sediment-velocity line. A few second arrivals can be interpreted as showing a velocity of 5.0 km/sec.

Station 19—The profile from 18 to 19 passed west of the pinnacle rocks at 15 km range, and station 19 was an anchor location on the southern edge of the flat in 29 meters of water. Extremely strong tidal currents were experienced, and the three hydrophones were probably lifted slightly off bottom by the current.

First arrivals give four layers with apparent velocities of 7.2, 4.7, and 2.6 km/sec on profile 19-north; all have good reverse fits with 18-south. Profile 19-south was two kilometers long, and confirmed the 2.6 km/sec sediment velocity. A velocity of 8.5 km/sec appears on 19-north as a strong second arrival on six shots.

ANALYSIS

Because "reversed profiles" are never truly reversed on all velocity segments, the details of structure and velocities obtained depend in part on the form of solution used and the assumptions made when treating a set of end-to-end profiles such as these. There are real changes of velocity in the upper layers along the line of shooting; there are changes in the computed velocities for the lower layers that may be either real or artifacts. As a result, strict adherence to standard computational methods for these lines either as "split" or reversed profiles can result in abrupt changes in layer depth that are due more to the form of computation than to the geology. The stations have, therefore, been analyzed in several different ways to see how many of the finer details of structure are due to the assumptions involved in any computational system. The structure sections given in figure 4 represent the results of analysis using the method of Ewing, Woollard, and Vine (1939) applied to each reversed pair of profiles independently in fig. 4(a) and then to the shallower layers as split profiles in fig. 4(b). Some gross mismatches in velocity and depth are apparent, due to inadequacy of the assumption of plane layers. A smoothed section correcting for the mismatching and using split profiles for the shallower layers near the stations is shown in figure 5.

The mismatches in depths and velocities at stations 16 and 17 are no greater than normal, and have been smoothed out in figure 5. The discrepancy in the intercept times for the crust arrival at station 18 is abnormally large; it can be explained in several ways, none of which is very satisfactory. One approach is to consider that there is present a fault or extremely steep dip just north or just south of the station. If the fault lies just south of the station, the delay time for 18-south should be the same as that for 18-north, which would then put the 7.0 km/sec layer at the sea floor on Gardner Bank and require the presence of a similar steep slope close in to station 19. Such a steep dip should cause greatly delayed crustal arrivals on the farthest shots of 18-south and 19-north. These shots are close to the crossover distance for the crust and mantle arrivals, and if the Mohorovičić discontinuity stays at approximately constant depth across the zone of crustal thinning, the first arrival would become a mantle arrival and a delay in the crustal arrival would not be noticed. This, then, remains a possibility and one can blame the discrepancy on an unfortunate choice of location for stations 18 and 19. This interpretation was used in a preliminary report on these stations (Shor, 1958).

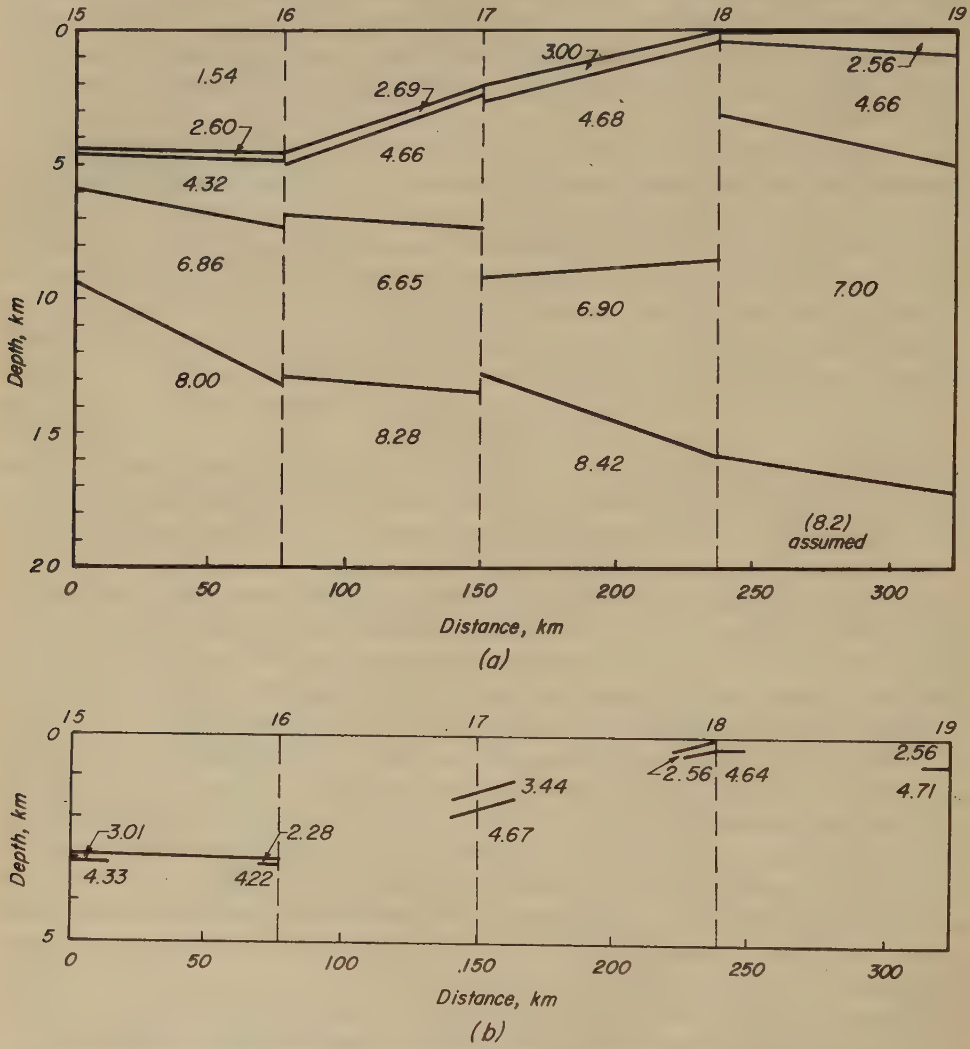

Fig. 4. Layer solutions, assuming plane layers: (a) As reversed profiles (b) As split profiles.

If a zone of steep dip lies just north of station 18 it would have to lie within the first 15 km. The delay time of the crustal arrival at 18 would be small, the top of the crust would be several kilometers deeper between stations 17 and 18, and a similar steep dip would have to be introduced close to station 17. This would make the crust extremely thin between 17 and 18.

A third interpretation could be based on the assumption that the 7.0 km/sec material observed on Gardner Bank is either a separated body lying within the 4.7 km/sec volcanics, or the remains of a central neck of high velocity material which has vertical or overhanging side boundaries. Such an interpretation, while admittedly special, is the only consistent one. It would eliminate the discrepancies in arrival times and give the structure shown in figure 5. A determination of the detailed structure would require further field work.

The presence of another layer with velocity near 5½ km/sec is suggested by some of the profiles (i.e., 16-north, 17-south, and 18-south). Such arrivals are indicated by dotted lines on figure 3. These arrivals cannot be found consistently and therefore cannot be used in a layer solution without an excessive number of assumptions. The inclusion of such a layer in the solution will not change the deep structure appreciably. Such a 5½ km/sec layer at depth was generally observed by Raitt (1954) at Bikini and Eniwetok.

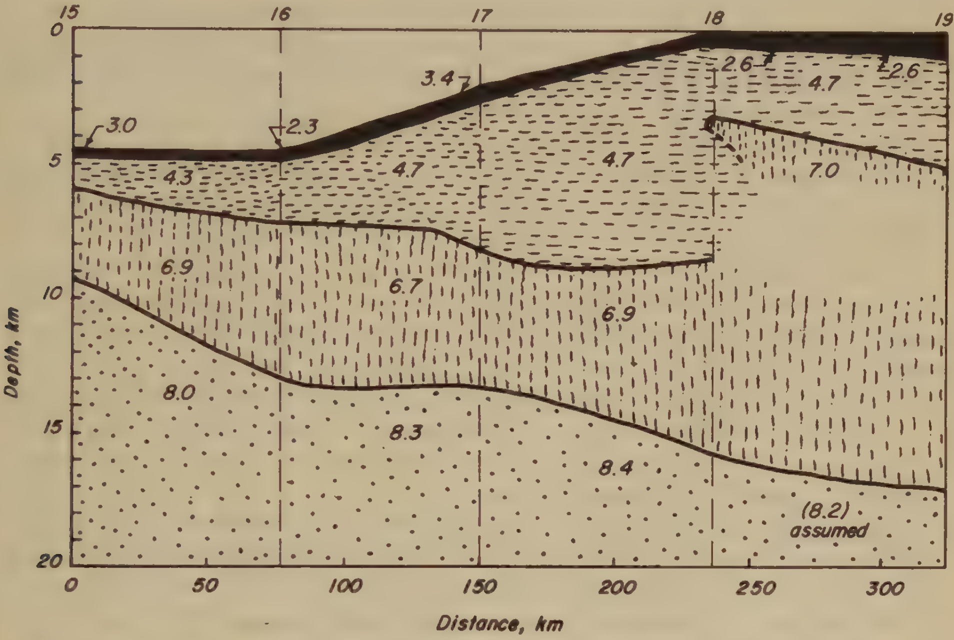

Fig. 5. Structural section, derived from Fig. 4. Velocities in kilometers per second.

INTERPRETATION

Seven major features of the structure, not dependent upon the form of interpretation, are:

1. A consistent set of layers can be carried through from one end of the profile to the other.

2. The Mohorovičić discontinuity is depressed to about 17 km below sea level beneath the ridge; this could represent either complete or partial isostatic compensation of the weight of the ridge depending on the densities of the layers.

3. The top of the oceanic crust dips beneath the Hawaiian Deep, then rises to less than normal oceanic depth under the center of the ridge; the velocity stays close to the normal oceanic $6\frac{3}{4}$ km/sec. Such a structure has been reported at Funafuti and possibly at Nukufetau (Gaskell and Swallow, 1953).

4. The portion of the ridge protruding above the sea floor consists primarily of material with a velocity of 4.7 km/sec and possibly more material with velocity about $5\frac{1}{2}$ km/sec, which are most probably volcanics (although they could remotely be carbonates). These are similar to the velocities found at Bikini and Eniwetok by Raitt (1954), Funafuti and Nukufetau by Gaskell and Swallow (1953), and Bermuda by Officer, Ewing, and Wuenschel (1952).

5. There are rapid changes of structure near the edge of the central flat.

6. The shallowest layer has significant variations in velocity; values range from 2 to over 3 km/sec. In the Hawaiian Deep, where it could be checked, the vertical and horizontal velocities are the same, indicating lack of compaction.

7. The shallow material at the station on the archipelagic apron has a velocity of 3 km/sec, higher than normal for oceanic sediment, and has an extremely high reflection coefficient. There may be a thin (up to 20-meter) layer of very low velocity material just below the sea floor, as shown by sub-bottom reflections.

According to Hamilton (1956) the genetically related Mid-Pacific Mountains (which join the Hawaiian Ridge about 400 km east of Gardner Pinnacles) were formed by extrusion of basalts and fragmental material and possibly of solid olivine basalt from fissures on the ocean floor to a height above Cretaceous sea level; isostatic adjustment largely took place before the highest peaks emerged. After planation of the highest peaks to sea level, subsidence, possibly caused by sub-crustal movements, carried the guyots down to depths between 500 and 1100 fathoms (0.94 and 2.06 km) below present sea level.

The features found at Gardner Pinnacles agree in general with Hamilton's interpretation for the Mid-Pacific Mountains. The flanks of the ridge (and probably its major volume) consist of material with velocity 4.7 km/sec, which is appropriate for vesicular basalt and fragmental material. The central volume with velocity 7.0 km/sec could be solid basalt from the oceanic crust.

The base of the 4.7 km/sec material is depressed beneath the flank of the ridge. While there is evidence of crustal thickening between stations 15 and 16, station 15 has a thinner crust than the average for the oceans. The crustal thicknesses at stations 15, 16, and 17 are all within the normal distribution for oceanic stations. There is a great thickening of the crustal material beneath the center of the ridge, unless the 7.0 km/sec velocity material is considered to be an isolated body overlying lower velocity volcanics.

If it is assumed that the first layer under the flat portion of Gardner Bank is coral and coral debris, the top of the volcanics would to some degree accord with the shallowest level of planation found by Hamilton in the Mid-Pacific Mountains, for at the south end of the bank the volcanics lie at a depth of 0.95 km.

The Hawaiian Deep is apparent on the fathograms (fig. 2) as a slight depression at this locale although it has been previously reported (Dietz and Menard, 1953; Hamilton, 1957) only farther to the southeast. The depression of the Mohorovičić discontinuity beneath the deep as well as the ridge lends support to the theory of "isobaric equilibrium" or regional isostatic compensation as proposed for the Hawaiian Ridge by Gunn (1943), and Vening Meinesz (1934).

The most unusual feature on these profiles is the presence of crustal material at shallow depth beneath the ridge. While the present form of this material as an overhanging neck, an isolated body, or a steep-sided block can only date back to the formation of the ridge, the presence of the extra crustal material may antedate the formation of the volcanic ridge. If so, the presence of a "line of weakness" giving rise to this linear mountain range may be related to the original presence of a welt of thickened crust.

References

Dietz, R. S., and H. W. Menard
1953. "Hawaiian Swell, Deep, and Arch, and Subsidence of the Hawaiian Islands," *Jour. Geol.*, 61: 99–113.
Ewing, M., G. P. Woollard, and A. C. Vine
1939. "Geophysical Investigations in the Emerged and Submerged Atlantic Coastal Plain, Part III: Barnegat Bay, New Jersey, Section," *Bull. Geol. Soc. Am.*, 50: 257–296.
Gaskell, T. F., and J. C. Swallow
1953. "Seismic Experiments on Two Pacific Atolls," *Occasional papers of the Challenger Society*, London, No. 3.
Gunn, R.
1943. "A Quantitative Study of Isobaric Equilibrium and Gravity Anomalies in the Hawaiian Islands," *Franklin Inst. Jour.*, 236: 373–390.
Hamilton, E. L.
1956. "Sunken Islands of the Mid-Pacific Mountains," Geol. Soc. Am., *Memoir 64*.
1957. "Marine Geology of the Southern Hawaiian Ridge," *Bull. Geol. Soc. Am.*, 68: 1011–1026.
Menard, H. W.
1956. "Archipelagic Aprons," *Bull. Am. Assoc. Petroleum Geologists*, 40: 2195–2210.
Officer, C. B., M. Ewing and P. C. Wuenschel
1952. "Seismic Refraction Measurements in the Atlantic Ocean, Part IV: Bermuda, Bermuda Rise and Nares Basin," *Bull. Geol. Soc. Am.*, 63: 777–808.
Raitt, R. W.
1952. "Geophysical Measurements," *Symposium on Oceanographic Instrumentation* (National Research Council) pp. 70–84.
1954. "Seismic Refraction Studies of Bikini and Kwajalein Atolls," U. S. Geol. Survey *Prof. Paper 260-K*, pp. 507–527.
Shor, G. G., Jr.
1958. "Crustal Structure Beneath the Western Hawaiian Ridge," (abstract) *Bull. Geol. Soc. Am.*, 69: 1705.
Vening Meinesz, F. A.
1934. *Gravity expeditions at sea*, vol. 2, Netherlands Geodetic Commission, p. 205.

University of California,
Marine Physical Laboratory of the Scripps Institution of Oceanography,
San Diego 52, California.
(Contribution from the Scripps Institution of Oceanography, New Series.)

(826)

THE WAVELENGTH DEPENDENCE OF PHOTOSYNTHESIS AND THE ROLE OF ACCESSORY PIGMENTS

FRANCIS T. HAXO
Scripps Institution of Oceanography, University of California, La Jolla, California

Reprinted from

COMPARATIVE BIOCHEMISTRY OF PHOTOREACTIVE SYSTEMS

COPYRIGHT ©, 1960

ACADEMIC PRESS INC., NEW YORK, NEW YORK
pp. 339-360

PRINTED IN THE UNITED STATES OF AMERICA

(827)

21

The Wavelength Dependence of Photosynthesis and the Rôle of Accessory Pigments

Francis T. Haxo

Scripps Institution of Oceanography, University of California, La Jolla, California

Introduction

Interest in the function of pigments accompanying chlorophyll in diversely-colored algae arose largely from efforts of botanists at the turn of the last century to interpret the vertical distribution of marine algae in reference to the available submarine light field. The well-known experiments of Engelmann (1882a, 1883, 1884) provided evidence that light absorbed by the masking pigments of brown algae, diatoms, red algae, and blue-green algae was available for photosynthesis, in addition to chlorophyll-absorbed light energy. In his view, these pigments represented evolutionary adaptations by which optical windows in the visible absorption spectrum of chlorophyll were effectively closed. For example, the presence of phycoerythrin in deep-growing red algae was interpreted as an adaptation permitting more effective absorption and utilization of the prevailing blue and green light. This interpretation met with an opposing view. Oltmanns and others argued that the observed vertical distribution of algae did not involve chromatic adaptation but rather a response to the prevailing light intensity gradient. In the modern view, the color and the intensity of light, as well as many other environmental factors, are recognized as interacting in complex ways to control the vertical distribution of algae.

Nevertheless, the essential premise upon which Engelmann's theory of complementary color adaptation was based proved correct. Rigorous investigations by more refined techniques over the past 20 years have confirmed his conclusion that fucoxanthin of diatoms (Dutton and Manning, 1941; Wassink and Kersten, 1946; Tanada, 1951) and of brown algae (Haxo and Blinks, 1950), phycocyanin of Cyanophyta (Emerson and Lewis, 1942), and phycoerythrin of the Rhodophyta (Haxo and Blinks, 1950) absorb light effectively for photosynthesis. Other studies have revealed something about the mechanism of accessory pigment participation in photosynthesis. Investigations by Dutton *et al.* (1943)

Contributions from the Scripps Institution of Oceanography, New Series, 1200

(829)

Reproduced by Permission

and by Wassink and Kersten (1944) on diatoms, by French and Young (1952) on red algae, and by Duysens (1952) on red and blue-green algae have shown that quanta absorbed by the dominant accessory pigments of these algae are able to excite chlorophyll fluorescence. Thus, a consistent and widely accepted picture seemed to emerge—the so-called energy transfer hypothesis—that accessory pigments function in photosynthesis only insofar as they are able to transfer the absorbed energy to chlorophyll *a*.

Indications of an additional role of accessory pigments have come from the recent studies conducted by Emerson and his co-workers* on the long-wavelength limit of photosynthesis in green algae and in red algae. These led to the important discovery that light absorbed by accessory pigments (for example chlorophyll *b*, in the case of *Chlorella*, and phycoerythrin, in the case of *Porphyridium*) improves the efficiency with which far-red light is used in photosynthesis. Thus, it would appear now that accessory pigments do something more than extend the absorption range of chlorophyll *a;* rather, they may be essential for its efficient operation.

The present paper will survey what is currently known concerning the wavelength dependence of photosynthesis in plants (other than the bacteria) representing the major types of pigment combinations. For additional discussions of various aspects of this problem, reference is made to the following reviewers: Rabinowitch (1945, 1951, 1956); Blinks (1954, 1955); French and Young (1956); Duysens (1956); Emerson (1958); and Haxo (1960).

A few comments should be made concerning the experimental methods employed to determine the photosynthetic activity of a given pigment and the limitations in interpreting these results. Two approaches have been used. Emerson and his collaborators have favored determinations of quantum yield as a function of wavelength, measured manometrically on partially or completely absorbing cell suspensions. Depressions in yield are indicative of inactive absorption by a given pigment or absorption by a less efficient pigment. The advantages of this method are: (*1*) errors in cell absorption measurements are minimized, particularly when totally absorbing suspensions are used; (*2*) quantitative information is obtained on pigment activity.

As a second approach, photosynthetic action spectra have been determined on partially absorbing thalli, using the polarographic technique for dissolved oxygen. The activity curves for photosynthetic oxygen production when plotted against thallus absorption provide, by the degree of correspondence and divergence of the superimposed curves, information on the relative activities of the individual pigments. The original design of the polarographic reaction vessel, which we owe largely to L. R. Blinks and C. M. Lewis (cf. Haxo and Blinks, 1950) has recently been modified by the present reviewer (Haxo, unpublished) to accommodate thin cell suspensions over a recessed, horizontal electrode, making possible comparative studies on a wide variety of unicellular algae. The advantages of the polarographic technique, as used by these workers, are the rapidity with which action spectra may be determined and the small size of the plant sample required. Its disadvantages are: (*1*) information is provided on the relative rates of photosynthesis only; (*2*) rates of respiration cannot be measured conveniently.

---

* See Emerson *et al.* (1956, 1957) and Emerson and Chalmers (1958).

Perhaps the most serious limitation in interpreting the photosynthetic activity of pigments follows from the difficulties in measuring the absorption spectra of individual plastid pigments in the living cells. Estimates of fractional absorption by component pigments have of necessity been reconstructed from measurements on extracts. This method has not proved entirely satisfactory because the extent to which pigment absorption *in vivo* is distorted by wavelength displacement and geometrical flattening can be estimated only approximately. Direct *in vivo* measurements of the absorption spectra of chlorophylls and other pigments (French, 1958) will doubtless prove helpful in this regard.

Plants Containing Chlorophyll *a*, Chlorophyll *b*, and Conventional Carotenoids (Chlorophyceae, Euglenophyceae, and Higher Plants)

We will first of all consider action spectra for typical grass-green colored plants. The Chlorophyta and the euglenids resemble higher plants most closely in pigment composition, containing chlorophyll *a* and chlorophyll *b*, β-carotene, and one or more xanthophylls. Spectral assimilation curves for the typical green-colored representatives of both algal groups, as determined by Engelmann, indicated that in gross features photosynthetic effectiveness follows the combined absorption curves of the chlorophylls.

This situation is seen clearly from the manometric studies of Emerson and Lewis (1943) on *Chlorella* (Fig. 1). Two additional features were noted. A decline in photosynthetic efficiency was observed beyond the chlorophyll *a* peak in the red, an effect which was originally unexplained other than to suggest that the energy of far-red quanta may be too low to activate the chlorophyll molecule for participation in subsequent dark reactions. We will return later to Emerson's recent interpretation of the long-wavelength decline in photosynthesis in *Chlorella* and other algae. A second feature is the divergence in the absorption and activity curves between 440 and 560 mμ, where carotenoids absorb. Duysens (1952) has estimated that 40–50% of the light absorbed by carotenoids is available for photosynthesis, although the exact extent to which these pigments are active remains uncertain (Emerson, 1958). The ubiquitous occurrence of carotenoids in the photosynthetic apparatus of plants suggests that they may play an important role other than that of trapping

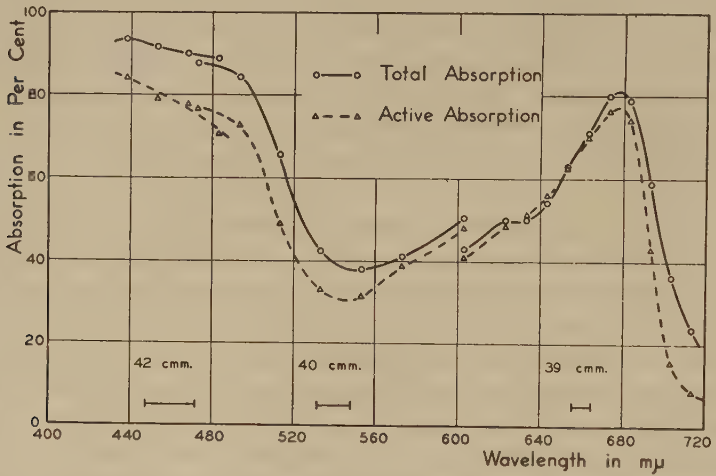

FIG. 1. Cell absorption and photosynthetic activity in *Chlorella* (Emerson and Lewis, 1943).

light for photosynthesis. This may be that of conferring protection against chlorophyll-catalyzed photo-oxidations, as suggested by the studies on the physiological effects of carotenoid deficiencies in photosynthetic bacteria (Sistrom *et al.*, 1956; Cohen-Bazire and Stanier, 1958; Stanier, 1958) and in *Chlorella* (Claes, 1954; Kandler and Schötz, 1956).

Using polarographic techniques, photosynthetic action spectra similar to those from manometric studies were obtained by Haxo and Blinks (1950) for the blade-type marine alga *Ulva* and more recently by Haxo (unpublished) for *Chlorella*. The latter results are presented in Fig. 2 and are of some interest since the photosynthetic action spectra obtained by the two methods are in substantial agreement.

In both Chlorophyta and Euglenophyta, representatives occur in which chlorophyll is masked by an abundance of extra-plastid carotenoids, most frequently either β-carotene or astaxanthin (Goodwin and Jamikorn, 1954). Engelmann (1882b) recognized that masking pigments of the so-called hematochrome-type, as found in *Haematococcus* and *Trentepohlia* (*Chroolepus*) reduce the amount of light available for photosynthesis. This situation has been clearly substantiated by quantitative studies of Yocum and Blinks (1954) for the red phases of *Haematococcus, Trentepohlia,* and *Dunaliella.* In *Trentepohlia* the masking effect of extra-plastid carotenoids is sufficiently great to suppress photosynthesis in blue light almost completely.

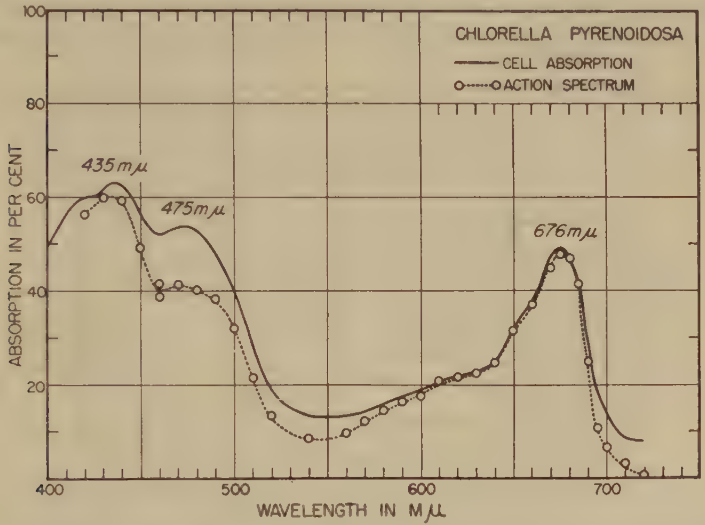

FIG. 2. Absorption and photosynthetic action spectra of *Chlorella pyrenoidosa* determined polarographically (Haxo, unpublished).

Only very limited data are available on the wavelength dependence of photosynthesis in higher plants. The action spectrum determined by Hoover (1937) for wheat plants in general resembles that of green algae. Differences may be attributed to the greater thickness and complexity of the tissue. This is further suggested by the fact that the action spectrum for the Hill reaction in isolated spinach chloroplasts is very similar to the action spectra for photosynthesis in *Chlorella* and in *Ulva* (Chen, 1952). We may refer here also to unpublished studies by M. Hommersand in the author's laboratory on the thin-leafed aquatic phanerogam *Elodea densa,* the detailed photosynthetic spectrum of which is almost an exact duplicate of the reported for *Ulva.*

Algae in Which Chlorophyll *a* Is Accompanied by Chlorophyll *c* and a Photosynthetically Efficient Carotenoid, Either Fucoxanthin or Peridinin (*Phaeophyceae, Bacillariophyceae,* and *Dinophyceae*)

In plant life in the ocean doubtless the two most abundant carotenoids are the polyoxy xanthophylls, fucoxanthin and peridinin. The former is characteristic of the diatoms and brown algae, the latter of dinoflagellates. Both pigments contribute strongly to cell absorption in the blue-green to green portion of the spectrum, and both occur within the plastid in company with chlorophylls *a* and *c* and other carotenoids. Evidence for fucoxanthin-sensitized photosynthesis in diatoms has come from the investigations of Dutton and Manning (1941), Wassink and Kersten (1946), and Tanada (1951). Tanada's study of quantum yield as a function of wavelength in *Navicula minima* provides the most detailed assessment of this situation (Fig. 3). Since the quantum yield was found to be practically constant (about 0.11) from 680 down to 530 mμ, where about 85% of the absorbed light could be attributed to fucoxanthin, Tanada concluded that this carotenoid was about as effective as the chlorophylls in sensitizing photosynthesis. Other carotenoids appeared to be inactive in this respect.

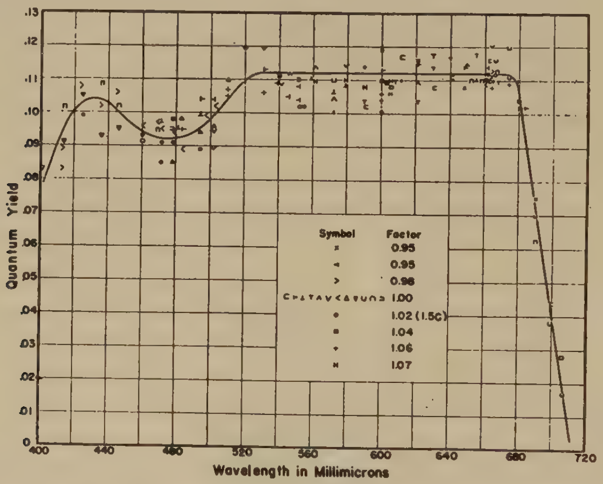

FIG. 3. Quantum yield of photosynthesis as a function of wavelength for *Navicula minima* (Tanada, 1951).

Studies by a number of workers using broad band-pass filters, in particular those of Montfort (1940) and Levring (1947), have all pointed to a high photosynthetic activity for fucoxanthin in brown algae as well. The more detailed study by Haxo and Blinks (1950) in the thin-bladed marine alga *Coilodesme* suggests this also, since the curves for photosynthetic activity and thallus absorption deviate only slightly in the region of strong fucoxanthin absorption (Fig. 4).

The dinoflagellates are of particular interest since they, together with the diatoms, constitute wide-spread and dominant components of marine phytoplankton populations. The recent study by Haxo (1959) provides evidence for believing that the function of peridinin in the photosynthesis of dinoflagellates is analogous to that of fucoxanthin in diatoms and brown algae. In *Gonyaulax polyedra* (Fig. 5), cell absorption and photosynthetic activity curves were found to be reasonably parallel in the region 520–560 mμ, where about 80% of the absorbed light could be attributed to peridinin. Other carotenoids appeared less active, as shown by the divergence between ca. 500 and 460 mμ. The marked decline in photosynthetic activity below 435 mμ was ascribed to inactive absorption by a pale yellow pigment which contributes most strongly to cell absorption in the near-ultraviolet.

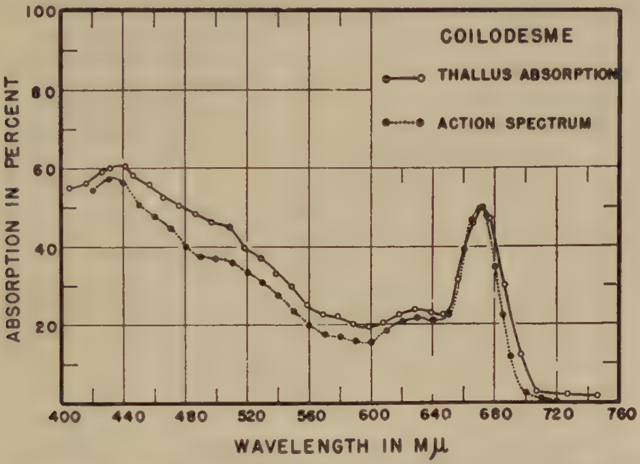

FIG. 4. Absorption and photosynthetic action spectra of the brown alga *Coilodesme californica* (Haxo and Blinks, 1950).

Algae in Which Phycobilins Accompany Chlorophyll *a* Alone or Possibly with Chlorophyll *d* (Principally Rhodophyta and Cyanophyta)

The red and blue-green algae have long attracted interest because of their abundant content of the red and blue chromoproteins, the phycoerythrins and the phycocyanins. In these algae, the presence of three phycoerythrins (R-, C-, and B-) and three phycocyanins (R-, C-, and allo-) has been established (cf. Haxo and ÓhEocha, 1960). All of these pigments with the exception of allophycocyanin, which has not been adequately studied from this viewpoint, have been shown to absorb light actively for photosynthesis.

The photosynthetic action spectrum reported by Haxo and Blinks (1950) for *Porphyra nereocystis* (Fig. 6) is typical of the results obtained by these workers for marine red algae containing predominantly R-phycoerythrin. The marked parallelism observable in the middle of the spectrum between photosynthetic activity and phycoerythrin absorption provides clear evidence of an accessory function of this pigment in confirmation of the conclusion reached by most earlier investigators of this problem.

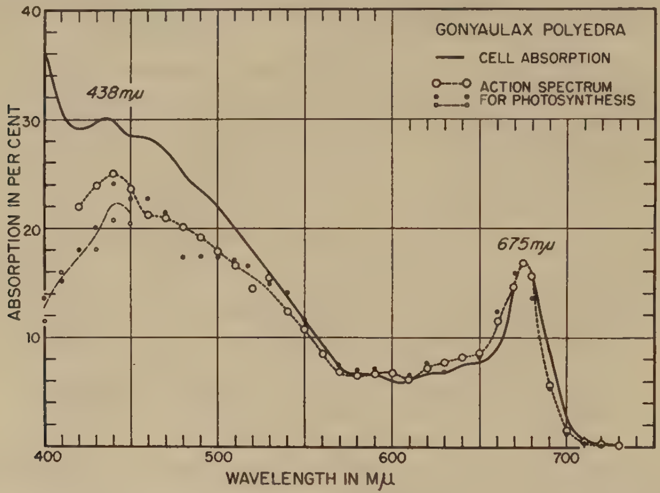

Fig. 5. Absorption and photosynthetic action spectra for the dinoflagellate *Gonyaulax polyedra* (Haxo, unpublished).

The marked depression in activity at both ends of the spectrum where absorption by chlorophyll *a* is high indicated a much lower effectiveness for light absorbed directly by chlorophyll. This situation was observed in all of the red algae studied by these workers and, with the additional studies of Yocum and Blinks (1954) and of Duysens (1952), led to the concept that a portion of the chlorophyll *a* in red algae exists in a physiologically inactive condition. This will be discussed subsequently in the light of Emerson's findings on the long-wavelength dependence of photosynthesis.

In general, these studies showed a low effectiveness for the carotenoids of most red algae, for example, *Porphyra* spp. and *Porphyridium* *cruentum*. However, a more detailed study of the deep-growing red algae may reveal a more active role for these pigments. This is suggested by the action spectra of *Myriogramme* and *Schizymenia* (Haxo and Blinks, 1950), which show a persistent parallelism between absorption and photosynthetic activity in the region 480–500 mu, where carotenoids may be expected to contribute significantly to thallus absorption.

The photosynthetic effectiveness of B-phycoerythrin which was later isolated in the pure form from *Porphyra naiadum* by Airth and Blinks (1956) was also demonstrated by Haxo and Blinks (1950). B-Phycoerythrin is very likely identical to the phycoerythrin present in the unicellular red alga *Porphyridium cruentum*, which has also been shown to be effective in photosynthesis (Duysens, 1952; Haxo and Norris, 1953). Duysens' studies of photosynthesis in *Porphyridium* are of particular interest since they were combined with quantitative estimates of absorption by component pigments (Fig. 7). Also included are points for the effectiveness spectrum for chlorophyll *a* excitation as determined by French and Young (1952). The latter agrees well with that of photosynthesis and of phycoerythrin absorption and indicates some of the evidence for the hypothesis that energy is transferred from accessory pigments to chlorophyll *a*.

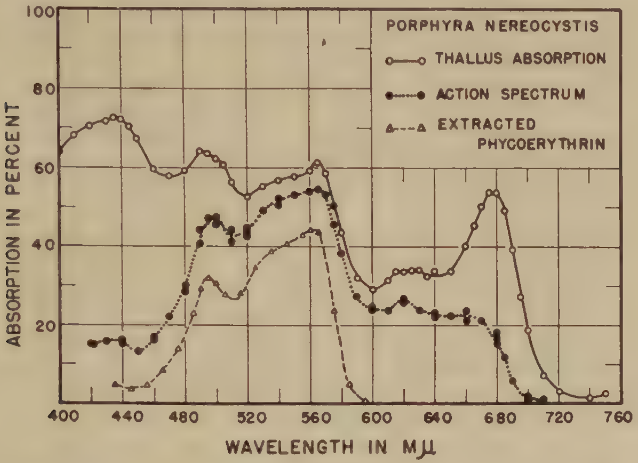

FIG. 6. Absorption and photosynthetic action spectra for the red alga *Porphyra nereocystis* (Haxo and Blinks, 1950).

A high photosynthetic activity for C-phycoerythrin (*in vivo* maximum at 565–570 mμ of blue-green algae was shown by an action spectrum analysis of the bright red filaments of *Phormidium ectocarpi* [(Fig.

8); Haxo and Norris, 1953] and this situation has been confirmed by these workers in unpublished studies of two other species of *Phormidium* (*P. fragile* and *P. persicinum*).

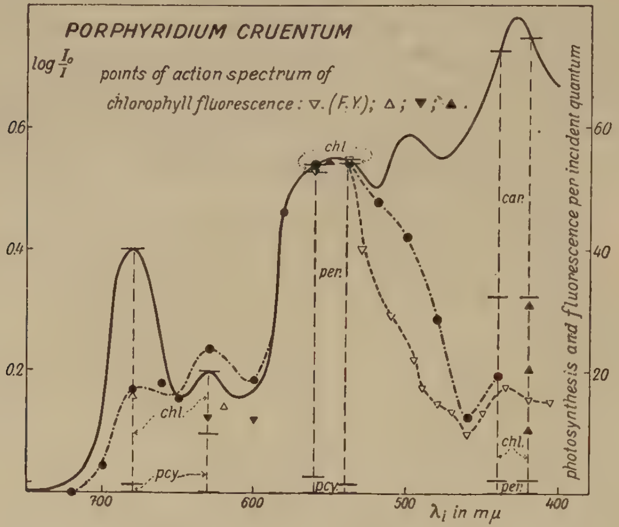

FIG. 7. Absorption spectrum (●—●), action spectrum for photosynthesis (●–·–●), and action spectrum for chlorophyll fluorescence (△------△) of the red alga *Porphyridium cruentum* (Duysens, 1952). The detailed fluorescence action spectrum is from French and Young (1952).

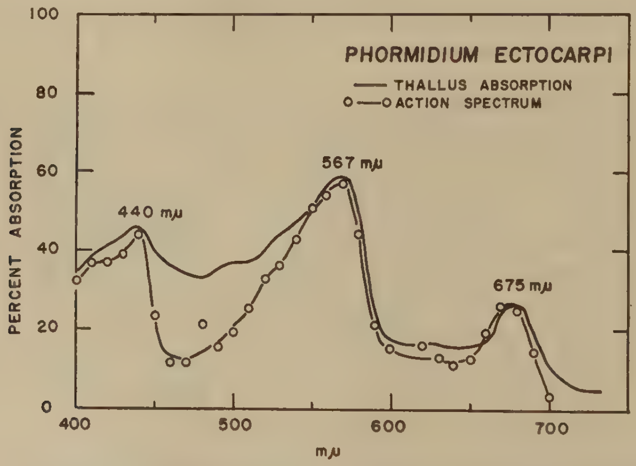

FIG. 8. Absorption and photosynthetic action spectra for the blue-green alga *Phormidium ectocarpi* (Haxo and Norris, 1953). The pronounced absorption peak at 567 mμ is attributable to C-phycoerythrin.

Rigorous assessment of the photosynthetic effectiveness of C-phycocyanin was first made by Emerson and Lewis (1942) in the case of the unicellular blue-green *Chroococcus*. The quantum yield of photosynthesis was found to be consistently high (about 0.08) throughout the region of strong phycocyanin absorption and to be equal to that of light absorbed directly by chlorophyll. Carotenoids, on the other hand, were found to be virtually inactive. The data of these workers for action spectra of partially absorbing suspensions are shown in Fig. 9.

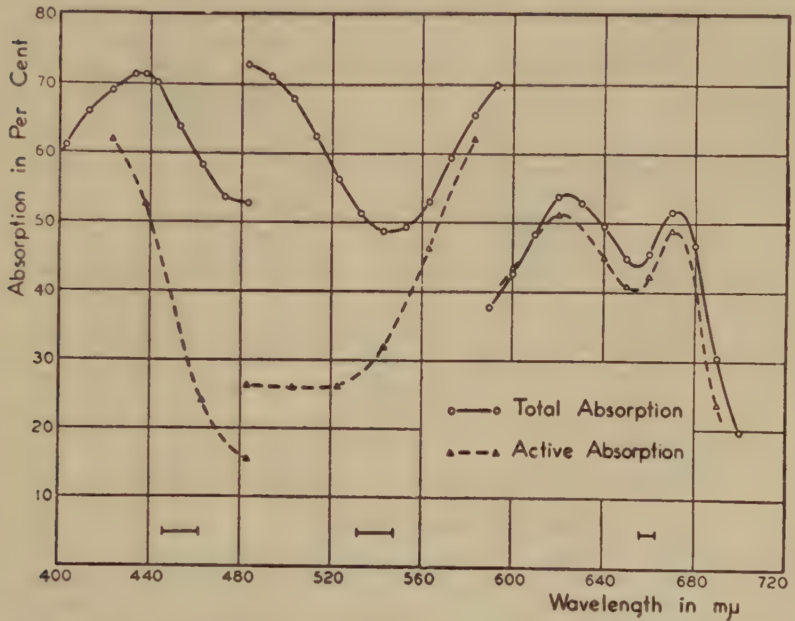

FIG. 9. Cell absorption and action spectra for photosynthesis in *Chroococcus*. Cell suspensions of different densities were used in the red, green, and blue regions of the spectrum (Emerson and Lewis, 1942).

Other phycocyanin-rich Cyanophyta, e.g., *Oscillatoria, Lyngbya, Anabaena,* and *Synechococcus,* resemble *Chroococcus* in containing a highly active phycocyanin but differ in showing appreciable (about one-half) inactive absorption by chlorophyll *a* (Haxo and Blinks, 1950; Duysens, 1952). A similar situation has been observed for C-phycocyanin in red algae, as shown in Fig. 10 for *Porphyridium aerugineum* (Haxo, unpublished), which lacks phycoerythrin.

Haxo and Allen (unpublished) have recently determined the photosynthetic action spectrum of the so-called "acid *Chlorella,*" *Cyanidium caldarium,* which, although showing morphological affinities to the green algae, resembles the blue-green algae in containing C-phycocyanin and chlorophyll *a* alone (Allen, 1959). Their data are shown in Fig. 11. The results are entirely comparable to those reported for most red and blue-green algae in that light absorbed directly by chlorophyll is inefficiently utilized.

No algae are known to contain R-phycocyanin as an exclusive phycobilin. However, this pigment occurs in abundance in the "green" thalli of the red alga *Porphyra perforata* and the corresponding broadening of the photosynthetic activity curve toward the orange-red part of the spectrum confirms its photosynthetic effectiveness (Haxo and Blinks, 1950).

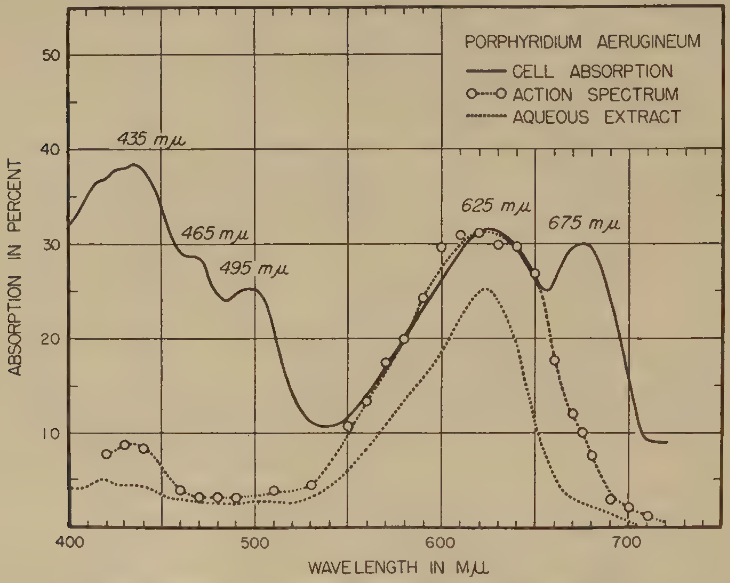

FIG. 10. Cell absorption and photosynthetic action spectra of the red alga *Porphyridium aerugineum*, which contains C-phycocyanin as its principal accessory pigment (Haxo, unpublished).

Algae in Which Chlorophyll *a* Is Accompanied by Chlorophyll *c* and by Phycobilins (Cryptophyceae)

The diversity in plastid pigmentation among photosynthetic members of the Cryptophyceae has long been noted. Indeed, this may be quite as great as that encountered in the Rhodophyta and the Cyanophyta. That this group of algal flagellates might contain water soluble pigments of the phycobilin type was only alluded to in the earlier literature (Geitler, 1924). Very recently investigations by Allen *et al.* (1959), by

Ó hEocha and Rafferty (1959), and by Haxo and Fork (1959) have all indicated that pigments of the phycoerythrin and phycocyanin type occur in the plastids of cryptomonads. Of additional interest is the fact that chlorophyll *c* appears to be a consistent component of the plastid pigments, in company with chlorophyll *a* and phycobilins. The presence of this accessory chlorophyll was suggested by the *in vivo* derivative spectra of *Cryptomonas ovata* as determined by French and Elliott (1958) and was established by isolation of the pure pigments from *Cryptomonas ovata, Rhodomonas lens,* and *Hemiselmis virescens* (Haxo and Fork, 1959). Thus, by contrast to the red and blue-green algae, the accessory pigment systems of cryptomonads are unusual in their content of both phycobilins and a second chlorophyll.

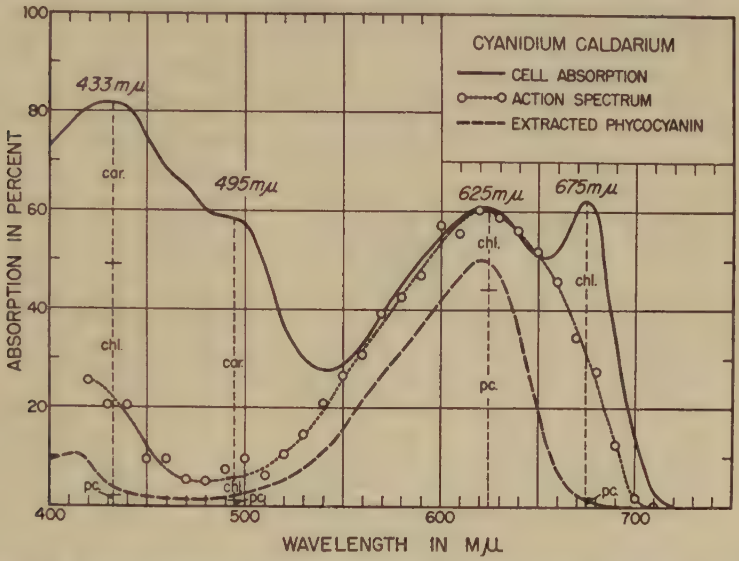

FIG. 11. Action spectrum for photosynthesis of *Cyanidium caldarium* compared with absorption spectra of intact cells and extracted C-phycocyanin. The relative contributions to cell absorption by chlorophyll *a* (chl.), phycocyanin (pc.) and by carotenoids (car.) are indicated by bars along the broken vertical lines (Haxo and Allen, unpublished).

The photosynthetic action spectra of *Rhodomonas* sp. (Haxo and Fork, 1959), a red-colored marine flagellate, and *Hemiselmis* (Haxo and Belser, unpublished), a blue flagellate, are therefore of some interest. Figures 12 and 13 both reveal that the phycobilins of these cryptomonads absorb light actively in photosynthesis and that light absorbed directly by chlorophyll *a* is by and large more active than in the red and blue-green algae, a situation which may be due to the presence of chlorophyll *c.*

The Emerson Effect (Photosynthetic Enhancement)

Having thus surveyed the wavelength dependence of photosynthesis in plants representing the major pigment combinations, we may return to an unusual feature revealed by these studies. This is the paradoxical situation observed in red algae and in most blue-green algae that light absorbed directly by chlorophyll *a* at the ends of the spectrum is utilized in photosynthesis less efficiently than light absorbed by accessory phycobilins (Haxo and Blinks, 1950; Duysens, 1952; Yocum and Blinks, 1954). With the demonstration by French and Young (1952) and by Duysens (1952) that an efficient energy transfer takes place between phycoerythrin and chlorophyll *a*, this situation seemed to receive adequate explanation from the postulate (Duysens, 1952; Yocum and Blinks, 1954) that two kinds of chlorophyll occur in red algae, one photosynthetically active and fluorescent, the other photosynthetically inactive and nonfluorescent, and, according to this postulate, phycoerythrin-absorbed light would be selectively transferred to active chlorophyll *a*.

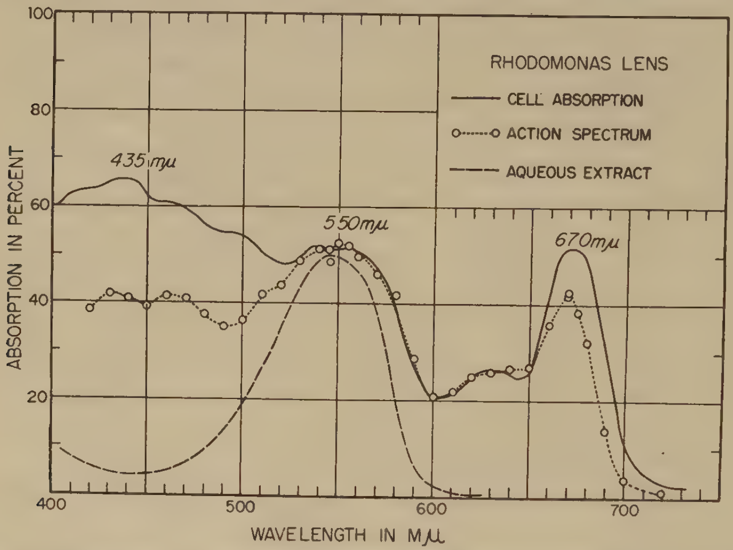

FIG. 12. Comparison of the action spectrum for photosynthesis in the red cryptomonad *Rhodomonas lens* with the absorption spectra of intact cells and extracted phycoerythrin. Chlorophyll *a*, chlorophyll *c*, and carotenoids also contribute to cell absorption (Haxo and Fork, 1959).

The recent studies of Emerson and his co-workers (1956–1958) on the effects of temperature and supplementary light on the long-wavelength limit of photosynthesis in variously colored algae reveal a new role for accessory pigments and have an important bearing on the problem of "inactive chlorophyll." In *Chlorella pyrenoidosa* and in *Porphyridium cruentum,* the far-red limit of photosynthesis could be extended to longer wavelengths by lowering the temperature from 20°C to 5°C. The data of Emerson *et al.* (1957) for *Chlorella* are shown in

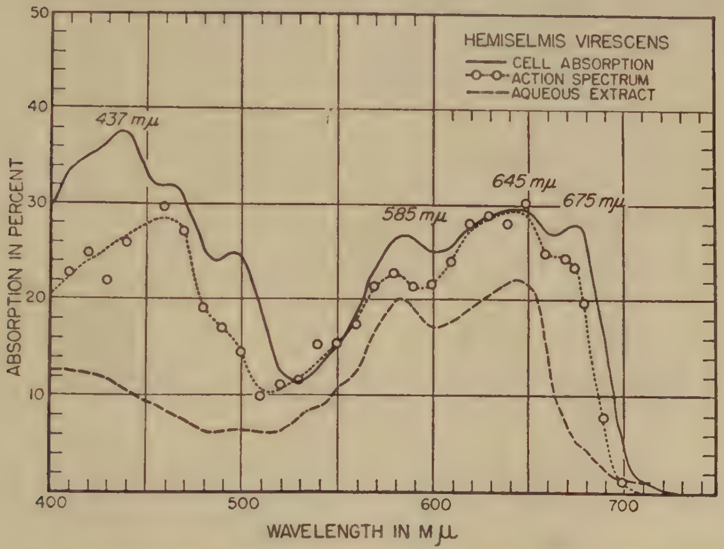

FIG. 13. Absorption and action spectra of the blue cryptomonad *Hemiselmis virescens.* The pigment of the aqueous extract is an aberrant phycocyanin (Haxo and Belser, unpublished).

Fig. 14. Even more striking results were obtained in *Porphyridium,* the range of full photosynthetic efficiency being extended from 650 to 670 mμ, which fell well within the red absorption band of chlorophyll *a.* This finding would seem to argue against the supposition that chlorophyll of red algae (and blue-green algae) has a uniquely lower efficiency than that of green algae, and this is supported by the recent quantum yield studies of Brody (1958) on *Porphyridium* in a region of the spectrum (644 mμ) where phycobilins and chlorophyll contribute about equally to cell absorption.

Supplementary light served to extend the high quantum yields in both red and green algae to even longer wavelengths than was possible with lowered temperatures. For *Porphyridium,* full photosynthetic effectiveness was extended to about 700 mμ (Brody, 1958) and to about the same wavelength for *Chlorella* (Fig. 14). Full efficiency could thus be obtained throughout almost the entire red absorption band of chlorophyll *a* in both groups of algae. Studies on the effectiveness of various wavelengths in improving the yield of photosynthesis in a band of far-red light (690 mμ and longer) in these and other algae suggested that enhancement follows the absorption spectrum of the characteristic accessory pigment(s) present (Emerson *et al.*, 1957; Emerson and Chalmers, 1958; Emerson, 1958a). In *Chlorella,* peaks of effectiveness were found at 480 and 655 mμ, giving a curve resembling chlorophyll *b* absorption; whereas in *Porphyridium* the action spectrum showed a single peak at the 546 mμ mercury line, in accordance with absorption by phycoerythrin (Fig. 15). For the diatom *Navicula,* peak effectiveness was at about 540 mμ and a second smaller maximum occurred at about 645 mμ, suggesting activity for both fucoxanthin and chlorophyll *c*. For the blue-green alga *Anacystis,* maximum effectiveness was at about 600 mμ, implicating C-phycocyanin.

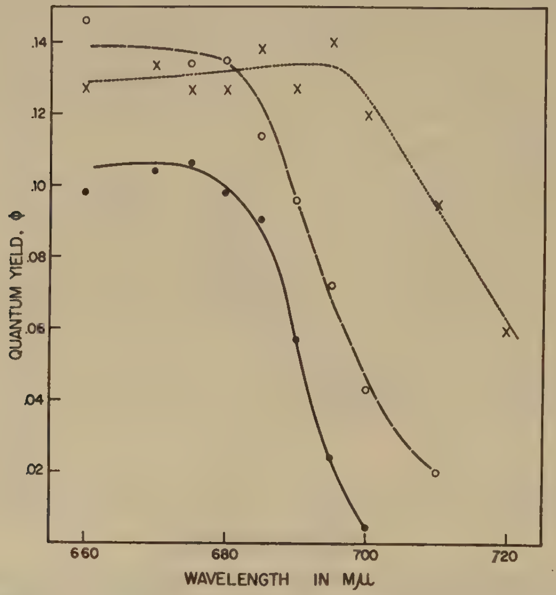

FIG. 14. Effect of temperature and supplementary light on quantum yield in *Chlorella*. The solid dots and continuous line are for 20°C; the open circles and dashed line for 5°C. The dotted curves and crosses are for measurements at 20°C with supplementary light (Emerson *et al.*, 1957).

That accessory pigments function in the enhancement of photosynthesis in far-red light has been confirmed in unpublished studies by

Myers and French for *Chlorella* and by Blinks for red algae. Similar action spectrum studies by David Fork in the author's laboratory are also consistent with this view and are of further interest because they include some of the marine algae studied by Haxo and Blinks. In *Ulva*, as in *Chlorella*, the action spectrum for enhancement resembles the absorption spectrum of chlorophyll *b*. The only brown alga studied, *Endarachne Binghamiae*, showed clear evidence for effectiveness of both fucoxanthin and chlorophyll *c*. In the red alga *Porphyra perforata* (Fig. 16, upper curve) photosynthetic enhancement was most effective in the middle of the spectrum where phycoerythrin contributes strongly to thallus absorption. Similar results were obtained with several other red algae examined.

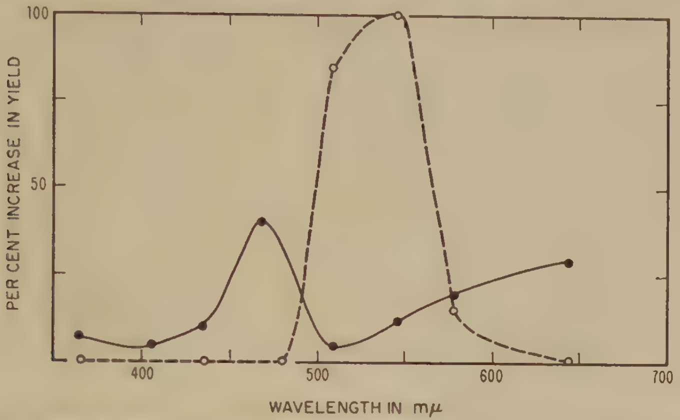

FIG. 15. Action spectra for the effect of supplementary light in enhancing photosynthesis in far-red light (690 mμ). KEY: —●—, *Chlorella;* —o—, *Porphyridium cruentum*. Plotted from the data of Emerson (1958a).

In order to explain the effect of supplementary light, Emerson suggested that maintenance of maximum photosynthetic efficiency in the far-red requires excitation of a pigment having an energy level higher than the first excited state of chlorophyll *a*. Thus, efficient photosynthesis would require simultaneous excitation of more than one photosynthetically active pigment. This function would be fulfilled by the accessory pigments—i.e., chlorophyll *b* in green algae, chlorophyll *c* in diatoms and brown algae, and phycobilins in red and blue-green algae. In this connection, Franck (1958) has theorized that a cooperation between the first excited singlet state of chlorophyll *a* and its metastable triplet state is a requirement for efficient photosynthesis. Rabinowitch (1959) has recently suggested that interpretation of the enhancement effect could be sought either in different photochemical functions of the several cell pigments, or in the existence of two or more forms of excited chlorophyll *a*. One of these would result from direct absorption in the far-red part of the spectrum, while the other could be obtained either by direct absorption of higher frequency quanta by chlorophyll *a* or by resonance transfer of the energy of the quanta from the excited accessory pigments.

Although the studies of Emerson and co-workers stressed chlorophyll *a* inefficiency as a long-wavelength phenomenon, the possibility was also considered that all the light absorbed by chlorophyll *a*—at long wavelengths and also at short wavelengths—must be supplemented by light absorbed by some accessory pigment to sustain maximum yields. In support of this, preliminary studies by Emerson and Chalmers (1958) with *Tribonema,* which lacked accessory pigments, failed to show enhancement in the far-red and showed a low quantum yield throughout the spectrum. Nevertheless, from the experimental evidence at hand it was unclear whether the low efficiency of chlorophyll *a* is a property of its absorption of low energy quanta in the far-red (a long-wavelength decline) or whether it is an intrinsic feature of chlorophyll *a*–sensitized photosynthesis and could thus be expected in any region of the spectrum in which chlorophyll *a* excitation takes place without appreciable excitation of accessory pigments.

In a direct test of the latter possibility, David Fork has recently demonstrated photosynthetic enhancement in the blue end of the spectrum in several species of marine red algae.* These offer the advantage over green algae of having low absorption by accessory pigments in the blue, as well as the red absorption band of chlorophyll *a*. Irradiation of *Porphyra perforata, Cryptopleura crispa,* and *Cryptonemia* sp. with the 436 and 546 mμ mercury lines, separately and paired, revealed an enhancement of photosynthesis at 436 mμ quite comparable to that observed when the 546 mμ line was paired with far-red light of wavelengths greater than 690 mμ. The action spectra for photosynthetic enhancement in the blue follow the absorption spectrum of phycoerythrin, in particular, and are quite similar to those obtained for enhancement in the far red. The results for *Porphyra perforata* are shown in Fig. 16.

Since it is possible in red algae to improve the effectiveness of utilization of quanta absorbed by chlorophyll *a* at both ends of the spectrum, it is unlikely that the Emerson Effect is dependent upon provision of higher energy quanta *per se*. The situation would seem to be restricted to the alternative proposed by Emerson that efficient photosynthesis is possible only by the simultaneous excitation of chlorophyll *a* and an accessory pigment. The apparent restriction of inefficient photosynthesis in green algae to long wavelengths would, accordingly, be a reflection of the fact that this is the one region of the spectrum where the activity of chlorophyll *a* can be assessed in the absence of chlorophyll *b* excitation.

---

* *Note added in proof:* This effect has been confirmed by Blinks [(1959). Personal communication; (1960). *Proc. Natl. Acad. Sci. U.S.* **46**, 327-333.]

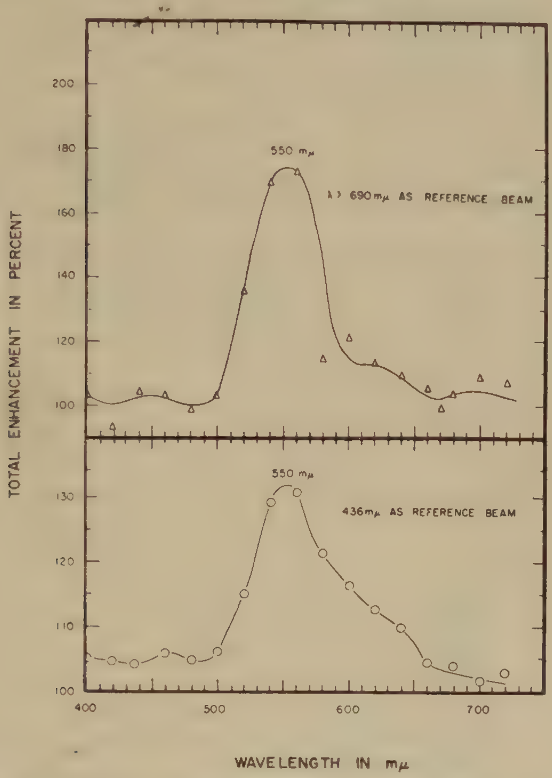

FIG. 16. Action spectra for photosynthetic enhancement by supplementary light in the red alga *Porphyra perforata*. In the upper curve, far-red light (wavelengths greater than 690 mμ) served as the reference beam. In the lower curve, the reference beam was the 436 mμ mercury line (Fork, unpublished).

This would also account for the low effectiveness in photosynthesis of chlorophyll-absorbed light at *both ends* of the spectrum in red and blue-green algae. It remains for future experimentation and consideration of other lines of evidence to reveal whether the low efficiency of chlorophyll *a*–absorbed light can best be explained in terms of a homogeneous chlorophyll *a* of intrinsically low effectiveness, or whether the concept of active and inactive chlorophyll *a* moieties should be retained.

REFERENCES

Airth, R. L., and Blinks, L. R. (1956). *Biol. Bull.* **111**, 321-327.

Allen, M. B. (1959). *Arch. Mikrobiol.* **32**, 270-277.

Allen, M. B., Dougherty, E. C., and McLaughlin, J. J. A. (1959). *Nature* **184**, 1047-1049.

Blinks, L. R. (1954). *In* "Autotrophic Microorganisms" (B. A. Fry and J. L. Peel, eds.), p. 224. Cambridge Univ. Press, London and New York.

Blinks, L. R. (1955). *Ann. Rev. Plant Physiol.* **5**, 93-114.

Brody, M. (1958). Doctoral Thesis, University of Illinois, Urbana, Illinois.

Chen, S. L. (1952). *Plant Physiol.* **27**, 35-48.

Claes, H. (1954). *Z. Naturforsch.* **9b**, 461-469.

Cohen-Bazire, G., and Stanier, R. Y. (1958). *Nature* **181**, 250-254.

Dutton, H. J., and Manning, W. M. (1941). *Am. J. Botany* **28**, 516-526.

Dutton, H. J., Manning, W. M., and Duggar, B. M. (1943). *J. Phys. Chem.* **47**, 308-313.

Duysens, L. N. M. (1952). Doctoral Thesis. University of Utrecht, Holland.

Duysens, L. N. M. (1956). *Ann. Rev. Plant Physiol.* **7**, 25-50.

Duysens, L. N. M. (1959). *In* "The Photochemical Apparatus: Its Structure and Function." *Brookhaven Symposia in Biol.* **11**, 10-25.

Emerson, R. (1958). *Ann. Rev. Plant Physiol.* **9**, 1-24.

Emerson, R. (1958a). *Science* **127**, 1059-1060.

Emerson, R., and Chalmers, R. (1958). *Phycol. Soc. Am. News Bull.* **11**, 51-56.

Emerson, R., and Lewis, C. M. (1942). *J. Gen. Physiol.* **25**, 579-595.

Emerson, R., and Lewis, C. M. (1943). *Am. J. Botany* **30**, 165-178.

Emerson, R., Chalmers, R., Cederstrand, C., and Brody, M. (1956). *Science* **123**, 673.

Emerson, R., Chalmers, R., and Cederstrand, C. (1957). *Proc. Natl. Acad. Sci. U.S.* **43**, 133-143.

Engelmann, T. W. (1882a). *Botan. Z.* **40**, 419-422.

Engelmann, T. W. (1882b). *Botan. Z.* **40**, 663-669.

Engelmann, T. W. (1883). *Botan. Z.* **41**, 1-29.

Engelmann, T. W. (1884). *Botan. Z.* **42**, 81-105.

Franck, J. (1958). *Proc. Natl. Acad. Sci. U.S.* **44**, 941-948.

French, C. S. (1958). *In* "Photobiology," Proc. 19th Ann. Biol. Colloquium, p. 52-64. Oregon State College, Corvallis, Oregon.

French, C. S., and Elliott, R. F. (1958). *Carnegie Inst. Wash. Year Book* **57**, 278-286.

French, C. S., and Young, V. K. (1952). *J. Gen. Physiol.* **35**, 873-890.

French, C. S., and Young, V. K. (1956). *In* "Radiation Biology" (A. Hollaender, ed.), Vol. 3, pp. 343-391. McGraw-Hill, New York.

Geitler, L. (1924). *Rev. Algol.* **1**, 357-375.

Goodwin, T. W., and Jamikorn, M. (1954). *Biochem. J.* **57**, 376-381.

Haxo, F. T. (1959). *Proc. Intern. Botan. Congr., 9th Congr., Montreal, 1959* pp. 154-155.

Haxo, F. T. (1960). *In* "Handbuch der Pflanzenhpysiologie" (W. Ruhland, ed.), Vol. 5, pp. 349-363. Springer, Berlin.

Haxo, F. T., and Blinks, L. R. (1950). *J. Gen. Physiol.* **33**, 389-422.

Haxo, F. T., and Fork, D. C. (1959). *Nature* **184**, 1051-1052.

Haxo, F. T., and Norris, P. S. (1953). *Biol. Bull.* **105**, 374.

Haxo, F. T., and Ó hEocha, C. (1960). *In* "Handbuch der Pflanzenphysiologie" (W. Ruhland, ed.), Vol. 5, pp. 479-510. Springer, Berlin.

Hoover, W. H. (1937). *Smithsonian Inst. Publ. Misc. Collections* **95**, No. 21.

Kandler, O., and Schötz, F. (1956). *Z. Naturforsch.* **11b**, 708-718.

Levring, T. (1947). *Göteborgs Kgl. Vetenskaps-Vitterhets-Samhäll. Handl.* **5**, 1-89.

Montfort, C. (1940). *Z. physiol. Chem., Hoppe-Seyler's* **186**, 57-93.

Ó hEocha, C., and Rafferty, M. (1959). *Nature* **184**, 1049-1051.

Rabinowitch, E. I. (1945). "Photosynthesis and Related Processes," Vol. I. Interscience, New York.

Rabinowitch, E. I. (1951). "Photosynthesis and Related Processes," Vol. II, Part 1. Interscience, New York.

Rabinowitch, E. I. (1956). "Photosynthesis and Related Processes," Vol. II, Part 2. Interscience, New York.

Rabinowitch, E. I. (1959). *Plant Physiol.* **34**, 179-184.

Sistrom, W. R., Griffith, M., and Stanier, R. Y. (1956). *J. Cellular Comp. Physiol.* **48**, 473-515.

Stanier, R. Y. (1958). *In* "The Photochemical Apparatus. Its Structure and Function." *Brookhaven Symp. Biol.* **11**, 43-53.

Tanada, T. (1951). *Am. J. Botany* **38**, 276-283.

Wassink, E. C., and Kersten, J. A. H. (1944). *Enzymologia* **11**, 282-312.

Wassink, E. C., and Kersten, J. A. H. (1946). *Enzymologia* **12**, 3-32.

Yocum, C., and Blinks, L. R. (1954). *J. Gen. Physiol.* **38**, 1-16.

DISCUSSION

FOX: If we entertain for a moment the assumption that photosynthetic plants had their beginnings in aqueous shallow regions, what is the evolutionary position of the bilichromoproteins? We do not see them in higher plants, do we?

HAXO: Well, I think most people would start their evolutionary scheme with chlorophyll *a* and, accepting Emerson's viewpoint, this would, in the absence of accessory pigments, have only moderate efficiency. In time, as accessory pigments came into the picture, they not only closed optical windows but they actually enhanced the activity of chlorophyll *a*.

FRENCH: I think there is a good deal of question as to how this enhancement effect comes about. I do not think we have much of an idea as to why we get an enhancement effect. One idea is that it might be in the pigment system, that is is part of the photochemistry that activating one pigment makes another one more able to work effectively. Another possibility is that the things come together at the chemical level some time after the photochemical part of it, that different products are made by chlorophyll *b* photosynthesis and chlorophyll *a* photosynthesis, and that these two things somehow get together and give more effective photosynthesis. But this must be in the oxygen-evolving part, because these are oxygen evolution measurements. Now there is one experiment of Jack Myers' that bears on this a little bit. He found that it was possible to give the two beams not only simultaneously to get enhancement, but to give one after the other up to 15 second intervals: 15 seconds of one, 15 seconds of the other. With a few seconds of one and a few seconds of the other you got almost as good an effect as you did with the two given together. Now that makes it look as though it were not highly immediate photochemistry with time constants that were very small, but the time constants of this thing were in the order of seconds. Now another thing that came out from your slides very nicely, I think, is that the enhancement effect requires activation of two pigments, one of which is chlorophyll *b*—let us just talk about *Chlorella* for a moment—one of which is chlorophyll *b* and possibly also the 670 form of chlorophyll *a*, and we have a slide that shows the same sort of an action with a hump at 670 mμ, so that apparently chlorophyll *b* and chlorophyll *a* 670 may be tied together. Perhaps we have energy transfer within that complex but that complex does one job and the long wavelength form of chlorophyll *a*, the 695 stuff, does another.

WEBER: In the same vein as Dr. French, it would be very interesting to have action spectra on the photosynthetic bacteria. I wonder how one would go about this, since they do not have such an easy indication of their activity. The second pigment may be connected with the oxygen-evolution mechanism which is photochemically activated because you always find these two pigments when you get oxygen evolution, while in the photosynthetic bacteria you find only one pigment and you do not have oxygen evolution.

HAXO: I am sure this would be a very interesting problem; however, I do not have any suggestions as to how to proceed with rapid measurements of action spectra in photosynthetic bacteria.

(850)

REPRINTED FROM
COMPARATIVE BIOCHEMISTRY OF PHOTOREACTIVE SYSTEMS
COPYRIGHT ©, 1960
ACADEMIC PRESS INC., NEW YORK
pp. 11-31

2

Pigments of Plant Origin in Animal Phyla*

Denis L. Fox

Division of Marine Biochemistry, Scripps Institution of Oceanography, University of California, La Jolla, California

The observed contrasts in size, morphology, and complexity among living species are fundamentally of biochemical origin. But it is equally true that certain basic physiological properties of all cells rest upon common chemical foundations. Responsible for interspecific differences are the constituent proteins, which vary widely through permutations in the relative proportions and the linear bonding sequences of two or three dozen amino acids.

The "green universe of plants" and its contained "red kingdom of animals" utilize much the same basic fuels in respiration, and store similar chemical types of reserves. And, whereas essentially all organisms, so far as we know, seem capable of synthesizing the tetrapyrrole nucleus, the green plants have elaborated therefrom chlorophyll compounds and have thus become autotrophic, while the vertebrates and some invertebrate animals build hemoglobin as an oxygen-conveyer. Other porphyrins, such as the cytochromes, catalase, and other peroxidases are biocatalysts common to both plants and animals. Moreover, the porphyrin skeleton, once synthesized, possesses considerable chemical stability. Identifiable derivatives of hems and especially of chlorophylls may persist as biochemical fossils of great antiquity. A paper concerning these, as well as others such as carotenoids, will be presented in more detail by another contributor to this symposium.†

Colored molecules offer much of interest in the realm of comparative biochemistry, and invite plant and animal biologists to common meeting grounds. In the plant world, for example, there are countless instances of the heritable capacity to synthesize carotenoid biochromes in certain tissues, e.g., as in poppies with white or yellow corollae, red versus pale yellow tomatoes or grapefruit, or orange contrasted with colorless fungal mycelia, as in *Neurospora* mutants. Again, the elaboration of carotenoids may depend, in kind or in degree, upon environmental factors (Good-

---

* Contribution, Scripps Institution of Oceanography, University of California, La Jolla, New Series. 1201

† See Paper No. 7 by J. R. Vallentyne.

Reproduced by Permission

win, 1955). Successive blooms of the California poppy may be observed to exhibit paler yellow-orange to yellow corollae with the advance of warm summer days, in contrast to the rich orange hues of the first spring blossoms; and all are familiar with the accumulation of carotenoids in many ripening fruits. The "red-snow" alga *Hematococcus pluvialis* has been demonstrated to elaborate large quantities of β-carotene when supplied with acetate (Lwoff and Lwoff, 1930). The halophilic algal flagellate *Dunaliella salina,* cosmopolitan in natural or industrial salterns the world over, is brick-red in saturated NaCl solutions, contains much β-carotene, little α-carotene and but traces of lutein and chlorophyll; in less concentrated media (12 to 15% NaCl), the cells are green with much chlorophyll, and contain far less β-carotene and minor quantities of α-carotene and lutein (Fox and Sargent, 1938).

Animals, deriving their carotenoids directly or indirectly from plant sources, exert different kinds of fractionation upon these molecules, whether through selective control of their assimilation within the lumen or walls of the alimentary tract, or in other tissues. Differences may reflect kinds, concentrations or activity of oxidase (perhaps lipoxidase) systems within the animal.

While there are indeed but few if any biochromes synthesized *de novo* only by animals,* there are several classes, in addition to the tetrapyrroles cited above, that are generated by both animals and plants, e.g., the indigoids, arising from the metabolism of tryptophan, the melanins deriving from that of tyrosine, and the pterins which are pyrimidopyrazine compounds. Beyond these and a few other examples, however, there is a wide array of pigments synthesized only by plants. Of these, a few are assimilated by animals in their nutrition. Passing references will be given to the flavins and quinones, after which we shall return to the prominence of the carotenoids.

Flavins

Riboflavin, variously called lacto-, cyto- or ovoflavin, is benzisoalloxazine-6,7-dimethyl-9, D-riboflavin, synthesized by most higher plants, notably in growing leaves, and by a number of microorganisms. Its physical and chemical properties have been well established and have been recorded rather extensively elsewhere (see Fox, 1953, pp. 282 *et seq.*) and its occurrence in very minute amounts in nearly all animal tissues is well known; likewise the fact that, as one of the B vitamins, it is an indispensable factor in cellular respiration. Moreover, riboflavin and the flavoproteins may occupy a significant position in photoreception, leading to photokinesis in certain plants (Goodwin, 1959), and perhaps are involved in the biochemistry of vision. Riboflavin is known to exercise some deterring influence over the incidence of cataract (Hogan, 1939).

---

* Even the few non-hem metalloproteins of animals, e.g., hemocyanin, hemerythrin, etc., can hardly be regarded as more than borderline exceptions, since animals depend upon ultimate plant sources for certain essential amino acids involved in protein synthesis.

Flavoproteins in the skin of certain fishes (e.g., eels) are localized in areas bearing carotenoids and melanophores, but are absent from the white, guanine-laden parts. While these observations have suggested a possible intermediary role of flavins in melanin formation, the demonstrated photoinactivation of tyrosinase and other biocatalysts by riboflavin indicates that it may possibly control rather than accelerate photically-induced melanogenesis (Fox, 1953, p. 287).

Quinones

NAPHTHOQUINONES

The naphthoquinones, encountered in many plants, are of various yellow, orange, red, or purple colors. Their appearance in animals is very limited; numerous species of echinoid (sea urchins, sand dollars, and the like) display them as red, purple, or in some instances green polyhydroxy derivatives known as echinochromes, in calcareous spines, in shell, and in thin ectodermal and endodermal tissues. The same pigments are to be found in the elaeocytes of the body fluid, in the lining of the alimentary tract, in nervous tissues, and in some instances within the egg-jelly (see Fox, 1953, Chapter VIII).

Incidentally the sea otter *Enhydra lutris* acquires pink and purple calcareous echinochrome deposits in its skull, teeth, and other skeletal parts from the eating of large numbers of sea urchins in their natural surroundings (see Fox, 1953, p. 195).

Certain members of a second echinoderm class, the crinoids (featherstars or sea-lilies), assimilate echinochromes. The pigments have been identified both in fossil species and in the living tissues of the free-swimming crinoid *Antedon bifida* (Dimelow, 1958).

Nothing is known with certainty of the physiological position of the naphthoquinones. Their chemical similarity to vitamin K has been ascertained, and a possible role has been suggested for them as respiratory stimulants for the eggs, and as activator of the sperm of certain echinoids. The careful experiments of Millott and his colleagues (Millott, 1957; Millott and Yoshida, 1957) lead one to suspect not only that echinochromes may act synergistically with melanins in screening out injurious light rays, but also that they may share with carotenoids the role of photoeffectors in the shading reaction.

ANTHRAQUINONES

The red polyhydroxyanthraquinone carboxylic acids (as well as glucosides and methyl or ethyl esters thereof) including carminic, kermesic, and laccaic acids, are doubtless derived by the respective scale-insects cochineal, kermes, and lac (lakh) from their plant hosts. The pigment, whether in the so-called fat-body of the cochineal or in the waxy excrescence of the (female) lac insect, represents, in all likelihood, a relatively inert residue or a secretory material; it has no recognized physiological function in the animal (Fox, 1953, pp. 205-208).

Recently another red anthraquinone has been discovered, occurring in red crinoids of the genus *Comatula*. Its investigators, Sutherland and Wells (1959), have called it rhodocomatulin, but have not to date ventured a guess as to its source or its potential biological function. The very fact of seemingly extravagant biochromy in some of these animals, through pigments deriving ultimately from plants, presents an enigma. Why do a few animal species assimilate and store the pigments while others, consuming the same food, do not? And do those which store the colored labile molecules utilize them anywhere in their over-all economy, e.g., in redox systems or as photoeffectors?

Carotenoids

This ubiquitous class of plant-synthesized polyene compounds emphasizes the questions raised above. For not only are the carotenoids of virtually universal occurrence in animals from the protozoan phylum to the highest vertebrates, but they are concentrated chiefly in three types of tissue: exposed integumentary surfaces, gonads (including immature spermaries and maturing eggs), and other glandular parts. Moreover the carotenoids themselves, and certain animal-produced derivatives of some of them, i.e., the A vitamins, have long been known to possess important physiological attributes. We have been aware, since the work of McCollum and Davis, and that of Osborne and Mendel, both in 1913, of the indispensability of vitamin A as a growth-promoting compound in vertebrates. A few years later its antixerotic or anti-keratosis properties were revealed by the studies of a whole series of workers in many laboratories. It was Moore who, in 1929, established the biochemical derivation of the vitamin from certain yellow carotenoids; nearly two decades later it was first demonstrated, in England by Glover and associates (1947) and in this country by Deuel and his colleagues (Mattson *et al.*, 1947; Wiese *et al.*, 1947) that the site of conversion of carotene into vitamin A is in the small intestine (of rats). Moreover, dietary carotene is converted into vitamin A by the cod *Gadus callarias* and by the lobster *Homarus americanus* (Neilands, 1947); and Kon and his associates in Reading have demonstrated the storage of relatively high concentrations of vitamin A, nearly exclusively in the eye-stalks, by numerous marine microcrustaceans of the euphausiid family, including "krill," the forms consumed in vast numbers by whales, which subsequently store vitamin-A-rich oil in their livers (Fisher *et al.*, 1955). It was demonstrated many years ago that mammals, even those storing but traces of carotenoids (e.g., swine), require them or vitamin A itself for successful reproduction.

The stimulating effects of the purified carotenoids, astaxanthin and, to a lesser extent, β-carotene, found in the egg-oil of the rainbow trout *Salmo irideus* upon the sperm of the same species, have been reported by Hartman *et al.* (1947), who found lutein and lactoflavin, both also present in the egg-oil, to be without any such effect.

VISION AND PHOTOKINESIS

Wald and his associates, among others, studying visual processes during the past quarter-century, have illuminated the unique position of the A vitamins in the visual pigmentary apparatus. The remarkable role of this carotenoid-fission product, derived by and functional in animals as a photolabile purple or red protein-conjugant, would appear to be an evolutionary biochemical advance from a basic and perhaps spectrally more restricted property of full-chain-length carotenoids. For we know that various molecules of this type in some way induce photokinesis, i.e., orientation or locomotion either toward or away from light-stimuli (Goodwin, 1959). This holds in both green and achlorophyllous plants; moreover, many animals, including eyeless invertebrate species, appear to have "borrowed" the same molecules, utilizing for similar purposes the carotenoids originally synthesized only in the plant world. The photosensitivity spectrum of some of these organisms has been observed to match closely the range of maximal light absorption by the carotenoids in their tissues. An interesting example is that of the sea-star *Marthasterias glacialis*,* in which Millott and Vevers (1955) have studied the carotenoid pigments of the optic cushion, a structure resembling a kind of "saddle" across the base of the small azygos tentacular finger at the tip of each arm or ray. The optic cushion bears some 150 deeply pigmented, so-called optic cups, and yields orange and reddish-orange carotenoids, the latter being prominent in the cups themselves. The pigments are labile *in vitro* if air is present, and are readily decomposed by light. The prominent pigments in the optic cushion seemed to be β-carotene and esterified astaxanthin, although Vevers and Millott (1957) found 8 chromatographic carotenoid fractions in the general skin of this star. One fraction exhibited the properties of β-carotene, another behaved like a neutral keto-carotenoid, while a hypophasic component resembled lutein; astaxanthin also was present, both free and esterified. Another important discovery made by these workers was that no traces of vitamin A itself were detectable in the animal. There is therefore the strong implication that asteroids may utilize full-length (40 C-atom), colored carotenoids as photoreceptors in their eye-spots or optic cushions. Moreover, in view of the exclusively carnivorous habit of most asteroid species, their carotenoid supplies are acquired from the ultimate plant source in an indirect way.

---

* Rockstein (1956) and Rockstein and Rubenstein (1957) also report the finding of photosensitive pigments in the terminal eyespots and skin of an asteroid, *Asterias forbesi.*

DISPOSITION OF CAROTENOIDS

Ingested carotenoids are subject to several alternative but not necessarily mutually exclusive fates in the animal body, as follows:

1. Discharge with feces, in chemically unaltered condition;
2. Assimilation and storage, chemically unchanged;
3. Assimilation and conversion into other carotenoids, e.g., A vitamins, astaxanthin, "canary xanthophyll," echinenone, or other special animal carotenoids;
4. Assimilated portions oxidatively consumed or otherwise converted to colorless substances;
5. Destruction in gut, whether by symbiotic microorganisms or by host's enzymes.

The many animals which have been included in a broad survey to date are classifiable into several groups and subgroups in accordance with their predominating metabolic disposition of ingested carotenoids (cf. Zechmeister, 1937; Fox, 1953), as follows.

I. Assimilation and storage *in statu quo:*
  1. Nonselective, e.g., man, frog (*Rana*), *Octopus*, echinoids, some insects
  2. Selective
    (*a*) Xanthophyll selectors: most fishes, some invertebrates, many birds
    (*b*) Carotene selectors: horse, cow, some sponges, some worms (e.g., *Thoracophelia*)

(856)

II. Production and storage of colored, oxidized derivatives, e.g., astaxanthin, from conventional dietary carotenoids: crustaceans, asteroid and ophiuroid echinoderms, nudibranch mollusks, some insects (locust), some coelenterates, certain birds (flamingo)

III. Excluders, by nonassimilation or through complete oxidation of carotenoids: carnivorous birds and mammals, pig, goat, guinea-pig, rabbit

Few if any generalities may be obvious in this condensed classification, but some definite trends exist. In the first place, carotene selectors tend to be herbivores or omnivores, and the same applies generally to the nonselective assimilators, although *Octopus bimaculatus,* a strict carnivore, is an exception (Fox and Crane, 1942). Moreover, the majority of animals in these two groups tend to store their carotenoids only internally and in small to moderate quantities. Certain sponges and bryozoans of brilliant colors provide exceptions to this generalization by depositing their carotenoids in the integument (although, considering the relative simplicity of their structure, they do not have much choice if they are to store the pigment at all). The vast majority of fishes examined carry solely or chiefly xanthophylls in their skin, liver, ovaries, or (rarely) flesh; carotenes, when present, are greatly in the minority, and in no published instance has the skin of any fish species yielded carotenes without xanthophylls. It will be remembered, also, that most fishes are carnivores, while many are omnivorous (Fox, 1957).

Mammals as a class are relatively poor in carotenoids; many store none of the colored members at all, although all demand a supply of vitamin or provitamin A. Some store carotenoids in plasma, liver, adipose tissue, adrenals, and corpus luteum. Of these, horses and cattle are outstanding carotene selectors (Palmer, 1922), which expel with the feces the xanthophylls not earlier degraded in the gut (Rogozinski, 1937). Other herbivorous mammals, such as sheep, goats, and swine, store no carotenoids or but the smallest traces, and, unlike cattle, secrete white instead of yellow butter-fat in their milk (Palmer, 1922). Rabbits (*Lepus cuniculus*) characteristically assimilate no carotenoids, and store white depot fat, save for a recessive strain whose adipose tissues are orange-yellow with xanthophyll (Pease, 1928; Willimott, 1928).

In contrast to numerous invertebrate carnivores, their mammalian dietary counterparts, e.g., the feline and canine families, store very little carotenoid in their bodies and, as in other mammals (save for some strains of cattle on a heavy diet of green food), none in the skin. Even omnivorous mammals such as rats are poor in carotenoids, while man remains an exception, depositing, notably in his body fat, portions of any carotenoid or combinations thereof from his recent diet. Indeed the extravagant consumption of carotenoid-rich foods, such as oranges or pumpkins, has been observed to confer upon the skin of children a distinctly yellow color, known variously as carotenemia, xanthemia, or false jaundice. The condition is not pathogenic, and is directly controllable by altering the diet (Fox, 1953, p. 174).

The blue whale, feeding upon such planktonic crustaceans as *Calanus* and *Euphausia*, stores much astaxanthin in its oil; indeed, according to Schmidt-Nielsen *et al.* (1932), an occasional reddish specimen of this whale may be seen, wherein the red carotenoid has been distributed into the tissues generally, rather than remaining only in the usual depots. The whale's supplies of vitamin A are supposedly obtained from the relatively rich amounts found in the eye-stalks of the crustaceans swallowed as food, although there is a persistent idea that the whale may, like certain other animals (see below) be capable of converting astaxanthin into vitamin A.

Secretion or Excrescence to the Exterior

Examples wherein carotenoids are secreted to the outside are to be found in some animal phyla. Many crustaceans mobilize astaxanthin from their thin, pigment-rich hypoderm into the chitinous carapace, and something similar may be observed in certain insects, notably the lady-beetle *Coccinella septempunctata*, which secretes lycopene as well as α- and β-carotenes into its elytra (or hard wing-covers). The honey-bee, *Apis mellifera*, deposits its pollen-derived carotenoids in its various products; β-carotene has been recovered from amber-colored honey, and carotenoids have been recognized also in the wax, while several fractions, including β-carotene and a lutein ester have been recovered from propolis or bee-glue (Schuette and Bott, 1928; Zechmeister, 1937).

Examples of carotenoids in the yolky parts of eggs are so numerous as to require here no more than passing reference, save for an interesting example in an insect, *Colias philodice*, whose caterpillar is either blue or green, depending upon a recessive gene which confers failure to assimilate and store yellow carotenoids from the common diet of green clover; the adults of this genotype lay colorless eggs which hatch into larvae colored blue (due to the presence of a tetrapyrrole from the degradation of chlorophyll), while the dominant green type lays yellow eggs, giving rise to larvae colored green from the presence of both the blue tetrapyrrole and the yellow carotenoid. Moreover, the latter coloration serves an incidentally useful role, for the carotenoid-assimilating, green-colored larvae enjoy a measurable degree of chromatic protection from predation by English sparrows, denied to their blue siblings against the natural background of green clover (Gerould, 1921).

Some insects secrete carotenoids into the silk of their cocoons. A well-known example is the larval stage of the silk-moth *Bombyx mori* which depends upon two genes for the spinning of yellow rather than white silk: C for assimilation of mulberry-leaf carotenoids to give yellow blood, and Y for the secretion of such xanthophylls as taraxanthin, violaxanthin, and lutein into the silk (Uda, 1919; Oku, 1929, 1930, 1932, 1933; Manunta, 1933, 1935, 1937). Another instance is that of a hemipteran or sucking-bug *Apanteles flaviconchae* which, preying upon the *Colias* caterpillars mentioned above, ultimately secretes cocoon-silk of a golden color if feeding upon the blood of the green type, and a white silk if nourished by that of the blue, carotenoid-free form (Gerould, 1921).

The cephalopod *Octopus bimaculatus*, assimilating either or both carotenes and xanthophylls, including astaxanthin, in its large "liver" or hepatopancreas, secretes into the closely adjacent ink-sac free and esterified xanthophylls but no carotenes (Fox and Crane, 1942).

Among the chordates, some ascidians or sea-squirts deposit rich stores of carotenoid, largely xanthophylls including astaxanthin, in the tunicin material of the outer cloak or test (Lederer, 1934). Certain brilliantly colored fishes, notably the marine dorado *Beryx decadactylus*, have mucus of a bright red color, due to the presence of astaxanthin, in the mouth and gills (Lederer, 1935). Among the reptiles the male spiny-tailed iguanid *Ctenosaura hemilopha* exudes a red, orange, or yellow waxy substance from its multiple femoral pits in the ventral skin of the thigh. The preponderant carotenoid is an esterified alcohol closely resembling taraxanthin (Fox, 1953, p. 158).

An account of the carotenoids secreted by bird species into their feathers would constitute an extensive chapter by itself, and must be deferred here, save for some special considerations below.

In mammals, apart from the presence of carotenoids in the milk of cattle and some other ruminants, as well as in the milk and particularly the colostrum of humans, there are but few instances of carotenoid secretion. An instance, however, is the ear-wax of cattle, the chief polyene of which appears to be β-carotene (Palmer and Eckles, 1914).

From a brief survey of the comparative secretion of carotenoids in animals, one might be tempted to draw some analogies with the known role of vitamin A in maintaining the status of mucous surfaces. Current difficulties are, however, that some fishes, crustaceans, anemones, and other animals may elaborate mucus containing carotenoids while others do not; moreover, we require far more study of the total constitution and physiology of mucus and other secreted materials before our thinking may advance much further.

Many animals store in various tissues what appears to be merely the excess of ingested carotenoids in chemically unaltered condition, e.g., among fishes, amphibians, reptiles, birds and mammals; although there remains the perplexing question of selective fractionation in many instances, the metabolic economy of carotenoids in these creatures still is obscure save for the importance of the A vitamins.

Biochemical Modification of Dietary Carotenoids

There remain the two other classes, i.e. (*1*) animals lacking or very poor in carotenoids, selecting but little and/or destroying essentially all of the pigment ingested save for that converted to vitamin A, and (*2*) the richly colored kinds, capable of converting assimilated carotenoids into partially oxidized derivatives often red in color.

We know little indeed about the biochemical fate of carotenoids consumed by animals of the first, relatively destructive category. And, while we have learned also but little of the pathways of carotenoid metabolism in the oxidative modifiers in the latter class, some account of a few empirical findings may stimulate further interest.

In a search for a possible astaxanthin precursor in the large marine crayfish *Panulirus interruptus*, marked and segregated specimens were maintained on a basic diet containing: in one group, no colored carotenoids; in a second, only carotenes; and in the last, only a taraxanthin-like xanthophyll ester. During the experimental period of many months in laboratory aquaria, several animals moulted the carapace. Cast carapaces and whole animals from the three groups were analyzed for total astaxanthin content, the values for which decreased with the passing of time; thus no evidence was forthcoming as to a potential carotenoid source of the red crustacean pigment (Fox and Kritzler, unpublished experiments, 1946-1947). But soon afterward Goodwin (1949, 1952) reported that 40% of the β-carotene, the only polyene found in newly laid eggs of the locusts *Locusta migratoria migratorioides* and *Schistocerca gregaria*, was replaced by astaxanthin by the time of hatching. He concluded that an oxidase must be present to effect this conversion, and that such conditions should ensure the equipment of the newly hatched hoppers with a means of photoreception, since no vitamin A was detected in these locusts and since astaxanthin has been cited as a likely photokinetic carotenoid in animals which do not synthesize the vitamin itself (Wald, 1943).

Indeed vitamin A, derived from certain precursors by all vertebrates, is lacking in many invertebrate species, including not only certain generally photosensitive forms, e.g., among the asteroids and echinoids, but even in kinds which possess functional eyes, notably most insects and many crustaceans. The relative obscurity of the visual processes in insects is emphasized by Fisher and Kon (1959), who remind us that no requirement for vitamin A has been detected by various workers in several species, e.g., the fruit fly *Drosophila melanogaster*, the flour beetle *Tribolium confusum*, the meal worm *Tenebrio molitor*, the clothes moth *Tineola biseliella* or the cockroach *Blatella germanica*. Likewise Goldsmith (1958) cites the failure of the grasshopper *Melanoplus* and the dragonfly *Sympetrum* to yield vitamin A in extracts of their heads; but his researches on the honeybee *Apis mellifera* revealed the presence of retinene$_1$ in the eyes (actually the whole heads) but not from the headless bodies similarly extracted. Addition of $SbCl_3$ to the retinene yielded a bright blue compound with an absorption maximum at 664 mμ, characteristic of retinene$_1$, while reduction of the terminal aldehyde group with potassium borohydride gave vitamin A which, treated with $SbCl_3$, manifested its blue product, absorbing maximally at 618 mμ. Similarly, Wolken (1959) has detected A vitamins in the heads of houseflies.

The extensive survey of Kon and his associates at Reading would suggest that in the arthropod phylum we encounter a kind of border area with respect to the synthesis of vitamin A and the compounds involved in vision; for, in view of the comparatively high concentrations of the vitamin in the eyes of numerous euphausiid species and its plentiful distribution between eyes and hepatopancreas in several groups of decapods, it is surprising that the compound should be completely lacking from most copepods examined, from several branchiopods (e.g., species of the "water-flea" *Daphnia* and the "fairy shrimp" or "brine shrimp" *Artemia salina*), and from all save 2 out of some 54 species of amphipods examined. The lack of vitamin A from adult cirripeds (barnacles) is less surprising since these sessile animals lie head-down within a shell; however they react to abrupt changes in incident light intensity by withdrawing the feeding appendages and closing the shell's aperture. Occurrence of the vitamin was found to be quite variable among the isopods and mysids examined. Moreover, in the decapod order, its presence varied not only between species but in some instances even among individuals within a species (Fisher and Kon, 1959; and Dr. Kon, personal communication, 1959). While it is certain that vitamin A serves a visual function in some Crustacea, it would appear likely that those species which do not store it consistently or which carry it in the body but not in the eyes must, like those seeing animals which completely lack the vitamin, employ instead an alternative chromophoric molecule such as astaxanthin in the visual cycle. Crustaceans commonly store astaxanthin, and notably in the eyes, whether or not accompanied therein by vitamin A. Wald (1943) has pointed out the degree of correlation between the absorption maximum of astaxanthin (ca. 490 mμ in castor oil) and the spectral range of sensitivity for photokinetic responses in several different species. In this connection, however, it will be borne in mind that the wavelength range of light perceived is likely to find more correlation with the absorption spectrum of the carotenoid-protein complex than with that of merely the pigmented moiety dissolved in an oil.

Some challenging riddles remain in the comparative biochemistry of photokinesis, and notably of vision. One of these poses the question: while all vertebrates and many invertebrates utilize vitamin A-protein conjugants in their retinal processes, how do invertebrates, closely related to this type but lacking vitamin A, effect ocular photoreception? If a colored 40-carbon carotenoid such as astaxanthin is present instead, are there photolabile, reversible carotenoid-protein conjugation systems involved, corresponding in function with the biochemical visual apparatus which is operative in the conventional A-vitamin-protein systems of many animals? We know that natural astaxanthin-protein complexes may assume any of several different colors, and that these conjugated chromoproteins may be carefully and reversibly dissociated by certain procedures. It would be interesting if it could be shown that such a colored complex, occurring in the eyes of dark-adapted, vitamin A-lacking crustacean species, might undergo photically induced reversible dissociation with changes of color (cf. Wald, 1943, p. 213).

Fisher and Goldie (1959) report that the euphausiid crustacean *Meganyctiphanes norvegica*, a prominent component of the "krill" eaten by whales, relies for its food in Loch Fyne during spring, almost exclusively upon copepods, which supply no vitamin A, but astaxanthin as the chief if not the only carotenoid. It was during that season, however, that the vitamin A concentrations in the euphausiids' eyes increased most rapidly. This species stores about 85% of the total supply of the vitamin in the inner ends of the ommatidia where the rhabdomes are situated (Fisher and Kon, 1959). It would be interesting to learn whether there might be differences in visual acuity and the color-spectrum thereof between arthropods storing only astaxanthin in the eyes and those which carry vitamin A there as well.

It has been found by Grangaud and Massonet (1955) that the mosquito-fish *Gambusia holbrooki*, rendered completely lacking in vitamin A through a restricted diet, exhibits characteristic signs of the deficiency, including emaciation and fraying of the caudal and other fins and an arciform flexure of the spine, but that the supplementation of the vitamin A-free diet with chromatographically separated astaxanthin ester at an advanced period of the regime will preclude the appearance of any aspect of the syndrome, and will later bring about restoration of vitamin A, notably in the eyes of the fish.

Thus there are the vertebrates in addition to certain insects and crustaceans which utilize vitamin A in their visual processes, and which obtain the vitamin either directly by eating other animals supplied with it, or through the splitting of any of several alternative precursors, e.g., α-, β-, or γ-carotenes, cryptoxanthin, echinenone, or 5,6-5′,6′-diepioxy-β-carotene (Fisher *et al.*, 1954). There are arthropods, some of which seem to utilize only astaxanthin in their photoreceptive chromophores, while others may use vitamin A as well or instead. Finally, certain fishes are able to convert astaxanthin into vitamin A.

Moreover, in order to form the vitamin A or the astaxanthin from their precursors, different biochemical processes are required on the part of the respective organisms. The genesis of vitamin A from carotene, bearing some resemblance to a simple hydrolysis through the introduction of one hydrogen atom and one hydroxyl radical linked to the same carbon atom

$$(\tfrac{1}{2}\ \beta\text{-carotene or } C_{20}\,H_{28}\ \ldots\ \xrightarrow[\text{OH}]{\text{H}}\ \text{Vitamin A or } C_{20}H_{30}O)$$

actually involves the conversion of a hydrocarbon radical with 6 double bonds to a primary alcohol with but 5. The formation of vitamin A_2 would involve an oxidation, however, since the net effect is not only to add an oxygen atom but to remove two hydrogen atoms from the cyclohexenyl ring, thereby conferring another site of unsaturation. Concerning the elaboration of astaxanthin, an example cited above was the locust which, while developing within the egg, oxidizes β-carotene, $C_{40}H_{56}$, to its symmetrical dihydroxy-diketo derivative $C_{40}H_{52}O_4$. If a copepod, having achieved this oxidation, is consumed by the euphausiid *Meganyctiphanes norvegica,* this predator then reduces the astaxanthin to vitamin A by introducing hydrogen, thus saturating double bonds, and by removal of oxygen. The fish *Gambusia* seemingly effects the same reduction. Studies with radioisotopic carbon might tell us whether certain crustaceans, storing both vitamin A and astaxanthin in their eyes, first oxidize plant carotenoids to astaxanthin and then reduce this, with splitting, to give the vitamin. One would like to know also whether some of the lower animals might be able to utilize tetrahydroxyxanthophylls, e.g., taraxanthin, or more likely dinoxanthin or a spectrally similar xanthophyll, which occurs widely in fishes (Fox, 1953, 1957), as precursors to astaxanthin or other red, oxidized carotenoids.

Instances are known wherein fishes oxidize carotene to a yellow xanthophyll, in contradistinction to *Gambusia*'s reduction of astaxanthin to vitamin A. Early researches of Sumner and Fox (1933, 1935) indicated that the Pacific killifish *Fundulus parvipinnis,* and in all likelihood the long-jawed goby *Gillichthys mirabilis* as well, are capable of increasing their body stores of xanthophyll during growth on diets containing no xanthophylls at all but β-carotene as the only recognizable carotenoid.

We know too that somewhat similar oxidations occur in birds, of which two or three examples should suffice here. Canaries, *Serinus canaria canaria,* investigated *inter alia* by Brockmann and Völker (1934), were fed on rations free from colored carotenoids until the new feathers emerged white; the birds were then given diets supplemented by known individual carotenoids. The hydrocarbons β-carotene and lycopene were neither altered nor assimilated; violaxanthin was chemically changed in the gut but not subsequently deposited in any organs, egg-yolk, or feathers; zeaxanthin was assimilated, partly unaltered and partly modified chemically, in egg-yolk and in feathers, conferring upon the latter a golden yellow color tinged with red-orange; and lutein, assimilated and stored unchanged in liver, egg-yolk and fat, emerged in the plumage as a new, bright yellow pigment called by the authors "canary-xanthophyll," with absorption maxima reminiscent of taraxanthin (472, 443 mμ in petroleum ether) rather than its precursor, whose spectrum exhibits peaks at 477.5 and 447.5 mμ in the same solvent. This retrogression of absorption maxima toward the shorter wavelengths suggests that an oxidation must have occurred.

According to Kritzler (1943), wild bishop birds, *Euplectes franciscanus* and *E. nigroventris,* deposited in their new feathers a unique red carotenoid with absorption maxima at 495 and 450 mμ (in carbon disulfide) as a result of a diet supplemented with mixed tomato carotenoids. Failure of other common carotenoids substituted in the diet to elicit this response led to the conclusion that lycopene in the tomato was the precursor of the new pigment. A third species, *E. taha,* manifested in its new plumage no chromatic response to the tomato diet.

Recent studies by the writer (Fox, 1955; and unpublished investigations) and by Völker (1958) have shown that several species of flamingo, notably the so-called American or West Indian and most brightly colored form, *Phoenicopterus ruber,* convert the yellow carotenoids of green plants into unique red derivatives which give characteristic pink or vermilion colors to the bird's feathers, naked leg-skin, and depot fat. The mesenterial fat, plasma, and adrenals are often of an orange or apricot color, while the liver, gonad, and other glands and the egg-yolk yield much carotenoid material as well. However, most of the ingested carotenoid is destroyed in the gut, partly doubtless by symbiotic bacteria; the voided feces yield no carotenoids. Captive specimens apparently must receive a diet rich in the pigment if an excess is to be deposited in skin and plumage.

Investigations by the writer, using a flock of flamingos at the San Diego Zoo, and observations by Conway (1958, 1959; personal communications, 1958-1960) at the New York Zoo, have confirmed the ability of *Ph. ruber* to convert various carotenoids into the characteristic oxidized products; Conway administers a diet enriched with oil extracted from carrots and therefore containing β-carotene as the chief pigment, while at San Diego the flamingos receive as a part of their diet shrimps, ground crayfish shell, and red salmon flesh as the principal sources of carotenoid, in this instance astaxanthin. This carotenoid reappears, at least in part, among the unique neutral red carotenoids of feathers and leg-skin, while the egg-yolk, blood plasma, fat, and other internal tissues have yielded no astaxanthin among the rich supplies of other carotenoids. Some deeply colored feathers, grown by American flamingos on the carrot-oil supplemented diet in New York and sent out to La Jolla by Mr. Conway have been found to yield, among other carotenoid fractions: (*a*) a substantial component which remains persistently epiphasic in petroleum ether over 90 to 95% methanol, in contrast to the mere traces of this fraction recoverable from feathers of the San Diego flock (this is not carotene, but a unique derivative with absorption maximum at 448 to 450 mμ and an inflexion at 468 mμ in petroleum ether); (*b*) more surprisingly, hydrolysis of the feathers yielded also a minor quantity of astacene, reminiscent of the other flock receiving astaxanthin in their regime; moreover, pyridine extracts of the feathers yielded minor quantities of astaxanthin itself. This notwithstanding the fact that the oily mash fed to the New York flock yields no traces of astaxanthin, and it is extremely unlikely that the New York birds might have adventitious sources of this carotenoid. Both colonies stored in their feathers a major carotenoid fraction chromatographically and spectrophotometrically indistinguishable from the red carotenoid canthaxanthin, recoverable from the pink mushroom *Cantharellus cinnabarinus* (Haxo, 1950) and shown by Petracek and Zechmeister (1956) to be the neutral 4,4′-diketo-β-carotene.

The initially edematous legs of the newly hatched, downy-whiteplumed flamingo chick are bright red or pink from hemoglobin beneath the thin epidermal layer. This skin turns black, however, on about the eighth day as the chick prepares to leave the shelter of the nest and the hovering parents. This rapid melanization, perhaps induced by multiple short exposures to solar rays, may, in the bird's native habitat, serve as an aid in protecting the thin skin and the delicate underlying tissues from injury due to unavoidable exposure to the blazing tropical sunlight. As time passes, a thick cuticle grows over the leg-skin; this skin later gradually loses its melanin, replacing it by red carotenoids. Whether these carotenoids, through their moderate absorption of light in the critical, erythemogenic fraction (ca. 295 to 320 mμ) may afford some continuing protection, notably over the flexible hock and over the toes, remains to be determined.

A final example may suffice for the purposes of this brief comparative survey. The oceanic siphonophore *Velella lata* exhibits striking blue colors in both mantle and tentacles, reflecting the presence of astaxanthin conjugated with protein (Fox and Haxo, 1958). Clear blue aqueous systems of the fresh mantle pigment manifest a smooth, rounded absorption profile with a broad maximum in the yellow region around 585 to 588 mμ, while like preparations from the blue tentacles exhibit a curve of very similar shape, but with maximal absorption in the orange at about 610 mμ, thus suggesting differences in the kind or ratio of protein conjugated with the same chromophore.

A typical coelenterate in its carnivorous habits, *Velella* may derive its supplies of astaxanthin from its known consumption of planktonic crustacean species and their floating eggs. The digestive tissues and the hanging medusa buds harbor an abundance of minute yellow-brown algal cells or zooxanthellae. These algae contain no astaxanthin, but a full complement of photosynthetic pigments, e.g., chlorophyll *a*, common carotenes, and several algal xanthophylls. The fresh mantle tissue, examined through dorsal and ventral surfaces and including the thin intermediary alga-laden endoderm, exhibit a rounded absorption maximum at 590 mμ, contributed by the astaxanthin-protein complex, and a secondary, minor peak at 675 mμ from the algal chlorophyll.

The members of this plant-animal association would appear to afford each other some features of mutual advantage. The algal cells within the tissues of the siphonophore receive harborage against consumption by filtering or particulate feeders, and perhaps also against their sinking into darkness; moreover, they reside in a site favorable for their assimilation of soluble metabolic wastes and digestive products of the host. And the animal's blue translucent canopy, while shading the plant cells against excessive sunlight at the ocean surface, demonstrably admits ample light for photosynthetic needs. The zooxanthellae, on their part, evolve *in situ* photosynthetic oxygen in excess of the respiratory requirements of the association. Free excess gas, perhaps relatively high in oxygen content, is therefore normally present in the chambers beneath the upper mantle surface. The siphonophore colony, consequently remaining afloat, occupies a region of adequate food supply, e.g., buoyant eggs, microscopic animals feeding upon particulate organic detritus or leptopel, often in the region of extensive surface "slicks." This floating facility, implemented by the entrapped gases, may not only reduce the likelihood of detection by nectonic predators but, augmented by the erect sail, should provide for the colony's transportation by prevailing winds toward or in company with surface concentrations of food materials.

* * *

Continued investigations should reveal increasing evidence of the vital importance of colored molecules, synthesized originally by plants and borrowed by animals, whether directly or through serial food-chains, often chemically modified in the process, and sometimes not without incidental usefulness to associated representatives of the original synthesizers.

Various animals may modify plant carotenoids for use in generalized or regionally focused photoreception. There remains the possibility that, in invertebrates and perhaps in some fishes, 40-carbon-atom xanthophylls may occupy roles somewhat parallel to those fulfilled by vitamin A in terrestrial vertebrates, e.g., in embryonic development and growth, in the maintenance of moist surfaces, including the elaboration and secretion of mucus and ink, and perhaps also in the deposition of chitinous skeletal structures.

Returning to the systems of invertebrates with eyes, it should be of interest to determine whether arthropod species lacking vitamin A may employ instead photolabile protein complexes of alternative polar carotenoids for perceiving light in certain spectral regions. Astaxanthin, the wide occurrence in arthropod eyes and the chemical properties of which would suggest it as a candidate for such a role, is a polar molecule, 3,3′-dihydroxy-4,4′-diketo-β-carotene, capable through enolization of acting as a weak acid and thus combining with metallic ions to form salts; alternatively, behaving as a secondary keto alcohol, it is esterifiable with fatty acids. Moreover, enolic astaxanthin occurs conjugated with proteins to give various blue, green, purple, grey, red, or brown complexes; and these are reversibly dissociable by gently warming and promptly re-cooling in aqueous media, or alternatively by rendering their electrolytic solutions slightly acidic, followed by early neutralization. Under such conditions a blue astaxanthin-protein association will progress gradually and reversibly through blue-purple and red-purple to red, e.g., on warming the chromoprotein from lobster shells (Wald *et al.*, 1948) or from *Velella lata* (Fox and Haxo, 1958). Denaturation of the protein moiety by heating to 100°C or by the addition of mineral acids, alcohol, acetone, or pyridine sets free the red-orange carotenoid. How chemically extensive or physiologically active photic energy might prove to be when allowed to impinge upon (dark-adapted) optical systems involving astaxanthin-protein compounds would now appear to be a demanding issue.

In the meanwhile, any direct correlation between the biochemical kind of visual equipment an animal possesses and the brightness or shadiness of its environment would appear, from surveys by Kon and his colleagues, to be nearly ruled out. But the suggested biochemical investigations might be undertaken with a view toward discovering any possible correlations between (*a*) action-spectra of acuity in visual response, (*b*) morphology of the visual apparatus, and (*c*) polarity and chemical reactivity of chromogens involved in photokinesis.

Answers derived from any such studies would, in all probability, leave us still puzzled about some insects which reportedly lack vitamin A and can be raised to normal adults of a second generation on diets lacking the vitamin or any other carotenoid (cited by Fox, 1953, p. 136).

References

Brockmann, H., and Völker, O. (1934). *Z. physiol. Chem.* **224**, 195-215.

Conway, W. G. (1958). *Animal Kingdom* **16**, 159-173.

Conway, W. G. (1959). The Avicult. Mag., Jul.-Oct., pp. 108-111.

Dimelow, E. J. (1958). *Nature* **182**, 812.

Fisher, L. R., and Goldie, E. H. (1959). *J. Marine Biol. Assoc. United Kingdom* **38**, 291-312.

Fisher, L. R., and Kon, S. K. (1959). *Biol. Revs. Cambridge Phil. Soc.* **34**, 1-36.

Fisher, L. R., Kon, S. K., and Thompson, S. Y. (1954). *J. Marine Biol. Assoc. United Kingdom* **33**, 589-612.

Fisher, L. R., Kon, S. K., and Thompson, S. Y. (1955). *J. Marine Biol. Assoc. United Kingdom* **34**, 81-100.

Fox, D. L. (1953). "Animal Biochromes." Cambridge Univ. Press, London and New York.

Fox, D. L. (1955). *Nature* **175**, 942-943.

Fox, D. L. (1957). *In* "The Physiology of Fishes" (M. E. Brown, ed.), Vol. II, pp. 367-385. Academic Press, New York.

Fox, D. L., and Crane, S. C. (1942). *Biol. Bull.* **82**, 284-291.

Fox, D. L., and Haxo, F. T. (1958). *15th Intern. Congr. Zool. London Sect. III, Paper 2* pp. 280-282.

Fox, D. L., and Sargent, M. C. (1938). *Chem. & Ind. (London)* **57**, 1111.

Gerould, J. H. (1921). *J. Exptl. Zool.* **34**, 385-415.

Glover, J., Goodwin, T. W., and Morton, R. A. (1947). *Biochem. J.* **41**, xlv.

Goldsmith, T. H. (1958). *Proc. Natl. Acad. Sci. (U.S.)* **44**, 123-126.

Goodwin, T. W. (1949). *Biochem. J.* **45**, 472-479.

Goodwin, T. W. (1952). *Biol. Revs. Cambridge Phil. Soc.* **27**, 439-460.

Goodwin, T. W. (1955). *Ann. Rev. Biochem.* **24**, 497-522.

Goodwin, T. W. (1959). *Advances in Enzymol.* **21**, 295-368.

Grangaud, R., and Massonet, R. (1955). *Arch. sci. physiol.* **9**, 245-256.

Hartman, M., Medem, F. G., Kuhn, R., and Bielig, H. J. (1947). *Z. Naturforsch.* **2b**, 330-349.

Haxo, F. (1950). *Botan. Gaz.* **112**, 228-232.

Hogan, A. G. (1939). *In* "The Vitamins" (M. Fishbein, ed.), pp. 280-281. Am. Med. Assoc., Chicago, Illinois.

Kritzler, H. (1943). *Physiol. Zoöl.* **16**, 241-255.

Lederer, E. (1934). *Compt. rend. soc. biol.* **117**, 1086-1088.

Lederer, E. (1935). "Les Carotenoides des Animaux." Hermann, Paris.

Lwoff, M., and Lwoff, A. (1930). *Compt. rend. soc. biol.* **105**, 454-456.

Manunta, C. (1933). *Boll. soc. ital. biol. sper.* **8**, 1278-1282.

Manunta, C. (1935). *Atti soc. nat. e mat. Modena* **66**, 104-113.

Manunta, C. (1937). *Boll. soc. ital. biol. sper.* **12**, 31-34, 626-628, 698-699.

Mattson, F. H., Mehl, J. W., and Deuel, H. J., Jr. (1947). *Arch. Biochem.* **15**, 65-73.

Millott, N. (1957). *Proc. Roy. Soc.* **129**, 263-272.

Millott, N., and Vevers, H. G. (1955). *J. Marine Biol. Assoc. United Kingdom* **34**, 279-287.

Millott, N., and Yoshida, M. (1957). *J. Exptl. Biol.* **34**, 394-401.

Neilands, J. B. (1947). *Arch. Biochem.* **13**, 415-419.

Oku, S. (1929). *Bull. Agr. Chem. Soc. Japan* **5**, 81-83.

Oku, S. (1930). *Bull. Agr. Chem. Soc. Japan* **6**, 104-105.

Oku, S. (1932). *Bull. Agr. Chem. Soc. Japan* **8**, 7-8; 89.

Oku, S. (1933). *Bull. Agr. Chem. Soc. Japan* **9**, 91-92.

Palmer, L. S. (1922). "Carotinoids and Related Pigments," pp. 125-137. Am. Chem. Soc. Monograph Ser. No. 9. Chemical Catalog Co., New York.

Palmer, L. S., and Eckles, C. H. (1914). *J. Biol. Chem.* **17**, 211-221.

Pease, M. (1928). *Z. Induktive Abstammungs- u. Vererbslehre Suppl.* **2**, 1153-1156; *Biol. Abstr.* **3**, 1121.

Petracek, F. J., and Zechmeister, L. (1956). *Arch. Biochem. Biophys.* **61**, 137-139.

Rockstein, M. (1956). *Nature* **177**, 341-342.

Rockstein, M., and Rubenstein, M. (1957). *Biol. Bull.* **113**, 353-354.

Rogozinski, F. (1937). *Bull. Inst. Acad. Cracovie*, Classe Sci., Math. Nat. B. 2, 183-193; *Chem. Abstr.* **32**, 1760.

Schmidt-Nielsen, S., Sørensen, N. A., and Trumpy, B. (1932). *Kgl. Norske Videnskab. Selskabs Forh.* **5** (30), 118-121.

Schuette, H. A., and Bott, P. A. (1928). *J. Am. Chem. Soc.* **50**, 1998.

Sumner, F. B., and Fox, D. L. (1933). *J. Exptl. Zool.* **66**, 263-301.

Sumner, F. B., and Fox, D. L. (1935). *Proc. Natl. Acad. Sci. U. S.* **21**, 330-340.

Sutherland, M. D., and Wells, J. W. (1959). *Chem. & Ind. (London)* **78**, 291-292.

Uda, H. (1919). *Genetics* **4**, 395-416.

Vevers, H. G., and Millott, N. (1957). *Proc. Zool. Soc. London* **129**, 75-80.

Völker, O. (1958). *J. Ornithol.* **99**, 209-217.

Wald, G. (1943). *Vitamins and Hormones* **1**, 195-227.

Wald, G., Nathanson, N., Jencks, W. P., and Tarr, E. (1948). *Biol. Bull.* **95**, 249-250.

Wiese, C. E., Mehl, J. W., and Deuel, H. J., Jr. (1947). *Arch. Biochem.* **15**, 75-79.

Willimott, S. G. (1928). *Biochem. J.* **22**, 157-159.

Wolken, J. J. (1959). Personal communication.

Zechmeister, L. (1937). *Ergeb. Physiol. biol. Chem. u. exptl. Pharmakol.* **39**, 117-191.

DISCUSSION

FRENCH: I am interested in your breeding experiment with the fish. I wonder if any comparable experiments have been done with lobsters; can you raise a white lobster by taking away carotenoids from his diet when he is changing shells?

FOX: We tried very hard to do that. Henry Fisk and I worked more than a year to find out what the precursor of astaxanthin was. We failed. The lobster got paler and paler, we got less and less astaxanthin in the carapaces as they were shed, but we never got to the end point. However, sometimes when they are kept for a long time in an aquarium on white food, the carapace is a kind of tan color instead of being red. It never gets white.

FRENCH: And how about the Echinida. Is it possible to raise those?

FOX: No, I have never tried that. You know they are not ideal laboratory specimens; they drop their spines. One of the first things that happens if you give them a dietary insufficiency is they begin to drop their spines and go to pieces.

FRENCH: Are these pigments essential to the animal or do they just pile them up because they have no use for them?

FOX: Both, I expect. I am on the spot here; I do not know. We do know, however, or we have every reason to suspect with all likelihood of being right, that they use some of these chromoproteins for vision.

FRENCH: Aside from vision and Vitamin A, is there any function of carotenoids known?

FOX: I do not know. I was thinking about mucus secretion and secretion of shells, but I do not know. They simply seem to occur together.

MILLOTT: The question might be answered another way. You were thinking of metabolic function. Of course, in natural history, there is an entirely different function. Carotenoids are extremely important as sexual colors.

MACKINNEY: If you had enough time and patience and raised the male and female exclusively on Vitamin A so they did not develop this sexual dichromatism, would you get normal mating, would you suspect?

FOX: Yes, I would suspect that you would. In the forms without eyes, it does not make any difference, of course. In G. K. Noble's experiments with fishes, he found out that with the female on one side of the glass and the male on the other side of the glass, she did not deposit eggs just because he was brightly colored, she deposited eggs if he were brightly colored and went through the proper ceremonies, went through a lot of movements. If there was a dull colored male who went through the right motions and a brightly colored male who was idle, she responded to the former, not the latter, although she did have color vision.

MILLOTT: I would like to refer to the rather peculiar and particular condition of starfish. We could not find Vitamin A in starfish and *Marthasterias*. We then referred to Fisher and Conrad Reddings who are experts in this matter, and Fisher has recently confirmed that he has been unable to find Vitamin A. In the meantime there was a note in *Nature* by a man called Rockstein stating that he had examined the eyespots of an American asteroid and had found there a pigment which behaved like rhodopsin; it was photosensitive, and he claimed to find tests for vitamin A. Now there is a complete impasse—there is Fisher and Vevers and myself who cannot find Vitamin A, while Rockstein has found in the eyespots a pigment of the rhodopsin type which seems to be based on Vitamin A.

Now in the case of the eyespots which Professor Fox mentioned, we found β-carotene and astaxanthin, but there was another point which I would like to take this opportunity to mention and that is in the starfish there has been dispute as to where the photosensitive parts are in this organism. Some say it is the eyespots, others say it is the skin. Still others have sought to compromise by saying that the eyespots permit more precise orientation but the animal's skin is light sensitive. Now the interesting thing was that Vevers and I found β-carotene and astaxanthin in the eyespots of *Marthasterias* and β-carotene and astaxanthin in the skin as well. Now this was a most suggestive observation that the animal probably has skin sensitivity. Now you may ask: how do you know that the starfish has a genuinely sensitive eyespot? There's one outstanding proof of that, I think, and that was of Hartline, who, in a paper, just gave a tracing, giving no experimental details at all, but showing that when you illuminated the eyespot of what he calls *Asterias* (whatever that may be, no species defined) you get a potential difference, a slow potential difference; in other words here is beautiful electrophysiological evidence. I do not know how he did it, because the eyespots are exceedingly minute. So starfishes seem to stand fair and square at the crossroads. Maybe it is a vitamin A rhodopsin type of thing; maybe it is specialized skin sensitivity, based upon β-carotene.

One last point. I have just come upon a paper by Rosenberg in which he has shown that β-carotene is photoconductive to a remarkable degree. And he asked the same fundamental question that has been asked time and time again: is there any need for a pigmented body to break down during vision? Why aren't you considering photoconduction?

Reprint from

Eclogae geol. Helv. 1958	Vol. 51	No. 3	Page 598—608	Basel, December 1959

18. – FRANCIS P. SHEPARD (University of California Scripps Institution of Oceanography La Jolla, California): **Sediment Environments of the Northwest Gulf of Mexico**[1]**.** With 6 text figures.

ABSTRACT

Study of a large suite of samples from the shallow water areas of the northwest Gulf of Mexico has provided criteria which should be helpful in determining the environments of dep-

---

[1] This investigation was supported by a grant from the American Petroleum Institute, Project 51.

Contributions from the Scripps Institution of Oceanography, New Series, 1202

(874) **Reproduced by Permission** of the editor, Eclogae geologicae Helvetiae (Swiss Geological Society).

osition of many ancient sediments. Among the criteria which have proven most useful for identifying bays are the oyster reefs, the interfingering silty clays and clayey sands, and the small number of species compared to the open shelf. The barrier islands are characterized by their high sand content and their mixture of open shelf and bay faunas. The continental shelf sediments are distinguished by their content of glauconite, echinoid fragments, and planktonic Foraminifera (outer shelf), all of which are very scarce in the bays. The deposits around the mouths of rivers are characterized by their high wood content, their abundance of mica, and their good lamination.

INTRODUCTION

Starting in 1951 the sediments of the northwestern Gulf of Mexico have been studied intensively under a project given to Scripps Institution of Oceanography by the American Petroleum Institute. In the seven years that have followed, numerous field trips have been made to collect several thousand samples, mostly cores. These samples have been studied by a group at Scripps Institution with some help from other scientists.

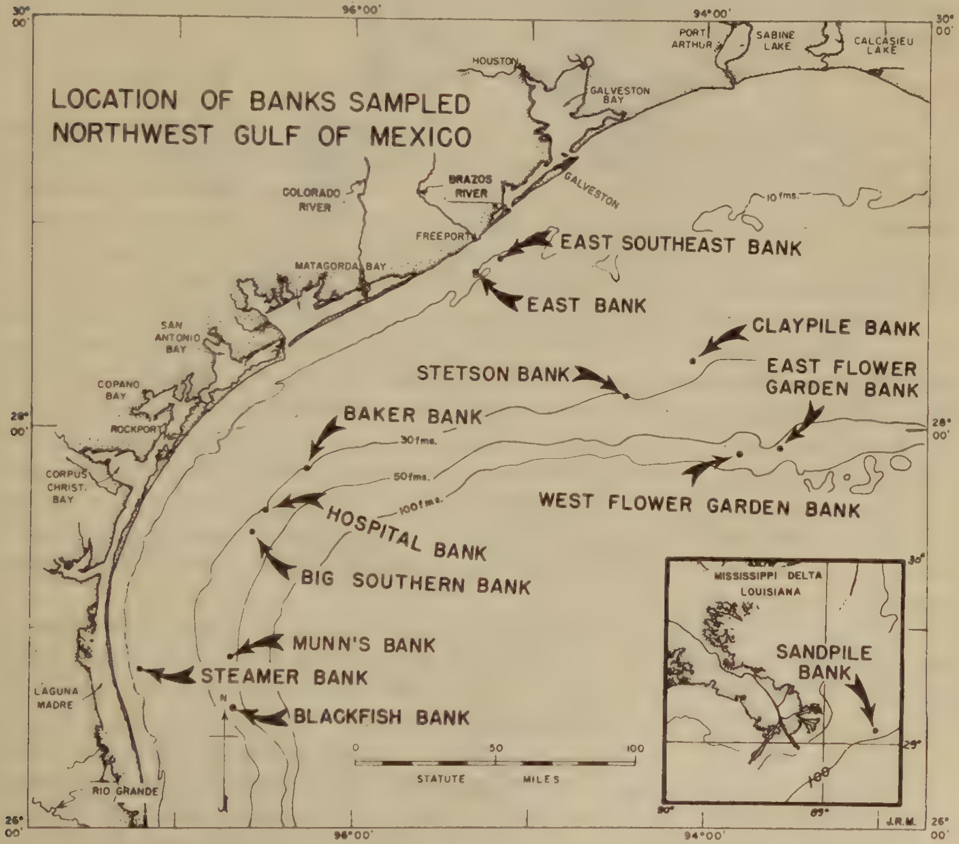
30° 00'
96°00'
94°00'
30° 00'
PORT ARTHUR
SABINE LAKE
CALCASIEU LAKE
HOUSTON
LOCATION OF BANKS SAMPLED
NORTHWEST GULF OF MEXICO
GALVESTON BAY
BRAZOS RIVER
COLORADO RIVER
GALVESTON
10 fms.
FREEPORT
EAST SOUTHEAST BANK
MATAGORDA BAY
EAST BANK
CLAYPILE BANK
SAN ANTONIO BAY
STETSON BANK
EAST FLOWER GARDEN BANK
COPANO BAY
BAKER BANK
28° 00'
ROCKPORT
30 fms.
28° 00'
CORPUS CHRIST. BAY
50 fms.
WEST FLOWER GARDEN BANK
100 fms.
HOSPITAL BANK
BIG SOUTHERN BANK
MISSISSIPPI DELTA
LOUISIANA
30°
MUNN'S BANK
SANDPILE BANK
STEAMER BANK
LAGUNA MADRE
N
BLACKFISH BANK
0
50
100
STATUTE MILES
29°
100
RIO GRANDE
90°
89°
J.R.M.
26° 00'
96°00'
94°00'
26° 00'

Fig. 1. Showing the general area from which samples were derived. Note that there is a gap of 150 miles between the main chart and the inset showing the Mississippi Delta.

Areas for field collections included: 1° the margins of the Mississippi Dalta, 2° the bays and barrier islands of the central Texas Coast, 3° the Laguna Madre, an elongate lagoon of southern Texas, and 4° the continental shelf from the Mississippi Delta to the Mexican border (see Fig. 1). These were chosen because they represent contrasting facies of deposition in the same general area, where subsidence has led to the formation of a sedimentary column with an average thickness under the present coast of at least 5,000 meters. The Mississippi Delta margin is an area of particularly rapid deposition where the huge river enters the sea. The bays of the central Texas coast are receiving smaller amounts of sediment from streams and from the barrier islands which border them. These bays differ from the Laguna Madre to the south in having relatively low salinity whereas the Laguna in a semiarid area has high salinity and no entering streams of appreciable size. The continental shelf receives only small supplies of sediments except relatively near the four large rivers which empty directly into the Gulf rather than into bays. Currents and waves play an important role in distributing the shelf sediments but are much less effective in the protected bays. Also the stable salinity and temperatures in the shelf waters form a marked contrast to the other environments.

MISSISSIPPI DELTA MARGIN

The Mississippi is the only large river in the world which has built a delta completely across the continental shelf. In the past 70 years it has advanced about eight miles into the Gulf over a wide area on the northeast side of the birdfoot-shaped delta (Fig. 2). It is building forward with a gentle foreset slope, not over one-half degree in inclination. On the shelf beyond the foreset slope much slower deposition is occurring both to the east and to the west of the delta.

The deltaic deposits seem best divided onto topset, foreset, and bottomset (Fig. 3). The topset beds are forming as natural levees, as marsh deposits, as shallow interdistributary bay deposits (between the levees), and as delta front platform deposits in a narrow band around the advancing distributaries. Except for the marsh deposits most of the topset beds are well laminated, consisting of alternating silty clay and very fine sand or coarse silt. Where distributaries have been abandoned, the waves along the coast are converting these mud and sand deposits to well-sorted fine sands which have become barrier beaches and in some cases barrier islands. Otherwise the delta marginal deposits have a conspicuous scarcity of clean sands.

The foreset beds differ from the topset in having a much higher content of silt and clay. Also the lamination is virtually absent in the slope deposits. The bottomset beds are largely silty clays, but they differ trom the topset and foreset in having a much higher content of Foraminifera, echinoid fragments, and shells, all of which are very scarce in the more rapidly accumulating deposits nearer the delta.

All of the deltaic sediments are conspicuous in their high content of wood fibres and other plant materials. Mica is much more common than in the non-deltaic sediments of the Gulf coast. Small orange-colored aggregates are found abundantly among the constituents of the coarse fraction. Each of these three items becomes very scarce out beyond the margin of the deltaic deposits.

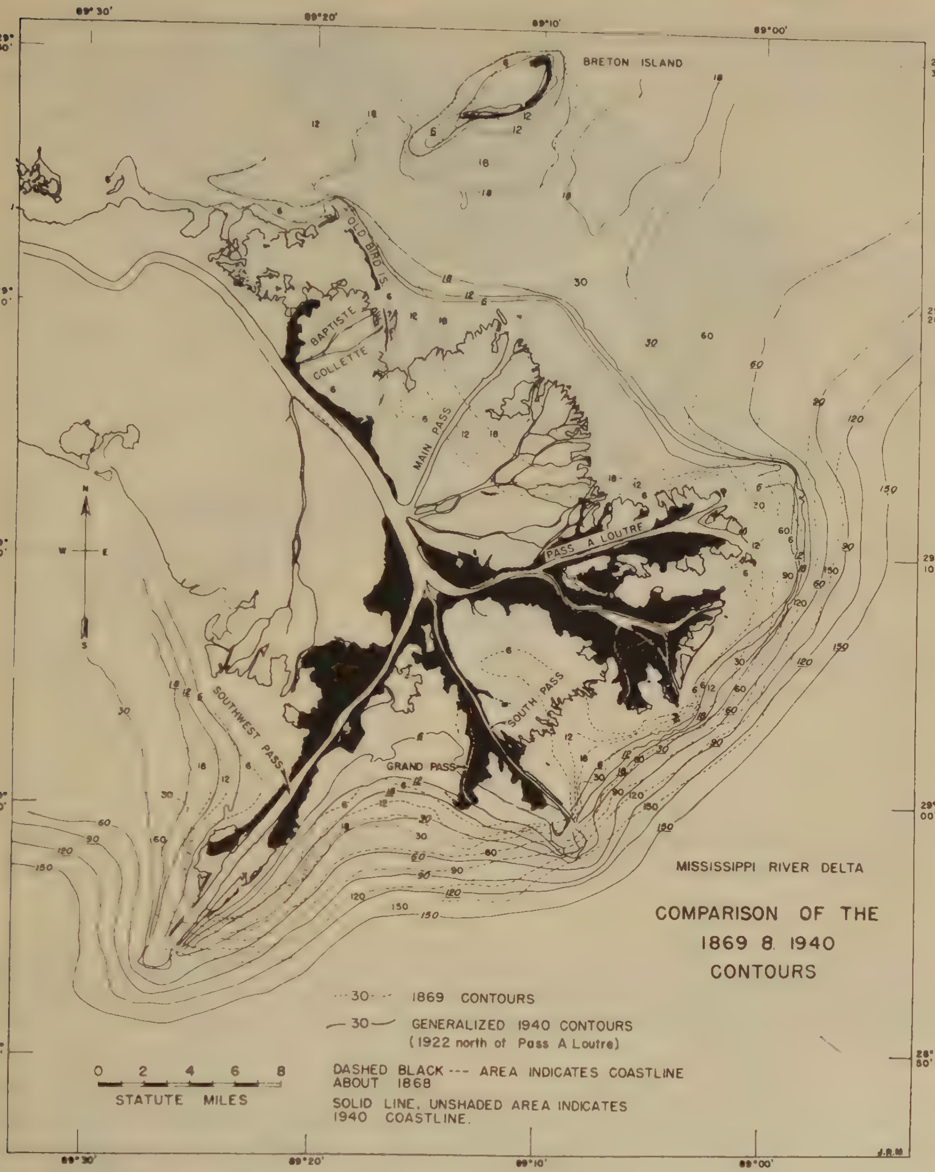
89°30'
89°20'
89°10'
89°00'
29° 30'
29° 20'
29° 10'
29° 00'
28° 50'
BRETON ISLAND
OLD BIRD IS.
BAPTISTE
COLLETTE
MAIN PASS
PASS A LOUTRE
SOUTH PASS
SOUTHWEST PASS
GRAND PASS
N
W
E
S
MISSISSIPPI RIVER DELTA
COMPARISON OF THE
1869 & 1940
CONTOURS
30 1869 CONTOURS
30 GENERALIZED 1940 CONTOURS
(1922 north of Pass A Loutre)
DASHED BLACK --- AREA INDICATES COASTLINE ABOUT 1868
SOLID LINE, UNSHADED AREA INDICATES 1940 COASTLINE.
0 2 4 6 8
STATUTE MILES
J.R.M.

Fig. 2. Showing the growth of the Mississippi Delta since 1869, along with generalized depth changes on the adjacent sea floor.

Borings in the Mississippi Delta have shown various cycles of deposition related to the changing sea levels of the Pleistocene and to a general subsidence of the deltaic area. From a series of these borings made by the Engineers Corps of the U.S. Army, we have been able to determine the sequence of events during the rising sea level at the end of the last glacial stage. The sea first advanced over

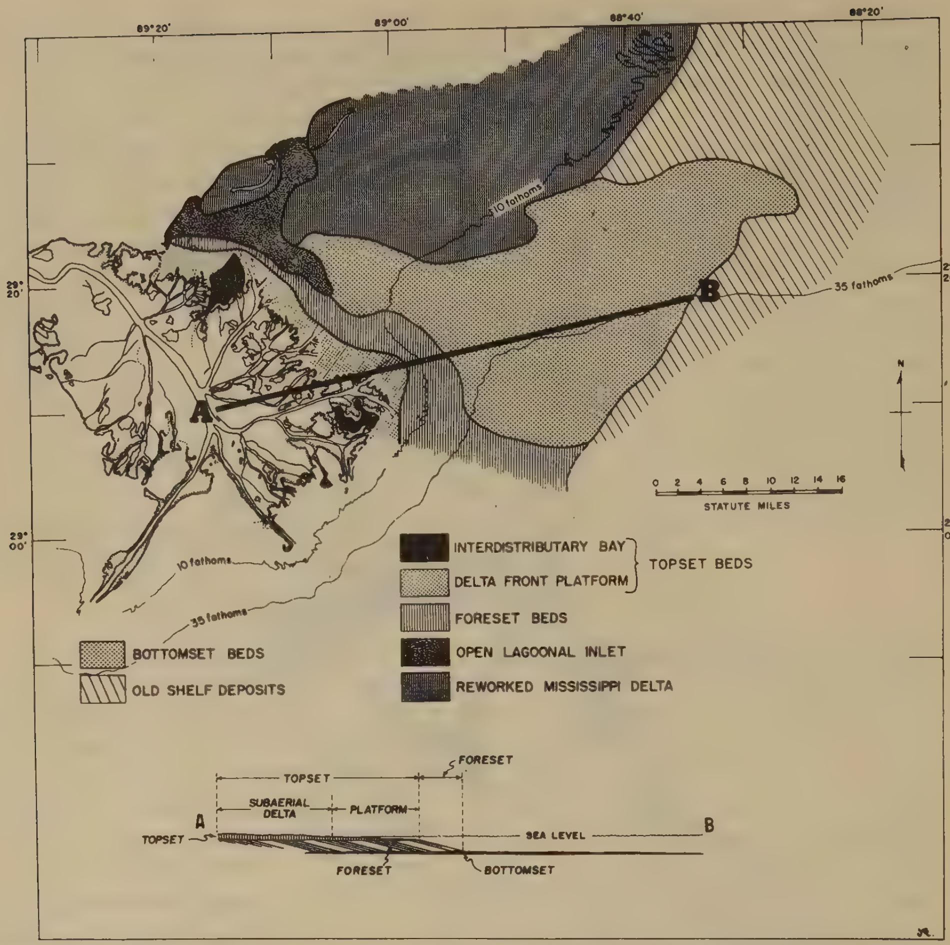
89°20'
89°00'
88°40'
88°20'
29° 20'
29° 00'
10 fathoms
35 fathoms
A
B
N
0 2 4 6 8 10 12 14 16
STATUTE MILES
INTERDISTRIBUTARY BAY
DELTA FRONT PLATFORM
TOPSET BEDS
FORESET BEDS
OPEN LAGOONAL INLET
REWORKED MISSISSIPPI DELTA
BOTTOMSET BEDS
OLD SHELF DEPOSITS
TOPSET
FORESET
SUBAERIAL DELTA
PLATFORM
SEA LEVEL
TOPSET
FORESET
BOTTOMSET

Fig. 3. Illustrating the depositional environments to the east of the Mississippi Delta. The cross section illustrates the relationship of these environments to the topset, foreset, and bottomset beds. The vertical is considerably exaggerated in this profile.

the area on the east side of the delta so that continental shelf deposits were forming. Then the river built out onto the shelf and formed a delta. After the abandonment of this delta about 2,000 years ago a portion was slowly submerged and covered by sound deposits, whereas the outer delta has been converted into sandy barrier islands which have built upward to keep pace with the submergence forming the Chandeleur Islands and Breton Island.

CENTRAL TEXAS BAYS

The bays along the Texas coast inside the barrier islands have a depth which is rarely greater than three meters. These bays include lagoons which extend along the coast directly inside the barrier islands, and estuaries which occur at the mouths of a number of the Texas rivers. Each of these rivers, however, is engaged in filling the estuaries. In addition the fill within the bays, aside from the advancing deltas, averages approximately 0.3 meters per century so that from the combined causes the virtual elimination of the bays in a few hundred years can be anticipated unless the fill is offset by a sea level rise or land subsidence.

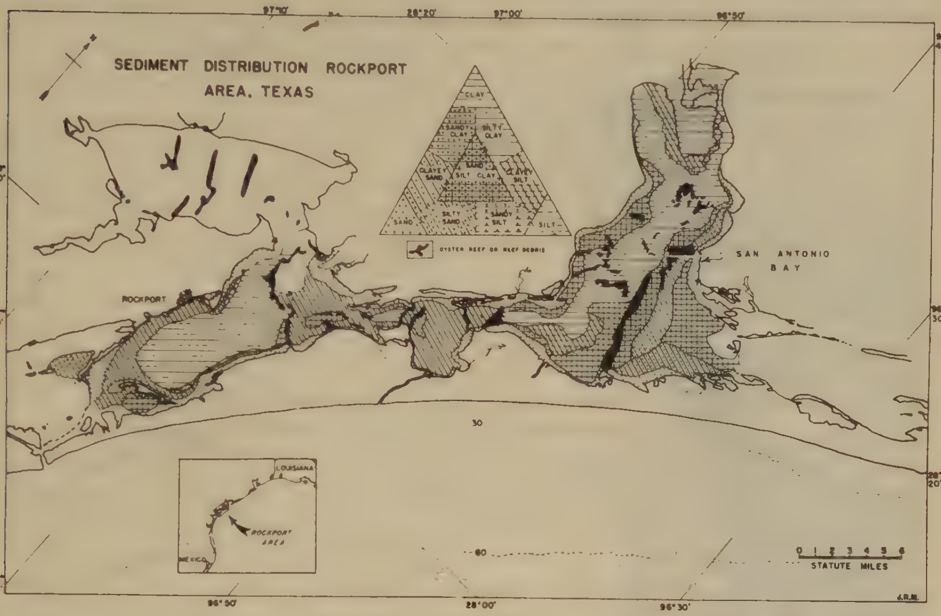
SEDIMENT DISTRIBUTION ROCKPORT AREA, TEXAS
CLAY
SANDY CLAY
SILTY CLAY
CLAYEY SAND
SAND SILT CLAY
CLAYEY SILT
SAND
SILTY SAND
SANDY SILT
SILT
OYSTER REEF OR REEF DEBRIS
ROCKPORT
SAN ANTONIO BAY
30
60
LOUISIANA
ROCKPORT AREA
MEXICO
0 1 2 3 4 5 6
STATUTE MILES
97°10'
28°20'
97°00'
96°50'
96°40'
28°00'
97°10'
96°30'
28°20'
97°00'
96°50'
28°00'
96°30'

Fig. 4. Showing the nature of the sediments in the bays of a central Texas area. Types are related to percentages of sand, silt, and clay as shown in the triangle diagram. Locations of oyster reefs are also indicated.

The bay deposits (Fig. 4) are commonly silty clays except near the barrier island inlets or at places where washovers from the Gulf have occurred during hurricanes when the sea level rose and crossed the low divides of the islands. As a result the outer or lower bays have sandy sediments with considerable quantity of clay and shells, but very little silt.

Most of the bay deposits are unstratified. Lamination occurs only near the river mouths. The stratification and lamination in the rest of the bays are apparently eliminated by bottom-living organisms which churn up the sediment and destroy the stratification. Near the river mouths, however, the fresh water inhibits the growth of the organisms and also the deposition is somewhat faster so that the stratification may be preserved, although it is not always found in the cores.

The oyster reefs are features particularly characteristic of the central portions of the bays where the salinity is intermediate between river and ocean water. These form ridges consisting of oyster shells and mud. Many of the reefs rise to the surface and form shell islands while others form shoals which are hard to avoid in navigating in small boats through the bays. The reefs should form an impure limestone if they are converted into rock. A considerable percentage of the muds brought into many of the bays by the rivers consist of particulate calcium carbonate, having been transported as the erosion product of the chalk formations, and this adds to the high carbonate content of the oyster reefs.

Borings show that the bay deposits have considerable thickness. Under San Antonio Bay oyster reefs have been traced to a depth of 60 feet and silty clays with bay faunas occur at depths of as much as 80 feet. During part of this deposition the bays were apparently more connected to the open Gulf than at present.

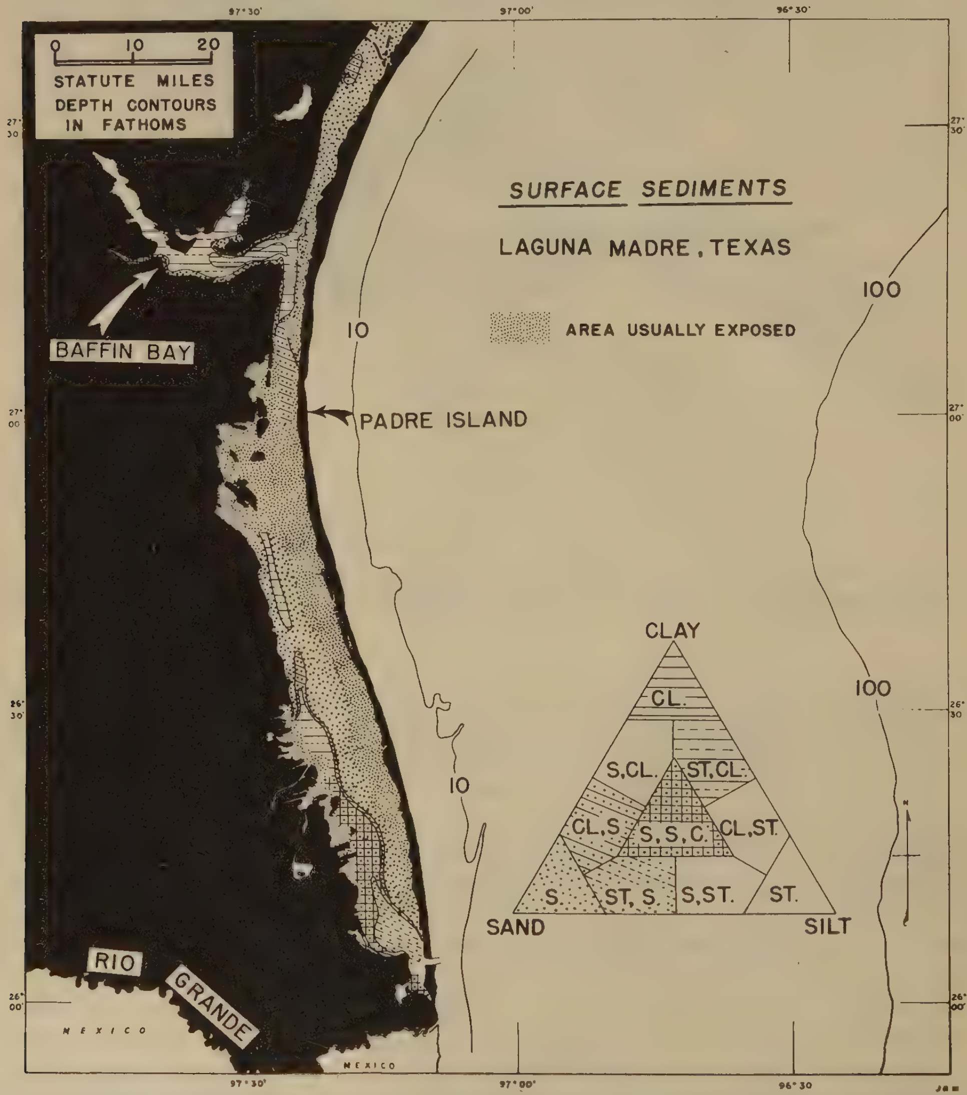
97°30'
97°00'
96°30'
0 10 20
STATUTE MILES
DEPTH CONTOURS IN FATHOMS
27° 30'
27° 00'
26° 30'
26° 00'
SURFACE SEDIMENTS
LAGUNA MADRE, TEXAS
100
10
AREA USUALLY EXPOSED
BAFFIN BAY
PADRE ISLAND
CLAY
CL.
S,CL.
ST,CL.
CL,S
S,S,C.
CL,ST
S.
ST, S.
S,ST.
ST.
SAND
SILT
RIO GRANDE
MEXICO
N

Fig. 5. Sediment distribution in the Laguna Madre based on sand-silt-clay content. Note that the central part of the Laguna Madre is usually exposed, being covered only during strong southerly winds.

LAGUNA MADRE

Inside Padre Island a lagoon extends for 200 kilometers along the southern coast of Texas (Fig. 5). The central part of this lagoon has recently become filled so that it is covered by water only during unusual wind conditions. The only continuous water connection along the length of the Laguna Madre is, therefore, the intracoastal canal in which a channel is maintained to a depth of four meters. To the south the Laguna is connected to the ocean through the inlet at Port Isabel. The northern Laguna is connected with Corpus Christi Bay and, hence, to the Gulf at Aransas Pass. The considerable distance between inlets combined with the semiarid condition and the absence of major streams entering the Laguna, results in high salinity. Much of the bay has salinity of 60 parts per thousand or more, with particularly high measurements being obtained in Baffin Bay, an estuary without any entering stream. Despite the high salinity, fish are very abundant in the Laguna, in fact, it is the best source of fish along the entire Texas coast.

The sediments of Laguna Madre which have been studied by G. A. Rusnak of Scripps Institution differ from those of the central Texas bays in having a much higher content of sand. The chief transporting agent is the wind which blows sand in from the dunes of Padre Island. In addition occasional washovers from the Gulf occur during times of high sea level, mostly hurricanes. A few of the deeper portions of the Laguna and of Baffin Bay have muddy sediments, part of which have more than 75 per cent of clay. Among the sands there are many grains which are coated with calcium carbonate and in some places oolites are found with a quartz nucleus. Several feet below the bottom gypsum rosettes have been dredged and these are exposed in the spoil banks along the intracoastal canal. Stratification is much less disturbed in the Laguna Madre sediments because the bottom conditions are not generally favorable to burrowing organisms which abound in the other bays. In some of the shallow portions an algal mat has formed on the surface which causes stagnant conditions and the production of H_2S and black colors underneath.

BARRIER ISLANDS

Wide barrier islands (formerly referred to as offshore bars) extend along almost the entire Texas coast (Figs. 1, 6). Where they are missing a river has filled in the lagoon behind a former barrier island. The Texas barriers consist of three divisions: the beach which is always present on the Gulf side of the island; the dune belt which is much wider than the beach, often a mile or more across; and the barrier flats found on the lagoon side of most of the barrier islands which also constitute a wide area including marshes and lakes (Fig. 6). The predominant sediment of the barriers is sand. Both the beaches and dunes have well sorted sand, usually with less than one per cent of silt and clay. The dune sands are ordinarily more rounded than those of the beaches, although the difference is small and there is some overlap between the two. Typical eolian cross-bedding in the dunes contrasts with the more even lamination of the beaches. The barrier flats are due largely to the washing over of sand from the outer beach during storms when the sea level is elevated. In addition some sand and silt are blown onto the flats from the interior of the islands. When the water of the lagoons is at a high stage the flats are inundated. At such times muddy sediments are introduced from the lagoons As a result the barrier flat sediments, while predominantly sand, contain some five to ten per cent of silt and clay. Due to evaporation during low water some calcareous deposition takes place on the flats forming small calcareous aggregates. Because of the vegetation on the flats organic matter is quite abundant in the deposits, and peat is formed in some places in the marshes.

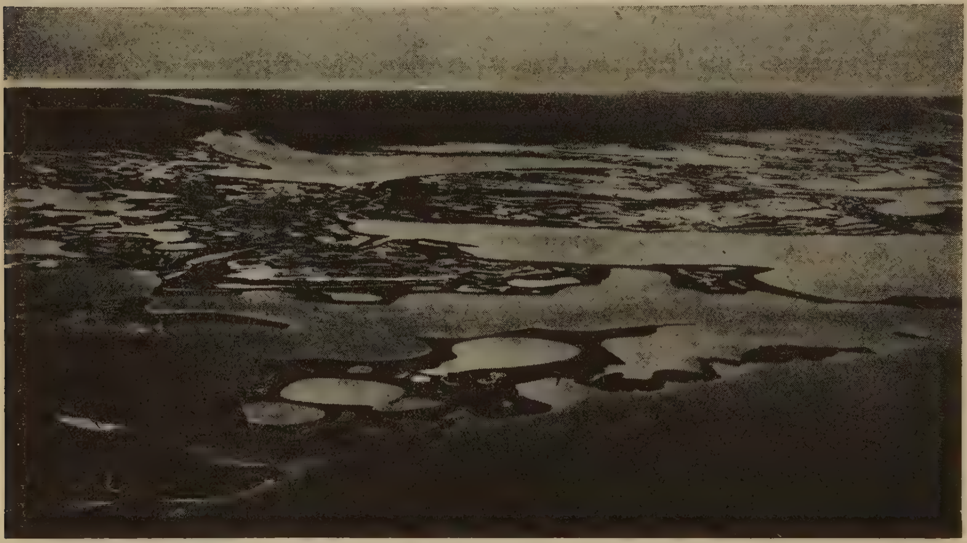

Fig. 6. Air view of a barrier island along the Texas coast with an unusually well developed series of lakes and channels on the lagoon side. The black portion in the intermediate section represents dunes largely covered with vegetation. The white portion in the distance is the beach along the Gulf Coast.

The barrier islands appear to have formed along a coast of submergence (due principally to postglacial sea level rise). Some of the barriers grew upward as the sea level rose. In other cases the barriers may have developed after the rise and grown from the mainland as spits extending along the shore. Barrier island sands up to 60 feet in thickness have been found in some borings.

CONTINENTAL SHELF

The shelf along the coast of Texas and Louisiana has an average width of about 60 miles, narrowing to the south off the Rio Grande Delta and to the northeast off the Mississippi Delta. The shelf has a considerable number of banks rising above its general level (Fig. 1). These consist of: 1° low ridges which probably represent barrier islands drowned by the postglacial rise in sea level, and 2° oval banks with calcareous cover and in some cases with bedrock outcrops. These banks may be partly bioherms, but some at least are definitely salt domes which have pushed the shelf up into shallow depths. One of them has outcrops of Miocene rock indicating that there has been a penetration of the salt dome through at least 3,000 meters of post-Miocene deposits.

The sediments on the shelf, which have been studied by J. R. CURRAY and others, show the influence of the deltas, particularly the Mississippi. According to TJ. H. VAN ANDEL, the Mississippi suite of minerals can be traced in the muddy sediments for about 400 kilometers west of the delta itself. Farther west the mineral suite indicates old Pleistocene deltas, which may come from the drainage basin of the Colorado of Texas, or from that of the Brazos River. To the south the Rio Grande mineral suites appear, here again partly related to the Pleistocene drainage system. The shelf sediments differ from those of the bays in containing an abundance of echinoid fragments and of glauconite in smaller quantities. Both of these are very rare in the bay sediments.

An extensive area of sand and silty sand with abundant shells is found on the outer shelf off Galveston. This appears to be a product of Pleistocene deposition during stages of low sea level. Some of the shells have been dated by Carbon 14 as old as 13,000 years. Portions of the sands resemble the barrier islands along the present coast although some of the relief of the outer barriers has been subdued by reworking which is still going on. A core of 1.5 meters in sand showed Foraminifera related to present day sea level conditions all along its length. This appears to indicate that the sand has been reworked to that depth under present conditions. Heavy mineral assemblages also suggest recent migration of sands along the outer shelf.

The cores obtained on the continental shelf, like those in the central Texas bays, have little stratification. Just outside the sandy zone along the coast most of the cores have irregular sand laminae or partings in the muds, although in no case is there the good lamination characterizing the topset beds of the Mississippi Delta. No stratification was seen in the outer silty clay deposits nor is there much stratification in the reworked sands of the middle and outer shelf.

BIOLOGICAL FACIES

The extensive study of the Gulf Coast Foraminifera by F. B. PHLEGER, F. L. PARKER, and R. R. LANKFORD, of the macroorganisms by R. H. PARKER, and of the Ostracoda by F. M. SWAIN (see bibliography) has allowed an unusually good classification of the biota in the environments. It is possible to distinguish between most bay and shelf environments by means of the faunas. In general the bays have larger numbers of a few species in contrast to smaller numbers of many species on the open shelf. This is interpreted as due to the greater variations in salinity, temperature, and other factors within the bays than on the shelf, which results in limiting the number of species which can stand the extremes of conditions. Also some of the species are restricted to the zones of low salinity characterizing the upper bays or the river mouths where the rivers empty into the Gulf. Certain species of the larger invertebrates are found only along the outer shores of the barrier islands where they survive because of their ability to burrow into the sands.

The faunas of the continental shelf have depth assemblages which characterize similar sediments in the older strata at least during the Tertiary. Along the Gulf coast there is also a progressive increase in the ratio of planktonic to benthonic Foraminifera going out across the shelf. On the outer shelf most samples show a preponderance of planktonics whereas on the inner shelf planktonics are rare and even more rare within the bays.

The ratio of living to dead species in samples of equivalent weight has been studied rather extensively from these sediments. Among the findings has been 1° in areas where deposition is thought to be rapid the live to dead ratios are generally high whereas they are generally low in areas of presumed slow deposition, 2° on the shelf dead Foraminifera and macroorganisms are found out at greater depths than living members of the same species. This last finding indicates either that there is relict sediment left uncovered during the rising sea levels or that the species are moved to greater depths by wave and current action. The gentle slopes make the latter interpretation rather unlikely.

BIBLIOGRAPHY OF THE PRINCIPAL PROJECT WORKS PUBLISHED TO DATE

Curray, J.R. (1956): *Dimensional grain orientation studies of Recent coastal sands.* Bull. Amer. Assoc. Petrol. Geol. *40*, no. 10, pp. 2440–2456.

Grim, R.E., & Johns, W.D. (1955): *Clay mineral investigation of sediments in the northern Gulf of Mexico.* 2nd natl. Conf. on Clays and Clay Minerals, natl. Res. Council, pp. 81–103.

Moore, D.G., & Scrutçn, P.C. (1957): *Minor internal structures of some recent unconsolidated sediments.* Amer. Assoc. Petrol. Geol. *41*, no. 12, pp. 2723–2751.

Parker, F.L., Phleger, F.B., & Peirson, J.F. (1953): *Ecology of Foraminifera from San Antonio Bay and environs, southwest Texas.* Cushm. Found. Spec. Publ. No. 2, 75 pp.

Parker, R.H. (1955): *Changes in the invertebrate fauna, apparently attributable to salinity changes, in the bays of central Texas.* J. Paleontol. *29*, no. 2, pp. 193–211.

– (1956): *Macro-invertebrate assemblages as indicators of sedimentary environments in East Mississippi Delta region.* Bull. Amer. Assoc. Petrol. Geol. *40*, no. 2, pp. 295–376.

Parker, R.H., & Curray, J.R. (1956): *Fauna and bathymetry of banks on continental shelf, northwest Gulf of Mexico.* Bull. Amer. Assoc. Petrol. Geol. *40*, no. 10, pp. 2428–2439.

Phleger, F.B. (1955): *Ecology of Foraminifera in southeastern Mississippi Delta area.* Bull. Amer. Assoc. Petrol. Geol. *39*, no. 5, pp. 712–752.

– (1956): *Significance of living foraminiferal populations along the central Texas coast.* Cushm. Found. Foram. Res. *7*, part 4, pp. 106–151.

Phleger, F.B., & Lankford R.R. (1957): *Seasonal occurrences of living benthonic Foraminifera in some Texas bays.* Cushm. Found. Foram. Res. *8*, part 3, pp. 93–105.

Scruton, P.C.(1956): *Oceanography of Mississippi Delta sedimentary environments.* Bull. Amer. Assoc. Petrol. Geol. *40*, no. 12, pp. 2864–2952.

Shepard, F.P. (1953): *Sedimentation rates in Texas estuaries and lagoons.* Bull. Amer. Assoc. Petrol. Geol. *37*, no. 8, pp. 1919–1934.

Shepard, F.P., & Moore, D.G. (1954): *Sedimentary environments differentiated by coarse-fraction studies.* Bull. Amer. Assoc. Petrol. Geol. *38*, no. 8, pp. 1792–1802.

– (1955): *Central Texas coast sedimentation: characteristics of sedimentary environment, recent history, and diagenesis.* Bull. Amer. Assoc. Petrol. Geol. *39*, no. 8, pp. 1463–1593.

Shepard, F.P. (1956): *Marginal sediments of Mississippi Delta.* Bull. Amer. Assoc. Petrol. Geol. *40*, no. 11, pp. 2537–2623.

Shepard, F.P. & Rusnak, G.A. (1957): *Texas bay sediments.* Inst. Mar. Sci. *4*, no. 2, pp. 5–13.

Swain, F.M. (1955): *Ostracoda of San Antonio Bay, Texas.* Paleont. *29*, no. 4, pp. 561–646.

(*Reprinted from Nature, Vol.* 187, *No.* 4736, *pp.* 480–482,
August 6, 1960)

FALL-OUT CÆSIUM IN SURFACE SEA WATER OFF THE CALIFORNIA COAST (1959–60) BY GAMMA-RAY MEASUREMENTS

By Dr. THEODORE R. FOLSOM, Dr. G. J. MOHANRAO and PERRIN WINCHELL

Scripps Institution of Oceanography, University of California,
La Jolla, California

STRONTIUM-90 and cæsium-137 decay at very similar rates and relatively slowly, half in about thirty years, or less than 2 per cent a year. The rate at which fall-out is reaching the land surface has been followed by extensive measurement[1] of these nuclides in soil specimens and in various rain samples. On the other hand, the collection of similar data concerning fall-out entering the sea has been seriously limited by measurement difficulties, arising mainly from the excessive dilution and from the presence in sea water of relatively larger amounts of natural radioactivities and relatively enormous amounts of stable nuclides that interfere with chemical concentration and purification.

Fortunately for study of fall-out phenomena, the dispersal of these long-lived fission products after they have entered the sea is also of great interest in the study of food-chains, especially those directly influencing fisheries, and also in the oceanographic study of water movements and mixing. Yamagata has developed a successful technique for measuring cæsium-137 in sea water through its beta-ray after numerous steps of chemical purification ; recently he has reported[2] his measurements of the recent distribution of cæsium-137 in waters close to the coast of Japan. Bowen and Sugihara, of Woods Hole Oceanographic Institution, have studied fall-out constituents in the sea for several years and have reported[3] recently on the horizontal and vertical distribution of strontium-90 in the Atlantic Ocean. They point out that their vertical profiles indicate downward mixing to depths of 300–700 metres at a rate much more rapid than might be predicted from existing radiocarbon measurements. They show that a significant amount of strontium-90 has penetrated even to a depth of 1,000 metres.

Contributions from the Scripps Institution of Oceanography, **New Series,**
1203
Reproduced by Permission

The oceans are very large, and many more of this sort of data must be collected before generalizations regarding either the arrival or dispersal of fall-out become convincing. Efforts at the Scripps Institution, therefore, have centred around simplifying the chemical assay required, adapting it to shipboard use, and the application of electronic aids wherever possible. Whereas strontium-90 emits only beta-rays and its assay in sea water is tedious, cæsium-137 (which falls into the sea at about the same rate) has both beta- and gamma-emission. To utilize the beta-ray as Yamagata and others have done, the trace of radiocæsium must be chemically separated from the large amount of potassium present in sea water, including the natural beta-emitter potassium-40. On the other hand, the modern scintillation spectrometer has no trouble resolving the gamma-ray of cæsium-137 (0·66 MeV.) in the presence of much larger amounts of potassium-40 (1·46 MeV.). The assay problem, therefore, reduces to one of concentrating sea water cæsium in a way convenient for gamma-ray spectrometry. Gustafson, Marinelli and Brar[4] at the Argonne National Laboratory have shown how low-level gamma-ray assays can be made from bulky specimens by use of large scintillation detectors. It was found at Scripps that the radiocæsium in a barrel of sea water, brought down together with roughly 30 per cent of the potassium by the mere addition of sodium cobaltinitrite, could be collected as a precipitate having a volume of about 250 ml. This wet material, placed near a 3-in. diameter sodium iodide scintillation crystal, gave accurate and reproducible measure of the cæsium content as could be established by adding known amounts of radiocæsium to controls. For this sort of work, a 256-channel gamma-ray spectrometer is now available at Scripps ; a digital computer accessory developed at Scripps now permits storage of information on short magnetic tape loops and gives means for the rapid comparison between gamma spectra and the elimination of background effects. At present the precipitate is allowed to settle overnight, collected after decantation and then exposed to a 3-in. crystal, generally overnight. It is expected that gamma spectrographs will be made in less than 2 hr. by the use of larger crystals ; and it is planned to have the initial precipitation carried out on board the research ship so that only the concentrated precipitate need be brought back from the longer expeditions.

Details of the procedure will appear elsewhere. Satisfactory reproduction of results has been demonstrated ; the difference between the assays of five

Table 1. CONCENTRATION OF CÆSIUM-137 IN SEA WATER FROM SCRIPPS PIER

No.	Date collected	CsCl carrier mgm./l.	Cs-137 $\mu\mu$c./kl.
1	11/30/59	0	76
2	12/ 2/59	0	123
3	12/ 3/59	0	104
4	12/11/59	100	163
5	1/ 2/60	0	67
6	1/16/60	0	90
7	1/23/60	20	135
8	2/ 3/60	30	145
9	2/ 4/60	0	108
10	2/12/60	25	108
11	2/15/60	0	108
12	3/ 4/60	0	99
13	3/12/60	0	45
14	3/17/60	0	46
15	3/18/60	0	67
16	3/25/60	0	79
17	4/ 9/60	0	76
18	4/15/60	0	71
19	4/22/60	0	86
20	4/27/60	0	138
		Average	97

200-litre replicate controls was less than 11 per cent. It now appears unnecessary to resort to the use of such large samples; nevertheless, several uncertainties in the early work were avoided by this means. For example, storage in full-sized steel oil drums for one month was found to cause a loss of about 20 per cent of the radiocæsium to the walls; and storage for one week in a rubber barrel caused a loss of about 13 per cent. Losses of this sort may be serious when small samples are stored for a long period, but, of course, are eliminated by immediate chemical precipitation.

Table 1 gives the results of twenty preliminary assays made on 200-litre sea water samples taken just beyond the surf zone (300 metres from shore) at Scripps pier. Serial 10 was deliberately taken when the water was brown with terrestrial mud from a heavy local rain; it is not significantly exceptional in cæsium content.

The average cæsium-137 is 97 micromicrocuries per kilo litre (97 $\mu\mu$c./kl.).

Table 2 shows the results for water carefully collected in 200-litre aliquots in the open sea many miles from shore. The average concentration is 138 $\mu\mu$c./kl.

For comparison there are two groups of measurements made by Yamagata[3] concerning Japanese waters. He deduced from industrial salt concentrates that coastal waters early in 1958 contained cæsium-137 in the amounts 70–150 $\mu\mu$c./kl. Later, by direct low-level beta technique, he measured the concentration in 1959 surface sea water taken from salt

Table 2. CONCENTRATION OF CÆSIUM-137 IN SAMPLES FROM THE OPEN SEA

Serial No.	Date collected	Position Lat. N.	Position Long. W.	Distance from coast, miles	Cs-137 $\mu\mu c./kl.$
1	12/10/59	33° 55′	121° 49′	75	81
2	12/17/59	31° 08′	120° 55′	215	163
3	12/17/59	31° 07′	122° 26′	300	161
4	1/31/60	38° 02′	127° 50′	200	152
5	1/31/60	38° 02′	127° 50′	200	124
6	3/8/60	30° 53′	116° 59′	35	87
7	3/15/60	24° 40′	114° 02′	100	144
8	3/18/60	31° 05′	122° 39′	300	150
9	3/19/60	30° 31′	122° 13′	300	141
10	3/21/60	26° 18′	118° 27′	200	230
11	3/22/60	29° 42′	120° 44′	250	120
12	3/25/60	28° 14′	119° 28′	220	100
				Average	138

Sample No. 5 was collected in a neoprene drum. The rest in steel drums.

works, reporting the average cæsium-137 from fifteen samples as 380 μμc./kl.

Of course, too much should not be expected from cursory comparisons between these preliminary sets of measurements. It is believed that the oceanographic phenomenon called ‘upwelling’ does not occur in the region where the samples of Table 2 were taken; nevertheless, these waters may have been influenced by local vertical mixing of some sort, perhaps at a place thousands of miles to the north of the sampling position. The range of variation in concentrations which appear in these tables as well as in Yamagata’s 1959 measurements (240–650 μμc./kl.) should be a warning to those who might hope to establish for specific oceanic areas the average vertical profile of radiocæsium (or radiostrontium or any other water tag) with only a few measurements.

The increase reported in cæsium in Japanese waters between 1958 and 1959 corresponds to an increase in weapon-testing activity and to a world-wide increase in fall-out. However, the difference between the California and the Japanese surface concentrations might be due to several factors; certainly to be considered are the reports of consistently higher local fall-out in Japan, and also are the differences of positions of Japan and California in the general circulation of the Pacific relative to the weapons proving-grounds. Certainly, the behaviour of a water tag in surface-water must be explored first, but these waters move faster horizontally; much more information concerning transport and mixing can be obtained when samples from several depths can be examined. Plans therefore have been made to sample Pacific waters to depths where there is little motion.

Arrival of fall-out, being associated with rainfall, is at best spotty. However, during the past eighteen months there has been a moratorium in weapons tests ; and over this period there have not appeared the large peak values witnessed during the previous years. Advantage, of course, should be taken of this simplifying circumstance to establish background values related to the ocean. Another factor arising from the moratorium should be mentioned as it concerns the measurement of radiocæsium in sea water. During the past year the shorter-lived fission products have become so attenuated that essentially nothing needs to be done now to eliminate their interference with cæsium-137 in a gamma-ray spectral analysis. Prior to this recent, happy period, the obscuring effects of fresh fall-out constituents were combated at Scripps either by additional chemical treatment, or by fullest use of the digital computer already mentioned and developed for just this purpose.

The matter of vertical biological transport cannot be overlooked. However, one can present an argument for neglecting the biological transport of radiocæsium perhaps as strong as that offered by Bowen and Sugihara for ignoring this contribution in the case of radiostrontium. They argued that biological transport cannot be important because of the presence of large amounts of stable strontium and calcium in sea water. Cæsium, too, is notably soluble ; only traces of the radionuclide enter as fall-out and these must share with large amounts (about 0·002 mgm./litre) of stable cæsium ; and also there is present in sea water much larger amounts of potassium (about 380 mgm./litre). It is common experience that potassium and cæsium are found together in many reactions—organic and inorganic. Still, a considerable loss of radiocæsium to surfaces has been observed in the actual handling of sea water specimens, and too little is now known about the behaviour of stable cæsium in the actual seas. Fortunately, the chemical behaviour of cæsium is quite different from that of strontium ; exploration based upon the progress of fall-out in the ocean should exploit this. At the outset, sampling of radiostrontium should go along with that for radiocæsium.

Various aspects of this work have been supported by the United States Atomic Energy Commission (Contract No. AT(11-1)-34, Project Agreement No. 56), and by the United States Office of Naval Research (Contract 233(34), Amendments No. 7,8,9). We are grateful for suggestions that have come personally from Drs. V. T. Bowen, T. T. Sugihara and N. Yamagata. We wish to thank D. C. Martin

for related preliminary studies, and also Barbara Edwards, William Hartin and Richard Schwartzlose for skilful technical assistance.

[1] Gustafson, P. F., *Science*, **130**, 1404 (1959).
[2] Yamagata, N., *Nature*, **184**, 1813 (1959).
[3] Bowen, V. T., and Sugihara, T. T., *Nature*, **186**, 71 (1960).
[4] Gustafson, P. F., Marinelli, L. D., and Brar, S. S., *Science*, **127**, 1240 (1958).

Printed in Great Britain by Fisher, Knight & Co., Ltd., St. Albans.

(890)

JOURNAL OF GEOPHYSICAL RESEARCH VOLUME 65, NO. 9 SEPTEMBER 1960

On the Nonseasonal Variations in Sea Level along the West Coast of North America[1]

GUNNAR I. RODEN

Scripps Institution of Oceanography
La Jolla, Californa

Abstract. Spectra of monthly sea level anomalies are investigated for the frequency range between 0 and 6 cycles per year. It is found that most of the power is concentrated at low frequencies. There is a good coherence between anomalies of sea level and atmospheric pressure at almost all frequencies, indicating a fast response between these variables. The coherence between anomalies of sea level and sea surface temperature is moderate to poor depending upon the particular environment of the tide gage station. There is some coherence between anomalies of sea level and the south component of the geostrophic wind, owing to the influence of the Coriolis force. In river mouths the anomalies in sea level largely reflect the anomalies in river discharge. A fairly successful estimate of the sea level anomaly of the present month can be made from the present anomalies of atmospheric pressure and sea surface temperature. Statistical prediction of sea level anomalies is less successful.

Introduction. For many years careful records have been kept of the sea level at various tide gage stations around the periphery of the Pacific and on a few ocean islands. The mean seasonal variation of such records was studied by *Nomitsu and Okamoto* [1927] and by *La Fond* [1939] and *Patullo, Munk, Revelle, and Strong* [1955]. Day to day variations in sea level were investigated by *Groves* [1956, 1957] and *Shoji* [1957], and a brief study of large scale irregular variations was made by *Stewart, Zetler, and Taylor* [1958]. Recently *Haubrich and Munk* [1959] made a statistical study of the sea level in connection with the pole tide. The main conclusions that can be drawn from the above-mentioned investigations are that (1) the mean annual variation of sea level shows a more or less close relation to the mean annual variations in atmospheric pressure and the average heat content of the water, (2) the response of sea level to atmospheric pressure is instantaneous and inverse for periods larger than a day, (3) the variations in sea level are coherent over distances of several hundred kilometers, and (4) there are no periodicities in the spectra.

In this paper the regular seasonal variation is eliminated by taking differences between the monthly mean and long-term mean for the same month. The resulting anomalies are then used to compute the autocorrelations and the cross correlations and from them the power spectral densities, coherence, and phase, using Fourier transforms. In performing these calculations it has been assumed that the anomaly records are stationary, at least in the wide sense, so that the correlation functions depend only upon the correlation interval and are not bound to any origin in time.

The location and environment of the tide gage stations together with some information on the statistics of the various records are given in Table 1 and Figure 1. It is seen that most tide gage stations are located in harbors and bays and that there are only very few stations along the open coast. The tide gage station at Astoria is located in the mouth of the Columbia River; this station has been included in order to show the effect of river discharge upon the sea level.

The length of the sea level records used varies from 72 months to 444 months. The particular length chosen was based upon the availability of simultaneous records of sea level, sea level atmospheric pressure, and sea surface temperature. The number of spectral estimates or correlation intervals was chosen so that the degrees of freedom, ν, defined by $\nu = 2n/m$, where n

---

[1] Contribution from the Scripps Institution of Oceanography, New Series. 1204

Reproduced by Permission

TABLE 1. Location and Environment of Tide Gage Stations (n = total record length in months; m = number of spectral estimates; ν = degrees of freedom)

Tide Gage Station	N-Lat.	W-Long.	Environment	n	m	ν
Hawaii						
Honolulu	21°18′	157°52′	Harbor	408	24	34
Mexico						
Salina Cruz	16°10′	95°12′	Harbor	80	9	18
Acapulco	16°51′	99°55′	Harbor	84	9	19
Mazatlan	23°11′	106°26′	Harbor	72	9	16
La Paz	24°10′	110°19′	Bay channel	84	9	19
Guaymas	27°55′	110°55′	Harbor	77	9	17
California						
La Jolla	32°52′	117°15′	Open coast	408	24	34
Los Angeles	33°43′	118°16′	Harbor	420	24	35
Avila	35°10′	120°44′	Open coast	150	12	25
San Francisco	37°48′	122°28′	Bay entrance	408	24	34
Crescent City	41°45′	124°12′	Harbor	300	24	25
Oregon						
Astoria	46°13′	123°46′	River mouth	372	24	31
Washington						
Neah Bay	48°22′	124°37′	Small bay	276	24	23
Seattle	47°36′	122°20′	Sound	408	24	34
British Columbia						
Victoria	48°25′	123°22′	Harbor	192	24	16
Alert Bay	50°36′	126°56′	Strait	126	12	21
Alaska						
Ketchikan	55°20′	131°38′	Narrow strait	444	24	37
Sitka	57°03′	135°20′	Harbor	192	24	16
Yakutat	59°33′	139°44′	Small bay	216	24	18
Womans Bay, Kodiak	57°43′	152°31′	Small bay	108	12	18

is the total number of observations and m the number of spectral estimates, was at least 15.

Data. Monthly mean sea levels were obtained from the U. S. Coast and Geodetic Survey, the Canadian Hydrographic Survey, and the Instituto de Geofisica UNAM, Mexico, for stations in the respective countries. The monthly means were computed from daily means of hourly heights according to $z = 1/24(h_0 + h_1 + \dots h_{23})$, where z is the daily mean and h refers to the hourly value. This particular kind of averaging largely eliminates the influence of diurnal, semidiurnal, and shorter tidal components, but it does not discriminate against long-period tides. The latter are of such a small amplitude, however, that they may be neglected in the first approximation. Much more serious contamination of daily sea levels can be expected in semienclosed bays and harbors, but the elimination of these is difficult and has not been attempted here. The accuracy of a single hourly sea level reading is estimated to be 1.5 cm.

Monthly mean sea level atmospheric pressures were obtained from the U. S. Weather Bureau [*Monthly Weather Review*, 1872–1949; *Climatological Data, National Summary*, 1950–present], the Canadian Department of Transport, and the Servicio Meteorologico Mexicano. For the Canadian and United States stations the monthly averages are computed from four equidistant daily readings at 0000, 0600, 1200, and 1800 GMT, and for Mexican stations from three daily readings at 0300, 1300, and 2000 GMT. The accuracy of a particular reading is estimated to be 0.2 mb.

Monthly mean sea surface temperatures were obtained from the *U. S. Coast and Geodetic Survey* [1956]. They represent, for the most part, averages of one daily reading taken at a random hour during the forenoon. The accuracy of a single reading is about 0.3°C.

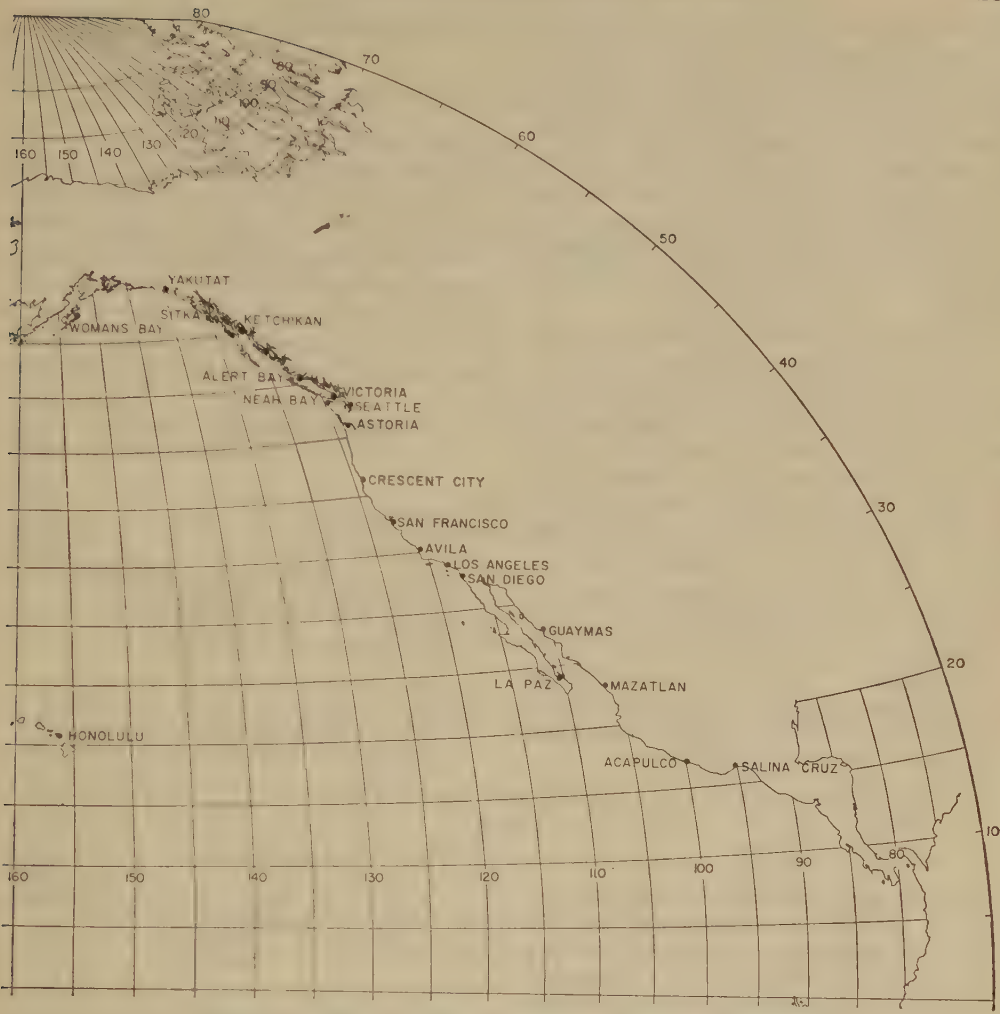
80
70
60
50
40
30
20
10
160
150
140
130
120
110
100
90
80
YAKUTAT
SITKA
KETCHIKAN
WOMANS BAY
ALERT BAY
NEAH BAY
VICTORIA
SEATTLE
ASTORIA
CRESCENT CITY
SAN FRANCISCO
AVILA
LOS ANGELES
SAN DIEGO
GUAYMAS
LA PAZ
MAZATLAN
HONOLULU
ACAPULCO
SALINA CRUZ

Fig. 1. Location of tide gage station used in this investigation.

Runoff records for the Columbia River were published by the *U. S. Geological Survey* [1958]. The averages are obtained from daily readings. The accuracy of a single determination is difficult to estimate, but should be of the order of 1000 ft^3/sec.

The observed sea level anomalies are illustrated in Figures 2*a* to 2*d*. Although the details of these records vary, a few preliminary results can be obtained from a visual inspection of them; (*a*) the magnitude of the anomalies increases toward the north, (*b*) the maximum amplitude of the anomalies appears to be in the neighborhood of 30 cm, (*c*) there are no obvious periodicities discernible, (*d*) the anomalies are similar over distances of several hundred kilometers, and (*e*) for the majority of stations the mean of the record does not change appreciably.

The probability distribution of sea level, atmospheric pressure, and sea surface temperature anomalies is shown in Figure 3. It is seen that the distribution is approximately normal, except at the extremes.

The standard deviations and extreme ranges of the anomalies for each of the stations are given in Table 2. For sea level and atmospheric pressure anomalies these are seen to increase from south to north, the increase being by a factor of roughly 2 for the former and about 6 for the latter. For sea surface temperature anomalies there is no dependence upon latitude; the anomalies appear, however, to be larger for stations located in shallow bays and harbors than for those situated in straits and sounds, suggesting that tidal mixing may be important in reducing the amplitude of the temperature variation.

The standard deviation of the sea level anomalies can, in many cases, be reduced by eliminating the static effect of atmospheric pressure from the sea level records. If this is done (noting that an excess of pressure of 1 mb decreases the sea level by 1 cm) the resulting standard deviation of the 'corrected' sea level is seen in the last column of Table 2 to depend very little upon latitude. However, a significant difference between the observed and corrected sea level anomalies exists in the northern part of the region only.

Computational procedures. Let $z(t)$ and $p(t)$ denote anomalies of sea level and atmospheric pressure. Then the autocorrelations and cross correlations are defined by

$$\phi_{zz}(\tau) = \langle z(t)z(t+\tau)\rangle, \qquad \phi_{zp}(\tau) = \langle z(t)p(t+\tau)\rangle \tag{1}$$

respectively, provided the records are stationary. Here ⟨ ⟩ denotes the time average over the entire record length, and τ the time lag in months.

The power spectral densities and cross-power spectral densities are obtained from a Fourier transform of the correlation functions:

$$E_{zz}(\omega) = \frac{2}{\pi}\int_0^\infty \phi_{zz}(\tau)\cos\omega\tau d\tau, \qquad E_{zp}(\omega) = \frac{1}{\pi}\int_{-\infty}^\infty \phi_{zp}(\tau)e^{i\omega\tau}\,d\tau \tag{2}$$

Practical methods for evaluating the power spectra are given by *Blackman and Tukey* [1958] and *Munk, Snodgrass, and Tucker* [1959].

The coherence between $z(t)$ and $p(t)$ is defined by

$$R_{zp}(\omega) = \frac{E_{zz}(\omega)}{[E_{zz}(\omega)E_{pp}(\omega)]^{1/2}} \tag{3}$$

and must lie between the values 0 and 1.

The phase lag of $z(t)$ over $p(t)$ is defined by

$$\pi_{zp}(\omega) = \arctan\frac{E_{zp} - E_{pz}}{E_{zp} + E_{pz}} \tag{4}$$

provided that for a positive $E_{zp} - E_{pz}$ $0 \leq \pi \leq 180$ and for a negative numerator $180 \leq \pi \leq 360$

It should be noted that the autocorrelations, and therefore also the spectral densities, depend upon the amount of smoothing or averaging performed upon the original data. In the case of a Markov process, the autocorrelation is improved by an increased amount of averaging [*Munk, Snodgrass, and Tucker*, 1960]. Thus a valid com-

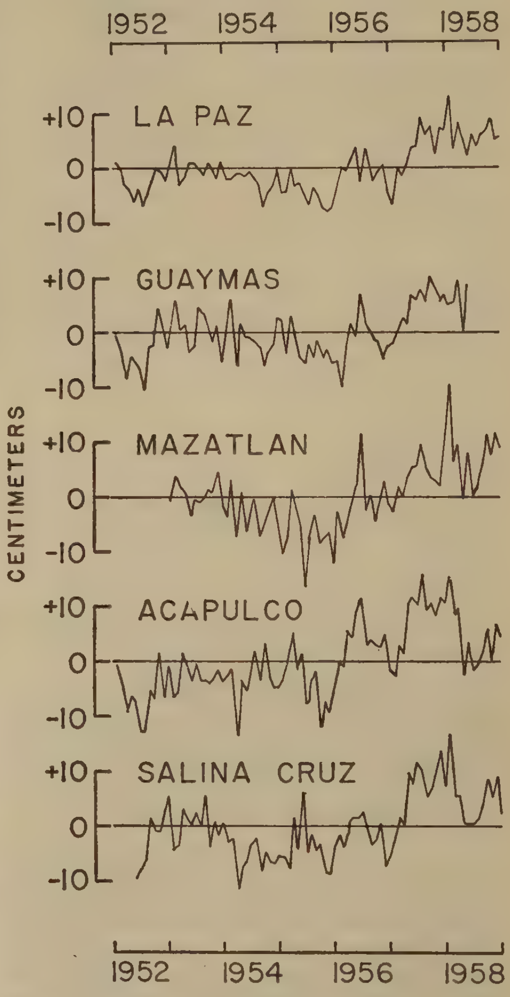

Fig. 2*a*. Sea level anomalies along the coast of Mexico.

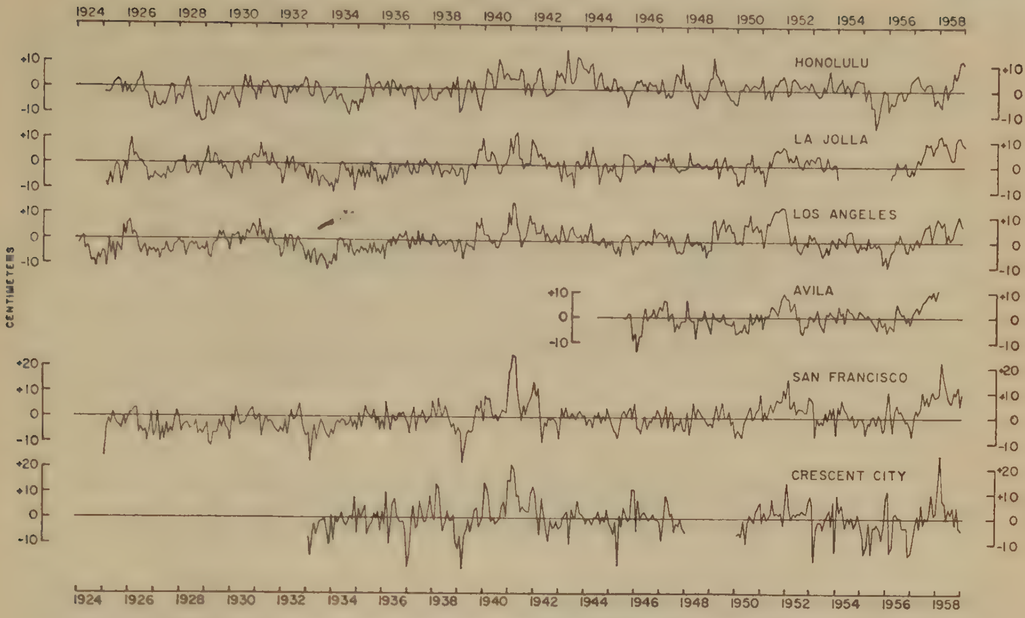

Fig. 2*b*. Sea level anomalies along the coast of California and Hawaii.

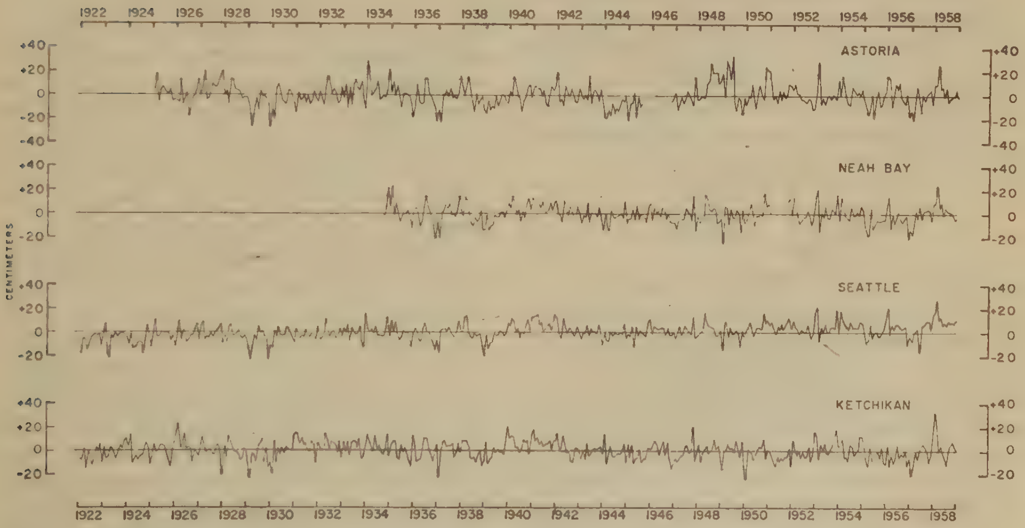

Fig. 2*c*. Sea level anomalies along the coasts of Oregon, Washington, and Alaska.

parison between autocorrelations or spectral densities can be made only if the data are averaged in the same way. In the present case the averaging was the same for each variable at all stations, though different for different variables. The discussion below is therefore limited to differences between stations.

The 95 per cent confidence limits for the power spectra coherence and phase are given in Table 3. They are based on the assumption

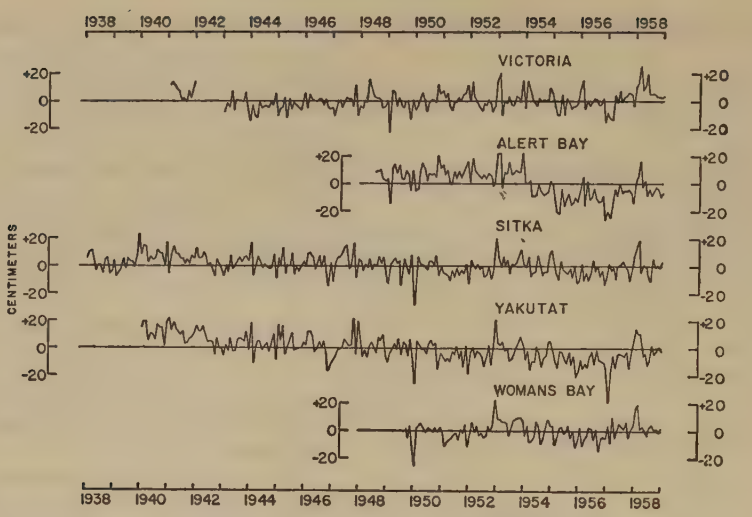

Fig. 2*d*. Sea level anomalies along the coast of British Columbia and Alaska.

that the anomalies are normally distributed and also possess a joint normal distribution. The confidence limits for the coherence and phase computed by *Goodman* [1957], have recently been questioned by Tick (personal communication). For the autocorrelation *Laning and Battin* [1956] give the following inequality from which the standard deviation σ of the observed autocorrelation from the true autocorrelation of an infinite record can be obtained:

$$\sigma \leq \left[\frac{4}{n}\int_0^\infty \phi^2(t)\,dt\right]^{1/2} \qquad (5)$$

where n denotes the total record length.

Response between sea level and atmospheric pressure anomalies. The time required for the sea surface to come into equilibrium with the field of atmospheric pressure has received considerable attention recently. In the case of an infinite and homogeneous ocean, *Sarkisyan* [1957*a*, *b*] computed the equilibrium time to be of the order of 1 to 2 months. For an inhomogeneous ocean *Veronis and Stommel* [1956] found that at least 100 years would be required to reach equilibrium. It appears, therefore, that for periods shorter than a month the sea surface does not adjust itself completely to the field of atmospheric pressure, regardless of whether an isotropic or baroclinic ocean is considered.

Once the equilibrium is established the departure of the sea surface from equilibrium can be computed from the Bernoulli equation

$$\eta = -p_0/\rho g - \mathbf{v}^2/2g \qquad (6)$$

where $\mathbf{v}$ is the vector velocity, ρ the density, g the acceleration of gravity, p_0 the atmospheric pressure, and η the height of sea level above the equilibrium surface. This equation has been derived on the assumption that the flow is irrotational and takes place on a resting earth. If the rotation of the earth is also considered, the integrated Coriolis term must be added.

The first term represents the effect of atmospheric pressure upon sea level; in particular it shows that, in the absence of motion ($\mathbf{v} = 0$), the sea level is depressed by approximately 1 cm for every millibar of pressure increase. The second term takes into account the dynamic effect, and it can be seen that if the atmospheric pressure is constant the sea level is lowered 1 cm for every increase in current of about 45 cm/sec. Such current changes are seldom observed, however, and the dynamic term, being much smaller than the static term, is generally neglected.

On a rotating earth, the sea level is further influenced by the Coriolis force; a rough estimate of the magnitude of this effect can be obtained by considering a current flowing northward along the west coast of North America,

(896)

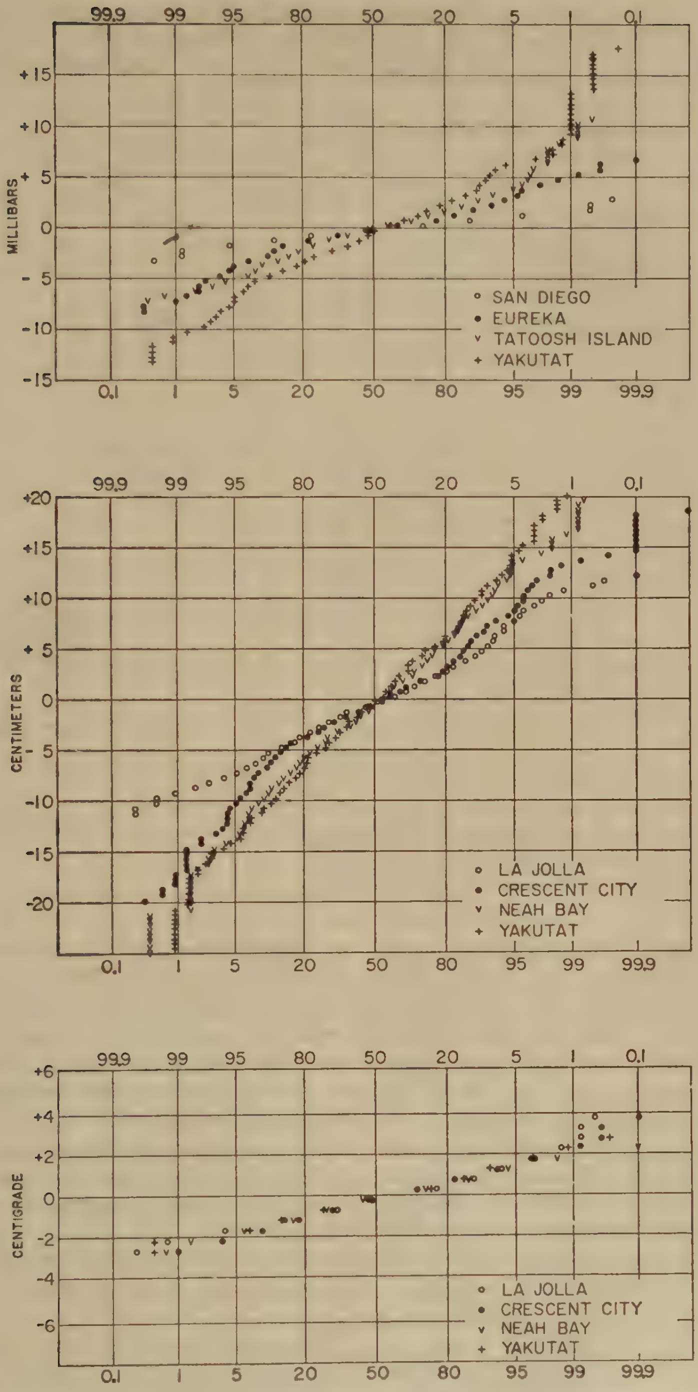

Fig. 3. Probability distribution of atmospheric pressure, sea level and sea surface temperature anomalies. Dots refer to 0.5 unit class intervals.

TABLE 2. Standard Deviations (σ) and Extreme Ranges (r) of Anomalies of Sea Level (z) Atmospheric Pressure (ρ), and Sea Surface Tempreature (θ)

Station	σ_z, cm	σ_ρ, mb	σ_θ, °C	r_z, cm	r_ρ, mb	r_θ, °C	(σ_z) corr., cm
Hawaii							
Honolulu	4.6	1.2	0.5	30	8	3	4.6
Mexico							
Salina Cruz	5.7	0.8	1.4	28	4	5	5.5
Acapulco	6.5	0.8	0.9	29	4	4	6.2
Mazatlan	6.5	0.7	1.7	32	3	6	6.4
La Paz	4.3	0.7	0.8	21	4	4	4.2
Guaymas	4.6	0.6	1.1	20	4	4	4.6
California							
La Jolla-San Diego*	4.2	0.9	1.0	24	8	6	4.0
Los Angeles	4.6	0.9	1.1	27	6	7	4.2
Avila-Santa Maria	4.1	0.9	0.6	25	5	3	4.0
San Francisco	5.5	1.5	0.8	43	12	5	5.0
Crescent City-Eureka	6.1	2.1	1.1	45	14	6	5.0
Oregon							
Astoria-North Head	9.2	2.6	1.0	64	15	7	7.9
Washington							
Neah Bay-Tatoosh Island	7.7	2.7	1.0	49	18	5	5.6
Seattle	6.7	2.4	0.8	45	16	5	5.2
British Columbia							
Victoria†	6.7	2.7	0.5	47	18	3	4.9
Alert Bay‡ Port Hardy	10.0	3.0	0.5	48	14	3	8.8
Alaska							
Ketchikan-Annette	7.6	3.5	0.8	57	23	4	5.6
Sitka-Juneau	6.5	3.9	0.8	48	24	4	4.4
Yakutat	8.5	4.1	1.0	60	31	6	6.8
Womans Bay, Kodiak Island	6.8	5.3	0.9	49	36	4	5.6

* Where two names occur, the first refers to tide gage stations, the second to meteorological ones.

† Sea surface temperature measured at Race Rocks, B.C.

‡ Sea surface temperature measured at Pine Island, B.C.

with an average width of 100 km and an average velocity of 10 cm/sec, assumed to be constant from top to bottom. The rise in sea level due solely to the Coriolis force would be about 10 cm. It is thus seen that relatively small changes in the average current speed can lead to appreciable changes in sea level. Fortunately, the known changes in the speed of the average current along the west coast of North America over a time period of a month are not very large, mostly within 20 cm/sec, and therefore excessively large sea level variations due to the Coriolis force alone are not to be expected.

Autocorrelation and power spectral density. The autocorrelation of sea level anomalies is shown in Figure 4. The dots refer to the observed anomalies, the crosses to those from which the atmospheric pressure effect has been eliminated. The dashed line refers to the standard deviation of the computed autocorrelation from the true one of an infinite record. It is seen that the persistence of the anomalies adjusted for the atmospheric pressure effect is improved over the persistence of the unadjusted anomalies, particularly at latitudes north of San Francisco. The autocorrelation differs significantly from zero for lag times between 0 and 4 to 16 months, depending upon the individual station but not upon latitude. Most of the autocorrelations suggest an exponential decay of the sea level anomaly with time, at least for the first few lags.

The spectral density of the anomalies for the frequency range between 0 and 6 cycles per year (cpy) is shown in Figure 5, where the dots refer, as previously, to the observed anomalies,

TABLE 3. Confrence Limits (95 %) for the Power Spectra (E), the Coherence (R), and the Phase (π)

Station	E, cm^2/cpy	R	π, deg.
Hawaii			
Honolulu	0.66–1.71	0.34	41
Mexico			
Salina Cruz	0.57–2.19	0.47	38
Acapulco	0.58–2.13	0.46	38
Mazatlan	0.56–2.31	0.50	37
La Paz	0.58–2.13	0.46	38
Guaymas	0.56–2.26	0.48	38
California			
La Jolla	0.66–1.71	0.34	41
Los Angeles	0.66–1.69	0.34	41
Avila	0.62–1.90	0.40	40
San Francisco	0.66–1.71	0.34	41
Crescent City	0.62–1.90	0.40	40
Oregon			
Astoria	0.64–1.78	0.36	41
Washington			
Neah Bay	0.60–1.97	0.42	39
Seattle	0.66–1.71	0.34	41
British Columbia			
Victoria	0.56–2.31	0.50	37
Alert Bay	0.59–2.04	0.44	39
Alaska			
Ketchikan	0.66–1.67	0.33	41
Sitka	0.56–2.31	0.50	37
Yakutat	0.57–2.19	0.47	38
Womans Bay, Kodiak Island	0.57–2.19	0.47	38

the crosses to those adjusted for the atmospheric pressure effect. The main feature in the spectra is that they contain most of their power in the low-frequency part and almost nothing at higher frequencies. As can be expected from the autocorrelations, the spectrum of the anomalies from which the atmospheric pressure effect has been eliminated contains less power than the spectrum of the observed anomalies, indicating that a substantial part of the sea level variations north of San Francisco is really due to variations in atmospheric pressure. It is also noteworthy that there are no significant peaks in the spectra, which emphasizes the absence of periodicities, a fact already mentioned by *Haubrich and Munk* [1959].

The autocorrelations and power spectral densities of atmospheric pressure anomalies (not shown here) indicate a persistence of less than a month and a distribution of power almost independent of frequency. For sea surface temperature anomalies the autocorrelations and spectral densities are similar to those in sea level anomalies; the persistence varies between 4 and 6 months and is independent of latitude; most of the power is found at frequencies between 0 and 2 cpy.

Coherence and phase between sea level and atmospheric pressure anomalies. The coherence spectrum is interesting from two points of view. It shows that the coherence along the coast becomes better toward the north and that at most stations the coherence depends very little upon frequency (Figs. 6 and 7). The latter may be interpreted to mean that sea level adjusts itself rather quickly to variations in atmospheric pressure, certainly in less than 2 months. The highest values of the coherence are about 0.8, indicating that about 64 per cent of the sea level anomalies can be accounted for in terms of atmospheric pressure anomalies. In the southern part of the region the coherence varies around 0.4, showing that only 16 per cent of the sea level anomalies are related to atmospheric pressure variations. The phase between these variables is 180° and, for all except the Mexican stations, varies very little with frequency. This indicates that the sea level responds to atmospheric pressure like an 'inverted barometer,' for most stations investigated here. Why the phase scatters so much at the Mexican stations is difficult to explain; it is possible that the nonseasonal atmospheric pressure variations are small and therefore have no effect upon sea level.

One of the most interesting and yet unexplained results is the ratio of the energy of sea level anomalies to the energy of atmospheric pressure anomalies as a function of frequency (Table 4).

It is seen that that ratio decreases sharply with increasing frequency and that the ratios at low frequencies are much smaller in the northern than in the southern part of the region. This suggests that something other than atmospheric pressure must also influence sea level. If it were not so, the ratio should be equal to 1 at all frequencies.

Coherence and phase between sea level and sea surface temperature anomalies. The coherence spectra (Fig. 8) do not show a relation to latitude, but seem rather to depend

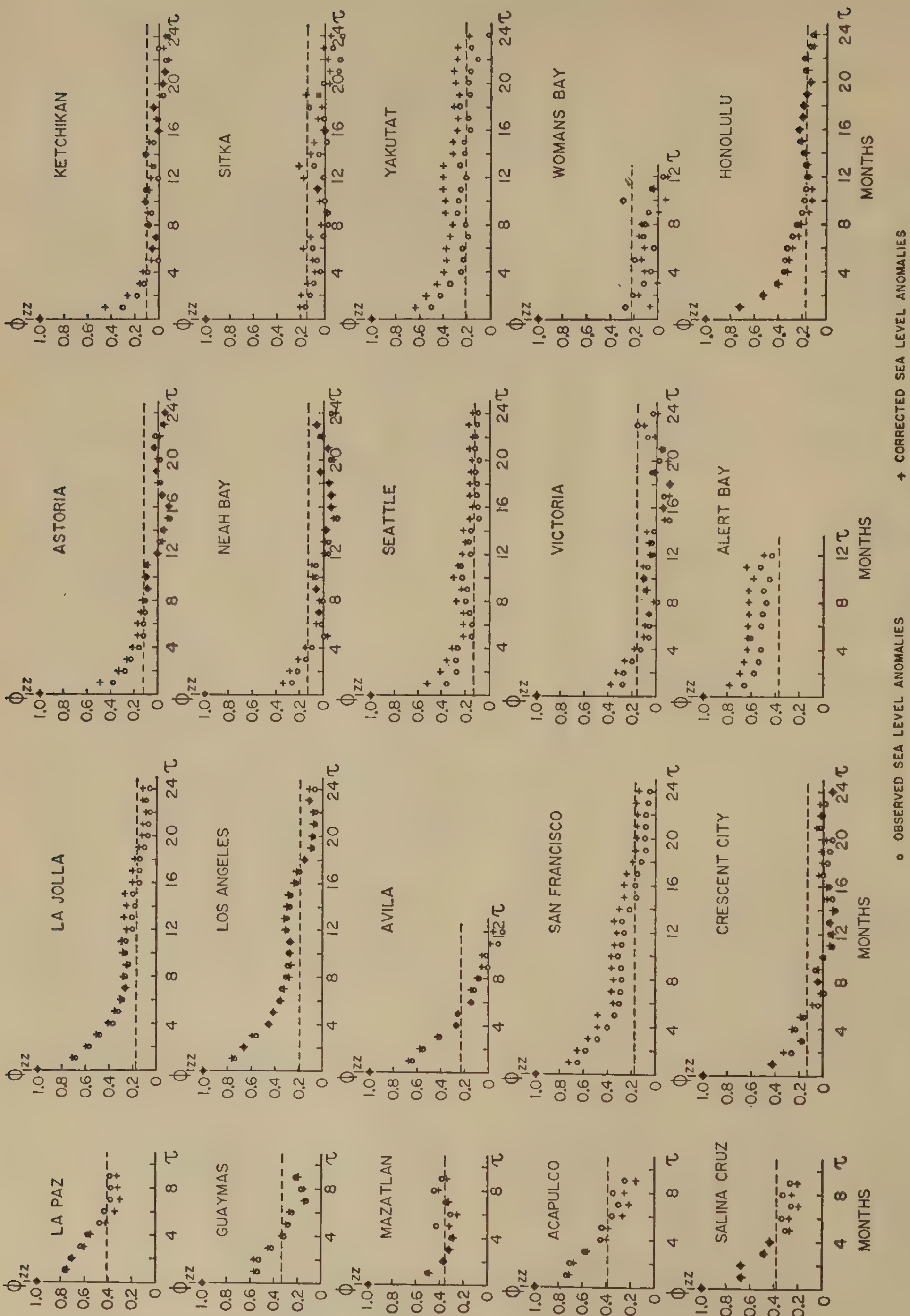

Fig. 4. Autocorrelation of sea level anomalies.

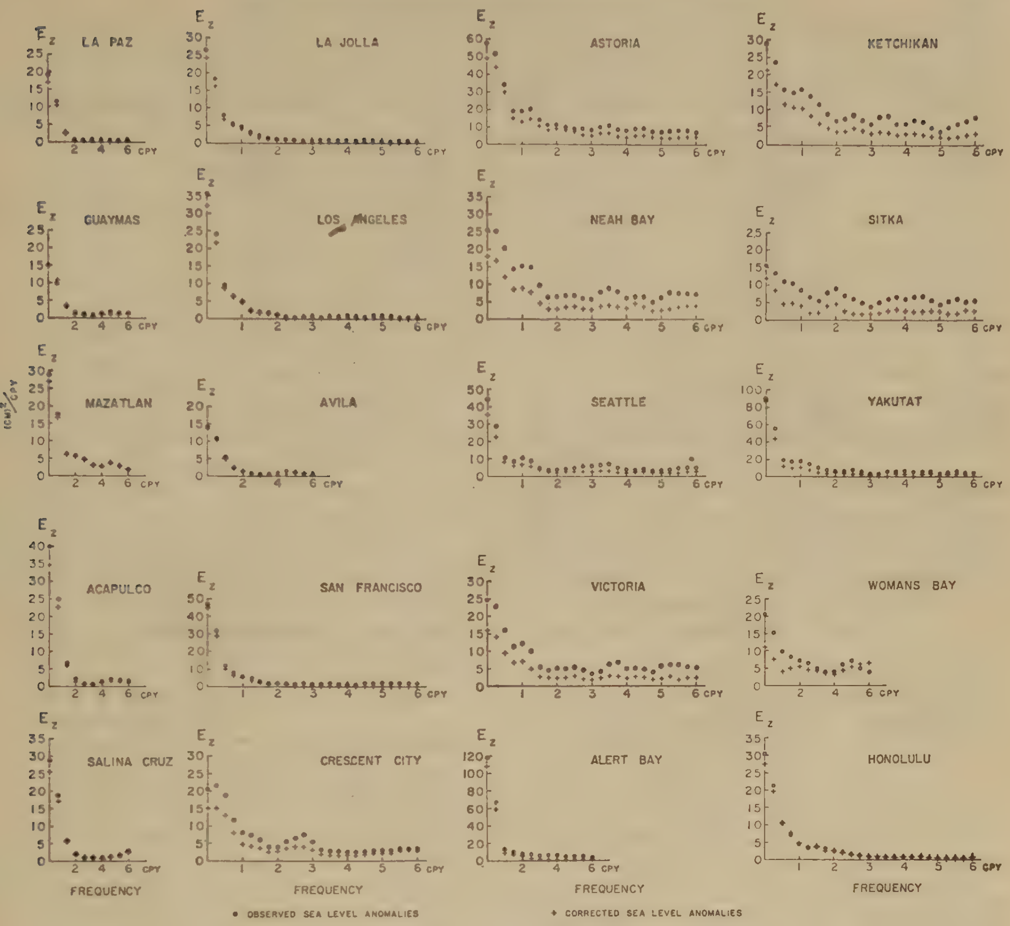

Fig. 5. Energy of sea level anomalies.

upon the particular environment in which the tide gage station is located. A relatively good coherence is found in most shallow bays and harbors, such as Los Angeles, Neah Bay, and Yakutat, whereas the coherence is poor in such places as river mouths (Astoria), and straits and sounds (Victoria, Seattle). Even along the open coast (La Jolla) the coherence is only moderate. In many cases the coherence is seen to depend on frequency, but the relation is not clear cut. On an average, less than 20 per cent of the sea level anomalies appear to be due to anomalies in sea surface temperature (Fig. 9). The phase between these anomalies is zero where the coherence is high and indicates a direct relation between the height of sea level and local warming. In places where tidal mixing is considerable, such as in straits and sounds, there is much scatter in the phase.

Coherence and phase between sea level and wind anomalies. The coherence between anomalies in the south component of the geostrophic wind and the sea level has been investigated for three places along the west coast of the United States in order to find out whether the Coriolis force has any effect upon sea level (Fig. 10). It is seen that the coherence is rather poor off Southern California, and somewhat better near Cape Mendocino and Cape Flattery. But even in the best cases not more than about one-third of the sea level variations can be related to variations in the wind. The phase between

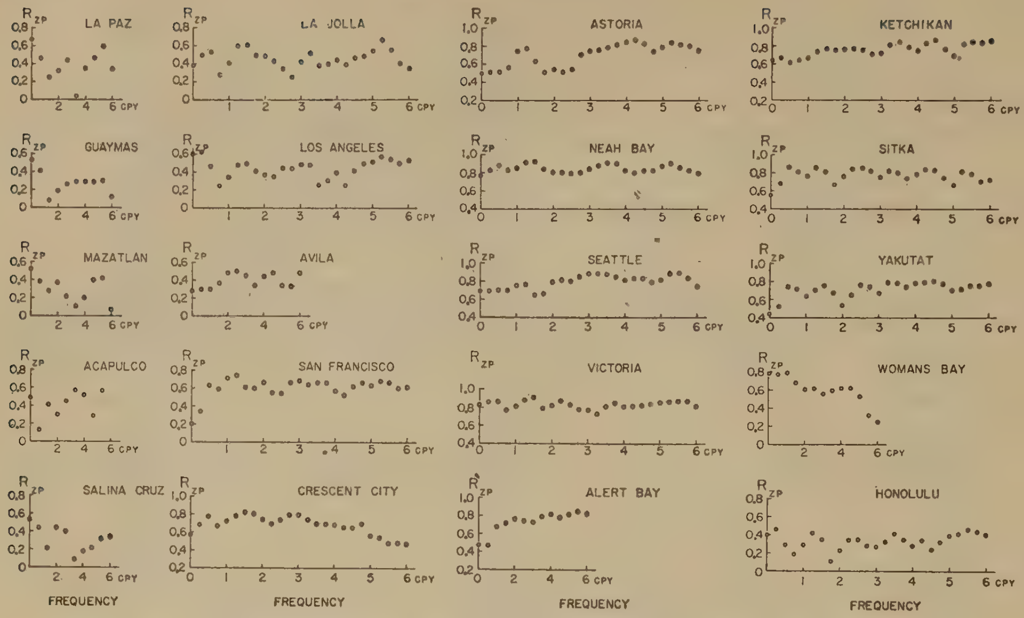

Fig. 6. Coherence between sea level and atmospheric pressure anomalies.

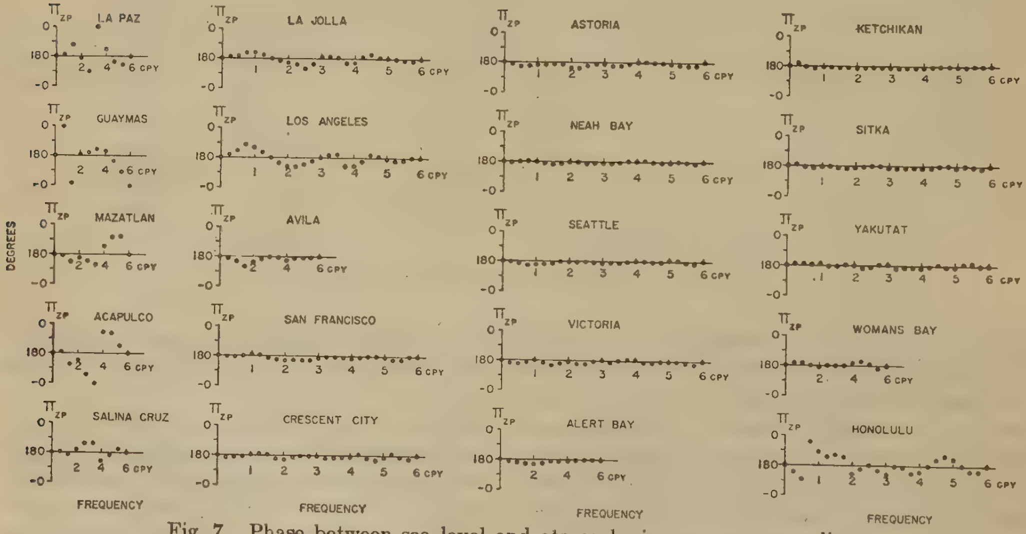

Fig. 7. Phase between sea level and atmospheric pressure anomalies.

these variables is 0° in the northern part of the region, indicating that a south wind leads to high sea levels, as can be expected from the deviating force of the earth's rotation. It is noteworthy that the phase in the north is almost constant with frequency. Off Southern California the phase is also zero where the coherence is high, but since the winds there are mostly northerly this indicates that the sea level is lowered when the winds are strong. It may be concluded that the Coriolis force has a small but recognizable effect upon sea level along the west coast of the United States.

Coherence and phase between sea level and

TABLE 4. The Ratio E_s/E_p as a Function of Frequency

	Tide Station				
Frequency, cpy	Honolulu	La Jolla	San Francisco	Neah Bay	Ketchikan
0	37.58	74.07	44.79	20.42	15.54
1	16.48	20.72	12.25	11.41	7.38
2	11.47	9.91	6.04	4.64	3.56
3	7.12	5.00	4.70	5.17	2.60
4	5.59	6.84	4.77	6.96	3.32
5	3.10	5.39	4.99	4.44	2.64
6	3.28	5.54	5.60	6.14	3.06

runoff anomalies. The considerable influence of the discharge of the Columbia River upon the sea level at Astoria, Oregon, is illustrated by the relatively high coherence, particularly at low frequencies (Fig. 11). Depending upon frequency, between 15 per cent and 50 per cent of the sea level variations can be related to variations in discharge. The phase scatters around zero showing that the variables are directly related. This indicates that tide gage stations in river mouths are not representative and cannot be used in studies of sea level variations on a larger than local scale.

Statistical prediction of sea level anomalies. Let the predicted sea level anomaly z^* at any future month α be a linear combination of the present and past anomalies of sea level, atmospheric pressure, and sea surface temperature. Then

$$z^*(t+\alpha) = \sum_{i=0}^{n} [a_i z(t-i) + \lambda_{zp} b_i p(t-i) + \lambda_{z\theta} c_i \theta(t-i)] \qquad (7)$$

where a_i, b_i, c_i are weighting coefficients to be determined by the method of least squares and n is the number of past months taken into account, and where the constants

$$\lambda_{zp} = \left[\frac{\langle z^2\rangle}{\langle p^2\rangle}\right]^{1/2} \qquad \lambda_{z\theta} = \left[\frac{\langle z^2\rangle}{\langle \theta^2\rangle}\right]^{1/2}$$

are introduced to keep the weighting coefficients dimensionless. The success or failure of the prediction can be described in terms of the mean-square error ϵ^2, defined by

$$\epsilon^2 = \frac{\langle [z^* - z]^2\rangle}{\langle z^2\rangle} \qquad (8)$$

Methods for the computation of the weighting coefficients and the mean-square error are discussed elsewhere [*Roden and Groves*, 1960] and will not be repeated.

Here only two simple cases will be considered. The first case concerns the estimation of the present sea level anomaly from the present anomalies of atmospheric pressure and sea surface temperature. Instead of equation 6 we have

TABLE 5. Coefficients and Mean-Square Error for an Estimate of the Present Sea Level Anomaly from the Present Anomalies of Atmospheric Pressure and Sea Surface Temperature

	λ_{zp}, cm/mb	$\lambda_{z\theta}$, cm/°C	b_0	c_0	ϵ^2
Hawaii					
Honolulu	3.8	9.2	0.07	0.21	0.98
Mexico					
Acapulco	8.1	7.2	−0.28	0.61	0.58
La Paz	6.1	5.4	−0.33	0.36	0.76
California					
La Jolla	4.7	4.2	−0.27	0.65	0.63
Los Angeles	5.1	4.2	−0.20	0.77	0.51
Avila	4.6	6.8	−0.24	0.49	0.73
San Francisco	3.7	6.9	−0.44	0.39	0.67
Crescent City	2.9	5.5	−0.62	0.44	0.44
Oregon					
Astoria	3.5	9.2	−0.54	0.02	0.71
Washington					
Neah Bay	2.8	7.7	−0.74	0.67	0.06
Seattle	2.8	8.4	−0.73	0.04	0.47
British Columbia					
Victoria	2.5	11.2	−0.78	0.27	0.31
Alert Bay	3.3	20.0	−0.56	0.16	0.66
Alaska					
Ketchikan	2.2	9.5	−0.69	0.28	0.44
Sitka	1.7	8.1	−0.72	0.38	0.34
Yakutat	2.1	8.5	−0.58	0.54	0.39

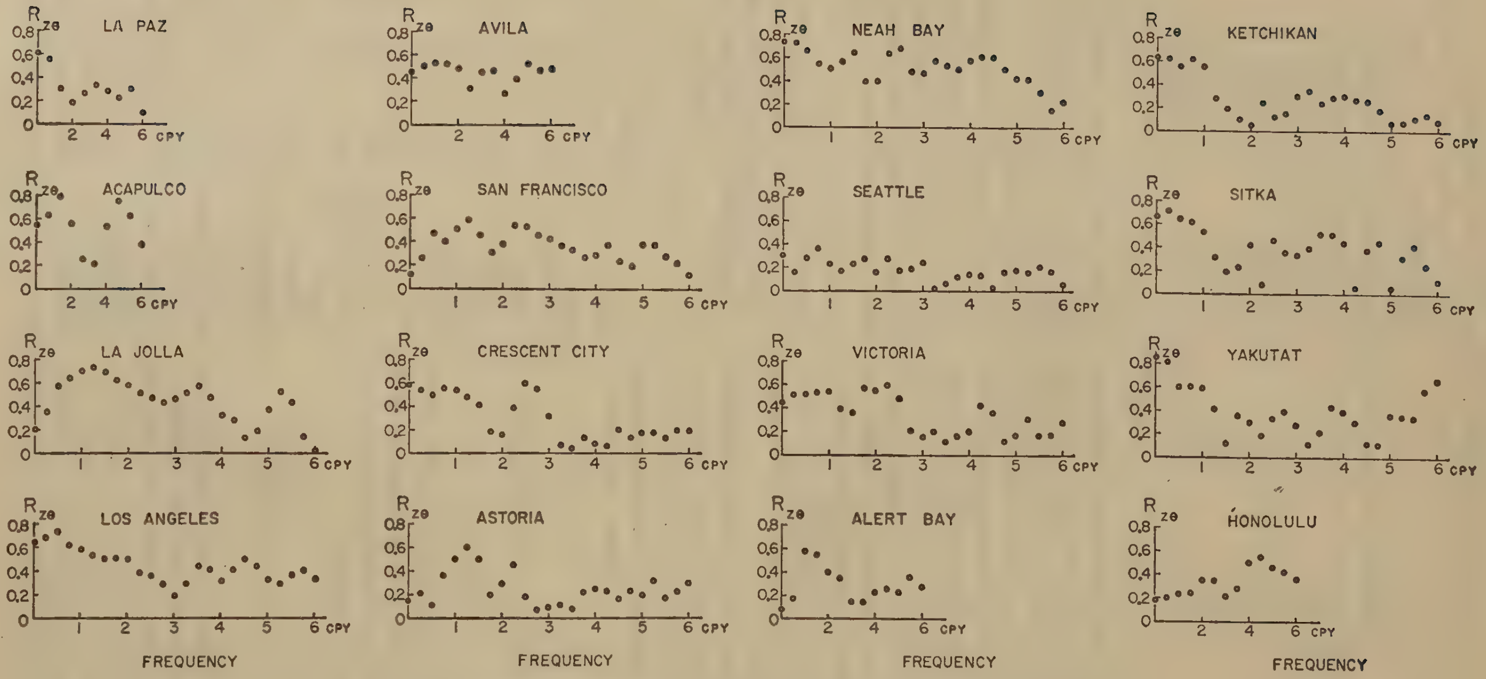

Fig. 8. Coherence between sea level and sea surface temperature anomalies.

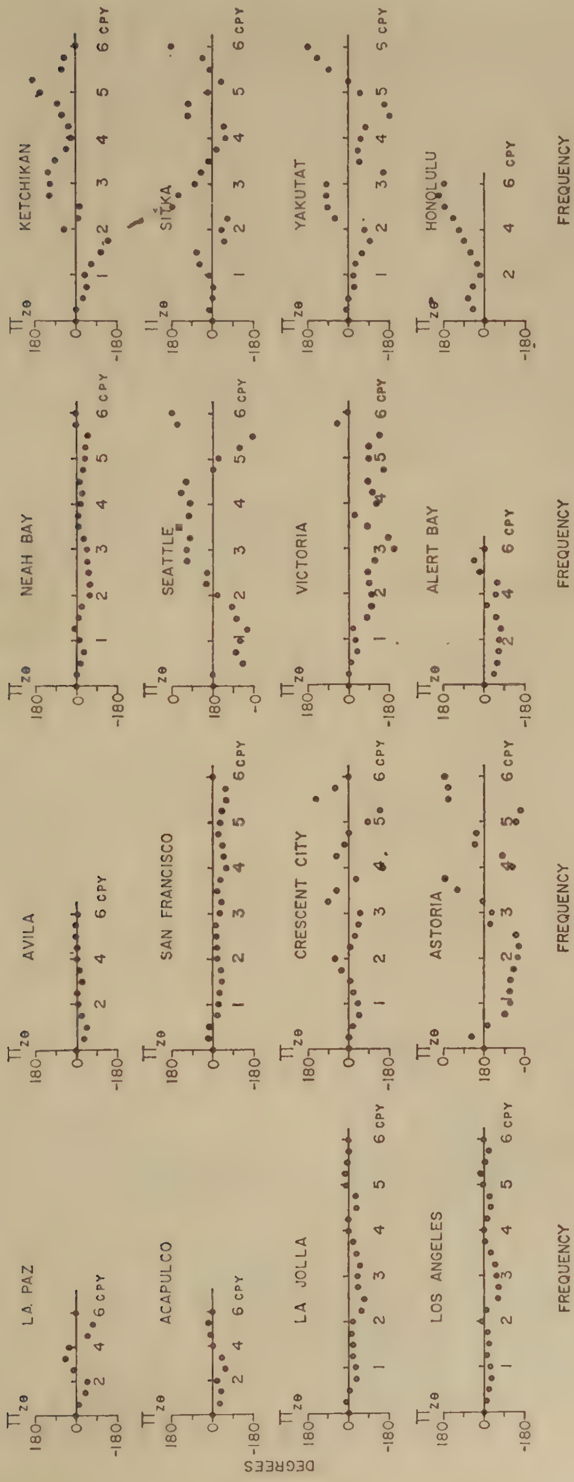

Fig. 9. Phase between sea level and sea surface temperature anomalies.

$$z^*(0) = \lambda_{zp} b_0 p(0) + \lambda_{z\theta} c_0 \theta(0) \tag{9}$$

The coefficients and the mean-square error are given in Table 5. It is seen that for stations north of San Francisco a fairly good estimate of the sea level anomaly can be made; on an average more than 50 per cent can be related to anomalies in atmospheric pressure and sea surface temperature. In the case of Neah Bay, Washington, this percentage is as high as 94 per cent. For stations in Mexico and Southern California the estimates are less good, and for Honolulu, Hawaii, the method fails altogether.

The second case concerns the prediction of the sea level anomaly a few months into the future from the present anomaly of sea level, atmospheric pressure, and sea surface temperature. We have the equation

$$z^*(\alpha) = a(\alpha)z(0) + \lambda_{zp} b(\alpha) p(0) + \lambda_{z\theta} c(\alpha) \theta(0) \tag{10}$$

The coefficients and the mean-square error are shown in Table 6. It is seen that the present sea level anomaly has the greatest weight, and that the other coefficients are relatively small, indicating that the prediction depends almost entirely upon the persistence of the sea level anomalies. Since the persistence is indicated by a Markov-type autocorrelation, the future value depends only upon the present and is independent of the past. Thus the inclusion of more past values of sea level anomalies in our prediction scheme would not lead to better results than we have already obtained. We must therefore conclude that prediction of sea level anomalies by the statistical method does not appear very promising.

Acknowledgments. I have benefited considerably from many fruitful discussions with Walter H. Munk. Maurice Blackburn, Gordon W. Groves, John D. Isaacs, and Joseph L. Reid, Jr., read the manuscript and offered many helpful suggestions.

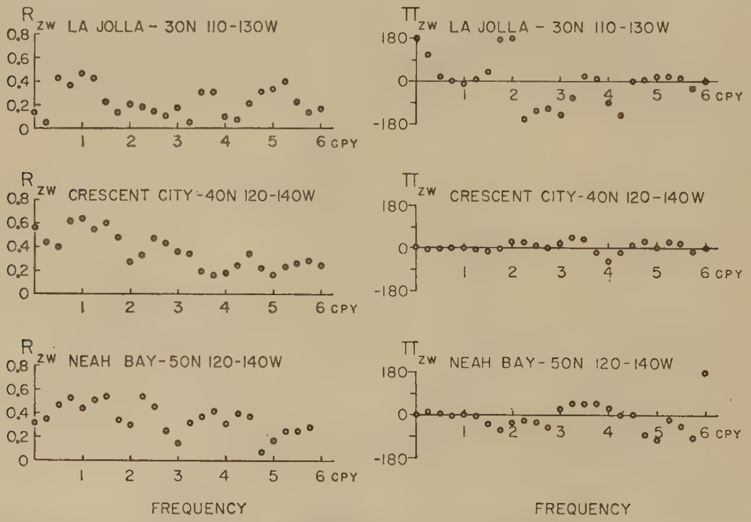

Fig. 10. Coherence and phase between anomalies of sea level and the south component of the geostrophic wind at the latitude and longitude stated.

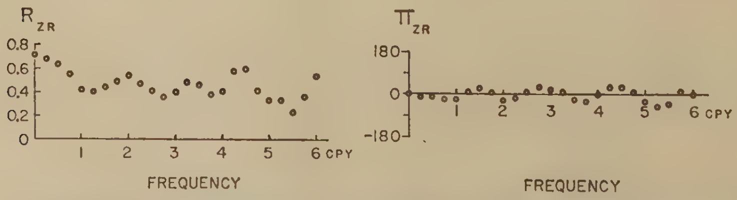

Fig. 11. Coherence and phase between sea level and runoff anomalies at Astoria, Oregon.

TABLE 6. Prediction Coefficients and Mean-Square Error for Prediction from Present Anomalies of Sea Level, Atmospheric Pressure, and Sea Surface Temperature

	$\lambda_{\zeta p}$ cm/mb	$\lambda_{\zeta \theta}$ cm/°C	a	b	c	ϵ^2	a	b	c	ϵ^2
			(α = 1 month ahead)				(α = 2 months ahead)			
Hawaii										
Honolulu	3.8	9.2	0.63	0.02	0.18	0.57	0.42	0.01	0.09	0.82
Mexico										
Acapulco	8.1	7.2	0.78	−0.08	−0.17	0.44	0.78	−0.20	−0.25	0.40
La Paz	6.1	5.4	0.77	0.04	0.00	0.43	0.76	0.04	−0.07	0.48
California										
La Jolla	4.7	4.2	0.73	0.09	−0.03	0.52	0.64	0.06	−0.09	0.66
Los Angeles	5.1	4.2	0.77	0.11	−0.02	0.46	0.71	0.11	−0.05	0.56
Avila	4.6	6.8	0.72	0.05	−0.12	0.53	0.64	0.05	−0.19	0.68
San Francisco	3.7	6.9	0.75	0.18	−0.04	0.55	0.69	0.07	−0.04	0.61
Crescent City	2.9	5.5	0.37	−0.02	0.10	0.81	0.32	0.10	0.06	0.92
Oregon										
Astoria	3.5	9.2	0.47	−0.10	−0.11	0.80	0.34	0.10	−0.12	0.90
Washington										
Neah Bay	2.8	7.7	0.41	0.27	0.00	0.93	0.36	0.18	0.05	0.95
Seattle	2.8	8.4	0.58	0.30	0.02	0.83	0.45	0.21	0.08	0.90
British Columbia										
Victoria	2.5	11.2	0.36	0.12	0.06	0.91	0.27	0.00	0.09	0.92
Alert Bay	3.3	20.0	0.79	0.40	−0.09	0.56	0.73	0.27	−0.12	0.62
Alaska										
Ketchikan	2.2	9.5	0.40	0.20	0.11	0.88	0.29	0.13	0.04	0.96
Sitka	1.7	8.1	0.34	−0.05	0.22	0.87	0.14	0.16	0.22	0.92
Yakutat	2.1	8.5	0.52	0.45	0.19	0.72	0.52	0.29	0.17	0.72

I am also indebted to Gaylord Miller and the Western Data Processing Center of the University of California, Los Angeles. The remaining desk computations were painstakingly done by Joan Connell.

This work was supported in part by the Marine Life Research and the Scripps Tuna Oceanography Research programs. Funds for the latter project were provided by the U. S. Bureau of Commercial Fisheries, Department of the Interior, Contract 14-19-008-9354.

REFERENCES

Canada, Fisheries Research Board, Observations of sea water temperature and salinity on the Pacific Coast of Canada, *Pacific Oceanic Group*, Nanaimo, B. C., 1957–1958.

Blackman, R. B., and J. W. Tukey, The measurement of power spectra from the point of view of communications engineering, *Bell System Tech. J., 37*, 185–282 and 485–509, 1958.

Goodman, N. R., On the joint estimation of the spectra, conspectrum and quadrature spectrum of a two dimensional Gaussian process, *N. Y. Univ., Engineering Statistics Lab. Sci. Paper 10*, 1957.

Groves, G. W., Periodic variation in sea level induced by equatorial waves in the easterlies, *Deep-Sea Research, 3*(4), 248–252, 1956.

Groves, G. W., Day to day variation in sea level, *Meteorol. Monographs, 2*(10), 32–45, 1957.

Haubrich, R., and W. H. Munk, The pole tide, *J. Geophys. Research, 64*(12), 2373–2388, 1959.

LaFond, E. C., Variations of sea level on the Pacific Coast of the United States, *J. Marine Research, Sears Foundation, 2*, 17–29, 1939.

Laning, J. H., and R. H. Battin, Random processes in automatic control, *McGraw-Hill Book Co.*, 434 pp., 1956.

Munk, W. H., F. E. Snodgrass, and M. J. Tucker, Spectra of low frequency ocean waves, *Bull. Scripps Inst. of Oceanog. Univ. Calif.*, 7(4), 283–362, 1959.

Munk, W. H., F. E. Snodgrass, and M. J. Tucker, Smoothing and peristence, *J. Meteorol., 17*(1), 92–93, 1960.

Mexico, Universidad Nacional Autonoma de Mexico Instituto de Geofisica, Observaciones mareograficas en la Republica Mexicana, Costa del Pacifico, *Boletin No. 5.*, 1958.

Nomitsu, T., and M. Okamoto, The causes of the annual variation of the mean sea level along the Japanese Coast, *Mem. Coll. Sci. Univ. Kyoto., Ser. A, 10*(3), 125–161, 1927.

Patullo, June, W. H. Munk, R. Revelle, and E. Strong, The seasonal oscillation in sea level, *J. Marine Research, Sears Foundation, 14*(1), 88–155, 1955.

Roden, G. I., and G. W. Groves, On the statistical prediction of ocean temperatures, *J. Geophys. Research, 65*(1), 249–264, 1960.

Sarkisyan, A. S., Nonstationary wind driven currents in a homogeneous ocean, *Izvest. Akad. Nauk SSSR Ser. Geofiz,* (8), 1008–1019, 1957*a*.

Sarkisyan, A. S., Theory of transient wind currents in an isotropic ocean. *Izvest. Akad. Nauk. SSSR Ser. Geofiz.,* (10), 1232–1237, 1957*b*.

Shoji, Daitaro, On the variation of daily mean sea levels and the Kuroshio from 1954 to 1955, *Proc. UNESCO Symposium on physical oceanography and Japan Society for the promotion of Science,* 130–136, 1957.

Stewart, H. B., B. D. Zetler, and C. B. Taylor, Recent increases of coastal water temperature and sea level. California to Alaska, *Tech. Bull.* (3), *U. S. Coast and Geodetic Survey.,* Washington, D. C., 1958.

U. S. Coast and Geodetic Survey, *Surface Water Temperatures at Tide Stations, Pacific Coast, North and South America and Pacific Ocean Islands,* Fifth Ed., Washington 25, D. C., 1956.

U. S. Coast and Geodetic Survey, Monthly mean sea levels at tide stations along the Pacific Coast of the United States, unpublished.

U. S. Geological Survey, Compilation of surface water records. Pacific Slope Basins in Oregon and the Lower Columbia River Basin (1318), Washington 25, D. C., 1958.

U. S. Weather Bureau, Monthly mean weather maps for the northern hemisphere, 1899–1958, unpublished.

U. S. Weather Bureau, *Monthly Weather Rev.,* Washington 25, D. C., 1872–1949.

U. S. Weather Bureau, *Climatological Data, National Summary,* Washington 25, D. C., 1950–1958.

Veronis, G., and H. Stommel, The action of variable wind stresses on a stratified ocean. *J. Marine Research, Sears Foundation, 15,* 43–75, 1956.

(Manuscript received June 2, 1960.)

CHEMISTS AND THE OCEANS

EDWARD D. GOLDBERG*

MAN has an unrelenting curiosity about his environment and especially about those factors that influence his everyday living. Man's interest in the waters of the world stems not only from their vast disposition over the surface of the earth but also—and perhaps more significantly—from his constant struggle to maintain his home and industries against the ravages of water.

Questions concerning the origin and behavior of natural waters were answered in the religious writings and legends of the first peoples for which we have recorded histories. The Greek civilizations provided the first atmosphere for the naturalistic interpretations of man's surroundings by separating thought from religious ritual. For over two thousand years the opinions of the Greek philosophers provided the focal points for argument and speculation.

As the various scientific disciplines developed, the characteristics of natural waters, especially the oceans, were sought. Initially, academic curiosity motivated the studies, but later on such problems as the origin of life, climates, the formation of continents, and the evolution of organisms directed many investigators to the study of the seas. And more often than not, knowledge about the chemistry of the oceans was needed in order to understand some of the strange phenomena that occur on the surface of the earth.

The paths of marine chemistry have also been fashioned by the advances of chemistry itself. During recent times the elements that can be analyzed, as well as the more intimate description of this complex fluid, have been limited by the theories and techniques of the day. Whereas in the nineteenth century but twenty elements in sea water had been adequately assayed, today a knowledge of the concentration of fifty or sixty has been established and attention is now centering upon the distribution of isotopes of the elements.

The marine chemist has enjoyed the relative homogeneity of marine waters, which has simplified his analytical procedures as compared to those of the rock chemist. But the problems arising from changes in chemical composition through evaporation or biological and chemical activity have forced him to transfer his laboratory from land to boats. Today, another great change is in the offing—the replacement of the seagoing chemist by machines that will carry out the analyses *in situ* more accurately and more rapidly.

---

* Scripps Institution of Oceanography, University of California, La Jolla, California.

Contributions from the Scripps Institution of Oceanography, New Series, 1205

Reproduced by Permission, Chymia, v. 6, 1960. pp. 162-179.

The following outline of the more important advances in marine chemistry since its inception evolved from the preparation of a bibliography of chemical analyses on ocean water in collaboration with Mr. Claude Michaux and Dr. L. H. N. Cooper. It has been impossible to cite all the important papers in this field. Only those contributions which are thought to represent consequential breakthroughs or the thinking of a given period have been included, yet omissions owing to oversight undoubtedly exist. The author acknowledges the extremely helpful assistance of Dr. Norris Rakestraw.

THE ORIGINS OF MODERN MARINE CHEMISTRY

The birth of marine chemistry was a natural byproduct of the scientific revolution that promoted chemistry as an integrated discipline during the latter part of the eighteenth century. The roots of this new endeavor in earth sciences may be found in the dilemmas concerning the very nature of water that confronted the pioneer chemists. The four-element theory of matter (Empedokles, 6th century B.C.), which taught that all substances were produced by combination of different proportions of the four elements, earth, air, fire, and water, permeated the scientific atmosphere. Although a vast reservoir of empirical knowledge was accumulated from the time of the Greeks to the eighteenth century, no definitive questioning of this thesis was made and each new fact was fitted into the inherited pattern. Fish and plants grew solely from water. Water could be transmuted into earth.

The emergence of *controlled experimentation to test* these doctrinaire concepts encouraged a new vigor in the thinking of chemists and allowed the foundations of modern chemistry to be laid. Antoine Laurent Lavoisier (1743–1794) and Torbern Bergman (1735–1784) were not only two key figures in this revolution but were the first scientists to seek out the composition of sea water.

The first researches of Lavoisier were concerned with the composition of the surface waters of France and were motivated by the chronic shortage of water in Paris. He was stimulated by the work of his contemporary, Pierre Joseph Macquer, to pursue hydrometry, the only quantitative method of assay of the salt contents of waters. He was further interested in this technique in the direct determination of the alcoholic content of beverages, inasmuch as he was a member of the tax-collecting company, *Ferme Generale*, which placed levies upon the production of spirits.

His researches kindled a strong curiosity concerning the nature of water and eventually resulted in experiments and theories indicating that water could not be transmuted into other substances and was compounded of the gases, hydrogen and oxygen. He was led to more elegant and elaborate procedures to replace the quite inadequate hydrometric techniques for the assay of dissolved substances in waters. In 1776 he published the first analysis of sea water and prefaced it with the following remarks:

> La partie de la Chimie qui porte le nom de *Halotechnie*, celle qui traite des Sels, est une des dernières qui semble avoir fixé l'attention des anciens Chimistes; l'analyse des Eaux minérales, qui appartient essentiellement à cette partie, s'est ressentie de ce retard; à peine y a-t-il cinquante ans que les Chimistes commencent à acquérir des idées nettes sur les différéntes substances qui entrent dans leur composition, encore est-ce de nos jours que ces progrès ont été les plus repides.
>
> La difficulté de l'analyse des Eaux minérales, consiste principalement à séparer les différentes substances qui s'y rencontrent, à purifier les sels qui souvent sont imprégnés d'eau-mère, de matières extractives, ou de parties bitumineuses.

Lavoisier evaporated the sea water slowly to dryness. During this process calcium carbonate and calcium sulphate were precipitated and were withdrawn. The dried saline mass was extracted with alcohol and magnesium chloride entered the liquid phase. The residue was heated with two parts of alcohol and one part of water until complete solution occurred. Upon cooling, sodium sulphate and magnesium sulphate crystallized from the solution. The aqueous phase retained only some magnesium chloride and sodium chloride (Table 1).

TABLE 1. THE COMPOSITION OF SEA WATER OF LAVOISIER (1776)

Substances	*Weight per Pound of Water, grains*
Sodium chloride	126
Magnesium chloride	14¾
Calcium and magnesium chlorides	23
Sodium and magnesium sulphates	7
Calcium carbonate and sulphate	8

Lavoisier extended the chemistry of the hydrosphere to the hypersaline waters in collaboration with Macquer (1781) and Sage by analyses of Dead Sea samples given to them by Guettard. The adequacy of their techniques is shown by their finding the water to be high in sodium and magnesium chlorides with a virtual absence of sulphates and carbonates. These results were confirmed over seventy-five years later by Boussingault (1856).

Lavoisier recognized the importance of the geochemical role played by water in the main sedimentary cycle:

> L'eau de mer est le résultat du lavage de toute la surface du globe; ce sont en quelque façon les rincures du grand laboratoire de la Nature, on doit donc

s'attendre à trouver réunis dans cette eau, tous les sels qui peuvent se rencontrer dans le règne minéral, et c'est ce qui arrive en effet: comme cette eau est la plus compliquée de toutes celles que j'ai eu occasion d'examiner, je l'ai choisie pour donner un exemple de l'application de l'esprit-de-vin à l'analyse des eaux minérales.

Lavoisier's concern with the geological implications of his work came from his initial schooling in geology with the mineralogist and surveyer Jean Etienne Guettard, his teacher, one of the founders of modern geology, who used the young Lavoisier as an assistant in the field during his preparation of a geological map of France. The influence of this background first appears in Lavoisier's papers on the composition of rivers, in which he attempts to relate the observed abundances of salts with the geological nature of the terrains involved. It is curious that Lavoisier's contributions to geochemistry have escaped notice in the historical introductions to textbooks in this field.

Bergman, on the other hand, complemented his initial training in mathematics and chemistry with studies in natural history. His first published paper was on the ovum of a species of leech. As a chemist he contributed to a broad spectrum of endeavors—mineralogical chemistry, the chemistry of carbon dioxide, the composition of alloys, and quantitative and qualitative analyses. One of his outstanding contributions was the analysis of natural waters. He devised a scheme for the qualitative analyses of many of the dissolved substances in the hydrosphere after carefully carrying through a thorough survey of the work of others on various tests and reagents for the detection of particular constituents. His results were collated in 1778 in a paper on the analysis of the surface waters of Europe. That same year he published his analyses on sea water taken from "a very great depth," 60 fathoms, and described the qualities of this water (Table 2). The chloride of magnesia was separated from the solid contents, obtained from the evaporation of sea water, by extraction with alcohol; the common salt by extraction into cold water and the gypsum by extraction into hot water. He also noted the alkaline nature of ocean waters, by the turning of Brasil-wood paper blue.

TABLE 2. THE COMPOSITION OF SEA WATER ACCORDING TO BERGMAN (1788)

Substances	*Weight per Swedish kanne (about 6½ pints)*		
	Ounces		*Grains*
Sodium chloride	2	and	433
Calcium sulphate	0	and	45
Magnesium chloride	0	and	380

Bergman was impressed by the ocean as a medium for life:

> If sea water taken from a considerable depth be always of the same nature with that above examined, we may conclude that such water is free from the ordinary nauseous flavour; and this supposition also agrees with other phenomena; for the innumerable croud of fish, insects, and vegetables, that grow, live, and perish in the water, as soon as they begin to grow putrid, swell, and rise to the surface, or at least such parts of them as are extracted by the water: on the surface these meet with a sufficient quantity of salt, and free access of air, circumstances which wonderfully promote putrefaction. This destruction is a necessary part of the economy of nature; and thus many circumstances with joint force, contribute to this operation; the necessary consequence of which I apprehend is, that nauseous and loathsome taste occasioned by the putrid particles near the surface.

Thus, biological and geological flavors were given marine chemistry during its birth. It is interesting to note that both these works preceded the acceptance of the hypothesis that water was not an element but a compound. As we now proceed towards the second phase of marine chemistry, the definitive analytical work of Dittmar in the 1880's, we shall see that marine chemistry will draw some of the outstanding personages in chemistry to its fold and will continue to maintain a close liaison with the developments of pure chemistry.

ELEMENTAL ABUNDANCES IN MARINE WATERS

The beginning of the nineteenth century saw the scientists groping for explanations for the widely discordant analyses of sea water. Although many believed that these discrepancies were based upon analytical procedures, others sought refuge in speculations upon the very nature of sea water. F. D. Lichtenberg (1811), one of the first scientists to analyze the carbon dioxide content of sea water, proposed: "Oder herrscht in dem Meere eine Thätigkeit, ein Leben gleichsam, das, obwohl immer dieses bestimmte Leben sich doch unter stets neuen Gestalten zeigt, je nach der Verkettung, in die es mit den Dingen ausser sich kommt?" He sought, to his credit, interlaboratory comparisons and studies on the relationship between wind direction and the salt content of the underlaying waters. Or again, E. J. Bouillon-Lagrange and H. A. Vogel (1813), state: "Quoique les trois mers, dont nous avons fait l'analyse de l'eau, communiquent entre elles, nous avons supposé une différence par rapport au degré de latitude, . . . "

John Murray (1818), formulated the modern methods of water analysis by advocating the determination of the "acids and bases" in solution rather than the minerals left by the removal of the water. He claimed that the latter method gave results more indicative of the operations than of the actual constitution of the inorganic components of natural waters. He realized that the entire separation of salts by crystallization was difficult if not impossible, and "that nothing is easier, for example than to estimate the total quantity of sulphuric acid by the precipitation by barytes, or of lime by precipitation by oxalic acid." He concludes: "In a like manner, it has often been a subject of controversy, whether sea water contains sulphate of soda with sulphate of magnesia (see for example A. Vogel, 1817). All such discussions, however, are superfluous. The salts procured are not necessarily the real ingredients, but in part, at least, are products of the operation, liable, therefore, to be obtained or not, or to be obtained in different proportions, according to the method employed. And all that can be done with precision, is to estimate the elements, and then to exhibit their binary combinations according to whatever may be the most probable view of the real composition."

Four of the techniques that Murray proposed have survived in modified form to the present time: the determination of sulphate as its insoluble barium salt, of calcium and magnesium as the respective oxalate and pyrophosphate, and of chloride by precipitation with silver ion. He relied solely upon gravimetry. His values for the dissolved constituents of marine waters are presented in Table 3.

TABLE 3. The First Analysis of Sea Water Based upon the Dissolved Species Present Murray (1818)

Chemical Species	*Grains in One Pint of Sea Water*
Calcium	2.9
Magnesium	14.8
Sodium	96.3
Sulphate as sulphuric acid	14.4
Chloride as hydrochloric acid	97.7

J. L. Gay-Lussac (1778–1850), the noted French chemist, is remembered by earth scientists for his work with von Humboldt upon the constancy of the composition of the atmosphere. He was also intrigued by the conflicting results upon the composition of sea water and chose to examine solely the salinity and densities of waters collected between France and South America to resolve this difficulty (Gay-Lussac, 1817). It was quite fortunate that he arrived at this decision, inasmuch as he readily recognized and recorded many of the significant parameters associated with the salinity of marine waters:

1. The reflection of density upon the stability of water masses and the temperature-density relationships: "Pour que les eaux de la mer

ne se mêlent pas entr'elles et restent en équilibre, il faut que les couches de niveau aient la même densité: or a cause de l'inégalité de température de l'équateur aux poles, qui seule ferait varier la densitié de l'eau, on a conclu que l'eau de la mer devait contenir d'autant plus de matières salines que sa température est éleveé."

2. Fresh water influx: "Le long des côtes, les fleuves versent annuellement des quantités considérables d'eau douce qui ne se répandent pas rapidement dans la masse des mers."
3. Currents: "Mais les courans continuels que l'on sait exister dans les mers tendent toujours à rétablir l'équilibre de salure."
4. Evaporation versus precipitation: "La différence entre la quantité de l'évaporation et celle de la pluie pourrait bien aussi contribuer à faire varier la salure des mers; et on ne purrait en douter s'il était démontré que ces deux quantités sont inégales."

Gay-Lussac's insight on the nature of oceanographic processes becomes more impressive when it is realized that the sparse amount of data he worked with (besides his own) could not be critically analyzed with respect to accuracy. Further, there was no evidence for temperature changes with depth in the ocean, and this inadequacy led to the erroneous conclusion that the salinity of sea waters was independent of depth. Nevertheless, he concluded from his experimental work, years before the development of the ionic theory, that there would be no separation of the dissolved substances owing to density differences (Gay-Lussac, 1818).

The continuing discoveries of new elements during the nineteenth century gave impetus to the increase of the knowledge regarding the composition of the oceans. Some scientists continued to believe that all the known elements would be found. Marcet (1822), suggested: "For the ocean having communication with every part of the earth through the rivers, all of which ultimately pour their waters into it; and soluble substances, even such as are theoretically incompatible with each other, being almost in every instance capable of co-existing in solution, I could see no reason why the ocean should not be a general receptacle of all bodies which can be held in solution." Marcet sought out mercury in his laboratory, but found none. He was forced to conclude that at least this one element would not be observed.

The discovery of bromine and iodine are both directly related to marine sciences. Their isolation and subsequent determination in sea water are illustrative of the concurrent advances of pure and marine chemistry.

In 1811 (reported in the literature in 1813), B. Courtois discovered iodine in the ash of marine algae. In 1825 iodine was detected in Baltic Sea water by Pfaff and it was observed in French coastal water by Laurens in 1835. The approach to the accepted value of iodine in marine waters (circa 50 micrograms/liter), reflected the improvements in analytical techniques and controlled experimentation of the times. The first quantitative assay resulted in an upper limit of 0.017 micrograms/liter (Macadam, 1852). This was followed by 8000 (Marchand, 1885); 1950 (Sonstadt, 1872); 20 (Koettstorfer, 1878); 20 (Dittmar, 1884); 0.36 (Kallie, 1889); 3.44 (Stanford, 1894); and 2360 (Gautier, 1899), in units of micrograms/liter.

The iodine problem was resolved by L. W. Winkler (1916) who not only arrived at a realistic iodine content (38 micrograms/liter) but also was able to show the partition of the element between the ionic states, iodide and iodate (8 and 30 micrograms/liter respectively). In some of the previous papers cited, analysts, probably influenced by the biophilic character of this element, had reported high concentrations of organic iodine compounds in ocean water. Winkler was further able to show that no detectable iodine was associated with the organic phases of sea water.

In 1824, the youthful French chemist Antoine-Jerome Balard treated the bittern from the deposits of common salt with chlorine and discovered in the distillate the element bromine (Weeks, 1939). The first attempt at a quantitative determination was made by Göbel in 1838 who found 4.5 and 3.0 mg. of Br./l. of sea water in Black Sea and Azov Sea samples respectively. The values fluctuated between 10.4 and 432 mg./l. between this work and that of Thorpe and Morton (1871), who first demonstrated by precise techniques the presently accepted value of 65 mg./l. It is interesting to note that an adequate method of assay was achieved much earlier for bromine than for iodine. This probably results from the fact bromine is 1,000 times more abundant in sea water than iodine.

The improvements in analytical techniques, combined with an ever-increasing curiosity about the distribution of elements on the earth's surface, led scientists to assay such elements as boron, potassium, fluorine, aluminum, manganese, iron, copper, and zinc in marine water during the latter part of the nineteenth century. Although these works are primarily of historical interest, they do emphasize the academic motivation of the workers. However, the analyses of two of the coinage metals in sea water, gold and silver, provided some scientists with an economic incentive. William E. Caldwell (1938), in a survey of gold in the ocean states: "Numerous investigators have analyzed sea water for its gold content, and much variance is noted in their reported results. Nearly fifty patents on methods of securing gold from sea water are on record as from several countries. Fraudulent promoters, or overly hopeful persons, have many times organized companies and sold stock therein, which companies, it was speculated, were to profitably extract gold from sea water."

The saga of noble metal analyses in ocean waters begins with the analysis of E. Sonstadt (1872), who found around 65 mg. of gold/metric ton of sea water. Chr. A. Münster (1892), found but 5 mg./metric ton but proposed placing two iron electrodes between two islands where the water flow was around 4 meters per minute. The electrodes were to be 2 meters by 3 meters and were to be placed in banks of 60 at 30° to the current. Liversidge (1895), observed between 10 and 66 mg./metric ton but commented: "It would probably not pay to extract the gold by itself, although it might as a by-product in the manufacture of salt, bromine, etc." Pack (1898), assayer at the U. S. Mint in San Francisco, proposed operating upon the bitterns from salt manufacture to obtain the gold. Cautionary notes were added by Loevy (1905), who found less than 1 mg./metric ton and elaborated: "Erklarlicherweise hat sich in Amerika auch die schwindelhafte Spekulation dieser Angelegenheit bemächtigt und einige ganz wunderbare, echt amerikanische Blüten gezeitigt."

Many other papers appeared on this problem but both the gold content of sea water and its economic potentialities were yet to be ascertained. Following World War I, the famed German scientist Fritz Haber tackled the problem with the explicit hope of success in order to repay the war debt obligations of his homeland. As his precision and care in his analytical procedures improved, Haber (1928), found less and less gold in sea water. He finally concluded there was around 0.004 mg./metric ton. Today at $35.00 per ounce of gold each ton of sea water is worth 0.01 cent for its gold on the basis of Haber's results.

Nonetheless, Haber's work did not settle the matter. Putnam (1953), summarized the gold analyses made subsequent to Haber's work, and concluded that the concentration of gold in sea water is extremely variable and ranges from 0.003 to at least 44 mg./cubic meter. Apparent confirmation of his ideas may be found in the recent paper of Robineau and Desbois (1955). Both studies emphasize the dependence of gold concentration upon the particular water mass and biological activity. Putnam claims to have collected gold upon an amalgamated silver-zinc couple and concludes "continuation of the work will make possible the location and charting of the movement of the richer bodies of gold bearing sea water from which gold could be economically recovered. Not only should such a study yield valuable geochemical information, but the profitable extraction of gold from sea water could lead to a better foundation for the currencies of the world."

Returning to the nineteenth century, confidence and insight in the analytical techniques, combined with an ever-increasing knowledge of the behavior of elements in solutions, were directing workers not only to the true constitution of ocean water with respect to its main constituents, but also to the formulation of questions concerning the biochemical and geochemical processes that occur in the marine *milieu.* Although scores of papers appeared during the second half of the nineteenth century, the works of Forchhammer and of Dittmar are best illustrative both of the

(918)

extreme care in assay in order to obtain unequivocal results and of the initial attempts at a three-dimensional survey of the hydrosphere.

Georg Forchhammer undertook his labors more as a geologist than as a chemist. His prime interest lay in the "mutual chemical decompositions and combinations, which, partly depending upon organic life, partly upon inorganic mechanical and chemical forces, play such a great part in the changes of the earth." He began his work in 1843 but was so occupied with the formidable tasks of his analyses for over twenty years that he found little leisure to interpret his results. The pattern of his methodology had been cast by Murray. He sought gravimetrically chloride, sulphate, magnesium, calcium and potassium, while sodium was obtained by difference. One hundred pounds of sea water were necessary. Forchhammer was aware of alteration of his samples in the laboratory through evaporation and organic decompositions, and did not try to ascertain the nature and quantity of the dissolved gases. He did, however, mark the neck of the flasks to determine the amounts of evaporation between collection time and the initiation of his analytical procedures.

Probably the principal consequence of Forchhammer's work (1865) is the proposition that, although sea waters exhibit marked regional differences in salinity, the ratios of the dissolved constituents to one another are almost invariable. He attempted to utilize the salinity differences for the tracing of water masses and the influences of melting ice masses and rivers upon the oceans.

He also posed in an elegant form the "geochemical balance" problem arising from the major sedimentary cycle: "Thus the quantity of the different elements in sea water is not proportional to the quantity of elements which river water pours into the sea, but inversely proportional to the facility with which the elements in sea water are made insoluble by general chemical or organo-chemical actions in the sea." He reached this conclusion by noting that, although calcium and silicon were often principal constituents of river waters, they were depleted in the oceans. He correctly attributed the deficiency of silicon to diatoms and other siliceous organisms but erroneously believed that calcium concentrations were regulated by carbonate-depositing animals.

W. Dittmar, professor of chemistry at Anderson's College in Glasgow, made exacting analyses on 77 samples of sea water, collected from the surface to great depths during the world encircling cruise of H.M.S. Challenger. His refinements included the use of the Volhard volumetric titration of the halides, and the calculation of potassium by difference following conversion of all cations to the sulphate form. Forchhammer, on the other hand, assumed the cations and anions neutralized one another but neglected the carbonate and bicarbonate ions in his difference calculation for potassium. Dittmar (1884) firmly established Forchhammer's conclusion concerning the constancy of the relative ionic composition of sea water with his own results which, "fairly agreeing with Forchhammer's were in still closer accordance with one another, and thus showed that Forchhammer's proposition may be extended to ocean waters obtained from all depths."

Changes in atomic weights and minor improvements in analytical procedures have brought but slight changes between the original values of Dittmar and the values that are presently accepted (Table 4). His remarkable attentiveness to accuracy through controlled experimentation resulted in oceanographic chemical standards that his successors have attempted to maintain.

TABLE 4. A Comparison of Dittmar's Values for the Components of Sea Water with the Modern Values (Sverdrup, Johnson and Fleming, 1946)

Species	*Values in Grams per Kilogram* *Dittmar*	 *Modern*
Cl^-	18.971	18.980
Br^-	0.065	0.065
SO_4^{--}	2.639	2.649
CO_3^{--}	0.071	
HCO_3^-		0.140
F^-		0.001
H_3BO_3		0.026
Mg^{++}	1.278	1.272
Ca^{++}	0.411	0.400
Sr^{++}		0.013
K^+	0.379	0.380
Na^+	10.497	10.556

Dittmar must also be credited with some excellent analyses on the dissolved gases in marine water. Mr. J. Y. Buchanan, the shipboard chemist during the Challenger Expedition, extracted from ½- to 1-liter samples the dissolved gases which were given to Dittmar at the conclusion of the expedition. Dittmar, although apparently not enthusiastic about this added work burden, devised an elegant gas train in which the carbon dioxide was removed with potassium hydroxide, the oxygen determined by combustion with hydrogen and the nitrogen ascertained by difference. Dittmar rightly applied to nitrogen the relationship between the solubility of gases in solution as a function of the partial pressure of the gases in the atmosphere of the system and found his results to be in manifest agreement with the theory. Oxygen and carbon dioxide gave anomalous values. Although Dittmar pointed out that processes of oxidation could reduce the quantities of oxygen in deep waters, the very small values of oxygen at great and moderate depths annoyed rather than stimulated him. He suspected technical difficulties in the gas extraction apparatus rather than the more consequential organic oxidation reactions.

The works of Forchhammer and Dittmar, the careful chemical analyses on large numbers of samples from different regions and from all depths, brought to a climax one phase of marine chemistry. Although future workers were to determine more elements and their isotopic constitutions, and were to obtain more precise results, questions upon the processes and factors which determine the composition of ocean waters were to motivate their work. Two general fields of inquiry were to be the more stimulating: the interactions of the marine biosphere with ocean waters and the role of the oceans in the major sedimentary cycle.

LIFE PROCESSES AND THE CHEMISTRY OF THE OCEANS

The possibility that life in the sea might govern the concentrations of some of the inorganic constituents in the oceans would have appeared strange to the pioneer marine chemists. Although they were cognizant of the remnants of sea creatures as decomposing organic matter, the presence and influence of the large photosynthesizing biomass escaped them.

By the middle of the nineteenth century observations on the chemical composition of the marine biosphere began to appear in spurts. Forchhammer realized that analyses of marine plants and animals offered a method of showing the existence in sea water of elements impossible to assay by chemical tests. He wrote: "It is now well known that the organic beings collect substances which are necessary for their existence and thus offer the means to the chemist of ascertaining that these substances were present in the medium in which the organisms lived, and from which they collected their food." Copper, lead, zinc, cobalt, nickel, and barium were found by him in living matter but not in the sea water. He sensed the importance of marine life by proposing that the constancy of the oceanic composition is maintained by the uptake by organisms of the materials introduced into the oceans by river run-off. This implies a constantly increasing biomass in the oceans. but Forchhammer did not pursue this problem to any such end.

As the analyses of dissolved oxygen and carbon dioxide became fashionable, the evidence of some deficiency of the former and an excess of the latter in deep waters prompted questions as to the effect upon animal life. Thus W. B. Carpenter (1872), found in two deep stations in the Mediterranean that "nearly the whole available oxygen had been converted into carbonic acid—fully adequate to account for the paucity of animal life on the deep bottom. . . . "

But it remained until 1909, nearly 100 years after the more general aspects of photosynthesis had been uncovered, for Legendre (1909) to relate variations in the oxygen content of surface waters to the activity of plants. He observed that the oxygen content of surface waters reached a maximum near midday—this increase could not be explained by any physical factors. He proposed that the daily variation is due to the influence of light upon photosynthetic processes and that the relative changes are in direct proportion to the abundance of the flora. J. P. Jacobsen (1912), stimulated by the work of Legendre, confirmed his findings, utilizing the more sensitive "Winkler" method for the determination of dissolved oxygen. Besides confirming the diurnal variation, he noted supersaturations of oxygen occurring in the summertime at depths between 25 and 75 meters, which were attributed to the activity of marine plants. He firmly established the presence of the oxygen minimum and related it to the consumption of oxygen by organic oxidation processes. Simultaneously, Brennecke (1909) encountered similar distributions of oxygen in the Atlantic Ocean. Thus, the oceans were to be considered as a medium in which plants and animals can exert a measureable influence upon the concentrations of the various components. The influence of both photosynthesis and oxidation processes upon the hydrogen ion and the carbonic acid concentrations was sought and found. The importance of primary production by marine plants became a primary influence in directing the researches of marine chemists in the second decade of the twentieth century. Were there other chemical species in the oceans that were related to the photosynthetic process? Why were the phytoplanktonic species more abundant in some areas?

In 1899 K. Brandt (quoted in Harvey, 1928, p. 20) had observed that the mineral species, nitrate and phosphate, were required by photosynthesizing plants and were built up into proteins. This finding, coupled with the realization that the minute ubiquitous plants of the eutrophic zones in the sea could alter the concentrations of oxygen, hydrogen ion and carbon dioxide, was suggestive that the concentrations of certain nutrient anions might be regulated by photosynthetic activity. This surmise was first borne out by the work of Raben (*op. cit.*) in the first decades of the twentieth century. He found that the North Sea waters displayed more phosphate and nitrate in the winter than in the more productive summer months and that these nutrients were depleted in the upper layers of the oceans. In 1926 Atkins and Harvey showed that much of the silica in the surface waters was removed by the diatoms in the formation of their tests. These works initiated a long series of researches that elaborated upon the relative fertilities of waters with respect to the nutrients, silicate, nitrate, and phosphate as a function of time of year, depth, and locality. Many of these pioneering investigations emanated from the Marine Biological Laboratory of the United Kingdom in Plymouth, England.

The accumulating evidence was crystallized into the objectives of the extensive chemical program of the "Meteor Expedition" of 1925 under the direction of Hermann Wattenberg. (An excellent summary of Wattenberg's life and contributions has been prepared by Rakestraw (1956).) He asked how the living organisms were distributed in relation to the inorganic nutrients and how the processes of respiration and inorganic decomposition may be reflected in the composition of sea water. He carried out thousands of analyses upon dissolved oxygen, pH, phosphate, carbon dioxide, and oxygen in 310 stations in the South Atlantic Ocean, and the resulting collection of data even today forms one of the foundations of marine chemical literature. He extracted from his analyses the causal relationships between the production of carbon dioxide and the nutrient anions and the consumption of oxygen at depths in the ocean. The richness of marine life off the African coast was traced to high concentrations of the nutrients in up-welled deep waters. Another contribution was his finding that most of the upper layers of the ocean were supersaturated with respect to calcium carbonate and that at the ocean floor calcareous deposits were undergoing solution. These results evolved from his work on the solubility of calcium carbonate in sea water.

But perhaps of significance equal to that of his scientific results was his recognition of the importance of doing chemical work at sea. He designed one of the first sea-going laboratories and demonstrated the practicality of carrying out the entire chemical program of a lengthy expedition in the rolling laboratory of a ship. He set precedents for the design of analytical equipment that could survive the abuses of the ocean.

A deeper insight into the cycle of nutrients, uptake during primary production, and return to the hydrosphere during respiratory and oxidative processes, was gained in the ensuing years. (A survey of this problem may be found in Harvey (1955).) The temporal presence of nitrites and ammonium ions in the upper layers of the ocean was shown to evolve from the degradation of nitrogenous organic debris (Cooper, 1933). A number of investigators have come to suspect that iron and manganese may be essential to plant growth in the oceans and that the distributions of these elements may partially delimit productive areas. Growth factors, such as vitamins, have been detected in the oceans. At the present time we are by no means certain as to all the chemical species required in primary production, but advances both in the mechanisms of photosynthesis and in the analytical methodology of marine chemistry promise to provide at least partial answers in the very near future.

THE MAJOR SEDIMENTARY CYCLE

The more general considerations of the mechanisms that regulate the composition of marine waters were initiated by studies upon the role of the oceans in the major sedimentary cycle. Early workers recognized the processes of rock weathering, of the transport to the oceans of dissolved and particulate substances, and of the subsequent deposition through physical or biological agencies. Quantitative calculations on the amounts of elements involved in the sedimentary cycle were initiated by Joly (1899), but it remained for Goldschmidt and his colleagues, who founded the modern school of geochemistry in Göttingen during the second and third decades of the twentieth century, to seek out the chemical parameters that control the distribution of some elements in the marine hydrosphere during this cycle (Goldschmidt, 1937).

Before studies on regulatory processes could be started, however, there remained the determinations of elements representative of those parts of the periodic table that were missing in oceanic abundance tables. Thus Goldschmidt and his co-workers, using highly refined spectroscopic techniques, analyzed a host of elements, many of them in the parts per billion range and many for the first time. The oceanic concentrations of lithium, boron, vanadium, nickel, selenium, molybdenum, strontium, yttrium, rubidium, cesium, barium, lanthanum, cerium, and mercury were revealed.

A geochemical balance sheet was prepared in which was tabulated the amount of a given element potentially available to the hydrosphere through igneous rock weathering, the amount actually observed, and the amount in sedimentary materials. From such data was established the utility of the ionic potential, the ratio of the ionic charge to the ionic radius, as an indicator of the behavior of elements during the sedimentary cycle. Three concentration domains, as a function of ionic potential, were observed. Substances with low ionic potentials, such as sodium, potassium, calcium, and magnesium, remain in solution in the oceans. Over 50 per cent of the sodium that has been released during the breakdown of igneous rocks now resides in ionic form in the hydrosphere. Those with intermediate values, including aluminum, silicon, titanium, and beryllium, tend to be readily precipitated from sea water as components of the sediments. Finally, the elements with high ionic potentials, which form the anionic Brönsted bases, stay in solution. From consideration on the amounts of the anions in sea water, such as chloride, bromide, and the carbonates, Goldschmidt was able to show that their derivation from igneous rocks was improbable. He suggested the possibility of large supplies of these materials from volcanic gases and springs.

Such contributions firmly established the usefulness of modern concepts in the atomic and ionic properties of matter in studying the chemistry of the ocean. Goldschmidt, for example, elaborated upon the phenomenon of the sorption of ions upon the particulate phases in the marine environment, an idea that was later used to advantage in the study of the uranium decay series. The concentration of uranium in sea water had been found to approach a few micrograms per liter, apparently stabilized by complexing of the hexavalent ions with carbonate (Piggot and Urry, 1941). However, radium and ionium, two of the decay products in the uranium series, were present in amounts far below those expected for radioactive equilibrium (recently determined to be under 2 per cent of the equilibrium amount for ionium (Koczy, *et al.*, 1957), yet it was present in marine sediments at rather high levels. This led Pettersson (1939), to postulate that ionium, a predecessor of radium, was removed from sea water by sorption on ferric hydroxide sols to the sedimentary deposits.

An interesting aftermath of these studies has recently appeared in the suggestion that a part of the radium, which arises from the ionium in the sedimentary deposits, returns to the oceans. This induction evolved from the evidence that radium shows a marked increase with water depth in a number of oceanic stations (Pettersson, 1955).

The influence of Goldschmidt's broad outlook upon chemistry of the ocean in relation to processes occurring on the earth's surface was undoubtedly responsible for the extensive quantitative studies by the Noddacks (1939), upon the distribution of heavy metals between sea water and marine animals. In the course of this work, such elements as bismuth, gallium, chromium, etc., were assayed for the first time.

Today, many of the general advances in the study of marine chemistry reflect the geochemical patterns inaugurated by Goldschmidt. More and more papers on the chemical analyses of the minor elements in sea water are complemented with analyses of sediments and marine organisms. The geological and biological implications of the chemist's work upon sea water have become an accepted part of his program.

REFERENCES

Atkins, W. R. G., and H. W. Harvey, "The variation with depth of certain salts utilized in plant growth in the sea." *Nature,* **116,** 784–785 (1926).

Bergman, Torbern, "Physical and Chemical Essays." Translated from the original Latin by Edmund Cullen. London, 1788.

Bouillon-Lagrange, E. J., and H. A. Vogel, "Mémoire sur l'eau des mers qui baignent les côtes de l'Empire française, considerée sous le point de vue chimique et médical." *Ann. chim.* (*Paris*), **87,** 190–214 (1813).

Boussingault, J. B., *Compte rend.*, **42,** 1233 (1856).

Brennecke, W., "*Forschungsreise S. M. S. Plante,* 1906–7," 1909.

Caldwell, William E., "The gold content of sea water." *J. Chem. Educ.*, **15,** 507–510 (1938).

Carpenter, W. B., "Report on scientific researches carried on during the months of August, September and October 1871 in H.M. surveying ship 'Shearwater.'" *Proc. Roy. Soc. London,* **1872,** 535–644.

Cooper, L. H. N., "Chemical constituents of biological importance in the English Channel, November, 1930 to January, 1932. Part. I. Phosphate, silicate, nitrate, nitrite, ammonia." *J. Mar. Biol. Assoc. United Kingdom,* **18,** 677–754 (1933).

Courtois, B., "Decouverte d'un substance nouvelle dans le Vareck." *Ann. chim. (Paris),* **88,** 304–310 (1813).

Dittmar, William, "Report on researches into the composition of ocean water, collected by H.M.S. Challenger, during the years 1873–1876." *Rept. Sci. Results Voyage H.M.S. Challenger (Phys. and Chem.),* **1,** 1–251 (1884).

Forchhammer, Georg, "On the composition of sea water in the different parts of the ocean." *Phil. Trans.,* **155,** 203–262 (1865).

Gautier, Armand, "L'iode dans l'eau de mer." *Compt. rend.,* **128,** 1069–75 (1899).

Gay-Lussac, J. L., "Note sur la salure de l'Océan atlantique." *Ann. chim. phys.,* **6,** 426–436 (1817).

Gay-Lussac, J. L., "Supplément à la note sur la salure de la mer, imprimée dans le sixième volume des annales de chimie et de physique, p. 426." *Ann. chim. phys.,* **7,** 79–83 (1818).

Göbel, Friedemann, "Reise in die Steppen des südlichen Russlands unternommen von Dr. Fr. Göbel." Vol. 2, 372 pp. Dorpat, 1838.

Goldschmidt, V. M., "The principles of distribution of chemical elements in minerals and rocks." *J. Chem. Soc.,* **1937,** 655–673.

Haber, Fritz, "Das Gold im Meere." *Z. Ges. Erdkunde Berlin,* **3,** 1–12 (1928).

Harvey, H. W., "Biological chemistry and physics of sea water." 194 pp. Cambridge, 1928.

Harvey, H. W., "The chemistry and fertility of sea waters." 224 pp. Cambridge, 1955.

Kallie, L. van., "Über das Vorkommen von Jodium in 'Fucus vesiculosus' und 'Chrondus crispus.'" *Arch. Pharm.,* **227,** 1132–1134 (1889).

Jacobsen, J. P., "The amount of oxygen in the water of the Mediterranean." *Rept. Danish Oceanographical Expedition 1908–10,* **1,** 207–236 (1912).

Joly, J., "An estimate of the geological age of the earth." *Sci. Trans. Roy. Soc. Dublin,* **7,** 23 (1899).

Koczy, F. F., E. Picciotto, G. Poulaert, and S. Wilgain, "Mesure des isotopes du thorium dans l'eau de mer." *Geochim. Cosmochim. Acta,* **11,** 103–129 (1957).

Koettstorfer, J., "Zum Nachweis von Jod im Meerwasser." *Z. anal. Chem.,* **17,** 305–309 (1878).

Laurens, G., "Analyse de la partie de la Mediterranée qui baigne les côtes de Marseille." *J. pharm. sci. accessories,* **21,** 90–92 (1835).

Lavoisier, A., "Mémoire sur l'usage de l'esprit-de-vin dans l'analyse des eaux minérales." *Mém. Acad. Roy. Sci.,* **1772,** Pt. 2, 555–563 (1776).

Legendre, R., "Recherches sur les variation de température, de densité et de teneur en oxygène de l'eau de la côte à Archachon." *Bull. Station biologique d'Archachon,* 29 pp., 1909.

Lichtenberg, F. D., "Chemische Untersuchung des Ostsee-Wassers." *J. für Chemie und Physik,* **2,** 252–257 (1811).

Liversidge, Archibald, "On the amount of gold and silver in sea water." *J. Proc. Roy. Soc. N. S. Wales,* **29,** 335–349 (1895).

Loevy, Julius, "Gold im Meerwasser." *Chem. Ztg.,* **29,** 213 (1905).

Macadam, Stevenson, "On the presence of iodine in various plants with some remarks on its general distribution." *Chem. Gaz.,* **10,** 281–286 (1852).

(926)

Macquer, P. J., A. Lavoisier, and B. G. Sage, "Analyse de l'eau du Lac Asphaltite." *Mém. Acad. Roy, Sci.*, **1778,** 69–72 (1781).

Marcet, Alexander, "Some experiments and researches on the saline contents of sea water, undertaken with a view to correct and improve its chemical analyses." *Phil. Trans. Roy. Soc.* (*London*), **1822,** 448–456.

Marchand, Eugène, "Des eaux potables en général considérées dans leur constitution physique et chimique et dans leurs rapports avec la physique du globe, la géologie, la physiologie générale et l'hygiene publique, ainsi que dans leurs applications à l'industrie et à l'agriculture; en particulier des eaux utilisées dans les arrondissements du Harvre et d'Yvetot." *Mém. Acad. Méd.* (*Paris*), **19,** 121–318 (1855).

Münster, Chr. A., "On the possibility of extracting precious metals from sea water." *Norsk Tek. Tiddskr.*, **10,** 13–20 (1892).

Murray, John, "A general formula for the analysis of mineral waters." *Trans. Roy. Soc. Edinburgh*, **8,** 259–280 (1818).

Noddack, Ida and Walter Noddack, "Die Häufigkeiten der Schwermetalle in Meerestieren." *Arkiv. Zool.*, **32A,** 1–35 (1939).

Pack, John W., "Gold from sea water." *Mining Sci. Press*, **77,** 154–155 (1898).

Pettersson, Hans, "Die radioactiven Elemente im Meere." *Rapp. Proc. Verb. Conseil Permanent Intern. Explor. Mer.*, **109,** No. 9, 66 (1939).

Pettersson, Hans, "Manganese nodules and oceanic radium." *Pap. Mar. Biol. and Oceanography, Deep-Sea Res.*, suppl. to Vol. 3, 335–346 (1955).

Pfaff, Chr., "Über die Kalisalze, den Salmiak- und Iode-Gehalt des Ostseewassers." *Jahrb. Chem. Phys.*, **15,** 378–382 (1825).

Piggot, C. S. and Wm. Urry, "Radioactivity of ocean sediments III. Radioactive relations in ocean water and bottom sediments." *Am. J. Sci.*, **239,** 81 (1941).

Putnam, Garth L., "The gold content of sea water." *J. Chem. Educ.*, **30,** 576–579 (1953).

Rakestraw, Norris W., "Hermann Wattenberg: a pioneer in a new field of exploration." *J. Chem. Educ.*, **33,** 217–222 (1956).

Robineau, Ch. and Ch. Desbois, "Étude sur la presence de l'or dans l'eau de mer." *Trav. centre recherches et d'études oceanographiques*, **2,** No. 3, 4 pp. (1955).

Sonstadt, Edward, "On the presence of iodate of calcium in sea water." *Chem. News*, **25,** 196–198, 231–232, and 241–242 (1872).

Sonstadt, Edward, "On the presence of gold in sea water." *Chem. News*, **26,** 159–161 (1872).

Stanford, Edward C., "The president's address." *J. Soc. Chem. Ind.* (*London*), **13,** 697 (1894).

Sverdrup, H. U., M. W. Johnson, and R. H. Fleming, "The Oceans." 1087 pp. New York, 1946.

Thorpe, Thomas E. and E. H. Morton, "On the composition of the water of the Irish Sea." *Mem. Lit. Phil. Soc. Manchester*, **4,** 287–302 (1871).

Vogel, A., "Analyse de Seewasser aus dem Canal." *J. für Chemie und Physik*, **8,** 344–351 (1817).

Weeks, Mary, "Discovery of the elements." 470 pp., 1939.

Winkler, L. W., "Der Jodid- und Jodat Iogehalt des Meerwassers." *Z. angew. Chem.*, **29,** 205–207 (1916).

(927)

(928)

JOURNAL OF GEOPHYSICAL RESEARCH VOLUME 65, No. 11 NOVEMBER 1960

A Low-Frequency Microbarograph[1]

WM. G. VAN DORN

Scripps Institution of Oceanography
La Jolla, California

Abstract. A sensitive band-pass microbarograph has been designed to assist in the interpretation of records of surface water waves of low frequency made at isolated Pacific island stations. The instrument employs a hydraulic resistance-capacitance filter network to attenuate high-frequency gusts and the atmospheric tide. Sensitivity can be adjusted to as little as 0.1 millibar full-scale, but the recorder normally operates at the much lower sensitivity of ± 5.0 mb at oceanic stations, with a resolution of ± 0.05 mb (± 50 dynes/cm^2).

An example is cited of a one-to-one correspondence between barometric pressure and sea surface elevation during the passage of an anomalous barometric disturbance.

Introduction. During the summer of 1960 the Scripps Institution of Oceanography will install three permanent recording stations at Wake, Johnston, and Canton islands in the mid-Pacific for the continuous monitoring of low-frequency water surface waves [*Van Dorn,* 1960]. While temporary stations of this type were used in the past to study waves from nuclear explosions and submarine earthquakes it was found that the great abundance of signals in the low-frequency spectrum were undoubtedly associated with barometric fluctuations in the lower atmosphere. In particular, the passage of typhoons within several hundred miles of these stations resulted invariably in long-period forerunners which preceded the ordinary wind waves by one or two days. It soon became obvious that interpretation of the sea-wave records depended for the most part on a knowledge of the local meteorological situation, and to a much more refined degree than was possible from the data available from local weather stations. Although much pioneering work of this nature has been carried out by *Donn* [1958] and *Gossard and Munk* [1955], it was believed that a microbarograph specifically designed to have the same spectral response characteristics as the long-wave recorder would greatly simplify the work of analysis of data.

Accordingly, essentially the same components utilized in the latter instrument were adapted to the device described below, resulting in a remarkably simple, thermally stable unit, the output from which can be recorded simultaneously with the water waves at similar amplitude levels and with perfect time synchronization.

Description of the microbarograph. A schematic diagram of the microbarograph is shown in Figure 1, and Figure 2 shows its construction details. It consists of a lower cylindrical plexiglass chamber 4 inches in diameter filled with silicone oil (Dow Corning DC-200, 1000 centistokes viscosity) connected through a capillary restriction to an identical upper chamber half full of oil and open to the atmosphere. The lower chamber also connects through another capillary to one side of an electric pressure transducer (Statham P5-0.2 psid). The other side of the differential transducer is open to the atmosphere. The lower chamber is also filled to a depth of about ¼ inch with mercury, which is in direct connection with a 1-inch diameter cylindrical glass flask evacuated and closed at its upper end and elevated about 30 inches above the base so as to produce a Torricelli vacuum above the mercury. In essence, the lower chamber and the elevated flask comprises an ordinary mercury barometer, the position of which is sensed by the pressure transducer. Within the region of interest in the barometric frequency spectrum the response is unity and the phase-shift zero. Response to frequencies outside this region is governed by low- and high-pass filters, which act to attenuate gusts and the barometric tides, respectively. Battery power (1.3 volts d-c) and signals are transmitted via a 4-conductor electric cable to a control panel containing balancing and calibrating networks, and recorded

---

[1] Contribution from the Scripps Institution of Oceanography, new series. 1206

Reproduced by Permission

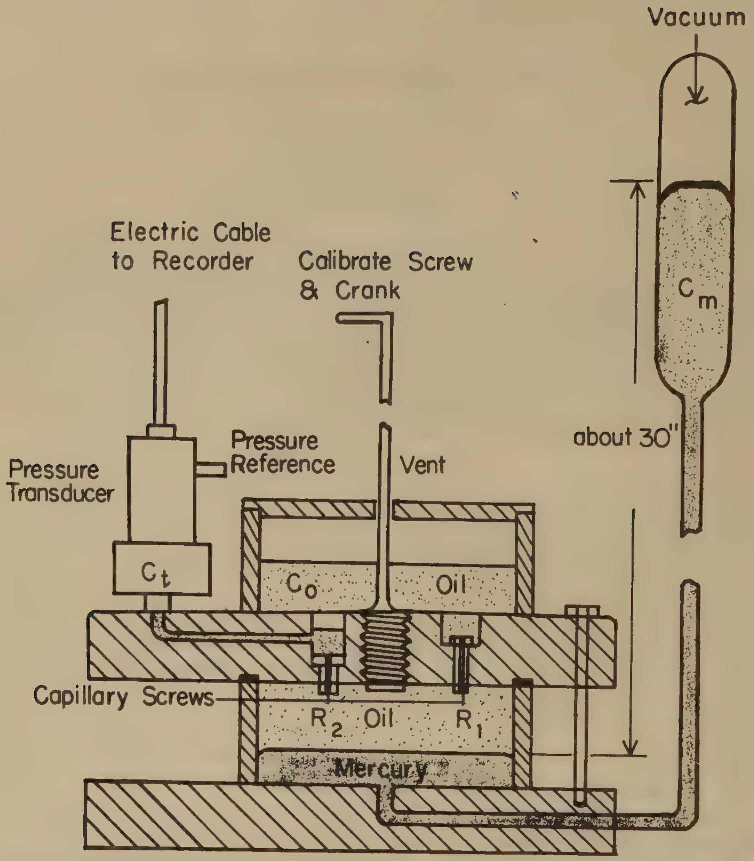
Vacuum
Electric Cable to Recorder
Calibrate Screw & Crank
C_m
Pressure Reference
Vent
about 30"
Pressure Transducer
C_t
C_0
Oil
Capillary Screws
R_2
Oil
R_1
Mercury

Fig. 1. Schematic drawing of the microbarograph. The abundant use of plexiglass facilitates machining, assembly, and inspection. The mercury flask and its stem are pyrex glass and are filled under vacuum.

TABLE 1. Circuit Constants for the Hydraulic Filter

Symbol	Component	Length, cm	Radius, cm	Circuit Constant (at 25°C)*
R_1	Capillary	1.59	0.080	7.40×10^5 dyne sec/cm^5
R_2	Capillary	0.935	0.046	5.26×10^6 dyne sec/cm^5
C_m	Mercury flask	20	1.27	3.46×10^{-4} cm^3/(dyne/cm^2)
C_t	Transducer bellows			8.78×10^{-6} cm^3/(dyne/cm^2)
C_0	Upper chamber	7.5	5.08	8.23×10^{-2} cm^3/(dyne/cm^2)

* Using 1000 centistoke (9.73 poise) silicone oil.

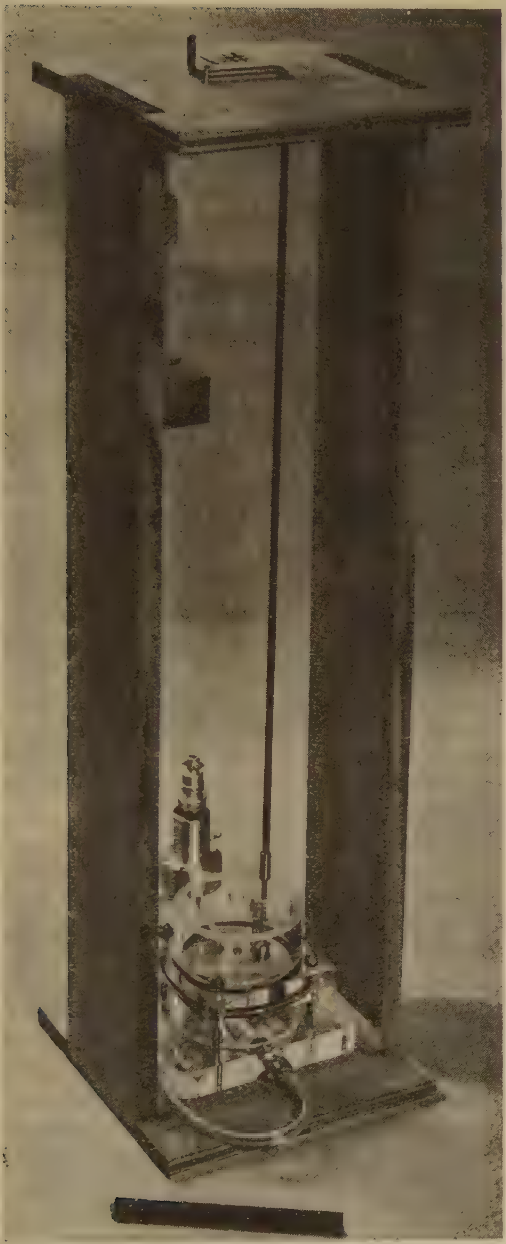

Fig. 2. The microbarograph in its wooden supporting rack. The 4-wire electric cable (not shown) connects to the upper end of the transducer.

on a Leeds and Northrup 10-millivolt Speedomax strip-chart recorder.

The dynamical frequency response of this system and its theory of operation are virtually identical with that already described [*Van Dorn*, 1960], except that the low-pass capacitance C_2, instead of being a mercury manometer, makes use of the compliance of the small bellows within the transducer itself. Figure 3 shows both the amplitude response of the microbarograph to a constant amplitude sine-wave input of variable frequency and its equivalent electrical analog circuit. Table 1 gives the circuit constants and the dimensions of the pertinent components.

Initial calibration of the microbarograph is accomplished in the laboratory by filling the upper (reference) opening of the transducer with oil and connecting it by a short plastic tube to the upper chamber. Then a brass cylinder is raised and lowered sinusoidally into the upper chamber by a pulley system coupled to a variable-frequency sine generator. In the field, calibration is accomplished by advancing a calibrating screw between the upper and lower chambers by one revolution through a long crank arm extending through the top of the wooden rack which supports the various components. Advancing the screw imparts a steplike increase in pressure to the lower chamber, corresponding to a sudden reduction in atmospheric pressure in normal operation.

In the field the rack-mounted instrument (Fig. 4) is lowered into a vertical well and in an area far away from the dynamical pressure effects induced by the presence of buildings, etc. The well is equipped with an airtight lid, and atmospheric pressure is admitted through an omnidirectional diffuser, consisting of a short vertical length of 1-inch pipe through which a multiplicity of ⅛-inch holes are drilled in staggered rows. Atop the diffuser is a sun shield, and thermal stability is further insured by filling the space above the rack with a plastic-encased kapok pillow, such that diurnal ambient temperature fluctuations within the well are reduced to about 1 per cent of their surface values. Thermal sensitivity of the system arises from differential rates of thermal expansion of the silicone oil and the lower chamber walls. This effect was minimized by the choice of plexiglass for the wall material, and laboratory tests indicate that even without the benefit of additional thermal insulation the system is stable to less than 1 per cent of its full-scale sensitivity over a 10°C diurnal variation but shows small signals from alternating exposure to darkness and direct sunlight.

Field experience. A prototype model of the

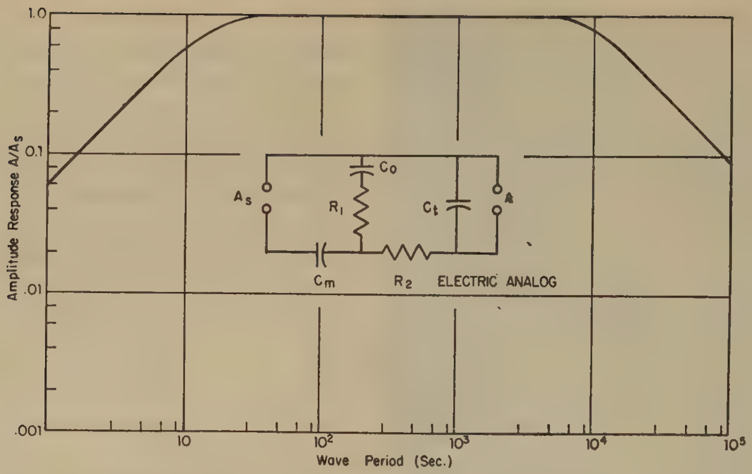

Fig. 3. Frequency response of the microbarograph to a unit sine-wave input, and the electrical analog of the hydraulic filter. The effective band width is easily adjusted by varying the capillaries R_1 and R_2.

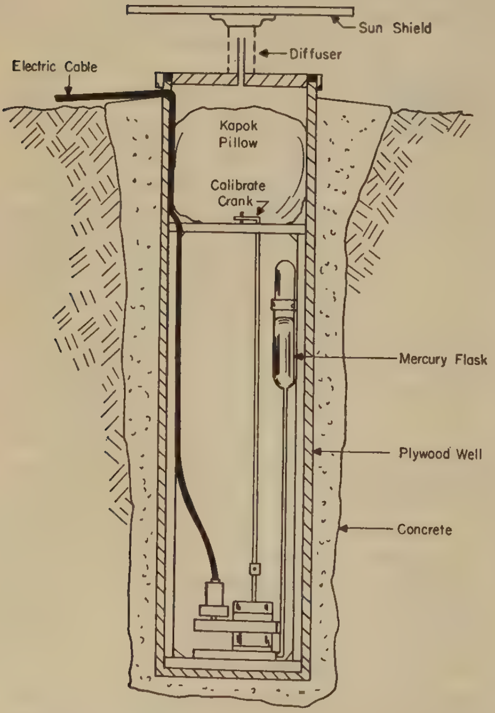

Fig. 4. Schematic drawing of the microbarograph rack installed in its well. The wooden well is coated with fiberglas outside, and serves as a shipping container before installation.

low-frequency microbarograph was installed on Marcus Island in January 1958, together with three long-wave recorders—one on each side of the triangular island—and a wind speed and direction recorder. The signals from all these instruments were recorded against time on a single six-channel Speedomax recorder. The objective for this station was to study the influence of the island on surface water waves approaching from various directions.

It soon became apparent that barometric fluctuations associated with the passage of local disturbances were often reflected by corresponding depressions and elevations of the water surface at all three wave recorders. Since the wave recorders are insensitive to barometric pressure changes, such coherence can only be due to atmospheric coupling. An excellent example of this coherence is shown in Figure 5, which is a direct tracing from the original record for February 26, 1958. In the top curve the microbarograph exhibits at the beginning of the sample quasi-periodic fluctuations of 10–20 minute period and amplitudes of the order of 0.5 mb superimposed on the diurnal atmospheric tide. Such a record is typical during the seasons of strong trade winds with bands of scattered cumulus clouds and occasional intense rain squalls. Suddenly two deep barometric depressions appear, separated by an interval of about 22 minutes, and bounding an unusually high peak; over-all maximum pressure change was 2.8 mb, and it occurred within

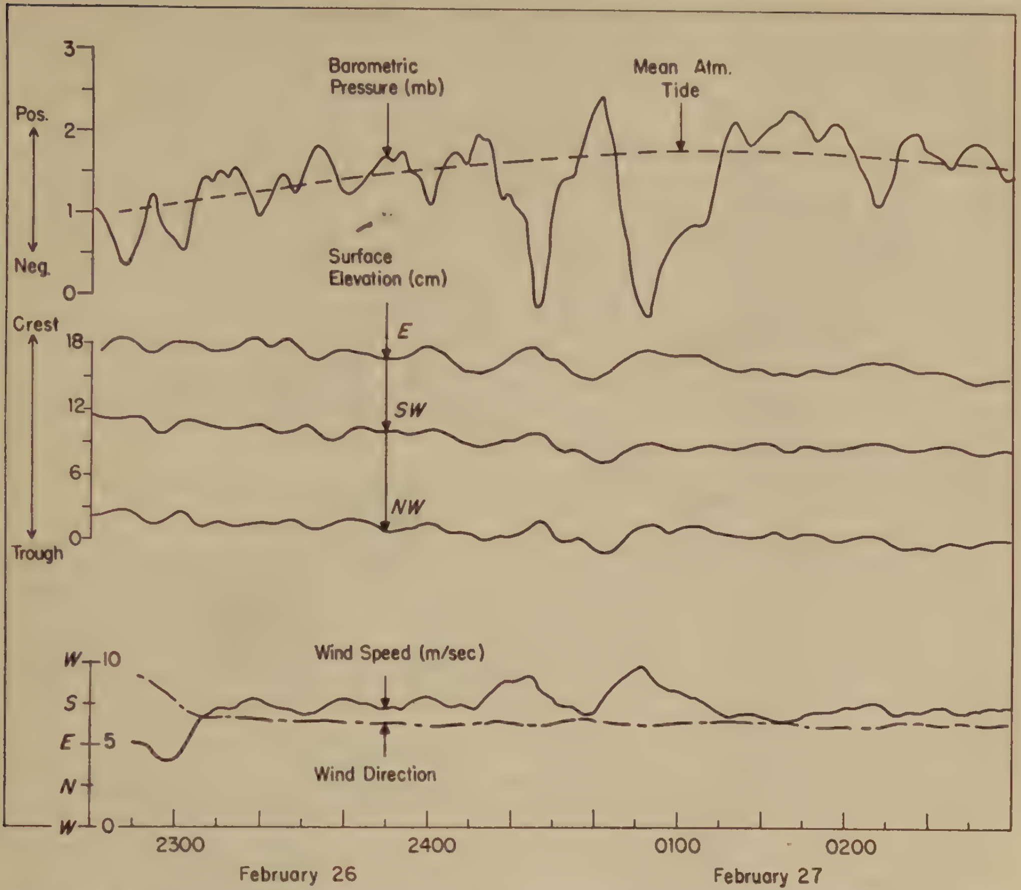

Fig. 5. Record sample from Marcus Island, showing passage of double pressure-jump, as construed from combined records of microbarometric pressure, sea level at three stations, and wind speed and direction.

8 minutes. Following this unusual disturbance the trace returns to normal activity. Corresponding to the barometric changes, the sea surface was elevated and depressed anomalously by about 3 cm, or by roughly the amount of the barometric change at all three stations. Two clear maxima occurred in the wind speed at the time of the depressions, and there was virtually no change in the wind direction.

Reconstruction of the probable sequence of events which resulted in this meteorological singularity[3] is possible through analysis of the above record and consideration of Figure 6, which shows the outline of Marcus Island and the geographical distribution of the instrumentation. The long-wave recorders were installed near the center of each leg of the triangular island. The anemometer and microbarograph were located on the east side of the island near the east long-wave station. The prevailing wind had been blowing at about 7.5 m/sec from ESE for about 2 hours. The first barometric depression, preceded by a relatively minor pressure increase, was accompanied by an increase in wind speed to 10 m/sec. The disturbance propagated unchanged in form across the island with the mean wind speed and in the prevailing wind direction, as evidenced by the displacement in time of the long-wave records at the SW and NW stations and the nearly identical anomalous sea-level

---

[3] Although some coherence between the sea level and barograph records was almost always present, only two such extreme examples were observed in 3 months of records at Marcus Island.

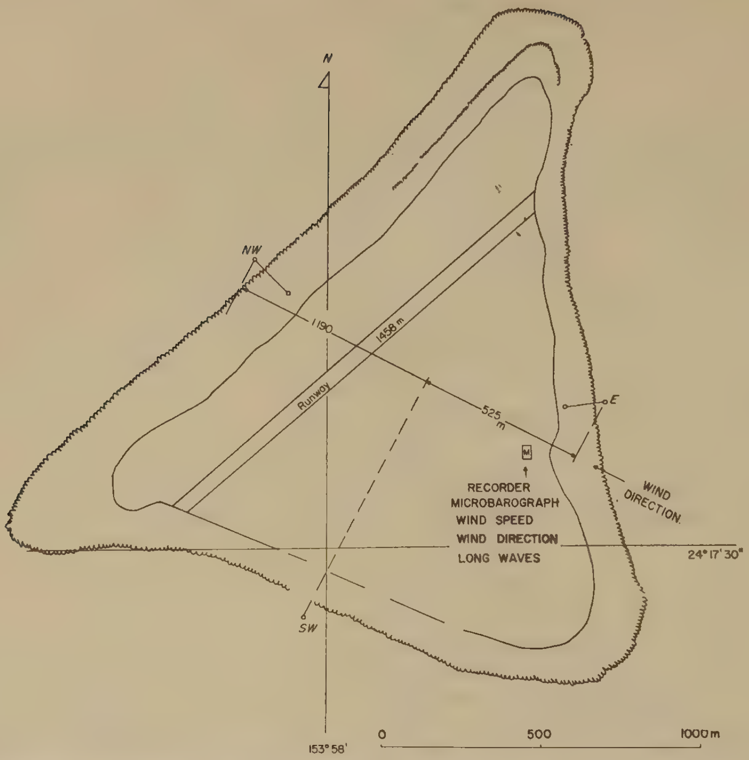

Fig. 6. Instrument installations at Marcus Island. The microbarograph and anemometer were installed at the east side of the island, adjacent to the east sea-level station.

fluctuations. The situation described bears a certain similarity to the 'pressure jump' often accompanying line squalls, as described by *Tepper* [1950], wherein an advancing line squall is preceded by one or more pressure jumps originating along the linear front at several centers of local impulsive horizontal acceleration. In such cases geostrophic conditions are overshadowed by the strong pressure gradient, and the wind blows normal to and away from the advancing front with a velocity which depends on the local gradient. The present situation may be likened to this model, save that pressure jumps are normally steplike increases in pressure, whereas the significant pressure changes here were negative. It is left to those experienced in tropical meteorology to find a more convincing explanation. The point to be made here is that without the barograph the disturbance observed in the wave records might have been interpreted as a progressive system of free waves, instead of a closely coupled response to a barometric anomaly propagating at the mean wind speed.

Conclusions. The simple band-pass microbarograph described above has proved to be a valuable adjunctive tool for the study of water surface disturbances. Its simplicity of construction and freedom from thermal variation suggest its use in other areas of meteorology.

Acknowledgment. This research was sponsored by the Office of Naval Research under contract Nonr 233(35).

REFERENCES

Donn, W. L., The microbarovariograph: A new instrument for measuring minute atmospheric pressure variations, *Trans. Am. Geophys. Union, 39,* 366–368, 1958.

Gossard, Earl, and Walter Munk, Gravity waves in the atmosphere, *Quart. J. Roy. Meteorol. Soc., 81,* 484–487, 1955.

Tepper, Morris, A proposed mechanism of squall lines: The pressure jump line, *J. Meteorol. 7,* 21–29, 1950.

Van Dorn, W. G., A new long-period wave recorder, *J. Geophys. Research, 65,* 1007–1012, 1960.

(Manuscript received May 20, 1960; revised September 1, 1960.)

Reprinted from SCIENCE, December 9, 1960, Vol. 132, No. 3441, pages 1737-1746

The East Pacific Rise

Recent marine geophysical measurements have shed some light on processes acting in the earth's mantle.

H. W. Menard

The sea floor slopes downward from California to Hawaii, and there is no obvious reason why it should. Ten years ago it seemed not unreasonable that the floor of an ocean basin should slope downward from the continental margin to the center. True, the deepest parts of the oceans are at the margins, but in many places, notably the east coast of North America, a great apron of continental debris forms a transitional slope between continent and ocean. As cores of sediment and seismic stations measuring the thickness of sediment accumulated, it became apparent that, off southern California, the apron of continental debris is either very narrow or nonexistent, and the sediment of the deep-sea floor is of relatively uniform thickness. The underlying layers in the earth's crust are also of relatively uniform thickness, and consequently the top of the mantle is parallel to the sea bottom. The slope between California and Hawaii is apparently produced by some variation in the mantle itself.

The fact that this was not an isolated problem was established immediately before and during the International Geophysical Year, when the Scripps Institution of Oceanography undertook to explore the East Pacific Rise. This rise, a vast bulge in the sea floor, extends through the remotest waters on earth and was little known; even the general outlines of the topography had only just been established by U.S. Navy ships during Operations Highjump and Deepfreeze. Scripps geological expeditions had already reached the fringes of the rise in regions east of the Marquesas Islands and west of Central America and found abnormal heat flow in both places and abnormal seismic velocities in the mantle at one of them. Comparable anomalies had been found in the North Atlantic, where the Mid-Atlantic Ridge is conveniently located for exploration. Maurice Ewing (*1*) and his collaborators at Lamont Geological Observatory found abnormal seismic velocities, and Sir Edward Bullard of Cambridge University found very high heat flow at the crest of the ridge. Were these few values characteristic of oceanic rises and ridges in general?

Another question to be investigated was raised by a hypothesis just then proposed by Ewing and Bruce Heezen. It had been known for many years that the Mid-Atlantic Ridge, the Mid-Indian Ridge, and the various ridges and rises of the Pacific basin form an almost continuous topographical feature marked by shallow earthquakes. Heezen and Ewing discovered a central rift valley associated with the seismic belt at the crest of the Mid-Atlantic Ridge in the North Atlantic, and they proposed (*2*) that the earthquakes originated in the rift valley and, since the topographic highs and the seismic zone extended through the oceans, that the rift must be continuous for 80,000 kilometers. If so, it would be present in the area to be studied in the parts of the East Pacific Rise which were about to be explored.

The Scripps Expedition Downwind was designed as a field experiment to investigate the known questions about topography, crustal structure, and heat flow of the East Pacific Rise as well as a number of problems of physical oceanography, geochemistry, and biology. The results (*3*) of this expedition and of others before and after (Fig. 1) can be combined to give a progress report on research on the East Pacific Rise. Attention is focused here on three questions. Does the rise extend under western North America? Are transverse wrench (tear) faults part of the rise structure? What is the origin of the rise?

Location and Topography

The East Pacific Rise is a vast low bulge of the sea floor comparable in size to North and South America (Fig. 2). The average relief is 2 to 3 kilometers, exclusive of the additional local relief of features such as volcanoes. The rise is 2000 to 4000 kilometers wide, and from Mexico to New Zealand it is 13,000 kilometers long.

Transverse to the East Pacific Rise are a number of long straight bands of mountainous topography called fracture zones (*4*). The crust of the rise is offset or changes trend in several places where it is intersected by fracture zones. In addition, the whole width of the rise has been displaced vertically by several hundred meters along some fracture zones. Thus, it appears that the vast bulge of the rise has been sliced

---

The author is associate professor of marine geology, Institute of Marine Resources and Department of Earth Sciences, University of California, La Jolla.

Contributions from the Scripps Institution of Oceanography, New Series, 1207

Reproduced by Permission

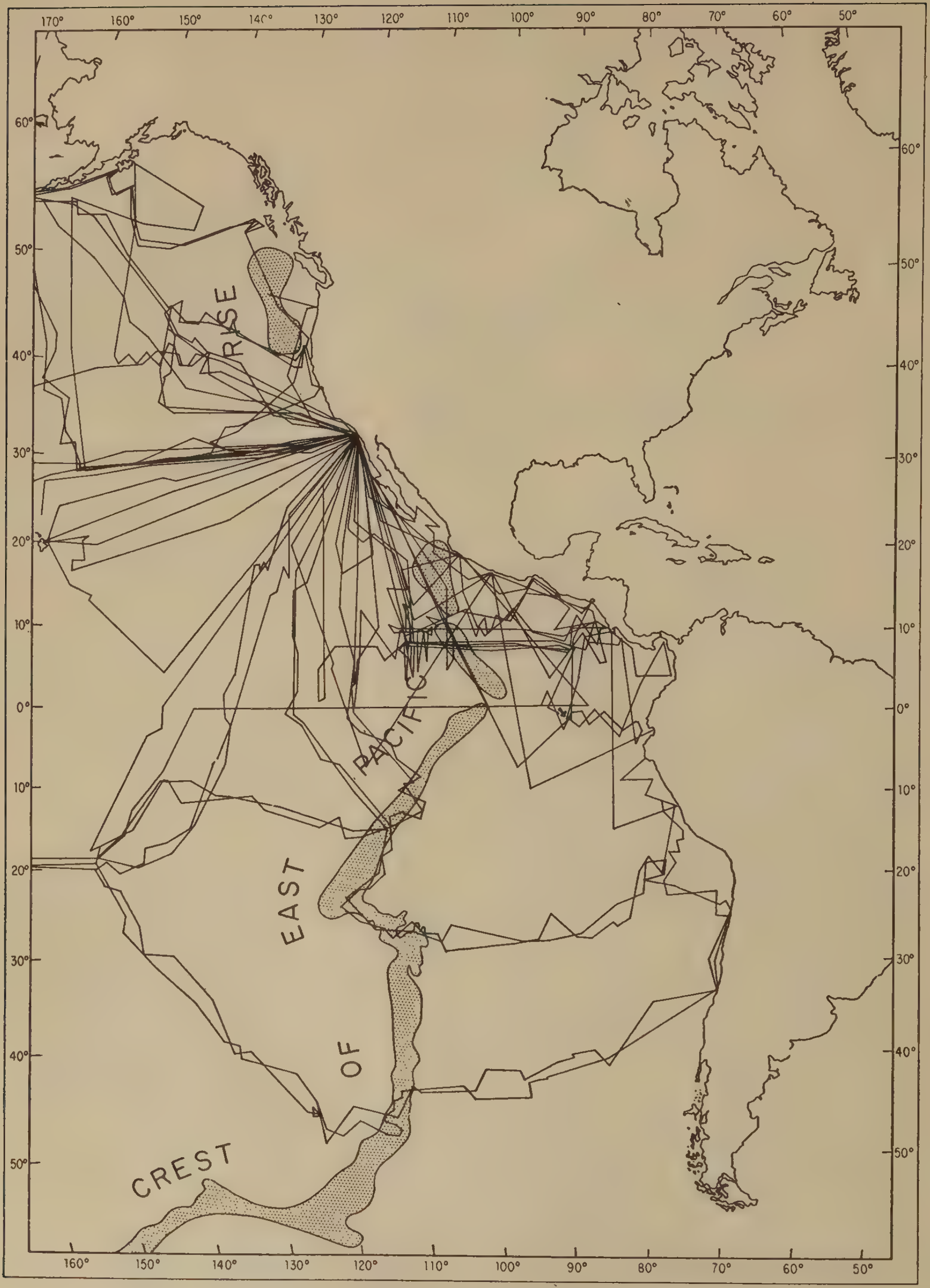
EAST OF PACIFIC RISE CREST
170° 160° 150° 140° 130° 120° 110° 100° 90° 80° 70° 60° 50°
60° 50° 40° 30° 20° 10° 0° 10° 20° 30° 40° 50°

Fig. 1. Scripps Institution of Oceanography sounding and sampling lines in the eastern Pacific.

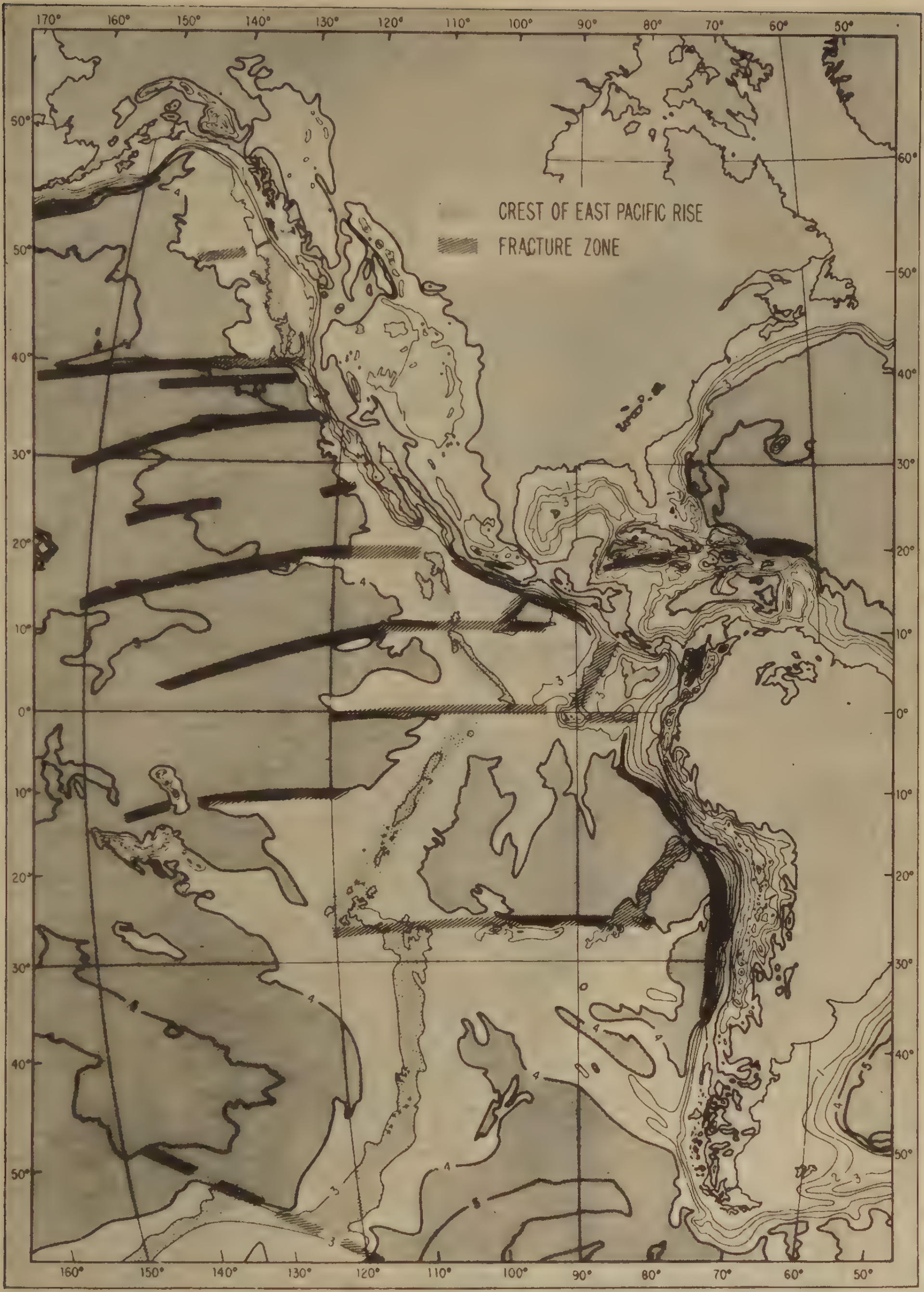
CREST OF EAST PACIFIC RISE
FRACTURE ZONE
170°
160°
150°
140°
130°
120°
110°
100°
90°
80°
70°
60°
50°
60°
50°
40°
30°
20°
10°
0°
10°
20°
30°
40°
50°
1
2
3
4
5

Fig. 2. Topography of the eastern Pacific and the Americas (depths and elevations in kilometers). Areas shallower than 4 kilometers in the ocean or higher than 1 kilometer on land are shown in white and are considered anomalous. On this basis the crest of the East Pacific Rise appears to extend for some distance through western North America, and the western slope of the rise is continuous as far north as Alaska.

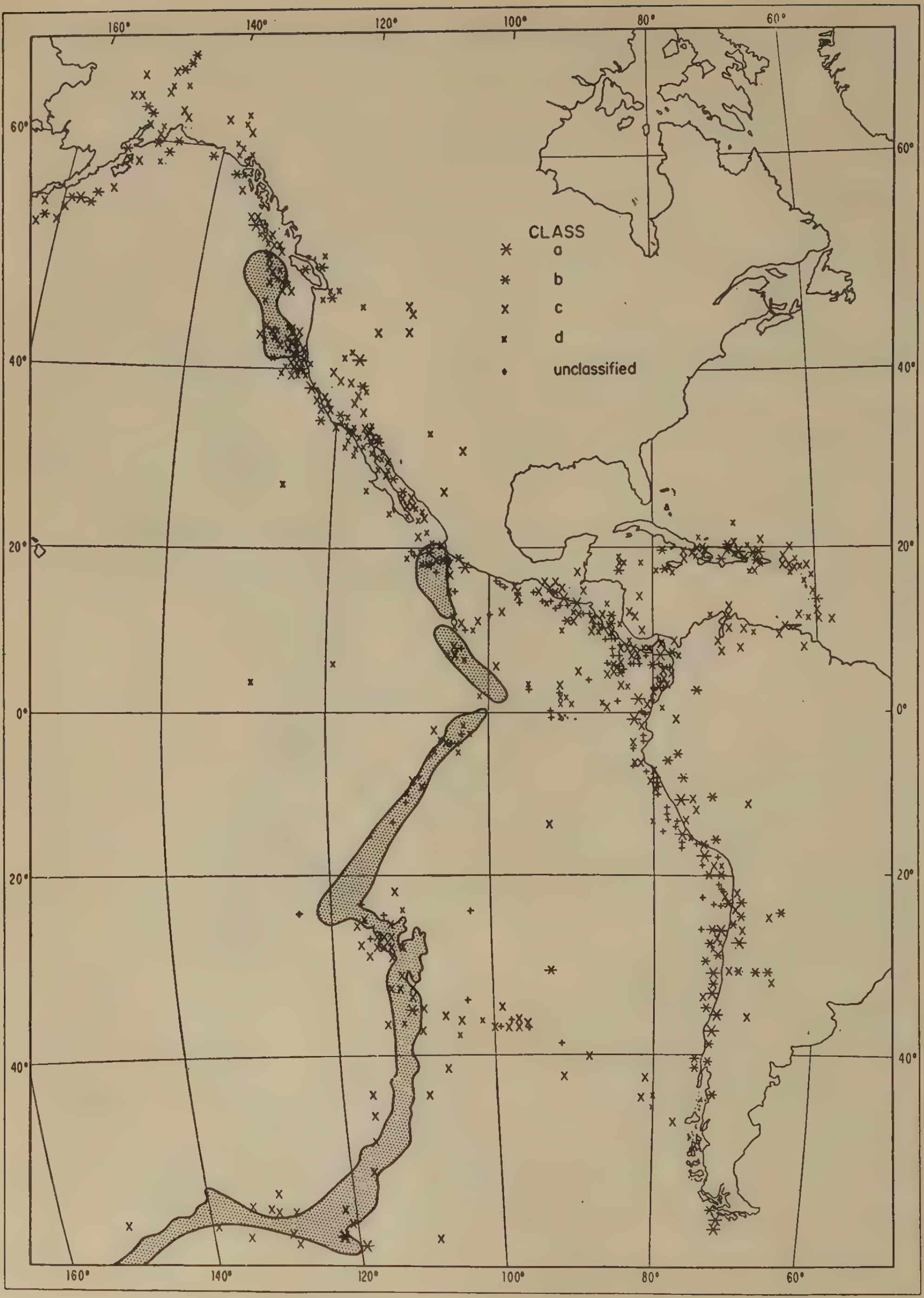
160°
140°
120°
100°
80°
60°
60°
40°
20°
0°
20°
40°
CLASS
a
b
c
d
unclassified

Fig. 3. Distribution of shallow earthquakes along the East Pacific Rise.

into sections which have been moved.

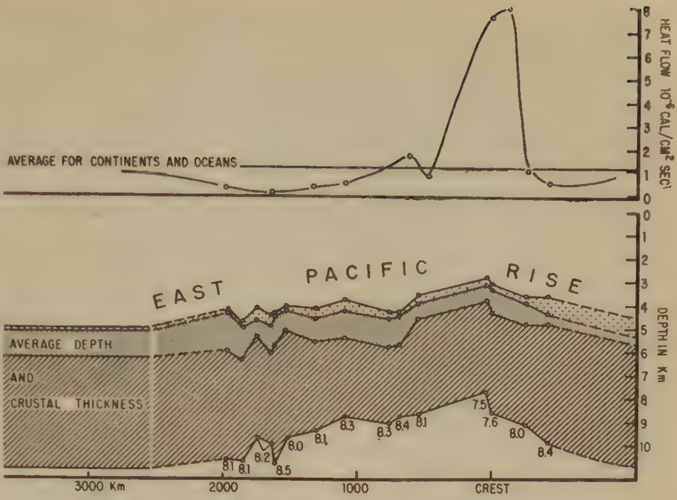

Fig. 4. Crustal section and heat flow profiles of the East Pacific Rise. Velocities below the "crust" are in kilometers per second. The crust is thinned under most of the rise, but the region of very high heat flow and anomalous "mantle" velocities is confined to a narrow band on the crest.

The fracture zones of the eastern Pacific characteristically have a relief of a few kilometers, a width of a few hundred kilometers, and a length of several thousand kilometers. Basically, they can be visualized as broad welts separating regions with different depths. Very long straight faults parallel to the welt have cut the center of each welt. The straightness of the faults suggests that the dominant displacement has been wrenching or horizontal movement. However, the only displacements evident from topography in most places are vertical ones, which have more of a tendency to produce relief. The central parts of the welts have been broken up in one of two ways. Typically, on the eastern ends of the fracture zones, only half of a welt is evident, and it is bounded by a cliff as much as 3 kilometers high. In contrast, the western parts of the fracture zones generally have a welt with the center collapsed in a band of elongate fault blocks forming ridges and troughs (graben). Large submarine volcanoes and islands are also common in fracture zones. For example, the Clarion fracture zones grade from west to east, from a welt with a central graben, to a graben interrupted in places by volcanoes, to a group of volcanic islands. On shore, along the same trend, are the line of great volcanoes of central Mexico. Fracture zones also separate topographic provinces in which volcanoes are common from provinces in which they are rare.

The oceanographers of Lamont Geological Observatory have now traced the median rift system discovered by Ewing and Heezen in the North Atlantic through the South Atlantic, where more than one rift exists, and into the Indian Ocean. English and German oceanographers have found gaps in the rift in some places in the North Atlantic, and in other places detailed surveys have shown it to be discontinuous. Results of the search for a rift in the East Pacific Rise during Downwind, Dolphin, and Doldrums, the three Scripps IGY expeditions, have been negative, despite repeated crossings of the crest of the rise. Indeed, in the Southern Hemisphere the crest of the East Pacific Rise is exceptionally smooth compared with the normal hilly or mountainous local relief of the sea floor. In other places the crests of median elevations of the ocean basins typically have been faulted into graben and horsts trending roughly parallel to the rises. This type of topography is prominent in the Ridge and Trough province off Oregon and Washington.

Seismicity

Shallow earthquakes are common along the crest of the East Pacific Rise (Fig. 3). Uncertainties in fixing epicenters in the southeastern Pacific make it impossible to establish whether the earthquakes are precisely aligned along the crest. Ewing and Heezen have found a very close correspondence between epicenters and the crest of the Mid-Atlantic and Mid-Indian ridges, and they have suggested a similar relationship in the Pacific. I have pointed out that earthquakes are more common within fracture zones than elsewhere in the eastern Pacific basin, but it now appears that this may be an incidental effect of the intersection of the East Pacifiic Rise seismic belt with transverse fault structures.

Crustal Section

An extensive network of shipborne seismic stations has been occupied by the Scripps geophysicists R. W. Raitt (*5*) and G. G. Shor in the eastern part of the Pacific Ocean. Results obtained at these stations show that the topographic bulge of the East Pacific Rise is matched by a very similar bulge of the mantle. However, it appears from present data that the mantle bulge has somewhat greater relief (Fig. 4). The oceanic crustal section consists almost everywhere of a layer of unconsolidated sediment a few hundred meters thick, a "second layer" of consolidated sediment and volcanic rock which is variable but, roughly, 1 kilometer thick, and a "third layer" or oceanic crust proper, which is separated from the mantle by the Mohorovičić discontinuity. The average thickness of the third layer at the 21 seismic stations within the Pacific basin, as defined by the andesite line, but off the East Pacific Rise is 4.9 kilometers. On the other hand, the average thickness of the third layer at seven stations within 1400 kilometers of the crest of the rise is only 3.7 kilometers. An additional group of five stations very near the crest of the rise does not obtain normal mantle velocities (8 km/sec or more) below the third layer, and there is a question about calling the third layer the "crust." However, the third layer, as such, at all 12 stations within 1400 kilometers of the crest, has an average thickness of only 3.8 kilometers, or 1 kilometer less than that found at an average station elsewhere in the Pacific basin.

Heat Flow

The intensity of heat flow through the crust of the East Pacific Rise has a close correlation with the topography, according to numerous observations by Richard von Herzen (*6*), Arthur Maxwell, and Roger Revelle. Average heat flow on continents and in ocean basins away from rises is about 1.1×10^{-6} cal/cm^2 sec. Along the crest of the rise the heat flow ranges between 2 and 8×10^{-6} cal/cm^2 sec in a band a few hundred kilometers wide and 10,000 kilometers long (Fig. 5). Similarly, high heat flow occurs on the crest of the Mid-Atlantic Ridge. In marked contrast, an area as much as 3000 kilometers wide and 6000 kilometers long on the west flank of the rise has low heat flow, with values of 0.14 to 0.97×10^{-6} cal/cm^2 sec. Another belt of low heat flow appears to exist on the east flank of the rise, but there have not been enough observations for us to be sure. The Downwind expedition was designed to investigate a suspected correlation of high heat flow with the crest of the East Pacific Rise, and this has been confirmed. The belt, or belts, of low heat flow had not been suspected, and another expedition will be required to work out the pattern in the eastern Pacific.

Does the Rise Extend under Western North America?

Now that the general characteristics of the East Pacific Rise have been described, the question of its continuation under western North America may be considered.

With regard to topography, it should be emphasized that this rise is only the Pacific section of a system of mid-ocean elevations which extends around Antarctica into the Indian and Atlantic oceans. An abrupt end to the system off Mexico would thus be all the more remarkable. However, the maps show that, although the crest of the rise can be traced as a distinct submarine feature only as far north as the latitude of Mexico, the western flank continues up to Alaska, and the crestal type of topography reappears off Oregon and Washington as the Ridge and Trough province. The puzzling slope between California and Hawaii is the west flank of the rise, and much of the geological exploration of the eastern Pacific has been on different parts of the same great feature. Where the crest and east flank of the rise intersect Mexico are found the plateau of Mexico, the Colorado Plateau, and the Basin Ranges, comprising a topographic bulge of the continent comparable in scale to the bulge of the sea floor. Similar plateau highlands exist only in central Asia and in east Africa, and the latter occurrence lies along a continuation of the rise in the Indian Ocean.

As for seismicity, the continuity of a belt of shallow earthquakes from the the crest of the East Pacific Rise south of Mexico, through the Gulf of California and California, to the Ridge and Trough province cannot be questioned. In California, however, many of the earthquakes are along the San Andreas fault, which may be unrelated to the stresses producing the rise faulting.

The typical thin oceanic crust of the rise reappears in the Ridge and Trough province, according to preliminary shipboard calculations by Raitt. This type of crust cannot, of course, be identified in the intervening continent.

The high heat flow characteristic of the East Pacific Rise south of Mexico has also been found by von Herzen in the Gulf of California, in the continental borderland off southern California, and in the Ridge and Trough province. The discontinuity under California appears to be a relatively trivial break in this long belt of high heat flow associated with the crest of the rise.

In summary, the East Pacific Rise, identifiable as an elevated region with a seismically active crest and high heat flow, extends from the south Pacific, under western North America, into the northeasternmost Pacific. The corresponding elevation of the mantle that is found in the oceanic regions has not been found under the intervening continent.

Possible Genetic Relationship between Rise and Fracture Zones

The great structures of the eastern Pacific basin are the East Pacific Rise and the system of intersecting fracture zones. Various lines of evidence suggest that the structures are genetically related—namely, similar geographical position, similar scale of crustal displacement, and interaction.

The fracture zones of the eastern Pacific form a pattern of rather regularly spaced and approximately parallel lines distributed in an area of about 10 percent of the earth's surface. As more sounding lines are collected it appears increasingly definite that most of the fracture zones do not extend as prominent features beyond the flanks of the East Pacific Rise, thus suggesting a genetic relationship. However, the possibility remains that these very extensive fractures are part of an ancient global system which has been rejuvenated and accentuated in the eastern Pacific. Lineations resembling fracture zones have been described in many places in the world, and the whole pattern in China is strikingly similar. Various worldwide fracture systems have been described, notably by F. A. Vening Meinesz (*7*), but the east Pacific zones, as a group, do not fit into any such pattern as yet proposed.

A comparison of crustal displacements associated with fracture zones and deduced from the structure of the rise requires a detailed description of available observations. Topography alone merely suggests that fracture zones are wrench faults, but a series of remarkable maps of the earth's magnetic field in the northeastern Pacific, prepared by Scripps geophysicists, not only proves the direction of faulting but gives the amount along several fracture zones. The first maps made by Ronald Mason (*8*) show a very extensive pattern of distinctive magnetic anomalies trending very close to north-south. The pattern is offset 150 kilometers in a right-lateral direction at the Murray fracture zone (which may now properly be called a fault). Stimulated by this discovery, Victor Vacquier began a series of magnetic surveys to establish whether displacements could be measured on other fracture zones. To date, he has found a 250-kilometer, left-lateral displacement of the Pioneer fault and a 1200-kilometer left-lateral displacement on the Mendocino fault (Fig. 6). This last displacement is by far the largest that has been measured on earth. Indeed, it is difficult to see how such large displacements could be established except in the very favorable circumstances which exist in the eastern Pacific basin. A similar displacement would tear a continent in half.

Depth contours in the area of the magnetic maps are offset in the same directions as the magnetic anomalies. To a remarkable degree, the amount of offset is also similar. The coincidence in offset is best demonstrated by the 4500-meter contour, which is least affected by the deposition of sediment near the

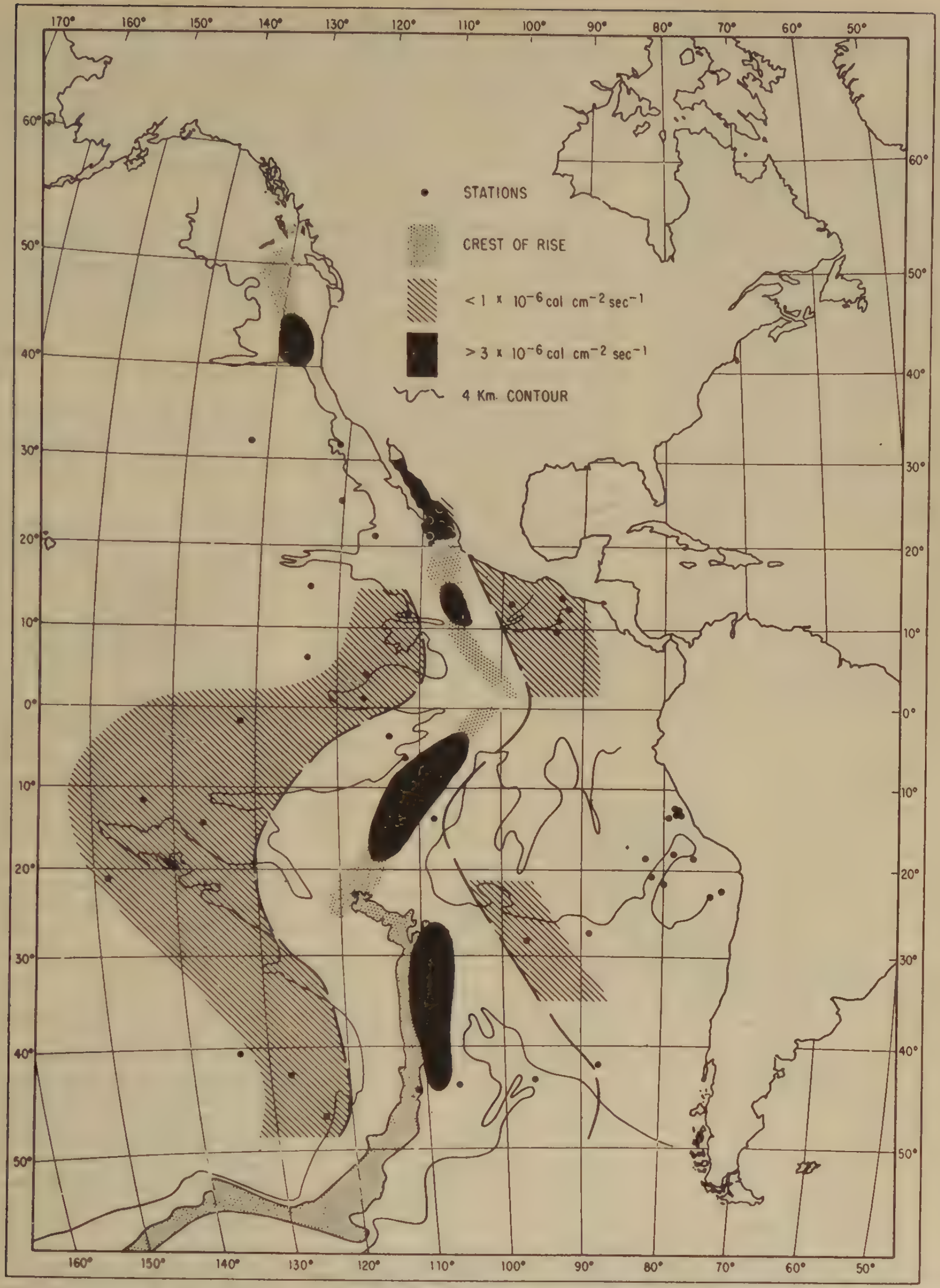

170° 160° 150° 140° 130° 120° 110° 100° 90° 80° 70° 60° 50°
60° 50° 40° 30° 20° 10° 0° 10° 20° 30° 40° 50°
● STATIONS
CREST OF RISE
< 1 × 10⁻⁶ cal cm⁻² sec⁻¹
> 3 × 10⁻⁶ cal cm⁻² sec⁻¹
4 Km. CONTOUR
160° 150° 140° 130° 120° 110° 100° 90° 80° 70° 60° 50°

Fig. 5. Correspondence in position of the crest of the East Pacific Rise and a pattern of heat flow. The points off the United States are based on unpublished observations by von Herzen. The band of high heat flow, like the crest of the rise, appears to pass through the western United States.

continent. It is difficult to escape the conclusions that the sea floor was sloping before the offsets occurred and that the displacements were almost exactly level.

The crustal blocks between fracture zones have areas of a few million square kilometers, but they are hardly more distorted by displacement than small blocks of wood. The magnetic anomaly pattern shows little evidence of compression, extension, rotation, or shearing, except within the fracture zones. However, a distinctive pattern of minor lineations (*9*) suggests a uniform stress within each block but different stresses in adjacent blocks. The lineations consist of elongate volcanoes, lines of volcanoes, and mountains produced by block faulting. These are features characteristically associated with crustal tension. It would appear that all the crustal blocks were in tension while the eastern Pacific was being sliced, or after it had been sliced, by fracture zones.

The enormous displacements of marine crustal blocks are not matched on the adjacent continent. The Mendocino fracture zone offsets the continental slope 100 kilometers in northern California, but the displacement is right-lateral—that is, in the opposite direction from the displacement of the deep-sea floor farther to the west. The continental slope is not offset by the Murray fracture zone, but the Channel Islands and the transverse ranges of California appear to mark an extension of the fracture zone on land. Wrench faults with the trend of the Murray fracture zone are common in these islands and ranges. Displacements are as much as 15 kilometers, but they are generally left-lateral—once again in the opposite direction from the displacement of the sea floor. It appears that some zone of discontinuity is parallel to, and near, the continental slope off California; that crustal blocks on opposite sides of the zone move in different directions; and that movement on the continental side of the zone is much less than on the oceanic side. However, the ages of the varying displacements are not known, and it is equally possible that wholly unrelated stresses produced movement in different directions at different times along the same zone of weakness.

To turn to wrench faulting deduced from the structure of the rise, if the boundary between crust and mantle marks chemically different rocks, the thin crust of the rise probably has been stretched. Arching of the crust would produce some thinning, but the amount is trivial. The region which is now 3.8 kilometers thick has an average width of 2800 kilometers. If it once had a thickness of 4.9 kilometers, which is typical of the Pacific basin outside the rise, then the width was 2200 kilometers, and the crust on the flanks of the rise has been translated laterally for 600 kilometers. Changes in direction of the crest require differential movement of sections of the rise, with wrench faults between sections. Moreover, wrench (tear) faults are commonly associated with large horizontal crustal displacements, both on land and in the ocean basins. Thus, the development on the rise of a thin crust seems to require wrench faults with the location and magnitude of displacement found in fracture zones.

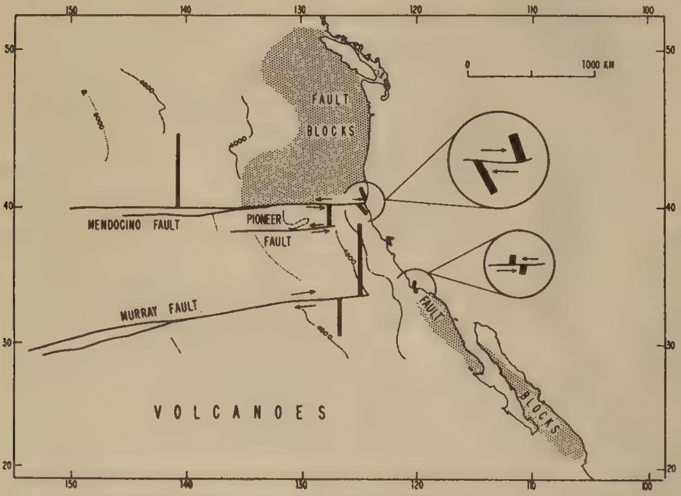

Fig. 6. Horizontal fault offsets off California. The sense of movement is reversed near shore on two faults. Points of no movement appear to lie near the East Pacific Rise crest. Crustal blocks which have been translated westward have provinces of minor fault blocks near the crest of the rise, suggesting crustal stretching and thinning. The width of the provinces is roughly proportional to the translation.

Interaction of rise and fracture zones in space and time is strongly suggested by the seismicity and topography. The crest of the rise is seismically active at present, indicating that it is still being deformed. The fracture zones appear to be active only where the crestal seismic zone intersects them, suggesting that their apparent seismicity is coincidental. However, the fracture zones are very straight, and the crustal blocks are undistorted, despite their great translation; the wrench faults may be almost completely frictionless discontinuities in the crust. Perhaps faulting occurs after only very small strain accumulates, with resulting earthquakes below the normal level of detection. George Shor is planning to build small seismometers which can be placed on the sea floor in the fracture zones to detect small earthquakes if they exist. Meanwhile it would be quite intriguing to employ a bathyscaphe and look for sinuous bends along the old submarine telegraph cable crossing the fracture zones.

Even if the fracture zones are not now active, they appear to have been since the rise first began to develop. The crest of the rise is offset or changes direction at the intersection of the fractures, suggesting horizontal movement; the flanks of the rise change depth along fracture zones, suggesting vertical or horizontal movement; and between the Mendocino and Murray fracture zones the flank of the rise is horizontally offset in the same direction and by about the same amount as the magnetic anomalies. If an anticlinal fold on land were offset by wrench faults in this manner it would be obvious that the wrenching had occurred after the

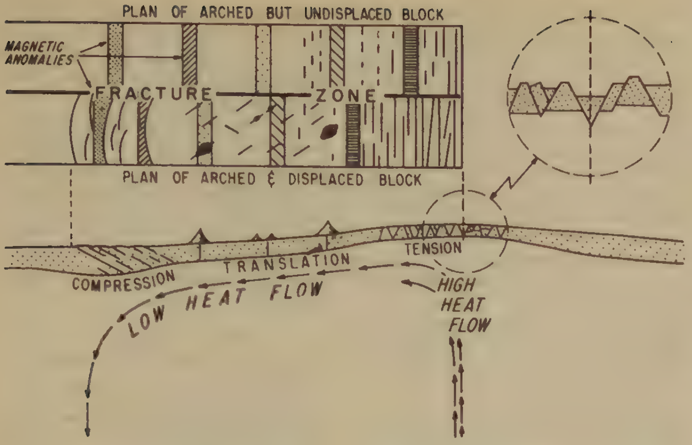

Fig. 7. A diagrammatic presentation of the convection-current hypothesis for the origin of various features associated with the East Pacific Rise.

folding or else that they were contemporaneous. It is difficult to escape the same conclusion regarding the enormous, undated, and little known structures of the sea floor.

Although no single line of evidence is wholly conclusive, the rise and fractures probably are genetically related. The thinning of the rise crust seems to require large horizontal movements on the flanks with differential movement between blocks. The fracture zones have the required geographical distribution and magnitude of displacement to be the boundaries between the displaced blocks; they have been active since the rise began to form, and the rise, at least, is seismically active and may still be developing.

Origin of the East Pacific Rise

Inasmuch as the facts available about oceanic rises are few and new information is being accumulated very rapidly, hypotheses about the origin of the rises are modified frequently or abandoned for new ones. Consequently, an elaborate discussion of present working hypotheses does not appear warranted, but a brief outline may serve the useful purpose of relating otherwise disconnected facts. The following facts are known about the East Pacific Rise.

A belt about 800 kilometers wide along the crest of the rise is anomalous in almost every respect: (i) The topography is characterized in some places by ridges and troughs trending parallel to the rise; (ii) the belt is seismically active; (iii) the heat flow is several times the normal flow; (iv) the third layer (crust) is thin; and (v) the seismic velocities are much less than mantle velocities at a depth where the mantle normally is found. This highly abnormal belt occupies about one-fifth the width of the rise.

Beyond the central anomalous belt and to about the midlines of the two flanks of the rise—at least on the better-known, western flank—the crust remains thin but the heat flow is abnormally low and the velocities in the mantle are normal. Little is known about the local topography in this region, but it appears to consist of volcanoes, low domes, and troughs with adjacent tilted fault blocks trending at various angles to the crest of the rise.

On the outer half of the western flank, the crustal thickness and mantle velocities are normal for the ocean basins, and the only abnormalities are low heat flow and the existence of the rise itself.

Fracture zones cut across the whole width of the rise and displace or change the trend of the rise. Both vertical and horizontal offsets occur, and the horizontal offsets are reversed at the continental margin.

The position of the rise along part of its length is at the edge rather than in the middle of the ocean basin, and the crest appears to pass under western North America.

A hypothesis of a youthful convection current in the mantle, suggested by Bullard, Maxwell, and Revelle (*10*) to explain high oceanic heat flow, offers a simple qualitative explanation of all the facts given above. A rising hot material, marked by high heat flow, produces an upward bulge of the mantle because of thermal expansion or physical-chemical changes (Fig. 7). The mantle bulge arches the overlying crust and forms a system of tension cracks parallel to the rise. Arching stretches and thins the crust, but the observed thinning is so great that translation of the crust toward the flanks of the rise is also required. Accordingly, the horizontal limb of the convection cell moves the crust outward and thins it at the crest of the rise by normal faulting along the tension cracks. Blocks are displaced different distances by wrench faulting on fracture zones because of variations in intensity of convection along the rise. Displacements on fracture zones have opposite directions on the two sides of the crest because convecting material moves in all directions from a rising hot center. Farther out on the flanks of the rise the convection current moves the crust between fracture zones as a unit (the displaced magnetic anomalies are not distorted as they are near the crest). On the outermost flanks the sinking convection current, marked by low heat flow, defines the outer limit of wrench faulting and, presumably, the crust is thickened by thrust faulting.

The East Pacific Rise is only one part of a world-girdling oceanic mountain system, and one may wonder whether the obvious implication of a single origin is correct. However, despite their continuity, the oceanic rises and ridges are not all alike. Compared with the Mid-Atlantic Ridge, the East Pacific Rise is much broader, has gentler slopes, and in most places is far less faulted on the crest. It may be that these differences only mark different stages of development and different times of origin. There is some evidence that the life of an oceanic rise may be rather short, and rises may be in different stages of development at the same time. All the ocean basins have median elevations except the Pacific, which, instead, has a line of atolls and guyots (different types of deeply submerged former islands) rising from a series of narrow, steep-sided ridges. If a broad oceanic rise, faulted at the crest and capped by volcanic islands, were to subside, the only evidence that it once existed might be such a line of drowned former islands and linear ridges (*11*). The guyots of the central Pacific were islands roughly 100 million years ago, and if they mark a former rise, the period of its subsidence must have been quite short compared with the age of the earth.

The East Pacific Rise differs from most broad oceanic elevations in another respect: the northern part is at the margin of an ocean basin rather than in the center. Thus, although all ocean basins have oceanic rises or former oceanic rises in the middle, not all ocean rises are in the middle of basins. In Africa and western North America the rises appear to penetrate continents. In fact, a feature as broad and low as an oceanic rise is difficult to recognize unless there is a large, relatively flat ocean basin on each side. Several marginal oceanic regions with anomalous levels, such as Melanesia and Indonesia, may have the same mantle and crustal structure as oceanic rises.

Continental drift, as suggested by the parallelism of the Atlantic coast lines and the crest of the Mid-Atlantic Ridge, has been a very attractive concept for continental geologists, particularly since it was revitalized by the paleomagnetic evidence for polar shifts and possible drift. Marine geologists, on the other hand, have been reluctant to accept the concept of continental drift because they find no evidence for it in the geology of the sea floor. Indeed, the existence of rises centered in the Indian and Pacific oceans seemed to eliminate the possibility that Africa and South America had moved away from the Mid-Atlantic Ridge. However, if a random distribution of relatively short-lived "oceanic" rises is accepted, the picture is entirely different. If all rises were in the center of ocean basins it would not be clear whether the convection current, or another agent, which produced the rise centered itself relative to the margins of the basin or created the basin. With rises bordering the Pacific and penetrating Africa, it appears more probable that most rises are centered because the margins of the basin have been adjusted by convection currents moving out from the center. If so, the African and East Pacific rises may mark relatively young or rejuvenated currents which have not yet had time to produce much continental displacement. Even so, east Africa is being torn by deep rifts and Baja California has almost been separated from North America along the crest of the East Pacific Rise.

It is apparent that the study of oceanic rises and ridges, which was accelerated by the IGY, is one of the most fruitful fields in geology and geophysics. According to present planning there will be few, if any, months during the next three years when there will not be oceanographers at sea attempting to advance this study (*12*).

References and Notes

1. J. Ewing and M. Ewing, *Bull. Geol. Soc. Am.* **70**, 291 (1959).
2. M. Ewing and B. C. Heezen, *Geophys. Monographs No. 1* (1956), pp. 75–81.
3. I am indebted to my colleagues at the Scripps Institution of Oceanography for permission to use unpublished data.
4. H. W. Menard, *Bull. Geol. Soc. Am.* **66**, 1149 (1955).
5. R. W. Raitt, *ibid.* **67**, 1963 (1956).
6. R. von Herzen, *Nature* **183**, 882 (1959).
7. F. A. Vening Meinesz, *Trans. Am. Geophys. Union* **28**, 1 (1947).
8. R. G. Mason, *Geophys. J.* **1**, 320 (1958).
9. H. W. Menard, *Bull. Geol. Soc. Am.* **70**, 1491 (1959).
10. E. C. Bullard, A. E. Maxwell, R. Revelle, *Advances in Geophys.* **3**, 153 (1956).
11. H. W. Menard, *Bull. Geol. Soc. Am.* **69**, 1179 (1958).
12. Almost all the field work has been supported by the Office of Naval Research and the National Science Foundation under various contracts.

Proceedings of
the United States
National Museum

SMITHSONIAN INSTITUTION • WASHINGTON, D.C.

Volume 112 1960 Number 3439

THE PELAGIC AMPHIPOD GENUS PARATHEMISTO (HYPERIIDEA : HYPERIIDAE) IN THE NORTH PACIFIC AND ADJACENT ARCTIC OCEAN

By Thomas E. Bowman

Among the marine planktonic Crustacea, the amphipods frequently play an important role in the economy of the sea. In general they rank third in numerical abundance; they are far exceeded by the copepods and euphausiids. In tropical and subtropical regions pelagic amphipods are not usually found in large numbers, but in the cooler parts of the oceans they are often extremely abundant. Members of the genus *Parathemisto* (=*Themisto* auct.) overwhelmingly dominate the cool-water epipelagic amphipod fauna, and their importance in the north Atlantic (including the Arctic Atlantic) has been pointed out by Bigelow (1926), Bigelow and Sears (1939), Stephensen (1923, 1924), and Dunbar (1946, 1957). Only cursory attention has been given to north Pacific representatives. The present paper is an attempt to fill in a few gaps in our knowledge of the distribution and life history of species of *Parathemisto* in the north Pacific and the Arctic Ocean north of Alaska and western Canada.

The amphipods upon which this report is based were obtained from plankton collections from several sources: (1) Off the Pacific coast of the United States from the latitude of the Columbia River to that of Punta Eugenia in middle Baja California, in connection with the California Cooperative Oceanic Fisheries Investigation (CCOFI). (2)

Contributions from the Scripps Institution of Oceanography, New Series, 1219

Reproduced by Permission

The *Northern Holiday* Expedition of the Scripps Institution of Oceanography, August and September 1951. (3) Cruises of the United States Fisheries steamer *Albatross* in the northern Pacific. (4) Cruises of the U.S.S. *Burton Island* to the Chukchi and Beaufort Seas during August 1950 and August and September 1951, and to Amundsen Gulf and Prince of Wales Strait during August 1953. (5) Northern Pacific stations of cruise VII of the *Carnegie*, 1928–29. (6) Samples from Japanese waters, sent to me by Dr. Sigeru Motoda and Mr. Zinziro Nakai. (7) Samples from Korean waters provided by Mr. Won Tack Yang.

Five species of *Parathemisto* were obtained from these collections. Each species is considered separately below with respect to its taxonomy, distribution, and ecology. A sixth species, doubtfully identified from the Yellow Sea by Yamada, is also considered.

Much of the work reported herein was carried out under the supervision of Dr. Martin W. Johnson, Scripps Institution of Oceanography, to whom I am grateful for many valuable suggestions and for forwarding to me the amphipods from the 1951 *Burton Island* Cruise. Dr. Robert Bieri, Antioch College, kindly sent me the amphipods from the 1953 *Burton Island* Cruise. I also wish to thank Dr. Sigeru Motoda, Hokkaido University, and Mr. Zinziro Nakai, Tokai Regional Research Laboratory, for sending me specimens of *Parathemisto* from Japanese waters. Mr. Won Tack Yang, Central Fisheries Experiment Station, Pusan, obligingly sent me specimens from several localities around Korea. Dr. Isabella Gordon, British Museum (Natural History), made it possible for me to examine *Challenger* specimens of *Parathemisto pacifica* Stebbing.

Genus *Parathemisto* Boeck

Themisto Guérin, 1825, p. 772.—Stephensen, 1923, p. 19; 1924, p. 94.
Parathemisto Boeck, 1870, p. 87.—Bovallius, 1889, p. 248.—Barnard, 1930, p. 419.
Euthemisto Bovallius, 1887, p. 21; 1889, p. 275.

DIAGNOSIS (FAMILY CHARACTERS OMITTED): Head moderately large, globular. P1 (pereopod 1) simple. P2 chelate; carpal process narrow, concave on anterior margin. Carpus of P3 and P4 more or less dilated, forming a prehensile organ with propodus. P5–7 longer than P3 and P4. Uropods narrow, elongate. Type species, by monotypy, *Themisto gaudichaudii* Guérin.

In 1870 Boeck established the genus *Parathemisto*, which was to be distinguished from *Themisto* Guérin by P5 not being much longer than P6 or P7. Noting that *Themisto* had been preoccupied in 1815 by a nudibranch mollusk, Bovallius (1887) changed the amphipod name to *Euthemisto*. Stephensen (1924) combined the two genera, since the relative lengths of P5–7 of the male of *Themisto gracilipes* Norman

(946)

placed it in *Euthemisto*, while the female had to be referred to *Parathemisto*. In combining the two genera, Stephensen returned to the oldest generic name, apparently not realizing that it had been preoccupied. K. H. Barnard (1930) pointed out that *Themisto* was not available and that Boeck's name had to be used. In spite of this, some authors continue to refer to the genus as *Themisto*.

K. H. Barnard (1930) retains *Parathemisto* and *Euthemisto* as subgenera of *Parathemisto*, a course which is followed by Hurley (1955) and Vinogradov (1956). I believe this is the most satisfactory way to deal with this group of amphipods. Although the differences between *Euthemisto* and *Parathemisto* are sufficiently clear cut so that there is no difficulty in assigning all the known species to one or the other, they are not as great as those which separate the other genera of the family Hyperiidae.

Keys to species of *Parathemisto* have been given by Barnard (1930, p. 420), Stephensen (1923, p. 19, European species), and Hurley (1955, New Zealand species).

Subgenus *Parathemisto* Boeck

Dorsal spines absent. Flagellum of female antenna 1 slender, straight. Carpus of P3–4 only slightly expanded. P5–7 subequal in length. Peduncle of uropod 3 strongly produced at inner distal angle. Inner ramus of uropod 3 serrate on medial and lateral margins. Type species, by subsequent designation, *Parathemisto abyssorum* Boeck.

Key to the Species of the Subgenus *Parathemisto*

1. In length P5>P7>P6; dactyls not pectinate. Posterior margin of P1 propodus bearing several long setae. Maxilliped without a distal row of setae on basal plate . . . . **abyssorum** Boeck
   In length P6>P7>P5; dactyls of P5–6 pectinate at base. Posterior margin of P1 propodus serrate but without setae on distal margin. Maxilliped with distal row of long setae on basal plate 2
2. Antennae 1 and 2 of female subequal. Length of adult 4.5–8.5 mm. **pacifica** Stebbing
   Antenna 2 longer than antenna 1. Length of adult 9–17 mm. **japonica** Bovallius

Parathemisto (*Parathemisto*) *pacifica* Stebbing

Figures 1; 2,*a*,*j*–*k*; 3,*a*–*e*; 4–10

Parathemisto pacifica Stebbing, 1888, pp, 1420–1423 [no figures].—Bovallius, 1889, p. 263.

Parathemisto oblivia (Krøyer), Holmes, 1904, p. 233.

Themisto abyssorum (Boeck), Shoemaker, 1930, pp. 132–133 [specimens from Nanaimo, British Columbia only].—Wailes, 1929, p. 5.

Parathemisto abyssorum (Boeck), Thorsteinson, 1941, pp. 90–91.
Parathemisto japonica Bovallius, Hurley, 1956, pp. 15–16.—Vinogradov, 1956, pp. 211–212.

Diagnosis: Total length of adult ♀, excluding antennae, 4.5–8.5 mm. Body more chunky in appearance than in most species of *Parathemisto*. Dorsal to antennal groove head is less roundly produced in lateral view than in *P. abyssorum*, i.e., slope of this part of head is directed more posteriad than in *P. abyssorum*. Pleonites with a few minute teeth along ventral margins, posterior lateral corners produced into small points. Female antenna 2 about as long as antenna 1, slightly shorter than head plus first 2 pereonites. Molar process of mandible about twice as long as incisor process. Maxilliped with row of long spines at distal end of basal plate. Propodus of P1 serrate but not spinous on posterior margin. In length P6>P7>P5. Posterior distal corners of carpus of P6–7, but not of P5, with conspicuous spines. Dactyls of P5–6 pectinate at base. Peduncle of uropod 3 from 2 to 2.5 times as long as telson.

Remarks: K. H. Barnard (1930, p. 419) suggested that Stebbing's *P. pacifica* was a synonym of *P. japonica*. Barnard did not have specimens of either species, and his conclusion was a reasonable one to draw from a comparison of the descriptions by Bovallius and Stebbing. I suspect that Stebbing would have reached the same conclusion, for at the time he described *P. pacifica*, Bovallius had published only a brief, unillustrated description of *P. japonica*. If Bovallius' more detailed and illustrated description published in 1889 had been available to Stebbing, he might not have described *P. pacifica* as a separate species, for the differences emphasized by Stebbing and listed below are actually not valid for distinguishing the two species:

1. The propodus of P3 of *P. pacifica* is longer than the carpus and is pectinate rather than smooth on the posterior margin. While Bovallius (1889) states that the propodus is a little shorter than the carpus, he also says that the propodus is finely pectinated, and in his figure 35, plate 12, it is shown as pectinate and slightly longer than the carpus.

2. In *P. pacifica*, the outer ramus of uropod 3 is shorter than the inner ramus. Although Bovallius (1889) states that the two rami are of equal length in *P. japonica*, his figure 43, plate 12, shows the outer one to be slightly shorter. Stebbing does not say how much shorter the outer ramus of *P. pacifica* is, and provides no figures. In my specimens of *P. japonica* and *P. pacifica*, the outer ramus is slightly shorter.

Although the above criteria are worthless for distinguishing between *P. pacifica* and *P. japonica*, I nevertheless consider them as distinct

(948)

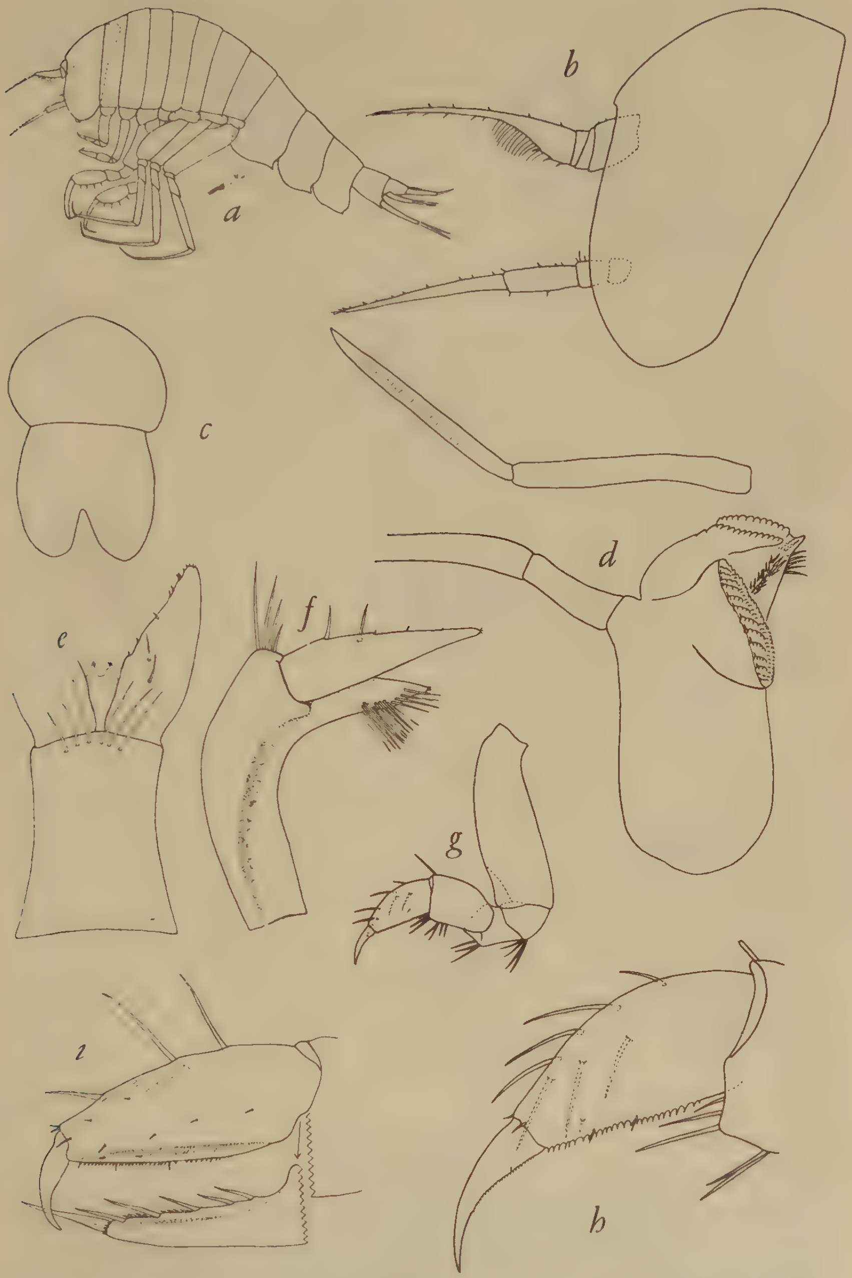

FIGURE 1.—*Parathemisto pacifica* Stebbing: *a*, Lateral view of female, 5.0 mm. in length; *b*, head and antennae, lateral view; *c*, labrum, male; *d*, left mandible, male; *e*, maxilliped, posterior surface; *f*, maxilliped, lateral view; *g*, *h*, pereopod 1, female; *i*, pereopod 2, female. Scales various.

(949)

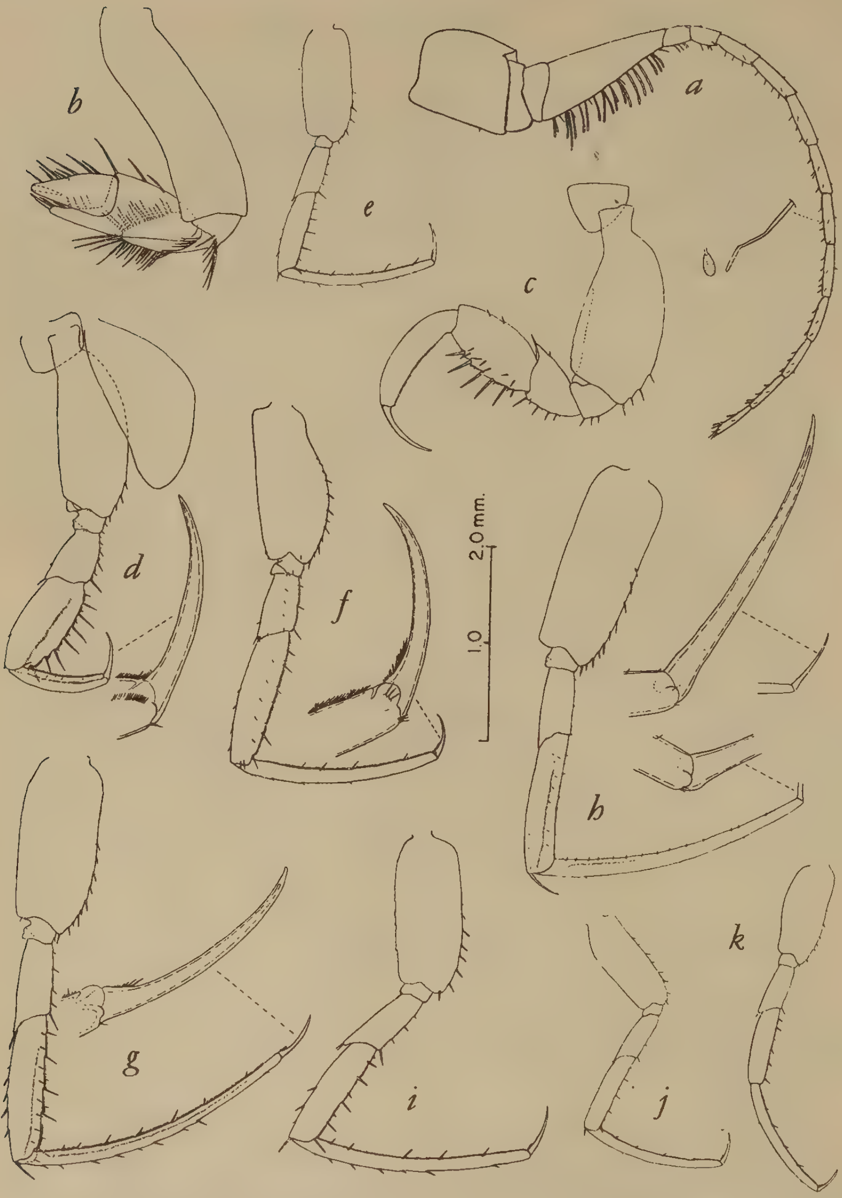

FIGURE 2.—*Parathemisto pacifica* Stebbing: *a*, Antenna 1, adult male, off California. *Parathemisto japonica* Bovallius, *b*, *c*, *f*, *g*, *h*, from adult female, 11.0 mm. in length, southern Sea of Okhotsk: *b*, Pereopod 2; *c*, pereopod 3; *d*, pereopod 4, slightly smaller female; *e*, pereopod 6, juvenile female, 6.7 mm., off Cape Esan, Japan; *f*, pereopod 5; *g*, pereopod 6; *h*, pereopod 7, dactyl broken, undamaged dactyl drawn from slightly smaller specimen, same locality; *i*, pereopod 6, ovigerous female, 9.5 mm., off Cape Esan. *Parathemisto pacifica* Stebbing, pereopod 6: *j*, Ovigerous female, 7.0 mm., off Cape Esan; *k*, adolescent female, 6.7 mm., Bering Sea. Scale same for *c*-*k*; enlargement 3.8 times greater in *a*, and 1.5 times greater in *b*.

(950)

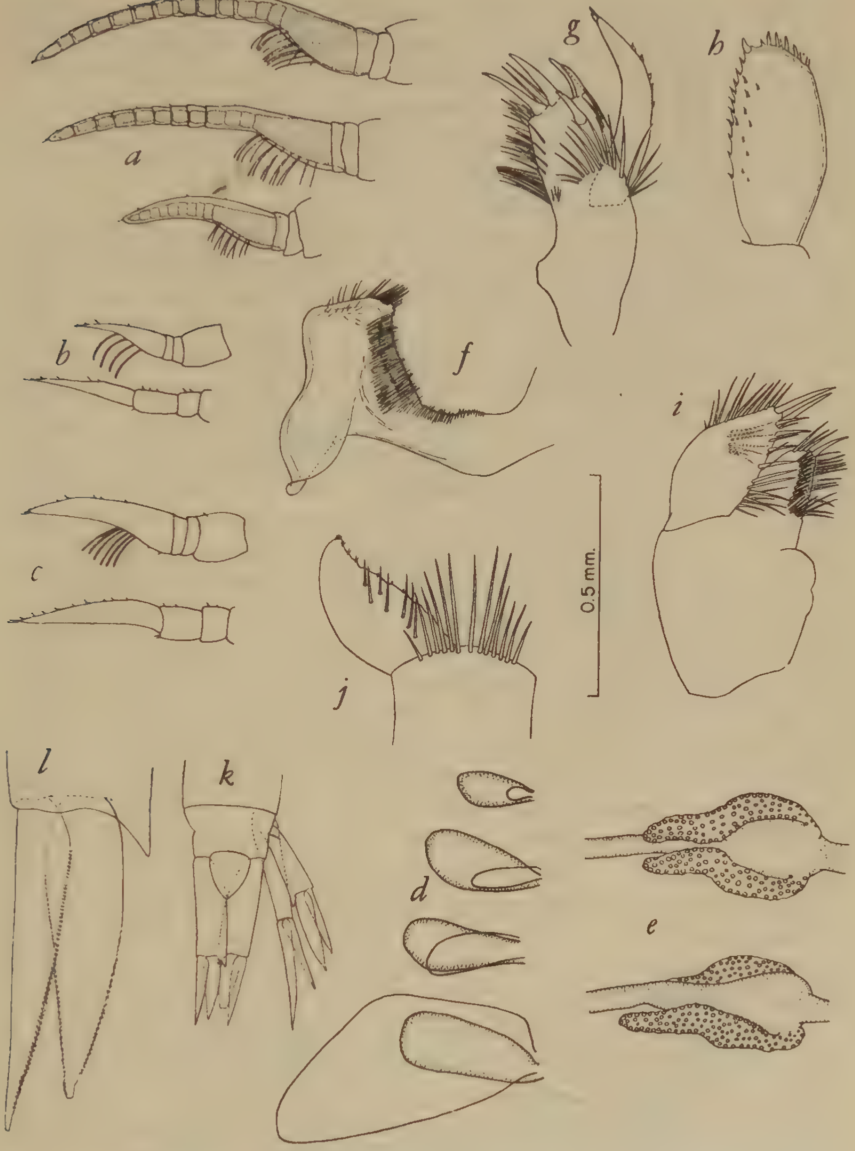

FIGURE 3.—*Parathemisto pacifica* Stebbing: *a*, Three stages in the development of male antenna 1, from specimens 3.8, 4.5, and 5.0 mm. in length, off California; *b*, antennae 1 and 2 of very young female; *c*, same of very young male; *d*, four stages in the development of oostegites (unshaded outline) showing size relative to gills (shaded outline); *e*, dorsal (above) and dorsolateral views of portion of digestive system, showing origin of digestive caecae from anterior part of midgut. *Parathemisto japonica* Bovallius: *f*, Labium; *g*, maxilla 1; *h*, palp of maxilla 1, flattened; *i*, maxilla 2; *j*, maxilliped, inner plate and left outer plate omitted; *k*, uropods and telson; *l*, uropod 3, distal end. Scale applies to *f–j*.

but very closely related species, which may be told apart by the larger size, greater development of the pereopodal setae, and unequal antennae of *P. japonica*. In addition to the small morphological differences, the two species have different geographical distributions. *P. japonica* occurs in the Japan and Okhotsk Seas and in a limited region east of Japan and the southern Kuriles; *P. pacifica* inhabits subarctic water in the rest of the Pacific.

The type material of *P. pacifica* consisted of 7 specimens, 3 females and 4 males, taken at the surface at *Challenger* station 240 (32°20′ N., 153°39′ E.). Stebbing's description was based on a male which seems not to be extant, for I am informed by Dr. Isabella Gordon (in litt.) that the collections of the British Museum (Natural History) contain 3 females and 3 males but no dissected male. Through her kindness I have been able to examine a male and a female with ova from the *Challenger* material. The female, 6.7 mm. in length, has fully developed oostegites and subequal antennae 1 and 2. The male, measuring 6.5 mm., is not fully mature, for the antennae are only slightly longer than the height of the head. Since Stebbing did not select a holotype, the *Challenger* specimens are all syntypes. The above mature female is herewith designated as the lectotype of *P. pacifica*.

COLOR: Eyes red, with black centers. General body color purplish red due to rather large, dark-red chromatophores, which are visible through the transparent cuticle. The chromatophores are most abundant on the pereon, and make it quite dark. Food in the gut may add to the darkness of the pereon. On the pleon the chromatophores occur slightly less than halfway down the sides of the pleonites and on the middle of the dorsal surface of the third and sometimes also the second pleonite. One or two chromatophores are located on the dorsal surface of the peduncle of uropod 3. The mouthparts have a reddish appearance. P1–2 have a few chromatophores, and P3–4 may have chromatophores at the distal end of the basipods. P5–7 are without chromatophores.

DISTRIBUTION: The distribution of *P. pacifica* will be considered in three sections: (1) in the area surveyed by CCOFI, off the coasts of California and Baja California; (2) in the northwestern Pacific Ocean adjacent to Japan and the Kurile Islands; (3) in the north Pacific Ocean as a whole.

1. CCOFI Area: Figures 4 to 7 show the distribution of *P. pacifica* encountered during four CCOFI cruises. At the stations shown, oblique hauls of 20 minutes duration were made with one-meter plankton nets from a depth of about 70 m. (140 m. in cruise 20 except for the northernmost line of stations) to the surface. Details of net construction and methods by which the hauls were made are given by Ahlstrom (1948, 1952). The volume of water strained during a haul was meas-

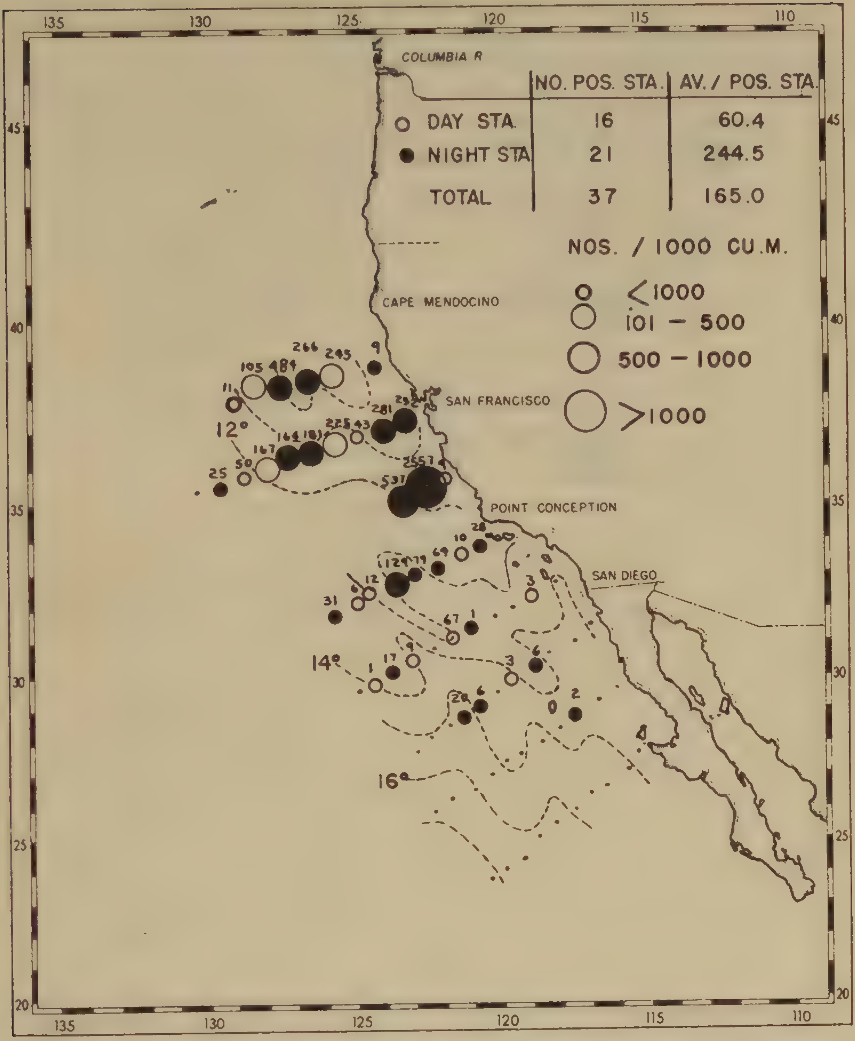
COLUMBIA R
NO. POS. STA.
AV. / POS. STA.
○ DAY STA. 16 60.4
● NIGHT STA 21 244.5
TOTAL 37 165.0
NOS. / 1000 CU.M.
<100
101 – 500
500 – 1000
>1000
CAPE MENDOCINO
SAN FRANCISCO
POINT CONCEPTION
SAN DIEGO
12°
14°
16°
135
130
125
120
115
110
45
40
35
30
25
20

Figure 4.—*Parathemisto pacifica* Stebbing, distribution in March 1949, CCOFI cruise 1.

ured with an Atlas-type current meter fastened in the center of the mouth of the net. This measure has been used to correct the counts of the numbers of amphipods in the samples studied to numbers per 1,000 cubic m. of water.

In the CCOFI area *P. pacifica* is by far the most abundant amphipod. The southern extent of its range lies within the CCOFI area, and by comparing the southern boundaries with the superimposed isotherms at a depth of 30 m., it is possible to estimate the limiting temperatures. In cruise 1 this temperature is estimated to be about

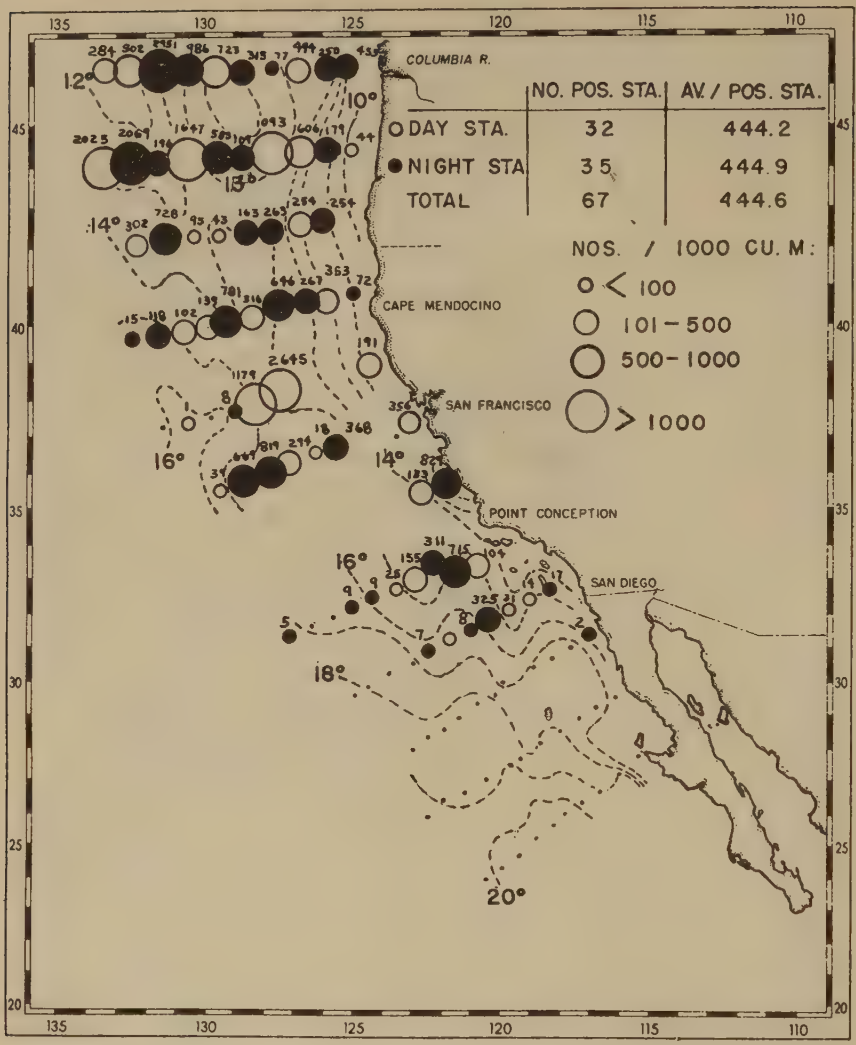
135
130
125
120
115
110
45
40
35
30
25
20
COLUMBIA R.
CAPE MENDOCINO
SAN FRANCISCO
POINT CONCEPTION
SAN DIEGO
10°
12°
13°
14°
16°
18°
20°
NOS. / 1000 CU. M:
○ < 100
○ 101 – 500
○ 500 – 1000
○ > 1000
284
302
2451
986
723
345
77
444
250
453
2025
2069
1647
1093
44
728
302
93
43
163
263
254
254
363
72
646
267
781
139
102
15
118
191
2645
1179
8
356
18
368
819
294
827
133
311
715
155
104
325
17
5
9
7
2

	NO. POS. STA.	AV. / POS. STA.
○ DAY STA.	32	444.2
● NIGHT STA	35	444.9
TOTAL	67	444.6

FIGURE 5.—*Parathemisto pacifica* Stebbing, distribution in July 1949, CCOFI cruise 5.

15° C., and for cruises 5 and 9 about 17°. The data of cruise 20 are very limited, but here the 18° isotherm may be limiting.

The numbers found at the different stations of a cruise vary considerably. Near the southern limits the numbers decrease somewhat, but elsewhere the variation appears to be random and not related to available measurements of oceanographic conditions. An unsuccessful attempt was made to determine the causes behind this variation in numbers in cruise 5. Using the northern four lines of stations in order to eliminate the limiting effect of higher temperatures to the

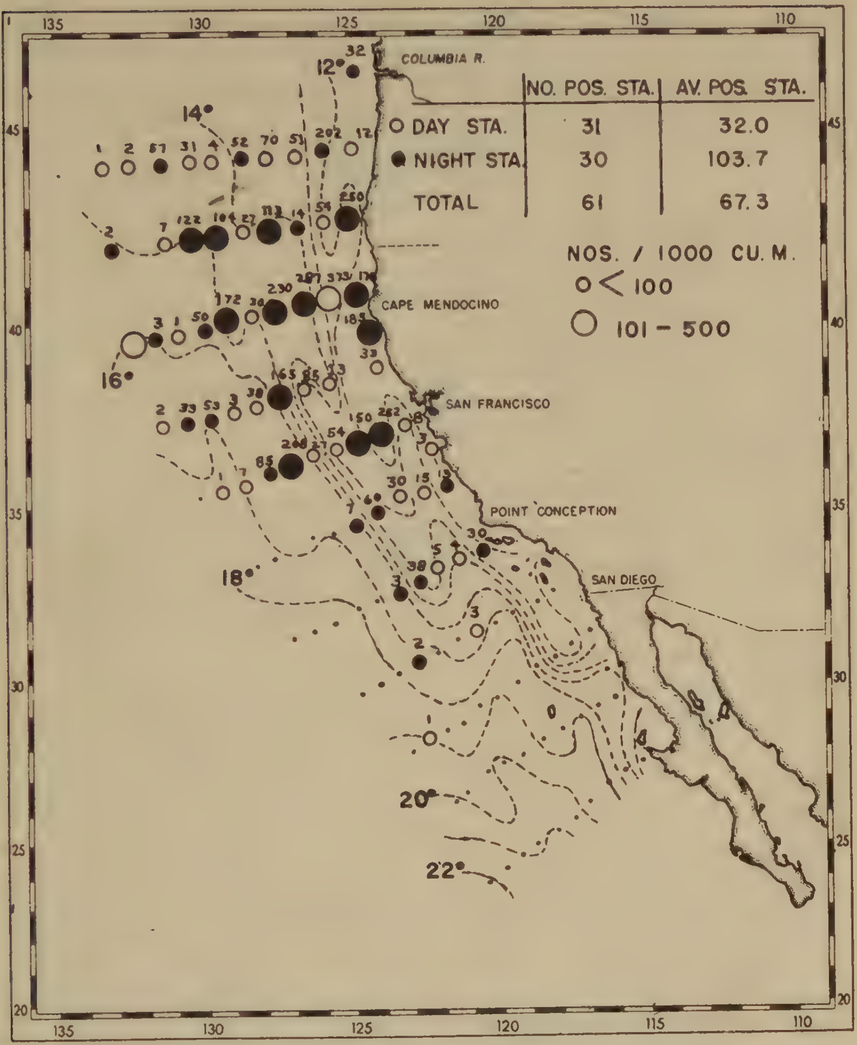
COLUMBIA R.
NO. POS. STA.
AV. POS. STA.
○ DAY STA. 31 32.0
● NIGHT STA. 30 103.7
TOTAL 61 67.3
NOS. / 1000 CU. M.
○ < 100
○ 101 - 500
CAPE MENDOCINO
SAN FRANCISCO
POINT CONCEPTION
SAN DIEGO
12°
14°
16°
18°
20°
22°
135
130
125
120
115
110
45
40
35
30
25
20

Figure 6.—*Parathemisto pacifica* Stebbing, distribution in November 1949, CCOFI cruise 9.

south, it was not possible to find any relation between the numbers taken at a station and the temperature, salinity, depth of haul, depth of thermocline, or the percent of the haul which was made below the thermocline.

The seasonal variation in numbers is of considerable interest. The average number per 1,000 cubic m. at the positive stations in 1949 increased from 165 in March to 445 in July, and then decreased to only 67 in November. Part of the March–July increase may be at-

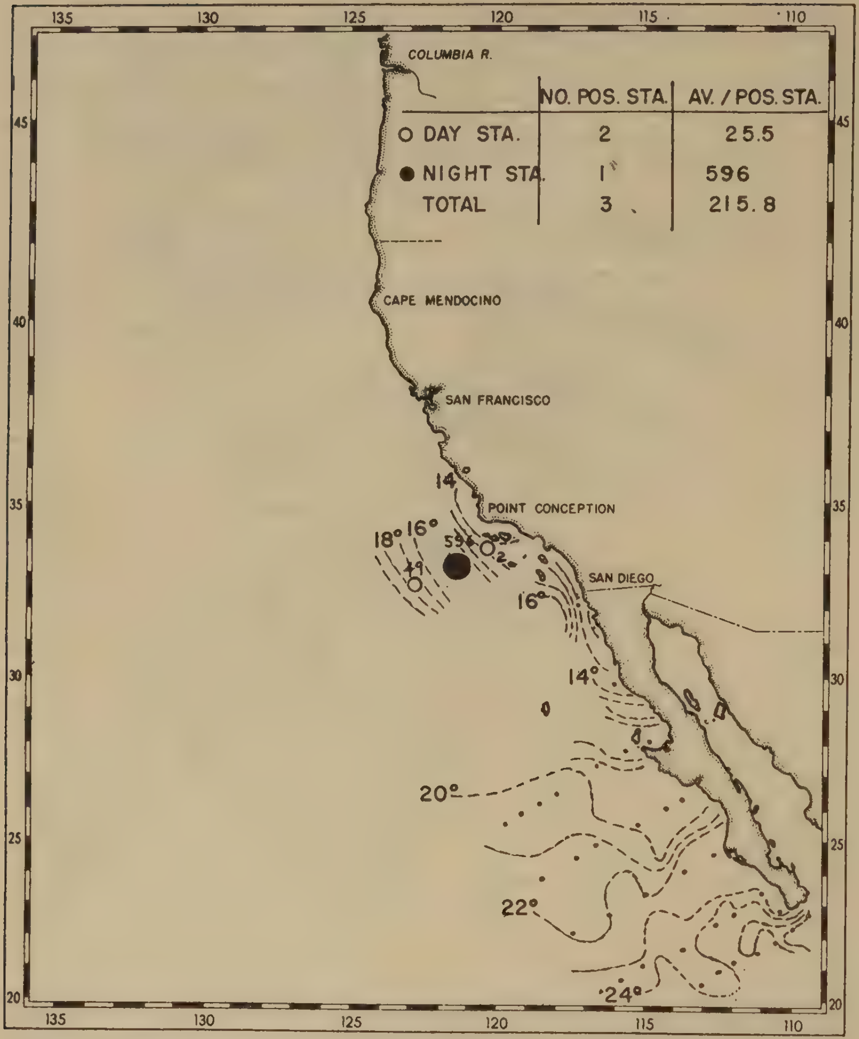
135
130
125
120
115
110
45
40
35
30
25
20
COLUMBIA R.
NO. POS. STA.
AV. / POS. STA.
○ DAY STA. 2 25.5
● NIGHT STA. 1 596
TOTAL 3 215.8
CAPE MENDOCINO
SAN FRANCISCO
14
POINT CONCEPTION
18°
16°
59
2
49
SAN DIEGO
16°
14°
20°
22°
24°

FIGURE 7.—*Parathemisto pacifica* Stebbing, distribution in November 1950, CCOFI cruise 20.

tributed to the fact that in March the four northernmost lines of stations were not occupied, and the average number is more heavily affected by the small numbers in the southernmost lines. But even if we consider only lines 5–8 of cruise 1, the mean number per station is increased only to 229, which still falls far short of the mean number for July, 445, or the mean number for lines 5–8 in July, 404. In November not only is there a notable decrease in numbers, but the range is slightly more restricted because of the higher temperatures of offshore waters.

Part of the variation in numbers may be caused by seasonal changes in the intensity of breeding. However, females with ova or embryos in the brood pouch were abundant at all but the southernmost stations on all three cruises. Juveniles which had recently left the brood pouch were also widespread, and it is apparent that breeding goes on during most if not all of the year.

Another possible explanation for the seasonal change in catch is that the population inhabited deeper water in March and November than in July. Some evidence for this is found in a comparison of day and night hauls. In both March and November the mean number per positive haul was much greater for the night hauls than for the day hauls, nearly five times as great in March and more than three times as great in November. These differences suggest that diurnal vertical movements were occurring during these months, and that during the day part of the population was below the level of the net hauls. In July, however, there was almost no difference between the mean number per station for the day hauls and that for the night hauls. Here diurnal vertical migrations were very limited or lacking, and probably at least most of the populations were living at depths not greater than 70 meters.

2. Northwestern Pacific: I have been able to examine a limited number of plankton samples from the northwestern Pacific. In addition to *Albatross* samples, principally from the Sea of Japan, I have studied specimens from *Carnegie* stations, material sent to me by Motoda, Nakai, and Yang, and a few specimens from salmon stomachs forwarded to me by William Aaron of the University of Washington.

All the samples from the Japan and Okhotsk Seas contained *P. japonica.* In addition *P. japonica* was found at *Albatross* stations 4805 (east of Iturup Island, Kuriles) and 4806 (east of Cape Yerimo, Hokkaido), and in one of Motoda's samples from east of Cape Esan, Hokkaido. In these latter three samples *P. pacifica* also occurred, but in much smaller numbers than *P. japonica.*

Further east only *P. pacifica* occurs. Detailed planktonic surveys are needed to establish the eastern boundary of *P. japonica. P. pacifica* extends to Japanese coastal waters, but does not occur in the Japan Sea and probably not in the Sea of Okhotsk, where it is replaced by the larger *P. japonica.*

In 1948 Irie reported on the distribution of a number of pelagic amphipods in waters adjacent to Japan, including a species of *Parathemisto* which was listed as "*Parathemisto* sp. A." In a later paper (1957b) this species is illustrated under the name *Themisto gracilipes* Norman, but the illustrations are clearly of *Parathemisto japonica.* Probably both *P. japonica* and *P. pacifica* were present in Irie's collections, and possibly *P. gracilipes* in the stations south of Japan.

In figure 8 I have plotted the distribution of *Parathemisto* in the vicinity of Japan from Irie's data. To these data I have added some *Albatross* and *Carnegie* stations as well as the localities reported by Nakai (1955). While the occurrences in the Japan and Okhotsk Seas are undoubtedly *P. japonica*, those east of Japan probably include both *P. japonica* and *P. pacifica*. Since the temperatures limiting southward penetration are similar for *P. japonica* in the Japan Sea (see p. 366) and for *P. pacifica* along the California coast, Irie's data on the occurrence of *Parathemisto* east of Japan can be applied to both *P. japonica* and *P. pacifica*. His data show that these species are most abundant north of Japan. Irie (1948) states that *Parathemisto* is abundant between 40° and 50° N., common between 35° and 40° N., but very rare between 25° and 35° N. Figure 8 indicates that the southern boundary falls at about 36° N.

P. pacifica inhabits cold water, and the extent of its southern penetration along the eastern coast of Japan must depend on the relative influences of the Kuroshio and the Oyashio. The warm Kuroshio leaves the coast of Japan and turns east or northeast at Cape Inubozaki (35°40′ N.), with a variable amount of north-south meandering (Masuzawa, 1955). Koizumi (1953) reported on the temperature variations at 39° N., 153° E., a locality which is sometimes covered with water of Kuroshio origin, at other times with cold water of Oyashio origin. Here the temperature at a depth of 25 m. in 1948 varied from 10.80° C. in March to 21.64° C. in September. Clearly the southern boundary of the Oyashio and of its inhabitants, including *P. japonica* and *P. pacifica*, is subject to fluctuation.

In the region where the two current systems meet, the Oyashio may underlie the Kuroshio to a limited extent. Tanaka (1953) observed that in the waters near the Izu Peninsula the warm-water copepod species of the Kuroshio were confined to the upper 200 m., while the cold-water species of the Oyashio were obtained chiefly from below 200 m.

Recently several Russian biologists of plankton have set up faunal zones and zoogeographic boundaries in the region east of Japan and southeast of the Kurile Islands. This work is summarized by Beklemishev and Semina (1956) and by Bogorov (1958). *P. japonica* (=*P. japonica* + *P. pacifica*) is listed by Bogorov and Vinogradov (1955) as an inhabitant of their boreal epipelagic zone, extending south to about 40–42° N. and having surface temperatures of from 9–15° C. This zone is also characterized by the copepods *Calanus tonsus* and the chaetognaths *Sagitta elegans* and *Eukrohnia hamata*. Brodsky (1955a) refers to it as the "*Calanus tonsus* Zone," and it undoubtedly corresponds to Hida's (1957) "Subarctic Zone" in the mid-Pacific.

(958)

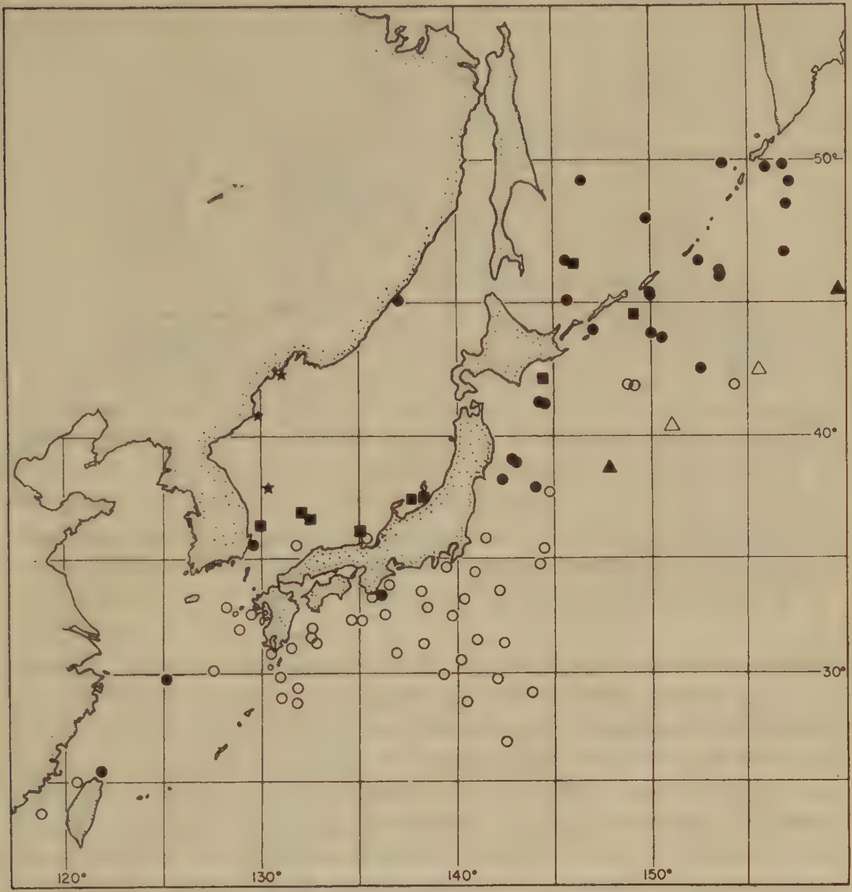

FIGURE 8.—Distribution of *Parathemisto pacifica* and *P. japonica* in the northwestern Pacific. Positive stations indicated by solid symbols, negative stations by open symbols. Circles, stations reported by Irie (1948). Squares, *Albatross* stations. Stars, stations reported by Nakai (1955). Triangles, *Carnegie* Stations. The two southernmost stations reported by Irie probably had *P. gracilipes*. Only *P. japonica* was present at the *Albatross* stations in the Japan and Okhotsk Seas; both *P. japonica* and *P. pacifica* at the two *Albatross* stations east of Japan; only *P. pacifica* at the *Carnegie* stations.

3. North Pacific Ocean: In figure 9 I have attempted to show the probable limits of distribution of *P. pacifica* across the entire North Pacific. The approximate southern boundary east of about 160° W. is based not only on CCOFI material, but also on samples from cruise VII of the *Carnegie* and the *Northern Holiday* Expedition of the Scripps Institution of Oceanography. In the region between 170° E. and 160° W., no collections have been made available to me, but extensions of the boundaries in the CCOFI area and in the northwestern

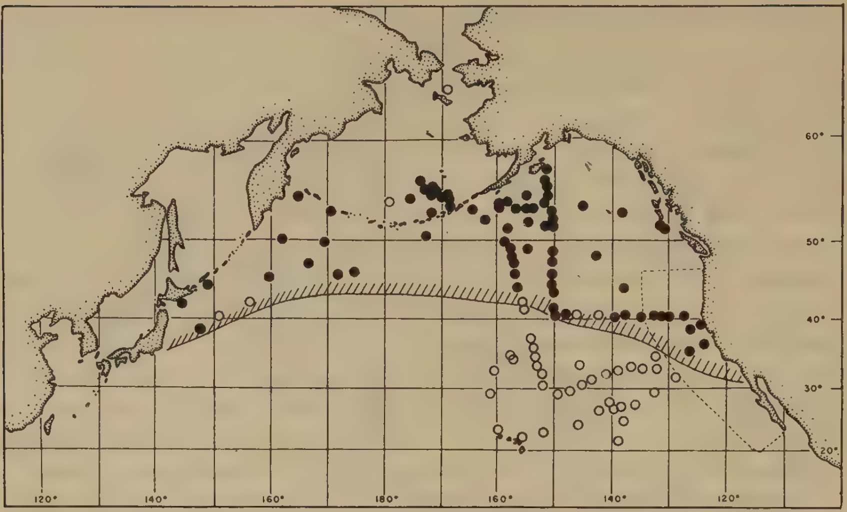

Figure 9.—Distribution of *Parathemisto pacifica* Stebbing. Solid circles, positive stations; open circles, negative stations. CCOFI area outlined by dashed line. Approximate southern limit of distribution shown by hachured line.

Pacific gives us a boundary line in the north central Pacific between latitudes 42° and 43° N. On the basis of an analysis of the distribution of chaetognaths and pteropods in about the same region (22°–50° N., 170° E.–145° W.), Hida (1957) established the Subarctic Zone, the southern limit of which was defined by the occurrence in abundance of the chaetognaths *Sagitta elegans* and *Eukrohnia hamata.* Hida found this boundary to lie between 43° and 45° N.; this finding agrees reasonably well with my suggested boundary for *Parathemisto pacifica.* It has already been mentioned that Bogorov and Vinogradov (1955) cited *P. japonica* as well as the above-mentioned chaetognaths as characteristic species of a faunal zone corresponding to Hida's Subarctic Zone. In Brodsky's (1955b) scheme for dividing the north Pacific into zoogeographical provinces according to the copepod faunas, *P. pacifica* fits roughly into his epipelagic temperate province. However, *P. pacifica* extends somewhat farther south and not so far to the north, for Brodsky's temperate province includes the southern part of the Chukchi Sea.

The northern limits of the area inhabited by *P. pacifica* are not known in detail. The species has not been reported from the Arctic Ocean, and I have not found it in any of the plankton samples which I have examined from the Beaufort and Chukchi Seas. Three investigators have reported it from the Bering Sea as *P. japonica* (Behning, 1939; Bulycheva, 1955, Vinogradov, 1956). Further collections in the

Bering Sea are needed to determine its northern boundary. The investigations of Johnson (1934, 1953, 1956) and Stepanova (1937) show that certain zooplanktonic species characteristic of the Bering Sea and north Pacific Ocean may be carried into the Chukchi Sea by the northward drift through the Bering Strait. *P. pacifica* does not seem to undergo such transport.

The boundaries of the area inhabited by *P. pacifica*, described above and shown in figure 9, are in fairly close agreement with the boundaries of north Pacific Subarctic Water as described and illustrated by Sverdrup et al (1946, p. 712, figures 202, 209*a*). It is apparent that *P. pacifica*, like *Sagitta elegans* and *Eukrohnia hamata*, is by virtue of its temperature requirements an inhabitant of sub-Arctic Water, and like these chaetognaths can serve as a biological indicator of this cold water of low salinity. However, its distribution differs from that *Sagitta elegans*, recently charted by Bieri (1959), in that it penetrates farther to the south and does not enter the Arctic Ocean, where *S. elegans* is common. The euphausiid, *Euphausia pacifica* Hansen, judging from the details given by Boden, Johnson, and Brinton (1955), has a distribution more nearly like that of *P. pacifica* than does *S. elegans*.

TEMPERATURE AND BODY SIZE: It is well known that the size of marine poikilotherms is related to the temperature of the water in which they develop (Sverdrup et al., 1946, pp. 855–857; Marshall and Orr, 1955, pp. 81–89). This relationship has been investigated for *P. pacifica*, and is summarized in figure 10. The mean length of the adult females was determined for each station and plotted against the temperature at a depth of 30 meters.

The results show a slight trend toward greater size at lower temperatures. Coefficients of correlation for cruises 1, 5, and 9 are respectively −0.526, −0.571 and −0.582. For the numbers of pairs of observations, 14, 20, and 19, the values of r required at the 5 percent level of significance are 0.532, 0.444, and 0.456. On this basis the correlation between *Parathemisto* body length and 30-meter temperature is significant for cruises 5 and 9, and nearly significant for cruise 1.

It can be seen from figure 10 that in July (cruise 5) *Parathemisto* averaged somewhat larger than in March or November. The mean length of adult female *Parathemisto* from all stations of a cruise was 5.07 mm. in March, 6.22 mm. in July, and 5.25 mm. in November. Several explanations are possible for this seasonable variation in length:

1. The *Parathemisto* populations sampled during the three cruises may belong to successive generations, the July generation having developed under conditions which resulted in greater size at maturity

than the March or November generations. If this explanation is correct, it means that several generations are produced each year, with each generation living only a few months or less. In contrast, Dunbar (1957) proposes a life cycle of 18 months to 2 years for *P. libellula* in the eastern Canadian Arctic, and Bogorov (1940) gives evidence for a 2-year life cycle for *P. abyssorum* in the Barents Sea.

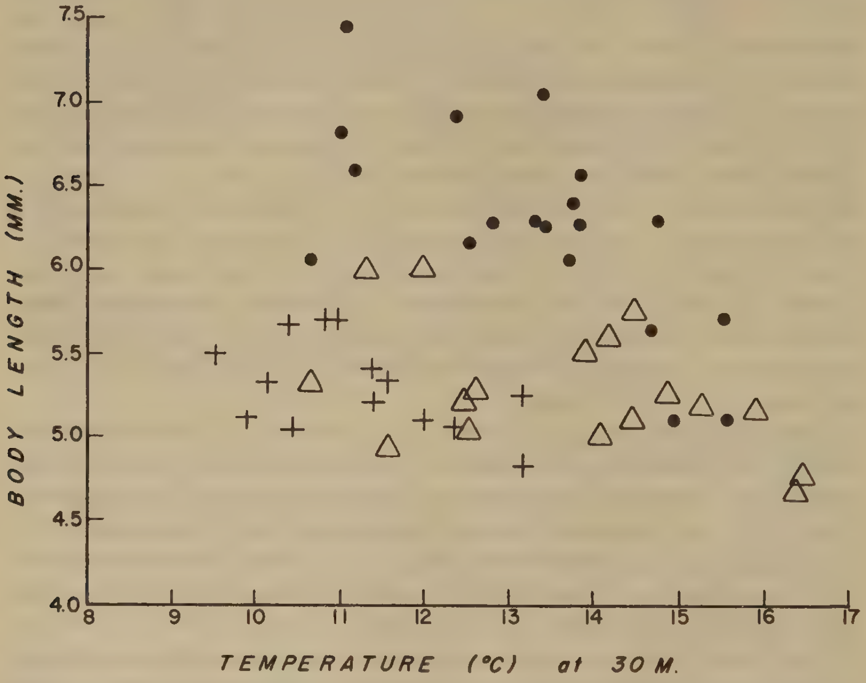

FIGURE 10.—*Parathemisto pacifica* Stebbing, relation between body length and temperature at a depth of 30 meters. Plus signs, cruise 1, March 1949; circles, cruise 5, July, 1949; triangles, cruise 9, November 1949. Each symbol represents the average length of the adult females from one station.

However, there is considerable evidence, much of it summarized by Dunbar, that marine poikilotherms from warm water grow to maturity more rapidly than do those from cold water. It is reasonable to suppose that *P. pacifica* passes through its life cycle more quickly than its Arctic relatives.

2. The *Parathemisto* population sampled in July may be older, hence larger individuals of the generation sampled in March. The November population, composed of smaller individuals than the July population, must represent a different generation. This interpretation requires that an individual breed more than once during its lifetime. Dunbar concluded that *P. libellula* breeds only once and then dies, but

this finding is not necessarily true for *P. pacifica.* On the contrary, examination of the ovaries of females with eggs or young in the brood pouch provides strong evidence that more than one generation of offspring is produced by the individual female. The ovaries can be readily seen through the transparent ventral body wall of the pereon; they lie on either side of the posterior midgut and anterior hindgut, above and in close association with the digestive diverticulae. In the ovigerous females that I examined, I saw new groups of eggs developing in the ovaries. The presence of a second group of eggs indicated that another clutch of eggs would be laid.

The above evidence indicates that the individual *P: pacifica,* in contrast to *P. libellula,* produces at least two and perhaps more sets of offspring during its lifetime. It is therefore possible that the July-breeding females are the older and larger members of the generation sampled in March, and that they have already produced one or more litters.

3. Because of a seasonal difference in vertical distribution, larger specimens, which lived in deeper water in March, were within the range of the nets in July. Earlier in this paper it was deduced from a comparison of day and night hauls that the *Parathemisto* population lives nearer the surface in July than in March or September. This habit would account for the larger average length as well as the larger numbers of the specimens collected in July. It is well established that in most, but not all zooplankters, the adults live at greater depths than the juveniles, and adults from deeper water average larger than those nearer the surface. Bogorov (1940) found that the young of *P. abyssorum* in the Barents Sea prefer the upper water layers, but according to Dunbar (1946), *P. libellula* has a marked phototropism and stays near the surface, especially on sunny days. In the Gulf of Maine the young *P. gaudichaudii* are most numerous near the surface, while adults occur mainly in net hauls made below the surface (Bigelow, 1926, p. 163).

4. The larger individuals collected in July lived in colder waters to the north in March and were carried south by the California Current. This hypothesis would not account for the smaller size of the November specimens, which would have to belong to a different generation. The California Current is slow and meandering, and has numerous eddies. It seems unlikely that any considerable segment of the *Parathemisto* population that inhabits the California Current is unable to maintain itself latitudinally against the southward flow. I regard this explanation as highly improbable.

It is improbable that any of the above explanations can, by itself, fully account for the observed seasonal variation in size of *P. pacifica.* The cruises from which I have studied material are too widely separated in time to provide the details needed for a satisfactory explanation.

Development: As in almost all amphipods, the eggs and early juveniles are carried loosely in the marsupium between the ventral wall of the pereon and the oostegites. Counts made of the number of eggs ranged from 20 to 60, with an average number of about 35. Behning (1939) found up to 200 eggs per female in the much larger (8.5–17 mm.) *P. japonica.*

When the young leave the marsupium there is almost no difference between the sexes. The young are miniature editions of the adults, except that there are fewer setae on the pereopods, and the flagella of antennae 1 and 2 are unisegmental in both sexes. Of course the oostegites are entirely absent from the female.

Even at this early stage it is possible to distinguish males from females in almost all cases by the shapes of the antennal flagellae, especially those of antennae 1. In the early juvenile male the flagellum of antenna 1 is longer and broader; the portion distal to the sensory filaments, which in the female is shorter and sharply pointed, tapers more gradually and is half the length of the whole flagellum. The flagellum of antenna 2 is also longer and heavier in the male.

As development proceeds, the male flagellum becomes segmented. In males about to molt, the segmentation which the flagellum will have during the following instar can be seen through the cuticle. Consequently it has been possible to estimate the number of instars from the last stage characterized by a unisegmental flagellum to the adult male stage.

The instars may be defined as follows:

1. Flagellum of antenna 1 short, unisegmental.
2. Flagellum slightly shorter than height of head, 8–10 segmented.
3. Flagellum about as long as pereonites 1–5 combined, 11–12 segmented.
4. Adult male, flagellum about as long as pereon, 13–15 segmented.

The additional segments are added from the distal end of the long first flagellar segment. In the male about to molt, it can be seen that two or three segments are formed here. The segments distal to the first one apparently do not divide further after being formed.

This method of forming additional segments differs from that of the gammarids *Pontoporeia affinis* Lindström (Segerstråle, 1937) and *Gammarus chevreuxi* Sexton (Sexton, 1924). In *Pontoporeia* males, new segments are formed, as in *Parathemisto*, by division of the proximal segment. At first this is the only method, but later the remaining segments begin to divide into two, after which they do not divide again. In the female the distal segments do not divide, and the process is essentially similar to that in *Parathemisto.* In

Gammarus new segments are formed by division of the two (or three in older animals) proximal flagellar segments with the result that two (or three) new segments are added at each molt. Segerstråle found that the antennal segments of the male *Pontoporeia* become greatly lengthened at the last molt; lengthening at this time must also occur in *Parathemisto* (compare figs. 2*a* and 3*a*).

It is apparent that after an unknown number of instars during which the antennal flagellum remains unisegmental, the male *Parathemisto* passes through a minimum of three additional instars. According to Mogk (1926), the male *Phronima sedentaria* (Forskål) passes through five instars with an unsegmented flagellum. Segments first appear in the sixth instar, and the male reaches maturity in the seventh instar. In *Phronima atlantica* Guérin segmentation is also first apparent in the sixth instar, but the adult condition is not reached until the eighth instar.

In the first stage after leaving the marsupium, the flagellum of antenna 1 of *Gammarus chevreuxi* Sexton (Sexton, 1924), *G. fasciatus* Say (Clemens, 1950), and *Pontoporeia affinis* Lindström (Segerstråle, 1937) consists of four segments. By the fourth stage the segments number 8 for *G. chevreuxi* and 9 for *G. fasciatus;* and in the fifth postmarsupial instar there are 10 and 9 segments, respectively. On the assumption that the first instar of *P. pacifica* with segmented flagella corresponds to the fourth or fifth instar of *Gammarus*, we can postulate that there are 3 or 4 postmarsupial instars of *Parathemisto* with unsegmented flagellae, or a total of 5 to 6 postmarsupial molts required to attain sexual maturity. In gammarideans which have been studied, from 7–14 molts are required (Sexton, 1924, 1928; Roux, 1933; Clemens, 1950; Kinne, 1953, 1959).

Oostegites first appear in the female when she is quite small (3.1 mm. in the earliest stage illustrated). At this stage, the oostegites are very small lobes arising mediad to the gills and only about one-third the length of the gills. During subsequent molts the oostegites increase in size, and in the adult they are transparent, membranous and much larger than the gills. No marginal setae are present. Development of the oostegites in *P. libellula* is identical (Dunbar, 1957).

The size at which maturity is reached varies widely. As an example, 382 females and 491 males from station 702, cruise 1, were examined for maturity, judged in the males by the elongate antennae and in the females by the presence of fully developed oostegites. The results are given in table 1.

The males attain maturity at a slightly smaller size than the females, though not necessarily at a younger age.

Food: Reports of the food habits of *P. gaudichaudii* and *P. libellula* have been given by Bigelow (1926, p. 107) and Dunbar (1946) respec-

TABLE 1.—*Length and maturity in* Parathemisto pacifica.

Specimens	*Length (mm.)*											
	3.6	*3.8*	*4.0*	*4.2*	*4.4*	*4.6*	*4.8*	*5.0*	*5.2*	*5.4*	*5.6*	*5.8*
Females:												
Number examined	–	165	32	37	24	23	29	24	20	17	11	7
Percent mature	–	0	3	0	13	35	48	83	90	77	82	100
Males:												
Number examined	165	55	60	63	51	26	26	20	6	7	–	–
Percent mature	0	2	0	21	41	74	90	100	83	100	–	–

tively. Both species are predominately carnivorous, sometimes cannibalistic, but also ingest some vegetable matter.

I have examined the midgut contents of a few specimens of *P. pacifica.* Consisting of minute greenish or brownish particles, much of the material was unrecognizable, but some fragments of diatoms and crustaceans were identified. The crustacean parts included copepod swimming legs and mouthparts (one mandible was recognizable), spines of undetermined origin, and crystalline cones from compound eyes. It seems reasonable to conclude that the food habits of *P. pacifica* are similar to those of *P. gaudichaudii* and *P. libellula.*

ANATOMY OF DIGESTIVE TRACT: The structure of the alimentary canal of *P. libellula* is considered briefly by Dunbar (1946). He describes an interesting "gastric apparatus" formed of dorsolateral and ventral sheets projecting backward in the midgut, which he compares with the peritrophic membrane of insects and onychophorans. Dunbar also states that there are no caeca or diverticula of any kind. On this point my findings do not agree with his.

In *P. pacifica* a pair of caecae arise laterally from the midgut near its anterior end. They extend posteriorly along the entire length of the pereon and run along in close association with the lateral parts of the midgut and with the gonads which lie dorsal to them. The caecae usually have a coarsely vesicular appearance; in section the vesicles are seen to be large vacuolate cells. The vacuoles are filled with an oily or fatty material, and vary greatly in size. In some individuals the vacuolate cells are so large that the lumena of the caecae are nearly obliterated; in others the vacuoles are small and the lumena well defined.

Contrary to Dunbar's statement, a pair of caecae is also present in *P. libellula.* Because they are closely applied to and partially fused with the gut wall, their true nature is not obvious in dissected specimens, and if the lumen is sufficiently encroached on by the large vacuolate cells, it may be difficult to interpret the caecae correctly in sectioned material. I have also found the same caecae in *P. gaudichaudii* from the Gulf of Maine, and they are probably characteristic of all species of *Parathemisto*.

Although I have not made a detailed study of the histology of the digestive caecae, it seems reasonable to suppose that their principal function is the storage of reserve food supplies. The large fat cells can scarcely be interpreted otherwise. In some specimens of *P. gaudichaudii* which had been stored in alcohol for a long period, the caecae have the appearance of a foamy network, and must be made up almost completely of fat cells. I have found no structure in *Parathemisto* comparable to the fat body of gammarids, and the storage of reserve food in this genus is probably carried out by the digestive diverticula. It is interesting to note that Nakai (1955) found the crude fat content of *P. japonica* from Korean waters to be nearly 40 percent of the dry weight.

***Parathemisto (Parathemisto) japonica* Bovallius**

FIGURES 2,*b–i;* 3,*f–l;* 8; 16,*c*

Parathemisto japonica Bovallius, 1887, p. 21; 1889, pp. 258–263, pl. 12, figs. 17–43.—Behning, 1939, pp. 362–363, fig. 1.

Parathemisto sp. (11) Yamada, 1933, p. 7, pl. 2, fig. 10,*a–g*.

Parathemisto sp. Nakai, 1955, pp. 14–15.

Parathemisto sp. A. Irie, 1948, p. 36.

Themisto gracilipes Norman, Irie, 1957b, p. 353, figs. 16–1, 16–2.

Themisto japonica, Irie, 1959, pp. 20, ff.

DIAGNOSIS: Total length of adult ♀, excluding antennae, 9–17 mm. Identical with *P. pacifica* in almost all characters except size, but female antenna 2 much longer than antenna 1, slightly longer than head plus first 3 pereonites. Setae of pereopods more conspicuous, more numerous on gnathopods.

REMARKS: While I am not unalterably convinced that *P. japonica* and *P. pacifica* are distinct species, all the evidence at my disposal leads to this conclusion. Except for mutilated specimens, I have had almost no difficulty in assigning specimens to one or the other species. The geographic ranges are different, with some overlap east of northern Japan and the southern Kuriles. In the three samples where both species occurred, I have found no intergrades, and thus no evidence of interbreeding.

Since the number of pereopodal setae increases with age in some species of hyperiids (unpublished observation), it may be argued that *P. japonica* is an older and larger form of *P. pacifica*. However, it is possible to distinguish the young stages of the two species. Antenna 2 is longer than antenna 1 even in very young specimens of *P. japonica*. The difference in the development of setae on pereopod 6,

(967)

especially on the posterior margin of the propodus, is shown in figure 2*j* of a 7.0 mm. adult female *P. pacifica* and figure 2*e* of a 6.7 mm. juvenile *P. japonicus*, both of which were taken in the same net tow off Cape Esan, Hokkaido, Japan.

The correlation between temperature and body length in *P. pacifica* raises the possibility that the large size of *P. japonica* is attributable to the low temperatures at which it lives. *P. pacifica* is abundant in the Gulf of Alaska, where adult females commonly measure 6.0–7.0 mm. in length. This size is much smaller than the size of *P. japonica*, and yet surface temperatures in the Gulf of Alaska are similar to those in the colder parts of the Sea of Japan (compare Robinson, 1957, fig. 18, and Uda, 1934, figs. 5 and 9).

With this evidence, the best course is to treat *P. japonica* and *P. pacifica* as closely related, but distinct, species. If intensive collections from the region of overlapping distributions should reveal extensive intergradation, it would then be necessary to reduce their status to that of subspecies. In the limited number of samples at my disposal, however, there is no indication of such intergradation.

The Japanese zoologist Zinziro Nakai believes that the hyperiid which I have described as *P. japonica* Bovallius is an undescribed species of *Parathemisto*. He has assigned to it the Japanese name "Usumurasaki-uminomi" (light purple sea flea) and intends to describe it as a new species (Nakai, 1955). Nakai states (in litt., Oct. 23, 1954) that his decision is based on many discrepancies between Bovallius' descriptions and the structure of specimens from Japanese waters, and on Bovallius' statement (1889) that *P. japonica* occurs in the subtropical region as well as in the northern temperate region of the Pacific. Nakai believes that *P. japonica* is distributed south of Japan and has not been discovered since Bovallius' description of 1889, while "usumurasaki-uminomi" is the common species found north of Japan.

In my opinion, Nakai places too much confidence in the detailed accuracy of Bovallius' descriptions and illustrations. I believe the differences that Nakai finds between Bovallius' account of *P. japonica* and "usumurasaki-uminomi" can be explained as inaccuracies of Bovallius or as variations in the structure of *P. japonica*.

DISTRIBUTION: Okhotsk Sea, Sea of Japan, western north Pacific off the east coasts of northern Japan and the southern Kuriles.

East of Japan and the southern Kuriles, *P. japonica*, like *P. pacifica*, inhabits Subarctic Water and penetrates about as far south along the Japanese coast as the cold Oyashio. The extent of its eastward distribution is unknown, but at some distance it is replaced by *P. pacifica*.

In the Sea of Japan the scattered records from *Albatross* stations show that *P. japonica* extends south nearly to the Straits of Korea.

The findings of Yamada (1933) are more instructive. In his report on plankton collected from a series of stations off both coasts of Korea, he found *P. japonica* present off the east coast south to nearly 38°, but absent from the Tusima Straits and the Yellow Sea. This distribution correlates well with the hydrography of the Sea of Japan. As Uda (1934) has shown, the water on the Asiatic mainland side is much colder than that on the Japanese side. The cold water flows south along the mainland coast (Liman Current) to the latitude of about 36°–38° N. and forms several counterclockwise eddies as it flows. Only a small amount of mixing occurs between this cold water, presumably formed by excessive cooling in winter, and the warm, north-flowing water of the Tusima Current, a branch of the Kuroshio.

Yamada's findings suggest that *P. japonica* is distributed in the Sea of Japan according to the extent of the cold water, as Tokioka (1940) found for the chaetognath, *Sagitta elegans*. The occurrence of *P. japonica* at *Albatross* stations along the west coast of Honshu makes this hypothesis improbable. Uda's (1934) isotherm charts show that in June most of the Sea of Japan is characterized by temperatures at least as low as those of the southern boundary of the Oyashio. The Oyashio boundary temperatures in Uda's charts are 17°–19° C. at the surface and at 25 m., about 17° at 50 m., and about 15° at 100 m. Most of the water of the Sea of Japan at these depths is as cold or colder, while the water of the southward-flowing current in the west is considerably colder. Hence a wide distribution of *P. japonica* in the Sea of Japan is to be expected from our knowledge of its distribution off the east coast of Japan.

It is reasonable to believe that *P. japonica* evolved from *P. pacifica* or from a common ancestor of both species as a result of geographical isolation. The current patterns in the Japan Sea provide little opportunity for *P. pacifica* to enter from the Pacific Ocean. Almost all the water entering the Sea of Japan is warm water derived from the Kuroshio; only a very small quantity of cold water enters through Tartary Strait between the Asiatic coast and Sakhalin Island. Water leaves the Japan Sea by way of the Straits of Soya (La Pérouse) and Tsugaru, north and south of Hokkaido, respectively. Information concerning water movements in the Okhotsk Sea is still scanty. According to Bruns (1958) there is some exchange of water with the Pacific Ocean through the Kuriles. The very limited collections available to me indicate that this exchange of water has been insufficient to allow *P. pacifica* to become established in the Okhotsk Sea.

Actually, therefore, the *P. japonica* population in the Okhotsk Sea and especially in the Sea of Japan is effectively isolated from extensive gene flow from the *P. pacifica* population. The three northwestern Pacific occurrences of *P. japonica* reported in this paper may be explained as being derived from the Japan or Okhotsk Seas. For some as yet unknown reason, *P. japonica* has not been able to extend its range far beyond the immediate vicinity of its site of origin.

Parathemisto (Parathemisto) abyssorum Boeck

FIGURE 11,*j–k*; 12–13

Parathemisto abyssorum Boeck, 1870, p. 87(7).—Barnard, 1959, pp. 125–127, pls. 17–19.

Themisto abyssorum (Boeck), Stephensen, 1923, pp. 20–24, chart 4; 1924, pp. 95–97, figs. 36–38; 1944, p. 12.—Shoemaker, 1930, pp. 132–133; 1955, p. 72.

DIAGNOSIS: Length of adult 10–21 mm. Larger and more slender than *P. pacifica*, and head more roundly produced. Maxilliped without a distal row of setae on the basal plate. P1–4 with more surface setae than in *P. pacifica*; posterior margin of propodus of P1 serrate and bearing several long setae. Carpal process of P2 with long end spine. In length P5>P7>P6; no long spines at posterior distal corners of carpi; dactyls not pectinate. Peduncle of uropod 3 about 3 times as long as telson.

DISTRIBUTION: Ekman (1953, p. 340) mentions *P. abyssorum* as an example of an "arctic-bathy-subarctic" species. In this category he includes plankters which live primarily in Arctic waters, but are also found in deep water in lower latitudes. A detailed discussion of the distribution of *P. abyssorum* in the Atlantic is given by Stephensen (1923, pp. 22–24, chart 4). Found throughout the Arctic and Sub-Arctic Atlantic, it is very common in the vicinity of Greenland and between Norway and Iceland. Stephensen believes that Bonnier's (1896) record of 9 mm. ovigerous *P. oblivia* taken at a depth of 950 m. in the Bay of Biscay should be referred to this species. On the western side of the Atlantic it occurs occasionally in the Gulf of Maine (Bigelow, 1926) and is widely distributed in and around the Gulf of St. Lawrence (Shoemaker, 1930; Bousfield, 1951). Bousfield believes that the permanent deep layer of very cold water in the Gulf of St. Lawrence enables the species to breed there successfully, as evidenced by the large numbers of young and immature stages taken near the surface.

I have not found *P. abyssorum* in any plankton collections from the Pacific Ocean. It was, however, the most commonly collected amphipod during the 1950 and 1951 expeditions of the *Burton Island* to the Beaufort Sea and in the 1953 expedition to Amundsen Gulf and Prince of Wales Strait. Station positions and locality records for *P. abyssorum* are shown in figure 12. Plankton hauls were made vertically with a one-half-meter Nansen type plankton net. In 1950 the hauls were made from various depths, usually 100–0 m., and in 1951 all

(970)

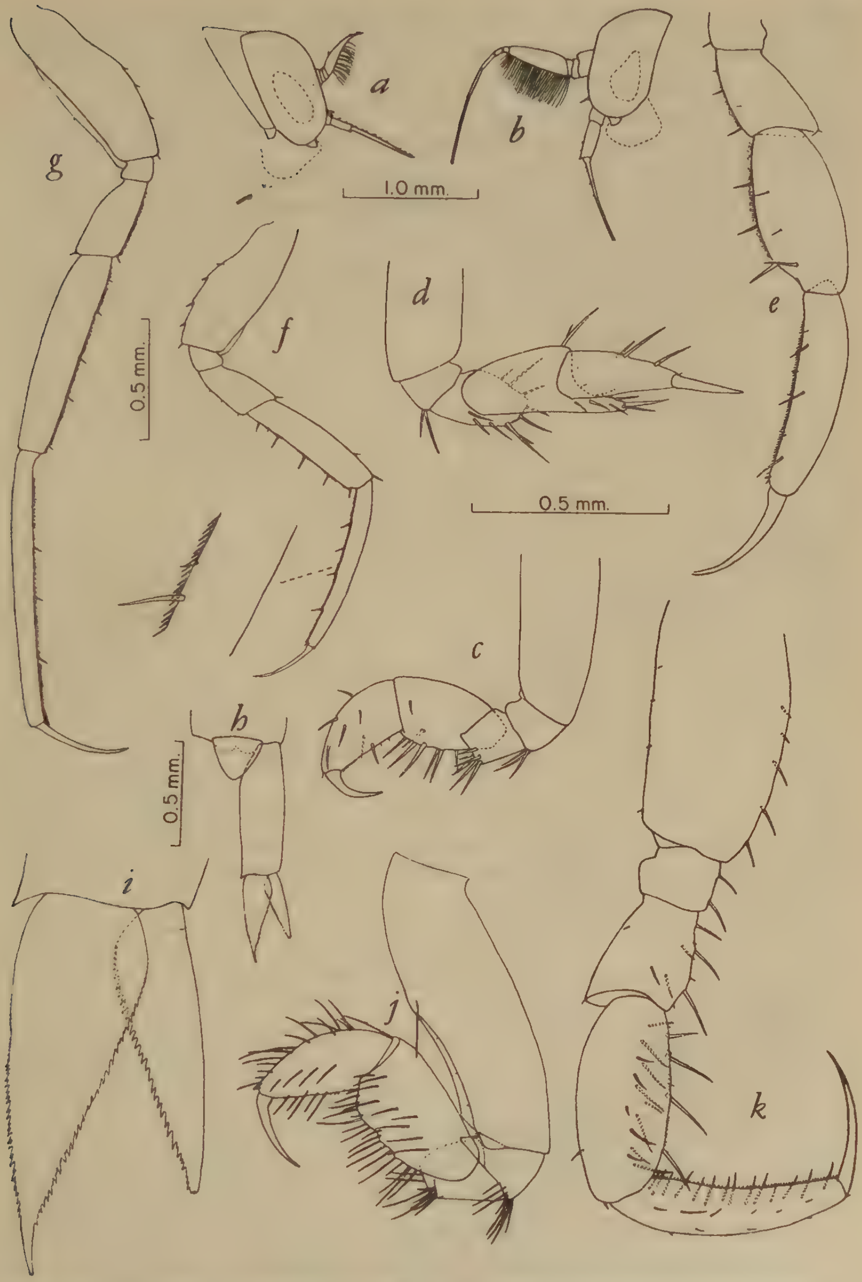

FIGURE 11.—*Parathemisto gracilipes* (Norman), Eastern Sea, west of Kyusyu, Japan: *a*, Head, female; *b*, head, male; *c*, pereopod 1, male; *d*, pereopod 2, male; *e*, pereopod 3, male; *f*, pereopod 5, female; *g*, pereopod 5, male; *h*, uropod 3 and telson, female; *i*, distal end of uropod 3, female. *Parathemisto abyssorum* Boeck, juvenile female, Beaufort Sea, west of Banks Island, U.S.S. *Burton Island* 1950 cruise, station 44: *j*, Pereopod 1; *k*, pereopod 3. Scale same for *a–b*, *c–e*, and *f–g*.

hauls were 100–0 m. except where the depth of the water was less than 100 m. In 1953 hauls were made from the bottom (usually less than 100 m.) to the surface.

In both 1950 and 1951 *P. abyssorum* occurred at about half the stations occupied and in about the same numbers. The average number per station (adjusted to 100 m. vertical tow) was 2.3 in 1950 and 2.6 in 1951. Distribution in the Beaufort Sea appeared not to be associated with variations in temperature or salinity.

P. abyssorum was somewhat less numerous in the 1953 *Burton Island* samples, and was captured at only 4 of the 25 stations in the Prince of Wales Strait. The average number per station was 0.75; the average number per positive station, 1.50.

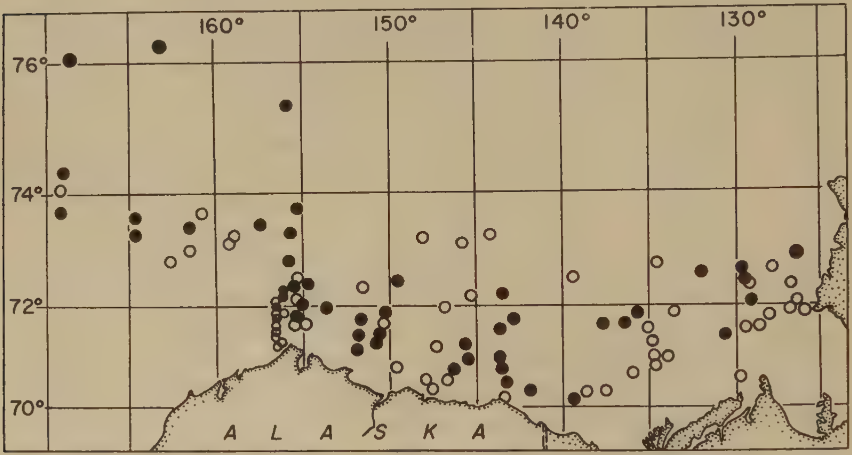

Figure 12.—*Parathemisto abyssorum* Boeck, distribution in the Chukchi and Beaufort Seas, U.S.S. *Burton Island* 1950 and 1951 cruises combined. Solid circles, positive stations; open circles, negative stations.

All the specimens of *P. abyssorum* collected on the *Burton Island* cruises were juvenile, with the exception of one ovigerous female, 14 mm. in length, taken at station 3, off Cape Parry, in a tow from 420 m. to the surface, August 8, 1953.

Little is known about the life history of *P. abyssorum.* Bogorov (1940) studied the life cycle in the Barents Sea and concluded that spawning occurs in "the second half of the winter season (about February)." He further concluded that the individual requires 2 years to grow to maturity, breeds once, and dies. The breeding season appears to be more prolonged than indicated by Bogorov, since at least some breeding occurs in the Beaufort Sea in August (see above), and Stephensen (1933) reported ovigerous females taken June 12 and

July 14 in waters west of Greenland. In the collections of the U.S. National Museum is a lot consisting of three adult males, 13, 14, and 14.5 mm. in length, and a female 14.8 mm., with fully developed oostegites, taken on May 18, 1902, between the Shetland and Faroe Islands.

Several records of *P. abyssorum* or *P. oblivia* in the Pacific Ocean are probably erroneous, since the authors almost certainly had *P. pacifica* or *P. japonica*. These include the records of Shoemaker (1930) and Thorsteinson (1941) from near Nanaimo, British Columbia, and that of Holmes (1904) from Humboldt Bay, Popof Island, Alaska (about 55° N., 161° W.). Possibly the specimens of "*P. oblivia*" from stations 13 and 14 of the Canadian Arctic Expedition (Shoemaker, 1920) were *P. japonica*, and those from stations 21 and 27 were *P. abyssorum*. Irie's (1957a) record from the Tusima Straits is probably *P. japonica*.

The puzzling thing about the distribution of *P. abyssorum* is that it has not been able to establish itself in the Pacific (fig. 13). This absence cannot be simply a matter of temperature, since the Okhotsk Sea and the western Bering Sea are regions of very low temperatures. In fact *P. libellula*, an Arctic species which does not penetrate as far to the south in the Atlantic as *P. abyssorum*, occurs in the Bering and Okhotsk Seas.

Three possible explanations may be given for the absence of *P. abyssorum* from the Pacific:

1. The current flow through the Bering Strait has made it mechanically impossible for *P. abyssorum* to enter the Pacific Ocean. The hydrographic evidence for a northward flow of water from the Bering Sea into the Chukchi Sea (Barnes and Thompson, 1938; LaFond and Pritchard, 1952) is corroborated by Johnson's (1956) report of the presence of characteristic Bering Sea copepods in the Chukchi Sea (*Eucalanus bungii bungii* Johnson, *Metridia lucens* Boeck). While the penetration of Arctic plankters into the Pacific would be retarded by this northward current, it is unreasonable to suppose that it would be completely inhibited. On the extreme west of Bering Strait there appears to be some movement of water southward, and Sewell (1948, pp. 399–401) believes that this movement has carried certain Arctic planktonic copepods into the north Pacific.

2. *P. abyssorum* is unable to compete successfully with the closely related north Pacific species, *P. japonica* and *P. pacifica*. All three species are very similar in structure and probably occupy similar if not identical ecologic niches. Possibly the Pacific species evolved during a time of isolation of the Pacific from the Arctic by emergence of Bering Strait. Bering Strait has been above sea level during much of geologic history. Hopkins (1959) has recently reviewed the Cenozoic history of the Bering Land Bridge. Evidence of the

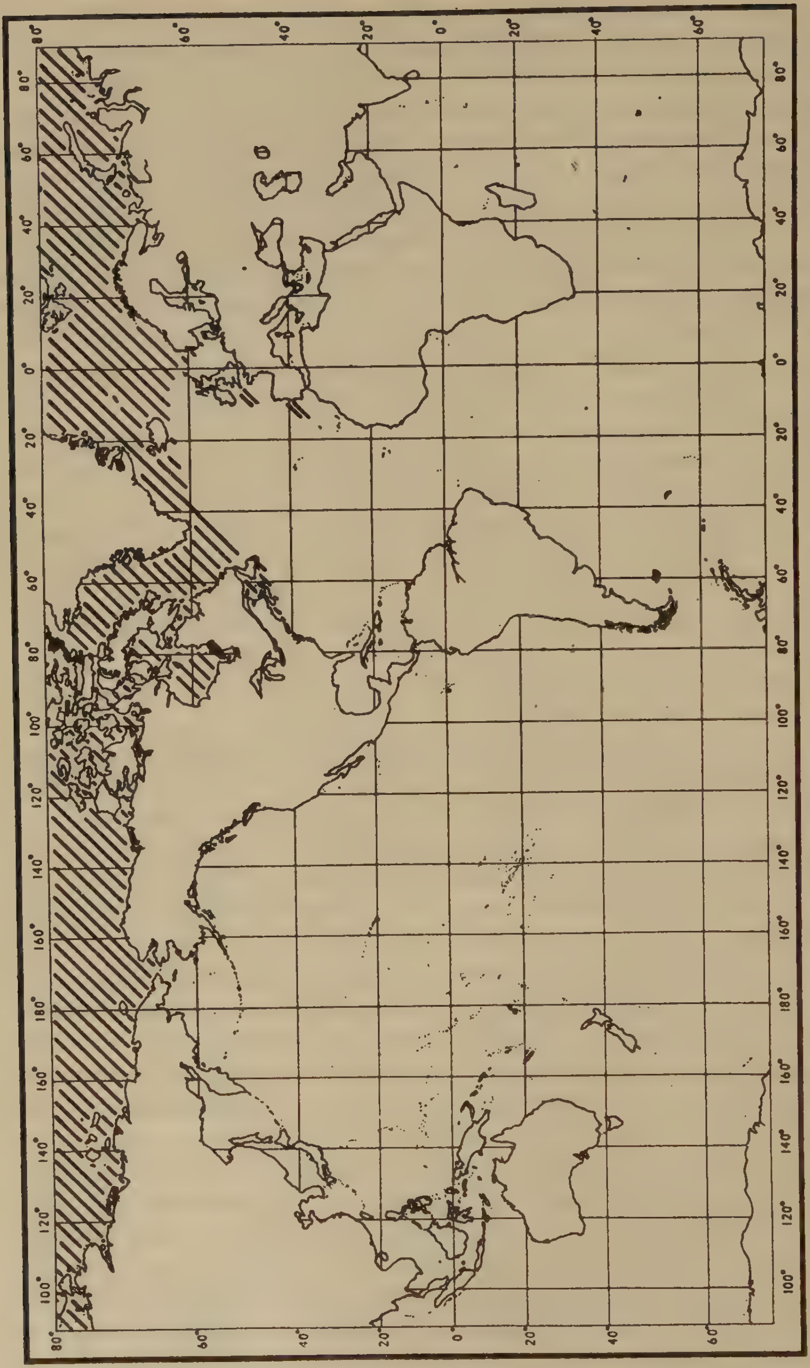
80°
60°
40°
20°
0°
20°
40°
60°
80°
100°
120°
140°
160°
180°
160°
140°
120°
100°
80°

FIGURE 13.—*Parathemisto abyssorum* Boeck, world distribution. The records south of Ireland and west of Portugal are from deep water.

interchange of land mammals strongly suggests that the bridge was submerged during middle Eocene time (Simpson, 1947a, 1947b), although physical evidence in support of this submergence has not yet been found in Alaska or the islands of the Bering Sea. During most of the remainder of the Tertiary Period the bridge was above sea level. After middle Pleiocene time but before the beginning of the Pleistocene epoch, the bridge was again submerged. The bridge emerged during each glacial interval and submerged during each interglacial interval of the Pleistocene; it sank below sea level for the last time between 11,000 and 12,000 years ago. There has thus been ample opportunity for the evolution of species in the north Pacific differing from their arctic relatives. If the northward flow of the current in the Bering Strait severely limits the numbers of *P. abyssorum* entering the Bering Sea, it is evident that this species would be markedly handicapped in establishing itself in competition with the abundant *P. pacifica*.

3. *P. abyssorum* avoids shallow water, hence does not enter the shallow Bering Strait. As suggested by the specific name, *P. abyssorum*, according to Stephensen (1923, p. 23), is found, as a rule, where the depth of the sea is considerable, 400–3,127 meters. It occurs in shallower water, as in the Gulf of St. Lawrence, where Bousfield (1951) reports it from stations where the water was less than 100 m. deep, though it was rare in the shallow water inside the Belle Isle Strait. Curiously, Bousfield found that *P. abyssorum* was an indicator of the relatively warm Gulf of St. Lawrence water, rather than, as might be expected of an Arctic species, of the cold water of the Labrador Current, which enters the gulf on the north side of the Belle Isle Strait. It is most abundant at the deep water stations of the gulf, which do not happen to be in the region influenced by the Labrador Current. It probably enters the gulf through Cabot Strait, rather than through the shallow Belle Isle Strait; this entrance also accounts for the larger numbers at the stations in the southern part of the gulf.

The depths of the sea at the stations in the Beaufort and Chukchi Seas occupied by the *U.S.S. Burton Island* ranged from 18 to 4,050 m. The depths at which *P. abyssorum* occurred are summarized in table 2.

The shallowest station at which *P. abyssorum* was taken was 53 m. The entire Bering Strait is less than 50 m. deep, much of it considerably less, and this shallowness may be an important factor in preventing *P. abyssorum* from gaining entrance to the Pacific Ocean. The comparative scarcity of *P. abyssorum* in the Prince of Wales Strait may be related to the shallowness of the water there; the deepest station was 150 m., and only five stations were more than 100 m.

Probably none of the three explanations given above can by itself account for the absence of *P. abyssorum* from the Pacific Ocean. A combination of them may, however, be effective, the shallowness of the Bering Strait and the northward set of the currents preventing all but a small number from entering the Bering Sea, while competition with *P. pacifica* prevents those that do enter from establishing themselves.

TABLE 2.—*Depth of the water and occurrence of* Parathemisto abyssorum *in the Beaufort and Chukchi Seas, 1950 and 1951* Burton Island *Cruises combined.*

Stations	*Depth (meters)*			
	0–100	*101–200*	*201–500*	*500*
Number occupied	23	18	20	44
Number positive	5	7	8	28
Percent positive	21. 7	38. 9	40. 0	63. 6

Subgenus *Euthemisto* Bovallius

Dorsal spines present or absent. Flagellum of female antenna 1 curved, heavier than in subgenus *Parathemisto* (except in *P.* (*E.*) *libellula*). Carpus of P3–4 usually more expanded than in subgenus *Parathemisto*. P5 much longer than P6–7 (except in some females of *P.* (*E.*) *gracilipes*). Peduncle of uropod 3 only slightly produced at inner distal end.

Key to the Species of the Subgenus *Euthemisto*

(Modified from Barnard, 1930)

1. Female antenna 1 slender, straight. Dactyls of P5–7 pectinate at base. **libellula** Lichtenstein
Female antenna 1 stouter, hooked. Dactyls of P5–7 unarmed at base . . 2
2. Inner ramus of uropod 3 serrate only on outer margin. **gaudichaudii** (Guérin)
Inner ramus of uropod 3 serrate on both margins 3
3. Inner margin of uropod 3 peduncle smooth throughout. **gracilipes** (Norman)
Inner margin of uropod 3 peduncle distally serrulate. **australis** (Stebbing)

Hurley (1955) discusses in detail the difficulties in distinguishing between *australis*, *gracilipes*, and *gaudichaudii* in collections from New Zealand waters. The three species show clear differences in general appearances, but these are very difficult to set down in words. Hurley notes that *P. australis* is shorter and stockier than the other species, with no sign of dorsal spines, and with coarse serrations on the inner ramus of uropod 3. *P. gaudichaudii* is characterized by larger size (up to 18 mm.), very distinct dorsal spination in adults, and the lack of serration along the inner margin of uropod 3 inner ramus and peduncle. In *P. gracilipes* the peduncle of uropod 3 of the very largest specimens appears serrulate when viewed under very high power, but is not at all comparable to that of *P. australis*. The serration of uropod 3 inner ramus is poorly developed in the female of *P. gracilipes*.

Parathemisto (Euthemisto) gracilipes (Norman)

FIGURES 11,*a–i*; 14–15; 16,*b*

Hyperia gracilipes and (?) *H. oblivia* Norman, 1869, p. 287.

Themisto gracilipes (Norman), Stephensen, 1924, pp. 97–103, figs. 39–42 [lit. and syn.]; 1949, p. 54.—Pirlot, 1929, p. 128.—Candeias, 1934, pp. 4–5, fig. 4.

Parathemisto (*Euthemisto*) *gracilipes* (Norman), Barnard, 1930, p. 421.—Hurley, 1955, pp. 153–161, figs. 133, 158, 176, 178.

[?] *Parathemisto* sp. (12), Yamada, 1933, p. 8, pl. 2, fig. 12a–e.

DIAGNOSIS: Total length of adult, excluding antennae, 4–7 mm., rarely up to 9 mm. (Stephensen, Mediterranean and Atlantic specimens); 6.5–14 mm. (Hurley, New Zealand specimens); 4.1–5.6 mm. (specimens from Tusima Straits and Eastern Sea). Only slight tendency to dorsal spination. Carpus of P2 extends about two-thirds along propodus, has one stout end spine. Uropod 3, inner ramus pectinate on both margins; inner margin of peduncle finely toothed in male (teeth very inconspicuous or absent in female).

REMARKS: The above diagnosis is based largely on that of Hurley (1955, p. 153), who has studied abundant material of *P. gracilipes*, *P. gaudichaudii*, and *P. australis* from New Zealand waters. I have had at my disposal a limited number of specimens from two surface-plankton tows—one made in Tusima Straits (34°20.7′ N., 130°47.3′ E.) and the other in the East China Sea west of Kyusyu, Japan (32°06.4′ N., 128°57.0′ E.), kindly sent to me by Zinziro Nakai. In addition, Won Tack Yang sent me three lots from off the southern coast of Korea. The characters which Hurley regards as diagnostic for *P. gracilipes* are found in these specimens. The Japanese specimens are small; two adult females measure 4.8 and 5.4 mm., and eight adult males range in length from 4.1–5.6 mm. and average 4.9 mm. The setal armature of the pereopods resembles Stephensen's (1924, figs. 39–41) rather than Hurley's drawings (1955, text-figs. 8–9). This fact may be attributed to the larger size of the New Zealand specimens.

In the Japanese specimens the serrulations of the inner margin of the male and female uropod 3 peduncle are barely discernible under high (×440) magnification, even less evident than that figured by

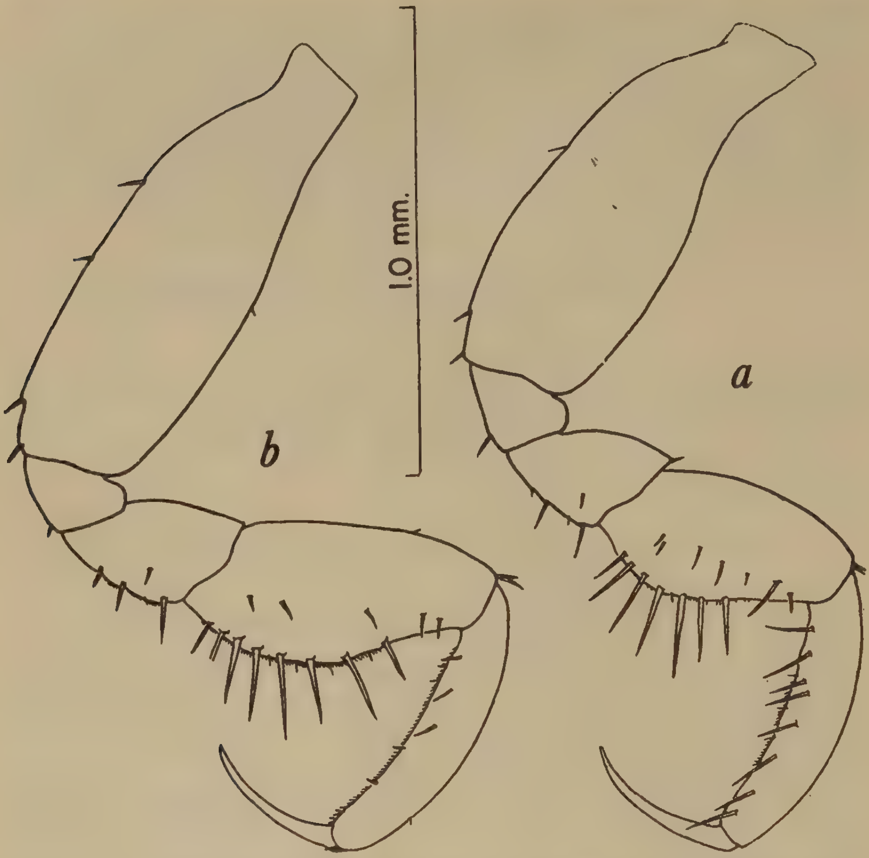

FIGURE 14.—*Parathemisto gracilipes* (Norman), "long-legged" form, adult female from Yellow Sea, west of Mok Po, Korea: *a*, Pereopod 3; *b*, pereopod 4.

Hurley. This near absence of serrulations is also probably due to the small size of the Japanese specimens. As in Hurley's description, the inner margin of uropod 3 inner ramus is more finely serrate in the female than in the male. In the female P5 and P7 are subequal, slightly longer than P6. In the male, P5 is relatively longer; the distal end of P6 propodus reaches about three-fourths to the distal end of P5 propodus.

The Korean specimens agree in general with the Japanese ones, which appear to represent Stephensen's (1924) "short-legged" form, but one lot collected west of Mok Po (34°30′ N., 125°0′ E.), consisting of an adult female and a juvenile, agrees with Stephensen's "long-legged" form, except in the shape of the carpus of P3–4. In the adult female, P6 extends one-fourth the distance down the propodus of P5 and has a high comb of setae on its anterior margin. P3–4 carpus (fig. 6) are of the form typical for *P. gaudichaudii* forma *bispinosa* (=*antarctica*), in which the carpus is wide proximally and narrows distally; the posterior margin is convex in the proximal part and becomes straight or slightly concave distally. A tendency toward this form is evident in the New Zealand specimens illustrated by Hurley (1955, text-fig. 9, Nos. 155–156). According to Stephensen, there are no fine teeth along the posterior margin between the long setae in the female, but these are present in both the New Zealand and Korean specimens.

Yamada (1933) illustrates a "*Parathemisto* sp. (12)" which he found to be widely distributed in the Yellow Sea. Although he did not identify it specifically, he stated that using Barnard's key (1930) the specimens keyed out to *P. gaudichaudii*. This statement implies that the inner margin of the inner ramus of uropod 3 appeared smooth to him. In my Korean "long-legged" *P. gracilipes*, the serrations of this margin are quite weak, and it is possible that they escaped Yamada's notice. If so, his "*Parathemisto* sp. (12)" is *P. gracilipes* rather than *P. gaudichaudii*, for in other respects "*Parathemisto* sp. (12)" agrees reasonably well with my" long-legged" *P. gracilipes*. Yamada's specimens attained a length of 7–8 mm.; this length is short for *P. gaudichaudii*, but about right for *P. gracilipes*. Moreover, on the basis of the temperatures at which they live in other regions, *P. gracilipes*, rather than *P. gaudichaudii*, would be expected to occur in the East China and Yellow Seas.

Although it thus seems probable that Yamada's "*Parathemisto* sp. (12)" is *P. gracilipes*, the possibility remains that his tentative identification of it as *P. gaudichaudii* was correct. This problem cannot be solved until extensive collections from the Yellow Sea are available.

DISTRIBUTION: Figure 15 shows the known distribution of *P. gracilipes*. It is evident that much remains to be learned about its distribution, especially in the southern hemisphere. The record of Stewart (1913) from off Brazil is probably erroneous, since members of the genus *Parathemisto* are not known to inhabit tropical waters. Stephensen (1949) regarded his identification of specimens from Tristan da Cunha as doubtful.

The collections of the U.S. National Museum contain 7 specimens of *P. gracilipes* collected in the vicinity of the Juan Fernandez Islands by the yacht *Vagabondia*. Comparable in size to Hurley's New Zealand specimens, these specimens range from 7.9–8.5 mm. in length and agree well with Hurley's description.

P. gracilipes lives in warmer water than *P. gaudichaudii*. This preference is clearly shown in the distribution of the two species in the north Atlantic (see figs. 15 and 17; see also Stephensen, 1923 and

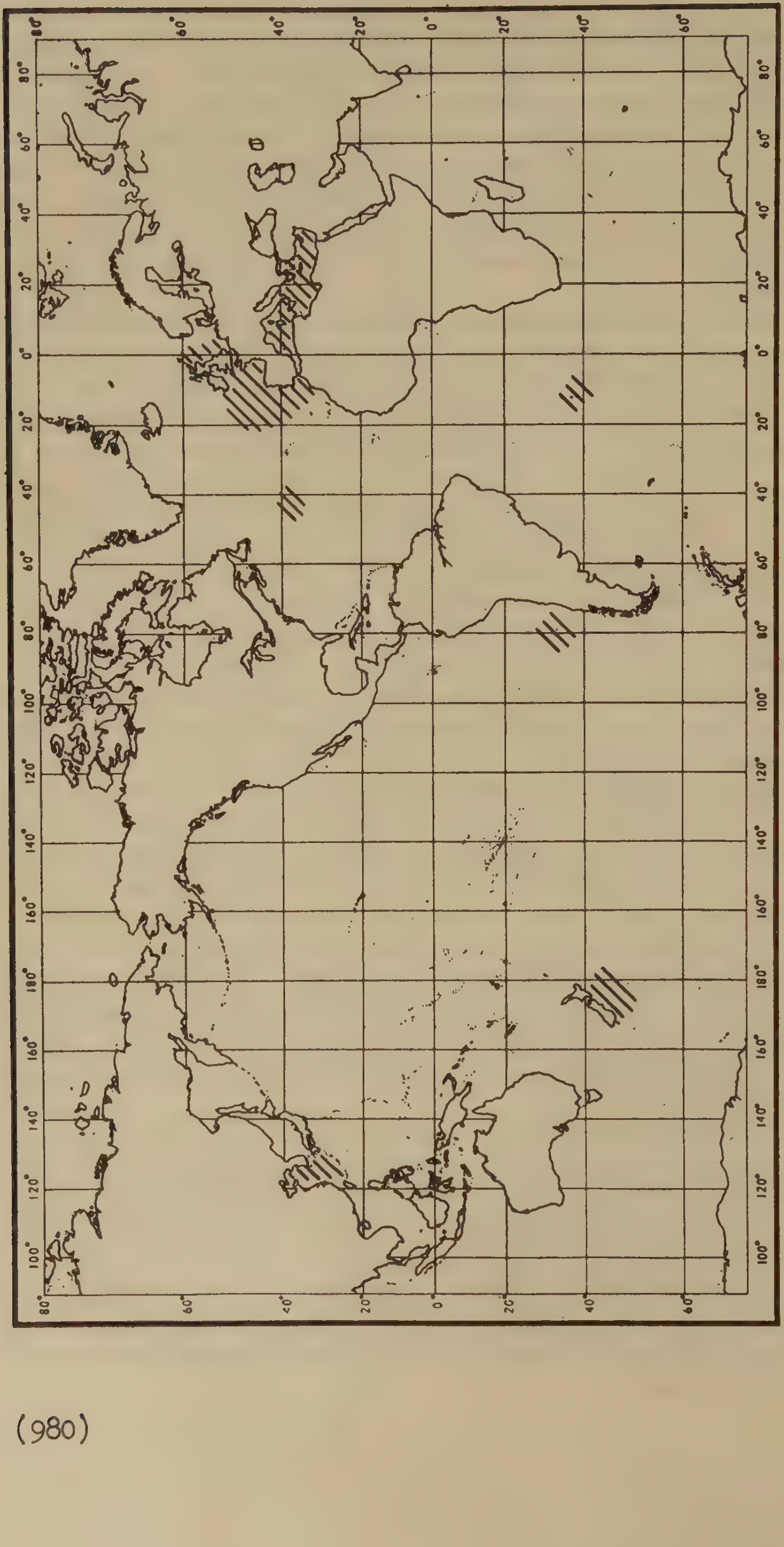
80°
60°
40°
20°
0°
20°
40°
60°
80°
100°
120°
140°
160°
180°
160°
140°
120°
100°
80°

FIGURE 15.—*Parathemisto gracilipes* (Norman), world distribution.

(980)

1924 and Pirlot, 1939). Bary (1959) showed a similar difference in temperature preference in southern New Zealand waters. The absence of *P. gracilipes* from the Atlantic coast of the United States results from the rapid change of temperature over the range inhabited by *P. gracilipes* so that it literally has no living room. Hurley (1955) pointed out that *P. gracilipes* inhabits more neritic water than *P. gaudichaudii* in the New Zealand area, and Bary's (1959) detailed analysis confirms this view. In the north Pacific the occurrence of *P. gracilipes* in the east China and Yellow Seas may reflect its preference for coastal waters. Both of these seas are shallow and subject to much runoff from rivers.

In the vicinity of Plymouth, England, *P. gracilipes* undergoes a diurnal vertical migration; it moves close to the surface at night and descends during the day (Russell, 1925). Bary's data show evidence of a similar migration in New Zealand waters.

Parathemisto (Euthemisto) gaudichaudii **(Guérin)**

FIGURES 16,*a*; 17

Themisto gaudichaudii Guérin, 1825, p. 774.
Themisto compressa Goës, Stephensen, 1924, pp. 103–110, figs. 43–49.
Euthemisto compressa (Goës), Chevreux, 1935, pp. 191–192.
Euthemisto bispinosa Boeck, Chevreux, 1935, p. 191.
Themisto gaudichaudii Guérin, Stephensen, 1933, pp. 63–64; 1944, pp. 10–12; 1947, pp. 76–77; 1949, p. 54.—Pirlot, 1939, p. 39.
Parathemisto (Euthemisto) gaudichaudii (Guérin), Barnard, 1930, p. 420; 1932, pp. 280–282 (synonomy).—Hurley, 1955, pp. 161–164, figs. 159–174.
[?] *Parathemisto* sp. (12) Yamada, 1933, p. 8, pl. 2, fig. 12, *a–e*.
Euthemisto antarctica (Dana), Ealey and Chittleborough, 1956, p. 22.

DIAGNOSIS (SLIGHTLY ALTERED FROM HURLEY, 1955): Length of adult, 7–25 mm. Strong dorsal spines in animals of more than 10 mm. total length. Carpus of P2 extends three-fourths along propodus. P3 male carpus widest proximally, width nearly one-half the length; like *P. gracilipes*, but rather more spines on surface and margin; carpus and propodus subequal. P4 male carpus oblong-ovate, width slightly more than one-half the length, fringe of small even bristles on posterior margin; about 12 strong spines. Uropod 2 outer ramus about three-fifths length of inner. Uropod 3 outer ramus two-thirds length of inner; inner ramus with smooth inner margin; inner margin of peduncle entirely smooth. P3 female carpus oblong-ovate and widest proximally, width about two-thirds the length; numerous fine surface spines, 10 marginal spines, marginal bristles throughout. P4 female has about 18 surface spines on carpus.

REMARKS: As Hurley has pointed out, the most dependable criterion by which *P. gaudichaudii* can be identified is the completely smooth inner margins of the peduncle and inner ramus of uropod 3.

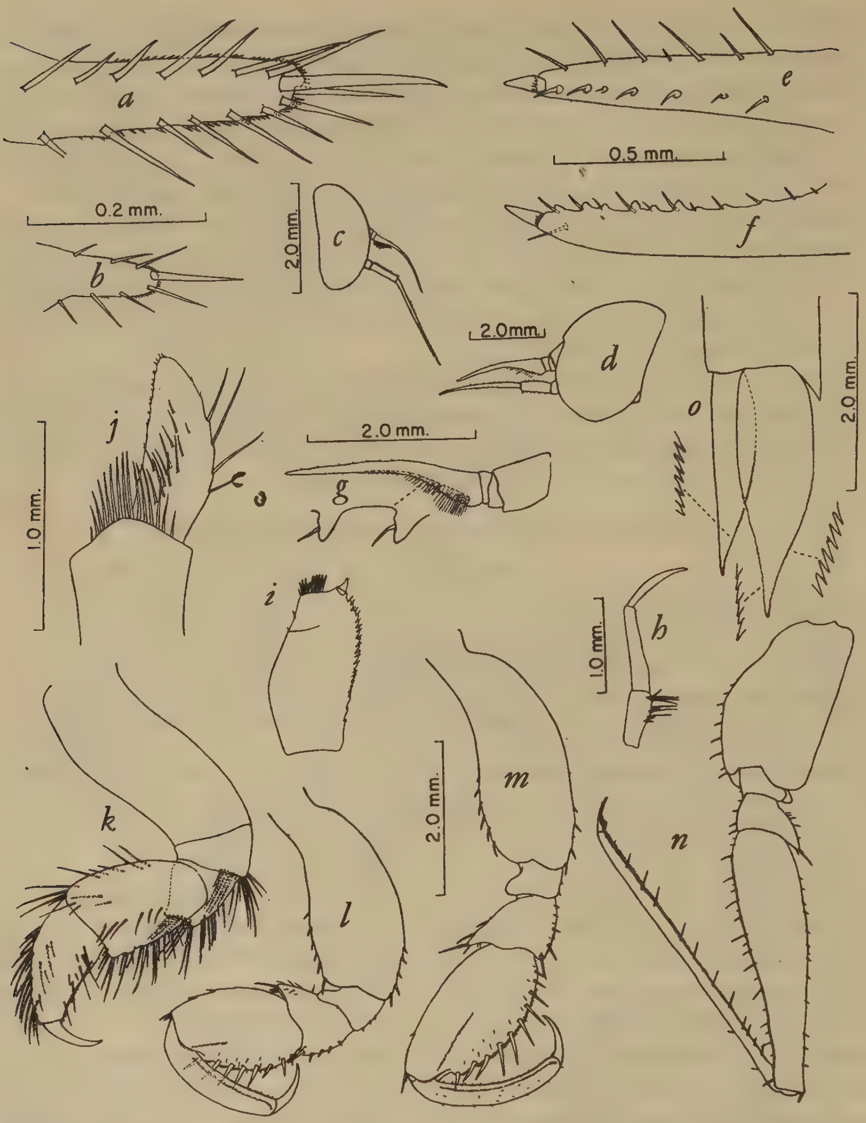

FIGURE 16.—*Parathemisto gaudichaudii* (Guérin), Gulf of Maine: *a*, Pereopod 2, carpal process, seen from above. *Parathemisto gracilipes* (Norman), west of Kyusyu, Japan: *b*, Same. *Parathemisto japonica* Bovallius, off Cape Esan, Japan: *c*, Head and antennae female. *Parathemisto libellula* (Lichtenstein), Point Barrow, Alaska: *d*, Same; *e*, pereopod 2, carpal process, seen from above; *f*, same, lateral view; *g*, antenna 1, lateral view; *h*, mandibular palp; *i*, maxilla 1, palp; *j*, maxilliped, inner plate and right outer plate omitted; *k*, pereopod 1; *l*, pereopod 3; *m*, pereopod 4; *n*, pereopod 5; *o*, distal end of uropod 3. Scale same for *a–b*, *e–f*, *i–j*, and *l–m*.

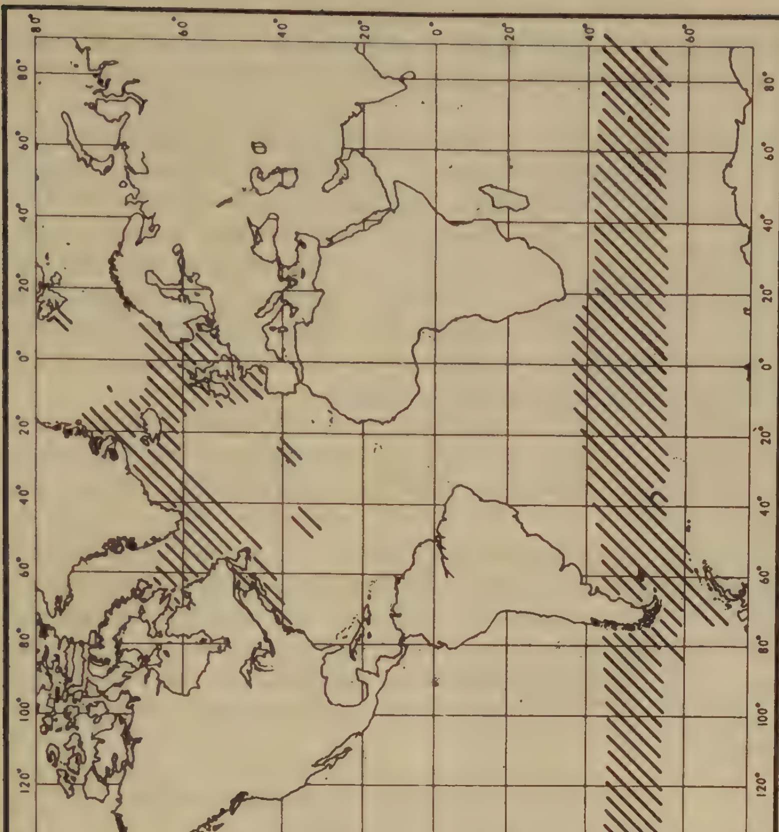
80°
60°
40°
20°
0°
20°
40°
60°
80°
60°
40°
20°
0°
20°
40°
60°
80°
100°
120°
140°
160°
180°
160°
140°
120°
100°

FIGURE 17.—*Parathemisto gaudichaudii* (Guérin), world distribution. The poleward limits in the southern hemisphere are uncertain.

Some care must be exercised, since Hurley observed that some female *P. gracilipes* have nearly smooth inner margins on the inner rami of uropod 3; these margins are nearly smooth in North Pacific specimens also.

According to Hurley's diagnoses, the carpal process of *P. gaudichaudii* P2 has several end spines, while that of *P. gracilipes* has one stout end spine. The carpal processes of these species are shown in figures 16*a–b*, looking down on the concave surface. Each has one large, stout spine inserted near the distal end, and a series of shorter, more slender spines distributed along the margins. The carpal process of the large specimen of *P. gaudichaudii* has about twice as many marginal spines as that of the small *P. gracilipes*, and the process is longer in relation to its breadth.

I have not seen any specimens of *P. gaudichaudii* from the North Pacific, and it is included in this paper because of the possibility, discussed under *P. gracilipes*, that Yamada's "*Parathemisto* sp. (12)" may belong here.

Distribution: As shown in figure 17, *P. gaudichaudii* is widely distributed in the cooler part of the north Atlantic with a few scattered records from warm water. Records in the southern hemisphere are less complete than in the north Atlantic, but it probably occurs throughout the Antarctic Ocean; i.e., the area between the Antarctic Continent and the Antarctic Convergence (Sverdrup, Johnson, and Fleming, 1942).

Parathemisto (Euthemisto) libellula (Lichtenstein)

Figures 16, *d–o*; 18; 19

Gammarus libellula Lichtenstein, *in* Mandt, 1822, p. 32.
Themisto libellula (Mandt), Stephensen, 1923, pp. 24–26, chart 5 [distribution].—Shoemaker, 1926, p. 4; 1955, p. 72.—Dunbar, 1946; 1957 [biology].
Euthemisto libellula (Mandt), Bovallius, 1889, pp. 281–283, pl. 12, figs. 1–31.—Sars, 1895, pp. 13–14, pl. 6, fig. 1.—Shoemaker, 1920, pp. 23–24, 28.
Parathemisto libellula (Mandt), Vinogradov, 1956, p. 211, fig. 10 [distribution].—Barnard, 1959, pp. 123, 125, pls. 22–23.

Diagnosis: The largest species of *Parathemisto*, reaching a length of 60 mm. Body segments not produced into spines dorsally. Female antennae 1 and 2 subequal; antenna 1 slender, straight, lower margin of flagellum serrate. First segment of mandibular palp setiferous. Maxilliped with distal row of long setae on basal plate and several long setae on lateral margins of outer plates. Carpal process of P2 with short end-spine and rounded lobes behind the spines on the lateral margins. P5 much longer than P6; P7 slightly shorter than P6; dactyls of P5–7 strongly pectinate at their bases. Inner ramus of uropod 3 serrate on both margins; peduncle strongly produced at inner distal corner.

(984)

REMARKS: The straight antenna 1 and the produced inner distal corner of uropod 3 are characteristic of subgenus *Parathemisto*, but the elongate P5 places *P. libellula* in subgenus *Euthemisto*. The species is easily recognized by the pectinate dactyls of P5–7.

Although Mandt has always been cited as the author of this species, Mandt expressly states that the name and description were prepared by Lichtenstein. The name "*libellula*" must therefore be attributed to Lichtenstein rather than to Mandt.

DISTRIBUTION (FIGURES 18, 19): Circumpolar in the Arctic Ocean. Its distribution in the eastern part of the north Atlantic is given in detail by Stephensen (1923). He reports it from many localities near Greenland and Iceland. In the Norwegian Sea it is not found below 70° N. In the western North Atlantic the southernmost records are from the Gulf of St. Lawrence and the east coast of Newfoundland. In the Pacific Ocean Behning (1939) records it from the Bering Sea and from the Okhotsk Sea as far south as about 46° N. (southeast of Sakhalin Island). Bulycheva (1955) also reports it from the Bering and Okhotsk Seas. I have identified specimens taken in September 1958 at four stations in the vicinity of Afognak Island, Alaska, by the University of Washington M/V *Brown Bear*. No other records from the Gulf of Alaska are known to me. Vinogradov (1956) summarizes the known distributional records in his figure 10.

Aside from *P. abyssorum*, *P. libellula* was the only commonly collected amphipod in the 1950, 1951, and 1953 expeditions of the *Burton Island*. In 1950 it occurred at about one-third and in 1951 at about one-fifth of the stations occupied. The average number per station (100 m. vertical tow) was 0.66 in 1950 and 0.30 in 1951. The average number per positive station was 2.2 in 1950 and 1.5 in 1951. No correlation with variations in temperature or salinity was found.

P. libellula was taken at 5 of the 25 *Burton Island* stations in the Prince of Wales Strait in 1953. The average number per station was 1.13; the average number per positive station was 1.80.

LIFE HISTORY: The life history has been studied in some detail by Dunbar (1946, 1957), who points out the importance of *P. libellula* in the ecology of the eastern Canadian Arctic. It is fed on heavily by the Arctic char and especially by the ringed seal. Dunbar postulates a life cycle of 2 years, with spawning beginning in September of the second year and extending through the winter until some time in May or June. The individual is believed to breed once and then to die. If this alternating or 2-phase breeding cycle remained undisturbed, adjacent year classes would be reproductively isolated. There is evidence that a few juveniles of each year breed the following winter, so reproductive isolation of the two coexisting year classes is not complete.

All the specimens taken in the net-tow collections of the *Burton Island* were juveniles ranging in length from 4.5 to 21.5 mm. None of the females had even rudimentary oostegites. The 1950 and 1953 collections were made in August, but the 1951 collections were made from August 12 to September 21. Thus the *Burton Island* collections give no evidence for breeding in August or September, although they may not be truly representative of the *P. libelulla* population. Dunbar (1957) found maturing females in ringed seal stomachs in August 1953 and July 1954, but a 2-meter stramin net hauled at 3 knots failed to collect maturing females during these months.

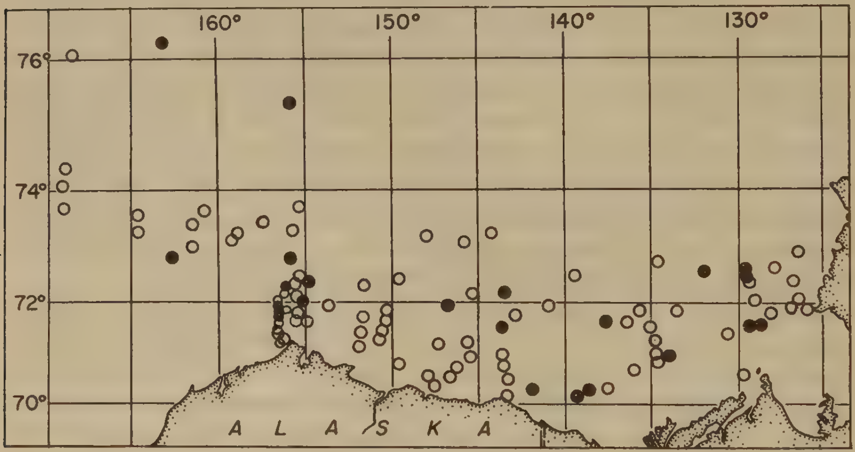

FIGURE 18.—*Parathemisto libellula* (Lichtenstein), distribution in the Chukchi and Beaufort Seas, U.S.S. *Burton Island* 1950 and 1951 cruises combined. Solid circles, positive stations; open circles, negative stations.

Shoemaker (1955) reports a collection of about 1,000 specimens washed ashore at Point Barrow, Alaska, September 12, 1949. I have examined and measured 100 specimens from this lot. They vary in length from 19 to 29 mm., with a mode of 24 mm. Most of the females have minute oostegites less than half the size of those figured by Dunbar (1957, fig. 9) to illustrate the "adolescent" female stage. The males are juveniles with segmented antennae only slightly longer than the head in the largest individuals. Some males as large as 25 mm. had unsegmented antennae. Apparently the breeding season had not arrived.

Several small lots of *P. libellula* from the Bering Sea are present in the collections of the U.S. National Museum, mostly *Albatross* collections made in early August 1893. Juveniles, adolescents, and

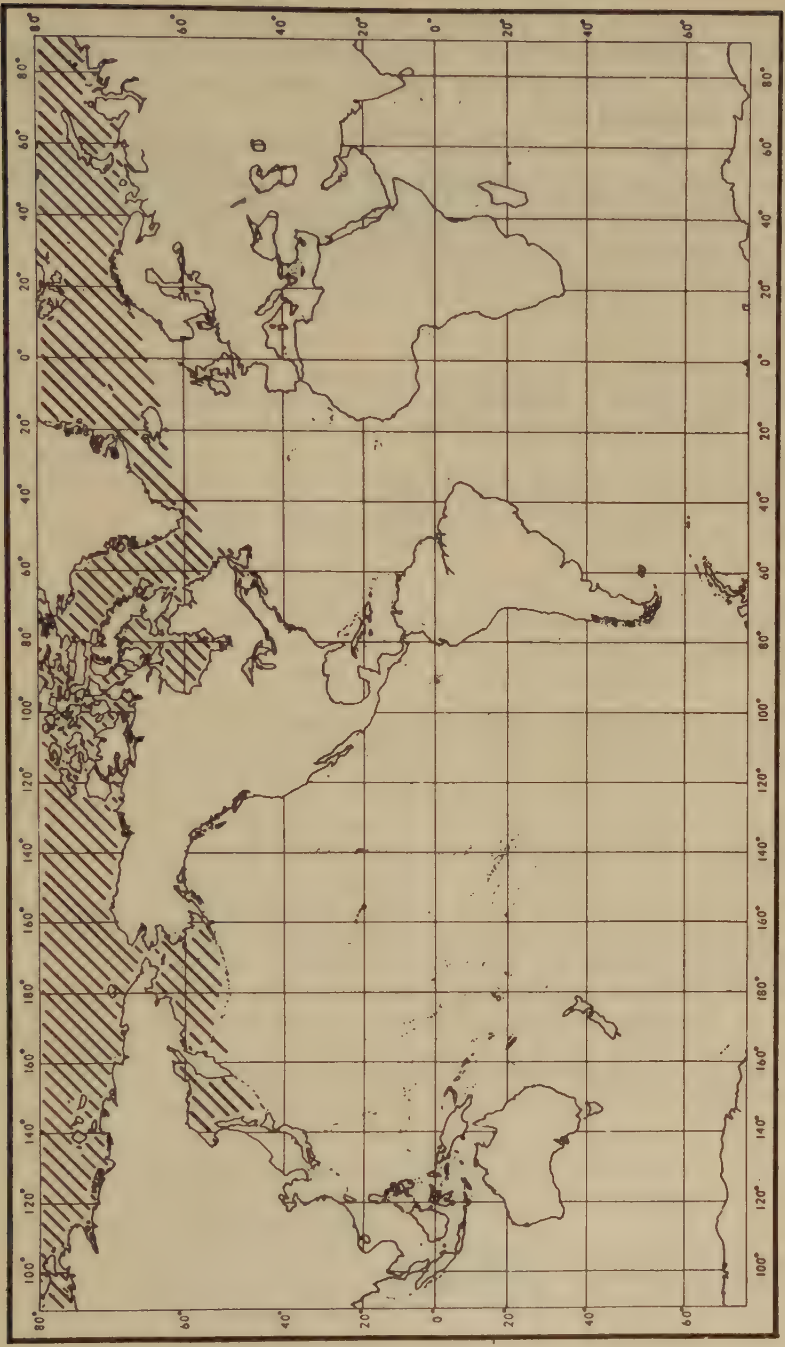
80°
60°
40°
20°
0°
20°
40°
60°
80°
60°
40°
20°
0°
20°
40°
60°
80°
100°
120°
140°
160°
180°
160°
140°
120°
100°

FIGURE 19.—*Parathemisto libellula* (Lichtenstein), world distribution.

maturing females are all present, and at Station 3518 (60°22′ N., 171°42′ W., August 3, 1893) an ovigerous female, 30 mm. in length, was collected. Evidently some breeding takes place during early August in the Bering Sea.

Dunbar's work on the life history of *P. libellula* and his proposed breeding cycle are of considerable interest. Much additional collecting, especially in the winter months, is needed before the validity of his conclusions can be adequately assessed.

Literature Cited

AHLSTROM, ELBERT H.

1948. A record of pilchard eggs and larvae collected during surveys made in 1939 to 1941. U.S. Fish and Wildlife Service, Spec. Sci. Rep., Fisheries, no. 54, pp. 1–76.

1952. Pilchard eggs and larvae and other fish larvae, Pacific Coast, 1950. U.S. Fish and Wildlife Service, Spec. Sci. Rep., Fisheries, no. 80, pp. 1–58.

BARNARD, J. LAURENS

1959. Epipelagic and under-ice Amphipoda of the central Arctic basin. Geophys: Res. Pap. no. 63, Scientific Studies at Fletcher's Ice Island, T-3, 1952–1955, vol. 1, pp. 115–152, pls. 1–23.

BARNARD, K. H.

1930. Crustacea. Part XI. Amphipoda. British Antarctic (*Terra Nova*) Expedition 1910, Nat. Hist. Rep., Zool., vol. 8, no. 4, pp. 307–454.

1932. Amphipoda. *Discovery* reports, vol. 5, pp. 1–326, figs. 1–174 in text, pl. 1 (in color).

BARNES, C. A., and THOMPSON, T. G.

1938. Physical and chemical investigations in Bering Sea and portions of the North Pacific Ocean. Univ. Washington Publ. Oceanog., vol. 3, no. 2, pp. 35–79.

BARY, B. M.

1959. Ecology and distribution of some pelagic Hyperiidea (Crustacea, Amphipoda) from New Zealand waters. Pacific Science, vol. 13, no. 4, pp. 317–334.

BEHNING, A.

1939. Die Amphipoda-Hyperiidea der den Fernen Osten der Ud. SSR umgrenzenden Meere. Intern. Rev. Ges. Hydrobiol. Hydrogr., vol. 38, pp. 353–367, figs. 1–6.

BEKLEMISHEV, K. V., and SEMINA, G. L.

1956. On the structure of the biogeographical boundary between the boreal and tropical regions in the pelagial of the northwestern Pacific Ocean. Doklady Akademii Nauk SSSR, vol. 108, no. 6, pp. 1057–1060 (in Russian, translation by W. G. Van Campen).

BIERI, ROBERT

1959. The distribution of the planktonic Chaetognatha in the Pacific and their relationship to the water masses. Limnol. and Oceanogr., vol. 4, no. 1, pp. 1–28.

BIGELOW, H. B.

1926. Plankton of the offshore waters of the Gulf of Maine. Bull. U.S. Bureau of Fisheries, vol. 40 (1924), pt. 2, pp. 1–509.

BIGELOW, H. B., and SEARS, MARY

1939. Studies of the waters of the Continental Shelf, Cape Cod to Chesapeake Bay, III. A volumetric study of the zooplankton. Mem. Mus. Comp. Zool., vol. 70, pp. 429–581.

Boden, Brian P., Johnson, Martin W., and Brinton, Edward

1955. The Euphausiacea (Crustacea) of the North Pacific. Bull. Scripps Inst. Oceanogr. Univ. California, vol. 6, no. 8, pp. 287–400.

Boeck, Axel.

1870. Crustacea Amphipoda borealia et arctica. Vidensk. Selsk. Forh., pp. 81–200.

Bogorov, B. G.

1940. Longevity and ecological characteristics of *Themisto abyssorum* in the Barents Sea. Doklady Akademii Nauk SSSR, vol. 27, no. 1, pp. 68–70.

1958. Biogeographical regions of the plankton of the north-western Pacific Ocean and their influence on the deep sea. Deep-Sea Research, vol. 5, no. 2, pp. 149–161.

Bogorov, B. G., and Vinogradov, M. E.

1955. On zooplankton of the northwestern part of the Pacific Ocean. Doklady Akademii Nauk SSSR, vol. 102, no. 5, pp. 835–838 (in Russian).

Bonnier, Jules

1896. "Edriophthalmes." Résultats scientifiques de la campagne du "Caudan" dans le Golfe de Gascogne, Août-Septembre, 1895. Ann. Univ. Lyon, vol. 26, pp. 527–689.

Bousfield, E. L.

1951. Pelagic Amphipoda of the Belle Isle Strait region. Journ. Fish. Res. Board Canada, vol. 8, no. 3, pp. 134–163.

Bovallius, Carl

1887. Systematical list of the Amphipoda Hyperiidea. Svenska Vet. Akad. Handl., vol. 11, no. 16, pp. 1–50.

1889. Contributions to a monograph of the Amphipoda Hyperiidea. Pt. I, 2. The families Cyllopodidae, Paraphronimidae, Thaumatopsidae, Mimonectidae, Hyperiidae, Phronimidae, and Anchylomeridae. Svenska Vet. Akad. Handl., vol. 22, pp. 1–434, pls. 1–18.

Brodsky, K. A.

1955a. On the distribution of plankton in the northwestern part of the Pacific Ocean. Doklady Akademii Nauk SSSR, vol. 101, no. 5, pp. 961–964 (in Russian).

1955b. Zoogeographical provinces of the pelagial of far eastern seas and the northern part of the Pacific Ocean. Doklady Akademii Nauk SSSR, vol. 102, no. 3, pp. 649–652 (in Russian).

Bruns, Erich

1958. Ozeanologie. Band I. Einführung in die Ozeanologie. Ozeanographie, Berlin, pp. 1–420.

Bulycheva, A. I.

1955. Hyperiids (Amphipoda-Hyperiidea) of the northwestern part of the Pacific Ocean. Doklady Akademii Nauk SSSR, vol. 102, no. 5, pp. 1047–1050 (in Russian).

Candeias, A.

1934. Crustáceos planctónicos das Costas de Portugal. Mem. Mus. Zool. Univ. Coimbra, ser. 1, no. 75, pp. 1–8.

Chevreux, Edouard

1935. Amphipodes provenant des campagnes scientifiques du Prince Albert I^{er} de Monaco. Résultats des campagnes scientifiques accomplies sur son yacht par Albert I^{er}, Prince Souverain de Monaco, Fasc. 90, pp. 1–214, pls. 1–16.

CLEMENS, HOWARD P.

1950. Life cycle and ecology of *Gammarus fasciatus* Say. Franz Theodore Stone Institute of Hydrobiology, Ohio State Univ., Contrib. no. 12, pp. 1–63.

DUNBAR, M. J.

1946. On *Themisto libellula* in Baffin Land coastal waters. Journ. Fish. Res. Board Canada, vol. 6, no.6, pp. 419–434.

1957. The determinants of production in northern seas: A study of the biology of *Themisto libellula* Mandt. "Calanus" series no 14. Canadian Journ. Zool., vol. 35, no. 6, pp. 797–819.

EALEY, E. H. M., and CHITTLEBOROUGH, R. G.

1956. Plankton, hydrology and marine fouling at Heard Island. Australian National Antarctic Research Expeditions Interim Reports, no. 15, pp. 1–81.

EKMAN, SVEN

1953. Zoogeography of the sea, London, Sidgwick and Jackson, xii + 417 pp.

GUÉRIN, F. E.

1825. Encyclopédie méthodique histoire naturelle. Entomologie ou histoire naturelle des crustacés, des arachnides et des insects. Tome dixième, par MM. Latreille, Le Peletier de Saint-Fargeau, Serville, et Guérin, Paris.

HIDA, THOMAS S.

1957. Chaetognaths and pteropods as biological indicators in the North Pacific. U.S. Fish and Wildlife Service, Spec. Sci. Rep., Fisheries, no. 215, pp. 1–13.

HOLMES, SAMUEL J.

1904. Amphipod crustaceans of the expedition. Harriman Alaska Expedition, vol. 10, pp. 233–246.

HOPKINS, DAVID M.

1959. Cenozoic history of the Bering land bridge. Science, vol. 129, no. 3362, pp. 1519–1528.

HURLEY, DESMOND E.

1955. Pelagic amphipods of the sub-order Hyperiidea in New Zealand waters. 1. Systematics. Trans. Roy. Soc. New Zealand, vol. 33, pt. 1, pp. 119–194.

1956. Bathypelagic and other Hyperiidea from California waters. Occ. Pap. Allan Hancock Foundation, no. 18, pp. 1–25.

IRIE, HARUHIKO

1948. Preliminary report on pelagic amphipods in the adjacent seas of Japan. Journ. Fac. Agric. Kyushu Univ., vol. 9, no. 1, pp. 33–40.

1957a. Pelagic amphipods in the western seas of Kyusyu. Bull. Fac. Fish. Nagasaki Univ., no. 5, pp. 41–52.

1957b. 25 species of pelagic amphipods, Hyperiidea, in the adjacent seas of Japan, Suisangaku Shusei, March 1957, Tokyo Univ. Press, pp. 345–355.

1959. Studies on pelagic amphipods in the adjacent seas of Japan. Bull. Fac. Fish. Nagasaki Univ., no. 8, pp. 20–42.

JOHNSON, MARTIN W.

1934. The production and distribution of zooplankton in the surface waters of Bering Sea and Bering Strait, pt. II, *in* Report of oceanographic cruise U.S. Coast Guard Cutter *Chelan*, 1934, pp. 45–82 (mimeographed).

Johnson, Martin W.

1953. Studies on plankton of the Bering and Chukchi Seas and adjacent areas. Proc. 7th Pacific Sci. Congress (1949), vol. 4, Zoology, pp. 480–500.

1956. The plankton of the Beaufort and Chukchi Sea areas of the Arctic and its relation to the hydrography. Arctic Inst. North America Tech. Pap. no. 1, pp. 1–32.

Kinne, Otto

1953. Zur Biologie und Physiologie von *Gammàrus duebeni* Lillj., I. Zeitschr. Wiss. Zool., vol. 157, pp. 427–491.

1959. Ecological data on the amphipod *Gammarus duebeni*. Monograph, Veröff. Inst. Meeresforschung Bremerhaven, vol. 6, pp. 177–202.

Koizumi, Masami

1953. On the annual variation in oceanographical elements at a fixed point (39° N, 153° E) in the Pacific Ocean. Rec. Oceanogr. Works Japan, n.s., vol. 1, no. 1, pp. 36–43.

Lafond, E. C., and Pritchard, D.W.

1952. Physical oceanographic investigations in the eastern Bering and Chukchi Seas during the summer of 1947. Journ. Marine Res., vol. 11, no. 1, pp. 69–86.

Mandt, Martin W.

1822. Observationes in historium naturalem et anatomiam comparatum in itinere Groenlandico factae, Dissertatio inauguralis, Berlin, viii + 40 pp.

Marshall, Sheina M., and Orr, A. P.

1955. The biology of a marine copepod, *Calanus finmarchicus* (Gunnerus), London, Oliver and Boyd, viii + 186 pp.

Masuzawa, Jotaro

1955. Preliminary report on the Kuroshio in the Eastern Sea of Japan (currents and water masses of the Kuroshio system III). Rec. Oceanogr. Works Japan, n.s., vol. 2, no. 1, pp. 132–140.

Mogk, H.

1926. Versuch einer Formanalyze bei Hyperiden. (Zugleich ein Beitrag zu einer neuer Methode der Artbeschreibung). I. Vorarbeiten an der Gattung *Phronima*. Intern. Rev. Ges. Hydrobiol. Hydrogr., vol. 14, pp. 276–311.

Nakai, Zinziro

1955. The chemical composition, volume, weight, and size of the important marine plankton. Tokai Regional Fisheries Research Laboratory, Spec. Publ. no. 5, pp. 12–24.

Norman, A. M.

1869. Last report on dredging among the Shetland Isles. Pt. 2. Crustacea. Rep. British Assoc. Adv. Sci. for 1868, pp. 247–336.

Pirlot, Jean M.

1929. Résultats zoologiques de la croisière *Atlantique* de l' *Armauer Hansen* (Mai-Juin 1922). 1. Les amphipodes hypérides. Travaux de l'Institut Université de Liége, fasc. 1., pp. 1–196. [Memoires de la Societé royale des Sciences de Liége 3ᵉ série, tome 15, fasc. 2].

1939. Sur des amphipodes hypérides provenant des croisières du Prince Albert Iᵉʳ der Monaco. Résultats des campagnes scientifiques accomplies sur son yacht par Albert Iᵉʳ, Prince Souverain de Monaco, fasc. 102, pp. 1–63, pls. 1–2.

(992)

ROBINSON, MARGARET K.

1957. Sea temperature in the Gulf of Alaska and in the northeast Pacific Ocean, 1941–1952. Bull. Scripps Inst. Oceanogr., vol. 7, no. 1, pp. 1–98, figs. 1–61, 1 chart.

ROUX, M. L. le,

1933. Recherches sur la sexualité des gammariens. Croissance, reproduction, determinisme des caractères sexuels secondaires. Bull. Biol. France Belg. Supp. no. 16, pp. 1–138.

RUSSELL, F. S.

1925. The vertical distribution of marine macroplankton. An observation of diurnal changes. Journ. Mar. Biol. Assoc., n.s., vol. 12, no. 4, pp. 769–809.

SARS, G. O.

1895. An account of the Crustacea of Norway, vol. 1, Amphipoda, pp. 1–711, pls. 1–240, suppl. pls. 1–8.

SEGERSTRÅLE, SVEN G.

1937. Studien über die Bodentierwelt in südfinnländischen Küstengewassern III. Zur Morphologie und Biologie des Amphipoden *Pontoporeia affinis*, nebst einer Revision der *Pontoporeia*-Systematik. Soc. Sci. Fennica Commentationes Biol., vol. 7, no. 1, pp. 1–183, pls. 1–19.

SEWELL, R. B. SEYMOUR

1948. The free-swimming planktonic Copepoda, geographical distribution. John Murray Exped., Sci. Rep., vol. 8, no. 3, pp. 317–592, 2 charts.

SEXTON, E. W.

1924. The moulting and growth stages of *Gammarus*, with descriptions of the normals and intersexes of *G. chevreuxi*. Journ. Mar. Biol. Assoc., n.s., vol. 13, pp. 340–397, pls. 1–21.

1928. On the rearing and breeding of *Gammarus* in laboratory conditions. Journ. Mar. Biol. Assoc., n.s., vol. 15, pp. 33–55.

SHOEMAKER, CLARENCE R.

1920. Crustacea. Part E: Amphipods. Rep. Canadian Arctic Exped. 1913–18, vol. 7, pp. 1–30.

1926. Report on the marine amphipods collected in Hudson and James Bays by Fritz Johansen in the summer of 1920. Contrib. Canadian Biol. and Fish., vol. 3, no. 1, pp. 1–11.

1930. The amphipods of the Cheticamp Expedition of 1917. Contrib. Canadian Biol. and Fish., vol. 5, no. 10, pp. 221–359.

1955. Amphipoda collected at the Arctic Laboratory, Office of Naval Research, Point Barrow, Alaska, by G. E. MacGinitie. Smithsonian Misc. Coll., vol. 128, no. 1, pp. 1–78.

SIMPSON, GEORGE GAYLORD

1947a. Evolution, interchange, and resemblance of the North American and Eurasian Cenozoic mammalian faunas. Evolution, vol. 1, no. 3, pp. 213–220.

1947b. Holarctic mammalian faunas and continental relationships during the Cenozoic. Bull. Geol. Soc. Amer., vol. 58, pp. 613–687.

STEBBING, T. R. R.

1888. Report on the Amphipoda collected by H. M. S. *Challenger* during the years 1873–1876. Rep. Sci. Res. Voyage of H.M.S. *Challenger*, Zool., vol. 29, pt. 67, xxiv+1737 pp., 210 pls., 1 map.

STEPANOVA, V.
1937. Biologische Zeichnungen der Stromungen im Nordischen Teil des Bering und im Sudlichen Teil des Tschuktschen Meeres. Publ. Hydrol. Inst. Lenningrad, no. 5, pp. 176–216.

STEPHENSEN, K.
1923. Crustacea Malacostraca V (Amphipoda I). The Danish *Ingolf* Exped., vol. 3, pt. 8, pp. 1–100, figs. 1–22.
1924. Hyperiidea—Amphipoda (pt. 2: Paraphronimidae, Hyperiidae, Dairellidae, Phronimidae, Anchylomeridae). Rep. Danish Oceanographic Exped. 1908–1910 to the Mediterranean and adjacent seas, vol. 2, D. 4, pp. 71–149.
1933. Amphipoda. The Godthaab Expedition 1928. Medd. Grønland, vol. 79, no. 7, pp. 1–88.
1944. Amphipoda. Zoology of East Greenland. Medd. om Grønland, vol. 121, no. 14, pp. 1–165.
1947. Tanaidacea, Isopoda, Amphipoda, and Pycnogonida. Sci. Res. Norwegian Antarctic Exped. 1927–1928 et seq., no. 27, pp. 1–90.
1949. The Amphipoda of Tristan da Cunha. Res. Norwegian Sci. Exped. to Tristan da Cunha 1937–1938, no. 19, pp. 1–61.

STEWART, DORTHY
1913. A report on the Extra-Antarctic Amphipoda Hyperiidea collected by the *Discovery*. Ann. Mag. Nat. Hist., ser. 8, vol. 12, pp. 245–265, pls. 4–7.

SVERDRUP, H. U.; JOHNSON, MARTIN W.; AND FLEMING, RICHARD H.
1946. The oceans, their physics, chemistry, and general biology, x+1087 pp., 7 charts.

TANAKA, OTOHIKO
1953. The pelagic copepods of the Izu region. Rec. Oceanogr. Works Japan, n.s., vol. 1, no. 1, pp. 126–137.

THORSTEINSON, ELSA D.
1941. New or noteworthy amphipods from the North Pacific coast. Univ. Washington Publ. Oceanogr., vol. 4, pp. 50–94.

TOKIOKA, TAKASI
1940. The chaetognath fauna of the waters of western Japan. Rec. Oceanogr. Works Japan, vol. 12, no. 1, pp. 1–22, charts 1–3.

UDA, MITITAKA
1934. Hydrographical studies based on simultaneous oceanographical surveys made in the Japan Sea and in its adjacent waters during May and June, 1932. Rec. Oceanogr. Works Japan, vol. 6, no. 1, pp. 19–107.

VINOGRADOV, M. E.
1956. Hyperiids (Amphipoda-Hyperiidea) of the western Bering Sea. Zool. Journ. Acad. Nauk SSSR, vol. 35, fasc. 2, pp. 194–218 (in Russian).

WAILES, G. H.
1929. Marine zoo-plankton of British Columbia. Museum and Art Notes, Vancouver, vol. 4, pp. 1–9.

YAMADA, TETUO
1933. Report on the distributions of the plankton in the neighboring seas of Tyosen in June, 1932. Ann. Rep. Hydrographical Observations, Fishery Experiment Station, Government General of Tyosen, no. 7, appendix (in Japanese).

(994)

U.S. GOVERNMENT PRINTING OFFICE: 1960

Reprinted by permission from

McGRAW-HILL ENCYCLOPEDIA OF SCIENCE AND TECHNOLOGY

Copyright © 1960 McGraw-Hill Book Co., Inc.

PACIFIC OCEAN

By

Joseph Reid

Pacific Ocean

The Pacific Ocean has an area of 165,000,000 square kilometers and a mean depth of 4282 km. It covers 32% of the earth's surface and 46% of the surface of all oceans and seas, and its area is greater than that of all the land areas combined. Its mean depth is the greatest of the three oceans and its volume is 53% of the total of all oceans. Its greatest depths in the Marianas and Japan trenches are the world's deepest, more than 10 km (Fig. 1).

Surface currents. The two major wind systems driving the waters of the ocean are the westerlies which lie about 40–50° latitude in both hemispheres (the "roaring forties") and the trade winds from the east which dominate in the region between 20°N and 20°S. These give momentum directly to the west wind drift (flow to the east) in high latitudes and to the equatorial currents which flow to the west. At the continents there is flow of water from one system to the other and huge circulatory systems result (Fig. 2).

The swiftest flow (greater than 2 knots) is found in the Kuroshio Current near Japan. It forms the northwestern part of a huge clockwise gyral whose north edge lies in the west wind drift centered at about 40°N, whose eastern part is the south-flowing California Current, and whose southern part is the North Equatorial Current.

Part of the west wind drift turns northward into the Gulf of Alaska, thence westward again and into the Bering Sea, returning southward off Kamchatka and northern Japan where it is called the Oyashio Current.

H. U. Sverdrup (1942) has reported estimates of the flow in the North Pacific in the upper 1500 meters. The Kuroshio carries about 65,000,000 m^3/sec at its greatest strength off Japan. The west wind drift in mid-ocean carries about 35,000,000, the California Current east of 135°W carries about 15,000,000, and the North Equatorial Countercurrent about 45,000,000.

A gyral corresponding to the Kuroshio-California-North Equatorial current gyral is found in the Southern Hemisphere. Its rotation is counterclockwise, with the highest speeds (about 2 knots) in the Southeast Australia Current at about 30°S. The current turns eastward and flows around New Zealand to South America, where it turns northward. Along this coast it has been called the Humboldt or the Peru Current. It turns westward at the Equator and is known as the South Equatorial Current in its westward flow. It is to be remarked that the northwestern edge of this gyral is severely confused by the chain of islands extending southeastward from New Guinea to New Zealand, which partly isolate the Coral and Tasman Seas from the rest of the South Pacific, so that the western equatorial edge of the gyral is not so regular in shape nor so clearly defined as its northern counterpart. *See* SOUTHEAST ASIAN WATERS.

In the region of the west wind drift in the South Pacific the ocean is open both to the Indian and the Atlantic, although the eastward passage to the Atlantic through Drake Passage is narrower and shallower than the region between Australia and Antarctica. Part of the water flows, however, all around Antarctica with the wind behind it, and it receives more momentum than its northern counter-

Contributions from the Scripps Institution of Oceanography, New Series, 1220

Reproduced by Permission

part. The total transport is several times greater. G. E. R. Deacon (1937) has estimated the transport to the east in the South Pacific part of the west wind drift as more than 100,000,000 m^3/sec in the upper 3000 m. Sverdrup estimates only about 35,000,000 m^3/sec for the upper 1500 m in the North Pacific west wind drift. The gyral corresponding to the Oyashio-Gulf of Alaska gyral of the North Pacific is thus vaster in transport and area, since much of it passes around Antarctica. *See* ANTARCTIC OCEAN; INDIAN OCEAN.

Between the two subtropical anticyclones (Kuroshio-California-North Equatorial Current and the Southeast Australia-Peru-South Equatorial Current) lies an east-flowing current between about 5° and 10°N, called the Equatorial Countercurrent. Sverdrup has estimates of flow of 25,000,000 m^3/sec for this current. Some of the observed set and drift of vessels in the area suggest that there is also an eastward flow along 10°S from 155°E to 180° from November through April.

Within the upper 1000 m the flow of water is generally parallel to the surface flow, but slower. Certain important exceptions occur. Beneath the surface waters of the California and Peru Currents, at depths of 200 m and below, countercurrents have been found, in which some part of the tropical waters are carried poleward. In the California Current this flow reaches to the surface in December, January, and February, and it is known as the Davidson Current north of 35°N. It is not known whether a surface poleward flow occurs in southern winter in the Peru Current.

Recent direct measurements at the Equator and 140°W have revealed that a subsurface flow to the east is found at least from 140°W to 90°W, with highest velocities at depths of about 100 m. Speeds as high as 2–3.5 knots to the east were found at

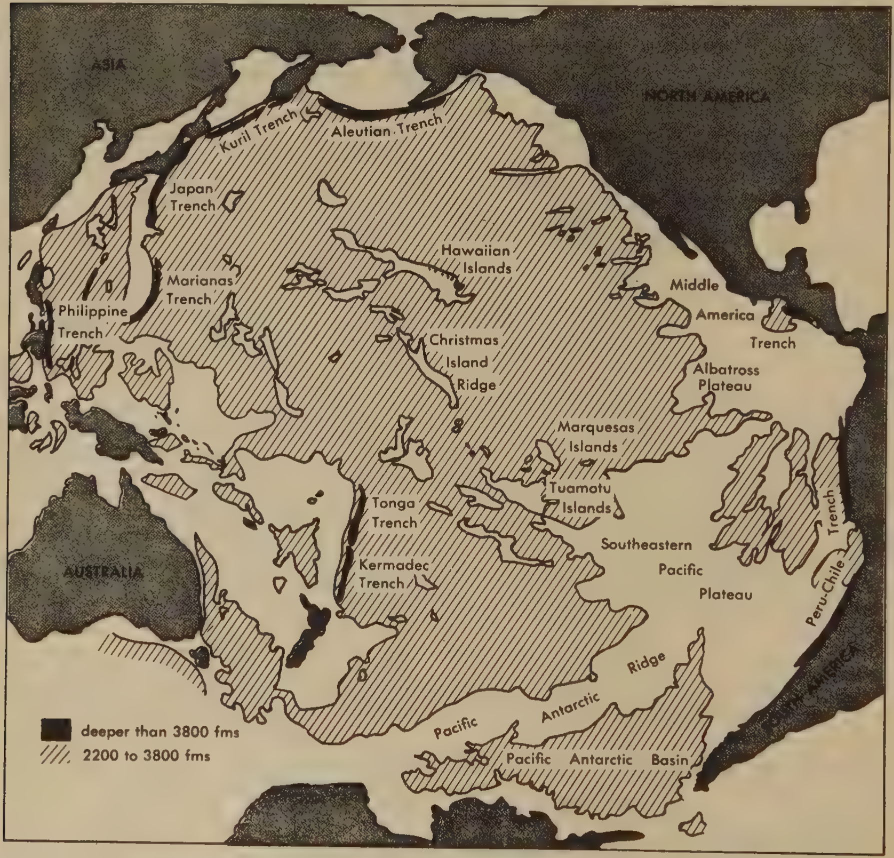
ASIA
NORTH AMERICA
Kuril Trench
Aleutian Trench
Japan Trench
Hawaiian Islands
Marianas Trench
Philippine Trench
Middle America Trench
Christmas Island Ridge
Albatross Plateau
Marquesas Islands
Tuamotu Islands
Tonga Trench
Kermadec Trench
Southeastern Pacific Plateau
Peru-Chile Trench
AUSTRALIA
Pacific Antarctic Ridge
Pacific Antarctic Basin
SOUTH AMERICA
■ deeper than 3800 fms
▨ 2200 to 3800 fms

Fig. 1. The principal relief features of the Pacific Ocean. Trenches slightly exaggerated in scale. (From *F. P. Shepard, The Earth Beneath the Sea, Johns Hopkins, 1959*)

this level while the upper waters (South Equatorial Current) were flowing west at 0.5–1.5 knots. It has been suggested that this equatorial undercurrent be called the Cromwell Current, after its discoverer. *See* OCEAN CURRENTS.

Temperature at the sea surface. Equatorward of 30° latitude the heat received from the sun exceeds that lost by reflection and back radiation, and surface waters flowing into these latitudes from higher latitudes (California and Peru Currents) increase in temperature as they flow equatorward and turn west with the Equatorial Current System. They carry heat poleward in the Kuroshio and Southeast Australia Currents and transfer part of it to the high-latitude cyclones (Oyashio-Gulf of Alaska Gyral and Antarctic Circumpolar Current) along the west wind drift. The temperature of the equatorward currents along the eastern boundaries of the subtropical anticyclones is thus much lower than that of the currents of their western boundaries at the same latitudes. Heat is accumulated, and the highest temperatures (more than 28°C) are found at the western end of the equatorial region (Fig. 3). Along the Equator itself somewhat lower temperatures are found. The cold Peru Current contributes to its eastern end, and there is apparent upwelling of deeper, colder water at the Equator, especially at its eastern end (as low as 19°C in February at 90°W) as a result of the divergence in the wind field.

Upwelling also occurs at the edge of the eastern boundary currents of the subtropical anticyclones. When the winds blow strongly equatorward (in summer) the surface waters are driven offshore, and the deeper colder waters rise to the surface and further reduce the low temperatures of these equatorward-flowing currents. The effect of these seasonal variations in the winds is thus to reduce the seasonal range of temperature, since the upwelling occurs in spring and summer. The seasonal range of nearshore surface temperature of the California Current at 35°N is less than 4C° (9–13°C), though the latitudinal mean is about 10°C. The equatorward winds off Japan occur in winter and the poleward in summer, so that seasonal range is increased at that latitude to more than 16C° (10–26°C).

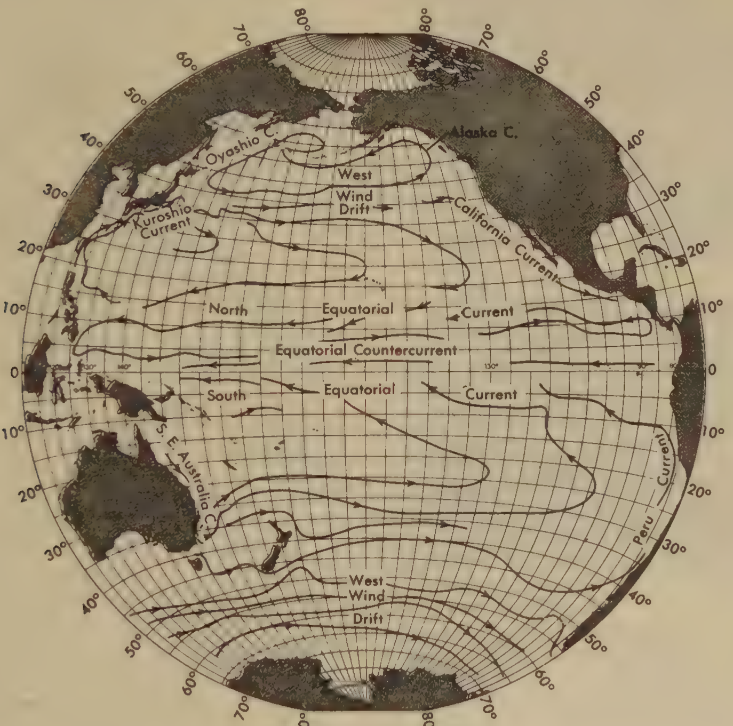

Fig. 2. The principal currents of the Pacific Ocean. Prepared from computations of geostrophic flow at the sea surface relative to 1000 decibars, using data from the NORPAC, EQUAPAC, *Carnegie*, and *Discovery* expeditions.

The temperatures at the surface of the South Pacific Ocean have not been nearly so well documented, since most of the information comes from measurements made by merchant vessels, and the commercial shipping lines cover but a small part of its great extent. It may be reasoned that most of the temperature characteristics of the North Pacific will have analogies in the Southern Hemisphere. The damped seasonal variation of the California Current seems to occur in the Peru Current as well. But the temperatures of the Southeast Australia Current do not seem to vary so widely through the year as those of the Kuroshio, probably because of the restrictions upon the flow which are imposed by the islands.

The limiting temperature in high latitudes is that of freezing. Ice is formed at the surface at temperatures slightly less than −1°C depending upon the salinity; further loss of heat is retarded by its insulating effect. The ice field covers the northern and eastern parts of the Bering Sea in winter, and most of the Sea of Okhotsk, including that part adjacent to Hokkaido (the north island of Japan). Summer temperatures, however, reach as high as 6°C in the northern Bering Sea and as high as 10° in the northern part of the Sea of Okhotsk.

Pack ice reaches to about 62°S from Antarctica in October and to about 70°S in March, with icebergs reaching as far as 50°S. *See* Bering Sea; Iceberg; Sea ice.

Salinity at the sea surface. The highest values of salinity observed in the Pacific Ocean are slightly greater than 35.5 and 36.5 parts per thousand (‰), found respectively in the surface water of the centers of the north and south subtropical anticyclones. These anticyclones cover the latitudes in which evaporation exceeds precipitation, and the overlying anticyclonic winds oppose outward flow at the sea surface. The three regions where precipitation most strongly exceeds evaporation are found poleward of 40° latitude and in the eastern tropical Pacific. The result is that the high-latitude cyclones are regions of low salinity (as low as 32.5 ‰ in the north, 33.8 in the south) which, through mixing with the anticyclones in the region of the west

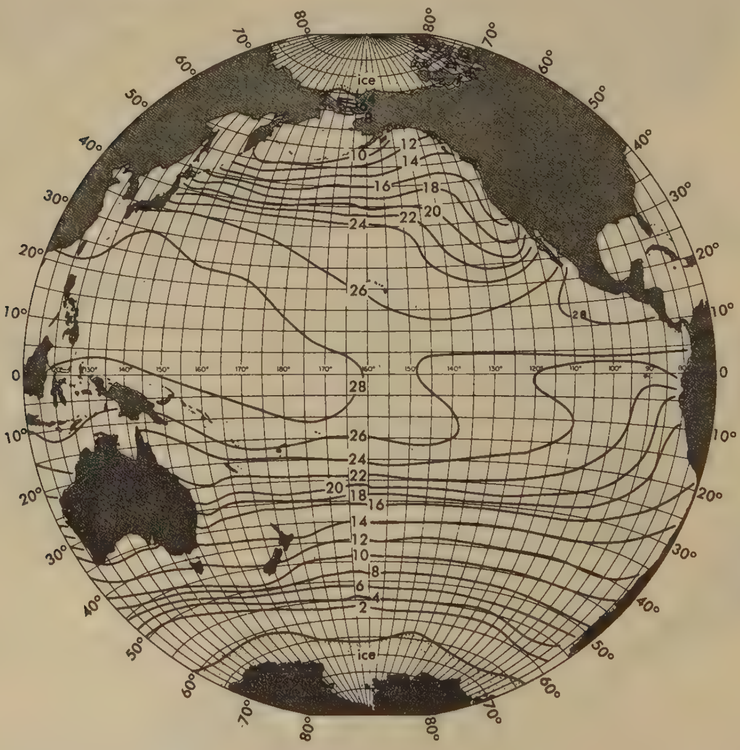

Fig. 3. Temperature at the sea surface in August in degrees C. (*Adapted from U.S. Navy Hydrographic Office, H. O. Publ. 225, 1948*)

wind drift, contribute water of low salinity to the eastern boundary currents (off California and South America). The greater part of the effect of the eastern tropical precipitation is found at the surface of the North Equatorial Current and Countercurrent. Near Central America the values are less than 33 ‰ at 10°N, but they rise nearly to 34.5 near the Philippine Islands.

Dissolved oxygen at the sea surface. Above the thermocline the water is in continual overturn and is thus in constant contact with the atmosphere. Oxygen from the atmosphere dissolves in the water until equilibrium is established, and over most of the Pacific the upper layer is very close to saturation in oxygen content with typical values from about 98 to 103% of the saturation value. *See* THERMOCLINE.

The saturated value of dissolved oxygen rises as both the temperature and salinity fall, but the range of surface temperature in the ocean accounts for a wider variation in saturated value than does that of surface salinity, and it is principally the variation in space and time of surface temperature which accounts for the oxygen values at the surface. Values greater than 7 ml/liter are found in the cold waters of high latitudes and less than 5 in the warm regions near the Equator.

Nutrients at the sea surface. Nutrients such as inorganic phosphate-phosphorus, silicate-silicon, and nitrate generally increase from the sea surface downward, since photosynthesis and growth in the upper mixed layer tend to use such quantities as are there, and diffusion upward from the higher concentrations is limited by the great stability usually found immediately below the surface layer. At the surface phosphate-phosphorus varies from less than 0.25 microgram-atoms (μg-atoms) per liter in the centers of the anticyclones to more than 1.5 in the high-latitude cyclones. High values are also found in the California and Peru Currents. In a manner similar to the low temperatures found there, their high concentrations are partly the result of transport of mixed water from the cyclones and partly the result of upwelling at the coasts under equatorward winds. Values greater than 1 μg-atom/liter are found in both areas during the summer period of upwelling. At the Equator in the eastern Pacific upwelling raises the values to more than 1 throughout the year.

Silicate-silicon has not been so extensively measured. It also is low in value at the surface and increases with depth. Surface values range from as high as 40 μg-atoms/liter in the high-latitude cyclones and 12 in the upwelling regions of the California Current, to 4 or less in the center of the anticyclones and to values too small to be detected near the Equator in the eastern region.

Distribution of properties with depth. The surface waters in high latitudes are colder and heavier than those in low latitudes. As a result some of the high-latitude waters sink below the surface and spread equatorward, mixing mostly with water of their own density as they move and eventually providing the dominant water type (in terms of salinity and temperature) of that density over vast regions (Fig. 4).

The deep and bottom water of all oceans is believed to be formed in the Atlantic high latitudes

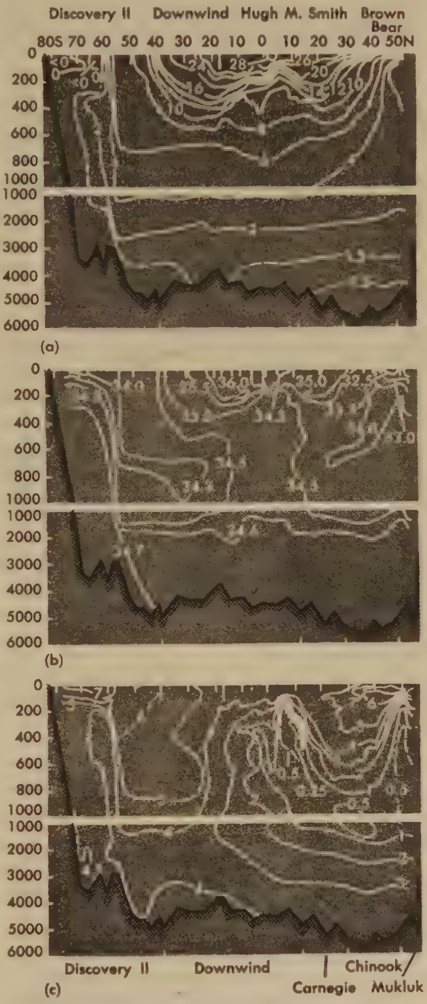

Fig. 4. Vertical sections of (a) temperature in degrees C, (b) salinity in parts per thousand, and (c) dissolved oxygen in milliliters per liter in the central Pacific Ocean, approximately along the meridian 160°W, from Alaska (right) to Antarctica (left). Depths are in meters. Depth scale is expanded in upper 1000 meters. Data from *Carnegie* expedition, NORPAC and EQUAPAC expeditions, *Discovery* expeditions, and Chinook, Mukluk, and Downwind expeditions.

off Greenland and in the Weddell Sea. It arrives in the South Pacific with temperature less than 2°C, salinity about 34.65–34.7‰, and oxygen about 4.5 ml/liter. The waters filling the Pacific below 3000 m retain these values of temperature and salinity everywhere, but in the northern part the oxygen is reduced to values between 2.5 and 3.5. This would be consistent with depletion by decay and respiration during a slow movement to the north.

Over most of the North Pacific Ocean the temperature does not decrease all the way to the bottom, but beneath a minimum value at about 3800–4000 m it rises again. The increase in temperature is probably in close balance with that in pressure, since no evidence has been found of instability. Two possible explanations for the temperature maximum at the bottom are the flow of heat upward from the ocean floor and an adiabatic rise in temperature as the water flows downward into the deeper basins.

The most conspicuous water masses formed in the Pacific are the Intermediate Waters of the North and of the South Pacific, which on the vertical sections include the two huge tongues of low salinity extending equatorward beneath the surface from about 55°S and from about 45°N. The southern tongue is higher in salinity and density and lies at a greater depth, since the surface waters of the high-latitude cyclone are more saline in the south than in the north.

It has been observed that the higher salinities are found at the surface in the anticyclones. The highest values are in the equatorward halves of the anticyclones. High values penetrate the base of the mixed layer, and tongues of high salinity extend in the thermocline toward the Equator from both north and south.

Beneath the mixed layer the waters are not in contact with the atmosphere and the oxygen consumed cannot be replaced directly from the atmosphere. The oxygen quickly falls below the saturated value. Even where high values of oxygen accompany the sinking of water masses, as in the South Pacific Intermediate Water, the oxygen is not in saturation below 300 m.

Between the saturated waters of the surface and the cold bottom waters entering from the south lies a minimum value of oxygen. Beneath the tongue of high oxygen associated with the South Pacific Intermediate Water the minimum is only a little less than 4 ml/liter. Beneath the North Pacific Intermediate Water, however, no water as high as 3.5 is found, and in the minimum itself values less than 0.5 occur over large areas. The values of oxygen beneath the surface are the result of consumption by organisms and replenishment by mixing and renewal of the water. Since at any position the values are nearly constant in time, consumption must everywhere equal replenishment by both flow and diffusion.

Phosphate-phosphorus increases rapidly beneath the sea surface to a maximum which usually lies beneath the oxygen minimum. In regions of upwelling and divergence, higher values of phosphate and other nutrients from depth may from time to time be brought to the surface and thus made available to the plants. Such regions (California and Peru Currents, South Equatorial Current) are highly productive. The values gradually diminish beneath the maximum, to about 2.5 μg-atoms/liter at the bottom in the north and slightly less than 2 in the south. The maximum value is greater than 3.5 in the north and between 2 and 2.5 in the south.

It is to be noted that the Pacific Ocean is higher in phosphate concentration than the Atlantic or Indian oceans, exceeding the Atlantic by about 1 μg-atom/liter on the average, though the values at the surface do not differ so much. This excess, like the lower value of oxygen, is undoubtedly related to the deep circulation.

Nitrate-nitrogen is present in the ratio of approximately 8:1 by weight of phosphate-phosphorus in those areas where it has been measured, but otherwise the details of its distribution are not so well known.

Silicate-silicon has also not been adequately sampled. Its vertical distribution parallels that of phosphate-phosphorus except that beneath the level of the phosphate maximum it remains nearly constant, at about 170 μg-atoms/liter in the center of the northern anticyclone, as high as 220 in the Bering Sea, about 130 in the center of the southern anticyclone. Silicate-silicon, like phosphate-phosphorus, is more highly concentrated in the Pacific than in the Indian and Atlantic oceans. *See* MARINE SEDIMENTS; OCEANOGRAPHY; SEA WATER; SEA WATER FERTILITY; SUBMARINE TOPOGRAPHY.

[J.L.R.]

Bibliography: G. E. R. Deacon, *Discovery Reports*, vol. 15, 1937; *Discovery Investigations Station List 1931–1933*, vol. 21, 1941; J. A. Fleming et al., *Scientific Results of Cruise VII of the Carnegie during 1928–29*, Carnegie Inst. Washington Publ. 545, Oceanog. vol. I-B, 1945; E. Kossinna, *Die Tiefen des Weltmeeres*, 1921; NORPAC committee, *Oceanic Observations of the Pacific: 1955*, 1959; *Oceanic Observations of the Pacific: -1956* (The EQUAPAC data), in press; *Oceanic Observations of the Pacific: 1956, 1957, 1958* (The Chinook, Mukluk and Downwind data), in press; H. U. Sverdrup, M. W. Johnson, and R. H. Fleming, *The Oceans*, 1942.

Reprinted from Copeia, 1960(2), June 29, 1960: 101-112, figs. 1-6, pl. 1. Reprint 546.

Potamarius, a new Genus of Ariid Catfishes from the Fresh Waters of Middle America[1]

CARL L. HUBBS AND ROBERT RUSH MILLER

(1001)

(1002)

Potamarius, a new Genus of Ariid Catfishes from the Fresh Waters of Middle America[1]

Carl L. Hubbs and Robert Rush Miller

INCREASING knowledge of the fish fauna of the peninsula-like connection between North and South America supports the concept of a distinctive Middle American fauna (Miller, 1959). Within this area great richness and diversity characterize the widespread Poeciliidae and, in a more limited region, the endemic family Goodeidae; also, to a lesser extent, cichlids referred to *Cichlasoma* and derived genera, freshwater atherinids (especially *Chirostoma*), and pimelodid catfishes of the genus *Rhamdia*. Although endemic genera and species of ictalurid catfishes have been described from México, no indigenous genus of the essentially marine Ariidae has heretofore been named from Middle America.

In addition to derivatives of immigrants from Nearctic and Neotropical regions, the faunally unsaturated fresh waters of Middle America have become populated by fishes from adjacent marine waters. Notable among these are the atherinids and very possibly the goodeids, already mentioned, and a considerable number of representatives of other families, including at least two hemiramphids, a peculiar gerrid described as *Gerres mexicanus* Steindachner, several eleotrid gobies and several pipefishes (Syngnathidae), the endemic toadfish (*Batrachoides goldmani* Evermann and Goldsborough), and several clingfishes of the genus *Gobiesox* (Briggs and Miller, 1960). In addition to the wholly or essentially freshwater species *Arius melanopus* Günther, with subspecies *A. m. melanopus* and *A. m. aguadulce* (Meek), the marine Ariidae have contributed to the Middle American freshwater fauna the peculiar genus herein described.

The new genus comprises two species, one of which has been misplaced by most workers in the South American pimelodid genus *Conorhynchos*. Breder (1935:161–162), however, referred it to the Ariidae, and Gosline (1945:9), on the advice of the senior author, indicated that it represents a distinct genus of that family.

Potamarius, gen. nov.

Type species.—Conorhynchos nelsoni Evermann and Goldsborough, 1902.

---

[1] Contributions from the Scripps Institution of Oceanography, New Series, and from the Museum of Zoology of the University of Michigan.

Contributions from the Scripps Institution of Oceanography, New Series, 1221

Reproduced by Permission

Diagnosis.—Ariid catfishes having the minute conical teeth restricted to rather short villous bands on premaxillaries and dentaries; the snout particularly narrow, depressed, and elongate (as long as or longer than the postorbital), not at all gibbous, produced, or elevated above the thick upper lip; lower jaw sharply included, with heavy lips; mouth narrow and small, with essentially transverse gape; barbels (one maxillary pair and two mental pairs) short; eye small, above middle of head; gill-membranes broadly V-shaped, but with a wide free border medially; rakers of moderate length and number (14 to 18 on first arch, with 8 to 11 below the angle); dorsal with strong spine, smooth along front and with obsolescent denticulations behind (the minute denticulations barely project out of the posterior furrow of the spine), and with 6 soft-rays (the last double); adipose moderately large, originating somewhat behind the anal origin; anal fin short and high, with 15 to 21 rays; principal caudal rays 7 + 8 = 15; pectoral rays I, 10 (rarely I, 9); pelvic rays 6; vertebrae 52 to 54 (including five modified vertebrae and the hypural complex).

Range.—Quiet fresh waters of Middle America: through the Río Usumacinta system of Guatemala and México and in Lago de Izabal on the east coast of Guatemala (Fig. 6).

Distinction from Conorhynchos.—*Potamarius* differs from *Conorhynchos*, in which South American pimelodid genus the type species (*nelsoni*) has almost consistently been misplaced, in many features of major systematic import (the comparison is made with a single adult female of *Conorhynchos conirostris* (Valenciennes), 402 mm. in standard length, UMMZ 147403, from lakes of Caripós, Pernambuco, Brazil). The anterior and posterior nostrils of each side are much less widely separated, by an interval only about as great as the length of either nostril, with no intervening bone; the principal caudal rays number 15 (7 + 8) instead of 17 (8 + 9); there is a transverse system of lateral-line neuromasts, which is lacking in *Conorhynchos* and all other pimelodids; the ovaries are more baglike and the ova are few and extremely large, instead of numerous and minute; the pelvic fin of the female is modified for the transfer of the eggs into the mouth of the male; there is an axillary pore (lacking in *Conorhynchos*); the body posteriorly is subterete instead of sharply compressed; the anal fin is shorter and relatively higher; the adipose fin originates over the front rather than the rear part of the anal base; the serrulations of the dorsal spine are obsolescent; the dorsal soft-rays number 6 instead of 5 (last two elements counted as one ray); the muzzle though narrow is depressed and straight, instead of being tubelike and decurved; the gill-membranes medially are broadly V-shaped instead of abruptly U-shaped and have a well-developed rather than incipient free fold. The resemblances in the edentulous palate, long and narrow snout, thick lips, small mouth, and short barbels are surely minor convergences, not indicative of direct phylogenetic relationship. Several of the trenchant differences denote not only generic but also family separation.

Reference to Ariidae.—*Potamarius* agrees with the diagnoses of the Ariidae by Regan (1911:557–558) and by Weber and de Beaufort (1913:271), but not with that of Berg (1940:447), since the palate is not toothed. But this region is edentulous also in several genera of certain Old World regions, for example, India (Day, 1878–88:440–468), the East Indies (Weber and de Beaufort, 1913: 272), and Thailand (Smith, 1945:404). Characteristics of the Ariidae, all shared by both species of *Potamarius*, include: (1) the anterior and posterior nostrils of each side are separated only by the respective valves and a narrow bridge of boneless tissue; (2) there are no nasal barbels; (3) oral gestation is practiced by males (in most if not all species of the family); (4) in correlation with the oral gestation, the buccal cavity of the males becomes greatly enlarged (Fig. 1); (5) the pelvic fins of the mature females are modified by hard, transitory protuberant ridges that presumably facilitate the passage of the eggs from the oviduct to the mouth of the males; (6) the ovaries are baglike and the ova are relatively immense; (7) transverse branches of the lateral line are marked by single files of neuromasts, and in life by rows of silvery specks (Fig. 2) that run across the body above and below; and (8) the gill-membranes are united, and are attached to the isthmus so as to leave a wide, free fold. The 6-rayed pelvics may be another, but not exclusive family character, and some of the other ray numbers, particularly of the caudal and dorsal soft-rays, may prove to have broad systematic value. As a group, the ariids occur chiefly along sandy and muddy shores and in coastal lagoons and estuaries, in tropical and subtropical regions. Some species freely enter fresh waters and a few, like the two species

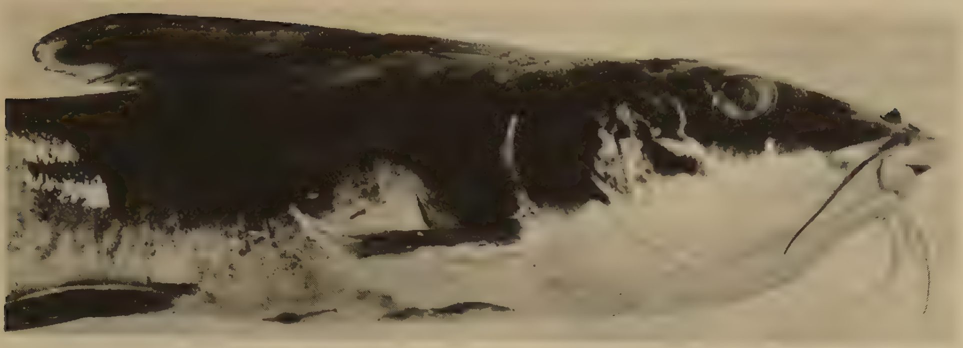

FIG. 1.—Lateral view of anterior parts of a brooding male of *Potamarius izabalensis* (USNM 134346), 313 mm. long. Photograph by Smithsonian Institution.

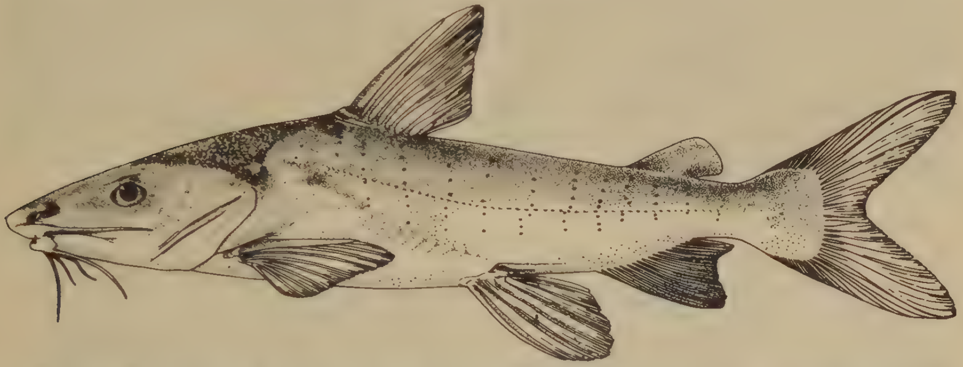

FIG. 2.—*Potamarius izabalensis*, new species. Lateral view of holotype, a female 386 mm. in standard length (the spots were added from a juvenile, with paper tag no. 16, USNM 179837, 286 mm. long).

of *Potamarius*, seem to be permanently restricted to fresh water.

Comparison with other ariid genera.—*Potamarius* is readily distinguishable from all previously established New World genera of Ariidae by its edentulous palate, narrowed and elongate snout, thick lips, small mouth, and short barbels—the characters in which it and *Conorhynchos* are convergent. From Old World genera with an edentulous palate, as described by Weber and de Beaufort (1913:272–329), it is also obviously distinct; and we assume that it originated independently from a different species of *Arius*, or from a genus closely related to *Arius*.

From *Katengus* it differs sharply in the essentially transverse, anterior, and smallish mouth, with the gape not nearly reaching to below the eye, and in having bands of minute conical teeth on the jaws, rather than a single series of incisors.

From *Tetranesodon* it is separated by having definite bands of many teeth instead of a small patch of a very few teeth on each side of each jaw; a flat rather than rotund and produced snout; and a scarcely serrulate dorsal spine.

From *Nedystoma* it is distinguished by having the teeth in bands instead of 1 or 2 series; only 8 to 11 shortish rakers instead of more than 20 long ones on the lower limb of the first arch; and the gill-membranes with a free posterior border.

From *Hemipimelodus*, which it seems to resemble most closely in such characters as dentition, it differs in having the snout flat, instead of being gibbous and more or less prominent or even projecting beyond the upper lip; the denticulations of the dorsal spine obsolescent; the free border of the gill-membranes wide medially; and the origin of the adipose fin somewhat behind rather than over or before the anal origin.

From all or nearly all Old World species of *Arius*, or of other closely related genera with teeth on the palate, if these be separated, the species of *Potamarius* differ further in the narrowness and/or the production of the snout. In one or the other of these respects some of the Old World forms do approach *Potamarius*. For example, the Indian species *Arius burmanicus* (Day) has the much depressed snout as long as in *Potamarius nelsoni*, but its snout is broad and the species is otherwise very different (Day, 1878–88:458, pl. 105, fig. 4).

In all probability trenchant osteological characters will be found to distinguish *Potamarius* from other ariid genera. Numerous cranial differences between *P. nelsoni* and *Galeichthys felis* are evident (pp. 109–110).

Etymology.—The name *Potamarius* is derived from ποτᾰμὸς, river, and *Arius* (probably from the Greek αριος, a warrior, through the Latin *Arius*). The gender is masculine.

Species.—In addition to *Potamarius nelsoni* (Evermann and Goldsborough), the type species, we find that the genus contains another species, here described as *P. izabalensis*. The two are distinguished by the several characters outlined in Table I.

Potamarius izabalensis, sp. nov.

(Figs. 1–4, 6)

Holotype.—USNM 134347, an adult female 386 mm. in standard length (Fig. 2), collected by Robert R. Miller and Ancil D. Holloway in Lago de Izabal, Guatemala, on April 6–7, 1946. It was caught on a 100-yard trot-line set overnight on the north shore of the lake about 1 mile west of El Paraíso, at a depth of not over 5 feet. Field tag U42-602, collection M46-43.

Paratopotypes.—USNM 134346, 8 immature to adult specimens (males and females), 254–394 mm. long to caudal base, from gill-nets set in Lago de Izabal near the mouth of Río Polochic, 5:30 to 8:30 P.M., April 7, 1946, by Miller and Holloway. UMMZ 177251, 5, immature to adult, males and females, 190–370 mm. long, with same data.

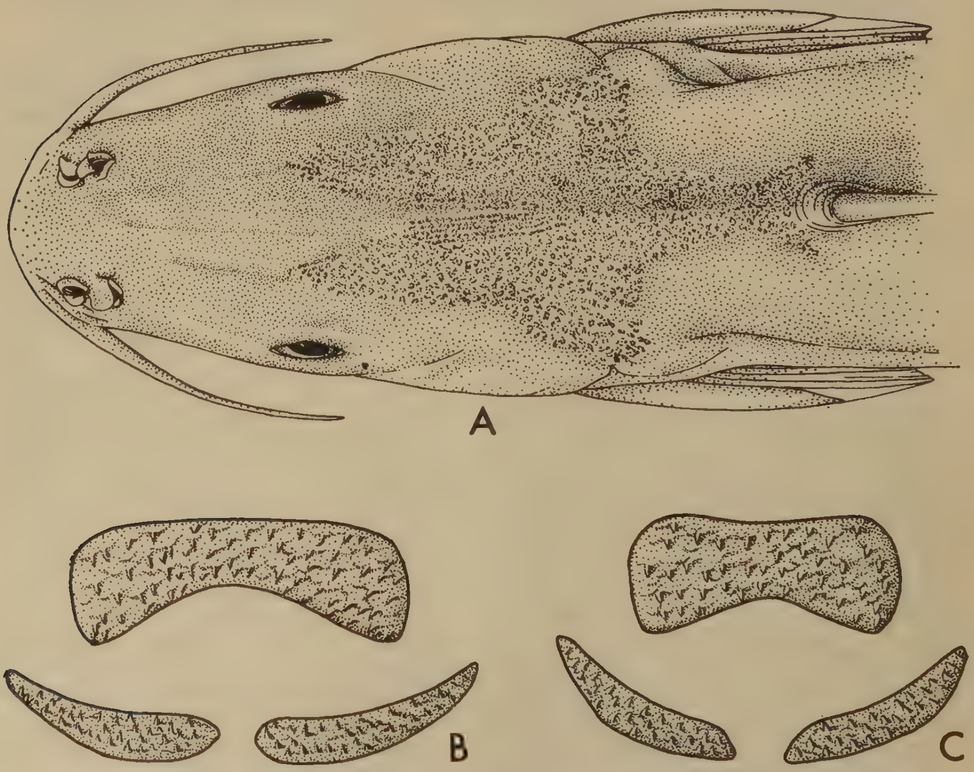

Fig. 3.—*Potamarius*, a new genus of *Ariidae*. A, Dorsal view of anterior part of holotype of *P. izabalensis*. B. Dentition (premaxillary and dentary) of a paratopotype of *P. izabalensis*, an adult female 370 mm. long. C, Dentition (premaxillary and dentary) of *P. nelsoni*, an adult male 360 mm. long.

(1006)

TABLE I

COMPARISON OF THE TWO SPECIES OF *Potamarius*

Proportional measurements are for subadult and adult specimens less than 400 mm. in standard length. For details see Table II.

Character	*P. izabalensis*	*P. nelsoni*
Gill-rakers, lower limb	9, seldom 8 or 10	10, occasionally 11
Gill-rakers, total	14 to 16	16 to 18
Maxillary barbel	Longer, extending posteriorly beyond eye; 1.65 to 2.1 in head length	Shorter, not extending posteriorly beyond middle of eye; 2.25 to 2.8 in head length
Snout into postorbital	0.9 to 1.05	0.7 to 0.9 (0.9 in 1 specimen)
Dorsal spine into head	1.3 to 1.9	1.8 to 2.3
Pectoral spine into head	1.55 to 2.0	2.05 to 2.4
Average differences:		
Head length	3.05 to 3.45	2.8 to 3.25
Predorsal length	2.35 to 2.7	2.25 to 2.55
Interorbital	2.5 to 3.05	2.8 to 3.25
Adipose base	3.2 to 3.95	3.0 to 3.5
Head width	1.5 to 1.7	1.6 to 1.85
Distribution	Lago de Izabal, Guatemala, and probably the lower Río Polochic	Lakes and quiet portions of large rivers in the Río Usumacinta basin, Guatemala (El Petén, Alta Vera Paz) and México (Tabasco, Chiapas)

USNM 139837, 3, 1 immature, 2 females, 286–440 mm., with same data as holotype. USNM 134348, 1 immature, 217 mm., from north shore of Lago de Izabal (gill-net in embayment about 3 miles west of El Estor), between 7:30 P.M. and 8:30 A.M., April 8–9, 1946, Miller and Holloway. USNM 114500, 22 young, from mouths of brooding males secured in gill-nets in Lago de Izabal, April 24–28, 1947, Miller and Holloway. UMMZ 177252, 2 young, with same data (Fig. 4).

The record stations, defining the distribution of the species, are shown on Fig. 6.

Diagnosis.— A species of *Potamarius* distinguished from its only known close relative, *P. nelsoni*, by its larger tooth patches (Fig. 3), fewer gill-rakers on the lower limb and in total count (Table I), and in various proportions (Tables I–II): rather consistently, the maxillary barbel is longer (in half-grown and adult specimens this barbel, when pressed backward against the head, reaches well behind the eye in 15 specimens of *P. izabalensis* and just beyond the eye in 2, whereas in *P. nelsoni* the barbel reaches back to any point from just in front of orbit to middle of orbit); the snout is shorter; the dorsal and pectoral spines are longer and heavier; on the average, with a wide overlap, the head, the predorsal length, and the adipose base are shorter; and the interorbital and head are less excessively narrowed as compared with most ariids (the head width varies widely, from slightly to much greater than maximum head depth). In most respects, *P. izabalensis* appears to be less extreme and more primitive than *P. nelsoni*.

Additional characters.—Several of the characters of *P. izabalensis* that are not specific are indicated in the account of the genus. The general body form and proportions of the adults, the dentition, and the appearance of the young, are well portrayed on Figs. 1–4. Proportional measurements are indicated in Table II. Sexual dimorphism in proportions is evident only in the greater length of the pelvic fins in females, and in the enlarged buccal cavity of brooding males (Fig. 1).

Meristic counts.—Dorsal invariably I, 6 (in the dorsal and anal fins the last two elements, approximated but separate at the base, are counted as a single ray). Anal 16–21 (in the 24 newborn young and in some of the larger specimens the count was determined from radiographs; in the remainder, a precise count was insured by incising the skin at the fin base). The counts were constant in the other fins: caudal (principal rays)

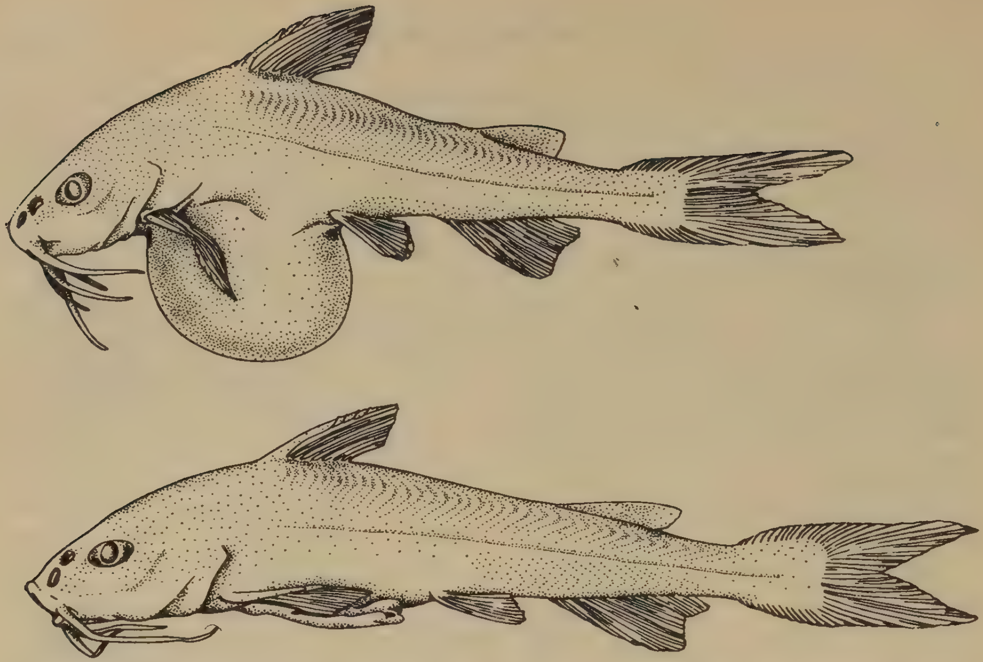

Fig. 4.—Young of *Potamarius izabalensis*, 45.0 and 51.5 mm. long, taken from mouths of brooding males.

Table II

Proportional Measurements of Two Species of *Potamarius*

The ratios were obtained by stepping the given measurement over the curve of the body or head with dividers, under appropriate magnification.

Item	*Potamarius izabalensis*			*P. nelsoni*	
Standard length in mm.	386[1]	190–394	440	138	276–388
Sex and no. of specimens	♀	4 ♂s, 6 ♀s, 7 imm.	♀	imm.	6 ♂s, 4 ♀s, 7 imm.
Into standard length:					
Head length	3.1	3.05–3.45	3.0	3.75	2.8–3.35
Body depth	5.0	4.5–5.1	4.5	5.3	4.3–5.3
Predorsal length	2.4	2.35–2.7	2.4	2.8	2.25–2.6
D origin to adipose origin	2.8	2.5–2.9	2.5	2.55	2.5–2.95
A origin to C base	3.6	3.2–3.6	3.75	2.95	3.3–3.6–
Into head length:					
Snout length	2.15	2.1–2.3	2.1	2.25	2.0–2.15
Maxillary barbel	2.0+	1.65–2.1	2.0+	1.75	2.25–2.8
Least fleshy interorbital	2.65	2.5–3.05	2.5	3.35	2.8–3.25
Dorsal spine	1.9	1.3–1.9	2.1–	1.8	1.8–2.3
Pectoral spine	2.0+	1.55–2.0	(2.5–)[2]	1.95	1.8–2.4
Dorsal base	3.35	2.8–3.2	3.2	2.4	2.8–3.6
Adipose base	3.9	3.2–3.95	4.3+	2.4	3.0–3.5
Anal base	2.5	2.0–2.5	2.7	1.5	1.95–2.6
Head width	1.65	1.5–1.7	1.75	1.6	1.6–1.85
Pelvic length					
Males[3]	...	2.0–2.05	...	...	1.95–2.2
Females[4]	1.5	1.5–1.6	1.6–	...	1.55–1.7+
Into postorbital length:					
Eye length	3.6	2.4–3.7	4.0	1.65	2.5–3.6
Snout length	0.95	0.9–1.05	0.95	0.75	0.7–0.9

---

[1] Holotype.

[2] The pectoral spine in this large specimen is interpreted as having been broken.

[3] In 4 males of *P. izabalensis* 301–320 mm. long, and in 6 males of *P. nelsoni* 317–385 mm. long.

[4] In 6 females of *P. izabalensis* 287–440 mm. long, and in 4 females of *P. nelsoni* 295–388 mm. long.

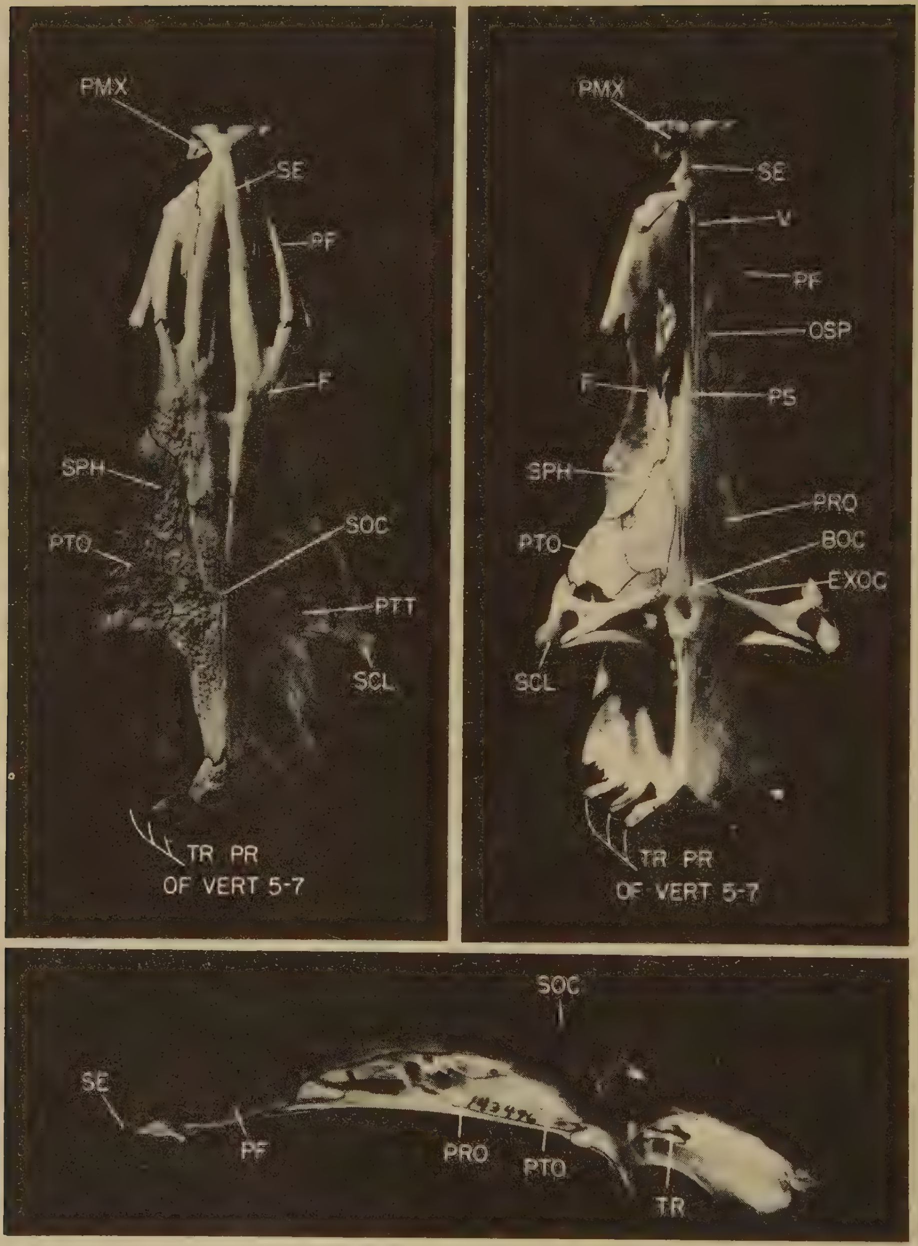
PMX
SE
PF
F
SPH
PTO
SOC
PTT
SCL
TR PR
OF VERT 5-7
PMX
SE
V
PF
OSP
F
PS
SPH
PRO
PTO
BOC
EXOC
SCL
TR PR
OF VERT 5-7
SOC
SE
PF
PRO
PTO
TR
143496

PLATE I

Potamarius nelsoni. Skull of adult (UMMZ 143496—S in dorsal, ventral, and lateral views (overall length of skull 143 mm.). BOC, Basioccipital; EXOC, exoccipital; F, frontal; OSP, orbitosphenoid; PF, prefrontal; PMX, premaxillary; PRO, prootic; PS, parasphenoid; PTO, pterotic; PTT, posttemporal; SCL, supracleithrum; SE, supraethmoid; SOC, supraoccipital; SPH, sphenotic; TR, tripus; TR PR, transverse process; V, vomer.

7 + 8 = 15; pectorals I, 10; pelvics 6. Gillrakers 5 to 7 + 9 or 10 = 14 to 16 (5 + 9 = 14 in one, 6 + 9 = 15 in twelve, 6 + 10 = 16 in one, 7 + 9 = 16 in three). Vertebrae 52 (3), 53 (13), 54 (2), in 18 (4 adults and 14 young), counting the vertebrae incorporated into the Weberian apparatus as 5 and including the hypural complex as one vertebra (the greatly expanded bialate transverse process is interpreted, as it was by Gregory (1933: fig. 79 on p. 193), as pertaining to the fourth vertebra).

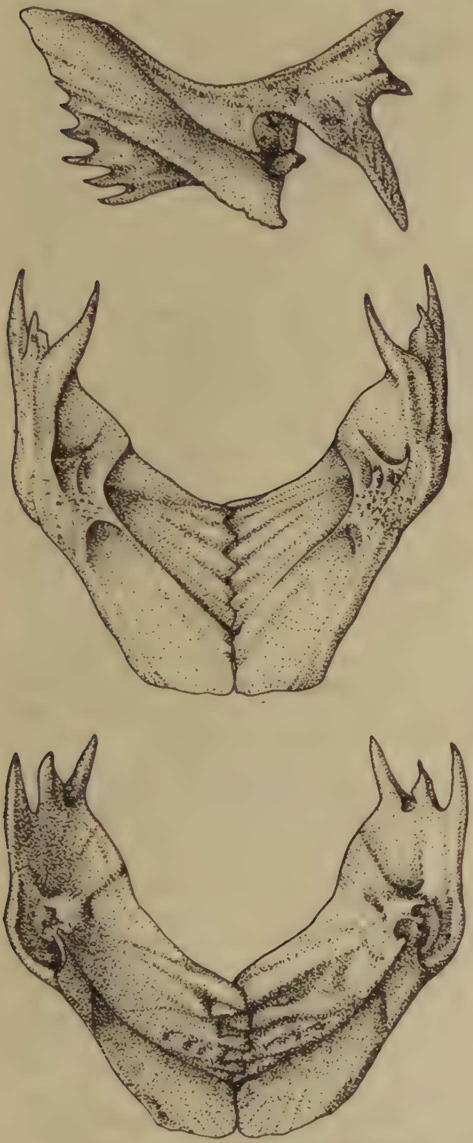

FIG. 5.—*Potamarius nelsoni*. Cleithrum of adult (UMMZ 143496—S) in three views, for comparison with figures for *Galeichthys felis* given by Merriman (1940: fig. 8).

Range.—So far as known this species is confined to Lago de Izabal, including a distributary of the Río Polochic. It no doubt occurs in the lower reaches of that stream.

Associates.—The fish fauna of Lago de Izabal is now known to total 48 species, referable to 38 genera (Holloway, 1950:114, in listing 37 genera, entered *Carlhubbsia* as *Phallichthys* and omitted *Diapterus*). Eleven of the species (23 percent) are endemic. Although fresh, except possibly at its mouth near San Felipe (Holloway, 1950: map 2), the lake contains such marine types as a shark, a sawfish, tarpon, anchovies, needlefish, a sparid, a croaker, and numerous gobbies.

Lago de Izabal is inhabited by five species of catfishes: *Galeichthys assimilis* (Günther), *Arius melanopus* Günther, *Bagre marinus* (Mitchill), and *Potamarius izabalensis*—all of the Ariidae—and *Rhamdia guatemalensis* (Günther), of the Pimelodidae. None is eaten by the natives, who shun scaleless fishes, although ariids are excellent food. *P. nelsoni* is relished by the natives in El Petén and in México, and was regarded by E. W. Nelson as the best freshwater food fish in México (Evermann and Goldsborough, 1902:146). The tastiness of the species of *Potamarius* has been verified by the authors. All the species except *Rhamdia guatemalensis* were taken in experimental gill-nets, on trot-lines, or in a 600 × 16 foot commercial seine (*Rhamdia* was caught in smaller seines; *Bagre* was the least abundant).

Lago de Izabal is also inhabited by a shrimp, *Palaemon pandaliformis* (Stimpson), which ranges widely in fresh and brackish waters of the tropical western Atlantic (identification and information furnished by L. B. Holthuis and Fenner A. Chace, Jr.).

Potamarius nelsoni (Evermann and Goldsborough)

(Pl. I and Figs. 3C, 5–6)

Conorhynchos nelsoni.—Evermann and Goldsborough, 1902:140–146, fig. 1 (original description; oral brooding; "Rio Usumacinta, Montecristo, Yucatan [=Tabasco]." Meek, 1904:19, fig. 3 (description and figure; "Atlantic streams from Chiapas to Brazil"). Eigenmann, 1910:390 ("Rio Usumacinta, Montecristo, Chiapas"). Jor-

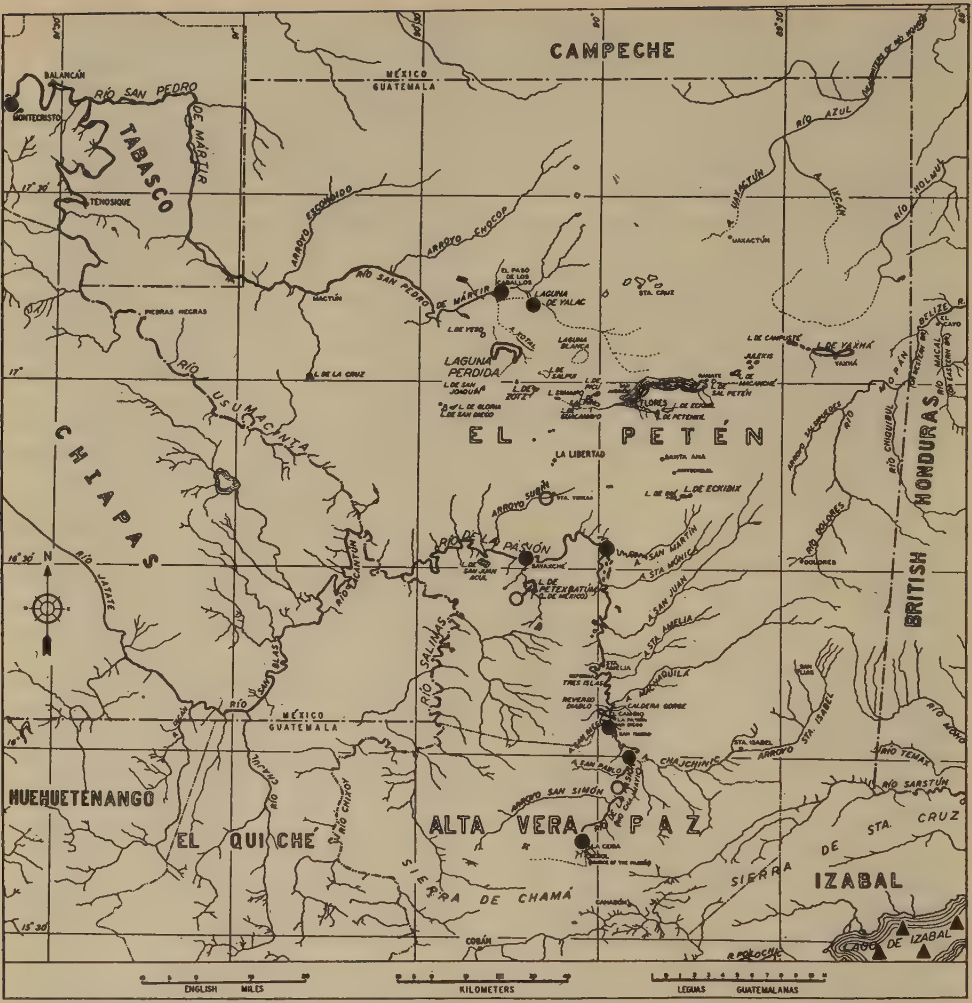
CAMPECHE
MÉXICO
GUATEMALA
BALANCÁN
MONTECRISTO
RÍO SAN PEDRO
DE MÁRTIR
TABASCO
TENOSIQUE
ARROYO ESCONDIDO
ARROYO CHOCOP
RÍO SAN PEDRO DE MÁRTIR
EL PASO DE LOS CABALLOS
LAGUNA DE YALAC
MACTÚN
PIEDRAS NEGRAS
RÍO USUMACINTA
L. DE LA CRUZ
LAGUNA PERDIDA
L. DE SAN JOAQUÍN
L. DE ZOTZ
LAGUNA BLANCA
STA. CRUZ
RÍO AZUL
RÍO HOLMUL
RÍO YAXACTÚN
R. IXCÁN
UAXACTÚN
L. DE CAMPUSTE
L. DE YAXHÁ
YAXHÁ
FLORES
L. DE PETÉN
SAL PETÉN
EL PETÉN
LA LIBERTAD
SANTA ANA
L. DE ECKIBIX
CHIAPAS
ARROYO SUBÍN
RÍO DE LA PASIÓN
SAYAXCHÉ
L. DE PETEXBATÚN
RÍO LACANTÚN
RÍO JATATE
RÍO SAN MARTÍN
A. STA. MÓNICA
A. SAN JUAN
A. STA. AMELIA
RÍO SALINAS
RÍO SANTO DOMINGO
RÍO MOPÁN
RÍO CHIQUIBUL
RÍO DOLORES
DOLORES
BRITISH HONDURAS
RÍO BELIZE
EL CAYO
TRES ISLAS
REVERSO DIABLO
CALDERA GORGE
RÍO MACHAQUILÁ
MÉXICO
GUATEMALA
ARROYO STA. ISABEL
STA. ISABEL
RÍO TEMASH
RÍO SARSTÚN
RÍO MOHO
RÍO SAN PABLO
RÍO CHAJCHINIC
ARROYO SAN SIMÓN
HUEHUETENANGO
EL QUICHÉ
RÍO CHIXOY
RÍO CHAJUL
ALTA VERA PAZ
LA CEIBA
SIERRA DE CHAMÁ
SIERRA DE STA. CRUZ
IZABAL
CAHABÓN
COBÁN
R. POLOCHIC
LAGO DE IZABAL
N
ENGLISH MILES
KILOMETERS
LEGUAS GUATEMALANAS

FIG. 6.—Distribution by record stations of the two species of *Potamarius: P. nelsoni* in the Río Usumacinta system and *P. izabalensis* in Lago de Izabal. Hollow circles represent records not verified by preserved specimens. Base map compiled by Carl L. Hubbs and Henry van der Schalie in 1937.

dan, Evermann and Clark, 1930:156 ("Rio Usumacinta, Yucatan"). De Buen, 1940:26 ("Rio Usumacinta, en Montecristo, Chiapas"). Alvarez, 1950:34 (characters in key; "Rio Usumacinta").

Conorhynchus nelsoni.—Regan, 1906–08:138 (characters; Rio Usumacinta in Chiapas). Breder, 1935:161–162 (referred to Ariidae).

.... *nelsoni*.—Gosline, 1945:9 ("Chiapas, México").

Material.—This species has been recorded in the literature only on the basis of the type material from the Río Usumacinta in Tabasco, México. The type locality was misplaced as in "Yucatan" by Evermann and Goldsborough and by Jordan, Evermann, and Clark, and as in "Chiapas" by Meek, Regan, Eigenmann, Gosline, and de Buen. Misled by the erroneous reference of the species to the Brazilian genus *Conorhynchos*, Meek indicated the range of *nelsoni* as "Atlantic streams from Chiapas to Brazil." (For references see synonymy.)

In 1935 the senior author and Henry van der Schalie collected in Guatemala 19 additional specimens (all in the University of Michigan Museum of Zoology), as follows: 143496, 2 adult males 360 and 388 mm. in standard length, and skeleton of one adult (prepared in field), saved from several caught in gill-net in Río de la Pasión across and near mouth of Arroyo del Petexbatum, Sayaxché, El Petén, April 22–24. 143497, 1 half-grown and 1 adult female, 138 and 388 mm. long (one still larger escaped), from gill-net in mouth of Arroyo Chajchinic (tributary to Río de la Pasión), on line between El Petén and Alta Vera Paz, April 17–18. 143498, 8 half-grown to adult, 195 and 276–322 mm. long, from gill-net and trot-line in Laguna de Yalac, in course of Río San Pedro de Mártir, about 6 leagues by river above El Paso de los Caballos, El Petén, March 16–17. 144267, 1 adult female, 342 mm. long, from gill-net in Río de la Pasión, at San Diego, on line between El Petén and Alta Vera Paz, between El Cambio and Chajchinic, May 18. 144269, 1 subadult male, 306 mm. long, 1 adult male 336 mm. long, and 1 adult female 362 mm. long (1 other discarded in field), from gill-net in Río de la Pasión near head, at Ceiba, Alta Vera Paz, April 10–12. 144270, 1 adult female, 295 mm. long, from gill-net in lagoon-like arm of Río San Pedro de Mártir, at El Paso de los Caballos, El Petén, March 10–12. 144271, 1 adult male 318 mm. long, from gill-net about junction of Arroyo San Martín with Río de la Pasión, east of Sayaxché, El Petén, April 21–22.

Proportional measurements. — Measurements of *Potamarius nelsoni* are presented in comparison with those of *P. izabalensis* in Tables I and II. Oddly, the head seems to increase in relative length with age. Marked sexual dimorphism in proportions seems to be restricted to the enlarged buccal cavity of brooding males and the enlarged pelvic fins of adult females.

Meristic counts (18 specimens).—Dorsal invariably I, 6. Anal 15–20. Caudal (principal rays) invariably $7 + 8 = 15$. Pectorals I, 10 (except I, 9 in one). Pelvics invariably 6. Gill-rakers 6 or $7 + 10$ or $11 = 16$ to 18 ($6 + 10 = 16$ in fifteen, $6 + 11 = 17$ in two, $7 + 11 = 18$ in one). Vertebrae 52(7), 53(3), 54(4) (counted as for *P. izabalensis*).

Skeletal characters.—The proportions and form of the skull are shown in Plate I, which illustrates its distinctively narrow anterior parts and its markedly domed outline. On comparison with a skull of the same length of *Galeichthys felis*, numerous striking differences are apparent. The comparison is made between a skull of *Potamarius nelsoni* (UMMZ 143496–S) from Río de la Pasión at Sayaxché, El Petén, and one of the same length of *G. felis* (University of Miami Marine Laboratory, no. 601) from Biscayne Bay, Florida, supplemented by the skeleton of a smaller specimen from the same locality, by Merriman's (1940) text and figures of the skeletons of *G. felis* and *Bagre marinus*, and by Gregory's (1933:197, fig. 79) account of the skull of *Arius* sp. In part we follow the conventional osteological nomenclature used by Merriman, and in part the newer terms advocated by Harrington (1955).

In dorsal view the skull of *Potamarius nelsoni* differs trenchantly from that of *Galeichthys felis* in the following respects, among others: (1) The median fontanelle is divided by a bridge of bone into a smaller posterior part as it is in *Bagre marinus*, as figured by Merriman, but with less closure. (2) The prefrontals (lateral ethmoids) are narrow and elongate, lack conspicuous anterior wings, and project backward almost to opposite the posterior end of the anterior lateral foramina. (3) The suture between prefrontal and frontal, just outside the anterior lateral foramen, remains open. (4) The posterior lateral foramina (between pterotic, posttemporal, and supracleithrum) are well developed, rather than absent; these foramina are indicated as present in *B. marinus*, though smaller than in *P. nelsoni*. (5) The supraethmoid (dermethmoid) is much narrower than in *G. felis* and is less arched in anterior profile.

In ventral aspect other differences appear: (6) The premaxillaries are much more expanded posteriorly. (7) The lateral wing of the vomer (prevomer) bridges over, on each side in the frontal plane, a conspicuous opening not present in *Galeichthys felis*. (7) The long needle-like shaft of the vomer is not fused with the parasphenoid posteriorly nor with the interdigitating parasphenoid and supraethmoids anteriorly, and the vomer is elsewhere delimited by distinct sutures, whereas in *G. felis* the shaft of the vomer and the posterior processes of the supraethmoid are fused with the parasphenoid, and the vomer elsewhere is almost completely anchylosed with the surrounding bones. (8) The prefrontal has an anterolateral expansion with a small elongate condyle unrepresented in *G. felis*, and the posterolateral margin of the supraethmoid forms a narrow and strongly curved definitive condyle, rather than an irregular articulating surface. (9) Medially the several bones of the skull are not expanded into conspicuous wings such as are developed in *G. felis*. (10) The fused

(1013)

Weberian complex bears a midventral keel that is not evident in *G. felis*. There are many other, detailed differences.

How many of these characters will prove useful in generic analysis can not be assured, pending a more complete osteological survey of the family.

Range (Fig. 6) and habitat.—Potamarius nelsoni no doubt inhabits most of the larger and medium-sized streams of the Río Usumacinta system. In addition to the type locality (Montecristo—also called Emiliano Zapata) on the lower Usumacinta in eastern Tabasco, México, we report the species, on the basis of specimens, from Laguna de Yalac on the upper Río San Pedro de Mártir and from various points on the Río de la Pasión in El Petén and Alta Vera Paz in Guatemala. In addition, we can record reports of the occurrence of this locally well-known species in Arroyo Subín (a northern tributary of the Pasión) and in Laguna de Petexbatum (south of Sayaxché). A large adult escaped from a net set in Río de la Pasión between the mouths of arroyos San Pablo and San Simón. It was not taken and presumably does not occur in smaller creeks, nor in Laguna de Petén, where extensive collections were made. In February, 1959, Sr. Jorge Carranza (Director of the Estación de Biología Marina, Veracruz) told one of us (R.R.M.) that the species does not occur in Laguna de Términos, Campeche (near the mouth of the Río Usumacinta), where he has studied the catches of commercial fishermen. It may avoid the coastal lagoons in general.

In the lakes and larger streams within its range, *P. nelsoni* exhibits little habitat selection. Where it was taken the water varied from rather silty to clear, in color from chalky blue (in the Pasión) to blackish (in Laguna de Yalac) and opaque olive-yellow. The bottom graded from bedrock to soft mud and clay; the vegetation was absent to scanty; the depth varied from about 1 to 7 meters.

Habits and vernacular names.—At Laguna de Yalac in March, 1935, the senior author noted that *Potamarius nelsoni*, like other ariids, is adept at noise production. Here both this species, locally known as "curuco" (likely an onomatopoetic word) and *Arius melanopus* Günther (which is known throughout El Petén as "cabeza-fierro"—equivalent of "steelhead"), were heard producing a "quack" with the pectoral spine, as well as a "ronk," which is issued from their mouths. Both noises were often produced simultaneously, with one compound twitch. The "quack" is higher in pitch than the "ronk," and both noises are higher in pitch in the "curuco" than in the "cabeza-fierro." *Ictalurus meridionalis* Günther, known in El Petén as "bo-bo" (obviously onomatopoetic), also "quacks" and "ronks." the "bo-bo" has a quick, relatively soft "quack," and its "ronk" is not so loud as that of the two other siluroids. The *Ictalurus* is known in Río de la Pasión also as a "jolote."

At the source of the Río de la Pasión the senior author obtained from Don Carlos Vidaurre and his Indian laborers the Quiché names of the common fishes, including "box" for both ariids and "lu" for the *Ictalurus*.

Buccal brooding by this species was reported by Evermann and Goldsborough (1902) and was observed on the Río de la Pasión on April 22–24, when a very dark male was found to have embryo-containing eggs in its strikingly enlarged buccal cavity.

The nocturnal activity of this fish is suggested by the fact that most specimens were taken in overnight gill-net sets.

NOMENCLATURAL REMARKS ON THE FAMILY ARIIDAE AND ON THE GENUS *Conorhynchos*

Most authors have named the major family of marine catfishes Ariidae, but some have applied the name Tachysuridae (based on *Tachysurus* Lacépède, 1803). We reject that name in favor of Ariidae (based on *Arius* Valenciennes, 1840), for the sound reasons given by Regan (1906–08:125–126). In effect, the fish to which the name *Tachysurus* has been applied is unidentifiable from the original description, which is based solely on a Chinese painting. Its generic status, therefore, apparently can not be determined.

Some nomenclatural complications have arisen regarding the generic name *Conorhynchos*, which was established by Bleeker in 1858, with *Pimelodus conirostris* Valenciennes of Brazil as the type species. Regan (1906–08:138) used the spelling *Conorhynchus*, proposed by Bleeker (1862:12) as an emendation of *Conorhynchos*. Both Regan and Neave (1939, *Nomenclator Zoologicus*, 1:822) cited a later paper by Bleeker (1863, *Ned. Tijdschr. Dierk. Amst.*, 1:102) as his first proposal of *Conorhynchus;* that name has been proposed no fewer than five times, twice in fishes (see Neave). Bleeker proposed *Conorhynchos* as a substitute name for *Conostomus* (accredited to Duméril, 1856) because he regarded the latter as preoccupied in birds (*Conostoma*) and in bryozoans (*Conostomum*). But, as Neave indicated, Duméril used the spelling *Conostoma*, as Hodgson had for a genus of birds (in 1842).

Subsequently, Regan (1906–08: 192) substituted *Conorhynchichthys* because *Conorhynchus* Bleeker is preoccupied by the same name in Coleoptera (*Conorhynchus* Motschoulsky, 1860). Since *Conorhynchichthys* Regan has the same type species as *Conorhynchus* Bleeker and *Conorhynchos* Bleeker, Regan's name is not available for the Middle American ariid. The South American pimelodid is still properly referred to *Conorhynchos*, but, as Gosline (1945:9, 47) indicated, on the basis of our findings, a new generic name is needed for *C. nelsoni*.

Acknowledgments.—Field work by the senior author in El Petén was conducted as the fourth Carnegie Institution – University of Michigan expedition into Mayan America. Appropriate acknowledgment of aid has already been made (Goodrich and van der Schalie, 1937:10), but we want especially to express thanks to O. A. Taintor, whose hospitality and eagerness to be of service contributed much to the success of the expedition. We are very grateful also to Henry van der Schalie, the senior author's cooperative companion on the expedition. The junior author's field work in Guatemala was sponsored jointly by the U. S. Fish and Wildlife Service, the Guatemalan government, the Smithsonian Institution, and the U. S. State Department. We wish especially to thank Ancil D. Holloway and Señor Julio Midence for assistance in collecting. For the loan of material we are grateful to Leonard P. Schultz, United States National Museum; James E. Böhlke, Academy of Natural Sciences of Philadelphia; and C. Richard Robins, University of Miami Marine Laboratory. Mrs. Elizabeth M. Anthony and Mrs. James D. Hall made the drawings, the Smithsonian Institution provided the photograph (Fig. 1), William L. Brudon prepared Plate I, and Teruya Uyeno entered the record-station symbols on the map.

LITERATURE CITED

ALVAREZ, JOSÉ. 1950. Claves para la determinación de especies en los peces de las aguas continentales mexicanas. *Sec. Marina, Dir. Gen. Pesca e Industrias Conexas, México, Pp. 1–144, Figs. 1–16.*

BERG, LEO S. 1940. Classification of fishes both Recent and fossil. *Akademiia Nauk, Leningrad, 1940:87–517, illus.*

BLEEKER, P. 1862. Atlas ichthyologique des Indes Orientales Nééderlandaises. Vol. II. Siluroïdes, Chacoïdes et Hétérobranchoïdes. *Amsterdam, F. Muller, Ed., 1862:1–112.*

BREDER, C. M., JR. 1935. The reproductive habits of the common catfish, *Ameiurus nebulosus* (Le Sueur), with a discussion of their significance in ontogeny and phylogeny. *Zoologica, 19(4):143–179, Figs. 12–23.*

BRIGGS, JOHN C., AND ROBERT RUSH MILLER. 1960. Two new freshwater clingfishes of the genus *Gobiesox* from southern Mexico. *Occ. Pap. Mus. Zool. Univ. Mich., 616:1–15, Fig. 1, Pls. 1–4.*

DAY, FRANCIS. 1878–88. The fishes of India. *London, Vol. 2 (Atlas), Pls. 1–195.*

DEBUEN, FERNANDO. 1940. Lista de peces de agua dulce de México. En preparación de su catálogo. *Estacion Limnologica Pátzcuaro, Trabajos Num. 2:1–66 (mimeo.).*

EIGENMANN, C. H. 1910. Catalogue of the freshwater fishes of tropical and south temperate America. *Repts. Princeton Univ. Exped. Patagonia, 1896–1899, 3* (Zool.), *Pt. 4:375–511, 1 map.*

EVERMANN, BARTON WARREN, AND EDMUND LEE GOLDSBOROUGH. 1902. A report on fishes collected in Mexico and Central America, with notes and descriptions of five new species. *Bull. U. S. Fish Comm., 21 (1901):137–159, Figs. 1–8.*

GOODRICH, CALVIN, AND HENRY VAN DER SCHALIE. 1937. Mollusca of Petén and north Alta Vera Paz, Guatemala. *Univ. Mich. Mus. Zool. Misc. Publ. 34:1–50, Fig. 1, Pl. 1, Map 1.*

GOSLINE, WILLIAM A. 1945. Catálogo dos nematognatos de água-doce da América do Sul e Central. *Bol. Mus. Nacional Brasil, N.S., No. 33:1–138.*

GREGORY, WILLIAM K. 1933. Fish skulls: A study of the evolution of natural mechanisms. *Trans. Amer. Philos. Soc., 23(2):vii + 75–481, Figs. 1–302.*

HARRINGTON, ROBERT W., JR. 1955. The osteocranium of the American cyprinid fish, *Notropis bifrenatus*, with an annotated synonymy of teleost skull bones. COPEIA, *1955(4):267–290, Figs. 1–8.*

HOLLOWAY, ANCIL D. 1950. Recommendations for the development of the fishery resources of Guatemala. *In:* A fish and wildlife survey of Guatemala. *U. S. Fish and Wildlife Serv., Spec. Sci. Rept.: Wildlife No. 5:99–140, Maps 1–3.*

JORDAN, DAVID STARR, BARTON WARREN EVERMANN, AND HOWARD WALTON CLARK. 1930. Check list of the fishes and fishlike vertebrates of North and Middle America north of the northern boundary of Venezuela and Colombia. *Rept. U. S. Comm. Fish., 1928* (2)*:i–iv, 1–670.*

MEEK, SETH EUGENE. 1904. The fresh-water fishes of Mexico north of the Isthmus of Tehuantepec. *Field Col. Mus., 93* (*Zool. Ser., Publ. 5*)*:i–lxiii, 1–252, Figs. 1–72, Pls. 1–17, 1 map.*

MERRIMAN, DANIEL. 1940. Morphological and embryological studies on two species of marine catfish, *Bagre marinus* and *Galeichthys felis. Zoologica, 25 (2):221–248, Figs. 1–9, Pls. 1–5.*

MILLER, ROBERT RUSH. 1959. Origin and affinities of the freshwater fish fauna of western North America. *In:* Zoogeography. *Amer. Assoc. Adv. Sci., Publ. 51* (*1958*)*: 187–222, Figs. 1–19.*

Regan, C. Tate. 1906–08. Pisces. *In:* Biologia Centrali-Americana, *8:i–xxxiii, 1–203, 12 figs., Maps 1–2, Pls. 1–26 (119 figs.).*

———. 1911. The classification of the teleostean fishes of the order Ostariophysi.—2. Siluroidea. *Ann. and Mag. Nat. Hist., Ser. 8, Vol. 8:553–577, Figs. 1–3, Pl. 2.*

Smith, Hugh M. 1945. The fresh-water fishes of Siam, or Thailand. *U. S. Nat. Mus., Bull. 188:i–xi, 1–622, Figs. 1–107, Pls. 1–9.*

Weber, Max, and L. F. de Beaufort. 1913. The fishes of the Indo-Australian Archipelago. *Leiden, 2:xx + 404, Figs. 1–151, frontis.*

Scripps Institution of Oceanography, La Jolla, California and Museum of Zoology, University of Michigan, Ann Arbor, Michigan.

(1016)

SHORTER COMMUNICATION

Tertiary sediments from the floor of the Indian Ocean

(*Received* 9 *June* 1960)

UNTIL last year, the only known occurrence of Tertiary strata on the floor of the Indian Ocean was an Eocene to Oligocene basaltic agglomerate dredged from 744 fathoms (1362 metres) on the west side of Providence Reef in 9° 25·8′ S, 50° 56·8′ E by H.M.S. *Sealark* in 1905 (GARDINER, 1907, p. 147). WISEMAN (1936) has described the chemistry, petrology and paleoentology of some of the rocks from this dredge haul, and suggested that part of the foundation of Providence Reef originated through a basaltic eruption of Eocene to Oligocene age. The rock composed of fragmental basaltic material set in a matrix of calcite (British Museum registered No. 1959, 440a (31)) was apparently the first to give direct evidence about the nature of the reef foundations. In this connection it is interesting to recall that drilling on Eniwetok Atoll in the Pacific Ocean revealed basalt at a depth of 692 fms (1266 m) below an Eocene limestone (LADD *et al.*, 1953).

In twelve sediment cores collected from the floor of the tropical Indian Ocean, RIEDEL (1951) found no evidence from the Radiolaria of outcropping Tertiary sediment. Last year, however, Tertiary microfossils were found in two samples collected at or near the sediment surface by early expeditions in the Indian Ocean. These samples are : (1) sounding No. 10 of H.M.S. *Egeria*, collected 22 October 1887, from a depth of 2582 fms (4722 m) at 20° 40′ S, 85° 29′ E, and (2) a sample collected by S.M.S. *Planet* from a depth of 2310 fms (4220 m) at 8° 45′ S, 64° 52′ E.

Egeria sounding No. 10 (British Museum registered No. M3781), originally described as a red clay (Anon., 1888), is one of a series of samples discussed by Sir JOHN MURRAY (1889, 1910) in connection with the dissolution of calcium carbonate in the deeper parts of the ocean. MURRAY indicated on his charts that this sample is a red clay, but a recent analysis (J.D.H.W.) of the material preserved in the British Museum (Natural History) revealed that the carbonate content is about 74 per cent. It is likely that the original material had a higher carbonate content, because the majority of the Foraminifera have apparently been removed from this sample. Although the exact carbonate content of the original material cannot be given, it is clear that it was a highly calcareous ooze and not a red clay. In the Murray Library (section 2, box 12, enclosure 136) there is a manuscript note (author unknown) giving a list of the Foraminifera in *Egeria* sounding No. 10 (*Globorotalia menardii*, *Globorotalia tumida*, *Globigerinoides sacculifera*) ; in addition it is stated that the carbonate content is about 40 per cent and that coccoliths are abundant. The most plausible explanation of this discrepancy is that MURRAY merely assumed that the calcium carbonate content of this sample was low, being misled by its original description in 1888, by its colour, and by the fact that nearby samples from comparable depths (2570 and 2564 fms, i.e., 4700 and 4690 m) contained practically no carbonate.

Coccoliths and discoasters, determined by Dr. M. N. BRAMLETTE to be Upper Eocene in age (personal communication), account for a large proportion of the calcium carbonate in *Egeria* sounding No. 10. It is possible that Eocene calcareous ooze outcrops at this locality, or it may be thinly covered by the somewhat phillipsitic clay which is the normal Quaternary sediment at depths greater than 2570 fms (4700 m) in this area. It is clearly desirable that highly calcareous sediments collected below the carbonate compensation level should be examined for Tertiary microfossils. Another example of a similar occurrence is a highly calcareous ooze (British Museum registered No. 1959, 42) collected by R.V. *Horizon* on Scripps Institution of Oceanography's ' Dolphin ' expedition from a depth of 2728 fms (5000 m) in the South Pacific at 12° 00′ S, 144° 21′ W. In this core the carbonate content at a depth of 52–56 cm below the sediment surface is 95·5 per cent ; late Tertiary coccoliths

Contributions from the Scripps Institution of Oceanography, New Series, 1222

Reproduced by Permission (1017)

and discoasters, together with a few admixed early Tertiary forms, account for most of this carbonate (microfossils dated by Dr. M. N. BRAMLETTE, personal communication).

The *Planet* sample is not so well documented as *Egeria* sounding No. 10. The German microscopist ALBERT ELGER kindly prepared and allowed us to examine a microscope slide of picked Radiolaria, bearing the locality data mentioned above. These locality data indicate that the sample is from station No. 127 of the *Planet* expedition of 1906–1907 ; this sample is described in the expedition report as *Globigerina* ooze (BRENNECKE, 1909). In addition to Quaternary species, the slide bears some Eocene forms – *Heliodiscus humboldti* (Ehrenberg), *Periphaena decora* Ehr., *Eusyringium fistuligerum* (Ehr.), *Podocyrtis triacantha* Ehr., *Podocyrtis papalis* Ehr., *Anthocyrtium* aff. *hispidum* (Ehr.), etc. There can be little doubt that fossiliferous Eocene occurs at or near the sediment surface in the vicinity of this *Planet* locality.

Although little can at present be determined regarding the conditions of the occurrence of these Eocene microfossils, the findings are recorded in the hope that the sea floor at these localities may be intensively sampled by oceanographic expeditions which will visit the Indian Ocean during the next year or two. It is also desired to draw attention to the necessity of keeping in an orderly and careful way both old (even if there is only a small amount of material available) and recently collected samples from the sea floor : the Tertiary samples noted in this paper were collected 73, 55 and 54 years ago. Because of the cost and difficulty of re-collecting geological samples from remote deep-sea localities, all precautions should be taken to preserve such material, free from any possibility of contamination, in order that it may be reliably used for a number of different types of investigations over a long period of time. Moreover, it is desirable that deep-sea geological samples be indexed geographically, on the basis of a grid of rectangles of 10° of latitude and longitude, as is the collection in the British Museum (Natural History) ; without this index and the facilities of the John Murray Library which has recently been reorganized, *Egeria* sounding No. 10 would not have been re-examined by the authors.

Finally, a word might be said regarding the implications of occurrences of Tertiary sediments at or near the surface of the sea floor. In 1951 one of us (W.R.R.) speculated that the exposure of Tertiary sediments to Quaternary agencies of erosion on the floor of the Pacific was to a considerable extent dependent on Tertiary and Quaternary tectonic movements. This view must be modified as a result of more recent findings. Where biogenous Tertiary sediments are covered by slowly accumulating non-fossiliferous Quaternary clays, the Quaternary cover may be only one or two metres thick. In such areas, no great tectonic movement is needed to expose at least late Tertiary material to agencies of erosion and transportation : this could easily be accomplised by a small slump or a localized current, in an area of relatively low topographic relief.

One of the authors (W.R.R.) wishes to acknowledge financial support from the Trustees of the British Museum, the U.S. Office of Naval Research, and the University of California, which made it possible for him to examine some of the sediment samples in the British Museum (Natural History).

†*British Museum (Natural History),*
London, S.W.7.
**Scripps Institution of Oceanography,*
La Jolla. California.

JOHN D. H. WISEMAN†
WILLIAM R. RIEDEL*

Contribution from Scripps Institution of Oceanography.

REFERENCES

ANON. (1888) Deep sea soundings and serial temperature observations obtained in the Indian Ocean by Captain PELHAM ALDRICH, H.M. Surveying Vessel *Egeria*, 1887. Hydrographic Department, Admiralty, London, March 1888.

BRENNECKE, W. (1909) Die Ergebnisse der Tiefseelotungen. Forschungsreise S.M.S. *Planet* 1906–07, 3, 21–47.

GARDINER, J. STANLEY (1907) Description of the Expedition – Part 2. Mauritius to Seychelles. *Trans. Linn. Soc. London*, ser. 2, *Zoology*, **12** (9), 111–175, pls. 14–18.

LADD, H. S., INGERSON, E., TOWNSEND, R. C., RUSSELL, M. and STEPHENSON, H. K. (1953) Drilling on Eniwetok Atoll, Marshall Islands. *Bull. Amer. Assoc. Petrol. Geol.*, **37** (10), 2257–2280.

MURRAY, J. (1889) On marine deposits in the Indian, Southern and Antarctic Oceans. *Scottish Geogr. Mag.*, 1889, **5**, 405–436, 1 map.

MURRAY, J. (1910) On the depth and marine deposits of the Indian Ocean, with description of deposit samples collected by Mr. J. STANLEY GARDINER in 1905. *Trans. Linn. Soc. London*, ser. 2, *Zoology*, **13** (3), 355–396, pls. 22–24.

RIEDEL, W. R. (1951) Sedimentation in the tropical Indian Ocean . *Nature, Lond.* **168**, 737.

WISEMAN, J. D. H. (1936) The petrography and significance of a rock dredged from a depth of 744 fathoms, near to Providence Reef, Indian Ocean. *Trans. Linn. Soc. London*, ser. 2, *Zoology*, **19** (4), 437–443.

Printed in Great Britain by The Salisbury Press Ltd., Publicity House, Wilton Road, Salisbury, Wilts. (25955)

(1019)

RATES OF MARINE EROSION OF TEPHRA AND LAVA AT ISLA SAN BENEDICTO, MEXICO

By ADRIAN F. RICHARDS

Reprinted from the Report of the

International Geological Congress, XXI Session, Norden, 1960

Part X.,

Submarine Geology

COPENHAGEN 1960

(1021)

(1022)

RATES OF MARINE EROSION OF TEPHRA AND LAVA AT ISLA SAN BENEDICTO, MEXICO*

By **ADRIAN F. RICHARDS**

U.S.A.

ABSTRACT

The southeastern shoreline on the leeward side of Isla San Benedicto, Mexico, was extended about 900 m seaward by tephra and lava during the life of Volcán Bárcena, which was born on August 1, 1952, and became inactive in early 1953. Effects of marine erosion were followed from 1952 until 1957 by photographic flights and visits by ship to the island. An estimated 7×10^5 m^3 (about 17,000 m^3/day) of tephra was eroded by wave action from Volcán Bárcena between August 11 and September 20, 1952. The bulge of Bárcena cone which extended farthest out to sea was eroded at a rate of slightly less than one meter day during this period. Lava flowed about 650 m out to sea from Bárcena between December 1952 and March 1953. The seaward 18 m of flow tongues exposed to wave attack were eroded away during the summer storm season between observations made on April 16 and September 21, 1953. This represents an average rate of about 11 cm/day, but erosion probably procedeed at varying rates depending on storms. Vertical cliffing of the flow tongues occurred during this period and subsequent erosion was relatively slight.

INTRODUCTION

In August 1952 the birth and subsequent development of a new terrestrial volcano, named Bárcena, near the shore of Isla San Benedicto, Mexico, produced marked constructional changes in the insular shoreline. Even before volcanic activity had stopped, currents and waves began an erosional and depositional process that continues today. Photogrammetric measurements of the amount and rate of erosion of the tephra† cone and lava flow during a three-year period of time are summarized in this paper. A final paper is in preparation on the effects of both terrestrial and marine erosion.

A remote and uninhabited oceanic island, San Benedicto is located about 550 km west of Cabo Corrientes on the Mexican mainland (Fig. 1). It and the other three members of the Islas Revillagigedo archipelago [Richards and Brattstrom, 1959] are located on the Clarión Fracture Zone, which appears to be a seaward continuation of the Trans-Mexico Volcanic Axis that includes Popocatépetl, Parícutin, and Colima volcanoes [Menard, 1955]. San Benedicto and Isla Socorro, directly south, are situated at the intersection of the Clarión Fracture Zone and a south-trending

---

* This paper represents results of research carried out by the University of California in part under contract with the Office of Naval Research and the Bureau of Ships. Reproduction in whole or in part is permitted for any purpose by the United States Government. The opinions and assertions contained in this paper are those of the writer and are not officially endorsed by the Hydrographic Office or U.S. Navy. The author is associated with the U.S. Hydrographic Office.

† A collective term for all fragmental volcanic material ejected through the air from a volcano (Thorarinsson, 1944, p. 210;1956).

Contributions from the Scripps Institution of Oceanography, New Series, 1223

Reproduced by Permission

submarine mountain range that extends nearly to Clipperton Island [Richards, 1957].

The investigation of the effects of marine erosion at Volcán Bárcena began in mid-September 1952, forty-one days after the volcano made its appearance, and continued until April 1957. Twelve U.S. Air Force and Navy photographic and observation flights and five visits by ship were made to San Benedicto during this period. Flights after 1952 were sponsored by the Office of Naval Research. Four of the cruises were expeditions of the Scripps Institution of Oceanography, University of California.

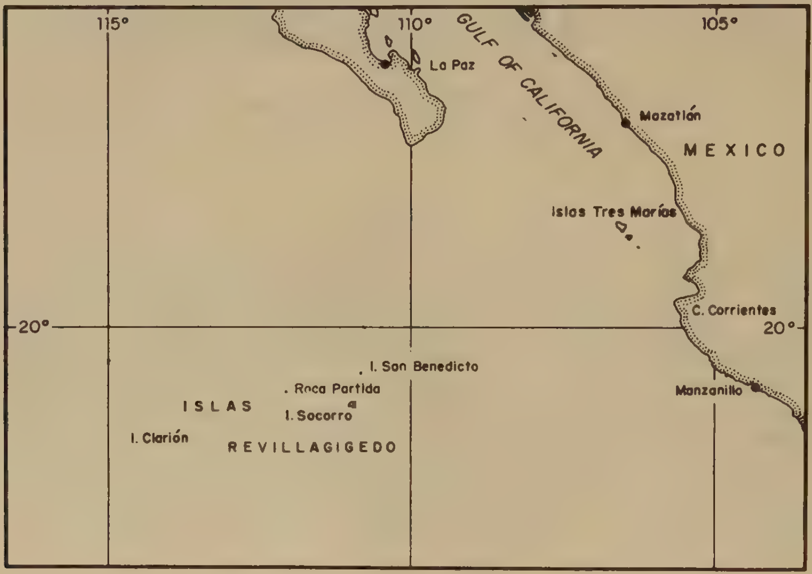
115°
110°
105°
GULF OF CALIFORNIA
La Paz
Mazatlán
MEXICO
Islas Tres Marías
C. Corrientes
20°
20°
I. San Benedicto
Roca Partida
ISLAS
I. Socorro
I. Clarión
REVILLAGIGEDO
Manzanillo

Fig. 1.—*Location map.*

The writer is indebted to all of the persons, unfortunately too numerous to mention individually, who assisted in this investigation. He is particularly appreciative of the continued encouragement and guidance of Dr. Robert S. Dietz, U.S. Navy Electronics Laboratory in San Diego, California, who conducted the study of Volcán Bárcena up to November 1952.

SYNOPSIS OF VOLCANIC ACTIVITY

Volcán Bárcena was born on August 1, 1952, on the north-eastern flank of Montículo Cinerítico, an eroded tephra cone. By August 12 a cone of soda trachyte tephra had been formed, which was nearly 335 m high and extended over 270 m seaward of the Montículo Cinerítico shoreline. Cone formation ceased by mid-September. Blocky, soda trachyte lava was extruded into Bárcena crater between November and December. Lava began to flow out to sea through the southeastern base of Bárcena in December. This flow, named the Delta Lávico because of its shape, extended about 650 m seaward of the December Bárcena shoreline by March 1953 (Fig. 2), at which time the volcano became inactive. The eruption is estimated to have produced about 270 million cubic meters of tephra and 27 million cubic meters of lava. Much of the tephra fell into the sea and some pumice from the eruption drifted across the Pacific Ocean in the North Equatorial Current [Richards, 1958]. A preliminary description of the activity of Volcán Bárcena has been published by Richards and Dietz (1956) and a final account by the writer is in press.

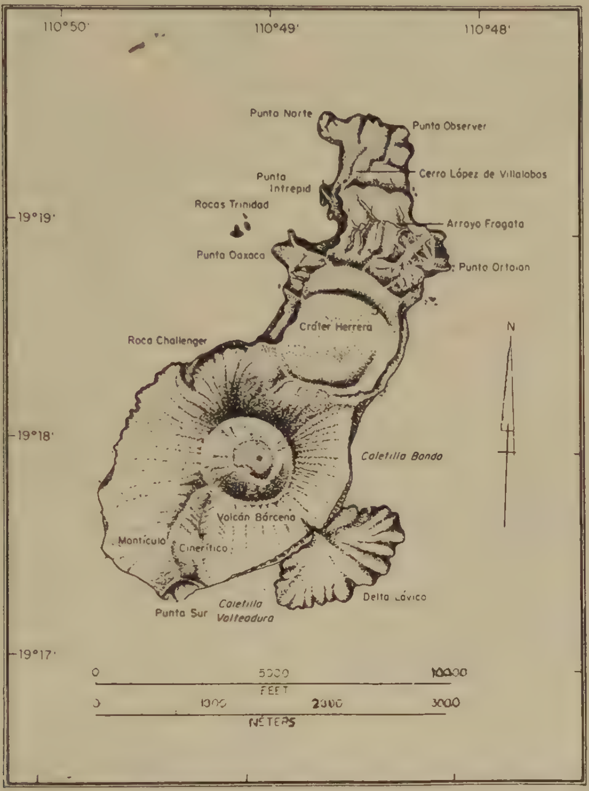
110°50'
110°49'
110°48'
Punta Norte
Punta Observer
Cerro López de Villalobos
Punta Intrepid
Rocas Trinidad
19°19'
Arroyo Fragata
Punta Oaxaca
Punta Ortolan
Cráter Herrera
N
Roca Challenger
19°18'
Caletilla Bonda
Volcán Bárcena
Montículo Cinerítico
Delta Lávico
Punta Sur
Caletilla Volteadura
19°17'
0
5000
10000
FEET
0
1000
2000
3000
METERS

FIG. 2.—*Map of Isla San Benedicto.*

EROSION OF BÁRCENA TEPHRA CONE

Bárcena continued to grow rapidly out to sea in the two weeks of very vigorous eruptive activity following its birth. Tephra in the cone predominantly consisted of unconsolidated volcanic dust or fine-grained ash. A random sample of tephra from the northeastern base of the cone that was mechanically analyzed had a median grain diameter of 38.5 microns.

Wave erosion of the volcano is considered to have been relatively negligible, compared to the rate of subaerial deposition, until at least August 11 or 12. From the

11th until about September 20 wave erosion probably proceeded at an accelerated rate. The first vertical air photographs of the volcano, taken on the 20th, show that a prominent sea cliff existed at the base of the cone, although a beach had not yet formed except near Cráter Herrera. Bárcena again was photographed from the air on November 15. On this date a small beach due east of Bárcena, at the base of the sea cliff, extended seaward about 90 m, and indicated that marine deposition had started to accompany erosion.

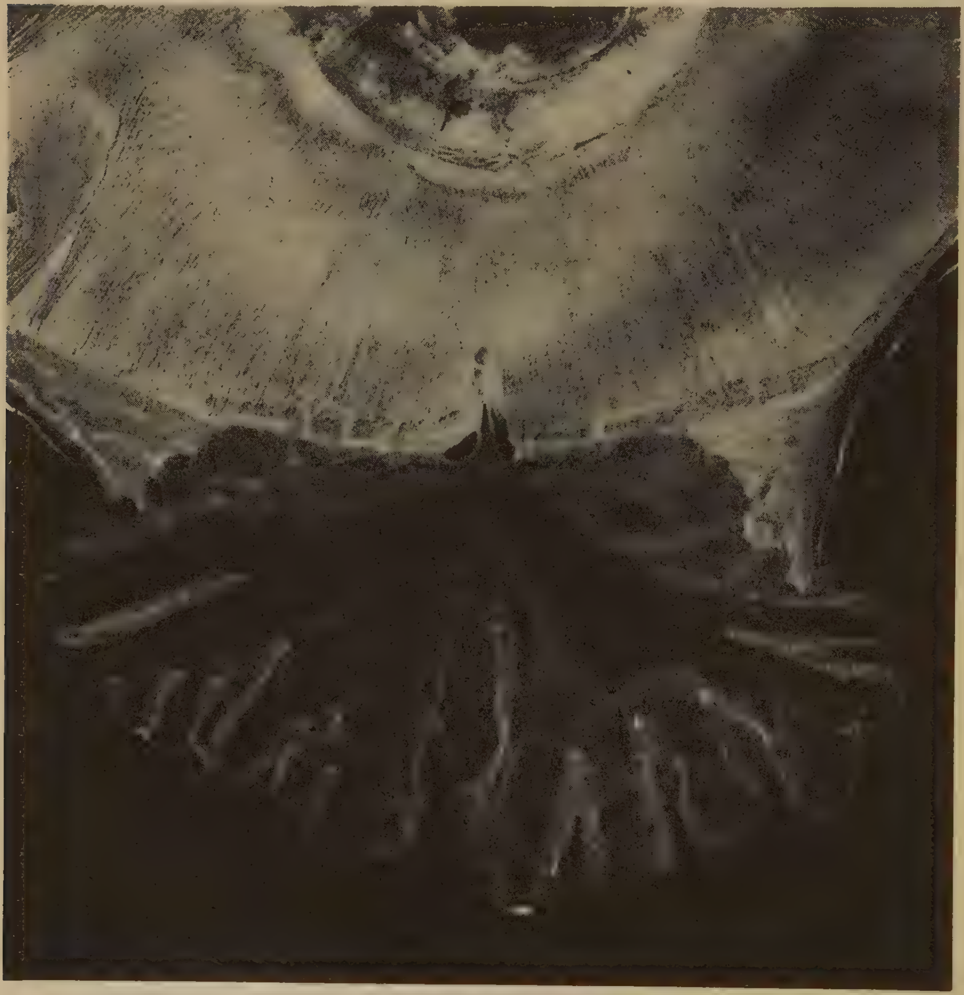

FIG. 3.—*Vertical air photograph of Volcán Bárcena and the Delta Lávico taken on April* 16, 1953. *Official U.S. Navy photograph.*

Calculations based on the 33° exterior slope of Bárcena, height of the sea cliff, and width of the beach on different dates indicate that between August 11 and December 10 the average rate of landward erosion of the east-southeast side of the cone was slightly less than one meter per day. After December 10 the cone in this area was protected from further erosion by the Delta Lávico.

It is estimated that about 700 thousand cubic meters of tephra were eroded, predominantly by wave attack, from the base of Bárcena cone in the 40 days between August 11 and September 20, or an average of about 17.5 thousand cubic meters per day. In comparison, during a period of about 225 days, wave and current erosion and transportation of unconsolidated volcanic ash from Falcon Island in the tradewind belt of the southwestern Pacific Ocean [Hoffmeister, et al, 1929] was 3.6 times the rate of erosion at Bárcena.

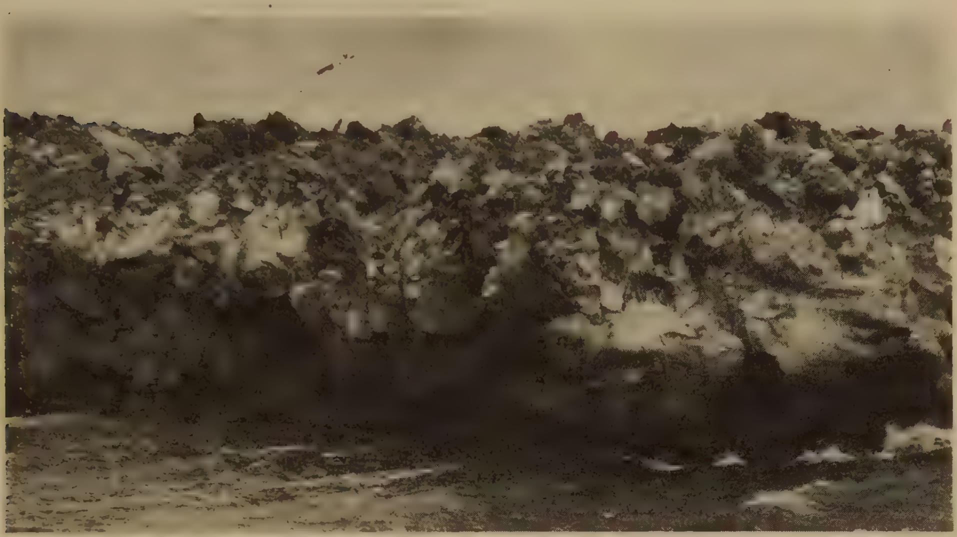

FIG. 4. *Photograph of the seaward edge of a Delta Lávico flow tongue taken from a ship in May* 1955. *R. M. Gilmore photograph.*

EROSION OF THE DELTA LÁVICO

Scoriaceous block lava flowed from the southeastern base of Volcán Bárcena between December 8, 1952, and the end of February 1953. A visit by ship in early March 1953 and vertical air photographs taken on the flight of April 16 (Fig. 3) show that wave erosion of the flow tongues was negligible or non-existent up to the latter date. These tongues of lava on the seaward side of the Delta Lávico had a subaerial slope of 28° in March; the submarine slope was virtually identical.

Photogrammetric comparison between vertical air photographs taken on the flights of April 16 and May 20, 1953, shows that wave erosion of clinker from the ends of flow tongues located on the southeastern side of the Delta Lávico occurred at an average rate of 30 cm per day during this 34-day period. It is likely that the existence of a submarine ridge on the southeastern side of the Delta resulted in a concentration of wave energy in this area. Wave erosion elsewhere on the Delta was undetected.

Additional photographic flights in 1953, 1954, and 1955 showed that relatively little erosion of the Delta Lávico occurred after September 21, 1953, when virtually all flow tongues were vertically cliffed (Fig. 4). In the 158 days between April 16 and September 21 the maximum rate of erosion of the most prominent flow tongue on the southeastern side of the Delta occurred at about 18 cm per day. A more conservative figure for all of the flow tongues which were exposed to wave attack is about 11 cm per day. This latter figure is based on an average horizontal distance of 18 m of lava eroded from the seaward ends of flow tongues. It should be emphasized that these rates are not meant to imply that erosion proceeded more or less continuously. On the contrary, it is believed that most of the erosion occurred relatively rapidly during one or more periods of high waves resulting from summer storms, some of which are known to be very severe, in the region between the Islas Revillagigedo and Mexico or Central America.

REFERENCES

Hoffmeister, J. E., Ladd, H. S., and Alling, H. L. (1929): Falcon Island. *American Jour. Sci.*, vol. 218, pp. 461–471.

Menard, H. W. (1955): Deformation of the northeastern Pacific basin and the west coast of North America. *Geol. Soc. America Bull.*, vol. 64, pp. 1149–1198.

Richards, A. F. (1957): Geology of the Islas Revillagigedo, Mexico. *Geol. Soc. America Bull.*, vol. 68, p. 1843 (abstract).

Richards, A. F. (1958): Transpacific distribution of floating pumice from Isla San Benedicto, Mexico. *Deep-sea Res.*, vol. 5, pp. 29–35.

Richards, A. F. (1960): Geology of the Islas Revillagigedo, Mexico 1. Birth and development of Volcán Bárcena, Isla San Benedicto. *Bull. Volcanologique*, ser. 2, vol. 22, pp. 73-123.

Richards, A. F., and Brattstrom, B. H. (1959): Bibliography, cartography, discovery, and exploration of the Islas Revillagigedo. *California Acad. Sci. Proc.*, 4th ser., vol. 29, pp. 315–360.

Richards, A. F., and Dietz, R. S. (1956): Eruption of Bárcena Volcano, San Benedicto Island, Mexico. *Eighth Pacific Sci. Congr. Proc.*, vol. 2, pp. 157–176.

Thorarinsson, S. (1944): Tefrokronologiska studier på Island. *Geog. Ann.*, vol. 26, 217 pp.

Thorarinsson, S. (1956): On the rhyolitic volcanic eruption in Iceland in post Glacial time. *Resumenes Trabajos Pres.*, XX Intern. Geol. Congr., Mexico, p. 20 (abstract).

[*Manuscript received Sept. 1st*, 1959]

Reprinted from
DEEP-SEA RESEARCH
Vol. 7, No. 2, pp. 100–116

ALEXA BANK, A DROWNED ATOLL ON THE MELANESIAN BORDER PLATEAU

RHODES W. FAIRBRIDGE* and HARRIS B. STEWART, Jr.**
*Columbia University, New York 27, New York.
**U.S. Coast and Geodetic Survey, Washington 25, D.C.

PERGAMON PRESS
NEW YORK OXFORD LONDON
PARIS
1960

(1029)

Deep-Sea Research, 1960, Vol. 7, pp. 100 to 116. Pergamon Press Ltd., London. Printed in Great Britain

Alexa Bank, a drowned atoll on the Melanesian Border Plateau

RHODES W. FAIRBRIDGE* and HARRIS B. STEWART, JR.**

(*Received* 13 *June* 1958)

Abstract—The Melanesian Border Plateau covers an area 1000 by 200 miles along the north-eastern edge of Melanesia, facing the Central Pacific Basin, with an average depth of 1500 fm (2700 m). It trends E–W, but is broken up into a series of narrow ridges and troughs *en échelon* trending NW–SE, each approximately 250 miles long and 100 miles from ridge crest to crest. The troughs rarely exceed 2200 fm (4000 m) in depth. Some are closed basins and others open out in a funnel shape, sloping gradually down into the Central Pacific Basin (2700 fm or 5000 m). Although the Border Plateau is bounded by the ' Andesite Line ' there is an anomalous absence of any belt of deep trenches on the Basin margin. The échelon ridges of the Plateau are mostly less than 1000 fm (1800 m) deep. They are capped by a few small volcanic islands and a large number of slightly submerged (10–15 fm or 18–27 m) atolls of dead, ' drowned ' corals. Alexa Bank is a characteristic example. The cause of coral death is a mystery; vulcanism and foul upwelling are possible explanations.

INTRODUCTION

ONE OF the most curious sectors of the Pacific margin is the Melanesian Border Plateau (Fig. 1). This area extends from about 170 °E to 175 °W longitude, between latitudes 10° and 14 °S, and is thus roughly 200 to 500 miles NW. to NE. of the Fiji Islands. Politically, the Wallis and Horne Islands belong to the French Dependencies in Oceania. Rotuma comes under the British colonial administration of Fiji, Nurakita is classified with the British colony of the Gilbert and Ellice Islands, while in the far west Anuda (or Cherry) and Mitre Islands belong administratively to the New Hebrides condominium.

The thousand-mile length of the Border Plateau is peculiar on several counts :

(a) It is oriented E–W, an altogether unusual pattern in the broad picture of the western border of the Pacific which runs roughly N–S.

(b) Its E–W trend is broken up into numerous NW–SE segments *en échelon*, little ridges and troughs, averaging 250 miles long and 100 miles from crest to crest, which, as bathymetric features, appear to be almost unique in the world oceans.

(c) It is bounded on the north by the ' Andesite Line,' but one island (Wallis) near its outermost edge, is regarded as having ' Atlantic-type ' (i.e. oceanic) lavas.

(d) The ' Andesite Line ' and Pacific margin is not bounded by a zone of deep ocean trenches as elsewhere, but generally only by a gentle slope†.

---

*Columbia University, New York 27, New York.

**U.S. Coast and Geodetic Survey, Washington 25, D.C.

†After these lines were written, the Soviet research ship, *Vitiaz* discovered a 6140 m deep trench, the *Vitiaz* Trench at 10° 25′S, 170° 16′E about 75 miles NNE of Anuda (Cherry) I. A modified interpretation of the feature is suggested in FIG. 1, in preference to the E–W trough depicted by UDINTSEV (1958).

Contributions from the Scripps Institution of Oceanography, New Series, 1224

Reproduced by Permission

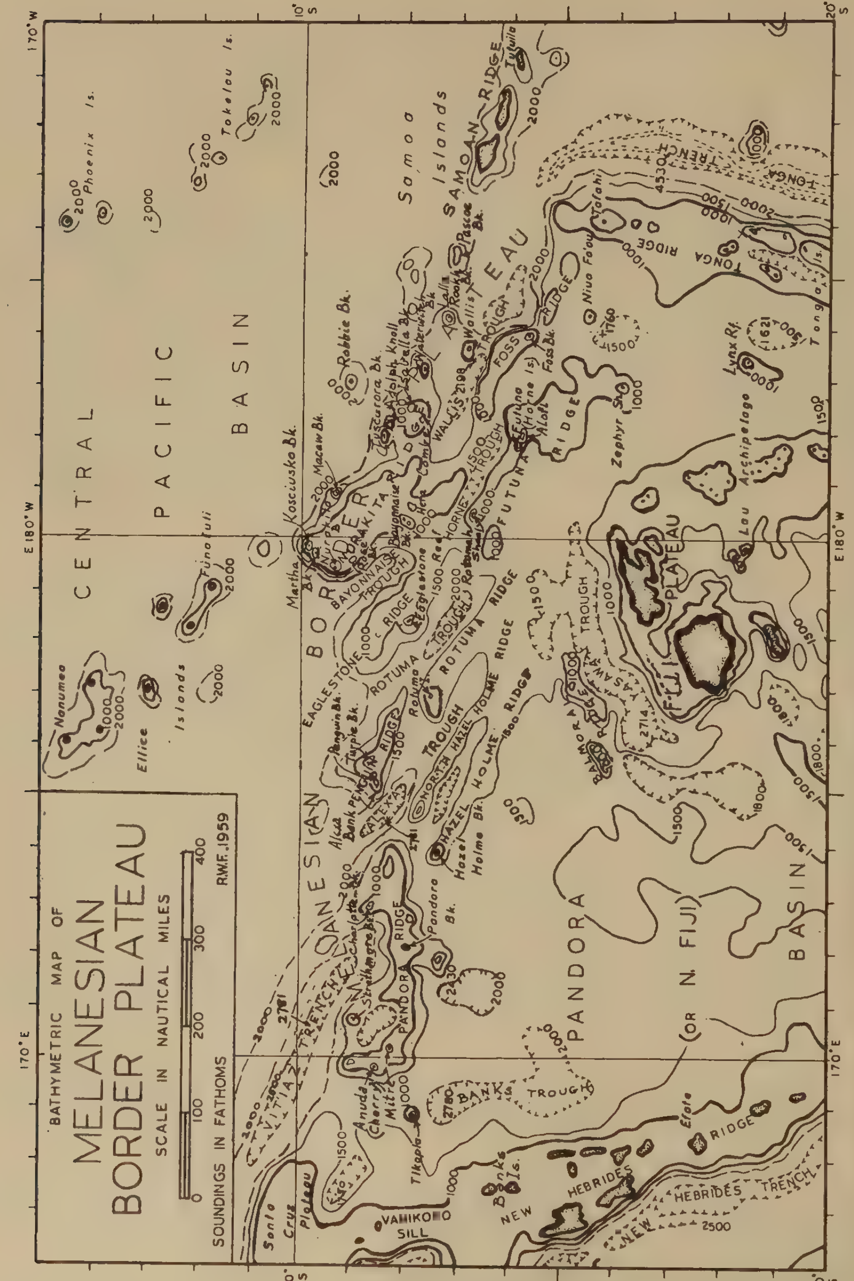
BATHYMETRIC MAP OF
MELANESIAN BORDER PLATEAU
SCALE IN NAUTICAL MILES
0 100 200 300 400
SOUNDINGS IN FATHOMS
R.W.F. 1959
170° W
E 180° W
170° E
10° S
20° S
CENTRAL PACIFIC BASIN
Phoenix Is.
Tokelau Is.
Ellice Islands
Nanumea
Funafuti
Samoa Islands
SAMOAN RIDGE
Tutuila
TONGA TRENCH
TONGA RIDGE
Tonga Is.
Tofahi
Niuo Fo'ou
Lynx Rf.
Lau Archipelago
Zephyr Sh.
FIJI PLATEAU
MELANESIAN BORDER PLATEAU
Kosciusko Bk.
Macaw Bk.
Robbie Bk.
Tuscarora Bk.
Adolph Knoll
Isabella Bk.
Wallis
Pascoe Bk.
FUTUNA TROUGH
FOSS TROUGH
HORNE TROUGH
Futuna (Horne Is.)
Alofi
Foss Bk.
Martha Bk.
BAYONNAISE TROUGH
Bayonnaise Bk.
EAGLESTONE RIDGE
Eaglestone Bk.
ROTUMA TROUGH
ROTUMA RIDGE
Rotuma
HOLME RIDGE
Holme Bk.
HAZEL HOLME TROUGH
Hazel Bk.
Penguin Bk.
Turpie Bk.
Alexa Bank
TEXAS RIDGE
Pandora Bk.
PANDORA RIDGE
Charlotte Bk.
Strathmore Bk.
BALMORAL REEF
YASAWA TROUGH
VITIAZ TRENCH
Anuda
Cherry
Mitre
Tikopia
Santa Cruz Plateau
VANIKORO SILL
BANKS TROUGH
Banks Is.
NEW HEBRIDES
RIDGE
Efate
NEW HEBRIDES TRENCH
PANDORA (OR N. FIJI) BASIN
1000
1500
2000
2500
2714
2781
4530

FIG. 1. Bathymetric chart of the Melanesian Border Plateau (see definition in introduction), showing location of echelon ridges and troughs, and banks representing probable drowned atolls.

(e) The *échelon* ridges are spotted by numerous ' banks ' at 10–15 fm (18–27 m) which are interpreted as ' drowned ' atolls. The cause of death of the corals is not yet clear.

The purpose of the present paper is to report on an echo-sounding survey of the Pacific slope, several banks (notably, Alexa Bank, also Penguin Bank and Tur[illegible] Bank, Figs. 2–3), and traverses over the Rotuma and Alexa Basins, and over Rotuma and Hazel Holme Ridges. These were carried out on Expedition CAPRICORN of the Scripps Institution of Oceanography, by the Research Vessels *Spencer F. Baird* and *Horizon* in December, 1952.

The two ships were equipped with high-frequency EDO echo-sounders reading by a vertical recording on a shoal scale of 0–600 ft, and deeper scales in 600 fm stages to over 5000 fm to an accuracy of 10 fm (18 m). Normal crusing speed was 11 knots. The ships navigated, as far as possible, on parallel courses 10–50 nautical miles apart.

A generalized contouring of the bathymetry of the Melanesian Border Plateau was carried out by the senior author at the Scripps Institution of Oceanography, La Jolla, in July–August 1954. The field work aboard the *Horizon* and the detailed map of Alexa Bank were completed by the junior author. The senior author joined the expedition at Fiji.

Our appreciation for encouragement and assistance is due to Dr. ROGER REVELLE, Director of the Scripps Institution of Oceanography and leader of the CAPRICORN expedition and to many individual members of the Scripps Institution, notably R. L. FISHER and H. W. MENARD.

BATHYMETRIC FEATURES OF MELANESIAN BORDER PLATEAU

The Melanesian Border Plateau (Fig. 1) measures approximately 1000 miles (E–W) by 100 to 300 miles (N–S). Depths of the basins are 1600 to 2200 fm (2900–4000 m) while the ridges are more or less flat-topped at 300–600 fm (556–1100 m). The mean depths of the plateau range from 1000 down to 1500 fm (1800–2700 m).

The name Melanesian Border Plateau was proposed (FAIRBRIDGE, 1960)* to designate the partially raised ' rim ' of the Melanesian region. It forms the northern limit of the Pandora Basin (or the ' North Fiji Basin ' of WISEMAN and OVEY, 1955, p. 101), and is separated from the Fiji Plateau (of Sir JOHN MURRAY, 1895) by the Balmoral Ridge and the Yasawa Trough (FAIRBRIDGE, 1960).

The contouring of this large and very poorly known area presents many difficulties of interpretation that cannot be satisfactorily solved until more detailed echo-sounding surveys are carried out. In the meantime, the details provided by the CAPRICORN tapes permit the establishment of a working hypothesis, *i.e.* that the basic trends or the Border Plateau are NW–SE, and not E–W as might reasonably have been assumed. With this assumption the pattern begins to unfold in a logical manner and a structural meaning appears for many isolated soundings.

However, it should be reiterated that these interpretations are based on a general hypothesis. It is not, for example, always possible to see whether an isolated shoal sounding represents a submerged bank on a general ridge or a seamount rising from considerable depths. With these reservations, therefore, the ridges and troughs are now described for the first time.

---

*Formal publication of this and other new names in this area first appeared in 1958, on Plate 10 of Bartholemew's Times Atlas (Mid-Century Edition), on the basis of ms. maps supplied by the senior author.

Among the more important *Ridges* are the following :

(a) *Pandora Ridge* is 250 miles in length (E–W) extending from 11° 45′S to 12° 30′S and 169° 30′E to 174° 30′E. It apparently consists of a series of minor NW–SE elevations 50 to 70 miles long and joined together *en échelon*. It forms the most westerly element of the Melanesian Border Plateau, being separated from the Santa Cruz Plateau by a 50 miles opening which connects the northwest end of the Pandora Basin (or N. Fiji Basin) with the Central Pacific Basin. Pandora Ridge is named after the Pandora Bank which lies in the middle of the ridge. This bank in turn was named after its discoverer H.M.S. *Pandora* under Captain E. EDWARDS. *Pandora* played a historic part in the search for the Bounty mutineers (1791) as well as in Pacific exploration. Other features of the ridge include Anuda (Cherry) and Mitre Islands, Strathmore, Charlotte and numerous unnamed banks and shoals, mostly of 10-15 fm (18–27 m).

(b) *Penguin Ridge* is 130 miles in length (NW–SE) and is separated from Pandora Ridge by the Alexa Trough with only 20–30 miles between the two. It is separated from the Rotuma Ridge to the southeast by a narrow sill that separates the Alexa and Rotuma Troughs. Penguin Ridge is surmounted by a number of banks and shoals, all submerged by 13–17 fm (24–31 m), and including Alexa, Penguin, and Turpie Banks (Figs. 2–3). Detailed soundings made by the *Baird* and *Horizon* indicate that the banks have saucer-shaped tops, suggestive of ‘drowned atolls’ (Fig. 3, also H.O. Chart 1984A, B.A. Chart 2901)*. The ridge is named for the middle of the three banks and also honours H.M.S. *Penguin*, which, under the command of Capt. A. M. FIELD, carried out the pioneer hydrographic surveys in this region during the year 1896.

(c) *Eaglestone Ridge* is 140 miles in length and lies some 50 miles east of Penguin Ridge. It is similar in form to the latter and can be defined by the 1000 fm (1800 m) contour. Eaglestone Reef could not be located by H.M.S. *Penguin* after a protracted search in 1896, but in 1943 a 5 fm (9 m) bank was sounded at 9° 43′S, 176° 36′E. However, although the ridge has not been thoroughly surveyed, it has an extensive top of depths of 400–600 fm (700–1100 m), so there is every possibility that other banks may be situated along the ridge. The feature is separated on the southwest by the Rotuma Trough from the Penguin-Rotuma Ridges and on the east by the Bayonnaise Trough from the Nurakita Ridge.

(d) *Nurakita Ridge* lies 50 miles north-east of the Eaglestone Ridge and trends equally NW–SE. It is 300 miles in length with a mean depth of 700 fm (1300 m) but is separated into more subsidiary rises, domes and furrows than most of the other ridges. It should be noted that it forms the extreme north-eastern limit of the Melanesian Border Plateau, paralleling the border of the

---

*H.O. refers to U.S. Navy Hydrographic Office charts and B.A. to British Admiralty charts.

Central Pacific Basin which drops sharply away to 2500–3000 fm (4500–5500 m). The Nurakita Ridge is crowned by two islands, Nurakita at the extreme north-western end and Wallis in the extreme southeast. Between, there are numerous banks and shoals, including Rose, Martha, Kosciusko, Macaw, Bayonnaise, Tuscarora, Adolph, Hera, Coombe, Isabella, Waterwitch, and Lalla Rookh. An interesting feature of these, and other unnamed banks is that they all rise to the very constant depth of 10–16 fm (18–29 m), approximately the same depth as the banks crowning Pandora and Penguin Ridges (H.O. Charts 0087, 1993; B.A. Charts, 1829; 1830).

(e) *Foss Ridge* lies south-east of the Nurakita Ridge and may be interpreted possibly as a long-distance extension of Eaglestone Ridge. As here defined it is 200 miles long, trending NW–SE with mean depths ranging from 800–1100 fm (1500–2000 m), generally about 900 fm (1645 m), thus notably lower than the western ridges. Foss Ridge, like Nurakita, forms the edge of the Melanesian Border Plateau and is separated from the parallel Samoan Ridge which lies less than 100 miles to the NE across an enclave of the South–West Pacific Basin. The only shoals that nearly reach the surface of the Foss Ridge are Foss Bank, with 22 fm (40 m), and another bank (reported in 1943) just south of it rising to 4½ fm (8 m) (B.A. Charts 1829, 1830).

(f) *Hazel Holme Ridge* forms one of a second series of *échelon* ridges and troughs that lie about 50–100 miles south of the series Pandora–Penguin–Eaglestone–Nurakita. Hazel Holme Ridge is about 250 miles long trending WNW–ESE with apparently two parallel crests separated by a narrow furrow; northerly one is distinguished as ‘ NORTH HAZEL HOLME RIDGE.’ The *Baird* and *Horizon* crossed these features on two traverses. Mean depths of the ridges are about 1000 kms (1800 m), and only one bank, Hazel Holme itself, rises to 17 fms (31 m); this bank has the same ‘ drowned atoll ’ form as the banks of the Penguin Ridge type (see H.O. Chart 1984B, or B.A. Chart 2901).

(g) *Rotuma Ridge* lies 25–50 miles east of Hazel Holme Ridge, trending WNW–ESE. It is 200 miles long with mean depths of the order of 1000 fms (1800 m) and is crowned by Rotuma Island and an unnamed 14 fm (25 m) bank, both at the north-west end. It is well defined by the 1500 fm (2700 m) contour. The traverses by the *Horizon* over the northern side of the ridge to Rotuma confirmed a remarkably steep off-shore profile (H.O. Chart 1984; B.A. Chart 1829).

(h) *Futuna Ridge* lies farther to the east and may perhaps be regarded as an extension of both Hazel Holme and Rotuma Ridges. It is of irregular shape extending roughly NW–SE for 250 miles in depths of 700–900 fms (1280–1450 m) (B.A. Chart 1829). It is crowned by the Horne Islands of Futuna and Alofi, with isolated shoals including Rotumah Shoal* in the north-west, and others including the Zephyr Shoal in the south-east. Rising as an isolated cone 50 miles to the east is the intermittently active volcano

---

*Not to be confused with Rotuma Island, 200 miles to the west.

Niua Fo'ou (' Tin Can Island '); however, it is doubtful if this island lies on the Futuna Ridge.

Turning next to the minor basins, troughs, or furrows between the elevated ridges of the Melanesian Border Plateau, there may be distinguished the following :

(i) *Alexa Trough* is a narrow depression, 200 miles long, trending NW–SE between Pandora and Hazel Holme Ridges in the south-west and Penguin and Rotuma Ridges on the north-east. There are also east–west furrows separating each ridge of each pair. The floor of the trough slopes down from 1500 fms (2700 m) in the south–west to 2200 fms (4000 m) in the north–west, where it reaches 2781 fm (5084 m). The basin is named after Alexa Bank to the north whence it falls away very sharply (Fig. 7a).

(ii) *Rotuma Trough* is parallel to and generally similar to the Alexa Trough, though somewhat broader, lying between Rotuma Ridge and Eaglestone Ridge. It is 150 miles long and includes a closed area east of Rotuma of more than 2000 fm (3650 m). To the north–west it opens into the Central Pacific Basin. R. V. *Horizon* traversing this part of the trough found a very even gradient down into the Central Pacific Basin (at about 10 fms per mile, or 1 : 100). This clearly is a case of an axially tilted trough where an emergence would expose a ' rias ' coastline (the British National Committee on Ocean Bottom Features informally suggested ' seafirth ' for such features, but the term has not found much favour).

(iii) *Bayonnaise Trough* is a third parallel furrow, separating Eaglestone from Nurakita Ridges. It is broader and shorter than the other troughs, being only 100 miles long and 50 miles wide. Its floor slopes from 1500 fms (2700 m) in the south–east to 2400 fms (4400 m) at the opening into the Central Pacific Basin. This is another case where the term ' trough ' or ' basin ' may well be replaced by another generic term, such as ' seabight.'

(iv) *Wallis Trough* lies in the same trend as Bayonnaise some 150 miles to the east–south–east. Its central part is a very narrow depression, completely closed by the 2000 fm (3656 m) contour, lying south–west of Wallis Island and north of the Foss Ridge. It is about 180 miles long and though the deep portion is only about 20 miles across, it widens out as it shallows to the west. Its eastern end is not well known.

(v) *Horne Trough* is oriented in a similar way and situated to the southwest and located to the north west of the Horne Islands (Futuna and Alofi). It is a very narrow depression with a portion of over 1800 fms (3290 m) completely closed. It extends over 100 miles in length and is only 10–20 miles wide.

TOPOGRAPHY OF ALEXA AND OTHER BANKS

Alexa Bank is well illustrated on B.A. Chart 2901 (H.O. 1984A) and numerous traverses by Expedition CAPRICORN add considerably to the detail (Figs. 2 and 3). Echo traces also disclose topographic features previously unknown. As shown in the illustrations (Figs. 4–7) the bank clearly has a raised ' rim.' This is generally

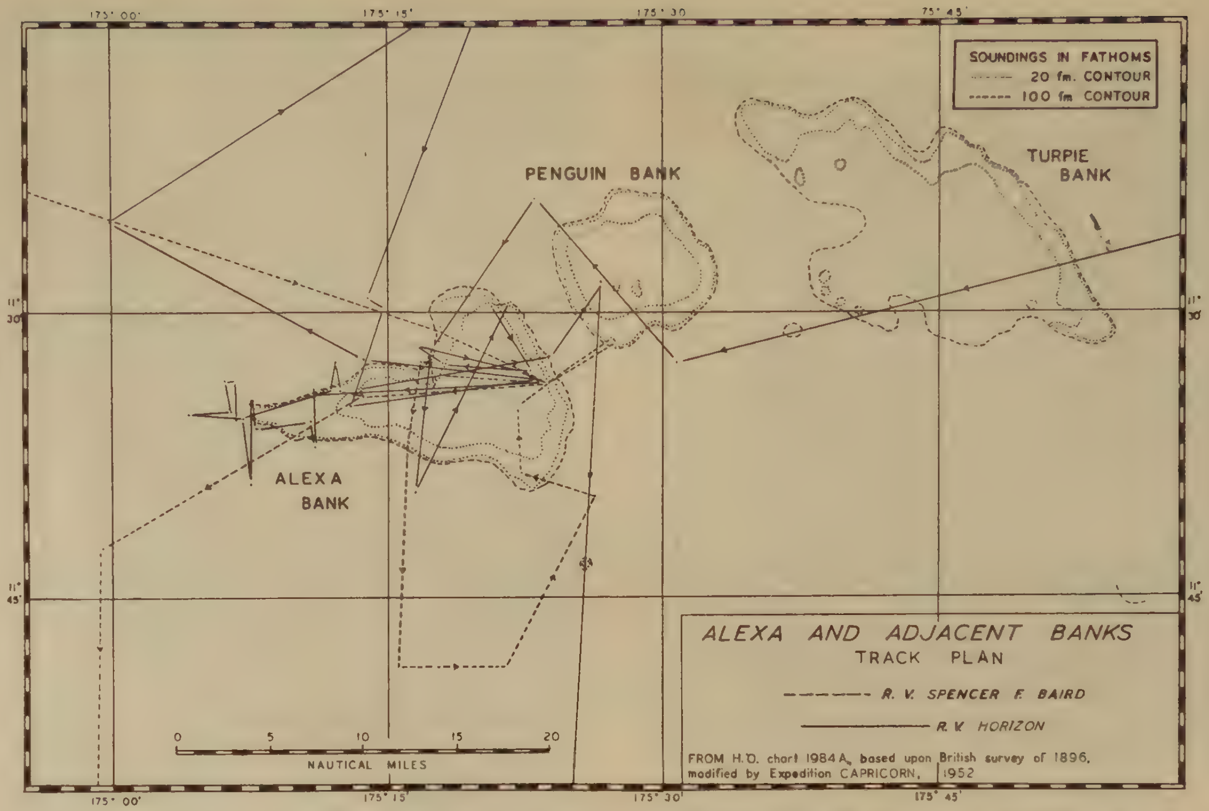
175° 00'
175° 15'
175° 30'
175° 45'
11° 30'
11° 45'
SOUNDINGS IN FATHOMS
20 fm. CONTOUR
100 fm CONTOUR
TURPIE BANK
PENGUIN BANK
ALEXA BANK
0
5
10
15
20
NAUTICAL MILES
ALEXA AND ADJACENT BANKS
TRACK PLAN
R. V. SPENCER F. BAIRD
R. V. HORIZON
FROM H.O. chart 1984 A, based upon British survey of 1896, modified by Expedition CAPRICORN, 1952

FIG. 2. Track plan for Alexa Bank area, showing routes of R. V. *Spencer*, F. *Baird* and R. V. *Horizon* on Expedition CAPRICORN, 1952. These banks are situated on Penguin Ridge (FIG. 1).

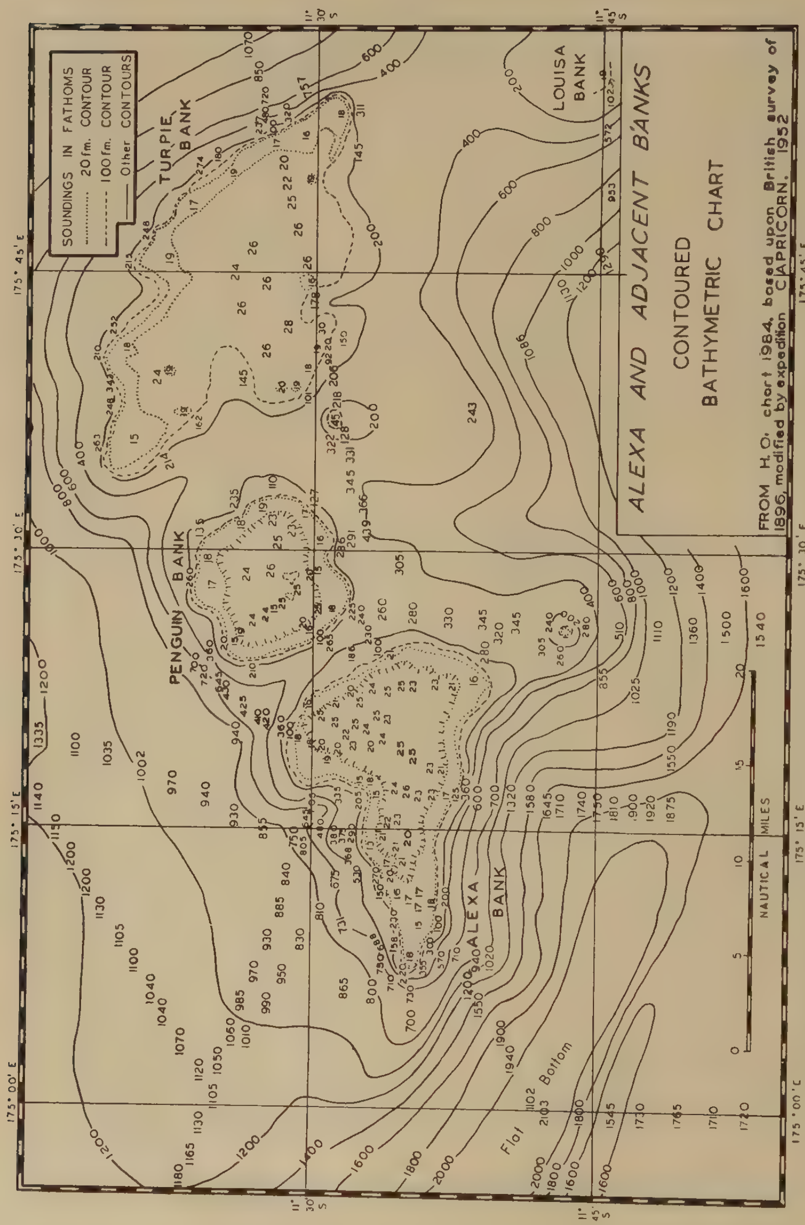
ALEXA AND ADJACENT BANKS
CONTOURED BATHYMETRIC CHART
SOUNDINGS IN FATHOMS
20 fm. CONTOUR
100 fm. CONTOUR
Other CONTOURS
FROM H.O. chart 1984, based upon British survey of 1896, modified by expedition CAPRICORN, 1952
TURPIE BANK
PENGUIN BANK
ALEXA BANK
LOUISA BANK
Flat Bottom
NAUTICAL MILES
0
5
10
15
20
175° 00' E
175° 15' E
175° 30' E
175° 45' E
11° 30' S
11° 45' S

FIG. 3. Contoured bathymetric chart of Alexa and adjacent banks, based on early surveys and CAPRICORN echo soundings. These banks are situated on Penguin Ridge (FIG. 1).

FIG. 4 (a). Surface of Alexa Bank, showing giant fan corals growing from an otherwise ' dead ' surface, covered with fine calcareous mud and algal covered boulders. ' Aqualung ' diver is Prof. WALTER MUNK. Photograph by Scripps Institution of Oceanography.

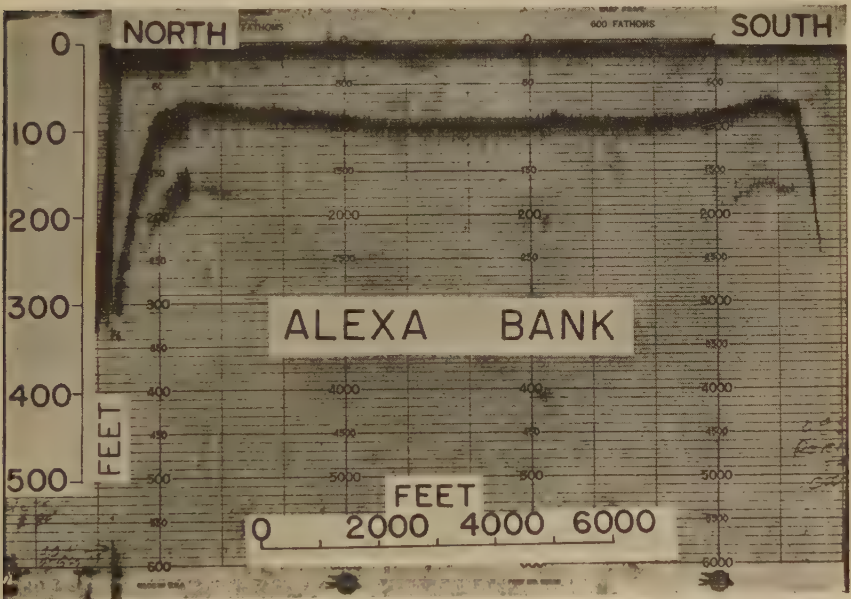

FIG. 4 (b). Echo-sounding trace by R. V. *Horizon* across the top of Alexa Bank, near the west end. Note rims of the bank at 60–70 ft, with saucer-shaped depression at 90 ft.

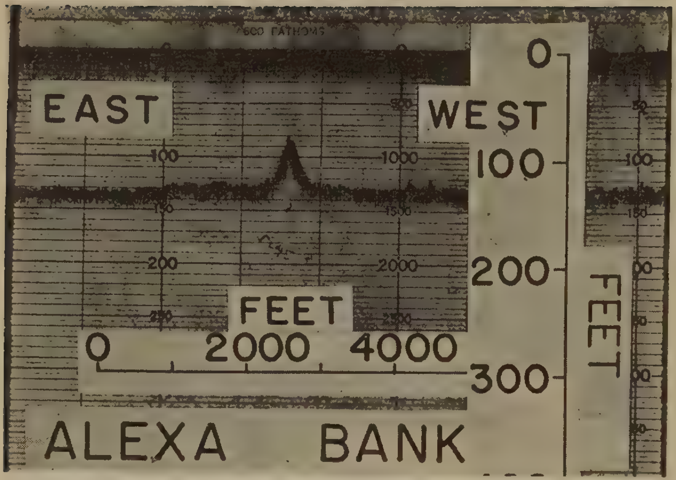

FIG. 5 (a). Surface of Alexa Bank, echo-trace by R.V. *Baird* in the deepest sector near the east center : average depth here 130 ft. Pinnacle rising 30 ft from floor may be interpreted either as a coral knoll that has grown up, or as a karst residual.

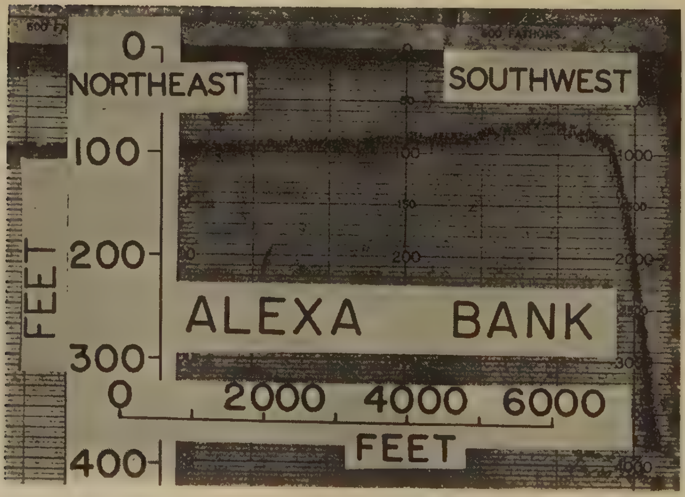

FIG. 5 (b). Detail of southwest rim of Alexa Bank, echo-trace by R.V. *Baird*, showing humped shape of rim 1800 ft wide, and abrupt offshore slope, dropping 500 ft in 900 ft of traverse, a gradient of 1 : 18 (30°).

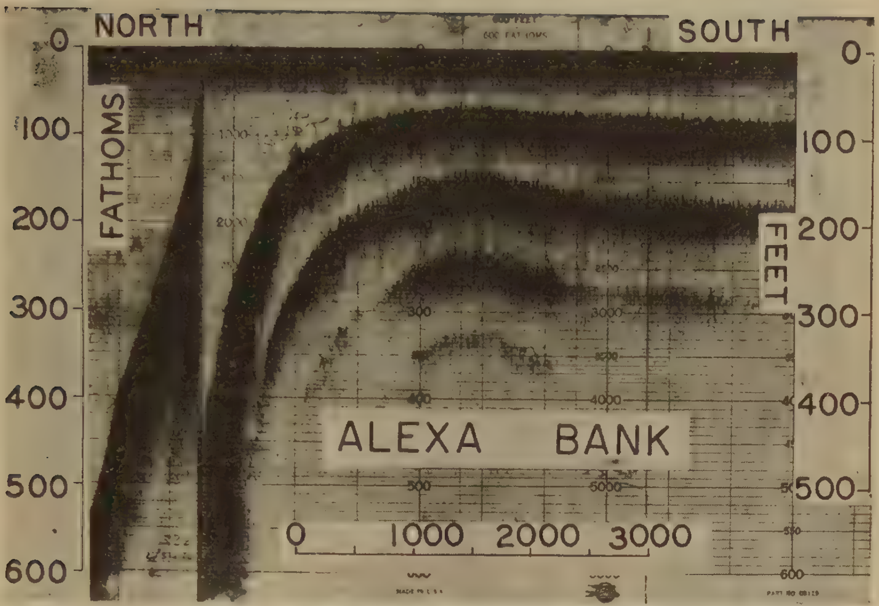

Fig. 6 (a). Northern rim of Alexa Bank, showing unusual rounded profile, with rim at 65 ft, dropping to 80 ft towards the interior of the saucer. Small coral heads seem to mark the outer edge in 70–120 ft. Offshore gradient (on fm scale) is 36° steepening at 1000 fm (course change) to 40°.

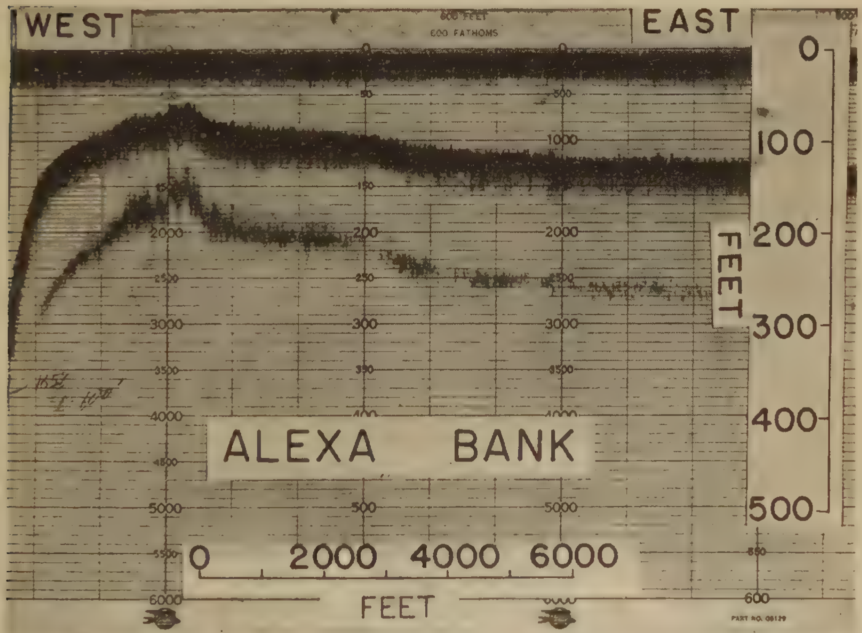

Fig. 6 (b). Northwest rim of Alexa Bank, showing traces of two terraces levels in saucer-like platform, the rim at 70 ft, rising in pinnacles to 60 ft, an inner terrace at 90 ft, and the platform floor at 120–130 ft.

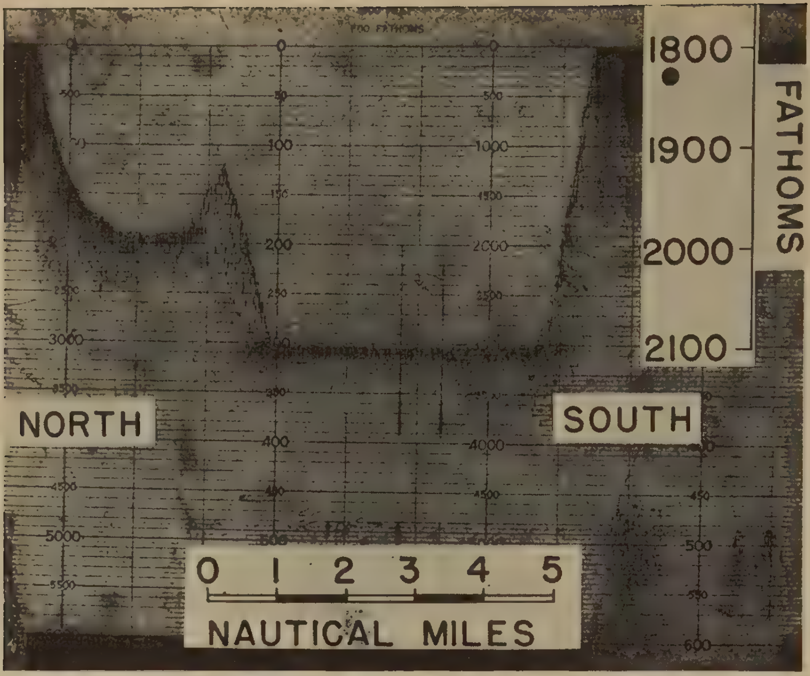

FIG. 7 (a). Section of the flat floor of the Alexa Trough at 2100 fms. The lower slopes of the trough exhibit a gradient of 1 : 25 (22°). An intermediate step is shown at 2000 fm, sediment being apparently dammed back by a low ridge.

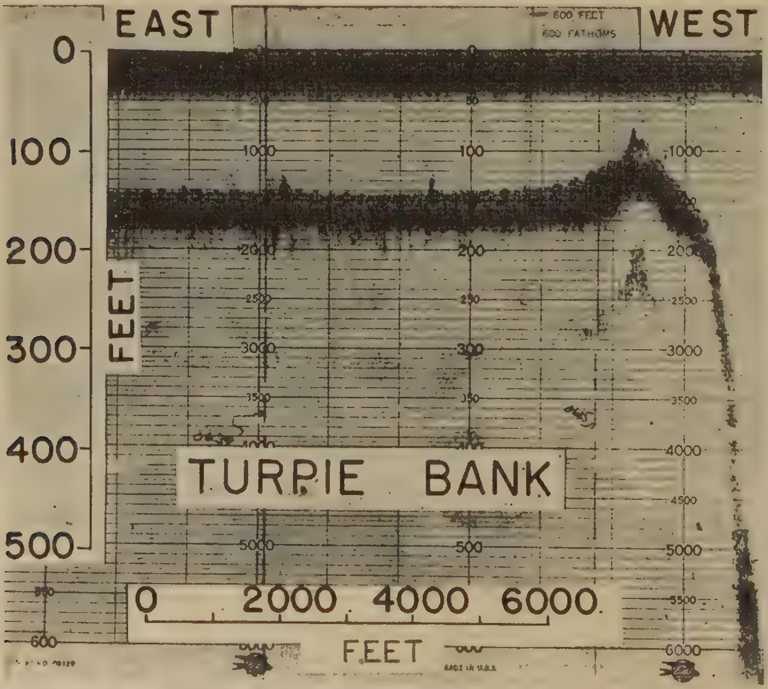

FIG. 7 (b). Margin of Turpie Bank, another drowned atoll on Penguin Ridge. Note that the inner side of the bank is steeper than at Alexa Bank, dropping from 70 ft rather steeply to a uniform floor at 140 ft, punctuated by small coral heads or knolls rising 10–20 ft above the floor.

1000–2000 feet wide and is 30–60 feet above the level of the flat saucer-like depression over the centre of the bank. There appear to be three distinctive levels : (a) 60–70 ft (10–12 fm or 18–21 m), the ' Rim ' ; (b) 90 ft (15 fm or 27 m), an intermediate terrace, on the inside it is about 2000–3000 ft in width, but on the outside it is 0–300 ft in width; (c) 120–130 ft (20–22 fm or 36–40 m), the main terrace (floor) of the bank

In places over the surface of the rim and on the floor of the bank there are pinnacles or knolls rising 10–20 ft. Investigations with the aid of an ' aqualung ' proved that these were in part living coral heads, but that the rest of the bank was covered by dead coral boulders encrusted with algae and covered with a white calcareous (foraminiferal) mud.

Some pinnacles of exceptional size, 30 ft high or more (Fig. 5a) could represent living coral heads, but, lacking confirmation, an alternative hypothesis must also be entertained. If the banks are essentially erosional features (see below, ' Pleistocene Karst Effects '), the pinnacles may in part be erosional remnants of karst solution.

The outer margins of Alexa Bank steepen very sharply and drop away to great depths at remarkably steep gradients. Angles of 30–40° are maintained on these slopes for thousands of feet. Dredging was unsuccessful on these slopes, but there seems no doubt that the only rock type strong enough to stand up at such angles without collapsing would be a massive coral limestone. Admittedly the spine of a volcanic cone will maintain steeper slopes, but the size of Alexa and other banks here (5–20 miles across) precludes a simple volcanic plug. We have no sample or geophysical evidence* which would indicate whether or not there is a volcanic core to each of the banks but the fact that several volcanic plugs (Anuda, Wallis, Horne, etc.) do occur in the area is suggestive.

Expedition CAPRICORN traversed Alexa, Penguin and Turpie Banks, which were all of the same type. The hydrographic charts suggest that there are more than forty such banks in the Melanesian Border Plateau. In dimensions, Alexa Bank is an average one measuring 10 miles by 5 miles across; Penguin Bank is about 4 miles by 4 miles.

Turpie Bank is also 10 miles by 5 miles, but most of its rim on the south–west side is missing; the rim terrace is mostly at 15–20 fm, and the main bank 26–27 fm. Tuscarora Bank is about 12 miles by 8 miles and its rim is broken in many places, and is of similar depths. Robbie is about 10 miles by 10 miles, has a perfect rim at 10–12 fm and an interior flat about 26–27 fm. Pascoe is nearly 30 miles long but only 2–5 miles across, with a rim at about 10 fm and interior terraces at 20 and 27 fm. Most of the others show this sort of pattern, though a few rise to 4–5 fm.

SUBMARINE BANK TERRACES

Hitherto the only author to comment at any length on the banks of the Melanesian Border Plateau was R. A. DALY (1934, p. 241 ff.), who concluded that the accordance of terrace depths between these (and other platforms in different parts of the world) required a common explanation. He suggested that low-sea level planation during Pleistocene glacial stages was the only acceptable hypothesis; local subsidence seems to require altogether too remarkable coincidences over such a very broad area.

---

*Dr. Russell Raitt (personal communication) notes that his incomplete seismic data suggests a volcanic core to Alexa " roughly similar to Funafuti atoll."

We agree with DALY's interpretation in general, but with some modifications. There appear to have been not one but several periods of planation, as there are several distinctive terrace levels. They are so wide-spread that they probably call for a eustatic explanation; 10–12 fm (18–21 m), 14–17 fm (25–30 m), and 25–27 fm (46–50 m) seem most constant.

Some local, but minor tectonic forces may be involved in some of the areas, where a slight tilt or segmentation seems to be involved. The region is now almost completely free from recordable seismicity and vulcanicity, although some of the steep lower slopes, *e.g.*, the 22° slope dropping straight down into Alexa Trough (Fig. 7a), are indicative of at least a potential instability.

There are no direct data for the terraces but if they are rather youthful there may not have been time for slow secular tectonic changes to become obvious. That the terraces are indeed youthful is suggested by the smooth fresh surfaces and the relative freedom from youthful coral overgrowth.

Recent studies by one of us (FAIRBRIDGE, 1958) assisted by radiocarbon datings, carried out by the Lamont Geological Observatory, Yale Geochronometric Laboratory and the U.S. Geological Survey, clearly indicate that important eustatic oscillations and still-stands occurred even during the post Glacial (Recent) epoch, notably at minus 3–4 m or 1½–2 fm (in several oscillations dating back to 4300 B.P.*), at about — 21 m or 12 fm (8500 B.P.), at — 32 m or 18 fm (11,000 B.P.) and at — 46 m or 25 fm (12,500 B.P.).

From the evidence available it would seem that deeper eustatic terraces ranging from 20 to 75 fm are to be correlated with low sea-levels of the last Glacial (Wisconsin/Würm), as may be seen from the data of the Mississippi delta, where a factor of local subsidence is also recordable (FISK and MCFARLAN, 1955). Consideration of the general, secular drop of sea level through the Quaternary (ZEUNER, 1952) suggests that the low sea-levels of glacial stages earlier than the Wisconsin would not have reached much lower than the present sea-level. This concept is quite contrary to that of DALY (1934) who visualized an equal drop of sea-level for each successive glacial age. Some evidence, admittedly not conclusive, is presented by EMERY (1958) for terrace cutting in southern California earlier than the Wisconsin but here the picture is considerably complicated by warping. EMERY has also provided a valuable bibliography of recent data on submarine terraces that confirms our first impression that the levels observed on Alexa and adjacent banks are to be found repeated in many parts of the world, and are therefore most reasonably interpreted as eustatic.

PLEISTOCENE KARST EFFECTS

There is little doubt that coral banks subject to late Pleistocene exposure due to a drop in sea-level underwent intensive karst solution. Such effects are most striking in reefs associated with the marginal latitudes of the coral-favoring environments : thus Bermuda (32°N), Bahamas (25°N.), Pescadores (23°N), Houtman's Abrolhos (29°S). Submarine terraces, channels and ‘ ocean holes ’ are characteristic features. In the days of the MURRAY-DARWIN controversy the solution effects were taken (by the MURRAY school) to be the product of contemporary erosion by sea-water. Following A. AGASSIZ (1903, p. 412) : ‘ The existence of honeycombed pinnacles of limestone within the lagoons of atolls, as shoals, islands, or islets, shows the extent of the solvent action of the sea upon land areas, having formerly a greater extension than at the present day.' But according to modern studies, carbonate solution by sea-water seems possible only in the intertidal belt, except under special circumstances (Revelle and Fairbridge, 1957).

---

*B.P. = before the present (datum year A.D. 1950).

Subaerial solution is thus inevitable. In any hypothesis it is therefore essential to provide for the total emergence of any coral platform to permit deep-reaching karst solution. ' Ocean holes ' (karst sink holes) dropping down hundreds of feet are observed in the Bahamas (Agassiz, 1894) and in the Houtman's Abrolhos (Fairbridge, 1948, see esp. pl. 3), and Jordan (1954) has described similar features at 140–150 fm on the east Florida shelf.

To quote from the Abrolhos description (Fairbridge, 1948, p. 30): ' During the Würm exposure, the island must have stood up as a fairly high eminence, about 350 ft above sea level. Deep reaching karst erosion set in and the whole of this limestone mountain became riddled with sink-holes, underground streams, caverns, stalactite caves, and the like. It is probable that the margins of this table-topped mountain were higher than the centre, though the rim may well have had gaps in the north.'

The development of submerged terraces on coral banks and atolls is particularly striking (as opposed to the less obvious terracing of continental shelves) because of the low rate of sedimentation in oceanic areas. Certain continental areas with marginal to arid hinterlands also show the same features but they are less usual (see the West Australian shelf profiles, Carrigy and Fairbridge, 1954).

Fine examples of bank terraces are to be seen in the Tonga Islands, especially north of Tongatabu and west of Ha'apai, both of which were traversed by Expedition Capricorn. Well-developed examples can be seen also in the South China Sea, e.g. Macclesfield Bank and Tizard Bank (Spratley Is. or Tua Sha Is.) where they are described by Wharton (1888) and Kuo (1948); also in the East Indies, e.g. Tijger and Paternoster Banks (Molengraaff, 1930; Kuenen, 1933, 1947; Umbgrove, 1947); again in the Maldives and Laccadives (Gardiner, 1903). Few, however, demonstrate such barren simplicity as those of the Melanesian Border.

In a laboratory tank, Hoffmeister and Ladd (1945) subjected an exposed block of limestone (with a flat-cut top) to a continuous shower of dilute acid, to simulate rainfall during the last Glacial low sea-level period. The similarity to the effects of subaerial solution was remarkable : the block became lined with characteristic karst runnels down the sides, but the top was only slightly lowered and in a *saucer-shape*. An atoll-like rim was thus produced by a purely solvent process. Many elevated islands have precisely this form today (Hoffmeister and Ladd, 1935). MacNiel (1954) proposed that such solution effects produced during low sea-level stands could explain the form of modern atolls generally. This may be true, but owing to the heavy post-Glacial overgrowth of coral on the rims and accumulation of sediment in the lagoons, it cannot always be demonstrated.

Special consideration is needed to explain how terraces occur on the rims of modern, growing atolls (e.g. Bikini; see Emery *et al.*, 1954), of emerged atolls (*e.g.* on Kita and Minami Daito or N. and S. Borodino Islands : see Nugent, 1948; Saplis and Flint, 1949; Fairbridge, 1950b), and of submerged atolls, such as on the Melanesian Border Plateau. If, after the last Glacial low period, as the sea rose to a still-stand at 8 fm (9000 B.P.), coral grew vigorously over the old eroded rim to the new level, it would then spread out to the limit of the foundation, within the depth range for the organism concerned. The sea-level then dropped to 12 fm (at 8500 B.P.). For several centuries the margins of the rim were then eroded, and became notched, forming terraces. At the same time new reef fringes built up these terraces at their periphery. Those coral communities facing the interior of the atoll built up more rapidly than those facing the outer margin, contrary to popular belief. Wider reef flats are found on the inner side, because the bottom is shallow there and permits rapid lateral growth while on the outer face the floor drops away steeply and much outward growth is impossible. This tendency has been confirmed by ground studies and from air photographs of many reef platforms (FAIRBRIDGE, 1950a; TEICHERT and FAIRBRIDGE, 1950); in the waters of atoll lagoons, which are changed daily by tidal currents, there is no convincing evidence of greatly restricted coral metabolism due to nutritional deficiency (thanks largely to the photosynthetic activity of the symbiotic algae, zooxanthellae : SARGENT and AUSTIN, 1954).

Coral upgrowth with rising sea-level continued after 8500 B.P. This was followed by alternate periods of terrace-cutting and lateral growth, repeated several times with diminishing amplitude to make the steep-like margins of atolls.

The reason for failure of most of the coral banks on the Melanesian Border Plateau to maintain up-growth to the present level is still a mystery. The terracing of the rims is not as sharp as is usual on emerged atolls and perhaps indicates a poverty of coral growth during the still-stands. Some of the profiles are very similar to HOFFMEISTER and LADD's (1945 and to MACNIEL's (1954) sketches, suggesting that solution has greatly dominated over coral growth during the last 15,000 years.

DISCUSSION : THE DROWNING ATOLLS

W. A. SETCHELL (1928, p. 325) once remarked : ' the general, although tacit, assumption that the submerged reef is living seems to be taken for granted,' indeed, without any real grounds at all. SETCHELL (1928) found that many of the submerged reefs, particularly in Hawaii, the Fijis and Tonga, were just as dead as the emerged reefs. Corals can be killed by a few hours of exposure above tide level, but it is not always appreciated that they can be wiped out almost as easily by a rapid submergence which may bring them into depths that are too cool or too dark for normal growth. This may be due either to local subsidence or to a very sudden eustatic rise in sea level. Such a rise took place near the beginning of the Recent epoch, when apparently the sea level rose 90 ft within a period of a few hundred years (according to recent radiocarbon dates). This may have exceeded the growth and adaptation rates of the corals concerned. Some of the subsequent, though smaller sea-level changes were even more rapid (FAIRBRIDGE, 1958). Under such conditions one speaks of corals as having been ' drowned,' but the physiological and environmental factors responsible for this are not well established. Under favourable conditions a number of coral species have an astonishing temperature and depth tolerance, as witness the deepwater reefs of the coast of Norway, Ireland and Spain (PRATJE, 1924; TEICHERT, 1958).

The ' drowned ' coral banks of the Melanesian Border Plateau lie between 11° and 13°S and thus are clearly equatorial. It is therefore improbable that their death reefs could be explained by lower sea temperatures during the last Glacial age. Coral farther from the equator (say 25–30°N and S) may well have been affected in that way, but the Melanesian Border Plateau is hardly a marginal latitude with respect to coral habitat.

DALY (1934) visualized Pleistocene planation by wave action as more vigorous than today. Furthermore the large amount of sediment in suspension would inhibit much of coral growth (DALY, 1934). In the continental shelf areas near the ecologic limits of coral growth this concept seems well-substantiated, but sediment suspensions are not to be expected in this part of Melanesia, many hundreds of miles even from the nearest major island groups (Fiji and New Herbrides) and 1500 miles or more from the nearest continental rivers in eastern Australia.

Quite distinct from the killing and erosion of the coral communities during the last Glacial stage is the major problem why, during the subsequent rise of sea-level, corals did not colonize the eroded platforms and grow upwards to form contemporary atolls and living coral banks. The scattered coral colonies on the surface of the banks today suggest a highly improverished or only recently colonized habitat.

There are at least five possible explanations worth considering :

(a) During the last major drop of sea-level, fringing reefs failed to maintain themselves on the margins of the coral banks. These were certainly very steep and offered an extremely restricted and narrow biotope. Block-faulting and landslides could have carried many colonies down into cold, dark, inhibitory depths. During the subsequent rise in sea-level there were no established colonies to generate upward growth to develop and maintain a normal atoll.

(b) The location of the Melanesian Border Plateau is an isolated region, not easily replenished by young coral planulae from protected, favourable 'nurseries' (GUPPY, 1903–06; WELLS, 1957). It lies within the South Equatorial Current which skirts the islandless region north of the Marquesas, Tahiti and Samoa, swinging southwestwards into Melanesia. In Glacial times this current may have been much cooler than today. Isotope temperature determinations by EMILIANI (1955) suggest 5° to 8° lower mean surface water temperatures. An additional factor to the general lowering of solar radiation was the contribution in the east from the cold Humboldt (Peru) Current, fed by the great Pleistocene glaciers of the Chilean Andes and the advanced ice-front of Antarctica.

(c) The Melanesian Border Plateau is situated in the region of the Southeast Trade Winds, which are only periodically reversed in summer by the northerlies or Northeast trades. This would mean that most of the time (especially in the cool Pleistocene period) it would be downwind of the volcanoes of Tonga and Niua Fo'ou; some of the youthful volcanic sources of Fiji or the Wallis Islands (now extinct) may also then have had active phases. Showers of volcanic dust coupled with a lowering of sea-level would be deleterious to coral growth. However, experimental work by YONGE (1940) and colleagues on the British Museum's Great Barrier Reef Expedition suggests that the importance of sedimentation in discouraging coral growth has been exaggerated in the past. This ' explanation ' is therefore discounted.

(d) As noted above, the narrow *échelon* troughs of the Melanesian Border Plateau are almost unique in contemporary marine geology. They compare most obviously with the ' Continental Borderland ' of southern California. Even the newly discovered *Vitiaz* Trench (Fig. 8), with its oceanside rim higher than the floor of the Central Pacific Basin, suggest ' borderland ' tectonics, rather than the marginal trench characteristic of the western Pacific. These borderland trenches and troughs include numerous narrow closed depressions, which would favour the development of foul bottom in black mud facies inhabited only by anaerobic bacteria. The production of H_2S by the latter would probably lead to periodic upwelling of lethal waters (Brongersma-Sanders, 1957).

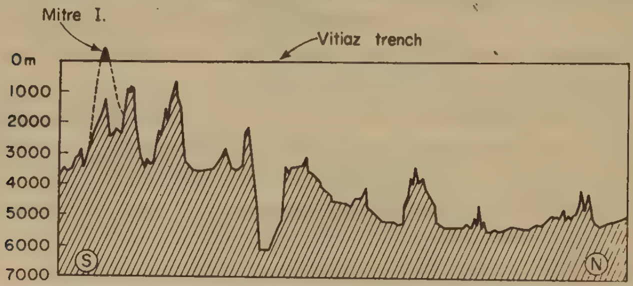

Fig. 8. North-south profile through the Melanesian Border Plateau along long. 170° 16′E, crossing Pandora Ridge just east of Mitre Island, and the newly discovered *Vitiaz* Trench (from Udintsev, 1958). Note the location of the trench *within* the borderland.

(e) Another possible form of upwelling is the type due to the impact of onshore currents on steeply rising continental margins (Sverdrup, 1938; Fleming and Revelle, 1939). The Melanesian Border Plateau is in fact a continental margin. Here the Central Pacific Basin is about 2700–2000 fm deep, and the bottom slopes steadily up to the banks of the Plateau. The South Equatorial Current flows southwesterly here, thus directly onto the *échelon* slopes of the banks which extend NW–SE. Unfortunately we lack water samples and temperature observations in the critical areas to prove the existence of such upwelling.

TECTONIC POSITION OF THE MELANESIAN BORDER PLATEAU

The situation and structural pattern of the Melanesian Border Plateau is anomalous from many points of view. According to Marshall (1911), Born (1933) and others it represents the subcontinental margin of the Pacific and is bounded by the ' Andesite Line.' Volcanic material in Fiji, and in the few volcanic islands of the Border Plateau mostly point to ' Pacific Suite ' (*i.e.* Pacific margin) petrology. Bryan (1944), however, drew his ' Marshall Line ' rather differently from Born (1933) to exclude the Melanesian Border Plateau, swinging it around Fiji and the New Hebrides, and leaving the Pandora Basin and the whole Border Plateau in the Mid-Pacific province. It is doubtful if Bryan was correct, however, as the shallow ridge and basin areas can hardly be classified as typically ' mid-Pacific.' The lavas from most of the islands confirms Born's (1933) viewpoint. Earlier reports by Viala (1919), De La Rue (1935) and Lacroix (1941) suggested that all the volcanics were of the Circum–Pacific olivine basalt.

However, MacDonald (1945, p. 870) demonstrated that a single centre, the Wallis Islands (notably Uvea), ' undoubtedly belong to the alkaline suite of the central Pacific volcanoes ' (*i.e.* ' Atlantic Suite ' of Harker). This is unusual since the Wallis Islands are situated within the Border Plateau. However, the orientation of the echelon ridges here exactly parallels that of the Samoan Ridge and other WNW–ESE mid-Pacific volcanoes (Cook, Tahiti, Hawaii). It is surmised therefore that some of these structures are related to deep crustal fractures, of considerable age, and less related to the new orogenic belts of the Melanesian subcontinent than to the old Pacific thlassocraton*.

In tectonic geology, it is tempting to interpret a zone of echelon structures as normal faults or short strike-slip shears, symptomatic of a great linear transcurrent (strike-slip) fault at depth. Since the *échelon* structures are oriented NW–SE or WNW–ESE, this would indicate an E–W trans-current basement fracture, of sinistral or left-lateral displacement. Thus, it would be complimentary in character to the Great Alpine Fault of New Zealand, to the San Andreas Fault of California and many others.

However, the similarity ends here, and in several outstanding points there is a marked contrast. The fundamental E–W orientation of the Melanesian Border Plateau is essentially out of line with the general NNE and NW trends of the western Pacific. It is an almost aseismic zone. It is not paralleled by a belt of deep sea trenches. It seems to fit into the broad picture of old Pacific shear patterns, but it apparently is no longer an active tectonic belt. This is supported by the geomorphologic evidence of a long period of stability in the Wallis Islands (Stearns, 1945).

Columbia University,
New York.

Contribution from the Scripps Institution of Oceanography, New Series. This paper represents one of the results of research on the Expedition Capricorn *of the Scripps Institution of Oceanography which was supported by the Office of Naval Research and the Bureau of Ships of the U.S. Navy Department. Participation of the senior author was supported also by a scientific fund from the Commonwealth of Australia.*

REFERENCES

Agassiz, A. (1894) A reconnaissance of the Bahamas and of the elevated reefs of Cuba. *Bull. Mus. Comp. Zool. (Harvard)*, **26**, 1–203.

Agassiz, A. (1903) On the formation of barrier reefs and of the different types of atolls. *Proc. Roy. Soc. (London)*, **71**, 412–414.

Born, A. (1933) Der geologische Aufbau der Erde. *Handbuch der Geophysik, Berlin*, **2**, 565–867.

Brongersma-Sanders, M. (1957) Mass mortality in the sea. *In* Treatise on Marine Ecology and Paleocology, vol. 1, *Geol. Soc. Amer. Mem.* **67**, 941–1010.

Bryan, W. H. (1944) The relationship of the Australian continent to the Pacific Ocean—now and in the past. *J. and Proc. Roy. Soc. N.S.W.*, **78**, 42–62.

Carrigy, M. A. and Fairbridge, R. W. (1954) Recent sedimentation physiography and structure of the continental shelves of Western Australia. *J. Roy. Soc., Western Australia.* **38**, 65–95.

Daly, R. A. (1934) *The changing world of the Ice Age.* Yale Univ. Press, New Haven, 271 pp.

Emery, K. O. (1958) Shallow submerged marine terraces of southern California. *Bull. Geol. Soc. Amer.*, **69**, 39–60.

---

*A term introduced by the senior author to cover the stable, oceanic type of crust (Fairbridge, 1955, p. 42).

Emery, K. O., Tracey, J. I. Jr. and Ladd, H. S. (1954) Geology of Bikini and nearby atolls. Part I, Geology. *U.S. Geol. Surv., Prof. Pap.* 260-A, 265 pp.

Emiliani, C. (1955) Pleistocene temperatures. *J. Geol.*, **63**, 538–578.

Fairbridge, R. W. (1948) Notes on the geomorphology of the Pelsart Group of the Houtman's Abrolhos Islands. *J. Roy. Soc. Western Australia*, **33** (for 1946–47), 1–43.

Fairbridge, R. W. (1950a), Recent and Pleistocene coral reefs of Australia. *J. Geol.*, **58**, 330–401.

Fairbridge, R. W. (1950b) Landslide patterns on oceanic volcanoes and atolls. *Geogr. J. (London)*, **115**, 84–88.

Fairbridge, R. W. (1955) Warm marine carbonate environments and dolomitization. *Tulsa Geol. Soc. Digest*, **23**, 39–48.

Fairbridge, R. W. (1958) Dating the latest movements of the Quaternary sea level. *Trans. N.Y. Acad. Sci.*, ser. 2, **20**, 471–482.

Fairbridge, R. W. (1960) Bathymetric features of the Melanesian region. (in preparation).

Fisk, H. N. and McFarlan, E. Jr. (1955) Late Quaternary deltaic deposits of the Mississippi River. *Geol. Soc. Amer. Sp. Pap.*, **62**, 279–302.

Fleming, R. H. and Revelle, R. (1939) Physical processes in the oceans. *In Recent Marine Sediments* (Tulsa, Okla., A.A.P.G. publ.) 48–141.

Gardiner, J. S. (1903–06) *The fauna and geography of Maldive and Laccadive archipelagoes*. Cambridge, 2 vols.

Gaskell, T. F. and Ritchie, G. S. (1953) H.M.S. *Challenger's* world voyage 1950–52. Part 1, Atlantic and Pacific Oceans. *Int. Hydrogr. Rev.* **30**, 111–123.

Guppy, H. B. (1903–06) *Observations of a naturalist in the Pacific between* 1896 *and* 1899. London, Macmillan and Co., 2 vols.

Hoffmeister, J. E. and Ladd, H. S. (1935) The foundations of atolls : a discussion. *J. Geol.*, **43**, 653–665.

Hoffmeister, J. E. and Ladd, H. S. (1945) Solution effects on elevated limestone terraces. *Bull. Geol. Soc. Am.*, **56**, 809–817.

Jordan, G. F. (1954) Large sink holes in Strait of Florida. *Bull. Amer. Assoc. Petr. Geol.*, **38**, 1810–1817.

Kuenen, P. H. (1933) Geology of coral reefs. *The Snellius Expedition*, v. 5, (Geological Results) (2) 124 pp.

Kuenen, P. H. (1947) Two problems of marine geology : atolls and canyons. *Verh. Kon. Ned. Akad. Wet.* (Amsterdam), *Afd. Nat.*, sec. 2, **43**, (3), 68 pp.

Kuo, L. C. (1948) Geomorphology of the Tizard Bank and Reefs, Nan-Sha Island, China. *Acta. Geol. Taiwanica*, **2**, 45–54.

Lacroix, A. (1941) Composition minéralogiques et chimique des laves des volcans des îles de l'Ocean Pacifiques situées entre l'Equateur et le Tropique Caprecorne, le 175° de longitude Ouest et le 165° de longitude Est. *Mém. Acad. Sci. Paris*, **63**, 2, 1–98.

MacDonald, G. A. (1945) Petrography of the Wallis Islands. *Bull. Geol. Soc. Amer.*, **56**, 861–872.

MacNeil, F. S. (1954) The shape of atolls : an inheritance from subaerial erosion forms. *Amer. J. Sci.*, **252**, 402–427.

Marshall, P. (1911) Oceania. *Handbuch der regionalen Geologie* (v. VII), Heidelberg, Carl Winter, 36 pp.

Molengraaff, G. A. F. (1930) The coral reefs in the East Indian Archipelago, their distribution and mode of development. *Proc. Pac. Sci. Congr.* (4th, Java, 1929) 2A & B, 58-89, 989–1021.

Murray, J. (1895) A Summary of the Scientific Results (in two parts). *Rept. Sci. Res. Voy.* H.M.S. *Challenger* 1872–76 (London).

Nugent, L. E. (1948) Elevated phosphate islands in Micronesia. *Bull. Geol. Soc. Amer.* **59**, 977–994.

Pratje, O. (1924) Korallenbanke in tiefem und kühlem Wasser. *Zentralbl. f. Min. Geol. Pal.*, 410–415.

Revelle, R. (ed.) (1953) *Shipboard Report, Capricorn Expedition*. Scripps Inst. Oceanography (U. of Calif), Ref. 53–15. (Unpublished manuscript).

Revelle, R. and Emery, K. O. (1957) Chemical erosion of beach rock and exposed reef rock. (Bikini and nearby atolls, Marshall Islands). *U.S. Geol. Surv., Prof. Pap.* 260–T, 699–709.

Revelle, R. and Fairbridge, R. W. (1957) Carbonates and carbon dioxide. *Geol. Soc. Amer. Mem.* 67. (Treatise on marine ecology and paleoecology) **1**, 239–296.

(1050)

ROTSCHI, H. (1953) Expedition océanographique CAPRICORN de la Scripps Institution of Oceanography. *Bull. d'Information, C.O.E.C.*, Serv. Cent. Hydr. (Paris), 10, 439–466.

RÜE, E. M. A. DE LA (1935) La constitution géologique des îles Wallis et Futuna. *C. R. Acad. Sci., Paris*, **200**, 328–330.

SAPLIS, R. A. and FLINT, D. E. (1949) Ramparts on the elevated atoll of Kito Daito Jima. *Bull. Geol. Soc. Amer.*, **60**, 1974 (Abs.).

SARGENT, M. C. and AUSTIN, T. S. (1954) Bikini and nearby atolls. Pt. 2 Oceanography (biologic) : Biologic economy of coral reefs. *U.S. Geol. Surv.*, Prof. Paper **260**–E, 293–300.

SETCHELL, W. A. (1928) The Coral Reef problem in the Pacific. *Proc. Pacific Sci. Congr.*, (3rd, Tokyo, 1926) **1**, 323–329.

STEARNS, H. T. (1945) Geology of the Wallis Islands. *Bull. Geol. Soc. Amer.*, **56**, 849–860.

SVERDRUP, H. U. (1938) On the process of upwelling. *J. Mar. Res.*, **1**, 155–164.

TEICHERT, C. (1958) Cold and deep water coral banks. *Bull. Amer. Assoc. Petrol. Geol.*, **42**, 5.

TEICHERT, C. and FAIRBRIDGE, R. W. (1950) Photo-interpretation of coral reefs. *Photogrammetric Engineering*, **16**, 744–755.

UDINSTEV, G. B. (1958) Okrytie glubokovodnogo zheloba v zapadnoy chasti tikhogo okeana (Discovery of a deep sea trench in the western part of the Pacific Ocean). *Priroda* (Moscow) (7), 85–88.

UMBGROVE, J. H. F. (1947) Coral Reefs of the East Indies. *Bull. Geol. Soc. Am.*, **58**, 729–778.

VIALA, M. (1919) Les îles Wallis et Horn. *Bull. Soc. Neuchateloise de Géog.*, **28**, 209–283.

WELLS, J. W. (1957) Coral Reefs. *In* Treatise on Marine Ecology and Paleoecology, 1, *Geol. Soc. Amer. Mem.*, **67**, 609–632.

WHARTON, W. L. (1888), Coral formations. *Nature, Lond.* **37**, 393–395.

WISEMAN, J. D. H. and OVEY, C. D. (1955a) Proposed names of features on the deep-sea floor. 1. The Pacific Ocean. *Deep-Sea Res.*, **2**, 93–106.

WISEMAN, J. D. H. and OVEY, C. D. (1955b) Proposed names of features on the deep-sea floor. 2. General principles governing the allocation of names. *Deep-Sea Res.*, **2**, 261–263.

YONGE, C. M. (1930) The biology of reef-building corals. Great Barrier Reef Expedition 1928–29. *British Museum (Nat. Hist.) Sci. Repts.*, **1**, 13, 353–391.

ZEUNER, F. E. (1952) *Dating the past; an introduction to geochronology*, Methuen, London (3rd ed.), 495 pp.

Printed in Great Britain by The Salisbury Press Ltd., Publicity House, Wilton Road, Salisbury, Wilts. (25134)

(1051)

CONGRESO GEOLOGICO INTERNACIONAL

XXª Sesión — Ciudad de México, 1956

G. G. SHOR, Jr. and R. W. RAITT

SEISMIC STUDIES IN THE SOUTHERN CALIFORNIA CONTINENTAL BORDERLAND

Sobretiro de la

Sección IX — Geofísica Aplicada
(Segundo Tomo)

243
págs. ~~253~~-259, 7 figs.

MEXICO, D. F.
1958

(1053)

SEISMIC STUDIES IN THE SOUTHERN CALIFORNIA CONTINENTAL BORDERLAND[*]

G. G. Shor, Jr.[**] and R. W. Raitt[**]

ABSTRACT

Crustal structure in the Continental Borderland of southern California has been determined by seismic refraction methods. Beneath the Catalina Basin the crustal thickness approaches that found under the continents, being less by an amount obtainable assuming Airy-method isostatic compensation. In a similar depth of water, at the upper edge of the Patton Escarpment (the outer continental slope), the total thickness of the crust is much less. The depth to the Mohorovicic discontinuity systematically increases from ocean basic to continent.

Thickness of unconsolidated sediment is greater under some of the basins and the continental shelf than under the neighboring ridges. A relatively small prism of sediment is found at the base of the outer continental slope.

Crustal material with a velocity of 6.7 km/sec, considered typical of the oceanic crust, is found at depths of 3 to 10 km below sea level from the ocean basin across the Continental Borderland to the continent, and most of the increase in crustal thickness is found within this layer. This is in contrast to lower velocities generally accepted as typical of the continental crust, and suggests that this region may represent a transition between the continental and oceanic crusts. Upper crustal material, with more typical continental velocities, is found under some of the ridges and basins.

INTRODUCTION

The Continental Borderland of southern California is unusual among the acean margins of the world. Instead of having a flat shelf bordered on its outer margin by a steep slope, southern California and northern Baja California have a marginal structure consisting of a narrow inner continental shelf, a series

---

[*] *Formerly titled "Seismic Refraction Studies of the Pacific Ocean Margin, Part I, Southern California Continental Borderland."*

[**] *University of California, Marine Physical Laboratory, Scripps Institution of Oceanography, La Jolla, California.*

Contributions from the Scripps Institution of Oceanography, New Series, 1225

Reproduced by Permission

of basins 1/2 to 2 km. deep separated by islands and banks, and finally on the seaward edge an extremely steep outer slope dropping rapidly ot water 3-1/2 km. deep. (Fig. 1).

The nature of the Borderland is not well understood. On the basis of topography it can well be considered as a region of fault blocks similar to the Basin Range province of the western United States and Mexico. From another aspect, in can be considered a subcontinental area with ridges of continental structure and the basins oceanic. To attempt to unravel something of the structure of the region, studies by seismic refraction methods have been made.

This Continental Borderland as delimited by Shepard and Emery (1941) extends from Point Conception in southern California, U. S. A., to Punta Eugenia, Baja California, Mexico. The topography of the California portion has been mapped in detail by the U. S. Coast and Geodetic Survey and the results interpreted and published by Shepard and Emery; the Baja California half is less well known and appears to merge at its southern end into the more typical Pacific trench margin. Work reported in the present papel deals only with the California section.

The area is far from ideal for the determination of deep crustal structure by seismic refraction methods. Ridges and basins are generally narrow and rarely of sufficient length for a refraction line that would assure deep penetration. They trend generally parallel to the coastline and to the outer slope, although where the slope and coastline converge near the Santa Barbara Channel Islands, the inner basins become parallel to the coast and away from the north-northwest trend of the outer slope. The surface geology of the islande is varied, indicating similar variation beneath the submerged ridges and basins. Nowhere is there any long flat area except in the bottoms of the basins, and there pronounced irregularities in the basement rocks exist beneath the smooth surface of the sedimentary fill.

Work on the area has been carried out on numerous trips between December 1948 and October 1955. The first trips were in part tests of methods and equipment; later trips have been planned specifically to study the problem of the crustal transition from continent to ocean.

ACKNOWLEDGMENTS

Because of the long period over which the studies have continued, many persons have been involved in the work and it is impossible to make adequate acknowledgments. All of the ships belonging to the Scripps Institution of Oceanography and the U. S. Navy Electronics Laboratory have participated in the work at least once; instrumentation has been developed at the Marine

Physical Laboratory of the Scripps Institution with aid from the U. S. Navy Electronics Laboratory. Personnel from Scripps Institution (especially the Marine Physical Laboratory) have made the observations and computed the results. The long-continued participation of Alan Jones, Willard North, and Gloria Slack is especially appreciated.

OPERATING PROCEDURE

Refraction lines have been determined using a single recording point and numerous shots. On a few early trips charges were detonated electrically with the firing ship stopped. All subsequent works has been done with the firing ship underway; TNT, Tetryl, and Tetrytol charges in 1/2 to 320 pound units are dropped with time fuse cut to detonate the charge at predetermined depth. The sound of the shot and the bottom reflection is detected by the firing ship's fathometer and transmitted by radio to the receiving ship. At the receiving ship the radio transmission, chronometer marks, and hydrophone outputs are recorded on a 17-channel photographic oscillograph and a 3-channel pen-and-ink recorder. On a few trips records were taken only on the pen-and-ink recorder. Normally detectors are modified Brush AX-58C hydrophones, suspended at a depth of approximately 50 meters. The filtered and amplified hydrophone outputs are recorded on high frequency high gain and low gain, intermediate frequency, and low frequency high gain and low gain channels. Detail of instrumentation and frequency response have been generally described by Raitt (1952).

INTERPRETATION

Arrival times of refracted waves are read to the hundredth of a second from the low frequency channels. When multiple hydrophones have been used, detection of weak first arrivals is aided by correlation of movements on all of the low frequency traces. Water-borne arrivals, both direct and bottom-reflected, are read from the high frequency traces and used to determine shot-to-hydrophone distance.

Velocities of sound in water for determination of distance have been computed using Kuwahara's (1939) tables. Temperature and salinity data for computation are obtained from bathythermograph observations at the time of shooting and from detailed regional hydrographic data in the files of Scripps Institution. In cases when bathythermograph data were not obtained, a velocity of sound in water. 1.5km/sec has been assumed. Computed velocities when data were available are between. 1.47 and 1.50 km/sec.

Travel times have been corrected for the delay between firing and reception of the firing signal at the shooting ship, and then corrected for depth of water beneath the shot and hydrophones. This procedure gives the travel times observed if shot and hydrophones had been on the bottom. This is necessary on most borderland lines because of the extreme variations of bottom depht.

Interpretation in terms of the "dipping layer" solution of Ewing. Woollard and Vine (1939) has been tried in a few cases, but the obvious variations in sediment thickness disclosed by the shorter profiles have made this method in general inapplicable. In most cases the determination of layer thicknesses has been point-by-point, either for every shot or for key positions such as the ends of lines and intersections of velocity segments. Many irregularities of layer thicknesses are disclosed by this method. When data have been lacking for determination of depths at individual points, and it has been necessary to extrapolate, assumptions of either constant layer thikness, constant depth below sea level to a given layer, or linear variation of layer thickness between known points have been made.

Velocity determination in the crustal layers on reversed profiles are made when possible by using plots of difference in travel time against difference in distance for shots on the same velocity segment and the same position on bottom. This serves to remove effects of local irregularities in the layers. Elsewhere harmonic means of apparent velocities from lines shot in apposite directions have been used, whether they were truly reversed or closely parallel. In some cases well-determined velocities from short reversed profiles have been used to determine intercept time on nearby unreversed profiles or long reversed profiles.

On lines in water over one kilometer deep, no direct determination of sediment velocity has been possible because of lack of first arrivals or reliable second arrivals through the sediments. A velocity of 2.8 km/sec has been used in many of the deep-water lines to represent sedimentary fill. Such a velocity has been found near some of the outer islands and on shallow banks. On lines near San Diego on the continental shelf, the inner continental slope, and the San Diego Trough a different velocity has been assumed as noted below. The nominal velocity of 2.8 km/sec is obviously high for unconsolitated sediments at the watersediment interface, whose velocity in this area has been found by Shumway (1956) to be very close to 1.5 km/sec. For a kilometer or more of sediment of varying degrees of consolidation, 2.8 km/sec may be nearly correct. For a section containing an appreciable percentage of consolidati

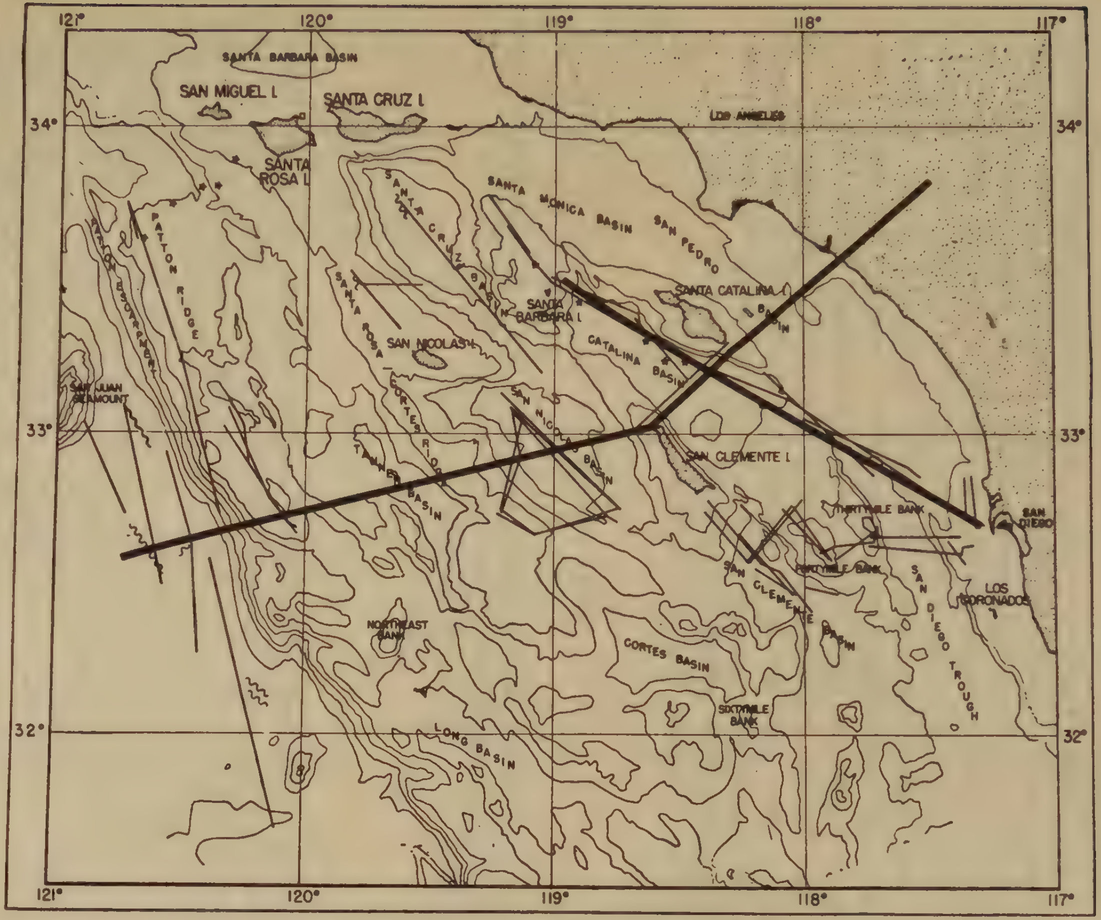
121°
120°
119°
118°
117°
34°
33°
32°
SANTA BARBARA BASIN
SAN MIGUEL I.
SANTA CRUZ I.
SANTA ROSA I.
LOS ANGELES
SANTA MONICA BASIN
SAN PEDRO
SANTA CATALINA I.
BASIN
SANTA CRUZ BASIN
SANTA BARBARA I.
CATALINA BASIN
SANTA ROSA
SAN NICOLAS I.
CORTES RIDGE
SAN NICOLAS BASIN
PATTON RIDGE
PATTON ESCARPMENT
SAN JUAN SEAMOUNT
TANNER BASIN
SAN CLEMENTE I.
THIRTYMILE BANK
SAN DIEGO
FORTYMILE BANK
SAN CLEMENTE BASIN
SAN DIEGO TROUGH
LOS CORONADOS
NORTHEAST BANK
CORTES BASIN
SIXTYMILE BANK
LONG BASIN

Fig. 1. Continental Borderland of southern California. Refraction profiles are indicated by narrow lines; the two broad lines indicate the sections of Fig. 2 and 7.

(1059)

ed sediment or volcanics with velocities of 4 km/sec and above, it would be low. The errors of determination of sediment thickness may well be as much as 20 per cent.

It is realized that for any set of seismic refraction data, an infinity of interpretations is possible, depending on the complexity of structure assumed. In most cases the data available are sufficient to show that the simplest structural model does not apply, but are insufficient to determine completely all aspects of a more complex model suggested. It has therefore been necessary to select that structural model that involves the smallest number of special assumptions, conforms best to the interpretatinos derivable from nearby refraction lines, and most nearly fits the observed travel times. This method is akin to that used by a field geologist trying ot determine a structural map and section from a small number of outcrops. It is not implied that each structure section presented herein represents the only possible interpretation of the data at hand. The data would be entirely sufficient in an area of low complexity; in this area they serve only as a beginning.

ANALYSIS OF AREAS

Many observations have been made in a series of regions across the Continental Borderland and are shown as lines in Fig. 1. Those forming the cross-section of Fig. 2 are described here.

Ocean Floor

The western end of the line of section lies at the foot of the Patton Escarpment (the outer continental slope). Here on two trips a total of four stations were occupied. Two of the stations form a roughly reversed profile 15 to 25 km west of the base of the escarpment. The other two were both split profiles located at the foot of the slope. On one profile penetration to the mantle was obtained; on the other crustal velocities only were observed. The second profile gives a reversal on the crustal layers of the first. A summary of the layer thicknesses on these stations is shown in Fig .2. The reversed portion of the profiles at the foot of the slope has also been used to stduy variation of sediment thickness along the line of shooting. The result, shown in Fig. 3 shows thinning of sediment over a small rise and a maximum sedimentary thickness of 1.4 km to be compared with the value of 0.6 km on the seaward profile.

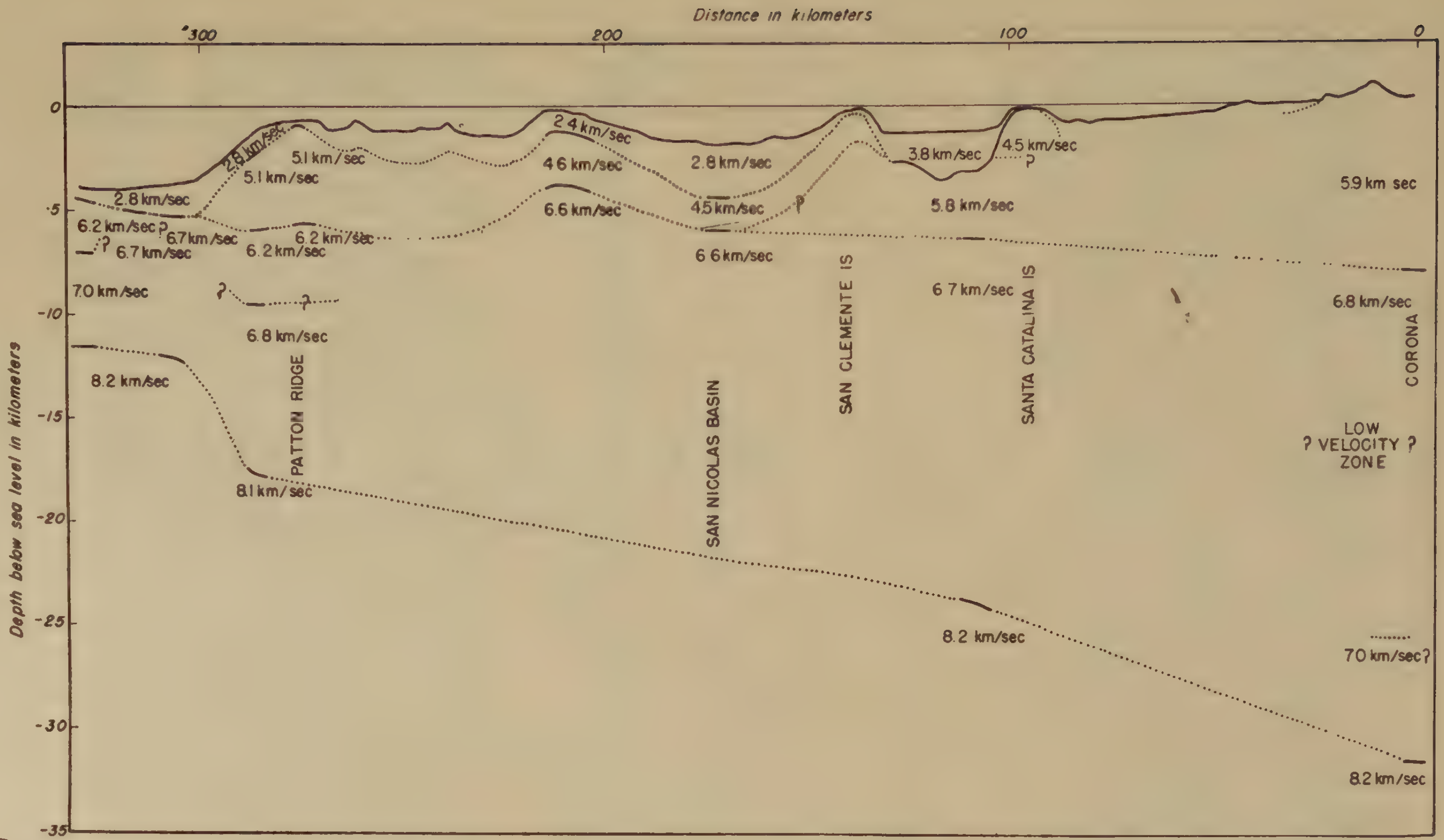

Fig. 2. Structural section from the Pacific Ocean Basin (left) to Peninsular Ranges (right). Dotted lines indicate areas where data are lacking.

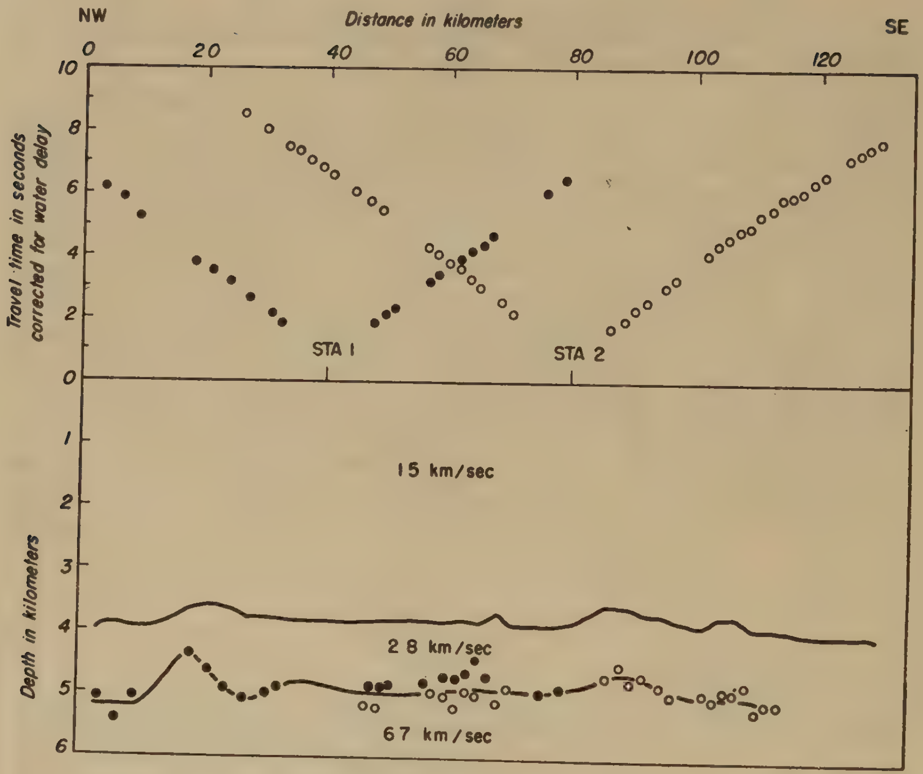

Fig. 3. Shallow structure at base of Patton Escarpment. Sediment velocity assumed.

PATTON RIDGE

At the top of the Patton Escarpment is a continuous ridge at a depth of approximately one kilometer below sea level. This ridge is unnamed on the charts; it is here referred to as the Patton Ridge. Four stations were occupied. Two of them were on the shallowest portion of the ridge, and had reversal on the shallowest crustal leyers only. The other two stations were subsequently occupied in such a manner that the reversal was on the arrivals from the deepest part of the crust and the mantle, and the zone of reversal was close to the position of the earlier short lines. Data from the short lines give the section of Fig. 4; here velocities could be accurately determined from time-difference plots in the zone of reversal.

The longer lines shot on the later trip were slightly west of the short lines, in 1.2 km of water. Shallow layer velocities observed were the same as those obtained on the short lines. Deep crustal and mantle arrivals with apparent velocities indicating pronounced dip to the north were obtained in the zone of reversal. The dip is probably related to a sharp bend in the Patton Escarpment near the point where the deep arrivals were obtained. Layering has been computed for a short zone at the north end of the line of shooting where maximum control was available. It is migrated along the contours and plotted as the western Patton Ridge poin int Fig. 2. The depth to the Mohorovicic discontinuaity of 17-1/2 km below sea level given for this point does not prevail over the entire line of shooting there is some evidence for a minimum depth between 14 and 15-1/2 km below sea level at the edge of the escarpment near the bend.

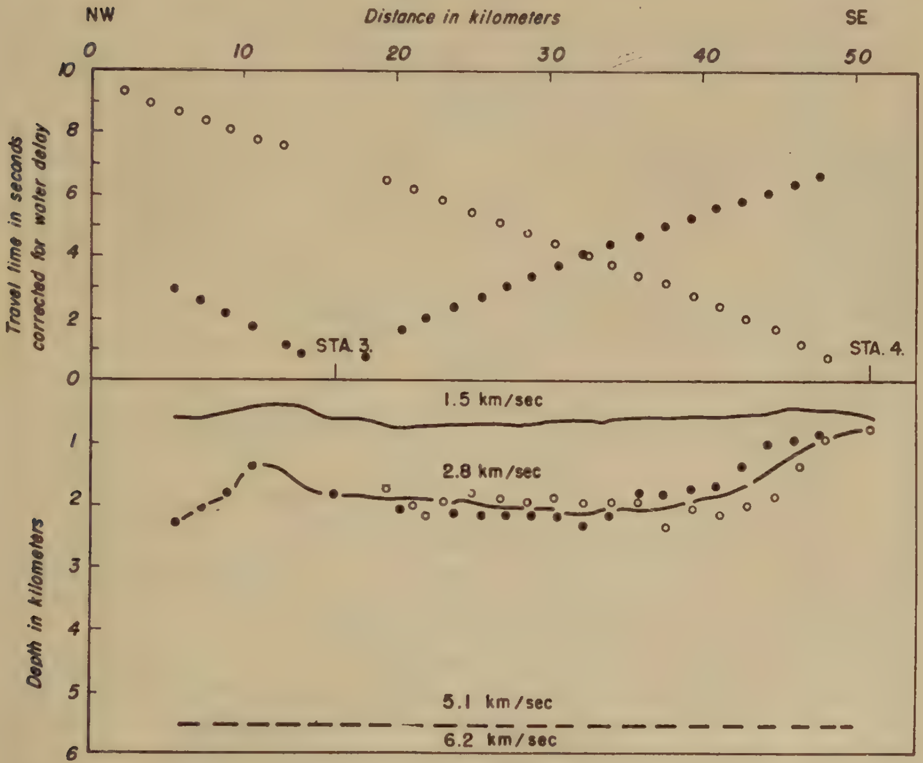

Fig. 4. Shallow structure along highest part of Patton Ridge.

INTERMEDIATE BASINS AND RIDGES

Lines shot in the Santa Cruz and San Nicolas Basins and on the Santa Rosa-Cortes Ridge could not be long enough to obtain arrivals from the mantle, but do give crustal velocities and sediment thickness. A reversed profile across the deepest part of the Santa Cruz Basin and through the saddle between Santa Barbara Island an San Nicolas Island gives a profile of sediment thickness from the center to the flank of the basin (Fig. 5) and a velocity of 6.2 km/sec for the material underlying the sediment. A reversed profile in the deepest part of the San Nicolas Basin has been solved in terms of a simple set of dipping layers for the section in Fig. 6. Here it is notable that arrivals with velocity 4.6 km/sec, normal for either volcanics or consolidated sedimnts,

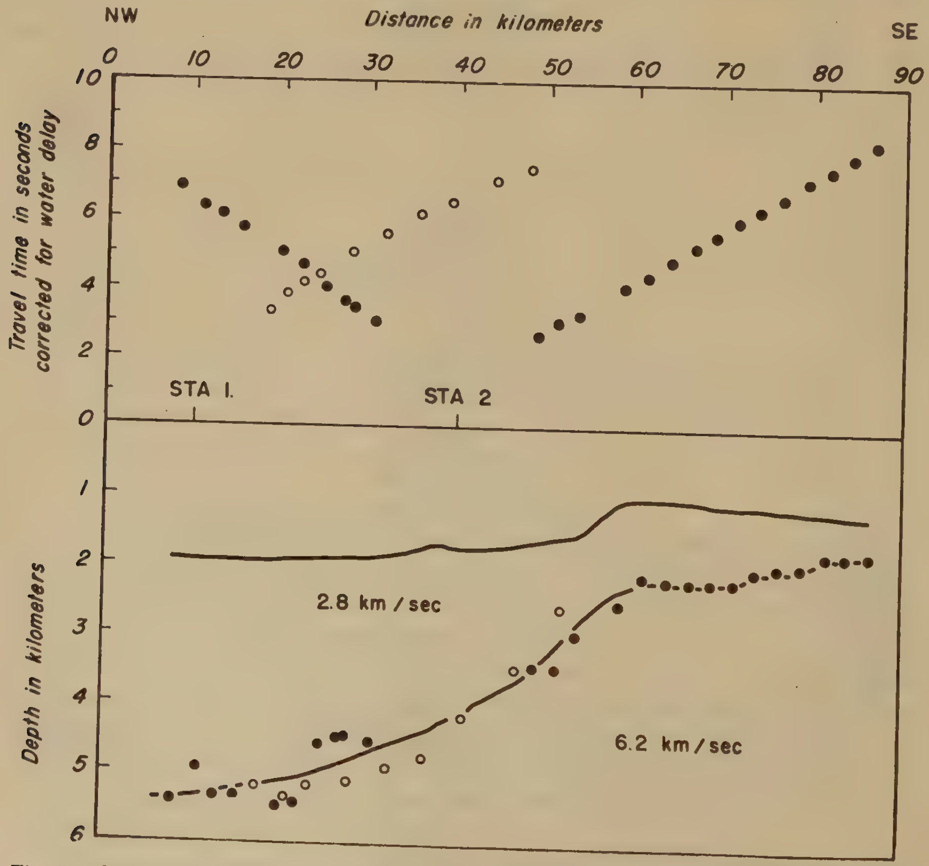

Fig. 5. Shallow structure from bottom of Santa Cruz Basin to saddle between Santa Cruz and San Nicolas Basins. Sediment velocity assumed.

are obtained from beneath the sediments, and that below these lies material with a well determined velocity of 6.65 km/sec, which is within the range of values normally found for the oceanic crust.

CATALINA BASIN - SAN DIEGO TROUGH

The longest available area of relatively constant depth for refraction work close to the coast is the combined length of the Catalina Basin and the northern

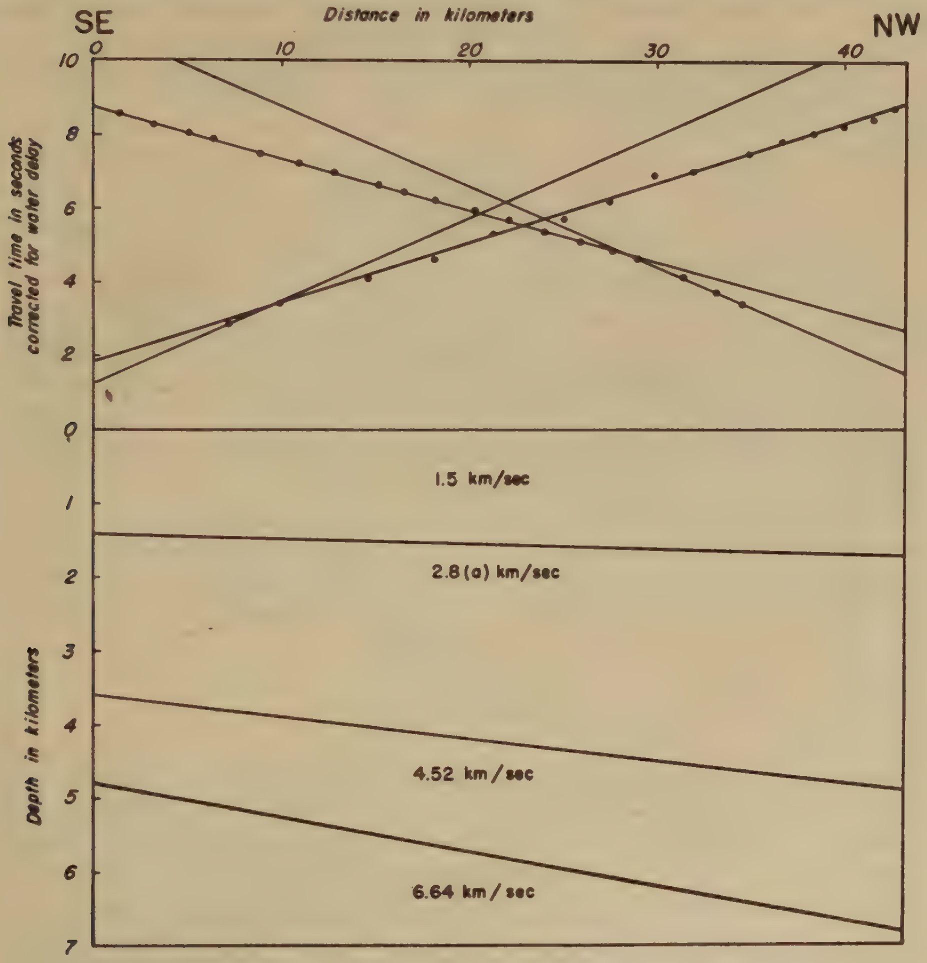

Fig. 6. Shallow structure across San Nicolas Basin assuming plane layers. Sediment velocity assumed.

part of the San Diego Trough. These two areas have a maximum depth of 1.3 km and are separated by a saddle one kilometer below sea level. Extensive refraction shooting has been done in the area, with a total of 14 individual lines of varying lengths constituting a multiply reversed profile from Point Loma to Santa Barbara Island.

Because of the rapid changes in topography at the two ends of the line there is no reason to believe that layers should change thickness uniformly along the full length of the profile. Point-by-point interpretation using the intercept method has been used, with data on the shallower layers at each point taken from the short reversed lines to provide corrections for the long lines. On deeper layers where data from only a few lines have been available, the assumption of constant depth of interface at shot and recording points has been made where necesary.

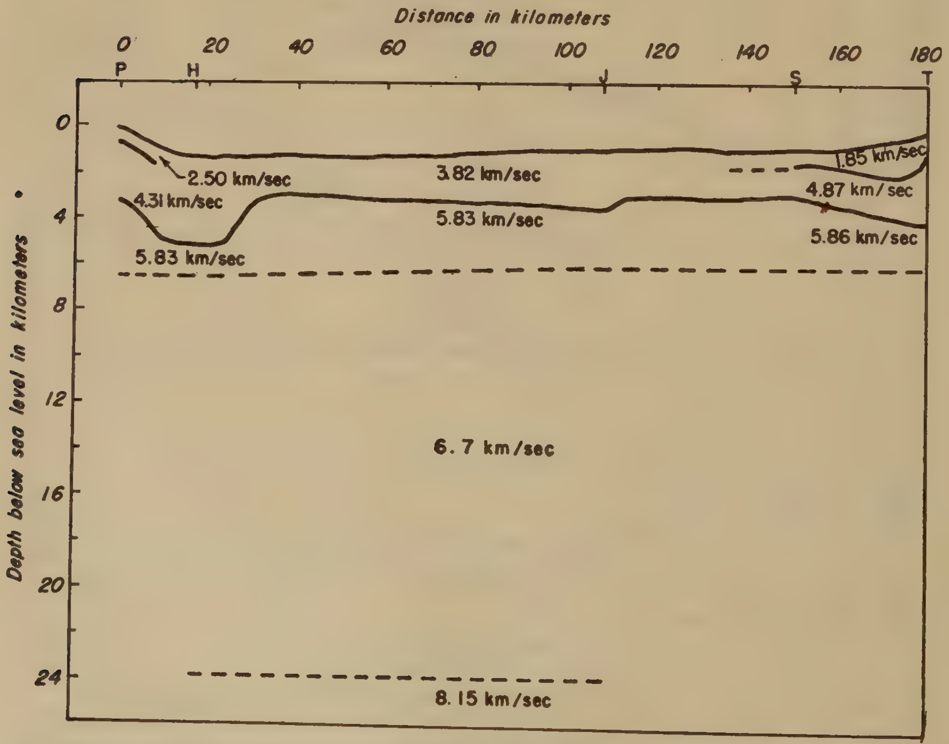
Distance in kilometers
0
20
40
60
80
100
120
140
160
180
P
H
J
S
T
0
4
8
12
16
20
24
Depth below sea level in kilometers
2.50 km/sec
3.82 km/sec
1.85 km/sec
4.87 km/sec
4.31 km/sec
5.83 km/sec
5.83 km/sec
5.86 km/sec
6.7 km/sec
8.15 km/sec

Fig. 7. Structural section from Santa Barbara Island (left) to Point Loma, San Diego (right), through the Catalina Basin and San Diego Trough. Mohorovicic discontinuity assumed horizontal for computation.

The upper layers at the ends of this section are obtained from observation; the upper layer in the central portion cannot be observed as a first arrival on the travel time plot because of the depth of water in the trough, and a velocity has had to be assumed. The velocity used is that which would give an equivalent single layer corresponding in travel times and thickness to the two layers observed a the ends. The deeper layers are all derived from observed velocities and intercepts of the refracted arrivals. A cross-section derived from these lines is shown in Fig. 7.

Peninsular Range

Data for the landward end of the section in Fig. 2 are derived from observations of blats at the Corona quarry of the Minnesota Mining and Manufacturing Company by personnel from the Carnegie Institution of Washiington, the California Institute of Technology, and the Scripps Institution of Oceanography, including the authors. Data from the blasts have been studied by Tatel, Adams, and Tuve (1953), buy Gutenberg (1951), and Shor (1954).

The pertinent observations consist of an unreversed refraction line extending south from Corona to the Mexican border, and a reflection record obtained at the quarry. The refraction data alone give a depth to the Mohorovicic discontinuity of 30 km below sea level; addition of the reflection data implies the presence of a low velocity layer within the crust and a depth below sea level of 32 km. The Corona data, although unreversed, suggests trongly that the crust in this area consists of an upper layer having velocity 5.9 km/sec overlying a layer having velocity 6.8, with a lower velocity zone probably present within the latter layer. No proof of the presence or absence of a low velocity layer is obtainable from the oceanic refraction data; otherwise the velocity structure is remarkably similar.

DISCUSSION

Seismic data at a number of key points in the Continental Borderland demonstrate the presence of structural variations in the shallow layers on a scale that is small compared with the length of the refraction lines. This is not surprising in view of the variation of the surficial geology as depicted on the Geologic Map of California (Jenkis 1938). More surprising is the uniformity of deep structure disclosed

In none of the areas of deep water can refracted arrivals from the unconsolidated sediments be detected using present methods of operation. Their presence is proven, however, by the delay in arrivals from deeper layers. The presence of material with velocity between 4.3 and 5.1 km/sec is demonstrated on all of the shallow water lines (on the continental shelf and on ridges within the borderland) and on lines in the San Nicolas Basin. This material could also be present on lines in the Santa Cruz Basin and west of the Patton Escarpment where it is not detected as a first arrival. If this is true, the thickness of the low velocity material (unconsolidated sediment) would be decreased and the total thickness of unconsolidated sediment plus consolidated sediment or volcanics would be increased. The fact that the 4.3 to 5.1 km/sec arrival is not present as a first arrival on these lines does indicate, however, that the low velocity sediment is a relatively large part of the total. Without further field observation by methods capable of separating the shallow layers, only a few generalizations can be drawn.

West of the Patton Escarpment a small prism of sediment 0.6 to about 2 km is found. Presumably this thins to the west to the value of less than 1/2 km found on the deep sea floor by Raitt (in press). This prism is much smaller than that reported on the Atlantic Coats by Worzel and Shurbet (1955).

Withing the borderland thickness of unconsolidated sediment is much less on the ridges and banks than in the adjacent basins, and in many cases pinancles of volcanics or consolidated sediments either outcrop or lie beneath a thin cover under small hills. Sedimentary fill in many of the basins is great. In the Los Angeles Basin depth to basement has been estimated as greater than 6 km by Woodford *et al* (1955). In the Santa Cruz Basin it is about 5 km below sea level; in the deepest part of the San Nicolás Basin it is 5 to 7 km below sea level, depending on whether the 4.5 or 6.6 km/sec material is considered to be basement. The San Diego Trough and Catalina Basin in contrast have the base of the unconsolidated sediment at 1-1/2 km and the base of the next layer at 3 km except at the northwest end of the Catalina Basin where the base of the second layer drops to 5.2 km below sea level. It is interesting to note that the depth to the base of the combined unconsolidated sediment and consolidated sediment or volcanics in these four deep areas is of the same magnitude as the depth to basement in the deep ocean west of the Patton Escarpment.

Under the continental shelf off Point Loma the unconsolidated sediment thicknes, and at the edge of the shelf the base of this layer is deeper than it is under the San Diego trough, suggesting that the continental shelf has been built out across the trough.

Identification of the layers is based on scanty evidence. The material inmediately below the sea floor has been frenquently sampled by coring by groups at Scripps Institution, University of Southern California, and the

U. S. Navy Electronics Laboratory and found to consist of Recent sediments. The entire layer with velocity observed as 1.8 km/sec at Point Loma, 2.5 km/sec at Santa Barbara Island, 2.4 km/sec at Tanner Bank and 2.8 km/sec at Patton Ridge probably consists of sediments ranging in age from Recent well down into the Tertiary. At Santa Barbara Island, the island is composed of Miocene volcanics with small amounts of Miocene sediments, so the material found on the adjacent shelf might be either of these or Recent sediment.

Material with velocity 4.9 km/sec found under the continental shelf at Point Loma (San Diego) has a dip that if extended would make it outcrop in the exposed Eocene and Cretaceous of Poin Loma and La Joya. The distinction between consolidated sediments and volcanisc cannot be made on the basis of velocity alone, and the presence of volcanic material in test wells on Point Loma and a basalt dike the coast at La Jolla (Hertlein and Grant, 1939) indicate that the material found beneath the continental shelf might possibly be volcanic. A velocity of 5.1 km/sec found under the Patton Ridge might be correlated with the 4.3 to 4.9 km/sec arrivals nearer shore although it approaches velocities typical of igneous intrusive rocks.

Material with velocity 5.9 to 6.2 km/sec is found as the upper layer of the crystalline crust under the Point Loma continental shelf, the San Diego Trough, Catalina Basin, Santa Cruz Basin, Patton Ridge, and in the Peninsular ranges, where it is exposed at the surface in the form of granodiorite and allied rocks of the Southern California Batholith (Larsen, 1948). A deeper layer with velocity near 6.7 km/sec has been found throughout the area wherever long enough refraction profiles were shot; it carries through continuously from the Peninsular Ranges to the ocean floor west of the Patton Escarpment, and forms the "basement" below the sediments in the San Nicolas Basin and the ocean floor.

The Mohorovicic discontinuity is at oceanic depth (9 to 11 km) as close to the base of the outer continental slope as it can be measured; on the inner edge of the slope it sinks to a depth between 14 and (more probably) 17-1/2 km in water only about 1 km deep. Depth to the discontinuity has not been traced through the intermediate basins, but under the Catalina Basin-San Diego Trough area, an inshore basin, it is at a depth of 24 km, and under the Peninsular ranges at a depth of 32 km. Most of this increase in depth is accounted for by the thickening of the 6.7 km/sec "oceanic crust" landward.

Computation of the depth at which the Mohorovicic discontinuity should lie beneath the Catalina Basin, using the densities given by Worzel and Shurbet (1955) gives a value of 26 Km assuming isostatic equilibrium, which is surprisingly close to the observed value of 24 km. The depths at the top and base of the Patton Escarpment do not agree nearly as well with the computed values.

SUMMARY

The significant results of this study are:

1. Trickness of unconsolidated sediment is small on the ridges, great under portions of the interior basins and the inner continental shelf.
2. The upper continental crust is present under some of the ridges and basins.
3. The typical oceanic crust with velocity 6.7 km/sec is continuously present across the borderland.
4. The Mohorovicic discontinuity systematically increases in depth toward the continent, with most of the depth increase accounted for by thickening of the oceanic (lower continental) crust.

BIBLIOGRAPHY

EWING, M., G. P. WOOLLARD AND A. C. VINE. 1939. Geophysical Investigations in the Emerged and Sumberged Atlantic Coastal Plain. *Bull. Geol. Soc.* America, 50:257-296.

GUTENBERG, B. 1951. Waves from Blasts Recorded in Southern California. *Trans. American Geophys. Union,* 33:427-431.

HERTLEIN, L. G. AND U. S. GRANT. 1939. Geology and oil possibilities of southwestern San Diego County. *California Jour. Mines and Geol.,* 35:57-78.

JENKINS, O. P. 1938. *Geologic Map of California.* California Div. of Mines.

KUWAHARA, S. 1939. Velocity of Sound in Sea Water and Calculation of the Velocity for Use in Sonic Sounding. *Hydrographic Rev.,* 16:127-140.

LARSEN, E. S. 1948. Batholith and associated rocks of Corona, Elsinore, and San Luis Rey quadrangles, southern California. *Geol. Soc. America, Mem.* 29.

RAITT, R. W. 1952. Geophysical Measurements. *Symposium on Oceanographic Instrumentation,* National Research Council, pp. 70-84.

——(in press). Seismic Refraction Studies of the Pacific Ocean Basin, Pt. 1, Crustal Thickness of the Central Equatorial Pacific.

SHEPARD, F. P. AND K. O. EMERY. 1941. Submarine Topography of the California Coast. *Geol. Soc. America, Spec. Paper* 31.

SHOR, G. G. 1954. Reflections from the Mohorovicic discontinuity and crustal structure in southern California. Unpublished thesis, California Inst. Technol.

SHUMWAY, G. 1956. A resonant chamber method for sound velocity and atenuation measurements in sediments. *Geophysics V,* XII (2):305-319.

TATEL, H. E., L. H. ADAMS AND M. A. TUVE. Studies of the Earth's Crust using waves from explosions. *Proc. American Phil. Soc.*, 97(6):658-669.

WOODFORD, A. O., J. E. SCHOELLHAMER, J. G. VEDDER AND R. F. YERKE 1955. Geology of the Los Angeles Basin. *Bull California Div. Mines*, 170:65-81.

WORZEL, J. L. AND G. L. SHURBERT. 1955. Gravity Anomalies at Continental Margins. *Proc. U. S. Nat. Acad. Sci.*, 41:458-469.

(1071)

(1072)

Reprinted from Annals of The New York Academy of Sciences
Volume 90, Article 3, Pages 617-621
November 17, 1960

PERSPECTIVES IN MARINE BIOCHEMISTRY

Denis L. Fox
Scripps Institution of Oceanography of the University of California, La Jolla, Calif.

How far back into time should one try to retreat, and then where should he endeavor to focus his sights on the vast marine world in order to present a few guiding perspectives in marine biochemistry? Different biologists or biochemists would react to these queries with their own various individual responses. I shall try to present a few basic panoramic views for your thinking and criticism.

The marine environment has, since primordial times, provided a moist, chemically polar reaction-medium containing dissolved electrolytes and characterized by conditions of temperature, movement, and innumerable diversified interfaces, all favorable to many kinds of prebiochemical events and syntheses. Moreover, there were the factors of time and the mass law, favoring reactions between molecules adsorbed to and thus concentrated at various kinds of inorganic colloidal and other surfaces; also there were general screening or buffering effects against sudden photic, thermal, chemical, or mechanical changes bearing upon labile compounds. Such features doubtless would have promoted marine waters as the medium of the earliest organisms and, as time passed, an environment wherein the widest permutations could occur, leading toward the greatest variations in size, shape, constitution, and functions of evolved living things.

The marine milieu and its enormous diversity of inhabitants must be regarded as having evolved together. Today the total surface area of the world's oceans exceeds that of the exposed land by about 2.4-fold, while the estimated *volume* of the marine biocycle bears to the combined volumes of terrestrial and fresh water biocycles a ratio of about 300:1.[1] And the greatest diversity and numbers of animal species are still to be found in the oceans. Indeed, several whole groups are exclusively marine, for example, echinoderms and tunicates, amphineuran, scaphopod, and cephalopod mollusks, brachiopods and gephyrean worms, while few save the insects and amphibian vertebrates are to be regarded as strictly nonmarine classes.

The oceans themselves gradually increased not only in volume but in concentrations of dissolved gases and salts; the concentrations and ratios of ions in today's marine, fresh-water, and terrestrial vertebrates are regarded as reflecting closely the electrolytic conditions prevailing in the seas at the time of the ancestral vertebrates' emergence in the evolutionary scale.[2]

The total mass of loose parts lying about has always exceeded that of the finished products entering the evolutionary procession; and while there is no estimating either the diversity of kinds or the preponderance in weight or numbers of inanimate organic molecules over reproducing entities at any past era in time, it should be useful to review a few conservative assumptions about qualitative diversity and relative concentrations in today's seas.

It is logical to regard abiogenesis as having had its day long ago, since the current world harbors organisms of incalculably diversified biochemical habits

Contributions from the Scripps Institution of Oceanography, New Series, 1226
Reproduced by Permission

and capacities, ready to assimilate any simple organic molecules that conceivably might emerge to build their own way toward systems of greater complexity. Hence all organic detritus of today's world (discounting a few metallic carbides, cyanide minerals, and the like) is of direct biological origin, whether from dead bodies of plants, animals, and microbes, or from their excreted or otherwise discarded materials. While the chemical variety of such organic molecules obviously must be very large, the present-day assortment can offer no challenge to compare with the vast assemblage and diversification that must have prevailed in prebiological times. Nevertheless, the ever-present unorganized, nonliving material, for example, in the oceans of today, constitutes the basic source of food supply for countless billions of omnivorous marine animals, not to mention, for the moment, the biomass of bacterial and fungal flora. This is true whether the detritophagous feeders obtain their food by ciliary, mucous, or setous filtration, or through combinations of these; by scraping adsorbed films of slime from immersed surfaces, or by ingesting masses of bottom sand, mud, or other relatively fine material to obtain therefrom associated organic matter, as does the earthworm in land soils. All of this applies also whether the creatures elaborate and secrete all of their own necessary digestive enzymes or, alternatively, like some land forms, harbor in their alimentary tracts specific microflora capable of hydrolyzing certain of the more refractory components. Indeed, this field is a marine nutritional area concerning which little indeed is yet known and therefore calls urgently for serious biochemical and microbiological attention.

Let us for the present exclude consideration of the strict carnivores, for example, the coelenterates, asteroid echinoderms, cephalopod mollusks, and many of the fishes, as well as the exclusively herbivorous species that devour fresh seaweed material, as do numerous gastropods and certain fishes. Let us contemplate instead some true scavengers, or feeders largely upon inanimate organic detritus.[8]

Filter feeders, removing from the water and swallowing marine leptopel, that is, colloidal and other finely particulate organic matter, not excluding adsorbed bacteria and other microscopic organisms, are represented among the setous screeners, such as barnacles, copepods, and some fishes supplied with gill-rakers. The mucociliary operators, elaborating sheets of mucus over extensive surfaces supplied with countless fine, hairlike cilia sweeping the mucus and its adsorbed complement of detritus toward the mouth, are found among the bivalve mollusks, such as oysters, clams, and mussels, as well as tunicates, crinoid echinoderms, and many microcrustaceans; the latter group may combine the setous and mucous functions.

So-called scrapers are represented chiefly by marine snails bearing a tough, horny tongue or radula, operated as a kind of rasp by strong buccal muscles that often exhibit the red colors of hemoglobin. True, the scrapers inevitably consume both plant and small-animal organisms along with the slimy inanimate component, just as filter-feeders swallow many such microorganisms with the leptopel. A few primitive animals are provided with sucking mechanisms for removing the so-called sapropel, pelogloea, or muddy slime.

Finally, the shovelers propel whole mud or sand into the mouth by pharyngeal muscular action (such as in many worms), by circumoral tentacles supplied with adhesive, distal pads (in some holothurians), by adhesive walking feet and seizing mouth-parts (of ophiuroids), or by tubular, sucking mouths, as in some bottom-feeding fish that consume sapropel, the viscous, slimy carpet of organic detrital material covering the bottom surface of some regions.

To achieve some general idea of the vast amounts of organic leptopel suspended in ocean waters, we may take a conservative figure of 1 ppm* as its average, over-all concentration, omitting the substantial fractions adsorbed to solid surfaces as pelogloea or resting on the floors as sapropel, and notably the large concentrations of organic matter that characterize foreshores the world over. Assigning the organic leptopel a density value approximating that of water (62.4 lb./cu. ft.) and, using the accepted value of 330 × 10^6 mi.^{3} as the total additive volume of the world's oceans, we obtain a product of $(5280)^3 \times 330 \times 62.4 = 31 \times 10^{14}$ lb., or 1.5×10^{12} tons of suspended organic matter, serving directly or potentially, via bacteria, as a raw food source in the perpetual metabolic cycles in the marine world. The figure exceeds by a whole order of magnitude the estimated value of 1.5×10^{11} tons of organic matter synthesized annually by marine phytoplankton, as derived from surveys by Riley and others.[9,10] And this latter value, in turn, exceeds by nearly tenfold the estimated total annual productivity of land plants, and surely by a greater ratio the total mass of animal life. Since plants are the primary producers in any community, a comparison between the foregoing estimates emphasizes the conclusion that the standing crop of organic leptopel must exceed by at least tenfold (perhaps 100-fold) the annual synthesis or standing crop of total living marine organisms.

Let us now look for a moment at the nutritional activities of three representative marine detritus feeders: (1) the California mussel, *Mytilus californianus*, representing the filterers; (2) an intertidal polychaete worm, *Thoracophelia mucronata*, characterizing the shovelers or wholesale swallowers of finely divided bottom material; and (3) a common, intertidal periwinkle, *Littorina planaxis*, as an illustration of the scrapers.

Earlier researches at La Jolla[3] indicate that a moderate colony of 10^6 mussels will, during their second year, filter the leptopel from some 22 × 10^6 tons of environmental water, or from a volume equivalent to a stratum 1 mile square by 25 feet deep. If the organic matter suspended in this near-shore water amounts to a year-round, average value of 1.5 ppm, the mollusks must remove about 33 tons of such material. The animals gain collectively about 4 tons of tissue (on a dry, ash-free basis), thus indicating an "efficiency" or ratio of assimilated to ingested material of about 12 per cent. Moreover, since considerable proportions of the available organic material are relatively inert and indigestible, such as chitin, cellulose, humus, and similar refractory products, and since a part of the total may be adsorbed to inorganic bodies rejected by the animal due to large size or rough shape, the above figure, in all probability, is low. Indeed, the efficiency of these mussels, based upon dry, ash-free organic weight-increment of new tissue and dry, ash-free content of intaken material as measured in the feces, gives the high but still probably conservative quotient of 17.6 per cent.

---

* Concentrations vary widely with latitude,[3] depth, season, distance from shore, and biochemical activity; deep waters (600 m.) may yield as little as 0.25 ppm, while surface waters, notably in the area of marine slicks, may contain 140-fold as much.

A beach sand bed occupying 1 square mile, aggregating 500 miles in length, 10 feet wide and 1 foot deep, harboring the burrowing annelid *Thoracophelia* in populations of about 3000 per square foot, will therefore contain approximately 8×10^{10} individuals weighing an aggregate of 3500 tons, and will amount to 1.4×10^{6} tons of sand (dry weight), involving hardly more than 1 per cent organic matter. The worms, swallowing 2100-fold their own weight of sand annually, will therefore cycle about 7.3×10^{6} tons of their substrate each year, or the entire quantity of sand in the total worm-bed once every 10 weeks. Of the estimated 7×10^{4} tons of organic matter available in the sand, the worms will convert 700 tons into new tissue, assuming an annual life cycle. A two-year life cycle, believed to be more likely in this species, would therefore indicate an efficiency of only about 0.5 per cent for these representative, relatively wasteful scavengers.

Turning to the third example, the intertidal gastropod *Littorina*, one finds that this little periwinkle achieves a much higher efficiency than that calculated for the annelid worm, and rather close to that found in the mussel. It scrapes and swallows impacted Eocene and Cretaceous siltstone bearing attached algae and pelogloeal materials in quantities amounting to about 2.6 per cent of organic matter by weight. An estimated population of 8.6×10^{8} snails on a square mile of wet siltstone will remove approximately 2200 tons annually, fixing as new tissue some 6.82 of the total 57.2 tons of organic matter available, thus demonstrating an efficiency of nearly 12 per cent.

So much for the numerically great but proportionately infinitesimal fractions of marine organic detritus cycled by these scavengers. It may be of additional interest to review the rather contrasting metabolic fractionation of certain known molecular constituents (that is, the carotenoids) of the omnivorous and, for practical purposes, almost identical basic diet of these and some other detritophagous marine animals.

Marine detritus, whether suspended in the upper waters as leptopel or adsorbed to solid interfaces as pelogloea, contains both the hydrocarbon (prominently β- and secondarily α-carotenes) and alcoholic types (various algal xanthophylls) of polyene pigments characteristic of phytoplankton and other marine plants. In plant cells, in the detritus derived largely therefrom, and in the majority of marine animals, the xanthophylls preponderate greatly over the carotenes, for example, by ratios of 9:1 or greater in plants, while some animals store exclusively members of the xanthophyll class. But there are exceptions among the animals, of which the worm *Thoracophelia* happens to be an outstanding one, since it not only assimilates selectively the hydrocarbon type of carotenoid, but solely the β-carotene, rejecting the α-isomer; moreover, the xanthophylls not only are not assimilated as such, but are destroyed during the brief interval during which the sand traverses the length of the worm's alimentary tract. *Thoracophelia* stores several fluorescent chromolipoids and is believed to employ active lipoxidases in its metabolism of fat-soluble materials.[4]

The mussel manages a contrasting biochemical performance, completely rejecting the dietary carotenes, assimilating the xanthophylls and converting some fraction of the carotenoid intake, presumably by oxidation, into a new acidic pigment, named mytiloxanthin by Scheer,[5] who discovered and isolated the compound in my laboratory many years ago.

The periwinkle *Littorina* seems, by contrast with the foregoing species, to be relatively conventional and unoriginal, storing what appears to be a full complement of the carotenes and algal xanthophylls from its natural diet.[6] The sea-cucumber *Stichopus parvimensis*, feeding as does *Thoracophelia* upon sand grains thinly coated with pelogloeal matter, is rather unselective of the kinds of lipochromes assimilated, storing members of both chief classes, although in very small quantities, while other echinoderms consuming bottom detritus, such as the ophiuroids or serpent stars *Ophiopterus papillosa*, *Ophiothrix spiculata*, and *O. rudis*, store no carotenes whatever, but only free and esterified xanthophylls, including several unique, very labile members.[7] Pelagic crustaceans, including euphausiids and some copepods, feeding upon leptopel, convert part of the ingested carotenoid material into the red, acidogenic, ketoxanthophyll astaxanthin. In addition, numerous euphausiids contain vitamin A derived from carotene or, perhaps in some instances, from astaxanthin, concentrated largely in the eye stalks.[8]

These few vignettes will, it is hoped, serve to emphasize the vast wealth of marine biochemical problems and the great contrasts in the nutritional habits of marine animals and in their biochemical metabolism of labile, colored molecules of the carotenoid group, obtained originally from plants. One hardly may wonder at the differences in metabolic efficiency, enzyme action, and the rich assortment of endogenous nitrogen compounds, some of them toxic, still encountered in the long evolutionary chains represented among marine animals.

References

1. Sverdrup, H. U., M. W. Johnson & R. H. Fleming. 1942. The Oceans. Their Physics, Chemistry, and General Biology. Prentice-Hall. New York, N. Y.
2. Baldwin, E. 1949. An Introduction to Comparative Biochemistry. Cambridge Univ. Press. Cambridge, England.
3. Fox, D. L. 1955. Organic detritus in the metabolism of the sea. Sci. Monthly. **80:** 256–259.
4. Fox, D. L., S. C. Crane & B. H. McConnaughey. 1948. A biochemical study of the marine annelid worm, *Thoracophelia mucronata*. Its food, biochromes, and carotenoid metabolism. J. Marine Research. **7:** 567–585.
5. Scheer, B. T. 1940. Some features of the metabolism of the carotenoid pigments in the California sea mussel (*Mytilus californianus*). J. Biol. Chem. **136:** 275–299.
6. North, W. J. 1953. Biometric, ecological and quantitative metabolic studies on the intertidal snails, *Littorina planaxis* and *L. scutulata*. Doctoral dissertation. Univ. of Calif. Los Angeles, Calif.
7. Fox, D. L. 1953. Animal Biochromes. Cambridge Univ. Press. Cambridge, England.
8. Fisher, L. R. & S. K. Kon. 1959. Vitamin A in the invertebrates. Biol. Rev. **34:** 1–36.
9. Riley, G. A. 1953. J. conseil, Conseil permanent intern. exploration mer. Letter to the Editor. **19:** 85–89.
10. Riley, G. A. 1944. The carbon metabolism and photosynthetic efficiency of the earth as a whole. Am. Scientist. **32:** 129–134.

(1078)

PIGMENTS AND ALGAL COMMENSALISM IN THE BLUE OCEANIC SIPHONOPHORE *VELELLA LATA*

Denis L. Fox and Francis T. Haxo
Scripps Institution of Oceanography, La Jolla, California, U.S.A.

The striking blue colour in the mantle and tentacles of *Velella lata*, the Pacific oceanic siphonophore, is due to the presence of a carotenoid, astaxanthin, conjugated with protein. Analogous instances of this condition are also prominent in crustaceans, wherein the astaxanthin–protein complexes confer green, purple, blue, grey or other colours upon carapaces, eggs and hypodermis. In all such instances, denaturation by heat, alcohol or other common means quickly destroys the natural colour of the complex (e.g. the blue in *Velella*) and unmasks the red of the liberated carotenoid. The very careful application of moderate heat for short periods, alternated with rapid re-cooling, demonstrates the reversibility of this dissociation between the protein and its coloured moiety by displaying blue through purple to reddish colours during the heating, and the reverse series of changes upon cooling.

A clear, blue, aqueous extract of fresh mantle tissue yielded a smooth, rounded absorption curve with a single broad maximum at 585–588mμ, while similar extracts of the tentacles exhibited a spectrum of like profile, showing a single maximum at about 610 mμ, thus suggesting possible differences in the character or proportion of protein involved in the complex. The carotenoid involved proved, through the identity of absorption spectra and through mixed chromatography, to be the same chemical individual, whether isolated from mantle or from tentacular tissue.

Unconjugated chromatographically separated *Velella* astaxanthin exhibited the characteristic single rounded maximum in the blue region, i.e. 488–490 mμ in pyridine, 472 mμ in light petroleum, and about 507 mμ in carbon disulphide. Its oxidized derivative, astacene, manifested its single rounded maximum at 495–496 mμ in pyridine, and 507–509 mμ in carbon disulphide. Again, spectrophotometric agreement and mixed chromatography demonstrated the identity between the astacene derived from *Velella* tissues and that recovered from the carapace of the crayfish *Panulirus interruptus*.

An obvious supply of astaxanthin for *Velella* (unless the pigments should be actually synthesized therein) is available in the many microcrustacean species and their eggs consumed by this colonial coelenterate in large numbers at the surface of the sea. According to Mr. Robert Bieri, the crustacean materials are primarily euphausiid eggs and copepods, although fish eggs are also taken, as well as decapod, amphipod and cladoceran materials and barnacle larvae.

Contributions from the Scripps Institution of Oceanography, New Series, 1227

Reproduced by Permission

The endodermal tissues of the digestive apparatus, as well as the medusa buds of the gonozoids, contain abundant minute yellow-brown algal cells, or zooxanthellae, which yield no astaxanthin, but copious chlorophyll *a*, conventional carotenes and several algal xanthophylls.

The living mantle tissue, examined through both dorsal and ventral surfaces and including the thin intermediary layer of zooxanthellae-laden endoderm, showed a rounded maximum with centre at 590 mμ, due to the astaxanthin–protein complex, and a minor but definite secondary peak at 675 mμ, arising from the presence of the algal chlorophyll.

It is attractive to contemplate some of the reciprocal benefits potentially derivable by the plant and the animal parties to the association. For example, the siphonophore colony affords the contained algae protection against grazing by filtering or particulate feeders, and perhaps also against the plant cells' sinking into darkness; moreover, the algae are stored in a site optimally favorable for their assimilation of the host's catabolic wastes, and perhaps also even certain soluble products of digestion. Again, the animal's blue "canopy" or window, while shading the algal cells against excessive sunlight at the ocean surface, has been shown to admit ample light for their active photosynthesis.

Furthermore, to resume our contemplative survey, it has been shown that in bright light the algae *in situ* evolve photosynthetic oxygen in excess of the respiratory needs of the association. Free excess gas, perhaps relatively high in oxygen, is normally present beneath the animal's mantle; the siphonophore, thus remaining afloat upon the ocean surface, occupies a region of adequate food supply, e.g. buoyant eggs, microcrustaceans feeding on detrital matter and other materials associated with the water–air interface, where extensive organic "slicks" often occur. This floating adaptation, aided by the entrapped gas, may not only effectively reduce the incidence of detection and attack by nectonic predators, but, augmented by the remarkable sail, should provide for the colony's transport, by prevailing winds, toward, or along with, surface concentrations of food materials. An obvious hazard in the sailing habit lies in the occasional wind-transport of *Velella* to shore, where it perishes by the thousands.